2014

ANNUAL PROGRESS REPORT

DOE Hydrogen and Fuel Cells Program

U.S. DEPARTMENT OF ENERGY

DOE/GO-102014-4504
November 2014

U.S. Department of Energy
1000 Independence Avenue, S.W.
Washington, D.C. 20585-0121

FY 2014
PROGRESS REPORT FOR THE DOE HYDROGEN AND FUEL CELLS PROGRAM

November 2014

DOE/GO-102014-4504

Approved by Sunita Satyapal, Director, Hydrogen and Fuel Cells Program

NOTICE

This report was prepared as an account of work sponsored by an agency of the United States government. Neither the United States government nor any agency thereof, nor any of their employees, makes any warranty, express or implied, or assumes any legal liability or responsibility for the accuracy, completeness, or usefulness of any information, apparatus, product, or process disclosed, or represents that its use would not infringe privately owned rights. Reference herein to any specific commercial product, process, or service by trade name, trademark, manufacturer, or otherwise does not necessarily constitute or imply its endorsement, recommendation, or favoring by the United States government or any agency thereof. The views and opinions of authors expressed herein do not necessarily state or reflect those of the United States government or any agency thereof.

Available electronically at http://www.osti.gov/bridge

Available for a processing fee to U.S. Department of Energy
and its contractors, in paper, from:

U.S. Department of Energy
Office of Scientific and Technical Information
P.O. Box 62
Oak Ridge, TN 37831-0062
Phone: (865) 576-8401
Fax: (865) 576-5728
E-mail: mailto:reports@adonis.osti.gov

Available for sale to the public, in paper, from:

U.S. Department of Commerce
National Technical Information Service
5285 Port Royal Road
Springfield, VA 22161
Phone: (800) 553-6847
Fax: (703) 605-6900
E-mail: orders@ntis.fedworld.gov
Online ordering: http://www.ntis.gov/ordering.htm

Printed on paper containing at least 50% wastepaper, including 20% postconsumer waste

Table of Contents

I. Introduction I-1

II. Hydrogen Production II-1

II.0 Hydrogen Production Program Overview II-3

II.A Hydrogen Production Analysis II-11

II.A.1 Strategic Analysis, Inc.: Hydrogen Pathways Analysis for Polymer Electrolyte Membrane (PEM) Electrolysis II-11

II.B Electrolysis II-17

II.B.1 National Renewable Energy Laboratory: Renewable Electrolysis Integrated Systems Development and Testing II-17

II.B.2 Proton OnSite: Economical Production of Hydrogen through Development of Novel, High-Efficiency Electrocatalysts for Alkaline Membrane Electrolysis II-21

II.B.3 Proton OnSite: Low-Noble-Metal-Content Catalysts/Electrodes for Hydrogen Production by Water Electrolysis II-24

II.B.4 Giner, Inc.: High-Performance, Long-Lifetime Catalysts for Proton Exchange Membrane Electrolysis II-28

II.C Solar Thermochemical II-33

II.C.1 University of Colorado: Solar-Thermal Redox-Based Water Splitting Cycles II-33

II.C.2 Sandia National Laboratories: Solar Hydrogen Production with a Metal Oxide-Based Thermochemical Cycle II-39

II.C.3 Savannah River National Laboratory: Electrolyzer Development for the HyS Thermochemical Cycle II-45

II.D Photoelectrochemical II-48

II.D.1 National Renewable Energy Laboratory: Semiconductor Materials for Photoelectrolysis II-48

II.D.2 Midwest Optoelectronics, LLC: Critical Research for Cost-Effective Photoelectrochemical Production of Hydrogen II-53

II.D.3 Lawrence Livermore National Laboratory: Characterization and Optimization of Photoelectrode Surfaces for Solar-to-Chemical Fuel Conversion II-58

II.E Biological II-63

II.E.1 University of California, Berkeley: Maximizing Light Utilization Efficiency and Hydrogen Production in Microalgal Cultures II-63

II.E.2 National Renewable Energy Laboratory: Biological Systems for Algal Hydrogen Photoproduction II-67

II.E.3 National Renewable Energy Laboratory: Fermentation and Electrohydrogenic Approaches to Hydrogen Production II-71

II.E.4 National Renewable Energy Laboratory: Probing O2-Tolerant CBS Hydrogenase for Hydrogen Production II-76

II.F Separations II-81

II.F.1 TDA Research: Bio-Fueled Solid Oxide Fuel Cells II-81

II.G Basic Energy Sciences II-85

II.G.1 University of Arizona: Semiconductor Nanorod/Metal(Metal Oxide) Hybrid Materials: Characterization of Frontier Orbital Energies and Charge Injection Processes Using Unique Combinations of Photoemission Spectroscopies and Waveguide Spectroelectrochemistries II-85

II.G.2 University of Rochester: Real-Time Atomistic Simulation of Light Harvesting and Charge Transport for Solar Hydrogen Production II-89

II.G.3 National Renewable Energy Laboratory: Oxidatively Stable Nanoporous Silicon Photocathodes for Photoelectrochemical Hydrogen Evolution II-92

II. Hydrogen Production (Continued)

II.G BES (Continued)

II.G.4 Argonne National Laboratory: Fundamental Design and Mechanisms for Solar Hydrogen Production in Natural and Artificial Photosynthetic Systems II-94

II.G.5 Arizona State: Electrochemical Characterization of the Oxygen-Tolerant Soluble Hydrogenase I from Pyrococcus furiosus II-97

II.G.6 University of Georgia: Hyperthermophilic Multiprotein Complexes and Pathways for Energy Conservation and Catalysis II-100

II.G.7 National Renewable Energy Laboratory: Photobiohybrid Solar Fuels II-103

II.G.8 Brookhaven National Laboratory: Heterogeneous Water Oxidation Catalysis With Molecular Catalysts II-106

II.G.9 Brookhaven National Laboratory: Proton-Coupled Electron Transfer in Artificial Photosynthesis II-108

II.G.10 Lawrence Berkeley National Laboratory: Joint Center for Artificial Photosynthesis: An Overview. II-111

II.G.11 Lawrence Berkeley National Laboratory: Joint Center for Artificial Photosynthesis: Corrosion Protection Schemes to Enable Durable Solar Water Splitting Devices II-115

II.G.12 Caltech: Joint Center for Artificial Photosynthesis: High Throughput Experimentation for Electrocatalyst and Photoabsorber Discovery II-119

II.G.13 University of Arizona: Center for Interface Science: Solar-Electric Materials (CISSEM). II-123

II.G.14 National Renewable Energy Laboratory: Photobiohybrid Solar Fuels – Nanoparticle-Hydrogenase Complexes II-125

II.G.15 Stanford University: Center on Nanostructuring for Efficient Energy Conversion (CNEEC) II-128

II.G.16 Arizona State: Artificial Hydrogenases: Utilization of Redox Non-Innocent Ligands in Iron Complexes for Hydrogen Production II-131

II.G.17 Caltech: Joint Center for Artificial Photosynthesis: Benchmarking Electrocatalysts for the Oxygen Evolution Reaction II-134

II.G.18 Caltech: Joint Center for Artificial Photosynthesis: Si Microwire-Based Solar Water Splitting Devices II-137

II.G.19 Northwestern University: Argonne-Northwestern Solar Energy Research (ANSER) Center II-141

II.G.20 Lawrence Berkeley National Laboratory: Joint Center for Artificial Photosynthesis: Modeling and Simulation Team II-144

III Hydrogen Delivery III-1

III.0 Hydrogen Delivery Sub-Program Overview III-3

III.1 Argonne National Laboratory: Hydrogen Delivery Infrastructure Analysis III-11

III.2 Mohawk Innovative Technologies, Inc.: Oil-Free Centrifugal Hydrogen Compression Technology Demonstration III-16

III.3 Hexagon Lincoln: Development of High-Pressure Hydrogen Storage Tank for Storage and Gaseous Truck Delivery III-21

III.4 Savannah River National Laboratory: Fiber Reinforced Composite Pipeline. III-24

III.5 Sandia National Laboratories: Hydrogen Embrittlement of Structural Steels. III-31

III.6 FuelCell Energy, Inc.: Electrochemical Hydrogen Compressor III-36

III.7 Oak Ridge National Laboratory: Vessel Design and Fabrication Technology for Stationary High-Pressure Hydrogen Storage III-39

III.8 Lawrence Livermore National Laboratory: Preliminary Testing of LLNL/Linde 875-bar Liquid Hydrogen Pump III-45

III.9 Concepts NREC: Development of a Centrifugal Hydrogen Pipeline Gas Compressor III-49

III.10 Pacific Northwest National Laboratory: Investigation of H2 Diaphragm Compressors to Enable Low-Cost Long-Life Operation III-54

III.11 National Renewable Energy Laboratory: 700-Bar Hydrogen Dispenser Hose Reliability Improvement III-58

IV Hydrogen Storage IV-1
IV.0 Hydrogen Storage Sub-Program Overview IV-3
IV.A Testing and Analysis IV-11
IV.A.1 Argonne National Laboratory: System Analysis of Physical and Materials-Based Hydrogen Storage Options IV-11
IV.A.2 Strategic Analysis, Inc.: Hydrogen Storage Cost Analysis IV-17
IV.B Engineering – HSECoE IV-22
IV.B.1 Savannah River National Laboratory: Hydrogen Storage Engineering Center of Excellence IV-22
IV.B.2 Pacific Northwest National Laboratory: Systems Engineering of Chemical Hydrogen Storage, Pressure Vessel, and Balance of Plant for Onboard Hydrogen Storage IV-30
IV.B.3 United Technologies Research Center: Advancement of Systems Designs and Key Engineering Technologies for Materials-Based Hydrogen Storage IV-36
IV.B.4 Los Alamos National Laboratory: Chemical Hydride Rate Modeling, Validation, and System Demonstration IV-43
IV.B.5 National Renewable Energy Laboratory: System Design, Analysis, Modeling, and Media Engineering Properties for Hydrogen Energy Storage IV-47
IV.B.6 General Motors Company: Thermal Management of Onboard Cryogenic Hydrogen Storage Systems IV-52
IV.B.7 Ford Motor Company: Ford/BASF-SE/UM Activities in Support of the Hydrogen Storage Engineering Center of Excellence IV-56
IV.B.8 Oregon State University: Microscale Enhancement of Heat and Mass Transfer for Hydrogen Energy Storage IV-61
IV.B.9 Hexagon Lincoln: Development of Improved Composite Pressure Vessels for Hydrogen Storage . . IV-65
IV.C Materials – Sorption IV-68
IV.C.1 National Renewable Energy Laboratory: Hydrogen Sorbent Measurement Qualification and Characterization IV-68
IV.C.2 Lawrence Berkeley National Laboratory: Hydrogen Storage in Metal-Organic Frameworks IV-73
IV.C.3 Pennsylvania State University: Hydrogen Trapping through Designer Hydrogen Spillover Molecules with Reversible Temperature and Pressure-Induced Switching IV-79
IV.C.4 University of Missouri: Multiply Surface-Functionalized Nanoporous Carbon for Vehicular Hydrogen Storage IV-86
IV.D Materials – Metal Hydrides IV-92
IV.D.1 Northwestern University: Design of Novel Multi-Component Metal Hydride-Based Mixtures for Hydrogen Storage IV-92
IV.D.2 Delaware State University: Hydrogen Storage Materials for Fuel Cell-Powered Vehicles IV-95
IV.D.3 National Institute of Standards and Technology: Neutron Characterization in Support of the DOE Hydrogen Storage Program IV-100
IV.E Materials – Chemical IV-105
IV.E.1 Boston College: Novel Carbon(C)-Boron(B)-Nitrogen(N)-Containing H2 Storage Materials IV-105
IV.E.2 Brookhaven National Laboratory: Aluminum Hydride: the Organo-Metallic Approach IV-111
IV.E.3 Savannah River National Laboratory: Electrochemical Reversible Formation of Alane IV-114
IV.F Advanced Tanks IV-118
IV.F.1 Oak Ridge National Laboratory: Melt Processable PAN Precursor for High-Strength, Low-Cost Carbon Fibers (Phase II) IV-118
IV.F.2 Oak Ridge National Laboratory: Development of Low-Cost, High-Strength Commercial Textile Precursor (PAN-MA) IV-124
IV.F.3 Pacific Northwest National Laboratory: Synergistically Enhanced Materials and Design Parameters for Reducing the Cost of Hydrogen Storage Tanks IV-131
IV.F.4 Lawrence Livermore National Laboratory: Thermomechanical Cycling of Thin-Liner High-Fiber-Fraction Cryogenic Pressure Vessels Rapidly Refueled a by LH2 pump to 700 bar . . . IV-136

IV Hydrogen Storage (Continued)

IV.F Advanced Tanks (Continued)

IV.F.5 Savannah River National Laboratory: Load-Sharing Polymeric Liner for Hydrogen Storage Composite Tanks IV-140

V Fuel Cells V-1

V.0 Fuel Cells Sub-Program Overview V-3

V.A Catalysts V-9

V.A.1 3M Company: Durable Catalysts for Fuel Cell Protection during Transient Conditions V-9

V.A.2 National Renewable Energy Laboratory: Extended, Continuous Pt Nanostructures in Thick, Dispersed Electrodes V-15

V.A.3 Argonne National Laboratory: Nanosegregated Cathode Catalysts with Ultra-Low Platinum Loading V-19

V.A.4 Brookhaven National Laboratory: Contiguous Platinum Monolayer Oxygen Reduction Electrocatalysts on High-Stability Low-Cost Supports V-25

V.A.5 Los Alamos National Laboratory: The Science and Engineering of Durable Ultra-Low PGM Catalysts V-30

V.A.6 National Renewable Energy Laboratory: Tungsten Oxide and Heteropoly Acid-Based System for Ultra-High Activity and Stability of Pt Catalysts in Proton Exchange Membrane Fuel Cell Cathodes V-36

V.A.7 Illinois Institute of Technology: Synthesis and Characterization of Mixed-Conducting Corrosion-Resistant Oxide Supports V-46

V.A.8 Northeastern University: Development of Novel Non-PGM Electrocatalysts for Proton Exchange Membrane Fuel Cell Applications V-50

V.A.9 General Motors Company: High-Activity Dealloyed Catalysts V-56

V.A.10 University of South Carolina: Development of Ultra-Low Platinum Alloy Cathode Catalysts for PEM Fuel Cells V-62

V.A.11 Los Alamos National Laboratory: Non-Precious Metal Fuel Cell Cathodes: Catalyst Development and Electrode Structure Design V-69

V.A.12 Argonne National Laboratory: Non-PGM Cathode Catalysts using ZIF-Based Precursors with Nanonetwork Architecture V-74

V.B Membranes V-79

V.B.1 Giner, Inc.: Dimensionally Stable High Performance Membrane V-79

V.C Membranes/Electrolytes V-83

V.C.1 3M Company: New Fuel Cell Membranes with Improved Durability and Performance V-83

V.C.2 Colorado School of Mines: Advanced Hybrid Membranes for Next Generation PEMFC Automotive Applications V-87

V.C.3 Los Alamos National Laboratory: Resonance-Stabilized Anion Exchange Polymer Electrolytes V-91

V.D MEA Integration V-95

V.D.1 3M Company: High-Performance, Durable, Low-Cost Membrane Electrode Assemblies for Transportation Applications V-95

V.D.2 Argonne National Laboratory: Rationally Designed Catalyst Layers for PEMFC Performance Optimization V-100

V.E Degradation Studies V-105

V.E.1 Los Alamos National Laboratory: Durability Improvements through Degradation Mechanism Studies V-105

V.E.2 Los Alamos National Laboratory: Accelerated Testing Validation V-111

V.E.3 National Renewable Energy Laboratory: Fuel Cell Technology Status—Cost and Price Status V-118

V.E.4 Ballard Power Systems: Open-Source PEMFC-Performance and Durability Model Consideration of Membrane Properties on Cathode Degradation V-122

V. Fuel Cells (Continued)

V.F Impurities V-128
V.F.1 National Renewable Energy Laboratory: Effect of System Contaminants on PEMFC Performance and Durability V-128
V.F.2 Hawaii Natural Energy Institute: The Effect of Airborne Contaminants on Fuel Cell Performance and Durability V-133

V.G Transport Studies V-140
V.G.1 Lawrence Berkeley National Laboratory: Fuel Cell Fundamentals at Low and Subzero Temperatures V-140
V.G.2 Giner, Inc.: Transport in Proton Exchange Membrane Fuel Cells V-146
V.G.3 General Motors Company: Investigation of Micro- and Macro-Scale Transport Processes for Improved Fuel Cell Performance V-151

V.H Balance of Plant V-158
V.H.1 Tetramer Technologies, LLC: New High-Performance Water Vapor Membranes To Improve Fuel Cell Balance-of-Plant Efficiency and Lower Costs (SBIR Phase II) V-158
V.H.2 Eaton Corporation: Roots Air Management System with Integrated Expander V-162

V.I Analysis/Characterization V-167
V.I.1 Argonne National Laboratory: Performance of Advanced Automotive Fuel Cell Systems with Heat Rejection Constraints V-167
V.I.2 Strategic Analysis, Inc.: Fuel Cell Transportation Cost Analysis V-173
V.I.3 Oak Ridge National Laboratory: Characterization of Fuel Cell Materials V-178
V.I.4 National Institute of Standards and Technology: Neutron Imaging Study of the Water Transport in Operating Fuel Cells V-184
V.I.5 National Renewable Energy Laboratory: Enlarging the Potential Market for Stationary Fuel Cells through System Design Optimization V-190
V.I.6 Battelle: Stationary and Emerging Market Fuel Cell System Cost Analysis - Material Handling Equipment V-193
V.I.7 Lawrence Berkeley National Laboratory: A Total Cost of Ownership Model for PEM Fuel Cells in Combined Heat and Power and Backup Power Applications V-196

V.J Portable Power V-201
V.J.1 Los Alamos National Laboratory: Advanced Materials and Concepts for Portable Power Fuel Cells V-201

V.K Stationary Power V-208
V.K.1 InnovaTek, Inc.: Power Generation from an Integrated Biomass Reformer and Solid Oxide Fuel Cell (SBIR Phase III Xlerator Program) V-208

V.L Alkaline Fuel Cells V-211
V.L.1 National Renewable Energy Laboratory: Advanced Ionomers and MEAs for Alkaline Membrane Fuel Cells V-211

V.M Testing and Technical Assessment V-215
V.M.1 National Renewable Energy Laboratory: Best Practices and Benchmark Activities for ORR Measurements by the Rotating Disk Electrode Technique V-215

VI Manufacturing R&D VI-1
VI.0 Manufacturing R&D Sub-Program Overview VI-3
VI.1 National Renewable Energy Laboratory: Fuel Cell Membrane Electrode Assembly Manufacturing R&D VI-7
VI.2 W. L. Gore & Associates, Inc.: Manufacturing of Low-Cost, Durable Membrane Electrode Assemblies Engineered for Rapid Conditioning VI-11
VI.3 Quantum Fuel Systems Technologies Worldwide, Inc.: Development of Advanced Manufacturing Technologies for Low-Cost Hydrogen Storage Vessels VI-15

VII Technology Validation VII-1
VII.0 Technology Validation Sub-Program Overview VII-3
VII.1 National Renewable Energy Laboratory: Technology Validation: Fuel Cell Bus Evaluations VII-9
VII.2 National Renewable Energy Laboratory: Stationary Fuel Cell Evaluation VII-14
VII.3 H2Pump LLC: Hydrogen Recycling System Evaluation and Data Collection VII-18
VII.4 National Renewable Energy Laboratory: Hydrogen Component Validation VII-22
VII.5 Proton OnSite: Validation of an Advanced High-Pressure PEM Electrolyzer and Composite Hydrogen Storage, with Data Reporting, for SunHydro Stations VII-26
VII.6 National Renewable Energy Laboratory: Forklift and Backup Power Data Collection and Analysis VII-31
VII.7 National Renewable Energy Laboratory: Fuel Cell Electric Vehicle Evaluation VII-37
VII.8 National Renewable Energy Laboratory: Next Generation Hydrogen Infrastructure Evaluation . . VII-41
VII.9 California Air Resources Board: Data Collection and Validation of Newport Beach Hydrogen Station Performance VII-46
VII.10 California State University, Los Angeles: California State University Los Angeles Hydrogen Refueling Facility Performance Evaluation and Optimization VII-49
VII.11 Gas Technology Institute: Performance Evaluation of Delivered Hydrogen Fueling Stations VII-52
VII.12 Sandia National Laboratories: Hydrogen Fueling Infrastructure Research and Station Technology VII-57
VII.13 Acumentrics: Demonstration of SOFC Generator Fueled by Propane to Provide Electrical Power to Real World Applications VII-59
VII.14 Plug Power Inc.: Accelerating Acceptance of Fuel Cell Backup Power Systems VII-63
VII.15 California Fuel Cell Partnership : H2-FCEV Commercialization - Facilitating Collaboration, Obtaining Real World Expertise, and Developing New Analysis Tools VII-66

VIII Safety, Codes & Standards VIII-1
VIII.0 Safety, Codes & Standards Sub-Program Overview VIII-3
VIII.1 National Renewable Energy Laboratory: Fuel Cell Technologies National Codes and Standards Development and Outreach VIII-9
VIII.2 National Renewable Energy Laboratory: Component Standard Research and Development. VIII-13
VIII.3 Los Alamos National Laboratory: Hydrogen Safety, Codes and Standards: Sensors VIII-16
VIII.4 Sandia National Laboratories: R&D for Safety, Codes and Standards: Materials and Components Compatibility. VIII-23
VIII.5 Los Alamos National Laboratory: Hydrogen Fuel Quality VIII-28
VIII.6 Sandia National Laboratories: R&D for Safety Codes and Standards: Hydrogen Release Behavior and Risk Assessment VIII-34
VIII.7 Pacific Northwest National Laboratory: Hydrogen Emergency Response Training for First Responders VIII-40
VIII.8 Pacific Northwest National Laboratory: Hydrogen Safety Panel and Hydrogen Safety Knowledge Tools VIII-43
VIII.9 National Renewable Energy Laboratory: NREL Hydrogen Sensor Testing Laboratory VIII-49
VIII.10 Lawrence Livermore National Laboratory: Hands-on Hydrogen Safety Training VIII-54

IX Market Transformation IX-1
IX.0 Market Transformation Sub-Program Overview IX-3
IX.1 Pacific Northwest National Laboratory: Fuel Cell Combined Heat and Power Commercial Demonstration IX-7
IX.2 Advanced Technology International: Landfill Gas-to-Hydrogen IX-12
IX.3 Hawaii Natural Energy Institute: Hydrogen Energy Systems as a Grid Management Tool IX-15
IX.4 Plug Power Inc.: Ground Support Equipment Demonstration IX-20
IX.5 Sandia National Laboratories: Maritime Fuel Cell Generator Project. IX-23

IX Market Transformation (Continued)

IX.6 Pacific Northwest National Laboratory: Fuel Cell-Based Auxiliary Power Unit for Refrigerated Trucks IX-26

X Systems Analysis X-1

X.0 Systems Analysis Sub-Program Overview X-3

X.1 Oak Ridge National Laboratory: Analysis of Optimal Onboard Storage Pressure for Hydrogen Fuel Cell Vehicles X-13

X.2 Argonne National Laboratory: Employment Impacts of Infrastructure Development for Hydrogen and Fuel Cell Technologies X-19

X.3 National Renewable Energy Laboratory: Pathway Analysis: Projected Cost, Life-Cycle Energy Use and Emissions of Future Hydrogen Technologies X-22

X.4 Argonne National Laboratory: Life-Cycle Analysis of Water Use for Hydrogen Production Pathways X-27

X.5 Argonne National Laboratory: Impact of Fuel Cell System Peak Efficiency on Fuel Consumption and Cost X-30

X.6 Argonne National Laboratory: Analysis of Incremental Fueling Pressure Cost X-36

X.7 Oak Ridge National Laboratory: Hydrogen Station Economics and Business (HySEB)--Preliminary Results X-40

X.8 University of California, Irvine: Tri-Generation Fuel Cell Technologies for Location-Specific Applications X-44

X.9 National Renewable Energy Laboratory: Electricity Market Valuation for Hydrogen Technologies X-46

XI SBIR . . . . .

XI.0 Small Business Innovation Research (SBIR) Fuel Cell Technologies Office New Projects Awarded in FY 2014 . . . . . XI-3

Phase I Projects XI-4

XI.1 Ionomer Dispersion Impact on Advanced Fuel Cell and Electrolyzer Performance and Durability XI-4

XI.2 Demonstration of a Prototype Fuel Cell-Battery Electric Hybrid Truck for Waste Transportation . . . XI-4

XI.3 Demonstration of a Prototype Fuel Cell Electric Truck for Waste Transportation XI-4

XI.4 Flexible Barrier Coatings for Harsh Environments XI-4

XI.5 New Approaches to Improved PEM Electrolyzer Ion Exchange Membranes XI-5

XI.6 High-Performance Proton Exchange Membranes for Electrolysis Cells XI-5

XI.7 High-Temperature High-Efficiency PEM Electrolysis XI-5

Phase II Projects XI-6

XI.8 Optimizing the Cost and Performance of Composite Cylinders for H2 Storage using a Graded Construction XI-6

XI.9 Novel Structured Metal Bipolar Plates for Low-Cost Manufacturing XI-6

XI.10 Cryogenically Flexible, Low Permeability Thoraeus Rubber Hydrogen Dispenser Hose XI-7

XII Acronyms, Abbreviations and Definitions XII-1

XIII Primary Contacts Index XIII-1

XIV Hydrogen and Fuel Cells Program Contacts XIV-1

XV Project Listings by State XV-1

XVI Project Listings by Organization XVI-1

I. INTRODUCTION

I.0 Introduction

The U.S. Department of Energy's Hydrogen and Fuel Cells Program (the Program) conducts comprehensive efforts across a range of technical and non-technical areas to enable the widespread commercialization of hydrogen and fuel cell technologies in diverse sectors of the economy. The Program is coordinated across the U.S. Department of Energy (DOE or the Department), incorporating activities in the offices of Energy Efficiency and Renewable Energy (EERE) led through the Fuel Cell Technologies Office (FCTO), Science (SC), Nuclear Energy (NE), and Fossil Energy (FE). The Program's efforts are aligned with the Administration's "all-of-the-above" approach to energy and the President's Climate Action Plan and will spark the type of innovation that drives economic growth and creates American jobs, while moving our economy toward cleaner, more efficient forms of energy that will cut our reliance on foreign oil.

With emphasis on applications that will most effectively strengthen our nation's energy security and improve our efforts to cut carbon pollution, the Program engages in research, development, and demonstration (RD&D) of critical improvements in hydrogen and fuel cell technologies, as well as diverse activities to overcome economic and institutional obstacles to commercialization. The Program addresses the full range of challenges facing the development and deployment of the technologies by integrating basic and applied research, technology development and demonstration, and other supporting activities.

In Fiscal Year (FY) 2014, Congress appropriated approximately $120 million for the DOE Hydrogen and Fuel Cells Program. The Program is organized into distinct areas of RD&D, as well as other activities to address non-technical challenges. More detailed discussions of Program activities and plans can be found in the Hydrogen and Fuel Cells Program Plan, as well as in the plans of the program offices—FCTO's Multi-Year RD&D Plan; FE's Hydrogen from Coal RD&D Plan; and SC's Basic Research Needs for the Hydrogen Economy. All of these documents are available at www.hydrogen.energy.gov/roadmaps_vision.html.

In the past year, the Program made substantial progress toward its goals and objectives. In addition to summarizing examples of key technical accomplishments, this report highlights major programmatic accomplishments such as the launch of a new project called Hydrogen Fueling Infrastructure Research and Station Technology (H2FIRST) that leverages the capabilities of the national laboratories in direct support of H2USA, a public private partnership formed in 2013 to overcome the barriers of hydrogen infrastructure.

PROGRESS AND ACCOMPLISHMENTS BY PROGRAM

This report documents more than 1,000 pages of accomplishments achieved by DOE-funded projects in the last year. The following summaries include only a few examples. More details can be found in the individual sub-program introductions, subsequent project reports, and in the corresponding 2014 Annual Merit Review and Peer Evaluation Report, which can be found at http://www.hydrogen.energy.gov/annual_review14_report.html.

Fuel Cells

The Fuel Cell sub-program's goal is to advance fuel cell technologies primarily for transportation, as well as early markets such as stationary and portable applications, to make them competitive in the marketplace in terms of cost, durability, and performance, while ensuring maximum environmental and energy-security benefits. Cost reductions and improvements in durability continue to be the key challenges facing fuel cell technologies.

The sub-program tracks cost of automotive fuel cells on an annual basis through system design and cost analysis projects at Argonne National Laboratory (ANL) and Strategic Analysis, Inc. The 2014 cost status for 80-kW automotive fuel cell systems was determined to be $55 kW. The cost model used the same core technology as used in 2013, resulting in a final cost that was within one dollar of the 2013 cost. Recent technological advancements are planned for inclusion in the 2015 cost model.

A major achievement in 2014 was synthesis of platinum nickel alloy nanoframe catalysts that showed a more than 30 times increase in activity compared to conventional platinum on carbon catalysts. Scientists initially created Pt-Ni crystalline polyhedra particles that were left under ambient conditions in a solvent exposed to air for two weeks. Surprising changes in the structure and composition were noted—the particles had spontaneously dealloyed into a more Pt-rich alloy and transformed into hollow nanoframe structures. Recognizing the potential relevance of these new structures for catalysis, the researchers teamed up with electrochemical experts. They optimized the synthesis process,

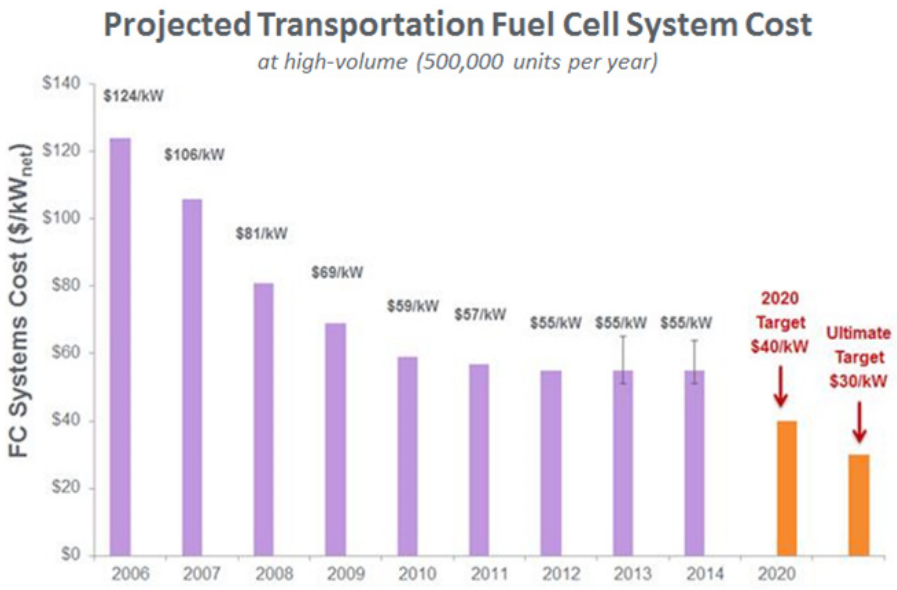

FIGURE 1. Projected transportation fuel cell system cost.

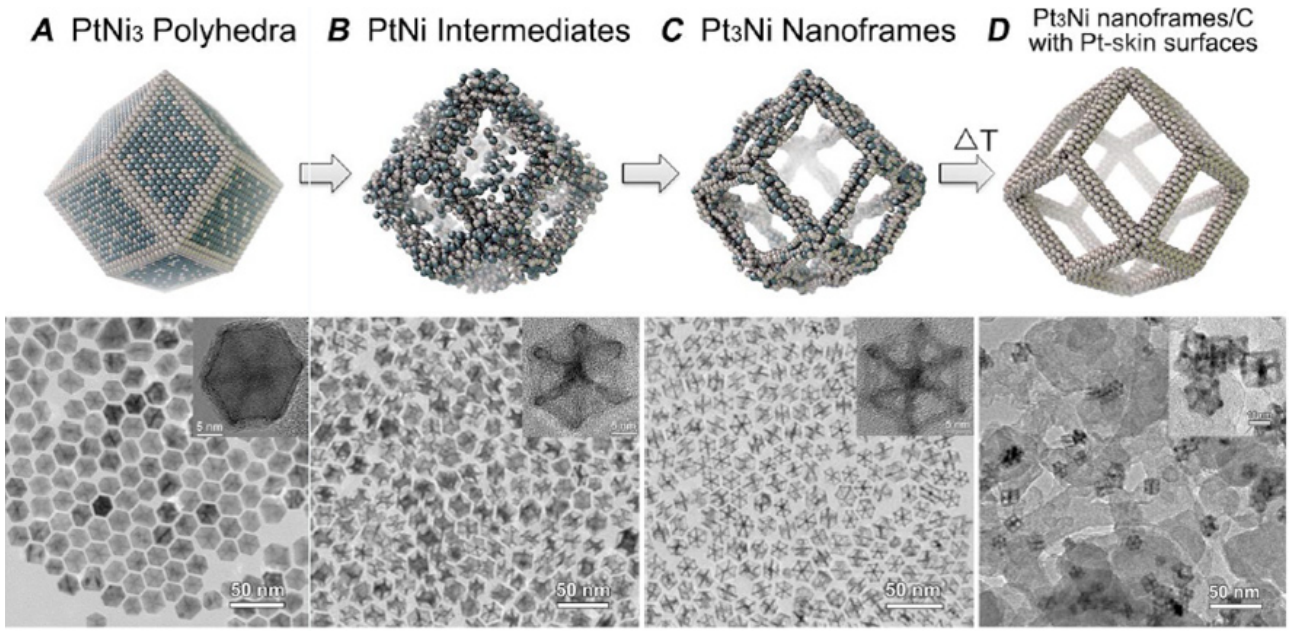

FIGURE 2. A new catalyst synthesized in 2014, which consists of a platinum-nickel alloy nanoframe covered by a thin platinum skin, has a performance more than 30 times higher than conventional platinum on carbon catalysts.

resulting in a catalyst that can be prepared in only a few hours with an activity that outstrips all previous fuel cell catalysts in ex situ testing.

Also in 2014, advances in catalyst synthesis and electrode optimization allowed PtCo and PtNi dealloyed catalysts, which have already met DOE targets for mass activity and durability of mass activity, to achieve good durability of high-current performance for the first time. These catalysts achieved the same H_2/air fuel cell performance as a 0.4 mg_{Pt}/cm^2 electrode, but with only one-fourth the platinum-group metal (PGM) loading. The performance improvements were confirmed in a full-active-area automotive stack. Up to 60,000 cycles between 0.6 and 0.925 V were performed with only 20 mV loss at 1.5 A/cm^2.

Protocols and best practices for rotating disk electrode (RDE) catalyst testing also were prepared. Initial screening of fuel cell catalyst activity is typically performed ex situ using RDE. These experiments are performed with little standardization between laboratories, leading to large discrepancies in reported activity values for the same catalysts and undermining the validity and usefulness of RDE data. Improvements in technique that allowed for higher and more reproducible activity have been reported recently, but have not yet been widely adopted. Therefore, FCTO issued a request for information on RDE best practices, discussed the issue at meetings of the catalysis and durability working groups, and supported a collaborative effort between researchers at ANL and the National Renewable Energy Laboratory (NREL) to use the resulting input to develop protocols and best practices for RDE testing. This effort established a standard protocol and test methodology for measurement of electrochemical area (ECA), oxygen reduction reaction (ORR) activity, and durability, and evaluated three electrocatalysts using identical protocols and electrode preparation in three laboratories. Comparison of the results verified the reproducibility of measured ECA, ORR activity, durability between the labs, demonstrating the validity of the newly issued protocols.

Improvements in membrane electrode assemblies (MEAs) containing PtNi nano-structured thin film catalysts have enabled performance improvement at high current densities, resulting in catalyst specific power levels at 0.69 V as high as 6.3 kW/g_{PGM} at 150 kPa_{abs}, meeting the 2014 milestone and on track to meet the 2020 target of 8.0 kW/g_{PGM}. When compared to catalyst specific power measured at 0.69 V in previous years, this year's results mark a 25% and a 6% improvement since 2012 and 2013, respectively. During voltage cycling accelerated stress tests, these catalysts lose 66% of their initial activity over the course of 30,000 cycles, falling short of the targeted 40% degradation level. MEAs with earlier generation catalysts met the durability target, but fell short of the catalyst specific power target. Further R&D work is under way to meet both targets with the same MEA.

Hydrogen Production

In FY 2014, the Hydrogen Production sub-program continued to focus on developing technologies to enable the long-term viability of hydrogen as an energy carrier for a range of applications with a focus on hydrogen from low-carbon and renewable sources. Progress continued in several key areas, including electrolysis, photoelectrochemical (PEC), biological, and solar-thermochemical hydrogen production.

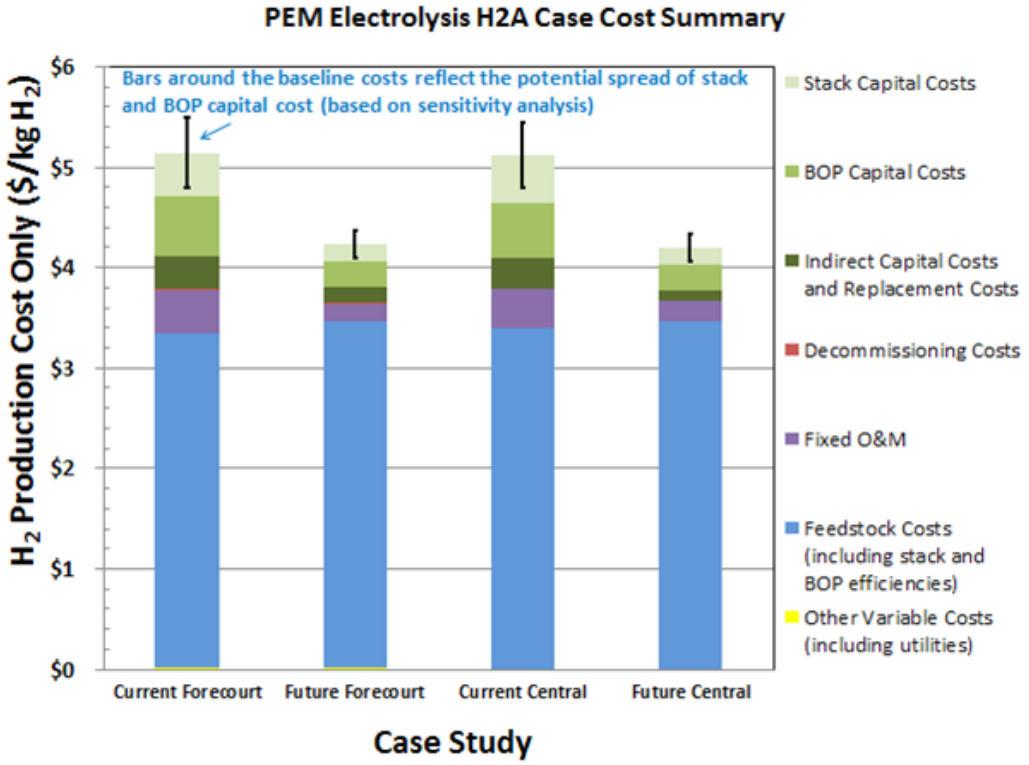

Figure 3. PEM electrolysis hydrogen production cost contributions (2007$/kg) for four case studies, showing of projected high volume untaxed costs ranging from ~$4 to $5.80/kg, broken down in terms of the major cost contributing factors.

In FY 2014, the major emphasis of the electrolysis activities were cost reduction and efficiency improvement through leveraging fuel cell catalyst development. Building off of work done by the Advanced Research Projects Agency – Energy (ARPA-E), a lead-ruthenium pyrochlore alkaline electrolysis membrane catalyst was synthesized and shown to have a mass activity 2,000 times greater than the nickel-cobalt baseline. In addition, an improved drying technique was developed with the potential to reduce drying losses in electrolyzers to less than 3.5% (compared with 11-8% in commercial systems) while operating on a variable (wind or solar) stack power profile. Testing is in progress to verify that the new drying technique meets SAE International J2719 specifications for water content (<5 ppm).

In the area of PEC hydrogen production, semiconductor tandem devices were shown to have more than 300 hours of stability at ~15 mA/cm^2 in III-V, showing a significant improvement over the previous year's 115 hours at 10 mA/cm^2. This result represents an important step toward demonstration of stabilized solar-to-hydrogen conversion efficiencies >20% using PEC devices.

In the area of biological hydrogen production, a larger, more scalable microbial reverse-electrodialysis cell design demonstrated a 0.9 L/L-reactor/day hydrogen production rate, a 12.5% increase over the 2013 demonstrated rate, using a salinity gradient instead of grid electricity.

Efforts in solar-thermochemical hydrogen characterized the performance of water splitting by novel, non-volatile metal-oxide based reaction materials and developed new reactor concepts to optimize efficiency of the reaction cycles. A thermodynamic model was developed for novel perovskite reaction materials that predicts the optimal operating temperature, O_2 pressure, and heat recovery effectiveness required for a solar to hydrogen conversion efficiency >20%; and derived performance criteria and thermodynamic properties for an "ideal" non-stoichiometric oxide reaction material were also developed.

The H2A v3 Production Model was applied to the PEM Electrolysis production pathway to analyze hydrogen costs ($/kg H2) and cost sensitivities. The case studies calculated a levelized cost of hydrogen production ranging from $4-5/kg for both distributed and central electrolyis; and identified the primary cost drivers as: (1) electricity cost; (2) electrolyzer electrical efficiency; and (3) electrolyzer capital cost.[1]

In June 2014, FCTO announced almost $13 million for six new research and development projects to address critical challenges and barriers for hydrogen production technology development, and specifically the long-term goal of hydrogen production at <$2/kg hydrogen. Selected projects are located in Connecticut, Washington, Colorado, Hawaii, and California.[2]

Hydrogen Delivery

The goal of the Hydrogen Delivery sub-program is to reduce the costs associated with delivering hydrogen to a point at which its use as an energy carrier in fuel cell applications is competitive with alternative transportation and power generation technologies. In FY 2014, the Hydrogen Delivery sub-program saw significant progress in RD&D activities. For example, a fueling strategy to improve station capacities during peak hours was developed. This strategy involves the use of a cascade of tubes in the tube trailers, wherein hydrogen gas is consolidated into one tube during peak fueling times. The high-pressure tube is then used directly for vehicle fueling while the compressor is used to either pressurize the gas in the other tubes or replenish buffer storage. This technique reduces on-site compression requirements, enabling a 10 kg/hr compressor to serve a 450 kg/day station, three times the capacity of 150 kg/day it could otherwise serve. This resulted in a 14% cost reduction for tube trailer delivery from $3.30/gasoline gallon equivalent (gge) to $2.85/gge delivered and dispensed for 700-bar refueling.

Other highlights include the Second International Workshop on Hydrogen Infrastructure and Transportation. This workshop, organized by Germany's National Organization of Hydrogen and Fuel Cell Technologies (NOW), Japan's National Energy and Industrial Technology Development Organization (NEDO), and DOE was held in June of 2014 and hosted by Toyota at the Toyota Motor Sales Corporate Accessory Center in Torrance, California. This workshop included members of industry and government from Japan, Germany, the European Union, Scandinavia, and the United States. Participants identified the major challenges and RD&D needs of hydrogen fueling protocols, metering, hydrogen fuel quality, and forecourt hardware. Additional detail will be available in the workshop proceedings when they are published later in calendar year 2014.

In June 2014, FCTO announced more than $7 million for five new awards, three selected from the FY 2014 Hydrogen Delivery Funding Opportunity Announcement (FOA) and two from Small Business Innovation Research

[1] DOE Hydrogen and Fuel Cells Program Record #14004 Hydrogen Cost from PEM Electrolysis is available at http://hydrogen.energy.gov/pdfs/14004_h2_production_cost_pem_electrolysis.pdf

[2] http://energy.gov/eere/articles/energy-department-invests-20-million-advance-hydrogen-production-and-delivery

(SBIR), for projects on compression, storage, and dispensing technologies. Selected projects are located in Texas, Massachusetts, Tennessee, and Virginia.[3]

Hydrogen Storage

In FY 2014, the Hydrogen Storage sub-program continued its focus on development of lower cost precursors for low-cost, high-strength carbon fibers to lower the cost of high-pressure compressed hydrogen systems, system engineering for transportation applications and advanced material R &D efforts, including for metal hydrides, chemical hydrogen storage materials, and hydrogen sorbents.

The Hydrogen Storage sub-program continued carrying out technoeconomic assessments of hydrogen storage technologies. System models were developed and top-down analyses was used to determine thermodynamic properties of sorbent materials needed to meet onboard system and offboard well-to-engine efficiency targets.

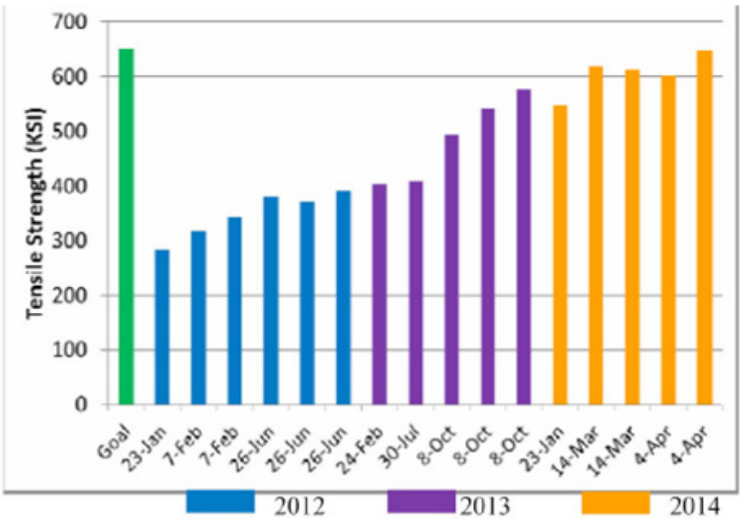

FIGURE 4. Tensile strength as a function of time for the F2350 precursor. (ORNL)

In the area of high pressure storage, the sub-program continued to reduce the cost of compressed hydrogen gas storage tanks. Progress included an increase of tensile strength from 405 KSI to 649 KSI, and tensile modulus from 33 MSI to 38 MSI for carbon fibers produced from polyacrylonitrile with methyl acrylate (PAN/MA) precursor fibers manufactured on high-volume, textile lines. FY 2014 analysis also projected a 52% mass reduction and 30% cost reduction in compressed hydrogen storage systems with 5.6 kg hydrogen usable capacity, at 500 bar and ~200 K, operating conditions, compared to baseline 700-bar ambient systems.

Of particular note, the FCTO-supported efforts delivered over 9 kg of MOF-5 to Hydrogen Storage Engineering Center of Excellence (HSECoE) partners for Phase III testing, with scaled-up batch material achieving performance within 10% of lab-scale batch material, and demonstrated 20x improvement in MOF-5 thermal conductivity using an enhanced natural graphite layering approach compared to random loading. Finally, the Hydrogen Storage sub-program established the HSECoE model website page (http://hsecoe.org/models.html) and posted the metal hydride (MH) acceptability envelope, MH finite element model, hydrogen tank mass and cost estimator, and hydrogen vehicle simulation framework models for public availability.

Manufacturing R&D

The Manufacturing R&D sub-program supports activities needed to reduce the cost of manufacturing hydrogen and fuel cell systems and components. FY 2014 saw a number of advancements in the manufacturing of fuel cells and hydrogen storage systems, including the assembly of infrared/direct current equipment on an industrial electrode coating line. Data was collected on three coating runs and defects were successfully detected at speed at the drying oven exit.

FCTO spearheaded a cross-cutting workshop, along with other offices within EERE, on quality control/metrology to leverage diagnostic capabilities and identify synergies and opportunities across other technologies. The purpose of the workshop was to convene government, industry, and other stakeholders to discuss the current status of quality control and metrology in manufacturing processes relevant to the EERE offices; note gaps in which current techniques are inadequate or missing; discuss similarities in materials inspection and metrology needs across technologies; and identify opportunities for collaboration across EERE offices to address shared challenges. Additional participating offices included Solar Energy, Vehicle, and Building Technologies and the Advanced Manufacturing Office and the Proceedings are available online.[4]

[3] http://energy.gov/eere/articles/energy-department-invests-20-million-advance-hydrogen-production-and-delivery
[4] http://energy.gov/eere/fuelcells/eere-quality-control-workshop

In May 2014 FCTO released a FOA for up to $2 million focused on *Clean Energy Supply Chain and Manufacturing Competitiveness Analysis for Hydrogen and Fuel Cell Technologies*. This funding will support projects that focus on scaling up the production of today's hydrogen and fuel cell components and systems. The topics included outreach to develop strategies and new approaches to facilitate expansion of the domestic supply chain of hydrogen and fuel cell related components in the U.S., and global manufacturing competitive analysis for hydrogen and fuel cell-related technologies.[5]

Basic Research

The Basic Energy Sciences program in the DOE Office of Science supports fundamental scientific research addressing critical challenges related to hydrogen storage, hydrogen production, and fuel cells. These basic research efforts complement the applied R&D projects supported by the other offices in the Program. Progress in any one area of basic science is likely to spill over to other areas and bring advances on more than one front.

The subjects of basic research most relevant to the Program's key technologies are:

- Hydrogen Storage: Nanostructured materials; theory, modeling, and simulation to predict behavior and design new materials; and novel analytical and characterization tools.
- Fuel Cells: Nanostructured catalysts and materials; integrated nanoscale architecture; novel fuel cell membranes; innovative synthetic techniques; theory, modeling, and simulation of catalytic pathways, membranes, and fuel cells; and novel characterization techniques.
- Hydrogen Production: Approaches such as photobiological and direct photochemical production of hydrogen.

By maintaining close coordination between basic science research and applied R&D, the Program ensures that discoveries and related conceptual breakthroughs achieved in basic research programs will provide a foundation for the innovative design of materials and processes that will lead to improvements in the performance, cost, and reliability of fuel cell technologies and technologies for hydrogen production and storage. This is accomplished in various ways—for example, through bi-monthly coordination meetings between the participating offices within DOE, and at the researcher level by having joint meetings with participation from principal investigators who are funded by the participating offices.

In June 2014, the Program included 20 presentations and posters from Basic Energy Sciences-funded researchers on fundamental science related topics in conjunction with presentations by EERE and ARPA-E funded researchers.

Technology Validation

The Technology Validation sub-program demonstrates, tests, and validates hydrogen and fuel cell technologies and uses the results to provide feedback to FCTO's R&D activities. In addition to validating fuel cell electric vehicle (FCEV) and hydrogen infrastructure technologies, continuing efforts include the real-world evaluation of fuel cell bus technologies at various transit authorities and monitoring performance of fuel cells in stationary power, backup power, and material handling equipment (MHE) applications.

Six major original equipment manufacturers (OEMs) were awarded $5.5M in FY 2014 to demonstrate advanced light-duty FCEVs, where data will be collected from up to 90 vehicles. The first composite data product will be published on NREL's website in December 2014.

A hydrogen fueling station at California State University in Los Angeles (CSULA) was commissioned in May 2014 and stations in West Sacramento and San Juan Capistrano are expected to be installed and commissioned by the third and fourth quarters of 2014, respectively. Data is being collected from these state-of-the-art fueling facilities to validate technology performance under real-word use. The CSULA project also serves educational purposes, as it provides a "living lab" environment for engineering and technology students.

During FY 2014, data from four fuel cell electric bus (FCEB) demonstrations at three transit agencies were collected and analyzed; AC Transit (Oakland, California), SunLine (Thousand Palms, California), and BC Transit (Whistler, Canada). Fuel cell buses continue to show improved fuel economy (ranging from 1.8 to 2.4 times higher) compared to baseline (diesel and compressed natural gas—CNG) buses in similar service. Fuel economy for the FCEBs ranged from 5.8 mi/diesel gallon equivalent (DGE), up to 7.3 mi/DGE (for an average of 6.8 mi/DGE), approaching the Federal Transit Administration's performance target for FCEB fuel economy of 8 mi/DGE.

[5] http://energy.gov/eere/articles/energy-department-announces-2-million-develop-supply-chain-manufacturing

Early market application of fuel cell technologies includes validating MHE and backup power fuel cell performance through analysis and reporting of real-world operation and value proposition metrics. By the fourth quarter of 2013, more than 850 backup power units were in operation as part of the Technology Validation sub-program efforts. These units were found to be operating with average availability of about 99.5 percent in 23 states. By the fourth quarter of FY 2013, almost 500 MHE fuel cell units were in operation as part of the data collection efforts, filling-up on average in 2.3 minutes, and operating an average of 4.4 hours between fills.

Safety, Codes and Standards

The Safety, Codes and Standards (SCS) sub-program identifies needs and performs high-priority R&D to provide an experimentally validated, fundamental understanding of the relevant physics, critical data, and safety information needed to define the requirements for technically sound and defensible codes and standards. In FY 2014, the sub-program continued to identify and evaluate safety and risk management measures that can be used to define the requirements and close the gaps in codes and standards in a timely manner.

In the area of hydrogen behavior, risk assessment, and materials compatibility, an initial test matrix was completed to determine the fatigue life of stainless steel 21Cr-6Ni-9Mn in 103 MPa hydrogen gas, satisfying the need to quantitatively evaluate methods published in CSA CHMC1 standard and to generate qualification data for lower-cost stainless steels.

Additionally, the sub-program released a first-of-its kind iPad/iPhone app to enhance utility and integration of the safety knowledge tools with other safety planning resources. As of May 2014, there have been more than 940 downloads of the app.

As hydrogen station deployment ramps up, the siting of hydrogen dispensers at existing stations is gaining interest. The SCS sub-program supported a study showing that 20% of 70 gasoline stations evaluated in California could accommodate hydrogen.[6]

Finally, a major milestone in FY 2014, also supported over several years by the SCS sub-program, and led by industry, was the standardization and publication of two SAE International standards: J2799 Standard for 70 MPa Compressed Hydrogen Surface Vehicle Fuelling Connection Device and Optional Vehicle to Station Communications and J2601 Standard Fueling Protocols for Light-Duty Gaseous Hydrogen Surface Vehicles.

Education

The Education sub-program facilitates hydrogen and fuel cell demonstrations and supports commercialization by providing technically accurate and objective information to key target audiences both directly and indirectly involved in the use of hydrogen and fuel cells. Funding from prior appropriations supported the sub-program's activities.

In FY 2014 FCTO published more than 80 success stories through news articles, blogs, press releases, and media announcements and conducted more than 15 webinars, averaging more than 150 attendees per webinar. Activities reached at least 3,000 people at key conferences and meetings. The sub-program is also continuing to train middle school and high school teachers based on prior years' funding through "H2 Educate!" reaching a cumulative of 12,000 teachers, in 35 states; 90% of participants have stated that the training resources increased the effectiveness of their lesson plans.

Market Transformation

To ensure that the benefits of the Program's efforts are realized in the marketplace, in FY 2014 the Market Transformation program continued to facilitate the growth of early markets for fuel cells used in stationary, specialty-vehicle and truck fleet applications. Market Transformation activities are helping to reduce the cost of fuel cells by enabling economies of scale through early market deployments; these early deployments also help to overcome a number of barriers, including the lack of operating performance data, the need for applicable codes and standards, and the need for user acceptance. Market Transformation also partners with other federal agencies and stakeholders to deploy fuel cell systems in applications such as marine cargo transport operations.

Current key objectives of the Market Transformation program are to build on past successes in MHE (e.g., lift trucks or forklifts) and emergency backup power applications by exploring other emerging applications for market viability. FY 2014 accomplishments included designing a commercial viable fuel cell-powered airport ground support baggage tractors, developing fuel cell-powered electric medium-duty hybrid trucks for parcel delivery applications,

[6] http://energy.sandia.gov/wp/wp-content/gallery/uploads/SAND_2014-3416-SCS-Metrics-Development_distribution.pdf

completing the design development of fuel cell auxiliary power systems for refrigerated trucks, and completing the design for a maritime auxiliary power system. These projects are highly leveraged, with an average of more than half of the projects' funds being provided by DOE's partners.

Affordable hydrogen in accessible locations is another key goal; Market Transformation is supporting this by a landfill-gas-to-hydrogen project at a working manufacturing facility and using curtailed renewable power to electrolyze water on another project.

A potential new activity that could be initiated subject to Congressional appropriations is the design and deployment of fuel cell battery-powered hybrid light-duty vehicles for parcel delivery or passenger transportation applications.

Systems Analysis

The Systems Analysis sub-program focuses on examining the economics, benefits, opportunities, and impacts of hydrogen and fuel cells through a consistent, comprehensive, analytical framework. Analysis conducted in FY 2014 included socio-economic impacts such as increased employment from early market infrastructure development, life-cycle analysis of various vehicle platforms including FCEVs with EERE's Bio-Energy Technologies and Vehicle Technologies Offices, hydrogen use for energy storage, fuel cell system cost impact to improve fuel cell efficiency, life cycle impacts of water use of hydrogen production pathways, identification of early markets for fuel cells, and options to reduce infrastructure cost through the application of tri-generation fuel cell systems.

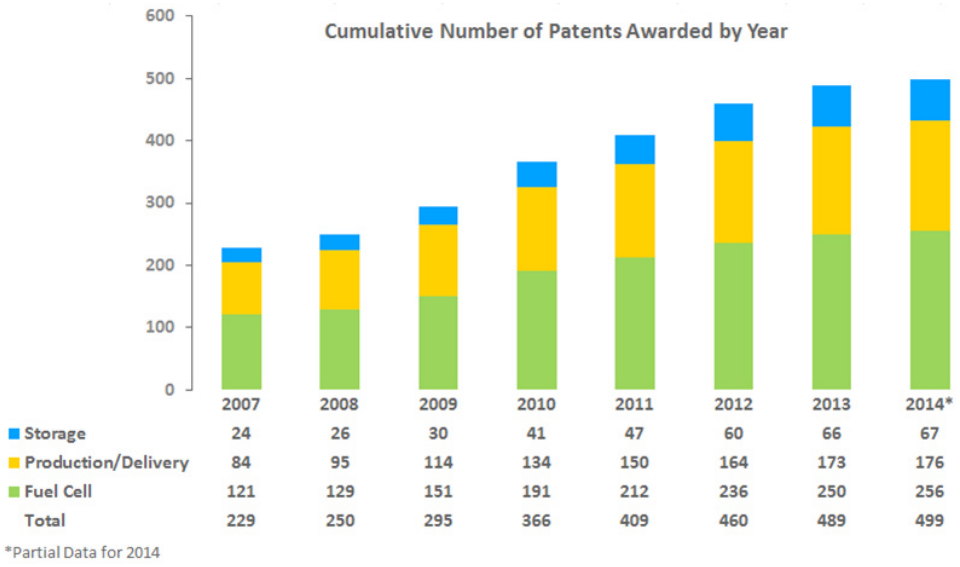

FIGURE 5. Number of issued patents as a result of FCTO funding. (PNNL)

The commercial benefits of FCTO were analyzed by tracking the commercial products and technologies, and patents developed from R&D funding. The benefits of DOE funded projects continue to grow. FY 2014 tracking showed 499 cumulative patents issued as a result of FCTO funding. In addition, 45 FCTO-funded were in the market and 65 were identified to be commercialized within three to five years.[7]

In FY 2014, the GREET (Greenhouse gases, Regulated Emissions and Energy use in Transportation) model's life cycle analysis capabilities were enhanced to include water consumption for hydrogen production and delivery pathways from natural gas, water electrolysis, and other fuels such as gasoline and ethanol. The analysis includes the water use assessment of pathway components including feedstocks such as natural gas and crude oil and energy use such as electricity, and biofeedstocks such as corn and cellulosic sources. Converting these conventional and new feedstocks to fuels require additional water consumption. The results of the analysis shown in the figure below show that water

[7] http://energy.gov/eere/fuelcells/market-analysis-reports#mkt_pathways

for irrigation, cooling water for electricity generation, and evaporation associated with hydropower generation has the greatest impact on life cycle water consumption of E85 (85% ethanol, 15% gasoline) fuel, hydrogen fuel cell, and electric vehicles.

The impact of different fuel cell targets on the vehicle energy consumption and cost were also studied using the Autonomie model and compared to conventional gasoline internal combustion powertrains. In addition, the impact of fuel cell system improvements on the potential on-board storage requirements and cost were analyzed. The findings of the study indicate the fuel economy of the FCEV could be improved by 10-14% by increasing the fuel cell peak efficiency from 60 to 68%. When the FCEV improvements are compared to conventional vehicle, the FCEV fuel economy was found to be 4 times higher (139 mpg unadjusted) than the 2013 conventional vehicle in the 2030 timeframe.

American Recovery and Reinvestment Act Projects

The American Recovery and Reinvestment Act of 2009 (Recovery Act or ARRA) has been a critical component of the Program's efforts to accelerate the commercialization and deployment of fuel cells in the marketplace. As of October 2014, all of the original twelve projects have been successfully completed, and over 96% of the Recovery Act project funds have been invoiced by the projects. A total of 1,330 fuel cell units were deployed, 824 fuel cell backup power system for cellular communication towers, 504 fuel cell lift trucks, and 2 stationary power systems, surpassing the original deployment goal of up to 1,000 fuel cells. NREL's National Fuel Cell Technology Evaluation Center (NFCTEC) has established data reporting protocols and Composite Data Products (CDPs) and Detailed Data Products showing progress to date have been prepared. The CDPs are available on the NREL NFCTEC website.[8]

Notable accomplishments in FY 2014 included design and construction of a 250-W propane-fueled, portable solid oxide fuel cell (SOFC) units successfully operated over 4 days (on a single 20-lb propane bottle) to power television cameras at NASCAR events; and successful backup operation of three propane-fueled, 5-kW, GenSys fuel cells to provide lighting to a building during a 30 minute, simulated outage at Ft Irwin, California.

Successful DOE deployments of fuel cells (including deployments from ARRA funding as well as Market Transformation projects) have led to industry orders of more than 7,500 fuel cell forklifts and more than 4,000 fuel cell backup power systems, with no additional DOE funding.[9,10]

OTHER PROGRAM ACTIVITIES AND HIGHLIGHTS FROM FY 2014

Tracking Commercialization

One indicator of the robustness and innovative vitality of an RD&D program is the number of patents granted, as well as the number of technologies commercialized. The Program continued to assess the commercial benefits of funding by tracking the commercial products and technologies developed with the support of FCTO. R&D efforts funded by FCTO have resulted in 499 patents, 45 commercial technologies in the market, and 65 technologies that are projected to be commercialized within three to five years (as of October 2014).[11]

In addition, EERE's investment of $95 million in specific hydrogen and fuel cell projects led to more than $400 million in revenue and investments of approximately $70 million in specific projects led to a nearly $390 million in additional private investment.

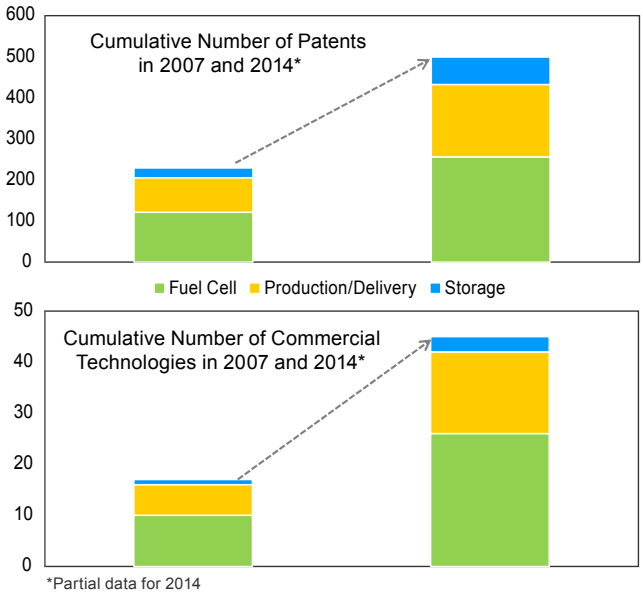

FIGURE 6. Patents and commercial products as a result of FCTO funding.

[8] http://www.nrel.gov/hydrogen/facilities_nfctec.html
[9] http://hydrogen.energy.gov/pdfs/14009_industry_bup_deployments.pdf
[10] http://hydrogen.energy.gov/pdfs/14010_industry_lift_truck_deployments.pdf
[11] http://energy.gov/eere/fuelcells/market-analysis-reports#mkt_pathways

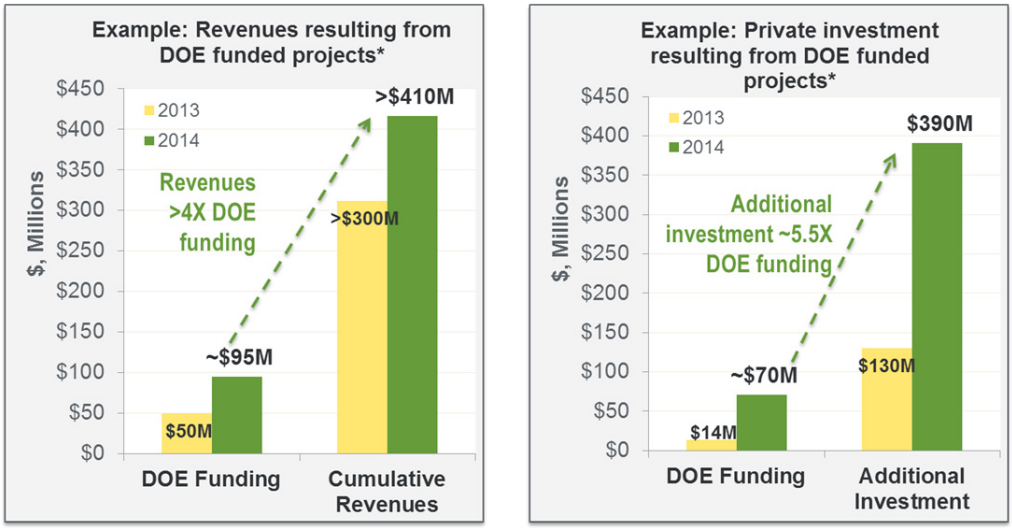

FIGURE 7. Revenues and private investment as a result of specific FCTO funding of projects.

Awards & Distinctions

During the last year, a number of researchers within the Program were recognized through various awards. For example:

- Dr. Adam Weber of the Energy Department's Lawrence Berkeley National Laboratory was honored with a Presidential Early Career Awards for Scientists and Engineers (PECASE), the federal government's highest honor for science and engineering professionals in the early stages of their careers. This follows last year's PECASE award to FCTO-funded Professor Tom Jaramillo of Stanford University and makes the only two PECASE awards within all of EERE. Dr. Weber also received the 2014 Charles W. Tobias Young Investigator Award.
- Dr. Maria Ghirardi was named to NREL's Research Fellows Council, the laboratory's top advisory council comprised of internationally recognized NREL scientists and engineers.
- The Women Chemists Committee of the American Chemical Society selected Katherine Ayers of Proton OnSite to be a recipient of the 2014 Women Chemists Committee Rising Star award.
- Northeastern chemistry professor Sanjeev Mukerjee was named a Fellow of The Electrochemical Society.
- James Miller and Riccardo Scarcelli of ANL's Energy Systems division are 2014 recipients of the prestigious McFarland Award from SAE International.
- The ACS Division of Inorganic Chemistry announced Jeffrey Long, University of California, Berkeley, as the winner of the second Inorganic Chemistry Lectureship Award.
- Dr. Piotr Zelenay of Los Alamos National Laboratory (LANL) was named a Fellow of The Electrochemical Society.
- Thomson Reuters has included University of South Carolina professor Branko N. Popov as one of the 2014 World's Most Influential Scientific Minds and one of our nation's most highly cited researchers from 2002 to 2014.
- Jennifer Kurtz and Keith Wipke from NREL and Daniel Dedrick from Sandia National Laboratories (SNL) have won prestigious Federal Lab Consortia 2014 Far West Regional Awards.

Key Reports/ Publications

Every year, the Program commissions a number of key reports, providing vital information to industry and the research community. Some of these are released on an annual basis—such as the Market Report (2013 Fuel Cell Technologies Market Report), the commercialization report (2013 Pathways to Commercial Success: Technologies and Products Supported by FCTO), and the State of the States: Fuel Cells in America 2014 report—while others are published when studies are complete, projects have ended, or key milestones have been reached. Key examples include:

- The ***Hydrogen Production Expert Panel (HPEP)***, a Hydrogen and Fuel Cell Technical Advisory Committee (HTAC) subcommittee, published major findings from their May 10–12, 2012 workshop which was launched with opening remarks by the previous Energy Secretary. Tasked with providing recommendations to enable the widespread production of affordable, low-carbon hydrogen, HPEP collected input from experts from industry, academia, and national laboratories during the workshop and developed recommendations based on that input. http://www.hydrogen.energy.gov/advisory_htac.html#reports
- The ***2013 Fuel Cell Technologies Market Report*** finds that there is continued growth in fuel cell commercial deployments, including MHE such as forklifts as well as combined heat and power systems and backup and auxiliary power units. Nationally, U.S. fuel cell shipments grew from 1,000 units in 2008 to nearly 5,000 units in 2013, while domestic manufacturing increased by more than 60% from 2012 to 2013. http://energy.gov/eere/fuelcells/market-analysis-reports#mkt_program
- ***States of the States: Fuel Cells in America 2013***, the fifth annual report on state activities, details fuel cell and hydrogen activities and policies in the 50 states and the District of Columbia. http://energy.gov/eere/fuelcells/market-analysis-reports#mkt_state
- ***Pathways to Commercial Success: Technologies and Products Supported by the Fuel Cell Technologies Office***, the Program's annual commercialization report, indicates that FCTO efforts have successfully generated more than 450 patents, 40 commercial technologies, and 65 technologies that are expected to reach commercial scale within the next three to five years, and issue more than 450 U.S. patents. http://energy.gov/eere/fuelcells/market-analysis-reports#mkt_pathways
- The ***Business Case for Fuel Cells*** illustrates how top American companies are using fuel cells in their business operations to advance their sustainability goals, save millions of dollars in electricity costs, and reduce carbon emissions by hundreds of thousands of metric tons per year. http://energy.gov/eere/fuelcells/market-analysis-reports#mkt_business
- ***Hydrogen Station Compression, Storage, and Dispensing Technical Status and Costs*** detail the findings of an independent review of hydrogen compression, storage, and dispensing for pipeline delivery of hydrogen and forecourt hydrogen production. http://www.hydrogen.energy.gov/peer_reviews.html
- ***Twenty new fact sheets*** on the models and tools used for system analysis of hydrogen and fuel cells were published. The models and tools summarized in the fact sheets are used by FCTO's System Analysis sub-program to perform hydrogen/fuel cell-related calculations, evaluations, and environmental assessments. This template was subsequently used by EERE's Vehicle Technologies Office (VTO) to document VTO-sponsored models and tools as well. http://energy.gov/eere/fuelcells/downloads/analysis-models-and-tools-systems-analysis-hydrogen-and-fuel-cells
- An inter-agency and inter-office report titled ***Hydrogen Fueling Station in Honolulu, Hawaii Feasibility Analysis*** assesses the technical and economic feasibility of developing a vacant, undeveloped General Services Administration-owned property into an income-producing site equipped with a hydrogen fueling station and a covered 175-stall parking structure with roof-top solar panels. http://energy.gov/eere/fuelcells/downloads/hydrogen-fueling-station-honolulu-hawaii-feasibility-analysis

Workshops and Proceedings

- On November 4, 2013, FCTO held its first ***Early Market Fuel Cell Showcase and Project Review*** in New York City at the New York Times building. This event was held for potential investors, business partners, and other stakeholders through presentations and a poster session in an effort to facilitate industry and investor awareness of these emerging and innovative technology areas. Attendees included Steve Chalk, Deputy Assistant Secretary of Renewable Energy; Congressman Paul Tonko (D-NY); and Richard Kauffman, Chairman of Energy and Finance for New York State.
- On April 15, 2014, FCTO held its ***Clean Energy Technology Showcase Review*** featuring fuel cells, flow batteries, and related energy efficiency technologies at Stanford University. Reviewers provided feedback to FCTO as well as Advanced Manufacturing Office (AMO) and ARPA-E on the projects presented. The event was launched by the Office of Energy Efficiency and Renewable Energy's Assistant Secretary Dr. David Danielson.
- The ***proceedings from the Biological Hydrogen Production Workshop*** that took place September 23–24, 2013, were released in November. The objective of the Biological Hydrogen Production Workshop was to share

information and identify issues, barriers, and R&D needs for biological hydrogen production to enable hydrogen production that meets cost goals. http://energy.gov/eere/fuelcells/biological-hydrogen-production-workshop

- The ***EERE Quality Control Workshop proceedings*** detail the activities of a workshop held December 9 and 10, 2013 and convened government, industry, and other stakeholders to discuss the current status of quality control and metrology in manufacturing processes relevant to the EERE offices. http://energy.gov/eere/fuelcells/articles/eere-quality-control-workshop-proceedings-released
- The ***2014 Hydrogen Transmission and Distribution Workshop proceedings*** and final summary report provide details on a workshop held February 25–26, 2014 that brought together experts from the industrial gas and energy industries, national laboratories, academia, and the National Institute of Standards and Technology to discuss and share information on the RD&D needs and challenges for low-cost, effective hydrogen transmission and distribution from centralized production facilities to the point of use. http://energy.gov/eere/fuelcells/downloads/hydrogen-transmission-and-distribution-workshop
- The ***2014 Electrolytic Hydrogen Production Workshop proceedings and final summary report*** shares information compiled during a workshop held on February 27–28, 2014 on the RD&D needs for enabling low-cost, effective hydrogen production from all types of water electrolysis systems, both centralized and forecourt. http://energy.gov/eere/fuelcells/downloads/electrolytic-hydrogen-production-workshop

New FOAs and Awards

- **$7 million** for four projects that will help bring cost-effective, advanced hydrogen and fuel cell technologies online faster through early market applications such as delivery vans. Selected projects are located in Georgia, Kansas, Pennsylvania, and Tennessee.
- **$3 million** to advance U.S. competitiveness in molten carbonate technology. The selected project is located in Connecticut.
- **$7 million** was awarded for six projects to develop lightweight, compact, and inexpensive advanced hydrogen storage systems that will enable longer driving ranges and help make fuel cell systems competitive for different platforms and sizes of vehicles. Selected projects are located in California and North Carolina.
- **$20 million** was awarded for 10 new research and development projects to advance hydrogen production and delivery technologies. Selected projects are located in Connecticut, Washington, Colorado, Hawaii, California, Texas, Massachusetts, Tennessee, and Virginia.
- **National Science Foundation (NSF)** funding, through the first ever Memorandum of Understanding between FCTO and NSF, to address discovery and development of advanced materials systems and chemical processes for direct photochemical and/or thermochemical water splitting for application in the solar production of hydrogen fuel. Four projects were announced in September 2014.
- **$2 million** to develop supply chain manufacturing competitiveness analysis for hydrogen and fuel cell technologies. This FOA closed on June 30, 2014.
- **$4.6 million** in incubator funding to identify potentially impactful technologies that are not already addressed in FCTO's strategic plan or project portfolio. Full responses were due September 3, 2014.

The Program participated in a number of SBIR FOAs and awards.

- Fuel cell project selected through a new **EERE SBIR Technology Transfer Opportunity topic** that moves existing inventions developed at DOE's national laboratories to the marketplace and accelerates the pace of commercialization. This was the first ever SBIR in EERE and provided national laboratory patents for small businesses to commercialize. The selected project is located in Massachusetts.
- **SBIR/Small Business Technology Transfer (STTR) Phase II** Release 1 Award Winners included two hydrogen and fuel cell projects. Topics include "optimizing the cost and performance of composite cylinders for hydrogen storage using a graded construction" and "novel structured metal bipolar plates for low cost manufacturing."
- **SBIR/STTR Phase I** Release 2 Technical Topics Announced for FY 2014, include prototype fuel cell-battery electric hybrid trucks for waste transportation and novel membranes and non-platinum group metal catalysts for direct methanol as well as hydrogen fuel cells.

- **2015 SBIR/STTR Phase I** Release 1 FOA includes hydrogen and fuel cell topics. Applications are due October 14, 2014. Topics include "non-platinum group metal catalysts for fuel cells" and "understanding of material behavior for detection of hydrogen contaminants."

The Program also coordinated with other offices and the following FOAs from FY 2014 were relevant.

- **$70 million** in AMO funding to a new Advanced Composite Manufacturing Institute to target continuous or discontinuous carbon and glass fiber composites. This FOA closed on June 24, 2014.
- **$33 million** in ARPA-E funding for intermediate-temperature fuel cell systems for distributed generation.[12]
- **$15 million** in FE funding for improved reliability of solid oxide fuel cell systems**.** This FOA closed on March 31, 2014.
- **$6.4 million** in FE funding for R&D support of the solid oxide fuel cell core technology program. This FOA closed on March 31, 2014.

Requests for Information (RFIs)

The Program uses RFIs to solicit feedback from the stakeholder community in an open and transparent process which serves to inform the Program and develop future plans. Key examples included collecting feedback on:

- Strategies for a robust market introduction of hydrogen supply, infrastructure, and FCEVs.The input received will augment financing strategies that DOE analyzes for public deployment of infrastructure for supporting FCEV introduction in U.S. markets. Such financing strategies should maximize financing, for example, with debt and equity, while minimizing public incentives. (January 31, 2014)
- Biological hydrogen production R&D pathways, barriers, issues and opportunities for development of technologies that can ultimately produce low cost hydrogen that meets DOE goals. (February 28, 2014)
- Existing and potential hydrogen contamination detectors and related factors such as performance characteristics, system integration requirements, costs, deployment guidance, and R&D needs. (May 19, 2014)
- Technical and economic feasibility of commercializing fuel cell range extenders as onboard power generators for all-electric vehicles in the United States market. (August 7, 2014)

[12] http://arpa-e.energy.gov/?q=arpa-e-news-item/arpa-e-announces-30-million-distributed-generation-technologies

The Program also held a number of webinars throughout the year.[13]

DATE	TITLE	DESCRIPTION
September 11, 2014	Introduction to SAE Hydrogen Fueling Standardization	This webinar provided an overview of the SAE International Standards J2601 and J2799 and how they are applied to hydrogen fueling for FCEVs. Validated in the lab and proven in the field over the last decade, the SAE J2601 hydrogen fueling protocol standard, coupled with the SAE J2799 FCEV communications standard, provide the basis for hydrogen fueling in the first generation of infrastructure worldwide.
August 19, 2014	Increasing Renewable Energy with Hydrogen Storage and Fuel Cell Technologies	This webinar featured representatives from NREL discussing a unique opportunity for the integration of multiple sectors including transportation, industrial, heating fuel, and electric sectors on hydrogen. This presentation looked at the architecture of hydrogen storage systems and economic competitiveness for those systems when compared with conventional systems.
July 29, 2014	Supporting a Hawaii Hydrogen Economy	During this webinar the Hawaii Natural Energy Institute (HNEI) discussed the status of current and planned hydrogen projects in Hawaii. HNEI has worked to reduce Hawaii's dependence on fossil fuels and increase energy security, serving as the implementing organization for several large-scale public-private partnerships to develop, deploy, and demonstrate renewable energy systems.
June 24, 2014	Hydrogen Fueling for Current and Anticipated Fuel Cell Electric Vehicles	This webinar featured representatives from the California Energy Commission who discussed their recently announced Notice of Proposed Award for 28 hydrogen fueling stations, the evaluation criteria, and the variety of competitions. In addition, representatives from ANL discussed a new tool for estimating the economic impacts of hydrogen infrastructure for early market fuel cell electric vehicles. The tool, titled JOBS and economic impacts of Hydrogen (JOBS H2), estimates the jobs, earnings, and economic output created by deploying hydrogen fueling stations.
May 27, 2014	NREL's Fuel Cell Contaminant Database	This webinar focused on the NREL's online data tool for fuel cell system-derived contaminants. NREL has led a multi-year project studying the effect of system-derived contaminants on the performance and durability of polymer electrolyte membrane fuel cells. The webinar provided an overview of data obtained during the project and a tutorial on how to use the Web-based data tool to access project results.
April 17, 2014	Fuel Cells at NASCAR	This webinar focused on fuel cell use at NASCAR Green. Presentations by NASCAR and Acumentrics described the use of SOFC generators for use in powering broadcast cameras for NASCAR. Recently, Acumentrics Corporation completed a field test program with NASCAR to replace small portable gasoline generators with SOFC units operational on commercial propane.
March 11, 2014	National Fuel Cell Technology Evaluation Center (NFCTEC)	This webinar focused on the NFCTEC, which is dedicated to the independent analysis of advanced hydrogen and fuel cell technologies at the Energy Department's Energy Systems Integration Facility located at the NREL in Golden, Colorado. The presentation by NREL highlighted the efforts of NFCTEC to accelerate the commercialization of fuel cell technologies through analysis of technologies operating under real-world conditions and comparison to technical targets.
February 11, 2014	Additive Manufacturing for Fuel Cells	This webinar focused on additive manufacturing to stimulate discussion in the hydrogen and fuel cell community on the application of additive manufacturing to prototyping and production. Presentations by Eaton and Nuvera highlight Eaton's experience using additive manufacturing for prototype development and recent developments in additive manufacturing for full scale production being employed at Nuvera.
January 16, 2014	Energy 101: Fuel Cells Discussion	This Google+ Hangout discussion focused on audience questions about fuel cells. Several experts answered questions and discussed fuel cells in front of a live online audience. Expert panelists included Dr. Sunita Satyapal, Director of the Energy Department's Fuel Cell Technologies Office; Daniel Dedrick, Manager of Hydrogen and Combustion Technologies at SNL; Anthony Eggert, Executive Director of the UC Davis Policy Institute for Energy, Environment and the Economy; and Charlie Freese, Executive Director of Global Fuel Cell Activities at General Motors.
January 14, 2014	2014 Hydrogen Student Design Contest	This webinar focused on the winning entries of the 2013 Hydrogen Student Design Contest from the University of Kyushu and University of Birmingham. This year, teams were challenged to develop hydrogen fueling infrastructure plans for the Northeast and mid-Atlantic for the 2013-2025 timeframe. During the webinar the theme for the 2014 contest—Designing a Drop-in Fueling Station—was also discussed.
December 16, 2013	International Hydrogen Infrastructure Challenges Workshop Summary – NOW, NEDO, and DOE	This webinar summarized the international information exchange on the hydrogen refueling infrastructure challenges and potential solutions to support the successful global commercialization of hydrogen fuel cell electric vehicles. The information exchange took place in June 2013 at the German Ministry of Transport, in Berlin.
November 19, 2013	Micro-structural Mitigation Strategies for PEM Fuel Cells	This webinar highlighted micro-structural mitigation strategies for polymer electrolyte membrane (PEM) fuel cells focusing on morphological simulations and experimental approaches. Presented by Ballard Power Systems, the webinar highlighted an open-source fuel cell simulation package funded by EERE that allows users to simulate both the performance and durability of a PEM fuel cell membrane electrode assembly. In this webinar, the details of the model were discussed with a focus on the theory, background, and validation/results of the simulation package.

[13] http://energy.gov/eere/fuelcells/2014-webinar-archives

The Program published multiple EERE blogs focused on hydrogen and fuel cell activities.

DATE	TITLE	SUMMARY
September 30, 2014	And the Oscar for Sustainable Mobile Lighting Goes to…. Lighting Up Operations with Hydrogen and Fuel Cell Technology[1]	An Energy Department-supported project is addressing these problems by designing, building, and testing a mobile lighting tower powered by hydrogen fuel cell technology, which is quiet and emits nothing but water while generating electricity.
September 26, 2014	Hyundai Tucson Fuel Cell Electric Vehicle visits Department of Energy[2]	From researchers to project managers to technical experts, there are dozens of EERE staff dedicated to supporting the research, development, and deployment of fuel cells.
September 11, 2014	Highlighting Hydrogen: Hawaii's Success with Fuel Cell Electric Vehicles Offers Opportunity Nationwide[3]	Engineers from the Energy Department's Idaho National Laboratory and NREL identified a new way to launch economically viable hydrogen fueling stations for FCEVs in Honolulu, Hawaii, based on a report titled "Hydrogen Fueling Station in Honolulu, Hawaii." The report's findings could also have a broad national impact, accelerating the pace of America's growing clean energy economy.
May 13, 2014	Research Leads to Improved Fuel Yields from Smaller Antenna Algae[4]	A study funded by the Energy Department could lead to big improvements in alternative fuel production. Researchers at the University of California, Berkeley have discovered that if particular genes are missing in certain strains of algae, the algae can produce more hydrogen and other fuel from full sunlight than the ordinary algae.
April 29, 2014	Small Catalyst Finding Could Lead to Big Breakthrough for Fuel Cell Deployment[5]	Researchers at the Energy Department's national labs have developed a new catalyst that could make fuel cells cost-competitive with other power generators.
March 28, 2014	Interested in Hydrogen and Fuel Cell Technologies? Help Shape the H2Refuel H-Prize Competition[6]	The Energy Department recently posted a blog about the H-Prize H2 Refuel Competition, which involves designing a small-scale hydrogen refueler system for homes, community centers, or businesses.
February 24, 2014	NASCAR Green Gets First Place in Daytona 500[7]	A story about how fuel cell generators were used at the Daytona 500 is currently posted on the Energy Department's blog.
February 4, 2014	Nebraska Company Expands to Meet Demand for Hydrogen Fuel[8]	Hexagon Lincoln develops carbon fiber composite fuel tanks that help deliver hydrogen to fleets throughout the country. The company has more than doubled its workforce to accommodate growing demand for the tanks.
January 28, 2014	You Asked, We're Answering Your Fuel Cell Questions[9]	The Energy Department posted a blog with answers to some of the fuel cell questions that didn't get covered during the Energy 101 Google+ Hangout on January 16.
January 9, 2014	Help Design the Hydrogen Fueling Station of Tomorrow[10]	As the hydrogen industry expands, refueling infrastructure needs to be developed to keep fuel cell electric vehicles powered and moving on America's roadways. University students can play a big role in this through the Hydrogen Education Foundation's Hydrogen Student Design Contest, supported by the Energy Department.
December 20, 2013	Your Holidays … Brought to You by Fuel Cells[11]	A story about how fuel cells are helping bring the holidays to you is currently posted on the Energy Department's Blog.

[1] http://energy.gov/eere/articles/and-oscar-sustainable-mobile-lighting-goes-lighting-operations-hydrogen-and-fuel-cell
[2] http://energy.gov/eere/articles/hyundai-tucson-fuel-cell-electric-vehicle-visits-department-energy
[3] http://energy.gov/eere/articles/highlighting-hydrogen-hawaii-s-success-fuel-cell-electric-vehicles-offers-opportunity
[4] http://energy.gov/eere/articles/research-leads-improved-fuel-yields-smaller-antenna-algae
[5] http://energy.gov/articles/small-catalyst-finding-could-lead-big-breakthrough-fuel-cell-deployment
[6] http://energy.gov/eere/fuelcells/articles/interested-hydrogen-and-fuel-cell-technologies-help-shape-h2-refuel-h-prize
[7] http://energy.gov/eere/fuelcells/articles/nascar-green-gets-first-place-daytona-500
[8] http://energy.gov/eere/articles/nebraska-company-expands-meet-demand-hydrogen-fuel
[9] http://energy.gov/eere/fuelcells/articles/you-asked-were-answering-your-fuel-cell-questions
[10] http://energy.gov/eere/fuelcells/articles/help-design-hydrogen-fueling-station-tomorrow-0
[11] http://energy.gov/eere/fuelcells/articles/your-holidaysbrought-you-fuel-cells

INTERNATIONAL ACTIVITIES

International Partnership for Hydrogen and Fuel Cells in the Economy

The International Partnership for Hydrogen and Fuel Cells in the Economy (IPHE) includes 17 member countries (Australia, Austria, Brazil, Canada, China, France, Germany, Iceland, India, Italy, Japan, Norway, the Republic of Korea, the Russian Federation, South Africa, the United Kingdom, and the United States) and the European Commission. The IPHE is a forum for governments to work together to advance worldwide progress in hydrogen and

fuel cell technologies. IPHE also offers a mechanism for international R&D managers, researchers, and policymakers to share program strategies. IPHE members embarked upon a second 10-year term in November 2013. The Chair of the IPHE is currently Japan, with the United States and Germany serving as Vice Chairs.[14]

In FY 2014, IPHE members met in Fukuoka, Japan (November 2013) and in Oslo, Norway (May 2014) to share progress and plans related to hydrogen and to discuss plans for the IPHE Secretariat. IPHE-related workshop topics in FY 2014 included energy storage and hydrogen infrastructure.

International Energy Agency

The United States is also involved in international collaboration on hydrogen and fuel cell R&D through the International Energy Agency (IEA) implementing agreements; the United States is a member of both the Advanced Fuel Cells Implementing Agreement (AFCIA) and the Hydrogen Implementing Agreement (HIA). These agreements provide a mechanism for member countries to share the results of R&D and analysis activities. The AFCIA is in a unique position to provide an overview of the status of fuel cell technology, deployment, and the opportunities and barriers faced within the member countries. The AFCIA has several annexes: Molten Carbonate Fuel Cells, Polymer Electrolyte Fuel Cells, Solid Oxide Fuel Cells, Fuel Cells for Stationary Applications, Fuel Cells for Transportation, Fuel Cells for Portable Power, and Systems Analysis. Participating countries include Australia, Austria, Belgium, Denmark, Finland, France, Germany, Israel, Italy, Japan, Korea, Mexico, Sweden, Switzerland, and the United States. The IEA HIA is focused on RD&D and analysis of hydrogen technologies. Tasks include Hydrogen Safety, Renewable Hydrogen, Fundamental and Applied Hydrogen Storage Materials Development, Small-Scale Reformers for On-site Hydrogen Supply, Large Scale Hydrogen Delivery Infrastructure, Distributed and Community Hydrogen for Remote Communities, and Global Hydrogen Systems Analysis. Members of the HIA include Australia, Denmark, the European Commission, Finland, France, Germany, Greece, Italy, Japan, Korea, Lithuania, New Zealand, Norway, Spain, Sweden, Switzerland, Turkey, Taiwan, and the United States. Additional sponsor members include Shell, Germany's National Organisation Hydrogen and Fuel Cell Technology, and Hy-SAFE Technology. The United States is a strong contributor to numerous IEA tasks and activities. During FY 2014 the United States hosted a workshop to solicit input to IEA's Roadmap activities related to hydrogen and fuel cells.

EXTERNAL COORDINATION, INPUT, AND ASSESSMENTS

H2USA Partnership

While hydrogen infrastructure remains a key challenge to the widespread adoption of FCEVS, states like California continue to show their commitment to this clean energy technology. A series of major announcements in 2014 shows increased momentum in overcoming obstacles.

On May 1, Governor Brown of California signed on to join H2USA, a public-private partnership led by the Energy Department and industry partners. H2USA was launched in May 2013 to address the challenge of hydrogen infrastructure, bringing together Federal agencies, state agencies, hydrogen providers, energy companies, technology developers, national labs, academia, and other trade associations or non-profit organizations. The partnership provides a platform for the United States similar to the public-private partnerships in other countries focused on hydrogen, particularly Germany, Japan and the UK. H2USA has more than tripled its partners in the last year and currently consists of 37 participants.

On April 30, the Energy Department announced the launch of a new project leveraging the capabilities of its national laboratories in direct support of H2USA. The project is led by NREL and SNL and will tackle the technical challenges related to hydrogen fueling infrastructure. The Hydrogen Fueling Infrastructure Research and Station Technology (H2FIRST) project is designed to reduce the cost and time of fueling station construction, increase station availability, and improve reliability by creating opportunities for industry partners to pool knowledge and resources to overcome hurdles. The project was established by FCTO, drawing on existing and emerging core capabilities at the national labs.

Hydrogen and Fuel Cells Technical Advisory Committee (HTAC)

As required by the Energy Policy Act of 2005, HTAC was created in 2006 to advise the Secretary of Energy on issues related to the development of hydrogen and fuel cell technologies and to provide recommendations regarding DOE's programs, plans, and activities, as well as on the safety, economic, and environmental issues related to hydrogen

[14] http://www.iphe.net/

and fuel cells. HTAC members include representatives of domestic industry, academia, professional societies, government agencies, financial organizations, and environmental groups, as well as experts in the area of hydrogen safety. HTAC met twice in FY 2014. In June 2014, HTAC released its sixth annual report, which summarizes hydrogen and fuel cell technology, domestic and international progress in RD&D projects, commercialization activities, and policy initiatives.[15]

Currently, the Committee has two established subcommittees, both started in late 2013. The Advanced Manufacturing Subcommittee is conducting an assessment of the state-of-manufacturing techniques that are, or could be, used to benefit commercialization in the fuel cell and hydrogen generation industries. The Retail Infrastructure Subcommittee will track the progress of the worldwide rollout of FCEVs and examine the evolving business case for retail hydrogen fueling stations, including the effects of technology advancement and government policy. It is anticipated that both subcommittees will prepare written reports detailing their accomplishments and findings to the full Committee during FY 2015.

Federal Inter-Agency Coordination

The Hydrogen and Fuel Cell Interagency Task Force (ITF), mandated by the Energy Policy Act of 2005, includes senior representatives from federal agencies supporting hydrogen and fuel cell activities, with the DOE/EERE serving as chair. The Hydrogen and Fuel Cell Interagency Working Group (IWG), also chaired by DOE, supports the initiatives and actions passed down by the ITF. The IWG meets monthly to share expertise and information about ongoing programs and results, to coordinate the activities of federal entities involved in hydrogen and fuel cell RD&D, and to ensure efficient use of taxpayer resources. A key example of interagency collaboration included work with the Environmental Protection Agency's (EPA) Diesel Emission Reduction Act program to broaden program rules to allow fuel cell alternatives. DOE worked with EPA to show how fuel cell applications can replace diesel power trains. DOE also worked with EPA to further refine the interpretation of a qualified renewable fuel under their Renewable Fuel Standard Program, resulting in the acceptance of biogas derived hydrogen for transportation within the program. In addition, the Office developed an interagency federal fleet strategy that provides a strategic, coordinated set of agency roles to help ensure a successful rollout of FCEVs to early markets. Finally, further collaboration with the Department of Agriculture and the Department of Defense to identify locations for future hydrogen stations is also helping support the early FCEV and hydrogen fuel infrastructure market.

The National Academies

The National Research Council (NRC) of the National Academies provides ongoing technical and programmatic reviews and input to the Hydrogen and Fuel Cells Program. The NRC has conducted independent reviews of both the Program and the R&D activities of the U.S. DRIVE partnership. Formerly known as the FreedomCAR and Fuel Partnership, the U.S. DRIVE partnership advances an extensive portfolio of advanced automotive and energy infrastructure technologies, including batteries and electric-drive components, advanced combustion engines, lightweight materials, and hydrogen and fuel cell technologies. Plans were developed for future reviews.

Clean Energy Manufacturing Initiative

The Clean Energy Manufacturing Initiative (CEMI) is a strategic integration and commitment of manufacturing efforts across EERE's clean energy technology offices and AMO, focusing on American competitiveness in clean energy manufacturing. The objectives are to increase U.S. competitiveness in the production of clean energy products by strategically investing in technologies that leverage American advantages and overcome disadvantages, and increase U.S. manufacturing competitiveness by strategically investing in technologies and practices to enable U.S. manufacturers to increase their competitiveness through energy efficiency, combined heat and power, and taking advantage of low-cost domestic energy sources.

The Office is an active participant in CEMI activities, leveraging opportunities for hydrogen and fuel cell manufacturing. In FY 2014, AMO released a request for information on Clean Energy Manufacturing Topics for a new National Network of Manufacturing Innovation Institute. Topics included materials discovery, next gen electric machines, high value-add roll-to-roll manufacturing, and manufacturing with biomaterials.

On September 17, 2014, as part of the American Energy and Manufacturing Competitiveness (AEMC) Partnership, CEMI, and the Council of Competitiveness co-hosted the Second Annual AEMC Summit. The Summit brought together perspectives from industry, government, academia, national laboratories, labor, and policy organizations

[15] http://www.hydrogen.energy.gov/advisory_htac.html

dedicated to the competitiveness of U.S. clean energy products and increasing U.S. energy productivity across the board. Also in FY 2014, CEMI held a regional summit in San Francisco, and two dialogue events in Santa Clara and in Berkeley, California.

FY 2014 Annual Merit Review and Peer Evaluation

The Program's AMR took place June 16-20 in Washington, DC, and provided an opportunity for the Program to obtain expert peer reviews of the projects it supports and to report its accomplishments and progress. For the sixth time, this meeting was held in conjunction with the annual review of DOE's Vehicle Technologies Office. During the AMR, reviewers evaluate the Program's projects and make recommendations; DOE uses these evaluations, along with other review processes, to make project funding decisions for the upcoming FY. The review also provides a forum for promoting collaborations, the exchange of ideas, and technology transfer. This year, approximately 1,800 participants attended, and more than 100 experts peer-reviewed 100 of the Program's projects—conducting a total of more than 600 individual project reviews, with an average of more than six reviewers per project. The report summarizing the results and comments from these reviews is available at www.hydrogen.energy.gov/annual_review14_report.html. The 2015 Annual Merit Review and Peer Evaluation Meeting will be held June 8–12, in Arlington, Virginia.

Funds Saved through Active Project Management

The AMR is a key part of the Program's comprehensive approach toward active management of its projects. Termination of underperforming projects—identified through the AMR as well as through other Go/No-Go decisions (with criteria defined in the project scope of work)—helped the Program redirect $3.0 million in funding in FY 2014, $7.6 million in FY 2013, and over $35 million over the past five years.

DOE Cross-Cutting Activities

Grid Integration: Increasing capacity for variable renewable energy technologies (e.g. wind and solar) on the grid is going to be a major challenge facing future deployment as these technologies make up a larger portion of the power generation portfolio. With the appropriate secure communication technology, electrolyzers can participate in energy markets to help balance the variability of these renewable energy sources by modulating the production of hydrogen to reduce or increase overall energy consumption within the electric grid. Further benefits include the ability of stationary fuel cells to effectively contribute to a grid market by increasing their visibility and controllability. Changing fuel cell generation from a variable source to a controllable source increases there value to the grid and makes stationary fuel cell systems more economical, especially in small-scale (e.g. residential applications) where electricity and heat demand is highly variable. EERE is working to address some of these issues through a new cross-cutting initiative focused on integrating clean energy technologies into the energy system in a safe, reliable, and cost effective manner at a relevant scale to support the nation's goals of 80% clean electricity by 2035 and reducing oil imports by 33% by 2025. All of the participating technologies offices, including FCTO, are determining the high impact RD&D necessary to enable the integration of energy efficiency and renewable energy technologies into the energy system at a scale necessary to realize this vision.

Carbon Fiber: Carbon fiber composites are expected to play an important role across many clean energy technologies, such as in high-efficiency, longer wind turbine blades; lighter-weight, higher fuel economy vehicles; and high-pressure gaseous fuel storage systems. EERE's cross-cutting carbon fiber initiative aims to lower the cost of carbon fiber for clean energy applications through higher energy efficiency manufacture, higher piece production throughput, lower-cost raw materials and increased recyclability. For high-pressure gaseous fuel storage systems, such as for hydrogen and compressed natural gas, high-strength carbon fiber is required and is a major contributor to cost of the storage systems. The PAN precursor fibers used to produce high-strength carbon fiber accounts for over 50% of the final carbon fiber costs. An approach FCTO has taken to lower the cost of carbon fibers has been to focus on alternative, lower-cost PAN precursors. Two projects have made significant advancements in this past year on demonstrating potential of lower cost precursors. One project is projected to have a 25% reduction in high-strength carbon fiber costs through use of a melt-spinning process to produce PAN fibers versus the conventional wet-spinning process. A second project has demonstrated that PAN fibers co-monomered with MA and produced in high volume on traditional high-volume textile-based manufacturing lines can be converted into high-strength carbon fiber. Cost modeling has estimated an approximate 17% reduction in the carbon fiber cost.

Wide Bandgap Semiconductors for Clean Energy Initiative: Wide bandgap (WBG) semiconductor materials allow power electronic components to be smaller, faster, more reliable, and more efficient than their silicon-based

counterparts. These capabilities make it possible to reduce weight, volume, and life-cycle costs in a wide range of power applications. EERE's technology offices, through AMO, are working together to harness these capabilities to lead to dramatic energy savings in industrial processing and consumer appliances. In support of this cross-cutting initiative, the Program has initiated cross-office and cross-agency R&D collaborations for innovative applications of WBG products. Numerous applications of hydrogen and fuel cell technologies could benefit from the development of next-generation WBG power electronics, including fuel cell-powered MHE and FCEVs in the transportation section; and large scale grid integration of fuel cells and electrolyzers in the stationary power sector. The Program is working with leading innovators in the WBG electronics industry to explore opportunities for product development responsive to the market pull of the hydrogen and fuel cell technology applications.

Materials Genome Initiative for Clean Energy: In FY 2014, FCTO initiated an effort to explore the use of high-throughput computational and experimental methods toward the accelerated discovery and development of critical materials for hydrogen and fuel cell technologies. This approach represents one of the leading pilot efforts at DOE in the cross-cutting Materials Genome Initiative (MGI) for Clean Energy. Consistent with the White House Office of Science and Technology Policy's Materials Genome Initiative strategic plan and with Advanced Manufacturing Partnership 2.0 recommendations, MGI for Clean Energy has become a core pillar of the Advanced Materials Manufacturing focus in the DOE Clean Energy Manufacturing Initiative. One important thrust of the FCTO pilot effort is the in situ development and optimization of alternative low-cost, high-performance non-PGM catalysts integrated into membrane electrode assemblies for PEM fuel cells and electrolyzers. Another activity is the combinatorial discovery and development of low-cost compound oxides (such as perovskites) for solar-thermochemical and photoelectrochemical hydrogen production technologies. The MGI-related efforts at FCTO, which have been kick-started by roundtable meetings of experts, RFIs and workshops, are expected to continue through FY 2015 and beyond.

IN CLOSING …

The need for clean, sustainable energy, combined with the need to reduce emissions, has come together to form a global imperative—one that demands new technologies and new approaches for the way we produce and use energy. Widespread use of hydrogen and fuel cells can play a substantial role in a portfolio of clean energy technologies that will overcome key energy challenges. In addition, growing interest and investment among leading world economies, such as Germany, Japan, and South Korea, underscores the global market potential for these technologies.

In 2013, worldwide fuel cell industry sales surpassed $1 billion for the first time, reaching $1.3 billion. In 2013 there was an approximately 30% increase in fuel cell systems shipments worldwide, continuing to achieve a consistent 30% annual market growth rate over the last few years. There were more than 35,000 fuel cell units shipped worldwide in 2013, making a total of 170 MW, nearly a 20% increase over 2012. This includes 80 MW shipped by the United States alone. Independent analyses have shown global markets could mature over the next 10–20 years, producing revenues of $14–$31 billion per year for stationary power, $11 billion per year for portable power, and $18–$97 billion per year for transportation. The global hydrogen market is also robust with over 55 Mtons produced in 2011 and over 70 Mtons projected in 2016, a >30% increase.

Another indicator of the robustness and innovative vitality of a thriving market is the number of patents granted, and the number of technologies commercialized. The number of patents in clean energy technologies continues to grow. The U.S. produced 44% of fuel cell patents followed by Japan with 33% from 2002 to 2012.[16] EERE-funded R&D has resulted in 499 patents, 45 commercial technologies, and 65 technologies that are projected to be commercialized within three to five years.[17] In addition, EERE's investment of $95 million in specific hydrogen and fuel cell projects led to more than $410 million in revenue and investments of approximately $70 million in specific projects led to a nearly $390 million in additional private investment.

With so much FCTO-supported activity in the last year, only a few are highlighted below.

At this year's Daytona 500, four fuel cell generators powered some of the broadcast cameras around the track, demonstrating how the technology could help NASCAR save money on fuel costs. As part of the FCTO-supported project, two 250-watt SOFCs were used to power some of the remote broadcast cameras and two 1-kilowatt SOFCs will be used to power lights in pit row.

[16] Clean Energy Patent Growth Index http://www.cepgi.com/2014/07/the-clean-energy-patent-growth-index-cepgi-published-quarterly-by-the-cleantech-groupat-heslin-rothenberg-farley.html

[17] http://energy.gov/eere/fuelcells/market-analysis-reports#mkt_pathways

Hexagon Lincoln, of Lincoln, Nebraska, more than doubled its workforce and added a fourth shift for 24-hour/7-days-a-week operation to accommodate growing demand for its carbon fiber composite tanks. With FCTO support, Hexagon developed a new trailer that uses high-strength composite vessels to carry more than 720 kg of hydrogen, thus transporting 2.5 times more compressed hydrogen gas than traditional steel tube trailers. With the increase in demand for their products for use on cars, trucks, and buses, and as large capacity tube trailers for delivering hydrogen and natural gas, the company has expanded annual sales from $33 million to $88 million and more than doubled their employees from 119 to 269 since 2010.

FCTO also completed a demonstration of landfill gas (LFG) as a source of renewable hydrogen production, using BMW's assembly plant in South Carolina as the host site. This project represents a first-of-its-kind LFG-to-hydrogen production project in the nation and is expected to serve as a model for future adoption of renewable biogas as a feedstock for hydrogen production. The hydrogen produced by this project could be used to power BMW's 300+ MHE fleet, the largest in the world to date.

While hydrogen infrastructure remains a key challenge to the widespread adoption of FCEVs, states like California continue to show their commitment. A series of major announcements in 2014 shows increased momentum in overcoming obstacles. For example, on April 30, the DOE announced the launch of a new project leveraging the capabilities of its national laboratories in direct support of H2USA. The project is led by NREL and SNL and will tackle the technical challenges related to hydrogen fueling infrastructure. The H2FIRST project is designed to reduce the cost and time of fueling station construction, increase station availability, and improve reliability by creating opportunities for industry partners to pool knowledge and resources to overcome hurdles.

FY 2014 brought with it a focus on technology transfer aligned with Assistant Secretary David Danielson's National Lab impact initiative. During the year, FCTO held two very successful financial forums that introduced DOE's early market projects to potential investors, business partners, and other stakeholders through presentations and a poster session in an effort to facilitate industry and investor awareness of these emerging and innovative technology areas.

EERE also recently announced the selection of small businesses for new SBIR awards that total nearly $6.3 million. Among the selections is a first-of-its-kind award under a new EERE SBIR technology-to-market topic that moves existing inventions developed at DOE's national laboratories to the marketplace and accelerates the pace of commercialization. Newton, Massachusetts-based Giner Inc. will use technology patented by LANL along with the company's well-established dimensionally-stabilized membrane technology to develop advanced, high-performance, and durable PEM electrode assemblies for fuel cell and electrolysis applications.

EERE cross-cutting activities proved successful as well. DOE researchers won 31 of the 100 awards given out this year by *R&D Magazine* for the most outstanding technology developments with promising commercial potential. PNNL was recognized for the Solar Thermochemical Advanced Reactor System, or STARS, that converts natural gas and sunlight into a more energy-rich fuel (syngas), which power plants can burn to make electricity. Initial funding was provided by FCTO to develop compact micro-meso-channel reactors and heat exchangers for the production of hydrogen from hydrocarbon fuels for use in automotive fuel cells. EERE's Solar Energy Technologies Office then supported an initial on-sun demonstration of the STARS concept—an evolution of the micro- and meso-channel concept—plus improvements that have achieved nearly 70% solar-to-chemical energy conversion. The group is now advancing the technology toward a commercial power generation application.

At the Washington Auto Show in January, Secretary Moniz highlighted the Energy Department's role in developing the next generation of fuel-efficient and electric vehicles and visited some of the latest vehicles that have benefitted from Energy Department R&D. Featured FCEVs included Hyundai's Tucson Fuel Cell that became available in Spring 2014, and a Toyota fuel cell vehicle that will be available in 2015.

In addition to the technical progress, education and outreach are critical and FCTO efforts have reached more than 30,000 code officials and first responders, 12,000 teachers, and more than 10,000 stakeholders per month through its monthly newsletter.[18] DOE also actively participated in the Senate and House Hydrogen and Fuel Cell Caucus events in FY 2014, including a ride and drive at which Deputy Secretary Poneman drove an FCEV. This event was followed by an EERE blog posting.[19]

This is a critical time for fuel cells and hydrogen. The DOE Hydrogen and Fuel Cell Program will continue to work in close collaboration with key stakeholders, and will continue its strong commitment to effective stewardship of

[18] http://energy.gov/eere/fuelcells/fuel-cell-technologies-office-newsletter

[19] http://energy.gov/eere/articles/hyundai-tucson-fuel-cell-electric-vehicle-visits-department-energy

tax payer dollars in support of its mission to enable the energy, environmental, and economic security of the Nation. In support of these efforts, the following nearly 1,000 pages document the results and impacts of the Program in the last year.

Sunita Satyapal
Director
Fuel Cell Technologies Office
U.S. Department of Energy

II. HYDROGEN PRODUCTION

II.0 Hydrogen Production Sub-Program Overview

INTRODUCTION

The Hydrogen Production sub-program supports research and development (R&D) of technologies that will enable the long-term viability of hydrogen as an energy carrier for a diverse range of end-use applications including transportation (e.g., specialty vehicles, cars, trucks, and buses), stationary power (e.g., backup power and combined-heat-and-power systems), and portable power. A portfolio of hydrogen production technology pathways utilizing a variety of renewable energy sources and renewable feedstocks is being developed under this sub-program.

Multiple DOE offices are engaged in R&D relevant to hydrogen production, including:

- The Fuel Cell Technologies Office (FCTO), within the Office of Energy Efficiency and Renewable Energy (EERE), is developing technologies for distributed and centralized renewable production of hydrogen. Distributed production options under development include reforming of bio-derived renewable liquids and electrolysis of water. Centralized renewable production options include water electrolysis integrated with renewable power generation (e.g., wind, solar, hydroelectric, and geothermal power), biomass gasification, solar-driven high-temperature thermochemical water splitting, direct photoelectrochemical water splitting, and biological processes.
- The Office of Fossil Energy (FE) has been advancing the technologies needed to produce hydrogen from coal-derived synthesis gas, including co-production of hydrogen and electricity. Separate from the Hydrogen and Fuel Cells Program, FE is also developing technologies for carbon capture, utilization, and storage, which will ultimately enable hydrogen production from coal to be a near-zero-emissions pathway.
- The Office of Science's Basic Energy Sciences (BES) program conducts research to expand the fundamental understanding of biological and biomimetic hydrogen production, photoelectrochemical water splitting, catalysis, and membranes for gas separation.
- The Office of Nuclear Energy (NE) is currently collaborating with EERE on a study of nuclear-renewable hybrid energy systems. Many of the systems being evaluated by this study use hydrogen production as a form of energy storage or as an input to industrial processes. The previous major hydrogen activity in NE, the Nuclear Hydrogen Initiative, was discontinued in Fiscal Year (FY) 2009 after steam electrolysis was chosen as the hydrogen production pathway most compatible with the next generation nuclear power.

GOAL

The goal of the Hydrogen Production sub-program is to develop low-cost, highly efficient hydrogen production technologies that utilize diverse domestic sources of energy, including renewable resources (EERE), coal with sequestration (FE), and nuclear power (NE).

OBJECTIVES

The objective of the Hydrogen Production sub-program is to reduce the cost of hydrogen dispensed at the pump to a cost that is competitive on a cents-per-mile basis with competing vehicle technologies. Based on current analysis, this translates to a hydrogen threshold cost of <$4 per kg hydrogen (produced, delivered, and dispensed, but untaxed) by 2020,[1] apportioned to <$2/kg for production only.[2] Technologies are being developed to achieve this goal in timeframes appropriate to their current stages of development.

The objectives of FE's efforts in hydrogen production are documented in the *Hydrogen from Coal Program Research, Development, and Demonstration Plan*.[3] They include proving the feasibility of a near-zero emissions, high-efficiency plant that will produce both hydrogen and electricity from coal and reduce the cost of hydrogen from coal by 25% compared with current technology by 2016. The objectives of NE's efforts in hydrogen production have been

[1] *Hydrogen Threshold Cost Calculation*, Program Record (Office of Fuel Cell Technologies) 11007, US Department of Energy, 2012, http://www.hydrogen.energy.gov/pdfs/11007_h2_threshold_costs.pdf

[2] *Hydrogen Production and Delivery Cost Apportionment*, Program Record (Office of Fuel Cell Technologies) 12001, US Department of Energy, 2012, http://hydrogen.energy.gov/pdfs/12001_h2_pd_cost_apportionment.pdf

[3] *Hydrogen from Coal Program Research Development and Demonstration Plan*, Office of Fossil Energy, US Department of Energy, September 2010, http://fossil.energy.gov/programs/fuels/hydrogen/2010_Draft_H2fromCoal_RDD_final.pdf

documented in the *Technology Roadmap for Generation IV Nuclear Energy Systems* (December 2002).[4] They include the development of high-temperature processes for hydrogen production compatible with next generation nuclear plants.

FY 2014 TECHNOLOGY STATUS AND ACCOMPLISHMENTS

In FY 2014, significant progress was made by the Hydrogen Production sub-program on several important fronts. For example:

- A Funding Opportunity Announcement (FOA) was released in November 2013, covering three hydrogen production topics: (1) novel systems using natural gas combined with renewable or low-carbon resources to produce hydrogen with greenhouse gas emissions significantly reduced when compared to traditional steam methane reforming; (2) hydrogen production from bio-derived liquids such as bio-oils, sugars, and alcohols using integrated system technologies for thermochemical conversion; and (3) advanced materials-based systems for direct solar water splitting. Six selected projects were announced in June 2014, as described in the following section.
- A joint solicitation with the National Science Foundation (NSF) was released in November 2013 for applications addressing discovery and development of advanced materials systems and chemical processes for direct photochemical and/or thermochemical water splitting for application in the solar production of hydrogen fuel. The selections were announced in August 2014.
- An Electrolytic Hydrogen Production Workshop was held in February 2014 to identify key R&D needs, and market and manufacturing challenges and opportunities. A report was posted on the website in July 2014, and a Request for Information (RFI) will be released to solicit public input.
- A Biological Hydrogen Production Workshop report was posted to the website in November 2013, and an RFI will be released to solicit public input.
- H2A v3 case studies for polymer electrolyte membrane (PEM) electrolysis were completed and posted,[5] and Hydrogen and Fuel Cells Program Record #14004 was published based on the results of the case studies.[6]

Hydrogen Production Cost Status

Recent and current status for the projected cost of hydrogen production for several of the near- to mid-term pathways is shown in Figure 1.

Detailed FY 2014 progress on numerous fronts in the Hydrogen Production sub-program is described in the following.

New Project Selections

In November 2014, a FOA was released to support R&D efforts to address critical challenges and barriers for hydrogen production technology development, and specifically the long-term goal of hydrogen production at <$2/kg hydrogen. Innovative materials, processes, and systems are needed to establish the technical and cost feasibility for renewable and low-carbon hydrogen production. With this FOA, DOE through FCTO sought to fund hydrogen production R&D projects to move technologies towards reaching the hydrogen production cost goal of <$2/kg. The six selected projects, announced at the 2014 Hydrogen and Fuel Cells Program Annual Merit Review and Peer Evaluation Meeting in June 2014, are:

- FuelCell Energy Inc. ($900K), Danbury, Connecticut; *Novel hybrid system for low-cost, low-greenhouse-gas hydrogen production.*
- Pacific Northwest National Laboratory ($2.2M), Richland, Washington; *Scalable, compact piston-type reactor for hydrogen production from bio-derived liquids.*

[4] *A Technology Roadmap for Generation IV Nuclear Energy Systems*, Office of Nuclear Energy, US Department of Energy, December 2002, http://curie.ornl.gov/system/files/documents/167/gen_iv_roadmap.pdf http://curie.ornl.gov/system/files/documents/167/gen_iv_roadmap.pdf

[5] Case studies available at http://www.hydrogen.energy.gov/h2a_prod_studies.html; supporting documents available at http://www.hydrogen.energy.gov/h2a_production_documentation.html

[6] DOE Hydrogen and Fuel Cells Program Record #14004 *Hydrogen Cost from PEM Electrolysis* is available at http://hydrogen.energy.gov/pdfs/14004_h2_production_cost_pem_electrolysis.pdf

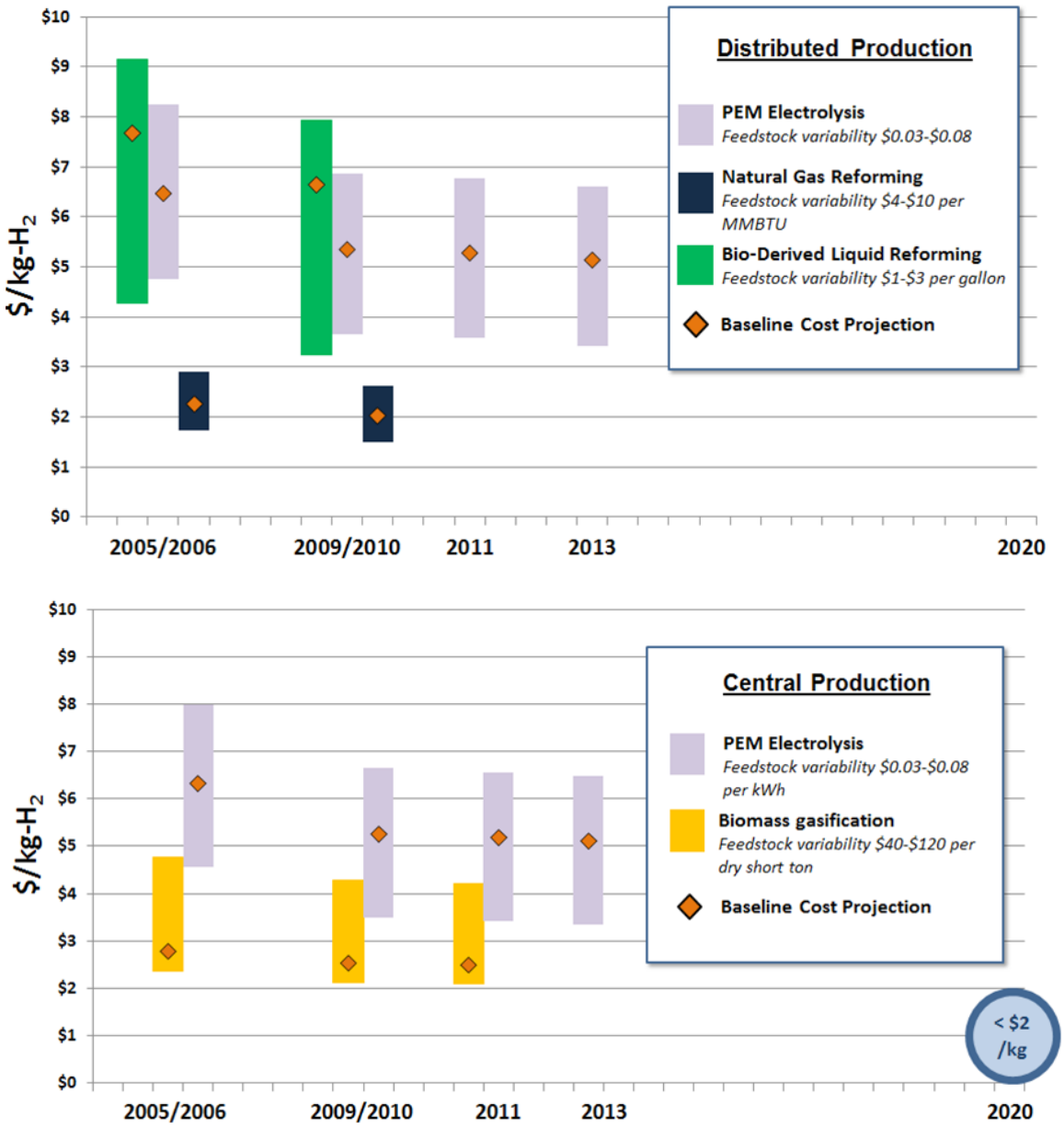

FIGURE 1. Range of hydrogen production costs, untaxed, for near- to mid-term distributed and centralized pathways. The high end of each bar represents a pathway-specific high feedstock cost as well as an escalation of capital cost; while the low end reflects a low end on feedstock costs and no capital escalation. Bars for different years in the same pathway represent improvements in the costs of the specific pathway, based on specific reference data for the appropriate year and pathway. Detailed information is included in the DOE Hydrogen and Fuel Cells Program Record #14005.[7]

- National Renewable Energy Laboratory (NREL) ($3M), Golden, Colorado; *High-efficiency tandem absorbers based on novel semiconductor materials that can produce hydrogen from water using solar energy.*
- University of Hawaii ($3M), Honolulu, Hawaii; *Photoelectrodes for direct solar water splitting.*
- Sandia National Laboratories (SNL) ($2.2M), Livermore, California; *An innovative high-efficiency solar thermochemical reactor for solar hydrogen production.*
- University of Colorado, Boulder ($2M), Boulder, Colorado; *A novel solar-thermal reactor to split water with concentrated sunlight.*

[7] DOE Hydrogen and Fuel Cells Program Record #14005 *Hydrogen Production Status 2006-2013*, under development.

PEM Electrolysis Case Studies

Industry-vetted case studies of hydrogen production costs via PEM electrolysis were completed and made publically available on the DOE website in FY 2014.[8] These cases modeled representative PEM electrolyzer systems and are based on input from several key industry collaborators with commercial experience. Four cases were analyzed, comprising two technology years, Current (2013) and Future (2025), and two production capacities, Distributed Forecourt (500-1,500 kg/day) and Centralized (50,000 kg/day). The process to evaluate the cases began with soliciting relevant, detailed information from the companies followed by synthesizing and amalgamating the data into base parameters for cases. The base parameters and sensitivity limits were vetted by the companies, and the data was then used to populate the four H2A v3 cases, which were run to project the hydrogen price.

The results of the Distributed and Centralized case studies indicated a current range of projected high-volume untaxed cost of hydrogen production via PEM electrolysis of ~$4.80/kg to $5.50/kg (Figure 2). Key cost drivers were identified and quantified, including electricity cost, electrolyzer efficiency, and capital cost. These results were documented in a DOE Hydrogen and Fuel Cells Program Record.[9]

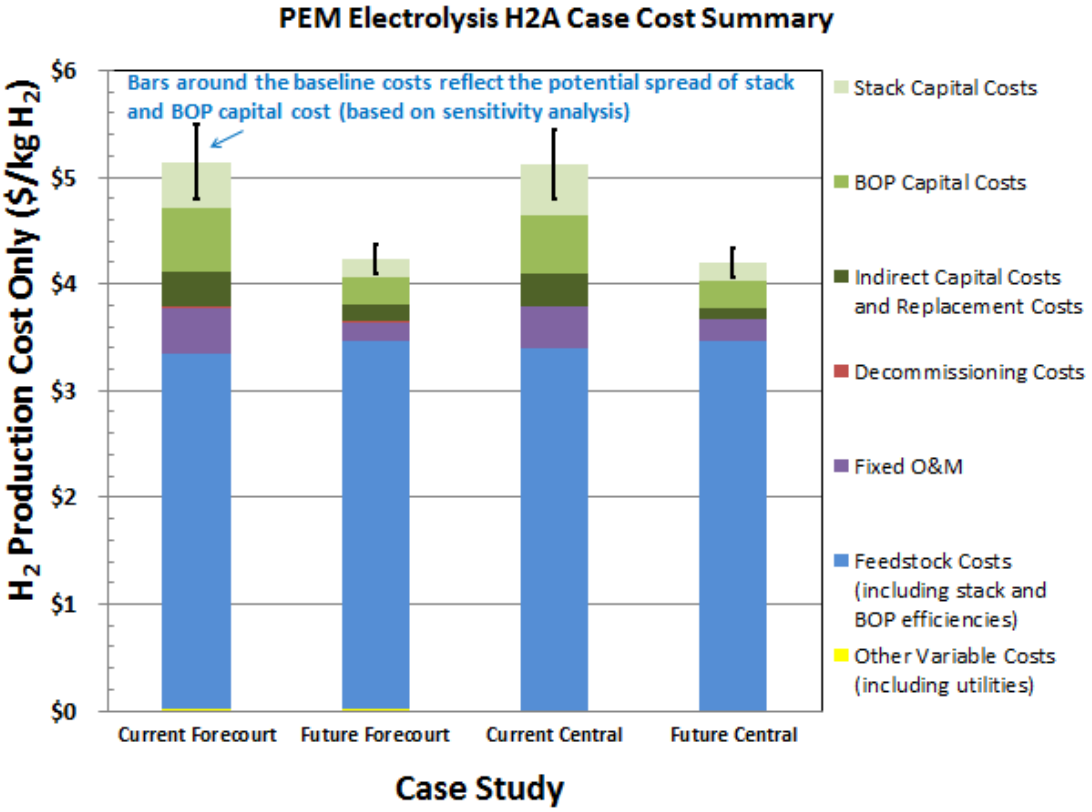

BOP - balance of plant; O&M - operations and maintenance

FIGURE 2. PEM electrolysis hydrogen production cost contributions (2007$/kg) for four case studies,[10] showing of projected high-volume untaxed costs ranging from ~$4.80 to $5.50/kg, broken down in terms of the major cost contributing factors.

[8] Case studies available at http://www.hydrogen.energy.gov/h2a_prod_studies.html; supporting documents available at http://www.hydrogen.energy.gov/h2a_production_documentation.html.
[9] DOE Hydrogen and Fuel Cells Program Record #14005, Hydrogen Cost from PEM Electrolysis available at http://hydrogen.energy.gov/pdfs/14004_h2_production_cost_pem_electrolysis.pdf
[10] Based on case-dependent electricity prices of 6.12¢/kWh, 6.88¢/kWh, 6.22¢/kWh and 6.89¢/kWh, respectively.

Separation Processes

Membrane separations research, development, and demonstration continued through the Small Business Innovation Research program and FE. Technical progress included:

- A sorbent bed was developed, through a Phase III Small Business Innovation Research project, to operate downstream of a bulk desulfurization system as a polishing bed to provide essentially sulfur-free biogas to a solid oxide fuel cell. In FY 2014, the design of an interface to connect the biogas cleanup skid to a 2-kWe solid oxide fuel cell skid was successfully completed. A field demonstration of the integrated system and an economic assessment of the technology is planned for late FY 2014. (TDA Research, Inc.)
- FE is funding projects to carry out comprehensive engineering design of advanced hydrogen-carbon dioxide Pd and Pd-alloy composite membrane separations for hydrogen production from syngas derived from coal or coal-biomass mixtures. The primary goal is to demonstrate the separation of hydrogen from coal- or coal-biomass-derived syngas via membranes at the pre-engineering/pilot scale to enable the use of coal for hydrogen production with reduced carbon dioxide emissions. The teams evaluated membrane performance based on flux, sulfur tolerance, water-gas shift activity, and hydrogen purity under syngas conditions expected from coal gasification. Five project teams successfully designed, constructed, and tested membranes with operating gasifier and/or simulated syngas mixtures that produced 2 lb/day of hydrogen. A down-select process has resulted in two project teams that were awarded projects to augment successful completion of their designs. The project teams plan to construct membrane separation modules with the capacity to produce up to 50 lbs/day of hydrogen.

Electrolysis Hydrogen Production

The major emphasis of the electrolysis projects was on cost reduction and efficiency improvement through leveraging catalyst development. Work on alkaline membrane electrolysis is showing promise to deliver electrolyzer systems with very low platinum-group metal (PGM) loading. Additional work focused on electrolyzer system cost reductions by minimizing balance-of-plant losses. Technical progress included:

- The manufacture of core shell catalyst technology developed by Brookhaven National Laboratory was successfully transferred to its facility and achieved equivalent cathode performance at $1/10^{th}$ of the cathode PGM loading relative to the 2013 baseline. (Proton OnSite)
- A nano-structured thin film catalyst anode technology was tested under electrolysis conditions and demonstrated comparable performance at $1/16^{th}$ of the anode PGM loading relative to a 2013 baseline. (Giner, Inc. and 3M)
- An improved drying technique was developed with the potential to reduce drying losses in electrolyzers to less than 3.5% (compared with 11-8% in commercial systems) while operating on a variable (wind or solar) stack power profile. Testing is in progress to verify that the new technique meets SAE International Standard J2719 specifications for water content (<5 ppm). (NREL)

Photoelectrochemical Hydrogen Production

The broad focus of projects in this area was on utilizing state-of-the-art theory, synthesis, and characterization tools to develop viable photoelectrochemical material systems and prototypes with improved efficiency and durability. Technical progress included:

- Greater than 300 hours of stability were demonstrated at ~15 mA/cm^2 in III-V semiconductor photoelectrochemical tandem devices, representing a significant improvement over the previous year's 115 hours at 10 mA/cm^2. This result represents an important step forward toward demonstration of stabilized solar-to-hydrogen conversion efficiencies >20% using photoelectrochemical devices. (NREL)
- Joint theoretical/experimental studies were continued on III-V photoelectrochemical electrode surfaces, including the development of a theoretical hydrogen evolution model relevant to photoelectrochemical hydrogen production that incorporates hydrogen diffusion; this resulted in the discovery that a low hydrogen diffusion barrier and low Heyrovsky barrier on a semiconductor surface can activate additional hydrogen evolution reaction channels to improve overall kinetics. (Lawrence Livermore National Laboratory and the NREL Surface Validation Team)
- Midwest Optoelectronics, LLC is working towards commercial-size photoelectrochemical electrodes; achieved 3.3% solar-to-hydrogen conversion efficiency for immersion-type photoelectrochemical cells of 4-inch by 4-inch size using low-cost electroplated Ni hydrogen evolution reaction catalysts. (Midwest Optoelectronics, LLC)

Biological Hydrogen Production

The broad focus of the projects in the biological hydrogen production portfolio addressed key barriers such as oxygen sensitivity and feedstock utilization using molecular biology and genetic engineering techniques along with improved systems engineering. Technical progress included:

- Increased activity of the Chlamydomonas strain was demonstrated expressing the Ca1 hydrogenase from 2% to about 11% of the native hydrogenase, with a duration of 30 minutes or more. (NREL)
- An average hydrogen production rate of 466 mL/L-reactor/day from fermentation of pretreated corn stover (a realistic lignocellulosic feedstock for industrial biofuel production), rather than the pure cellulosic feedstock previously used, was demonstrated with no indication of lignin inhibition. Additionally, a larger, more scalable microbial reverse-electrodialysis cell design demonstrated a 0.9 L/L-reactor/day hydrogen production rate, a 12.5% increase over the 2013 demonstrated rate, using a salinity gradient instead of grid electricity. (NREL)
- The genome of the bacterium Rubrivivax gelatinosus Casa Bonita Strain (CBS) was examined for candidate genes to transfer to the cyanobacteria Synechocystis to improve the expression and activity of the non-native CBS hydrogenase enzyme. The researchers identified slyD, involved in binding and inserting Ni into the hydrogenase active site, as a likely gene as it is present in CBS but absent in Synechocystis. Researchers also improved the Synechocystis expression of the CBS maturation protein HypF, which is involved in assembling the active hydrogenase enzyme, up to nine-fold. (NREL)
- The truncated light-harvesting antenna concept was applied to cyanobacteria, demonstrating that a Δcpc strain of *Synechocystis*, which is missing the phycobilisome portion of the photosynthetic antenna, can reach higher light levels before saturation than the wild type and has 55-60% greater rates of biomass accumulation. (University of California, Berkeley)

Solar-Thermochemical Hydrogen Production

Efforts in these projects were directed toward performance characterization of water splitting by novel, non-volatile metal-oxide based reaction materials and developing new reactor concepts to optimize efficiency of the reaction cycles. Technical progress included:

- A thermodynamic model was developed for Sr- and Mn-doped $LaAlO_3$ perovskite reaction materials that predicts the optimal operating temperature, oxygen pressure, and heat recovery effectiveness required for a solar-to-hydrogen conversion efficiency >20%; and derived performance criteria and thermodynamic properties for an "ideal" non-stoichiometric oxide reaction material. (SNL)
- Over three times improvement in hydrogen production was demonstrated relative to 2013 results of 100 micromole/g for isothermal operation at 1,350ºC for hercynite cycle materials using near-isothermal reduction/oxidation cycling. (University of Colorado, Boulder)
- Integration of major components into a pressurized button cell test facility was completed for the electrolysis step of the Hybrid Sulfur thermochemical cycle that will allow testing of catalysts and membranes at pressures up to 1 MPa and temperatures of 130ºC. The team identified and screened electrocatalysts with the potential to reduce oxidation overpotential by >20 mV versus the state-of-the-art platinum catalyst. Savannah River National Laboratory (SRNL) also tested thin-film electrodes as candidate anode electrocatalysts, including Pt, Pd, Ir, Au, PtAu, and PtV. Au, PtAu and PtV showed 28 mV, 46 mV, and 13 mV reduction, respectively, on the anode polarization versus state-of-the-art Pt catalyst. (SRNL)

Hydrogen Production Pathway Analysis

The focus of the analysis efforts was on establishing standardized procedures for hydrogen production pathway technoeconomic case studies utilizing the H2A v3 tool with technical inputs from production pathway experts, applying the procedures toward the completion of a series of PEM electrolysis case studies, and initiating bio-fermentation and high-temperature solid oxide electrolysis case studies. Technical accomplishments included:

- New technoeconomic case studies were completed specifically for the PEM electrolysis production pathway, applying the H2A v3 Production Model to analyze hydrogen costs ($/kg hydrogen) and cost sensitivities. The results of the Distributed and Centralized case studies indicated a current range of projected high-volume untaxed cost of hydrogen production via PEM electrolysis of ~$4.80/kg to $5.50/kg. (Strategic Analysis, Inc., NREL, Argonne National Laboratory, ANL)

- Technical questionnaires were distributed to experts in the fields of bio-fermentation and high-temperature solid oxide electrolysis to initiate the H2A v3 case studies of these pathways. (Strategic Analysis, Inc., NREL, and ANL)

BUDGET

The FY 2014 appropriation for the Hydrogen Production and Hydrogen Delivery sub-programs was $21 million. Funding was distributed approximately evenly between Production and Delivery, representing an increase in funding to Delivery relative to past years, when funding was distributed with approximately two thirds to Production and one third to Delivery. This distribution reflects the current FCTO emphasis on hydrogen infrastructure technology R&D. The request for Production and Delivery in FY 2015 is $21 million. The estimated budget breakdown for Production funding in FY 2014 and FY 2015 is shown in Figure 3. Production has increasingly focused in past years on long-term, renewable pathways such as photoelectrochemical, biological, and solar-thermochemical hydrogen production. This trend generally continued in FY 2014 with several new projects selected from funding opportunities falling into the photoelectrochemical and solar-thermochemical hydrogen categories, supplemented by two newly selected projects in the nearer-term distributed renewable production category. The emphasis on a balanced portfolio of long-term and nearer-term renewable technologies is expected to continue into FY 2015.

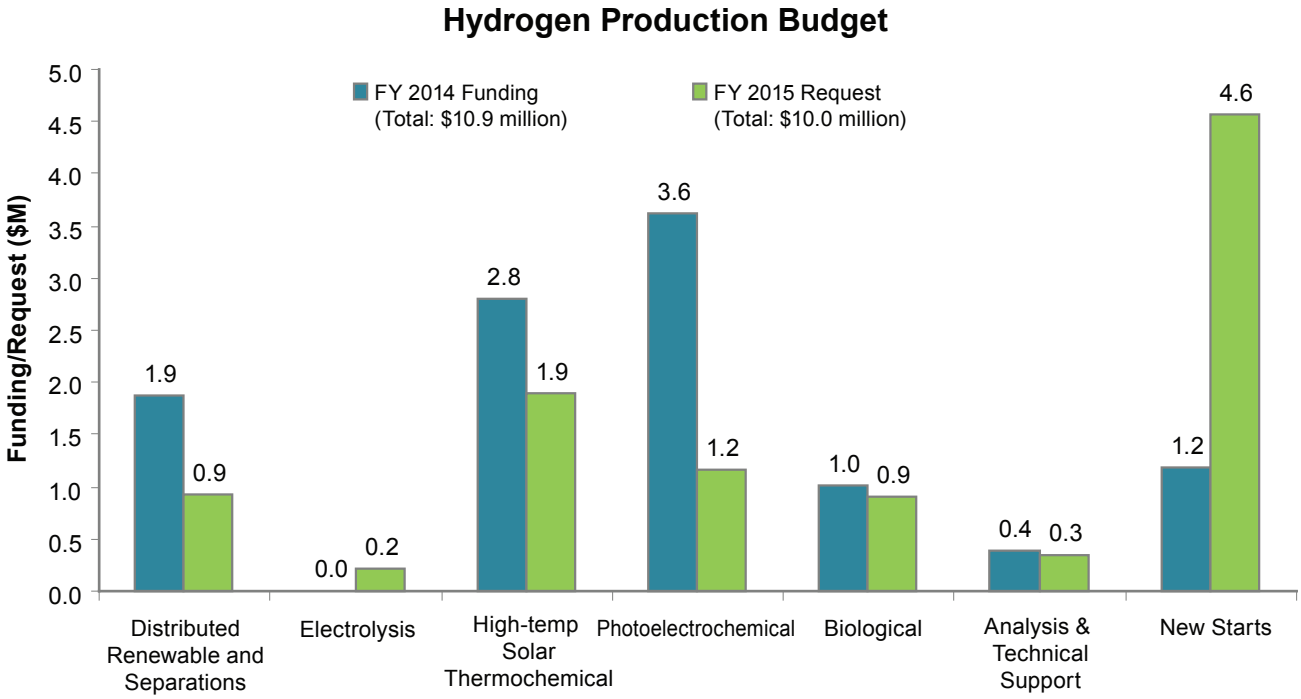

* Subject to appropriations, project go/no-go decisions, and competitive selections. Exact amounts will be determined based on research and development progress in each area.

FIGURE 3. Hydrogen Production Budget. Budget amounts for FY 2014 and projected amounts for FY 2015, contingent upon appropriations, are shown broken down by the different production pathways. Exact distribution of funds in FY 2015 will not be defined until funds have been appropriated and new projects selected.

FY 2015 PLANS

General Hydrogen Production sub-program plans for FY 2015 include:

- Demonstrate substantial initial progress in the six new projects selected under the 2014 Hydrogen Production FOA.
- Continue emphasis on materials durability, production efficiency, and process optimization for all pathways, and develop and refine materials characterization protocols and performance metrics for early development technologies.

- Continue to develop and update hydrogen production pathways analyses with the H2A v3 tool developing case studies on bio-fermentation and high-temperature solid oxide electrolysis and establishing cost and performance baselines for new project starts.
- Continue coordination with the Office of Science and NSF, which fund fundamental and use-inspired research related to hydrogen and fuel cell technologies. Leveraging BES and NSF activities improves the understanding of scientific issues related to hydrogen production (particularly in the longer-term R&D areas of photoelectrochemical and biological processes), and can help address the fundamental challenges of hydrogen production. Coordination of FCTO's systems-oriented hydrogen production R&D with the solar-hydrogen-related fundamental research activities in the Office of Science's Solar Fuels Innovation Hub and with the use-inspired projects selected under the joint NSF/EERE solicitation "Renewable Hydrogen Fuel Production via Solar Water Splitting" will remain a high priority.
- Release an RFI inviting further input on the 2014 Electrolytic Hydrogen Production Workshop Report, and prepare and post an Addendum to the Workshop Report based on RFI responses. Outcomes of the workshop and responses to the RFI will be used to inform programmatic planning.

Important pathway-specific milestones planned for FY 2015 in the Hydrogen Production sub-program projects include:

- Demonstrate fermentation of deacetylated corn stover lignocellulose in a sequencing fed-batch bioreactor and obtain a hydrogen production rate of 450 mL H_2/L/d with a total hydrogen output of 80% of that of avicel cellulose based on the same amount of cellulose loading (5 g/L).
- Deliver 100 feet of roll-to-roll produced electrolysis catalyst with a durability of <20 mV drop after 1,000 hours of operation at 1.5 A/cm^2, and with a total PGM loading of less than 0.5 mg/cm^2.
- Demonstrate the viability of stabilized photoelectrochemical systems with >15% solar-to-hydrogen efficiency using advanced tandem devices based on either III-V crystalline semiconductor or chalcopyrite thin-film semiconductor materials.
- Develop a monolith reactor concept for integration of steam reforming reactions with in situ carbon dioxide capture and heat transfer for high-throughput hydrogen production from bio-oils. Identify optimum reforming catalysts and sorbents for >80% of equilibrium hydrogen yield at T <500°C, and >90% carbon dioxide capture under reaction conditions.
- Continue development of conceptual designs for fully integrated solar thermochemical prototype reactors and synthesis and evaluation of perovskite and hercynite reaction materials. Demonstrate the production of spray-dried active materials that produce at least 150 µmol H_2/g total and reduction of at least 1 gram of oxidized spray-dried active materials under vacuum pumping to remove released O_2, and oxidation of at least 1 gram reduced spray-dried active materials with steam to produce hydrogen.
- Completion of H2A v3 case studies for bio-fermentation and high-temperature solid oxide electrolysis hydrogen production pathways.

Sara Dillich
Hydrogen Production & Delivery Program Manager
Fuel Cell Technologies Office
U.S. Department of Energy
1000 Independence Ave., SW
Washington, D.C. 20585-0121
Phone: (202) 586-7925
Email: Sara.Dillich@ee.doe.gov

II.A.1 Hydrogen Pathways Analysis for Polymer Electrolyte Membrane (PEM) Electrolysis

Brian D. James (Primary Contact),
Whitney G. Colella, Jennie M. Moton
Strategic Analysis, Inc.
4075 Wilson Blvd, Suite 200
Arlington, VA 22203
Phone: (703) 778-7114
Email: bjames@sainc.com

DOE Managers
Eric Miller
Phone: (202) 287-5829
Email: Eric.Miller@ee.doe.gov
Katie Randolph
Phone: (720) 356-1759
Email: Katie.Randolph@ee.doe.gov

Contract Number: DE-EE0006231

Project Start Date: March 15, 2013
Project End Date: March 14, 2016

Overall Objectives

- Analyze hydrogen production and delivery (P&D) pathways and provide case studies to DOE for enabling informed evaluation of the most economical, environmentally benign, and societally feasible paths for the P&D of hydrogen fuel for fuel cell vehicles (FCVs).
- Identify key "bottlenecks" to the success of these pathways, primary cost drivers, and remaining R&D challenges.
- Assess technical progress, benefits and limitations, levelized hydrogen costs, and potential to meet DOE P&D cost goals of $2 to $4 per gasoline gallon equivalent (gge) (dispensed, untaxed) by 2020.
- Provide analyses that assist DOE in setting research priorities.
- Apply the H2A Production Model as the primary analysis tool for projection of levelized hydrogen costs (U.S. dollars per kilogram of hydrogen [$/kg hydrogen]) and cost sensitivities.

Fiscal Year (FY) 2014 Objectives

- Develop a hydrogen pathway validation case based on hydrogen generation with grid-powered PEM electrolyzers.
- Select additional hydrogen pathways for analysis, gather information on those hydrogen pathways, and define those hydrogen pathways.
- Initiate a hydrogen pathway case based on hydrogen generation via dark fermentation of bio-feedstocks.
- Initiate a hydrogen pathway case based on hydrogen generation via high-temperature electrolysis using solid oxide electrolysis cells (SOECs).

Technical Barriers

This project addresses the following technical barriers from the Hydrogen Production section of the Fuel Cell Technologies Office Multi-Year Research, Development, and Demonstration Plan:

Hydrogen Generation by Water Electrolysis

(F) Capital Cost

(G) System Efficiency and Electricity Cost

(K) Manufacturing

Dark Fermentative Hydrogen Production

(AX) Hydrogen Molar Yield

(AY) Feedstock Costs

(AZ) Systems Engineering

Technical Targets

This project conducts cost modeling to attain realistic cost estimates for the production and delivery of hydrogen fuel for FCVs. These values can help inform future technical targets.

- DOE P&D cost goals: $2 to $4/gge of hydrogen (dispensed, untaxed) by 2020

FY 2014 Accomplishments

- Completed a validation case for hydrogen generation with grid-powered, distributed and central, PEM electrolyzers using the H2A Production Model (Version 3) (Year 1, Milestone 2).
  - Developed PEM electrolysis case materials and supporting documentation and made them publicly available and downloadable from the website: http://www.hydrogen.energy.gov/h2a_prod_studies.html
  - Developed four PEM electrolysis public cases that reflect a $4/kg to $5/kg hydrogen production cost, based on an average cost of electricity of 6.1¢ to

6.9¢/kWh. Found electricity costs to be the primary cost driver.

  - Quantitatively demonstrated that the three main cost drivers for the levelized hydrogen cost from PEM electrolysis are (1) electricity price, (2) electrolyzer electrical efficiency, and (3) electrolyzer capital cost.
  - Described the PEM electrolysis capital cost breakdown in detail, which is a unique contribution of this work.
- Initiated hydrogen pathway cases based on hydrogen generation from dark fermentation of biomass.
  - Developed a questionnaire to solicit case parameter information from industry and researcher experts.
  - Distributed questionnaire and collected data.
- Initiated hydrogen pathway cases based on hydrogen generation from SOEC.
  - Developed a questionnaire to solicit case parameter information from industry and researcher experts.
  - Distributed questionnaire and collected data.

INTRODUCTION

This report reflects work conducted in the first year of a three-year project to analyze innovative hydrogen production and delivery pathways and their potential to meet the DOE P&D cost goal of $2/gge to $4/gge by 2020. To date, work has concentrated on a validation case based on PEM electrolysis technology. The purpose of the validation case is to demonstrate the successful application of the analysis procedure to a near-term technology for which some measure of information is known and against which modeling results can be compared. After validation, the analysis methodology can be applied to less developed technologies with greater confidence in the results. The analysis methodology utilizes DOE's H2A Distributed and Central Hydrogen Production models.[1] Those models provide a transparent modeling framework and apply standard mass, energy, and economic analysis methods agreed upon by DOE's Hydrogen and Fuel Cells Program.

APPROACH

The following approach was applied to the PEM electrolysis case study and is the model for future analyses:

- Conduct literature review
- Develop, circulate, and analyze results from an industry questionnaire covering the targeted technology (i.e., PEM electrolysis)
- Define generalized cases for systems of different sizes and technology readiness levels (TRLs)
- Run H2A models with general case input data to calculate the levelized cost of hydrogen ($/kg hydrogen)
- Perform sensitivity analyses (including tornado and waterfall charts) to identify key cost drivers
- Document case study results
- Vet case study results with DOE, industry, and team partners
- Repeat these steps until agreement is attained among project partners

A questionnaire spreadsheet was circulated to four electrolyzer companies (Giner Inc., Hydrogenics Inc., ITM Power LLC, and Proton Onsite Inc.) to gather data on PEM electrolyzer performance. Collected data included H2A model input parameters necessary for developing cases and covered engineering system definition, stack and balance-of-plant (BOP) capital costs, and other economic factors. The research team analyzed this data and used it to synthesize generalized cases, so as not to reveal any one company's sensitive technical information. Four public generalized cases were developed.

- Current Forecourt
- Current Central
- Future Forecourt
- Future Central

Data from the four generalized cases were used to populate the H2A Model (Version 3.0) and to generate estimates of the levelized hydrogen cost. The four eletrolyzer companies vetted the generalized cases, H2A model results, sensitivity limit parameters and results, and resulting documentation.

Two hydrogen production plant sizes are considered: Forecourt[2] at 1,500 kg hydrogen/day and Central at 50,000 kg hydrogen/day. Two technology development time horizons are considered: Current for year 2013 TRL and Future for year 2025 TRL. Current cases assume a short-term technology readiness projection from technology that has been demonstrated already in the lab. Future cases project the development of the technology with better materials, capabilities, efficiencies, lifetimes, and costs than that currently demonstrated. A fifth non-public case was also developed based on existing PEM electrolyzer TRL performance (i.e., using commercially available products). However, results are not disclosed due to corporate sensitivities.

[1] http://www.hydrogen.energy.gov/h2a_analysis.html

[2] Hydrogen production cost is the focus of the case study. For the Forecourt cases, compression, storage, and dispensing computations are included in the base H2A spreadsheet, and thus they are also reported in the case study.

Analyses were also initiated for hydrogen production via dark fermentation and high temperature SOEC. The dark fermentation case study considers three types of biomass feedstock, an energy crop (e.g., corn stover), a waste stream (e.g., agricultural waste), and a refined bioproduct (e.g., alcohol or sugar). For both analyses, the team conducted a literature review, cultivated a list of experts to serve as questionnaire respondents (including the European Institute for Energy Research for the SOEC analysis), created a detailed techno-economic questionnaire, revised the questionnaire in response to expert technical feedback from DOE and from the Idaho National Laboratory (INL) for the SOEC analysis, circulated the questionnaire to the list of experts, pursued non-disclosure agreements at the request of experts, and collected initial questionnaire responses from several entities. Draft case studies are in the process of being created but analysis results are not yet available.

RESULTS

Figure 1 shows the cost results for the four public H2A Production PEM electrolysis cases. The y-axis shows the levelized cost of producing hydrogen and the cost breakdown. All cases reflect a $4/kg to $5/kg hydrogen production cost, based on an average cost of electricity of 6.1¢/kWh to 6.9¢/kWh. The primary cost driver is the feedstock cost, which is mainly the cost of electricity expenditures for operation of the PEM stack[3]. These feedstock costs can be reduced through either lower electricity prices or higher electrolyzer efficiencies. The second most important cost driver is the electrolyzer equipment capital cost, which includes the costs of the stack and associated BOP. The figure also shows that the reduction in hydrogen cost is estimated to be larger in moving from a Current to a Future case, compared with moving from a Forecourt to a Central case. Although the data is not shown publicly for the Existing case, it is important to note that large capital cost reductions are predicted between Existing and Current systems, and between Current and Future systems. The vertical bars at the top of the figure reflect the low and high projections based solely on low and high sensitivity limits for uninstalled capital costs (including stack and BOP costs) that were agreed upon by industry. Also, in addition to the levelized hydrogen production cost shown on the y-axis, the cost of compression, storage, and dispensing is expected to add between 37% and 47% in the Forecourt cases.

[3] Water is technically the only feedstock. However, electricity is tabulated under feedstock cost, and not utility cost, to match past analyses.

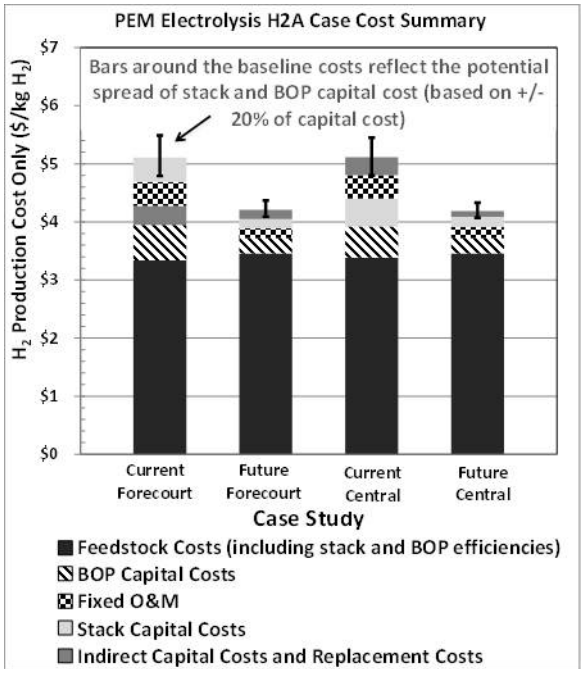

FIGURE 1. H2A Production PEM Electrolysis Breakdown (cost results reported in 2007$; average electricity prices for all cases range between 6.1 cents/kWh and 6.9 cents/kWh)

A unique contribution of this work is the detailed capital cost breakdown, which is shown for the Current Forecourt Case in Figure 2. The stack constitutes ~41% of system capital cost, and is the primary cost driver for system capital costs in all cases. For the Current Forecourt Case, ~60% of the stack capital costs can be attributed to the combined costs of the membrane, catalyst, anode, and cathode.

Figures 3 and 4 show waterfall charts for the Forecourt and Central cases. The waterfall charts graphically show the cumulative change in hydrogen production cost on the y-axis corresponding to each change in input parameter on the x-axis in moving from the Current case on the left to the Future case on the right. The charts show that the increase in electricity price expected over time is expected to be

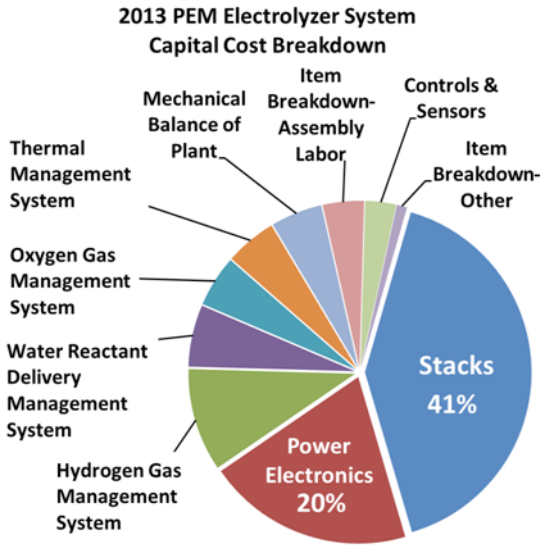

FIGURE 2. Capital Cost Breakdown for Current Forecourt Case

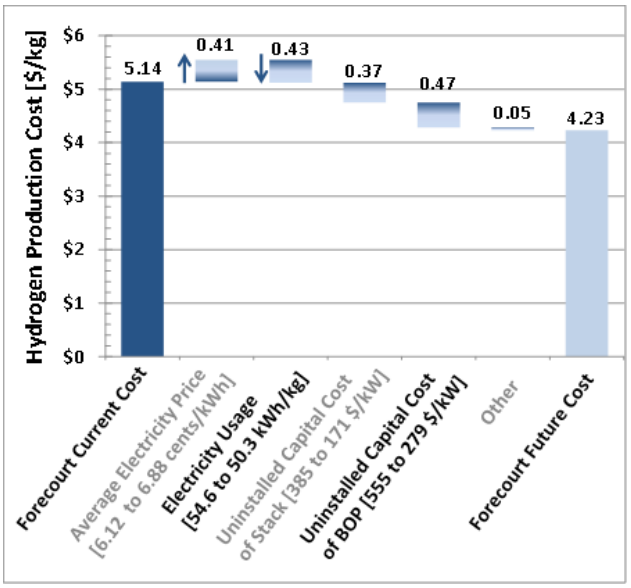

FIGURE 3. Waterfall Chart for the Forecourt Case

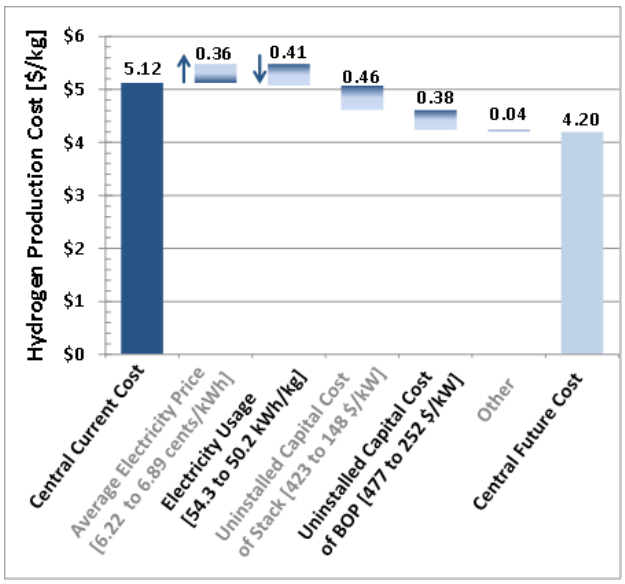

FIGURE 4. Waterfall Chart for the Central Case

counteracted by the increase in electrical efficiency of the electrolyzer stack over time. Because the model's electricity prices follow the Annual Energy Outlook projections, which vary by year, and because the Current and Future cases cover different timespans, an increase in electricity price is expected between Current and Future cases, and therefore electricity expenditures increase, as shown in the chart's second column from the left. At the same time, the increase in electrical efficiency expected in the future reduces net electricity expenditures and brings down the hydrogen production cost. This counteractive effect is shown in the third column from the left in each chart.

All of the case studies correspond to futuristic scenarios since PEM electrolyzer are not currently mass-produced. Consequently, direct comparisons between case study results here and existing system costs do not constitute an apples-to-apples comparison. However, to the extent possible, the methodology, input variables, and results for the PEM electrolyzer were vetted by the four electrolyzer companies, judged to be reasonable, and thus informally validated for purposes of application to future case studies.

CONCLUSIONS AND FUTURE DIRECTIONS

In its first year, this project made key observations and important achievements.

- A Validation Case was completed for hydrogen generation with grid-powered PEM electrolyzers using the H2A Production Model (V3).
- Four PEM electrolysis companies were asked to fill out questionnaires inquiring about engineering and economic information for PEM electrolyzers, and five generalized cases were developed (four public, one non-public).
- Large capital cost reductions are predicted between Existing and Current systems, and between Current and Future systems.
- All PEM Electrolysis cases reflect a $4/kg to $5/kg hydrogen production cost, based on an average cost of electricity of 6.1¢ to 6.9¢/kWh. Electricity costs are the primary cost driver.
- The hydrogen cost reduction is greater in moving from a Current to a Future case, compared with moving from a Forecourt to a Central case.
- The three main cost drivers for the levelized hydrogen cost are (1) electricity price, (2) electrolyzer electrical efficiency, and (3) electrolyzer capital cost.
- A unique contribution of this work is the detailed capital cost breakdown.
- Compression, storage and dispensing costs are expected to add ~37% to ~47% to the levelized hydrogen production cost in the Forecourt Cases.
- Analysis of dark fermentation of biomass and SOEC electrolysis was initiated. Results are not yet available.

SPECIAL RECOGNITIONS & AWARDS/ PATENTS ISSUED

1. Hydrogen and Fuel Cells Program Award. Awarded to Brian D. James by the Director of the Fuel Cell Technologies Office, Sunita Satyapal, June 17th 2014.

FY 2014 PUBLICATIONS/PRESENTATIONS

Web-Posted PEM Electrolysis Case Studies and Supporting Documentation

H2A Production Version 3 Excel Models: http://www.hydrogen.energy.gov/h2a_prod_studies.html

- *Central Electrolysis*
  - Current Central Hydrogen Production from PEM Electrolysis Version 3.0
  - Future Central Hydrogen Production from PEM Electrolysis Version 3.0
- Forecourt (Distributed) Electrolysis
  - Current Forecourt Hydrogen Production from PEM Electrolysis Version 3.0
  - Future Forecourt Hydrogen Production from PEM Electrolysis Version 3.0

Supporting Documentation

- Report: James, B.D., Colella, W.G., Moton, J.M., Saur, G., Ramsden, T.G., *PEM Electrolysis H2A Production Case Study Documentation*, report for the U.S. DOE EERE FCT program, December 2013: http://www.hydrogen.energy.gov/pdfs/h2a_pem_electrolysis_case_study_documentation.pdf
- Slide presentation: Colella, W.G., James, B.D., Moton, J.M., "Hydrogen Pathways Analysis for Polymer Electrolyte Membrane (PEM) Electrolysis," *2014 DOE Hydrogen and Fuel Cells Program and Vehicle Technologies Office Annual Merit Review and Peer Evaluation Meeting*, Washington, D.C., June 16th-20th, 2014. http://www.hydrogen.energy.gov/pdfs/review14/pd102_james_2014_o.pdf
- DOE program record, http://www.hydrogen.energy.gov/pdfs/14004_h2_production_cost_pem_electrolysis.pdf

Peer-Reviewed Journal Articles and Conference Proceedings

1. Colella, W. G., James, B. D., Moton, J. M., Saur, G., Ramsden, T., "Next Generation Hydrogen Production Systems Using Proton Exchange Membrane Electrolysis," *Proceedings of the ASME 2014 12th Fuel Cell Science, Engineering and Technology Conference*, June 30th-July 2nd, 2014, Boston, Massachusetts, USA, ESFuelCell2014-6649.

2. Colella, W.G., Moton, J.M., James, B.D. "Techno-Economic Analysis of Advanced Approaches for Generating Hydrogen Fuel for Vehicles," *Proceedings of the Fifth European Fuel Cell Technology & Applications Conference - Piero Lunghi Conference and Exhibition (EFC2013)*, Rome, Italy, Dec. 11th-13th, 2013 (EFC13-180).

3. Colella, W.G., "Reducing Energy, Environmental, and Economic Constraints in Global Transport Supply Chains with Novel Fuel Cell and Hydrogen Technologies," *Proceedings of the Fifth European Fuel Cell Technology & Applications Conference - Piero Lunghi Conference and Exhibition (EFC2013)*, Rome, Italy, Dec. 11th-13th, 2013 (EFC13-178).

4. Colella, W.G. "Resolving Constraints in Global Energy Supply with Cogenerative, Polygenerative, and Fast Ramping Fuel Cells," *Proceedings of the Fifth European Fuel Cell Technology & Applications Conference - Piero Lunghi Conference and Exhibition (EFC2013)*, Rome, Italy, Dec. 11th-13th, 2013 (EFC13-177).

Peer-Reviewed Reports

1. James, B. D., Colella, W. G., Moton, J. M., Saur, G., Ramsden, T., *PEM Electrolysis H2A Production Case Study Documentation*, report for the U.S. DOE EERE FCT program, Revised and Publicly Re-Released June 2014.

2. James, B. D., Colella, W. G., Moton, J. M., Saur, G., Ramsden, T., *ADDENDUM to the PEM Electrolysis H2A Production Case Study Documentation*, report for the U.S. DOE EERE FCT program, Revised and Re-Submitted June 2014.

Plenary Oral Conference Presentations

1. Colella, W.G., James, B.D., Moton, J.M., Saur, G., Ramsden, T.G., "Techno-economic Analysis of PEM Electrolysis," *Electrolytic Hydrogen Production Workshop*, U.S. DOE EERE FCT Office and the National Renewable Energy Laboratory (NREL), Golden, Colorado, Feb. 27th-28th, 2014.

Oral Conference Presentations

1. Colella, W.G., James, B. D., Moton, J.M., "Hydrogen Pathways Analysis for Polymer Electrolyte Membrane (PEM) Electrolysis," *2014 DOE Hydrogen and Fuel Cells Program and Vehicle Technologies Office Annual Merit Review and Peer Evaluation Meeting*, Washington, D.C., June 16th-20th, 2014.

2. Colella, W.G., Moton, J.M., James, B.D. "Techno-Economic Analysis of Advanced Approaches for Generating Hydrogen Fuel for Vehicles," *Fifth European Fuel Cell Technology & Applications Conference - Piero Lunghi Conference and Exhibition (EFC2013)*, Rome, Italy, Dec. 11th-13th, 2013 (EFC13-180).

3. Colella, W.G., "Reducing Energy, Environmental, and Economic Constraints in Global Transport Supply Chains with Novel Fuel Cell and Hydrogen Technologies," *Fifth European Fuel Cell Technology & Applications Conference - Piero Lunghi Conference and Exhibition (EFC2013)*, Rome, Italy, Dec. 11th-13th, 2013 (EFC13-178).

4. Colella, W.G., James, B.D., Spisak, A.B., Moton, J.M., "Next Generation Electrochemical Systems," *American Institute of Chemical Engineers (AIChE) Annual Meeting*, San Francisco, CA, Nov. 3th-8th, 2013.

5. Colella, W.G., Moton, J.M., James, B.D., "Analysis of Emerging Hydrogen Production and Delivery Pathways," *2013 Fuel Cell Seminar*, Session STA33 Hydrogen Production & Storage, Paper Number 266, Greater Columbus Convention Center, Columbus, Ohio, October 21st-24th, 2013.

Invited Talks

1. Colella, W.G., James, B.D., Moton, J.M., Saur, G., Ramsden, T.G., "Thermo-economic Analysis of Producing Hydrogen with Proton Exchange Membrane Electrolyzers," *International Energy Agency (IEA) Advanced Fuel Cells Annex 25 Meeting No 10*, SOFC-POWER Inc. premises in Trento, Italy, April 23rd-24th 2014 (delivered remotely via webinar.)

2. James, B. D., Colella, W. G., Moton, J. M., Saur, G., Ramsden, T., *Techno-Economic Analysis of Hydrogen Production by PEM Electrolysis,* Hydrogen Production Technical Team (HPTT) Meeting, delivered remotely from Arlington, VA, Dec. 3rd, 2013.

3. James, B. D., Colella, W. G., Moton, J. M., *Techno-Economic Analysis of Hydrogen Production Pathways,* DOE Hydrogen and Fuel Cell Technical Advisory Committee (HTAC) Meeting, NREL, Golden, Colorado, delivered remotely from Arlington, VA, Oct. 30th, 2013.

4. James, B. D., Colella, W. G., Moton, J. M., Saur, G., Ramsden, T., "Analysis of Hydrogen Costs from Proton Exchange Membrane (PEM) Electrolyzers." Presentation to the U.S. Department of Energy Office of Energy Efficiency & Renewable Energy Fuel Cell Technologies Program, Washington, D.C., September 27th, 2013.

Poster Presentations

1. Colella, W.G., "Reducing Energy, Environmental, and Economic Constraints in Global Transport Supply Chains with Novel Fuel Cell and Hydrogen Technologies," *Fifth European Fuel Cell Technology & Applications Conference - Piero Lunghi Conference and Exhibition (EFC2013)*, Rome, Italy, Dec. 11th-13th, 2013 (EFC13-178).

2. Colella, W.G., Moton, J.M., James, B.D., "Analysis of Emerging Hydrogen Production and Delivery Pathways," *2013 Fuel Cell Seminar*, Session STA33 Hydrogen Production & Storage, Paper Number 266, Greater Columbus Convention Center, Columbus, Ohio, October 21st-24th, 2013.

3. Colella, W.G., "Resolving Bottlenecks in Transportation Supply Chains with Next Generation Fuel Cell and Hydrogen Energy Systems," *2013 Fuel Cell Seminar*, Greater Columbus Convention Center, Columbus, Ohio, October 21st-24th, 2013.

II.B.1 Renewable Electrolysis Integrated Systems Development and Testing

Kevin Harrison (Primary Contact) and Mike Peters
National Renewable Energy Laboratory (NREL)
15013 Denver West Parkway
Golden, CO 80401-3305
Phone: (303) 384-7091
Email: Kevin.Harrison@nrel.gov

DOE Manager
David Peterson
Phone: (720) 356-1747
Email: David.Peterson@ee.doe.gov

Subcontractor
Spectrum Automation Controls, Arvada, CO

Project Start Date: October 1, 2003
Project End Date: Project continuation and direction determined annually by DOE

Overall Objectives

- Collaborate with industry to research, develop and demonstrate improved integration opportunities for renewable electrolysis systems for energy storage, vehicle refueling, grid support, and industrial gas end-uses
- Design, develop, and test advanced experimental and analytical methods to validate electrolyzer stack and system efficiency; including contributions of sub-system losses (e.g., power conversion, drying, electrochemical compression) of advanced electrolysis systems

Fiscal Year (FY) 2014 Objectives

- Baseline first 2,000 hours of constant powered testing on two Proton OnSite proton exchange membrane (PEM) electrolyzer stacks and run variable testing to 5,000 hours comparing stack decay rates of the two operational modes
- Improve system efficiency and operation cost to the electrolyzer end-user by:
  - Testing NREL's novel drying technique to reduce drying losses below 3.5%
  - Demonstrating electrolyzer's capability to participate in grid ancillary services
- Report on industry collaborations to ensure research goals align with industry needs

Technical Barriers

This project addresses the following technical barriers from the Hydrogen Production section of the Fuel Cell Technologies Office Multi-Year Research, Development, and Demonstration (MYRD&D) Plan, section 3.1.5:

(G) System Efficiency and Electricity Cost

(J) Renewable Electricity Generation Integration (for central production)

(M) Control and Safety

Technical Targets

This project is conducting applied research, development, and demonstration (RD&D) to reduce the cost of hydrogen production via renewable electrolysis for both distributed and central production pathways to help meet the following DOE hydrogen production and delivery targets found in the MYRD&D Plan:

Technical Targets: Central Water Electrolysis using Green Electricity (Table 3.1.5)

- Stack Efficiency:
  - 44 kWh/kg H_2 (76% lower heating value, LHV) by 2015
  - 43 kWh/kg H_2 (78% LHV) by 2020
- System Efficiency:
  - 46 kWh/kg H_2 (73% LHV) by 2015
  - 44.7 kWh/kg H_2 (75% LHV) by 2020
- By 2015 reduce the cost of central production of hydrogen from water electrolysis using renewable power to $3.00/gasoline gallon equivalent (gge) at the plant gate. By 2020, reduce the cost of central production of hydrogen from water electrolysis using renewable power to ≤$2.00/gge at the plant gate.

FY 2014 Accomplishments

- Completed 2,000 hours of constant-powered testing on two Proton OnSite PEM electrolyzer stacks. Decay rate for both stacks was at 9.5 (μV/cell-h).
  - On-going testing to 5,000 hours with one stack operating with a variable-powered profile and the other remaining with a constant powered profile
  - Decay rates expected to continue to decline below the 9.5 (μV/cell-h) as more hours are put on the stacks

  - A new generation PEM electrolyzer stack from Proton OnSite has been procured and will be installed late FY 2014 which will allow comparison of a newer generation of stack from Proton OnSite.
- Demonstrated hydrogen production moisture content and drying losses of a commercially available electrolyzer (Proton OnSite H-Series, 13 kg/day, 40 kW). This testing provides a baseline to inform design and implementation of NREL's novel drying technique aiming to reduce drying losses below 3.5% of rated flow.
  - Baseline results indicated drying losses of 11% at full stack power, 14% at 80% of rated stack power, and 18% at 60% of rated stack power
- Demonstrated PEM electrolyzer's ability to quickly respond and closely match a command signal sent from grid to participate in grid ancillary services
- By end of FY 2014: Report on current and potential industry partnerships including how future work will correspond with projects for industry formed through other internal NREL projects (e.g., INTEGRATE)

INTRODUCTION

The capital cost of commercially available water electrolyzer systems, along with the high cost of electricity in many regions, limits widespread adoption of electrolysis technology to deliver low-cost hydrogen production. PEM electrolyzer manufacturers are working to scale up into the megawatt range to improve their system energy efficiency. Along with capital cost reductions and efficiency improvements, both technologies are developing utility-scale electrolyzers capable of advanced grid integration functionality and better integration with renewable electricity sources. An integrated system with advanced sensing and communications will enable grid operators to take advantage of the controllable nature of distributed and central water electrolysis systems to maintain grid stability. Electrolytic production of hydrogen, where fossil fuels are the primary electricity source, will not lead to significant carbon emission reduction without carbon sequestration technologies.

Renewable electrolysis is inherently distributed, but large-scale wind and solar installations are being planned to take advantage of economies of scale and achieve system-level energy efficiencies less than 50 kWh/kg. Renewable electricity sources, such as wind and solar, can be closely- and in some cases directly-coupled to the hydrogen-producing stacks of electrolyzers to reduce energy conversion losses and capital costs investment of this near-zero-carbon pathway.

APPROACH

Results and insights gained from this RD&D project aim to benefit the hydrogen industry and relevant stakeholders as the market for water electrolyzers expands. Results from the project have demonstrated opportunities to improve efficiency and capital cost of an integrated renewably coupled electrolysis system.

The Xcel Energy/NREL Wind-to-Hydrogen and Energy Systems Integration Laboratory RD&D project is advancing the integration of renewable electricity sources with state-of-the-art electrolyzer technology. Real-world data from 24/7 daily operation are demonstrating opportunities for improved system design and novel hardware configurations to advance the commercialization of this technology. Lessons learned and data-driven results provide feedback to industry and to the analytical components of this project. Finally, this project provides independent testing and verification of the technical readiness of advanced electrolyzer systems by operating them on both grid and renewable electricity sources.

RESULTS

Stack Decay Comparison: Variable Versus Constant Powered

NREL is conducting side-by-side testing and comparison of stack voltage decay rates between constant and variable power operation of electrolyzer stacks. Two 34-cell stacks for the H-Series PEM electrolyzer from Proton Onsite were obtained in June 2013. The stacks were operated in a constant full-powered mode for the first 2,000 hours of their lifetime to obtain baseline decay rate at constant power. Table 1 shows the stack decay rates for both stacks after 2,000 hours of operation. The stacks showed the same decay rate over the first 2,000 hours so it was determined to start operating one in variable mode while the other stays at constant power for a decay rate comparison.

TABLE 1. Stack Decay Rate of two Proton OnSite 10-kW Stacks after 2,000 Hours of Operation

Stack Operating Mode	Stack Identifier	Decay Rate (μV/cell-h)
Constant Power	Stack A	9.5
Constant Power	Stack B	9.5

A varying wind power profile is currently being run on one of the stacks to achieve a milestone of 5,000 hours of total operation (2,000 hrs constant powered with 3,000 variable-powered hours versus 5,000 constant-powered hours). NREL has procured a third stack from Proton OnSite to allow comparison of newer stack technology operating alongside an older stack, both running on variable power. Once the stack from Proton OnSite is installed, it will be operated at constant power for the first 2,000 hours, like

the other two, before being switched to variable-powered operation.

Baseline Testing for Variable Flow Drying Technique

A dual-bed pressure swing absorption drying system consists of a handful of control valves and two desiccant beds combined in parallel at the output of the H_2/H_2O phase separator. A back-pressure regulator maintains constant pressure on the pressure swing absorption system and stack. The water vapor saturated hydrogen comes out of the hydrogen phase separator and travels through one of the desiccant tubes; the goal of the first tube is to dry the hydrogen to less than 5 parts per million by volume (ppmv) of H_2O in H_2. At the outlet of the desiccant tube being used for drying, an orifice allows a percentage of dry hydrogen to sweep out (dry) the bed being regenerated (inactive bed). The orifice between the two desiccant beds allows a fixed amount of hydrogen to flow and dry the inactive bed. The flow of dry hydrogen through the inactive bed is a function of the orifice size and the back pressure regulator setting. The hydrogen used to dry the desiccant bed is not recoverable and is vented out of the system; this is what is considered the electrolyzer drying losses.

The typical drying approach results in the same amount of hydrogen being lost regardless of the stack power. This approach decreases system efficiency at lower than rated stack power levels because the amount of hydrogen lost due to drying is a higher overall percentage of the flow rate. This concept was validated experimentally using NREL's Proton OnSite H-Series and is described in Table 2. The table shows the drying losses as a percentage of rated hydrogen flow at three stack power levels. As expected, the drying losses are constant at 0.07 kg/hr for each test. However, when stack power is being decreased, the product hydrogen flow decreases, and thus there is a higher percentage of drying loss.

TABLE 2. Proton OnSite H-Series Drying Losses with Variable Stack Power

Drying Losses	100% Stack Power	80% Stack Power	60% Stack Power
Flow (kg/hr)	0.07	0.07	0.07
% of Rated Flow	11	14	18

* Relatively Small Sample Size n = 5 for each test

SAE International (SAE) J2719 sets standards for fuel quality for station providers in the hydrogen dispensing market; they have set their standard for moisture content to less than 5 ppmv H_2O so for hydrogen vehicle fueling applications the electrolyzer drying system must be able to achieve this specification. Dry hydrogen ensures that impurities are not delivered to fuel cell units when the hydrogen is converted back to electricity.

The electrolyzer output was instrumented with a dew point sensor, pressure gauge, pressure transducer and resistive temperature device to measure the parameters needed to calculate moisture content in the hydrogen. First, a series of start-ups was tested to determine how quickly the electrolyzer reached the SAE J2719 tolerance. During this testing the electrolyzer consistently provided hydrogen below the 5 ppmv tolerance in less than 5 minutes. The second test looked at the hydrogen output moisture content versus stack current. It was established that the moisture content was unaffected by stack current, however, drying losses increased as a percentage as stack current dropped. Figure 1 shows a graph of three stack current levels (blue) and the resulting hydrogen moisture content (red).

NREL's variable flow drying technique aims to reduce the percentage of hydrogen lost due to drying by replacing the fixed orifice between the two desiccant beds with a variable flow orifice. Unlike the fixed flow orifice which allows the same amount of flow through the inactive

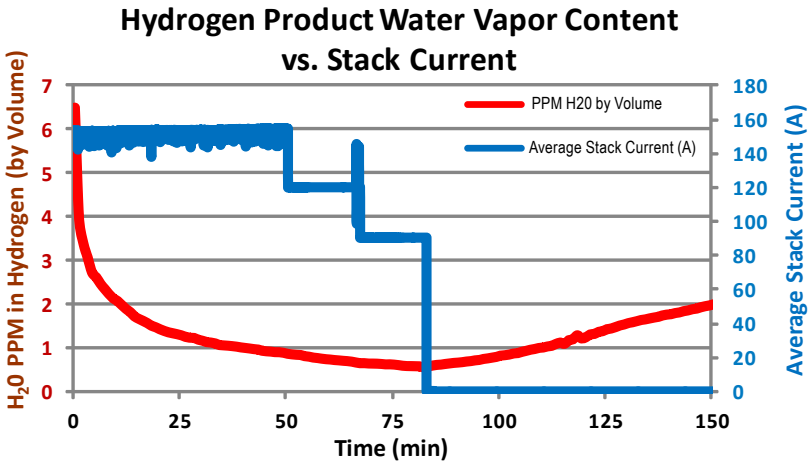

FIGURE 1. Water Vapor Content versus Stack Current

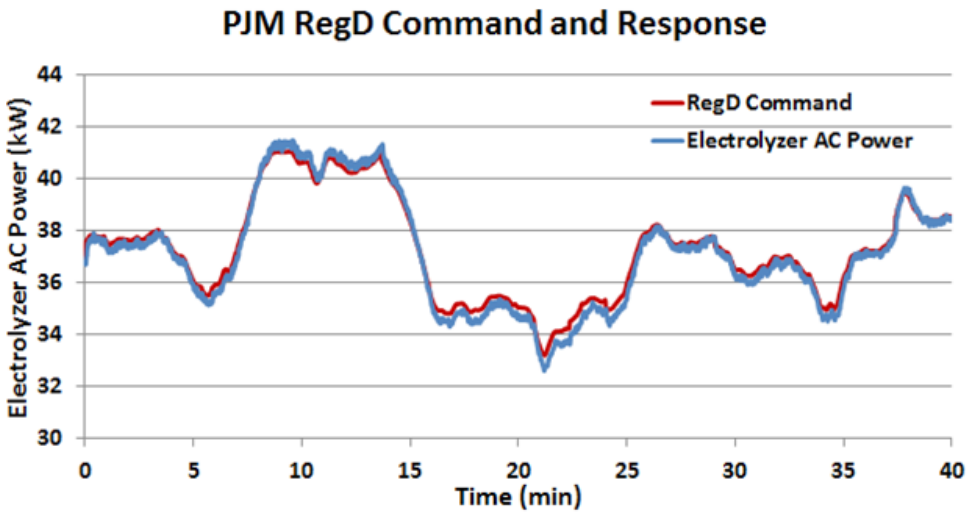

FIGURE 2 - Dynamic Regulation of Proton OnSite H-Series

desiccant bed, the variable flow orifice will be capable of adjusting with stack power to maintain the same percentage of hydrogen lost through drying. This approach will increase electrolyzer system efficiency while still maintaining the necessary hydrogen dryness required by SAE J2719.

PEM Electrolyzer Participating in Grid Ancillary Services

NREL demonstrated the ability of the Proton OnSite H-Series to react to a quickly changing command similar to those provided in grid ancillary service markets. PJM Interconnection, a regional transmission organization that coordinates the movement of electricity in 13 states and Washington D.C., has regulation tests that electricity assets need to pass before they can bid into the regulation market. The H-Series electrolyzer was tested with a standard regulation signal (RegA) and a dynamic regulation signal (RegD) both provided by PJM Interconnection. Figure 2 shows the results of the RegD dynamic regulation test which is the harder of the two tests to pass. Although results were not sent to PJM for an official grade, compared to other examples provided by PJM the electrolyzer response to the command signal was very good. This testing demonstrated that future electrolyzers should be able to bid into the regulation market, providing an additional revenue source.

CONCLUSIONS AND FUTURE DIRECTIONS

- **Conclusion:** Completed 2,000 hours of constant-powered testing on two Proton OnSite PEM electrolyzer stacks. Decay rate for both stacks was at 9.5 (μV/cell-h).
  - **Future:** Continue long-duration testing to compare constant versus variable powered operation
- **Conclusion:** Baseline results of Proton OnSite H-Series drying losses of 11% but quickly (less than 5 min) achieves the SAE J2719 moisture content tolerance
  - **Future:** Continue testing NREL variable flow drying technique aiming to reduce drying losses below 3.5% at rated power
- **Future:** Leverage other NREL projects to characterize electrolyzer system improvements, grid integration, and advanced stack efficiency

SPECIAL RECOGNITIONS & AWARDS/ PATENTS ISSUED

1. DOE special recognition awards to Chris Ainscough and Kevin Harrison for the work completed in FY 2013 on the Giner/Parker Hannifin electrolyzer testing

FY 2014 PUBLICATIONS/PRESENTATIONS

1. Harrison, K. (May 2013). "Renewable Electrolysis: Integrated System Testing." Keynote presentation at the 2nd Annual ADvanced ELectrolysis (ADEL) International Workshop, Corsica, France, May 2013.

2. Harrison, K. (October 2013). "Integrated Systems Testing PEM/ Alkaline." Presentation at F-Cell Conference. Stuttgart, Berlin. October 2013

3. Harrison, K. (February 2014). "Renewables and Grid Integration." Presentation at DOE Electrolytic Hydrogen Production Workshop. Golden, CO. February 2014

4. Peters, M. & Harrison, K. (June 2014) "Innovative Drying Technique for Wind and Solar Powered Electrolysis." ASME 2014 12th Fuel Cell Science, Engineering & Technology Conference. Boston, MA. June 2014.

5. Eichman, J., Harrison, K. and Peters, M. "Novel Applications for Electrolyzers: Providing more than just hydrogen." NREL Publication. Under Review. Golden, CO

II.B.2 Economical Production of Hydrogen through Development of Novel, High-Efficiency Electrocatalysts for Alkaline Membrane Electroysis

Dr. Katherine Ayers (Primary Contact), Chris Capuano

Proton Energy Systems d/b/a Proton OnSite
10 Technology Drive
Wallingford, CT 06492
Phone: (203) 678-2190
Email: kayers@protononsite.com

DOE Manager

David Peterson
Phone: (720) 356-1747
Email: David.Peterson@ee.doe.gov

Contract Number: DE-SC0007574

Subcontractor

Illinois Institute of Technology (IIT), Chicago, IL

Project Start Date: February 20, 2012 (Phase 1)
Project End Date: April 21, 2015 (with Phase 2 continuation)

Overall Objectives

- Determine how the composition (choice of A, B and A/B ratio) influences pyrochlore microstructure and physical properties
- Understand how the intrinsic activity of pyrochlore catalysts for the oxygen reduction/evolution reaction changes with composition and processing induced changes in microstructure
- Determine the impact of key anion exchange membrane (AEM) properties (conductivity, water uptake, gas crossover) on AEM performance
- Derivatize hydrocarbon or fluorocarbon backbones with basic cations to form new AEMs and characterize said AEMs for mechanical and electrochemical properties
- Select the electrolyte (deionized water or carbonate) based on understanding of the influence on ion conductivity and stability of the AEM in electrolysis conditions
- Process promising membrane and catalyst materials into membrane electrode assemblies/gas diffusion electrodes (MEAs/GDEs) and test in operational cells
- Down-select a final electrode configuration for the cell stack for durability testing
- Develop a prototype system package with the option of incorporating carbonate in the electrolyte fluid stream and perform testing of up to 500 hours
- Provide a product cost analysis demonstrating the cost saving for the lab-scale generator and H2A modeling for a large scale AEM electrolysis system

Fiscal Year (FY) 2014 Objectives

- Complete material assessment of alkaline compatible system/stack materials (cost and strength)
- Determine optimal electrode composition for increased durability
- Evaluate alternative cathode catalyst for AEM
- Complete cell stack fluid calculations to quantify maximum cell capacity of 28-cm^2 design
- Create computer-aided design models and assemble cost-reduced prototype AEM lab-scale electrolyzer
- Report elucidating fundamental degradation pathways in AEM as ascertained using two-dimensional nuclear magnetic resonance

Technical Barriers

This project addresses the following technical barriers from the Production section of the Fuel Cell Technologies Office Multi-Year Research, Development, and Demonstration Plan:

(G) Capital Cost

(H) System Efficiency

Technical Targets

TABLE 1. Proton OnSite Progress towards Meeting Technical Targets for Distributed Water Electrolysis Hydrogen Production

Characteristics	Units	2011 Status	2015 Target	2020 Target	Proton Status
Hydrogen Levelized Cost	$/kg	4.2	3.9	2.3	3.46
Electrolyzer System Capital Cost	$/kg $/kW	0.70 430	0.50 300	0.50 300	0.64
Stack Energy Efficiency	% (LHV) kWh/kg	74 45	76 44	77 43	67

gge - gasoline gallon equivalent; LHV - lower heating value
Note: Estimates are based on H2A v2.1, for electrolysis only (compression-storage-delivery not included). Model assumes $0.05/kWh.
Electrolyzer cost based on 1,500 kg/day capacity, 500 units/year; Efficiency based on system projections and demonstrated stack efficiency of 74% LHV efficiency

FY 2014 Accomplishments

- System components procured, assembled, and functionally verified
- Prototype unit operational testing initiated
- Demonstrated improved operational stability through the introduction of carbonate into AEM system
- Completed cost and strength analysis of materials for cost reduction of alkaline system/stack
- Stack maximum cell count calculations completed

✧ ✧ ✧ ✧ ✧

INTRODUCTION

The project aims to address some of the barriers associated with the strategic development of a hydrogen infrastructure. This is viewed as a major impediment to the wide spread deployment of hydrogen-fueled vehicles. All of the world's major automotive companies have hydrogen vehicle programs and are poised to roll out the next generation of vehicles, with plans that number in the thousands of units by 2015. Hydrogen is also an ideal storage medium for renewable energy and stationary power applications. However, economical and environmentally benign production and storage of hydrogen for energy markets remains a challenge. The project leverages anion exchange membranes, enabling elimination of the highest expense materials in the cell stack, while the new catalyst formulations provide higher efficiencies than existing state of the art. The project would culminate in a commercial fidelity prototype to demonstrate the cost improvements.

APPROACH

The project addresses both of the following issues by replacing the proton exchange membrane with an AEM and exploring new pyrochlore-based catalysts for oxygen evolution.

- The high capital expense associated with expensive catalysts and flow field materials of construction, required for the acidic environment associated with proton exchange membrane electrolyzers
- Improving operational efficiency, to reduce the $/kg H_2

Moving to an anion exchange membrane platform enables flow fields made of lower cost nickel or stainless steel. In addition, the classes of catalyst materials which are stable in the alkaline membrane environment are expanded vs. the acid environment. This project will thus advance development of higher efficiency hydrogen and oxygen production at lower cost than existing electrolysis methods.

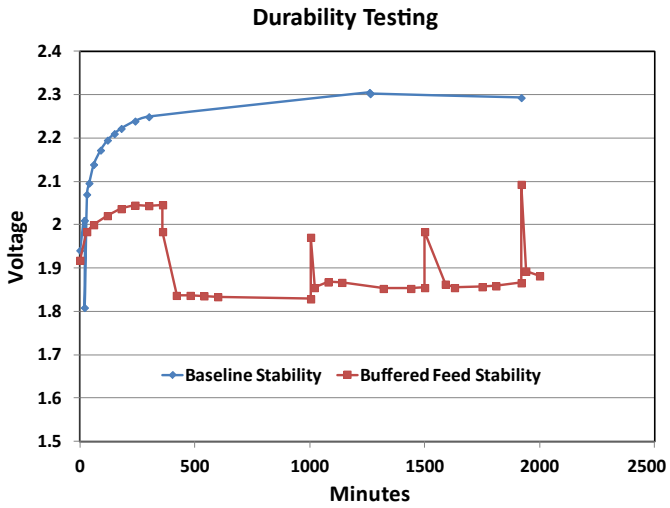

FIGURE 1. Improved Performance with the Introduction of Carbonate to the AEM System

The Phase 2 project has continued material exploration initiated in Phase 1, furthering the development of an optimized catalyst formulation based on the theory developed in Phase 1. The ionomer is also being tailored for stability in the electrolysis environment, leveraging added carbonate if necessary. Gas diffusion electrode configurations and manufacturing approaches have been explored, as a means to improve operational durability. A prototype system concept is being developed with manufacture pending as an initial step to commercialization, as well as cost validation and durability testing.

RESULTS

Building from initial Phase I studies, progress has been made towards scale up production of the non-noble metal catalyst being explored. This scale up in synthesis is critical in producing quantities large enough for full-scale cell stack testing from a single batch. Additionally, improvements in electrode performance were realized through the introduction of carbonate to the electrolyzer feed water. Cell potential was reduced through the use of carbonate, as shown in Figure 1. This is thought to improve durability as well.

Non-noble metal catalysts synthesized at IIT were operated in an electrochemical cell at Proton and demonstrated significantly improved efficiency over the baseline configuration. With the optimized composition, an ~8% gain in efficiency was calculated at 500 mA/cm^2 when using the LHV of hydrogen. This result is shown in Figure 2. Durability testing is being pursued through the incorporation of these catalyst powders with a variety of binders known to work well in proton exchange membrane systems, and through the pursuit of alternative deposition techniques, focused on creating both GDEs and catalyst-

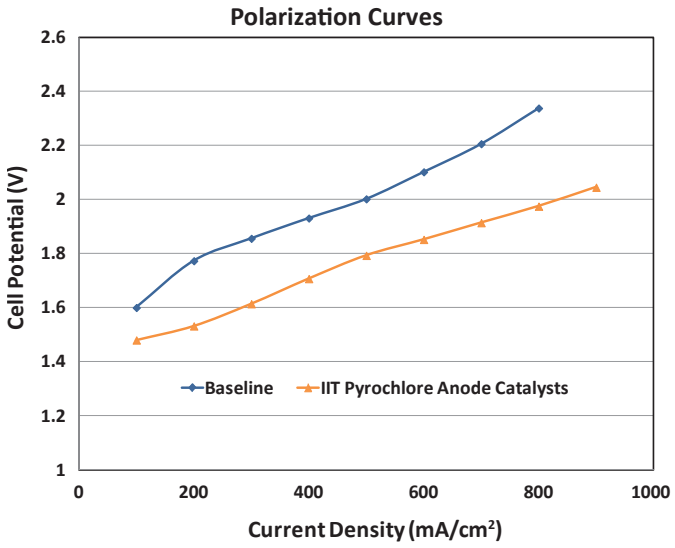

FIGURE 2. Performance of the IIT Pyrochlore Catalyst vs. Baseline

coated membranes. In addition to the development of a robust electrode, work at Proton has also been conducted on in-house synthesis of non-precious metal oxygen evolution catalysts. Work to date has not produced materials exceeding the performance of the IIT synthesized powders, but is being reviewed for possible iteration on the compositions to improve the activity.

System development has been initiated, with operational verification completed for the unit. Additional control capability is expected by August 2014, which will allow unattended durability testing of multi-cell configurations at various current densities. The electrochemical module is designed to be removable, so testing of specific configurations and materials can be switched without risk of cross-contamination of materials. The design of this system will also enable the generation of electrochemically pressurized hydrogen, up to 8 bar. This system prototype is shown in Figure 3 during verification testing. Cell hardware has been manufactured at this scale, including the AEM MEA for planned durability testing.

CONCLUSIONS AND FUTURE DIRECTIONS

- Scale up to production type quantities demonstrated for non-noble metal catalysts:
  - Performance improvement shown with durability and repeatability tests on-going
- Operational testing of catalyst powders with alternative binder formulations in process:
  - Compositional testing of Proton synthesized powders in progress at MEA level
  - IIT catalysts evaluated and undergoing compositional optimization
- Electrode and stack scale up initiated:
  - Parts manufactured and assembled into Proton commercial cell stack
  - Bench testing initiated to verify stack integrity
- Initial prototype system assembled:
  - Removable electrolysis module tested
  - Additional balance of plant being integrated to add operational parameter control and gas drying
  - Conduct material analysis
  - Update with MEA electrical efficiencies and operational data as testing progresses, with capital and operating cost impacts reported.

FY 2014 PUBLICATIONS/PRESENTATIONS

1. 2014 DOE AMR presentation: pd094_ayers_2014.

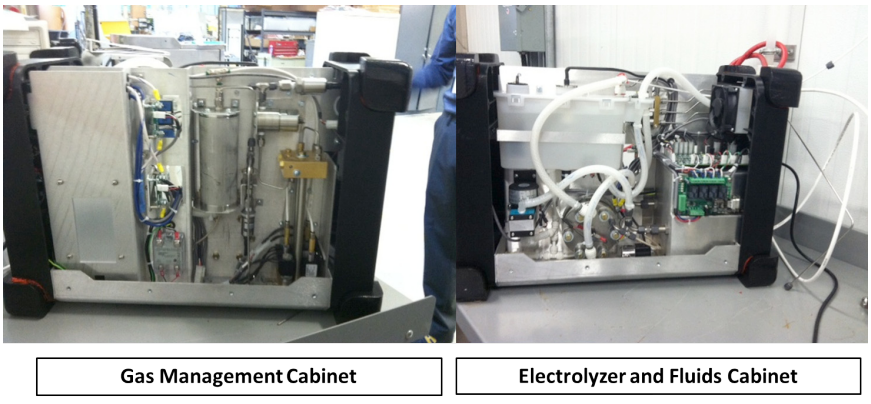

FIGURE 3. Full System being Evaluated for Durability Testing

II.B.3 Low-Noble-Metal-Content Catalysts/Electrodes for Hydrogen Production by Water Electrolysis

Katherine Ayers (Primary Contact), Julie Renner
Proton Energy Systems d/b/a Proton OnSite
10 Technology Drive
Wallingford, CT 06492
Phone: (203) 678-2190
Email: kayers@protononsite.com

DOE Manager
David Peterson
Phone: (720) 356-1747
Email: David.Peterson@ee.doe.gov

Contract Number: DE-FG02-12ER86531

Subcontractor
Brookhaven National Laboratory (BNL), Upton, NY

Project Start Date: June 28, 2012 (Phase 1)
Project End Date: August 13, 2015

Overall Objectives

- Translate catalyst synthesis to a manufacturable process at Proton
- Develop a robust technique for manufacturable electrodes
- Demonstrate feasibility for 80% cost reduction in the anode catalyst
- Downselect promising anode electrode configurations to achieve >100 hrs durability
- Achieve 500 hrs of operation in production hardware using cost-reduced electrodes
- Evaluate the cost benefits of new materials

Fiscal Year (FY) 2014 Objectives

- Demonstrate uniform and robust catalyst layer on anode gas diffusion layers (GDLs)
- Complete scale up synthesis of cathode catalysts to 10–100 g batch level
- Complete cell design analysis for cathode configuration
- Downselect optimal cathode material and process for reliable production
- Demonstrate improved activity and durability of selected anode gas diffusion electrode (GDE) samples in cell
- Provide initial cost assessment via H2A model
- Identify key issues for enhancing durability

Technical Barriers

This project addresses the following technical barriers from the Hydrogen Production section of the Fuel Cell Technologies Office Multi-Year Research, Development, and Demonstration Plan:

(F) Capital Cost

(G) System Efficiency and Electricity Cost

Technical Targets

Technical targets are presented in Table 1.

TABLE 1. Technical Targets for Distributed Forecourt Water Electrolysis Hydrogen Production [1]

Characteristics	Units	2011 Status	2015 Target	2020 Target
Hydrogen Levelized Cost	$/kg	4.2	3.9	2.3
Electrolyzer System Capital Cost	$/kg $/kW	0.70 430	0.50 300	0.50 300
Stack Energy Efficiency	% (LHV) kWh/kg	74 45	76 44	77 43

LHV – lower heating value

Ultra-Low Catalyst Loading

This project is developing methods to reduce the amount of platinum group metals (PGMs) used in the membrane electrode assembly (MEA). Advancements made in this project will

- Reduce the capital cost of the system by requiring less precious materials while simultaneously reducing sensitivity to market fluctuations in precious metal cost
- Increase stack efficiency and lower total cost by establishing more uniform electrode layers, enabling thinner membranes.

FY 2014 Accomplishments

- Achieved technology transfer of the BNL core-shell synthesis technique with equivalent cathode performance at <1/10 commercial loading
- Showed feasibility for an alternative deposition technique which could result in more automated GDE manufacturing

- Showed >500 hrs durability with ultra-low-loaded Proton-made cathode
- TiOx-supported Ru-Ir catalysts were manufactured and characterized
- Uniform and stable anode GDEs were manufactured at lower loadings, and baseline performance was obtained with IrOx

INTRODUCTION

The economical use of hydrogen as a transportation and stationary power fuel remains a long-term Department of Energy objective. Energy storage applications in Europe such as wind capture and improved biogas conversion efficiency are also driving significant interest in hydrogen production from renewable sources. New and efficient catalytic processes for hydrogen generation are therefore needed to achieve production targets for hydrogen cost. In the Phase 1 project, Proton Energy Systems (d/b/a Proton OnSite), in collaboration with BNL, demonstrated feasibility for development of low-noble-metal-content catalysts/electrodes for proton exchange membrane electrolyzers, through design and synthesis of core-shell nanocatalysts. In Phase 2, continued development of the anode formulation is being performed for reproducible and stable electrode fabrication, while technology transfer and scale up from BNL to Proton is occurring for the cathode electrode fabrication. The Phase 2 project is strategically important because reduction of noble metal content is a significant opportunity for cost reduction to address large-scale opportunities for hydrogen-based energy storage and hydrogen fueling.

APPROACH

The Phase 2 project will continue maturation of the catalyst structures and electrode processing initiated in Phase 1, to develop a manufacturable electrode at relevant scale and ultra-low catalyst loadings. The overall technical approach will include development of the manufacturing process for the cathode electrode as well as cell stack validation for the alternative electrode configuration. For the anode, work will focus on continued optimization of catalyst application and GDL structure for reproducible and durable performance equal to or exceeding the current baseline. Additionally, catalyst composition will be refined for high activity and durability. The impact of these advancements will be quantified using the H2A model.

RESULTS

Core-shell nanoparticles were synthesized at Proton after on-site training at BNL and follow-up training at Proton. As a result, Proton has developed a detailed written protocol to guide the synthesis process. Consultation with BNL provided a number of specifications to judge the quality of the process (Table 2). Additional feedback from BNL was provided in terms of set up and refined in-process measurements, which were applied to trials #4 and #5, resulting in all targets being met.

BNL's current method for manufacturing the cathode GDL involves hand application of the electrode ink to the surface. To replicate the previous results, Proton manufactured a GDE via hand application with nanocatalyst from trial 4 at 1/25th the PGM/cm^2 loading compared to baseline loadings in the MEA and GDE configurations. Polarization curves showed that the ultra-low-loaded cathode cell had equivalent performance to the baselines (Figure 1). It should be noted that the variance seen between the samples is typical of the variance seen in Proton's production-quality MEAs; however, a deeper investigation of slightly higher resistance in the new GDE material is underway. Proton allowed the 3-cell stack with the ultra-low-loaded Proton-made cathode to run for 917 hrs (Figure 2). No noticeable decay in performance was observed, and the voltage trended similarly to the baselines. This indicates that the core-shell structure is stable in the electrolysis environment.

While transfer of the BNL GDE manufacturing method to Proton shows substantial benefit as an implementation pathway (through elimination of over 90% of the catalyst material as well as some labor content), the end goal is to transition to a more automated, higher speed manufacturing

TABLE 2. Proton Synthesis Trials of Nanocatalysts Showing On-Target Specifications *(italics)* and Off-Target Specifications (grey)

Synthesis Trial	Color (green)	Soln. pH (5-7)	Weight (±5% of target)	Pt soln. pH (<1)	Final Weight (within ±5% of target)
1	*green*	10	200%	terminated	terminated
2	*green*	9	-20%	terminated	terminated
3	*green*	8	-20%	terminated	terminated
4	*green*	***5***	***2.0%***	***0.3***	***0.2%***
5	*green*	***5***	***-0.10%***	***0.4***	***3%***

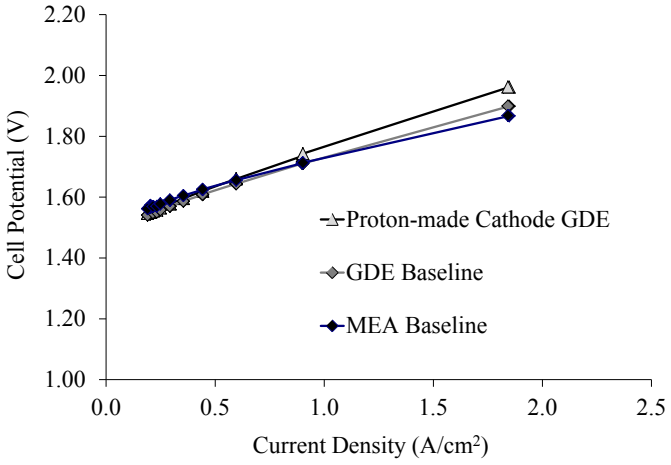

FIGURE 1. Cathode GDEs manufactured at Proton with Proton-made nanocatalyst demonstrated high performance nearly equivalent to baseline at 1/25th the precious metal loading.

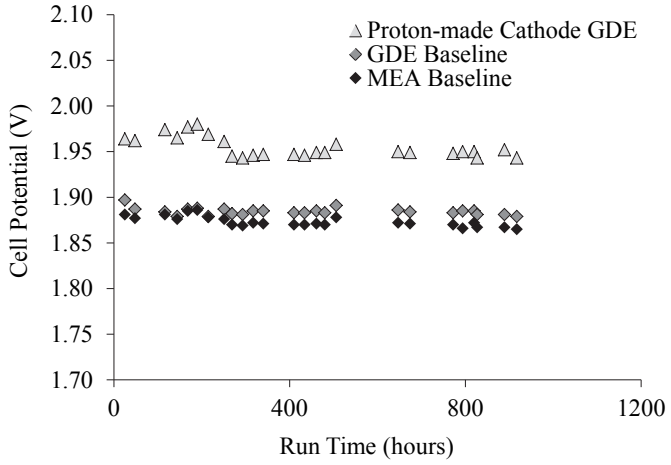

FIGURE 2. Ultra-low-loaded Proton-made cathode shows durability for 917 hrs.

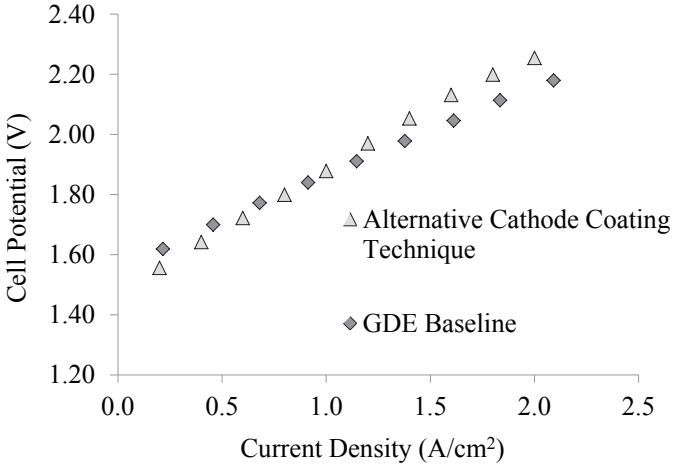

FIGURE 3. Performance of an alternatively manufactured cathode with Proton-made nanocatalyst at 1/100th the precious metal loading.

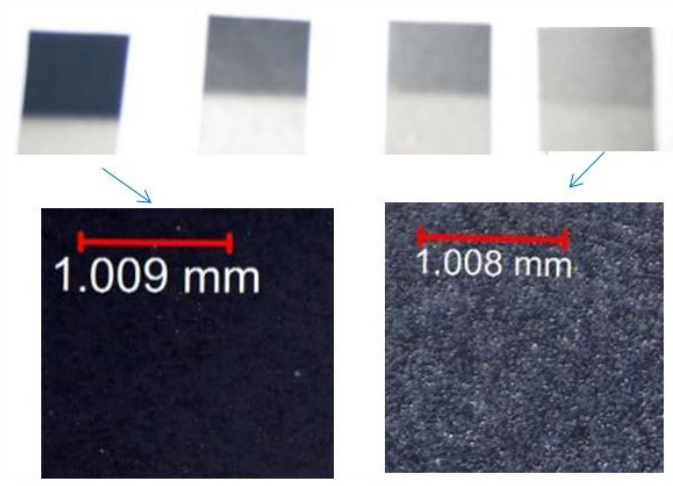

FIGURE 4. Photos and optical images of catalyst-coated anode GDLs with ~1, 1/2, 1/4, and 1/10 of the loading compared to baseline anodes show uniform distribution.

process. Therefore, Proton and BNL engaged suppliers of alternative catalyst coating machines capable of high-throughput automated processing. A sample GDE at 1/100th the PGM loading compared to baseline was manufactured. The coated GDE was operated in Proton's 25-cm^2 bench-scale hardware to assess performance at 50ºC (Figure 3). At 1.8 A/cm^2, the coated GDE was only ~85 mV higher, showing roughly equivalent performance to the baseline and proof-of-concept for the alternative manufacturing technique.

For anode development, BNL synthesized and characterized Ru-Ir core-shell nanocatalysts on TiO_2 supports. X-ray diffraction was used to confirm the nanocatalyst synthesis. Performance was similar to unsupported catalysts, and the results indicated that the interaction with the anode GDL may be important. Initially, BNL reported weak adhesion with the anode catalysts on the GDL when testing in solution, as well as difficulty in obtaining uniform, reproducible samples. BNL has overcome these issues by using a printing method as well as post-processing to make a uniform and stable catalyst coating on the anode GDL. Figure 4 shows photos and optical images of catalyst-coated anode GDLs. In Proton's current process, even distribution of catalyst is difficult without using higher loadings. The electrodes manufactured by BNL show uniformity at 1/10th the loading, representing a significant achievement. Baseline performance was measured in solution via an electrochemical cell using standalone GDE strips.

CONCLUSIONS AND FUTURE DIRECTIONS

- The procedure for synthesis of nanocatalysts and GDEs has been transferred from BNL. Proton has scaled the nanocatalyst synthesis process from 1 g to a relevant production capacity of 10 g and is currently testing the material in cells.
- Proton-made cathodes demonstrated >900 hrs durability in production-quality hardware while achieving the milestone performance of <2.0 V at 1.8 A/cm^2. Proton will also work to identify an optimum cathode and anode GDL materials to increase the efficiency and maintain durability.
- The scale up of the GDE manufacturing process is feasible using a more automated coating technique. Proton will continue to explore this process as a viable manufacturing alternative.
- TiOx-supported nanocatalysts were manufactured and characterized. BNL is developing an anode nanocatalyst with improved durability with two parallel approaches.
- Uniform and stable anode GDEs were manufactured, and baseline performance was obtained. BNL will develop ways to enhance the catalyst-GDL interaction as well as study the impact of the GDLs on the oxygen evolution performance.
- The H2A model and Proton's electrochemical interface model will be used to refine the impact of design changes developed in this Phase 2 project on the $/kg of H_2.

REFERENCES

1. The Fuel Cell Technologies Office Multi-Year Research, Development, and Demonstration Plan, 2012. http://energy.gov/eere/fuelcells/fuel-cell-technologies-office-multi-year-research-development-and-demonstration-plan

II.B.4 High-Performance, Long-Lifetime Catalysts for Proton Exchange Membrane Electrolysis

Hui Xu (Primary Contact), Brian Rasimick, and Allison Stocks (Giner)
Bryan Pivovar, Shaun Alia, and K. C. Neyerlin (NREL)
Krzysztof Lewinski and Sean Luopa (3M)
Giner, Inc.
89 Rumford Ave.
Newton, MA 02466
Phone: (781) 529-0573
Email: hxu@ginerinc.com

DOE Manager
David Peterson
Phone: (720) 356-1747
Email: David.Peterson@ee.doe.gov

Contract Number: DE-SC0007471

Subcontractors
- National Renewable National Laboratory (NREL), Golden, CO
- 3M Company, St. Paul, MN

Project Start Date: April 22, 2013
Project End Date: April 21, 2015

Overall Objectives

- Develop various synthetic routes to make iridium (Ir)-based oxygen evolution reaction (OER) catalysts with enhanced surface area, oxidation resistance, performance and durability
- Screen the OER catalyst powders via rotating disk electrode (RDE) to determine corrosion resistance and initial catalytic activity
- Physically characterize the catalysts with good RDE activity using microscopy and X-ray techniques to elucidate their structure and particle size distribution
- Evaluate the performance and the durability of membrane electrode assemblies (MEAs) (1,000 hours) in Giner's laboratory and commercial electrolyzers
- Determine one category of catalyst that is most efficient and economically feasible

Fiscal Year (FY) 2014 Objectives

- Develop three synthetic routes to make Ir-based OER catalysts that may help to lower Ir loading or enhance proton exchange membrane (PEM) water electrolysis efficiency
- Screen the OER catalysts via RDE to determine corrosion resistance and initial catalytic activity
- Characterize the catalysts with good RDE activity using microscopy and X-ray techniques to elucidate their structure and particle size distribution
- Evaluate the performance of catalysts synthesized from three routes in operating PEM electrolyzers and select the best catalysts for future short production

Technical Barriers

This project addresses the following technical barriers from the Production section of Fuel Cell Technologies Office Multi-Year Research, Development, and Demonstration Plan:

(F) Capital Cost

(G) System Efficiency and Electricity Cost

Technical Targets

The targets of this project are to develop high-performance and long-lifetime OER catalysts that may help meet the technical targets of DOE distributed forecourt water electrolysis as shown in Table 1. Included in this table is Giner's status as of 2013.

FY 2014 Accomplishments

- Synthesized Ir supported on tungsten (W)-doped titanium dioxide (TiO_2) that demonstrated excellent oxidation resistance (up to 1.8 V) and 3 times higher OER activity compared to commercial Ir black in RDE tests.
- Developed Ir/metal (Ag, Fe or Co) nanowire OER catalysts that enhance mass activity and specific activity simultaneously by 4 times, compared to commercial Ir black in RDE tests.
- Giner's Ir/W-TiO_2 catalysts demonstrated excellent performance in a PEM electrolyzer:
  - Catalytic activity increased by 3 times compared with standard Ir black
  - Matches Giner baseline performance with reduced Ir loading by 5 times
- 3M Ir NSTF demonstrated superior performance in a PEM electrolyzer:

TABLE 1. Technical Targets: Distributed Forecourt Water Electrolysis [1]

Characteristics		Units	2015	2020	Giner Status (2013)
Hydrogen Levelized Cost[2]		$/kg-$H_2$	3.90	<2.30	3.64[3] (5.11)[4]
Electrolyzer Cap. Cost		$/kg-$H_2$	0.50	0.50	1.30 (0.74)[5]
Efficiency	System	%LHV (kWh/kg)	72 (46)	75 (44)	65 (51)
	Stack	%LHV (kWh/kg)	76 (44)	77 (43)	74 (45)

[1] 2012 MYRDD Plan. [2]Production Only. [3]Utilizing H2A Ver.2. [4]Utilizing H2A Ver.3 (Electric costs increased to $0.057/kW from 0.039$/kW) . [5] Stack Only

LHV - lower heating value

- Comparable performance with Giner baseline but at 8 times lower Ir loading
- Stable operation for 100 hours: 1.675 V at 1.5 A/cm^2

INTRODUCTION

Current hydrogen production from electrolysis is only a small fraction of the global hydrogen market, due to the high cost that results from expensive materials (membrane, catalyst, and bipolar plate) and electricity consumption. The two largest efficiency losses in PEM electrolysis are the anode overpotential and the ohmic losses from the membrane resistance. Anode overpotential is a source of major inefficiency in the entire region of current densities, originating from poor OER kinetics. The only way to lower the overpotential at the anode is to utilize a better catalyst, increase the catalyst loading, or operate at a higher temperature. Iridium and its oxide (IrO_2) represent the current state of the art for oxygen evolution catalysts in electrolysis applications where both performance and durability are important. State-of-the-art PEM electrolyzers relying heavily on Ir black have high Ir loading and low system efficiency (high electricity consumption/kg H_2). Therefore, our project aims to develop advanced Ir-based catalysts that may enhance OER catalyst and the efficiency of PEM electrolysis.

APPROACH

This project is a strong collaboration between Giner, 3M, and NREL. Giner, NREL, and 3M will each develop a different approach to synthesize the OER catalysts, which will be compared to select the best catalysts for short production (see Figure 1).

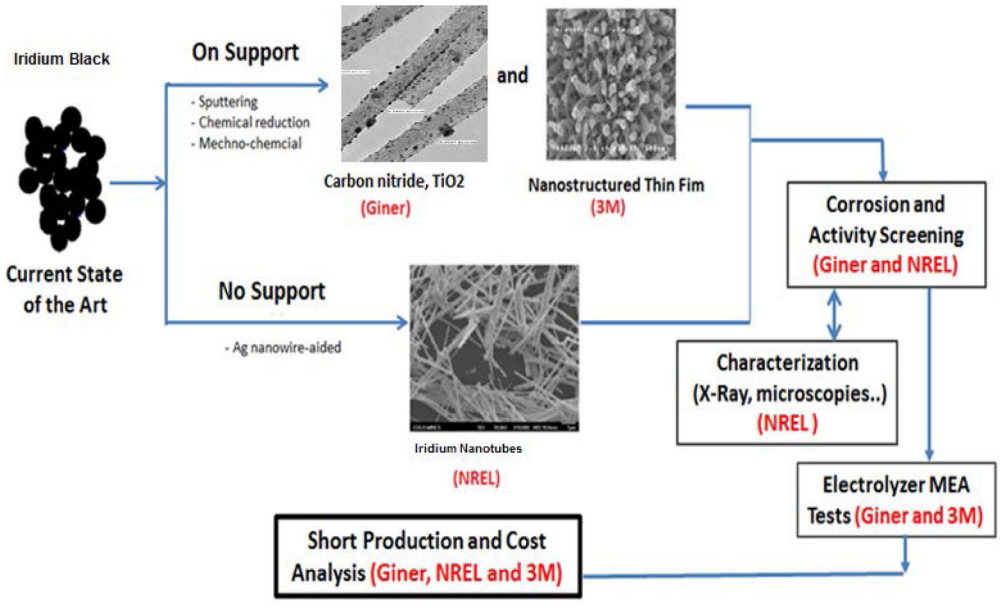

FIGURE 1. Illustration of Synergistic PEM Electrolysis Catalyst Development

The first approach is IrO_2 dispersed on a corrosion-resistant support (e.g. carbon nitride, doped titanium oxide) (Giner). The second approach is iridium nanostructured thin film (NSTF) from 3M that is derived from their platinum NSTF successfully used in PEM fuel cells. The third approach uses NREL's iridium nanotube technology, which may be used to greatly improve performance and/or decrease loading while maintaining high durability at higher electrode loadings. The developed catalysts will be first screened by RDE for corrosion resistance and activity and selected catalysts will be made into MEAs and tested in Giner's state-of-the-art electrolyzer test stations. Finally, scaled-up production of selected catalysts will be conducted and the cost of the catalysts as a function of production volume will be analyzed.

RESULTS

Giner has investigated a broad variety of supports for iridium, including titanium nitride, titanium carbide, indium tin oxide (ITO), TiO_2, W-doped TiO_2 (W-TiO_2), carbon nitrides. W-TiO_2 ($W_{0.1}Ti_{0.9}O_2$) nanoparticles and TiO_2 nanowires have been selected as supports. In particular, W-TiO_2 not only demonstrates high oxidation resistance, but also possesses fair electronic conductivity. Ir nanoparticles were deposited on these supports via chemical reduction of Ir precursors and the resulted particle size of 2-3 nm was confirmed by transmission electron microscopy. The activity and durability of supported catalysts are shown in Figure 2.

In the RDE tests, the Ir/W-TiO_2 catalyst improves the OER activity by a factor of 3 compared with commercial Ir black (Figure 2a). The Ir/ W-TiO_2 catalyst also demonstrates good stability during voltage cycling from 1.4 to 1.8 V; it retains 95% of its original OER activity even after 10,000 cycles (Figure 2b). Ir/W-TiO_2 also exhibits outstanding performance in a real PEM electrolyzer (Figure 2c). At 0.4 mg/cm^2 Ir loading, it nearly matches the performance of a Giner standard anode (2 mg/cm^2 Ir + 2 mg/cm^2 Pt) while reducing Ir loading by a factor of 5 and precious metal

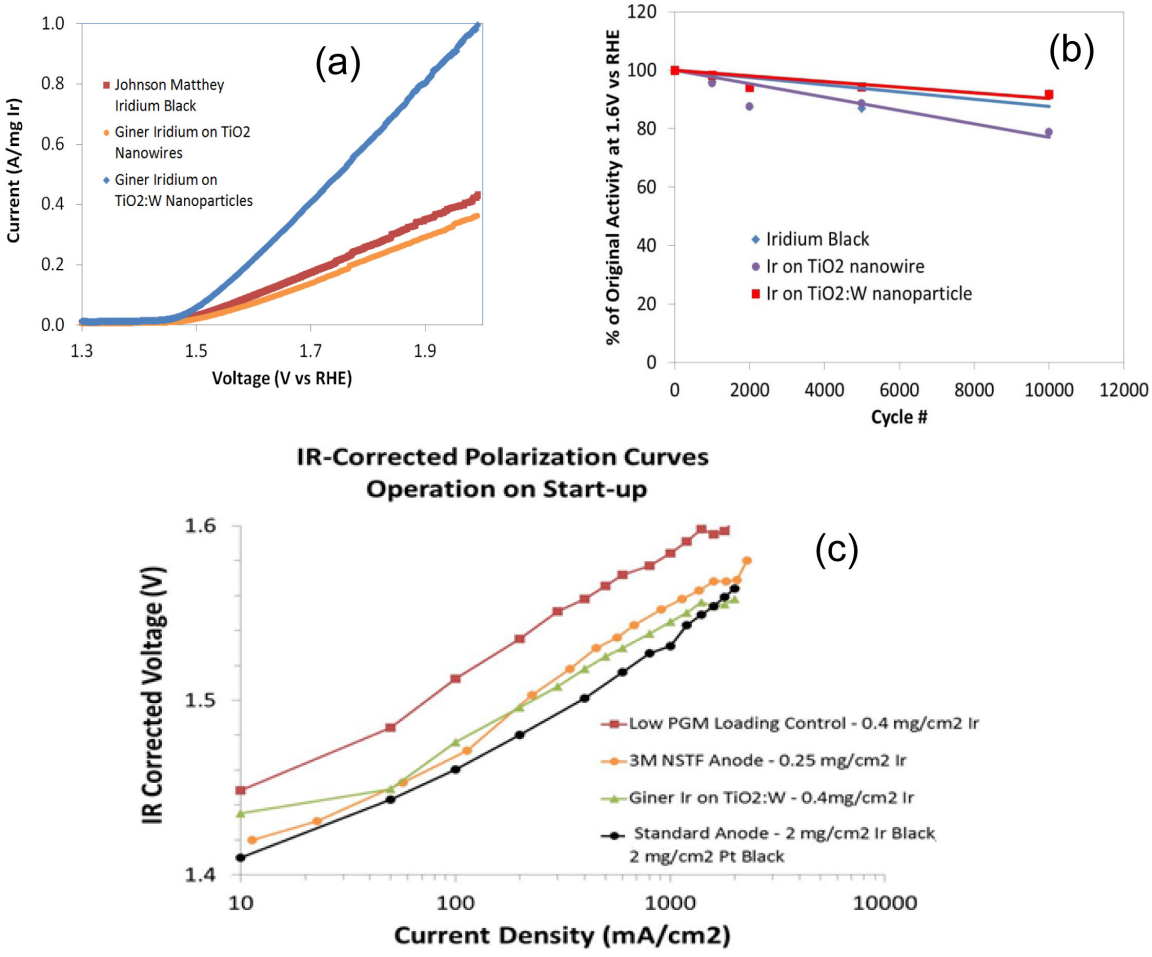

FIGURE 2. Performance of Giner Ir supported on two TiO_2 supports (a) OER activity of in a RDE (scan rate: 20 mV/s; RPM: 2,500 rpm; Ir loading: 40 μg/cm^2; 0.1 M $HClO_4$); (b) catalyst durability during voltage cycling from 1.4 V to 1.8 V vs RHE; (c) PEM electrolyzer performance of Ir/W-TiO_2 at 80°C

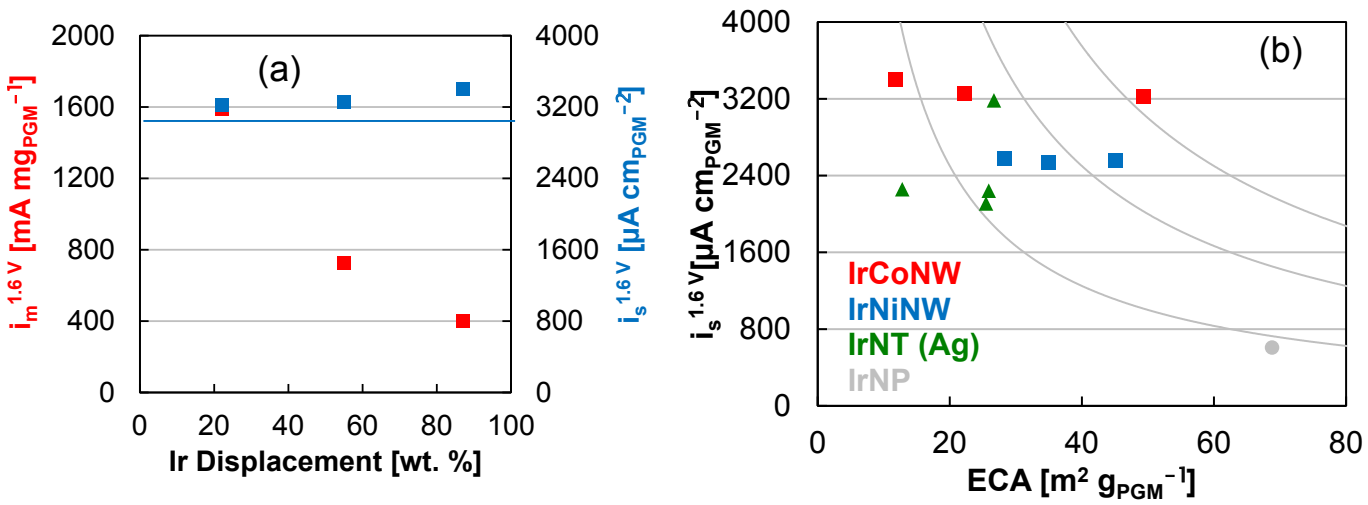

FIGURE 3. Performance of NREL Ir/metal nanowires in RDE tests (a) OER activity of Ir/Co nanowire vs. Ir loading in the nanowire; (b) OER activity comparison of different Ir/metal nanowires vs. the Ir ECSA

loading by a factor of 8. In a comparison with 0.4 mg/cm^2 Ir black, Ir/W-TiO_2 improves the OER activity (current density at a fixed voltage 1.8 V) by a factor of 3. The improved OER activity is directly correlated to decreased Ir particle size. Ir is well dispersed on W-TiO_2 which may increase the electrochemical surface area (ECSA) of Ir particles.

NREL attempted to make iridium nanotubes using different nanowires as a scaffold material. Iridium was deposited onto metal nanowire (Ag, Co or Ni) using partial galvanic displacement. In a typical experiment, iridium cobalt nanowires were synthesized by the galvanic displacement of cobalt with iridium chloride. Synthesis was completed in water to ensure that all iridium reduction occurred at the expense of cobalt. Excess iridium precursor was supplied and experiments were conducted with and without the presence of nitric acid. Iridium content in the cobalt nanowires can be varied. The addition of nitric acid increased the iridium content to 98.4 wt%. The OER activity of these Ir/metal nanowires is shown in Figure 3. Figure 3a illustrates the impact of Ir displacement in the Ir/Co nanowire on the mass and specific activity using a RDE. It can be seen that, as the Ir loading increases, the mass activity of the Ir/Co nanowire catalyst increases but its specific activity remains nearly constant. Figure 3b plots the OER activity of Ir/various metal (Ag, Ni or Co) nanowires against the Ir ECSA that was measured by a mercury under-potential deposition [2]. Contour lines are of constant mass OER activity (500, 1,000, 1,500 mA mg_{PGM}^{-1}) and Y-axis represents the specific activity. Ir/Co nanowire catalyst demonstrates the highest activity: 3.8 times greater specific activity than Ir black and 3 times greater mass activity than Ir black. The durability of these catalysts was also measured by the voltage cycling and it was found that the higher Ir loading, the lower OER activity, the better durability (data not shown). The acid leaching of the Ir/metal nanowire catalysts increase their durability.

3M has created a new NSTF anode that uses iridium without any platinum. This is different from the first generation NSTF anode, where iridium is supported on platinum deposited on the NSTF. The catalyst loading is 0.25 mg/cm^2. The novel anode is pressed onto a MEA along with a NSTF cathode containing 0.25 mg/cm^2 platinum. The membrane material was a 50-μm thick sheet of 3M 800 equivalent weight ionomer. The MEA is assembled in Giner's proprietary electrolyzer hardware (flow field and diffusion media) and tested performance is shown in Figure 4. The effect of Ir loading on the electrolyzer performance is shown in Figure 4a and found that the optimum Ir loading appears to be around 0.2-0.4 mg/cm^2 PGM. In comparison, the NSTF MEA performed nearly as well as a standard MEA despite having only 25% of the iridium and 12.5% of the total PGM. Preliminary durability testing of the NSTF was also conducted by 3M. Two MEAs were subjected to extended operation at 1.65 V. Both MEAs showed no sign of significant performance degradation after 200 hours (Figure 4b). This has met Milestone 3: PGM loading of less the 0.5 mg/cm^2; electrochemical stability at 1.8 V; voltage below 1.7 V @ 1 A/cm^2.

CONCLUSIONS AND FUTURE DIRECTIONS

Conclusions

- Ir-based OER catalysts for PEM electrolysis have been successfully synthesized and characterized at NREL, 3M, and Giner and RDE data show promising activity of developed catalysts compared to commercial Ir black:
  - Giner: various supports and Ir nanotubes
  - NREL: Ir/metal nanowires

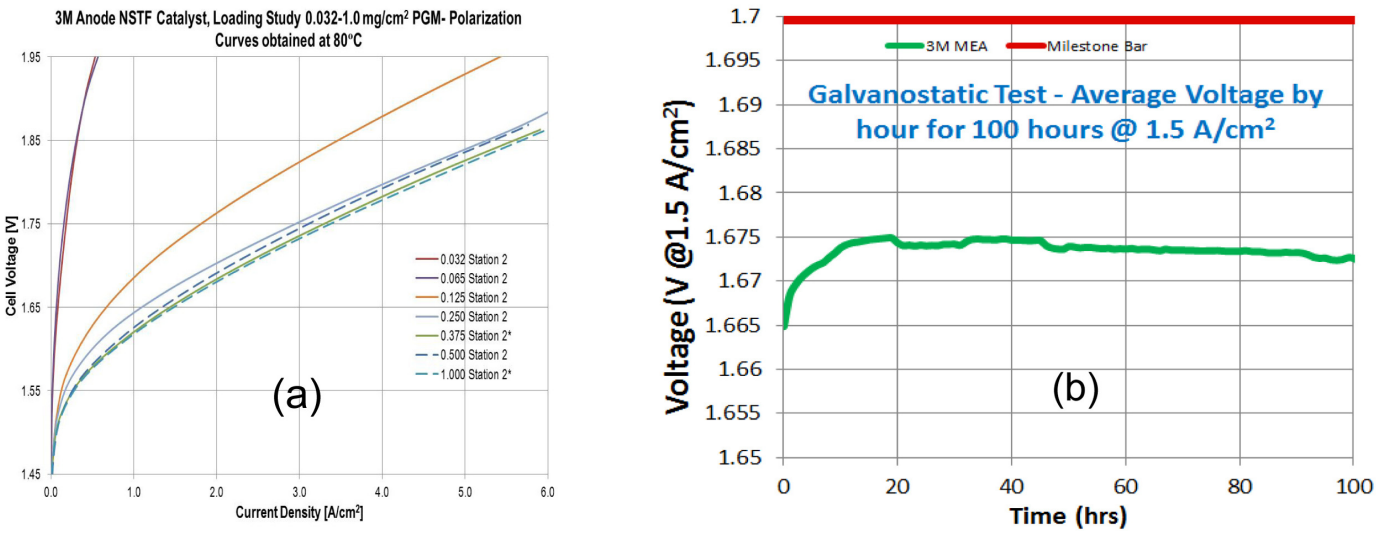

FIGURE 4. Performance of 3M Ir NSTF catalysts (a) impact of Ir loading in the IrNSTF on the electrolyzer performance; (b) a 100-hour durability test of the IrNSTF catalyst (at a current density of 1.5 A/cm^2)

  - 3M: Ir NTSF
- 3M NSTF catalyst-based MEA demonstrates superior performance:
  - Comparable performance to standard Ir black catalyst but at 8 times lower Ir loading
  - 1.675 V at 1.5 A/cm^2 for 100 hours, with Ir loading <0.5 mg/cm^2
  - Significantly exceeding the milestone set for July 2014
- Giner Ir/W-TiO_2 catalyst MEA demonstrates excellent performance:
  - Catalytic activity increased by 3 times compared with Ir black with same loading
  - Nearly matches Giner baseline performance but reduce Ir loading by 5 times
  - Approaches the performance of 3M NSTF OER catalyst

Future Directions

- Test the duality of the developed catalysts in PEM electrolyzers
- Develop economic analysis of materials and system:
  - Catalyst and MEA cost from short production
  - Electrolyzer system cost and efficiency

FY 2014 PUBLICATIONS/PRESENTATIONS

1. Xu, H., "High-Performance, Long-Lifetime Catalysts for Proton Exchange Membrane Electrolysis", Presentation in DOE Hydrogen and Fuel Cell merit review meeting, Arlington, VA, June 2014.

2. Xu, H, B Rasimick, A Stocks, S Alia, B Pivovar, "High-Performance, Long-Lifetime Catalysts for Proton Exchange Membrane Electrolysis" Prog Rpt, DOE Phase II DE-SC0007471, August 2013.

3. Xu, H., B. Rasimick, A. Stocks, B. Pivovar, and K. Lewinski, "High-Performance, Long-Lifetime Catalysts for Proton Exchange Membrane Electrolysis," Progress Report, U.S. Department of Energy Phase II Grant No. DE-SC0007471, January 2014.

REFERENCES

1. Hamden, M., "PEM Electrolyzer Incorporating an Advanced Low Cost Membrane". Presentation in DOE 2012 H2 and Fuel cells AMR meeting, http://www.hydrogen.energy.gov /pdfs/review12/ pd030_hamdan_2012_o.pdf (2012)

2. Kounaves, K.P and Buffle, J. "Deposition and Stripping Properties of Mercury on Iridium Electrodes", J. Electrochem. Soc. 13, 2495-2498 (1986).

II.C.1 Solar-Thermal Redox-Based Water Splitting Cycles

Christopher Muhich, Janna Martinek, Brian Ehrhart, Kayla Weston, Darwin Arifin, Ibraheam Al-Shankiti, Charles Musgrave and Alan W. Weimer (Primary Contact)
University of Colorado
Campus Box 596
Boulder, CO 80309-0596
Phone: (303) 492-3759
Email: alan.weimer@colorado.edu

DOE Manager
Sara Dillich
Phone: (202) 586-7925
Email: Sara.Dillich@ee.doe.gov

Contract Number: DE-FC36-05GO15044

Project Start Date: March 31, 2005
Project End Date: September 30, 2014

Overall Objectives

- Develop efficient robust materials and operation methods for a two-step thermochemical redox cycle that will achieve the DOE cost targets for solar hydrogen
- Develop a scalable solar-thermal reactor design that will achieve the DOE cost targets for solar hydrogen

Fiscal Year (FY) 2014 Objectives

- Synthesize hercynite redox materials that are >80% active by mass
- Characterize "pseudo-isothermal" redox chemistry in a stagnation flow reactor to demonstrate a hydrogen productivity greater than 150 µmole/gram total
- Investigate isothermal and/or "near-isothermal" redox in the High Flux Solar Furnace at the National Renewable Energy Laboratory, demonstrating a hydrogen productivity greater than 150 µmole/gram total on-sun
- Perform robustness testing of "hercynite cycle" redox at ETH Zurich, demonstrating a hydrogen productivity of greater than 150 µmole/g total after 100 cycles.
- Develop an understanding of temperature-swing vs. isothermal redox and the relative efficiency for carrying out each

Technical Barriers

This project addresses the following technical barriers from the Hydrogen Production section of the Fuel Cell Technologies Office Multi-Year Research, Development, and Demonstration Plan:

(S) High-Temperature Robust Materials

(T) Coupling Concentrated Solar Energy and Thermochemical Cycles

(U) Concentrated Solar Energy Capital Cost

Technical Targets

TABLE 1. Technical Targets for Solar-Driven High-Temperature Thermochemical Hydrogen Production

Characteristics	Units	2020 Target	Ultimate
Plant Gate H_2 Cost	\$/gge H_2	3.70	2.00
Chemical Tower Capital Cost (installed cost)	\$/TPD H_2	2.3 MM	1.1 MM
Annual Reaction Material Cost	\$/yr.-TPD H_2	89,000	11,000
Solar to H_2 Energy Conversion	%	20	26

gge – gasoline gallon equivalent; TPD – tons per day; MM - million

FY 2014 Accomplishments

- Completed computer model for thermodynamic efficiency calculations for isothermal and near-isothermal for cerium oxide
- Demonstrated over 3× H_2 production from "hercynite cycle" materials using near-isothermal Red/Ox cycling (basis of 100 micromole H_2/g in 2013)
- Determined kinetic model and mechanism for CO_2 splitting for "hercynite cycle"
- Performed computational fluid dynamic modeling on SurroundSun™ reactor

✧ ✧ ✧ ✧ ✧

INTRODUCTION

Two-step solar thermochemical processes based on non-volatile metal oxide cycles, as shown in Equations 1 and 2, have the potential to operate at high thermal efficiencies, are chemically simple, and require less land and water to operate than competing biomass, artificial photosynthesis and photovoltaic-driven electrolysis. Traditionally, two types of non-volatile metal oxide redox chemistries are utilized in solar thermochemical H_2O splitting. The first is based on non-stoichiometric oxides of which ceria is a representative example. Such redox materials are thermally reduced without undergoing phase change, as the lattice is able to accommodate the strain induced by oxygen vacancy

formation. These materials are thermally quite stable, although the extent of reduction, and hence cycle capacity, is small compared to other reducible oxides.

$$MO_x \rightarrow MO_{x-\delta} + \delta/2\ O_2 \quad (1)$$

$$MO_{x-\delta} + \delta\ H_2O \rightarrow MO_x + \delta\ H_2 \quad (2)$$

The second prototypical chemistry utilizes materials of the spinel structure that form solid solutions upon reduction. The most common are ferrites where Fe^{3+} in $M_xFe_{3-x}O_4$ is partially reduced to Fe^{2+}; here M can be any number of transition metals that form spinel type oxides with Fe though Co, Zn, and Ni are the most studied. In these redox cycles, the ferrite spinel is heated until it decomposes into a mixture of metal oxide solid solutions that are thermodynamically stable at temperatures above which the spinel decomposes. While these materials theoretically exhibit greater redox potential than non-stoichiometric oxides, in practice deactivation induced by irreversible processes such as sintering or the formation of liquid phases and metal vaporization lead to loss of active oxide.

APPROACH

Our approach is to develop an efficient cost-effective hydrogen process through (1) an understanding of Red/Ox thermal cycling conditions, (2) the development of improved robust active materials, and (3) a scalable solar thermal reactor system that is optimal for the materials that we develop. First, a thorough understanding of the activity of Red/Ox materials and its impact on type of cycling (isothermal, near-isothermal, and temperature-swing) and reactor efficiency is needed to understand how to produce hydrogen in the most efficient way. This will depend on the specific material being used, as well as different practical and economic constraints on operating conditions. In addition to the reaction cycling conditions, it is important to develop a more detailed understanding of Red/Ox materials mechanisms and, hence, methods to improve materials performance. Different materials and mechanisms (i.e., displacement or oxygen vacancy) can benefit from different operating conditions, and so understanding these fundamental differences is important. Finally, a reactor must be designed which is scalable to large sizes, is comprised of suitable containment materials, and is tunable for specific active materials. This will allow for flexibility in operating the Red/Ox cycle in the most efficient way possible and allow for the hydrogen production process to take advantage of economies of scale.

RESULTS

Determining the most efficient way to operate is an important consideration for solar thermochemical water splitting. Ermanoski et al. and other groups have suggested different ways of finding the overall solar-to-hydrogen efficiency [1], and we have expanded upon the model of Ermanoski et al. in our own analysis. Some of our results are shown in Figure 1, and indicate that isothermal cycling is theoretically the most efficient way to operate ceria Red/Ox, assuming perfect gas-gas heat recuperation. This gas-gas heat recuperation efficiency is an important factor in the overall solar-to-hydrogen efficiency, and in determining the best possible combination of operational parameters. This heat recuperation deals with the water entering the system into the oxidation reactor, some of which reacts to form hydrogen and then exits the oxidation reactor along with any excess steam and is cooled to ambient temperatures. The

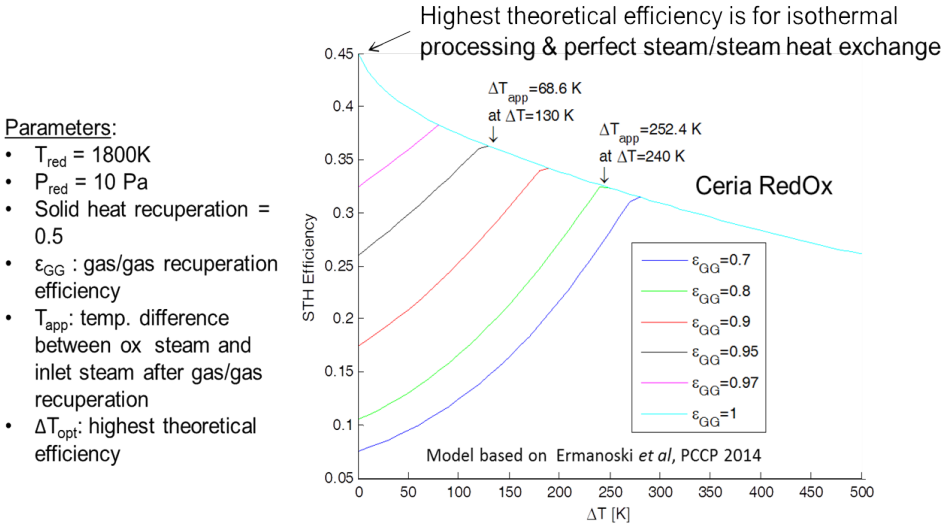

FIGURE 1. Solar-to-hydrogen efficiency calculations for cerium oxide based on thermodynamic compositions for a single reduction temperature and pressure with different oxidation temperatures and gas-gas heat recuperation efficiencies.

gas-gas heat recuperation efficiency is a lumped parameter of how much heat form the cooling of the steam/H_2 mixture can be used to pre-heat the water. Here we show that for ceria, as the heat recuperation approach temperature between the steam to be fed to the oxidizer and the exiting steam/H_2 mixture is minimized and approaches zero (meaning the gas-gas heat recuperation efficiency approaches 100%), the overall efficiency of the process is improved and more isothermal-like operating temperatures are suggested.

Achieving very high gas-gas heat recuperation efficiencies is a considerable challenge. Metal alloy heat exchangers are able to heat the steam from ambient to 1,000°C using high-temperature Ni alloys, such as Inconel. These would be followed by ceramic heat exchangers that are being developed by a number of companies to take the steam to even higher temperatures in order to minimize the approach temperature, or the difference in temperature between the hot steam and hydrogen entering the heat exchanger and the fresh water leaving the heat exchanger. We've contacted some of these companies and have been told that heating gases to 1,200°C is almost guaranteed, 1,300°C should work, 1,500°C should be possible and even hotter may be possible. This would then become an economic argument (as with everything else in the system), and the cost/benefit tradeoffs will need to be considered.

As discussed in the previous section, it may be desirable to operate in a near-isothermal mode, where the temperature difference between the oxidation and reduction steps is relatively small (<150°C). This will minimize simultaneous Red/Ox formation of O_2 and H_2 while increasing theoretical efficiency if the perfect gas/gas heat exchange is not achieved. Therefore, we experimentally investigated the hydrogen production capacity under near isothermal conditions where the reduction step is carried out at 1,350, 1,400, 1,450, and 1,500°C while oxidation occurred at 1,350°C. This was done using 85% active hercynite skeletal material. As expected, we were able to achieve ~100 µmol H_2/total gram of material for 1,350°C isothermal water splitting, and as we increased the reduction temperature we were able to increase the H_2 produced, achieving over 350 µmole H_2/total gram of material under 1,500°C reduction, as seen in Figure 2. The increased reduction temperature increases the extent of hercynite material reduction, thereby increasing the hydrogen production capacity, while the high 1,350°C oxidation temperature reduces the deleterious kinetic effects of lower oxidation temperatures, leading to the high quantity of hydrogen generated.

In the past fiscal year, we studied isothermal carbon dioxide splitting using the laser assisted stagnation flow reactor at the Livermore branch of Sandia National Laboratories. We collected data using "hercynite cycle" material for isothermal operation with temperatures of 1,280-1,420°C and partial pressures of CO_2 in the range of 316-576 Torr. During experimental runs catalytic CO_2 splitting occurred along the inside of the reactor walls at the high operating temperatures. In order to correct for this material-independent splitting, blanks were run at each of the experimental conditions. The CO curves generated with the blanks were subtracted from the overall signal in order to determine corrected CO generation data. The corrected curves were then used to model the CO_2 splitting behavior of the "hercynite cycle" material and the dispersion of CO as the gas moves through the analytics section as outlined by Scheffe et al. [2]. However, because of the catalytic CO_2 splitting and O_2 uptake by the hercynite materials from O_2 resulting from CO_2 splitting on the walls of the reactor, we were unable to fit the CO_2 production curves using only one of the traditional solid state reaction models (F1, F2, D1, D2, etc.) shown in Equation 3, where α is the extent of reaction (in this case the extent of re-oxidation), t is time, k_0 is kinetic rate coefficient, Y is the CO_2 concentration, γ is the reaction order with respect to the CO_2 concentration, and f(α) is the reaction model.

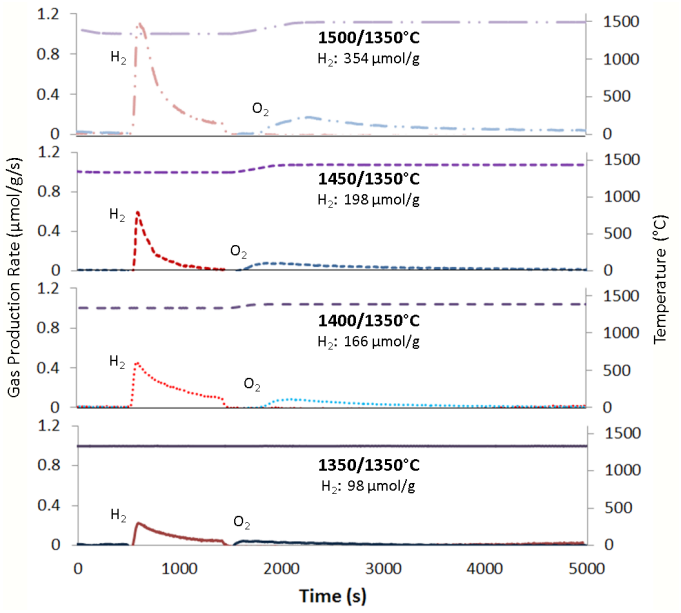

FIGURE 2. Near isothermal water splitting gas production. The H_2 and O_2 generation rates under isothermal or near isothermal water splitting conditions for reduction temperatures of 1,350-1,500°C and an oxidation temperature of 1,350°C.

$$\frac{d\alpha}{dt} = \kappa_0 Y_{CO_2}^{\gamma} f(\alpha) \quad (3)$$

The models had to be expanded to include the reaction of O_2 produced on the walls, along with that produced by the "hercynite cycle" active materials and catalytic CO_2 splitting. The overall rate expression for material re-oxidation is shown in Equation 4, where the first and second terms are the CO_2 and O_2 oxidation contributions, respectively.

$$\frac{d\alpha_o}{dt} = \kappa_1 Y_{CO_2}^{\gamma}(1-\alpha_0)^{n_1} + \kappa_3{}^{1} Y_{CO_2}^{\gamma_3}(1-\alpha_0)^{n_3} \quad (4)$$

We have complete modeling of isothermal CO_2 splitting based on surface limited models (Equation 2) and system dispersion as can be seen in Figures 3 a-d. The surface limited models give reasonably good fits to the experimental data. Additionally, Figures 3f-g shows the reaction progression without dispersion effects. Overall, we found that the CO_2 reaction is roughly third and second order with respect to the CO_2 pressure, and material respectively, and the O_2 reaction is roughly first and second order with respect to the O_2 pressure, and material respectively.

Over the past several years, we have developed the SurroundSun™ reactor design which is simple to operate and maintain. In this design, the active material is fixed within heated reaction tubes which are themselves housed in an insulating cavity. Concentrated sunlight enters through a window and directly irradiates the tubes containing

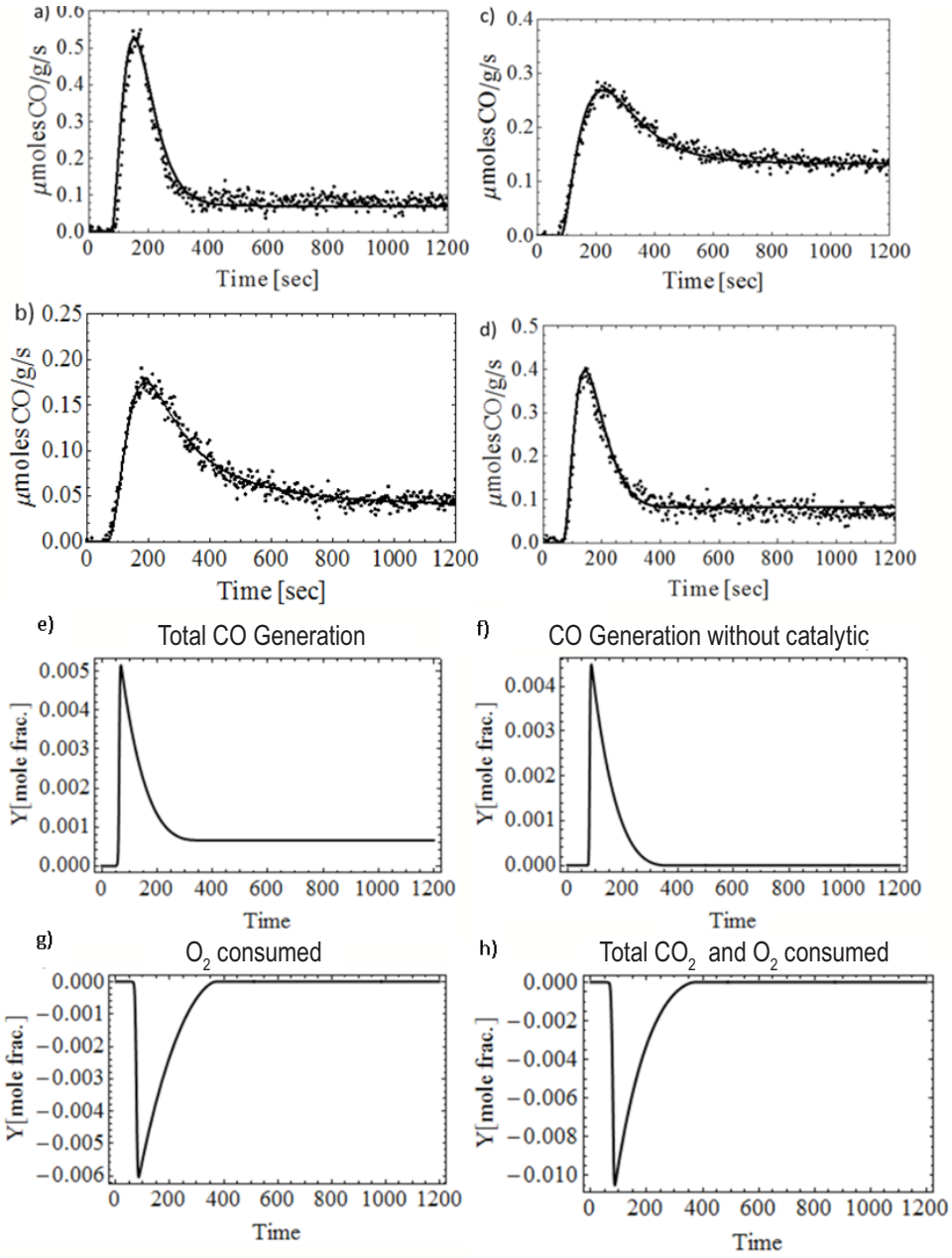

FIGURE 3. Result of kinetic molding analysis for isothermal CO_2 splitting using hercynite materials. CO_2 production curves as experimentally observed (dots) and modeled (straight lines) for a) 1,420°C and b) 1,280°C at 450 Torr CO_2, and at 1,350°C under c) 576 and d) 310 Torr. Modeled CO_2 production curves as modeled using Equation 2 for isothermal splitting at 1,350°C under 310 Torr. e) total CO generated, f) CO generated without including the catalytic activity, g) O_2 oxidation and h) total O_2 and CO_2 oxidation. These curves are un-corrected for dispersion.

the active materials, as shown in Figure 4. One great benefit to this design is that there are no moving parts. For temperature-swing operation, the concentrated sunlight is moved from one half of the reaction tubes to the other with reduction occurring in the irradiated tubes while steam is fed to the other, oxidizing tubes producing H_2. For isothermal operation, concentrated sunlight is directed such that all reaction tubes are heated uniformly and the steam is fed into the desired tubes to drive oxidation. This past year we carried out detailed computational fluid dynamics modeling of the operation of this reactor design under isothermal and temperature swing conditions, which indicate major challenges in the operation of this reactor design. For temperature swing operation, it is impossible to achieve substantial differences in temperature between the reduction and oxidation reaction tubes, while for isothermal operation there is a substantial temperature variation with the tubes, thus preventing all of the active material to hold at a constant temperature. This indicates two major drawbacks of the SurroundSun™ design: 1) limited control over the operating temperature within the reactor, as indicated by the small temperature change achieved during temperature swing operations modeling; and 2) inefficient use of the material because it is not efficiently heated all the way through to the center of the reducing tubes, as illustrated by the large temperature gradients across individual reaction tubes undergoing reduction under both temperature swing and isothermal water splitting operation. Based on these results, we have concluded that a new reactor design should be considered based on the following principles: 1) flowing particles to enable even material heating, 2) separate reduction/oxidation reaction containment and 3) decoupled reduction/oxidation times.

CONCLUSIONS AND FUTURE DIRECTIONS

- Determined that isothermal Red/Ox is possible, enabling large design space for optimization
- Determined that optimal change in temperature (ΔT) is dependent on active materials, gas/gas heat transfer efficiency and temperature of H_2/H_2O separation
- Developed oxidation kinetics for high temperature CO_2 splitting

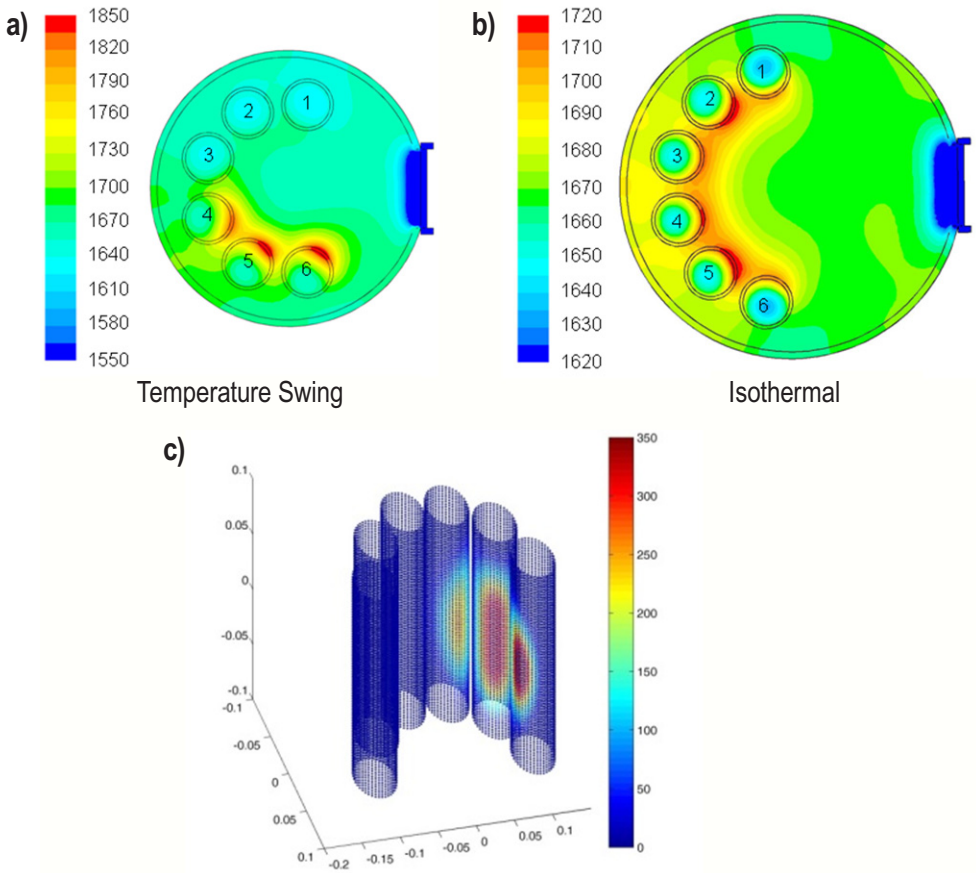

FIGURE 4. Computational fluid dynamics modeling results of SurroundSun™ reactor. a) and b) show the temperature profile with in the reactor under temperature swing and isothermal conditions. c) shows the directional focus of the concentrated sunlight during temperature swing operations.

- Determined that "near-isothermal" processing enables high reduction extent and rapid oxidation kinetics without simultaneous reduction/oxidation occurring
- Determined that a packed bed, stationary tube, SurroundSun™ reactor does not enable considerable ΔT, and materials heating is uneven across the reactant tubes
- Will incorporate Red/Ox extents from "hercynite cycle" and new materials into model to determine "optimal" ΔT
- Will develop improved "hercynite cycle" and perovskite materials using high through-put screening methods and investigate extent of reduction for various P_{O2} and P_{H2O}

FY 2014 PUBLICATIONS/PRESENTATIONS

1. Martinek, J., R. Viger, and A.W. Weimer, "Transient Simulation of a Tubular Packed Bed Solar Receiver for Hydrogen Generation via Metal Oxide Thermochemical Cycles," Solar Energy, 105, 613-631 (2014).

2. Saade, E., D.E. Clough, and A.W. Weimer, "Use of Image-Based Direct Normal Irradiance Forecasts in the Model Predictive Control of a Solar-Thermal Reactor," Journal of Solar Energy Engineering – Transactions of the ASME, 136 (1), Article 010905 (February, 2014).

3. Saade, E., D.E. Clough, and A.W. Weimer, "Model Predictive Control of a Solar – thermal Reactor," Solar Energy, 102, 31-44 (2014).

REFERENCES

1. I. Ermanoski, *et al.*, "Efficiency maximization in solar-thermochemical fuel production: challenging the concept of isothermal water splitting," Physical Chemistry Chemical Physics, **16**, pp. 8418-8427, 2014.

2. J.R. Scheffe, *et al.*, "Kinetics and mechanism of solar-thermochemical H2 production by oxidation of a cobalt ferrite-zirconia composite," *Energy & Environmental Science*, **6**, pp. 963-973, 2013.

ACKNOWLEDGEMENT

The authors would like to thank Dr. Anthony McDaniel at Sandia National Laboratories – Livermore for the use of his laser-assisted stagnation flow reactor equipment and his input into the fundamental understanding of the chemistry.

II.C.2 Solar Hydrogen Production with a Metal Oxide-Based Thermochemical Cycle

Anthony McDaniel
Sandia National Laboratories
MS9052
PO Box 969
Livermore, CA 94550
Phone: (925) 294-1440
Email: amcdani@sandia.gov

DOE Manager
Sara Dillich
Phone: (202) 586-7925
Email: Sara.Dillich@ee.doe.gov

Subcontractors
- Nathan Siegel, Bucknell University, Lewisburg, PA
- Jianhua Tong, Colorado School of Mines, Golden, CO
- Alan Weimer, University of Colorado, Boulder, CO

Project Start Date: October 1, 2008
Project End Date: Project continuation and direction determined annually by DOE

Overall Objectives

- Verify the potential for a solar thermochemical hydrogen production cycle based on a two-step, non-volatile metal oxide to be competitive in the long term.
- Develop a high-temperature solar receiver-reactor (SRR) and redox material for hydrogen production with a projected cost of $3.70/gasoline gallon equivalent at the plant gate by 2020.

Fiscal Year (FY) 2014 Objectives

- Discover and characterize novel perovskite materials for a two-step, non-volatile metal oxide water-splitting thermochemical cycle.
- Calculate theoretical system efficiency for various SRR operating scenarios that meet or exceed a solar-to-hydrogen (STH) conversion ratio of 26%.
- Formulate and refine particle-based SRR designs and assess feasibility.
- Construct an engineering test stand and evaluate particle conveyance and pressure separation concepts under vacuum at elevated temperature.
- Conduct H2Av3 analysis of a central receiver-based particle SRR producing 100,000 kg H_2/day and identify a clear path towards meeting DOE projected cost targets for hydrogen.

Technical Barriers

This project addresses the following technical barriers from the Hydrogen Production section of the Fuel Cell Technologies Office Multi-Year Research, Development, and Demonstration Plan:

(S) High-Temperature Robust Materials

(T) Coupling Concentrated Solar Energy and Thermochemical Cycles

(X) Chemical Reactor Development and Capital Costs

(AC) Solar Receiver and Reactor Interface Development

Technical Targets

This project is conducting fundamental studies on materials for use in concentrated solar power applications and designing reactor concepts that, when combined, will produce H_2 from thermochemical water-splitting (WS) cycles. Insights gained from these studies will be applied toward the design and optimization of an SRR that meets the following ultimate DOE hydrogen production targets:

- Hydrogen Cost: <$2/kg H_2
- Material of Reaction Cost: ≤$11K/yr tons/day H_2
- STH Conversion Ratio: ≥26%
- 1-Sun Hydrogen Production Rate: $\geq 2.1\times10^{-6}$ kg/s m^2

FY 2014 Accomplishments

- Synthesized 30 different redox materials using AB(Mn or Fe)O_3 perovskite oxides (A = Ca, La, Sr, or mixtures thereof; B = Ce, Ti, or Zr). Compounds were screened for water-splitting activity using thermogravimetric analysis (TGA) methodologies. Finding a more effective redox material increases the likelihood of meeting the DOE targets for material cost and STH conversion ratio.
- Developed a thermodynamic model for $Sr_xLa_{1-x}Mn_yAl_{1-y}O_3$ perovskite compositions (SLMA2) based on P_{O2}-δ-T data. Predicted the optimal operating temperature (ΔT), O_2 pressure (vacuum), and heat recovery effectiveness required for SLMA2 to meet or exceed a STH conversion ratio greater than 20%. We predict that near-term DOE technical targets for solar H_2 can be achieved in a two-step high-temperature thermochemical cycle using SLMA2.

- Derived performance criteria and thermodynamic properties for an "ideal" non-stoichiometric oxide. This hypothetical material strikes a balance between the solar energy required to heat oxide versus steam, and thus is predicted to cycle at an *optimal* reactor efficiency. Identifying such criteria is key to meeting the long-term DOE STH conversion ratio target of 26%.
- Advanced Sandia's particle bed reactor concept to include a novel and game-changing approach—cascading pressure thermal reduction—enabling ultra-low O_2 pressure under thermal reduction in vacuum. This discovery is critical to achieving a STH conversion ratio greater than 20% for state-of-the-art perovskites.
- Designed a particle elevator for a 3-5 kW-scale engineering test stand. Construction is under way. When completed, it will be integrated into a fully functioning SRR. Knowledge gained from operating this reactor will be used to analytically up-scale our technology to a 100,000 kg H_2/day centralized plant.
- Analyzed H_2 cost for a central receiver-based particle SRR operating at 100,000 kg H_2/day capacity. Plant design incorporates a full field beam-down optical layout for each of many 5 MW central receivers. Analysis reveals the importance of reactor efficiency to meeting DOE ultimate cost targets due to the high capital cost of solar collection.

INTRODUCTION

This research and development project is focused on the advancement of a technology that produces hydrogen at a cost that is competitive with fossil-based fuels for transportation. A two-step, solar-driven WS thermochemical cycle is theoretically capable of achieving a STH conversion ratio (i.e. conversion efficiency) that exceeds the DOE target of 26% at a scale large enough to support an industrialized economy [1]. The challenge is to transition this technology from the laboratory to the marketplace and produce H_2 at a cost that meets or exceeds the DOE target of <$2/kg H_2.

Conceptually, heat derived from concentrated solar energy can be used to reduce a metal oxide at high temperature producing O_2 (Step 1). The reduced metal oxide is then taken "off sun" and re-oxidized at lower temperature by exposure to H_2O, thus producing H_2 (Step 2) and completing the cycle. The ultimate commercial success of solar thermochemical H_2 production is contingent upon developing suitable redox active materials and incorporating them into an efficient SRR. There are numerous material chemistries that have attributes suitable for inclusion in a thermochemical H_2 production system [2-4]. The challenge is to identify an optimally performing material. In addition, the development of redox material and SRR are not mutually exclusive, but must be conducted in parallel [5]. To maximize the probability of success, this project also addresses the reactor- and system-level challenges related to the design of an efficient particle-based SRR concept [6].

APPROACH

Thermochemical WS reactors are heat engines that convert concentrated solar energy (heat) to chemical work. Our approach is to discover novel materials to accomplish the WS chemistry and pair these with a novel SRR that, when combined, can achieve an unprecedented STH conversion ratio. The material discovery work involves expanding our understanding of the underlying thermodynamics and kinetics in order to make performance improvements and/or formulate new, more redox-active compositions. Sandia's patented SRR technology is based on a moving bed of packed particles that embodies all of the design attributes essential for achieving high efficiency operation: (1) sensible heat recovery; (2) spatial separation of pressure, temperature, and reaction products; (3) continuous on sun operation; and (4) direct absorption of solar radiation by the redox-active material. Research efforts are focused on validating design concepts and deriving optimal operating conditions through detailed systems modeling.

RESULTS

In this project year, Sandia advanced the understanding of perovskite oxides as a class of materials for solar H_2 production, as well as identified the characteristics of an ideal redox material that can be incorporated into Sandia's SRR. Thirty different perovskite formulations were synthesized and screened. Our principle focus in FY 2014 was on chemical modifications of Mn- and Fe- based perovskites according to the following elemental substitutions: AB(Mn or Fe)O_3 oxides; A = Ca, La, Sr, or mixtures thereof; B = Ce, Ti, or Zr. We found that many of these compounds readily reduce at temperatures well below that of CeO_2 (T_{RED}<1,000°C), and possess redox capacities in excess of CeO_2 (i.e., reduce more deeply, $\delta >> 0.1$). Unfortunately, none of these materials performed WS chemistry better than the family of SLMA compounds we discovered last year [4]. Nonetheless, we are encouraged by the fact that simple modifications of AB(Mn or Fe)O_3 oxides yield redox-active materials, and maintain the position that perovskite oxides hold great promise for meeting DOE targets.

In FY 2014, we developed specifications for an ideal non-stoichiometric oxide for use in high-temperature WS cycles (summarized in Figure 1a). Here, seven key characteristics of redox-active materials are defined, such as WS temperature (T_{WS}), extent of oxygen non-stoichiometry in reduction (δ), H_2O/H_2 ratio during WS, etc. These values (or limiting ranges) were determined by high-level theoretical analysis of

(a)

prop.	SLMA	IDEAL	CeO_2
T_{OR}	865°C	900-1200°C	1220°C
T_{WS}	900°C	750-900°C	1000°C
δ	0.30	SLMA	0.08
H_2O/H_2	200/1	CeO_2	10/1
*$Rate_{WS}$	~0.04 s^{-1}	CeO_2	~0.01 s^{-1}
*ΔH_{TR}	220-320	350-400	400-500
*ΔS_{TR}	100-130	~CeO_2	200-300

* Rate=pseudo first order, ΔH(δ)=kJ/mol O, ΔS(δ)=J/K mol O

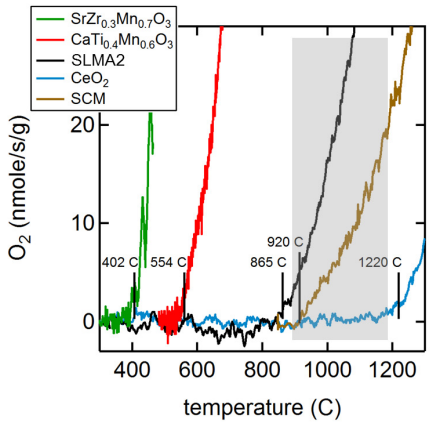

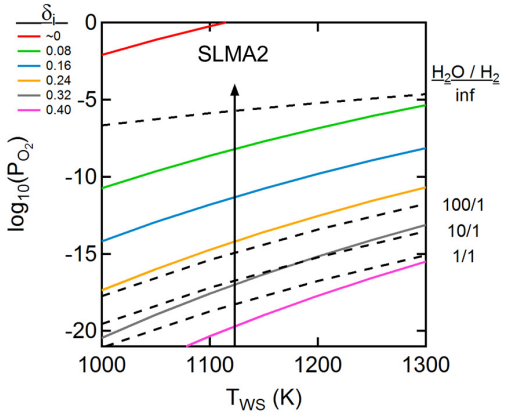

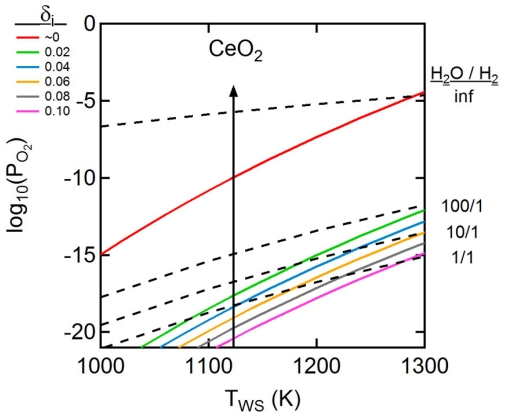

η_{STH} dominated by steam heating.

η_{STH} dominated by oxide heating.

FIGURE 1. (a) Range of material properties derived for an ideal non-stoichiometric oxide (see text). (b) O_2 production rate, normalized to material mass, as a function of temperature measured during thermal reduction under a flow of He gas for several representative perovskite formulations (see legend). Dark vertical lines denote the onset temperature for O_2 evolution, which strongly correlates to the reduction enthalpy (ΔH_{TR}) and WS activity. Shaded box represents a temperature region where the ideal material will begin to evolve O_2. (c, d) Thermodynamic data for SLMA2, CeO_2, and H_2O plotted as a function of WS temperature (T_{WS}), oxygen non-stoichiometry (δ), and H_2O/H_2 ratio. For H_2 production (i.e., water splitting) to be thermodynamically favored at a particular H_2O/H_2 ratio and temperature, the solid colored lines for the final state δ must lie below the dashed lines (see text).

Sandia's SRR using known properties for CeO_2 and SLMA2 that revealed the controlling factors for STH conversion ratio. With CeO_2, efficiency is dominated by oxide heating. For SLMA2, it is dominated by steam heating. Therefore, we postulate that the ideal material properties lie between these two.

We also discovered a new descriptor to aid in material screening, defined as "T_{OR}." This is the temperature at which O_2 begins to evolve from the solid and is strongly correlated to reduction enthalpy, WS activity, and process viability. With this descriptor, we can accelerate screening in both the TGA and stagnation flow reactor. Shown in Figure 1b is the O_2 evolution rate measured as a function of temperature during thermal reduction for several perovskite formulations tested in FY 2014. It is clear that some of our newest Mn-based compounds readily reduce, as evidenced by a T_{OR}<600°C that is well below SLMA2 or CeO_2. We also know that the reduction enthalpy for SLMA2<CeO_2, and therefore deduce that high T_{OR} suggest high reduction enthalpy. Not surprisingly, T_{OR} also strongly correlates to WS activity. The data in Figures 1c and 1d provide evidence for this. Equilibrium data for SLMA2 and CeO_2 under various WS conditions are shown in these two plots. For an oxygen atom from a H_2O molecule to go into the solid (thereby making H_2), the end-state δ curve (colored lines) must lie below that of a dashed curve for a specific WS condition (T_{WS} and H_2O/H_2 ratio). Ceria's T_{OR} (1,220°C) is higher than SLMA2 (865°C). And by comparison, a larger collection of colored lines for CeO_2 (Figure 1d) lie below a H_2O/H_2 ratio of 10/1 than for SLMA2 (Figure 1c). This implies that

the driving force for WS on reduced CeO_2 is greater than SLMA2. Therefore, high T_{OR} *also* indicates high WS activity. More importantly from a screening perspective, if T_{OR} is too low (below 700°C), as is the case for $SrZr_{0.3}Mn_{0.7}O_3$ and $CaTi_{0.4}Mn_{0.6}O_3$, the oxide will not split water. We believe that the ideal redox material will have a T_{OR} bounded by the grey shaded area in Figure 1b.

This year we derived a thermodynamic expression for SLMA2 from fitting a solid solution model to TGA measurements. The results, presented in Figure 2a, allow us to calculate the chemical state of SLMA2(P_{O2}, δ, T_{TR}) given any two of these parameters. The model also predicts enthalpy and entropy of reduction as a function of oxygen non-stoichiometry. With this model we have mapped the theoretical STH efficiency for SLMA2, shown in Figure 2b, as a function of temperature separation (ΔT), heat recuperation effectiveness (ε_{GG} and ε_R), and O_2 pressure in reduction (p_{TR} Pa) at T_{TR} = 1,450°C. It is evident from the efficiency profiles in Figure 2b that SLMA2 can meet or exceed the 2020 DOE target for STH conversion efficiency in Sandia's SRR. By using SLMA2 to decrease the thermal reduction temperature (T_{TR}) while maintaining a $\Delta\delta > CeO_2$, we achieve high STH efficiency without relying on solid-solid heat recovery (ε_R=0); a much less demanding reactor condition than proposed for high-STH operation with CeO_2 [6]. In addition, the gas-gas heat recovery effectiveness (ε_{GG}) has been limited to exchanger temperatures less than 1,000°C, an important design consideration given the difficulty of ultra-high temperature heat exchange.

In FY 2014, we made a groundbreaking improvement to the packed bed reactor design; the invention of a multi-stage thermal reduction process via pressure cascade [7] (shown schematically in Figure 3). This approach enables hitherto unfeasibly low thermal reduction pressures (i.e., high vacuum). Achieving ultra-low O_2 pressure (p_{TR}) during reduction is critically important to high STH efficiency operation (see Figure 2b). The practical challenges to reaching low p_{TR} are extremely large O_2 flow velocities, and correspondingly large pumping speeds, required for a multi-MW tower SRR. In fact, the desired extent of reduction requires p_{TR}<10 Pa, a physical impossibility in a single-chambered reactor using existing pumping technology. The improved cascade approach performs the thermal reduction in multiple chambers, each operating at a successively lower pressure. The packed particle bed design inherently provides for the required pneumatic sealing between chambers. The data in Figure 3b show the outstanding potential for decreasing p_{TR} via cascading pressure thermal reduction. One order of magnitude p_{TR} decrease can be achieved in only five stages, each operating at the same pumping speed. In a ceria based cycle for example, a 10-fold p_{TR} decrease corresponds to a 45% relative efficiency increase. Furthermore, because ultra-low p_{TR} is accessible via the new cascade approach, technically challenging high-temperature solid-solid heat recovery is no longer vital for efficient reactor

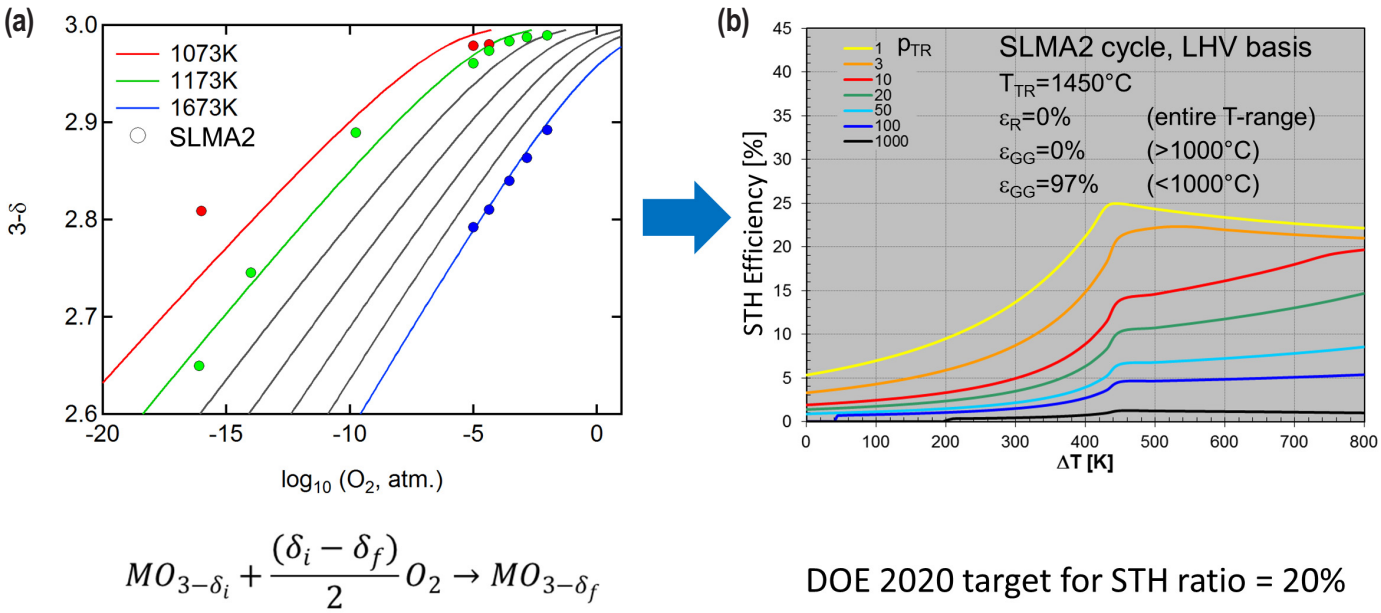

FIGURE 2. (a) P_{O2}-δ-T relationship map for SLMA2. Solid markers are experimental data measured by TGA, lines are fits to a solid solution model. (b) Predicted STH efficiency as a function of the temperature difference between T_{RED} and T_{OXD} (ΔT) for SLMA2 at various O_2 partial pressures under reduction (p_{TR}, Pa). Practical limits are assigned to the gas-gas (ε_{GG}) heat recovery effectiveness, and no credit is taken for solid-solid (ε_R) heat recovery (see inset). The thermodynamic model derived for SLMA2 was incorporated into this calculation [8]. At a p_{TR}<3 Pa, SLMA2 is predicted to exceed the DOE 2020 STH efficiency target in Sandia's particle-based SRR.

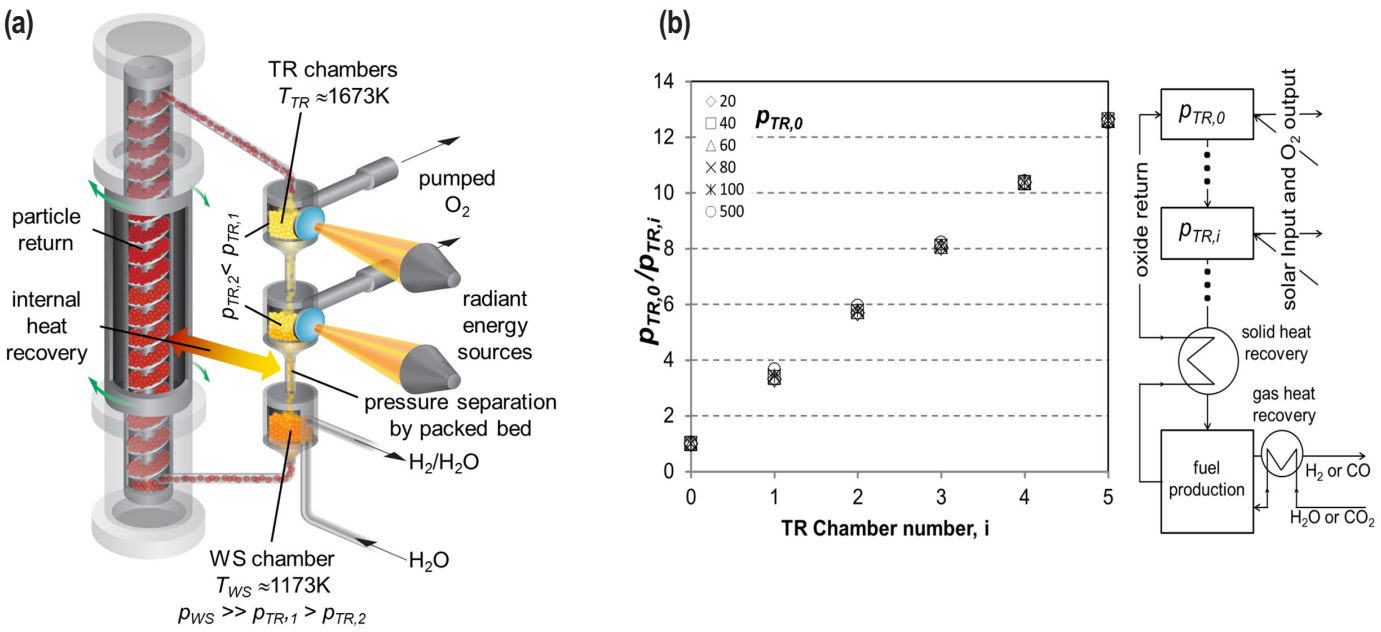

FIGURE 3. (a) Conceptual schematic of the 3-5 kW-scale engineering test stand under construction at Sandia. The sketch shows salient features of the device including two thermal reduction chambers and the particle elevator. (b) A simple schematic illustration of a cascading pressure reactor along with a graph showing the pumping advantage realized by using a multi-chambered approach. The ratio of $p_{TR,0}/p_{TR,i}$ (where TR,0 is the first chamber) is plotted as a function of the number of reduction chambers (i). One order of magnitude reduction in p_{TR} is achieved using only five chambers (calculation based on CeO_2 and other limiting factors such as solar concentration ratio and practical gas pumping speeds.)

design, representing a significant design innovation and simplification.

Finally, in FY 2014 we incorporated our extensive theoretical understanding of this process into the design of a 3-5 kW-scale engineering test stand. The particle elevator and apparatus for testing radiative heat transfer into particle beds is shown in Figure 4. When completed, this prototype will be used to evaluate all reactor functions, first individually and then within a fully integrated system inclusive of continuous operation and hydrogen production under simulated solar radiation. Data collected from this instrument will be used to further refine reactor designs, and analytically up-scale Sandia's technology to a 5-MW centralized tower system.

CONCLUSIONS AND FUTURE DIRECTIONS

- Discover additional perovskite and phase-change type oxides with ideal properties identified in FY 2014 for improved WS activity.
- Construct and test a functional SRR test stand sized for 3-5 kW with two reduction chambers.
- Design tower and field configurations compatible with multiple reduction chambers.

FY 2014 PUBLICATIONS/PRESENTATIONS

1. "Cascading Pressure Thermal Reduction for Efficient Solar Fuel Production", I. Ermanoski, *International Journal of Hydrogen Energy*, (2014) DOI:10.1016/j.ijhydene.2014.06.143.

2. "Efficiency Maximization in Solar Thermochemical Fuel Production: Challenging the Concept of Isothermal Water Splitting", I. Ermanoski, J.E. Miller, M.D. Allendorf, *Physical Chemistry Chemical Physics*, **16** (2014) 8418.

3. "Annual Average Efficiency of a Solar-Thermochemical Reactor", I. Ermanoski and N.P. Siegel, *Energy Procedia*, **49** (2014) 1932.

4. "Advancing Oxide Materials for Thermochemical Production of Solar Fuels", J.E. Miller, A. Ambrosini, E.N. Coker, M.D. Allendorf, A.H. McDaniel, *Energy Procedia*, **49** (2014) 2019.

5. "Nonstoichiometric Perovskite Oxides for Solar Thermochemical H_2 and CO Production", A.H. McDaniel, A. Ambrosini, E.N. Coker, J.E. Miller, W.C. Chueh, R. O'Hayre, J. Tong, *Energy Procedia,* **49** (2014) 2009.

6. "Considerations in the Design of Materials for Solar-Driven Fuel Production Using Metal-Oxide Thermochemical Cycles", J.E. Miller, A.H. McDaniel, M.D. Allendorf, *Advanced Energy Materials,* **4,** (2), (2014) 1300469. DOI:10.1002/aenm.201300469.

7. "Perovskite-Type Oxides for Efficient Energy Conversion and Storage", J. Tong. Invited seminar at Institute of Engineering Thermophysics, Chinese Academy of Sciences, China, 23 June, 2014.

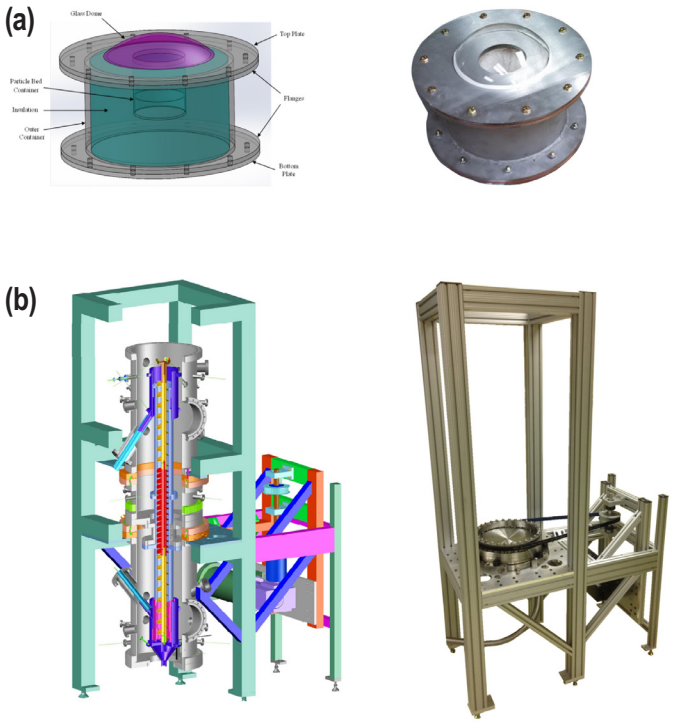

FIGURE 4. (a) Schematic and image of Bucknell's test platform designed to study radiant heat transfer into particle beds. The platform consists of a windowed aperture (hemispherical quartz dome) attached to an insulated housing, and operates under vacuum with minimal attenuation of incident radiant energy. Approximately 100 cm^3 of particles can be placed in the cavity. (b) Schematic and image of Sandia's particle elevator. When complete, approximately 10 kg of redox-active particles can be transported, under vacuum at high temperature (<1,000°C), to adjacent oxidation and reduction chambers (not shown). The moving packed particle bed is key to achieving ultra-low O_2 pressure during reduction and continuous on-sun operation.

8. "Solar Thermochemical Water Splitting: Advances in Materials and Methods", A.H. McDaniel, M.D. Allendorf, I. Ermanoski, A. Ambrosini, E.N. Coker and J.E. Miller, W.C. Chueh, R. O'Hayre, J. Tong. Invited seminar at CIMTEC 2014 6th Forum on New Materials, Montecatini Terme, Italy, 15–19 June, 2014.

9. "Solar Chemistry and Fuel Production", N.P. Siegel. Presented at the Chemical Engineering Spring Seminar Series, Bucknell University, Lewisburg, PA, USA, 25 February, 2014.

10. "The Water Splitting Kinetics of Two-Step Solar Thermochemical Process With CeO_2", D. Arifin, A.H. McDaniel, A.W. Weimer. Presented at the annual meeting of the AIChE, San Francisco, CA, USA, 3–8 November, 2013.

11. "A Detailed Mechanism of Solar Thermochemical Carbon Dioxide Splitting With CeO_2", D. Arifin, A.H. McDaniel, A.W. Weimer. Presented at the annual meeting of the AIChE, San Francisco, CA, USA, 3–8 November, 2013.

12. "High Temperature Solar Fuel Production Using Solid State Ionic Materials", J. Tong, R. O'Hayre. Presented at the annual meeting of Center for Revolutionary Photoconversion, Denver, CO, USA, 12–15 August 2013.

REFERENCES

1. N.P. Siegel, J.E. Miller, I. Ermanoski, R.B. Diver, and E.B. Stechel, *Ind. Eng. Chem. Res.*, **52**, 3276–3286 (2013).

2. W.C. Chueh and S.M. Haile, *Philos. Trans. R. Soc. Math. Phys. Eng. Sci.*, **368**, 3269–3294 (2010).

3. R.B. Diver, J.E. Miller, M.D. Allendorf, N.P. Siegel, and R.E. Hogan, *J. Sol. Energy Eng.*, **130**, 041001(1)–041001(8) (2008).

4. A.H. McDaniel, E.C. Miller, D. Arifin, A. Ambrosini, E.N. Coker, R. O'Hayre, W.C. Chueh, and J. Tong, *Energy Environ. Sci.*, **6**, 2424–2428 (2013).

5. J.E. Miller, A.H. McDaniel, and M.D. Allendorf, *Adv. Energy Mater.*, **4**, 1300469 (2014).

6. I. Ermanoski, N.P. Siegel, and E.B. Stechel, *J. Sol. Energy Eng.*, **135**, 031002 (2013).

7. I. Ermanoski, *Int. J. Hydrog. Energy* (2014) http://dx.doi.org/10.1016/j.ijhydene.2014.06.143.

8. I. Ermanoski, J.E. Miller, and M.D. Allendorf, *Phys. Chem. Chem. Phys.*, **16**, 8418 (2014).

II.C.3 Electrolyzer Development for the HyS Thermochemical Cycle

Héctor Colón-Mercado (Primary Contact),
William A. Summers
Savannah River National Laboratory
Building 999-2W
Aiken, SC 29808
Phone: (803) 645-7819
Email: Hector.Colon-Mercado@srnl.doe.gov

DOE Manager
Sara Dillich
Phone: (202) 586-7925
Email: Sara.Dillich@ee.doe.gov

Project Start Date: June 1, 2013
Project End Date: Project continuation and direction determined annually by DOE

Overall Objectives

- Identify and quantify anode electrocatalysts and advanced proton-exchange membranes to improve the performance and lower the capital and operating costs for the electrolysis step of the Hybrid Sulfur (HyS) thermochemical water-splitting process
- Demonstrate electrolyzer operation at elevated temperature and pressure up to 140°C and 2 MPa
- Improve electrolyzer efficiency to achieve 600 mV cell potential at current density of 500 mA/cm^2 or higher

Fiscal Year (FY) 2014 Objectives

- Complete integration of major components into the Pressurized Button Cell Test Facility (PBCTF) that will ultimately allow testing of catalysts and membranes at pressures up to 1 MPa and temperatures of 130°C. Major components include anolyte tank, electrolyzer cell, hydrogen storage tank, and anolyte pump.
- Identify and screen electrocatalysts with the potential to reduce oxidation overpotential by >20 mV versus the state-of-the-art platinum catalyst.
- Characterize three or more anode catalysts in conditions of sulfur-dioxide-saturated solutions of 30-50 wt% H_2SO_4.

Technical Barriers

This project addresses the following technical barriers from the Hydrogen Production section of the Fuel Cell Technologies Office Multi-Year Research, Development, and Demonstration (RD&D) Plan:

(T) Coupling Concentrated Solar Energy and Thermochemical Cycles

(W) Materials and Catalysts Development

(X) Chemical Reactor Development and Capital Costs

Technical Targets

This project is conducting studies to improve the performance and lower the capital and operating costs for the electrolysis step of the HyS thermochemical cycle. Insights gained from these studies will be applied toward the design and demonstration of a solar-driven HyS thermochemical cycle that meets the following DOE 2020 hydrogen production targets for high-temperature, solar-driven, thermochemical processes, as given in Table 3.1.7 of the Multi-Year RD&D Plan:

- Hydrogen Cost: $3.70/kg
- Solar to Hydrogen Energy Conversion Ratio: 20%

FY 2014 Accomplishments

- Identified and purchased tantalum-coated parts as a more cost-effective alternative instead of custom-made zirconium fittings for construction of the metal parts of the PBCTF.
- Finished modification of the original piping and instrumentation diagram as well as finished construction of the set-up from earlier large-scale testing to accommodate the changes in size and type of parts to be used in the PBCTF.
- Finished construction and integration of all components.
- Tested thin-film electrodes as candidate anode electrocatalysts, including Pt, Pd, Ir, Au, PtAu, and PtV. Au, PtAu and PtV showed 28 mV, 46 mV, and 13 mV reduction, respectively, on the anode polarization versus state-of-the-art Pt catalyst.

INTRODUCTION

Solar thermochemical hydrogen (STCH) cycles have the potential to produce hydrogen at competitive costs. The DOE is supporting research on STCH cycles for hydrogen production that can be competitive in the long-term and by 2020 be developed to produce hydrogen with a projected cost of $3.70/gasoline gallon equivalent at the plant gate. The HyS process is a promising sulfur-based STCH cycle that depends on a simple, two-step chemical process with

all-fluid reactants. It contains a low-energy electrolysis step, making it a thermo/electrochemical hybrid process. In this process, sulfuric acid (H_2SO_4) is thermally decomposed by solar energy at high temperature (>800ºC), producing SO_2, O_2, and steam. Sulfuric acid saturated with SO_2 is then pumped into a sulfur dioxide-depolarized electrolyzer (SDE) that electrochemically oxidizes sulfur dioxide with water to form sulfuric acid at the anode and reduces protons to form hydrogen at the cathode. The reversible cell potential for this electrochemical process is -0.158 V (standard hydrogen electrode, SHE) versus -1.229 V (SHE) for low-temperature water electrolysis [1]. The overall electrochemical reaction consists of the production of H_2SO_4 and H_2, while the entire cycle produces H_2 and O_2 from H_2O with no side products.

The SDE is the major developmental technology in this cycle, and the objective of the research is to identify, develop, and demonstrate new SDE components to improve the efficiency and lower the costs of this key step. The focus of the research is on the anode electrocatalyst and the proton exchange membrane. New research has shown that Pt alloys with transition metals, gold, and gold alloys can decrease the overpotential for the SO_2 oxidation reaction [2]. Another major goal of the research is to develop membranes that can operate at elevated temperature and pressure (140°C and 2 MPa) for extended periods without degradation of performance. Higher-temperature operation is expected to reduce kinetic polarization losses at the anode and permit the use of advanced high-temperature membranes (versus Nafion®). Previous low-temperature results indicate that the advanced membranes can also reduce the crossover of SO_2 through the membrane to the cathode, thereby eliminating or minimizing elemental sulfur formation that can reduce cell performance and operating lifetime.

APPROACH

There are two main approaches that were studied for performance improvements on the SDE: anode electrocatalysts and expanded operating conditions (operating temperatures up to 130ºC and pressures up to 1 MPa). Electrocatalyst anode materials that can provide higher activity for the SO_2 oxidation were investigated. Materials are expected to provide similar amount of corrosion resistance as state-of-the-art Pt electrocatalysts, while increasing the kinetic current at comparable operating potentials. This approach will not only improve the overall performance of the PBCTF system, but will also reduce the amount of precious metals used in the SDE.

Operation at expanded operating conditions will allow the system to operate at a higher efficiency by reducing kinetic and ionic/mass transfer losses. The system is being redesigned for operation at higher temperatures and pressures in order to get baseline performance of state-of-the-art materials (i.e., catalysts consisting of Pt/C and Nafion® membranes) at different operating conditions. This information will be useful for establishing and making performance comparisons when using next-generation membranes and electrocatalysts.

RESULTS

Depending on the operating conditions, around 70% of the losses in efficiency in the electrolyzer arise from the kinetic losses associated with the anode electrode. Improvements in anode performance are being sought as a way to improve overall electrochemical performance of the electrolyzer. Over the past, the SDE research has been focused on Pt electrocatalysts. However, new research has shown that Pt alloys with transition metals, Au, and Au alloys can decrease the overpotential for the SO_2 oxidation reaction [2]. Catalytic thin films were prepared by sputter deposition on corrosion-resistant coupons for the materials of interest (Pt, Au, Pd, Ir, etc.) and were evaluated in sulfur-dioxide-saturated sulfuric acid solutions. Figure 1 shows the typical Tafel plots for the electrolysis of SO_2 by Pt. As observed in Figure 1, the performance consists of two curved lines coming together to form a point. The top curved line gives an indication of the reaction rate far from equilibrium potentials. This top curved line is representative of the current region where the electrolyzer will be operated. In other words, a shift to the lower right side of the plot will indicate significant improvement in the electrocatalyst performance that will translate to higher plant efficiency. The shaded area under the dashed lines indicates the milestone target of ≥20 mV performance improvement over un-modified Pt catalysts. The performance of the catalysts tested away from equilibrium conditions is plotted in Figure 2 at the current

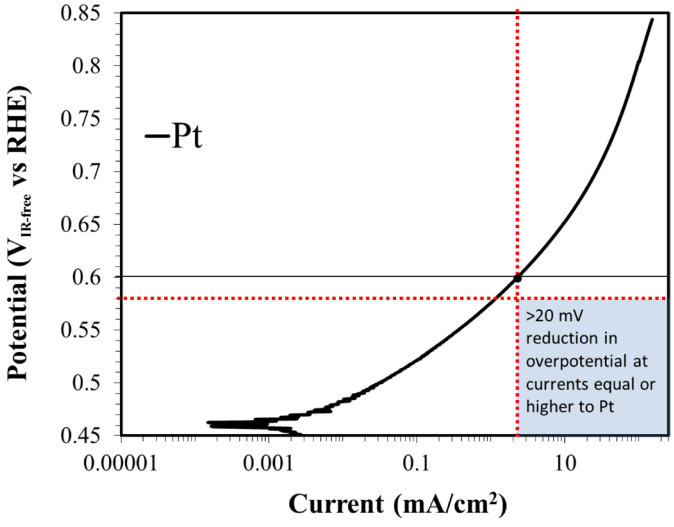

FIGURE 1. Typical consecutive Tafel plots for the electrolysis of SO_2 by Pt. Test performed in SO_2 saturated with 30 wt% sulfuric acid at room temperature. Shaded area indicates FY 2013 milestone performance target.

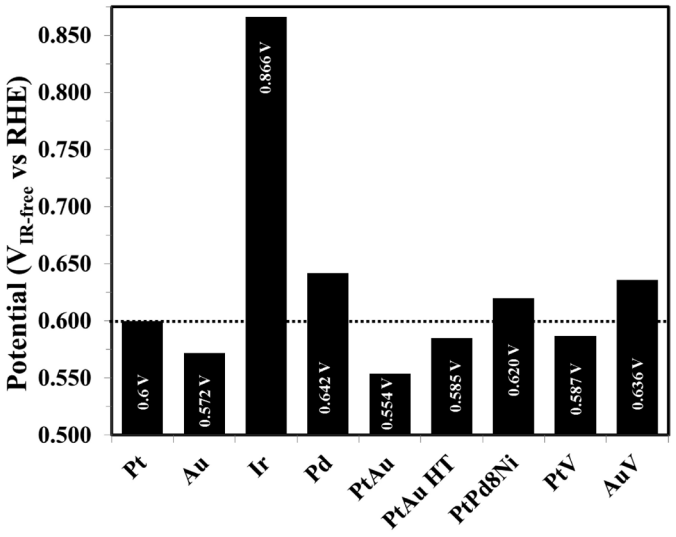

FIGURE 2. Operation Potential of the Different Catalysts Working at the Current Density of Pt Operated at 600 mV

density 2.3 mA/cm^2. The use of Au or the addition of Au or V to the Pt catalysts decreases the operational voltage (better performance). The catalysts with performance better than Pt (0.6 V or lower voltage): are observed by PtAu alloy (0.554 V) > Au (0.572 V) > PtAu-HT (0.587 V) > PtV (0.587 V).

In addition to improvements in catalyst activity, operation of the electrolyzer at higher temperatures and pressures will facilitate the kinetics and mass transfer and allow the use of high-temperature membranes, and, therefore, will improve overall performance. Fabrication of the PBCTF will facilitate the testing of anode electrocatalysts and high-temperature membranes at improved SDE-relevant conditions. Because of the corrosive nature of the sulfuric acid, specialty instruments and materials need to be used. Previous experience has indicated that metals such as zirconium and tantalum can provide both mechanical and chemical resistance. Polymer use is limited to uses such as liners due to the operating temperatures and pressures. Design, procurement, and fabrication were completed. Major fabrication items include the SO_2 acid anolyte tank and the electrochemical cell. All metal-wetted parts of the anolyte tank are made of Zircalloy, while the wetted parts of the electrochemical cell are made of graphite and fluoro-polymers. To integrate all the different components, tantalum-wetted fittings were used. Figure 3 shows the complete integration of all the components. With the setup completed, baseline performance of state-of-the-art materials, such as Nafion® and platinized carbon, will be assessed followed by testing of the advanced materials.

CONCLUSIONS AND FUTURE DIRECTIONS

- Identified and procured tantalum-coated parts as a more cost-effective alternative instead of custom-made zirconium fittings for construction of the metal parts of the PBCTF.
- Finished modification of the original piping and instrumentation diagram as well as finished fabrication of parts to be used in the PBCTF.
- Finished construction and integration of all components.
- Tested thin-film electrodes as candidate anode electrocatalysts, including Pt, Pd, Ir, Au, PtAu, and PtV. Au, PtAu, and PtV showed 28 mV, 46 mV, and 13 mV reduction on the anode polarization, respectively, versus state-of-the-art Pt catalyst.
- Future work will establish baseline performance of state-of-the-art materials and start studying the performance of new high-temperature membranes.

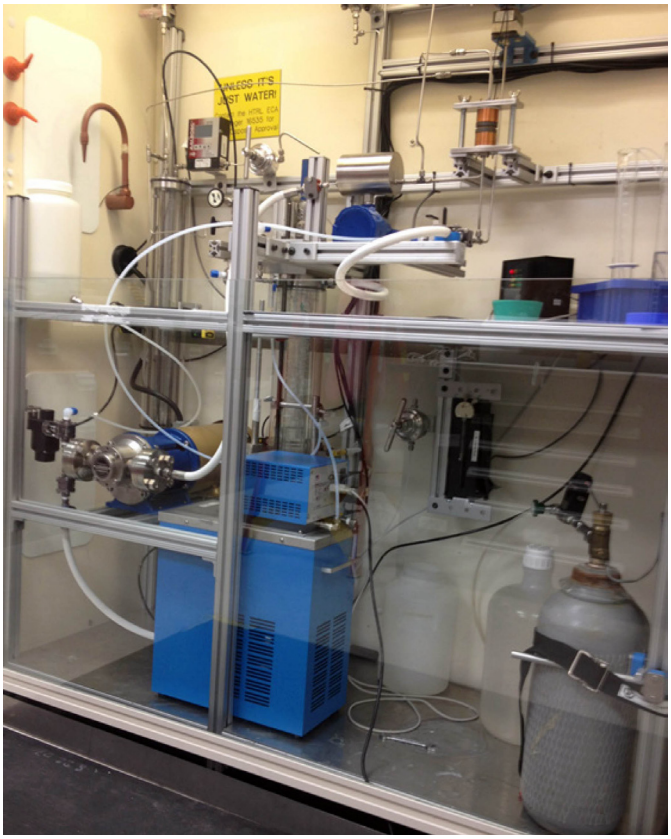

FIGURE 3. Photograph of Completed System

REFERENCES

1. Gorensek, M.B.; Staser, J.A.; Stanford, T.G.; Weidner, J.W., A thermodynamic analysis of the SO_2/H_2SO_4 system in SO_2-depolarized electrolysis. *International Journal of Hydrogen Energy* 2009, 34 (15), 6089-6095.

2. O'Brien, J.A.; Chemistry, U. o. N. S. o., *Solar Hydrogen: A Fundamental and Applied Electrochemical Investigation of the Hybrid Sulfur Cycle Electrolyser.* University of Newcastle: 2011.

II.D.1 Semiconductor Materials for Photoelectrolysis

Todd Deutsch (Primary Contact), John Turner, Heli Wang, Huyen Dinh
National Renewable Energy Laboratory (NREL)
15013 Denver West Parkway
Golden, CO 80401
Phone: (303) 275-3727
Email: Todd.Deutsch@nrel.gov

DOE Manager
Eric Miller
Phone: (202) 287-5829
Email: Eric.Miller@ee.doe.gov

Subcontractor
University of Nevada, Las Vegas, Las Vegas, NV

Project Start Date: 2005
Project End Date: Project continuation and direction determined annually by DOE

Overall Objectives

Identify, synthesize, and characterize new semiconductor materials that have the capability of meeting the criteria for a viable photoelectrochemical (PEC) hydrogen-producing device, either as a single absorber or as part of a high-efficiency multijunction device.

Fiscal Year (FY) 2014 Objectives

- Design tandem III-V semiconductor structures with lower bandgaps than $GaInP_2$/GaAs that have the potential to push the boundaries on achievable solar-to-hydrogen (STH) efficiencies.
- Demonstrate surface modification for passivation against corrosion to improve durability for lower-bandgap III-V semiconductor electrodes at high current densities.

Technical Barriers

This project addresses the following technical barriers from the Hydrogen Production section of the Fuel Cell Technologies Office Multi-Year Research, Development, and Demonstration Plan:

(AE) Materials Efficiency – Bulk and Interface

(AF) Materials Durability – Bulk and Interface

(AG) Integrated Device Configurations

(AI) Auxiliary Materials

Technical Targets

This project is a materials discovery investigation to identify a single semiconductor material that meets the technical targets for efficiency and stability. The 2015 technical targets from the Multi-Year Research, Development, and Demonstration Plan PEC hydrogen production goals in Table 3.1.8.A are the following:

- 15% STH conversion efficiency
- 900-hour replacement lifetime (1/2 year at 20% capacity factor)
- $\$300/m^2$ PEC electrode cost.

FY 2014 Accomplishments

- We contributed to getting the Springer brief, *Photoelectrochemical Water Splitting: Standards, Experimental Methods, and Protocols*, published.
- We performed outdoor testing with surface-treated tandem electrodes in a photoreactor mounted on a solar tracker with moderate optical concentration. We measured the product gases and found less than unity Faradaic yields for hydrogen and oxygen. The electrodes exhibited corrosion after only four hours of operation, suggesting that the surface passivation treatment needs further optimization for these high current conditions.
- We confirmed that our two-step surface passivation, involving nitrogen ion implantation and flash sputtering with a noble metal alloy, protects p-InP surfaces under very high rates of hydrogen evolution. No surface corrosion was observed after testing at -25 mA/cm^2 for 24 hours in 3 M H_2SO_4, demonstrating that this treatment we developed on $GaInP_2$ works not only on other III-V materials, but is also viable at the elevated current densities necessary for high-efficiency solar water-splitting.
- We made quantitative measurements of the PtRu loading in the nitridation/sputtering surface passivation treatment. Scanning transmission electron microscopy indicates the morphology of the PtRu is partially aggregated particles with dimensions on the order of 5 nm covering about 30% of the surface. Inductively coupled plasma mass-spectrometry reveals that the equivalent surface coverage (if the morphology was a continuous film) of PtRu is between 1 and 2 nm.
- We generated a waterfall chart (presented at the Annual Merit Review) projecting cost reductions in PEC hydrogen production by making serial iterations of the H2A Future Central Hydrogen Production from

Photoelectrochemical Type 4 Version 3.0 case study with our anticipated progress toward technical targets.

- We designed a p-GaAs:n/p-GaAs stacked tandem configuration that should be able to generate 2.0 V at open circuit and is theoretically capable of nearly 20% STH. Using a thinned top cell splits photons in the solar spectrum with energies above the 1.42-eV bandgap. Preliminary testing of this device shows it is capable of unbiased water splitting.

INTRODUCTION

Photoelectrochemistry combines a light-harvesting system and a water-splitting system into a single, monolithic device. The catalyzed surface of a semiconductor is the light-harvesting component as well as one part of the water-splitting system, with the balance consisting of a spatially separated counter electrode. Discovering a semiconductor system that can efficiently and sustainably collect solar energy and direct it toward the water-splitting reaction could provide renewable and economically competitive fuel for the hydrogen economy.

The goal of this work is to develop a semiconductor material set or device configuration that (i) splits water into hydrogen and oxygen spontaneously upon illumination without an external bias, (ii) has a STH efficiency of at least 10% with a clear pathway to exceed 20%, and (iii) can ultimately be synthesized via high-volume manufacturing techniques with a final hydrogen production cost below $2/kg.

APPROACH

Our approach is to study the current material sets used in commercial solar cells as well as related materials that meet near-term STH efficiency targets and to extend their durability by surface-passivation techniques. The surface-passivation treatments are engineered to stabilize the semiconductor at the electrolyte interface, but also, to maintain the high native efficiencies by ensuring that charge transfer is not compromised. To help us identify the steps that initiate corrosion reactions and develop mitigation strategies, we collaborate with partners who apply state-of-the-art spectroscopic characterization skills and theory to better observe and understand our system. Another area of focus is to investigate new materials that have lower bandgaps and high quantum efficiencies that could allow them to achieve DOE's ultimate STH efficiency target, which is very high.

RESULTS

Outdoor Photoreactor Testing

We performed outdoor testing with treated p-$GaInP_2$: n/p-GaAs tandem electrodes in a photoreactor mounted on a solar tracker with moderate (~4x) optical concentration provided by a cylindrical lens attached to a Plexiglas® window (Figure 1). We tested three different electrodes and all exhibited similar efficiency and durability behavior; the following results for one of the tested samples are representative of all three. The cathodic photocurrent at short circuit started at -33 mA/cm^2, but decayed to about -11 mA/cm^2 in less than a minute. To maintain a reasonable current sufficient to generate measureable product gases, the semiconductor electrode was biased at -1 V (vs. Pt black counter-electrode), but the current still declined from -47 mA/cm^2 to -13.7 mA/cm^2 over the 4-hour course of testing. A total charge of -37.111 Coulombs was passed during the test, which should have generated 5.80 mL of

FIGURE 1. Photograph of the photoreactor mounted on a solar tracker. A cylindrical lens was affixed to the front window and focused the sunlight onto the semiconductor photoelectrode. Captured hydrogen and oxygen gas was measured in inverted pipettes to determine the Faradaic yield over the 4-hour test runs.

hydrogen gas at ambient conditions. The 4.40 mL of H_2 and 1.90 mL of O_2 represent Faradaic yields of 75% and 66%, respectively. The low Faradaic yields could be from leaks in the prototype photoreactor or surfactant foaming that prevented accurate measurements of gas volume. The sample also exhibited damage indicative of corrosion at the conclusion of testing.

Durability Testing on p-InP at High Current Densities

We applied a protective surface modification that we had previously developed for p-$GaInP_2$ (nitrogen implantation and/or PtRu or Ru sputtering) to p-InP and observed dramatically improved photocorrosion resistance. The bandgap of InP is 1.33 eV, compared with 1.81 eV for $GaInP_2$, allowing greater utilization of the solar spectrum and higher theoretical STH efficiencies in an optimized tandem configuration. NREL's III-V group synthesized a 2-inch-diameter, 4-µm-thick, p-InP epilayer by metal-organic chemical vapor deposition. The wafer was subdivided into four quarters, with three quarters subjected to different surface treatments. One quarter received our standard nitrogen ion implantation followed by a PtRu alloy sputtering. Neither of the other two quarters were ion implanted; they only received a sputtering treatment, one with PtRu and the other just Ru. Each quarter was cut into smaller pieces and mounted to make electrodes with surface areas on the order of 0.1 cm^2. Photoelectrodes were galvanostatically tested for durability in 3 M H_2SO_4 electrolytes with the fluorosurfactant Zonyl FSN-100, with the galvanostat maintaining a constant photocurrent density of -25 mA/cm^2 for 24 hours. Electrodes were illuminated by a 250-watt tungsten light source calibrated to Air Mass 1.5 Global with a 1.1-eV-bandgap Si reference cell. All of the tests were accomplished in a two-terminal configuration with water oxidation occurring at a 5-cm^2 platinum counter-electrode.

After the 24-hour tests, the electrodes were deconstructed and the semiconductor surfaces were qualitatively evaluated with low-magnification optical photomicroscopy (Figure 2). The degree of surface etching was also determined with optical profilometry. Inductively coupled plasma mass spectrometry (ICP-MS) was used to quantitatively assess indium concentrations in the electrolytes used for each durability test. The analytes were detected in parts per billion quantities and converted to nanomoles per Coulomb to account for variations in electrolyte volume in the testing cell and electrode surface areas.

All of the untreated InP electrodes and four of the treated electrodes exhibited dramatically altered surfaces after durability testing. All of the "failed" electrodes had a similar appearance, with the surface transformed from a specular reflective smooth surface to a metallic-looking one (Figure 2, bottom) in the electrochemically active areas. Most of the treated electrodes had no obvious signs of degradation, with surfaces similar to the one on the top of Figure 2.

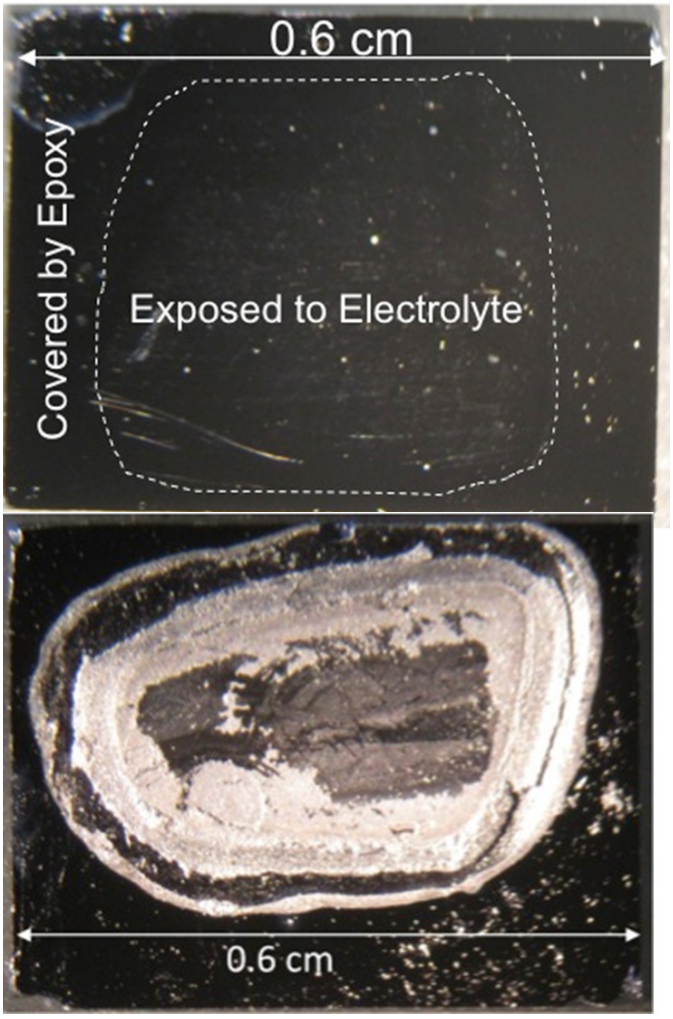

FIGURE 2. Photographs of p-InP surfaces after 24 hours of testing at -25 mA/cm^2 in 3 M H_2SO_4. The electrode on the top had nitrogen ion implantation and PtRu sputtering and there is no obvious difference between the exposed area and the portion masked by epoxy during testing. The electrode on the bottom was untreated and experienced significant damage in the area exposed to the electrolyte.

The physical degradation that was apparent on the failed electrodes was confirmed with optical profilometry. The electrodes that failed experienced removal of 3–4 µm of InP from their surfaces over the course of the durability testing. Optical profilometry was unable to detect any etching on electrodes that exhibited protection. The area exposed to electrolyte was indistinguishable from the native surface, with both having features varying by only a few nanometers.

The concentration of indium detected in durability electrolytes by ICP-MS correlated well with the degree of degradation observed (Figure 3). Phosphorous was not analyzed because background levels made this measurement unreliable. The normalized indium values for the controls and treated electrodes that failed are well above the others

that had no obvious signs of corrosion. Out of 21 treated p-InP electrodes tested at -25 mA/cm^2 for 24 hours, 17 electrodes had no visible signs of degradation and only trace quantities of indium (~25 ppb) in their durability electrolytes. Conversely, similarly tested untreated p-InP had several microns of material removed from their surfaces and indium concentrations in durability electrolytes greater than two orders of magnitude higher than the treated electrodes (~4 ppm vs. ~25 ppb). Of the 15 samples that were treated with PtRu, 14 of the samples were successfully protected from corrosion. The average normalized value for all seven N-ion implanted and PtRu sputtered samples (0.0183 nanomoles/C) was almost identical to the average of the seven successfully protected (out of eight) PtRu sputtered-only electrodes (0.0185 nanomoles/C). The three Ru sputtered-only electrodes that survived testing have normalized indium values that are slightly higher than the other two treatments, averaging 0.0321 nanomoles/C, but well below the average of the untreated electrodes (3.20 nanomoles/C). The failure rate of the Ru-only electrodes was 50%, suggesting that platinum is a necessary component of a successful surface-passivation treatment. Of the 15 treatments that incorporated PtRu sputtering, only one failed, resulting in 93% of the electrodes successfully resisting corrosion under these testing conditions. These results demonstrate that III-V surfaces can be protected against corrosion under the high flux conditions that accompany the high-efficiency DOE target of 25% STH.

CONCLUSIONS AND FUTURE DIRECTIONS

- The surface passivation treatment that we developed for p-GaInP$_2$ significantly improves the durability of p-InP electrode surfaces at high water-splitting current densities, demonstrating that it is able to protect other III-V surfaces and is viable for stabilizing future, higher-efficiency tandem devices.
- To meet STH efficiency targets beyond 20%, we need to develop new tandem architectures that have a lower bottom-cell bandgap that allows greater utilization of the solar spectrum. We will design, synthesize, and characterize these novel device configurations in the next year.
- We generated a waterfall chart from the H2A Future Central Hydrogen Production from Photoelectrochemical Type 4 Version 3.0 that shows a pathway to meeting the DOE target of PEC hydrogen for <$2/kg through continued achievable improvements in efficiency, durability, and absorber costs.

SPECIAL RECOGNITIONS & AWARDS/ PATENTS ISSUED

1. 2014 DOE Hydrogen & Fuel Cells Program R&D Award, presented at the Annual Merit Review as part of a team award to Todd Deutsch (NREL), Clemens Heske (UNLV), and Tadashi Ogitsu (LLNL) for III-V surface validation efforts.

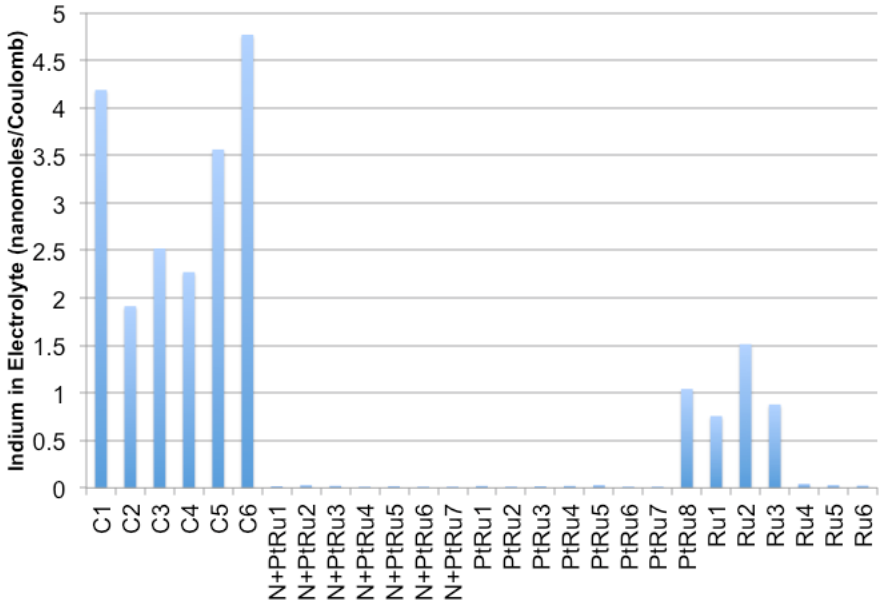

FIGURE 3. Indium present in 3 M H_2SO_4 durability solutions detected by ICP-MS for InP electrodes that were untreated (C), nitrogen ion implanted and PtRu sputtered (N + PtRu), PtRu sputtered only (PtRu), and Ru sputtered only (Ru). Each data point is for an individual electrode run at -25 mA/cm^2 for 24 hours. Lower values for the treated electrodes compared with the untreated samples confirm qualitative stability observations. Electrode N+PtRu5 corresponds with the top image in Figure 2.

2. "Stable Photoelectrode Surfaces and Methods," U.S. patent application 14/276,425 filed on May 13, 2014, *pending.*

FY 2014 PUBLICATIONS

1. "Photoelectrochemical Reduction of Nitrates at the Illuminated p-$GaInP_2$ Photoelectrode," H. Wang and J. A. Turner, *Energy Environ. Sci.* **6**(6), 1802–1805 (2013).

2. Photoelectrochemical Water Splitting: Standards, Experimental Methods, and Protocols, Z. Chen, H.N. Dinh, E. Miller, T.G. Deutsch, K. Domen, K. Emery, A.J. Forman, N. Gaillard, R. Garland, C. Heske, T.F. Jaramillo, A. Kleiman-Shwarsctein, K. Takanabe, J. Turner, eds: Z. Chen, H.N. Dinh, E. Miller. New York: Springer, 2013.

3. "Solar Fuel Production for a Sustainable Energy Future: Highlights of a Symposium on Renewable Fuels from Sunlight and Electricity," H. Wang, D. Chu, and E.L. Miller, *Interface*, Summer 2013, 69–71.

4. "New Visible Light Absorbing Materials for Solar Fuels, $Ga(Sb_x)N_{1-x}$," S. Sunkara, V.K. Vendra, J.B. Jasinski, T. Deutsch, A.N. Andriotis, K. Rajan, and M. K. Sunkara, *Adv. Mater.* **26**, 2878–2882 (2014).

5. "Sunlight Absorption in Water – Efficiency and Design Implications for Photoelectrochemical Devices," H. Döscher, J.F. Geisz, T.G. Deutsch, and J.A. Turner, *Energy Environ. Sci.*, **7**(9), 2951–2956 (2014).

PRESENTATIONS

1. "Photoelectrochemistry and the Hydrogen Economy," DFG SPP 1613, Summer School, Schoenenberg Ellwangen, Germany, October 8, 2013 (Turner) *Invited.*

2. "Enabling a Sustainable Energy Future Through Hydrogen," Science Undergraduate Laboratory Internship seminar, NREL, October 9, 2013. (Deutsch) *Invited.*

3. "III-V Nitrides and Tandem Cells for Photoelectrochemical Water Splitting," 224th Electrochemical Society Meeting, October 28, 2013 (Turner) *Invited.*

4. "Materials for Photoelectrochemical Water Splitting," 224th Meeting of the Electrochemical Society, San Francisco, CA. October 28, 2013. (Wang) *Contributed.*

5. "Hydrogen production: Overview," Hydrogen Technical Advisory Committee meeting, October 30, 2013 (Turner) *Invited*

6. "Semiconductor Materials for Photoelectrolysis: Requirements, Challenges and Opportunities," Parthenope University of Naples, Naples, Italy, December 9, 2013. (Deutsch) *Invited.*

7. "III-V Surface Treatments and Catalysis for Photoelectrochemical Water Splitting," 2014 MRS Spring Meeting, April 22, 2014, San Francisco, CA. (Turner) *Invited.*

8. "Materials for Efficient Photoelectrochemical Water Splitting: The U.S. Department of Energy PEC Working Group," 2014 MRS Spring Meeting, April 22, 2014, San Francisco, CA. (Wang) *Invited.*

II.D.2 Critical Research for Cost-Effective Photoelectrochemical Production of Hydrogen

Liwei Xu[1], Changyong Chen[2], Anke Abken[1], Yanfa Yan[2], John Turner[3], Wenhui Du[1], Aarohi Vijh[4], Xunming Deng[1,2]

[1]Midwest Optoelectronics, LLC (MWOE)
2801 W. Bancroft Street
Mail Stop 230
Toledo, OH 43606
Phone: (419) 215-8583
Email: xu@mwoe.com

DOE Managers
Eric Miller
Phone: (202) 287-5829
Email: Eric.Miller@ee.doe.gov
David Peterson
Phone: (720) 356-1747
Email: David.Peterson@ee.doe.gov

Contract Number: DE-FG36-05GO15028

Subcontractors
[2] University of Toledo (UT), Toledo, OH
[3] National Renewable Energy Laboratory (NREL), Golden, CO
[4] Xunlight Corporation (Xunlight), Toledo, OH

Project Start Date: April 1, 2005
Project End Date: July 31, 2014

Overall Objectives

To develop critical technologies required for cost-effective production of hydrogen from sunlight and water using thin film (tf)-Si-based photoelectrodes.

Fiscal Year (FY) 2014 Objectives

- Focus on immersion-type photoelectrochemical (PEC) systems. Further improve the performance of the photoelectrode with the corrosion-resistant transparent protective (CRTP)/corrosion-resistant conducting catalytic (CRCC) novel layer design in an effort to improve the solar-to-hydrogen (STH) conversion efficiency and the durability to achieve a cost-effective PEC system.
- Complete techno-economic analysis of MWOE's PEC system.
- Explore new kinds of transparent, conducting, and corrosion-resistant (TCCR) coating material to improve the durability of the electrode.
- Work towards commercial-size PEC electrodes and PEC systems, and improve their efficiency and lifetime performance.

Technical Barriers

This project addresses the following technical barriers from the Hydrogen Production section (3.1.5) of the Fuel Cell Technologies Office Multi-Year Research, Development, and Demonstration Plan:

(AE) Materials Efficiency - Bulk and Interface

(AF) Materials Durability - Bulk and Interface

(AG) Integrated Device Configurations

(AI) Auxiliary Materials

(AJ) Synthesis and Manufacturing

Technical Targets

This project focuses on the development of low-cost photoelectrode materials and systems using triple junction tf-Si-based PEC cells to split water and generate hydrogen using sunlight.

FY 2014 Accomplishments

- Worked on the novel design for immersion-type PEC cells, where the illuminated side of the PEC electrode is divided into areas coated with a CRTP layer for light absorption and areas coated with a CRCC layer for oxygen generation.
- Investigated the use of electroplated Pt as the CRCC layer in a CRCC/CRTP device.
- Developed an electroplated Ni/Pt bi-layer as the CRCC layer in a CRCC/CRTP device.
- Studied the sputter deposition of thick Co_3O_4 layer in selective regions for the CRCC layer in a CRCC/CRTP device.
- Studied the use of a sputter-deposited SiO_2 layer as the CRTP layer for both a CRCC (Ni/Pt)/CRTP (SiO_2) device and a CRCC (Co_3O_4)/CRTP (SiO_2) device. Studies included the first deposition of CRCC then CRTP, or, the first deposition of CRTP then CRCC layers.
- Investigated the use of TiO_2 as a CRTP layer in a CRCC/CRTP device.
- Performed techno-economic analysis of MWOE's PEC system using DOE's H2A model. The results indicate that with 50-ton-per-day ("TPD") production capacity,

our system has the potential to achieve a hydrogen generation cost of $2/gasoline gallon equivalent (gge).

- Worked towards commercial-size PEC electrodes; achieved 3.3% STH conversion efficiency for immersion-type PEC cells of 4-inch x 4-inch size using low-cost electroplated Ni hydrogen evolution reaction (HER).
- Worked with different PEC groups around the world to supply both standard and custom-made triple-junction solar cells and to further PEC research. Sent a triple-junction PEC device to Caltech for collaboration.
- Fabricated p-i-n structure solar cells (different from our normal n-i-p device) for PEC application so that the HER would take place on the front surface and the oxygen evolution reaction (OER) would take place on the back surface.

INTRODUCTION

In this project, MWOE and its subcontractors are jointly developing critical technologies for cost-effective production of hydrogen from sunlight and water using tf-Si-based photoelectrodes. Triple-junction a-Si/a-SiGe/a-SiGe solar cells are an ideal material for making cost-effective PEC systems for hydrogen generation. They have the following key features: (1) an open-circuit voltage (V_{oc}) of ~2.3 V and an operating voltage around 1.6 V, ideal for water splitting; (2) they can be put on a conducting stainless steel substrate which serves as an electrode; (3) they can be produced on large rolls of 3-ft-wide and up to 5,000-ft-long stainless steel web in a 25 MW roll-to-roll production equipment, so that the corresponding PEC electrodes and systems can be made at very low cost. However, the tf-Si solar cell is not highly stable in a strongly acidic or strongly basic electrolyte, which is typically needed for efficient and simultaneous evolution of oxygen and hydrogen. The tf-Si layers could be corroded by such electrolytes, especially under light working conditions. In order to develop a PEC system using triple-junction tf-Si solar cells, we need to develop a coating that can be applied onto the solar cell surface and that has the following features: 1) transparent, so that the light can pass through the coating and reach the solar cells; 2) conducting, so that the voltage generated by the solar cell under sunlight can be applied to the electrolyte-electrode interface and generate oxygen and hydrogen; 3) corrosion-resistant, so that it can protect the solar cell surface from being corroded in the electrolyte; and 4) capable of being deposited onto the solar cell surface at 200°C or lower, since the solar cell could be damaged if the temperature is higher than 200°C. In addition, it needs to act as either an OER catalyst (for n-i-p structure) or an HER catalyst (for p-i-n structure).

APPROACH

Three technical tasks were performed during this reporting period:

- Development of TCCR coating for triple-junction tf-Si-based photoelectrodes.
- Understanding and characterization of photo-electrochemistry.
- Development of device designs for low-cost, durable, and efficient immersion-type PEC cells and systems.

RESULTS

Development of a Durable PEC Device Having a CRCC/CRTP Structure

Development of a Pt/Ni Plated Layer as a CRCC

We investigated coating the Pt electrode as a CRCC layer/OER catalyst on top of Co_3O_4 coated on a a-Si triple-junction solar cell, using H_2PtCl_6 as the electrolyte (pH ~1) and a Pt mesh as the counter electrode. It is found that corrosion of Co_3O_4 starts after 90 seconds of electrodeposition. A similar plating process on the stainless steel back side as the HER catalyst was successful. When the pH level was increased to ~6, minimal corrosion occurred. We explored the plating of Pt onto Co_3O_4 coated with a-Si with varying plating current densities and varying plating times. A typical plating condition used is 8 mA/cm^2 for 60 sec. In order to form a Pt coating in certain areas for a CRCC layer and expose certain other areas for the application of a CRTP layer, Kapton® tapes are applied to areas to prevent Pt plating. A clear coating used in the automotive industry is used to create the CRTP layer region. Certain overlap of CRCC and CRTP areas are designed into the process to avoid undercut corrosion. The effort in generating a CRCC/CRTP structure using plated Pt is challenged by device shunting issues, as the plating process corrodes the transparent conductive oxide layer and the a-Si device. Future effort will be focused on plating deposition of Pt on a-Si films under less acidic conditions.

We then explored the use of plated Ni as a buffer layer prior to the plating of the Pt layer. We investigated plating of Ni films on Co_3O_4 coating a a-Si device using $NiSO_4/NiCl_2$ electrolyte with a pH of ~3. A typical plating condition used is 20 mA/cm^2 current for 30-180 sec. Again, Kapton® tapes are used to pre-define areas for plating so that the clear coat can be applied to create CRTP regions. The device structure in the CRCC region is stainless steel (SS)/a-Si triple cell/indium tin oxide/Co_3O_4/Ni/Pt. Many sets of PEC electrodes with such a structure were fabricated and studied. The results show that a Pt/Ni-coated device is more stable than a Pt-coated device, with an initial STH efficiency of 3.7%.

The performance drops 50% after approximately 5 hours of operation. It is interesting to notice that after the sample is kept overnight in the dark, the STH efficiency is recovered almost back to its initial value (see Figure 1). This repeats for five consecutive days. The mechanism for the degradation of STH efficiency under light and the recovery of efficiency in dark needs to be further understood.

Development of Co_3O_4 as the CRCC Layer

As electroplating an OER catalyst layer exposes the semiconductor under corrosive environment, a vacuum coating process is used to deposit a CRCC layer using sputter deposition. In this approach, we explored the use of a thick Co_3O_4 layer as the OER catalyst. Thick Co_3O_4 is deposited on top of a thin Co_3O_4 layer. A thick Co_3O_4 layer is acceptable even though its transparency is not high, since only a partial area of the device front surface is covered with the thick Co_3O_4 layer. An automotive clear coat, with a thickness of around 0.5 mm, is used as the CRTP layer. Kapton® tape is used to define the areas for clear coat coverage. Alternatively, a sputter-deposited SiO_2 layer is used as the CRTP layer. Certain overlap of CRCC and CRTP areas are designed into the process to avoid undercut corrosion.

Specifically, we deposited Co_3O_4 layers with a thickness in the range of 500 nm and 1,500 nm as the CRCC layer, over the 70 nm Co_3O_4 coating that covers all areas, using magnetron sputter deposition with a power density of around 100 W over a 3" round sputter target. Various devices with such a Co_3O_4 (CRCC) and clear coat (CRTP) combination were fabricated. Initial results show an initial STH efficiency of 3.5% and performance degraded 50% after 55 hours. Studies of the degraded samples show a change of color in the clear coat CRTP layer, suggesting the lifetime of the Co_3O_4 layer may be much longer.

In order to have a stable CRTP layer, we used magnetron sputtering process to deposit the SiO_2 layer. This is done for both CRCC layers made using electroplated Ni/Pt layers and a sputter-deposited Co_3O_4 layer. For CRCC (Ni/Pt)/CRTP (SiO_2) combination, the initial STH efficiency is around 3.5%, and the STH efficiency drops 50% in about 12 hours, representing an improvement from CRCC (Ni/Pt)/CRTP (clear coat). It is also observed that the STH efficiency recovers to 90% of its initial value after the sample is kept in the dark overnight.

A device structure with CRCC (sputtered-Co_3O_4)/CRTP (sputtered-SiO_2) was also explored. Two approaches were studied: (1) first SiO_2, then Co_3O_4 (the "SiO_2/Co_3O_4" device); and (2) first Co_3O_4, then SiO_2 (the "Co_3O_4/SiO_2" device). Kapton® tapes were used to mask out the area during sputtering so that the deposition would not occur in the unwanted areas. The Kapton® tapes were applied in such a way to allow certain overlap of Co_3O_4 and SiO_2 layers to avoid undercut corrosion. The Co_3O_4/SiO_2 device showed less durability, with the device failing after around 30 hours of PEC operation. The SiO_2/Co_3O_4 device showed an interesting increase in STH efficiency during the first 250 hours of run time, followed by a drop after 300 hours (Figure 2). Further research is needed to understand such an increase in STH efficiency.

Use of TiO_2 as a CRTP Layer

We have previously investigated TiO_2 as a TCCR material. However, the conductivity of TiO_2 limits the performance of the PEC device. In this study, TiO_2 is used as the CRTP layer, where the conductivity is not a requirement due to the unique CRCC/CRTP design. After various baseline depositions on various substrates and various deposition conditions, a device with CRCC (sputtered-Co_3O_4)/CRTP (sputtered-TiO_2) was fabricated. The device has shown

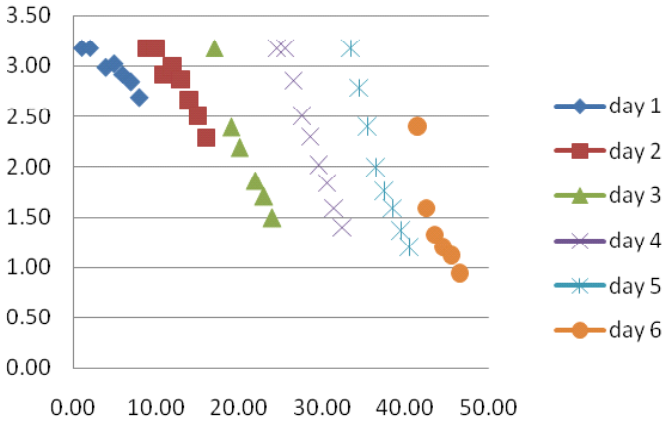

FIGURE 1. STH efficiency (%) as a function of PEC hydrogen production time (in hours) for a CRCC (electroplated Ni/Pt)/CRTP (clear coat) device, showing the recovery of its degradation when the sample is placed in the dark

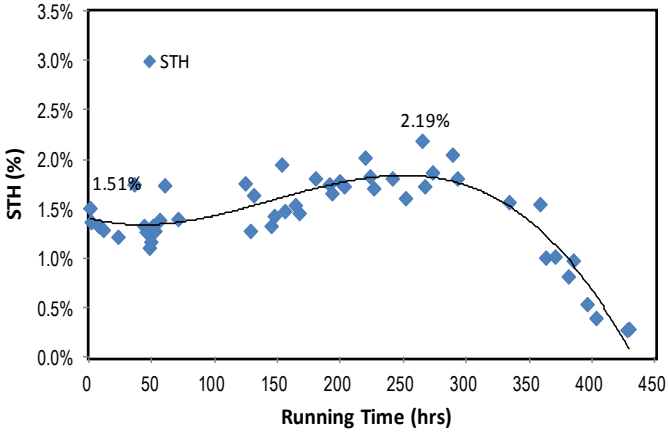

FIGURE 2. STH efficiency (%) as a function of PEC hydrogen production time (in hours) for a CRCC (Co_3O_4)/CRTP (SiO_2) device, showing an increase in STH efficiency during the first 200 hours of operation

improved stability, with performance down to 50% at ~40 hours and with >1% STH efficiency even after 100 hours.

Development of a Large-Area PEC Device

Our most efficient PEC device with STH efficiency of 5.7% was obtained on a 1.5" x 1.5" device with a Co_3O_4 OER catalyst and a Ru HER catalyst. A standard lower-cost Ni HER led to a STH efficiency of around 4.1%. During this year, effort was made to produce a larger-area PEC device, with an active area of 4" x 4". One objective is to see whether a larger device would show reduced performance due to shunting and degradation, or, size-related reduction in performance. Results show that the larger 4" x 4" device exhibits a 3.3% STH efficiency with electroplated Ni as the HER catalyst, which is about 25% lower than the STH efficiency obtained on smaller-size devices. The device lifetime is also reduced to around 40 hours (>1% STH efficiency), which is reduced from the previously obtained 170 hours for smaller devices. Further work is needed to reduce the size dependence of the STH efficiency.

Development of Techno-Economic Analysis Using the H2A Model

During this period, we have performed the techno-economic analysis of MWOE's immersion-type PEC system using the H2A model provided by DOE. The a-Si triple-junction photovoltaic cells, coated with appropriate corrosion-resistant catalyst material and/or protective coatings, are in direct contact with the electrolyte and produce oxygen gas on the anode side and hydrogen gas on the cathode side. Circulation pumps are used to maintain electrolyte concentration and to provide filtration. The evolved hydrogen is compressed, water is allowed to condense, and the stream is passed through an intercooler system to provide cool, dry hydrogen at 300 psi at the factory gate.

The current variable manufacturing costs of triple-junction solar cells on a stainless steel substrate are in the range of $\$25/m^2$ (assuming full production of a 25 MW plant), and many technology improvements and the use of alternative materials will lead to a reduction of variable manufacturing cost down to about $\$15/m^2$ by 2017 (with expanded capacity). We expect that the corrosion-resistant catalytic coatings and durable protective layers will add some additional cost, but no more than $\$15/m^2$, for a total PEC electrode cost less than $\$30/m^2$. The electrode will be contained in a polymeric housing. The cost of the housing, electrical terminals, etc. is expected to be approximately $\$10/m^2$, which is a reasonable assumption given the packaging costs of current (2014) commercially available photovoltaic panels. For example, current 8% a-Si modules are reported to have a manufacturing cost around \$0.5/Watt, corresponding to a panel cost of $\$40/m^2$ for a fully encapsulated and framed panel with junction box and all other functional components.

We anticipate that some electrodes will require refurbishment/catalyst regeneration every two years, at a cost of $\$6/m^2$ (i.e., 20% of the PEC electrode cost).

We also assume 10% STH conversion efficiency and 1,825 hours of standard sunlight per year. Land costs are taken to be \$500/acre, and 50% coverage is assumed due to the use of tilt structures. The plant is designed for 1 TPD, and costs have been scaled to 50 tons/day using a "learning factor" of 0.78 (supported by Williams et al. 2007). Balance-of-system costs are based on a Type 3 PEC example system in a report by Strategic Analysis, Inc. with a projected reduction in installation costs due to modular design.

This calculation demonstrates that by Year 2017, the 1 TPD system will be able to produce hydrogen at a cost of approximately \$5/gge with an electrode lifetime of 2 years before refurbishment. Scaling the system by a factor of 50 using a 0.78 learning factor, to 50 TPD, is projected to reduce costs to under \$2/gge, thus meeting DOE's goal. Table 1 summarizes H2A Model parameters and results stated above.

From the model calculation, about 73% of hydrogen generation cost results from direct capital cost and 26% from operation and maintenance. As shown in Figure 3, the cost of PEC cells accounts for about 37% of total direct capital costs, which is about \$2.2M for a plant of 1 TPD production scale. The second most costly item is installation, and most of it is for the PEC reactors. The installation cost does not depend on the total installed wattage, but on the number of panels installed. If the STH efficiency is improved by 10%, it is

TABLE 1. H2A Model Parameters and Results for MWOE's PEC System

Parameter	2017 (1TPD)	Ultimate Case (50 TPD)
Solar to Hydrogen Conversion Ratio	10%	10%
Plant Size	1 TPD	50 TPD
PEC Electrode Cost	$\$30.00/m^2$	$\$12.80/ m^2$
PEC refurbishment/Catalyst Regeneration Cost	$\$6.00/ m^2$	$\$2.56/ m^2$
Catalyst Replacement Schedule	2 years (expected)	2 years
Balance of Plant Cost	\$2.8 million	\$1.2 million/1 TPD base
Cost of Hydrogen	\$4.97/gge	\$1.95/gge

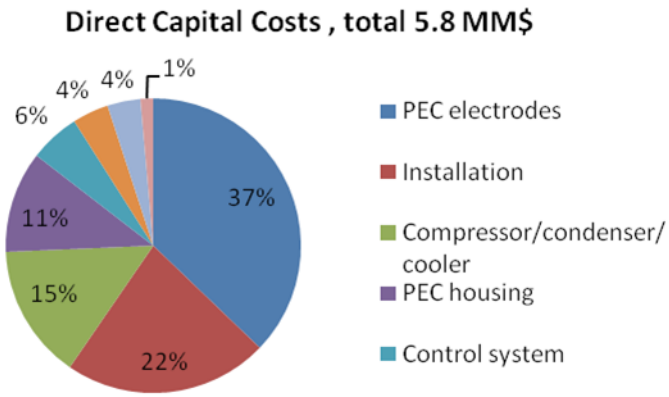

FIGURE 3. The Capital Cost Allocation for a Flat PEC Array (for a production scale of 1 TPD)

expected that the installation cost will drop roughly by 10% because PEC reactors are reduced by 10%. The rest of the capital cost allocation is also shown in Figure 3.

CONCLUSIONS

- The novel design for immersion-type PEC cells where the illuminated side of the PEC electrode is divided into areas coated with a CRTP layer for light absorption and areas coated with a CRCC layer for oxygen generation has shown promising results.
- Techno-economic analysis using DOE's H2A model indicates that MWOE's immersion-type PEC system based on triple-junction a-Si solar cells has the potential to achieve a hydrogen generation cost of $2/gge.
- Effective TCCR material, oxygen and hydrogen generation catalyst material, and a PEC electrode fabrication method have been developed, and a potentially low-cost PEC system is made possible using these materials and approaches.
- The team collaborated with different research groups around the world to further extend PEC hydrogen generation research and development.
- As this project is approaching its final phase, we documented progress made and lessons learned to position for further research and commercialization in the future.

FY 2014 PUBLICATIONS/PRESENTATIONS

1. Xu, L., Deng, X., Abken, A.E., Chen, C., Turner, J., "Critical Research for Cost-effective Photoelectrochemical Production of Hydrogen", 2014 DOE Hydrogen Program and Vehicle Technologies Program Annual Merit Review and Peer Evaluation Meeting, Oral presentation, Washington Marriott Wardman Park, Washington, D.C., June 19, 2014.

II.D.3 Characterization and Optimization of Photoelectrode Surfaces for Solar-to-Chemical Fuel Conversion

Tadashi Ogitsu (Primary Contact), Woon Ih Choi, Brandon Wood
Lawrence Livermore National Laboratory
7000 East Ave., L-413
Livermore, CA 94550
Phone: (925) 422-8511
Email: ogitsu@llnl.gov

DOE Manager
Eric Miller
Phone: (202) 287-5829
Email: Eric.Miller@ee.doe.gov

Project Start Date: March 1, 2010
Project End Date: Project continuation and direction determined annually by DOE

Overall Objectives

- Develop theoretical tool chest for modeling photoelectrochemical (PEC) materials to be used for synergistic theory, characterization, and synthesis activities.
- Uncover underlying mechanisms of surface corrosion and hydrogen evolution at the water-photoelectrode interface.
- Elucidate relationship between stability and efficiency.
- Use derived structure-property relationships to develop device improvement strategies.

Fiscal Year (FY) 2014 Objectives

- Summarize the ab initio studies of water-InP and water-GaP interfaces, the development of ab initio-derived Model Hamiltonian for rapid screening of catalyst materials, and the interpretation of X-ray spectroscopic data relevant for corrosion mitigation mechanism, publish in peer-reviewed journals.
- Analyze the N/Ru/Pt based surface treatment experimental results provided by the National Renewable Energy Laboratory (NREL) and the University of Nevada, Las Vegas (UNLV) and develop a research and development plan for an effective corrosion mitigation method with the surface validation (SV) team members.
- Develop a theoretical hydrogen evolution reaction (HER) model, which takes hydrogen diffusion at the interface between III-V and electrolyte into account. The model is to design an optimized co-catalyst arrangement for a cost-effective photoelectrode.
- Compile knowledge database of existing research on PEC electrode materials (ex. III-Vs and GIGS), interfaces and the other relevant subjects such as catalyst and X-ray spectroscopy.

Technical Barriers

This project addresses the following technical barriers from the Hydrogen Production, Photoelectrochemical Hydrogen Production section of the Fuel Cell Technologies Office Multi-Year Research, Development, and Demonstration Plan:

(AE) Materials Efficiency – Bulk and Interface

(AF) Materials Durability – Bulk and Interface

Technical Targets

This project is conducting fundamental theoretical studies of mechanisms of corrosion and catalysis in semiconductor-based photoelectrode materials for PEC hydrogen production. Insights gained from these studies will be applied toward the optimization and design of semiconductor materials that meet the following DOE 2015 PEC hydrogen production targets (Table 3.1.8A in ref. [1]):

- Solar-to-Hydrogen (STH) Energy Conversion Ratio: 15%
- Electrode Replacement Lifetime: 0.5 year

FY 2014 Accomplishments

- Continued with compilation, review, and sharing of available information on III-V electrode materials, catalysts, and related subjects (ongoing).
- Three publications in peer reviewed journals.
- A novel hydrogen evolution reaction model, which takes hydrogen diffusion at the interface between III-V electrode and electrolyte into account, has been proposed.
  - The model might open up a new design strategy for improved STH conversion efficiency and optimal co-catalyst use (i.e. reduced cost).
- Continued collaborations with unfunded external collaborators to develop theoretical tool chest for PEC hydrogen research.
- Continued joint theoretical/experimental X-ray spectroscopy study on III-V electrode surface (continue through FY 2014 and beyond).

INTRODUCTION

Certain III-V-based PEC cells, notably the $GaInP_2$/GaAs tandem cell developed at NREL, are known to demonstrate high STH conversion efficiencies that are close to the DOE FY 2015 goal [1]. However, durability of these cells has remained the key unresolved issue so far. The primary purpose of this project is to perform a detailed investigation into the microscopic properties of the water-electrode interface, and to use this information to identify correlations with device performance, as measured in terms of STH conversion efficiency and corrosion resistance. The results will provide key feedback to collaborators at NREL, helping them develop a coherent performance optimization scheme for III-V-based photoelectrodes. State-of-art X-ray spectroscopic measurements performed by the UNLV team will bridge remaining gaps in the knowledge obtained from our atomistic modeling, facilitating comparison with actual electrode properties. In FY 2014, we had three major accomplishments. First, the results on III-V surface and interfaces as well as development of ab initio-derived Model Hamiltonian method for catalyst screening have been summarized and published as three papers in peer reviewed journals. Second, potential importance of interfacial H diffusion (publication 2) has led to development of a novel HER model, which could be used to investigate on a better surface treatment and co-catalyst arrangement. Third, as a part of the SV team, we have contributed in improved understanding of the relevant control parameter for $GaInP_2$ surface treatment based on nitrogen and Cu/Pt impurity.

APPROACH

Further progress in semiconductor-based PEC photoelectrodes requires in-depth understanding of the complex relationship between surface stability and catalytic activity. This in turn relies on knowledge of the fundamental nature of the electrode-water interface, and of the chemical pathways explored during surface-active hydrogen evolution. As such, we are carrying out finite-temperature ab initio molecular dynamics simulations and energetics calculations based on density-functional theory to understand the chemical, structural, and electronic properties of water/electrode interfaces under equilibrium conditions, as well as to understand the competing chemical reaction pathways visited during photocatalysis. Our approach uses (001) surfaces of InP, GaP and $GaInP_2$ as model semiconductor electrodes. We are investigating on the effect of the foreign chemical species on the stability and reactivity of the electrode surfaces, as suggested by our collaborators in J. Turner and T. Deutsch's group at NREL [2], as well as independent reports in the literature that surface oxygen may play a key role in motivating both the surface photocorrosion and the catalytic water splitting reaction [3,4]. Accordingly, we are evaluating the stability, structure and reactivity of the III-V(001)/water interfaces in the presence of surface oxygen, hydroxyl, and nitrogen, in order to correlate the results to experimentally observed surface compositions and morphologies. We also provided ab initio derived X-ray spectroscopic data to enable direct comparison with experimental results from Prof. C. Heske's group at UNLV. This information is intended to suggest a strategy for device improvement.

RESULTS

About 1,750 papers relevant for PEC hydrogen research have been collected, indexed, and stored. Important information for the NREL/UNLV collaborators was summarized and shared using online tools such as email or photoelectrochemical.sharepointsite.net (Contact: Heli Wang of NREL). Comprehensive analysis on the acquired knowledge from literatures combined with detailed information on the experimental condition provided by NREL and with the UNLV spectroscopic information [7] led to identification of a few possible causes of performance variability: partial segregation of $GaInP_2$ into thin layers of InP and GaP [5, 6] and co-existence of ordered/disordered phases of $GaInP_2$ [8-12]. The former was primarily motivated by the results of photoemission spectroscopy and inverse photoemission spectroscopy measurements, where careful non-destructive surface cleaning using low energy ion sputtering was performed simultaneously. The $GaInP_2$ sample provided by NREL, after the cleaning, has shown that the surface band gap of about 1.3 eV [7], significantly smaller than known value of E_g ~1.8-2 eV [8-12] for $GaInP_2$. This value is rather close to that of InP. It is known that $GaInP_2$ is not thermodynamically stable against segregation into GaP and InP [5,6], therefore, it was conjectured that the photelectrode used by NREL might have the segregation problem, which might have contributed partly to the performance reproducibility issue. Also, it was discussed that the disordered phase has a higher conduction band edge position and the wider band gap [8-12], which is an advantage for the top absorber for tandem PEC cell, however, at the expense of shorter charger carrier lifetime [13]. There are many conflicting material behaviors, and therefore, it is very important to have comprehensive understanding of basic material properties in order to develop an effective research plan.

The research based on ab initio simulations of III-V surfaces and interfaces as well as on ab initio-derived model Hamiltonian for catalytic reactions being conducted for FY 2010-2013 [14-17] were summarized and published as three papers in peer reviewed journals. In publication 3, it was shown that behavior of a water molecule at the water-semiconductor interface is fundamentally different from that of a water molecule adsorbed on a semiconductor surface

due to the presence/absence of H-bonds around the water molecule. In publication 2, it was shown that H diffusion at the water-InP interface is significantly higher than that at water-GaP interfaces, and combined with the experimental evidences, it was proposed that facile H diffusion at the water-semiconductor interface might activate additional HER pathways, which, in turn, might enhance overall STH conversion efficiency. An experimental observation consistent with our proposition has been reported on a silicon-based metal-insulator-semiconductor device by Esposito et al. in 2013 [18].

The discovery of potential relevance of H diffusion at the interface led to further development of a novel HER model, which ncorporates the interface diffusion into account (Figure 1). Such a computational model will open up a new design strategy for highly cost-effective photoelectrodes via choice of semiconductor surface treatment which will take full advantage of H diffusion that activates additional HER channels, and via optimal co-catalyst arrangement (for example, minimize use of platinum without sacrificing overall STH conversion efficiency).

In FY 2012, the NREL collaborators have demonstrated that the nitrogen bombardment of $GaInP_2$ photoelectrode surface improves corrosion resistance. In the following year, detailed characterization of the nitrogen treated photoelectrode by the UNLV team led to discovery of un-intentional metal impurities (Pt and Ru), and they are found to be crucial for the improved durability. Accordingly, the focus of SV team shifted from nitrogen alone to separating the role of these impurities. A systematic experimental study on the correlation between corrosion resistance and combination of Pt/Ru/N treatment has been designed by the SV team, and executed by the NREL team [19]. The results have led to a significantly clearer understanding on the extent of correlation between the treatments and the corrosion resistance, however, it also revealed that there are yet to be identified factors that affect corrosion resistance.

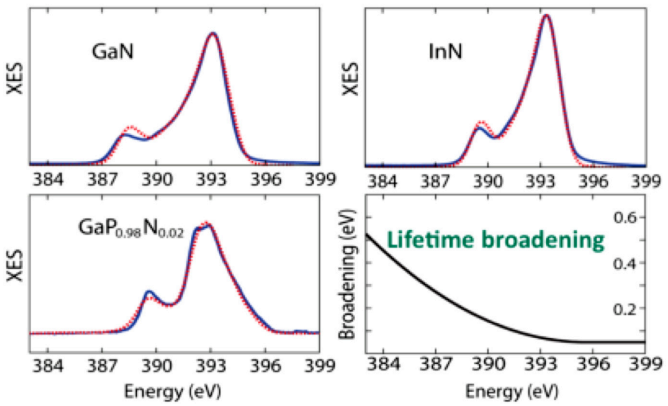

FIGURE 2. Experimental (blue lines) and theoretical (red dash lines) N K-edge XES of three nitride compounds: GaN, InN, and $GaP_{0.98}N_{0.02}$, as well as the energy dependent lifetime broadening profile used for the theoretical spectrum.

The SV team is currently in the process of developing a new research plan for precise determination of control parameters for the surface treatment. As a part of this effort, we have been investigating on the N K-edge X-ray emission spectrum (XES) of nitrogen-bombarded $GaInP_2$. In FY 2013, we have established the calculation procedure and identified several nitrogen defect complexes, which are major contributors to the measured spectrum. During this process, we have learned that the experimental XES spectra of InN published in literature show slight disagreement. Since they were critical for calibrating theoretical spectrum, the UNLV team has performed additional measurements on N K-edge XES of high quality InN, GaN, $GaP_{0.98}N_{0.02}$ samples provided by the LANL collaborator, Todd Williamson. After careful assessments, theoretical analysis was repeated, and concluded that the FY 2013 results are robust (Figure 2 and 3). We are now in the process of addressing an issue stemming from uncertainty in lifetime broadening, and preparing the draft paper on the characterization of nitrogen impurity states in $GaInP_2$ photoelectrode.

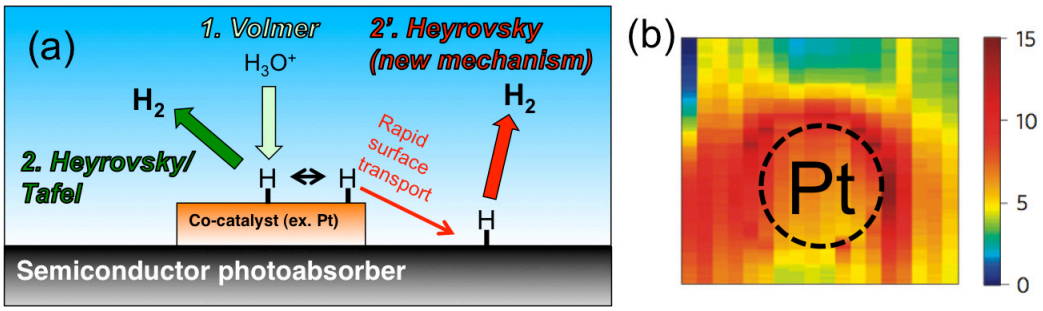

FIGURE 1. (a) Schematics of the novel HER model proposed in the FY 2013 publication 3. In addition to the conventional HER taking place on Pt co-catalyst, facile H diffusion (and reasonably low Heyrovsky barrier) on the semiconductor surface will enable additional HER pathway (red arrow). (b) H_2 evolution activity on the Si-based MIS device reported in ref [18]. Pt catalyst (dashed circle) was found to activate HER in surrounding SiO_2 surface, which is consistent with our model described in (a). Copyright 2013: Macmillan Publisher Ltd: Nature Material.

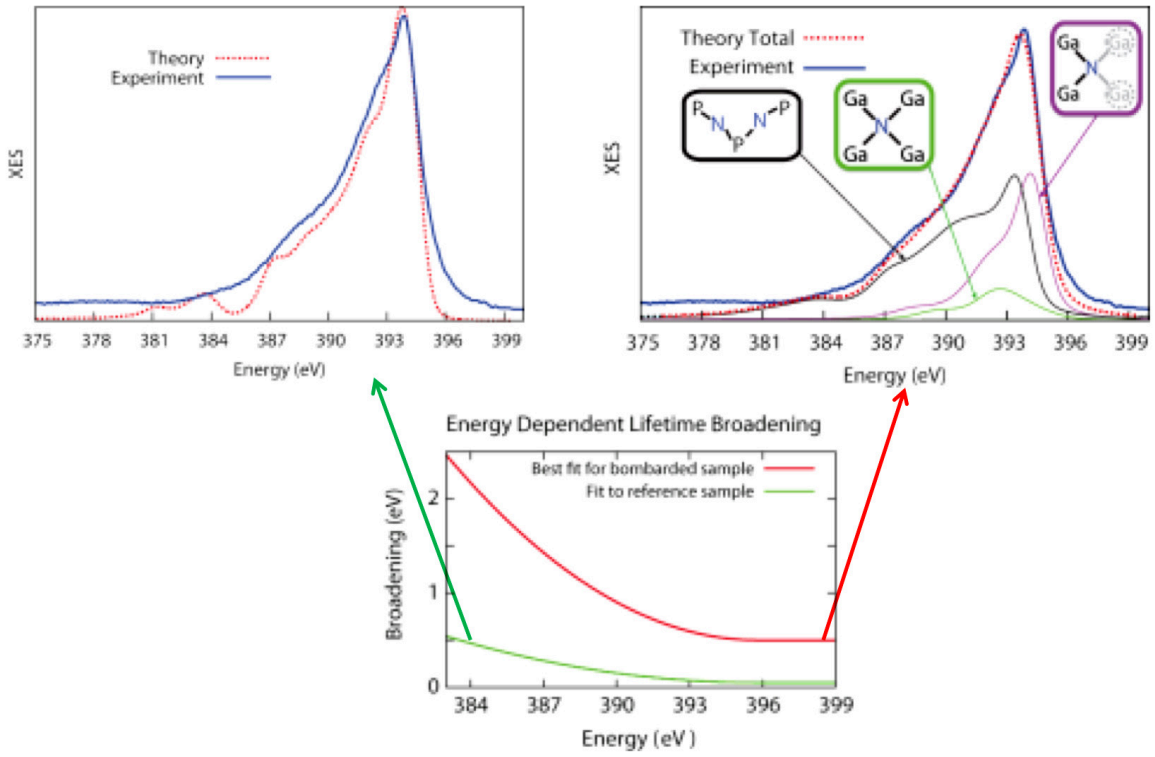

FIGURE 3. Simulated XESs of nitrogen bombarded $GaInP_2$. The left plot was generated with the lifetime broadening used in Figure 2, while in the right plot, the lifetime broadening profile was adjusted so as to obtain the best fit to the UNLV results (blue lines). In general, lifetime of electronic excitation will be decreased by introduction of defects (i.e. larger lifetime broadening), which is expected in the nitrogen bombarded sample used in the UNLV measurements. However, the extent of change in lifetime broadening is not known. Nevertheless, the types of nitrogen defects complex used to generate these theoretical XESs are essentially the same, while the rates of contributions are slightly different.

CONCLUSIONS AND FUTURE DIRECTIONS

- A few potential causes of performance variability problems were identified through the SV team discussions and the PEC literature database development.
- Ab initio study of III-V surfaces and interfaces as well as the development of ab initio-derived Model Hamiltonian for catalyst screening were summarized and published as three papers in peer reviewed journals.
- A novel HER model, which account for H diffusion at the semiconductor-electrolyte interface, has been developed. This model could be used to design a cost-effective PEC electrode, therefore, continuation of the model development is desirable.
- As a part of the SV team, systematic investigation on effective surface treatment for improved electrode durability has been conducted. Unambiguous identification of the control parameters and development of better corrosion mitigation strategy will be the priority for the SV team activity in near future.

SPECIAL RECOGNITIONS & AWARDS/ PATENTS ISSUED

1. 2014 DOE Hydrogen and Fuel Cells Program R&D Award.

FY 2014 PUBLICATIONS/PRESENTATIONS

Publications

1. W.-I. Choi, B.C. Wood, E. Schwegler, and T. Ogitsu, "Site-Dependent Free Energy Barrier for Proton Reduction on MoS_2 Edges." J. Phys. Chem. C. **117**, 21772 (2013).

2. B.C. Wood, E. Schwegler, W.-I. Choi, and T. Ogitsu, "Hydrogen-Bond Dynamics of Water at the Interface with InP/GaP(001) and the Implications for Photoelectrochemistry." J. Am. Chem. Soc. **135**, 15774 (2013).

3. B.C. Wood, E. Schwegler, W.-I. Choi, and T. Ogitsu, "Surface chemistry of GaP(001) and InP(001) in contact with water." J. Phys. Chem. C **118**, 1062 (2014).

4. W.-I. Choi, M. Weir, T. Deutsch, T. Williamson, L. Weinhardt, A. Benkert, M. Blum, F. Meyer, M. Bar, K. George, B.C. Wood, D. Prendergast, J. Turner, C. Heske, and T. Ogitsu, "Chemical Envrionment of Implanted Nitrogen Into $GaInP_2$: Characterized with X-ray Emission Spectroscopy." to be submitted.

5. T. Ogitsu, B. Wood, W. Choi, *DOE Fuel Cell Technology Hydrogen Program Annual Merit Review* (2014).

6. Y. Liu, K. Hackenberg, W.-I. Choi, T. Ogitsu, M. Wang, K. Ajayan, B. Yakobson, and B.C. Wood, "Towards surface-active metal dichalcogenides for efficient hydrogen production." submitted.

Presentations

1. Electrochemical Society 224th Meeting, San Francisco, CA, Oct 2013 (one invited, one oral).

2. Invited lecture at Brigham Young University, Provo, UT, Nov 2013.

3. Invited seminar at Rice University, Huston, TX, April 2014.

4. Invited seminar at MIT, Cambridge, MA, May 2014.

5. 2014 Materials Research Society Spring Meeting, San Francisco, CA, April 2014 (poster).

6. DOE Hydrogen and Fuel Cells Program Annual Merit Review, DC, June 2014 (oral).

7. ICMR Workshop on Ab-initio description of charged systems and solid/liquid interfaces for semiconductors and electrochemistry, Santa Barbara, July 2014 (oral).

REFERENCES

1. DOE EERE Fuel Cell Technologies Office Multi-Year Research, Development, and Demonstration Plan, 3.1 Hydrogen Production, 2012, http://www1.eere.energy.gov/hydrogenandfuelcells/mypp

2. T.G. Deutsch, C.A. Koval, and J.A. Turner, "III-V nitride epilayers for photoelectrochemical water splitting: GaPN and GaAsPN," *J. Phys. Chem. B* **110**, 25297 (2006).

3. A. Heller, "Hydrogen evolving solar cells," *Science* **223**, 1141 (1984).

4. J. Vigneron, M. Herlem, E.M. Khoumri, and A. Etcheberry, *Appl. Surf. Sci.* **201**, 51 (2002).

5. R. Osorio, J.E. Bernard, S. Froyen, and A. Zunger, "Ordering thermodynamics of surface and subsurface layers in the $Ga_{1-x}In_xP$ alloy," *Phys Rev B* **45**, 11173 (1992).

6. J. Jiang, A.K. Schaper, Z. Spika, and W. Stolz, Morphological aspects of continuous and modulated epitaxial growth of (GaIn)P, *J Appl Phys* **88**, 3341 (2000).

7. C. Heske, DOE Fuel Cell Technology Hydrogen Program Annual Merit Review (2012).

8. A. Gomyo, T. Suzuki, and S. Iijima, "Observation of Strong Ordering in $Ga_xIn_{1-X}P$ Alloy Semiconductors," *Phys Rev Lett* **60**, 2645 (1988).

9. A. Mascarenhas, S. Kurtz, A. Kibbler, and J.M. Olson, "Polarized band-edge photoluminescence and ordering in $Ga_{0.52}In_{0.48}P$," *Phys Rev Lett* **63**, 2108 (1989).

10. P. Ernst, C. Geng, F. Scholz, H. Schweizer, Y. Zhang, and A. Mascarenhas, "Band-gap reduction and valence-band splitting of ordered $GaInP_2$," *Appl Phys Lett* **67**, 2347 (1995).

11. S.-H. Wei and A. Zunger, "Band gaps and spin-orbit splitting of ordered and disordered $Al_xGa_{1-x}As$ and $GaAs_xSb_{1-x}$ alloys," *Phys Rev* B **39**, 3279 (1989).

12. A. Gomyo, T. Suzuki, S. Iijima, K. Kobayashi, S. Kawata, H. Fujii, and I. Hino, "Observation of a superstructure in $Ga_{0.5}In_{0.5}P$ with an anomalously low band-gap energy and substrate orientation effects on the formation of the structure," *J Electron Mater* **17**, S5 (1988).

13. A. Sasaki, K. Tsuchida, Y. Narukawa, Y. Kawakami, S. Fujita, Y. Hsu, and G.B. Stringfellow, "Ordering dependence of carrier lifetimes and ordered states of $Ga_{0.52}In_{0.48}P$/GaAs with degree of order <= 0.55," *J Appl Phys* **89**, 343 (2001).

14. T. Ogitsu, B. Wood, *DOE Fuel Cell Technology Hydrogen Program Annual Merit Review* (2010).

15. T. Ogitsu, B. Wood, W. Choi, *DOE Fuel Cell Technology Hydrogen Program Annual Merit Review* (2011).

16. T. Ogitsu, B. Wood, W. Choi, *DOE Fuel Cell Technology Hydrogen Program Annual Merit Review* (2012).

17. T. Ogitsu, B. Wood, W. Choi, *DOE Fuel Cell Technology Hydrogen Program Annual Merit Review* (2013).

18. D.V. Esposito, I. Levin, T.P. Moffat, and A.A. Talin, "H_2 evolution at Si-based metal–insulator–semiconductor photoelectrodes enhanced by inversion channel charge collection and H spillover," *Nat Mater* **12**, 562 (2013).

19. T. Deutsch, *DOE Hydrogen and Fuel Cells Program Annual Merit Review* (2014).

II.E.1 Maximizing Light Utilization Efficiency and Hydrogen Production in Microalgal Cultures

Tasios Melis
University of California, Berkeley
Dept. of Plant & Microbial Biology
111 Koshland Hall
Berkeley, CA 94720-3102
Phone: (510) 642-8166
Email: melis@berkeley.edu

DOE Manager
Katie Randolph
Phone: (720) 356-1759
Email: Katie.Randolph@ee.doe.gov

Contract Number: DE-FG36-05GO15041

Start Date: December 1, 2004
End Date: September 30, 2014

Overall Objectives

- Minimize, or truncate, the chlorophyll antenna size in green algae, and the phycobilisome antenna size in cyanobacteria to maximize culture photobiological solar energy conversion efficiency and H_2 production.
- Demonstrate that a truncated light-harvesting antenna (TLA) minimizes absorption and wasteful dissipation of bright sunlight by individual cells, resulting in better light utilization efficiency and greater photosynthetic productivity in high-density mass cultures.

Fiscal Year (FY) 2014 Objectives

Apply the TLA concept in cyanobacteria and test for improved culture productivity.

Technical Barriers

The project addresses the following technical barriers from the Biological Hydrogen Production section of the Production section of the Fuel Cell Technologies Office Multi-Year Research, Development, and Demonstration Plan:

(AN) Light Utilization Efficiency

Technical Targets

The Fuel Cell Technologies Office Multi-Year Plan technical target for this project was to apply the TLA concept in cyanobacteria and to test for the premise of improved culture productivity. The cyanobacterial project was competed on schedule. The technical targets for this project are listed in Table 1.

FY 2014 Accomplishments (TLA effort in cyanobacteria)

- Work on the application of the TLA concept in cyanobacteria was completed. The work provided first-time direct evidence of the applicability of the TLA concept in cyanobacteria, entailing substantial improvements in the photosynthetic efficiency and

TABLE 1. Microalgal Technical Targets, Milestones and Progress (Sunlight utilization efficiency is shown as percent of incident solar energy. Maximum possible based on PAR=30%. Maximum possible based on e-PAR=40%.)

	2000	2003	2005	2007	2008	2010	2011	2012	2015
Targets (Light utilization efficiency)	3%	10%				15%			20%
Tla strain with the highest efficiency identified	3% (WT)	10% TLA1	15% TLA2		25% TLA3				
Gene cloning from the TLA strains				TLA1: Mov34 MPN			TLA2: FTSY	TLA3: SRP43	

productivity of mass cultures upon minimizing the phycobilisome light-harvesting antenna size.

- A patent application was filed.
- A peer-reviewed paper was published with the following citation:
  - Kirst, H., Formighieri, C., Melis, A. (2014) Maximizing photosynthetic efficiency and culture productivity in cyanobacteria upon minimizing the phycobilisome light-harvesting antenna size. Biochimica et Biophysica Acta, Bioenergetics DOI: 10.1016/j.bbabio.2014.07.009

✧ ✧ ✧ ✧ ✧

INTRODUCTION

The goal of the research is to generate green algal and cyanobacterial strains with enhanced photosynthetic productivity and H_2 production under mass culture conditions. To achieve this goal, it is necessary to optimize the light absorption and utilization properties of the cells [1]. A cost-effective way to achieve this goal is to reduce the number of chlorophyll (Chl) molecules (green microalgae) or phycobilins (cyanobacteria) that function in the apparatus of photosynthesis.

The rationale for this work is that a truncated light-harvesting antenna size in green algae or cyanobacteria will prevent individual cells at the surface of a high-density culture from over-absorbing sunlight and wastefully dissipating most of it (Figure 1). A truncated antenna size will permit sunlight to penetrate deeper into the culture, thus enabling many more cells to contribute to useful photosynthesis and H_2 production (Figure 2). It has been shown that a truncated Chl antenna size will enable about 3-4 times greater solar energy conversion efficiency and photosynthetic productivity than could be achieved with fully pigmented green microalgal cells [2].

APPROACH

A phycocyanin-deletion mutant of *Synechocystis* (cyanobacteria) was generated upon replacement of the *CPC*-operon with a kanamycin resistance cassette.

RESULTS

The *Δcpc* transformant strains (*Δcpc*) exhibited a green phenotype, compared to the blue-green of the wild type (WT), lacked the distinct phycocyanin absorbance at 625 nm, had a lower Chl per cell content, and a lower Photosystem I/ Photosystem II reaction center ratio compared to the WT. Molecular and genetic analyses showed replacement of all WT copies of the *Synechocystis* DNA with the transgenic version, thereby achieving genomic DNA homoplasmy. Biochemical analyses showed absence of the phycocyanin α- and β-subunits, and overexpression of the kanamycin resistance NPTI protein in the *Δcpc*. Physiological analyses revealed a higher, by a factor of about 2, intensity for the saturation of photosynthesis in the *Δcpc* compared to the WT. Under limiting intensities of illumination, growth of the *Δcpc* was slower than that of the WT. This difference in the rate of cell duplication diminished gradually as growth irradiance increased. Identical rates of cell duplication of about 13 h for both WT and the *Δcpc* were observed at about 800 µmol photons m^{-2} s^{-1} or greater. (Note: Full sunlight intensity at sea level is about 2,200 mmol photons m^{-2} s^{-1}.) Culture productivity analyses under simulated bright sunlight and high cell-density conditions showed that biomass accumulation by the *Δcpc* was 1.57 times greater than that achieved by the WT. Results were published in Kirst et al. (2014) Biochim Biophys Acta DOI: 10.1016/j.bbabio.2014.07.009.

CONCLUSIONS

Cyanobacterial TLA Project

The work provided first-time direct evidence of substantial improvements in the biomass productivity of mass cultures upon minimizing the phycobilisome light-harvesting antenna size in cyanobacteria.

Green Microalgal TLA Project

The following green microalgal ***tla*** strains have been deposited and are available to the public from the Chalmydomonas Resource Center (<chlamycollection.org>).

CC-4473 tla3 mt+

CC-4474 tla4 mt+

CC-4475 tla5 mt+

CC-4472 tla2-ΔFtsY (cw15) mt+

CC-4476 tla2-ΔFtsY (CW15+) mt+

CC-4561 tla3-Δcpsrp43 (cw+) mt+

CC-4562 tla3-Δcpsrp43 (cw+) mt-

CC-4169 tla1 cw15 sr-u-2-60 mt+ Chromosome: 05Locus: TLA1

CC-4170 tla1 nr-u-2-1 mt- Chromosome: 05Locus: TLA1

e-PAR Project

In silico work was conducted to advance exploration of the "*extended Photosynthetically Active Radiation*" (e-PAR) concept. Proprietary preliminary information on the molecular genetic design was arrived at but not disclosed. Successful implementation of the e-PAR concept is a long-term project, one that could not be further pursued under the auspices of this contract.

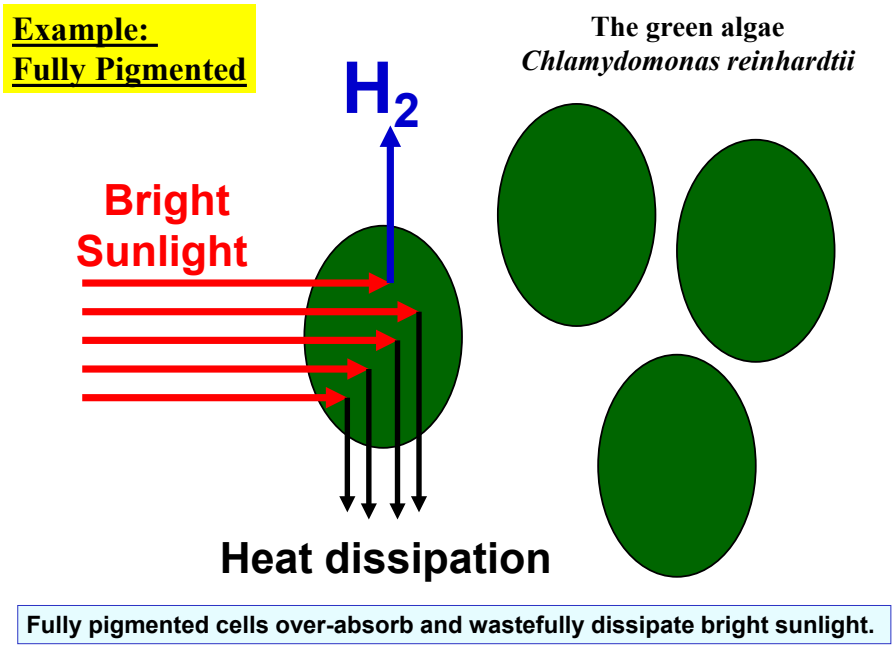

FIGURE 1. Schematic presentation of the fate of absorbed sunlight in fully pigmented (dark green) algae. Individual cells at the surface of the culture over-absorb incoming sunlight, i.e., they absorb more than can be utilized by photosynthesis, and 'heat dissipate' most of it. Note that a high probability of absorption by the first layer of cells would cause shading of cells deeper in the culture.

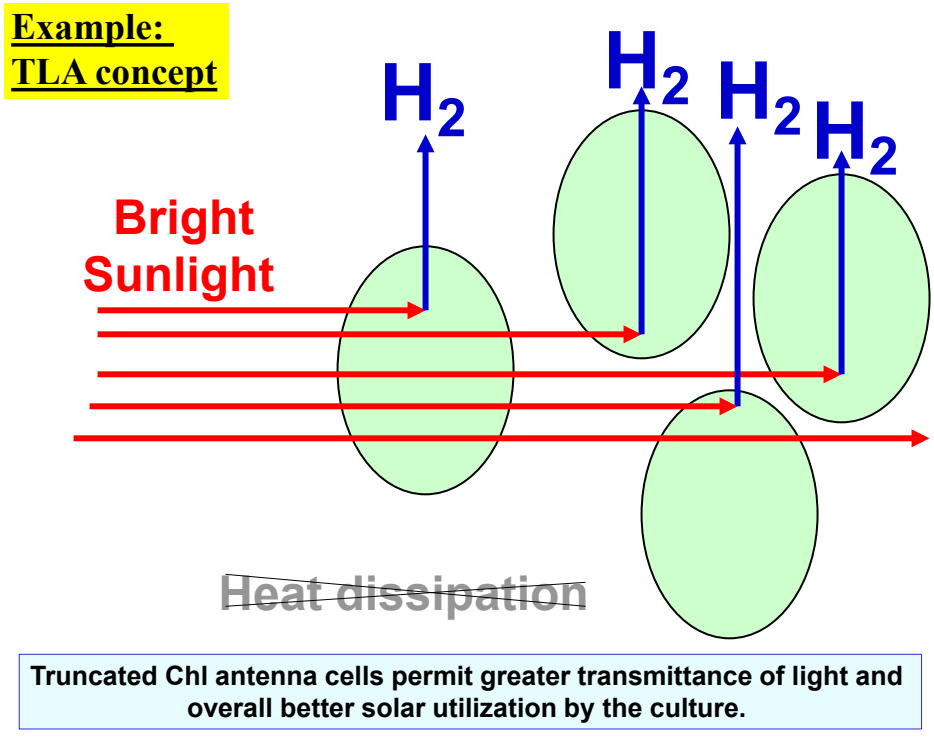

FIGURE 2. Schematic of sunlight penetration through cells with a truncated chlorophyll antenna size. Individual cells have a diminished probability of absorbing sunlight, thereby permitting penetration of irradiance and H2 production by cells deeper in the culture.

FUTURE DIRECTIONS

This project has achieved all its objectives and is about to be officially terminated at the end of September 2014.

FY 2014 PUBLICATIONS

1. Kirst H, Melis A (2014) The chloroplast *Signal Recognition Particle* pathway (CpSRP) as a tool to minimize chlorophyll antenna size and maximize photosynthetic productivity. Biotechnology Advances 32: 66–72 DOI: 10.1016/j.biotechadv.2013.08.018.

2. Kirst H, Formighieri C, Melis A (2014) Maximizing photosynthetic efficiency and culture productivity in cyanobacteria upon minimizing the phycobilisome light-harvesting antenna size. Biochim Biophys Acta - Bioenergetics DOI: 10.1016/j.bbabio.2014.07.009 in press.

REFERENCES

1. Kok B (1953) Experiments on photosynthesis by *Chlorella* in flashing light. In: Burlew JS (ed), Algal culture: from laboratory to pilot plant. Carnegie Institution of Washington, Washington D.C., pp 63-75.

2. Melis A, Neidhardt J, Benemann JR (1999) *Dunaliella salina* (Chlorophyta) with small chlorophyll antenna sizes exhibit higher photosynthetic productivities and photon use efficiencies than normally pigmented cells. J. appl. Phycol. 10: 515-525

II.E.2 Biological Systems for Algal Hydrogen Photoproduction

Maria L. Ghirardi
National Renewable Energy Laboratory (NREL)
15013 Denver West Parkway
Golden, CO 80401
Phone: (303) 384-6312
Email: maria.ghirardi@nrel.gov

DOE Manager
Katie Randolph
Phone: (720) 356-1759
Email: Katie.Randolph@ee.doe.gov

Project Start Date: October 1, 2013
Project End Date: December 31, 2014

Overall Objectives

Develop photobiological systems for large-scale, low-cost, and efficient H_2 production from water to meet DOE's targets (see Table 1).

Fiscal Year (FY) 2014 Objectives

- Quantify the initial and final rates, as well as total H_2 yield following a 30-min illumination of wild-type versus a transformant expressing the more O_2-tolerant *Clostridium acetobutylicum* Ca1 hydrogenase.
- Measure the light conversion efficiency of wild-type and Ca1 transformant under solar intensities.
- Initiate genetic crosses to introduce additional traits to the best H_2-producing Ca1 transformant in order to further enhance its H_2 production capability.

Technical Barriers

This project addresses the following technical barriers from the Hydrogen Production section of the Fuel Cell Technologies Office Multi-Year Research, Development, and Demonstration Plan:

(AO) Rate of Hydrogen Production

(AP) Oxygen Accumulation

Technical Targets

The technical targets for this project are listed in Table 1.

TABLE 1. Progress towards Meeting Technical Targets for Photobiological Algal Hydrogen Production

Characteristic	2014 Status	2015 Target	2020 Target	Ultimate target
Duration of continuous H_2 production under full sunlight intensity	7-30 min[a]	30 min	4 h	8 h
Solar-to-Hydrogen (STH) Energy Conversion Ratio	0.12%	2%	5%	17%

[a]Data variability is responsible for the wide range of values.

FY 2014 Accomplishments

- Demonstrated initial rates of H_2 photoproduction for the Ca1 transformant strain 55 that correspond to about 8% of wild-type, final rates of 10% of wild-type and final net H_2 yield equal to 90% of that measured with the wild-type strain upon 30 min continuous illumination equivalent to solar intensities.
- Estimated a solar conversion efficiency of 0.12% for the mutant versus 0.75% for wild-type strain under solar intensities.
- Demonstrated a 3.6-fold higher average rate of H_2 photoproduction using strains transformed with a linear plasmid containing the Ca1 gene versus strain 55 (transformed with a circular plasmid).

INTRODUCTION

Hydrogen photoproduction is a characteristic of certain microbes, including photosynthetic green algae. *Chlamydomonas reinhardtii* has been a model green alga that has been used to increase our understanding of the H_2 photoproduction process and to test hypotheses regarding factors that need to be addressed to increase and sustain algal H_2 photoproduction capability. One of these factors is the sensitivity of hydrogenases to O_2, a necessary by-product of photosynthetic water oxidation. Other factors include (a) competition for photosynthetic reductant between carbon fixation and hydrogen production, (b) regulatory mechanisms that inhibit electron transport from water to the hydrogenase in the absence of carbon fixation, and (c) the low light saturation of photosynthesis due to the large number of light-harvesting molecules associated with its photosynthetic apparatus.

NREL's approach to address the barriers to H_2 photoproduction consisted of introducing the gene encoding the more O_2-tolerant hydrogenase from the anaerobic bacterium *Clostridium acetobutylicum* into *Chlamydomonas*, followed by integration of known genetic traits that address the other barriers to efficient and sustained H_2 photoproduction.

APPROACH

In previous funding periods, we developed methods to introduce and stably express the Ca1 hydrogenase in a Chlamydomonas strain, *hyd-*, in which the native hydrogenase genes, *HYDA1* and *HYDA2* had been genetically knocked out. We observed that various samples with a positive phenotype (H_2-production measured with the GFP assay[1]) had to undergo a couple of rounds of re-plating to yield homogeneous single colonies. This year, we tested the effect of introducing different combinations of introns into the deoxyribonucleic acid (DNA) construct carrying the Ca1 gene, as well as the efficacy of using linear versus circular plasmid in Ca1 expression. Both approaches have been shown to increase expression of heterologous genes in *Chlamydomonas*. Concomitantly, we started genetic crosses to introduce the *pgrl1* and *tla3* mutations into the *hyd- Chlamydomonas* strain for future crosses with the Ca1 transformant. The *pgrl1* strain was reported to exhibit higher rates of H_2 photoproduction due to the lack of cyclic electron transport (Tolleter, D., et al.) [1]; the *tla3* mutant has a truncated light-harvesting antenna and its photosynthetic rates saturate at much higher light intensities than the wild-type strain (Kirst, H., et al.) [2].

RESULTS

The first milestone for FY 2014 required us to benchmark the STH conversion efficiency and duration of H_2 production using wild-type versus our best transformant which, at the time, was strain 55. We performed our experiments in the Clark electrode chamber, under illumination from LEDs that emitted 2,000 µEinsteins m^{-2} s^{-1}, which is the equivalent to the photosynthetic active radiation region at one sun intensity (2,500 J/m^{-2} s^{-1}). The uncoupler carbonyl cyanide-p-trifluoromethoxyphenol hydrozone (FCCP) was used to eliminate the down-regulation of electron transport by non-dissipation of the proton gradient. We measured the effect of cell density (represented by Chl concentration) on H_2 photoproduction rates and converted the rates into STH, using the value of 242 kJ for each mole of H_2. Figure 1 shows an STH value of about 0.75% for the wild-type strain and about 0.12% for strain 55. Although the reported STH values are low compared to the programmatic targets, it must be noted that the measurements were done under less than optimal conditions, using a 2 ml-volume "photobioreactor" with an essentially zero headspace, due to technical challenges involved in measuring low rates. The latter prevented fast equilibration of gases between the liquid and gaseous phase, and may have limited the observed rates. Indeed, Kosourov et al. [3] demonstrated that increases in the gas/liquid volume ratio have a significant effect on the rates of H_2 photoproduction.

In order to complete the second quarter Go/No-Go milestone for FY 2014, we measured H_2 photoproduction by wild-type and strain 55 (our best H_2-producing strain from a pool of transformants generated by introduction of a circular plasmid containing the Ca1 gene under regulation of the PsaD promoter) for a total of 30 minutes and estimated initial and final rates, as well as total H_2 yield. The results, which are shown in Table 2, reflect the variability of the measurements, with very high standard deviations. In summary, the initial rate target of 11 mmoles H_2 mg Chl^{-1} h^{-1} was met, the final rate target of 0.06 mmoles H_2 mg Chl^{-1} h^{-1} was not, and the final net H_2 yield value was slightly lower than the target value (equal or higher than wild type, WT). As a result the decision was a No-Go. The high data variability for WT and mutant strain is not very well understood; we have attempted to optimize growth and induction conditions, as well as the experimental set-up, without much success, so far, and this needs to be addressed more carefully in the future.

TABLE 2. Estimated Parameters for WT and Ca1-Expressing Strain 55; Standard Deviations were Calculated from 6 WT and 13 Strain 55 Individual Curves

Strain	Initial Rate	Final rate	Total H_2 Yield
WT (D66)	160 ± 35	-0.47 ± 0.14	0.36 ± 0.20
Strain 55	13.25 ± 7.56	-0.05 ± 0.21	0.31 ± 0.20

As an alternative approach to increase the activity of the Ca1 transformants, we used our previous expression construct (PsaD Ca1+) and added three introns into the Ca1 open reading frame. We also used two commercial plasmids (from Invitrogen) under the regulation of the Hsp70A/RbcS2 promoter/terminators that induce high constitutive expression levels. Into one of the commercial plasmids, we introduced the codon-optimized Ca1 gene carrying an intron in its 5'UTR (pChlamy Ca1); the second plasmid carried additional three introns into the Ca1 open reading frame (pChlamyCa1 introns), similarly to the PsaD $Ca1^+$ construct. Unfortunately, neither of the new intron-containing plasmids resulted in higher Ca1-expressing strains (not shown).

Our next alternative used an excised plasmid (linear) containing no introns, under the regulation of the PsaD promoter ($PsaD_{excised}$). We introduced it into the *hyd- Chlamydomonas* strain, screened transformants using the GFP assay, and selected transformants with high H_2 production rates as measure by the Clark electrode. Two of them were further re-plated and underwent another round of

[1] Green fluorescent protein-based H_2-sensing assay developed by NREL (Wecker et al., Biotechnol. Bioeng. 111, 1332-1340).

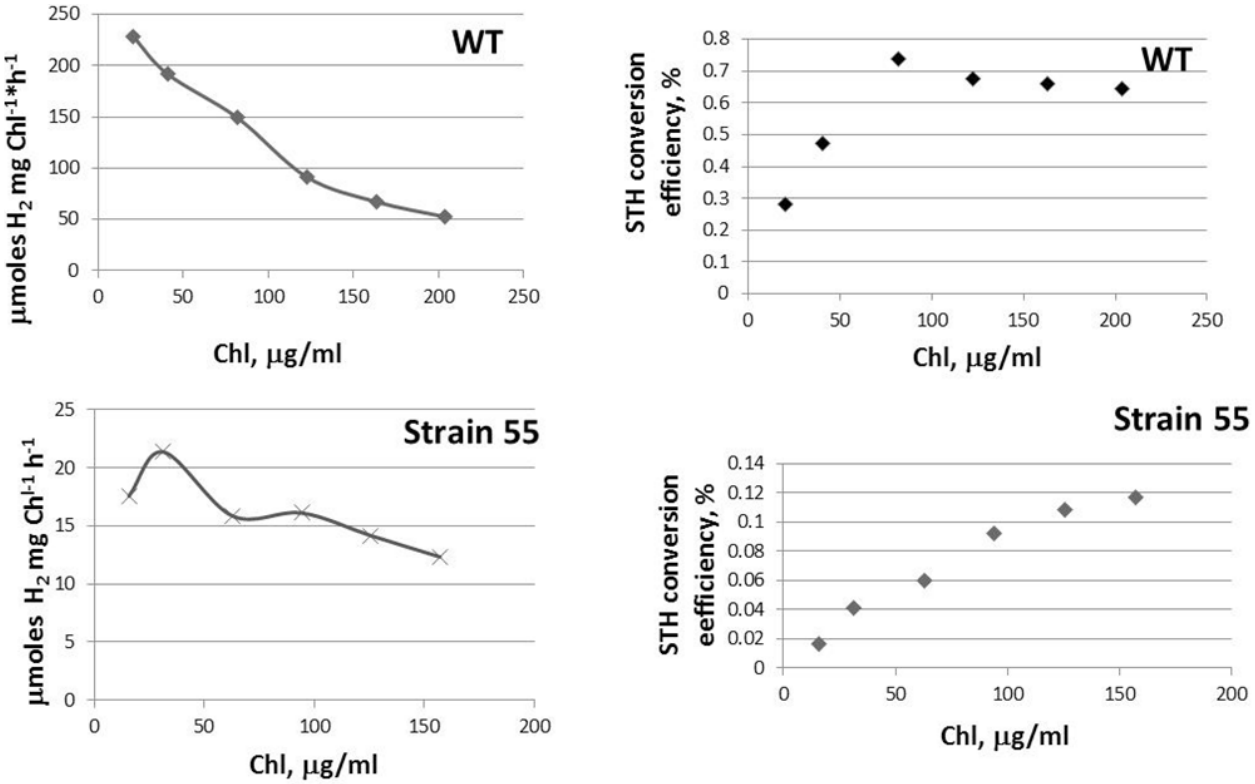

FIGURE 1. Left: Rates of H_2 production (µmoles H_2 mg Chl^{-1} s^{-1}) by representative WT (top) and strain 55 (bottom) as a function of the Chl concentration in the electrode chamber. Right: Estimated STH conversion efficiency of WT (top) and strain 55 (bottom) as a function of Chl concentration in the electrode chamber.

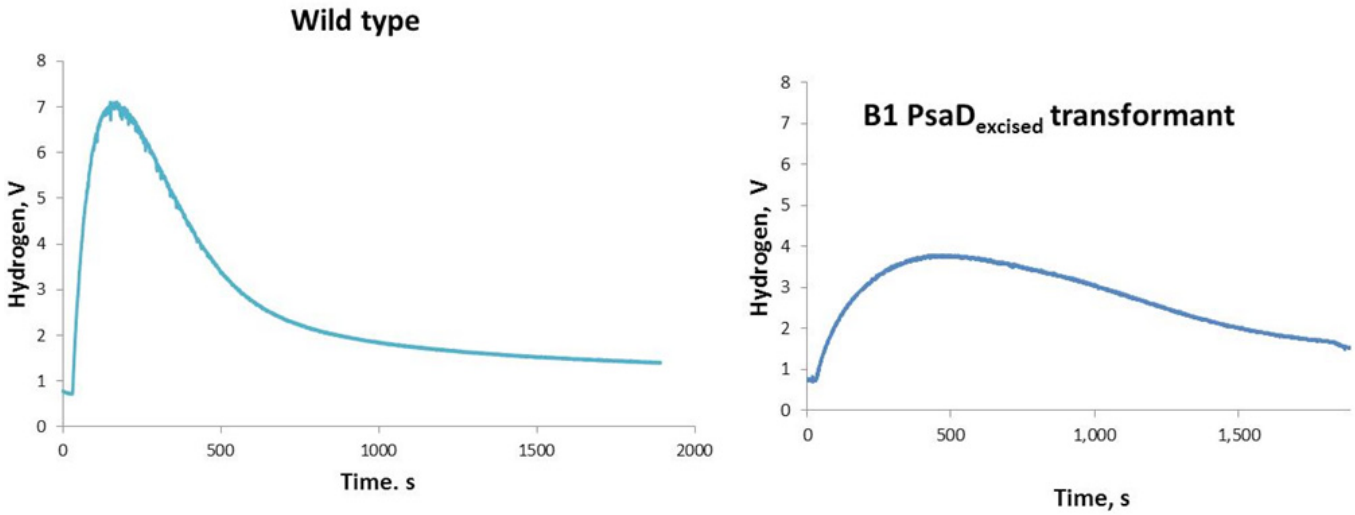

FIGURE 2. Hydrogen levels (measured as volts) in the Clark electrode chamber during a 30-min illumination period. WT (left) and B1 transformant (right). Initial rates were estimated from the slope of the curves during the initial 100 s; final rates represent the slopes during the last 500 s; total H_2 yield was determined by subtracting the voltage at the beginning of the illumination to that at the end of the illumination period and converting the number into moles H_2 per Chl concentration, as discussed in the text. Estimated initial rates determined from the representative curves are 163 and 49.5 mmoles H_2 mg Chl^{-1} s^{-1} for WT and the B1 transformant, respectively.

GFP selection. Transformants B1 and C2 exhibited average rates 3.5-fold higher than strain 55 (transformed with a circular plasmid) and 29% of the average WT initial rates (Figure 2 and Table 3). However, there is considerable H_2

uptake during the 30-min experiment, resulting in a total final H_2 yield that is similar to those of the WT and strain 55. We will use either of the two transformants in our final genetic cross. Nevertheless, the maximum H_2 peak occurs at longer times than that recorded for the WT strain, at about 7.2 vs. 2.6 min, demonstrating that the phenotype of the Ca1-expressing mutant is indeed different from that of the WT strain.

TABLE 3. Total H_2 Yield, Initial and Final Rates of H_2 Photoproduction by Mutant Strains Carrying Excised Plasmid

Strain	Initial rate (µmoles H_2 mg Chl^{-1} h^{-1})	Final rate (µmoles H_2 mg Chl^{-1} h^{-1})	Total H_2 yield/Chl (µmoles H_2 mg Chl^{-1})
B1	29	-0.488	0.102
	49.5	-1.59	0.317
C2	78	-2.336	0.554
	30.6	-1.036	0.24
Average all	**46.8**	**-1.36**	**0.303**
% average WT[1]	29	289	84
% average strain 55[1]	350	2,700	98

[1] See Table 2 for average values used here

CONCLUSIONS AND FUTURE DIRECTIONS

- The data show that it is possible to generate Ca1-expressing mutants with final net H_2 yields comparable to those of the WT strain. The best transformants to date (strains B1 and C2) show initial rates equivalent to about 29% of WT, but do not exhibit significantly higher final net H_2 yields/Chl, although peak production occurs at later timepoints.
- The STH conversion efficiency of mutant (strain 55) and WT strains are currently very low (0.12 and 0.75%, respectively) but could be increased through reactor engineering approaches. We have not yet measure the STH of our latest mutants.
- Intron-containing constructs did not increase the levels of Ca1 expression by *Chlamydomonas*, but the use of linear versus circular plasmids resulted in an average 3.6-fold increase in the initial rates.
- This project will be terminated at the end of the first quarter of FY 2015. The work remaining to be completed in FY 2015 focuses on generating and characterizing the final transformant strain, *pgrl1 tla3 hyd*- Ca1. We expect that the results will direct future research towards improving algal H_2 photoproduction.

FY 2014 PUBLICATIONS/PRESENTATIONS

1. Presentation to the Hydrogen Production Tech Team at PNNL (July 2013).

2. Poster presentation at the International Photosynthesis Conference, St. Louis (August 2013).

3. Invited speaker at the University of Rochester, NY (Dec. 2013).

4. Invited seminar presentation at the University of Colorado (Jan. 2014).

REFERENCES

1. Tolleter, D., Ghysels, B., Alric, J., Petroutsos, D., Tolstygina I., Krawitz, D., Happe, T., Auroy, P., Adriano J., Beyly A., Cuine, S., Piet, J., Reiter, I., Genty, B., Cournac, L., Hippler, M., and Peltier, G. (2011) Plant Cell 23, 2619-2630.

2. Kirst, H., Garcia-Cerdan J., Zurbriggen A., Ruehle, T. and Melis, A. *Plant Physiol.* 160, 2251-2260.

3. Kosourov, S., Ghirardi, M.L. and Seibert, M. (2011) *Int. J. Hydrogen Res.* 36, 2044-2048.

II.E.3 Fermentation and Electrohydrogenic Approaches to Hydrogen Production

Pin-Ching Maness (Primary Contact), Katherine Chou, and Lauren Magnusson
National Renewable Energy Laboratory (NREL)
15013 Denver West Parkway
Golden, CO 80401
Phone: (303) 384-6114
Email: pinching.maness@nrel.gov

DOE Manager
Katie Randolph
Phone: (720) 356-1759
Email: Katie.Randolph@ee.doe.gov

Subcontractor:
Bruce Logan, Pennsylvania State University

Start Date: October 1, 2004
Projected End Date: Project continuation and direction determined annually by DOE

Overall Objectives

- Optimize rates and yields of hydrogen production in a sequencing fed-batch bioreactor by varying hydraulic retention time (HRT) and reactor volume replacement
- Optimize genetic tools to transform *Clostridium thermocellum* and obtain mutants lacking the targeted competing pathway to improve hydrogen molar yield
- Demonstrate hydrogen production from the NREL fermentation effluent and harness the energy in a chemical gradient to improve overall energy efficiency in hydrogen production using a microbial electrolysis cell (MEC) reactor

Fiscal Year (FY) 2014 Objectives

- Optimize sequencing fed-batch parameters and convert corn stover lignocellulose to hydrogen by the cellulolytic bacterium *Clostridium thermocellum*, aimed to lower feedstock cost.
- Use the genetic tools developed at NREL tailored for *C. thermocellum* and delete the competing ethanol pathway, aimed to improve hydrogen molar yield via fermentation.
- Redesign a microbial reverse-electrodialysis electrolysis cell (MREC) to examine the scalability of the MREC for hydrogen production from fermentation effluent without an external energy input, aimed to improve H_2 molar yield.

Technical Barriers

This project supports research and development on DOE Technical Task 6, subtasks Molecular and Systems Engineering for Dark Fermentative Hydrogen Production and Molecular and Systems Engineering for MEC and it addresses barriers AX, AY, and AZ.

(AX) H_2 Molar Yield

(AY) Feedstock Cost

(AZ) System Engineering

Technical Targets

Technical targets for this project are listed in Table 1.

TABLE 1. Progress toward Meeting DOE Technical Targets in Dark Fermentation

Characteristics	Units	Current Status	2015 Target	2020 Target
Yield of H_2 from glucose	Mole H_2/mole glucose	2–3.2	6*	--
Feedstock cost	Cents/lb glucose	13.5	10	8
Duration of continuous production (fermentation)	Time	17 days	3 months	6 months
MEC cost of electrodes	$/m^2	$2,400	$300	$50
MEC production rate	L-H_2/L-reactor-d	1	1	4

*Yield of H_2 from glucose: DOE has a 2015 target of an H_2 molar yield of 6 (4 from fermentation and 2 from MEC) from each mole of glucose as the feedstock, derived from cellulose.

Feedstock cost: The DOE Bioenergy Technologies Office is conducting research to meet its 2015 target of 10 cents/lb biomass-derived glucose. NREL's approach is to use cellulolytic microbes to ferment cellulose and hemicellulose directly, which will result in lower feedstock costs.

FY 2014 Accomplishments

- Conducted sequencing fed-batch reactor experiments and demonstrated that by using a HRT of 48 h and displacing 50% of the reactor liquid every 24 h, *C. thermocellum* converted corn stover lignocellulose (5 g/L loading based on cellulose content) to H_2 with a maximal rate of 1,102 mL $H_2/L_{reactor}$/d. The accumulation of up to 28 g lignin/L did not inhibit rate of H_2 production, a promising finding for using lignocellulosic biomass.

- Both total and specific rate of H_2 production was increased by nearly 1.5-fold in log-phase *C. thermocellum* culture when its formate competing pathway was deleted using the NREL proprietary genetic tools. This mutant yielded 1.6-fold more ethanol, which prompted its deletion, an ongoing effort in FY 2014 to further improve H_2 output.
- Obtained a volumetric current density of 78–110 A/m^3 by treating NREL fermentation wastewater in an MREC with an 8 h HRT and a reverse electrodialysis stack potential of 0.6–0.75 V. The maximum hydrogen production rate was 0.9 L-H_2 $L_{reactor}^{-1}$ d^{-1} with a chemical oxygen demand (COD) removal of 60% and an H_2 yield of 1.0 L H_2/g COD. Increased HRT to 24 h resulted in an increase in COD removal to 73%, but decreased H_2 production rates to 0.3 L-H_2 $L_{reactor}^{-1}$ d^{-1} and H_2 yields to 0.8 L H_2/g COD.

INTRODUCTION

Biomass-derived glucose feedstock is a major operating cost driver for economic hydrogen production via fermentation. The DOE Fuel Cell Technologies Office is taking advantage of the DOE Bioenergy Technology Office's investment in developing less expensive glucose from biomass to meet its cost target of 10 cents/lb by 2015. Meanwhile, one alternative and viable approach to addressing the glucose feedstock technical barrier (AZ) is to use certain cellulose-degrading microbes that can ferment biomass-derived cellulose directly for hydrogen production. One such model microbe is the cellulose-degrading bacterium *Clostridium thermocellum*, which was reported to exhibit one of the highest growth rates using crystalline cellulose [1]. Another technical barrier to fermentation is the relatively low molar yield of hydrogen from glucose (mol H_2/mol sugar; technical barrier AX), which results from the simultaneous production of waste organic acids and solvents. Biological pathways maximally yield 4 moles of H_2 per 1 mole of glucose (the biological maximum) [2]. However, most laboratories have reported a molar yield of 2 or less [3,4]. Molecular engineering to block competing pathways is a viable option toward improving H_2 molar yield. This strategy had resulted in improved H_2 molar yield in *Enterobacter aerogenes* [5].

A promising parallel approach to move past the biological fermentation limit has been developed by a team of scientists led by Prof. Bruce Logan at Pennsylvania State University. In the absence of O_2, and by adding a slight amount of negative potential (–250 mV) to the circuit, Logan's group has produced hydrogen from acetate (a fermentation byproduct) at a molar yield of 2.9–3.8 (versus a theoretical maximum of 4) in a modified microbial fuel cell called an MEC [6]. It demonstrates for the first time a potential route for producing eight or more moles of hydrogen per mole glucose when coupled to a dark fermentation process. In FY 2009 the team reported a combined molar yield of 9.95 when fermentation was coupled to MEC in an integrated system [7]. Combining fermentation with MEC could therefore address technical barrier AX and improve the techno-economic feasibility of hydrogen production via fermentation.

APPROACH

NREL's approach to addressing feedstock cost is to optimize the performance of the cellulose-degrading bacterium *C. thermocellum* using corn stover lignocellulose as the feedstock. To achieve this goal, we are optimizing the various parameters in a sequencing fed-batch reactor to improve longevity, yield, and rate of H_2 production. To improve H_2 molar yield, we are selectively blocking competing metabolic pathways in this organism via genetic methods. Through a subcontract, Pennsylvania State University is testing the performance of an MEC and MREC using both a synthetic effluent and the real waste stream from lignocellulosic fermentation generated at NREL.

RESULTS

Lignocellulose Fermentation

Lignocellulose is a solid substrate, and, with continuous feeding, the system will eventually suffer from clogging of feed lines and over-exhaustion of the feed pump. A more feasible strategy for lignocellulose fermentation is to feed the substrate at a predetermined interval instead of using continuous feeding. This strategy can be realized via the use of a sequencing fed-batch bioreactor. This method also simultaneously retains the acclimated microbes to increase the H_2 production rate. We carried out the experiment in a Sartorius bioreactor with a working volume of 2 L. The medium was continuously sparged with N_2 at a flow rate of 16 ccm and agitated at 100 rpm. We used an HRT of 48 h, a liquid displacement of 50% working volume every 24 h, and four cycles each of carbon loadings of 2.5, 5.0, or 10 g/L of cellulose (with lignocellulose feedstock concentration adjusted based on cellulose content). The pretreated lignocellulose material contained 59% glucan, 3.9% xylan and 27.5% lignin, generated via acid hydrolysis, kindly supplied by the NREL National Bioenergy Center. In general the rate of H_2 increased proportionally when the cellulose substrate was increased from 2.5 g/L/d to 10 g/L/d, despite an accumulation of the undigested lignin, up to 28 g/L (Table 2). This finding is promising and suggests that lignin does not inhibit fermentation, a concern when fermenting lignocellulosic biomass. Total H_2 produced at 10 g/L/d feeding, however, was not proportional to that at

5 g/L/d, suggesting not all carbon substrate is consumed at this feeding.

TABLE 2. Rate and Yield of Hydrogen Production in Sequencing Fed-Batch Bioreactor with *Clostridium thermocellum* Fermenting Corn Stover Lignocellulose

Pretreated Corn Stover ($gL^{-1}d^{-1}$)	HRT (h)	Displacement volume (%)	Average H_2 Production ($mL\ L^{-1}\ D^{-1}$)	Maximum H_2 Production ($mL\ L^{-1}\ d^{-1}$)
2.5	**48**	50	239	474
5.0	**48**	50	550	974
10	**48**	50	902	1,466

Metabolic Engineering

The ultimate goal of this approach is to develop tools to inactivate genes encoding competing metabolic pathways, thus redirecting more cellular flux, i.e., electrons, to improve H_2 molar yield. Transformation in *C. thermocellum* has been challenging, likely due to either an inefficiency of the plasmids used or an incompatibility of the DNA restriction system between the host and the plasmid [8]. To circumvent both challenges, we have achieved the following: (1) redesigned an in-house plasmid with a gram-positive origin of replication suitable for *C. thermocellum*; (2) deleted the *dcm* gene in the *E. coli* host used for cloning purpose; and (3) used *C. thermocellum* strain DSM 1313 as the model cellulose-degrader. Following the protocols developed by Argyros et al. [9], we have created a mutant lacking the gene of interest encoding a specific competing pathway. The mutant yielded nearly 60% more ethanol. We have since used this strain as the recipient to delete the bifunctional acetaldehyde/ethanol dehydrogenase encoded by the *adhE* gene. We have undergone one round of selection based on resistance to the thiamphenicol antibiotic (indicating introduction of the plasmid), followed by two rounds of counter-selections using two suicide substrates (leading to gene knockout and loss of the plasmid). Work is ongoing to confirm the genotype via polymerase chain reaction, followed by phenotyping to quantify both ethanol and H_2 in the triple mutant lines.

Microbial Reverse-Electrodialysis Electrolysis Cell

The larger, redesigned MREC (Figure 1) had a total (anode and cathode chamber) volume of 315 mL. The reactor was initially fed and tested using a sodium acetate (0.8 g COD/L) amended 100 mM sodium bicarbonate buffer solution, followed by a synthetic fermentation effluent (1.2 g COD/L) containing glucose, lactate, ethanol, and bovine serum albumin in addition to the acetate. Following that, the substrate was shifted to diluted fermentation wastewater (1.2 g COD/L) provided by NREL. The catholyte was 1 M sodium bicarbonate (55 mS/cm) which was recycled at a rate of 8 mL/min. The reverse electrodialysis stack (10 cell pairs)

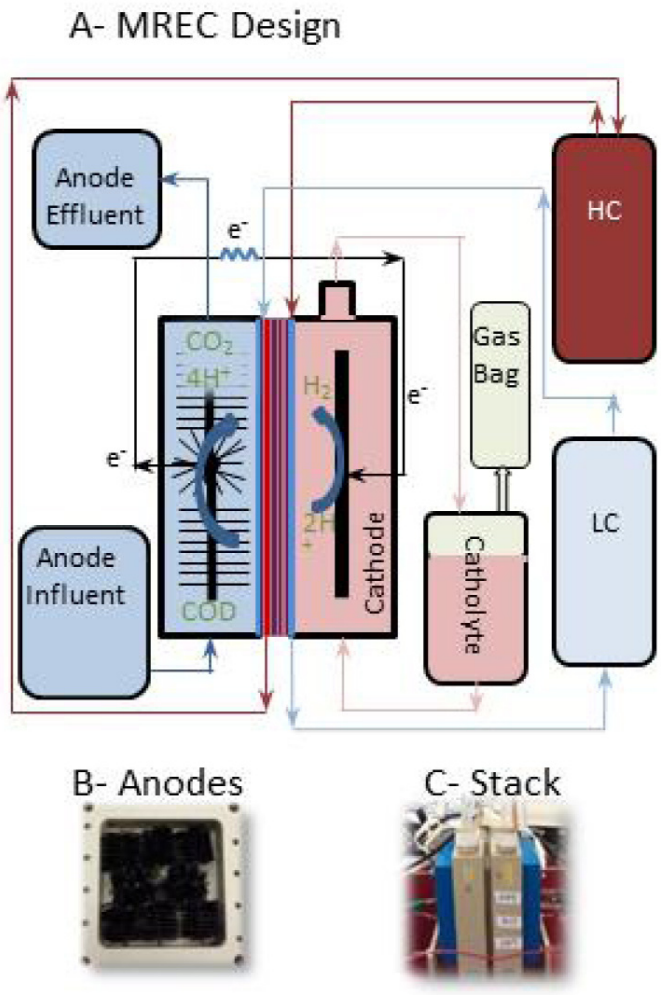

FIGURE 1. MREC Flow Diagram

was operated with 10 L of 1.4 M ammonium bicarbonate (90 mS/cm) as the high concentrate solution and distilled water (1 µS/cm) as the low concentrate solution, which were fed through the stack and recycled at a flow rate of 300 mL/min until the stack potential dropped to a point where there was minimal H_2 production. The anolyte HRT was varied between 8, 12 and 24 h.

At higher HRT (24 h), the anode potential was unstable, but at the shorter HRT (8 h), the anode potential stabilized and the MREC produced higher current densities, suggesting that there is a level where low COD along the length of the anode chamber severely limits current density (Figure 2). The maximum volumetric current densities obtained with fermentation wastewater (78–110 A/m^3, 8 h HRT, 0.6–0.75 V stack potential) decreased slightly compared to that obtained with the synthetic wastewater (100–130 A/m^3). H_2 production rate increased from 0.3 to 0.9 $L\text{-}H_2\ L_{reactor}^{-1}\ d^{-1}$ and H_2 yields increased from 0.8 to 1.0 L/g COD when HRT was decreased from 24 h to 8 h (Figure 3). The composition of gas collected

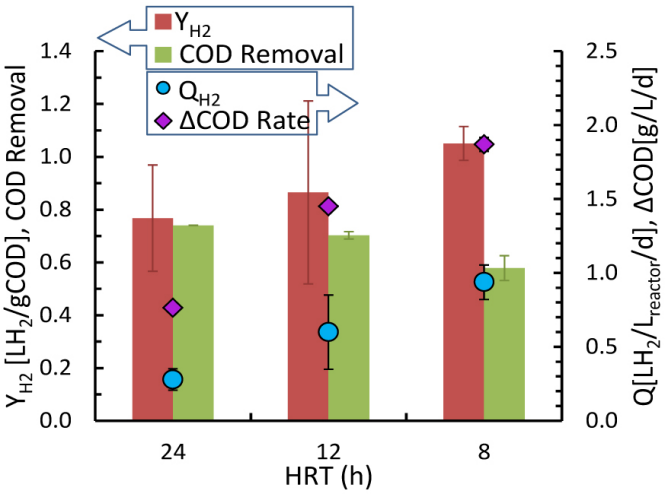

FIGURE 2. Current Generation from Continuous flow MREC using Fermentation Wastewater at HRTs of 8, 12 and 24 h

was 93–96% H_2 with the balance as CO_2. COD removal decreased from 73% to 60% with the decrease in HRT, but the rate at which COD was removed increased from 0.8 g/L/d to 1.9 g/L/d (Figure 3).

Protein Removal

MEC anodes were conditioned separately to degrade acetate or protein in order to increase the protein removal while maximizing H_2 production by utilizing a system with two reactors in series. Acetate fed anodes would not produce appreciable current, and current levels in protein fed reactors were limited on startup, in 100 mM sodium bicarbonate at pH 8.2 to 9. At a buffer pH of 7.6, all anodes started to acclimate rapidly to produce current. Optimal HRT is being tested for both acetate and protein removal and then the reactors will be tested in series.

CONCLUSIONS AND FUTURE DIRECTION

- Using corn stover lignocellulose (2.5-10 g/L based on cellulose content) as the substrate in a sequencing fed-batch reactor, an HRT of 48 h, and displacing 50% of the reactor liquid volume at 24 h intervals, rate of H_2 was proportional to the amount of substrate feeding. The outcomes also indicate that the accumulation of up to 28 g lignin/L does not inhibit rate of H_2 production, a promising finding for using lignocellulose as the feedstock.
- Following published protocols and using the NREL proprietary plasmid, we deleted the gene of interest. Its phenotype of increased ethanol production guided the design to delete the ethanol competing pathway. Work is ongoing toward making this triple mutant and quantifying ethanol and H_2 production. The outcome should aid in future site-directed mutagenesis effort by deleting multiple competing pathways to improve hydrogen molar yield.

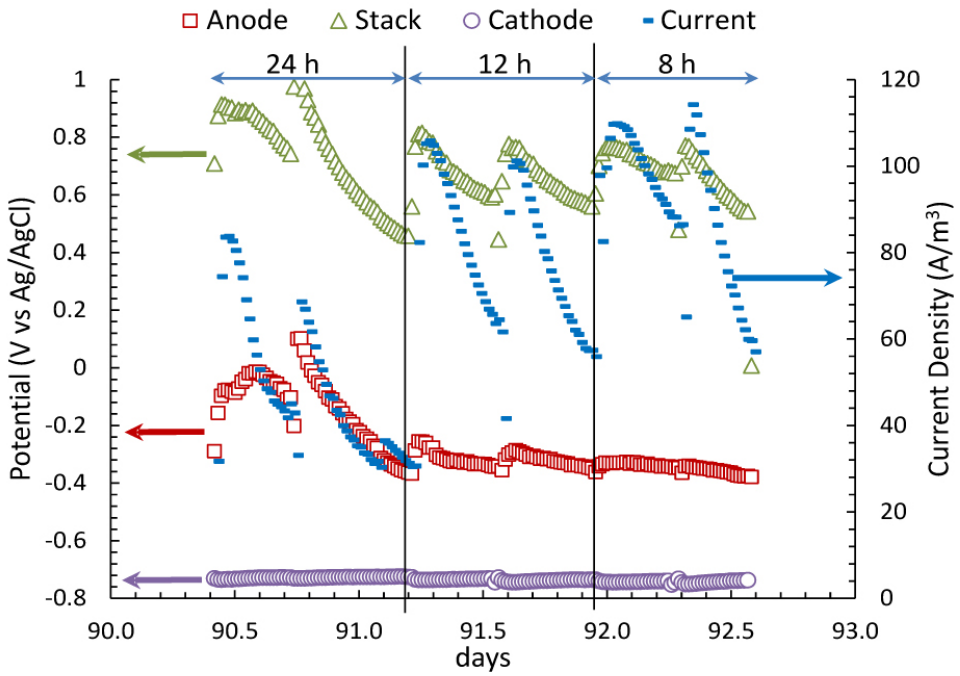

FIGURE 3. Hydrogen Generation and COD Removal from Continuous Flow MREC Treating Fermentation Wastewater at HRTs of 8, 12 and 24 h

- Larger scale MRECs can be used to produce H_2 without net use of electrical grid energy. HRT has a significant impact on the anode potential and the current produced in the MREC. There is a level where the COD drop within the anode chamber negatively impacts the anode potential and severely limits current density and hydrogen production, suggesting the use of a two stage system for increased COD removal with maximum H_2 production rates.

In the future, we will operate the fed-batch bioreactor fermenting corn stover lignocellulose generated from a de-acetylated process vs. the acid-hydrolysis pretreatment used at present. De-acetylation reaction is a milder pretreatment process and hence eliminates the non-specific binding of lignin to cellulose. The latter has rendered the lignocellulose less fermentable. We will determine ethanol and H_2 production profiles in the triple mutants with the outcomes guiding future mutagenesis efforts to delete multiple competing pathways, aimed to improve H_2 molar yield. In the future, we will continue to evaluate the performance of reactors in series, operated at different HRTs and applied potentials, for COD and protein removal efficiency as well as H_2 production rates. We will also be looking at maximizing H_2 production rates while decreasing the electrode cost by exploring the use of non-precious metal cathodes.

FY 2014 PUBLICATIONS/PRESENTATIONS

1. Wei, H., Y. Fu, L. Magnusson, J.O. Baker, P.C. Maness, Q. Xu, S. Yang, A. Bowersox, I. Bogorad, W. Wang, M.P. Tucker, M.E. Himmel, and S-Y. Ding. 2014. Comparison of transcriptional profiles of *Clostridium thermocellum* grown on cellobiose and pretreated yellow poplar using RNA-Seq. Frontiers in Microbiology 5: Article 142.(doi: 10.3389/fmicb.2014.00142).

2. Nam, J.-Y., M. Yates, Z. Zaybak, and B.E. Logan. Factors affecting protein degradability in a continuous microbial electrolysis cell treating fermentation wastewater. *Bioresource. Technol. Submitted* July 2014.

3. Watson, V.J. and B.E. Logan. Effect of hydraulic retention time on hydrogen production and organics removal from fermentation effluent using a continuous flow microbial reverse-electrodialysis electrolysis cell. Kappe Environmental Engineering Seminar, Penn State University, March 6, 2014.

4. "Metabolic engineering of *Clostridium thermocellum* for H_2 production", oral presentation at the MGCB2 annual review (collaboration with and paid for by the Genome Canada Program). March 18, 2014, Winnipeg, Canada (Chou).

5. Watson, V.J., M. Hatzell, and B.E. Logan. Hydrogen production from fermentation effluent using a continuous flow microbial reverse-electrodialysis electrolysis cell. Poster presentation at NA-ISMET Conference, Penn State University, May 14–15, 2014.

6. "Hydrogen Production from Cellulose in *Clostridium thermocellum*", poster presentation at the 114th General Meeting of the American Society for Microbiology, May 17–20, 2014, Boston (Chou).

7. Maness, P.C. and Logan, B. 2014. DOE Fuel Cell Technology Office Annual Merit Review, June 19 2014, Washington, DC. Presentation PD038.

REFERENCES

1. Zhang, Y.P.; Lynd, L.R. (2005). Cellulose utilization by *Clostridium thermocellum*: bioenergetics and hydrolysis product assimilation. *Proc. Natl. Acad. Sci. USA* **102**, 7321–7325.

2. Hawkes, F.R.; Dinsdale, R.; Hawkes, D.L.; Hussy, I. (2002). Sustainable fermentative hydrogen production: Challenges for process optimisation. *Intl. J. Hydrogen Energy* **27**, 1339–1347.

3. Logan, B.E.; Oh, S.E.; Kim, I.S.; Van Ginkel, S. (2002). Biological hydrogen production measured in batch anaerobic respirometers. *Environ. Sci. Technol.* **36**, 2530–2535.

4. Van Ginkel, S.; Sung, S. (2001). Biohydrogen production as a function of pH and substrate concentration. *Environ. Sci. Technol.* **35**, 4726–4730.

5. Rachman, M.A.; Furutani, Y.; Nakashimada, Y.; Kakizono, T.; Nishio, N. (1997). Enhanced hydrogen production in altered mixed acid fermentation of glucose by *Enterobacter aerogenes. J. Ferm. Eng.* **83**, 358–363.

6. Cheng, S.; Logan, B. E. (2007). Sustainable and efficient biohydrogen production via electrogenesis. *Proc. Natl. Acad. Sci. USA.* **104**, 18871–18873.

7. Lalaurette, E.; Thammannagowda, S.; Mohagheghi, A.; Maness, P.C.; Logan, B.E. (2009). Hydrogen production from cellulose in a two-stage process combining fermentation and electrohydrogenesis. *Intl. J. Hydrogen Energy* **34**, 6201–6210.

8. Guss, A.; Olson, D.G.; Caiazza, N.C.; Lynd, L.R. (2012). Dcm methylation is detrimental to plasmid transformation in *Clostridium thermocellum*. *Biotechnol. Biofuels* **5**, 30–41.

9. Argyros, D.; Tripathi, S.A.; Barrett, T.F.; Rogers, S.R.; Feinberg, L.F.; Olson, D.G.; Foden, J.M.; Miller, B.B.; Lynd, L.R.; Hogsett, D.A.; Caiazza, N.C. (2011). High ethanol titers from cellulose by using metabolically engineered thermophilic anaerobic microbes. *Appl. Environ. Microbiol.* **77**, 8288–8294.

II.E.4 Probing O_2-Tolerant CBS Hydrogenase for Hydrogen Production

Pin-Ching Maness (Primary Contact), Carrie Eckert, Scott Noble, and Jianping Yu
National Renewable Energy Laboratory (NREL)
15013 Denver West Parkway
Golden, CO 80401
Phone: (303) 381-6114
Email: pinching.maness@nrel.gov

DOE Manager
Katie Randolph
Phone: (720) 356-1759
Email: Katie.Randolph@ee.doe.gov

Project Start Date: May 1, 2005
Project End Date: Continuation and direction determined annually by DOE

Overall Objectives

- Decipher the maturation machinery of the O_2-tolerant hydrogenase in *Rubrivivax gelatinosus* to transfer the correct number of genes to build a cyanobacterial recombinant.
- Construct a cyanobacterial recombinant by expressing four hydrogenase genes and six maturation genes from *R. gelatinosus* for sustained H_2 production.
- Demonstrate H_2 production in the cyanobacterial recombinant during photosynthesis for photolytic H_2 production.

Fiscal Year (FY) 2014 Objective

Develop an O_2-tolerant cyanobacterial system for sustained and continuous light-driven H_2 production from water.

Technical Barrier

This project addresses the following technical barrier from the Hydrogen Production section (3.1.4) of the Fuel Cell Technologies Office Multi-Year Research, Development, and Demonstration Plan:

(AP) Oxygen Accumulation

Technical Targets

Characteristics	Units	2011 Target	2015 Target	2020 Target	Ultimate Target
Duration of continuous H_2 production at full sunlight intensity	Time units	2 min	30 min	4 h	8 h

FY 2014 Accomplishments

- Based on amino acid homology comparison of the newly sequenced genome, we uncovered additional hydrogenase maturation genes in *Rubrivivax gelatinosus* Casa Bonita strain (hereafter "CBS"). They are *slyD* and *carAB*; the former is responsible for Ni insertion and the latter for the synthesis of carbon-nitrogen ligand. Both are likely involved in assembling the CBS hydrogenase active site. *Synechocystis* contains *carAB*, but not *slydD*; hence, only *slyD* will be genetically transferred into *Synechocystis* to assemble the O_2-tolerant CBS hydrogenase.
- We used the strong *psbA* promoter to drive the expression of CBS hydrogenase maturation gene *hypF*, in a *Synechocystis* recombinant already expressing CBS hydrogenase and five of the maturation genes (*hypABCDE*). When compared to the original weaker *petE* promoter, HypF protein levels increased by near 9-fold with the strong *psbA* promoter. Yet, the *Synechocystis* recombinant still failed to yield hydrogenase activity, warranting the refactoring of the genetic construct to afford activity.

✧ ✧ ✧ ✧ ✧

INTRODUCTION

Photobiological processes are attractive routes to renewable H_2 production. With the input of solar energy, photosynthetic microbes such as cyanobacteria and green algae carry out oxygenic photosynthesis using solar energy to extract reducing equivalents (electrons) from water. The resulting reducing equivalents can be fed to a hydrogenase system yielding H_2. However, one major barrier is that most hydrogen-evolving hydrogenases are inhibited by O_2, which is an inherent byproduct of oxygenic photosynthesis. The rate and duration of H_2 production is thus limited. Certain photosynthetic bacteria are reported to have an O_2-tolerant, H_2-evolving hydrogenase, yet these microbes do not split water and require other more expensive feedstock.

To overcome these technical barriers, we propose to construct novel microbial hybrids by genetically transferring O_2-tolerant hydrogenases from other bacteria into cyanobacteria. These hybrids will use the photosynthetic machinery of the cyanobacterial hosts to perform the water-oxidation reaction with the input of solar energy, and couple the resulting reducing equivalents to the O_2-tolerant bacterial hydrogenase, all within the same microbe. By overcoming the sensitivity of the hydrogenase enzyme to O_2, we address one of the key technological hurdles (barrier AP) to cost-effective photobiological H_2 production, which currently limits the production of H_2 in photolytic systems.

APPROACH

Our goal is to construct a novel microbial recombinant, taking advantage of the most desirable properties of both cyanobacteria and other bacteria, to serve as the basis for technology to produce renewable H_2 from water and solar energy. To achieve this goal, we transfer known O_2-tolerant hydrogenase from CBS to the model cyanobacterium *Synechocystis* sp. PCC 6803.

RESULTS

Probing Hydrogenase Maturation Machinery in CBS

The overarching goal is to construct a cyanobacterial recombinant harboring the O_2-tolerant hydrogenase from CBS using *Synechocystis* sp. PCC 6803 as a model host for sustained photolytic H_2 production. A prerequisite for success is to gain better understanding of the CBS hydrogenase and its underlying maturation machinery to ensure transfer of the correct genes into *Synechocystis* to confer hydrogenase activity. CBS genome was sequenced and annotated in FY 2013 by Michigan State University and Pacific Biosciences. Using the Basic Local Alignment Search Tool – Protein (BLASTP) tool, we uncovered a second set of hydrogenase maturation genes (*hyp2*) in the CBS genome, which is different from the set of hydrogenase maturation genes found earlier (*hyp1*). This raises the question as to which set of maturation genes is responsible for building an active CBS hydrogenase and needs to be co-transformed along with the CBS hydrogenase into *Synechocystis*. As such we conducted a detailed comparison of CBS *hyp1* with *hyp2*, as well as with other known hydrogenase maturation proteins. These data will provide the blueprint to guide genetic engineering effort toward constructing a *Synechocystis* recombinant harboring O_2-tolerant hydrogenase activity. The homology comparison in Table 1 using BLASTP reveals that CBS *hyp1* is quite different from CBS *hyp2* based on low level of identity (34–58%). Data from Table 2 show the homology comparison of CBS *hyp1* and CBS *hyp2* with the *hyp* genes known to be involved in the maturation of a well-studied uptake hydrogenase in *Ralstonia eutropha* (Re). The higher level of identity between Re *hyp* genes with CBS *hyp2* (60% to near 80%), but not with *hyp1,* clearly supports that CBS *hyp2* genes are involved in the maturation of the uptake hydrogenase in CBS, while the CBS *hyp1* genes are involved in the maturation of the O_2-tolerant evolving hydrogenase.

TABLE 1. Homology Comparison (% amino acid identity) of CBS Hyp1 with Hyp2 Proteins

CBS Hyp Proteins	Hyp1 vs. Hyp2 (%)
HypA	34.5
HypB	53.6
HypC	39.2
HypD	50.9
HypE	53.8
HypF	37.2

TABLE 2. Homology Comparison (% amino acid identity) of the Hyp proteins from *Ralstonia eutropha* with the respective Hyp1 and Hyp2 proteins from CBS

Ralstonia eutropha	CBS Hyp1 (%)	CBS Hyp2 (%)
HypA	31.0	65.5
HypB	52.3	67.4
HypC	38.4	59.5
HypD	47.4	77.3
hypE	54.0	74.4
HypF	38.4	60.2

Moreover, after careful search of the CBS genome, we identified a single *slyD* homolog which displays 33% amino acid identity to its counterpart in *E. coli,* which was used as the model system to probe maturation of NiFe-hydrogenases. *Synechocystis* genome does not contain a SlyD homolog based on a BLASTP search. Studies in *E. coli* suggest that carbamoyl phosphate synthase (encoded by *carAB*) is necessary for hydrogenase maturation. This enzyme complex synthesizes carbamoyl phosphate, the precursor for carbon-nitrogen ligand, which is an integral component of the hydrogenase active site. A search of the CBS genome revealed *carA* and *carB* homologs with 64% and 70% identity, respectively, to the homologs in *E. coli*. CarA and CarB homologs with 51% and 60% identity, respectively, are present in *Synechocystis.* Therefore, we may need to minimally evaluate the expression of CBS *slyD* in addition to the *hyp1* genes in order to obtain a more active CBS hydrogenase in *Synechocystis*.

Expression of the CBS Hydrogenase in *Synechocystis*

One strategy to increase H_2 production is to increase the amount of active CBS hydrogenase expressed in *Synechocystis* by using stronger promoters. We have systematically re-engineered the *Synechocystis* recombinant using the strong *psbA* promoter to drive the expression of

cooLXUH (encoding CBS hydrogenase) and *psbA2* promoter to drive the expression of *hyp1ABCDE*. The resultant recombinant is *psbA-LXUH/psbA2-ABCDE*. Moreover, we incorporated the CBS maturation gene *hypF* in the above recombinant driven by the strong *psbA* promoter. We first produced a plasmid where the weak promoter *petE* was replaced with *psbA* promoter, with its replacement confirmed by restriction digest analysis and sequencing. We then transformed this plasmid into *Synechocystis* (*psbA-LXUH/psbA2-ABCDE)* and confirmed the integration of *psbA-hypF* into the *Synechocystis* genome via colony polymerase chain reaction (PCR) in 8 out of 18 colonies tested (Figure 1A). Expression of HypF protein was determined via protein immunoblots. We detected that HypF expression was enhanced from 1.7- to 8.9-fold in these strains (*psbA-LXUH/psbA2-ABCDE/psbA-hypF*) when driven by the strong *psbA* promoter, when compared to expression using the weak *petE* promoter (Figure 1B). Yet, the engineered strain failed to yield hydrogenase activity.

To troubleshoot, expression levels need to be carefully quantified for further improvements. Therefore, we performed quantitative protein immunoblots of CooLXUH and Hyp1EF (based on available antibodies) to compare levels of each CBS protein in CBS to that in *psbA-LXUH/psbA2-hypABCDE/psbA-hypF.* It was clear from the results that only CooU, CooH, and HypE1 were expressed at detectable levels in the *Synechocystis* strain, and levels were much lower than those seen in CBS, the latter loaded with two-third less protein (data not shown). This imbalanced protein expression prompted us to redesign the expression construct (Figure 2) that employs the strong *trc* promoter from *E. coli,* which has shown up to 80 times higher expression levels in *Synechocystis* when compared to native promoters [1]. In addition, we also integrated a consensus ribosomal binding site from *Synechococcus* 7002 (cpcB gene) shown to have high levels of expression in *Synechocystis* [2] in front of each gene to be expressed to maximize translational efficiencies. Because we may need to break up the expression constructs

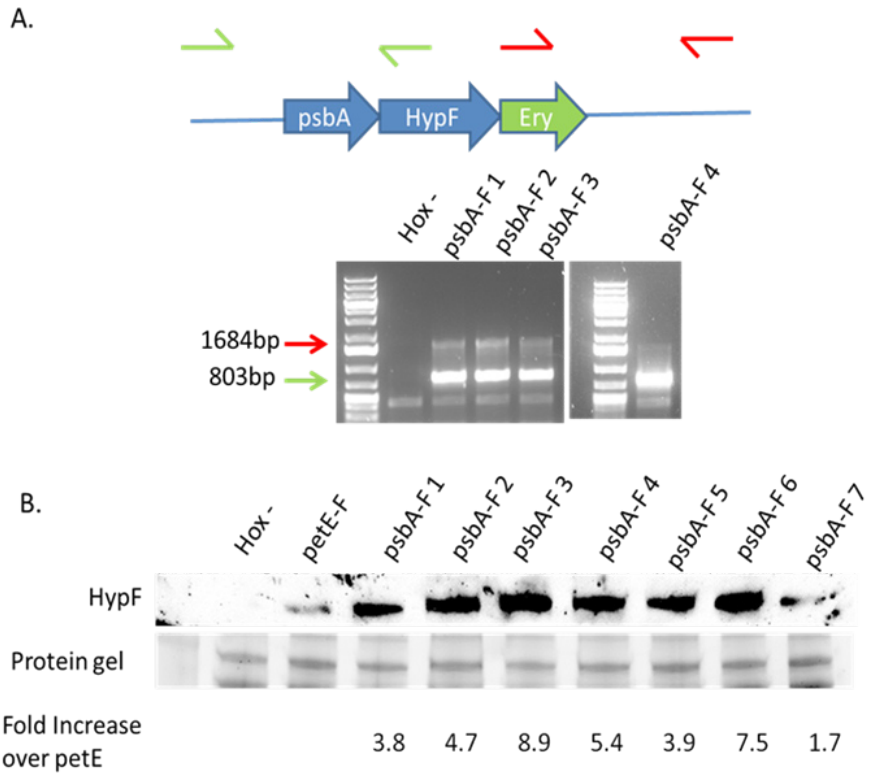

FIGURE 1. Integration and Enhanced Expression of HypF in ***psbA-LXUH/psbA2-ABCDE/psbA-hypF*** Strains—Panel A shows colony PCR confirming the integration of *psbA-hypF* into the *Synechocystis* genome. Primers upstream, downstream, and within the integrated construct (red and green arrows denoting forward and reverse primers) should produce two products of 803 bp and 1648 bp in size. PCR of colonies confirmed the correct integration of the construct into the *Synechocystis* genome. Panel B shows a western immunoblot against the CBS HypF protein. The new recombinants containing the *psbA-hypF* construct displayed a higher level of expression compared to that of the control with *petE-hypF*. Fold increase was calculated by normalizing to a constant band in the protein gel and comparing levels of *psbA-hypF* to the *petE-hypF* recombinant.

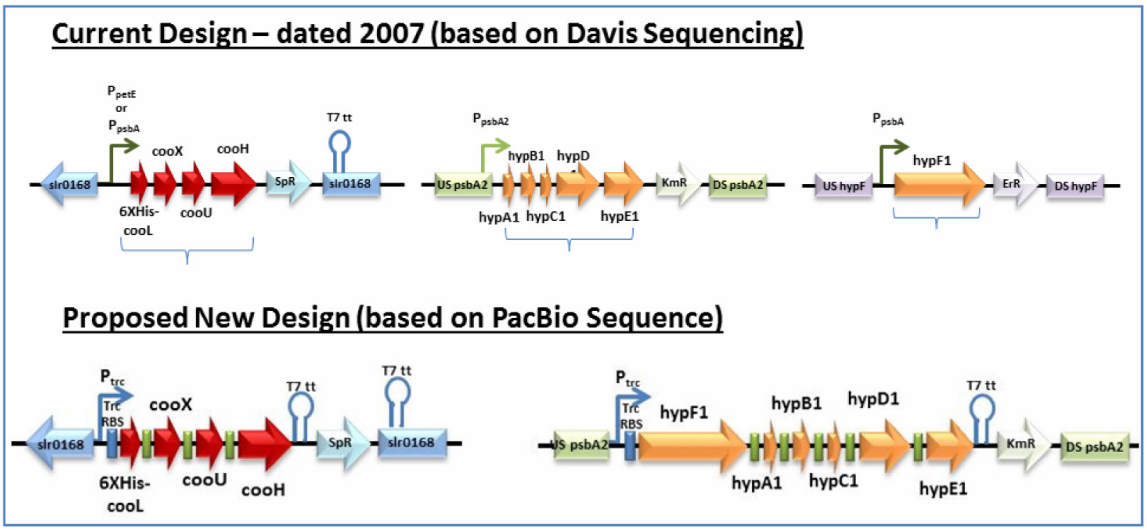

FIGURE 2. Current and Proposed New Design to Express the CBS Hydrogenase and Maturation Genes in *Synechocystis*

into smaller number of genes expressed per promoter, we have also inserted unique restriction sites between each gene to allow for the insertion of additional promoters if necessary. The new design is modular, affording flexibility in tuning and balancing gene expression individually, on a need basis, to ultimately afford O_2-tolerant hydrogenase activity in *Synechocystis*.

CONCLUSIONS AND FUTURE DIRECTIONS

Conclusions

- Amino acid homology comparison reveals that *hyp1* and *hyp2* are dissimilar, with *hyp2* displaying high level of homology with the *hyp* genes in *R. eutropha*, known to assemble its H_2-uptake hydrogenase. As such, *hyp1* likely assembles the O_2-tolerant CBS hydrogenase. *slyD*, which has a putative role in Ni insertion, was identified in CBS also, but not in *Synechocystis*. Initial work will focus on expressing *hyp1* and *slyD* genes along with CBS hydrogenase in *Synechocystis*.
- Use of the strong *psbA* promoter dramatically enhanced CBS hydrogenase maturation protein HypF expression levels by near 9-fold in *Synechocystis*, yet the recombinant still lacks hydrogenase activity. We propose to re-engineer the CBS gene construct to incorporate strong *trc* promoter and proven ribosome binding sites to afford hydrogenase activity.

Future Directions

- Further investigate the roles of CBS *hyp1* and *hyp2* in hydrogenase maturation by directly examining CO uptake and H_2 production in the *hyp1* and *hyp2* single and double mutants.
- Transform the new designs containing *cooLXUH*, followed by *hyp1* operons to ensure balanced protein expression. If the protein expression is not balanced, we will troubleshoot by inserting more frequent *trc* promoters in between each gene to tune expression. In conjunction with this iterative approach, we will perform in vitro hydrogenase activity assay using reduced methyl viologen as the mediator.

FY 2014 PUBLICATIONS/PRESENTATIONS

1. Ghirardi, M.L.; King, P.W.; Mulder, D.W.; Eckert, C.; Dubini, A.; Maness, P.C.; Yu, J. 2013. "Hydrogen production by water biophotolysis." *Microbial Bioenergy: Hydrogen Production*, Advances in Photosynthesis and Respiration series (D. Zannoni and R. De Philippis, eds.), p. 101-135.

2. Maness, P.C. "Genetic analysis of the Hox hydrogenase in the cyanobacterium *Synechocystis* sp. PCC 6803." Oral presentation at the 10th International Hydrogenase Conference, July 8-12, 2013, Szeged, Hungary.

3. Maness, P.C. "Hydrogen from water in a novel recombinant O_2-tolerant cyanobacterial system." Presentation at the Hydrogen Production Tech Team Review. July 30, 2013, PNNL, Richland, WA.

4. Maness, P.C. "Improving cyanobacterial O_2-tolerance using CBS hydrogenase for hydrogen production." Presentation at the DOE Hydrogen and Fuel Cells Annual Merit Review, June 19, 2014, Washington, DC (PD095).

REFERENCES

1. Huang, H.-H., D. Camsund, P. Lindblad, and T. Heidorn. 2010. Design and characterization of molecular biology tools for a synthetic biology approach towards developing cyanobacterial biotechnology. Nucleic Acids Res. 38: 2577-2593.

2. Abe, K., K. Miyake, M. Nakamura, K. Kojima, S. Ferri, K. Ikebukuro, and K. Sode. 2014. Engineering a green-light inducible expression system in *Synechocystis* sp. PCC 6803. Microbial Biotech., 7: 177-183.

II.F.1 Bio-Fueled Solid Oxide Fuel Cells

Gökhan Alptekin (Primary Contact),
Ambal Jayaraman
TDA Research, Inc.
12345 W 52nd Ave
Wheat Ridge, CO 80033
Phone: (303) 940-2349
Email: galptekin@tda.com

DOE Manager
Sara Dillich
Phone: (202) 586-7925
Email: Sara.Dillich@ee.doe.gov

Contract Number: DE-EE0004537

Subcontractors
- FuelCell Energy (FCE), Danbury, CT
- Sacramento Municipal Utility District (SMUD), Sacramento, CA

Project Start Date: October 1, 2010
Project End Date: September 30, 2014

Overall Objectives

Demonstrate the operation of a bio-fueled solid oxide fuel cell (SOFC) integrated with a cost-effective contaminant control system in a waste-to-energy application

Fiscal Year (FY) 2014 Objectives

- Complete the fabrication of the 2-kW_e bio-fueled SOFC module
- Integrate the biogas cleanup skid and the SOFC skid and carry out a successful field demonstration with biogas at the Cal-Denier Dairy Farm
- Prepare a detailed cost analysis and economic assessment of the biogas-fueled SOFC system

Technical Barriers

This project addresses the following technical barriers from the Hydrogen Production section of the Fuel Cell Technologies Office Multi-Year Research, Development, and Demonstration Plan:

- Cost Effective Separation of Impurities and High-Efficiency Electricity Production from Renewable Feed Stocks
- SOFCs are known to provide the highest possible net efficiency for Combined Heat and Power (CHP) applications. Hence, there is a need to demonstrate successful operation of SOFC on biogas and this project serves this need
- Impurities present in biogas (such as organic sulfur species and siloxanes) poison the catalysts and SOFC stacks, reducing their efficiency and lifetime, and must be removed to a concentration of less than 10 ppbv

Technical Targets

This project will demonstrate the operation of a bio-fueled SOFC integrated with a cost-effective contaminant control system in a waste-to-energy application. The specific targets/goals are:

- Develop and demonstrate the efficacy of a sorbent-based gas clean-up system to remove harmful impurities from biogas such as sulfur and siloxane to less than 0.1 ppmv
- Demonstrate operation of a 2-kW_e biogas-fueled SOFC stack integrated with a biogas cleanup system in a waste-to-energy application
- Demonstrate the economic viability of our biogas cleanup technology

FY 2014 Accomplishments

- Project partner FCE has completed the fabrication of the 2-kW_e SOFC module, which is currently being tested at their facility using simulated gases
- Interface requirements between the biogas cleanup skid and SOFC skid have been identified and TDA has completed the design of the interface skid
- TDA in collaboration with SMUD has completed an assessment of the site modifications needed at the Cal-Denier Dairy test site
- Integrated field tests with cleanup and SOFC skids are scheduled to start at the Cal Denier Dairy Farm in August 2014

✧ ✧ ✧ ✧ ✧

INTRODUCTION

The energy potentially available from bio-waste approaches 1.46 quadrillion Btu, only a small amount of which is currently utilized. The use of this domestic renewable source will reduce U.S. dependence on fossil fuels and greenhouse gas emissions. Fuel cells have a great potential for immediate use in biogas based distributed hydrogen and power generation systems, if cost-effective gas clean up system were available. Distributed fuel cell power generation is becoming a viable alternative to buying

power from a central grid, particularly for dairy farms, food industries and waste water treatment plants that produce anaerobic digester gas (ADG). However, impurities (such as organic sulfur species and siloxanes contaminants in the ADG) must be removed from the ADG to prevent degradation of the fuel cell stacks and poisoning of the catalysts used in the fuel processor. Even for the more sulfur-tolerant SOFCs, the sulfur and siloxane concentrations must be reduced to less than 0.1 ppmv.

In the previous SBIR Phase I and Phase II projects, TDA developed a low-cost, high-capacity sorbent that can remove sulfur-bearing odorants from natural gas and liquefied petroleum gas. TDA demonstrated the performance of the desulfurization sorbent first in bench scale and then in the field, integrated with fuel cell systems (with fuel cell stacks, fuel processor and all auxiliary items). The technology was commercialized under the SulfaTrap™ name, and spun-off SulfaTrap, LLC as a separate business in 2013 and are now supplying multi-ton quantities to fuel cell generators operating around the world on natural gas and liquefied petroleum gas. In this Phase III research TDA in collaboration with FCE, will demonstrate the ability of our sorbent to operate in a regenerable manner to carry out bulk desulfurization of biogas, which will then be used in a 2-kW_e bio-fueled SOFC generator. Successful demonstration of the integrated system will enable widespread adoption of small-scale high-efficiency bio-fueled SOFC-based combined heat and power systems.

APPROACH

TDA's approach is to use an ambient temperature gas clean-up system to remove all contaminants to ppbv levels. The purification system includes a bulk desulfurization system (regenerable) followed by an expendable polisher (Figure 1). The key requirement for the sorbent is tolerance to high levels of moisture (biogas is expected to have at least 4,000 ppmv moisture) to eliminate the energy penalty for biogas compression and chilling that are needed with conventional gas cleanup systems. The commercial systems are also known to contribute to the formation of very complex sulfur species that are difficult to remove, such as the di- and tri-sulfides. TDA's polishing bed is designed to remove siloxanes and the organic sulfur species. In collaboration with SMUD integrated field tests with a 2-kW_e bio-fueled SOFC module from FCE will be carried out with TDA biogas desulfurization sorbents at Cal-DeNier Dairy, Grand Valley, CA.

RESULTS

Prototype Biogas Cleanup Unit

The regenerable desulfurizer demonstration skid is designed to test TDA's regenerable sulfur sorbent from a gas treatment slipstream. Suitable slipstreams could come from landfills, waste water treatment plants or dairy farms (ADG), or natural gas pipelines. The flowrate through the skid is adjustable, but system design was based on a nominal 50 scfm. The system is equipped with an online H_2S sensor that can be manually set to measure H_2S concentration at the inlet or outlet of the regenerable beds, or downstream of the polisher bed. Other instrumentation includes the O_2 sensor for verifying that post-regeneration purge has been completed, as well as and various pressure and temperature transmitters and indicators.

The fabrication of the prototype system was completed in FY 2013. Figure 2 shows the picture of the prototype test system. The entire system is compactly mounted on a powder-coated steel skid that is 8 feet long and 4 feet wide. The height of the skid is roughly 6 feet. All electrical components have been constructed for a Class 1, Div 2 hazardous location with a Z-purge on the electronics boxes. The skid is designed to be operated outdoors in any weather. System automation is implemented with LabVIEW software running on a National Instruments cRIO controller. The automation is headless, meaning there is no laptop or other computer required for the system to operate. All data will be logged to a file for later viewing and analysis. The user can also connect wirelessly to the system to view the current system state and change settings such as adsorption time or temperature.

In FY 2014, shakedown and system checkout were performed, verifying all aspects of the safety systems, normal operations and regeneration capabilities of the demonstration unit with the reactors fully loaded with the

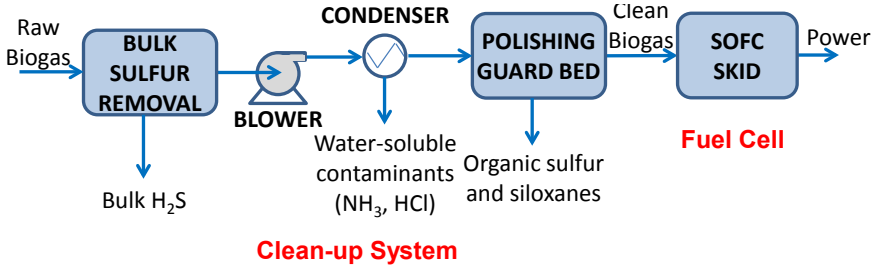

FIGURE 1. TDA's Biogas Clean-Up System Integrated with a SOFC

FIGURE 2. TDA's Biogas Clean-Up Skid

SulfaTrap™ sorbent. The final system automation program modifications that are needed for remotely controlling and monitoring the desulfurizer skid have been completed and verified. The skid will operate in an autonomous manner, but can be viewed either locally or through the internet with this program. The skid-mounted cellular router makes this remote connection possible; it also allows data retrieval.

SOFC Module Development at FCE

FCE completed the fabrication of the 2-kW_e bio-fueled SOFC skid. Figure 3 shows FCE's integrated 2-kW_e bio-fueled SOFC skid with the tilted façade feature. The electrical balance of plant was assembled concurrently with mechanical balance of plant and the hot components section (fuel cell, reformer, anode gas oxidizer) was completed subsequently. Prior to completion of the hot components section both the 16-cell SOFC stack and the 25-cell SOFC stack were tested for gas tightness. The 16-cell stack was then compressed and installed in the hot components section. FCE has completed the programming of the programmable logic controller. Full functional test of the power conversion system was completed by FCE. The power conversion system consists of a DC/DC converter that boosts the fuel cell output of 10-13 VDC to regulated 24 VDC, useful for the second power conversion system stage. The second

FIGURE 3. FCE's Integrated 2-kW_e Bio-Fueled SOFC Skid

stage consists of a DC/AC inverter that converts 24 VDC to 120/240 VAC. This inverter is a commercial device originally designed for solar photovoltaic applications and FCE had made appropriate modifications to operate it with a fuel cell power source. Functional testing of the DC/DC converter had verified the high efficiency of power conversion as stated by the manufacturer. Power quality was verified as well as minimum input voltage necessary for operation. Functional testing of the DC/AC inverter showed that the inverter could be grid-connected with power export and sell capability. Testing also showed that the inverter supports island mode operation where the unit is disconnected from the grid and is powered internally from the fuel cell. The HMI for the bio-fueled SOFC had been completed.

The 2-kW_e bio-fueled SOFC skid is undergoing factory testing at FCE. Prior to factory testing, which is a live testing procedure, the unit is being dry tested (functional testing). This initially consists of instrument checkout and major component testing, where natural gas fuel is not involved. This testing is now complete and successful. The next step will be testing with natural gas and then a change out of SOFC stacks. The 16-cell SOFC will be replaced by a 25-cell SOFC prior to shipment to the SMUD demonstration site.

Site Conditioning

In order to demonstrate the capabilities of the regenerable desulfurizer skid, the apparatus will be taken to the Cal-Denier Dairy farm in Galt, California. In preparation for this we completed an assessment of the plumbing and electrical modification requirements at the site. TDA has designed an interface skid that will be built on-site to tie the two skids, i.e., TDA's desulfurization skid and FCE's SOFC

FIGURE 4. Cal-Denier Demonstration Pad

skid. Figure 4 shows the enclosed building and covered demonstration pad area of the farm. The electrical service to the building is 480-VAC 3-phase power and a spare 150 amp circuit breaker is available to power the demonstration skid. The electrical requirements of the skid are 50 mp of 480-VAC 3-phase so there is excess power already available on-site. The far side of the pad has an I-Power Energy Systems ENI 65-kW combined heat and power generator that is currently operating and generating electricity with the biogas from the digester pond. The raw biogas is compressed to about 1-2 psig with a regenerative blower in the enclosed area in the demonstration pad, which has been identified as the place for locating the two demonstration skids. We have identified the outlet of the regenerative blower as a convenient place to tee in a supply line to the desulfurizer skid. The outlet from the desulfurization skid can either be fed to the SOFC skid (during integrated testing) or flared (during stand-alone operation). A sample of the biogas H_2S level was conducted and the levels were between 2,000 and 2,500 ppmv. TDA's desulfurization skid was shipped to the site on July 24, 2014. We will install the "interface skid" onsite in the week of August 4, 2014 and will commence stand-alone operation in the week of August 11, 2014.

CONCLUSIONS AND FUTURE DIRECTIONS

Successful demonstration is key for wide spread utilization of the SOFCs and TDA's biogas clean-up technologies in biogas applications. The remaining activities include:

- Integration of the biogas cleanup skid and the SOFC skid
- Successful field demonstration with biogas at Cal DeNier Dairy Farm
- Detailed cost analysis and economic assessment of the biogas-fueled SOFC system

FY 2014 PUBLICATIONS/PRESENTATIONS

1. Jayaraman, A., Alptekin, G., Schaefer, M., Cates, M., Ware, M., Hunt, J., Tiangco, V.M. "Novel Sorbents to Clean Up Biogas for Fuel Cell CHP Systems" at the 2013 Fuel Cell Seminar & Exposition held between October 21–24, 2013 in Columbus, OH.

2. Jayaraman A., Alptekin, G., "Bio-Fueled Solid Oxide Fuel Cells" at the DOE EERE Annual Merit Review Meeting held between June 16–20, 2014 in Washington, D.C.

II.G.1 Semiconductor Nanorod/Metal(Metal Oxide) Hybrid Materials: Characterization of Frontier Orbital Energies and Charge Injection Processes Using Unique Combinations of Photoemission Spectroscopies and Waveguide Spectroelectrochemistries

Principal Investigators: Neal R. Armstrong; Jeffry Pyun, S. Scott Saavedra

University of Arizona,
Department of Chemistry/Biochemistry,
Tucson, Arizona 85721
Phone: (520) 621-8242
Email: nra@email.arizona.edu; jpyun@email.arizona.edu; saavedra@email.arizona.edu

Names of Team Members: Ramanan Ehamparam, Nicholas Pavlopoulos, Michael W. Liao, Lawrence J. Hill (all graduate students supported in part by this BES award)

University of Arizona,
Department of Chemistry/Biochemistry,
Tucson, Arizona 85721

DOE Program Manager: Dr. Mark Spitler,

Chemical Sciences, Geosciences and Biosciences Division,
Office of Science,
Email: mark.spitler@science.doe.gov

Objectives

We are focused on the development of new semiconductor nanomaterials which are prototypical for systems that may be ultimately used to photoelectrochemically produce fuels from sunlight, and in understanding how the introduction of catalytic sites (e.g. metallic tips on a semiconductor nanorod) can alter the band edge energies (E_{VB}/E_{CB}) and the dynamics of electron transfer to/from these nanomaterials.

Technical Barriers

Producing rod-like semiconductor materials, tipped with catalysts at nanometer length scales, with good control over composition, size and energetic dispersity, is extremely challenging. Arranging these materials in interconnected assemblies without loss of function is even more challenging. We also need (and are developing) new ways of characterizing band edge energies of these materials, and rates of electron transfer, in motifs that apply to their use in energy conversion platforms – even more challenging! A key target and technical question is whether the conjugation of cobalt oxide nanoparticles onto semiconductor nanorods offers a route to preparing photosensitized cobalt oxide NPs for OER.

Abstract

This talk will review our multi-PI study of the formation of unique semiconductor nanorods (NRs) and NRs decorated with metallic or oxide catalytic sites, and the characterization of their band edge energies as catalytic sites are introduced.[1-5] We demonstrate new approaches to a) the characterization of valence band energies using photoemission spectroscopies, which for the first time fully take into account local vacuum level shifts (due to the dipolar nature of the NR), and b) conduction band energies (E_{CB}) using waveguide-based spectroelectrochemical approaches to determine the potentials (versus vacuum) for electron injection into the NC or NR. Both approaches show significant shifts in band edge energies, and the rates of electron transfer (ET), when NCs and NRs are decorated with metallic and oxide catalytic sites at the NR tip. Even small Au nano-tips on CdSe NRs, where the metallic component is less than 1% of the total atomic content of the NR, introduces shifts in E_{VB} and E_{CB} which are predicted to alter efficiencies of photoelectrochemically driven water splitting and related formation pathways toward solar fuels. This work underpins the rational design of new photocatalytic materials, and is a necessary step toward a complete understanding of the effects of modification and interconnection of NR assemblies on both energetics and dynamics of ET in these materials.

Progress Report

1. Formation of new semiconductor nanorods with metallic and oxide catalytic tips:

We have created a series of new semiconductor NR materials which have been tipped at both end, or one end, with catalytic sites, either metallic in nature (Pt, Au) or oxides such as Co_xO_y. The synthetic methods developed under this project allow the installation of a photosensitizing semiconductor nanorod (either CdSe@CdS, CdS, CdSe) with metallic (Au, Pt), or metal oxide (Co_xO_y) NP tips. The modularity of this approach enables spatial and energetic control in this photoactive nanocomposite. Heterostructured nanorods based on CdSe@CdS have served as model systems to develop these synthetic methods, with an emphasis on installing one, or two NP tips per nanorod. To facilitate spectroelectrochemical measurements, we have also prepared

heterostructured CdSe nanorods that incorporate Au, Co and Co_xO_y tips. Our work has focused on these CdSe NRs which have high bandgap energies and afford ease of synthesis and tuning of the NR size, shape and functionalization in ways which leads to insights about their energetics which we think will be generalizable across a number of material platforms. Figure 1 at right shows a recent TEM characterization ofi individual NRs, Au-tipped NRs and Au-NR fused assemblies which show intriguing linkages between NRs which, if controlled, might lead to vectoral charge transport – a perquisite for photoelectrocatalytic assemblies.

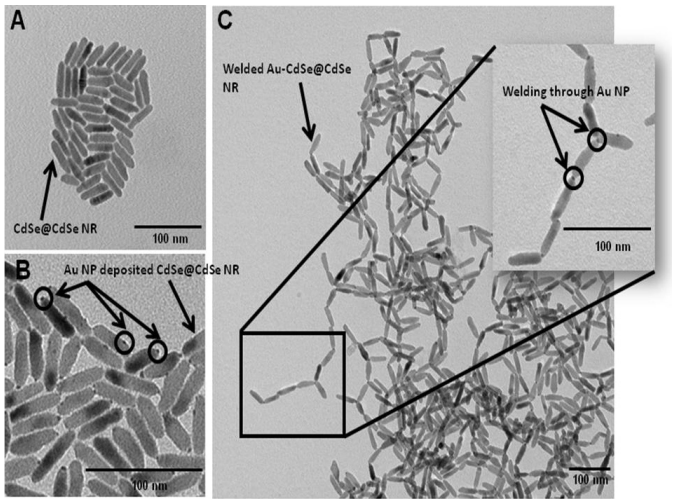

FIGURE 1. TEM images of (A) synthesized CdSe@CdSe nanorod heterostructures (L = 40.1 ± 4.1 nm; D = 9.6 ± 1.2 nm). (B) Au-CdSe@CdSe heterostructures exhibiting matchstick and dumbbell morphologies, with some lateral deposition of AuNP observed. (C) Fused Au-CdSe@CdSe nanorod networks formed by coalescence of AuNP tips. Fusion of CdSe@CdSe NRs occurs through Au NPs.

2. Characterization of valence band energies in NCs and NRs using photoemission spectroscopies, effect of metallic tips on E_{VB}:

We have recently developed a unique approach to the characterization of NC and NR band edge energies (E_{VB} directly, E_{CB} from E_{VB} and the optical band gap), using UV-photoemission spectroscopies (He I and He II UPS) for NC and NR thin films on highly ordered pryolitic graphite (HOPG), accompanied by removal of He satellite emission lines and secondary electron background, and correction for local shifts in vacuum levels due to the dipolar nature of these NC and NRs. This approach gives us for the first time good accuracy for determination of E_{VB}, and confidence in the shifts we see in E_{VB} as NRs are modified with metallic and oxide catalytic sites. Figure 2 shows, for example, that there are significant decreases in E_{VB} (and E_{CB})for Au-tipping of CdSe NRs, and even larger decreases in E_{VB}/E_{CB} when these NRs are fused through their tips, both effects are predicted to increase the driving force for proton reduction on these assemblies, and will factor into the design of new semiconductor nanomaterials.

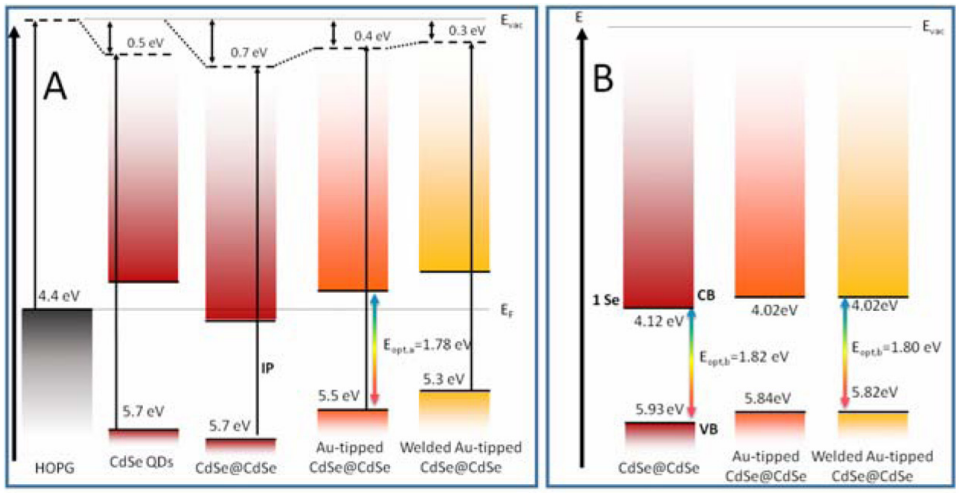

FIGURE 2. Estimates of EVB and ECB from UV-photoemission studies (UPS) of NC and NR thin films on HOPG (A) and waveguide spectroelectrochemical studies of electron injection (B). In the UPS studies we were able to uniquely correct for shifts in local vacuum levels (critical) and show that addition of Au tips to the NR, and NR fusion through the Au tpis, lead to demonstrable decreases in E_{VB}/E_{CB}. These changes in band energies are confirmed in the spectroelectrochemical studies of electron injection into E_{CB}, in contact with electrolyte solutions.

3. Characterization of conduction band energies and rates of heterogeneous ET in NCs and NRs using waveguide-based spectroelectrochemistries:

We have also recently demonstrated that waveguide-based spectroelectrochemical techniques can be used to monitor injection of electrons into the conduction band of both NCs and NRs, at coverages on the waveguide that ensure isolation of the NR or NC, or at coverages where strong interactions exist between these nano-objects, this time in contact with electrolyte solutions. As shown in Figure 3A, we can uniquely monitor the bleaching of the lowest energy excitonic features in these NRs, as electron injection proceeds, at potentials which can be translated to the vacuum scale and compared with PES measurements in Figure 2. Furthermore, by modulating the potential applied to the NR assembly and poising at the excitonic wavelength, we obtain estimates of rates of electron injection/extraction from optical impedance data (Figure 3B) which show that electronic coupling to the substrate electrode, and rates of ET, are greatly improved by introduction of Au tips and fusion of NRs through these tips.

Future Directions

We are in the process of expanding the scope of this work by: *i)* varying tip composition of the semiconductor NR, adding catalytic sites that function for both hydrogen evolution (HER) and oxygen evolution (OER), with both symmetric (dumbbell) and asymmetric (matchstick) motives; *ii)* interconnecting the asymmetric assemblies to create a network which retains the asymmetry (critical for photoelectrochemical water splitting and related processes), iii) systematic characterization of the energetics and dynamics of electron transfer to/from these NR materials, as isolated nano-objects, and as a function of tip modification and interconnection, using both photoemission and spectroelectrochemical protocols.

Recent publications

1. Shallcross, R.C.; D'Ambruoso, G.D.; Korth, B.D.; Hall, H.K.; Zheng, Z.P.; Pyun, J.; Armstrong, N.R. Poly(3,4-ethylenedioxythiophene) - Semiconductor nanoparticle composite thin films tethered to indium tin oxide substrates via electropolymerization. *Journal of the American Chemical Society* **2007**, *129*, 11310-+.

2. Shallcross, R.C.; D'Ambruoso, G.D.; Pyun, J.; Armstrong, N.R. Photoelectrochemical Processes in Polymer-Tethered CdSe Nanocrystals. *Journal of the American Chemical Society* **2010**, *132*, 2622-2632.

3. Kim, B.Y.; Shim, I.B.; Araci, Z.O.; Saavedra, S.S.; Monti, O.L.A.; Armstrong, N.R.; Sahoo, R.; Srivastava, D.N.; Pyun, J. Synthesis and Colloidal Polymerization of Ferromagnetic Au-Co Nanoparticles into Au-Co3O4 Nanowires. *Journal of the American Chemical Society* **2010**, *132*, 3234-+.

4. Keng, P.Y.; Bull, M.M.; Shim, I.B.; Nebesny, K.G.; Armstrong, N.R.; Sung, Y.; Char, K.; Pyun, J. Colloidal Polymerization of Polymer-Coated Ferromagnetic Cobalt Nanoparticles into Pt-Co3O4 Nanowires. *Chemistry of Materials* **2011**, *23*, 1120-1129.

5. Hill, L.J.; Bull, M.M.; Sung, Y.; Simmonds, A.G.; Dirlam, P.T.; Richey, N.E.; DeRosa, S.E.; Shim, I.-B.; Guin, D.; Costanzo, P.J.; Pinna, N.; Willinger, M.-G.; Vogel, W.; Char, K.; Pyun, J. Directing the Deposition of Ferromagnetic Cobalt onto Pt-Tipped CdSe@CdS Nanorods: Synthetic and Mechanistic Insights. *ACS Nano* **2012**, *6*, 8632-8645.

6. Hill, L.J.; Richey, N.E.; Sung, Y.-H.; Dirlam, P.T.; Lavoie-Higgins, E.; Shim, I.-B.; Pinna, N.; Willinger, M.-G.; Vogel, W.; Char, K.; Pyun, J. Colloidal Polymers via Dipolar Assembly of Heterostructured Co-tipped CdSe@CdS Nanorods. *ACS Nano* **2014**, 8, 3272-3284

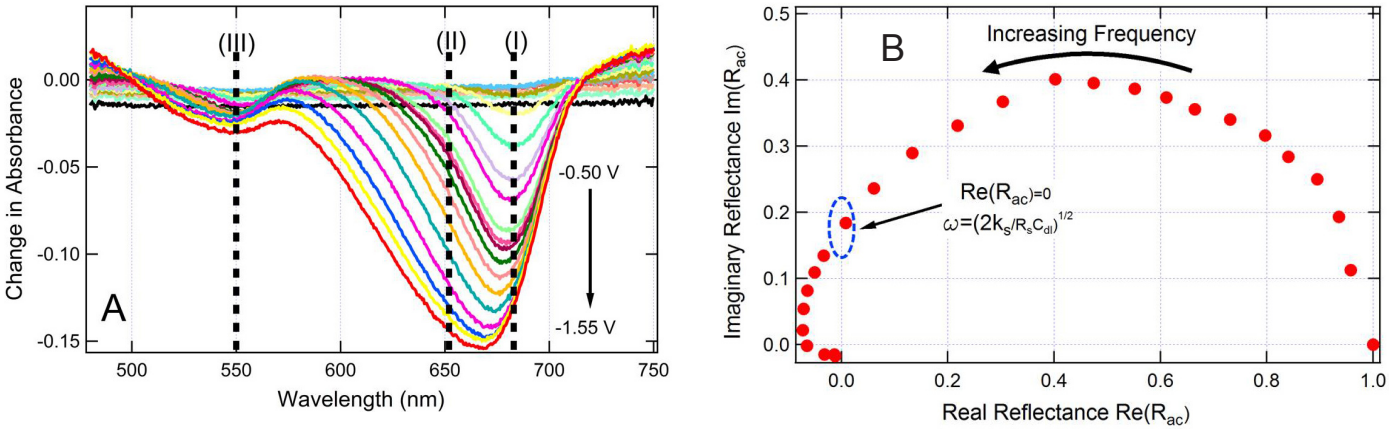

FIGURE 3. (A) Bleaching spectra for CdSe NRs on a waveguide spectroelectrochemical substrate, showing the loss of the excitonic band feature as electrons are injected into the conduction band, the potential for this process defines E_{CB}; (B) PM-ATR optical impedance data (imaginary versus real components of the optical bleach) as a function of frequency, which can be used to estimate the rate of electron injection/extraction ($k_{s,app}$) for these NR assemblies.

7. Hill, L.J.; Pyun, J. Colloidal Polymers via Dipolar Assembly of Magnetic Nanoparticle Monomers. *ACS Applied Interfaces* **2014**, *ASAP*, DOI: 10.1021/am405786u http://dx.doi.org/10.1021/am405786u

8. Hill, L.J.; Richey, N.E.; Sung, Y.-H.; Dirlam, P.T.; Lavoie-Higgins, E.; Shim, I-.B.; Pinna, N.; Willinger, M.-G.; Vogel, W.; Char, K.; Pyun, J. Synthesis and Dipolar Assembly of Heterostructured Cobalt Tipped CdSe@CdS Nanorods. *Cryst. Eng. Comm.* **2014**, DOI: 10.1039/C4CE00680A

9. Ehamparam, Ramanan, Pavlopoulos, Nicholas, Liao, Michael, Hill, Lawerence J., Armstrong, N.R., Pyun, Jeffrey, Saavedra, S. Scott, Characterization of Frontier Orbital Energies and Charge Injection Processes in Au-CdSe Hybrid Nanostructures: Waveguide Spectroelectrochemistry and Photoemission Spectroscopies of Nanorod Monolayers and Multilayers, manuscript in preparation for submission to Journal of the American Chemical Society.

10. Liao, Michael, Ehamparam, Ramanan, Pavlopoulos, Nicholas, Hill, Lawerence J., Armstrong, N.R., Pyun, Jeffry, Saavedra, S. Scott, Characterization of Frontier Orbital Energies and Charge Injection Processes in Pt-CdSe@CdS Hybrid Nanostructures: Waveguide Spectroelectrochemistry and Photoemission Spectroscopies of Nanorod Monolayers and Multilayers, manuscript in preparation for submission to J. Phys. Chem. Lett.

11. Hill, L; Sung, Y.; J.; Char, K.H.; Pyun, J. Colloidal Polymerization: A New Concept in Polymer Science. *Prog. Polym. Sci.* **2014** *in preparation*

II.G.2 Real-Time Atomistic Simulation of Light Harvesting and Charge Transport for Solar Hydrogen Production

Principal Investigator: Oleg V. Prezhdo
Department of Chemistry
University of Rochester
Rochester, NY 14627
Phone: (585) 275-4231
Email: oleg.prezhdo@rochester.edu

Names of Team Members
- Alexey V. Akimov; Email: alexvakimov@gmail.com
- Amanda J. Neukirch; Email: ajneuk@pas.rochester.edu
- Run Long; Email: runlong.anh@gmail.com

DOE Program Manager: Mark Spittler
Phone: (301) 903-4568
Email: mark.spitler@science.doe.gov

Objectives

Develop novel approaches for studying photo-induced electron-nuclear dynamics in nanoscale materials and investigate excited state processes in photovoltaic and photo-catalytic systems for solar hydrogen production.

Technical Barriers

Theoretical and computational approaches are needed, capable of accurate description of non-equilibrium electron-nuclear dynamics, including nuclear quantum effects, and applicable to systems composed of hundreds of atoms.

Abstract

The growing need for renewable, clean and abundant energy sources constitutes one of the highest priority problems of the humankind. If a small fraction of the Sun energy can be accumulated and transformed into a convenient form, the problem can be solved. Therefore, search for novel photovoltaic and photocatalytic materials is an actively developing field of chemistry. Rational design of solar materials requires thorough understanding of the charge separation and photochemical processes, in competition with charge recombination and energy losses to heat. Many key steps occur on ultrafast timescales and are best understood by direct non-equilibrium time-domain simulation. I will present the non-adiabatic molecular dynamics (NA-MD) approach for studying quantum dynamics of solar energy nanoscale materials. The recent implementation of NA-MD within the open-source package, PYXAID, will be introduced.[1,2] Then, two important applications will be considered.[3,4]

Progress Report

Sub Topic 1: Non-adiabatic dynamics of singlet fission in organic photovoltaic materials

The first application focuses on the dynamics of singlet fission (SF) and charge transfer (CT) at a pentacene/C_{60} photovoltaic heterojunction.[4] In the early works on singlet fission the mechanism involving optically dark multi-exciton (ME) state has been proposed. According to the scheme, initially prepared singly excited state, S_1, the natural product of direct photoexchitation, is gradually transformed in otherwise inaccessible ME state. The existence of the ME state has later been confirmed experimentally, however it was found that decay of S_1 and accumulation of ME states are not directly correlated. The coherent mechanism of the SF has been suggested, according to which both ME and S_1 configurations are excited simultaneously, as the components of a true wavefunction of multielectron Hamiltonian. In our work we have performed atomistic time-domain NA-MD simulations to better understand the nature of the SF process.

In our work we develop a minimalistic model that is capable of describing singlet fission and charge transfer in the pentacene/C_{60} heterojunciton. The model includes six types of states – single pentacene exciton (S_1), pentacene multiexciton (ME), pair of coupled triplets (Tx2) – a predecessor of a charge-multiplied state, and three types of charge transfer between heterojunction components (CT_0, CT_1, and CT_2). With the minimalistic set of these diabatic states we propose a comprehensive kinetic scheme that yields electron transfer timescales in agreement with experimental observations. The kinetic scheme is parameterized by energy levels of participating states and by the non-adiabatic

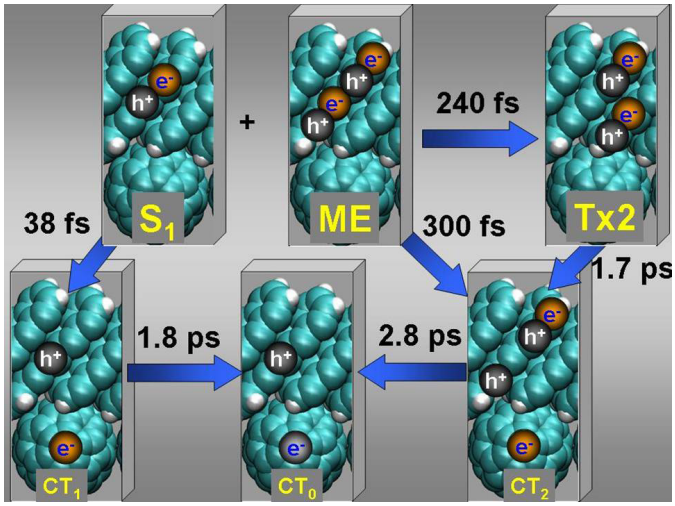

coupling between each their pair. The energy levels of the states are chosen on the basis of judicious examination of comprehensive experimental and theoretical data. For singly-excited states they agree with our DFT calculations, while for doubly excited states the differences are substantial, pointing to importance of electrostatic and exchange-correlation interaction, which are absent at the level of single Slater determinants. The non-adiabatic couplings are computed explicitly using NA-MD approach and real time TD-DFT simulations. These calculations indicate that the coupling between S_1 and ME states is negligible, making them effectively decoupled from each other. As a result, the ME state can not be populated by a decay of S_1 state, supporting the hypothesis of the coherent mechanism of SF.

By direct examination, we find that alternative kinetic schemes fail to reproduce the timescales of one or more kinetic processes. This implies some restrictions on the order and difference of the involved energy levels, helping us to resolve some inconsistencies among the available experimental and theoretical results. On the basis of analysis of the energy levels and the magnitudes of non-adiabatic couplings, we propose that the intermediate doubly-excited states of charge-transfer character are crucially important for dissociation of the ME state into a pair of coupled triples, Tx2. Without the corresponding intermediate states, the direct coupling between ME and Tx2 is vanishing and singlet fission can not proceed efficiently. The model predicts that the SF efficiency relies strongly on the availability of the intermediate states and on its competition with the CT processes.

Sub Topic 2: Non-adiabatic dynamics of holes in photocatalytic water splitting

The second application concerns photocatalytic water splitting at GaN semiconductor. Photochemical water splitting is a promising avenue to sustainable, clean energy and fuel production. Gallium nitride (GaN) and its solid solutions are excellent photocatalytic materials; however, the efficiency of the process is low on pure GaN, and co-catalysts are required to increase the yields.

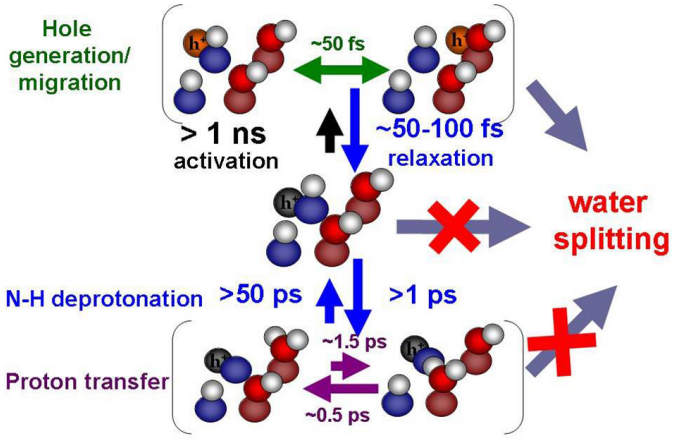

We present the first time-domain theoretical study of the initial steps of photocatalytic water splitting on a GaN surface. Our state-of-the-art simulation technique, combining NA-MD and time-dependent density functional theory (TD-DFT), allows us to characterize the mechanisms and timescales of the evolution of the photogenerated positive charge (hole) and the subsequent proton transfer at the GaN/water interface. The calculations show that the hole loses its excess energy within 100 fs and localizes primarily on the nitrogen atoms of the GaN surface, initiating a sequence of proton transfer events from the surface N-H group to the nearby OH groups and bulk water molecules. Water splitting requires hole localization on oxygen rather than on nitrogen, necessitating non-adiabatic transitions uphill in energy on pure GaN. These transitions occur infrequently, resulting in low yields of the photocatalytic water splitting observed experimentally. We conclude that efficient co-catalysts should favor localization of the photogenerated hole on oxygen-containing species at the semiconductor/water interface.

Future Directions

We will investigate novel, promising materials for solar hydrogen production, and will continue developing efficient theoretical and computational approaches for this purpose.

Publication list (including patents) acknowledging the DOE grant or contract

Publications cited in this document that acknowledge DOE grant or contract:

1. Akimov, A.V.; Prezhdo, O.V. The PYXAID Program for Non-Adiabatic Molecular Dynamics in Condensed Matter Systems. *J. Chem. Theory Comput.* **2013**, *9*, 4959.

2. Akimov, A.V.; Prezhdo, O.V. Advanced Capabilities of the PYXAID Program: Integration Schemes, Decoherence Effects, Multiexcitonic States, and Field-Matter Interaction. *J. Chem. Theory Comput.* **2014**, *10*, 789.

3. Akimov, A.V.; Muckerman, J.T.; Prezhdo, O.V. Nonadiabatic Dynamics of Positive Charge during Photocatalytic Water Splitting on GaN(10-10) Surface: Charge Localization Governs Splitting Efficiency. *J. Am. Chem. Soc.* **2013**, *135*, 8682.

4. Akimov, A.V.; Prezhdo, O.V. Nonadiabatic Dynamics of Charge Transfer and Singlet Fission at the pentacene/C60 Interface. *J. Am. Chem. Soc.* **2014**, *136*, 1599.

Additional publications that acknowledge the DOE grant or contract:

Reviews

1. A.J. Neukirch, K. Hyeon-Deuk, O.V. Prezhdo, "A time-domain ab initio view of excitation dynamics in quantum dots", *Coord. Chem. Rev.* **2014**, 263-264, 161.

2. A.V. Akimov, A.J. Neukirch, O.V. Prezhdo "Theoretical insights into photoinduced charge transfer and catalysis at metal oxide surfaces", *Chem. Rev.*, **2013**, 113, 4496.

3. H.M. Jaeger, K. Hyeon-Deuk, O.V. Prezhdo "Exciton multiplication from first principles", *Acc. Chem. Res.* **2013**, 46, 1280.

Original papers

1. A.V. Akimov, R. Long, O.V. Prezhdo, "Coherence penalty functional: A simple method for adding decoherence in Ehrenfest dynamics", *J Chem. Phys.*, **2014**, in press

2. D.N. Tafen, R. Long, O.V. Prezhdo "Dimensionality of nanoscale TiO_2 determines the mechanism of photoinduced electron injection from a CdSe nanoparticle", *Nano Lett.* **2014**, 14, 1790

3. H. Zhu, Y. Yang, K. Hyeon-Deuk, M. Califano, N. Song, Y. Wang, W. Zhang, O.V. Prezhdo, T. Lian "Auger-assisted electron transfer from photoexcited semiconductor quantum dots", *Nano Lett.* **2014**, 14, 1263.

4. A.J. Neukirch, L.C. Shamberger, E. Abad, B.J. Haycock, H. Wang, J. Ortega, O.V. Prezhdo, and J.P. Lewis, "Nonadiabatic ensemble simulations of cis-stilbene and cis-azobenzene photoisomerization, *J. Chem. Theory and Comp.* **2014**, 10, 14.

6. M. Trimithioti, A.V. Akimov, O.V. Prezhdo, S.C. Hayes "Analysis of depolarization ratios of $ClNO_2$ dissolved in methanol", *J. Chem. Phys.* **2014**, 140, 014301.

6. R. Long, N.J. English, O.V. Prezhdo "Defects are needed for fast photo-induced electron transfer from a nanocrystal to a molecule: Time-domain ab initio analysis", *J. Am. Chem. Soc.* **2013**, 135, 18892.

7. A.V. Akimov, O.V. Prezhdo "Persistent electronic coherence despite rapid loss of electron-nuclear correlation", *J. Phys. Chem. Lett.* **2013**, 4, 3857.

8. L.J. Wang, A.V. Akimov, L.P. Chen, O.V. Prezhdo "Quantized Hamiltonian dynamics captures the low-temperature regime of charge transport in molecular crystals", *J. Chem. Phys.* **2013**, 139, 174109.

9. J. Liu, A.J. Neukirch, O.V. Prezhdo "Phonon-induced pure-dephasing of luminescence, multiple exciton generation, and fission in silicon clusters", *J. Chem. Phys.* **2013**, 139, 164303.

10. S.V. Kilina, A.J. Neukirch, B.F. Habenicht, D.S. Kilin, O.V. Prezhdo "Quantum Zeno effect rationalizes the phonon bottleneck in semiconductor quantum dots", *Phys. Rev. Lett.* **2013**, 110, 180404.

II.G.3 Oxidatively Stable Nanoporous Silicon Photocathodes for Photoelectrochemical Hydrogen Evolution

Principal Investigator: Nathan R. Neale
National Renewable Energy Laboratory
15013 Denver West Parkway
Golden, CO 80401
Phone: (303) 384-6165
Email: Nathan.Neale@nrel.gov

Yixin Zhao,[‡] Kai Zhu,[a] Jihun Oh,[b]
Jao van de Lagemaat,[a] Hao-Chih Yuan,[a]
Howard M. Branz[a]

[‡] Present address: Shanghai Jiao Tong University, Shanghai, China
[a] National Renewable Energy Laboratory
[b] Korea Advanced Institute of Technology, Daejeon, South Korea

DOE Program Manager: Dr. Mark T. Spitler
Phone: (301) 903-4568
Email: Mark.Spitler@science.doe.gov

Objectives

Within our BES Solar Photochemistry program, we are developing improved understanding of the interactions at the liquid-solid interface during catalyzed photoelectrochemistry using nanostructured photoelectrodes. To understand basic issues critical to increasing the photocarrier-driven fuel-producing chemical reaction rates and their selectivity over parasitic reactions, we apply catalysts to photocathodes of well-understood, near-ideal semiconductors into which we can build random or controlled nanostructures through novel metal-assisted chemistries. The application of well-understood single-crystal semiconductors like silicon allows us to separate out and study the important new photoelectrochemical (PEC) science introduced by nanostructuring and the interactions of catalysts with the nanostructured surface.

Technical Barriers

- Understand how to control fundamental interactions such as light absorption in molecules and solids, charge transport and recombination, interfacial electron transfer, and coupled transfer of multiple electrons and protons through a catalyst.
- Based on this knowledge, develop efficient semiconductor photoelectrodes stable to both photo-assisted and dark corrosion processes.

Abstract

Stable and high-performance nanoporous "black silicon" photoelectrodes with electrolessly deposited Pt nanoparticle (NP) catalysts are made with two metal-assisted etching steps. Doubly etched samples exhibit >20 mA/cm^2 photocurrent density at +0.2 V vs. reversible hydrogen electrode (RHE) for photoelectrochemical hydrogen evolution under 1 sun illumination.

We find that the photocurrent onset voltage of black Si photocathodes prepared from single-crystal planar Si wafers increases in oxidative environments (e.g., aqueous electrolyte) owing to a positive flat-band potential shift caused by surface oxidation. However, this beneficial oxide layer becomes a kinetic barrier to proton reduction that inhibits hydrogen production after just 24 h. To mitigate this problem, we developed a novel second Pt-assisted etch process that buries the Pt NPs deeper into the nanoporous Si surface. This second etch shifts the onset voltage positively, from +0.25 V to +0.4 V vs. RHE, and reduces the charge-transfer resistance with no performance decrease seen for at least two months.

Progress Report

Recently, nanostructured Si photocathodes have been developed for hydrogen production due to their advantages of low reflectivity and a higher surface area compared to bulk planar Si, which improves charge collection, exchange current density, and hydrogen gas surface-desorption. Our group and others have focused on the metal-assisted solution etching of planar Si to prepare nanostructured Si—also called "black Si"—a process that is suitable for large-scale manufacture and has been applied to make high-efficiency Si solar cells.

But the performance of Si electrodes used in any aqueous PEC system normally deteriorates from surface oxidation, an effect that appears to be unavoidable because of the high reactivity of Si with O_2, especially in the presence of water. In a deployed PEC hydrogen production system, surface oxidation might be expected during the night and at other times when photoelectrons are not providing cathodic protection against surface oxidation. Although the deposition of a surface-adsorbed catalyst such as Pt can help reduce the kinetic barrier for proton reduction, the PEC properties of Pt-deposited Si photoelectrodes are also found to degrade significantly upon surface oxidation.

Here we find that our black Si photoelectrodes with electrolessly deposited Pt NP catalysts (Pt/b-Si) exhibit improved PEC hydrogen production performance relative

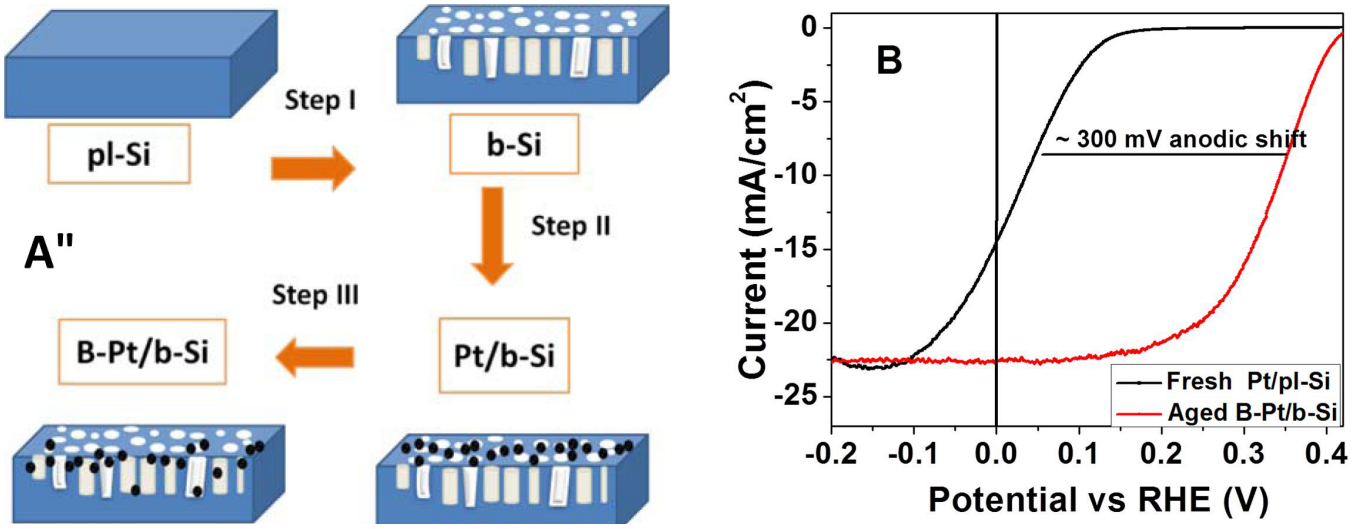

FIGURE 1. (A) Schematic of the preparation process for air-stable high-performance nanoporous B-Pt/b-Si photocathodes. (B) Comparison of J–V curves for the photoelectrochemical production of hydrogen at 0.5 M H2SO4 and 100 mW/cm2 irradiation for a fresh Pt/plSi photocathode (black curve) and a B-Pt/b-Si photocathode aged for 1 month in air (red curve).

to planar Si (pl-Si) electrodes. In particular, the deleterious effect of air exposure for more than 1 h on pl-Si or catalyst-free black Si (b-Si) electrodes are not observed in Pt/b-Si at aging times greater than 24 h. Instead, the nanoporous Pt/b-Si electrode exhibits a positive onset potential shift (by ~200 mV) upon aging for 24 h that improves its PEC performance. To explore the mechanism for the positive onset potential shift of nanoporous b-Si after exposure to air, Mott-Schottky (MS) plots of the pl-Si, b-Si, and Pt/b-Si electrodes were measured in 0.5 M H_2SO_4 after different aging times. The MS data confirm that oxide growth results in a positive flat-band potential shift for the Si photocathodes, which initially improves PEC performance but eventually degrades it with further oxide growth.

To address this issue, we have developed a novel re-etching process as described in Fig. 1A. This process results in high PEC performance despite the presence of surface oxide. These black Si photoelectrodes with buried Pt NP catalysts (B-Pt/b-Si) exhibit an ~300 mV positive shift for hydrogen evolution compared to a Pt-modified planar Si photoelectrode and are stable even after months of air exposure (Fig. 1B). Electrochemical impedance studies reveal that the second etch leads to a considerably smaller interfacial charge-transfer resistance than samples without the additional etch, suggesting that burying the Pt NPs improves the interfacial contact between the black Si surface and the Pt catalysts.

Future Directions

We plan fundamental experiments to probe the nature of the interface between Pt and b-Si using high-resolution transmission electron microscopy, scanning tunneling microscopy, x-ray absorption spectroscopy, and related techniques. Utilizing this secondary etching treatment with buried p-n junction photocathodes may reduce the overpotential for hydrogen evolution and make possible tandem overall water splitting devices using this photocathode and an appropriately matched photoanode such as bismuth vanadate.

Selected Publications

1. Anti-Reflective Nanoporous Silicon For Efficient Hydrogen Production, US Patent No. US 2012/0103825 A1, Jihun Oh, Howard Branz

2. Oh, J.; Deutsch, T.G.; Yuan, H.-C.; Branz, H.M., Nanoporous Black Silicon Photocathode for H_2 Production by Photoelectrochemical Water Splitting. *Energy Environ. Sci.* **2011**, *4* (5), 1690-1694.

3. Seabold, J.A.; Zhu, K.; Neale, N.R., Efficient Solar Photoelectrolysis by Nanoporous Mo:$BiVO_4$ Through Controlled Electron Transport. *Phys. Chem. Chem. Phys.* **2014**, *16* (3), 1121-1131.

4. Zhao, Y.; Neale, N.R.; Zhu, K.; Oh, J.; van de Lagemaat, J.; Yuan, H.-C.; Branz, H.M., Oxidatively Stable Nanoporous Silicon Photocathodes with Enhanced Onset Voltage for Photoelectrochemical Hydrogen Evolution. *Submitted* **2014**.

II.G.4 Fundamental Design and Mechanisms for Solar Hydrogen Production in Natural and Artificial Photosynthetic Systems

Principal Investigator: David M. Tiede

Chemical Sciences and Engineering Division
Argonne National Laboratory
9700 South Cass Ave
Argonne, IL 60439
Phone: (630) 252-3539
Email: tiede@anl.gov

- Lisa M. Utschig
  Phone: (630) 252-3544; Email: utschig@anl.gov
- Karen L. Mulfort
  Phone: (630) 252-3545; Email: mulfort@anl.gov)
- Oleg G. Poluektov
  Phone: (630) 252-3546; Email: poluektov@anl.gov)
- Lin X. Chen
  Phone: (630) 252-3533; Email: lchen@anl.gov)

Chemical Sciences and Engineering Division,
Argonne National Laboratory, 9700 South Cass Ave,
Argonne, IL 60439

- Phani R. Pokkuluri

Biosciences Division, Argonne National Laboratory,
9700 South Cass Ave, Argonne, IL 60439
Phone: (630) 252-4197; Email: rajp@anl.gov)

Subcontractors

Michael R. Wasielewski, Department of Chemistry,
Northwestern University, Evanston, IL 60208-3113
Phone: (847) 467-1423
Email: m-wasielewski@northwestern.edu)

DOE Program Manager

Mark T. Spitler, Solar Photochemistry Program
Phone: (301) 903-4568
Email: Mark.Spitler@science.doe.gov)

Gail McLean, Photosynthetic Systems
Phone: (301) 903-7807
Email: Gail.McLean@science.doe.gov)

Objectives

The goal of our program in Solar Photochemistry is to resolve fundamental mechanisms for solar energy capture and conversion in artificial photosynthesis and photosynthetic model compounds. Research goals focus on i) investigation of the interplay between structure, ground and excited-state electronic couplings, and photoinduced energy and electron transfer processes in linked light-harvesting and electron donor-acceptor systems, ii) the phenomena of excited state delocalization and electronic coupling/spin coherence across different parts of molecular and supramolecular systems, and their roles in coupling single photon events to multiple electron redox processes, and iii) the design, synthesis and structure-function analyses of photosensitizer-catalyst assemblies.

The goal of our program in Photosynthetic Systems is to resolve fundamental mechanisms for light-harvesting and coupling of excited-state photochemistry to proton-coupled electron transfer, water oxidation, and chemical energy conversion in photosynthesis, and to test design concepts in photosynthesis using photosynthetic hybrid systems. Photosynthetic hybrids are developed that include the coupling of abiotic catalytic cofactors to electron transfer within photosynthetic protein complexes, and the insertion of abiotic light-harvesting photochemistry and catalytic functions within redox protein frameworks.

Technical Barriers

A key challenge in solar energy conversion lies in understanding how to efficiently couple light-generated, transient, single-electron excited states to long-lived charge separation and multi-electron, proton-coupled fuels catalysis.

Abstract

This program investigates fundamental mechanisms for coupling photons to fuels in natural and artificial photosynthesis, and tests strategies for the design of sustainable photosynthetic systems for solar energy conversion. The comparison between natural and artificial photosynthesis is used to identify fundamental principles for solar energy conversion and to develop strategies for the design of sustainable photosynthetic systems for solar energy conversion. This presentation will provide examples of chemically-inspired biohybrid designs for multi-electron solar fuels catalysis, and present results on X-ray characterization of amorphous oxide water-oxidation catalyst films as an approach for resolving metal-oxo coordination chemistry underlying solar fuels-dependent water-splitting.

Progress Report

Program highlights accomplished in FY2013-2014 include the following.

1. Design of linked light-harvesting, hydrogen-evolving catalyst supramolecular assemblies. Key problems for the design of supramolecular assemblies for efficient solar hydrogen production include creating designs that promote efficient photosensitizer-to-catalyst excited-state charge transfer. We succeeded in demonstrating the first example of a dyad assembly, **1**, which accomplishes this transfer in less than 1 ps (Mulfort et. al. 2013 PCCP). The results

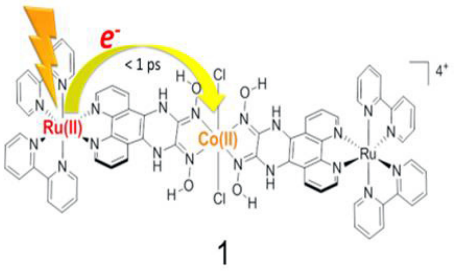

1

are remarkable since they demonstrate a metal-to-metal delocalized excited state analogous to the primary excited state in photosynthesis, and establish a ligand architecture for the design for photo-hydrogen generation.

2. Photosynthetic bio-hybrids for solar hydrogen production. We demonstrated biohybrids that use Photosystem I (PSI) to drive solar fuel production from a nickel diphosphine molecular catalyst (Utschig et. al. JACS 2013). Upon exposure to visible light, a self-assembled PSI-$[Ni(P_2^{Ph}N_2^{Ph})2](BF_4)_2$ hybrid generates H_2 at a rate 2 orders of magnitude greater than rates reported for synthetic systems using the same catalyst. In addition, this work developed a strategy for incorporating the Ni molecular catalyst using the native acceptor protein of PSI, flavodoxin. Photocatalysis experiments with this modified flavodoxin demonstrate a new mechanism for biohybrid creation that involves protein-directed delivery of a molecular catalyst to the reducing side of Photosystem I for light-driven catalysis. This work further establishes strategies for constructing functional, inexpensive, earth abundant solar fuel-producing PSI hybrids that use light to rapidly produce hydrogen directly from water.

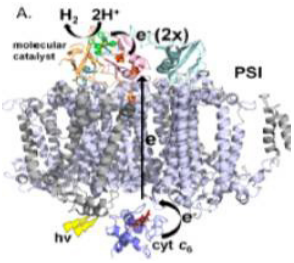

3. Redox protein biohybrids. Current research points to the challenges of creating architectures that support the multiple electron and proton transfers needed for solar fuels catalysis, while avoiding a variety of excited-state quenching and charge recombination pathways. This program demonstrated opportunities to exploit the tri-heme cytochromes c7 from *Geobacter sulfurreducens* as "molecular wire" components in supramolecular biohybrid synthesis (Tiede et. al Biochem. 2014). This work has mapped out site-dependent photo-sensitized electron transfer to cofactor hemes using $Ru(bpy)_3$ derivatives that are covalently linked to cysteine residues placed at a variety of positions on the cytochrome c7 surface through site-directed mutagenesis. Rates of electron transfer were found to vary from 10^{11} s^{-1} to 10^6 s^{-1} depending upon the site and pathway for electron transfer. Photochemical quenching processes are found to track in parallel the site-dependent electron transfer, indicating that both processes follow similar pathway dependences. These results establish criteria for constructing photocatalytic pathways in multi-heme proteins, one that requires multi-step electron transfer to prevent heme-based sensitizer quenching and rapid charge recombination pathways.

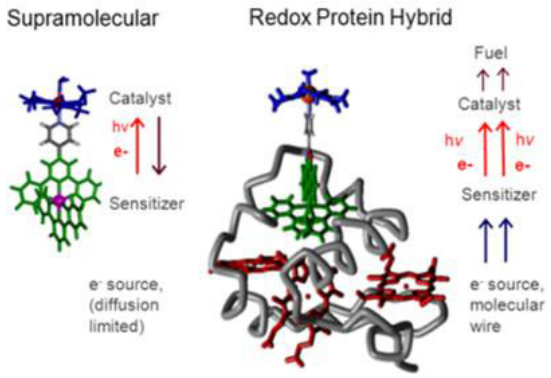

4. Amorphous oxides as models for deciphering the chemistry underlying photosynthetic water-splitting and interfacial photochemistry. Amorphous thin film oxygen evolving catalysts (OECs) of first-row transition metals are of wide-spread interest for artificial leaf applications, and further serve as models for investigating metal-oxo coordination chemistry underlying photosynthetic water-splitting. We have developed X-ray atomic pair distribution function analysis techniques for the characterization of the "molecular-dimensioned" domain structures within amorphous oxide water-oxidation catalyst films (Tiede et. al. PCCP 2014). Our recent work has extended these measurements to electrode-supported films to resolve structure linked to photochemical energy conversion at electrode interfaces and to develop capabilities that can be extended to molecular-based systems.

Future Directions

Future research will include the following: i) Biomimetic assembly of photocatalyst modules, ii) the development of new redox-active chromophore modules, iii) the development of homogeneous metal-oxide water oxidation catalytic clusters, and iv) Metal-organic frameworks (MOFs) as heterogeneous platforms for solar energy conversion. Within each thrust, we will also describe high-resolution structural and physical characterization techniques which will be critical for in-depth knowledge of the structural factors at the atomic, molecular, and supramolecular levels which impact processes relevant to photocatalysis such as light absorption, photoinduced electron transfer, charge separation and recombination.

Publication list for D.M. Tiede, 2011-2014, acknowledging the DOE grant or contract:

1. Oxyanion Determined Domain Structure for Electrodeposited Amorphous Cobalt Oxide Oxygen Evolving Catalyst Films, Du, P., Ali Han, G. Kwon, O. Kokhan, K.W. Chapman, P.J. Chupas, and D.M. Tiede, (2014) *J.Phys. Chem. Letts. submitted.*

2. Multimerization of Solution-State Proteins by Tetrakis(4-Sulfonatophenyl) Porphyrin. O. Kokhan, N. Ponomarenko, P. Raj Pokkuluri, M. Schiffer, and D.M. Tiede*, (2014) *Biochemistry, in press.*

3. Resolving the Domain Structure for the Amorphous Iridium-oxide Water Oxidation Catalyst by X-ray Pair Distribution Function Analysis, J. Huang, J.D. Blakemore, O. Kokhan, N.D. Schley, R.H. Crabtree,* G.W. Brudvig,* and D.M. Tiede*, (2014) *Phys. Chem. Chem. Phys., 16(5): 1814-1819.*

4. Detection of a charge-separated catalyst precursor state in a linked photosensitizer-catalyst assembly, A. Mukherjee, O. Kokhan, J. Huang, J. Niklas, L.X. Chen, D.M. Tiede, K.L. Mulfort* (2013) *Phys. Chem. Chem. Phys., **15**, 21070-21076.*

5. "Protein Delivery of a Ni Catalyst to Photosystem I for Light-Driven Hydrogen Production", Silver, S.C., Niklas, J., Du, P., Poluektov, O.G., Tiede, D.M., and Utschig, L.M, J. Amer. Chem. Soc., (2013) 135(36) 13246-13249.

6. Nanostructured TiO2/Polypyrrole for Visible Light Photocatalysis, Dimitrijevic, N.M.; Tepavcevic, S.; Liu, Y.; Rajh, T.; Silver, S.C.; Tiede, D.M. (2013) *J. Phys. Chem. C* **117**: 15540-15544.

7. Artificial Photosynthesis as a Frontier Technology for Energy Sustainability, T. Faunce, S. Styring, M. R Wasielewski, G.W. Brudvig, A.W. Rutherford, J. Messinger, A.F. Lee, C.L. Hill, H. deGroot, M. Fontecave, D.R. MacFarlane, B. Hankamer, D.G. Nocera, D.M. Tiede, H. Dau, W. Hillier, L. Wang (2013) *Energy Environ. Sci., 6, 1074–1076*

8. Characterization of an amorphous iridium water oxidation catalyst electrodeposited from organometallic precursors, J.D. Blakemore, M.W. Mara, M.N. Kushner-Lenhoff,† N.D. Schley, S.J. Konezny, I. Rivalta, C.F.A. Negre, R.C. Snoeberger, O. Huang, A. Stickrath, L.A. Tran, M.L. Parr, L.X. Chen,* D.M. Tiede,* V.S. Batista,* R. Crabtree,* and G.W. Brudvig*, (2013) *Inorgan. Chem*. **52**: 1860-1871.

9. Structure-based analysis of solar fuels catalysts using *in-situ* X-ray scattering analyses, Karen L. Mulfort*, Anusree Mukherjee, Oleksandr Kokhan, Pingwu Du, David M. Tiede* (2013) *Chem. Soc. Rev. **42,*** 2215-2227.

10. A novel ruthenium(II)–cobaloxime supramolecular complex for photocatalytic H_2 evolution: synthesis, characterisation and mechanistic studies, D.M. Cropek, A. Metz, A.M. Müller, H.B. Gray, T. Horne, D.C. Horton, O. Poluektov, D.M. Tiede, R.T. Weber, W.L. Jarrett, J.D. Phillips and A.A. Holder (2012) *Dalton Trans.*, **41**, 13060-13073.

11. Elucidating the Domain Structure of the Cobalt-oxide Water Splitting Catalyst by X-ray Pair Distribution Function Analysis, P. Du, O. Kokhan, K.W. Chapman, P.J. Chupas, and D.M. Tiede* (2012) *J. Am. Chem. Soc.* **134(27)**:11096-11099.

12. Resolution of Cofactor-Specific Excited States and Charge Separation Pathways in Photosynthetic Reaction Centers by Single Crystal Spectroscopy, L. Huang, N. Ponomarenko, G.P. Wiederrecht, and D.M. Tiede (2012) *Proc. Nat. Acad. Sci. USA* **109(13)**, 4851-4856.

13. X-ray Capabilities on the Picosecond Timescale at the Advanced Photon Source, B. Adams, M. Borland, L.X. Chen, P. Chupas, N. Dashdor, G. Doumy, E. Dufresne, S. Durbin, H. Düurr, P. Evans, T. Graber, R. Henning, E.P. Kanter, D. Keavney, C. Kurtz, Y. Li, A.M. March, K. Moffat, A. Nassiri, S.H. Southworth, V. Srajer, D.M. Tiede, D. Walko, J. Wang, H. Wen, L. Young, X. Zhang, and A. Zholents, (2012) *Synchrotron Rad. News* **25(2)**: 6-10.

14. Highly Efficient Ultrafast Electron Injection from the Singlet MLCT Excited State of CuI-Diimine Complexes to TiO2 Nanoparticles, J. Huang, O. Buyukcakir, M.W. Mara, A. Coskun, N.M. Dimitrijevic, G. Barin, O. Kokhan, A.B. Stickrath, R. Ruppert, D.M. Tiede, J.F. Stoddart, J.-P. Sauvage, and L.X. Chen, *Angew. Chem. Intl. Ed.* 51, 12711–12715. (2012).

15. The Hydrogen Catalyst Cobaloxime – a Multifrequency EPR and DFT Study of Cobaloxime's Electronic Structure, Niklas, J., Mulfort, K.L., Rakhimov, R.R, Mardis, K.L., Tiede, D.M., and Poluektov, O.G. (2012) *J. Phys. Chem. B*, **116**, 2943-2957.

16. Nature-Driven Photochemistry for Catalytic Solar Hydrogen Production: A Photosystem I–Transition Metal Catalyst Hybrid, L.M. Utschig, S.C. Silver, K.L. Mulfort, and D.M. Tiede (2011) *J. Am. Chem. Soc.* **133**:16334-16337.

17. Metal Nanoparticle Plasmon-Enhanced Light-Harvesting in a Photosystem I Thin Film, I. Kim, S.L. Bender, J. Hranisavljevic, L.M. Utschig, L. Huang, G.P. Wiederrecht, and D.M. Tiede (2011) *Nano Letts***. 11 (8)**: 3091–3098.

18. Comparing Photosynthetic and Photovoltaic Efficiencies and Recognizing the Potential for Improvement, R. E. Blankenship*, D.M. Tiede*, J. Barber, G.W. Brudvig, G. Fleming, M. Ghirardi, M.R. Gunner, W. Junge, D.M. Kramer, A. Melis, T.A. Moore, C.C. Moser, D.G. Nocera, A.J. Nozik, D.R. Ort, W.W. Parson, R.C. Prince, R.T. Sayre (2011) *Science* **332**: 805-809.

19. Photocatalytic Hydrogen Production from Noncovalent Biohybrid Photosystem I/Pt Nanoparticle Complexes, L.M. Utschig, N.M. Dimitrijevic, O.G. Poluektov, S.D. Chemerisov, K.L. Mulfort, and D.M. Tiede (2011) J. Phys. Chem. Letts. *2:* 236-241. *Highlighted in Chemical & Engineering News, **2011**, 89(5), 44-45.*

II.G.5 Electrochemical Characterization of the Oxygen-Tolerant Soluble Hydrogenase I from *Pyrococcus furiosus*

Principal Investigator: Anne Katherine Jones
Department of Chemistry and Biochemistry
Arizona State University
Tempe, AZ 85287
Phone: (480) 965-0356
Email: jonesak@asu.edu

Names of Team Members
Chelsea L. McIntosh[a] (clmcinto@asu.edu),
Patrick Kwan[a] (Patrick.Kwan@asu.edu), R. Chris Hopkins[b],
Michael W.W. Adams[b] (adams@bmb.uga.edu)

[a] Department of Chemistry and Biochemistry, Arizona State University, Tempe, AZ 85287
[b] Department of Biochemistry, The University of Georgia, Athens, GA 30602

DOE Program Manager: Robert Stack
Phone: (301) 903-5652
Email: Robert.Stack@science.doe.gov

Objectives

The long term goal of this project is to characterize the reactivity of soluble [NiFe]-hydrogenases (SH) as a model for energetically relevant multielectron redox catalysis and to understand what factors control bias towards hydrogen production (or oxidation) and competing reactions with oxygen.

Technical Barriers

Although membrane bound [NiFe]-hydrogenases (MBH) have been extensively characterized via electrochemical methods, soluble [NiFe]-hydrogenases have remained largely unstudied due to difficulty in obtaining stable enzyme samples and functional attachment to electrode surfaces.

Abstract

The soluble hydrogenase I from *Pyrococcus furiosus* (SHI) is the first oxygen-tolerant soluble hydrogenase to be electrochemically characterized. We demonstrate that the electrocatalytic activity is highly sensitive to temperature with the ratio of proton reduction activity to hydrogen oxidation activity shifting dramatically in favor of proton reduction with increased temperature. Similarly, reactions of the active site with oxygen are dependent both on the length of time the enzyme is exposed to oxygen and the temperature of the reaction. We show that SHI is an oxygen-tolerant electrocatalyst, but its catalytic properties are different from the more commonly studied membrane bound [NiFe]-hydrogenases and the mechanisms of oxygen tolerance are likely different.

Progress Report

Pyrococcus furiosus is a hyperthermophilic, strictly anaerobic archaeon that grows optimally at 100 ºC by fermentation of carbohydrates. It produces three [NiFe]-hydrogenases: two soluble group 3 enzymes (SHI and SHII)

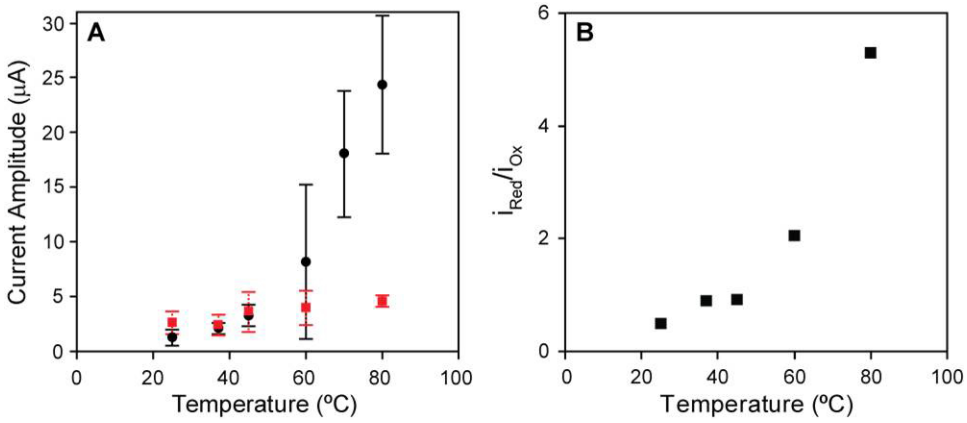

FIGURE 1. Temperature Dependence of (●) H^+ reduction and (●) hydrogen oxidation catalytic currents and the ratio of the two activities from adsorbed *Pf*SHI. Experiments were performed in a mixed buffer with pH = 6.5 at the indicated temperatures with electrode rotation at 2000 rpm.

and a group 4 H_2-evolving membrane-bound hydrogenase (MBH). SHI is a heterotetrameric enzyme believed to produce hydrogen physiologically.

Protein film electrochemistry (PFE) is a technique in which a redox protein is functionally adsorbed to an electrode surface and electron transfer can be observed as current without the addition of a chemical mediator. This method allows exquisite control of electrochemical potential and has proven invaluable in the study of group 1 membrane-bound hydrogenases. However, the reactions of an oxygen-tolerant group 3 SH have not been characterized eletrochemically. Herein, we describe the characterization of SHI using PFE.

Electrocatalysis by SHI immobilized at graphite: catalytic bias

SHI is functional as both a hydrogen oxidation and a proton reduction catalyst when immobilized at a pyrolytic graphite electrode. Solution assays of SHI have shown that the activity is highly dependent on temperature. Thus the electrocatalytic activity of adsorbed SHI was probed at pH 6.5 at temperature in the range 25-80 ºC. Figure 1 shows the electrocatalytic currents, proportional to turnover frequency, for both proton reduction and hydrogen oxidation as well as the ratio of the two catalytic activities. Both hydrogen oxidation and proton reduction activities

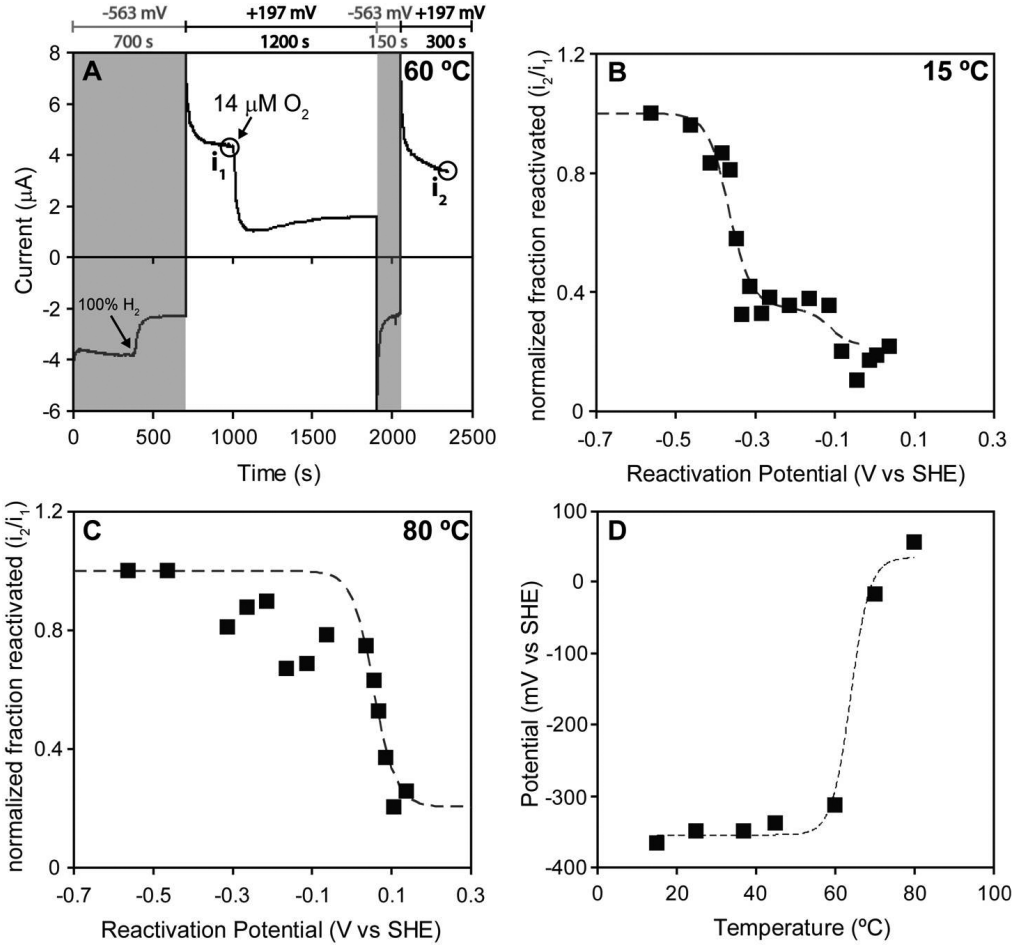

FIGURE 2. SHI reacts with O_2 to form two inactive states that are distinguished by the electrochemical potential required to reactivate them. These reactivation profiles shift to less reducing potentials with increasing temperature. (A) Current-time trace for a chronoamperometry experiment evaluating the catalytic activity of *Pf*SHI in the presence of different gases and at different reduction potentials. The potentials and durations of the various electrochemical steps are noted above the figure. Grey background denotes portions of the experiment in which the potential was more reducing than the hydrogen couple and white background indicates periods in which the working electrode potential was more oxidizing than the hydrogen couple. Changes in the gas composition in the experimental apparatus are indicated by arrows on the current trace. The times at which the currents in later panels were evaluated are indicated by circles. Introduction of hydrogen is continuous, but oxygen was introduced via injection so that it is only transiently present in solution. Control experiments indicate that after injection, 200 s are required for the oxygen concentration to decrease to an undetectable level.

increase directly with temperature. However, the increase of proton reduction activity is far more dramatic. The result of this uneven response is a shift in the catalytic bias of the enzyme towards a marked preference for proton reduction at higher temperatures. Typically, [NiFe]-hydrogenases have been thought of as "uptake" hydrogenases, meaning their activity is higher for the oxidation direction. These results demonstrate that this is clearly an oversimplified understanding of their activities.

Reactions of SHI with oxygen

Prototypical [NiFe]-hydrogenases are known to be reversibly inactivated by both oxidative anaerobic and aerobic conditions. In constrast, so-called oxygen-tolerant [NiFe]-hydrogenases are defined by their ability to maintain some level of hydrogen oxidation activity in the presence of oxygen. Chronamperometry experiments were used to probe the impact of oxygen on the hydrogen oxidation activity of SHI. As shown in Figure 2A, exposure of an enzyme film to oxygen results in an immediate decrease in hydrogen oxidation activity. Although the current decrease is dramatic, the activity drops to a non-zero level. This is in contrast to standard [NiFe]-hydrogenases that are completely inactived by transient exposure to oxygen. Furthermore, after the experimental conditions were returned to anaerobiosis, the immobilized sample spontaneously regained some catalytic activity. Similarly, when the potential was dropped to more reducing conditions, the activity of the enzyme was regained on a timescale of seconds. This reductive reactivation is far faster than that of aerobically inactivated MBHs. Panel 2D shows that the potential of this reduction reactivation, like catalytic bias, was also very sensitive to temperature. It appears that it is thermodynamically easier to reactivate inactive enzyme at more physiologically relevant temperatures.

In addtion to probing the response of SHI to transient exposure to oxygen, we also evaluated the impact of prolonged exposure to oxygen on hydrogen oxidation activity. Figure 3A shows a chronoamperometric trace demonstrating the impact of constant exposure over 900 s to 1% oxygen on hydrogen oxidation catalysis. The catalytic activity drops to zero until the experiment is returned to anaerobic conditions. Following removal of oxygen, a small amount (<2%) of catalytic activity is regained without exposure to reducing conditions. As in the experiments with transient exposure to oxygen, larger fractions of the activity could be recovered by short exposures to reducing conditions. This activity, like the other activities of SHI, also showed a marked temperature dependence (Figure 3B). At higher temperatures, longer exposure to oxygen was necessary to observe complete inactivation. Suprisingly, the inactive form also required longer reduction to regain catalytic activity. This suggests that two inactive forms are generated upon long-term exposure to oxygen, and the ratio of the populations of the two states is highly sensitive to temperature.

Future Directions

SHI clearly demonstrates oxygen-tolerance and is the first oxygen-tolerance soluble hydrogenase to be electrochemically characterize. Oxygen-tolerance in MBHs is thought to arise from the presence of an unusual [4Fe3S] cluster, but phylogenetic analysis suggests that SHs do not possess such a cluster. Thus the explanation of the reactivity of SHI must lie elsewhere. Future studies will target the molecule details of this mechanism.

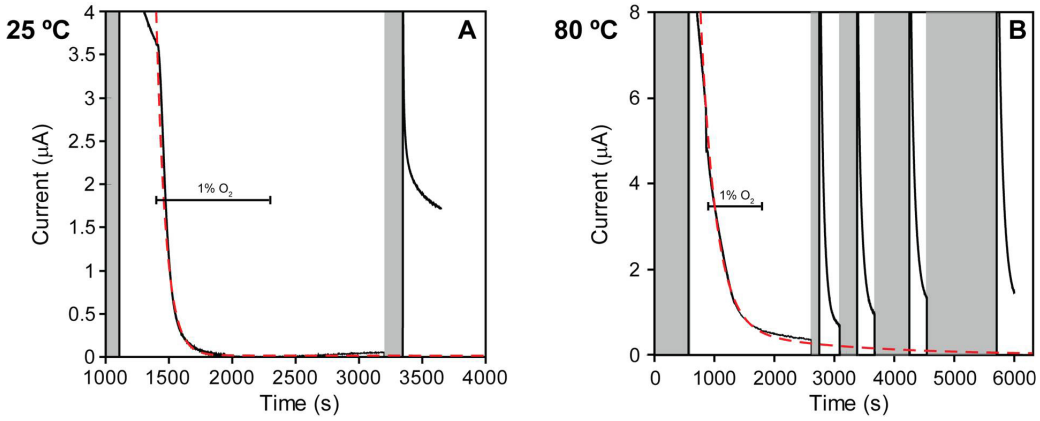

FIGURE 3. Hydrogen oxidation activity under prolonged O_2 exposure at 25 ºC (A) and 80 ºC (B). Gray panels in **(A)** and **(B)** indicate periods where the electrode was held at reducing (-563 mV) potential and white panels indicate periods where the electrode was held at oxidizing (+197 mV) potentials. Unless otherwise indicated, the electrochemical cell is under 100% H_2. At time indicated by the bracketed line, the gas in the electrochemical cell was switched to 1% O_2 in 99% H_2 while simultaneously injecting an air-saturated buffer into the electrochemical cell for a final O_2 concentration of 14 µM. Aerobic inactivation of the enzyme was observed in the form of decreasing H_2-oxidation current.

II.G.6 Hyperthermophilic Multiprotein Complexes and Pathways for Energy Conservation and Catalysis

Principal Investigator: Michael W.W. Adams
Department of Biochemistry and Molecular Biology
University of Georgia
Athens, GA 30602
Phone: (706) 542-2060
Email: adams@bmb.uga.edu

DOE Program Manager: Dr. Robert J. Stack
Phone: (301) 903-5652
Email: robert.stack@science.doe.gov

Objectives

We are investigating the mechanisms of assembly of energy transducing systems, the processes that regulate energy-relevant chemical reactions, the architecture of biopolymers, and the active site protein chemistry leading to efficient bio-inspired catalysts. The novel protein complexes under study have the remarkable property of being synthesized (self-assembling) at temperatures near 100°C in a so-called hyperthermophilic microorganism. Moreover, the novel complexes are involved in the conversion of low potential reducing equivalents into gaseous end products such as hydrogen and hydrogen sulfide, or the oxidation of C1 compounds such as formate and CO, with the concomitant conservation of energy in the form of ion gradients. This is particularly relevant to the DOE mission since a fundamental problem in all photosynthetic reaction systems is the conversion of low potential reductant to a useable form of energy such as an ion motive force.

Technical Barriers

The model microbial system that is being used to study the energy conservation complexes is *Pyrococcus furiosus*. This archaeon grows optimally at 100°C and is also a strict anaerobe that grows in the absence of oxygen.

Abstract

P. furiosus obtains carbon and energy for growth by fermenting carbohydrates and producing H_2 and by reducing elemental sulfur (S°) to H_2S. It has a respiratory metabolism in which it couples H_2 production by a ferredoxin-dependent, membrane-bound hydrogenase (MBH) to ion translocation and formation of a membrane potential that *P. furiosus* utilizes to synthesize ATP. *P. furiosus* also contains a cytoplasmic hydrogenase (SHI) that has the rare property of evolving H_2 from NADPH, a reaction of utility in H_2 production systems. Addition of S° to *P. furiosus* prevents the synthesis of MBH and SHI, and induces the synthesis of a highly homologous membrane complex which we term MBX. MBX is proposed to oxidize ferredoxin, reduce S° and conserve energy by an as yet unknown mechanism. The specific aims of this research are: 1) to characterize the novel energy-conserving complex MBH, 2) to characterize the novel energy-conserving complex MBX, and 3) to structurally characterize native SHI and minimal forms of SHI and MBH. We are taking advantage of our recent development of a genetic system in *P. furiosus* to generate strains containing deletions of key genes, affinity-tagged enzymes and/or over-expressed forms of the enzymes of interest. We are also heterologously expressing in *P. furiosus* H_2-evolving membrane complexes from related archaea that are analogous to MBH. The results of this research will provide a fundamental understanding of energy conservation in *P. furiosus* that involve the metabolism of H_2 gas.

Progress Report

1. Engineering P. furiosus to overproduce its cytoplasmic [NiFe] hydrogenase SHI. SHI is a complex heterotetrameric enzyme that contains flavin and multiple iron-sulfur clusters (Figure 1). Using the new genetic system [1] we have generated a strain of *P. furiosus* that yields approximately10-

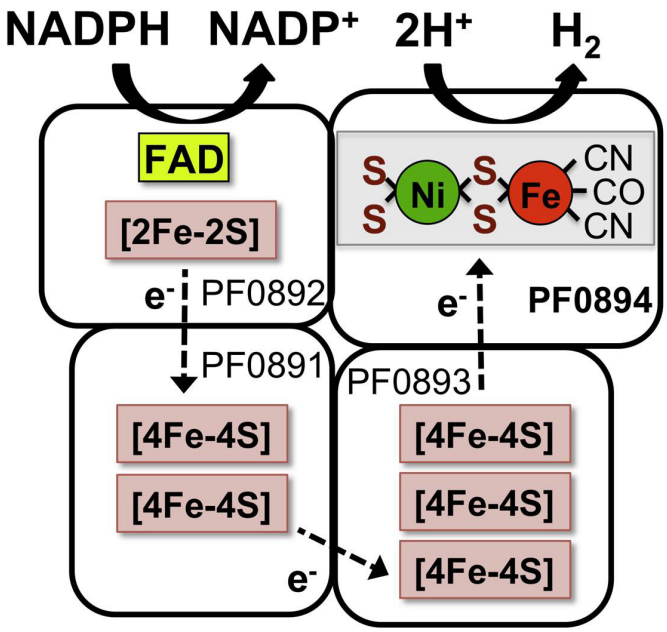

FIGURE 1. Proposed structure and cofactor content of hydrogenase I (SHI).

fold higher amounts of SHI compared to the native purification and produces the affinity-tagged enzyme containing a Step tag to facilitate purification [2].

2. Obtaining deletion strains of P. furiosus lacking both soluble hydrogenases or lacking the membrane-bound hydrogenase and construction of enzyme variants. A deletion mutant lacking both hydrogenases SHI and SHII has been obtained and this shows no phenotype [3]. This means that these enzymes are not essential for growth and we can, therefore, generate a range of 'minimal' and other variants of both enzymes. In addition, a deletion mutant of MBH was obtained and this strain, as expected, only grows in the presence of sulfur [3].

3. Evidence for the membrane-bound hydrogenase of P. furiosus as an ancestral H_2-evolving ion-pumping complex. The 14-subunit membrane-bound [NiFe] hydrogenase (MBH) of *P. furiosus* links the thermodynamically favorable oxidation of ferredoxin with the formation of hydrogen and conserves energy in the form of an ion gradient thereby representing a simple respiratory system within a single complex (Figure 2). This hydrogenase shows a modular composition represented by a Na^+/H^+ antiporter domain (Mrp) and a [NiFe] hydrogenase domain (Mbh). With the availability of a large number of microbial genome sequences, we have shown that homologs of Mbh and Mrp are ubiquitous in the microbial world and some species contain additional domains that catalyze the oxidation of formate, CO or NAD(P)H. The respiratory-type MBH of *P. furiosus* appears to be closely related to the common ancestor of complex I and [NiFe]-hydrogenases in general [4].

4. Purification of the Intact Functional Fourteen-Subunit Respiratory Membrane Bound [NiFe]-Hydrogenase Complex (MBH) of P. furiosus. MBH is encoded by a 14-gene operon with both hydrogenase and Na+/H+ antiporter modules. A His-tagged form MBH with the tag at the N-subunit (Figure 2) was expressed in *P. furiosus* and the detergent-solubilized complex purified under anaerobic conditions by affinity chromatography (unpublished data). Purified MBH contained all 14 subunits by electrophoretic analysis (13 subunits were also identified by mass spectrometry) and had a measured Fe:Ni ratio of 15:1, resembling the predicted value of 13:1. The as-purified enzyme exhibited a rhombic EPR signal characteristic of the ready Ni-B state. The purified and membrane bound forms of MBH both preferentially evolved H_2 with the physiological donor (reduced ferredoxin) as well as with standard dyes. The O_2 sensitivities of the two forms were similar (half-lives of ~15 hr in air), but the purified enzyme was more thermolabile (half-lives at 90 degrees C of 1 hr and 25 hr, respectively). Structural analysis of purified MBH (with John A Tainer, Lawrence Berkeley National Laboratory) by small angle x-ray scattering (SAXS) indicated a Z-shaped structure with a mass of 310 kDa, resembling the predicted value (298 kDa). The SAXS analyses reinforce and extend the conserved sequence relationships of group 4 enzymes and Complex I (NADH quinone oxidoreductase). This is the first report on the properties of a solubilized form of an intact respiratory MBH complex that is proposed to evolve H_2 and pump Na+ ions.

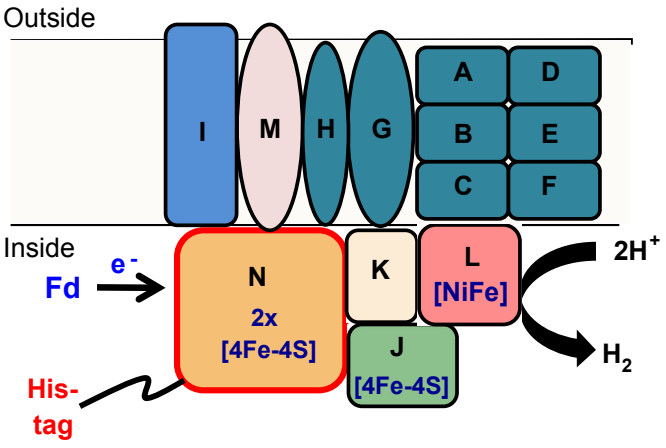

FIGURE 2. Proposed structure of the 14-subunit membrane-bound hydrogenase (MBH).

5. Engineering Hydrogen Gas Production from Formate in P. furiosus by Heterologous Production of an 18-Subunit Membrane-Bound Complex. Although H_2 gas has enormous potential as a source of reductant for the microbial production of biofuels, its low solubility and poor gas mass transfer rates are limiting factors. These limitations could be circumvented by engineering biofuel production in microorganisms that are also capable of generating H_2 from highly soluble chemicals such as formate, which can function as an electron donor. We have now engineered *P. furiosus,* which grows by fermenting sugars to produce H_2, has been engineered to also efficiently convert formate to H_2. Using a bacterial artificial chromosome vector, the 16.9 kb 18-gene cluster encoding the membrane-bound, respiratory formate hydrogen lyase (FHL) complex of *Thermococcus onnurineus* (Figure 3) was inserted into the *P. furiosus* chromosome and expressed as a functional unit [5]. This enabled *P. furiosus* to utilize formate as well as sugars as an H_2 source, and to do so at both 80° and 95°C, near the optimum growth temperature of the donor (*T. onnurineus*) and engineered host (*P. furiosus*), respectively. This accomplishment also demonstrates the versatility of *P. furiosus* for metabolic engineering purposes [5].

6. P. furiosus grows in the presence of oxygen. This organism had always been regarded as an obligate anaerobe that grows by fermenting carbohydrates to H_2, CO_2 and acetate. We have now shown [6] show that it is surprisingly tolerant to oxygen, growing well in the presence of 8% O_2 (v/v). Cell growth and acetate production were not affected by O_2 but H_2 production was reduced by 50%. Analysis of

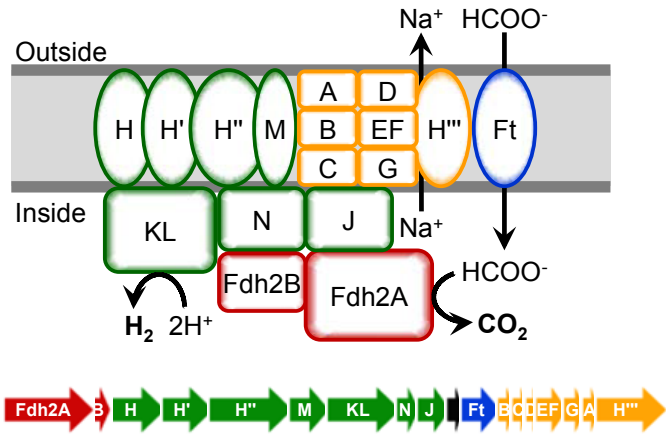

FIGURE 3. The formate hydrogen lyase (FHL) of *T. onnurineus* expressed in *P. furiosus* [5]. Colors represent the hydrogenase (green), formate dehydrogenase (red), the formate transporter (blue) and the Na^+/H^+ antiporter (yellow) modules of this multiprotein complex. The color-coded 18-gene operon that encodes FHL is also shown.

deletion mutants showed that electrons from fermentation are diverted to relieve O_2 stress at the level of reduced ferredoxin before H_2 production occurs. Superoxide reductase and flavo-diiron protein A were shown to play primary roles in removing O_2. These results bode well for using *P. furiosus* to obtain recombinant forms of O_2-requiring or utilizing enzymes [6].

7. Regulation of iron metabolism in P. furiosus. Iron is a key component of the enzymes of interest in *P. furiosus,* namely SHI, MBH and MBX, but how iron assimilation is regulated is completely unknown. Understanding this issue is important in order to ensure that highly up-regulated iron-containing enzymes are not limited for iron. In this work [7] we showed using DNA microarrays of deletion strains grown under iron-sufficient and -limiting conditions, in combination with *in vitro* DNA binding analyses, that DtxR is the key iron-responsive transcriptional regulator. DtxR regulates the expression of the genes encoding two putative iron transporters, Ftr1 and FeoAB while the expected regulator, Fur, was not functional [7].

Future Directions

In the future this research will focus on the characterization of solubilized MBH, the solubilization of the analogous MBX complex from *P. furiosus,* and on the characterization of analogous complexes from other hyperthermophilic archaea that are heterologously-expressed in *P. furiosus.*

Publication list acknowledging DOE grant FG05-95ER20175

1. Bridger, S.L, Lancaster, W.A., Poole, F.L., Schut, G.J. and Adams, M.W.W. Genome sequencing of a genetically-tractable *Pyrococcus furiosus* strain reveals a highly dynamic genome. *J. Bacteriol.* **2012,** *194,* 4097-4106

2. Chandrayan, S.K., McTernan, P.M., Hopkins, R.C., Sun, J., Jenney, F.E. and Adams, M.W.W. Engineering the hyperthermophilic archaeon *Pyrococcus furiosus* to overproduce its cytoplasmic [NiFe]-Hydrogenase. *J. Biol. Chem.* **2012,** *287,* 3257-3264

3. Schut, G.J., Nixon, W.J., Lipscomb, G.L., Scott, R.A. and Adams, M.W.W. Mutational analyses of the enzymes involved in the metabolism of hydrogen by the hyperthermophilic archaeon *Pyrococcus furiosus*. *Frontiers in Microbiology* **2012,** *3,* 163 (1-6)

4. Schut, G.J., Boyd, E.S., Peters, J.W and Adams, M.W.W. The modular respiratory complexes involved in hydrogen and sulfur metabolism by heterotrophic hyperthermophilic archaea and their evolutionary implications. *FEMS Microbiol. Rev.***2013,** *37,* 182-203

5. Lipscomb, G.L., Schut, G.J., Thorgersen, M.P., Nixon, W.J., Kelly, R.M. and Adams, M.W.W. Engineering hydrogen gas production from formate in a hyperthermophile by heterologous production of an 18-subunit membrane-bound complex. *J. Biol. Chem.* **2014,** *289,* 2873-2879

6. Thorgersen, M.P., Stirrett, K., Scott, R.A. and Adams, M.W.W. Mechanism of oxygen detoxification by the surprisingly oxygen-tolerant hyperthermophilic archaeon, *Pyrococcus furiosus. Proc. Natl. Acad. Sci. USA* **2012,** *109,* 18547-18552

7. Zhu, Y., Kumar, S., Menon, A.L., Scott, R.A. and Adams, M.W.W. (2013) "Regulation of Iron Metabolism by *Pyrococcus furiosus*" *J. Bacteriol.* **2014,** *195,* 2400-2407

II.G.7 Photobiohybrid Solar Fuels

Principal Investigator: Paul W. King
NREL
15013 Denver West Parkway
Golden, CO
Phone: (303) 384-6277
Email: paul.king@nrel.gov

Team Members

- Katherine A. Brown (Scientist)
  NREL, Phone: (303) 384-7721
  Email: kate.brown@nrel.gov
- David W. Mulder (Scientist)
  NREL, Phone: (303) 384-7486,
  Email: david.mulder@nrel.gov
- Michael W. Ratzloff (Scientist)
  NREL, Phone: (303) 384-7861,
  Email: mike.ratzloff@nrel.gov

DOE Program Manager: Gail McLean
Phone: (301) 903-7807
Email: Gail.McLean@science.doe.gov

Objectives

The long-term objective of this project is to understand energy transduction in photochemical systems that combine the light harvesting, charge-separation of nanoparticles (NP) with catalytic H_2 activation by hydrogenases as models for solar energy conversion. Light-driven production of H_2 occurs naturally in photosynthetic microbes, where hydrogenases couple to low potential reductant pools and help to maintain electron flow under anaerobic-aerobic transitions. The ubiquitous role of H_2 as an energy carrier in microbial systems is underscored by significant structural-functional diversity among the different hydrogenase enzyme classes. Structural properties including active site coordination, substrate transfer pathways and cofactor compositions of hydrogenases are being investigated towards developing a broad understanding of the determinants that control enzymatic function.

Technical Barriers

The efficiencies of coupling natural or artificial photosynthesis to production of reduced chemical and fuels require a more fundamental understanding of the factors controlling energy transduction reactions, how this process couples to downstream enzymatic reactions, and the catalytic mechanisms. These aims of this project are to investigate the physical, thermodynamic and kinetic parameters of light-harvesting, charge-transfer and catalysis in molecular systems for solar hydrogen production.

Abstract

Photosynthetic light-capture and conversion efficiencies in plant-type systems are constrained at ~12.5% photon-to-fuel due to narrow spectral bandwidth, low-light saturation kinetics and thermodynamic losses during energy transduction. Together these limitations can constrain enzymatic rates to levels that are below full turnover capacities. Semiconducting nanomaterials exhibit a wider spectral response and higher saturation intensities and are promising for use in next generation photovoltaics and for solar harvesting in artificial photosynthetic schemes. To create and control the essential charge-transfer interactions between synthetic chromophores and biocatalysts requires developing a broader understanding of energy transduction processes at molecular junctions. This project integrates fundamental research on structure-function mechanisms of enzymatic H_2 activation, with steady-state and ultrafast measurements of photochemical conversion in enzyme-NP hybrids. The knowledge will be used to help elucidate the physical, thermodynamic and kinetic control of light-harvesting, charge-transfer and catalysis in molecular systems for solar hydrogen production.

Progress Report

Biophysical analysis of [FeFe]-hydrogenase and modeling of the catalytic mechanism

The [FeFe]-hydrogenase from the green alga *Chlamydomonas reinhardtii*, consisting of only the catalytic H-cluster, was analyzed using EPR and FTIR spectroscopy of enzymes poised under reducing and oxidizing conditions. The spectra revealed new paramagnetic signals and IR bands under various reductive treatments. Collectively these results have provided new insights on the electronic structure of the H-cluster, and the basis for a revised catalytic scheme (summarized in Figure 1) for [FeFe]-hydrogenases. The model incorporates electron exchange steps between the two H-cluster ($[4Fe\text{-}4S]_H$ and $2Fe_H$) sub-sites during enzymatic turnover. It has been proposed that oxidation of the $2Fe_H$ sub-site is concomitant with H_2 binding and activation, and necessary for intermolecular electron-transfer reactions to soluble electron carriers.

Solar energy conversion and catalysis in photobiohybrid complexes

We have shown that clostridial [FeFe]-hydrogenase can self-assemble with mercaptopropionic acid (MPA) capped CdS/CdTe quantum dots into photocatalytic complexes (Figure 2). Under illumination, NP light adsorption and charge-separation leads to interfacial electron-transfer into the bound hydrogenase via the ferredoxin-binding site

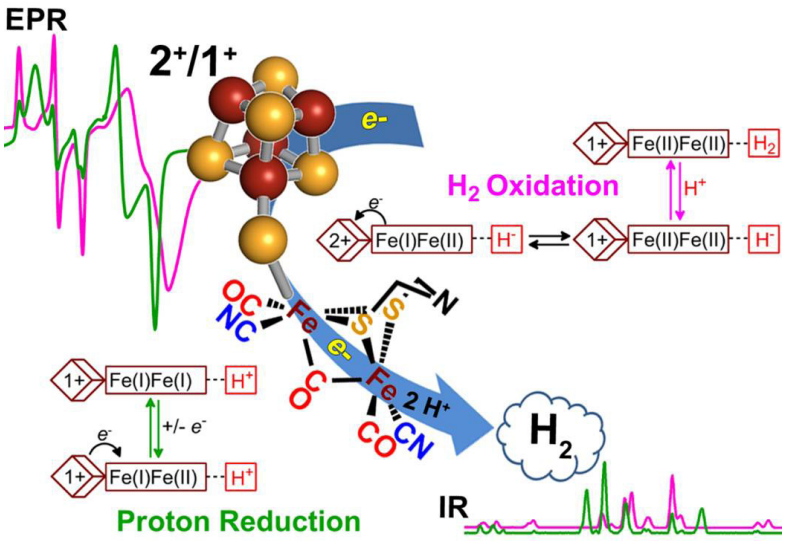

FIGURE 1. EPR (top-left) and IR (bottom-right) spectra of the reduced (green) and H activated (magenta) H-cluster (center) of [FeFe]-hydrogenases are shown along with the proposed models for reversible H_2 catalysis (bottom-left, top-right).

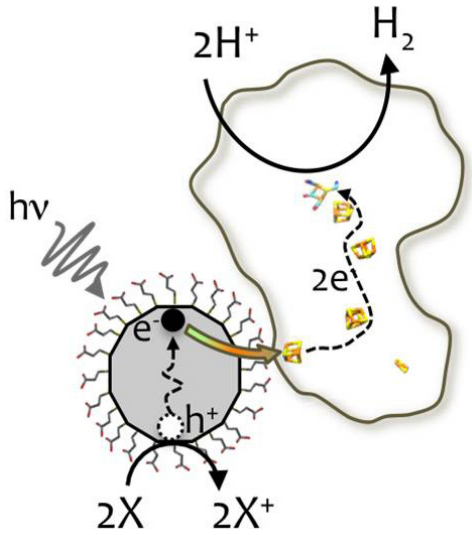

FIGURE 2. NP-hydrogenase complex. Photoexcited electrons from the nanoparticle are injected into hydrogenase to drive H_2 production.

adjacent to a surface localized [4Fe-4S]-cluster. Ultrafast measurements showed photoexcited, interfacial electron-transfer from NPs leads to injection of electrons into the [4Fe-4S] cluster at a rate of ~10^7 s^{-1}. We are currently investigating how altering the kinetics of competing reactions (e.g., NP charge recombination), and the free-energy of the electron-transfer step, affect the quantum yields of H_2 production. Changing NP dimension (e.g., diameter) provides a means to control these properties. The interplay of kinetic/thermodynamic effects are complex, and are further complicated by the inherent heterogeneity of molecular compositions. Resolving the details of each of these effects will help to understand the mechanisms that control energy transduction in nanoparticle-based complexes.

Computational modeling of proton-transfer in [FeFe]-hydrogenase

The free energies along proton-transfer (PT) pathways in [FeFe]-hydrogenase were investigated using QM/MM and umbrella sampling techniques. Key residues were identified along with pK_a estimations from a thermodynamics integration method and used to model PT profiles to the H-cluster.

Single-molecule resolution measurements of enzyme turnover

In collaboration with the Moore and Gust group at ASU, clostridial [FeFe]-hydrogenase was studied on Au electrodes bearing self-assembled thiol monolayers (SAMs). Binding was mediated between positively charged patches on the hydrogenase and carboxylate groups on the SAM. Single-molecule images were obtained in an electrochemical STM and showed the tunneling currents increased under an applied bias, which led to an estimated lower limit k_{cat} value of 20,000 s^{-1}, in combination by macroscopic voltammetry.

Future Directions

- Theoretical calculations on QM/MM H-cluster models poised under different protonation and redox states are being completed towards identifying candidate structures for discrete catalytic intermediates and the relevant vibrational spectra.
- Investigate algal [FeFe]-hydrogenase proton-transfer mutants using FTIR, Mossbauer, HYSCORE and EPR spectroscopy. Current FTIR results indicate disruption of proton-transfer results in the selective enrichment of catalytic site intermediates under reduction. Future work will aim to resolve assignments of IR bands, Fe oxidation levels, H-cluster spin-states in the context of reduction and H_2 oxidation.
- We have been characterizing the electron-transfer and photocatalytic properties of complexes between [FeFe]-hydrogenase and CdS, CdSe and CdTe nanoparticles. These efforts will be aimed at revealing how the physical compositions and dimensions of NPs control electron-transfer rates using ultrafast time-resolved spectroscopy, and measurement of H_2 production quantum yields, towards understanding the thermodynamic and kinetic control of solar conversion in these systems.

- Collaborative studies with Prof Dukovic's group at CU-Boulder are aimed towards developing a comprehensive NP-hydrogenase charge-transfer framework model, and the effects of interfacial ligands (i.e., chain length, head-group chemistry) on k_{ET} dynamics.

Publication list (including patents) acknowledging the DOE grant or contract

1. McDonald, T.J., Svedruzic, D., Kim, Y-H., Blackburn, J.L., Zhang, S. B., King P.W., and Heben, M.J. "Wiring up hydrogenase with single-walled carbon nanotubes." **2007,** *Nano Letts. 7*:3528.

2. Hamourger, M., Gervaldo, M., Svedruzic, D., King, P.W., Gust, D., Ghirardi, M., Moore, A.L. and Moore, T.A. "[FeFe]-hydrogenase-catalyzed H_2 production in a photoelectrochemical biofuel cell." **2008**, *J. Am. Chem. Soc. 130*(6):2015.

3. Chang, C.H., and Kim, K. "Density functional theory calculation of bonding and charge parameters for molecular dynamics studies on [FeFe]-hydrogenases." **2009**, *J. Chem. Theory Comput. 5*(4):1137.

4. Brown, K.A., Dayal, S., Ai, X., Rumbles, G. and King, P.W. "Controlled assembly of hydrogenase-CdTe nanocrystal hybrids for solar hydrogen production." **2010**, *J. Am. Chem. Soc. 132*(28):9672.

5. Yacoby, I., Pochekailov, S., Tiporik, H., Ghirardi, M.L., King, P.W., and Zhang, S. "Photosynthetic electron partitioning between [FeFe]-hydrogenase and ferredoxin:$NADP^+$-oxidoreductase (FNR) enzymes *in vitro*." *Proc. Natl. Acad. Sci. U.S.A.* **2011,** *108*:9396.

6. Chang, C.H. "Computational chemical analysis of [FeFe] hydrogenase H-cluster analogs to discern catalytically relevant features of the natural diatomic ligand configuration." *J. Phys. Chem. A.* **2011,** *115*(31):8691.

7. Madden, C., Vaughn, M.D., Diez-Perez, I., Brown, K.A., King, P.W., Gust, D., Moore, A.L. and Moore, T.A. "Catalytic turnover of [FeFe]-hydrogenase based on single-molecule imaging." *J. Am. Chem. Soc*. **2012***, 134*:1577.

8. Brown, K.A., Wilker, M.B., Boehm, M., Dukovic, G., and King, P.W. "Characterization of photochemical processes of H_2 production by CdS nanorod-[FeFe] hydrogenase complexes." *J. Am. Chem. Soc.* **2012**, *134*(12):5627.

9. Yacoby, I., Tegler, L.T., Pochekailov, S., Zhang, S. and King, P.W. "Optimized expression and purification for high-activity preparations of algal [FeFe]-hydrogenase." *PLoS ONE.* **2012**, e0035886.

10. Mulder, D.W., Ratzloff, M.W., Shepard, E.M., Byer, A.S., Noone, S.M., Peters, J.W., Broderick, J.B., and King, P.W. "EPR and FTIR analysis on the mechanism of H_2 activation by [FeFe]-hydrogenase HydA1 from *Chlamydomonas reinhardtii*." *J. Am. Chem. Soc*. **2013**, *135*(8):6921.

12. King, P.W. "Designing interfaces of hydrogenase-nanomaterial hybrids for efficient solar conversion." *Biochim. Biophys. ACTA-Bioenergetics*. **2013**, *1827*(8-9):949.

13. Long, H., King, P.W., and Chang, C.H. "Proton Transport in *Clostridium pasteurianum* [FeFe] hydrogenase I:A computational study." *J. Phys. Chem. B.* **2014,** *118:*890.

14. Wilker, M.B., Shiopoulos, K., Brown, K.A., Mulder, D.W., King, P.W., and Dukovic, G. "Electron transfer kinetics in CdS Nanorod-[FeFe]-hydrogenase complexes and implications for photochemical H_2 generation." *J. Am. Chem. Soc.* **2014,** *136*:4316.

II.G.8 Heterogeneous Water Oxidation Catalysis With Molecular Catalysts

Principal Investigator: Javier J. Concepcion

Brookhaven National Laboratory
Chemistry Department
Bldg. 555A
P.O. Box 5000
Upton, NY 11973-5000
Phone: (631) 344-4369
Email: jconcepc@bnl.gov

Names of Team Members

- Etsuko Fujita
  Brookhaven National Laboratory
  Chemistry Department
  Bldg. 555A
  P.O. Box 5000
  Upton, NY 11973-5000
  Phone: (631) 344-4356
  Email: fujita@bnl.gov
- James Muckerman
  Brookhaven National Laboratory
  Chemistry Department
  Bldg. 555A
  P.O. Box 5000
  Upton, NY 11973-5000
  Phone: (631) 344-4368
  Email: muckerma@bnl.gov

DOE Program Manager: Mark Spitler

Phone: (301) 903-4568
Email: Mark.Spitler@science.doe.gov

Objectives

- **Development of fast, efficient and robust molecular water oxidation catalysts:** Design, synthesis and characterization of molecular water oxidation catalysts capable of carrying up this reaction with high turnover frequencies (fast) at low overpotentials (efficient) and with high turnover numbers (robust).
- **Deep understanding of the mechanism(s) of water oxidation:** Mechanistic studies using a combination of experimental techniques and DFT calculations to gain insight into the interplay of thermodynamics and kinetics in water oxidation catalysis.
- **Development of stable anchoring groups/ heterogenization:** Incorporation of anchoring groups on molecular water oxidation catalysts for attachment to planar and high surface area electrodes. Evaluation of catalytic activity in a true device configuration.

Technical Barriers

- The development of efficient water oxidation catalysts is one of the limiting factors in solar fuels production via artificial photosynthesis.
- Water oxidation is a complex process involving multi-electron, multi-proton steps. Isolation/characterization of intermediates is difficult due to the harsh conditions used to study this reaction. Progress has been made but a better mechanistic understanding is needed, especially on metal oxide surfaces in a true device configuration.
- Available/known anchoring groups from dye-sensitized solar cells are usually stable in organic solvents but not in aqueous solutions under water oxidation conditions.

Abstract

Water oxidation to oxygen in nature's photosynthesis is the source of most of the energy we use today. It is also anticipated to be the source of most of the energy we use in the future through artificial photosynthesis. For the latter, one of the main challenges is the development of efficient and robust water oxidation catalysts. We are developing new water oxidation catalysts and performing detailed mechanistic studies using a combination of experimental and theoretical tools. In addition, we are combining studies with catalysts in solution using sacrificial oxidants and electrochemical techniques with studies of "heterogeneous" catalysis with the catalysts anchored to planar and high surface area electrodes. We have discovered significant differences in both catalytic activity and mechanistic details between solution and surface studies. Furthermore, there are also significant differences between catalytic behavior in planar and high surface area electrodes. These results emphasized the need to study water oxidation catalysis under true device configuration conditions.

Progress Report

We have developed a series of catalysts that can efficiently oxidize water to oxygen, Figure 1. These catalysts seem to follow catalytic cycles involving seven coordinate intermediates, although different mechanisms are operative for the different families of catalysts. We have also developed anchoring groups that are appropriate for these catalyst's structural motifs.

We have used a combination of experimental techniques and DFT calculations to understand how these catalysts oxidize water. One of the most powerful tools to study water oxidation catalysis is electrochemistry. We have

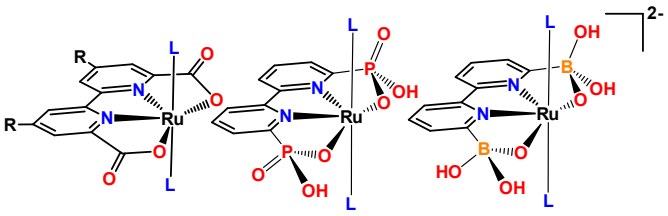

FIGURE 1. Representative structures of catalysts

used this technique to generate intermediates that have been characterized by X-ray crystallography. In addition, combining surface anchoring to metal oxide electrodes with rotating ring-disc electrode techniques has allowed us to study water oxidation catalysis in a true device configuration. These experiments provide all the required information regarding catalytic activity but in addition they also provide mechanistic insight.

We have employed high surface area transparent conductive metal oxide electrodes to perform spectroelectrochemistry of surface-bound water oxidation catalysts. We have been able to identify key intermediates in the water oxidation cycle using this technique by comparison with calculated absorption spectra from time-dependent DFT calculations.

Future Directions

We are currently developing new catalysts based on the gained knowledge from previous experiments and DFT calculations. We are also developing new approaches for "surface synthesis" of highly efficient molecular water oxidation catalysts with long-term surface stability. These approaches also take into account the combination of catalysts and chromophores for incorporation into solar cells for light-driven water splitting.

II.G.9 Proton-Coupled Electron Transfer in Artificial Photosynthesis

Principal Investigator: Dmitry Polyansky
Department of Chemistry
Brookhaven National Laboratory
Upton, New York 11973-5000
Phone: (631) 344-3415
Email: dep@bnl.gov

David Grills, Javier Concepcion,
James T. Muckerman and Etsuko Fujita
Department of Chemistry, Brookhaven National Laboratory
Upton, New York 11973-5000

DOE Program Manager: Mark T. Spitler
Email: Mark.Spitler@science.doe.gov

Abstract

Artificial photosynthetic systems exploit a variety of photochemical transformations with the ultimate result of efficient conversion of the energy of photons into chemical bonds. The efficiency of these transformations strongly depends on how successfully PCET processes are implemented. In this part of our program we focus on mechanistic understanding of the role of PCET in reactions such as: (1) photochemical formation and reactivity of NADPH-like transition metal complexes; (2) hydrogen atom transfer (HAT) in the excited states of transition metal systems; and (3) light-driven water oxidation catalyzed by transition metal complexes.

Progress Report

Photochemical formation and reactivity of NADPH-like transition metal complexes

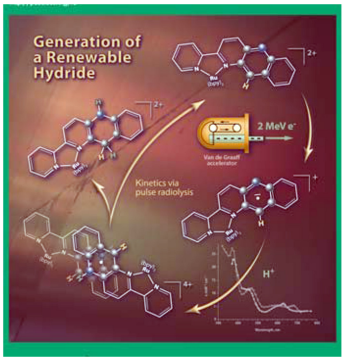

Understanding the ability of NADPH model compounds to shuttle charge in a manner that is coupled to the proton movement in reactions such as HAT or hydride ion transfer is crucial for development of efficient systems involving light-induced charge separation, charge transfer and catalytic systems. In our early work, we found that the renewable hydride donor $[Ru(bpy)_2(pbnHH)]^{2+}$ (bpy = 2,2′-bipyridine, pbn = 2-(2-pyridyl)benzo[*b*]-1,5-naphthyridine) can be

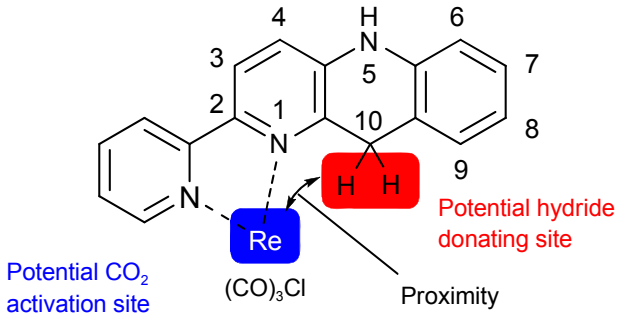

generated photochemically in high yields (quantum yield ca. 21% at 355 nm and quantitative chemical yield) and its formation in the low pH region is mainly achieved through disproportionation of a π-stacking dimer via an intermolecular PCET reaction [1,2]. The net hydride ion transfer reaction from photo-generated hydride donors was found to be controlled by steric factors around the hydride donor sites [4]. The hydride donor ability of the produced organic hydrides was not sufficient to reduce uncoordinated CO_2, however the further photogenerated one-electron reduced form shows reactivity towards $[CpRe^{I}(NO)(CO)_2]^{+}$ (CO and CH_4 products were observed) [5]. We have also investigated the effect of combining both a CO_2 activation site and a hydride donating site in the same coordination sphere of *fac*-Re(pbn)$(CO)_3$Cl on catalytic CO_2 reduction. It was found that the second reduction potential (–1.65 V under Ar) shifted in a positive direction to –1.44 V under CO_2 atmosphere (acetonitrile solution containing Re(pbn)$(CO)_3$Cl and ~0.3 M water, indicating a chemical process, i.e., CO_2 binding to the complex. A 12-fold current enhancement was observed at –2.11 V with 0.26 M CO_2 in the presence of water in acetonitrile solution. The rate constant for CO_2 reduction was estimated as ~300 M^{-1} s^{-1}. Controlled potential electrolysis of Re(pbn)$(CO)_3$Cl at –2.11 V produced CO with a Faradaic efficiency of ~70 %.[8]

Hydrogen atom transfer in the excited states of transition metal systems

Within the scope of this project we study light-driven CPET reactions between a series of NAD^+ model compounds, such as $[Ru(bpy)_2(pbn)]^{2+}$, $[Ru(bpy)_2(bpz)]^{2+}$, $[Ru(bpz)_3]^{2+}$ (bpy = 2,2′-bipyridine, pbn = 2-(2-pyridyl) benzo[*b*]-1,5-naphthyridine, bpz = 2,2′-bipyrazine) and hydrogen atom donors, such as substituted hydroquinones and para-substituted phenols. We found that in solvents with high donor numbers (e.g., acetonitrile), the strong hydrogen bonding between phenol donors and solvent molecules results in significant kinetic solvent effects (KSEs). It is necessary to account for these effects if any mechanistic conclusions are based on the rate analysis.

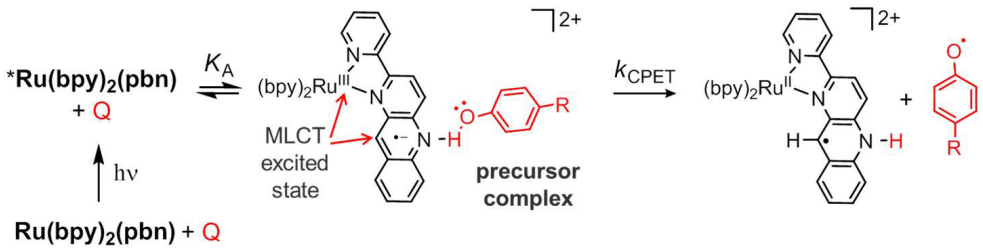

The use of low coordinating solvents such as dichloromethane enabled the measurements of CPET rate constants with minimum contribution from KSE. Based on the transient spectra and observation of substantial kinetic isotope effects (KIEs) the quenching of the excited state of all metal complexes by *para*-substituted phenols proceeds through a CPET mechanism except for the $[Ru(bpz)_3]^{2+}$ / *para*-nitrophenol pair, which follows an electron-transfer (ET) mechanism. The analysis of activation parameters for CPET is indicative of zero or slightly negative activation energy, with significant negative activation entropies contributing to the overall free energy barrier. On the other hand, in the case of the ET reaction a positive activation energy and virtually zero activation entropy are observed making it distinctly different from CPET. The analysis of kinetic data using Marcus theory provides deeper insight into how the mechanism of CPET compares to ET reactions.

Light-driven water oxidation catalyzed by transition metal complexes

Another aspect of our work is related to studies of light-induced catalytic reactions. A system in which a water oxidation catalyst interacts directly in uni- or bi-molecular fashion with photoinduced charges can provide valuable mechanistic insights. In our recent work, we have demonstrated that the mononuclear ruthenium catalyst $[Ru(NPM)(pic)_2]^{2+}$ (**1**) (NPM = 4-*t*-butyl-2,6-di-1',8'-(naphthyrid-2'-yl)-pyridine, pic = 4-picoline) can promote light-driven water oxidation with 9% quantum efficiency in homogeneous aqueous solution in the presence of $[Ru(bpy)_3]^{2+}$ and $[S_2O_8]^{2-}$ [6]. With complex **1**, we were able to reach a TON and TOF of > 103 and 0.12 s^{-1}, respectively. These values render catalyst **1** to be one of the most active mononuclear ruthenium-based catalysts for light-driven water oxidation in a homogeneous system. According to the previously proposed mechanism for water oxidation catalyzed by **1**, a low-energy pathway for O–O bond formation via the $[Ru^{IV}=O]^{2+}$ intermediate can be achieved at neutral pH [3], thus enabling the use of a mild oxidant such as photogenerated (1.26 V vs NHE) $[Ru(bpy)_3]^{3+}$. Our work demonstrates that catalytic pathways for complex **1** can be tuned by a simple change of proton concentration, and that the more efficient low energy "direct pathway" enables photochemical water oxidation using $[Ru(bpy)_3]^{2+}$ with persulfate . In addition, we have established a comprehensive model for the accurate description of similar reactions involving catalyst/sensitizer/quencher systems [7]. We are planning to extend this work to other catalytic systems in order to explore their advantages and limitations under photochemical conditions.

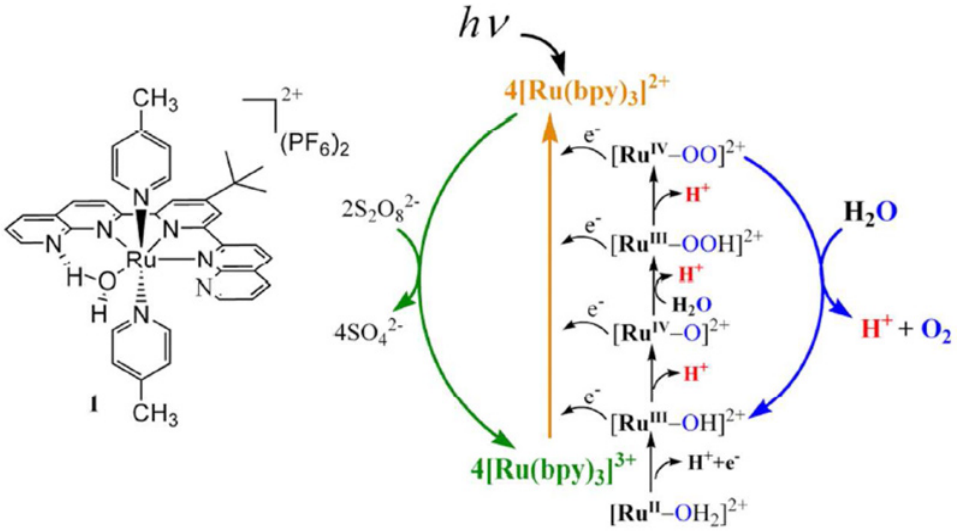

Publication list acknowledging the DOE grant or contract

1. Doherty, MD.; Grills, D. C.; Muckerman, J.T.; Polyansky, D.E.; Fujita, E. "Toward More Efficient Photochemical CO_2 Reduction: Use of $scCO_2$ or Photogenerated Hydrides," *Coord. Chem. Rev.* **2010**, *254,* 2472-2482.

2. Cohen, B.W.; Polyansky, D.E.; Zong, R.; Zhou, H.; Ouk, T.; Cabelli, D.; Thummel, R.P.; Fujita, E. "Differences of pH-Dependent Mechanisms on Generation of Hydride Donors using Ru(II) Complexes Containing Geometric Isomers of NAD^+ Model Ligands: NMR and Radiolysis Studies in Aqueous Solution," *Inorg. Chem.* **2010**, *49*, 8034-8044.

3. Polyansky, D.E.; Muckerman, J.T.; Rochford, J.; Zong, R.; Thummel. R.P.; Fujita, E. "Water Oxidation by a Mononuclear Ruthenium Catalyst: Characterization of the Intermediates," *J. Am. Chem. Soc.* **2011**, *133*, 14649-14665.

4. Cohen, B.W.; Polyansky, D.E.; Achord, A.; Cabelli, D.; Muckerman, J.T.; Tanaka, K.; Thummel, R.P.; Zong, R.; Fujita, E. "Steric Effect for Proton, Hydrogen-Atom, and Hydride Transfer Reactions with Geometric Isomers of NADH-Model Ruthenium Complexes," *Faraday Discuss.* **2012**, *155*, 129-144.

5. Muckerman, J.T.; Achord, P.; Creutz, C.A.; Polyansky, D.E.; Fujita, E. "Calculation of Thermodynamic Hydricities and the Design of Hydride Donors for CO_2 Reduction," *Proc. Nat. Acad. Sci. USA* **2012**, *109*, 15657-15662.

6. Lewandowska-Andralojc, A.; Polyansky, D.E.; Zong, R.; Thummel, R.P.; Fujita, E. Enabling Light-Driven Water Oxidation via a Low Energy Ru^{IV}=O Intermediate, *Phys. Chem. Chem. Phys.* ***2013,*** *15, 14058-14068.*

7. Lewandowska-Andralojc, A. and Polyansky, D.E. "Mechanism of the Quenching of the Tris(bipyridine)ruthenium(II) Emission by Persulfate: Implications for Photo-Induced Oxidation Reactions" *J. Phys Chem. A* **2013**, *117*, 10311–10319.

8. Matsubara, Y.; Hightower, S.H.; Chen, J.; Grills, D.C.; Polyansky, D.E.; Muckerman, J.T.; Tanaka, K.; Fujita, E. "Reactivity of a *fac*-ReCl(α-diimine)$(CO)_3$ complex with an NAD+ model ligand toward CO_2 reduction" *Chem. Commun.* **2014**, *50*, 728-730.

II.G.10 Joint Center for Artificial Photosynthesis: An Overview

Principal Investigator: Carl Koval
California Institute of Technology, Pasadena, CA

Team Members
Hans J. Lewerenz and Frances Houle (Department Heads), Nate Lewis (Scientific Director), Xenia Amashukeli and Will Royea (Asst. Directors), Cliff Kubiak, Don Tilley, Alex Bell, John Hemminger, Manny Soriaga, Joel Ager, Nate Lewis, Harry Atwater, Nate Lynd, Tom Jaramillo, Jonas Peters, John Gregoire, Heinz Frei, Jian Jin, C.X. Xiang, Ian Sharp, Chris Karp, Bill Goddard, Martin Head-Gordon, Lin-Wang Wang, Robert Nielsen, Adam Weber, Carl Koval, Frances Houle, Junko Yano (Project and Team Leads and Co-leads). Institutions: California Institute of Technology, Lawrence Berkeley National Laboratory, SLAC National Laboratory, UC Irvine, UC San Diego

DOE Program Manager: Gail McLean
Phone: (301) 903-7807
Email: gail.mclean@science.doe.gov

Objectives

The mission of the Joint Center for Artificial Photosynthesis (JCAP) is to produce fundamental scientific discoveries and major technological breakthroughs to enable the development of energy-efficient, cost-effective, and commercially viable processes for the large-scale conversion of sunlight directly to fuels. JCAP's 5-year goal is discovery of robust, Earth-abundant light absorbers, catalysts, linkers, membranes, and scale-up science required to assemble the components into a complete artificial photosynthetic system.

Technical Barriers

While a substantial advances in materials components and subassemblies that demonstrate water splitting have been reported in the literature, the work has been focused primarily on making scientific progress rather than creation of efficient, stable, durable, and scalable solar fuels generator systems. JCAP's work aims to bridge that gap.

Abstract

JCAP's technical program spans discovery science through early technology demonstration. In this talk an overview of the Center is presented, highlighting unique capabilities developed by JCAP, and briefly summarizing recent scientific advances.

Progress Report

A cartoon of JCAP's target, a fully integrated photoelectrochemical device architecture, is shown in Figure 1. The assembly is a tandem semiconductor microwire array embedded in a conductive gas-separation membrane and decorated with catalysts for water splitting and/or carbon dioxide reduction. The assembly is immersed in 1 Molar aqueous acid or base to support photoelectrochemical device efficiency. The diversity of science and engineering research challenges that must be met to achieve JCAP's mission of building and demonstrating such a device is extremely broad. In order to focus its portfolio, JCAP's approach is to start with development of robust concepts for complete solar-fuels generators containing the devices, then to break them down into essential assemblies of active components, and finally to adapt or discover the materials needed to fabricate those assemblies, as illustrated in Figure 2.

Prototypes

JCAP's prototyping strategy is to use robust engineering principles and processes to design, model, assemble, test and analyze prototypes of complete artificial photosynthetic systems. As a result, JCAP's prototyping team is able to (a) evaluate component-level performance within integrated systems under realistic operating conditions; (b) utilize

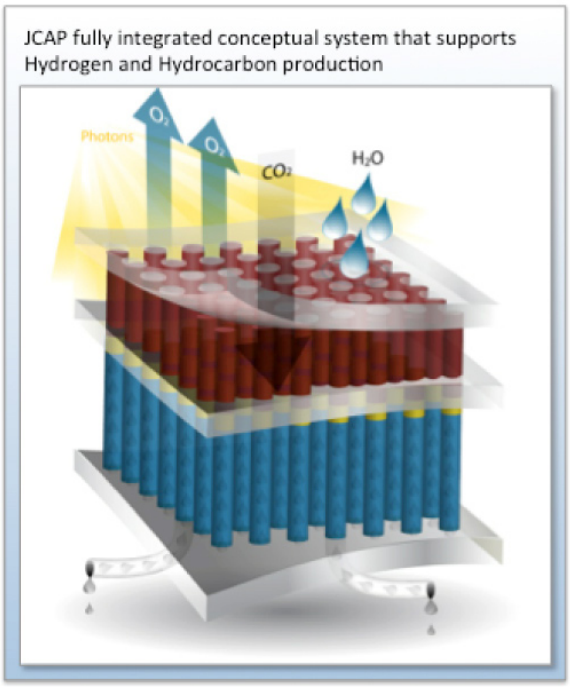

FIGURE 1. JCAP solar fuels device concept

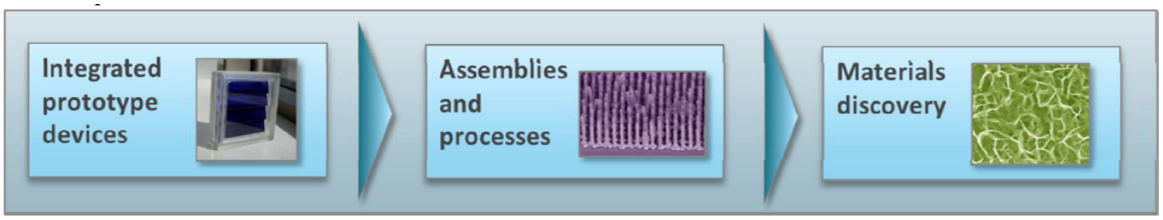

FIGURE 2. Schematic of JCAP's research and development flow.

3-D and 2-D modeling tools to develop and characterize prototype modules; (c) gain insight into which scientific and engineering approaches prove to be more robust and are therefore preferable; and (d) inform the R&D agenda on key bottlenecks associated with JCAP's technology. Specific focus areas are material selection, assembly and integration strategies, with evaluation of stability, performance, and ultimately cost. In the past year, JCAP has initiated analytical studies aimed at understanding requirements for solar-fuels generating facilities at the GW scale, and also manufacturing strategies for solar water-splitting modules.

Materials Integration and processing

In order to assemble solar-fuels generators, JCAP needs to develop and understand the integration of materials and processes over a wide range of length scales. One of JCAP's most important accomplishments has been the development of n-p+-Si/n-WO_3 and n-p+-Si/n-TiO_2 core-shell microwire devices for solar water splitting in acidic and basic electrolytes. These are embodiments of the concept in Figure 1. Preparation of these complex structures requires optimization and control of a series of processing techniques and instruments. Furthermore, even after the procedures for making highly integrated materials is accomplished at a laboratory scale (< 1 cm^2), there are many other additional challenges associated with scaleup and characterization of these processes to dimensions that are necessary for prototypes (10 cm^2 or larger). Another critical integration issue is the ability to protect materials from corrosion and other damaging processes during operation in extreme pH in a complete device. JCAP has made significant progress in the ability to use atomic layer deposition (ALD) and nanostructuring to protect both photocathodes and photoanodes for up to hundreds of hours under hydrogen evolution reaction (HER) and oxygen evolution reaction (OER) conditions, respectively, in highly acidic and basic electrolytes. The performance and stability of individual material components also greatly depend on the integrity of their interfaces. JCAP is addressing the knowledge gaps in the field of heterogeneous catalyst-light absorber interfaces by systematically investigating the effect of catalyst deposition strategies on photoelectrochemical energy-conversion, product selectivity, and stability for different classes of photoanodes and photocathodes to determine how and why certain physical attachment techniques work. Advanced spectromicroscopy and surface mapping techniques are being utilized to investigate, at the nanoscale, the surface potential and conductivity of various catalyst and light capture systems to understand their properties and to identify why some materials form good contacts while others do not. The findings will increase understanding of the criteria necessary for effective device integration and allow for optimization of the catalyst-semiconductor assemblies. JCAP is also investigating the stable attachment of molecular catalysts on photocathodes and photoanodes in aqueous electrolytes without adversely influencing the performance of the semiconductor light absorber or catalyst.

Discovery, characterization and understanding of materials

Many of the materials required for integrated, efficient, and stable solar-fuels generators do not yet exist. Therefore the Hub is accelerating the needed discovery process by utilizing both traditional (i.e.,directed) and high-throughput synthesis and characterization methods, and by appropriate use of computational theory and DOE User Facilities. JCAP materials discovery and characterization efforts have resulted in the development of entirely new capabilities and techniques that benefit the entire solar-fuels community.

Objective performance characterization of the most promising catalyst and light absorbing materials is critical facilitating of comparisons of newly discovered materials to existing ones in a meaningful way. JCAP Benchmarking develops and implements uniform methods and protocols for characterizing the activities of OER, HER, and carbon dioxide reduction reaction (CO2RR) catalysts under solar-fuels generator operating conditions.

To complement JCAP's directed approach toward material development, the Hub is heavily invested in the accelerated, high throughput synthesis and analysis of promising materials by the High-Throughput Experimentation Project. The HTE project demonstrated significant breakthroughs in instrumentation innovation and has enabled discovery of new classes of water oxidation catalysts.

JCAP has a portfolio of research projects aimed at the directed discovery, characterization and understanding of light absorber, catalyst and membrane materials. JCAP's

computational theory effort elucidates how the composition and structure of molecular and heterogeneous catalysts affect their activity for the HER, OER and CO2RR. JCAP is focused on identifying either a single or a tandem combination of stable, scalable, and efficient light absorbers that provide the required photovoltage to produce fuels from sunlight. JCAP has developed suitable materials choices for photocathodes, including Si and WSe_2, that are relatively stable and have demonstrated high efficiency for the solar-driven production of H_2 from H_2O. However, a major technology gap is to obtain a stable earth-abundant light absorber having a band gap in the 1.7–2.3 eV range, to either complement these materials in a tandem structure as a photoanode, or to autonomously enable the direct production of fuel from sunlight. New photoanodes are identified through a variety of routes. JCAP has aimed a significant and fundamental theory effort at this gap, and is working to predict, using ab initio calculations, the synthesis conditions, performance, and stability of promising photoanode materials. Guided by a detailed understanding of optical interactions, researchers from JCAP and the Center for Energy Nanoscience, a DOE Energy Frontier Research Center, demonstrated that a sparse array of GaAs nanowires (<10% areal coverage) has nearly 100% photoelectrochemical charge conversion efficiency. JCAP has discovered and characterized a new class of light absorbers, $ZnSn_xGe_{1-x}N_2$, whose direct band gap can be tuned from 2 eV to 3.1 eV by simple control of the composition. Two new and scalable thin-film deposition methods for $BiVO_4$, a photoanode material composed of earth-abundant elements, were developed. Both methods provide control of stoichiometry, which is important for their use. It also enables understanding of the basic properties of the materials and maximizing OER performance through learning how to work with complex oxide film stacks.

Each half reaction in solar water-splitting requires discovery of stable catalysts that promote the oxidation of water and the reduction of protons at low overpotentials. The challenge is to identify earth-abundant elements for use as catalysts that are comparable or superior in activity to rare and precious metals. JCAP's Heterogeneous Catalysis project is addressing these technical gaps by performing characterization of the physical and chemical properties of catalytic materials using state-of-the-art in surface science and beamline capabilities, and participates in the work of the HTE project to discover completely new catalyst systems. JCAP is also investigating molecular catalysts for CO2RR, because no catalysts (molecular or heterogeneous) exist at present that can selectively reduce CO_2 at rates and efficiencies required by a JCAP solar-fuels device.

A fully integrated solar-fuels generator requires separation of gaseous products for both safety and efficiency, while maintaining sufficient ion-conduction between the reduction and oxidation chambers. JCAP is developing mechanically stable ion conducting and gas impermeable membranes that can be fully integrated with assemblies of photocatalytic units and enable their efficient function.

Future Directions

Work in progress in JCAP places strong focus on continuing the discovery of new photoanode materials, corrosion protection schemes, and acid-stable oxygen evolution reaction catalysts in order to demonstrate stable devices capable of 10% hydrogen generation efficiency from water splitting. Catalyst studies have also expanded to include heterogeneous CO_2 reduction catalysts with a specific focus on understanding the reaction mechanisms so that selective catalysts can be designed.

Publication list (including patents) acknowledging the DOE grant or contract

(please note – JCAP has over 100 papers published and submitted since October 2010. The following are a selection. Please see the other JCAP abstracts in this collection for additional key publications.)

1. Chen, S.Y.; Wang, L.W., Thermodynamic Oxidation and Reduction Potentials of Photocatalytic Semiconductors in Aqueous Solution. *Chemistry of Materials* **2012**, *24*, 3659-3666

2. Haussener, S.; Xiang, C.X.; Spurgeon, J.M.; Ardo, S.; Lewis, N.S.; Weber, A.Z., Modeling, simulation, and design criteria for photoelectrochemical water-splitting systems. *Energy & Environmental Science* **2012**, *5*, 9922-9935.

3. Casalongue, H.S.; Kaya, S.; Viswanathan, V.; Miller, D.J.; Friebel, D.; Hansen, H.A.; Norskov, J.K.; Nilsson, A.; Ogasawara, H., Direct observation of the oxygenated species during oxygen reduction on a platinum fuel cell cathode. *Nature Communications* **2013**, *4*, 6

4. Hu, S.; Chi, C.Y.; Fountaine, K.T.; Yao, M.Q.; Atwater, H.A.; Dapkus, P.D.; Lewis, N.S.; Zhou, C.W., Optical, electrical, and solar energy-conversion properties of gallium arsenide nanowire array photoanodes. *Energy & Environmental Science* **2013**, *6*, 1879-1890.

5. Hu, S.; Xiang, C.X.; Haussener, S.; Berger, A.D.; Lewis, N.S., An analysis of the optimal band gaps of light absorbers in integrated tandem photoelectrochemical water-splitting systems. *Energy & Environmental Science* **2013**, *6*, 2984-2993

6. Sampson, M.D.; Froehlich, J.D.; Smieja, J.M.; Benson, E.E.; Sharp, I.D.; Kubiak, C.P., Direct observation of the reduction of carbon dioxide by rhenium bipyridine catalysts. *Energy & Environmental Science* **2013**, *6*, 3748-3755

7. Schneider, Y.; Modestino, M.A.; McCulloch, B.L.; Hoarfrost, M.L.; Hess, R.W.; Segalman, R.A., Ionic Conduction in Nanostructured Membranes Based on Polymerized Protic Ionic Liquids. *Macromolecules* **2013**, *46*, 1543-1548

8. Zhai, P.; Haussener, S.; Ager, J.; Sathre, R.; Walczak, K.; Greenblatt, J.; McKone, T., Net primary energy balance of a solar driven photoelectrochemical water-splitting device. *Energy & Environmental Science* **2013**, *6*, 2380-2389

9. Modestino, M.A.; Walczak, K.A.; Berger, A.; Evans, C.M.; Haussener, S.; Koval, C.; Newman, J.S.; Ager, J.W.; Segalman, R.A., Robust production of purified H_2 in a stable, self regulating, and continuously operating solar fuel generator. *Energy & Environmental Science* **2014**, *7*, 297-301

II.G.11 Joint Center for Artificial Photosynthesis: Corrosion Protection Schemes to Enable Durable Solar Water Splitting Devices

Principal Investigator: Carl Koval
California Institute of Technology, Pasadena, CA

Team Members

- Ian Sharp (idsharp@lbl.gov, Team Lead), Jinhui Yang, Yongjing Lin, Ali Javey, Joel Ager (Project Lead)
  Lawrence Berkeley National Laboratory
- Shu Hu, Michael Lichterman, Nate Lewis (Scientific Director and Project Lead)
  California Institute of Technology

DOE Program Manager: Gail McLean
Phone: (301) 903-7807
Email: gail.mclean@science.doe.gov

Objectives

The mission of the Joint Center for Artificial Photosynthesis (JCAP) is to produce fundamental scientific discoveries and major technological breakthroughs to enable the development of energy-efficient, cost-effective, and commercially viable processes for the large-scale conversion of sunlight directly to fuels. In pursuit of this mission, JCAP has initiated a focused activity devoted to the development of methods for stabilizing otherwise unstable semiconductor light absorbers under harsh acidic or alkaline conditions. This cross-cutting effort, involving multiple JCAP projects and investigators, aims to greatly expand the range of materials available for integrated solar water splitting devices by providing a broadly applicable portfolio of corrosion protection solutions.

Technical Barriers

A basic requirement for scalable solar fuel systems is safety; eliminating the possibility of forming explosive product mixtures necessitates incorporation of membranes in current integrated architectures and imposes a constraint for operation under extreme pH conditions, either acidic or alkaline, in order to eliminate pH gradients in the absence of recirculation.[1] At present, the central challenge of artificial photosynthesis is the availability of photoelectrodes that are capable of supporting high efficiency operation and possess long term durability under these harsh aqueous conditions. Indeed, many materials that are energetically well suited for driving water oxidation and reduction reactions rapidly degrade in aqueous environments. Stabilization of existing semiconductors against corrosion would have a significant impact on photoelectrochemical energy conversion and enable the development of a new generation of robust integrated devices for efficient solar water splitting.

Abstract

Fabrication of overall water splitting devices requires the incorporation of all elements - catalysts, light absorbers, membranes, and interfacial layers - into an integrated system in which all materials are stable under identical conditions. Durability and compatibility of materials remain critical hurdles in the field. In addition to the discovery of new materials, a primary strategy for overcoming this limitation is aimed at utilizing thin film surface coatings for preventing corrosion of photoelectrodes, while also allowing efficient charge transfer between the semiconductor light absorber and catalysts. Here, we present a series of case examples highlighting approaches for thin film corrosion protection that enable sustained operation of both photocathodes and photoanodes. Each of these examples represents a significant technical advancement and provides complimentary insight into the important roles of interfacial energetics, physical and chemical structure, photon management, and defect engineering.

Progress Report

Strategies for stabilizing photoanodes against corrosion and photocorrosion have been widely explored in recent years._ENREF_21 General approaches involve introducing thin corrosion protection layers that allow interfacial charge transfer of photogenerated minority carriers while physically protecting the light-absorbers. In an alternative approach, recent advances in direct conformal deposition of catalytically active surface layers have been leveraged for providing corrosion protection without need for an interfacial later. Case examples of advanced corrosion protection schemes developed within JCAP and their implications for development of integrated systems for photoelectrochemical energy conversion will be presented.

Photocathode protection using atomic layer deposited TiO_2

Favorable band alignment of chemically robust TiO_2 with a variety of photocathodes enables direct minority carrier injection into its conduction band with minimal interfacial resistance losses. Therefore, deposition of conformal TiO_2 layers onto photocathodes using processes that are substrate-compatible provides a powerful opportunity for facile corrosion protection. While initial literature demonstrations were performed on planar, single crystalline substrates, researchers at JCAP have extended this strategy

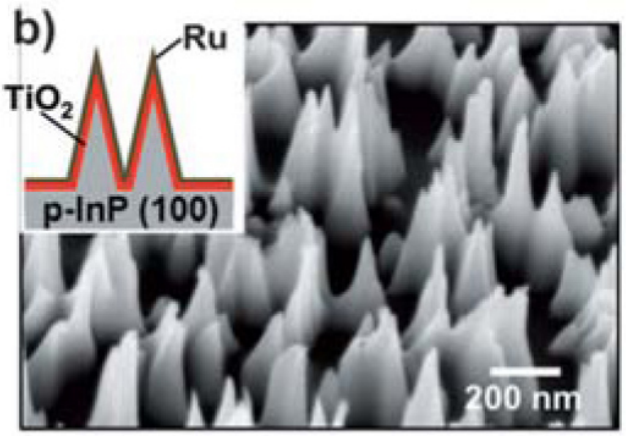

FIGURE 1. SEM image of p-InP nanopillar array formed by reactive ion etching. The inset shows a schematic of the protected structure, which incorporates a thin, conformal ALD TiO_2 layer.[2]

to encompass high surface area photocathodes. For example, p-InP nanopillared (NPL) arrays exhibit improved solar-driven hydrogen generation compared to planar controls due to a combination of reduced reflectivity and promoted H_2 bubble desorption. However, gradual loss of NPL fidelity, and corresponding hydrogen generation efficiency, over time was observed. Stable photocathodes were formed by introducing a thin interfacial layer of ALD TiO_2 (Fig. 1).[2] Given that mesostructured materials with high surface areas are desired for achieving reaction rates that take full advantage of the solar energy flux and reducing ionic transport lengths, the demonstration that ALD TiO_2 provides sufficient conformality for long-term corrosion protection of high surface area photoelectrodes represents an important advancement.

In complimentary work, JCAP researchers sought to extend photocathode protection to amorphous Si (a-Si) solar cells. In this study, the possibility of replacing ALD with reactively co-sputtered TiO_2, which is an inherently scalable deposition process, was investigated.[3] The resulting structure provided a stable onset potential of 930 mV vs. RHE, one of the highest reported to date. Furthermore, the integration of inexpensive NiMo hydrogen evolution catalysts to replace precious metal catalyst, such as Pt or Ru, was accomplished with minimal efficiency loss. The demonstration of high voltage photocathodes that are entirely formed using Earth-abundant elements and low-cost manufacturing processes represents an important advance in the drive towards scalable solar water splitting technologies.

Photoanode protection using atomic layer deposited TiO_2

Although many traditional semiconductors are energetically well-suited for efficient solar-driven water splitting, these materials are unstable when operated under photoanodic conditions in aqueous electrolytes. Recently, JCAP researchers demonstrated a stabilization method that enables the use of an entire class of existing, technologically important semiconductors with optimal band gaps for solar energy conversion as viable photoanodes in solar-driven water-splitting schemes.[4] In this work, Si, GaAs and GaP photoanodes were stabilized against photocorrosion and photopassivation in aqueous alkaline media by ALD of thick, chemically stable, electronically defective TiO_2 overlayers, combined with a Ni catalyst for driving the oxygen evolution reaction. Unlike photocathodes, where electrons can be expected to inject into the conduction band of stoichiometric TiO_2, the TiO_2 in this study should present a tunneling barrier for holes in the valence band. However, the key to enabling conduction of holes across the thick TiO_2 protective layers was the use of unannealed ALD-TiO_2 which combines

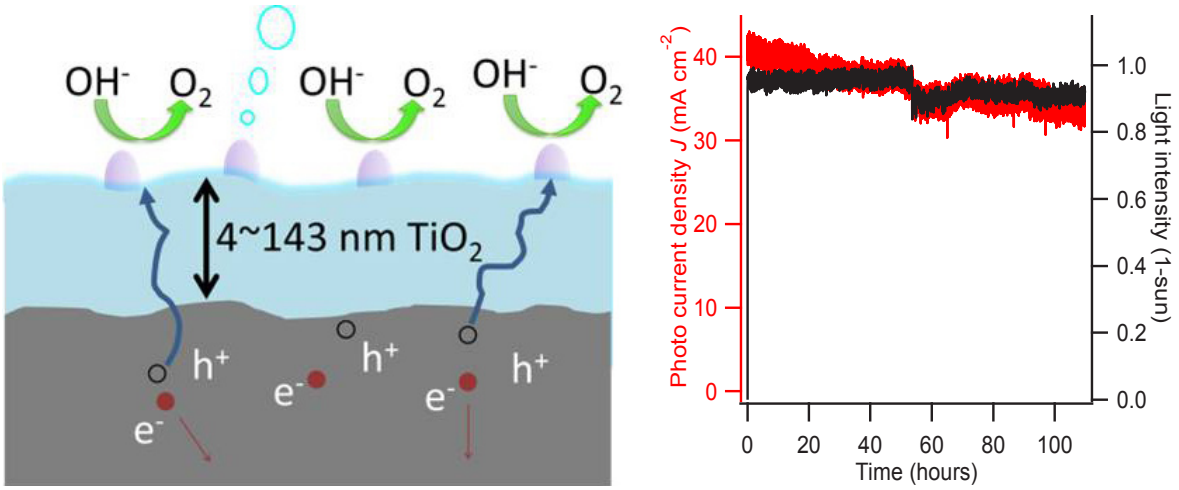

FIGURE 2. (left) Schematic representation of the corrosion protection scheme based on thick, defective TiO_2 layers, together with Ni catalyst, on photoanode surfaces. (right) Stability of Si in 1M KOH(aq) is demonstrated for over 100 h using this approach.[4]

optical transparency and high electrical conductivity to both electrons and holes. The resulting films were electronically defective and thus highly conductive with the exception of a thin insulating barrier layer at the surface of the as-grown film. Importantly, intermixing of the deposited Ni catalyst provided electrical contact through the insulating surface layer, thus allowing the thick ALD-TiO_2 films to act as a highly effective corrosion barrier while facilitating interfacial charge transport with minimal resistance loss. The thick ALD-TiO_2 films were formed without pinholes and can thus protect semiconductor material over macroscopic areas. In addition to enabling a wide range of existing materials to be further developed for incorporation in autonomous solar water splitting devices, these results demonstrate the power of film and defect engineering, as well as interfacial chemistry, on controlling interfacial charge transport.

Photoanode protection via direct catalyst deposition

As an alternate approach to photoanode protection, JCAP researchers have explored the possibility of photoelectrode stabilization via direct deposition of the catalyst onto the semiconductor light absorber. Although the precursors and processes for ALD of many catalytically active materials are available, the properties of atomic layer deposited materials can differ significantly from those of films fabricated with more traditional methods. Therefore, it is essential to understand the structures and morphologies of the deposited films, the effect of ALD on availability of catalytically active surface sites, and the physical and chemical properties of the interfaces between catalysts and underlying semiconductors. Here, two recent examples of cobalt oxide (CoO_x) ALD onto model photoanode materials, $BiVO_4$ and Si, are discussed.

$BiVO_4$ is a 2.4-eV band gap n-type semiconductor that is comprised of Earth-abundant elements but is kinetically sluggish for water oxidation, which leads to poor photoelectrical performance and photocorrosion in alkaline media. Within JCAP, this material has been selected as a model metal oxide photoanode for detailed study; it exhibits many of the complexities associated with this class of material and can be used to guide understanding that is expected to be useful in the development of next generation oxide semiconductors for photocatalysis. Recently, JCAP researchers demonstrated that the use of ALD to form thin layers of cobalt oxide on n-type $BiVO_4$ produced photoanodes capable of water oxidation with essentially 100% faradaic efficiency in alkaline electrolytes.[5] While improved performance was observed upon thin CoO_x deposition, decreased performance was found with slightly thicker layers. This finding highlights a critical consideration that is central to corrosion protection of photoanode materials: in the absence of a buried junction, the semiconductor/electrolyte junction provides the driving force for charge separation within the photoelectrode and conformal layers for corrosion protection and catalysis must be optimized to ensure that the interfacial electronic structure is not adversely affected.

In a separate study, plasma-enhanced ALD of cobalt oxide directly onto p+n-Si devices was investigated as a function of surface pre-treatment.6 As shown in Fig. 4, a combined nanotexturing and ALD process enabled efficient photoelectrochemical water oxidation and effective protection of Si from corrosion at high pH (pH 13.6). Physical sputtering of the Si surface prior to catalyst deposition led to nanometer scale texturing that was critical to defining the crystallinity of the deposited catalyst and its electronic registry with the light absorber. In particular, this process provided regions of reduced interfacial silica thickness that improved tunneling probability and dramatically reduced the interfacial charge transfer resistance. Furthermore, texturing the surface inhibited crystallization of CoO_x and enabled formation of a highly conformal amorphous catalyst layer with reduced pinhole densities in inter-grain regions compared to crystalline materials. This work revealed that

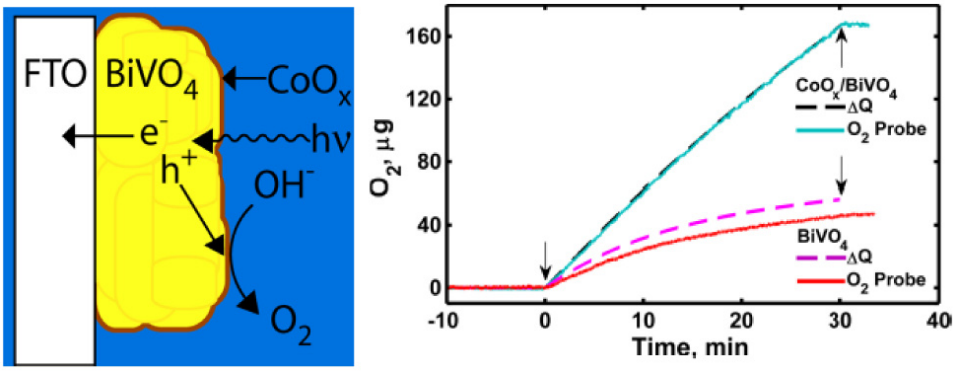

FIGURE 3. (left) Schematic illustration of conformal ALD CoO_x on $BiVO_4$ photoanode, which provides enhanced catalytic activity and stability to the material. (right) Oxygen production as detected by probe and coulometry at 0.97 V vs RHE in pH 13 KOH(aq), AM 1.5G illumination. Arrows mark the beginning and end of current flow from the potentiostat.[5]

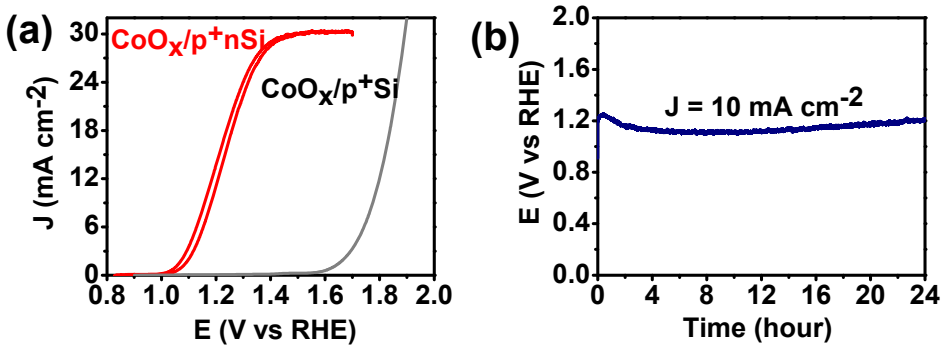

FIGURE 4. Photoelectrochemical behavior of nanotextured CoO_x/p^+n-Si photoanode in aqueous 1.0 M NaOH under 100 mW/cm^2 of simulated solar illumination. **(a)** *J–E* response of CoO_x/p^+n-Si (red) under illumination and CoO_x/p^+ Si (grey) in the dark. **(b)** Chronopotentiometry of nanotextured CoO_x/p^+n-Si photoanode at a constant current density of 10 mA/cm^2.[6]

specific engineering of the interface is essential to improving catalytic activity and enhancing long term durability.

Future Directions

The results presented here highlight the significant potential for utilization of high efficiency semiconductors in systems for overall water splitting. Ongoing work is devoted to integrating materials and processes for assessment of these corrosion protection schemes in functional demonstration devices, to deep studies aimed at understanding the fundamental physical and chemical processes that govern interfacial charge transport, and to identification and elimination of deleterious failure mechanisms. Furthermore, with the demonstration of long-term stability, the need to develop general protocols for accelerated testing and failure analysis becomes more urgent. Mechanistic understanding of factors affecting efficiency and durability, as well as their sensitivities to processing and environment, will enable the fabrication of scaled prototypes. Ultimately, application of these concepts to monolithically integrated mesostructured materials systems will enable the next generation of high efficiency solar photoreactors.

Publication list (including patents) acknowledging the DOE grant or contract

1. Modestino, M.A.; Walczak, K.A.; Berger, A.; Evans, C.M.; Haussener, S.; Koval, C.; Newman, J.S.; Ager, J.W.; Segalman, R.A., Robust Production of Purified H_2 in a Stable, Self-regulating, and Continuously Operating Solar Fuel Generator, *Energy Environ. Sci.* **2014**, *7*, 297.

2. Lee, M.H.; Takei, K.; Zhang, J.; Kapadia, R.; Zheng, M.; Chen, Y.-Z.; Nah, J.; Matthews, T.S.; Chueh, Y.-L.; Ager, J.W.; Javey, A., p-Type InP Nanopillar Photocathodes for Efficient Solar-Driven Hydrogen Production, *Angewandte Chemie* **2012**, *124*, 10918.

3. Lin, Y.; Battaglia, C.; Boccard, M.; Hettick, M.; Yu, Z.; Ballif, C.; Ager, J.W.; Javey, A., Amorphous Si Thin Film Based Photocathodes with High Photovoltage for Efficient Hydrogen Production, *Nano Lett.* **2013**, *13*, 5615.

4. Hu, S.; Lichterman, M.; Lewis, N.S. *Science* **2014** *in press.*

5. Lichterman, M.F.; Shaner, M.R.; Handler, S.G.; Brunschwig, B.S.; Gray, H.B.; Lewis, N.S.; Spurgeon, J.M., Enhanced Stability and Activity for Water Oxidation in Alkaline Media with Bismuth Vanadate Photoelectrodes Modified with a Cobalt Oxide Catalytic Layer Produced by Atomic Layer Deposition, *J. Phys. Chem. Lett.* **2013**, *4*, 4188.

6. Yang, J.; Walczak, K.; Anzenberg, E.; Toma, F.M.; Yuan, G.; Beeman, J.; Schwartzberg, A.; Lin, Y.; Hettick, M.; Javey, A.; Ager, J.W.; Yano, J.; Frei, H.M.; Sharp, I.D., Efficient and sustained photoelectrochemical water oxidation by cobalt oxide/silicon photoanodes with nanotextured interfaces, *J. Am. Chem. Soc.* **2014**, *136*, 6191.

II.G.12 Joint Center for Artificial Photosynthesis: High Throughput Experimentation for Electrocatalyst and Photoabsorber Discovery

Principal Investigator: Carl Koval
California Institute of Technology, Pasadena, CA
Email: ckoval@caltech.edu

Names of Team Members
J.M. Gregoire (Project Lead, gregoire@caltech.edu), J. Jin (Project Co-lead), M. Marcin, S. Mitrovic, E. Cornell, C. Xiang, E. Soedarmadji, S. Suram, K. Kan, J. Haber, P. Newhouse, D. Guevarra, R. Jones, N. Becerra, M. Pesenson, L. Zhou, A. Shinde
California Institute of Technology, Pasadena, CA

DOE Program Manager: Gail McLean,
Phone: (301) 903-7807
Email: gail.mclean@science.doe.gov

Objectives

The mission of the Joint Center for Artificial Photosynthesis (JCAP) is to produce fundamental scientific discoveries and major technological breakthroughs to enable the development of energy-efficient, cost-effective, and commercially viable processes for the large-scale conversion of sunlight directly to fuels. JCAP's 5-year goal is discovery of robust, Earth-abundant light absorbers, catalysts, linkers, membranes, and scale-up science required to assemble the components into a complete artificial photosynthetic system. The High Throughput Experimentation (HTE) project develops state of the art high throughput techniques and applies them to efficient screening of earth-abundant composition spaces to identify new electrocatalyst and light absorber materials.

Technical Barriers

To identify materials that can operate in a solar fuels device, material screening must be performed under technologically-relevant conditions. High throughput instruments that adhere to these conditions must be developed and then automated to provide robust high throughput operation. This screening strategy must then be embedded in a high throughput pipeline that includes high quality materials synthesis and characterization. While operation of this pipeline can identify new promising materials and accelerated discovery, development and deployment of materials can only be attained by integrating the high throughput pipeline into a larger consortium that includes benchmarking, directed research and prototyping efforts. Successful implementation of this research paradigm also requires interplay with theory efforts. JCAP is boldly solving these exciting technical and research integration challenges.

Abstract

JCAP-HTE performs accelerated discovery of new earth-abundant photoabsorbers and electrocatalysts through operation of a high throughput pipeline for the synthesis, screening and characterization of photoelectrochemical materials. To establish the pipeline, several new screening instruments for high throughput (photo-)electrochemical measurements have been invented. These instruments are not only optimized for screening against solar fuels requirements, but also provide new tools for the broader combinatorial materials science community. Operation of the pipeline and its embedment into the solar fuels hub has yielded the high throughput discovery, follow-on verification, and device implementation of a new quaternary metal oxide catalyst. This rapid technology development from discovery to device implementation is a hallmark of the multi-faceted JCAP research effort.

Progress Report

The widespread deployment of new energy technologies requires discovery and development of new functional materials [Energy Environ Sci 2013, 6, 1983]. Artificial photosynthesis is a promising energy technology with several substantial materials challenges [Chem Reviews 2010, 110, 6446]. Proposed designs for an artificial photosynthesis device, or solar fuel generator, involve coupling electrocatalysts to light absorbing semiconductors to provide solar-driven photoelectrochemical reactions. Successful development of such a device requires discovery of both photoabsorbers and electrocatalysts for the pertinent reactions. Desirable traits for new high performance materials include high earth abundance, facile synthesis methods and insensitivity to small variations in composition. To identify new photoabsorbers and electrocatalysts with these traits, we are building a high throughput pipeline for accelerated materials discovery.

The development of this pipeline within the solar to fuels energy innovation hub provides very powerful capabilities for accelerated discovery. The performance screening metrics employed in the pipeline are developed according to the specifications of the directed research and device prototype experts. Another important capability is the rapid incorporation of newly discovered materials into a solar fuels testbed. This capability shortens the time lapse between high

throughput discovery and technology demonstration from years to weeks.

The JCAP-HTE accelerated discovery pipeline contains 4 primary sectors as shown in Figure 1, three of which involve the development of new experimental equipment and techniques: Materials synthesis, (Light-absorber and Electrocatalyst) screening, and Characterization. The fourth sector is Data informatics and distribution and involves the data connectivity to the other sectors and to users.

Performance Screening

The heart of the high throughput pipeline is the evaluation of new materials as either electrocatalysts for solar fuels reactions or solar light absorbers. To create a high throughput screening platform, semi-quantitative parallel screening is used to rapidly identify composition regions of interest, followed by more detailed serial screening on select samples.

The JCAP-HTE parallel catalyst screening instrument is based on bubble imaging, a conceptually simple but technically nuanced technique[1]. The JCAP-HTE bubble screening instrument (see Figure 2) images the oxygen and hydrogen bubbles produced by the Oxygen Evolution Reaction (OER) and Hydrogen Evolution Reaction (HER). The bubble screening method can function in all pH conditions and is suitable for the combinatorial search of catalysts for any gas evolving reaction, most notably the OER and HER solar fuels reactions.

To provide more detailed electrochemical screening, JCAP-HTE developed a scanning droplet cell (SDC)[2] _ENREF_2. The JCAP SDC provides a 3-electrode cell for an individual 1 mm^2 sample with no o-rings or other physical contact to the working electrode, other than the electrolyte solution. The SDC is used to provide quantitative screening at throughput of less than 10 s per sample. Carefully designed software allows for real time data analysis so that high performance materials can be automatically evaluated with subsequent measurements, of typically longer duration, to ascertain stability.

For the screening of photoabsorbers, JCAP-HTE is continuing its development of novel instrumentation for parallel and serial screening for optical properties, but the key innovation in light absorber screening has moved beyond this to fill the technology gap between optical characterization and photoelectrochemical water splitting. With the expectation that the best photoanode absorber will not also be the best OER catalysts, a solar fuels photoanode is typically made by coupling a catalyst and absorber. To discover photoabsorbers which are not photocatalysts, a new screening tool needed to be developed. JCAP's recently published solution to this technology gap is another example of a conceptually simple but technically nuanced instrument. To alleviate the catalytic requirement, n-type/p-type photoabsorbers are screened by measuring the photo-oxidation/reduction of facile redox couples. To mitigate dark currents, a multiplexed counter electrode is coupled with the sample-indexed illumination, and to mitigate shunting of the photocurrent, a carefully engineered thin layer cell is established.

Discovery of a new class of rare earth-rich OER catalysts in unpredicted composition spaces

The discovery of Ce-rich OER catalysts was recently reported[3] and followed by a detailed investigation describing its unique electrochemical performance. The pseudo-quaternary (Ni-Fe-Co-Ce)O_x library was deposited as an array of 5456 discrete compositions at 3.3 at% composition steps using inkjet printing of four separate metal precursor inks. The relative electrocatalytic performance of each composition was screened using several different figures of merit (FOM). The most informative FOM for photoelectrochemical water-splitting devices is the overpotential (η) for the OER at 10 mA/cm^2, which is mapped in Figure 3A for the entire composition space. The most active regions can be seen near the Ni-Fe edge and on the Ni-Co-Ce face of the tetrahedron. To visualize the

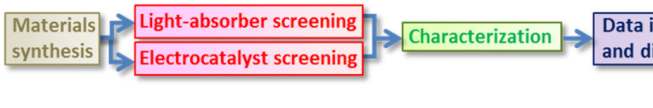

FIGURE 1. Sectors of the accelerated discovery pipeline, with the screening sector split for the 2 general material functions of light absorption and electrocatalysis.

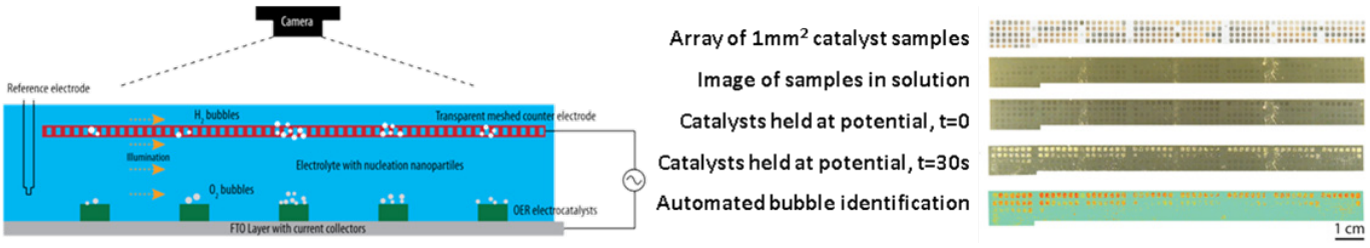

FIGURE 2. Summary of the bubble screening technique. Bubbles of evolved gas appear as white dots above active catalysts. Simultaneous imaging of all samples and automated image processing yields rapid identification of the most active catalyst compositions.

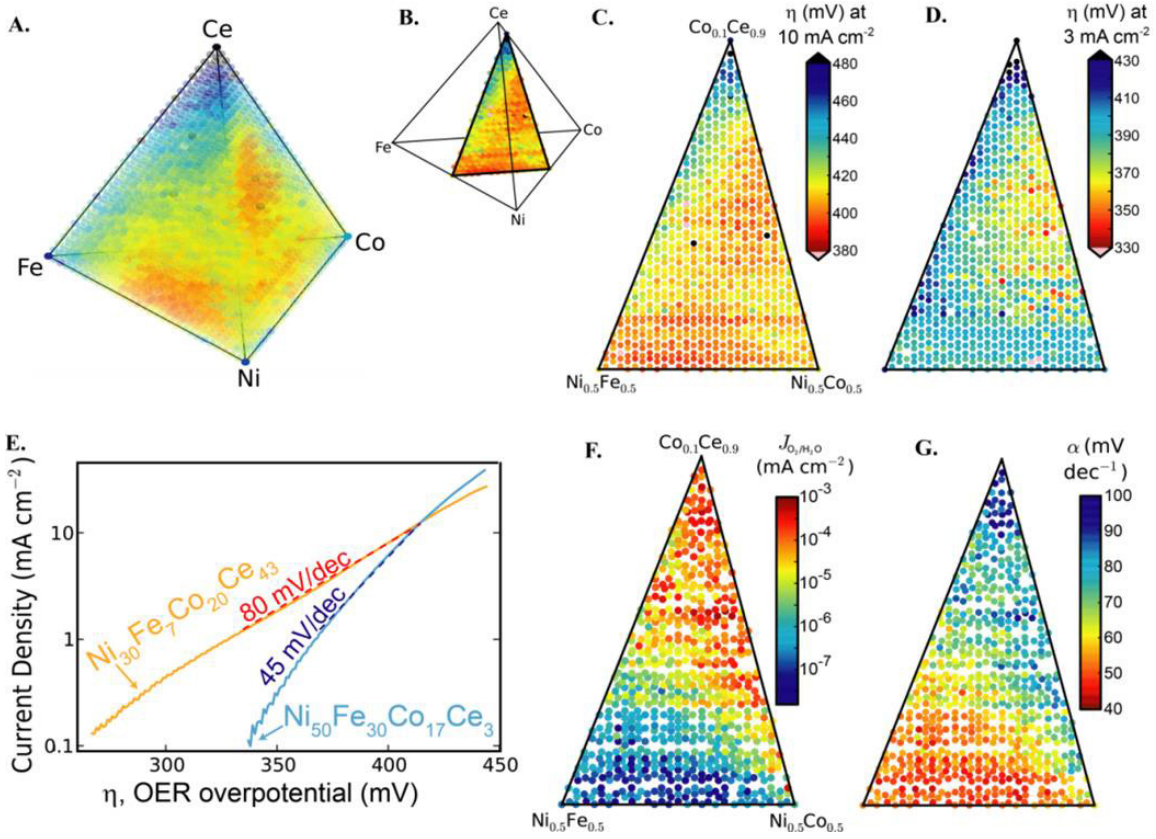

FIGURE 3. The OER overpotential for 10 mA/cm^{-2} is shown for the entire quaternary composition space (A) and for a pseudo-ternary cross section (B-C). A different composition trend is observed with the OER overpotential for 3 mA/cm^{-2} (D). This is due to the different catalytic behavior of the newly discovered high-Ce catalyst compared to known catalysts (E), prompting exploration of the trends in Tafel parameters (F-G).

relationship between these composition regions, Figure 3B demonstrates the extraction of a pseudo-ternary cross section of the data in Figure 3A, which is plotted in Figure 3C. For these same compositions, the overpotential (η) for the OER at 3 mA/cm^2 is mapped in Figure 3D. This figure demonstrates that the newly discovered high-Ce catalysts are far superior to the known Ni-Fe catalysts at low current density. To further demonstrate this relative performance, Figure 3E shows the catalytic current for representative compositions ($Ni_{0.5}Fe_{0.3}Co_{0.17}Ce_{0.03}O_x$ and $Ni_{0.3}Fe_{0.07}Co_{0.2}Ce_{0.43}O_x$), the former being a low-Ce composition similar to the known Ni-Fe catalysts, and the latter being a newly discovered high-Ce composition. Figure 3E also shows that these 2 compositions have different characteristic Tafel slopes and corresponding exchange current densities (Figure 3F-3G). Detailed composition measurements of these representative samples both before and after electrochemical testing demonstrate the fidelity of the inkjet printing synthesis and the stability of the catalysts. Using the JCAP rapid technology development platform, this catalyst and its performance have been verified by benchmarking, improved by directed research, demonstrated in a prototype device, and understood by extensive characterization.

Characterization and Data Informatics

The importance of characterization and informatics in materials discovery and understanding cannot be overstated. It is through the characterization of materials that composition-processing-structure-property relationships can be developed. Material characterization also facilitates interactions with theory efforts. Data informatics enables automated identification of unforeseen trends and completes a learning feedback loop for identification of superior materials. By developing state of the art techniques in these sectors, JCAP-HTE is foundational in using high throughput methods as tools for performing basic energy science.

Publication list

1. Xiang, C.; Suram, S.K.; Haber, J.A.; Guevarra, D.W.; Jin, J.; Gregoire, J.M., A High Throughput Bubble Screening Method for Combinatorial Discovery of Electrocatalysts for Water Splitting. *ACS Comb. Sci.* **2014,** *16* (2), 47-52.

2. Gregoire, J.M.; Xiang, C.; Liu, X.; Marcin, M.; Jin, J., Scanning Droplet Cell for High Throughput Electrochemical and Photoelectrochemical Measurements. *Review of Scientific Instruments* **2013,** *84* (2), 024102.

3. Haber, J.A.; Cai, Y.; Jung, S.; Xiang, C.; Mitrovic, S.; Jin, J.; Bell, A.T.; Gregoire, J.M., Discovering Ce-rich oxygen evolution catalysts, from high throughput screening to water electrolysis. *Energ Environ Sci* **2014,** *7* (2), 682-688.

4. Haber, J.A.; Xiang, C.; Guevarra, D.; Jung, S.; Jin, J.; Gregoire, J.M., High-Throughput Mapping of the Electrochemical Properties of (Ni-Fe-Co-Ce) Ox Oxygen-Evolution Catalysts. *ChemElectroChem* **2014** *1* (3) 524-528.

5. Gregoire, J.M.; Xiang, C.; Mitrovic, S.; Liu, X.; Marcin, M.; Cornell, E.W.; Jin, J., Combined Catalysis and Optical Screening for High Throughput Discovery of Solar Fuels Catalysts *Journal of the Electrochemical Society* **2013,** *160* (4), F337

6. Xiang, C.; Haber, J.; Marcin, M.; Mitrovic, S.; Jin, J.; Gregoire, J.M., Mapping Quantum Yield for (Fe–Zn–Sn–Ti)Ox Photoabsorbers Using a High Throughput Photoelectrochemical Screening System. *ACS Combinatorial Science* **2014**

7. Patent Application: Scanning Drop Sensor, May 31, 2013, J. Jin, C, Xiang, J. M. Gregoire.

II.G.13 Center for Interface Science: Solar-Electric Materials (CISSEM)

Presenter: Scott Saavedra
University of Arizona

Abstract

CISSEM was established on August 1, 2009 as an EFRC funded by the U.S. DOE, Office of Science, Basic Energy Sciences, under Award Number DE-SC0001084. We combine research groups at The University of Arizona (the lead institution), Georgia Institute of Technology, Princeton University, the University of Washington and NREL in a coordinated and integrated multi-investigator program. CISSEM's mission is to advance the understanding of interface science underlying solar energy conversion technologies based on organic and organic-inorganic hybrid materials; and to inspire, recruit and train future scientists and leaders in the basic science of solar electric energy conversion.

Continued improvement of thin-film photovoltaic (PV) energy conversion technologies –underpinned by basic science – is an exciting challenge that engages CISSEM. For "printable" solar cells based on hybrids of polymers, small molecules and semiconductor nanocrystals, the open-circuit photovoltage is limited by: *i)* the work function difference between two contacts, which is affected by the composition, structure and energetics at both contact/active layer interfaces; *ii)* the competition between charge harvesting and charge recombination, both in the active layer itself, and at the interfaces between electrical contacts and active layer components; and *iii)* other detrimental processes such as charge back injection from the contacts. By incorporating thin *interlayers* of appropriate inorganic or organic materials between each contact and the active layer, we can increase device efficiency by providing thermodynamic and/or kinetic barriers to help facilitate the desired preferential or 'selective' charge harvesting of either electrons or holes at each contact, while also minimizing charge back injection.

This poster highlights our experimental and theoretical research focused on understanding the principles of efficient charge harvesting, and providing a molecule/atomic scale understanding of how interface composition, structure, energetics and rates of charge extraction versus recombination control PV efficiency, i.e., through better contact and interlayer design and more efficient charge extraction. CISSEM research should ultimately provide design principles to help create a wide array of new energy conversion platforms, including the new perovskite-based PV platform, and the scientific foundations for thin-film PV technologies and our nation's pursuit of lowering costs to transform the sun's energy into electricity.

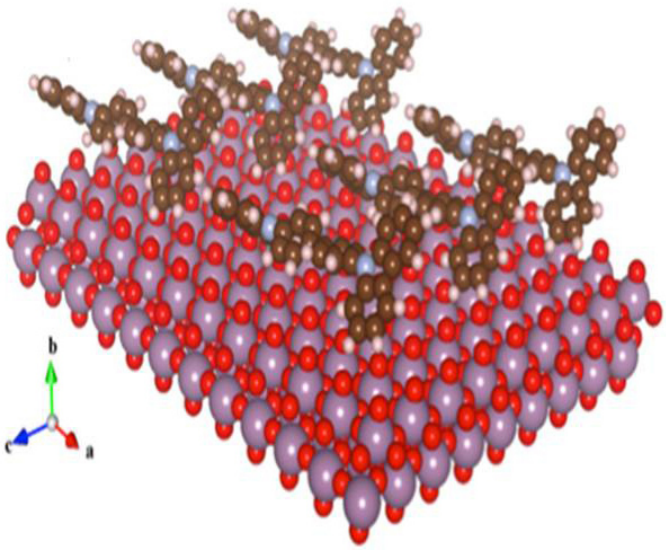

Above: Theoretical modeling of the organic hole-transport layer 4,4′-N,N′-dicarbazole-biphenyl physisorbed on the important, transition metal oxide surface MoO3 (010) – part of a combined theoretical and experimental study of facile hole collection and injection. [DOI: 10.1002/adfm.201301466]

Next Page: Using photoemission spectroscopy at SLAC to investigate the electronic structure and carrier dynamics at a model zinc oxide/fullerene (C_{60}) interface, like those used to selectively harvest electron in OPV platforms. Hybrid interface states form in both the ground and excited state manifold. Using resonant photoemission spectroscopy, we are able to observe ultrafast carrier delocalization in bare ZnO, with electrons scattering into bulk states on the time-scale of less than 500 as. In the presence of C_{60} (and hybridization between C_{60} and ZnO), the resulting interface state formation leads to carrier localization and long-lived excited states in the vicinity of the conduction band minimum. [*manuscript submitted*]

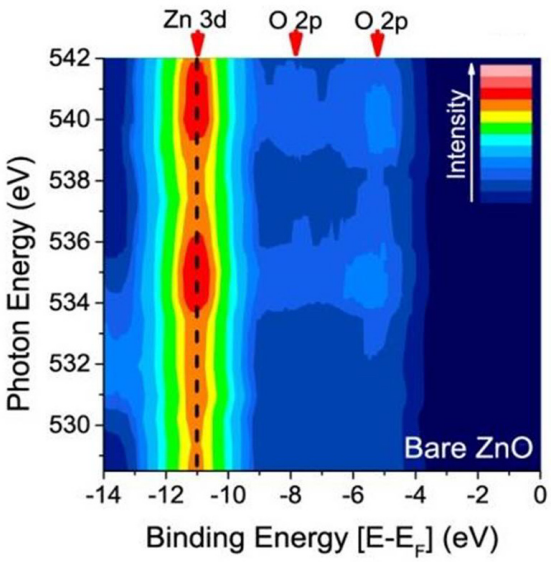
Zn 3d
O 2p
O 2p
Photon Energy (eV)
542
540
538
536
534
532
530
Intensity
Bare ZnO
-14
-12
-10
-8
-6
-4
-2
0
Binding Energy [E-E$_F$] (eV)

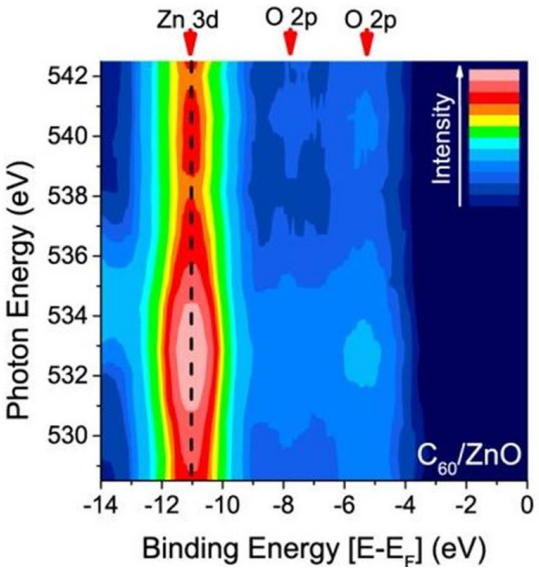
Zn 3d
O 2p
O 2p
Photon Energy (eV)
542
540
538
536
534
532
530
Intensity
C$_{60}$/ZnO
-14
-12
-10
-8
-6
-4
-2
0
Binding Energy [E-E$_F$] (eV)

II.G.14 Photobiohybrid Solar Fuels – Nanoparticle-Hydrogenase Complexes

Principal Investigator: Paul W. King
NREL, 15013 Denver West Parkway
Phone: (303) 384-6277
Email: paul.king@nrel.gov

Team Members

- Katherine A. Brown (Scientist)
  NREL, 15013 Denver West Parkway
  Phone: (303) 384-7721, Email: kate.brown@nrel.gov
- David W. Mulder (Scientist)
  NREL, 15013 Denver West Parkway
  Phone: (303) 384-7486, Email: david.mulder@nrel.gov
- Michael W. Ratzloff (Scientist)
  NREL, 15013 Denver West Parkway
  Phone: (303) 384-7861, Email: mike.ratzloff@nrel.gov

DOE Program Manager: Gail McLean
Phone: (301) 903-7807
Email: Gail.McLean@science.doe.gov

Objectives

The long-term objective of this project is to understand energy transduction in photochemical systems that combine the light harvesting, charge-separation of nanoparticles (NP) with catalytic H_2 activation by hydrogenases as models for solar energy conversion. By coupling hydrogenase catalysis to semiconductor nanoparticles, light driven H2 production can be achieved by transfer of the nanoparticle exciton electron into the electron transport network of the enzyme. Light-driven production of H_2 occurs naturally in photosynthetic microbes, where hydrogenases couple to low potential reductant pools and help to maintain electron flow under anaerobic-aerobic transitions. Integration of a nanoparticle with hydrogenase catalysis allows for control over reductant potential, and will contribute to developing a broad understanding of the determinants that control enzymatic function.

Technical Barriers

The efficiencies of coupling natural or artificial photosynthesis to production of reduced chemical and fuels require a more fundamental understanding of the factors controlling energy transduction reactions, how this process couples to downstream enzymatic reactions, and the catalytic mechanisms. The aims of this project are to investigate the physical, thermodynamic and kinetic parameters of light-harvesting, charge-transfer and catalysis in nanoparticle-hydrogenase systems for solar hydrogen production. Investigation of the assembly, charge transfer and catalytic properties are providing mechanistic insights into both nanoparticle and enzyme behavior, as well as design principles for optimizing artificial photosynthetic systems

Abstract

We have developed complexes of CdS and CdTe nanorods capped with 3-mercaptopropionic acid (MPA) coupled to Clostridium acetobutylicum [FeFe]-hydrogenase I (CaI) that photocatalyze reduction of H^+ to H_2 at photon conversion efficiencies of up to 20% under illumination at 405 nm. Characterization has focused the compositional and mechanistic aspects of complexes that control photochemical conversion of solar energy into H_2. Complexes self-assemble by an electrostatically driven association between nanoparticle ligands and the CaI surface. Production of H_2 by the complexes was observed only under illumination, and only in the presence of a sacrificial donor. Nanoparticle-to-CaI molar ratio, sacrificial donor concentration and light intensity each have a pronounced effect on photocatalytic H_2 production. Photocatalytic activity appears to depend on contributions from electron and hole transfer, exciton recombination, and photon absorption rate. Recent investigations have focused on electron transfer rate and the effect of exciton electron potential. Kinetics of electron transfer play a critical role in the overall photochemical reactivity, as the quantum efficiency of electron transfer defines the upper limit on the quantum yield of H_2 generation. We investigated the competitiveness of ET with the electron relaxation pathways in CdS nanoparticles by directly measuring the rate and quantum efficiency of ET from photoexcited CdS nanoparticles to CaI using transient absorption spectroscopy. We found that the electron transfer rate constant (k_{ET}) and the electron relaxation rate constant in CdS (k_{CdS}) were comparable, with values of $10^7\ s^{-1}$, resulting in a quantum efficiency of ET of 42% for complexes with the average CaI:CdS molar ratio of 1:1. Given the direct competition between the two processes that occur with similar rates, we propose that gains in efficiencies of H_2 production could be achieved by increasing k_{ET} and/or decreasing k_{CdS} through structural modifications of the nanocrystals (i.e., core-shell particles). We have also investigated the effect of exciton electron potential on electron transfer and H_2 production. By varying nanoparticle diameter, the band-gap and the conduction band potential can be controlled. The electron transfer rate into CaI from CdTe nanoparticles with diameters between 2.0 and 3.5 nm was measured using time-resolved photoluminescence. The k_{ET} values were constant across the diameter range, despite a decrease in the electron overpotential from 250 to 30 mV between 2.0 and 3.5 nm diameter nanoparticles. Photocatalytic H_2 production and photon conversion

efficiencies increased with increasing diameter despite lower overpotentials. Given the inverse trend in H_2 production and the insensitivity of k_{ET} to electron overpotential, we conclude that ΔG_{ET} is not a determining factor in photocatalysis by CdTe-CaI complexes, and contributions from other factors, including nanoparticle recombination rates, enzyme coverage, and exciton lifetimes, dominate photocatalytic behavior. Future studies will focus on further elucidation of the interdependent factors which contribute to photocatalysis in these systems.

Progress Report

Characterization of CdTe-CaI complexes [4]

- Molecular assembly CdTe-CaI complexes was mediated by electrostatic interactions and resulted in stable, enzymatically active complexes. The assembly kinetics were monitored by CdTe photoluminescence (PL) spectroscopy and exhibited first-order Langmuir adsorption behavior.
- Photocatalytic H_2 production required the presence of a sacrificial donor (ascorbic acid), and was found to be highly dependent on donor concentration and CdTe-to-CaI molar ratio.
- Nanoparticle photoluminescence efficiency affected H_2 production, likely due to competition for available exciton electrons.

Characterization of CdS-CaI complexes [2]

- Complex self-assembly resulted in CdS binding to the *in vivo* electron donor (ferredoxin, Fd) binding site, as evidenced by the inhibition of Fd-driven H_2 production by CdS. Competition assays yielded a ΔG_{ABS} in the regime between electrostatic and covalent interactions.
- Photocatalytic H_2 production was dependent on molar ratio, and the results were interpreted using a Poisson distribution. H_2 production efficiency maximized in solutions favoring a single CaI per nanorod. Higher CaI coverage appears to lead to competition of electrons and loss in efficiency due to back-electron-transfer.
- H_2 production was limited by light intensities at fluxes up to approximately 3x solar flux.
- The quantum yield of H_2 production measured for monochromatic 405nm light was 20%.

Electron transfer in CdS-CaI complexes [1]

- Electron transfer rates of 10^7 were measured by transient absorption. These rates are on the same order as the recombination rate of the nanoparticle. Quantum efficiency of electron trasnfer was measured at 42% for 1-to-1 molar ratios, and the efficiency increased with increasing CaI concentration.

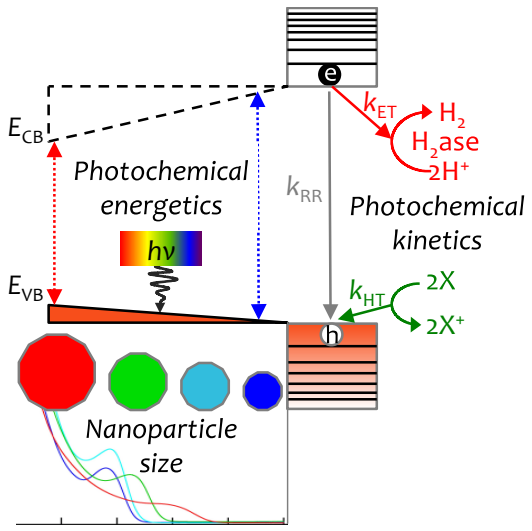

- It may be possible to enhance complex efficiency by manipulating the nanoparticle recombination rates such that ET is faster that recombination, improving the completion for exciton electrons.
- The electron transfer rate was unaffected by catalytic inhibition of CaI, indicating electron transfer occurs between the CdS and an accessory Fe-S cluster of the CaI, followed by transfer through the enzyme electron transfer pathway to the active site.

CdTe nanoparticle size manuscript in preparation)

- Electron transfer rates are insensitive the nanoparticle size, despite increasing electron overpotential with decreasing nanoparticle diameter.
- Photocatalytic H_2 production rates and quantum efficiencies increasing with increasing diameter, with a maximum quantum efficiency for 3.5 nm CdTe of 12%.
- CdTe-CaI electron transfer and photocatalytic H_2 production rates are insensitive to electron overpotential and likely depend on combination of other factors, including nanoparticle recombination rates, enzyme coverage, and exciton lifetime.

Future Directions

- Investigate the photocatalytic properties of nanoparticle/Ni-N_2P_2 complexes in collaboration with Dr. Wendy Shaw at PNNL.
- Continue collaborative studies with CU-Boulder on developing a nanoparticle/-hydrogenase charge-transfer framework model, effects of interfacial ligands on k_{ET} dynamics, and core-shell complexes.
- Integrate metallic nanoparticles into nanoparticle-hydrogenase complexes to investigate the impact

of surface plasmon enhancement on artificial photosynthesis in these systems.

Publication list (including patents) acknowledging the DOE grant or contract

1. Wilker, M.B., Shiopoulos, K., Brown, K.A., Mulder, D.W., King, P.W., and Dukovic, G. "Electron transfer kinetics in CdS Nanorod-[FeFe]-hydrogenase complexes and implications for photochemical H_2 generation." *J. Am. Chem. Soc.* 2014, *136*:4316.

2. Brown, K.A., Wilker, M.B., Boehm, M., Dukovic, G., and King, P.W. "Characterization of photochemical processes of H_2 production by CdS nanorod-[FeFe] hydrogenase complexes." *J. Am. Chem. Soc.* **2012**, *134*(12):5627.

3. Madden, C., Vaughn, M.D., Diez-Perez, I., Brown, K.A., King, P.W., Gust, D., Moore, A.L. and Moore, T.A. "Catalytic turnover of [FeFe]-hydrogenase based on single-molecule imaging." *J. Am. Chem. Soc.* **2012***, 134*:1577.

4. Brown, K.A., Dayal, S., Ai, X., Rumbles, G. and King, P.W. "Controlled assembly of hydrogenase-CdTe nanocrystal hybrids for solar hydrogen production." 2010, *J. Am. Chem. Soc. 132*(28):9672.

II.G.15 Center on Nanostructuring for Efficient Energy Conversion (CNEEC)

Principal Investigator: Fritz B. Prinz

Finmeccanica Professor in the School of Engineering
Professor of Mechanical Engineering
Professor of Materials Science and Engineering
Stanford University, Stanford, CA 94305,
Phone: (650) 725-2018, Email: fbp@cdr.stanford.edu

Stacey F. Bent

Jagdeep & Roshni Singh Professor of Engineering
Senior Fellow at the Precourt Institute
Professor of Chemical Engineering
Stanford University, Stanford, CA 94305
Phone: (650) 723-0385, Email: sbent@stanford.edu

Names of Team Members

- Mark L. Brongersma
  Stanford University,
  Geballe Laboratory for Advanced Materials,
  Department of Materials Science and Engineering,
  McCullough Building, Room 349, 476 Lomita Mall,
  Stanford University, Stanford, CA 94305-4045
  Pone: (650) 736-2152, Email: Brongersma@stanford.edu
- Bruce Clemens
  Walter B. Reinhold Professor of Engineering, and
  Professor of Photon Science at SLAC
  Department of Materials Science and Engineering
  Stanford University, Stanford, CA 94305
  Phone: (650) 725-7455, Email: bmc@stanford.edu
- Yi Cui
  Department of Materials Science and Engineering, and
  Photon Science (SLAC)
  Stanford University, Stanford, CA 94305
  Email: yicui@stanford.edu
- David Goldhaber-Gordon
  Department of Physics
  Geballe Laboratory for Advanced Materials
  McCullough Building Rm. 346, 476 Lomita Mall
  Stanford University, Stanford, California 94305
  Phone: (650) 724-3709
  Email: goldhaber-gordon@stanford.edu
- Shanhui Fan
  Department of Electrical Engineering
  Stanford University, Stanford, CA 94305
  Phone: (650) 724-4759, Email: shanhui@stanford.edu
- Thomas F. Jaramillo
  Dept. of Chemical Engineering
  Stanford University, Stanford CA 94305-5025
  Phone: (650) 498-6879, Email: Jaramillo@stanford.edu
- Jens K. Nørskov
  Department of Chemical Engineering,
  Stanford University, Photon Science, SLAC National
  Accelerator Laboratory
  Stanford, CA 94305
  Phone: (650) 926-3647, Email: norskov@stanford.edu
- Robert Sinclair
  Charles M. Pigott Professor of Engineering
  Department of Materials Science and Engineering
  Stanford University, Stanford, CA 94305
  Pone: (650) 723-1102, Email: bobsinc@stanford,edu
- Xiaolin Zheng
  Department of Mechanical Engineering
  Stanford University, Stanford, CA 94305
  Pone: (650) 736-8953, Email: xlzheng@stanford.edu

Subcontractors

- Carnegie Institute: Arthur Grossman
  Department of Plant Biology, The Carnegie Institution
  Stanford, CA 94305
  Pone: (650) 325-1521 x212, Email: arthurg@stanford.edu
- Denmark Technical University: Karsten W. Jacobsen
  Department of Physics, Director of CAMD
  Technical University of Denmark
  Fysikvej Building 307 2800, Kongens Lyngby
  Phone: +45 45253186. Email: kwj@fysik.dtu.dk

DOE Program Manager: Christopher Fecko

Email: Christopher.Fecko@science.doe.gov

Objectives

CNEEC's mission is to understand how nanostructuring can enhance efficiency for solar energy conversion to produce hydrogen fuel and to solve fundamental cross-cutting problems.

The overarching goal is to increase conversion efficiency by manipulating materials at the nanometer scale. We develop advanced synthesis, fabrication and characterization methodologies to understand how nanostructuring can optimize light absorption through quantum and optical confinement and improve catalysis through theory-driven and bio-inspired design. Each is manipulated to improve performance and efficiency in solar energy conversion to hydrogen fuel for storage.

Our research helps understand and expand the scientific foundation of the underlying physical and chemical phenomena that can lead to break-out high-efficiency, cost-effective energy technologies. This multi-disciplinary approach is enabled by the Center structure that provides the intellectual environment and the facilities infrastructure critical to carry out the research projects. A team of CNEEC

researchers assembled across disciplines and institutions (see Fig. 1) bring their complementary expertise to bear on these complex but fundamental issues that cut across not just conversion of sunlight to hydrogen fuel, but also many energy conversion and storage devices. To pursue its mission, CNEEC has organized its research activities in two interconnected projects:

- Project 1. Optical and quantum confinement for light absorption.
- Project 2. Atomic-scale engineering for catalysis.

Technical Barriers

The two projects collectively aim to tackle two primary technical barriers: (1) the efficient absorption of sunlight and (2) subsequent conversion it to stored energy in the form of hydrogen fuel. The project teams work closely together to integrate the best absorbers from Project 1 with the best catalysts from Project 2 and test their solar-to-chemical conversion efficiency.

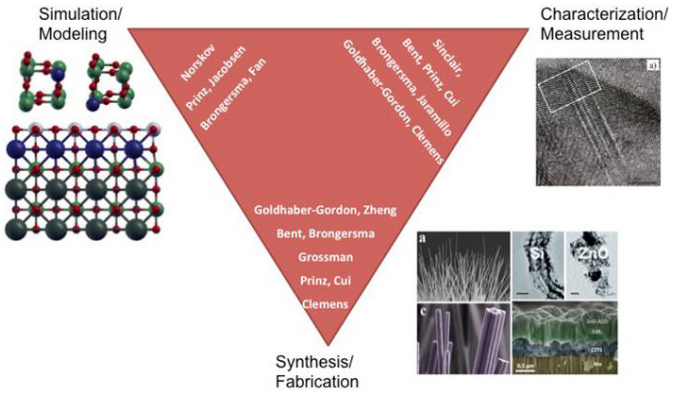

FIGURE 1. CNEEC model.

Abstract

This poster will cover selected CNEEC highlights from both Project #1 and Project #2, as well as their integrations, Fig. 2. In particular, the poster will describe our efforts to establish nanoconfinement effects, to utilize photonic concepts for enhanced light absorption, and to develop sophisticated fabrication and observation platforms to advance the field of photoelectrochemical (PEC) water-splitting. The poster will also describe our efforts in catalyst engineering at the atomic scale in order to develop active catalysts for both the hydrogen evolution reaction (HER) and the oxygen evolution reaction (OER). We will also show our latest results in developing active, stable, low-cost photoelectrodes for PEC water-splitting.

Progress Report

Selected key accomplishments in CNEEC during this past year:

- Demonstrated interparticle electronic coupling between closely spaced quantum dots using electron energy loss spectroscopy in the transmission electron microscope (STEM-EELS).
- Demonstrated the ability to engineer band energy positions of PbS quantum dots through passivation by ligands with different dipole moments.
- Used atomic layer deposition (ALD) to form engineered PbS quantum dots and Al_2O_3 barrier layers to improve charge collection of photo-induced carriers; tested using quantum dot-sensitized solar cell platform.

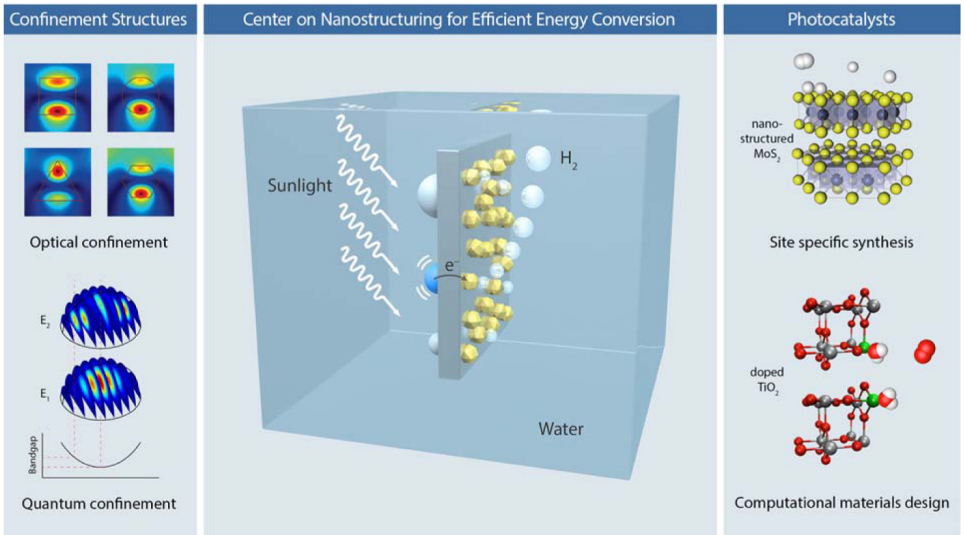

FIGURE 2. Schematic depiction of CNEEC research projects.

- Accomplished record absorption coefficients for visible light using self-assembled plasmonic arrays tuned by atomic layer deposition.
- Used optical simulations to demonstrate that judiciously engineered iron oxide photoanodes based on nanocone arrays can achieve total above-band-gap solar absorption.
- Developed new types of transparent electrodes consisting of mesoscale and nanoscale metal nanowires achieving a sheet resistance of 0.36 Ohm/sq and transmittance of 92%.
- Demonstrated large-area nanopatterned photoelectrodes that capitalize on optical (Mie) resonances to boost the rate of water splitting reactions by a factor of 3.
- Developed models for the performance limits on PEC water-splitting based on the current state of materials research, providing insights into avenues of greatest impact to improve performance.
- Identified the surface structure of manganese oxide catalysts under OER and ORR operating conditions using in-situ synchrotron spectroscopies.
- Engineered improved catalysts by interfacing manganese oxide with gold, and explored their interactions with *ex-situ* and *in-situ* synchrotron spectroscopies.
- Developed precious-metal free regenerative fuel cells for energy storage by means of water electrolysis, based on CNEEC-developed OER catalysts.
- Identified how MoS_2 surface structure impacts its semiconductor properties for PEC water-splitting.
- Employed theory to identify transition metal selenides for HER and to understand trends in reactivity based on the electronic structure.
- Developed methods to calculate Pourbaix diagrams to assess material stability under PEC water-splitting conditions, expanding screening-space to include layered perovskites, double perovskites, and 2400 additional known materials from the ICSD database, leading to the identification by theory of several new promising materials for visible light absorption and catalysis.
- Identified new promising catalyst materials by means of a computational DFT screening study of several hundred ABO_3 perovskite oxides, including strain-induced systems.
- Developed ternary oxide OER electrocatalysts deposited by ALD, complementing theoretical predictions on mixed metal oxide catalysts made by Nørskov and coworkers in CNEEC.
- Integrated atomically-engineered molybdenum sulfide catalysts onto silicon to produce highly active, and stable photocathodes for PEC water-splitting without precious metals.

Future Directions

CNEEC will continue forward with its mission is to understand how nanostructuring can enhance efficiency for solar energy conversion to produce hydrogen fuel and to solve fundamental cross-cutting problems. By manipulating materials at the nanometer scale through advanced synthesis, fabrication and characterization methodologies we will impact optical and catalytic properties of materials to produce fundamental advancements that can ultimately enable technology in this field.

Selected publications acknowledging the DOE grant or contract

1. Ng, J.W.D.; Gorlin, Y.; Hatsukade, T.; and Jaramillo, T.F.A PRECIOUS-METAL FREE REGENERATIVE FUEL CELL FOR STORING RENEWABLE ELECTRICITY, *Advanced Energy Materials*, (2013).

2. Hsu, P.C.; Wang, S.; Wu, H.; Narasimhan, V.K.; Kong, D.S.; Lee, Hye Ryoung; and Cui, Y. PERFORMANCE ENHANCEMENT OF METAL NANOWIRE TRANSPARENT CONDUCTING ELECTRODES BY MESOSCALE METAL WIRES, *Nature Communications*, **4**, 2522-1 (2013). [10.1038/ncomms3522]

3. Hagglund, C.; Zeltzer, G.; Thomann, I.; Lee, H.B.R.; Brongersma, M.L.; and Bent, S.F. SELF-ASSEMBLY BASED PLASMONIC ARRAYS TUNED BY ATOMIC LAYER DEPOSITION FOR EXTREME VISIBLE LIGHT ABSORPTION, *Nano Lett*, **13**, 3352-3357 (2013). [10.1021/nl401641v]

4. Cho, I.S.; Lee, C.H.; Feng, Y.Z.; Logar, M.; Rao, P.M.; Cai, L.L.; Kim, D.R.; Sinclair, R.; and Zheng, X.L. CODOPING TIO2 NANOWIRES WITH (W, C) FOR ENHANCING PHOTOELECTROCHEMICAL PERFORMANCE, *Nature Communications*, (2013).

5. Jung, H.J.; Dasgupta, N.P.; Van Stockum, P.B.; Koh, A.L.; Sinclair, R.; and Prinz, F.B. SPATIAL VARIATION OF AVAILABLE ELECTRONIC EXCITATIONS WITHIN INDIVIDUAL QUANTUM DOTS, *Nano Letters*, **13**, 716-721 (2013). [10.1021/nl304400c]

6. Castelli, I.E.; Garcia-Lastra, J.M.; Huser, F.; Thygesen, K.S.; Jacobsen, K.W.; and , STABILITY AND BANDGAPS OF LAYERED PEROVSKITES FOR ONE- AND TWO-PHOTON WATER SPLITTING, *New Journal of Physics*, **15**, 105026 (2013). [10.1088/1367-2630/15/10/105026]

7. Heinnickel, Mark L.; and Grossman, Arthur R. THE GREEN CUT: RE-EVALUATION OF PHYSIOLOGICAL ROLE OF PREVIOUSLY STUDIED PROTEINS AND POTENTIAL NOVEL PROTEIN FUNCTIONS (REVIEW), *Photosynth. Res.*, **116**, 427-436 (2013). [10.1007/s11120-013-9882-6]

8. Gorlin, Y.; Lassalle-Kaiser, B.; Benck, J.D.; Gul, S.; Webb, S.M.; Yachandra, V.; Yano, Junko; and Jaramillo, T.F. IN-SITU X-RAY ABSORPTION SPECTROSCOPY (XAS) INVESTIGATION OF A BI-FUNCTIONAL MANGANESE OXIDE CATALYST WITH HIGH ACTIVITY FOR ELECTROCHEMICAL WATER OXIDATION AND OXYGEN REDUCTION, *Journal of the American Chemical Society*, **135**, 8525–8534 (2013). [10.1021/ja3104632]

II.G.16 Artificial Hydrogenases: Utilization of Redox Non-Innocent Ligands in Iron Complexes for Hydrogen Production

Principal Investigator: Anne Katherine Jones
Center for Bio-Inspired Solar Fuel Production
Arizona State University
Tempe, AZ 85287
Phone: (480) 965-0356
Email: jonesak@asu.edu

Souvik Roy (sroy11@asu.edu), Lu Gan (Lu.Gan.1@asu.edu), Shobeir K.S. Mazinani (Shobeir.Khezrseddigh@asu.edu), Thomas L. Groy (Tgroy@asu.edu), Pilarisetty Tarakeshwar (tarakesh@asu.edu), Vladimiro Mujica (vmujica@asu.edu)
Center for Bio-Inspired Solar Fuel Production,
Arizona State University, Tempe, AZ 85287
Phone: (480) 965-0356

DOE Program Manager: Christopher J. Fecko
Phone: (301) 903-1303
Email: Christopher.Fecko@science.doe.gov

Objectives

The primary barrier to widescale electrocatalytic production of hydrogen from water is development of efficient catalysts for this transformation using only earth abundant transition metals. The objective of this project is to employ chemical principles gleaned from hydrogenases, biological hydrogen production catalysts, to construct fast and efficient hydrogen production catalysts based on iron.

Technical Barriers

Iron-based molecular proton reduction catalysts usually require substantial basicity at the metal site for fast catalysis. However, the price for this basicity is electrochemical overpotential, i.e. high activation energy, for the electrocatalysis. In this project, we have sought to break this link by constructing bio-inspired complexes employing redox non-innocent, chelating and sterically demanding ligands.

Abstract

Here we report the synthesis and characterization of functional models of hydrogenases for electrocatalytic prouduction of hydrogen from weak acids. The complexes employ iron in bio-inspired coordination environments yielding catalysts that are fast and require very little electrochemical overpotential to support turnover.

Progress Report

Electrocatalysis by an Asymmetrically Disubstituted Diiron Complex with a Redox-Active 2,2'-bipyridyl Ligand

Organometallic complexes of the (μ-$S(CH_2)_3S$) $Fe_2(CO)_4L_2$ family of biomimetic models of [FeFe]-hydrogenases are capable of electrocatalytic production of hydrogen from weak acids, but they typically require substantial overpotential to achieve the catalytically competent Fe(I)Fe(0) redox state. This is especially true if L is a strongly donating ligand that enhances the basicity of the coordinated metal.

In this project, we have employed the chelating, strongly electron donating, redox active 2,2'-bipyridyl (bpy) ligand to construct (μ-$S(CH_2)_3S$)$Fe_2(CO)_4(\kappa^2$-bpy) (**1**) as shown in Figure 1. At room termperature in the presence of excess HBF_4-OEt_2, an acetonitrile solution of **1** changes color from green to light brown. As shown in Figure 2, the reaction was monitored by FTIR spectroscopy. Upon addition of acid, three new bands appeared in the ν_{CO} region at 2098, 2044, and 1970 cm^{-1} with concomitant decrease of the bands associated with **1**. The shift of an average of 92 cm^{-1} to higher wavenumbers is consistent with protonation of the Fe-Fe bond to form a bridging hydride. A ^1H NMR resonance associated with hydride formation could also be detected providing further evidence that $[1H]^+$ is a bridging hydride complex.

Cyclic voltammetry was employed to characterize the redox properties of 1 and the impact of the redox non-innocent ligand on electrocatalytic proton reduction. Controlled potential coulometry showed that a reduction observed as -2.06 V vs. Fc^+/Fc is a two-electron process. By analogy to related complexes and since complexes in this family are not usually able to form an Fe(0)Fe(0) state, we hypothesize that one of the reductions occurs at the metal forming an Fe(I)Fe(0) complex and the

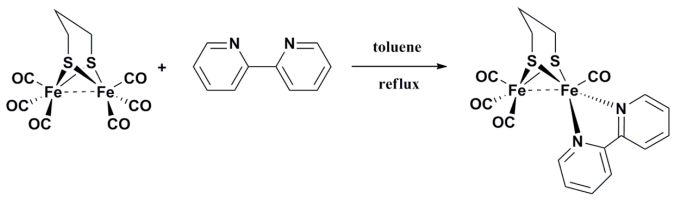

FIGURE 1. Synthetic route to (μ-S(CH2)$_3$S)Fe_2(CO)4(κ^2-bpy).

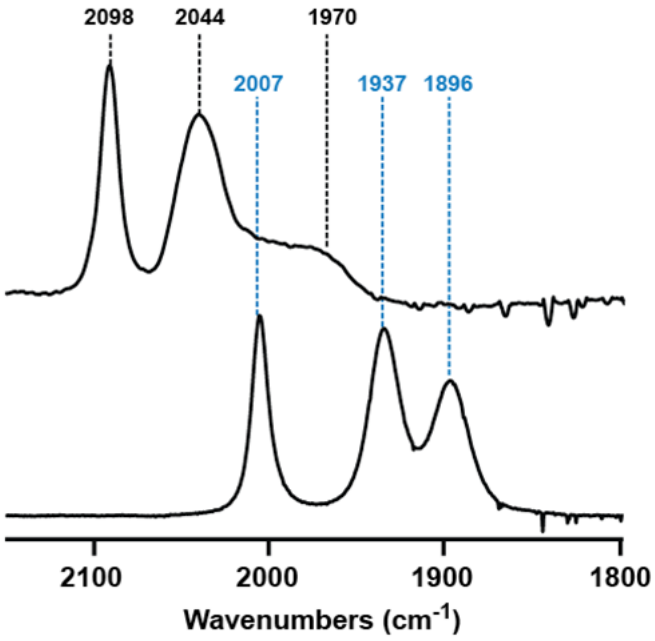

FIGURE 2. FTIR spectra of **1** before (bottom) and after (top) the addition of HBF_4-OEt_2.

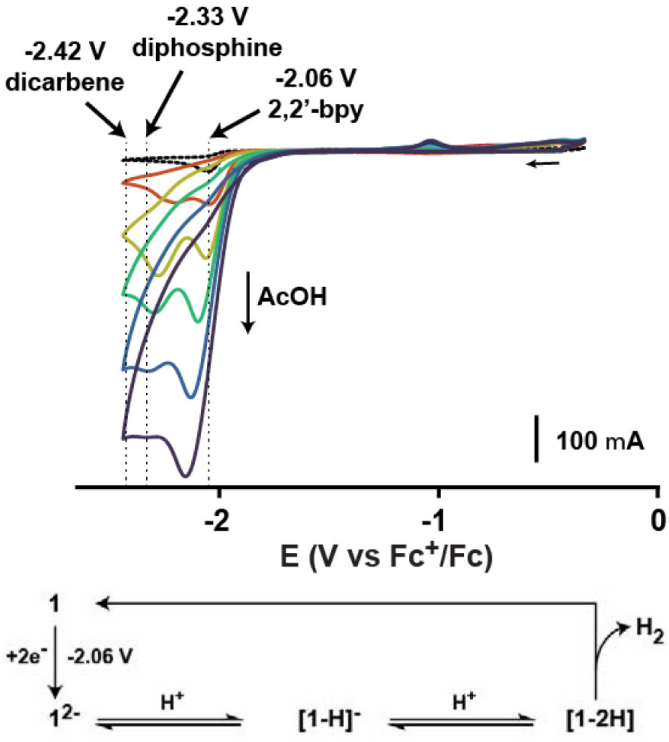

FIGURE 3. Cyclic voltammograms demonstrating electrocatalytic proton reduction by 1 from acetic acid and a hypothetical EECC catalytic scheme that accounts for all data. Dotted lines indicate potentials of electrocatalysis by related complexes with different chelating ligands.

other corresponds to the bpy^0/bpy^{1-} couple. As shown in Figure 3, addition of 1-30 equivalents of the weak acid acetic acid results in a 12-fold enhancement of the reductive current indicating electrocatalytic reduction of protons to hydrogen. The overpotential of this process, defined as the difference between the standard potential for reduction of the acid and the half-wave potential for catalytic proton reduction, was 0.68 V. On the basis of these and other electrochemical results, an EECC mechanism such as that depicted in Figure 3 is thought to be operational. Perhaps most importantly, although this mechanism is not unusual for diiron carbonyl complexes, the low overpotential of the catalysis is. Ordinarily, there is a strong correlation between the CO stretching frequency and the potential of catalysis. For **1**, this connection has been partially broken, and, compared to complexes with similar CO stretching frequencies, catalysis is observed at a less reducing potential. This unexpectedly mild overpotential may be a result of the redox non-innocence of the chelating bpy ligand.

Catalytic Hydrogen Evolution by Fe(II) Carbonyls Featuring a Redox Non-innocent Dithiolate and Chelating Phosphine

Figure 4 shows the synthetic route to two new pentacoordinate Fe(II) complexes: (κ^2-dppf)Fe(CO)(κ^2-bdt) (**2**) and (κ^2-NP_2)Fe(CO)(κ^2-bdt) (**3**) where dppf is 1,1'-bis(diphenylphosphino)ferrocene, bdt is benzene-1,2-dithiol, and NP_2 is methyl-2-{bis(diphenylphosphinomethyl) amino}-acetate. The bdt ligand was employed both for its strong donating propensity and its redox non-innocence. The dppf and NP_2 ligands are both chelating phosphines, but dppf has an extraordinarily large bite angle and comparatively little flexibility. The structures of **2** and **3** were determined by single-crystal X-ray diffraction. Suprisingly, **2** features a trigonal bipyramidal geometry with phosphorous and sulfur in the apical positions. On the other hand, **3** is in a distorted square pyramidal geometry with an axial CO ligand. Importantly, in both structures, the C-C bond lengths of the bdt show an alternating pattern of two shorter C-C bonds and four longer ones. Similarly, the two C-S bonds are not equivalent. This suggests that the C-S bond orders are greater than one and the bdt possesses substantial 1,2-dithiobenzosemiquinonate, π-radical character. The structural results could also be confirmed via DFT calculations of the electronic structure of the complexes.

To establish whether the open coordation site of complexes **2** and **3** is available for external ligand binding, the reactions of **2** and **3** with CO were studied. Although coordinatively unsaturated, both complexes display only weak, reversible binding of CO (data not shown). However, ligand centered protonation of **2** by HBF_4-OEt_2 triggers

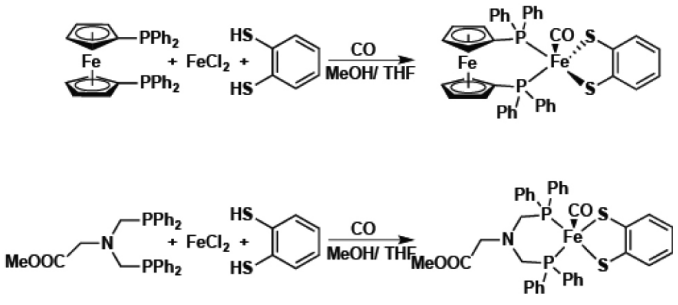

FIGURE 4. Synthetic route to Fe(II) carbonyl complexes.

quantitative, reversible uptake of CO. This reactivity is very similar to that observed for [FeFe]-hydrogenases. DFT calculations suggest that ligand protonation disrupts the extensive electronic delocalization between the Fe and bdt of **2** making it more susceptible to ligand uptake.

As shown in Figure 5, electrochemical investigation shows that both complexes catalyze electocatalytic proton reduction from acetic acid at mild overpotentials, 0.17 and 0.38 V for **2** and **3**, respectively. The unusually low overpotential for catalysis by **2** is likely a result of the geometric strain imposed by dppf and the stabilization of significant electron density at the iron site by the redox non-innocence of bdt.

Future Directions

Future research will investigate the impact of redox non-innocent ligands on proton reduction catalysts employing other first row transition metals including nickel. Decreasing the overpotential to even more energetically favorable values will be attempted by tuning the electron donating propensities of the ligands.

Publication list

1. Jones, Anne K.; McIntosh, Chelsea L.; Dutta, Arnab; Kwan, Patrick; Roy, Souvik; Yang, Sijie. Bioelectrocatalysis of hydrogen oxidation/production by hydrogenases, In *Enzymatic Fuel Cells: From Fundamentals to Applications*. Edited by H. Luckarift, G Johnson, and P. Attanasov, Wiley-VCH, Weinheim, Germany, **2014**.

2. Roy, Souvik; Groy, Thomas; Jones, Anne K. Biomimetic model for [FeFe]-hydrogenase: Asummetrically disubstituted diiron complex with a redox-active 2,2'-bipyridyl ligand. *Dalton Trans.* **2013**, *42*.

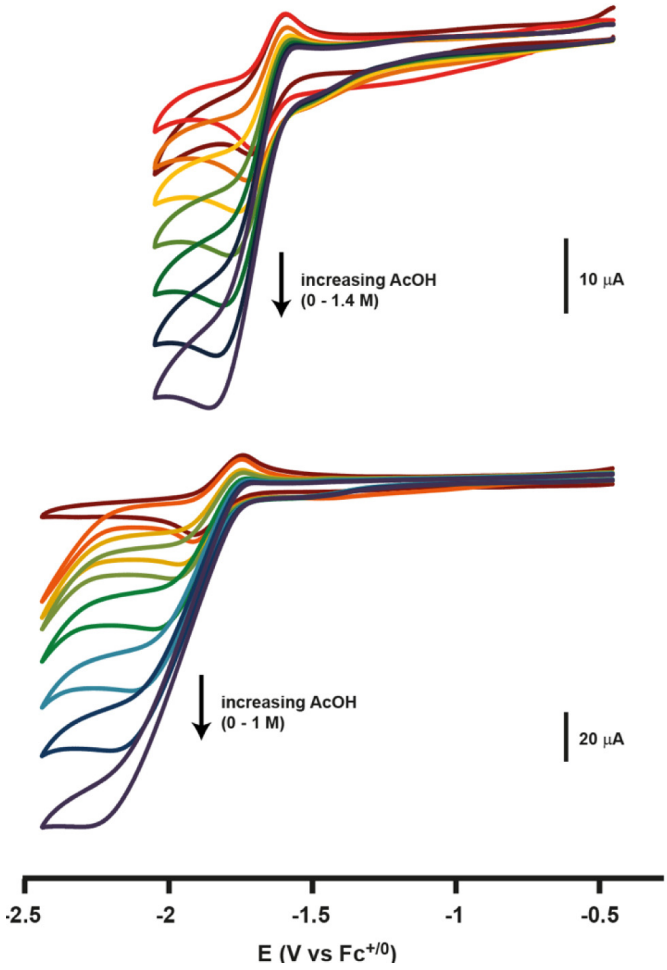

FIGURE 5. Cyclic voltammograms demonstrating proton reduction electrocatalysis by **2** (top) and **3** (bottom).

3. Dutta, Arnab; Flores, Marco; Roy, Souvik; Schmitt, Jennifer; Hamilton, George A.; Hartnett, Hilairy E.; Shearer, Jason; Jones, Anne K. Sequential Oxidation of Thiolates and the Cobalt Metallocenter in a Synthetic Metallopeptide: Implications for the Biosynthesis of Nitrile Hydratase, *Inorg. Chem.*, **2013**, *52*.

4. Dutta, Arnab; Hamilton, George A.; Hartnett, Hilairy, E.; Jones, Anne K. Construction of Heterometallic Clusters in a Small Peptide Scaffold as [NiFe]-hydrogenase Models: Development of a Synthetic Methodology, *Inorg. Chem.*, **2012**, *51*.

II.G.17 Joint Center for Artificial Photosynthesis: Benchmarking Electrocatalysts for the Oxygen Evolution Reaction

Principal Investigator: Carl A. Koval
California Institute of Technology
Pasadena, CA
Email: ckoval@caltech.edu

Team Members

- Thomas F. Jaramillo (Project Lead)
  Stanford University, Stanford, CA
  Email: jaramillo@stanford.edu
- Jonas C. Peters (Project Lead)
  California Institute of Technology, Pasadena, CA
  Email: jpeters@caltech.edu
- Charles C.L. McCrory
  California Institute of Technology, Pasadena, CA
  Phone: (626) 395-2815, Email: cmccrory@caltech.edu
- Suho Jung
  California Institute of Technology, Pasadena, CA
  Phone: (626) 395-2820, Email: suho.jung@caltech.edu

DOE Program Manager: Gail McLean
Phone: (301) 903-7807, Email: gail.mclean@science.doe.gov

Objectives

The JCAP benchmarking project involves the development and implementation of uniform protocols for characterizing the performance of catalysts for the oxygen evolution reaction (OER), the hydrogen evolution reaction (HER), and carbon dioxide reduction reaction (CO_2RR) under standard conditions relevant to the design of a water-splitting device. To this end, the benchmarking team identifies standard reaction conditions relevant to integrated solar fuels devices, determines standard measurement protocols that adequately and efficiently test catalytic activity and stability, and present pertinent data to the community in a concise and transparent way. By employing standard measurement protocols, unbiased evaluation by the JCAP benchmarking team will provide comparisons that are as accurate as possible between electrocatalytic materials under a uniquely defined set of conditions.

Technical Barriers

The identification of efficient electrocatalysts for the oxygen evolution reaction remains an important challenge in the development of integrated solar-fuels generators.[1-3] However, objective evaluation of the efficiency of OER catalysts is complicated by a lack of standardization both in the measurement and reporting of electrocatalytic data. The protocol we have developed in this study has allowed us to evaluate and compare 10 different non-noble metal catalysts for OER.

Abstract

We have developed a procedure for evaluating the activity, stability, electrochemically-active surface area, and Faradaic efficiency of electrodeposited catalysts for the oxygen-evolution reaction (OER). The primary figure of merit used is the overpotential necessary to achieve 10 mA cm^{-2} current density, roughly the current density expected for a 10% efficient integrated solar-to-fuels device under 1 sun illumination.[4-6] This benchmarking protocol was used to examine the oxygen-evolution activity of the following representative set of Ni- and Co-based metal oxide catalysts in acidic and alkaline solution: CoO_x,[7] CoP_i,[8,9] $CoFeO_x$,[7] NiO_x,[10] $NiCeO_x$,[10] $NiCoO_x$,[11] $NiFeO_x$,[7] and $NiLaO_x$.[10] An electrodeposited IrO_x catalyst was also investigated for comparison.[12,13] We have developed a graphical representation of relevant electrocatalytic parameters in order to facilitate the comparison of catalytic performance of multiple catalysts. Two general observations were made from comparing the performance of these catalysts: 1) every system but IrO_x was unstable under oxidative conditions in acidic solution and 2) every non-noble metal system achieved 10 mA cm^{-2} current density at similar operating overpotentials between 0.35 and 0.43 V in basic solution.

Progress Report

We have developed a procedure for evaluating the activity, stability, electrochemically-active surface area, and Faradaic efficiency of electrodeposited catalysts for the oxygen-evolution reaction (OER) shown in Figure 1. Rotating disk voltammetry (RDV) is used to explore the electrocatalytic activity of electrodeposited catalysts. Rotating the electrode in solution ensures rapid product removal and minimizes bubble formation at the electrode surface. All measurements are made at 1600 rpm under 1 atm O_2 using a commercial saturated-calomel reference electrode and a carbon-rod auxiliary electrode. Ferrocenecarboxylic acid at pH 7 is used as an external reference. The activity and stability of each catalyst system is measured at room temperature in two of the solutions relevant to an integrated solar water-splitting device: 1 M H_2SO_4 and 1 M NaOH. The figure of merit for electrocatalytic activity is the overpotential η required to achieve a 10 mA cm^{-2} current density per geometric area.

The procedure for measuring electrocatalytic activity is as follows: first, the solution resistance is estimated

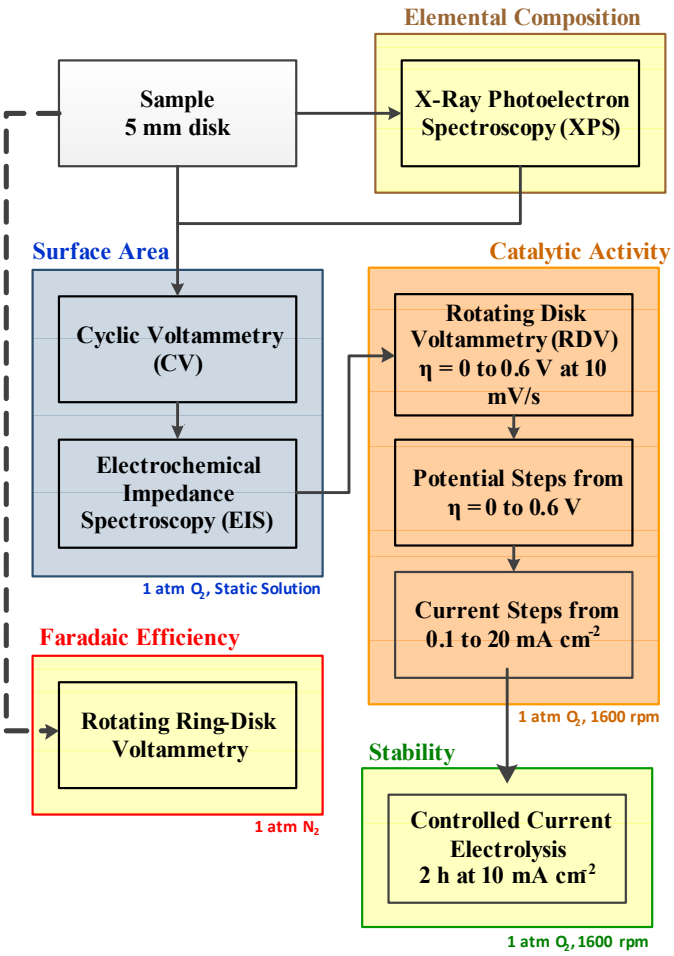

FIGURE 1. Protocol for measuring the electrochemically-active surface area, catalytic activity, stability, and Faradaic efficiency of heterogeneous electrocatalysts for OER. (Reprinted with permission from McCrory, C.C.L.; Jung, S.; Peters, J.C.; Jaramillo, T.F. *J. Am. Chem. Soc.* 2013, *135*, 16977-16987. Copyright 2013 American Chemical Society.)

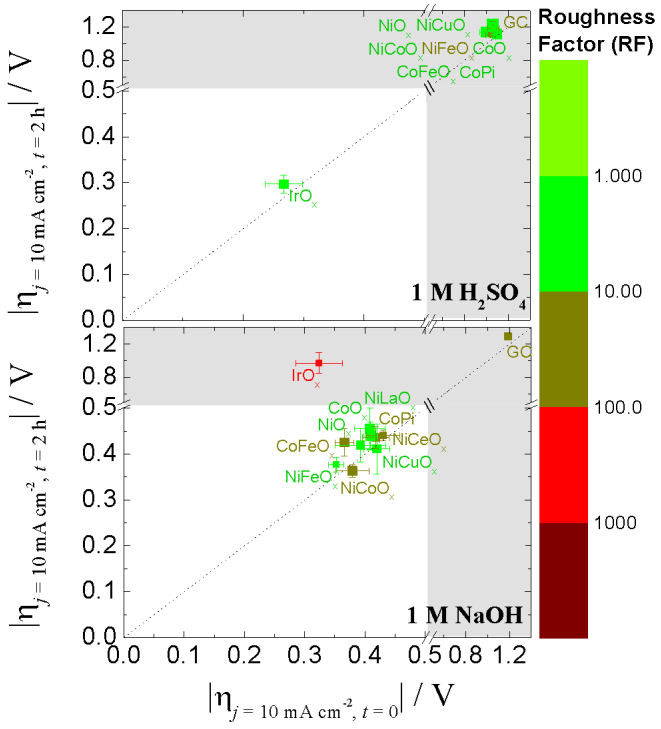

FIGURE 2. Comprehensive plots of catalytic activity, stability, and electrochemically-active surface area for OER electrocatalysts in acidic (top) and alkaline (bottom) solutions. The x-axis is the overpotential required to achieve 10 mA cm-2 per geometric area at time t = 0. The y-axis is the overpotential required to achieve 10 mA cm^{-2} per geometric area at time t = 2 h. The diagonal dashed line is the expected response for a stable catalyst. The color of the each point represents the roughness factor (RF) of the catalyst with a bin size of one order of magnitude with light green representing RF = 1, and dark red representing RF > 10^3. The size of each point is inversely proportional to the standard deviation in the ECSA measurements. The region of interest for benchmarking is the unshaded white region of the plot where the overpotential required to achieve 10 mA cm^{-2} per geometric area at time t = 0 and t = 2 h is less than 0.5 V. There is a break and change in scale in both axes at overpotentials > 0.5 V, and the corresponding region of the plot is shown in gray. (Reprinted with permission from McCrory, C.C.L.; Jung, S.; Peters, J.C.; Jaramillo, T.F. *J. Am. Chem. Soc.* 2013, *135*, 16977-16987. Copyright 2013 American Chemical Society.)

from a high-frequency impedance measurement and every subsequent measurement is IR compensated at 85%. This is followed by a set of activity measurements including linear sweep voltammograms at 0.01 V/s, current steps from 0.01 to 20 mA cm^{-2} per geometric area, and potential steps. Short-term stability measurements are conducted by stepping and holding the current at 10 mA cm^{-2} per geometric area for 2 h and observing the change in operating potential as a function of time. A comprehensive plot that contains information regarding catalyst activity, stability, and specific activity is shown in Figure 2. In general, the best catalyst are expected to achieve 10 mA cm^{-2} current densities at low overpotential, maintain constant activity over time, and have low surface roughness (i.e. high specific activity). Here, the surface roughness is estimated from measuring the non-Faradaic capacitive current associated with double-layer charging from the scan-rate dependence of cyclic voltammograms[14,15] and from measuring the frequency-dependent impedance of the system using electrochemical-impedance spectroscopy (EIS).[16-18]

Two general observations are made from comparing the performance of these catalysts. First, every system investigated with the exception of IrO_x was unstable under oxidative conditions in acidic solution. Although this study focused on a comparatively small subset of OER catalysts, nevertheless this result highlights the need for additional research towards the discovery of non-noble metal acid-stable OER catalysts. Secondly, every non-noble metal system studied achieved 10 mA cm^{-2} current density per geometric area at similar operating overpotentials between 0.35 and 0.43 V in 1 M NaOH. This suggests that several

existing OER catalysts may be attractive for incorporation into devices from an activity and stability standpoint, although the measurements here do not take into account other considerations such as thickness and absorptivity of the catalysts which may have a significant impact on the performance of an integrated catalyst-semiconductor photoanode.

Future Directions

The procedure reported here was initially used to compare the performance of 10 OER catalysts. We are currently expanding the scope of this work to compare the activity and stability of roughly 50 electrocatalysts for HER and OER. This includes developing extended-stability tests for select catalysts that show particular promise based on the initial activity and stability measurements. Moreover, we are currently developing protocols to benchmark the activity, stability, and product distribution of CO_2RR electrocatalyst and integrated semiconductor-catalyst photoelectrodes for HER and OER.

References

1. Eisenberg, R.; Gray, H.B. *Inorg. Chem.* **2008**, *47*, 1697-1699.

2. Lewis, N.S. *Science* **2007**, *315*, 798-801.

3. Lewis, N.S.; Crabtree, G.; Nozik, A.J.; Wasielewski, M.R.; Alivisatos, A.P. *Basic Research Needs for Solar Energy Utilization*, Department of Energy, 2005.

4. Weber, M.F.; Dignam, M.J. *J. Electrochem. Soc.* **1984**, *131*, 1258-1265.

5. Walter, M.G.; Warren, E.L.; McKone, J.R.; Boettcher, S.W.; Mi, Q.; Santori, E.A.; Lewis, N.S. *Chem. Rev.* **2010**, *110*, 6446-6473.

6. Gorlin, Y.; Jaramillo, T.F. *J. Am. Chem. Soc.* **2010**, *132*, 13612-13614.

7. Merrill, M.D.; Dougherty, R.C. *J. Phys. Chem. C* **2008**, *112*, 3655-3666.

8. Kanan, M.W.; Nocera, D.G. *Science* **2008**, *321*, 1072-1075.

9. Surendranath, Y.; Dincă, M.; Nocera, D.G. *J. Am. Chem. Soc.* **2009**, *131*, 2615-2620.

10. Corrigan, D.A.; Bendert, R.M. *J. Electrochem. Soc.* **1989**, *136*, 723-728.

11. Ho, J.C.K.; Piron, D.L. *J. Appl. Electrochem.* **1996**, *26*, 515-521.

12. Nakagawa, T.; Beasley, C.A.; Murray, R.W. *J. Phys. Chem. C* **2009**, *113*, 12958-12961.

13. Zhao, Y.; Hernandez-Pagan, E.A.; Vargas-Barbosa, N.M.; Dysart, J.L.; Mallouk, T.E. *J. Phys. Chem. Lett.* **2011**, *2*, 402-406.

14. Benck, J.D.; Chen, Z.; Kuritzky, L.Y.; Forman, A.J.; Jaramillo, T.F. *ACS Catalysis* **2012**, *2*, 1916-1923.

15. Trasatti, S.; Petrii, O.A. *Pure Appl. Chem.* **1991**, *63*, 711-734.

16. Orazem, M.E.; Tribollet, B. *Electrochemical Impedance Spectroscopy*; John Wiley & Sons, Inc.: Hoboken, NJ, 2008, p. 233-237.

17. Brug, G.J.; van den Eeden, A.L.G.; Sluyters-Rehbach, M.; Sluyters, J.H. *J. Electroanal. Chem.* **1984**, *176*, 275-295.

18. Huang, V.M.-W.; Vivier, V.; Orazem, M.E.; Pébère, N.; Tribollet, B. *J. Electrochem. Soc.* **2007**, *154*, C99-C107.

Publication list (including patents) acknowledging the DOE grant or contract

1. McCrory, Charles C.L.; Jung, Suho; Petres, Jonas C.; Jaramillo, Thomas F.; Benchmarking Heterogeneous Electrocatalysts for the Oxygen Evolution Reaction. *Journal of the American Chemical Society* **2013**, *135* (45), pp 16977-16987.

II.G.18 Joint Center for Artificial Photosynthesis: Si Microwire-Based Solar Water Splitting Devices

Principal Investigator: Carl Koval
California Institute of Technology
Pasadena, CA
Email: ckoval@caltech.edu

Names of Team Members
Harry A. Atwater (Project Lead, haa@caltech.edu),
Nathaniel A. Lynd (Project co-lead),
M. Shaner (mshaner@caltech.edu), K. Fountaine,
J. Spurgeon, I. Sharp, M. McDowell, S. Hu, K. Sun, S. Liang
California Institute of Technology, Pasadena, CA

DOE Program Manager: Gail McLean
Phone: (301) 903-7807, Email: gail.mclean@science.doe.gov

Objectives

The mission of the Joint Center for Artificial Photosynthesis (JCAP) is to produce fundamental scientific discoveries and major technological breakthroughs to enable the development of energy-efficient, cost-effective, and commercially viable processes for the large-scale conversion of sunlight directly to fuels. JCAP's 5-year goal is discovery of robust, Earth-abundant light absorbers, catalysts, linkers, membranes, and scale-up science required to assemble the components into a complete artificial photosynthetic system. The Membranes and Mesoscale group within JCAP is focused on membrane development for solar fuels devices and design, modeling, fabrication and characterization of integrated device components on the micro- and nano-scopic scale. One design currently being pursued and presented here is a tandem junction device based on Si microwire arrays and a second absorber conformally coating each individual microwire, which is all embedded and supported in an ionic transport membrane.

Abstract

Tandem junction (n–p^+-Si/ITO/WO_3/liquid) core–shell microwire devices for solar-driven water splitting have been designed, fabricated and investigated photoelectrochemically. The tandem devices exhibited open-circuit potentials of E_{OC} =-1.21 V versus $E^{0'}(O_2/H_2O)$, demonstrating additive voltages across the individual junctions (n–p^+-Si Eoc =0.5 V versus solution; WO_3/liquid E_{OC} =-0.73 V versus $E^{0'}(O_2/H_2O)$). Optical concentration (12x, AM1.5D) shifted the open-circuit potential to E_{OC} =1.27 V versus $E^{0'}(O_2/H_2O)$ and resulted in unassisted H_2 production during two-electrode measurements (anode: tandem device, cathode: Pt disc). The solar energy-conversion efficiencies were very low, 0.0068% and 0.0019% when the cathode compartment was saturated with Ar or H2, respectively, due to the non-optimal photovoltage and band-gap of the WO_3 that was used in the demonstration system to obtain stability of all of the system components under common operating conditions while also insuring product separation for safety purposes.

Introduction

Si microwire array photocathodes have been shown to generate photovoltages in excess of 500 mV in acidic aqueous environments, and provide a preferred geometry, relative to planar structures, for devices that effect the unassisted generation of fuels from sunlight. Microwire arrays benefit from orthogonalization of the directions of light absorption and minority-carrier collection, as well as from light-trapping effects, an increased surface area for catalyst loading per unit of geometric area, a small solution resistance as compared to planar designs, a reduced material usage through reusable substrates, and the ability to embed the microwires into ion-exchange membranes that exhibit little permeability to H_2 and O_2, thereby producing flexible devices that persistently separate the products of the water-splitting reaction. However, the voltage generated from single-junction Si microwire arrays is much lower than the 1.23 V required for solar-driven water splitting, so a wider band-gap partner light absorber must be introduced electrically in tandem (Si/partner tandem device), to generate useful current at voltages that exceed the thermodynamically required values for fuel production. Accordingly, tandem-junction devices offer the highest theoretical and experimentally realized efficiencies for solar-driven water splitting through additive voltages across two photoabsorbers that use the solar spectrum more effectively.

In addition to band gap considerations for a Si/partner tandem system, achieving the desired electronic behaviour at the interface between Si and its tandem partner presents a significant challenge for production of an integrated solar fuels generation device. The materials must be mutually compatible and generally must operate in a single, concentrated (1.0 M) aqueous electrolyte. TiO_2, WO_3, $BiVO_4$ and Fe_2O_3 are stable in concentrated aqueous electrolytes and form suitable tandem partners for Si. However, Si is stable only in acidic aqueous environments, limiting the presently available partner materials that are stable under such conditions to only TiO_2 and WO_3. WO_3 is the preferred material because of its smaller band gap (Eg = 2.6 eV) and significant photocurrent response to visible-light illumination. The electronic behaviour of the

Si/ WO_3 interface has recently been shown to be non-ohmic, but addition of an intermediate tin-doped indium oxide (ITO) layer has been shown to provide low resistance, ohmic behaviour between p-type, or p^+-type, Si and WO_3.

We present a tandem core–shell photoelectrochemical device that consists of a periodic array of buried homojunction n–p^+-Si microwires that have been sequentially coated with a radial sheath of ITO and WO_3. When immersed in air-saturated 1.0 M H_2SO_4, the dual radial-junction microwire structure enables efficient carrier collection from both the Si and WO_3 light absorbers, despite short minority-carrier diffusion lengths, i.e., ~10 micrometers in Si and ~1 micrometers in WO_3. A necessary feature of this tandem architecture is the incorporation of the ITO layer between the Si and WO_3 light-absorbing materials. This ohmic contact layer ensures facile, low-resistance carrier transport between the Si and $WO_3$and relaxes the requirements for proper band alignment between the p^+-Si emitter and the WO_3. Transparent conductive oxides, such as FTO or ITO, are commonly used as back contacts to semiconductor metal oxides; thus this design is expected to be robust towards implementation of newly discovered materials, because the ITO layer will be amenable to many different Si tandem partner absorbers.

Results

Fig. 1a–f depicts the process used to fabricate the on-wafer devices used herein. Fig. 1g displays an image of a completed wire-array device, while Fig. 1h shows a cross-section of a single wire demonstrating the layered device structure. The Si microwires were 40–70 micrometers in length, had a diameter of ~2 micrometers and had doping densities on the order of 10^{17} cm^{-3}. Secondary-ion mass spectrometry data from planar samples indicated that the p^+-Si emitter thickness was ~200 nm. The sequential, conformal layers of ITO and WO_3 were ~100 nm and ~400 nm, respectively.

Device operation proceeds through photoexcitation of electrons and holes where photoexcited majority-carrier electrons in the n-Si core are transported axially to the back contact through the degenerately doped substrate (n^+-Si) to perform the hydrogen-evolution reaction (HER) at a Pt counter electrode, while photoexcited minority-carrier holes are collected radially in the p^+-Si sheath. The holes in Si recombine with photoexcited majority-carrier electrons from the n-WO_3 at the ITO contact, while minority-carrier holes that are photoexcited in the n-WO_3 are collected at the liquid interface and drive the oxidation of water or anolyte.

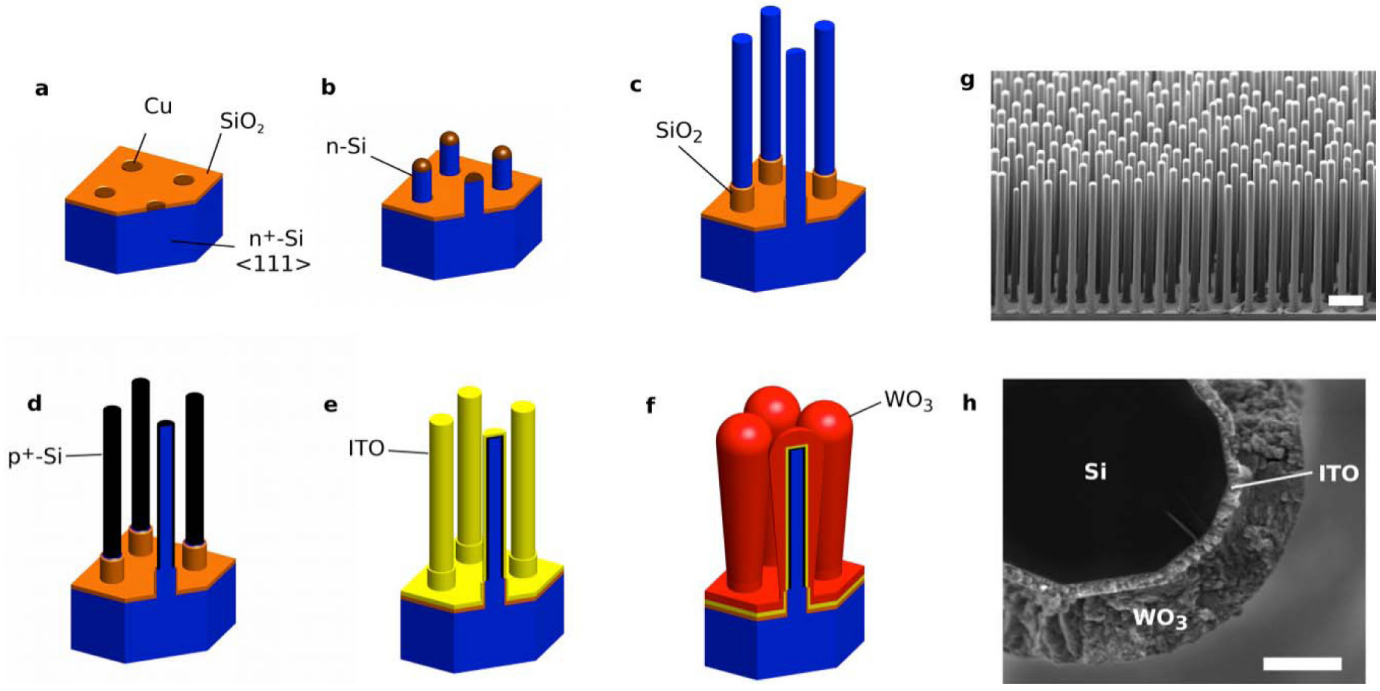

FIGURE 1. (a) Photolithographically patterned n^+-Si <111> wafer with a SiO_2 mask layer and Cu catalyst in the desired growth pattern. (b) VLS Cu-catalyzed growth of n-type Si microwires on an n^+-Si substrate followed by a metal etch (RCA 2). (c) SiO_2 diffusion barrier (boot) formation via SiO_2 growth, PDMS infill, HF etch and PDMS removal. (d) p^+-Si emitter drive-in from BCl_3 precursor at 950°C for 30 min in a CVD furnace. (e) Conformal DC sputter coating of ITO. (f) Conformal n-WO_3 electrodeposition and annealing at 400°C for 2 h. (g) Fully assembled tandem junction device array SEM (scale bar = 10 micrometers). (h) Cross-sectional SEM of a fully assembled tandem junction single wire demonstrating the layered structure of the device (scale bar = 500 nm).

Fig. 2 shows the photoelectrochemical behaviour of single junction (p-Si/ITO/n-WO_3/1.0 M H_2SO_4) and tandem junction (n-Si/p^+-Si/ITO/n-WO_3/1.0 M H_2SO_4) microwire array devices under simulated one Sun illumination conditions. The p-Si/ITO and p^+-Si/ITO contacts have been shown to produce ohmic behaviour allowing isolation of the n-WO_3/1.0 M H_2SO_4 liquid junction performance in the single junction case and efficient use of the buried n–p^+-Si junction in the tandem junction case. The single- and tandem-junction microwire devices exhibited J =0.50 mA cm^{-2} and J =0.58 mA cm^{-2}, respectively, at the formal potential for oxidation of water to O_2, $E^{0'}(O_2/H_2O)$. The first peak in photocurrent density is a dark redox process that results in the photochromism of WO_3, whereupon reverse scans the WO_3 film is reduced through proton intercalation, and is subsequently oxidized on the forward scan. The second peak is associated with photocurrent that results in actual solution redox reactions.

The open-circuit potentials were E_{OC} =-0.73 V vs. $E^{0'}(O_2/H_2O)$ and E_{OC} =-1.21 V vs. $E^{0'}(O_2/H_2O)$ for the single- and tandem-junction devices, respectively. The E_{OC} for the WO_3/liquid contact is in accord with expectations for WO_3 photoanodes operating under these conditions. The 0.48 V shift in E_{OC} of the tandem junction device relative to the single junction device is therefore attributable to the presence of the n–p^+-Si buried junction in the tandem device and is consistent with non-aqueous photoelectrochemical performance of n–p^+-Si buried junction microwire arrays.

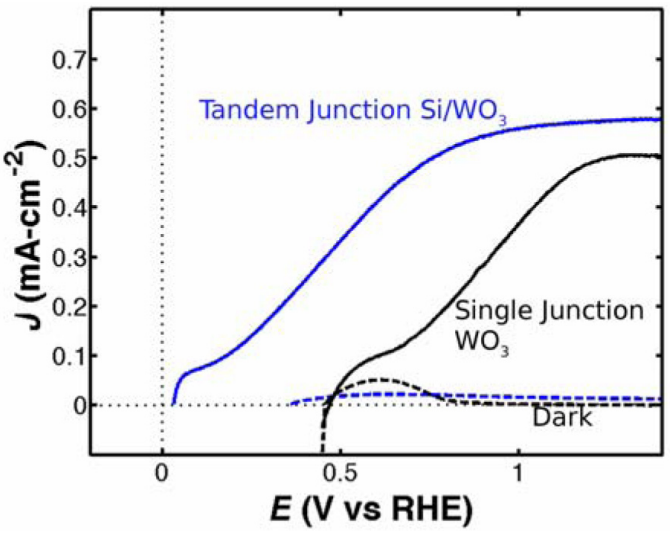

FIGURE 2. Three electrode photoelectrochemical (forward scan, scan rate = 20 mV s^{-1}) performance for single (black) and tandem (blue) junction microwire devices in contact with 1.0 M H_2SO_4(aq.). The single junction microwire device consisted of WO_3 supported on p-Si microwires that had been coated with ITO. Here the p-Si/ITO contact is ohmic so the only rectifying junction is at the WO_3/liquid junction. These data demonstrate the presence of an additive voltage from each junction, with 0.73 V and 0.5 V produced by the WO_3/liquid and n–p^+- Si buried junctions, respectively.

-Reproduced by permission of the Royal Society of Chemistry.

Under modest optical concentration (12 Suns, AM1.5D), tandem junction microwire-array devices exhibited E_{OC} =-1.27 V vs. $E^{0'}(O_2/H_2O)$, which exceeds the 1.23 V potential difference necessary for unassisted water splitting under standard-state conditions. Chronoamperometric measurements were performed with a two-electrode setup at 0 V applied bias between an illuminated tandem junction WO_3/Si microwire array device and a Pt disc electrode. The devices produced solar-to-hydrogen energy-conversion efficiencies of 0.0068% (6.5 x 10^{-3} mA, 0.060 mA-cm^{-2}) and 0.0019% (1.9 x 10^{-3} mA, 0.017 mA-cm^{-2}) when the Pt disc was in contact with Ar(g)- and H_2(g)-saturated solutions, respectively. Product analysis was performed separately on the oxidation and reduction products in 1.0 M H_2SO_4. In contact with H_2SO_4 (aq.), sulfate (SO_4^{2-}) is preferentially oxidized to peroxydisulfate ($S_2O_8^{2-}$) at the WO_3/liquid interface, which was confirmed as an oxidative product by ultraviolet-visible absorption spectroscopy as published previously. Although direct oxygen evolution was not realized due to the slow O_2 evolution kinetics of WO_3, peroxydisulfate has been shown to stoichiometrically evolve O_2 using Ag^+ as a catalyst. At the Pt disc cathode, H_2(g) production was detected by mass spectrometry of the reaction products when the operational current density was passed at the Pt disc electrode. Due to the small amount of H_2(g) produced, direct quantification of the faradaic efficiency was not performed, however no other products are expected due to the use of trace metal grade H_2SO_4.

Future

Integration of new photoanode materials in place of WO_3 has the potential to increase the performance of the tandem device by producing more negative E_{OC} values as well as much larger values of the current density at E = $E^{0'}(O_2/H_2O)$. To produce a more negative value of E_{OC}, the potential of the conduction band of the anode material must be more negative than the potential of the conduction band of WO_3, i.e. closer to the vacuum level, thereby increasing the barrier height at the semiconductor/ liquid junction. Recent studies of mixed-metal oxides have demonstrated photoanode materials with smaller electron affinities than WO_3. The production of increased current density at E = $E^{0'}(O_2/H_2O)$ will require lowering the recombination rates, by improving the material quality and passivating surface states, as well as the discovery of narrower band-gap materials that are stable under oxidizing conditions. Additionally the anodes must be stable under conditions where the cathode and membrane materials are stable, and under conditions where the membrane exhibits high transference numbers for protons, to allow for effective, passive neutralization of the pH gradient between the sites of water oxidation and water reduction while maintaining product separation for intrinsically safe operation of the system under varying levels of illumination.

Publication list (including patents) acknowledging the DOE grant or contract

1. Shaner, M.R. *et al.* Photoelectrochemistry of core–shell tandem junction n–p+-Si/n-WO3 microwire array photoelectrodes. *Energy Environ. Sci.* **2014,** 7 (779)

1. Patent Application: Semiconductor Structures for Fuel Generation, April 3, 2013, Shane Ardo, et. al.

II.G.19 Argonne-Northwestern Solar Energy Research (ANSER) Center

Michael R. Wasielewski, Director
Northwestern University
2145 Sheridan Rd.
Evanston, IL 60208
Phone: (847) 467-1423
Email: m-wasielewski@northwestern.edu

DOE Program Manager: Dr. Chris Fecko
Phone: (301) 903-1303
Email: Christopher.fecko@science.doe.gov

Objectives

The long-term vision of the ANSER Center is to develop the fundamental understanding, materials and methods necessary to create dramatically more efficient technologies for solar fuels and electricity production. ANSER will realize this vision by understanding and characterizing the basic phenomena of solar energy conversion dynamics, by designing and synthesizing new nanoscale and mesoscale architectures with extraordinary functionality, and by linking basic solar energy conversion phenomena across time and space to create emergent energy conversion systems operating with exceptional performance.

Technical Barriers

The ANSER Center's goals are to answer the following four fundamental questions essential to both solar fuels and solar electricity production:

Question 1: How can multi-scale predictive theory and computational modeling lead to the design and discovery of novel organic, inorganic, and hybrid systems?

Question 2: How do molecular and materials structure and order determine the efficiency of light capture, charge separation, and long-range charge transport?

Question 3: What are the fundamental multi-scale temporal and spatial requirements for efficient charge transport across interfaces to deliver multiple redox equivalents to catalysts and electrodes?

Question 4: How can molecular and materials properties be tailored to exploit hierarchical assembly for solar fuels and electricity systems scalable from the nanoscale to the mesoscale?

Abstract

ANSER is investigating coupling light-driven charge generation to multi-electron catalysts for H_2O splitting and H_2 production, focusing on how the structure of photodriven donor-acceptor-catalyst systems determines their charge transfer dynamics at all relevant time scales. Selected highlights of research accomplishments are presented here.

Progress Report

1. *Photodriven Proton Reduction Catalysts.* ANSER focused on understanding hydrogen evolution catalysts made from earth-abundant metals, e.g. the diiron dithiolato complexes found in natural hydrogenases, and providing them with photogenerated redox equivalents. One deficiency with traditional "bioinspired" systems is the photolability of the iron carbonyl group. ANSER discovered that diiron catalysts stabilized by diphosphine ligands are photostable. They also isolated and crystallized the long sought doubly-protonated catalytic intermediate in Fe_2S_2 hydrogenase mimics and showed it to be highly active for H_2 formation. The mixed valence intermediate was characterized by EPR and crystallographic studies, and remarkably the bridging hydride (**Fig. 1**) persisted throughout catalytic turnover.

ANSER developed photodriven H^+ reduction catalysts that mimic the active cofactor within hydrogenase enzymes, yet do so in simplified structures. For example, in the dithiolate diiron complex **1** in **Fig. 2**, the electron-withdrawing naphthalene monoimide (NMI) ligand makes the diiron complex among the most easily reduced hydrogenase mimics reported to date. In the presence of triflic acid, **1** shows electrocatalytic H_2 production. Selective femtosecond laser excitation of the Zn porphyrin in **2** yields charge separation and charge recombination dynamics of 20 ps and 62 ps, respectively. Time-resolved X-ray absorption spectroscopy (at the APS, Argonne) on the electrochemically-generated reduced Fe_2 complex shows that both the Fe-Fe and Fe-CO bonds lengthen as the complex is reduced.

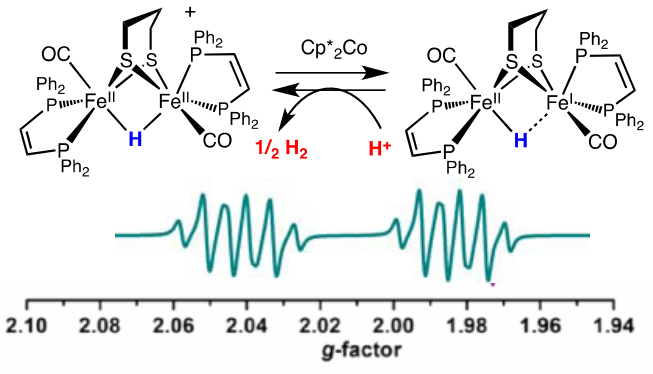

FIGURE 1. Fe-Fe hydrogenase mimic and the EPR spectrum of the Fe(II)-Fe(I) state.

To extend the lifetime of the reduced diiron state of **1**, an electron donor-acceptor triad (**Fig. 2, 3**) was prepared. Here, charge recombination occurs with τ_{CR} = 67 ns in CH_2Cl_2, an increase of >1000-fold relative to the dyad. These results show that rapid energy transfer from the photoexcited Zn porphyrin to the low-lying d-d states of the iron complexes does not compete with the desired photoreduction of NMI-$Fe_2S_2(CO)_6$. Photoexcitation of the triad in the presence of trifluoroacetic acid generates one mole of H_2 for every two photons absorbed.

2. ***Self-assembly of Hierarchical Systems for Photocatalytic Proton Reduction.*** ANSER developed a novel class of biomimetic chalcogenides, "chalcogels", which are air-stable porous, high surface area (150 m^2/g) materials resistant to hydrolysis. These gels have a high degree of synthetic flexibility, allowing a wide range of light-driven processes relevant to solar fuels production. For example, using a simple ion-exchange process, a $Ru(bpy)_3^{2+}$ photosensitizer was incorporated into a chalcogel containing a Fe_4S_4 cluster which serves as a H^+ reduction catalyst. Visible light irradiation results in H_2 evolution for days. Importantly, the chalcogel framework provides a flexible design scaffold for assembling integrated systems for solar fuels formation (**Fig. 3**), and this work was extended to high-performance FeMoS clusters, where the relevant transient redox states responsible for H_2 formation were identified. ANSER also examined the effect of third metal cations (in addition to the Fe_4S_4 clusters) on the electrochemical and electrocatalytic properties of the chalcogels. They found that ternary biomimetic chalcogels containing Ni or Co show increased efficiency in CO_2 to formate conversion and can be thought of as solid-state analogues of enzymatic NiFe or NiFeS reaction centers.

ANSER also demonstrated control of the electrochemical redox potential of biomimetic Fe_4S_4 clusters by varying the size of the bridge between them. As a result, the light to H_2 conversion efficiency of the dye-functionalized chalcogels, ($[Fe_4S_4]_x[Sn_nSn_{2n+2}]_y[Ru(bpy)_3]_z$) was enhanced by using three different Fe/S chalcogels with increasingly larger bridges of $[SnS_4]^{4-}$, $[Sn_2S_6]^{4-}$, and $[Sn_4S_{10}]^{4-}$ (ITS-cg1, ITS-cg2, and ITS-cg3, respectively, **Fig. 3**). The anion sizes define the inter-Fe_4S_4 cluster spacing and modulate the redox potentials. Transient spectroscopy shows that increased H_2 production for ITS-cg3 tracks the longer charge separation lifetime for this system.

A negatively-charged perylene-monoimide (PMI) carboxylate derivative and a positively charged polyelectrolyte was used to self-assemble hierarchically-ordered supramolecular membrane materials that strongly

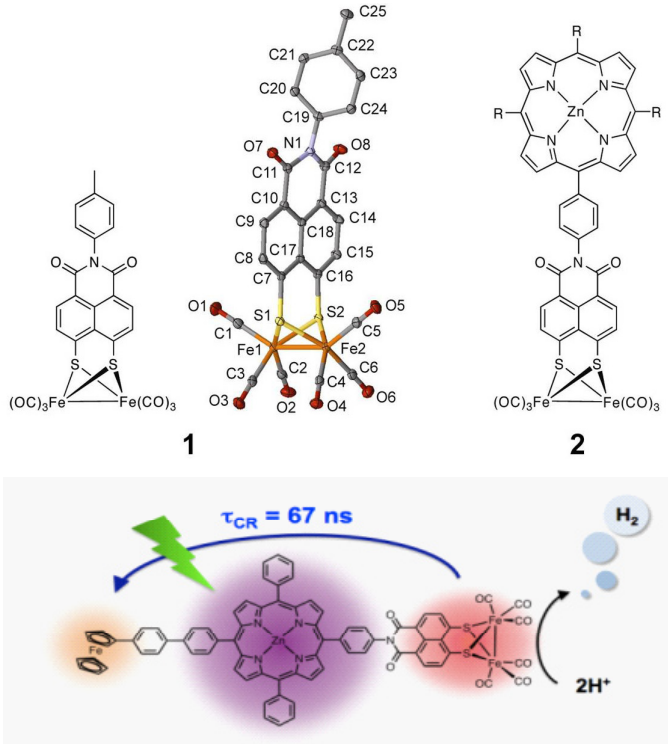

FIGURE 2. Top left: chemical structure of **1**. Top Center: X-ray structure of **1.** Top Right: chemical structure of **2** (R = *n*-C_5H_{11}). Bottom: chemical structure of **3**.

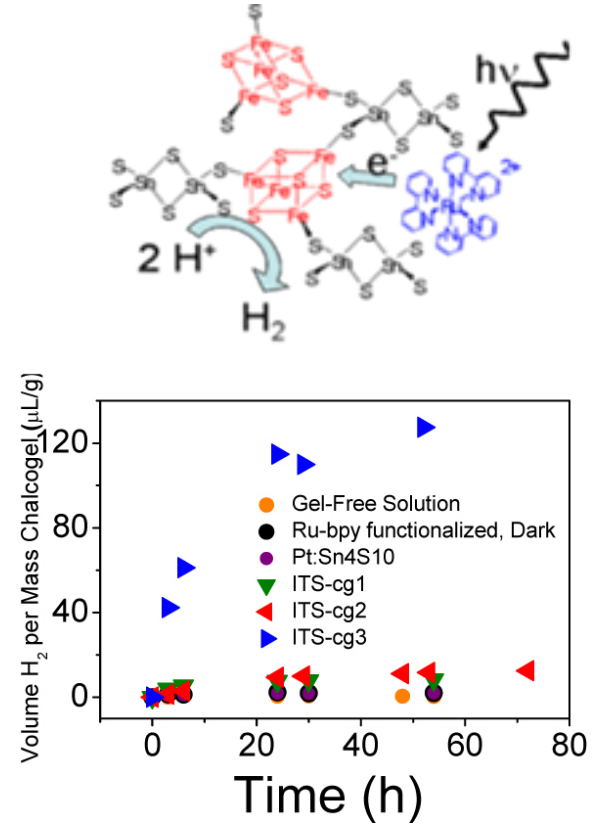

FIGURE 3. Top: Schematic of photo-sensitized of H_2 production using a Fe_4S_4-Sn_2S_6 chalcogel. Bottom: H_2 production as a function of photolysis time and cluster porosity.

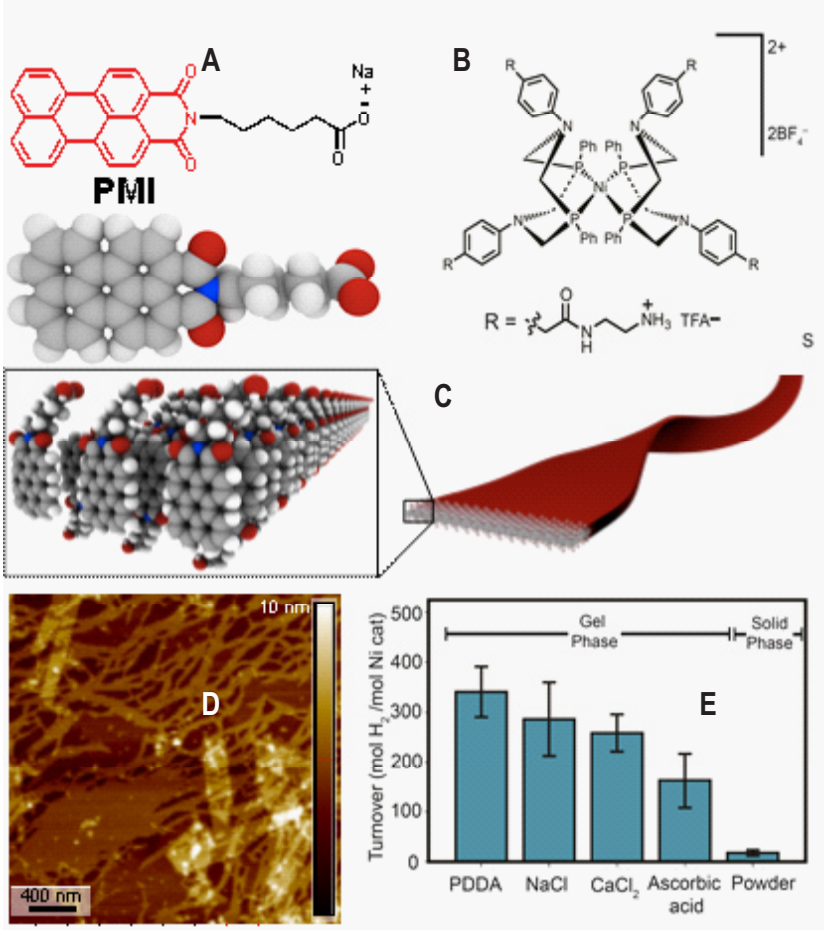

FIGURE 4. (A) Amphiphilic PMI photosensitizer; (B) Ni(II)-phosphine$_4$ catalyst; (C) schematic of self-assembled PMI ribbon; (D) AFM image of ribbons; (E) H_2 evolution in gels.

absorb visible light and are mechanically robust and acid stable (**Fig. 4A-E**). ANSER showed that the PMI carboxylate acts as a photosensitizer to drive photocatalytic H_2 production from H^+ and light with a positively-charged DuBois-type[7] Ni(II)-phosphine catalyst with a sacrificial donor (**Fig. 4E**). In fact, the cationic catalyst itself induces PMI ribbon formation as an emergent property. This result shows that it is possible to associate and compartmentalize catalysts in a self-assembled light-harvesting system to achieve photodriven catalytic H_2 evolution.

Future Directions

Our greatest challenge is efficient fuel production at acceptable rates and driving forces. The ANSER team will use a hierarchical approach to designing, synthesizing, modeling, characterizing, assessing, and understanding catalyst and photocatalyst function. The focus will be on theory-guided and hypothesis-driven design and discovery of superior catalysts, and integration of catalysts with light-harvesting/charge generation molecules and materials. Catalysts will span the range from molecules to clusters, nanoparticles, and bulk materials. Molecules and clusters offer the possibility of full atomic-scale characterization and investigation, while studies of bulk materials will point toward issues that may be relevant for eventual technologies. Nanoparticles provide a useful functional and conceptual bridge between these two limits. The work will be organized around four cross-cutting questions outlined under Technical Barriers.

Publication list (including patents)

See official list from www.energyfrontier.us website. As of April 30, 2014, there are 209 cumulative peer-reviewed publications acknowledging ANSER EFRC funding, resulting in 2750+ citations and an h-index of 32.

II.G.20 Joint Center for Artificial Photosynthesis: Modeling and Simulation Team

Principal Investigator: Carl Koval
California Institute of Technology
Pasadena, CA
Email: ckoval@caltech.edu

Names of Team Members
Adam Z. Weber (Team Lead, azweber@lbl.gov), Chengxiang (CX) Xiang, Alan Berger, John Newman, Meenesh Singh, Kate Fountaine, John Stevens, Katie Chen, Nate Lewis, Shu Hu

DOE Program Manager: Gail McLean
Phone: (301) 903-7807, Email: gail.mclean@science.doe.gov

Objectives

The mission of the Joint Center for Artificial Photosynthesis (JCAP) is to produce fundamental scientific discoveries and major technological breakthroughs to enable the development of energy-efficient, cost-effective, and commercially viable processes for the large-scale conversion of sunlight directly to fuels. JCAP's 5-year goal is discovery of robust, Earth-abundant light absorbers, catalysts, linkers, membranes, and scale-up science required to assemble the components into a complete artificial photosynthetic system. The Modeling and Simulation Team (MaST) develops state of the art multi-scale, multiphysics continuum models of the various processes occurring within the integrated photoelectrode cells.

Technical Barriers

To identify materials that can operate in a solar fuels device, material screening must be performed under technologically-relevant conditions. High throughput instruments that adhere to these conditions must be developed and then automated to provide robust high throughput operation. This screening strategy must then be imbedded in a high throughput pipeline that includes high quality materials synthesis and characterization. While operation of this pipeline can identify new promising materials, accelerated discovery, development and deployment of materials can only be attained by integrating the high throughput pipeline in a larger effort that includes benchmarking, directed research and prototyping efforts. Successful implementation of this research paradigm also requires interplay with theory efforts. JCAP is boldly solving these exciting technical and research integration challenges.

Abstract

Modeling and simulation at the continuum level has been used for years to help interpret and guide experimental investigations of electrochemical technologies, in particular, fuel cells and batteries. The same principles can be applied to new areas such as photoelectrochemical cells that produce fuels from sunlight. It is the objective of the Modeling and Simulation Team (MaST) at JCAP to provide such knowledge in this area. MaST provides guidance, examined tradeoff analysis between material and physical properties, helps to set design targets to the JCAP projects, guides experiments for model input and validation, provides scale-up and prototype guidance, and interacts with the external community with respect to modeling photoelectrochemical-cell phenomena. Specific issues to be discussed in this poster include examination of the design space for solar-fuel generators including alternate designs; the impact of operation at near-neutral pH, and optimization of component design targets.

Progress Report

Operation of PEC at near-neutral pH

There is a desire to operate PECs at neutral or near-neutral pH conditions in order to mitigate corrosion and enable easier fluid handling. This has been shown to be accomplished in single, stirred reactors through the use of buffers and supporting electrolyte so as not to increase ohmic losses in the system. However, there is also a need to minimize product crossover and thus generate pure hydrogen. Such separation necessitates the use of some kind of separator, typically an ion-exchange membrane like Nafion. Modeling and simulation is an ideal tool to explore the operation of such PECs and identify the feasibility of operation at near-neutral pH.

The overpotentials during operation can be seen as being due to the reaction overpotentials at the anode (oxygen evolution), cathode (hydrogen evolution), transport by diffusion, ohmic losses, and transport due to the protons (pH), which are reactive species at the electrodes. For a low-pH system (i.e., sulfuric acid) using state-of-the-art material properties and Nafion as a separator, continuum simulations can be used to show the breakdown of the overpotentials as shown in Figure 1a. From the figure, it is clear that one can theoretically operate at very high current densities (of course real operation in a PEC depends on how the load curve intersects with the PV power curve, which is ignored in this study). For comparison, Figure 1b shows

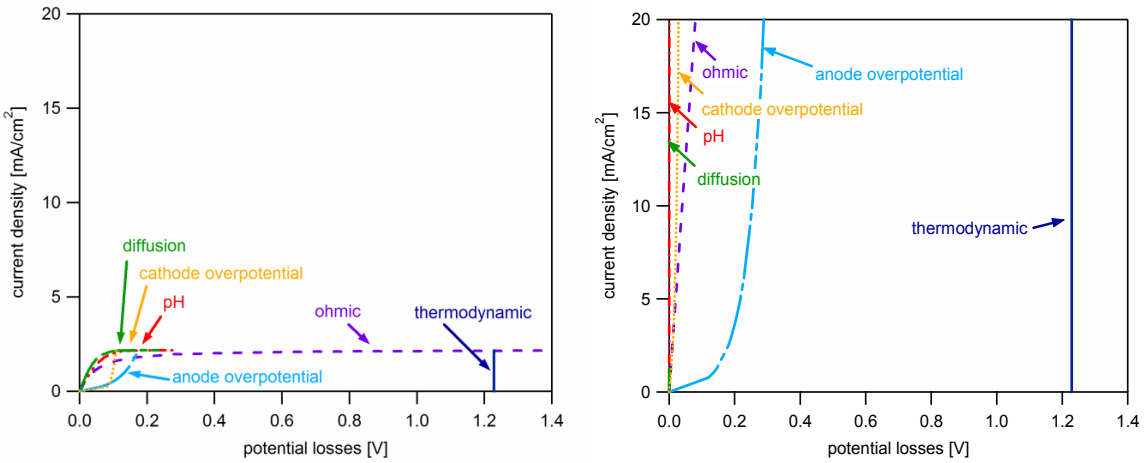

FIGURE 1. Overpotential losses at (a) pH = 0 for sulfuric acid and (b) pH = 9.2 for a borate buffer.

the same overpotential breakdown for the case of a borate buffer that operates around pH 9.2. As shown in the figure, the cell can no longer obtain higher current densities due to the very large ohmic potential that develops at steady state. The genesis of this overpotential can be understood in that during operation, electrodialysis of the solution occurs. Thus, the generation(consumption) of protons at the anode(cathode) results in more neutral acid in the anode and similarly more anions in the cathode, which drives the positive salt ions from the anode to the cathode. This cycle effectively decreases the number of charge carriers at the anode and thus results in larger ohmic losses. Similar electrodialysis effects will happen if one tries to use weak acids or supporting electrolyte, where the pH and diffusion losses can become limiting. The results of such simulations are shown in Figure 2, where one can see that operation at even moderate acid conditions results in small obtainable steady-state current densities. Finally, as shown in Figure 3, even if operating with a porous separator and the borate buffer, the pH at the electrodes will still be highly basic due to the migration and diffusion fluxes and the generation/consumption of hydroxide radicals.

PEC designs

Practical PECs are only now beginning to be fabricated and designed. Modeling and simulation can help greatly in examining tradeoffs of kinetics and ohmic losses, current efficiencies and crossover, and hence optimizing designs for various material properties. Such an example is shown in Figure 4, where a back-to-back louvered design is constructed virtually and the current lines and potential drops calculated. One can then use the model to examine

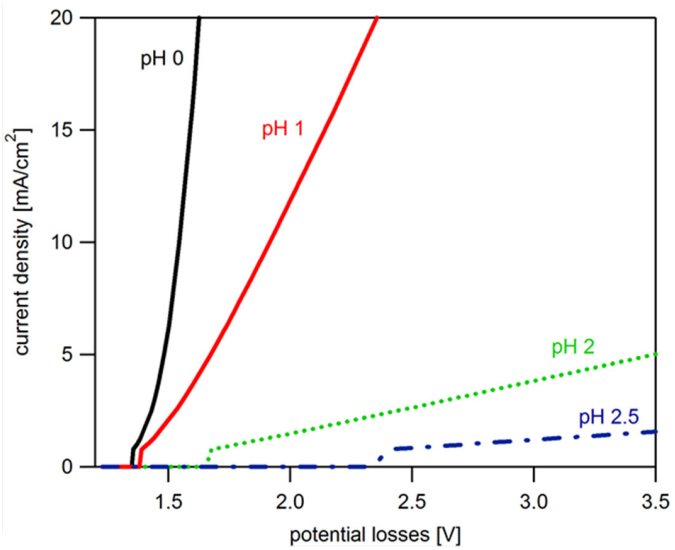

FIGURE 2. Current density as a function of potential losses at different operation pH

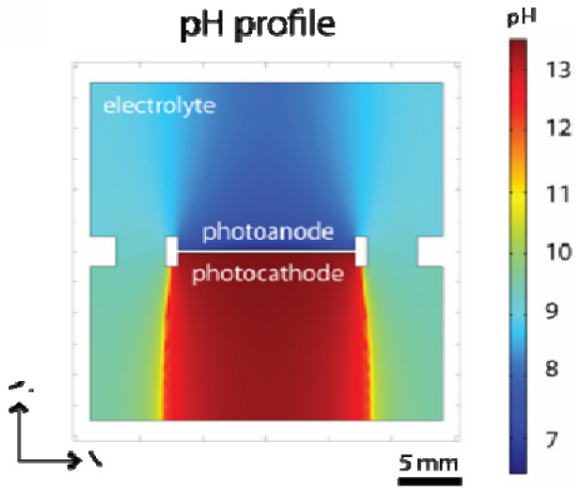

FIGURE 3. pH profile of operating PEC with borate buffer (pH = 9.2)

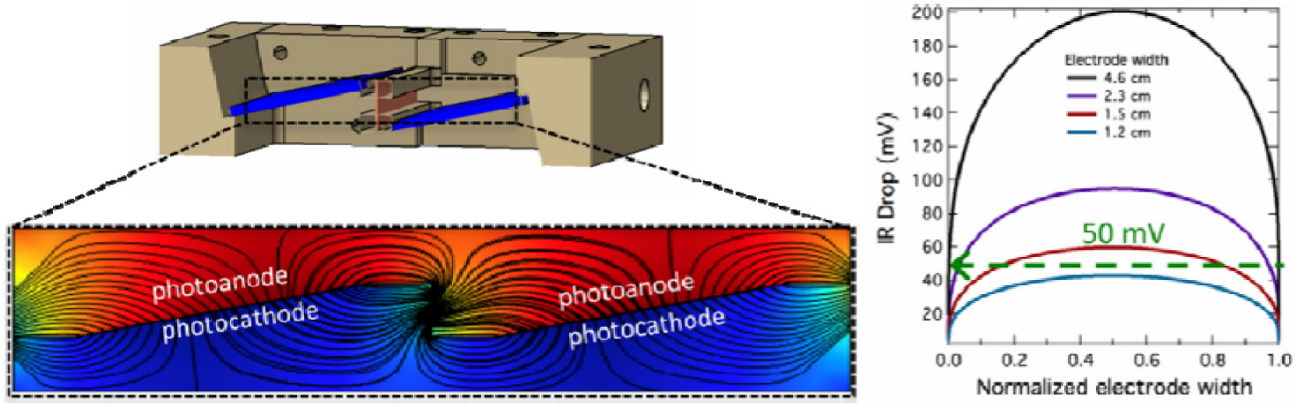

FIGURE 4. Simulated current and potential profiles for a louvered design and examination of the impact of electrode width of such a design on its ohmic losses.

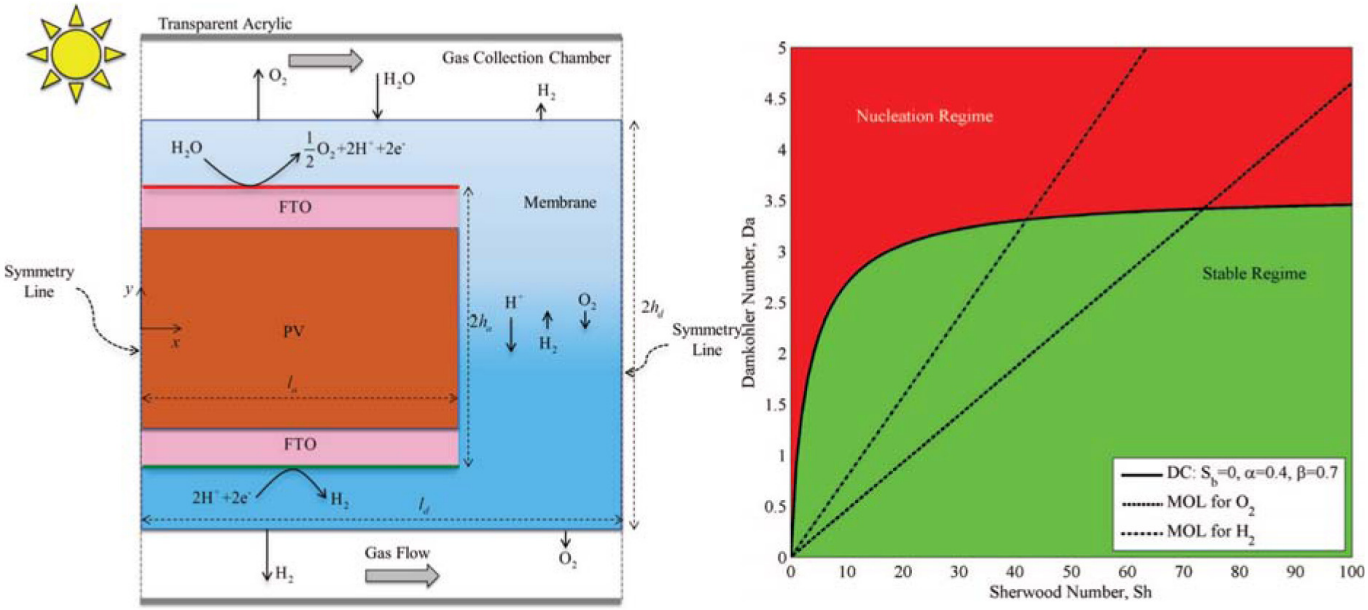

FIGURE 5. (left) Schematic of operation of a PEC with water vapor where the PV and catalyst assembly is embedded in an ion-conducting membrane. (right) Unstable and stable regimes based on material properties and operating conditions of Nafion specific to hydrogen and oxygen transport.

how the ohmic losses change with cell width as shown in the right-side of Figure 4. Here, it is clearly seen that larger electrode widths result in more nonuniform current densities and higher ohmic drops due to the longer proton path-length. In a similar manner, optimized cell dimensions for height, separator thickness, etc. can be derived.

In addition to analyzing current designs, the model has also been utilized to look at newer designs. As shown in Figure 5, one can envision operating on only water vapor instead of liquid water. This can occur because the necessary amount of water for operation at 10 mA/cm^2 (10% efficient conversion of the solar irradiance) is only 3.4 mg/cm^2/hr, which can be supplied by mist or wicks. Operation with vapor can also help to avoid pumping, corrosion, and bubble issues with liquid electrolyte. By simulating the transport of heat, water, protons, and gases through the membrane, one can determine the necessary design space for stable operation as shown in the right-side figure in Figure 5. In such a design, one is worried about supplying enough water for adequate reaction and conductivity, while also minimizing membrane thickness to avoid gas bubbles and delamination.

Examination of optimal band-gap combinations

As mentioned above, operation of a PEC occurs at the intersection of the PV power curve with the load curve as shown in Figure 6. Modeling this intersection and the

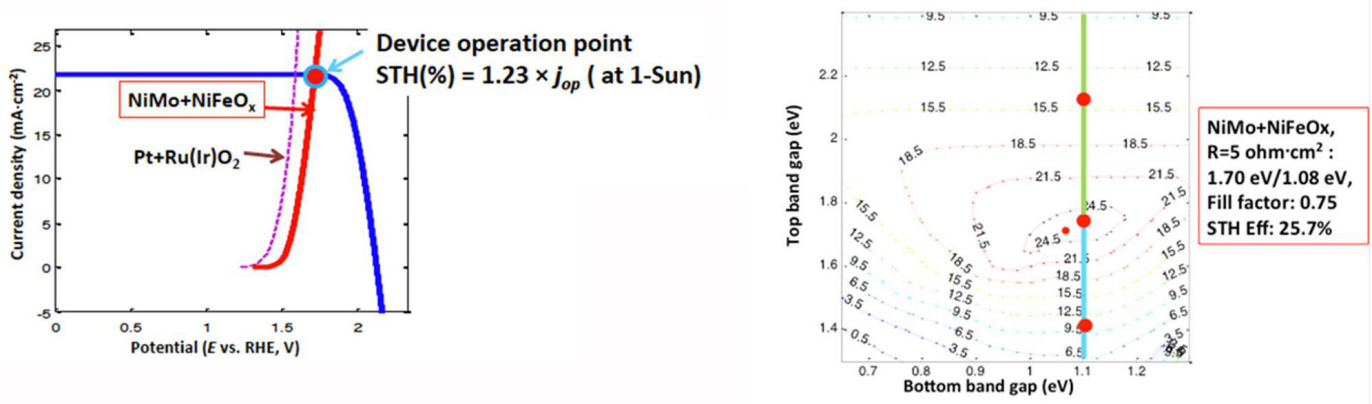

FIGURE 6. PEC operation and model results showing the current density for different bandgap combinations.

associated semiconductor physics along with the ion transport phenomena allows one to optimize and examine the impact of different material properties. Similar to the analysis above for water-vapor PEC, where one could examine the impact of different membrane properties, one can also examine the impact of the semiconductor properties. For example, as shown in Figure 6, for a tandem structure, the choice of the top and bottom bandgaps can be analyzed to set design targets for the material-development efforts within JCAP.

Future Directions

There are several issues that are planned to be addressed in the upcoming year by MaST, including:

- Complete multi-physics model incorporating light capture and semiconductor physics using cross-platform models and software
- Release of the JCAP Modeler to the external community to allow them usage of this resource
- Continued examination of new designs (e.g., concentrator) and phenomena (e.g., bubble existence)
- Sensitivity analysis of key parameters/properties

Selected publication list

1. Haussener, S., Hu, S., Xiang, C., Weber, A.Z., Lewis, N.S., 'Simulations of the Irradiation and Temperature Dependence of the Efficiency of Tandem Photoelectrochemical Water-Splitting Systems', *Energy and Environmental Science* **2013**, *6* (12), 3605-3618.

2. Haussener, S., Xiang, C., Spurgeon, J., Ardo, S., Lewis, N.S., Weber, A.Z., 'Modeling, Simulation, and Design Criteria for Photoelectrochemical Water-Splitting Systems,' *Energy and Environmental Science* **2012**, *5* (12), 9922-9935.

3. Hu, S., Xiang, C., Haussener, S., Berger, A.D., Lewis, N.S., 'An analysis of the optimal band gaps of light absorbers in integrated tandem photoelectrochemical water-splitting systems,' *Energy Environ. Sci.* **2013**, *6*, 2984-2993

4. Berger, A.D., Seglaman, R.A., Newman, J., 'Material Requirements for Membrane Separators in a Water-Splitting Photoelectrochemical Cell,' *Energy Environ. Sci.* **2014.**

5. Singh, M.R., Stevens, J.C, Weber, A.Z., 'Design of Membrane-Encapsulated Wireless Photoelectrochemical Cells for Hydrogen Production,' *J. Electrochem. Soc.* **2014**, in press.

6. Berger, A.D., Newman, J., 'An Integrated 1-Dimensional Model of a Photoelectrochemical Cell for Water Splitting', *J. Electrochem. Soc.* **2014**, in press.

7. Fountaine, K.T., Whitney, W.S., Atwater, H.A. 'Achieving near-unity broadband absorption in sparse arrays of GaAs nanowires via a fundamental understanding of localized radial modes', *Optics Express* **2014**.

8. Shaner, M.R., Fountaine, K.T., Lewerenz, H.J., 'Current-voltage characteristics of coupled photodiode-electrocatalyst devices', *Appl. Phys. Lett*. **2013**, *103*, 143905.

9. Xiang, C., Chen, Y., Lewis, N.S., 'Modeling an integrated photoelectrolysis system sustained by water vapor,' *Energy and Environmental Science* **2013**, *6* (12), 3713-3721.

III. HYDROGEN DELIVERY

III.0 Hydrogen Delivery Sub-Program Overview

INTRODUCTION

The Hydrogen Delivery sub-program addresses all hydrogen transmission and distribution activities from the point of production to the point of dispensing. Research and development activities address challenges to the widespread commercialization of hydrogen technologies in the near-term through development of tube trailer and liquid tanker technologies as well as forecourt compressors, dispensers, and bulk storage; and in the mid- to long-term through development of pipeline and advanced delivery technologies. Technoeconomic analysis is used by the sub-program to identify cost, performance, and market barriers to commercial deployment of hydrogen technologies, and to inform sub-program planning and portfolio development.

GOAL

The goal of this sub-program is to reduce the costs associated with delivering hydrogen to a point at which its use as an energy carrier in fuel cell applications is competitive with alternative transportation and power generation technologies.

OBJECTIVES

The objective of the Hydrogen Delivery sub-program is to reduce the cost of hydrogen dispensed at the pump to a cost that is competitive on a cents-per-mile basis with competing vehicle technologies. Based on current analysis, this translates to a hydrogen threshold cost of less than $4 per gallon gasoline equivalent (gge) (produced, delivered, and dispensed, but untaxed) by 2020,[1] apportioned to less than $2/gge for delivery and dispensing.[2] The sub-program plans to meet these objectives by developing low-cost, efficient, and safe technologies to deliver hydrogen from the point of production to the point of use, in both stationary fuel cells and fuel cell electric vehicles. This objective applies to all of the possible delivery pathways. Key objectives for specific delivery components include:

- **Tube Trailers:** Reduce the cost of compressed gas delivery via tube trailer by increasing vessel pressure to 520 bar and lowering trailer capital cost on a per-kilogram-of-hydrogen-transported basis to less than $575/kg by 2020.
- **Pipeline Technology:** Advance the development and acceptance of alternative composite pipe materials that can reduce installed pipeline costs through inclusion in the American Society of Mechanical Engineers (ASME) B31.12 code by 2015.
- **Liquid Delivery:** Reduce the capital and energy use of small-scale hydrogen liquefiers to less than $42M and less than 8 kWh/kg by 2015.
- **Forecourt Technologies:** Reduce the cost and improve the reliability of compression, storage and dispensing technologies to achieve a station cost contribution of less than $1.60/gge by 2015.

FISCAL YEAR (FY) 2014 TECHNOLOGY STATUS AND ACCOMPLISHMENTS

In FY 2014, the Hydrogen Delivery sub-program made five new awards, held two workshops, and saw significant progress in RD&D activities of existing projects. Significant accomplishments included:

- The release of Hydrogen and Fuel Cells Program Record #13013 documenting the changes in costs of hydrogen delivery technologies from 2005 to 2013, and projecting future costs.[3]
- Five new awards, three selected from the FY 2014 Hydrogen Delivery Funding Opportunity Announcement (FOA) and two from Small Business Innovation Research (SBIR) projects on compression, storage, and dispensing technologies.

---

[1] *Hydrogen Threshold Cost Calculation*, Program Record (Office of Fuel Cell Technologies) 11007, US Department of Energy, 2012, http://www.hydrogen.energy.gov/pdfs/11007_h2_threshold_costs.pdf

[2] *Hydrogen Production and Delivery Cost Apportionment*, Program Record (Office of Fuel Cell Technologies) 12001, US Department of Energy, 2012; http://hydrogen.energy.gov/pdfs/12001_h2_pd_cost_apportionment.pdf

[3] http://energy.gov/eere/fuelcells/downloads/fuel-cell-technologies-office-multi-year-research-development-and-14

- Two workshops to foster collaboration between industry, academia, and the international community in identifying the current challenges and RD&D needs of forecourt technologies to reduce costs and improve system reliability.
- The *Hydrogen Station Compression, Storage, and Dispensing Technical Status and Costs* report was published by the National Renewable Energy Laboratory (NREL) in 2014. This report is an independent panel review of the current status and RD&D needs of hydrogen delivery technologies.
- The Hydrogen Fueling Infrastructure Research and Station Technology (H2FIRST) project was initiated in April of 2014 to conduct RD&D on the development of a hydrogen infrastructure. The project is a collaboration between Sandia National Laboratories (SNL) and NREL and was developed to support H2USA.

Workshops

The first delivery workshop was the *Hydrogen Transmission and Distribution Workshop*, held in February of 2014. This workshop identified technical challenges in the transmission and distribution of hydrogen from the point of production to the point of use in consumer vehicles at a cost of <$3/gge by 2015 and <$2/gge by 2020.[4] Participants included experts from the natural gas industry, national laboratories, academia, and the National Institute of Standards and Technology. The workshop was divided into discussions on pipelines, including pipeline materials and compression, and over-road distribution, including gaseous, liquid, and hybrid distribution. The key challenges and RD&D requirements identified within these areas are summarized in Tables 1 and 2.

TABLE 1. Key Pipeline Areas Discussed

	Challenges	RD&D Needs
Pipeline Compression	Compressor reliability and maintenance requirements	Development of novel compressor systems. *Long-term*: Development of compressors with line packing capability.
	Optimization of performance and cost of high-pressure compressors	High-volume manufacturing of miniaturized parts. Integration of purification, cooling, and compression systems.
	Optimization of hydrogen transmission and distribution routes	Techno-economic models to optimize key variables, e.g. storage capacity and pressure. *Long-term:* A model addressing the interface between hydrogen pipelines and the electric grid.
	Evaluation and comparison of existing technologies	Facilities that provide third-party validation of compressor performance and define procedures to assess key metrics.
Pipeline Materials	Physical understanding of hydrogen-induced damage mechanisms	Research on the performance of high-strength steels and welds in hydrogen service and identification of the material properties that affect hydrogen embrittlement. *Long-term:* Development of a physics-based predictive fatigue crack growth model informed by testing.
	Joining technologies	Evaluation of existing non-metallic materials and development of new cost effective and reliable joining technologies for fiber-reinforced polymer (FRP) pipelines.
	Capital cost of pipeline installation	Demonstration of FRP in hydrogen transport at scale in a variety of soil types. *Long-term:* Development of a machine that can manufacture FRP in situ.
	Codes and standards adoption	Burst and fatigue testing of FRP in hydrogen, and measurement of permeation rates to develop the technical basis for factors of safety. Development of efficient inspection and monitoring techniques.

[4] The "Hydrogen Transmission and Distribution Workshop" proceedings are available here: http://energy.gov/sites/prod/files/2014/07/f17/fcto_2014_h2_trans_dist_wkshp_summary_report.pdf

TABLE 2. Key Over-Road Distribution Areas Discussed

	Challenges	RD&D Needs
Distribution via Gaseous Tube Trailers	Understanding of degradation mechanisms	Test procedures and acceptance criteria for polymers in hydrogen. Research on the degradation of polymers and composite vessels under high-pressure hydrogen cycles.
	High capital and operating costs	Discovery and qualification of low-cost, lightweight structural alloys for use in high-pressure trailers. Techno-economic analysis of supply chain models.
	Design limitations of tube trailers	Development of gaseous sorbent materials for low-pressure delivery. Design optimization of tube trailers.
Liquid and Hybrid Distribution	Energy intensity of liquefaction process	Efficiency improvements to pre-cooling, compression, cryo-cooling, expansion, and power recovery systems. Modular high-efficiency liquefaction technologies.
	Length of time required for standards and regulations development	Risk analysis of liquid hydrogen releases. Develop a comprehensive source for information on regulations, codes and standards.
	Increase truck payload	Carrier material development. Low-cost, lightweight structural alloys for low-temperature operation.

The *Second International Workshop on Hydrogen Infrastructure and Transportation,* organized by Germany's NOW (National Organisation Hydrogen and Fuel Cell Technology), Japan's NEDO (New Energy and Industrial Technology Development Organization), and DOE was held in June of 2014, hosted by Toyota at the Toyota Motor Sales Corporate Accessory Center in Torrance, California. This workshop included members of industry and government from Japan, Germany, the European Union, Scandinavia, and the United States. Participants identified the major challenges and RD&D needs of hydrogen fueling protocols, metering, hydrogen fuel quality, and forecourt hardware. The highest priority issues in each of these areas are summarized in Table 3. Additional detail will be available in the workshop proceedings when they are published later in calendar year 2014.

TABLE 3. Issues in International Hydrogen Infrastructure

Topic Area	Highest Priority Issue
Fueling	Development of procedures and hardware to enable certification of stations to SAE International technical specification J2601.
Metering	Agreement between metering accuracy requirements established by the National Institute of Standards and Technology and the International Organization of Legal Metrology, and communication of these requirements to industry.
Hydrogen fuel quality	Development of a low-cost method and hardware to continuously monitor hydrogen inline.
Forecourt hardware	Improve the reliability, durability, and cost of hydrogen compression.

Publications

In FY 2014, the Hydrogen Delivery sub-program released Hydrogen and Fuel Cells Program Record #13013 to document the changes in costs of hydrogen delivery technologies from 2005 to 2013, and to project future costs. The 2013 hydrogen delivery cost at 700 bar is between $3.23/gge and $4.84/gge (Figure 1), depending on the delivery pathway. To meet the 2020 target of <$2/gge, additional RD&D is needed across all aspects of delivery, as is discussed in the *Hydrogen Station Compression, Storage, and Dispensing Technical Status and Costs* independent panel report.

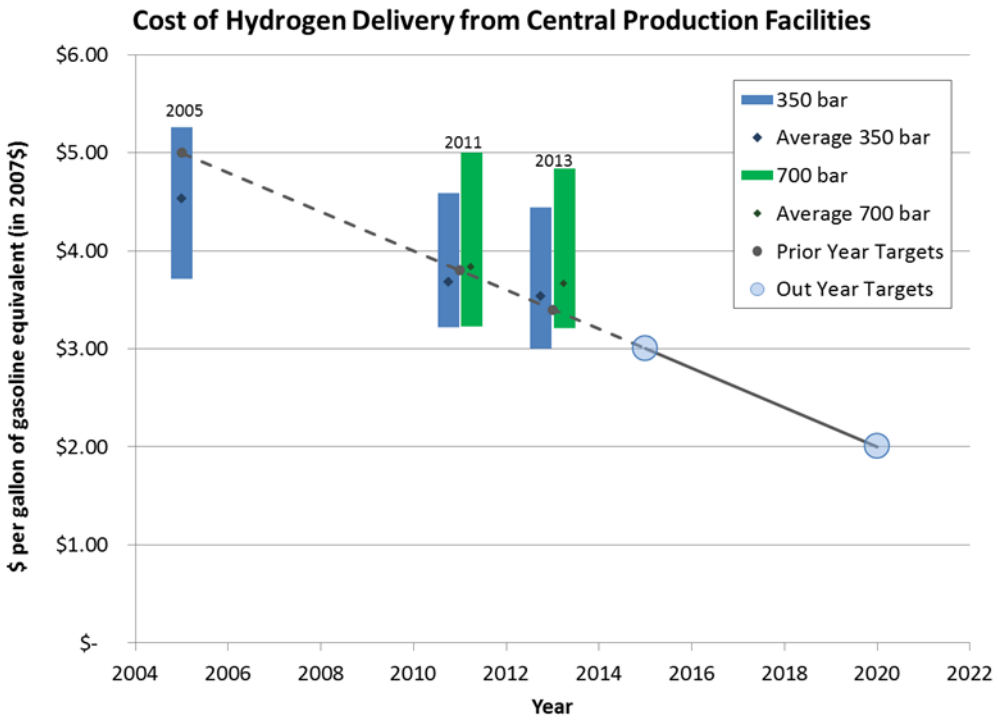

FIGURE 1. Cost of Hydrogen Delivery from Central Production Facilities. The cost statuses and targets of hydrogen delivery (transmission and distribution) have steadily declined since 2005. The ranges shown in this graph are based on simulations of three 350-bar scenarios: (1) transmission and distribution via pipelines, (2) transmission via pipelines and distribution via tube trailers, and (3) transmission and distribution via tube trailers; and five 700-bar scenarios: (1) transmission and distribution via pipelines, (2) transmission via pipelines and distribution via tube trailers, (3) transmission and distribution via tube trailers, (4) transmission via pipelines and distribution via liquid tankers, and (5) transmission and distribution via liquid tankers. Cost statuses for prior years were based on the technology readiness levels during those years. Cost projections are based on DOE targets and feasibility assumptions from technical experts.

For the conditions studied in the record, the lowest-cost transport method was identified as the use of tube trailers for both transmission and distribution. Tube trailers were also the lowest-cost delivery method identified in the *Hydrogen Station Compression, Storage, and Dispensing Technical Status and Costs* independent panel report. The record assumes hydrogen production takes place 100 km from the edge of a U.S. city of average size (Indianapolis was the basis for the analysis), with a market penetration of 10-15%, and a station dispensing rate of 750-1,000 kg/day.

Funding Opportunity Announcements

The Hydrogen Delivery Technologies FOA (DE-FOA-0000821) was announced in 2014, and three award selections are currently being negotiated. The FOA sought research on hydrogen compression, dispensing, and storage technologies that could help bring the cost of hydrogen delivery to less than $2/gge. The awards being made are:

- Southwest Research Institute® ($1.8M), Rockville, MD: *Linear Motor Reciprocating Compressor.* This project involves the design and development of a linear motor reciprocating compressor over the course of three years. In a linear motor reciprocating compressor, the piston contains a permanent magnet that interacts with electromagnetic windings in the cylinder to thrust the piston, and thereby compress the gas. The compressor design is advantageous because it has few moving parts and can be easily modularized.
- Wiretough Cylinders ($2.0M), Bristol, VA: *Low Cost Hydrogen Storage at 875 bar by using Steel Liner and Steel Wire Wrap.* This project involves the development and testing of Type II vessels that can store hydrogen at 875 bar at a cost of $650/kg of hydrogen, exceeding the DOE target of $1,000/kg by 2020.
- Oak Ridge National Laboratory (ORNL) ($2.0M), Oak Ridge, TN: *Low-Cost Steel Concrete Composite Vessel for Forecourt Hydrogen Storage at 875 Bar or Greater.* This project involves the design and development of a prototype of a steel concrete composite vessel that can store hydrogen at 875 bar at $800/kg, exceeding the DOE target of $1,000/kg by 2020.

Tube Trailers and Bulk Storage

Significant cost reduction at the forecourt can be achieved through the use of high-pressure tube trailers and low-cost on-site storage. Higher pressure tube trailers at the forecourt can move the gaseous compression upstream to the tube trailer terminals where economies of scale can reduce the cost of the compression. This year the following two projects have contributed to the cost reduction of the gaseous hydrogen delivery pathway.

- The development of the TITAN™V XL40 trailer configuration for hydrogen delivery was initiated. With a storage capacity of 890 kg of hydrogen and a 90% hauling efficiency, this configuration will increase delivery capacity by 11% over that of the TITAN™V Magnum. The first deployments of TITAN™V Magnum trailers were made in 2013 for compressed natural gas applications. (Hexagon Lincoln)
- A detailed cost analysis of steel/concrete composite vessels that demonstrates the technology's potential to exceed the DOE's 2015 storage cost target of $1,200/kg was completed. (ORNL)

Pipeline Technologies

Pipelines are an attractive delivery pathway for large market scenarios. Advances in both pipeline compression and FRP pipelines continue to improve the economics of the scenario, while work on hydrogen embrittlement of steel continues to improve our understanding of the performance of traditional pipeline materials in use in a hydrogen pipeline transmission and distribution network.

- The inclusion of FRP pipeline with a 50-year design life in the ASME B31.12 code was pursued, and it is expected to be complete by 2015. Fatigue testing has been underway since 2012 at a range of pressures and ratios to support codification efforts. The current data supports an increase in design life from 20 years to 50 years for FRP through a 5% decrease in fiber stress and a limit on fatigue life of 33,100 cycles at an R ratio of 0.5. Experimentation shows that the fatigue life of FRP is highly sensitive to R ratio. (Savannah River National Laboratory, SRNL)
- Triplicate measurements of fatigue crack growth in the base metal, fusion zone, and heat-affected zones of X65 pipeline steel in 21 MPa of hydrogen were collected. The data demonstrate that, at high values of ΔK, crack growth rates are very similar in all three zones. The data collected to date can also be used to determine inspection frequencies for pipelines based on their thicknesses. Experimentation has also been conducted to assess the effect of microstructure on crack growth rate. Crack growth was seen to be slower in banded pearlite microstructures. Further investigation is underway. (Sandia National Laboratories)
- Testing of a single-stage oil-free centrifugal hydrogen compressor in helium was completed in accordance with Industry Standard ASME PTC-10. Vibration of the compressor was very low, reaching a maximum of only 20% of the bearing clearance. The adiabatic efficiency, power requirements, and head of the compressor were additionally strongly correlated with theoretically determined values. Furthermore, the uninstalled capital cost of the compressor was reduced to ~$2M from $2.7M based on a 3,000 kWh motor rating. (Mohawk Innovative Technologies)

Forecourt Technologies

Forecourt technologies, in particular compression and onsite storage, are a key area of focus for the sub-program. Efforts in this area aim to improve the reliability and reduce the cost of the technologies.

- An 8-cell, 185-cm^2 electrochemical hydrogen compressor stack at a capacity of 2 lb/day with an outlet pressure of 3,000 psi for over 3,800 hours was demonstrated. The 185-cm^2 cell was also validated at over 8,500 hours of operation at current densities greater than or equal to 750 mA/$cm.^2$ The compressor cell design was additionally improved to enable a capital cost reduction of 60% in comparison to the original 2010 design. Design improvements included higher current densities, greater cell active area, increase in stack size, reduction in the number of cell parts, reduction in the cost of cell and stack materials, and reduction in the cost of fabrication. (Fuel Cell Energy)
- A 700-bar refueling hose was tested under simulated mature market conditions to determine the baseline reliability and failure mechanisms from which the technology can be improved. Burst testing has been completed, and the hose material properties have been assessed via spectroscopy, microscopy, calorimetry, and thermal analysis. The hose was found to have a burst pressure of 58,800 psig, more than 105% of its specification. (NREL)
- A fueling strategy to improve station capacities during peak hours was developed. This strategy involves the use of a cascade of tubes in the tube trailers, wherein hydrogen gas is consolidated into one tube during peak fueling times. The high-pressure tube is then used directly for vehicle fueling while the compressor is used to either

pressurize the gas in the other tubes or replenish buffer storage. This technique reduces on-site compression requirements, enabling a 10-kg/hr compressor to serve a 450-kg/day station, three times the capacity of 150 kg/day it could otherwise serve, that results in a 14% cost reduction for tube trailer delivery from $3.30/gge to $2.85/gge delivered and dispensed for 700-bar refueling. (Argonne National Laboratory)

- A Phase II award of $1M for the FY 2013 Small Business Innovation Research topic on hoses for hydrogen dispensing at 700 bar was made to Nanosonic Inc. The project objective is to develop a low-cost hose for dispensing hydrogen that can be operated reliably for more than 25,000 fuelings under the temperature and pressure cycles (-40°C and 875 bar) experienced during fueling of 700-bar tanks to the SAE J2601 type A fill. During phase I, the project selected polymers for hose construction that survived the low-temperature flexure test and exhibited ultra-low hydrogen permeance after severe bending. The team then used these materials to form hoses that were predicted to have burst pressures of 2,560 bar. During phase II, hoses made of the selected materials will be evaluated per American National Standards Institute/CSA HGV 4.2-2013 to verify their safety, compatibility for hydrogen service, and weatherability. (Nanosonic Inc.)
- A $150K Small Business Innovation Research award was made to GVD Corporation for the development and testing of a novel coating for plastic/elastomer seals used in hydrogen technologies. Seals have poor reliability and high cost because of their failure rates in extreme temperatures and high-pressure hydrogen. GVD's coating, which will be comprised of both inorganic and organic layers that will be generated by chemical vapor deposition technologies, will reduce hydrogen permeation into the seal by 10x over the uncoated baseline. (GVD Corporation)

BUDGET

The FY 2014 appropriation provided $21 million for the Hydrogen Production and Delivery sub-program, with approximately $9.7 million provided for Delivery RD&D. The estimated budget breakdown for Delivery in FY 2014 and FY 2015 is shown below. The request for Hydrogen Production and Delivery in FY 2015 is $21 million, with $11 million planned for Delivery RD&D, with an emphasis on reducing near-term technology costs, improving forecourt compressor reliability, and reducing onsite storage costs.

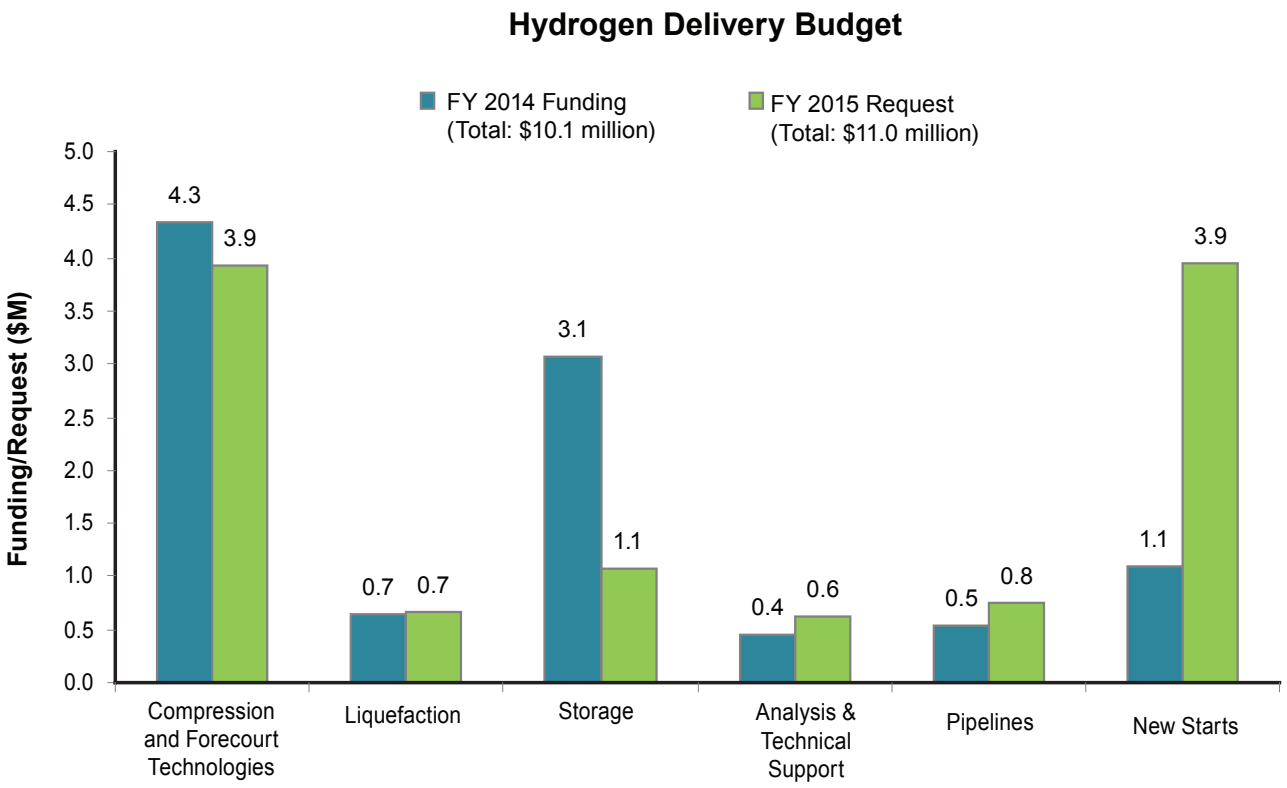

* Subject to appropriations, project go/no-go decisions, and competitive selections. Exact amounts will be determined based on research and development progress in each area.

FY 2015 PLANS

In FY 2015, the Hydrogen Delivery sub-program will focus on several key efforts:

- Release an updated version of the Hydrogen Delivery Scenario Analysis model. The results of a May 2014 Independent Panel Review Report on the current status of compression, storage, and dispensing technologies will be used to revise and release an updated version of the Hydrogen Delivery Scenario Analysis model by the end of 2014. The new version will include updated 700-bar and cryo-compressed dispensing scenarios from liquid hydrogen delivery, as well as updated cost indices.
- Complete data analysis and reporting to ASME B31.12 for inclusion of FRP into the code. The initial proposal for codification of FRP pipeline into ASME B31.12 was presented to the Code Committee in March 2014. Additional research is currently being conducted at SRNL to support codification. Fatigue testing is being conducted to support a 50-year design life for FRP, and non-mechanical joints are being evaluated. A demonstration of FRP in hydrogen service is also planned.
- Validate the steel concrete composite vessel cost and performance, through prototype testing, to demonstrate that it meets the 2015 cost and performance targets in the Multi-Year Research, Development, and Demonstration Plan.
- Continue to focus on forecourt RD&D through new awards and the H2FIRST project. H2FIRST is composed of many interdisciplinary initiatives to support early market infrastructure deployment. Specific efforts will include technoeconomic modeling of station requirements and market demands, and the development, optimization, and validation of technologies that address barriers to station operation and integrate hydrogen infrastructure to the electric grid.

Erika Sutherland
Hydrogen Production and Delivery Team
Technology Development Manager
Fuel Cell Technologies Office
U.S. Department of Energy
1000 Independence Ave., SW
Washington, D.C. 20585-0121
Phone: (202) 586-3152
Email: Erika.Sutherland@ee.doe.gov

III.1 Hydrogen Delivery Infrastructure Analysis

Amgad Elgowainy (Primary Contact),
Krishna Reddi and Marianne Mintz

Argonne National Laboratory
9700 South Cass Avenue
Argonne, IL 60439
Phone: (630) 252-3074
Email: aelgowainy@anl.gov

DOE Manager

Erika Sutherland
Phone: (202) 586-3152
Email: Erika.Sutherland@ee.doe.gov

Project Start Date: October 2007
Project End Date: Project continuation and direction determined annually by DOE

Overall Objectives

Evaluate hydrogen delivery and refueling concepts that can reduce hydrogen delivery cost towards meeting the delivery cost targets.

Fiscal Year (FY) 2014 Objectives

- Evaluate the potential of novel delivery concepts for refueling cost reduction
- Evaluate the role of high-pressure tube-trailers in reducing compression cost at hydrogen refueling stations (HRS)
- Incorporate limitations imposed by SAE International (SAE) J2601 refueling protocol in the modeling of HRS

Technical Barriers

This project directly addresses Technical Barriers A, B, and E in the Hydrogen Delivery section of the Fuel Cell Technologies Office (FCTO) Multi-Year Research, Development, and Demonstration (MYRD&D) Plan. These barriers are:

(A) Lack of Hydrogen/Carrier and Infrastructure Options Analysis

(B) Reliability and Costs of Gaseous Hydrogen Compression

(E) Gaseous Hydrogen Storage and Tube Trailer Delivery Costs

Technical Targets

The project employs the Hydrogen Delivery Scenario Analysis Model (HDSAM) and Hydrogen Station Cost Optimization & Performance Evaluation (H2SCOPE) simulation tools to investigate current and novel hydrogen delivery technologies and pathway options with the potential to meet the cost targets specified in the FCTO MYRD&D Plan, and to assist with defining R&D areas that can bridge current and future performance and cost targets of major delivery and refueling components.

Contribution to Achievement of DOE Hydrogen Delivery Milestones

This project contributes to achievement of the following DOE milestone from the Hydrogen Delivery section of the FCTO MYRD&D Plan:

- Task 2.5: Down select two to three H_2 pressurization and/or containment technologies that minimize delivery pathway cost for mid-term markets. (2Q, 2014)

FY 2014 Accomplishments

Developed and simulated a novel tube-trailer consolidation scheme that can reduce the capital cost of compression at refueling station by more than 50% of current values, working toward the DOE FCTO MYRD&D FY 2015 target of $360,000 for one forecourt compressor at a 1,000 kg/day station.

INTRODUCTION

From our previous analyses, the refueling station was found to contribute about half of total delivery cost in a mature fuel cell electric vehicle (FCEV) market where the station's capital investment is fully utilized. Furthermore, the refueling station compression constitutes about half of the station installed capital cost. Thus, the focus of our analysis this FY was on identifying opportunities at the refueling station that would reduce its capital cost by developing a significant part of the hydrogen compression upstream of the HRS where the compression equipment would benefit from economies of scale and improved utilization of the capital investment. Compressing hydrogen into tube trailers in terminals adjacent to hydrogen production would satisfy this purpose. Tube trailers are furthermore likely to be the primary means of hydrogen delivery in the near to mid term. This project examined the benefits of operating high-pressure tube trailers at hydrogen refueling stations using

the H2SCOPE model. H2SCOPE was developed from first principles by solving physical conservation laws to track temperature, pressure and mass at various points within a refueling station and also inside the FCEV's onboard storage tank. H2SCOPE allowed us to optimize the size of the compressor and cascade buffer storage system at the refueling station while following the SAE J2601 hydrogen fueling protocol. A novel tube trailer consolidation concept was developed and simulated to examine the potential reduction of compression cost at the refueling station through efficient management of the payload of the tube trailer.

We modeled the operation of the refueling station that includes a dispenser which connects and manages the hydrogen flow between the high-pressure buffer storage system and the vehicle tank, a refrigeration unit placed between the dispenser and the high pressure buffer storage system which pre-cools the hydrogen to -40°C for fast refueling, a 250-bar tube trailer that supplies hydrogen to the refueling station, and a compressor which draws hydrogen from the tube trailer to replenish the high-pressure cascade buffer storage system.

Accurate modeling of the compressor performance is key to generating reliable simulation results. Figure 1 shows the PDC 2500/7500 compressor performance curve which was employed in our modeling and analysis. The figure shows the variation in the compressor's throughput with suction pressures. The flow rate varies from about 100 Nm^3/hr @ 20 bar suction to about 900 Nm^3/hr @ 250 bar suction. Maintaining the minimum suction pressure at a high pressure, e.g., above 100 bar, ensures a flow rate above 400 Nm^3/hr, which is about 4 times the flow rate at the rated suction pressure of 20 bar. The proposed tube-trailer consolidation scheme aims to take advantage of this linear relationship between the compressor's suction pressure and flow rate. The consolidation concept maintains a high compressor suction pressure during peak demand hours, thus amplifying the compressor's throughput. A small compressor can therefore be employed to serve a station during its high demand periods, thus reducing the station's capital investment.

In this context, consolidation is the process of compressing hydrogen from one tube trailer vessel into another to maintain high pressure in at least one of the tube trailer vessels that supplies the compressor suction manifold. To maintain a high compressor suction pressure during peak hours, hydrogen is consolidated within the individual pressure vessels mounted on the tube trailer during off-peak hours. This occurs when the compressor is otherwise idle, thus improving the utilization of the compressor.

In general, hydrogen can be consolidated within the tube trailer, when the compressor and pressure vessels on the tube trailer are idle. To simplify the simulation and examine the extreme refueling conditions, we have divided each hour into two periods: A and B. For any hour with number of vehicles n expected to be filled within that hour, A represents the minimum time required to fill all the vehicles back-to-back within that hour, while period B represents the remaining time of that hour. Hydrogen is assumed to be consolidated during period B when all buffer storage banks are at their rated working pressure.

Figure 2 shows the operation of a refueling station with tube trailer consolidation capability during period A of each hour. The vehicle is fueled either by drawing hydrogen from the tube trailer or one of the high-pressure buffer storage banks, while the other (idle) cascade pressure vessel banks

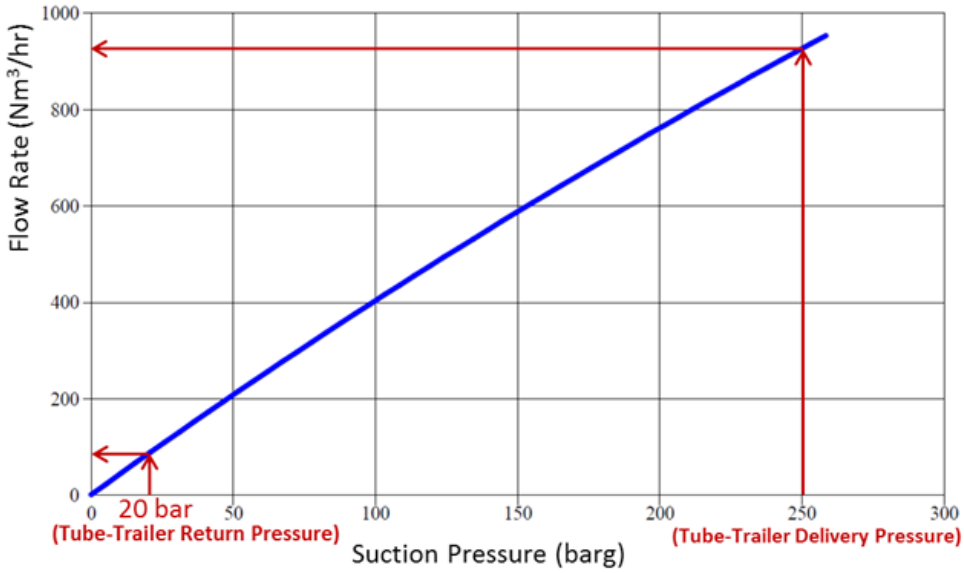

FIGURE 1. Flow Curve of PDC 2500/7500 Compressor

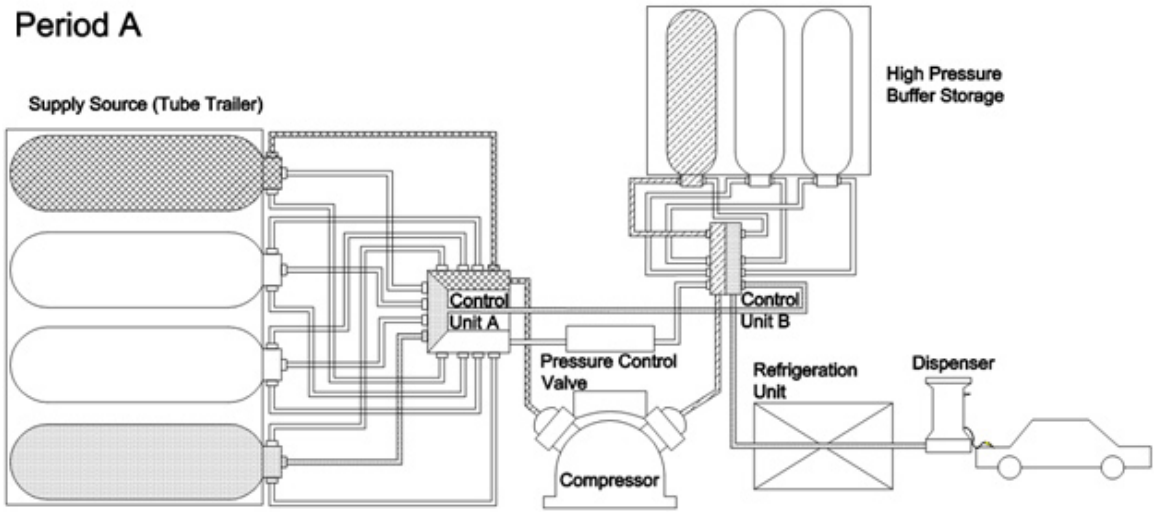

FIGURE 2. Schematic of Station Component Layout and Operation for Period A of Each Hour

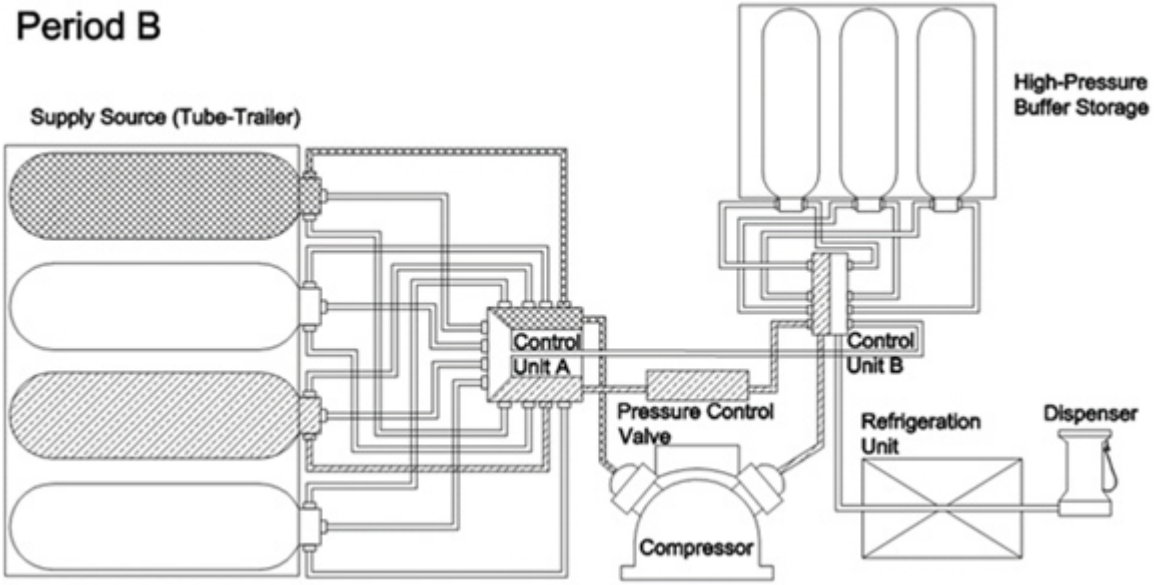

FIGURE 3. Schematic of Station Component Layout and Operation for Period B of Each Hour

are replenished by the compressor that draws hydrogen from the tube trailer vessels. During the period B hydrogen is consolidated in the pressure vessels on the tube trailer by moving hydrogen from the vessels with lower pressure to the vessels with higher pressure as shown in Figure 3. Table 1 shows a summary of the tube trailer operation strategy for a refueling station with and without tube trailer consolidation.

RESULTS

We performed simulations for station capacities of 100, 150, 200, 250, 300, 350, 400, and 450 kg per day. Implementation of the consolidation concept is shown in Figure 4, which illustrates the mass in each pressure vessel on the tube-trailer after every vehicle fill. The horizontal axis represents the number of vehicles filled during the operation of the refueling station, while the vertical axis represents the mass of hydrogen within each of the four vessels mounted on the trailer. An increase in hydrogen mass in a vessel indicates consolidation, while a decrease in hydrogen mass in a vessel indicates drawdown by the compressor to fill the buffer storage bank or to consolidate hydrogen to another vessel on the trailer.

TABLE 1. Summary of HRS Operation Strategy with and without Tube Trailer Consolidation

Operation Strategy Parameter	Tube Trailer Operation Strategy	
	Without Consolidation	With Consolidation
Tube trailer used for initial vehicle fill	No	Yes
Tube trailer hydrogen consolidation	No	Yes
Pressure of selected vessel on tube trailer to fill vehicle tank	NA	Max
Pressure of selected vessel on tube trailer to fill cascade buffer storage system	Min	Max (Period A) Min (Period B)
Pressure of selected vessel on tube trailer for H_2 consolidation	NA	Min
Number of tube trailer vessels	4	4
Tube trailer capacity (H_2 in kg)	640	640
Tube trailer capacity for refueling (vehicles)	123	123

TABLE 2. Summary of Number of Vehicle Fillings with and without Tube Trailer Consolidation

Daily HRS Capacity (kg/day)	# of Vehicles Filled (Tube Trailer Payload Utilization)	
	Without Consolidation	With Consolidation
100	121 (94%)	
150	121 (94%)	
200	21 (not capable of satisfying hourly demand)	110 (86%)
250		110 (86%)
300		110 (86%)
350		109 (85%)
400		109 (85%)
450		109 (85%)

Table 2 shows that a station can satisfy a refueling demand of up to 150 kg/day without tube trailer consolidation, but can satisfy a demand of up to 450 kg/day with tube trailer consolidation. The station operation with the consolidation strategy achieves a high tube-trailer payload utilization of 85% as shown in Table 2. For a 450 kg/day refueling station not employing the consolidation strategy, the compressor capacity at a tube-trailer return pressure of 20 bar would be about 400 Nm^3/h. Quotes from compressor manufacturers show compressor cost increases from about $300,000 for a 90 Nm^3/h compressor (with the consolidation strategy) to $750,000 for the 400 Nm^3/h compressor (without the consolidation strategy), implying a compression cost savings of $450,000 with tube trailer consolidation for that station capacity.

The tube trailer consolidation strategy improves the economics of the station through more efficient utilization of a station compressor that operates more steadily during peak and off-peak hours. The station cost-reduction benefits associated with the tube trailer consolidation concept can be multiplied further in early FCEV markets, in which

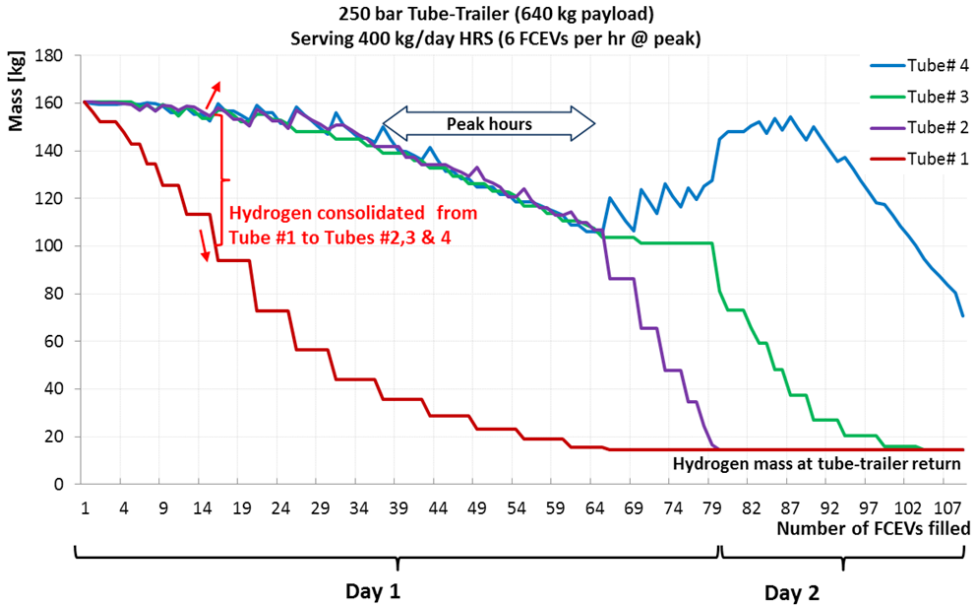

FIGURE 4. Status of Hydrogen Mass in Each of the Four Tube Trailer Vessels during Operation of the Refueling Station with the Consolidation Strategy

the cost of dispensed hydrogen is likely to be higher because underutilization of of the station equipment. The consolidation concept works in tandem with high-pressure tube trailer deliveries, which alone have the advantage of lowering the overall cost of compression by shifting a significant part of the process upstream to gas terminals; the economies of scale at terminals enable more efficient use of compression equipment than at the refueling station itself.

CONCLUSIONS AND FUTURE DIRECTIONS

By implementing consolidation strategy for managing hydrogen within tube-trailer vessels, the same station equipment can triple the station's capacity while satisfying peak demand with fast-fill rates (1.7 kg/min). For a given station capacity, the tube trailer consolidation strategy can reduce the compression cost at refueling sites by 60% and the total investment cost for refueling stations by 40%. Tube trailers with pressures higher than 250 bar (e.g., 350 bar and 500 bar) offer greater compression cost-reduction benefits with the consolidation strategy.

SPECIAL RECOGNITIONS AND AWARDS/ PATENTS

Patent Application

1. Elgowainy, A., Reddi, K., "ENHANCED METHODS FOR OPERATING REFUELING STATION TUBETRAILERS TO REDUCE REFUELING COST", Docket No.: ANL-IN-13-058, submitted to United States Patent and Trademark Office on September 27th 2013.

FY 2014 PUBLICATIONS/PRESENTATIONS

1. Reddi, K., Mintz, M., Elgowainy, A., Sutherland, E., "Challenges and opportunities of hydrogen delivery via pipeline, tube-trailer, Liquid tanker and methanation-natural gas grid", Wiley (in press).

2. Reddi, K., Elgowainy, A., Sutherland, E., 2014, "Hydrogen Refueling Station Compression and Storage Optimization with Tube Trailer Deliveries," Accepted for publication at the International Journal of Hydrogen Energy.

3. Reddi, K., Elgowainy, A., Sutherland, E., Joseck, F., 2014, "Tube-Trailer Consolidation Strategy for Reducing Hydrogen Refueling Station Costs," submitted for publication at the International Journal of Hydrogen Energy.

III.2 Oil-Free Centrifugal Hydrogen Compression Technology Demonstration

Hooshang Heshmat
Mohawk Innovative Technology, Inc. (MiTi®)
1037 Watervliet Shaker Road
Albany, NY 12205
Phone: (518) 862-4290
Email: HHeshmat@miti.cc

DOE Managers
Erika Sutherland
Phone: (202) 586-3152
Email: Erika.Sutherland@ee.doe.gov
Katie Randolph
Phone: (720) 356-1759
Email: Katie.Randolph@ee.doe.gov

Contract Number: DE-FG36-08GO18060

Subcontractor
Mitsubishi Heavy Industries, Ltd, Compressor Corporation, Hiroshima, Japan

Project Start Date: September 25, 2008
Project End Date: August 29, 2014

Overall Objectives

Design a reliable and cost-effective centrifugal compressor for hydrogen pipeline transport and delivery

- Eliminate sources of oil/lubricant contamination
- Increase efficiency by using high rotational speeds
- Reduce system cost and increase reliability

Fiscal Year (FY) 2014 Objectives

- Perform validation testing of single-stage compressor system in air and in helium per American Society of Mechanical Engineers (ASME) PTC-10
- Conduct system refinement of multi-stage system for pipeline compression

Technical Barriers

This project addresses the following technical barriers from the Hydrogen Delivery section of the Fuel Cell Technologies Office Multi-Year Research, Development, and Demonstration Plan:

(B) Reliability and Costs of Hydrogen Compression

(J) Hydrogen Leakage and Sensors

Technical Targets

This project is directed towards the design, fabrication and demonstration of the oil-free centrifugal compression technology for hydrogen delivery. This project will identify the key technological challenges for development and implementation of a full scale hydrogen/natural gas centrifugal compressor. The project addresses the DOE technical targets from the Hydrogen Delivery section of the Fuel Cell Technologies Office Multi-Year Research, Development, and Demonstration Plan (see Table 1).

ABLE 1. Technical Targets for Hydrogen Compression

Category	2005 Status	FY 2011 Status	FY 2015	FY 2020
Reliability	Low	Low	Improved	Improved
Isentropic Efficiency	88%	88%	>88%	>88%
Losses (% of H_2 throughput)	0.5	0.5	0.5	<0.5
Capital Investment (based on 3,000 kW motor rating)	$2.7M	$2.7M	$2.3M	$1.9M
Maintenance (% of Total Capital Investment)	4	4	3	2
Contamination	Varies by Design	Varies by Design	Varies by Design	None

NA – not applicable

FY 2014 Accomplishments

- Performed validation testing of single-stage compressor in helium per ASME PTC-10
- System refinement of multi-stage compressor system
- Final report has been written and reviewed for submission to the DOE

✧ ✧ ✧ ✧ ✧

INTRODUCTION

One of the key elements in realizing a mature market for hydrogen vehicles is the deployment of a safe, efficient hydrogen production and delivery infrastructure on a scale that can compete, economically, with current fuels. The challenge, however, is that hydrogen, the lightest and smallest of gases with a lower viscosity than natural gas, readily migrates through small spaces. While efficient and cost-effective compression technology is crucial to effective pipeline delivery of hydrogen, today's positive displacement

hydrogen compression technology is very costly, and has poor reliability and durability, especially for components subjected to wear (e.g., valves, rider bands, and piston rings). Even so called "oil-free" machines use oil lubricants that migrate into and contaminate the gas path. Due to the poor reliability of compressors, current hydrogen producers often install duplicate units in order to maintain on-line times of 98–99%. Such machine redundancy adds substantially to system capital costs. Additionally, current hydrogen compression often requires energy well in excess of the DOE goal. As such, low capital cost, reliable, efficient and oil-free advanced compressor technologies are needed.

APPROACH

The MiTi team has met program objectives by conducting compressor, bearing, and seal design studies; selecting components for validation testing; fabricating the selected centrifugal compressor stage and the corresponding oil-free bearings and seals; and testing of the high-speed, full-scale centrifugal compressor stage, and oil-free compliant foil bearings and seals under realistic pressures and flows in air and helium (used as a simulant gas for hydrogen). Specific tasks included (1) compressor design analysis for an oil-free, multi-stage, high-speed centrifugal compressor system; (2) mechanical component detailed design of oil-free bearings, seals, and shaft system; (3) detailed design and fabrication of a full-scale, single-stage centrifugal compressor for aerodynamic design verification and component reliability testing; (4) compressor performance testing with air and helium; (5) system design refinement; and (6) program management and reporting.

RESULTS

The MiTi® hydrogen compressor design consists of three identical frames, each with three compression stages operating in series at the same rotation speed of 56,414 rpm (1,600 fps). The system capacity is 500,000 kg/day with a total pressure ratio of approximately 2.4 to achieve the desired 1,200 psi discharge pressure. A full-scale, three-dimensional solid model of a single frame has been fabricated for visual reference as a design aid, shown in Figure 1A. A single compressor stage, identical to those in the multi-stage system, has been fabricated and tested to validate aerodynamics of the MiTi® oil-free, high-speed compressor system. The single-stage compressor with volute is shown in Figure 1B. Fabrication and installation of the single-stage compressor was previously conducted and the final compressor test facility is shown in Figure 1C. The single-stage compressor system is located in a reinforced test cell and features remote access so that the rest rig can be fully operated from a safe distance (Figure 1D). A high-resolution video camera is located in the cell, and used for monitoring and video recording. A custom graphical user interface using LabVIEW software (National Instruments) allows for direct command of motor speed control, monitoring of all pressure and temperature data, as well as high-frequency

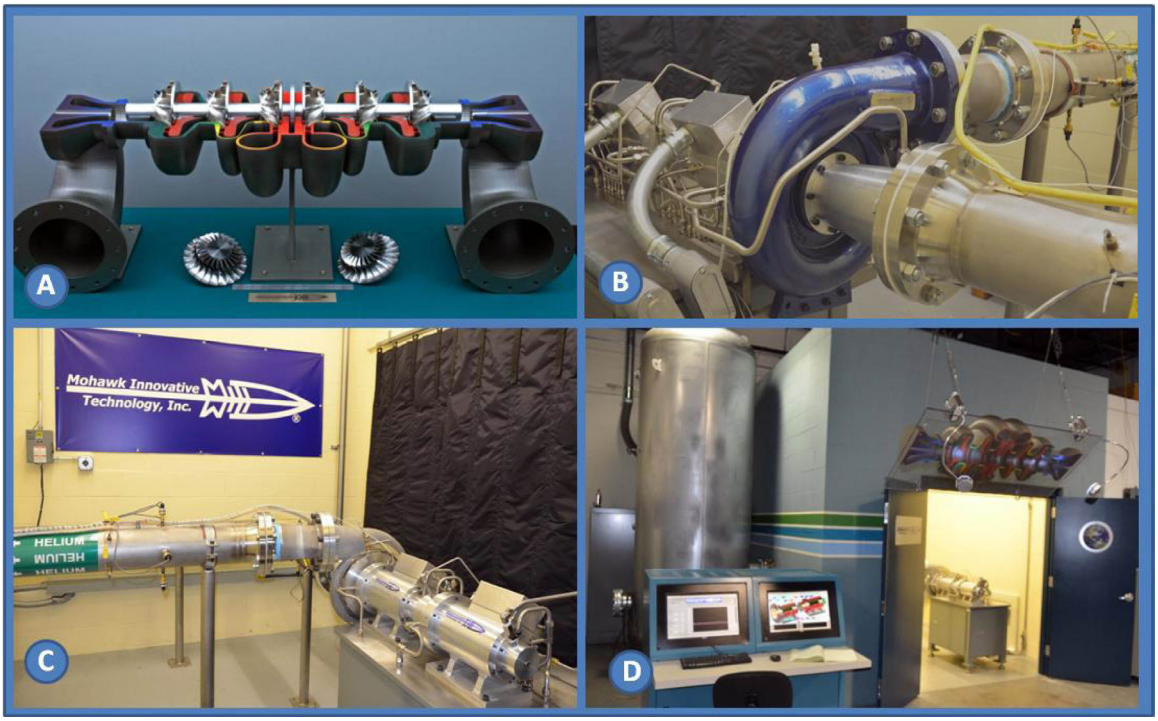

FIGURE 1. MiTi® Single-Stage Compressor System with Oil-Free, 60,000 RPM Motor Drive and Closed-Loop Helium Test Facility

spectral analysis of up to four proximity probes for vibration measurement.

In the past year, extensive aerodynamic performance testing was conducted in accordance with ASME PTC-10. The key function of a Type 2 test is to prove aerodymanic similutude of a compressor design when the exact design conditions are unable to be met. In this project it was not feasible to test in a hydrogen environment. Helium was therefore selected because it most closely matches the physical properties of hydrogen. In order to validate aerodynamic performance of a compressor for hydrogen, it is critical that four non-dimensional quantities be preserved in the test conditions. In Table 2, the list of required non-dimensional variables that must be held constant are shown in Column 1. The values of each variable in the first stage of the full-scale, multi-stage hydrogen compressor are listed in the column labeled "H_2 Design Point." In order to satisfy the requirments of the ASME test code, experimental results must fall within a predefined range, as described in PTC-10. The acceptable variability, as prescribed by PTC-10, is also listed in Table 2. Finally, the experimental results obtained by MiTi® for the single-stage testing conducted in helium are presented in the final column. It can be seen that all experimental results fall within the acceptable range prescribed by ASME PTC-10 and, therefore, validate the aerodynamic performance of the MiTi® hydrogen centrifugal compressor.

TABLE 2. Summary of Operating Conditions Met to Successfully Achieve ASME PTC-10 Type 2 Test Requirements

Quantity	H_2 Design Point	ASME Acceptable Test Variation	Experimental Results
Specific Volume Ratio	1.072	1.018–1.126	1.095
Flow Coefficient	0.125	0.120–0.130	0.126
Machine Mach No.	0.327	0.141–0.532	0.322
Machine Reynolds No.	$6.6e^5$	$6.6e^4$–$6.6e^6$	$8.0e^4$

In addition to the successful demonstration of the compressor at a single operating point, the machine was also operated across a wide range of flows and speeds in order to obtain a complete compressor map. The results of the compressor discharge head are shown in Figure 2. Experimental data points are plotted as individual points. Results were obtained at 20, 30, 40, and 45 krpm. For each operating speed condition, the predicted head is shown as a solid line. For all speed conditions, it can be seen that the experimental results exceed theoretical prediction by 5-10%. The compressor adiabatic efficiency ($\eta_{T\text{-}S}$) was also determined, and these results are shown in Figure 3. Again, theoretical prediction is shown as solid lines. At both 40 krpm and 45 krpm, experimentally measured adiabatic efficiency exceeds prediction, as well as DOE efficiency

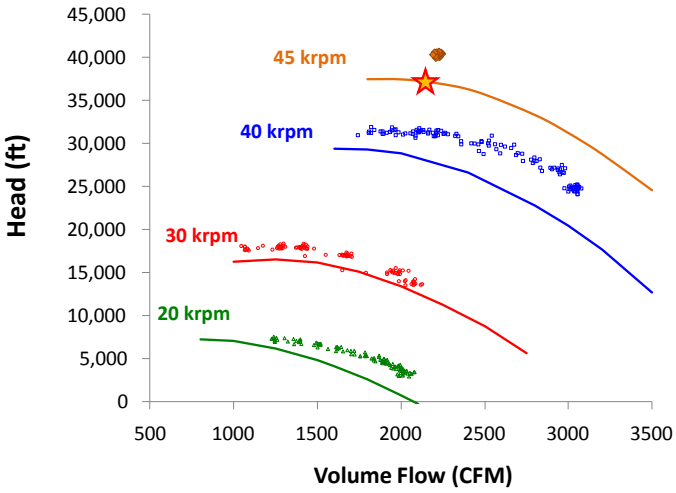

FIGURE 2. Comparison of Theoretical and Experimentally Measured Head for the Single-Stage Compressor (Design point condition indicated with a yellow star)

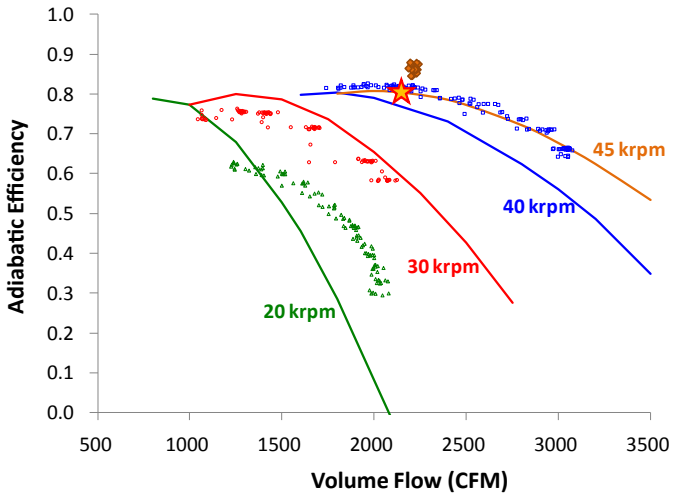

FIGURE 3. Comparison of Theoretical and Experimentally Measured Adiabatic Efficiency for the Single-Stage Compressor (Design point condition indicated with a yellow star)

goals. The experimental adiabatic efficiency (total-to-static) was calculated using the following equation:

$$\eta_{T-S} = \frac{\left(P_{2s}/P_{1t}\right)^{(k-1)/k} - 1}{\left(T_{2t}/T_{1t}\right) - 1}$$

where subscripts "1" and "2" refer to the compressor inlet and discharge, respectively. Subscripts "s" and "t" refer to the static or total thermodynamic condition of the test fluid. While the total-to-total adiabatic efficiency is slightly higher,

the use of total-to-static adiabatic efficiency is the most appropriate for evaluation of a single-stage compressor.

The dynamic performance of the compliant foil bearings in a hermetically sealed helium environment was also demonstrated in these tests. For all test conditions, no external cooling gas was passed through the compliant foil bearings which support the entire rotating shaft both radially and axially. A recirculation path exists in the compressor, whereby, a small fraction of compressed helium gas intentionally passes behind the compressor wheel, through the bearing cavities, along the entire length of the shaft and is then plumbed back to the compressor inlet. Compressor performance measurements, including discharge head and efficiency, were measured downstream of the bearing recirculation flow and its effects were already included in their calculation. In order to demonstrate the thermal stability of the compliant foil bearing, the differential temperature within the bearings is shown in Figure 4. Data from only the first thrust and first journal bearing are presented, as these bearings demonstrated the highest operating temperatures of all bearings. Differential bearing temperature is defined as the temperature of the bearing (thermocouple welded to bearing foils) minus the temperature of the compressor discharge (T_{OUT}), which is fed directly to the bearing. A bearing differential temperature greater than zero indicates that some heat from bearing losses is being added to the system. However, a bearing differential temperature less than zero assumes that bearing losses are minimal and more heat within the recirculation flow is lost to housing than is added from the bearing. Because the helium test facility is a closed-loop system and no heat exchanger is present, gas temperature within the system continues to rise as it is compressed. For this reason, it is necessary to discuss bearing differential temperature rather than absolute bearing temperature. From the results in Figure 4 we can see that, for all test points, the temperature of the complaint foil bearings do not exceed the compressor discharge by more than 15°F. The highest differential temperature occurs immediately following a change in compressor speed. Some heat from speed change is a result of power losses in the motor during acceleration or braking of the rotor and has nothing to do with bearing performance. Other causes of heat during change in speed are due to mechanical and thermal transients in the shaft. For each speed change, it can be seen that bearing differential temperatures stabilize and begin to fall after equilibrium is reached. These results indicate very low power loss and a high degree of thermal stability of the complaint foil bearing in a hermetically sealed helium environment. The heat capacity of hydrogen is nearly three times greater than helium. This implies that achieving thermal stability of the compliant foil bearing in the hydrogen environment will be less challenging.

CONCLUSIONS AND FUTURE DIRECTIONS

MiTi® has successfully completed performance testing of a single-stage, centrifugal hydrogen compressor per ASME PTC-10. The Type 2 test conducted in a similitude gas (helium) has shown that the centrifugal compressor stage is capable of exceeding the performance goals predicted by aerodynamic design software and computational fluid dynamics analysis. Experimental adiabatic efficiency was measured to be 86% and discharge head exceeded theoretical prediction by 10%. MiTi®'s compliant foil bearings demonstrated stable and reliable performance with extremely lower power loss. Thermal stability of the compliant foil bearings in a hermetically sealed helium environment was verified. There results provide high confidence in the

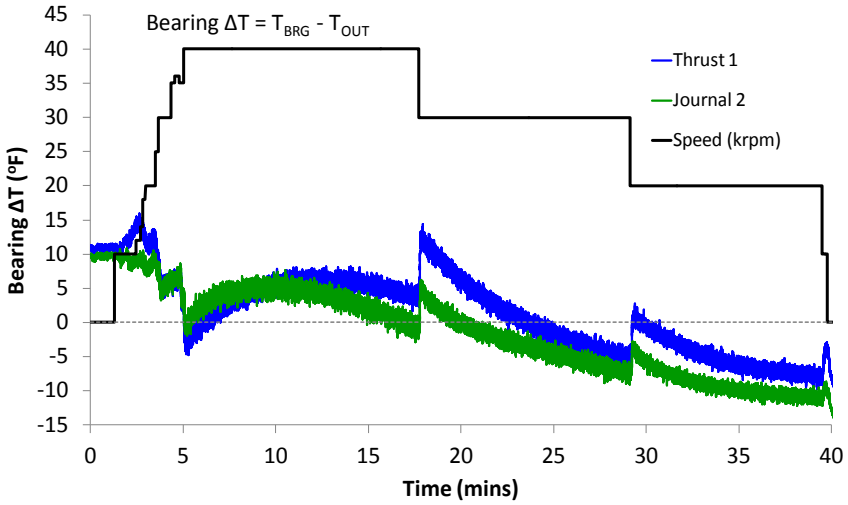

FIGURE 4. Experimental Thermal Performance of the Foil Thrust Bearings during Operation up to 40 krpm

feasibility of the proposed multi-stage centrifugal pipeline compressor concept to meet the DOE's need for 500,000 kg/day of hydrogen with a total pressure ratio of 2.4. The project has been successfully completed.

FY 2014 PUBLICATIONS/PRESENTATIONS

1. H. Heshmat, "Oil-Free Centrifugal Hydrogen Compression Technology Demonstration," DOE Hydrogen and Fuel Cells Program Annual Review and Peer Evaluation Meeting, June 17, 2014, Washington, D.C.

III.3 Development of High-Pressure Hydrogen Storage Tank for Storage and Gaseous Truck Delivery

Don Baldwin
Hexagon Lincoln (formerly Lincoln Composites Inc.)
5117 N.W. 40th Street
Lincoln, NE 68524
Phone: (402) 470-5017
Email: don.baldwin@hexagonlincoln.com

DOE Managers
Erika Sutherland
Phone: (202) 586-3152
Email: Erika.Sutherland@ee.doe.gov
Katie Randolph
Phone: (720) 356-1759
Email: Katie.Randolph@ee.doe.gov

Contract Number: DE-FG36-08GO18062

Project Start Date: July 1, 2008
Project End Date: June 30, 2015

Overall Objectives

The objective of this project is to design and develop the most effective bulk hauling and storage solution for compressed hydrogen gas (CHG) in terms of:

- Cost
- Safety
- Weight
- Volumetric Efficiency

FY 2014 Objectives

Project activity in 2014 is focused on:

- Continuing to investigate cost improvements
- Improving performance and reliability of safety system(s) through evaluation and adoption of new technologies
- Increasing volume/capacity per payload at operating pressure of 250 bar

Technical Barriers

This project addresses the following technical barriers from the Hydrogen Delivery section of the Fuel Cell Technologies Office Multi-Year Research, Development, and Demonstration Plan:

(E) Gaseous Hydrogen Storage and Tube Trailer Delivery Costs

(I) Other Fueling Site/Terminal Operations

Technical Targets

This project has focused primarily on the design and qualification of a 3,600-psi pressure vessel and International Organization for Standardization (ISO) frame system to yield a combined storage capacity solution of approximately 34,000 liters of water. The original scope of project was to increase working pressure in the current design. Together with DOE, the project focus has shifted towards increasing available volume at the 3,600-psi working pressure. Technical targets for this project are listed in Table 1.

FY 2014 Accomplishments

Completed the design, manufacture and assembly of integrated TITAN V Magnum trailer system capable of storing ~800 kg H_2 @ 3,600 psi. This new bulk hauling system was first deployed in compressed natural gas (CNG) service in 2013. Many improvements to the trailers were implemented in 2014 based on customer feedback from the field.

✧ ✧ ✧ ✧ ✧

INTRODUCTION

Successful commercialization of hydrogen fuel cell vehicles requires the creation of a hydrogen delivery infrastructure that provides the same level of safety, ease, and functionality as the existing gasoline and diesel fuel delivery infrastructure. Today, CHG is shipped in tube trailers at pressures up to 3,000 psi (about 200 bar). However, the low

TABLE 1. Progress towards Meeting Technical Targets for Hydrogen Storage

Characteristic	Units	2010 Target	2015 Target	2020 Target	Status	Comments
Storage Costs	$/kg	500	730	575	800	
Volumetric Capacity	kg/liter	0.030	>0.035		0.018	
Delivery Capacity, Trailer	kg	700	700	940	720	Titan5 Magnum trailer capacity is 800

hydrogen-carrying capacity of these tube trailers results in high delivery costs. Hydrogen rail delivery is currently economically feasible only for cryogenic liquid hydrogen; however, almost no hydrogen is transported by rail. Reasons include the lack of timely scheduling and transport to avoid excessive hydrogen boil-off and the lack of rail cars capable of handling cryogenic liquid hydrogen. Hydrogen transport by barge faces similar issues in that few vessels are designed to handle the transport of hydrogen over inland waterways. The Hexagon Lincoln TITAN ISO-format module will not only provide a technically feasible method to transport CHG over road, rail and water, but a more cost- and weight-efficient means as well.

APPROACH

In Phase 1 of this project, Hexagon Lincoln has designed and qualified a large composite pressure vessel and ISO frame that can be used for storage and transport of CHG over road, rail or water.

The baseline composite vessel has a 250 bar (3,626 psi) service pressure, an outer diameter of 42.8 inches and a length of 38.3 feet. The weight of this tank is approximately 2,485 kg. The internal volume is equal to 8,500 liters water capacity and will contain 150 kg of CHG. The contained hydrogen will be approximately 6.0% of the tank weight (5.7% of the combined weight).

Four of these tanks are mounted in a custom-designed ISO frame, resulting in an assembly with a combined capacity of 600 kg of hydrogen. Installing the vessels into an ISO frame offers a benefit of having one solution for both transportable and stationary storage. This decreases research and development costs as well as the amount of infrastructure and equipment needed for both applications.

The large size of the vessel also offers benefits. A limited number of large tanks is easier to package into the container and requires fewer valves and fittings. This results in higher system reliability and lower system cost. The larger diameter also means thicker tank walls, which will make the vessel more robust and damage tolerant.

Phase 2 of the project was originally scoped to evaluate vessel(s) of approximately the same size and ISO frame at elevated pressures. Trade studies performed in 2011 indicate optimization of hauling efficiency and system cost for CHG at 350 bar (5,076 psi). Due to differences in the compressibility of CHG and CNG, 350-bar operation is not an attractive option for CNG. The CHG market is difficult to forecast at this time and the cost to fully qualify a higher pressure module estimated at $5MM to complete. Based on insufficient CHG market definition to support a stand-alone business case for CHG, development of a 350-bar (5,076 psi) system has been placed on hold and will not be pursued under this project.

Consequently, it was determined that Hexagon Lincoln would work with our current 250-bar product and move forward with increasing the potential volume per load as well as improvements in safety. Increased volume has been achieved with the development of the TITAN V Magnum, an integrated trailer system with additional tankage. Other system improvements supported by the project include the evaluation, testing and qualification of an improved emergency venting systems as well as development and installation of laboratory capabilities to evaluate the effects of hydrogen on liner materials.

RESULTS

Hexagon Lincoln completed qualification of the TITAN pressure vessel and ISO frame in 2009. The baseline 250 bar system shown in Figure 1 has an internal volume of 34,000 liters water capacity and will contain 150 kg of CHG.

The initial Hexagon Lincoln TITAN V trailer prototype increased total payload capacity by 18% as compared with the baseline Titan module. This new integrated trailer utilized the same four 40’ TITAN cylinders with the addition of a single 30’ TITAN tank placed lower in the assembly to utilize space between the frame rails of the trailer.

Lincoln Composites has continued the design and evaluation of a more robust emergency venting system utilizing memory metal as a trigger mechanism for de-pressurizing the tank in the case of a fire. This technology

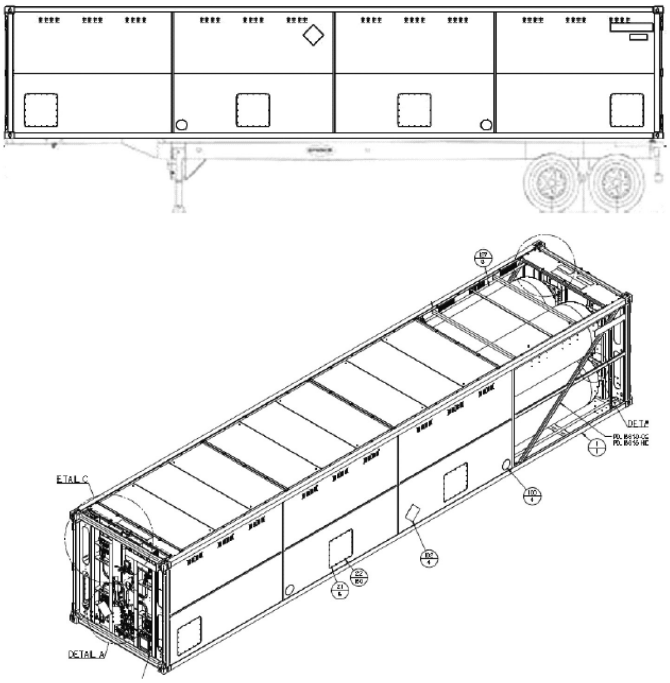

FIGURE 1. TITAN ISO-Format Module

greatly reduces the cost of the system in both components and labor for assembly. The reduction of components in the system affects the potential number of failure modes that could occur and thus making for a more reliable product.

The installation of a 100% hydrogen testing facility is complete. This laboratory will be used to fully investigate new materials with the potential for them to be integrated into liners. Specifically, these alternate materials will be quantified and qualified as a means to reduce the permeation rates that are present in current Type 4 cylinders.

To further enhance system volume, the development/design of the TITAN V Magnum trailer with additional tankage has been completed. This design utilizes the TITAN V as a baseline with the addition of up to nine smaller tanks on either side of the 30' single tank at the bottom of the module. See Figure 2 for illustration of this design. This configuration has increased capacity by 26% when compared to the standard 4-cylinder TITAN module. This translates to an overall payload of 775 kg of hydrogen. The TITAN V Magnum trailer system is currently deployed in CNG service in South and Central America as shown in Figure 3.

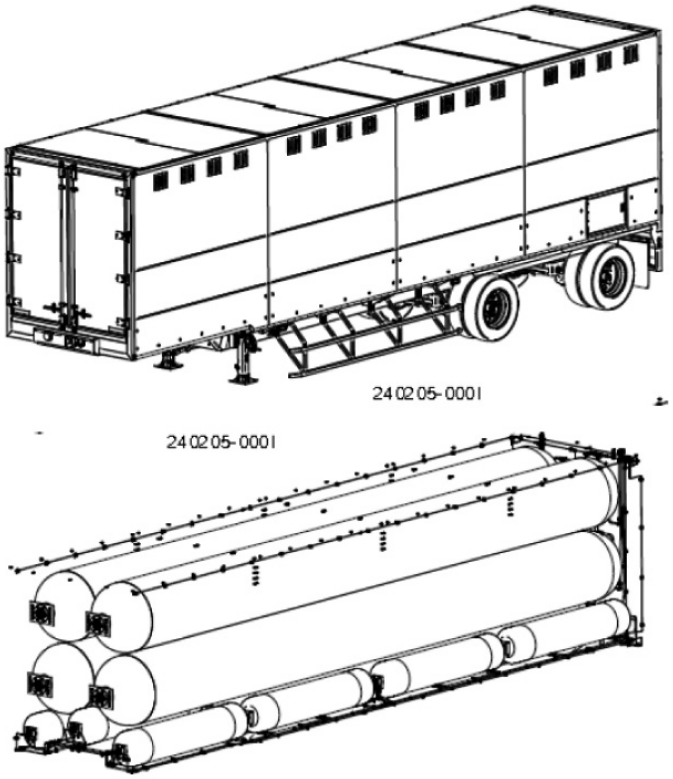

FIGURE 2. TITAN V Magnum Integrated Trailer System

CONCLUSIONS AND FUTURE DIRECTIONS

- The TITAN V Magnum integrated trailer configuration has an increased capacity of 26% when compared to the standard 4-cylinder TITAN module. This translates to an overall payload of 775 kg of hydrogen.
- Deep cycle testing of TITAN pressure vessels with CHG will be performed in the fourth quarter of 2014 and first quarter of 2015 to characterize CHG-specific operating protocols for use of TITAN systems in CHG service at 250 bar.
- Hexagon Lincoln will prepare and submit an application for Special Permit approval with the U.S. Department of Transportation for the manufacture, making, sale and use of TITAN V trailer systems in the United States. Initial discussions with the Department of Transportation indicate structural testing analogous to ISO 1496 will be required.

FY 2014 PUBLICATIONS/PRESENTATIONS

1. 2014 DOE Hydrogen Program Annual Merit Review, June 17, 2014

FIGURE 3. TITAN V Magnum Trailer in CNG Service

III.4 Fiber Reinforced Composite Pipeline

George Rawls
Savannah River National Laboratory (SRNL)
Materials Science & Technology
773-41A/173
Aiken, SC 29808
Phone: (803) 725-5658
Email: george.rawls@srnl.doe.gov

DOE Manager
Erika Sutherland
Phone: (202) 586-3152
Email: Erika.Sutherland@ee.doe.gov

Project Start Date: October 1, 2006
Project End Date: October 1, 2016

Project Objectives

Successfully adapt spoolable fiber reinforced polymer composite pipeline (FRP) currently used in the oil and natural gas industry for use in high-pressure hydrogen delivery systems and development of the data needed for codification of fiber reinforced composite piping into the American Society of Mechanical Engineers (ASME) B31.12 Hydrogen Piping Code.

Fiscal Year (FY) 2014 Objectives

- Perform fatigue testing of FRP at the product rated design pressure of 1,500 psig to determine the effect of R ratio on the cyclic life of fiber reinforced piping. Testing will be performed between a range of R values of 0.7 maximum and 0.3 minimum.
- Present the technical basis for FRP and a technical proposal for inclusion of FRP into the B31.12 Code to the Code Committee.
- Provide a technical evaluation for the extension of the design life of fiber reinforced piping from 20 years to 50 years.
- Provide a technical report evaluating concepts for improved FRP joints, with emphasis providing a more robust hydrogen seal and maintaining the structural integrity requirement for pressure retention.

Technical Barriers

This project addresses the following technical barriers from the Hydrogen Delivery section of the Fuel Cell Technologies Office Multi-Year Research, Development, and Demonstration Plan:

(D) High As-Installed Cost of Pipelines

(J) Hydrogen Leakage and Sensors

(K) Safety, Codes and Standards, Permitting

Technical Targets

This project is focused on the evaluation of FRP for hydrogen service applications. Assessment of the structural integrity of the FRP piping and the individual manufacturing components in hydrogen will be performed. Insights gained will support qualifications of these materials for hydrogen service including:

- Transmission pipeline reliability: Acceptable for hydrogen as a major energy carrier
- Transmission pipeline total capital cost $715k, per mile (2020)
- H2 delivery cost <$0.90/gasoline gallon equivalent
- H2 pipeline leakage: <780 kg/mi/y (2020)

FY 2014 Accomplishments

In FY 2014, the main activity at SRNL was to complete the required fatigue testing for the FRP project. During FY 2014 two additional samples were tested. The maximum pressure for each test was the 1,500 psi, rated FRP sample pressure. These tests were performed at a stress ratio or R-ratio values of 0.3 and 0.5. The fatigue test data directly support both FRP codification and the evaluation of a 50-year FRP design life.

A report providing the basis for extension for the design life for FRP was completed. The technical basis for codification of FRP material into the B31.12 Hydrogen Piping Code was expanded to include the results of the additional fatigue tests and the life extension evaluation. A separate effort in FY 2014 was the completion of a report to evaluate new concepts for improved FRP joints.

- FRP Fatigue Testing
  The fatigue tests were completed at a maximum pressure of 1,500 psi, the rated FRP sample pressure. These tests were performed at R-ratio values of 0.3 and 0.5.
- FRP Codification into ASME B31.12
  The initial proposal (Code Language) for codification into ASME B31.12 was presented to the Code Committee at a March 2014 meeting.
- Extension of Design Life of FRP
  A technical report providing a basis for the extension of the design life of FRP from 20 years to 50 years was completed.

- Improved Joint Concepts for FRP
  A technical report providing an evaluation of new FRP joint concepts with an improved hydrogen seal for the inner polyethylene liner was finalized.

✧ ✧ ✧ ✧ ✧

INTRODUCTION

The goal of the overall project is to successfully adapt spoolable FRP currently used in the oil industry for use in high-pressure hydrogen pipelines. The use of FRP materials for hydrogen service will rely on the demonstrated compatibility of these materials for pipeline service environments and operating conditions. The ability of the polymer piping to withstand degradation while in service, and development of the tools and data required for life management are imperative for successful implementation of these materials for hydrogen pipelines.

APPROACH

To achieve the objective an FRP life management plan was developed. The plan was a joint document developed by SRNL and the ASME to guide generation of a technical basis for safe use of FRP in delivery applications. The plan addresses the needed material evaluations and also focuses on the needed information for codification of FRP into the ASME B31 Code of Pressure Piping. The testing performed by SRNL has:

- Critically evaluated the current application of available FRP product standards through independent testing.
- Defined changes to the current FRP product standards to meet the ASME Code Methodology.
- Provided a body of data to support inclusion of FRP in the ASME B31.12 Hydrogen Piping Code.

RESULTS

Fatigue Testing

Fatigue testing of FRP was initiated at SRNL in FY 2012 and continued through 2014. During FY 2013 six fatigue tests were completed at pressure levels ranging from 750 psi to 3,000 psi. The pressure levels ranged from half to twice the rated pressure of the FRP product test samples. The range of test pressure was selected to provide sufficient data to understand the general shape of the FRP fatigue curve. All these tests were performed at a R- ratio of 0.1. The stress-ratio is defined as $R = \sigma_{min}/\sigma_{max}$. There σ_{min} is the minimum pipe stress and σ_{max} is the maximum pipe stress.

During FY 2014 two additional samples were tested. The maximum pressure for each test was 1,500 psi, the rated FRP sample pressure. These tests were performed at a stress ratio or R-ratio values of 0.3 and 0.5. The FY 2014 fatigue tests show that the FRP product is sensitive to R-ratio. The test data is shown in Figure 1. The fatigue test data directly support both FRP codification and a 50-year FRP design life.

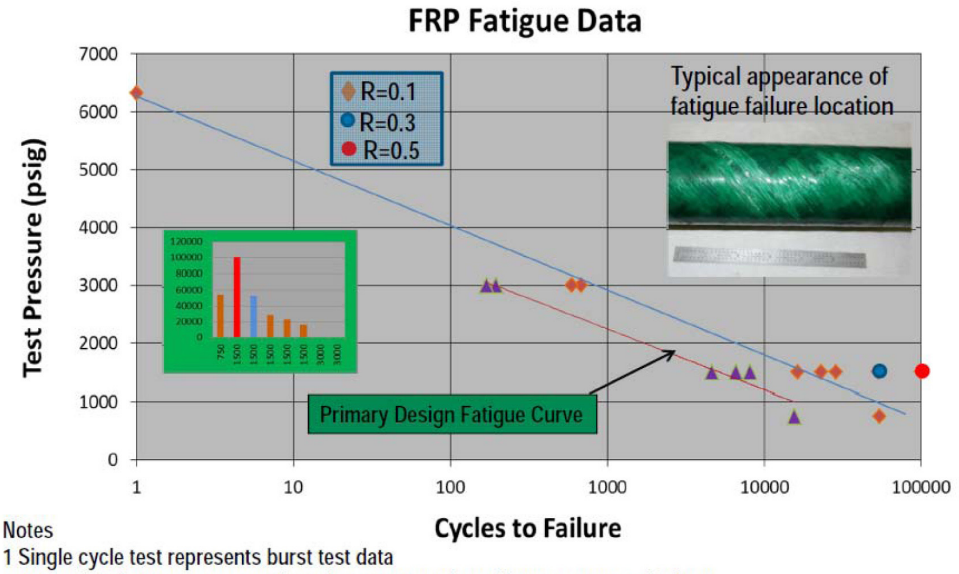

FIGURE 1. FRP Preliminary Fatigue Curve

FRP Codification into ASME B31.12

A report summarizing the FRP testing by SRNL and Oak Ridge National Laboratory has been completed. The report will become the basis for ASME Codification of FRP into the B31.12 Hydrogen Piping Code. In FY 2014 the report was expanded to include both the additional fatigue testing and the technical basis for a FRP 50-year design life. The initial proposal (code language) for codification into ASME B31.12 was presented to the Code Committee in March 2014.

Extension of Design Life of FRP

The evaluation project for FRP has reviewed the structural integrity of FRP for both the hydrostatic design basis that affects the long-term stress rupture of the glass fiber and the fatigue strength of the FRP product. Both of these modes of failure require review when increasing the design life.

Defining the effect on the stress rupture life or the hydrostatic design basis for the FRP is straight forward. The increase in design life is an increase in the total time the pipe is under maximum pressure. To evaluate the required change on hydrostatic design stress to increase the stress rupture life from 20 years to 50 years, stress rupture data for the FRP material was obtained. The design data and calculation procedure are expressed in hours of service. A plot of the D2992 stress rupture data is provided in Figure 2. A review of the graph shows that the stress rupture data can be reasonably modeled by a log-log least squares regression analysis as recommended by ASTM standard D2992.

Table 1 provides the calculation results showing the reduction in stress level in the glass fiber forming the structural layer of the FRP product required to increase design life from 20 to 50 years. The data shows that a decrease in the fiber stress level by 4.3% will provide the required increase in design life.

The data from the FRP fatigue tests completed by SRNL for the DOE Hydrogen Production and Delivery Program

TABLE 1. Rupture Stress vs. Time for FRP

Years	Time (hours)	Rupture Stress (psi)
1	8,760	42,113
20	175,200	36,465
50	438,000	34,894

shown in Figure 1. This set of data is for tests of FRP samples. The rated pressure of the FRP test specimens is 1,500 psi. The data for the failure curve is for testing that was performed for an R ratio of approximately 0.1.

The increase in fatigue life is more difficult to define because the number of operational cycles per time will depend on how the industrial gas suppliers operate the pipeline. The fatigue life is affected by both the total number of cycles and the magnitude of the cycles, and both of these parameters can be controlled.

The initial SRNL fatigue evaluation assumed one stress cycle per day for fatigue life. Based on the peak demand for the fueling stations occurring twice a day, corresponding to high demand occurring in both the morning, when the public is traveling to work and in the evening at the end of the work schedule, two cycles a day were assumed in this review. Current hydrogen pipelines are operated at much lower cyclic rates. If conservative equipment maintenance demands are considered the fatigue demand for FRP can be greatly reduced. The values provided in Table 2 below show these effects on required fatigue design life. The low R ratio tests at 1,500 psi pressure show that the fatigue life for FRP does not support the 50-year fatigue life based on refueling demand. The FY 2014 testing at higher R ratio values of 0.3 to 0.5 show much higher fatigue life for FRP. The current data for the 0.3 and 0.5 R ratio tests indicate that a small change in the stress level of the fiber may be needed for the fatigue life to reach the 50-year goal to reach the refueling demand level. The current FRP design will support a 50-year design life if

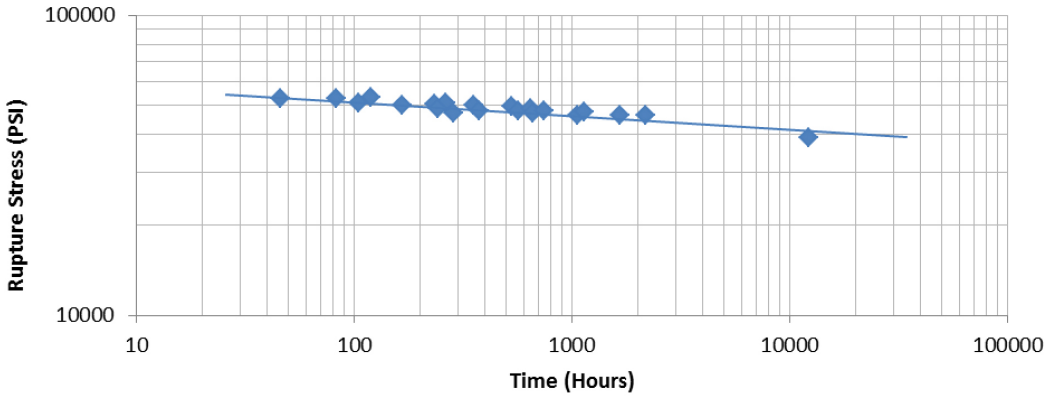

FIGURE 2. ASTM D2992 Data Set for FRP

the pressure rating is reduced from 1,500 psi to 1,400 psi and the pressure cycles are limited to 28,500 at an R ratio of 0.5.

TABLE 2. Design Life Values for Increase from 20 Years to 50 Years

Years	Equipment Maintenance Demand		Refueling Station Demand	
	Fatigue Life (@ 1 Cycle per Month)	Fatigue Life (@ 2 Cycles per Month)	Fatigue Life (@ 1 Cycle per Day)	Fatigue Life (@ 2 Cycles per Day)
1	12	24	365	730
20	240	480	7,300	14,600
50	600	1,200	18,250	36,500

Improved Joint Concepts for FRP

Three concepts have been developed for improving the existing FRP joint design. The emphasis for the new design is on a more robust seal for the polyethylene inner layer. The structural elements for the joint are fundamentally the same as for the existing design. The evaluation addressed elements of the joint that form the leakage connection to the polyethylene liner and the structural connection to the fiberglass structural layer. The specific requirements for FRP joints are as follows:

- Seal the inner layer so that leakage at the joint is $\leq 5 \times 10^{-4}$ STD CC H_2/Sec.
- The joint shall be rated to the full strength of the attached piping:
  - The burst strength of the joint shall exceed the burst strength of the FRP
  - The joint shall exceed the axial strength (tensile strength) of the FRP
- Metallic joint components shall be designed to the requirements of the ASME B31.12 Hydrogen Piping Code.

Fusion Bonded Joints

Polyethylene piping is commonly joined today using two types of fusion processes. These processes are heat fusion bonding and the electrofusion bonding. There is extensive successful experience joining polyethylene material with these fusion processes. The current polyethylene natural gas distribution system utilizes the heat fusion process for the majority of the systems installed today. Both these methods have specific requirements for installation procedures. Both methods are addressed by ASTM standards that provide the requirements for joining procedure qualification. A review of these techniques showed that these bonding processes are candidates for joining the inner polyethylene layer of FRP. Two concepts have been developed for improving the joint by fusion bonding the inner liner. The fusion bonding techniques are applied to bond the liner in these designs. Where the heat fusion joint is more like a butt weld connection the electrofusion joint is more like a brazed connection.

Heat Fusion FRP Joint

In the heat fusion concept, the fiberglass structural layer would be cut away exposing the polyethylene inner layer. The concept for the heat fusion design is shown in Figure 3.

The heat fusion joint will only require a very small section of the fiberglass structural layer to be removed. When whole spools of piping are used, the ends of the liner would be left unwrapped during manufacturing. The heat fusion process described above would be used to form a permanent leak tight joint in the inner polyethylene layer. The heat fusion bead is indicated by the yellow line shown in Figure 3. The internal diameter of the pressure fitting will be sized to have a small clearance above the outside diameter of the structural fiberglass layer. The pressure fitting will be centered on the joint. The gap at the weld bead will be filled with epoxy or other suitable material to provide radial transfer of the pressure load from the exposed section of polyethylene at the fusion bead to the pressure fitting. The pressure fitting will have threaded ends to accept a connector nut that would tighten onto the compression slip ring. The

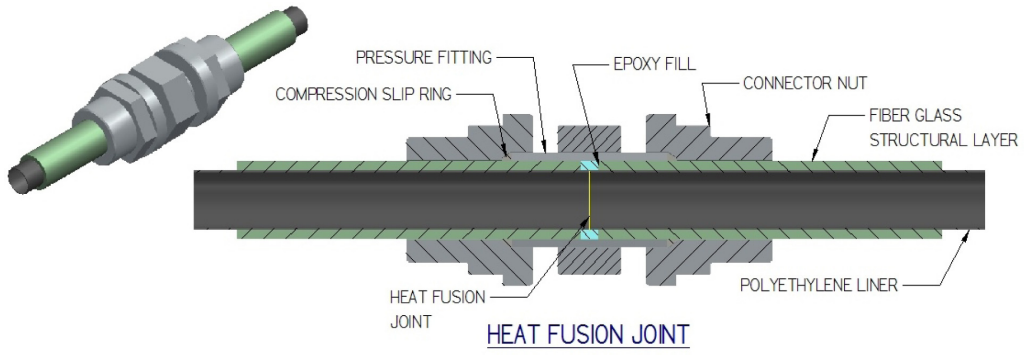

FIGURE 3. Heat Fusion Joint Concept

compression slip ring provides the axial load path across the joint. The compression slip ring is wedged into the pressure fitting, forcing it downward, generating a normal force between the ring and the pipe surface. The resulting frictional force transmits the load from the FRP to the metallic fitting.

Electrofusion FPR Joint

The electrofusion joint is similar in design to the heat fusion joint. The concept for the electrofusion joint is an integral fitting including the polyethylene electofusion fitting and the metallic pressure fitting. In the electrofusion design, a longer section of the fiberglass layer is required to be removed to allow the polyethylene liner to slip into the electrofusion fitting. The concept design is shown in Figure 4.

The development of this joint would entail combining the electrofusion fitting (purple section in Figure 4) with the metallic pressure fitting. The combining of the fusion fitting and the pressure fitting is a requirement for this joint type because ports have to be provided in the pressure fitting for the electrical connection to the electrofusion fitting (yellow section in Figure 4). Where there is an obvious gap requiring reinforcement at the fusion bead in the heat fusion design, additional development work is needed to determine the clearances and gaps in the electrofusion design. The required thickness of the polyethylene to accommodate the heating element will drive the dimensional requirements for this fitting concept. The thickness of the pressure fitting for the electrofusion concept will be fundamentally the same as for the heat fusion fitting, with some possible small increase in thickness required to reinforce the opening for the electrical ports. The ends of the pressure fitting will be threaded with the connector nut and compression slip ring providing for the same load transfer concept as in the heat fusion joint described above.

Welded FRP Joint

The FRP welded joint concept relies on the technology developed by Hexagon Lincoln Inc. The concept was developed for Lincoln's Tuffshell™ Tank product line. The concept is shown in Figure 5.

The aluminum boss is the specific part that will be modified to form the welded FRP joint. The metallic boss is injection molded into the polyethylene material. The keyways lock the metallic part into the polyethylene. To fabricate the joint for FRP the metallic part is reshaped to function in a tubular product form that would be integrally molded into a polyethylene tube, as shown in Figure 6. The concept is the same at the Hexagon Lincoln tank boss, in that keyways

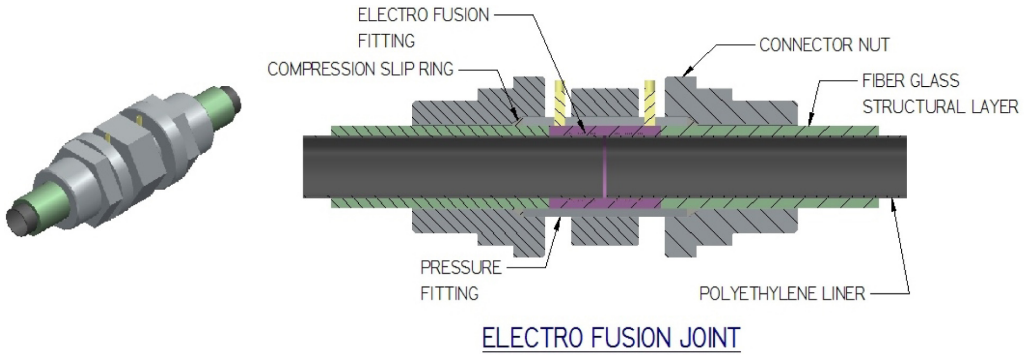

FIGURE 4. Electrofusion Joint Concept

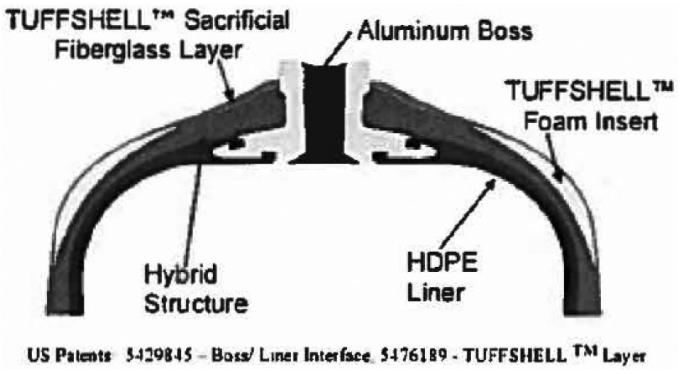

FIGURE 5. Hexagon Lincoln Aluminum Boss Design

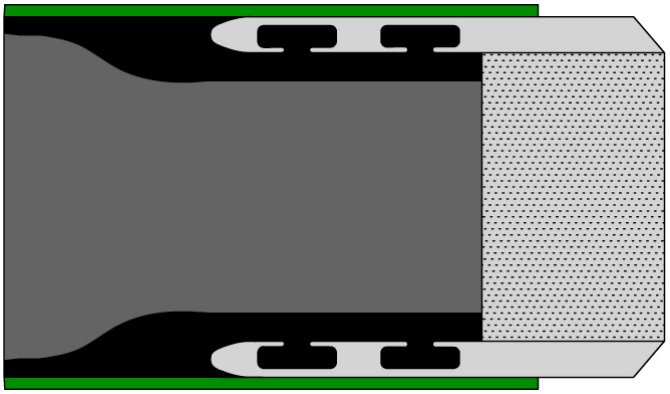

FIGURE 6. FRP Tubular Connector Design

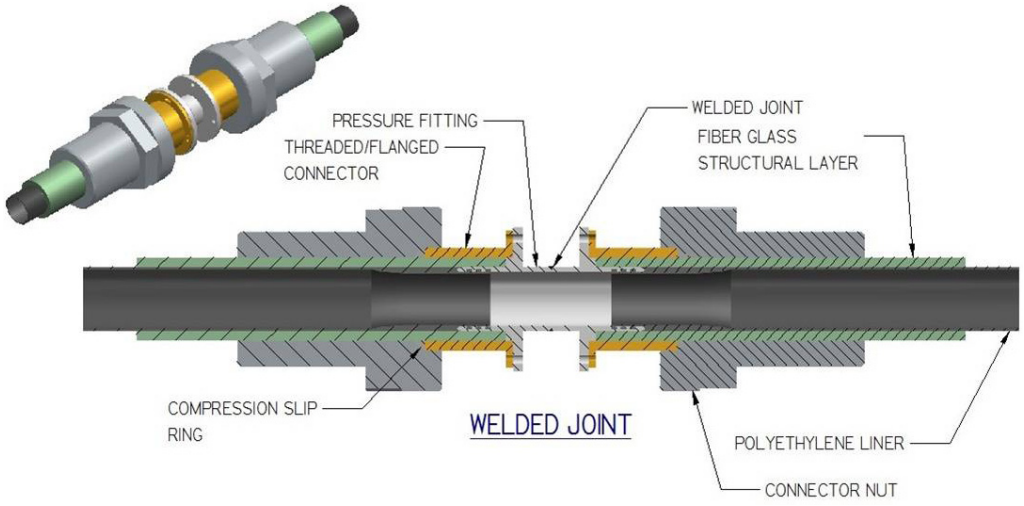

FIGURE 7. Welded Joint Concept

are used to form an integral metallic-polyethylene part that would be injection molded. These parts would be fusion welded to the polyethylene coil and wound into spoolable pipe with welded end connections.

The complete design concept for the welded FRP joint is shown in Figure 7. The pipe to pipe joint for this concept would be made with a standard butt weld. The butt weld would be made using accepted ASME welding practices. The pressure fitting is integral with the FRP section for the welded joint concept. The axial load path for this joint design functions in the same manner as the models shown for the fusion joints. The connector nut is tightened onto the compression slip ring to generate a frictional force to transfer the load across the discontinuity in the fiberglass structural layer. In the welded joint concept an additional part, identified as the thread/flanged connector in Figure 7, is used to link the connector nut to the pressure fitting and complete the axial load path. The length of the metal extending past the fiberglass layer will have to be sufficiently long to ensure that the polymer materials are not damaged by high temperature generated during welding.

The axial load path could also be developed for the welded joint design by placing a metallic sleeve over the metallic-polyethylene part. This sleeve design would be the same concept as the pressure fitting connector nut detail used for the heat fusion concept as shown in Figure 5. One disadvantage to the welded detail is that it is more applicable to FRP manufactured in standard lengths. As shown, the fiber reinforced layer is wrapped over the connection between the metallic-polyethylene part and the remaining FRP section. Achieving the continuity in the structural layer could be difficult to achieve in field fabrication. A technical report providing an evaluation of an improved hydrogen seal for the FPR inner polyethylene liner was finalized.

CONCLUSIONS AND FUTURE DIRECTIONS

Conclusions

- The design life evaluation supports that an increase in design life from 20 years to 50 years is feasible for FRP.
- The codification of FRP will proceed with a recommendation for a 50-year design life. The proposed fatigue testing provided in the B31.12 Code proposal is well suited to address the required fatigue life.
- Fatigue testing over the range of 750 psig to 3,000 psig was completed in FY 2013. The data provides an indication on the fatigue life of FRP. The FY 2013 tests were performed at an R- ratio of 0.1.
- Fatigue testing continued in FY 2014. The first fatigue test at an R ratio of approximately 0.5 has been tested to 100,000 cycles without failure. The second test with an R ratio of approximately 0.3 has been tested to 53,000 cycles. The testing shows that the FRP has a significant sensitivity to R-ratio.

Future Work

- Complete the FRP Codification into ASME B31.12
- Complete collaboration with Fiberspar to determine the variability in the fatigue data and effect of cycle frequency.
- Collect and document available service history data for FRP from literature and FRP manufacturers.
- Continue the evaluation of non-mechanical joints for FRP application.
- Development an in-service inspection criteria for FRP.
- Continue to support the development of an FRP demonstration project.

FY 2014 PUBLICATIONS/PRESENTATIONS

1. B31.12 Hydrogen Piping Committee Meeting, Portland, ME October 2013.

2. Hydrogen Delivery Workshop, Denver, CO, March 2014.

3. B31.12 Hydrogen Piping Committee Meeting, Washington, DC, March 2014.

III.5 Hydrogen Embrittlement of Structural Steels

Brian Somerday
Sandia National Laboratories
P.O. Box 969
Livermore, CA 94550
Phone: (925) 294-3141
Email: bpsomer@sandia.gov

DOE Manager
Erika Sutherland
Phone: (202) 586-3152
Email: Erika.Sutherland@ee.doe.gov

Project Start Date: January 2007
Project End Date: Project continuation and direction determined annually by DOE

Overall Objectives

- Demonstrate the reliability/integrity of steel hydrogen pipelines subjected to cyclic pressure operating conditions, emphasizing welded regions
- Identify pathways for reducing the cost of steel hydrogen pipelines without compromising reliability/integrity

Fiscal Year (FY) 2014 Objectives

- Complete triplicate measurements to establish reliable fatigue crack growth relationships for X65 girth weld fusion zone in 3,000 psi (21 MPa) hydrogen gas
- Complete duplicate measurements of fatigue crack growth relationships in hydrogen gas for model iron-carbon alloys with two different grain sizes in collaboration with the International Institute for Carbon-Neutral Energy Research

Technical Barriers

This project addresses the following technical barriers from the Hydrogen Delivery section of the Fuel Cell Technologies Office Multi-Year Research, Development, and Demonstration Plan (section 3.2.5):

(B) Reliability and Costs of Gaseous Hydrogen Compression

(D) High As-Installed Cost of Pipelines

(K) Safety, Codes and Standards, Permitting

Technical Targets

The principal target addressed by this project is Pipeline Reliability/Integrity (Table 3.2.4).

One salient reliability/integrity issue for steel hydrogen pipelines is hydrogen embrittlement. For steel pipelines, the central unresolved issue is the pipeline performance under extensive pressure cycling. One of the objectives of this project is to enable safety assessments of steel hydrogen pipelines subjected to pressure cycling through the use of structural integrity models in design codes, e.g., American Society of Mechanical Engineers (ASME) B31.12. This structural integrity analysis can determine limits on design and operating parameters such as the allowable number of pressure cycles and pipeline wall thickness. Efficiently specifying pipeline dimensions such as wall thickness also affects pipeline cost through the quantity of material required in the design.

FY 2014 Accomplishments

- Reproducible fatigue crack growth rate (da/dN) vs. stress-intensity factor range (ΔK) relationships were measured for X65 weld fusion zones in 3,000 psi (21 MPa) hydrogen gas. Comparing with results from FY 2013 suggests that the weld fusion zone and heat-affected zone are no more susceptible to hydrogen-accelerated fatigue crack growth compared to the base metal.
- Modified specimen geometry ESE(T) (eccentrically loaded, single edge tension) used in this study expands fatigue crack growth testing capabilities by allowing thinner walled pipes to be examined as well as different orientations of materials that would otherwise be precluded by employing the conventional C(T) (compact tension) specimen.

INTRODUCTION

Carbon-manganese steels are candidates for the structural materials in hydrogen gas pipelines; however, it is well known that these steels are susceptible to hydrogen embrittlement. Decades of research and industrial experience have established that hydrogen embrittlement compromises the structural integrity of steel components. This experience has also helped identify the failure modes that can operate in hydrogen containment structures. As a result, there are tangible ideas for managing hydrogen embrittlement in steels and quantifying safety margins for steel hydrogen containment structures. For example, fatigue crack growth aided by hydrogen embrittlement is a well-established failure mode for steel hydrogen containment structures subjected to pressure cycling. This pressure cycling represents one of the key differences in operating conditions between current

hydrogen pipelines and those anticipated in a hydrogen delivery infrastructure. Applying structural integrity models in design codes coupled with measurement of relevant material properties allows quantification of the reliability/integrity of steel hydrogen pipelines subjected to pressure cycling. Furthermore, application of these structural integrity models is aided by the development of physics-based predictive models, which provide important insights such as the effects of microstructure on hydrogen-assisted fatigue crack growth. Successful implementation of these structural integrity and physics-based models enhances confidence in the design codes and enables decisions about materials selection and operating conditions for reliable and efficient steel hydrogen pipelines.

APPROACH

The approach of this project is to apply the core capability in materials characterization at Sandia to measure the fatigue crack growth rates of technologically relevant pipeline steels in high-pressure hydrogen gas. These properties must be measured for the base materials as well as the welds, which are likely to be most vulnerable to hydrogen embrittlement. Such measurements are necessary to enable the application of structural integrity models in design codes. For example, the new ASME B31.12 code for hydrogen pipelines includes a fracture mechanics-based integrity management option, which requires material property inputs such as the fatigue crack growth relationship in hydrogen gas.

Following the establishment of reliable fatigue crack growth relationships for pipeline steel base metal, weld heat-affected zone, and weld fusion zone in hydrogen gas, a secondary approach of this project is to apply analytical techniques such as electron microscopy to define the mechanisms of hydrogen embrittlement for the purpose of developing physics-based predictive models. Such predictive models can provide quantitative insight into the effects of environmental, material, and mechanical variables on hydrogen embrittlement. For example, quantifying the effect of microstructure on hydrogen-accelerated fatigue crack growth can aid in the qualification of line pipe steels and their welds for hydrogen service.

RESULTS

The da/dN vs. ΔK relationship is a necessary material-property input into structural integrity models applied to steel hydrogen pipelines. One such integrity assessment methodology for steel hydrogen pipelines was recently published in the ASME B31.12 code. The measurement of fatigue crack growth relationships in this task supports the objective of establishing the reliability/integrity of steel hydrogen pipelines by enabling application of the ASME B31.12 code.

Low-strength line pipe steels such as X52, X60, and X65 were selected for this task because of their stakeholder-recognized technological relevance for hydrogen pipelines. Generally, lower-strength steels are selected for hydrogen pipelines since these steels are less susceptible to hydrogen embrittlement. A section of X65 steel pipe containing a girth-oriented gas metal arc weld was provided by an industry partner. An optical-microscope image revealing the base metal (BM), weld fusion zone (FZ), and weld heat-affected zone (HAZ) is shown in Figure 1. This image demonstrates that the material regions have distinctly different metallurgical structures, particularly the base metal and fusion zone. In FY 2013, the da/dN vs. ΔK relationships for the HAZ in 3,000 psi (21 MPa) hydrogen gas were measured and compared to the base metal. The emphasis for FY 2014 was measurement of the weld fusion zone (FZ) in 3,000 psi (21 MPa) hydrogen gas. As specified in ASME B31.12, the da/dN vs. ΔK relationship was measured following ASTM Standard E647. Since the maximum pressure specified for hydrogen gas pipelines in the ASME B31.12 code is 3,000 psi (21 MPa), this upper-bound pressure was selected for the testing. The load-cycle frequency selected for the testing was 1 Hz, consistent with previous testing on X52 line pipe steel in high-pressure hydrogen gas.

As demonstrated in FY 2013, non-uniform crack fronts were observed in HAZ and FZ C(T) specimens. To mitigate deviation of the crack fronts during testing, C(T) specimens were thinned from their original 0.5 in (13 mm) to 0.25 in (6 mm) for the HAZ and FZ specimens. While this specimen

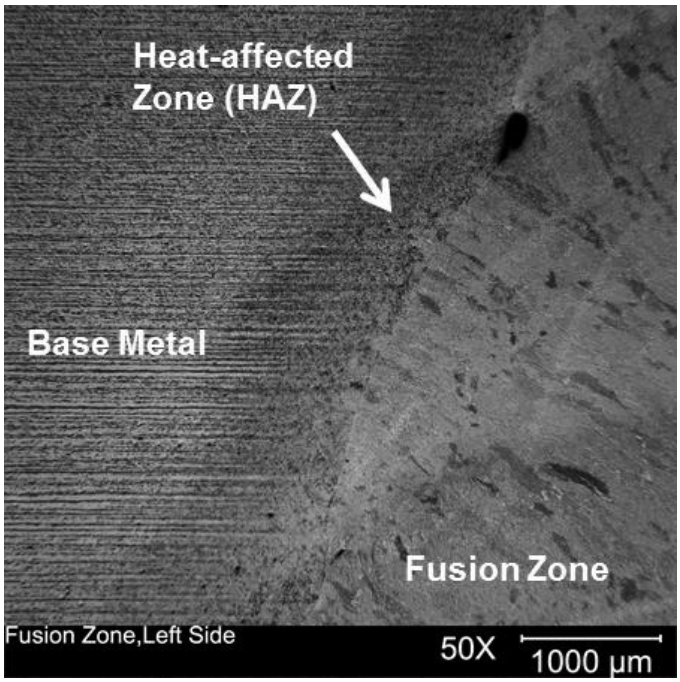

FIGURE 1. Optical-microscope image showing base metal, fusion zone, and HAZ of X65 weld.

modification improved results for the HAZ C(T) specimens, this thinning did not rectify non-uniform crack advance in the FZ C(T) specimens; therefore, both an alternate specimen geometry, i.e., the ESE(T), and crack propagation direction were adopted for the weld FZ, which improved crack front uniformity. Non-uniform crack fronts in the FZ were attributed to residual stress gradients [1] across the crack front. Figure 2 shows a schematic of the orientations and specimen geometries tested in this study with respect to the welded pipe. The first letter in parenthesis refers to the direction of applied load and the second letter refers to the crack propagation direction. Because of the residual stress gradient, the preferred orientation for the FZ specimens was longitudinal-radial (L-R). The ESE(T) specimens were extracted not only from the FZ but also from the BM (L-R and longitudinal-circumferential [L-C] orientations) for comparison. Uniform crack fronts were observed in all ESE(T) specimens.

The results from testing the X65 BM, HAZ, and FZ in 3,000 psi (21 MPa) hydrogen gas are shown in Figure 3. Tests performed in air at 10 Hz are also shown for comparison. The specimen orientation relative to the pipe is identified in parenthesis for each specimen tested and can be referenced in Figure 2, and tests performed in triplicate are identified by (x3). The FZ and BM circumferential-longitudinal (C-L) exhibited similar fatigue crack growth rates (FCGR) in hydrogen gas over the entire ΔK range. The HAZ exhibited slightly lower crack growth rates in hydrogen gas for the lower ΔK range but shows similar trends to the BM (C-L) and FZ in the higher range of ΔK. These results indicate that the weld FZ and HAZ are no more susceptible to hydrogen-accelerated fatigue crack growth than the base metal.

The effect of orientation on hydrogen-assisted FCGR is not well documented for line pipe steels, mainly because geometrical constraints preclude testing in all orientations; however, the ESE(T) specimen geometry allows for BM samples to be extracted in the L-R orientation (see Figure 2). Additional tests were performed on BM ESE(T) specimens for the L-R orientation in both air and hydrogen gas as shown in Figure 3. The FCGR of BM (L-R) was 2 to 4 times lower in air and nearly an order of magnitude lower in hydrogen throughout the ΔK range as compared to BM (C-L) tests in the respective environments. Microstructural banding is prevalent in pipeline steels with features elongated in the longitudinal and circumferential directions. Cracks propagating perpendicular to the banding (i.e., in L-R orientation) will encounter sequential planes of ferrite and pearlite which may affect FCGR. Previous work [2] showed lower hydrogen-assisted FCGR in fully pearlitic microstructures as compared to pure iron. This microstructural banding appears to play an important role in hydrogen-assisted FCGR for the X65 base metal when crack growth is perpendicular to the banded direction as demonstrated by the significantly lower FCGR in the BM (L-R) orientation.

In collaboration with the International Institute for Carbon-Neutral Energy Research, custom heats of two high-purity Fe-C materials were procured and delivered to Kyushu University (Fukuoka, Japan), a fine grain size (15 μm) heat and a coarse grain size (70 μm) heat. The goal was to assess whether the grain size in these model ferrite-pearlite steels

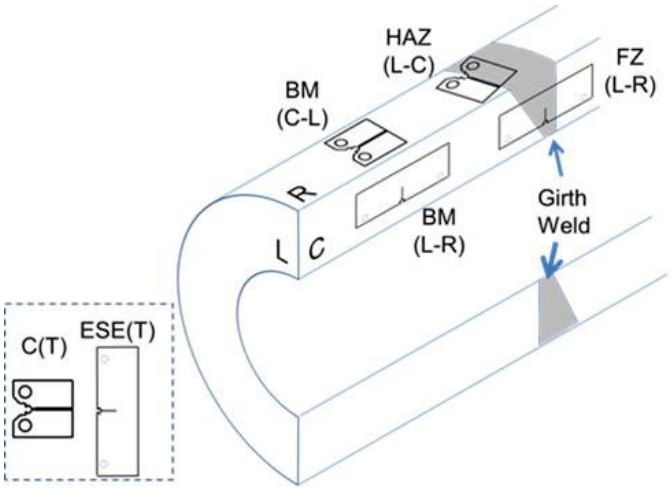

FIGURE 2. Schematic of gas metal arc welded pipeline with ESE(T) and C(T) specimens superimposed to show orientation tested for BM, HAZ, and FZ.

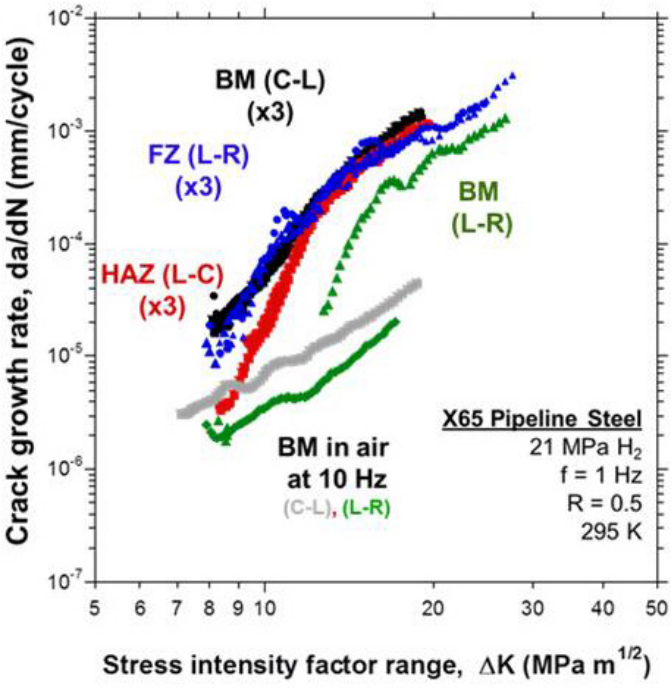

FIGURE 3. Fatigue crack growth rate relationships for X65 BM, HAZ, and FZ in 3,000 psi (21 MPa) hydrogen gas. The results are compared to measurements for X65 BM in air.

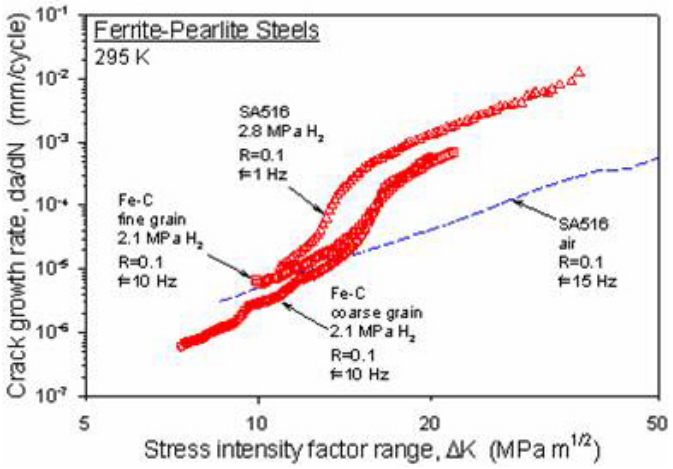

FIGURE 4. Fatigue crack growth rate relationships for fine and coarse grained model ferrite-pearlite steels. Data for a commercial ferrite-pearlite steel (SA516) is shown for comparison in air and hydrogen gas.

affects the onset of hydrogen-accelerated cracking. Tests on the model steels were performed at 10 Hz and R=0.1 in 2.1 MPa hydrogen gas. Figure 4 shows the FCGR curves for the fine and coarse grain size steels along with data for a commercial ferrite-pearlite steel (SA516) in both air (15 Hz) and hydrogen gas (1 Hz) for comparison. Both model ferrite-pearlite steels exhibited the onset of hydrogen-accelerated fatigue crack growth at similar ΔK ranges, suggesting that grain size does not have a pronounced effect. However, further testing (e.g., at higher load ratio, R) is required to conclusively demonstrate such insensitivity of hydrogen-assisted FCGR to grain size.

CONCLUSIONS AND FUTURE DIRECTIONS

- Reliable da/dN vs. ΔK relationships were measured for the X65 weld FZ in 3,000 psi (21 MPa) hydrogen gas. Comparison of results shows that weld FZ and HAZ are no more susceptible to hydrogen-accelerated fatigue crack growth compared to the base metal.
- (future) Orientation was shown to have a pronounced effect on crack growth rate, therefore, in order to compare the BM and HAZ results directly similar orientations should be tested. Tests on C(T) specimens from the BM in L-C orientation will provide a more direct comparison to results from completed tests on C(T) specimens in the HAZ.
- (future) ESE(T) specimens will be extracted from a friction stir welded X52 pipe provided by Oak Ridge National Laboratory for triplicate testing in 3,000 psi (21 MPa) hydrogen gas.

SPECIAL RECOGNITIONS & AWARDS/ PATENTS ISSUED

1. Best Poster Award: "Assessing Hydrogen Pipeline Reliability: Quantifying Susceptibility of Pipeline Steels to Hydrogen Gas-Accelerated Fatigue Crack Growth," Brian Somerday and Joe Ronevich, ASME 12th Fuel Cell Science, Engineering and Technology Conference Boston, MA, June 30 - July 2, 2014.

2. Brian Somerday and Chris San Marchi, DOE Hydrogen and Fuel Cells Program Awards, Hydrogen Delivery and Safety, Codes and Standards, 2014.

FY 2014 PUBLICATIONS/PRESENTATIONS

1. "Effect of Hydrogen Gas Impurities on the Hydrogen Dissociation on Iron Surface", A. Staykov, J. Yamabe, and B.P. Somerday, *International Journal of Quantum Chemistry*, vol. 114, 2014, pp. 626-635.

2. "Measurement of Fatigue Crack Growth Relationships for Steel Pipeline Welds in High-Pressure Hydrogen Gas", J.A. Ronevich and B.P. Somerday, submitted to Second International Conference on Metals & Hydrogen, 2014.

3. "Measurements of H_2-Assisted Crack Growth in Pipeline Steels at SNL", J. Ronevich, B. Somerday, C. San Marchi, and K. Nibur, Joint DOC/DOE/DOT Meeting on Hydrogen Fuel Research, NIST, Boulder, CO, Dec. 2013.

4. (invited) "Modeling of Gaseous Impurity Inhibition of Hydrogen Environment Embrittlement", B. Somerday, A. Staykov, P. Sofronis, and R. Kirchheim, TMS 2014 Annual Meeting & Exhibition, San Diego, CA, Feb. 2014.

5. "Structural Materials Challenges in the Deployment of Hydrogen Pipelines", B. Somerday, Hydrogen Transmission and Distribution Workshop, National Renewable Energy Laboratory, Golden, CO, Feb. 2014.

6. (invited) "Addressing Critical Issues for Hydrogen Gas-Accelerated Fatigue Crack Growth in Pipeline Steels: Effects of Welds and Oxygen Gas Impurities", B. Somerday, University of Virginia, Charlottesville, VA, March 2014.

7. "Assessing Hydrogen Pipeline Reliability: Quantifying Susceptibility of Pipeline Steels to Hydrogen Gas-Accelerated Fatigue Crack Growth", B.P. Somerday and J.A. Ronevich, ASME 12th Fuel Cell Science, Engineering and Technology Conference Boston, MA, June 30 – July 2, 2014.

REFERENCES

1. Neeraj, T., Gnaupel-Herold, T., Prask, H.J., Ayer, R., "Residual stresses in girth welds of carbon steel pipes: neutron diffraction analysis," Science and Technology of Welding and Joining. Vol. 16, No.3, pp. 249-253, 2011.

2. Cialone, H.J. and Holbrook, J.H. "Microstructure and fractographic features of hydrogen-accelerated fatigue crack growth in steels" in Microstructural Science Vol. 14, Eds. M.R. Louthan, I. LeMay, and G.F. Vander Voort, ASM, Metals Park, OH, (1987) pp. 407-422.

Sandia National Laboratories is a multi-program laboratory managed and operated by Sandia Corporation, a wholly owned subsidiary of Lockheed Martin Corporation, for the U.S. Department of Energy's National Nuclear Security Administration under contract DE-AC04-94AL85000

III.6 Electrochemical Hydrogen Compressor

Ludwig Lipp (Primary Contact), Pinakin Patel
FuelCell Energy, Inc. (FCE)
3 Great Pasture Road
Danbury, CT 06813
Phone: (203) 205-2492
Email: llipp@fce.com

DOE Managers
Erika Sutherland
Phone: (202) 586-3152
Email: Erika.Sutherland@ee.doe.gov
David Peterson
Phone: (720) 356-1747
Email: David.Peterson@ee.doe.gov

Contract Number: DE-EE0003727

Subcontractor
Sustainable Innovations, LLC, Glastonbury, CT

Start Date: July 15, 2010
End Date: October 14, 2014

Overall Objectives

- Demonstrate the capability of electrochemical hydrogen compression (EHC) technology to meet the DOE targets for small compressors for refueling sites.
- Quantify EHC cell performance and durability.
- Reduce capital cost to demonstrate the potential to meet DOE cost targets for hydrogen compression, storage, and delivery.

Fiscal Year (FY) 2014 Objectives

- Develop a solid-state EHC building block capable of compressing 2 lb/day hydrogen from near-atmospheric pressure to 2,000-3,000 psi.
- Scale up the EHC stack active cell area by >100%.
- Increase compression efficiency (isentropic) to 73% (DOE 2015 Target).

Technical Barriers

This project addresses the following technical barrier from the Hydrogen Delivery section (3.2) of the Fuel Cell Technologies Office Multi-Year Research, Development, and Demonstration Plan:

- (B) Reliability and Costs of Gaseous Hydrogen Compression

Technical Targets

Technical targets are presented in Table 1.

TABLE 1. FCE Progress towards Meeting Technical Targets for Small Compressors for Fueling Sites [1]

Characteristic	Units	DOE 2015 Target	FCE Status
Reliability	-	Improved	>10,900 hours
Compressor Efficiency	%	73% isentropic	<5 kWh/kg at 200 bar
Losses (% of H_2 throughput)	%	0.5	1
Uninstalled Capital Cost	$	400,000	300,000 projected for EHC stack
Outlet Pressure Capability	bar	860	Up to 880
Contamination	-	Varies by design	None

FY 2014 Accomplishments

- Design: Reduced electrochemical compressor cell part count by ~75% compared to baseline design (Figure 1).
- EHC Stack Scale Up: Scaled up stack height in 185 cm^2 design from one to eight cells.
- Hydrogen Capacity: Increased EHC capacity to 2 lb/day, meeting a major program goal (Table 2).
- Capital Cost: Achieved 60% decrease in single production unit cost compared to baseline design by lowering part count and increasing the cell active area.

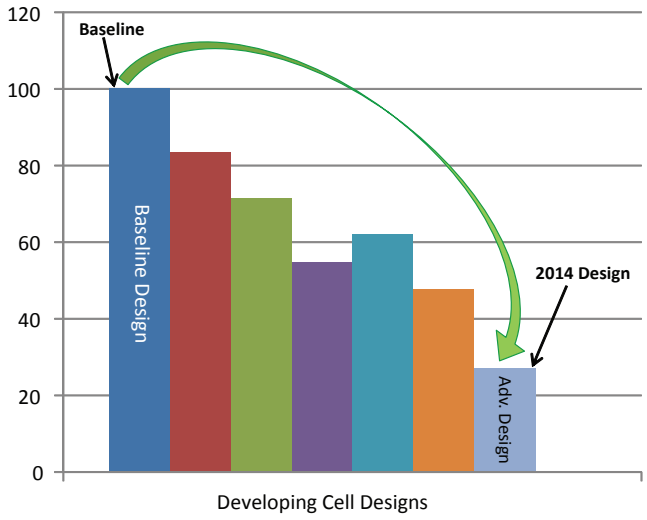

FIGURE 1. Decreased Cell Part Count for EHC Cost Reduction

- Efficiency: Validated lower specific energy consumption of <5 kWh/kg H_2 at 3,000 psi in 185 cm^2 design (Figure 2).
- Durability: Demonstrated >10,900 hour operation in larger area 185 cm^2 cell at >95% hydrogen recovery (Figure 3).

INTRODUCTION

With the depletion of fossil fuel reserves and a global requirement for the development of a sustainable economy, hydrogen-based energy is becoming increasingly important. Production, purification, and compression of hydrogen represent key technical challenges for the widespread commercialization of hydrogen fuel cell technologies. In the transportation sector, onboard storage of pure hydrogen is required at pressures up to 10,000 psi and compression of the hydrogen fuel up to 12,700 psi.

The level of maturity of current hydrogen compressor technology is not adequate to meet projected infrastructure demands. Existing compressors are inefficient and have many moving parts, resulting in significant component wear and therefore excessive maintenance. New technologies that achieve higher operational efficiencies, are low in cost, safe, and easy to operate are therefore required. This project addresses high-pressure hydrogen needs by developing a solid-state electrochemical hydrogen compressor.

APPROACH

The approach to address the project goals consists of the following major elements:

- Increase hydrogen recovery efficiency by improving flow field design.
- Reduce capital cost by increasing the hydrogen flux.
- Reduce operating cost by improving membrane and electrode design.
- Increase compressor capacity by increasing cell active area and stack height.

To this end, the approach includes the design, fabrication and evaluation of improved cell architecture, and the development and demonstration of critical sealing technology to contain the high-pressure hydrogen within the EHC.

RESULTS

A major activity this year was to reduce the capital cost of the EHC design for 2,000-3,000 psi hydrogen product pressure. This was addressed by reducing the cell part count, as well as scaling up the cell active area and transitioning to a short stack. A number of design innovations were implemented in the advanced EHC design. The number of parts has been reduced in a stepwise process as shown in Figure 1. Compared to 2013, the number of parts was reduced by 50%. Compared to the original baseline design, a 75% reduction has been achieved. The reduced part count results in a lower cost to fabricate EHC cells. This contributes to the overall reduction in capital cost. Potential for mass manufacturability was maintained with the improved cell components. Preliminary cost projections show a stack cost of $300,000 can be achieved at 160 bar with further scale up from 185 to 400 cm^2 active area, increased current density to 2 A/cm^2, increased stack height to 10-50 cells per stack and a moderate production volume of 10,000 stacks per year. This compares favorably to the DOE FY 2015 cost target of $360,000-$400,000 for small compressors. Additional cost reduction is expected by further increasing stack height and production volume. Improved cell stack materials and components to meet these projections are under development, including repeating and non-repeating stack hardware.

To demonstrate increased hydrogen capacity, an eight-cell stack using the scaled-up 185-cm^2 hardware was fabricated. Procedures were developed to operate the stack continuously at a product pressure of 3,000 psi. A direct current up to 133 A was applied to the stack, thus achieving a capacity of 2 lb/day hydrogen, as shown in Table 2. Hence a major milestone in the project is met. The stack was operated at various conditions, reaching total operating time of >3,000 hours to date.

TABLE 2. Increased Hydrogen Capacity by 7x to Meet Project Target of 2 lb/day

Characteristic	Units	2014 Result
DC Load	A	133
Average Cell Voltage	V	0.373
Hydrogen Flux Rate	slpm	7.6
Power Input	Watts	397
Production Rate	lb H_2/day	2

The EHC efficiency is measured by the hydrogen recovery as well as the specific energy consumption. Figure 2 shows the specific energy consumption of a number of recent EHC cells. Efforts in previous years reduced the specific energy consumption to below that of state-of-the-art multi-stage mechanical compressors, first at hydrogen product pressures of 2,000 psi and then at 3,000 psi. This development was carried out in 81-cm^2 EHC hardware. This year the lowest specific energy consumption of <5 kWh/kg at 3,000 psi was reproduced in a scaled-up 185-cm^2 cell. This indicates a successful cell area scale up.

Durability and reliability are significant barriers for mechanical compressors, and major incentives for pursuing electrochemical compression. Therefore, emphasis was

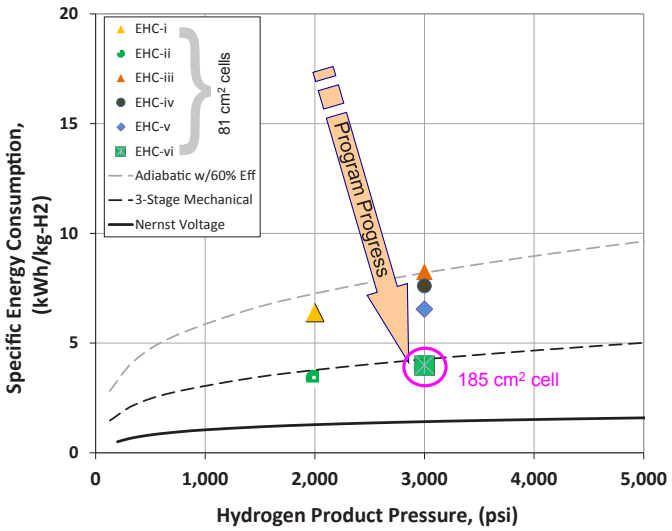

FIGURE 2. Maintained Lower Specific Energy Consumption at 3,000 psi in Scaled-Up EHC (185 cm^2 active area)

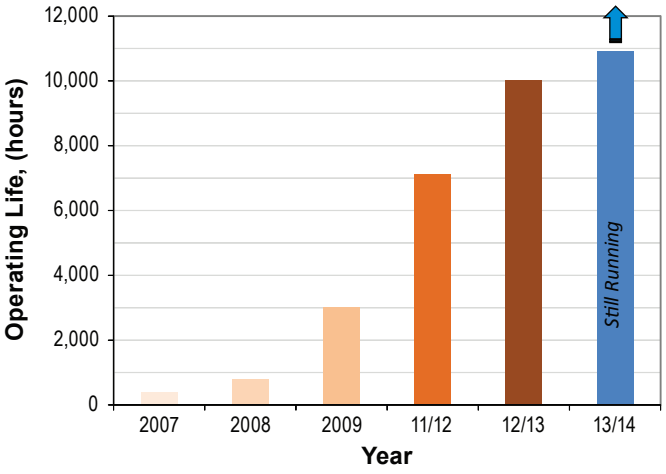

FIGURE 3. 10,900 Hour Endurance Demonstrated in Scaled-Up EHC at >95% Hydrogen Recovery

placed on endurance testing the EHC. 81-cm^2 cells were operated up to 10,000 hours at 3,000 psi, as reported in the last annual progress report. This year, a 185-cm^2 cell has reached 10,900 hours of operation, as shown in Figure 3. Its hydrogen recovery was in excess of 95%. Cell operation is continuing. This result is further confirmation of the robustness of the EHC, even with increased cell active area. Therefore, EHC is expected to be able to meet the DOE target for high compressor reliability.

CONCLUSIONS AND FUTURE DIRECTIONS

The EHC capacity has been increased by a factor of seven to meet the project target of 2 lb/day hydrogen. The cell part count was reduced by 50% to 25% of the original baseline cell, in an effort to reduce EHC capital cost. A specific energy consumption below that of state-of-the-art mechanical compressors has been maintained with the scaled-up cell hardware. Durability of the scaled-up cell architecture has been demonstrated in a 10,900 hour test, confirming its robustness. The following summarizes critical performance parameters that were advanced during this reporting period:

Parameter	2013 Value	2014 Value
Percent of Original Part Count	50	25
EHC hydrogen capacity	0.3 lb/day	2 lb/day
Specific energy consumption at 3,000 psi	<5 kWh/kg in 81 cm^2	<5 kWh/kg in 185 cm^2
Endurance	10,000 hours	10,900 hours

Future efforts will include continued endurance testing of a 185-cm^2 EHC cell, as well as fabrication and testing of a taller EHC stack.

FY 2014 PUBLICATIONS/PRESENTATIONS

1. L. Lipp, "Electrochemical Hydrogen Compressor", 2014 DOE Hydrogen Program Merit Review and Peer Evaluation Meeting, Washington, DC, June 16–20, 2014.

REFERENCES

1. DOE Office of Energy Efficiency and Renewable Energy (EERE) Fuel Cell Technologies Office Multi-Year Research, Development and Demonstration (MYRD&D) Plan, Table 3.2.4 "Technical Targets for Hydrogen Delivery Components", section on Small Compressors, page 3.2-16.

III.7 Vessel Design and Fabrication Technology for Stationary High-Pressure Hydrogen Storage

Zhili Feng (Primary Contact), Yanli Wang, Yong Chae Lim, Lawrence Anovitz and John Wang
Oak Ridge National Laboratory (ORNL)
1 Bethel Valley Rd, PO Box 2008, MS 6095
Oak Ridge, TN 37831
Phone: (865) 576-3797
Email: fengz@ornl.gov

DOE Manager
Erika Sutherland
Phone: (202) 586-3152
Email: Erika.Sutherland@ee.doe.gov

Subcontractors
- Global Engineering and Technology LLC, Camas, WA
- Ben C. Gerwick Inc., Oakland, CA
- MegaStir Technologies LLC, Provo, UT
- Kobe Steel, LTD., Japan

Project Start Date: October 1, 2010
Project End Date: Project continuation and direction determined annually by DOE

Overall Objectives

- To address the significant safety and cost challenges in high-pressure stationary hydrogen storage technology
- To develop and demonstrate a novel steel/concrete composite vessel (SCCV) design and fabrication technology for stationary hydrogen storage systems

Fiscal Year (FY) 2014 Objectives

- Validate that SCCVs can reduce the cost of stationary hydrogen storage and meet the DOE 2015 cost target of $1,200/kg stored at 860 bar
- Demonstrate friction stir welding scale-up manufacturing process for multiple-layer steels with wall thickness of 1.5 inch
- Design, engineer and manufacture a representative ¼-sized mock-up SCCV capable of storing 90 kg gaseous hydrogen at 430 bar, capturing all major features of SCCV design and fabricability with today's manufacturing technologies and code/standard requirements

Technical Barriers

This project addresses the following technical barriers from the Hydrogen Delivery section (3.2) of the Fuel Cell Technologies Office Multi-Year Research, Development, and Demonstration Plan:

(E) Gaseous Hydrogen Storage and Tube Trailer Delivery Costs

Technical Targets

This project aims to develop and demonstrate the novel design and fabrication technology for low-cost and high-safety SCCVs for stationary gaseous hydrogen storage. The flexible and scalable composite vessel design can meet different stationary storage needs (e.g., capacity and pressure) at hydrogen fueling stations, renewable energy hydrogen production sites, and other non-transport storage sites. As shown in Table 1, the current generation composite vessel made using the existing design and manufacturing technology can readily exceed DOE's 2015 cost target. Moreover, with the successful development of advanced manufacturing technology such as the highly-automated friction-stir welding (FSW) process, the next generation vessel has a high potential to meet DOE's 2020 capital cost target. Details of the cost analysis are given in Zhang, et al [1].

TABLE 1. Progress towards Meeting Technical Targets for Stationary Gaseous Hydrogen Storage Tanks (for fueling sites, terminals, or other non-transport storage needs)

Pressure	DOE 2015 Target	Current SCCV	DOE 2020 Target	Next generation SCCV
Low Pressure (160 bar) Purchased Capital Cost ($/kg of hydrogen stored)	850	681	700	652
Moderate Pressure (430 bar) Purchased Capital Cost ($/kg of hydrogen stored)	900	713	750	684
High Pressure (860 bar) Purchased Capital Cost ($/kg of hydrogen stored)	1,200	957	1,000	919

FY 2014 Accomplishments

- Validated that SCCVs can reduce the cost of stationary hydrogen storage by more than 15% and meet the DOE 2015 cost target of $1,200/kg-stored at 860 bar through detailed vessel design and supplier quotes.

- Completed the demonstration of friction stir welding scale up process for a multiple layer high strength steel with total thickness of 1.5 inch.
- Completed detailed engineering design and fabrication specifications for the ¼-sized mock-up composite SCCV capable of storing 90 kg gaseous hydrogen at 430 bar. Fabrication of the inner steel vessel is underway. Finalized procurement of concrete forming and pre-stressing. Made detailed plans on the follow up vessel testing and demonstration.

INTRODUCTION

Low-cost infrastructure is critical to successful market penetration of hydrogen-based transportation technologies such as off-board bulk stationary hydrogen storage. Stationary storage is needed in many locations ranging from hydrogen production plants to refueling stations. The design capacity and pressure of the stationary storage vessel are expected to vary considerably depending on the intended usage, the location, and other economic and logistic considerations. For example, storage vessels at a hydrogen refueling station may have higher pressures but smaller storage capacity when compared to that at a renewable energy hydrogen production site. Therefore, it is important the make storage vessel design flexible and scalable in order to meet different storage needs. Moreover, as it provides the surge capacity to handle hourly, daily, and seasonal demand variations, the stationary storage vessel endures repeated charging/discharging cycles. Therefore, the hydrogen embrittlement in structural materials, especially the accelerated crack growth due to fatigue cycling, needs to be mitigated to ensure the vessel safety. Therefore, safety and economics are two prevailing drivers behind the composite hydrogen storage technology.

In this project, ORNL leads a diverse multidisciplinary team consisting of industry and academia to develop and demonstrate an integrated design and fabrication technology for cost-effective high-pressure steel/concrete composite storage vessel that can meet different stationary hydrogen storage needs.

APPROACH

A novel SCCV has been specifically designed and engineered for stationary high-pressure gaseous hydrogen storage applications. SCCV has several inherent features aimed at solving the two critical limitations and challenges of today's high-pressure hydrogen storage vessels—the high capital cost and the safety concerns of hydrogen embrittlement of high-strength steel vessels.

The basic concept of SCCV is illustrated in Figure 1. SCCV comprises four major innovations: (1) flexible modular design for storage stations for scalability to meet

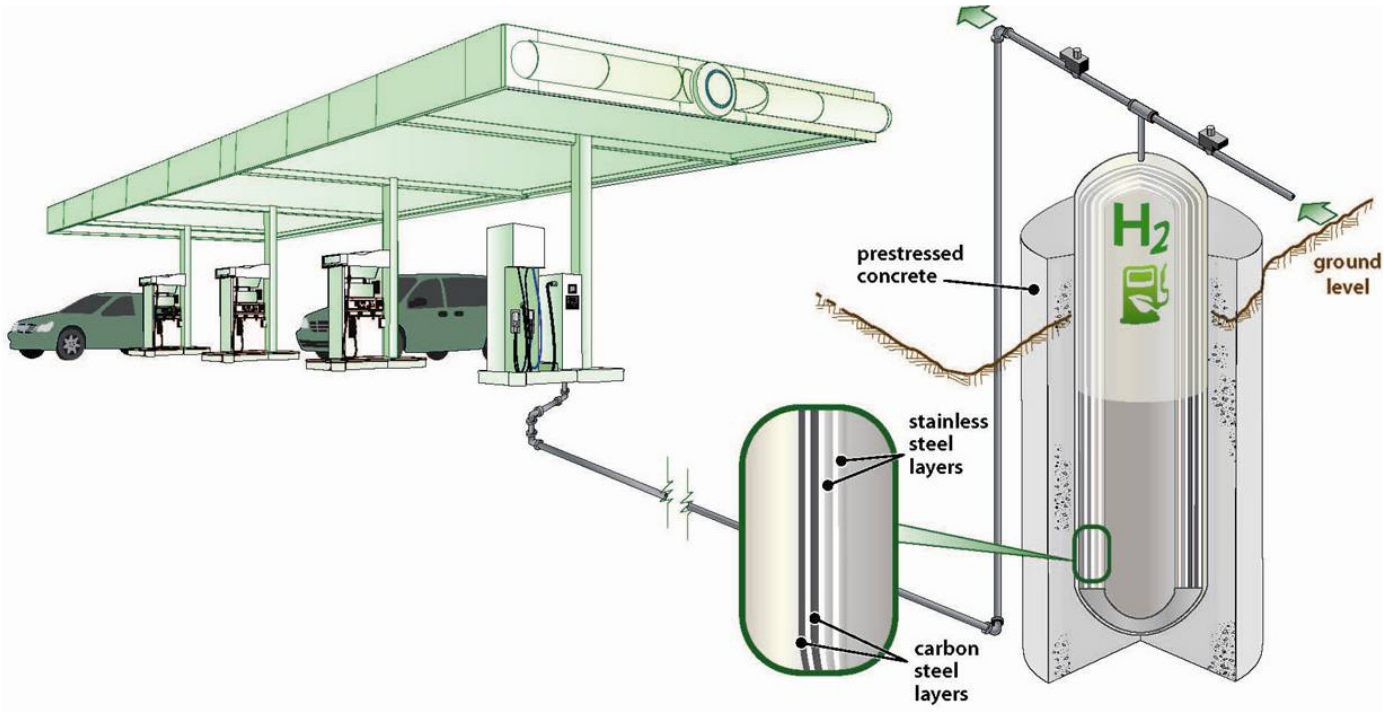

FIGURE 1. Schematic showing the design of a steel/concrete composite vessel comprising inner layered steel tanks and outer pre-stressed concrete confinement.

different storage pressure and capacity needs, flexibility for cost optimization, and system reliability and safety; (2) composite storage vessel design and construction with a inner steel vessel encased in a pre-stressed outer concrete reinforcement; (3) layered steel vessel wall and vent holes to solve the hydrogen embrittlement problem by design; and (4) integrated sensor system to monitor the structural integrity and operation status of the storage system. Together, these innovations form an integrated approach to make the SCCV cost competitive and inherently safe for stationary high-pressure hydrogen storage services. The inner steel vessel is a multi-layer design with strategically placed vent holes to prevent the intake and accumulation of hydrogen in the steel layers except the innermost layer. This effectively solves the hydrogen embrittlement problem by design and frees up the selection of steel for cost optimization. Furthermore, the novel steel/concrete composite vessel design allows for the stresses or the structural load from the high-pressure hydrogen to be shared between the inner steel vessel and the pre-stressed outer concrete reinforcement, thereby offering the flexibility to optimize the use of low-cost commodity materials (such as structural steels and concretes) and industry accepted fabrication technologies for cost reduction. For example, the layered steel vessel technology is proven and accepted in industry standards and codes (e.g., American Society of Mechanical Engineers [ASME] Boiler and Pressure Vessel Code). Moreover, the layered steel vessel is amiable to the advanced fabrication technology based on FSW for further reducing fabrication cost.

RESULTS

The major tasks in FY 2014 include (1) validate the SCCV design can reduce the cost of stationary hydrogen storage by more than 15% and meet the DOE 2015 cost target; (2) demonstrate ORNL-patented multi-pass, multi-layer (MM)-FSW for joining a multiple-layer ASME A516 Grade 70 steel to a total thickness of 1.5 inch; and (3) design and fabricate a ¼-size mock-up composite vessel capable of storing 90 kg gaseous hydrogen at 430 bar, while capturing all major features of SCCV design and fabricability with today's manufacturing technologies and code/standard requirements. The key results from this year's substantial development are as follows.

Validation on Cost Reduction of SCCV at 860 bar

The high-fidelity cost analysis tool developed in this project was used to optimize the design and engineering of the SCCV to achieve DOE's cost target. Since SCCVs can be fabricated with relatively mature technologies, it was possible to obtain cost figures for fabrication of SCCVs from commercial manufacturing vendors. A number of industry manufacturing vendors were surveyed, and a detailed cost breakdown of fabricating different parts of the SCCV structure was obtained under the assumption of moderate to high-volume production scenario. These cost figures were used as the basis for design and engineering optimization to meet the DOE cost target. A thorough study was performed to optimize the design and fabrication cost of SCCVs for hydrogen storage. The details of the cost analysis are summarized in an ORNL Technical Report [1].

The cost analysis results show that the 50/50 SCCV design is economically viable and technically feasible for storing compressed gaseous hydrogen. The design specifications were based on a 1,500 kg hydrogen station storage capacity design capable of refilling 250 to 300 cars per week, in moderate volume production (24 identical vessels per order). The unit cost breakdowns are listed in Table 1. As shown in this table, the steel vessel constitutes around 73% of the total SCCV cost. In other words, the pre-stressed concrete enclosure bears half of the total structural load at a cost that is only 37% of the steel vessel which bears the other half of the load. Hence, it is cost-effective to use the low-cost pre-stressed concrete enclosure to bear 50% of the structural load when compared to the current industry-standard steel-only pressure vessel.

In addition, further cost reduction can be achieved for the construction of the layered steel vessel. The detailed cost analysis shows that a major pathway for further reducing the total composite SCCV cost is the development of an advanced welding process to replace labor-intensive conventional arc welding of steel shells. ORNL has successfully developed a novel MM-FSW process (US Patent 7,762,447 B2) and high-strength steel plates fabricated by multi-pass FSW are demonstrated to show better or equivalent mechanical properties than the base metal. The highly automated FSW process is expected to significantly reduce labor costs while improving weld quality.

Table 1. Unit Cost Breakdowns for the 860-bar SCCV

Steel vessel (unit price $ per kg of stored hydrogen)	
Bill of materials	386
Labor (conventional arc welding)	251
Labor (FSW)	213
Consumables and others	33
Pre-stressed concrete enclosure (unit price $ per kg of stored hydrogen)	
Concrete	14
Rebar	4
Pre-stressing wire	269
Total SCCV unit cost ($ per kg of stored hydrogen)	
SCCV	957
SCCV with FSW	919

Note: The unit cost of SCCV utilizing FSW for layered steel shell manufacturing is projected by reducing the inner steel vessel manufacturing labor cost by 15%.

Figure 2 summarizes the projected total SCCV costs at 860-bar pressure from the detailed comparison of the

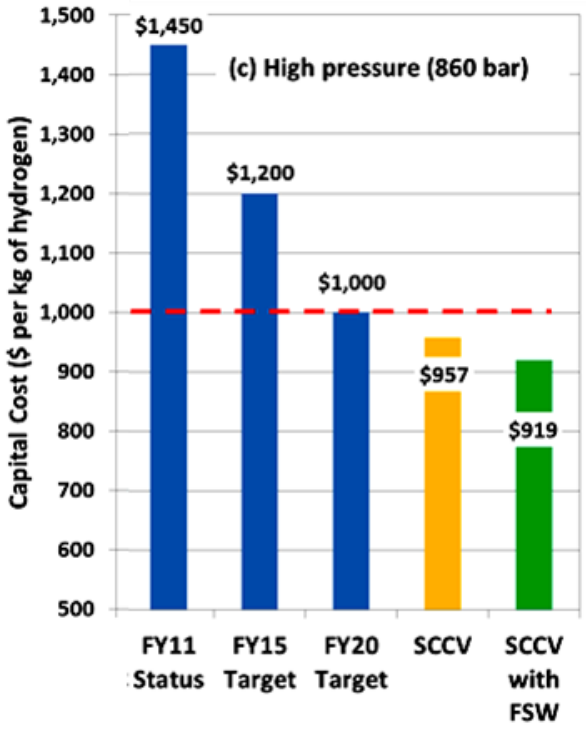

FIGURE 2. Comparison between SCCV unit costs and DOE technical targets for hydrogen pressures of 860 bar.

current cost status, DOE FY 2015 target, and DOE FY 2020 target. As shown in this figure, the projected cost of SCCV technology exceeds the DOE FY 2015 cost targets by about 20%, and potentially by 23% if FSW technology is commercialized and used. Furthermore, the SCCV technology exceeds the DOE FY 2020 cost targets by about 4%, and by 9% with the FSW technology.

Scale Up Demonstration of Friction Stir Welding Technology

In FY 2014, the feasibility of MM-FSW technique was successfully demonstrated on 15-mm thick three-layer pressure vessel steel (ASTM International technical specification 572 G50) plates and steel pipes [2]. This year, MM-FSW was further scaled up on 1.5-in (38.1-mm) thick, six-layer high-strength low-alloy steel (ASTM A516 Grade 70). The six-layer FSW was tested for transverse weld tensile and Charpy V-notch impact toughness as a function of temperature. Microstructure characterizations and digital image correlation technique were used during transverse weld tensile test to understand the local deformation and failure associated with the improvement in weld mechanical properties.

Consistent with our previous research on FSW of high-strength steels [2,3], the transverse weld tensile test revealed that the failure was in the base metal, far away from the FSW region (Figure 3), for defect-free welds produced

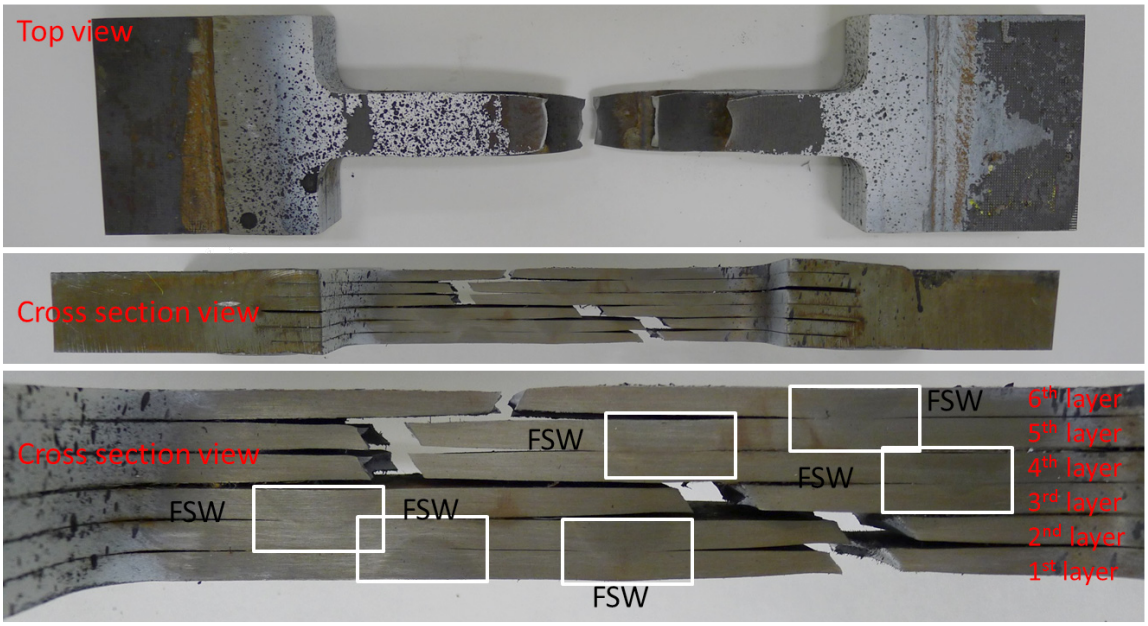

FIGURE 3. A six-layer MM-FSW sample after transverse tensile test. (a) top view image showing broken specimen. (b) Cross-sectional view of failed sample with each layer. Failure location for each layer was at the base metal. Note that a white box indicates friction stir weld (lightly etched with Nital solution) at each layer.

in this project (as determined by an X-ray non-destructive evaluation method). In addition, the Charpy V-notch impact toughness in both the stir zone and the heat affected zone of the friction stir welds are consistently higher than that of the base metal over the entire temperature range tested (-50 to 20°C).

Mock-Up SCCV Fabrication

A ¼-size mockup SCCV is under construction and expected to be completed in FY 2015 due to the relatively long leadtime (10 months) associated with the one-of-a-kind design. As shown in Figure 4, the mock-up vessel has all the essential features and functionality of the full-size SCCV. It contains the inner steel vessel and the outer pre-stressed concrete reinforcement containment. This mock-up vessel is designed to store 89 kg of hydrogen compressed to 430 bar (6,250 psi, or 43 MPa). The steel has a stainless steel inner layer as the hydrogen permeation barrier, hydrogen charging and discharging ports, and trunions for tank handling during the concrete construction and in-service installation. In addition, a manway on the top is added to the mock-up vessel, as it is an essential feature in the construction, inspection, and repair of the full-size steel vessel. The reinforcement skirt has a 6 inch thick concrete layer and five layers of pre-stressing wires.

The inner steel vessel will be built, inspected and hydro-tested in accordance to the ASME Boiler and Pressure Vessel Code Section VIII Division 2 (2013 Edition), and will be code stamped for high-pressure service, as expected for future commercial SCCV for high-pressure hydrogen storage. The pre-stressed concrete outer reinforcement is designed and constructed by ACI design allowables. The entire completed vessel will be hydro-static tested at 1.4 times the design pressure as part of code acceptance. A cyclic hydrogen

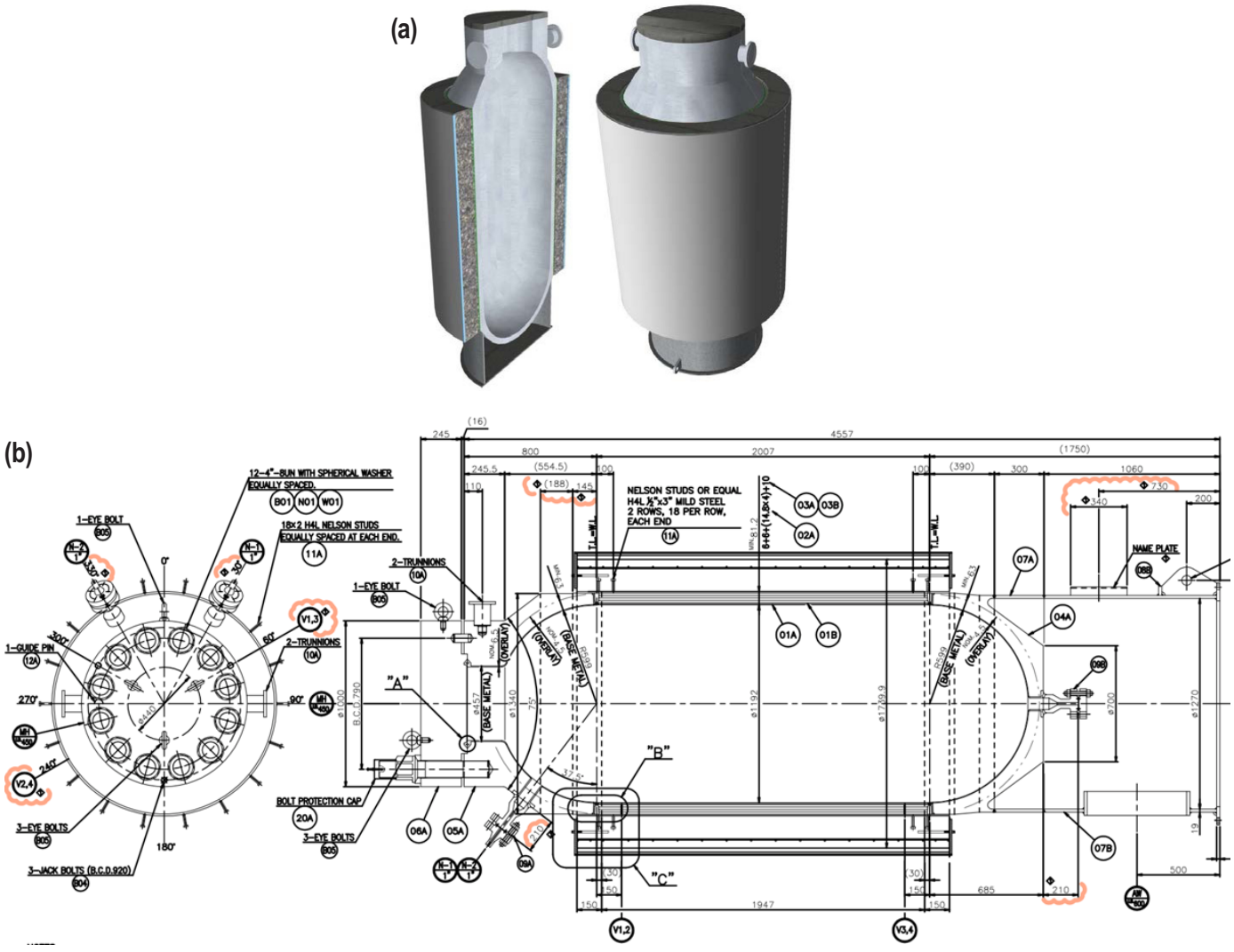

FIGURE 4. (a) Rendition of the mock-up design with all essential features of a SCCV for high-pressure hydrogen storage. (b) Detailed engineering drawing.

pressure loading test simulating hydrogen storage service conditions is planned to be completed.

CONCLUSIONS AND FUTURE DIRECTIONS

- The SCCV design was validated to reduce the cost of stationary hydrogen storage by more than 15% and meet the DOE 2015 cost target of $1,200/kg-stored at 860 bar. Further cost reduction concepts will be evaluated.
- The FSW scale-up process was demonstrated for a multiple layer high-strength steel with total thickness of 1.5 inch. This confirms the potential of using this technique as a future cost reduction element for hydrogen storage vessels.
- The fabrication of the ¼-sized mock-up SCCV capable of storing 90 kg gaseous hydrogen at 430 bar is ongoing.
- Testing of the mock-up SCCV under high-pressure hydrogen including long-term performance evaluation under cyclic hydrogen pressure loading is planned in FY 2015 to demonstrate both the constructability and performance of the SCCV for hydrogen storage.

FY 2014 PUBLICATIONS/PRESENTATIONS

1. Y.C. Lim, S. Sanderson, M. Mahoney, Y. Wang, and Z. Feng, "Mechanical properties and characterization of friction stir welded/root arc welded pipe steel," abstract accepted, 2014 MS&T conference.

2. Y. Wang, Y.C. Lim, F. Ren, W. Zhang, M. Jawad, F. Vossoughi and Z. Feng, 2014. "Steel-Concrete Composite Vessel for Stationary High-Pressure Hydrogen Storage," ASME 2014 12th Fuel Cell Science, Engineering & Technology Conference, Boston, MA, June 30 – July 2, 2014.

3. Y. Wang, Y.C. Lim, J-A Wang, L. Anovitz, W. Zhang, and Z. Feng, 2014. "Evaluation of Mechanical Property Testing Procedures and Techniques for Materials used for Hydrogen Storage and Distribution," ASME 2014 12th Fuel Cell Science, Engineering & Technology Conference, Boston, MA, June 30 – July 2, 2014.

4. Z. Feng, F. Ren, W. Zhang, Y. Wang, Y. C. Lim, and J. Wang, 2013 DOE Annual Merit Review, Fuel Cell Technologies Program, Washington, DC, June 2014.

5. Y.C. Lim, S. Sanderson, M. Mahoney, X. Yu, Y. Wang and Z. Feng, 2014. "Characterization of Multilayered Multipass Friction Stir Weld on ASTM A572 G50 Steel," Welding Journal, in press.

6. Y.C. Lim, S. Sanderson, M. Mahoney, Y. Wang and Z. Feng, 2014, "Friction Stir Welding High Strength Low Alloy Steel using a Multilayer Approach," 10th International Friction Stir Symposium, Beijing, China, May 20–23, 2014.

REFERENCES

1. W. Zhang, F. Ren, Z. Feng, and J. Wang, "Manufacturing Cost Analysis of Novel Steel/Concrete Composite Vessel for Stationary Storage of High-Pressure Hydrogen", Oak Ridge National Laboratory Report, ORNL/TM-2013/113, Oak Ridge National Laboratory, Oak Ridge, TN, Mar. 2013.

2. Y.C. Lim, S. Sanderson, M. Murray, X. Yu, D. Qiao, Y. Wang, W. Zhang, Z. Feng, "Characterization of Multilayered-Multipass Friction-Stir Weld on ASTM A572 G50 steel" in press, Welding Journal.

3. Feng, Z, Steel, RJ, Packer, SM, and David, SA. (2009), "Friction Stir Welding of API Grade 65 Steel Pipes," in Proceedings of the ASME Pressure Vessels and Piping Conference, Vol 6, pp. 775-779.

III.8 Preliminary Testing of LLNL/Linde 875-bar Liquid Hydrogen Pump

Salvador M. Aceves (Primary Contact), Gene Berry, Francisco Espinosa-Loza, Guillaume Petitpas, Vernon Switzer
Lawrence Livermore National Laboratory (LLNL)
7000 East Avenue, L-792
Livermore, CA 94551
Phone: (925) 422 0864
Email: saceves@llnl.gov

DOE Manager
Erika Sutherland
Phone: (202) 586-3152
Email: Erika.Sutherland@ee.doe.gov

Subcontractor
Linde LLC, Hayward, CA

Start Date: October 1, 2009
End Date: September 30, 2013

Overall Objectives

- Demonstrate rapid (100 kg H_2/hr) refueling of cryogenic vessels
- Refuel cryogenic vessels even when warm and/or pressurized
- Refuel at high density (up to 80 kg H_2/m^3)

Fiscal Year 2013 Objectives

Measure refuel performance of liquid hydrogen pump at 350 bar

Technical Barriers

This project addresses the following technical barrier from the Hydrogen Delivery section of the Fuel Cell Technologies Office Multi-Year Research, Development, and Demonstration Plan:

(C) Reliability and Cost of Liquid Hydrogen Pumping

TABLE 1. Progress toward Meeting DOE Hydrogen Delivery Technical Targets for Liquid Hydrogen Pumps

Liquid hydrogen pumps			
Characteristic	**Units**	**2015/2020 targets**	**LLNL 2014 status**
Uninstalled capital cost (870 bar, 100 kg/hr)	$	150,000/150,000	1,300,000

FY 2014 Accomplishments

Operated pump and conducted 350-bar refuel experiments:

- Verified 100 kg/hr hydrogen flow rate
- Measured <1.5 kWh/kg electricity consumption
- Refueling density of 70 g/L achieved at 340 bar, 62 K

INTRODUCTION

Unlike existing technologies (liquid and compressed hydrogen) that remain at nearly constant temperature during operation, cryogenic pressurized storage drifts in temperature and pressure depending on use patterns. Practical cryogenic pressurized storage demands rapid refueling under any initial operating condition, even as the vessel warms up and pressurizes due to long parking periods. Liquid hydrogen pumping promises to meet the challenge of practical cryogenic pressurized storage refueling.

APPROACH

LLNL is researching a liquid hydrogen (LH_2) pump for cryogenic pressure vessel refueling. Manufactured by Linde, a leading supplier of cryogenic equipment, this pump takes liquid hydrogen at low pressure (near atmospheric) and delivers it at high pressure (up to 875 bar), high flow rate (100 kg/hour), low temperature (30-60 K), high density (up to 80 g/L), and low evaporation at the pump (less than 3% of dispensed hydrogen). Evaporation at the pump does not result in hydrogen venting because evaporated hydrogen is recycled into the Dewar to maintain its pressurization. Pumped hydrogen can be directly dispensed into a cryogenic pressure vessel, even when warm and/or pressurized. As a part of this project, LLNL has installed a LH_2 pump and is planning to demonstrate its virtues for rapid and efficient cryogenic vessel refueling [1,2].

RESULTS

In FY 2013, LLNL and Linde installed an LH_2 pump at the Lawrence Livermore campus (Figure 1). FY 2013´s annual progress report [3] covers all phases of construction, installation, and commissioning. We now report preliminary results of pump operation conducted on an existing cryogenic pressure vessel with 151 liters of capacity and 350-bar rating.

Table 2 shows technical data for the first 11 refuel experiments conducted with the pump. These experiments

FIGURE 1. Liquid Hydrogen Pump Installed at the LLNL Campus

are preliminary because thermal insulation on the high-pressure delivery line was lacking, the pump was not fully instrumented, and the cryogenic vessel is only rated for 350 bar vs. the 875 bar pump rating.

From Table 2, we can observe the following results.

1. Refuel density is lower than expected. In a previous year [4], LLNL developed a thermodynamic fill model that was validated by comparison with experimental data collected by BMW on a similar liquid hydrogen pump manufactured by Linde and rated at 300 bar. Preliminary results with the LLNL pump show lower refuel density than predicted by the thermodynamic fill model (Figure 2). There may be several reasons for this: (1) the LLNL delivery line was uninsulated, resulting in considerable heating of the delivered hydrogen (estimated at 3 kW); (2) due to differences between U.S. and European standards, the LLNL pump is located relatively far from the Dewar (6 meters), potentially introducing losses in the liquid hydrogen transfer line between the Dewar and the pump; (3) higher pressure lines in LLNL's 875-bar pump demand foam insulated delivery lines vs. vacuum insulated lines in BMW's 300-bar pump. Further research in oncoming years should help in developing a better understanding of how pump conditions affect refuel density.
2. The pump succeeded in delivering the target flow rate of 100 kg per hour for most experiments, and is within the experimental margin of error for the others. This is a key result that minimizes refueling cost; rapid vehicle refueling enables amortization of liquid hydrogen pump cost over many refueled vehicles.
3. Electricity consumption is higher than expected (1.5 kWh/kg H_2 measured vs. 1 kWh/kg H_2 anticipated). New instrumentation and thermal insulation in the delivery line may bring experimental results closer to anticipated values.

CONCLUSIONS AND FUTURE DIRECTIONS

- Rapid refueling of cryogenic vessels is possible through pressurized LH_2 dispensing.
- LLNL installed a cryogenic high-pressure liquid hydrogen pump and Dewar and conducted preliminary refuel experiments to 350 bar.
- Experiments confirm the pump target refueling rate (100 kg H_2/hr). However, pump delivery density is lower than expected, and electricity consumption is higher than expected. Further experiments are necessary to fully understand these deviations.

TABLE 2. Summary of the first 11 experiments conducted with the liquid hydrogen pump with an uninsulated delivery line on a 350-bar, 151-liter cryogenic pressure vessel. Experiments marked in blue indicate starting conditions within the two-phase region.

Experiment	Initial T K	Initial Pressure bar	Initial density g/L	Final T K	Final pressure bar	Final density g/L	H_2 mass pumped kg	Refuel time minutes	Average flow rate kg/hr	Steady flow rate Kg/hr	Refuel energy kWh	Refuel energy kWh/kg
1	288	18.93	1.58	219	166.5	16.4	2.24	5	26.8		6	2.62
2	204	85.1	9.52	153	330	38.6	4.39	6.5	40.5	103	7	1.58
3	95	1.25	0.32	87	333	58.5	8.78	6.5	81.1	108	11	1.22
4	21	1.25	5	74	340	64.7	9.0	7	77.3	94.2	13	1.45
5	21	1.25	12.5	67	338	67.9	8.4	6.25	80.3	94.8	12	1.48
6	63.2	51.3	22.4	84.6	338	59.9	5.67	4.38	77.6	97.2	8	1.43
7	21	1.25	4.13	71.4	338	65.8	9.31	6.46	86.5	110	13	1.39
8	21	1.25	11.4	67.1	338	67.8	8.52	5.8	88.1	111	11	1.29
9	21	1.25	18	64	338	69.3	7.75	5.6	83	106	10	1.28
10	21	1.25	22	61.9	339	70.4	7.31	5.26	83.4	106	10	1.37
11	21	1.25	22	61.9	339	70.4	7.31	5.13	85.5	108	10	1.37

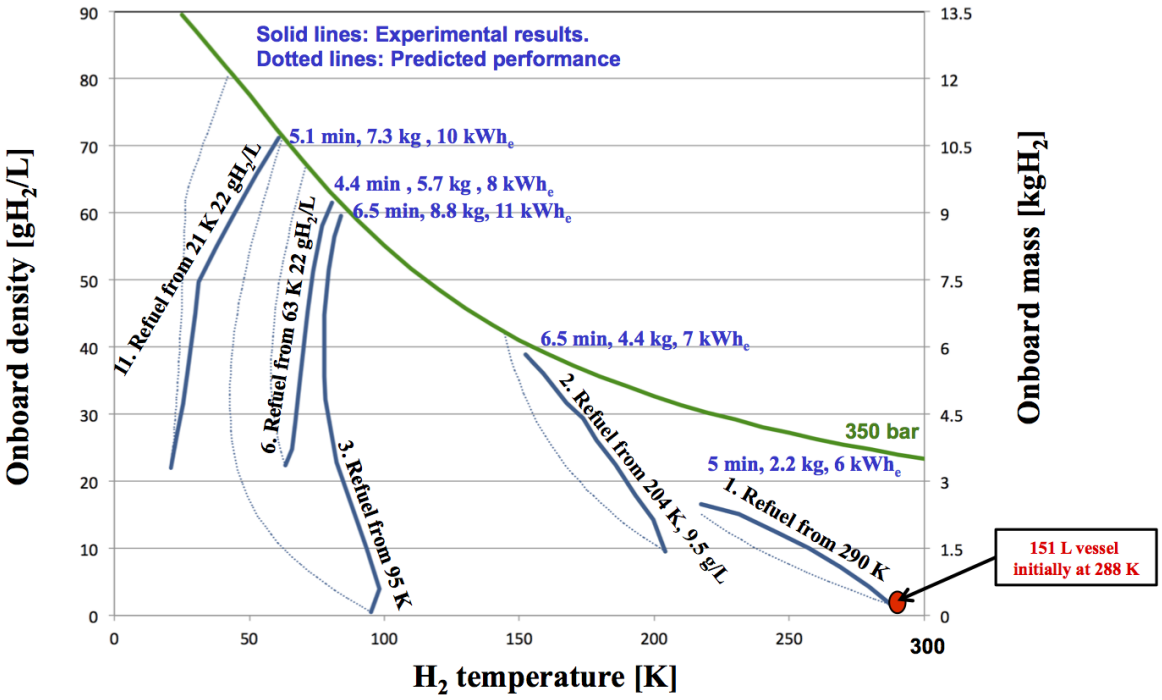

FIGURE 2. Onboard density vs. temperature during five refuel experiments (1, 2, 3, 6 and 11) listed in Table 2. The figure shows experimental (blue solid lines) as well as numerical (dotted lines) results for the five refuel experiments. Numerical results were obtained with a thermodynamic fill model validated by comparison with experimental data provided by BMW for a similar pump rated at 300 bar. The figure also shows a green line with density vs. temperature for 350-bar storage.

- Pump characterization to full pressure range (875 bar) will demand construction of a stronger experimental pressure vessel. This is planned for FY 2014.

FY 2014 PUBLICATIONS/PRESENTATIONS

1. Compact Hydrogen Storage in Cryogenic Pressure Vessels, Salvador M. Aceves, Francisco Espinosa-Loza, Elias Ledesma-Orozco, Guillaume Petitpas, in Handbook of Hydrogen Energy, Edited by S.A. Sherif, E.K. Stefanakos, and D.Y. Goswami, CRC Press, Taylor & Francis, ISBN-13: 978-1420054477, 2013.

2. Hydrogen Storage in Pressure Vessels: Liquid, Cryogenic, and Compressed Gas, Guillaume Petitpas and Salvador Aceves, in Hydrogen Storage Technology: Materials and Applications, Edited by Leonard E. Klebanoff, CRC Press, Taylor & Francis, Chapter 4, pp. 91-107, 2013.

3. Cold Hydrogen Delivery in Glass Fiber Composite Pressure Vessels: Analysis, Manufacture, and Testing, Andrew H. Weisberg, Salvador M. Aceves, Francisco Espinosa-Loza, Elias Ledesma-Orozco, Blake Myers, Brian Spencer, International Journal of Hydrogen Energy, Vol. 38, pp. 9271-9284, 2013.

4. Modeling of sudden hydrogen expansion from cryogenic pressure vessel failure, Petitpas, G. and Aceves, S.M., International Journal of Hydrogen Energy, Vol. 38, pp. 8190-8198, 2013**.**

5. Web-Based Resources Enhance Hydrogen Safety Knowledge, Weiner, S.C., Fassbender, L.L., Blake, C., Aceves, S.M., Somerday, B.P., and Ruiz, A., International Journal of Hydrogen Energy, Vol. 38, pp. 7583-7593, 2013.

6. Safe, long range, inexpensive and rapidly refuelable hydrogen vehicles with cryogenic pressure vessels, SM Aceves, G Petitpas, F Espinosa-Loza, MJ Matthews, E Ledesma-Orozco, International Journal of Hydrogen Energy, Vol. 38, pp. 2480-2489, 2013.

7. A Comparative Analysis of the Cryo-Compression and Cryo-Adsorption Hydrogen Storage Methods, G. Petitpas, P. Benard, L.E. Klebanoff, J. Xiao, S. Aceves, International Journal of Hydrogen Energy, 2014.

8. Para-H2 to ortho-H2 conversion in a full-scale automotive cryogenic pressurized hydrogen storage up to 345 bar, Guillaume Petitpas, Salvador M. Aceves, Manyalibo J. Matthews, James R. Smith, International Journal of Hydrogen Energy, Vol. 39, pp. 6533-6547, 2014.

REFERENCES

1. Aceves, S.M., Espinosa-Loza, F., Ledesma-Orozco, E., Ross, T.O., Weisberg, A.H., Brunner, T.C., Kircher, O., "High-density automotive hydrogen storage with cryogenic capable pressure vessels," International Journal of Hydrogen Energy, Vol. 35, pp. 1219-1226, 2010.

2. Ahluwalia, R.K. Hua, T.Q. Peng, J.-K. Lasher. S, McKenney. K. Sinha, J., Gardiner. M. "Technical assessment of cryo-compressed hydrogen storage tank systems for automotive applications," International journal of hydrogen energy, Vol. 35, pp. 4171–4184, 2010.

3. Aceves, S.M., Berry, G., Espinosa-Loza, F., Petitpas, G., Switzer, V. "Rapid High Pressure Liquid Hydrogen Refueling for Maximum Range and Dormancy," FY 2013 Annual Progress Report, DOE Hydrogen Program, Washington, DC, 2013.

4. Aceves, S.M., Berry, G., Espinosa-Loza, F., Petitpas, G., Switzer, V. Tuholski, S., "LLNL/Linde 875 bar Liquid Hydrogen Pump for High Density Cryogenic Vessel Refueling," FY 2012 Annual Progress Report, DOE Hydrogen Program, Washington, DC, 2012.

III.9 Development of a Centrifugal Hydrogen Pipeline Gas Compressor

Francis A. Di Bella, P.E.
Concepts ETI, Inc., d.b.a. Concepts NREC
285 Billerica Road, Suite 102
Chelmsford, MA 01824-4174
Phone: (781) 937-4718
Email: fdibella@conceptsnrec.com

DOE Managers
Erika Sutherland
Phone: (202) 586-3152
Email: Erika.Sutherland@ee.doe.gov
Katie Randolph
Phone: (720) 356-1759
Email: Katie.Randolph@ee.doe.gov

Contract Number: DE-FG36-08GO18059

Subcontractors
- Texas A&M University, College Station, TX
- HyGen Industries, Eureka, CA

Project Start Date: June 1, 2008
Project End Date: December, 2014

Overall Project Objectives

- Develop and demonstrate an advanced centrifugal compressor system for high-pressure hydrogen pipeline transport to support DOE's hydrogen infrastructure targets. The technical targets of the compressor are:
  1. Delivery of 100,000 to 1,000,000 kg/day of 99.99% hydrogen gas.
  2. Compression from 350 psig to 1,000 psig or greater.
  3. Initial installed system equipment cost of less than $9M (compressor package of $5.4M) for 240,000 kg/day system.
- Reduce package footprint and improve packaging design.
- Reduce maintenance cost to below 3% of total capital investment. Increase system reliability to avoid purchasing redundant systems.

Fiscal Year (FY) 2014 Objectives

- Procure custom gearbox
- Assemble single-stage prototype components
- Prepare test plan for prototype testing
- Coordinate the use of the prototype as a testing platform in a national lab doing research with hydrogen

Technical Barriers

This project addresses the following technical barriers from the Delivery section (3) of the Fuel Cell Technologies Office Multi-Year Research, Development, and Demonstration Plan [1]:

(B) Reliability and Costs of Hydrogen Compression

Technical Targets

The project has met the following DOE targets as presented the Fuel Cell Technologies Office Multi-Year Research, Development, and Demonstration Plan [1] (see Table 1).

The original DOE proposal requirements were satisfied with the detailed design of a pipeline hydrogen compressor that utilizes all state-of-the-art and commercially available

TABLE 1. Progress towards Meeting Technical Targets for Delivery of Hydrogen via Centrifugal Pipeline Compression

Progress Towards Meeting Technical Targets for Delivery of Hydrogen via Centrifugal Pipeline Compression				
{Note: Letters correspond to DOE's 2007 Technical Plan-Delivery Sec. 3.2-page 16}				
Characteristic	**Units**	**DOE Target**	**Project Accomplishment**	**STATUS**
Hydrogen Efficiency (f)	[btu/btu]	98%	98%	Objective Met
Hydrogen Capacity (g)	kg/day	100,000 to 1,000,000	240,000	Objective Met
Hydrogen Leakage (d)	%	< .5	0.2 (per Flowserve Shaft Seal Spec)	Objective Met
Hydrogen Purity (h)	%	99.99	99.99 (per Flowserve Shaft Seal Spec)	Objective Met
Discharge Pressure (g)	psig	>1000	1285	Objective Met
Comp. Package Cost (g)	$M	6.0 +/- 1	4.5 +/- 0.75	Objective Met
Main. Cost (Table 3.2.2)	$/kWhr	0.007	0.005 (per *CN* Analysis Model)	Objective Met
Package Size (g)	sq. ft.	350 (per HyGen Study)	260 (per *CN* Design)	Objective Met
Reliability (e)	# Sys.s Req.d	Eliminate redundent system	Modular sys.s with 240K kg/day with no redundency req.d	Objective Met

components, including: high-speed centrifugal compressor, gearbox, intercooler, tilt-pad bearings, and oil-free dry gas shaft seal and controls.

Accomplishments for Phases I and II (completed from 2008 to 2011) and Phase III (in progress)

Developed computer models to aid in analysis of hydrogen compressor:

- System Cost and Performance Model
  - Identifies hydrogen compressor package performance and component cost with respect to a variety of compressor-gearbox configurations
- System Reliability and Maintenance Cost Model
  - Estimates comparative reliabilities for piston and centrifugal compressors for pipeline compressors developed
    - Failure mode and effects analysis for component risk and reliability assessment
  - Estimates operation and maintenance costs for compressor system
    - Uses Federal Energy Regulatory Commission operation and maintenance database as the basis for determining the maintenance costs for a centrifugal compressor
- Anti-surge algorithm developed to assist in controls analysis and component selection of preliminary design (completed) and detailed design of pipeline compressor module (in progress), including:
  - Compressor design conditions confirmed by project collaborators
    - P_{inlet} = 350 psig, P_{outlet} = 1,285 psig; flow rate = 240,000 kg/day
    - A six-stage, 60,000 revolutions per minute, 3.6 (max) pressure ratio compressor with a mechanical assembly of integrally geared, overhung compressor impellers
    - Stress analysis completed
    - Volute (compressor housing) design completed for two-stage prototype
    - Rotordynamics completed to verify shaft-seal-bearing integrity at operating speeds
- Completed critical component development (compressor rotor, shaft seal, bearings, gearing, safety systems) and specifications for near-term manufacturing availability
- Completed detailed design and cost analysis of a complete pipeline compressor and a laboratory-scale prototype for future performance lab verification testing
- Procured all remaining system components for one-stage prototype compressor including the longest lead item: the single-speed step gearbox
- Completed the pre-assembly of the hydrogen compressor to determine interferences

INTRODUCTION

The DOE has prepared a Multi-Year Research, Development, and Demonstration Plan to provide hydrogen as a viable fuel for transportation after 2020, in order to reduce the consumption of limited fossil fuels in the transportation industry. Hydrogen fuel can be derived from a variety of renewable energy sources and has a very high BTU energy content per kg, equivalent to the BTU content in a gallon of gasoline. The switch to hydrogen-based fuel requires the development of an infrastructure to produce, deliver, store, and refuel vehicles. This technology development is the responsibility of the Production and Delivery Programs within the DOE. The least expensive delivery option for hydrogen to refueling stations in a mature market would be via pipelines. Pipelines use compressor stations to maintain the flow of gas. Compressors account for a significant portion of the delivery cost, and the DOE has therefore set a goal that compression (capital, installation, and operation) accounts for <$2/gasoline gallon equivalent by 2020.

The delivery cost target can be met if the compressor system can be made more reliable (to reduce maintenance costs), more efficient (to reduce operation costs), and be a smaller, more complete modular package (to reduce the compressor system equipment, shipment, and its installation costs). To meet these goals, the DOE has commissioned Concepts NREC with the project entitled: The Development of a Centrifugal Hydrogen Pipeline Gas Compressor.

APPROACH

A three-phase approach has been programmed to implement the technical solutions required to complete a viable hydrogen compressor for pipeline delivery of hydrogen. The three phases include: Phase I - Preliminary Design, Phase II - Detailed Design of Both a Full-scale and Prototype Hydrogen Compressor, and Phase III - The Assembly and Testing of the Prototype Compressor.

The technical approach used by Concepts NREC to accomplish these goals is to utilize state-of-the-art aerodynamic/structural analyses to develop a high-performance centrifugal compressor system for pipeline service. The centrifugal-type compressor is able to provide high pressure ratios under acceptable material stresses for relatively high capacities—flow rates that are higher than

what a piston compressor can provide. Concepts NREC's technical approach also includes the decision to utilize commercially available, and thus, proven bearings, shaft seal technology, and high-speed gearing to reduce developmental risk and increase system reliability at a competitive cost.

The engineering challenge to implement this technical approach is to design a compressor stage that maximizes pressure ratio and thermodynamic efficiency per stage, and minimizes the number of stages and the impeller diameter. The largest constraint to the design is the stress capability of the impeller material. This constraint is further aggravated by the need for the material selection to account for the effects of hydrogen embrittlement. The selection of a rotor material that can enable the high tip speeds to be achieved while avoiding damage from hydrogen embrittlement was determined to be the major technical challenge for the project.

Concepts NREC has met all of these engineering challenges in order to provide a pipeline compressor system that meets DOE's specifications for near-term deployment.

The project team includes researchers at Texas A&M, led by Dr. Hong Liang, who are collaborating with Concepts NREC to confirm the viability of aluminum alloys for this compressor application. Also providing unfunded assistance were several national labs, including: Sandia National Laboratories (fracture mechanics testing; Chris San Marchi), Savannah River National Laboratory (specimen "charging" with hydrogen plus tensile testing with hydrogen; Andrew Duncan and Thad Adams), and Argonne National Laboratory (George Fenske).

RESULTS

The engineering analysis has resulted in the design of the pipeline compressor package shown in Figure 1. The complete modular compressor package is 29 ft long x 10 ft tall x 6 ft wide at the base x 8 ft wide at the control panel, which is approximately one-half of the footprint of a piston-type, hydrogen compressor.

The compressor selection uses six stages, each operating at 60,000 rpm, with an impeller tip speed of less than 2,100 ft/s. Each compressor rotor and drive shaft is 8 inches in diameter and has an overall stage efficiency of between 79.5 and 80.5%, for an overall compressor efficiency of 80.3%. The first and last stages have a slightly different length, which helps to improve the rotordynamics for the last stages. Each compressor impeller is a single overhung

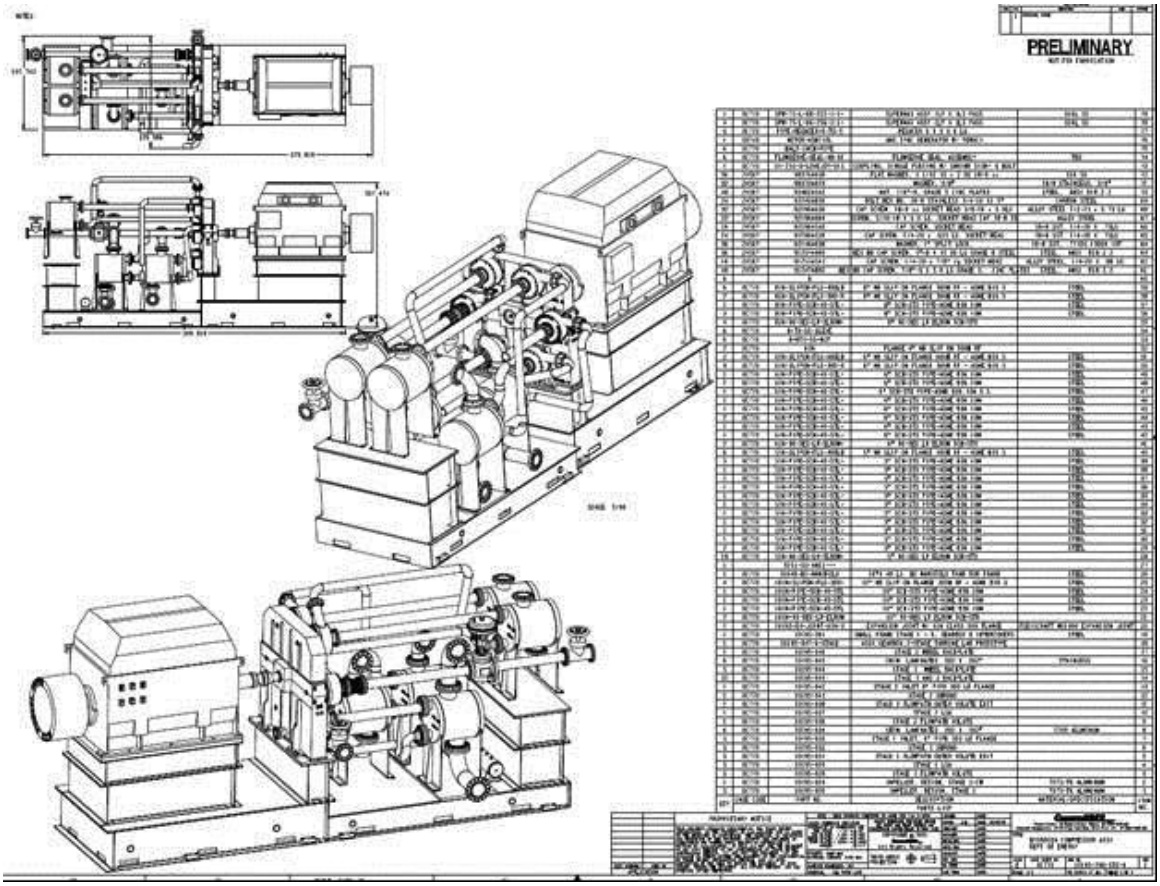

FIGURE 1. Pipeline Hydrogen Centrifugal Compressor: 240,000 kg/day; 350 to 1,285 psig

(cantilevered) impeller attached to a drive shaft that includes a shaft seal, bearing, and drive pinion (Figure 2) integrated with the gearbox drive. The impeller rotor is designed without a bored hub, in order to reduce the hub "hoop" stresses. This requires the impeller to be mechanically attached to the high-strength steel alloy, a drive shaft with a patented design attachment system that enables the rotor to be removed from the gearbox without removing the drive shaft, so it does not disturb the shaft seal and bearings. A gas face seal will provide the isolation of the hydrogen from the lubricating oil. The 1,400 hp per stage can be sustained by using two tilting pad hydrodynamic bearings on either side of a 2.5-inch-long drive-pinion gear. The face seal and bearings are commercially available from Flowserve and KMC, respectively. The pinion and bull gear is part of a custom gearbox manufactured by Artec Machine Systems representing NOVAGEAR (Zurich, Switzerland) and utilizes commercially available gear materials that are subjected to stresses and pitch line speeds that meet acceptable engineering practice.

The material chosen for the compressor rotor and volute is an aluminum alloy: 7075-T6 alloy. The choice is based on its mechanical strength-to-density ratio or (S_{yield}/ρ), which can be shown to be a characteristic of the material's ability to withstand centrifugal forces. This aluminum alloy has a strength-to-density ratio that is similar to titanium and high-strength steels at the 140°F (max) operating temperatures that will be experienced by the hydrogen compressor. However, unlike titanium and most steels, aluminum is recognized by the industry as being very compatible with hydrogen.

Aluminum also helps to reduce the weight of the rotor, which leads to an improved rotordynamic stability at the 60,000 rpm operating speed. A rotor stability and critical speed analysis has confirmed that the overhung design is viable. The first stage compressor rotor has been manufactured and successfully spun to 110% of its 60,000 rpm operating speed. A subsequent fluorescent penetrant inspection and strain measurements of the rotor after the spin test indicated no creep or micro-crack design flaws as a result of the test.

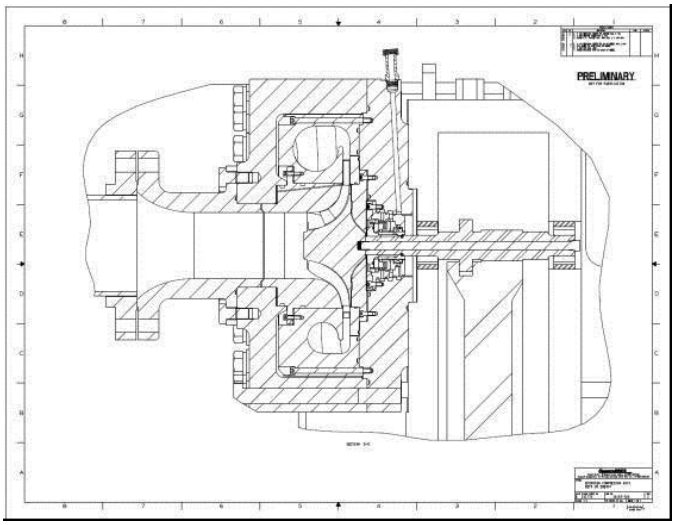

FIGURE 2. Mechanical Detailed Assembly of One-Stage, Prototype Compressor

The one-stage prototype compressor has been chosen for laboratory testing in Phase III of the project. The laboratory prototype is shown in Figure 3. The compressor components are being manufactured, and the balance of the system components are being purchased. The system will be assembled and tested in the fall of 2014.

CONCLUSIONS AND FUTURE DIRECTIONS

The advanced, six-stage, intercooled, centrifugal compressor-based system can provide 240,000 kg/day of hydrogen from 350 to 1,285 psig high (6,300 kWe) for pipeline-grade service. The original DOE proposal requirements were satisfied with the detailed design of a pipeline hydrogen compressor that utilizes all state-of-the-art and commercially available components, including: high-speed centrifugal compressor, gearbox, intercooler, tilt-pad bearings, oil-free dry gas shaft seal and controls. As a result of the sponsored research and development, a pipeline-capacity, hydrogen centrifugal compressor can be made available now to meet the hydrogen infrastructure needs of the future!

OBJECTIVES FOR THIS YEAR

Phase III System Component Procurement, Construction, and Validation Testing

Continue component procurement for the one-stage prototype hydrogen compressor system

- Complete assembly of the one-stage centrifugal compressor system (Figure 4)
- Conduct mechanical shakedown and aerodynamic testing and assessment of mechanical integrity of the compressor system
- Prepare a plan for field evaluation of the prototype compressor, including deployment in a national laboratory or a university research laboratory

REFERENCES

1. DOE Multi-Year Research, Development, and Demonstration Plan.

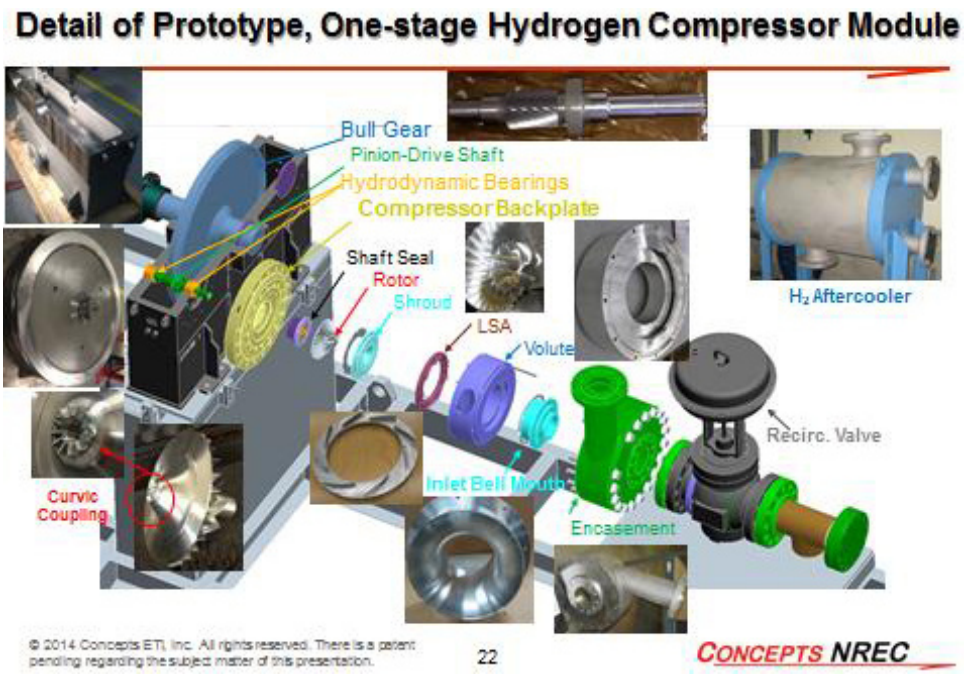

FIGURE 3. Detailed Specification for the One-Stage Prototype Compressor

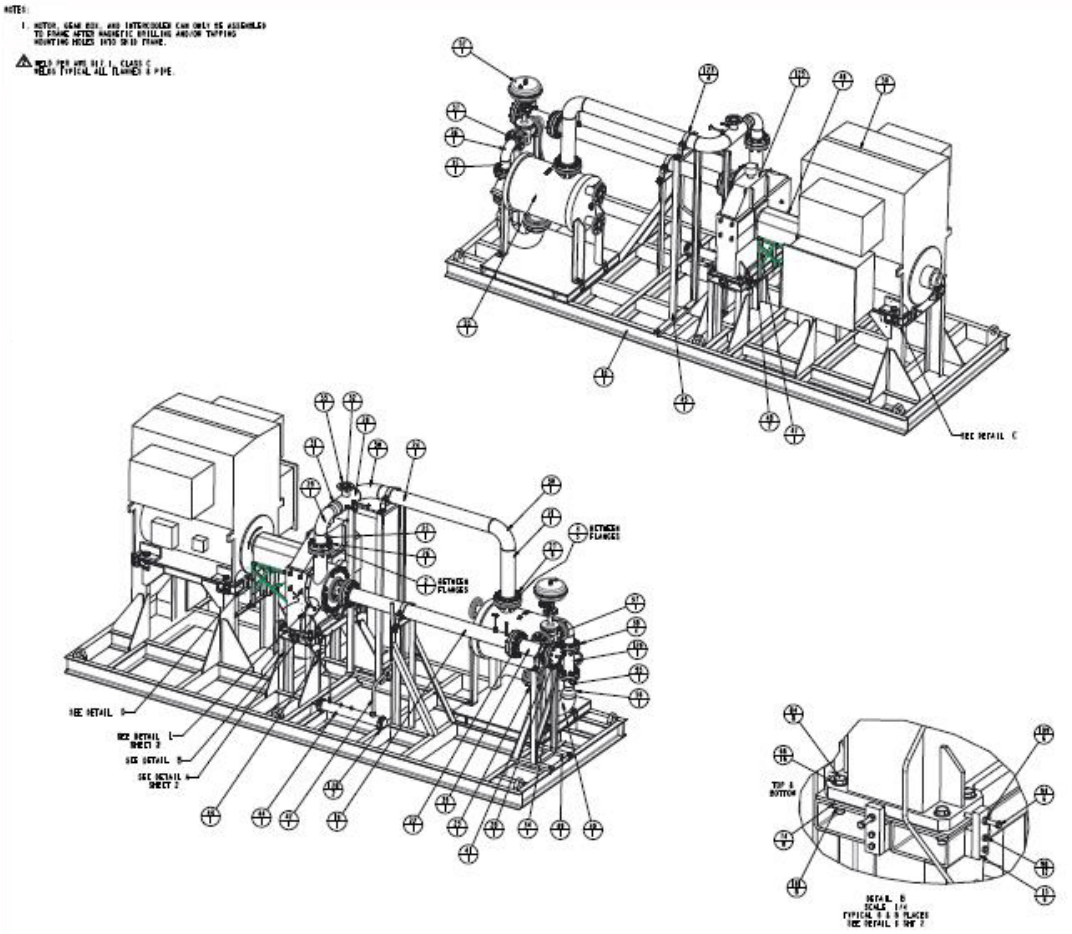

FIGURE 4. Detail of Prototype, One-Stage Hydrogen Compressor Module

III.10 Investigation of H_2 Diaphragm Compressors to Enable Low-Cost Long-Life Operation

Aashish Rohatgi (Primary Contact), Ken Johnson, Naveen Karri, Ayoub Soulami
Pacific Northwest National Laboratory (PNNL)
902 Battelle Blvd.
Richland, WA 99352
Phone: (509) 372-6047
Email: aashish.rohatgi@pnnl.gov

DOE Managers
Erika Sutherland
Phone: (202) 586-3152
Email: Erika.Sutherland@ee.doe.gov
Katie Randolph
Phone: (720) 356-1759
Email: Katie.Randolph@ee.doe.gov

Project Start Date: June 1, 2013
Project End Date: December 31, 2013

Overall Objectives

Reduce compressor operation and maintenance cost by reducing instances of diaphragm failure and the resulting need for repair of hydrogen gas compressors

Fiscal Year (FY) 2013 Objectives

- Identify the causes for the reduced lifetime of the diaphragm compressors operated under start-stop mode
- Develop material and compressor design solutions to enhance the lifetime of diaphragm compressors

Technical Barriers

This project addresses the barrier "B" from the Hydrogen Delivery section from the Fuel Cell Technologies Office Multi-Year Research, Development, and Demonstration Plan:

(B) Reliability and Costs of Gaseous Hydrogen Compression

Technical Targets

This project conducted research to decrease compressor operations and maintenance costs by improving the reliability of hydrogen compressors. Understanding gained from this work will be applied to future compressors to enable them to meet DOE 2015 compressor targets:

- 2.5% of installed capital cost for maintenance
- Improved reliability and life

Accomplishments

This project was developed in conjunction with PDC Machines, Inc., a commercial supplier of diaphragm hydrogen compressors. The project accomplishments are:

- Contamination/debris in the H_2 gas and improper priming procedures when restarting a compressor after stopping have been identified as two important factors that adversely affect the life of the diaphragm.
- A finite element model (FEM) of the diaphragm was developed to predict the location on the diaphragm where the maximum stress and maximum contact sliding occur relative to the compressor process head. Both the maximum stress and maximum contact sliding occur where failures are typically observed in PDC's compressor diaphragms.
- A second FEM was developed to estimate the contact and residual stresses that could occur if debris is trapped against the head profile during the compression stroke. The results showed that the operating pressure is high enough to cause local plastic deformation around trapped hard particles leaving residual stresses that could reduce the fatigue life of the diaphragm.
- The location and orientation of the primary crack in a failed diaphragm, taken out of service, indicated the importance of radial stresses in the diaphragm failure. Significant plastic deformation could be seen in the primary crack region while numerous stringers, oriented in the sheet rolling direction, were also observed in the sheet cross section.

INTRODUCTION

The goal of this project is to reduce the instances of diaphragm failures and the resulting need for repair of hydrogen gas compressors. Achieving this goal will help enable economical operation of hydrogen vending stations in support of DOE's goal of developing a hydrogen distribution network. The short life of compressor diaphragms subjected to intermittent operation is a key hurdle in developing an economical hydrogen distribution network. This hurdle exists because the repair costs and the down time associated with repeated compressor breakdown may substantially increase the costs for fueling stations for hydrogen fuel cell vehicles. Consequently, there is a need to enhance the life of hydrogen compressors to successfully establish a wide-spread hydrogen distribution network via the existing gas stations and new

hydrogen stations. For this project, PNNL has partnered with PDC Machines, Inc., a leader in hydrogen compressor technology, to develop materials and engineering solutions to the problem of repeated breakdown of hydrogen compressors. The team investigated the diaphragm failures through finite element modeling of the diaphragm, and through materials characterization of commercially manufactured diaphragms.

APPROACH

Material characterization and engineering stress analysis were performed to study why diaphragm compressors require more frequent maintenance when they are operated intermittently than when they are operated continuously. PNNL worked with PDC Machines, Inc. to analyze the design and operating performance of one of PDC's commercially available diaphragm compressors. FEMs (using ANSYS software) were developed to understand the diaphragm deformation and stresses as it bears against the compressor cavity during the compression stroke. A second model was developed to predict the contact stresses and plastic damage that may occur if contaminant particles were trapped and compressed between the diaphragm and the compressor head. A scoping study was also initiated to develop a combined Eulerian-Lagrangian model of the dynamic oil flow and local pressure distribution and deformation of the diaphragm.

The materials characterization effort comprised analysis of commercial diaphragm materials provided by PDC Machines. A failed diaphragm taken out of service was examined using optical and electron microscopy. The location and orientation of the crack was examined and related to the stress distribution predicted by finite element analysis. The microstructure of the diaphragm materials was analyzed using optical microscopy and the electron backscatter diffraction technique. Finally, the crack and adjoining microscale features were analyzed using scanning electron microscopy (SEM).

RESULTS

Figure 1 shows a used PDC diaphragm that was removed from service due to cracking. The diaphragm shows a ring of black deposit, possibly generated from impurities in the H_2 gas, which is suspected to be one cause of reduced diaphragm life. The finite element analysis (Figure 2) showed that both the maximum sliding displacement and the maximum radial stresses occur in the same location where diaphragm cracking is typically observed. This is close to the ring of black deposit in Figure 1, which could potentially be a site for fretting damage and subsequent failure, especially in the presence of any debris. Finite element analysis showed that the operating pressure is high enough that contact stresses from debris compressed against the diaphragm could cause plastic surface damage with accompanied high residual stresses that could lead to surface wear and reduced fatigue life.

FIGURE 1. Picture of a PDC diaphragm taken out of service, showing the ring of black deposit suspected to be a cause of reduced diaphragm life. The location of the crack, where the diaphragm leaked, is circled with a black marker.

Examination of the failed diaphragm showed that the primary crack was approximately perpendicular to the radial direction, suggesting that mode I fracture under high radial stresses was the likely cause of diaphragm failure. Multiple microcracks were also observed adjacent to the primary crack and were found to be oriented perpendicular to the sheet rolling direction. At places, the surface of the diaphragm appeared to stretch across the primary crack, suggesting significant plastic deformation associated with the failure (e.g. see Figure 3). Microstructural analysis in the sheet through-thickness direction showed numerous oriented stringers (see Figure 4) that were formed during the sheet's prior thermo-mechanical treatment. Such 2nd phase particles can have an adverse effect on the diaphragm's fatigue life.

CONCLUSIONS AND FUTURE DIRECTIONS

This project has enabled PNNL to begin developing a fundamental understanding of design, materials and operational issues that affect the diaphragm life. The FEM approach was successful, to a first approximation, in predicting potential failure locations that matched closely with the observed failure location. The FEM results also emphasize the importance of diaphragm sizing, the inner contour of the compressor head and debris on the stress distribution in the diaphragm and the potential for failure. Microstructural analysis of the diaphragm provided insights into how failure was affected by the stress distribution and

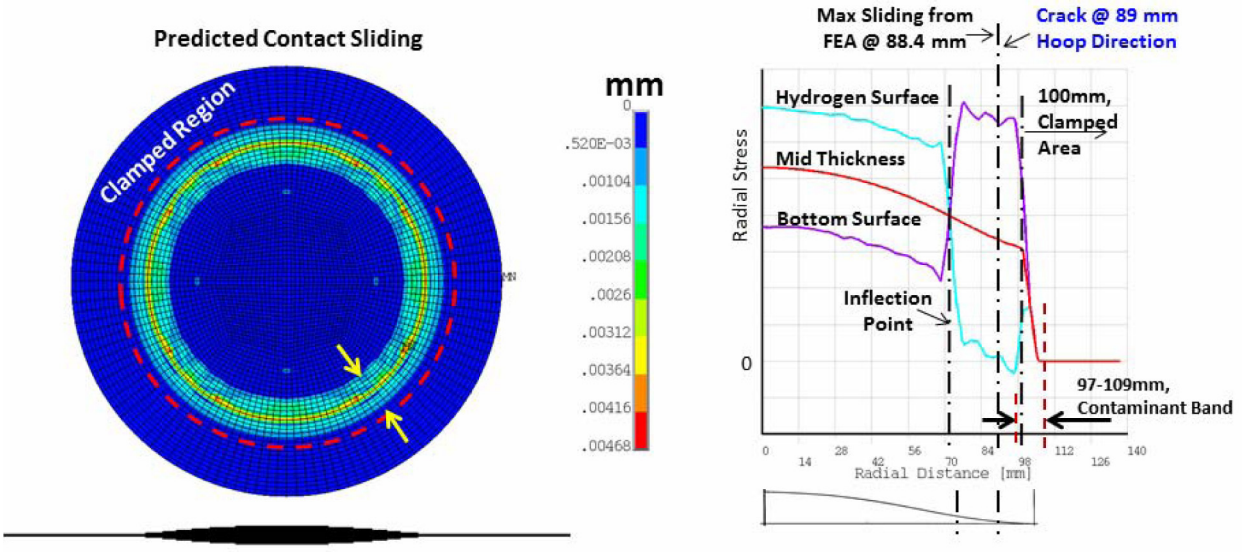

FIGURE 2. Left: The yellow contour band indicates the radial location of maximum sliding, which coincides with the ring of black deposit in Figure 1. Right: Maximum stress also coincides with maximum sliding and location of fracture in the diaphragm (stress magnitudes are PDC proprietary).

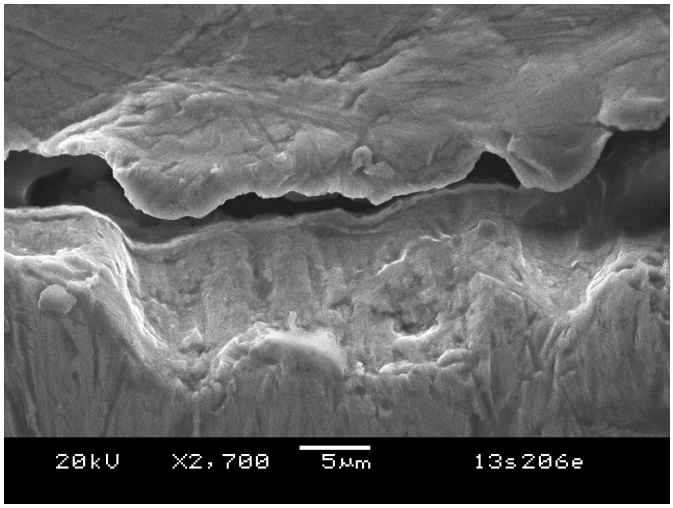

FIGURE 3. A SEM image of a portion of the crack (from diaphragm shown in Figure 1) showing plastic deformation in the diaphragm associated with the crack.

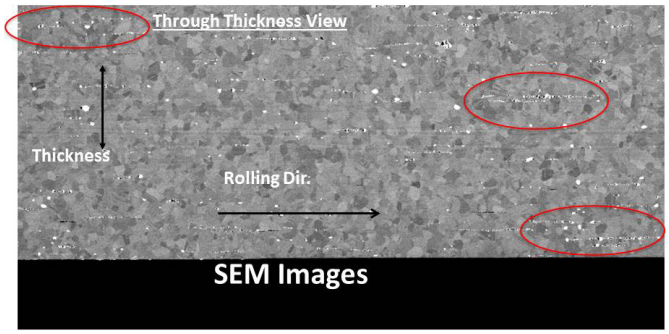

FIGURE 4. A through thickness back-scatter electron image of a diaphragm showing numerous stringer particles (bright features enclosed within the ellipses) that are aligned along the sheet rolling direction. (Grain size is PDC proprietary.)

potentially deleterious features in the microstructure and surface texture.

We anticipate that this partnership and information and knowledge exchange between the industry and a national laboratory will be critical in helping DOE achieve its targets for improving compressor reliability, increase diaphragm life and reduced maintenance costs. The following are three potential areas for further research to enable long life for H_2 compressors:

- Understanding the role of diaphragm microstructure in controlling its operational life.
- Design tools for evaluating interactions between compressor design, fluid flow, and diaphragm response.
- The effect of impurities and debris on fatigue life of the diaphragm.

FY 2014 PUBLICATIONS/PRESENTATIONS

1. Aashish Rohatgi, Ken Johnson, Naveen Karri, Ayoub Soulami, Jamie Holladay, Kareem Afzal, *"Investigation of H2 Diaphragm Compressors to Enable Low-Cost Long-Life Operation."* Presented at the Hydrogen Delivery Tech Team meeting, September 12, 2013, Sandia National Laboratories.

2. KI Johnson, A Rohatgi, and NK Karri. *"A Modeling and Microstructural Investigation of H2 Diaphragm Compressors to Enable Low-Cost, Long-Life Operation."* PNNL-SA-103662. Poster presented at the ASME 12th Fuel Cell Science, Engineering and Technology Conference, June 30 – July 3, 2014. Boston, MA.

III.11 700-Bar Hydrogen Dispenser Hose Reliability and Improvement

Kevin Harrison (Primary Contact), Michael Peters, Owen Smith, Huyen Dinh, Clay Macomber and Svitlana Pylypenko
National Renewable Energy Laboratory (NREL)
15013 Denver West Parkway
Golden, CO 80401-3305
Phone: (303) 384-7091
Email: Kevin.Harrison@nrel.gov

DOE Manager
Erika Sutherland
Phone: (202) 586-3152
Email: Erika.Sutherland@ee.doe.gov

Subcontractor
Spectrum Automation Controls, Arvada, CO

Project Start Date: July 2013
Project End Date: Project continuation and direction determined annually by DOE

Overall Objectives

By working closely with the original equipment manufacturer, Spir Star, NREL's 700-bar hydrogen fueling hose reliability R&D project aims to characterize, improve the reliability, and ultimately reduce the cost of dispensing hydrogen to fuel cell electric vehicles.

The high-cycling autonomous test apparatus is designed to reveal the compounding impacts of high-volume 700-bar fuel cell electric vehicle refueling that has yet to be experienced in today's low-volume market. The project scope includes performing physical and chemical analysis on the inner hose material before and after cycling to understand the relative changes in its bulk properties and material degradation mechanisms.

Fiscal Year (FY) 2014 Objectives

- Design, build, and begin operation of a test apparatus that unifies the stresses to which the hose is subjected during high volume back-to-back fueling events.
  - The stresses include use of hydrogen gas, high-pressure (up to 875 bar), low-temperature (≥ -40°C), 3–5 minute refueling time and automated mechanical bending and twisting of the hose assembly to simulate the refueling process.
- Specify, down select and complete chemical and physical material analysis of inner hose material prior to cycling. This analysis will reveal chemical and property changes of the material between the pre- and post-cycle testing of the inner hose material.

Technical Barriers and Targets

This project is conducting applied research, development, and demonstration to reduce the cost of hydrogen delivery systems. This project addresses the following technical barriers from the Hydrogen Delivery section of the Fuel Cell Technologies Office Multi-Year Research, Development, and Demonstration Plan:

(I) Other Fueling Site/Terminal Operations

(J) Hydrogen Leakage and Sensors

FY 2014 Accomplishments

- Completed multiple chemical and physical analysis techniques, using donated hoses and hose material from Spir Star, to establish the baseline (pre-cycled) characterization of the inner hose material.
  - The inner hose material was found to be polyoxymethylene and matched perfectly with a standard spectra provided by the literature.
- Completed burst testing of one of the donated hoses at Sandia National Laboratories.
  - The 9' long hose failed roughly in the middle at 58,800 psig.
- Designed, built and performed automatic cycling of a development robotics system interfaced to a main controller that operated valves and other system functions.
  - System cycled without operator intervention for over 1,000 cycles (goal was 100 cycles).
- Designed the high-pressure, low-temperature automated system by leveraging the NREL-funded 700-bar hydrogen refueling system and existing infrastructure at the Energy Systems Integration Facility (ESIF).
  - Hose cycling will begin in FY 2014 and post chemical analysis early in FY 2015.

INTRODUCTION

NREL operates and maintains a unique user facility known as the ESIF. The ESIF houses a broad array of capabilities and laboratories focused on energy integration research. Fast and flexible swapping of research test articles is a hallmark of the facility.

NREL partners with DOE, industry, and market stakeholders from throughout the hydrogen, fuel cell, and utility industries in order to provide critical testing, validation, and refinement stages in the product research and development process. NREL's approach to integrated systems testing simplifies the interfaces between hydrogen production, compression, storage, delivery, and end use systems.

Operation and maintenance costs of compression, storage, and dispensing are significant, and NREL has found that about 19% of maintenance hours for 350-bar hydrogen fueling infrastructure are associated with dispensers. This data can be found in NREL's material handling equipment Composite Data Products MHE #52 and MHE #66 [1]. Stations dispensing at 350 bar are much more heavily used today than those dispensing at 700 bar. These composite data products provide an early look at maintenance and reliability issues of the prospective 700-bar vehicle refueling stations.

APPROACH

This project aims to perform long-duration accelerated life testing using high-pressure, low-temperature hydrogen. This work is unique in that it simultaneously stresses the hose assembly with realistic fueling conditions (hydrogen gas, pressure ramp rates, delays, low temperature, and time). In addition, the project applies mechanical stress (bending/twisting) to the hose and nozzle assembly to simulate people refueling vehicles. Finally, the system automatically completes the full fueling process by connecting and disconnecting the nozzle to the receptacle.

The project will perform accelerated life testing of hydrogen refueling hose assemblies by accomplishing the following:

- Long duration, unattended operation of an autonomous system
- 3–5 minute fills closely following SAE International technical specification SAE J2601 pressure profile
- Type A fills using low volumes of hydrogen (at -40°C)
- Simulation of the mechanical stress of a routine consumer refueling event, including the connection and disconnection of the nozzle to the vehicle receptacle, using a 6-axis robot.
- Leak monitoring around hose/nozzle connections to detect excessive leaking and failure.

The project will also include analysis of the physical and chemical property changes to the inner hose material after cycling. The following methods will be used:

- Burst testing the entire hose assembly with crimped connection fittings.
- Fourier transform infrared spectroscopy, attenuated total reflectance (FTIR-ATR) – Identifies molecular bonding and functional groups of molecules in solids, powders, gases, and liquids. ATR identifies the bulk property of the material.
- Thermogravimetric analysis (TGA) – Thermal analysis method that accurately monitors mass changes of materials during controlled temperature profiles. Unlike FTIR, TGA does not give detailed chemical information, but provides insight into the material degradation mechanism.
- Differential scanning calorimeter (DSC) – Thermal analysis method that accurately monitors changes of heat flow in/out of a material to identify physical transformations like melting points, glass transition and recrystallization. The heats at which these transformations take place allow for identification of the material. TGA is complementary to DSC and allows for decomposition of the material at higher temperatures.
- Scanning electron microscopy (SEM) – This analysis reveals changes of the inner hose material morphology between the pre- and post-cycle testing.
- Energy dispersive X-ray spectroscopy (EDX) – This analysis technique provides bulk elemental composition. EDX coupled with SEM provides a mapping of elements in the hose material.
- X-ray photoelectron spectroscopy (XPS) – XPS reveals changes in surface properties after testing with high pressure and low temperature in the hydrogen environment. Surface reactions, like embrittlement, of the polymer would be seen using this technique.

RESULTS

Automated Hose Cycling

A development robot was interfaced with a main controller to perform automated mating, activation and cycling using low-pressure nitrogen. The system was designed, built and cycled using 350-bar nozzle and completed over 1,000 cycles without operator intervention. The automatic cycling was terminated with a controlled user-initiated stop request once the milestone goal was exceeded by an order of magnitude. Furthermore, the system testing showed that the nozzle and receptacle mating, nozzle activation (i.e., 180° rotation), and required valve sequencing was sufficiently repeatable to enable unattended operation inside the ESIF's High Pressure Test Bay (HPTB).

Lessons learned, software, and safety systems provided by this development work were transferred to the 700-bar (nominal) system design. The new design will utilize a smaller robot and full suite of 700-bar (nominally rated) equipment that will be installed in the 10'x10' footprint of the HPTB.

Baseline (Pre-Cycled) Inner Hose Material Chemical and Physical Analysis

Spir Star donated three hose assemblies and a section of hose material—all from the same batch of material. One of the hose assemblies, complete with standard crimp end connectors, was given to Sandia National Laboratories for burst testing. The hose failed at 58,800 psig in the middle of its 9' length. Spir Star's burst rating specification is 50,800 psig with a 5% tolerance due to manufacturing and material variability.

A sample of the inner hose material was characterized by identifying and quantifying bulk and molecular species present through the implementation of a suite of analytical instrumentation and analysis techniques. The inner hose material was identified using FTIR to be polyoxymethylene and found to be a match with a standard spectra provided by literature. The black curve of Figure 1 is the spectra of the pre-cycled inner hose material and the red curve is the standard spectra for polyoxymethylene. FTIR testing of post-cycled inner hose material will expose any changes in the bonding structure.

A summary of the other chemical analysis results are:

- TGA resulted in 100% inner hose material being decomposed in two concurrent steps with a decomposition temperature of 302°C. TGA of post-cycled hose material revealed shifts in the decomposition temperature, indicating polymer composition changes.
- DSC shows melting temperature of polyoxymethylene in the range of 162–169°C, which matches the range provided by literature. During the cooling period of the test, the hose material recrystallized at 143°C. If the post-cycled hose material changes, by taking on impurities or hydrogen for example, DSC will identify the change because the melting point will likely also change.
- SEM shows the structure of new inner hose material resembling wrinkles/folds at 2,000 magnification. Post-cycled SEM scans will provide visual proof of pitting, embrittlement, or other surface morphology degradation.
- XPS analysis revealed that the inner hose material consists of carbon-carbon and carbon-oxygen bonds. EDX analysis showed that the bulk elemental composition of the inner and outer hose liner was 60–64% carbon and 39–36% oxygen.

CONCLUSIONS AND FUTURE DIRECTIONS

- **Conclusion:** Development of the controls, interfacing, and automated nozzle to receptacle process is very repeatable. Lessons learned from the 350-bar system were transferred to the 700-bar full system design, build, and operation.
  - **Future:** The system will be continuously cycled in unattended mode to achieve accelerated life testing of the hose assembly in the ESIF's HPTB using high-pressure, low-temperature hydrogen gas.
- **Conclusion:** Chemical and physical material analysis, aimed at revealing material changes between pre- and post-cycled hose material, was completed. Baseline (pre-cycled) chemical analysis identified the inner hose material to be polyoxymethylene. Burst test was completed with hose failing at 58,800 psig; well above the specification (50,800, ±5% psig) from Spir Star.

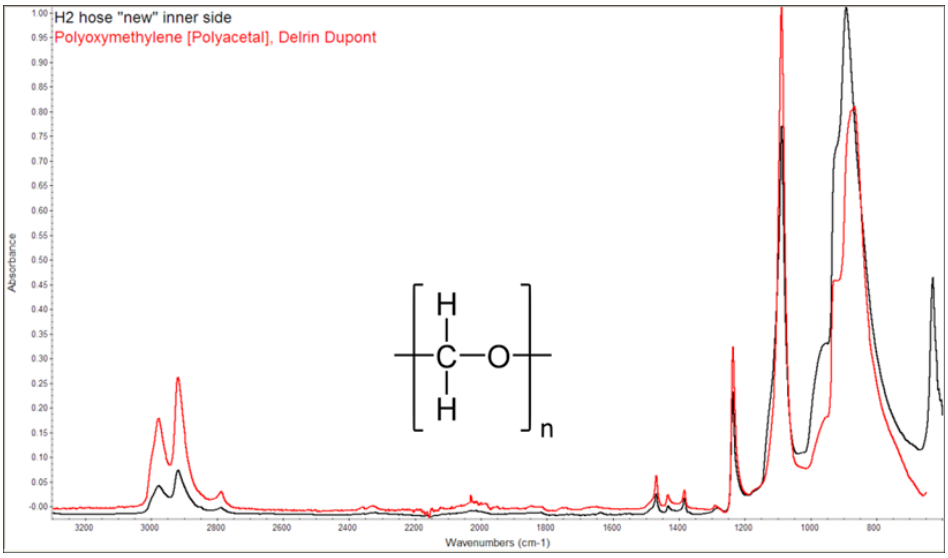

FIGURE 1. FTIR shows molecular bonding of inner hose material consistent with Polyoxymethylene

  - **Future:** Perform the same suite of analytic techniques on inner hose material after cycling with hydrogen at high pressure, low temperature and repeated bending/twisting to (potentially) reveal changes in bulk properties and elemental material composition.

- **Future:** Continue to work with industry partners like NanoSonic to test prototype hoses from their Small Business Innovation Research Phase II project, "Cryogenically Flexible, Low Permeability Thoraeus Rubber™ Hydrogen Dispenser Hose."

FY 2014 PUBLICATIONS/PRESENTATIONS

1. 1-Page Fact Sheet - http://www.nrel.gov/docs/fy14osti/61091.pdf

2. YouTube Video - http://www.youtube.com/watch?v=Rbc7f01oP8kA

REFERENCES

1. http://www.nrel.gov/hydrogen/proj_fc_market_demo.html

IV. HYDROGEN STORAGE

IV.0 Hydrogen Storage Sub-Program Overview

INTRODUCTION

The Hydrogen Storage sub-program supports research and development (R&D) of materials and technologies for compact, lightweight, and inexpensive storage of hydrogen for automotive, portable, and material handling equipment (MHE) applications. The Hydrogen Storage sub-program has developed a dual strategy, with a near-term focus on improving performance and lowering the cost of high-pressure compressed hydrogen storage systems and a long-term focus on developing advanced cold/cryo-compressed and materials-based hydrogen storage system technologies.

In Fiscal Year (FY) 2014, the sub-program continued its focus on development of lower-cost precursors for high-strength carbon fibers to lower the cost of high-pressure compressed hydrogen systems, system engineering for transportation applications, and advanced material R&D efforts, including for metal hydrides, chemical hydrogen storage materials, and hydrogen sorbents.

GOAL

The sub-program's goal is to develop and demonstrate advanced hydrogen storage technologies to enable successful commercialization of fuel cell products in transportation, portable, and MHE applications.

OBJECTIVES

The Hydrogen Storage sub-program's objective is to develop technologies that provide sufficient onboard hydrogen storage to allow fuel cell devices to provide the performance and run-time demanded by the application. For light-duty vehicles this means providing a driving range of more than 300 miles (500 km), while meeting packaging, cost, safety, and performance requirements to be competitive with current vehicles. Although some fuel cell electric vehicles (FCEVs) have been demonstrated to travel more than 300 miles on a single fill using high-pressure tanks, this driving range must be achievable across the full range of vehicle models without compromising space, performance, or cost. The Hydrogen Storage sub-program has developed comprehensive sets of hydrogen storage performance targets for onboard automotive, portable power, and MHE applications. The targets can be found in the *Multi-Year Research, Development, and Demonstration* (MYRD&D) *Plan*.[1]

By 2020, the sub-program aims to develop and verify onboard automotive hydrogen storage systems achieving the following targets that will allow some hydrogen-fueled vehicle platforms to meet customer performance expectations:

- 1.8 kWh/kg system (5.5 wt%)
- 1.3 kWh/L system (0.040 kg hydrogen/L)
- $10/kWh ($333/kg hydrogen storage capacity)

To achieve wide-spread commercialization of hydrogen FCEVs across the full range of light-duty vehicle platforms, the sub-program has established the following onboard hydrogen storage targets to ultimately meet the needs for full fleet adoption:

- 2.5 kWh/kg system (7.5 wt%)
- 2.3 kWh/L system (0.070 kg hydrogen/L)
- $8/kWh ($266/kg stored hydrogen capacity)

Tables that include the complete sets of near-term and longer-term targets for onboard automotive, portable power, and MHE applications can be found in the MYRD&D Plan.

FY 2014 TECHNOLOGY STATUS AND ACCOMPLISHMENTS

The status of the various storage technologies pursued is evaluated through techno-economic analyses within individual projects, but also through independent analyses carried out for the sub-program.

[1] http://energy.gov/eere/fuelcells/fuel-cell-technologies-office-multi-year-research-development-and-demonstration-plan

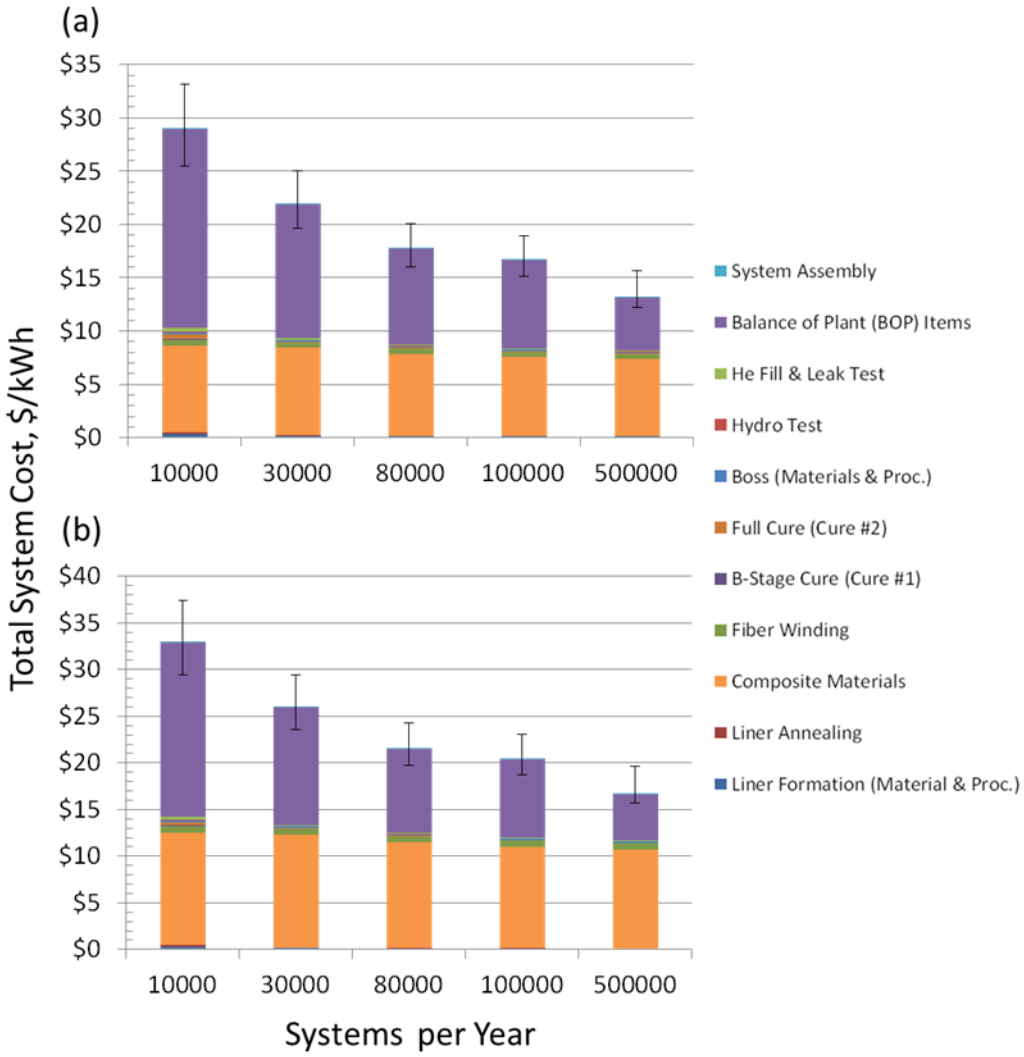

FIGURE 1. Projected costs in 2007$, at various annual manufacturing volumes, for (a) 350 bar and (b) 700 bar compressed hydrogen storage systems, sized to deliver 5.6 kg of hydrogen to the vehicle fuel cell powerplant. Cost analysis performed by Strategic Analysis Inc. in 2013.

In the near term, automotive companies plan to commercialize FCEVs that use compressed hydrogen systems onboard, with system cost being one of the most important challenges to commercialization. The sub-program, working with automotive original equipment manufacturers through the United States Driving Research and Innovation for Vehicle efficiency and Energy sustainability Partnership, established onboard automotive hydrogen storage system cost targets of $10/kWh of usable stored hydrogen to be reached by 2020, and $8/kWh of usable stored hydrogen as an Ultimate Full Fleet target. In 2013, Strategic Analysis Inc., working with Argonne National Laboratory (ANL) and the National Renewable Energy Laboratory (NREL), using a Design for Manufacturing and Assembly (DFMA®) methodology, completed a thorough cost analysis for baseline Type IV 350- and 700-bar compressed hydrogen storage systems, for both single- and multi-tank configurations. Figure 1 shows the projected variable volume manufacturing costs for 700-bar, Type IV onboard systems with a 5.6 kg hydrogen usable capacity, including component breakdown costs. While the cost for the carbon fiber composite must be reduced to meet the ultimate cost targets, at lower manufacturing volumes, the cost of the balance-of-plant (BOP) components was shown to be the largest cost contributor. Therefore, in 2014, the Strategic Analysis Inc. team was tasked with carrying out a detailed failure mode and effects analysis of the BOP to understand the major cost contributors. Figure 2 shows the projected cost breakdown for 700-bar system BOP at 500,000 units per year. The piping/fittings, integrated in-tank valve, and pressure regulator were found to be the largest three cost contributors. These results will be used to develop strategies to reduce BOP costs.

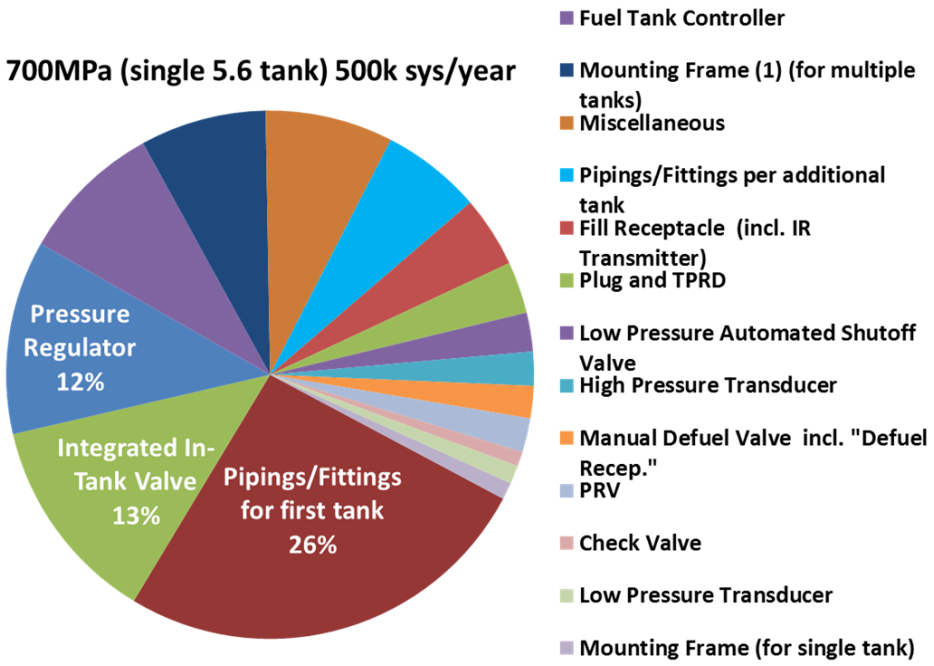

IR - infrared; TPRD - temperature/pressure relief device; PRV - pressure relief valve

FIGURE 2. Projected costs, in 2013$, for BOP components for 700-bar compressed hydrogen storage systems produced at 500,000 systems per year.

As a longer-term strategy, the Hydrogen Storage sub-program continues to pursue less mature hydrogen storage technologies that have the potential to satisfy all onboard hydrogen storage targets. These technologies include cold (sub-ambient temperatures as low as ~150-200 K) and cryo-compressed (temperatures <150 K) hydrogen and materials-based storage technologies. The materials-based efforts include total systems engineering and hydrogen storage materials development, including adsorbents, metal hydrides, and chemical hydrogen storage materials. A major effort in this area the last several years has been through the Hydrogen Storage Engineering Center of Excellence (HSECoE). In 2014, the HSECoE transitioned into Phase III—sub-scale system prototype development and evaluation. The Phase II–III transition decisions included the phase-out of activities on chemical hydrogen storage materials systems and continuing with prototype evaluation of two sorbent systems with differing heat exchanger design—a flow-through system with a hexagonal honey-comb aluminum (hexcell) heat exchanger and a liquid-nitrogen-cooled design with the "Module Adsorption Tank Insert" (MATI) heat exchanger. Figure 3 shows the modeled systems performance at the end of Phase II for the hexcell sorbent and alane chemical systems, respectively. Neither system is projected to meet all of the DOE targets for onboard hydrogen storage with currently available materials. However, these efforts are able to help define the material properties that are needed for a complete system to meet the targets. While the chemical systems are projected to be able to meet most of the 2020 storage targets, the decision to discontinue work on these systems was partially based on the lack of any practical materials on the foreseeable horizon available at low initial cost and with low-cost, energy-efficient regeneration processes. Therefore, it was decided to not continue towards sub-scale system prototype evaluation until materials are available that are projected to be low-cost and are able to be efficiently regenerated.

Testing & Analysis

In FY 2014, the Hydrogen Storage sub-program continued carrying out techno-economic assessments of hydrogen storage technologies. Technical analysis and cost modeling of Type IV pressure vessel systems remained a critical focus during FY 2014, with detailed analyses to determine costs for BOP components and validation of the low-volume costs through comparisons with compressed natural gas (CNG) tank data. Additionally, analyses were performed to "reverse engineer" sorbent system performance to identify adsorbent material property requirements to meet DOE system-level performance targets.

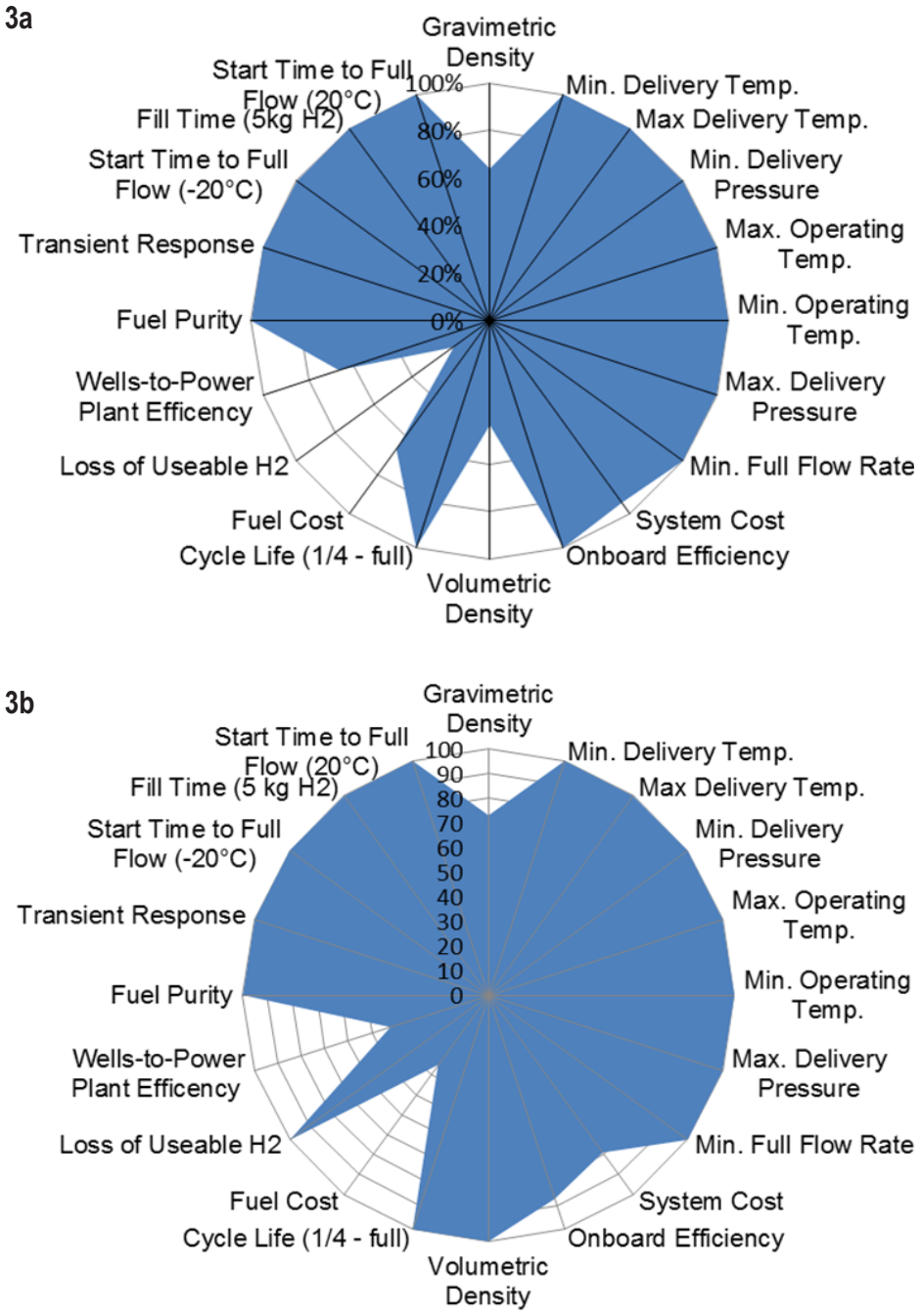

FIGURE 3. (3a) Status of projected sorbent (hexcell) and chemical hydrogen storage (50 wt% alane slurry); (3b) system performance versus 2020 onboard system targets. Note that the systems were sized to provide 5.6 kg of usable hydrogen.

Specific accomplishments include:

- Completed a DFMA® analysis of high-pressure (>825 bar [>12 kpsi]) and low-pressure (<28 bar [<400 psi]) hydrogen fittings and for the integrated valve.
- Validated the hydrogen pressure vessel DFMA® cost model at a low production rate by using it to model a CNG pressure vessel, and obtained close agreement with CNG industry quotations for the same size tank at an annual production rate of 1,000 vessels per year.

- Formulated system models and performed reverse engineering to determine thermodynamic properties of sorbent materials needed to meet onboard system and off-board well-to-engine efficiency targets. (ANL)
- The "Recommended Best Practices for the Characterization of Storage Properties of Hydrogen Storage Materials" document was completed, which now contains the following sections: Introduction, Capacity, Kinetics, Thermodynamics, Cycle-Life, Thermal Properties, and Mechanical Properties measurements. (NREL)

Advanced Physical Storage

In FY 2014, the sub-program continued to reduce the cost of compressed hydrogen gas storage tanks with efforts focused on low-cost, high-strength carbon fiber precursors and advanced tank designs. Lightweight compressed gas storage vessels requiring a composite overwrap to contain hydrogen gas are considered the most likely near-term hydrogen storage solution for the initial commercialization of FCEVs, as well as for other early market applications. Carbon fiber composite overwraps can currently contribute as much as 75% or more to the overall cost of advanced Type IV tanks. The Hydrogen Storage sub-program supported efforts at the Oak Ridge National Laboratory (ORNL) to reduce the cost of polyacrylonitrile (PAN)-based fibers used as precursors to produce high-strength carbon fibers. ORNL efforts focused on advanced precursor materials and processing since precursors have been shown to contribute over 50% of the total cost of high-strength carbon fibers. The team investigated the use of low-cost textile-grade fibers made from PAN blended with a methyl acrylate comonomer (PAN-MA) as lower-cost precursors and continued to improve on the development of melt-spinnable PAN precursors and processing techniques to replace the current more costly wet processing methods. Additionally, a team led by the Pacific Northwest National Laboratory (PNNL) focused on reducing the cost of a Type IV tank system by developing novel alternative resins and resin matrix modification, modifying the carbon fiber surface to improve composite translational efficiency, developing methods for alternative fiber placement and enhanced operating conditions that demonstrated routes to increase carbon fiber usage efficiency.

One new Small Business Innovation Research Phase II award was made that focuses on a graded construction approach of using a lower-cost, lower-performance carbon fiber in the outer layers where fibers are exposed to lower stress due to the thick wall effect with 700-bar Type IV tanks. Three new sub-program awards were made:

- Materia Inc. will investigate use of a low-viscosity resin and a vacuum-assisted resin transfer molding process as alternatives to the traditional epoxy resin and wet-wind manufacturing process for Type IV tanks.
- PPG Industries Inc. will investigate the production scale-up of an ultra-high-strength glass fiber (≥5,500 MPa) and evaluate its performance in composites and a low-cost alternative to carbon fiber in Type III and IV tanks.
- Sandia National Laboratories (SNL) will screen alternative metal alloys for use in place of 316/316L stainless steel for materials of construction in balance of plant and other hydrogen applications, leading to lower costs and lower mass.

Specific accomplishments include:

- Increased tensile strength from 405 KSI to 649 KSI and tensile modulus from 33 MSI to 38 MSI for carbon fibers produced from PAN-MA precursor fibers manufactured on high-volume textile lines. (ORNL)
- Projected a 52% mass reduction and 30% cost reduction in compressed hydrogen storage systems with 5.6 kg hydrogen usable capacity, at 500 bar and cold (approximately 200 K) operating conditions, compared to baseline 700-bar ambient systems. (PNNL)
- Initiated preliminary testing of the liquid hydrogen cryo-pump installation, with 875-bar capability. (Lawrence Livermore National Laboratory, LLNL)
- Carried out initial testing of thermotropic liquid crystal polymers as potential load-bearing, thermally conducting liner materials as an alternative to high-density polyethylene liners and with potential to reduce carbon fiber composites in Type IV tanks. (Savannah River National Laboratory, SRNL)

Advanced Materials Development

In FY 2014, the sub-program continued efforts in developing and improving hydrogen storage materials with potential to meet the 2020 onboard storage targets in addition to the 2015 portable power and MHE targets. In the area of metal hydrides, efforts emphasized material discovery coupled with reducing desorption temperatures and improving kinetics. For chemical hydrogen storage materials, much of the focus was on developing reversible or

regenerable liquid-phase materials, and also increasing efficiency of regeneration routes for solid-phase materials. For hydrogen sorbents, efforts were focused on increasing the isosteric heat of adsorption, mainly through inclusion of open metal centers or boron doping, to increase the adsorbed capacity at higher temperatures and improving standard measurement practices for hydrogen capacity. Also in FY 2014, the Hydrogen Storage sub-program maintained efforts to collect and disseminate materials data on advanced hydrogen storage materials through the hydrogen storage materials database (http://hydrogenmaterialssearch.govtools.us/).

Three new awards were initiated in FY 2014:

- HRL Laboratories, with partners SNL and University of Missouri-St. Louis, will investigate two material systems, mixed metal borohydrides and lithiated boranes, with potential to offer high gravimetric capacity with fast kinetics at temperatures and pressures relevant to automotive applications.
- LLNL, with partners SNL, Georgia Tech, and University of Michigan, will use a combined multi-scale computational and experimental approach to develop and validate strategies to improve the performance of $Mg(BH_4)_2$, a material with potential for 14 wt% reversible hydrogen storage.
- Ardica Technologies, with partner SRI, will transition and scale up a version of the SRNL-developed electrochemical method of alane (AlH_3) production/regeneration from the laboratory to production to significantly lower the cost of alane compared to conventional solution synthesis methods.

Specific accomplishments include:

- Hydrogen desorption and decomposition pathways were studied for 2 $LiBH_4$ + 5 $Mg(BH_4)_2$ using nuclear magnetic resonance; experimentally observed reaction products were consistent with theoretically predicted B_2H_6 anion. Using a combination of experiments and density functional theory, all but one reaction product was able to be assigned. (Northwestern University)
- Developed the M_2(4,6- dioxido benzene 1,3-dicarboxylate) (known as m-dobdc) (M = Mg, Mn, Fe, Co, Ni) series of metal organic frameworks via a new structural isomer that shows a significantly improved hydrogen binding enthalpy as compared to the regular M_2(dobdc) for the Mn, Fe, Co, and Ni analogues. The open metal coordination sites are shown to have a greater positive charge in M_2(m-dobdc) than in M_2(dobdc), leading to the experimentally determined higher isosteric heats of H_2 adsorption (~1.0 kJ/mol higher on average) and up to 40% increase in adsorption enthalpy. (Lawrence Berkeley National Laboratory, LBNL)
- Demonstrated a volumetric capacity for Ni_2(m-dobdc) at room temperature and 100 bar of 12.1 g/L, which is the highest demonstrated to date and 50% greater than H_2 gas. (LBNL)
- Developed recommended volumetric capacity definitions and measurement protocols to help the research community better report and understand their volumetric capacity material results. (NREL)

Engineering

In FY 2014, the HSECoE developed prototype designs and evaluation plans for each of the hexcell and MATI sorbent systems using a 2-L Type I (all metal) aluminum pressure vessel. The MATI system is being constructed and modeled by partner Oregon State University, with evaluations to be done by SRNL. The hexcell system will be constructed and evaluated by partner University of Quebec-Three Rivers, with SRNL modeling the system. Efforts this past year included designing, constructing, and modifying test apparatuses at University of Quebec-Three Rivers and SRNL for evaluating the larger prototype systems. Additionally, the HSECoE completed evaluation work on chemical hydrogen storage material systems, demonstrating use of up to a 60% mass-loaded alane slurry, and refined their validated system models. These results were used to "reverse engineer" the chemical hydrogen storage material property requirements for a system to meet the full set of onboard storage targets. The models are posted on the models page of the HSECoE website (http://hsecoe.org/models.html) and are publically available for use by the hydrogen storage R&D community.

Specific accomplishments include the following:

- Demonstrated hydrogen release through a flow-through auger reactor with up to 60% mass-loaded slurries of alane. (Los Alamos National Laboratory, LANL)
- Developed and validated a single chemical hydrogen storage system model that combines exothermic and endothermic materials. Preparing it for public release through the HSECoE model website page. (PNNL)

- Quantified chemical hydrogen storage material property requirements to be able to meet all onboard hydrogen storage targets and submitted as a manuscript to Journal of Power Sources. (LANL and PNNL)
- Demonstrated that use of a liquid-nitrogen-cooled wall tank concept could significantly reduce the amount of hydrogen needed to be used with flow-through sorbent systems. (PNNL, Hexagon Lincoln)
- Tested at pressure and validated a computational fluid dynamics model of a gas-liquid separator uniquely designed for use with chemical hydrogen storage systems capable of separating hydrogen from liquids up to a peak power level of 80 kW_e. (UTRC)
- Successfully completed design, cycle, and burst (ambient and cryogenic) testing of a 2-L, Type I aluminum three-piece pressure vessel for use in Phase III prototype sorbent system evaluations. (Hexagon Lincoln)
- Delivered over 9 kg of MOF-5 adsorbent to HSECoE partners for Phase III testing, with scaled-up batch material achieving performance within 10% of lab-scale batch material. (Ford)
- Demonstrated 20x improvement in MOF-5 thermal conductivity using an enhanced natural graphite layering approach compared to random loading. (Ford)
- Completed experimental verification of the fast-fill and discharge dynamics of a cryo-adsorbent bed, enabling validation of the transport models. (General Motors)
- Completed design and assembly of the MATI for 2-L prototype system testing. (Oregon State University)
- Completed design and commenced construction of two test stations for evaluating the hexcell and MATI 2-L sorbent system prototypes. (SRNL, University of Quebec-Three Rivers)
- Established the HSECoE model website page[2] and posted metal hydride acceptability envelope, metal hydride finite element model, hydrogen tank mass and cost estimator, and hydrogen vehicle simulation framework models for public availability. (NREL)

BUDGET

$15.6 million from the FY 2015 budget request is planned for hydrogen storage—consistent with $15.6 million from the FY 2014 congressional appropriation. In FY 2015, the Hydrogen Storage sub-program will continue to focus on nearer-term R&D to lower the cost of high-pressure storage systems and longer-term technology development including cold/cryo-compressed hydrogen and materials discovery and system engineering for materials-based storage technologies. The sub-program will also continue to carry out systems analyses. The sub-program plans to initiate new activities in these areas for onboard automotive and non-automotive applications.

[2] http://hsecoe.org/models.html

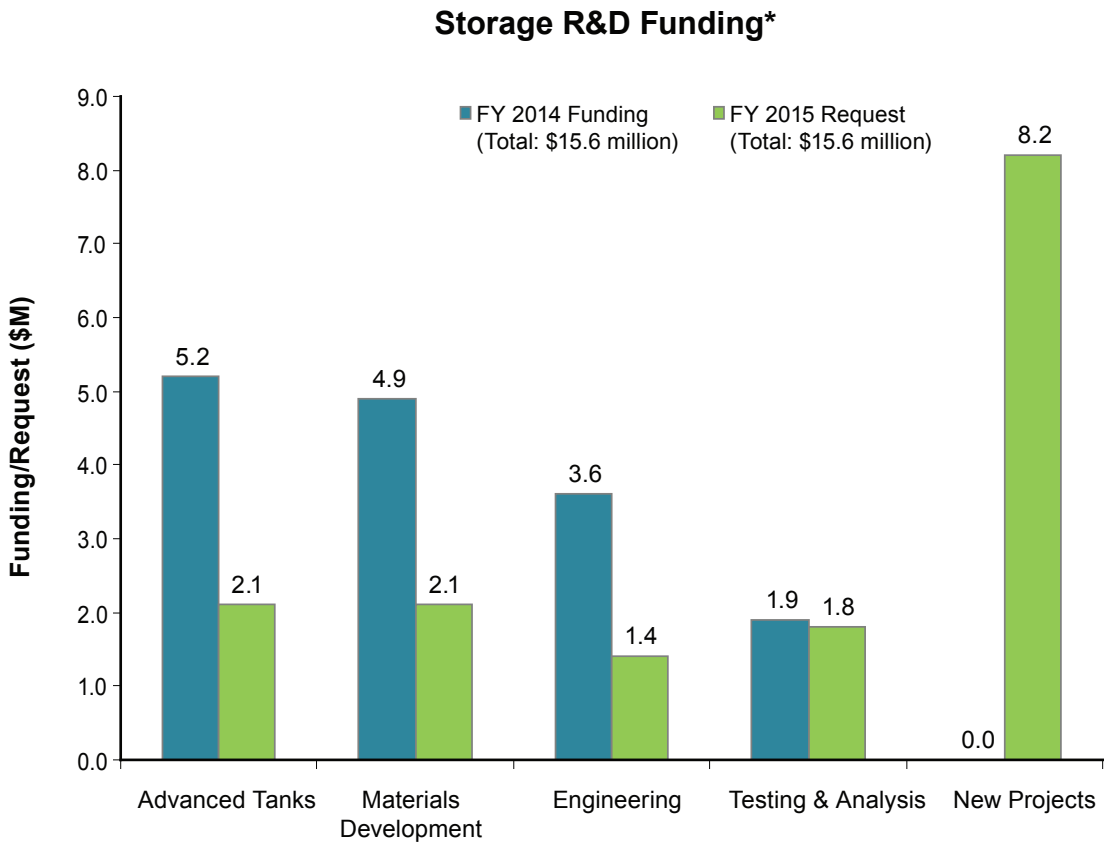

* Subject to appropriations, project go/no-go decisions, and competitive selections. Exact amounts will be determined based on research and development progress in each area.

FY 2015 PLANS

The technology portfolio for Hydrogen Storage emphasizes materials R&D to meet system targets for onboard automotive and non-automotive applications. While a focus on light-duty vehicle applications will continue, increased emphasis will be placed on new materials and novel concepts to meet performance requirements for portable power and MHE applications. The emphasis on developing lower-cost physical storage technologies will continue and be coordinated with related activities through the Vehicle Technologies and Advanced Manufacturing Offices of Energy Efficiency and Renewable Energy. Specifically, the sub-program will coordinate with and leverage other efforts through the planned Advanced Manufacturing Office Advanced Composites Institute and Vehicle Technologies Office efforts on CNG storage to develop approaches to produce low-cost compressed gas storage systems. System engineering and analysis will continue through the HSECoE, ANL, and Strategic Analysis Inc. Coordination with basic science efforts, including theory, characterization, and novel concepts, will be pursued during FY 2015.

Ned Stetson
Hydrogen Storage Program Manager
Fuel Cell Technologies Office
Office of Energy Efficiency and Renewable Energy
U.S. Department of Energy
1000 Independence Ave., SW
Washington, D.C. 20585-0121
Phone: (202) 586-9995
Email: Ned.Stetson@ee.doe.gov

IV.A.1 System Analysis of Physical and Materials-Based Hydrogen Storage

Rajesh K. Ahluwalia (Primary Contact), T.Q. Hua, J-K Peng, and Hee Seok Roh
Argonne National Laboratory
9700 South Cass Avenue
Argonne, IL 60439
Phone: (630) 252-5979
Email: walia@anl.gov

DOE Manager
Grace Ordaz
Phone: (202) 586-8350
Email: Grace.Ordaz@ee.doe.gov

Start Date: October 1, 2004
Projected End Date: Project continuation and direction determined annually by DOE

Overall Objectives

- Model various developmental hydrogen storage systems.
- Provide results to the Hydrogen Storage Engineering Center of Excellence for assessment of performance targets and goals.
- Develop models to "reverse-engineer" particular approaches.
- Identify interface issues, opportunities, and data needs for technology development.

Fiscal Year (FY) 2014 Objectives

- Perform impact damage analysis for Type 4 hydrogen storage tanks.
- Determine potential reduction in carbon fiber (CF) requirement with advanced resins.
- Determined gravimetric and volumetric capacities, and CF requirement with cold hydrogen storage.
- Establish sorbent properties needed to satisfy onboard and off-board storage system targets.

Technical Barriers

This project addresses the following technical barriers from the Hydrogen Storage section of the Fuel Cell Technologies Office Multi-Year Research, Development, and Demonstration Plan:

(A) System Weight and Volume

(B) System Cost

(C) Efficiency

(E) Charging/Discharging Rates

(J) Thermal Management

(K) System Life-Cycle Assessments

Technical Targets

This project is conducting system level analyses to address the DOE 2017 technical targets for onboard hydrogen storage systems:

- System gravimetric capacity: 1.8 kWh/kg
- System volumetric capacity: 1.3 kWh/L
- Minimum H_2 delivery pressure: 5 bar
- Refueling rate: 1.5 kg/min
- Minimum full flow rate of H_2: 0.02 g/s/kW

FY 2014 Accomplishments

- Conducted ABAQUS/Explicit analysis of impact damage in a fiber composite plate and validated the damage model with experimental data. Simulated horizontal and 45° drop tests of Type 4 tanks per SAE International (SAE) J2579 protocol. Determined the damage volume in Type 4 tanks with and without advanced resins and with and without foam protection in the dome.
- Performed MultiMech analysis to determine the mechanical properties of nanocomposite resins and CF composites with advanced resins. Calibrated and validated MultiMech model against experimental data.
- Analyzed cold gas storage option that achieved ~50% reduction in CF and ~30% increase in gravimetric capacity (if a Type 4 tank can be used) compared to ambient 700-bar tanks. Identified off-board issues related to cryogenic cooling and insulated Type 3 vessels for trailer tubes and cascade refueling.
- Formulated models and performed reverse engineering to determine thermodynamic properties of sorbent materials needed to meet onboard system and off-board well-to-engine efficiency targets.

INTRODUCTION

Several different approaches are being pursued to develop onboard hydrogen storage systems with the goal of meeting the DOE targets for light-duty vehicle applications. Each approach has unique characteristics, such as the thermal energy and temperature of charge and discharge,

kinetics of the physical and chemical process steps involved, and requirements for the materials and energy interfaces between the storage system and the fuel supply system, on the one hand, and the fuel user on the other. Other storage system design and operating parameters influence the projected system costs as well. We are developing models to understand the characteristics of storage systems based on the various approaches, and to evaluate their potential to meet the DOE targets for onboard applications, including the off-board targets for energy efficiency.

APPROACH

Our approach is to develop thermodynamic, kinetic, and engineering models of the various hydrogen storage systems being developed under DOE sponsorship. We then use these models to identify significant component and performance issues, and to assist DOE and its contractors in evaluating alternative system configurations and design and operating parameters. We establish performance criteria that may be used, for example, in developing storage system cost models. We refine and validate the models as data become available from the various developers. We work with the Hydrogen Storage Systems Analysis Working Group to coordinate our research activities with other analysis projects to assure consistency and to avoid duplication. An important aspect of our work is to develop overall systems models that include the interfaces between hydrogen production and delivery, hydrogen storage, and the fuel cell.

RESULTS

Physical Storage

We developed a model to investigate impact energy absorption and damage of the composite overwrap in Type 4 tanks. We used this model to determine the minimum CF requirement for a Type 4 tank to pass the drop tests. We used ABAQUS/Explicit to model the transient dynamic response of the composite layer by layer. We simulated the drop tests for a full-sized Type 4 tank as defined in SAE J2579 [1], including horizontal drop impacting the cylinder, and 45° drop impacting the dome. In both cases, the center of mass is located at 1.8 m above ground. The tank was modeled with conventional 90° hoop winding and 15° helical winding. It was wound with sufficient CF composite to meet the 2.25 safety factor for 70 MPa nominal storage pressure. The impact analysis included three damage criteria: (1) matrix cracking, (2) layer delamination, and (3) fiber breakage. For horizontal drop, results from our analysis indicated that the matrix on the surface cracked but there was no internal damage to the matrix or the fiber. There was no delamination. Surface matrix cracking can be prevented with a thin layer of glass fiber over the CF composite overwrap. For 45° drop, our model predicted matrix damages through the composite thickness near the impact area. The calculated damage volume was 73 cm^3. There was no fiber breakage.

We investigated the effect of matrix dominant properties on impact resistance by varying each of the three properties (transverse tensile, transverse compressive, and shear strengths) independently of the other two. Simulation results show that the impact damage resistance is highly correlated to the shear strength with only small effects of the transverse tensile and compressive strengths. We simulated the 45° drop test for a full-sized Type 4 tank using advanced resins in the composite to determine the tank performance relative to one with neat resins. The advanced resins selected for this analysis is similar to the Applied Nanotech resins that include 1 wt% carbon nanotubes and 0.25 wt% SiO_2 which show ~20% improvement in tensile, compressive, and shear strengths over neat resins [2]. Figure 1a shows the reduction in the damage volume for 10 to 30% enhancement in the matrix dominant properties. We predicted a 35% reduction in damage volume with 30% enhancement in transverse tensile, transverse compressive, and shear strengths. We also investigated the effect of placing a foam "cap" over the CF composite overwrapped pressure vessel and then applying a thin layer of glass fiber overwrap over it all. Figure 1b shows that 1 cm of polyurethane foam can reduce the damage volume by 50%. A 2.5-cm foam can completely prevent damage to the dome in the 45° drop test. While foam is significantly more effective in protecting the dome from impact damage, advanced resins can provide protection in areas without foam such as near the boss and in the cylinder section.

We analyzed the off-board and onboard performance of the cold hydrogen storage option. We evaluated one scenario for hydrogen production (central steam methane

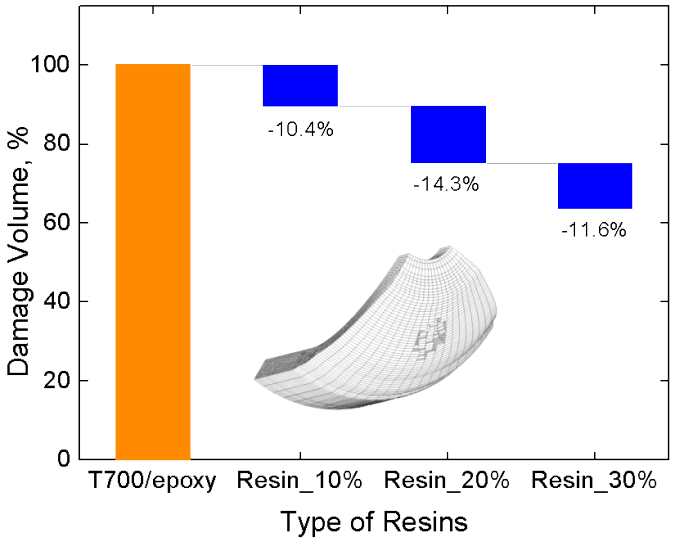

FIGURE 1a. Damage Volume Reduction with Enhancement in Matrix Dominant Properties

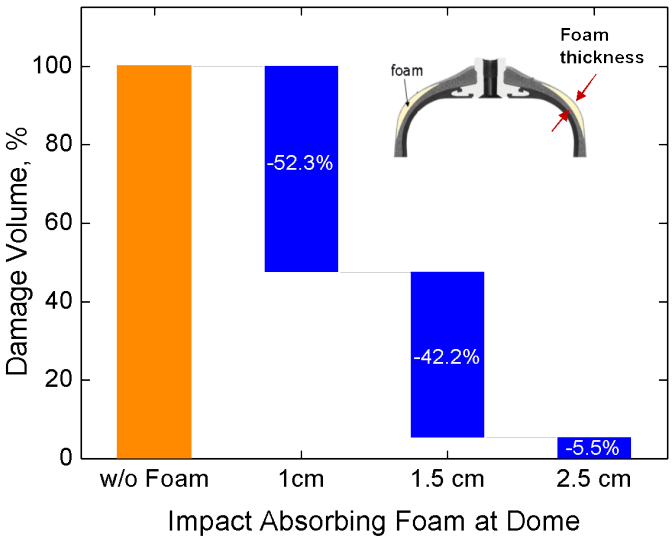

FIGURE 1b. Damage Volume in Dome With and Without Foam "Cap"

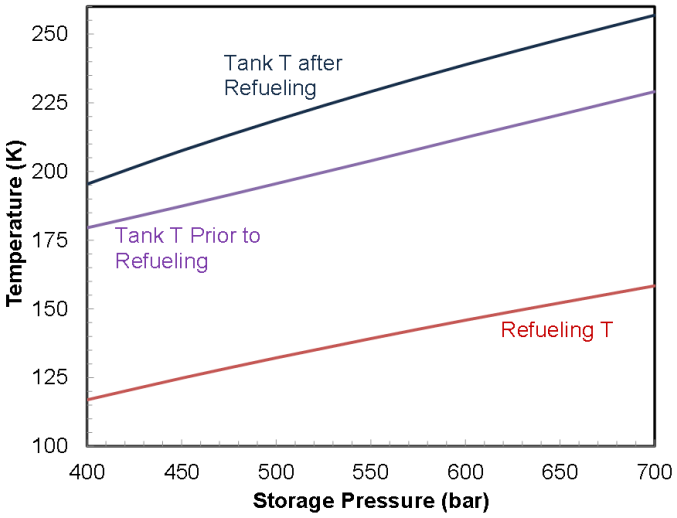

FIGURE 2a. Operating Temperatures as a Function of Storage Pressures

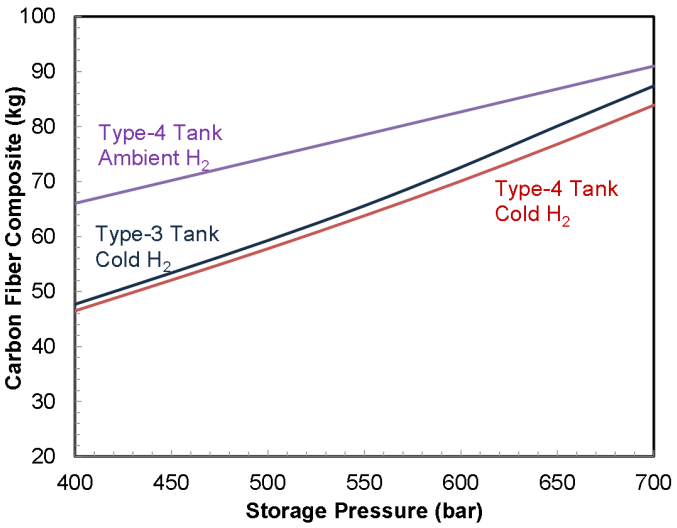

FIGURE 2b. CF Composite Requirements for Ambient and Cold Hydrogen Storage Options

reformation), refrigeration (liquid nitrogen cooling at the city gate), and delivery (transmitted via pipeline to the city gate, insulated Type 3 tube trailers for trucking of compressed cold hydrogen to the refueling station). At the forecourt, the cold hydrogen is stored in Type 1 tube banks and dispensed using a cascade refueling system. For this scenario, we estimate a well-to-tank (WTT) efficiency of 47.4%, which is 13% lower than 54.2% WTT efficiency of the baseline ambient temperature 700-bar compressed hydrogen storage option.

The onboard storage system is adapted from the cryo-compressed system configuration [3] except that we analyzed the options of storing hydrogen in both Type 3 and Type 4 insulated tanks. The composite pressure vessel consists of T700S CF composite (2,550 MPa tensile strength) wound on an Al 6061-T6 alloy liner (Type 3), or high-density polyethylene (HDPE) liner (Type 4) and it is thermally insulated with multi-layer vacuum super insulation encased in a 3-mm-thick Al alloy vacuum shell. For Type 3 tanks, we conducted fatigue analyses to estimate the required metal liner thickness to meet the target life of 5,500 pressure cycles (SAE J2579 requirement). The thickness of the insulation was determined so as to limit the heat transfer rate from the ambient to 5 W.

Figure 2a shows the dependence of the operating temperatures on the storage pressure. It includes the temperature of the refueled cold gas, initially at 90 K and 340 bar in the tube trailer, compressed to 135% of the storage pressure in one stage with 65% isentropic efficiency. It also includes the tank temperatures prior to refueling and after discharging of 5.6 kg hydrogen, allowing for a 50 W-d heat gain from the ambient and the pressure/volume work. At 400 bar, the storage temperatures are above the HDPE glass transition temperature but below the ductile to fragile transition temperature.

Figure 2b indicates that nearly 50% reduction in CF composite (from 91 kg in baseline 700-bar Type 4 tank) is possible if cold gas (fixed 90 K nominal tube trailer temperature) is stored at 400 bar. There is only a small difference in CF composite requirements for Type 3 and Type 4 tanks storing cold gas. The projected CF usage is based on fiber strengths that are independent of storage temperature and translation efficiencies that only depend on storage pressure.

Figure 3a indicates that the volumetric capacity of the cold gas option with fixed 90 K tube trailer temperature

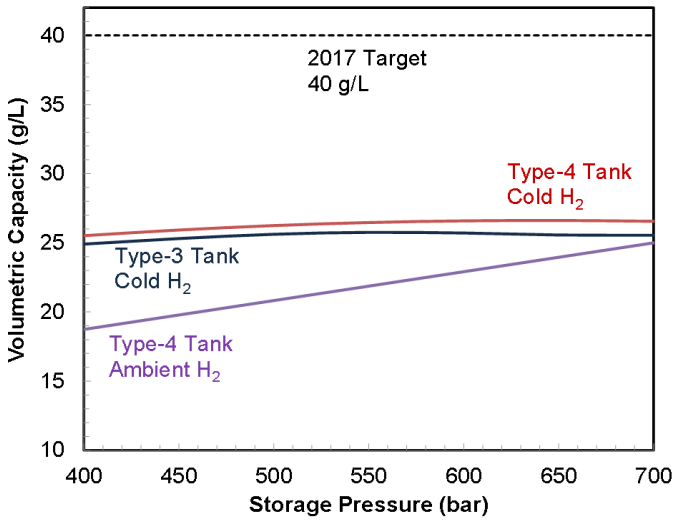

FIGURE 3a. Volumetric Capacity for Ambient and Cold Hydrogen Storage Options

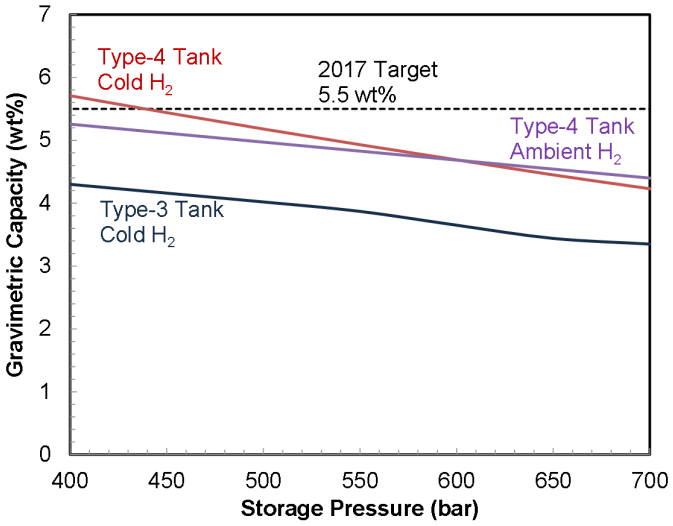

FIGURE 3b. Gravimetric Capacity for Ambient and Cold Hydrogen Storage Options

is nearly the same for Type 3 and Type 4 tanks, is nearly independent of the storage pressure, and is marginally (2-6%) higher than the volumetric capacity (25 g/L) of the baseline ambient temperature 700-bar compressed hydrogen system. Figure 3b suggests that it may be possible to meet the 5.5 wt% 2017 gravimetric capacity target with cold hydrogen storage in Type 4 tanks at storage pressures below 450 bar.

In summary, compared to the baseline 700-bar compressed hydrogen option, cold hydrogen storage (90 K nominal tube trailer temperature) at 400 bar in insulated Type 4 tanks has the potential of achieving 30% increase in gravimetric capacity (without sacrificing the volumetric

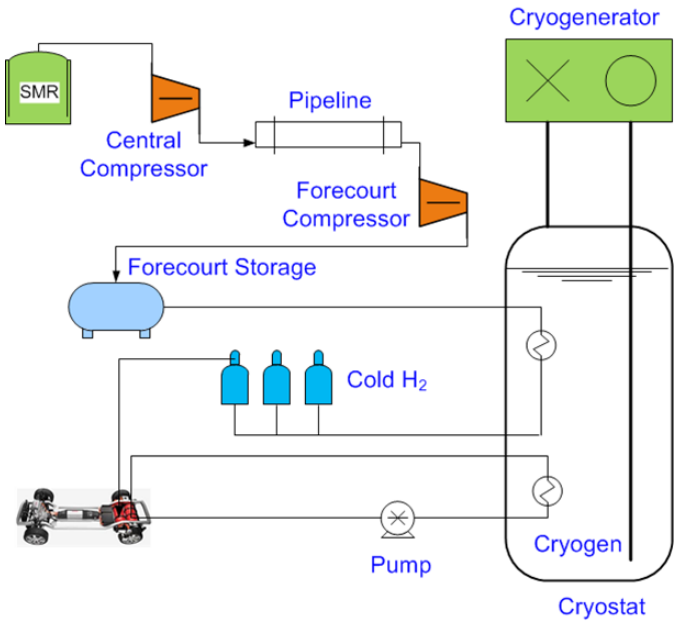

FIGURE 4a. Hydrogen Production, Delivery and Forecourt Scenario

capacity) and 50% saving in CF composite. The penalty is that the required cooling with liquid nitrogen incurs a 13% decrease in WTT efficiency.

Hydrogen Storage in Sorbents

We conducted a "reverse engineering" analysis to determine the minimal material requirements for a sorbent storage system to meet the DOE 2017 performance targets. We first conducted a literature search to develop an empirical correlation for coefficient of performance of cryogenic systems as a function of the refrigeration temperature and plant size. We used this correlation to formulate a simple model that determines the allowable cooling duty for specified coolant temperature and target WTT efficiency for a hydrogen production, delivery, and forecourt scenario outlined in Figure 4a.

Figure 4b shows the reference onboard system used in the reverse engineering analysis. A model was developed to determine the performance of this system in terms of the sorbent sorption properties and the operating conditions. The system model uses a single-Langmuir equation to describe the adsorption isotherms, a model for thermodynamic of adsorption, a correlation for bed thermal conductivity as function of additive weight fraction and fill factor, transient heat transfer module for refueling and discharge, and a containment module for liner thickness and CF requirement.

Table 1 summarizes the results of the reverse engineering analysis. The main conclusion is that a promising sorbent should have >120 g-H_2/kg excess sorption capacity at 150 K or higher temperature and 100 bar, when compacted to 420 kg/m^3 bulk density, and mixed with 10-20% expanded

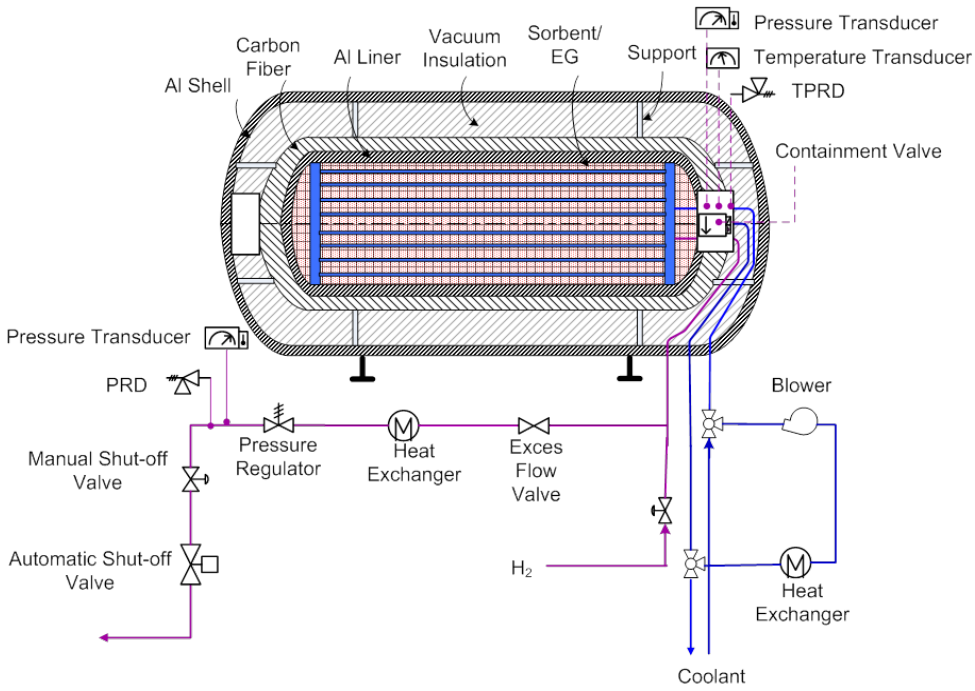

FIGURE 4b. Schematic of Onboard System for Hydrogen Storage in Sorbents

natural graphite or other conductivity enhancement materials to reach 1 W/m·K bed thermal conductivity. A material with ΔH^o of 5 kJ/mol will need to have a minimum excess capacity of 190 g-H_2/kg-sorbent at 77 K for the system to meet the 5.5 wt% gravimetric capacity target. The off-board coolant temperature needs to be above 135 K to reach the study target of >55% WTT efficiency. Adsorbents with $\Delta H°$ >7.5 kJ/mol are especially appealing as they may lead to higher storage temperatures, lower storage pressures, and 60% WTT efficiency.

CONCLUSIONS AND FUTURE DIRECTIONS

- We estimate that the damage volume in the dome for a Type 4 tank holding 5.6 kg usable hydrogen is 73 cm^3 when it is dropped at 45° from a height of 1.8 m. The damage volume can be reduced with advanced resins in the composite, or by placing a foam "cap" over the CF composite overwrapped pressure vessel. A 2.5-cm foam "cap" can completely prevent damage to the dome in the 45° drop test.

TABLE 1. Reference Values for Meeting Onboard Targets

Independent Variables	Related Variables	Reference Values	Constraints
Material Properties			
Excess Uptake at 77 K	DH^o = 5 kJ/mol	190 g-H_2/kg-sorbent	5.5 wt% gravimetric capacity
Fill Ratio	Bulk Density	67% bed porosity	40 g/L volumetric capacity
		420 kg/m^3 sorbent bulk density	
	Thermal Conductivity	1 W/m.K bed conductivity	
Operating Temperatures			
Off-board Coolant	WTT Efficiency	135 K	>55% WTT efficiency
Storage Temperature		155 K	
Temperature Swing	Usable H_2	60 K	95% usable H_2
System Variables			
Mass of Sorbent	Mass of Expanded	42 kg sorbent	5.6 kg usable H_2
	Graphite	8.4 kg ENG	
HX Tube Spacing	Number of HX Tubes	r_2/r_1 = 3.4	1.5 kg/min refueling rate
		112 U tubes	

HX – heat exchanger

- We project that cold hydrogen storage at 400 bar and 180-195 K can achieve ~50% reduction in CF and ~30% increase in gravimetric capacity (if Type 4 tanks can be used at these service temperatures) compared to ambient 700-bar tanks. The WTT efficiency, however, would be 13% lower to 47.4% because of the liquid nitrogen needed to cool the hydrogen to 90 K at the city gate.
- We suggest that a sorbent needs to have $\Delta H° > 5$ kJ/mol and an excess uptake >190 g-H_2/kg at 77 K for the storage system to meet the 5.5 wt% gravimetric capacity target at 150 K and >55% WTT efficiency. The sorbent material should be capable of being compacted to >420 kg/m^3 bulk density for >40 g/L system volumetric capacity. The sorbent compact should also have thermal conductivity >1 W/m.K, when mixed with up to 10-20 wt% conductivity enhancement additives, for 1.5 kg-H_2/min refueling rate.
- In FY 2015, we will continue to run ABAQUS simulations to analyze hydrogen storage in near term, Type 4 700-bar CF-wound pressure vessels. We will simulate local dome winding as an alternate to the endcap concept and investigate helical angle tailoring in the cylinder section to optimize CF performance.
- In FY 2015, we will perform independent analyses to determine the optimal storage pressures and temperatures for physical storage with respect to cost and driving range. We will conduct the analysis for both onboard Type 3 and Type 4 CF wound storage tanks. We will work with the Analysis and Delivery Team personnel to include results for off-board cost and energy consumption.
- In FY 2015, we will analyze the data obtained by the Hydrogen Storage Engineering Center of Excellence for alane slurries of up to 60 wt% loadings. We will use the data to improve, calibrate, and validate the models for dehydrogenation kinetics, component size and volume, and storage system. We will conduct onboard system analysis to evaluate the viability of chemical hydrogen storage and identify the technology gaps for meeting the DOE 2017 performance targets.

FY 2014 PUBLICATIONS/PRESENTATIONS

1. H.S. Roh, T.Q. Hua, and R.K. Ahluwalia, " Optimization of Carbon Fiber Usage in Type-4 Hydrogen Storage Tanks for Fuel Cell Automobiles," International Journal of Hydrogen Energy, 38 (2013) 12795-12802,

2. J.K. Peng and R.K. Ahluwalia, "Enhanced Dormancy due to Para-to-Ortho Hydrogen Conversion in Insulated Cryogenic Pressure Vessels for Automotive Applications," International Journal of Hydrogen Energy, 38 (2013) 13664-1367.

3. R.K. Ahluwalia, J.K. Peng, and T.Q. Hua, "Bounding Material Properties for Automotive Storage of Hydrogen in Metal Hydrides for Low-Temperature Fuel Cells," Accepted for publication in International Journal of Hydrogen Energy.

4. R.K. Ahluwalia and T.Q. Hua, "Onboard Safety," Data, Facts and Figures on Fuel Cells, Detlef Stolten and Remzi Samsun (Editors), Wiley-VCH, to be published in 2014,

5. R.K. Ahluwalia and T.Q. Hua, "Pressurized System," Data, Facts and Figures on Fuel Cells, Detlef Stolten and Remzi Samsun (Editors), Wiley-VCH, to be published in 2014.

6. R.K. Ahluwalia, T.Q. Hua, J.K. Peng, and H.S. Roh, "System Level Analysis of Hydrogen Storage Options," Hydrogen Storage Tech Team Meeting, Southfield, MI, February 20, 2014.

7. H.S. Roh, T.Q. Hua, and R.K. Ahluwalia, "Effect of Resin Properties on Impact Damage Tolerance in Carbon Fiber Composite Tanks," Storage System Analysis Working Group Meeting, Webinar, April 10 2014.

REFERENCES

1. SAE J2579, Technical Information Report for Fuel Systems in Fuel Cell and Other Hydrogen Vehicles. SAE International, 2013.

2. Dongsheng Mao, "Ultra Lightweight High Pressure Hydrogen Fuel Tanks Reinforced with Carbon Nanotube," 2013 DOE Hydrogen Program review, Washington, DC, May 2013.

3. R.K. Ahluwalia, T.Q. Hua, J.K. Peng, D. Papadias, and R. Kumar, "System Level Analysis of Hydrogen Storage Options," 2011 DOE Hydrogen Program review, Washington, DC, May 2011.

IV.A.2 Hydrogen Storage Cost Analysis

Brian D. James (Primary Contact),
Whitney G. Colella, Jennie M. Moton
Strategic Analysis, Inc. (SA)
4075 Wilson Blvd., Suite 200
Arlington, VA 22203
Phone: (703) 778-7114
Email: bjames@sainc.com

DOE Managers
Grace Ordaz
Phone: (202) 586-8350
Email: Grace.Ordaz@ee.doe.gov
Katie Randolph
Phone: (720) 356-1759
Email: Katie.Randolph@ee.doe.gov

Contract Number: DE-EE0005253

Project Start Date: September 30, 2012
Project End Date: September 29, 2016

Overall Objectives

- Identify and/or update the configuration and performance of a variety of hydrogen storage systems for both vehicular and stationary applications.
- Conduct rigorous cost estimates of multiple hydrogen storage systems to reflect optimized components for the specific application and manufacturing processes at various rates of production.
- Explore cost parameter sensitivity to gain understanding of system cost drivers and future pathways to lower system cost.

Fiscal Year (FY) 2014 Objectives

- Update and expand the cost analysis of onboard hydrogen storage in pressurized carbon composite (fiber and resin) pressure vessels.
- Validate the cost analysis methodology and results as a function of manufacturing rate against a Type IV compressed natural gas (CNG) storage tank. Compare CNG storage tank Design for Manufacturing and Assembly (DFMA®) cost modeling results with industry estimates for higher volume tanks currently produced, thereby increasing confidence in the hydrogen pressure vessel storage cost estimates.
- Exploration of high cost balance-of-plant (BOP) components using DFMA® analysis.
- Assess cost and performance impact of Pacific Northwest National Laboratory enhanced materials and design concepts for pressurized hydrogen storage.
- Identify cost drivers and future pathways to lower cost.
- Document all analysis results and assumptions.

Technical Barriers

This project addresses the following technical barriers from the Hydrogen Storage section of the Fuel Cell Technologies Office Multi-Year Research, Development, and Demonstration Plan:

(B) System Cost

(H) Balance-of-Plant (BOP) Components

(K) System Life-Cycle Assessments

Technical Targets

This project conducts cost modeling to attain realistic, process-based system costs for a variety of hydrogen storage systems. These values can inform future technical targets for system storage cost.

- System Storage Cost: <$12/kWh net (2017 target)

FY 2014 Accomplishments

- Validated the Strategic Analysis Inc. hydrogen pressure vessel DFMA® cost model by using it to model a CNG pressure vessel and then comparing the CNG vessel predicted cost with industry quotations. These CNG model results showed agreement with industry quotations (between 2 and 20%) for the same size tank at an annual production rate of 1,000 vessels per year.
- Completed a DFMA® analysis of high-pressure (HP, >12 kpsi) and low-pressure (LP, <400 psi) hydrogen fittings.
- The accuracy of DFMA® cost analysis methodology to assess solenoid valve cost was tested by modeling a CNG integrated valve and comparing the results to vendor quotations. Excellent agreement between the DFMA® analysis predictions and vendor quotations was achieved (within ~6% of vendor quotation)
- The CNG integrated valve DFMA® analysis was modified to represent a hydrogen integrated valve (adjusted for higher pressure, materials, and construction). The projected results were generally lower than previous hydrogen integrated valve price projections and the limited set of vendor quotes available.

- Initiated a cost and performance validation of the Pacific Northwest National Laboratory cold gas storage concept system.
- Refined assumptions, models, and analysis based on expert feedback.

INTRODUCTION

The Fuel Cell Technologies Office (FCTO) states that hydrogen storage is a key enabling technology for the advancement of hydrogen and fuel cell power technologies in transportation, stationary, and portable applications. Consequently, the FCTO has established a goal of developing and demonstrating viable hydrogen storage technologies for transportation and stationary applications. This cost assessment project supports the FCTO goals by identifying the current technology system components, performance levels, and manufacturing/assembly techniques most likely to lead to the lowest system storage cost. Furthermore, the project forecasts the cost of these systems at a variety of annual manufacturing rates to allow comparison to the overall 2017 and "Ultimate" DOE cost targets. The cost breakdown of the system components and manufacturing steps can then be used to guide future R&D decisions.

During the second year of the project, onboard hydrogen storage in pressurized carbon composite pressure vessels was selected for continued analysis. While this system has been previously analyzed by DOE, the objective is to update and expand the cost analysis while also validating the cost analysis methodology and results against industry estimates, thereby increasing confidence for future cost analysis projects. Key BOP components were selected for an in-depth analysis as they constitute a significant portion of the storage system cost.

APPROACH

To generate cost estimates for the compressed hydrogen pressure vessel system, a DFMA®-style analysis was conducted. Key system design parameters and an engineering system diagram describing process flows were obtained from a combination of industry partners, Argonne National Laboratory (ANL), and members of the Hydrogen Storage Engineering Center of Excellence [1]. From this system design, the physical embodiment of the system was developed, including materials, scaling, dimensions, and design. Based on this physical embodiment, the manufacturing process train was modeled to attain the cost to manufacture each part. Industry partners were consulted to assess current and future manufacturing procedures and parameters. Cost was based on the capital cost of the manufacturing equipment, machine rate of the equipment, equipment tooling amortization, part material costs, and other financial assumptions. Once the cost model was complete for the system design, sensitivity data for the modeled technology was obtained by varying the key parameters. These results were shared with ANL, the National Renewable Energy Laboratory, and industry partners to obtain feedback and further refine the model.

The analysis explicitly includes fixed factory expenses such as equipment depreciation, tooling amortization, utilities, and maintenance as well as variable direct costs such as materials and labor. However, because this analysis is intended to model manufacturing costs, a number of components that usually contribute to the original equipment manufacturer price are explicitly not included in the modeling. These costs are excluded in this analysis: profit and markup, one-time costs such as non-recurring research/design/engineering, and general expenses such as general and administrative costs, warranties, advertising, and sales taxes.

In the case of compressed hydrogen pressure vessel BOP components, there are a limited number (if any) of industry vendors that manufacture hydrogen components in high volumes. For example, the integrated in-tank valve incorporates many individual components currently made in industry, but there are very few companies that commercially produce the complete integrated in-tank valves for hydrogen fuel cell systems in high volumes. However, there are multiple manufacturers that have developed similar valves for CNG light-duty vehicles. Consequently, whenever appropriate, DFMA® models of CNG components were generated and the cost projections compared to quotations as a method of validating and improving cost projection accuracy. Then the models were altered to reflect their hydrogen system analog. From this approach, a more accurate projection of hydrogen storage system BOP component costs is achieved.

RESULTS

A validation study of the hydrogen pressure vessel cost model was completed this year by adapting the cost model to represent a CNG pressure vessel and then comparing the projected results to actual vendor high-production CNG quotes. CNG pressure vessels are manufactured in a very similar way to compressed hydrogen Type IV tanks: a polymer liner overwrapped by continuous carbon fiber filament. For this comparison, a 270-liter (internal water volume) CNG tank (sizing for light-duty trucks) was selected for modeling based on discussions with CNG industry professionals who suggested that this size tank is currently produced at 500 to 1,000 units per year. While the Honda Civic CNG tank (120-liter water volume) is produced at higher manufacturing rates (5,000 systems/year) by Structural Composite Industries (SCI)/Worthington Cylinders, the vessels are Type III tanks (metal lined,

waist wrapped) rather than the Type IV tanks assumed for current hydrogen storage pressure vessels. Consequently, the Honda Civic-based tanks by SCI were rejected for the CNG validation basis.

After a tank size was selected, ANL used ABAQUS™ finite element analysis modeling tool to identify material weights, masses, and dimensions: these served as input values for SA's DFMA® pressure vessel cost model. Results from the cost analysis were then compared to price quotations acquired from CNG tank manufacturers (Quantum Technologies, 3M, and Hexagon Lincoln), so as to validate the cost modeling approach. The final analysis results shown in Table 1 compare price quotations provided by manufacturers with the corresponding assumed markup schemes to allow comparison to DFMA® cost results. SA's results align quite well with Quantum and 3M quotation base tank costs. However the Hexagon Lincoln costs are 15% lower, most likely due to Hexagon Lincoln's higher total tank production volume (i.e. production total of all size vessels not just the DFMA® modeled size). Additionally, Hexagon Lincoln's interior tank volume is lower than the other manufacturers in part due to their addition of fiberglass to both the outer tank wrapping (for abrasion and chemical resistance) and to the inner fiber wrapping (for impact resistance). Quantum and 3M restrict fiberglass to the outside of the tank only, thereby providing a higher internal volume for the same outer tank dimensions. During this analysis, it was noted that the DFMA® cost projection is quite sensitive to production rate. Thus, minor assumption differences in annual production rate can lead to significant changes in projected cost.

BOP components have been identified as costly components worthy of further detailed examination, and DOE has directed SA to make BOP cost analysis a focus of the FY 2014 effort. According to SA's 2013 analysis, the two most significant cost drivers for the BOP are the fittings and the integrated in-tank valve. These two elements account for almost 40% of the total BOP costs for a single tank system, at a production rate of 500,000 tank systems per year.

Price quotations were solicited from high-pressure fitting manufacturers for two main types of fittings: 1) Metal-on metal cone/thread sealing fittings (e.g. Swagelok or EV Metal fittings), and 2) O-ring face seal fittings (e.g. Parker Hannifin Seal-Lok™ fittings). A wide variation in fitting cost quotation exists for both types of fittings. Additionally, cost quotations were not available for quantities greater than 50,000 parts although demand is expected to be approximately 3 million fittings per year (for system production 500,000 systems/yr). It is anticipated that fitting cost would decrease with purchase quantity due to both a reduction in production cost and a reduction in manufacturer markup rate. That some distributers did not indicate a purchasing quantity discount is felt to be a reflection of their inability or unwillingness to project the sales price at such high purchase quantities, and not that fitting cost is truly constant with production rate.

For the 2014 analysis, a DFMA® cost analysis was conducted on two representative hydrogen fittings: Parker Hannifin Seal-Lok™ type fittings (4 F57OLO-SS H2U 990549 for HP at 12 kpsi and 4-6 F57OLO-SS H2U for LP at 400 psi). Figure 1 details the projected cost breakdown of the HP fitting at 500,000 systems/yr (6 HP units per system at 3 million units per year). The total fitting cost for both HP and LP fittings at 500,000 systems/yr is approximately $12/fitting. The fitting body cost and individual testing costs are observed to be the most expensive (they include materials, manufacturing, testing equipment needed, and labor). Overall, the 2014 DFMA® analysis predicts total

TABLE 1. CNG Storage Tank Cost Parameters for Three Manufacturers and SA's DFMA® Cost Model Results (Text in red denotes vendor price quotes or DFMA cost modeling results.)

CNG Storage Tank Cost Parameter	Quantum	3M	SA DFMA	Hexagon Lincoln
Annual Purchase Quantity (vessels per year)	Not Spec. (But est. at 1,000)	Not Spec. (But est. at 1,000)	1,000 (prod. Rate)	500
Tank Interior Volume (liters)	274	279	275	251
Tank Mass (kg)	60.8	59.4	65.5	92.1
Tank Cost before markup($/tank)	$2,800	$2,260 - $2,730	$2,852	$2,420
Tank Manufacturer Markup %	15%	15%	15%	15%
Tank Cost after markup ($/tank)	$3,220	$2,600 - $3,140	$3,280	$2,785
Authorized Installer Markup %	10%	8-13%	10%	10%
Tank Cost after markup ($/tank)	$3,500	$2,800 - $3,550	$3,607	$3,030

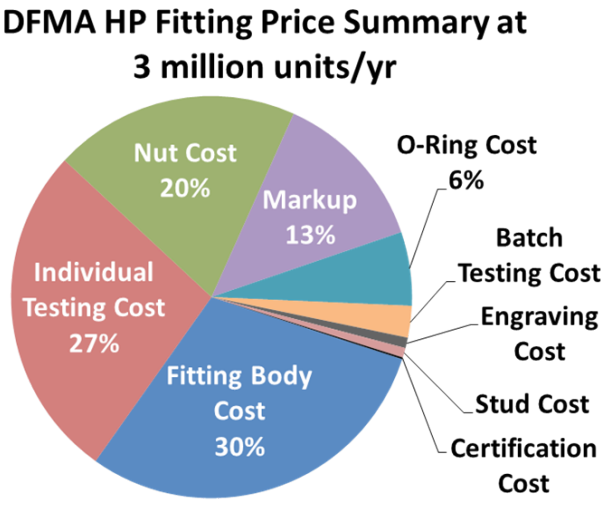

FIGURE 1. DFMA® Results for Breakdown of Fitting Price Based on Six High-Pressure Fittings per System at 500,000 Systems/Yr

fitting and piping system cost to be 11% less (on average over all manufacturing rates) than 2013 levels.

As currently envisioned, the integrated valve body is an in-tank pressure gas solenoid valve that has the additional functionalities of a temperature activated pressure relief device, excess flow valve, particle filter, port provision, a valve for manual override (to allow manual tank depressurization), and a temperature sensor. For the 2013 analysis, the cost of this integrated in-tank valve was assessed by summing the cost contribution of each functional aspect. The sum of these costs was compared to an auto manufacturer's proprietary cost estimates at 10,000 and 100,000 per year and judged reasonable. For the 2014 analysis, a DFMA® analysis was conducted on the integrated valve to more fully understand cost related issues and scaling with manufacturing rate. CNG integrated valves were also considered as they are currently produced in relatively high quantities and therefore provide an opportunity to calibrate the cost estimation procedure.

A full DFMA® analysis was completed for a CNG integrated valve to understand and compare to quotations of existing units at low production rates (10,000 systems/yr). The CNG integrated valve design concept used by SA as the basis for the DFMA® cost analysis is based on an internal flow concept detailed in a GFI patent [2], and uses valve dimensions similar to the OMB Saleri Lyra CV valve (one of the most widely used integrated valves and used on Quantum Technologies, 3M, and Hexagon Lincoln CNG tanks). Price quotations were acquired from CNG BOP component manufacturers (OMB and Tomasetto) and are displayed on the left side of Figure 2 along with the results of the DFMA® analysis. Price quotations were acquired from Tomasetto at an unknown production volume, but are estimated to be between 1,000 and 4,000 units/year. Markup was added to the DFMA® cost results (10-20% depending on production volume) to allow direct comparison to the price quotations. At 17,000 units/year, the DFMA® cost of a CNG integrated valve with markup aligns well with price projections for the currently produced Lyra CV CNG integrated valve ($130/valve).

With confirmation that a DFMA® analysis can successfully be applied to a CNG integrated tank valve product, a similar DFMA® analysis was applied to an hydrogen integrated in-tank valve. While functionality is similar, there are multiple component differences between a CNG and hydrogen integrated valve. The following five differences were identified for this analysis: 1) The operating pressure for CNG valves is typically 3,600 psi while the pressure for hydrogen valves is 10,000 psi (leading to a higher cost due to thicker walls and higher tolerances). 2) The solenoid valve is internal to the hydrogen tank and external to CNG tank. 3) The temperature transducer and filter are included on the hydrogen valve, but are not included on the CNG valve. 4) CNG valves can be composed of

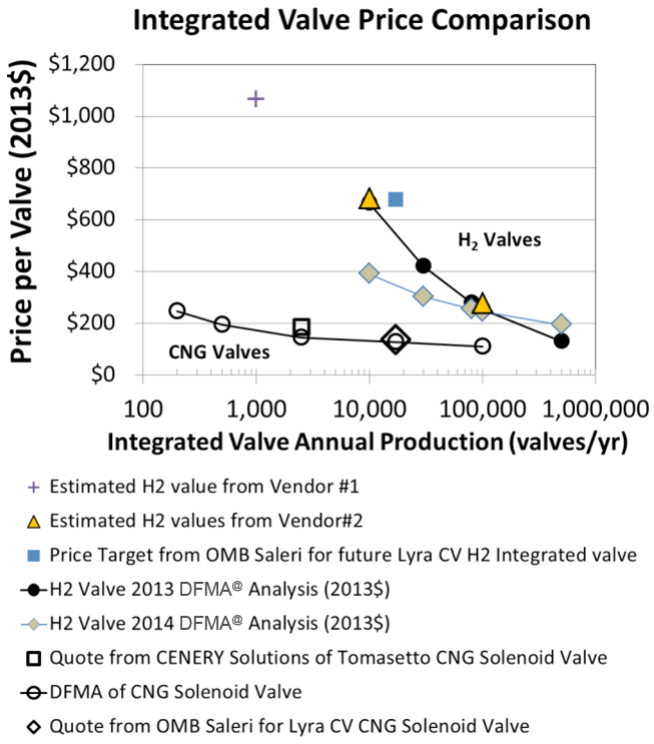

FIGURE 2. Price Quotations Compared to 2014 DFMA® Analysis on CNG (left) and Hydrogen (right) Tank Integrated Valves

aluminum or brass while hydrogen valves are typically made of stainless steel. 5) The typical neck opening is 2 inches in diameter on a CNG tank and 1.5 inches on a (higher pressure) hydrogen tank.

The design and sizing used for the hydrogen integrated valve DFMA® are loosely based on Quantum Technology's in-tank valve. Informal discussions with OMB Saleri suggest the current cost of a hydrogen integrated valve is around $2,000/valve. OMB Saleri is working to reduce the cost of the valve, and has set a future target of $675/valve (at an unknown production volume). The results from the 2014 DFMA® analysis for the hydrogen integrated valve are shown on the right side of Figure 2, and show a shallower slope in valve cost with production volume compared to the 2013 analysis. The OMB Saleri cost target for a hydrogen integrated valve is close to the 10,000 systems/yr cost projection from the 2013 analysis. However, this $675/valve may have different internal components and functionality than what has been defined for SA's hydrogen integrated valve design. Furthermore, the production volume is unknown, but is assumed to be similar to the CNG Lyra CV valves OMB Saleri produces at 17,000 units/yr.

After investigating the BOP components for the hydrogen pressure vessel, the total BOP price changes between the 2013 analysis and 2014 analysis are very small at the high manufacturing rates, but differ by about 18% at

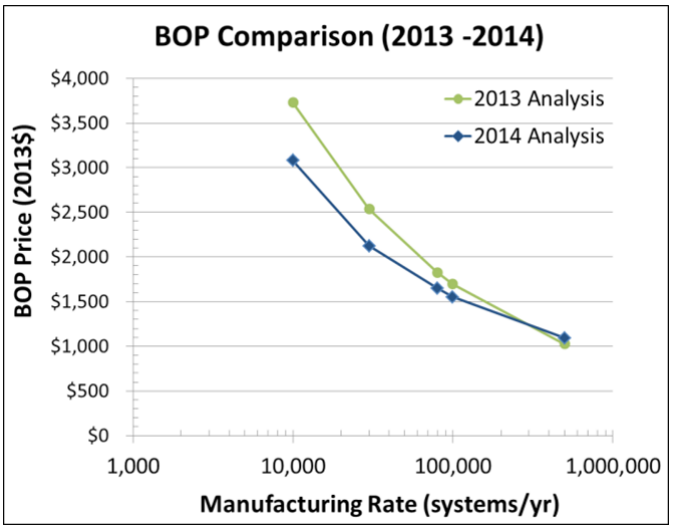

FIGURE 3. Graph of Total BOP Price for 2013 and 2014 Analyses (All prices are in 2013$.)

10,000 systems/yr (this includes the DFMA® cost results for fittings and integrated in-tank valves and quotations for pressure regulators). Figure 3 shows this comparison between 10,000 and 500,000 systems per year.

CONCLUSIONS AND FUTURE DIRECTIONS

Based upon work from this year, the following conclusions and future directions are revealed:

- Validation of the hydrogen pressure vessel DFMA® cost model by adaptation of the DFMA® model to project CNG pressure vessel cost and subsequent agreement between model projected costs and vendor quotations (at 1,000 tanks/year).
- Identification of the BOP components as major contributors to total system cost and identification of fittings and the integrated in-tank valve as key cost drivers of the BOP subsystem.
- DFMA® analysis of both fittings and integrated in-tank valve suggest a small change in cost compared to 2013 analysis at 500,000 systems/yr, but an 18% lower cost at 10,000 systems/yr.

Future work will:

- Continue to refine the hydrogen pressure vessel cost analysis
- Gather further original equipment manufacturer data on BOP component costs
- Explore BOP component simplification and combined functionality as a pathway to lower cost
- Assess the cost impact of advanced tankage concepts such as use of strength-graded fibers, carbon nanotube addition between fiber layers to increase translational strength, and cold hydrogen storage (200 K)
- Conduct a DFMA® cost assessment of the Hawaii Hydrogen Carrier metal hydride storage system for fork lift applications
- Conduct a DFMA® cost assessment of an alane chemical hydrogen storage system used onboard a vehicle
- Conduct a DFMA® cost assessment of the sorbent based onboard systems as investigated by the Hydrogen Storage Engineering Center of Excellence

SPECIAL RECOGNITIONS & AWARDS/ PATENTS ISSUED

1. Hydrogen and Fuel Cells Program Award. Awarded to Brian D. James by the Director of the Fuel Cell Technologies Office, Sunita Satyapal June 17th 2014.

FY 2014 PUBLICATIONS/PRESENTATIONS

1. James, B.D., Moton, J.M., Colella, W.G., "Ongoing Validation of the H_2 Pressure Vessel Storage System Cost Model," Presentation to the 2014 Hydrogen Storage Technical Team, presented remotely from Strategic Analysis Office in Arlington, Virginia, April 17, 2014.

2. James, B. D., Moton, J.M., Colella, W. G., "Ongoing Analysis of H_2 Storage System Costs," U.S. DOE's 2014 Annual Merit Review and Peer Evaluation Meeting (AMR) for the Hydrogen and Fuel Cells Program, Washington, D.C., June 16–20, 2014, Project ID ST100.

3. Moton, J.M., James, B.D., Colella, W.G. "Advances in Electrochemical Compression of Hydrogen," *Proceedings of the ASME 2014 8th International Conference on Energy Sustainability & 12th Fuel Cell Science, Engineering and Technology Conference (ESFuelCell2014)*, Boston, Massachusetts, June 30th- July 2nd , 2014 (ESFuelCell2014-6641).

4. Moton, J.M., James, B.D., Colella, W.G. "Advances in Electrochemical Compression of Hydrogen," *Presentation given at the ASME 2014 8th International Conference on Energy Sustainability & 12th Fuel Cell Science, Engineering and Technology Conference (ESFuelCell2014)*, Boston, Massachusetts, June 30th – July 2nd, 2014.

REFERENCES

1. "Technical assessment of compressed hydrogen storage tank systems for automotive applications," T.Q. Hua, R.K. Ahluwalia, J.-K. Peng, M. Kromer, S. Lasher, K. McKenney, K. Law, J. Sinha, International Journal of Hydrogen Energy 36 (2011) 3037-3049. (doi:10.1016/j.ijhydene.2010.11.090)

2. European Patent (EP 0805295 B1).

IV.B.1 Hydrogen Storage Engineering Center of Excellence (HSCoE)

Donald L Anton (Primary Contact),
Theodore Motyka, Bruce J Hardy,
David A Tamburello and Claudio Corgnale
Savannah River National Laboratory (SRNL)
Bldg. 999-2W
Aiken, SC 29808
Phone: (803) 507-8551
Email: DONALD.ANTON@SRNL.DOE.GOV

DOE Managers
Ned Stetson
Phone: (202) 586-9995
Email: Ned.Stetson@ee.doe.gov
Jesse Adams
Phone: (720) 356-1421
Email: Jesse.Adams@ee.doe.gov

Technical Advisor
Robert Bowman
Phone: 818-354-7941
Email: rcbjr1967@gmail.com

Subcontractors
- Pacific Northwest National Laboratory (PNNL), Richland, WA
- United Technologies Research Center (UTRC), E. Hartford, CT
- General Motors Corporation (GM), Dearborn, MI
- Ford Motor Corporation (Ford), Dearborn, MI
- The National Renewable Energy Laboratory (NREL), Golden, CO
- Los Alamos National Laboratory (LANL), Los Almaos, NM
- The Jet Propulsion Laboratory (JPL), Pasadena, CA
- The University of Michigan (UM), Ann Arbor, MI
- The California Institute of Technology (Cal Tech), Pasadena, CA
- Oregon State University (OSU), Corvallis, OR
- Hexagon Lincoln LLC, Lincoln, NB
- University of Québec, Trios Rivieres (UQTR), Trois Rivieres, QC, Canada

Project Start Date: February 1, 2009
Project End Date: June 30, 2015

Overall Objectives

- Develop system models that will lend insight into overall fuel cycle efficiency.
- Compile all relevant materials data for candidate storage media and define future data requirements.
- Develop engineering and design models to further the understanding of onboard storage energy management requirements.
- Develop innovative onboard system concepts for metal hydride, chemical hydrogen storage, and adsorbent materials-based storage technologies.
- Design components and experimental test fixtures to evaluate the innovative storage devices and subsystem design concepts, validate model predictions, and improve both component design and predictive capability.
- Design, fabricate, test, and decommission the subscale prototype components and systems of each materials-based technology (adsorbents, metal hydrides, and chemical hydrogen storage materials).

Fiscal Year (FY) 2014 Objectives

Management Work Scope

- Coordination and facilitation of partner's activities:
  - Organize and conduct one face-to-face Center Technical Meeting
  - Organize and participate in Tech Team Review
  - Publish Integrated model on the HSECoE website
  - Complete construction of Phase 3 prototypes
- Updated prototype system testing plan for both adsorbent and chemical hydrogen systems

Technical Work Scope

- Design and construct two hydrogen cryo-adsorbent test stations capable of evaluating the performance of a 2-liter prototype operating between 80-160 K and 5-100 bar.
  - Test Station #1 – Flow-through cooling concept with a resistance-based heater
  - Test Station #2 – Isolated-fluid cooling/heating concept
- Design and construct two 2-liter adsorbent subscale prototypes:
  - Hexagonal heat exchanger (HexCell) Design – Flow-through cooling concept with a resistance-based hexagonal heat exchanger developed for powder adsorbent
  - Modular Adsorption Tank Insert (MATI) Design – Isolated-fluid cooling/heating concept developed for compacted adsorbent
- Complete test matrix for evaluation of the 2-liter adsorbent system.

- Update the cryo-adsorbent system models with Phase 3 performance data, integrate the models into the framework, document the models, and release them to the public.
- Refine the detailed models (validate) for scale up and alternative hydrogen storage applications.
- Determine minimally acceptable adsorbent material properties to meet the 2017 and ultimate system targets.

Technical Barriers

This project addresses the following technical barriers from the Hydrogen Storage section of the Fuel Cell Technologies Office Multi-Year Research, Development, and Demonstration Plan:

(A) System Weight and Volume

(B) System Cost

(C) Efficiency

(D) Durability/Operability

(E) Charging/Discharging Rates

(G) Materials of Construction

(H) Balance-of-Plant (BOP) Components

(J) Thermal Management

(K) System Life-Cycle Assessments

(L) Lack of Tank Performance Data and Understanding of Failure Mechanisms

(O) Lack of Understanding of Hydrogen Physisorption and Chemisorption

(R) By-Product/Spent Material Removal

Technical Targets

This project directs the modeling, design, build, and demonstration of prototype hydrogen storage systems for each material class (metal hydride, chemical hydrogen storage and hydrogen adsorbent) meeting as many of the DOE Technical Targets for light-duty vehicular hydrogen storage. The current status of these systems versus the Onboard Hydrogen Storage System Technical Targets as of the end of Phase 2 is given in Table 1.

Center Wide Accomplishments

The following are landmark innovations that the HSECoE can claim to have lead which have changed the way we think about hydrogen storage systems and the materials which are used in them. Overall, the DOE Technical Targets

TABLE 1. System Status vs. Technical Targets

			Adsorbent System			Chemical Systyem		
			Phase 2 *Actual (automotive scale)*			Projected System HSECoE Go/No-Go*What could be built in the future (full scale)*		
Target	Units	2017 DOE Goal (System)	Phase 2 HSECoE Targets (Material)	Phase 2 HSECoE Targets (BOP only)	Phase 2 HSECoE Targets (System)	Phase 2 HSECoE Targets (Material)	Phase 2 HSECoE Targets (BOP only)	Phase 2 HSECoE Targets (System)
Gravametric Capacity	kg H2/kg system	0.055	0.187	0.10	0.0352	0.0872	0.15	0.055
mass	*kg*	*102*		*16.1*	159			*102*
Volumetric Capacity	kg H2/L system	0.04	0.03	0.053	0.0175	0.078	0.132	0.049
Volumetric	*liters*	*140*		*16.9*	320			*114*
System Cost	$/kWh net	6	3.5	5.62	12.74			
	$	*1,119*		*1048*	2376			
Fuel Cost	$/gge at pump	2-6			4.89			
Min Operating Temp	°C	-40			-40			-20
Max Operating Temp	°C	60			60			60
Min Delivery Temp	°C	-40			-40			-20
Max Delivery Temp	°C	85			85			85
Cycle Life	Cycles	1500			1500			1000
Min Delivery Pressure	bar	5			5			5
Max Delivery Pressure	bar	12			12			12
Onboard Efficiency	%	90			92			95
Well to Power Plant Efficiency	%	60			39.2			37
System Fill Time	min	3.3			3.3			2.9
Min Full Flow Rate	(g/s/kW)	0.02			0.02			0.02
	g/s	*1.6*			*1.6*			*1.6*
Start Time to Full Flow (20°C)	sec	5			5			1
Start Time to Full Flow (-20°C)	sec	15			15			1
Transient Response	sec	0.75			0.75			0.5
Fuel Purity	% H2	99.97			99.99			99.97
Permeation, Toxicity, Safety	Scc/h	Meets or Exceeds Standards			s			s
Loss of Useable Hydrogen	(g/h)/kg H2 stored	0.05			0.44			0.05

were prioritized showing that volumetric density is more important than gravimetric density when range and space are considered. Integration of the hydrogen storage system models including the fuel cell, balance of plant, and vehicle drive cycles were used to determine the empty tank status under the US06 drive cycle.

For metal hydride storage, a metal hydride acceptability envelope showing the interrelationship of the enthalpy, specific heat, thermal conductivity, and gravimetric density in a postulated material's ability to meet the refueling target was accomplished. A microchannel catalytic burner was demonstrated achieving a volumetric density record for oxidizing hydrogen and return the available heat in a useful form to the storage system.

For chemical hydrogen storage the HSECoE identified that a slurry was needed to transport the hydrogen carrier material into and out of a controlled temperature reactor. The definition of slurry storage material characteristics necessary to meet the DOE Technical Targets was identified. An Auger reactor for slurries and a helical reactor for neat liquids allowing the uniform transport of the chemical hydrogen carrier into a thermally controlled reactor for dehydrogenation were shown. Demonstration of a viable 60 wt% alane slurry into an auger reactor with controlled hydrogen discharge.

For adsorbent storage the HSECoE identified the requirement for a liquid nitrogen jacket tank cooling strategy which rapidly dissipates the enthalpy of adsorption and cools the adsorbent allowing achievement of the three minute refueling time technical target. Demonstration of a novel low-cost flow-through heat exchanger design which allows for the rapid cooling of the adsorbent media during refueling and even heat distribution during operation was also shown. Combined metal organic framework (MOF) compaction and augmentation with thermal conductivity enhancements achieved hydrogen adsorption densities 50% greater than conventional powder packing had previously achieved. Development of a microchannel heat exchanger design allowing for the use of compacted adsorbent media achieving a 10% reduction total system volume. Development of the adsorbent acceptability envelope outlines the necessary adsorbent properties using the UNILAN model showing the necessity for adsorbed hydrogen density of ≥120 mol/Kg and an isosteric heat of 4.6 KJ/mol.

Technical Accomplishments

Small-scale (0.5-liter flanged vessel with a HexCell HX) experiments and models for powder MOF-5:

- Verification that physical processes are properly included/represented
- Flow-through cooling hydrogen charging experiments were completed and models were validated
- Resistive heating rod hydrogen discharging experiments were completed and models were validated

- Phase 3 HexCell experiments and model validation:
  - Prototype test station at UQTR was built and tested
  - 2-liter vessel with resistive rod heater within a hexagonal heat exchanger
    - Design completed
    - Assembled and instrumented at UQTR
  - Model for the 2-liter tank in three-dimensional geometry with 90° symmetry
    - Model running successfully with preliminary test cases
    - Leveraged previous experience from the 0.5-liter tank
  - Test matrix completed
  - Preliminary experiments at UQTR have begun
- Phase 3 MATI experiments and model validation:
  - Prototype design has been completed with OSU
  - Prototype test station at SRNL design completed
    - All components purchased and on site
    - Test station is 80% assembled with electrical left to complete
  - Preliminary test matrix completed

INTRODUCTION

The HSECoE brings together all of the materials and hydrogen storage technology efforts to address onboard hydrogen storage in light-duty vehicle applications. The effort began with a heavy emphasis on modeling and data gathering to determine the state of the art in hydrogen storage systems. This effort spanned the design space of vehicle requirements, power plant and balance of plant requirements, storage system components, and materials engineering efforts. These data and models will then be used to design components and sub-scale prototypes of hydrogen storage systems which will be evaluated and tested to determine the status of potential systems against the DOE 2017 and Ultimate Full Fleet Technical Targets for Hydrogen Storage Systems for Light-Duty Vehicles.

APPROACH

A team of leading North American national laboratories, universities, and industrial laboratories, each with a high

degree of hydrogen storage engineering expertise cultivated through prior DOE, international, and privately sponsored projects has been assembled to study and analyze the engineering aspects of condensed phase hydrogen storage as applied to automotive applications. The technical activities of the HSCoE are divided into three System Architectures: adsorbent, chemical hydrogen storage and metal hydride matrixed with six technology areas: Performance Analysis, Integrated Power Plant/Storage System Analysis, Materials Operating Requirements, Transport Phenomena, Enabling Technologies and Subscale Prototype Construction, Testing and Evaluation. The project is divided into three phases; Phase 1: System Requirements and Novel Concepts, Phase 2: Novel Concept Modeling Design and Evaluation, and Phas 3: Subscale System Design, Testing, and Evaluation.

RESULTS

SRNL and UQTR to date have met and or exceeded their FY 2014 objectives for all of their major technical goals within the HSECoE. These objectives fall within the areas of Transport Phenomena, Adsorbent System Level Modeling, Material Operating Requirements, and System Architecture. Transport Phenomena and Adsorbent System Modeling results are shown below for adsorbent systems.

Transport Phenomena

- Component level experiments for MOF-5 charging and discharging in a 0.5-liter flow-through cooling system were conducted.
  - Flow-through cooling was demonstrated for the charging process.
  - Heating via a resistance rod imbedded in an aluminum hexagon was used for the discharge process.
    - Heating (discharge) experiments along with computational comparisons completed for multiple configurations including heating experiments with empty HexCells, heating experiments with alumina-filled HexCells, and heating experiments with MOF-5 powder-filled HexCells.
- Models developed/applied by SRNL replicate the experimental conditions
  - Validation of models against the 0.5-liter experimental data for several flow-through cooling and resistance heater desorption experiments to verify that the physical processes are properly included/represented.
  - Figure 1 shows representative results between the experimental data and computational model for powder MOF-5, initially at 3.5 MPa hydrogen, 77 K at vessel surface, and no outflow.
    - The HexCell HX distributes thermal energy well.
    - Results are shown for a uniform heater power profile; comparisons are also good for a parabolic heater power profile.
  - Both experimental measurements and numerical models of the heating/discharge technique showed that the HexCell HX distributes thermal energy well.
- 2-liter HexCell prototype experiments and models
  - Designed and assembled vessel and internal components of the 2-liter prototype (as shown in Figure 2) and the HexCell prototype test stand (as shown in Figure 3).
    - The prototype test facility has been completed, with capabilities of hydrogen flow rates up to 1,000 splm.
  - Developed a test matrix
  - Conducted preliminary experiments in ambient temperature and above
  - Created a three-dimensional computational model geometry with a 90^{o} symmetry (as shown in Figure 2), which is successfully running and shows good agreement with the preliminary ambient temperature experiments.
  - Currently working on solutions for the 2-liter vessel seal leak issue at cryogenic temperatures.
- 2-liter MATI prototype experiments and models
  - Assisted OSU in the design of the 2-liter prototype and its internal components (shown in Figure 4).
  - Designed and began assembly of the MATI prototype test stand, shown in Figure 4, with the following capabilities:
    - Gas supplies:
      - H_2 at 80 K and >100 slpm
      - LN_2 at ~7 bar and 80 K
      - N_2 at >373 K and >100 slpm
    - Data acquisition:
      - Pressure and temperature at all tank inlets/outlets
      - Mass flow control and measurements of all gas/liquid flows
  - Began construction of the MATI prototype test stand, with completion scheduled for August, 2014.

Adsorbent System Level Modeling

- The MATLAB®-version of the cryo-adsorbent system models has been updated to reflect the latest input from all HSECoE partners for both of the HexCell and

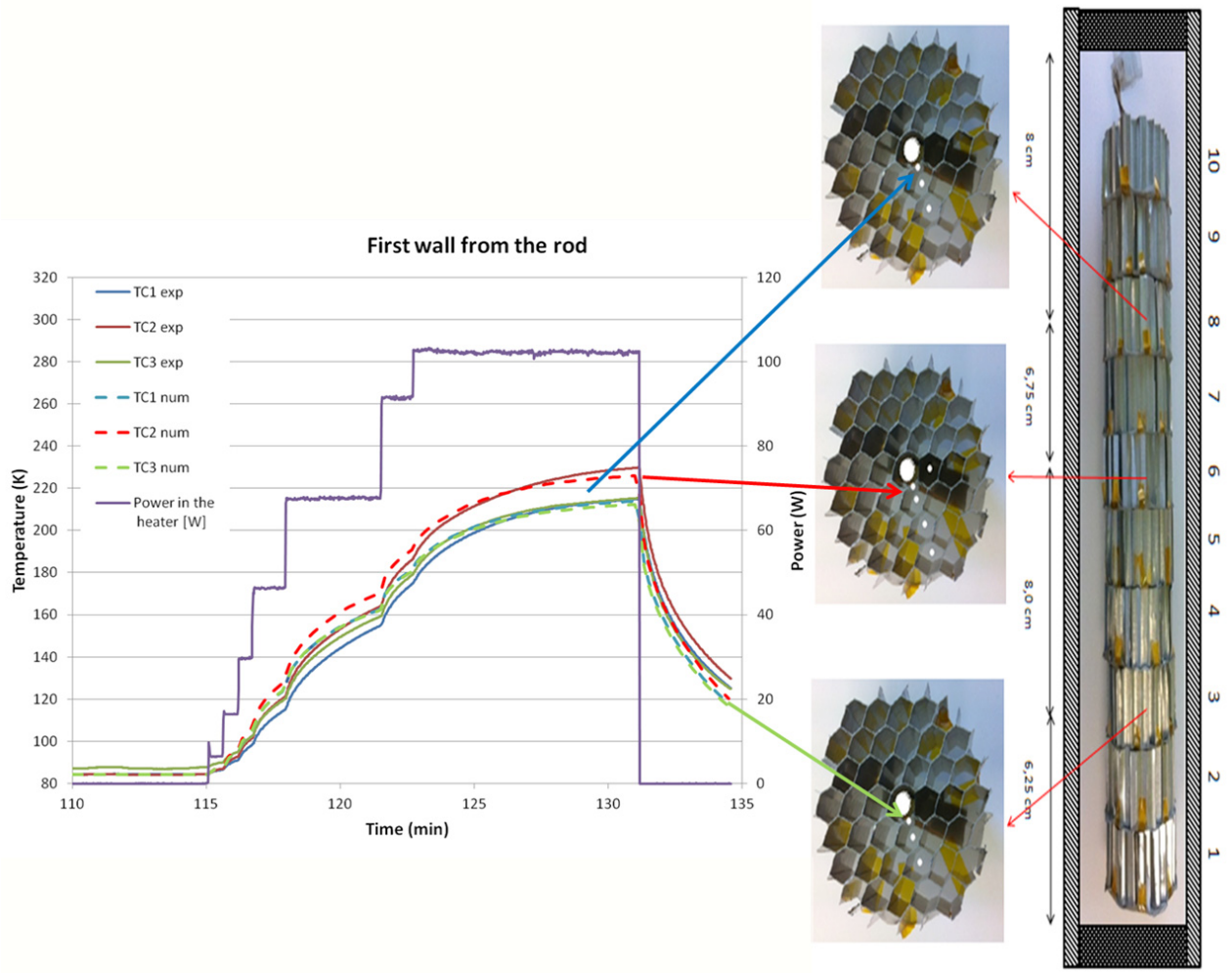

FIGURE 1. 0.5-Liter Vessel Experimental Data and Model Comparison

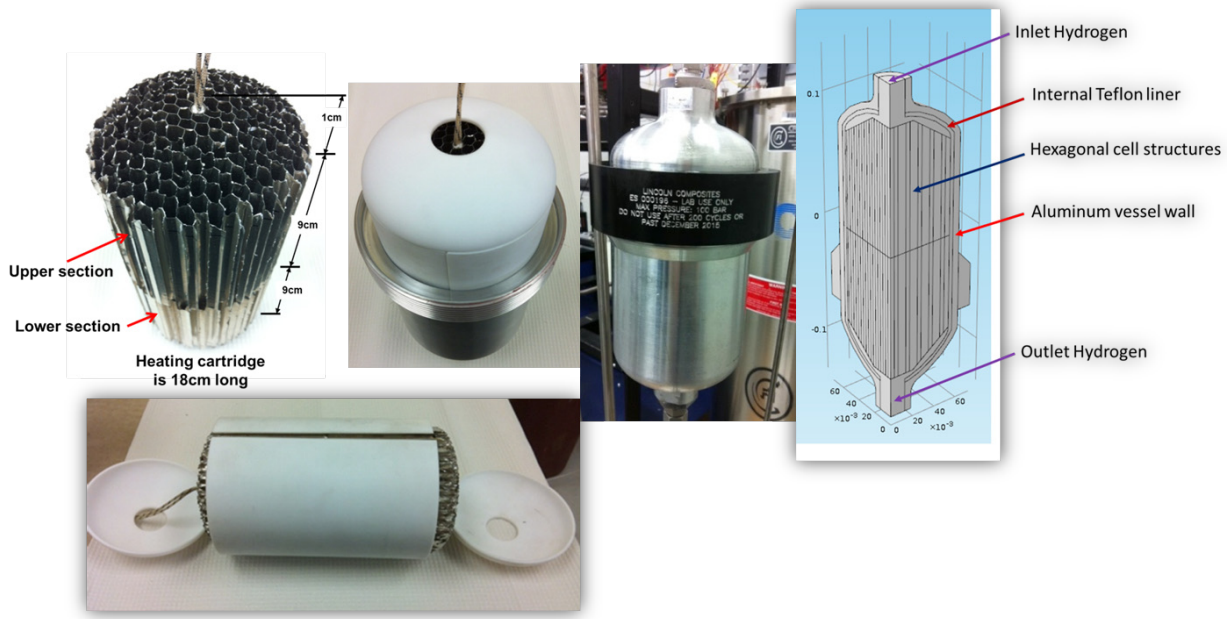

FIGURE 2. 2-Liter HexCell Prototype Assembly and Computational Model

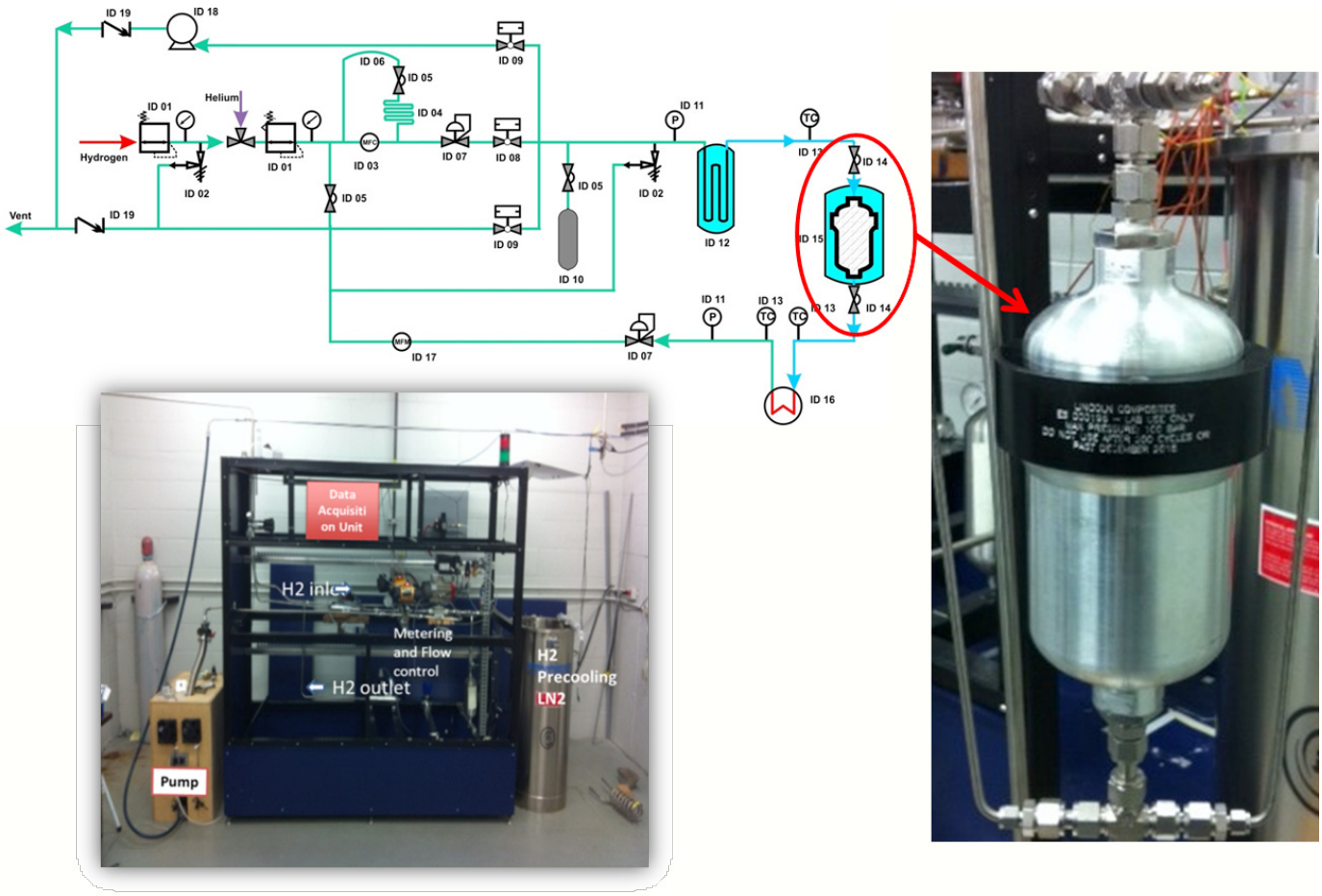

FIGURE 3. 2-Liter HexCell Prototype Test Stand

MATI system designs. Note that the system models have the following capabilities, with all subroutines having expansion abilities should additional options/improvements be available/desirable:

- First-order system and individual component cost estimates.
- Overall system ranks based on a value algorithm developed by Ford that incorporates the system cost, gravimetric capacity, and volumetric capacity.
- Dubinin-Astakhov parameters for hydrogen storage within several cryo-adsorbents (single and multi-component versions are available).
- Internal tank heat exchanger concepts, where the mass and volume of the heat exchanger is adaptable based on the properties (and amount) of the cryo-adsorbent.
- A tank design algorithm, with a wide variety of material and dimensional options, which was developed by PNNL with input from SRNL and Hexagon Lincoln.
- A wide range of thermo-physical property correlations for 0.1 bar < P < 450 bar and 20 K < T < 450 K.
- Excluding pressure and temperature, there are a total of over 60,000 system parameter option combinations.

• The Simulink® version of the cryo-adsorbent system models is being updated from the MATLAB-version in preparation for its inclusion in "Models on the Web."

CONCLUSIONS AND FUTURE DIRECTIONS

Metal hydride efforts were terminated based on the judgment that no known material was capable of meeting either the 2017 or ultimate targets in a system configuration. Ultimately, a metal hydride is needed which will have a capacity of 10-11 wt% hydrogen and an enthalpy of 25-27 KJ/mole H_2 to avoid the requirement of consuming a significant portion of the stored hydrogen. No metal hydride is currently foreseen that meets this very demanding target.

Chemical hydrogen storage efforts were centered on slurry/solvent materials utilizing flow through reactor

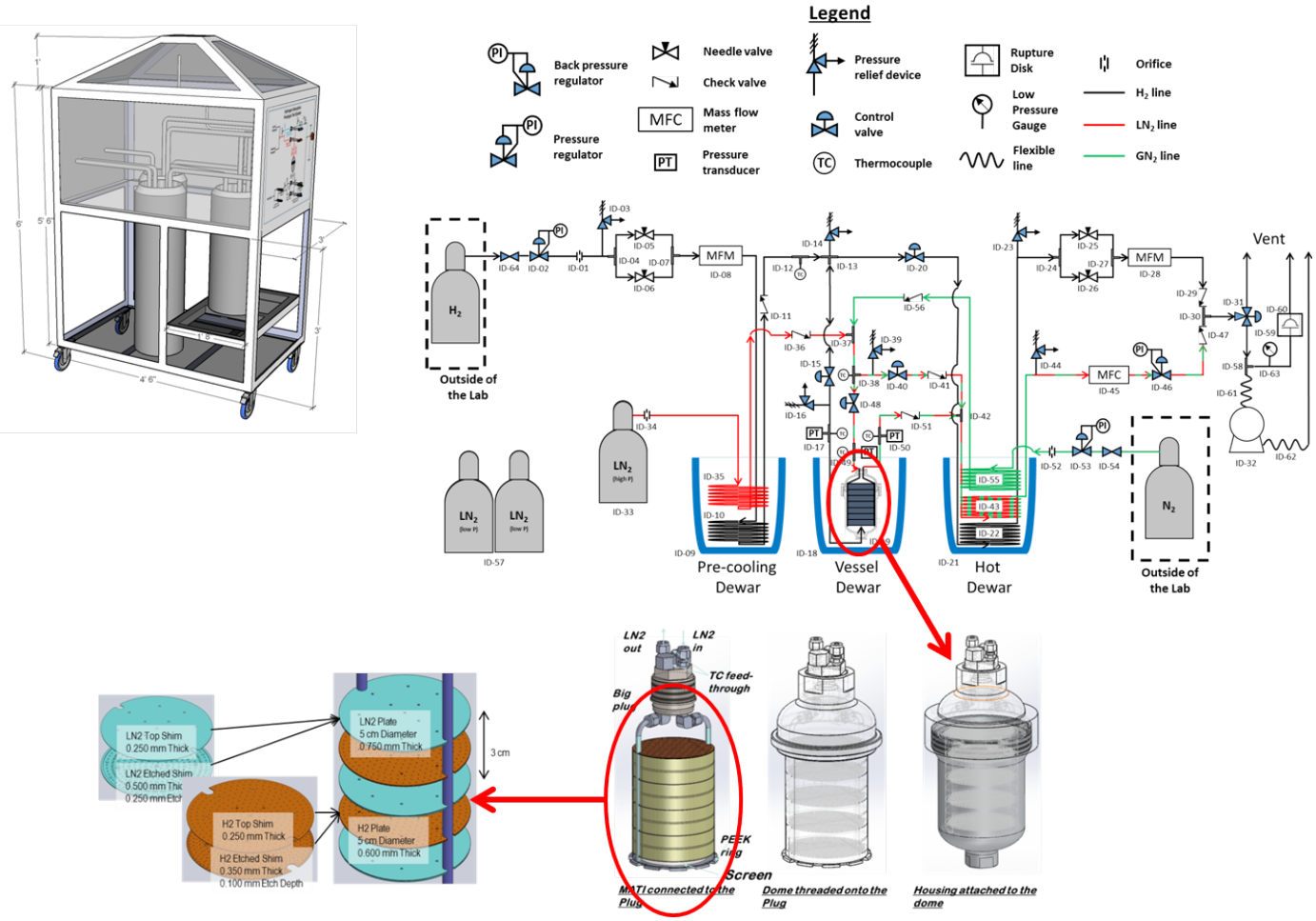

FIGURE 4. 2-Liter MATI Prototype Test Stand

development with dynamic temperature control, high-flow gas liquid separation and impurity trapping. Further studies were conducted on endothermic vs. exothermic chemical hydrogen storage materials with the identification of various start-stop cycles deeply inhibiting attainment of the onboard efficiency target. Ultimately, the chemical hydrogen storage materials efforts were terminated based on the regeneration costs and other associated technology factors outside of the HSECoE scope.

Adsorbent system efforts are concentrated on Phase 3 prototype design, assembly, testing, and modeling, including test station design, construction, and capabilities verification. Two prototypes are being tested (and modeled) in Phase 3; (1) powder MOF-5 in a HexCell that utilizes flow-through cooling during refueling and resistance heating during discharge will be tested at UQTR and modeled at SRNL, and (2) compacted MOF-5 in a MATI utilizing isolated liquid nitrogen during refueling and isolated hydrogen during discharge will be tested at SRNL and modeled at OSU. Several factors affected this selection, including the detailed model analyses with experimental validation, the overall system performance projections, the projected costs, the projected interaction with the forecourt, and the future direction of adsorbent material research.

Future technical work by SRNL in the adsorbent area will include:

- Continue to verify and determine solutions for the 2-liter vessel seal leak issue at cryogenic temperatures.
- Preliminary test plan for the HexCell prototype:
  - Pressure tests the 2-liter vessel without the HexCell structure inside the tank to check the characteristics of the tank (volume, thermal mass, etc.)
  - Performance evaluation of the heating rod (temperature profiles)
  - Flow-through cooling/charging tests with powder MOF-5
  - Heating/desorption tests with powder MOF-5
  - Cycle testing, with charge-discharge-charge, etc.

- Complete construction and capabilities verification of the MATI prototype test stand.
- Preliminary test plan for the MATI prototype:
  - Pressure test the 2-liter vessel without the MATI structure inside the tank to check the characteristics of the tank (volume, thermal mass, etc.)
  - Performance evaluation of the MATI (temperature profiles)
  - Cooling/adsorption tests with compacted MOF-5
  - Heating/desorption tests with compacted MOF-5
  - Cycle testing, with charge-discharge-charge, etc.
- Update Simulink cryo-adsorbent system models to predict full-scale system performance.
  - Make updated system models available for "models on the Web."

FY 2014 PUBLICATIONS/PRESENTATIONS BY SRNL/UQTR

1. Hardy B, Corgnale C, Tamburello D, Anton D. "Acceptability envelope for adsorption based hydrogen storage" Invited presentation at MCARE 2014, Clearwater (FL), USA.

2. Pasini JM, Corgnale C, Van Hassel B, Motyka T., Kumar S, Simmons K. "Metal hydride material requirements for automotive hydrogen storage systems" International Journal of Hydrogen Energy, Volume 38, Issue 23, 2013, Pages 9755–9765

3. "Hydrogen Storage Materials: A System Perspective as to What Is Needed for Transportation Applications", D.L. Anton Invited Presentation at Gordon Conference 2013, Barga, Italy.

FY 2014 PATENTS BY SRNL/UQTR

1. Tamburello et. al., Heat Transfer Unit Method for Prefabricated Vessel, 61/905,557, 12/12/2013.

IV.B.2 Systems Engineering of Chemical Hydrogen Storage, Pressure Vessel, and Balance of Plant for Onboard Hydrogen Storage

Kriston P. Brooks (Primary Contact),
Kevin L. Simmons, Mark R. Weimar
Pacific Northwest National Laboratory (PNNL)
P.O. Box 999/K6-28
Richland, WA 99352
Phone: (509) 372-4343
Email: Kriston.brooks@pnnl.gov

DOE Managers
Ned Stetson
Phone: (202) 586-9995
Email: Ned.Stetson@ee.doe.gov
Jesse Adams
Phone: (720) 356-1421
Email: Jesse.Adams@ee.doe.gov

Project Start Date: February 1, 2009
Project End Date: June 30, 2015

Overall Objectives

- Develop hydrogen storage systems that meet DOE 2017 targets for light-duty vehicles based on cryo-adsorbent and chemical hydrogen storage materials.
- Identify, develop and validate critical components of the chemical hydrogen and cryo-adsorbent-based materials for performance, mass, volume, and cost.
- Develop and validate models for a chemical hydrogen storage system to further the understanding of onboard storage energy management requirements.
- Work with our partners to integrate our validated models into system framework that will lend insight into overall fuel cycle efficiency.
- Reduce system volume and mass while optimizing system storage capability and performance through value engineering of heat exchangers and balance-of-plant (BOP) components.
- Mitigate materials incompatibility issues associated with hydrogen embrittlement, corrosion, and permeability through suitable materials selection for vessel materials, heat exchangers, plumbing and BOP components.

Fiscal Year (FY) 2014 Objectives

- Chemical Hydrogen Storage Design
  - Develop system models for exothermic and endothermic systems to predict mass, volume, performance
  - Validate models via experimentation
  - Perform cost modeling and manufacturing analysis for the endothermic system design
- Cryo-Adsorbent Hydrogen Storage Design
  - Develop and validate the LN_2-cooled wall approach to refueling and dormancy
  - Perform value engineering of BOP to minimize cost, volume and mass
  - Guide design and technology down selection via cost modeling and manufacturing analysis

Technical Barriers

This project addressed the following technical barriers this last year for Hydrogen Storage from the Fuel Cell Technologies Office Multi-Year Research, Development, and Demonstration Plan:

(A) System Weight and Volume

(B System Cost

(C) Efficiency

(D) Durability

(E) Charging/Discharging Rates

(G) Materials of Construction

(H) Balance of Plant (BOP) Components

(J) Thermal Management

(O) Hydrogen Boil-Off

Technical Targets

The current status of the chemical hydride and cryo-sorption material systems versus the DOE Onboard Hydrogen Storage System Technical Targets as of the end of Phase 2 is given in Table 1.

FY 2014 Accomplishments

- Developed a cost analysis for the endothermic chemical hydrogen storage materials using alane as a surrogate. Projected system costs of $4,127 or $22/kWh at 500,000 units were calculated.
- Developed a chemical hydrogen storage system model that combines exothermic and endothermic models into a single system and validated it using experimental data from reactor studies performed with ammonia borane (AB) and alane at Los Alamos National Laboratory (LANL).

TABLE 1. Progress towards Meeting DOE Technical Targets for Hydrogen Storage

			Adsorbent System			Chemical Systyem		
			Phase 2 *Actual (automotive scale)*			Projected System HSECoE Go/No-Go*What could be built in the future (full scale)*		
Target	Units	2017 DOE Goal (System)	Phase 2 HSECoE Targets (Material)	Phase 2 HSECoE Targets (BOP only)	Phase 2 HSECoE Targets (System)	Phase 2 HSECoE Targets (Material)	Phase 2 HSECoE Targets (BOP only)	Phase 2 HSECoE Targets (System)
Gravametric Capacity	kg H2/kg system	0.055	0.187	0.10	0.0352	0.0872	0.15	0.055
mass	*kg*	*102*		*16.1*	159			*102*
Volumetric Capacity	kg H2/L system	0.04	0.03	0.053	0.0175	0.078	0.132	0.049
Volumetric	*liters*	*140*		*16.9*	320			*114*
System Cost	$/kWh net	6	3.5	5.62	12.74			
	$	*1,119*		*1048*	2376			
Fuel Cost	$/gge at pump	2-6			4.89			
Min Operating Temp	°C	-40			-40			-20
Max Operating Temp	°C	60			60			60
Min Delivery Temp	°C	-40			-40			-20
Max Delivery Temp	°C	85			85			85
Cycle Life	Cycles	1500			1500			1000
Min Delivery Pressure	bar	5			5			5
Max Delivery Pressure	bar	12			12			12
Onboard Efficiency	%	90			92			95
Well to Power Plant Efficiency	%	60			39.2			37
System Fill Time	min	3.3			3.3			2.9
Min Full Flow Rate	(g/s/kW)	0.02			0.02			0.02
	g/s	*1.6*			*1.6*			*1.6*
Start Time to Full Flow (20°C)	sec	5			5			1
Start Time to Full Flow (-20°C)	sec	15			15			1
Transient Response	sec	0.75			0.75			0.5
Fuel Purity	%H2	99.97			99.99			99.97
Permeation, Toxicity, Safety	Scc/h	Meets or Exceeds Standards			s			s
Loss of Useable Hydrogen	(g/h)/kg H2 stored	0.05			0.44			0.05

- Reduced the BOP part count, mass and volume in the design of a consolidated BOP component that combined eight valves and sensors into a single device. Mass and volume of this device was reduced from 5.7 kg and 4.1 liters to 3.9 kg and 0.6 liters.
- Performed proof-of-concept testing for the LN_2-cooled wall concept and measured the estimated cooling rate. Demonstrated the concept's feasibility experimentally and scaled up the results to the full-scale tank design.

INTRODUCTION

Multiple onboard vehicle-scale hydrogen storage demonstrations have been done, including several studies to examine characteristics that impact systems engineering. However, none of these demonstrations have simultaneously met all of the DOE hydrogen storage program goals. Additionally, engineering of new chemical hydrogen storage approaches is in its infancy, with ample opportunity to develop novel systems capable of reaching the DOE targets for storage capacity. The goal of the Hydrogen Storage Engineering Center of Excellence (HSECoE), led by Savannah River National Laboratory, is to develop and demonstrate low-cost, high-performing, onboard hydrogen storage through a fully integrated systems design and engineering approach. Toward this end, PNNL is working with HSECoE partners to design and evaluate systems based on slurry chemical and cryo-adsorbent hydrogen storage media.

APPROACH

As part of the HSECoE, PNNL as a center partner has actively contributed to the design and testing of hydrogen storage systems. This work involves the development of system designs using both slurry chemical hydrogen and cryo-adsorbent hydrogen storage media. As these designs

are developed, efforts are made to minimize mass, volume, and cost, in an effort to achieve the DOE technical targets. PNNL's specific responsibility is to identify BOP components for these systems. This year's work has focused on reducing the mass and volume of these BOP components for the cryo-sorbent hydrogen storage systems. As the BOP is developed, PNNL considers the materials incompatibility issues associated with H_2 embrittlement, corrosion and permeability. The Center also develops engineering solutions to overcome deficiencies identified during system development. This year PNNL developed and tested a concept for cooling the walls of the tank during cryo-adsorbent refueling. By cooling the outer walls of the tank with liquid nitrogen, less cold hydrogen has to recirculate through the bed during the refueling. This engineering solution will reduce the cost of refueling.

Once the systems have been designed, the center has developed models to describe the performance of these systems under a variety of drive cycle scenarios. The PNNL work has focused on the development of the chemical hydrogen storage models. These models as well as the design are validated experimentally by testing the key components of the system and comparing them to expected results in the model. The models that have been developed can be used to not only to predict the performance of AB and alane as they are now, but they can also help researchers predict the performance of yet-to-be-developed materials relative to DOE's technical targets for light-duty vehicles. In addition to performance modeling, cost modeling is also performed. This is done with a combination of top-down and bottom-up manufacturing analysis. Production rates between 10,000 and 500,000 have been estimated for each system that is developed.

RESULTS

Cryo-Sorbent Hydrogen Storage

PNNL's cryo-sorbent work in the Center has focused on minimizing mass of the BOP and developing a concept for cooling the outer tank wall for faster refueling. In an effort to minimize the BOP cost, mass, and volume, for the cryo-sorbent hydrogen storage system, 11 of the valves and instrumentation interfacing with the storage tank were combined into a single housing. This consolidated BOP component included ports to attach pressure relief valves, a check valve, pressure and temperature sensors, pressure regulators, and isolations valves. By combining these components together, the system installation time is reduced and the system cost minimized. To reduce the housing mass, unnecessary material was removed from the block. The original design had a mass and volume of 5.7 kg and 4.1 L; this was reduced to 3.9 kg and 0.6 L, respectively. The current design installs this consolidated BOP component directly on the top of the tank and is shown in Figure 1.

A structural analysis was performed on this component to understand the impact of pressure and thermal stresses. Evaluating the smallest bridge sections between ports, the system design appears to be adequate for pressure stresses with a demand to capacity ratio of 0.77. Additionally, the thermal gradients and the resultant thermal stresses are small because the heat transfer rates associated with boiling of the liquid nitrogen in the boundary layer are smaller than the heat transfer associated with heat movement through high thermally conductive aluminum.

One approach to refueling the cryo-adsorbent tank uses cold hydrogen in a flow-through mode to cool the tank from an expected 110 K to the required 80 K. Modeling of this process during refueling has demonstrated that while the adsorbent material can be cooled relatively easily, the tank wall remains warm. As a result, it was estimated that 11.4 kg of hydrogen would be required for cooling the adsorbent and tank wall in addition to the 5.6 kg of required for the fill. To address this shortcoming, PNNL and Hexagon Lincoln have developed the LN_2-cooled wall approach that utilizes the flow of liquid nitrogen in an annulus between the tank and its insulation to cool the tank wall during refueling and reduce the waste of hydrogen fuel. The concept is shown in Figure 2.

Work was performed this year to quantify the performance of this approach using a simple proof-of-concept test. A 2" diameter pipe with the same wall thickness expected in the full-scale tank was fabricated to allow liquid nitrogen flow in an annulus on the outside of the pipe. The starting temperature, mass flow rate of LN_2, and annulus thickness could be varied during the experiment and the temperature axially and radially along the pipe were measured during the cooling process. The results of these experiments were analyzed to determine pipe cooling rate. Cooling rate (kW) was normalized by dividing it by the LN_2 mass flow rate (kg/s), yielding kW-s/kg. The results of the

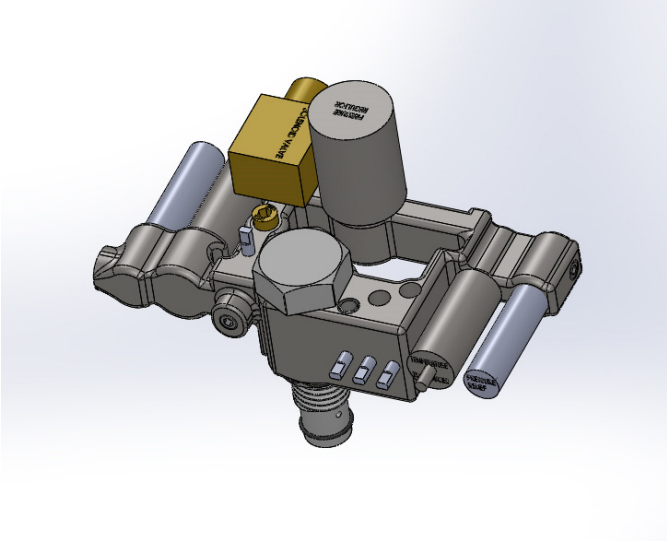

FIGURE 1. Reduced Mass Consolidated BOP Component

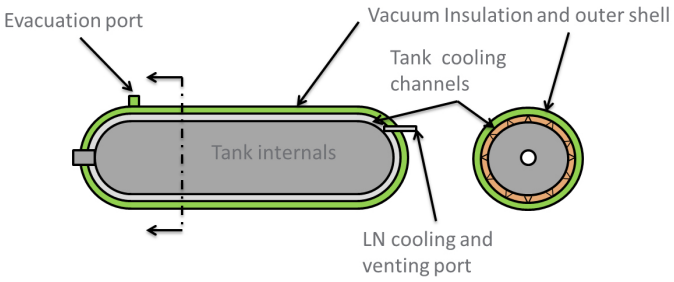

FIGURE 2. LN_2-Cooled Wall Tank Concept for Cooling the Wall of the Cryo-Adsorption Tank

tests indicate two phases of cooling. There is an initial lower cooling rate of ~70 kW-s/kg that is relatively constant as the temperature in the pipe drops until it reaches approximately 130K at which point the cooling rate rises sharply to ~130 kW-s/kg (see Figure 3). This higher cooling rate is associated with nucleate boiling and quickly cools the pipe to its required 77 K. The results of this analysis indicated that higher flows of liquid nitrogen will bring the tank to the higher cooling nucleate boiling regime more quickly and reduce the overall cooling time.

The results of these proof-of-concept tests were extrapolated to estimate the amount of liquid nitrogen to cool a 163 liter full-scale tank from 110 K to 80 K in four minutes. The results of this analysis are shown in Table 2. In addition this analysis demonstrated that combining the initial internal cooling with hydrogen and later cooling with liquid nitrogen will result in an overall reduction in the total gases required.

The use of liquid nitrogen in the tank annulus resulted in concerns relative to the fatigue of the tank wall. As a result, a fatigue stress calculation was performed based on the experimental results. During testing, a maximum of 10°C/inch gradient was observed in the pipe during the cooling process. The stress in the aluminum wall was calculated using finite element analysis and the results indicated a peak thermal stress of 3.2 MPa (von Mises) or 3.4 MPa (stress intensity). The fatigue strength of the aluminum alloy is 100 MPa for 5,000 cycles. These results indicate that significantly higher temperature gradients are needed to challenge the material's fatigue limit.

TABLE 2. Predicted Liquid Nitrogen Usage for 163-L LN_2-Cooled Wall Tank Design

Cooling Rate Assumptions	Cooling Rate (W-s/kg)	Required LN_2 Only (kg)	Required LN_2 + H_2 for 163 L tank (kg)
Average Test	87.1k	66	41 kg N_2 + 5.5 kg H_2
Ideal LN_2 Boiling + Gas Cooling	241k	24	15 kg N_2 + 2 kg H_2

Chemical Hydrogen Storage

With the DOE's decision that chemical hydrogen storage materials would not move into Phase 3, the work in this area was reduced to completion of previous work and final documentation of the center results. In addition the cost modeling done in FY 2013 for the system developed for AB was expanded to provide an estimate for alane. The storage

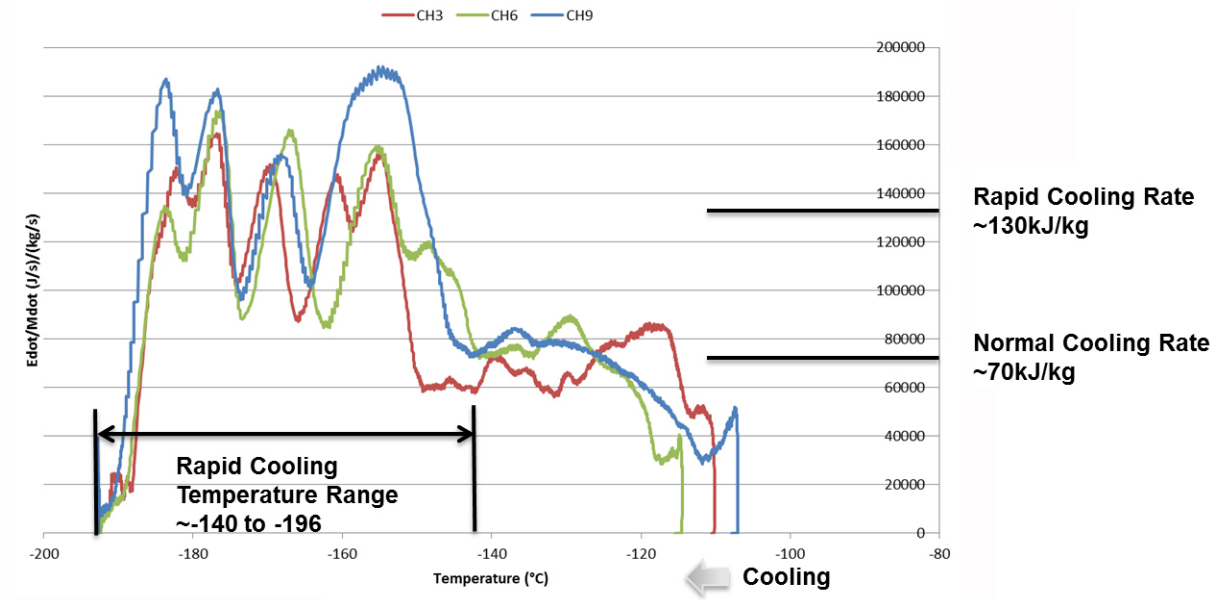

FIGURE 3. Pipe Cooling Rate as a Function of Temperature for the Proof-of-Concept LN_2-Cooled Wall Testing

system models for AB and alane were also completed and incorporated into the vehicle-level model framework.

Using the cost model developed for a slurried AB, only minor changes were required to predict the costs for an alane-based system. Alane does not produce significant impurities during its thermolysis, as a result, borazine and ammonia scrubbers were removed. Furthermore, the alane system uses a recuperator rather than recycle to preheat the feed. The most significant cost increase was the larger amount of alane and slurrying agent required because of its lower hydrogen content. The cost of an alane system for 500,000 units is compared to other automotive systems in Figure 4. The cost of the alane ($26/kg) was significantly higher than the other systems considered. There is, however, considerable uncertainty in its first time production cost.

The chemical hydrogen storage models were finalized and documented. Rather than have separate exothermic and endothermic models using AB and alane as the representative materials, respectively, a single model was developed. Because the systems are very similar, most of the system components are identical. To switch between models, a flag can be set to toggle between the two system configurations and include a recuperator or a recycle stream and to include or not include the impurities clean-up system.

These models were evaluated relative to data sets generated at LANL for a small scale flow-through reactor system. Tests were performed with alane over a range of solids loadings, residence times, auger speeds, and reaction temperatures. The model fit the experimental data reasonably well for alane and AB at low temperatures. The model did not fit the experimental data for AB at high temperatures. As a result, the AB kinetic model was refit to represent the higher temperature experimental data produced at LANL. These models were then documented and incorporated into the vehicle level framework.

CONCLUSIONS AND FUTURE DIRECTIONS

The conclusions of the FY 2014 work are as follows:

- A consolidated BOP component was developed resulting in reduced cost, mass and volume over separate individual components.
- Testing of the LN_2-cooled wall tank concept indicate significant reduction in hydrogen usage to cool the tank during refueling.
- Estimates of the alane-based chemical hydrogen storage system were made for 10,000 to 500,000 units. The 500,000 unit cost of $4,127/system was significantly higher than slurry AB and the cryo-adsorbent systems.
- The transient models developed to predict performance of AB and alane were compared to experimental data and validated before being incorporated in the vehicle level model.

The future direction of this work during FY 2015 is as follows:

- Update cost models and write up cost results for the MATI and Hexcell cryo-adsorbent systems based on addition of consolidated BOP component as well as additional system design detail.

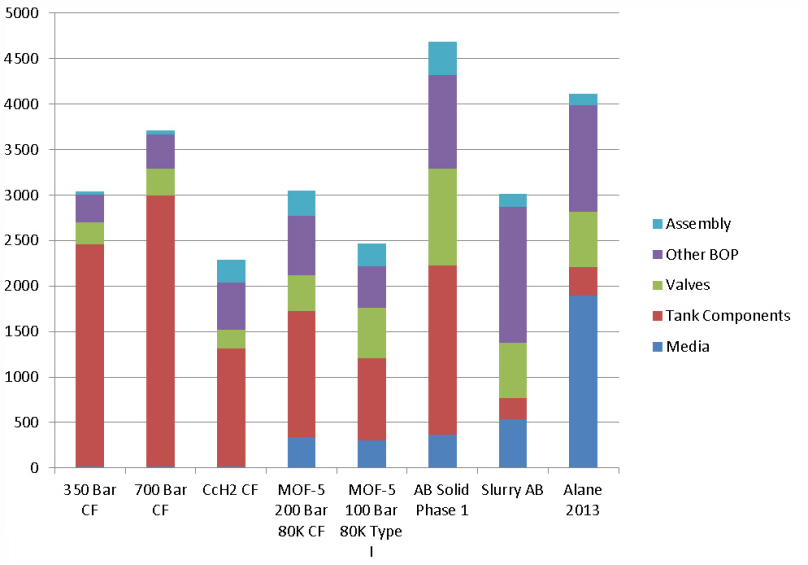

FIGURE 4. Estimated Cost for 500,000 Units Assuming Various Hydrogen Storage Systems

- Design and fabricate the 2-liter scale LN_2-cooled wall tank perform flow through and dormancy tests with and without a surrogate adsorbent material.
- The results of the 2-liter scale LN_2-cooled wall tank tests will be used to estimate the refueling time and dormancy losses for a full-scale tank.
- PNNL will work with other center partners to compile a final report for the cryo-adsorbent work which was performed over the course of the HSECoE.

PATENTS PENDING

1. Newhouse, Norm, John Makinson, and Kevin Simmons, "Thermal Insulation Shell System For Composite Pressure Vessel," U.S. Provisional Patent Application No. 61/822,580, May 2013.

FY 2014 PUBLICATIONS/PRESENTATIONS

Publications

1. Choi, Young Joon, Ewa C. E. Rönnebro, Scot Rassat, Abhi Karkamkar, Gary Maupin, Jamie Holladay, Kevin Simmons and Kriston Brooks, "Kinetics study of solid ammonia borane hydrogen release – modeling and experimental validation for chemical hydrogen storage," *Phys. Chem. Chem. Phys*., Vol. 16, 7959-7968.

2. Brooks, Kriston P., Troy A. Semelsberger, Kevin L. Simmons, and Bart van Hassel, "Slurry-Based Chemical Hydrogen Storage Systems for Automotive Fuel Cell Applications," *Journal of Power Sources*, Vol. 268, 950-959.

3. Semelsberger, Troy A., Brooks, Kriston P., "Chemical Hydrogen Storage Material Property Guidelines for Automotive Applications," *Journal of Power Sources*, submitted May 2014.

4. Brooks, Kriston P., Richard P. Pires, Kevin L. Simmons, "Development and Validation of a Slurry Model for Chemical Hydrogen Storage in Fuel Cell Vehicle Applications," *Journal of Power Sources*, submitted June 2014.

5. Choi, Young Joon, Matthew Westman, Abhi Karkamkar, Jaehun Chun and Ewa Rönnebro, "Synthesis and Engineering Materials Properties of Fluid Phase Chemical Hydrides for Automotive Applications," *Energy Fuels*, submitted August 2014.

6. Westman, Matthew, Ewa Ronnebro, Jaehun Chun, Abhi Karkamkar, Jacob Ishibashi, Shih-Yuan Liu, "Scale-up of fluid phase chemical hydrogen storage materials and materials engineering properties", *Energy Fuels*, submitted August 2014.

Presentations

1. Brooks, Kriston P., R.P. Pires and J.D. Holladay, "Development and Experimental Validation of An Automotive System Model for Slurry-Based Chemical Hydrogen Storage Materials," Fuel Cell Seminar & Energy Exposition 2013, Columbus, OH, October 2013.

2. Brooks, Kriston P., R.P. Pires and J.D. Holladay, "Development and Experimental Validation of An Automotive System Model for Slurry-Based Chemical Hydrogen Storage Materials," Innovations of Green Process Engineering for Sustainable Energy and Environment, AIChE Annual Meeting, November 2013.

IV.B.3 Advancement of Systems Designs and Key Engineering Technologies for Materials-Based Hydrogen Storage

Bart van Hassel (Primary Contact),
Jose Miguel Pasini, Reddy Karra, Ron Brown,
Randy McGee, Allen Murray and Shiling Zhang.
United Technologies Research Center (UTRC)
411 Silver Lane
East Hartford, CT 06108
Phone: (860) 610-7701
Email: vanhasba@utrc.utc.com

DOE Managers
Ned T. Stetson
Phone: (202) 586-9995
Email: Ned.Stetson@ee.doe.gov
Jesse Adams
Phone: (720) 356-1421
Email: Jesse.Adams@ee.doe.gov

Contract Number: DE-FC36-09GO19006

Project Start Date: February 1, 2009
Project End Date: June 30, 2015 (including 1-year no-cost extension)

Overall Objectives

UTRC's overall objectives mirror those of the Hydrogen Storage Engineering Center of Excellence (HSECoE) to advance hydrogen storage system technologies toward the DOE Hydrogen Storage Program's 2017 storage targets. Outcomes of this project will include:

- A more detailed understanding of storage system requirements
- Development of higher performance and enabling technologies such as novel approaches to heat exchange, onboard purification and compacted storage material structures
- Component/system design optimization for prototype demonstration

Fiscal Year (FY) 2014 Objectives

- Develop vehicle/power plant/storage system integrated system modeling elements to improve specification of storage system requirements and to predict performance for candidate designs
- Engineer and test specialty components for materials-based hydrogen storage systems
- Assess the viability of onboard purification for various storage material classes and purification approaches
- Collaborate closely with the HSECoE partners to advance materials-based hydrogen storage system technologies

Technical Barriers

This project addresses the following technical barriers from the Storage section (3.3.4) of the Fuel Cell Technologies Office Multi-Year Research, Development, and Demonstration Plan:

(A) System Weight and Volume

(D) Durability/Operability

(H) Balance-of-Plant (BOP) Components

Technical Targets

The goals of this project mirror those of the HSECoE to advance hydrogen storage system technologies toward the DOE Hydrogen Storage Program's 2017 storage targets [1]. UTRC reduced the mass and volume of its contribution to the BOP components from 28% to <5% by mass and from 12% to <3% by volume of the total chemical hydrogen storage system. Thereby the gravimetric capacity of the chemical hydrogen storage system was improved from 31 g H_2/kg system to 41 g H_2/kg system which is somewhat below the 2017 gravimetric capacity target of 55 g H_2/kg system. Thereby the volumetric capacity of the chemical hydrogen storage system was improved from 36 gram H_2/L system to 40 gram H_2/L system, which is the 2017 target. The status of UTRC's technical targets is documented in Table 1.

FY 2014 Accomplishments

Accomplishments during the current project period include:

- Collaborated with HSECoE partners on disseminating the Simulink® Framework with a graphical user interface (GUI) on the Web.
- Implemented Pacific Northwest National Laboratory's (PNNL's) chemical hydrogen storage (CH) system model in the Simulink® Framework and made it available for beta testing.
- Tested, at high pressure (12-16 bar), the performance of a compact gas/liquid separator (GLS) that was designed for the CH system. The GLS is capable of separating hydrogen gas from the fluid up to a peak power level of 80 kWe, as required for a light-duty vehicle.

TABLE 1. UTRC's Progress towards Meeting Technical Targets for Onboard H_2 Storage Systems

	Characteristic	Units	2017 Target	UTRC
Chemical H_2 storage system	Gravimetric capacity	kWh/kg ($kg\ H_2$/ kg system)	1.8 (0.055)	1.3 (0.041)
	Volumetric capacity	kWh/L ($kg\ H_2$/L system)	1.3 (0.04)	1.3 (0.04)
Cryo-adsorbent H_2 storage system	H_2 Quality	% H_2	SAE J2719 and ISO/PDTS 14687-2 (99.97% dry basis)	Meets

SAE – SAE International (automotive standards association)
ISO – International Organization for Standardization

- Validated a computational fluid dynamics (CFD) model of the GLS by measuring the critical gas velocity and the droplet size distribution at the outlet of the GLS.
- Identified and quantified impurities that result from using silicone oil AR20 as the liquid for making a slurry with ammonia borane (NH_3BH_3) or alane (AlH_3). Identified fluids with a significant lower vapor pressure and higher thermal stability, which may be more suitable than AR20.
- Characterized metal-organic framework-5 (MOF-5) particulate filters for the cryo-adsorbent hydrogen storage system in terms of particulate filtration efficiency, darcy flow coefficient and thermal shock resistance.

INTRODUCTION

Physical storage of hydrogen through compressed gas and cryogenic liquid approaches is well established, but has drawbacks regarding weight, volume, cost and efficiency which motivate the development of alternative, low-pressure materials-based methods of hydrogen storage. Recent worldwide research efforts for improved storage materials have produced novel candidates and continue in the pursuit of materials with overall viability. While the characteristics of the storage materials are of primary importance, the additional system components required for the materials to function as desired can have a significant impact on the overall performance and cost. Definition, analysis and improvement of such systems components and architectures, both for specific materials and for generalized material classes, are important technical elements to advance in the development of superior methods of hydrogen storage.

APPROACH

UTRC's approach is to leverage in-house expertise in various engineering disciplines and prior experience with metal hydride system prototyping to advance materials-based hydrogen storage for automotive applications. During the fifth year of the HSECoE project, UTRC continued the successful development of the Simulink® modeling framework for comparing H_2 storage systems on a common basis, which can now be downloaded from the National Renewable Energy Laboratory (NREL)-hosted website at www.hsecoe.org. UTRC completed its contribution to the chemical hydrogen storage system development in an orderly fashion when DOE decided to discontinue the development of such a system after the Phase 2 to Phase 3 Go/No-Go meeting in March, 2013. Through experimental work, UTRC determined the critical velocity of a compact GLS at elevated pressure with a surrogate gas (N_2). The result show that this particular GLS design was capable of separating H_2 gas from the fluid at a power level of up to 80 kWe, which is the full-scale capacity for a light-duty automotive system. UTRC also developed a CFD model of the GLS in order to predict the liquid carryover as a function of operating conditions. The model was validated with the experimental results of liquid carryover rate as a function of gas flow rate and through the measurement of the droplet size distribution at the outlet of the vortex finder. UTRC demonstrated through simulated distillation and vapor pressure measurements with an isoteniscope that the silicone oil AR20 had an unacceptable high vapor pressure for this application and recommended alternate fluids with a significant lower vapor pressure and higher boiling point but similar viscosity. For the cryo-adsorption system, UTRC evaluated several particulate filters for the mitigation of MOF-5 particulates and demonstrated that those filters did remove particulates between 0.2 um and 32 um to concentrations that were orders of magnitude lower than the SAE guideline [2]. The filters were also tested for their flow resistance and their ability to withstand thermal cycling between room temperature and 77 K. It is expected that the allowable pressure drop in the system will ultimately determine how much particulate filter area needs to be installed.

RESULTS

The Simulink® Framework with a GUI was disseminated on the Web through NREL's website at www.hsecoe.org. It contains models of the 350-bar and 700-bar compressed gas storage systems and the model of the ideal metal hydride. Users can vary the metal hydride amount and the buffer

volume when simulating different drive cycles. UTRC also incorporated PNNL's chemical hydrogen storage system into the framework. It will first be beta-tested before it will become available on the website. A diagram of the GUI is shown in Figure 1.

A chemical hydrogen storage system that uses a liquid hydrogen carrier requires a GLS in order to separate the hydrogen gas from the spent liquid hydrogen carrier. UTRC relentlessly reduced the weight and volume of the GLS in order to substantially improve the gravimetric and volumetric capacity of the chemical hydrogen storage system from 31 g H_2/kg system to 41 g H_2/kg system and from 36 gram H_2/L system to 40 gram H_2/L system, which is the 2017 volumetric capacity target. The compact GLS with a low profile was tested at high pressure (12 and 16 bar) and at a capacity that is required for a full size automotive chemical hydrogen storage system that can support a peak fuel cell power of 80 kWe. Figure 2 shows the excellent performance of the GLS at two different pressures (12 and 16 bar) and two different silicone oil AR20 flow rates as a function of the flow rate of the surrogate gas (N_2 instead of H_2). The GLS meets the S*M*A*R*T milestone requirements with its critical N_2 gas flow rate of about 300 slpm under those experimental conditions. The critical gas velocity for H_2 gas

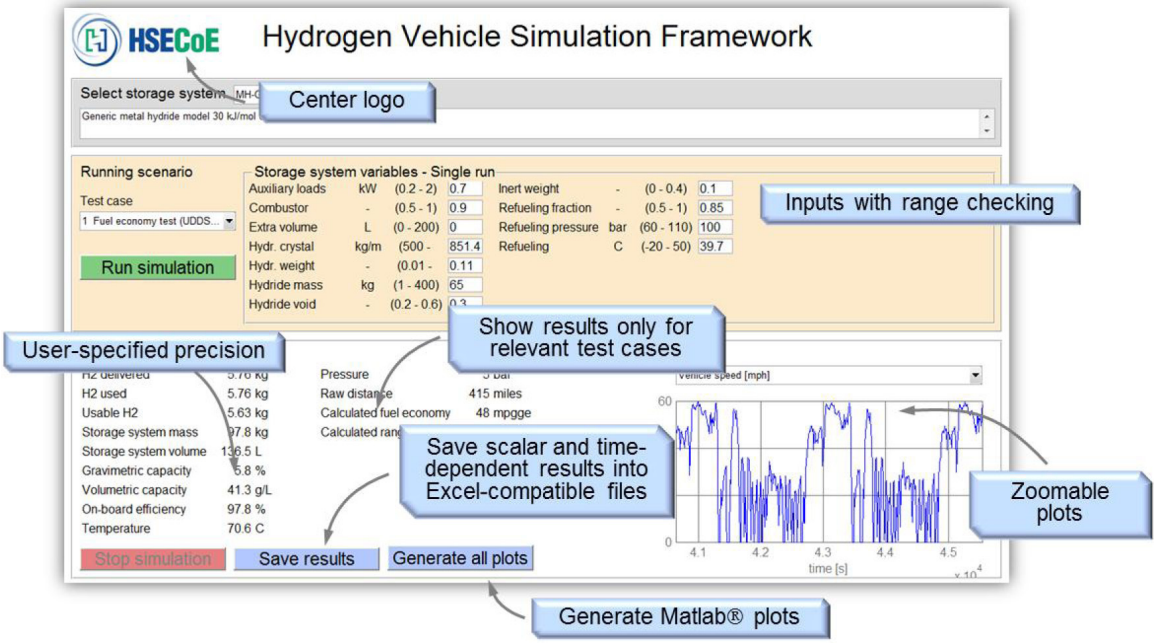

FIGURE 1. Example of GUI of Simulink® modeling framework.

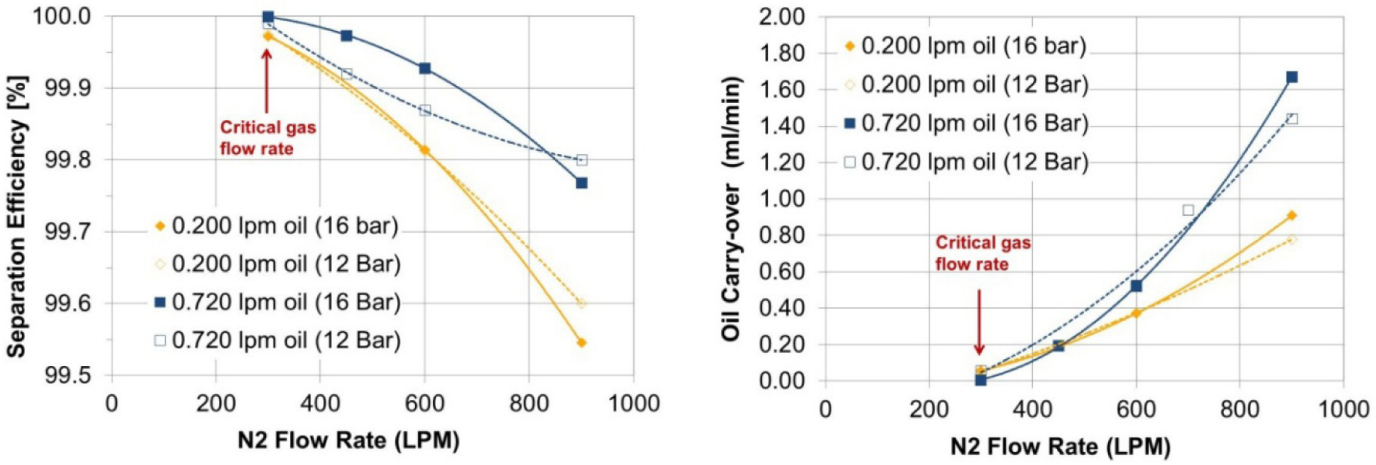

FIGURE 2. Silicone oil AR20 carryover rate (ml/min) as a function of the N_2 gas flow rate (slpm) at 70°C and elevated pressure (12-16 bar) for two different silicone oil flow rates.

is expected to be a factor 3.75 higher than for N_2 gas. This means that this GLS will be able to separate H_2 from silicone oil up to an electrical power level of about 80 kWe by the proton exchange membrane fuel cell. In other words, the GLS that was developed and tested has a capacity that is sufficient for this light-duty vehicle application.

The GLS is such an important unit operation in the chemical hydrogen storage system that a CFD model was developed of this component in order to develop the capability to size it for different capacities, e.g. for the capacity that would have been required for the Phase 3 sub-scale prototype. Figure 3 shows the streamlines of droplets in the GLS. Droplets that hit the wall will form an oil film that will drain. Dry gas is extracted from the center of the vortex with a vortex finder. The model correctly predicted the critical gas flow rate below which the liquid carryover rate is negligible. The CFD model predicted an outlet droplet size distribution in the size range of 10-50 micrometer but droplet size distribution measurements showed a droplet size distribution in the range of 100-500 micrometer, as shown in Figure 4. A more detailed computational analysis showed that the 10-50 micrometer droplets would form an oil film on the inside surface of the vortex finder and the oil film would breakup into 100-200 micrometer droplets due to the high gas flow rate in the vortex finder.

Delivering hydrogen from a materials-based hydrogen storage system at a high quality is of key importance for the long-term stability of the expensive proton exchange membrane fuel cell. UTRC noticed during tests with the GLS that the silicone oil AR20 posed significant challenges as the optical window for droplet size distribution measurements quickly became contaminated with an oil film. This prompted an investigation of the boiling point range and vapor pressure of silicone oil AR20, as shown in Figure 5. Simulated distillation showed a relative low boiling point range in comparison to the expected operating conditions in the thermolysis reactor (120-200°C) and measurements with the isoteniscope showed a high vapor pressure, which is clearly undesired. Dow Chemical assisted with additional qualitative and quantitative measurements of the different siloxane species that are present in the gas phase, as documented in Table 2. These impurities would need to be adsorbed similar to the other impurities like borazine, diborane and ammonia when using a fluid form of AB. A better approach is to select fluids with a much lower vapor pressure and higher boiling temperature range. Several of such oils have been identified and were included in Figure 5 but it will need to be determined how well (chemical) hydrogen storage material will disperse in such fluids.

In the good spirit of the HSECoE, UTRC also contributed to the development of the cryo-adsorbent system by evaluating the performance of porous metal particulate filters when exposed to MOF-5 adsorbent. The sorbent was located in the bottom of a transparent pressure vessel at the start of the experiment and fluidized by nitrogen gas, as a surrogate for hydrogen gas. Gradually MOF-5 particulates would start accumulating on the filter surface and form a filter cake. Filter cake formation caused a drop in the Darcy

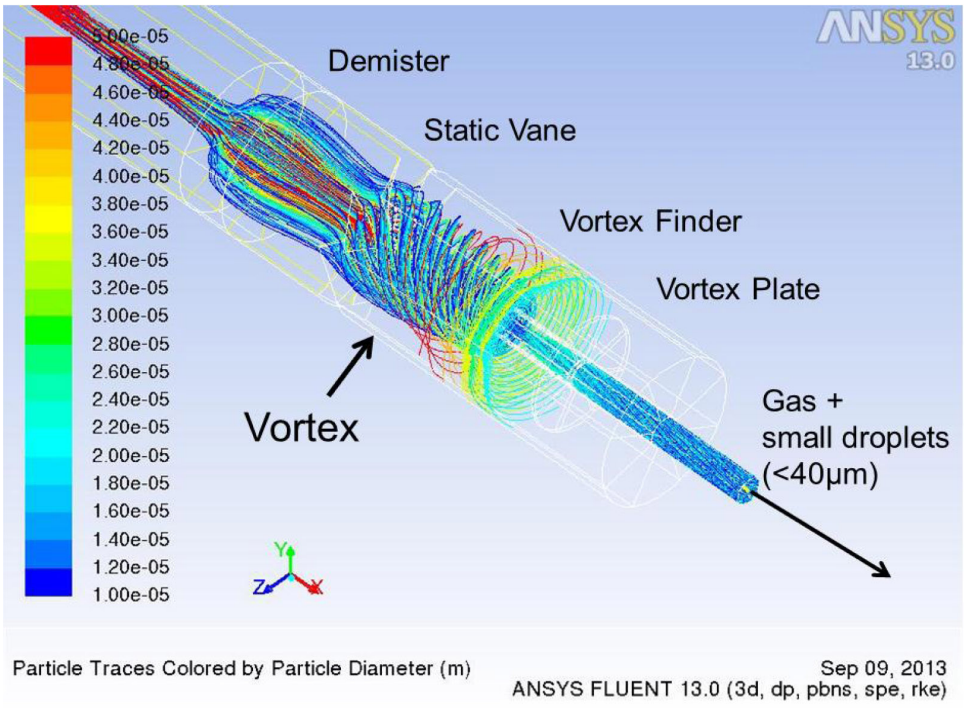

FIGURE 3. CFD model of the GLS. The streamlines of the droplets have been colored by their droplet size.

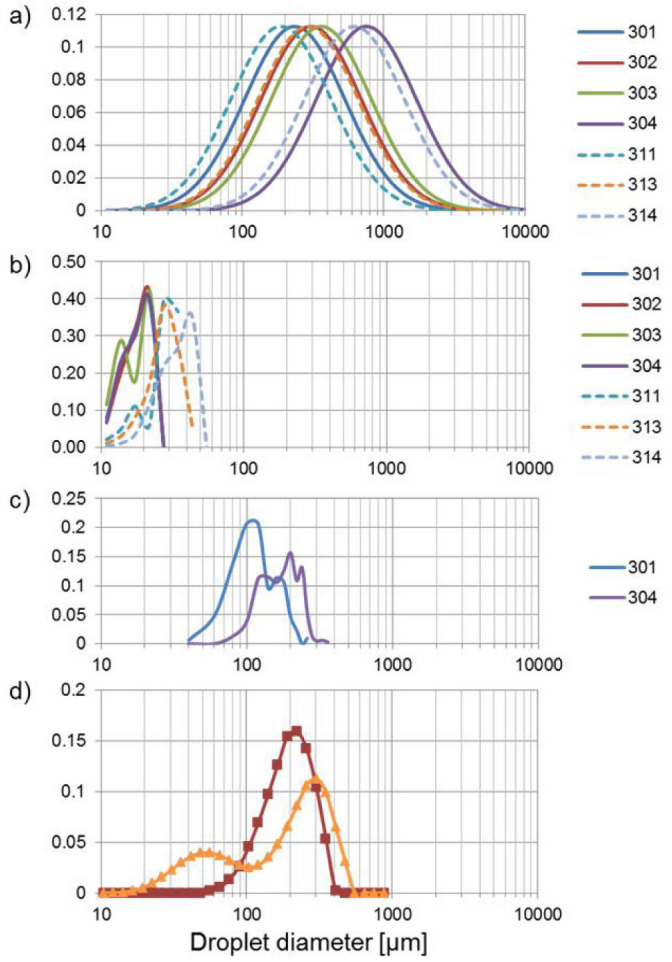

FIGURE 4. Droplet size distributions at 70°C, 12 bar and various N_2 and silicone AR-20 flow rates (Table 2): a) Inlet of the GLS, b) Outlet of the GLS (no filming), c) Outlet of the GLS with filming inside the vortex finder, d) Two representative but distinctly different experimental droplet size distributions at a N_2 gas flow rate of 600 slpm and a silicone oil AR20 flow rate of 0.365 lpm.

TABLE 2. Quantitative Results of Headspace Gas Chromatography with Flame Ionization Detection Of Silicone Oil AR20 at 70°C, as used in the AB Slurry of the Chemical Hydrogen Storage System

Component	MW (g/mol)	ppm by weight	ppm by volume (25°C, 1 atm)
Me_3SiOH	90	318	106
$Me_3SiOSiMe_2OH$	164	86	16
$Me_3Si(OSiMe_2)OSiMe_2OH$	238	20	2
$Me_3Si(OSiMe_2)_2OSiMe_2OH$	312	7	0.7
$Me_3Si(OSiMe_2)_3OSiMe_2OH$	386	12	0.9
$cyclo(OSiMe_2)_4(OSiMePh)$??	432	33	2
$cyclo(OSiMe_2)_5(OSiMePh)$??	506	23	1

flow permeability of the filter (Figure 6), which needs to be considered in the overall system analysis of a cryo-adsorbent system. The porous metal filters were able to reduce the particulate content well below the SAE guideline of 1,000 µg/m^3, as shown in Figure 7. The porous metal filters did also withstand rapid thermal cycles between room temperature and 77 K as evidenced by no change in physical appearance or Darcy flow permeability. The Darcy flow permeability can be used to right-size the particulate filter area for flow through cooling when the team determines a value for the allowable pressure drop.

CONCLUSIONS AND FUTURE DIRECTIONS

Conclusions derived from the work in FY 2014 are:

- Users of the Simulink® modeling framework will benefit from having access to more hydrogen storage system model parameters in the GUI.

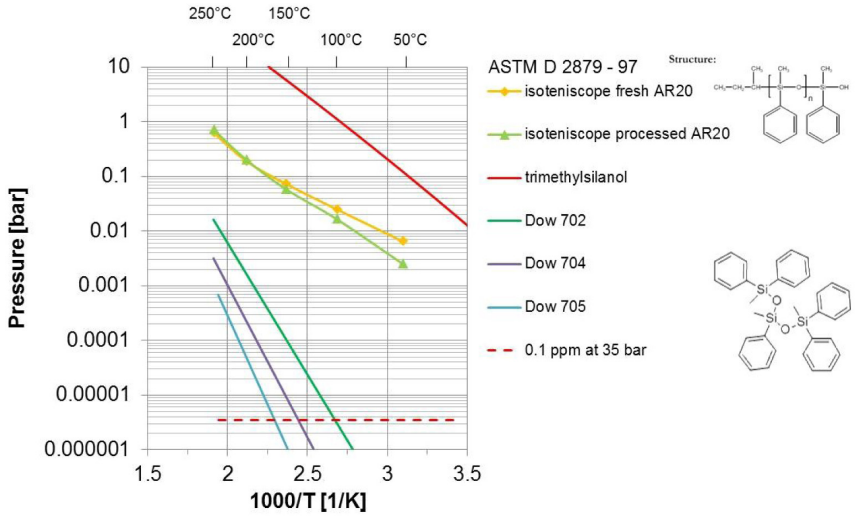

FIGURE 5. Boiling temperature range (simulated distillation) and vapor pressure (isoteniscope) of silicone oil AR20 as a function of temperature.

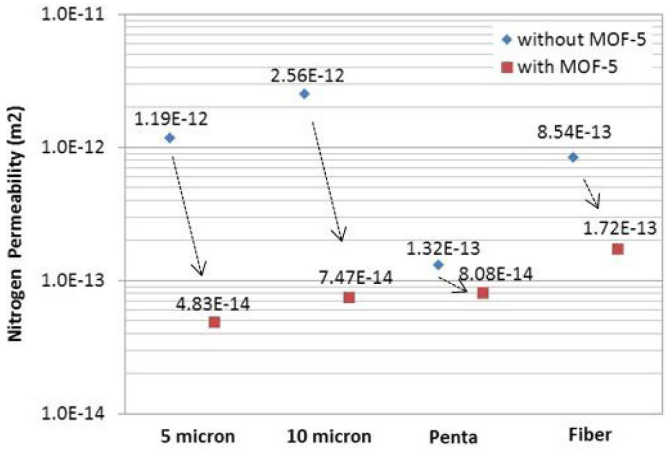

FIGURE 6. Drop in Darcy flow parameter due to filter cake formation for four different porous metal filters.

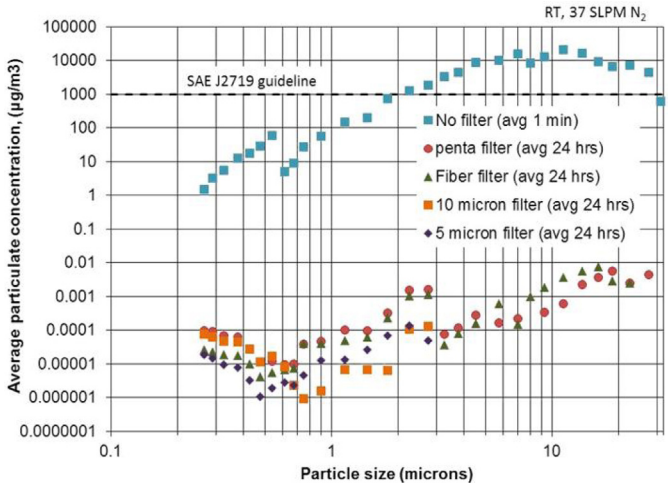

FIGURE 7. Particulate concentration at the outlet of the particulate filters when exposed to MOF-5 particulates.

- Silicone oil AR20 is unsuitable for turning AB into a slurry as its boiling point is too low. This causes a very high vapor pressure and contamination of the hydrogen gas that is liberated in the thermolysis reactor.
- Gas liquid separators that use a combination of gravitational settling, coalescence and a centrifugal force enable an efficient separation of gas and liquid for systems with fluid-phase chemical hydrogen storage materials.
- Surface filters on which MOF-5 particulates will form a filter cake are suitable for reducing the particulate concentration to levels that are well below the SAE guideline and it is the allowable pressure drop that will ultimately determine how much filter area needs to be installed.

Future work in Phase 3 will comprise:

- Lead Integrated Power Plant/Storage System Modeling technical area.
- Collaborate with Savannah River National Laboratory and NREL on making the newest version of the Simulink® Framework available on the HSECoE website.
- Incorporate updated CH system model in Simulink® Framework after Los Alamos National Laboratory/ PNNL have collected and analyzed their latest kinetic data.
- Update high level models to reflect the as-fabricated behavior of the cryo-adsorption system and assess its impact on the power plant performance.
- Document results in final reports about UTRC's contribution to the metal hydride, chemical hydride and the cryo-adsorption system developments.

FY 2014 PUBLICATIONS/PRESENTATIONS

1. Bart A. van Hassel, Jagadeswara R. Karra, Jose Santana, Salvatore Saita, Allen Murray and Daniel Goberman, Richard Chahine and Daniel Cossement, Ammonia Sorbent Development for On-Board H_2 Purification, Accepted by Separation and Purification Technology.

2. Igor I. Fedchenia, Bart A. van Hassel and Ron Brown, Solution of Inverse Thermal Problem for Assessment of Thermal Parameters of Engineered H_2 Storage Materials, Accepted by Inverse Problems in Science & Engineering.

3. Bart A. van Hassel, Jagadeswara. R. Karra , David Gerlach, and Igor I. Fedchenia, Dynamics of fixed-bed adsorption of ammonia on impregnated activated carbon for hydrogen purification, To be submitted to Separation and Purification Technology, In Preparation.

4. B.A. van Hassel, R. McGee, R. Karra, A. Murray, I. Fedchenia, D. Gerlach, and Jose Miguel Pasini, Engineering Aspects of Materials Based Hydrogen Storage Systems, IEA Task 32, Heraklion, Greece, April 22–25, 2013.

5. B.A. van Hassel, Hydrogen Storage Systems for Mobile Applications, IEA Task 32, Key Largo, Florida, USA, December 8–12, 2013.

6. B.A. van Hassel, Hydrogen Storage for Mobile Applications in US, I2CNER International Workshop, Hydrogen Storage, Kyushu University, Fukuoka, Japan, January 31, 2014, Invited Talk.

7. Bart A. van Hassel, Randy McGee, Allen Murray and Shiling Zhang, Engineering Technologies for Fluid Chemical Hydrogen Storage System, MCARE 2014, Clearwater, Florida, February 17–20, 2014, Invited Talk.

8. K.P. Brooks, T.A. Semelsberger, K.L. Simmons and B.A. van Hassel, Slurry-based chemical hydrogen storage systems for automotive fuel cell applications, Submitted to Energy & Fuels Journal.

REFERENCES

1. http://www1.eere.energy.gov/hydrogenandfuelcells/mypp/pdfs/storage.pdf

2. Information Report on the Development of a Hydrogen Quality Guideline for Fuel Cell Vehicles, SAE International Surface Vehicle Information Report, J2719 APR2008, Revised 2008-04.

IV.B.4 Chemical Hydride Rate Modeling, Validation, and System Demonstration

Troy A. Semelsberger (Primary Contact), and Jose I. Tafoya
Los Alamos National Laboratory (LANL)
MS J579, P.O. Box 1663
Los Alamos, NM 87545
Phone: (505) 665-4766
Email: troy@lanl.gov

DOE Managers
Ned Stetson
Phone: (202) 586-9995
Email: Ned.Stetson@ee.doe.gov
Jesse Adams
Phone: (720) 356-1421
Email: Jesse.Adams@ee.doe.gov

Project Start Date: February 2009
Project End Date: February 2015

Overall Objectives

- Develop an automotive chemical hydrogen storage system capable of meeting all of the 2017 DOE targets simultaneously
- Develop and validate chemical hydrogen storage system models
- Quantify viable chemical hydrogen storage material properties that will meet DOE 2017 technical targets with our current system
- Develop and demonstrate "advanced"(non-prototypical) engineering concepts

Fiscal Year (FY) 2014 Objectives

- Quantify chemical hydrogen storage material properties meeting the DOE 2017 technical targets
- Design, build, and demonstrate advanced dehydrogenation reactors

Technical Barriers

This project addresses the following technical barriers from the Hydrogen Storage section of the Fuel Cell Technologies Office Multi-Year Research, Development, and Demonstration Plan:

(A) System Weight and Volume

(B) System Cost

(C) Efficiency

(D) Durability/Operability

(E) Charging/Discharging Rate

(F) Codes and Standards

(G) Materials of Construction

(H) Balance-of-Plant (BOP) Components

(J) Thermal Management

(K) System Life-Cycle Assessment

(R) By-Product/Spent Material Removal

Technical Targets

The summary of our progress in relation to the DOE 2017 technical targets for both ammonia borane and alane can be seen in Figure 1. The cost target was assumed to be seven dollars per kilogram of hydrogen. The projections are based on the Hydrogen Storage Engineering Center of Excellence's chemical hydrogen storage system design. Both systems assume 50 wt% slurry loadings for ammonia borane and alane.

FY 2014 Accomplishments

- Developed chemical hydrogen storage material property guidelines
- Demonstrated 50 and 60 wt% alane slurries in flow through reactor

✧ ✧ ✧ ✧ ✧

INTRODUCTION

Hydrogen storage systems based on chemical hydrides require a chemical reactor to release the hydrogen from the storage media, which is a fundamental difference from the other modes of hydrogen storage, adsorbents, and metal hydrides. This hydrogen-release reactor is crucial to the performance of the overall storage system, especially in meeting the DOE targets for hydrogen generation rate, transient operation, and startup times. The reactor must be designed to achieve these targets while meeting the constraints of the overall system volume and weight targets.

LANL will also address the unique requirements of onboard automotive hydrogen storage systems. For example, these systems require fast startup, operation over a wide dynamic range (10:1 turndown or greater), and fast transient

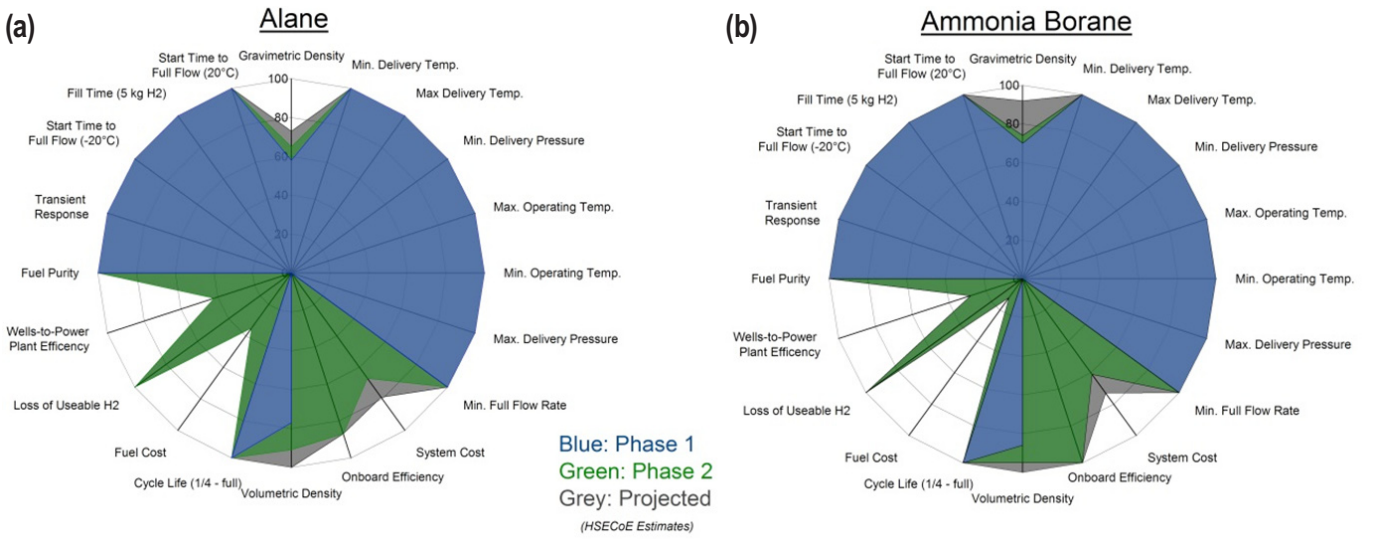

FIGURE 1. Spider chart summarizing our progress in meeting the DOE 2017 technical targets for (a) 50 wt% alane slurry and (b) 50 wt% ammonia borane slurry (note: values are Hydrogen Storage Engineering Center of Excellence estimates).

response to meet the demands of a drive cycle. The LANL team will develop novel reactor designs and operation strategies to meet these transient demands. In addition, the shelf life and stability of the hydrogen storage media is crucial for an automotive system, especially pertaining to safety and cost. Starting with the kinetics models, the LANL team will develop mathematical models for the aging characteristics of candidate hydrogen storage media (for example, complex metal hydrides or chemical hydrogen storage materials) subjected to a range of environmental factors. These models can be incorporated into system-level models of performance and cost and also used for the development of accelerated aging protocols necessary for later testing.

RESULTS

Chemical Hydrogen Storage Material Property Guidelines

Our objective was to develop a set of fluid-phase chemical hydrogen storage material property guidelines for automotive applications meeting the 2017 DOE technical targets. The fluid-phase chemical hydrogen storage media considered in the study were neat liquids, solutions, and non-settling homogeneous slurries. The fluid-phase material property guidelines are expected to aid material researchers in their materials development and/or discovery efforts. Until now, the materials researchers relied on system level targets to guide their materials research. Consequently, providing the materials research community with a viable set of chemical hydrogen storage materials properties fills a critical knowledge gap. Although the quantified set of material properties is not exhaustive, it is a necessary first step.

The ammonia borane system design developed by the Hydrogen Storage Engineering Center of Excellence was used as the boilerplate system design. The boilerplate system is presumed to contain the necessary components that will be common to all realizable fluid-phase chemical hydrogen storage media. Components of the ammonia borane system were identified as system independent (e.g., fuel cost), BOP/material independent (e.g., valves and pumps), and material-dependent (e.g., reactor).

System independent components are components invariant to the system design and vice-versa—examples include fuel cost and regeneration efficiency. Material-dependent components (MDC) include pumps, sensors, valves, tubing, etc. Because the BOP components were presumed to be material independent, the BOP components were grouped and treated as a constant with respect to mass, volume, durability, and operability. MDC are the components whose mass and volume are reliant upon the material properties, kinetics, and thermodynamics of the chemical hydrogen storage media. MDC of interest are reactor, heat exchanger, volume displacement tank, and hydrogen purification. To calculate viable material properties, the masses and volumes of the MDC were sized independent of the material. Given the *a priori* sizing of the MDC and the BOP sizing, the minimum gravimetric and volumetric hydrogen capacities for slurries, solutions and neat liquids were calculated that would meet the DOE 2017 gravimetric and volumetric system target. *A priori* sizing of the MDC permitted the calculation of material properties (e.g., kinetics and heat of reaction) that meet the mass and volume estimates of those components. The quantified list of chemical hydrogen storage material properties can be seen in Table 1.

TABLE 1. Chemical Hydrogen Storage Material Property Guidelines

Parameter	Symbol	Units	Range*	Assumptions
Minimum Material Capacity (liquids)	γ_{mat}	$g_{H2}/g_{material}$	~0.078 (*0.085*)†	• System mass (excludes media) = 30.6 kg (36.3 kg) • 5.6 kg of H_2 stored • Liquid media (neat) • Media density = 1.0 g/mL
Minimum Material Capacity (solutions)	γ_{mat}	$g_{H2}/g_{material}$	~0.098 (*0.106*) †	• System mass (excludes media) = 30.6 kg (36.3 kg) • Solute mass fraction = 0.35 ~ 0.80 • Solution density = 1.0 g/mL
Minimum Material Capacity (slurries)	γ_{mat}	$g_{H2}/g_{material}$	~0.112 (*0.121*) †	• System mass (excludes media) = 30.6 kg (36.3 kg) • Non-settling homogeneous slurry • Slurry mass fraction = 0.35 ~ 0.70 • Slurry volume fraction = 0 ~ 0.5 • Slurry density = 1.0 g/mL
Kinetics: Activation Energy	E_a	kJ/mol	117-150	• $V_{reactor}$ ≤ 4 L • Shelf life ≥ 60 days • Reaction order, n = 0 – 1
Kinetics: Pre-exponential Factor	A		$4 \times 10^9 – 1 \times 10^{16}$	
Endothermic Heat of Reaction	ΔH_{rxn}	kJ/mol H_2	≤ +17 (*15*) †	• Onboard Efficiency = 90% • # Cold Startups = 4 • ΔT = 150°C with no heat recovery • neat liquid (C_p = 1.6 J/g K) • Reactor mass = 2.5 kg SS (5.0 kg SS)
Exothermic Heat of Reaction	ΔH_{rxn}	kJ/mol H_2	≤ -27	• T_{max} = 250°C • Recycle ratio @ 50%
Maximum Reactor Outlet Temperature	T_{outlet}	°C	250	• Liquid Radiator = 2.08 kg • Gas Radiator = 0.3 kg • Ballast Tank = 2.6 kg
Impurities Concentration	y_i	ppm	No *a priori* estimates can be quantified	• $m_{adsorbent}$ ≤3.2 kg
Media H_2 Density	$(\gamma_{mat})(\phi_m)(\rho_{mat})$	kg H_2/L	≥0.07	• Heavy-duty polyethylene tank ≤ 6.2 kg
Regeneration Efficiency	η_{regen}	%	≥66.6%	• Onboard Efficiency = 90% • Well-to-power plant efficiency = 60%
Viscosity	η	cP	≤1,500	None

* (a) Parameter values are based on a specific system design and component performance with fixed masses and volumes. (b) Values outside these ranges do not imply that a material is not capable of meeting the system performance targets. (c) The material property ranges are subject to change as new or alternate technologies and/or new system designs are developed. (d) The minimum material capacities are subject to change as the density of the composition changes due to reductions in the mass and volume of the storage tank or reductions in system mass are realized.

† Values outside of parentheses are the values that correlate to the idealized system design (i.e., 30.6 kg) and the values in parentheses are those that correlate to the baseline system design (36.3 kg).

Flow-Through Reactor Studies with 50 and 60 wt% Alane Slurries

Alane is an attractive chemical hydrogen storage media because of its high net-usable hydrogen capacity of 10 wt%. Dehydrogenation of neat alane also produces impurity free, fuel cell-grade hydrogen. The disadvantage of alane is the fact that it is a solid; thus, resulting in a cumbersome technological task of moving solids onboard and off-board. Alane slurries offer a means to retain the advantages of alane dehydrogenation (i.e., hydrogen purity) but also a more facile means of moving the chemical hydrogen storage media onboard and off-board. The disadvantage of alane slurries (or any slurry) is the fact that the non-hydrogen bearing fluidizing media lowers the overall hydrogen capacity of the media composition. In order to achieve a net-usable hydrogen capacity of the alane slurry, alane loadings must approach 75-80 wt%. Shown in Figure 2 are the results of our flow-through reactor studies with 50 and 60 wt% alane loadings. High alane conversions (~90%) were achieved at the highest space-time (tau = 7.6 min), highest temperature (T = 210°C) and the lowest auger speed (auger = 12 rpm) for the 50 wt% alane slurry in silicon oil (Figure 2a). Impurities were observed when silicon oil was used as the fluidizing media. Chemical incompatibilities of alane and silicon oil resulted in a gas-phase impurity with "Si-H" infrared transitions. Alane slurries with silicon oil require reactor temperatures below 200°C in order to prevent the undesired side reactions.

Using mechanical pump fluid and the fluidizing media for alane slurries eliminated the production of the gas-phase impurity with the Si-H infrared transitions; thus, demonstrating the importance of slurry carrier. However, gas-phase impurities were still observed with 60 wt% alane

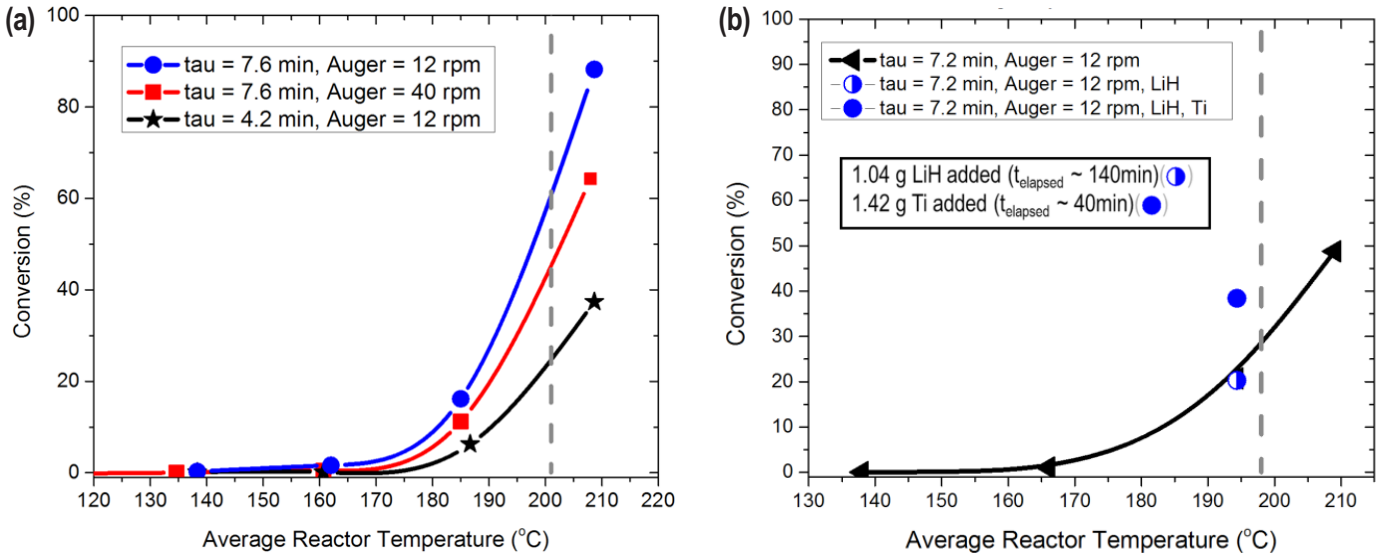

FIGURE 2. (a) Alane conversion as function of reactor temperature, space-time (tau), and auger speed for a 50 wt% alane slurry in silicon oil and (b) alane conversion as a function of reactor temperature, lithium hydride dopant, and titanium dopant for a 60 wt% alane slurry in mechanical pump fluid.

slurry in mechanical pump fluid. The highest conversion observed with the 60 wt% alane slurry was around 50% at 210°C (Figure 2b). Doping alane with LiH alone did not result in an increase the dehydrogenation kinetics. However, adding Ti (after doping with LiH) nearly doubled the conversion at an average reactor temperature of 195°C. Dopants and fluidizing media play an important role in alane slurry compositions. Optimizing alane slurries with respect to the carrier and dopants will prove critical in the further development of alane slurries.

SUMMARY

- Quantified chemical hydrogen storage material property guidelines
- Demonstrated 50 and 60 wt% alane slurries in flow through auger reactor

FY 2014 PUBLICATIONS AND PRESENTATIONS

1. K.P. Brooks,T.A. Semelsberger, K.L. Simmons, B.A. van Hassel, *Slurry-Based Chemical Hydrogen Storage Systems for Automotive Fuel Cell Applications*, Journal of Power Sources, DOI: 10.1016/j.jpowsour.2014.05.145.

2. T.A. Semelsberger, K.P. Brooks, *Chemical Hydrogen Storage Material Property Guidelines for Automotive Applications, Journal of Power Sources*, submitted.

3. T.A. Semelsberger, B.D. Rekken, B. Paik, E.L. Brosha, J.I. Tafoya, *Chemical Hydride Rate Modeling, Validation, and System Demonstration*, 2014 Annual Merit Review, Washington, D.C., June 2014.

IV.B.5 System Design, Analysis, Modeling, and Media Engineering Properties for Hydrogen Energy Storage

Matthew Thornton (Primary Contact), Jeff Gonder, Aaron Brooker, and Jonathon Cosgrove

National Renewable Energy Laboratory
1617 Cole Boulevard
Golden, CO 80401
Phone: (303) 275-4273
Email: Matthew.Thornton@nrel.gov

DOE Managers

Ned Stetson
Phone: (202) 586-9995
Email: Ned.Stetson@ee.doe.gov

Jesse Adams
Phone: (720) 356-1421
Email: Jesse.Adams@ee.doe.gov

Subcontractors

- Strategic Analysis Inc., VA
- Mark Pastor, MD

Project Start Date: February 2, 2009
Project End Date: June 30, 2015

Overall Objectives

- Perform vehicle-level modeling and simulations of various storage systems configurations.
- Lead the storage system energy analysis and provide results.
- Compile and obtain media engineering properties for adsorbent materials.
- Coordinate the public access of select Hydrogen Storage Engineering Center of Excellence (HSECoE) models, including web posting documentation and tracking downloads and Web activity.

FY 2014 Objectives

Coordinate the public access of select HSECoE models, including Web posting documentation and tracking downloads and Web activity.

Technical Barriers

This project addresses the following technical barriers from the Hydrogen Storage section of the Fuel Cell Technologies Office Multi-Year Research, Development, and Demonstration Plan:

(A) System Weight and Volume

(B) System Cost

(C) Efficiency

(E) Charging/Discharging Rates

(I) Dispensing Technology

(K) Systems Life-Cycle Assessments

Technical Targets

This project is conducting simulation and modeling studies of advanced onboard materials-based hydrogen storage technologies. Insights gleaned from these studies are being applied toward the design and synthesis of hydrogen storage vessels that meet the following DOE 2015 hydrogen storage for light-duty vehicle targets:

- Cost: to be determined
- Specific energy: 0.055 kg H_2/kg system
- Energy density: 0.040 kg H_2/L system
- Charging/discharging rates: 3.3 min
- Well-to-powerplant efficiency: 60%

FY 2014 Accomplishments

- Updated and integrated several center storage system models with the modeling framework and posted them on the website portal. These included a 700-bar physical storage model, a metal hydride model and two chemical hydride models.
- Completed documentation updates for the posted models (including website text and downloadable user manual).
- Developed disclaimer language to post alongside the models.
- Completed migration and link updates from the old SRNL.gov site to the current hsecoe.org site for all model postings.
- Performed vehicle-level tradeoff analyses to better understand the impact of key engineering designs, for example, the tradeoff between mass, onboard hydrogen storage capacity, and vehicle range.

INTRODUCTION

Overcoming challenges associated with onboard hydrogen storage is critical to the widespread adoption of hydrogen-fueled vehicles. The overarching challenge is identifying a means to store enough hydrogen onboard to enable a driving range greater than 300 miles within vehicle-related packaging, cost, safety, and performance constraints. By means of systems analysis and modeling, hydrogen storage system requirements for light-duty vehicles can be assessed. With these findings and through collaboration with our HSECoE partners, optimal pathways for successful hydrogen storage system technology can be identified to enable future commercialization of hydrogen-fueled vehicles. At this stage of the project the focus of activities has moved from the model application and analysis to model validation and making select models developed under the HSECoE publicly available and accessible to other researcher.

APPROACH

An array of tools and experience at NREL are being used to meet the objectives of the HSECoE. Specifically, extensive knowledge of multiple vehicle simulations, well-to-wheels analysis, and optimization are being employed and integrated with fuel cell and material-based hydrogen storage system models developed by other HSECoE partners. This integrated model framework allows for the evaluation of various hydrogen storage options on a common basis. Engineering requirements are defined from these studies thus enabling the design of hydrogen storage vessels that could meet DOE performance and cost targets in a vehicle system context. The approach for FY 2014 is to now update, validate, troubleshoot, de-bug, and document these framework and other models to that they can be made accessible and used by other research organizations.

RESULTS

The following will provide results from work completed this year to support the HSECoE with a focus on the coordination of the public access of select HSECoE models, including Web posting documentation and tracking downloads and web activity. In collaboration with several HSECoE partners, NREL (1) worked on the validation, refinement, Graphical User Interface (GUI) development, troubleshooting, and documentation of models selected for Web posting and (2) executed website migration, logistics, model posting and monitoring/tracking.

Model validation work on the HSECoE MH standalone acceptability envelope, MH finite element, the tank volume/cost models and the compressed gas, MH and CH framework models have been completed. Documentation and users guides for all of these HSECoE models have also been completed this year and all are currently or will soon be available via the HSECoE website (hsecoe.org). Figure 1 shows a screen caption of the current HSECoE home page which has direct links to the documentation, user guides, and download area for all available models.

Table 1 shows all of the select HSECoE models that are either available or that will be available on the website.

TABLE 1. HSECoE Models Available on Web Portal and Model Posting Status

Model Name	HSECoE Lead	Status
MH Acceptability Envelop	SRNL	Complete
MH Finite Element Model	SRNL	Complete
Tank Volume/Cost Model	PNNL	Complete
MH Framework Model	UTRC/NREL	Complete
CH Framework Model	PNNL/UTRC/NREL	In progress
AD Framework Model	SRNL/UTRC/NREL	9/2014
AD Finite Element Model	SRNL	3/2015

In addition to the validation, documentation, user guide, and posting activities this year, efforts were also focused on the development of a graphical user interface for the framework model in order to make the models more user friendly. In FY 2014 UTRC, NREL, and other HSECoE

FIGURE 1. HSECoE Web Home Page

partners teamed up on the GUI development effort. Figure 2 shows the current framework model GUI developed by UTRC. In this figure are the model selection pull down menu, the parameter settings location, and the model output and plot area.

Now that several HSECoE models are available to a wider research audience via the HSECoE web page, the final task for this year has been to track and document website activity and model downloads. Figure 3 shows the website activity from when the site was migrated to the new location in March through August. As can be seen the site has received over 700 visitors since the migration and of those 75% are new visitors. The bounce rate, which indicates sessions under 10 seconds, is 53% which meant that 47% of the visitors stay longer than 10 seconds and stay over four minutes on average.

Figure 4 shows the geographic locations of the visitors to the website. As expected most of the activity originated in the U.S., but there was also significant activity from Europe, Japan, Brazil, and Australia.

FUTURE DIRECTION

- Work with center partners to continue to make select center developed models available and accessible to the broader research and academic community through a controlled Web-based access portal and track downloads and website activity.
- Continue to run vehicle simulations to support Phase III engineering designs for adsorbent systems as needed:
  - Run vehicle simulations to support high-level storage system design and engineering tradeoffs.
  - Run vehicle simulations to support storage systems sizing analyses.

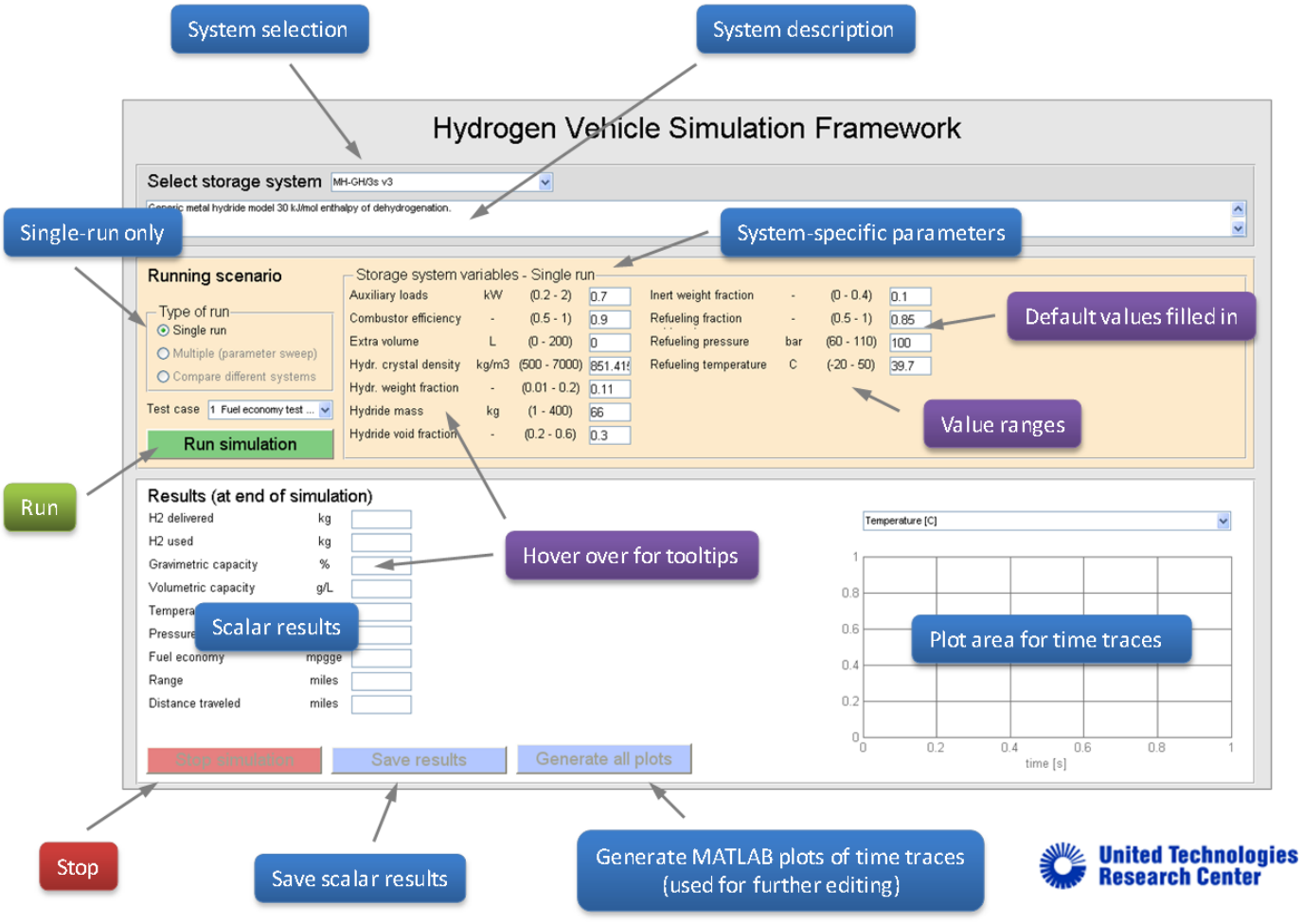

FIGURE 2. HSECoE Web Models Documentation and Download Page

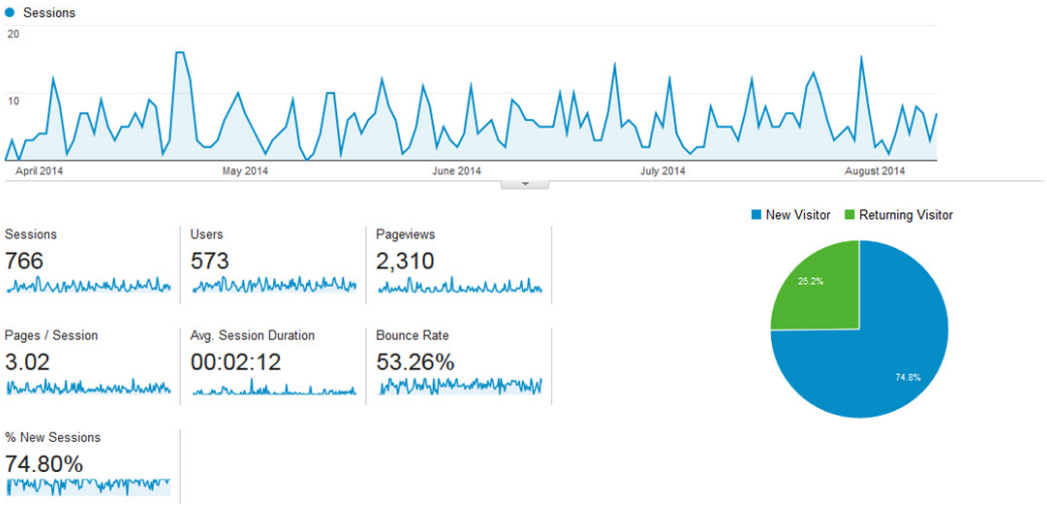

FIGURE 3. HSECoE Framework Model GUI

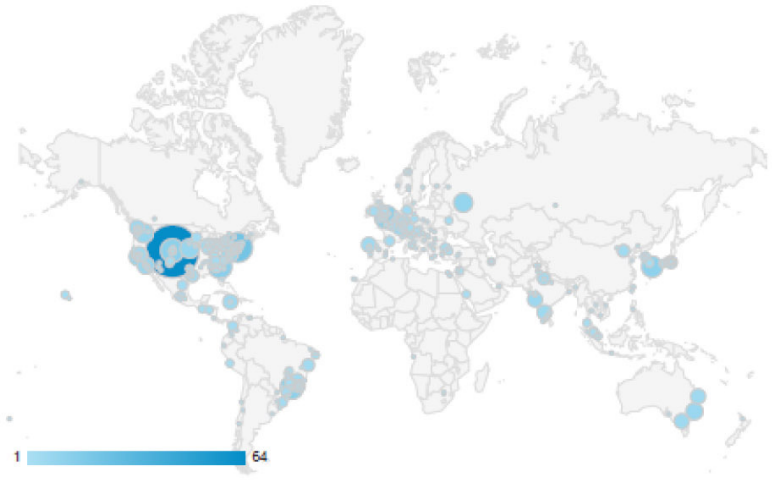

City	Acquisition			Behavior			Conversions		
	Sessions	% New Sessions	New Users	Bounce Rate	Pages / Session	Avg. Session Duration	Goal Conversion Rate	Goal Completions	Goal Value
	766 % of Total: 100.00% (766)	74.80% Site Avg: 74.80% (0.00%)	573 % of Total: 100.00% (573)	53.26% Site Avg: 53.26% (0.00%)	3.02 Site Avg: 3.02 (0.00%)	00:02:12 Site Avg: 00:02:12 (0.00%)	0.00% Site Avg: 0.00% (0.00%)	0 % of Total: 0.00% (0)	$0.00 % of Total: 0.00% ($0.00)
1. West Pleasant View	64 (8.38%)	18.75%	12 (2.09%)	28.12%	3.42	00:03:35	0.00%	0 (0.00%)	$0.00 (0.00%)
2. (not set)	43 (5.61%)	81.40%	35 (6.11%)	79.07%	2.21	00:01:00	0.00%	0 (0.00%)	$0.00 (0.00%)
3. Stratford	21 (2.74%)	23.81%	5 (0.87%)	9.52%	3.38	00:05:54	0.00%	0 (0.00%)	$0.00 (0.00%)
4. Aiken	13 (1.70%)	61.54%	8 (1.40%)	23.08%	2.69	00:00:24	0.00%	0 (0.00%)	$0.00 (0.00%)
5. Sao Paulo	12 (1.57%)	100.00%	12 (2.09%)	100.00%	1.00	00:00:00	0.00%	0 (0.00%)	$0.00 (0.00%)
6. London	12 (1.57%)	66.67%	8 (1.40%)	50.00%	3.33	00:05:58	0.00%	0 (0.00%)	$0.00 (0.00%)
7. Boulder	12 (1.57%)	8.33%	1 (0.17%)	83.33%	1.50	00:02:50	0.00%	0 (0.00%)	$0.00 (0.00%)
8. Fukuoka	11 (1.44%)	18.18%	2 (0.35%)	100.00%	1.00	00:00:00	0.00%	0 (0.00%)	$0.00 (0.00%)
9. Moscow	9 (1.17%)	100.00%	9 (1.57%)	44.44%	2.67	00:03:40	0.00%	0 (0.00%)	$0.00 (0.00%)
10. Livermore	9 (1.17%)	44.44%	4 (0.70%)	33.33%	4.78	00:02:49	0.00%	0 (0.00%)	$0.00 (0.00%)

FIGURE 4. HSECoE Web Analytics: Site Activity Metrics

FY 2014 PUBLICATIONS/PRESENTATIONS

1. System Design, Analysis, Modeling, and Media Engineering Properties for Hydrogen Energy Storage, Matthew Thornton, DOE Annual Merit Review Meeting, June 18, 2014, Washington, D.C.

2. Development of a Vehicle-Level Simulation Model for Evaluating the Trade-Off between Various Advanced On-Board Hydrogen Storage Technologies for Fuel Cell Vehicles, Matthew Thornton, Jon Cosgrove, Aaron Brooker and Jeff Gonder, 1st International Symposium on Energy Challenges and Mechanics, Aberdeen Scotland, July 10, 2014.

IV.B.6 Thermal Management of Onboard Cryogenic Hydrogen Storage Systems

Mei Cai (Primary contact), Peter Hou, Jerome Ortmann, and Martin Sulic (currently SRNL)
General Motors R&D Center (GM)
30500 Mound Road
Warren, MI 48090
Phone: (586) 596-4392
Email: mei.cai@gm.com

DOE Managers
Jesse Adams
Phone: (720) 356-1421
Email: Jesse.Adams@ee.doe.gov
Ned Stetson
Phone: (202) 586-9995
Email: Ned.Stetson@ee.doe.gov

Contract Number: DE-FC36-09GO19003

Project Start Date: February 1, 2009
Project End Date: June 30, 2015

Overall Objectives

- Develop system simulation models and detailed transport models for onboard hydrogen storage systems using adsorbent materials, and to determine system compliance with the DOE technical targets
- Design, build, and test an experimental vessel for validation of cryo-adsorption models and determine the fast-fill and discharge dynamics of cryo-adsorbent storage systems

Fiscal Year (FY) 2014 Objectives

- Demonstrate 3-minute scaled refueling by an internal flow-through cooling system based on powder media
- Demonstrate scaled H_2 release rate of 0.02 (g H_2/s)/kW by an internal heating system (<6.5 kg and 6 L)
- Participate in Phase III of the project as an original equipment manufacturer consultant in face-to-face meetings and coordinating council telecons; indicate technical or programmatic areas the Hydrogen Storage Engineering Center of Excellence (HSECoE) should be pursuing with more emphasis

Technical Barriers

This project addresses the following technical barriers from the Hydrogen Storage section of the Fuel Cell Technologies Office Multi-Year Research, Development, and Demonstration Plan:

(A) System Weight and Volume

(C) Efficiency

(E) Charging/Discharging Rates

(J) Thermal Management

Technical Targets

In this project, studies are being conducted to develop metal-organic framework (MOF)-5-based storage media with optimized engineering properties. This material has the potential to meet the 2017 technical targets for onboard hydrogen storage shown in Table 1.

TABLE 1. Project Technical Targets

Storage Parameter	2017 Target
System Gravimetric Capacity	0.055 (kg H_2/kg system)
System Volumetric Capacity	0.040 (kg H_2/L system)

FY 2014 Accomplishments

- Completed work on the experimental verification of the fast-fill and discharge dynamics of a cryo-adsorbent bed. The experimental data obtained with the cryo-apparatus enabled GM and the HSECoE to validate the transport models for these processes.
- Conducted additional experiments and model simulations while varying several operating conditions to improve upon the flow-through method of cooling the MOF-5 bed.
- The helical coil electric resistance heater design was tested successfully in the experimental program, reaching the targeted H_2 release rate.
- Obtained performance and operational data of MOF-5 powder/heat exchanger system.

INTRODUCTION

The DOE is supporting research to demonstrate viable materials for onboard hydrogen storage. Onboard hydrogen storage systems based on cryo-adsorbents are of particular interest due to the high gravimetric hydrogen capacity and fast kinetics of the sorbent materials at low temperatures and moderate pressure. However, cryo-adsorbents are generally characterized by low density and unsatisfactory thermal

properties. As part of the HSECoE team, the GM team is building system models and detailed transport models to optimize a cryo-absorbent fuel tank. A laboratory-scale cryogenic vessel was designed, built, and tested to determine the charging and discharging capabilities of an actual, operational system.

APPROACH

The 3-liter stainless steel cryogenic test vessel is sealed in an evacuated chamber that is temperature controlled down to cryogenic temperatures to best establish adiabatic conditions. Approximately 525 g of pure MOF-5 powder is packed into the 3-liter test vessel resulting in an adsorbent bed density of 0.18 g/cm^3. When pressurized to 60 bar, the adsorbent bed contains 96 g of hydrogen resulting in a weight fraction of 0.16 kg H_2/(kg MOF + H_2) and a volumetric density of 0.032 kg H_2/L of MOF. Mass flow rates in and out of the adsorption vessel are measured with a number of selectable orifice meters to allow accurate measurement over a large range of flow rates (0.005 to 0.75 g/s). A GM-designed helical coil heater with a center heating element is installed in the vessel to supply heat to the adsorbent bed during discharge. The vessel can be pressurized by either controlling the outlet flow rate or closing the outlet. A total of 32 high precision resistive temperatures devices and associated data acquisition channels are used to measure temperatures throughout the system and in the adsorption bed. Twenty-two of the resistive temperatures devices are devoted to measuring temperatures throughout the bed and at the inlet and outlet ports. The remaining 10 are associated with monitoring thermal conditions of hydrogen gas flow throughout the apparatus.

Three-dimensional adsorption and desorption models of the 3-liter cryogenic test vessel were developed using COMSOL Multiphysics® software. COMSOL contains application modes allowing for fluid flow through a porous media. The porous and fluid media are treated as a single medium having volume-averaged variables such as the flow velocity, pressure, and density. The gas and the solid bed are assumed to be in thermal equilibrium. Real gas properties of hydrogen are calculated using equations for a compressibility factor. Properties that are temperature or pressure dependent (and time-varying), such as the heat capacity of the MOF-5 bed and the heat of adsorption, are calculated at each time step. The amount of adsorbed hydrogen was quantified by employing a Dubinin-Astakhov isotherm. Model simulations were performed for the charging and discharging processes for the 3-liter cryogenic vessel. The flow in the system was modeled with Free and Porous Media Flow physics, and the heat transfer process was modeled with Heat Transfer with Porous Media. Pressure drop and flow velocity fields can be calculated with the former physics, and the process of heat transfer in the solids, fluids, and porous media can be investigated with the latter one.

RESULTS

A. Cryogenic Test Vessel – Charging Tests

During hydrogen charging, the exothermic adsorption process will produce heat as the hydrogen is introduced into the vessel. For fast hydrogen charging, this adsorption heat must be removed from the storage vessel as quickly and efficiently as possible or the rate of adsorption will decrease significantly. Experiments were performed to control the heat removal by varying the hydrogen outlet flow rate during flow-through cooling. Outlet flow rates of 0.4 and 0.52 g/s were used to determine if the faster rate would be more efficient at cooling the MOF-5 bed. For the 0.4 g/s case, the outlet flow rate had to be increased to 0.58 g/s at time 160 or the target pressure of 60 bar would have been exceeded. The initial bed temperature was approximately 102 K. Pressure was ramped from 5 bar to 60 bar within 60 seconds. The inlet hydrogen temperature was maintained at 82 K and the inlet flow rate was 0.65 g/s. The effect of the outlet flow rate on the average bed temperature profile is shown in Figure 1. After an initial rapid increase in temperature due to the heat produced by adsorption, the run with the faster outlet flow rate of 0.52 g/s maintains a lower temperature for the majority of the run until the temperatures eventually converge. The faster outlet flow rate helps to speed up the removal of the heated hydrogen gas. However, the final temperature of 104 K is still well above the desired temperature of 82 K.

The flow-through cooling method tested previously was found to have several inefficiencies. For example, the mass flow rate required to bring the 150 K MOF-5 bed to a temperature of 80 K would require an extremely large amount of hydrogen to pass through the vessel. Cooling the bed from an initial temperature of 150 K to 80 K by flowing hydrogen that is at the target temperature is also inefficient. Another issue with flow-through cooling is that

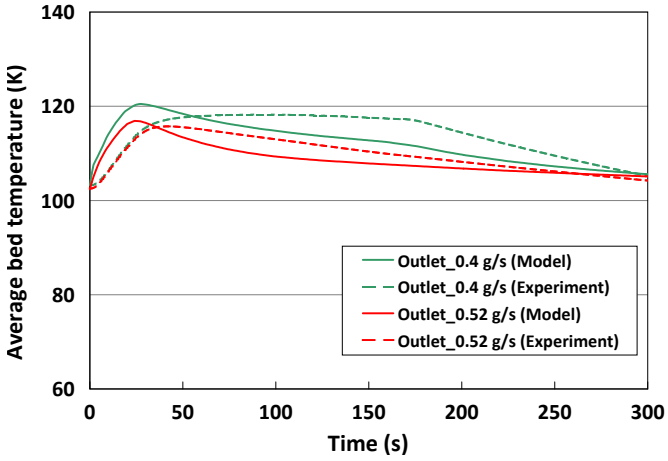

FIGURE 1. Effect of Outlet Flow Rate on Average Bed Temperature during Flow-Through Cooling

its effectiveness could suffer from possible channeling in the MOF-5 powder bed. This could cause some areas of the bed to be bypassed by the cold stream of hydrogen, making it very difficult to cool down these regions.

In order to address the issues associated with the flow-through cooling method, an alternative experimental method was devised for cooling the MOF-5 bed during charging. In this rapid charge/discharge method, the outlet of the cryogenic test vessel was initially closed while hydrogen flowed into the vessel. After a rapid temperature increase due to the adsorption heat, the outlet was opened to discharge the heated gas and depressurize the vessel. After a pressure of 5 bar was reached, along with a corresponding drop in temperature, the outlet was then closed and a new charge/discharge cycle was begun. For the first experiment a series of five charge/discharge cycles was performed with an initial bed temperature of 150 K. While each subsequent cycle achieved lower temperatures, the average bed temperature failed to reach the 80 K target, although it did decrease approximately 45 K from the initial temperature. For a second experiment, an initial bed temperature of 115 K was used. The results of this experiment are shown in Figure 2. The minimum temperature reached was 73 K, well below the inlet hydrogen temperature of 80 K. This shows that the cycling method can cool certain regions of the bed to a temperature lower than that of the inlet hydrogen, making it possible to store more hydrogen. This is a definite improvement over the flow-through cooling method, which could not achieve these low temperatures.

The cryogenic test vessel had been situated for horizontal gas flow for the entire set of experiments performed with it. This was the logical orientation for testing, since a full-size storage vessel would have to be placed horizontally in a vehicle. In order to test the effect of the vessel orientation on the experimental results, a run was performed in which the vessel was placed in the vertical position. The temperature profiles along the center line of the vessel matched closely for comparable charging tests performed with the vessel in the horizontal and vertical positions. The repeatability of the temperature profiles indicates that the orientation of the vessel had a negligible effect on the results.

B. Cryogenic Test Vessel: Discharging Experiments and Modeling

Previous discharge experiments with the cryogenic vessel demonstrated that a continuously running helical coil heater supplies adequate heat to maintain desorption and release hydrogen at the desired target rate of 0.02 g H_2/sec. Energy savings might be attained if it is possible to avoid powering the heater continuously when driving the vehicle. To test this hypothesis, the effect of delaying the introduction of heating power to the helical coil was investigated for the discharge process. The initial pressure of 60 bar can be used to extract hydrogen from the vessel without supplying heat. However, due to the endothermic effect of hydrogen desorption, the bed temperature will decrease. Extra heat must eventually be provided to warm up the bed. There are potential benefits to this mode of operation. If hydrogen in the vessel is not going to be used in a short period of time, the temperature drop in the vessel can be helpful for prolonging the dormancy period. If the hydrogen that remains in the tank can be warmed up by heat transfer from the warmer ambient air during parking time, less heating power is needed for the discharge and energy can be saved.

Figure 3 shows the change of average bed temperature in the vessel when heat is not provided until 2,160 s. The discharge rate was 0.02 g/s, supplied heating power 39 W, and heat flux 978 W/m^2. It can be seen that the average bed temperature drops during the discharge process. The lowest average bed temperature reached was 75 K. The

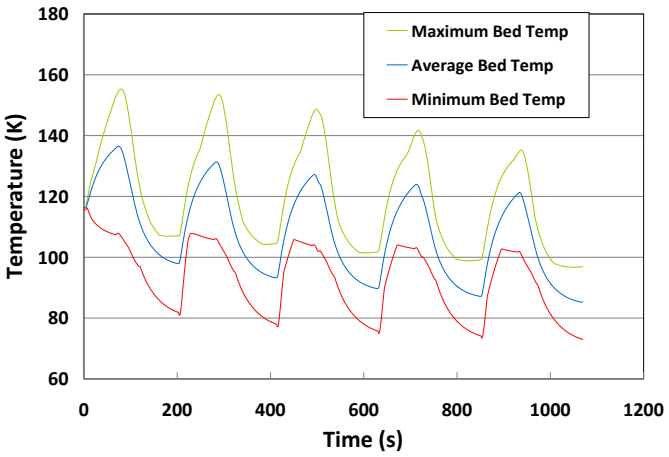

FIGURE 2. Rapid Cooling for the Charging Process with Initial Bed Temperature of 115 K

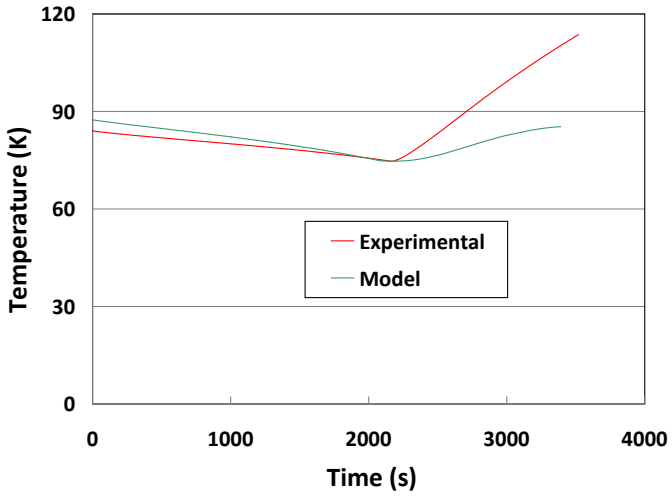

FIGURE 3. Effect of Delayed Heat Supply during Discharge on Average Bed Temperatures

inconsistency in average bed temperatures between the experiment and the model at the latter part of discharge is mainly due to the fact that the temperatures beyond the ends of the heating element were not detected and recorded. In the discharge process, temperatures in those two regions tend to be lower due to the endothermic effect of desorption. The average bed temperature in the model is integrated over the entire volume of the bed; thus, it tends to be lower than the values obtained in the experiment. The corresponding pressures in the vessel are shown in Figure 4. Delaying the supply of heating power to the helical coil causes the pressure to drop far more rapidly than the case with a continuously running heater. Although the delayed heating case runs for a slightly shorter amount of time, most likely due to additional hydrogen remaining adsorbed, the experiments show that leaving the heating power off for certain periods may be beneficial. With the use of better electronics controlling the system during driving, it may be possible to obtain significant energy savings.

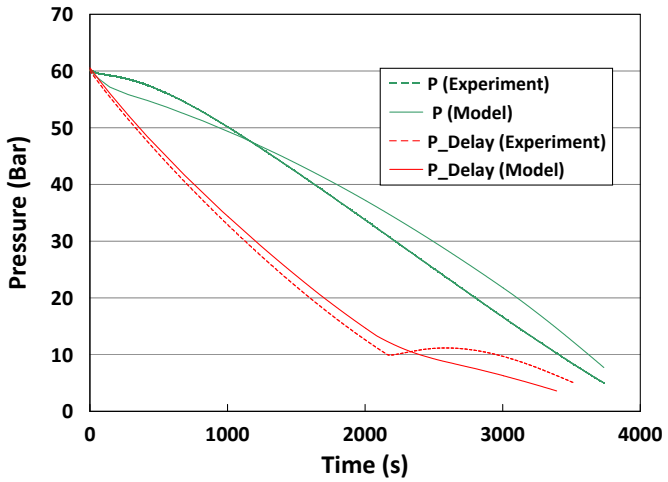

FIGURE 4. Effect of Delayed Heat Supply during Discharge on Pressure

CONCLUSIONS AND FUTURE DIRECTION

- The GM team completed its Phase II work on the experimental verification of the fast-fill and discharge dynamics of a cryo-adsorbent bed. The experimental data obtained with the cryo-apparatus enabled GM and the HSECoE to validate the transport models for these processes.
- The flow-through cooling concept for removal of heat during charging was validated experimentally, within the limits of the test apparatus. In addition, the helical coil electric resistance heater design was tested successfully in the experimental project.
- GM will continue to participate in Phase III as an original equipment manufacturer consultant to the HSECoE team. No additional experimental work is planned for Phase III.

FY 2014 PUBLICATIONS/PRESENTATIONS

1. M. Cai, et al. (2014), Testing and Modeling of a Cryogenic Hydrogen Storage System with a Helical Coil Electric Heater, presented at the 2014 DOE Hydrogen Program Annual Merit Review Meeting, Washington, D.C.

2. P. Hou, J.P. Ortmann, M. Sulic, A. Chakraborty, M. Cai, Experimental and numerical investigation of the cryogenic hydrogen storage processes over MOF-5, submitted to IJHE.

IV.B.7 Ford/BASF SE/UM Activities in Support of the Hydrogen Storage Engineering Center of Excellence

Michael Veenstra (Primary Contact, Ford),
Jun Yang (Ford), Chunchuan Xu (Ford),
Donald Siegel (UM), Yang Ming (UM),
Manuela Gaab (BASF SE), Lena Arnold (BASF SE),
and Ulrich Müller (BASF SE)

Ford Motor Company
1201 Village Road
Dearborn, MI 48124
Phone: (313) 322-3148
Email: mveenstr@ford.com

DOE Managers

Ned Stetson
Phone: (202) 586-9995
Email: Ned.Stetson@ee.doe.gov

Jesse Adams
Phone: (720) 356-1421
Email: Jesse.Adams@ee.doe.gov

Contract Number: DE-FC36-GO19002

Subcontractors
- University of Michigan (UM), Ann Arbor, MI
- BASF SE, Ludwigshafen, Germany

Project Start Date: February 1, 2009
Project End Date: June 30, 2015

Overall Objectives

This project addresses three of the key technical obstacles associated with the development of a viable hydrogen storage system for automotive applications:

- (Task 1) Create accurate system models that account for realistic interactions between the fuel system and the vehicle powerplant.
- (Task 2) Develop robust cost projections for various hydrogen storage system configurations.
- (Task 3) Assess and optimize the effective engineering properties of framework-based hydrogen storage media (such as metal-organic frameworks [MOFs]).

Fiscal Year (FY) 2014 Objectives

The project focus during FY 2014 was to complete the following objectives:

- Conduct a scale up of the MOF-5 manufacturing process to deliver >9 kg of material while maintaining performance, as measured by surface area, particle size, and hydrogen uptake, to within 10% of lab-scale procedure.
- Explore approaches to optimize MOF-5 engineering properties, such as thermal conductivity, mass transport, and safety.

Technical Barriers

This project addresses the following technical barriers from the Hydrogen Storage section of the Fuel Cell Technologies Office Multi-Year Research, Development, and Demonstration Plan:

(A) System Weight and Volume

(B) System Cost

(C) Efficiency

(D) Durability/Operability

(E) Charging/Discharging Rates

(H) Balance-of-Plant (BOP) Components

(J) Thermal Management

Technical Targets

The outcomes of this project provide input to vehicle and system level models, cost projections, and also contribute to the assessment and optimization of materials properties. Insights gained from these studies are applied towards the engineering of hydrogen storage systems that attempt to meet the DOE 2017 and ultimate hydrogen storage targets, shown in Table 1. As a status based on the cooperative analysis within the HSECoE, the current adsorbent systems are also shown in Table 1 based on powder and compacted MOF-5.

FY 2014 Accomplishments

- Task 1. System Modeling
  - Led the Hydrogen Storage Engineering Center of Excellence (HSECoE) adsorbent system effort by serving as the system architect and provided guidance from an original equipment manufacturer perspective to identify and prioritize the design direction.
  - Contributed to development of the Hydrogen Vehicle Simulation Model based on validated powertrain data and participated in development of the storage system model.

TABLE 1. Technical Targets and Current Adsorbent Systems

Storage Parameter	Units	DOE 2017 Target	DOE Ultimate Target	HexCell MOF-5 powder	MATI MOF-5 compact
System Gravimetric Capacity	$kg \cdot H_2/kg$	0.055	0.075	0.035	0.034
System Volumetric Capacity	$kg \cdot H_2/L$	0.040	0.070	0.018	0.021
Storage System Cost	$\$/kWh_{net}$	12	8	12.7	15.5
System Fill Time (for 5 kg H_2)	min	3.3	2.5	3-5	3-5
Minimum Full Flow Rate	(g/s)/kW	0.02	0.02	0.02	0.02
Min/Max Delivery Temperature	ºC	-40/85	-40/85	-40/85	-40/85
Min. Delivery Pressure (Fuel Cell)	Atm	5	3	5	5

  - Initiated design verification plan to align the failure mode and effects analysis action items with the Phase 3 test results. These activities were aimed at reducing the occurrence of failure modes in the adsorbent system.
- Task 2. Cost Analysis
  - Contributed to trade-off studies and integration analysis of BOP componentry. In collaboration with HSECoE partners, assessed cost-saving opportunities for a full-scale adsorbent storage system.
- Task 3. Assessment/Optimization of Framework-Based Storage Media
  - Delivered 9.3 kg of MOF-5 to HSECoE partners for Phase 3 system testing. Demonstrated successful scale up of material synthesis with delivered material achieving performance levels within 10% of lab-scale material properties.
  - Used high-throughput computational screening to assess the hydrogen storage capacity of ~4,000 porous metal-organic compounds mined from the Cambridge Structural Database. Identified trends in performance, and pinpointed several over-looked, yet promising MOFs that exhibit high volumetric and gravimetric hydrogen densities simultaneously.
  - Demonstrated a 20x improvement in MOF-5 thermal conductivity using an enhanced natural graphite (ENG) layering approach (compared to an equivalent MOF-5/ENG composite with random ENG loading).
  - Initiated degradation MOF-5 impurity cycle testing and conducted additional hydrogen flow parameter testing through powders.
  - Completed the formation of over 50 MATI half pucks using a novel embedded thermocouples technique with high dimensional and density consistency.

✧ ✧ ✧ ✧ ✧

INTRODUCTION

Widespread adoption of hydrogen as a vehicular fuel depends critically on the development of low-cost, onboard hydrogen storage technologies capable of achieving high energy densities and fast kinetics for hydrogen uptake and release. Since present-day technology based on compression and liquefaction is unlikely to attain established DOE targets, development of materials-based storage approaches has garnered increasing attention. To hasten development of these 'hydride' materials, the DOE previously established three centers of excellence for materials-based hydrogen storage research. While the centers have made substantial progress in developing new storage materials, challenges associated with the engineering of the storage system around a candidate storage material have received much less attention.

APPROACH

Ford-UM-BASF is conducting a multi-faceted research project that addresses the key challenges associated with the development of materials-based hydrogen storage systems. As in previous years, we continue to be engaged in system modeling (Task 1), with the objective of a public release of the HSECoE Hydrogen Vehicle Simulation Model. Work also continues in the system cost analysis effort (Task 2). During the past year, the majority of our effort has been focused on sorbent media (Task 3), with the primary goal of characterizing the "effective engineering properties" of MOFs in order to guide the development of optimal strategies for their use in an adsorbent system. In particular, we projected the performance for several thousand sorbent materials, conducted scale up of the MOF-5 synthesis process, and explored approaches for optimization of MOF-5 adsorbent media. Additional details are provided in the following section.

RESULTS

Following is a description of our technical results for certain key accomplishments and how these results relate to achieving the DOE targets.

Sorbent Media Performance Potential

As a response to project reviewers, we performed an analysis to determine the performance potential of sorbent media. Rather than considering theoretical MOF structures, we sought to identify promising known MOFs whose crystal structures reside within the Cambridge Structural Database. Many of these compounds have not been assessed as hydrogen storage materials. We developed an approach based on data mining and automated structure analysis to identify, "cleanup," and rapidly predict the hydrogen storage properties of these compounds. Approximately 20,000 candidate compounds were generated from the Cambridge Structural Database using an algorithm that removes solvent/guest molecules. These compounds were then characterized with respect to their surface area and porosity. Employing the empirical relationship between excess hydrogen uptake and surface area, we predict the theoretical total hydrogen storage capacity for the subset of ~4,000 compounds exhibiting nontrivial internal porosity (see Figure 1).

Our screening identified several overlooked compounds having high volumetric and gravimetric hydrogen capacities simultaneously; these compounds are suggested as targets of opportunity for additional experimental characterization. More importantly, our screening revealed that the relationship between gravimetric and volumetric hydrogen density is concave downward, Figure 1, with maximal volumetric performance occurring for surface areas of 3,100−4,800 m^2/g. We conclude that hydrogen storage in MOFs will not benefit from further improvements in surface area alone. Rather, discovery efforts should aim to achieve moderate mass densities and surface areas simultaneously, while ensuring framework stability upon solvent removal.

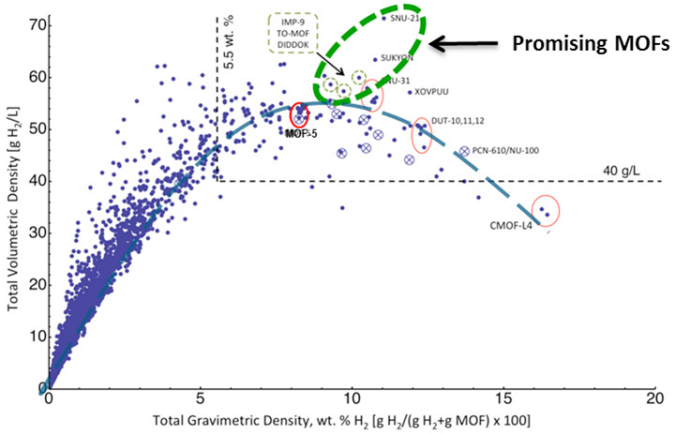

FIGURE 1. Theoretical Total (adsorbed + gas phase hydrogen at 77 K and 35 bar) Volumetric and Gravimetric Density of Stored Hydrogen in ~4,000 MOFs Mined from the Cambridge Structural Database.

Sorbent Media Scale Up

The scale up MOF-5 synthesis from a small-scale reactor (60 liters) to series-production representative reactors (200 liters) was successfully demonstrated. A total of 9.3 kg of MOF-5 powder was synthesized and subsequently characterized to ensure the scaled-up material could achieve a level of performance—as measured by surface area and particle size—to within 10% of lab-scale procedure. As shown in Table 1, the scaled-up material mix (GP0378) achieved the desired 10% of lab-scale material (GP0326). In fact, the Brunauer-Emmett-Teller (BET) surface area of the scaled-up material was increased by about 1% relative to the 60-liter (lab-scale) batch. The crystal size comparison between batches was found to be comparable using scanning electron microscopy analysis. The microscopy evaluation provided an assessment of the MOF-5 crystal attributes (i.e., roughness) as an effect from the scale-up synthesis steps (i.e., washing time). The particle size was extensively evaluated using laser diffraction based on International Organization for Standardization technical specification ISO 13320. The cumulative distribution measurement of particle size indicates a consistent particle size among the batches, with the particle size of the scaled-up material within 7% of the lab-scale batch.

TABLE 1. Surface Area, Crystal Size, and Particle Size Comparison of 200 Liter Scale-Up Material (GP0378) to 60 Liter Lab-Scale Material (GP0326)

Batch Code	Reactor Size (L)	Amount (kg)	BET (m2/g)	Zn (wt%)	C (wt%)	Crystal size (μm)	Particle size (mm)
GP0372	200	3.1	2937	32	37	0.2-2.0	
GP0374	200	3.5	2870	34	37	0.2-2.0	
GP0375	200	3.2	2955	34	37	0.2-2.0	
GP0378	Mix of above	9.3	2937	30	37	0.2-2.6	0.1-1.3
GP0326	60	1	2905	34	37	0.2-3.0	0.1-1.4

In addition to comparing physical properties of the powders produced by different synthesis methods, the hydrogen uptake was also compared. As shown in Figure 2, the 200-liter batch provides the same excess adsorption as the 60-liter material, consistent with their similar surface areas. Multiple measurements were taken for both powder and 0.5 g/cc compacted pellets, and the good agreement between batches was maintained across these systems.

Sorbent Media Assessment and Optimization

MOF-5 has an extremely low thermal conductivity, suggesting that enhancement strategies may be needed to enable efficient heat exchange designs within the adsorbent system. To increase the thermal conductivity of MOF-5 we explored the addition of ENG to MOF-5 pellets. In this

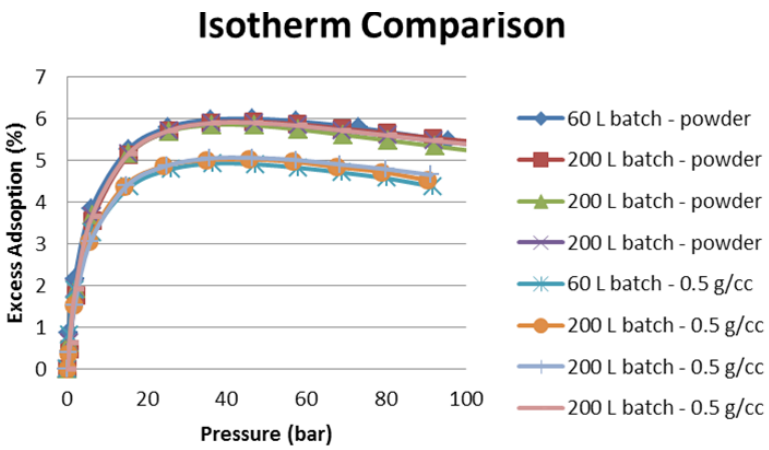

FIGURE 2. Excess Adsorption Comparison of the 200 Liter Scaled-Up Material versus 60 Liter Lab-Scale Material Synthesis

approach the ENG is typically mixed randomly into the MOF-5 powder. For cylindrical pellets, the ENG particles tend to lie perpendicular to the press direction, resulting in anisotropic thermal conductivity in the radial vs. axial directions. In previous work we determined that the thermal conductivity along directions parallel to the ENG alignment is two to three times higher than that in the perpendicular direction.

Our more recent work has demonstrated that additional improvement to thermal conductivity can be achieved by layering the ENG within the MOF-5 pellet. The pellet in Figure 3 (left) was formed by filling the die with alternating layers of MOF-5 and ENG. The die was tapped after each new layer was added. When all the layers were filled the pellet was pressed. The ENG appears to form a series of connected layers across the pellet. The resulting thermal conductivity as shown in Figure 3 (right) has 20 times improvement over the thermal conductivity measured in a pellet of comparable density and random ENG loading.

As a follow-up to the previous permeation flow testing with compacted pellets, we conducted flow testing through a bed of MOF-5 powder. The results align with the trend of an exponential increase in permeation with decrease of the sample density. The conclusion is that the hydrogen permeability of MOF-5 with density at 0.20 g/ml is over 100 times higher than that with density of 0.30g/ml. The testing was repeated with powders that were slightly compacted in the holder at a density of 0.25 g/cc and 0.29 g/cc which follow the expected trend.

CONCLUSIONS AND FUTURE DIRECTIONS

- Task 1. System Modeling
  - Evaluate the cryo-adsorbent system model based on Phase 3 performance data; support the integration into the framework; and document and release models to the public.

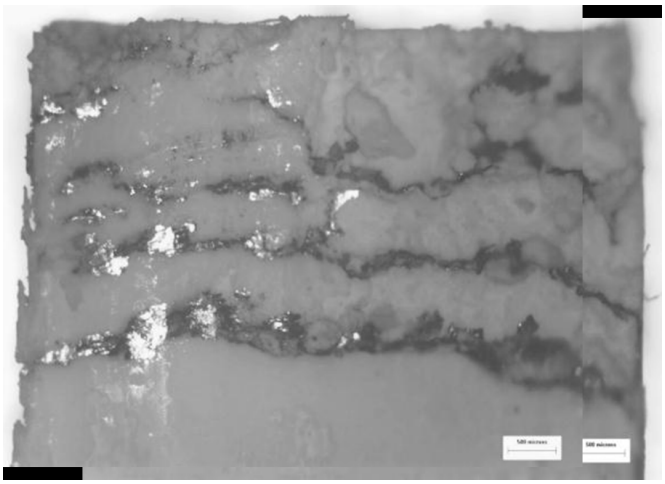

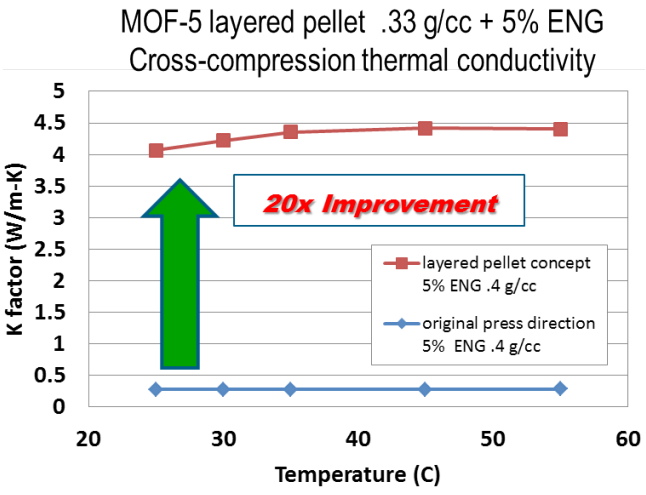

FIGURE 3. Layered Pellet Micrograph (Left) and Thermal Conductivity Measurement (Right)

  - Complete the failure mode and effects analysis associated with real-world operating conditions for a MOF-5-based system, for both HexCell and Modular Adsorbent Tank Insert concepts based on the Phase 3 test results. Reduce the risk priority numbers from the Phase 2 peak/mean and identify key failure modes.
- Task 2. Cost Analysis
  - Support further integration of the system BOP components for the cost analysis, and prepare for HSECoE project summary documentation to guide material researchers.
- Task 3. Sorbent Media Assessment and Optimization
  - Complete MOF-5 degradation cycle testing based on impurity levels as stated in SAE International technical specification SAE J2719 and report on the ability to mitigate to less than 10%.
  - Complete the optimization approaches to enhance thermal conductivity, mass transport, and density variations in formed pucks.

FY 2014 PUBLICATIONS/PRESENTATIONS

1. J. Goldsmith, A.G. Wong-Foy, M.J. Cafarella, and D.J. Siegel, Theoretical Limits of Hydrogen Storage in Metal-Organic Frameworks: Opportunities and Challenges, Chem. Mater., ASAP Article, (2013). DOI: 10.1021/cm401978e.

2. Y. Ming, J. Purewal, D. Liu, A. Sudik, C. Xu, J. Yang, M. Veenstra, K. Rodes, R. Soltis, J. Warner, M. Gaab, U. Muller, and D.J. Siegel, *Thermophysical Properties of MOF-5 Powders*, Microporous Mesoporous Mater., **185**, 235 (2014). DOI:10.1016/j.micromeso.2013.11.015

3. Y. Ming, H. Chi, R. Blaser, C. Xu, J. Yang, M. Veenstra, M. Gaab, U. Müller, C. Uher, and D. Siegel, *Aniostropic Thermal Transport in MOF-5 Composites,* International Journal of Heat and Mass Transfer, submitted.

4. M. Veenstra. "MOF-5 Development in Support of the Hydrogen Storage Engineering Center of Excellence," USDRIVE Hydrogen Storage Technical Team, March 19, 2014.

5. D.J. Siegel. "Adsorbent System Overview," Phase 3 Go/No-Go Milestone Review, March 19, 2014.

6. M. Veenstra, "Ford/BASF/UM Activities in Support of the Hydrogen Storage Engineering Center of Excellence", 2013 DOE Hydrogen Program Annual Merit Review Meeting, Washington, June 18, 2014.

IV.B.8 Microscale Enhancement of Heat and Mass Transfer for Hydrogen Energy Storage

Kevin Drost (Primary Contact), Goran Jovanovic, Vinod Narayanan, Brian Paul, Christopher Loeb, Mohammad Ghazvini, Agnieszka Truszkowska, and Hailei Wang

School of Mechanical, Industrial and Manufacturing Engineering
Rogers Hall
Oregon State University (OSU)
Corvallis, OR 97331
Phone: (541) 713-1344
Email: Kevin.Drost@oregonstate.edu

DOE Managers

Ned Stetson
Phone: (202) 586-9995
Email: Ned.Stetson@ee.doe.gov

Jesse Adams
Phone: (720) 356-1421
Email: Jesse.Adams@ee.doe.gov

Contract Number: DE-FC36-08GO19005

Project Start Date: February 1, 2009
Project End Date: June 30, 2015

Overall Objectives

Use microchannel processing techniques to:

- Demonstrate reduction in size and weight of hydrogen storage systems
- Improve charge/discharge rates of hydrogen storage systems
- Reduce size and weight and increase performance of thermal balance of plant components

Fiscal Year (FY) 2014 Objectives

Demonstrate 2-liter Modular Absorption Tank Insert (MATI)

Technical Barriers

This project addresses the following technical barriers from the Fuel Cell Technologies Office Multi-Year Research, Development, and Demonstration Plan:

(A) System Weight and Volume

(E) Charging/Discharging Rates

(H) Balance of Plant (BOP) Components

Technical Targets

The Phase 3 technical targets for the Microscale Enhancement of Heat and Mass Transfer for Hydrogen Energy Storage project are shown in Table 1.

TABLE 1. Project Technical Targets

Characteristic	Units	2014 Project Milestones	Status
MATI Weight	Kg	9.4	6.0
MATI Volume	Liter	4.2	3.0

Accomplishments

Key developments and technical accomplishments for the reporting period are:

- Completed design and assembly of the 2-liter MATI prototype (Barriers A and E).
- Completed assembly of the test facility for the 2-liter MATI (Barriers A and E).
- Completed model development for the charge and discharge cycle for the 2-liter MATI to prototype (Barriers A and E).

INTRODUCTION

Hydrogen storage involves coupled heat and mass transfer processes that are significantly impacted by size, weight, cost, and performance of system components. Micro-technology devices that contain channels of 10-500 microns in characteristic length offer substantial heat and mass transfer enhancements by greatly increasing the surface-to-volume ratio and by reducing the distance that heat or molecules must traverse. These enhancements often result in a reduction in the size of energy and chemical systems by a factor of 5 to 10 over conventional designs, while attaining substantially higher heat and mass transfer efficiency. We are developing micro-technology based advanced adsorption tank inserts (MATI) for high media utilization and enhanced heat and mass transfer during charge and discharge of adsorbent hydrogen storage systems.

APPROACH

Our technical approach to meet Phase 3 goals is that for each high-priority component, we will use microchannel

technology to reduce the relevant barriers to heat and mass transfer. Our approach involves (1) optimizing the performance of a single unit cell, i.e., an individual microchannel, and then "numbering up" using appropriate simulation tools that we then validate by experimental investigation; and (2) developing microlamination methods as a path to numbering up by low-cost, high-volume manufacturing.

RESULTS

In Phase 3 we are focused on the demonstration of high-value applications of microchannel technology: MATI for cooling during charging, heating during discharging, and hydrogen distribution. The MATI concept integrates storage media, microchannel heat exchangers, and microchannel hydrogen distribution plates in such a way that allows convenient use of densified adsorption media in excess of 94% of the tank volume. The concept separates the cooling process from the charging process, allowing flexibility in cooling strategies; in addition, MATI can provide heating during discharge, avoiding the need to use electric energy for discharge heating. A schematic of a single cell is presented in Figure 1. The full-sized MATI would consist of a number of cells, along with headers for cooling fluid and distributing hydrogen (see Figure 2).

At the end of Phase 2, MATI was selected for inclusion in Phase 3 of the Hydrogen Storage Engineering Center of Excellence research scope. In Phase 3 we are engaged in demonstration of MATI, specifically, in the design, assembly, and testing of a multi-cell MATI contained in a 2-liter pressure vessel. Testing will measure heat removal rates, hydrogen distribution, and durability. After acceptance testing at OSU, MATI will be supplied to Savannah River National Laboratory (SRNL) for independent testing. Progress to date on the development of the microchannel-based tank insert includes:

- Completed design and assembly of the 2-liter MATI prototype. The design of the 2-liter MATI prototype was completed during the reporting period (see Figure 2). The prototype will have five unit cells, each consisting of two cooling plates, two "pucks" of densified metal-organic framework-5 (MOF-5), and a hydrogen distribution region. The design includes (1) a pressure vessel developed in collaboration with Hexagon Lincoln, (2) the monolithic densified MOF-5 or "puck" developed in collaboration with Ford and University of Michigan, (3) the microchannel cooling plate, and

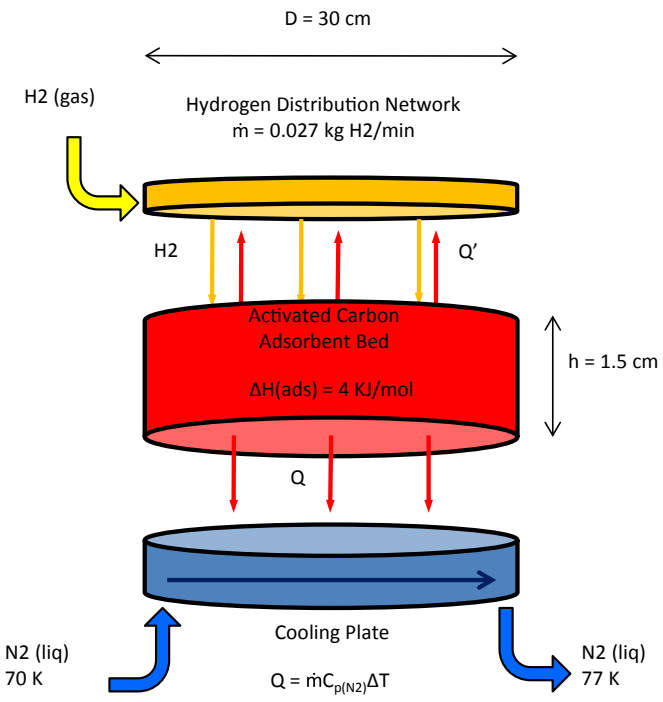

FIGURE 1. MATI Concept

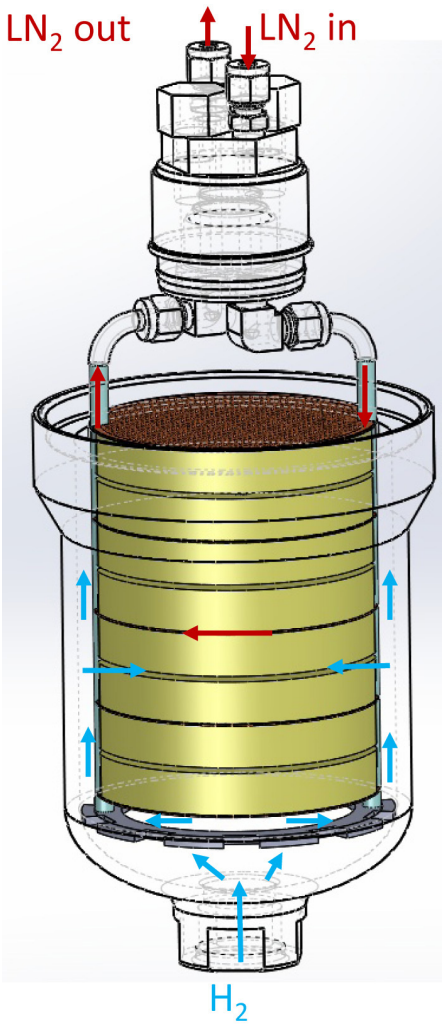

FIGURE 2. 2 Liter Prototype MATI Design

4) the headers for distributing the liquid nitrogen to the cooling plate. The design of the cooling plates was based on our Phase 2 design yet modified to achieve improved flow distribution. Based on both simulation and flow visualization, we have achieved the desired degree of uniform flow distribution in the cooling plate. Figure 3 shows the results of simulation of the flow distribution in a typical cooling plate. The design of the 2-liter MATI prototype was the subject of an external design review conducted by other center members, and recommended design modifications were incorporated into the prototype. Fabrication techniques for bonding the headers to the cooling plates have been developed and demonstrated. Initially we had difficulty brazing the cooling plates to the headers, but after investigating alternative approaches, we are now able to braze the cooling plates to the headers with a high degree of confidence. Figure 4 shows a complete unit cell with cooling plates, headers, and MOF-5 pucks. We are currently assembling the first 2-liter MATI prototype, and this will be used to start up our acceptance test apparatus.

- Completed assembly of the test facility for the 2-liter MATI. OSU will conduct limited testing on the 2-liter MATI prototype to ensure that it is functioning properly before shipping the device to SRNL for comprehensive testing. To facilitate testing, a cryogenic acceptance testing apparatus was designed, and a test plan was developed for acceptance testing. The test apparatus includes both the system for testing MATI and the conditioning systems for cooling the inlet hydrogen and liquid nitrogen to the appropriate inlet conditions. The design and test plan were the subject of an external design review conducted by other center members, and recommended design modifications were incorporated into the test apparatus and test plan. The apparatus will be used for experimental investigations of charging and discharging a 2-liter prototype MATI. Acceptance testing involves experimental investigations of the complete charging and discharge cycles, including hydrogen distribution and adsorption and the removal of the heat of adsorption using liquid nitrogen. We have completed assembly of the test apparatus and will be starting up the device in the next month.

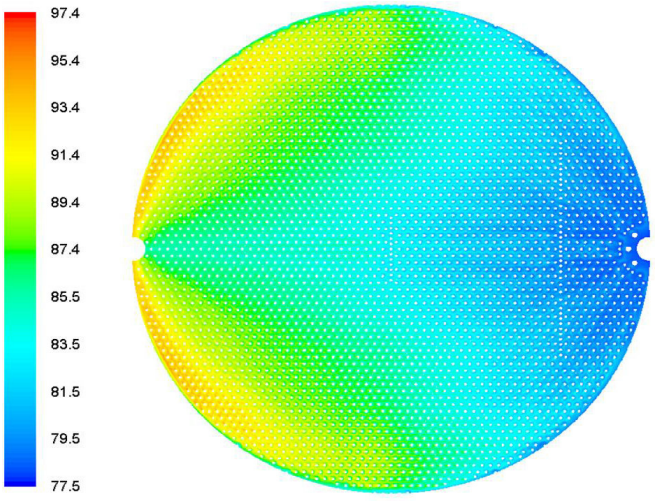

FIGURE 3. Simulation Results for Flow Distribution in a MATI Prototype Cooling Plate

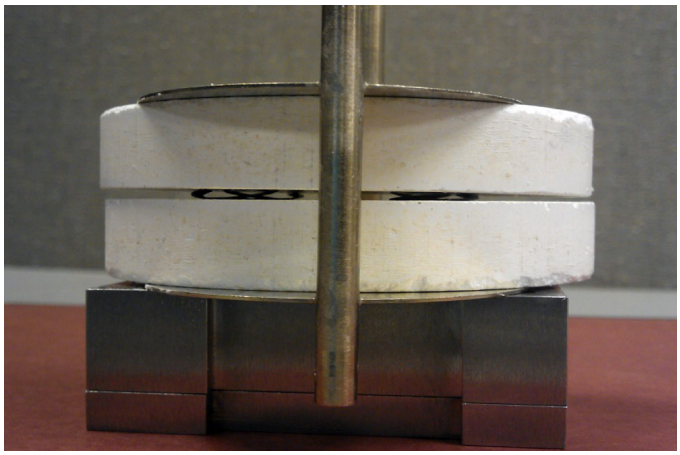

FIGURE 4. Assembled MATI Unit Cell

- Completed model development for the charge and discharge cycle for the 2-liter MATI to prototype. Simulation models have been developed to model all relevant phenomena associated with the charging and discharging of the MATI. During Phase 2 the models were validated against the experimental results of our integrated testing. Overall, the average error between experiment and simulation results was between 4% and 5% with the maximum error being between 8% and 9%. Based on these validation results, we were confident that we could accurately model the adsorption and desorption behavior of a single puck. However, to further improve our modeling capability, we worked with SRNL to incorporate several advanced features used by SRNL. With these modifications we have reduced the average error in our comparison with experimental data from 5.9% to 3.5%. We have completed the assembly of an eight-zone model that will model the complete MATI, including the pressure vessel during both the charge and discharge cycles. As data become available from the SRNL comprehensive testing, we will use the eight-zone model for model validation and support of the experimental investigations being conducted at both OSU and SRNL.

Extending beyond the formal Phase 3 scope of work, OSU made promising advances in commercializing the microchannel combustor/heat exchanger concept for a

number of heating applications, with the inventor winning the Transformational Idea award at the FLoW competition at Caltech on May 7, 2014. This technology was developed for hydrogen storage applications in earlier phases of the project.

CONCLUSIONS AND FUTURE DIRECTIONS

Key conclusions resulting from our research are as follows.

- The use of the modular adsorption tank insert allows convenient use of densified adsorption media in excess of 94% of the tank volume. The concept separates the cooling process from the charging process, allowing flexibility in cooling strategies, and MATI can provide both cooling during charging and heating during discharge with a weight under 9.5 kg for a hydrogen storage system containing 5.6 kg of hydrogen.
- The design of the 2-liter MATI has been completed and peer reviewed, as have the design of the test apparatus and our test plans.

The next step in our research is to complete the demonstration of MATI that includes (1) final assembly of the test article at OSU, (2) acceptance testing at OSU, (3) comprehensive testing at SRNL, and (4) model validation. In addition, if monolithic densified media, "pucks," are available with conduction enhancements, these will be tested in FY 2015.

SPECIAL RECOGNITIONS & AWARDS/ PATENTS ISSUED

Mohammad Ghazvini, a post-doctoral researcher in OSU's School of Mechanical Industrial and Manufacturing Engineering, won the Transformational Idea award at the FLoW competition at Caltech on May 7, 2014, for the microchannel combustor/heat exchanger developed as part of this project. The $5,000 award is given to groundbreaking pre-commercial research with large potential impact on energy sustainability and efficiency. The FLoW competition is held every year in Los Angeles, California, and is supported by the Department of Energy. FLoW's mission is to support the development of entrepreneurial talent within American universities and to accelerate the movement of leading-edge technologies out of the lab and into the marketplace

FY 2014 PUBLICATIONS/PRESENTATIONS

1. E. Rasouli and V. Narayanan, "Single-phase cryogenic flows through microchannel heat sinks," Proceedings of ICNMM2014-21275, ASME international conference of nanochannels, microchannels, and minichannels, Chicago, Illinois, 2014.

2. C. Loeb and G. Jovanovic, "Improved storage capacity of a MOF-5 hydrogen storage system using a novel microchannel heat exchange device," 23rd International Symposium on Chemical Reaction Engineering and 7th Asia-Pacific Chemical Reaction Engineering Symposium, Bangkok, Thailand, 2014.

3. C. Loeb, A. Truszkowska, G. Jovanovic, "Increasing hydrogen storage in compressed MOF-5 system using a microchannel thermal management device: experiment and simulation," Advances in Chemical Engineering and Science, 2014 (in review).

4. E.D. Truong, E. Rasouli, and V. Narayanan, "Cryogenic single-phase heat transfer in a microscale pin fin heat sink," Proceedings of SHTC 2013-17660, ASME summer heat transfer conference, Minneapolis, Minnesota, 2013.

IV.B.9 Development of Improved Composite Pressure Vessels for Hydrogen Storage

Norman Newhouse (Primary Contact), Jon Knudsen, Alex Vaipan
Hexagon Lincoln Inc. (formerly Lincoln Composites, Inc.)
5117 NW 40th Street
Lincoln, NE 68524
Phone: (402) 470-5035
Email: norman.newhouse@hexagonlincoln.com

DOE Managers
Ned Stetson
Phone: (202) 586-9995
Email: Ned.Stetson@ee.doe.gov
Jesse Adams
Phone: (720) 356-1421
Email: Jesse.Adams@ee.doe.gov

Contract Number: DE-FC36-09GO19004

Project Start Date: February 1, 2009
Project End Date: June 30, 2015

Overall Objectives

- Improve the performance characteristics, including weight, volumetric efficiency, and cost, of composite pressure vessels used to contain hydrogen in adsorbants.
- Evaluate design, materials, or manufacturing process improvements necessary for containing adsorbants.
- Demonstrate these improvements in prototype systems through fabrication, testing, and evaluation.

Fiscal Year (FY) 2014 Objectives

- Select the best tank size and design option to use for Phase 3 testing.
- Manufacture prototype tanks and distribute to Hydrogen Storage Engineering Center of Excellence (HSECoE) partners requesting them.
- Demonstrate alternate tank designs with improved performance.

Technical Barriers

This project addresses the following technical barriers from the Hydrogen Storage section of the Fuel Cell Technologies Office Multi-Year Research, Development, and Demonstration Plan:

(A) System Weight and Volume

(B) System Cost

(G) Materials of Construction

Technical Targets

This project is conducting studies for the development of improved composite pressure vessels for hydrogen storage, and developing an optimized vessel for use by HSECoE partners in demonstrating a functioning vehicle storage system using adsorbant materials. The targets apply to the storage system, of which the vessel is a part. Insights gained from these studies will be applied toward the design and manufacturing of hydrogen storage vessels that meet the following DOE hydrogen storage targets:

TABLE 1. Project Technical Targets

	2017
Gravimetric capacity	>5.5%
Volumetric capacity	>0.040 kg H_2/L
Storage system cost	<$12/kWh

FY 2014 Accomplishments

- HSECoE partners confirmed operating requirements for the Phase 3 test vessel, including a confirmation of the 100-bar operating pressure, and an internal volume of 2 L.
- The Phase 3 test vessel, of 3-piece Type 1 construction, was designed to have the same internal contour as the Phase 2 vessel, but thinner walls to make it more cost and weight efficient.
- The Phase 3 test vessel was subjected to 200 pressure cycles and a burst test, achieving 292 bar at ambient temperature, and 380 bar at 77 K, which confirmed the design and safety for use. A Type 1 vessel is about 20% to 40% heavier than a Type 4 vessel, but about 30% to 50% lower in cost at 100 bar.
- Phase 3 test vessels were distributed to HSECoE partners as requested. An internal thermal insulation layer was also provided.
- Subscale Type 1, Type 3, and Type 4 tanks are being designed to evaluate further improvement possibilities in alternate designs.
- Toughened resin systems continue to be evaluated as a means to improve composite performance by improving response to impact loading.

INTRODUCTION

Hexagon Lincoln is conducting research to meet DOE 2017 Hydrogen Storage goals for a storage system by identifying appropriate materials and design approaches for the hydrogen container. At the same time, the pressure vessels must continue to maintain durability, operability and safety characteristics that already meet current industry guidelines. There is a continuation of work with HSECoE partners to identify pressure vessel characteristics and opportunities for performance improvement. Hexagon Lincoln is working to develop high-pressure vessels as are required to enable tank design approaches to meet weight and volume goals and to allow adsorbant materials that operate at cryogenic temperatures to operate efficiently.

APPROACH

Hexagon Lincoln established a baseline design for full-scale and test tank using HSECoE team operating criteria as a means to compare and evaluate potential improvements in design, materials and process to achieve cylinder performance improvements for weight, volume and cost. Hexagon Lincoln selected the most promising engineering concepts to meet Go/No-Go requirements for moving forward. The emphasis was on demonstrated technology to ensure ability of HSECoE partners to test their system components.

In Phase 3, operating conditions have been confirmed, and a reduced weight laboratory test vessel was designed and tested. This three-piece Type 1 tank is designed for safety and re-usability. Studies are continuing to identify designs and materials that may result in lighter weight and/or less expensive tanks.

RESULTS

HSECoE partners confirmed operation at 100-bar service pressure, with an operating temperature range from 80 K to 160 K, and a non-operating limit of 373 K. A test vessel configuration with three-piece Type 1 construction, a 2-liter volume, and reduced wall thickness was also established to demonstrate component technology. Test vessels were designed, manufactured, tested, and distributed to HSECoE partners to facilitate Phase 3 testing of prototype components.

The Phase 3 Type 1 test vessel was designed using aluminum alloy 6061-T6 and a three-piece construction (Figure 1). The three-piece construction allowed HSECoE partners to remove and replace components in the vessel between tests. A Type 1 vessel is about 20% to 40% heavier than Type 4 construction, but about 30% to 50% lower

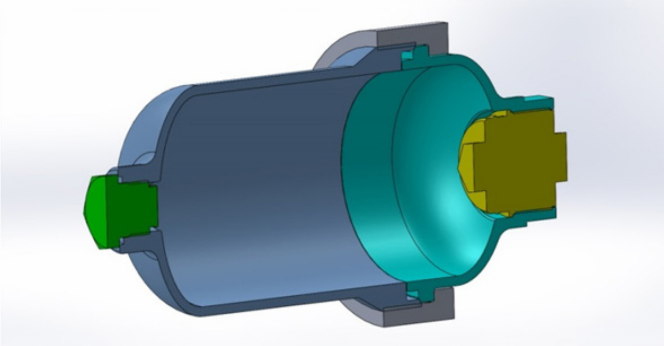

FIGURE 1. Phase 3 T1 Test Tank

FIGURE 2. Tank after Cryo Burst

in cost at 100 bar. The Phase 3 prototype, with reduced wall thickness compared with the Phase 2 prototype, was 15% lighter in weight. A burst test to 290 bar at ambient temperature confirmed safety. A test vessel was also subjected to 200 cycles to service pressure at 80 K, then burst at 380 bar (Figure 2). This test confirmed safety for use by HSECoE partners in laboratory testing.

A Teflon® liner was fabricated as internal thermal insulation for the subscale tank. The liner has a thickness of 1/8 inch. The liner allows the completed tank to be submerged in liquid nitrogen to cool the apparatus, and then adding heat to drive off the hydrogen in the adsorbant material, without the added heat being absorbed totally by the liquid nitrogen.

Designs were prepared for a single-piece Type 1 tank to be made of 6061-T6 aluminum, and a Type 3 tank using the same material as a liner, and using carbon/epoxy reinforcement. The inside of the two tanks would have approximately the same dimensions as the 3-piece Type 1 tank. A supplier for the tank and liner has been identified and an order placed for the components. Efforts are continuing

to design a Type 4 tank that is compatible with the cold operating conditions that have been specified.

HSECoE partners have begun using the three-piece Type 1 tanks to demonstrate system components. A problem developed with leaking seals. It appears this problem will be resolved with the use of crushable metal washer type seals.

Additional cooling experiments were conducted to evaluate the external insulation system that will also be used for cooling the shell at time of fill. It was determined that a 3-mm gap between the outside of the tank and the inside of the insulating shell would be sufficient for use on the prototype system.

A task to evaluate toughened epoxy resin has been continued from Phase 2. Six different technologies have been selected for toughening the epoxy resin used in hydrogen pressure vessels. Table 2 shows results of initial screening. The glass transition temperature must remain above 105°C to maintain environmental stability in use, and the maximum viscosity for ease of manufacture is 2,500 cP.

TABLE 2. Results of Initial Screening

Material	Glass transition temperature (°C)	Room Temperature Viscosity (cP)
Baseline	118.3	916
ATBN	116.8	1,530
Core shell rubber	118.3	1,460
Nanosilica	118.2	1,070
Surface Modified Silica	117.3	960
Titanium Dioxide	118.4	930
Phase separating rubber	118.1	1,080

Neat resin coupons (Figure 3) were then fabricated and tested for tensile strength. The top four resin formulation showing the greatest increase in toughness will continue in the evaluation using composite rings and subscale tanks.

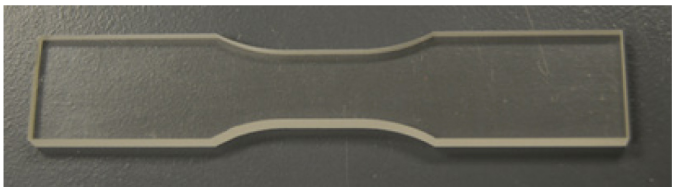

FIGURE 3. Resin Coupon

CONCLUSIONS AND FUTURE DIRECTIONS

- A Type 1 tank can meet the pressure and temperature requirements for Phase 3 testing and component development, and has the lowest program risk. A revised design of lighter weight was developed and tested.
- Subscale 1-piece Type 1, Type 3, and Type 4 tanks will be designed and fabricated to achieve higher performance than the three-piece Type 1 tank, and suitable for cryogenic service. The Type 1 tank and Type 3 tank liner have been ordered.
- The concept for insulating and pre-cooling the tank has been tested using prototype components. A full-scale component will be designed and modeled. A subscale unit will be manufactured and tested.
- Toughened resins that may further improve performance of Type 3 and Type 4 composite tanks are being developed and tested.

SPECIAL RECOGNITIONS & AWARDS/ PATENTS ISSUED

1. A patent application was filed on the concept for a thermal insulation shell system that would also allow cooling of the tank prior to refilling.

FY 2014 PUBLICATIONS/PRESENTATIONS

1. 2014 DOE Hydrogen Program Annual Merit Review, June 18, 2014.

IV.C.1 Hydrogen Sorbent Measurement Qualification and Characterization

Philip A. Parilla (Primary Contact), Katherine Hurst, Chaiwait Engtrakul, Thomas Gennett

National Renewable Energy Laboratory (NREL)
15013 Denver West Pkwy.
MS 3211
Golden, CO 80228
Phone: (303) 384-6506
Email: Philip.Parilla@nrel.gov

DOE Managers

Jesse Adams
Phone: (720) 356-1421
Email: Jesse.Adams@ee.doe.gov

Channing Ahn
Phone: (202) 586-9490
Email: Channing.Ahn@ee.doe.gov

Subcontractor

H2 Technology Consulting LLC, Karl Gross, CA

Collaborators

- Oak Ridge National Laboratory (ORNL) and University of Missouri – Raina Olsen group
- University of Missouri – Peter Pfeifer group
- National Institute of Standards and Technology, Facility for Adsorbent Characterization and Testing – ARPA-E Project
- National Institute of Standards and Technology – Laura Espinal group
- FBK, Italy – M. Testi and L. Crema
- University of South Alabama – J. Burress group

Project Start Date: October 1, 2012
Project End Date: Project continuation and direction determined annually by DOE

Overall Objectives

- Provide validation measurements for the hydrogen capacity of storage materials.
- Develop and disseminate measurement best practices and recommended protocols and data analysis procedures for hydrogen capacity measurements.
- Assist research groups within the hydrogen storage community to perform robust and accurate measurements of hydrogen storage capacity.
- Analyze for, identify, and recommend corrective actions for major sources of measurement error in volumetric and temperature-programmed desorption (TPD) systems.

Fiscal Year (FY) 2014 Objectives

- Develop volumetric capacity protocols and recommend their implementation to the hydrogen storage community so that material properties can be reported in a uniform and unambiguous manner.
  - Compile a complete list of volumetric capacity definitions and options needed to develop a standardized methodology to measure, calculate, interpret, and report on volumetric capacity.
  - Propose protocols for the determination of volumetric capacity of sorbent materials.
  - Submit a report that will be disseminated to the scientific community (pending at the time of this report).
- Assist materials research groups to characterize and qualify their samples for hydrogen storage properties.
  - Measure external samples at NREL to compare results with source group's and/or third-party's results.
  - Discover sources of measurement discrepancies and advise on corrective actions, if needed, for source group.
- Analyze for, identify, and recommend corrective actions for major sources of measurement error in volumetric and TPD systems.
  - Analyze realistic models for random and systematic errors.
  - Identify the major error sources that will dominate the measurement.
  - Recommend improved instrumentation and procedures to minimize such errors.

Technical Barriers

This project addresses the following technical barriers from the Hydrogen Storage section of the Fuel Cell Technologies Office Multi-Year Research, Development, and Demonstration Plan:

(A) System Weight and Volume

(B) System Cost

(C) Efficiency

(E) Charging/Discharging Rates

(K) System Life-Cycle Assessments

(O) Lack of Understanding of Hydrogen Physisorption and Chemisorption

(P) Reproducibility of Performance

Technical Targets

This project supports the following overall DOE objective: "Capacity measurements for hydrogen storage materials must be based on valid and accurate results to ensure proper identification of promising materials for DOE support." This project focuses on this through the FY 2014 objectives as listed previously. Insights gained from these studies will be applied toward the design and synthesis of hydrogen storage material systems that meet the following 2017 DOE hydrogen storage targets:

- Cost: $12/kWh net
- Specific energy: 1.8 kWh/kg
- Energy density: 1.3 kWh/L

The specific technical objectives include the following:

- Disseminate measurement qualification and validation improvements to the hydrogen community.
- Work with hydrogen-storage material-synthesis researchers to measure at least two external samples.

FY 2014 Accomplishments

- Developed recommended volumetric capacity definitions and protocols.
- Measured two external samples from outside laboratories, and we anticipate measuring two more external samples before the end of FY 2014. This surpasses the milestone of measuring three external samples.
- Collaborated with outside labs to investigate and verify operation of their hydrogen capacity equipment.
- Continued to develop realistic models for the data analysis for volumetric systems, both for isothermal and non-isothermal conditions. Used models to understand both systematic and random error sensitivities. Initiated efforts to identify these and possible other methodological/error analysis issues for differential volumetric systems. Discussed the major error sources that dominate the measurement; determined that the most dominant errors are still systematic errors. Reported detailed findings and recommendations on hydrogen capacity measurements at the International Energy Agency-Hydrogen Implementing Agreement Task 22 meeting in February 2014.
- Continued to manage and collaborate on the "Best Practices" project with its seven sections: Introduction, Capacity, Kinetics, Thermodynamics, Cycle-Life, Thermal Properties, and Mechanical Properties measurements. With the completion of the Mechanical Properties section, this will complete the Best Practice document [1].

INTRODUCTION

The ultimate goal of the Hydrogen Storage program is the development of hydrogen storage systems that meet or exceed the DOE's goals for onboard storage in hydrogen-powered vehicles. In order to develop new materials to meet these goals, it is extremely critical to accurately, uniformly, and precisely measure the materials' properties relevant to the specific goals; otherwise, the metrics are meaningless and achieving of goals, uncertain. In particular, capacity measurements for hydrogen storage materials must be based on valid and accurate results to ensure proper identification of promising materials for DOE support. A previous round-robin study discovered major discrepancies among the different participating laboratories for capacity measurements on a standard material, both for room-temperature and liquid-nitrogen capacity determinations [2]. This study emphasizes the importance of maintaining a quality assurance effort within the hydrogen storage community. This project focuses on maintaining a world-class measurement facility for determining hydrogen storage capacities of novel research materials; understanding the experimental issues, procedures, and analysis to ensure accurate measurements; and assisting the hydrogen storage community in performing and understanding these measurements. NREL's main focus is on the volumetric capacity measurement technique; this is also known as the manometric and Sieverts technique. NREL also has extensive experience in the TPD (or thermal desorption spectroscopy) technique.

APPROACH

NREL continues with a multi-year, intensive effort to improve measurement quality and accuracy, understand the sources of and correct for measurement error, work with external groups to provide measurements and verify results, collaborate with the hydrogen community to improve measurements, and manage and coordinate with the "Best Practices" project to disseminate recommended practices and procedures. In previous FYs, this effort was folded into the main materials-development program. This effort has its roots even before the Hydrogen Sorption Center of Excellence (HSCoE), but the effort accelerated during its existence as NREL was the main measurement resource for the HSCoE. The approach can be divided into three components: 1) work with external groups to measure samples and to examine their measurement techniques and procedures; 2) in general, analyze for, identify, and recommend corrective actions for major sources of measurement error in volumetric systems;

and 3) develop standardized procedures and protocols so that data and results are reported in a uniform manner to allow direct comparison of material performance.

With respect to working with external groups, NREL actively seeks out collaborations for comparison studies, helps out with DOE projects to ensure robust measurements, and tests very promising results for verification. Additionally, NREL works with external groups to discover sources of measurement discrepancies and advise on corrective actions, if needed. This entails sending standardized samples to external labs to test instrumentation and experimental procedures, examining data and data analysis protocols to discover possible avenues to improve measurement techniques, and making recommendations to labs for improvements. In FY 2014, NREL has developed definitions and implementations for determining volumetric capacity of hydrogen storage materials. With respect to measurement error, NREL analyzes realistic models for random and systematic errors, identifies the major error sources that will dominate the measurement, and recommends improved instrumentation, protocols, and data analysis to minimize such errors.

RESULTS

1. Developed recommended volumetric capacity (VC) definitions and protocols. VC determinations ultimately involve a separate accounting of hydrogen in a storage vessel or system and a separate accounting of quantifying the volume of said vessel or system and dividing the former by the latter. Different accountings for hydrogen and volumes define different figures of merit (FOMs), and depending on the goals of the project with corresponding emphasis of different merits, the best FOM to use to quantify those merits will change with the emphasis. Figures 1 and 2 give examples of how this accounting can occur for hydrogen and volumes, respectively.

   For a VC FOM that emphasizes materials, we recommend the total hydrogen capacity divided by the bulk volume of the sample. This includes all the hydrogen in the pores and adsorbed on the surface. The bulk volume is identical to the packing volume in Figure 2 with no subtraction of the skeletal volume. This material-centric FOM can be used to maximize total capacity, minimize skeletal volume, and maximize compaction-adsorption characteristics. Because this includes the free hydrogen in the pores and voids, this is also a useful engineering-centric FOM.

   For a VC FOM that emphasizes systems, we recommend the total hydrogen capacity divided by the system volume. This engineering-centric FOM includes all the hydrogen in the pores and adsorbed on the surface. The system volume includes the entire volume of materials, tanks, insulation, and balance of plant.

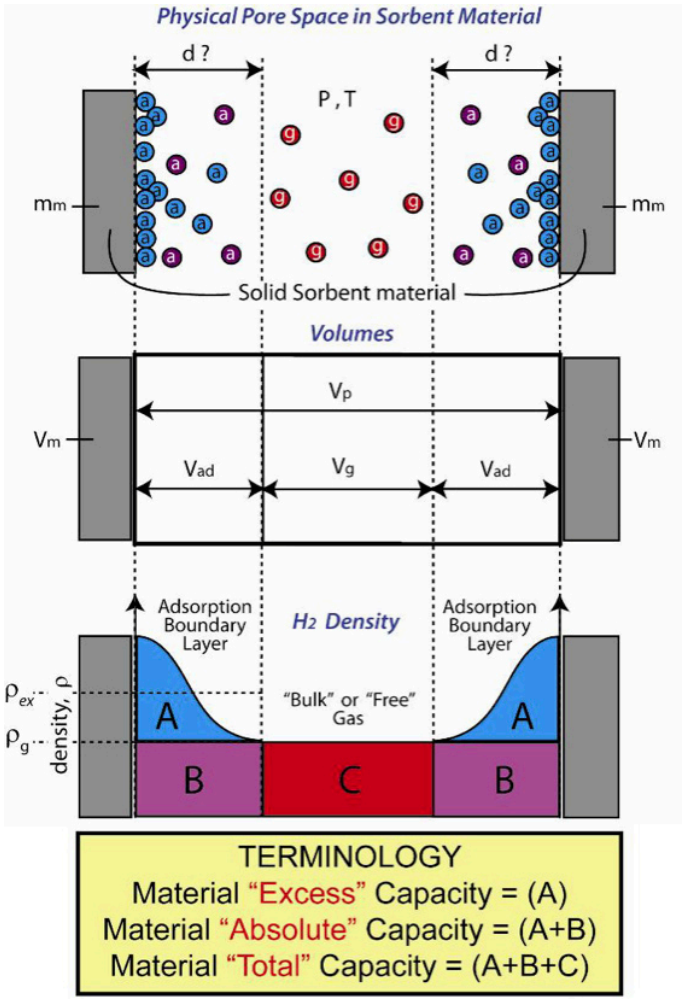

FIGURE 1. The Common Concepts Used to Label Stored Hydrogen (Figure source: adapted from Figure 81, [1])

2. Measured two external samples from other laboratories and are collaborating to have two more samples measured before the end of this FY for a total of four samples. This surpasses the milestone of measuring three external samples. Each sample undergoes approximately five measurements using different techniques in the course of a typical analysis. Techniques include multiple pressure-concentration-temperature (PCT) isotherms, Brunauer-Emmett-Teller isotherm for surface-area analysis, TPD during degas, TPD after PCT, and density and cycle-life PCT. Sample material types included high-surface-area carbons with and without catalysts, boron-substituted carbon material with and without catalysts, and metal-organic frameworks with and without catalysts. Data from these external samples are considered proprietary.
3. Collaborated with other laboratories to investigate and verify operation of their hydrogen capacity equipment. When discrepancies were found, we worked with the

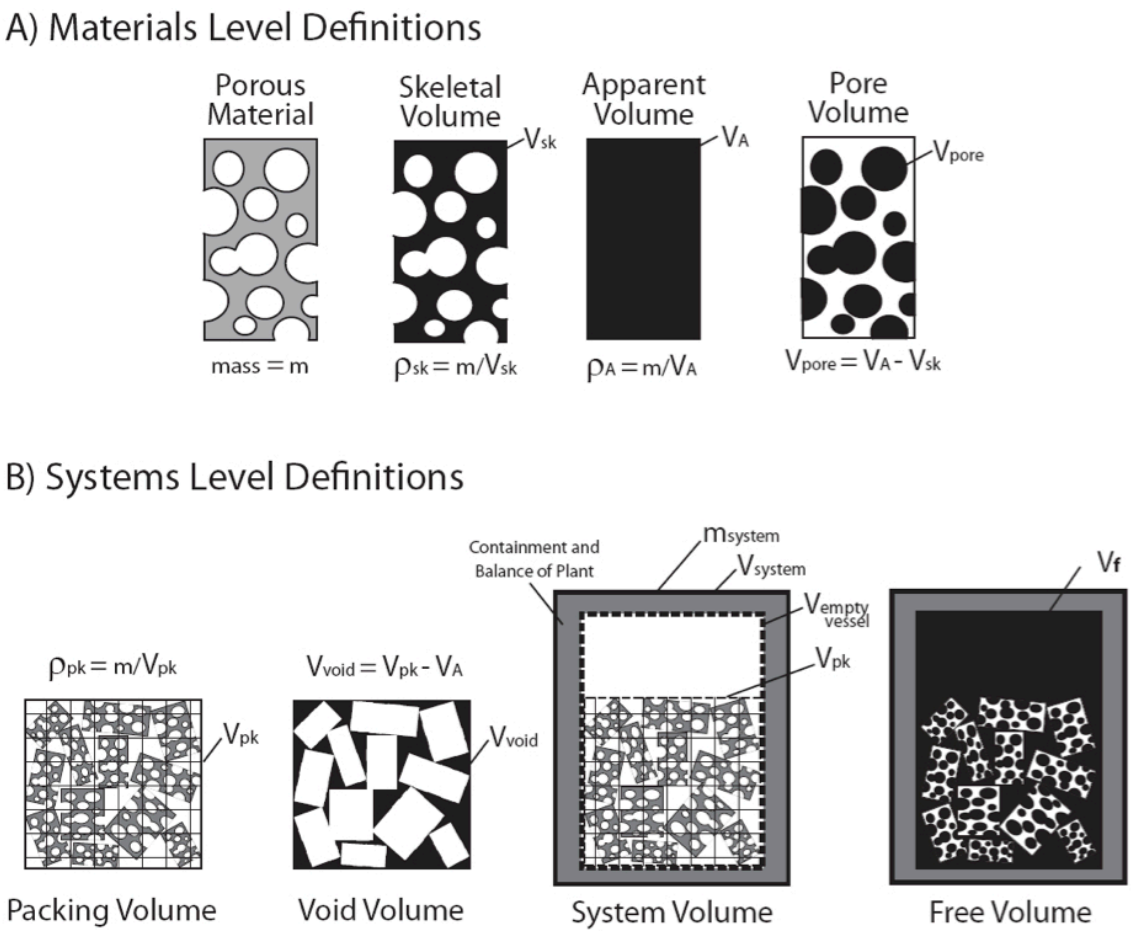

FIGURE 2. The Different Kinds of Volume Concepts and Considerations That Can Be Applied to Volumetric Capacity Definitions (Figure source: Figure 84, [1])

lab to discover the source of the discrepancy and made suggestions to remedy.

4. Continued to develop realistic models for the data analysis for volumetric systems, both for isothermal and non-isothermal conditions. The importance of using realistic models should not be underestimated. Volumetric mass-balance models in the scientific literature, although correct for ideal conditions, typically do not account for real-world measurement situations. Most volumetric systems contain many more moles in the gas phase than the moles sorbed onto the sample, thus requiring very accurate mass-balance accounting. Examples of real-world issues absent in the models include valves that change volume with operation and can transport gas between volumes; assumptions of non-measured pressure values; and the absence of temperature gradients or unrealistic temperature gradients. We conclude that the most dominant errors are still systematic errors! The main sources of systematic error are improper "null" calibration, inadequate data analysis models (mass-balance models), ignorance of the large error associated with non-uniform temperature fluctuations, and importance of having adequate sample mass and inexperience leading to acceptance of vendor number (black-box syndrome). Overall, the null calibration is the main factor in determining the accuracy of the mass-balance accounting.

CONCLUSIONS AND FUTURE DIRECTIONS

- The hydrogen storage community will benefit from efforts to ensure accurate capacity measurements. Increased quality control efforts will ensure that the proper emphasis will be placed on new hydrogen storage materials. There is sufficient cause to believe that inaccurate measurements may have misdirected emphasis.
- Direct collaboration among the laboratories performing capacity measurements has improved measurement accuracy and the quality of published results, thereby allowing for more effective utilization of the available research and development resources.

- Several key aspects of the measurement equipment and protocols have been identified to minimize experimental error. Recommendations addressing these issues have been made to improve measurement quality. We have initiated an investigation of these and possible other issues for differential volumetric systems.
- The hydrogen storage community will continue to benefit from these efforts in the future, which help ensure high-quality research. NREL will continue to assist in these efforts and provide expertise for the hydrogen storage community. NREL will adjust its measurement program to meet the needs of the DOE program, such as expanding its capabilities towards a wider range of temperatures and/or pressures or facilitating discovery of new materials.
- With the recent advances in developing prototype systems within the Hydrogen Storage Engineering Center of Excellence, it has become clear that besides hydrogen capacity (both volumetric and gravimetric) being a critical property for storage media, the thermal conductivity of these materials is also critical, as the heats of sorption/desorption must be managed within any hydrogen storage system and the material's thermal conductivity drastically affects the system design and cost. This is especially true for the sorption cycle (refueling); it is highly desirable that the refueling occur rapidly, and this exacerbates the heat removal issues. As this kind of measurement capability is uncommon, we feel the need exists to provide a facility where these measurements can occur for various types of materials, in several form factors (powder, pucks, etc.), as a function of gas pressure and sample temperature.

FY 2014 PUBLICATIONS/PRESENTATIONS

1. "Recommended Volumetric Capacity Definitions and Protocols for Accurate and Standardized Metrics for Hydrogen Storage Materials", P.A. Parilla et al., in preparation.

2. "The Evaluation of a Multi-laboratory Analysis of the Gravimetric and Volumetric Hydrogen Sorption Properties of Sorbent Materials", K.E. Hurst, T. Gennett, P.A. Parilla, in preparation.

3. "Realistic modeling and error analysis for volumetric apparatus", P.A. Parilla et al., in preparation.

4. "Water-Mediated Cooperative Migration of Chemisorbed Hydrogen on Graphene", Y. Zhao and T. Gennett, Phys. Rev. Lett. 112, 076101 (2014).

5. Invited Talk: Task 32 IEA HIA Expert Meeting, December, 2013, Key Largo, FL – P.A. Parilla, "Protocols and Conventions for Volumetric Capacity Determination."

6. Invited Talk: June 2014, 2014 U.S. DOE Hydrogen and Fuel Cells Program Annual Merit Review and Peer Evaluation Meeting – P.A. Parilla, "Hydrogen Sorbent Measurement Qualification and Characterization."

7. Talk: MRS Spring 2014 Meeting, San Francisco, CA; Symposium QQ: Computationally Enabled Discoveries in Synthesis, Structure and Properties of Nanoscale Materials – Yufeng Zhao, Thomas Gennett, "Water-Mediated Cooperative Migration of Chemisorbed Hydrogen on Graphene."

REFERENCES

1. http://www1.eere.energy.gov/hydrogenandfuelcells/pdfs/best_practices_hydrogen_storage.pdf

2. Zlotea et. al., International Journal of Hydrogen Energy 34 (2009) 3044.

IV.C.2 Hydrogen Storage in Metal-Organic Frameworks

Jeffrey Long (Primary Contact),
Martin Head-Gordon

Lawrence Berkeley National Laboratory (LBNL)
1 Cyclotron Road
Berkeley, CA 95720
Phone: (510) 642-0860
Email: jrlong@berkeley.edu

DOE Managers

Jesse Adams
Phone: (720) 356-1421
Email: Jesse.Adams@ee.doe.gov

Channing Ahn
Phone: (202) 586-9490
Email: Channing.Ahn@ee.doe.gov

Subcontractors

- National Institute of Standards and Technology (NIST), Gaithersburg, MD (Craig Brown)
- General Motors Corporation (GM), Warren, MI (Anne Dailly)

Project Start Date: April 1, 2012
Project End Date: March 31, 2015

Overall Objectives

- Research and development of onboard systems that allow for a driving range greater than 300 miles
- Materials sought with the potential for meeting the DOE system targets of reversible uptake:
  - 2017 targets: 5.5% H_2 by mass, volumetric capacity of 40 g/L
  - "Ultimate full fleet" targets: 7.5% H_2 by mass, 70 g/L
- Synthesize new metal-organic frameworks (MOFs) capable of approaching the -20 kJ/mol adsorption enthalpy required for use as hydrogen storage materials operating under 100 bar at ambient temperatures

Fiscal Year (FY) 2014 Objectives

- Synthesize MOFs exhibiting reversible excess H_2 uptake greater than 2.5 wt% at room temperature
- Prepare a high-valent MOF with an initial H_2 adsorption enthalpy greater than 12 kJ/mol
- Synthesize new MOFs with the multifunctional ligands prepared in year 1
- Demonstrate the post-synthetic insertion of metals into the open chelate sites of these new materials
- Prepare at least two MOFs with the optimal 7 Å between opposing pore surfaces as predicted with *in silico* screening techniques
- Demonstrate that improved understanding of MOF-H_2 interactions through inelastic neutron scattering experiments and that new approaches to calculate observed spectra provide new insight into the governing physics of adsorption in porous media
- Demonstrate the ability to determine H_2-metal interactions in model systems containing low-coordinate metal cations
- Demonstrate a correlation between high-pressure measurements and theoretical and spectroscopic predictions
- Demonstrate the ability to measure H_2 adsorption in a test material up to 10 cycles at 298 K

Technical Barriers

This project addresses the following technical barriers from the Hydrogen Storage section of the Fuel Cell Technologies Office Multi-Year Research, Development, and Demonstration Plan:

(A) System Weight and Volume

Technical Targets

Specific efforts are focused on the research and development of onboard systems that allow for a driving range greater than 300 miles. Materials are sought with the potential for meeting the 2017 DOE targets for reversible uptake and, subsequently, the "ultimate full fleet" targets (see Table 1).

FY 2014 Accomplishments

- High-pressure H_2 adsorption measurements were completed on the M_2(dioxido-biphenyl-dicarboxylate, known as dobpdc) structure family. These materials and their expanded analogs are approaching the 2.5 wt% target.
- A new Zr^{4+}-based framework featuring charge-balancing chelating ligands functionalized with a pyridine and a hydroxyl group and enhanced stability has been synthesized in gram-scale quantities. These MOFs have subsequently been metalated with high crystallinity. Charge balance is key to enhancing the H_2 binding enthalpy at open metal centers on these ligands as well as allowing for multiple H_2 molecules to bind to a single metal center, which will drastically increase both

TABLE 1. Progress towards Meeting Technical Targets for Onboard Hydrogen Storage for Light-Duty Vehicles

Storage Parameter	Units	2017 Target	Ultimate Target	2012 Status†	2013 Status†	2014 Status†
System Gravimetric Capacity*: Usable specific energy from H_2 (net useful energy/max system mass)**	kWh/kg (kg H_2/kg system)	1.8 (0.055)	2.5 (0.075)	(0.016 kg H_2/kg adsorbent)	(0.016 kg H_2/kg adsorbent)	(0.016 kg H_2/kg adsorbent)
System Volumetric Capacity*: Usable energy density from H_2 (net useful energy/max system volume)	kWh/L (kg H_2/L system)	1.3 (0.040)	2.3 (0.070)	(0.011 kg H_2/L adsorbent)	(0.011 kg H_2/L adsorbent)	(0.013 kg H_2/L adsorbent)

* Room temperature, total adsorption capacity
** Generally the full mass (including hydrogen) is used; for systems that gain weight, the highest mass during discharge is used. All capacities are net useable capacity able to be delivered to the power plant. Capacities must be met at end of service life.
† Since the project deals with the development of storage materials, the performance status is given in terms of storage capacity for storage materials, not the whole storage system.

gravimetric and volumetric H_2 uptake approaching the DOE targets.

- H_2 high-pressure adsorption was measured on Ni_2(4,6-dioxido benzene 1,3-dicarboxylate, known as *m*-dobdc) and Co_2(*m*-dobdc), with the former showing the highest known volumetric capacity for H_2 at room temperature and 100 bar.
- We have determined the structure of D_2 adsorbed in the 2-ring extended linker variant of MOF-74, M_2(dobpdc). These expanded variants of the M_2(2,5-dioxido benzene-1,4-dicarboxylate, known as dobdc) structure type show improvement of ~0.5 kJ/mol in H_2 binding enthalpy as compared to the M_2(dobdc) analogues.
- We have determined the rotational character of H_2 adsorbed to the metal center in Co_2(m-dobdc). This shows that we have a firm understanding of the ways in which H_2 interacts with metal centers and can interpret the results from neutron diffraction.
- First principle calculations have shown that catechol-style ligands with divalent di-coordinated metals are promising candidates to achieve hydrogen binding energies in a suitable range as well as allow for more than one bound H_2 per metal, which would help approach the DOE capacity targets.
- Adsorption enthalpies were measured to 320 bar at ambient temperature on extended MOF-74 analogues. The adsorption enthalpy was observed to be 40% higher for the 2-ring extended MOF-74 compared to the standard MOF-74.
- We have shown that expanded versions of the cobalt and nickel MOF-74 have larger excess adsorption enthalpies at ambient temperature.

INTRODUCTION

MOFs are promising solid sorbents for storage of H_2 at room temperature. They can be tailored to incorporate a large number of selected metal ions, thereby tuning the H_2 binding energy. The overall aim of the project is to synthesize new MOFs capable of achieving the 20 kJ/mol adsorption enthalpy required for use as hydrogen storage materials operating under 100 bar at ambient temperatures.

APPROACH

This research involves investigators with a range of capabilities—including synthesis and characterization of new materials, electronic structure calculations, neutron diffraction and scattering studies, and high-pressure gas sorption measurements. The team performs work in four areas: Task 1) Synthesis of Metal-Organic Frameworks (Long-LBNL), Task 2) Characterization of Framework-H_2 Interactions (Brown-NIST), Task 3) First-Principles Calculations of Hydrogen Binding Enthalpies (Head-Gordon-LBNL), and Task 4) High-Pressure H_2 Adsorption Measurements (Dailly-GM).

RESULTS

Introduction

The approach taken in this past year is a multi-pronged approach. Conventional MOFs are still being targeted as materials that can adsorb large quantities of hydrogen. In addition to these more conventional strategies of improving binding enthalpy, gravimetric capacity, and volumetric capacity through framework modifications and the design of new materials, alternate strategies are being employed. The main focus of these strategies is to synthesize frameworks with a very high density of open metal coordination sites, either as part of the structure of the framework or as post-synthetically bound metal centers. The advantage of having non-structural metals bind in a MOF is that they could potentially be desolvated to expose multiple coordination sites and bind up to four H_2 molecules per metal center, giving a dramatic and groundbreaking boost in capacity as compared to currently known frameworks.

M_2(*m*-dobdc) with Increased H_2 Binding Enthalpy

The first strategy is that of modifying conventional frameworks. In the last year, we have gained a complete understanding of the M_2(*m*-dobdc) (M = Mg, Mn, Fe, Co, Ni) series of frameworks that our lab has discovered. This MOF is a structural isomer of the well-known M_2(dobdc) series, yet shows a significantly improved H_2 binding enthalpy as compared to the regular M_2(dobdc) for the Mn, Fe, Co, and Ni analogues. The open metal coordination sites are shown to have a greater positive charge in M_2(*m*-dobdc) than in M_2(dobdc), leading to the experimentally determined higher isosteric heats of H_2 adsorption (~1.0 kJ/mol higher on average, as seen in Figure 1) [1]. This is quite a significant increase by simply changing to a structural isomer of the linker, so this was investigated further.

Quasi-elastic and inelastic neutron scattering measurements were used to locate H_2 molecules in Co_2(m-dobdc) (Figure 2). Two-dimensional inelastic neutron scattering was further used to demonstrate improved understanding of MOF-H_2 interactions. The extracted intensities for different loadings of H_2 distinguish between the spatial dependence of the rotations/phonons and here were used to determine that all of the observed transitions are rotational in nature, as expected based on the neutron diffraction data [2].

Further experiments involving infrared spectroscopy with bound H_2 were completed. It can be seen from looking at the H_2 stretch in these experiments that the H_2 is bound more strongly in the Ni_2(*m*-dobdc) and Co_2(*m*-dobdc) frameworks as compared to their respective Ni_2(dobdc) and Co_2(dobdc) counterparts. This shift to a lower-energy stretching frequency is expected based on the higher isosteric heats of adsorption from the obtained isotherms. It is worth noting that the secondary binding sites saw no change in H_2 stretching frequency between the M_2(*m*-dobdc) and M_2(dobdc) series, indicating that the change in binding enthalpy is solely due to a change in the electronic structure at the open metal coordination site. Variable-temperature infrared spectroscopy experiments were used to probe the site-specific binding enthalpies at the open metal center, which were calculated to be as high as 13.7 kJ/mol for Ni_2(*m*-dobdc), which is the highest reliably-obtained isosteric heat of adsorption in a MOF thus far.

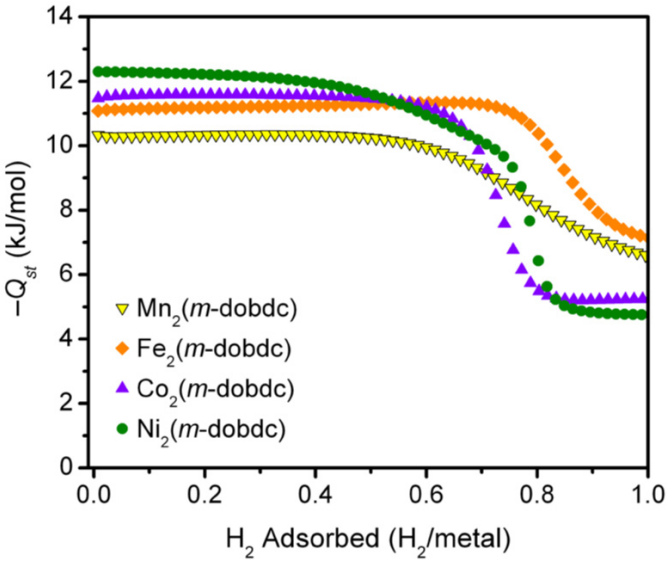

FIGURE 1. H_2 Isosteric Heat of Adsorption Curves for the M_2(*m*-dobdc) Series of Frameworks, as a Function of the Amount Adsorbed

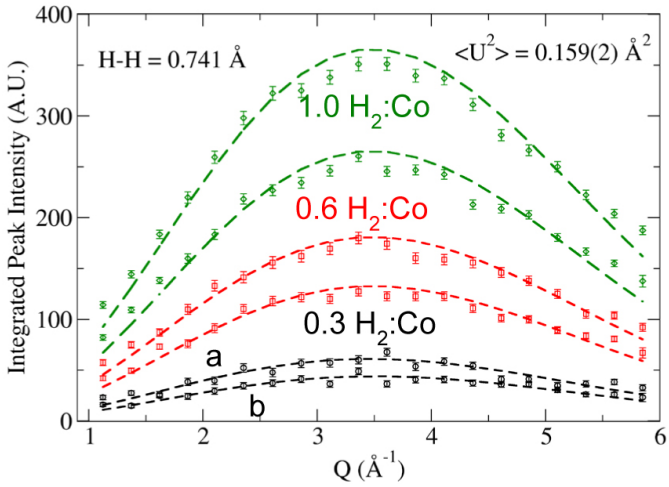

FIGURE 2. Extracted Rotational Level Areas for Different Loadings Fit to a Model Indicating the Classical Nature of the Adsorbed Molecule

High-Pressure H_2 Isotherms

Further studies were completed on the expanded M_2(dobpdc) series of frameworks. These were shown to have a higher binding enthalpy than their M_2(dobdc) analogues; the larger pores have a positive effect on the binding enthalpy, despite having similar open metal coordination site geometries. Additionally, powder neutron diffraction showed five unique binding sites in the pores of the framework, which is significantly more than the three unique sites seen in the M_2(dobdc) series. The high-pressure volumetric uptake of these frameworks was shown to be greater than that of pure H_2 compressed in a tank, which is also advantageous and is working toward the volumetric hydrogen storage goals set forth by the DOE. By further expanding the pores of this same series of frameworks, it is believed that even higher capacities can be reached at 298 K and room temperature, approaching the DOE target of 1.3 kg H_2/L system. While we did not demonstrate an increase in the excess uptake as compared to the literature standard, Co_2(DiOxido-TerPhenyl-DiCarboxylate) (the Co_2(dobdc) analogue with three aromatic rings in the linker) has a total uptake of 2.5 wt% at 298 K and 140 bar as well as at 273 K and 100 bar. The Ni_2(dobpdc)

framework had a gravimetric uptake of 10.0 g/L at 298 K and 100 bar, which is approaching state of the art. The Ni_2(*m*-dobdc) framework mentioned before surpassed this and set a record for volumetric hydrogen storage with a capacity of 12.5 g/L at 298 K and 100 bar. This is higher than the previous state-of-the-art framework, Mn-1,3,5-BenzeneTrisTetrazole.

High-pressure adsorption isotherms were also measured at GM up to 320 bar. A method for determining the adsorption enthalpy from a single isotherm was developed by applying the van't Hoff formula directly to the Dubinin-Astakohov model. This led to benchmark results that were consistent with expectations for these materials. Subsequently, the Ni_2(dobdc) and Ni_2(*m*-dobdc) frameworks were measured and shown to be very similar in their H_2 uptake. The Ni_2(*m*-dobdc) framework was then cycled between 50 bar and 320 bar 10 times at 298 K; the variability in each isotherm was shown to have no correlation with the cycle, meaning that the results are reproducible.

Computational Work

To gain a fundamental view into the adsorption of hydrogen in MOFs, we study and analyze the adsorption of hydrogen into "standard," i.e., undecorated, linkers. Although the binding enthalpies are not expected to be significant for storage purposes, they exist in any MOF and contribute to the overall adsorption. We study the adsorption of hydrogen with several molecules that are commonly used as a building block for MOF linkers. For each one, we optimize the structure, calculate binding enthalpy, and analyze the fundamental linker-hydrogen interaction. It is found that hydrogen adsorption enthalpies could be as high as 3 to 5 kJ/mol, which could contribute significantly to the adsorption enthalpy. Most of the enthalpy stems from the "frozen interaction," which indicates both van der Waals interactions and non-induced electrostatic interactions. Surprisingly, and contrary to conventional wisdom, it was found that charge transfer interaction (i.e., the formation of a dative chemical interaction) makes a significant contribution to the adsorption of hydrogen on these conjugated organics—with hydrogen accepting charge to its anti-bonding vacant orbital. This charge transfer interaction corresponds to about 30% of the total hydrogen-linker interaction.

We also completed work on larger systems and investigated hydrogen adsorption on several MOF ligands that were reported in the scientific literature (or prepared by the Long group) to be metalated. For each of the ligands, we optimize the structure, calculate interaction energy, and analyze the result in order to provide a rational explanation of the hydrogen adsorption capacity. We modeled a MOF consisting of bpy ligands that was prepared and metalated with $CuCl_2$ by the Long group. The optimized structure is shown in Figure 3. The calculated adsorption energy is 9.1 kJ/mol, and the charge transfer interaction is again found to dominate. This could also be inferred (or confirmed) by observing that the hydrogen molecule is placed "side-on" to the transition-metal cation, in order to maximize donation from the σ bonding orbital onto a diffuse orbital on the cation.

Recently, a MOF containing a catechol ligand was prepared and metalated by Fe^{3+} and Cr^{3+}. This MOF was modeled using a catechol molecule metallated by Al^{3+} and one F^- counterion—this combination has a special interest, since AlF_3 was found to have a strong interaction with H_2 of about 20 kJ/mol. It is therefore interesting to estimate the same interaction in a realistic system. Interaction energy is 8.7 kJ/mol, which is considerably smaller than -21.7 predicted for AlF_3, mostly due to a reduced polarization component of the interaction. Since metals in planar and tetrahedral coordination were found to have insufficient hydrogen adsorption, we began to study systems that are expected to develop a strong dipole moment. The systems based on the catechol ligand (or its sulfur-based analog) have been prepared in experiments and are expected to have strong dipole moments. The calculated binding energies are close to 20 kJ/mol, and adsorption of a second hydrogen molecule is also feasible, with only a small decrease in interaction energy with respect to the first hydrogen molecule.

To conclude, we find that planar and tetrahedral coordination of the metallic ion have an intrinsic limitation of not being able to polarize H_2 to a sufficient extent such that

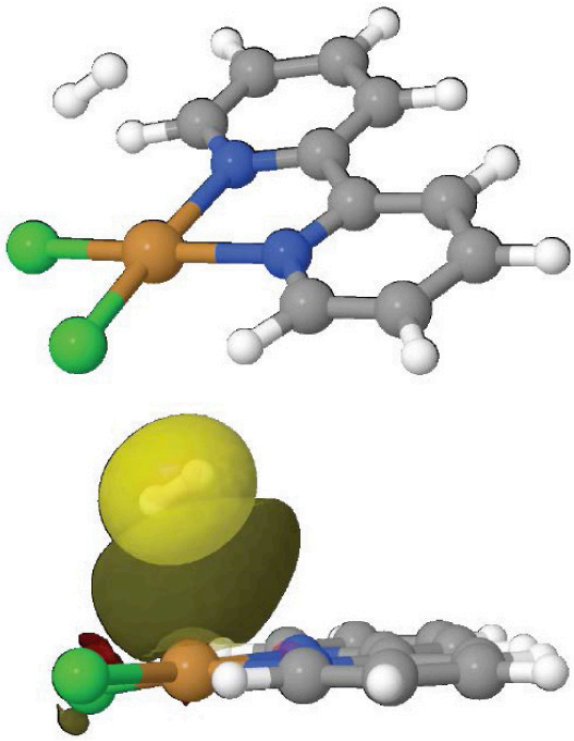

FIGURE 3. Optimized Structure of bpy-$CuCl_2$

an adequate adsorption energy for hydrogen can be attained. By contrast, a metal attached to a linker with a coordination number of two, or another arrangement of the coordination environment of the metal that results in a strong local dipole moment, appears to give hydrogen binding energies in a suitable range. As examples, the catechol-style ligands with divalent di-coordinated metals such as those we investigated above are promising candidates. Overall, this work demonstrates our understanding of H_2-metal interactions in a variety of model systems containing low-coordinate metal cations.

Multiple H_2 per Metal Center

As previously mentioned, our approach includes both studying conventional MOFs as well as attempting to synthesize MOFs with the ability to bind additional metal centers and subsequently bind H_2 both more strongly and with a higher density than currently known MOFs. This is quite a challenging task, as there are many challenges to synthesizing these materials. However, a potential breakthrough could be reached if multiple H_2 molecules could be bound per metal center, with uptakes as high as 6.6 wt% excess uptake possible at room temperature if four H_2 molecules were bound to a metal center bound to a catechol within a framework. This would also result in a significant improvement in volumetric capacity.

One framework we have synthesized that can bind additional metal centers is the UIO-67-Bipyridine dicarboxylate (bpydc) framework, which has a bipyridine in the linker (Figure 4). This framework bpydc has been metalated with a variety of metal salts and investigated for its H_2 storage properties. It was anticipated that metalation with metals that form square planar complexes with the ligand would leave available hydrogen binding sites in the axial positions on the metal center. It was found from single-crystal X-ray diffraction that the metal center distorts from square planar for several of these complexes, however, and that the anticipated binding sites may not be available (Figure 4). Nonetheless, several samples show higher uptake than the bare framework at selected pressures, most notably the $PdCl_2$- and $CuCl_2$-metalated samples. It is estimated that, based on the excess H_2 adsorption at 1 bar and 77 K, there are 2.6 and 1.5 H_2 molecules per metal center for the $PdCl_2$ and $CuCl_2$ samples, respectively.

Another framework that has been synthesized is the UIO-67-pyOHdc framework, which has a single pyridine and a hydroxyl group in the linker rather than a bipyridine. This functional group affords charge balance to the metal center to which it binds, which will allow for the easier desolvation of this framework. This framework has been prepared in gram-scale quantities with high crystallinity and surface area. After synthesis of the bare framework, these frameworks have been metalated with a variety of metal species, but the H_2 uptake was not improved over the bare framework.

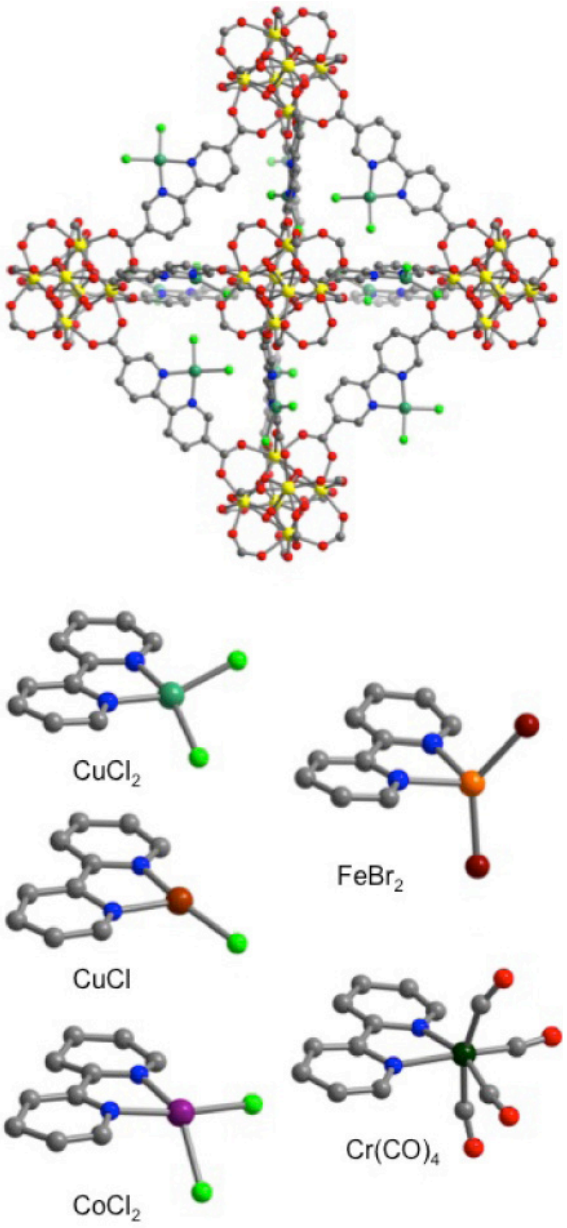

FIGURE 4. Structure of the Metalated UIO-67-bpydc, Showing the Partial Crystal Structures of Several of the Incorporated Metals

Further metalation is underway with other metal salts with more labile ligands.

Overall, we have laid a basis with this work for understanding the best methods for synthesizing frameworks that can post-synthetically bind metal centers. With this understanding, we are poised for a breakthrough in room-temperature hydrogen storage by binding multiple H_2 molecules per metal center and quite significantly improving the volumetric and gravimetric H_2 densities that are possible in MOFs.

CONCLUSIONS AND FUTURE DIRECTIONS

Overall, much work was completed during FY 2014 toward the DOE hydrogen storage targets. The M_2(*m*-dobdc) series of frameworks was completely studied, and its higher H_2 binding enthalpy was determined to be from a higher positive charge at the open metal centers. Powder neutron diffraction and inelastic neutron scattering were used to study a variety of systems and learn more about MOF-H_2 interactions as well as methods for doing high-pressure, high-temperature powder neutron diffraction of D_2-dosed samples. Several samples were measured on the high-pressure system at GM, which is now operating at full potential and is fully calibrated. Many systems were studied for understanding metal-H_2 interactions in order to guide synthetic efforts for binding multiple H_2 molecules per metal center. Finally, many synthetic efforts were completed in order to attempt to bind two H_2 molecules per metal center.

Moving forward, we believe that the most probable method for achieving the DOE hydrogen storage targets is post-synthetic incorporation of metal centers into ligands and use of these centers to interact with multiple H_2 molecules. All future synthetic efforts will be concentrated on this target, which will provide a huge breakthrough in the capacities for hydrogen storage. The following goals will be targeted in FY 2015:

- Further study metalated UIO-67-bpydc samples and determine if any of the samples are binding multiple H_2 molecules per metal center.
- Develop the UIO-67-pyOHdc framework and metalate this framework with metal sources that contain significantly more labile ligands than those we have previously used.
- Synthesize more ligands with charge-balancing functionalities for optimal metal binding properties.
- Explore other possible functional groups for protecting and deprotecting these charge-balancing functionalities.

FY 2014 PUBLICATIONS/PRESENTATIONS

Publications

1. "Structure and spectroscopy of hydrogen adsorbed in a nickel metal-organic framework", C.M. Brown, A.J. Ramirez-Cuesta, J.-H. Her, P.S. Wheatley, R.E. Morris, Chem Phys. 2013, 427, 3.

2. "Adsorption Enthalpy Calculations of Hydrogen Adsorption at Ambient Temperature and Pressures Exceeding 300 bar", M. Beckner, A. Dailly, Am. J. Anal. Chem. 2013, 10C, 8-16.

3. "Kinetic trapping of D_2 in MIL-53(Al) observed using neutron scattering", R.A. Pollock, J.-H. Her, C.M. Brown, Y. Liu, A. Dailly, J. Phys. Chem. C [DOI: 10.1021/jp504870n].

4. "Hydrogen and Natural Gas Storage in Adsorbent Materials for Automotive Applications", M. Beckner, A. Dailly, Proceedings of the 13th International Conference on Clean Energy, June 2014, Istanbul, Turkey.

5. "M_2(*m*-dobdc) (M = Mg, Mn, Fe, Co, Ni) Metal-Organic Frameworks Exhibiting Increased Charge Density and Enhanced H_2 Binding at the Open Metal Sites", M.T. Kapelewski, S.J. Geier, M.R. Hudson, D. Stuck, J.A. Mason, J.N. Nelson, D.J. Xiao, Z. Hulvey, E. Gilmour, S.A. FitzGerald, M. Head-Gordon, C.M. Brown, J.R. Long. *J. Am. Chem. Soc. Article ASAP.*

Presentations

1. "Hydrogen and Natural Gas Storage in Adsorbent Materials for Automotive Applications", M. Beckner, A. Dailly, Proceedings of the 13th International Conference on Clean Energy, June 2014, Istanbul, Turkey.

2. "Neutron Powder Diffraction: D_2 vs H_2", Z. Hulvey, C.M. Brown, IAEA experts meeting, Key Largo, Florida, Dec. 2013.

3. "High-pressure, ambient temperature hydrogen storage in metal-organic frameworks and porous carbon", M. Beckner, A. Dailly, APS March Meeting 2014, Denver, Colorado, March 2014.

4. "Hydrogen and Natural Gas Storage in Adsorbent Materials for Automotive Applications", M. Beckner, A. Dailly, 13th International Conference on Clean Energy, June 2014, Istanbul, Turkey.

REFERENCES

1. Zhou, W.; Wu, H.; Yildirim, T. *J. Am. Chem. Soc.* **2008**, *130*, 15268

2. Liu, Y.; Kabbour, H.; Brown, C.M.; Neumann, D.A.; Ahn, C.C. *Langmuir* **2008**, *24*, 4772.

IV.C.3 Hydrogen Trapping through Designer Hydrogen Spillover Molecules with Reversible Temperature and Pressure-Induced Switching

Angela D. Lueking (Primary Contact), Jing Li, Cheng-Yu Wang, Yonggang Zhao, Haohan Wu, Qihan Gong

The Pennsylvania State University
120 Hosler Building
University Park, PA 16802
Phone: (814) 863-6256
Email: adl11@psu.edu

DOE Managers

Jesse Adams
Phone: (720) 356-1421
Email: Jesse.Adams@ee.doe.gov

Channing Ahn
Phone: (202) 586-9490
Email: Channing.Ahn@ee.doe.gov

Contract Number: DE-FG36-08GO18139

Subcontractor
Rutgers University, Piscataway, NJ

Project Start Date: January 1, 2009
Project End Date: June 30, 2014

Overall Objectives

- Synthesize designer microporous metal-organic frameworks (MMOFs) mixed with catalysts to enable H-spillover for H_2 storage at 300 K-400 K and moderate pressures
- Develop methods to reliably introduce catalyst into MMOFs
- Demonstrate spectroscopic evidence for hydrogen spillover

Fiscal Year (FY) 2014 Objectives

- Determine high-pressure stability of Cu_3(2,4,6-tris(3,5-dicarboxylphenylamino)-1,3,5-triazine)$(H_2O)_3$ (CuTDPAT)
- Finalize control tests and interpretation of spectroscopic data for identification of H binding sites to CuTDPAT populated via spillover
- Assess thermal stability of Pt-doped CuTDPAT in H_2
- Assess role of MMOF structural defects in propagating room temperature hydrogenation of CuTDPAT
- Reporting: Submit four research papers to peer-reviewed journals, finalize doctoral theses of two students, finish reporting requirements

Technical Barriers

This project addresses the following technical barriers from the Hydrogen Storage section of the Fuel Cell Technologies Office Multi-Year Research, Development and Demonstration Plan:

(A) System Weight and Volume

(D) Durability/Operability

(E) Charging/Discharging rates

(O) Lack of Understanding of Hydrogen Physisorption and Chemisorption

(P) Reproducibility of Performance

Technical Targets

Technical targets for this project are listed in Table 1. The Go/No-Go milestones for this project are listed as follows.

1. Exceed 3.0 wt% reversible (<80°C, <30 minutes) hydrogen storage through the use of the "hydrogen spillover" mechanism, metal-organic framework (MOF) material, or a combination of the two as proposed at moderate temperatures and pressure (i.e. 300-400 K and 100 bar).
2. Demonstrate hydrogen spillover mechanism provides a means to increase ambient temperature hydrogen uptake of the MOF and/or carbon support by 50%.

FY 2014 Accomplishments

- Reproducibility: Demonstrated 2-7-fold increase in measurement sensitivity, i.e. within 0.05 wt% for a 100-mg sample. Published peer-reviewed paper [1] demonstrating improved adsorption methodology to minimize error due to experimental volume calibrations for low-density samples.
- Reproducibility: Demonstrated PB-doping technique maintains MMOF structure, surface area, and porosity. Retains structure at temperatures up to 20-25°C below the undoped MMOF material. (Published in peer-reviewed journal [2].)
- System Weight and Reproducibility: Demonstrated both MMOF structural defects and dissociation catalyst may increase room temperature H_2 adsorption (submitted to peer-reviewed journal).

TABLE 1. Progress towards Meeting Technical Targets for Hydrogen Storage

Characteristic	Units	2017 Target for Light-Duty Fuel Cell Vehicles	Status
Gravimetric Capacity	kg/kg	5.5 wt%	0.6-0.8 wt% (Uptake incomplete after 40-60 hours)
Durability/Operability Operating temperature	°C	-40/60	25°C tested
Charging/Discharging Rates System fill time	min	3.3	>80 Hours
Lack of Understanding of Physisorption versus Chemisorption	--	--	Chemisorption sites identified via spectroscopy, Reversible dehydrogenation between 25-125°C.
Reproducibility of Performance	--	--	Method to introduce catalytic sites into MMOFs developed; reproducible at low pressure. Thermal stability of MMOF retained after catalytic doping. MMOF studied is unstable at high-pressure (even prior to catalyst addition).

- Lack of Understanding of Physisorption vs. Chemisorption: Identified three chemisorption sites on CuTDPAT MMOF populated via high-pressure hydrogen spillover. Spectroscopic identification confirmed with theoretical calculations. (Submitted to peer-reviewed journal.)

INTRODUCTION

The term hydrogen spillover has been used to describe a synergistic effect between high-surface area adsorbents and associated catalysts. The associated catalyst dissociates molecular H_2 into atomic H species, which may then diffuse to and chemisorb to the support. This process occurs at moderate temperature (i.e. 300 K) and may lead to a much higher uptake than expected for the metal catalyst or high-surface area adsorbent alone under comparable conditions. Spillover materials using MMOFs have been reported to have high uptake at ambient temperature: bridged ('br') PtAC/IRMOF8 (AC=activated carbon) achieved 4 wt% excess adsorption at 100 bar and 298 K [3]. (The structure of IRMOF8 is illustrated in Figure 1A.) Independent groups have demonstrated up to 4.2 wt% at 6.9 MPa after extended equilibration for brPtAC/IRMOF-8 [4]. Subsequent reports on spillover materials at room temperature have varied from less than physisorption to almost 9 wt%, demonstrating difficulties in reproducibility and invoking controversy. These uptakes approach DOE goals at ambient temperature; however, as the process is highly dependent upon synthesis, measurement, and catalytic particle size, [5,6] the process remains poorly understood. It is anticipated that optimization of the MMOF structure, surface chemistry, and porosity will further increase uptake via spillover. Meeting DOE hydrogen storage targets at moderate temperature will have significant engineering advantages for mobile applications, as temperature of operation has implications for system weight.

In prior years of this project, we have developed and tested some 20 new MMOF structures with incorporated

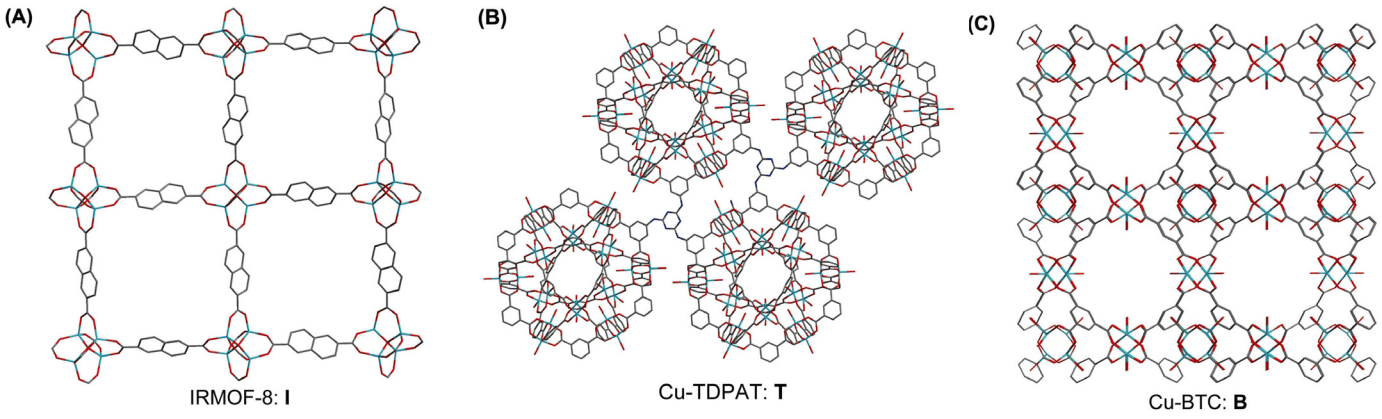

FIGURE 1. Diagram of **I**RMOF8 (**I**), Cu**T**DPAT (**T**), and Cu**B**TC (**B**), in which zinc (for **I**) and copper paddlewheel (for **T** and **B**) structure work as metal clusters, while the organic ligand (**I**: 2,6-naphthalenedicarboxylate, **T**: TDPAT, **B**: BTC) connects with metal cluster to form the long-range order MOF structure. TDPAT contains nitrogen in the center rings as well as three branches stretching from the center ring, similar to melamine. (Gray: C, Red: O, Cyan: Cu or Zn, Blue: N)

catalysts, determined MMOF stability after various catalytic doping techniques, worked to reproducibly optimize the uptake of carbon-based Pt/AC catalysts, developed techniques to verify spillover to specific surface sites on MMOFs with spectroscopy, conducted extensive reproducibility tests on standard samples including the effect of measurement, synthesis, and pretreatment conditions, and quantitatively validated our differential adsorption measurement. In FY 2013, CuTDPAT (Figure 1B) was selected for more extensive studies due to its structure, stability, and baseline H_2 uptake at 300 K (0.61 [excess] and 1.04 [total] wt%, at 298 K and 60 bar, measured by Rutgers University). CuTDPAT is the smallest member of (3,24)-connect nets of *rht* topology made of a three-armed hexacarboxylate ligand and 24 $M_2(COO)_4$ paddle-wheel based supramolecular building blocks. The CuTDPAT framework is highly porous and contains three different types of cages, cuboctahedron, truncated tetrahedron, and truncated octahedron. The pore volume, Brunauer-Emmett-Teller (BET) and Langmuir surface areas are estimated to be 0.93 cc/g, 1,938 and 2,608 m^2/g, respectively, calculated from N_2 adsorption isotherms at 77 K. CuTDPAT is featured with a high density of both open metal sites (1.76/nm^3) and Lewis basic sites (3.52/nm^3), as well as high thermal and water stability.

APPROACH

The project relates to materials development and optimization of catalyst, surface chemistry, crystal and pore structure, and system parameters for the hydrogen spillover phenomenon. For surface chemistry, three different MMOFs were doped with catalyst to test hydrogen storage and the effect of functional groups, namely IRMOF8, CuTDPAT, and Cu_3(1,3,5-benzenetricarboxylate [BTC])$_2(H_2O)_3$ (CuBTC) (see Figure 1). Novel methods to incorporate a hydrogen dissociation catalyst into MMOFs were evaluated, by focusing on methods that lead to well dispersed catalytic entities without compromising the original pore structure and surface area of the MMOF. The current 'pre-bridge' (PB) technique is adapted from methods published previously [7,8] with adaptation to use an optimized hydrogenation catalyst and MMOFs with various structures and surface chemistry. Hydrogen uptake is quantified utilizing both gravimetric and differential volumetric adsorption methods (detailed elsewhere [1]); the former allows for precise catalyst activation whereas the latter allows for high-pressure measurements and is more accurate than conventional volumetric techniques. Complementary spectroscopic techniques are being used to identify the active sites that bind with spilled over hydrogen.

RESULTS

In FY 2013, we reported successful insertion of a Pt/AC catalyst was inserted into CuTDPAT via a solvothermal PB doping technique [7,8], with almost complete retention of surface area and structure for four preparations. At 1 bar and 298 K, the hydrogen uptake of PB-CuTDPAT was enhanced 7.8-fold relative to the 'as-received' CuTDPAT (i.e. 4.9 cc/g versus 0.6 cc/g for CuTDPAT), and the increase was attributed to hydrogen spillover from the catalyst to the CuTDPAT substrate. Low-pressure 300 K isotherms were reversible and cyclable. Spectroscopic results confirmed hydrogenation of N groups on the TPAT ligand. At high-pressure (70 bar), the uptake of PB-CuTDPAT exceeded that of the undoped CuTDPAT precursor for five measurements, but the uptake was less than ~1 wt% (excess) after 40-60 hours (but still increasing), demonstrating slow kinetics would render this material unsuitable for meeting DOE targets (see Table 1). Subsequent testing demonstrated undoped CuTDPAT was unstable in high-pressure hydrogen, which may have contributed to the slow adsorption kinetics.

As PB-CuTDPAT did not meet targets, and ultimately undoped CuTDPAT was not stable in high-pressure H_2, the focus in FY 2014 has been on reproducibility and mechanistic studies to better understand the hydrogen spillover mechanism for potential application to other substrates. Specifically, our focus in FY 2014 has turned to (I) a more mechanistic understanding of the hydrogen spillover process (Technical Barrier O), and (II) determining how the PB doping technique alters the thermal stability and structural integrity of MMOFs (Technical Barrier P) so that the technique could possibly be applied to future material development. Topic I has included (A) extensive analysis of spectroscopic data and micrographs of three PB-MOF materials after hydrogenation, (B) control tests to ascertain the role of introduced defects on the 300 K enhancement, and (C) development/implementation of methodology to assess structural defects in Cu-type MOFs in order to quantify their effect on 300 K hydrogen uptake. Topic II has included: (D) thermal stability testing of IRMOF8 and CuTDPAT doped via the 'pre-bridge' doping methodology, and (E) additional characterization tests of PB-CuTDPAT, PB-IRMOF8, and PB-CuBTC to ascertain the effect of surface chemistry and structure on spillover. Each of these subtasks is summarized breifly in subsequent paragraphs.

(O) Lack of Understanding of Hydrogen Physisorption and Chemisorption

IA: Analysis of Spectroscopic Data for PB-MOFs. In FY 2013, we reported X-ray photoelectron spectra (XPS) demonstrating reversible (at T <400 K) hydrogenation of the N surface sites in PB-CuTDPAT after H_2 exposure at 70 bar. This reversible N hydrogenation was not observed in undoped CuTDPAT after H_2 exposure at any temperature or pressure studied. With more extensive analysis, we were able to assign the XPS features specifically to (1) the sp^2 N aromatic heterocycles in the center ring, and (2) the secondary-amine type NH in the branches (as detailed in Ref. Wang 2014a).

The latter assignment led us to revisit density functional theory (DFT) model calculations suggesting hydrogenation at this site was endothermic for the TDPAT ligand, and we were able to resolve this apparent discrepancy by considering the potential role of defects and charged ligands in the CuTDPAT structure. This demonstrates experimental and theoretical studies must be done in concert, as ultimately, truncated or analog model structures may not represent real materials. Experimentally, additional evidence for hydrogen chemisorption within CuTDPAT was found at (3) the Cu-O-C bond that connects the TDPAT ligand to the Cu paddlewheel. (A fourth potential binding site was the carbon atoms present in the TDPAT ligand, but the characterization techniques were relatively insensitive to C-H modes.) Subseuqent DFT calculations identified hydrogenated Cu paddlewheel structures that were consistent with the experimetnal resutls, and exothermic with respect to molecular H_2.

Overall, these spectroscopic techniques provided evidence for hydrogenation of the TDPAT ligand at 300 K without full dissociation of CuTDPAT to Cu metal and H_6TDPAT, and provided strong support for the hydrogen spillover mechanism, as comparable hydrogenation was not observed in the absence of the Pt catalyst. The ability to detect hydrogenation sites with ex situ characterization techniques confirmed hydrogen spillover is a hydrogneation process, consistent with our prevous results for carbon-based materials, including reversible (at 300 K) hydrogenation identified with in situ spectroscpy [9], and detailed DFT calculations [9,10]. Interestingly, spectroscpic evidence of hydrogenation of the TDPAT ligand was observed only after higher pressure (70 bar) H_2 exposure, consistent with several previous experimental isotherms found in the literature showing hydrogen spillover isotherms may not plateu at pressures up to 10 MPa. Combined with the partial degradation of CuTDPAT observed after high-pressure measurements, as well as the DFT calculations that demonstrate exotehrmic hydrogenation of N sites only for a charged ligand, the observed high-pressure hydrogenation may be associated with defect creation.

IB: Role of Defects to Enhance 300 K Hydrogen Chemisorption. To further explore the potential role of MMOF structural defects in the enhanced hydrogen uptake of PB-CuTDPAT, AC-T was prepared as an analog to PB-CuTDPAT, but the Pt transition metal was excluded. In other words, the AC support was inserted into the CuTDPAT structure during synthesis, omitting the Pt nanoparticles on the Pt/AC catalyst that was inserted into PB-CuTDPAT. At 1 bar and 300 K, the hydrogen excess adsorption of AC-**T** exceeded that expected for physisorption to its components by a factor of 4, whereas the uptake of PB-CuTDPAT exceeded that expected for physisorption by a factor of 8 (Figure 2A). This strongly suggests defects play a role in enhancing the room temperature uptake, however, we cannot rule out the effect of Pt as the textural properties of AC-**T** were generally more favorable than PB-CuTDPAT for both physisorption (i.e. the BET surface area was higher) and hydrogenation of external crystallite edge sites (based on external surface area determinations, XPS, X-ray diffraction (XRD), and electron micrographs). As mentioned above, complementary DFT calculations demonstrate N hydrogenation of the NH amine sites on the H_6TDPAT is highly endothermic, whereas hydrogenation of a charged H_6TDPAT ligand is exothermic. Similarly, previous calculations demonstrated structural defects would propagate the hydrogen spillover

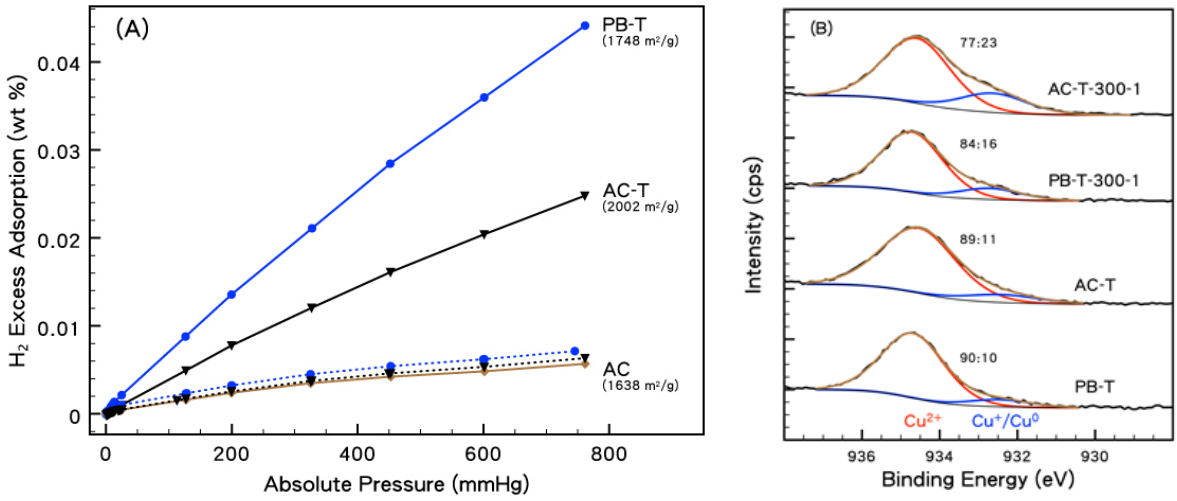

FIGURE 2. (A) Hydrogen 300 K 1 bar excess isotherms of Maxsorb AC, AC in Cu-TDPAT (**T**) via PB method (AC-**T**), and pre-bridged Cu-TDPAT with Pt/AC (PB-**T**), with expected uptake (dotted lines) based on weighted average versus experimental data (solid line). (B) The XPS spectra of Cu 2p 3/2 of AC-**T** and PB-**T**DPAT, before (bottom two) and after (top two) hydrogen exposure at 300 K and 1 bar, demonstrates reduction of Cu after mild H_2 exposure, which is more pronounced for AC-**T.**

mechanism via a hole-mediated effect [11]. Perhaps notably then, the Cu paddlewheel showed reduction after 300 K, 1 bar exposure, and the effect was more pronounced for AC-T than for PB-TDPAT (Figure 2B). The reduction of the Cu paddlewheel may be associated with partial charging of the ligand, resulting in more thermodynamically favorable hydrogenation of the ligand.

IC: Further Characterization of Defects. The potential increase in 300 K hydrogen adsorption by the introduction of defects and/or partial ligand charging of AC-T required further experimental validation. However, the readily available characterization methods (i.e. XPS, Fourier transform infrared [FTIR], XRD, and N_2 physisorption) were relatively insensitive probes of MMOF defects. Although Cu XPS demonstrated some reduction after H_2 exposure for AC-T (Figure 2B), and this has been associated with defects [12], this technique is not a well-established probe of defects in Cu-paddlewheel MOFs. Thus, we attempted to extend in situ FTIR probes of CO adsorption to CuBTC [12-14] to CuTDPAT, as both have the same Cu paddlewheel building unit. However, the CO signal in FTIR after CO adsorption/desorption to CuTDPAT at 150 K was notably different than adsorption to CuBTC controls that were conducted in parallel measurements. Whereas CO adsorption to CuBTC gave rise to perturbation of the CO spectra at ~2,170 and ~2,120 cm^{-1} (which are associated with adsorption at Cu^{2+} axial positions and defect sites, respectively [12-14]), both of these features were absent in CuTDPAT at all conditions studied. Additional control studies ruled out the effect of retention of the coordinated solvent, pretreatment conditions, sample preparation conditions, and thermal degradation. It seems that the lack of CO perturbation in CuTDPAT is associated with either the electron withdrawing nature of the TDPAT ligand (vs. the BTC ligand in CuBTC) or the equilibrium distance between CO and the Cu Paddlewheel site, which would be affected by differences in porosity of the two Cu-type MOFs. Thus, a more quantitative assessment of the role of introduced or induced defects on 300 K H_2 adsorption to CuTDPAT was not possible before project conclusion.

(P) Reproducibility of Performance

IID: Thermal Stability. As discussed above, CuTDPAT was degraded in high-pressure H_2, even prior to introduction of a catalyst. Although PB-CuTDPAT was ultimately found not to be a good candidate to meet DOE targets, we were interested in whether the PB doping technique may be used for other MMOFs (or other porous coordiantion polymers), and the effect the doping would have on the thermal stability of the materials. We compared the thermogravimetric analysis profiles of PB-CuTDPAT and PB-IRMOF8 to their undoped coutnerparts, in both N_2 and H_2, and found the PB doping technique had only a modest effect on the thermal stability of these two MMOFs. In brief, the onset of thermal degradation was reduced by 10-25 K, relative to the undoped MMOF precursor. PB-IRMOF8 was stable up to 660 K in H_2 (vs. 680 K for IRMOF8) and weight loss was <0.1%/hr at 573 K in long time (i.e. 5 hr) experiments. PB-CuTDPAT was stable up to 540 K in H_2 (vs. 550 K for CuTDPAT) and weight loss was <0.1%/hr in the long term stability tests up to 473 K. However, despite apparent thermal stability at 473 K, PB-CuTDPAT exhibited a loss of BET surface area after heating to 473 K. Additional evidence for hydrogen chemisorption to PB-CuTDPAT was found in these tests, and likely contributed to the observed decrease in BET surface area.

IIE: Role of Other Parameters in Reproducibility of 300K H_2 Adsorption in Catalyzed MMOFs. At project onset, the primary goal of this project was to investigate the role of surface chemistry and porosity on enhancing hydrogen uptake in catalyzed MMOFs via hydrogen spillover. Due to reproducibility issues in the broader field, however, the project was restructured in Year 2 to focus more on reproducibility and validation of the spillover mechanism,with a focus on one particular MMOF (namely, CuTDPAT). As we return to the initial question at project conclusion, we find that surface chemistry and porosity play a secondary role to catalyst-MMOF connectivity. This is illustrated by the comparison of the low pressure 300 K isotherm of three MMOFs (IRMOF8, CuBTC, and CuTDPAT), all doped with Pt/AC via the PB doping teqhnique. Although the surface chemistry and structure of these three MMOFs are very different (see Figure 1 A-C), these factors played very little role in dictating the hydrogen isotherms.

Specifically, the hydrogen isotherms at 300 K of the PB-MOF composites (solid lines, Figure 3A) are compared to the weighted average of their components (dotted lines, Figure 3A). The PB-CuTDPAT and PB-IRMOF8 samples show significant enhancement in hydrogen uptake relative to those of the weighted average of their components, whereas PB-CuBTC mirrors the uptake expected from the weighted average. In fact, the hydrogen uptake of PB-CuTDPAT at 1 bar exceeds (by ~25%) that of Pt/AC, despite having a fraction (~$1/20^{th}$) of the introduced catalyst. Furthermore, the slope of the H_2 isotherms for PB-CuTDPAT and PB-IRMOF8 are increased relative to the undoped precursors. These effects cannot be attributed to surface chemistry or porosity; rather, they correlate to observations of catalyst encapsulation via visual microscopy, increased mesoporosity (as determined from N_2 adsorption), and slightly expanded d-spacing in the XRD of PB-CuTDPAT and PB-IRMOF8. In contrast, the lack of enhancement seen for PB-CuBTC can be attributed to the fact that the Pt/AC catalyst was not effectively incorporated into the CuBTC matrix, judging from the optical microscopy, XRD, and decreased N_2 adsorption. We believe this is due to the smaller particle size of the methodology used to produce CuBTC. To better quantify this enhancement, we introduce a spillover efficiency parameter, η, defined as:

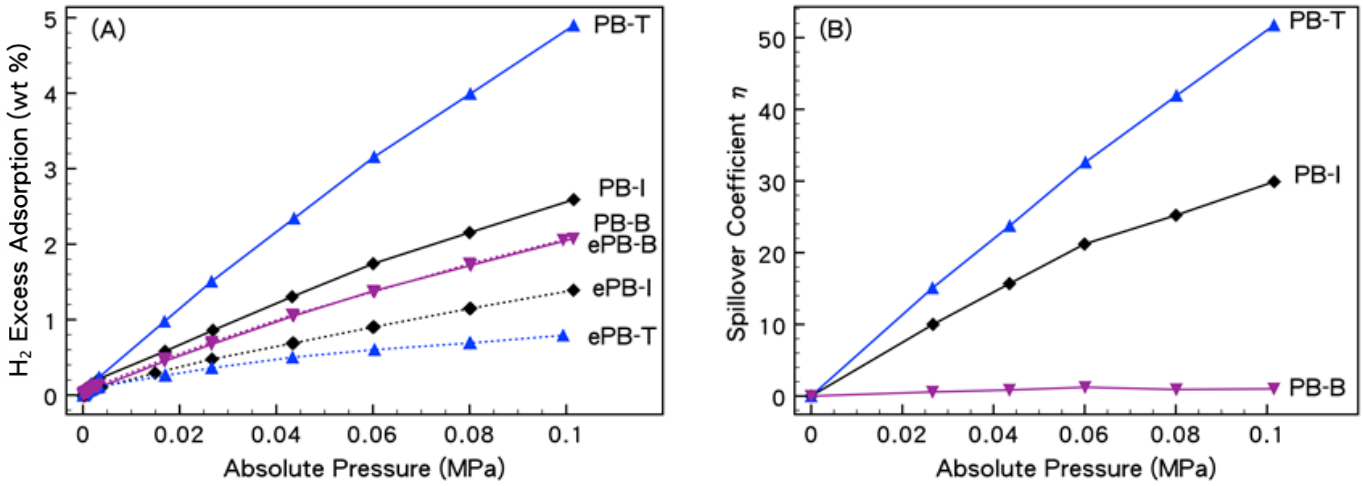

FIGURE 3. (A) Hydrogen 300 K 1 bar excess isotherms of expected (dotted line) PB-MOF samples vs. experimental data (solid line). The expected isotherms are shown based on the weighted average of each component in the composite. (B) Spillover efficiency η (see Eq 1) at 300 K of pre-bridged MOFs. Sample names have been abbreviated as PB-T, PB-I, and PB-B for PB-CuTDPAT, PB-IRMOF8, and PB-CuBTC, respectively.

$$\eta \equiv \frac{H}{M_S} = \frac{H}{M_T \cdot D} = \frac{\mu}{D} \qquad \text{Equation 1}$$

Where H is the amount of hydrogen adsorbed above and beyond adsorption to the components measured independently, M_S is the active Pt surface metal determined from H_2 measurements of the corresponding Pt/AC, M_T is the total Pt metal content, and D is the dispersion of the metal (i.e. ratio of surface sites to total metal atoms). A spillover efficiency exceeding 1 would be an indication of hydrogen spillover, and use of the active metal sites in its calculation helps to account for differences between the activities of the Pt/AC catalysts used in the synthesis of the different materials. The data clearly shows PB-Cu**T**DPAT has the highest spillover efficiency, whereas the spillover effect in PB-Cu**B**TC is negligible. For PB-**T**DPAT and PB-**I**RMOF8, spillover efficiency increases with pressure, suggesting greater access of H to the MMOF at increased pressure. The increased spillover efficiency seen for PB-**T**DPAT and PB-**I**RMOF8 may be associated with porosity, as PB-**T**DPAT shows broad pore size distribution from 8-20 Å, and this has previously been associated with H_2 transport to the catalyst [15-18] with a particular emphasis on pores within a fractal network that are greater than 3.2 nm [19]. Large pores would facilitate gaseous H_2 diffusion to the catalyst and subsequent spillover; in contrast, gaseous H_2 diffusion to catalysts embedded in micropores would be slowed.

The high uptake of PB-**T**DPAT (relative to PB-**I**RMOF8) cannot be attributed to surface chemistry, as DFT predictions actually indicate the chemical functionalities of the H_6TDPAT ligand are unfavorable for hydrogen diffusion and hydrogenation [20]. The textural properties of CuTDPAT and IRMOF8 do not differ enough to warrant the differences seen in the H_2 uptake, and the surface areas are similar (BET = 1,640 and 1,380 m^2/g, respectively). Thus, it seems likely that the high uptake seen for PB-CuTDPAT is associated with the creation of defects, and complementary XPS results suggest this structure is particularly susceptible to defect formation. Furthermore, the uptake can be completely eliminated, as in the case of PB-CuBTC, by insufficient catalyst-MMOF contact, which has been emphasized previously.

CONCLUSIONS AND FUTURE DIRECTIONS

- A PB doping technique reproducibility incorporated catalytic entities into MMOFs, while retaining structure and textural properties of the MMOF. The thermal stability of the MMOF was within 10-25 K of the precursor (for IRMOF8 and CuTDPAT).
- The PB technique led to reproducible hydrogen uptake at low pressure for two MMOFs (IRMOF8, CuTDPAT). The high H_2 uptake of PB-CuTDPAT was attributed to both the creation of defects and the introduction of Pt catalyst. Porosity, surface area, and/or surface chemistry of the MMOF did not correlate to high hydrogen uptake. Enhancement due to hydrogen spillover was eliminated when there was insufficient contact between the inserted catalyst and the MMOF (for PB-CuBTC).
- At high pressure, the uptake of PB-CuTDPAT exceeded that of the CuTDPAT precursor in five cases, but was extremely slow (i.e. in excess of 20-40 hours). Further tests at high pressure for CuTDPAT were aborted due to inherent mechanical instability of CuTDPAT (even prior to catalytic doping) in H_2.
- Spectroscopic evidence for hydrogen spillover to PB-CuTDPAT showed hydrogenation of the TDPAT ligand

and the Cu-O-C site, verifying the hydrogen spillover mechanism, and further demonstrating hydrogen spillover occurs through the process of weak chemisorption.

The project concluded on June 30, 2014. Open issues remaining include:

- Introduced or inherent defects within MMOF play a pivotal role in 300 K hydrogen uptake, and may contribute to propagation of hydrogen introduce via a catalyst. We were not fully able to quantify defects within the project timeframe, due to unexpected results when a probe of defects was extended from CuBTC to CuTDPAT.
- More direct contact between the inserted catalyst and the substrate (which acts as a reservoir for hydrogen) would be needed to overcome the slow kinetics observed at high pressure. Yet, prior studies from our laboratory suggest many 'traditional' methods to catalytically dope MMOFs lead to structural degradation of the MMOF.
- Thus, it is difficult to see how reproducible hydrogen uptake via spillover will be achieved with MOFs doped with transition metals. Perhaps catalytic sites could be incorporated directly into the MMOF framework. Or, novel metal-carbon structures may be more appropriate. For reversible hydrogen uptake, a hydrogenation reaction with a small ΔG (Gibbs Free Energy) is required, but unique to hydrogen spillover, the activation energy for surface diffusion from each surface site must also be considered in material design. A theoretical study of ~20 model surfaces demonstrates the relationship between surface binding energy and the barrier for diffusion are not correlated [10], contrary to common "rules of thumb" in the literature. (However, these rules of thumb serve to provide initial estimates to correlate the two parameters.)
- It is not clear why the rates of hydrogen spillover were impeded at high pressure (for PB-CuTDPAT), but this was observed in previous reports in this field as well. Once again, the barrier for surface diffusion must be considered in the design of hydrogen spillover materials.

FY 2014 PUBLICATIONS/PRESENTATIONS

1. Wang, C.Y., Gray, J.L., Gong, Q., Zhao, Y., Li, J. Klontzas, E., Psofogiannakis, G., Froudakis, G., Lueking, A.D., "Hydrogen Storage with Spectroscopic Identification of Chemisorption Sites in Cu-TDPAT via Spillover from a Pt/Activated carbon catalyst", J. Phys. Chem. C., Submitted 2014.

2. Sircar, S., Pramanik, S., Li, J., Cole, M., Lueking, A.D., Corresponding States Interpretation of Adsorption in Gate-Opening Metal-Organic Framework Cu(dhbc)2(4,4í-bpy), J. Phys. Chem. C, Submitted, 2014.

3. Sircar, S., Lueking, A.D., Adsorption Rates in Gate-Opening Metal Organic Frameworks: Development of a Combined Relaxation and Diffusion Model", Langmuir, Submitted, 2014.

4. Wang, C.Y., Gong, Q., Zhao, Y., Li, J. Lueking, A.D., "Stability and Catalytic Activity of Metal-Organic Frameworks Prepared via Different Catalyst Doping Methods", J. Catal., 2014, In Press.

5. Sircar, S., Wang, C.Y., Lueking, A.D., "Design of High Pressure Differential Volumetric Adsorption Measurements with Increased Accuracy", Adsorption, 19 (6), 1211-1234, 2013. DOI: 10.1007/s10450-013-9558-8.

REFERENCES

1. Sircar, S.; Wang, C.-Y.; and Lueking, A.D. *Adsorption*. **2013**, 1-24.

2. Wang, C.Y.; Gong, Q.; Zhao, Y.; Li, J.; and Lueking, A.D. *J. Catal.* **2014.**

3. Li, Y. and Yang, R.T. *J. Am. Chem. Soc.* **2006**, *128*, 8136-8137.

4. Tsao, C.S.; Yu, M.S.; Wang, C.Y.; Liao, P.Y.; Chen, H.L.; Jeng, U.S.; Tzeng, Y.R.; Chung, T.Y.; and Wu, H.C. *J. Am. Chem. Soc.* **2009**, *131*, 1404-1406.

5. Stadie, N.P.; Purewal, J.J.; Ahn, C.C.; and Fultz, B. *Langmuir.* **2010**, *26*, 15481-15485.

6. Stuckert, N.R.; Wang, L.; and Yang, R.T. *Langmuir.* **2010**, *26*, 11963-11971.

7. Yang, S.J.; Cho, J.H.; Nahm, K.S.; and Park, C.R. *Int. J. Hydorgen Energ.* **2010**, *35*, 13062-13067.

8. Lee, S.Y. and Park, S.J. *Int. J. Hydorgen Energ.* **2011**, *36*, 8381-8387.

9. Liu, X.M.; Tang, Y.; Xu, E.S.; Fitzgibbons, T.C.; Larsen, G.S.; Gutierrez, H.R.; Tseng, H.H.; Yu, M.S.; Tsao, C.S.; Badding, J.V.; Crespi, V.H.; and Lueking, A.D. *Nano Lett.* **2013**, *13*, 137-41.

10. Lueking, A.D.; Psofogiannakis, G.; and Froudakis, G.E. *J. Phys. Chem. C.* **2013**, *117*, 6312−6319.

11. Lee, K.; Kim, Y.H.; Sun, Y.Y.; West, D.; Zhao, Y.; Chen, Z.; and Zhang, S.B. *Physical Review Letters.* **2010**, *104*, 236101.

12. St Petkov, P.; Vayssilov, G.N.; Liu, J.; Shekhah, O.; Wang, Y.; Wöll, C.; and Heine, T. *Chemphyschem.* **2012**, *13*, 2025-2029.

13. Drenchev, N.; Ivanova, E.; Mihaylov, M.; and Hadjiivanov, K. *Phys. Chem. Chem. Phys.* **2010**, *12*, 6423-7.

14. Szanyi, J.; Daturi, M.; Clet, G.; Baer, D.R.; and Peden, C.H. *Phys. Chem. Chem. Phys.* **2012**, *14*, 4383-90.

15. Li, Y. and Yang, R.T. *J. Phys. Chem. C.* **2007**, *111*, 11086-11094.

16. Conner, W.C. and Falconer, J.L. *Chem. Rev.* **1995**, *95*, 759-788.

17. Boudart, M.; Aldag, A.W.; and Vannice, M.A. *J. Catal.* **1970**, *18*, 46-51.

18. Chen, H.; Wang, L.; Yang, J.; and Yang, R.T. *J. Phys. Chem. C.* **2013**, *117*, 7565-7576.

19. Tsao, C.S.; Yu, M.S.; Chung, T.Y.; Wu, H.C.; Wang, C.Y.; Chang, K.S.; and Chen, H.L. *J. Am. Chem. Soc.* **2007**, *129*, 15997-16004.

20. Wang, C.Y.; Gray, J.L.; Gong, Q.; Zhao, Y.; Li, J.; Klontzas, E.; Psofogiannakis, G.; Froudakis, F.; and Lueking, A.D. *J. Phys. Chem. C.* **2014.**

IV.C.4 Multiply Surface-Functionalized Nanoporous Carbon for Vehicular Hydrogen Storage

P. Pfeifer (Primary Contact), L. Firlej, B. Kuchta, M. Lee, C. Wexler, P. Yu, D. Robertson
University of Missouri
223 Physics Building
Columbia, MO 65211
Phone: (573) 882-2335
Email: pfeiferp@missouri.edu

DOE Managers
Ned Stetson
Phone: (202) 586-9995
Email: Ned.Stetson@ee.doe.gov
Jesse Adams
Phone: (720) 356-1421
Email: Jesse.Adams@ee.doe.gov

Contract Number: DE-FG36-08GO18142

Project Start Date: September 1, 2008
Project End Date: November 30, 2014

Overall Objectives

- Fabricate high surface area, multiply surface-functionalized carbon ("substituted materials") for reversible hydrogen storage with superior storage capacity by physisorption.
- Characterize materials and storage performance. Evaluate efficacy of surface functionalization, experimentally and computationally, for fabrication of materials with deep potential wells for hydrogen adsorption, indicating high binding energies.
- Optimize gravimetric and volumetric storage capacity by optimizing pore architecture and surface composition ("engineered nanospaces").

Fiscal Year (FY) 2014 Objectives

- Fabricate boron-doped nanoporous carbon (particulate and monoliths), using decaborane ($B_{10}H_{14}$) as boron carrier, for high-capacity reversible hydrogen storage.
- Establish high surface areas, low void fractions, and boron concentration maps in materials.
- Quantify complete substitution of boron in carbon lattice, enhanced binding energies of hydrogen on doped materials, and enhanced adsorption of hydrogen on doped materials. Establish reproducibility of enhanced performance.

Technical Barriers

This project addresses the following technical barriers from the Hydrogen Storage section of the Fuel Cell Technologies Office Multi-Year Research, Development, and Demonstration Plan:

(A) System Weight and Volume

(B) System Cost

(E) Charging/Discharging Rates

(J) Thermal Management

(O) Lack of Understanding of Hydrogen Physisorption and Chemisorption

Technical Targets

Structural and energetic targets are surface-engineered carbons, made from low-cost raw materials, which simultaneously host high surface areas (2,700 m^2/g or higher), high binding energies for hydrogen (12 kJ/mol or higher), and low void fractions (0.70 or less). Progress towards materials that meet DOE performance targets for hydrogen storage (technical targets in the Multi-Year Research, Development, and Demonstration Plan) is summarized in Table 1. Performance of University of Missouri materials at liquid-nitrogen temperature, 77 K, and room temperature, 296 K, is compared with storage targets for vehicles and portable equipment, respectively, because cryogenic tanks are under active consideration by the DOE for vehicles, but are unlikely for portable power supplies.

FY 2014 Accomplishments

- Reproducibly synthesized high-performing precursor and doped carbon powders.
- Developed quantitative X-ray photoelectron spectroscopy (XPS) analysis for simultaneous fitting of spectra.
- Demonstrated the existence of sp^2-bonded boron (high-binding-energy sites, "correctly coordinated boron" [1]).
- Demonstrated that the desired structure (sp^2 B-C bonds) leads to increases in low coverage binding energy as high as 9.2 kJ/mol.

✧ ✧ ✧ ✧ ✧

INTRODUCTION

Graphene-like high surface area carbons, as developed by our team from low-cost raw materials (e.g., corncob), are

TABLE 1. Progress towards meeting 2017 and 2015 DOE targets for hydrogen storage. University of Missouri sorbent is 5K-0280 (undoped carbon powder, [2] and Table 2). Reported gravimetric and volumetric storage capacities are for material, not system. Experimental data for the reported storage capacities, including excess adsorption, are listed in Table 2. Storage material cost is based on $5.20/kg sorbent (raw material and chemicals) and respective gravimetric storage capacity. Referenced targets for portable equipment are for single-use equipment.

Storage Parameter	Onboard Storage for Light-Duty Vehicles, 2017	Storage Material Handling Equipment, 2015	U. Missouri 2014 Status (77 K, 190 bar)
Gravimetric Storage Capacity	0.055 kg H_2/kg system	N/A	0.164 kg H_2/kg sorbent
Volumetric Storage Capacity	0.040 kg H_2/L system	0.030 kg H_2/L system	0.054 kg H_2/L sorbent
Storage Cost	$400/kg H_2 stored	$667/kg H_2 stored	$39/kg H_2 stored (storage material cost)

Storage Parameter	Storage for Low Power Portable Equipment	Storage for Medium Power Portable Equipment	U. Missouri 2014 Status (296 K, 190 bar)
Gravimetric Capacity	0.020 kg H_2/kg system	0.020 kg H_2/kg system	0.046 kg H_2/kg sorbent
Volumetric Capacity	0.030 kg H_2/L system	0.030 kg H_2/L system	0.015 kg H_2/L sorbent
Storage Cost	$3/g H_2 stored	$6.70/g H_2 stored	$0.15/g H_2 stored (storage material cost)

NA - not applicable

outstanding starting materials for functionalized materials that store hydrogen by adsorption at high gravimetric and volumetric storage capacity. A recent carbon exhibited a gravimetric storage capacity of 0.164 kg H_2/kg carbon and 0.054 kg H_2/L carbon at 77 K and 190 bar (Table 1). This project is a systematic effort to achieve comparable results at 300 K, by maintaining current surface areas, ~2,700 m^2g, and substituting carbon with boron and other chemistries to increase the binding energy for hydrogen (electron donation from H_2 to electron-deficient B, and other charge-transfer mechanisms). In the DOE Hydrogen Sorption Center of Excellence, one of the program final recommendations stated [1]: "*...it became clear that only correctly coordinated boron substituted in graphitic carbon is a viable route to improved hydrogen storage for substituted carbon materials... the Center recommends that researchers should develop substituted/heterogeneous materials that can be used to enhance dihydrogen isosteric heats of adsorption in the range of 10–25 kJ/mol ... Development efforts should focus on creating materials with the appropriate chemical and electronic structures, sufficient composition, and high specific-surface areas....*" High binding energies are also hosted by sub-nanometer pores in narrowly spaced stacks of graphene sheets. Boron-substituted materials are manufactured by thermolysis of volatile $B_{10}H_{14}$ in pores of stacks of graphene sheets. A significant effort of the project goes into conversion of these materials, most of which are powders, into monoliths, without loss of surface area and high-binding-energy sites. Monoliths have lower porosity and, as a result, higher volumetric storage capacity than powders.

APPROACH

The approach is an integrated fabrication, characterization, and computational effort. Structural characterization includes determination of surface areas, pore size distributions, and pore shapes. Storage characterization includes measurements of hydrogen sorption isotherms, enthalpies of adsorption (isosteric heats), and binding energies. Computational work includes adsorption potentials and simulations of adsorbed films for thermodynamic analysis of experimental isotherms. Comparison of computed and experimental isotherms validates theoretical adsorption potentials and experimental structure data.

RESULTS

In 2013-14, approximately 150 new carbon samples were prepared as high-surface-area, graphene-like carbon and precursors for boron-doped materials, using varied KOH:C ratios, affecting the pore structures and defect ratios of the precursor. The carbons were fully characterized and tested for reproducibility of material composition and performance. The best performing materials are summarized in Table 2. Precursor carbons were boron-doped by decomposition of $B_{10}H_{14}$ according to temperature and pressure protocols described in [2]. Hydrogen adsorption properties of doped materials were analyzed at low and high pressures, and at cryogenic and room temperatures. Linear isotherms at low pressure and 77 K and 87 K (Figure 1a) gave binding energies, E_B (depth of the adsorption potential), which could be compared with new theoretical estimates of the energy from quantum-chemical computations (Figure 1b). The agreement between experimental binding energies of B-doped carbons, 6.5–9.2 kJ/mol, and computed binding energies, 7.4-12 kJ/mol, was excellent. Binding energies from Henry's law were determined from ratios of gravimetric excess adsorption at temperatures T_1 and T_2,

$$G_{ex}(p,T_1)/G_{ex}(p,T_2) = \chi(T_1)/\chi(T_2) = (T_2/T_1)^{1/2}\cdot\exp\{E_B(T_2-T_1)/[(T_1T_2)R]\} \quad (1)$$

evaluated for the Langmuir model in the limit of zero pressure, with Langmuir constant $\chi(T)$ [3]. They were found

TABLE 2. Best performing, reproducible U. Missouri carbons 2013-14 (undoped, doped, powders, and monoliths) at liquid-nitrogen temperature (77 K) and room temperature (296 K), high-lighted in yellow. Performance metrics are: gravimetric storage capacity, G_{st}; volumetric storage capacity, V_{st}; binding energy, E_B; and enthalpy of adsorption, ΔH. Specific surface areas, Σ, and void fractions, ϕ, are from N_2 adsorption at 77 K. Gravimetric and volumetric storage capacities are calculated from experimental gravimetric excess adsorption, G_{ex}, and void fraction according to Ref. [4], Eqs. (1, 2). Void fraction is related to bulk density by $\rho_{bulk} = (1 - \phi)\ \rho_{skel}$, where the skeletal density is 2.0 g/cm^3 for University of Missouri carbons. The reported maximum values of gravimetric excess adsorption, Max. G_{ex}, are for the pressure interval 0-190 bar. The maximum occurs at 40-50 bar for 77 K, and at 190 bar for 296 K.

	Sample	Σ (m^2/g)	ϕ	Max. G_{ex} (wt%)	G_{st} (wt%)	V_{st} (g/L)	ΔH, E_B (kJ / mol)
Nanoporous Graphene-like Carbons	5K-0280 (77 K, 190 bar) (296 K, 190 bar)	2,700	0.84	5.9 0.9	14 4.4	54 15	5.8, N/A
	4K-0284 (77 K, 190 bar) (296 K, 190 bar)	2,600	0.81	5.6 1.0	13 3.9	54 15	4.7, N/A
B-Doped Graphene-like Carbons	4K-0246 (B=4%) (77 K, 190 bar) (296 K, 190 bar)	2,400	0.81	5.1 0.9	12 3.8	52 15	5.5, 7.5
	5K-0215 (B=8%) (77 K, 190 bar) (296 K, 190 bar)	1,900	0.79	4.3 0.7	11 3.3	50 14	6.2, 9.2
Synthetic Nanoporous Carbons	HS;0B-20 (77 K, 190 bar)	940	0.46	2.5	3.5	40	6.6, 9.4
	PVDC-0400 (77 K, 190 bar)	780	0.49	2.0	3.7	28	7.8, 10.8
Monoliths	4K Monolith (297 K, 100 bar)	2,100		0.9	2.5	9.5	-
	BR-0311 (77 K, 190 bar) (296 K, 190 bar)	2,300	0.74	4.3 0.9	9.0 2.9	51 15	5.6, N/A
Commercial Carbon	MSC-30 (77 K, 190 bar) (296 K, 190 bar)	2,700	0.80	5.3 0.9	12 3.6	53 15	5.0, N/A

to increase with increasing boron concentration, while isosteric heats ΔH as a function of boron concentration exhibited only insignificant variation (Figure 2a). This demonstrates that B-doped samples typically host a whole distribution of binding energies and that different metrics, such as E_B and ΔH, probe different components of the distribution.

To better understand the chemistry of $B_{10}H_{14}$ decomposition and the resulting environment of boron in the carbon matrix, the process was monitored by XPS. Boron XPS spectra exhibited a strong dependence on B concentration: at low concentration the spectrum consists only of a B-O peak, with residual oxygen from undoped, incompletely deoxygenated carbon precursor, and no measureable B-B or B-C. At higher concentration, the B-O peak splits into a B-B and a sp^2-bonded B-C peak ("correctly coordinated" boron atoms), allowing us to estimate the concentration of B-O, B-B, B-C, and C-O from an analysis of three simultaneous spectra—B, C, O (Figure 3). From the B-C spectrum we obtained the concentration of sp^2-bonded boron. While the concentration of sp^2-bonded boron is low in the investigated samples, with approximately one sp^2-bonded boron atom per total of 5-7 boron atoms (Figure 3, left), the binding energy is already at 9.2 kJ/mol at 1.7 wt% sp^2-bonded boron (Figure 2, right). This suggests that improved deposition and annealing methods in samples yet to be investigated, are likely to generate high binding energies, E_B = 11-12 kJ/mol, both on individual adsorption sites and for the average binding energy, $E_{B,av}$.

CONCLUSIONS AND FUTURE DIRECTIONS

- Quantitative XPS analysis demonstrates that the total amount of sp^2-bonded boron increases approximately linearly with total boron.

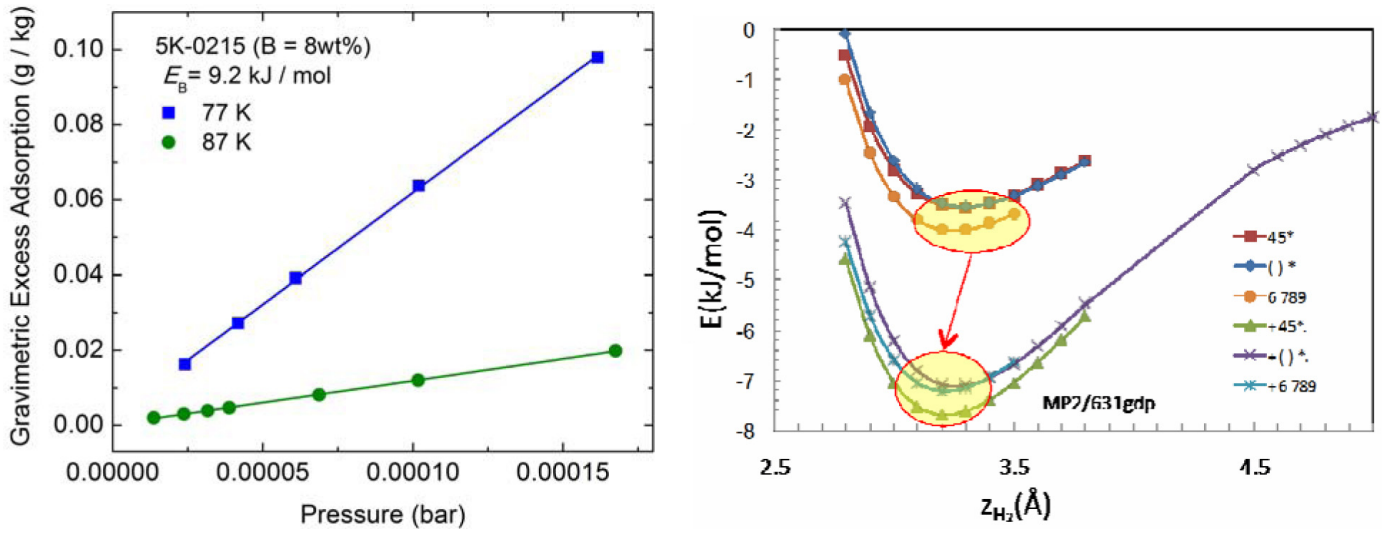

FIGURE 1. *Left:* Adsorption increases linearly with increasing pressure at sufficiently low pressure (Henry's law), here for sample 5K-0215 and p = 0–0.15 mbar. The slope of the isotherm grows exponentially with the binding energy E_B. For fixed binding energy, the ratio of the slopes at two different temperatures gives E_B, Eq. (1), here E_B = 9.2.kJ/mol. The linear behavior of the isotherm and the value of the slope were highly repeatable for all samples, also on different instruments. *Right:* Binding energy of graphene with one carbon atom substituted by anionic boron, B^-, and an unspecified cation, from ab initio calculations of the potential energy of a H_2 molecule as a function of distance from the boron atom. For a single B atom, E_B = 7.8 kJ/mol, and rises to E_B = 11-12 kJ/mol for B~10 wt%. About 50% of the enhanced binding energy is attributable to the negative charge distribution near B^-.

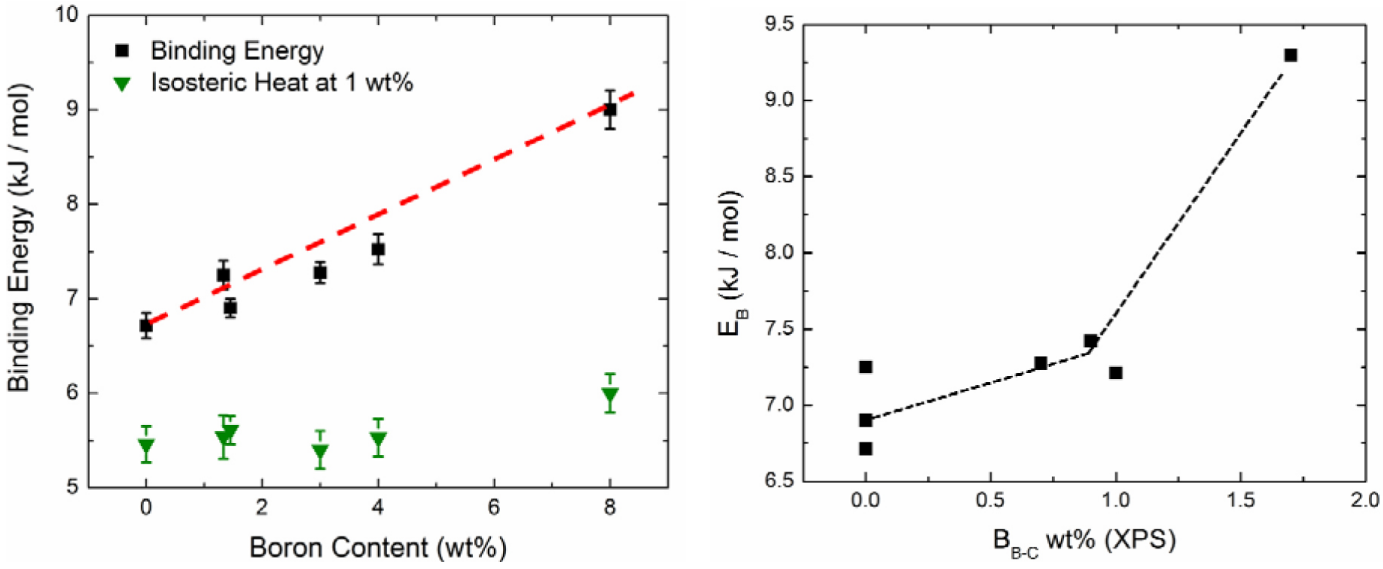

FIGURE 2. *Left:* Binding energies, from Henry's law (Figure 1a), increase linearly with increasing boron concentration: E_B = 6.7-9.2 kJ/mol. Isosteric heats, ΔH, from high H_2 coverage, 1.0 wt%, and isosteres from four different temperatures, increase insignificantly with B wt%: 5.5-6.0 kJ/mol. This indicates an insignificant increase of average binding energy, $E_{B,av}$. The two results are entirely consistent because Henry's law probes binding energies in the limit of zero coverage (highest binding energies present in the material), while ΔH at high coverage is sensitive only to the average binding energy, $E_{B,av}$, which may be low because only a few boron atoms may be present, or only a few "correctly coordinated" boron atoms —sp^2-bonded boron (B-C bonds, high-binding-energy sites) are present. *Right:* XPS analysis of sp^2-bonded boron (Figure 3) indicates that only 0.0-1.7 wt% sp^2-bonded boron is present on the samples analyzed. Equivalently, only up to 1 out 5 boron atoms present in the sample is sp^2-bonded. The graph of E_B vs. B_{B-C} wt% (right) shows that E_B = 9.2 kJ/mol is already reached at 1.7 B_{B-C} wt%.

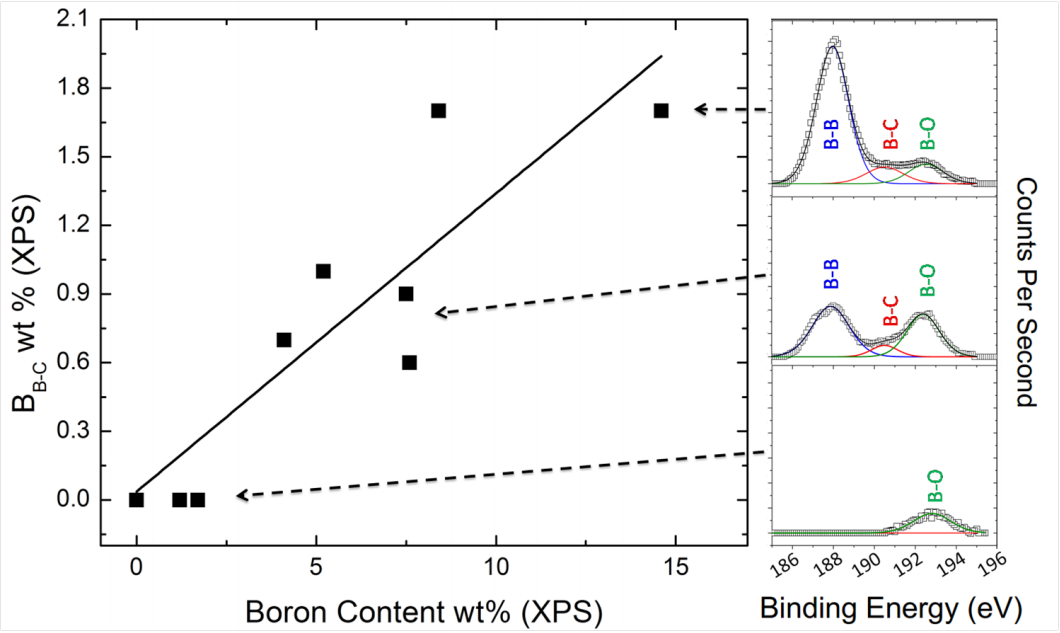

FIGURE 3. *Left:* Concentration of sp^2-bonded boron (B-C bonds, high-binding-energy sites) in different samples as a function of total boron concentration in the samples. XPS spectra for boron, carbon, and oxygen were simultaneously fit to determine amounts of sp^2-bonded boron in doped carbon samples. The concentration of sp^2-bonded boron increases with increasing total boron content. *Bottom Right:* Boron spectrum for sample 4K-0244. This spectrum is representative of all samples with boron content <2 wt%. In this range, the decomposition of $B_{10}H_{14}$ readily forms B-O bonds. No B-C bonds are observed. *Middle Right:* Boron spectrum for sample 3K-0211. This spectrum is representative of samples with 2 <B wt% <7. In this range, peak splitting is observed as B-B and B-C bonds emerge in addition to the formation of B-O bonds. *Top Right:* Boron spectrum for sample 3K-0208. This spectrum is representative of samples with B wt% >7. The B-B peak is most prominent in this spectrum due to the larger quantity of total boron in the sample. Further, the area under the B-C peak increased to be approximately equal to that under the B-O peak, indicating a larger amount of sp^2-bonded boron (1.7 wt%) in the sample. The spectra are normalized such that the area under the combined B-B, B-C, and B-O peaks corresponds to the total B concentration present in each sample.

- Binding energies were shown to increase both with increasing total boron content and with increasing sp^2-bonded boron, in quantitative agreement with the binding energy calculations in Figure 1. The increase with increasing sp^2-bonded boron appears to be non-linear, with a rapid rise observed between 1 and 2 wt% sp^2-bonded boron (Figure 2, right) and expected saturation at 11-12 kJ/mol around 10 wt% sp^2-bonded boron. This demonstrates that B-doping of nano-engineered carbon by vapor deposition and pyrolysis of decaborane has the capability of delivering materials with surface areas in excess of 2,000 m^2/g [2], average binding energies in excess of 10 kJ/mol, and accordingly enhanced gravimetric and volumetric storage capacities.
- Test higher annealing temperatures for possibly higher (% of sp^2-bonded boron)/(% of total boron).
- Conduct solid-state nuclear magnetic resonance work (^{11}B spectra) of boron-doped materials and compare with XPS.

SPECIAL RECOGNITIONS & AWARDS/ PATENTS ISSUED

1. P. Pfeifer, G.J. Suppes, P. Shah, J.W. Burress, "High surface area carbon and process for its production." U.S. Patent No. 8,691,177, issued Apr. 8, 2014.

FY 2014 PUBLICATIONS/PRESENTATIONS

1. L. Firlej, P. Pfeifer, and B. Kuchta, "Understanding universal adsorption limits for hydrogen storage in nanoporous systems." Adv. Mater. **25**, 5971-5974 (2013).

2. L. Firlej, M. Beckner, J. Romanos, P. Pfeifer, and B. Kuchta, "Different Approach to Estimation of Hydrogen-Binding Energy in Nanospace-Engineered Activated Carbons." J. Phys. Chem. C **118**, 955-961 (2014).

3. P. Pfeifer, A. Gillespie, E. Dohnke, and Y.Soo, "Hydrogen densities greater than liquid hydrogen at 77 K in engineered carbon nanospaces." In: *Materials Challenges in Alternative & Renewable Energy, Conference Program* (American Ceramic Society, Columbus, OH, 2014), MCARE-166-2014, p. 36.

4. A. Gillespie, E. Dohnke, J. Schaeperkoetter, D. Stalla, and P. Pfeifer, "Adsorption Enthalpies of Hydrogen on Chemically Enhanced Carbon Nanospaces." Bull. Am. Phys. Soc. 59, M22.00005 (2014).

5. E. Dohnke, A. Gillespie, and P. Pfeifer, "Liquid-like hydrogen densities in engineered carbon nanospaces" Bull. Am. Phys. Soc. 59, M22.00003 (2014).

6. C. Wexler, A. St. John, and M. Connolly, "Energetics of Boron Doping of Carbon Pores." Bull. Am. Phys. Soc. **59**, Z37.00007 (2014).

7. M. Connolly and C. Wexler, "Adsorption-Induced Breathing in Nanoporous Carbon." Bull. Am. Phys. Soc. **59**, Z37.00011 (2014).

8. P. Pfeifer, C. Wexler, P. Yu, M. Lee, D. Robertson, L. Firlej, and B. Kuchta, "Multiply Surface-Functionalized Nanoporous Carbon for Vehicular Hydrogen Storage." In: *Proceedings of the 2014 DOE Hydrogen and Fuel Cells Program Annual Merit Review and Peer Evaluation,* Washington, DC, June 16–20, 2014.

REFERENCES

1. L. Simpson, *DOE Hydrogen Sorption Center of Excellence, Final Report Executive Summary,* NREL, (2010), p. 36.

2. P. Pfeifer et al., in: *2014 DOE Hydrogen and Fuel Cells Program Annual Merit Review and Peer Evaluation,* Washington, DC, June 16–20, 2014.

3. J. Burress, M. Kraus, M. Beckner, R. Cepel, G. Suppes, C. Wexler, and P. Pfeifer, *Nanotechnology* 20, 204026 (2009).

4. P. Pfeifer et al., In: *DOE Hydrogen Program, FY 2009 Annual Progress Report*, ed. by S. Satyapal (U.S. Department of Energy, Washington, DC, 2009), p. 646-651.

IV.D.1 Design of Novel Multi-Component Metal Hydride-Based Mixtures for Hydrogen Storage

Christopher Wolverton (Primary Contact), Harold H. Kung, Vidvuds Ozolins (University of California, Los Angeles), Jun Yang (Ford Motor Company)
Department of Materials Science & Engineering
Northwestern University
Evanston, IL 60208
Phone: 847-467-0593
Email: c-wolverton@northwestern.edu

DOE Managers
Katie Randolph
Phone: (720) 356-1759
Email: Katie.Randolph@ee.doe.gov
Ned Stetson
Phone: (202) 586-9995
Email: Ned.Stetson@ee.doe.gov

Subcontractors
- University of California, Los Angeles, Los Angeles, CA
- Ford Motor Company, Dearborn, MI

Contract Number: DE-FC36-08GO18136

Project Start Date: September 1, 2008
Project End Date: August 31, 2014

Overall Objectives

- Discover novel mixed hydrides for hydrogen storage, which enable the DOE system-level goals
- Discover a material that has thermodynamics which allow desorbtion of 8.5 wt% hydrogen or more at temperatures below 85°C
- Via the combination of first-principles calculations of reaction thermodynamics and kinetics with material and catalyst synthesis, testing, and characterization, search for combinations of materials from distinct categories to form novel multicomponent reactions

Fiscal Year (FY) 2014 Objectives

- Determine storage capacities, kinetics, and reversibility for reactions predicted to have high capacity and suitable thermodynamics for hydrogen storage applications, $2LiBH_4 + 5Mg(BH_4)_2$ and $B_{20}H_{16}$
- Use combined density functional theory (DFT) and experiment to characterize reaction products from $2LiBH_4 + 5Mg(BH_4)_2$
- Synthesize $B_{20}H_{16}$ and determine hydrogen desorption properties and reaction products
- Develop computational methods to extend calculation of kinetics beyond mass transport to predict dissociation, surface diffusion, and other kinetic barriers

Technical Barriers

This project addresses the following technical barriers from the Hydrogen Storage section of the Fuel Cell Technologies Office Multi-Year Research, Development, and Demonstration Plan:

(O) Lack of Understanding of Hydrogen Physisorption and Chemisorption

(A) System Weight and Volume

(E) Charging/Discharging Rates

Technical Targets

This study is aimed at fundamental insights into new materials and the thermodynamic and kinetic aspects of hydrogen release and reabsorption from them. Insights gained from these studies will be applied toward the design and synthesis of hydrogen storage materials that meet the following DOE 2010 hydrogen storage targets:

- Specific energy: 1.5 kWh/kg
- Energy density: 0.9 kWh/L

FY 2014 Accomplishments

- Used computational tools and high-throughput machinery to survey high-capacity, thermodynamically reversible reactions
- Focused efforts on two main reactions predicted to have high capacity and suitable thermodynamics for hydrogen storage applications, $2LiBH_4 + 5Mg(BH_4)_2$ and $B_{20}H_{16}$
- Determined $B_{20}H_{16}$ to be promising—only known hydrogen storage reaction with high capacity, good thermodynamics, and computational predicted fast mass transport kinetics
- Theoretically predicted that mass transport in $B_{20}H_{16}$ is fast. Subcontract at OSU focused on synthesis of $B_{20}H_{16}$ compound (synthesis and nuclear magnetic resonance [NMR] characterization performed; project ran out of time/funds before full desorption, kinetics, and reaction products could be performed)

- Studied hydrogen desporption and decomposition pathways have been studied in $2LiBH_4 + 5Mg(BH_4)_2$ using NMR; reaction products consistent with theoretically predicted B_2H_6 anion. Using combination of experiments and DFT, able to assign almost all reaction products. Still one uncertain product (~25 ppm).
- Completed computational survey of dopants that lower surface dissociation or diffusion for MgB_2 rehydrogenation
- Confirmed the addition of $ZnCl_2$ (and carbon) to $LiBH_4$+$Mg(BH_4)_2$ mixture results in (slight) increase in hydrogen desorption at lower temperatures

INTRODUCTION

The long-term DOE targets for hydrogen storage systems are very challenging, and cannot be met with existing materials. The vast majority of the work to date has delineated materials into various classes, e.g., complex and metal hydrides, chemical hydrides, and sorbents. However, very recent studies indicate that mixtures of storage materials, particularly mixtures between various classes, hold promise to achieve technological attributes that materials within an individual class cannot reach. Our project involves a systematic, rational approach to designing novel multicomponent mixtures of materials with fast hydrogenation/dehydrogenation kinetics and favorable thermodynamics using a combination of state-of-the-art scientific computing and experimentation. Specifically, we focus on combinations of materials from distinct categories to form novel multicomponent reactions.

APPROACH

We use the accurate predictive power of first-principles modeling to understand the thermodynamic and microscopic kinetic processes involved in hydrogen release and uptake and to design new material/catalyst systems with improved properties. Detailed characterization and atomic-scale catalysis experiments elucidate the effect of dopants and nanoscale catalysts in achieving fast kinetics and reversibility. And, state-of-the-art storage experiments give key storage attributes of the investigated reactions, validate computational predictions, and help guide and improve computational methods. In sum, our approach involves a powerful blend of (1) hydrogen storage measurements and characterization, (2) state-of-the-art computational modeling, (3) detailed catalysis experiments, and (4) an in-depth automotive perspective.

FUTURE DIRECTIONS

This project is complete. $B_{20}H_{16}$ is unique and potentially very interesting as the only hydrogen storage reaction of a known compound with (1) high capacity, (2) good thermodynamics, and (3) predicted fast mass transport kinetics. Of course, there are drawbacks, but because of this unique combination of characteristics, recommend that more future work on this reaction is warranted. Synthesis of $B_{20}H_{16}$ proved difficult, with low yield. However, based on our project accomplishments, we can make several recommendations for future directions for this area.

- Validate future experimental work should try to validate predicted beneficial attributes of $B_{20}H_{16}$ material; if validated, more focused effort should be performed to overcome any potential drawbacks (e.g., low yield synthesis, low-cost synthesis, possible kinetic limitations)
- Perform computations of observed reaction products to confirm results and provide predictions of thermodynamics/kinetics
- Extend NMR experiments and DFT-NMR calculations to "recharged" $2LiBH_4$+$5Mg(BH_4)_2$ samples, to determine portion(s) of the reaction that are reversible
- Explore the potentially promising avenue for "fast kinetics" borohydrides: low melting point combinations (i.e., low-lying eutectics); direct some computational effort to finding these low-lying eutectics (AIMD and λ-integration)

PUBLICATIONS

1. *Theoretical prediction of different decomposition paths for $Ca(BH_4)_2$ and $Mg(BH_4)_2$* Yongsheng Zhang, Eric Majzoub, Vidvuds Ozolins and C. Wolverton Phys. Rev. B **82**, 174107 (2010)

2. *First-principles prediction of phase stability and crystal structures in Li-Zn and Na-Zn mixed-metal borohydrides* Dilpuneet S. Aidhy and C. Wolverton Phys. Rev. B **83**, 144111 (2011)

3. *Prediction of a $Ca(BH_4)(NH_2)$ quaternary hydrogen storage compound from first-principles calculations* Dilpuneet S. Aidhy, Yongsheng Zhang and C. Wolverton Phys. Rev. B **84**, 134103 (2011)

4. *First-principles prediction of high-capacity, thermodynamically reversible hydrogen storage reactions based on (NH4)2B12H12* W.H. Sun, C. Wolverton, A.R. Akbarzadeh and V. Ozolins Phys. Rev. B 83, 064112 (2011)

5. *Transition Metal-Decorated Activated carbon Catalysts for Dehydrogenation of NaAlH4*, Sean S.-Y. Lin, Jun Yang, and Harold H. Kung, Int. J. Hydrogen Energy **37**, 2737 (2012)

6. Theoretical prediction of metastable intermediates in the decomposition of $Mg(BH_4)_2$ Yongsheng Zhang, Eric Majzoub, Vidvuds Ozolins and C. Wolverton J. Phys. Chem. C **116**, 10522 (2012)

7. *Crystal structures, phase stabilities, and hydrogen storage properties of metal amidoboranes* Yongsheng Zhang and C. Wolverton J. Phys. Chem. C **116**, 14224 (2012)

8. *First-principles insight into the degeneracy of ground state $LiBH_4$ structures* Yongsheng Zhang, Yongli Wang, Kyle Michel and C. Wolverton Phys. Rev. B **86**, 094111 (2012)

9. *Structure determination of an amorphous compound AlB_4H_{11}* Xuenian Chen, Yongsheng Zhang, Yongli Wang, Wei Zhou, Douglas A. Knight, Teshome B. Yisgedu, Zhenguo Huang, Hima K. Lingam, Beau Billet, Terrence J. Udovic, Terrence J. Udovic, Gibert M. Brown, Sheldon G. Shore, Christopher M. Wolverton and Ji-Cheng Zhao Chem. Sci. **3**, 3183 (2012)

10. *First-principles studies at intermediate products in the decomposition of metal amidoboranes* Yongsheng Zhang, Tom Autrey and C. Wolverton J. Phys. Chem. C **116**, 26728 (2012)

11. *The kinetics of mass transport in $B_{20}H_{16}$* Kyle Michel, Yongsheng Zhang and C. Wolverton J. Phys. Chem. C **117**, 19295 (2013)

12. *First principles studies of phase stability and crystal structures in Li-Zn mixed-metal borohydrides* Yongli Wang, Yongsheng Zhang and C. Wolverton Phys. Rev. B **88**, 024119 (2013)

13. *Hydrogen Storage Properties of Complex Metal Hydride-Carbon Materials* Sean S.-Y. Lin, Jun Yang, Harold H. Kung, Mayfair C. Kung Topics in Catalysis 56, 1937 (2013)

14. *Crystal structure, phase stability, and decomposition of the quaternary Mg-B-N-H hydrogen storage system* Yongsheng Zhang, David Farrell, Jun Yang, Andrea Sudik and C. Wolverton, J. Phys. Chem. C 118, 11193 (2014)

15. *Stability of transition metals on the Mg-terminated MgB2 (0001) surface and their effects on hydrogen dissociation and diffusion* Yongli Wang, Kyle Michel, Yongsheng Zhang and C. Wolverton, submitted to Phys. Rev. B (2014)

16. *Hydrogen diffusion in MgB2 bulk* Y.L. Wang, K. Michel, and C. Wolverton, in prep. (2014)

17. *A strategy for designing hydrogen storage materials with moderate thermodynamic properties* Y.L. Wang, K. Michel, and C. Wolverton, in prep. (2014)

IV.D.2 Hydrogen Storage Materials for Fuel Cell-Powered Vehicles

Andrew Goudy
Delaware State University
1200 N. Dupont Highway
Dover, DE 19901
Phone: (302) 857-6534
Email: agoudy@desu.edu

DOE Managers
Ned Stetson
Phone: (202) 586-9995
Email: Ned.Stetson@ee.doe.gov.
Katie Randolph
Phone: (720) 356-1759
Email: Katie.Randolph@ee.doe.gov

Contract Number: DE-FC36-06GO86046

Subcontractor
University of Delaware, Newark, DE

Start Date: July 1, 2006
Projected End Date: September 30, 2014

Overall Objectives

The objectives of this project are to:

- Identify complex hydrides that have great hydrogen storage potential.
- Develop new catalysts and engineering techniques for increasing reaction rates and lowering reaction temperatures.
- Perform kinetic modeling studies that will identify the rate-controlling processes in the hydrogen desorption reactions.
- Evaluate the parameters that affect the ability of metal-organic frameworks (MOFs) to adsorb gases.

Fiscal Year (FY) 2014 Objectives

- Perform absorption and desorption kinetics on the $LiNH_2/MgH_2$ system using RbH as a catalytic additive.
- Perform kinetic modeling studies on both absorption and desorption reactions to identify the rate-controlling processes in the $LiNH_2/MgH_2$ system.
- Perform absorption/desorption cycling measurements to determine the cyclic stability of the $LiNH_2/MgH_2$ system.
- Evaluate the parameters that affect the ability of selected MOFs to adsorb gases such as H_2, CH_4 and CO_2.
- Determine the effect of nano-confinement on the hydrogen sorption capacity of the $LiNH_2/MgH_2$ system.

Technical Barriers

This project addresses the following technical barriers from the Hydrogen Storage section of the Fuel Cell Technologies Office Multi-Year Research, Development, and Demonstration Plan:

(A) System Weight and Volume

(D) Durability/Operability

(E) Charging/Discharging Rates

Technical Targets

This project is conducting fundamental studies of complex amide materials and other promising hydrogen storage materials. Insights gained from these studies will be applied toward the design and synthesis of hydrogen storage materials that meet DOE's 2015 gravimetric goal of 5.5 wt% hydrogen storage for the system. Table 1 summarizes the targets.

TABLE 1. Project Technical Targets

Storage Parameter	Target	$LiNH_2/MgH_2$
System Gravimetric Capacity:	0.055 kg H_2/kg System	To Be Determined
System Volumetric Capacity:	0.040 kg H_2/L System	To Be Determined

FY 2014 Accomplishments

- Have developed a reactive ball milling method for synthesizing RbH and CsH catalysts for the $MgH_2/LiNH_2$ system.
- Cycling studies have been done in which absorption and desorption pressure-concentration-temperature isotherms were constructed for the RbH-doped mixtures after every 10 cycles. The results showed that the absorption plateau pressure increased during cycling while the desorption plateau pressure decreased. Also the amount of hydrogen absorbed and desorbed gradually decreased during cycling.
- The absorption and desorption kinetics of the RbH-catalyzed mixtures were compared at 160°C and at the same thermodynamic driving forces. Under these conditions, absorption reaction proceeds faster than the desorption reaction.
- Since many MOFs have been found to adsorb more gas than expected based on surface areas, sticking efficiencies (θ) were determined to see how this could

be explained. The MOFs that were studied include: Zn-NDC, Zn-BDC, Zn-Mim, Cu-BTC, Fe-BTC and Mil-53(Al). NDC is naphthalenedicarboxylic acid; BDC is benzenedicarboxylic acid; Mim is methyl imidazole and BTC is benzenetricarboxylic acid. Since three of the MOFs contain the same metal and different linkers, whereas two others contain the same linker but different metals, it was possible to determine the possible effects of type of metal and linker on θ.

- The three gases studied include: H_2, CH_4 and CO_2. Results show that of the three Zn-containing MOFs, Zn-NDC has the highest sticking efficiency. Therefore it was concluded that NDC is a more effective linker than BDC and Mim when it comes to gas adsorption. Results also show that Cu is a more effective metal than Fe for gas adsorption.
- Results also show that θ can be correlated with the isosteric heat of adsorption. Thus it seems as though the binding strength can be just as important as surface area in gas adsorptions.
- Experiments were also done to determine how nano-confinement of complex hydrides in MOFs would affect hydrogen desorption temperature. It was found that nano-confinement of a $2LiNH_2/MgH_2$ mixture in isoreticular MOF-8 (IRMOF-8) results in a lowering of the desorption temperature of the mixture.

✧ ✧ ✧ ✧ ✧

INTRODUCTION

The $2LiNH_2/MgH_2$ system has been identified as an important "near-term" system for hydrogen storage. This is because of its good long-term cycling behavior and high hydrogen capacity. Current efforts in our research lab are focused on performing hydrogen storage studies on this system. We have developed methods for the synthesis, characterization, and modeling of this system. New catalysts and engineering techniques for increasing reaction rates and lowering reaction temperatures have also been developed. We have also extended these studies to include MOFs as potential hydrogen storage materials. Once a suitable material has been identified for hydrogen storage it will be necessary to design, fabricate and test a hydride-based hydrogen storage system for fuel cell applications.

APPROACH

To achieve the project objectives, it was first necessary to design suitable methods for synthesizing, characterizing, and testing the materials. These methods included synthesis of new materials by mechanical alloying using ball milling, determining thermal stability using thermal gravimetric analysis or thermally programmed desorption (TPD), using X-ray diffraction to determine phase purity and crystal structure, using pressure-composition isotherm (PCI) analyses to determine thermodynamic stability, finding catalysts for making the hydriding faster and reversible, determining kinetic rate curves using constant pressure driving forces, and performing modeling to gain understanding of the mechanism.

RESULTS

The thermodynamics and kinetics of the $2LiNH_2/MgH_2$ system have been reported but it is also necessary to know how stable the system is upon continuous pressurizations and depressurizations. Therefore a series of absorption/desorption cycling measurements were done on this system at 200°C. Figure 1 (left) contains a pair of absorption/desorption

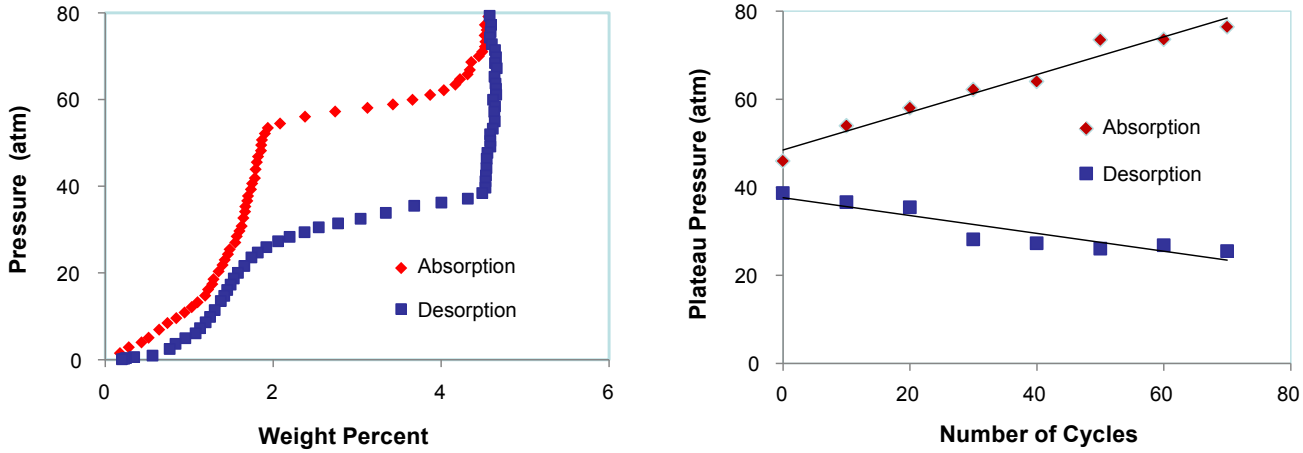

FIGURE 1. Cycling Study for the $LiNH_2/MgH_2$ System – The absorption and desorption PCIs shown above on the left were done at 160°C after 20 cycles. The plots show that there is a significant amount of hysteresis. The graph on the right gives the absorption and desorption plateau pressures after every 10 cycles up to 70 cycles. It is evident that the hysteresis increases as a result of cycling.

isotherms that were obtained at 200°C after 20 cycles. The plots show that there is a significant amount of hysteresis. Figure 1 (right) gives the absorption and desorption plateau pressures after every 10 cycles up to 70 cycles. It is evident that the hysteresis increases as a result of cycling. Since the amount of hysteresis usually remains fairly constant, regardless of cycling, this was an unexpected result. Additional measurements using other catalysts such as KH will also be done to determine if similar effects exist. It was also found that the hydrogen capacity decreased by about 25% during the course of 70 cycles.

The kinetics of hydrogen uptake and release from the $2LiNH_2/MgH_2$ system was also measured in the two-phase region. The absorption and desorption kinetics of the RbH catalyzed mixtures were compared at 160°C using a constant pressure thermodynamic driving force. This was achieved by using a ratio of the plateau pressure to the applied hydrogen pressure of 3 (desorption) or a ratio of the applied pressure to the plateau pressure of 3 (absorption). Figure 2 contains plots for the rates of hydrogen absorption and desorption from the RbH-catalyzed mixtures. The results show that absorption occurs faster than desorption under the same conditions. It takes ~350 minutes to attain 90% absorption whereas ~740 minutes are required for 90% desorption.

An attempt was also made to determine the rate-controlling process in these samples by doing kinetic modeling. The theoretical equations that were used are shown below:

$$\frac{t}{\tau} = 1 - (1 - X_B)^{1/3} \quad (1)$$

$$\frac{t}{\tau} = 1 - 3(1 - X_B)^{2/3} + 2(1 - X_B) \quad (2)$$

Where τ is a constant that depends on several parameters such as the initial radius of the hydride particles, the gas phase concentration of reactant, the density of the metal hydride, etc.

The model based on Eq. (1) will have chemical reaction at the phase boundary controlling the reaction rate whereas a model based on Eq. (2) is one in which diffusion controls the overall reaction rate. Both equations were fitted to the kinetic data for $LiNH_2/MgH_2$ system. Figure 2 (right) contains modeling plots for the $2LiNH_2/MgH_2$ system catalyzed by RbH. In the graph, one curve is an experimental curve, a second curve is based on the overall rate being controlled by diffusion, and a third curve is calculated based on chemical reaction controlling the rate. The results show a good fit between the experimental curve and the diffusion controlled curve. This indicates that diffusion controls the rate of absorption over the entire course of the reaction. The desorption reaction (curves are not shown) is also diffusion controlled but only during the first 50% of reaction.

Since many MOFs have been found to adsorb more gas than expected based on surface areas alone, sticking efficiencies were determined to see how this could be explained. Sticking efficiencies were determined based on a newly developed parameter called the sticking factor (θ). The sticking factor (θ) can be calculated based on the following equation:

$$\theta = \frac{\%\ \text{Hydrogen Adsorbed X Avogadro's No.}}{\text{Surface Area}\left(\frac{m^2}{g}\right) \text{X Mol. Wt.}} \quad (3)$$

The MOFs that were studied include: Zn-NDC, Zn-BDC, Zn-Mim, Cu-BTC, Fe-BTC and Mil-53(Al). Since three of the MOFs contain the same metal and different linkers whereas two others contain the same linker but different metals, it was possible to determine the possible effect of metal and linker on θ. The three gases studied include: H_2, CH_4 and CO_2. Results show that in the three Zn-containing

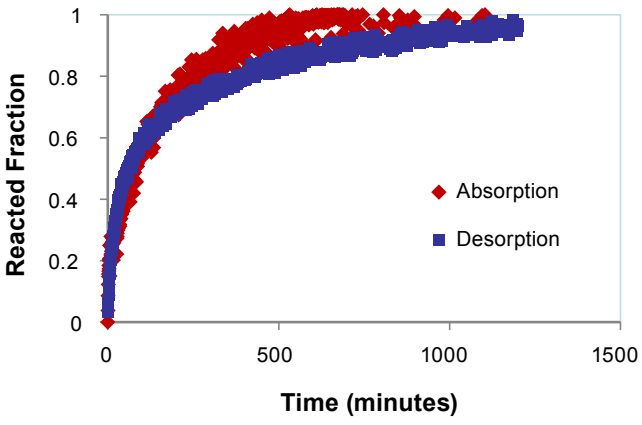

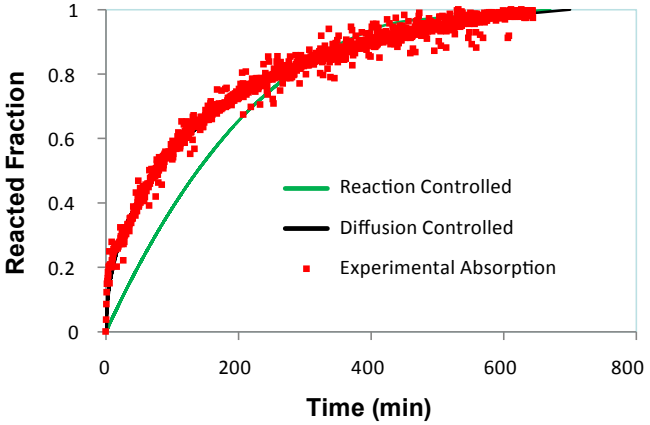

FIGURE 2. Kinetics and Modeling for the RbH-Doped $LiNH_2/MgH_2$ System – Kinetics were done in the two-phase region at 160°C and N=3. The graph on the left shows that absorption occurs faster than desorption under the same conditions. It takes ~350 minutes to attain 90% absorption whereas ~740 minutes are required for 90% desorption. The graph on the right contains absorption modeling results for the system. The experimental curve fits the diffusion controlled curve over the entire course of the reaction.

MOFs, Zn-NDC has the highest sticking efficiency. Therefore it was concluded that NDC is a more effective linker than BDC or Mim. Results also showed that Cu is a more effective metal than Fe for gas adsorption. Measurements of adsorption enthalpies showed that θ can be correlated with the isosteric heat of adsorption. The graph on the top left of Figure 3 shows that (θ) for H_2 adsorption on the various MOFs correlates well with adsorption enthalpy. The graph on the top right shows that the same correlation exists for CH_4 adsorption on the MOFs, while the graph on the bottom right shows that a similar correlation exists for CO_2. Thus it seems as though the binding strength can be just as important as surface area in gas adsorptions.

Experiments were also done to determine how nano-confinement of complex hydrides in MOFs would affect hydrogen desorption temperature. The TPD in Figure 4 shows that nano-confinement of $LiNH_2/MgH_2$ in IRMOF-8 causes hydrogen to be released at a lower temperature. Doping with RbH produces a further lowering of the desorption temperature.

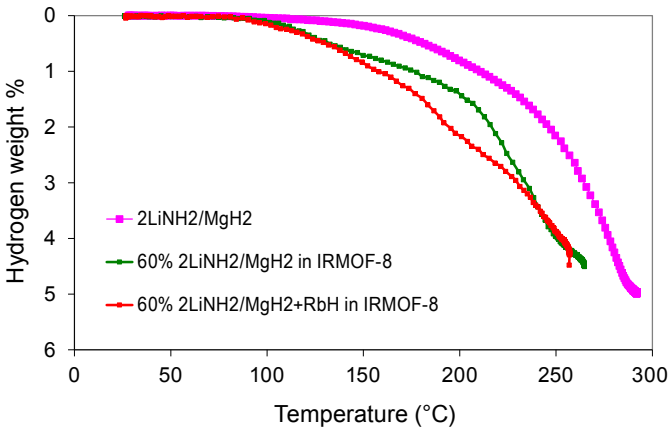

FIGURE 4. Nano-Confinement of $LiNH_2/MgH_2$ in IRMOF-8 – The TPD plots show that nano-confinement of $LiNH_2/MgH_2$ in IRMOF-8 causes hydrogen to be released at a lower temperature. Doping with RbH_2 produces a further lowering of the desorption temperature.

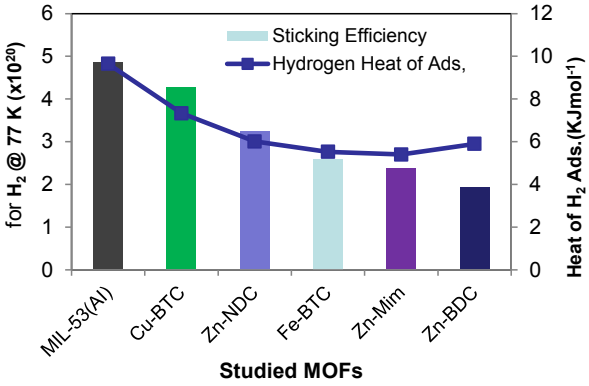

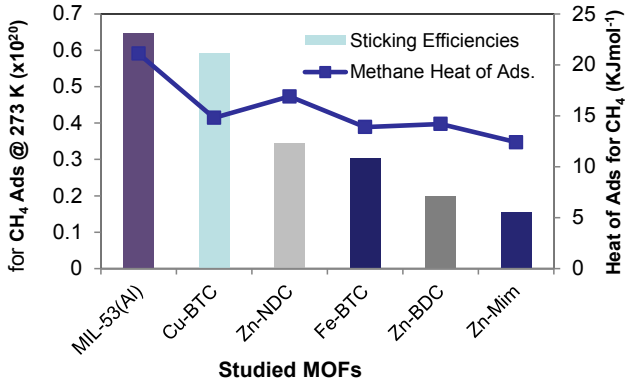

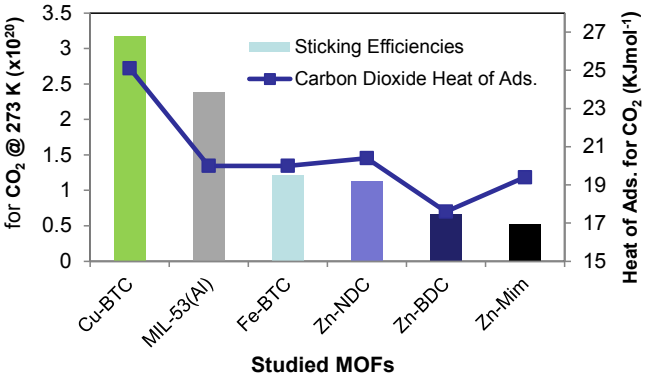

- $\theta = \dfrac{\%\ \text{Hydrogen Adsorbed X Avogadro's No.}}{\text{Surface Area}\left(\frac{m^2}{g}\right)\text{X Mol. Wt.}}$
- Sticking factors (θ) were calculated from the above equation.

FIGURE 3. Relationship between Sticking Efficiency and Heat of Adsorption – The graph on the top left shows that (θ) for H_2 adsorption on the various MOFs correlates well with adsorption enthalpy. The graph on the top right shows that the same correlation exists for CH_4 adsorption on the MOFs. The graph on the bottom right shows that the same correlation exists for CO_2 adsorption on the MOFs.

CONCLUSIONS

- The results of this study show that hydrogen absorption in the RbH catalyzed $2LiNH_2/MgH_2$ system occurs about twice as fast as desorption under the same conditions.
- Absorption/desorption cycling results in an increase in the amount of hysteresis in the RbH-catalyzed $2LiNH_2/MgH_2$ system with a decrease in hydrogen absorption capacity of 25% during the first 70 cycles.
- Modeling studies using the shrinking core model indicated that the absorption and desorption reaction rates are controlled by diffusion in the two-phase plateau region.
- It was found that in the three MOFs containing a common metal but different linkers, the Zn-NDC had the highest sticking efficiency. Therefore it appears that NDC (naphthalene dicarboxylic) acid is the most effective linker for hydrogen adsorption.
- In the two MOFs with the same linker but different metals the Cu-BTC had a greater sticking efficiency than Fe-BTC. Therefore it seems that Cu was a more effective metal than Fe in increasing adsorption capacity.
- Since there is a direct correlation between sticking efficiency and adsorption enthalpy this indicates that the strength of hydrogen adsorption on the surface is an important parameter in determining the quantity of gas adsorption.
- Nano-confinement studies showed that confinement of $2LiNH_2/MgH_2$ in the pores of IRMOF-8 results in a decrease in the dehydriding temperature of the complex hydride. The addition of RbH further decreases the temperature.

FUTURE DIRECTIONS

Although financial support for this work is ending in September 2014, the following future work is planned:

- Continue to perform kinetics and modeling studies on the $MgH_2/LiNH_2$ system based destabilized systems using our newly developed RbH catalytic additive as well as KH and CsH additives. We will focus on absorption studies, including modeling work, since most of the work to date has been on desorption kinetics.
- Continue the cycling studies on the KH and CsH catalyzed $MgH_2/LiNH_2$ system.
- Continue to study nano-confinement of complex hydrides in other lightweight MOFs such as Mil-53(Al).
- Continue to study sticking factors as a way to explain different adsorption behaviors in MOFs.
- Continue collaborating with the University of Delaware on the design, fabrication and demonstration of a hydride-based hydrogen storage system.

PATENT ISSUED

1. A Rubidium Hydride Catalyzed Lithium Amide/Magnesium Hydride System for Hydrogen Storage Applications, EFS ID 19061394.

FY 2014 PUBLICATIONS/PRESENTATIONS

1. J. Hayes, T. Durojaiye and A.J. Goudy, "Hydriding and Dehydriding Kinetics of the rubidium hydride doped lithium amide/magnesium hydride system", J. Alloys Compds (Submitted).

2. Esosa Iriowen, Samuel Orefuwa, Yang Hongwei, Andrew Goudy, "Comparative Studies of Sticking Efficiencies in Gas Adsorptions Analysis on Selected Metal Organic Frameworks", J. Alloys Compds, (Submitted).

3. Samuel Orefuwa, Esosa Iriowen, Hongwei Yang, Bryan Wakefield and Andrew Goudy, "Effects of Nitro-Functionalization on the Gas Sorption Properties of Isoreticular Metal-Organic Framework-Eight (IRMOF-8)", Micropor. Mesopor. Mater., 177 (2013) 82-90.

4. Durojaiye T, Hayes, J, and Goudy A, "Rubidium Hydride – A Highly Effective Dehydrogenation Catalyst for the lithium amide/magnesium hydride system" J. Phys Chem C, 117 (2013) 6554 – 6560.

5. J. Hayes, T. Durojaiye and A.J. Goudy, "Effects of Alkali Metal Hydrides on $2LiNH_2/MgH_2$ System", Gordon Conference, Lucca, Italy, 2013.

6. E. Iriowen, S.A. Abidemi, H. Yang and A.J. Goudy, "Sticking Efficiencies of Different Gases on Metal Organic Frameworks", Gordon Conference, Lucca, Italy, 2013.

IV.D.3 Neutron Characterization in Support of the DOE Hydrogen Storage Program

Terrence J. Udovic (Primary Contact),
Craig M. Brown, Dan A. Neumann
NIST Center for Neutron Research
National Institute of Standards & Technology
100 Bureau Dr., MS 6102
Gaithersburg, MD 20899-6102
Phone: (301) 975-6241
Email: udovic@nist.gov

DOE Managers
Channing Ahn
Phone: (202) 586-9490
Email: Channing.Ahn@ee.doe.gov
Ned Stetson
Phone: (202) 586-9995
Email: Ned.Stetson@ee.doe.gov

Project Start Date: October 2010
Project End Date: Project continuation and direction determined annually by DOE

Overall Objectives

- Support the DOE-funded hydrogen-storage projects by providing timely, comprehensive characterization of materials and storage systems using state-of-the-art neutron methods.
- Direct partner synthesis efforts based on the understanding gained through the use of these methods.
- Demonstrate the fundamental characteristics of useful hydrogen-storage materials.

Fiscal Year (FY) 2014 Objectives

- Synthesize and characterize the structure and dehydrogenation properties of the Na and K analog compounds of lithium hydrazinoborane, $LiN_2H_3BH_3$.
- Investigate how halide substitution in $NaBH_4$ perturbs the parent structure and BH_4^- anion mobilities.
- Complete our investigations concerning previously unknown order-disorder phase transitions in $LiBH_4$ and $NaBH_4$ dehydrogenation by-products $Li_2B_{12}H_{12}$ and $Na_2B_{12}H_{12}$.
- Elucidate the conductivities of disordered, cation-vacancy-rich $Li_2B_{12}H_{12}$ and $Na_2B_{12}H_{12}$.

Technical Barriers

This project addresses the following technical barriers from the Hydrogen Storage section of the Fuel Cell Technologies Office Multi-Year Research, Development, and Demonstration Plan:

(A) System Weight and Volume

(O) Lack of Understanding of Hydrogen Physisorption and Chemisorption

Technical Targets

NIST provides important materials metrologies for DOE-funded projects using neutron-scattering measurements to understand and characterize hydrogen-substrate interactions of interest in a variety of materials ranging from H_2 adsorbed in nanoporous materials to H chemically bonded in complex-hydride materials. Insights gained from these studies will be applied toward the design and synthesis of hydrogen-storage materials that meet the following DOE 2017 storage targets:

- Specific energy: 1.8 kWh/kg
- Energy density: 1.3 kWh/L
- Cost: $12/kWh

FY 2014 Accomplishments

- Manuscript published on two alkali metal hydride modifications of hydrazine borane for improved dehydrogenation properties.
- Manuscript published on detailed quasielastic neutron scattering (QENS) study of confinement effects on $LiBH_4$ nanosequestered in both ordered (columnar-pore) carbon frameworks and carbon aerogels.
- Four manuscripts published on the structural modifications, anion and cation dynamics, and cationic conductivity associated with the order-disorder phase transitions in $Li_2B_{12}H_{12}$ and $Na_2B_{12}H_{12}$.
- Manuscript published on the structure and spectroscopy of H_2 adsorbed in a nickel metal-organic framework (MOF).

INTRODUCTION

To obtain the DOE levels of hydrogen storage in a timely manner, it is imperative that trial-and-error testing of materials be avoided. Thus, the focus must be upon

the rational design of new systems. From a thorough understanding of the physics and chemistry that governs the hydrogen-substrate interactions, we will be able to make a more concerted effort to push the frontiers of new materials. The key to improving materials is a detailed understanding of the atomic-scale locations of hydrogen and determining how it gets there and how it gets out. Neutron scattering is perhaps the premier technique for studying hydrogen, and the NIST Center for Neutron Research is currently the leading facility in the U.S. for studying these materials.

APPROACH

NIST provides important materials characterization for DOE-funded, hydrogen storage projects using neutron-scattering measurements to probe the amount, location, bonding states, dynamics, and morphological aspects of (i) molecular hydrogen in carbon-based materials such as polymers, MOFs, and carbonaceous materials such as carbon nanohorns and (ii) atomic hydrogen in a variety of complex hydride materials including those containing boron and nitrogen, as well as their intermediates and by-products. NIST works directly with DOE and other partners that produce novel hydrogen-storage materials to analyze the most promising samples and to help determine and resolve the fundamental issues that need to be addressed.

RESULTS

In collaboration with the University of Maryland, Dalian Institute of Chemical Physics, and Sichuan University, two new alkali metal hydrazidotrihydridoborates, $NaN_2H_3BH_3$ and $KN_2H_3BH_3$, were synthesized via a liquid approach [1]. The crystal structures were determined by X-ray diffraction and corroborated by neutron vibrational spectroscopy (NVS) measurements of the phonon densities of states in conjunction with density functional theory (DFT) calculations (Figure 1). There was a clear correlation between the sizes of the metal cations and their corresponding melting and dehydrogenation temperatures. Upon approaching the melting points, alkali metal hydrazidotrihydridoborates dehydrogenated rapidly in the first step, giving rise to the formation of intermediates that possessed N_2BH_2, N_2BH, and NBH_3 species. Further increases in temperature led to the release of additional H_2 and the formation of N_2BH species. Compared to pristine $N_2H_4BH_3$, the alkali-metal-substituted hydrazidotrihydridoborates showed markedly improved dehydrogenation behavior with no N_2H_4 emission and greatly suppressed NH_3 release.

In collaboration with the University of Maryland and the Institute of Metal Physics-Ekaterinburg, the effect of partial Cl^- anion substitution in $NaBH_4$ on the reorientational dynamics of the BH_4^- anions was investigated by QENS. 1:1 $Na^{11}BH_4$-NaCl solid solutions were made by ball-milling the pure components. The elastic incoherent structure factor

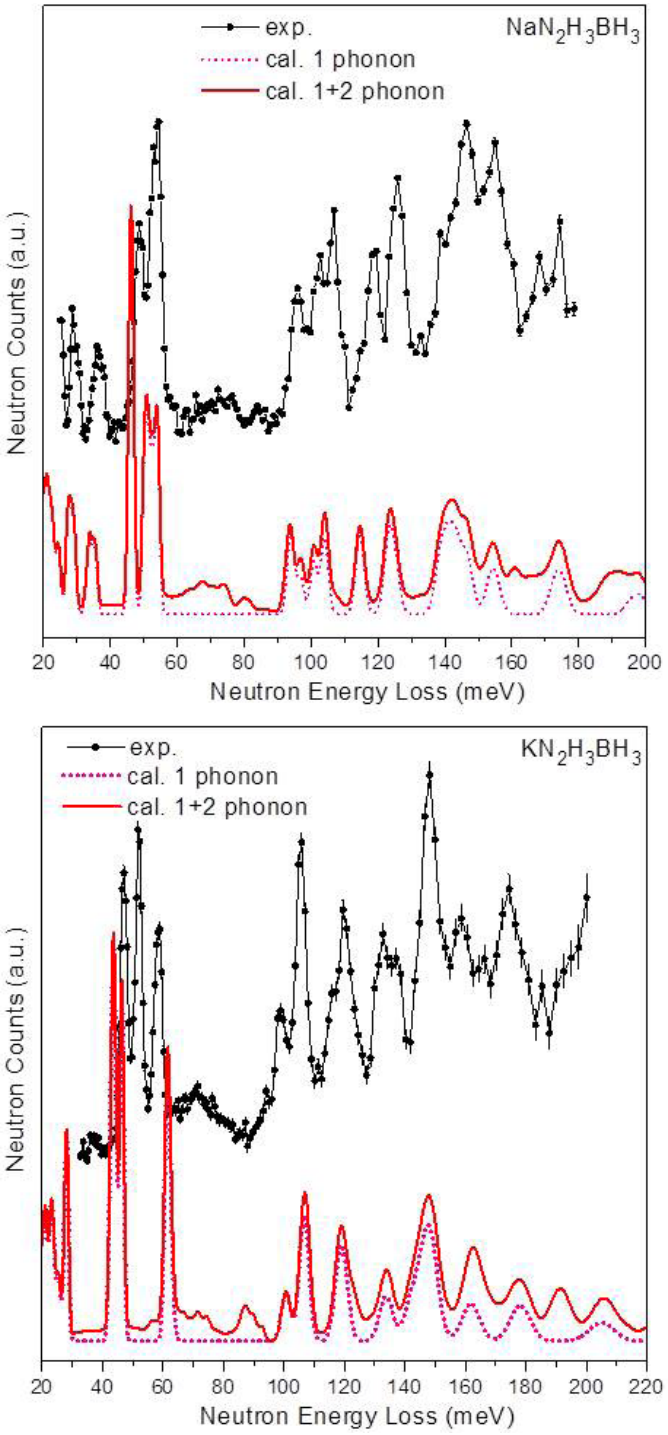

FIGURE 1. The NVS-measured (4 K) and DFT-calculated vibrational spectra for $NaN_2H_3BH_3$ and $KN_2H_3BH_3$ (from Ref. 1).

behavior with neutron momentum transfer Q at 450 K (Figure 2) indicated that the BH_4^- anions in the disordered structure were undergoing reorientational "cubic" tumbling motions such that the four H atoms associated with each B atom were visiting all eight corners of a cube. Since Cl^-

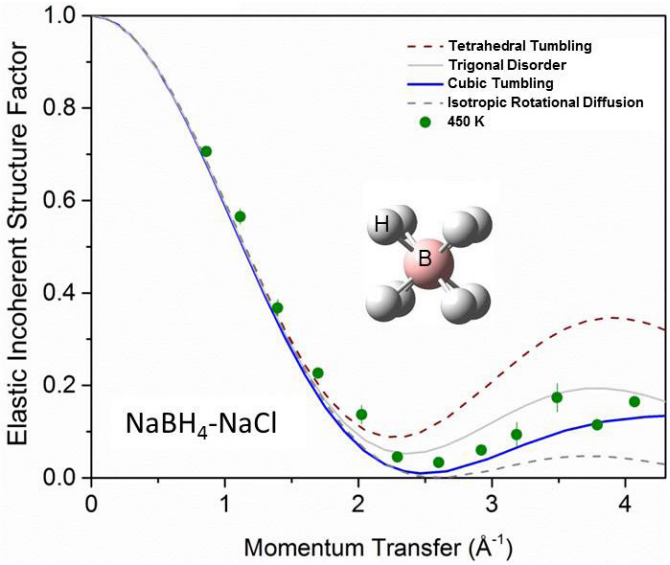

FIGURE 2. EISFs derived from QENS measurements for $NaBH_4$-NaCl at 450 K (green circles) compared with several BH_4^- reorientational jump models. A schematic of BH_4^- disordered cubic site geometry is depicted in the inset.

anions are smaller than BH_4^- anions, the mixed compound had a reduced lattice constant, and thus a smaller lattice volume, to accommodate each BH_4^- anion and lower anion rotational mobility compared with pristine $NaBH_4$. The activation energy for reorientation for $NaBH_4$-NaCl was found to be 114(4) meV which is similar to that observed for $NaBH_4$. Preliminary neutron elastic scattering fixed-window scans indicated that replacing Cl^- with the relatively larger I^- anion results in a BH_4^- rotational mobility surpassing that of both $NaBH_4$-NaCl and $NaBH_4$.

In collaboration with the University of Maryland, GE, Sandia National Laboratories, the Institute of Metal Physics-Ekaterinburg, and Tohoku University, we discovered by X-ray diffraction and neutron powder diffraction that $Li_2B_{12}H_{12}$ and $Na_2B_{12}H_{12}$ undergo phase transitions at ~615 K and 529 K, respectively, upon heating from known low-temperature ordered structures to high-temperature, entropically-driven, highly-disordered cubic structures with orientationally mobile anions and vacancy-rich cation sublattices [2]. These new high-temperature structures have to be considered in any future thermodynamic analyses of Li-B-H and Na-B-H systems. The disordered $Na_2B_{12}H_{12}$ phase (Figure 3) was found to be stable and more amenable to study than the disordered $Li_2B_{12}H_{12}$ phase. Nuclear magnetic resonance (NMR) and QENS studies [2-4] were performed to characterize the Na^+ cation translational mobility and the $B_{12}H_{12}^{2-}$ anion reorientational mobility of the disordered $Na_2B_{12}H_{12}$ phase. Measurements of the ^{23}Na NMR spectra and spin−lattice relaxation rates showed that the transition from the ordered to the disordered phase of $Na_2B_{12}H_{12}$ was accompanied by the onset of fast translational diffusion of the Na^+ cations. Just above the phase transition, the lower limit of the Na^+ jump rate was estimated to be ~2×10^8 s^{-1}, and the corresponding activation energy for Na^+ diffusion was ~410 meV. QENS and NMR measurements also indicated a two-orders-of-magnitude enhancement in $B_{12}H_{12}^{2-}$ anion reorientational mobility upon transitioning to the disordered phase, with a reorientational jump rate on the order of 10^{11} s^{-1}. The predominant mechanism at 580 K appeared to be small-angle, uniaxial reorientational jumps, with the best overall fit to the elastic incoherent structure factor at high temperature being six-fold or greater reorientations around one of the anion C_3 symmetry axes. The average activation energy for reorientation was determined to be about 770(20) meV for the ordered phase and about 260(20) meV for the disordered phase. Subsequent AC impedance measurements [5] (Figure 3) confirmed that disordered $Na_2B_{12}H_{12}$ was superionic, with a conductivity of about 0.1 S cm^{-1} near 550 K, which greatly exceeds that of all other complex-hydride materials to date. This conductivity rivals that of sodium beta alumina, the current commercial electrolyte for Na-ion batteries operating in this temperature region. It is believed that the overly large anions facilitate the high conductivity by providing large intralattice diffusion pathways for the much smaller cations.

In collaboration with the University of Delaware, University of Maryland, Oak Ridge National Laboratory, and University of St. Andrews, the structure of the MOF, Ni_2(dobdc) (dobdc = 2,5-dioxido-1,4-benzenedicarboxylate), as a function of D_2 adsorption was determined by in situ neutron powder diffraction, and the local adsorption potential for hydrogen at each site was probed using NVS [6]. At the lowest loadings, the D_2 molecules were located 2.20(1) Å from the open metal centers. The Ni^{2+} variant showed the shortest D_2-metal distance in the M_2(dobdc) series (M = Mg, Zn, Co, Fe) studied thus far and is consistent with the high initial H_2 adsorption enthalpy of 13.5 kJ mol^{-1}. The secondary adsorption sites were located close to the framework oxygen and carbon, respectively. NVS revealed detailed interactions of the adsorbed para-H_2 with the framework and its response to further H_2 adsorption. The adsorbed H_2 interconverts between ortho- and para-H_2, depending on the sample temperature. The transitions between rotational energy levels were determined for the three adsorption sites, with the transitions shifting slightly with increased adsorption levels.

CONCLUSIONS AND FUTURE DIRECTIONS

- Neutron methods have provided crucial, non-destructive characterization tools for the DOE Hydrogen Storage Program.
- Agreement between NVS and DFT corroborates the recently synthesized $NaN_2H_3BH_3$ and $KN_2H_3BH_3$ structures that were determined by diffraction methods.

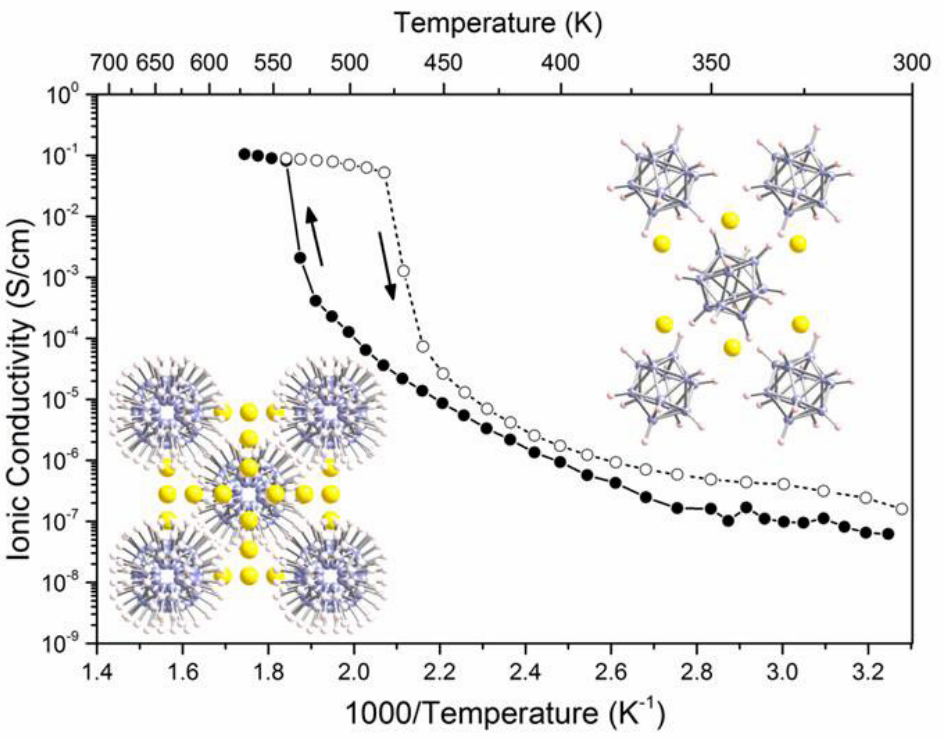

FIGURE 3. Depictions of the low-temperature ordered and high-temperature disordered structures of $Na_2B_{12}H_{12}$ and the corresponding Na^+ conductivity behavior vs. temperature upon heating and cooling. Conductivity hysteresis coincides with the observed order-disorder structural hysteresis (from Ref. 5).

- Compared to $N_2H_4BH_3$, the alkali-metal substituted hydrazidotrihydridoborates display improved dehydrogenation behavior with no N_2H_4 emission and greatly suppressed NH_3 release.
- Neutron-scattering fixed-window scans are shown to be valuable for making relative comparisons of BH_4^- anion rotational mobilities in bulk and halide-substituted $NaBH_4$.
- The cubic tumbling mechanism, where the H atoms jump to the eight corners of a cube, is in best agreement with the QENS data for NaCl-$NaBH_4$ solid solution above room temperature.
- $Li_2B_{12}H_{12}$ and $Na_2B_{12}H_{12}$ undergo order-disorder phase transitions at ~615 K and 529 K, respectively, resulting in orientationally mobile anions and vacancy-rich cation sublattices.
- $Na_2B_{12}H_{12}$ exhibits dramatic superionicity above its order-disorder phase transition, aided by the large mobile anions and the appearance of cation vacancies.
- The Ni^{2+} variant in the MOF M_2(dobdc) series (M = Mg, Zn, Co, Fe) displayed the shortest adsorbed D_2-metal distance (2.20[1] Å) of all studied variants, which is consistent with the high initial H_2 adsorption enthalpy.
- We will start characterization work on new hydrogenated metal silicides ($M_x[SiH_3]_y$).
- We will investigate properties of alkali (A) and alkaline-earth (Ae) metal decahydro-*closo*-decaborates $A_2B_{10}H_{10}$ and $AeB_{10}H_{10}$.
- We will continue to perform neutron-based structural and spectroscopic characterizations of new materials in conjunction with the needs of the DOE-funded projects, including novel bulk and nanoconfined complex hydride materials.

SPECIAL RECOGNITIONS & AWARDS/ PATENTS ISSUED

1. W.S. Tang: Highly Commended Poster Award for "Altering the Structural Properties of $A_2B_{12}H_{12}$ Compounds via Cation and Anion Modifications" at the 14th International Symposium on Metal-Hydrogen Systems: Fundamentals and Applications (MH2014), Manchester, UK.

FY 2014 PUBLICATIONS/PRESENTATIONS

1. C.M. Brown, A.J. Ramirez-Cuesta, J.-H. Her, P.S. Wheatley, and R.E. Morris, "Structure and Spectroscopy of Hydrogen Adsorbed in a Nickel Metal-Organic Framework," Chem. Phys. 427, 3-8 (2013).

2. T.J. Udovic, N. Verdal, J.J. Rush, D.J. De Vries, M.R. Hartman, J.J. Vajo, A.F. Gross, and A.V. Skripov, "Mapping Trends in the Reorientational Mobilities of Tetrahydroborate Anions via Neutron-Scattering Fixed-Window Scans," J. Alloys Compds. 580, S47-S50 (2013).

3. X. Liu, E.H. Majzoub, V. Stavila, R.K. Bhakta, M.D. Allendorf, D.T. Shane, M.S. Conradi, N. Verdal, T.J. Udovic, and S.-J. Hwang, "Probing the Unusual Anion Mobility of $LiBH_4$ Confined in Highly Ordered Nanoporous Carbon Frameworks via Solid State NMR and Quasielastic Neutron Scattering," J. Mater. Chem. A 1, 9935-9941 (2013).

4. N. Verdal, T.J. Udovic, J.J. Rush, X. Liu, E.H. Majzoub, J.J. Vajo, and A.F. Gross, "Dynamical Perturbations of Tetrahydroborate Anions in $LiBH_4$ due to Nanoconfinement in Controlled-pore Carbon Scaffolds," J. Phys. Chem. C 117, 17983-17995 (2013).

5. A.V. Skripov, O.A. Babanova, A.V. Soloninin, V. Stavila, N. Verdal, T.J. Udovic, and J.J. Rush, "Nuclear Magnetic Resonance Study of Atomic Motion in $A_2B_{12}H_{12}$ (A = Na, K, Rb, Cs): Anion Reorientations and Na^+ Mobility," J. Phys. Chem. C 117, 25961-25968 (2013).

6. N. Verdal, J.-H. Her, V. Stavila, A.V. Soloninin, O.A. Babanova, A.V. Skripov, T.J. Udovic, and J.J. Rush, "Complex High-Temperature Phase Transitions in $Li_2B_{12}H_{12}$ and $Na_2B_{12}H_{12}$," J. Solid State Chem. 212, 81-91 (2014).

7. A.V. Skripov, V. Paul-Boncour, T.J. Udovic, and J.J. Rush, "Hydrogen Dynamics in Laves-Phase Hydride $YFe_2H_{2.6}$: Inelastic and Quasielastic Neutron Scattering Studies," J. Alloys Compds. 595, 28-32 (2014).

8. Y.S. Chua, Q. Pei, X. Ju, W. Zhou, T.J. Udovic, G. Wu, Z. Xiong, P. Chen, and H. Wu, "Alkali Metal Hydride Modification on Hydrazine Borane for Improved Dehydrogenation," J. Phys. Chem. C 118, 11244-11251 (2014).

9. N. Verdal, T.J. Udovic, V. Stavila, W.S. Tang, J.J. Rush, and A.V. Skripov, "Anion Reorientations in the Superionic Conducting Phase of $Na_2B_{12}H_{12}$," 118, 17483-17489 (2014).

10. T.J. Udovic, M. Matsuo, A. Unemoto, N. Verdal, V. Stavila, A.V. Skripov, J.J. Rush, H. Takamura, and S.-I. Orimo, "Sodium Superionic Conduction in $Na_2B_{12}H_{12}$," Chem. Commun. 50, 3750-3752 (2014).

11. M.R. Hudson, "*In-situ* Powder Diffraction for Industrial Gas Separations," User Science Lecture, Advanced Photon Source, Argonne National Laboratory, Argonne, IL, May 2013. (invited)

12. H. Wu, "Development of Novel Gas Storage Materials," Dalian Institute of Chemical Physics, Chinese Academy of Sciences, Dalian, China, May 2013. (invited)

13. C.M. Brown "Applications of Neutron Scattering to Understanding Structure and Gas Storage Properties of Metal-Organic Frameworks and Related Materials," American Chemical Society National Meeting, Indianapolis, IN, Aug. 2013. (invited)

14. H. Wu, "Novel Gas Storage Materials and Related Structural Studies," IUPAC 9th International Conference on Novel Materials and Synthesis (NMS-IX), Shanghai, China, Oct. 2013. (invited)

15. Y.S. Chua, Q. Pei, X. Ju, W. Zhou, T.J. Udovic, G. Wu, Z. Xiong, P. Chen, and H. Wu, "Alkali Metal Hydrazinoboranes for Hydrogen Storage," American Chemical Society Spring Meeting, Dallas, TX, Mar. 2014.

16. C.M. Brown, "Gas Adsorption in Microporous Materials," Chemistry Seminar, Drexel University, Philadelphia, PA, May 2014. (invited)

17. T.J. Udovic, C.M. Brown, D.A. Neumann, "Neutron Characterization in Support of the DOE Hydrogen Storage Sub-Program," DOE EERE Annual Merit Review, Washington, DC, Jun. 2014. (invited)

18. H. Wu, "Novel Complex Hydrides for Hydrogen Storage and Related Structural Studies," 14th International Symposium on Metal-Hydrogen Systems: Fundamentals and Applications (MH2014), Manchester, UK, Jul. 2014. (invited)

19. T.J. Udovic, N. Verdal, J.J. Rush, W.S. Tang, A.V. Skripov, and V. Stavila, "Probing Hydroborate Polyanion Reorientations via Quasielastic Neutron Scattering," 14th International Symposium on Metal-Hydrogen Systems: Fundamentals and Applications (MH2014), Manchester, UK, Jul. 2014. (invited)

20. C.M. Brown, "Neutron Studies of Hydrogen Adsorption in Porous Materials," 14th International Symposium on Metal-Hydrogen Systems: Fundamentals and Applications (MH2014), Manchester, UK, Jul. 2014. (invited)

21. S. Orimo, "Cool Hydrides! - Research Topics and Trends in Japan," 14th International Symposium on Metal-Hydrogen Systems: Fundamentals and Applications (MH2014), Manchester, UK, Jul. 2014. (plenary)

22. M. Matsuo, H. Oguchi, A. Unemoto, T. Ikeshoji, H. Takamura, T. Vegge, A. Remhof, A. Borgshulte, A. Züttel, T.J. Udovic, A.V. Skripov, and S. Orimo, "Fast Ionic Conduction in Complex Hydrides," 14th International Symposium on Metal-Hydrogen Systems: Fundamentals and Applications (MH2014), Manchester, UK, Jul. 2014. (invited)

23. A.V. Skripov, "Nuclear Magnetic Resonance Studies of Atomic Motion in Borohydride-Based Materials," 14th International Symposium on Metal-Hydrogen Systems: Fundamentals and Applications (MH2014), Manchester, UK, Jul. 2014. (invited)

24. W.S. Tang, T.J. Udovic, N. Verdal, J.J. Rush, A.V. Skripov, V. Stavila, M. Matsuo, and S. Orimo, "Altering the Structural Properties of $A_2B_{12}H_{12}$ Compounds via Cation and Anion Modifications," 14th International Symposium on Metal-Hydrogen Systems: Fundamentals and Applications (MH2014), Manchester, UK, Jul. 2014.

25. T.J. Udovic, "Sodium Superionic Conduction Discovered in Disordered Sodium Borohydride Compounds," IEA HIA Expert Meeting of Task 32 – Hydrogen-Based Energy Storage, Manchester, UK, Jul. 2014. (invited)

REFERENCES

1. Y.S. Chua *et al.*, J. Phys. Chem. C **118**, 11244 (2014).

2. N. Verdal *et al.*, J. Solid State Chem. **212**, 81 (2014).

3. A.V. Skripov *et al.*, J. Phys. Chem. C **117**, 25961 (2013).

4. N.Verdal *et al.*, J. Phys. Chem. C **118**, 17483 (2014).

5. T.J. Udovic *et al.*, Chem. Commun. **50**, 3750 (2014).

6. C.M. Brown *et al.*, Chem. Phys. **427**, 3 (2013).

IV.E.1 Novel Carbon(C)-Boron(B)-Nitrogen(N)-Containing H_2 Storage Materials

Shih-Yuan Liu
Boston College
Department of Chemistry
2609 Beacon Street
Chestnut Hill, MA 02467
Phone: (617) 552-8543
Email: shihyuan.liu@bc.edu

In collaboration with

- Dr. Frank Tsung, Boston College
- Dr. Tom Autrey, Dr. Abhi Karkamkar, Dr. Mark Bowden, Dr. Sean Whittemore and Dr. Kriston Brooks, Pacific Northwest National Laboratory
- Dr. David Dixon, The University of Alabama
- Dr. Paul Osenar, Dr. Jim Sisco, Protonex Technology Corporation

DOE Managers
Grace Ordaz
Phone: (202) 586-8350
Email: Grace.Ordaz@ee.doe.gov
Katie Randolph
Phone: (720) 356-1759
Email: Katie.Randolph@ee.doe.gov

Contract Number: DE-EE0005658

Project Start Date: March 5, 2012
Project End Date: August 14, 2015

Overall Objectives

Develop new carbon-boron-nitrogen (CBN)-based chemical hydrogen storage materials that have the potential to meet the DOE technical targets for vehicular and non-automotive applications

Fiscal Year (FY) 2014 Objectives

- Continue to optimize fuel blends with respect to capacity, melting point, and stability
- Synthesize compound **E** and its derivatives
- Continue the potential energy surface calculations of the various pathways of H_2 desorption from CBN compounds

Technical Barriers

This project addresses the following technical barriers from the Hydrogen Storage section of the Fuel Cell Technologies Office Multi-Year Research, Development, and Demonstration Plan:

(A) System Weight and Volume

(C) Efficiency

(E) Charging/Discharging Rates

Technical Targets

This project is developing and characterizing new CBN materials for hydrogen storage. Insights gained from these studies will be applied toward the design and synthesis of hydrogen storage materials that meet the following DOE 2017 hydrogen storage system targets:

- Specific energy: 1.8 kWh/kg (5.5 wt%)
- Energy density: 1.3 kWh/L (4.0 vol%)

FY 2014 Accomplishments

- Investigated liquid fuel blends of compound **B** and ammonia borane (AB) with different ratios to maximize hydrogen release while minimizing borazine formation
- Full characterization of compound **B** regarding thermal stability
- Synthesized a series of compound **E** derivatives
- Calculated important thermodynamic and kinetic parameters and molecular properties to help develop an understanding of the hydrogen desorption mechanism

INTRODUCTION

Approaches to store H_2 in chemical bonds provide a means for attaining high energy densities. Molecular complexes containing protic and hydridic hydrogen such as AB provide between 8 to 16 wt% H_2 at acceptable temperatures in a kinetically controlled decomposition. AB shows promise to meet a number of important technological targets such as high volumetric and gravimetric density of H_2, fast kinetics, thermal stability, facile synthesis at large scale and safe handling under atmospheric conditions. Some of the challenges involving AB include volatile impurities (e.g., ammonia, diborane, borazine) and the economics of spent fuel regeneration [1-4].

This project is developing hydrogen storage materials that contain the element carbon in addition to boron and nitrogen. The inclusion of carbon can be advantageous for

developing chemical H_2 storage materials that are structurally well defined, thus have good potential to be liquid phase, exhibit thermodynamic properties conducive to reversibility, and demonstrate good storage capacities.

APPROACH

This project is developing new CBN H_2 storage materials that have the potential to meet the DOE targets for motive and non-motive applications. Specifically, we are focusing on on three basic systems, (1) liquid-phase systems that release H_2 in a well-defined and high-yield fashion, minimizing the formation of NH_3 and $B_3N_3H_6$; (2) reversible storage systems that could potentially be regenerated onboard; and (3) high H_2-content storage systems that can be used in slurries and regenerated off-board (Figure 1). Computational chemistry studies help direct our research. Finally, we will demonstrate the developed material as a fuel in a fuel cell device. These new materials are prepared and characterized by our interdisciplinary team comprised of Boston College, The University of Alabama, Pacific Northwest National Laboratory, and Protonex Technology Corporation (Southborough, MA, a small business fuel cell manufacturer). Note: This project has moved from the University of Oregon to Boston College at the end of FY 2013.

RESULTS

Characterization of the Liquid Carrier B and its Fuel Blends

In FY 2013, we performed additional characterization studies of compound **B** that are relevant to H_2 storage applications. This year, we investigated liquid fuel blends of compound **B** and AB to maximize hydrogen while minimizing borazine content. We determined that the solubility of AB in **B** is approximately 16 mol% (**B**:AB ~5:1). Consequently, a ratio of **B**:AB (2:1) is a suspension at room temperature that, however, has relatively low viscosity. Upon dehydrogenation, the product is a clear liquid at room temperature.

We have investigated different ratios of compound **B** and AB to determine how fuel composition affects borazine production. We measured borazine released at 110°C with blends of **B** and AB**,** ranging from 1:1 to 4:1 molar ratios. We synthesized pure borazine and calibrated its residual gas analysis traces by comparing the signal intensity with the reported vapor pressure at different temperatures. The concentration of borazine drops substantially with increasing fraction of **B**, as shown in Figure 2a. The results are compared to borazine formation of AB in tetraglyme solution. The 3:1 and 4:1 **B**:AB blends reduced the concentration of borazine by factors of 21 and 46, respectively. The presence of a catalyst allowed hydrogen release at a lower temperature and resulted in a dramatic

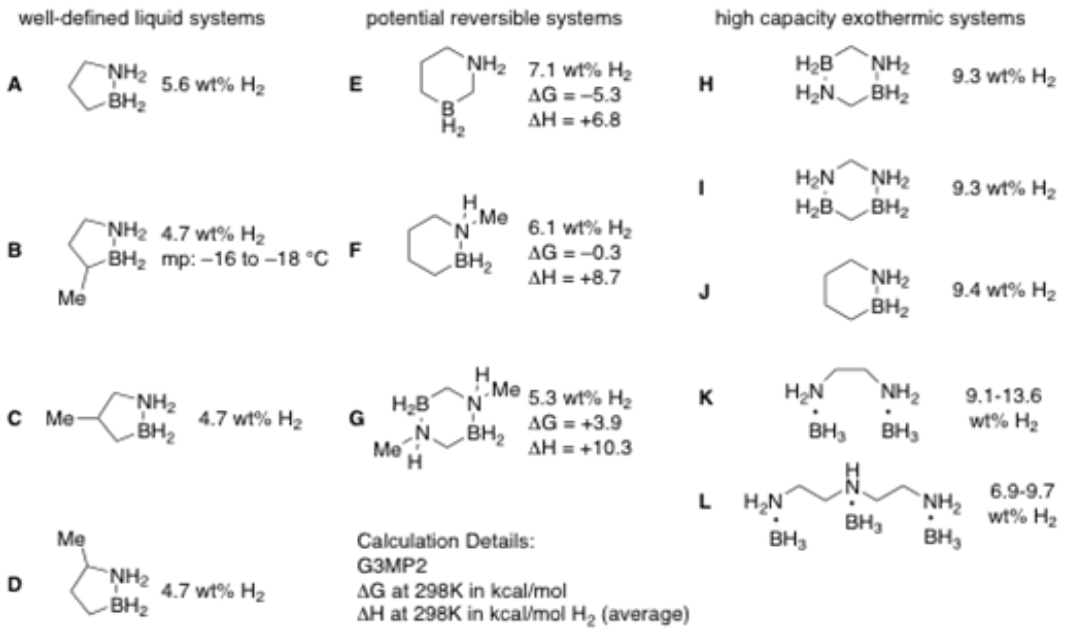

FIGURE 1. Selected Synthetic Targets and their Potential Storage Capacities and Predicted Thermodynamic Parameters

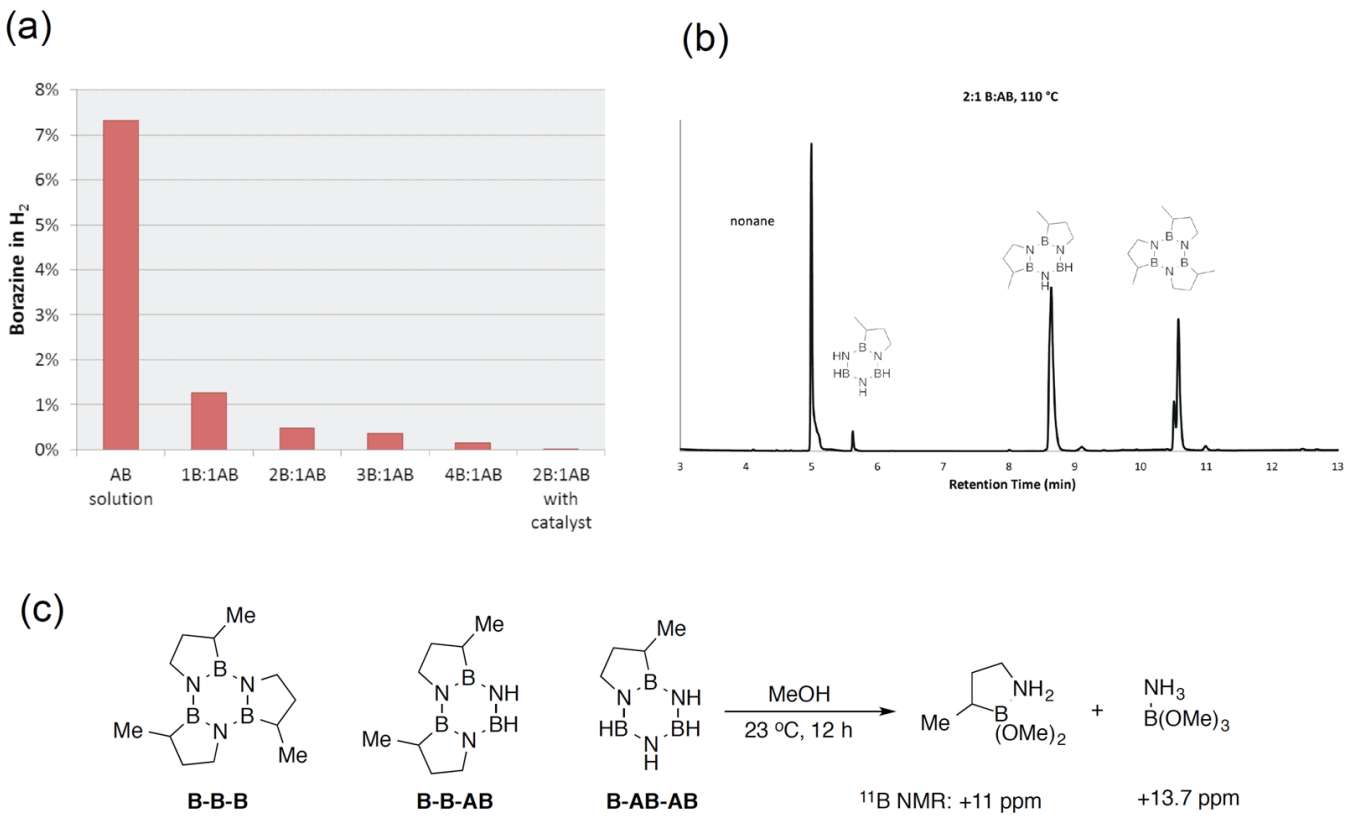

FIGURE 2. (a) Concentration of borazine in gas stream from **B**:AB blends measured by residual gas analysis, compared to a solution of AB in tetraglyme. Dehydrogenation was carried out at 110°C, except for the catalyzed (Pt/Ni on C) sample, which was conducted 80°C. (b) GC/MS trace of the dehydrogenation products at 110°C of a **B**:AB (2:1) blend. The two signals for the B trimer at ca. 10.6 minutes originate from the different diastereomers. (c) Methanolysis of the spent fuel mixture.

reduction in borazine concentration to 0.01%, 670 times lower than the corresponding AB in tetraglyme sample.

The ^{11}B nuclear magnetic resonance (NMR) spectra of the dehydrogenation products showed signals at +31 ppm and +41 ppm, consistent with the formation of 6-membered B-N rings. This could arise from a mixture of separate molecules of borazine and the trimeric product from dehydrogenation of **B**, or from individual molecules containing fragments of both of these compounds. Gas chromatography/mass spectrometry (GC/MS) results demonstrated that the spent fuel products contained mixed trimers. Figure 2b shows the GC/MS trace obtained after dehydrogenation of a **B**:AB (2:1) blend at 110°C. The largest signal, at a retention time of ca. 8.7 min, had a mass corresponding to a trimer containing **B-B-**AB fragments. The **B-B-B** and **B-AB-**AB trimers were also observed. The relative quantities of these trimers varied in the expected way with different starting compositions in the fuel blend, suggesting that the products were a statistical mixture of the possible trimeric compounds.

With respect to regeneration of spent fuel, we have shown previously that the **B** trimer can be digested in methanol to protonate the N atom and form a dimethoxy borate ester [5]. The ester can be subsequently treated with metal hydrides to regenerate compound **B**. Our initial experiments suggest that this regeneration scheme would also work for the mixed trimeric dehydrogenation products identified above. ^{11}B NMR spectra shown that the spent fuel is completely reacted after methanolysis. The borate ester of compound **B** is identified by the resonance at +11 ppm, and the resonance at +13.7 ppm is believed to arise from $NH_3B(OMe)_3$ (Figure 2c). Reduction of this mixture is therefore likely to regenerate the mixture of **B** and AB.

Thermal Stability of Compound B and the Spent Fuel

We measured the thermal stability of compound **B** at 50°C using a gas burette. Figure 3a (red trace) shows that compound **B** evolves gas at this temperature, at an initial rate of ca. 0.3 equivalents H_2/day. The rate drops with time, reaching a plateau when 1 equivalent of H_2 was released after approximately one week. The second equivalent of hydrogen is not released at 50°C. We also recorded the ^{11}B NMR spectrum of the product after one week and found the formation of a species consistent with a cyclodiborazane dimer which has ca. 2.3 wt% H_2 capacity. We also measured

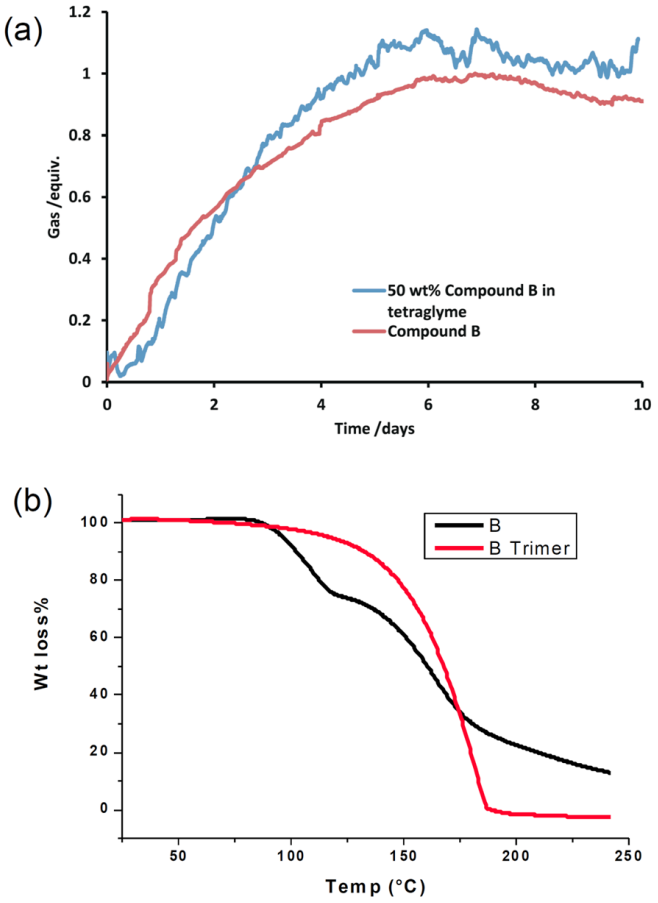

FIGURE 3. (a) Gas evolution from **B** with and without tetraglyme at 50°C, measured by gas burette. (b) TGA traces for compound **B** (black) and the spent fuel trimer of compound B (red).

the stability of compound **B** in tetraglyme solution (50 wt%). Despite the dilution, the rate of gas evolution (Figure 3a, blue trace) was not significantly changed indicating that tetraglyme is not effective at stabilizing compound **B**.

The thermal stability of compound **B** and its spent fuel was also measured by thermogravimetric analysis (TGA), at a heating rate of 1°C/min (Figure 3b, black trace). The loss of 4.7 wt% H_2 at ca. 100°C coincided with an additional weight loss of ca. 20 wt%, probably due to the high vapor pressure of compound **B**. Above 120°C, a more substantial weight loss took place such that nearly all the sample had volatized by 180°C. The weight loss above 120°C is attributed to the vaporization of the spent fuel trimer, confirmed by TGA of an authentic trimer sample (Figure 3b, red trace).

We have made a No-Go decision on compound **B** blends due to the thermal stability issue. Current efforts are geared toward understanding the factors that improve thermal stability.

Compound E and its Derivatives

We attempted to synthesize compound **E** and its derivatives, which may activate and release H_2 reversibly via the frustrated Lewis pair-type reactivity. For the parent compound **E**, however, there is a potential for dimerization after dehydrogenation, which needs to be be prevented (potentially by introducing bulky groups at boron and/or nitrogen positions). Thus, we designed compounds **3** and **6** (Figure 4) for that purpose. The synthesis of the key intermediate, compound **1**, is straightforward by using the protocol reported by our group in 2011 [6].

Replacement of the B-diisopropylamino group in compound **1** with the acetoxy group followed by treatment with lithium aluminum tetrahydride ($LiAlH_4$) yielded compound **2**. Hydrogenation of compound **2** in the presence of 10 mol% of Pd/C cleanly transformed **2** into **3**, which however, formed dimer **4** and unidentified oligomers instantly. Accordingly, compound **6**, which has a bulkier substituent at boron, was proposed as a better candidate. Following a similar synthetic route, compound **6** could potentially be obtained through hydrogenation of compound **5**. In fact, the reduction of compound **5** with H_2 (45 psi) was accomplished efficiently in the presence of 20 mol% of Pd/C as catalyst at 100°C for 14 h. However, both ^{11}B and ^{1}H NMR indicated the formation of dimer **7** instead of the expected product **6**, suggesting an even bulkier group is needed on either boron or nitrogen to prevent the dimerization. Consequently, we proposed compound **9**, which has the 2,4,6-triisopropylphenyl (Tip) group on boron. However, all attempts to place the Tip group on the boron center to prepare compound **8** through established protocols were unsuccessful, most likely due to the significant steric hindrance between the two reagents (Figure 4).

We have made a No-Go decision on compound **E** because we were only able to partially hydrogenate its spent fuel, and dimer formation prevents its full potential.

Investigation of CBN Systems with Computational Chemistry

We have continued to perform mechanistic studies of H_2 desorption from CBN materials using computational chemistry. A range of potential energy surfaces for H_2 release and dimer and trimer formation have been obtained at a reliable correlated molecular orbital theory G3MP2 level. In addition, we calculated molecular properties of various CBN materials. The ^{11}B NMR chemical shifts (Figure 5) for a range of compounds containing B-N bonds were calculated, and the results are being used to aid the experimental identification of intermediates in dehydrogenation processes. Thermodynamic properties of a broad range of compounds including spent fuel derivatives have been calculated in the gas phase and in the liquid phase together with boiling points.

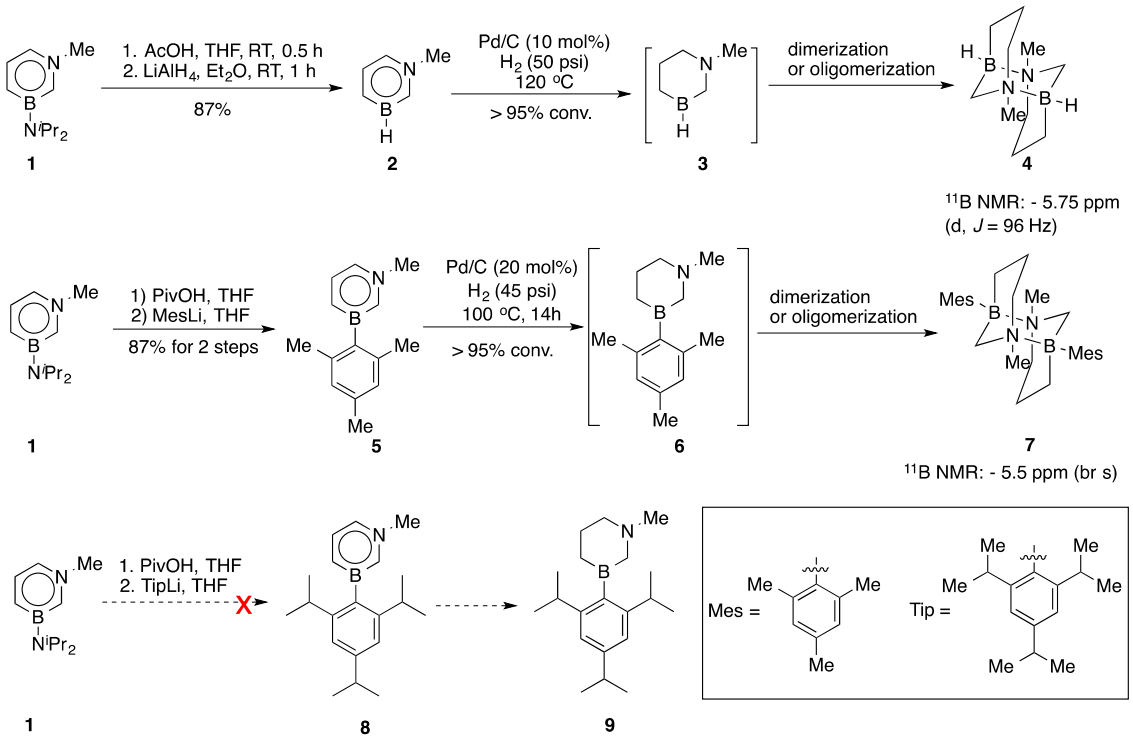

FIGURE 4. Attempts to Synthesize Compound **E** Derivatives as Reversible Hydrogen Storage Materials

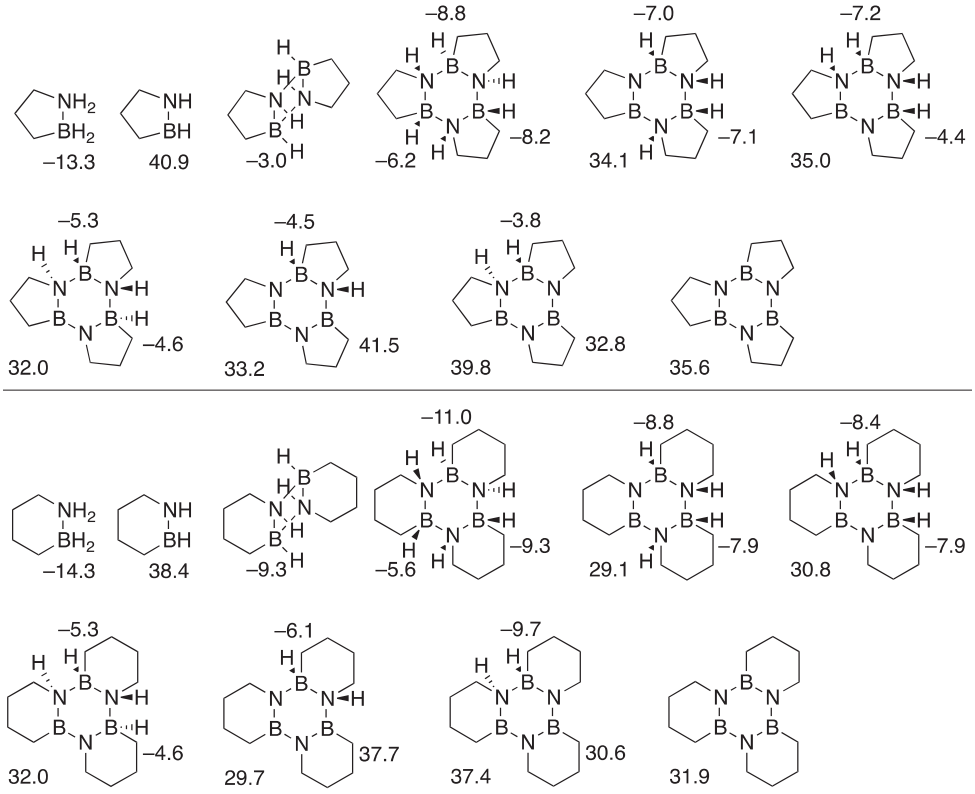

FIGURE 5. Predicted ^{11}B NMR Chemical Shifts for Select Compounds in PPM (against BH_3•THF Standard)

CONCLUSIONS AND FUTURE DIRECTIONS

This year, we investigated liquid fuel blends of compound **B** and AB to maximize hydrogen release while minimizing borazine formation. Characterization of compound **B** with respect to thermal stability was also carried out. We were able to synthesize a series of compound **E** derivatives, however dimerization or oligomerization of the partially hydrogenated compounds prevented the full potential of this class of compounds. Additionally, we calculated molecular properties such as ^{11}B NMR chemical shifts which are helpful in aiding the experimental identification of intermediates in dehydrogenation processes. Our future goals are to:

- Achieve hydrogen desorption from the carbon portion of CBN
- Determine the mechanism for H_2 desorption for CBN materials by both experiment and computation
- Further characterize and determine thermodynamics and kinetics for the desorption of compound **H**
- Achieve 4-5 equivalent of H_2 release for compound **H** (9.3 wt% - 11.6 wt%)
- Develop thermally stable CBN compounds as H_2 storage material
- Continue theory support for property predictions including thermodynamics and spectroscopy, and finalize the desorption mechanism of CBN compounds

SPECIAL RECOGNITIONS & AWARDS/ PATENTS ISSUED

1. D.A. Dixon named in ACS Fellow at the 2013 Fall American Chemical Society National Meeting, Indianapolis, IN

FY 2013 PUBLICATIONS/PRESENTATIONS

1. "Development of a Single-Component Liquid-Phase Hydrogen Storage Material"; Singapore, 15th Asian Chemical Congress 2013, Asia America Chemical Symposium on "Advanced Materials, August **2013**. (Presentation, Liu)

2. "An Extremely Stable Chemical Hydrogen Storage Material: Synthesis, Structure and Potential Application of 1,4-Diazonia-2,5-Diboratacyclohexanes"; Newark NJ, *Boron in the Americas XIV*, June 16, 2014. (poster presentation: Gang Chen, Lev Zakharov, Shih-Yuan Liu)

3. "Novel Carbon(C)-Boron(B)-Nitrogen(N)-Containing H_2 Storage Materials "; Washington, DC, DOE Annual Merit Review, June 17, **2014**. (Presentation, Tom Autrey)

4. "Exploring the use of carbon, nitrogen, and boron containing heterocycles in liquid hydrogen storage"; Dallas TX, 247th American Chemical Society National Meeting & Exposition, March 16, **2014**. (Presentation, Sean Whittemore, PNNL)

REFERENCES

1. McWhorter, S.C. Read, G. Ordaz, N. Stetson. "Materials-Based Hydrogen Storage: Attributes for Near-Term, Early Market PEM Fuel Cells" *Current Opin. Sol. State Mat. Sci.* **2011**, *15*, 29.

2. Staubitz, A.; Robertson, A.P.; Manners, I. "Ammonia-borane and related compounds as dihydrogen sources" *Chem. Rev.* **2010**, *110*, 4079.

3. Aardahl, C.L.; Rassat, D. "Overview of systems considerations for on-board chemical hydrogen storage" *Int. J. Hydrogen. Energy.* **2009**, *34*, 6676.

4. Sutton, A.D.; Burrell, A.K.; Dixon, D.A.; Garner, III, E.B.; Gordon, J.C.; Nakagawa, T.; Ott, K.C.; Robinson, J.P.; Vasiliu, M. "Regeneration of Ammonia Borane Spent Fuel by Direct Reaction with Hydrazine and Liquid Ammonia" *Science,* **2011**, *331*, 1426.

5. Luo, W.; Campbell, P.G.; Zakharov, L.N.; Liu, S.-Y. "A Single-Component Liquid-Phase Hydrogen Storage Material"*J. Am. Chem. Soc.* **2011**, *133*, 19326–19329.

6. Xu, S.; Zakharov, L.N.; Liu, S.-Y. "A 1,3-Dihydro-1,3-azaborine Debuts" *J. Am. Chem. Soc.* **2011**, *133*, 20152.

IV.E.2 Aluminum Hydride: the Organic-Metallic Approach

James Wegrzyn (Primary Contact), Chengbao Ni, Wei Min Zhou
Brookhaven National Laboratory (BNL)
Building 815
Upton, NY 11973
Phone: (631) 344-7917
Email: jwegrzyn@bnl.gov

DOE Managers
Ned Stetson
Phone: (202) 586-9995
Email: Ned.Stetson@ee.doe.gov
Channing Ahn
Phone: (202) 586-9490
Email: Channing.Ahn@ee.doe.gov

Project Start Date: October 1, 2011
Project End Date: September 30, 2014

Overall Objectives

Develop onboard vehicle storage systems using aluminum hydride that meets all of DOE's targets for the proton exchange membrane fuel cell vehicle.

- Produce aluminum hydride material with a hydrogen gravimetric storage capacity greater than 9.7% (kg-H_2/kg) and volumetric storage capacity of (0.13 kg-H_2/L).
- Identifying solvent substitutions in the chemical synthesis of aluminum hydride.

Fiscal Year (FY) 2014 Objectives

Develop practical and economical processes for regenerating aluminum hydride.

Technical Barriers

This project addresses the following technical barriers from the Hydrogen Storage section of the Fuel Cell Technologies Office Multi-Year Research, Development, and Demonstration Plan:

(A) System Weight and Volume

(B) System Cost

(C) Efficiency

(Q) Regeneration Processes

Technical Targets

Table 1 is a listing of the 2015 EERE hydrogen storage targets along with BNL's current aluminum hydride project status. The well-to-wheels efficiency listed in the table under the column for Status was taken from an independent analysis by Argonne National Laboratory on the alane adduct (AlH_3:triethylamine) storage system. The 0.0582 gravimetric storage parameter listed in Table 1 was a measured value obtained by decomposing 60-wt% alane slurries. The slurries consisted of aluminum hydride particles having a hydrogen content of 9.7 wt% that were suspended in liquid glycol. The gravimetric storage parameter was hydrogen material weight only, and did not take into account the balance of plant weight.

TABLE 1. Progress in Meeting Technical Hydrogen Storage Targets

Storage Parameter	Units	Target	Status
Gravimetric	wt% H_2	0.055	0.0582
Volumetric	kg-H_2/L	0.040	0.070
Fuel Flow Rate (temperature)	(g/s)/kW °C	0.02 80	0.02 80
Well-to-Wheels Efficiency	kW-H_2/kW	60%	>55%
Refueling Time	min	3.3	To be determined

FY 2014 Accomplishments

- The chemical synthesis of the alane adduct (2-MeTHF:AlH_3) by directly reacting γ-AlH_3 in a solution of 2-MeTHF.
- Recovery of donor-free alpha aluminum hydride in high yields by combining vacuum distillation with thermal drying methods, starting with a solution of 2-MeTHF:AlH_3.

✧ ✧ ✧ ✧ ✧

INTRODUCTION

Past research on developing hydrogen storage materials for proton exchange membrane fuel cells have focused primarily on stable-reversible metal hydrides. However all reversible metal hydrides with high hydrogen content also have reaction enthalpies greater than 30 kJ/H_2-mol. Therefore they require operating temperatures greater than 150°C when delivering hydrogen at acceptable fueling rates (>0.02 g H_2/s/kW). Kinetically stabilized (metastable) hydrides, on the other hand, represent a class of hydrogen storage materials receiving much less attention. This lack of attention, placed on metastable hydrides, can be attributed to the technical and cost challenges of achieving chemical

reversibility. However, if the regeneration-reversibility problem could be solved, metastable hydrides would have clear hydrogen delivery advantages over more stable reversible metal hydrides. Of the many metastable hydrides, aluminum hydride is of interest because its volumetric hydrogen density of 148 g H_2/L is twice that of liquid hydrogen, and its gravimetric hydrogen density exceeds 10 wt%. Aluminum hydride also exhibits a low heat of reaction (7 kJ/mol H_2) and has demonstrated acceptable hydrogen delivery rates at temperatures much less than 100°C. Since aluminum hydride is not thermodynamically but instead kinetically stable, previous studies was focused mainly on stabilizing the material (tailoring particle size and coatings) to extend its shelf life from months to decades. Figure 1 shows four electron microscope slides of aluminum hydride. These samples have been prepared by either a wet or dry synthesis using diethyl ether as the solvent. The dry method of making aluminum hydride results in nanometer size particles, and the wet crystal growth procedure yields micron size particles. Micron-size particles are preferred over the nanometer size material. Shown in Figure 1 are micron size donor free aluminum hydride particles produced by DOW, ATK and BNL by wet crystal growth in a diethyl ether-toluene mixture. In FY 2014 the work focuses on investigating various solvent substitutions for replacing the use of diethyl ether as the solvent in the synthesis of donor free aluminum hydride.

APPROACH

The main challenge of using alane as a storage medium is finding methods for the cost- and energy-effective hydrogenation of aluminum back to donor-free AlH_3. Several synthetic methods that include reaction of $AlCl_3$ with alkali alanates, electrochemical synthesis from $LiAlH_4$ and $NaAlH_4$, and direct hydrogenation of Al metal all involve either expensive materials or very high H_2 pressures. All these methods for producing materials are very challenging when manufacturing aluminum hydride on a large commercial scale. In addressing this challenge, work at Brookhaven has shown a three-step alane regeneration pathway. This regeneration procedure involves hydrogenating titanium catalyzed aluminum metal under moderate hydrogen pressure using tertiary amines to form various amine:alane adducts in diethyl ether and tetrahydrofuran (THF) solvents. The approach for FY 2014 is to further improve the synthesis of donor free aluminum hydride by replacing the use of diethyl ether or THF solvent/electrolyte with 2-MeTHF.

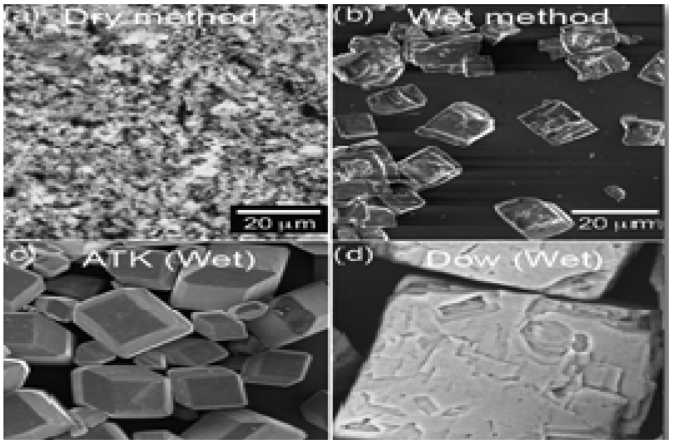

FIGURE 1. Figure 1shows four electron microscope pictures of donor-free AlH_3; a) dry BNL, b) wet BNL, c) wet ATK, d) wet DOW. The wet samples are from crystal growth, dry samples are from vacuum distillation and thermal drying.

RESULTS

Alane formation, using the organo-metallic approach, requires the use of aprotic solvents. In past studies we have exclusively used either THF or diethyl ether as the aprotic solvents of choice. This year we have explored the advantages of using of 2-MeTHF as a replacement solvent for THF and/or Et_2O. The solvent properties of 2-MeTHF is between THF and ET_2O in solvent polarity and Lewis base strength. Table 2 lists these solvent properties [1].

TABLE 2. Solvent Properties

Property	MeTHF	THF	ET_2O
Dielectric constant	6.97	7.5	4.42
Dipole moment, Debye	1.38	1.69	1.11
Water solubility, g/100g	4	miscible	1.2
Hildebrand parameter	16.9	18.7	15.5
Solvation energy, kcal/mol	0.6	0	2.3
Donor number	18	20.5	19.2

Attractive features of 2-MeTHF are that it is available in bulk and derivable from renewable resources. Another important feature is its solubility decreases with increasing temperature. This fact allows for a 70% reduction in energy requirements for drying 2-MeTHF compared to THF. It also has received DOE approval as an additive to gasoline. To our knowledge, 2-MeTHF:Alane is a newly synthesized compound whose properties are now being tabulated at BNL. However the alane adduct (THF:Alane) has been previously studied [2], and its crystal structures and infrared spectrum are available in the open literature. However, there appears to be no consistent terminology for alane adducts. Figure 2 shows the three accepted structures for alane adducts. They are referred to as 1:1 (for both Structures I and II) and the 1:2 bis-compounds (Structure III). For THF:Alane the 1:2 bis-compound is formed when THF is in excess. As the excess THF is removed the 1:2 bis-compound is converted to the 1:1 dimer compound. Some confusion arises because the 1:1 compound has two types of structures (I and II).

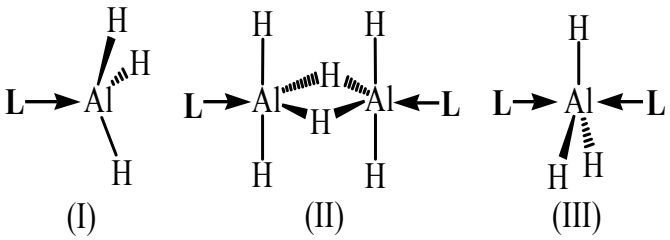

FIGURE 2. Figure 2 shows the three structure types of mono-dentate Lewis base alane compounds; (I) mono, (II) dimer, (III) bis.

To avoid this confusion we prefer to discuss the Fourier transform infrared spectrum for alane compound in terms of either terminal or bridging hydrogen bonds. The Type III bis-compound has three terminal hydrogen bonds and an absorption peak at 1727 wavenumber, while the Type II dimer compound having two bridging hydrogen bonds and an absorption peak at 1803 wavenumber. This year work has been towards evaluating 2-MeTHF as the adduct in forming 2-MeTHF:Alane, and comparing its structure and properties against other ether adducts such as; THF:Alane and Et_2O:Alane. Figure 3 is a section of the FTIR spectrum for 2-MeTHF:Alane. The spectrum shows two absorption peaks at wavenumbers 1727 and 1803. These peaks overlap with the THF:Alane peaks, and confirms that 2-MeTHF:Alane compound has similar structures as THF:Alane. These two structures are the hydrogen bridging dimer-compound and a bis-compound consisting of three terminal hydrogen bonds. Figure 4 is the X-ray diffraction spectrum of donor-free aluminum hydride by recovery from 2-MeTHF:Alane.

CONCLUSIONS AND FUTURE DIRECTIONS

The result of this year study on the properties of 2-MeTHF identified its usefulness both as a solvent and an electrolyte in the synthesis of donor-free aluminum hydride. Future work will investigate the conditions for producing micron size donor free aluminum hydride by the crystal growth method in a saturated 2-MeTHF:Alane/Toluene mixed solution. Also during this year the research application has shifted to portable power because of the selection of compressed hydrogen storage as the fuel cell vehicle storage system of choice. The future direction of this work therefore will address a different set of targets than those associated with hydrogen storage (Table 1) for the fuel cell vehicle. Instead, the new challenge is developing aluminum hydride storage systems that meets DOE's 2015 hydrogen cost target of \$6.7/g-H_2 (primary) and \$33/g-H_2 (rechargeable) for medium portable power applications.

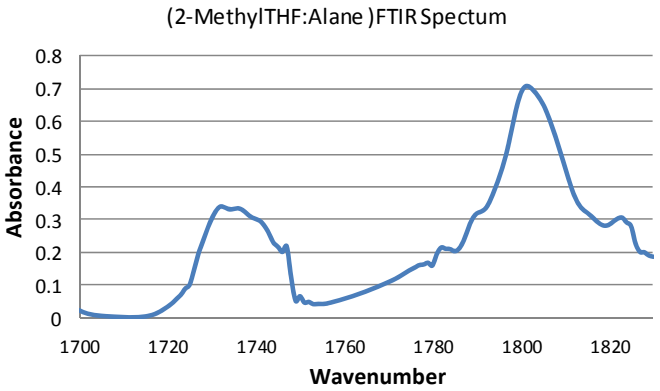

FIGURE 3. Figure 3 is the Fourier transform infrared spectrum of 2-MeTHF:Alane showing the 1727 wavenumber peak for the bis-compound and the 1803 wavenumber for the mono or dimer compound.

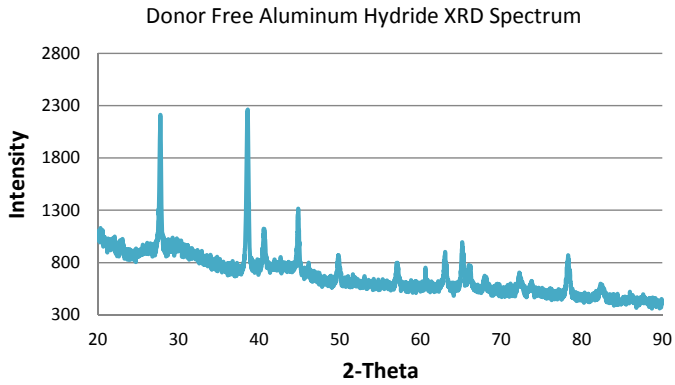

FIGURE 4. Figure 4 is the X-ray diffraction spectrum of donor free alane recovered from 2-MeTHF:Alane.

FY 2014 PUBLICATIONS/PRESENTATIONS

1. Ni, Chengbao; Yang L.; 'Reaction pathways and roles of N-Alkylmorphine in amine-alane transamination: A mechanistic study', *Int. J Hydrogen Energy*, March (2014), p 5003.

REFERENCES

1. Aycock, D. F., *Organic Processes R&D*, Vol 11, 2007.

2. I.B. Gorrell. *et. al*., *J. Chem. Soc., Chem. Commun.*, 1993.

IV.E.3 Electrochemical Reversible Formation of Alane

Ragaiy Zidan (Primary Contact), Joe Teprovich, Patrick Ward, Scott Greenway
Savannah River National Laboratory (SRNL)
999-2W Room 121
Savannah River Site
Aiken, SC 29808
Phone: (803) 646-8876
Email: ragaiy.zidan@srnl.doe.gov

DOE Managers
Ned Stetson
Phone: (202) 586-9995
Email: Ned.Stetson@ee.doe.gov
Channing Ahn
Phone: (202) 586-9490
Email: Channing.Ahn@ee.doe.gov

Project Start Date: October 1, 2011
Project End Date: Project continuation and direction determined annually by DOE

Overall Objectives

- Develop methods of alane (AlH_3) production and regeneration that lower the cost of alane production to less than $10/kg
- Demonstrate and characterize alane production system that lower the cost of alane production with the lowest possible capital and operating costs
- Identify and quantify fundamental properties of alane production chemistry and physics that will lead to improved design and modeling of systems for alane production and use

Fiscal Year (FY) 2014 Objectives

- Demonstrate improved synthesis of alane using the dry method, and identify improved reaction conditions for improved yield and crystal size.
- Demonstrate $NaAlH_4$ electrolyte recycling with a reaction yield above 70% in a system where at least 5 g of $NaAlH_4$ can be produced.
- Synthesis of AlH_3 in a divided cell with an electrolyte containing $NaAlH_4$. Synthesis will produce at least 1 g of AlH_3 that can be isolated and products at the sodium electrode will be characterized to demonstrate the potential for electrolyte recycling.
- $NaAlH_4$ and $LiAlH_4$ electrolyte recycling. Identification of low-cost catalyst formulations and catalyst loadings necessary to achieve yields above 80%.

Technical Barriers

This project addresses the following technical barriers from the Hydrogen Storage section of the Fuel Cell Technologies Office Multi-Year Research, Development, and Demonstration Plan:

(A) System Weight and Volume

(B) System Cost

(C) Efficiency

(Q) Regeneration Processes

Technical Targets

In this project studies are being conducted to lower cost and improve efficiency of the electrochemical method to form AlH_3. This material has the potential to meet long-term and near-term targets for automotive and portable power applications [1,2]. The research performed as part of this contract is equally applicable to both areas.

- By 2015, develop and verify a single-use hydrogen storage system for portable power applications achieving 0.7 kWh/kg system (2.0 wt% hydrogen) and 1.0 kWh/L system (0.030 kg hydrogen/L) at a cost of $0.09/Whnet ($3/g H_2 stored).
- By 2017, develop and verify onboard automotive hydrogen storage systems achieving 1.8 kWh/kg system (5.5 wt% hydrogen) and 1.3 kWh/L system (0.040 kg hydrogen/L) at a cost of $12/kWh ($400/kg H_2 stored).

FY 2014 Accomplishments

- Developed projections for AlH_3 cost
- Demonstrated synthesis of AlH_3 by the dry method with $NaAlH_4$ precursors
- Demonstrated regeneration of $NaAlH_4$ electrolyte for electrochemical alane generation is possible with a cheaper catalyst to enable low cost alane recycling
- Synthesized alane by the electrochemical method and developing novel adduct removal techniques
- Demonstrated improved $NaAlH_4$ recycling with yields above 80% and production of over 5 grams of material.

INTRODUCTION

The DOE is supporting research to demonstrate viable materials for onboard hydrogen storage. Aluminum hydride (alane, AlH_3), having a gravimetric capacity of 10 wt% and volumetric capacity of 149 g H_2/L and a desorption temperature of ~60°C to 175°C (depending on particle size and the addition of catalysts) has the potential to meet the 2015 and 2017 DOE targets for automotive and portable power applications. The main draw back for using alane as a hydrogen storage material is unfavorable thermodynamics towards hydrogenation. Zidan et al. [3] were the first to show a reversible cycle utilizing electrochemistry and direct hydrogenation, where gram quantities of alane were produced, isolated, and characterized. This regeneration method is based on a complete cycle that uses electrolysis and catalytic hydrogenation of spent Al(s). This cycle avoids the impractical high pressure needed to form AlH_3 and the chemical reaction route of AlH_3 that leads to the formation of alkali halide salts, such as LiCl or NaCl, which become a thermodynamic sink because of their stability.

During FY 2014, research has continued to demonstrate methods that will improve the generation of alane. This work has been done in collaboration with Ardica Technologies and has focused on improving dry methods of alane synthesis that can reduce costs from solvent removal and product recovery along with improvements in the electrochemical method that will allow more efficient generation of alane. This research seeks to solve real-world problems in using alane as a hydrogen carrier and make it a more cost effective material for transportation and portable power systems.

APPROACH

The electrochemical generation of alane has been show by Zidan et al. [3,4] to be capable of generating high purity material using methods that can be developed into a fueling cycle for hydrogen vehicles, portable power systems, or other applications. This research has demonstrated the system electrochemistry and improvements have been made to improve the efficiency of the electrochemical alane production reactions. The regeneration of the electrolyte from spent materials and improvements in the separations process are equally as important in developing overall alane production and reprocessing schemes. SRNL has developed and demonstrated a method to regenerate the electrolyte for the electrochemical cell with materials present in electrochemical cell cathode, dehydrogenated alane, and hydrogen gas. Improvements to the electrochemical cell design have also been realized to allow improved separation of the cell products to enable electrolyte generation and separation of alane.

RESULTS

SRNL has investigated the use of $NaAlH_4$ in the dry method for the synthesis of alane in order to achieve cost reductions in its manufacture. Figure 1 displays an X-ray

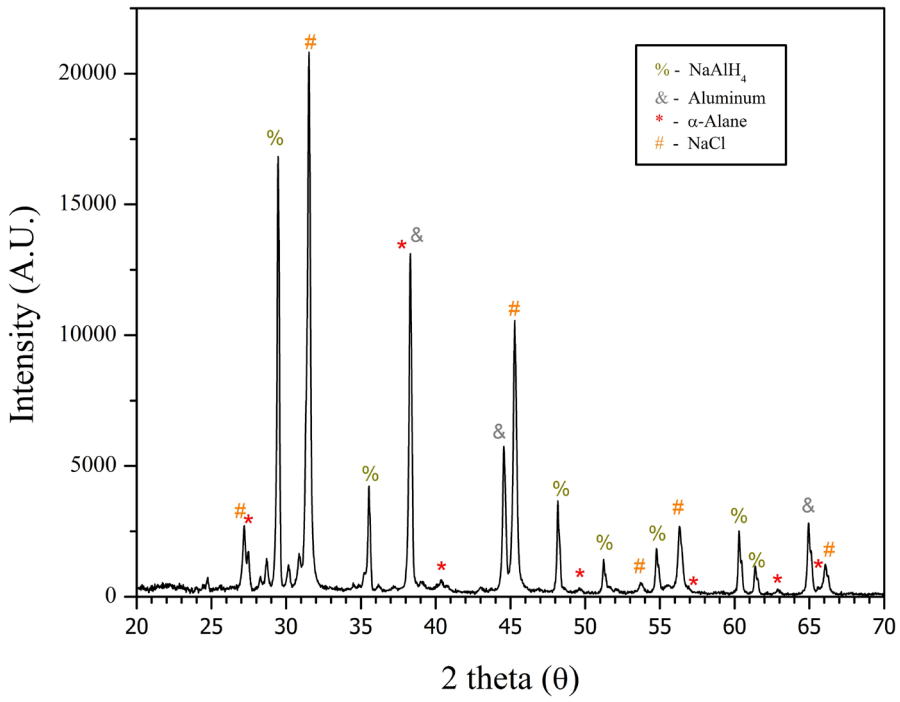

FIGURE 1. XRD spectrum of the unwashed product formed from annealing $NaAlH_4$ and $AlCl_3$ in the solid state.

diffraction (XRD) measurement of the crude reaction product from the dry method synthesis using $NaAlH_4$. A diffraction pattern confirming the production of α-alane is observed. A novel variation of the dry method to produce alane with $NaAlH_4$ has also been accomplished. This process is currently being optimized to increase yields.

Recycling the $NaAlH_4$ electrolyte in tetrahydrofuran can potentially reduce the cost of the electrolyte that is used in the electrochemical cell. $NaAlH_4$ regeneration resulting in a percent yield over 80% was conducted by lengthening the reaction time and the hydrogen pressure in the reactor. This reaction was conducted on a scale to produce more than 5 grams of material. Table 1 shows the $NaAlH_4$ yield for various operating conditions and using two different catalysts. $TiCl_3$ is a well-known catalyst for this reaction and displays the highest regeneration yields, but the new catalyst is nearly two orders of magnitude cheaper than $TiCl_3$. Figure 2 shows the diffraction pattern for regenerated $NaAlH_4$ with no detectable impurities from both catalysts used. These results demonstrate that high purity $NaAlH_4$ can be regenerated from spent alane using both catalysts. These experiments were conducted in a Parr vessel with simple hydrogen overpressure. In this reactor configuration, the slow step in the reaction is the diffusion of hydrogen into the solution because it is limited by Henry's law. The results suggest that if a reactor with better two-phase mixing of the hydrogen would likely be able to lower the hydrogen pressure that is needed and reduce the reaction time. The yield can likely be further increased, while retaining high purity, by developing a flow reactor with better gas, liquid, solid mixing.

TABLE 1. Percent yield of $NaAlH_4$ at different pressures, temperatures and catalyst utilization. The highest percent yield of 84.2% was acquired by increasing the duration of the reaction to 42.5 hours

Temperature and H_2 Pressure	Percent Yield with New Catalyst (5 mol%)	Percent Yield with $TiCl_3$ (5 mol%)
70°C, 1,400 psi	17.0%	31.8%
120°C, 1,400 psi	28.2%	56.6%
150°C, 1,400 psi	55.5%	65.5%
150°C, 1,800 psi	57.1%	84.2%

Crystallization of the product from the electrochemical reaction of alane is important for being able to get the desired storage lifetime and hydrogen release characteristics. Left over electrolyte from the electrochemical cell containing AlH_3 product after the reaction was used to crystallize over 1 g of alane. $LiAlH_4$ assists in the adduct removal process by thermal decomposition. This electrolyte can be easily separated by washing with diethyl ether and then reused for alane production. The alane can then be washed with dilute hydrochloric acid solution to passivate the surface and remove residual aluminum. This passivation process increases the shelf life of the material. Alternative adduct removal techniques have been theorized and the equipment necessary to conduct these experiments has been constructed. This theoretical adduct removal approach could result in further cost reductions for the synthesis of alane.

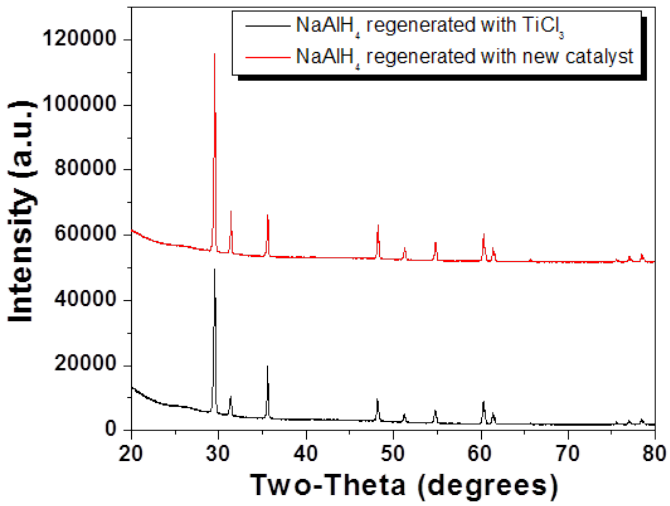

FIGURE 2. XRD pattern of regenerated $NaAlH_4$ from utilization of both catalysts displaying a pure product in both cases.

CONCLUSIONS AND FUTURE DIRECTIONS

- Improved dry methods that work with $NaAlH_4$ and allow simple product separation.
- Regeneration of $NaAlH_4$ electrolyte for the electrochemical cell was demonstrated with a yield greater than 80% producing more than 5 grams of material.
- The recycled $NaAlH_4$ electrolyte was produced without detectable impurities and it is hypothesized that optimization of the reactor can increase the yield while lowering the reaction time and pressure.
- Crystallization of alane from the electrolyte of the electrochemical cell has shown control of crystal size and demonstrated that a product with desirable storage and hydrogen release characteristics can be synthesized from the electrochemical cell product.
- Characterization of the electrode material is currently underway and its composition should be confirmed soon.
- Optimization of the regeneration conditions for $LiAlH_4$ to produce yields above 80% is currently being investigated.

SPECIAL RECOGNITIONS & AWARDS/ PATENTS ISSUED

1. Ragaiy Zidan, Douglas A. Knight, Long V. Dinh; Novel Methods for Synthesizing Alane without the Formation of Adducts and Free of Halides US20120141363 Feb 2013.

2. Ragaiy Zidan; Electrochemical Process and Production of Novel Complex Hydrides US8,470,156B2 Jun 2013.

FY 2014 PUBLICATIONS/PRESENTATIONS

1. Ragaiy Zidan" Development and characterization of novel hydrogen storage materials", Oct 27 2012 International Energy Agency (IEA) HIA Task 22 Meeting Kyoto Japan. [PR]

2. Novel Materials and New Methods for Hydrogen Storage" International Symposium on Metal-Hydrogen Systems 2012, Oct 21 Kyoto, Japan Invited Speaker. [PR]

REFERENCES

1. Teprovich, J.A., T. Motyka, and R. Zidan, International Journal of Hydrogen Energy, 2012. **37**(2): p. 1594-1603.

2. Graetz, J. and J.J. Reilly, J. Phys. Chem. B, 2005. **109**(47): p. 22181-22185.

3. Zidan, R., et al., Chemical Communications, 2009(25): p. 3717-3719.

4. Martinez-Rodriguez, M.J., et al., Appl. Phys. A-Mater. Sci. Process., 2012. **106**(3): p. 545-550.

IV.F.1 Melt Processable PAN Precursor for High-Strength, Low-Cost Carbon Fibers (Phase II)

Felix L. Paulauskas, Bob Norris (Primary Contact), Ken Yarborough, and Fue Xiong
Oak Ridge National Laboratory (ORNL)
MS 6053
Oak Ridge, TN 37831-6053
Phone: (865) 576-1179
Email: norrisrejr@ornl.gov

DOE Manager
Grace Ordaz
Phone: (202) 586-8350
Email: Grace.Ordaz@ee.doe.gov

Subcontractor
Virginia Polytechnic Institute and State University, Blacksburg, VA; Donald G. Baird, Judy Riffle, Sue Mecham, Jianhua Huang

Project Start Date: October 2013
Project End Date: September 2016

Overall Objectives

- Demonstrate means to achieve cost reduction of ≥25% in the manufacture of carbon fiber meeting properties of industry baseline carbon fiber utilized in fabrication of composite vessels for 700-bar hydrogen storage.
- Develop and demonstrate new chemistry and spinning techniques and assess capability for advanced conversion technologies to meet needs in reducing carbon fiber manufacturing costs for fiber meeting program performance goals.

Fiscal Year (FY) 2014 Objectives

- Procure, install, and initiate operations with a spinning system capable of melt spinning continuous precursor polyacrylonitrile (PAN) fiber tows of several hundred appropriately sized filaments with a length >100 m that can be easily spooled and later de-spooled for conversion at ORNL's Precursor Development System.
- Restart chemical formulation work focused on advancing polyacrylonitrile co-polymerized with methyl acrylate (PAN-MA) formulations with appropriate plasticizers and monomers to facilitate spinning precursors with characteristics such as molecular weight, molecular weight distribution, orientation, fiber size, fiber mechanicals, etc. consistent with conversion to high-performance carbon fiber with economic advantages over conventional approaches. (Formulation development had been deferred in late Phase I in order to demonstrate feasibility of melt spinning and converting compounds based on polyacrylonitrile with vinyl acetate [PAN-VA] formulations that were easier to process but not likely capable of meeting longer-term program performance goals.)

Technical Barriers

High-strength carbon fibers account for approximately 65% of the cost of the high-pressure storage tanks. This project addresses the following technical barriers from the Hydrogen Storage section of the Fuel Cell Technologies Office Multi-Year Research, Development, and Demonstration Plan [1]:

(A) System Weight and Volume

(B) System Cost

(D) Durability/Operability

(G) Materials of Construction

High-strength carbon fiber enables the manufacture of durable, lightweight, compressed hydrogen storage vessels for use in high-pressure storage. Unfortunately, current high-strength carbon fiber products are far too expensive to meet DOE goals for storage system costs.

Technical Targets

Working targets are in approximate equivalence with Toray T-700 at substantially reduced production costs:

- 700 ksi ultimate tensile strength
- 33 Msi tensile modulus
- Production cost reduction of at least 25% versus baseline

FY 2014 Accomplishments

- The extruder system needed to produce precursor fiber quantities for continuous conversion processing has been procured and is being set up for operation. Related design and procurements for a metering pump, spin packs, spinnerets, drawing system, etc., are underway based on recent experimental data from ongoing spinning demonstrations utilizing a much smaller scale rheometer. An additional rheometer is being refurbished to facilitate transitioning formulation alternatives to fiber spinning. Most of this equipment is expected to be delivered by the end of FY 2014 while critical supporting activities are ongoing with existing equipment.

- The project has effectively transitioned from demonstrating spinning PAN-VA formulations for feasibility demonstration purposes to advancing PAN-MA formulations projected to be pathway to ultimate cost and performance targets for project. At the conclusion of this time period, precursor fiber properties with melt spun PAN-MA have essentially matched those achieved with PAN-VA formulations in late Phase I.

INTRODUCTION

High-strength carbon fiber enables the manufacture of durable, lightweight, compressed hydrogen storage vessels for use in high-pressure storage. Unfortunately, current high-strength carbon fiber products are too expensive to meet DOE goals for storage system costs. Developing and demonstrating a melt-spun PAN approach to producing precursor for carbon fiber will provide a more cost-effective route to achieving performance necessary for high-pressure gas storage. Melt spinning removes significant costs in handling and recovering solvents involved in solution spinning as well as eliminating a significant bottleneck in production rates required by the time, space, and energy utilized in the solvent recovery steps. Although somewhat similar processes have been demonstrated in the past, no PAN-based carbon fiber is produced currently utilizing this approach due to specific materials employed in the previously demonstrated process and lack of investment from industry to revisit and revamp that process. It is anticipated that the melt-spinning approach could save 25% of cost involved in producing carbon fiber for high-pressure gas storage systems and that additional savings may be possible in combination with ORNL advanced conversion approaches. It is also projected that the melt spinning process would be more attractive for PAN fiber production in the U.S., possibly helping to revitalize some of the acrylic fiber business lost due to environmental concerns.

A major milestone was achieved during latter portions of Phase I with demonstration of carbon fiber properties exceeding the Go/No-Go point established at 15 Msi modulus and 150 ksi strength. Properties meeting follow-on milestone levels up to 25 Msi modulus and 250 ksi strength were also achieved. These properties were achieved with melt spun PAN produced at Virginia Tech and utilizing conversion protocol developed by ORNL. The conversion protocol consists of a number of steps in simulating oxidation with differential scanning calorimetry testing and then preliminary tensioning experiments in batch mode utilizing the customized ORNL precursor evaluation system. Small tows as spun at Virginia Tech were combined at ORNL to obtain a tow with ample number of filaments (~100) to enable progressive tensioning during multiple oxidative stabilization steps and specific shrinkage management in low and high temperature carbonization. During the last year, Phase I has been completed and activities in Phase II are now underway with resumption of the broader approach evaluating new chemical formulations, advanced spinning techniques, and novel conversion processes.

APPROACH

This project is structured into tasks focused on precursor development and conversion process improvements. Development and demonstration of melt-spinnable PAN is the project's primary precursor option. If successful, melt spinning is projected to be significantly less costly than wet spinning with capability to produce high-quality, relatively defect-free precursor. This requires concurrent activities in both development of melt-stable PAN copolymer and blends as well as the processes necessary to successfully spin the formulations into filamentary tows. Melt processing of PAN is a difficult issue, although Virginia Tech and others have made modest progress over the last decade [2-6]. One of the principal problems is that polyacrylonitrile degrades (cross-links) even without main chain scission or weight loss, and this essentially precludes melt processing. Reactions of the side groups have been discussed in many reports [7-10]. These degradative reactions can take place both in an intra-molecular manner, but also via inter-molecular branching and gelation, which quickly alters the capacity for these materials to be melt fabricated. At 200-220°C, the material can quickly increase in viscosity, thus rendering an intractable material in a very short time. Ideally, one would like to maintain constant viscosity for a required period, and practical considerations suggest that this should be at least 30 minutes or longer.

The following have been identified as key elements of the project approach:

- Melt-spun precursors are being formulated for evaluation. The optimum formulation of polyacrylonitrile, methyl acrylate, and a ter-monomer will be determined based upon small scale spinning trials.
- Methods for handling, melting, and spinning the polymer developed in Task 1 above are being developed to produce precursor fiber for the oxidative stabilization and carbonization conversion processes. Critical will be development of the spinning process, including temperature, speed, pressure, and draw profiles.
- Processing of the new polymer into finished carbon fiber will be necessary beginning with conventional processes. By applying conventional processes, a good estimate of the cost benefit of the change in precursor alone will be obtainable and the technology will be developed to allow for introduction of the precursor into current commercial processing lines.

- Processing of the new polymer into finished carbon fiber using the alternative manufacturing processes will be assessed. By applying the alternative processes, the synergistic cost savings of a less expensive precursor along with less expensive processing technologies will be obtainable.

RESULTS

During this period, the project team has focused on upgrading the capabilities necessary to produce adequate quality and quantities of precursor fiber necessary to establish stable, continuous conversion processes, restarting the chemical formulation development work, and transitioning from the PAN-VA formulations utilized to demonstrate feasibility to PAN-MA formulations projected to be necessary to achieve both economic and performance goals. A Randcastle 5/8" extruder as shown in Figure 1 has been procured specifically to support spinning work at Virginia Tech. Related design and procurements for a metering pump, spin packs, spinnerets, drawing system, etc., are underway based on recent experimental data from ongoing spinning demonstrations utilizing a much smaller scale rheometer. An additional rheometer is being refurbished to facilitate transitioning formulation alternatives to fiber spinning. Most of this equipment is expected to be delivered by the end of FY 2014 while critical supporting activities are ongoing with existing equipment.

FIGURE 1. Randcastle 5/8" Screw Extruder in the Processing Lab at Virginia Tech

The synthesis efforts at Virginia Tech have focused on the preparation of high acrylonitrile (AN) content poly(AN-*co*-methyl acrylate) materials for small scale spinning trials. The parameters to be controlled in the synthesis are the molecular weight and molecular weight distribution and the AN content. All of these parameters, in conjunction with the plasticizer type and content and spinning parameters will determine the spinnability of a particular composition. The current objectives are to provide trial materials with approximately 95 wt% AN and 5 wt% methyl acrylate. The materials will be screened in the standard rheometer and/or the modified capillary rheometer spinning apparatus using plasticizers such as water and acetonitrile to determine the spinnability. The feedback on spinnability will be used to define a target molecular weight for scaling up a batch to be used for extruder trials.

One current objective is to identify an optimum molecular weight for a high AN copolymer for melt spinning. A second objective is to develop a scalable process for such materials so that this composition can be scaled to sufficient quantities for spinning and carbonization studies. A series of copolymers with approximately 95/5 wt/wt AN/MA were synthesized by emulsion free radical polymerization (Table 1) and this work remains in progress. Entry 1 in the table was prepared at a lower temperature and lower percent solids relative to the other samples. For Entry 1, ammonium persulfate was combined with sodium metabisulfite as an activator. All of the remaining samples were prepared by conventional free radical emulsion polymerization using ammonium persulfate as the initiator. Based on our results to date, it appears that an optimum molecular weight range (M_w) lies somewhere between 70 and 140 kg/mole. Thus, the team is working to develop a scalable process for polymers in this molecular weight range and to determine the sensitivity of molecular weight on various reaction parameters, particularly temperature, concentration of initiator, and concentration of the chain transfer agent. Please notice that entry MJ-114 in Table 1 has a M_w in the targeted range, but that this copolymer precipitated during synthesis, and this would make this "non-scalable." There are numerous reports of precipitation polymerization for high AN copolymers in the literature so this is not entirely unexpected, but we need to move away from these reaction parameters to develop a robust and scalable process. Nevertheless, MJ-114 may provide insight into "spinnability" of copolymers with this composition in this molecular weight range. Once spinnable polymers with known molecular weight and high AN composition have been developed, the impact of molecular weight on the mechanical characteristics of the melt spun precursor and carbon fibers can be determined.

Table 2 demonstrates parameters from recent spinning trails utilized to effectively transition from the use of PAN-VA formulations for demonstration purposes to the PAN-MA formulations as focus for the Phase II portion of this work.

TABLE 1. Synthetic Parameters for Scaling Trials

Sample ID	Temp.	[Initiator][a] Mol%	[CTA][b] Mol %	% solids	[Surfac Tant] [c]	Time	AN/MA ^{1}H NMR (wt%)	SEC Mw (kg/mol)[d]	Comments
PPP-135*	45	0.12 + 0.02 activator	0.20	20	1.6 wt%	3 h	95/5	70	Filaments failed during spinning
PPP-131	70	0.05	0	25	1 wt%	16 h	95/5	573	Viscosity too high – not spinnable
PPP-133	70	0.05	0.15	25	1 wt%	3 h	95/5	140	Viscosity too high – not spinnable
PPP-129	70	0.1	0.5	25	1 wt%	16 h	94/6	60	filaments failed during spinning;
MJ-114	70	0.1	0.4	25	1 wt%	40 min	96/4	118	Precipitated during synthesis
MJ-131	70	0.1	0.4	25	1 wt%	40 min	96/4	45	Precipitated during synthesis
MJ-121	70	0.1	0.4	28	1 wt%	40 min	96/4	56	

*Synthesized at low temperature using ammonium persulfate activated by sodium metabisulfite

TABLE 2. List of VT PAN Precursor Fibers Generated in this Quarter

Sample ID	VT 04-13	VT 04-14A	VT 04-14B
Polymer mol/mol	PAN-VA 93/7	PAN-MA 95/5	PAN-MA 95/5
Water wt%	12	14	14
AN wt%	12	14	14
Spinning Temp	165°C	165°C	165°C
Draw Ratio	1.7	1.8	1.8
Pressure of FFZ	150 psi	100 psi	50 psi
2nd Draw ratio	4.4	3.8	3.8
Steam condition	19 psi/125C	19 psi/125°C	19 psi/125°C
Fiber diameter	17.8 µm	18.8 µm	18.5 µm
Filament number	14	14	13
Filament length	580 ft (177 m)	542 ft (165 m)	440 ft (134 m)

FFZ - fiber formation zone

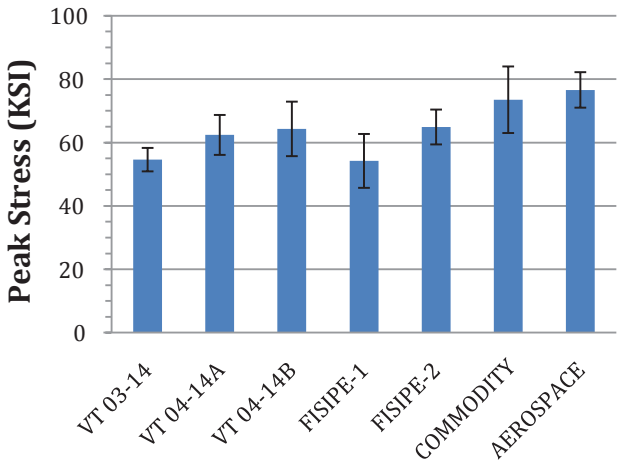

FIGURE 2. Tensile Strength of PAN Precursor Fibers

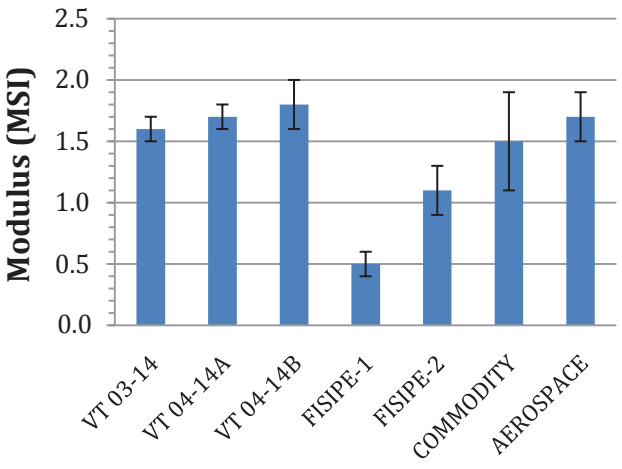

FIGURE 3. Tensile Modulus of PAN Precursor Fibers

Tensile mechanical properties of the new precursor fibers as well as the commercial wet-spun products are presented in Figures 2-4 for comparison. It can be seen that the strength of the new precursor fibers is close to those of FISIPE-1 and 2 (textile-based PAN fibers produced several years ago as an introduction to a precursor alternative for another project) but a little bit lower than those of the commodity or aerospace products. In contrast, the modulus of our precursor is the same or even higher than that of the wet-spun products including the commodity and aerospace products. The elongation-at-break of our precursor is lower than that of the wet-spun products.

The new Virginia Tech precursor fibers have all been converted to carbon fibers at ORNL. The tensile strength, modulus, elongation (strain at break), and diameter of the carbon fibers are shown in Figures 5-8. Compared to the

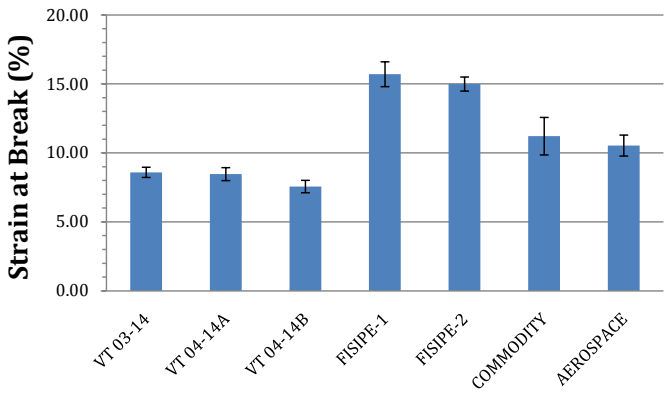

FIGURE 4. Elongation of PAN Precursor Fibers

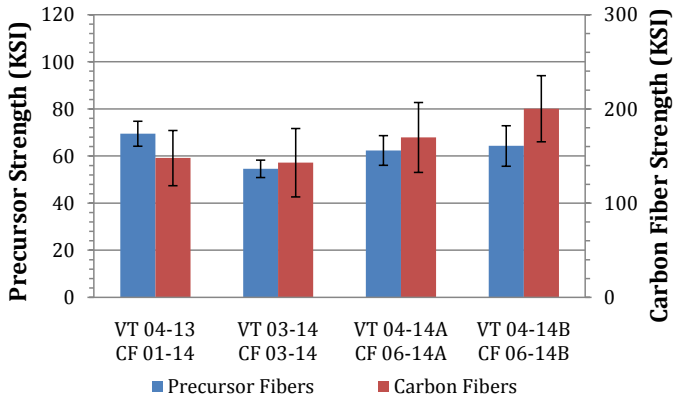

FIGURE 5. Tensile Strength Of Carbonized Virginia Tech PAN Fibers

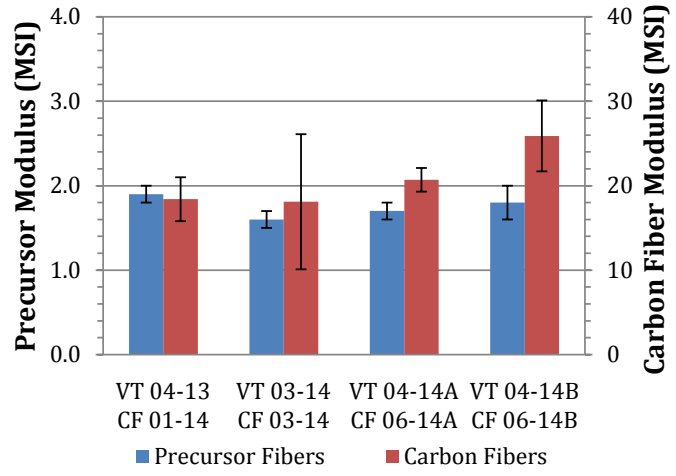

FIGURE 6. Tensile Modulus of Carbonized Virginia Tech PAN Fibers

carbon fibers converted from PAN-VA precursor fibers, the carbon fibers converted from PAN-MA precursor fibers have higher tensile strength and modulus. This may be attributed to the fact that PAN-MA we were using has higher AN content, higher molecular weight and more favorable co-

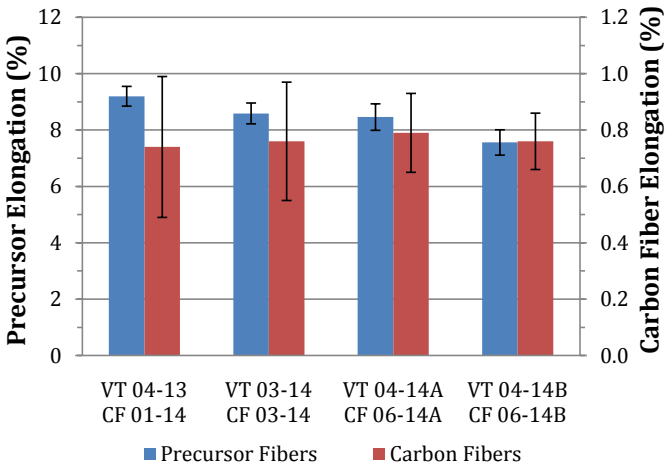

FIGURE 7. Elongation of Carbonized Virginia Tech PAN Fibers

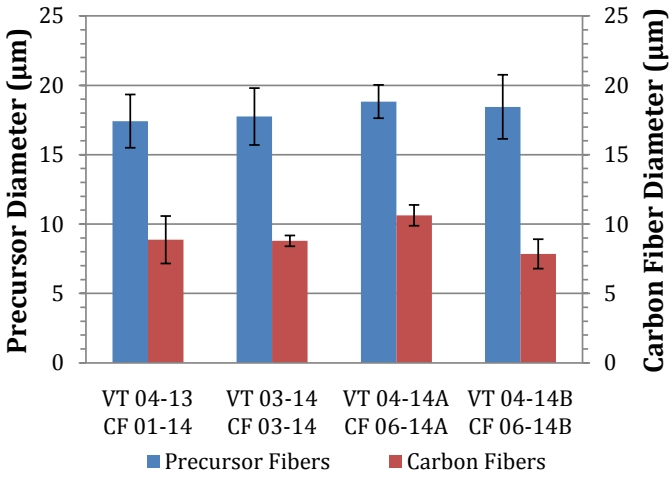

FIGURE 8. Diameter of Carbonized Virginia Tech PAN Fibers

monomer compared to PAN-VA copolymer. The modulus of carbon fibers converted from Virginia Tech 04-14B precursor has a modulus of over 25 Msi which meets our target at the present time. The strength of the carbon fibers is still lower than our target (300 Ksi). The elongation of all carbon fibers is very similar.

CONCLUSIONS AND FUTURE DIRECTIONS

Significant progress has been made in demonstrating and improving melt spinning processes and producing precursor fiber in sufficient quality and minimum quantity to begin carbon fiber conversion investigations. Mechanical properties of the melt spun precursor fiber are comparable to commercially produced fibers. Initial conversion protocols have been developed and demonstrated indicating that we are indeed taking an effective approach and making progress towards project goals.

Near-term objectives are for Virginia Tech to produce longer and more uniform tows that are then drawn in a secondary step as previously described. ORNL will characterize fiber and conduct more extensive conversion trials on precursor filaments generated using its precursor evaluation system. Working on the precursor chemistry necessary to enhance baseline properties and move towards the ultimate goals of 33 Msi modulus and 700 Ksi strength has been resumed and is making progress. Equipment necessary to scale the spinning processes up so that the team can work with larger tow sizes and more continuous tows in further enhancing the conversion processes and providing feedback to the chemistry and fiber forming development has either been obtained or is on order. The filaments at various steps of the conversion process will be fully characterized and the data used to commence optimization of precursor chemistry and the filament generation process. In order to fully address application requirements, the team will also need to evaluate and implement appropriate post treatment operations including surface treatment and sizing for the fiber. Plans are also in place to evaluate whether advanced plasma-based conversion processes (oxidative stabilization and carbonization) under development at ORNL are appropriate for these fibers in reducing costs while meeting performance goals. As the technology is being successfully demonstrated at the Carbon Fiber Technology Facility in Oak Ridge, ORNL will concentrate on the commercialization strategy for technology transfer and implementation.

FY 2014 PUBLICATIONS/PRESENTATIONS

1. Bob Norris, Soydan Ozcan, and Felix Paulauskas, "Carbon Fiber and Nanostructured Material Systems for Manufacturing for High Pressure Hydrogen and Natural Gas Storage", Nanomaterials for Industry Conference, April 6–9, 2014.

2. Felix L. Paulauskas and Bob Norris, "Melt Processable PAN Precursor for High Strength, Low-Cost Carbon Fibers", presentation at Hydrogen Storage Tech Team Meeting, April 17, 2014.

3. Jianhua Huang, Donald G. Baird and Felix L. Paulauskas, "Thermal and rheological behavior of plasticized polyacrylonitrile and melt spinning of precursor fibers" ANTEC® 2014 - Proceedings of the Technical Conference & Exhibition, April 28–30, 2014.

4. Felix L. Paulauskas and Bob Norris, "Melt Processable PAN Precursor for High Strength, Low-Cost Carbon Fibers", presentation at 2014 DOE Hydrogen Program and Vehicle Technologies Annual Merit Review and Peer Evaluation Meeting, June 17, 2014.

REFERENCES

1. Hydrogen, Fuel Cells and Infrastructure Technologies Program Multi-Year Research, Development and Demonstration Plan Planned program activities for 2005-2015, October 2007 update.

2. Wiles, K.B., V.A. Bhanu, A.J. Pasquale, T.E. Long, and J.E. McGrath, Journal of Polymer Science: Part A: Polymer Chemistry, Vol. 42, 2994-3001 (2004).

3. Bhanu, V.A., P. Rangarajan, K. Wiles, M. Bortner, S. Sankarapandian, D. Godshall, T.E. Glass, A.K. Banthia, J. Yang, G. Wilkes, D. Baird, and J.E. McGrath, Polymer, 43, 4841-4850, (2002).

4. Godshall, D., P. Rangarajan, D.G. Baird, G.L. Wilkes, V.A. Bhanu, and J.E. McGrath, "Polymer 44 (2003), 4221-4228.

5. Rangarajan, P., V.A. Bhanu, D. Godshall, G.L. Wilkes, J.E. McGrath, and D.G. Baird, Polymer 43, 2699-2709 (2002).

6. Bortner, Michael J., Vinayak Bhanu, James E. McGrath, and Donald G. Baird, Journal of Applied Polymer Science, 93(6), 2856-2865 (2004).

7. Peng, Fred M., "Acrylonitrile Polymers," in Mark, Herman F.; Bikales, Norbert M.; Overberger, Charles G.; Menges, Georg; Editors. Encyclopedia of Polymer Science and Engineering, Vol. 1: A to Amorphous Polymers. (1986), 843 pp, pages 426-470, and references therein.

8. Back, Hartwig, C, and Knorr, Raymond S. "Acrylic Fibers," in Mark, Herman F.; Bikales, Norbert M.; Overberger, Charles G.; Menges, Georg; Editors. Encyclopedia of Polymer Science and Engineering, Vol. 1: A to Amorphous Polymers. (1986), 843 pp, pages 334-388, and references therein.

9. Capone, Gary J.; Masson, James C. Fibers, acrylic. Kirk-Othmer Encyclopedia of Chemical Technology (5th Edition) (2005), 11 188-224

10. Frushour, Bruce G.; Knorr, Raymond S. Acrylic fibers. International Fiber Science and Technology Series (2007), 16(Handbook of Fiber Chemistry (3rd Edition)), 811-973.

IV.F.2 Development of Low-Cost, High-Strength Commercial Textile Precursor (PAN-MA)

C.D. Warren and Felix L. Paulauskas
Oak Ridge National Laboratory (ORNL)
1 Bethel Valley Road
Oak Ridge, TN 37831
Phone: (865) 574-9693
Email: warrencd@ornl.gov
Email: paulauskasfl@ornl.gov

DOE Manager
Grace Ordaz
Phone: (202) 586-8350
Email: Grace.Ordaz@ee.doe.gov

Contributors
Hippolyte Grappe, Fue Xiong, Ken Yarborough, Ana Paula Vidigal

Project Start Date: April 21, 2011
Project End Date: December 31, 2014

Overall Objectives

- Develop a carbon fiber precursor that yields carbon fiber that is 25% less expensive to manufacture than commercially available carbon fibers and has a strength of at least 650 KSI and a modulus of at least 35 MSI.
- Down-select from 11 polymer candidate polymer compositions to three for spinning fibers.
- Evaluate three fiber compositions to yield guidance for selecting the best fiber composition.
- Demonstrate at least 300 KSI breaking strength and 30 MSI modulus by mid project. (Gate Milestone)
- Optimize the conversion protocol to achieve at least a 650 KSI ultimate strength fiber.
- Conduct a cost study to establish a baseline manufacturing costs for aerospace grade carbon fiber manufacturing.
- Evaluate the cost of manufacturing carbon fiber from the precursor developed in this project and compare to the baseline manufacturing costs.
- Assist manufacturer in implementing the technology in a precursor production facility and a carbon fiber manufacturing facility.

Fiscal Year (FY 2014) Objectives

- Optimize the previously selected fiber composition.
- Increase finished carbon fiber tensile strength from 400 KSI to 650 KSI.
- Increase finished carbon fiber tensile modulus from 32 MSI to 35 MSI.
- Establish a firm commercialization commitment if final target properties are met at the end of the project.
- Establish a baseline cost model for the manufacture of aerospace grade carbon fiber.
- Determine the cost savings in the manufacture of carbon fiber from the newly developed precursor and compare to the baseline cost model.

Technical Barriers

This project addresses the following technical barriers from the 3.3 section of the Fuel Cell Technologies Office Multi-Year Research, Development, and Demonstration Plan:

(B) System Cost

(A) System Weight and Volume

Technical Targets

The cost of the carbon fiber in hydrogen storage systems is 60-80% of the total system cost (Figure 1). Precursors account for 55% of the total cost of the carbon fiber (Figure 2). The precursor alone can account for 33-44% of the cost of the tank. The hydrogen storage team has been conducting projects to develop lower cost carbon fiber precursors to reduce the cost of carbon fiber for hydrogen

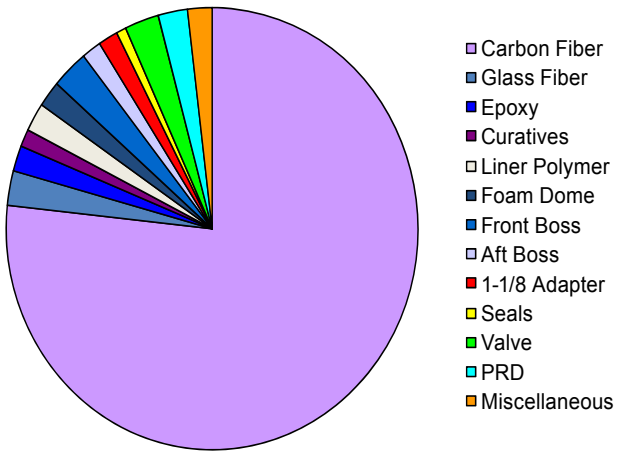

FIGURE 1. Cost of Hydrogen Storage System Broken Out by Major Components and Materials

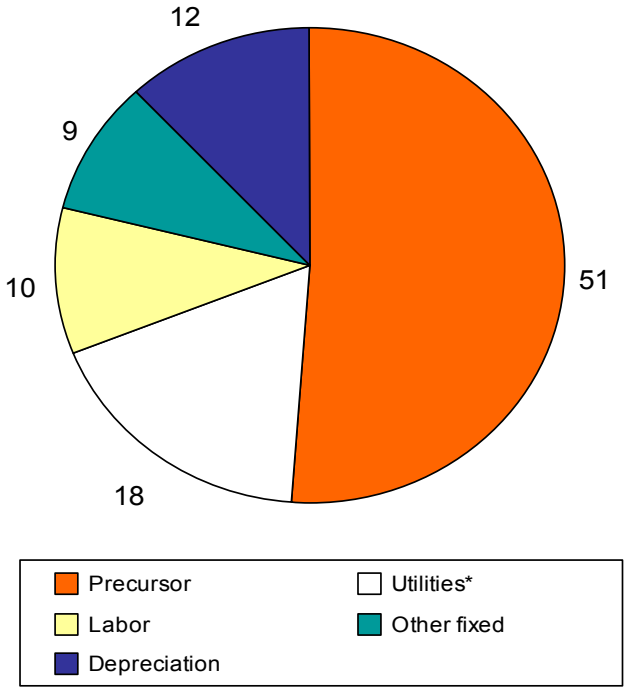

FIGURE 2. Carbon Fiber Production Costs

storage tanks. This effort is to develop a solution spun textile grade polyacrylonitrile with methyl acrylate (PAN-MA) precursor with strengths in the range of 650-700 KSI. This project is a shorter term, lower risk approach to addressing the same issue as is being addressed by the melt-spun polyacrylonitrile (PAN) project. The fiber developed in this proposal will be ready for commercialization within one to two years.

TABLE 1. Progress towards Meeting Technical Targets for PAN-MA Based Lower Cost Carbon Fiber for Hydrogen Storage Tanks

	Strength (KSI)	Modulus (MSI)	Estimated Production Costs
Current Market Fibers	750	38	$15-20/lb
Target	650-700	35-38	$10-12/lb
Status of Developmental Precursor	648	38	$10-12/lb

FY 2014 Accomplishments (as of July 1, 2014)

- Completed 19 of 21 steps for optimizing selected fiber composition conversion conditions.
- Increased finished carbon fiber tensile strength from 405 KSI to 649 KSI.
- Increased finished carbon fiber tensile modulus from 33 MSI to 38 MSI.
- Developed a baseline cost model for the manufacture of aerospace grade carbon fiber.
- Partner is finalizing refinement of conversion conditions for their plant and has agreed to provide fiber for sampling to a tank manufacturer.

INTRODUCTION

In previous years, the Vehicle Technologies Office developed technologies for the production of lower cost carbon fiber for use in body and chassis applications in automobiles. Program goals target materials that have tensile strengths in excess of 250 KSI and modulus of at least 25 MSI. Past work included the development of a vinyl-acetate co-monomered, lower cost precursor and methods for manufacturing precursors into finished carbon fiber. The basic premise of the project was to be able to use PAN material produced in a high volume textile production process for a carbon fiber precursor rather than the specialty material that is typically used for carbon fiber precursors. A textile line that formerly made knitting yarn has been retrofitted and that precursor is being commercialized.

The previously developed fiber had strengths slightly below 500 KSI, which is far above strengths suitable for automotive structural applications but insufficient for many higher demanding applications with higher performance requirements such as the manufacture of hydrogen storage tanks. In order to preserve the cost advantages of using a high-volume PAN fiber and simultaneously meet the needs of higher performance applications, it was proposed to develop the capability to use methyl-acrylate based, textile grade, PAN as a carbon fiber precursor and to manufacture that precursor on a textile line.

The purpose of this current project is to take one precursor technology, textile-based PAN, while using a higher performance chemical formulation, from the technical feasibility stage and scale up to technology demonstration. This project has resulted in the determination of the best polymer formulation and conversion protocol (time-temperature-tension profiles) to produce the best carbon fiber while the precursor is readily and inexpensively manufacturable in existing textile PAN plants. Successful completion of this project resulted in defining the precursor formulation and manufacturing methods to produce carbon fiber. SGL Carbon Fibers is the partner for this work and has both the commitment and ability to commercialize the technology. SGL purchased FISIPE after FISIPE's involvement in the development of the first precursor. Therefore the team that developed the first textile based precursor is involved in this work. Deliverables include spools of fully carbonized, surface treated and sized carbon fiber. This project is on the critical path for the development of lower cost carbon fiber.

APPROACH

The first step to developing a new precursor is to define and analyze candidate precursor formulations. Those are then down-selected and multiple candidate polymer formulations are produced. For this project, SGL/FISIPE down-selected to 11 candidate formulations. Those polymer formulations were sent to ORNL for evaluation from which three polymer formulations were selected to be spun into precursor fiber for attempted conversion into carbon fiber. SGL/FISIPE worked to determine how to spin each of those three formulations into precursor fiber tows and sent them to ORNL for conversion trials. Developing uniformly round fibers and maintaining fiber consistency from fiber to fiber and along the length of each fiber were critical parameters.

Upon receipt of the precursor spools, ORNL began the thermal evaluations to pinpoint conversion temperatures of the precursor, particularly the temperatures to be used for oxidative stabilization. The next step was to determine the limits of fiber stretching that can be achieved in each of the oxidative stabilization stages. As a general rule, higher levels of tension (i.e., percentage of stretching) will promote better polymer chain alignment along the axis of the fiber and will result in higher breaking strengths of the fiber. It is therefore necessary to apply the maximum tension to the fiber, especially during the early stages of oxidative stabilization, without breaking the filaments and without damaging the filaments.

The amount of stretching in each stage of conversion, the optimum temperatures for conversion and the time that the precursor is exposed to those conditions must be developed for each of the seven stages (Prestretching, Oxidation 1, Oxidation 2, Oxidation 3, Oxidation 4, Low Temperature Carbonization and High Temperature Carbonization) of processing. These must be done sequentially, completing each processing step before proceeding to the next. Only after completing all of these steps, can the final properties of the fiber be determined. The plan was to evaluate the three formulations, pinpointing processing parameters in approximate ranges and then down-select to one final formulation. For that formulation, all spinning and conversion parameters are now being optimized. That down-selection has been made to the F2350 formulation.

The main challenges to be addressed in optimizing the performance of the selected precursor are:

- Adapting high-speed processes for producing fiber containing higher acrylonitrile (AN) concentrations.
- Adapting high-speed processes for producing fiber containing methyl-acrylate (MA) co-monomers.
- Adapting high-speed processes for producing fiber with increased chemical purity in order to minimize defects.
- Spinning of round fibers rather than the kidney shaped fibers that are typically produced during textile fiber production.
- Improving the fiber consistency from fiber to fiber and along the fiber length without sacrificing production speed and throughput.
- Determining the optimal conversion protocol by balancing residence time, temperature and applied tension during each of the multiple steps in precursor conversion to carbon fiber.

RESULTS

The down-selection of chemical compositions and fiber formulations started in April of 2011. The main issue related to achieving the proper formulation was the generation of the PAN-polymer with a higher AN content and with a MA comonomer. Dealing with MA co-monomered polymer required some changes to SGL/FISIPE's equipment and standard practices, which required three months. SGL/FISIPE generated 11 candidate compositions. Those 11 compositions were sent to ORNL for evaluation. Differential scanning calorimetry (DSC) curves and other technical data for those compositions were generated for comparison to each other and to known aerospace and industrial grade precursors. The research team then selected three fiber compositions from the first 11 formulations for fiber spinning and preliminary evaluation trials.

Upon receipt of the three fiber candidates, ORNL began the thermal evaluations to pinpoint conversion temperatures of the precursor, particularly the temperatures to be used for oxidative stabilization. Two features are prominent and were expected from the thermal evaluations: (1) the onset of the exotherm occurs at a slightly different temperature from traditional precursors indicating a different starting

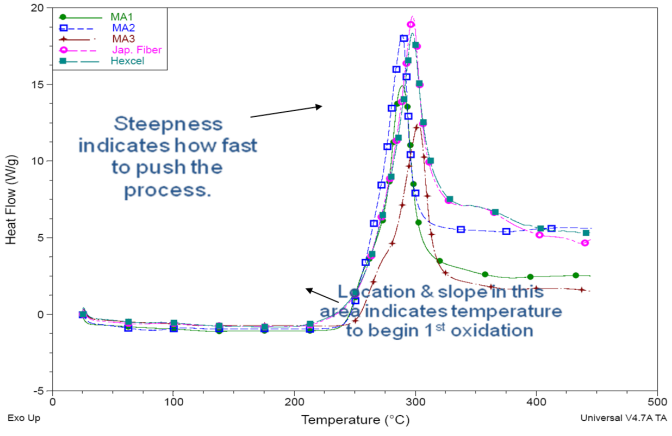

FIGURE 3. DSC Scans of the Three Fiber Compositions Compared to Aerospace and Industrial Grade Precursors

temperature for oxidative stabilization; (2) the exothermic curve is steeper for the PAN-MA precursors than it is for the PAN-VA precursors indicating a slower temperature ramp up being necessary during oxidative stabilization.

The next step was to determine the limits of fiber stretching that can be achieved in each of the stages during oxidative stabilization. As a general rule, higher levels of tension (i.e., percentage of stretching) will promote better polymer chain alignment along the axis of the fiber and will result in high breaking strength of the fiber. It is therefore necessary to apply the maximum tension to the fiber, especially during the early stages of oxidative stabilization, without breaking the filaments. Damage to the filaments that is hidden can also be induced by the tensioning. That damage many not show up until later processing stages. After determining the temperature and tension limits for processing, precursor conversion trials were conducted for those three fiber formulations. The results of those trials are shown below in Table 2. The F2000 formulation was selected for full program development but due to a further refinement by FISIPE was changed to the F2350 formulation. Filament diameters for the new precursor were measured at 11.7 microns which is within the desired range for an oxidized precursor. Normal ranges are 11-12 microns which, after carbonization, produce an ~7 micron diameter carbonized fiber.

Table 2. Final Fiber Properties for Three Candidate Precursor Systems

Fiber Designation	Tensile Strength (KSI)	Tensile Modulus (MSI)
F1921	324.7	26.9
F2000	372.8	36.0
F2027	252.7	27.2

At this point precursor optimization began. Using the three spools of laboratory-produced F2000 that ORNL had, temperature profiles during oxidation were then determined. The temperature profiles are the temperature setting of each of the oxidation ovens and dwell times before significant polymer stretching (tensioning) is applied. Figure 4 shows the DSC curves used for that evaluation. Axis data labels are intentionally omitted for this and all DSC curves in this report due to export control restrictions. The closeness of the Stage 1 and Stage 2 curves is indicative of further improvements that can still be made in the oxidation temperature profile.

The processing parameters (temperature, time at that temperature, and tension applied during oxidative stabilization) during oxidation are interdependent. If any one of the processing conditions in the first stage of oxidation is changed, then the processing conditions that will be optimal in Stage 2 are altered. If Stage 2 parameters are changed then Stage 3 will be altered, etc. As a result, it is critical when optimizing a precursor to finish each processing stage in series rather than in parallel. As an example, if the

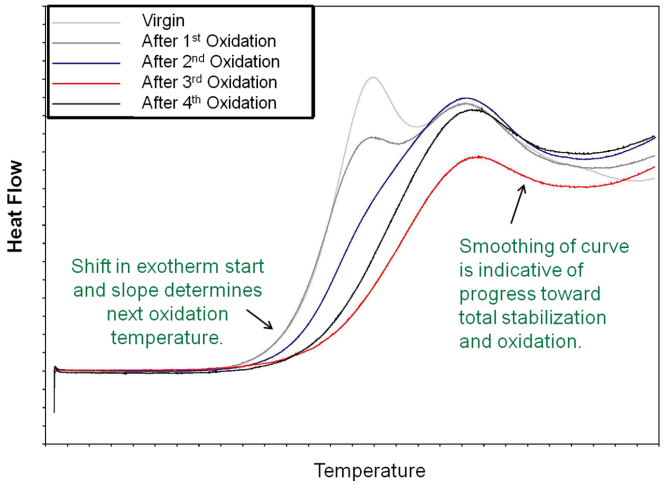

FIGURE 4. DSC Curves for the F2000 Precursor after Various Stages of Oxidative Stabilization

temperature is increased during one stage of oxidation, or the residence time at temperature is increased, then the resulting material will be more highly crosslinked and the amount of oxygen diffusion into the fiber will have increased as will the degree of polymer crosslinking. Likewise, if the fiber is more highly stretched, then the fiber diameter will have decreased, affecting oxygen diffusion into the fiber. For each of these parameters—time, tension and degree of stretch—there is an optimal processing condition for each production step. Too little of each of these and the fibers final properties are compromised. Too much of each of these and the fibers are damaged. Fortunately, once these conditions are optimized, as long as the precursor chemistry is not changed, the processing conditions will not change either.

After determining these beginning temperatures, the amount of stretch that can be given to the precursors during each stage of processing had to be determined. This is done by systematically adding tension to precursors that have been processed through all earlier stages until the breaking point of the precursor at the next temperature is achieved. Figure 5 shows the tension and percent stretching for fibers after exposure to the temperatures determined in the previous step. Of particular interest are the ends of each curve which indicate the upper tension limit of the processing window for these precursors. The closeness of the first and second stage curves indicates that not much progress was being made during the first stage oxidation so either the temperature or the residence time will have to be increased. Since the goal of this effort is to develop a lower cost carbon fiber, a temperature increase of just a few degrees Celsius was used to combat this problem. The closeness of data and the magnitude of the data after the third and fourth stages is indicative of damage during earlier stages, likely due to over stretching the fibers. Export control restrictions require that all tension loads, stretching percentages, oven temperatures

and residence times not be publicly disclosed, therefore axis values are intentionally left off of these charts.

One issue that had to be dealt with for these precursors was "fuzzing" of the fiber tow during processing. Figure 6 shows an example of this. Fiber fuzzing is typically due to small, not fully developed "baby" fibers present in the precursor. Upon tensioning, these fibers see a higher than average stress, exceed their strength and break. This issue has been resolved.

As second issue that had to be dealt with was the cross-sectional geometry of the fibers. Typical textile production processes yield fibers that are kidney bean in shape (Figure 7A). These are fine and even preferable for making carpet fiber or knitting yarn but not for carbon fiber. Carbon fiber properties are enhanced by having uniformly round fibers (Figure 7B). To solve this problem a slightly different configuration for spinning the precursor into the solvent bath during solution spinning of the precursor had to be adopted. The details are proprietary.

Determination of the residence time, stretch percentage and oven temperatures for all oxidation stages has been completed. Determination of 19 of the 21 processing parameters for conversion of the precursor to the final carbon fiber has been completed. The remaining parameters are stretch percentage in low-temperature carbonization, stretch percentage in high-temperature carbonization and the optimum high-temperature carbonization temperature.

Figures 8 and 9 are the property as a function of time charts for tracking precursor progress. Each data point is the average of 18 tests. Blue indicates properties in 2012, purple indicates properties in 2013 and gold the properties in 2014.

Another task to be accomplished is to develop a baseline cost model for production of high-strength carbon fiber (700 KSI) based upon the technologies currently employed in industry today. The expected cost benefits of using the precursor that is being developed under this project will then be evaluated using that cost model and the processing conditions determined in this project. The baseline cost

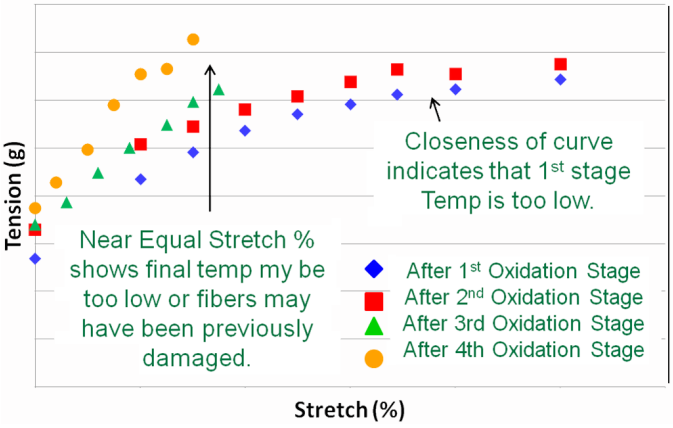

FIGURE 5. Stretch – Break Curves for F2000 Precursor

FIGURE 6. Top: "Fuzzing" of Filament Tow during Oxidative Stabilization; Bottom: Tow not exhibiting "Fuzzing"

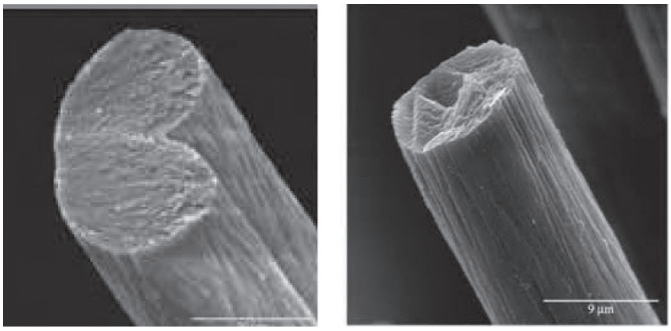

FIGURE 7. (A) Typical Textile Produced PAN Fibers; (B) Carbon Fiber Grade PAN Fibers

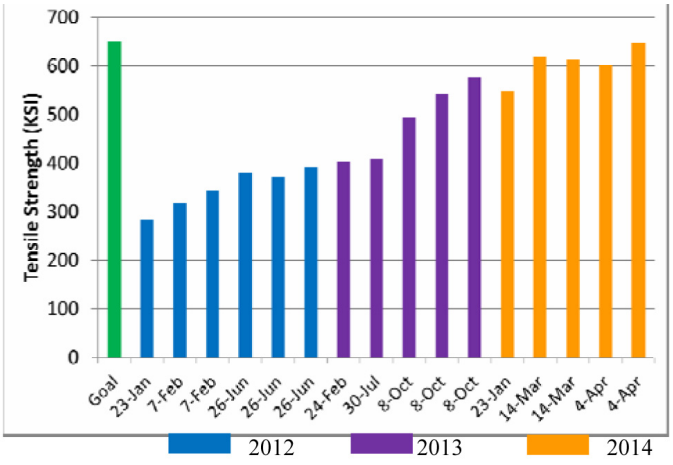

FIGURE 8. Tensile Strength as a Function of Time for the F2350 Precursor

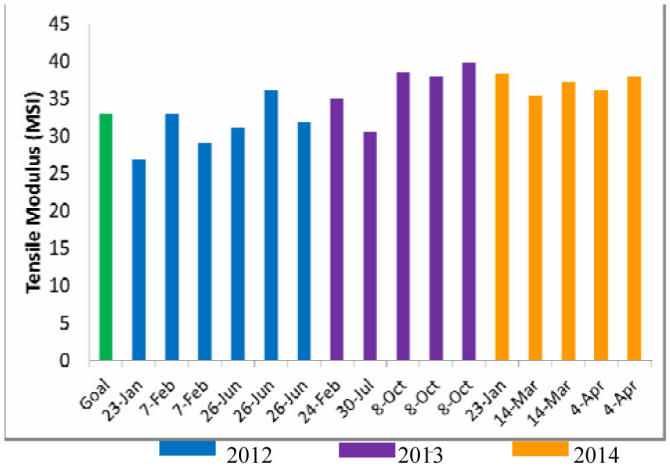

FIGURE 9. Tensile Modulus as a Function of Time for the F2350 Precursor

model nearing completion and preliminary results are presented in Figures 10 and 11.

While we have not yet achieved Hydrogen Storage Program goals, the properties achieved thus far are sufficient for this precursor to go into production for lower performance applications. As a result, SGL/FISIPE is now moving to produce the precursor that they are supplying for this work on their full-scale production line

CONCLUSIONS AND FUTURE DIRECTIONS

The gate milestone for project continuation has been met. The original 11 polymer compositions have now been selected down to one final composition. That material is being produced on full-scale production lines while optimization of the conversion protocol is occurring. To

Precursor Cost $6.40/Kg ($2.91/pound)

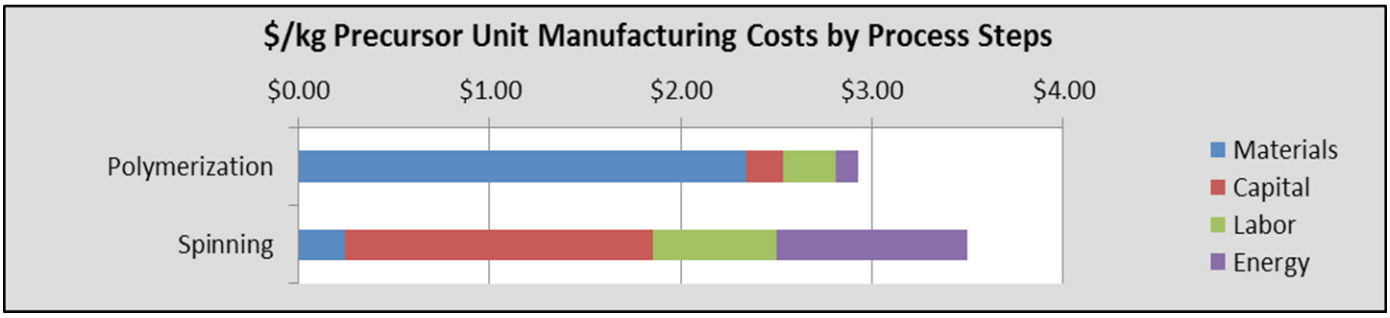

FIGURE 10. Baseline Precursor Cost for High-Performance Carbon Fiber (2.1 lbs of Precursor is required to make 1.0 lbs of Carbon Fiber)

Carbon Fiber Cost $29.40/Kg ($13.36/pound)

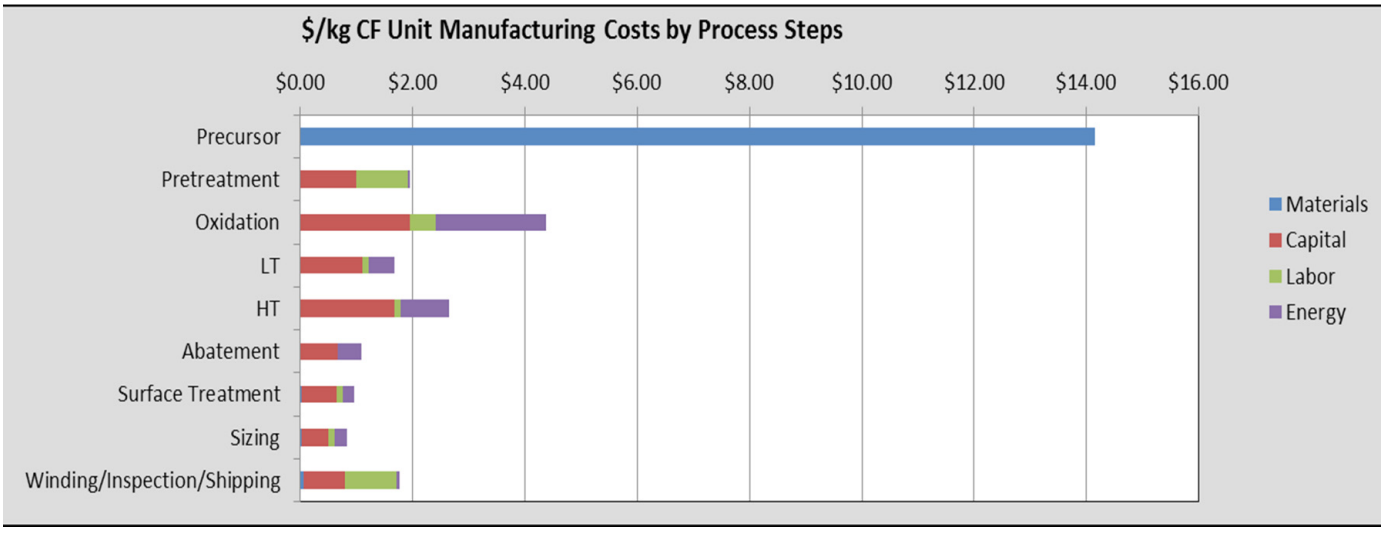

FIGURE 11. Baseline Carbon Fiber Cost for High-Performance Carbon Fiber

date, we are approximately half-way through the conversion protocol optimization phase. Work to improve fiber consistency from filament to filament and along the lengths of the filaments has mostly been completed. This is a task that manufacturers will continue throughout the production life of the precursor since it is critical to pushing the final carbon fiber properties higher.

FY 2014 PUBLICATIONS

1. Warren, C.D., Wheatley, A. and Das S., "Low Cost Carbon Fibre for Automotive Applications Part 1: Low Cost Carbon Fibre Development", Chapter 3 in Advanced Composite Materials for Automotive Applications: Structural Integrity and Crashworthiness, (in final editing) Publisher: Wiley, Edited by: Ahmed Elmarkbi. (2013).

2. Warren, C.D., Wheatley, A. and Das S., "Low Cost Carbon Fibre for Automotive Applications Part 2: Applications, Performance and Cost Reduction Models" Chapter 17 in Advanced Composite Materials for Automotive Applications: Structural Integrity and Crashworthiness, (in final editing) Publisher: Wiley, Edited by: Ahmed Elmarkbi. (2013).

IV.F.3 Synergistically Enhanced Materials and Design Parameters for Reducing the Cost of Hydrogen Storage Tanks

Kevin L. Simmons
Pacific Northwest National Laboratory
PO Box 999, MSIN K2-44
Richland, WA 99352
Phone: (509) 376-3651
Email: kevin.simmons@pnnl.gov

DOE Manager
Grace Ordaz
Phone: (202) 586-8350
Email: grace.ordaz@ee.doe.gov

Subcontractors
- Hexagon Lincoln, Lincoln, NE
- Ford Motor Company, Dearborn, MI
- Toray Composites America, Decatur, AL
- AOC, LLC, Collierville, TN

Project Start Date: January 18, 2012
Project End Date: September 30, 2015

Overall Objectives

- Reduce carbon fiber usage and hydrogen tank cost through a series of combined material and design approaches for a cumulative 37% cost savings.
- Reduce tank cost by reducing composite mass through: (A) resin matrix modifications and alternatives, (B) carbon fiber surface properties that increase load translational efficiency, (C) alternate carbon fiber placement and materials, and (D) enhanced operating conditions to increase the energy density vs. pressure.
- Demonstrate the combined carbon fiber as well as cost reductions through modeling, materials, and burst testing.

Fiscal Year (FY) 2014 Objectives

- Develop a feasible pathway through cold gas enhanced operating conditions to achieve at least an additional 20% ($3.4/Kwh) (mass reduction of 18.7 kg composite or 13.3 kg carbon fiber) cost reduction for compressed hydrogen storage tank above the 15% (13.5 kg composite, 9.6 kg carbon fiber) accomplished in FY 2013 through resin modification and fiber placement. This will be demonstrated through thermal and cost modeling of low-cost thermal insulating approaches. Percent improvements are based on a 2013 projected high-volume baseline (composite mass 93.6 kg, carbon fiber mass 66.3 kg) cost of $17/kWh for 70-MPa compressed hydrogen storage tanks.
- Conduct material testing of resin modifications with higher filler concentrations.
- Complete modeling of tank dormancy for cold gas storage.
- Model tank to redesign for cold gas storage.
- Complete tooling for baseline tank fabrication.
- Fabricate baseline sub-scale prototype tank.
- Accomplish burst testing of baseline sub-scale tank.

Technical Barriers

This project addresses the following technical barriers from the Hydrogen Storage section of the Fuel Cell Technologies Office Multi-Year Research, Development, and Demonstration Plan:

(A) System Weight and Volume

(B) System Cost

(G) Materials of Construction

(H) Balance-of-Plant (BOP) Components

Technical Targets

This project contributes to achieving the following DOE milestone from the Manufacturing R&D section of the Fuel Cell Technologies Office Multi-Year Research, Development, and Demonstration Plan:

- By 2017, develop and verify onboard automotive hydrogen storage systems achieving 1.8 kWh/kg system (5.5 wt% hydrogen) and 1.3 kWh/L system (0.040 kg hydrogen/L) at a cost of $12/kWh ($400/kg $H_{2\ stored}$). Progress toward targets is shown in Table 1.

TABLE 1. Progress toward Meeting Technical Targets for Onboard Hydrogen Storage for Light-Duty Fuel Cell Vehicles

Technical System Targets: Onboard Hydrogen Storage for Light-Duty Fuel Cell Vehicles			
Storage Parameter	**Units**	**2017 Targets**	**PNNL 2014 Status**
System Gravimetric Capacity	kg H2/kg system	0.055	0.051
System Volumetric Capacity	kg H2/L system	0.040	.027
Storage System Cost	$/kWh net	12	15.37

FY 2014 Accomplishments

- Completed testing of material modification enhancements with higher concentrations of nanofillers.
- Fabricated tanks with baseline geometry with alternate fiber placement and several fiber types.
- Fabricated baseline tank geometry with material property enhancements.
- Completed matrix of burst tests.
- Identified additional 38% tank composite mass reduction through lower pressure cold gas storage, which is greater than the required Go/No-Go of 20% additional reduction. Total mass reduction of all design enhancements is 52% of the baseline.
- Identified a path to 30% tank cost reduction with combined efficiencies of 1) lower cost resins, 2) improved nanofilled resins, 3) alternative fibers and winding patterns, and 4) cold gas storage. through……, as well as via/through….. Accomplished modeling to identify the following potential cost savings:
  - 500-bar pressure vessel design with enhanced operating conditions (37% cost reduction).
  - Low-cost insulation for enhanced cold gas operation (7% cost).
- Total savings after cost model analysis is 30%.

INTRODUCTION

The ultimate DOE goal of this research is to reduce the cost of compressed hydrogen storage vessels by at least 50% from the current high-volume projections of $15.4/kWh to $6/kWh for commercialization in early-market and light-duty hydrogen fuel cell vehicles. The cost and performance baseline comparisons are the current 70-MPa Type IV pressure vessel (high-strength, standard modulus carbon fiber in an epoxy matrix filament wound on a high density polyethylene liner). The high-strength carbon fiber composite can account for nearly 70-80% of the overall tank costs. Therefore, our research objective is to reduce carbon fiber usage and associated tank cost through a series of combined material and design improvements that are estimated to total nearly 30% of the project initial baseline tank cost. The project has identified through modeling a series of material design optimizations and experiments that achieve the cost savings goal. It is probable that these cost savings, combined with future reductions in carbon fiber cost could lead to the 50% cost reduction toward the ultimate DOE target.

APPROACH

The project takes a holistic approach to improve performance by lowering the required gas pressure at lower operating temperature, refining the tank composite design with local reinforcement and hybrid layups, plus increasing the composite translation efficiency with material modifications at the composite constituent level. The project team includes industry experts in each of the following focus areas of improvement: enhanced operating conditions to improve energy density/pressure ratios, load translational efficiency improvements by carbon fiber surface modification, resin matrix modifications and alternatives, and alternate fiber placement and materials. We expect these savings approaches to be compatible and additive.

RESULTS

The following Go/No-Go Milestone was specified for FY 2014:

> "PNNL, along with partner Ford, will demonstrate a feasible path to reduce the overall carbon fiber composite weight by 20% (composite savings of 18.7 kg from the 2013 baseline estimate of 93.6 kg) of a composite overwrapped pressure vessel through modeling of cold gas (200 K) enhanced operation."

The waterfall plot in Figure 1 shows the progressive savings of the composite material and tank design improvements studied in this project. These results were calculated using the tank mass and cost model developed by Ford and PNNL during the first year. For the baseline 145-liter Type IV composite pressure vessel (5.8 kg of total hydrogen at 288 K (15°C) and 70 MPa), this model predicts a tank composite mass of 93.6 kg compared to 91 kg estimated by the DOE model by Strategic Analysis, Inc (3% difference). In the first year, the engineering cost analysis estimated that 12% of the $3,171 tank cost (and 14% of the 93.6 kg composite mass) could be saved with low cost reinforced resins combined with improved fiber placement and winding efficiencies. Analysis of the reduced pressure, cold-gas operating condition in the second year estimated that the tank mass could be further reduced by 38% (52% total mass reduction) with a total cost reduction including insulation of 30% from the baseline. The additional 38% mass savings is significantly greater than the 20% composite mass reduction required by the Go/No-Go Milestone.

The net cost of the tank at cold-gas conditions must include the insulation system required to maintain cold-gas dormancy. Comparing the estimated 37% cost reduction with the 30% project goal leaves 7% or $222 for the insulation system. PNNL performed thermal analysis of the vacuum insulation system used by Lawrence Livermore National Laboratory on their cryo-compressed hydrogen tank. The model was validated against the measured thermal

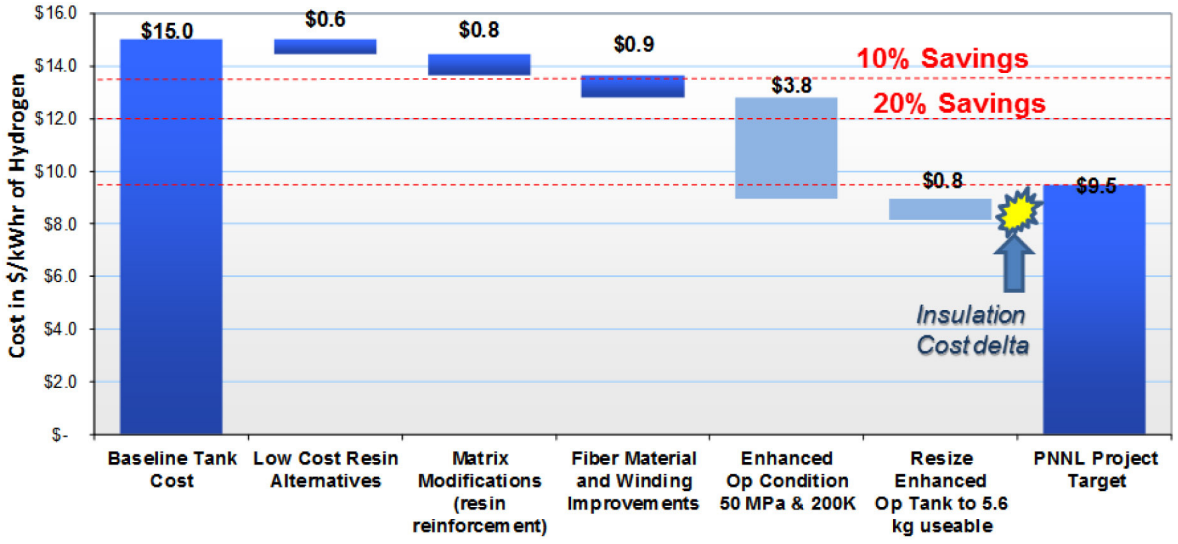

FIGURE 1. Waterfall Plot of Progressive Cost Reductions from Tank Material and Design Improvements

performance and then used to estimate the dormancy time of a similar vacuum vessel at the cold-gas conditions. The analysis estimated that 18 days of dormancy could be achieved before the 50-MPa rated pressure increased to the 125% maximum operating pressure (62.5 MPa). Published cost analysis of the cryo-compressed tank [1] estimated the vacuum vessel cost to be about $290, which is similar to our $222 insulation margin. Reducing the tank volume to 141 L at cold conditions (vs. the 151-L cryo-compressed tank) and designing for a shorter dormancy (i.e., 7 days) may reduce the insulation system cost. High-performance physical insulations will also be tested in the coming year to compare cost and thermal performance with vacuum insulation.

Resin Matrix Modifications

Resin fillers or additives can improve load translation in the composite by increasing the resin modulus and strength to be more compatible with the fiber transverse modulus, as well as some improvement in matrix elongation at break. Detailed finite element calculations, including elastic/plastic matrix deformation with damage, were performed for a composite tank cylinder to estimate the effect of nano-additives on composite strength and burst pressure. Tensile test models of the matrix alone agreed within 5% of particle strengthening effects reported in the literature. Based on these calculations, we estimate that a 15% improvement in matrix modulus with an accompanying 12% increase in material strength can achieve to an increased burst pressure of approximately 8%. This is equivalent to an 8% reduction in carbon fiber usage. Because this is direct modification of the resin matrix properties and not the fiber, we expect additional strength improvement with the carbon fiber modification for a combined savings.

Based on expected cost and performance to date, we have down-selected to two very different nanofiller morphologies: 1) a silica nanofiber (SNF) with very high aspect ratio, and a nanoscale graphite material (N307 by Asbury) similar to graphene platelets (Figure 2). Here we report findings of the relative tensile properties of the T015 system doped with SNF. Figure 3 shows the tensile strength and modulus data taken from samples machined from neat and nanofilled resin panels. The addition of the SNF improved the modulus of the resin as compared to the T015, but resulted in a simultaneous drop in strength. Since both parameters are important to improving tank burst pressure, we have been working on addressing improvements in strength of the nanofilled resin. Issues can arise in nanofilled systems due to either poor dispersion or poor interfacial adhesion with the nanomaterial and the resin. Poor dispersion was indicated by the presence of clumping in scanning electron microscope images of the fractured edges of the SNF containing resins. To correct this we modify the SNF fiber surface using silane (3-(Trimethoxysilyl)propyl methacrylate) to improve wetting, dispersion, and interfacial adhesion; and we used ultrasonic mixing to improve dispersion.

Figures 3 shows both the sonication and surface modification have increased the strength and modulus of the nanofilled resins. In fact, the strength of the surface modified nanofilled resin is nearly that of the neat resin, while the modulus is significantly improved. It is likely that additional sonication (up to a point) will further increase properties as dispersion is improved. Beyond a certain point the sonication will start to break up the nanofibers and the properties will again decrease. It is likely that the two combined effects will result in a resin that exceeds both the strength and modulus of the neat resin. In the next phase of work, we will continue to improve the dispersion and interfacial adhesion

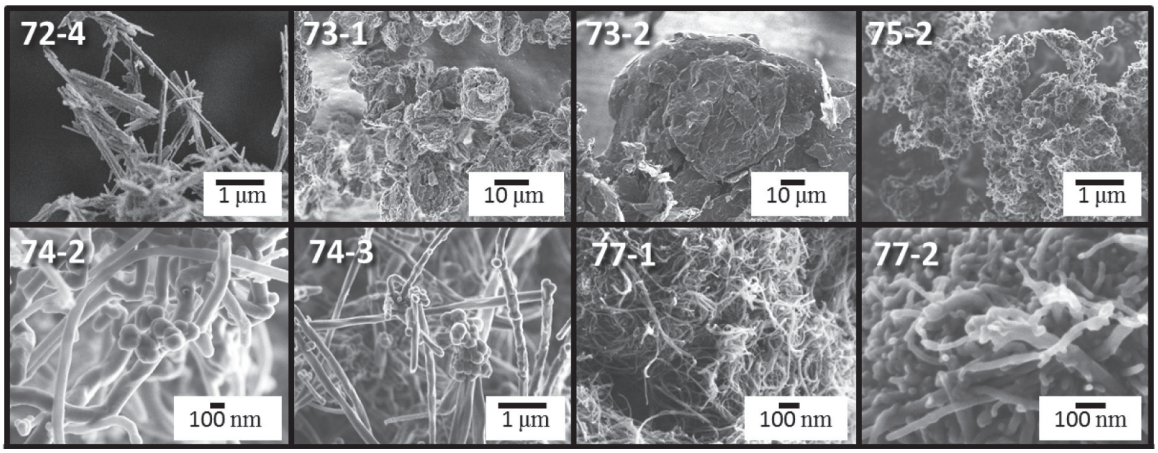

FIGURE 2. Scanning Electron Microscope Images of Nanoscale Material: (left) Silica Nanofibers, (right) N307 Nano-Graphite

by optimizing the sonication for surface modified SNF resins and in the new resin systems with the new peroxide. In addition, we will adopt the same approach for the N307 material.

Composite Layup Optimization Study

From the modeling study in FY 2013, a series of prototype tanks have been wound for experimental validation. The study includes alternative fibers, fiber combinations, and alternate laminate designs in the construction of 70-MPa all-composite pressure vessels. Vessel cost and mass are the primary and secondary evaluation parameters. A finite element model of an axisymmetric cylinder wall was used to guide the tank design selection. There are over 60 pressure vessel tanks currently being evaluated.

The tanks being wound include a single fiber design comparison of T700, T720, and T800 fibers. Hybrid combinations of the currently available commercial fibers are also included. Although these did not show a significant cost reduction, several layup combinations showed a significant reduction in the tank mass. Most notable was the combination of 51% T720 inside and 49% T700 outside with a 23% predicted mass reduction without impacting the tank cost.

Other tank experiments include altering the typical layup design approach for wind angle and sequencing. The modeling study showed that tailoring the wind angles has the potential to reduce cost and mass by 3% to 14%. Increasing the stresses in the low angle helical (near axial) fibers could potentially reduce cost and mass by 7% to 16%. Implementing these alternate layup designs will require more detailed composites analysis of the tank, including the need for local reinforcement in the dome. Wind angle tailoring has higher risk with processing challenges that will be assessed through our experimental validation.

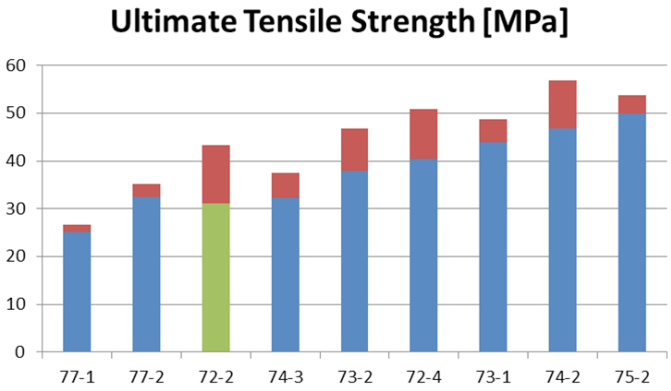

FIGURE3. Strength and Modulus of SNF Reinforced Resins

Conclusions and Future Directions

Research during FY 2014 has demonstrated cost reductions totaling 30% (including insulation for cold-gas) through combined material improvements, composite layup design, and cold-gas operation. The model also estimates that cold-gas operation will save an additional 38% composite mass by shifting from 70 MPa at room temperature to 50 MPa at 200 K. This is nearly double the 20% mass savings required by the Go/No-Go.

Work in the next year will focus on demonstrating these improvements through burst testing of prototype tanks with alternative resins and reduced carbon fiber mass. High-performance physical insulations will also be tested to compare cost, formability, and thermal performance.

FUTURE WORK

- Fabricate and burst test prototype baseline T700S carbon fiber plus epoxy tanks rated for 50 MPa and 70 MPa.

- Perform material testing of T700S fiber treatments and alternate filled resins at room temperature and cold-gas operating temperature for comparison with T700S carbon fiber and epoxy composite used in the baseline prototype tank.
- High-performance physical insulations will also be tested to compare cost, formability and thermal performance.
- Fabricate and burst test 50-MPa prototype tanks using the standard T700S carbon fiber plus AOC alternate resins reinforced with nano-particle additives.
- Report project results of modeling, material testing, and tank fabrication and burst testing.

FY 2013 PUBLICATIONS/PRESENTATIONS

1. K.L. Simmons. 2014. "Enhanced Materials and Design Parameters for Reducing the Cost of Hydrogen Storage Tanks." Project ID# ST101. DOE Fuel Cells Office Annual Merit Review, June 16-20, 2014, Washington, DC. Pacific Northwest National Laboratory, Richland, WA.

REFERENCES

1. Ahluwalia, RK, TQ Hua, JK Peng, S Lasher, K McKenney, J Sinha, and M Gardiner. 2010. *Technical assessment of cryo-compressed hydrogen storage tank systems for automotive applications.* International Journal of Hydrogen Energy. Elsevier, Vol. 35, pp. 4177-4184.

IV.F.4 Thermomechanical Cycling of Thin-Liner High-Fiber-Fraction Cryogenic Pressure Vessels Rapidly Refueled by a LH_2 Pump to 700 Bar

Salvador M. Aceves (Primary Contact), Gene Berry, Francisco Espinosa-Loza, Guillaume Petitpas, Vernon Switzer

Lawrence Livermore National Laboratory
7000 East Avenue, L-792
Livermore, CA 94551
Phone: (925) 422 0864
Email: saceves@llnl.gov

DOE Manager

Jesse Adams
Phone: (720) 356-1421
Email: Jesse.Adams@ee.doe.gov

Subcontractors

- Linde LLC, Hayward, CA
- Spencer Composites Corporation, Sacramento, CA
- BMW, Munich, Germany

Start Date: January 1, 2014
End Date: December 31, 2016

Overall Objectives

- Demonstrate small (60 liters internal volume), high aspect ratio (35 cm outer diameter and 110 cm length) cryogenic pressure vessels with high volumetric and gravimetric hydrogen storage performance (50 gH_2/L and 9% H_2 weight fraction)
- Demonstrate durability (1,500 thermomechanical cycles) of thin-lined high-fiber-fraction pressure vessels
- Measure liquid hydrogen (LH_2) pump performance after 5,000 refuelings (24 tonnes of LH_2)

Fiscal Year (FY) 2014 Objectives

- Write a safety plan and receive DOE operational approval
- Complete fabrication drawings for pressure vessel test facility
- Manufacture a vacuum jacket cryogenic pressure vessel with 163 liter capacity
- Conduct cryo-pump testing at 700 bar with 163 liter vessel
- Fabricate the first thin-lined high-fiber-fraction vessel
- Pressure test the thin-lined high-fiber-fraction vessel (Go/No-Go)

Technical Barriers

This project addresses the following technical barriers from the Hydrogen Storage section of the Fuel Cell Technologies Office Multi-Year Research, Development, and Demonstration Plan:

(A) System Weight and Volume

(D) Durability/Operability

(E) Charging/Discharging Rates

(N) Hydrogen Venting

TABLE 1. Progress toward Meeting DOE Hydrogen Storage Technical Targets

Cryogenic Pressurized Storage			
Characteristic	**Units**	**2017/ultimate targets**	**LLNL 2014 status**
System gravimetric capacity	kWh/kg	1.8/2.5	2.45
System volumetric capacity	kWh/L	1.3/2.3	1.51
Storage system cost	$/kWh	12/8	12

FY 2014 Accomplishments

- Demonstrated weldability of candidate liner material by performing tension tests of welded dog bones
- Completed site design and construction-ready drawings for a pressure vessel test facility
- Wrote the preliminary version of a safety plan

INTRODUCTION

Cryogenic pressure vessels have demonstrated the highest performance for automotive hydrogen storage, with density (43 gH_2/L), weight fraction (7.3%), cost ($12/kWh), and safety advantages (~8X lower expansion energy than compressed gas and secondary protection from vacuum jacket) [1,2]. This project will explore the potential for reaching high volumetric (50 gH_2/L target) and gravimetric (9% hydrogen weight fraction target) storage performance within a small (60 liters internal volume), high aspect ratio (35 cm outer diameter and 110 cm length) cryogenic pressure vessel with long durability (1,500 thermomechanical cycles) refueled by a liquid hydrogen pump to be tested for degradation after delivery of 24 tonnes of LH_2.

APPROACH

Reaching the very challenging weight and volume targets set for this project demands an innovative cryogenic pressure vessel design. Spencer Composites Corporation, in collaboration with LLNL, will develop thin-lined, high-fiber-fraction cryogenic pressure vessels. At a target liner thickness of 1.5 mm and 80% fiber fraction, these thin-walled, vessels may be able to reach the targets when installed within a thin vacuum gap and refueled at high density (up to 80 gH_2/liter) with the LH_2 pump.

RESULTS

The first seven months (January-July 2014) of this project have focused on the three initial tasks described next.

1. Development of Thin-Lined, High-Fiber-Fraction Vessels. In collaboration with Spencer Composites Corporation, LLNL selected appropriate liner materials for high-pressure cryogenic operation that can withstand compression from the composite overwrap without buckling. At 1.5 mm target thickness, the focus is on hydrogen-compatible stainless steels (316). Recent experiments have helped establish weldability. Dog bones were made from the baseline material, and then cut in half and TIG welded with and without welding rods. The results have been very satisfactory. Little loss in strength (10%, (Figures 1 and 2), resulted from welding, and all dog bones failed at the heat-affected zone indicating a high quality weld.
2. Construction Planning. Experimental vessels to be built by Spencer Composites Corporation are not certified and therefore cannot be tested in a manned area according to LLNL pressure safety standards. Extensive cycling and pressurization of these experimental vessels therefore demands a pressure vessel test facility where the vessels can be tested within the confines of an appropriately sized containment vessel that guarantees safe operation. The Facilities group at LLNL has produced a package of construction-ready drawings for the test facility (Figure 3), and construction is projected to start in FY 2015.
3. Safety Plan. Aside from extensive safety reviews internal to LLNL, DOE demands a comprehensive safety plan to be reviewed by DOE´s Safety Panel. These reviews are especially important for this project due to extensive pressure and cycle testing with hydrogen. A preliminary safety plan including all construction and system component details has been produced and is being reviewed by the Safety Panel.

CONCLUSIONS AND FUTURE DIRECTIONS

- This project attempts to identify volumetric and gravimetric performance limits for cryogenic pressurized storage at small size (60 liters) and high aspect ratio (35 cm outer diameter and 110 cm length)
- Performance targets demand thin walled vessels, and these are being developed in collaboration with Spencer Composites Corporation
- Vessel durability over 1,500 thermomechanical cycles will be demonstrated before pressure testing to minimum burst pressure
- Pump durability will also be demonstrated by measuring performance after pumping 24 tonnes of LH_2

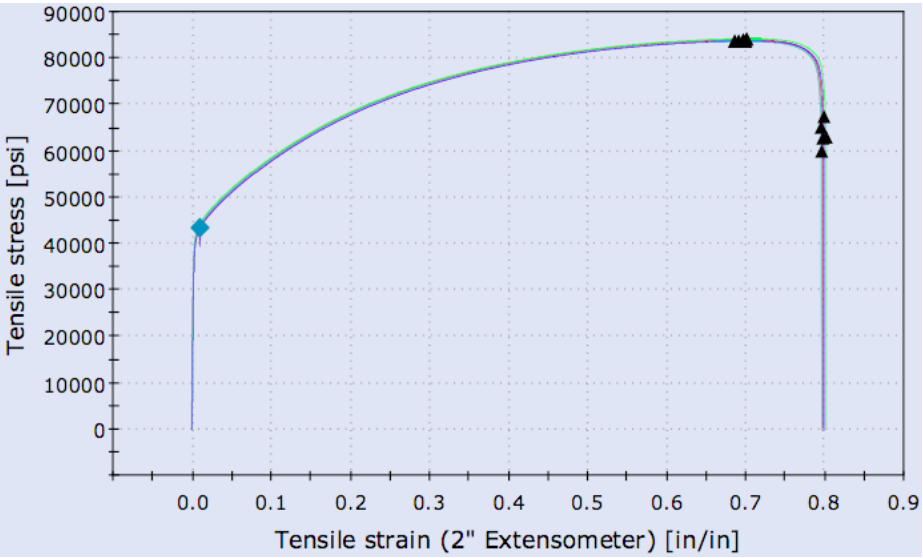

FIGURE 1. Stress-Strain for Stainless Steel 316 for a Dog Bone made of the Parent Material and No Welds

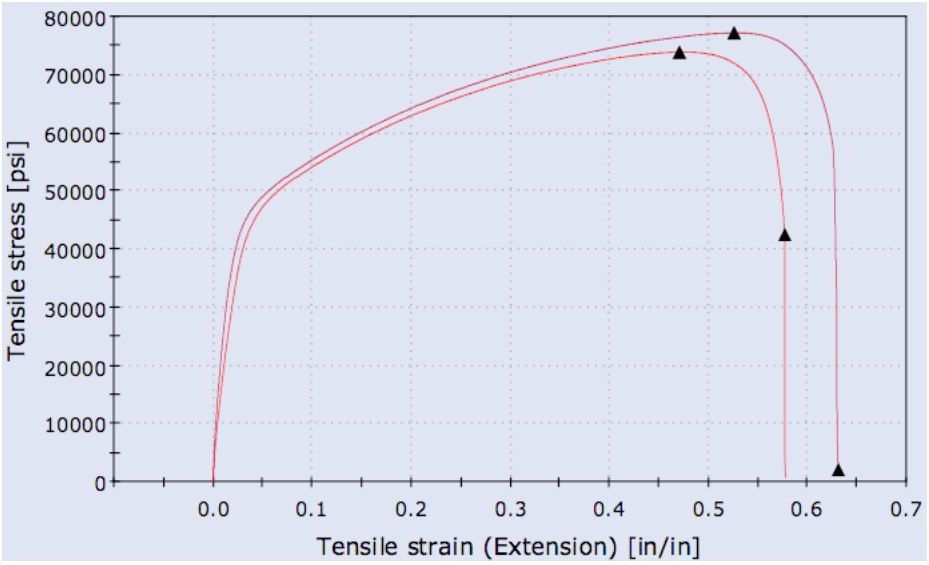

FIGURE 2. Stress-Strain for Stainless Steel 316 for a Dog Bone Welded with No Welding Rod

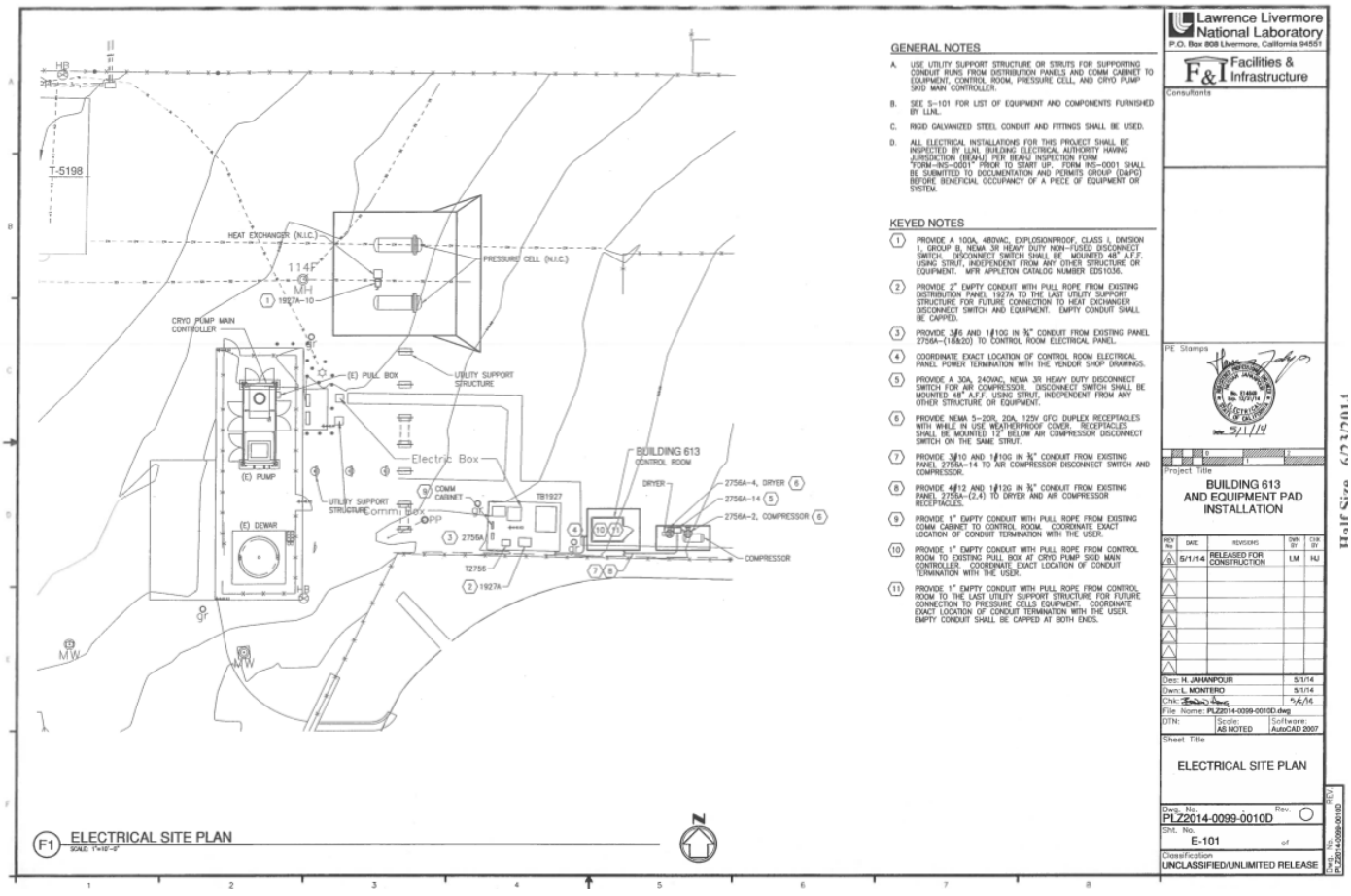

FIGURE 3. Electrical Site Plan for the Future LLNL Pressure Vessel Test Facility

SPECIAL RECOGNITIONS AND AWARDS/ PATENTS ISSUED

1. Methods for tape fabrication of continuous filament composite parts and articles of manufacture thereof. Weisberg AH. United States Patent US 8545657 B2, November 2013.

FY 2014 PUBLICATIONS/PRESENTATIONS

1. Compact Hydrogen Storage in Cryogenic Pressure Vessels, Salvador M. Aceves, Francisco Espinosa-Loza, Elias Ledesma-Orozco, Guillaume Petitpas, in Handbook of Hydrogen Energy, Edited by S.A. Sherif, E.K. Stefanakos, and D.Y. Goswami, CRC Press, Taylor & Francis, ISBN-13: 978-1420054477, 2013.

2. Hydrogen Storage in Pressure Vessels: Liquid, Cryogenic, and Compressed Gas, Guillaume Petitpas and Salvador Aceves, in Hydrogen Storage Technology: Materials and Applications, Edited by Leonard E. Klebanoff, CRC Press, Taylor & Francis, Chapter 4, pp. 91-107, 2013.

3. Cold Hydrogen Delivery in Glass Fiber Composite Pressure Vessels: Analysis, Manufacture, and Testing, Andrew H. Weisberg, Salvador M. Aceves, Francisco Espinosa-Loza, Elias Ledesma-Orozco, Blake Myers, Brian Spencer, International Journal of Hydrogen Energy, Vol. 38, pp. 9271-9284, 2013.

4. Modeling of sudden hydrogen expansion from cryogenic pressure vessel failure, Petitpas, G. and Aceves, S.M., International Journal of Hydrogen Energy, Vol. 38, pp. 8190-8198, 2013**.**

5. Web-Based Resources Enhance Hydrogen Safety Knowledge, Weiner, S.C., Fassbender, L.L., Blake, C., Aceves, S.M., Somerday, B.P., and Ruiz, A., International Journal of Hydrogen Energy, Vol. 38, pp. 7583-7593, 2013.

6. Safe, long range, inexpensive and rapidly refuelable hydrogen vehicles with cryogenic pressure vessels, SM Aceves, G Petitpas, F Espinosa-Loza, MJ Matthews, E Ledesma-Orozco, International Journal of Hydrogen Energy, Vol. 38, pp. 2480-2489, 2013.

7. A Comparative Analysis of the Cryo-Compression and Cryo-Adsorption Hydrogen Storage Methods, G. Petitpas, P. Benard, L.E. Klebanoff, J. Xiao, S. Aceves, International Journal of Hydrogen Energy, 2014.

8. Para-H2 to ortho-H2 conversion in a full-scale automotive cryogenic pressurized hydrogen storage up to 345 bar, Guillaume Petitpas, Salvador M. Aceves, Manyalibo J. Matthews, James R. Smith, International Journal of Hydrogen Energy, Vol. 39, pp. 6533-6547, 2014.

REFERENCES

1. Aceves, S.M., Espinosa-Loza, F., Ledesma-Orozco, E., Ross, T.O., Weisberg, A.H., Brunner, T.C., Kircher, O., "High-density automotive hydrogen storage with cryogenic capable pressure vessels," International Journal of Hydrogen Energy, Vol. 35, pp. 1219-1226, 2010.

2. Ahluwalia, R.K. Hua, T.Q. Peng, J.-K. Lasher. S, McKenney. K. Sinha, J., Gardiner. M. "Technical assessment of cryo-compressed hydrogen storage tank systems for automotive applications," International journal of hydrogen energy, Vol. 35, pp. 4171–4184, 2010.

IV.F.5 Load-Sharing Polymeric Liner for Hydrogen Storage Composite Tanks

Scott McWhorter (Primary Contact), T. Adams, G. Rawls
Savannah River National Laboratory
Hydrogen Technology Research Laboratory
Aiken, SC 29808
Phone: (803) 761-1109
Email: scott.mcwhorter@srnl.doe.gov

DOE Manager
Ned Stetson
Phone: (202) 586-9995
Email: Ned.Stetson@ee.doe.gov

Subcontractor
Virginia Polytechnic Institute and State University, Blacksburg, VA

Project Start Date: October 1, 2013
Project End Date: September 30, 2014

Overall and Fiscal Year (FY) 2014 Objectives

- Reduce cost of compressed hydrogen storage tanks
- Develop basis for using load-sharing liner to displace expensive carbon fiber
- Enhance mechanical properties of polymer
- Reduce off-board impact of fast-fill refueling
- Increase thermal conductivity of polymer to allow better heat transfer

Technical Barriers

This project addresses the following technical barriers from the Hydrogen Storage section of the Fuel Cell Technologies Office Multi-Year Research, Development, and Demonstration Plan:

(B) System Cost

(E) Charging/Discharging Rates

(G) Materials of Construction

(J) Thermal Management

Technical Targets

This project is addressing the needs of compressed gas storage through fundamental material development that shows potential to meet the targets. The goal of the project was to investigate the idea of using nanofilled thermotropic liquid crystalline polymers (TLCPs) for advanced liners and collect data to demonstrate concept feasibility and not to explicitly address specific targets. However, insights gained from these studies will be applied toward the design and synthesis of advanced polymeric liner materials that meet the following DOE 2017 hydrogen storage targets:

- Storage System Cost $12 kWh_{net}
- Min/Max Delivery Temp -40/85°C
- System fill time (5 kg) 3.3 min
- Loss of Usable H_2 0.05 (g/H_2)/kg H_2 stored

INTRODUCTION

Currently, Type IV hydrogen storage tanks, are designed for operational pressures between 350 and 700 bar of compressed gas service that utilize a composite overwrap for reinforcement that is fabricated using expensive aerospace-grade carbon fiber, such as Toray T700S, around a no-load bearing polymeric liner, commonly high density polyethylene (HDPE). While the use of carbon fiber composite overwraps coupled with lightweight, inexpensive no-load bearing liners can significantly lower the weight of high-pressure cylinders compared to all-metallic, analyses have shown that the cost of the carbon fiber composite layer [1] and the limited heat transfer of the liner [2] can add significant cost and complexity to the tank and off-board refueling processes. Furthermore, hydrogen exhibits a reverse Joule-Thomson effect during 700-bar refueling from high-pressure stationary tanks causing heating of the gas, especially during fast-fill protocols that require 5.6-kg of hydrogen be transferred in 3.3 min where the gas temperature inside the tank can rise over 50ºC; adversely affecting the liner and composite integrity when starting at ambient conditions [3]. To compensate for the increase in gas temperature, the gas must be precooled to -40ºC and the tank overpressurized to ensure a complete fill once equilibrium is reached which adds costs from additional energy for refrigeration and compression of more than 20% of the nominal work of compression. Analysis by the Argonne National Laboratory [2] has demonstrated the effect of liner thermal conductivity on gas temperature during a 700-bar fast-fill scenario and projected that a five- to ten-fold increase in the HDPE liner thermal conductivity would have the potential to reduce the liner and gas temperatures by up to 20ºC.

The focus of this project is to demonstrate a viable method to producing a low-cost, high-strength, polymeric load-sharing liner that will allow displacement of expensive aerospace-grade carbon fiber, reducing the cost and mass of the tank, as well as increasing the thermal conductivity of the liner material compared to that of HDPE, thus reducing the impact of precooling and overpressurizing hydrogen during fast-fill refueling to 700-bar.

APPROACH

TLCP liner plaques and bottles (material samples) were injection stretch blow molded by Virginia Tech under various conditions. Zenite is a class of TLCPs originally developed by DuPont™, then bought by Ticona/Celanese. Zenite molecules contain various amounts of 4-hydroxy benzoic acid, terephthalic acid and hydroquinone, but the detailed monomer contents belong to the proprietor. Three grades of Zenite series were used in this project: HX-8000 has a melting temperature of 280°C, HX-3000 and HX-6000 are high melting grades, with melting points around 330°C. Fiber-reinforced Vectra materials were kindly supplied by Ticona/Celanese. Both Vectra A130 and Vectra A230 are based on the same matrix, Vectra A950. Vectra A130 contains 30 wt% short glass fibers, while Vectra A230 is reinforced by 30 wt% short carbon fibers. The composite matrix, Vectra A950, is probably the most extensively discussed commercial TLCP in the literature, which is a copolyester composed of 73 mol% 4-hydroxy benzoic acid and 27 mol% 2-hydroxy-6-naphthoic acid. Due to the lack of a nondisclosure agreement with Celanese in this project, Vectra A950 was not available.

For the samples, three rates of fill (chosen by Virginia Tech) were selected to demonstrate the influence on the initial orientation of the TLCPs. A subsection of samples were heated and subjected to moderate and substantial degrees of stretch in both the axial (machine) direction and the transverse (hoop) direction to generate samples with varying strength as a function of orientation. Samples were also fabricated with varying concentrations of carbon nano-tube and glass fillers to provide initial data on the effect of nanofillers on the mechanical strength of injection molded TLCPs while simultaneously increasing the thermal conductivity. The mechanical and thermal properties of the plaques were measured by Virginia Tech and SRNL using dynamic mechanical analysis, tensile testing and thermal diffusivity, to assess the effect of the processing variables described above.

FY 2014 ACCOMPLISHMENTS

To understand the influence of processing histories on the mechanical properties of unfilled and fiber-reinforced TLCP materials, three materials were injection molded: HX-8000, Vectra A130 and Vectra A230 and mechanical data are shown in Figure 1a-f. Significant tensile property anisotropy can be observed from the mechanical measurements, which could be problematic in hydrogen fuel storage. It seems the longitudinal properties decrease as extrusion speed is increased (Figures 1a and 1d). The injection molded plaques were found to consist of three main sublayers: two skin layers

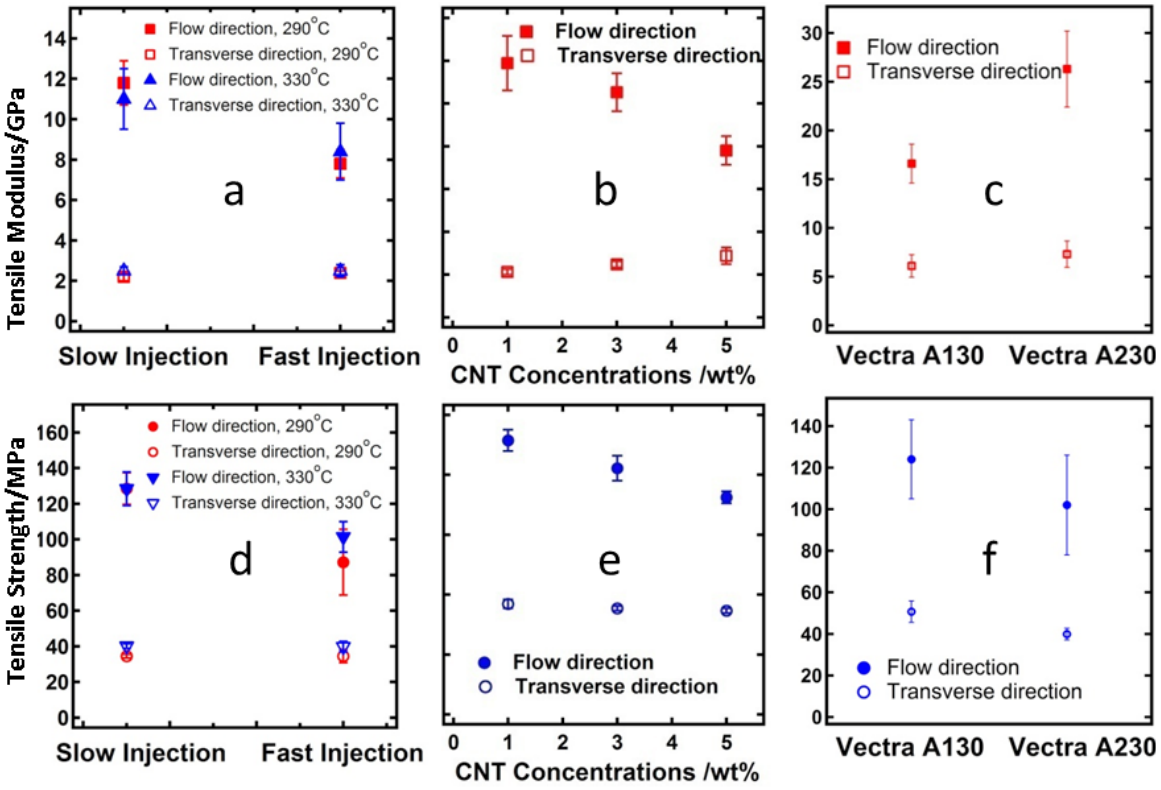

FIGURE 1. Tensile properties of initial blending and extrusion of TLCPs; (a/d) effect of injection speed on unfilled HX-8000, (b/e) effect of nanofiller addition to HX-8000 and (c/f) glass-filled Vectra A130 and A230.

with more oriented molecules and a more isotropic core layer in between, each layer accounted for approximately one-third of the total thickness. High shear stress near the mold wall and the elongation flow field at the flow front ("fountain" flow) are responsible for the formation of the highly oriented skin layers. On the other hand, the core region possesses an overall in-plane random orientation. The tensile modulus in the machine direction shows an increasing trend with slower injection speed and lower barrel temperature (closer to nominal melting point) (Figure 1a). Intuitively, higher injection speeds lead to a higher degree of orientation. However, it is worth noting that the higher injection speeds require a longer time to cool the melt, which leaves the nematic melt more time for orientation relaxation. The relaxed orientation leads to reduced mechanical properties at higher injection speeds as observed in Figure 1a/d.

To determine effect of nanofillers, the maximum carbon nanotube (CNT) concentration is mainly limited by the CNT induced viscosity increment and the CNT concentration gradient in the hopper (low CNT bulk density). For TLCP nanocomposites, the low viscosity of the matrix benefits the extrusion. However, in the hopper the low-density CNTs float above the polymer pellets bed, making extrusion at high CNT concentrations rather challenging so that 5 wt% is the highest possible concentration for $scCO_2$-treated Nanocyl CNT. Shown in Figures 1b/e, as CNT concentrations increase, the modulus and strength in the flow direction exhibits a decreasing trend. The only improvement is observed in the transverse modulus. Lack of surface interaction between the CNT and the polymer matrix is speculated to be the cause for the worse mechanical properties. Thus surface modification of CNTs might be necessary.

Although the lack of unfilled Vectra A130/230 makes the fiber induced property increments difficult to calculate, our objective was to choose materials with superior properties and use them for extrusion blow molding. Thus it is still fair to take the properties of HX-8000 as reference. As clearly indicated in Figure 1c/f, fiber reinforced grades exhibit much better modulus in the flow direction than HX-8000, especially for the carbon fiber composite. Moreover, the transverse moduli are much higher for Vectra A130/230 as well. For overall strength, the fiber reinforced grades are only slightly better. However, the higher melt strength of these materials could be advantageous over the unfilled grades.

Determining the most appropriate die temperature serves as a key to the success of blow molding. The die temperature has to be lower than the melting temperatures of the TLCPs, thus the parisons are in their supercooled state to obtain enough melt strength. On the other hand, if the die temperature is too low, the parisons start to solidify, which makes completion of inflation impossible. The HX-8000 bottles were successfully blow molded and are pictured in Figure 3. With the mold that is currently used, the blow up ratio (bottle diameter to parison diameter) is 1.75.

Thermal conductivity in polymers is predominantly transferred by lattice vibrations with electron transport also occurring slightly. The factors that affect the thermal conductivity in a polymer composite are the filler size, shape, concentration, dispersion (degree of mixing), orientation, bonding between the filler and polymer matrix, thermal conductivity of the constituents (filler and matrix) and the crystallinity of the polymer (increasing crystallinity improves thermal conductivity). Studies were initiated in FY 2014 to determine the thermal conductivity of the unfilled and filled

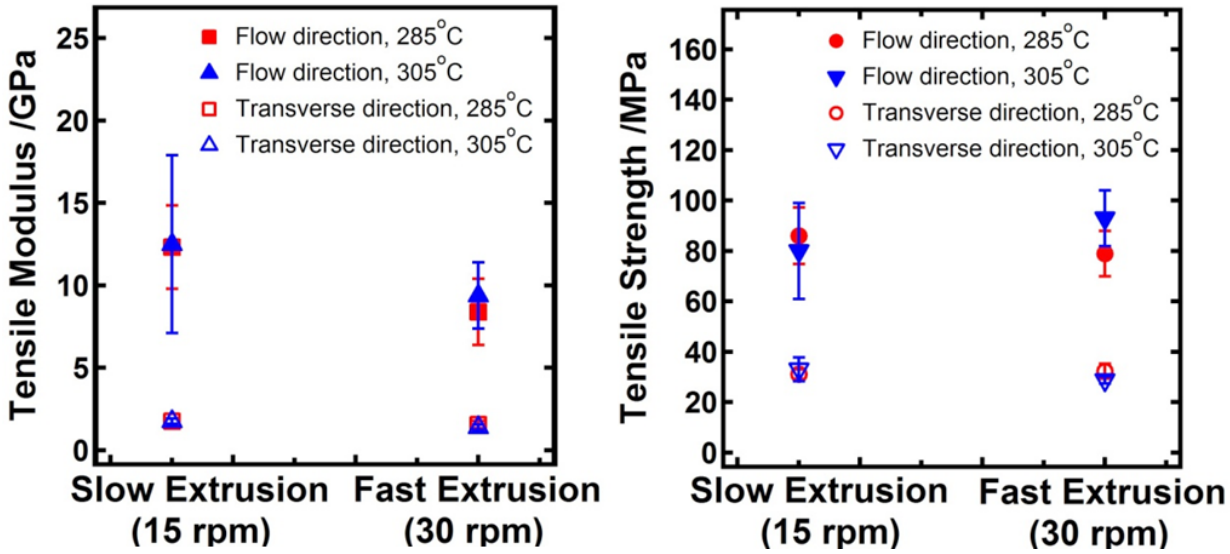

FIGURE 2. Tensile properties, (a) modulus and (b) strength, of blow-molded HX-8000 bottles as a function of extrusion barrel temperatures and extrusion speed.

FIGURE 3. Images of a stretch blow-molded HX-8000 bottle showing the weld lines at mold interfaces. Blow-up ratio (bottle diameter to parison diameter) of 1.75.

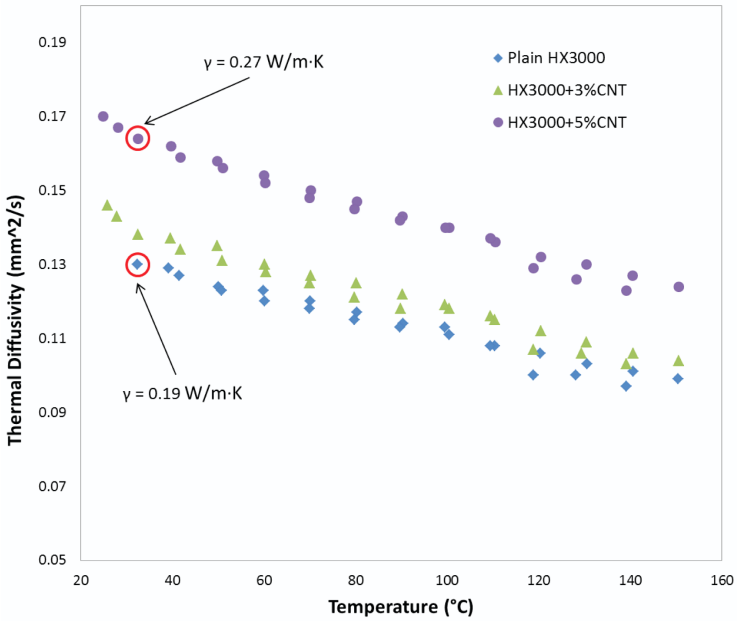

FIGURE 4. Thermal diffusivity of unfilled and CNT-filled HX-3000 between room temperature and 140°C, measured using laser flash diffusivity.

TLCP plaques created for mechanical property improvement and develop a path to increasing the thermal conductivity of the materials. In this case, laser flash thermal diffusivity was used to measure the conductance of heat through 10-mm rounds of TLCP (HX-3000 polymer was chosen due to availability) samples with the data shown in Figure 4. The samples demonstrated a significant increase in the thermal diffusivity which could be indicative of the orientational alignment due to stretching and incorporation of the CNT fillers. However, the magnitude of the highest sample tested at the time of the report (5 wt% CNT loading, 0.27 W/m-K) was almost half of the calculated thermal conductivity of HDPE (0.45 W/m-K) when measured at 23°C. Increasing the blow up ratio and optimizing nanofiller incorporation are expected to give further increases in thermal conductivity creating highly oriented crystal structure that would exceed the values of HDPE.

In summary, the accomplishments of the SRNL and Virginia Tech team during FY 2014 were the following;

- Demonstrated injection molding parameters for initial nanofiller-modified TLCP plaques that show increases in mechanical and thermal properties; however, voids limit properties.
- Demonstrated stretch blow molding parameters to produce nearly void free bottles from base TLCPs that show reasonable tensile properties.
- Initiated thermal diffusivity measurements to characterize the through-plane thermal conductivity of the nanofiller enhanced TLCPs and established a route to increase the thermal conductivity of the TLCPs.

FUTURE DIRECTIONS

- Injection mold TLCP plaques with up to 15 wt% CNT for further thermal diffusivity screening.
- Demonstrate processing parameters to stretch blow mold nanofiller modified TLCP bottles with high blow ratios.
- Demonstrate processing parameters to stretch blow mold modified TLCP blends.
- Continue measuring tensile and thermal properties of nanofiller modified stretch blow molded TLCP bottles.
- Document findings in final report to serve as a basis for future efforts in advanced liner materials.

FY 2014 PUBLICATIONS/PRESENTATIONS

1. McWhorter, S., Baird, D.B., Adams, T., Rawls, G. "Load-sharing Polymeric Liner for Hydrogen Storage Composite Tanks." *2014 US DOE Hydrogen and Fuel Cells Program Annual Merit Review.* Washington, DC: June 2014.

REFERENCES

1. James, B.D., Moton, J.M., Colella, W.G. "Hydrogen Storage Cost Analysis." *Proceedings of the 2013 US DOE Hydrogen and Fuel Cells Program Annual Merit Review*. Crystal City, VA: June 2013. [Online]. [Accessed July 2014] Available: http://www.hydrogen.energy.gov/pdfs/review13/st100_james_2013_o.pdf.

2. Ahluwalia, R.K., Hua, T.Q., Peng, J-K., Roh, H.S. "System Level Analysis of Hydrogen Storage Options" *Proceedings of the 2012 US DOE Hydrogen and Fuel Cells Program Annual Merit Review*. Crystal City, VA: June 2013. [Online][Accessed July 2014]. Available: http://www.hydrogen.energy.gov/pdfs/review12/st001_ahluwalia_2012_o.pdf.

3. Zhang, J., Fisher, T.S., Ramachandran, P.V., Gore, J.P. and Mudawar, I., "A Review of Heat Transfer Issues in Hydrogen Storage Technologies," J. of Heat Transfer (2005), 127: 1391.

V. FUEL CELLS

V.0 Fuel Cells Sub-Program Overview

INTRODUCTION

The Fuel Cells sub-program supports research, development, and demonstration of fuel cell technologies for a variety of transportation, stationary, and portable applications, with a primary focus on reducing cost and improving durability. These efforts include research and development (R&D) of fuel cell stack components, system balance-of-plant components, and subsystems, as well as system integration. The sub-program seeks a balanced, comprehensive approach to fuel cells for near-, mid-, and longer-term applications. Existing early markets and near-term markets include portable power, backup power, auxiliary power units, and specialty applications such as material handling equipment. In the mid- to long-term, development of fuel cells for transportation applications is a primary goal due to the nation's significantly reduced energy and petroleum requirements and the subsequent increase of available high-efficiency fuel cell electric vehicles. Development of fuel cells for distributed power generation (e.g., combined heat and power (CHP) for residential and commercial applications) is also underway. The sub-program's portfolio of projects covers a broad range of technologies including polymer electrolyte membrane (PEM) fuel cells, direct methanol fuel cells, alkaline membrane fuel cells, and molten carbonate fuel cells.

The sub-program's fuel cell tasks in the *Fuel Cell Technologies Office Multi-Year Research, Development, and Demonstration Plan* are organized around development of components, stacks, sub-systems, and systems; supporting analysis; and testing, technical assessment, and characterization activities.[1] Task areas for fuel cell system and fuel processor sub-system development for stationary power generation applications are included, as are those for early market fuel cell applications, and for the development of innovative concepts for fuel cell systems.

GOAL

The sub-program's goal is to advance fuel cell technologies for transportation, stationary, and portable applications to make them competitive in the marketplace in terms of cost, durability, and performance, while ensuring maximum environmental and energy-security benefits.

OBJECTIVES[2]

The sub-program's key objectives include:

- Develop a 60% peak-efficient, direct-hydrogen fuel cell power system for transportation, with 5,000-hour durability, that can be mass-produced at a cost of $30/kW ($40/kW by 2020).
- Develop distributed generation and micro-CHP fuel cell systems (5 kW) operating on natural gas or liquid petroleum gas that achieve 45% electrical efficiency and 60,000-hour durability at an equipment cost of $1,500/kW by 2020.
- Develop medium-scale CHP fuel cell systems (100 kW–3 MW) by 2020 that achieve 50% electrical efficiency, 90% CHP efficiency, and 80,000-hour durability at a cost of $1,500/kW for operation on natural gas and $2,100/kW when configured for operation on biogas.
- Develop a fuel cell system for auxiliary power units (1–10 kW) with a specific power of 45 W/kg and a power density of 40 W/L at a cost of $1,000/kW by 2020.

FISCAL YEAR (FY) 2014 TECHNOLOGY STATUS AND ACCOMPLISHMENTS

Cost reductions and improvements in durability continue to be the key challenges facing fuel cell technologies. In addition, advances in air, thermal, and water management are necessary for improving fuel cell performance; some stationary applications would benefit from increased fuel flexibility; and, while fuel cells are approaching their targets for power density and specific power, further progress is required to achieve system packaging requirements necessary for commercialization.

[1] http://energy.gov/eere/fuelcells/downloads/fuel-cell-technologies-office-multi-year-research-development-and-16

[2] Note: Targets and milestones were recently revised; therefore, individual project progress reports may reference prior targets.

One of the most important metrics is the projected high-volume manufacturing cost for automotive fuel cells, which the sub-program tracks on an annual basis. The cost analysis in 2014 was based on similar technologies as used in 2013, including a Pt-Co-Mn nanostructured thin film cathode catalyst developed through an earlier DOE-funded project, and therefore the 2014 costs status of $55/kW is the same as the 2013 status, as depicted in Figure 1. Examination of more advanced catalyst technology developed more recently by the sub-program, including de-alloyed PtNi catalysts, is planned for future year analyses.

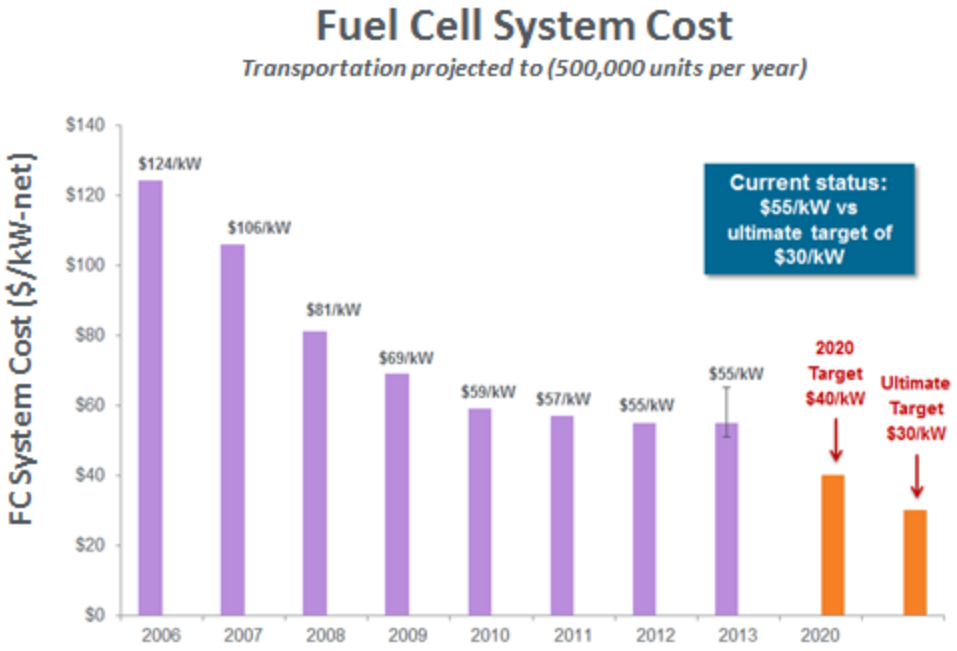

FIGURE 1. Modeled cost of an 80-kW automotive fuel cell system based on projection to high-volume manufacturing (500,000 units/year).[3]

To enable vehicle commercialization, the sub-program is targeting a cost reduction to $40/kW by 2020. Long-term competitiveness with alternative powertrains is expected to require further cost reduction to $30/kW, which represents the sub-program's ultimate cost target.

The sub-program sponsors technical working groups on the topics of durability, transport modeling, and catalysis. These working groups, composed of representatives from DOE-funded R&D projects, met in 2014 to exchange information, create synergies, share experimental and computational results, and collaboratively develop methodologies for and understanding of further R&D needs in the topical areas. Additional issues addressed in 2014 include an examination of non-platinum-grade metal (PGM) catalyst targets by the catalysis working group, which led to development of a new non-PGM activity target adopted by the Fuel Cell Tech Team and planned for adoption by the Fuel Cell Technologies Office.

Catalysts

Argonne National Laboratory (ANL) adapted a synthetic procedure originally developed at Lawrence Berkeley National Laboratory (LBNL) to produce a new platinum-nickel (Pt-Ni) catalyst with unprecedented activity. Scientists at LBNL initially created Pt-Ni crystalline polyhedra particles that were left under ambient conditions in a solvent exposed to air for two weeks. Surprising changes in the structure and composition were noted—the particles had spontaneously dealloyed into a more Pt-rich alloy and transformed into hollow nanoframe structures. Recognizing the potential relevance of these new structures for catalysis, the LBNL researchers teamed up with electrochemical experts at ANL. ANL optimized the synthesis process, resulting in a catalyst that can be prepared in only a few hours with an

[3] DOE Hydrogen and Fuel Cells Program Record #13012, http://hydrogen.energy.gov/pdfs/13012_fuel_cell_system_cost.pdf.

activity that outstrips all previous fuel cell catalysts in ex situ testing. Encapsulating a protic ionic liquid inside the nanoframe catalyst resulted in a further increase in activity, yielding more than 30X the mass activity of a conventional platinum catalyst in rotating disk electrode (RDE) testing. The nanoframes showed no decrease in activity after 10,000 cycles of accelerated stress testing, demonstrating high durability. ANL is now scaling up synthesis of the catalyst for testing in a fuel cell, a critical step to assess viability in practical applications (Figure 2). (ANL)

In 2014, advances in catalyst synthesis and electrode optimization allowed PtCo and PtNi dealloyed catalysts, which have already met DOE targets for mass activity and durability of mass activity, to achieve good durability of high-current performance for the first time. These catalysts achieved the same H_2/air fuel cell performance as a 0.4 mg_{Pt}/cm^2 electrode, but with only one-fourth the PGM loading. The performance improvements were confirmed in a full-active-area automotive stack. Up to 60,000 cycles between 0.6 and 0.925 V were performed with only 20 mV loss at 1.5 A/cm^2 (Figure 3). (General Motors)

Anode-protection catalysts based on the oxygen evolution reaction (OER catalysts), which prevent oxidative degradation of anode catalysts and supports under-cell reversal, have been developed by 3M, but until now these catalysts were degraded by typical startup/shutdown conditions, in which H_2/air fronts move through the anode. In 2014 this problem was solved by incorporating a refractory metal interlayer between the anode catalyst and the OER catalyst, serving to isolate the OER catalysts from the localized destructive effects of H_2/air fronts. These interlayer-modified catalysts have demonstrated the ability to continue protecting the anode during more than 10 hours of cell reversal even after being exposed to 200 cycles of hydrogen/air switching (Figure 4). (3M)

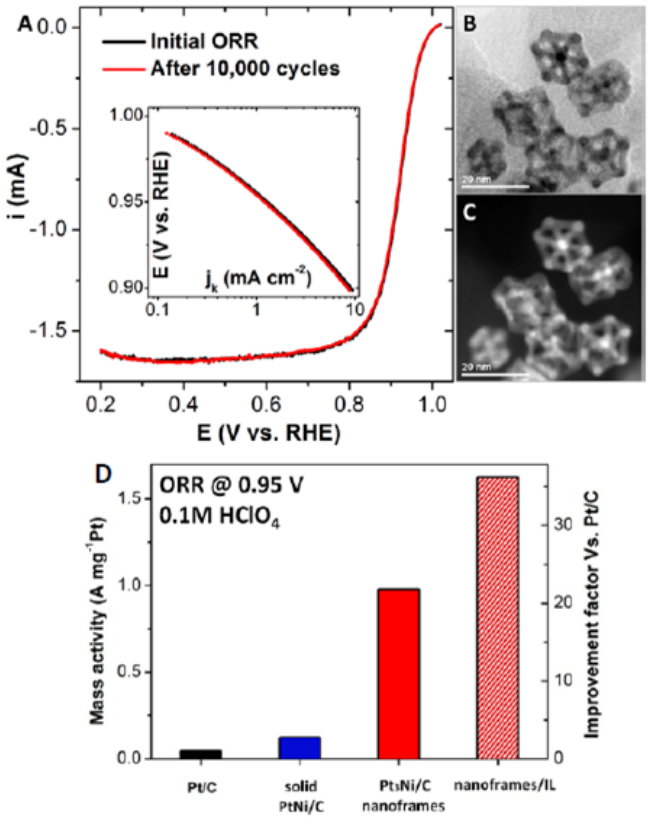

FIGURE 2. Multimetallic nanoframes with three-dimensional surfaces: (A) Oxygen reduction reaction (ORR) performance before and after 10,000 cycles between 0.6-1.0 V (reference hydrogen electrode, RHE); (B-C) preserved morphology of nanoframes after durability test; (D) superior mass activity.

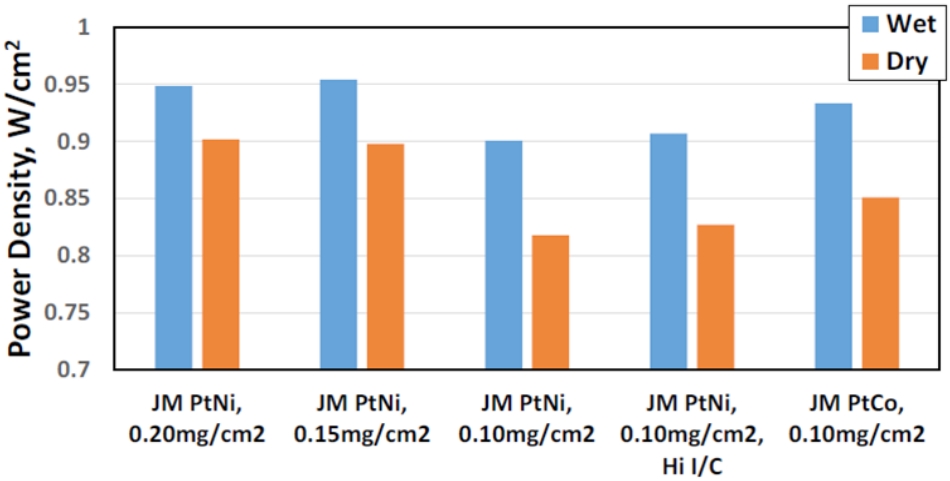

FIGURE 3. Full-active-area stack high-power performance of the dealloyed $PtNi_3$ and $PtCo_3$ catalysts under Fuel Cell Tech Team recommended conditions.

Protocols and best practices for RDE catalyst testing were prepared. Initial screening of fuel cell catalyst activity is typically performed ex situ using an RDE. RDE experiments are performed with little standardization between laboratories, leading to large discrepancies in reported activity values for the same catalysts and undermining the validity and usefulness of RDE data. Improvements in technique that allowed for higher and more reproducible activity have been reported recently, but have not yet been widely adopted. Therefore, Fuel Cell Technologies Office issued a request for information on RDE best practices, discussed the issue at meetings of the catalysis and durability working groups, and supported a collaborative effort between researchers at ANL and the National Renewable Energy Laboratory (NREL) to use the resulting input to develop protocols and best practices for RDE testing. This effort established a standard protocol and test methodology for measurement of electrochemical area (ECA), ORR activity, and durability, and evaluated three electrocatalysts using identical protocols and electrode preparation in three laboratories. Comparison of the results verified the reproducibility of measured ECA, ORR activity, durability between the labs, demonstrating the validity of the newly issued protocols (Figure 5). (ANL and NREL)

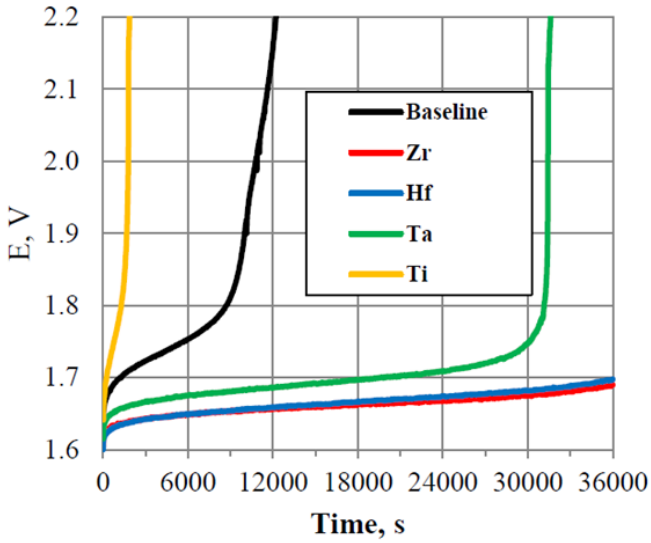

FIGURE 4. Cell reversal durability after 200 gas switches in addition to 200 pulses at 200 mA/cm^2. Reversal potential of the four refractory metals added as a sandwich between Pt and the Ir OER catalyst.

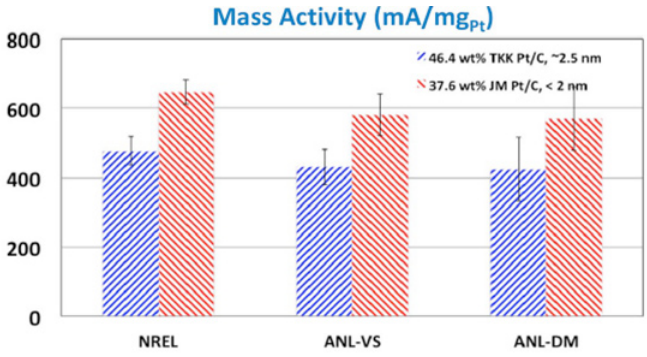

FIGURE 5. Comparison of mass activity between laboratories of two Pt/C electrocatalysts in 0.1M $HClO_4$ at 25°C and 100 kPa conducted at 20 mV/s in the anodic sweep.

Membranes

A new project begun in FY 2014 is further advancing performance and durability of membranes under hot and dry operating conditions by improving and combining components developed under earlier projects. Perfluoroimide acid ionomers previously developed have met many performance and durability targets, but ionomer improvement and membrane thickness reduction are required to simultaneously meet all DOE membrane targets. Modifications to the ionomer chemical structure, combined with incorporation of inert nanofiber supports developed by Vanderbilt University, has enabled the new membranes to meet chemical and mechanical durability targets while approaching all membrane resistance targets. (3M)

Membrane Electrode Assembly (MEA) Integration

Improvements in MEAs containing PtNi nano-structured thin film catalysts have enabled performance improvement at high current densities, resulting in PGM total content levels as low as 0.16 g/kW at 150 kPa_{abs}. This measurement was obtained at a high operating temperature of 90°C and voltage of 0.69 V, conditions that satisfy the DOE heat rejection target, $Q/\Delta T \leq 1.45$. When compared to PGM total content measured at 0.69 V in previous years, this year's results mark a 25% and a 6% improvement since 2012 and 2013, respectively. Further development is required to achieve DOE's target level of 0.125 g/kW, and to simultaneously meet durability targets (Figure 6). (3M)

BUDGET

The FY 2015 budget request calls for approximately $33.0 million for the Fuel Cells sub-program, which is at approximately the same level as the FY 2014 appropriation.

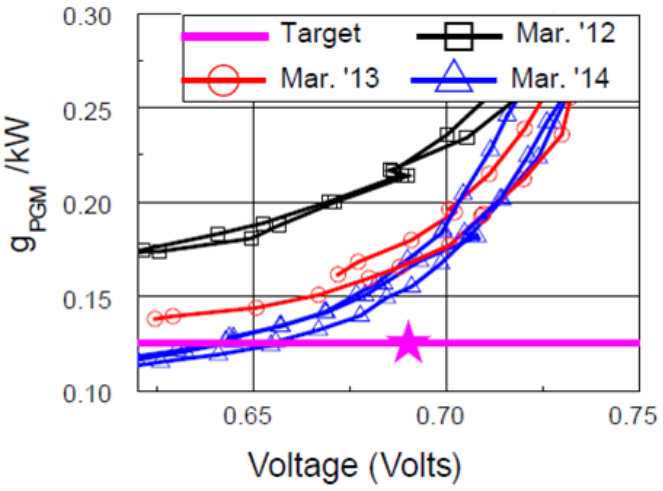

FIGURE 6. Total PGM content in PtNi nano-structured thin film-based MEAs operating at 90°C. At this temperature, an operating voltage of 0.69 V or higher is required to meet the DOE heat rejection target.

Figure 7 shows the budget breakdown by R&D area for the FY 2014 congressional appropriation of $33.5 million and the FY 2015 budget request. The sub-program continues to focus on reducing costs and improving durability with an emphasis on fuel cell stack components. New projects were initiated in FY 2014 for R&D on membranes, and molten carbonate fuel cells. In FY 2015, the Fuel Cells sub-program plans to facilitate the development of non-

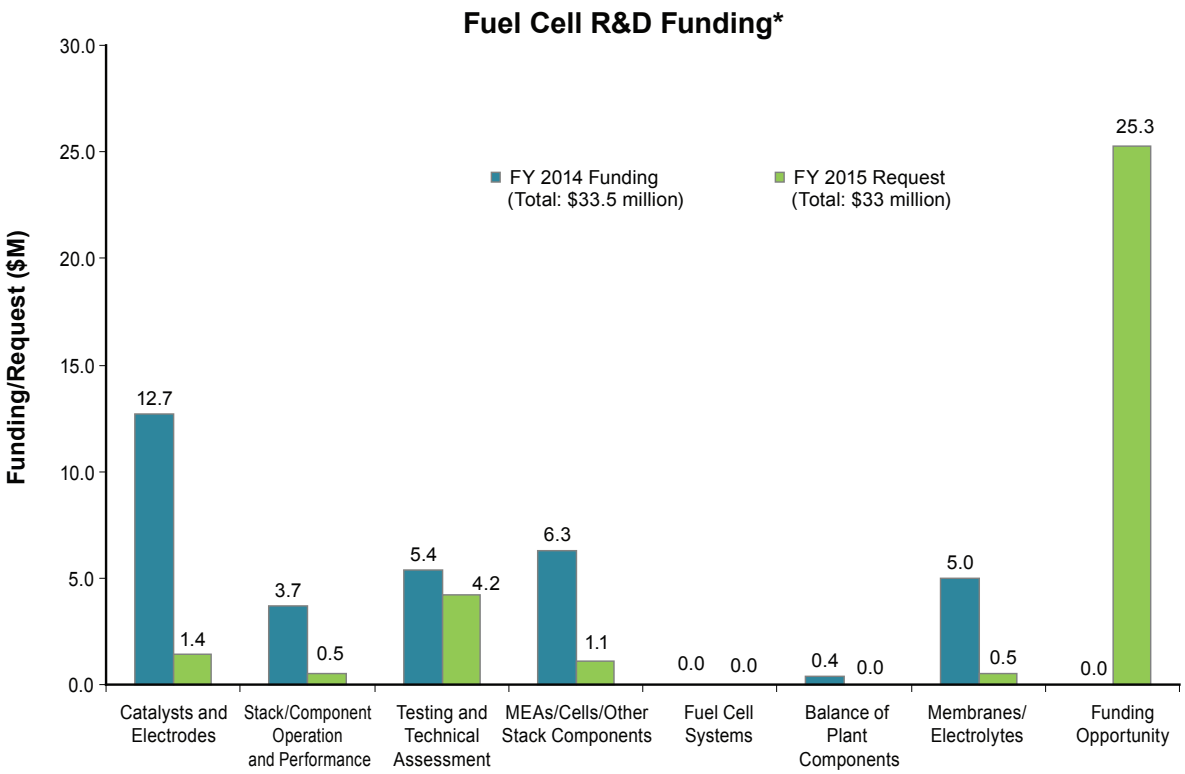

* Subject to appropriations, project go/no-go decisions, and competitive selections. Exact amounts will be determined based on research and development progress in each area and the relative merit and applicability of projects competitively selected through planned funding opportunity announcements.

FIGURE 7. Budget Breakdown for FY 2014 and FY 2015

PGM catalyst containing MEAs through a center of excellence approach addressing improved modeling for materials development, high-throughput screening, and advanced characterization. The Fuel Cells sub-program plans to issue a funding opportunity announcement for awards funded in FY 2015.

FY 2015 PLANS

In FY 2015, the Fuel Cells sub-program will continue R&D efforts on fuel cells and fuel cell systems for diverse applications, using a variety of technologies (including PEM and alkaline membrane fuel cells) and a range of fuels (including hydrogen, natural gas, and bio-derived renewable fuels). Support will continue for R&D that addresses critical issues with electrolytes, catalysts, electrodes, and modes of operation, with an emphasis on cost reduction and durability improvement. The sub-program will also continue its emphasis on science and engineering with a focus on component integration at the cell and stack level, as well as on integration and component interactions at the system level. Ongoing support of modeling will guide component R&D, benchmarking complete systems before they are built and enabling exploration of alternate system components and configurations. Cost analysis efforts include studies of PEM fuel cell technology for transportation applications, as well as PEM fuel cell and alternative technologies for distributed power generation systems (including CHP) and systems for emerging markets; further detailed results of these analyses are expected in FY 2015. Updates to target values will be released in a revision of the *Multi-Year Research, Development, and Demonstration Plan*, which is scheduled for release in FY 2015.

Dr. Dimitrios Papageorgopoulos
Fuel Cells Program Manager
Fuel Cell Technologies Office
Office of Energy Efficiency and Renewable Energy
U.S. Department of Energy
1000 Independence Ave., SW
Washington, D.C. 20585-0121
Phone: (202) 586-9995
Email: Dimitrios.Papageorgopoulos@ee.doe.gov

V.A.1 Durable Catalysts for Fuel Cell Protection during Transient Conditions

Radoslav T. Atanasoski (Primary Contact), Dennis van der Vliet, Gregory M. Haugen, Jimmy Wong, Theresa M. Watschke, Andy Armstrong, Ljiljana L. Atanasoska

Energy Components Program, 3M Company
3M Center, Building 201-2N-05
St. Paul, MN 55144-1000
Phone: (651) 733-9441
Email: rtatanasoski@mmm.com

- Timothy C. Crowtz, Jessie E. Harlow, Robbie J. Sanderson, David A. Stevens, Jeff R. Dahn
  Dalhousie University, Halifax, Nova Scotia, Canada
- David A. Cullen, Karren L. More, Shawn Reeves
  Oak Ridge National Laboratory, Oak Ridge, TN
- Deborah J. Myers, A. Jeremy Kropf, Vojislav R. Stamenkovic, Nenad M. Markovic
  Argonne National Laboratory, LeMont, IL
- Hao Zhang, Sumit Kundu, Wendy Lee
  AFCC (Automotive Fuel Cell Cooperation) Corporation
  Burnaby, BC, Canada

DOE Managers

Jacob Spendelow
Phone: (202) 586-4796
Email: Jacob.Spendelow@ee.doe.gov

David Peterson
Phone: (720) 356-1747
Email: David.Peterson@ee.doe.gov

Technical Advisors

Thomas Benjamin
Phone: (630) 252-1632
Email: Benjamin@cmt.anl.gov

John P. Kopasz
Phone: (630) 252-7531
Email: kopasz@anl.gov

Contract Number: DE-EE0000456

Subcontractors and Federally Funded Research and Development Centers:

- Dalhousie University, Halifax, Nova Scotia, Canada
- Oak Ridge National Laboratory, Oak Ridge, TN
- AFCC Corporation, Burnaby, BC, Canada
- Argonne National Laboratory, Argonne, IL

Project Start Date: August 1, 2009
Projected End Date: December 31, 2013

Overall Objectives

- Develop catalysts that will enable proton exchange membrane (PEM) fuel cell systems to weather the damaging conditions in the fuel cell at voltages beyond the thermodynamic stability of water during the transient periods of fuel starvation.
- Demonstrate that these catalysts will not substantially interfere with the performance of nor add much to the cost of the existing catalysts.

Fiscal Year (FY) 2014 Objectives

- Expand the catalyst evaluation towards 'real life' application with emphasis on hydrogen – air gas switching.
- Perform root cause analysis and develop working hypothesis of the impact of gas switching.
- Mitigate the impact of gas switching on the oxygen evolution reaction (OER) catalyst stability.
- Synthesize modified OER catalysts and narrow composition and construction parameters.
- Establish fundamentals of the activity and stability of the modified OER catalysts.

Technical Barriers

This project addresses the following technical barriers from the Fuel Cells section of the Fuel Cell Technologies Office Multi-Year Research, Development, and Demonstration Plan:

(A) Durability

(C) Performance

Technical Targets

The DOE-approved technical target for the final year had the following milestone:

- 2014 Milestone: After 200 gas switches, achieve cell reversal of 10 hours at -0.2 A/cm^2 at <1.7 V with <0.035 mg/cm^2 platinum group metal (PGM).

Accomplishments

The final-year project milestone has been achieved:

- Constructs with additional refractory metals have fulfilled the cell reversal requirement after gas switching

within the 2014 program milestone voltage limit, <1.7 V, and PGM loading, <0.035 mg/cm².

In addition:

- The hypothesis that separating the OER catalyst from atomic proximity of Pt may alleviate the impact of gas switching was proven.
- As an added benefit of the separating layer, improved OER activity was achieved.
- Fundamental materials studies aimed at understanding the extraordinary durability of the new OER-Pt/nano-structured thin-film (NSTF) constructs have converged to conclude that stabilizing the Pt and Ir oxides is paramount to increasing reversal endurance.

INTRODUCTION

The project addresses a key issue of importance for successful transition of PEM fuel cell technology from development to the pre-commercial phase (2010-2015). This issue is the failure of the catalyst and the other thermodynamically unstable membrane electrode assembly (MEA) components at the anode during start-up/shut-down (SU/SD) and local fuel starvation, commonly referred to as transient conditions. During these periods, the electrodes can reach potentials up to 2 V. One way to minimize the damage from such transient events is to lower the potential seen by the electrodes. At lower positive potentials, increased stability of the catalysts themselves and reduced degradation of the other MEA components are expected.

APPROACH

This project tries to alleviate the damaging effects during transient conditions from within the fuel cells via improvements to the existing catalyst materials. We are modifying both the anode and the cathode catalysts to favor the oxidation of water over carbon corrosion by maintaining the cathode potential close to the onset potential for water oxidation. The presence of a highly active OER catalyst on the cathode reduces the overpotential for a given current demand, thus reducing the driving force for carbon and platinum dissolution. In addition, inhibition of the oxygen reduction reaction (ORR) on the anode side lowers the ORR current through reduced proton demand, which in turn decreases the OER current on the cathode, resulting in reduced cathode potential.

A key requirement for both concepts is to implement the added catalyst with negligible inhibition of the fuel cell performance and with minimal increment of PGM.

RESULTS

Durable Oxygen Evolution Reaction Catalysts. During the previous four years, we have developed and integrated Ir and IrRu OER components with Pt catalyst on 3M NSTF support [1-4]. The catalyst was tested via the electrochemical equivalent to start-up conditions, sustaining up to 5,000 pulses to <1.5 V. However, the *same catalyst, when applied on the anode side for cell reversal mitigation, lost its OER activity when exposed to real gas switching (GS) from hydrogen to air.* In Figure 1, the difference in the cell reversal durability is illustrated by comparing the baseline OER-Pt/NSTF (20 μg/cm^2 Pt + 15 μg/cm^2 Ir) after the 200 GS cycles with the same catalyst after the electrochemical equivalent of 200 pulses. It is obvious that the gas switches are detrimental to the OER. The initial hold potential of the GS-cycled catalyst is about 50 mV higher than without the GS, and the decay to MEA failure happens 2.5 hours sooner. Clearly, gas switches are damaging the MEA in a way that the electrochemical equivalent of 200 pulses (designed to simulate SU/SD cycles) did not predict.

Root Cause Hypothesis. *High electrode potential* is usually the first cause to be associated with the catalyst failure during SU/SD. However, the *GS does not provoke a high anode potential;* the maximum potential that can be reached under air is about 1 V (Figure 2A). Numerous tests performed during the past three years have proven that the OER catalyst is stable up to 1.75 V, with simulated pulses (Figure 2B) integrated into the testing to confirm the catalyst stability during SU/SD events. This precludes high potential during GS as the cause of the OER catalyst degradation.

The only other plausible explanation involves the *hydrogen-air direct recombination on the anode catalyst.*

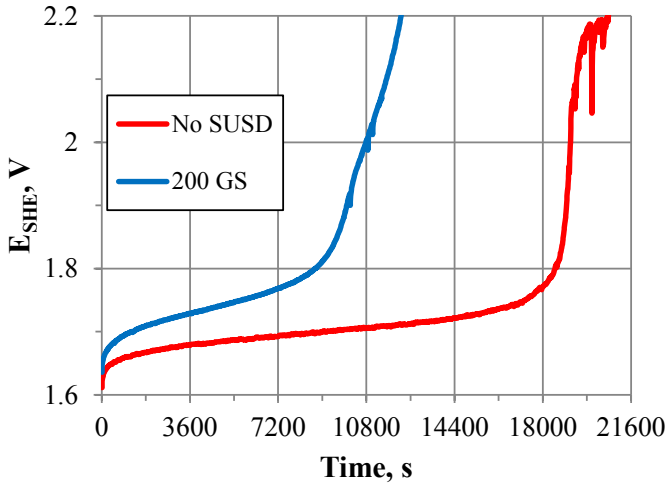

FIGURE 1. Effect of GS on reversal durability: potential as a function of time at 200 mA/cm^2 galvanostatic hold. The blue line represents reversal durability after 200 gas switches on IrPt/NSTF (20 μg/cm^2 Pt + 15 μg/cm^2 Ir); 50-cm^2 MEA under nitrogen/1% hydrogen, 70°C, fully saturated.

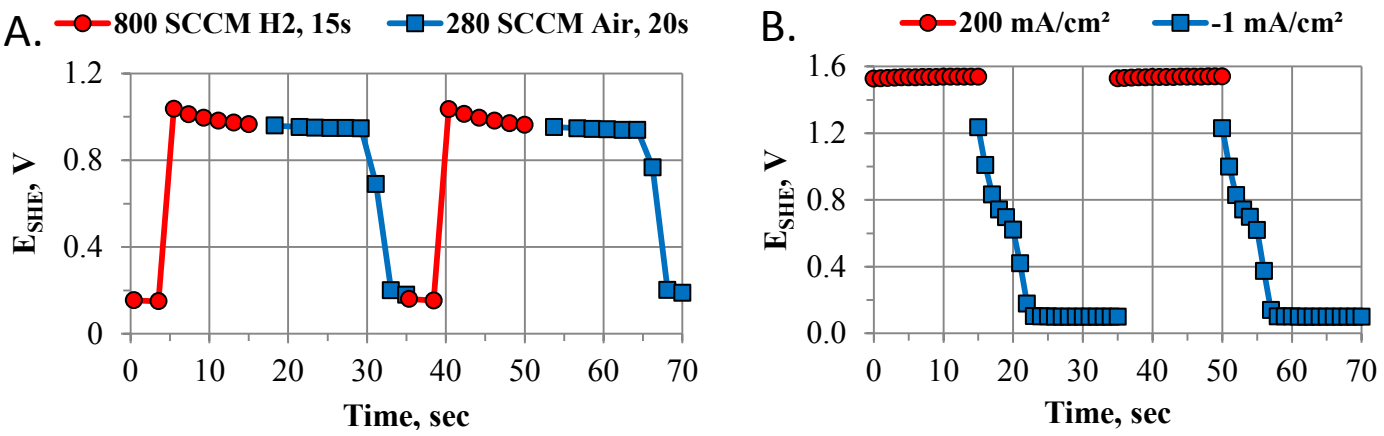

FIGURE 2. Potential Profiles of the Anode During Gas Switching (A) and During Electrochemically Simulated Pulses (B)

This mechanism came into consideration based on the key observation that the otherwise inferior conventional, dispersed OER-added catalyst—*admixed* IrRu catalyst with dispersed Pt—did not lose much of its performance due to GS. As is well known, hydrogen and oxygen (in the air) can directly react, and the reaction can be vigorous in the presence of platinum. This reaction produces *heat and a variety of radicals*. The OER-Pt/NSTF construct is such that the OER catalyst is in *atomic proximity* of the Pt reaction sites. Therefore, both the heat and the reactive radicals can directly impact the thin-film OER catalyst before the heat is dissipated and the radicals recombined. This is in contrast to the dispersed catalyst, where the two catalyst components, Pt/C for hydrogen oxidation reaction (HOR) and IrRu for OER, are well separated on the atomic scale. Therefore, the OER catalyst within the dispersed anode suffers very little from the SU/SD event, while the durability of the OER-Pt/NSTF is quickly compromised. Based on this hypothesis, the concept and the strategy for diminishing the damaging effect of the gas switching were based on two principles:

- *Slowing down the rate of the chemical reaction between hydrogen and oxygen,* while leaving the electrocatalytic HOR unaffected. This will decrease the rate of both the release of heat and the creation of radicals. Whereas the reaction is chemical in nature, the fact that the recombination of the two elements needs catalytic sites to proceed provides a theoretical background upon which the approach of this proposal can be justified. Specifically, we would block a sufficient number of the platinum active sites in a fashion similar to the inhibition of the ORR [4]. Since the incoming hydrogen molecules during startup will react with the adsorbed oxygen, a substantial reduction in the number of the sites where oxygen can be adsorbed and subsequently radicals formed will effectively reduce the rate of the HOR.
- *Inducing a physical separation of Pt from the OER*, which will reduce both the number of radicals and the extent of heat transfer from the Pt sites where they are generated to the OER where they cause degradation.

This concept is material-based, just like the OER-modified anode. The concept fits into the philosophy of a protection from within the MEA and as such is always 'on.' The success of the concept would depend on

- finding a material that is stable when exposed to high potentials during cell reversal
- implementing an amount sufficient to inhibit the undesired H_2–O_2 reaction without compromising the anode performance
- manufacturing via processes compatible with the existing Pt/NSTF anode fabrication
- adding little, preferably not at all, to the PGM loading.

Materials with the required stability were found in *the group of transition elements known as refractory metals.* Due to the high affinity for oxygen, these metals form extremely inert oxide films on their surfaces, which is the source of their high stability. These elements are inexpensive compared to the PGMs and can be sputter-deposited in a vacuum while their compounds can be generated via reactive sputtering or by using a sputtering target of the desired composition. Most of these elements and their oxides are known inhibitors for the ORR; therefore, their application will not only inhibit the HOR but will also enhance the protection of the cathode during SU/SD. As we have shown in this project [4], using the deposition of tantalum (Ta) on Pt, a relatively small coverage of Ta reduces the ORR substantially without any noticeable adverse effect on the HOR.

Four metals from the group of refractory metals were selected for rather rigorous evaluation: Zr, Hf, Ti, and Ta. The catalyst fabrication and evaluation were intended to

- Determine the range of added elements
- Ascertain the stability of the added element in PEMs

- Establish testing procedures and protocols
- Evaluate the performance for cell reversal
- Understand the fundamentals of the impact of the added elements.

The cell reversal test protocol as described in [4] was added by

- GS cycling (20 sec air, 15 sec H_2)
- High current reversal hold up to 10 hours (-200 mA/cm², to 2.2 V)

and it was carried out using 50-cm^2 MEAs at 70°C, A/C N_2/1% H_2 @ 1,000 SCCM, 110% relative humidity.

The *constructs with zirconium* were tested first, and the results were such that eventually zirconium was considered as a *model system*. This material was studied in detail to understand the fundamentals of the mechanism with which the refractory metal oxides can mitigate the degradation through gas switching. It became clear from Zr study that the layer thickness and position within the PtIr anode is of great importance. Fundamental characterization of the PtZrIr model system using advanced analytical techniques, including X-ray photoelectron spectroscopy and scanning transmission electron microscopy (STEM), allowed for better understanding of how to improve durability.

The greatest impact to increasing reversal durability after GS was with *Zr deposited between Pt and Ir* (Figure 3A), forming a M-Ox interlayer ('sandwich') construction, validating our starting hypothesis that a physical separation of Pt from the OER catalyst is key in mitigating GS degradation. The best-of-class interlayer constructs for all four elements is represented in Figure 3B, from which we concluded that planar equivalent of 250 Å Zr and Hf gave the highest reversal durability performance, reaching 10 hours under 1.7 V.

Finally, in Figure 4, comparative STEM images of IrPt/NSTF and Ir*Zr*Pt/NSTF are presented at different stages of the durability test protocol. These images illustrate well the considerably improved retention of the Ir catalyst when Zr is present between Pt and Ir, as result of which a better cell reversal durability was observed. Along with the other techniques used in this period, the understanding of the extraordinary durability of the new OER-Pt/NSTF constructs has converged to conclude that stabilizing the Pt and Ir oxides is paramount to increasing the reversal endurance.

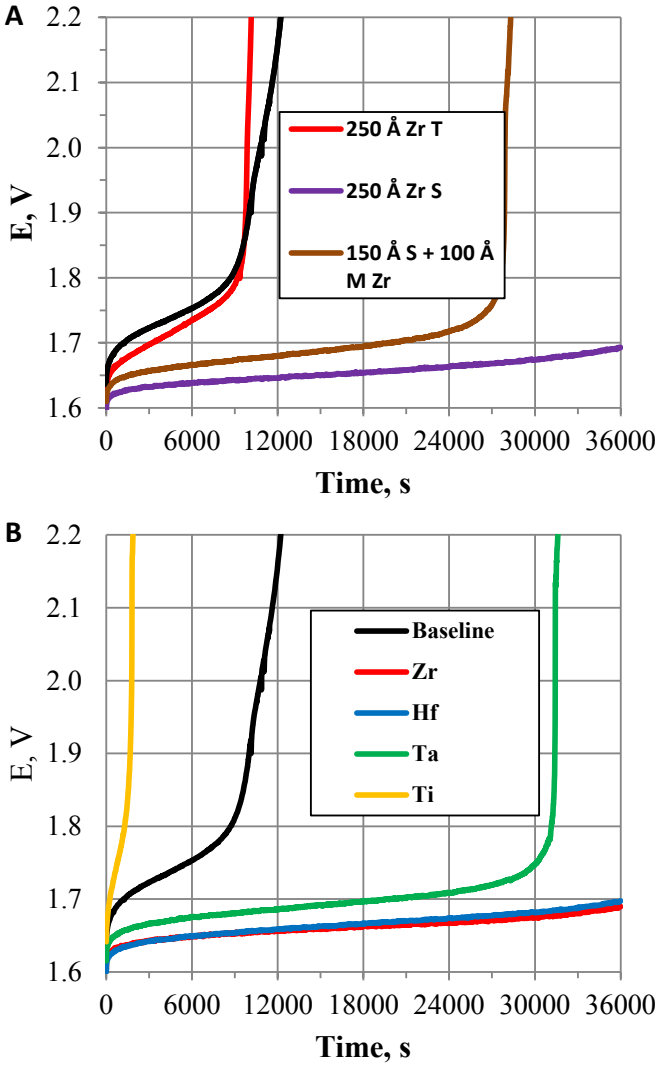

FIGURE 3. Cell reversal durability after 200 gas switches in addition to 200 pulses at 200 mA/cm^2. (A) Three different constructs of 250-Å Zr added to the Pt/NSTF: atop deposited Zr (T); Zr sandwiched between Pt and Ir (S). 150-Å Zr deposited on top of Pt, followed by 100-Å Zr intermixed with Ir (M); Black line: baseline IrPt/NSTF. (B) Reversal potential of the four refractory metals added as a sandwich between Pt and Ir.

FY 2014 PUBLICATIONS/PRESENTATIONS

Papers

1. Vincent Lee, Darija Susac, Sumit Kundu, Viatcheslav Berejnov, Radoslav T. Atanasoski, Adam P. Hitchcock, Jürgen Stumper: "STXM Characterization of Nanostructured Thin Film Anode Before and After Start-up Shut-down and Reversal Tests", *Transaction of the Electrochemical Society* 58 (2013) 473-479.

2. LL Atanasoska, DA Cullen, RT Atanasoski: "XPS and STEM of the interface formation between ultra-thin Ru and Ir OER catalyst layers and Perylene Red support whiskers", *J. Serb. Chem. Soc. 78 (12) 1993–2005 (2013).*

3. Vincent Lee, Adam P. Hitchcock, Marcia West, Viatcheslav Berejnov, Sumit Kundu, Darija Susac, Juergen Stumper, Radoslav Atanasoski and Mark Debe: "STXM Investigations of Nano Structured Thin Film Catalysts for Proton-Exchange-Membrane Fuel Cell Applications", *J. Power Sources* 263, 163 - 174 (2014).

4. Timothy Crowtz, David Stevens, Robbie Sanderson, Jessie Harlow, George Vernstrom, Ljiljana Atanasoska, Greg Haugen, and

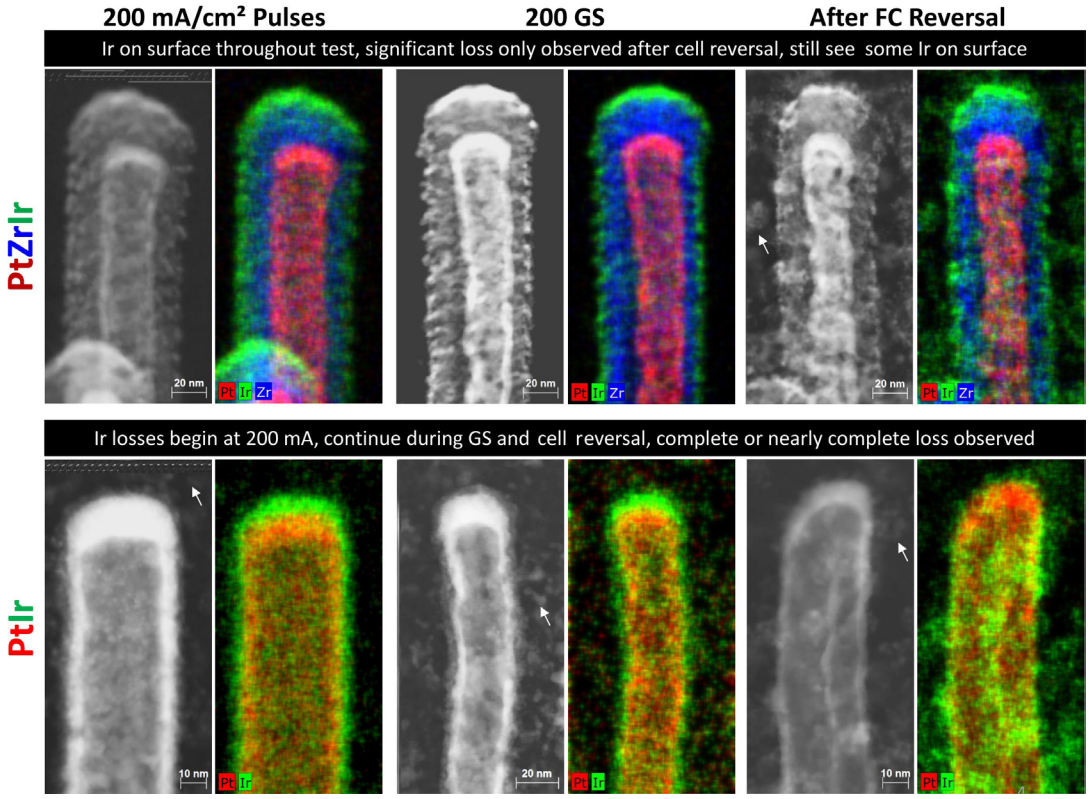

FIGURE 4. Comparative STEM images and elemental maps of IrPt/NSTF and Ir*Zr*Pt/NSTF at different stages of the durability test protocol. Left panel: after 200 pulses at 200 mA/cm^2. Middle panel: after 200 gas switches. Right panel: after the cell reversal durability test at 200 mA/cm^2. Note that IrPt/NSTF endured only 3.3 hours *vs.* a full 10 hours for IrZrPt/NSTF. Zr catalyst constructs: 250-Å Zr sandwiched between Ir and Pt.

Radoslav Atanasoski, Jeff Dahn: "The effect of Ru or Ir addition on Nano-Structured-Thin-Film supported Pt fuel cell catalysts under rotating disk electrode simulated start-up shut-down", *J. Electrochem.* Soc. 161 (10) F961-F968 (2014).

5. DA Cullen, KL More, LL Atanasoska, RT Atanasoski: "Impact of IrRu Oxygen Evolution Reaction Catalysts on Pt Nanostructured Thin Films under Start-Up/Shutdown Cycling", *J. Power Sources* 269, 671-681, 2014.

Presentations

1. GM Haugen, GD Vernstrom, LL Atanasoska, and RT Atanasoski: "SU/SD, a Materials Solution", Abstract #1279, 224th ECS Meeting (oral presentation).

2. T.C. Crowtz, D.A. Stevens, R.J. Sanderson, C.W. Watson, J.E. Harlow, and J.R. Dahn: "An RDE assessment of sputtered Ir-Ru-Pt overlayer nanostructured thin film catalysts for protection of PEM fuel cell cathodes against start-up and shut-down: The durability of oxygen reduction activity", Abstract #1552 (oral presentation).

3. Vincent Lee, Darija Susac, Sumit Kundu, Viatcheslav Berejnov, Radoslav T. Atanasoski, Adam P. Hitchcock, Jürgen Stumper: "STXM Characterization of Nanostructured Thin Film Anode Before and After Start-up Shut-down and Reversal Tests", Abstract #1322, 224th ECS Meeting (oral presentation).

Presentations to DOE

1. "Durable Catalysts for Fuel Cell Protection during Transient Conditions" Project progress Review, presented to DOE (internal), November, 2013, St. Paul, Minnesota.

2. "Durable Catalysts for Fuel Cell Protection during Transient Conditions" Project progress Review, presented to DOE (internal), Web conf., April, 2014.

3. "Durable Catalysts for Fuel Cell Protection during Transient Conditions" presented at the FC Tech Team, Detroit, April, 2014.

4. "Durable Catalysts for Fuel Cell Protection during Transient Conditions" presented at the DOE 2014 AMR, June, 2014, Washington, D.C.

REFERENCES

1. RT Atanasoski, DA Cullen, GD Vernstrom, GM Haugen, and LL Atanasoska: "A Materials-Based Mitigation Strategy for SU/SD in PEM Fuel Cells: Properties and Performance-Specific Testing of IrRu OER Catalysts", *ECS Electrochem. Lett.*, 2 (3) F25-F28, 2013.

2. RT Atanasoski, LL Atanasoska, DA Cullen: "Efficient Oxygen Evolution Reaction Catalysts for Cell Reversal and Start/Stop Tolerance" in M. Shao ed., "*Electrocatalysis in Fuel Cells: A Non and Low Platinum Approach*", Chapter 22, Springer, March, 2013.

3. RT Atanasoski, LL Atanasoska, DA Cullen, GM Haugen, KL More, GD Vernstrom: "Fuel Cells Catalyst for Start-up and Shutdown Conditions: Electrochemical, XPS, and TEM Evaluation of Sputter-Deposited Ru, Ir, and Ti on Pt-Nano-Structured Thin Film (NSTF) Support", *Electrocatalysis*, 3, 284–297, 2012.

4. R.T. Atanasoski, Project review at the DOE Vehicle Technologies and Hydrogen Programs Annual Merit Review, 2010 - 2014, Washington, D.C., FC# 003.

V.A.2 Extended, Continuous Pt Nanostructures in Thick, Dispersed Electrodes

Bryan Pivovar (Primary Contact), Shyam Kocha, KC Neyerlin, Jason Zack, Shaun Alia, Arrelaine Dameron

National Renewable Energy Laboratory
15013 Denver West Parkway
Golden, CO 80401
Phone: (303) 275-3809
Email: Bryan.Pivovar@nrel.gov

DOE Manager

David Peterson
Phone: (720) 356-1747
Email: David.Peterson@ee.doe.gov

Subcontractors

- Dave Cullen: Oak Ridge National Laboratory, Oak Ridge, TN
- Yushan Yan: University of Delaware, Newark, DE
- Svitlana Pylypenko, Dave Diercks, Colorado School of Mines (CSM), Golden, CO
- (In-kind) Fumiaki Ogura: Tanaka Kikinzoku Kogyo, Hiratsuka, Japan
- Anusorn Kongkanand: General Motors Corporation, Pontiac, MI

Project Start Date: July 20, 2009
Project End Date: Project continuation and direction determined annually by DOE

Overall Objectives

- Increasing mass activity and durability of Pt-based electrocatalysts through the implementation of high surface area extended surface electrocatalysts.
- Optimize fuel cell performance of extended surface electrocatalysts.
- Demonstrate DOE 2020 target performance and durability in fuel cell tests.

Fiscal Year (FY) 2014 Objectives

- Demonstrate an initial performance of >0.66 A mg_{Pt}^{-1} @ 900 mV (internal resistance [IR]-free) (50% increase over the DOE 2020 Target), and <30% loss in initial mass activity (25% improvement on DOE 2020 Target).
- Develop membrance electrode assemblies (MEAs) using novel electrocatalysts that show less than 10% mass activity loss in electrocatalyst support stability tests.
- Go/No-Go decision for annealing. No-go if mass activity gain is less than 10% of unannealed samples and durability gain is less than 25% compared to unannealled samples.
- Demonstrate fuel cell performance using novel electrocatalysts of 0.44 A mg_{Pt}^{-1} @ 900 mV (IR-free, DOE 2020 Target).

Technical Barriers

This project addresses the following technical barriers from the Fuel Cells section (3.4.4) of the Fuel Cell Technologies Office Multi-Year Research, Development, and Demonstration Plan:

(A) Durability (of catalysts and membrane electrode assemblies)

(B) Cost (of catalysts and membrane electrode assemblies)

(C) Performance (of catalysts and membrane electrode assemblies)

Technical Targets

This project synthesizes novel extended thin film electrocatalyst structures (ETFECS) and incorporates these catalysts into electrodes with and without carbon for further study. The project has targets outlined in the Multi-Year Research, Development, and Demonstration Plan for both electrocatalysts for transportation applications (Table 3.4.13) and MEAs (Table 3.4.14). The specific targets and status of highest relevance are presented in Table 1.

TABLE 1. Technical Targets for Electrocatalysts for Transportation Applications

Characteristic	Units	2017/2020 Targets	Status
Mass Activity (150 kPa H_2/O_2 80°C 100% relative humidity)	A/mg-Pt @ 900mV	0.44/0.44	0.45
Electro catalyst support stability	% mass activity loss	<10/<10	<10
Loss in initial catalytic activity	% mass activity loss	<40/<40	<10

FY 2014 Accomplishments

- Go decision for annealing as a method to improve catalyst activity.
- Demonstrated mass activities of ETFECS as high as 2,400 mA mg_{Pt}^{-1} @ 900 mV in rotating disc electrode (RDE) tests.

- Reduced leaching of the Ni template by annealing catalyst in oxygen (<2% following break-in, <2% following durability in RDE half-cells).
- Demonstrated ETFECS with mass activities (RDE) prior to and following durability testing of 1,963 and 1,564 mA mg_{Pt}^{-1}. The initial activity represents a 446% increase over the DOE 2020 target and the final activity was a 20% loss from initial activity (355% increase over the DOE 2020 target).
- Demonstrated fuel cell mass activity using ETFECS 50% higher than that of Pt/C baseline materials.
- Demonstrated greatly improved durability using ETFECS when exposed to carbon corrosion cycling.

INTRODUCTION

Conventional nanoparticle Pt/C electrocatalysts (2–5 nm) used in automotive fuel cells appear to have plateaued in terms of electrochemical area and catalytic activity. ETFECS offers the possibility of higher specific activities, comparable to that of bulk poly-Pt. ETFECS materials formed by direct deposition traditionally exhibit lower electrochemical surface areas (ECAs), and lower mass activities; synthesis by galvanic displacement, however, has in cases allowed for a thrifting of the noble metal layer, and for ECAs comparable to conventional nanoparticle catalysts. Although these materials exceed the 2020 activity target following durability testing (in RDE half-cells), durability are somewhat limited by the high template metal (Ni, Co) content which is more susceptible to leaching. By investigating post-synthesis processing conditions, we expect to: form Pt Ni alloys with improved specific activity (comparable to that observed in the Pt Co system); to minimize leaching during electrochemical testing; and to improve retention of ECA and activity following durability testing.

APPROACH

Our overall approach is towards developing extended surface Pt catalysts with high mass activity and durability, and incorporating these structures into robust, high-efficiency MEAs. This approach has focused on the synthesis of novel ETFECS formed by spontaneous galvanic displacement, specifically with Ni and Co templates. These materials have demonstrated high specific activity and durability, as well as surface areas significantly larger than traditionally found in extended surface Pt catalysts (3M [1], others [2]). In our work, we examine post-synthesis annealing in oxygen to improve catalyst durability and annealing to improve activity, potentially by an alloying effect.

RESULTS

We have completed detailed studies on Co nanowires (NWs) galvanically displaced with Pt, shown in Figure 1. This completed the study initially presented in FY 2013, by examining additional compositions or degrees of partial displacement. Pt-coated Co NWs reached a mass activity of 800 mA mg_{Pt}^{-1} at a Pt composition of 5.5 wt%. These materials, however, produced significantly lower ECAs (30 m^2 g_{Pt}^{-1}) than the Pt-Ni system and the gains in activity are therefore primarily due to the specific activity. This improvement was also correlated to Pt lattice compression, where the specific activity generally increased with an increased degree of alloying (at lower Pt content). Following durability testing (30,000 cycles, 0.6–1.0 V in RDE), these materials exceeded mass activities of 600 mA mg_{Pt}^{-1}. Future work will focus on improving the retention of activity (and ECA) following durability testing by post synthesis processing (as completed in FY 2014 on Pt-Ni NWs).

We have examined annealing of Pt-Ni NWs in oxygen to reduce Ni leaching during electrochemical testing and to improve the retention of activity following durability testing. As shown in Figure 2, annealing in oxygen significantly reduced Ni leaching. At a temperature of 200°C, less than 2% of the Ni was lost into the RDE electrolyte (<4% total including durability testing). At this temperature, the initial activity of the Pt-Ni NWs was slightly reduced but the retention of activity (and ECA) dramatically improved. As shown in Figure 2, the ECA of Pt-Ni NWs (200°C) improved in durability testing (3%); the mass activity increased as well (6%).

Novel, next-generation Pt NWs (NG Pt NWs) were also synthesized in FY 2014. As shown in Figure 3, catalysts were produced with mass activities as high as 2,400 mA mg_{Pt}^{-1}, a 5x improvement over the 2020 DOE target. These novel

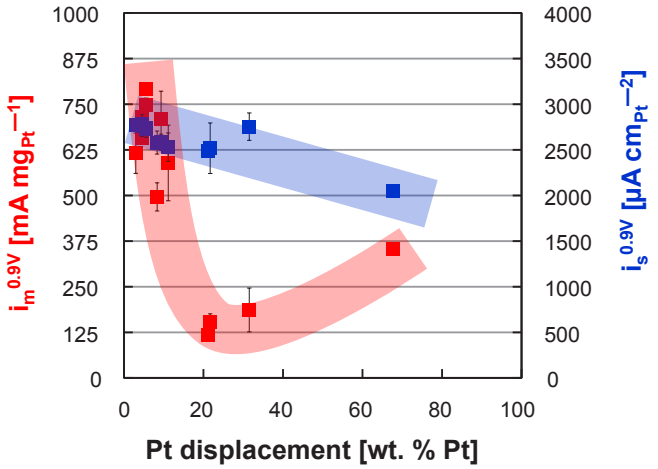

FIGURE 1. Mass and specific activity of Pt-Co NWs as a function of displacement.

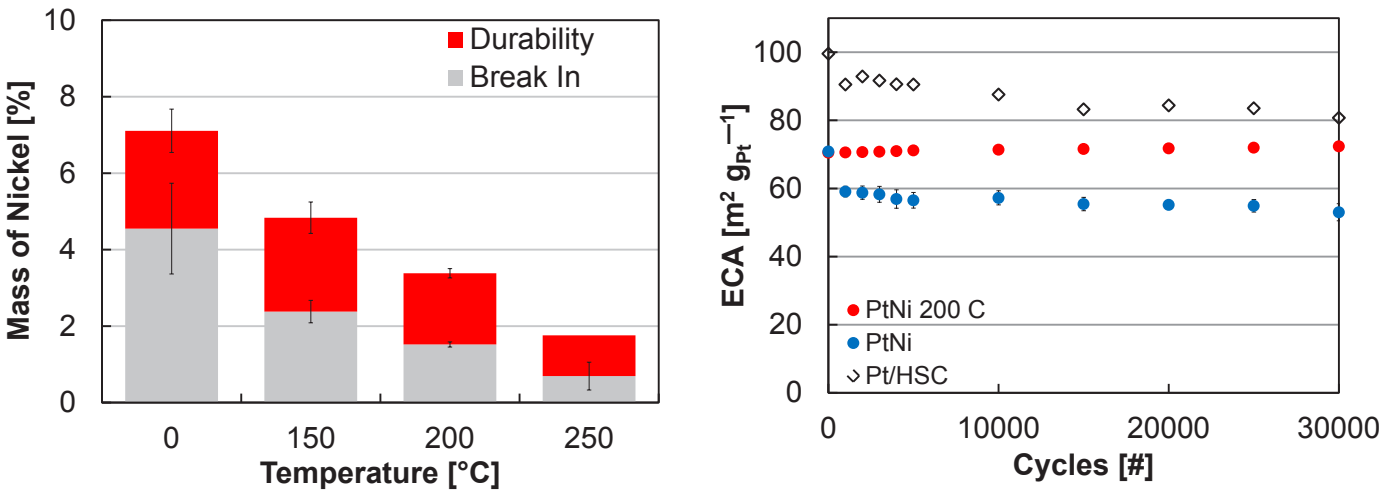

FIGURE 2. Percent loss of Ni (following RDE break-in and durability testing) as a function of annealing temperature in oxygen. ECA of catalysts (Pt Ni NWs annealed and untreated, Pt nanoparticles supported on high surface area carbon, Pt/HSC) as a function of durability cycle.

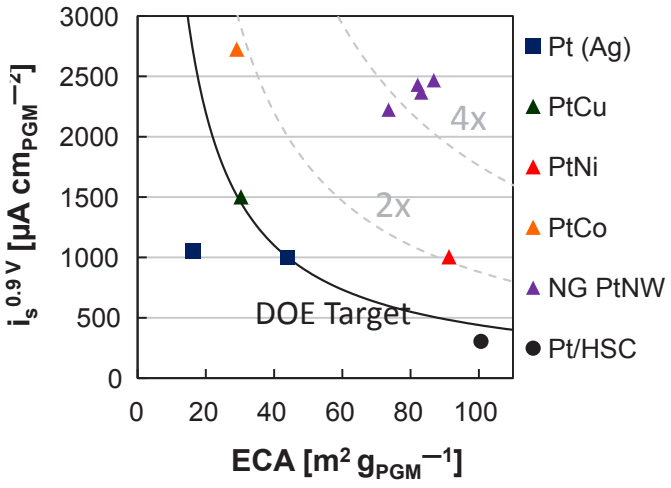

FIGURE 3. ECA and specific activities (i_s) summary of past synthesis routes and currently developed materials (NG Pt NW), lines of constant mass activity shown for DOE 2020 target, and 2 and 4 times the DOE 2020 target.

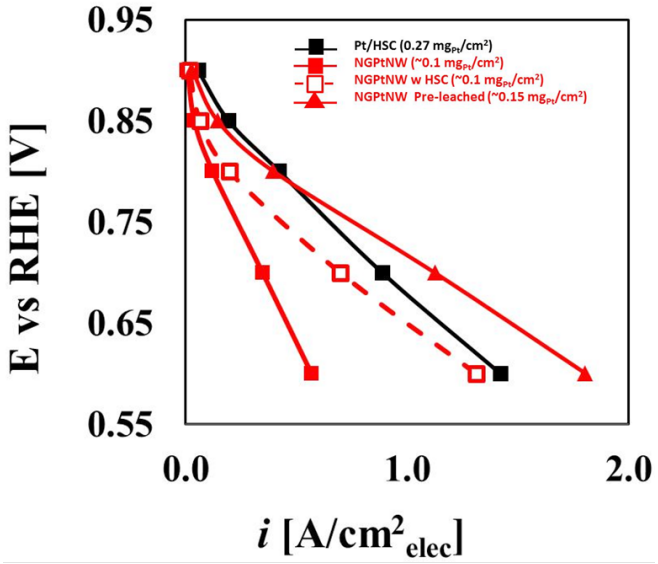

FIGURE 4. Fuel cell polarization curves of Pt NWs compared to Pt/C baseline material.

catalysts also showed the ability to maintain performance following potential cycling. The catalyst shown in Figure 3 with an initial activity of 1,963 mA mg_{Pt}^{-1} (446% increase over the DOE 2020 target in RDE half-cells) demonstrated a final activity of 1,564 mA mg_{Pt}^{-1} (20% loss from initial activity, 355% increase over the DOE 2020 target in RDE half-cells).

We have substantially increased our efforts to demonstrate our novel materials in fuel cell testing. We have scaled up synthesis and explored different fabrication routes. Figure 4 shows polarization curves and loadings for four different fuel cell tests. Pt/C has been included as a baseline comparison. The fuel cell performances presented represent improvements over time in both the catalysts themselves and in our ability to fabricate improved performance MEAs. The NG Pt NW MEA shows increased performance compared to Pt/C, in spite of lower catalyst loading, and all Pt NW samples show significantly improved durability when evaluated by potential cycling in the region of carbon corrosion. The observed Pt NW MEA performances are still far below the observed properties of RDE tests. The difference in performance is most pronounced at high voltage where the Pt NW samples

demonstrate lower specific activities than anticipated relative to lower voltage operation.

CONCLUSIONS AND FUTURE DIRECTIONS

The project has synthesized many novel catalysts using materials, geometries, and approaches not previously demonstrated. We improved upon the activity of Pt Ni NWs reported in FY 2013, reaching mass activities of 2,400 mA mg_{Pt}^{-1}. We have further demonstrated ETFECS catalysts with a high initial mass activity (2,400 mA mg_{Pt}^{-1}) and a high level of activity following durability testing (20% loss). Our efforts going forward will seek to further increase catalyst activity and optimize MEA performance in order to maintain RDE activity in fuel cell tests by focusing on the following.

- Electrocatalyst synthesis:
  - Focus on durability and the role of transition metals.
  - Continued investigation of oxide layer role in passivation of transition metal components.
  - Selective removal of transition metals to limit impact of performance loss.
- Fuel cell studies:
  - Optimization of fuel cell performance (ECA) using ETFECS with a focus on catalyst ink dispersions and composition.
  - Isolation of overpotential losses in MEA electrodes made with ETFECS materials (separation of mass transfer, ohmic, kinetic losses).
  - Durability studies to quantify and reduce impact of performance loss with specific emphasis on transition metal leaching.

FY 2014 PUBLICATIONS/PRESENTATIONS

1. Shaun M. Alia, Svitlana Pylypenko, K.C. Neyerlin, David A. Cullen, Shyam S. Kocha, Bryan S. Pivovar, "Platinum-Coated Cobalt Nanowires as Oxygen Reduction Reaction Electrocatalysts" ACS Catalysis 2014, 4, 2680.

2. K.C. Neyerlin, Brian A. Larsen, Svitlana Pylypenko, Shyam S. Kocha, Bryan S. Pivovar "Activity of Pt Extended Network Electrocatalyst Structures Made from Spontaneous Galvanic Displacement" ECS Transactions 2013, 50, 1405.

3. Justin Bult, K.C. Neyerlin, Steven Christensen, Arrelaine Dameron, Shyam S. Kocha, Jason W Zack, Bryan S. Pivovar, Katherine Hurst "Synthesis and Electrochemical Characterization of Carbon Supported Platinum Grown by Template Assisted Gas Phase Deposition," ECS Transactions 2013, 50, 1723.

4. Kazuma Shinozaki, Bryan S Pivovar, Shyam S Kocha "Enhanced Oxygen Reduction Activity on Pt/C for Nafion-free, Thin, Uniform Films in Rotating Disk Electrode Studies," ECS Transactions 2013, 58, 15.

5. Alexander B. Papandrew, Robert W. Atkinson III, Gabriel A. Goenaga, Shyam S. Kocha, Jason W. Zack, Bryan S. Pivovar, Thomas A. Zawodzinski Jr. "Oxygen Reduction Activity of Vapor-Grown Platinum Nanotubes," Journal of the Electrochemical Society 2013, 160, F848.

6. Alexander B. Papandrew, Robert W. Atkinson, Gabriel A. Goenaga, David L. Wilson, Shyam S. Kocha, K.C. Neyerlin, Jason W. Zack, Bryan S. Pivovar, Thomas A. Zawodzinski Jr. "Oxygen Reduction Activity of Vapor-Grown Platinum Nanotubes," ECS Transactions 2013, 50, 1397.

7. Shaun M. Alia, Kathylene Duong, Toby Liu, Kurt Jensen, Yushan Yan, "Palladium and Gold Nanotubes as Oxygen Reduction and Alcohol Oxidation Reaction Catalysts in Base" ChemSusChem 2014, 7, 1739.

8. Shaun M. Alia, Brian A. Larsen, Svitlana Pylypenko, David A. Cullen, David R. Diercks, K.C. Neyerlin, Shyam S. Kocha, Bryan S. Pivovar, "Platinum Coated Nickel Nanowires as Oxygen Reducing Electrocatalysts" ACS Catalysis 2014, 4, 1114.

9. Shaun M. Alia, Bryan S. Pivovar, Yushan Yan "Platinum Coated Copper Nanowires with High Activity for Hydrogen Oxidation Reaction in Base" Journal of the American Chemical Society 2013, 135, 13473. DOI: 10.1021/ja405598a

10. Shyam S. Kocha, Jason W. Zack, Shaun M. Alia, K.C. Neyerlin, Bryan S. Pivovar, "Influence of Ink Composition on the Electrochemical Properties of Pt/C Electrocatalysts" ECS Transactions 2013, 50, 1475.

11. Shaun M. Alia, Svitlana Pylypenko, K.C. Neyerlin, Brian A. Larsen, Shyam S. Kocha, Bryan S. Pivovar "Platinum Coated Cobalt Nanowires," November 3–8, San Francisco, California, AIChE Annual Meeting 2013, Abstract 729c.

12. Shaun M. Alia, Brian A. Larsen, Svitlana Pylypenko, David A. Cullen, David R. Diercks, K.C. Neyerlin, Shyam S. Kocha, Bryan S. Pivovar "Platinum Coated Nickel Nanowires as Oxygen Reducing Electrocatalysts," October 27 – November 1, San Francisco, California, 224th ECS Meeting 2013, Abstract 1308.

13. Kazuma Shinozaki, Bryan S. Pivovar, Shyam S. Kocha "Influence of Film Morphology on the Oxygen Reduction Reaction Activity in Rotating Disk Electrode Studies," October 27-November 1, San Francisco, California, 224th ECS Meeting 2013, Abstract 1239.

14. Bryan S Pivovar, K.C. Neyerlin, Shaun M Alia, Brian A Larsen, Svitlana Pylypenko, David A Cullen, David R Diercks, Shyam S Kocha "Extended Surface Pt Electrocatalysts: Synthesis and Challenges in Fuel Cell Applications," October 27 – November 1, San Francisco, California, 224th ECS Meeting 2013, Abstract 1245.

15. Pivovar, B.; Larsen, B.; Alia, S.; Pylypenko, S.; Zack, J.; Neyerlin, K.C.; Kocha, S. (September 2013). "Extended Surface Pt Electrocatalysts Synthesized by Galvanic Displacement." Presented at the 64th International Society of Electrochemistry Meeting, Queretaro, Mexico, September 18, 2013.

REFERENCES

1. http://www.hydrogen.energy.gov/pdfs/review08/fc_1_debe.pdf.

2. Z. Chen, W. Li, M. Waje, Y.S. Yan, *Angew. Chem. Int. Ed.* 2007, 46:4060-4063.

V.A.3 Nanosegregated Cathode Alloy Catalysts with Ultra-Low Platinum Loading

Vojislav R. Stamenkovic and Nenad M. Markovic
Argonne National Laboratory
9700 S. Cass Avenue
Argonne, IL 60439
Phone: (630) 252-5181
Email: vrstamenkovic@anl.gov; nmmarkovic@anl.gov

DOE Manager
Nancy Garland
Phone: (202) 586-5673
Email:Nancy.Garland@ee.doe.gov

Subcontractors
- Karren More (Oak Ridge National Laboratory, Oak Ridge, TN)
- Shuoheng Sun (Brown University, Providence, RI)
- Guofeng Wang (University of Pittsburgh, Pittsburgh, PA)
- Radoslav Atanasoski (3M Company, St. Paul, MN)

Project Start Date: September 2009
Project End Date: September 2014

Overall Objectives

- Fundamental understanding of the oxygen reduction reaction (ORR) on multimetallic PtM (M = Co, Ni, Fe, Mn, Cr, V, and Ti) and PtM_1N_2 (M_1 =Co or Ni; N_2 = Fe, Mn, Cr, V, and Ti) materials.
- Develop highly-efficient, durable, nanosegregated Pt-skin PtM and PtM_1N_2 catalysts with ultra-low Pt content.
- Develop highly-active and durable Au/PtM_3 nanoparticles with ultra-low Pt content.
- Find relationships between activity/stability of well-characterized bulk alloys and real nanoparticles.
- Develop novel chemical and physical methods for synthesis of monodispersed PtM and PtM_1N_2 alloy nanoparticles and thin metal films.
- Resolve electronic/atomic structure and segregation profile of PtM and PtM_1N_2 systems.
- Resolve composition effects of PtM and PtM_1N_2 systems.
- Demonstrate mass activity and stability improvement of PtM and PtM_1N_2 alloy nanomaterials in rotating disk electrodes (RDEs) and membrane electrode assemblies (MEAs).
- Use computational methods as the basis to form any predictive ability in tailor-making binary and ternary systems to have desirable reactivity and durability properties.
- Develop and synthesize highly active and durable practical catalyst with ultra-low content of precious metals.

Fiscal Year (FY) 2014 Objectives

- Optimization of synthesis methods to produce larger volumes of catalysts in a single batch.
- Implementation of the advanced protocols for surfactant removal for different classes of nanomaterials.
- Synthesis and characterization of the most active and durable PtM_1N_2 alloy nanoparticles with controlled particle size and elemental distribution.
- Evaluation of the nanosegregated compositional profile in the most active and durable systems.
- Employment of high crystallinity in nanoscale materials.
- Design and synthesis of multimetallic three-dimensional (3-D) nanowire-based material with controlled length, width and composition.
- Evaluation of catalyst properties in an MEA.

Technical Barriers

This project addresses the following technical barriers from the Fuel Cells section of the, Fuel Cell Technologies Office Multi-Year Research, Development, and Demonstration Plan:

(A) Durability
  - Reduce precious metal loading of catalysts
  - Increase the specific and mass activities of catalysts
  - Increase the durability/stability of catalysts with cycling
  - Test and characterize catalysts

Technical Targets

This project is conducting fundamental studies of the ORR on Pt-based PtM (M= Ni, Co, Fe, Cr, V, and Ti) binary and PtM_1N_2 (nanomaterials = Fe, Co, and/or Ni) catalysts as well as on Au/Pt_3M ternary nanoparticles. Insights gained from these studies will be applied toward the design and synthesis of highly efficient, durable, nanosegregated Pt-skin catalysts with ultra-low Pt content that meet or exceed the following DOE 2015 targets:

- Specific activity @ 0.9 V (iR-free): 720 mA/cm^2
- Mass activity @ 0.9 V: 0.44 A/mg$_{Pt}$
- Catalyst support loss: <30% over 30,000 potential cycles
- Platinum group metal total content: 0.2 g/kW
- Total loading: 0.2 mg/cm^2
- Durability with/cycling (80°C): 5,000 hrs

FY 2014 Accomplishments

- Developed experimental protocol to synthesize novel class of core/interlayer/bi-metallic-shell nanoparticles with Pt-"pseudo-skin" and established concentration profile for core/interlayer/shell.
- Evaluated surface Au vs. subsurface Au effect in multimetallic systems.
- Synthesis and characterization of the core/shell Au/CoPt$_3$ nanoparticles.
- Optimized compositional profile of the Ni-core/Au-interlayer/NiPt-shell nanoparticles for the maximal catalytic activity, superior durability and minimal loading of precious metals.
- Performed 10,000 potential cycles by RDE for activity/durability evaluations of core-interlayer/shell nanoparticles.
- Developed protocols for synthesis of highly crystalline multimetallic nanoframes with 3-D network of catalytically active surfaces, well-defined size, shape, composition, and surface structure.
- Performed detailed in situ and ex situ structural characterization of nanoframes and established compositional profile of nanoframes and tuned their surface composition towards multi-layered Pt-skin.
- Demonstrated high thermal stability of nanoframes. Established electrochemical pretreatment for nanoframe particles and optimized catalyst loading into high-surface-area carbon and performed detailed electrochemical characterization by establishing the activity/stability signature for nanoframe catalysts before and after 10,000 potential cycles.
- Implemented ionic-liquid approach into the nanoframe catalyst and performed detailed structural and electrochemical evaluations by high-resolution transmission electron (TEM) microscope and RDE.
- PtNi nanoframe catalyst achieved the highest specific and mass activity for the ORR ever measured for practical nanoscale electrocatalysts.

INTRODUCTION

In the quest to make the polymer electrolyte membrane fuel cell a competitive force, one of the major limitations is to reduce the significant overpotential for the ORR and minimize dissolution of the cathode catalysts. Here, we report on progress for FY 2014 in experimental and theoretical studies to addressing the importance of alloying Pt with 3-D elements (M= Ni, Co, Fe, etc.) in order to form catalytically active materials with so-called *nanosegregated profile* [1]. In our previous work we have identified that the nanosegregated surfaces are superior with both exceptional catalytic activity for the ORR and improved stability of Pt surface atoms.

APPROACH

In order to address the challenges that are listed as the DOE targets for the Hydrogen and Fuel Cells Program we rely on our materials-by-design approach [1-8]. This involves four major steps: (i) advanced chemical and physical methods for synthesis of novel nano/mesoscale materials, which enables control of their size, composition, morphology and structure; (ii) characterization of atomic and electronic properties by ex situ and in situ surface specific tools and theoretical methods; (iii) resolving the surface electronic and crystal structures at atomic/molecular level that govern efficient kinetics of the ORR; and (iv) synthesis/fabrication (scale up) of the highly efficient practical catalysts, which are guided by the fundamental understanding of structure-function relationships.

RESULTS

The effect of surface Au vs. subsurface Au on the ORR electrocatalysis. In Pt-alloy nanoparticle electrocatalysts, Au can have both catalytic and durability roles owing to its high redox potential. Its effectiveness for both is greatly affected by the nanoparticle structure as well as compositional profile, and therefore, proper electrocatalyst design requires a fundamental understanding of the structure-function relationship, specifically how Au placement can affect the catalytic properties of Pt-alloys. Two different cases were considered, one in which Au is deposited on the surface of PtNi nanoparticles, PtNi-Au, and the other one in which Au is located beneath the surface, Au@PtN. The ORR activity trend associated with Au placement results in lower specific activity where 10% surface coverage of Au leads to a decrease in half-wave by 40 mV while 50% surface coverage leads to a loss of over 100 mV in the half-wave potential and a significant decrease in the diffusion limited current, suggesting a partial shift from 4-electron toward 2-electron oxygen reduction mechanism. From these results it is clear that the beneficial effects of Au are best realized in Pt-Au-Ni ternary system when Au is located beneath the

surface, not directly being exposed to the reactive species. In principle, core-shell transition metal@Pt catalysts can minimize the mass of buried, electrocatalytically inactive Pt; however, if the core itself is high in precious metal content, such as Au, it fails to effectively address the cost per kW in polymer electrolyte membrane fuel cells. All of the above points towards a unique multilayered compositional profile where the core is entirely composed of an inexpensive transition metal while the interface between the core and Pt alloy shell contains an optimal amount of Au to enhance durability and limit the total mass of precious metals within the catalyst. Nanomaterials with such distinct compositional profile are termed as core/interlayer/shell nanoparticles.

Synthesis and characterization of Ni-Core, Au-interlayer, NiPt-shell nanoparticles. Through a controlled layer-by-layer growth mechanism, we add Au to the interface between the nanoscale core and shell. In brief, 3.1 nm ($\sigma < 5\%$) Ni nanoparticles are synthesized and used as core, Figure 1, to deposit Au in a desired quantity, forming an intermediate Ni@Au core/shell nanostructure. The final step is deposition of a PtNi shell with the thickness of approximately 1 nm (~6 MLs) which forms the desirable nanosegregated Ni@Au@PtNi nanoparticles with a diameter of 5.0 nm ($\sigma = 6\%$), as shown in Figure 1. The scanning transmission electron microscopy (STEM) images (Figure 1c and d) show that after exposure to acidic electrolyte, the core-shell structure and the Ni core are preserved, and the line scan of energy-dispersive X-ray spectroscopy (EDX) confirms the formation of the Pt-skeleton surface (Figure 1e). In our previous study, the durability enhancement in Au/FePt ternary core/shell electrocatalyst was ascribed to the hindered place-exchange mechanism [7]. Subsurface Au content equivalent to 0.25 ML in the underlying atomic layer of a Pt surface reduce the adsorption strength of subsurface oxygen at all relevant potentials for the ORR. The presence of subsurface oxygen drives the place-exchange mechanism which is responsible for bringing transition metals to the surface as well as being the dominant mechanism by which Pt is dissolved. Therefore, placement of Au atoms with higher redox potential in the near-surface region lowers the probability for both transition metal (Fe, Co and/or Ni) and Pt dissolution. We determined that the amount of interlayered Au that surrounds the Ni core can be successfully controlled from a complete monolayer down to 0.25 ML. Detailed electrochemical evaluation revealed that after 10,000 potential cycles in 0.1 M $HClO_4$ between 0.6 and 1.1 V vs. RHE, there is a negligible loss in activity for all of the nanoparticles containing some quantity of subsurface Au, as revealed in Figure 2. The amount of Au was varied from a solid Au core where Au makes up 47 at% of the nanoparticle, to an equivalent of ~1 ML over the Ni core where Au is 28 at% of the crystal down to a Au content of 5 at% which is close to 0.25 ML on the Ni core. The ORR activity of Ni@Au@PtNi/C electrocatalysts is tested and compared with commercial Pt/C and PtNi/C electrocatalysts. As shown in Figure 2, the Ni@Au@PtNi/C electrocatalysts possess great durability towards the ORR without noticeable loss in either electrochemically active surface area (ECSA) or specific activity. The specific and mass activity enhancement of Ni@Au@PtNi/C is over 8-fold versus the Pt/C and outperforms multilayered Pt-skin PtNi/C due to the Ni replacement of expensive Pt in the core. Figure 2d shows TEM images of Pt/C, PtNi-Skeleton/C, and Ni@Au@PtNi/C nanoparticles before and after 10,000 cycles. After potential cycling, the

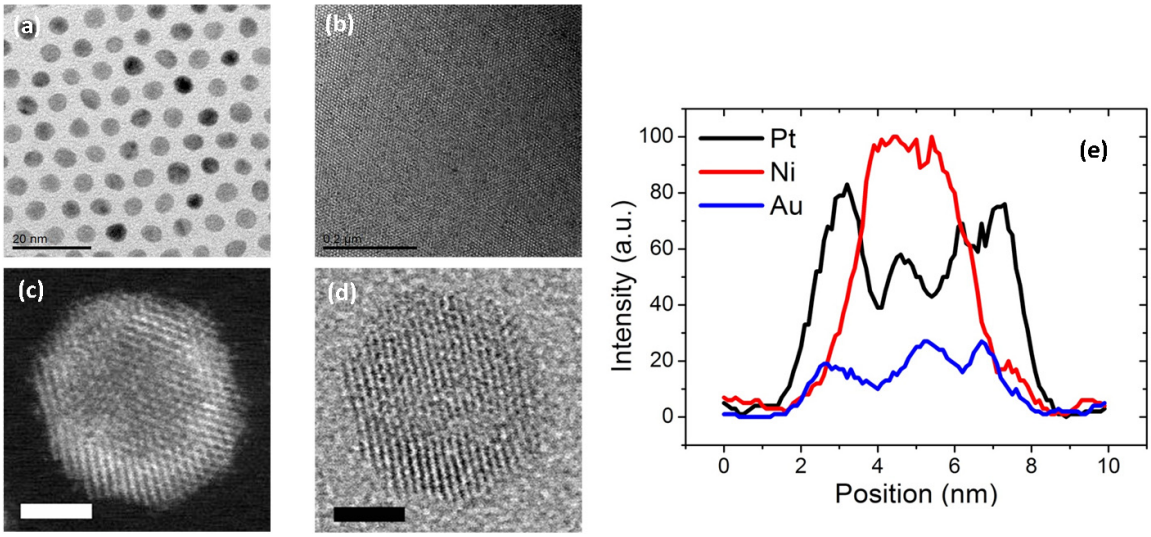

FIGURE 1. TEM images of (a-b) as-synthesized Ni nanoparticles (c) Ni/Au/NiPt core/interlayer/shell nanoparticle bright-field STEM images; d) dark-field STEM images, e) EDX data clearly show the core-shell structure; and (f) the EDX line profile shows a Pt-rich skeleton structure over the Au-coated Ni core. Scale bars: a) 0.2 μm, b) 20 nm, c, d) 2 nm.

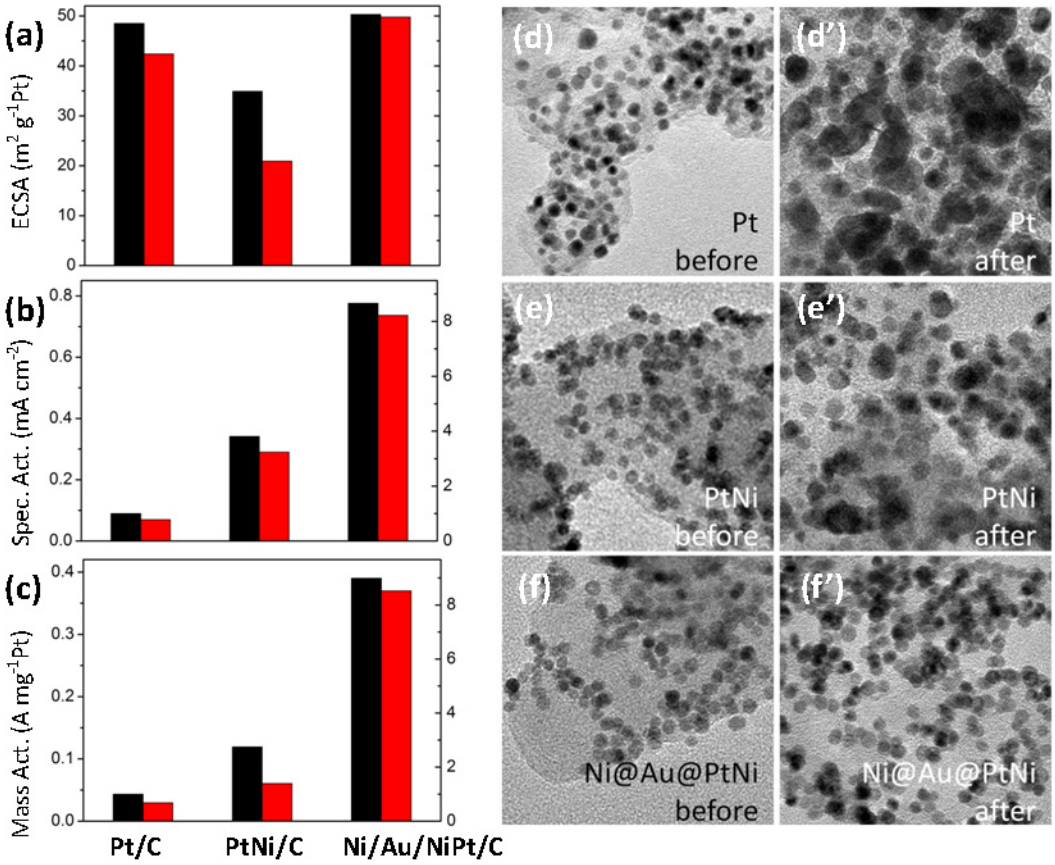

FIGURE 2. Bar charts showing a) electrochemically active surface areas, b) specific activities, and c) mass activities of Pt/C, PtNi/C (with Pt-Skeleton), and Ni@Au@PtNi/C (with pseudo Pt-Skin) electrocatalysts before and after 10,000 cycles of electrochemical cycling up to 1.1 V. The activity is normalized kinetic current density measured at 0.95 V. The specific activity is the activity normalized to the ECSA measured by CO-stripping. (d-f) TEM images of Pt, PtNi, and Ni@Au@PtNi nanoparticles before and (d'-f') after 10,000 cycles up to 1.1 V. All the images are at size of 100 nm × 100 nm.

sizes of Pt and PtNi nanoparticles are significantly changed: big particles (>10 nm) and small particles (<5 nm) are observed instead of the initial ~5 nm size, indicating that Pt and PtNi are affected by the well-known Ostwald ripening process under the potential cycling. However, such change in size and shape is not observed on Ni@Au@PtNi, again demonstrating the synergy between high activity and high durability of Ni@Au@PtNi/C electrocatalysts.

Highly crystalline multimetallic nanoframes as electrocatalysts. An entirely new class of catalysts was synthesized from $PtNi_3$ polyhedra in oleylamine that had a uniform rhombic dodecahedron morphology and size (20.1 ± 1.9 nm), as observed in Figure 3. Initially, the oleylamine-capped $PtNi_3$ polyhedra were dispersed in nonpolar solvents, during which time they transformed into Pt_3Ni nanoframes, with unchanged symmetry and size. Solid nanostructures gradually eroded into hollow frames, and the bulk composition changed from $PtNi_3$ to PtNi and eventually Pt_3Ni, as evidenced by X-ray diffraction and EDX spectra. After dispersion of nanoframes onto a high-surface-area carbon support (VULCAN® XC72) and subsequent thermal treatment in inert gas (Ar) atmosphere between 370 and 400°C, most nanoframes developed the smooth Pt-skin type of structure. The electrocatalytic properties of Pt_3Ni nanoframes were evaluated and compared to PtNi/C and commercial state-of-the-art Pt/C nanoscale electrocatalysts (Figure 3). The polarization curves shown in Figure 3b show an increase in ORR activity in the following order: Pt/C < PtNi/C << Pt_3Ni nanoframes. The ratio between ECSA values determined by integrated charge from CO-stripping and underpotentially deposited hydrogen (H_{upd}) was 1.52 for the Pt_3Ni nanoframes, strongly suggesting formation of a Pt-skin terminated (111)-like surface structure. Moreover, EDX line profiles confirmed the presence of Pt-skin on the nanoframe surfaces with a thickness of at least two Pt monolayers. As a result, the specific activity of Pt_3Ni nanoframes at 0.95 V exhibited an improvement factor of over 16 versus commercial Pt/C electrocatalyst (Figure 3c). The synergy between specific activity and the open architecture of the Pt_3Ni nanoframes that enables access of reactants to both the

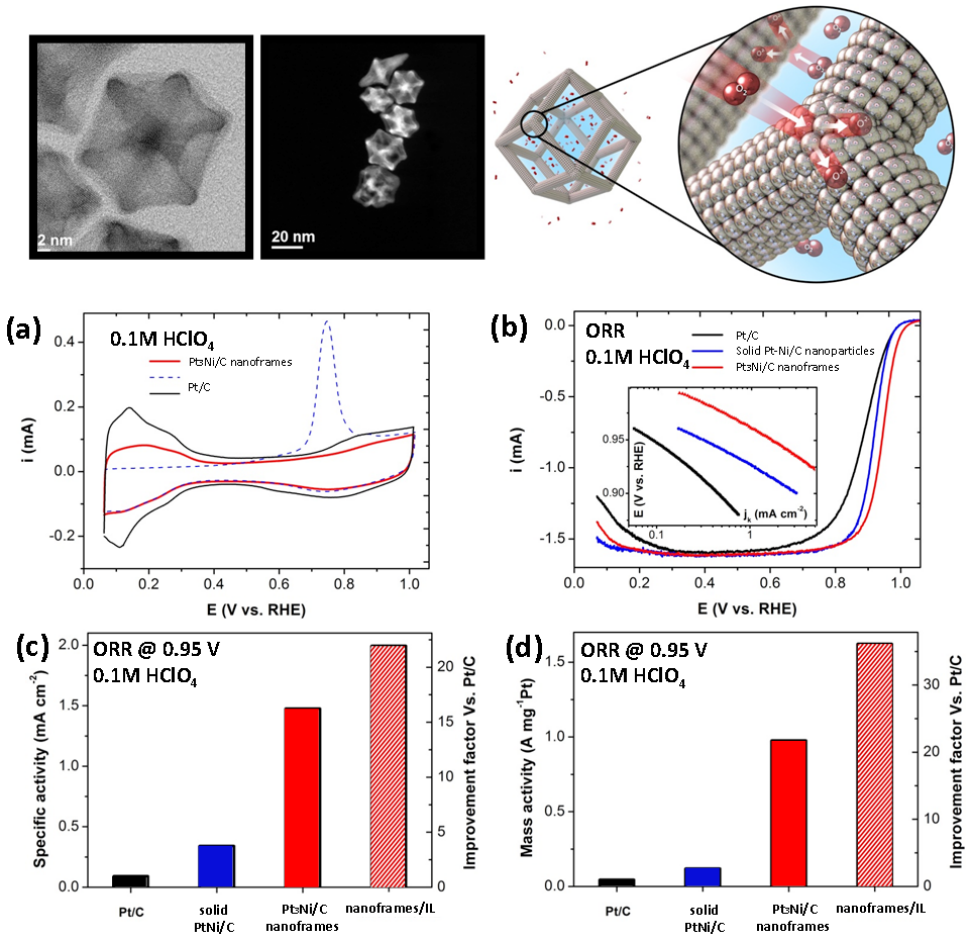

FIGURE 3. High-resolution TEM images of Pt_3Ni nanoframes. (a) cyclic voltammograms of Pt/C and Pt_3Ni nanoframes signify the difference in surface coverage by H_{upd} and OH_{ad}. ECSA of the nanoframes is determined by integrated charge of adsorbed CO electrooxidation curve; (b) The ORR polarization curves and corresponding Tafel plots; (c) specific activities and (d) mass activities measured at 0.95 V and improvement factors versus Pt/C catalysts. Because of the high intrinsic activity of the Pt_3Ni nanoframes the ORR activity values are given at 0.95 V in order to avoid the extensive error margin introduced by the close proximity of current values at 0.9 V to the diffusion limited current.

internal and external surfaces led to an unprecedented 22-fold enhancement in the mass activity vs. Pt/C (Figure 3d). The mass activity calculated at 0.9 V (5.7 A mg^{-1}Pt) is over one order of magnitude higher than the DOE's 2017 target (0.44 A mg^{-1}Pt), making the Pt_3Ni nanoframes the most efficient electrocatalyst for the ORR. In addition to the high intrinsic and mass activities, the Pt_3Ni nanoframes exhibited remarkable durability throughout electrochemical operation, i.e., STEM (dark field and bright field) images confirmed that the frame structure was preserved while activity loss was negligible after 10,000 potential cycles. The enhanced durability is ascribed to the electronic structure of the Pt-skin surface resulting in a lower coverage of oxygenated intermediates because of the weaker oxygen binding strength, which diminishes the probability of Pt dissolution, plus, the optimized Pt-skin thickness of at least 2 MLs hinders the loss of subsurface transition metal through the place-exchange mechanism during electrochemical operation consequently preserving the high intrinsic activity [8]. In addition, protic ionic liquids (ILs) were integrated into a porous nanoframe catalyst, where the high O_2 solubility of IL increases the O_2 concentration at the catalyst surface, resulting in higher attempt frequencies for the ORR and consequently higher activity. The [MTBD][NTf_2] protic-liquid was used that has an O_2 solubility ($C_{O2,[MTBD][NTf2]} = 2.28 \pm 0.12$ mM), approximately twice that of the common electrolyte $HClO_4$. Capillary forces exerted by the Pt_3Ni nanoframes pulled the IL inside the frames and prevented it from being washed away by electrolyte. The IL-encapsulated Pt_3Ni nanoframes showed sustained superior activity upon prolonged (10,000) potential cycling without noticeable decay in performance. As depicted in Figure 3, the IL-encapsulated Pt_3Ni nanoframes exhibited a 36-fold enhancement in mass activity and 22-fold enhancement in specific activity compared with

Pt/C, which is the highest activity ever measured for practical nanoscale catalysts.

CONCLUSIONS AND FUTURE DIRECTIONS

- PtM and $Pt_3M_1N_2$ nanoparticles cathode catalysts obtained from the organic solvo-thermal synthesis exhibit superior activity and stability than those prepared by the conventional methods. The method to synthesize of Pt_3MN nanoparticles with highly active Pt-skin morphology is being further established.
- Ternary core-interlayer/shell systems operate through the same mode of action of improving the catalytic properties and durability as core/shell particles.
- Nanoframes with 3-D network of electrocatalytically active surface possess superior specific, mass activities with outstanding durability.
- Future effort will be dedicated to the scale up synthesis of the nanoframes and MEA evaluation.

FY 2014 PUBLICATIONS/PRESENTATIONS

1. S. Guo, D.Li, H.Zhu,S.Zhang, N.M.Markovic, V.R.Stamenkovic, S.Sun *FePt and CoPt Nanowires as Efficient Catalysts for the Oxygen Reduction Reaction* Angewandte Chemie International Edition, 52(2013)3465.

2. C.Chen, Y.Kang, Ziyang Huo, Zhongwei Zhu, Wenyu Huang, Huolin L. Xin, Joshua D. Snyder, Dongguo Li, Jeffrey A. Herron, Manos Mavrikakis, Miaofang Chi, Karren L. More, Yadong Li, N.M.Markovic, G.Somorjai, Peidong Yang, V.R.Stamenkovic *Highly Crystalline Multimetallic Nanoframes with Three-Dimensional Electrocatalytic Surfaces* Science, 343(2014)1339.

3. D. Strmcnik, N. Markovic and V. Stamenkovic *Advanced Electrocatalysts* Fourth Regional ISE Symposium on Electrochemistry, May 2013, Ljubljana, Slovenia.

4. Y. Kang, D. Li, N.M.Markovic and V. Stamenkovic *Exploiting high activity and durability by tuning nanostructure for electrocatalytic applications* 245th American Chemical Society Spring Meeting, April 2013, New Orleans, LA.

5. C. Wang, N. Markovic and V. Stamenkovic *Design and Synthesis of Advanced Electrocatalysts* 246th American Chemical Society National Meeting, September 2013, Indianapolis, IN.

6. Yijin Kang, Dongguo Li, Nenad M. Markovic and V. Stamenkovic *Design of Highly Active and Durable Electrocatalysts by Tuning Nanostructure* 224th Electrochemical Society Meeting, October 2013, San Francisco, CA.

7. Joshua Snyder, Yijin Kang, Dongguo Li, Nenad M. Markovic and V. Stamenkovic *Mesostructured Multimetallic Thin Films as Electrocatalysts for Fuel Cells* 224th Electrochemical Society Meeting, October 2013, San Francisco, CA.

8. Joshua Snyder, Yijin Kang, Dongguo Li, Nenad M. Markovic and V. Stamenkovic *Advanced Electrocatalysts for Fuel Cells* 225th Electrochemical Society Meeting, May 2014, Orlando, FL.

REFERENCES

1. V. Stamenkovic, B. Fowler, B.S. Mun, G. Wang, P.N. Ross, C. Lucas, N.M. Markovic, "Improved Oxygen Reduction Activity on $Pt_3Ni(111)$ via Increased Surface Site Availability ", *Science,* **315** (2007) 493-497.

2. V.Stamenkovic and N.M.Markovic, "Electrocatalysis on Model Metallic and Bimetallic Single Crystal Surfaces, Model Systems in Catalysis: From Single Crystals and Size Selected Clusters", Editor: Robert M. Rioux, Harvard University, USA; Publisher: Elsevier Science, The Netherlands, *2009.*

3. K.J.J.Mayrhofer, B.B. Blizanac, M. Arenz, V. Stamenkovic, P.N. Ross, N.M. Markovic, "The Impact of Geometric and Surface Electronic Properties of Ptcatalysts on the Particle Size Effect in Electrocatalysis", *J. Phys. Chem B,* **109** (2005) 14433-14440.

4. C. Wang, D. van der Vliet, K.C. Chang, H. You, D. Strmcnik, J.A. Schlueter, N.M. Markovic, V.R. Stamenkovic, "Monodisperse Pt_3Co Nanoparticles as a Catalyst for the Oxygen Reduction Reaction: Size Dependent Activity", *J. Phys. Chem. C.,* **113** (2009)19365.

5. C. Wang, D. van der Vliet, K.C. Chang, N.M. Markovic, V.R. Stamenkovic, "Monodisperse Pt_3Co Nanoparticles as Electrocatlyst: the Effect of Particle Size and Pretreatment on Electrocatalytic Reduction of Oxygen"*, Phys.Chem.Chem.Phys*., **12** (2010)6933-6939.

6. V. Stamenkovic, B.S. Mun, M. Arenz, K.J.J.Mayrhofer, C. Lucas, G. Wang, P.N. Ross, N.M. Markovic, "Trends in Electrocatalysis on Extended and Nanoscale Ptbimetallic Alloy Surfaces", *Nature Materials,* **6** (2007) 241-247.

7. C. Wang, D.van derVliet, K.L. More, N.J. Zaluzec, S. Peng, S. Sun, H. Daimon, G. Wang, J. Greeley, J. Pearson, A.P. Paulikas, G. Karapetrov, D. Strmcnik, N.M.Markovic, V.R.Stamenkovic "MultimetallicAu/$FePt_3$ Nanoparticles as Highly Durable Electrocatalysts", *Nano Letters*, **11** (2011)919-928.

8. C. Wang, M.Chi, D. Li, D. Strmcnik, D.van derVliet, G. Wang, V. Komanicky, K.-C. Chang, A.P. Paulikas, D. Tripkovic, J. Pearson, K.L. More, N.M. Markovic, V.R. Stamenkovic, "Design and Synthesis of Bimetallic Electrocatalyst with Multilayered Pt-Skin Surfaces"*, Journal of American Chemical Society*, **133** (2011)14396.

9. C. Wang, M.Chi, D. Li, D.van derVliet, G. Wang, Q. Lin, J.F. Mitchell, K.L. More, N.M. Markovic, V.R.Stamenkovic, "Synthesis of Homogenious Pt-Bimetallic Nanoparticles as Highly Efficient Electrocatalysts"*, ACS Catalysis*, **1** (2011)1355.

10. D.van derVliet, C. Wang, M.K. Debe, R.T. Atanasoski, N.M.Markovic, V.R.Stamenkovic, "Platinum Alloy Nanostructured Thin Film Catalysts for the Oxygen Reduction Reaction"*, Electrochimica Acta*, **56**,24 (2011)8695.

11. D.van derVliet, C. Wang, D.Tripkovic, D.Strmcnik, X.F.Zhang, M.K. Debe, R.T. Atanasoski, N.M.Markovic, V.R.Stamenkovic, "Mesostructured Thin Films as Electrocatalysts with Tunable Composition and Surface Morphology" *Nature Materials*, 11(2012)1051.

V.A.4 Contiguous Platinum Monolayer Oxygen Reduction Electrocatalysts on High-Stability Low-Cost Supports

Radoslav Adzic (Primary Contact), Jia Wang, Miomir Vukmirovic, Kotaro Sasaki
Brookhaven National Laboratory (BNL)
Bldg. 555
Upton, NY 11973-5000
Phone: (631) 344-4522
Email: adzic@bnl.gov

DOE Manager
Nancy Garland
Phone: (202) 586-5673
Email: Nancy.Garland@ee.doe.gov

Project Start Date: July 1, 2009
Project End Date: Project continuation and direction determined annually by DOE

Overall Objectives

- Synthesizing high-performance Pt monolayer (ML) on stable, inexpensive metal or alloy nanostructured fuel cell electrocatalysts for the oxygen reduction reaction (ORR).
- Increasing activity and stability of Pt ML shell and stability of supporting cores, while reducing noble metal contents.

Fiscal Year (FY) 2014 Objectives

Scale-up of syntheses of three catalysts including:

- Pt ML on Pd hollow nanoparticles; Pt ML on WNi nanoparticles, and Pt ML on Pd_9Au_1 nanoparticles
- Obtaining perfect Pt ML deposition and achieving 100% utilization of Pt
- New methods for increasing stability of core-shell nanoparticles, while reducing the Pt-group metal (PGM) contents
- Delivering a 300-cm^2 membrane electrode assembly (MEA) for testing at General Motors

Technical Barriers

This project addresses the following technical barriers from the Fuel Cells section of the Fuel Cell Technologies Office Multi-Year Research, Development, and Demonstration Plan:

(A) Durability

(B) Cost

(C) Performance

Technical Targets

We are focusing on simplifying synthetic processes to obtain better catalyst activity, higher Pt utilization, lower content of PGM and more simple MEA formation (see Table 1).

TABLE 1. Progress toward Meeting DOE Fuel Cell Electrocatalysts Technical Targets

Characteristic	Units	Target 2017	Achieved 2014
PGM total loading	mg PGM/cm^2 electrode area	0.125	0.05 (Pt/PdAu, Pt/PdWNi/gas diffusion layer)
Mass activity	A/mg Pt @ 900 $mV_{iR\text{-}free}$	0.44	1.7 (Pt/PdAu nanowires)
Specific activity	mA/cm^2 @ 900 $mV_{iR\text{-}free}$	0.72	1.4 (Pt/hollow Pd)
PGM mass activity	A/mg PGM @ 900 $mV_{iR\text{-}free}$	0.44	0.5 (Pt/hollow Pd)
Loss in initial catalytic activity	% mass activity loss over 30,000 cycles	<48	No significant loss in activity in 200,000 cycles (Pt/PdAu)

FY 2014 Accomplishments

New methodologies for improving activity and stability of Pt ML catalysts:

- Synthesis of monodisperse cores
- Forming atomically ordered, sharp core-shell interfaces
- Gold promoting the formation of ordered intermetallic compounds (The AuPdCo compound is a Pt-free catalyst with activity approaching that of Pt. It can serve as an excellent core supporting Pt ML.)
- Nitrating non–noble metal cores constituents (Both ordered intermetallic compounds and nitrated.)

INTRODUCTION

Further developments of oxygen reduction electrocatalysts are inevitable to lessen the remaining technological difficulties that hamper automotive applications of fuel cells, and we thus have focused on reducing Pt, or PGM contents in our Pt ML electrocatalysts, while increasing their stability and activity. The understanding of

the properties of Pt ML electrocatalysts, and of a broader class of core-shell electrocatalysts, has considerably grown up. Optimizing the properties of nano-structured cores by varying their composition, size and shape can improve Pt ML catalysts to make them ready for applications.

APPROACH

Improving Pt ML using novel core compositions and new synthetic methods including:

- Depositing nearly perfect Pt MLs on various cores
- Ordering core-ML shell interface structure
- Synthetizing monodisperse, smooth cores, or hollow cores
- Nitrating non-noble metal core components for increased stability
- Electrodeposition and underpotential deposition of cores (refractory metal alloys) to optimize their composition and maximize catalyst utilization
- Ordered intermetallic compounds with high activity without Pt
- Reactive spray deposition method to synthesize novel low cost cores

RESULTS

We describe four results illustrating the new methods developed in FY 2014 for improving Pt ML catalysts for the ORR.

Synthesis of Atomically Perfect Ru(core)-Pt(shell) Nanoparticles

We developed a new method to produce an atomically sharp, ordered core-shell interface by avoiding partial alloying of Ru-rich cores and Pt-rich shells. We verified the interface structure using high-resolution scanning transmission electron microscopy techniques. For Ru(core)-Pt(bilayer) particles, we show, by overlapping the Ru-specific electron energy loss signal with the high-angle annular dark field image (Figure 1b), that the Ru core was completely encapsulated by uniformly thin Pt shells. More importantly, an atomically-resolved scanning transmission electron microscopy image (Figure 1c) shows that the measured lattice structure (white dots) matches well with the theoretically calculated structure for an perfectly ordered phase-transition between the hexagonal close packed (hcp) Ru core and a face-centered cubic (fcc) Pt shell. Attaining such a level of structural perfection is unprecedented. Thus, Ballard Power Systems evaluates its application as the anode catalysts for hydrogen and reformate polymer electrolyte membrane fuel cells (PEMFCs). A similar method also produced a uniform coating of a Pt ML or bilayer on Pd cores, as is evident in Figure 1d, and 1e.

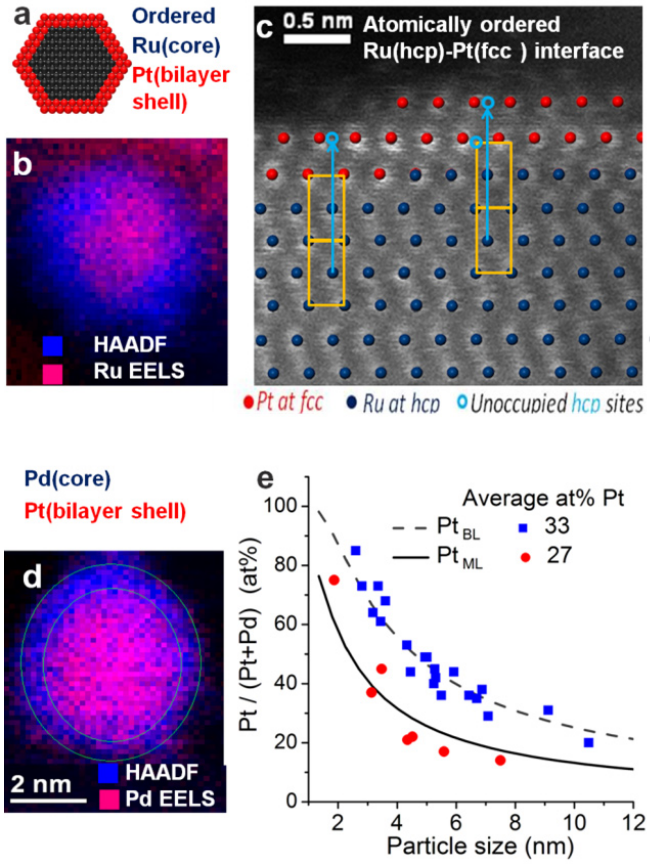

FIGURE 1. Structural schematics (a) and scanning transmission electron microcopy data for atomically perfect Ru(core)-Pt(bilayer shell) nanoparticles (b,c), and for Pd(core)-Pt(shell) nanoparticles (d,e).

Ru(core)-Pt(bilayer) Particles as the Anode Catalysts for PEMFCs

Currently, the anode Pt loading is targeted at 0.05 mg cm^{-2} for hydrogen PEMFCs using Pt nanoparticle catalysts based on the state-of-the-art technologies. With ordered Ru-Pt core-shell particles, the amount of Pt can be further reduced by half because the Pt specific surface area nearly doubles for a Pt bilayer catalyst compared to the commonly used Pt nanoparticles. In addition, the ordered Ru-Pt core-shell catalysts are highly uniform, stable, and resistant to airborne contamination. For applications in PEMFCs, we, in collaboration with Ballard Power Systems, further tested the catalysts' stability against potential cycles up to 0.95 V. Figure 2a shows the polarization curves measured before and after 2,500 startup/shutdown cycles (~65 hrs) that alternated the anode's potential between 0.02 and 0.95 V. The performance was unaffected with a loading as low as 0.025 mg cm^{-2} Pt and 10 mg cm^{-2} Ru.

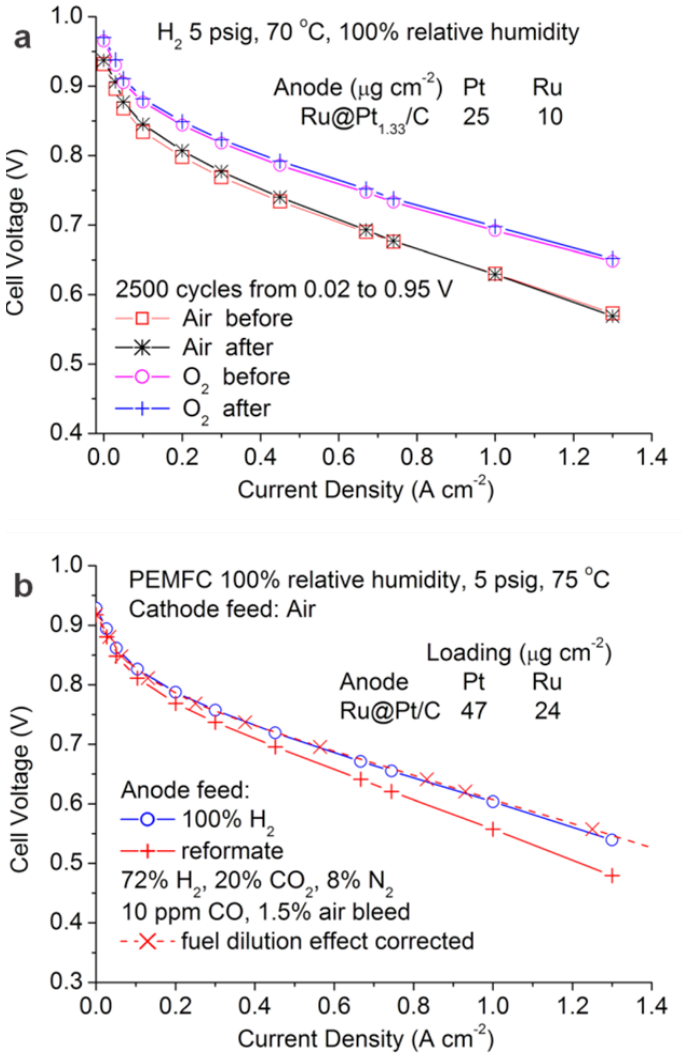

FIGURE 2. Results on anode durability (a), and CO tolerance (b) test for atomically perfect Ru(core)-Pt(shell) nanocatalysts.

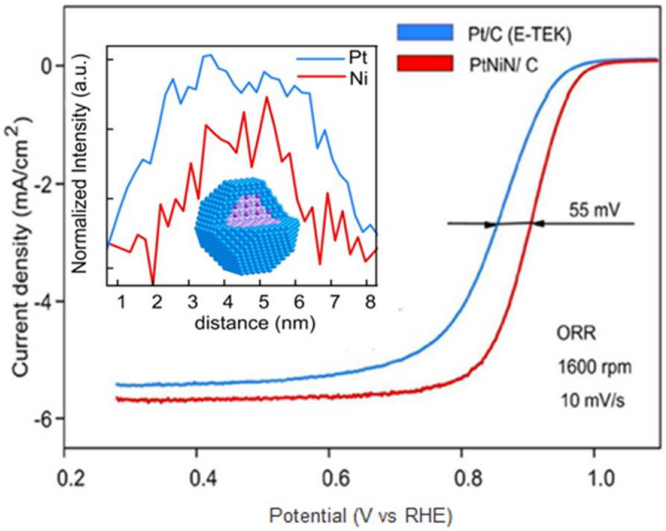

FIGURE 3. ORR polarization curves of PtNiN/C and Pt/C catalysts on a rotating disk electrode in 0.1 M $HClO_4$. Also shown is electron energy loss signal line-scan profiles of Pt and Ni in a single PtNiN nanoparticle (blue, Pt; gray, Ni; purple, N).

Nitride-Stabilized Pt-M Core-Shell Catalysts in Acid Media

We developed novel nitride-stabilized PtM core−shell catalysts (M = Fe, Co, and Ni) with low-Pt-content shells and inexpensive metal-nitride cores having high activity and stability for the ORR. The synthesis involves nitriding metal nanoparticles (e.g., Ni_4N) and simultaneously encapsulating it by 2−4 ML-thick Pt shell (the inset of Figure 3). The PtM nitride catalysts showed 3 to 4 times higher mass activity and 3 to 7 times higher specific activity than that of Pt/C (Figure 3). The Pt mass and specific activity of PtNiN in the rotating disk electrode tests was 0.84 A/mg and 1.64 mA/cm^2, respectively. The order of both the activity is PtNiN/C > PtFeN/C > PtCoN/C > Pt/C. The accelerated stability tests for PtMN/C catalysts showed little loss in its electrochemical surface area and half-wave potential after 35,000 cycling tests, demonstrating that all the nitride cores improved the stability of the catalysts, and in particular the PtCoN catalyst showed the best durability among the catalysts. The experimental data and the density functional theory calculations indicated that nitride has the bifunctional effect that facilitates formation of the core−shell structures and improves the performance of the Pt shell by inducing both geometric and electronic effects.

Au–Promoted Formation of Structurally Ordered Intermetallic PdCo Nanoparticles

We established an innovative but simple methodology for synthesizing structurally ordered AuPdCo that exhibits comparable activity to Pt/C in both acid and alkaline media. Electron microscopic techniques demonstrate that by addition of Au atoms PdCo nanoparticles undergo at elevated temperatures an atomic structural transition from core-shell to a rare intermetallic ordered structure with twin boundaries forming stable {111}, {110} and {100} facets (the inset of Figure 4). The AuPdCo nanoparticles are a promising Pt-free catalyst that shows comparable ORR activity with commercial Pt/C but much better long-term stability in alkaline medium (Figure 4). The superior stability over Pt/C in potential cycling tests in alkaline media is specially attributed to the atomic structural order of PdCo nanoparticles along with protective effect of clusters of Au atoms on the surface. Since we use a simple and cost-effective strategy to make structurally ordered intermetallic PdCo nanoparticles, it is believed that this approach offers numerous possibilities in tailoring other transition metal intermetallic nanocatalysts.

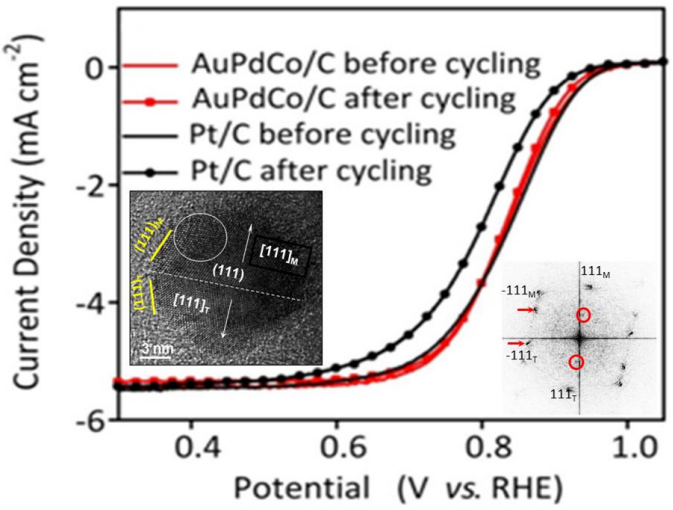

FIGURE 4. ORR polarization curves of AuPdCo/C-intermetallic and Pt/C catalysts before and after 10,000 cycle test between 0.6 and 1.0 V in 0.1 M KOH. Also shown is a high-resolution transmission electron microscope image and its diffractogram of a single AuPdCo intermetallic particle. Superlattice spots are visible in the diffractogram as indicated by the red circles.

CONCLUSIONS AND FUTURE DIRECTIONS

Further improvements of Pt ML catalysts aimed at reducing the cost of the Pd core, increasing stability and improving syntheses efficiency have been achieved. Further testing of Pt ML electrocatalysts demonstrated their attractive features, their application readiness, and the versatility of the core shell approach. New methodologies for improving activity and stability of these catalysts include:

- Synthesis of monodisperse cores.
- Forming atomically ordered, sharp core-shell interfaces.
- Gold promoting the formation of ordered intermetallic compounds.
- Nitrating non–noble metal cores constituents that demonstrate their attractive features, their application readiness, and the versatility of the core shell approach for designing catalysts are discussed in this report.

FUTURE DIRECTIONS

Future work will focus on:

- MEA and stack tests of selected catalysts.
- Electrodeposition from non-aqueous solvents to obtain new cores.
- Reactive spray deposition technology is another method to obtain cores unattainable so far with conventional syntheses.
- Modifying Pt-water interactions and enhance the ORR efficiency.
- Developing new non-noble-metal nitride and/or carbide (e.g., WN, WC, etc.) cores for Pt ML/shell to enhance the activity and stability for the ORR.
- Searching new ordered intermetallic compounds for Pt-free catalysts and supporting cores for Pt ML.

SPECIAL RECOGNITIONS AND AWARDS/ PATENTS ISSUED

1. R. Adzic, Member, Editorial Board, Scientific Reports; Nature.com.

2. R. Adzic, Member, International Academy of Electrochemical Energy Science, 2014,

3. R. Adzic, Distinguished Lecture, Hong Kong University of Science and Engineering, April 2014.

4. R. Adzic, Distinguished Lecture Xiamen University, April 2014.

5. R. Adzic, Invited talk, ECS-ECS meeting, Shanghai, China., April 2014.

6. R. Adzic, Plenary talk at International Symposium on Clean Energy from Ethanol, Rzeszow, Poland, 2014.

Patents

1. Two patent applications have been submitted in 2013-2014.

FY 2014 PUBLICATIONS/PRESENTATIONS

1. Tuning the Catalytic Activity of Ru@Pt Core-Shell Nanoparticles for the Oxygen Reduction Reaction by Varying the Shell Thickness, L. Yang, M. Vukmirovic, D. Su, K. Sasaki, J.A. Herron, M. Mavrikakis, S. Liao, R.R. Adzic, *J. Phys. Chem.,* 117, 1748-1753, 2013.

2. Ordered bilayer ruthenium-platinum core-shell nanoparticles. Y. Hsieh, Y. Zhang, D. Su, V. Volkov, R. Si, L. Wu, Y. Zhu, W. An, P. Liu, P. He, S. Ye, R.R. Adzic, J. Wang, Nat. Commun. 4:2466, 2013.

3. Hollow core supported Pt monolayer catalysts for oxygen reduction, Yu Zhang, Chao Ma, Zhu, Y., Rui Si, Yun Cai, Jia X. Wang, J.X., Adzic, R.R., Catalysis Today, 202, 50–54, 2013.

4. Au-Promoted Structurally Ordered Intermetallic PdCo Nanoparticles for the Oxygen Reduction Reaction, K.A. Kuttiyiel, K. Sasaki, D. Su, L. Wu, Y. Zhu, R.R. Adzic, Nat. Commun., in press.

5. Pt monolayer shell on hollow Pd core electrocatalysts: scale up synthesis, structure, and activity for the oxygen reduction reaction, Miomir B. Vukmirovic, Yu Zhang, Jia X. Wang, David Buceta, Lijun Wu and Radoslav R. Adzic, J. Serb. Chem. Soc. 18, 1983-1992, 2013.

6. Pt Monolayer on Au-Stabilized PdNi Core-Shell Nanoparticles for Oxygen Reduction Reaction, K.A. Kuttiyiel, K. Sasaki, D. Su, M.B. Vukmirovic, N.S. Marinkovic, R.R. Adzic, Electrochimica Acta, 110, 267-272, 2013.

7. Flame Based Synthesis of Core-Shell Structures using Pd-Ru and Pd Cores Prepared from the Vapor Phase with Reactive Spray Deposition Technology, Justin M. Roller, Haoran Yu, Dr. Miomir B. Vukmirovic, Dr. C.B. Carter, Dr. Radoslav R. Adzic, and Dr. Radenka Maric, presented at the 224nd ECS Meeting, San Francisco, California, October 27 – November 1, 2013.

8. Investigation of structural features in Pd nanoparticle cores comprising a shell layer of Pt , Justin Roller, M.J. Arellano-Jimenez, Miomir Vukmirovic, Radoslav Adzic, Paul Kotula, Radenka Maric and C. Barry Carter, 2013 MRS Fall Meeting & Exhibit, December 1–6, 2013, Boston, MA.

9. Core-Shell, Hollow-Structured Iridium-Nickel NitrideNanoparticles for the Hydrogen Evolution Reaction, K.A. Kuttiyiel,K. Sasaki, W.-F. Chen, R.R. Adzic, Journal of Materials Chemistry A, 3, 593-594,2014

V.A.5 The Science and Engineering of Durable Ultra-Low PGM Catalysts

Fernando H. Garzon (Primary Contact),
Jose-Maria Sansiñena, Mahlon Wilson,
Jerzy Chlistunoff, Ivana Matanovic, Neil Henson,
and Eric L. Brosha
Los Alamos National Laboratory
MPA-11, MS. D429
Los Alamos, NM 87545
Phone: (505) 667-6643
Email: garzon@lanl.gov

DOE Manager
Nancy Garland
Phone: (202) 586-5673
Email: Nancy.Garland@ee.doe.gov

Subcontractors
- Yushan Yan, University of Delaware, Newark, DE
- Abhaya Datye and S. Michael Stewart, University of New Mexico, Albuquerque, NM
- Siyu Ye and David Harvey, Ballard Fuel Cells, Burnaby, BC, Canada

Project Start Date: October, 2009
Project End Date: March, 2014

Overall Objectives

- Development of durable, high mass activity platinum group metal (PGM) cathode catalysts enabling lower cost fuel cells
- Elucidation of the fundamental relationships between PGM catalyst shape, particle size and activity to help design better catalysts
- Optimization of the cathode electrode layer to maximize the performance of PGM catalysts—improving fuel cell performance and lowering cost
- Understanding the performance degradation mechanisms of high mass activity cathode catalysts—provide insights to better catalyst design
- Development and testing of fuel cells using ultra-low loading high activity PGM catalysts—validation of advanced concepts

Fiscal Year (FY) 2014 Objectives

- Optimization of Pt supported on pyrolyzed polypyrrole nanowire catalysts for fuel cell testing
- Quantification of Pt supported on pyrolyzed polypyrrole nanowire cathode fuel cell performance
- Optimization of ceria doping for high performance, low free radical generation cathode catalysts
- Demonstration of lifetime improvement of ceria nanoparticle stabilized fuel cells measured by accelerated stress testing

Technical Barriers

For fuel cells and fuel cell systems to be commercially viable, significant reduction in cost is required. Materials and manufacturing costs for stack components need to be reduced. Low-cost, high-performance catalysts enabling ultra-low precious metal loading, and lower cost, are required to make fuel cell stacks competitive. Polymer electrolyte membrane fuel cells, polybenzimidazole-type fuel cells, and phosphoric acid fuel cells suffer from the necessity of relatively high PGM loading.

- PGM catalysts are difficult to synthesize on high performance alternative corrosion resistant supports
- PGM area specific activity may decrease with decreasing particle size
- Durability may decrease with use of smaller catalyst particles that possess greater PGM surface area to mass ratios

The technical targets for catalyst loading are indicated in Table 1. These targets were formulated with the assumption that fuel cell durability and impurity tolerance would not be impacted by the decreased Pt loadings used in the fuel cells.

TABLE 1. Technical Targets

Characteristic	Units	2011 Status	Targets	
			2017	2020
PGM total content (both electrodes)	g/kW (rated)	0.19	0.125	0.125
PGM total loading	mg PGM/cm^2 electrode area	0.15	0.125	0.125

FY 2014 Accomplishments

- Accomplished large batch synthesis (>2 g) of novel nanowire PGM catalysts
- Completed ceria nanoparticle migration study using advanced photon source synchrotron X-ray microprobe
- Completed oxygen-free radical decomposition catalysis studies for Pr-, Gd- and Zr-doped ceria
- Completed accelerated stress testing of fuel cell membrane electrode assemblies (MEAs) incorporating ceria free-radical scavengers

- Completed characterization of LANL catalyst materials delivered to Ballard Fuel Cells for validation testing
- Performed fuel cell testing using novel nanowire PGM catalysts demonstrating 50-cm^2 single-cell performance with <<0.1 mg Pt/cm^2 that equals or exceeds conventional MEAs with 0.2 mg Pt/cm^2

INTRODUCTION

Minimizing the quantity of PGMs used in polymer electrolyte membrane fuel cells is one of the remaining challenges for fuel cell commercialization. Tremendous progress has been achieved over the last two decades in decreasing the Pt loading required for efficient fuel cell performance. Unfortunately, the fluctuations in the price of Pt represent a substantial barrier to the economics of widespread fuel cell use. Durability and impurity tolerance are also challenges that are tightly coupled to fuel cell Pt electrode loading. Polymer electrolyte fuel cell membrane durability is limited by free radical attack generated from oxygen reduction processes. The creation of peroxide via two electron oxygen reduction and subsequent decomposition into hydroxyl and/or hydroperoxyl free radicals may be the major source of nonmetallic fuel cell component chemical degradation. The addition of Ce^{+3} by ion exchange has greatly improved the durability of polymer electrolyte fuel cells. The cerium cations decompose the free radical species at high rates, thus limiting membrane damage and carbon support oxidation. However our recent studies show the Ce ions are very mobile [1]. An alternative approach is the addition of cerium oxide nanoparticles as free radical scavengers. The surfaces of CeO_2 nanoparticles contain appreciable concentrations of Ce^{+3} and Ce^{+4} that may act as catalytic sites for free radical decomposition. However little is known about the effects of particle size and doping on the free radical scavenging rates, and the selectivity towards peroxide decomposition versus secondary free radical generation has not been previously studied. The mobility of cerium generated from the decomposition of the nanoparticles is also unknown. The results of our FY 2014 work are published in greater detail in the references [1-3] listed at the end of this report.

APPROACH

Our approach to new PGM catalyst design is multi-tiered**.** We are designing new low platinum loading catalysts on novel support materials to improve fuel cell performance. Novel shapes; nanoparticles, nanotubes and nanowires are being synthesized in a variety of sizes. We are using contemporary theoretical modeling and advanced computational methods to understand and engineer the new catalysts. We are also modeling and designing appropriate catalyst architectures to maximize the performance of our novel catalysts. Catalyst-support interactions and their effects on durability and mass activity are also investigated. New methods to reduce the free radical attack on fuel cell components, such as catalytic nanoparticle free radical scavengers, are being studied. We also study and test the performance of the catalysts in electrochemical cells, single-cell fuel cells and fuel cell stacks. The new catalysts are be extensively characterized before and after fuel cell operation. The synthesis and characterization of Pt catalysts on carbon nanowires derived from pyrolyzed polypyrrole were reported on last year. In FY 2014 we scaled up the production and delivered catalyst quantities sufficient for Ballard fuel cell testing. The testing results are summarized in our DOE-EERE-FCT FC010 Annual Merit Review presentation. The catalysts showed much superior performance to conventional materials at low loadings, ~0.05 mg Pt/cm^2 and low relative humidity (RH) (30%) conditions.

Ceria and doped ceria nanoparticles were synthesized using acetate solution precursors [2]. Cerium(III)acetate (Strem Chemicals) and Pr or Zr acetates were dissolved in deionized water acidified to obtain a solution of 0.1 M metal ions (Ce + *M*). To the mixture concentrated nitric acid (Fisher) was added until both the cerium and *M* acetates were dissolved. Once both metal acetates were dissolved, a 50 % ammonium hydroxide solution (Alfa Aesar) was added to the solution while it was manually agitated until the solution turned white and opaque. The dried samples were subsequently transferred to a ceramic boat and heated under air at between 200-800°C for 1 hour to achieve a range of particles sizes from 5 to 40 nm. Phase purity, crystal structure, lattice parameters and crystallite size were determined by powder X-ray diffraction measurements. Specific (normalized by Brunauer-Emmett-Teller gas adsorption surface area) hydrogen peroxide decomposition rates were determined by volumetric determination of catalytic oxygen production. To determine the peroxide decomposition to free radical production selectivity, a 6-carboxyfluoroscein dye coupled with ultraviolet visible spectroscopy was used. Fluorine ion emission rates were determined by fluorine ion specific electrode measurements (Orion). Inks were made by mixing a 2% Nafion© solution with a TKK platinum supported on carbon catalyst (47.9 wt% Pt). If pure or doped ceria (2% of the weight of platinum) were also added to the cathode inks, they were incorporated after catalyst mixing. Decals were made by painting catalyst inks onto polymer substrates. The loading of platinum as well as the platinum to cerium ratio was verified using X-ray fluorescence (XRF) spectroscopy; all cathode decal loadings were 0.23 mg Pt/cm^2 and the anode decal loading were 0.18 mg Pt/cm^2.

All MEAs were assembled using 50-cm^2 Dupont™ XL proton exchange membranes. To create un-stabilized MEAs,

the XL membranes were first boiled in NaOH. The washed membranes were partially dried at 80°C for 10 minutes, then hot pressed between the decals at 120 psi/cm^2 at 212°C for 5 minutes, then allowed to cool to room temperature in air. The pressed MEAs were then boiled in 1 M sulfuric acid to remove the cerium cations. The removal of the silica and cerium ions was confirmed by XRF and energy dispersive spectrometer measurements. Fuel cells were assembled using a SGL 25BC gas diffusion layer (SGL Group) with graphite current collectors.

Open circuit voltage testing at low RH is well known to accelerate membrane degradation. Cells were conditioned by running at 80°C and 100 % RH overnight. Beginning of life testing was carried out after conditioning at both 30°C and 100% RH, and 80°C and 30% RH. For beginning-of-life testing, the high frequency resistance, limiting current, power-density, and impedance spectroscopy were performed with hydrogen. The cells were allowed to operate under open circuit at 80°C, 30% RH, except when tested every 24 to 72 hours to assess cell degradation. A jacketed condenser was used to remove water vapor from the exhaust gases so that the fluorine emission rate of both the anode and cathode could be measured. The accelerated stress test was stopped when open circuit potential dropped beneath 0.7 V, at which point impedance spectroscopy and limiting current measurements were impossible, or the crossover current appeared ohmic, which was indicative of a gas crossover leak in the cell.

Unmodified Dupont™ XL membranes were used as received, containing both cerium cations and silica fibers, and were also subjected to stress testing to determine baseline behavior. Unlike the unstabilized membranes, the control XL membranes were not pretreated by boiling in sodium hydroxide or sulfuric acid; the as-received membranes were used to fabricate MEAs using ink decal transfer, and then conditioned and tested the in the same manner as the other cells. An FEI Quanta 400F scanning electron microscope (SEM) equipped with an energy dispersive spectrometer was used to acquire scanning electron microscope images of membranes after conditioning and stress testing. 5 KeV electrons were used, and both backscattered and secondary electrons images were recorded.

RESULTS

Figures 1 and 2 show the inverse selectivity versus reactivity for praseodymium, zirconium, and doped cerium oxide, respectively. On each plot, the performance of cerium oxide is plotted in red for comparison. An ideal catalyst would be one that maximizes reactivity while minimizing inverse selectivity; the particle size that gives the fastest peroxide decomposition rate while producing the least free radicals.

Un-doped cerium oxide exhibits interesting trends in specific activity and inverse selectivity. The red markers representing the pure ceria samples, clearly show a trend of

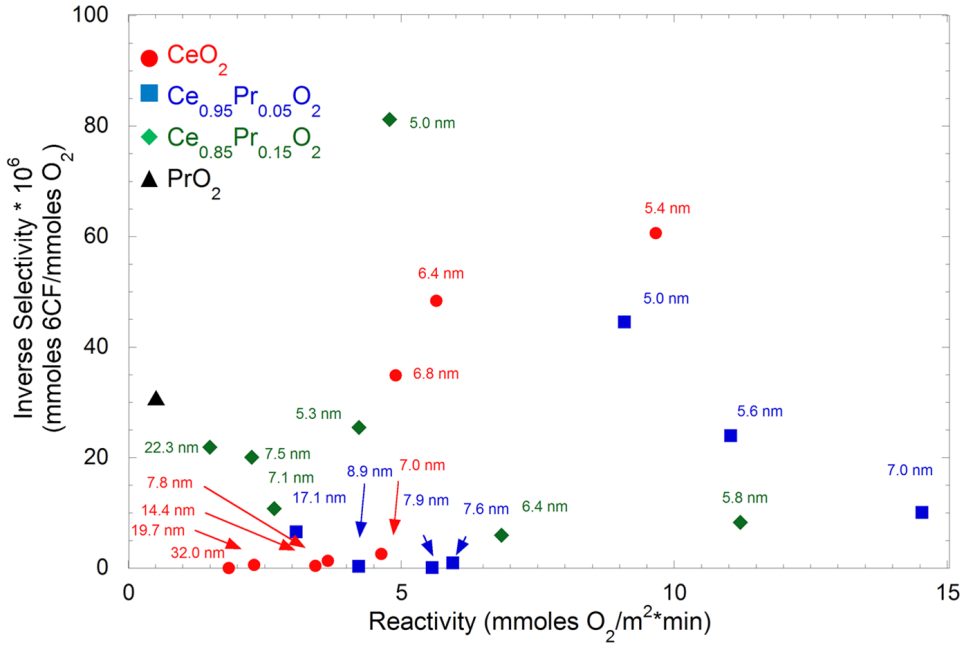

FIGURE 1. Inverse selectivity versus activity for peroxide decomposition by different particle sizes of cerium oxide (circle), $Ce_{0.95}Pr_{0.05}O_2$ (square), $Ce_{0.85}Pr_{0.15}O_2$ (diamond), and bulk PrO_2 (triangle). Particle sizes for the different doped and undoped cerium oxides are listed beside the data points [2].

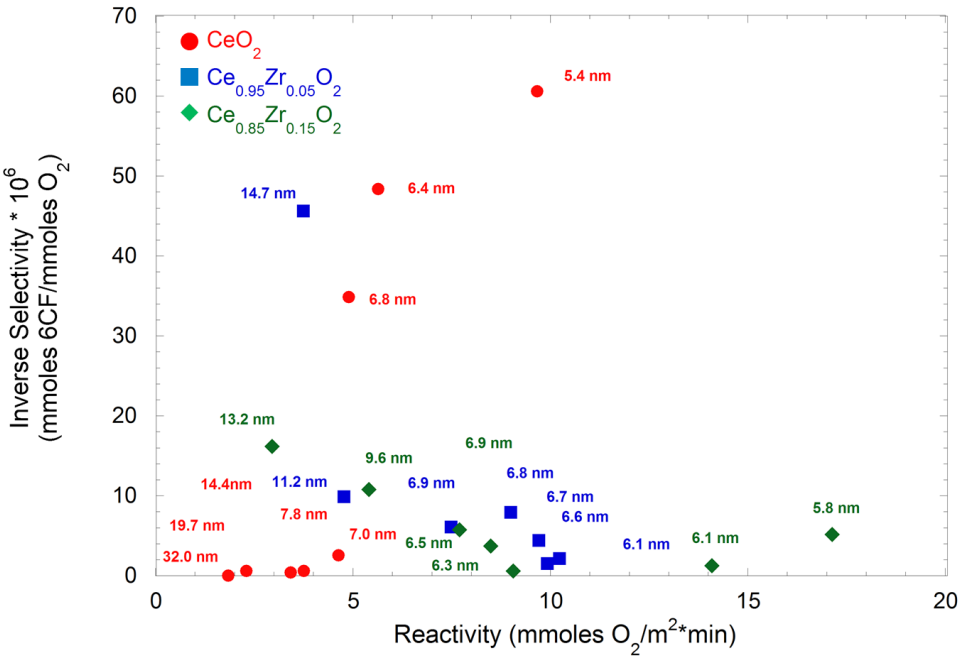

FIGURE 2. Inverse selectivity versus activity for peroxide decomposition by different particle sizes of cerium oxide (circle), $Ce_{0.95}Zr_{0.05}O_2$ (square), and $Ce_{0.85}Zr_{0.15}O_2$ (diamond). Particle sizes for the different doped and undoped cerium oxides are listed beside the data points [2].

increasing area specific activity with decreasing particle size, however the free radical production rate increases for the smaller ~8 to 5 nm particle size range. The largest particle sizes produce no measurable free radicals, however it is desirable for fuel cell performance to minimize the volume of MEA components that do not contribute to multiphase transport.

As compared to pure cerium oxide, when praseodymium is incorporated into the nanoparticle at 5 at%, the optimal reactivity is seen for circa 7 nm without any loss in selectivity, with smaller and larger crystallite sizes giving worse activity. Similarly for 15 at% Pr incorporation, the optimal crystallite size is closer to 6 nm with a loss of activity and selectivity seen above and below this crystallite size. For the 15 at% Pr particles, the activity and selectivity of the particles approaches that of pure praseodymium for the 22.3 nm particles, whereas the 5 at% Pr particles, while beginning to become less selective and active for larger crystallite sizes, do not reproduce the behavior of pure praseodymium at 17.1 nm. However, the 5 at% particles gave better performance over pure cerium oxide and 15 at% nanoparticles. For zirconium doping, unlike praseodymium, there is no loss in activity and selectivity with decreasing crystallite size as seen in Figure 2. In fact, decreasing particle size and increasing zirconia content improve both activity and selectivity in these nanoparticles, and suggests that any cerium-zirconium nanoparticles beneath 7 nm would be useful for selectively decomposing hydrogen peroxide.

When compared to an un-stabilized membrane cell, large cerium oxide nanoparticles have stabilizing effects, which results in a lower loss in performance over time. Both medium and small cerium oxide nanoparticles also show some initial stabilization. However, ultimately they have detrimental effect on the lifetime of the fuel cells during accelerated stress testing, causing an increase in hydrogen cross over, fluorine emission, and exponential loss in open circuit voltage. As predicted from selectivity and activity performance, ~7.0 nm pure cerium oxide nanoparticles incorporated in the cathode catalyst layer impart the same stabilization for fuel cells as cerium cations dispersed in the membrane; Figures 3 and 4 illustrate this effect. However, this improvement is short lived. The loss in performance in attributed to the loss of cerium oxide due to dissolution, which increases for decreasing particle size [3]. After 350 hrs the cerium oxide particle sizes become smaller, perhaps changing the energetics of the cerium oxide oxidation states, so that the selectivity of the cerium oxide for free radical decomposition becomes too low and the peroxide decomposition on cerium oxide, generates an increasing amount of free radicals. A parallel study by the authors using spatially resolved XRF observed cerium migration in both membrane ion-exchanged and ceria nanoparticle stabilized fuel cells after accelerated stress testing in very short time periods [1]. While future work remains on the stabilization effects of zirconium doped cerium oxide nanoparticles in fuel cells, research focusing on the changes in selectivity and activity of doped nanoparticles for hydrogen peroxide

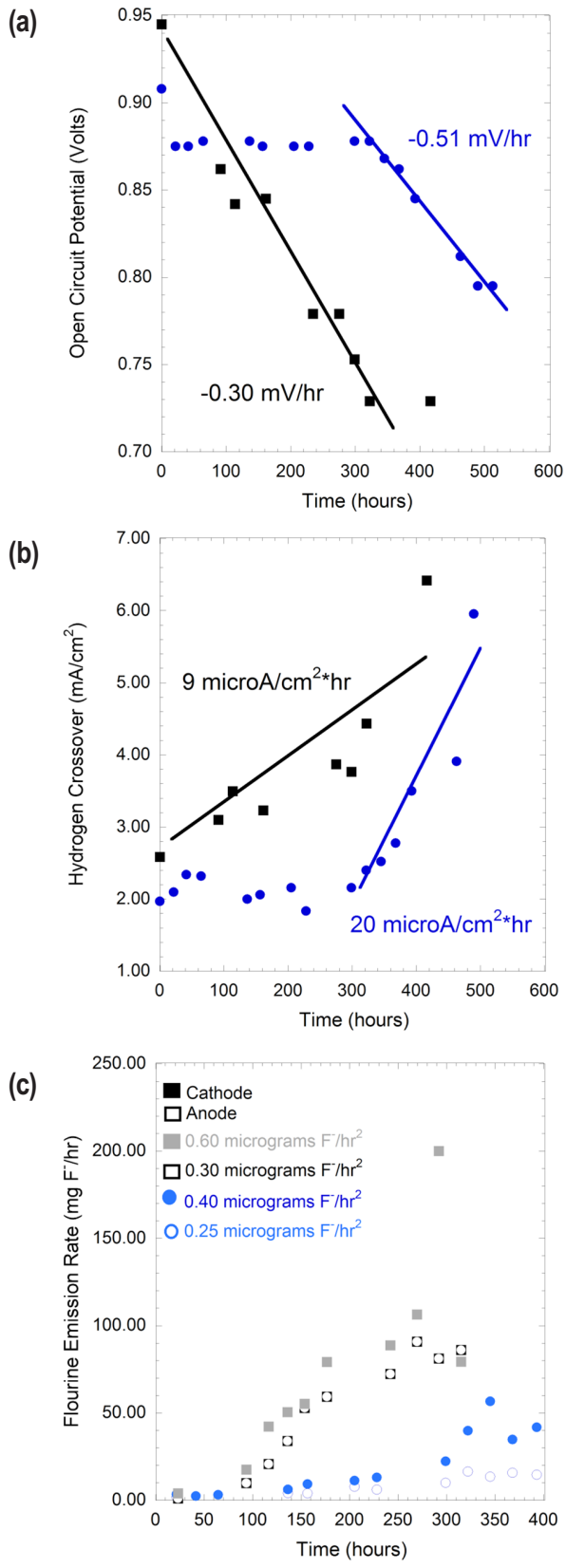

FIGURE 3. Un-stabilized membrane fuel cell open circuit voltage accelerated stress test with 7 nm ceria particles (circles) addition to cathode versus XL un-stabilized membrane fuel cell (squares) a) open circuit voltage, b) hydrogen crossover, c) fluorine ion emission [3].

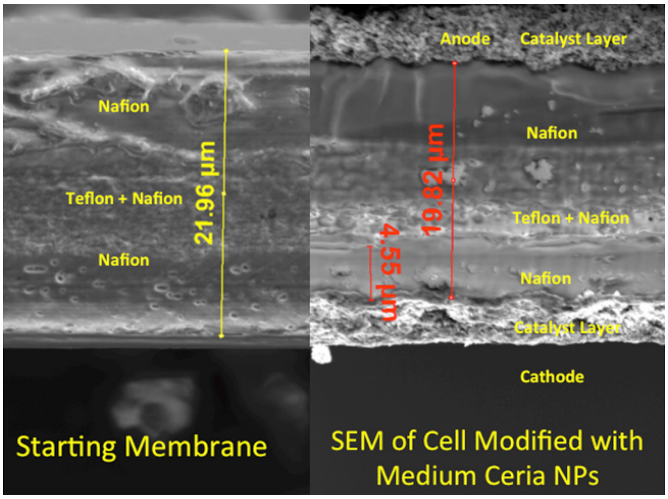

FIGURE 4. SEM images of fuel cell membrane electrode assembly before and after 500 hrs testing [4].

decomposition provides insight into their predicted behavior. Of the two dopants, zirconium cations are the only dopants that demonstrate ideal behavior for fuel cell dopants; increasing selectivity and activity with decreasing particles size, with no lower limit on particle size. In summary, the nanoparticle additives were shown to decompose peroxide and in some cases, improve ionomer durability. The catalytic activity and reaction pathway of cerium oxide towards hydrogen peroxide decomposition was strongly influenced by the crystallite size and the doping of cerium oxide nanoparticles. For both cerium oxide and doped cerium oxide, the size and doping of ceria nanoparticles is also shown to play an important role on their ability to improve membrane durability.

CONCLUSIONS AND FUTURE DIRECTIONS

- Carbon nanowires derived from the pyrolysis of polypyrrole exhibited excellent properties for Pt fuel cell cathode performance optimization
- MEAs incorporating carbon nanowires will benefit from further optimization strategies
- The doping of ceria nanoparticles improves the stability and selectivity of the free radical scavenging catalyst
- The optimal concentration of doped ceria nanoparticles for fuel cell lifetime improvements needs to be determined

FY 2014 PUBLICATIONS/PRESENTATIONS

Publications

1. Stewart, S.M.; Spernjak, D.; Borup, R.; Datye, A.; Garzon, F., Cerium Migration through Hydrogen Fuel Cells during Accelerated Stress Testing. *ECS Electrochemistry Letters* **2014,** *3* (4), F19-F22.

2. Stewart, S.M.; Spernjak, D.; Borup, R.; Datye, A.; Garzon, F., Ceria and Doped Ceria Nanoparticle Additives for Polymer Fuel Cell Lifetime Improvement. Accepted for publication *ECS Transactions* **2014.**

3. Banham, D.; Ye, S.; Cheng, T.; Knights, S.; Stewart, S.M.; Wilson, M.; Garzon, F., Effect of CeOx Crystallite Size on the Chemical Stability of CeOx Nanoparticles. *Journal of The Electrochemical Society* **2014,** *161* (10), F1075-F1080.

4. Sansiñena, J.-M.; Wilson, M.S.; Garzon, F.H., Conductive Nanostructured Materials for Supported Metal Catalysts. *ECS Transactions* **2013,** *50* (2), 1693-1699.

5. Matanovic, I.; Kent, P.R.C.; Garzon, F.H.; Henson, N.J., Theoretical Study of the Structure, Stability and Oxygen Reduction Activity of Ultrathin Platinum Nanowires. *ECS Transactions* **2013,** *50* (2), 1385-1395.

6. Matanovic, I.; Kent, P.R.C.; Garzon, F.H.; Henson, N.J., Density Functional Study of the Structure, Stability and Oxygen Reduction Activity of Ultrathin Platinum Nanowires. *Journal of the Electrochemical Society* **2013,** *160* (6), F548-F553.

7. Alia, S.M.; Jensen, K.; Contreras, C.; Garzon, F.; Pivovar, B.; Yan, Y., Platinum Coated Copper Nanowires and Platinum Nanotubes as Oxygen Reduction Electrocatalysts. *ACS Catalysis* **2013,** *3* (3), 358-362.

8. Ogumi, Z.; Matsuoka, H.; Garzon, F.; Kim, H.; Wan, L.-J.; Tamao, K.; Nakamura, M., Electrochemistry 80th Anniversary Special Issue. *Electrochemistry* **2013,** *81* (3), 140-197.

Presentations

1. Banham, D.; Ye, S.; Cheng, T.; Knights, S.; Stewart, S.M.; Garzon, F.H., Impact of CeOx Additives On Cathode Catalyst Layer Poisoning. *ECS Meeting Abstracts* 2013**,** *MA2013-02* (15), 1303.

2. Mukundan, R.; Beattie, P.; Davey, J.R.; Langlois, D.A.; Spernjak, D.; Fairweather, J.D.; Torraco, D.; Garzon, F.; Weber, A.Z.; More, K. L.; Borup, R. L., Durability of PEM Fuel Cells and the Relevance of Accelerated Stress Tests. *ECS Meeting Abstracts* 2014**,** *MA2014-01* (18), 794.

V.A.6 Tungsten Oxide and Heteropoly Acid-Based System for Ultra-High Activity and Stability of Pt Catalysts in Proton Exchange Membrane Fuel Cell Cathodes

John A. Turner
National Renewable Energy Laboratory (NREL)
15013 Denver West Pkwy
Golden, CO 80401
Email: John.Turner@nrel.gov

DOE Manager
David Peterson
Phone: (720) 356-1747
Email: David.Peterson@ee.doe.gov

Subcontractors
University of Colorado, Boulder, CO
Colorado School of Mines, Golden, CO

Project Start Date: May 1, 2010
Project End Date: April 30, 2014

Overall Objectives

- Replace carbon in the fuel cell cathode with tungsten oxide (WO_X) to reduce support corrosion.
- Utilize heteropolyacid (HPA)-functionalized supports (carbon and WO_X), to increase platinum stability.

Fiscal Year (FY) 2014 Objectives

Quantify the mass activity, electrochemical active surface area and durability of HPA-functionalized carbon blacks

Technical Barriers

This project addresses the following technical barriers from the Fuel Cells section (3.4.4) of the Fuel Cell Technologies Office Multi-Year Research, Development, and Demonstration Plan:

(A) Durability (of catalysts and membrane electrode assemblies [MEAs])

(B) Cost (of catalysts and MEAs)

(C) Performance (of catalysts and MEAs)

Technical Targets

This project addresses the severe corrosion and fuel cell cathode electrode degradation that takes place when using carbon-black-supported Pt catalysts in automotive applications during unmitigated start-up and shut-down operations. The following are the targets that are being addressed.

- Mass Activity: >275 mA/mg_{Pt}
- Durability under start-up/shut-down cycling: electrochemical surface area (ECA) loss <40%

The cost of the fuel cell system will be lowered with system simplification if the fuel cell vehicle can be subject to start-stop cycles without any complex system mitigation involved.

INTRODUCTION

Conventional nanoparticle Pt/C electrocatalysts used in automotive fuel cells suffer significant degradation during start-up and shut-down operations. Under these conditions the potential at the cathode approaches ~1.5–1.6 V for short bursts of time leading to carbon support corrosion. In this project we evaluate alternative supports for Pt that might be more stable and corrosion-resistant than conventional carbon blacks. Developing such a support will allow the fuel cell system to be simplified, lowering the costs and simultaneously increasing the durability. Alternative supports such as WO_X as well as HPA-functionalized carbon blacks were synthesized and evaluated for improved corrosion resistance while maintaining or improving on the activity in comparison to conventional Pt/C. Studies were primarily conducted in half-cell rotating disk electrode (RDE) experimental set-ups due to the small quantity (tens of mg) of catalyst materials that were typically synthesized. Only catalysts that met the activity and durability target in RDE studies would be considered for further evaluation as MEAs in subscale proton exchange membrane fuel cells.

APPROACH

Oxide supports such as WO_X are grown using a hot-wire chemical vapor deposition (HWCVD) method and atomic layer deposition (ALD) or wet-chemistry is used to deposit Pt nanoparticles on the support. These oxide supports are inherently more stable than carbon black but have known drawbacks in terms of lower surface area and lower electronic conductivity as compared to conventional carbon black supports. Therefore, the electronic conductivity and the electrochemical activity of the supports and Pt-catalyzed supports as a function of small added quantities of highly

graphitized carbon blacks/fibers was studied in parallel with measurement of the oxygen reduction reaction (ORR) activity of the materials. The overall approach in terms of collaboration with the various subcontractors and institutions is schematically depicted in Figure 1. Durability cycling protocols that simulate start-up/shut-down were not available at the beginning of the project and were developed along with the DOE Durability Working Group to quantify the suppression of degradation achieved with the novel supports. We delineate the choice of protocols that were selected by the Durability Working Group for evaluating cyclic durability of the novel supports in comparison to carbon blacks in RDE studies.

Materials and Catalyst Synthesis and Scale-Up and Conductivity Measurements

Tungsten Oxide Hot Wire Deposition

Tungsten oxide nanostructures were synthesized by HWCVD in an atmosphere of argon and oxygen. Material synthesis employing sequential depositions at room temperature leads to rod-like nanostructure growth 10–50 nm in diameter, and up to microns in length. The yield of one batch was approximately 25 mg. We increased the WO_X HWCVD yield to 50 mg/synthesis by increasing the length of the reaction zone. Our initial synthetic runs resulted in the fabrication of mixed phases; fully (x=3) and sub-stoichiometric (x<3) WO_X material. The fabrication of the sub-stoichiometric material is more desirable owing to its higher electrical conductivity. We were able to decrease the amount of WO_3 by conditioning, or flowing current through the filament, in an Ar-only atmosphere prior to the addition of oxygen to the reaction zone. This generated sub-stoichiometric material, where the bulk WO_X synthesized was x=1.39 as determined by thermo-gravimetric analysis. The WO_X nanoparticle stoichiometry and crystalline structure can also be controlled by subsequent annealing in air, as demonstrated by the X-ray diffraction spectra in Figure 2a. Near edge X-ray absorption fine structure data were obtained from the Stanford Linear Accelerator Center to provide insight into oxygen bonding on tungsten oxide, illustrated in Figure 2b. However, in situ and post-synthetic attempts to increase the conductivity of the WO_X substrates were not observable in the electrochemical characterization.

Another method to produce tungsten oxide nanorods was the pyrolysis of the precursor compound $((C_4H_9)_4)N)_4W_{10}O_{32}$. The precursor compound, was synthesized by using $Na_2WO_4.2H_2O$ and tetrabutylammonium bromide as the starting materials. The precursor was recrystallized in hot dimethyl formamide to give yellow crystals. The pyrolysis of $((C_4H_9)_4)N)_4W_{10}O_{32}$ to synthesize WO_3 nanorods is carried as follows: 1 g of the precursor compound was taken in an alumina crucible and introduced inside a tubular furnace and heated at 450°C under an Ar atmosphere for 3 hours followed by heating under air atmosphere at the same temperature for 3 hours. Then it was gradually cooled to room temperature to obtain WO_3 nanorods. Scanning electron microscopy

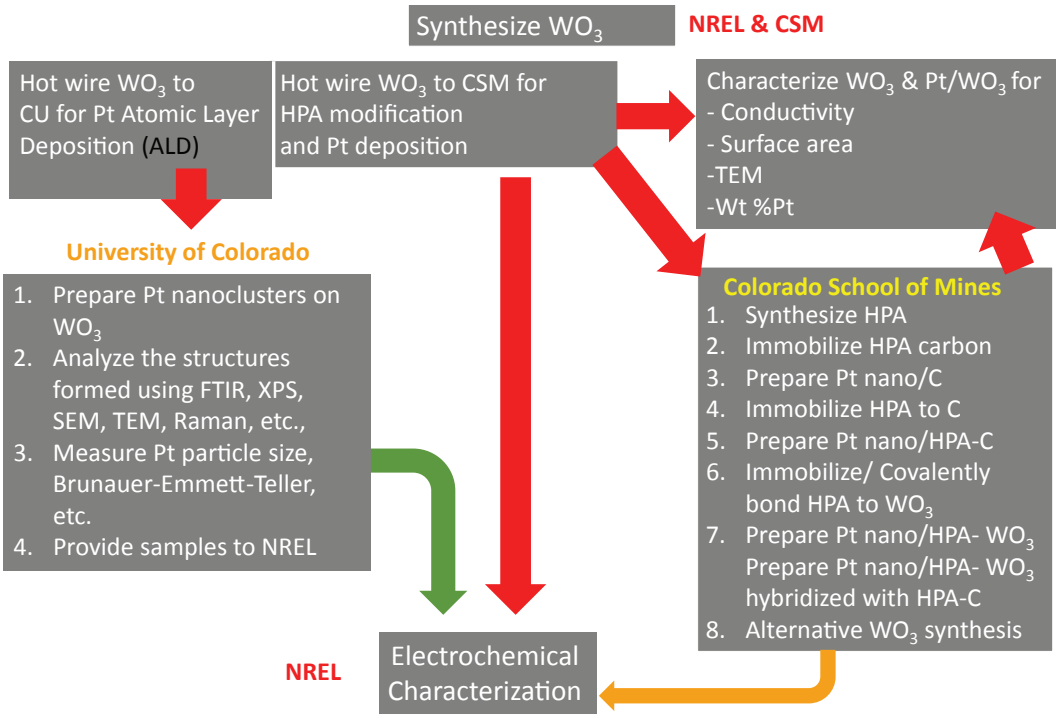

FIGURE 1. Operational Flow Diagram

was employed to observe the morphology of WO_3. The as-synthesized WO_3 showed the formation of one-dimensional nanorods (Figure 3) in high yields. The rods were poly-dispersed with an average width of 15 nm.

Vand der Pauw Technique

The bulk conductivity of the WO_X materials was investigated by four-point probe measurement in the Van der Pauw geometry. The as-produced materials were pressed into a pellet and the conductivity was measured over a range of pellet pressing pressures. The average conductivity was ~0.25 $(ohm\ cm)^{-1}$.

In-House Electronic-Conductivity Cell Measurements

Conductivity measurements were carried out in an in-house experimental set-up that consisted of Au-coated Cu plates. The density and conductivity of various support materials as well as supports mixed with various amounts of a graphitized carbon were determined at various loads and were reported previously. The challenges that result from

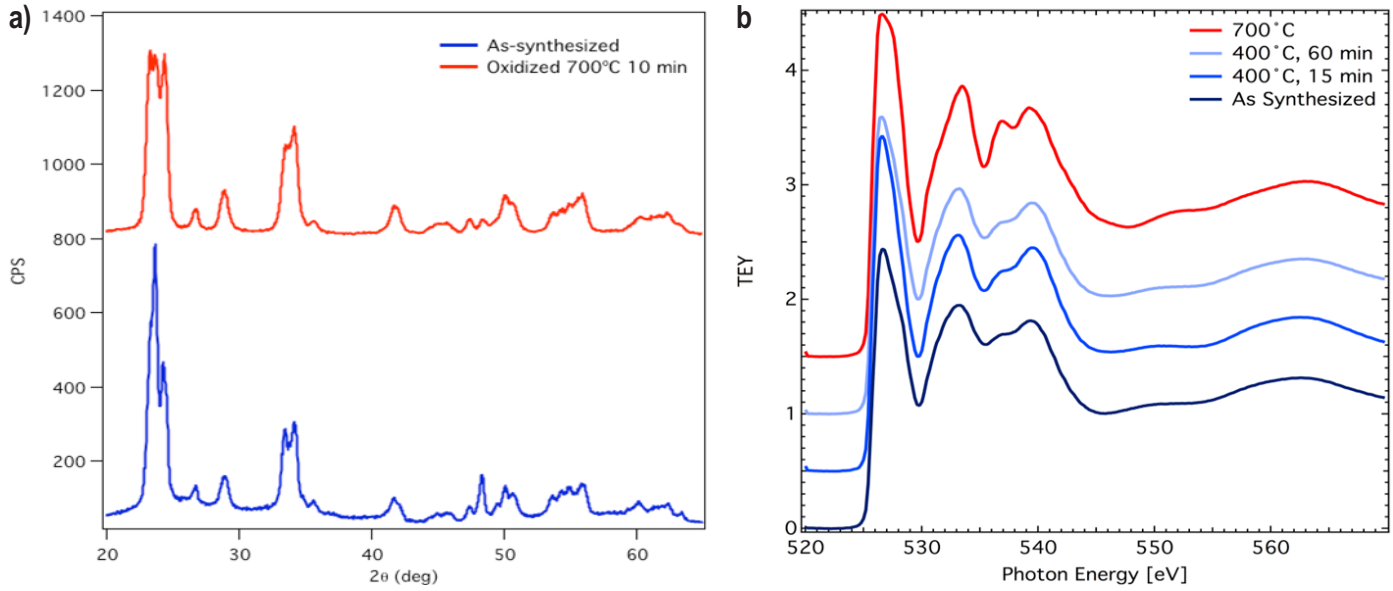

FIGURE 2. a) X-Ray Diffraction and b) Near Edge X-ray Absorption Fine Structure of HWCVD WO_X Materials

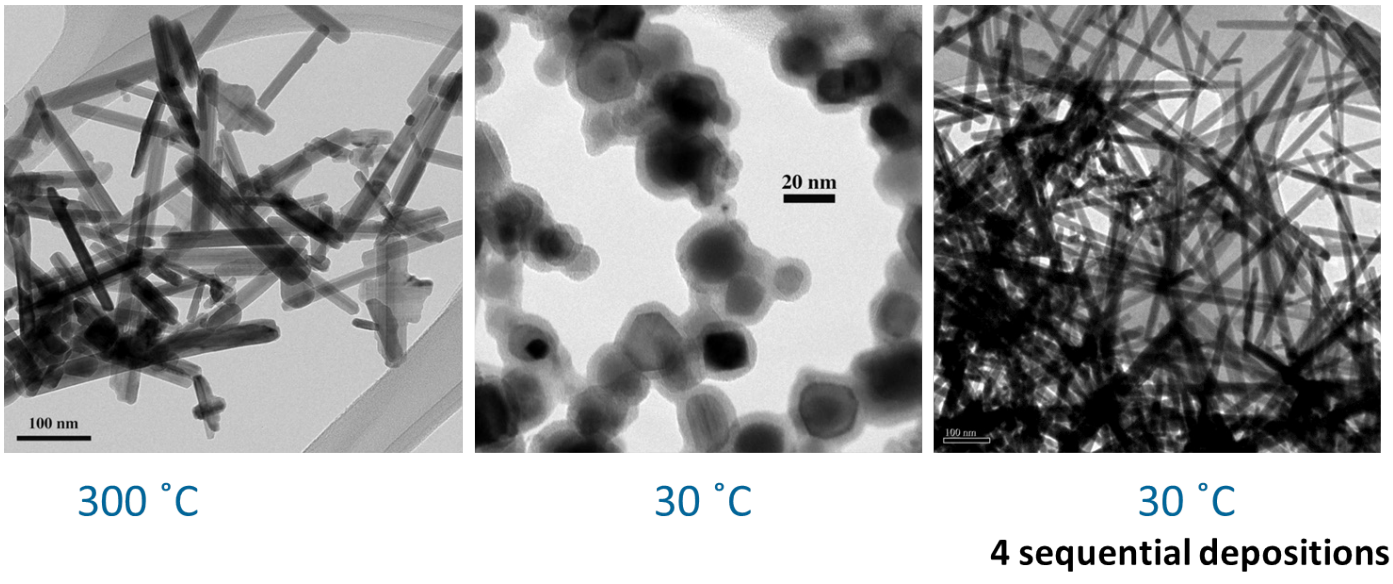

FIGURE 3. HWCVD production of tungsten oxide nanostructures. Synthesis at 150 Torr 4% O_2 in Ar, filament temperature ~2,000°C. Showing dramatic change in particle morphology with lower furnace temperature and that sequential depositions lead to rod growth.

the lower conductivity of alternative supports are illustrated in Figure 4a. Three electronic pathways are illustrated in the figure: i) electronic contact between Pt and the support or Pt and ionomer covered support; ii) conductivity through the bulk support, and iii) electronic pathway between Pt/support agglomerates through added carbon support. We note that, although currently used carbon black supports have extremely high electronic conductivity (~10-100 S/cm), novel corrosion resistance supports with lower conductivity in the range (~1-10 S/cm) might be acceptable, since the limiting resistance in the cathode catalyst layer of proton exchange membrane fuel cells are the result of protonic resistances of the ionomer (~0.1 S/cm). A micrograph of the mixture is given in Figure 4b.

ALD Deposition of Pt on WO_X

Platinum was deposited on the WO_X nanoparticles by ALD using sequential dosing of (methylcyclopentadienyl) trimethylplatinum IV ($Me_3PtMeCp$) precursor and oxygen. We investigated different methods to alter the morphology of the Pt deposition. Our initial ALD work resulted in a high Pt loading with large particle sizes and agglomeration. By increasing the precursor temperature, a higher flux of Pt enabled more uniform nucleation, leading to smaller particles throughout the sample. Uniform deposition of Pt nanoparticles on tungsten oxide, with a diameter distribution of 2-4 nm is shown in Figure 5. We developed control of uniform deposition in the range of 0-60 wt% Pt loadings. For high loadings of Pt, the particles almost reach full coverage the WO_X surface as shown in Figure 6a. This has been achieved by performing ALD in a stop-flow configuration with increased dosing time of the platinum precursor as well as increased soak times during deposition. The ALD deposition process was scaled up to accommodate gram size quantities of WO_X with new capabilities at NREL using a rotary ALD system.

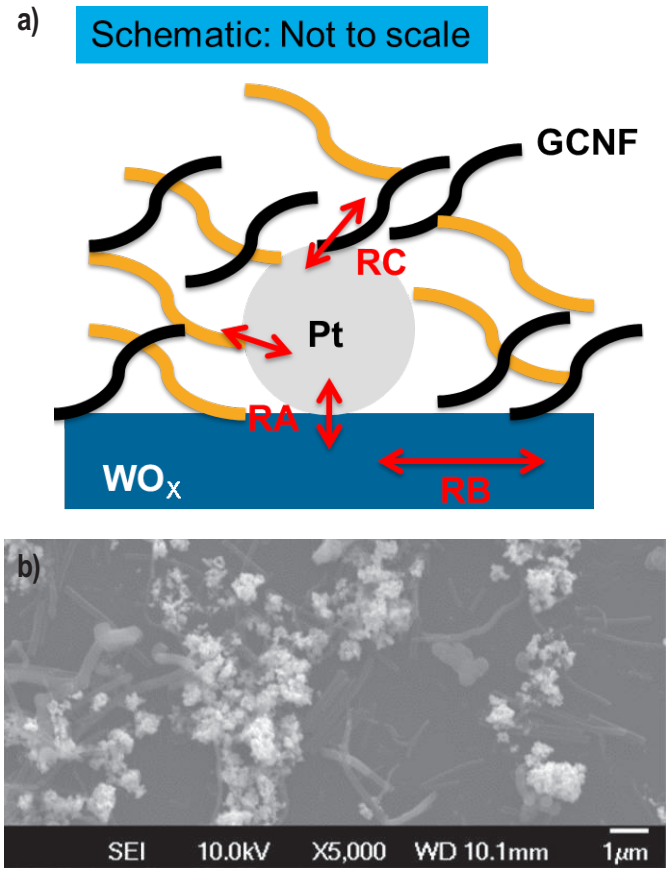

FIGURE 4. a) Electronic pathways in a Pt/support mixed with carbon black structure; RA: electronic contact between Pt and the support or Pt and ionomer covered support; RB: conductivity through the bulk support; and RC: electronic pathway between Pt/support agglomerates through added carbon support GCNF. b) Micrograph of WO_X/Pt/GCNF.

The effect of temperature is demonstrated by performing the same deposition conditions, (number of cycles, precursor temperature, flow rates, and dose and soak times) with changing the reactor temperature. Figures 6a and 6b show 20 cycles of Pt deposition on WO_X substrates for the reactor temperature of 270°C and 300°C, respectively. The Pt deposited at higher temperature results in rounder particles owing to the greater mobility and higher surface energy of Pt. ALD of thin Pt films was also attempted on the WO_X substrates. Wetting of a Pt film on a substrate, however, requires a material with higher surface energy such as W metal. Therefore, a thin W layer was deposited using WF_6+Si_2H_6 on the WO_X substrate prior to Pt ALD.

The use of Pt II hexafluoroacetylacetonate, $Pt(hfac)_2$, precursor was also considered. This work was done by the University of Colorado. Our intent was to use the hfac ligand chemistry as site-blocking species to enable greater control over the spacing and Pt particle size. This concept was previously demonstrated for the deposition of Pd particles using $Pd(hfac)_2$. This method was scaled up from the initial synthesis of mg samples to gram size samples by the use of a rotary ALD system. However, high metal loadings were difficult to achieve using this precursor. Although novel chemistry of Pt ALD was demonstrated, it was shown that this was not an efficient route for fuel cell catalyst development. The addition of a plasma source to the ALD rotary system may provide a route to increase Pt loadings.

Deposition of Pt Nanoparticles on HPA-Functionalized Carbon Black

HPA functionalization of carbon was carried out to i) shield carbon against corrosion, ii) stabilize nano-metallic particles, iii) decompose peroxide, iv) alter electrochemistry at the Pt surface, and v) conduct protons. These functionalized carbons were used as supports for depositing Pt nanoparticles that were synthesized using a colloidal preparation. A literature recipe was modified significantly to synthesize small controlled Pt nanoparticles by decreasing the temperature to 80°C, bubbling dilute CO into solution,

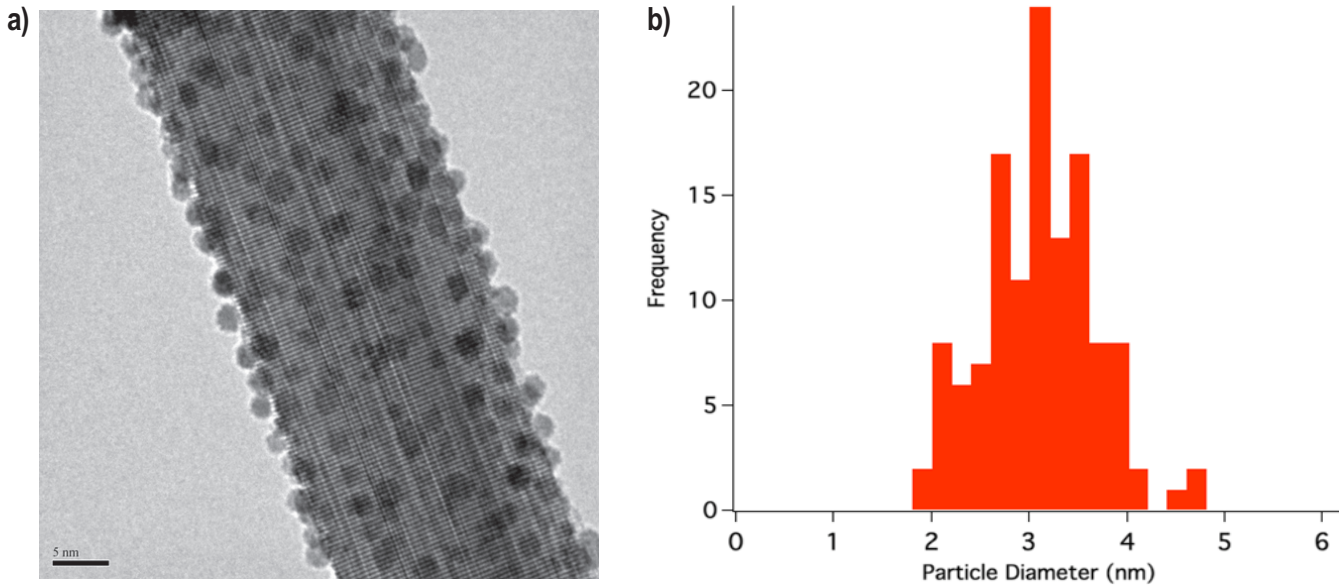

FIGURE 5. (A) TEM Image of Pt ALD on WO_x and (B) Associated Particle Size Distribution

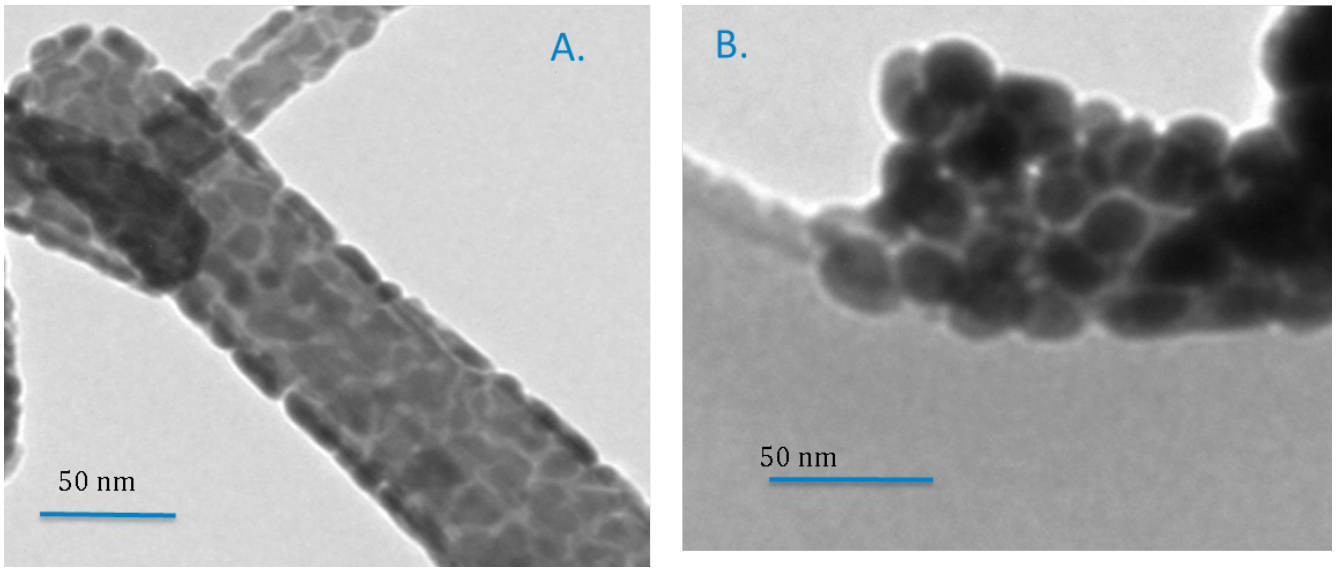

FIGURE 6. For high loadings of Pt, the particles almost reach full coverage of the WO_x surface. 20 cycles of Pt ALD deposited on WO_x with a reactor temperature at A). 300°C and B) 270°C.

and gradually adding 0.25M NaOH over 3 hours. Figure 7a illustrates the transmission electron micrograph (TEM) and particle size distribution of the synthesized colloids that were deposited onto the HPA-functionalized carbon by the following process: (i) dispersion of HPA-C material in water via 20 min ultrasonication; (ii) addition of Pt colloid followed by ultrasonication for an additional 20 min; (iii) catalyst separation via Buechner filtration; and (iv) drying at 200°C for 2 hours. Figure 7b illustrates the Z-contrast scanning TEM (STEM) image of Pt/SiW11-C showing spatial distribution of Pt (bright white spots ~3-5 nm) and SiW11 (~1 nm dull gray spots).

Electrochemical Characterization and Analysis

Prior to evaluating novel materials for electrochemical ORR activity, we established benchmarks for the activity of baseline commercial Pt/C materials. The ORR activity and ECA of the novel synthesized materials were then compared to the benchmarks to determine if they performed well enough to be taken to the next stage of scale up of synthesis

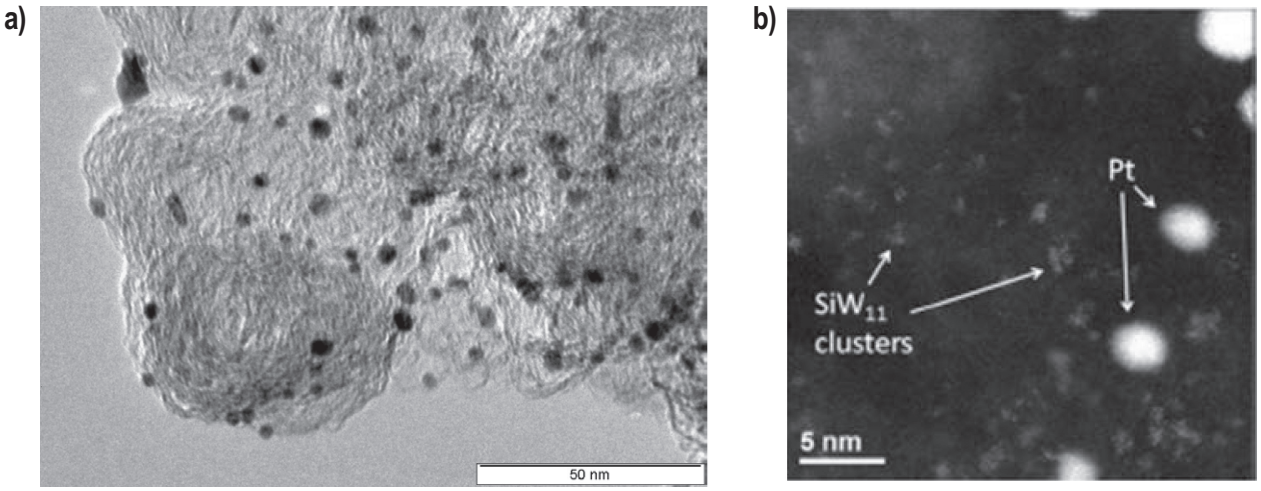

FIGURE 7. (a) Illustrates the TEM and particle size distribution of the synthesized colloids that were deposited onto the HPA-functionalized carbon. Scaled up to produce 1 g of electrocatalyst for MEA preparation. (b) Z-contrast STEM image of Pt/SiW_{11}-C showing spatial distribution of Pt (bright white spots ~3-5 nm) and SiW_{11} (~1 nm dull gray spots).

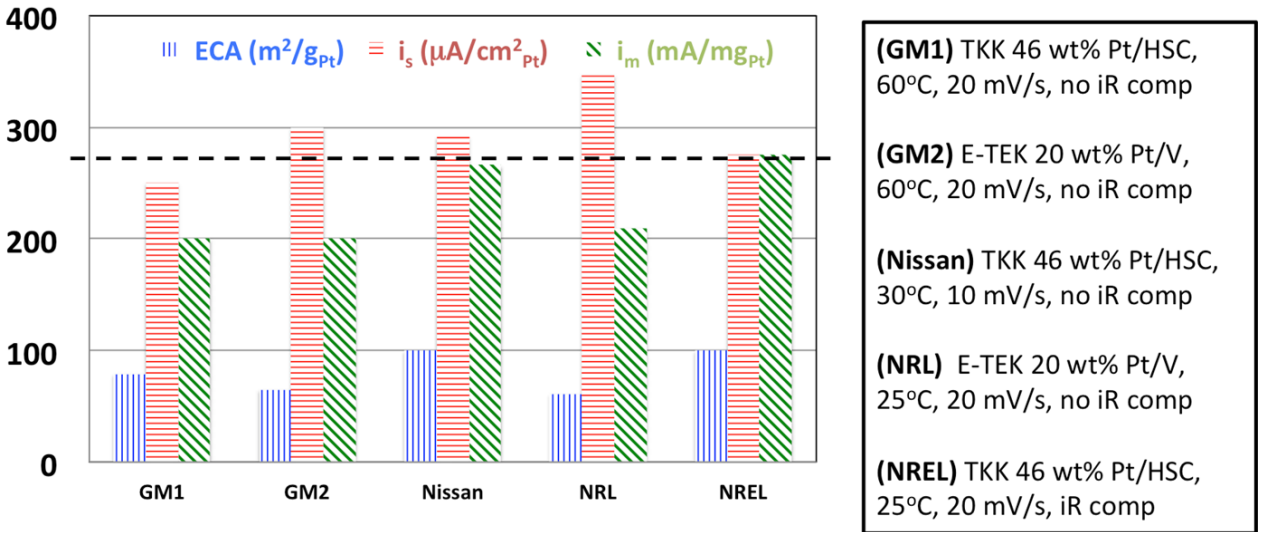

FIGURE 8. Baseline Pt/C Activity Benchmarks in RDE at NREL and Other Labs

and evaluation of material durability. Figure 8 illustrates the performance of the baseline Pt/C materials and comparison to other values in the literature for measurements conducted under approximately similar conditions.

Because of the formation of tungsten bronzes that produces a peak in the same voltage domain as hydrogen underpotential deposition, the accurate determination of the ECA of Pt/WO_X becomes difficult. We have used CO stripping as well as Cu underpotential deposition to determine the Pt area for these electrocatalysts. Cu underpotential deposition is preferred since CO appears to get oxidized and shows an anodic peak that complicates the determination of a good baseline for CO stripping area.

Durability protocols were established for evaluating the corrosion resistance of alternate supports in collaboration with the DOE Durability Working Group. Figure 9a depicts the durability protocol that simulated start-stop degradation in the voltage range 1–1.6 V. Nissan and NREL protocols result in comparable losses for ECA, i_s and i_m (Figure 9b). Nissan protocol (60°C) takes only 8 hours due to higher temperature accelerant. NREL protocol is conducted at room temperature and takes 24 hours using low-scan-rate accelerant and was selected due to environmental, health and safety issues of making measurements at temperature at NREL.

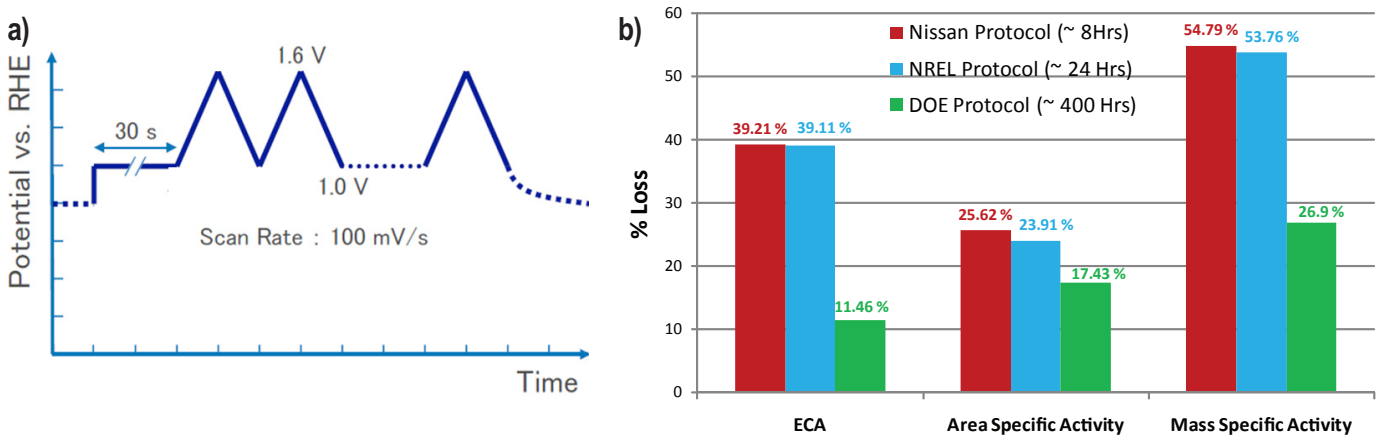

FIGURE 9. a) Illustrates the durability protocol that simulated start-stop degradation in the voltage range 1–1.6 V (start-up/shut-down regime) used to evaluate the corrosion resistance of alternative supports. b) Two equivalent protocols for measurements at room temperature and 60°C. DOE protocol is 1.2 V constant hold for 400 hr.

Corrosion of Supports

Corrosion studies were carried out in RDE cells and the working electrodes were subjected to high potentials reaching 1.8 V in perchloric acid. The onset and magnitude of corrosion currents was determined and compared. Figures 10 and 11 depict the conductivity and corrosion currents for the set of support materials that were evaluated. TiO_2, TaC and WO_3 exhibited the highest corrosion resistances while TiC had the lowest corrosion resistance. WC also exhibited less than ideal behavior. The preferred materials are those that possess both a high electronic conductivity and corrosion resistance.

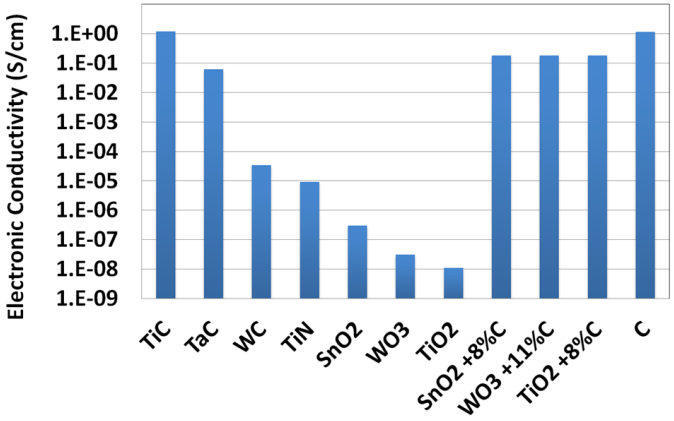

FIGURE 10. Electronic Conductivity for Various Support Material Candidates

Pt/WO_x

Based on the conductivity measurements of WO_x, it was clear that the conductivity of WO_x was significantly lower than that of carbon black. As a result, electrochemical measurements were performed using catalyst inks with and without incorporation of carbon black. The results with the incorporation of carbon black would allow us to estimate the losses incurred due to electronic conductivity issues.

Pt/WO_x was scaled up to g quantities using ALD deposition on HWCVD WO_x. The mass activity of Pt/WO_x was found to be ~175 mA/mg when measured in RDE half-cells (WO_x). This is a significant improvement but falls short of the activity of baseline Pt/C. The lower activity of Pt/WO_x is primarily due to the low electronic conductivity of the WO_x as seen by the doubling in activity with the addition of 50 wt% carbon black to it. Based on these results further work on Pt/WO_x was discontinued and alternative paths were deemed appropriate at the end of FY 2013.

Pt Black/WO_x

Although conductivity studies provide some insight into the potential of using a support material, actual mixtures of Pt black, (an unsupported catalyst) with various amounts of tungsten oxide and carbon black allows us to evaluate the materials electrochemically for ORR activity. To support the conductivity studies and verify the necessity of carbon black addition to achieve high mass activities, we conducted a study that evaluated Pt black mixed with various amounts of carbon black. The detailed studies revealed that only for very thin films (low catalyst loadings), was it possible to meet the baseline Pt/C ORR activity values. The results indicated that electronic resistance of the support would be an impediment when WO_x or other corrosion-resistant oxide supports are used as a support due to their low electronic conductivity. Extremely low loadings/thin films/high added carbon black content would be necessary for the catalyst to perform at acceptable levels of activity. Figure 13 indicates that the

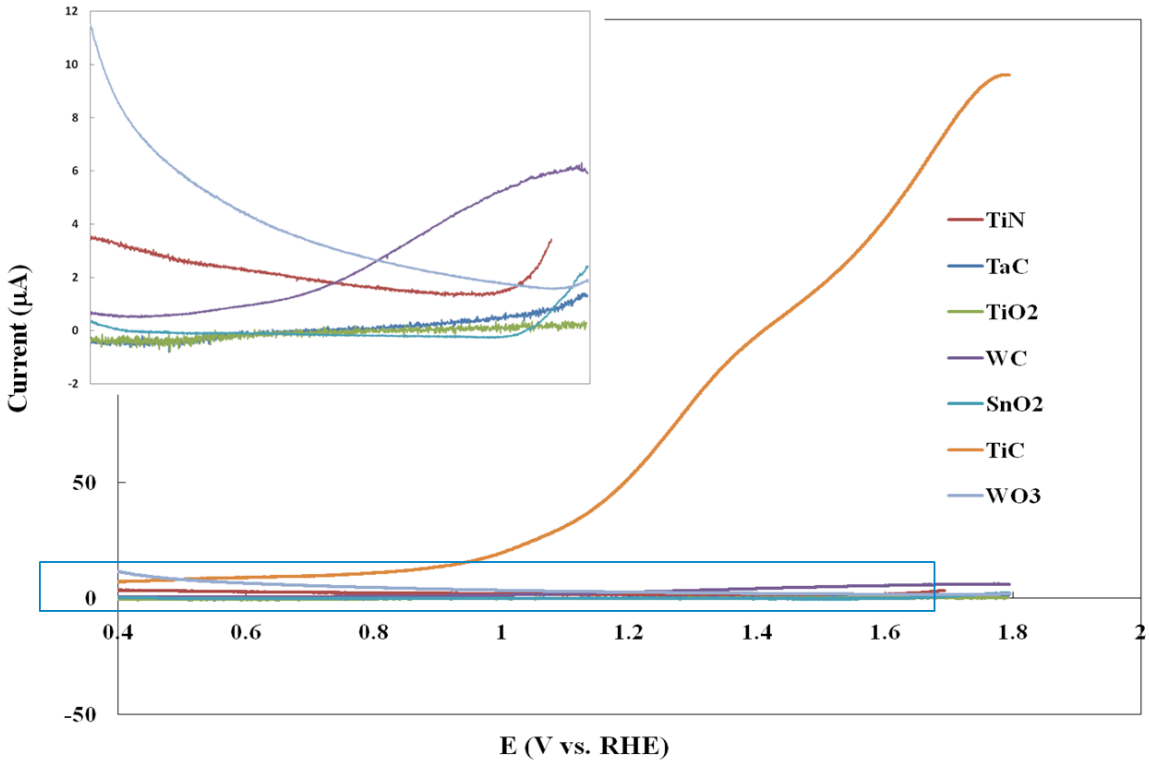

FIGURE 11. Corrosion Currents for Various Support Material Candidates

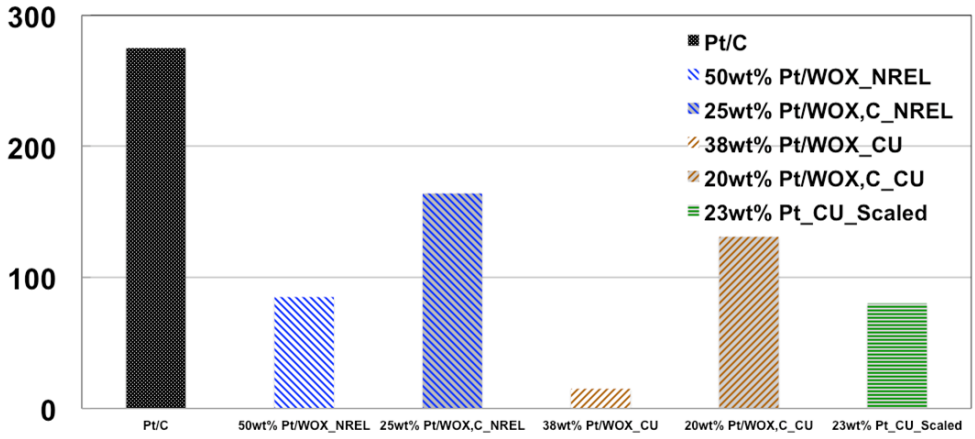

FIGURE 12. Mass Activity of Various Pt/WO_x in Comparison to Baseline Pt/C

durability of Pt/GCNF as well as the best case of Pt black/graphitized carbon nano-fibers (GCNFs)/WO_X has higher durability than baseline Pt/C.

Pt/SnO_2

Since the mass activity of Pt/WO_X had not yet met the benchmark values for commercial Pt/C in RDE studies, we investigated the performance of a Pt/SnO_2 electrocatalyst produced by a commercial catalyst manufacturer (TKK). For these catalysts, with the addition of a graphitized carbon black to enhance conductivity, values close to benchmark Pt/C of 275 mA/mgPt were achieved. The ORR activities were found to be even higher for ink formulations that were Nafion®-free. The catalyst was spray-coated onto Nafion® membranes and evaluated in subscale fuel cells. Initial results were lower than that found in RDE, and ink optimization and modification were attempted without success to attain the same activity as in RDE studies

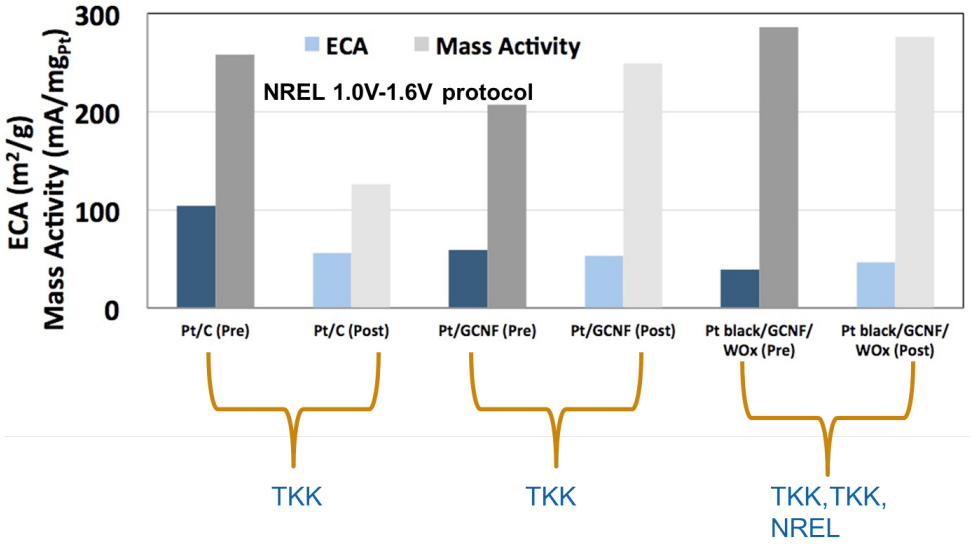

FIGURE 13. Mass Activity and Durability of Pt Black/GCNF/WO_x Mixtures

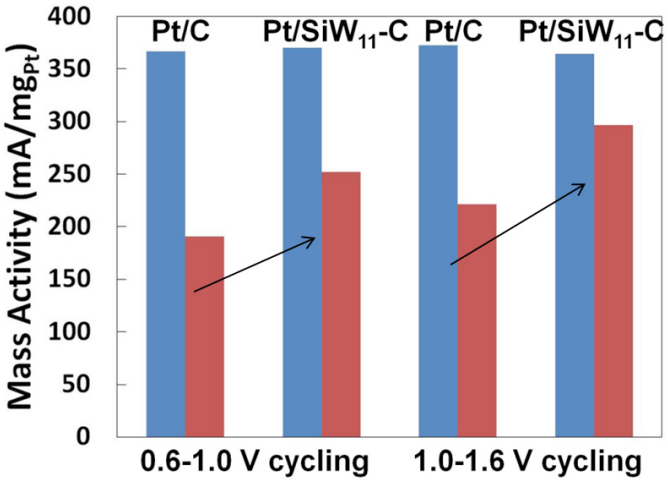

FIGURE 14. The 0.6-1.0 V cycling (30,000 cycles, 500 mV/s) was used to evaluate Pt dissolution, while 1.0-1.6 V cycling (6,000 cycles, 100 mV/s) evaluated support corrosion. HPA loading was chosen such that initial activity was near equal to Pt/C. In both cases, HPA helped maintain catalyst activity by slowing particle growth.

ECA (m^2/g_{Pt}); ECA Loss (%); EOL @ 5000 cycles

Pt/Ketjen Black Baseline:
BOL= 100 m^2/g_{Pt}; EOL= 46 m^2/g_{Pt}; 39.5% Loss

Pt/GCNF:
BOL= 82 m^2/g_{Pt}; EOL=71 m^2/g_{Pt}; 13.4% Loss

Pt/GCNF-HPA:
BOL= 68 m^2/g_{Pt}; EOL=52 m^2/g_{Pt}; 23.5% Loss

FIGURE 15. Cyclic Durability of Pt/C and Pt/C-HPA. Pt/GCNF exhibits improved durability compared to baseline, but post-HPA treatment, the losses are higher. HPA treatment does not result in an improvement on the durability of the catalyst system.

Pt/C-HPA

Durability results on Pt/HPA-C were conducted using previously developed protocols. Results of durability are shown in Figure 14. The 0.6–1.0 V cycling (30,000 cycles, 500 mV/s) was used to evaluate Pt dissolution, while 1.0–1.6 V cycling (6,000 cycles, 100 mV/s) evaluated support corrosion. HPA loading was chosen such that initial activity was nearly equal to Pt/C. In both cases, HPA helped maintain catalyst activity by slowing particle growth.

Graphitized carbons treated with HPA were the new focus of research during the first and second quarters of FY 2014. The expectation was that we might be able to maintain the activity similar to Pt/C-HPA while improving the durability even further with the use of more durable graphitized carbon blacks. Various graphitized carbon blacks were modified with HPA and Pt deposited on them using ALD or wet chemistry. Samples with Pt-ALD did not meet the activity requirements. Our results indicated that Pt deposited by wet-chemistry onto GCNFs, showed excellent activity and cyclic durability. Modifying the GCNF with HPA did not affect the activity significantly and actually lowered the cyclic durability. As a result, even though Pt/HPA-GCNF met the durability requirement, it was not a result of the HPA treatment and hence a No-Go decision was made as is not a viable option. Figure 15 summarizes the ECA loss for baseline Pt/C, Pt/GCNF and Pt/GCNF-HPA.

CONCLUSIONS

Pt deposited by ALD or wet chemistry technique on WO_X supports did not meet the ORR activity requirements of commercial Pt/C primarily due to the low electronic conductivity of WO_X. ECAs were also lower than conventional Pt/C. A higher Pt wt% on the support as well as incorporating carbon black to the catalyst resulted in improved ORR activities that were still lower than the baseline Pt/C materials. Pt deposited by wet chemistry on HPA modified conventional high surface area carbon (Ketjen Black) met the requirements for ORR activity in RDE studies. The most durable catalyst was wet chemistry Pt deposited on GCNFs from TKK. Pt/GCNF exhibited activity and durability in RDE studies that were significantly higher than Pt/Ketjen Black baseline materials. However, Pt deposited on HPA-modified graphitized carbons including GCNF did not show any additional improvements due to the HPA functionalization; the durability of these materials was slightly lower than untreated Pt/GCNF. As a result, even though Pt/HPA-GCNF met the durability requirement, it was not a result of the HPA treatment and hence a No-Go decision was made. HPA functionalized Pt/GCNF were not evaluated in subscale fuel cells, but Pt/GCNF based subscale cells were evaluated and compared to Pt/Ketjen Black to demonstrate improved durability under cyclic durability protocols.

2014 PUBLICATIONS AND PRESENTATIONS

1. "Atomic Layer Deposition of Platinum Particles on Titanium Oxide and Tungsten Oxide" Virginia R. Anderson, Noemi Leick, Joel W. Clancey, Katherine E. Hurst, Kim M. Jones, Anne C. Dillon, Steven M. George. Submitted to J. Phys Chem C. 2014.

2. Mason, K. Sykes, Kenneth C. Neyerlin, Mei-Chen Kuo, Kiersten C. Horning, Karren L. More, and Andrew M. Herring. "Investigation of a Silicotungstic Acid Functionalized Carbon on Pt Activity and Durability for the Oxygen Reduction Reaction." Journal of The Electrochemical Society 159, no. 12 (2012): F871-F879.

V.A.7 Synthesis and Characterization of Mixed-Conducting Corrosion-Resistant Oxide Supports

Vijay K. Ramani (Primary Contact), Jai Prakash
Illinois Institute of Technology (IIT)
10 W 33rd Street 127 PH
Chicago, IL 60616
Phone: (312) 567-3064
Email: ramani@iit.edu

DOE Managers
Jacob Spendelow
Phone: (202) 586-4796
Email: Jacob.Spendelow@ee.doe.gov
Gregory Kleen
Phone: (720) 356-1672
Email: Gregory.Kleen@ee.doe.gov

Contract Number: DE-EE0000461

Subcontractor
Nissan Technical Center, North America (NTCNA), Farmington Hills, MI

Project Start Date: September 1, 2010
Project End Date: January 31, 2015

Overall Objectives

- <40% electrochemical area (ECA) loss in electrocatalysts using the synthesized supports tested per the General Motors (GM) protocol.
- <30 mV electrocatalyst support loss in the synthesized supports after 100 h at 1.2 mV, tested using the GM protocol.

Fiscal Year (FY) 2014 Objectives

- Evaluate the suitability of titanium dioxide-ruthenium dioxide (RTO), indium tin oxide (ITO) as conducting catalyst supports for proton exchange membrane fuel cells (PEMFCs).
- Optimize the Pt deposition method on the above catalyst supports to improve PEMFC performance and durability.
- Demonstrate the performance and durability (under start-stop and load cycling protocols) of Pt deposited on titanium dioxide-ruthenium dioxide, ITO in a PEMFC.
- Prepare a preliminary cost model for new supports.

Technical Barriers

This project addresses the following technical barrier from the Fuel Cells section of the Fuel Cell Technologies Office Multi-Year Research, Development, and Demonstration Plan:

(A) Durability

Technical Targets

Identical to those listed under overall objectives.

FY 2014 Accomplishments

- Rotating disk electrode (RDE) testing showed that both 20% and 40% Pt/RTO had very similar mass activity (150-160 mA/mg_{Pt}), comparable to the mass activity of a commercial catalyst made by TKK, TEC10E50E-HT (~120-150 mA/mg_{Pt}).
- RDE testing of both 20% and 40% Pt/ITO showed mass activity of ~150 mA/mg_{Pt}, comparable to Pt/RTO.
- Pt/ITO was very stable under the start-up/shut-down accelerated degradation protocol. The electrochemical active surface area (ECSA) change was less than 4% over 10,000 cycles. The load cycling accelerated protocol (from 0.6 to 0.95 V vs. the standard hydrogen electrode) resulted in a loss of approximately 34% of the initial ECSA after 10,000 cycles.
- A cost model for RTO, ITO supports has been developed, and their durability benefits have been considered.

INTRODUCTION

Commercial carbon black currently used as support material for the Pt in the PEMFC electrocatalysts can undergo corrosion under fuel cell operational conditions [1]:

$C + 2H_2O \rightarrow CO_2 + 4H^+ + 4e^-$ $E_o^0 = 0.207$ V vs. the standard hydrogen electrode

This thermodynamically favorable reaction is very slow under normal operating conditions but can be accelerated during voltage transients occurring during start/stop and fuel starvation. This causes reverse currents in the fuel cell, which drives the potential at the cathode to as high as 1.5 volts [2,3]. The irreversible carbon corrosion leads to the aggregation of Pt, which results in a loss of ECSA. This contributes to significant and irreversible losses in fuel cell performance. To overcome

these obstacles, it is necessary to replace the carbon with high-electronic-conductivity, high-surface-area, porous support with high corrosion resistance under fuel cell operating conditions. In this project, we are evaluating the electrochemical stability and fuel cell performance of non-carbon supports.

APPROACH

To solve the problems associated with carbon corrosion, we have synthesized and evaluated electrical conducting mixed metal oxides (ITO) as supports for PEMFC catalyst during this year. Multiple approaches were used to prepare the ITO and catalyze the ITO. A concern expressed with metal-oxide-based supports is the cost of the material compared to conventional carbon supports, which are very inexpensive. So a cost model for RTO and ITO was considered. NTCNA has prepared a preliminary cost model for these non-carbon support materials considering their durability benefits.

RESULTS

Platinum Catalyzed Indium Tin Oxide (Pt/ITO)

We have found that the best Pt/ITO (ITO synthesized by co-precipitation) catalyst resulted from the reduction of hexachloroplatinic acid in presence of ethylene glycol. The cyclic voltammograms, ECA, and specific and mass activity values for 50% and 20% Pt on ITO samples are presented in Figure 1. The mass activity values obtained for both catalysts are almost equal (140–150 mA/mg_{Pt}), and they are comparable to what we have obtained for Pt/RTO and TEC10E50E-HT, which showed mass activity values of ~120–150 mA/mg_{Pt}.

Pt/ITO was a very resistant and durable catalyst and did not degrade during the simulated start-up/shut-down transients occurring in a PEMFC. Catalyst stability for 40% Pt/ITO (co-precipitation) was also evaluated following the same protocols (potential cycling from 1.0 to 1.5 V vs. the reference hydrogen electrode, RHE). The loss of ECSA was less than 4% after 10,000 cycles, whereas it was 40% for commercial Pt/C (Tanaka 46% Pt) after the same number of cycles (see Figure 2). The 40% Pt/ITO was also tested using the load cycling protocol (potential cycling from 0.6 to 0.95 V vs. RHE, using a square wave with a period of 6 seconds), and it was found that the loss of the ECSA for 40% Pt/ITO was about 30% after 10,000 cycles. However, the ECSA loss was 40% for commercial Pt/C (Tanaka 46% Pt) after the same number of cycles.

The fuel cell performance for a membrane electrode assembly (MEA) using Pt/ITO catalyst is shown in Figure 3. The performance was poor when compared with baseline data for 46% Pt/C (Tanaka). The maximum current density with hydrogen/air was only 100 mA/cm^2, whereas 1,500 mA/cm^2 was obtained with the 46% Pt/C commercial catalyst (at the same Pt loadings). We suspect the reason for the low performance is the low ECSA of the Pt/ITO catalyst. The ITO may also undergo structural changes under operating conditions. We are currently working to find the reasons for the low performance of ITO-based catalysts. Preliminary X-ray photoelectron spectroscopy measurements have shown that the formation of PtIn alloy and the formation of $In(OH)_3$ during the reduction process may affect the electrode resistivity and hence the fuel cell performance.

Cost Model for RTO and ITO Supports

The metal-oxide-based non-carbon supports may not be very cost-competitive to carbon supports when only material cost is considered, but owing to their excellent durability under automotive start-stop and load cycling accelerated tests, cost analysis of these non-carbon supports has indeed

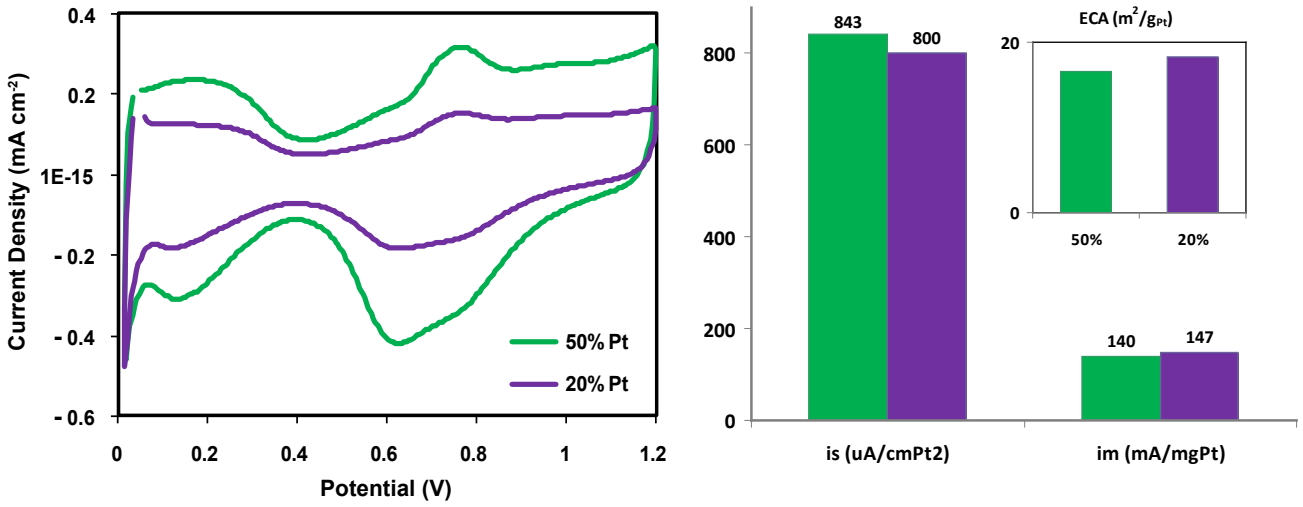

FIGURE 1. The Cyclic Voltammogram, ECA, Specific and Mass Activity Values for 50% and 20% Pt on ITO Samples

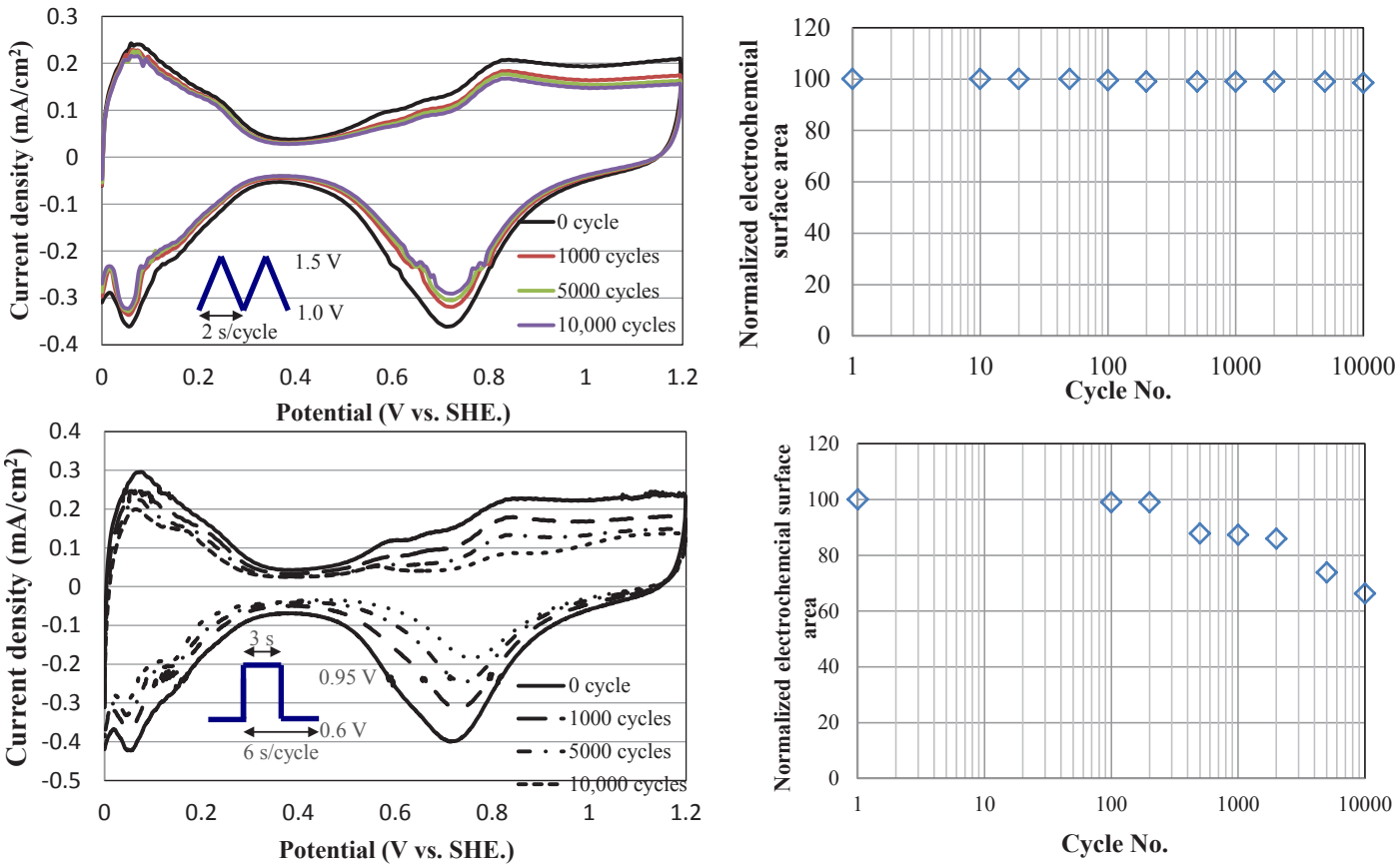

FIGURE 2. Support Corrosion Test and Platinum Dissolution Test for 40% Pt/ITO (Pt by reduction of $Pt(NH_3)_2Cl_2$ using $NaBH_4$)

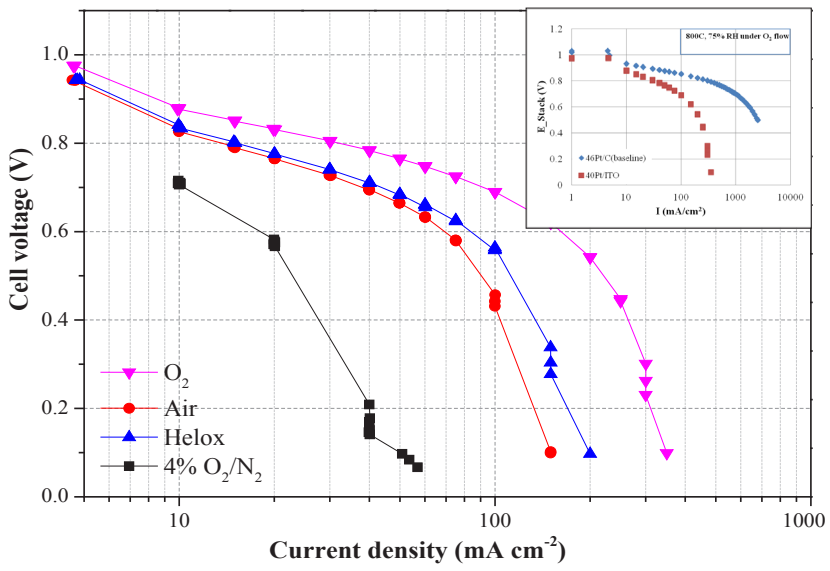

FIGURE 3. Fuel Cell Performance at 80°C for an MEA with 40% Pt/ITO Catalyst at Cathode and 46% Pt/C (Tanaka) at Anode with 30 wt% Nafion® Binder Loading

become essential. Cost modeling was done using the 2008 Pt price of $1,100/troy oz. for comparison with the 2008 DOE fuel cell cost system. The assumptions made to simplify this model were: a) except for the cathode, the rest of the MEA was identical; b) the rated power was at 80°C, 100% relative humidity; c) all the stacks in the cell were operating identically; d) the processing costs (ink manufacturing, catalyst application, etc.) were the same.

The material costs of the cathodes are compared in Figure 4. As shown in the figure, the RTO support was more expensive than ITO and Vulcan, but the total material costs were still dominated by platinum cost. Although ruthenium is considered a precious metal, its cost ($80-90/troy oz.) is far less than that of platinum ($1,100/troy oz. – DOE standard). It should also be noted that ruthenium only makes up 38% of the mass of the support, while the rest is relatively inexpensive TiO_2. This proportion can be further lowered. Furthermore, significant

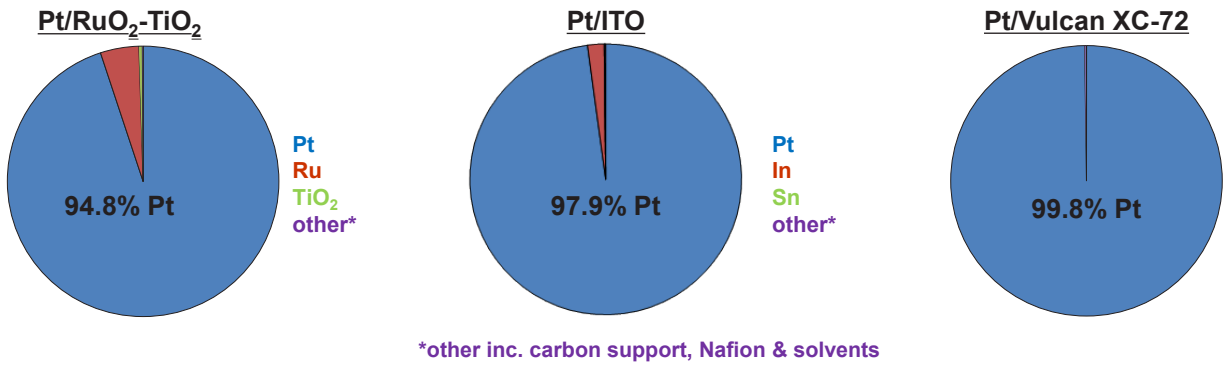

FIGURE 4. Cathode Material Cost Comparison Between Pt/Non-Carbon and Pt/Vulcan® XC72.

cost reduction can be achieved by reducing the cathode Pt loadings (cathode material costs were proportional to Pt loading).

The major advantage of using metal oxide supports at the cathode was their excellent resistance to degradation under start-stop cycling. This durability needs to be considered while doing the cost analysis. Based on the data obtained for Pt/RTO and Pt/Vulcan® XC72 under the Nissan start-stop durability cycling, a so-called "durability factor" was calculated using following equation:

$$\text{Durability Factor} = \frac{\text{Mass Activity Retention of Catalyst}}{\text{Mass Activity Retention of Pt/RuO}_2 - \text{TiO}_2}$$

Mass activity retention was chosen as a basis because the DOE target for catalyst support durability is defined in terms of mass activity. Pt/RTO retained 86% of its mass activity, while Pt/Vulcan® XC72 retained only 66% of its initial mass activity under Nissan start-stop durability cycling. Based on this protocol, Pt/Vulcan® XC72 is only 69% as durable as the Pt/RTO. After considering the durability advantages of Pt/RTO and assuming similar durability for Pt/ITO (justified thus far based on durability studies in the RDE), the preliminary cost model shows that even with almost double the Pt loading (0.35 vs. 0.18 mg Pt/cm^2), Pt/RTO and Pt/ITO are only 4% and 0.5% more expensive than Pt/Vulcan® XC72, respectively

CONCLUSIONS

- The mass activity values obtained for both 50% and 20% Pt on ITO sample were almost equal (140-150 mA/mg$_{Pt}$), and they were comparable to Pt/RTO and TEC10E50E-HT.
- 40% Pt/ITO catalyst had better electrochemical stability under start-stop cycling protocol than commercial Pt/C. The loss in the ECSA was less than 4% after 10,000 cycles, whereas it was 40% for commercial 46% Pt/C (after the same number of cycles).
- Fuel cell performance when using Pt/ITO at the cathode needs to be improved. Several approaches are being used to identify the possible causes and mitigating approaches.
- After considering the durability advantages of Pt/RTO, a preliminary cost model for Pt/RTO showed that it was only marginally more expensive than Pt/Vulcan® XC72.

FUTURE DIRECTIONS

- Optimize the Pt deposition method on ITO and evaluate the fuel cell performance and catalyst stability in a working PEMFC. Understand how to improve MEA performance of Pt/ITO.
- Prepare MEAs with best supports to deliver to DOE for independent evaluation.

FY 2014 PUBLICATIONS/PRESENTATIONS

1. J. Parrondo, T. Han, E. Niangar, C. Wang, N. Dale, K. Adjemian, and V. Ramani, "Pt supported on titanium-ruthenium oxide: A remarkably stable electrocatalyst for hydrogen fuel cell vehicles" Proceedings of the National Academy of Sciences, 111 (1) (2014) 45-50.

SPECIAL RECOGNITIONS & AWARDS/ PATENTS ISSUED

1. Patent Filed: "Non-Carbon Mixed-Metal Support for Electrocatlaysts"

REFERENCES

1. N. Takeuchi; T.F. Fuller, J. Electrochemical Society, 155 (2008) B770-B775.

2. Reiser, L. Bregoli, T.W. Patterson, J.S. Yi, J.D. Yang, M.L. Perry, T.D. Jarvi, Electrochem. Solid-State Lett. 8 (2005) A273-A276.

3. H. Tang, Z. Qi, M. Ramani, J.F. Elter, J. Power Sources 158 (2006) 1306-1312.

V.A.8 Development of Novel Non-PGM Electrocatalysts for Proton Exchange Membrane Fuel Cell Applications

Sanjeev Mukerjee
Department of Chemistry and Chemical Biology,
Northeastern University (NEU)
Boston, MA 02115
Phone: (617) 373-2382
Email: S.mukerjee@neu.edu

DOE Managers
Donna Ho
Phone: (202) 586-8000
Email: Donna.Ho@ee.doe.gov
David Peterson
Phone: (720) 356-1747
Email: David.Peterson@ee.doe.gov

Contract Number: DE-EE0000459

Subcontractors
- University of New Mexico (UNM), Albuquerque, NM (Plamen Atanassov)
- Michigan State University (MSU), East Lansing, MI (Scott Calabrese Barton)
- Nissan Technical Center, North America (NTCNA), Detroit, MI (Nilesh Dale)
- Pajarito Powder, Albuquerque, NM (Bar Halevi)
- Los Alamos National Laboratory (LANL), Los Alamos, NM (Piotr Zelenay)

Project Start Date: August 1, 2010
Project End Date: August 1, 2014

Overall Objectives and Objectives for Fiscal Year (FY) 2014

The objective of this project is to design non-platinum group metal (PGM)-based catalysts and supporting gas transport layer, both in the interfacial reaction layer between the electrode and membrane as well as in the underlying gas diffusion medium, for meeting and exceeding DOE goals for application in solid polymer electrolyte fuel cells. This project is focused on materials development and is assisted by advanced analytical tools, computation, and testing for improving the design via critical understanding of electrocatalysis in these novel structures. The principal target for the reporting FY was to take the project beyond the first phase, where the project's Go/No-Go milestone of 100 mA/cm^2 @ 0.8 V (internal resistance-free, iR-free) at 80^{o}C, pure H_2/O_2, with 1.5 bar total pressure was met. This reporting period, the principal objective was to transition the project from H_2/O_2 to H_2/air with slated target of 30 mA/cm^2 @ 0.8 V, 2.5 bar total pressure and an end-of-the-project target of 1 A/cm^2 @ 0.4 V (same total pressure), both under 100% relative humidity (RH). In a quarterly timeline basis, the target for scale up was to achieve 50 gm batch size by the 3rd quarter and 100 gm batch size at the end of the project (5th quarter). Both these scale-up targets had a quality control milestone of less than 5% variation of activity measured with H_2/air (2.5 bar total pressure) at 0.8 V. In addition, the project aimed at arriving at a unified understanding of the nature of active sites in these catalysts as well as some preliminary understanding of the mechanistic pathway.

Technical Barriers

This project addresses the following technical barriers from the Fuel Cells section of the Fuel Cell Technologies Office Multi-Year Research, Development, and Demonstration Plan:

(B) Cost (eliminate precious metal loading of catalysts)

(C) Performance (increase the specific and mass activities of catalysts)

(A) Durability (increase the durability/stability of catalysts with cycling)

Technical Targets

The technical targets for this project are listed in Table 1.

FY 2014 Accomplishments

1. Following our Go/No-Go decision target (successfully met in July 2013), our down-selected catalyst was from University of New Mexico, referred to as UNM-CTS (mechano-chemical approach using water insoluble nicarbazin) catalyst. In order to transition to areal performance with air, blends were prepared of this down-selected catalyst with previously developed catalyst from University of New Mexico referred to UNM-CBDZ (prepared using non-metal chelating approach using carbendazim material) to improve mass transport and durability. As per our milestones for areal activity in H_2/air (Table 1), we have successfully surpassed the low current density target (30 mA/cm^2 @ 0.8 V). Our current state of the art for high-current-density performance stands at 850 mA/cm^2 using the above-mentioned blends. In addition, emerging catalysts prepared using an Fe-encapsulated metal organic framework (MOF) chemistry approach referred to as NEU-Fe-MOF (from Northeastern University) show great promise for an alternative approach. Preliminary

TABLE 1. Progress towards Meeting Technical Targets for Non-PGM Electrocatalysts for Transportation Applications

Characteristic	Units	2015 Target	NEU 2014 status
Specific activity @ 80°C, 1.5 bar total pressure, H_2/O_2, 100% RH	A/cm^3	Volumetric activity of 300 A/cm^3 @ 0.8 V (iR-free) projected from ~10 mA/cm^2	400 A/cm^3
		Un-projected volumetric activity (no target set)	95 A/cm^3
2013 Go/No-Go target	A/cm^2	100 mA/cm^2 (iR-free)	100 mA/cm^2
Specific activity @ 80°C, 2.5 bar total pressure, H_2/Air, 100% RH	A/cm^2	Areal activity of 30 mA/cm^2 @ 0.8 V	70 mA/cm^2
2014 target		Areal activity of 1 A/cm^2 @ 0.4 V	800 mA/cm^2
Scale-up of catalyst	gms	50 gms	Target successfully met
Intra- and inter-batch variability	percent	5% variation for both inter- and intra-batch	Target successfully met
Durability at 80°C cycling: catalyst durability	% loss of activity	5	<1
Durability at 80°C cycling: carbon corrosion durability	% loss of activity	10	<50 Partially recoverable

measurements indicate that this has the potential of meeting both the low- and high-current-density areal activity targets in air. However, this is data using small batch synthesis (below 1 gm batch size). Our current efforts include approaches for scaling up the synthesis using low-cost precursors.

2. Our current efforts toward scale up performed by Pajarito Powders are on target based on the timelines for the slated milestones. At the end of the second quarter in the second phase of this project, we have successfully demonstrated less than 5% variability in performance at the low current density target potential (0.8 V) and approximately 5% variability at the higher current density (0.6 V). These variabilities include materials, reflecting both inter- and intra-batch measurements. This data is exclusively from areal activity measurements using single-cell data in air as per this project's slated operating conditions (2.5 bar total pressure in air, 100% humidification at 80°C).
3. Durability measurements conducted on the down-selected UNM-Fe-CTS catalysts show excellent tolerance to catalyst stability tests. Carbon corrosion tests, which involve load cycling to 1.5 V vs. the reference hydrogen electrode, however, indicated significant losses, similar to the losses with a PGM cathode.
4. Understanding of the nature of the active site was significantly advanced in this reporting period with identification of a dual site mechanism wherein the N_{2+2} site was responsible for the initial adsorption and reduction of oxygen to peroxide moieties followed by a second cascade step of further reduction of the peroxide in closely surrounding Fe-N_2 sites. Such formulation of the mechanism was supported with in situ X-ray absorption spectroscopy and targeted electrochemical probe measurements.

✧ ✧ ✧ ✧ ✧

INTRODUCTION

Recent reports [1,2] have clearly demonstrated the significant advancements made in enabling good oxygen reduction activity by Fe-based non-PGM catalysts. These so called Fe-N_x-based systems have evolved over several decades of intense work leading up to the current state of the art, reported recently in references [1,2]. This report provides for the first time a comprehensive view of (a) confluence of oxygen reduction reaction (ORR) activity derived from materials prepared using a variety of polymeric precursor materials viz. the current state of the art by three different university groups, (b) successful transition from previous operations in oxygen to air, (c) excellent durability in terms of catalyst stability (*vide* DOE and Nissan protocols), and (d) detailed understanding of the nature of active site and electrocatalytic pathway as distinct from the parallel pathway in alkaline electrolytes.

APPROACH

The approach adopted in this reporting period involved blends of materials derived using two separate approaches under the common ambit of the University of New Mexico group's silica templating methodology, referred to as the UNM-CTS and UNM-CBDZ. The former material (UNM-CTS) was derived using a mechano-chemical approach of ball milling an organic charge transfer salt (nicarbazin) in the presence of Fe salt and the latter using an aqueous formulation of a non-chelating material, carbendazim, with Fe salt, both in conjunction with silica support followed by several steps of pyrolysis and etching. Typical blends comprised a 1:1 mixture. The Northeastern University approach involved a one-pot synthesis of an MOF material

referred to as Zif8 in conjunction with chelated metal salt encapsulation.

These derived materials were tested in single cells (5 cm^2) using a commercial anode electrode (Alfa Aesar) containing 0.3 mg/cm^2 Pt loading. Typical cathode loading was 2 mg/cm^2, and the membrane used was Nafion® 211, with 50% Nafion® loading at the cathode. Tests were conducted under steady-state potentiostatic conditions with each point measured for a minimum of 60 s. Common test protocols are replicated at NTCNA and NEU. In this annual report, the data related to scale up efforts were exclusively conducted at Pajarito Powders Corp. Durability studies were performed on pre-scale-up catalysts at the Nissan Technical Center. Investigation of the nature of active site and ORR electrocatalysis steps was accomplished using in situ synchrotron spectroscopy at the Fe-K edge under actual cell *operando* conditions.

RESULTS

Pajarito Powder has scaled up formulations of the charge transfer salt (CTS) catalyst and a previously reported (Phase 1) derived UNM catalyst referred to as UNM-CBDZ in a 1:1 ratio. The approaches for both these catalysts are briefly described above in the approach section. The key purpose for this formulation was to (a) improve mass transport to meet the areal activity target in H_2/air as well as (b) provide higher durability under the two above-mentioned (see approach section) DOE-mandated protocols. The chemically intensive approach for scale up involved several key steps requiring optimization. The initial scale up effort was focused on a 10-20-gram batch (Phase 1, reported in the 2012-13 report), with the goal that the methods developed can be applied towards 30-50 gr, with trajectory towards 100-gram batches.

Demonstration of trajectory towards 100 grams per batch of the original Fe-CTS catalyst involved pre-treatment of precursors to reduce and eliminate precursors source and batch consistency effects on manufacturing. As mentioned above, the milestone was to meet the H_2/air areal performance target of 30 mA @ 0.8 V and 1,000 mA @ 0.4 V in 2.5 bar air, 80°C, 100% humidification.

The trajectory towards 100-gram batches was established through use of larger volume processing equipment, processing vessel materials changes, and tuning of processing parameters such as the pyrolysis temperature trajectory, etching times and agitations, and mixing times and intensity.

Increased manufacturability and production robustness due to pretreatment and conditioning of precursors is demonstrated in the performance of a 50-gram batch made using a 10-kg aliquot from a 100-kg key precursor conditioned and pretreated so the final catalyst matches catalysts made from different batches of the same key precursor sold in 100-gram containers.

A brief summary illustrating these developments is presented, showing a nearly 80% improvement in performance in air (compared to previous reporting period) with 70 mA @ 0.8 V and 800 mA @ 0.4 V achieved using 2.2 mg/cm^2 loading gas diffusion electrodes. Figure 1(a) shows two separate formulations (Gen 1 and Gen 2, blends) using variations in silica templates. Comparison of Gen 2 (100% CTS batch) and Gen 2A (CTS/CBDZ blend) with variation of the silica template shows remarkable inter-batch reproducibility in H_2/air. The low current density target of 30 mA/cm^2 at 0.8 V (uncorrected) has been met and exceeded with current state-of-the-art 70 mA/cm^2 current density. The higher current density target of 1 A/cm^2 at 0.4 V (uncorrected) (quarter 5, end-of-project target) is not yet met, with current activity at 0.8 A/cm^2. These performance figures are better delineated in the corresponding Tafel (semi-log) plot shown in Figure 1(b). Both these are reported without any internal resistance correction. Figure 1(c) reports intra-batch variations in performance using Gen 2 catalyst formulations. Over the upcoming period, further improvements to performance will continue, and modeling predictions from MSU will be combined with impedance and helium-oxygen testing at NEU to determine transport issues. In addition, NTCNA will be testing the improved Gen 2 catalyst.

A brief introduction to the NEU catalyst synthesis methodology is provided in Figure 2(a), wherein an iron-based non-PGM ORR electrocatalyst utilizes a MOF-based support that hosts a chelated iron complex within its pores. The MOF support was chosen in order to take advantage of the porosity and high surface area that are key features known to improve the catalytic activity and mass transport. A one-pot encapsulation procedure developed by NEU uses a zinc metal organic framework (ZIF-8 MOF) synthesized in the presence of the chelated Fe (or Co) precursors. The final product was dried in a vacuum oven for 4 hours at 70°C, followed by either one or two heat-treatments in argon at 1,050°C and ammonia at 950°C. Preliminary rotating disk electrode analysis, shown in Figure 2(b), shows performance exceeding that of Pt in alkaline electrolyte (0.1 M KOH) and a half-wave potential difference of 70 mV compared to Pt in acidic pH (0.1 M $HClO_4$). Non-Fe-containing MOF shows comparatively a 400 mV over-voltage, indicating predominant peroxide generation. Preliminary fuel cell measurements made using H_2/O_2 (1.5 bar total pressure), 80°C, 100% humidification indicated performance in excess of the DOE Phase 1 target of 100 mA/cm^2 at 0.8 V (iR corrected) with current state of the art at 170 mA/cm^2. More importantly, the H_2/air performance meets both the low (0.8 V iR uncorrected) and high current density (0.4 V iR uncorrected) values with current state of the art at 75 mA/cm^2 (at 0.8 V) and 1 A/cm^2 (at 0.4 V).

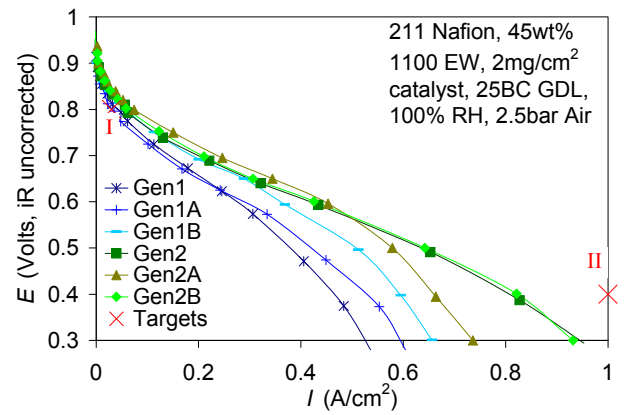

Catalyst formulations

	Organic Precursor	Silica
Gen1	CTS	L90
Gen1A	CTS	L90
Gen1B	CTS	L90
Gen2	CTS	LM150
Gen2A	CTS & CBDZ	LM150
Gen2B	CTS & CBDZ	LM150 & OX50

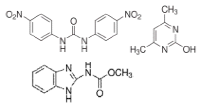

CTS

CBDZ

(a)

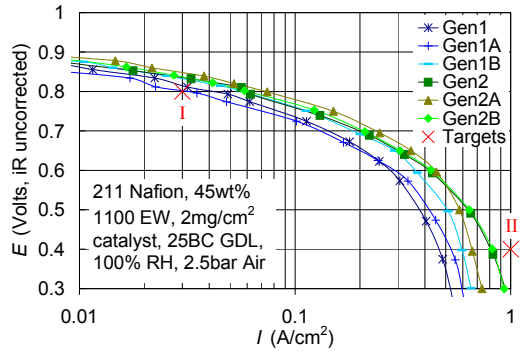

(b)

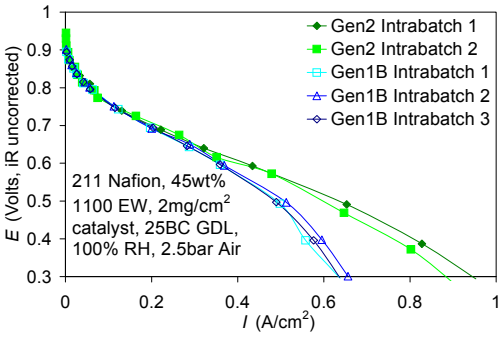

(c)

Figure 1 (a-c). Areal activity measured using 5-cm^2 single cells in H_2/air (2.5 bar total pressure), 80°C, 100% humidity, 2.2 mg/cm^2 non-PGM catalyst loading at the cathode and anode comprising a commercially obtained electrode (Alfa Aesar, 0.5 mg/cm^2 Pt loading on SGL substrate). The non-PGM catalyst depicted comprised both a pure UNM-CTS (Gen 1) and a formulation (1:1) of UNM-CTS and UNM-CBDZ (Gen 2) using different formulations of silica support (resultant pore formation). Here the batch sizes used were in excess of 50 gms. (a) Inter-batch variations between Gen 1 and Gen 2 and internal formulation effects using variation of silica support. (b) The corresponding Tafel slope showing performance in lieu of this project's milestones for both low- and high-current-density operation. (c) Intra-batch variations for both Gen 1 and 2 catalysts.

CONCLUSIONS

1. Catalyst blends (1:1) prepared by Pajarito Powders using 50+ gms batch sizes with UNM catalysts (UNM-CTS and UNM-CBDZ) show inter- and intra-batch variations below 5%. They also meet and exceed the low-current-density areal activity target in H_2/air (2.5 bar total pressure, 80°C, 100% RH). The high-current-density target of 1 A/cm^2 at 0.4 V (quarter 5, end-of-project target) is currently at 800 mA/cm^2. A separate MOF-based approach from NEU shows excellent areal activity under these performance metrics, exceeding the low-current-density benchmark and meeting the high-current-density target.
2. Detailed durability studies reported earlier on the UNM catalysts measured by NTCNA indicate excellent tolerance to catalyst stability tests and relatively poor resistance to carbon corrosion test protocols; the latter, however, is on par with those observed for PGM catalysts.

FUTURE DIRECTIONS

1. The principal focus of the group will be to meet the high-current-density areal activity target at 0.4 V (iR uncorrected) using both UNM blend formulations. Correlate impedance and helium-oxygen experiments with modeling to identify dominant polarization effects.

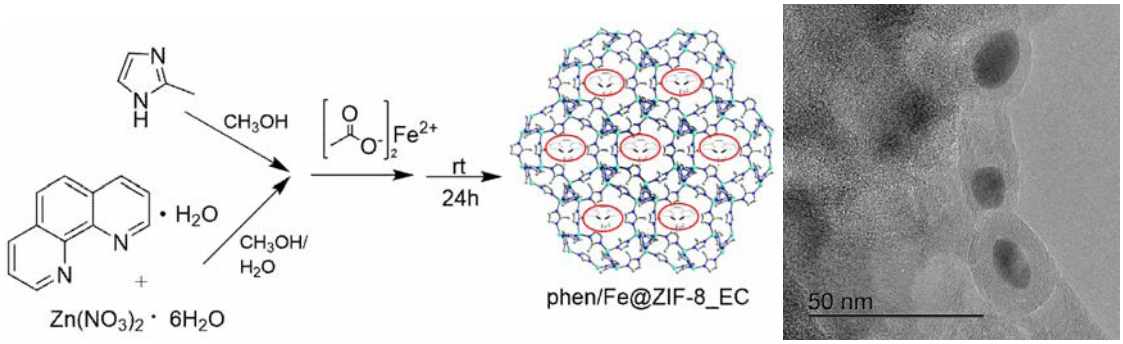

(a)

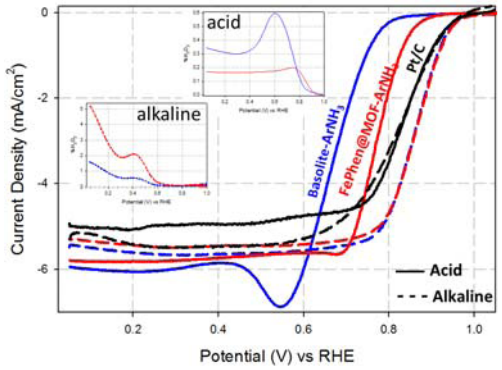

(b)

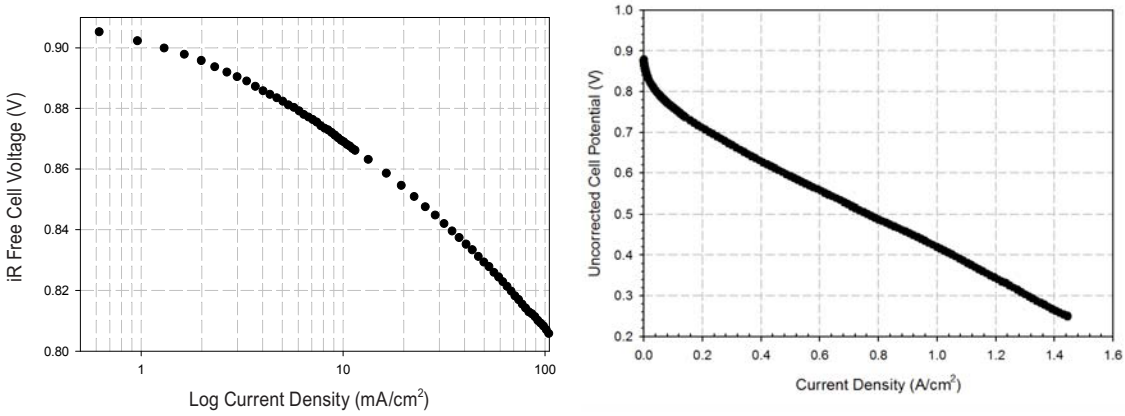

(c)

Figure 2 (a-c). (a) Schematic showing the one-pot synthetic approach for NEU MOF-based Fe-encapsulated catalysts. Scanning electron micrograph shows encapsulation and carbon fiber formation**.** (b) Rotating disk electrode comparison with Pt/C (Tanaka 30% Pt/C) in both acid and alkaline pH (0.1 M KOH and $HClO_4$). Also plotted is a non-Fe-containing catalyst referred to as Basolite. (c) Tafel plot for single-cell data (5 cm^2) in H_2/O_2 with 1.5 bar total pressure, 100% RH, 80°C. Also shown is the corresponding linear polarization data (iR uncorrected) in H_2/air showing the concomitant low- and high-current-density performance using 2.5 bar total pressure.

2. Optimize scale up and MEA fabrication for MOF-based catalysts from NEU.
3. Validate durability under DOE protocols with tests conducted at NTCNA.
4. Further test the validity of the proposed mechanism using final set of in situ and *operando* synchrotron X-ray absorption spectroscopy data in conjunction with density functional theory calculations. In addition, use the in situ spectroscopy to probe degradation pathways.

FY 2014 PUBLICATIONS

1. 'A mechanistic study of 4-aminoantipyrene and iron derived non-platinum group catalyst on the oxygen reduction reaction',

M. H. Robson, A. Serov, K. Artyushkova, and P. Atanassov, *Electrochimica Acta*, **90**, 656-665 (2013).

2. 'pH dependence of catalytic activity for ORR of the non PGM catalyst derived from heat treated Fe-phenanthroline', S. Brocato, A. Serov and P. Atanassov, *Electrochimica Acta*, **87**, 361-365 (2013).

3. 'Catalytic activity of Co-N_x/C electrocatalysts for oxygen reduction reaction: a density functional theory study', S. Kattel, P. Attanasov, and B. Kiefer, *Phy. Chem. Chem. Phys.,* **15,** 148-153 (2013).

4. 'Mechanistic studies of oxygen reduction Fe-PEI derived non PGM electrocatalysts, A. Serov, U. Tylus, K. Kartyushkova, S. Mukerjee and P. Atanassov, *App. Catal. B.,* **150-151**, 179-186 (2014).

5. 'Elucidating oxygen reduction active sites in pyrolyzed metal nitrogen coordinated non precious metal electrocatalysts systems', U. Tylus, Q. Jia, K. Strickland, N. Ramaswamy, A. Serov, P. Atanassov and S. Mukerjee, *J. Phys. Chem. C.,* **118 (17),** 8999-9008 (2014).

6. 'Fe-N-C oxygen reduction fuel cell catalyst derived from carbedazim', A Seriv, K. Kartyushkova and P. Atannasov, **4(10)**, July 2014, DOI 10.1002/aenm.201301735.

7. 'Activity descriptor identification for oxygen reduction on non precious electrocatalysts: linking surface science to coordination chemistry', N. Ramaswamy, U. Tylus, Q. Jia and S. Mukerjee, J. Amer**135(41)**, 15443-15449 (2013).

8. 'Carbon supports for non-precious metal oxygen reduction catalysts, *J. Electrochem. Soc.,* **160(8)**, F788-F792 (2013).

9. 'Impact of transition metal on nitrogen retention and activity of iron-nitrogen-carbon oxygen reduction catalysts.', S. Ganesan, N. Leonard and S.C. Barton, *Phys. Chem. Chem. Phys.*, **16**, 4576–4585 (2014). doi:10.1039/c3cp54751e.

REFERENCES

1. Wu, G.; More, K.L.; Johnston, C.M.; Zelenay, P. *Science* 2011, *332*, 443.

2. Lefèvre, M.; Proietti, E.; Jaouen, F.; Dodelet, J.-P. *Science* 2009, *324*, 71.

3. Saha, M.S.; Gullá, A.F.; Allen, R.J.; Mukerjee, S. *Electrochimica acta* 2006, *51*, 4680.

4. Haji, S. *Renewable Energy* 2011, *36*, 451.

5. Zhang, J.; Zhang, L.; Bezerra, C. W.; Li, H.; Xia, Z.; Zhang, J.; Marques, A.L.; Marques, E.P. *Electrochimica Acta* 2009, *54*, 1737.

6. Gasteiger, H.A.; Kocha, S.S.; Sompalli, B.; Wagner, F.T. *Applied Catalysis B: Environmental* 2005, *56*, 9.

V.A.9 High-Activity Dealloyed Catalysts

Anusorn Kongkanand
General Motors, LLC (GM)
895 Joslyn Ave
Pontiac, MI 48340-2920
Phone: (585) 953-5538
Email: anusorn.kongkanand@gm.com

DOE Managers
Dimitrios Papageorgopoulos
Phone: (202) 586-5463
Email: Dimitrios.Papageorgopoulos@ee.doe.gov
Gregory Kleen
Phone: (720) 356-1672
Email: Gregory.Kleen@ee.doe.gov

Contract Number: DE-EE0000458

Subcontractors
- David Ramaker, George Washington University (GWU), Washington, D.C.
- Rachel O'Malley, Johnson Matthey Fuel Cells (JMFC), Sonning Common, UK
- Yang Shao-Horn, Massachusetts Institute of Technology (MIT), Cambridge, MA
- Sanjeev Mukerjee, Northeastern University (NEU), Boston, MA
- Peter Strasser, Technical University Berlin (TUB), Berlin, Germany

Project Start Date: August 1, 2010
Project End Date: September 30, 2014

Overall Objectives

- Demonstrate, in 50-cm^2 membrane electrode assemblies (MEAs) in fuel cells using catalyst precursors prepared in large batch size, a dealloyed catalyst that satisfies DOE 2017 catalyst goals.
- Determine, at the atomic scale, where alloying-element atoms should reside with respect to the surface of the catalyst particle for simultaneously good activity, durability, and high-current density performance in air.
- Develop and demonstrate electrodes giving high current density performance in air adequate to meet the DOE platinum group metal (PGM) loading targets of <0.125 g_{PGM}/kW_{rated} and <0.125 mg_{Pt}/cm^2_{geo}.
- Scale up of synthesis and dealloying. Test durability of activity and power density in full-active-area cells.

Fiscal Year (FY) 2014 Objectives

- Improve understanding of where alloying-element atoms should reside with respect to the surface of the catalyst particle for simultaneously achieving good activity, durability, and high-current-density performance in air.
- Demonstrate electrodes made from dealloyed catalysts that give good high current density performance using air as the oxidant: >0.56 V at 1.5 A/cm^2 when tested with the DOE-targeted cathode loadings ≤0.1 mg_{PGM}/cm^2.
- Develop catalyst and optimize electrode to achieve >0.56 V at 1.5 A/cm^2 after durability testing.

Technical Barriers

This project addresses the following technical barriers from the Fuel Cells section of the Fuel Cell Technologies Office Multi-Year Research, Development, and Demonstration Plan:

(B) Cost

(A) Durability

(C) Performance

Technical Targets

Table 1. Progress towards Meeting Technical Targets for Electrocatalysts for Transportation Applications

Characteristic	Units	2017 DOE Stack Targets	Project 2014 Status (50 cm^2 at GM)
Mass activity	A/mg_{PGM} @ $900mV_{iR\text{-}free}$	≥0.44	0.6-0.75 (PtNi&PtCo)
Loss in catalytic (mass) activity	% lost after 30k cycles 0.6-1.0 V	≤40%	0-40% (PtNi&PtCo)
PGM Total Content	g_{PGM}/kW_{rated}	≤0.125	0.16 @1.5A/cm^2 in H_2/air (still 0.05 on anode)
PGM Total Loading	mg_{PGM}/cm^2_{geo}	≤0.125	0.15 (still 0.05 on anode)
Performance @ rated power	mW/cm^2	1,000	945
Performance @ 0.8 V	mA/cm^2	300	240

FY 2014 Accomplishments

- Developed several large-batch $PtNi_3$ and $PtCo_3$ catalysts achieving initial mass activities of 0.60-0.75 A/mg_{PGM}, substantially exceeding the target of 0.44 A/mg_{PGM}.

- The above catalysts lost only 0-40% of its initial activity after 30,000 cycles at 0.6-1.0 V, bettering the target of <40% loss.
- Achieved same H_2/air fuel cell performance as 0.4 mg_{Pt}/cm^2 electrode with one-fourth the PGM loading with newly developed catalysts. Confirmed improved performance of the newly developed catalyst in a full-active-area automotive stack.

INTRODUCTION

The amount of expensive platinum used as the oxygen reduction catalyst in fuel cells must be reduced at least 4-fold to make proton exchange membrane fuel cells cost competitive with other power sources. Pt-alloy catalysts, typically prepared with a composition of Pt_3M (M being a non-precious metal) have historically provided about half of the necessary activity gain vs. state-of-the-art pure-Pt/carbon catalysts. Prior to this project, team member Peter Strasser's group had shown, in small-scale laboratory experiments, that additional activity gains could be obtained by first synthesizing alloys with excess M and then removing most of the M by an electrochemical treatment [1]. They hypothesized that this treatment leaves the surface Pt atoms closer to one another than they are in pure Pt, causing electronic structure changes that accelerate the reduction of oxygen [2].

This project has developed manufacturable means of scaling up these dealloyed catalysts, confirming that most of the activity gains seen in ex situ laboratory experiments can also be achieved in practical fuel cells at GM, which satisfy the DOE catalyst initial activity target. However, we identified severe problems: (1) lack of durability and (2) poor performance in hydrogen/air fuel cells at high current density, associated with the use of the alloying element, copper, which had seemed most attractive in ex situ experiments. In FY 2012 we successfully shifted to other alloying elements, cobalt and nickel, which avoid one of the mechanisms whereby copper caused problems. We continue to pursue ideas to solve the durability shortfall that we have seen to date for the large-scale dealloyed $PtNi_3$ and $PtCo_3$ materials.

APPROACH

During FY 2012 and 2013, we successfully shifted to dealloyed $PtNi_3$ and $PtCo_3$ systems and demonstrated on several large-batch precursors their improved activity and durability in 50-cm^2 fuel cells exceeding DOE 2017 targets, and therefore passed the Go/No-Go gate in 2012. During FY 2013 and 2014, we extensively used advanced electron microscopy and synchrotron X-ray techniques in an attempt to correlate atomic-scale structure and composition with catalytic performance in order to improve our understanding in designing a better catalyst. On the other hand, as the loading of Pt in the cathode electrode is reduced, we observed larger voltage loss, especially at high power, than expected. This loss was attributed to low available Pt area for oxygen reduction reaction as Pt loading is reduced. Therefore, we continue to further develop our catalyst to have higher specific Pt area. Meanwhile, iterations of electrode optimization were done and selected catalysts were demonstrated in a full-active-area fuel cell stack.

RESULTS

We have showed record oxygen reduction reaction (ORR) activities even after accelerated voltage-cycling stability tests. These catalysts were prepared from large batch catalyst precursors from Johnson Matthey and were dealloyed using multiple acid-leaching conditions and post-leaching thermal annealing treatments at GM. A subset of those samples and their respective ORR activity changes with voltage-cycling tests is shown in Figure 1. As reported last year, catalysts made from the old $PtNi_3$ precursor (11/176 type) had poor particle size distribution and showed poor durability. However, catalysts made from the new $PtNi_3$ precursor (12/280 type) had good particle size distribution and showed excellent durability. GM generated MEA samples at different aging stages of these catalysts and sent to the partners for advanced characterization (MIT for transmission electron microscopy [TEM], NEU for extended X-ray absorption fine structure analysis [EXAFS], and GWU for X-ray absorption near-edge spectroscopy [XANES]) in an attempt to deepen our understanding of what is needed to make a high-activity and durable catalyst. Due to limited space, only a few achievements will be highlighted in this report.

The high activity of dealloyed Pt-Ni catalysts can be attributed to the compressive lattice strain of the Pt-shell surface due to the lattice and composition mismatch to the underlayer Ni-rich core. As the Pt shell grows thicker the lattice strain diminishes. On the other hand, certain Pt-shell thickness and quality are necessary to protect the Ni-rich core from degradation in an MEA environment. We have developed methods to evaluate the Pt-shell quality and to correlate micro-composition to the ORR activity.

Using the microscopic results from TEM at MIT and GM, the elemental measurement results from GM, and micro-composition analysis from EXAFS at NEU, GWU developed XANES delta mu technique to evaluate the quality of the Pt shell. They identified a specific feature in the XANES spectra that belongs to direct and indirect Ni-O bonds. Measuring this feature at different electrochemical potentials on the different catalysts after different aging stages, GWU found that it was easier for oxygen to penetrate through the Pt-shell on the catalyst made from the old

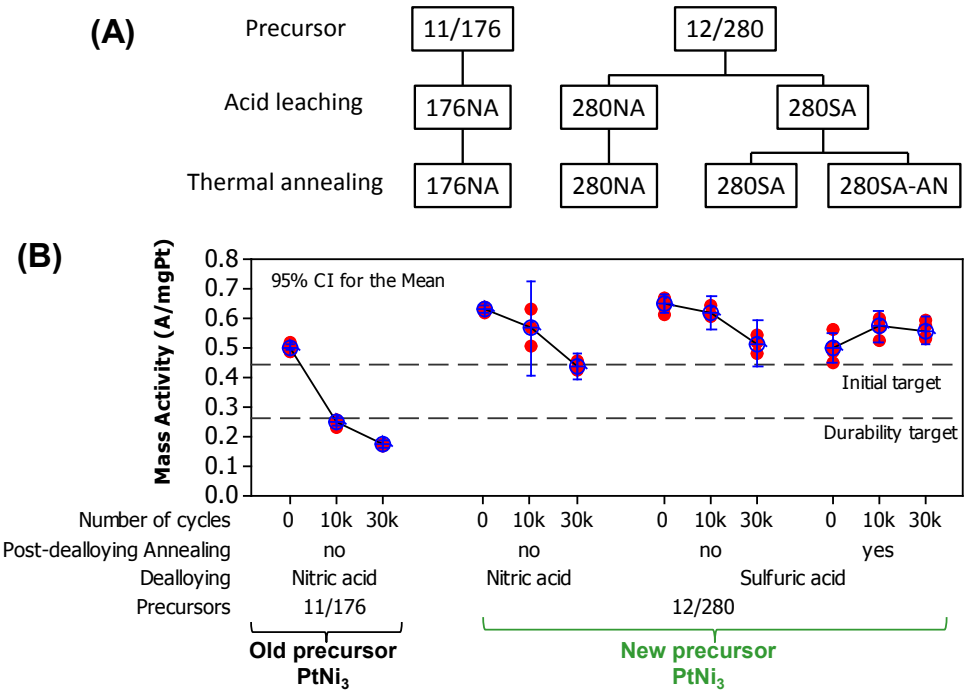

FIGURE 1. (A) Schematic showing selected catalysts. The precursors were either treated in: (1) 1 M nitric acid at 70°C for 24 h in air (176NA and 280NA) or, (2) 0.5 M sulfuric acid at 80°C for 24 h in nitrogen (280SA). After the dealloying, some 280SA catalysts were thermally annealed at 400°C for 4 h in 5% H_2 and 95% N_2, marked as 280SA-AN. (B) GM 50-cm^2 MEA mass-activity data for the different catalysts as a function of voltage cycles. Error bars represent 95% confidence intervals for the means.

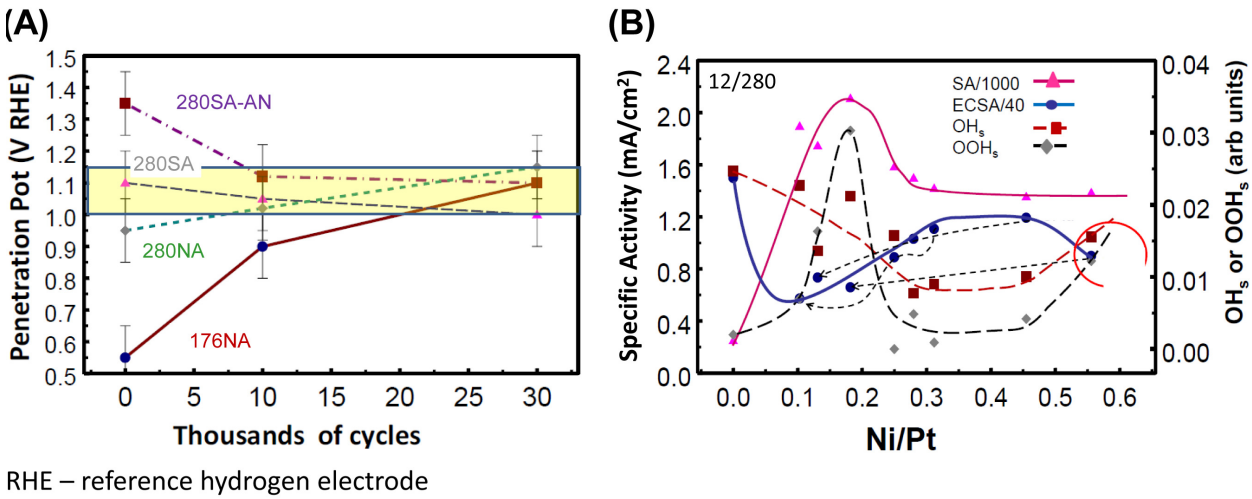

RHE – reference hydrogen electrode

FIGURE 2. (A) Potentials where indirect Ni-O interaction become dominant (penetration potentials) determined by Ni K edge XANES for the different catalysts. (B) Plot of δ|Δμ| for OOH_n* at 0.7 V in O_2 and |Δμ| for OH* at 0.9 V in N_2, along with the specific activity (mA/cm_{Pt}) at 0.9 V, as a function of Ni/Pt content.

precursor (176NA) than on those made from the new precursor (Figure 2A). Post-dealloying thermal annealing (280SA-AN) was also found to enhance Pt-shell quality. Interestingly, after extensive voltage cycling, all catalysts showed a similar characteristic shell quality. This may indicate the minimum Pt shell thickness needed for any catalyst to be sufficiently stable in a fuel cell environment.

Furthermore, XANES analysis on the Pt L_3 edge allows quantification of adsorbed species on the Pt surface. Of particular interest, adsorbed OH, OOH, and HOOH

are believed to strongly correlate with ORR activity. A comprehensive picture appeared when measurements on the different catalysts at different aging stages were done (Figure 2B). The specific activity measured in MEAs (pink solid line) correlates with OOH surface species in lieu of OH dominating. This points to a relatively lower Pt-O bond strength on the dealloyed catalysts. More importantly, it explains how the activity of the 12/280-type catalyst increases before it decreases as the Ni content decreases but the activity of the 11/176-type catalyst monotonically decreases. This suggests that the catalyst should start at a slightly high Ni content to maintain high activity for an extended period of time.

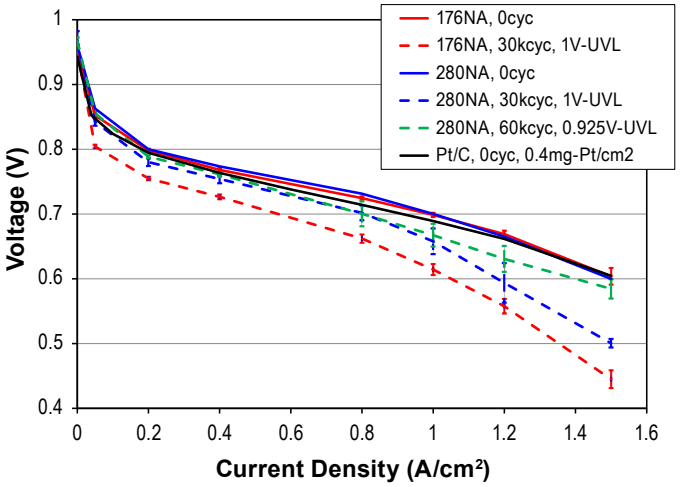

UVL – upper voltage limit

FIGURE 3. GM 50-cm^2 MEA polarization curves of D-PtNi$_3$ (color lines) and Pt/C (black line) catalysts, before (solid lines) and after (dashed lines) voltage-cycling tests as indicated in the legend. Operating conditions were H_2/air, 80°C, 100/100% relative humidity$_{in}$, stoichiometry 1.5/2, 170/170 kPa$_{abs}$.

In the previous year, we reported encouraging H_2/air fuel cell performance but noted that the high-power performance was still lower than what one would expect from such highly active catalysts. Since then, GM conducted multiple iterations of electrode optimization. Figure 3 shows comparative polarization curves of the different catalysts after optimization. Dealloyed catalysts 176NA (red solid line) and 280NA (blue solid line) at 0.1 mg$_{PGM}$/cm^2 cathode loading gave comparable performance as a Pt/C catalyst (black solid line) at four times the loading. This demonstrates good utilization of the new catalysts.

After 30,000 voltage cycles, 176NA lost more activity than 280NA (also showed in Figure 1, first and second triads) and hence larger voltage (red vs. blue dashed lines). Interestingly, we found that one could mitigate the performance loss by constraining the upper voltage limit during the voltage cycling from 1 V to 0.925 V. Doing so, we were able to mitigate the performance loss at 1.5 A/cm^2 to only 20 mV after 60,000 cycles. This highlights the highly intimate interaction between materials and system and the necessity of optimizing one in correlation with the other.

In an attempt to demonstrate the newly developed catalyst in a real fuel cell system, selected catalysts were integrated with other state-of-the-art components and were fabricated into a full-active-area stack. Figure 4 shows the power density for the dealloyed PtNi$_3$ and PtCo$_3$ catalysts tested under Fuel Cell Tech Team recommended conditions. Noticeable voltage loss at dry condition indicates needs for more electrode optimization. Note that one can easily boost the voltage by testing at higher pressure which was recently advised by DOE funded system modeling. We intend to test

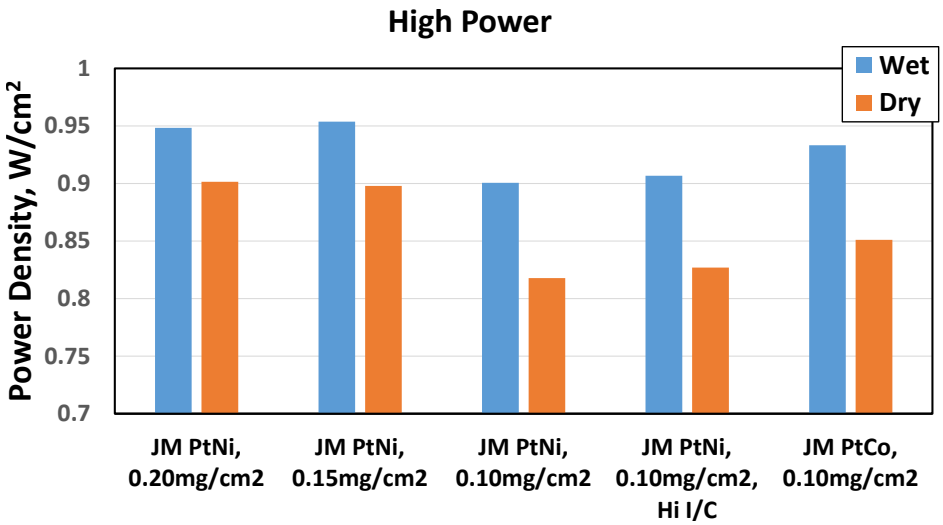

FIGURE 4. Full-active-area stack high-power performance of the dealloyed PtNi$_3$ and PtCo$_3$ catalysts under Fuel Cell Tech Team recommended conditions.

at this higher pressure in the near future. In addition, using a relatively high anode loading (0.05 mg_{Pt}/cm^2), we currently achieved a PGM total content of 0.16 g_{PGM}/kW (Table 1). If we reduced the anode loading to 0.025 mg_{Pt}/cm^2, we would approach the DOE target of 0.125 g_{PGM}/kW_{rated}.

CONCLUSIONS AND FUTURE DIRECTIONS

- Developed and used XAFS techniques to characterize Pt shell and subsurface metals in a fuel cell-relevant environment. Identified factors important in designing a durable highly-active catalyst.
- Demonstrated that dealloyed catalysts developed under this project might be sufficiently durable if we suppressed the upper-limit voltage.
- Successfully transferred and further developed catalyst technology from academia, to catalyst supplier, and to stack integrator in ~3 years. Confirmed improved performance of the newly developed catalyst in a full-active-area automotive stack.
- This project is ending in September FY 2014. However, some future activities will be focused on:
  - Perform durability testing on full-active-area stack.
  - Develop catalyst with higher surface area.
  - Consult with Argonne National Laboratory-led DOE project ("Rationally Designed Catalyst Layers for PEMFC Performance Optimization") to improve the understanding on the effect of leached Ni on fuel cell performance.

FY 2014 PUBLICATIONS/PRESENTATIONS

Presentations and Published Abstracts

1. D.E. Ramaker, X-ray Absorption Spectroscopy, an in operando probe of reactions in fuel cells and batteries, 245th ACS meeting, April 7–11, 2013, New Orleans, LA.

2. Invited talk: "X-ray absorption spectroscopy: An in operando probe of electrode reactions in fuel cells and batteries" D.E. Ramaker 245th National Meeting and Exposition of the American Chemical Society, April 7–11, 2013, New Orleans, LA

3. "Preparation of Dealloyed Catalysts with Durably High Oxygen Reduction Activity", J.E. Owejan, E.L. Thompson, A. Kongkanand, Z. Lui, J. Ziegelbauer, F.T. Wagner, A. Martinez, S. Thorpe, W. Turner, R. O'Malley, L. Gan, S. Rudi, C. Cui, P. Strasser, C. Carlton, A. Han, Y. Shao-Horn, Q. Jia, S. Mukerjee, K. Caldwell, and D.E. Ramaker, National Electrochemical Society Meeting, May 12–16, 2013 Toronto, CN.

4. "Understanding the Durability and ORR Reactivity of Four Different De-alloyed PtNi Cathodic Catalysts" David E. Ramaker, Keegan Caldwell, Qingying Jia, Sanjeev Mukerjee, and Joseph M. Ziegelbauer, Presentation at 224th ECS meeting, San Francisco, CA, Oct. 27 – Nov. 1, 2013.

5. "What we learned and paths forward on dealloyed catalysts" Anusorn Kongkanand, Presentation to Deborah Myers team at Argonne National Lab, Oct. 16, 2013.

6. "Advanced Fuel Cell Catalyst Development for Automotive Application" Anusorn Kongkanand, at University of Akron, Jan. 23, 2014 (small section on dealloyed catalysts).

7. "Characterization of Dealloyed Catalysts in PEMFC" A. Kongkanand, R. Kukreja, T.E. Moylan, J. Ziegelbauer, A. Martinez, S. Thorpe, W. Turner, R. O'Malley, L. Gan, S. Rudi, C. Cui, P. Strasser, C. Carlton, A. Han, Y. Shao-Horn, Q. Jia, S. Mukerjee, K. Caldwell, and D.E. Ramaker, National Electrochemical Society Meeting, May 11–16, 2014 Orlando, FL.

8. "Are we there yet? Pt-alloy catalysts" A. Kongkanand, S. Kumaraguru, at the DOE Catalyst and Durability Working Groups, Washington, DC, Jun. 16, 2014 (small section on dealloyed catalysts).

Publications

1. Q. Jia, D.E. Ramaker, J.M. Ziegelbauer, N. Ramaswamy, A. Halder, S. Mukerjee, Fundamental Aspects of ad-Metal Dissolution and Contamination in Low and Medium Temperature Fuel Cell Electrocatalysis: A Cu Based Case Study Using In Situ Electrochemical X-ray Absorption Spectroscopy, The Journal of Physical Chemistry C, 117 (2013) 4585-4596

2. Cui, C.; Ahmadi, M.; Behafarid, F.; Gan, L.; Neumann, M.; Heggen, M.; Cuenya, B. R.; Strasser, P.: Shape-selected bimetallic nanoparticle electrocatalysts: evolution of their atomic scale structure, chemical composition, and electrochemical reactivity under various chemical environments. Faraday Discuss. 2013, 162, 91-112.

3. L. Gan, S. Rudi, C. Cui, P. Strasser, Ni-Catalyzed Growth of Graphene Layers during Thermal Annealing: Implications for the Synthesis of Carbon-Supported Pt-Ni Fuel-Cell Catalysts. ChemCatChem, 2013, 5, 2691-2694.

4. D. Ramaker, K. Caldwell, Q. Jia, J. Ziegelbauer, S. Mukerjee, "Observed molecular adsorbates on Pt-bimetallic surfaces during electrocatalysis" Angew. Chem Int Ed.

5. Cui, C.; Gan, L.; Heggen, M.; Rudi, S.; Strasser, P.: Compositional segregation in shaped Pt alloy nanoparticles and their structural behaviour during electrocatalysis. Nat Mater 2013, 12, 765-771.

6. Lin Gan, Marc Heggen and Peter Strasser. Subsurface Enrichment of Highly Active Dealloyed Pt-Ni Catalyst Nanoparticles for Oxygen Reduction Reaction. ECS Trans. 2013 volume 50, issue 2, 1627-1631.

7. C. Cui, L. Gan, M., Neumann, M. Heggen, B. R. Cuenya, P. Strasser, J. Am. Chem. Soc. 2014, 136, 4813–4816.

8. A. Kongkanand, W. Gu, F.T. Wagner, Electrocatalyst Design in Proton Exchange Membrane Fuel Cells for Automotive Application, in: F. Tao, W. Schneider, P. Kamat (Eds.) Heterogeneous Catalysis at the Nanoscale for Energy Applications, Wiley-VCH, 2014. (one section on dealloyed catalyst)

9. Lin Gan, Chunhua Cui, Stefan Rudi, and Peter Strasser. Core-shell and nanoporous particle architectures and their effect on the

activity and stability of Pt ORR electrocatalysts. Topics in Catalysis 2014, 57, 236-244.

REFERENCES

1. Koh, S. and P. Strasser, *Electrocatalysis on bimetallic surfaces: Modifying catalytic reactivity for oxygen reduction by voltammetric surface dealloying.* Journal of the American Chemical Society, 2007. **129**(42): p. 12624-12625.

2. Strasser, P., et al., *Lattice-strain control of the activity in dealloyed core-shell fuel cell catalysts.* Nature Chemistry, 2010. **2**(6): p. 454-460.

V.A.10 Development of Ultra-Low Platinum Alloy Cathode Catalysts for PEM Fuel Cells

Branko N. Popov
University of South Carolina (USC)
301 Main Street
Columbia, SC 29208
Phone: (803) 777-7314
Email: popov@cec.sc.edu

DOE Managers
Donna Lee Ho
Phone: (202) 586-8000
Email: Donna.Ho@ee.doe.gov
David Peterson
Phone: (720) 356-1747
Email: David.Peterson@ee.doe.gov

Technical Advisor
Thomas Benjamin
Phone: (630) 252-1632
Email: benjamin@anl.gov

Contract Number: DE-EE0000460

Project Start Date: September 1, 2010
Project End Date: May 31, 2015

Overall Objectives

- Develop a cost-effective, high-volume synthesis procedure to manufacture highly stable and catalytically active partially graphitized carbon composite catalyst (CCC) and graphitized activated carbon composite catalyst (A-CCC) supports.
  - Achieve onset potential close to 0.9 V vs. the reference hydrogen electrode (RHE) for oxygen reduction reaction (ORR) with well-defined kinetic and mass transfer regions for CCC and A-CCC supports.
  - Achieve ≤30 mV loss at 0.8 A cm^{-2} in H_2/air fuel cell after 400 h potential holding (1.2 V).
- Develop low-cost procedures to synthesize a catalyst with enhanced activity due to the synergistic effect of non-metallic catalytic sites from the support and compressive Pt-lattice catalyst.
  - Demonstrate mass activity of ≥0.44 A mg_{PGM}^{-1} in H_2/O_2 fuel cell, initial high current performance under H_2/air (<0.125 g_{PGM} kW^{-1} rated power density) and stability of mass activity (≤ 40% loss) and stability of high current density performance (≤30 mV loss at 0.8 A cm^{-2}) under H_2/air using DOE potential cycling (0.6-1.0 V, 30k cycles, potential cycling (1.0-1.5 V), and potential holding tests (1.2 V, 400 h).
- Scale up synthesis of supports (CCC and A-CCC) and catalysts (Pt/CCC, doped-Pt/CCC, Pt/A-CCC, and doped-Pt/A-CCC).

Fiscal Year (FY) 2014 Objectives

- Synthesis and performance evaluation of Co-doped Pt/CCC catalyst using partially graphitized CCC support having Brunauer-Emmett-Teller (BET) surface area of 400 m^2 g^{-1} and well-defined pore-size and pore-size distribution.
  - Initial high kinetic mass activity under H_2-O_2
  - Initial high current density performance under H_2-air
  - Catalyst durability under potential cycling experimental conditions
- Synthesis and performance evaluation of Pt/A-CCC catalyst using graphitized A-CCC support having BET surface area 200 m^2 g^{-1} and well-defined pore-size and pore-size distribution.
  - Initial high kinetic mass activity under H_2-O_2
  - Initial high current density performance under H_2-air
  - Catalyst durability and support stability under potential cycling and potential holding experimental conditions, respectively

Technical Barriers

This project addresses the following technical barriers from the Fuel Cells section of the Fuel Cell Technologies Office Multi-Year Research, Development, and Demonstration Plan:

(A) Durability

(B) Cost

(C) Performance

Technical Targets

In this project, studies are being conducted to develop highly active and stable ultra-low Pt loading cathode catalysts for PEM fuel cells. The catalysts developed in this project are

Pt/CCC, doped-Pt/CCC, Pt/A-CCC, and doped-Pt/A-CCC using procedures developed at USC. These catalysts have the potential to meet the 2017 DOE technical target for electrocatalysts for automotive applications as shown in Table 1.

FY 2014 Accomplishments

- For the first time, USC has reported the development of Pt/A-CCC catalyst which shows high support stability both under 1.2 V potential holding and under 1.0-1.5 V potential cycling conditions. (BET surface area of the A-CCC support is 200 $m^2\ g^{-1}$.)
- Advances have been made in approaching the DOE 2017 power density (rated) target of 0.125 $g_{PGM}\ kW^{-1}$ with a Pt/A-CCC catalyst (0.196 $g_{PGM}\ kW^{-1}$).
- Achieved 24 mV loss at 1.5 A cm^{-2} after 5k cycles between 1.0 V and 1.5 V for the Pt/A-CCC catalyst which satisfies the 2017 DOE target for support stability (≤30 mV loss at 1.5 A cm^{-2}).
- Accomplished 32% mass activity loss and 30% ECSA loss, and 27 mV loss at 0.8 A cm^{-2} after 400 h potential holding (1.2 V) for the Pt/A-CCC catalyst. These values meet the 2017 DOE targets for support stability (≤40% loss of initial mass activity and <40% loss of initial ECSA after 400 h).
- Achieved initial mass activity of 0.44 A mg_{PGM}^{-1} (2017 DOE target is 0.44 A mg_{PGM}^{-1}) and 0.25 A mg_{PGM}^{-1} (2017 DOE target is 0.26 A mg_{PGM}^{-1}) after 30k cycles (0.6-1.0 V) for the doped-Pt/CCC catalyst. (BET surface area of the CCC support is 400 $m^2\ g^{-1}$.)
- Accomplished 32% ECSA loss (2017 DOE target is ≤40% loss) and 40 mV loss (iR-corrected) after 30k cycles (0.6-1.0 V) for the doped-Pt/CCC catalyst (2017 DOE target is ≤30 mV loss at 0.8 A cm^{-2}). (BET surface area of the CCC support is 400 $m^2\ g^{-1}$.)

INTRODUCTION

Novel methodologies were developed at USC to synthesize A-CCC and CCC [1-14] supports. Highly active and stable Pt/CCC, Pt/A-CCC, doped-Pt/CCC, and doped-Pt/A-CCC catalysts are developed that show higher performance than the commercial Pt/C at low loadings (≤0.1 mg cm^{-2}) [1-5]. These catalysts are a combination of non-metallic active site containing CCC and platinum or compressive Pt lattice catalyst, which shows higher activity for the ORR through synergistic effect. Pt catalyst deposited on CCC and A-CCC supports with high activity towards ORR was synthesized and its catalytic activity and stability were evaluated using potential cycling (0.6-1.0 V for 30k cycles) and potential holding (1.2 V for 400 h) experiments.

APPROACH

In order to develop ultra-low Pt loading catalyst for automotive applications, the research at USC was aimed at developing catalytically active and stable supports having 200-400 $m^2\ g^{-1}$ BET surface area with well-defined pore-size and pore-size distribution to sustain potential cycling and potential holding experiments. The CCC support was synthesized through (i) surface modification with acids and

TABLE 1. Progress towards Meeting Technical Targets for Electrocatalysts for Automotive Applications.

Characteristic	Units	2017 Targets	FY 2014 Status
PGM total content	g kW^{-1} (rated)	0.125	0.196 (Pt/A-CCC) 0.241 (Doped-Pt/CCC)
PGM total loading	mg cm^{-2}	0.125	0.2
Mass activity (H_2/O_2 (2/9.5 stoic.) 80°C, 100% RH, 150 kPa_{abs}.)	A mg_{Pt}^{-1} @ 0.9 $V_{iR\text{-}free}$	0.44	0.44 (Doped-Pt/CCC)
Catalyst durability (30k cycles, 0.6-1.0 V, 50 mV/s, 80°C, H_2/N_2, 100% RH, No back press.)	% Mass activity (MA) loss % ECSA loss mV loss @ 0.8 A cm^{-2}	≤40% ≤40% ≤30 mV	**Catalyst 1: Pt/A-CCC** 50% loss (MA) 41% loss (ECSA) 72 mV loss (H_2-air)
			Catalyst 2: Doped-Pt/CCC 43% loss (MA) 32% loss (ECSA) 40 mV loss (H_2-air)
Support stability (1.2 V for 400 h 80°C, H_2/N_2, 100% RH, 150 $kPa_{abs.}$)	% Mass activity (MA) loss % ECSA loss mV loss @ 0.8 A cm^{-2}	≤40% ≤40% ≤30 mV	**Catalyst 1: Pt/A-CCC** 32% loss (MA) 30% loss (ECSA) 27 mV loss (H_2-air)

RH – relative humidity

inclusion of oxygen groups, (ii) metal catalyzed pyrolysis, and (iii) chemical leaching to remove excess metal used to dope the support. The A-CCC support was synthesized through a stabilization process to remove electrochemically unstable amorphous carbon from the support. A novel surface modification process was developed to achieve uniform Pt deposition on the CCC and A-CCC supports. Pt deposition was carried out using a modified polyol process to synthesize Pt/CCC and Pt/A-CCC catalysts with particle size in the range 3-5 nm. A protective coating method was also developed to inhibit particle growth during heat treatment for the synthesis of doped-Pt/CCC and dope-Pt/A-CCC catalysts. The novelty of the method is that the doping metal is present within the CCC or A-CCC supports which diffuses during controlled heat treatment to form doped-Pt catalysts having compressive Pt lattices. A schematic of USC methodology of preparing Pt and doped-Pt catalysts is shown in Figure 1.

RESULTS

Our approach in FY 2013 was to synthesize ultra-low Pt loading catalysts by optimizing the properties of the support. Based on our previous experience in synthesizing various CCC supports, our target in FY 2014 was to synthesize A-CCC support with optimized BET surface area, pore size and pore-size distribution to sustain potential cycling and potential holding experiments.

The BET surface area, pore-size, and pore-size distribution of the partially graphitized CCC support was tailored using various procedures developed at USC. The CCC support showed BET surface area of 400 $m^2\ g^{-1}$ with pore-size distribution in the range between 4 nm and 7 nm. Furthermore, the CCC support showed very high activity with an onset potential of 0.87 V vs. RHE for ORR and well-defined kinetic and mass transfer regions (Results were reported in FY 2012 annual report).

Doped-Pt/CCC with an average particle size of ~4.0 nm was synthesized through a controlled heat-treatment procedure developed at USC. The catalyst durability of doped-Pt/CCC catalyst was evaluated using a potential cycling protocol (cycling between 0.6 V and 1.0 V). Figures 2a and 2b present the durability of mass activity and durability of H_2-air fuel cell performance of doped-Pt/CCC catalyst subjected to potential cycling in a 25 cm^2 membrane electrode assembly. The doped-Pt/CCC catalyst showed initial mass activity of 0.44 A mg_{PGM}^{-1} and 0.25 A mg_{PGM}^{-1} after 30k cycles corresponding to 43% loss. The ECSA decreased from 74 $m^2\ g_{Pt}^{-1}$ to 50 $m^2\ g_{Pt}^{-1}$ after 30k cycles (32% loss). The H_2-air fuel cell polarization test showed initial current density of 1.4 A cm^{-2} at 0.6 $V_{iR\text{-}free}$. The potential loss at 0.8 A cm^{-2} was used as a metric to evaluate the stability of the catalyst under potential cycling. Initially, the cell exhibited a cell voltage of 0.706 $V_{iR\text{-}free}$ and after 30k cycles, it decreased to 0.666 $V_{iR\text{-}free}$ at 0.8 A cm^{-2} with a cell potential loss of 40 mV. The cell potential loss is very close to that of 2017 DOE target (≤30 mV loss after 30k cycles). In the case of commercial Pt/C (46.7% Pt supported on high-surface-area carbon, Tanaka Kikinzoku Kogyo [TKK] Corporation, Japan), the mass activity loss and ECSA loss are 56% and 83%, respectively. The commercial Pt/C showed iR-corrected cell voltage loss of 284 mV at 0.7 A cm^{-2} after 30k cycles, since the polarization curve did not show any activity beyond 0.7 A cm^{-2} after 30k cycles. The catalyst durability study results of doped-Pt/CCC and commercial Pt/C catalysts are summarized in Table 2.

Based on our studies using the CCC support with BET surface area of 400 $m^2\ g^{-1}$, the following observation is made: In order to dope the Pt catalyst with transition metals, it is necessary to use high surface area carbon support which results in catalysts with very good catalyst stability under potential cycling conditions (0.6-1.0 V). The doped-Pt/CCC catalyst showed 100-120 mV loss in potential holding experiment and further optimization studies are in progress to improve the support stability at 1.2 V.

In order to further improve the support stability at high potentials, a novel process was developed to stabilize and activate the support through various treatments including a first heat treatment, leaching, and a second heat treatment to remove the electrochemically unstable amorphous carbon. The resulting graphitized A-CCC with a BET surface area

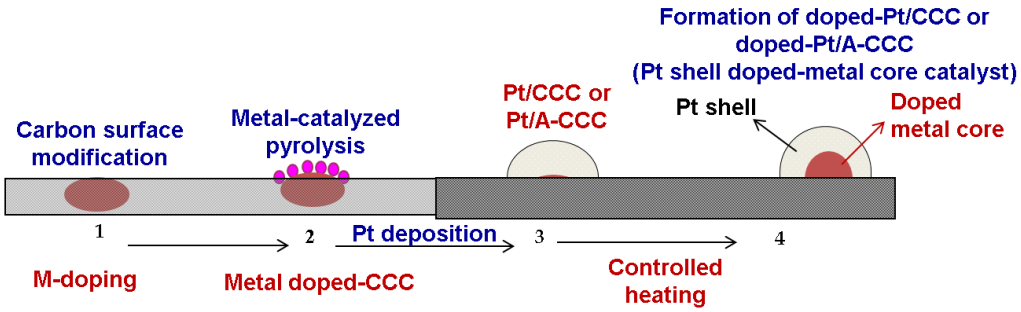

FIGURE 1. Schematic of synthesis procedure for Pt/CCC, Pt/A-CCC, doped-Pt/CCC, and doped-Pt/A-CCC catalysts developed at USC.

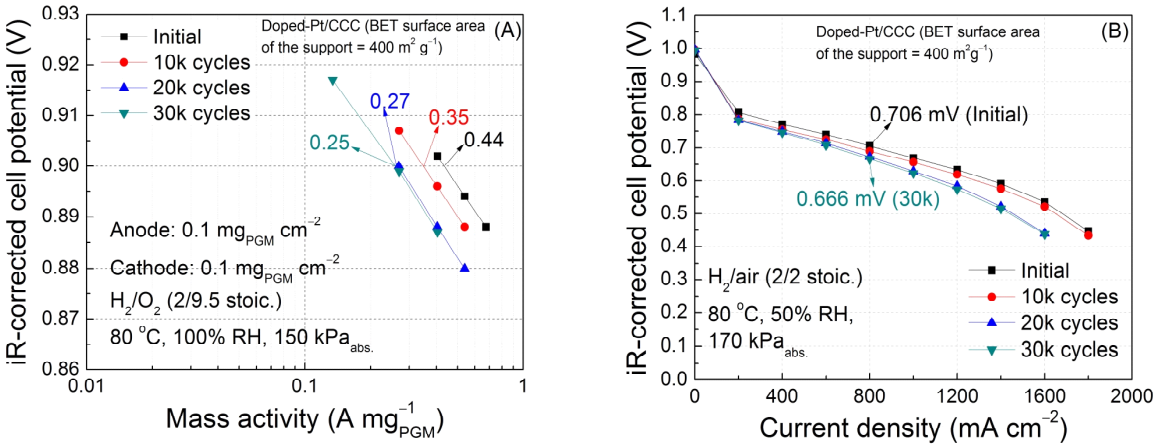

FIGURE 2. (A) Comparison of mass activities of doped-Pt/CCC catalyst before and after 30k potential cycling between 0.6 and 1.0 V. The catalyst loading is 0.1 mg_{PGM} cm^{-2} on both the anode and cathode electrodes. The fuel cell operating conditions are: H_2/O_2 (2.0/9.5), 80°C, 100% RH, 150 kPa_{abs} back pressure. Nafion® NRE 212 membrane is used as the electrolyte. (B) H_2/air fuel cell performance of doped Pt/CCC catalyst subjected to 30k potential cycling between 0.6 V and 1.0 V. The catalyst loading is 0.1 mg_{PGM} cm^{-2} on both the anode and cathode electrodes. The fuel cell operating conditions are: H_2/air (2/2 stoic.), 80°C, 50% RH, 170 $kPa_{abs.}$ back pressure. Nafion® NRE 212 membrane is used as the electrolyte.

TABLE 2. Summary of Catalyst Durability Test (30k potential cycling between 0.6 V and 1.0 V) for Doped-Pt/CCC and Commercial Pt/C Catalysts

Catalyst	Particle size (nm)	Mass activity (A mg_{Pt}^{-1})		ECSA (m^2 g^{-1})		Cell voltage loss at 0.8 A cm^{-2} (mV)	
		Initial	Final	Initial	Final	ΔV_{Cell}	$\Delta V_{iR\text{-}free}$
Doped-Pt/CCC	4.0	**0.44**	**0.25** (**43% loss**) (30k cycles)	**74**	**50** (**32% loss**) (30k cycles)	**36** (30k cycles)	**40** (30k cycles)
Pt/C	2.2	**0.18**	**0.08** (**56% loss**) (30k cycles)	**68**	**12** (**83% loss**) (30k cycles)	No activity (30k cycles)	No activity (30k cycles)

of 200 m^2 g^{-1}, high degree of graphitization, and improved hydrophobicity was used to synthesize Pt/A-CCC catalyst having an average Pt particle size of 3.1 nm.

The catalyst durability of Pt/A-CCC catalyst was evaluated using a potential cycling protocol (cycling between 0.6 and 1.0 V). Upon cycling, the catalyst showed mass activity loss and ECSA loss of 50% and 41%, respectively after 30k cycles. Initially, the single cell with Pt/A-CCC catalyst exhibited a cell voltage of 0.715 $V_{iR\text{-}free}$ at 0.8 A cm^{-2} which decreased to 0.643 $V_{iR\text{-}free}$ after 30k potential cycles corresponding to a loss of 72 mV (Figure 3).

The support stability of Pt/A-CCC catalyst was evaluated by applying a constant potential of 1.2 V for 400 h. The Pt/A-CCC catalyst showed mass activity loss of 32% and ECSA loss of 30% after 400 h. The initial H_2-air polarization curve and polarization curves obtained after 100 h, 200 h, and 400 h potential holding at 1.2 V for the Pt/A-CCC catalysts are compared in Figure 4. Figure 4 shows an initial potential of 689 mV at 0.8 A cm^{-2} and 662 mV at 0.8 A cm^{-2} after 400 h potential holding with a potential loss of 27 mV. The observed potential loss is less than the 2017 DOE target for support stability (≤30 mV loss after 400 h). Furthermore, the initial peak power density was 1,098 mW cm^{-2} which decreased to 958 mW cm^{-2} after 400 h stability tests corresponding to a loss of only 13%. The catalyst durability and support stability test results of Pt/A-CCC catalyst are summarized and compared with that of commercial Pt/C catalyst in Table 3.

The support stability test of Pt/A-CCC and commercial Pt/C (Pt deposited on high surface area carbon) catalysts was performed using "U.S DRIVE Fuel Cell Tech Team Cell Component Accelerated Stress Test and Polarization curve Protocols for PEM Fuel Cells" revised on January 14, 2013. Support durability test was carried out using triangular sweep cycles between 1.0 V and 1.5 V at 500 mV s^{-1} sweep rate for 5,000 cycles under H_2/N_2. The H_2-air polarization results after 0 and 5k cycles for the Pt/A-CCC catalyst is compared in Figure 5. The Pt/A-CCC catalyst showed 0.587 $V_{iR\text{-}free}$ at 1.5 A cm^{-2} which decreased to 0.563 $V_{iR\text{-}free}$ after 5k cycles

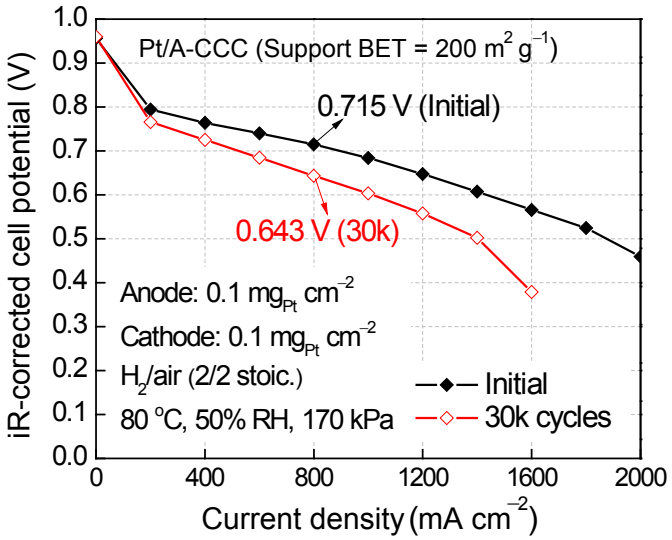

FIGURE 3. H_2/air fuel cell performance of Pt/A-CCC catalyst subjected to 30k potential cycling between 0.6 V and 1.0 V. The catalyst loading is 0.1 mg_{PGM} cm^{-2} on both the anode and cathode electrodes. The fuel cell operating conditions are: H_2/air (2/2 stoic.), 80°C, 50% RH, 170 $kPa_{abs.}$ back pressure. Nafion® NRE 212 membrane is used as the electrolyte.

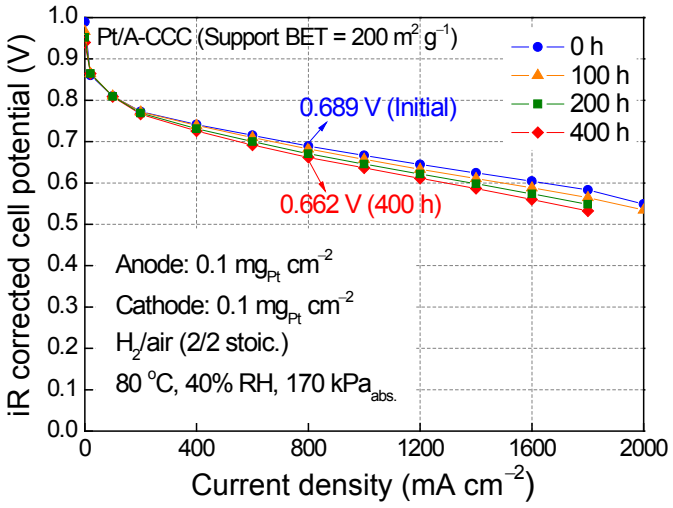

FIGURE 4. H_2/air fuel cell performance of Pt/A-CCC catalyst subjected to potential holding at 1.2 V for 400 h. The catalyst loading is 0.1 mg_{PGM} cm^{-2} on both the anode and cathode electrodes. The fuel cell operating conditions are: H_2/air (2/2 stoic.), 80°C, 40% RH, 170 kPa_{abs} back pressure. Nafion® NRE 212 membrane is used as the electrolyte.

TABLE 3. Summary of Catalyst Durability Test (30k Potential Cycling between 0.6 V and 1.0 V) and Support Stability Test (Potential Holding at 1.2 V for 400 h) for Pt/A-CCC and Commercial Pt/C Catalysts

Catalyst/Test	Particle size (nm)	Mass activity loss (%)	ECSA (m^2 g_{Pt}^{-1})		Cell voltage loss at 0.8 A cm^{-2} (mV)	
			Initial	Final	ΔV_{Cell}	$\Delta V_{iR\text{-}free}$
Pt/A-CCC						
Catalyst Durability	3.1	50	39	**23** (**41% loss**) (30k cycles)	**74** (30k cycles)	**72** (30k cycles)
Support Durability	3.1	32	40	**28** (**30% loss**) (400 h)	**29** (400 h)	**27** (400 h)
Pt/C						
Catalyst Durability	2.2	56	68	**12** (**83% loss**) (30k cycles)	No activity (30k cycles)	No activity (30k cycles)
Support Stability	2.2	72	68	**20** (**71% loss**) (**48h**)	No activity (48h)	No activity (48h)

with a potential loss of only 24 mV. The potential loss is less than the 2017 DOE target of ≤30 mV loss after 5k cycles (Figure 5). It has been reported that while high potentials effectively accelerate carbon corrosion, degradation of the catalyst due to Pt dissolution is minimized because of the oxide formation [15]. Drastic performance degradation was observed for the commercial Pt/C after 2k cycles due to severe carbon support corrosion at high potentials. The commercial Pt/C catalyst did not show any activity after 2k cycles.

Based on the studies carried out at USC for the past three years in developing various catalyst supports and catalysts, the following observations are made:

- Alloying Pt with transition metals helps increase the catalyst mass activity (measured under H_2/O_2). The enhanced mass activity does not translate to high current density performance of the catalyst under H_2-air. The effect of catalyst loading on catalyst mass activity has been previously studied at USC to understand the physical meaning of catalyst mass activity through

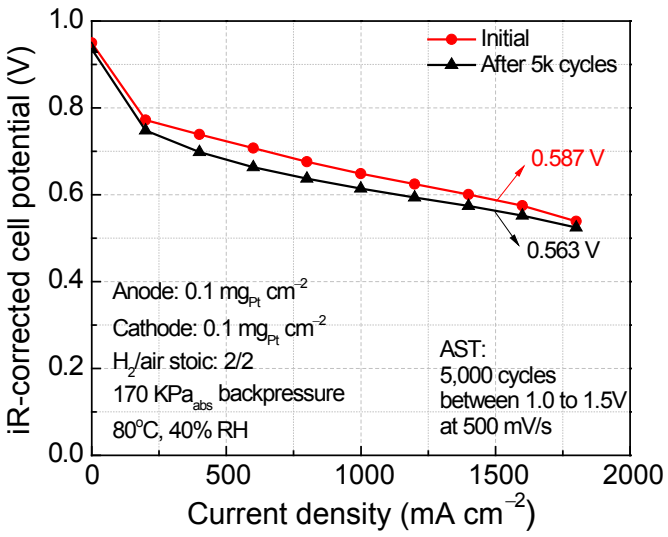

FIGURE 5. H_2/air fuel cell performance of Pt/A-CCC catalyst subjected to 5k potential cycling between 1.0 V and 1.5 V at 500 mV s^{-1}. The catalyst loading is 0.1 mg_{PGM} cm^{-2} on both the anode and cathode electrodes. The fuel cell operating conditions are: H_2/air (2/2 stoichiometry), 80°C, 40% RH, 170 kPa_{abs} back pressure. Nafion® NRE 212 membrane is used as the electrolyte.

mathematical modeling [16-18]. Our studies showed that alloying Pt with transition metals may contribute to the catalyst durability under potential cycling.

- According to our studies, in order to increase the mass activity, it is necessary to introduce three additional steps in the synthesis procedure to synthesize Pt-alloy/C catalysts from Pt/C:
  - Impregnation of excess amount of transition metal salt into Pt/C
  - Heat treatment at elevated temperatures (800-900 °C) for the alloy formation
  - Prolonged leaching (~12 h) in strong acid solution to remove excess transition metal

CONCLUSIONS AND FUTURE DIRECTIONS

Conclusions

- Accomplished rated power density of 0.196 g_{PGM} kW^{-1} for the Pt/A-CCC catalyst which is close to the 2017 DOE target of 0.125 g_{PGM} kW^{-1}.
- Accomplished 32% mass activity loss, 30% ECSA loss, and potential loss (iR-corrected) of 27 mV at 0.8 A cm^{-2} after 400 h potential holding (1.2 V) for the Pt/A-CCC catalyst which satisfy the 2017 DOE targets for support stability. (BET surface area of the A-CCC support is 200 m^2 g^{-1}.)
- Achieved 24 mV loss at 1.5 A cm^{-2} after 5k cycles between 1.0 V and 1.5 V for the Pt/A-CCC catalyst which satisfies the 2017 DOE target of ≤30 mV loss at 1.5 A cm^{-2}. (BET surface area of the A-CCC support is 200 m^2 g^{-1}.)
- Achieved initial mass activity of 0.44 A mg_{PGM}^{-1} and 0.25 A mg_{PGM}^{-1} after 30k cycles (0.6-1.0 V) for the doped-Pt/CCC catalyst corresponding to a loss of 43%. The initial mass activity satisfies the 2017 DOE target for initial mass activity (0.44 A g_{PGM}^{-1}) and stability of mass activity after 30k cycles is very close to that of the 2017 DOE target (0.26 A g_{PGM}^{-1}). (BET surface area of the CCC support is 400 m^2 g^{-1}.)
- Achieved 32% ECSA loss and potential loss (iR-corrected) of 40 mV after 30k cycles (0.6-1.0 V) for the Pt/CCC catalyst. The ECSA loss satisfies the 2017 DOE target (≤40% loss of initial ECSA) and the potential loss at 0.8 A cm^{-2} is very close to that of the 2017 DOE target (≤30 mV loss at 0.8 A cm^{-2}). (BET surface area of the CCC support is 400 m^2 g^{-1}.)

Future Anticipated Accomplishments

- Synthesis of highly stable and highly graphitized A-CCC support with BET surface area of 200-300 m^2 g^{-1} by optimizing the synthesis parameters such as heat treatment temperature and time.
- Study the structure-catalyst activity of doped-Pt/A-CCC catalysts through physical characterization studies such as high-resolution transmission electron microscopy and energy-dispersive X-ray spectroscopy, and fuel cell testing.
- Increase the performance of Pt-M/A-CCC catalysts by increasing the concentration of doped metal in the A-CCC support and pyrolysis conditions.
- Achieve stability of mass activity of ≤40% and stability of high current density (≤30 mV loss) after 30k potential cycling (between 0.6 and 1.0 V), potential holding (at 1.2 V for 400 h), and 5k potential cycling (between 1.0 and 1.5 V) experiments by optimizing the hydrophilic/hydrophobic properties of the support and introducing defects in the graphitic structure.
- The goal is to select a best performing catalyst which satisfies the 2017 DOE requirements of ≤40% loss of mass activity, ≤40% loss of ECSA and ≤30 mV loss at 0.8 A cm^{-2} under H_2-air after 30k potential cycling (between 0.6 and 1.0 V), potential holding (at 1.2 V for 400 h), and potential cycling (between 1.0 and 1.5 V, total 5k cycles) experiments.

FY 2014 PUBLICATIONS/PRESENTATIONS

Publications

1. Taekeun Kim, Tianyuan Xie, Wonsuk Jung, Francis Gadala-Maria, Prabhu Ganesan, and Branko N. Popov, Development

of Catalytically Active and Highly Stable Catalyst Supports for Polymer Electrolyte Membrane (PEM) Fuel Cells , *J. Power Sources*, July 2014. *Under Review.*

2. Ákos Kriston, Tianyuan Xie and Branko N. Popov, Impact of Ultra-low Platinum loading on Mass Activity and Mass Transport in H_2-Oxygen and H_2-Air PEM Fuel Cells, *Electrochim. Acta*, **121** (2014) 116-127.

3. Branko N. Popov, Tianyuan Xie, Taekeun Kim, Won Suk Jung, Joseph C. Rotchford, Akos Kriston, and Prabhu Ganesan, Development of Ultra-Low Loading Pt Alloy Cathode Catalyst for PEM Fuel Cells, *ECS Trans*., **58** (2013) 761-778.

4. Ákos Kriston, Tianyuan Xie, David Gamliel, Prabhu Ganesan, Branko N. Popov, "Effect of Ultra-Low Pt Loading on Mass Activity of PEM Fuel Cells," *J. Power Sources*, **243** (2013) 958-963.

5. Akos Kriston, Tianyuan Xie, Prabhu Ganesan, Branko N. Popov, "Effect of Pt Loading on Mass and Specific Activity in PEM Fuel Cells," *J. Electrochem. Soc*., **160** (2013) F406-F412.

Presentations

1. Tianyuan Xie, Taekeun Kim, Won Suk Jung, Prabhu Ganesan, and Branko N. Popov, Development of Ultra-Low Loading Pt Hybrid Catalyst for PEM Fuel Cells, *224th ECS Meeting*, San Francisco, CA, October 27 – November 01, 2013.

2. Branko N. Popov, Tianyuan Xie, Taekeun Kim, Won Suk Jung, and Prabhu Ganesan, Development of Ultra-Low Loading Pt Alloy Cathode Catalyst for PEM Fuel Cells, *224th ECS Meeting*, San Francisco, CA, October 27 – November 01, 2013.

3. Taekeun Kim, Won Suk Jung, and Prabhu Ganesan, Tianyuan Xie, and Branko N. Popov, Development of Ultra-Low Loading Pt/AGC Catalyst for PEM Fuel Cells, *224th ECS Meeting*, San Francisco, CA, October 27 – November 01, 2013.

REFERENCES

1. Taekeun Kim, Tianyuan Xie, Wonsuk Jung, Francis Gadala-Maria, Prabhu Ganesan, and Branko N. Popov, Development of Catalytically Active and Highly Stable Catalyst Supports for Polymer Electrolyte Membrane (PEM) Fuel Cells , *J. Power Sources*, July 2014. Under Review

2. Branko N. Popov, Tianyuan Xie, Taekeun Kim, Won Suk Jung, Joseph C. Rotchford, Akos Kriston, and Prabhu Ganesan, Development of Ultra-Low Loading Pt Alloy Cathode Catalyst for PEM Fuel Cells, *ECS Trans*., **58** (2013) 761-778.

3. B.N. Popov, X. Li and J. W. Lee, "Power source research at USC: Development of advanced electrocatalysts for polymer electrolyte membrane fuel cells," *Int. J. Hyd. Energy*, **36** (2011) 1794-1802.

4. Xuguang Li, Branko N. Popov, Takeo Kawahara, Hiroyuki Yanagi, "Non-precious metal catalysts synthesized from precursors of carbon, nitrogen, and transition metal for oxygen reduction in alkaline fuel cells," *J. Power Sources*, 196 (2011), 1717-1722.

5. Gang Liu, Xuguang Li, Jong-Won Lee and Branko Popov, "A Review of the Development of Nitrogen Modified Carbon-based catalyst for Oxygen Reduction at USC," *Catalysis Science & Technology,* 1, (2011) 207-217.

6. Xuguang Li, Gang Liu, Branko N. Popov, "Activity and stability of non-precious metal catalysts for oxygen reduction in acid and alkaline electrolytes," *J. Power Sources*, **195** (2010) 6373-6378.

7. Li, Xuguang, Park, Sehkyu, Popov, Branko N, "Highly stable Pt and PtPd hybrid catalysts supported on a nitrogen-modified carbon composite for fuel cell application," *J. Power Sources*, **195** (2010) 445-452.

8. Liu, Gang, Li, Xuguang, Ganesan, Prabhu, Popov, Branko N, "Studies of oxygen reduction reaction active sites and stability of nitrogen-modified carbon composite catalysts for PEM fuel cells," *Electrochim. Acta*, **55** (2010) 2853-2858.

9. Subramanian, Nalini P, Li, Xuguang, Nallathambi, Vijayadurda, Kumaraguru, Swaminatha P, Colon-Mercado, Hector, Wu, Gang, Lee, Jong-Won, Popov, Branko N, "Nitrogen-modified carbon-based catalysts for oxygen reduction reaction in polymer electrolyte membrane fuel cells," *J. Power Sources*, **188** (2009) 38-44.

10. Liu, Gang, Li, Xuguang, Ganesan, Prabhu, Popov, Branko N, Development of non-precious metal oxygen-reduction catalysts for PEM fuel cells based on N-doped ordered porous carbon," *Appl. Catal. B: Environmental,* **93** (2009) 156-165.

11. Nallathambi, Vijayadurga; Lee, Jong-Won; Kumaraguru, Swaminatha P, Wu, Gang; Popov, Branko N, "Development of high performance carbon composite catalyst for oxygen reduction reaction in PEM Proton Exchange Membrane fuel cells," *J. Power Sources*, **183** (2008) 34-42.

12. X. Li, H.R. Colon-Mercado, G. Wu, J.-W. Lee, B.N. Popov, "Development of Method for Synthesis of Pt-Co Cathode Catalysts for PEM Fuel Cells," *Electrochem. Solid-State Lett.*, **10** (2007) B201-B205.

13. N.P. Subramanian, S.P. Kumaraguru, H.R. Colon-Mercado, H. Kim, B.N. Popov, T. Black and D.A. Chen, "Studies on Co-Based Catalysts Supported on Modified Carbon Substrates for PEMFC Cathodes," *J. Power Sources*, **157** (2006) 56-63.

14. R.A. Sidik, A.B. Anderson, N.P. Subramanian, S.P. Kumaraguru and B.N. Popov, "O_2 Reduction on Graphite and Nitrogen-Doped Graphite: Experiment and Theory," *J. Phys. Chem. B*, **110** (2006) 1787-1793.

15. Inaba, Minoru, *ECS Trans*., **25** (2009) 573-581.

16. Ákos Kriston, Tianyuan Xie and Branko N. Popov, Impact of Ultra-low Platinum loading on Mass Activity and Mass Transport in H_2-Oxygen and H_2-Air PEM Fuel Cells, *Electrochim. Acta*, **121** (2014) 116-127.

17. Ákos Kriston, Tianyuan Xie, David Gamliel, Prabhu Ganesan, Branko N. Popov, "Effect of Ultra-Low Pt Loading on Mass Activity of PEM Fuel Cells," *J. Power Sources*, **243** (2013) 958-963.

18. Akos Kriston, Tianyuan Xie, Prabhu Ganesan, Branko N. Popov, "Effect of Pt Loading on Mass and Specific Activity in PEM Fuel Cells," *J. Electrochem. Soc*., **160** (2013) F406-F412.

V.A.11 Non-Precious Metal Fuel Cell Cathodes: Catalyst Development and Electrode Structure Design

Piotr Zelenay (Primary Contact), H. Chung, U. Martinez, G. Purdy, G. Wu

Materials Physics and Applications Division
Los Alamos National Laboratory (LANL)
Los Alamos, NM 87545
Phone: (505) 667-0197
Email: zelenay@lanl.gov

DOE Manager

Nancy Garland
Phone: (202) 586-5673
Email: Nancy.Garland@ee.doe.gov

Subcontractors

- J. Ziegelbauer, General Motors, Honeoye Falls, NY
- M. Odgaard and D. Schlueter, IRD Fuel Cells, Albuquerque, NM
- S. Litster and S.K. Babu, Carnegie Mellon University, Pittsburgh, PA
- M. Neidig and J. Kehl, J. Kneebone, University of Rochester, Rochester, NY
- Z. Chen, D. Higgins, and G. Jiang, M.-H. Seo, University of Waterloo, Waterloo, Canada
- K.L. More and D. Cullen, Oak Ridge National Laboratory, Oak Ridge, TN

Project Start Date: April 1, 2013
Project End Date: March 31, 2016

Overall Objectives

Advance non-precious-grade metal (non-PGM) cathode technology through the development and implementation of novel materials and concepts for oxygen reduction catalysts and electrode layers with:

- Oxygen reduction reaction (ORR) activity viable for practical fuel cell systems
- Much improved durability
- Sufficient ionic/electronic conductivity within the catalyst layer
- Adequate oxygen mass transport
- Effective removal of the product water

Fiscal Year (FY) 2014 Objectives

- Optimize the most active Fe-N-C catalysts by the heat-treatment approach for maximum hydrogen-air fuel cell performance
- Synthesize metal-free non-PGM catalysts
- Use surface probe approaches to identify the structure of active sites
- Optimize non-PGM cathodes using experimental and modeling tools
- Scale up membrane electrode assembly (MEA) to 50 cm^2

Technical Barriers

This project addresses the following technical barriers from the Fuel Cells section (3.4.5) of the Fuel Cell Technologies Office Multi-Year Research, Development, and Demonstration Plan [1]:

(A) Durability (catalysts, electrode layers)

(B) Cost (catalyst, MEAs)

(C) Performance (catalysts, electrodes, MEAs)

Technical Targets

Non-PGM fuel cell catalyst research in this project focuses on the DOE technical targets outlined in Table 3.4.13 in section 3.4.4 (Technical Challenges) of the Fuel Cell Technologies Office Multi-Year Research, Development, and Demonstration Plan [1]. The ultimate technical targets of the project are:

- Volumetric catalyst activity in an MEA at 0.80 V (iR-free[1]), 80°C: ≥ 300 A cm^{-3}
- Four-electron selectivity (rotating ring disc electrode): ≥ 99% (H_2O_2 ≤ 1%)
- MEA maximum power density at 80°C: ≥ 1.0 W cm^{-2}
- Performance loss at 0.80 A cm^{-2} after 30,000 cycles in N_2: ≤ 30 mV

[1] iR – internal resistance

FY 2014 Accomplishments

- A high-surface-area, graphene-rich polyaniline-iron-carbon catalyst was synthesized through a novel three-step heat-treatment strategy. It was tested in a fuel cell, reaching a current density of 0.19 A cm^{-2} at 0.80 V (iR-corrected) and a volumetric current density of 84 A cm^{-3} at 0.80 V (iR-corrected).
- A new "nanofoam" catalyst was developed using multiple nitrogen precursors, providing a microporous surface area of 1,585 $m^2 g^{-1}$ and significantly enhanced mass transport. In fuel cell testing, a power density of 0.87 W cm^{-2} was achieved at 1.0 bar O_2.

- A metal-free catalyst was developed, showing a $E_{½}$ of 0.32 V vs. the reference hydrogen electrode.
- Viability of the surface probe approach in combination with Mössbauer and nuclear resonance vibrational spectroscopy (NRVS) was demonstrated to identify the possible structure of active sites in Fe-based non-PGM catalysts.
- Computational simulation of transport process in a nano-X-ray tomography (nano-XRT) imaged non-PGM electrode was completed.

INTRODUCTION

Cost studies estimate that conventional Pt-based catalysts comprise almost half of the entire proton exchange fuel cell (PEFC) stack cost and as much as 20% of the overall system cost [2]. Since Pt is a precious metal resource, it will not benefit from economies of scale and is subject to volatile price fluctuations and monopolized global distributions. Reducing or ideally replacing expensive Pt catalysts in PEFC systems is highly desirable and has been a major focus of catalyst research and development efforts. Owing to the inherently slow ORR, the cathode requires much higher Pt content than the anode, at which the relatively fast anodic hydrogen oxidation reaction is taking place. Developing non-PGM catalysts for use at the cathode would provide the most significant economic advantage. However, hindering the successful elimination of Pt cathode catalysts in PEFC systems is the lack of non-PGM catalysts that can provide sufficiently high ORR activity and durability under fuel cell operative conditions.

APPROACH

In this multi-faceted research project we intend to accomplish major advancements in non-PGM cathode technology through the development and implementation of novel materials and concepts. Our catalyst development effort concentrates on novel synthesis methods, including heat-treated catalysts obtained using multiple nitrogen precursors, alternative supports for heat-treated catalysts, non-pyrolyzed phthalocyanine-derived catalysts and metal-free catalysts based on nitrogen-doped carbon nanostructures. Comprehensive testing of materials, including initial performance screening by in situ electrochemical techniques and ex situ characterization to assess catalyst activity and durability, identify catalytic sites and validate fuel cell performance of the most-promising materials, represents a substantial fraction of the efforts.

Since the use of non-PGM catalysts will almost certainly result in cathodes with greatly increased thickness compared to Pt-based cathodes, significant effort is required to address the resulting electrode design challenges. The key issues include oxygen mass transport, proton conductivity and the prevention of catalyst layer flooding. The research focuses initially on the validation of the General Motors electrode model for non-PGM electrodes and parameter estimation using in situ microstructured electrode scaffold diagnostics. Electrode optimization is based on insight obtained from the modeling, nano-XRT imaging, and advanced microscopy analysis. In parallel to the catalyst and electrode development components of this project, MEA fabrication, optimization and scale up will be performed to obtain a 50-cm^2 (or larger, if needed) MEA with the best-performing materials for independent testing and evaluation at a DOE-approved facility.

RESULTS

(a) Demonstrated $i_{0.8V}$ > 190 mA cm^{-2} and a volumetric activity of 84 A cm^{-3} at 0.80 V (iR-free) for non-PGM catalyst in single-cell MEA. High-surface-area polyaniline-iron-carbon (PANI-Fe-C) catalysts were prepared, optimized and tested for fuel cell performance. Using 30 wt% Fe in the catalyst and employing a three-step heating synthesis protocol, PANI-Fe-C allowed for an ORR current density of 190 mA cm^{-2} at a voltage of 0.80 V (iR-free) in fuel cell testing (Figure 1). This significantly surpasses the September 2014 ORR catalyst development milestone stating a specific activity of 150 mA cm^{-2}.

A new catalyst fabrication approach combining multiple nitrogen precursors was also applied to prepare a highly ORR-active non-PGM catalyst with a favorable micro- and meso-structure to facilitate mass transport through the catalyst layer. Improved mass transport is demonstrated by

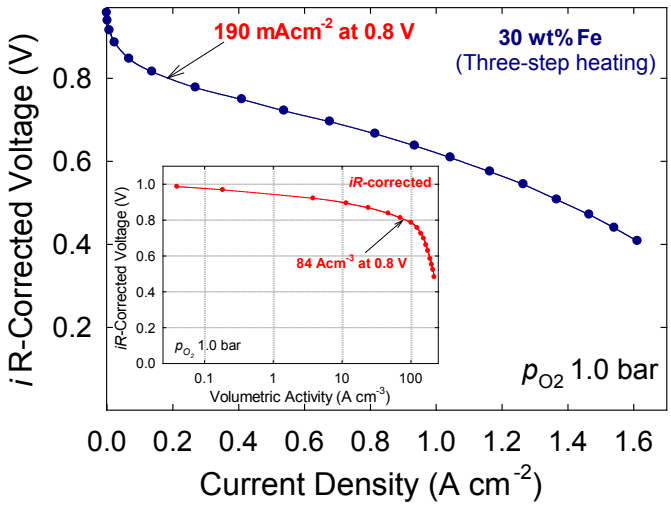

FIGURE 1. Fuel cell performance of a PANI-Fe-C non-PGM catalyst demonstrating ORR current density close to 190 mA cm^{-2} and volumetric current density of 84 A cm^3 at 0.80 V.

a current density >3.0 A cm^{-2} at a cell voltage of 0.20 V (iR-free) and O_2 partial pressure (p_{O2}) of 1.0 bar, with minimal performance enhancement realized with a further increase in the partial pressure to 2.0 bar (Figure 2). A current density of 160 mA cm^{-2} was achieved through fuel cell testing at 0.80 V (iR-free), reaching the September 2014 ORR catalyst development milestone, with another catalyst developed in this project. At 0.40 V and 1.0 bar O_2 partial pressure, a very high current density and a power density of 0.87 W cm^{-2} was obtained, due to the high catalyst activity and facile mass transport.

(b) Image three-dimensional structure of a state-of-the-art LANL electrode by nano-XRT and compute effective transport properties. Nano-XRT was used to image non-PGM electrodes (Figure 3a-c). The nano-XRT imaging provides the three-dimensional micro-scale and macro-scale structure of the electrode. Through image processing, computational reconstruction and numerical simulations, the nano-XRT data was used to extract the key morphological transport properties of the electrode (Figure 3d). The obtained information will be essential to

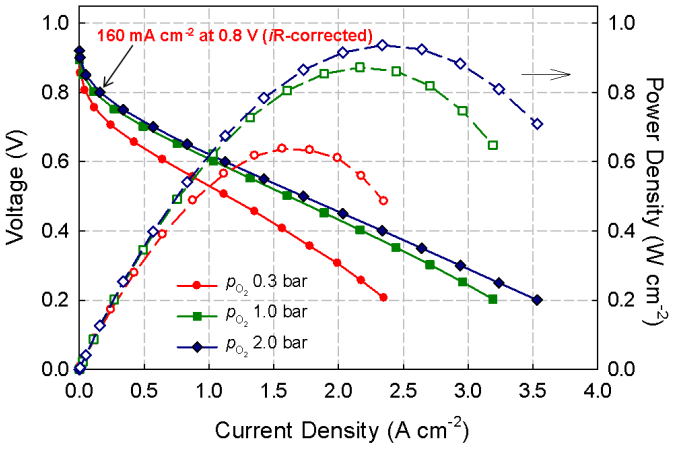

FIGURE 2. Fuel cell performance of the CM-PANI-Fe-C catalyst demonstrating (a) power density of 0.87 W cm^{-2} at 0.40 V and (b) ORR current density of 160 mA cm^{-2} at 0.80 V (iR-corrected). Anode: 0.5 mg cm^{-2} Pt (E-TEK) 1.0 bar (partial pressure), H_2 200 sccm; cathode: ~4.0 mg cm^2, 1.0 bar (partial pressure), O_2 200 sccm; membrane: Nafion® 211; cell: 80°C; 100% relative humidity.

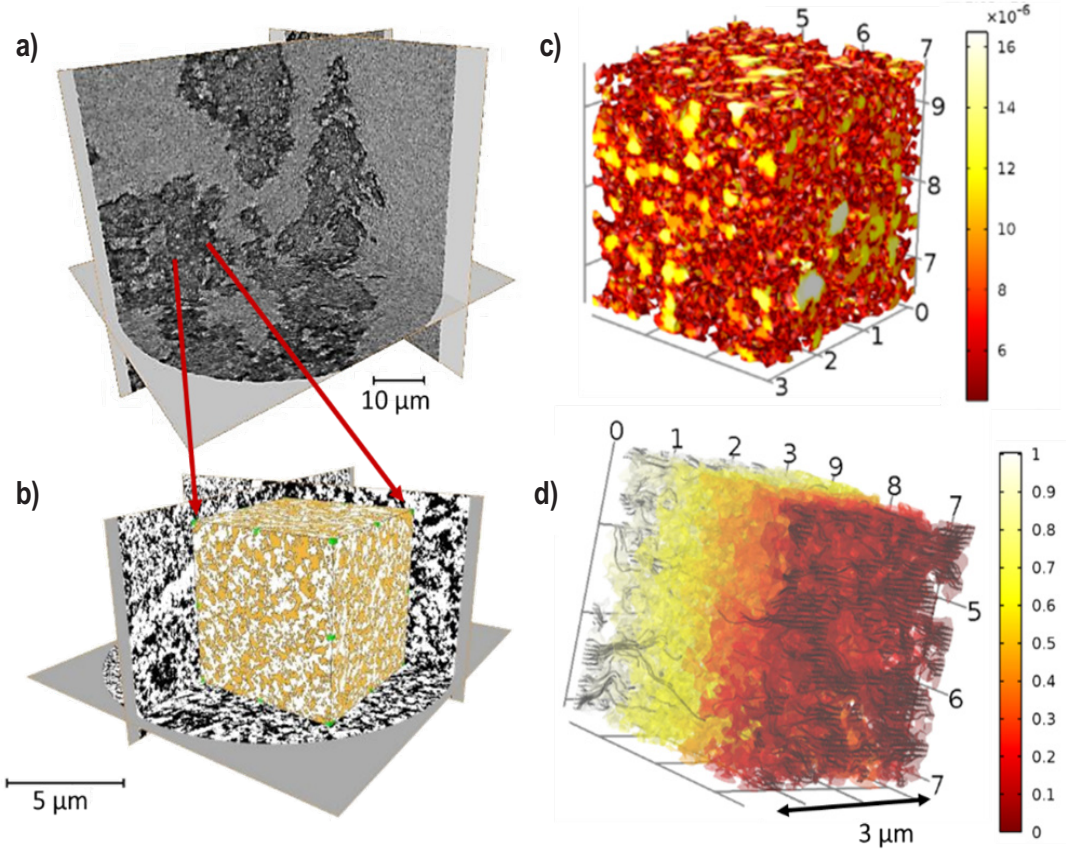

FIGURE 3. Ortho-slices from a large-field-of-view nano-XRT scan of the non-PGM electrode (a) and (b) the pore|solid phase segmented (pores white) data from a high resolution (50 nm) scan of the solid dense (dark) region in (a). (c) Three dimensionally reconstructed pore volume from the high resolution scan colored by the local oxygen diffusion coefficient calculated from local pore sizes. (d) Computational simulation of gas diffusion in the non-PGM electrode using pore geometry from nano-XRT imaging. Color is oxygen concentration.

future non-PGM electrode structure design and optimization. The March 2014 electrode design, integration and optimization milestone has been completed.

(c) Validate surface-probe approach for non-PGM catalysts using Mössbauer spectroscopy. Detection of surface iron based on perturbation by a gaseous probe provides a key advantage in that it allows for characterization of iron sites on the catalyst surface, accessible to gas phase reactants (i.e., oxygen). Mössbauer spectroscopy was used in combination with $NO_{(g)}$ probing to demonstrate the presence of Fe-species in PANI-Fe-C catalyst. Validation of the surface-probe approach with Mössbauer spectroscopy and previously with NRVS accomplishes the March 2014 characterization and active-site determination milestone. During the beam time at Advanced Photon Source (June, 2014), NRVS was used again to confirm the surface features of the same catalyst samples probed by Mössbauer spectroscopy. Reproducible data were obtained and relevant analysis is currently in progress.

(d) Electron microscopy analysis of state-of-the-art LANL catalysts and electrodes. Advanced scanning electron microscopy (SEM), transmission electron microscopy (TEM) and scanning transmission electron microscopy (STEM) were performed to study the new PANI-Fe-C materials in order to provide additional insight into the structure of high-performance catalysts with high surface area. As shown in Figure 4, the predominant morphology consisted of an intimate mixture of agglomerated Ketjenblack (KJ) particles and rumpled, multi-layered graphene sheets (Figure 4a). Fe particles, most likely FeS, were also occasionally identified (orange arrow, Figure 4a). An SEM image (Figure 4b) of the same region, shown in the TEM image in Figure 4a, also indicates that the rumpled, sheet-like morphology of the multi-layered graphene envelopes the KJ particles. An ADF-STEM image of a multi-layered graphene sheet and associated electron energy loss spectroscopy (EELS) analysis (Figure 4c) indicates that single Fe atoms are dispersed across the surface of the graphene. These Fe atoms were highly mobile under the electron beam, indicating that Fe is not incorporated within the carbon lattice. Additionally, EELS identified nitrogen in thicker areas of the layered graphene sheets.

The non-PGM catalysts, prepared by mixing nitrogen precursors, were integrated into electrodes containing Nafion® ionomer and studied using microscopy. A relatively thick (0.1-0.5 μm) ionomer film was found to surround CM-PANI-Fe-KJ catalyst agglomerates (Figure 4d), but very little ionomer penetrated inside the agglomerates. Elemental mapping (Figure 4e) shows fluorine (green, associated with ionomer) and sulfur (blue, associated with all carbon phases and ionomer). Areas where the imaged sulfur does not overlap with the fluorine can be attributed to ionomer-free carbon. These results suggest that the optimal dispersion of ionomer within carbon-based catalysts in the cathode is a key strategy to increasing catalyst utilization, thereby significantly improving catalyst performance.

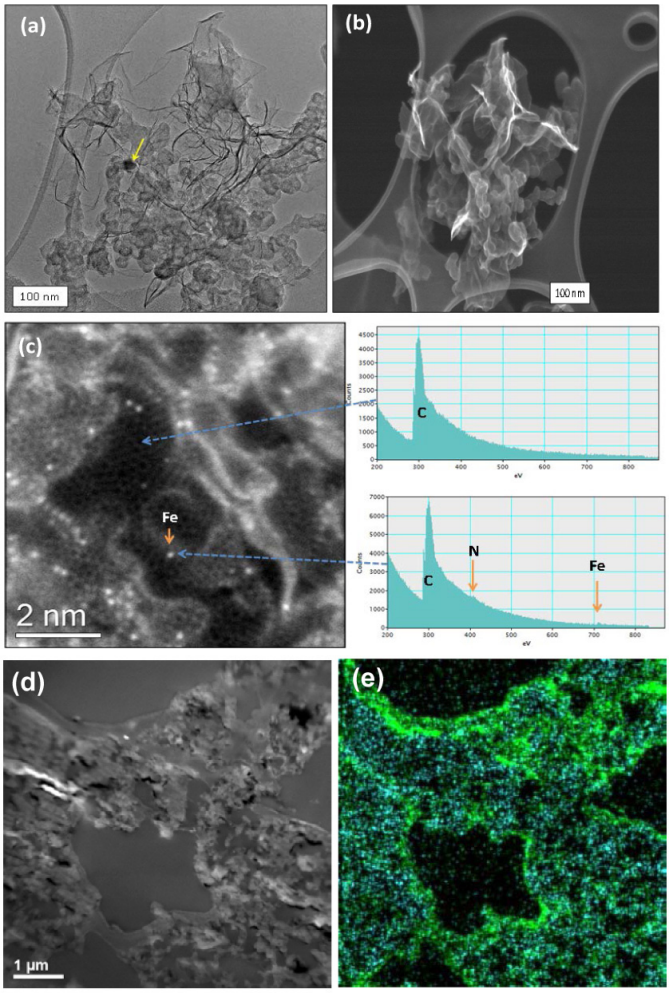

FIGURE 4. Microscopy studies for newly developed non-PGM catalysts and cathodes. (a) TEM image for PANI-Fe-C (30 wt% Fe) catalyst and (b) SEM image of the same agglomerated area showing KJ particles mixed with multi-layered graphene sheets. The yellow arrow indicates a large FeS particle. (c) Annular dark-field imaging-STEM of graphene sheet and associated electron energy loss spectra showing presence of single Fe atoms on surface of graphene. (d, e) Microstructure and chemistry of PANICM-Fe-KB + 35% Nafion® cathode in MEA: fluorine, associated with ionomer, is shown as green; and sulfur, predominantly associated with all carbon phases in catalysts, shown in blue.

CONCLUSIONS

- A high-surface-area, graphene-rich, polyaniline-derived catalyst was synthesized and tested in a fuel cell reaching a current density of 0.19 A cm^{-2} at 0.8 V (iR-free), exceeding the September 2014 current density milestone (150 mA cm^{-2}).
- A volumetric activity of 84 A cm^{-3} was achieved at 0.8 V (iR-free), an over 30% enhancement in the

volumetric current density compared to the 2011 baseline (60 A cm^{-3}), approaching the June 2014 catalyst activity milestone (100 A cm^{-3}).

- Computational simulation of transport processes in the nano-XRT imaged non-PGM electrode was completed, achieving the December 2013 electrode imaging milestone.
- Advanced electron microscopy provided insightful information about the catalyst structure at the atomic level, as well as about the ionomer dispersion in non-PGM cathodes.

FUTURE DIRECTIONS

- Synthesis of non-PGM catalysts supported on highly-graphitic carbon(s) as a way of enhancing active-site density and improving performance durability.
- Use of developed surface-probe approach to identify the non-PGM ORR active-site structures.
- Full implementation of advanced catalyst characterization methods (NRVS, magnetic circular dichroism, Mössbauer spectroscopy, microstructured electrode scaffold, low-voltage aberration-corrected STEM, nano-XCT, X-ray absorption, thermogravimetric analysis, porosimetry, etc.) in non-PGM catalysis studies.
- Initiation of the predictive model for non-PGM catalyst layers (ORR activity, conductivity, and O_2 transport); validation of the preliminary model.
- Fabrication of MEAs with optimized microstructure and morphology.
- Demonstration of Generation-1 spray-coated MEA with non-PGM cathode.

SPECIAL RECOGNITIONS & AWARDS/ PATENTS ISSUED

1. Piotr Zelenay has been named a Fellow of The Electrochemical Society, 2014.

FY 2014 PUBLICATIONS/PRESENTATIONS

(a) Peer-Reviewed Publications

1. W. Gao, G. Wu, M. Janicke, D. Cullen, R. Mukundan, J. Baldwin, E. Brosha, C. Galande, P. Ajayan, K. More, A. Dattelbaum, P. Zelenay, "Ozonated Graphene Oxide Film as a Proton Exchange Membrane", *Angew. Chemie Int. Ed.*, **53** (14), 3588-3593 (2014).

2. S. Litster, W. Epting, E. Wargo, S. Kalidindi, E. Kumbur, "Morphological Analyses of Polymer Electrolyte Fuel Cell Electrodes with Nano-Scale Computed Tomography Imaging", *Fuel Cells*, **13** (5), 935-945 (2013).

3. M. Seo, D. Higgins, G. Jiang, S. Choi, B. Han, Z. Chen, "Theoretical and experimental study of highly durable iron phthalocyanine derived non-precious catalyst for oxygen reduction reaction", *J. Mater. Chem. A.*, submitted (2014).

4. P. Zamani, D. Higgins, F. Hassan, J. Wu, S. Abureden, Z. Chen, "Electrospun Iron–Polyaniline–Polyacrylonitrile Derived Nanofibers as Non-Precious Oxygen Reduction Reaction Catalysts for PEM Fuel Cells", *Electrochim. Acta*, accepted, (2014).

5. D. Higgins, M.A. Hoque, F, Hassan, J.Y. Choi, B. Kim, Z. Chen, "Oxygen Reduction on Graphene-Carbon Nanotube Composites Doped Sequentially with Nitrogen and Sulfur" *ACS Catalysis*, accepted 2014.

6. Q. Li, G. Wu, D.A. Cullen, K.L. More, N.H. Mack, H.T. Chung, P. Zelenay "Phosphate-Tolerant Oxygen Reduction Catalysts" *ACS Catalysis*, accepted 2014.

(B) Conference Presentations

1. G. Wu, P. Zelenay, "Mn-Based Non-Precious Catalyst for the Polymer Electrolyte Fuel Cell Cathode", *225th Electrochemical Society Meeting*, Orlando, Florida, May 11-16 (2014).

2. U. Martinez, G. Purdy, M. Misra, N. Mack, D. Cullen, H. Chung, K. More, A. Dattelbaum, A. Mohite, P. Zelenay, G. Gupta, "Graphene-Oxide-Based Electrocatalysts for Oxygen Reduction Reaction", *225th Electrochemical Society Meeting*, Orlando, Florida, May 11-16 (2014).

3. H. Chung, G. Wu, U. Martinez, P. Zelenay, "Carbon-based catalysts for oxygen reduction in polymer electrolyte fuel cells", *247th American Chemical Society Meeting and Exposition*, Dallas, Texas, March 16-20 (2014) Invited lecture.

4. D. Kim, N. Zussblatt, P. Minoofar, R. Ganguli, P. Zelenay, B. Chmelka, "Effects of transition metals on oxygen reduction and oxygen evolution electrocatalytic activities of N-doped mesoporous carbon catalysts", *247th American Chemical Society Meeting and Exposition*, Dallas, Texas, March 16-20 (2014).

REFERENCES

1. *Multi-Year Research, Development and Demonstration Plan: Section 3.4 Fuel Cells*, Fuel Cell Technologies Program, 2011. http://www1.eere.energy.gov/hydrogenandfuelcells/mypp/pdfs/fuel_cells.pdf

2. James et al., DTI, Inc., 2010 DOE Hydrogen Program Review, Washington, DC, June 9, 2010

V.A.12 Non-PGM Cathode Catalysts using ZIF-Based Precursors with Nanonetwork Architecture

Di-Jia Liu (Primary Contact), Dan Zhao, Jianglan Shui, Lauren Grabstanowicz, Sean Commet

Argonne National Laboratory
9700 S. Cass Ave
Argonne, Il 60439
Phone: (630) 252-3533
Email: djliu@anl.gov

DOE Manager

Nancy Garland
Phone: (202) 586-5673
Email: Nancy.Garland@ee.doe.gov

Project Start Date: January 2, 2013
Project End Date: January 31, 2014

Overall Objectives

- To design, synthesize, and evaluate highly efficient zeolitic imidazolate framework (ZIF) based non-platinum group metal (non-PGM) cathode catalysts for the proton exchange membrane fuel cell (PEMFC) for transportation applications
- To maximize electron, heat and mass transports by incorporating the catalyst into the porous nano-network structure
- To support non-PGM catalyst development through advanced structural characterizations

Fiscal Year (FY) 2014 Objectives

- Develop and improve a one-pot method for ZIF-based non-PGM catalyst synthesis and demonstrate at least one oxygen reduction reaction (ORR) catalyst with onset potential >0.9 V.
- Characterize the surface property and chemical composition of ZIF-derived non-PGM catalysts and establish property-function relationships.
- Complete initial design and synthesis of nano-network catalysts and demonstrate significantly improved volumetric and areal current densities at the membrane electrode assembly (MEA)/single cell level.

Technical Barriers

This project addresses the following technical barriers from the Fuel Cells section of the Fuel Cell Technologies Office Multi-Year Research, Development, and Demonstration Plan:

(A) Durability

(B) Cost

(C) Performance

Technical Targets

This project aims at developing non-PGM high-efficiency materials, as the low-cost cathode catalyst replacements for platinum. Technical targets for this project are presented in Table 1.

TABLE 1. Current Status towards Meeting Technical Targets for non-PGM Electrocatalysts for Transportation Applications

Characteristic	Unit	2017/2020 Targets	ANL 2014 Status
Non-Pt catalyst activity per volume of supported catalyst	A/cm^3 @ 800 $mV_{iR\text{-}free}$ (iR – internal resistance)	300/300[a]	90.2[b]

[a] T = 80°C, fully humidified H_2/O_2, P = 150 KPa

[b] Measured in single fuel cell: $P_{O2} = P_{H2}$ = 2 bar; fully humidified at 80ºC, cathode loading = 2.0 mg/cm^2, anode loading = 0.3 mg_{Pt}/cm^2, Nafion® = 117.

FY 2014 Accomplishments

- A one-pot synthesis method for non-PGM catalyst was developed and four ZIF-derived catalysts with different organic ligands were produced. Three of the catalysts showed onset potential >0.9 V with half-wave potential as high as 0.81 V achieved.
- A process improvement of a ZIF-based catalyst yielded a high fuel cell areal current density of 178 mA/cm^2 @ 0.8 V under one bar oxygen pressure.
- An initial optimization of ZIF/nano-network catalyst was completed. The MEA with this catalyst at the cathode reached a volumetric current density of 90.2 A/cm^3 at 0.8 V and areal current density of 3 A/cm^2 at 0.2 V ($P_{O2} = P_{H2}$ = 2 bar).

INTRODUCTION

Finding inexpensive, earth-abundant materials to substitute the PGMs has been the ultimate goal for PEMFC catalyst research. Since the electrode/catalyst materials contribute to nearly half of a fuel cell stack cost, there is an urgent need to reduce or replace PGM usage in order to meet the DOE 2017/2020 cost target of $30/$kW_e$ for automotive

applications. Among all the non-PGM candidates explored so far, transition metal-doped nitrogen-carbon (TM-N-C) composites appear to be the most promising ones. Generally, these catalysts are prepared by applying TM-N_x molecular complexes over amorphous carbon support, followed by thermal activation. Since non-PGM catalysts are known to have lower turn-over frequency *per catalytic site* than platinum, their active site densities have to be substantially higher in order to deliver a comparable performance. Using carbon support dilutes the active site density and limits the potential of reaching higher performance. New approaches to circumvent such dilution include the uses of catalyst precursors such as metal-organic frameworks (MOFs) [1-3] and porous organic polymers (POPs) [4]. These precursors are intrinsically porous or porous after thermal activation. Since the potential active sites, TM-N_4, are adjacent to each other and uniformly distributed in MOFs and POPs, these rationally designed precursors have the promises to produce the highest catalytic site density therefore the most active catalysts.

At Argonne National Laboratory, we pioneered the approaches of using MOFs and POPs as precursors for preparing highly efficient non-PGM ORR catalysts [1,3,4]. MOF/POP syntheses were perceived as tedious and costly, due to multiple reaction steps and the use of chemicals for crystallization and separation. To address such concern, we recently developed a novel "one-pot" solid-state synthesis method for preparing ZIF-derived (a subclass of MOF) catalysts [5]. The new approach not only greatly simplifies the preparation of ZIF-based non-PGM electrocatalysts, rending it suitable for large-scale production at very low cost, but also paves the way of exploring a variety of ZIFs in searching for better catalysts.

APPROACH

The project includes two parallel approaches. The first approach focuses on optimizing the newly developed "one-pot" synthesis method for ZIF-derived non-PGM catalysts. This solid-state reaction uses imidazole as the ligand and zinc oxide as the secondary building unit, both are inexpensive commodity chemicals at the price range of $3/lb to $5/lb. The method is robust and applicable to a variety of imidazoles, therefore feasible for exploring ZIFs with different organic group substitution. Study on such substitutions could lead to better understanding on the impact of ligand structure to the final catalyst activity. The ZIF-precursors are converted to non-PGM catalyst through thermolysis. The heat-activation is crucial to the catalyst performance and needs also to be optimized.

The second approach is to improve mass and charge transfers of ZIF-derived catalysts through new electrode architecture. To compensate lower turn-over frequency of non-PGM catalysts by simply increasing the usage will cause higher mass and charge transfer resistances from the thicker electrode layer. To circumvent such a barrier, we developed a novel network electrode structure in which the catalytic sites are embedded in the micropores of the nanofibers. The charge transfer is accomplished by carbonaceous network whereas the mass transport is facilitated by the voids between the fibers. Such network nearly eliminates the presence of mesopores without affecting microporous surface area and the active sites density.

RESULTS

Four ZIF-based precursors containing ligands of 2-methylimidazole (HmIm), imidazole (HIm), 2-ethylimidazole (HeIm), as well as 4-azabenzimidazole (H4abIm) were prepared through solid-state reaction with zinc oxide in the presence of 5 wt% phenanthroline iron(II) perchlorate (TPI). The corresponding iron-doped ZIFs are named as $Zn(mIm)_2TPI$, $Zn(Im)_2TPI$, $Zn(eIm)_2TPI$ and $Zn(abIm)_2TPI$, respectively. The molecular structures of the imidazole ligands, the organometallic iron complex and the lattice structures of the four ZIF precursors are given in Figure 1. Upon thermal activation at elevated temperature, the organic ligands are converted to carbonaceous composite with much improved electro-conductivity and the catalytic activity. We also carried out extensive structural characterizations for these precursors before and after the activation using techniques such as powder X-ray diffraction, nitrogen sorption isotherms, X-ray photoelectron spectroscopy, scanning electron microscopy, transmission electron microscopy (TEM), and surface Raman spectroscopy. Figure 1 also shows the TEM images of the four catalysts after thermal conversion. We found, for example, nearly all the ZIFs, other than $Zn(eIm)_2TPI$, have no initial surface areas. The corresponding catalysts produced after the thermolysis, however, showed very high specific surface areas in the range of 800 to 1,200 m^2/g. Furthermore, they all possessed high fractions of micropores within the total pore volume. Both are important factors in controlling the overall catalytic activity.

The catalytic activity was tested at both rotating disk electrode (RDE) and MEA levels. Cathodic linear sweep voltammograms of all four catalysts were collected in an oxygen saturated $HClO_4$ (0.1 M) solution. All four samples exhibited prominent ORR activities with excellent onset (E_0) and half-wave potentials ($E_{½}$) potentials. We also found that the catalytic activity was sensitive to the processing condition. For example, by optimizing the processing parameters, we were able to improve onset potential from 0.91 to 0.96 V and half-wave potential from 0.75 to 0.81 V, respectively. Excellent catalytic activity was also demonstrated by the MEA/single cell measurement. Figure 2 shows (a) current-voltage polarization and (b) Tafel plot of iR-free potential as the function of areal current density

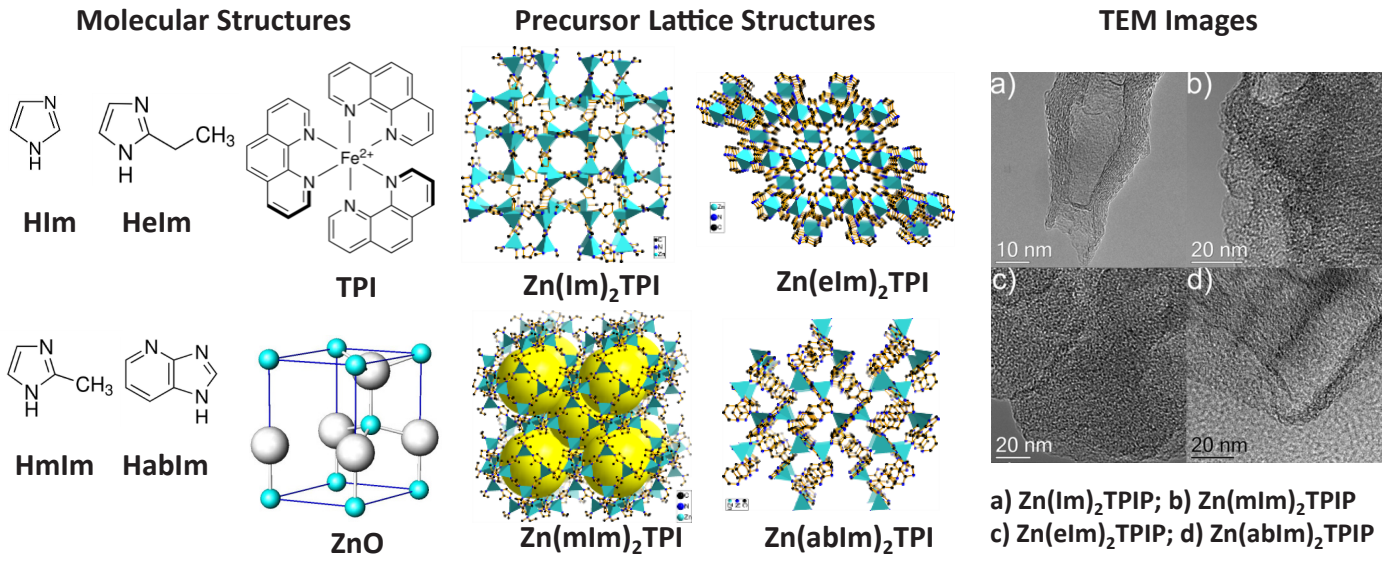

FIGURE 1. Left – molecular structure of four imidazole ligands, ZnO and iron organometallic complex; Center – lattice structures of four corresponding ZIF precursor containing iron complex (not shown); Right – TEM images of thermally activated ZIF catalysts.

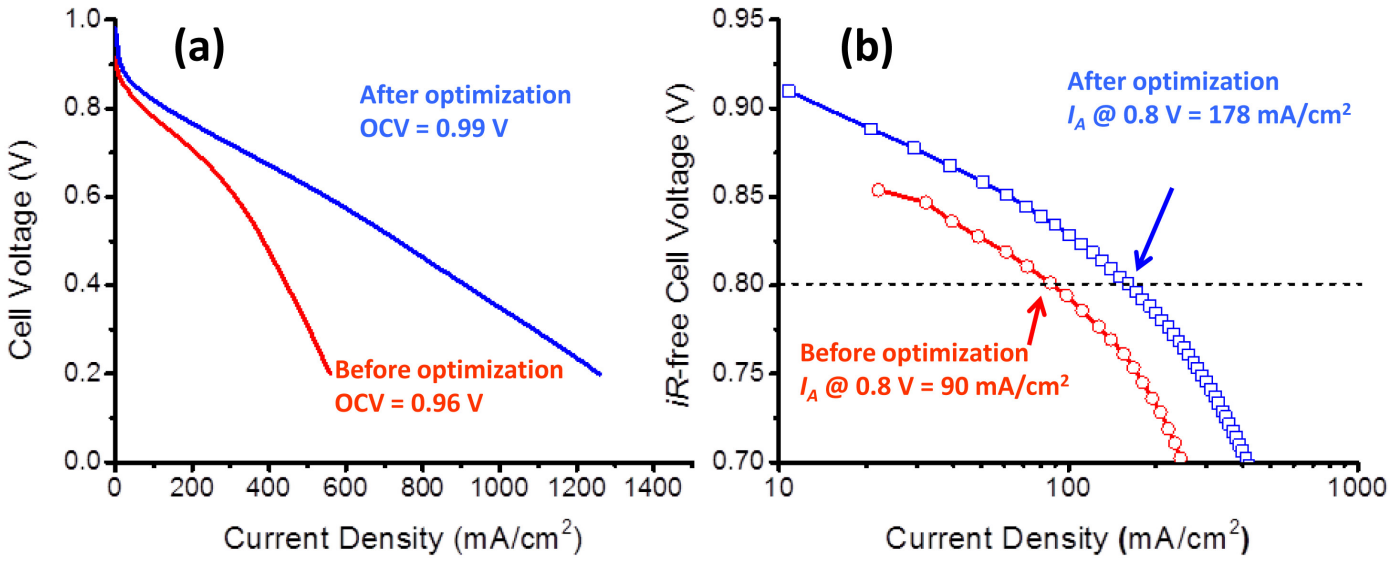

FIGURE 2. (a) Current-voltage polarizations and (b) Tafel plots of iR-free cell potential versus areal current density of MEAs/single fuel cells containing a ZIF-based non-PGM catalyst before and after post-treatment optimization. Condition: $P_{O2} = P_{H2}$ = 1 bar (back pressure = 7.3 psig) fully humidified; T = 80°C; N-211 membrane; 5 cm^2 MEA; cathode catalyst = 4 mg/cm^2, anode catalyst = 0.3 mg_{Pt}/cm^2.

of a single fuel cell containing a $Zn(mIm)_2TPI$ catalyst before and after the post-treatment optimization. Significant improvement in fuel cell performance was observed, with open-circuit potential increased from 0.96 V to 0.99 V and current density (@ 0.8 V) increased from 90 mA/cm^2 to 178 mA/cm^2, all under one bar oxygen pressure. These values are among the highest reported in the literature.

We also successfully improved formulation and parameters in processing the nanofibrous network electrode. The nano-network was prepared from a polymeric mixture containing catalyst precursor and fiber-forming reagents. Optimizing these ingredients is essential for the overall catalytic activity while maintaining good electronic conductivity and oxygen/water mass transports. We formulated multiple mixtures and obtained several catalysts

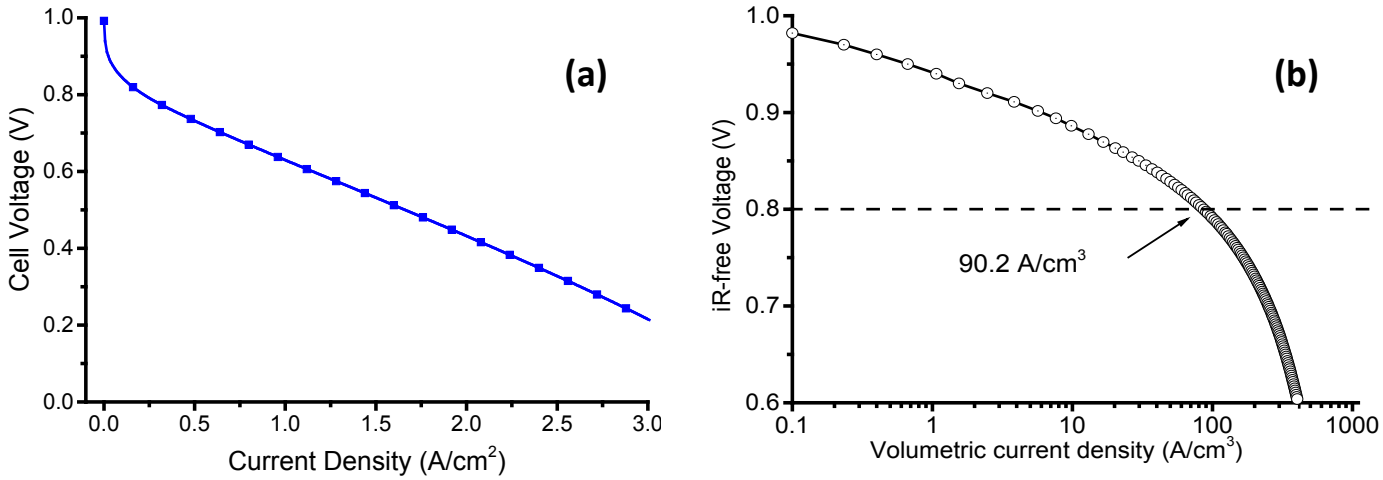

FIGURE 3. (a) Current-voltage polarization and (b) Tafel plot of iR-free cell potential versus volumetric current density of a MEA prepared with non-PGM nano-network cathode. Condition: P_{O2} = P_{H2} = 2 bar; fully humidified at 80ºC, cathode loading = 3.0 mg/cm^2, anode loading = 0.3 mg_{Pt}/cm^2, Nafion® = 211, active area = 5 cm^2; (b) iR-corrected volumetric current density under similar condition as (a) except Nafion® = 117, cathode catalyst loading = 2 mg/cm^2.

with excellent activity. These nanostructured catalysts were also integrated into the cathode layer of MEAs and tested by single fuel cells. Figure 3a shows an optimized current-voltage polarization obtained from a fuel cell test. Very high current density up to 3 A/cm^2 at 0.2 V was achieved where no flooding was observed. Figure 3b shows a Tafel plot of iR-corrected cell potential as the function of the volumetric current density in a separate MEA test under 2 bar oxygen pressure. A value of 90.2 A/cm^3 was obtained at 0.8 V.

CONCLUSIONS AND FUTURE DIRECTIONS

This one-year project is concluded with the following major accomplishments:

- A low-cost, "one-pot" synthesis method produced multiple ZIF-based catalysts with E_0 > 0.9 V and $E_{½}$ as high as 0.81 V, measured by RDE in O_2-saturated acidic electrolyte.
- A comprehensive characterization of the ZIF-derived catalysts demonstrated the good correlations between the precursor/catalyst surface structures and the performance.
- Process optimizations led to an improved non-PGM cathode performance achieving areal current density of 178 mA/cm^2 at 0.8 V under one bar O_2 pressure.
- Formulation improvement over the original ANL's ZIF/nano-network catalyst yielded a cathode volumetric current density of 90 A/cm^3 (@ 0.8 V, P_{O2} = 2 bar).

The approach of ZIF-derived nano-network electrode opens up new directions for further non-PGM fuel cell performance improvement, including:

- Better active site conversion and preservation through controlled process conditions.
- Higher catalytic activity through new organic ligand and organometallic additive designs.
- Higher overall electrode performance through nano-network morphological and composition optimization.

FY 2014 PUBLICATIONS/PRESENTATIONS

1. "Highly Efficient Non-Precious Metal Electrocatalysts Prepared from One-Pot Synthesized Zeolitic Imidazolate Frameworks (ZIFs)" Dan Zhao, Jiang-Lan Shui, Lauren R. Grabstanowicz, Chen Chen, Sean M. Commet, Tao Xu, Jun Lu, and Di-Jia Liu, *Advanced Materials*, 2014, *26*, 1093–1097 DOI: 10.1002/adma.201304238. (Frontpiece article)

2. "Highly-Active and "Support-free" Oxygen Reduction Catalyst Prepared from Ultrahigh Surface Area Porous Polyporphyrin" Shengwen Yuan, Jiang-Lan Shui, Lauren Grabstanowicz, Chen Chen, Sean Commet, Briana Reprogle, Tao Xu, Luping Yu and Di-Jia Liu, *Angew. Chem. Int. Ed.,* 2013, 52(32), 8349–8353 DOI: 10.1002/anie.201302924.

3. "New Approach to High-Efficiency Non-PGM Catalysts Using Rationally Designed Porous Organic Polymers" S. Yuan, G. Goenaga, L. Grabstanowicz, J. Shui, C. Chen, S. Commet, B. Reprogle and D.-J. Liu, ECS Transaction, 2013 58(1): 1671-1680.

4. "Non-PGM Cathode Catalysts using ZIF-based Precursors with Nanonetwork Architecture", Di-Jia Liu, Dan Zhao, Jianglan Shui, Lauren Grabstanowicz, Sean Commet, Poster presentation at 2014 DOE Hydrogen and Fuel Cells Program and Vehicle Technologies Office Annual Merit Review and Peer Evaluation Meeting, Washington, D.C., June 16–20, 2014.

5. "New Approach to High-Efficiency Non-PGM Catalysts Using Rationally Designed Porous Organic Polymers", Shengwen Yuan,

Jianglan Shui, Lauren Grabstanowicz, Chen Chen, Sean Commet, Briana Reprogle and Di-Jia Liu, Oral Presentation at 224nd Electrochemical Society Meeting, San Francisco, Oct 27 – Nov. 1, 2013.

REFERENCES

1. S. Ma, G. Goenaga, A. Call and D.-J. Liu, *Chemistry: A European Journal* **17,** 2063 (2011).

2. E. Proietti, F. Jaouen, M. Lefèvre, N. Larouche, J. Tian, J. Herranz and J.-P. Dodelet, *Nature Comm*. **2**, 416 (2011).

3. D. Zhao, J.-L. Shui, C. Chen, X. Chen, B. M. Reprogle, D. Wang and D.-J. Liu, *Chem. Sci.*, **3** (11), 3200 (2012).

4. S. Yuan, J.-L. Shui, L. Grabstanowicz, C. Chen, S. Commet, B. Reprogle, T. Xu, L. Yu and D.-J. Liu, *Angew. Chem. Int. Ed.*, **52**(32), 8349 (2013).

5. D. Zhao, J.-L. Shui, L.R. Grabstanowicz, C. Chen, S.M. Commet, T. Xu, J. Lu, and D.-J. Liu, *Advanced Materials*, **26** 1093 (2014).

6. F. Jaouen, J. Herranz, M. Lefèvre, J.P. Dodelet, U.I. Kramm, I. Herrmann, P. Bogdanoff, J. Maruyama, T. Nagaoka, A. Garsuch, J.R. Dahn, T. Olson, S. Pylypenko, P. Atanassov, E.A. Ustinov, *ACS Appl. Mater. Interfaces*, **1,** 1623; (2009).

V.B.1 Dimensionally Stable High Performance Membrane

Cortney Mittelsteadt (Primary Contact),
Avni A. Argun, Castro Laicer
Giner, Inc. / Giner Electrochemical Systems, LLC
89 Rumford Avenue
Newton, MA 02466
Phone: (781) 529-0529
Email: cmittelsteadt@ginerinc.com

DOE Manager
Donna Ho
Phone: (202) 586-8000
Email: Donna.Ho@ee.doe.gov

Contract Number: DE-EE0004533

Project Start Date: October 1, 2010
Project End Date: December 31, 2014

Overall Objectives

- Achieve mechanically supported, dimensionally stable, and highly conductive fuel cell membranes that meet the DOE performance and cost targets.
- Demonstrate a scalable and cost-effective roll-to-roll method for fabrication of membrane electrode assemblies.
- Commercialize Dimensionally Stable Membranes (DSM™) for use in fuel cells, electrolyzers, and other electrochemical applications that require thin and strong membranes.

Fiscal Year (FY) 2014 Objectives

- Optimize materials and process parameters for the selected DSM™ support fabrication that involves mechanical deformation of dimensionally stable polymers to obtain 5- to 10-µm-thick microporous DSM™ supports with 50% pore density.
- Develop and characterize membrane electrode assemblies using low equivalent weight (EW) ionomers embedded in the DSM™ supports.
- Demonstrate a scalable process and conduct a pilot roll-to-roll run to yield ~1,000 ft of DSM™ roll.

Technical Barriers

This project addresses the following technical barriers from the Fuel Cells and Manufacturing R&D sections of the Fuel Cell Technologies Office Multi-Year Research, Development, and Demonstration Plan:

Fuel Cells

(A) Durability

(B) Cost

(C) Performance

Manufacturing R&D

(A) Lack of High-Volume Membrane Electrode Assembly Processes

Technical Targets

Progress has been made in achieving the DOE targets listed in the Multi-Year Research, Development, and Demonstration Plan. Table 1 lists the DOE's technical targets and where our research and development efforts stand to date.

TABLE 1. DOE Technical Targets and GINER/GES Status

Characteristic	Unit	2017 Target	DSM™ Status
Oxygen Crossover	mA/cm^2	2	1.5[a]
Hydrogen Crossover	mA/cm^2	2	1.8[a]
Membrane Conductivity Operating Temperature 20°C -20°C	S/cm	 0.10 0.07	 0.093[b] 0.083 Not tested
Operating Temperature	°C	≤120°C	95°C
Area Resistance	$Ohm*cm^2$	0.02	0.03
Cost	$\$/m^2$	20	<100
Lifetime	hours	5,000	Untested
Durability with Cycling <80°C	cycles	20,000	20,000
Unassisted Start from Low Temperature	°C	-40	Untested
Thermal Cyclability in Presence of Condensed Water		Yes	Yes

[a]Crossover measured for 1 atm of pure H_2 and pure O_2 at 95°C and 50% relative humidity.
[b]For 1-µm DSM operating at 95°C with H_2/air at 20 psi. H_2/air stoichiometry of 1.1/2.0.

This project previously pursued multiple micromold-based DSM™ fabrication processes based on the criteria of fuel cell performance and cost reduction. Despite the favorable scalability of all processes for high-volume production, only the DSMs™ fabricated using the mechanical deformation method met the required performance characteristics to achieve the DOE targets:

- Area resistance: <0.02 $\Omega.cm^2$
- Cost: <\$20 m^2
- Lifetime: >5,000 hours
- Durability at 80°C: >20,000 cycles

FY 2014 Accomplishments

- A mechanical deformation method was developed to form DSM™ supports with round and square pores using a variety of dimensionally stable commodity polymers.
- A comprehensive optimization study was conducted to refine the mechanical deformation method to yield ~10-µm thick microporous DSM™ supports with 50% pore density. The process parameters were finalized for successful adaption to roll-to-roll trial.
- By improving the release process of polysulfone (PSU) from nickel micromolds using ultrathin fluoropolymer coatings, film porosity of over 50% has been demonstrated using the mold-assisted mechanical deformation route.
- A detailed route to achieve roll-to-roll production of DSM™ was identified and executed at a pilot size to yield ~ 1,000 ft roll of DSM™. This route involved the fabrication and surface treatment of nickel micromolds, attachment of micromolds onto a tooling belt to form a process drum, roll-coating of perfluorinated sulfonic acid (PFSA) and PSU layers on a 5,000-ft carrier film roll at various thickness values, and mechanical deformation of the PFSA/PSU layers by the process drum to form the final DSM™.

INTRODUCTION

In proton exchange membrane (PEM) fuel cells, attaining and maintaining high membrane conductivity at various operating conditions is crucial for the fuel cell performance and efficiency. Incorporating ionomers within highly porous, dimensionally stable PEM substrates increases the performance and longevity of PEM devices. Lowering the EW of perfluorinated ionomers is one of the few options available to improve membrane conductivity, especially in the low-relative-humidity regime. However, excessive changes in membrane dimensions upon application of wet/dry or freeze/thaw cycles yield catastrophic losses in membrane integrity, thus hindering their long-term durability. This is especially of concern when low-EW ionomers are used in thin membrane configurations to minimize resistive losses. Incorporating perfluorinated ionomers of low EW within highly porous, dimensionally stable support materials is an optimal method to achieve the DOE fuel cell membrane metrics for conductivity and durability. A scalable, cost-effective method to fabricate these composite membranes is also necessary to achieve the DOE membrane cost target of <$20/m^2. Giner/GES has developed DSM™ technology to provide mechanical support for the conductive ionomer. These composite membranes include a highly conductive and high-acid-content ionomer within a thin and durable polymer support with well-defined, "through" pores and high (50%) porosity. Utilizing high-strength engineering polymers, the DSM™ approach completely restrains the in-plane swelling of the ionomer. Providing a non-tortuous, through-plane path for ionic transport minimizes the conductivity penalty due to the support structure. Additionally, when filled with low-EW PFSA ionomers, the DSM™ meets nearly all of the DOE's 2017 durability and performance targets, including those for freeze/thaw cycling and wet/dry cycling operation.

As currently manufactured, DSM™ is far too expensive (~$100-1,000/m^2) for automotive and stationary applications. A scalable, continuous fabrication method is needed to reduce the cost down to or below the DOE's 2017 cost target of $20/m^2.

APPROACH

A major goal for this project is the identification and optimization of materials and processes for scalable and cost-effective manufacturing of DSMs™ consisting of low-EW PFSA ionomers. Giner had previously identified the optimum DSM™ support geometry to be a 5- to 10-µm-thick microporous support film with 20-µm pore diameter and 50% pore density. Specifically, the project has investigated in depth a laser ablation method along with three micromolding processes: Phase Inversion, UV Microreplication, and Mechanical Deformation. Giner has evaluated the feasibility of each process for scaled fabrication at low cost. The "Laser Micromachining" process was eliminated first due to issues with extremely slow process speeds, high capital instrumentation demand, and high operation cost. The remaining three micromolding processes rely on fabrication of electroformed nickel "pillar" molds as the initial stage. Figure 1 shows the cross-sectional illustration of the nickel micromold along with a scanning electron micrograph that shows the configuration of 10-µm pillar height pillars to yield 50% area coverage.

The "Phase Inversion" method, first used during Phase II of this project, aimed to develop a DSM™ support that is less expensive and easier to scale up compared to laser micromachining. It involves casting a polymer solution on a micromold followed by rapid precipitation of the polymer in a non-solvent to yield porous films. Despite its ease of application, the presence of residual solvent wastes hinder its widespread application. Additionally, the resulting porous films had poor mechanical properties due to microporosity of inversion-cast films. The "UV Microreplication" method, a soft lithography approach that uses imprint lithography principles, involves the use of a low-viscosity, ultraviolet (UV)-crosslinkable monomer solution placed between a micromold and a backing layer followed by its solidification to form a porous network. This is a highly scalable process that generates materials at low cost and high volume.

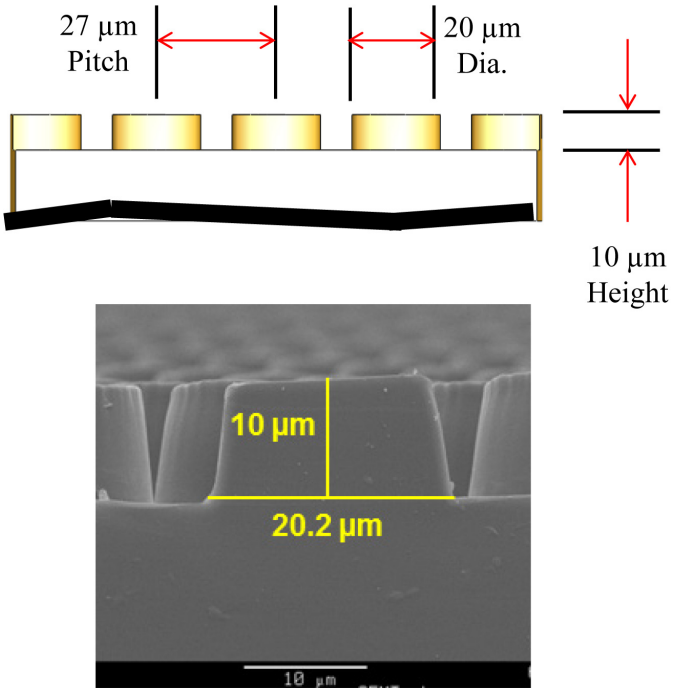

FIGURE 1. A scanning electron micrograph of a micromold pillar—cross-sectional view with dimensions.

However, the crosslinked polymers have failed to pass the durability and mechanical strength criteria during their evaluation as DSM™ support. Upon elimination of the Phase Inversion process due to complications with solvent waste and the UV Microreplication process due to inferior material properties, Giner has continued to investigate the Mechanical Deformation method, which relies on controlled puncturing of high strength engineering polymers with an array of high fidelity micropillars. By eliminating the material risks encountered in phase inversion and UV Microreplication methods , this process has proven to be readily scalable to generate a DSM™ support material at low cost.

RESULTS

During FY 2014, Giner/GES investigated the micromold-assisted mechanical deformation method for scaled and cost-effective fabrication of DSM™. This is a direct perforation route that involves puncturing a high-performance engineering polymer with micromolds to fabricate porous films. It is attractive because the resulting support structure has identical performance to the initial material unlike the case for UV-crosslinked films where further validation is required. This method can also utilize commodity polymers with very fast processing times allowing for roll-to-roll production.

Figure 2 shows the process flow that Giner has developed to apply the mechanical deformation concept to form DSM™ supports. First, a thermoplastic such as PSU is solution

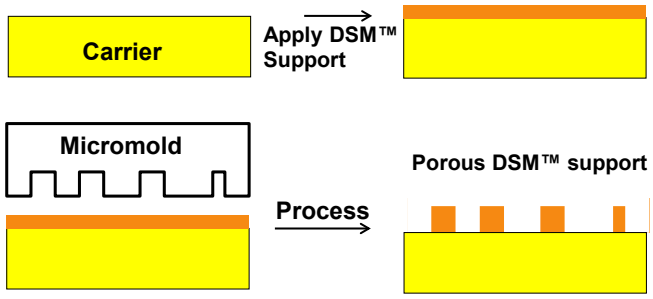

FIGURE 2. Giner's mechanical deformation process to form DSM™ supports (patent pending).

cast on a rigid backing layer. A nickel micromold treated with a low surface energy anti-stick coating is then applied. Upon completion of the process, the micromold is removed, resulting in a continuous DSM™ support with well-defined pores attached to the underlying carrier layer. Using the process scheme shown in Figure 2, Giner performed a series of batch perforation experiments and optimized process parameters to form PSU DSM™ supports with highly regular pores. Using the process flow shown in Figure 2, DSM™ supports were fabricated at two different configurations where the DSM™ support layer was perforated on a carrier film (Figure 3a) or on a PFSA/carrier layer (Figure 3b). Scanning electron micrographs obtained from these two configurations (Figure 3) clearly show the formation of pores without residual layers. Depending on the application, this approach can generate a porous network of PSU either directly on the carrier film or as a PSU/PFSA bilayer configuration. For example, if separation of the DSM™ support material from the underlying carrier layer proves difficult, a PFSA layer can be applied on the carrier polymer prior to the DSM™ support layer. Giner currently uses this bilayer approach to feature a thin (~1.5 µm) PFSA film on the carrier film followed by coating a 3-µm thick PSU film, which brings the total bilayer thickness to slightly below 5 µm. Upon processing the film with micromold pillars, the result is a 10-µm thick porous PSU/PFSA film as shown in Figure 3b. The next step would be to complete the DSM™ fabrication by adding another PFSA layer.

Figure 4 shows the schematic illustration of the continuous, roll-to-roll fabrication process. The carrier layer that is coated with the DSM™ support is fed continuously between a rotating conveyer and the process drum that contains the micromold. The distance between the rotating conveyer and the process drum is adjusted so that a pressure in a preferred range of 100-300 psi can be applied between micropillars and the DSM™ support layer. Once the process is complete, the resulting porous DSM™ support can be transferred to the next processing step to incorporate the ionomer layer. In collaboration with an industrial partner, we are currently implementing a pilot-size roll-to-roll method to

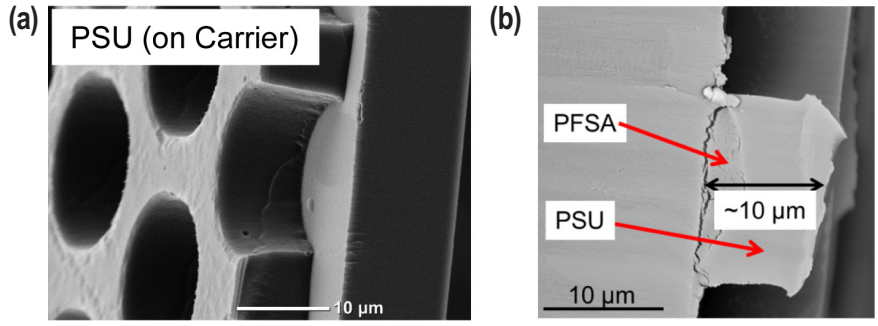

FIGURE 3. Two configurations of the mechanical deformation process. (a) PSU on carrier (b) PSU on PFSA/carrier.

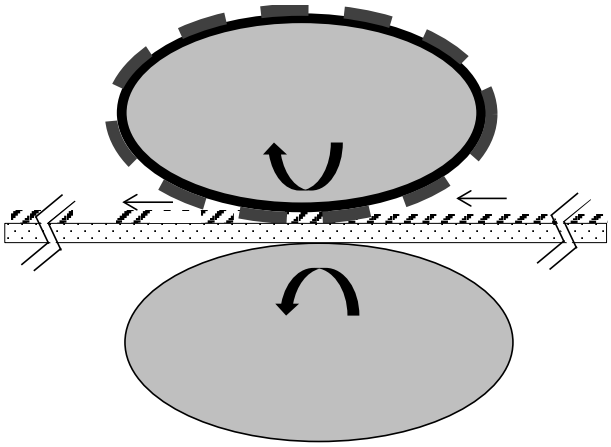

FIGURE 4. Schematic illustration of the roll-to-roll mechanical deformation process.

produce ~1,000 ft of DSM™ roll where each DSM is sized ~45 in^2 (~280 cm^2) between the seams.

CONCLUSIONS

The goal by the end of FY 2014 was to demonstrate the roll-to-roll adaption of the mechanical deformation method for cost-effective manufacturing of DSMs™ for fuel cells. The potential of this method is due to its very low material risk. Giner's process development effort has yielded a clear pathway for large-scale production of DSM™ support materials with targeted dimensional stabilities to allow for incorporation of low-EW ionomers in fuel cells. Upon qualification of these DSM™ supports by Giner in membrane electrode assemblies for fuel cells, the focus will be to extend the material width to 12" using larger micromolds and investigate effective ways to integrate the ionomer layers with DSM™ supports for continuous production of DSMs™.

SPECIAL RECOGNITIONS & AWARDS/ PATENTS ISSUED

1. Mittelsteadt C.K.; Argun, A.A.; Laicer, C.; Willey, J. "*Micromold Methods for Fabricating Perforated Substrates and for Preparing Solid Polymer Electrolyte Composite Membranes*" US Patent Application No. 14/120,353, filed on May 14, 2014.

FY 2014 PUBLICATIONS/PRESENTATIONS

1. Mittelsteadt, C.K., A. Argun, C. Laicer, J. Willey, P. Maxwell. "*2014 Annual Merit Review Proceedings– Fuel Cells* " June, 2014.

2. Mittelsteadt, C.K., A. Argun, C. Laicer. "*2014 Fuel Cells Tech Team* " February, 2014.

3. Mittelsteadt, C.K., A. Argun, and C. Laicer "Dimensionally Stable High Performance Membrane," Annual Progress Report, U.S. Department of Energy Phase III Xlerator Program Grant No. DE-EE0004533, December 2013.

V.C.1 New Fuel Cell Membranes with Improved Durability and Performance

Michael Yandrasits
3M Company
3M Center, Building 201-1W-28
St. Paul, MN 55144
Phone: (651) 736-5719
Email: mayandrasits@mmm.com

DOE Managers
Jacob Spendelow
Phone: (202) 586-4796
Email: Jacob.Spendelow@ee.doe.gov
David Peterson
Phone: (720) 356-1747
Email: David.Peterson@ee.doe.gov

Contract Number: DE - EE0006362

Subcontractors:
- General Motors Fuel Cell Activities, Pontiac MI – Craig Gittleman
- Vanderbilt University, Nashville, TN – Peter Pintauro

Project Start Date: October 1, 2013
Project End Date: September 30, 2016

Overall Objectives

- Meet all of the DOE Fuel Cell Technologies Office Multi-Year Research, Development, and Demonstration Plan membrane performance, durability, and cost targets simultaneously with a single membrane.
- Membranes will be based on multi-acid side chain (MASC) ionomers.
- Electrospun nanofiber structures will be developed to reinforce membranes.
- Peroxide scavenging additives will be used to enhance chemical stability.
- New membranes will have improved mechanical properties, low area specific resistance and excellent chemical stability compared to current state of the art.
- Experimental membranes will be integrated into membrane electrode assemblies and evaluated in single fuel cells and finally fuel cell stacks.

Fiscal Year (FY) 2014 Objectives

- Baseline performance of conventional membranes and demonstrate MASC ionomer conductivity of 0.1 S/cm at 80°C and 50% relative humidity (RH).
- Identify one or more polymer systems for use as reinforcing fibers made by electrospinning.
- Develop methods for making perfluoroimide acid (PFIA) electrospun fibers.
- Make a membrane in the lab that has improved performance over state-of-the-art membranes and meets DOE accelerated durability targets.

Technical Barriers

This project addresses the following technical barriers from the Fuel Cells section of the Fuel Cell Technologies Office Multi-Year Research, Development, and Demonstration Plan:

(A) Durability

(B) Cost

(C) Performance

Technical Targets

Technical targets are shown in Table 1 along with the comparative data to date. The conventional membranes listed are perfluorosulfonic acid-based membranes that are either unsupported (725 equivalent weight [EW]-20 μm) or supported with 3M's standard nanofiber material (725 EW-S-14 μm). The experimental PFIA is shown in both the unsupported (PFIA-20 μm) and supported (PFIA-S-14 μm) forms.

FY 2014 Accomplishments

- Successfully synthesized three lots of PFIA ionomer in the lab and demonstrated conductivity of 0.1 S/cm at 80°C and 50% RH.
- Initiate scale up efforts for PFIA ionomer.
- Fabricated 20 nanofiber support candidates and evaluated composite membranes for mechanical properties including swell in hot water.
- Developed a method for decoupling conductivity of the center composite layer from the pure ionomer skin layers of a supported membrane.
- Developed a method to electrospin PFIA ionomer.

INTRODUCTION

One of the key challenges for fuel cell membranes is the ability to meet the automotive industry targets for

TABLE 1. DOE Targets and Measured Data to Date

Characteristic	Units	2017 & 2020 Targets	725 EW (20 µm)	725 EW-S (14 µm)	PFIA (20 µm)	PFIA-S (14 µm)
Area specific proton resistance at:						
80°C and water partial pressures from 25 Kpa	Ohm cm^2	0.02	0.026	0.034	0.017	0.025
Durability						
Mechanical	Cycles with <10 sccm crossover hours	20,000	8,300	>20,000	12,000	26,300*
Chemical	hrs	>500				2,170*

*Durability samples made with 80/20 blend of PFIA and 825EW PFSA

area specific resistance, durability, and cost. One way to reduce membrane resistance is to use low EW ionomers. Unfortunately, membranes based on perfluorosulfonic acid polymers with equivalent weights of about 700 g/mol or lower have significant water soluble fractions and are not stable for long times in an operating fuel cell. New ionomers are needed that have improved conductivity, especially under hot and dry operating conditions, that are not water soluble. By increasing the number of acid groups per side chain, the proton conductivity can be increased while retaining the polymer backbone to resist solubility. However, increasing the bulk proton conductivity alone is likely not enough to meet the area specific resistance targets. Thinner membranes will also improve the resistance but they will compromise durability. In this case polymer fiber supports are needed to improve the mechanical strength, resist swelling in the x-y plane, and increase durability.

Previous projects have made significant advances in meeting many of the membrane targets but often the samples used to meet one milestone were different than those used to meet another. For example, a thin, unsupported, low EW ionomer membrane can meet many of the performance targets while falling short of the durability goals. Likewise, a fiber supported membrane can often meet the accelerated durability targets while having relatively poor performance. This project is focused on meeting all of the DOE goals with one membrane.

APPROACH

The goal of this project is to make a fuel cell membrane that meets all of the Department of Energy Fuel Cell Technologies Office targets for performance, durability and cost. The materials part of this project is split into two parts; ionomer development and nanofiber support development. The basis of the ionomer development is 3M's MASC polymers. The main candidate in this category is an ionomer that has two side-chain acid groups, a perfluoroimide and a sulfonic acid. Work is also underway to increase the number of acid groups per side chain to three or more by increasing the number of imide groups per side chain. The mechanical support part of the project relies on fibers made by an electrospinning process. These fibers will be made from fluoropolymers, aromatic polymers, or blends. Work at Vanderbilt University will also evaluate electropsun ionomer fibers and dual spun (ionomer with support fibers) membranes. The final membrane developed in this project will combine both new ionomer and nanofiber technology.

Membranes developed under this project are evaluated with both in-cell and out-of-cell testing. Mechanical properties testing are conducted at both 3M and General Motors (GM) laboratories with particular emphases placed on GM's blister test. Accelerated tests are underway to evaluate the mechanical failure mechanism based on a humidity cycle test [1] and chemical stability based on an open-circuit voltage hold test [2]. Fuel cell performance testing is being conducted with single-cell test stations and ultimately the new membrane will be demonstrated in a small stack.

RESULTS

The ionomers under development in this project are shown in Figure 1. The structure in Figure 1a is 3M's PFIA and has a calculated EW of 620 g/mol. This polymer was initially developed under a previous DOE-funded project [3] in small lab quantities (~100g) and will be made in pilot-scale quantities (~1-5 kg) as part of the current project. In the past three quarters preliminary work to establish reaction conditions, efficiency, safety, and quality control has been initiated. It is expected the first pilot-scale reaction will be run in the fourth quarter of this project.

Methods to increase the number of acid groups per side chain to three or more are under development. The structure shown in Figure 1b is an example of an ionene chain extended polymer with two imide groups and one acid group. Small quantities of this polymer have been made in the lab and are under evaluation.

Conductivity milestones have been established for this work of 100 mS/cm at 80°C and 50% RH at the end of the first quarter and 100 mS/cm at 80°C and 40% RH at the end of the fifth quarter. These milestones are shown in Figure 2 along with three lots of PFIA ionomer tested to date. It can be seen that the first milestone is within the 95% confidence

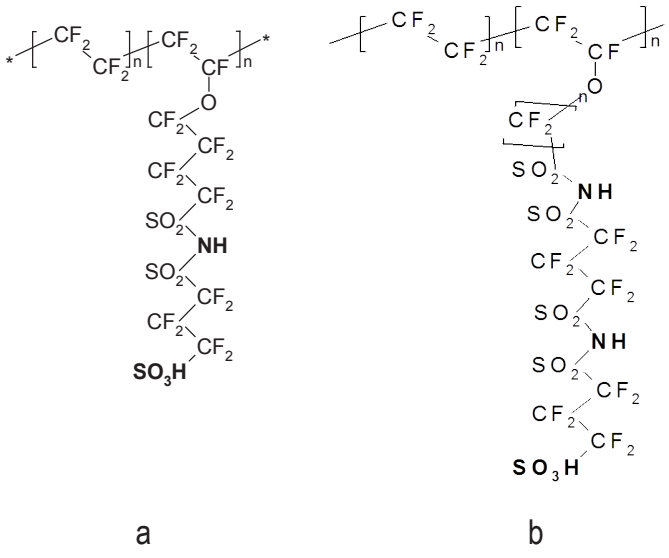

FIGURE 1. Multiacid side chain structures; a) PFIA and b) Perfluoroionene chain extended ionomers.

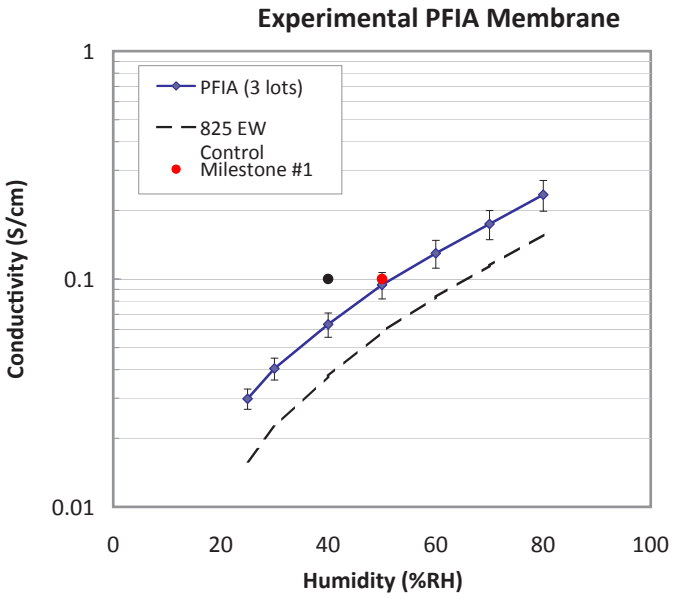

FIGURE 2. Conductivity versus RH for three lots of PFIA membrane with 95% confidence intervals. Standard 825 EW membrane indicted by dashed line. Project milestones indicated with circles.

range of three PFIA lots but the fifth milestone has not yet been met. It is our expectation that the perfluoroinonene chain extended polymers will be able to achieve the conductivity targets set out in milestone number five.

Several new nanofiber materials have been generated under this project. All of the materials have been made using electrospinning process and conventional fluoropolymers, aromatic hydrocarbon polymers, or blends. A key metric is the ability for the support to restrict the swell of the ionomer

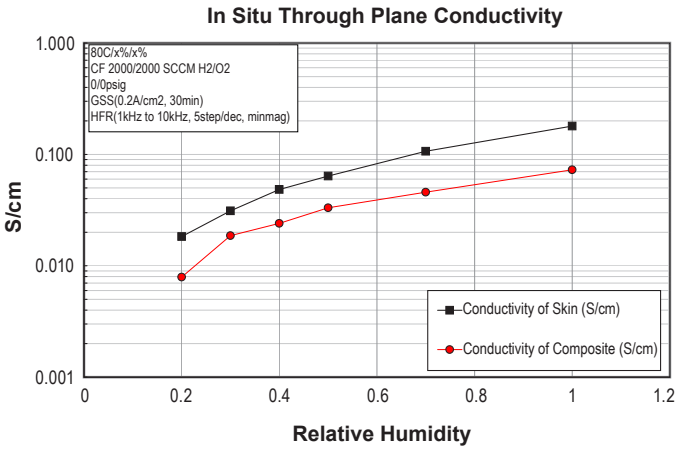

FIGURE 3. Through plane conductivity versus RH measured in-cell with contributions from the center composite layer decoupled from pure ionomer skin layer.

in the x-y plane to less than 5% in each direction. There have been 20 nanofiber samples generated in the first three quarters and the average fiber content required in a composite membrane to meet the 5% swell target is about 20% by volume in the down-web direction and about 35% in the cross-web direction.

A consequence of adding supporting fibers to an ionomer membrane is a reduction in the proton conductivity of the membrane. In order to better understand this impact, methods have been developed to measure the in-cell membrane resistance and to decouple the contribution of the center composite layer from the unsupported skin layers. This approach involves testing a series different thickness supported and unsupported membranes and extrapolating values to zero membrane thickness to obtain the non-membrane related resistance. Figure 3 shows the results of one of these experiments where the center composite layer has about half the conductivity of the pure ionomer. This is an encouraging result since the fiber content is about 50% by volume in this layer. It is expected that stiffer, stronger fibers could be developed that meet the mechanical property requirements at lower total fiber content and therefore, lower resistance loses.

In addition to new support fiber development, Vanderbilt University has developed methods to electrospin 3M ionomers including the PFIA ionomer. Figure 4 shows electron microscope images for one set of experiments. In order to make high quality fibers a spinning aid such as polyethylene oxide needs to be used. The series of images demonstrates the effect of increasing the polyethylene oxide content from 0 to 4 weight percent with 1% being the optimum. These conditions can be used to make dual-spun fiber membranes where the ionomer and a support fiber are spun at the same time resulting in a mixed fiber membrane. The ionomer can then be fused into a continuous phase

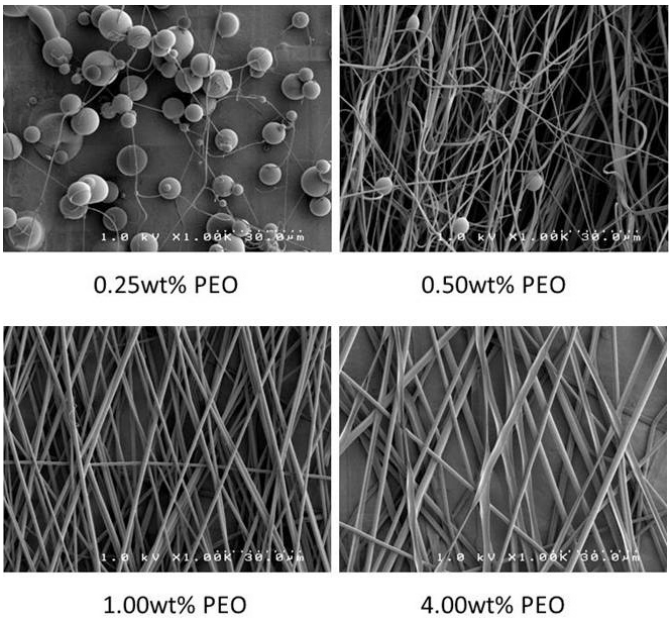

FIGURE 4. Electron microscope images of PFIA electrospinning experiments showing the effect of added polyethylene oxide (contribution from Vanderbilt University).

leaving the fiber support evenly distributed throughout the membrane.

CONCLUSIONS AND FUTURE DIRECTIONS

- 3M's PFIA shows good conductivity at 80°C and 50% RH and meets milestone #1 but falls short of milestone #5 (0.1 S/cm @ 80°C, 40% RH).
- Synthetic routes to ionene chain extended polymers are being developed. These polymers will have three or more acid groups per side chain.
- Fiber contents of about 20-35% by volume are needed to reduce swell in hot water of composite membranes to less than 5%.
- Experiments to decouple the resistance of the fiber composite center layer from the pure ionomer skin have shown that the conductivity is approximately proportional to the ionomer content.
- Work to scale up PFIA ionomer to 1-5 kg batches has been started.
- Membranes will be made in the second year of this project that incorporate PFIA ionomer and new nanofiber technology.

FY 2014 PUBLICATIONS/PRESENTATIONS

1. http://www.hydrogen.energy.gov/pdfs/review14/fc109_yandrasits_2014_o.pdf (M. Yandrasits 2014 Annual Merit Review Proceedings Fuel Cells).

REFERENCES

1. FOA DE-FOA-0000360 Appendix Table D-3: MEA Chemical Stability and Metrics.

2. FOA DE-FOA-0000360 Appendix Table D-4: Membrane Mechanical Cycle and Metrics.

3. http://www.hydrogen.energy.gov/pdfs/progress11/v_c_1_hamrock_2011.pdf). Status represents 3M PFIA membrane (S. Hamrock, U.S. Department of Energy Hydrogen and Fuel Cells Program 2011 Annual Progress Report).

V.C.2 Advanced Hybrid Membranes for Next Generation PEMFC Automotive Applications

Andrew M. Herring (Primary Contact),
Mei-Chen Kuo, James L. Horan, Andrew Motz

Colorado School of Mines
1500 Illinois Street
Golden, CO 80401
Phone: (303) 384-2082
Email: aherring@mines.edu

DOE Managers

Donna Ho
Phone: (202) 586-8000
Email: Donna.Ho@ee.doe.gov

Gregory Kleen
Phone: (720) 356-1672
Email: Gregory.Kleen@ee.doe.gov

Technical Advisor

John Kopasz
Phone: (630) 252-7531
Email: Kopasz@anl.gov

Contract Number: DE-EE0006363TDD

Subcontractors

- Bryan Pivovar, Michael Penev, National Renewable Energy Laboratory, Golden, CO
- Nilesh Dale, Nissan Technical Center North America, Farmington Hills, MI
- Steven Hamrock, 3M Fuel Cell Components Group, St. Paul, MN

Project Start Date: October 1, 2013
Project End Date: September 30, 2016

Overall Objectives

- Fabricate a low-cost, high-performance proton exchange membrane to operate at the temperature of an automotive fuel cell stack, and requiring no system inlet humidification
- Optimize the membrane to meet durability, cross-over, and electrical resistance targets
- Incorporate the membrane into a 50-cm^2 membrane electrode assembly

Fiscal Year (FY) 2014 Objectives

Show that heteropoly acid (HPA) containing films can be fabricated thin and have a low area-specific resistance (ASR) at the temperature of an automotive fuel cell stack

- Increase HPA loading and organization for maximum proton conduction in two different perfluorinated polymer systems
- Demonstrate that a zirconium phosphonate polymer system is competitive with HPA-based polymer systems

Technical Barriers

This project addresses the following technical barriers from the Fuel Cells section of the Fuel Cell Technologies Office Multi-Year Research, Development, and Demonstration Plan:

(A) Durability

(B) Cost

(C) Performance

Technical Targets

The technical targets are shown in Table 1

TABLE 1. Progress towards Meeting Technical Targets for Membranes for Transportation Applications

	DOE Target 2017 ASR, Ω cm^2	Result Ω cm^2	Thickness μm	Conditions
System I, TFVE-HPA	<=0.02	0.04	16	80ºC 95% RH
System II, Dyneon-HPA	<=0.02	<=0.02	5-27	80ºC 95% RH
System III, ZrP/VPA	<=0.02	0.05	149	60ºC 95% RH

RH – relative humidity; VPA - vinyl phosphoric acid

FY 2014 Accomplishments

- Showed that development of membranes that eliminate the need for the system humidification system will lower system costs to <$40/kW.
- Using highly purified trifluorovinyl ether (TFVE) monomers synthesized next generation HPA-based proton conductors.
- Showed that TFVE-HPA polymers fabricated from material stable to boiling water can be fabricated into thin films with low ASRs.
- Demonstrated HPA attachment to commercial Dyneon™ polymers with desirable mechanical properties.
- Showed that zirconium phophonate polymers can be fabricated into a novel proton conducting film with low ASR under vehicular operating conditions.

INTRODUCTION

The objective of this project is to fabricate a low-cost high-performance hybrid inorganic/polymer membrane that has a proton ASR <0.02 ohm cm^2 at the operating temperature of an automotive fuel cell stack (95-120°C) at water partial pressures from 40-80 kPa with good mechanical and chemical durability. Additionally the membrane will be optimized for low hydrogen and oxygen crossover with high electrical ASR at all temperatures and adequate proton ASR at lower temperatures. We also seek to gain valuable insights into rapid proton transport at the limit of proton hydration. Additional research will be performed to incorporate the membrane into a 50-cm^2 membrane electrode assembly (MEA). The materials at the start of this project are at a technology readiness level (TRL) of 2, as we have shown that they have proton conductivity under high and dry conditions, but we have not yet consistently shown that they will function in an operational fuel cell. At the project's end the materials will be at a TRL of 4 and will be integrated into an MEA, demonstrating that they can function with electrodes as a single fuel cell. This work will enable hydrogen-powered fuel cells as it will negate the need for costly and bulky external humidification unit operations in the fuel cell system. Additionally excess water will not be an issue for freeze or fuel cell reactant supply. The project is addressing the 2017 DOE technical targets for membranes for transportation applications.

APPROACH

In past funding from the Department of Energy/ National Science Foundation we have developed completely new ionomer systems based on incorporation of inorganic super acids into polymer systems, which have high proton conductivity under conditions of low humidity, higher temperature operation, high oxidative stability, and little swelling when wet. This project will perform the work to optimize the proton conductivity and mechanical properties in these materials to produce a robust thin film for proton exchange membrane (PEM) fuel cells in automotive applications. The technical concept is to use functionalized inorganic super acids that utilize little water for high proton conductivity, as the protogenic group covalently attached to a polymer backbone optimized for all other functions of the membrane.

Many composite inorganic/polymer films have been fabricated, but unless the particles have dimensions on the nano-scale there is no advantage as the improvement to film properties occurs at the particle polymer interface. The limit of this approach is to use molecules with high acidity as the highly activating functionalities, but to do this we must immobilize them, control the morphology of the proton conducting channel, and fabricate an amorphous material. The two moieties that have received the most attention and appear to greatly enhance proton transport are HPAs and zirconyl phosphonates. In previous work, we demonstrated both composite membranes and true inorganic/polymer hybrid materials with very high proton conductivity, but the inorganic super acid in the membrane was not immobilized and the inorganic/polymer hybrid material transformed into undesirable crystalline phases at low RH. These materials are not yet fuel cell ready. In this project, we will overcome all of these disadvantages with an innovative approach to amorphous materials to produce high proton conductivity and all other properties desired of a PEM.

RESULTS

Work was performed on three polymer systems that have all shown promising proton conductivities under automotive fuel cell operating conditions. Progress towards making fuel cell ready membranes for each is described below.

System I: TFVE-HPA

For the TFVE system to work well we needed very pure monomers as any material without a perfluorinated ether is not polymerizable. In the first quarter of the year we demonstrated that we could make these small molecules extremely pure. The HPA functionalized monomer is shown in Figure 1. This monomer is easily polymerized via a thermal process in which the perfluoro vinyl ethers combine to make perfluorocyclobutane linkages, as shown in Figure 1. The system is very versatile in that there are a large number of additional monomers that can be used to form co-polymerized materials which can be tailored to have desirable properties for incorporation into MEAs. We also have the option of forming the polymers in the presence of binders such as PVDF-HFP or perfluorinated sulfonic acid (PFSAs) such as the 3M ionomer. As our objective here is fuel cell ready materials all polymers made are first boiled in water to ensure that they will be stable to liquid water during operation. The resultant materials are then recast into thin films for further testing.

Some of our preliminary data is shown in Figure 2. These films are inherently brittle and so an easy way to form them into films is to blend them with other polymers with good film forming properties. Surprisingly the film using PVDF-HFP out performs the film fabricated with 733 equivalent weight 3M ionomer. The reasons for this are not clear, but may indicate that as the HPA mediates proton conduction differently than a PFSA that the PFSA may be slowing down proton transport in these films. Recently we have successfully made free standing films of the TFVE-HPA polymer by using a hot press. Thin films, <20 µm, have shown ASRs of 0.04 Ω cm^2.

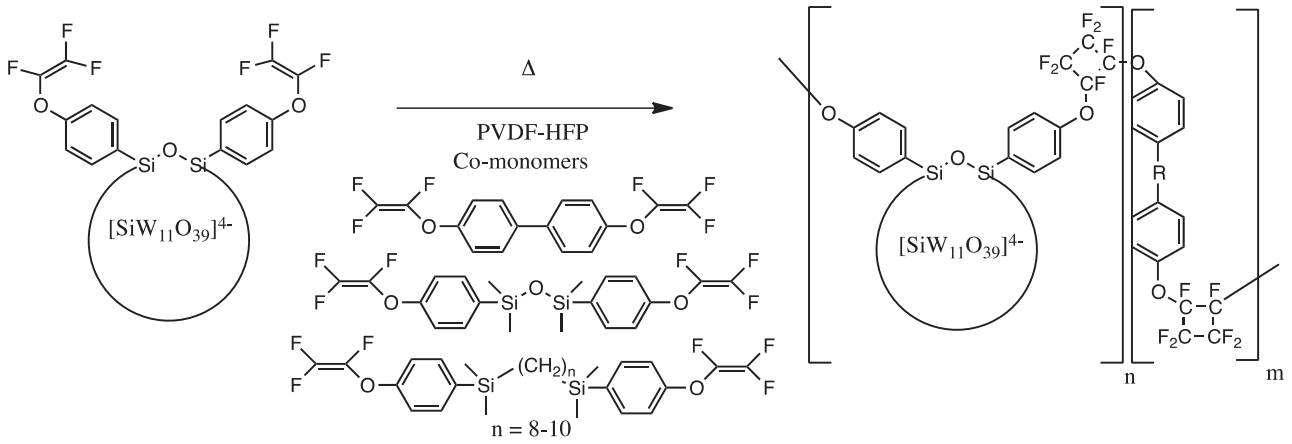

FIGURE 1. Monomers and the synthesis of the trifluorovinylether HPA functionalized polymer.

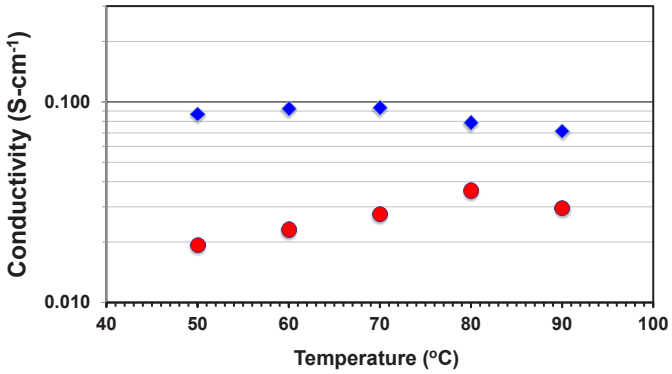

FIGURE 2. Proton conductivity data at 95% RH for 73% $H_8SiW_{11}0_{39}[(TFVE)_2O]$, 19% TFVE-C10 dimer, 8% PVDF-HFP, diamonds, 71% $H_8SiW_{11}0_{39}[(TFVE)_2O]$, 23% TFVE-C10 dimer, 6% 3M PFSA 733 equivalent weight, circles, both films >100 µm.

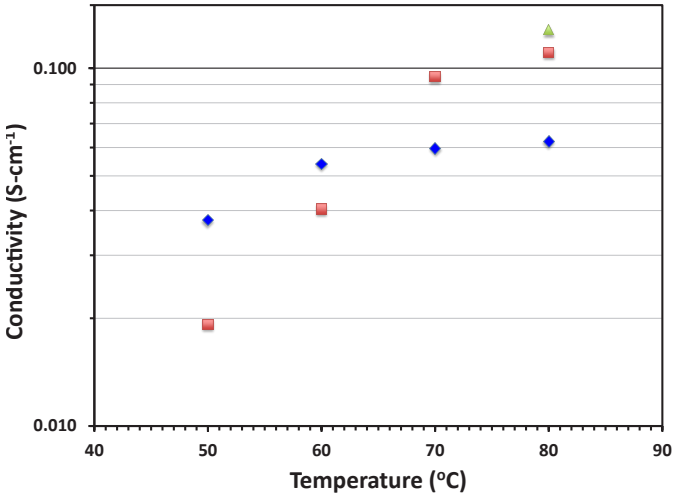

FIGURE 3. Proton conductivity data for a Hybrid HPA-3M Dyneon™ Ionomer, at 95% RH, progress in April (diamonds), August (squares) and membranes that passed the Year 1 Go/No-Go decision point (triangles).

System II: Dyneon-HPA

In the second system that we have been working on, we chemically modify the 3M material Dyneon™ so that we can attach HPAs to it. This is a multi-step process with manipulations to the polymer. We found this to be somewhat cumbersome so we are now initiating a procedure where a small molecule is built up first for attachment to the polymer in a final step. Nevertheless we were able to make HPA containing ionomer films using this approach. The biggest issue has been obtaining enough attachment points to have sufficient HPA in the material such that high proton conductivity can be obtained. As we are still concentrating on the chemistry in this system, we have not begun much film forming work and so the films are still generally thick, <100 µm. Data for one of the Dyneon™-HPA membranes is shown in Figure 3. The data shows high proton conductivity, but it is still not sufficiently high with our current methodology for polymer synthesis. Recent advances in polymer casting procedures have allowed us to fabricate films as thin as 10 microns.

System III: ZrP-VPA

We have shown that vinylzirconium phosphate can be polymerized with vinyl phosphonic acid to make nano-structured films in which the proton conductivity can be extraordinarily high [1]. Unfortunately, the stability of films to boiling water formed from this system is very variable. One possibility is to increase the amount of zirconium-based monomer in the film, but the issue is still that dispersing more than 20 wt% of this monomer is very hard to achieve. We show the typical high proton conductivity achieved for these films in Figure 4. These films are again thick and would have no problem reaching the DOE ASR targets at moderate film thicknesses of <50 µm. Because this system showed a

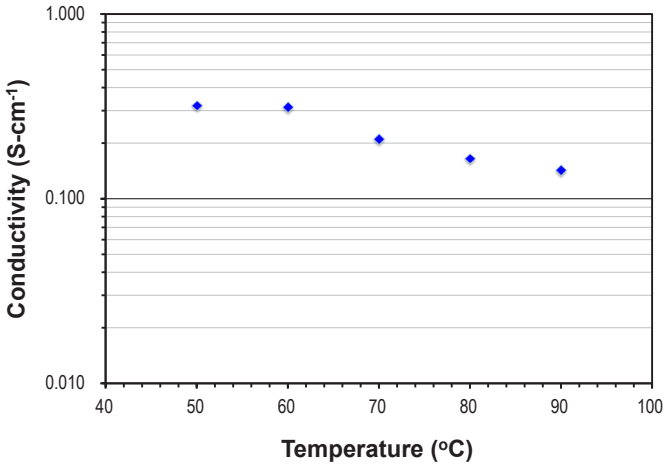

FIGURE 4. Proton conductivity data at 95% RH for a 20% vinyl zirconium phosphate –*co*- 80% vinylphosphonic acid film.

noticeable drop in performance at higher temperatures and could not be stabilized to boiling water, work on this material was terminated under this contract.

CONCLUSIONS AND FUTURE DIRECTIONS

- Demonstrated that TFVE-HPA films could be prepared that were stable to boiling and that low ASRs for these films will be achievable
- Demonstrated that the Dyneon™-HPA system can produce films with high proton conductivity
- Showed that the zirconium phophonate polymers have superior proton conductivity, but their stability to boiling water still provides issues
- Plan to fabricate thin TFVE-HPA polymers or Dyneon™-HPA materials and incorporate into MEAs

REFERENCES

1. "A Hybrid Organic/Inorganic Ionomer from the Copolymerization of Vinyl Phosphonic Acid and Zirconium Vinyl Phosphonate." G.J. Schlichting, J.L. Horan, J. Jessop, S. Nelson, S. Seifert, Y. Yang, and A.M. Herring,* *Macromol.*, **2012**, *45*, 3874.

V.C.3 Resonance-Stabilized Anion Exchange Polymer Electrolytes

Yu Seung Kim (Primary Contact), Kwan-Soo Lee
Los Alamos National Laboratory (LANL)
Materials Physics and Applications Division
Los Alamos, NM 87545
Phone: (505) 667-5782
Email: yskim@lanl.gov

DOE Manager
Nancy Garland
Phone: (202) 586-5673
Email: Nancy.Garland@ee.doe.gov

Project Start Date: October 1, 2012
Project End Date: September 30, 2013

Overall Objectives

- Synthesize highly conductive and stable perfluorinated anion exchange membranes.
- Prepare perfluorinated ionomer dispersions for the fabrication of fuel cell electrodes.
- Develop non-precious metal electro-catalysts for the hydrogen oxidation reaction (HOR) and oxygen reduction reaction (ORR).
- Demonstrate the single-cell performance of alkaline membrane fuel cells (AMFCs).
- Demonstrate the long-term AMFC performance under steady and accelerated stress conditions.

Fiscal Year (FY) 2014 Objectives

- Prepare tough and thin perfluorinated anion exchange membranes by new chemistry.
- Evaluate chemical stability of resonance stabilized perfluorinated membranes under high pH conditions.
- Characterize HOR and ORR behaviors at the Pt-perfluorinated polymer interface using a thin film-coated microelectrode.
- Demonstrate AMFC performance using the perfluorinated anion exchange ionomers.

Technical Barriers

This project addresses the following technical barriers from Section 3.4.4 of the Fuel Cell Technologies Office Multi-Year Research, Development, and Demonstration Plan:

(A) Durability (polymer electrolytes)

(B) Cost (non-precious metal catalysts)

(C) Performance (AMFCs)

Technical Targets

The purpose of this project is to investigate practical aspects of AMFCs for practical use in intermediate (10-50 kW) power applications. Insights gained from this project will be applied toward the next stage of advanced AMFC systems. Since there are no specific technical targets for AMFCs in the current U.S. DOE Fuel Cells Program, we modified technical targets for proton exchange membrane fuel cell (PEMFC) membranes from the DOE Multi-Year RD&D Plan [1] based on appropriate AMFC operating conditions (Table 1).

TABLE 1. DOE Membrane Targets for Transportation Applications

Technical Targets: Membrane for Transportation Applications				
Characteristics	**Units**	**2012 Status[a]**	**2017 Targets**	**LANL Status**
Area specific resistance at maximum operating temperature	Ohm cm^2	0.086	0.02	0.05
Hydroxide conductivity (σ)	mS/cm	70	100[b]	50
Membrane formation ability	μm	60	20[b]	25
Chemical stability after immersion in 0.5 M, NaOH at 80°C for 100 h	% σ decrease	75	0	33

[a] From our previous project: poly(phenylene) membrane (ATM-PP) [1]
[b] Based on PEMFC transportation application target; Corresponding areal resistance: <0.02 Ohm cm^2

FY 2014 Accomplishments

- Developed synthetic route to produce thin and tough perfluorinated anion exchange membranes with the thickness range from 20 to 50 μm and the elongation at break >200%.
- Demonstrated good hydroxide conductivity (30–80 mS/cm) at low water uptake <15% by introducing hydrophobic perfluorinated polymer backbone and guanidinium functional group.
- Improved chemical stability of perfluorinated membranes, ca. 3.3% conductivity loss after 120 hours 0.5 M NaOH treatment at 80°C by introducing more stable amide linkages between the perfluorinated polymer side chain and guanidinium functional group.
- Discovered superior HOR behaviors of Pt with perfluorinated ionomers to Pt with hydrocarbon ionomers from alkaline microelectrode experiments.

- Achieved excellent AMFC performance at 80°C using a perfluorinated anion exchange ionomer, ca. peak power density: 580 mW/cm^2.

INTRODUCTION

AMFCs are currently drawing tremendous attention because non-precious metal catalysts have shown good ORR activities under high pH environments. However, current AMFC performance using nonprecious metal catalyst is much inferior to their PEMFC counterparts. One of the reasons for this inferior performance is the unavailability of anion-conducting perfluorinated ionomers for AMFC systems. Perfluorinated ionomers have many desired properties for the use in fuel cell applications including good ionic conductivity, chemical stability, high oxygen permeability, hydrophobicity, less anion adsorption onto the catalyst, facile polymer chain mobility, the ability to create porous electrode structures. In the previous project (2008-2011), we first demonstrated stable perfluorinated hydroxide conducting ionomers from sequential reactions of Nafion® precursors. In the continuation of this effort, we report several updated research achievements to produce a series of perfluorinated hydroxide conducting polymers.

APPROACH

Our approach to achieve high performance AMFCs is to develop new hydroxide conducting perfluorinated membranes which have improved stability and conductivity compared to state-of-the-art benzyl ammonium-hydrocarbon based anion exchange membranes. The degradation of anion exchange membranes occurs not only at the cationic functional group and its linkage to the polymer but also at the polymer backbone itself [2]. In order to improve the polymer backbone stability, perfluorinated polymers are used. The hydrophobicity of the polymer backbone structure prevents the access of solubilized hydroxide ion and improves the alkaline stability. Resonance stabilized phenyl guanidinium is used for the cationic functional group. In order to enhance the stability of the functional group-polymer linkage, amide groups are used. The amide linkages are stable in both acid and base conditions. The general polymer structure is shown in Figure 1.

RESULTS

Synthesis: The synthesis of guanidinium functionalized perfluorinated polymers was accomplished with a three-step procedure: (i) attachment of tetramethyl guanidinium to Nafion®-COOH, (ii) functionalization of tetramethyl guanidinium, and (iii) methylation. We prepared a series of guanidinium functionalized perfluorinated polymers, PF-Amide-G1 to -G6, which have different amide and phenyl guanidinium groups. Cast membranes with thickness range from 20 to 50 μm were converted to hydroxide form. These cast membranes prepared from the reactions had excellent mechanical properties, e.g., tensile toughness is 19 MPa and elongation at break is >200% at 0% relative humidity and 50°C.

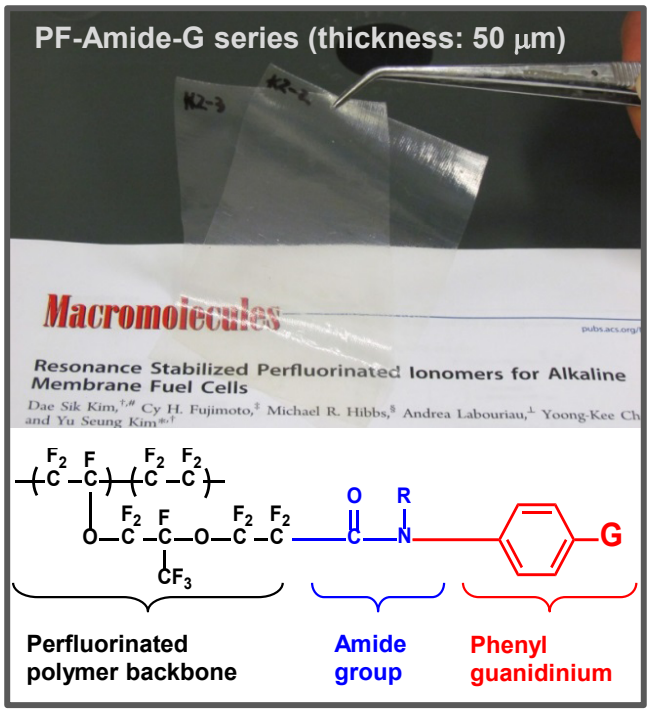

FIGURE 1. The Chemical Structure of PF-Amide-G Series Membranes

Hydroxide conductivity and water uptake: The hydroxide conductivity of the PF-Amide-G membranes was measured as a function of temperature. In order to avoid the possible (bi)carbonate formation, the hydroxide conductivity was measured in hydroxide-rich environment as described in the previous report [3]. Figure 2 shows the hydroxide conductivity of the PF-Amide-G membranes. The conductivity of PF-Amide-G membranes increases approximately 2-fold as the temperature increases from 30 to 80°C. The hydroxide conductivity of PF-Amide-G1 to G4 is comparable to that of the state-of-the-art benzyl trimethyl ammonium functionalized poly(phenylene) anion exchange membrane (ATM-PP). Improved conductivity was observed with for the PF-Amide-G5 and G6 membranes (40-60% higher than that of the reference ATM-PP polymer).

The water uptake of the PF-Amide-G membranes were less than 15 wt%, which was much lower than ATM-PP (~100 wt%). These extremely low water uptakes of the PF-Amide-G membranes were due to the hydrophobicity of perfluorinated polymer backbone and low hydration energy of guanidinium functional group. The low water uptake of the PF-Amide-G

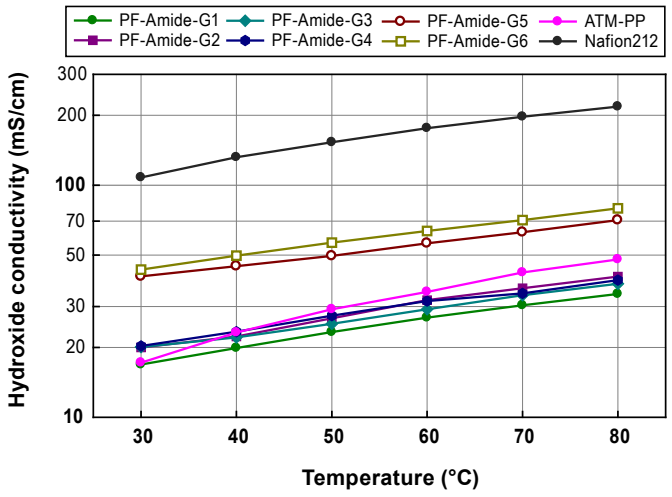

FIGURE 2. Hydroxide conductivity of PF-Amide-G series membranes as a function of temperature; proton conductivity of Nafion® 212 is drawn for comparison purpose.

membranes are desirable because (i) hydroxide conductivity can be further increased by increasing the ion exchange capacity of the membranes and (ii) the dimensional and membrane-electrode interfacial stability are better with low water swollen membranes.

Stabilities: The acid and alkaline stabilities of the PF-Amide-G membranes were investigated. The PF-Amide-G membranes exhibited excellent acid stability as we observed no chemical structural change of the membranes after acid treatment, 0.5 M H_2SO_4, 80°C for 24 h. The alkaline stability of the PF-Amide-G membranes was measured after alkaline treatment, 0.5 M NaOH, 80°C. The alkaline stability of the PF-Amide-G membranes strongly depends on the chemical structure of the amide linkage group since amide hydrolysis occurs before guanidinium cation degradation. The PF-Amide-G4 membrane showed 12.5% and 30.3% loss of the amide linkage after 120-h and 300-h NaOH treatments, respectively. The conductivity loss after stability test was 3.3% and 19.0% after 120 h and 300 h test, exceeding the FY 2014 milestone (<10% conductivity loss after 100 h in 0.5 M NaOH at 80°C).

Electrochemical activities: The electrochemical activity of an electro-catalyst in contact with the perfluorinated ionomer was examined using Pt microelectrode setup. We found that chain flexibility of ionomers is critically important for HOR behavior. The facile chain mobility of the perfluorinated ionomers allows diffusing the guanidinium cation group away from the Pt surface while the polymer stiffness of ATM-PP prevents the cation diffusion which brings quick readsorption upon applying low cell potential. As a result, the HOR current density of the PF-Amide-G2 ionomer coated with Pt is approximately 40% greater than that of ATM-PP coated with Pt (Figure 3). The microelectrode experiments also exhibited that the oxygen permeability of PF-Amide-G2 was 2.3×10^{12} mol s^{-1} cm^{-1} which was 2.5-fold greater than that of ATM-PP.

The AMFC performance and durability using PF-Amide-G2 was investigated. Figure 4 shows the hydrogen/oxygen AMFC performance of membrane electrode assemblies (MEAs) using PF-Amide-G2 and ATM-PP as an ionomeric binder in the AMFC electrodes at 80°C. The

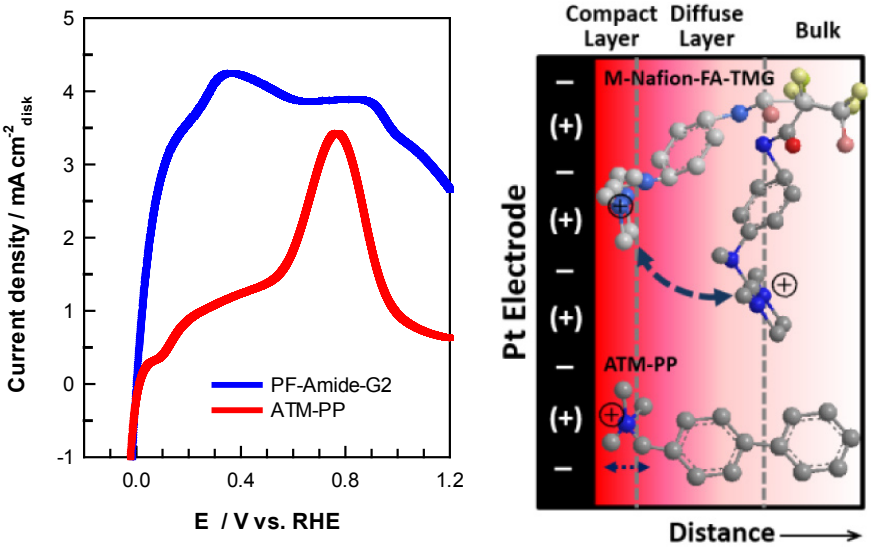

FIGURE 3. Hydrogen oxidation reaction of platinum in contact with PF-Amide-G2 and ATM-PP alkaline polymer electrolytes at 40°C after pre-conditioning at 1.4 V for 10s. Right figure: schematic diagram of ionomer relaxation on platinum surface during potential change.

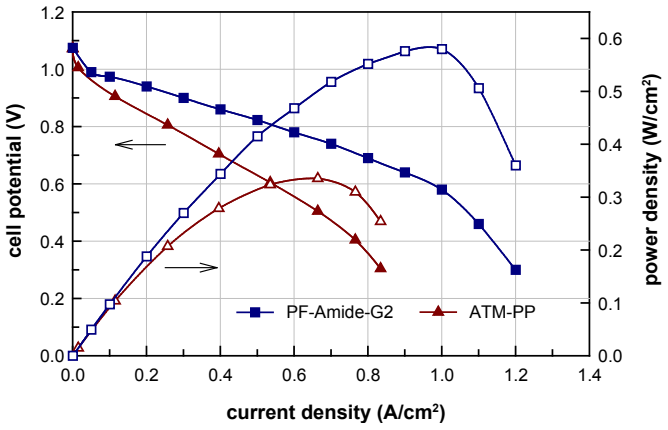

FIGURE 4. AMFC performance using ATM-PP and PF-Amide-G2 as the ionomeric binder for the electrode at 80°C; membrane: ATM-PP (50 μm thick); gas supply: H_2/O_2.

MEA using PF-Amide-G2 shows a maximum power density = 577 mW/cm^2 under H_2/O_2 conditions which is 172% of the maximum power density of a MEA using ATM-PP as an ionomeric binder under H_2/O_2 conditions. Higher oxygen permeability and lower cation adsorption potential of PF-Amide-G2 are the reasons for the better AMFC performance.

CONCLUSIONS AND FUTURE DIRECTIONS

- A series of perfluorinated anion exchange membranes (PF-Amide-G) were successfully prepared from Nafion®-COOH precursors and multi-step condensation reactions. The membranes prepared from newly developed chemistry have tough and ductile properties, e.g., the elongation at break of the membranes: >200% at 0% relative humidity, which is 10 times greater than that of the state-of-the-art ATM-PP.
- The hydroxide conductivity of the PF-Amide-G membranes ranged from 32 to 80 mS/cm at 80°C. The PF-Amide-G membranes had low water uptake, ca. six times lower water uptake at 30°C relative to the ATM-PP membranes having comparable hydroxide conductivity.
- The acid and alkaline stabilities of the PF-Amide-G membranes are excellent; no chemical degradation was observed after 0.5 M H_2SO_4 treatment at 80°C for 24 h. Only 3.4% hydroxide conductivity decreased after 0.5 M NaOH treatment at 80°C for 120 h, which exceeded the FY 2014 milestone.
- Excellent AMFC performance using PF-Amide-G2 ionomer was demonstrated. The Pt microelectrode experiments elucidated that the improved HOR kinetics and higher oxygen permeability of PF-Amide-G2 compared to ATM-PP.
- Further development of perfluorinated membranes having better stability and hydroxide conductivity and their performance and durability in AMFCs as a membrane as well as an ionomeric binder for the electrodes.

SPECIAL RECOGNITIONS & AWARDS/ PATENTS ISSUED

1. Anion Exchange Polymer Electrolytes, USP 8,492,049 B2 (2013)

2. Anion Exchange Polymer Electrolytes, USP 8,530,109 B2 (2013)

3. Poly(arylene)-based Anion Exchange Polymer Electrolytes, S-129,607, Patent pending (2014)

FY 2014 PUBLICATIONS/PRESENTATIONS

1. Hydrogen Oxidation and Oxygen Reduction Reaction at the Platinum-Alkaline Ionomer Interfaces, Sung-Dae Yim, Jerzy Chlistunoff, Hoon Chung, Yoong-Kee Choe, Tae-Hyun Yang, Yu Seung Kim, 225th ECS Meeting, May 11–16, 2014, Orlando, FL.

2. Molecular Design Aspect of Anion Exchange Polymer Electrolytes, Y.S. Kim, C. Fujimoto, M. Hibbs, Y.-K. Choe, D.-S. Kim, H. Chung, 224th ECS Meeting, Oct. 27 – Nov. 1, 2013, San Francisco, CA.

3. Resonance Stabilized Perfluorinated Ionomers for Alkaline Membrane Fuel Cells, D.S. Kim, C.H. Fujimoto, M.R. Hibbs, A. Labouriau, Y.-K. Choe, Y.S. Kim, *Macromolecules* 46, 7826-7833 (2013).

4. Alkaline Stability of Benzyl Trimethyl Ammonium Functionalized Polyaromatics: A Computational and Experimental Study, Y.-K. Choe, C. Fujimoto, K.-S. Lee, L. Dalton, K. Ayers, N.J. Henson, Y.S. Kim, manuscript submitted for publication (2014).

REFERENCES

1. Fuel Cell Technologies Office Multi-Year Research, Development and Demonstration Plan: Section 3.4 Fuel Cells, Fuel Cell Technologies Program, 2013. http://energy.gov/eere/fuelcells/fuel-cell-technologies-office-multi-year-research-development-and-demonstration-plan

2. C. Fujimoto, D.S. Kim, M. Hibbs, D. Wrobleski, Y.S. Kim, *J. Memb. Sci*. 423, 438 (2012).

3. D.S. Kim, A. Labouriau, M.D. Guiver, Y.S. Kim, *Chem. Mater.* 23, 3795 (2011).

V.D.1 High-Performance, Durable, Low-Cost Membrane Electrode Assemblies for Transportation Applications

Andrew Steinbach (Primary Contact),
Dennis van der Vliet, Cemal Duru, Andrei Komlev,
Darren Miller, Amy Hester, Mike Yandrasits,
Andrew Haug, John Abulu, and Matthew Pejsa
3M Company, Fuel Cell Components Program
3M Center, Building 201-2N-19
St. Paul, MN 55144-1000
Phone: (651) 737-0103
Email: ajsteinbach2@mmm.com

DOE Managers
Dimitrios Papageorgopoulos
Phone: (202) 586-5463
Email: Dimitrios.Papageorgopoulos@ee.doe.gov
Gregory Kleen
Phone: (720) 356-1672
Email: Gregory.Kleen@ee.doe.gov

Contract Number: DE-EE0005667

Subcontractors
- Johns Hopkins University, Baltimore, MD
- Michigan Technological University, Houghton, MI
- Lawrence Berkeley National Laboratory, Berkeley, CA
- General Motors Co., Pontiac, MI
- Argonne National Laboratory, Argonne, IL (collaborator)
- Los Alamos National Laboratory, Los Alamos, NM

Project Start Date: September 1, 2012
Project End Date: August 31, 2015

Overall Objectives

- Demonstrate a durable, low-cost, and high-performance membrane electrode assembly (MEA) for transportation applications, characterized by:
  - total platinum (Pt) group metal (PGM) loadings of ≤0.125 mg/cm^2 of MEA area,
  - performance at rated power of ≥1,000 mW/cm^2,
  - performance at ¼ power (0.8 V) of ≥0.3 A/cm^2,
  - durability of ≥5,000 hours under cycling conditions,
  - Q/ΔT of ≤1.45 kW/°C, and
  - cost of $5-9/kW, projected at high volume.
- Improve operational robustness to allow achievement of transient response, cold-startup, and freeze-startup system targets.

Fiscal Year (FY) 2014 Objectives

- Improve operational robustness via material optimization, characterization and modeling.
- Optimize post-processing of 3M Pt_3Ni_7 nanostructured thin film (NSTF) oxygen reduction reaction (ORR) cathode electrodes for improved MEA activity, durability, and rated-power capability.
- Integrate ultra-low PGM NSTF anode catalysts, NSTF cathode catalysts, and next-generation supported 3M polymer electrolyte membranes (PEMs) for improved MEA performance, durability, and cost.
- Identify key factors influencing NSTF MEA durability, with a primary focus on maintenance of rated power performance.

Technical Barriers

(A) Durability

(B) Cost

(C) Performance

Technical Targets

This project is focused on development of a durable, high-performance, low-cost, and robust MEA for transportation applications. Table 1 lists current project status against the DOE Technical Targets for Membrane Electrode Assemblies (Table 3.4.14) and a subset of Electrocatalyst Targets (Table 3.4.13) from the Multi-Year Research, Development and Demonstration Plan. The project status values are provided by results from the 2014 (March) Best of Class MEA, tested in duplicate and described at the bottom of Table 1. This MEA has achieved 91% of the performance at rated power and 42% of the performance @ 0.8 V characteristics, and PGM total content and Q/ΔT are higher than the allowable target by 3.2 and 5.5%, respectively. An estimate of total MEA cost is not available, but the PGM catalyst cost is estimated to be $5/kW. Durability with cycling status is not available.

FY 2014 Accomplishments

- Improved NSTF MEA operational robustness via development and integration of a durable, low PGM Pt/C interlayer which provides a 20°C improvement in minimum operating temperature for fast load transients up to 1 A/cm^2. Confirmed that the primary mechanism by which the anode GDL influences cold-startup

TABLE 1. Status against Technical Targets

Characteristic	Units	2017 Targets	3M 2014 Status*
Q/ΔT	kW/°C	1.45	1.53
Cost	$/kW	9	5 (PGM only @ $35/$g_{Pt}$)
Durability with cycling	hours	5,000	Not available
Performance @ 0.8 V	mA/cm^2	300	125
Performance @ rated power	mW/cm^2	1,000	907
Platinum group metal total content (both electrodes)	g/kW (rated)	0.125	0.143
PGM total loading	mg PGM/cm^2 electrode area	0.125	0.129

*3M Status with 2014 (March) Best of Class MEA:
0.019 mg_{PGM}/cm^2 PtCoMn/NSTF anode, 0.110 mg_{PGM}/cm^2 Pt_3Ni_7(TREATED)/NSTF cathode, 20μ 825 equivalent weight (EW) 3M PEM, 3M 2979 gas diffusion layers (GDLs), optimized flow fields. 90°C, 150 kPa H_2/air, 84°C dewpoints, 2.0/2.5 H_2/air stoichiometry.
Performance @ rated power, Q/ΔT characteristics calculated at 1.34 A/cm^2, 0.675 V.

capability of NSTF MEAs is its ability to influence MEA water balance.

- Developed chemical dealloying method for Pt_3Ni_7/NSTF cathodes which results in a 20% increase in MEA limiting current density over the baseline dealloying method. Demonstrated a 43% increase in rated power output per unit PGM (0.675 V) over 2012 pre-project status with the 3M 2014 (March) Best of Class MEA, directly reducing cost.
- Developed hypothesis that rated power degradation of NSTF MEA is most likely caused by generation of perfluorosulfonic acid (PFSA) PEM decomposition products which appear to irreversibly adsorb to the cathode electrode, leading to decreased ORR activity and electrode utilization.

✧ ✧ ✧ ✧ ✧

INTRODUCTION

While significant progress has been made, state-of-the-art PEM fuel cell MEAs utilized in today's prototype automotive traction fuel cell systems continue to suffer from significant limitations due to high cost, insufficient durability, and low robustness to off-nominal operating conditions. State-of-the-art MEAs based on conventional carbon-supported Pt nanoparticle catalysts currently incorporate precious metal loadings which are significantly above those needed to achieve MEA cost targets—performance, durability and/or robustness decrease significantly as loadings are reduced. This project focuses on integration of 3M's state-of-the-art NSTF anode and cathode catalysts with 3M's state-of-the-art PEMs, advanced and low-cost GDLs, and robustness-enhancing interfacial layers. At significantly lower precious metal content, the NSTF catalyst technology platform has several significant demonstrated benefits in performance, durability, and cost over conventional catalysts.

APPROACH

Optimize integration of advanced anode and cathode catalysts with next-generation PFSA PEMs, gas diffusion media, and flow fields for best overall MEA performance, durability, robustness, and cost by using a combined experimental and modeling approach.

RESULTS

One challenge of NSTF electrode MEA integration into automotive stacks has been its higher performance sensitivity to operating conditions than traditional thick dispersed electrode MEAs, especially at cool and wet conditions applicable to automotive startup. In previous work, we had shown that variation of the anode GDL can have an extraordinarily large positive influence [1], but the mechanism was unclear. This year, through combined materials characterization and modeling studies at 3M, Michigan Technological University and Lawrence Berkeley National Laboratory, several relevant factors have been identified. Spatial variation in the anode backing fiber density appears beneficial, possibly leading to higher limiting liquid water flux under cold-startup conditions (Figure 1A), higher retention of gas phase permeability (Figure 1B), both likely due to formation of preferential liquid/gas transport pathways and/or decreased water droplet detachment force [2], which ultimately results in decreased water content within the cathode electrode [3]. Based on these findings, anode backing optimization experiments with Freudenberg FCCT are currently in progress. In addition, we have also previously reported that integration of an interlayer (low-loaded Pt/C electrode between the NSTF cathode electrode and cathode GDL) improves NSTF MEAs' ability to rapidly transition from low- to high-current density under cool and wet operating conditions. This year, interlayer optimization studies have significantly improved the load transient capability at low temperature (passes at 30°C cell temperature with interlayer vs. 50°C without interlayer), with <0.02mg_{PGM}/cm^2 of interlayer loading [4]. The interlayer performance benefit has proven to be relatively durable. After 3,000 accelerated stress test voltage cycles up to 1.2 V, the mass activity was unchanged, the H_2/Air performance increased, and the load transient response improved (Figure 2).

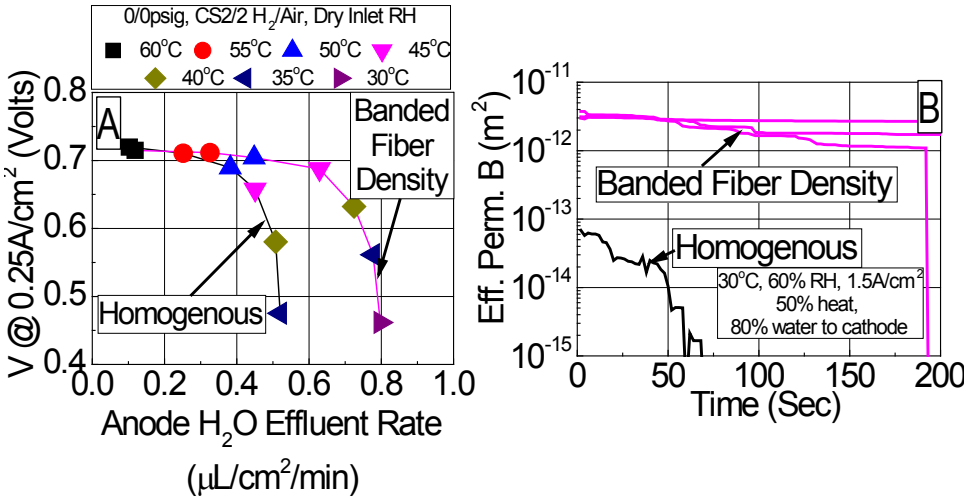

FIGURE 1. Influence of Anode GDL on Measured MEA Water Balance (A) and Modeled Gas Permeability (B) Under Cold-Startup Relevant Conditions

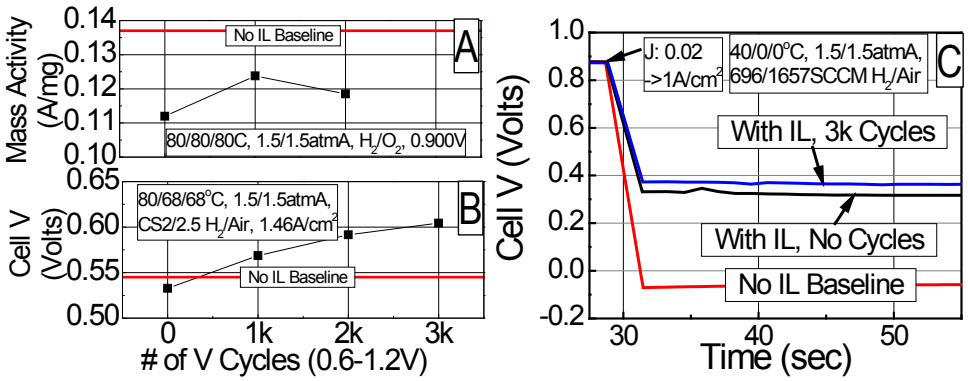

FIGURE 2. Performance of MEAs with Interim Downselected Cathode Interlayer as a Function of Number of Accelerated Stress Test Voltage Cycles (A): ORR Mass Activity. (B): Cell Voltage at 1.46A/cm^2, 150 kPa H_2/Air. (C): Stepwise Load Transient from 0.02 to 1.0 A/cm^2, at 40°C Cell Temperature. Accelerated Stress Test Cycles: 0.6-1.2 V vs. Reference Hydrogen Electrode, 20 mV/s, 70°C Cell Temperature.

Work has continued this year to improve the activity and rated power capability of Pt_3Ni_7/NSTF ORR cathode catalysts, through optimization of annealing and dealloying methods. Over the past year, development of an improved dealloying method at Johns Hopkins University has resulted in a ca. 20% increase in the H_2/air limiting current density over the baseline method [4]. High-angle annular dark-field (HAADF) scanning transmission electron microscopy (STEM) and X-ray photoelectron spectroscopy characterization at Oak Ridge National Laboratory has revealed that the dealloying transforms the Pt_3Ni_7/NSTF surface from NiO_x- to Pt-rich and forms nanoporosity [4]. HAADF STEM has also confirmed that annealing improves the process by which in situ nanoporosity develops during fuel cell operation, leading to 30% higher mass activity [4]. The dealloying development has enabled a significant improvement in rated power coincident with a PGM loading reduction. Figures 3A and 3B show measured polarization curves and PGM content per unit power output, respectively, for the pre-project baseline MEA (March 2012), the project Best of Class (BOC) MEA from last year (March 2013), and a further improved March 2014 BOC MEA. Compared to the pre-project baseline MEA, the March 2014 BOC MEA achieved a 60 mV gain in cell voltage at 1.41 A/cm^2 and reduced PGM content 14.5%, resulting in a 43% gain in power output per unit PGM at 0.675 V. Mass activity has been maintained at 0.38 A/mg. In addition, work has also been conducted to develop Pt_3Ni_7/NSTF cathode ORR kinetic and MEA performance models in collaboration with Argonne National Laboratory.

Extensive work has continued towards understanding the key factors which influence the durability of rated power performance with project MEAs. This year, additional

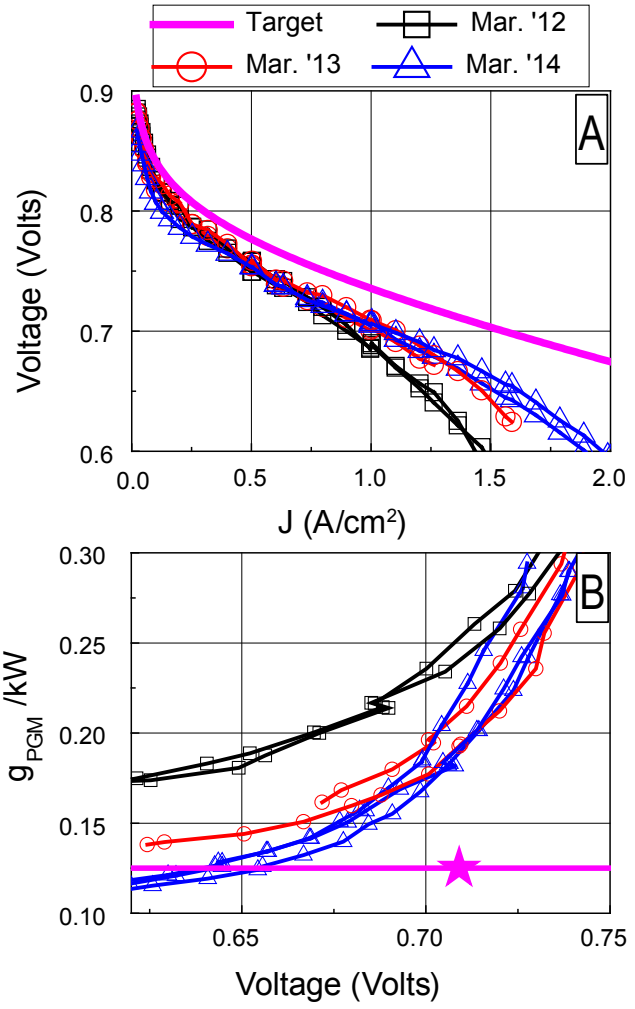

FIGURE 3. Performance Progression over Project for Integrated Project MEAs (A): Measured Polarization Curves. (B): PGM Content per Unit Power Output. Conditions: 90/84/84°C Cell/Anode/Cathode, 150/150 kPa H_2/Air, Stoichiometry 2.0/2.5.

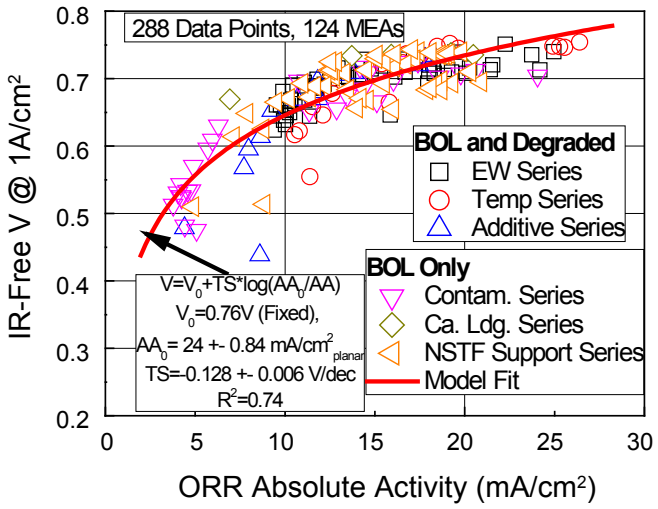

FIGURE 4. Relationship between H_2/Air Performance and ORR Absolute Activity for NSTF MEAs at Beginning of Life or After Degradation Due to Durability Testing—Conditions (H_2/Air): 80/68/68°C Cell/Anode/Cathode, 150/150 kPa H_2/Air, Stoichiometry 2.0/2.5. Conditions (ORR Activity): 80/80/80°C Cell/Anode/Cathode, 150/150 kPa H_2/O_2; After 17.5 minute hold at 0.900 V_{MEAS}.

diagnostic experiments have been conducted, efforts have been expanded to include studies at Los Alamos National Laboratory, and a primary hypothesis for the mechanism has been generated. Along with the operating temperature and PFSA EW effects noted last year [1], this year we have shown that presence of an ionomer chemical degradation mitigating agent decreases degradation rates 10x as compared to when the agent was not present in the MEA [4]. Cathode cyclic voltammetry indicates a correlation between performance degradation extent and the degree of cathode contamination by a (likely) anionic contaminant [4]. A correlation was identified between the H_2/Air cell voltage at 1 A/cm^2 and the cathode ORR activity, where the cell voltage decreases ca. 130 mV per decade of ORR absolute activity loss (Figure 4). With all factors taken into account, our hypothesis is that the loss of rated power performance is due to the (apparently) irreversible adsorption of PFSA PEM decomposition product(s) on the cathode electrocatalyst, resulting in substantial loss of ORR absolute activity and rated power.

Work has continued to integrate next generation PEMs with NSTF anode and cathode electrodes, including PEMs comprising mechanical supports and new ionomer types. In addition to the PEM-induced MEA areal-utilization losses noted last year [1], a factor was identified this year which resulted in substantial ORR activity and H_2/Air performance reduction with certain supported PFSA PEMs. Through extensive in-situ and ex situ diagnostic experiments, the loss mechanism was identified and the issue was resolved, leading to demonstration of expected performance. Additional work to integrate PEMs based on next generation 3M perfluoroimide acid and alternative PFSA ionomers, as well as the influence of PEM processing, is in progress.

CONCLUSIONS AND FUTURE DIRECTIONS

While significant progress has been made, considerable additional work is needed to achieve project performance, cost and durability targets and to improve operational robustness of NSTF MEAs. Primary future directions include:

- Demonstrate scale up feasibility of downselected Pt_3Ni_7 dealloying method, and incorporate best practice catalyst annealing for optimal MEA rated power and kinetic performance.
- Continue efforts towards improving NSTF MEA operational robustness, including materials optimization, characterization, and modeling of the anode gas

diffusion layer and further optimization of the cathode interlayer.

- Integrate advanced, thinner supported PEMs to increase performance and durability, and to reduce cost.
- Develop material and operational mitigation approaches to reduce rated-power degradation.

FY 2014 PUBLICATIONS/PRESENTATIONS

1. A.J. Steinbach and D.M. Peppin, "Polymer Electrolyte Membrane Fuel Cell Active Area Utilization Dependence on Relative Humidity Measured via AC Impedance High Frequency Resistance", *ECS Trans.* **58**(1) 1589-1600 (2013).

2. A. Steinbach, D. van der Vliet, S. Luopa, J. Erlebacher, and D. Cullen, "Dealloying and Annealing Optimization of High Mass Activity Pt_3Ni_7/NSTF ORR Cathodes for PEMFCs", 224th Electrochemical Society Meeting, Abstract #1350, San Francisco, CA, Oct. 2013.

3. A. Steinbach and D.M. Peppin, "PEMFC Active Area Utilization Dependence on Relative Humidity- Measured via AC Impedance High Frequency Resistance", 224th Electrochemical Society Meeting, Abstract #1579, San Francisco, CA, Oct. 2013.

4. A. Kusoglu and A.Z. Weber, "Morphology and Swelling of Perfluorosulfonic-acid (PFSA) Ionomer Thin Films," 224th Electrochemical Society Meeting, Abstract #1283, San Francisco, CA, Oct. 2013.

5. D.A. Cullen. "Optimizing fuel cell materials through electron microscopy and microanalysis", Annual Meeting of the Appalachian Regional Microscopy Society, Raleigh, NC, Nov. 15, 2013.

6. A. Kusoglu, A. Hexemer, and A. Weber, "Interfaces, Bulk, and Confinement in Nafion," Golden Gate Polymer Forum, San Francisco (invited), 2013.

7. Project Quarterly Report, Jan. 2014.

8. Project Quarterly Report, Apr. 2014.

9. P.K. Das, A. Santamaria, and A.Z. Weber, "Understanding liquid water and gas-diffusion layers," Grove Fuel Cell Science and Technology Conference, Amsterdam, 2014.

10. Andrew Steinbach, "High Performance, Durable, Low Cost Membrane Electrode Assemblies for Transportation Applications", Presentation FC104, 2014 DOE Annual Merit Review, Washington, DC, June 2014.

REFERENCES

1. Andrew J. Steinbach, Presentation FC104, 2013 Annual Merit Review, DOE Hydrogen and Fuel Cell Vehicles Technology Programs, May 2013, Washington, DC.

2. Adam Z. Weber, Presentation FC026, 2014 Annual Merit Review, DOE Hydrogen and Fuel Cell Vehicles Technology Programs, June 2014, Washington, DC.

3. Adam Z. Weber, Presentation FC026, 2013 Annual Merit Review, DOE Hydrogen and Fuel Cell Vehicles Technology Programs, May 2013, Washington, DC.

4. Andrew J. Steinbach, Presentation FC104, 2014 Annual Merit Review, DOE Hydrogen and Fuel Cell Vehicles Technology Programs, June 2014, Washington, DC.

V.D.2 Rationally Designed Catalyst Layers for PEMFC Performance Optimization

Debbie Myers (Primary Contact), Nancy Kariuki, Rajesh Ahluwalia, Xiaohua Wang, and Jui-Kun Peng

Argonne National Laboratory
9700 S. Cass Avenue
Lemont, IL 60439
Phone: (630) 252-4261
Email: dmyers@anl.gov

DOE Manager

Nancy Garland
Phone: (202) 586-5673
Email: Nancy.Garland@ee.doe.gov

Subcontractors

- Johnson Matthey Fuel Cells, Sonning Common, United Kingdom
  Jonathan Sharman, Alex Martinez, Dash Fongalland, Stephen Thorpe, Brian Theobald, L. Smith, D. Ozkaya, M. Gutierrez, Eleanor Dann, Graham Hards, and Willie Hall
- United Technologies Research Center (UTRC), East Hartford, CT
  Zhiwei Yang and Michael Perry
- University of Texas at Austin, Austin, TX
  Paulo Ferreira, Kang Yu, Somaye Rasouli, and Andres Godoy
- Indiana University - Purdue University Indianapolis (IUPUI), Indianapolis, IN
  Jian Xie, Chuankun Jia, Zhefei Li, Yun Zhou, and Fan Yang

Project Start Date: May 1, 2013
Project End Date: April 30, 2016

Overall Objectives

To realize the oxygen reduction reaction (ORR) mass activity benefits of dealloyed cathode electrocatalysts in membrane electrode assemblies (MEAs) and stacks operating at high current densities and on air and at low platinum group metal (PGM) loading ($\leq$0.1 mg_{Pt}/cm^2 on the cathode).

Fiscal Year (FY) 2014 Objectives

- Determine catalyst and cathode layer properties responsible for decline in dealloyed PtNi cathode air performance at >1 A/cm²
- Develop a cathode catalyst layer model for dealloyed catalyst
- Develop a method to impart proton conductivity to high surface area carbon supports

Technical Barriers

This project addresses the following technical barriers from the Fuel Cells section of the Fuel Cell Technologies Office Multi-Year Research, Development, and Demonstration Plan:

(A) Durability

(B) Cost

(C) Performance

Technical Targets

The technical targets for this project are listed in Table 1.

TABLE 1. Progress towards Meeting Technical Targets for Electrocatalysts and MEAs for Transportation Applications

Metric	Units	DOE 2020 Target	Project Status
ORR mass activity	A/mg_{PGM} @ 900 $mV_{iR\text{-}free}$	≥0.44	0.57
ORR specific activity	$\mu A/cm^2_{PGM}$	720	986
PGM total loading	mg_{PGM}/cm^2_{geo}	≤0.125	0.092 (cathode only)
MEA performance	mA/cm² @ 800 mV	≥300	298

FY 2014 Accomplishments

- Standard Pt/C, annealed Pt/C, and d-PtNi/C catalysts and catalyst-coated membranes (CCMs) containing approximately 0.1 mg Pt/cm² loading of these cathode catalysts have been fabricated, tested, and characterized.
- Three iterations of the d-PtNi with decreasing Ni content have been synthesized and fabricated into CCMs. Each iteration showed increasing ORR mass activity (0.53 A/mg-Pt to 0.57 A/mg-Pt) and improved H_2/air CCM performance at >1 A/cm².
- The best ORR mass activity obtained for the d-PtNi/C in a CCM was 0.57 A/mg-Pt, which exceeds the DOE 2020 target.
- Mass transport losses are higher with d-PtNi/C and annealed Pt/C-based cathodes as compared to conventional Pt/C.
- Modeling effort shows that mass transport losses are related to lower surface area enhancement factors (cathode catalyst electrochemically active surface area [ECA]/electrode area) of d-PtNi.

- Annealed Pt/C inks show smaller carbon agglomerates and a more branched and open secondary carbon structure than d-PtNi/C inks. This may impact interaction of ionomer with catalyst surface and consequently mass transport to catalytic sites.
- A functionalized carbon black with promising proton conductivity has been synthesized to address performance of low surface enhancement factor catalysts.

✧ ✧ ✧ ✧ ✧

INTRODUCTION

One of the major cost contributors to polymer electrolyte membrane fuel cell (PEMFC) systems for automotive and stationary power applications is the PGM cathode electrocatalyst [1]. The high cost of the cathode electrocatalyst results from the high loadings of catalyst necessary to overcome the limitations of low ORR activity, low utilization of PGM, and loss of activity with operating time. Alloying platinum with base metals (e.g., cobalt, iron, and nickel) is well known to improve its intrinsic ORR activity [2]. While ORR activities exceeding the DOE 2017 targets (>0.44 A/mg PGM and 720 μA/cm² @ 900 mV) have been demonstrated for high-surface-area-carbon-supported Pt alloy and core-shell nanoparticle catalysts in aqueous cell rotating disk electrode tests [3], some as high as 5.75 A/mg-Pt [4], the full activities and performance of these promising catalysts have yet to be achieved in MEAs, especially when operating at realistic current densities and on air rather than oxygen.

There are several possible reasons the full potentials of the advanced alloy, de-alloyed, and core-shell materials have not been realized in MEAs operating on air and at current densities >1 A/cm^2. One may arise from the complex requirements for full utilization of the electrocatalytic sites and for adequate reactant transport in the MEA cathode layer. These requirements are easily met in the fuel cell at low current densities in an oxygen environment where the electrocatalytic reaction rate dominates the voltage losses and demands on transport to the reactive sites are easily filled. Fulfillment of these requirements at high current densities in an MEA cathode relies on optimization of the electrode composition and structure to balance the structure of the proton-conducting phase, the electron-conducting phase, and the distribution and size of pores for reactant/product diffusion. This optimization is a lengthy, trial-and-error process and has taken several years for the traditional Pt-only cathode layers. The goal of this project is to optimize the electrode layer composition, structure, and materials properties of cathodes based on advanced alloy catalysts so their intrinsically high performance for the ORR can be translated into performances at high current densities and on air which exceed simultaneously the DOE performance, durability, and cost targets for PEMFCs for automotive applications.

APPROACH

The advanced Pt alloy catalyst chosen for this project consists of a range of dealloyed PtNi (d-PtNi) catalysts developed by Johnson Matthey Fuel Cells in the General Motors-led project (FC087). A range of PtNi alloys were chosen with different Pt:Ni ratios in order to investigate the impact of base metal content on mass activity and performance at high current density on air. The key catalyst characteristics and metrics are:

- Catalyst deposited as nanoparticles onto Ketjenblack® supports
- Catalyst deposition chemistry is proven and via methods scalable to commercial levels
- Mass activity exceeds DOE 2020 target
- Mass activity loss after 30,000—0.60 to 1.0 V cycles exceeds the DOE kinetic stability target.

This project is following a multi-pronged approach to achieving the goals. The approach to translating these high ORR mass activities to MEA performance at automotive-relevant high current densities is to first determine the property or properties of the electrode/catalyst that limit(s) the high current density/air performance of electrodes based on this catalyst type. The approach and techniques being used to elucidate these properties are:

- In-cell diagnostics of d-PtNi versus high-surface-area Pt (non-annealed Pt) and Pt of comparable ECA (annealed Pt).
- In situ and ex situ characterization: transmission electron microscopy (TEM), cryogenic TEM, dynamic light scattering, ultra-small angle X-ray scattering, and X-ray absorption spectroscopy to:
  - Study the dispersion of d-PtNi/C catalyst aggregates and the perfluorinated sulfonic acid ionomer particles in liquid media and in electrodes and compare them to Pt/C-based inks and electrodes.
  - Study the effects of solvent type and solvent removal processes on the agglomerate structure of the electrodes.
- Modeling to correlate electrode performance under a variety of conditions to electrode structure and morphology.

Once the performance-limiting properties are determined, the project approach is to use computational modeling to guide the design of the catalyst layer composition and structure and carbon support functionality to mitigate the performance limitations. Tools which can be used to modify the electrode structure are the use of alternative ink compositions and solvent removal processes to minimize Ni corrosion and result in the optimum agglomerate structure in d-PtNi/C-based electrodes. An

approach being pursued to allow greater flexibility in the design of the electrode structure is the decoupling of the proton-conducting and binder electrode components by imparting proton conductivity to the carbon support through functionalization.

RESULTS

Four iterations of the d-PtNi/C with decreasing Ni content were synthesized and fabricated into CCMs. Each iteration showed improved ORR mass activity (0.53 A/mg-Pt to 0.57 A/mg-Pt) and improved H_2/air performance at >1 A/cm² (Figure 1). The best ORR mass activity obtained for the d-PtNi/C in a CCM was 0.57 A/mg-Pt, which exceeds the DOE 2020 target (0.44 A/mg-Pt).

To determine the electrode property or properties limiting the performance of the d-PtNi/C-based cathode and decouple the effect of catalyst surface area from an effect unique to the base metal-containing catalysts, the standard Pt/C catalyst of 2.0 nm mean Pt particle diameter was annealed to grow the mean particle size to 5.8 nm which is comparable to that of the d-PtNi/C catalysts (5.1 to 5.8 nm). CCMs with cathodes comprised of standard Pt/C, annealed Pt/C, and d-PtNi/C at loadings of 0.1 mg Pt/cm² and an ionomer to carbon ratio of 0.8 were fabricated, tested, and characterized under a variety of test conditions and using numerous characterization techniques. The diagnostics included hydrogen pump, hydrogen crossover, ECA by CO stripping, cyclic voltammetry and impedance characterization under nitrogen and air atmospheres. The various test conditions included different oxygen concentrations on the cathode (pure oxygen to 1% oxygen), temperatures (60°C, 70°C, 80°C, and 90°C), back pressures (100, 150, 200, and 250 kPa_{abs}), and relative humidities (100, 85, 55, and 30%). The polarization curves for MEAs with d-PtNi/C, standard non-annealed Pt/C, and annealed Pt/C cathode catalysts are shown in Figure 2. Modeling of these data to determine the sources of the observed voltage losses (i.e., purely resistive, kinetic, or mass transport) showed that mass transport losses are higher with d-PtNi/C and annealed Pt/C-based cathodes as compared to standard non-annealed Pt/C, while the kinetic losses are lower for d-PtNi/C and standard non-annealed Pt/C as compared to the annealed Pt/C due to higher area-specific activity and higher ECA, respectively (Figure 3). The modeling effort showed that the mass transport losses, particularly under fully humidified conditions, are related to lower surface area enhancement

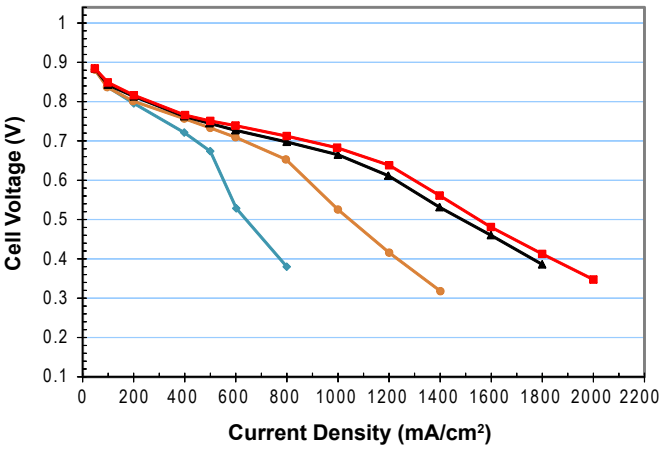

FIGURE 1. Hydrogen-air polarization curves at 80°C, 100% relative humidity, and 2 atm for MEAs with subsequent versions of the d-PtNi/C cathode catalyst (blue – first version; red – latest version) at a cathode loading of ~0.09 mgPt/cm².

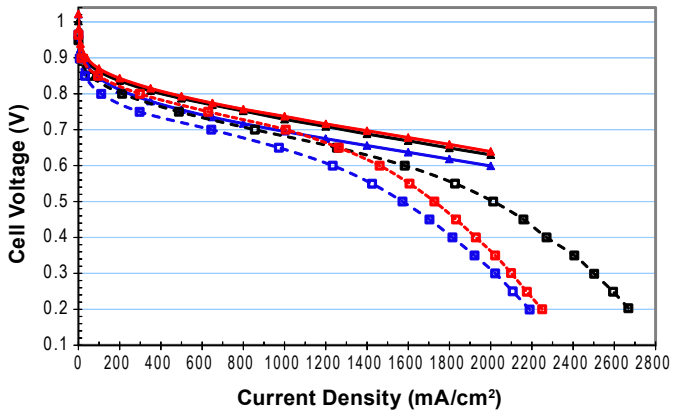

FIGURE 2. Hydrogen-oxygen (solid lines) and hydrogen-air (dashed lines) polarization curves at 80°C, 100% relative humidity, and 1.5 atm for MEAs with d-PtNi/C, non-annealed Pt/C, and annealed Pt/C cathode catalysts at a cathode loading of ~0.09 mgPt/cm².

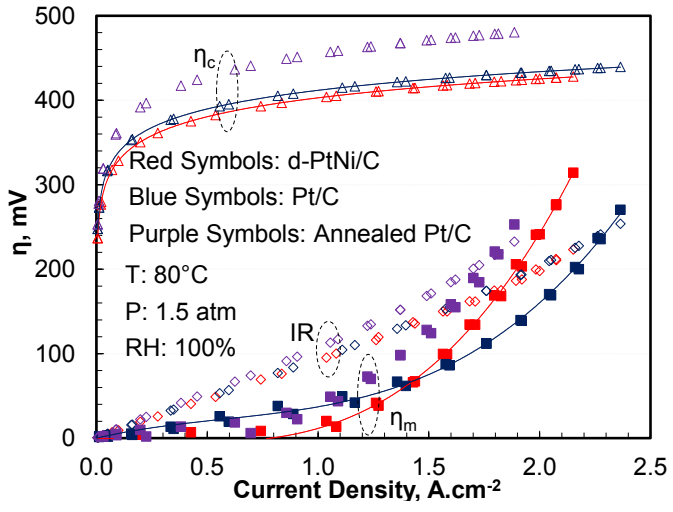

FIGURE 3. Breakdown of overpotentials for hydrogen-air polarization curves taken at 80°C, 100% relative humidity, and 1.5 atm for MEAs with d-PtNi/C (red), non-annealed Pt/C (blue), and annealed Pt/C (purple) cathode catalysts at a cathode loading of ~0.09 mgPt/cm².

factors (ECA/electrode area) of the d-PtNi/C-based cathodes and indicated a relatively minor role of Ni in the increased mass transport losses.

Catalyst-ionomer inks with ionomer to carbon ratios of 0.8, 1.0, and 1.2 and with varied concentration of solids and ink solvent (water or water-propanol mixtures) were characterized by dynamic light scattering, ultra-small angle X-ray scattering (USAXS), and cryogenic TEM to determine carbon-ionomer aggregate and agglomerate size distributions. As shown in Figure 4, the aqueous annealed Pt/C inks show smaller carbon agglomerates and a more branched and open secondary carbon structure than d-PtNi/C inks of equivalent formulation. It was also found, by USAXS, that the type of solvent in the inks changes the aggregate structure of the d-PtNi/C inks, but not that of the annealed Pt/C inks (Figure 4). This is an effect which can be exploited to improve the transport properties of the d-PtNi/C-based cathodes.

A diazonium coupling reaction was used to functionalize carbon black and catalyzed carbon black with sulfonate groups to impart proton conductivity to decrease the reliance on ionomer for adequate proton conductivity in the cathode layer [5]. Functionalization levels of 15 wt% for the annealed Pt/C catalyst were verified by thermogravimetric analysis. A proton conductivity of 0.05 S/cm was measured ex situ for a catalyst layer comprised of sulfonate-functionalized carbon black and a Teflon® binder.

CONCLUSIONS AND FUTURE DIRECTIONS

Conclusions

- Mass transport losses are higher with d-PtNi/C and annealed Pt/C-based cathodes as compared to conventional Pt/C.
- Modeling of the cell losses suggest that mass transport losses are related to the lower surface area enhancement factors (ECA/electrode area) of the d-PtNi and annealed Pt/C.
- Annealed Pt/C inks show smaller carbon agglomerates and a more branched and open secondary carbon structure than d-PtNi/C inks. This may impact interaction of ionomer with catalyst surface and consequently mass transport to catalytic sites.
- A functionalized carbon black with promising proton conductivity and low relative humidity performance has been synthesized to address performance of low-SEF catalysts.

Future Directions

- Determine if Ni leached from d-PtNi/C during electrode fabrication is impacting electrode structure/properties:

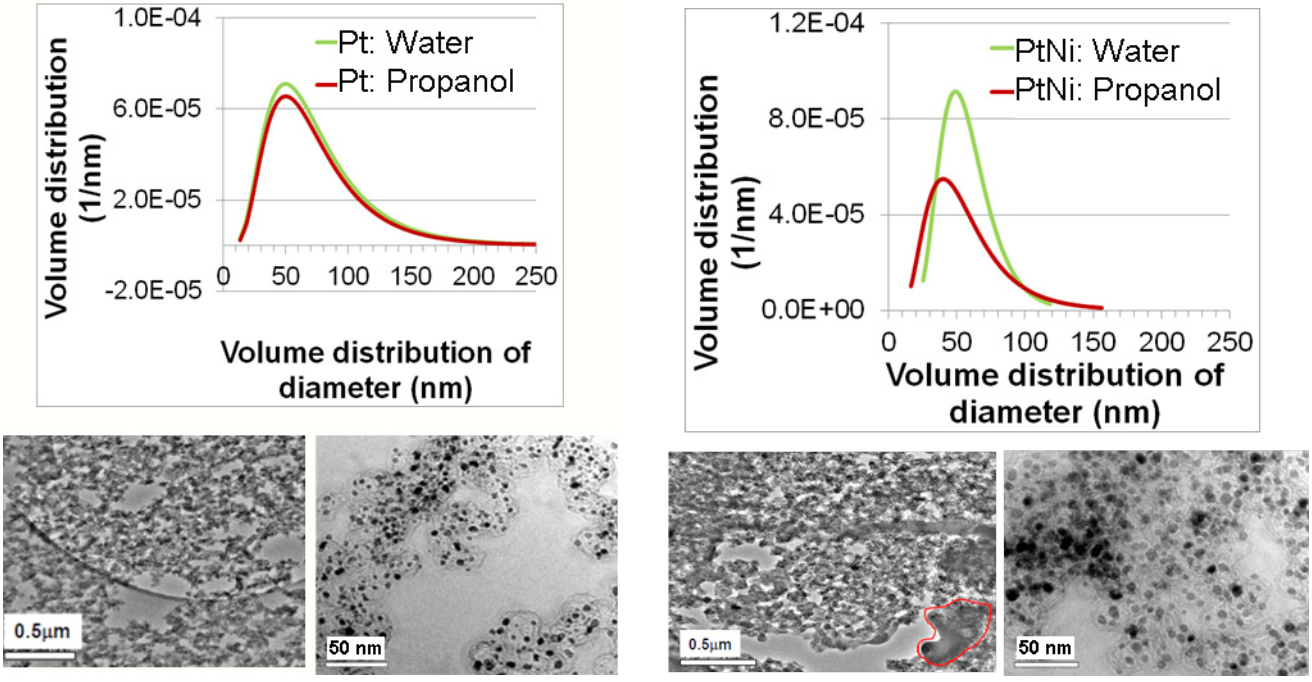

FIGURE 4. Ultra-small angle X-ray scattering-determined agglomerate distributions of water-ionomer and water-propanol-ionomer catalyst inks and cryogenic transmission electron micrographs of water-ionomer-catalyst inks: annealed Pt/C (left) vs. d-PtNi/C (right).

  - Experiments are planned to add Ni^{2+} to Pt/C electrode layers
- Improve performance at high current densities for low-SEF electrodes with different ionomer content, equivalent weight ionomer, ink solvent, and/or proton-conducting carbon supports:
  - d-PtNi/C-containing CCMs with new ionomer/carbon ratio have been delivered to UTRC for testing/diagnostics
  - Electrodes using proton-conducting supports are being fabricated by IUPUI
  - The effect of the testing conditions, such as cell pressure and cell temperature, will be examined.
- Complete USAXS, cryo-TEM, TEM analysis of ink and electrodes for input into the model of electrode structure.
- Additional analysis of diagnostic data for annealed Pt/C and d-PtNi/C electrode layers and CCMs:
  - Impedance spectroscopy for breakdown of mass transport overpotentials for GDL, catalyst layer pores, and ionomer.
  - Steady-state oxide coverage measurements, kinetics of oxide formation.
- Determine proton conductivity and electronic conductivity as a function of temperature and relative humidity (ex situ) for electrodes made from the various catalysts and inks.

FY 2014 PUBLICATIONS/PRESENTATIONS

1. Nancy Kariuki, Deborah Myers, and James Gilbert, "X-ray Scattering and Absorption Studies of Polymer Electrolyte Fuel Cell Cathode Electrocatalysts", Abstract and Invited Presentation, 248th American Chemical Society National Meeting, San Francisco, California, August 10–14, 2014.

2. Deborah Myers, James Gilbert, Nancy Kariuki, Xiaoping Wang, and A. Jeremy Kropf, "Durability of Low-Temperature Fuel Cell Electrocatalysts", Abstract and Invited Presentation, 225th Electrochemical Society Meeting, Orlando, Florida, May 11–16, 2014.

3. Deborah J. Myers, Nancy N. Kariuki, A. Jeremy Kropf, and James A. Gilbert, "In situ X-ray absorption and scattering studies of proton exchange membrane fuel cell electrocatalysts", Abstract and Invited Presentation, *In Situ Studies of Fuel Cell Materials and Devices Symposium,* 247th American Chemical Society National Meeting, Dallas, Texas, March 19, 2014.

4. Deborah Myers, Nancy Kariuki, and Xiaoping Wang, "The Effects of Polymer Electrolyte Fuel Cell Fabrication on Pt and Pt alloy Electrocatalysts", Abstract and Presentation, 224th Electrochemical Society Meeting, San Francisco, California, October 27 – November 1, 2013.

5. Lili Sun, Zhefei Li, Andrew Saab, and Jian Xie, "Improving MEA Kinetic Performance through Removing Nafion Ionomer Binders in a Catalyst Layer", Abstract and Presentation, 224th Electrochemical Society Meeting, San Francisco, California, October 27 – November 1, 2013.

REFERENCES

1. Papageorgopoulos, "Fuel Cells-Session Introduction", 2013 DOE Hydrogen and Fuel Cells Program and Vehicle Technologies Program Annual Merit Review and Peer Evaluation Meeting, Washington D.C., May 13–17, 2013.

2. (a) Gasteiger, H.A.; Kocha, S.S.; Sompalli, B.; Wagner, F.T., Activity benchmarks and requirements for Pt, Pt-alloy, and non-Pt oxygen reduction catalysts for PEMFCs. Appl Catal B-Environ 2005, 56 (1-2), 9-35; (b) Thompsett, D., Pt Alloys as Oxygen Reduction Catalysts. In Handbook of Fuel Cells: Fundamentals, Technology and Applications; Vol 3, Vielstich, W.; Lamm, A.; Gasteiger, H. A., Eds. John Wiley & Sons: Chichester, 2003; p 467.

3. (a) Zhang, J.; Lima, F.H.B.; Shao, M.H.; Sasaki, K.; Wang, J.X.; Hanson, J.; Adzic, R.R., "Platinum monolayer on non-noble metal-noble metal core-shell nanoparticle electrocatalysts for O_2 reduction", J Phys Chem B 2005, 109 (48), 22701-22704; (b) Wang, C.; van der Vilet, D.; Chang, K.C.; You, H.D.; Strmcnik, D.; Schlueter, J.A.; Markovic, N.M.; Stamenkovic, V.R., "Monodisperse Pt_3Co Nanoparticles as a Catalyst for the Oxygen Reduction Reaction: Size-Dependent Activity", J Phys Chem C 2009, 113 (45), 19365-19368; (c) Wang, C.; Wang, G.F.; van der Vliet, D.; Chang, K.C.; Markovic, N.M.; Stamenkovic, V.R., "Monodisperse Pt_3Co nanoparticles as electrocatalyst: the effects of particle size and pretreatment on electrocatalytic reduction of oxygen.", Phys Chem Chem Phys 2010, 12 (26), 6933-6939; (d) Markovic, N.; Stamenkovic, V., Nanosegregated Cathode Alloy Catalysts with Ultra-Low Platinum Loading. DOE Fuel Cell Technologies Annual Report 2012.; (f) Debe, M.K.; Steinbach, A.J.; Hendricks, S.M.; Kurkowski, M.J.; Vernstrom, G.D.; Atanasoski, R.T.; Hester, A.E.; Haug, A.T.; Lewinski, K.A.; Deppe, S.K., "Advanced Cathode Catalysts and Supports for PEM Fuel Cells", DOE Hydrogen Program 2012 Annual Report 2012; (g) Mani, P.; Srivastava, R.; Strasser, P., "Dealloyed Pt-Cu core-shell nanoparticle electrocatalysts for use in PEM fuel cell cathodes", J Phys Chem C 2008, 112 (7), 2770-2778.

4. (a) Markovic, N.; Stamenkovic, V., "Nanosegregated Cathode Alloy Catalysts with Ultra-Low Platinum Loading", DOE Hydrogen Program Annual Report 2013; (b) Chen, C.; Kang, Y.; Huo, Z.; Zhu, Z.; Huang, W.; Xin, H.L.; Snyder, J.D.; Li, D.; Herron, J.A.; Mavrikakis, M.; Chi, M.; More, K.L.; Li, Y.; Markovic, N.M.; Somorjai, G.A.; Yang, P.; Stamenkovic, V.R. "Highly Crystalline Multimetallic Nanoframes with Three-Dimensional Electrocatalytic Surfaces", Science 2014, 343 (6177), 1339-1343.

5. Xu, Fan; Wang, Mei-xian; Sun, Lili; Liu, Qi; Sun, Hong-fang; Stach, Eric A.; and Xie, Jian, "Enhanced Pt/C catalyst stability using pbenzensulfonic acid functionalized carbon blacks as catalyst supports", Electrochim. Acta 2013, 94, 172– 181.

V.E.1 Durability Improvements through Degradation Mechanism Studies

Rod Borup[1] (Primary Contact),
Rangachary Mukundan[1], Dusan Spernjak[1],
Roger Lujan[1], David Langlois[1], Fernando Garzon[1],
S. Michael Stewart[1], Rajesh Ahluwalia[2],
Xiaohua Wang[2], Adam Weber[3], Ahmet Kusoglu[3],
Karren More[4], Steve Grot[5]

[1]Los Alamos National Laboratory (LANL)
MS D429, P.O. Box 1663
Los Alamos, NM 87545
Phone: (505) 667-2823
Email: Borup@lanl.gov

DOE Manager
Nancy Garland
Phone: (202) 586-5673
Email: Nancy.Garland@ee.doe.gov

Subcontractors & Collaborators
[2] Argonne National Laboratory, Argonne, IL
[3] Lawrence Berkeley National Laboratory, Berkeley, CA
[4] Oak Ridge National Laboratory, Oak Ridge, TN
[5] Ion Power, New Castle, DE

Start Date: October, 2009
Project End Date: Project continuation and direction determined by DOE

Overall Objectives

- Identify and Quantify Degradation Mechanisms
  - Degradation measurements of components and component interfaces
  - Elucidation of component interactions, interfaces, and operations leading to degradation
  - Development of advanced in situ and ex situ characterization techniques
  - Discern the impact of electrode structure on durability and performance
    - Develop concepts for designing more stable electrode structures
- Develop Models Relating Components and Operating Conditions to Fuel Cell Durability
  - Individual degradation models of individual fuel cell components
  - Development and dissemination of an integrated comprehensive model of cell degradation
- Develop Methods to Mitigate Degradation of Components
  - Use degradation mechanisms to design new materials/structures to improve durability
  - Develop operating strategies to improve durability
  - Provide predictive comparisons for material durability related to operational aspects

Fiscal Year (FY) 2014 Objectives

- Quantify degree of cerium migration during fuel cell operation in membranes
- Quantify and compare the loss of pore volume after drive cycle tests of 0, 50, 100, 200, 400, and 1,000 hours
- Complete testing comparison of single type carbons and mixed carbons (high surface area carbon and graphitized) comparing the structure effect on mass transport losses
- Evaluate the effect of catalyst layer cracks on membrane durability during relative humidity (RH) cycling (wet/dry drive cycle tests)

Technical Barriers

This project addresses the following technical barriers from the Fuel Cells section of the Fuel Cell Technologies Office Multi-Year Research, Development, and Demonstration Plan:

(A) Durability

(B) Cost

Technical Targets

- Transportation Durability: 5,000 hours (with cycling)
  - Estimated start/stop cycles: 17,000
  - Estimated frozen cycles: 1,650
  - Estimated load cycles: 1,200,000
- Stationary Durability: 40,000 hours
  - Survivability: Stationary -35°C to 40°C
  - Cost: $25/kWe

FY 2014 ACCOMPLISHMENTS

INTRODUCTION

The durability of polymer electrolyte membrane (PEM) fuel cells is a major barrier to the commercialization of these systems for stationary and transportation power applications. By investigating component and cell degradation modes, thereby defining the fundamental degradation mechanisms of components and component interactions, new materials can be designed to improve durability. To achieve a deeper understanding of PEM fuel cell durability and component degradation mechanisms, we utilize a multi-institutional and multi-disciplinary team with significant experience investigating these phenomena.

APPROACH

Our approach to understanding durability and degradation mechanisms within fuel cells is structured in three areas: fuel cell testing (life testing, accelerated stress tests, ex situ aging), characterization of component properties as a function of aging time, and modeling (component aging and integrated degradation modeling). The modeling studies tie together what is learned during component characterization and allow better interpretation of the fuel cell studies. This approach and our team give us the greatest chance to increase the understanding of fuel cell degradation and to develop and employ materials that will overcome durability limitations in fuel cell systems. This work is also being coordinated with other funded projects examining durability through a DOE Durability Working Group.

RESULTS

Electrode Structural Changes

The cathode catalyst layer structure has been found previously in this project to change during operation. We have also experimentally shown that carbon corrosion exists at normal fuel cell operating conditions. This carbon corrosion (as measured by CO_2 evolution) is exacerbated by the voltage cycling inherent in the drive cycle. An example of how the cathode catalyst layer changes is shown by scanning transmission electron microscopy (STEM) in Figure 1 after utilizing a simulated drive cycle test prescribed by DOE/ Fuel Cell Tech Team [3]; in this case the drive cycle test RH was held continuously at 100%. STEM post-analysis shows gradual thinning of the catalyst layer during operation. The reduction in catalyst layer width can be due to the loss of carbon through carbon corrosion or due to compaction; both effects likely lead to a loss of void volume. A sharp decrease in catalyst layer thickness is observed within the first 100 hours of operation (30%), eventually reaching ~50% of its thickness after 1,000 hours. The reduction in catalyst layer thickness leads to increases in mass transport resistance as well as contributing to the loss of Pt electrochemical surface area (ECSA). While the cathode has thinning/compression, there is little evidence for carbon corrosion from the microscopic analysis:

- The majority of the VULCAN® retains its meso-graphitic structure
- Structure of the carbon support is unchanged (observe abundant VULCAN® graphitic structure)
- Little densification (banding) until 1,000 h, and even then it is minimal
- The cathode catalyst layer structural changes during the drive cycle are very different than that which is observed during carbon corrosion holds at 1.2 V
- There is also an increased Pt migration into the membrane with increased drive cycle time

The loss of catalyst layer void volume is shown by digitized STEM images in Figure 2. The estimation of pore shape and (area) volume percent is made from two-dimensional image "slices" taken of the catalyst layer.

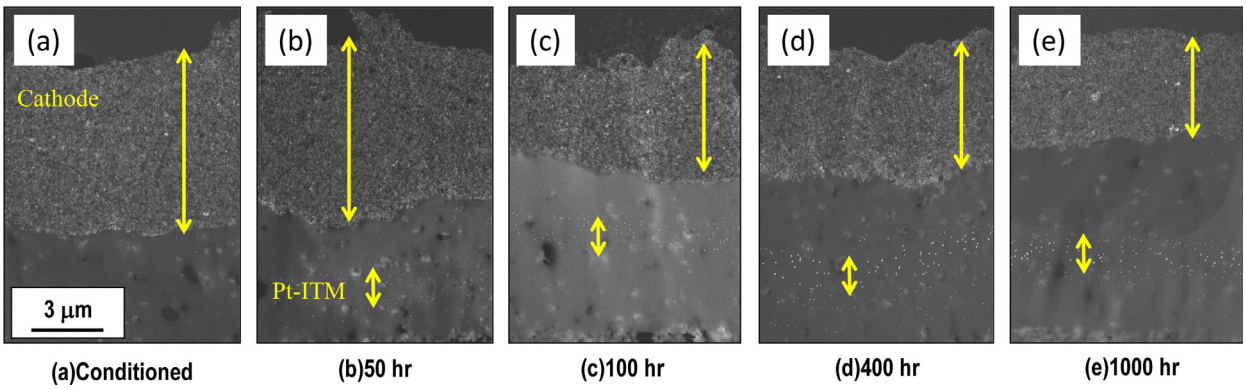

FIGURE 1. STEM images of the cathode catalyst layer and the membrane with VULCAN® Carbon (a) after conditioning (b) after 50 hours (c) after 100 hours (d) after 400 hours, and (e) after 1,000 hours of testing using the U.S. DRIVE Durability Drive Cycle Test operating at 100% RH.

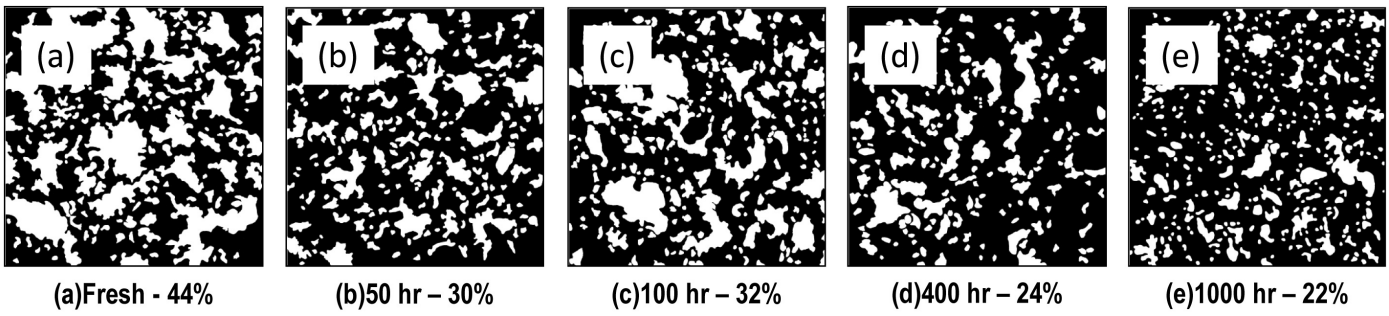

FIGURE 2. Digitized STEM images of the cathode catalyst layer examining the catalyst layer porosity with VULCAN® Carbon (a) after conditioning (b) after 50 hours (c) after 100 hours (d) after 400 hours, and (e) after 1,000 hours of testing using the U.S. DRIVE Durability Drive Cycle Test operating at 100% RH.

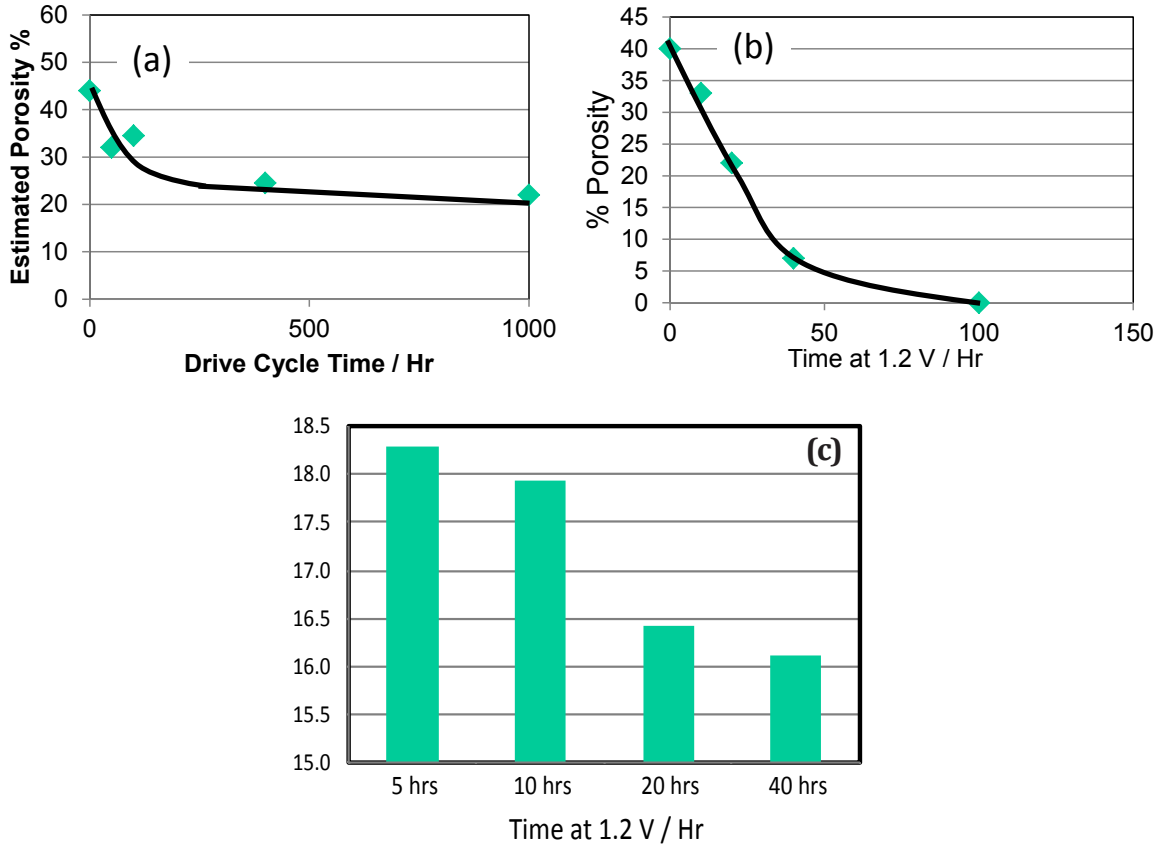

FIGURE 3. Cathode catalyst layer porosity during (a) drive-cycle operational time evaluated by STEM (b) during a carbon corrosion hold evaluated by STEM, and (c) during a carbon corrosion hold evaluated by MIP based on 0.01 to 0.2 micron pores.

The overall pore size and percent porosity decreases with increasing drive cycle time, with an initially large change followed by a gradual decline which appears to reach a limit. The void volume during the drive cycle time is shown in Figure 3a. An accelerated stress test (a potential hold of the cathode at 1.2 V inducing carbon corrosion) was used to evaluate the cathode support material Figures 3b and 3c show the changing catalyst layer porosity measured during carbon corrosion holds evaluated by digitized STEM images (3b) and mercury intrusion porosimetry (3c), where the void volume measured was limited to 0.01 to 0.2 micron sized pores. The mercury intrusion porosimetry (MIP) analysis was limited to these pore sizes as that is the predominant size of the pores in the electrode layer, as opposed to the membrane. Both the STEM and MIP show that the cathode catalyst layer porosity decreases rapidly during the carbon corrosion hold, contrasting to the initial rapid decrease but leveling off during drive cycle operations.

Cerium Migration

During the oxygen reduction reaction (ORR), whereby oxygen is converted to water, hydrogen peroxide and hydroxyl radicals are generated and are believed to be the principle cause of membrane chemical degradation. Cerium cations provide a viable option for inducing hydrogen peroxide decomposition as cerium plays a role in peroxide decomposition. Cerium cations can also facilitate the scavenging of radicals, which are generated during the decomposition process. We have measured the changes in the distribution of cerium cations during the lifetime of the fuel cell.

Figure 4a shows the initial cerium concentration in fresh DuPont™ XL membranes and how the cerium content of the membrane electrode assembly (MEA) decreases during operating time under OCV conditions (80°C and 100% RH). After 750 hours, only about 20% of the original cerium is left in the membrane. We have also observed that the cerium content decreases during normal fuel cell operation. The movement of cerium in the ionomer phase is quite quick as demonstrated by the results in Figure 4b where two Nafion® N211 membranes containing no cerium were hot/wet pressed with a DuPont™ XL membrane containing cerium. The cerium equilibrates between the N211 and XL membranes within the 10 minute pressing process at 90°C. During fuel cell operation, we have observed that cerium migrates from the membrane into both the anode and the cathode catalyst layer. Post-characterization shows that cerium in the cathode catalyst layer will migrate through the membrane to the anode catalyst layer, with little cerium remaining in the membrane.

CONCLUSIONS

We have measured and quantified catalyst layer thinning during both accelerated stress tests (inducing carbon corrosion) and voltage cycle tests mimicking vehicle operation (drive cycle). Carbon corrosion is observed during the normal operating cycle potentials, although in a significantly smaller amount than is induced by start/stop cycles. During drive cycle operations the catalyst layer thins in width, which is not due solely to carbon corrosion, although carbon corrosion likely plays a role. Most of this thinning must be from compaction of the material in the catalyst layer. This reduction in thickness leads to the loss of catalyst layer porosity, which increases performance losses due to mass transport.

Cerium cations are effective at reducing the chemical degradation of proton conducting membranes. However, the cerium cations are not stable in terms of distribution within the membrane. Loss of cerium during operations has been measured and the changes in the distribution of cerium within the membranes are very quick, with equilibration occurring within 10 minutes during pressing tests at 90°C.

FUTURE DIRECTIONS

Catalyst layer morphology effect on durability

- Quantify the relationship between carbon corrosion and resulting changes in cathode catalyst layer structure
  - Quantification of Pt/pore distributions, Pt utilization, and ECSA
  - High vs. low surface area carbon structures and mixed formulations

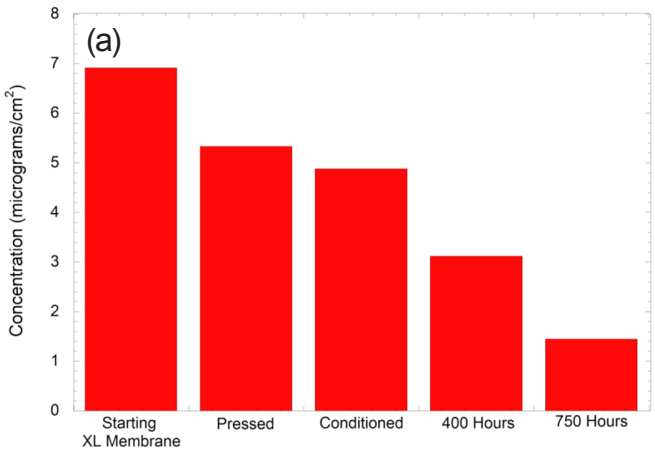

(a)Change in cerium concentration for DuPont™ XL membrane

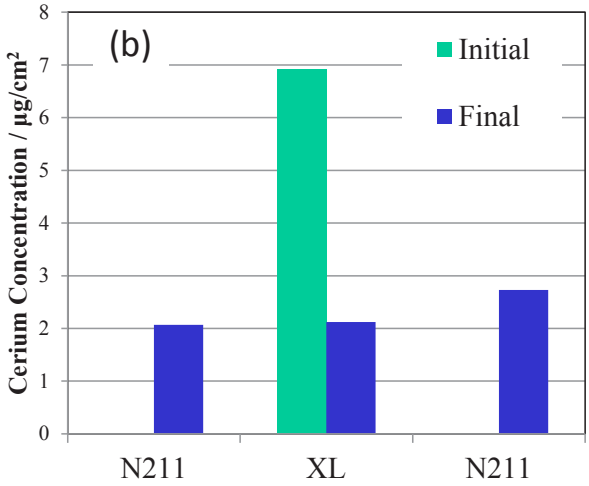

(b)Cerium Concentration Before/After 10 min Hot Press at 90°C

FIGURE 4. (a) Cerium concentration in DuPont™ XL membrane during operational time at open-circuit voltage conditions (80°C and 100% RH) (b) cerium concentration before and after pressing under hot/wet conditions for 10 minutes. Measured by X-ray diffraction.

- Effect of catalyst layer cracks and gaps; formation of cracks
  - Evaluate the effect of catalyst layer cracks on membrane durability
- Identify uniform methodology for measuring the real durability impact of start-up/shut-down and air cycling
  - Identify spatial/area performance variations over ageing

Durability evaluation of Pt alloys

- Define the effect of Pt and alloy migration on membrane durability
  - Experimentally define and model the dissolution of Pt at elevated temperatures and with a partial pressure of oxygen
  - Expand our previously developed models on Pt dissolution to incorporate alloy effects

Membrane structural changes and radical scavengers

- Effect of Ce (and other radical scavengers) movement on durability
  - Define best form of Ce for radical scavenging
  - Methods to stabilize Ce in both membrane and cell to prevent wash-out
- Evaluate changes in membrane crystallinity to determine both the durability effects and if these crystallinity changes affect more than water uptake.
- Examine membrane durability trade-offs with carbon corrosion
  - Compare membrane degradation at shut-down versus start-stop H_2 purging and carbon corrosion

Discern carbon/Nafion®/catalyst interactions and structure on durability

- Define catalyst layer porosity loss due to causes other than carbon corrosion
- Map the ionomer in the catalyst layer and define the ionomer chemical/structural changes in the catalyst layer
- Understand the structural effects of the catalyst layer on durability; different methods of forming catalyst layers
- Improve the durability/performance of low loaded MEAs (0.05 mg/cm^2)
  - Define the dependence of catalyst loading, MEAs, etc. on increases in mass transport resistance with fuel cell drive cycle testing

Mitigation of degradation

- Expand work on mitigation
  - Increasing catalyst layer transport and increase stability
    - Catalyst layer stability through the use of structure and stable materials
  - Stabilize cerium and/or other radical scavengers
  - Predict durability cost versus function of mitigation strategies

FY 2014 PUBLICATIONS/PRESENTATIONS

Publications

1. Ahluwalia, Rajesh K.; Arisetty, Srikanth; Peng, Jui-Kun; Subbaraman, Ram; Wang, Xiaoping; Kariuki, Nancy; Myers, Deborah J.; Mukundan, Rangachary; Borup, Rodney; Polevaya, Olga, Dynamics of particle growth and electrochemical surface area loss due to platinum dissolution, J. Electrochem. Soc. (2014), 161(3), F291-F304.

2. Papadias, Dionissios D.; Ahluwalia, Rajesh K.; Thomson, Jeffery K.; Meyer, Harry M., III; Brady, Michael P.; Wang, Heli; Turner, John A.; Mukundan, Rangachary; Borup, Rod, Degradation of SS316L bipolar plates in simulated fuel cell environment: Corrosion rate, barrier film formation kinetics and contact resistance, Journal of Power Sources (2014).

3. Dillet, J.; Spernjak, D.; Lamibrac, A.; Maranzana, G.; Mukundan, R.; Fairweather, J.; Didierjean, S.; Borup, R.L.; Lottin, O., Impact of flow rates and electrode specifications on degradations during repeated startups and shutdowns in polymer-electrolyte membrane fuel cells, J. Power Sources (2014), 250, 68-79.

4. Garzon, F., S. M. Stewart, R. Borup, M. Wilson, and A. Datye, Effects of Particles Size on Lifetime Improvement for Cerium (IV) Oxide in Hydrogen Fuel Cells, Accepted to J. Electrochem. Soc.

5. Stewart, S.M., R. Borup, M. Wilson, A. Datye, F. Garzon, Effects of Cerium (IV) Oxide Particle Size on Hydrogen Fuel Cell Durability During Accelerated Stress Testing, ECS Electrochemistry Letters (2014), 3(4), F19-F22.

6. Hwang G.S., H. Kim, R. Lujan, R. Mukundan, D. Spernjak, R.L. Borup, M. Kaviany M.H. Kim, and A.Z. Weber, Phase-Change-Related Degradation of Catalyst Layers in Proton-Exchange-Membrane Fuel Cells, Electrochimica Acta (2013), 95, 29-37.

7. Fairweather J., D. Spernjak, A.Z. Weber, D. Harvey, S. Wessel, D.S. Hussey, D.L. Jacobson, K. Artyushkova, R. Mukundan, and R.L. Borup, Effects of Cathode Corrosion on Through-Plane Water Transport in Proton Exchange Membrane Fuel Cells, J. Electrochem. Soc. (2013), 160(9), F980-F993.

8. Mishler, J.; Wang, Y.; Lujan, R.; Mukundan, R.; Borup, R.L., An experimental study of polymer electrolyte fuel cell operation at sub-freezing temperatures, J. Electrochem. Soc. (2013), 160(6), F514-F521.

9. Carnes, B.; Spernjak, D.; Luo, G.; Hao, L.; Chen, K.S.; Wang, C.-Y.; Mukundan, R.; Borup, R.L., Validation of a two-phase multidimensional polymer electrolyte membrane fuel cell computational model using current distribution measurements, J. Power Sources (2013), 236, 126-137.

10. Borup, R.L., R. Mukundan, J. Fairweather, D. Spernjak, D. Langlois, J. Davey, K. More, and K. Artyushkova, PEM Fuel Cell Catalyst Layer Structure Degradation During Carbon Corrosion, ECS Transactions (2013).

11. Rodgers M.P., L.J. Bonville, R. Mukundan, R. Borup, R. Ahluwalia, P. Beattie, R.P. Brooker, N. Mohajeri, H.R. Kunz, D.K. Slattery, J.M. Fenton, , Perfluorinated Sulfonic Acid Membrane and Membrane Electrode Assembly Degradation Correlating Accelerated Stress Testing and Lifetime Testing, ECS Transactions (2013).

12. Fairweather J.D., D. Spernjak, J. Spendelow, R. Mukundan, D. Hussey, D. Jacobson, and R.L. Borup, Evaluation of Transient Water Content During PEMFC Operational Cycles by Stroboscopic Neutron Imaging, ECS Transactions (2013).

13. Abbou S., J. Dillet, D. Spernjak, R. Mukundan, J. Fairweather, R.L. Borup, G. Maranzana, S. Didierjean, O. Lottin, Time Evolution of Local Potentials during PEM Fuel Cell Operation with Dead-Ended Anode, ECS Transactions (2013).

14. Mukundan, R., J. Davey, K. Rau, D. Langlois, D. Spernjak, K. Artyushkova, R. Schweiss, and R.L. Borup, Degradation of Gas Diffusion Layers in PEM fuel cells during drive cycle operation, ECS Transactions (2013).

15. Hussey D.S., D. Spernjak, G. Wu, D.L. Jacobson, D. Liu, B. Khaykovich, M.V. Gubarev, J. Fairweather, R. Mukundan, R. Lujan, P. Zelenay, and R.L. Borup, Neutron Imaging Of Water Transport In Polymer-Electrolyte Membranes And Membrane-Electrode Assemblies, ECS Trans. (2013).

Presentations (Invited only)

1. Borup, Rodney L., Rangachary Mukundan, Yu Seung Kim, Dusan Spernjak, David Langlois, Karren More, R. Ahluwalia, S. Arisetty, G. Maranzana, J. Dillet and O. Lottin, (Invited) PEM Fuel Cell MEA Degradation During Drive Cycle Operation, Spring ECS May 2014.

2. Borup, Rodney L., Rangachary Mukundan, Dusan Spernjak, David Langlois, Dennis Torraco, Karren More, R. Ahluwalia, S. Arisetty Laure Guetaz, (Invited) Electrocatalyst Layer Degradation of PEM Fuel Cells, Fall ECS October 2014.

3. Rodgers, M.P., L.J. Bonville, R. Mukundan, R. Borup, S. Knights, R. Ahluwalia, P. Beattie, R.P. Brooker, N. Mohajeri, H.R. Kunz, D.K. Slattery J.M. Fenton, (Invited Keynote), Perfluorinated Sulfonic Acid Membrane and Membrane Electrode Assembly Degradation Correlating Accelerated Stress Testing and Lifetime Testing, Fall ECS October 2013.

4. Borup, R.L., et al., Degradation Mechanisms and Accelerated Testing in PEM Fuel Cells, (Invited), KIER – Korean Institute for Energy Research, October 2013.

5. Borup, R.L., R. Mukundan,J, Fairweather, D, Spernjak, D, Langlois, J, Davey and K, More, K. Artyushkova, R. Ahluwalia, S. Arisetty, (Invited), Electrode Morphology and Carbon Support Changes During Catalyst and Electrode Durability Tests, Joint DOE Durability/Catalyst Working Group Meeting, Golden Colorado, Dec. 2013.

6. Borup, Rod et al., Durability Improvements Through Degradation Mechanism Studies, (Invited), FC Tech Team, Detroit MI, September 18, 2013.

7. Borup, Rod et al., Durability Improvements Through Degradation Mechanism Studies, (Invited), DOE Fuel Cell Technologies Annual Merit Review, Arlington, Va, May 13–17, 2013.

8. Borup Rodney L., Rangachary Mukundan, Yu Seung Kim, Dusan Spernjak, David Langlois, Karren More, N. Mack, M. Hawley, C. Welch, (Invited) PEM Fuel Cells: Microstructural Design and Durability at the Microstructural Level, LANL Materials by Design Workshop, July 17, 2013.

9. Borup, R.L., et al, PEM Fuel Cells: Design and Durability at the Microstructural Level, 2014 Los Alamos National Lab, (Invited) Materials Capability Review.

V.E.2 Accelerated Testing Validation

Rangachary Mukundan[1] (Primary Contact), Rod Borup [1], John Davey[1], Roger Lujan[1], Dennis Torraco[1], David Langlois[1], Fernando Garzon[1], Dusan Spernjak[1], Joe Fairweather[1], Adam Weber[2], Karren More[3], Paul Beattie[4], and Steve Grot[5]

[1]Los Alamos National Laboratory (LANL)
MS D429, P.O. Box 1663
Los Alamos, NM 87545
Phone: (505) 665-8523
Email: Mukundan@lanl.gov

DOE Manager

Nancy Garland
Phone: (202) 586-5673
Email: Nancy.Garland@ee.doe.gov

Subcontractors

[2] Lawrence Berkeley National Laboratory, Berkeley, CA
[3] Oak Ridge National Laboratory, Oak Ridge TN
[4] Ballard Power Systems, Burnaby, BC, Canada
[5] Ion Power, New Castle, DE

Project Start Date: October 2009
Project End Date: September 2014

Overall Objectives

- Correlation of the component lifetimes measured in an accelerated stress test (AST) to "real-world" behavior of that component
- Validation of existing component specific ASTs for electrocatalysts, catalyst supports and membranes (mechanical and chemical degradation)
- Development of new ASTs for gas diffusion layers (GDLs) and bipolar plates
- Co-ordinate effort with Fuel Cell Tech Team (FCTT) and Durability Working Group

Fiscal Year (FY) 2014 Objectives

- Compare the United States Driving Research and Innovation for Vehicle efficiency and Energy sustainability (U.S. DRIVE) FCTT's new AST for carbon corrosion (1- to 1.5-V cycle) with the U.S. DRIVE FCTT's old AST for carbon corrosion (1.2-V hold)
- Development of a new membrane AST that is representative of membrane degradation observed in the field and during the U.S. DRIVE FCTT "Protocol for Determining Cell/Stack Durability"
- Development and validation of new AST for GDL materials

Technical Barriers

This project addresses the following technical barriers from the Fuel Cells section (3.4.5) of the Fuel Cell Technologies Office Multi-Year Research, Development, and Demonstration Plan:

(A) Durability

(B) Cost

Technical Targets

Cost and durability are the major challenges to fuel cell commercialization. ASTs enable rapid screening of fuel cell materials and are critical in meeting the long life times required for stationary and automotive environments. Moreover these ASTs can also help predict the lifetime of the various components in "real-world" applications.

- Transportation Durability: 5,000 hours (with cycling)
  - Estimated start/stop cycles: 17,000
  - Estimated frozen cycles: 1,650
  - Estimated load cycles: 1,200,000
  - Cost ($30/kWe)
- Stationary Durability: 40,000 hours; (2015); 60,000 hours (2020)
  - Survivability: Stationary -35°C to 40°C
- Bus Durability: 12 years/500,000 miles (2016 and ultimate)
  - Power plant lifetime: 18,000 hours (2016), 25,000 hours (ultimate)
  - Power plant cost: $450,000 (2016), $200,000 (ultimate)
  - Range: 300 miles; Fuel Economy: 8 miles/gallon diesel equivalent

FY 2014 Accomplishments

- Completed the U.S. DRIVE FCTT 1- to 1.5-V cycling AST on membrane electrode assemblies (MEAs) utilizing three different carbon types
- Determined that 1- to 1.5-V cycling results in 1 order of magnitude greater carbon corrosion than the 1.2-V hold
- Determined that 1- to 1.5-V cycling results in approximately 100 times faster Pt growth rate and voltage decay rate than the 1.2-V hold

- Determined that 1- to 1.5-V cycling has the ability to clearly distinguish various carbon types with different degrees of graphitization
- Initiated development of a new membrane AST that has the ability to reproduce degradation mechanisms observed in the field and during simulated durability tests using the U.S. DRIVE FCTT "Protocol for Determining Cell/Stack Durability"
- Developed a GDL degradation AST that results in similar degradation to that observed during durability tests using the U.S. DRIVE FCTT "protocol for determining cell/stack durability"
- GDL fingerprinting, mercury intrusion porosimetry (MIP), and contact angle measurements utilized to quantify GDL degradation

INTRODUCTION

The durability of polymer electrolyte membrane fuel cells is a major barrier to the commercialization of these systems for stationary and transportation power applications [1]. Commercial viability depends on improving the durability of fuel cell components to increase the system reliability and to reduce system lifetime costs by reducing the stack replacement frequency. The need for ASTs can be quickly understood given the target lives for fuel cell systems: 5,000 hours (~7 months) for automotive, and 40,000 hrs (~4.6 years) for stationary systems. Thus testing methods that enable more rapid screening of individual components to determine their durability characteristics, such as off-line environmental testing, are needed for evaluating new component durability with a rapid turn-around time. This allows proposed improvements in a component to be evaluated rapidly and independently, subsequently allowing rapid advancement in polymer electrolyte membrane fuel cell durability. These tests are also crucial to developers in order to verify that durability is not sacrificed while making improvements in costs (e.g. lower platinum group metal loading) and performance (e.g. thinner membrane or a GDL with better water management properties).

DOE has suggested AST protocols for use in evaluating materials, but only for the catalyst layer components (electrocatalyst and support), and for the membrane [2,3]. The United States Fuel Cell Council has also suggested AST protocols for the same materials [4]. While these protocols have concentrated on the catalyst, catalyst support and membrane materials, to date, no accelerated degradation protocols have been suggested for GDL materials or MPL layers, bipolar plates or seals. In spite of recent advances in AST development, a main portion, which is deficient, is the quantitative correlation between the results of a given fuel cell AST, and the degradation rate or life in an operating fuel cell.

APPROACH

A main desired outcome of this project is the correlation of the component lifetimes measured in an AST to in situ behavior of that component in "real-world" situations. This requires testing of components via ASTs and in operating fuel cells, and delineating the various component contributions to the overall cell degradation. This will primarily be performed by using a simplified one-dimensional model that takes into account the different component contributions like membrane ionic conductivity, cathode catalyst layer kinetic losses and mass transport losses (catalyst layer and GDL) to the overall losses observed in operating cells [5]. This project will then attempt to correlate the performance losses observed due to a particular component in "real-world" situations with the degradation in AST metrics of that component. The correlation between AST and life data if state-of-the-art materials are used, in essence, gives one data point. Thus, for a reasonable correlation to be made, materials with different life spans are utilized in this project. The "real-world" data utilized in this project include field data from bus fleets provided by Ballard Power Systems and simulated drive cycle data obtained at LANL utilizing the U.S. DRIVE FCTT "Protocol for Determining Cell/Stack Durability" [6]. This work is also being coordinated with other funded projects examining durability through a DOE Durability Working Group.

RESULTS

The U.S. DRIVE FCTT recommended ASTs and "Protocol for Determining Cell/Stack Durability" [6] was performed on various MEA/GDLs using 50-cm^2 single- or quad-serpentine hardware purchased from Fuel Cell Technologies Inc. Polarization curves, electrochemically active surface area, mass activity, cross-over, shorting resistance and impedance measurements were performed at regular intervals to monitor the degradation rate. For carbon corrosion testing a California Analytical Instruments Inc. non-dispersive infrared (NDIR) instrument was attached to the outlet N_2 from the cathode side (after condensing the water) to monitor total amount of CO_2 evolved.

Catalyst Degradation

The U.S. DRIVE FCTT recommended 1- to 1.5-V cycle was performed on MEAs utilizing three different carbon types, viz: E carbon (high surface area), V carbon (VULCAN®) and EA carbon (graphitized low surface area). The NDIR analysis of the nitrogen at the cathode outlet clearly showed CO_2 corresponding to the corrosion of the carbon support in the cathode catalyst layer. Figure 1a) illustrates the CO_2 evolved from the MEA using the

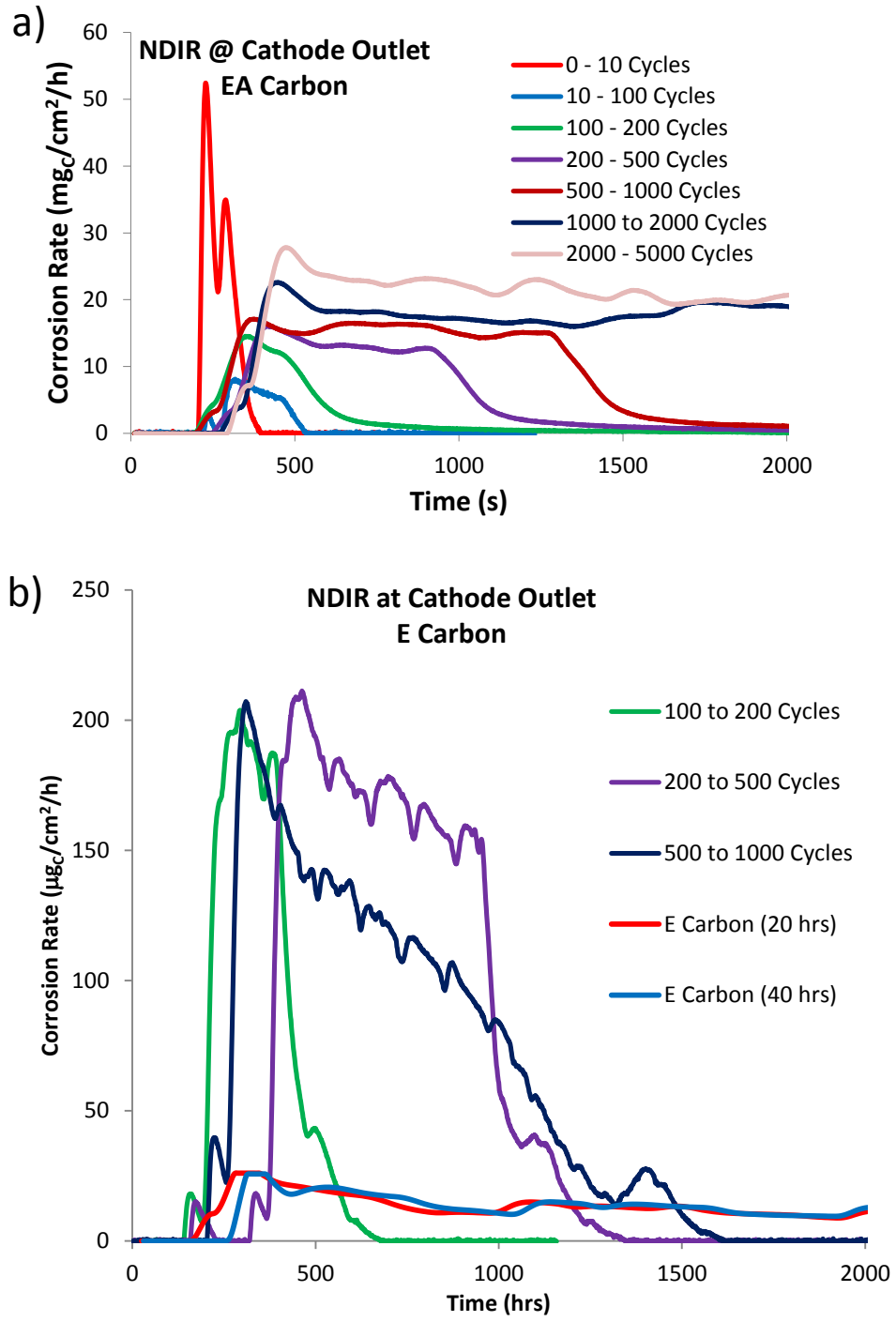

FIGURE 1. Carbon corrosion rate measured by the CO_2 concentration at the N_2 cathode (using non-dispersive infrared) during AST testing of MEAs utilizing Pt/C catalysts with a) low surface area graphitized carbon (EA-Carbon) and b) high surface area E-carbon.

EA-carbon support in the cathode catalyst layer. The CO_2 evolution steadily decreases over time as the number of cycles is increased. However, after characterization and resumption in testing an increased CO_2 evolution rate is observed. This is consistent with the formation of a passivation layer over time that can be reduced when the voltage is lowered below 1.0 V. NDIR results from the MEA utilizing the E-carbon (Figure 1b) show that the corrosion rate from the high surface area carbon is almost an order of magnitude larger than the corrosion from the graphitized carbon. Moreover the E-carbon also shows a dramatic lowering in the CO_2 evolution rate after 500 cycles,

consistent with the low amount of residual carbon in the catalyst layer (decreased catalyst layer thickness). This is also confirmed by large increases in mass transport losses in the MEA associated with catalyst layer compaction and loss in porosity. Figure 1b also shows a comparison of the CO_2 emission from the 1.2-V hold AST showing about an order of magnitude greater CO_2 emission from the 1- to 1.5-V cycling.

The MEA performance degradation observed during the 1.2-V hold and the 1- to 1.5-V cycling is compared in Figure 2a. The performance degradation rate during the 1- to 1.5-V cycling is at least 2 orders of magnitude greater (≈150x) than the degradation rate during the 1.2-V hold. For example the polarization curves for the MEA using the V-carbon are similar after 80 hours (200 hours) of 1.2-V hold and 1,000 cycles (2,000 cycles) from 1.0 to 1.5 V corresponding to a cycling time of 0.56 hours (1.11 hours). Similar behavior was also observed for the MEA with the E-carbon electrode where the performance after 32 hours and 96 hours of 1.2-V hold are similar to performance after 500 and 1,000 cycles from 1.0 to 1.5 V, respectively. Figure 2b shows the Pt particle size measured by X-ray diffraction (post testing) after various times of either the 1.2-V hold or 1- to 1.5-V cycling ASTs. The time of the 1- to 1.5-V cycling has been multiplied by 100 times, clearly showing the 100 times acceleration factor of Pt growth in the 1- to 1.5-V cycling AST. Both ASTs also show a lowering of the degradation rate with increasing time, consistent with the lower growth rate of the larger Pt particles [7].

Membrane Degradation

Membrane degradation (increase in membrane cross-over) could be observed during durability testing using the U.S. DRIVE "Protocol for Determining Cell/Stack Durability." While un-stabilized (both chemically and mechanically) membranes failed in <1,000 hours of this drive cycle testing, stabilized membranes showed excellent durability. For example the DuPont XL® membrane after 3,800 hours of this drive cycle showed only a 30% decrease in membrane thickness, but failed at the edges due to the absence of a sub-gasket. Figure 3a is a back-scattered scanning electron micrograph of the DuPont XL® membrane after 3,800 hours of durability testing showing thinning (originally 25 μm) on the cathode (bottom) side of the reinforcement. A stabilized membrane from another supplier also lasted >2,000 hours with no change in membrane thickness but the test was aborted due to test stand issues. Further testing with sub-gasketing of both these stabilized membranes is under progress to evaluate their lifetime during drive-cycle testing and should be close to the required 5,000-hour durability target. The testing of un-stabilized membranes revealed both chemical and mechanical degradation, as evidenced by global thinning and local tearing respectively. All membranes tested under this drive cycle failed due to mechanical degradation either at the edges (for stabilized membranes) or at the inlets/outlets (for un-stabilized membranes).

The current membrane ASTs fail to capture this failure mode and therefore a new relative humidity (RH) cycling test in H_2/air was developed to accelerate/simulate this membrane failure mechanism. The H_2/air RH cycling was performed initially at a cell temperature of 80°C with dry gases for 2 minutes and super saturated gases (dew point = 90°C) for 2 minutes and resulted in failure of unstabilized membranes in less than 300 hours (<5,000 cycles). However, stabilized membranes hardly showed any degradation under this testing with no thinning or increase in crossover observed even after 20,000 cycles (≈55 days). In order to further accelerate this test, the cell temperature was increased to 90°C with

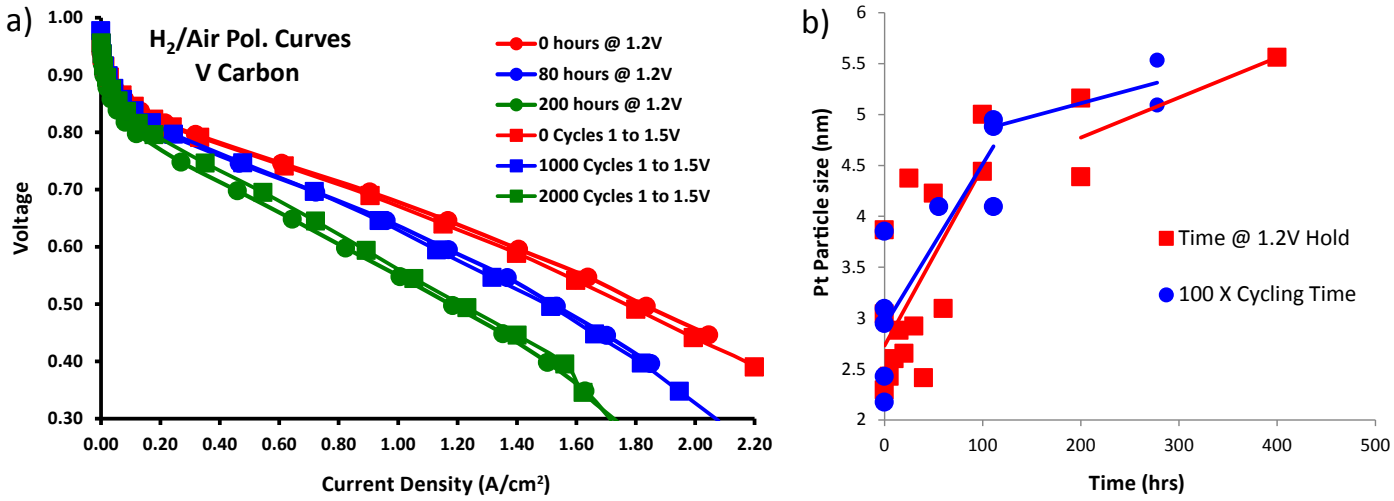

FIGURE 2. Comparison of a) polarization curves measured after various times and b) Pt particle size evolution over time, during two different U.S. DRIVE FCTT recommended carbon corrosion ASTs (1.2-V hold and 1.0- to 1.5-V cycling).

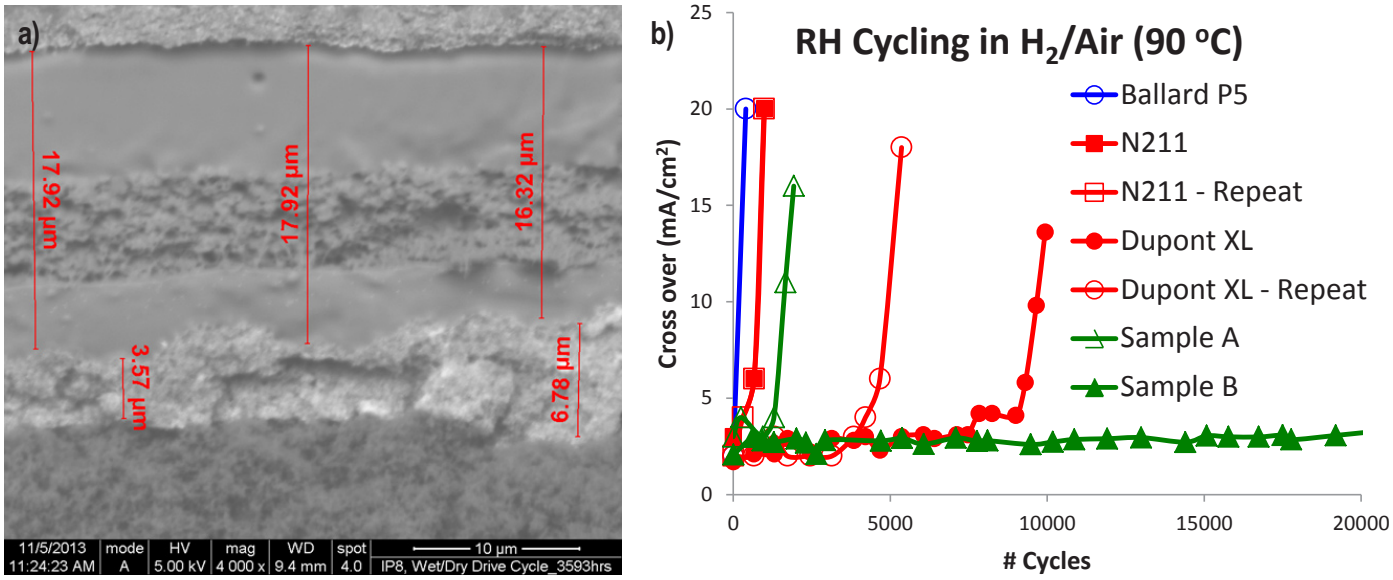

FIGURE 3. a) Backscattered scanning electron micrograph of DuPont XL® membrane after 3,800 hours of drive cycle testing, b) cross-over evolution of various membranes during RH cycling test in H_2/air at a cell temperature of 90°C.

2 minutes of dry and 2 minutes of super-saturated (dew point = 92°C) gases. The crossover of various stabilized and unstabilized membranes subjected to this test is presented in Figure 3b. The N211 membrane failed this test within 33 hours (1,000 cycles) and exhibited both global thinning (40% reduction in thickness) and local tearing (several pinholes/cracks in membrane). However, the stabilized DuPont XL® membrane showed no global thinning even after 600 hours of this testing (≈10,000 cycles) and showed increased crossover due to edge failure. Another stabilized membrane with a sub gasket also lasted >20,000 cycles with little increase in cross-over, indicating that further acceleration is required in order to evaluate state-of-the-art membranes. This AST is being refined further in order to increase chemical degradation with respect to mechanical degradation by decreasing the time during the wet part of the RH cycle.

GDL Degradation

GDL degradation has been observed during drive cycle testing of fuel cells and an ex situ AST for GDL durability was reported last year. The ex situ aging of GDLs was achieved by submerging them in a boiling solution of 30% hydrogen peroxide (H_2O_2) at 95°C for prolonged intervals up to 15 hours (this protocol was first reported by SGL as their part of the DECODE project). This test resulted in qualitatively similar degradation to that observed during drive-cycle testing, i.e. increase in mass transport resistance of MEAs using aged GDLs. This year we have developed tests to quantify this degradation both in terms of fuel cell performance and materials property changes in the GDL. MIP was used to monitor the changing average pore diameter and porosity of the GDL as a function of aging time (see Figure 4a). The decreasing porosity and average pore diameter can be used to quantify GDL degradation and are consistent with the observed mass transport increases in MEAs utilizing aged GDLs. A RH fingerprint test as first reported by D. L. Wood et al. [8] was utilized to quantify the performance changes observed due to GDL ageing. The performance of an MEA utilizing fresh and aged GDLs was monitored at a fixed voltage (selected to yield a current density of ≈1.5 A/cm^2) while varying the inlet dew point of the anode and cathode gases. The cell temperature was kept constant at 80°C while the inlet dew points of H_2/air were increased at 5°C intervals from 30°C to 80°C. The performance of MEAs using fresh and 7-hour aged GDLs during this test is illustrated in Figure 4b). While the fresh GDL shows increasing performance with increasing RH, the aged GDL shows improved performance at low inlet RHs and a loss in performance at high inlet RHs. These results are consistent with improved high-frequency resistance (HFR) and better membrane hydration with the aged GDLs and improved mass transport with the fresh GDLs. The contact angles measured as a function of ageing time at 95°C and 80°C are plotted in Figure 4c and illustrate the increasing hydrophilicity of the GDL with ageing. The oxidation of the carbon in the GDL material results in the formation of hydrophilic surface oxide groups which in turn result in improved performance under drier conditions (improved membrane HFR) and degraded performance under wetter conditions (increased mass transport resistance). These tests will be utilized to quantitatively correlate in situ GDL degradation in MEAs with ex situ AST degradation of

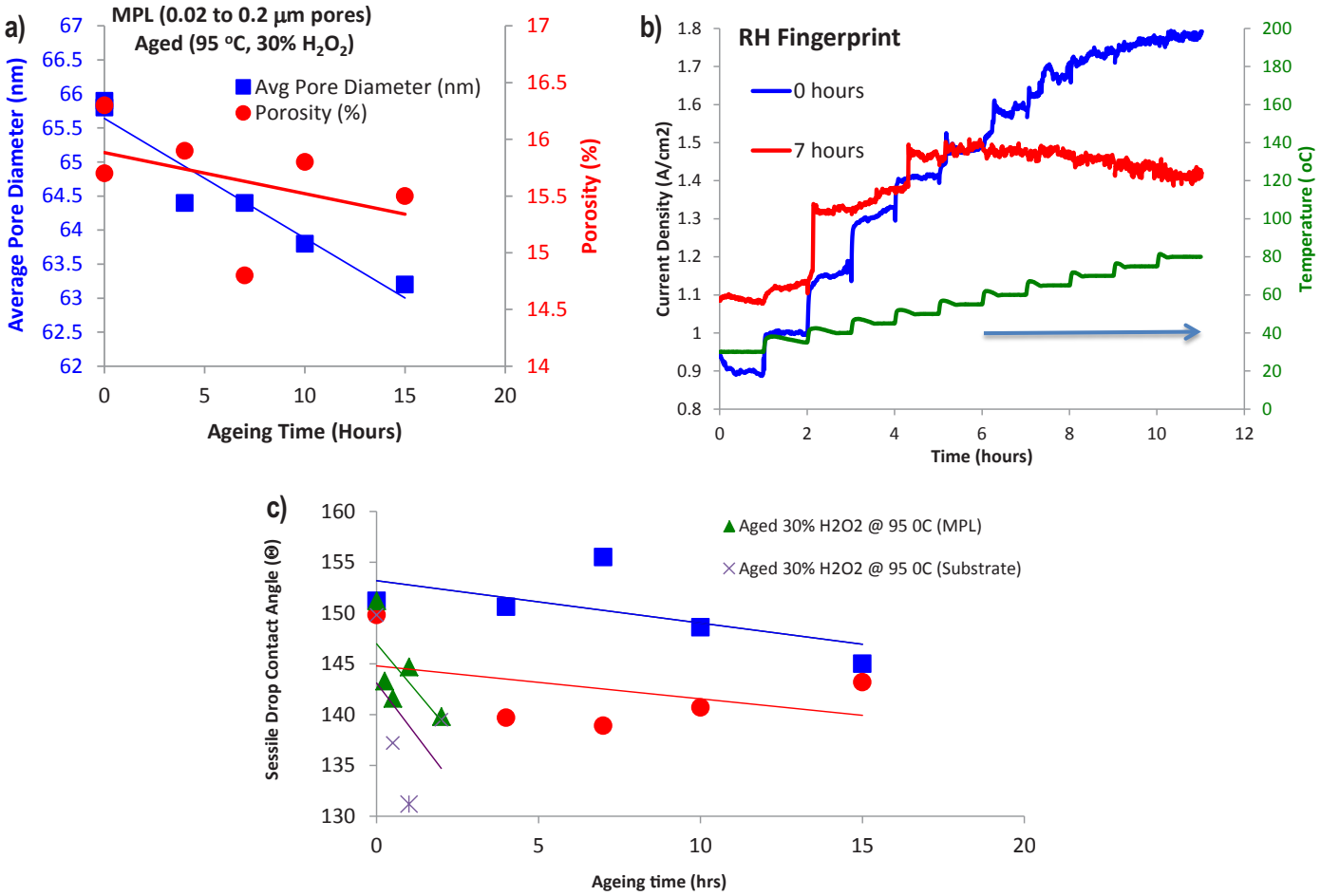

FIGURE 4. a) Decreasing porosity and average pore diameter of the GDL (measured using MIP) as a function of aging time, b) GDL RH fingerprint: performance (current at 0.55 V) of MEAs using fresh and 7-hour aged GDLs, as a function of cathode/anode inlet RHs, c) Sessile drop contact angles of substrate and GDL as a function of AST aging time.

GDLs. The ex situ aging time, temperature and peroxide composition will be varied to optimize this AST and correlate it to GDL ageing during dive cycle testing

CONCLUSIONS AND FUTURE DIRECTIONS

The electro-catalyst AST (0.6-V to 1.0-V cycling) was found to accurately capture the Pt electrochemically active surface area loss occurring during wet/dry drive cycle testing. However, this test needs further acceleration that can be achieved by increasing the voltage ramp rate. The U.S. DRIVE FCTT recommended new AST (1.0- to 1.5-V cycling) for carbon corrosion results in ten times greater carbon corrosion than the older 1.2-V hold AST. The new AST results in ≈100 times acceleration of the Pt growth rate and the observed voltage decay rate. A new H_2/air RH cycling AST, which better simulates membrane degradation observed in the field and during drive cycle operation was developed. However, this AST requires further acceleration of chemical degradation with respect to mechanical degradation which will be achieved by decreasing the duration of the wet portion of the RH cycle with respect to the dry portion. Ex situ GDL ageing in peroxide solutions was found to degrade GDLs similar to those observed during drive cycle operation. GDL fingerprint test was found to be effective in characterizing GDL degradation and will be utilized to refine the GDL AST and to define accelerating factors with respect to drive cycle testing.

- AST Testing
  - Further accelerate the catalyst cycling AST by speeding up the cycling rates from the current 50 mV/s. Perform an AST using a trapezoid wave with 0.5 s rise time from 0.6 V to 0.95 V, 2.5 s hold at 0.95 V, 0.5 s from 0.95 to 0.6 V, and 2.5 s hold at 0.6 V
  - Refine membrane AST to better simulate membrane degradation observed during durability testing using the U.S. DRIVE “Protocol for Determining Cell/Stack Durability”

- "Real-World" Testing
  - Perform simulated start/stop tests on MEAs utilizing three different carbon types
  - Perform the U.S. DRIVE "Protocol for determining Cell/Stack durability" on MEAs using different membrane and catalyst layer types
- Characterization of Materials
  - Perform ex situ characterization of catalyst particle size distribution, layer thickness, membrane thickness, and GDL hydrophobicity as a function of drive cycle and/or AST test time
- Correlation of AST to "Real-World" Data
  - Determine acceleration factors of the membrane AST with respect to the U.S. DRIVE "Protocol for Determining Cell/Stack Durability"
  - Determine acceleration factors of the 1- to 1.5-V cycling AST with respect to the simulated start/stop cycles

FY 2014 PUBLICATIONS/PRESENTATIONS

1. R. Mukundan, J.R. Davey, K. Rau, D.A. Langlois, D. Spernjak, J.D. Fairweather, K. Artyushkova, R. Schweiss, and R.L. Borup, "Degradation of Gas Diffusion Layers in PEM fuel cells during drive cycle operation," *ECS Transactions,* **V58(1)**, pp. 919-926 (2013).

2. M.P. Rodgers, L.J. Bonville, R. Mukundan, R.L. Borup, R. Ahluwalia, P. Beattie, R.P. Brooker, N. Mohajeri, H.R. Kunz, D.K. Slattery, and J.M. Fenton, "Perfluorinated Sulfonic Acid Membrane and Membrane Electrode Assembly Degradation Correlating Accelerated Stress Testing and Lifetime Testing," *ECS Transactions,* **V58(1)**, pp. 129-148 (2013).

3. R.K. Ahluwalia, S. Arisetty, J.-K. Peng, R. Subbaraman, X. Wang, N. Kariuki, D.J. Myers, R. Mukundan, R. Borup, and O. Polevaya, "Dynamics of Particle Growth and Electrochemical Surface Area Loss due to Platinum Dissolution," *Journal of The Electrochemical Society,* **V161**, pp. F291-F304 (2014).

4. R. Mukundan, J.R. Davey, K. Rau, D.A. Langlois, D. Spernjak, J.D. Fairweather, K. Artyushkova, R. Schweiss, and R.L. Borup, "Degradation of Gas Diffusion Layers in PEM fuel cells during drive cycle operation," 224th Meeting of the Electrochemical Society, Oct. 27–31, 2013.

5. M.P. Rodgers, L.J. Bonville, R. Mukundan, R. Borup, S. Knights, R. Ahluwalia,[e] P. Beattie, R.P. Brooker, N. Mohajeri, H.R. Kunz, D.K. Slattery, and J.M. Fenton, "The Chemistry of Membrane Degradation in PEM Fuel Cells" 225th Meeting of the Electrochemical Society, May 11–15, 2014 (Invited).

6. R. Mukundan, P. Beattie, J. Davey, D. Langlois, D. Spernjak, J. Fairweather, D. Torraco, F. Garzon, A.Z. Weber, K. More, and R.L. Borup, Durability of PEM fuel cells and the relevance of accelerated stress tests, 225th Meeting of the Electrochemical Society, May 11–15, 2014 (Invited).

REFERENCES

1. R. Borup, J. Meyers, B. Pivovar, et al., *Chemical Reviews*; **107(10)**, 3904 (2007).

2. T.G. Benjamin, Abstracts of the International Workshop On Degradation Issues in Fuel Cells, Hersonessos, Crete, Greece, (2007).

3. N.L. Garland, T.G. Benjamin, J.P. Kopasz, *ECS Trans.*, **V. 11 No. 1**, 923 (2007).

4. S. Knight, G. Escobedo, *Meeting Abstracts of 2006 Fuel Cell Seminar*, Honolulu, HI (2006).

5. A.Z. Weber, J. Newman, "Modeling Transport in Polymer-Electrolyte Fuel cells" *Chemical Reviews*, **V. 104**, 4679-4726 (2004).

6. FreedomCAR Fuel Cell Tech Team Cell Component AST and polarization curve Protocols for PEM Fuel Cells (Electrocatalysts, Supports, Membranes and MEAs), Revised December 16, 2010.

7. Z. Yang, S. Ball, D. Condit and M. Gummalla, J. Electrochem. Soc., **158(11)**, B1439-B1445 (2011).

8. D.L. Wood, R.L. Borup, "Degradation aspects of gas-diffusion and micro porous layers" in Polmer Electrolyte fuel cell durability. Ed. F.N. Buchi, M. Inaba and T.J. Schmidt, Springer, 159-198 (2009).

V.E.3 Fuel Cell Technology Status—Cost and Price Status

Jennifer Kurtz (Primary Contact) and Huyen Dinh
National Renewable Energy Laboratory (NREL)
15013 Denver West Parkway
Golden, CO 80401-3305
Phone: (303) 275-4061
Email: jennifer.kurtz@nrel.gov

DOE Manager
David Peterson
Phone: (720) 356-1747
Email: David.Peterson@ee.doe.gov

Project Start Date: July 01, 2009
Project End Date: Project continuation and direction determined annually by DOE

Overall Objectives

- Conduct an independent assessment to benchmark current fuel cell system cost and price in a non-proprietary method.
- Leverage the National Fuel Cell Technology Evaluation Center (NFCTEC).
- Collaborate with key fuel cell developers on the voluntary data share and NFCTEC analysis.

Fiscal Year (FY) 2014 Objectives

- Establish price data templates and pursue gathering current price data for fuel cell developer products.
- Publish aggregated, current fuel cell price by application.

Technical Barriers

This project addresses the following technical barriers from the Fuel Cells section of the Fuel Cell Technologies Office Multi-Year Research, Development, and Demonstration Plan:

(B) Cost (Lack of data for current fuel cell costs and status per targets)

Technical Targets

This project is conducting an independent assessment of the current cost and price of fuel cell systems. All results are aggregated to protect proprietary information and reported on by the system application. Per the Fuel Cells section of the Fuel Cell Technologies Office Multi-Year Research, Development, and Demonstration Plan:

- The 2017 transportation fuel cell system cost target is $30/kW
- The 2020 micro-combined heat and power (CHP) (5 kW) fuel cell system cost target is $1,500/kW
- The 2020 medium CHP (100 kW–3 MW) fuel cell system cost target is $1,000/kW for natural gas and $1,400/kW for biogas

FY 2014 Accomplishments

- Updated and published an information pamphlet with participation request and benefits as well as past fuel cell durability composite data products (CDPs) and example price/cost CDPs,
- Project benefits include
  - Current and accurate cost/price status for DOE to complement the high-volume model cost predictions
  - Realistic expectations for current fuel cell system price at low volume
  - Aggregate and individual benchmarking
  - Supports adoption of fuel cell technology.
- Presented project overview and data request in a DOE webinar on the NFCTEC.
- Created example results to support conversations with developers on how data would be aggregated and published.
- Created generic cost/price data template.
- Published a CDP on low-volume price by backup power, forklift, and prime power applications.

INTRODUCTION

The DOE has funded significant research and development activity with universities, national laboratories, and the fuel cell industry to improve the market competitiveness of fuel cells. System cost is a barrier to widespread market acceptance. There is a lack of data for current, low-volume system cost and price data. NREL is benchmarking the current fuel cell system cost and price through independent assessment of voluntarily supplied data. NREL's data processing, analysis, and reporting capitalize on capabilities developed in DOE's NFCTEC. Fuel cell system cost/price is reported every two years. A key component of this project is the collaborative effort with key fuel cell developers for the available data.

APPROACH

The project involves voluntary submission of data from relevant fuel cell developers. NREL is contacting fuel cell developers for cost and price data for multiple fuel cell types to either continue or begin a data sharing collaboration. A continuing effort is to include more data sets, types of fuel cells, quantity of units sold, and developers.

Raw and processed data are stored in NREL's NFCTEC. The NFCTEC is an off-network room with access provided to a small set of approved users. Processing capabilities are developed or modified for new data sets and then included in the analytical processing of NREL's Fleet Analysis Toolkit. The incoming raw data may be new or a continuation of data that have already been supplied to NREL. An internal analysis of all available data is completed annually and a set of technical CDPs is published every other year. Publications are uploaded to NREL's technology validation website [1] and presented at industry-relevant conferences. The CDPs present aggregated data across multiple systems, sites, and teams in order to protect proprietary data and summarize the performance of hundreds of fuel cell systems and thousands of data records. A review cycle is completed before the CDPs are published. This review cycle includes providing detailed data products (DDPs) of individual system- and site-performance results to the specific data provider. DDPs also identify the individual contribution to the CDPs. The Fleet Analysis Toolkit is an internally-developed tool for data processing and analysis structured for flexibility, growth, and simple addition of new applications. Analyses are created for general performance studies as well as application- or technology-specific studies.

RESULTS

The past years of this project aimed to gather, analyze, and report on state-of-the-art fuel cell durability. Project direction was modified, per DOE's request, in FY 2014 to focus on cost and then alternate with durability every other year. This enables the project team to report on the current status for the two leading technical barriers per the Fuel Cell Technologies Office Multi-Year Research, Development, and Demonstration Plan. FY 2014 was the first year for publishing data on the current cost and price of fuel cell systems sold at low volume. A request for both cost and price were made to leading fuel cell developers because it was unclear how the data would be voluntarily supplied. The data that was supplied for the FY 2014 published CDP was price data, as noted in the CDP. Cost will remain in the request in order to gain a better understanding of the system cost without markup.

With the new focus on cost and price data collection in FY 2014, the informational project pamphlet was updated to add examples for cost and price. A data template was also generated (Figure 1). The template includes pricing, product availability, application, and quantity/type of units sold. The generic data template is available to DOE to collect and deliver data to the NFCTEC. This template was also modified in order to generate specific templates for fuel cell developers per known available systems. Example results (Figures 2 and 3) were created to support conversations with developers on how data would be aggregated and published.

The first CDP was published in June 2014 for backup power, forklift, and prime power applications (Figure 4). Statistical details, specifically the median and 25th and 75th percentile range, were identified for each application in dollars per kilowatt. The data is in 2013 dollars without incentives and is from public information, American Recovery and Reinvestment Act deployments, and voluntarily supplied data from fuel cell developers. This includes more than 20 different data points from more than three fuel cell developers. One of the first trends from Figure 4 worth noting is the large span of data in the prime power category. Prime power price data supplied includes multiple system sizes, types, and fuels. The variety of systems in prime power is an important reason for the need to further breakdown the prime power category (e.g. residential and commercial). The number of data sets and providers did not allow for this breakdown, which is an objective for the next update. Another trend to note is that the 25th percentile value for all three applications is below $4,000 per kilowatt. While these values are above DOE's cost targets, the system prices have not yet realized cost reduction due to mass production. Figure 4 is the initial price benchmarking and provides a format that can be used to track progress in cost reduction in the next update, expected in FY 2016 per DOE's discretion. Planned updates include more data and new applications, addition of price versus the number of units sold, breakdown of prime power by commercial and residential scales, low-volume cost-reduction trends by time, and system cost status.

CONCLUSIONS AND FUTURE DIRECTIONS

This project has leveraged other technology validation projects and existing industry relationships to report on the current, low-volume fuel cell system price status with a relatively low investment from DOE. The data collection effort includes both domestic and international developers and it is an ongoing task to include new data sets, update data sets already included (if applicable), and include new fuel cell developers, applications, and types. An online interface provides information on the project, contact information for interested collaborators, and all publications [1]. The published CDP from June 2014 is the first publication and will be updated in 2016 per DOE's discretion. Future work includes the following:

- Continue cultivating existing collaboration and developing new collaborations with fuel cell developers

4/7/14

Note: The information you provide here will be shared with the NREL National Fuel Cell Technology Evaluation Center for independent analysis and may be published as composite data products after a 2 stage review and concurrence process with the data providers. The information will be treated as confidential.

Instructions -

Please fill in applicable requested information for each available product, with each product entered as a new column. Some information may have been filled in based on an internet search of your available product. Please correct as appropriate.

System	ProductName1	ProductName2	ProductName32	ProductName4	ProductName5	ProductName6
Current Price (US $)						
Availability						
Market						
Application						
Fuel Cell Type						
Fuel						
Comments						
Power Rating (kW)						
Other features						
# systems sold to date						
2010 Price (US $)						
2012 Price (US $)						
2014 Price (US $)						
Current system cost (US $)						
Current fuel cell stack cost (US $)						
System efficiency						
Cell count						
Active area						
Turndown capability						
Spec sheet link or Product brochure PDF attached						

	Availability	Application	Fuel Cell Type	Fuel	Other features	Markets
	Available	Stationary Prime	DMFC	Hydrogen	CHP	Europe
	Future product	Stationary Residential	PEMFC	Methanol	CHHP	Japan
	No longer available	Stationary Backup	SOFC	Reformate	Other (Please specify)	United States
	Other (Please specify)	Forklift	MCFC	Other (please specify)		All
		Automotive	PAFC	Natural Gas		Other (please specify)
		Bus	AEM	Propane		
		Portable	Other (please specify)			
		Auxiliary				
		Other (Please specify)				

FIGURE 1. Generic Cost and Price Data Template

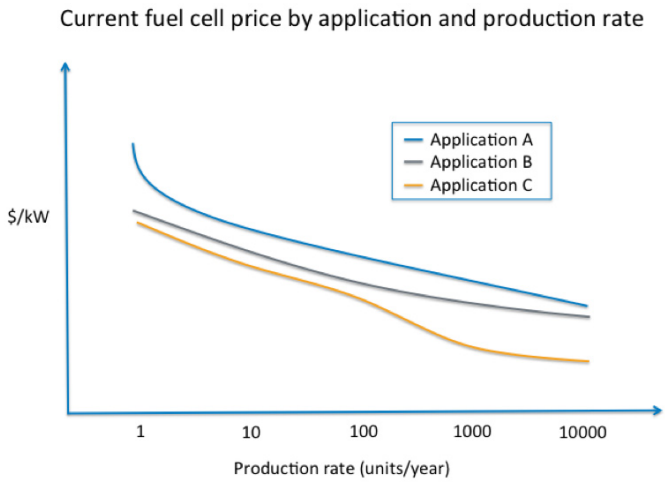

FIGURE 2. Example Result (Fake Data) for Current Fuel Cell Price By Application and Production Rate

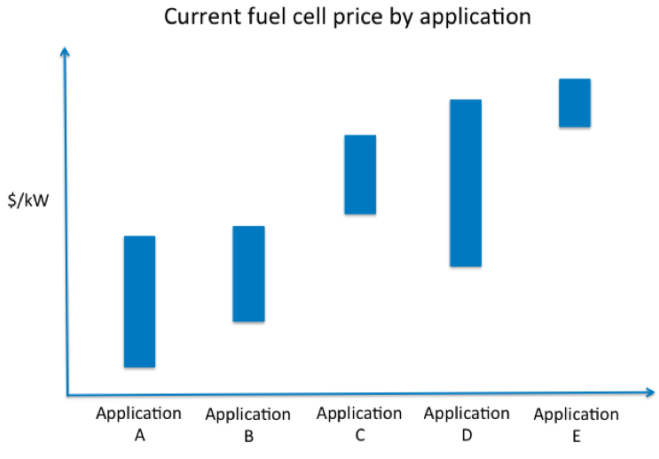

FIGURE 3. Example Result (Fake Data) for Current Fuel Cell Price by Application

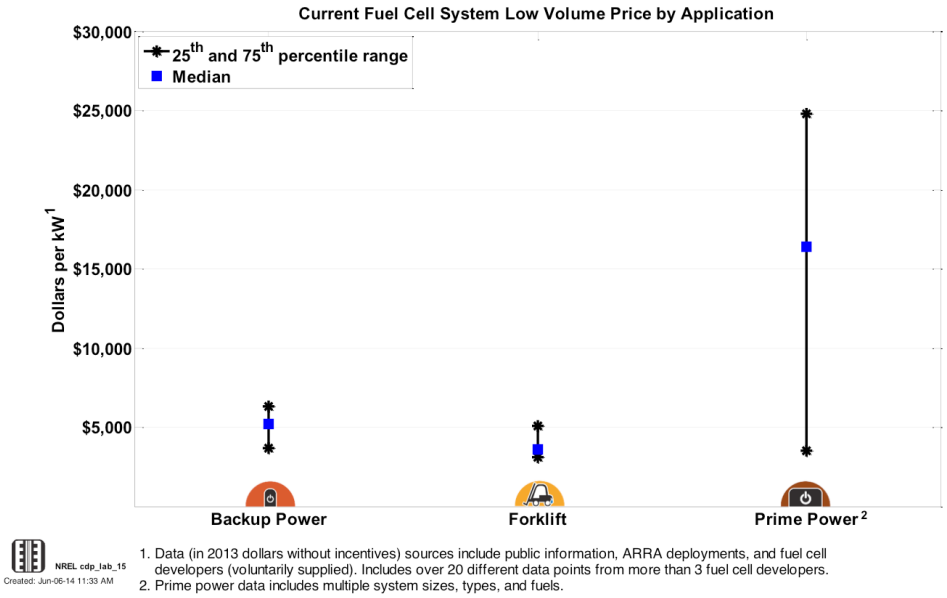

FIGURE 4. Current Fuel Cell System Low-Volume Price by Application (Published June 2014)

- Gathering, processing, and reporting on current fuel cell product cost and/or price
- Focusing on fuel cell durability data for expected publication of status in FY 2015.

FY 2014 PUBLICATIONS/PRESENTATIONS

1. Kurtz, J., Dinh, H., "Fuel Cell Technology Status – Cost & Price Status," Presented as a poster at the 2014 Annual Merit Review and Peer Evaluation Meeting, Washington, D.C. (June 2014)

2. Kurtz, J., Dinh, H., "Current Low Volume Fuel Cell System Price: 2014 Composite Data Product." (June 2014)

3. Kurtz, J., Sprik, S., "National Fuel Cell Technology Evaluation Centers." DOE webinar. (March 2014)

4. Kurtz, J., Dinh, H., Sprik, S., Saur, G., Ainscough, C., Peters, M., "Analysis of Laboratory Fuel Cell Technology Status – Voltage Degradation," Annual Progress Report. (August 2013)

REFERENCES

1. http://www.nrel.gov/hydrogen/proj_fc_analysis.html

V.E.4 Open-Source PEMFC-Performance and Durability Model Consideration of Membrane Properties on Cathode Degradation

David Harvey
Ballard Power Systems
9000 Glenlyon Parkway
Burnaby, B.C. V5J 5J8
Phone: (604) 453-3668
Email: david.harvey@ballard.com

DOE Managers
Donna Ho
Phone: (202) 586-8000
Email: Donna.Ho@ee.doe.gov
David Peterson
Phone: (720) 356-1747
Email: David.Peterson@ee.doe.gov

Technical Advisor
John Kopasz
Phone: (630) 252-7531
Email: kopasz@anl.gov

Contract Number: DE-EE0006375

Subcontractors
- University of Calgary, Calgary, Alberta, Canada (K. Karan)
- University of New Mexico, Albuquerque, NM (P. Atanassov)

Project Start Date: January 1, 2014
Project End Date: October 31, 2014

Overall Objective

Develop open-source, forward predictive models and conduct systematic cell degradation studies.

Fiscal Year (FY) 2014 Objectives

- Complete down selection of membrane types for analysis
- Measure and report material properties for down-selected membranes
- Evaluate beginning of test (BOT) performance and accelerated stress test (AST) behavior for down-selected membranes
- Evaluate BOT performance and AST behavior for membrane-AST-degraded membrane electrode assemblies (MEAs)
- Assess the membrane sub-model within FC-APOLLO and compare with assessment of to-be-implemented sub-model.
- Integrate the 'new' membrane sub-model into FC-APOLLO

Technical Barriers

This project addresses the following technical barriers from the Fuel Cells section of the DOE Fuel Technologies Office Multi-year Research, Development, and Demonstration Plan [1].

(A) Durability

Pt catalyst and Pt catalyst layer degradation

- Effect of cathode structure and composition
- Effect of operational conditions

(B) Performance

- Effect of cathode catalyst structure and composition

(C) Cost

Technical Targets

In this project, fundamental studies of the Pt/carbon catalyst degradation mechanisms and degradation rates are conducted and correlated with membrane transport properties and operational conditions. The fundamental studies are used to facilitate the development and refinement of membrane model implementation within the open-source software FC-APOLLO. Furthermore, the design curves generated both through model simulations and experimental work, will enable MEA designers to optimize performance, durability, and cost towards the 2020 targets for fuel cell commercialization [1]:

- System Durability (10% performance loss)
  - Transportation applications: 5,000 hours
  - Stationary applications (1-10 kW_e): 60,000 hours
- Electrocatalyst (transportation applications)
  - Support stability: <10% mass activity loss after 400 hrs @ 1.2 V in H_2/N_2
  - Electrochemical surface area (ECSA) loss: <40%
  - Pt group metal total loading: 0.125 mg /cm^2

FY 2014 Accomplishments

- Completed down selection of membranes, with inclusion for perfluorinated sulfonic acid (PFSA), reinforced-PFSA, and hydrocarbon-based materials
- Reported on BOT performance and cathode catalyst AST testing for MEAs with the down-selected membrane materials
- Generated data for membrane-AST degraded MEAs for BOT performance and cathode catalyst AST testing
- Completed assessment of to-be-implemented sub-model and respective material relationship and predictions

INTRODUCTION

Catalyst/catalyst layer degradation has been identified as a substantial contributor to fuel cell performance degradation and this contribution will most likely increase as MEAs are driven to lower Pt loadings in order to meet the cost targets for full-scale commercialization. Over the past few years significant progress has been made in identifying catalyst degradation mechanisms [2,3] and several key parameters that greatly influence the degradation rates, including electrode potentials, potential cycling, temperature, humidity, and reactant gas composition [2,4,5,6]. Despite these advancements, many gaps with respect to catalyst layer degradation and an understanding of its driving mechanisms still exist. In particular, acceleration of the mechanisms under different fuel cell operating conditions, due to different structural compositions/neighboring components, and as a function of the drive to lower Pt loadings remains an area not well understood. In order to close these gaps an understanding of the effect of the membrane properties on the local conditions within the catalyst layer and the subsequent manifestation of those local conditions on performance and durability, in particular the catalyst layer degradation mechanisms and degradation rates, is needed.

The focus of this project is to develop open-source, forward predictive models and conduct systematic cell degradation studies that enable quantification of the cathode catalyst layer degradation mechanisms and rates and to correlate those rates and the degradation-derived changes in catalyst properties/composition to the materials properties of the chosen membranes.

APPROACH

This project addresses the performance and durability of Pt catalysts and catalyst layers which have been identified as key technical barriers in the DOE Fuel Cell Technologies Office Multi-Year Research, Development, and Demonstration Plan. The project follows a parallel three-path approach of (1) theoretical simulations, (2) experimental investigations, and (3) material/component characterization (collaborative work) with the overall goal to advance the ability to simulate and design durable fuel cell products and subsequently reduce the iterative design/test cycle process for next generation fuel cell products.

The approach of the project includes: (1) Refinement of the membrane model that is an integral part of FC-APOLLO in order to describe changes in transport properties as a function of the change in membrane type (material characteristics); (2) Experimental assessment of the impact of membrane type, transport and materials properties on the MEA performance loss mechanisms and the Pt dissolution mechanism/rate; (3) Development of correlations that link membrane materials properties and catalyst layer effective properties to MEA/cathode performance and degradation loss mechanisms.

RESULTS

Model Development

During the first FY the review of the membrane models was the first step completed in order to facilitate integration into FC-APOLLO. To this end, several models within the literature were reviewed and partially implemented in a simplified framework in order to access the relational behavior of the parameters. Based on these reviews it was found that the existing membrane sub-models within the literature pose several challenges for use in unit-cell modelling. Many of the membrane sub-models are steady state and do not adequately describe the rate of exchange between liquid and and vapor phases. Furthermore, many of the existing models contain parameters which are difficult, if not impossible, to measure quantitatively; for example, thermodynamic arguments like pressure and concentration are not compatible within a fixed-proton conducting polymer electrolyte and the surface activities which are generally defined by either pressure for gases or concentration for liquids, are not captured when both occur at the same time.

While physics-based membrane models do exist in the literature, the inherent coefficients are generally not measurable [7]; thus, in order to validate the model the coefficients need to be related to membrane properties that can be physically quantified. We have started to adapt the steady-state model proposed by Weber and Newman [8] with the intent to generate a general transient, three-dimensional implementation in the context of a unit cell. As shown in Figure 1, the module attempts to encode physics for the known transport processes taking place in the membrane as adapted by the work published by Weber and Newman. This module applies an inner iteration process to determine the state of the membrane (i.e. proton conductivity, diffusivity,

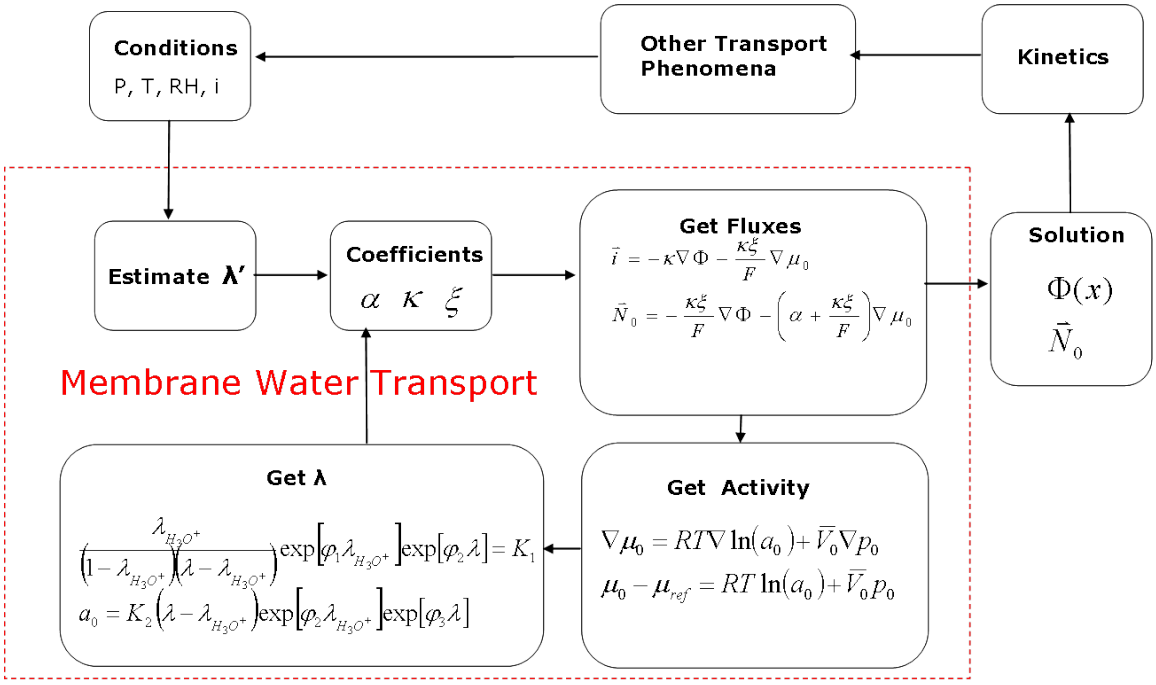

FIGURE 1. Membrane Water Modeling Approach

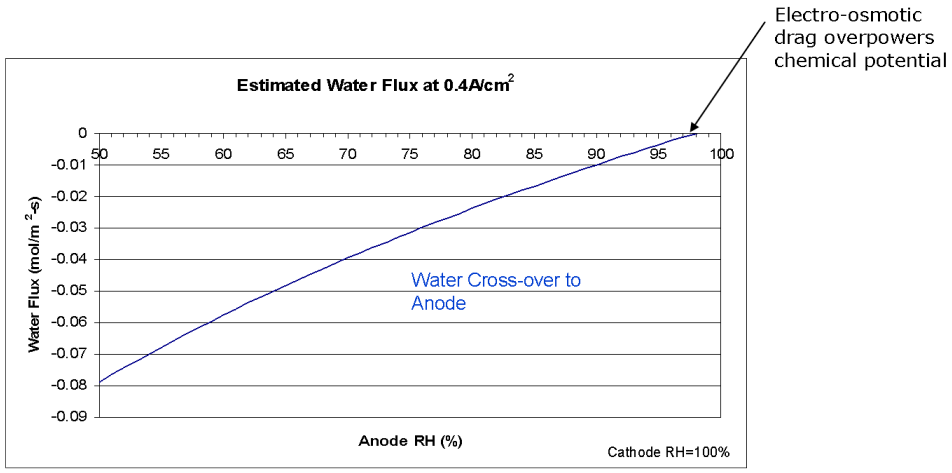

FIGURE 2. Simulated Water Flux

etc.) and an outer iteration to determine the solved variables (i.e. potential and fluxes) that external models, such as those for the oxygen reduction reaction kinetics, require.

An initial test to check the response of the numerical system and ensure that it behaved as expected is shown in Figure 2. In this test a current density of 0.4 A/cm^2 was applied at the membrane boundary with the water flux through the membrane determined as a function of anode relative humidity (RH), while the cathode RH was held constant. As expected, the current drove an electro osmotic flux which affected the net water flux to the anode as indicated by the adjusted "zero" water flux conditions occurring increasingly towards a lower anode RH.

Experimental Parametric Studies

Experimental testing and characterization within this FY was conducted on the following types of membranes Nafion®211 (baseline membrane), Nafion®212 (optional), experimental reinforced PFSA membranes with low and high equivalent weights (EWs), and reinforced partially fluorinated hydrocarbon membranes of high and low EWs. The intention of the testing in the project is to develop

characterization and validation data for the simulation and modelling work and to generate datasets that can be used to correlate MEA performance and durability to membrane properties and key transport parameters.

A table of key membrane properties/characteristics was extracted (Table 1) based on the theory/relationships of previous/existing/and to-be-implemented models and this was used to guide the selection of experimental tests that are being conducted within the characterization component of the project.

In addition to the characterization of the membranes for the properties shown in Table 1, in-cell testing consisting of steady-state polarizations, a membrane AST and a cathode catalyst AST are used to elucidate differences and effects due to the use of different membrane materials and the associated effects on the cathode catalyst layer local conditions. The baseline MEA, the test hardware, the cathode AST, and suite of diagnostic tools are described in detail in the previous project documentation.

The BOT performance results for the MEAs with three different membranes at relative humidities of 60% and 100% are shown in Figure 3. We see that each of the MEAs has similar performance at current densities less than 1 A/cm^2. However, at current densities greater than 1 A/cm^2 the baseline membrane exhibits larger performance losses than the other PFSA materials. At 2 A/cm^2 and 100% RH a performance loss of as much as 80 mV emerges between the baseline membrane and the low EW PFSA membrane materials. The performance difference can be explained in part due to variations in the thickness of the membrane materials as the baseline material is the thickest of the three shown, while the differences seen at low RH are likely a more complex mix of the water transport, water content, EW, and thickness.

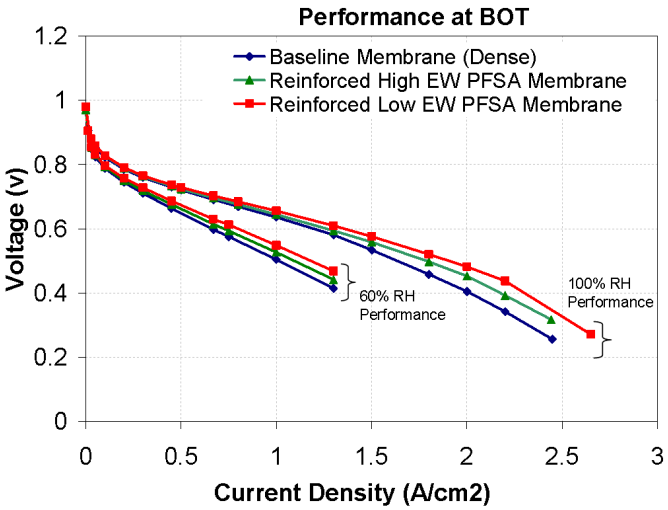

FIGURE 3. BOT Performance of MEAs with Different Membranes

After the BOT performance benchmark, the MEAs were subjected to a cathode AST for 4,700 cycles. As seen in Figure 4(a), the performance throughout the current density range is very similar for the three membranes. Figure 4(b) shows that the ECSA losses are systematically offset between the different membranes and this offset appears to potentially be a function of the equivalent weight. There are also higher voltage losses for the high EW PFSA membrane MEA compared to the baseline MEA, with a loss of ~90 mV vs. 60 mV at 2 A/cm^2. It is also of note that the low RH performance is further depressed for the low EW PFSA membrane compared to the other membranes, again

TABLE 1. Membrane Properties for Model Inputs

Membrane Properties	versus	Required	Optional
Ion Exchange Capacity (EW)		x	
Density	dry, RH	dry	RH
Thickness	dry, RH	dry, RH	
Water Uptake/Content	T, RH, EW, time (rate of from dry state)	RH, time	T, EW
Proton Conductivity	T, RH, time (rate of from dry state)	RH, time	T, EW
O2, H2 Gas/Dissolved Gas Diffusivity	dry, T, RH, EW		T, RH, EW
O2, H2 Solubility	T, RH, EW		T, RH, EW
PtOH solubility/Diffusivity	T, RH, EW		T, RH, EW
Reactant Cross-over	T, RH	T, RH, system pressure	EW
Water flux (Constant System Pressure Anode/Cathode)	T, RH, EW, Pressure (cathode/anode)	RH, T, Pressure	EW
Water Permeation (Differential Pressure Anode/Cathode)	V/V, V/L, L/V, L/L		V/V, V/L, L/V, L/L
Thermal Relaxation			x
Interfacial Ionic Resistance (Between Ionomeric Materials)	T, RH, EW		RH, T, EW

RH calclated from P_total, P_H2O, T

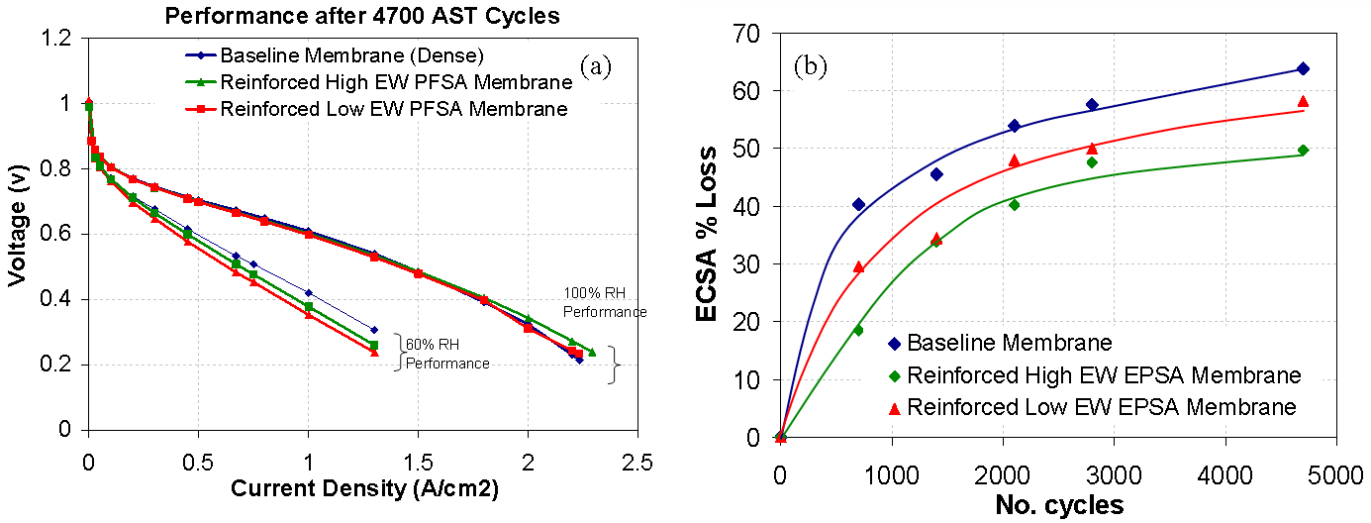

FIGURE 4. MEAs Containing Different Membranes after Exposure to Cathode AST, (a) EOT Performance, (b) ECSA Loss

indicating the potentially higher water content in the low EW PFSA membrane appears to be interacting with the catalyst layer degradation.

CONCLUSIONS AND FUTURE DIRECTIONS

The interim conclusions are:

- Platinum surface area losses appear to be affected by the EW of the membrane; this will be further explored within the project based on a set of theory in which the local solvation of the platinum complexes within the membrane are dependent on EW and may yield an increase or decrease in the amount of platinum complexes local to the catalyst thus affecting the driving force for the platinum dissolution reaction.
- Based on the results to date, the choice of membrane material results in differences in water-crossover and, subsequently, the local conditions around the platinum sites in the cathode catalyst layer. ECSA differences are observed over the course of AST cycling, however, the overall performance differences are not as large as was expected. This is due in part to a result that was observed from our previous project, in that the correlation between ECSA and cell performance showed a non-linear drop in performance which occurred for ECSA at ~80 or less. As a result, the current results and their impact on degraded performance are expected to be much more influential on lower loaded cathode catalyst layer designs, dependent on the membrane type used.

Future directions include:

- Complete implementation/revision of the "improved" membrane transport sub-model in FC-APOLLO
- Extend the Pt dissolution model to include coupling to address the water content effect and pH effect of different membranes
- Complete validation of FC-APOLLO with experimental data for the sub-model and cell performance/AST data
- Complete the membrane AST degraded, cathode catalyst AST testing for the various membranes
- Tabulate characterization data for membrane properties based on ex situ/in situ testing and compare to existing theory
- Release revised FC-APOLLO model to www.sourceforge.net/projects/fcapollo
- Develop design curves for catalyst degradation rates and catalyst changes to membrane transport properties

REFERENCES

1. Hydrogen, Fuel Cells & Infrastructure Technologies Program: Multi-Year Research, Development and Demonstration Plan, U.S. Department of Energy, Energy Efficiency and Renewable Energy, 2011 revision. http://www.eere.energy.gov/hydrogenandfuelcells/mypp/

2. J. Wu, X.Z. Yuan, J.J. Martin, H. Wang, J. Zhang, J. Shen, S. Wu, W. Merida, A Review of PEM Fuel Cell Durability: Degradation Mechanisms and Mitigation Strategies. Journal of Power Sources 184, 104-119.

3. R. Borup, J.P. Meyers, B. Pivovar, Y.S. Kim, R. Mukundan, N. Garland, D. Myers, M. Wilson, F. Garzon, D. Wood, P. Zelenay, K. More, K. Stroh, T. Zawodinski, J. Boncella, J.E. McGarth, M. Inaba, K. Miyatake, M. Hori, K. Ota, Z. Ogumi, S. Miyata, A. Nishikata, Z. Siroma, Y. Uchimoto, K. Yasuda, K. Kimijima, N. Iwashita, Scientific Aspects of Polymer Electrolyte Fuel Cell Durability and Degradation. Chemical Reviews 2007, 107, 3904-3951.

4. Y. Shao, G. Yin, Y. Gao, Understanding and Approaches for the Durability Issues of Pt-Based Catalysts for PEM Fuel Cell. Journal of Power Sources 2007, 171, 558-566.

5. M.S. Wilson, F. Garzon, K.E. Sickafus, S. Gottesfeld, Surface Area Loss of Supported Platinum in Polymer Electrolyte Fuel Cells. Journal of the Electrochemical Society 1993, 140, 2872-2876.

6. P.J. Ferreira, G.J. Ia O', Y. Shao-Horn, D. Morgan, R. Makharia, S. Kocha, H. Gasteiger, Instability of Pt/C Electrocatalysts Membrane Fuel Cells - A Mechanistic Investigation. Journal of the Electrochemical Society 2005, 152, A2256-A2271.

7. G.J.M. Janssen. "A phenomenological model of water transport in a proton exchange membrane fuel cell", ECS 148 (12) A1313-A1323 (2001).

8. Weber, A.Z. & J. Newman. "Transport in Polymer-Electrolyte Membranes II. Mathematical Model". ECS 151 (2) A311-A325 (2004).

V.F.1 Effect of System Contaminants on PEMFC Performance and Durability

Huyen N. Dinh (Primary Contact), Guido Bender, Clay Macomber, Heli Wang, Bryan Pivovar

National Renewable Energy Laboratory (NREL)
15013 Denver West Parkway
Golden, CO 80401-3305
Phone: (303) 275-3605
Email: Huyen.Dinh@nrel.gov

DOE Manager

David Peterson
Phone: (720) 356-1747
Email: David.Peterson@ee.doe.gov

Subcontractors

- Paul T. Yu, Balsu Lakshmanan, General Motors LLC, Honeoye Falls, NY
- John Weidner, John Van Zee, University of South Carolina, Columbia, SC
- Ryan Richards, Jason Christ, Colorado School of Mines, Golden, CO
- Steve Hamrock, Andrew Steinbach (in-kind partner), 3M, St. Paul, MN
- Paul Beattie (in-kind partner), Ballard Power Systems, Vancouver, BC, Canada
- Olga Polevaya (in-kind partner), Nuvera Fuel Cells Inc., Billerica, MA

Project Start Date: July 20, 2009
Project End Date: Project continuation and direction determined annually by DOE

Overall Objectives

Our overall objective is to decrease the cost associated with system components without compromising function, fuel cell performance, or durability. Our specific project objectives are to:

- Identify and quantify system-derived contaminants.
- Develop ex situ and in situ test methods to study contaminants derived from system components.
- Identify severity of system contaminants and impact of operating conditions.
- Identify contamination mechanisms.
- Develop models/predictive capability.
- Guide system developers on future material selection.
- Disseminate knowledge gained to the community.

Fiscal Year (FY) 2014 Objectives

- Identify impact of operating conditions.
- Develop a mechanistic model for contamination.
- Disseminate project information to the fuel cell community.
- Develop understanding of leaching conditions' impact on contaminant concentration.

Technical Barriers

This project addresses the following technical barriers from the Fuel Cells section (3.4.4) of the Fuel Cell Technologies Office Multi-Year Research, Development, and Demonstration Plan:

(A) Durability

(B) Cost

Technical Targets

This project focuses on quantifying the impact of system contaminants on fuel cell performance and durability. Insights gained from these studies will increase performance and durability by limiting contamination-related losses and decreasing overall fuel cell system costs by lowering balance-of-plant (BOP) material costs. Proper selection of BOP materials will help meet the following DOE 2020 targets:

- Cost: $30/kW for transportation; $1,000–1,700/kW for stationary
- Lifetime: 5,000 hours for transportation; 60,000 hours for stationary

FY 2014 Accomplishments

- Developed the leaching index as a quick material screening method.
- Identified impact of various fuel cell operating conditions (contaminant concentration, relative humidity, cell temperature, current density, and catalyst loading) on fuel cell performance and recovery for selected structural material extracts. This knowledge can help identify future mitigation strategies for contaminants.
- Developed a model for contamination mechanism based on experiments with model organic compounds.
- Improved NREL website (www.nrel.gov/hydrogen/contaminants.html) and interactive material data tool (www.nrel.gov/hydrogen/system_contaminants_data/) by adding more data (60 system component materials

total) and project information and improving user experience.

- Presented DOE webinar on "An Overview of NREL's Online Data Tool for Fuel Cell System-Derived Contaminants" [1].

INTRODUCTION

Cost and durability issues of polymer electrolyte membrane fuel cell (PEMFC) systems have been challenging for the fuel cell industry. The current status of fuel cell system costs is $55/kW, much lower than $124/kW in 2006, but still higher than the ultimate target of $30/kW [2]. As fuel cell systems become more commercially competitive, the impact of contaminants derived from fuel cell system component materials has risen in importance. Contaminants derived from fuel cell system component materials—structural materials, lubricants, greases, adhesives, sealants, and hoses—have been shown to affect the performance and durability of fuel cell systems. Lowering the cost of PEMFC system components requires understanding of the materials used in these components and the contaminants that are derived from them. Unfortunately, there are many possible contamination sources from system components [3-5]. Currently deployed, high-cost, limited-production systems use expensive materials for system components. In order to make fuel cell systems commercially competitive, the cost of BOP components needs to be lowered without sacrificing performance and durability. Fuel cell durability requirements limit the performance loss attributable to contaminants to at most a few mV over required lifetimes (thousands of hours), which means system contaminants must have a near-zero impact.

As catalyst loadings decrease and membranes are made thinner (both are current trends in automotive fuel cell research and development), operation of fuel cells becomes even more susceptible to contaminants. In consumer automotive markets, low-cost materials are usually required, but lower cost typically implies higher contamination potential. The results of this project will provide the information necessary to help the fuel cell industry make informed decisions regarding the cost of specific materials versus the potential contaminant impact on fuel cell performance and durability. The project results will also identify the impact of different operating conditions and possible mitigation strategies for contaminants.

APPROACH

Our goal is to provide an increased understanding of fuel cell system contaminants and to help guide the implementation and, where necessary, development of system materials to support fuel cell commercialization. While much attention has been paid to air and fuel contaminants, system contaminants have received limited public attention and very little research has been publicly reported [6-8]. Our approach is to perform parametric studies to characterize the effects of system contaminants on fuel cell performance, as well as to identify the severity of contamination, identify contamination mechanisms, develop a model, and disseminate information about material contamination potential that would benefit the fuel cell industry in making cost-benefit analyses for system components. The BOP materials selected for this study are commercially available commodity materials and are generally developed for other applications for which common additives/processing aids may not be a concern, but they may present problems for fuel cells. We studied leachates as well as model compounds that are capable of replicating the deleterious impact of system-based contaminants.

RESULTS

One of this year's accomplishments was expanding the BOP material data base and project information as well as improving the user experience on the NREL website. The screening results for 60 commercially available BOP materials (structural, hoses, assembly aids such as seals, gaskets, and adhesives), using multiple screening methods to identify and quantify system-derived contaminants, are archived and made publicly accessible on the NREL website. The NREL material screening data tool was designed to be interactive, easy to use and informative to the fuel cell community. Furthermore, a DOE webinar was presented by Dinh to give an overview of NREL's online data tool and provide a tutorial on how to use the Web-based tool to access project results [1].

General Motors (GM) screened and categorized 34 structural plastic materials into groups based on their basic polymer resin (e.g., polyamide or PA) and manufacturers. They found that the leaching index (LI), which is the sum of the solution conductivity and total organic carbon (TOC), is a quick way to screen plastic materials. The leaching index is an indicator of the amount of contaminants (organics, inorganics, and ions) leaching from the material. Figure 1 shows that higher leaching index generally results in higher cell voltage loss and is correlated with lower material cost. The implication is that fuel cell developers can do a quick screening of the BOP material candidates by carrying out the leaching experiment and measure the TOC and solution conductivity of the extract solution. These measurements are quick and easy to do. If some good material candidates are found, then further testing, such as electrochemistry, membrane conductivity, advanced analytical characterization, and in situ infusion experiments can be carried out to better understand what contaminant species are present and how they impact fuel cell performance.

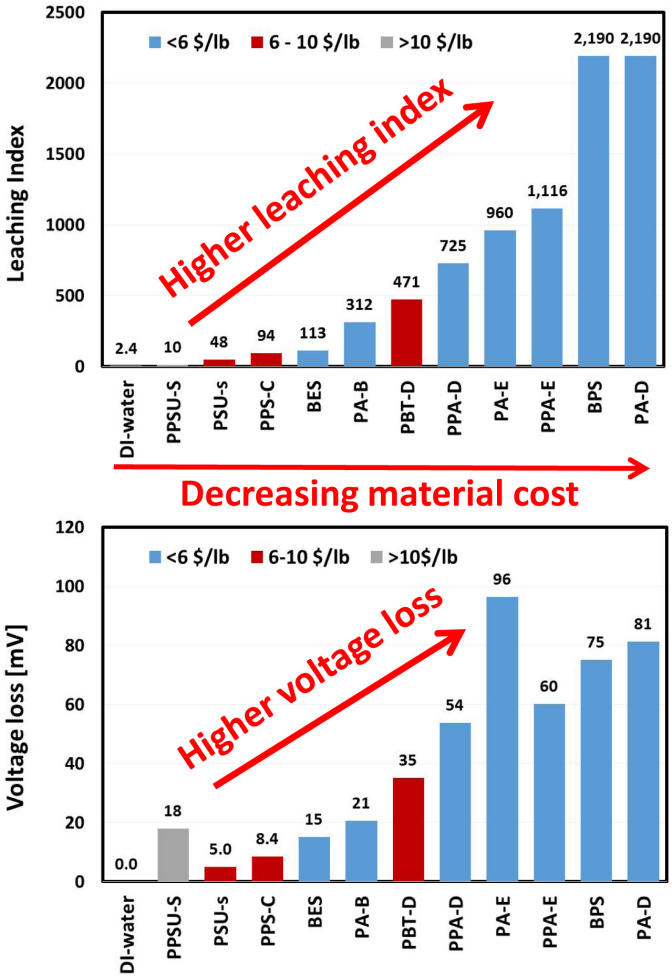

FIGURE 1. Higher leaching index (conductivity + total organic carbon) is generally correlated with higher fuel cell performance loss and lower material cost. BES = Bakelite epoxy-based material – Sumitomo; BPS = Bakelite phenolic-based material – Sumitomo; S = Solvay; C = Chevron Philips; B = BASF; D = DuPont; E = EMS; Information provided by GM.

From 34 structural plastic materials screened, three were selected for in situ infusion parametric studies to understand the effect of the polymer resin (PA and PPA or polyphthalamide), additive (e.g., percent of glass fiber added for plastic structural integrity), and different operating conditions (contaminant concentration, relative humidity (RH), cell temperature, current density (CD), and catalyst loading) on fuel cell performance and recovery. The parameters studied reflect 80% of typical fuel cell operating conditions. Figure 2 shows that the PA material (EMS-4), which has the highest LI, resulted in higher voltage loss than PPA materials. Furthermore, the PPA material that has the lower glass fiber (GF) content (30% GF for EMS-10 vs. 50% GF for EMS-7) resulted in a lower LI and lower fuel cell performance loss. These results imply that the polymer resin type and additives are important contaminant source considerations. In addition, Figure 2 shows that the in situ

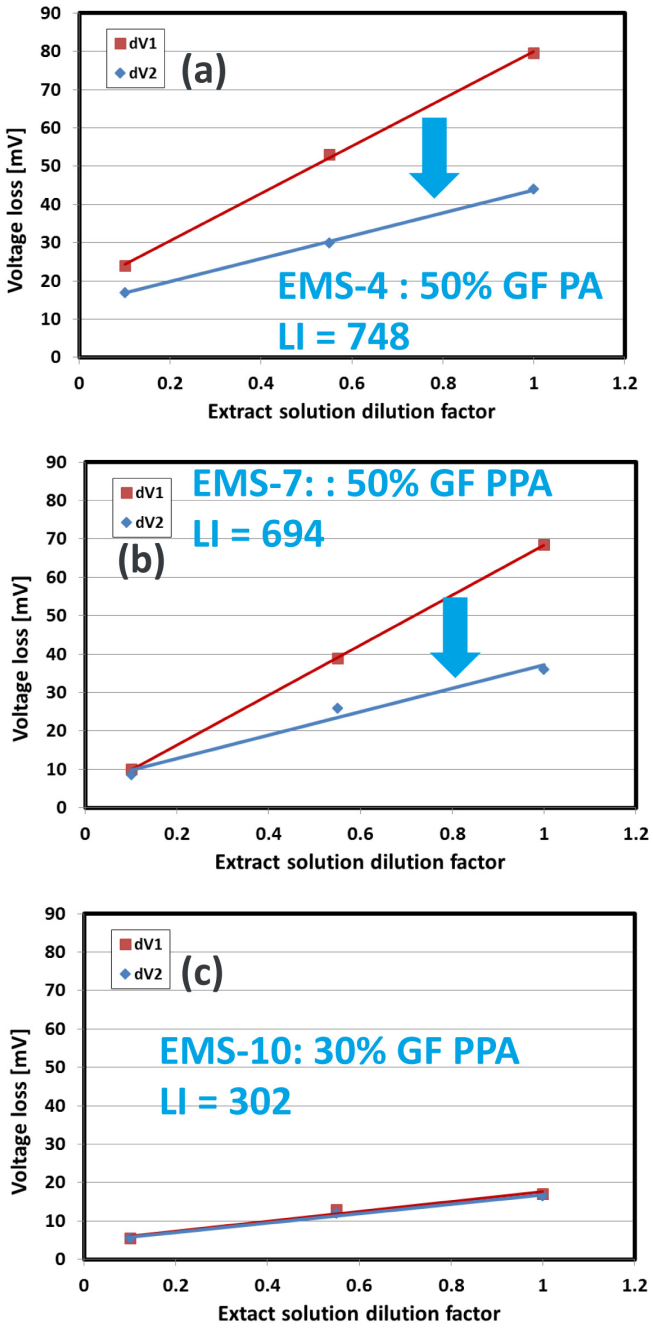

FIGURE 2. In situ fuel cell voltage loss due to contaminants (dV1) increases linearly as a function of structural material leachate concentration due to contamination of the fuel cell cathode: (a) EMS-4 50% glass fiber PA, (b) EMS-7 50% glass fiber PPA, and (c) EMS-10 30% glass fiber PPA. The voltage loss after passive recovery (dV2) is also shown. The plots also show that polymer resin type and additives in plastic materials matter. The LI for the different materials is also shown for comparison. Standard operating conditions (SOC): 80°C, 32/32% inlet RH, 0.2 A/cm^2, H_2/air stoichiometry = 2/2; 150/150 kPa; Information provided by GM.

fuel cell voltage loss due to contaminants (dV1) increases linearly as a function of leachate concentration (red line) and the contamination effect can be partially reversed in the absence of contaminants (blue line). A similar trend was observed for all three structural materials studied.

Figure 3 summarizes the main effect of different operating conditions (concentration, RH, CD, and catalyst loading) on fuel cell performance loss due to contamination (dV1) and recovery (dV2) in the absence of contaminants (also known as passive recovery). As expected, fuel cells with low Pt loading are more sensitive to BOP plastic leached contaminants and result in higher cell voltage loss, regardless of the material studied. Figure 3a shows that the voltage loss increases with increasing current density while RH appears to have a minimum effect on voltage loss. RH is a complicated factor since it controls the mole fraction of both water and contaminant into the fuel cell. As RH increases, more water vapor enters the fuel cell and can help flush out the contaminants. However, more water vapor also means more contaminants are brought into the fuel cell and results in higher voltage loss. These two phenomena may counter each other and lead to insensitivity of RH to fuel cell performance loss. Figure 3b shows that these four parameters have similar effect on the voltage loss after passive recovery (dV2), but the magnitude of the voltage loss is lower compared to dV1. These voltage losses were obtained during infusion at relatively low current density (0.2 A/cm^2). Analysis of the polarization curves before contamination (beginning of life) and after passive recovery showed that the trend on fuel cell voltage loss due to these operating parameters is similar at low and high current densities (e.g., 1.2 A/cm^2).

Statistical analysis of the parametric results showed that CD and/or dosage are/is the most significant factor(s) affecting cell performance, followed by leachate concentration, interaction of RH and Pt loading, Pt loading, and interaction of RH and concentration. It is important to note that interaction between different operating conditions should be considered with respect to contamination effect. For example, trends toward lower catalyst loadings may mean that fuel cells need to operate at higher RH since these two parameters interact with one another.

From the parametric study, we have identified several mitigation strategies to minimize the leachate concentration (leaching index). These strategies include minimizing the contact time and contact ratio of the plastic materials with water in the fuel cell, minimizing exposure of plastic material to high temperature, increasing the RH or increasing the RH and potential cycling (ex situ recovery), choosing clean BOP materials (usually more expensive, e.g., resin type and additive), and working with material suppliers to minimize contaminants (i.e., removing additives that are not applicable to fuel cells and using less or alternative additives that do not leach out contaminants). These strategies can minimize fuel cell performance loss due to system-derived contaminants.

CONCLUSIONS AND FUTURE DIRECTIONS

- We improved the NREL project website and interactive data tool by expanding the material database, enhancing user experience, archiving the results, and making them publicly accessible.
- We developed the leaching index as a good, quick screening method for potential system components. This data is also included on the NREL website.
- We found that cost, polymer resin type and additives need to be considered when selecting BOP plastic materials for fuel cell systems because the choice can have different degrees of contamination impact.

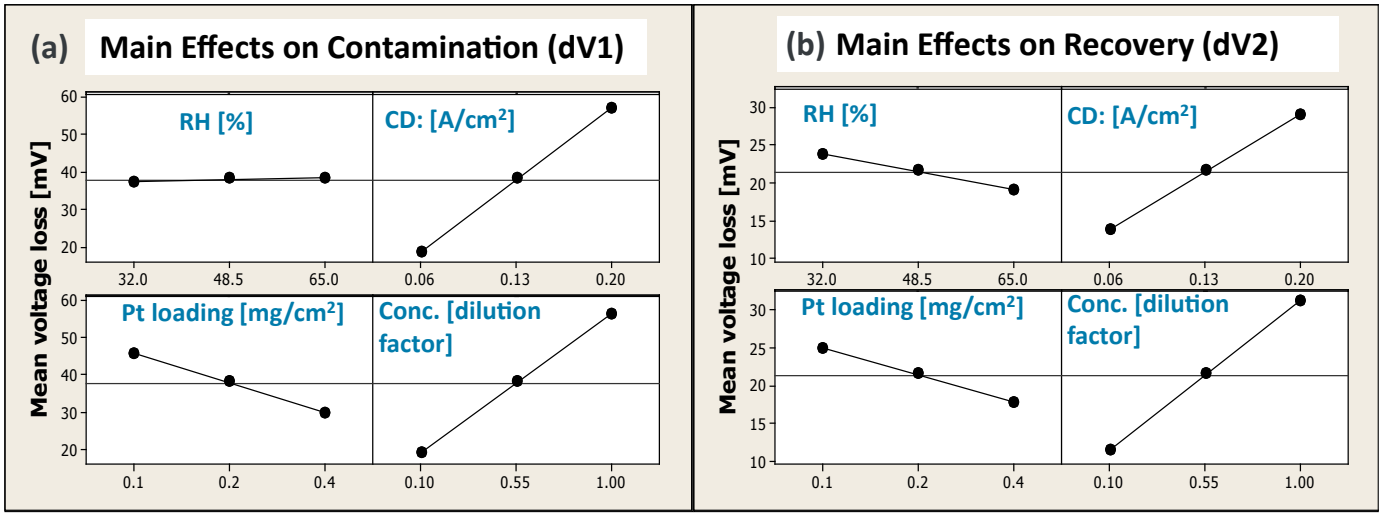

FIGURE 3. Summary of the effects of different operating conditions on fuel cell performance loss (dV1) and passive recovery (dV2). SOC were used.

- We found that contamination impact depends on fuel cell operating conditions (CD, concentration, Pt loading, RH interaction with Pt loading and concentration, temperature) and that interactions between different operating conditions need to be considered.
- We found that operating conditions (e.g., time, temperature) that cause more liquid/plastic contact need to be considered in developing a fuel cell system because they can lead to higher contaminant concentration (higher leaching index).
- We have identified several mitigation strategies to minimize the leaching index and hence minimize the performance loss.
- We will determine the fuel cell performance impact of lower leachate concentrations.
- We will develop analytical methods to measure soluble leachates in solution and volatiles in headspace.
- We will perform mechanistic studies on organic and ionic model compounds derived from structural plastics to understand the effect of individual and mixtures of compounds on fuel cell performance.
- We will disseminate project information via the NREL website, publications, reports, and presentations.

FY 2014 PUBLICATIONS/PRESENTATIONS

1. Wang, H.; Macomber, C.S.; Christ, J.; Bender, G.; Pivovar, B.; Dinh, H.N. "Evaluating the Influence of PEMFC System Contaminants on the Performance of Pt Catalyst via Cyclic Voltammetry." Electrocatalysis (5), 2014; pp. 62-67.

2. Yu, P.T.; Bonn, E.A.; Lakshmanan, B. "Impact of Structural Plastics as Balance of Plant Components on Polymer Electrolyte Membrane Fuel Cell Performance." *ECS Transactions* (58:1), 2013; pp. 665-680.

3. Dinh, H.N. "Effect of System Contaminants on PEMFC Performance and Durability." Section V.B.1. *2013 DOE Hydrogen and Fuel Cells Program Annual Progress Report*; pp. V129-V134.

4. Dinh, H.N. "Effect of System Contaminants on PEMFC Performance and Durability." DOE Fuel Cell Technologies Office Annual Merit Review, Washington, DC, June 2014.

5. Dinh, H.N. "An Overview of NREL's Online Data Tool for Fuel Cell System-Derived Contaminants." DOE Fuel Cell Technologies Office Webinar, May 27, 2014.

6. Christ, J.M. "Adsorption Characteristics of Polymer Electrolyte Membrane Chemical Degradation Products and their Impact on Oxygen Reduction Reaction Activity for Platinum Catalysts." Colorado School of Mines Chemistry Departmental Seminar, Golden, CO, April 2014.

7. Christ, J.M.; Neyerlin, K.C.; Richards, R.; Dinh, H.N. Presentation at the Electrochemistry Gordon Research Conference, Ventura, CA, January 2014.

8. Dinh, H.N.; Yu, P.T.; Weidner, J. "Effect of System Contaminants on PEMFC Performance and Durability." Presentation to the DOE Fuel Cell Tech Team, Southfield, MI, Jan. 15, 2014.

REFERENCES

1. Dinh, H.N. "An Overview of NREL's Online Data Tool for Fuel Cell System-Derived Contaminants." DOE Fuel Cell Technologies Office Webinar, May 27, 2014. http://energy.gov/sites/prod/files/2014/06/f16/webinarslides_fuel_cell_contaminants_052714.pdf.

2. http://www.hydrogen.energy.gov/pdfs/13012_fuel_cell_system_cost_2013.pdf.

3. D. Gerard. "Materials and Materials Challenges for Advanced Automotive Technologies Being Developed to Reduce Global Petroleum Consumption." 2007 Materials Science and Technology (Invited), Detroit, MI, September 16–20, 2007.

4. D.A. Masten, A.B. Bosco. *Handbook of Fuel Cells* (eds.: W. Vielstich, A. Lamm, H.A. Gasteiger), Wiley (2003): Vol. 4, Chapter 53, p. 714.

5. Q. Guo, R. Pollard, J. Ruby, T. Bendon, P. Graney, J. Elter. *ECS Trans.*, Vol. 5(1), p. 187 (2007).

6. G.A. James, et. al. "Prevention of Membrane Contamination in Electrochemical Fuel Cells." U.S. Patent Application US2005089746A.

7. R. Moses. "Materials Effects on Fuel Cell Performance." National Research Council Canada Institute for Fuel Cell Innovation, International Fuel Cell Testing Workshop, September 20–21, 2006.

8. K. O'Leary, B. Lakshmanan, M. Budinski. "Methodologies for Evaluating Automotive PEM Fuel Cell System Contaminants." 2009 Canada-USA PEM Network Research Workshop, February 16, 2009.

V.F.2 The Effect of Airborne Contaminants on Fuel Cell Performance and Durability

Jean St-Pierre (Primary Contact), Yunfeng Zhai, Junjie Ge, Tatyana Reshetenko, Michael Angelo, Trent Molter[1], Leonard Bonville[1], Ugur Pasaogullari[1], Xiaofeng Wang[1], Jing Qi[1], Ozan Ozdemir[1], Amman Uddin[1], Navvab Khajeh-Hosseini-Dalasm[1], Jaehyung Park[1], Selvarani Ganesan[1], William Collins[2], Silvia Wessel[3], Tommy Cheng[3]

Hawaii Natural Energy Institute
1680 East-West Road
Honolulu, HI 96822
Phone: (808) 956-3909
Email: jsp7@hawaii.edu

DOE Managers

Nancy Garland
Phone: (202) 586-5673
Email: Nancy.Garland@ee.doe.gov

Reg Tyler
Phone: (720) 356-1805
Email: Reginald.Tyler@ee.doe.gov

Technical Advisor

Tom Benjamin
Phone: (630) 252-1632
Email: benjamin@anl.gov

Contract Number: DE-EE0000467

Subcontractors

[1] University of Connecticut, Storrs, CT
[2] WPCSOL, East Windsor, CT
[3] Ballard Power Systems, Burnaby, BC, Canada

Project Start Date: April 1, 2010
Project End Date: March 31, 2015

Overall Objectives

- Identify and mitigate the adverse effects of airborne contaminants on fuel cell system performance and durability
- Provide contaminants and tolerance limits for filter specifications (preventive measure)
- Identify fuel cell stack's material, design, operation or maintenance changes to remove contaminant species and recover performance (recovery measure)

Fiscal Year (FY) 2014 Objectives

Quantify spatial variability of performance loss and identify principal poisoning mechanism for at least four different contaminants.

Technical Barriers

This project addresses the following technical barriers from the Fuel Cells section of the Fuel Cell Technologies Office Multi-Year Research, Development, and Demonstration Plan:

(A) Durability

(B) Cost

(C) Performance

Technical Targets

The following 2017 technical targets for automotive applications, 80-kW_e (net) integrated transportation fuel cell power systems operating on direct hydrogen, are considered:

- Durability: 5,000 hours in automotive drive cycle
- Cost: \$30/kW_e
- Performance: 60% energy efficiency at 25% of rated power

The effects of specific airborne contaminants are studied including a commercially relevant low-cathode-catalyst loading and the resulting information will be used to impact both preventive measures and recovery procedures:

- Airborne contaminant tolerance limits to support the development of filtering system component specifications and ensure negligible fuel cell performance losses
- Fuel cell stack material, design, operation, or maintenance changes to recover performance losses derived from contamination mechanisms

FY 2014 Accomplishments

- Completed characterization database using ex situ and in situ diagnostic techniques for seven airborne contaminants and one foreign cation to support the development of contamination mechanisms and recovery procedures that diminish the contamination impact on system durability and performance
- Assessed the effect of a decrease in cathode catalyst loading from 0.4 to a commercially relevant 0.1 mg Pt cm^{-2} on the steady-state cell voltage loss during contamination for seven airborne contaminants

- Developed a transient, one-dimensional, through the membrane/electrode assembly plane model for foreign cation contamination to isolate individual cell performance effects which are not experimentally accessible and advance the understanding of contamination mechanisms
- Evaluated and modeled the scavenging effect of product liquid water for two cases, contaminant dissolution and contaminant dissolution followed by dissociation reactions, to determine effective contaminant concentrations within the cell and increase the accuracy of cell performance loss correlations

✧ ✧ ✧ ✧ ✧

INTRODUCTION

The composition of atmospheric air cannot be controlled and typically includes contaminants, volatile compounds, as well as ions entrained by liquid water drops in the form of rain, mist, etc., especially near marine environments. Proton exchange membrane fuel cells operated with ambient air are therefore susceptible to deleterious effects which include decreased cell performance and durability [1,2]. Numerous air contaminants have not yet been tested in fuel cells and consequently their effects as well as recovery methods are unknown [2,3]. Furthermore, prevention is difficult to achieve because tolerance limits are also missing in most cases [2]. This increases the risk of failure for fuel cell systems and thus jeopardizes their introduction into the market.

Airborne contaminants and foreign ions have previously been selected using a cost-effective two-tiered approach combining qualitative and quantitative criteria [3]. Automotive fuel cells are used under a wide range of operating conditions resulting from changes in power demands (drive cycle). Temperature and current density impact fuel cell contamination the most [4]. The effect of contaminant concentration is also particularly important. Contaminant threshold concentrations for predetermined fuel cell performance losses were determined [5] to facilitate the definition of air filtering system tolerances (prevention). The effect of inlet reactant relative humidity is linked to the presence of liquid water within the cell which in turn may affect the effective contaminant concentration by dissolution and entrainment in water drops. This scavenging effect has not previously been considered. Cell design parameters also impact the severity of contamination. However, the effect of catalyst loading, which is important for cost reduction, has only been determined for a few species [2]. It is likely that prevention will be insufficient to avert all contaminant effects. Therefore, recovery procedures will also be needed, and these are more easily devised by understanding the origins of the contaminant effects (mechanisms). However for the case of foreign cations, present experimental methods are insufficient to separate the different contributions to cell performance loss (thermodynamic, kinetic, ohmic, mass transport) [2,6,7]. Mathematical modeling is a valuable substitute approach. However, existing models either need improvement [8] or are incomplete. A separation factor more accurately represents ion exchange processes [9,10] and the change in oxygen permeability in the ionomer due to the presence of a foreign cation has not previously been tackled [11,12].

APPROACH

Impedance spectroscopy was first used to classify airborne contaminant effects into different resistance losses to focus subsequent activities. As a second step, more detailed information was obtained using other diagnostics methods to unravel contamination mechanisms: rotating ring/disc electrode, membrane conductivity cell, segmented fuel cell for current/cell voltage distributions over the active area, and gas chromatography/mass spectrometry. Because many of these diagnostics methods are not applicable or are irrelevant to foreign ions partly due to their different state (in a liquid rather than a gaseous state) and behavior (salt precipitation within the fuel cell), other diagnostic methods were employed including photography, scanning electron microscopy and energy dispersive X-ray spectroscopy. Mathematical modeling was also exploited as experimental data obtained with many in situ diagnostic methods are subject to misinterpretations because the presence of foreign ions in the membrane and ionomer affects fuel cell resistance losses that invalidate assumptions needed to separate individual performance loss contributions.

The cathode catalyst loading impact was investigated under a single set of operating conditions. The scavenging effect of liquid water was studied with an inactive fuel cell to minimize the presence of side reactions. The contaminant was carried inside the fuel cell with a saturated and inert carrier gas whereas the water was transferred from the anode compartment by thermo-osmosis [13]. Water transfer was facilitated by avoiding the use of a gas diffusion layer on the anode side. The amount of water transferred was measured by collection at the fuel cell outlet. Methanol and sulfur dioxide were used as model contaminants that either only dissolve in water or hydrolizes and reacts to form a bisulfite ion. For methanol, outlet water samples were analyzed by cyclic voltammetry and total organic carbon. For sulfur dioxide, outlet gas samples were analyzed by gas chromatography.

RESULTS

Table 1 summarizes key metrics obtained from the in situ and ex situ diagnostic tests. Electrochemical catalyst areas and peroxide production currents indicate that the

TABLE 1. Summary of Ex Situ And In Situ Diagnostic Methods' Results for Seven Airborne Contaminants and One Foreign Cation To Resolve Contamination Mechanisms

Contaminant	Kinetic Current (% loss in air at 30°C and 0.9 V vs RHE)	Electrochemical Catalyst Area (% loss in N_2 at 30°C)	H_2O_2 Current (% gain in air at 30°C and 0.5 V vs RHE)[a]	Membrane Conductivity (% loss at 80°C and 50% relative humidity)	Dimensionless Local Current (maximum % loss and gain in air at 80°C)		Contaminant Conversion (% in air at 80°C)[b]
					Contamination Phase	Recovery Phase	
Acetonitrile	79-84 (16.9 mM)	>76 (16.9 mM)	850-1300 (16.9 mM)	0 (100 ppm), N product detected by ISE (IC tests planned)	Step change followed by a cell potential triggered evolution reaching –15 to 12 at steady state (20 ppm)	Traveling current wave reaching –28 to 22 to values approximately equal to initial values (20 ppm)	20 to 45 for 0.55 to 0.65 V (20 ppm)
Acetylene	100 (4,030 ppm)	100 (4,040 ppm)	2,700-3,800 (4,030 ppm)	1-2 (500 ppm)	Traveling current wave of –99 to 100 synchronized with voltage transient followed by –17 to 18 at steady state (300 ppm)	Step change to values approximately equal to initial values (300 ppm)	0.8 to 100 for 0.55 to 0.85 V (300 ppm)
Bromomethane	54 (400 ppm)	43 (400 ppm)	56 (400 ppm)	No ohmic loss in fuel cell	Gradual change starts after voltage steady state reaching –19 to 13 (5 ppm)	Trend continues reaching –21 to 21 (5 ppm)	0 for 0.1 to ~1 V (10 ppm)
Iso-propanol	12 (1 mM)	7 (1 mM)	18 (1 mM)	No ohmic loss in fuel cell	Step change of –9 to 5 (5,300 ppm)	Reverse step change (5,300 ppm)	Not applicable
Methyl methacrylate	65 (1 mM)	43 (H_{UPD}) and 82 (PtO reduction) (1 mM)	1,300 (1 mM)	No ohmic loss in fuel cell	Step change of –7 to 6 (20 ppm)	Reverse step change (20 ppm)	49 to 57 for 0.55 to 0.68 V (20 ppm)
Naphthalene	66 (sat soln)[c]	90 (sat soln)[c]	780 (sat soln)[c]	No ohmic loss in fuel cell	Traveling current wave of –25 to 14 synchronized with voltage transient (2.3 ppm)	Traveling current wave of –39 to 40 synchronized with voltage transient (2.3 ppm)	Detectable but not quantifiable for 0.5 to 0.85 V (1.4 ppm)
Propene	53 (1,010 ppm)	26 (H_{UPD}) and ~50 (PtO reduction) (1,010 ppm)	620-960 (1,010 ppm)	No ohmic loss in fuel cell	Step change of –8 to 6 (100 ppm)	Reverse step change (100 ppm)	43 to 89 for 0.55 to 0.85 V (100 ppm)
Ca^{2+}	37 (90 mM $Ca(ClO_4)_2$), 21 (5 ppm)[d]	2 (90 mM $Ca(ClO_4)_2$), 16-46 (5 ppm)[d]	660 (90 mM $Ca(ClO_4)_2$)	1.1-11 (5 ppm)[e]	Gradual change up to –50 to 20 (5 ppm)[f]	Gradual change up to –60 to 40 (5 ppm)[f]	-

[a] The total current is still mostly due to oxygen reduction in spite of a large peroxide production rate increase. [b] Observed products include: for acetonitrile, ammonia/amine; for acetylene, CO and CO_2; for iso-propanol, CO_2; for methyl methacrylate, CO_2; for naphthalene, 1,2,3,4-tetramethyl-benzene, 1,3,5,7-tetramethyl-adamantane, pentamethyl-benzene, 1-penten-3-one, 1-(2,6,6-trimethyl-1-cyclohexen-1-yl); for propene, CO_2. [c] 0.25 mM solubility at 25°C. [d] Derived from in situ polarization curve and cyclic voltammetry tests. [e] In situ result by current interrupt for 0.6-1 A cm^{-2} and 125% relative humidity before a steady state is reached at 100 h. [f] 0.6 rather than 1 A cm^{-2} and before a steady state is reached at 100 h. Figures in parentheses represent the contaminant concentration either in the gas phase (ppm) or liquid phase (M). Both concentration units are used for the Ca^{2+} ion. RHE – reference hydrogen electrode; GDE – gas diffusion electrode; IC - ion chromatography; ISE - ion selective electrode; TBD - to be determined; UPD - under-potential deposition.

change in kinetic resistance associated with contamination is not only due to a decrease in surface area but also to a modification of the oxygen reduction mechanism in favor of a 2 rather than a 4 electrons path leading to increased amounts of hydrogen peroxide. Only Ca^{2+} did not significantly affect the electrochemical surface area. Generally, organic contaminants undergo chemical or electrochemical reactions within the fuel cell as detected by gas chromatography/mass spectrometry analysis of outlet gases. Only bromomethane was inactive. Iso-propanol could not be analyzed because the sample gas stream drying step, which is necessary to avoid equipment damage, entrains a significant portion of iso-propanol. Ca^{2+} is not expected to be converted to Ca in the fuel cell because the electrode potentials are not sufficiently low. Acetonitrile and Ca^{2+} were the only contaminants that led to an ohmic resistance change. For acetonitrile, the change was ascribed to a decomposition product because the membrane conductivity measured ex situ was not affected by acetonitrile. Ammonium was detected in the fuel cell outlet water. It is possible that a nitrogen organic compound is also present because the ion selective electrode cannot discriminate between such species. For Ca^{2+}, ion exchange with the ionomer proton modifies ionic conductivity as well as other physico-chemical parameters. The current distribution was not affected by iso-propanol, methyl methacrylate and propene. This observation is consistent with relatively slow catalyst surface kinetics, rapid transport processes and a relatively uniform contaminant concentration across the cell. However, the other contaminants revealed varied behaviors that may be useful to facilitate mechanism identification and generalize contamination mechanisms [14]. It is hypothesized that a change in rate determining step along the contaminant transport to the catalyst surface, catalyst surface kinetics, contaminant and products transport away from the catalyst surface sequence is responsible for the change in behavior. The gas diffusion electrode water content

has not yet been measured because the increase in mass transport loss in the presence of organic contaminants was largely attributed to contaminant adsorption on the catalyst [15].

The presence of elevated levels of peroxide is expected to affect cell durability. The presence of contaminant products and the uneven current distribution may complicate performance recovery strategies.

Table 2 illustrates that a 75% reduction in Pt catalyst loading from 0.4 to 0.1 mg cm^{-2} leads to a decrease in cell voltage at steady state due to contamination (the difference between the cell voltage before contamination and during contamination) that generally exceeds 75% and reaches values of 92 to 6,325%. As a result, filter system specifications either need to be revised or should be determined for commercially relevant Pt catalyst loadings.

Figure 1A depicts a schematic representation of the one-dimensional (x direction) modeled membrane/electrode assembly portion. Figure 1B calculations show that the presence of a foreign cation in the catalyst layers' ionomer and membrane significantly affects the oxygen concentration distribution due to a smaller ionomer water content [16] and oxygen permeability [17]. The oxygen concentration gradient is steeper and the average oxygen concentration is lower than values in absence of foreign cation contamination. The lower oxygen concentration affects thermodynamic (Nernst equation), kinetic (oxygen reduction is a first order reaction) and mass transport contributions. The foreign cation contamination model also demonstrates that the change in oxygen permeability of the ionomer accounts for a significant fraction of the decrease in cell performance. This new information is important to focus activities aimed at minimizing the effect of foreign cation contamination on cell performance.

Figure 2A illustrates the cell and method used to measure the impact of liquid water scavenging on contaminant concentration. Figure 2B shows that the CH_3OH concentration at the cell outlet measured by two different methods acceptably fits the liquid water scavenging model over a stoichiometry range exceeding the normal operating regime of approximately 1.5 to 2.5. The same conclusion is reached from Figure 2C for the case of SO_2. However, for this particular case of a species hydrolizing and reacting by forming a bisulfite ion, the amount of species scavenged is concentration dependent which is important for predictive purposes. Figure 2C depicts the amount of SO_2 scavenged, which is the difference between the full line and the dash line. The amount of SO_2 scavenged increases with a decrease in inlet SO_2 concentration. Therefore, cell performance extrapolations to lower contaminant concentrations using only high concentration data while disregarding the scavenging effect are conservative.

The scavenging model reduces to a simple expression because a time-scale analysis of all relevant phenomena

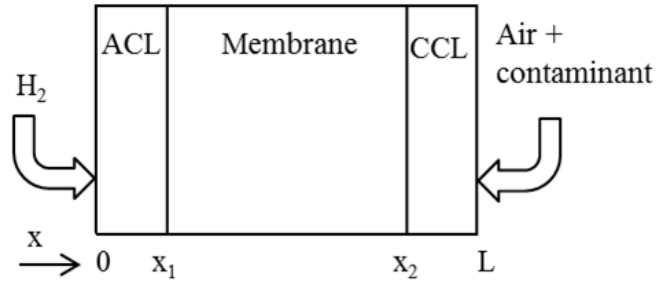

ACL – anode catalyst layer; CCL – cathode catalyst layer

FIGURE 1A. Schematic polymer electrolyte membrane fuel cell representation and X-axis definition. From M.A. Uddin, U. Pasaogullari, *J. Electrochem. Soc.*, **161** (2014) F1081 (reproduced by permission of The Electrochemical Society)

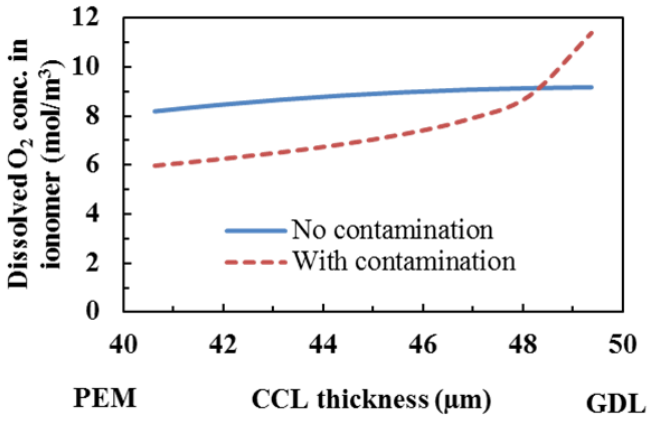

PEM – polymer electrolyte membrane; GDL – gas diffusion layer

FIGURE 1B. Model predictions for the dissolved oxygen concentration profile in the CCL contaminated with Na^+ (sulfonate site occupancy = 1 at the catalyst/GDL interface), 0.7 V, 80/100% anode/cathode relative humidity, 80°C. From M.A. Uddin, U. Pasaogullari, *J. Electrochem. Soc.*, **161** (2014) F1081 (reproduced by permission of The Electrochemical Society)

TABLE 2. Summary of the Impact of a Cathode Catalyst Loading Reduction on Steady-State Cell Performance Loss for Seven Airborne Contaminants

Contaminant	Acetonitrile	Acetylene	Bromomethane	Iso-propanol	Methyl methacrylate	Naphthalene	Propene
Cell voltage loss (% gain for a Pt loading reduction of 0.4 to 0.1 mg cm^{-2} in air at 80°C)	58 (20 ppm)	6,325 (100 ppm)	–10 (5 ppm)	92 (~8,000 ppm)	104 (20 ppm)	187 (1.4 ppm)	224 (100 ppm)

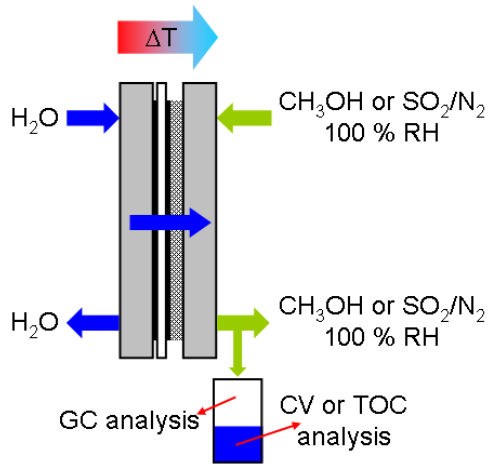

RH – relative humidity; GC – gas chromatograph; CV – cyclic voltammetry; TOC – total organic carbon

FIGURE 2A. Experimental setup schematic showing the transport of water through the PEMFC membrane/electrode assembly by thermo-osmosis, the injection of methanol and sulfur dioxide contaminants in a saturated and inert carrier gas, and the methods used to measure the amount of contaminant scavenged by liquid water. From J. St-Pierre, B. Wetton, Y. Zhai, J. Ge, *J. Electrochem. Soc.*, **161** (2014) E3357 (reproduced under the creative commons license terms, http://creativecommons.org/licenses/by-nc-nd/4.0/)

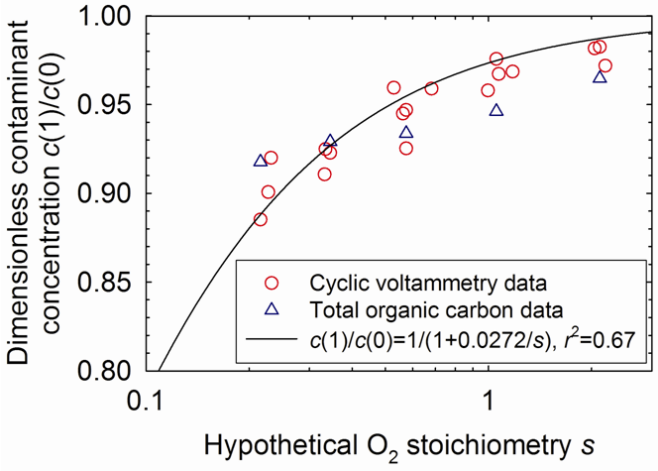

FIGURE 2B. Dimensionless methanol concentration $c(1)/c(0)$ in the PEMFC cathode outlet gas stream measured by two different methods as a function of the hypothetical oxygen stoichiometry s. c(1) and c(0) are respectively the cell outlet and inlet concentrations. The full line represents a curve fit to the mathematical model. Dimensionless contaminant inlet concentration c_{in}/c_a approximately 1,000 ppm methanol in N_2, 80°C, 48.3 kPag, 100% inlet relative humidity, c_r = 34.9 mol m^{-3}. From J. St-Pierre, B. Wetton, Y. Zhai, J. Ge, *J. Electrochem. Soc.*, **161** (2014) E3357 (reproduced under the creative commons license terms, http://creativecommons.org/licenses/by-nc-nd/4.0/)

revealed that liquid water accumulation within the cell is the slowest step. As a result, the liquid water is saturated by the contaminant, which simplified model derivation by eliminating the need to track individual water droplets. The

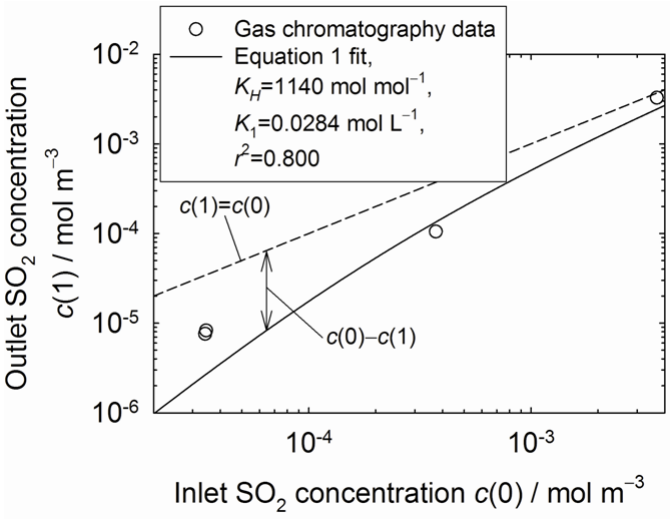

FIGURE 2C. SO_2 concentration $c(1)$ in the PEMFC cathode outlet gas stream as a function of contaminant inlet concentration $c(0)$ at a hypothetical oxygen stoichiometry s of approximately 2.5. 80°C, 48.3 kPag, 100% inlet relative humidity, c_r = 34.9 mol m^{-3}. K_H = 1,140 mol mol^{-1} (H = 0.021 m^3 mol^{-1}), K_1 = 0.0284 mol L^{-1} (H' = 0.00324 m$^{3/2}$ mol$^{-1/2}$) for equation 1. From J. St-Pierre, B. Wetton, Y. Zhai, J. Ge, *J. Electrochem. Soc.*, **161** (2014) E3357 (reproduced under the creative commons license terms, http://creativecommons.org/licenses/by-nc-nd/4.0/)

model expression, which depends on two dimensionless parameters is simple which facilitates its use to calculate effective concentrations and improve correlations with cell performance losses:

$$\frac{c(x)}{c(0)} = \left(\frac{-W_2 x}{1+W_1 x} + \sqrt{\frac{W_2^2 x^2}{(1+W_1 x)^2} + \frac{1}{1+W_1 x}} \right)^2, c(0) = \frac{c_{in} c_r}{c_a} \quad (1)$$

where c is the molar concentration of contaminant X in the gas phase (mol m^{-3}), x the dimensionless flow field channel length, c_{in} the inlet contaminant X concentration in the ambient air on a dry basis (mol m^{-3}), c_r the molar concentration of non vapor gases at saturation conditions within the fuel cell (mol m^{-3}), c_a the molar concentration of an ideal gas at a pressure of 1 atmosphere (mol m^{-3}), W_1 represents the dimensionless number characterizing the severity of the liquid water scavenging effect on the contaminant X, and W_2 represents the dimensionless number characterizing the severity of the liquid water scavenging effect on the contaminant X in the presence of dissociation reactions.

CONCLUSIONS AND FUTURE DIRECTIONS

- Contamination mechanisms for seven airborne contaminants and one foreign cation were refined by building a database using a variety of ex situ and in situ diagnostic methods

- The performance loss at steady state due to contamination is generally and proportionally larger than the decrease in cathode catalyst loading thus suggesting a revision of filter system specifications for commercially relevant low catalyst loadings
- For foreign cation contamination, the performance loss associated with the decrease in oxygen permeability through the ionomer is significant and cannot be ignored to minimize its impact
- Contaminant scavenging by liquid water was demonstrated and modeled to improve correlations between fuel cell performance losses and the effective contaminant concentration
- Complete long-term tests to assess the impact of increased peroxide production in the presence of airborne contaminants on fuel cell durability
- Develop mitigation strategies for the most important contaminants
- Continue to disseminate the large fuel cell contamination database

FY 2014 PUBLICATIONS/PRESENTATIONS

1. J. Ge, J. St-Pierre, Y. Zhai, 'PEMFC Cathode Catalyst Contamination Evaluation with a RRDE – Methyl Methacrylate', *Int. J. Hydrogen Energy*, accepted.

2. M.A. Uddin, U. Pasaogullari, 'Computational Modeling of Foreign Cation Contamination in PEFCs', *J. Electrochem. Soc.*, **161** (2014) F1081.

3. J. Ge, J. St-Pierre, Y. Zhai, *Electrochim. Acta*, **138** (2014) 437.

4. J. Ge, J. St-Pierre, Y. Zhai, *Electrochim. Acta*, **134** (2014) 272.

5. J. Ge, J. St-Pierre, Y. Zhai, *Electrochim. Acta*, **133** (2014) 65.

6. J. St-Pierre, B. Wetton, Y. Zhai, J. Ge, *J. Electrochem. Soc.*, **161** (2014) E3357.

7. X. Wang, J. Qi, O. Ozdemir, A. Uddin, U. Pasaogullari, L. J. Bonville, T. Molter, *J. Electrochem. Soc.*, **161** (2014) F1006.

8. J. St-Pierre, M. Angelo, K. Bethune, J. Ge, S. Higgins, T. Reshetenko, M. Virji, Y. Zhai, 'PEMFC Contamination – Fundamentals and Outlook', *Electrochem. Soc. Trans*., accepted.

9. M.A. Uddin, X. Wang, M.O. Ozdemir, J. Qi, L. Bonville, U. Pasaogullari, T. Molter, 'Distributed PEFC Performance during Cationic Contamination', *Electrochem. Soc. Trans*., accepted.

10. M.A. Uddin, J. Qi, X. Wang, M.O. Ozdemir, N. Khajeh-Hosseini-Dalasm, L. Bonville, U. Pasaogullari, T. Molter, 'Study of Through Plane Cation Contamination in Polymer Electrolyte Fuel Cell', *Electrochem. Soc. Trans*., accepted.

11. Y. Zhai, J. St-Pierre, J. Ge, 'PEMFC Cathode Contamination Evaluation with Membrane Conductivity Cell, CA, CP, CV, EIS, GC/MS and ISE – Acetonitrile', *Electrochem. Soc. Trans*., accepted.

12. M.A. Uddin, X. Wang, J. Qi, M.O. Ozdemir, L. Bonville, U. Pasaogullari, T. Molter, 224th Electrochemical Society meeting oral presentation, abstract 1334.

13. J. Qi, X. Wang, M.O. Ozdemir, M.A. Uddin, L. Bonville, U. Pasaogullari, T. Molter, 224th Electrochemical Society meeting oral presentation, abstract 1333.

14. X. Wang, J. Qi, O. Ozdemir, U. Pasaogullari, L.J. Bonville, T. Molter, 224th Electrochemical Society meeting oral presentation, abstract 1332.

15. J. St-Pierre, J. Ge, Y. Zhai, T. Reshetenko, M. Angelo, 224th Electrochemical Society meeting oral presentation, abstract 1330.

16. Y. Zhai, J. St-Pierre, J. Ge, 224th Electrochemical Society meeting oral presentation, abstract 1329.

17. T. Reshetenko, J. St-Pierre, 224th Electrochemical Society meeting oral presentation, abstract 1328.

18. J. Ge, Y. Zhai, J. St-Pierre, 224th Electrochemical Society meeting oral presentation, abstract 1302.

19. J. St-Pierre, 'The Effect of Airborne Contaminants on Fuel Cell Performance and Durability', USDRIVE Fuel Cell Tech Team meeting oral presentation, Southfield, MI, January 15, 2014.

20. J. St-Pierre, M. Angelo, K. Bethune, J. Ge, S. Higgins, T. Reshetenko, M. Virji, Y. Zhai, 225th Electrochemical Society meeting oral presentation, abstract 796.

21. M.A. Uddin, X. Wang, M.O. Ozdemir, J. Qi, L. Bonville, U. Pasaogullari, T. Molter, 225th Electrochemical Society meeting oral presentation, abstract 638.

22. M.A. Uddin, J. Qi, X. Wang, M.O. Ozdemir, N.K.H. Dalasm, L. Bonville, U. Pasaogullari, T. Molter, 225th Electrochemical Society meeting oral presentation, abstract 637.

23. J. St-Pierre, 'PEMFC Contamination – Fundamentals and Outlook', General Motors oral presentation, Pontiac, MI, June 9, 2014.

24. J. St-Pierre, 'PEMFC Contamination – Fundamentals and Outlook' and 'The Effect of Airborne Contaminants on Fuel Cell Performance and Durability', SAE International oral presentations, Troy, MI, June 10, 2014.

25. J. St-Pierre, 'The Effect of Airborne Contaminants on Fuel Cell Performance and Durability', United States Department of Energy 2014 Annual Merit Review meeting oral presentation, Washington, DC, June 18, 2014.

REFERENCES

1. J. St-Pierre, 'Air Impurities', in *Polymer Electrolyte Fuel Cell Durability*, Edited by F.N. Büchi, M. Inaba, T.J. Schmidt, Springer, 2009, p. 289.

2. J. St-Pierre, M. Angelo, K. Bethune, J. Ge, S. Higgins, T. Reshetenko, M. Virji, Y. Zhai, 'PEMFC Contamination – Fundamentals and Outlook', *Electrochem. Soc. Trans*., accepted.

3. J. St-Pierre, Y. Zhai, M.S. Angelo, *J. Electrochem. Soc.*, **161** (2014) F280.

4. J. St-Pierre, Y. Zhai, M. Angelo, *Int. J. Hydrogen Energy*, **37** (2012) 6784.

5. J. St-Pierre, Y. Zhai, J. Ge, M. Angelo, T. Reshetenko, T. Molter, L. Bonville, U. Pasaogullari, W. Collins, S. Wessel, DOE Hydrogen and Fuel Cells Program, FY 2013 Annual Progress Report, p. V-3.

6. B. L. Kienitz, H. Baskaran, T.A. Zawodzinski Jr., *Electrochim. Acta*, **54** (2009) 1671.

7. B. Kienitz, B. Pivovar, T. Zawodzinski, F.H. Garzon, *J. Electrochem. Soc*., **158** (2011) B1175.

8. M.F. Serincan, U. Pasaogullari, T. Molter, *Int. J. Hydrogen Energy*, **35** (2010) 5539.

9. J. St-Pierre, *Int. J. Hydrogen Energy*, **36** (2011) 5527.

10. J. St-Pierre, *J. Power Sources*, **196** (2011) 6274.

11. T. Okada, J. Dale, Y. Ayato, O.A. Asbjørnsen, M. Yuasa, I. Sekine, *Langmuir*, **15** (1999) 8490.

12. T. Okada, Y. Ayato, J. Dale, M. Yuasa, I. Sekine, O.A. Asbjornsen, *Phys. Chem. Chem. Phys*., **2** (2000) 3255.

13. R. Zaffou, J.S. Yi, H.R. Kunz, J.M. Fenton, *Electrochem. Solid-State Lett*., **9** (2006) A418.

14. T.V. Reshetenko, K. Bethune, M.A. Rubio, R. Rocheleau, *J. Power Sources*, **269** (2014) 344.

15. J. St-Pierre, J. Ge, Y. Zhai, T.V. Reshetenko, M. Angelo, *Electrochem. Soc. Trans*., **58**(1) (2013) 519.

16. K. Hongsirikarn, J.G. Goodwin Jr, S. Greenway, S. Creager, *J. Power Sources*, **195** (2010) 7213.

17. K. Broka, P. Ekdunge, *J. Appl. Electrochem*., **27** (1997) 117.

V.G.1 Fuel Cell Fundamentals at Low and Subzero Temperatures

Adam Z. Weber
Lawrence Berkeley National Laboratory
1 Cyclotron Rd., MS 70-108B
Berkeley, CA 94720
Phone: (510) 486-6308
Email: azweber@lbl.gov

DOE Manager
Donna Ho
Phone: (202) 586-8000
Email: Donna.Ho@ee.doe.gov

Subcontractors
- Los Alamos National Laboratory (LANL), Los Alamos, NM
- United Technologies Research Center (UTRC), East Hartford, CT
- 3M Company, St Paul, MN
- McGill University, Montreal, Quebec, Canada

Project Start Date: September 21, 2009
Project End Date: Project continuation and direction determined annually by DOE

Overall Objectives

- Fundamentally understand transport phenomena and water and thermal management at low and subzero temperatures
- Examine water (liquid and ice) management with nano-structured thin-film (NSTF) catalyst layers
- Develop diagnostic methods for critical properties for operation with liquid water
- Elucidate the associated degradation mechanisms due to subzero operation and enable mitigation strategies to be developed

Fiscal Year (FY) 2014 Objectives

- Develop transient models and use it to examine NSTF start-up performance as compared to experimental data
- Quantify performance changes with NSTF and at different temperatures and material sets
- Develop diagnostic methods for critical properties for operation with liquid water including analysis of gas diffusion layers (GDLs) and micro-porous layers (MPLs)
- Examine impact of freeze kinetics and ionomer morphology with traditional catalyst layers and thin-film model systems

Technical Barriers

This project addresses the following technical barriers from the Fuel Cells section of the Fuel Cell Technologies Office Multi-Year Research, Development, and Demonstration Plan:

(A) Durability

(C) Performance
  - Cell issues
  - Stack water management
  - System thermal and water management
  - System start-up and shut-down time and energy/ transient operation

Technical Targets

This project is conducting fundamental investigations into fuel cell operation at low and subzero temperatures. The knowledge gained will enable various metrics to be met or exceeded. These include those related to durability, performance, and cost:

- Durability
  - 5,000 hr (automotive) and 40,000 hr (stationary)
  - Thermal cycling ability with liquid water
- Performance
  - Unassisted start from −40°C
  - Cold start to 50% power in 30 seconds and with 5 MJ or less energy
  - Efficiency of 65% and 55% for 25% and 100% rated power, respectively
  - Stack power density of 2 kW/kg
  - Platinum group metal loading of 0.2 g/kW
- Cost: \$15/kW_e for 80-kW_e fuel cell stack operating on direct hydrogen

FY 2014 Accomplishments

- Analyzed NSTF performance with different anode GDLs to ascertain the mechanisms of improved performance at lower temperature due to more water out of the anode due to GDL structure and changes in droplet adhesion force
- Explored mechanism of liquid water movement through an MPL by development of MPL analogues, which is due to specific sites that are partially in liquid contact

- Measured current distribution using segmented cell for model validation and analysis
- Measured Nafion® morphology by direct imaging using cryo-transmission electron microscopy tomography
- Demonstrated that improved freeze kinetics predicts measured delay of cell failure in isothermal freeze experiments
- Measured and modeled isothermal and adiabatic cell performance, showing that NSTF cells can startup and operate better within a stack environment due to the different thermal boundary conditions
- Systematically investigated various casting and thermal treatment conditions on the morphology, swelling, and water-uptake behavior of ionomer thin films on various substrates

INTRODUCTION

Polymer-electrolyte fuel cells experience a range of different operating conditions. As part of that range, they are expected to be able to survive and start at low and subzero temperatures. Under these conditions, there is a large amount of liquid and perhaps frozen water due to the low vapor pressure of water. Thus, water and thermal management become critical to understanding and eventually optimizing operation at these conditions. Similarly, durability aspects due to freeze and low temperatures are somewhat unknown and need further study in order to identify mechanisms and mitigation strategies. In addition, it is known that thin-film catalyst layers such as the NSTF developed by 3M have issues with large amounts of liquid water due to their thinness. These layers provide routes towards meeting the DOE cost targets due to their high catalytic activities. This project directly focuses on the above aspects of operation at lower temperatures with both NSTF and traditional catalyst layers with the goal that improved understanding will allow for the DOE targets to be met with regard to cold start, survivability, performance, and cost.

APPROACH

The overall approach is to use a synergistic combination of cell, stack, and component diagnostic studies with advanced mathematical modeling at various locations (national laboratories, industry, and academia). Ex situ diagnostics are used to quantify transport properties and to delineate phenomena that are used in the modeling. The two-dimensional cell model is developed and validated by comparison of measured in situ cell performance using a variety of cell assemblies and in order to highlight specific controlling phenomena. To explore controlling phenomena and the impact of various layers, a systematic investigation at the component scale is accomplished including the development of a suite of advanced ex situ diagnostics that measure and evaluate the various critical material properties and transport-related phenomena.

RESULTS

As fuel cells operate at low and subzero conditions, liquid water and water management become more important. Thus, there is a need to study properties of the porous fuel cell layers in the presence of liquid water. It is also expected that this is exacerbated in thin-film catalyst layers such as NSTF catalyst layers (CLs) as shown previously with single-cell, low-temperature operation. To improve performance, it is thought that one needs to reduce the amount of water within the thin-film cathode, and thus increase it out of the anode. Such an analysis is shown in Figure 1a, where we plot the cell voltage at 0.25 A/cm^2 for different operating temperatures as a function of the fraction of water being removed from the anode. As can be seen, the larger the fraction removed, the better the performance at lower temperatures. Also, the performance decreases as temperature decreases. Shown in Figure 1 are cell test results with the cell having two different anode GDLs. The one with the improved GDL allows better performance at lower temperatures that is seemingly correlated to the ability of that anode GDL to remove more water. Characterization of the GDLs has shown that the improved one has a banded structure, and the main variable that this is seemingly impacting is the ease of water removal from its surface as shown in Figure 1b. Here, we developed a technique to measure the flow velocity in a channel needed to remove a water droplet from the GDL's top surface that was formed through bottom-inject of the water. Figure 1b shows that the improved GDL has a lower detachment velocity, thus meaning that for a given flowrate water can be more easily removed, which correlates with more water out of the anode and the improved performance seen in Figure 1a.

The above analysis is for a single cell, but in practice fuel cells are operated within a stack. To mimic such an impact, a single-cell fixture with limited thermal mass was designed since one major difference between a single cell and a cell within a stack is the thermal boundary condition. As shown in Figure 2a, the measured startup performance for such an adiabatic cell (i.e., one within a stack where the other cells insulate it) compared to the traditional isothermal one (i.e., where the temperature boundaries remain constant) shows that the cell has better transient and steady-state performance. To explore this, the LBNL two-dimensional performance model was made transient and the adiabatic and isothermal conditions compared. As shown in Figure 2b, the temperature increase provided by the adiabatic cell allows for the catalyst-layer water content to decrease since more can be removed in the vapor phase. The model can now be

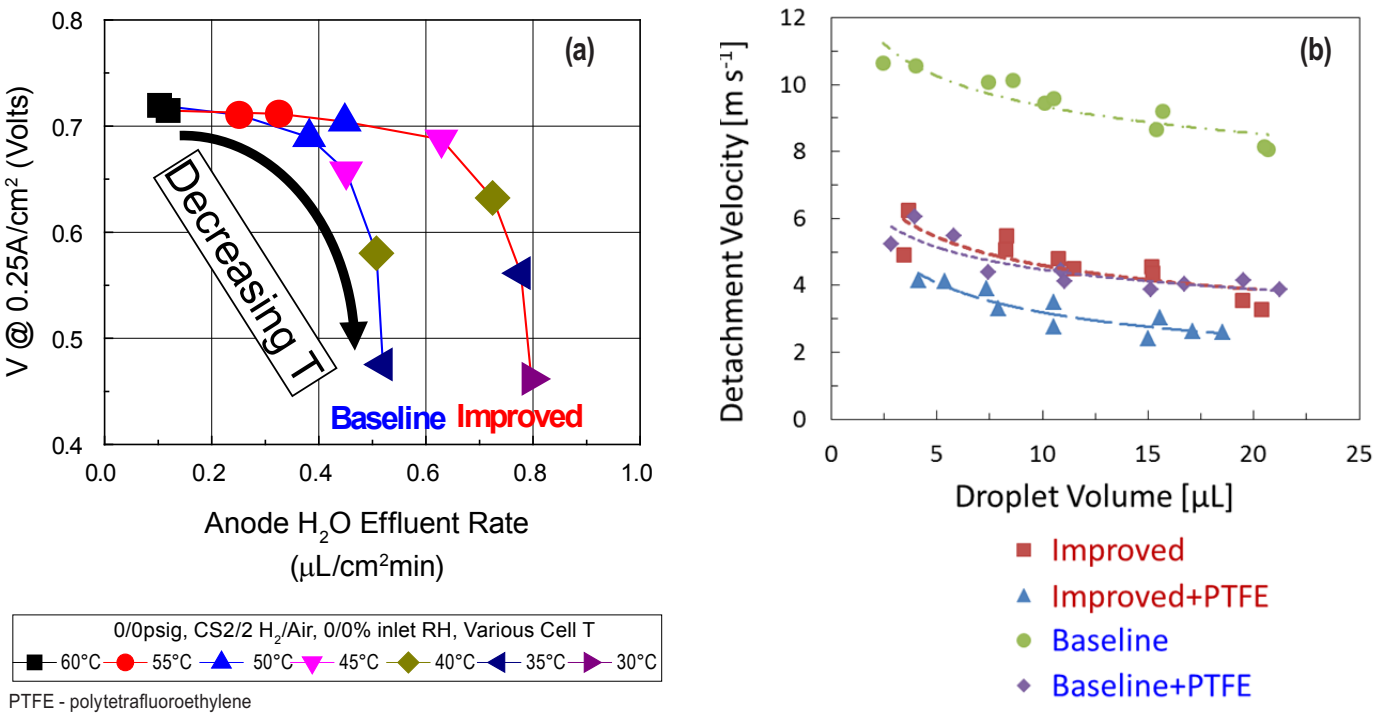

FIGURE 1. (a) Cell voltage at 0.25 A/cm^2 for an NSTF cell as a function of amount of water leaving the anode for two different anode GDLs. The different points correspond to different cell temperatures, and the cell conditions are no humidity or back pressure. (b) Measured detachment velocity as a function of droplet volume for a droplet emerged from different GDLs.

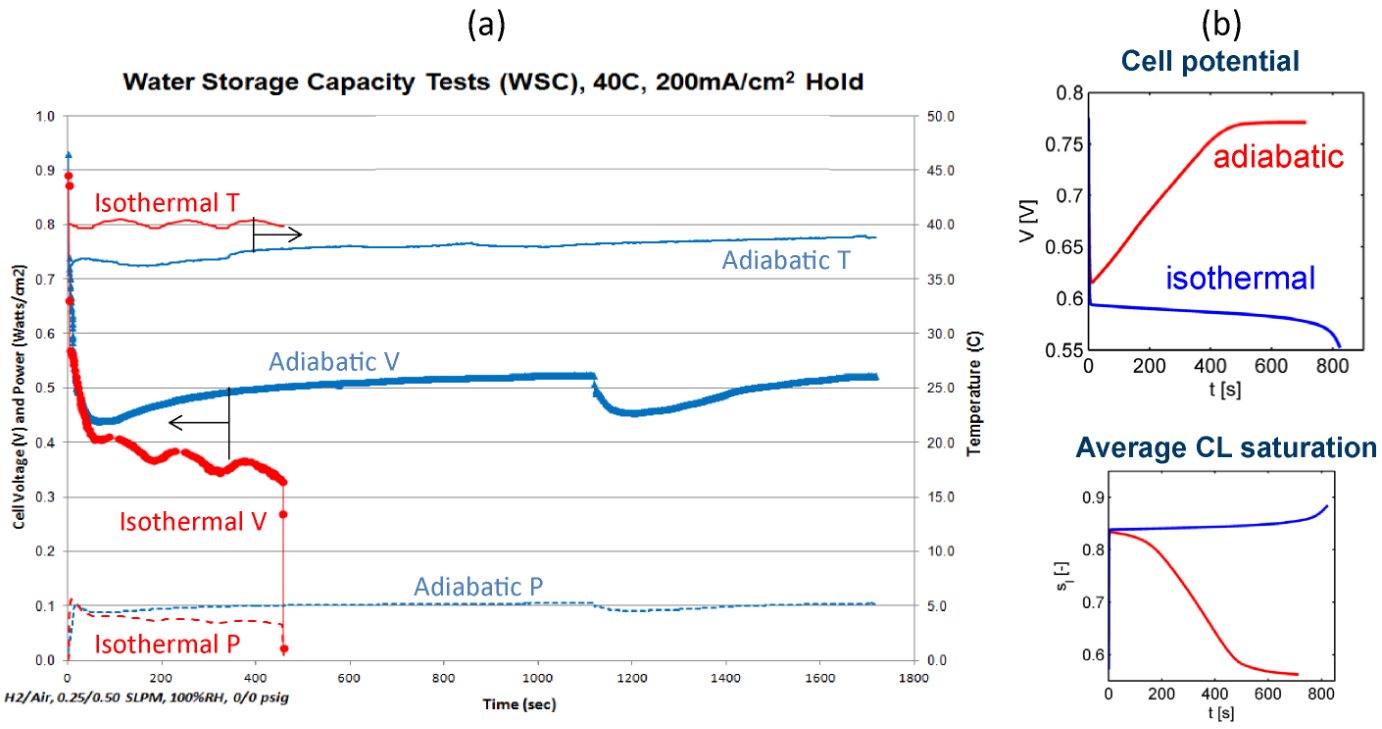

FIGURE 2. (a) Cell voltage as a function of time for both an isothermal and adiabatic single cell with NSTF catalyst layers. One can see that the adiabatic cell allows for increased performance and startup. (b) Transient two-dimensional simulation results for adiabatic and isothermal boundary conditions in terms of both cell potential and average catalyst-layer saturation as a function of time.

validated with the data and used to explore the importance of the thermal boundary condition (e.g., cell location in a stack) on performance and startup.

To understand further the emergence of water droplets and liquid water through the fuel cell porous backing layers (MPL and GDL), a setup was designed to measure the liquid-pressure response of the system rather than visualizing the liquid-water behavior. The droplet growth-detachment cycle and resultant pressure profile contains valuable information about the water configuration inside the GDL and MPL. This potential was explored more closely by studying GDLs with and without an MPL. Attempts are also made to mimic the behavior of the MPL using various water-impermeable masks with a variety of hole arrays, to mimic the cracks and blemishes typically found in real MPLs and elucidate the underlying transport mechanisms. To help interpret the observed experimental behavior, a model was developed that explains the sawtooth pressure profiles as seen in Figure 3. The figure shows that the model can accurately reproduce the experimental data, where a GDL has multiple entry sites whereas the MPL has a limited number of entry sites but also a small reservoir that is accessed through the changing liquid/vapor interfaces of the smaller domains. With the gained knowledge, better models and understanding can be obtained for liquid-water transport through these important layers.

Figure 4 shows the impact of subcooling or subzero temperature on isothermal-start experiments. As the subcooling becomes lower (i.e., temperature approaches 0°C), the time for cell failure (i.e., 0 V), drastically increases. As shown in the figure, a simple model of water and thermal transport through the cathode side of the cell captures this behavior when using our previously measured ex situ freeze kinetics in both the GDL and catalyst layers. The reason is that as the subcooling becomes less than 15°C or so, the formation of ice becomes nucleation limited. Furthermore, such behavior is not reproduced when using a traditional thermodynamic-based rate expressions, showing the importance of accounting for the ice-formation kinetics.

CONCLUSIONS AND FUTURE DIRECTIONS

The project focus this year was on developing and utilizing diagnostic methods for fuel cell components at low temperatures to elucidate routes for performance improvement including changing the anode GDL. Such

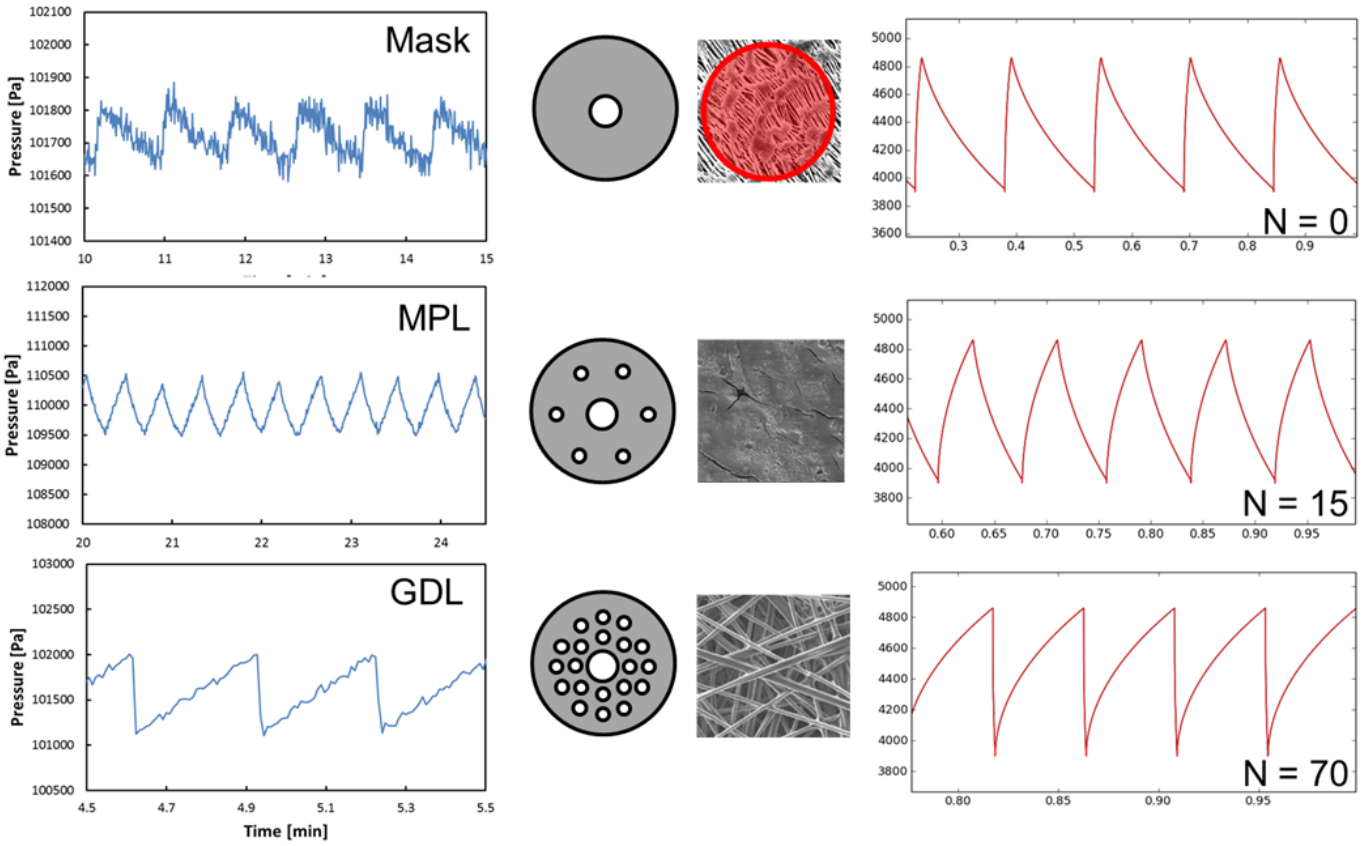

FIGURE 3. Analysis of liquid-water pressure as a function of time for a pendant droplet being formed and removed (by gravity) through different porous media of a mask/GDL, MPL/GDL, and bare GDL. The left side shows the pressure data, the middle shows the morphology used in a simple water-flow model used to generate the data on the right side. The model shows that a simple analysis of water entry points and interfacial reservoirs can explain the experimental data.

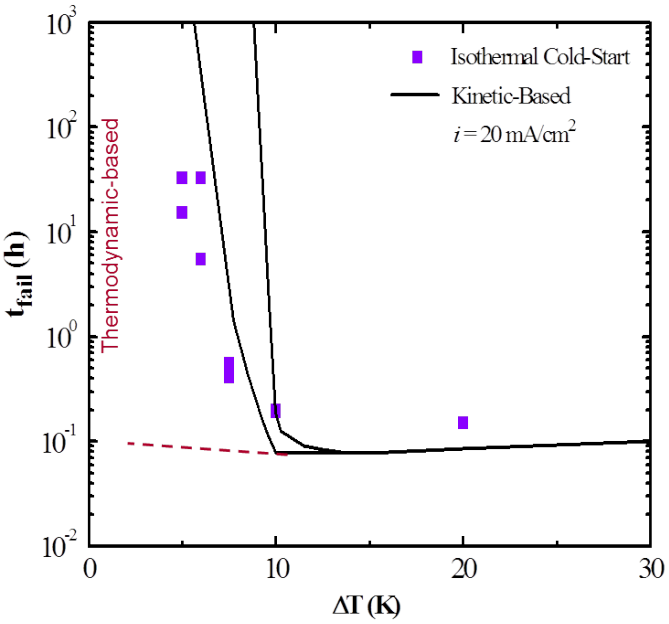

FIGURE 4. Measured isothermal cold-start data for single cells as a function of subcooling (temperature below 0°C), where the data are time to cell failure. The solid lines correspond to a simple water and thermal model using measured ice-formation kinetics, and the dotted lines to the typically used thermodynamic-based rate equation for ice formation.

activities also include incorporating the experimental observations into a transient performance model that can describe the observed changes. Several novel methods were developed and measurements for membranes, GDLs, and catalyst-layer ionomer were made. The results allow for a better understanding of liquid formation and movement within the cell, as well as limitations due to ionomer films at low catalyst loadings. In addition, single-cell testing of NSTF cells was accomplished with varying thermal boundary conditions to mimic cells within a stack.

In terms of future work, this can be summarized as follows:

- Cell Performance
  - UTRC to run tests with cool and cold starts including adiabatic and temperature transients
    - Both NSTF and low-loaded traditional CLs
  - LANL to run tests with both NSTF and traditional CL Gore cells with different GDLs and operation conditions
    - Segmented cell
    - Power transients
    - NIST high(er)- and low- (transient) resolution imaging
- Component Characterization
  - Traditional CLs
    - Examine gas-phase transport properties and uptake with low-equivalent weight ionomer and ionomer thin films
  - NSTF CLs
    - Determine proton conductivity on platinum
  - GDLs
    - Study the impact of bipolar plate structures on liquid-water movement out of the GDL
    - Measure effective transport properties (e.g., diffusivity, permeability, thermal conductivity)
    - Produce images of liquid water within and on the surface of the GDL
  - Membrane
    - Correlate interfacial resistance and membrane morphology in different environments
- Modeling
  - Use data from all partners to refine transient model
  - Develop bilayer or alternate approach for NSTF CLs
  - Develop down-the-channel model (two-dimensional + 1)
- Understand and increase the operating window with thin-film CLs
  - Focus on possible solutions and strategies as derived from the integrated model, as well as cell and component studies
- Solicit input and advice from original equipment manufacturers regarding areas to focus on and key issues they face with regard to low-temperature operation

SPECIAL RECOGNITIONS & AWARDS/ PATENTS ISSUED

1. Adam Z. Weber, Presidential Early Career Award for Scientists and Engineers (PECASE)

FY 2014 PUBLICATIONS

1. Gi Suk Hwang, Dilworth Y. Parkinson, Ahmet Kusoglu, Alastair A. MacDowell, and Adam Z. Weber, 'Understanding Water Uptake and Transport in Nafion using X-Ray Microtomography,' *ACS Macro Letters*, **2**, 288-291 (2013).

2. Ahmet Kusoglu, Kyu Taek Cho, Rafael A. Prato, and Adam Z. Weber, 'Structural and Transport Properties of Nafion in Hydrobromic-Acid Solutions', *Solid State Ionics*, **252**, 68-74 (2013).

3. Thomas J. Dursch, Greg J. Trigub, J. F. Liu, Clayton J. Radke, and Adam Z. Weber, 'Non-isothermal Melting of Ice in the Gas-Diffusion Layer of a Proton-Exchange-Membrane Fuel Cell,' *International Journal of Heat and Mass Transfer*, **67**, 896-901 (2013).

4. Thomas J. Dursch, Greg J. Trigub, Rodger Lujan, J. F. Liu, Rangachary Mukundan, Clayton J. Radke, and Adam Z. Weber, 'Ice-Crystallization Kinetics in the Catalyst Layer of a Proton-Exchange-Membrane Fuel Cell,' *Journal of the Electrochemical Society,* **161** (3), F199-F207 (2014).

5. Ahmet Kusoglu, Douglas Kushner, Devproshad K. Paul, Kunal Karan, Michael A. Hickner, and Adam Z. Weber, 'Impact of Substrate and Processing on Confinement of Nafion Thin Films,' *Advanced Functional Materials*, **24** (30), 4763-4774, (2014).

6. Kirt A. Page, Ahmet Kusoglu, Christopher M. Stafford, Sangcheol Kim, R. Joseph Kline, and Adam Z. Weber, 'Confinement-driven Increase in Ionomer Thin-Film Modulus,' *Nano Letters*, **14**, 2299-2304 (2014).

7. Thomas J. Dursch, Jianfeng F. Liu, Greg J. Trigub, Clayton J. Radke, and Adam Z. Weber, 'Ice-Crystallization During Cold-Start of a Proton-Exchange-Membrane Fuel Cell,' *ECS Transactions,* **58** (1), 897-905 (2013).

8. Adam Z. Weber, 'Macroscopic Modeling of Porous Electrodes,' in Electrochemical Engineering, Trung Nguyen, Editor in encyclopedia of applied electrochemistry, Robert Savinell, Ken-Ichiro Ota, Gerhard Kreysa, Editors, Springer, in press (2014). doi: 10.1007/978-1-4419-6996-5.

9. Adam Z. Weber, 'Thermal Effects in Electrochemical Systems,' in Electrochemical Engineering, Trung Nguyen, Editor in encyclopedia of applied electrochemistry, Robert Savinell, Ken-Ichiro Ota, Gerhard Kreysa, Editors, Springer, in press (2014). doi: 10.1007/978-1-4419-6996-5.

10. Fairweather J. D., D. Spernjak, J. Spendelow, R. Mukundan, D. Hussey, D. Jacobson, and R. L. Borup, "Evaluation of Transient Water Content During PEMFC Operational Cycles by Stroboscopic Neutron Imaging," *ECS Transactions* (2013)

11. J. Mishler, Y. Wang, R. Lujan, R. Mukundan, and R.L. Borup, "An experimental study of polymer electrolyte fuel cell operation at sub-freezing temperatures," *J. Electrochem. Soc.,* **160**, F514-F521 (2013).

FY 2014 PRESENTATIONS

1. A. Kusoglu, G.S. Hwang, and A.Z. Weber, "Water Uptake in PFSA Membranes," ECS Meeting, Tornto (2013). (invited tutorial).

2. Thomas J. Dursch, Clayton J. Radke, and Adam Z. Weber, "Phase Change and Water Movement in Fuel-Cell Porous Media," ASME Heat Transfer Conference, Minneapolis (2013). (invited keynote).

3. Adam Z Weber and Ahmet Kusoglu, "Structure/Function Relationships in Perfluorinated Sulfonic Acid Membranes", Solid State Ionics, Kyoto, (2013).

4. Ahmet Kusoglu, Adam Z. Weber, "Morphology and Swelling of Perfluorosulfonic-acid (PFSA) Ionomer Thin Films," ECS meeting, San Francisco.

4. Prodip K. Das and Adam Z. Weber, 'Water-Management in PEMFC with Ultra-Thin Catalyst-Layers," ASME Fuel Cell Conference, Minneapolis (2013).

5. T.J. Dursch, G.J. Trigub, J.F Liu, C.J. Radke, A.Z. Weber, "Effect of External Vibrations on Non-isothermal Ice-Nucleation Rates," AIChE meeting, San Francisco.

6. Thomas J. Dursch, Jianfeng F. Liu, Greg J. Trigub, Clayton J. Radke, and Adam Z. Weber, 'Ice-Crystallization Kinetics During Cold-Start of a Proton-Exchange-Membrane Fuel Cell,' ECS meeting, San Francisco.

7. Rangachary Mukundan, Dusan Spernjak, Roger Lujan, Daniel Hussey, David Jacobson, Andy Steinbach, Adam Weber, and Rodney L. Borup, "Neutron imaging and performance of PEM fuel cells with nanostructured thin film electrodes at low temperatures," ECS meeting, San Francisco.

8. Gi-suk Hwang, Joseph Grant, and Adam Z. Weber, "Effective Diffusivity Measurement of Partially-Saturated Diffusion Media," ECS meeting, San Francisco (2013).

9. Adam Z. Weber, Ahmet Kusoglu, "The Role of the Interface in Controlling Transport Phenomena in PFSAs," Water Phenomena in PEM Workshop, Norway (invited).

10. Rachid Zaffou, Mike L. Perry, Zhongfen Ding, "Performance of Polymer-Electrolyte Fuel Cells with Ultra-Low Catalyst Loadings under Low Temperature Operation," ECS Meeting, Toronto (2013).

11. Adam Weber, "Understanding Transport in and Properties of Nafion Across Length Scales," MII Symposium, Virginia Tech (invited).

12. Ahmet Kusoglu, Alex Hexemer, Adam Weber, "Interfaces, Bulk, and Confinement in Nafion," Golden Gate Polymer Forum, San Francisco (invited).

13. Adam Z Weber, "Macroscopic Modeling of Performance Concerns in Proton-Exchange-Membrane Fuel-Cell Catalyst Layers," IPAM Fuel Cell Modeling, Los Angeles (invited).

14. Prodip K Das, Anthony Santamaria, Adam Z. Weber, "Understanding liquid water and gas-diffusion layers," Grove Fuel Cell Science and Technology Conference, Amsterdam, (2014).

15. Ahmet Kusoglu and Adam Weber, "Impact of Interfacial Conditions on Perfluorosulfonic-acid (PFSA) Membranes and Thin Films," ECEE conference, Shanghai (2014). (invited)

V.G.2 Transport in Proton Exchange Membrane Fuel Cells

Cortney Mittelsteadt (Primary Contact), Hui Xu, Shelly Brawn (Giner)
Sirivatch Shimpalee, Visarn Lilavivat (USC)
James E. McGrath, Jarrett Rowler (VA Tech)
Don Conners, Guy Ebbrell (AvCarb)
Kevin Russell (Tech-Etch)
John W. Van Zee (U. of Alabama)

Giner, Inc./Giner Electrochemical Systems, LLC
89 Rumford Ave.
Newton, MA 02466
Phone: (781) 529-0529
Email: cmittelsteadt@ginerinc.com

DOE Managers

Donna Ho
Phone: (202) 586-8000
E-mail: Donna.Ho@ee.doe.gov

Gregory Kleen
Phone: (720) 356-1672
Email: Gregory.Kleen@ee.doe.gov

Contract Number: DE-EE0000471

Subcontractors

- Tech-Etch, Plymouth, MA
- Ballard Material Products, Inc., Lowell, MA
- Virginia Polytechnic and State University (VA Tech), Blacksburg, VA
- University of South Carolina (USC), Columbia, SC

Project Start Date: November 1, 2009
Project End Date: April 30, 2014

Overall Objectives

- Design fuel cell components (membranes, gas-diffusion media [GDM], bipolar plates and flow fields) that possess specific transport properties
- Establish a computational fluid dynamics (CFD) model to elucidate the effect of component variables on these transport properties
- Determine sensitivity of fuel cell performance to these component properties to identify limiting components for fuel cell transport loss

Fiscal Year (FY) 2014 Objectives

- Evaluate the performance of VA Tech membrane electrode assemblies (MEAs) and the impact of VA Tech membrane on water transport in operating fuel cells
- Perform CFD modeling of VA Tech membrane for fuel cell performance and water transport using measured water uptake and diffusivity and electro-osmotic drag coefficient
- Design GDM with varying substrate, diffusivity and micro-porous layer (MPL) and characterize their microstructures
- Test the performance of fuel cells using the above MEAs and correlate the microstructures of GDM to the fuel cell performance

Technical Barriers

This project addresses the following technical barriers from the Fuel Cells section of the Fuel Cell Technologies Office Multi-Year Research, Development, and Demonstration Plan:

(C) Performance

Technical Targets

The goals of this project are not to reach specific technical targets put forth by the DOE (i.e. target catalyst loading, target cost per kilowatt). Instead, this project aims to develop fuel cell components (i.e. membranes, GDM, bipolar plates and flow fields) that possess specific properties (i.e. water transport and conductivity). A CFD model will then be developed to elucidate the effect of certain parameters on these specific properties (i.e., the effect of membrane type and thickness on membrane water transport). Ultimately, the model will be used to determine sensitivity of fuel cell performance to component properties to determine limiting components and guide research.

FY 2014 Accomplishments

- Synthesized large batches of hexafluoro bisphenol a benzonitrile (6FPAEB)-bi phenyl sulfone: H form (BPSH) membranes, nitrile containing block copolymers for 50-cm^2 MEA fabrication
- Achieved good reproducibility of the VA Tech 6FPAEB-BPSH-based MEAs
- Successfully integrated VA Tech MEAs with current distribution board (CDB) to study the impact of VA Tech membranes on water transport in fuel cells
- Obtained 12 custom GDM with varying substrate, diffusivity and MPL and characterized their microstructures

- Tested the above GDM in operating fuel cells and illustrated how the microstructures of GDM impact fuel cell performance and water transport

INTRODUCTION

Many fuel cell component properties that influence water transport and thermal management are not well understood [1,2]. A better understanding of how water transport and thermal management can be controlled would represent a significant step forward in meeting the DOE's stated 2015 targets. This project aims for a better understanding of water transport and thermal management by tailoring fuel cell components to exhibit specific measurable transport properties. These transport properties are then used in a model, which will enable the prediction of the effect of changing component parameters on transport properties.

APPROACH

This project seeks to develop fuel cell components possessing specific transport properties. Membranes will be developed to achieve different ratios of water transport and conductivity. Bulk membrane properties (i.e. diffusivity, water uptake, conductivity) will be evaluated and modeled. Also, GDMs with varying substrate, diffusivity and micro-porous layer will be developed and tailored to illustrate specific differences in porosity, tortuosity and hydrophobicity. The fuel cell performance will be evaluated using these components and compared with the model. The model will be used to predict the effect of changing component parameters (i.e. changing membrane type and thickness, changing flow field configuration) on component transport properties and fuel cell performance.

RESULTS

VA Tech 6FPAEB-BPSH-based MEA was made at Giner and sent to USC for measuring local currents using current distribution board on a 50-cm² serpentine flow field. The experimental results were compared and validated with numerical predictions. Work focused on high humidity toward over saturation conditions, 100/125% relative humidity (RH) and 100/150% RH, as liquid water significantly affects the performance of proton exchange membrane fuel cells. The validation between modeling results and experimental data will give an accuracy level of modeling code for further analysis of water transport in the proton exchange membrane fuel cell single cell and stack.

Local polarization curves from CDB measurements and CFD modeling results are shown in Figure 1**:** (a) 100/125% RH; (b) 100/150% RH. The numbers 1 to 10 represent the segments associated to the flow direction. Both conditions reveal similar local performance profiles but 100/125% RH gives higher performance than 100/150% RH. To compare the experimental results with model predictions, the contour plot pattern was used. The experimental data were imported to plotting software for a contour plot. The comparison of current density between experiment and model predictions for two inlet humidity conditions is illustrated in Figure 1c and 1d. It can be seen that the model predictions agree with experimental data for very high humidity conditions. There is a significant drop in local performance around the middle toward the exit of the cell observed in both experiment and modeling results. This is because of the high flooding in those areas.

Figure 2 shows the prediction of liquid water film thickness on the cathode membrane surface for both conditions. It shows that the thickness of liquid water is higher with the inlet humidity of the cathode side is increased. As expected, the thicker the liquid water, the lower local performance is in those areas. It also presents that with this over saturated humidity condition on the cathode, the condensation of water vapor starts from the entrance event though there is a heat generated due to the high electrochemical reaction (data not shown).

Twelve custom GDMs from AvCarb have been tested under selected humidity conditions. There are three different carbon substrates. They are EP40, P50, and P75. All of them have differences in thickness and properties (e.g., bulk density, permeability, porosity, tortuosity, etc.). These substrates were modified by adding two MPLs. Each of these was then treated with two different methods to provide two different values of diffusivity (i.e. <0.15 cm^2/s and >0.35 cm^2/s). Moreover, two MPLs have been constructed with two different sizes of carbon particles (i.e. small and large). Table 1 shows a list of samples for experiment and comparison in this report using seven custom GDMs. In this table the measurement of MacNullin number from those GDMs is also provided.

The pore distribution and microstructures of these GDMs are shown in Figure 3. The pore size distribution in both accumulative pore volume and differential pore volume of the baseline GDM compared to custom GDMs is shown in Figure 3a. Adding two different MPLs greatly reduces the volume of large pores. The scanning electron microscope images on the EP 40 substrate surfaces and cross section of custom GDMs compared to baseline GDM are shown in Figure 3b.

The fuel cell performance measurements and predictions of three main substrate-based GDMs are shown in Figure 4 (i.e. P50, P75, and EP40, with large carbon particle in MP1 and small carbon particle in MP2). As shown in Figure 4a, EP40 exhibits the best performance compared with other types especially at dryer humidity conditions. When inlet humidity increases, the performance of those three GDMs

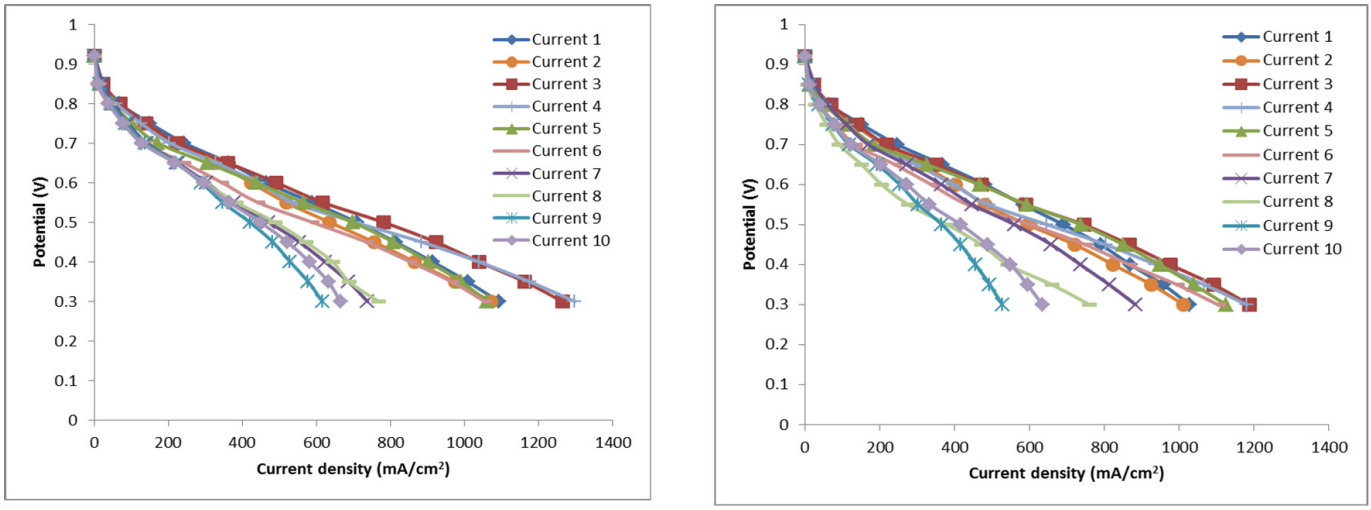

FIGURE 1. Local polarization curves of 6FPAEB-BPSH membrane from CDB measurements and CFD modeling for H_2 (anode)/air (cathode).

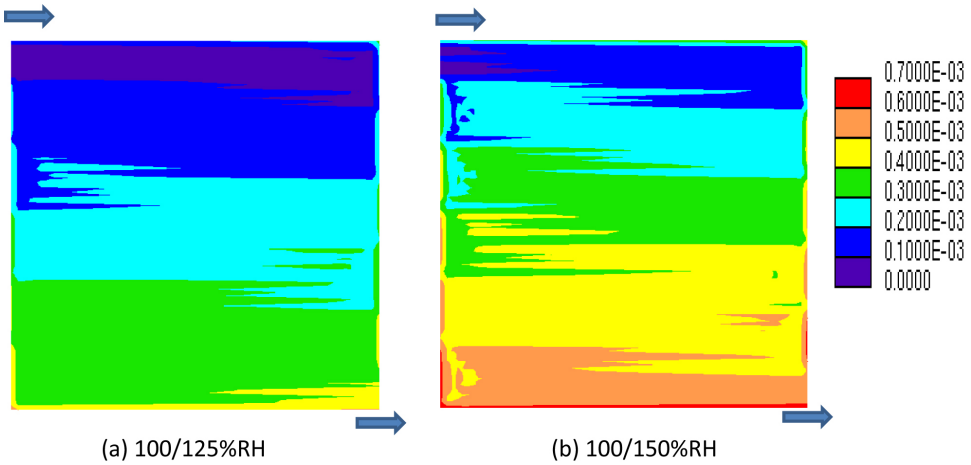

FIGURE 2. Predictions of liquid water film thickness on the cathode 6FPAEB-BPSH membrane surface for both RH conditions.

TABLE 1. GDM Design Matrix

Substrate	Diffusivity	MPL1	MPL2	MacMullin No.	Status
P50T				3.09	Done
P50	Low	Large	Small	2.63	Done
P50	High	Large	Small	2.18	Done
P50	Low	Small	Large	4.04	Done
P50	High	Small	Large	2.73	Done
P75T				4.43	Done
P75	Low	Large	Small	2.14	Done
P75	High	Large	Small	1.92	Done
P75	Low	Small	Large	11.11	Done
P75	High	Small	Large	2.63	Done
EP40T				3.70	Done
EP40	Low	Large	Small	5.18	Done
EP40	High	Large	Small	2.34	Done
EP40	Low	Small	Large	3.18	Done
EP40	High	Small	Large	2.62	Done

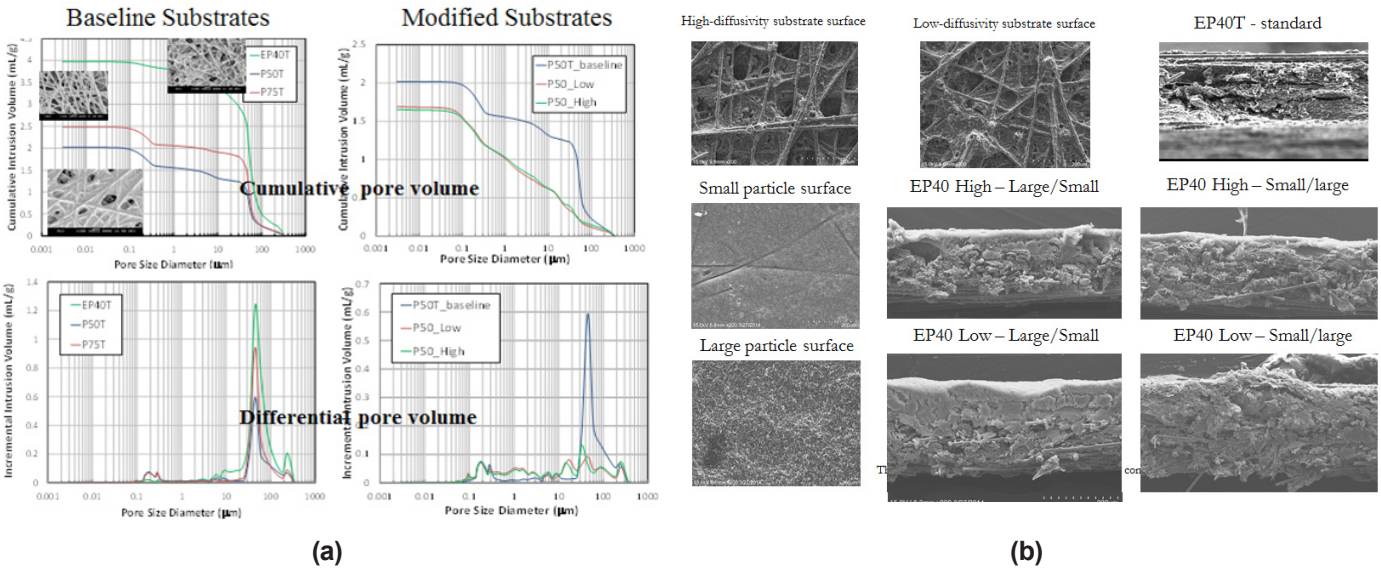

FIGURE 3. Pore distributions and microstructures of designed GDMs. (a) The pore size distribution in both accumulative pore volume and differential pore volume; (b) scanning electron microscope images on the EP40 substrate surfaces and cross section of EP40-based GDL.

are close to each other. GDM P50 and P75 show similar performance at low inlet humidity condition but P50 gives slightly higher performance than P75 at higher inlet humidity conditions. The current density distribution and membrane water content of custom GDMs via CFD simulation are depicted in Figure 4b**.** The simulation is for an average current density of 1 A/cm^2. P75 has the most non-uniform distribution and EP40 shows the most uniform distribution with a high value of membrane water content.

CONCLUSIONS AND FUTURE DIRECTIONS

- Fuel cell performance of hydrocarbon membranes integrated with CDBs has been evaluated and agrees well with the CFD simulations.
- Local distributions of water content in hydrocarbon membranes and liquid have been simulated; hydrocarbon membranes demonstrate more uniform water distribution along the MEA flow fields.
- Custom GDMs with varying substrate, diffusivity and MPLs have been designed and fabricated and their microstructures characterized.

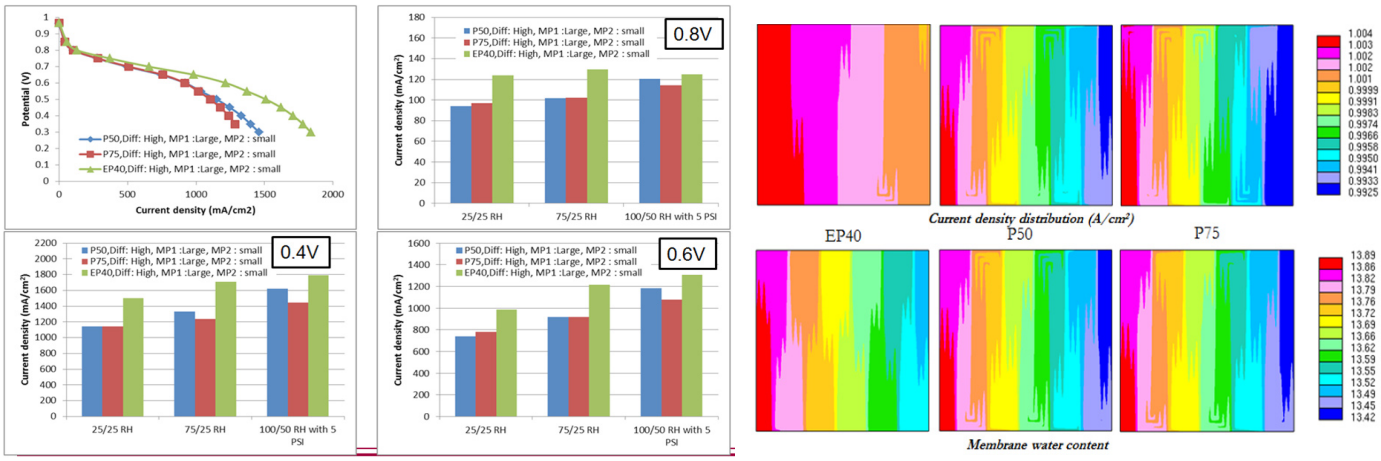

FIGURE 4. Fuel cell performance measurements and predictions of three main substrate-based GDLs. (a) Performance of different types of substrate, P50, P75, and EP40, with high diffusivity, large carbon particle of MP1 and small carbon particle of MP2. Conditions: 80°C; Stoichiometry # 1.5 (anode)/2.0 (cathode); RH (%): 25/25, 75/25 (voltage-current curves are shown), and 100/50 ; pressure: 5 psig. (b) Current density distribution and membrane water content of custom GDLs via CFD simulation.

- The substrate diffusivity and MPL pore structures significantly impacts the performance of MEAs and the GDM optimization has been achieved.
- In the future, the focus will be given to the impact of catalyst layer composition and structure (e.g., hydrocarbon ionomer and advanced catalysts) on fuel cell transport properties.

FY 2014 PUBLICATIONS/PRESENTATIONS

1. "Transport in PEMFC Stacks", Presented by Cortney Mittelsteadt in DOE Hydrogen and Fuel Cell merit review meeting, Arlington, VA, June 2014.

2. "Characterizing Water Transport Properties of Hydrocarbon Block Copolymer Proton Exchange Membranes", presented by Hui Xu in 222th meeting of ECS, Abstract #1344, San Francisco, October 2013.

3. Chen, Yu; Rowlett, Jarrett R.; Lee, Chang Hyun; Lane, Ozma R.; Van Houten, Desmond J.; Zhang, Mingqiang; Moore, Robert B.; McGrath, James E., "Synthesis and characterization of multiblock partially fluorinated hydrophobic poly(arylene ether sulfone)-hydrophilic disulfonated poly(arylene ether sulfone) copolymers for proton exchange membranes", *Journal of Polymer Science, Part A: Polymer Chemistry*, published online: DOI: 10.1002/pola.26618. (2013)

4. Y. Fan, C.J. Cornelius, H.S. Lee, J.E. McGrath, M. Zhang, R.B. Moore and C.L. Staiger, "The effect of block length upon structure, physical properties, and transport within a series of sulfonated poly(arylene ether sulfone)s", Y. Fan, C.J. Cornelius, H.S. Lee, J.E. McGrath, M. Zhang, R.B. Moore and C.L. Staiger, *Journal of Membrane Science* 430, 106-112. (2013)

5. Rowlett, J.R., Chen, Y., Shaver, A.T., Lane, O., Mittelsteadt, C., Xu, H., Zhang, McGrath, J.E., "Multiblock poly(arylene ether nitrile) disulfonated poly(arylene ether sulfone) copolymers for proton exchange membranes: Part 1 synthesis and characterization", *Polymer (United Kingdom)* 54 (23) PP. 6305 – 6313. (2013)

6. V. Lilavivat, S. Shimpalee, H. Xu, J.W. Van Zee, and C.K. Mittelsteadt, "Novel current distribution board for PEMFC," submitted to Intl J. of Hydrogen Energy. (2014).

REFERENCES

1. T.A. Zawodzinski, C. Derouin, S. Radzinski, R.J. Sherman, V.T. Smith, T.E. Springer and S. Gottesfeld, *J. Electrochem. Soc.*, **140**, 1041 (1993).

2. T.V. Nguyen and R.E. White, *J. Electrochem. Soc.*, **140**, 2178 (1993).

V.G.3 Investigation of Micro- and Macro-Scale Transport Processes for Improved Fuel Cell Performance

Wenbin Gu (Primary Contact), Matthew Mench, Michael Hickner, Satish Kandlikar, Thomas Trabold, Jeffrey Gagliardo, Anusorn Kongkanand, Vinod Kumar, Ruichun Jiang, Swami Kumaraguru
General Motors
895 Joslyn Ave.
Pontiac, MI 48340
Phone: (585) 953-5552
Email: wenbin.gu@gm.com

DOE Managers
Donna Ho
Phone: (202) 586-8000
Email: Donna.Ho@ee.doe.gov
David Peterson
Phone: (720) 356-1747
Email: David.Peterson@ee.doe.gov

Technical Advisor
John Kopasz
Phone: (630) 252-7531
Email: kopasz@anl.gov

Contract Number: DE-EE0000470

Subcontractors
- Penn State University, University Park, PA
- University of Tennessee, Knoxville, TN
- Rochester Institute of Technology, Rochester, NY
- University of Rochester, Rochester, NY

Project Start Date: June 1, 2010
Project End Date: May 31, 2014

Overall Objectives

Investigate and synthesize fundamental understanding of transport phenomena at both the macro- and micro-scales for the development of a down-the-channel model that accounts for all transport domains in a broad operating space.

Fiscal Year (FY) 2014 Objectives

- Characterize saturated relationships in state-of-the-art fuel cell materials.
- Obtain a comprehensive down-the-channel validation dataset for a parametric study material set.
- Develop multidimensional component models to output bulk and interfacial transport resistances.
- Demonstrate integrated transport resistances with a one plus one-dimension (1+1D) fuel cell model solved along a straight gas flow path.
- Identify critical parameters for low-cost material development.

Technical Barriers

This project addresses the following technical barriers from the Fuel Cells section of the Fuel Cell Technologies Office Multi-Year Research, Development, and Demonstration Plan:

(B) Cost

(C) Performance

Technical Targets

This project supports fundamental studies of fluid, proton and electron transport with a focus on saturated operating conditions. Insights gained from these studies are being used to develop modeling tools that capture fundamental transport physics under single and two-phase conditions. The primary deliverables are:

- Validated cell model including all component physical and chemical properties.
- Public dissemination of the model and instructions for exercise of the model.
- Compilation of the data generated in the course of model development and validation.
- Identification of rate-limiting steps and recommendations for improvements to the plate-to-plate fuel cell package.

FY 2014 Accomplishments

- Obtained validation data set for baseline materials with low Pt-loaded cathode
- Established or refined several one-dimensional relationships based on parametric and characterization methods developed within the project.
- Demonstrated improved down-the-channel 1+1D model prediction with new relationships integrated.
- Published validation, parametric studies, and characterization data to a project website at: www.pemfcdata.org.

INTRODUCTION

The transport physics associated with fuel cell operation are widely debated amongst researchers because comprehensive micro/nano-scale process validation is very difficult. Furthermore, fuel cell operation has a strong interdependence between components making it difficult to separate the key relationships required for predictive models with ex situ methods. Generally, a validated model that predicts operation based on known design parameters for fuel cell hardware and materials is highly desired by developers. Such a model has been proposed by many research groups for dry (less than 100% relative humidity exhaust) operation with moderate success; however these modelers unanimously assert that their ability to predict wet operation is limited by two-phase component-level understanding of transport processes. Additionally, as two-phase models continue to be refined, benchmarking progress is difficult due to incomplete validation datasets.

In the current work, our team is developing characterization tools for saturated relationships based on the evolution of a dry 1+1D model for accurate wet prediction [1]. To complement this work we are also developing a comprehensive validation dataset based on a wide proton exchange membrane fuel cell (PEMFC) operating space. As data and modeling reach a final form, these are uploaded to a project website at www.pemfcdata.org. All characterization and validation work is conducted with common material sets that represent current and next generations of PEMFC design.

APPROACH

This project is organized around baseline and next-generation material sets. These materials define parametric bounds for component and integrated down-the-channel modeling efforts. The baseline material set was chosen based on the commercial state of the art that exists today. The next-generation material set consists of transport impacting parametric changes that are in line with the DOE 2015 targets for reduced cost while improving durability and performance. For characterization and validation experiments, a standard protocol was also developed to enable the team to conduct experiments with the same boundary conditions.

The first phase of this project was experimentally focused on characterization work that is organized by transport domain, comprising thin film ionomers, bulk membranes, porous electrodes, gas diffusion layers (GDLs) and flow distribution channels. The specifics of these relationships were outlined previously [2]. In anticipation of this integrated model, validation data sets are being collected in parallel with small scale hardware specifically designed to include automotive stack constraints [3]. Currently with these experimental methods established, work becomes more modeling focused as the physical mechanisms that govern the observed transport phenomenon are described multi-dimensionally at the component level and evaluated with a 1+1D fully integrated model. This work continuously guides parametric studies with novel material changes.

RESULTS

Validation Data

In the auto-competitive material set tested for model validation, a number of parameters, including membrane thickness, anode GDL, cathode catalyst layer composition, flowfield land/channel geometry and manifold exit headers, are changed from the baseline material set. Hence, the performance difference between the two material sets represents a compounded effect of all changes being made at once. To de-convolute the effects of high diffusion resistance anode GDL and cell design differences used in DOE automotive competitive cell builds from low Pt-loaded cathode catalyst layer effects, a parametric study cell built with low Pt-loaded cathode and other baseline materials was tested using the standardized project protocol that varies outlet temperature, inlet relative humidity, outlet pressures, and current density [4]. Compared to the baseline cell, the parametric study cell yielded lower cell voltage and less product water to the cathode flowfield. The lower voltage results primarily from lower Pt loading and slightly higher high-frequency resistance (HFR). And less product water to the cathode flowfield appears to be consistent with higher temperature gradient caused by the lower cell voltage and thus higher heat generation rate. However, both baseline and parametric study cells demonstrate same trend in down-the-channel current distribution, suggesting that lower Pt-loaded cathode in the auto-competitive material set would not be responsible for the opposite trend in current distribution associated with the auto-competitive cell at low temperatures. Instead, the highly tortuous anode diffusion medium is most likely the cause.

Transport in Thin Ionomer Films

With focus on elucidating the structural features and transport properties of thin ionomer films, we have performed extensive gravimetric and volumetric swelling studies to understand how these thin films based on perfluorinated sulfonic acid (PFSA) ionomers uptake water and have compared the properties of thin ionomer films to what is known about PFSA-based membranes. The focus on water uptake and swelling is because the transport properties of these materials is determined in large part by their hydration. We have found that the water uptake of PFSA-based thin films varies with thickness, substrate type, and processing conditions. To understand the swelling processes in more depth, we have undertaken measurements of polymer chain alignment using Fourier transform infrared (FTIR) and ellipsometry. These techniques were chosen because they can be adapted to electrochemical measurements to study

the behavior of thin films under potential control, which is ongoing work. Shown in Figure 1 is the FTIR spectra of 50-nm and 5-nm Nafion® films. The SO_3/CF_3 side chain peaks are enhanced in the thin film spectra indicating alignment of these moieties towards the surface in the thinnest films [5]. Similar observations have been made by studying the birefringence of Nafion® films using spectroscopic ellipsometry [6]. Our goal is to be able to measure the dynamic behavior of these thin films as a function of potential, which can be detected by changes in their FTIR or ellipsometric spectra. These types of measurements focusing on the features of the ionomer-substrate interface may lead to a better understanding of why the oxygen transport resistance at low platinum loading occurs. This work on the structure of the thin films and how the structure correlates with swelling and ultimately other transport properties complements our collaborative work with Lawrence Berkeley National Laboratory on scattering studies [7] as a function of film processing conditions and substrate type.

Transport in Diffusion Materials

We developed an empirical relationship for effective thermal conductivity of partially saturated diffusion media via ex situ material testing [8]. Additionally, we experimentally determined capillary drainage functions of liquid water from the catalyst layer, micro-porous layer, and the interfacial domains [9]. Utilizing the high resolution neutron imaging facility at the National Institute of Standards and Technology, we completed extensive in situ characterization of the impacts of diffusion media design, flow-field interface architecture, and aging, covering an extremely wide range of operational test conditions. In particular, diffusion media aged in situ for over 2,500 hours has been tested with neutron imaging and show additional water storage during operation. The water balance was found to shift in the aged material from the anode to the cathode, as shown in Figure 2. To understand what has caused the change in water balance, energy dispersive X-ray spectroscopy and X-ray photoelectron spectroscopy were used to determine changes in chemical makeup and surface morphology. The results indicate an increase in carbon-oxygen bonding and increased surface functionalization. These oxygen groups can be responsible for increasing the hydrophilicity of the

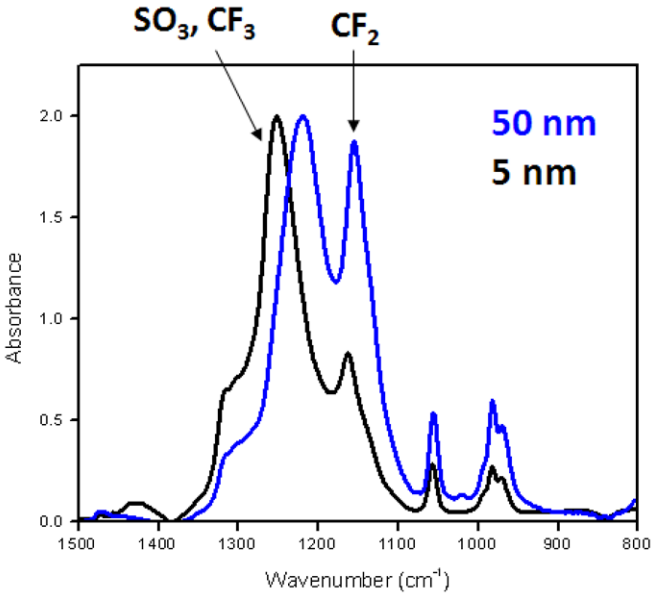

FIGURE 1. FTIR-Attenuated total reflectance spectrum of 50-nm thick and 5-nm thick Nafion® thin films showing the change in the CF_3 (backbone) and SO_3/CF_3 (side chain) peak ratios with thickness.

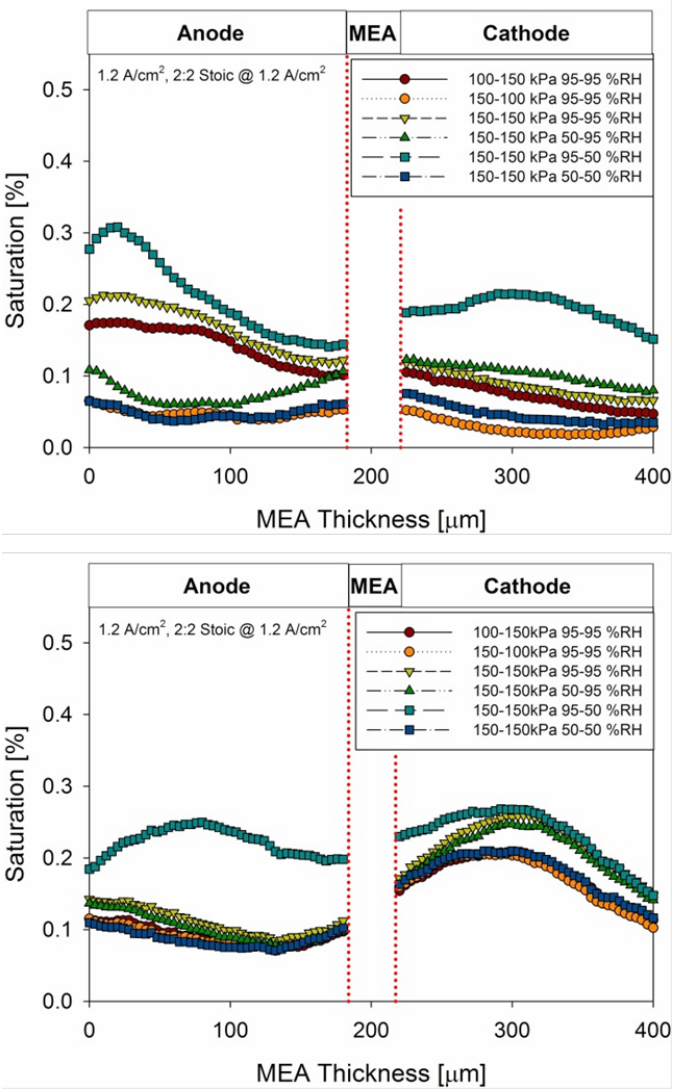

FIGURE 2. Saturation profiles for baseline fresh (upper) and 2,666 hr aged (lower) GDL/MEA packages at 60°C. Test conditions: 1.2 A/cm^2, 95|95% (An|Ca) constant inlet relative humidity for pressure tests, 150|150 kPa (An|Ca) constant exhaust pressure for concentration gradient tests, constant flow rate at an equivalent stoichiometry ratio of 2:2 at 1.2 A/cm^2. Profiles are summed along entire imaged area.

surface, increasing water retention and wicking action. Both anode and cathode GDLs were tested, and the cathode GDL was more affected by ageing. Finally, a GDL component level multi-phase computational model has been developed to address the need for meso-scale modeling within this media. A statistical approach using percolation theory was used to construct appropriate model porous domain structures, and a Lattice-Boltzman approach was used to determine the effective tortuosity and gas-diffusivity of these domains. Additionally, X-ray microscopy was used to determine the three-dimensional morphology of the GDL structure, which can then be directly used as the computational domain in the model. Future publications are being prepared based on the results which demonstrate the prediction of effective diffusivity and tortuosity for the real media morphology as a function of saturation. This result can then be correlated and linked with macroscopic performance models to obtain high-speed predictive performance modeling with greater GDL level transport fidelity.

Transport in Flow Distributor Channels

The emergence of droplets and their interaction with the reactant channel sidewall dictate trends of GDL-channel interface coverage, two-phase flow pressure drop, and transition of flow patterns. These trends are dependent on the corner filling of the channel by liquid water. We conducted ex situ experimentation to establish correlations to predict corner filling behavior as a function of channel design parameters and operating conditions [10]. Liquid water was injected into a single channel that was manufactured to match baseline and auto-competitive designs. The distance from water injection location on the GDL to the channel side wall, materials of GDL and channel walls, corner angle in an auto-competitive channel, and superficial air velocity in the channel were varied. A channel corner angle of 50° is suggested for improved water removal characteristics. Moreover, correlations were established to predict the corner filling behavior and two-phase flow pressure drop at the instant of droplet removal. A force balanced model has also been developed to provide further insight into the dynamics of the droplet at the time of its interaction with the channel side wall. Consequently, a channel design was suggested to minimize the buildup of liquid water.

Two-phase pressure drop studies from the literature have focused on the fundamental factors that influence the two-phase flow. However, the conditions in the PEMFC reactant channels are unique as there is consumption of gaseous reactants along the length and water is continuously introduced through the GDL. This results in a continuously changing quality of the two-phase mixture. There are temperature gradients both along the length of the channel as well as the cross section of the cell, resulting in evaporation and condensation-driven mass transport in these directions. A step-wise elemental modeling scheme that allows ease of integration into the down-the-channel performance model has been proposed, developed and validated for the prediction of two-phase pressure drop in the reactant channels. The modeling scheme has been tested with several fundamental pressure drop models available in the literature. It is found that the modified English and Kandlikar model [11] works best to predict two-phase pressure drop in PEMFC reactant channels. Figure 3 shows that it has a mean error of 11.6% and 40.2% for cathode and anode, respectively, over the entire range. A mean error of 5.2% was observed for the cathode with a fully humidified inlet.

In investigating channel-scale water transport and accumulation, both within the fuel cell active area and in the non-active areas extending all the way to the anode and

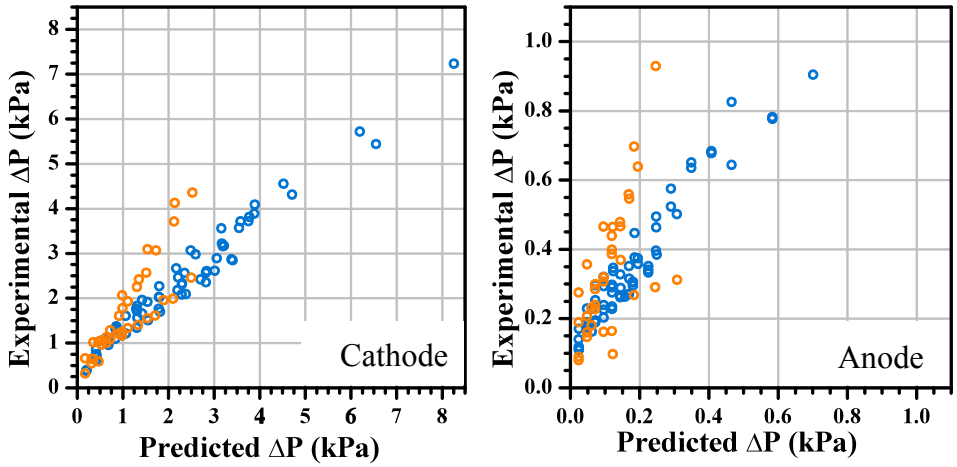

FIGURE 3. Comparison between the modified English and Kandlikar correlation and experimental data. Cell temperature 40°C, Orange – 0% relative humidity Inlet, Blue – 95% relative humidity Inlet, (left) Cathode Side Pressure Drop (right) Anode Side Pressure Drop.

cathode exit manifolds, we carried out ex situ two-phase flow experiments to understand pressure drop performance over a wide range of simulated operating conditions, coupled with in situ experiments applying neutron imaging to directly measure fuel cell water content under low temperature conditions in the range of 20 to 40°C [12]. It was observed that the active area water volume is strongly dependent on cell temperature, and temperature variation of as little as 0.5°C can produce a significant change in water accumulation, which is also reflected in the cell voltage. In general, active area water decreases with increasing current density. However, the water quantity is a function of both cell temperature and anode/cathode pressure. Conversely, the anode non-active water is weakly dependent on current density, presumably because in this region there is little driving force to remove water once it is present. This finding has obvious implications relative to fuel cell operation under freezing conditions, and is indicative of the difficulty of removing anode exit water during shut-down purge. Furthermore, a significant pressure drop was seen over non-active area. On average, the outlet region contributes more to the total (manifold-to-manifold) pressure drop for higher water flow rates, suggesting that water mitigation strategies should focus on outlet non-active area as well as channel-to-manifold interface, especially on anode side.

Modeling

The two-phase, 1+1D down-the-channel model has been improved and tested against the experimental data generated from baseline, baseline with low Pt-loaded cathode, and auto-competitive material sets. Due to lack of experimental data on liquid water saturation within an electrode, the electrodes are allowed to be supersaturated and water saturation therein is evaluated based on local relative humidity by an empirical correlation. Using a single set of parameters, the model agrees fairly well to all three data sets. Figure 4 compares the predicted down-the-channel current and HFR distributions with the measured ones. Significantly, the model captures the opposite trends in current density distribution observed for the automotive competitive and baseline materials plus low-loaded Pt material sets, that is caused by the highly tortuous anode diffusion media in the automotive competitive data set. However, the agreement for the automotive competitive material set comes with a compromise in the agreement for the baseline material set. More work is needed to achieve better quantitative agreement in down-the-channel distributions.

A parametric study was performed for cell component optimization based on the parametric study cell validation data using the two-phase, 1+1D down-the-channel model. The design for six sigma approach was employed to find optimal material properties for better cell performance [13]. Among numerous input parameters, eight were chosen to be the control factors. For the operating condition given in

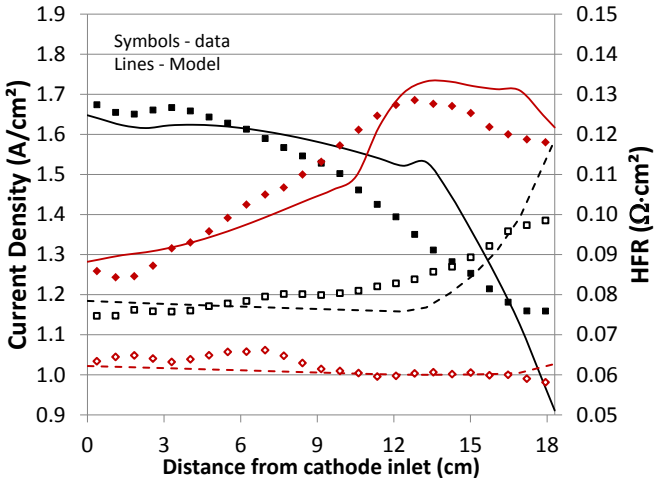

FIGURE 4. Comparisons between model and data for down-the-channel current and HFR distributions. Squares represent baseline materials with low Pt-loaded cathode (0.1 mgPt/cm^2); and diamonds stand for Auto-Competitive material set. The cell operates with H_2/Air at stoichimetry 1.5/2.0, 100/150 kPa-abs outlet pressure, 60°C coolant out temperature, 0/95% inlet relative humidity.

Figure 4, the following recommendation can be made for cell component properties in reference to the baseline materials:

- Thinner membrane (12 microns)
- 50% lower membrane water permeability
- 25% less tortuous supporting layer in the ePTFE-reinforced membrane
- 25% less tortuous GDL in the presence of liquid water
- 2X GDL thermal conductivity
- 2X MPL thermal conductivity
- 2X coolant-to-plate thermal resistance
- 50% lower local oxygen transport resistance

CONCLUSIONS AND FUTURE DIRECTIONS

A well-organized characterization, modeling and validation framework was developed early in this project. The first phase (FY 2011) of execution was largely focused on experimental development. The focus gradually shifted to model development while continuing to complete validation data. During the final phase of the project (FY 2014), results from these methods were described with multidimensional component models and summarized in a down-the-channel model that is compared to a comprehensive validation database. Specific highlights from FY 2014:

- A new validation data set based on the baseline materials with low Pt-loaded cathode added to the database for model validation.

- Coninued studies on thin ionomer films and ionomer-substrate interactions.
- Neutron imaging data on liquid water saturation within GDL for the effects of GDL type, aging, and flowfield shows the impact of GDL surface properties and heat transfer.
- Validated flowfield pressure drop model includes the effects of water droplet-channel corner interaction, liquid water flow pattern, and local operating condition.
- Significant pressure drop occurs in the non-active, channel-to-manifold region due to liquid water accumulation therein; peak active area water volume exists likely due to gas momentum and hydraulic force balance.
- Down-the-channel 1+1D model improved with new relationships integrated, and the opposite trend in down-the-channel current distribution associated with auto-competitive material set successfully captured.
- A parametric study performed for cell component optimization, and optimal material properties recommended for better cell performance.

The project ended in May 2014. A final report is forthcoming.

FY 2014 PUBLICATIONS/PRESENTATIONS

1. Petrina, S.A. "Water Sorption, Viscoelastic, and Optical Properties of Thin NAFION® Films." Ph.D. Dissertation, Pennsylvania State University, 2013.

2. Kusoglu, A., D. Kushner, D.K. Paul, K. Karan, M.A. Hickner, A.Z. Weber, "Impact of Substrate and Processing on Confinement of Nafion Thin Films," *Advanced Functional Materials* 2014, DOI: 10.1002/adfm.201304311.

3. Zimudzi, T.J., M.A. Hickner, "FTIR Analysis of Alignment in NAFION® Thin Films at SiO_2 and Au Interfaces," *submitted to J. Phys. Chem. B* (2014).

4. Kushner, D.I., M.A. Hickner, "FTIR Analysis of Alignment in NAFION® Thin Films at SiO_2 and Au Interfaces," *submitted to Langmuir* (2014).

5. LaManna, J.M., J.M. Bothe, F.Y. Zhang, and M.M. Mench, "Measurement of Capillary Pressure in Fuel Cell Diffusion Media, Micro-Porous Layers, Catalyst Layers, and Interfaces," *submitted to J. Power S*ources (2014).

6. LaManna, J.M., Chakraborty, S., Gagliardo, J.J., and Mench, M.M., "Isolation of transport mechanisms in PEFCs using high resolution neutron imaging," International Journal of Hydrogen Energy, 39(7), pp. 3387-3396 (2014).

7. Xu, G., LaManna, J.M., Clement, J.T., and Mench, M.M., "Direct measurement of through-plane thermal conductivity of partially saturated fuel cell diffusion media," Journal of Power Sources, 256, pp. 212-219 (2014).

8. Owejan, J.P., Trabold, T.A., and Mench, M.M., "Oxygen transport resistance correlated to liquid water saturation in the gas diffusion layer of PEM fuel cells," International Journal of Heat and Mass Transfer, 71(10), pp. 585-592 (2014).

9. Kandlikar, S.G., E.J.See, M. Koz, P. Gopalan, R. Banerjee, "Two-Phase Flow in GDL and Reactant Channels of a Proton Exchange Membrane Fuel Cell," International Journal of Hydrogen Energy, 39 (12), pp. 6620-6636 (2014).

10. Banerjee, R., and S.G. Kandlikar, "Liquid Water Quantification in the Cathode Side Gas Channels of a Proton Exchange Membrane Fuel Cell Through Two-Phase Flow Visualization," Journal of Power Sources, 247, pp. 9-19 (2014).

11. Gopalan, P., and S.G. Kandlikar, "Modeling Dynamic Interaction Between an Emerging Water Droplet and the Sidewall of a Trapezoidal Channel," Colloids and Surfaces A: Physicochemical and Engineering Aspects, 441, pp. 267-274 (2014).

12. Gopalan, P., and S.G. Kandlikar, "Effect of Channel Materials and Trapezoidal Corner Angles on Emerging Droplet Behavior in Proton Exchange Membrane Fuel Cell Gas Channels," Journal of Power Sources, 248, pp. 230-238 (2014).

13. Banerjee, R., E.J. See, and S.G. Kandlikar, "Pressure Drop and Voltage Response of PEMFC Operation under Transient Temperature and Loading Conditions," ECS Transactions, 58(1), pp. 1601-1611 (2013).

14. See, E.J., and S.G. Kandlikar, "Effect of GDL Material on Thermal Gradients along the Reactant Flow Channels in PEMFCs," ECS Transactions, 58(1), pp. 867-880 (2013).

15. Xu, G., LaManna, J., and Mench, M.M., "Measurement of Thermal Conductivity of Partially Saturated Diffusion Media under Compression," 2014 ECS Spring meeting, Toronto, Canada, May 12–16, 2014.

16. LaManna, Jacob M., Matthew M. Mench , " Flow Field and Diffusion Media Tortuosity Influences on PEFC Water Balance," Accepted for invited oral presentation. 2014 ECS and SMEQ Joint International Meeting, Cancun, Mexico, October 5–10, 2014.

17. LaManna,Jacob M., Daniel S. Hussey, David L. Jacobson, Matthew M. Mench, "Role of Land Drainage on Water Storage in Polymer Electrolyte Fuel Cells Using High Resolution Neutron Imaging," Accepted for poster presentation.10th World Conference on Neutron Radiography. Grindelwald, Switzerland, October 5–10, 2014.

18. Fenton, D.J., J.J. Gagliardo and T.A. Trabold, "Analysis of water morphology in the active area and channel-to-manifold transitions of a PEM fuelcell," submitted for publication in *Proceedings of the ASME 8th International Conference on Energy Sustainability & 12th International Fuel Cell Science, Engineering and Technology Conference,* Paper ESFuelCell2014-6565, Boston, MA, June 30 – July 2, 2014.

REFERENCES

1. Gu, W., Baker, D.R., Liu, Y., Gasteiger, H.A., "Proton exchange membrane fuel cell (PEMFC) down-the-channel performance model," *Handbook of Fuel Cells* - Volume 5, Prof. Dr. W. Vielstich *et al*. (Eds.), John Wiley & Sons Ltd. (2009).

2. Owejan, J.P., 2011 Annual Progress Report for the DOE Hydrogen and Fuel Cells Program (2011).

3. Owejan, J.P., Gagliardo, J.J., Sergi, J.M., Kandlikar, S.G., Trabold, T.A., "Water management studies in PEM fuel cells, Part I: Fuel cell design and in situ water distributions," *International Journal of Hydrogen Energy*, 34 (8), 3436-3444 (2009).

4. http://www.pemfcdata.org/data/Standard_Protocol.xls.

5. Zimudzi, T.J., M.A. Hickner, "FTIR Analysis of Alignment in NAFION® Thin Films at SiO2 and Au Interfaces," submitted to *J. Phys. Chem. B* (2014).

6. Kushner, D.I., M.A. Hickner, "FTIR Analysis of Alignment in NAFION® Thin Films at SiO2 and Au Interfaces," submitted to *Langmuir* (2014).

7. Kusoglu, A., D. Kushner, D.K. Paul, K. Karan, M.A. Hickner, A.Z. Weber, "Impact of Substrate and Processing on Confinement of Nafion Thin Films," *Advanced Functional Materials* 2014, DOI: 10.1002/adfm.201304311.

8. Xu, G., LaManna, J.M., Clement, J.T., and Mench, M.M., "Direct measurement of through-plane thermal conductivity of partially saturated fuel cell diffusion media," Journal of Power Sources, 256, pp. 212-219 (2014).

9. LaManna, J.M., J.M. Bothe, F.Y. Zhang, and M.M. Mench, "Measurement of Capillary Pressure in Fuel Cell Diffusion Media, Micro-Porous Layers, Catalyst Layers, and Interfaces," *submitted to J. Power S*ources (2014).

10. Gopalan, P., and S.G. Kandlikar, "Effect of Channel Materials and Trapezoidal Corner Angles on Emerging Droplet Behavior in Proton Exchange Membrane Fuel Cell Gas Channels," Journal of Power Sources, 248, pp. 230-238 (2014).

11. Grimm M., E.J. See, and S.G. Kandlikar, "Modeling gas flow in PEMFC channels: Part I – Flow pattern transitions and pressure drop in a simulated ex situ channel with uniform water injection through the GDL," Int. J. Hydrog. Energy, 37(17), pp. 12489-12503 (2012).

12. Fenton, D.J., J.J. Gagliardo and T.A. Trabold, "Analysis of water morphology in the active area and channel-to-manifold transitions of a PEM fuelcell," submitted for publication in *Proceedings of the ASME 8th International Conference on Energy Sustainability & 12th International Fuel Cell Science, Engineering and Technology Conference,* Paper ESFuelCell2014-6565, Boston, MA, June 30 – July 2, 2014.

13. Kai Yang and El Haik, *Design for Six Sigma*, McGraw-Hill, 2003.

V.H.1 New High-Performance Water Vapor Membranes To Improve Fuel Cell Balance-of-Plant Efficiency and Lower Costs (SBIR Phase II)

Earl H. Wagener (Primary Contact), Brad P. Morgan
Tetramer Technologies LLC
657 S. Mechanic St.
Pendleton, SC 29670
Phone: (864) 646-6282
Email: earl.wagener@tetramertechnologies.com

DOE Manager
Nancy Garland
Phone: (202) 586-5673
Email: Nancy.Garland@ee.doe.gov

Collaborators
- Dana Holding Corporation, Maumee, OH
- General Motors Corporation, Detroit, MI
- Membrane Technology and Research Incorporated, Newark, CA

Contract Number: DE-SC0006172

Project Start Date: September 17, 2012
Project End Date: September 16, 2014

Overall Objectives

- Develop improved low-cost water vapor membranes for cathode humidification modules in fuel cells.
- Synthesize new polymer molecular architectures, which avoid chemical degradation, increase water vapor transport and exhibit good mechanical durability at lower cost.
- Determine long-term stability of membranes through chemical resistance tests. In parallel, continue the synthesis of higher permeability polymer architectures.
- Down select best candidates for scale up and provide prototypes to collaborators.

Fiscal Year (FY) 2014 Objectives

- Performance of 3.32 g sec^{-1} m^{-2} with no chemical degradation over 5,000 hours
- Durability of 5,000 hours with <10% drop in performance
- Crossover leak rate of <5%
- Temperature durability of 90°C with excursions to >100°C
- Cost of <$10/$m^2$ at volumes of 500,000 systems per year

Technical Barriers

This project addresses the following technical barriers from the Fuel Cells section (3.4) of the Fuel Cell Technologies Office Multi-Year Research, Development, and Demonstration Plan:

(A) Durability

(B) Cost

(C) Performance

Technical Targets

- Ionomer membrane performance optimization through improvements in molecular architecture
- Durability improvement
- Scale up of high-performance materials to lower cost

FY 2014 Accomplishments

- Consistently met the target goal of crossover leak rate less than 5%.
- Passed the 20,000-cycle hour durability test.
- Scaled up the down-selected polymer to 2 kg to verify cost projections.
- Cost target of $20/$m^2$ for the ionomer achieved and $10/$m^2$ is on target.
- 12 m^2 of membrane has been successfully coated through a commercial roll coater.
- Industrial partner testing has expanded to involve significantly higher temperatures than DOE targets.

✧ ✧ ✧ ✧ ✧

INTRODUCTION

Hydrogen fuel cells are one of the more promising alternative energy and propulsion systems with the most promising type of fuel cell for automotive and stationary power applications being the proton exchange membrane (PEM) fuel cell. PEMs have the advantage of high power density at the low operating temperatures required for systems that will see frequent on/off cycling. One of the biggest challenges for PEM systems is the fact that PEMs perform much better with higher water environments to effectively conduct protons from the anode to the cathode of the cell. The design of a membrane humidifier unit as part of the balance of plant has been proposed and has

been emphasized by DOE in the Multi-Year Research, Development, and Demonstration Plan in Table 3.4.9 and Table 3.4.10 to utilize the water produced as a byproduct of the oxygen reduction reaction to humidify the inlet air to the fuel cell [1].

The use of membrane humidifiers for fuel cell applications represents a reasonable value proposition; however, expanding the accessible markets for these membranes to increase volumes and lower manufacturing cost is also beneficial, particularly when the new applications satisfy the overall DOE objectives of saving energy. Dehumidification of feed air to heating, ventilation, and air conditioning systems using these membranes can save as much as 40% of the energy required to condition air [2]. The membranes currently being commercialized do not meeting the desired size, weight and pressure drop requirements for automotive applications. More importantly the durability of current membranes have not been found to maintain performance due to degradation mechanisms of the membrane. In 2012, Gore reported that both their new perfluorinated sulfonic acid (PFSA) and hydrocarbon membranes suffered from detrimental loss in performance with a loss in permeance of up to 60% within 500 hours [3]. This loss in performance was attributed to the potential for anhydride formation and was confirmed using methods developed by Collette for PFSAs [4,5]. Gore also addressed a loss in performance from salt contamination where the membrane lost more than 70% of permeance after being converted to the corresponding sodium salt [3]. These possible means for loss in performance drove us to develop a more robust system, which alleviates these degradation mechanisms.

APPROACH

Nafion® has been found widely useful as an ion exchange membrane for chloroalkali cells, which has become a very profitable market and has kept the cost of the current PFSAs much higher than what would be needed for membranes within the fuel cell market. The demand for a cheaper membrane material that does not undergo detrimental side processes has been the inspiration for Tetramer's membrane development work. The evolution of Tetramer's basic ionomer technology with polymers designed for hydrogen ion transport in PEM fuel cells has led to a semifluorinated ionomer that has equaled or exceeded the incumbent PFSA with significant (>50%) cost and processing advantages.

The development of water vapor transfer membranes at Tetramer during this Small Business Innovation Research project has met the target of reproducibly producing a water flux of 2.58 g sec^{-1} m^{-2} with no chemical degradation. Since thin, unsupported membranes have been found to possess mechanical deficiencies, a supported configuration that increases the mechanical durability of the membrane with minimal detriment to overall flux has been implemented. New membranes with unique polymer design elements that emphasize high water transport while alleviating possible means of performance degradation have been proposed and are the driving force for this contract. The synthesis of these new monomers and polymers has been demonstrated; optimization of polymer architecture is in progress and characterization of long-term water vapor transport by both Tetramer and industry partners is currently being explored.

RESULTS

The need for a unique polymer design of a water vapor membrane has been addressed by Tetramer through a systematic approach in which four key polymer design elements were explored. These polymer design elements are summarized in Figure 1. The first and most critical parameter was to design a water permeability unit that consists of hydrophilic groups with ionic or intermolecular attractions. The selected polymer structures have potential for water transport without the possible side effects of anhydride formation. The need for mechanical strength has been addressed in our polymer design by incorporating rigid, hydrophobic structures that impart toughness and keep the material from becoming water soluble. The need for processability has received a great deal of attention especially within the membrane world. To make high quality uniform thin films, the need to either melt process or solution cast the polymer can be addressed by the inclusion of stereoisomeric structures to disrupt packing as well as solubilizing groups. The last parameter addressed has been stability in which specific functional groups have been chosen to ensure chemical resistance, as well as chemical groups that allow for crosslinking have been incorporated into the polymer design to impart an additional robustness for the material.

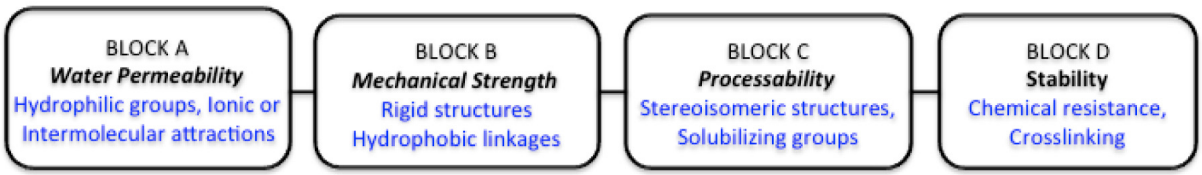

FIGURE 1. Water Vapor Membrane Polymer Design Elements

Tetramer membranes have been found to achieve the 2.58 g sec^{-1} m^{-2} target consistently and currently meet the need for minimal crossover and are being explored for loss in performance over time as well as meeting the highest durability temperature with the lowest cost.

To evaluate membranes for water vapor transport quickly without the need of assembling a full-scale fuel cell system, we have acquired a testing unit from one of our collaborators, MTR and have duplicated the testing conditions that General Motors (GM) used during automotive applications. GM has continued testing our membranes in in parallel, which has helped speed up our evaluations. Our current testing has focused on DOE conditions (dry air in: 0.23 SLPM/cm^2 dry gas flow, 183 kPa absolute, 80°C, 0% relative humidity [RH]; wet air in: 0.20 SLPM/cm^2 dry gas flow, 160 kPa absolute, 80°C, 85% RH) which are highlighted in the Fuel Cell Technologies Office Multi-Year Research, Development, and Demonstration Plan [1]. The progress of membrane performance is shown in Figure 2 in which membranes have improved from a water flux of 1.35 to 3.17 g sec^{-1} m^{-2}. Membranes from these improvements were then tested for anhydride formation using the methods developed by Collette [4,5] and no anhydride formation was found.

These membranes were recently tested by industrial partners under varying real world commercial conditions and found promising results in comparison to competitor membranes as seen in Figure 3. This testing was shown to expand our current conditions to significantly higher temperatures (>100°C) than the initial DOE conditions. Even at these higher temperatures and more extreme conditions Tetramer's membranes have been found to perform higher than multiple comparative suppliers.

During the exploration of more extreme conditions, which consisted of higher temperatures, it was found that commonly used casting solvents such as dimethylacetamide have strong interactions with sulfonic acid groups. This interaction then allows for the decomposition of the dimethylacetamide through acid hydrolysis to form dimethylamine, which is shown in Figure 4a. This dimethylamine can then form ammonium salts with the sulfonic acid groups on the polymer as seen in Figure 4b. To test the effect this amine has on the ionomer a film was treated with an amine and was found to decrease the water flux from 2.61 to 0.94 g sec^{-1} m^{-2}. The need for a solution to this formation of a detrimental performance loss was initially addressed by a post treatment of the membrane to ensure all the residual solvent was removed. Fourier transform infrared (FTIR) confirmed removal of the residual solvent as seen in Figure 4c.

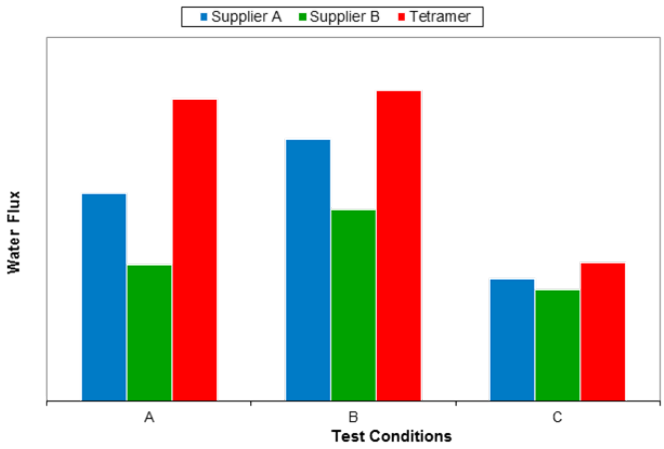

FIGURE 3. Comparison of Tetramer's Membranes vs. Commercial Competition

The development of these membranes is still being pursued and increasing the permeance of the current materials while maintaining these transport properties over long-term durability studies is critical to the success of the project. The down-selected materials from this study will continue to be tested by our industry partners under their conditions to ensure we meet the demands for today's humidification technology needs.

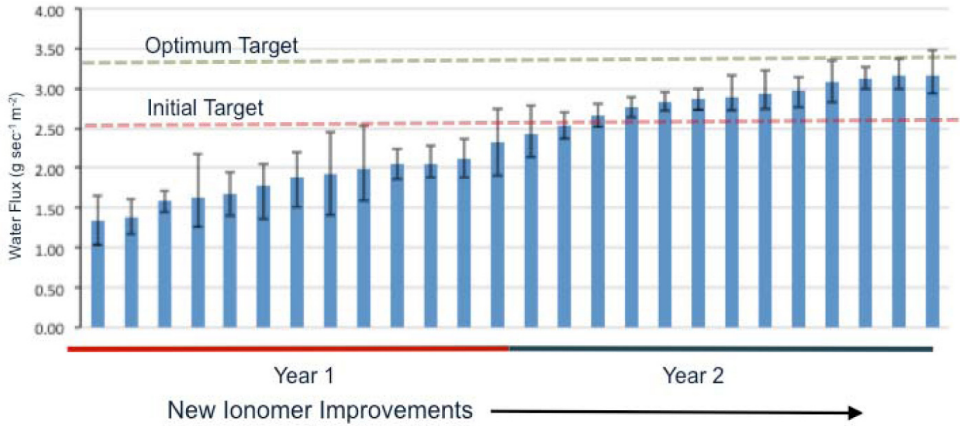

FIGURE 2. New Membrane Initial Performance

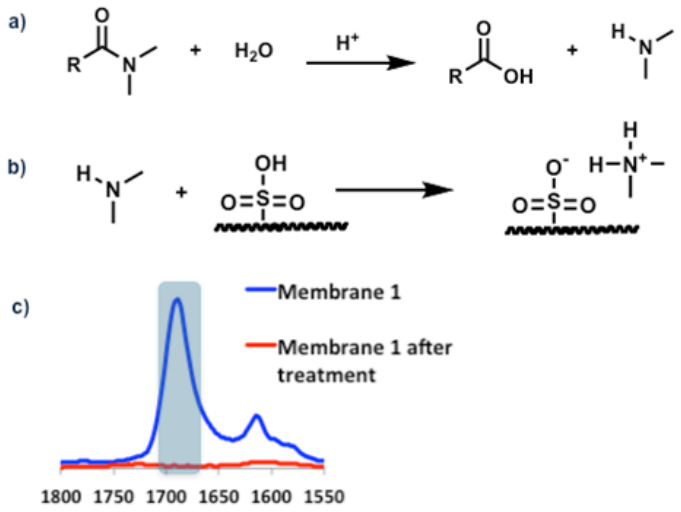

FIGURE 4. a) Decomposition of amide containing solvent such as dimethylacetamide to the corresponding acid and dimethylamine. b) Reaction of dimethylamine with polymer containing a sulfonic acid group to give the ammonium salt. c) FTIR of sulfonic acid polymer containing dimethylacetamide followed by a 24-hour soaking treatment for the membrane.

FUTURE DIRECTIONS

- Resolve solvent degradation issue
- Determine optimum support composite matrix
- Long-term testing
- Manufacture 400 m^2 at commercial roll coater
- Construct prototype water vapor transport module

FY 2014 PUBLICATIONS/PRESENTATIONS

1. Wagener, Earl H.; Morgan, Brad P. "New High Performance Water Vapor Membranes To Improve Fuel Cell Balance of Plant Efficiency and Lower Costs", DOE Annual Review, Washington DC, June 18, 2014, Oral Presentation FC102, available from www.hydrogen.energy.gov.

REFERENCES

1. Fuel Cell Technologies Office Multi-Year Research, Development and Demonstration Plan, Department of Energy Office of Energy Efficiency and Renewable Energy 3.4 – 24 (2012)

2. Zhang, Yinping; Jiang, Yi; Zhang, Li Zhi; Deng, Yuchun; Jin, Zhaofen "Analysis of thermal performance and energy savings of membrane based heat recovery ventilator", Energy, 25, 515-527 (2000).

3. Johnson, William. B. "Materials and Modules for Low-Cost, High Performance Fuel Cell Humidifiers", DOE Annual Review, Crystal City, VA, May 17, 2012, Oral Presentation FC067, available from www.hydrogen.evergy.gov.

4. Collette, Floraine M.; Lorentz, Chantal; Gebel, Gerard; Thominette, Francette, "Hygrothermal aging of Nafion", Journal of Membrane Science, 330(1-2), 21-29 (2009).

5. Collette, Floraine M.; Thominette, Francette; Escribano, Sylvie; Ravachol, Angèle; Morin, Arnaud; Gebel, G., "Fuel cell rejuvenation of hygrothermally aged Nafion", Journal of Power Sources, 202, 126-133 (2012).

V.H.2 Roots Air Management System with Integrated Expander

Dale Stretch (Primary Contact), William Eybergen, Brad Wright
Eaton Corporation
W126N7250 Flint Drive
Menomonee Falls, WI 53051-4404
Phone: (248) 226-6799
Email: DaleAStretch@Eaton.com

DOE Manager
Jason Marcinkoski
Phone: (202) 586-7466
Email: Jason.Marcinkoski@ee.doe.gov

Contract Number: DE-EE0005665

Subcontractors
- Ballard Power Systems, Burnaby, BC, Canada
- Kettering University, Flint, MI
- Electricore, Inc., Valencia, CA

Project Start Date: July 5, 2012
Project End Date: August 31, 2015

Overall Objectives

Primary Objectives

- 62/64% (base 2011) >65/70% (target 2017) compressor/expander efficiency at 25% of full flow
- 80% (base 2011) >90% (target 2017) combined motor/motor controller efficiency full flow
- 11.0/17.3 kW (base 2011) <8/14 kW (target 2017) compressor/expander input power at 100% of full flow

Secondary Objectives

- Meeting all 2017 project target objectives in Table 1.
- Conduct a cost reduction analysis to identify areas for additional possible cost reductions.

A fully tested and validated TRL 7 air management system hardware capable of meeting the 2017 Project Targets in Table 1 will be delivered at the conclusion of this project.

Fiscal Year (FY) 2014 Objectives

- Continue to optimize the peak efficiency island of the compressor and expander to best fit the primary objectives listed above.
- Continue to use computational fluid dynamics (CFD) capability to optimize the compressor and expander inlet, outlet and rotor geometry for peak efficiency.
- Continue to develop plastic expander rotors with required twist angles.
- Finalize the compressor/expander and motor design, create detailed drawing package and procure prototype hardware.
- Develop finalized production cost estimates.
- Conduct performance and validation testing on the complete air system per predefined test plan approved by the DOE.

Technical Barriers

This project addresses the following technical barriers from the Fuel Cells section of the Fuel Cell Technologies Office Multi-Year Research, Development, and Demonstration Plan:

(B) Cost: Reduce by ~50%

(C) Performance:

- Reduce power by ~30%
- Motor efficiency: Increase by ~40%
- Compressor efficiency: Increase by ~5%
- Expander efficiency: Increase by ~9%

Technical Targets

A fully tested and validated TRL 7 air management system hardware capable of meeting the 2017 project targets in Table 1 delivered at project conclusion.

FY 2014 Accomplishments

CFD Modeling

- CFD modeling of the compressors and expanders was perfected. Tool used to better understand the air flow through, and the performance of, various configurations of expanders and compressors.
- A total of 17 expander geometries and configurations were analyzed. The tool has served to identify the correct inlet and exhaust shape and timing to maximize the torque developed by the expander design.
- Two different compressor rotor geometries were analyzed, a three-lobe and a four-lobe. Significant information was gained on the three-lobe rotor compressor analysis. Lessons learned from modeling were incorporated into the final compressor design.

TABLE 1. 2015 and 2017 Project Targets

Characteristic	Units	Current Status	Project Target 2015	DOE Target 2017
Input power[a] at full flowb (with expander/without expander)	kWe	10.6/14.8	8/14	8/14
Combined motor and motor controller efficiency at full flow[b]	%	93	90	90
Compressor/expander efficiency at full flow (compressor/expander only)[b]	%	65/65	75/75	75/80
Input power at 25% flow[c] (with expander/without expander)	kWe	2.0/2.0	1.0/2.0	1.0/2.0
Combined motor and motor controller efficiency at 25% flow[c]	%	82	80	80
Compressor/expander efficiency at 25% flow[c]	%	65/51	65/70	65/70
Input power at idled (with/without expander)	We	405/405	200/200	200/200
Combined motor/motor controller efficiency at idle[d]	%	50	?	70
Compressor/expander efficiency at idle[d]	%	21	60/60	60/60
Turndown ratio (max/min flow rate)		20	20	20
Noise at maximum flow (excluding air flow noise at air inlet and exhaust)	dB(A) at 1 meter	65 (with enclosure and suppression)	65 (with enclosure and suppression)	65
Transient time for 10-90% of maximum airflow	sec	1	1	1
System volume[e]	liters	10.8	15	15
System weight[e]	kg	15.9	15	15
System cost[f]	$	984	500	500

[a] Electrical input power to motor controller when bench testing fully integrated system. Fully integrated system includes control system electronics, air filter, and any additional air flow that may be used for cooling.
[b] Compressor: 92 g/s flow rate, 2.5 bar (absolute) discharge pressure; 40°C, 25% relative humidity (RH) inlet conditions. Expander: 88 g/s flow rate, 2.2 bar (absolute) inlet pressure, 70°C, 100% RH inlet conditions.
[c] Compressor: 23 g/s flow rate, minimum 1.5 bar (absolute) discharge pressure; 40°C, 25% RH inlet conditions. Expander: 23 g/s flow rate, 1.4 bar (absolute) inlet pressure, 70°C, 100% RH inlet conditions.
[d] Compressor: 4.6 g/s flow rate, minimum 1.2 bar (absolute) discharge pressure; 40°C, 25% RH inlet conditions. Expander: 4.6 g/s flow rate, < compressor discharge pressure, 70°C, 20% RH inlet conditions.
[e] Weight and volume include the motor, motor controller and system enclosure.
[f] Cost target based on a manufacturing volume of 500,000 units per year.

Expander Plastic Rotor

- Procured straight rotor injection molding tool and rotor prototypes.
- Tested straight rotors in expander environment.
- Designed helical shape rotors and mold.

Design

- Designed compressor/expander with integrated motor system configuration was packaged with the finalized compressor and expander designs. The air management system built consists of a 260 compressor, a 210 expander, a 12-turn motor and a 30-kW motor controller. System volume and part count have been reduced over the first design iteration.
- Designed and detailed all part drawings for the optimized 260 compressor for hardware fabrication.
- Designed and detailed all part drawings for the optimized 210 expander for hardware fabrication.

Hardware Procurement

- Defined Ballard fuel cell module test specifications, procedures and acceptance criteria.
- Procured the Ballard fuel cell module.
- Ordered and received the 12-turn motors and 30-kw motor controllers.
- Fabricated the 260 compressor and 210 expander hardware per design.

Hardware Testing.

- Tested the 12-turn motor and controller hardware.

INTRODUCTION

Proton exchange membrane (PEM) fuel cells remain an emerging technology in the vehicle market with several cost and reliability challenges that must be overcome in order to increase market penetration and acceptance. The DOE has identified the lack of cost-effective, reliable,

and efficient air supply systems that meet the operational requirements of a pressurized PEM 80-kW fuel cell are some of the major technological barriers that must be overcome. This project will leverage roots blower advancements and develop and demonstrate an efficient and low-cost fuel cell air management system. Eaton will build upon our newly developed P-Series roots blower and shift the peak efficiency making it ideal for use on an 80-kW PEM module. Advantages to this solution include:

- Lower speed of the roots blower eliminates complex air bearings present on other systems.
- Broad efficiency map of roots systems provide an overall higher drive cycle fuel economy.
- Core roots machine technology has been developed and validated for other transportation applications.

Eaton will modify their novel R340 Twin Vortices Series (TVS) roots-type supercharger for this application. The TVS delivers more power and better fuel economy in a smaller package as compared to other supercharger technologies. By properly matching the helix angle with the rotor's physical aspect ratio the supercharger's peak efficiency can be moved to the operating range where it is most beneficial for the application. The compressor will be designed to meet the 92 g/s flow at a pressure ratio of 2.5, similar in design to the R-Series 340. A net shape plastic expander housing with integrated motor and compressor will significantly reduce the cost of the system.

APPROACH

The approach will be to leverage recent advancements to, and further develop, roots compressor and expander technology by leveraging the broad efficiency map of Eaton's TVS compressor to improve the overall fuel cell drive cycle fuel economy. In period 1, the project will optimize the expander and compressor individually at the specified requirements, with an integrated expander, compressor and motor concept as the final deliverable. The primary goal will be to meet the power and efficiency objects. The secondary objective is to reduce subsystem cost by keeping part count low by developing a net shape plastic expander housing and rotor. This work will be supplemented with CFD analysis to help optimize the expander and compressor performance and system analysis which will help optimize the integrated system

Period 2 will finalize the integrated concept, then build and test the integrated system and individual subsystems. The last phase (3) will be to incorporate the roots air management system with integrated expander into an overall hydrogen and fuel cells application. This will include designing, building and testing the complete system.

RESULTS

The team continued the development of the compressor and expander and finalized the system concept using both experimental and analytical methods.

Compressor Design

The 260 compressor design and fabrication was completed in the last year. The design included the following features:

- Rotors: The rotor set has been optimized for flow performance. High helix angles were used to achieve the higher pressure ratios required by the DOE. The rotors use Eaton's billet aluminum rotor technology to allow for reduced clearances driving up supercharger efficiency.
- Housing: The housing design will feature optimized outlet geometry and an integrated motor adaptor plate. The housing utilizes existing Eaton production seals, bearings, and gears. The timing gears used will be an existing Eaton steel design. Water cooling will be shared with the electric drive motor to increase durability at high pressure ratios.
- Inlet: The inlet has been designed to incorporate the bearing end plate and air inlet with sealed roller bearings into one compact part.

Expander Design

The 210 expander design and fabrication was completed in the last year. The design included the following features:

- Rotors: The rotor set was optimized for minimum leakage. This warranted the implementation of a larger rotor root radius and the use of a higher speed, smaller displacement expander. Two rotor materials will be assessed, a traditional aluminum extrusion construction to minimize complexity and reduce design risk and a new glass-filled plastic rotor over-molded on to a laminated aluminum core as an option to reduce cost and rotating inertia.
- Housing: The latest design incorporates provisions to manufacture the housing in glass reinforced plastic to reduce cost and weight. The housing also features other design improvements such as common shaft, bearing, and seal sizes as well as revised inlet geometry.
- Outlet: The outlet has been designed as a high-temperature plastic part that locates the shaft ends with two incorporated sealed roller bearings with plastic dust covers while maintaining the simplicity of a two-part mold capable part. The rotor outlet timing has been revised to provide for more favorable torque curve, per CFD analysis.
- Gears: The timing gears used will be an existing Eaton plastic/steel hybrid design.

Compressor/Expander with Integrated Motor

The compressor/expander with integrated motor system configuration proposed was achieved through iterative analysis between expander and compressor geometries utilizing actual test data while mathematically correcting for temperature and humidity according to the DOE-specified operating conditions. Effort was placed on effectively matching the expander operating speed to the compressor operating speed at each DOE-specified point. An analytical tool was developed to predict expander power production and operating speed given a known displacement and predicted operating efficiency. This tool compared various expander geometries to tested components in order to find the most appropriate compressor/expander.

Through this process the team concluded that a 260 compressor, a 210 expander, a 12-turn motor supplier motor, and a 30-kW motor supplier controller would be the optimal design that would meet the project technical objectives, Figure 1. This design will contain five shafts and three gears, a modification to the original two shafts and two-gear proposal.

The Phase I air management system performance estimates are listed in Table 1. The parameters listed in this table will be what the final hardware design will be measured against.

System Volume and Part Count

The component and system volumes are within specification and come in at 10.8 liters. The system weight is slightly higher than the targeted 15.0 kg by 0.9 kg but significantly lower than the benchmark weight of 22 kg.

System Design Cost

Eaton worked with Strategic Analysis in generating a preliminary cost for the Eaton air management system. Cost results were estimated at manufacturing rates of 1,000 and 500,000 systems per year. Assembly and manufacturing markup are included in the cost estimate, assuming a 15% markup on all the compressor and expander components and a 10% markup for the motor and motor controller components. The most expensive part of the compressor/expander with integrated motor is the motor controller and motor. The electric motor was considered a purchased component with its cost based on Eaton estimates. The costs for the 500k manufacturing rate are as follows: compressor: $116, expander: $77, motor: $167, motor controller: $360, full assembly and mark-up: $816.

Expander Plastic Rotor

The injection molding tool was completed in September 2013 and first shots occurred in October 2013. Parts filled as predicted in the mold flow analysis with no visual indication of delamination from the aluminum support structure.

Single-rotor testing was conducted at the end of 2013. A single rotor was spun at speeds of 15,000, 17,500 and 20,000 at a constant temperature. Testing was conducted at three temperature set points – 70°C, 90°C and 100°C with dwell times of 5 minutes. The over-molded rotor (Figure 2) was able to achieve the maximum rpm at maximum temperature (20,000 rpm at 110°C) with no evidence of delamination. The next round of testing will include testing to failure to understand material and design capabilities.

CONCLUSIONS AND FUTURE DIRECTIONS

Period 2 Conclusions

- Delivered a design and hardware of the fuel cell air management system (compressor/expander and motor per Figure 1) that is projected to meet the project

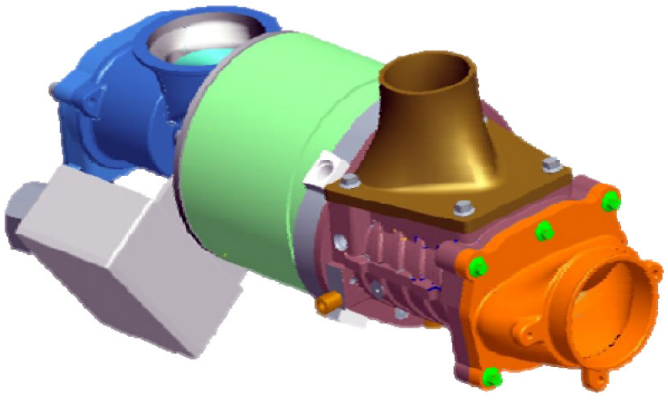

FIGURE 1. Fuel Cell Air System Design

FIGURE 2. As-Molded Rotors

performance targets as stated in the current status section of Table 1.

- Successfully demonstrated straight plastic rotors in compressor environment.
- Successfully demonstrated the capability to use CFD modeling on true dimensional models to predict compressor and expander performance.
- Delivered costing results for complete fuel cell air management system.

Future Directions

- Conduct performance and validation testing at Eaton:
  - Write test plan/determine test criteria
  - Measure and document using maps and Excel data sheets
  - Conduct test at the specified target conditions
  - Document results with performance maps
  - Measure system weight, and volume including motor, controller, and system enclosure
- Conduct performance and validation testing at Ballard:
  - Write test plan/determine test criteria
  - Integrate design, build, and debug unit on Ballard stack
  - Compressor/expander validation testing on Ballard stack
  - Write test report and review Ballard testing

FY 2014 PUBLICATIONS/PRESENTATIONS

Presentations

1. Stretch, Dale, Roots Air Management System with Integrated Expander, U.S. DRIVE Technical Meetings - Fuel Cell Tech Team (FCTT), April 9, 2014.

2. Stretch, Dale, Roots Air Management System with Integrated Expander, DOE Merit Review - Fuel Cell Tech Team (FCTT), June 18, 2014.

V.I.1 Performance of Advanced Automotive Fuel Cell Systems with Heat Rejection Constraints

Rajesh K. Ahluwalia (Primary Contact),
Xiaohua Wang
Argonne National Laboratory
9700 South Cass Avenue
Argonne, IL 60439
Phone: (630) 252-5979
Email: walia@anl.gov

DOE Manager
Nancy Garland
Phone: (202) 586-5673
Email: Nancy.Garland@ee.doe.gov

Project Start Date: October 1, 2003
Project End Date: Project continuation and direction determined annually by DOE

Overall Objectives

- Develop a validated model for automotive fuel cell systems, and use it to assess the status of the technology.
- Conduct studies to improve performance and packaging, to reduce cost, and to identify key R&D issues.
- Compare and assess alternative configurations and systems for transportation and stationary applications.
- Support DOE/U.S. Driving Research and Innovation for Vehicle efficiency and Energy sustainability (U.S. DRIVE) automotive fuel cell development efforts.

Fiscal Year (FY) 2014 Objectives

- Further develop and validate the stack model for membrane electrode assemblies (MEAs) with 3M's nanostructured thin-film (NSTF) catalysts for applicability to hotter and drier operating conditions.
- Develop a methodology to analyze the performance of automotive fuel cells subject to the recently imposed heat rejection constraint ($Q/\Delta T = 1.45$ kW/°C).
- Determine the optimum operating conditions for minimum system cost subject to the $Q/\Delta T$ constraint.
- Provide component specifications and operating conditions to the detailed fuel cell system cost study.

Technical Barriers

This project addresses the following technical barriers from the Fuel Cells section of the Fuel Cell Technologies Office Multi-Year Research, Development, and Demonstration Plan:

(B) Cost

(C) Performance

Technical Targets

This project is conducting system-level analyses to address the following DOE 2020 technical targets for automotive fuel cell power systems operating on direct hydrogen:

- Energy efficiency: 60% at 25% of rated power
- $Q/\Delta T$: 1.45 kW/°C
- Power density: 650 W/L for system, 2,500 W/L for stack
- Specific power: 650 W/kg for system, 2,000 W/kg for stack
- Transient response: 1 s from 10% to 90% of rated power
- Start-up time: 30 s from –20°C and 5 s from +20°C ambient temperature
- Precious metal content: 0.125 g/kW

FY 2014 Accomplishments

- Collaborated with 3M in taking cell data to validate the model for NSTF catalyst-based MEAs and stacks.
- Developed a correlation for limiting current densities for MEAs with PtCoMn/NSTF catalyst.
- Developed a rational model for mass transfer overpotentials in PtCoMn/NSTF cathode catalyst.
- Validated the cell model over a wide range of operating pressures, temperatures, relative humidities, and stoichiometries.
- Conducted a comprehensive study to investigate the impact of the heat rejection constraint ($Q/\Delta T$) on fuel cell system operation, performance, and cost.

INTRODUCTION

While different developers are addressing improvements in individual components and subsystems in automotive fuel cell propulsion systems (i.e., cells, stacks, balance-of-plant components), we are using modeling and analysis to address issues of thermal and water management, design-point and

part-load operation, and component-, system-, and vehicle-level efficiency and fuel economy. Such analyses are essential for effective system integration.

APPROACH

Two sets of models are being developed. The GCtool software is a stand-alone code with capabilities for design, off-design, steady-state, transient, and constrained optimization analyses of fuel cell systems. A companion code, GCtool-ENG, has an alternative set of models with a built-in procedure for translation to the MATLAB®/Simulink® platform commonly used in vehicle simulation codes, such as Autonomie.

RESULTS

In FY 2014, we continued to collaborate with 3M to obtain reference performance data on 50-cm^2 active-area single cells using MEAs that consisted of 3M 24-μm membrane (850 equivalent weight), ternary $Pt_{0.68}Co_{0.3}Mn_{0.02}$/NSTF catalyst, and 3M gas diffusion layers made by applying a hydrophobic treatment to a backing paper and a micro-porous layer [1]. The Pt loading was 0.050 mg·cm^{-2} in the anode and 0.054, 0.103, 0.146 or 0.186 mg·cm^{-2} in the cathode.

For applicability to hotter and drier conditions, we reanalyzed the available polarization data to develop a rational model for mass transfer overpotentials in ternary PtCoMn/NSTF catalysts. The approach was to first define a limiting current density (i_L) at which the mass transfer overpotential equals a set value of 0.45 V. This limiting current density was determined from the cell polarization data and was correlated as a function of the operating pressure (P), temperature (T), oxygen mole fraction (X_{O2}), relative humidity (RH) and gas velocity in flow channel. Figure 1a compares the i_L correlation with the experimental data for tests at different pressures and temperatures and 100% RH at cell exit. The accuracy of the correlation could be improved if the experimental data were obtained in differential cells or if the tests were run at high stoichiometries with one variable changing at a time.

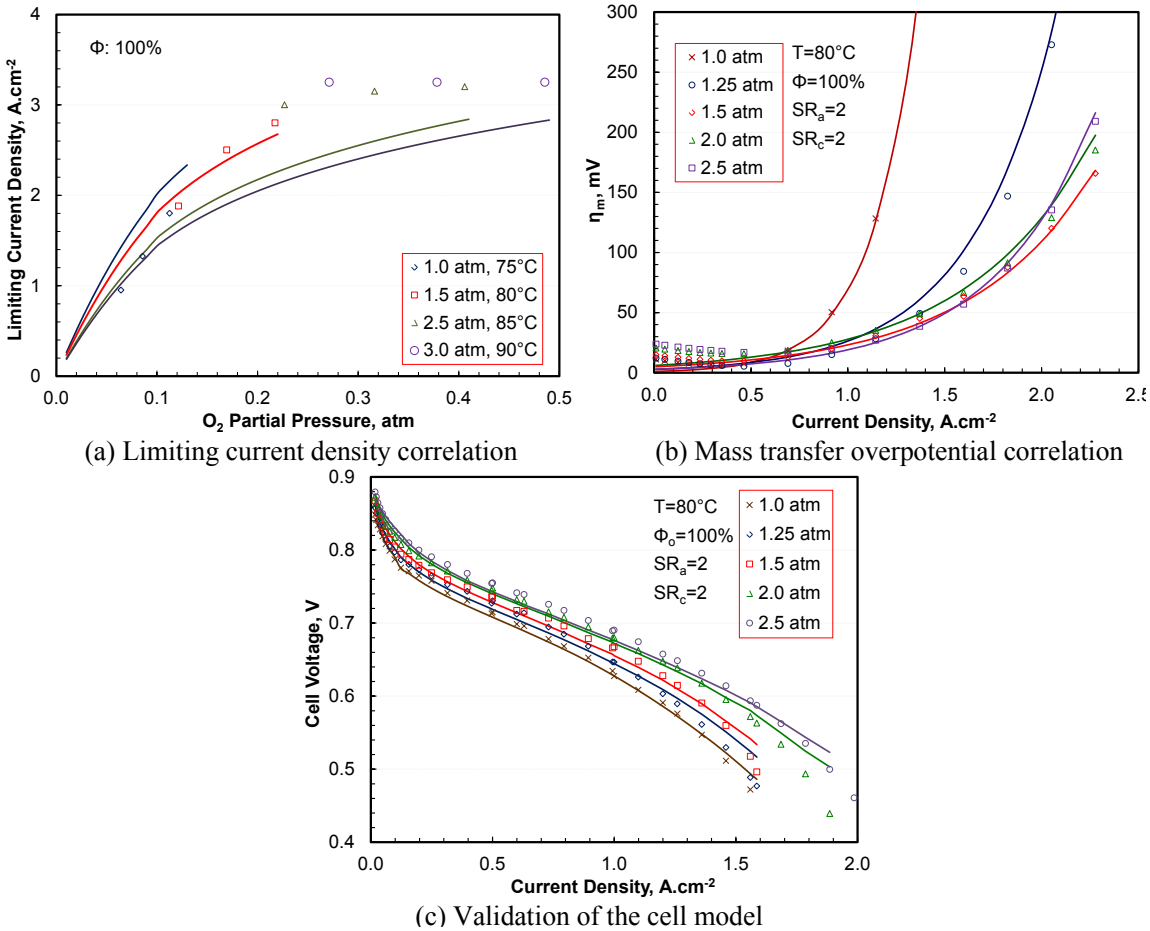

(a) Limiting current density correlation

(b) Mass transfer overpotential correlation

(c) Validation of the cell model

FIGURE 1. Development and validation of the cell performance model. The data are shown for 100% RH (Φ) and a cell with 3M MEA and ternary PtCoMn/NSTF catalysts. Pt loading is 0.104 mg_{Pt}·cm^{-2} in the cathode and 0.05 mg_{Pt}·cm^{-2} in the anode.

The second step was to correlate the mass transfer overpotential (η_m) in terms of the reduced current density (i/i_L), i.e., the current density (i) normalized by i_L. Second order terms were included in the η_m correlation to correct for P, T, X_{O2}, RH, and gas velocity. Figure 1b compares the correlation with the experimental data for one series of tests in which the exit pressure was changed from 1 atm to 2.5 atm. The comparison is equally good for other series of tests with T, RH, and anode/cathode stoichiometric ratio (SR) as variables.

The rational model for η_m was incorporated in the multi-nodal cell model that also has modules for calculating the activation overpotentials for the oxygen reduction reaction on cathode [1] and hydrogen oxidation reaction on anode [2]; anode mass transfer overpotentials because of nitrogen buildup; and ohmic overpotentials in the membrane, gas diffusion layer, and membrane/gas diffusion layer interface. Figure 1c compares the model results with the experimental polarization curves for the pressure series of tests as in Figure 1b. The comparison is equally good for other series of tests with T, RH, and anode/cathode SR as variables.

System Performance

The updated cell model was used to analyze the performance of an 80-kW_{net} fuel cell system (see Refs. [3,4] for system configuration) with ternary PtCoMn/NSTF catalysts in the polymer electrolyte fuel cell (PEFC) stack. Table 1 lists the important parameters of the components comprising the stack, fuel management system, air management system, heat rejection system, and water management system. An optimization study was conducted to determine the coolant exit temperature (limited to 95°C), dew point temperature of cathode air at stack inlet, and cell voltage for minimum system cost, subject to the Q/ΔT constraint of 1.45 kW/°C, for specified Pt loading in anode and cathode catalysts. Here Q is the stack heat load and ΔT is the difference between the coolant stack outlet temperature and the ambient (heat sink) temperature taken as 40°C. For comparison with previous results, the study was repeated for 100% stack exit RH.

The physical coupling of the PEFC stack and the upstream membrane humidifier determines the approach dew point temperature at cathode inlet and establishes the relationship between the optimum stack coolant exit temperature (T_c) and cathode stoichiometric ratio (SR_c) as a function of the stack operating pressure. For 100% stack exit RH, T_c is limited to 82°C at 1.5 atm, 87°C at 2 atm, 92°C at 2.5 atm, and 95°C at 3 atm, if SR_c is held at 1.5; T_c is lower, especially at low operating pressures (8°C lower at 1.5 atm), if SR_c is raised to 2.5. Without any restriction on stack exit RH, T_c increases to 90°C at 1.5 atm for a SR_c of 1.5.

Figure 2 shows the cell voltage and the corresponding system efficiency needed at rated power to satisfy the Q/ΔT constraint. The results indicate that low stack inlet pressures (1.5 atm) with 100% exit RH may not be acceptable because the coolant exit temperature is restricted to <82°C, ΔT to <42°C, and Q to <61 kW, so that the required cell voltage has to be >740 mV. The required cell voltage at 1.5 atm stack inlet pressure is 65 mV lower if the stack is operated hotter (90°C vs. 82°C) and drier (83% RH vs. 100% RH). Over the range of SR_c investigated, 1.5–2.5, the required cell voltage is lowest at SR_c of 1.5.

TABLE 1. Critical Parameters for Various Components of the Fuel Cell System

PEFC Stack
- 1.5 -3 atm at rated power
- 40 -67% O_2 utilization (SR_c: 1.5 -2.5)
- 50% H_2 consumption per pass
- Cell voltage at rated power: TBD
- 24 -μm 3M membrane at TBD temperature
- 3M ternary alloy: 0.1/0.05 mg -Pt/cm^2 on cathode/anode
- GDL: 235 -μm non - woven carbon fiber with MPL
- 1.1 -mm metal bipolar plates, each with cooling channels
- 17 cells/inch

Fuel Management System
- Hybrid ejector - recirculation pump
- 35% pump efficiency
- 3 psi pressure drop at rated power

Air Management System
- Compressor -expander module
- Liquid -cooled motor
- Efficiencies at rated power: 71% compressor, 73% expander, 89.5% motor, 89.5% controller
- Turn -down: 20
- 5 psi pressure drop at rated power

Heat Rejection System
- Two circuits: 75 -95 °C HT, 10 °C ΔT 65 °C LT coolant, 5° C ΔT
- 55% pump + 92% motor efficiency
- 45% blower + 92% motor efficiency
- 10 psi pressure drop in the stack and 5 psi pressure drop in the radiator

Water Management System
- Membrane humidifier, TBD dew -point temperature at rated power

TBD – to be determined; GDL – gas diffusion layer; LT – low temperature ; MPL - microporous layer; HT - high temperature

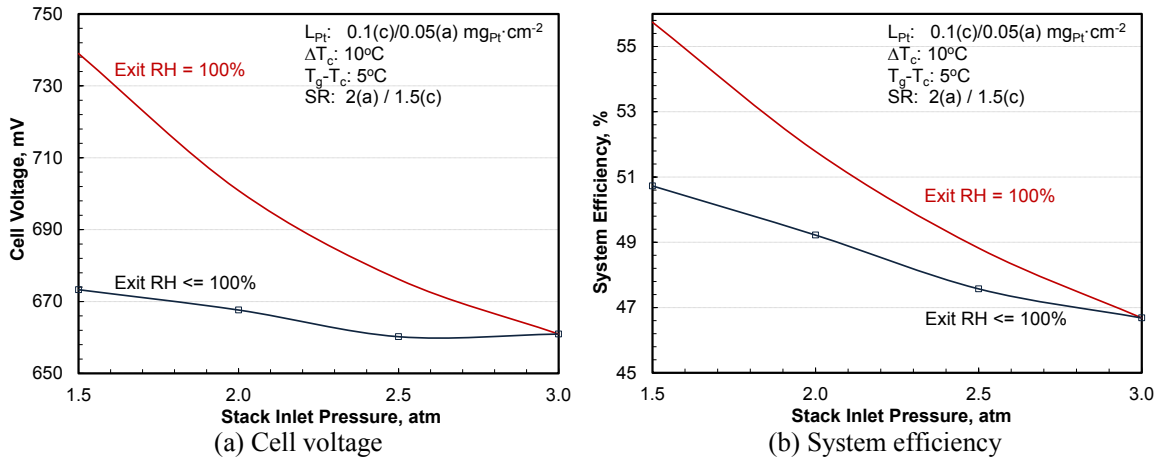

FIGURE 2. Cell Voltage and the Corresponding System Efficiency Needed to meet the Q/ΔT Constraint at Different Stack Inlet Pressures

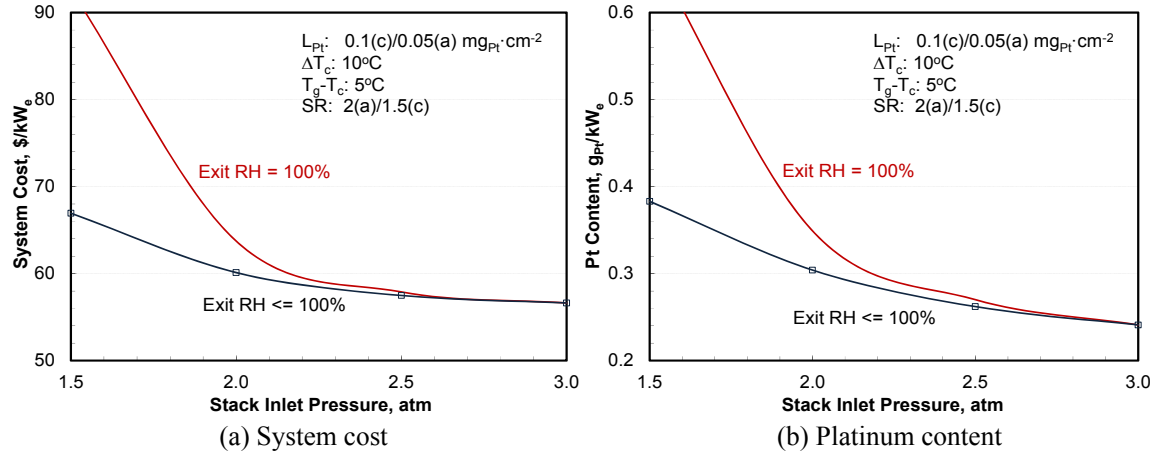

FIGURE 3. Results of an optimization study for minimum system cost subject to Q/ΔT constraint. The various symbols in the legend are for anode (a) and cathode (c) Pt loadings (L_{Pt}), coolant temperature rise in stack (ΔT_c), difference in MEA and coolant temperatures (T_g-T_c) and anode and cathode SRs.

Figure 2a indicates that, for 100% exit RH and SR_c of 1.5, the required cell voltage decreases sharply as the stack inlet pressure is raised from 1.5 atm to 3 atm. This decrease in required cell voltage is slower if the cathode exit RH is optimized and not restricted to 100%. The stack power density is <500 mW·cm^{-2} for stack operating pressures below 1.8 to 2 atm. The difference in power densities for restricted (100%) and unrestricted (<100%) RH diminishes as the stack inlet pressure is raised above 2.5 atm since, even without the RH restriction, the optimum cathode exit RH approaches 100%.

Figure 2b presents the power conversion efficiency (lower heating value basis) that the fuel cell system must have in order to meet the Q/ΔT constraint at rated power. Imposing the heat rejection constraint makes the system efficiency at rated power a function of the operating pressure. The required efficiency is lower (desired result) at higher stack inlet pressures or if the cathode exit RH is less than 100% (although there are durability implications). Note that the anode outlet may contain condensed water; the stack heat load includes this latent heat and the sensible heat loads due to rise in gas temperatures in addition to the waste heat generated (related to cell voltage) by the thermodynamic irreversibilities in the cell electrochemical reactions (i.e., cell overpotentials).

Figure 3 presents the system cost ($/kW$_e$) and Pt content (g/kW$_e$) under optimum operating conditions. The system cost in this study has been estimated using correlations provided by Strategic Analysis, Inc. for high-volume manufacturing (500,000 units/year) and a Pt price of $1,500/tr-oz [5]. Consistent with the results in Figure 2a, the differences in system cost and Pt content between saturated (RH = 100%) and superheated (RH < 100%) cathode exits are large at low operating pressures and diminish at higher

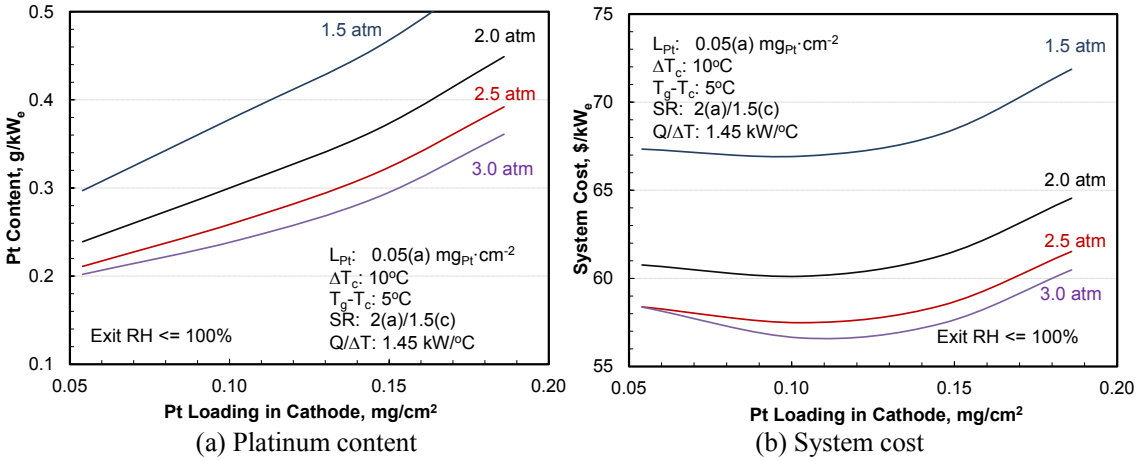

FIGURE 4. Pt Content and System Cost as Function of Pt Loading in Cathode Catalyst, 2.5-atm Stack Inlet Pressure

operating pressures. The lowest system cost is at 3-atm stack inlet pressure, although the cost saving is small compared to 2.5-atm stack inlet pressure. The optimum cathode exit RH is >95% if the stack inlet pressure is higher than 2.5 atm, and it is <83% if the inlet pressure is 1.5 atm.

A parametric study was conducted to determine the optimum Pt loading in the cathode catalyst for 2.5-atm stack inlet pressure. Figure 4a shows that the cathode with the smallest Pt loading considered in this study (0.054 $mg_{Pt}\cdot cm^{-2}$) has the lowest Pt content but also the lowest power density (see Table 2). The system cost is lowest for cathode Pt loading between 0.1 and 0.125 $mg\cdot cm^{-2}$, although the power density is highest for 0.146 $mg\cdot cm^{-2}$ Pt loading (see Table 2). The optimum Pt loading in cathode would be higher if the Pt price was $1,100/tr-oz rather than $1,500/tr-oz assumed in this study.

TABLE 2. Effect of Cathode Pt Loading on Stack Performance and Cost

Pt Loading	mg/cm^2	0.054	0.103	0.146	0.186
Power Density	mW/cm^2	541	641	679	660
Pt Cost	$\$/kW_e$	10.2	12.6	15.3	18.9
Stack Cost	$\$/kW_e$	28.8	29.2	31.1	35.1

CONCLUSIONS AND FUTURE DIRECTIONS

- Meeting the Q/ΔT constraint requires that the stack be operated hotter (coolant exit temperature >90°C), drier (stack exit RH <100%), and at elevated pressures (inlet pressures >2 atm).
- Under optimum conditions, the projected Pt content and cost of an 80-kWe fuel cell system that meets the 1.45 kW/ºC constraint are 0.27 g/kW_e and 57.9 $\$/kW_e$. The stack in this system has ternary PtCoMn/NSTF catalysts with Pt loading of 0.104 $mg\cdot cm^{-2}$ in the cathode and 0.05 $mg\cdot cm^{-2}$ in the anode.
- Stack durability under operating conditions needed to meet the heat rejection requirement is a concern. In FY 2015, we will develop a model to investigate the durability of NSTF MEAs under an automotive duty cycle that includes heat rejection at peak power.
- In FY 2015, we will continue to evaluate alternative advanced catalysts on NSTF and corrosion-resistant carbon supports. We will also continue our collaboration with Eaton on developing and modeling a Roots air management system.

FY 2014 PUBLICATIONS/PRESENTATIONS

1. R.K. Ahluwalia, S. Arisetty, J-K Peng, R. Subbaraman, X. Wang, N. Kariuki, D.J. Myers, R. Mukundan, R. Borup, and O. Polevaya, "Dynamics of Particle Growth and Electrochemical Surface Area Loss due to Platinum Dissolution," Journal of the Electrochemical Society, 161 (3) F291-F304 (2013).

2. S. Ahmed, D.P. Papadias, and R.K. Ahluwalia, "Configuring a Fuel Cell based Residential Combined Heat and Power System," Journal of Power Sources, 242, 884-894 (2013).

3. D.D. Papadias, R.K. Ahluwalia, J.K. Thomson, H.M. Meyer III, M.P. Brady, H. Wang, R. Mukundan, and R. Borup, "Degradation of SS316L Bipolar Plates in Fuel Cell Environment: Corrosion Rate, Barrier Film Formation Kinetics and Contact Resistance," accepted for publication in Journal of Power Sources, (2014).

4. T.Q. Hua, R.K. Ahluwalia, L. Eudy, G. Singer, B. Jermer, N. Asselin-Miller and T. Patterson, "Status of Hydrogen Fuel Cell Electric Buses Worldwide," submitted to Journal of Power Sources, (2014).

5. N. Garland and R.K. Ahluwalia, "Report from the Annexes: Annex 26," IEA AFC ExCo 46th Meeting, Salzburg, Austria, May 22-23, 2013.

REFERENCES

1. R.K. Ahluwalia, X. Wang, A. Lajunen, A.J. Steinbach, S.M. Hendricks, M.J. Kurkowski, and M.K. Debe, "Kinetics of Oxygen Reduction Reaction on Nanostructured Thin-Film Platinum Alloy Catalyst," J. Power Sources, 215, 77-88, 2012.

2. X. Wang, R.K. Ahluwalia, and A.J. Steinbach, "Kinetics of Hydrogen Oxidation and Hydrogen Evolution Reactions on Nanostructured Thin-Film Platinum Alloy Catalyst," J. Electrochemical Society, 160 (3) F251-F261, 2013.

3. R.K. Ahluwalia, X. Wang, J. Kwon, and A. Rousseau, "Drive-Cycle Performance and Life-Cycle Costs of Automotive Fuel Cell Systems," 2011 Fuel Cell Seminar & Exposition, Orlando, FL, October 31 – November 2, 2011.

4. R.K. Ahluwalia, X. Wang, J. Kwon, A. Rousseau, J. Kalinoski, B. James, and J. Marcinkoski, "Performance and Cost of Automotive Fuel Cell Systems with Ultra-Low Platinum Loadings," J. Power Sources, 196, 4619, 2011.

5. B.D. James, J.A. Kalinoski, and K.N. Baum, "Mass Production Cost Estimation for Direct H_2 PEM Fuel Cell Systems for Automotive Applications: 2009 Update," DTI Report GS-10F-0099J, January 2010.

V.I.2 Fuel Cell Transportation Cost Analysis

Brian D. James (Primary Contact), Jennie M. Moton, Whitney G. Colella
Strategic Analysis, Inc. (SA)
4075 Wilson Blvd., Suite 200
Arlington, VA 22203
Phone: (703) 778-7114
Email: bjames@sainc.com

DOE Managers
Jason Marcinkoski
Phone: (202) 586-7466
Email: Jason.Marcinkoski@ee.doe.gov
Reg Tyler
Phone: (720) 356-1805
Email: Reginald.Tyler@ee.doe.gov

Contract Number: DE-EE0005236

Project Start Date: September 30, 2011
Project End Date: September 30, 2016

Overall Objectives

- Define low-temperature proton exchange membrane (PEM) fuel cell power system operational and physical characteristics that reflect the current status of system performance and fabrication technologies.
- Estimate the production cost of the fuel cell systems (FCSs) for automotive and bus applications at multiple rates of annual production.
- Identify key cost drivers of these systems and pathways to further cost reduction.

Fiscal Year (FY) 2014 Objectives

- Update 2013 automotive and bus FCS cost projections to reflect latest performance data and system design information.
- Define design and analyze cost of alternate catalyst fabrication and application methods.
- Define design and analyze cost of alternate compressor-expander-motor (CEM) systems.

Technical Barriers

This project addresses the following technical barriers from the Fuel Cells section of the Fuel Cell Technologies Office Multi-Year Research, Development, and Demonstration Plan:

(B) Cost

Technical Targets

This project conducts cost modeling to attain realistic, process-based system costs estimates for integrated transportation FCSs operating on hydrogen. These values can help inform future technical targets:

- DOE fuel cell system cost target: $40/kWe in 2020
- DOE fuel cell system ultimate cost target: $30/kWe

FY 2014 Accomplishments

- Updated automotive FCS cost analysis to include the most up-to-date fuel cell stack performance data provided by Argonne National Laboratory (ANL).
- Projected the fuel cell power system cost for an 80-kW light-duty vehicle application using a Design for Manufacturing and Assembly (DFMA®) methodology at an annual production rate of 500,000 FCSs per year.
- Projected the cost of a 160 kilowatt-electric (kWe) FCS for a bus at 1,000 systems per year.
- Analyzed a platinum, nickel, and carbon (PtNiC) de-alloyed catalyst fabrication process with greater detail for Pt recycle cost.
- Analyzed an Eaton-style Roots technology air compressor unit for the automotive and bus systems.

INTRODUCTION

FCSs for transportation applications are a longstanding area of fuel cell product development. Numerous prototype vehicles exist for a variety of transportation applications and research continues into improving the competitiveness of fuel cells as compared to the internal combustion engine. To better assess the potential usefulness and market-worthiness of fuel cells for transportation applications, this work describes a DFMA®-style [1] analysis of the cost to manufacture two different transportation FCSs. The systems analyzed are low-temperature PEM FCSs with peak electrical capacities of 80 kWe for light-duty vehicle (automobile) applications and 160 kWe for 40-foot transit bus applications. The FCSs consume a hydrogen gas fuel stream from an onboard compressed hydrogen storage system (not part of this analysis). The impact of annual production rate on the cost of the automotive and bus systems is examined to assess the difference between a nascent and a mature product manufacturing base. The annual production rates analyzed are 1,000, 10,000, 30,000, 80,000, 100,000, and 500,000 FCSs per year for automotive systems and 200, 400, 800, and 1,000 systems per year for the bus systems.

This work focuses primarily on the efforts to update the existing DFMA® cost model of the automobile FCS as well as efforts to design and cost-model the bus FCS. These systems' stack and balance of plant designs and performance parameters are discussed and the methods of cost-modeling each explained. New technologies, materials data, and optimization modeling are incorporated to give an up-to-date value for system cost. Cost trends are evaluated in terms of the capital costs per unit of installed electrical capacity ($/kWe) and system annual production rate.

APPROACH

A DFMA®-style analysis is conducted to attain cost estimates of PEM FCSs for automobiles and buses at various manufacturing production rates. Fuel cell stack polarization performance is supplied by ANL and included in the PEM FCS performance and cost model. In addition, industry partners provide feedback on the design, materials, and manufacturing and assembly of FCS components and overall system. Fuel cell stack polarization performance is based on output from a detailed, first principals stack model created by ANL and validated against 3M nano-structured, thin film (NSTF) MEA performance. Output from the detailed ANL model is used to create a simplified stack polarization model that returns predicted current density for a specified cell voltage, stack pressure, cathode Pt catalyst loading, air stoichiometry, and stack outlet coolant temperature. This simplified 5-variable model is incorporated into the overall FCS cost model to allow complete flexibility in specification of stack operating conditions. A sweep over the entire potential stack operating condition design space can then be used to determine conditions that lead to the lowest system cost. The FCS is sized based on rated power operating parameters. System performance is based on performance estimates of individual components, built up into an overall system energy budget. Overall system and component performance are cross-checked against estimates made by the ANL detailed models [2].

DFMA® process-based cost estimation techniques are applied to the major system components (and other specialty components) such as the fuel cell stack, membrane humidifier, air CEM unit, and hydrogen recirculation ejectors. For each of these, a manufacturing process train detailed the specific manufacturing and assembly machinery, and processing conditions are identified and used to assess component cost. For the 2014 analysis, full DFMA® analyses were conducted on the PtNiC de-alloyed catalyst fabrication and on the Eaton-style CEM unit. (DFMA® analysis was not conducted on the motor component, rather, motor cost was based on a vendor quotation.)

For lower cost components such as valves, heat exchangers, sensors, and piping, a less detailed method of cost estimate is applied. These methods include simplified DFMA®-style techniques or price quotations from vendors. An approach of frequent communication with vendors to obtain price quotes, and to discuss component design characteristics and manufacturing methods, is used to ensure the validity of the assumptions used in the cost estimates.

RESULTS

The 2014 analysis is out of phase with the annual reporting schedule and thus 2014 final system costs are not yet available. This was also the case for last year's annual report. Consequently, this report documents a blend of the final 2013 cost results (reported for the first time) and 2014 component results. Substantial progress has been made on analyzing alternative component technologies, specifically a de-alloyed PtNiC catalyst and Roots-type air CEM.

The 2013 automotive and bus system models underwent significant changes since 2012. For the automotive system, changes are described in Table 1 with the changes leading to the largest cost impacts being 1) updated polarization data,

TABLE 1. List of Changes between the 2012 and 2013 Final Auto System Cost at 500,000 Systems/Year

Change	Comment	Change from previous value	Cost at 500k sys/year, ($/kW)
2012 Final Cost Estimate		NA	$46.95
Plate Frame Humidifier	Switch to lower volume membrane plate frame humidifier from tube humidifier	$0.51	$47.46
Improved Catalyst Deposition Modeling	Re-examination of NSTF application including wastage and Pt recycle	($0.20)	$47.26
Realigned Compressor and Expander Efficiencies	Air compressor: (75% to 71%) FC air exhaust gas expander: (80% to 73%) Motor: (85% to 80%)	$1.87	$49.13
Updated Material Costs	New 316 SS and other material price quotes	$0.13	$49.26
Updated Quality Control System	To ensure full functionality and improve cost realism	$0.00	$49.26
Increased Platinum Cost	Increase from $1100/oz t to $1500/oz t	$3.19	$52.45
Other Misc. Changes	Improve and correct model i.e. LT and HT loop, CEM, and membrane adjustments	($0.86)	$51.59
Updated Polarization Data, Stack Operating Condition Optimization, and Imposition of Radiator Area Constraints	Improved MEA performance data for 3M NSTF experimental results. Performed stack condition optimization to achieve lowest system cost. Limited radiator Q/ΔT for volume management within the auto.	$3.24	$54.83
Final 2013 Value		**$7.88**	**$54.83**

stack operating condition optimization and imposition of radiator volume constraints; and 2) increase in Pt cost from $1,100/troy ounce (Pt price used between 2006 and 2012) to $1,500/troy ounce (to align with market changes). The 2013 automotive system cost at 500,000 systems per year is $54.83/$kW_{net}$, higher than 2012's projected cost of $46.95/$kW_{net}$. Over the last several years, the projected cost of high-volume manufactured automotive FCS decreased from year to year, however in 2013, the system cost became more expensive.

Similar changes to the auto system were also made for the 160-kW_e bus system with an additional change in non-vertical integration. Vertical integration describes the extent to which a single company conducts many (or all) of the manufacturing/assembly steps from raw materials to finished product. High degrees of vertical integration can be cost efficient by decreasing transportation costs and turn-around times, and reducing nested layers of markup/profit. However, at low manufacturing rates, the advantages of vertical integration may be overwhelmed by the negative impact of low machinery utilization or poor quality control due to inexperience/lack-of-expertise with a particular manufacturing step. For the 2012 analysis, both the automotive and bus fuel cell power plants were cost modeled as if they were highly vertically integrated operations. However for the 2013 analysis, the automotive fuel cell system retains the assumption of high vertical integration but the bus system assumes a non-vertically integrated structure. This is consistent with the much lower production rates of the bus systems (200 to 1,000 systems/year) compared to the auto systems (1,000 to 500,000 systems/year). The effect of non-vertical integration reduced the total bus FCS cost between 2012 and 2013. However, other additional changes (including updated performance operating conditions) caused the total bus FCS cost to increase from $190/$kW_{net}$ to $270/$kW_{net}$ at a manufacturing rate of 1,000 systems per year between 2012 and 2013. As shown in Figure 1, the cost of the 2013 bus system is within the range of the UTC 2010 Target of $200-$350/kW_{net} at 1,000 systems per year.

In previous SA transportation FCS cost studies, the membrane electrode assemblies have been modeled as using a 3M NSTF Pt/cobalt/manganese catalyst. As an alternative to this ternary catalyst, a binary catalyst, de-alloyed PtNiC, was explored. The 3M PtCoMn NSTF remains the 2014 baseline catalyst although the analysis may switch to the de-alloyed PtNiC catalyst in future years after its cost and performance is further experimentally vetted. A flow diagram of the de-alloyed PtNiC processing steps is shown in Figure 2. Processing steps are based on open-source descriptions of Johnson-Matthey de-alloyed catalyst procedures combined with hypothesized materials and operations where information was missing. Thus the manufacturing steps should be viewed as Johnson-Matthey-inspired rather than a duplication of their exact procedures. As shown in Table 2, Pt material cost is the dominant catalyst cost contributor, and represents over 98% of the

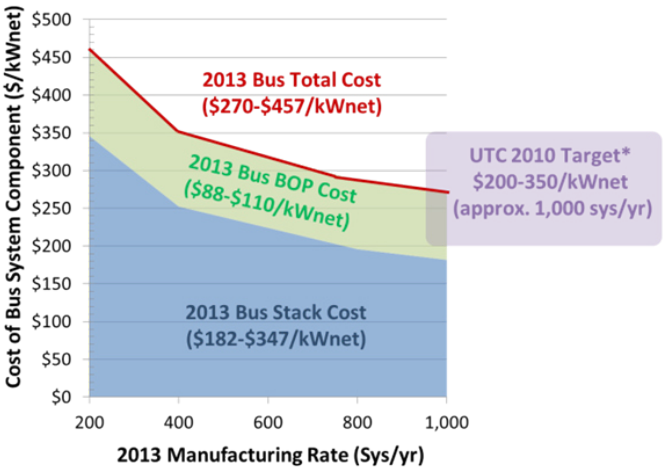

* 2010 DOE AMR Joint DOE/DOT Bus Workshop, "Progress and Challenges for PEM Transit Fleet Applications", Tom Madden, UTC, 7 June 2010: 2010 UTC Preliminary Bus Fleet Cost Target: $200-350/kW in 1,000's per year.

FIGURE 1. DFMA® Cost Results for the 2013 Final Bus System Cost between 200 and 1,000 Systems/Year

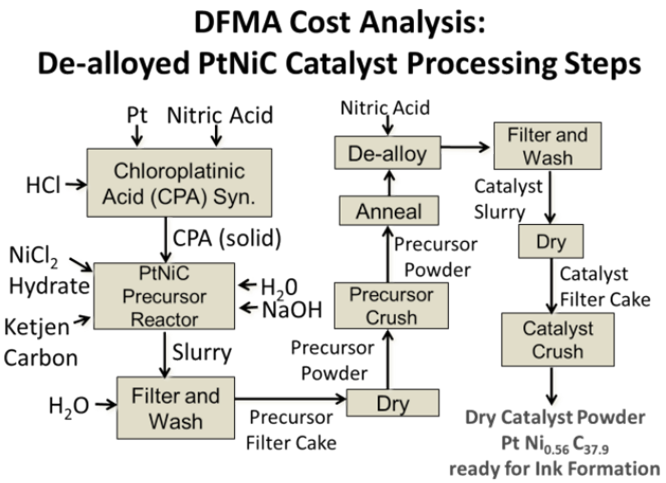

FIGURE 2. DFMA® Cost Analysis of De-Alloyed PtNiC Catalyst Processing Steps

total cost of the de-alloyed PtNiC powder. Other than the Pt material cost, the chloroplatinic acid synthesis and PtNiC precursor reaction (step 1) are the most expensive in materials ($4.26/system at 500,000 systems/year) and manufacturing ($2.75/system at 500,000 systems/year). To understand the possible range in cost for the de-alloyed catalyst fabrication process, a single-variable sensitivity was performed on the PtNiC de-alloyed catalyst system. From this sensitivity study, it is evident that many parameters have only a small impact on the bottom line cost. Vendor quotes indicate that the cost of chloroplatinic acid can be as high as $1/g, much higher than SA's DFMA® projection of ~$0.11/g. Recovering excess

TABLE 2. PtNiC Catalyst Processing Cost Breakdown ($/system)

Component Costs per 80kW$_{net}$ Fuel Cell System	All at 500k Systems per Year			
	Materials	Manuf.	Markup	Total
Platinum Cost	$1,190.35	$0.00	$0.00	$1,190.35
Step 1: Catalyst PtNiC Precursor	$4.26	$2.75	$2.80	$9.80
Step 2: Precursor Filtration	$0.00	$0.19	$0.08	$0.27
Step 3: Precursor Wash	$0.00	$0.03	$0.01	$0.04
Step 4: Precursor Drying	$0.00	$0.31	$0.13	$0.44
Step 5: Precursor Crushing	$0.00	$0.08	$0.03	$0.11
Step 6: Precursor Annealing	$0.00	$0.68	$0.27	$0.95
Step 7: Catalyst De-alloying	$0.99	$0.55	$0.62	$2.16
Step 8: Catalyst Filtration	$0.00	$0.19	$0.08	$0.26
Step 9: Catalyst Wash	$0.00	$0.03	$0.01	$0.04
Step 10: Catalyst Dry	$0.00	$0.22	$0.09	$0.31
Step 11: Catalyst Crushing	$0.00	$0.10	$0.04	$0.14
Total	$1,195.60	$5.13	$4.15	$1,204.88

Pt used in the fabrication process is also vital to the catalyst cost. If no Pt were to be recovered, it would add $0.97/kW$_{net}$ to the baseline cost.

The air compression system for the automotive power system is based on a Honeywell-style centrifugal air compressor mated to a radial inflow exhaust gas expander and a 165,000 rpm permanent magnet motor. In search for alternative and less expensive CEM units, an Eaton-style twin vortex, Roots-type air CEM was analyzed. A complete DFMA® analysis of the Eaton-style CEM was conducted based on a 5-shaft design (2 compressor drive shafts, 2 expander drive shafts, and a motor shaft) consisting of a motor, motor controller, compressor rotors, expander rotors, drive shafts, couplings, bearings, housing, and other components. The design represents SA's interpretation of Eaton technology applied to the particular specifications of the baseline automotive FCS. The baseline compressor is modeled on Eaton's R340 supercharger which is in Eaton's Twin Vortices Series. The unit is a Roots-type supercharger featuring 2 four-lobed rotors, high-flow inlet and outlet ports, and the capability to achieve high efficiency over a wide air flow range. The compressor is mechanically mated to a 20,000 rpm (max) high efficiency brushless motor. The auto Eaton-style air compressor unit (including motor and motor controller) is estimated at $816 at 500,000 units per year. This value incorporates material, manufacturing, and assembly with a 15% Tier 1 markup on compressor and expander components and a 10% Tier 1 markup on the motor and motor controller components.

A cost comparison of the Eaton-style Roots-technology CEM and the Honeywell-style centrifugal-technology CEM is shown in Figure 3. The Eaton-style CEM is observed to be less expensive at lower volumes (1,000 systems/year), and more expensive at higher volumes (500,000 systems/year). This comparison has the following stipulations:

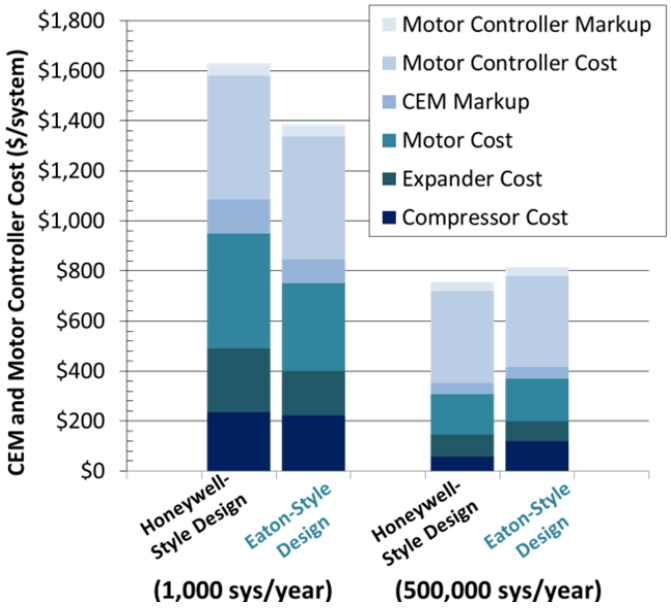

FIGURE 3. Comparison of the DFMA® Cost of Honeywell-Style and Eaton-Style Designs at 1,000 and 500,000 Systems/Year

- Both systems are modeled with the same efficiencies for the compressor, expander, motor, and motor controller.
- The motor controller costs are currently assessed at the same level even though the motors operate at different peak speeds (Eaton-style: 20,000 rpm, Honeywell-style: 165,000 rpm). Future analysis will investigate whether the controller for the Eaton-style system should be lower

cost as the insulated-gate, bipolar transistor switching frequency would be less stringent.

- Motor costs merit further scrutiny as the Eaton motor cost is based on scaled quotes rather than a DFMA® analysis as was used for the Honeywell-style system.

CONCLUSIONS AND FUTURE DIRECTIONS

- 2013 final auto and bus FCS cost results increased from 2012, due to a series of specific analysis and assumption improvements. The 2014 final system cost analysis for the automotive and bus systems are currently underway.
- The 2013 projected system cost of the 160-kWe low-temperature PEM bus FCS is ~$270/kW$_{net}$, and is consistent with other industry estimates. One of the main changes to the bus FCS for 2013 was the implementation of non-vertical integration.
- Other than Pt cost, the PtNiC de-alloyed catalyst cost is dominated by chloroplatinic acid synthesis cost. Pt recovery of greater than 80% is recommended to drive down cost. Future work on the de-alloyed catalyst includes the application to the membrane process and a final comparison to NSTF ternary catalysts, including the impact, if any, of polarization performance differences.
- The cost of the Eaton-style automotive CEM is projected to be $816 per system at 500,000 systems/year. Further 2014 analysis will update this value for recent dimensions and design changes suggested by Eaton.
- Projections of the overall fuel cell power system cost for both automotive and bus applications will be made for the 2014 analysis.

SPECIAL RECOGNITIONS & AWARDS/ PATENTS ISSUED

1. Hydrogen and Fuel Cells Program Award. Awarded to Brian D. James by the Director of the Fuel Cell Technologies Office, Sunita Satyapal, June 17th 2014.

FY 2014 PUBLICATIONS/PRESENTATIONS

1. "Mass Production Cost Estimation of Direct H_2 PEM Fuel Cell Systems for Transportation Applications: 2013 Update", Strategic Analysis Report prepared by Brian D. James, Jennie M. Moton, and Whitney G. Colella, January 2014.

2. James, B.D., Moton, J.M., Colella, W.G., "Fuel Cell Transportation Cost Analysis," Presented at U.S. Department of Energy's 2014 Annual Merit Review and Peer Evaluation Meeting for the Hydrogen and Fuel Cell Technologies Program in Washington, D.C., June 16th–20th, 2014.

3. James, B.D., Moton, J.M., Colella, W.G., "Fuel Cell Transportation Cost Analysis," Presented to DOE Fuel Cell Technology Team in Southfield, MI., July 16th, 2014.

4. James, B.D., Moton, J.M., Colella, W.G., "Design for Manufacturing and Assembly Analysis of Zero Emission Vehicular Power Plants," *Proceedings of the ASME 2014 8th International Conference on Energy Sustainability & 12th Fuel Cell Science, Engineering and Technology Conference (ESFuelCell2014)*, Boston, Massachusetts, June 30th – July 2nd, 2014 (ESFuelCell2014-6656).

5. James, B.D., Moton, J.M., Colella, W.G., "Definition and Cost Evaluation of Fuel Cell Bus and Passenger Vehicle Power Plants," *Presentation at the ASME 2014 8th International Conference on Energy Sustainability & 12th Fuel Cell Science, Engineering and Technology Conference (ESFuelCell2014)*, Boston, Massachusetts, June 30th – July 2nd, 2014.

REFERENCES

1. Boothroyd, G., P. Dewhurst, and W. Knight. "Product Design for Manufacture and Assembly, Second Edition," 2002.

2. Ahluwalia, R. "Fuel Cell Systems Analysis," Argonne National Laboratory, Presentation to DOE Fuel Cell Tech Team, 16 July 2014, Southfield, MI.

V.I.3 Characterization of Fuel Cell Materials

Karren L. More (Primary Contact) and
David A. Cullen
Oak Ridge National Laboratory (ORNL)
1 Bethel Valley Road
Oak Ridge, TN 37831-6064
Phone: (865) 574-7788
Email: morekl1@ornl.gov

DOE Manager
Donna Ho
Phone: (202) 586-8000
Email: Donna.Ho@ee.doe.gov

Project Start Date: October 1, 1999
Project End Date: Project continuation and direction determined annually by DOE

Overall Objectives

- Identify, develop, and optimize novel high-resolution imaging and compositional/chemical analysis techniques, and unique specimen preparation methodologies, for the μm- to sub-Å-scale characterization of material constituents comprising fuel cells (electrocatalysts, supports, ionomer films).
- Understand fundamental relationships between the material constituents within fuel cell membrane electrode assemblies (MEAs) and correlate these data with stability and performance as per guidance/input from the fuel cell community.
- Integrate microstructural characterization within other DOE fuel cell projects.
- Apply advanced analytical and imaging techniques for the evaluation of microstructural and microchemical changes to elucidate microstructure-related degradation mechanisms contributing to fuel cell performance loss.
- Make capabilities and expertise available to broad fuel cell research community.

Fiscal Year (FY) 2014 Objectives

- Establish several new collaborations with fuel cell manufacturers and researchers to identify and quantify fuel cell materials degradation mechanisms and to characterize new fuel cell materials.
- Follow-on to studies conducted in FY 2013 to image (map) and quantify the through-thickness distribution of ionomer thin films within catalyst layers.
- Study microstructural origin of compression/compaction observed in cathode catalyst layers during carbon corrosion accelerated stress tests (ASTs).
- Continue development of in situ electrochemical transmission electron microscopy methods to study degradation of catalyst and support materials.

Technical Barriers

This project addresses the following technical barriers from the Fuel Cells section of the Fuel Cell Technologies Office Multi-Year Research, Development, and Demonstration Plan:

(A) Durability

(C) Performance

Technical Targets

This project is focused on conducting fundamental characterization studies on the stability of individual material constituents comprising fuel cell MEAs. Of primary importance is relating electrode microstructural/material changes occurring during electrochemical aging with measured fuel cell durability and performance. Insights gained through extensive microstructural studies will be applied toward the design and manufacture of catalysts and catalyst supports that meet the DOE 2017 and 2020 targets for integrated proton exchange membrane (PEM) fuel cell power systems and fuel cell stacks operating on direct hydrogen for transportation applications (listed in Table 1).

TABLE 1. Technical Targets: Electrocatalysts for Transportation Applications

Characteristic	Unit	2011 Status	2017 Target	2020 Target
PGM Total Content (both electrodes)	g/kW (rated)	0.19	0.125	0.125
PGM Total Loading	mg PGM/cm^2 electrode area	0.15	0.125	0.125
Loss in Initial Catalytic Activity	% mass activity loss	48	<40	<40
Electrocatalyst Support Stability	% mass activity loss	<10	<10	<10
Mass Activity	A/mg Pt @ 900 mV	0.24	0.44	0.44
Non-PGM Catalyst Activity per Volume of Supported Catalyst	A/cm^2 @ 800 mV	60 (at 0.8 V) 165 (extrapolated from >0.85V)	300	300

PGM – Pt group metal

FY 2014 Accomplishments

- Completed parametric study with General Motors (GM) to identify the proper electron microscopy imaging and analysis conditions to compositionally map and quantify ionomer distributions at multiple length scales within MEAs, e.g., through-thickness distributions within catalyst layers (100-nm level) and surrounding individual pores within catalyst layers (<10-nm level). Results from this study have recently been accepted for publication in the *Journal of The Electrochemical Society* and represents a successful collaboration between ORNL, GM, and Clarkson University.
- Established a new collaboration with Ford to study catalyst dispersions on various catalyst support structures using X-ray photoelectron spectroscopy, high-resolution scanning transmission electron microscopy (STEM), and electron energy loss spectroscopy (EELS).
- Correlated initial Pt dispersions with localized regions of accelerated carbon corrosion in cathode catalyst layers subjected to ASTs, the results of which were used to further quantify observed differences in MEA performance based on the type of carbon support used and provided additional insight regarding cathode thinning mechanisms.
- Collaborated with FuelCell Energy to characterize novel PEM fuel cell membranes and identify degradation mechanisms as a function of aging protocols.
- Initiated collaboration with the University of Tennessee and 3M to characterize the effect of Pt loading on the stability and performance of MEAs prepared with low-surface-area carbon (LSAC) supports. Two students from Tom Zawodzinski's University of Tennessee group work at ORNL to conduct the microscopy studies to identify ionomer distrubutions, Pt dispersions, and degradation mechanisms as a function of Pt loading on LSAC.
- Demonstrated initial in situ electrochemical microscopy results for Pt/C in a dilute H_2SO_4 electrolyte (Pt supported on pyrolyzed carbon nanofibers prepared from polypyrrole supplied by Los Alamos National Laboratory); further optimization of the liquid cell is required to quantify electrochemical behavior.

INTRODUCTION

PEM fuel cells are being developed for future use as efficient, zero-emission power sources. However, the performance of PEM fuel cells degrades with time at elevated temperature and relative humidity during electrochemical aging in automotive and stationary applications. Performance degradation can be directly attributed to the durability of individual material constituents comprising the MEA, including the electrocatalyst, catalyst support, recast ionomer, polymer membrane, and gas diffusion layer/microporous layer. The structural and chemical degradation mechanisms contributing to performance loss have not been fully quantified. The Microstructural Characterization Project at ORNL has been focused on forming collaborative relationships with numerous industrial PEM fuel cell developers/manufacturers, universities, and national laboratories, to apply ORNL's advanced electron microscopy techniques and expertise to characterize as-fabricated (fresh) fuel cell materials (individual constituents and/or materials incorporated in fresh MEAs), MEAs subjected to ASTs designed to degrade specific MEA components, and field-aged MEAs, with the ultimate goal of establishing critical processing-microstructure-performance correlations to elucidate the individual materials changes contributing to measured MEA degradation, performance loss, and failure. Understanding the structural and compositional changes of the materials comprising MEAs during electrochemical aging will allow for the implementation of materials-based mitigation strategies required for optimizing PEM fuel cell durability and performance.

APPROACH

The microstructural characterization task utilizes advanced electron microscopy analysis techniques to characterize the individual material components comprising PEM fuel cells, before and after incorporation into an MEA, and after electrochemical aging. Our approach is focused on identifying and optimizing novel high-resolution imaging and compositional/chemical analysis techniques, and developing unique specimen preparation methodologies, for the µm-to-Å-scale characterization of the material constituents of fuel cell MEAs (electrocatalysts, catalyst supports, recast ionomer films, membranes, etc.) ORNL applies these advanced analytical and imaging techniques for the evaluation of the microstructural and microchemical characteristics of each material constituent and correlates these observations with fuel cell performance (aging studies are conducted at the collaborator's laboratories). These studies are designed to elucidate the materials-based microstructure-related degradation mechanisms contributing to fuel cell performance loss. Most importantly, ORNL is making the techniques and expertise available to fuel cell researchers outside of ORNL via several mechanisms (1) work for others (proprietary) research, (2) ORNL User Facilities (e.g., Center for Nanophase Materials Sciences), and (3) collaborative non-proprietary research projects via the Microstructural Characterization Project that are consistent with ORNL's research activities.

RESULTS

The primary focus of research conducted in FY 2014 has been on identifying the proper microscopy conditions to characterize ionomer distributions at multiple length scales (on the 100-nm scale and the ~5-nm scale) within catalyst layers through collaborations with GM and Ballard. This research was initiated in FY 2013 by studying model systems (Nafion® thin films supported on nanostructured thin film catalysts and silicon substrates) and continued through FY 2014 with studies focused on quantifying the distribution of ionomer layers within MEAs.

Model substrates were initially prepared to identify the proper microscopy imaging and analysis conditions that were required to minimize electron beam damage (primarily radiolysis) during evaluation of the ionomer. The primary microscope variables assessed were the effect of accelerating voltage, electron dose, and specimen temperature on F-loss. Figure 1 summarizes the results of this parametric study for thin Nafion® films (ranging from 5-25 nm thick) and clearly shows that analysis of ionomer films to minimize F-loss should be conducted at higher voltages (200 kV), low electron doses, and with cryogenic cooling (temperatures less than

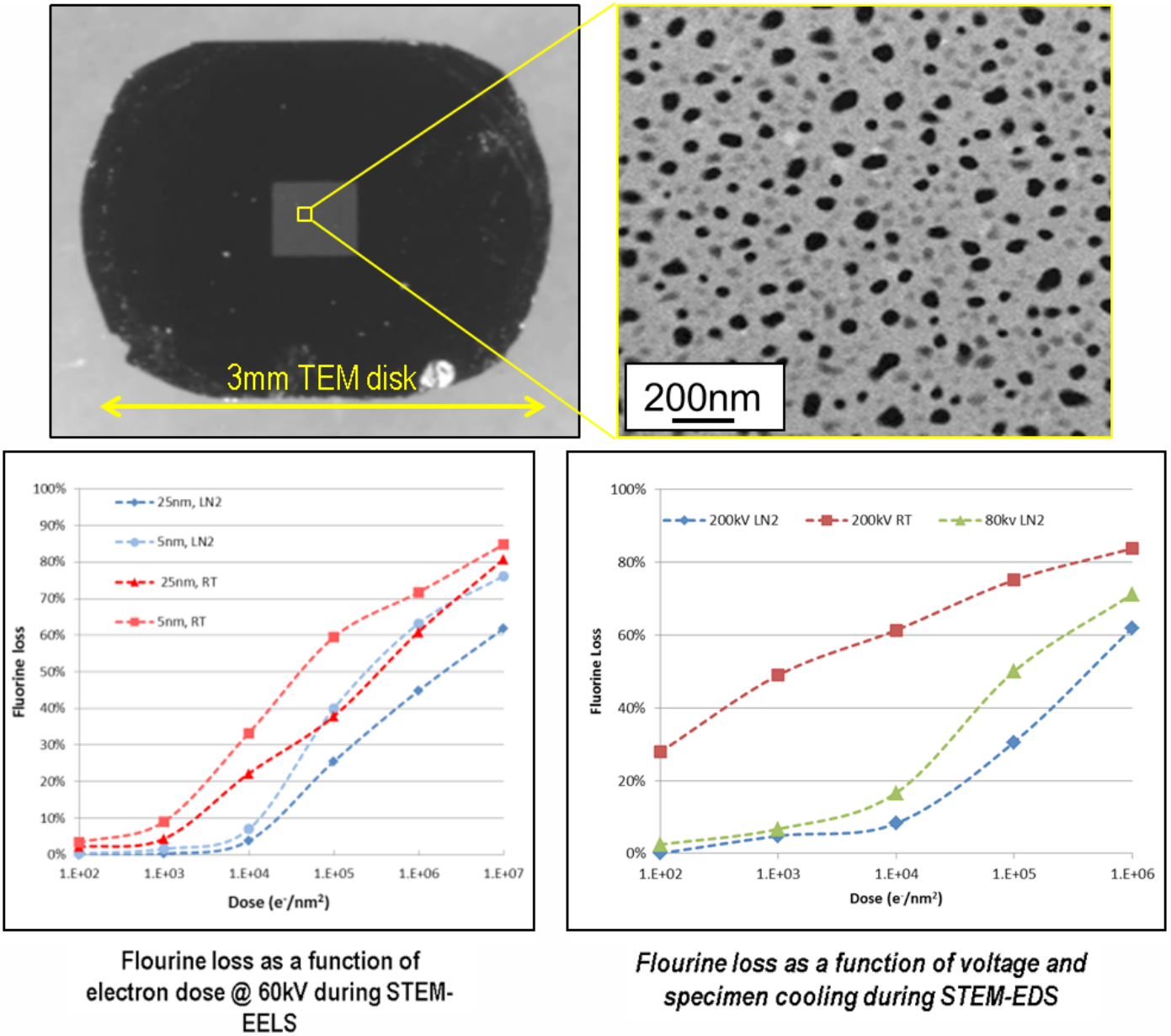

TEM - transmission electron microscope

FIGURE 1. STEM-EELS and STEM-EDS data acquired from Nafion® thin films suspended across nanoporour silicon—microscope parameters (accelerating voltage, electron dose, and specimen temperature) were varied to identify conditions to minimize fluorine loss.

-100°C). When combined, a 2-3X decrease in beam damage can be achieved.

As part of an ongoing collaboration with GM and using the "lessons learned" from the initial Nafion® thin film characterization study using model substrates, the through-electrode-loading variation of the ionomer distributions were studied for two different electrode geometries to understand the effect of underlying microporous layers on the ionomer distribution. The Pt/C electrode layers were coated either on a sacrificial ethylene-tetrafluoroethylene co-polymer decal (catalyst coating on decal or CCD) or directly on the diffusion media (catalyst coating on diffusion media or CCDM). The ionomer/carbon (I/C=1) ratio and the Pt loading were kept constant for both the CCD and CCDM electrodes (same ink formulation was used to prepare both electrodes). Thin cross-sections were prepared by ultramicrotomy, then cryogenically cooled to -105°C in the electron microscope to limit the rate of F-loss under the electron beam. Energy dispersive X-ray spectroscopy (EDS) spectrum images were recorded of each electrode, then quantified to determine the Pt:F ratio through the electrode layer thickness. As shown in Figure 2, two different I/C profiles were observed for the CCD and CCDM samples. The I/C profile for the CCD electrode (green) exhibits a bowed profile, with a higher ionomer loading at both the top and bottom surfaces of the electrode and a slightly lower ionomer content in the center. The CCDM electrode exhibits an overall lower ionomer content (I/C=0.6) as well as a lower local ionomer content at the diffusion media interface, indicating the ionomer is able to easily leach out the back of the electrode and move tens of microns deep into the diffusion media. This case study clearly demonstrates that quantitative ionomer measurements can be performed in STEM by mitigating electron beam damage through controlled electron beam dose, sample cooling, and using high accelerating voltages. This result is comparable to scanning transmission X-ray microscopy performed using a synchrotron source. We are currently working with Adam Hitchcock at McMaster University to directly compare STEM-based analyses with scanning transmission X-ray microscopy acquired on the exact same areas of microtomed samples.

Two spectroscopic techniques, STEM-based EELS and EDS, were used to map and quantify the ionomer distribution within fuel cell electrodes with high spatial resolution such that much finer scale features can be resolved. In collaboration with CEA-Grenoble, France, a large-solid-angle EDS system was used to map C, Pt, and F within a partially embedded CCD electrode with an I/C of 1.5 (Figure 3). Multivariate statistical analysis combined with principal component analysis (PCA) methods were applied to the EDS data to improve the ability to identify small-signal features and identify the chemically relevant components in the spectrum image. The score image or "PCA map" in Figure 3 shows clear resolution of the ionomer strands (less than 10 nm thick and shown for component #2 corresponding to fluorine in green) and larger regions of "clumped" ionomer

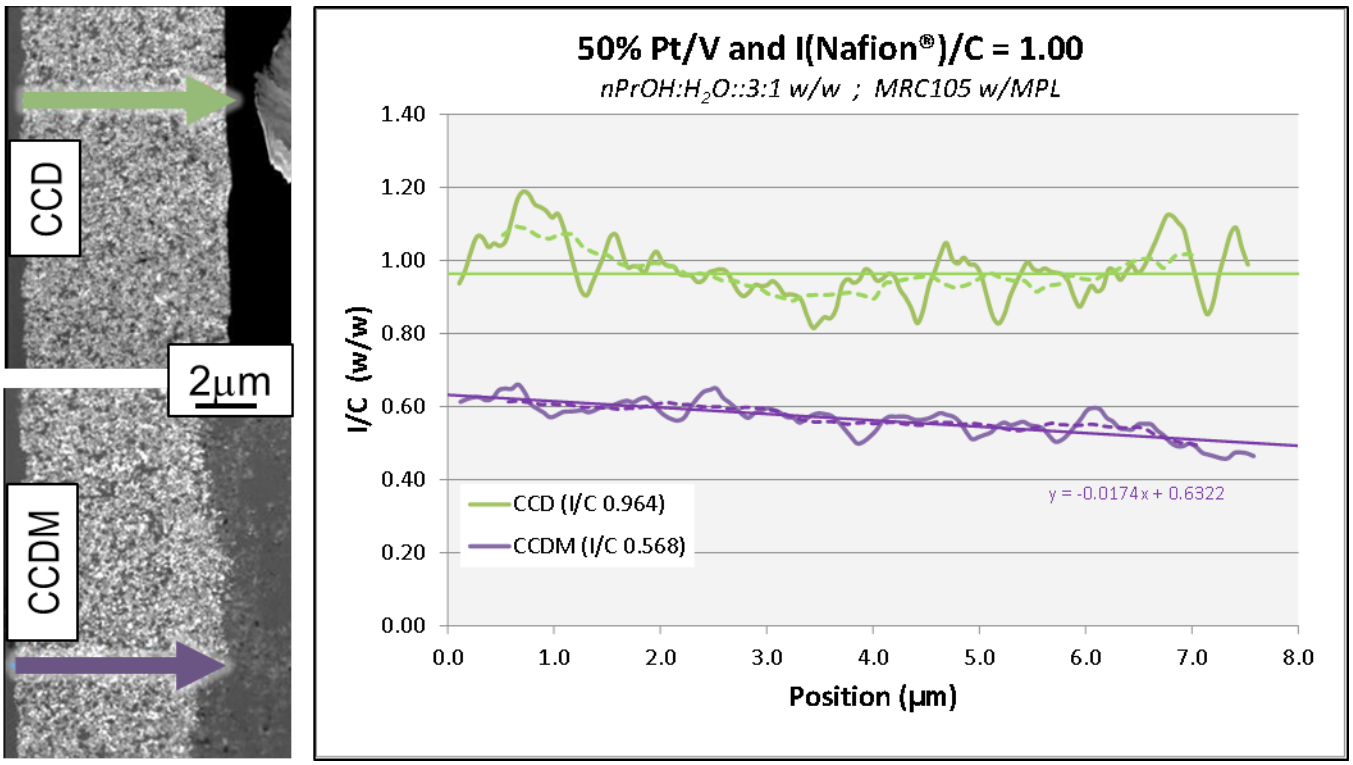

FIGURE 2. I/C profiles (STEM-EDS) acquired across the entire electrode thickness, comparing CCD and CCDM electrode profiles.

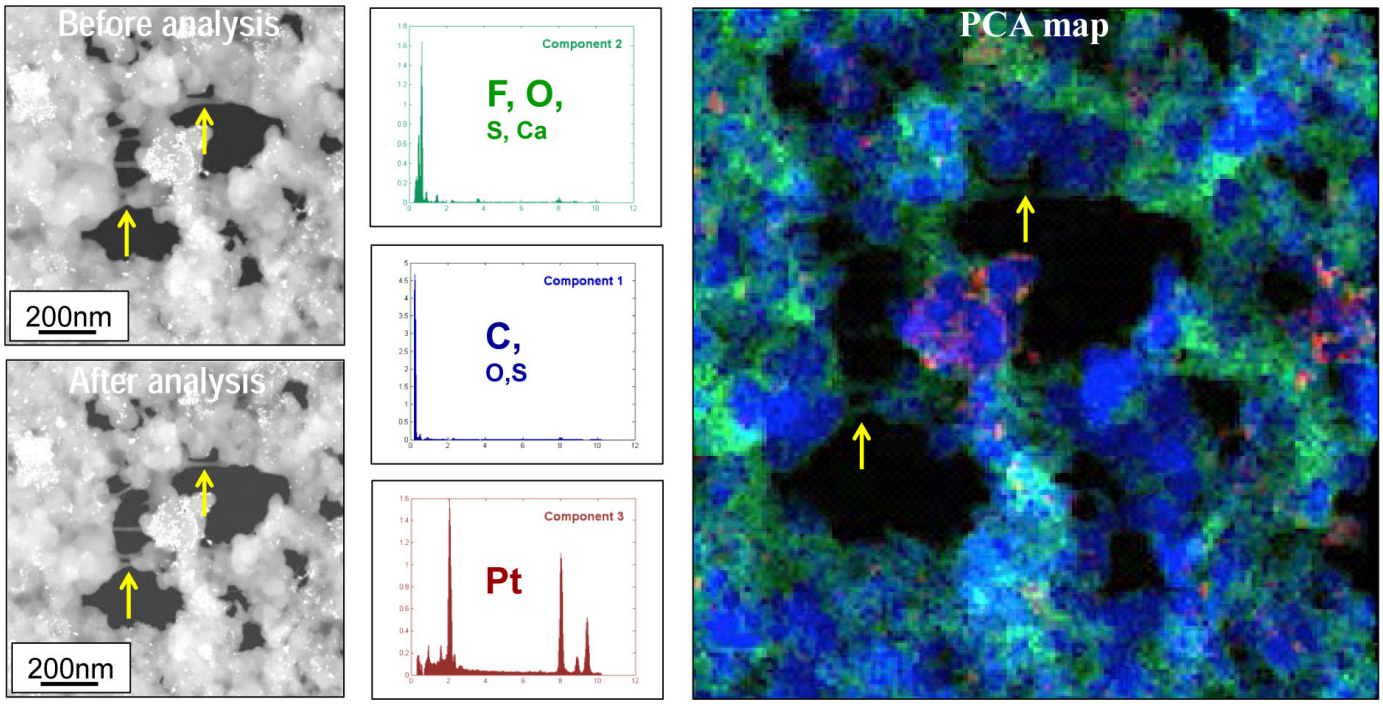

FIGURE 3. EDS Maps Acquired from a Region of a Partially Embedded CCD Electrode (Data acquired in an FEI Osirus TEM/STEM equipped with large solid-angle SDD with pixel size of 5 nm, 200-kV operating voltage, liquid nitrogen cooling, and electron dose of $4X10^6$ e^-/nm^2. Multivariate statistical analysis-PCA methods applied to "denoise" spectra).

and thicker ionomer films on the carbon support (also shown in green).

By utilizing a cryogenic specimen holder, the loss of F due to electron beam interactions was greatly reduced, such that thin strands (<10-nm) of ionomer could be detected and analyzed. By utilizing in-house expertise with PCA, very weak F signals could be amplified, leading to a much clearer view of the thin ionomer films within the electrode. These results show a significant step forward in mapping the ionomer distributions within the electrodes of MEAs with high spatial resolution (<10-nm) in the TEM/STEM.

CONCLUSIONS AND FUTURE DIRECTIONS

ORNL's microstructural studies continue to provide insight regarding the structural and compositional factors of MEA material components that ultimately contribute to the stability and durability of fuel cells. We have focused primarily on characterizing ionomer distributions within catalyst layers, further understanding carbon corrosion mechanisms, and electrocatalyst evaluation during FY 2014, and will continue to support these studies in FY 2015 through collaborations with industrial and academic partners while emphasizing new studies focused on optimizing electrocatalyst interactions and dispersion on novel carbon supports (e.g., LSAC):

- Continue to establish new collaborations with fuel cell manufacturers and researchers to identify and quantify fuel cell materials degradation mechanisms and to characterize new fuel cell materials. Input from the Fuel Cell Tech Team, reviewer comments from the Annual Merit Review, and collaborations are key to the success of this Microstructural Characterization Project and to identify critical research directions.
- Through a systematic study using model systems, the proper imaging and analysis conditions were established for studying ionomer layers and through-thickness ionomer distributions. This work will be expanded in FY 2015 to specifically focus on aging effects within cathode catalyst layers as well as electrode/membrane interfaces.
- Combine ionomer imaging and microanalysis with modeling efforts to identify ionomer interactions with different carbon surfaces (this task has already been initiated). Further characterize ionomer distributions through the use of high-resolution three-dimensional electron tomography studies (both structure and compositional tomography).
- Perform dispersion optimization studies for ionomer and Pt on LSAC.
- Continue the development, optimization, and application of in situ electrochemical TEM/STEM—correlate with bench-scale (rotating disk electrode) catalyst testing and

apply to other fuel cell material components (e.g., Pt on other supports, catalyst nucleation and growth studies, with/without ionomer, etc.).

FY 2014 PUBLICATIONS/PRESENTATIONS

1. G. Wu, K.L. More, P. Xu, H.L. Wang, M. Ferrandon, A.J. Kropf, D.J. Myers, S.G. Ma, C.M. Johnston, and P. Zelenay," *Chemical Communications* 49[32] 3291-3293 (2013).

2. Y. Garsany, A. Epshteyn, K.L. More, and K.E. Swider-Lyons, "Oxygen Electroreduction on a Nanoscale Pt/[$TaOPO_4$/VC] and Pt/[Ta_2O_5/VC] in Alkaline Electrolyte," *ECS Electrochemistry Letters* 2[10] H46-H50 (2013).

3. C.-N. Sun, K.L. More, G.M. Veith, and T.A. Zawodzinski, "Composition Dependence of the Pore Structure and Water Transport of Composite Catalyst Layers," *Journal of the Electrochemical Society* 160[9] F1000-F1005 (2013).

4. M. Li, D.A. Cullen, K. Sasaki, N.S. Marinkovic, K.L. More, and R.R. Adzic, "Ternary Electrocatalysts for Oxidizing Ethanol to Carbon Dioxide: Making Ir Capable of Splitting C-C," *Journal of The American Chemical Society* 135[1] 132-141 (2013).

5. S. Pylypenko, A. Borisevich, K.L. More, A.R. Corpuz, T. Holme, A.A. Dameron, T.S. Olson, H.N. Dihn, T. Gennett, and R. O'Hayre, "Nitrogen: Unraveling the Secret to Stable Carbon-supported Pt-alloy Electrocatalysts," *Energy & Environmental Science* 6[10] 2957-2964 (2013).

6. K.A. Perry, K.L. More, E.A. Payzant, R.A. Meisner, B.G. Sumpter, and B.C. Benicewicz, "A Comparative Study of Phosphoric Acid-doped m-PBI Membranes," *Journal of Polymer Science B* 52[1] 26-35 (2014).

7. C. Chen, Y.J. Kang, Z.Y. Huo, Z.W. Zhu, W.Y. Huang, H.L.L. Xin, J.D. Snyder, D.G. Li, J.A. Herron, M. Mavrikakis, M. Chi, K.L. More, Y.D. Li, N.M. Markovic, G.A. Somorjai, P.D. Yang, and V.R. Stamenkovic, "Highly Crystalline Multimetallic Nanoframes with 3D Electrocatalytic Surfaces," *Science* 343[6177] 1339-1343 (2014).

8. W. Gao, G. Wu, M.T. Janicke, D.A. Cullen, R. Mukundan, J.K. Baldwin, E.L. Brosha, C. Galande, P.M. Ajayan, K.L. More, A.M. Dattelbaum, and P. Zelenay, "Ozonated Graphene Oxide Film as a Proton Exchange Membrane," *Angewandte Chemie International Edition* 53[14] 3588-3593 (2014).

9. Invited Presentation: K.L. More, D.A. Cullen, and K.S. Reeves, "Application of Advanced Microscopy to Elucidate Materials Degradation Mechanisms in PEM Fuel Cells," TMS Pacific Rim Conference on Advanced Materials, Waikaloa, HI - August 4–8, 2013.

10. Invited Presentation: D.A. Cullen, H.M. Meyer, K.S. Reeves, D. Coffey, and K.L. More, "Developing Fuel Cell Technologies Through Electron Microscopy," Microscopy & Microanalysis 2013, Indianapolis, IN - August 4–8, 2013.

11. Invited Presentation: K.L. More, D.A. Cullen, and K.S. Reeves, "Characterization and Optimization of Cathode Materials for PEM Fuel Cells," 246th American Chemical Society National Meeting, Indianapolis, IN – September 8, 2013.

12. Contributed Presentation: D.A. Cullen, H. Meyer, K.L. More, R. Koestner, R. Kukreja, S. Minko, O. Trotsenko, A. Tokarev, and L. Guetaz, "Characterization of Thin Ionomer Films," 224th ECS Meeting, San Francisco, CA – October 27 – November 1, 2013.

13. Invited Presentation: K.L. More, D.A. Cullen, and K.S. Reeves, "Correlating Catalyst Stability and Degradation with Cathode Materials Interactions in PEM Fuel Cells," 2013 MRS Fall Meeting, Boston, MA – December 1–5, 2013.

14. Invited Presentation: K.L. More, D.A. Cullen, and K.S. Reeves, "Advanced Microscopy Methods to Understand Materials Degradation in PEM Fuel Cell MEAs," 556th WE-Herraeus Seminar Analytical Tools for Fuel Cells and Batteries, Bad Honnef, Germany – March 23–26, 2014.

15. Invited Presentation: K.L. More, D.A. Cullen, and K.S. Reeves, "Microscopy of Fuel Cell Catalyst and Catalyst Support Degradation," Spring Meeting of the Materials Research Society, San Francisco, CA - April 20–24, 2014.

16. Contributed Presentation: K.L. More, R.R. Unocic, and D.A. Cullen, "In Situ Electrochemical Microscopy of PEM Fuel Cell Materials," 225th Meeting of The Electrochemical Society, Orlando, FL – May 11–15, 2014.

17. Invited Presentation: K.L. More, D.A. Cullen, and K.S. Reeves, "Correlating Catalyst Stability with Improved Cathode Materials for PEM Fuel Cells," Fuel Cells Gordon Research Conference, Bryant University, Smithfield, RI – August 3–8, 2014.

18. Contributed Presentation: D.A. Cullen, K.L. More, M. Lopez-Haro, P. Bayle-Guillemaud, L. Guetaz, M.K. Debe, D.F. van der Vliet, and A.J Steinbach, "Fine Tuning Highly Active Pt_3Ni_7 Nanostructured Thin Films for Fuel Cell Cathodes," Microscopy & Microanalysis 2014 Annual Meeting, Hartford, CT – August 3–8, 2014.

V.I.4 Neutron Imaging Study of the Water Transport in Operating Fuel Cells

Muhammad Arif (Primary Contact),
David L. Jacobson, Daniel S. Hussey
National Institute of Standards and Technology (NIST)
100 Bureau Drive
Gaithersburg, MD 20899
Phone: (301) 975-6303
Email: arif@nist.gov

DOE Manager
Nancy Garland
Phone: (202) 586-5673
Email: Nancy.Garland@ee.doe.gov

Contract Number: DE-AI-01-01EE50660

Project Start Date: October 1, 2001
Project End Date: Project continuation and direction determined annually by DOE

Overall Objectives

- Provide state-of-the-art research and testing infrastructure to enable the fuel cell industry to design, test, and optimize prototype to commercial-grade fuel cells using in situ neutron imaging techniques.
- Provide a secure facility for proprietary research by industry. Provide beam time at no cost to non-proprietary research through a competitive proposal process. Make open research data available for beneficial use by the general fuel cell community.
- Continually improve and develop methods and technology to accommodate rapidly changing industry/academia needs.

Fiscal Year (FY) 2014 Objectives

- Collaborate and support groups from the DOE Hydrogen and Fuel Cells Program performing water transport measurements with neutron imaging at NIST.
- Improve fuel cell measurement infrastructure based on needs of the fuel cell community.
- Provide support to fuel cell infrastructure to enable testing of automotive-scale test sections.
- Explore and develop high-resolution neutron imaging methods to enable water transport studies of catalyst and membrane electrode assemblies (MEAs).
- Employ a high-resolution imaging method to achieve resolution approaching 1 micrometer to resolve water concentration in fuel cell electrodes.
- Determine and correct systematic effects due to spatial resolution effects.

Technical Barriers

This project addresses the following technical barriers from the Fuel Cells section of the Fuel Cell Technologies Office Multi-Year Research, Development, and Demonstration Plan:

(A) Durability

(B) Cost

(C) Performance

Technical Targets

This project is conducting fundamental studies of water transport in the fuel cell. Insights gained from these studies will be applied toward the design of components and operation strategies of proton exchange membrane fuel cells that meet the following DOE fuel cell targets:

- Durability with cycling at operating temperature of ≤80°C: 5,000 h
- System energy density: 650 W/L
- System specific power: 850 Watt/kg
- Energy efficiency: 60% at 25% rated power
- Cost: $30/kWe
- Start-up time to 50% power: 30 seconds from -20°C, 5 seconds from 20°C
- Assisted start from low temperatures: -40°C
- Durability with cycling: 5,000 hrs

FY 2014 Accomplishments

- Employed a high-resolution imaging method to achieve resolution approaching 1 μm
- Enhanced the fuel cell imaging analysis software to correct for systematic effects due to image blurring
- Developed the technical support infrastructure for testing of automotive-scale test sections
- Improved fuel cell high-resolution image time to improve the experimental throughput of the facility
- Standardized design of the high-resolution fuel cell test cell

INTRODUCTION

At NIST, we maintain the premier fuel cell neutron imaging facility in the world and continually seek to improve its capabilities to meet the changing needs of the fuel cell community. This facility provides researchers with a powerful and effective tool to visualize and quantify water transport inside operating fuel cells. Imaging the water dynamics of a fuel cell is carried out in real time with the required spatial resolution needed for fuel cells that are being developed today. From these images, with freely available NIST-developed image analysis routines, fuel cell industry personnel and researchers can obtain in situ, non-destructive, quantitative measurements of the water content of an operating fuel cell. Neutron imaging is the only in situ method for visualizing the water distribution in a "real-world" fuel cell. Unlike X-rays, whose interaction with materials increases with the number density of electrons, neutrons interact via the nuclear force, which varies somewhat randomly across the periodic table, and is isotopically sensitive. For instance, a neutron's interaction with hydrogen is approximately 100 times greater than that with aluminum, and 10 times greater than that with deuterium. It is this sensitivity to hydrogen (and insensitivity to many other materials) that is exploited in neutron imaging studies of water transport in operating fuel cells.

APPROACH

The typical length scales of interest in a fuel cell are: channels approximately 1 mm wide and 1 mm deep, the diffusion media are 0.1-mm to 0.3-mm thick, the membrane is 0.01-mm to 0.02-mm thick, and the active area of test sections can range from 2 cm^2 to 500 cm^2. Though the study of water transport within these length scales is technically very challenging, the unique capabilities of neutron imaging have already successfully addressed many of the questions. However, as fuel cell research matures, the water transport questions become increasingly more demanding, requiring for instance resolving the water content in catalyst layers. To meet these demands, based on fuel cell community feedback and need, we continue to develop new facilities and improve existing capabilities for obtaining higher spatial and temporal resolution neutron images. These improvements will enable users to perform even more detailed, nondestructive, and in situ studies of the water and hydrogen transport in fuel cells to meet DOE goals. In addition, employing mathematical models of neutron scattering, we will develop a software suite that enables users to obtain reliable, accurate, quantitative measurements of the water content in an operating fuel cell. Due to the complexity of fuel cells and the large number of remaining open questions regarding water transport, we will develop partnerships with industry, academia, and national laboratories to train them in the use of the facility, seek their feedback, and collaborate with them on research projects, to seek measurement breakthroughs that will facilitate the rapid, efficient, and robust development of fuel cells.

RESULTS

The NIST Neutron Imaging Facility provides year-to-year support for the DOE Hydrogen and Fuel Cells Program projects by providing beam time and by collaboration with users on a variety of related neutron imaging projects that support the DOE mission. For FY 2014 General Motors (GM), Nissan, Los Alamos National Laboratory, University of Connecticut, University of California, Davis, Commissariat à l'énergie atomique et aux énergies alternatives, and University of Tennessee, Knoxville have received project support for experiments at the facility accounting for more than 70 days of beam time. Published results from these and previous years experiments are reflected in the publication list attached to this report.

NIST now provides full support to full-sized commercial and automotive grade fuel cell testing at the facility with a large-scale fuel cell test stand. This stand was developed through the NIST partnership with GM. The facility technical staff has received extensive onsite training on calibration, operation and validation testing from our testing partners at GM. This test stand is capable of operating fuel cells and small stacks at 800 W, 6-1,000 A @ 0.2 V, 0 V–50 V, hydrogen: 0.065 slpm – 11.31 slpm, air: 0.239 slpm – 26.92 slpm. Further reports of this capability and tests made with this stand will be presented at future Annual Merit Reviews.

The fuel cell testing community has requested that NIST devise a standardized design for fuel cells used for high-resolution neutron imaging. These types of fuel cells can be difficult to design and field without experience. Through a collaborative effort with our testing partners at Los Alamos National Laboratory, we have identified a robust design that yields good fuel cell performance and image quality. MEAs for this cell design can be taken from existing MEAs, for instance enabling water transport studies during durability tests in 50 cm^2 (see Figure 1). The design uses poly-tetrafluoroethylene (PTFE) gaskets that have high neutron transmission and maintain geometry of the fuel cell very well. Maintaining the fuel cell geometry is critical in high-resolution fuel cell testing as small changes due to swelling of the membrane or lack of parallelism of the end-plates is very apparent. To ensure end-plate parallelism, the design includes cutouts for gauge blocks. Finally the use of porous metal foam flow fields is being investigated to avoid the wavy non-uniformities introduced as the MEA/diffusion media protruded into standard flow field designs.

Understanding flooding and degradation issues due to liquid water in catalysts is a critical step towards improving durability and cycling of fuel cells. This requires even better spatial resolution than what has been achieved to date.

Currently we can achieve near 13 μm, but to effectively study catalysts it will be necessary to achieve near 1 μm spatial resolution in one dimension of the image. This has pushed the need for innovation in neutron imaging that must go beyond the current limiting spatial resolution. This current resolution limit is due to the range of charged particles that are used to detect neutrons (3.5 μm–150 μm) and fundamentally limits the spatial resolution. To overcome this limit we have been exploring two methods. The first, called structured illumination, uses neutron absorbing slits nanofabricated into gratings that are ~2 μm or less in width to define the neutron path illuminating the fuel cell with high spatial resolution in one dimension. The grating can then be translated across the object to obtain a high-resolution image along the grating direction, overcoming the resolution limit of the detector. The resulting images can be combined to produce an image with spatial resolution defined by the slit width of the grating. This year a new apparatus (photo in Figure 2) was designed and tested that will enable fuel cell users to achieve sub 10-μm resolution. This new experimental system was deployed and tested at the facility and the results from a preliminary test are shown in Figure 3. In Figure 3 is plotted the liquid water distribution in an operating fuel cell with the grating and without the grating. The results show that the grating adjusted for 5-μm resolution allows one to differentiate far more detail of the liquid water distribution.

The data from the high-resolution fuel cell images show that improvements to the signal to noise ratio are necessary to improve the quality of the data. This can be achieved with longer integration times or more efficient detectors. Longer integration times will limit the number of fuel cell operating conditions that can be measured. Therefore emphasis has been placed on improving the detector efficiency in order to improve the signal quality. Gadox scintillators have similar spatial resolution and 4 times the stopping power of the microchannel plates currently used for high resolution imaging. However, Gadox produces little light for each stopped neutron and has not been used due to small signal to noise ratios. Modern image intensifiers have been developed that enable high image resolution with stable long-term performance and initial tests showed that an intensifier improved the signal to noise ratio by over a factor of 30. A new detector system based on an intensifier has been designed, and an image intensifier is being procured for fuel cell users. This new system is expected to be available at the

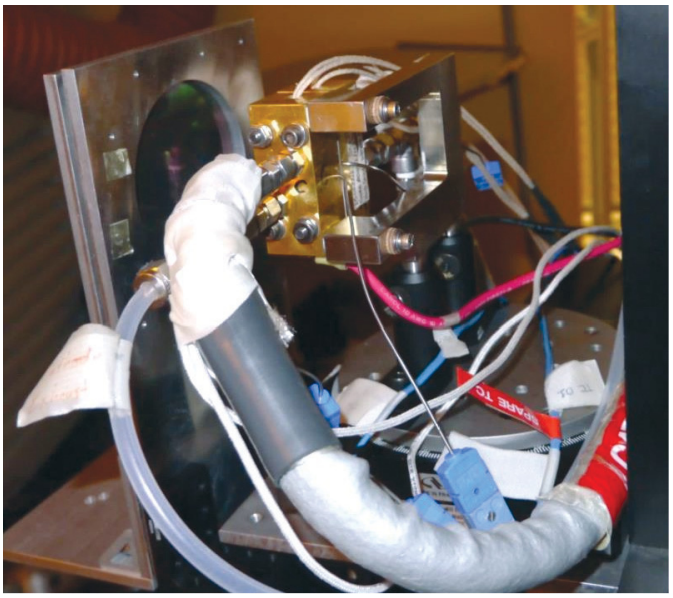

FIGURE 2. Grating set-up now available for users for high-resolution fuel cell testing.

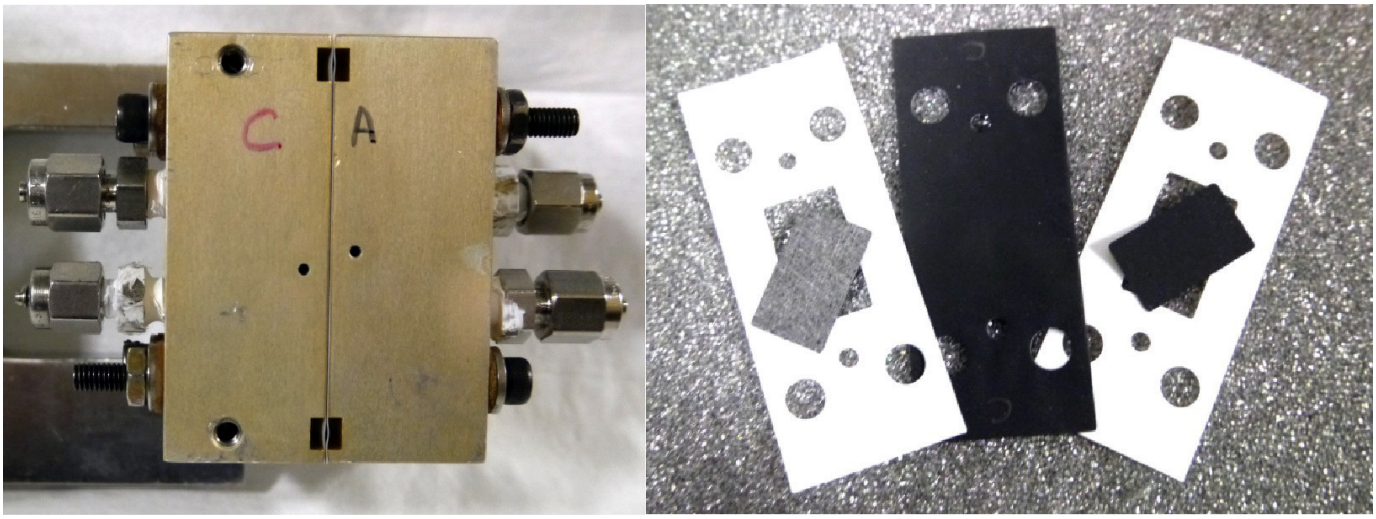

FIGURE 1. Left shows the standardized high-resolution test cell adopted from Los Alamos National Laboratory design. Right shows the MEA cut from existing 50-cm^2 MEA tested for durability shown with the hard PTFE seals.

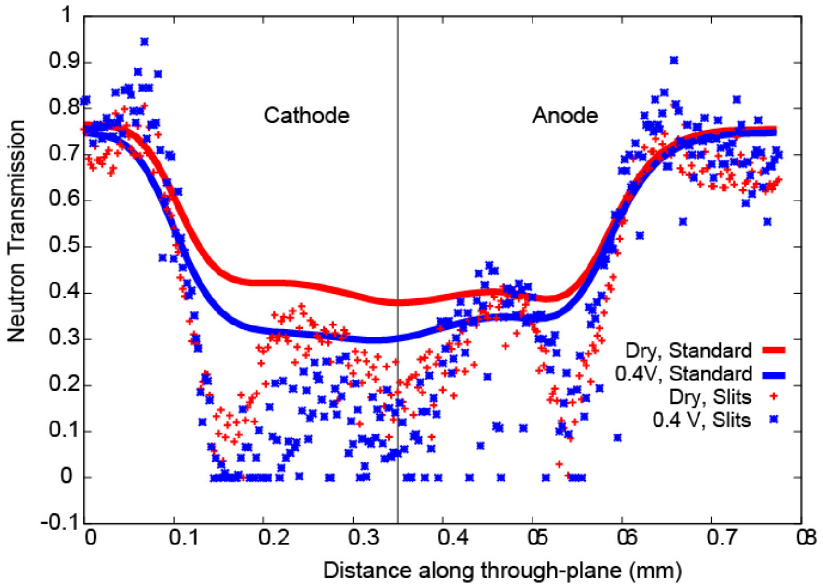

FIGURE 3. Data from initial tests of the gratings for high-resolution fuel cell testing. Solid line shows the standard water distribution measured without gratings. Data points are the spatially resolved liquid water distribution.

facility by January 2015 and is expected to increase the time resolution for high-resolution neutron imaging by a factor of 4 due to the increased neutron detection efficiency.

It could be possible to increase the neutron intensity by 50 to 100 times than currently available using a neutron lens. Previously, practical lenses for neutrons have not been available due to the low neutron refractive power of all materials. However, a new X-ray lens technology developed by the National Aeronautics and Space Administration has shown great promise to provide a practical lens for neutron imaging. This year NIST committed to developing a neutron microscope with a milestone to provide a 1:1 lens with greater than 50 times increase in signal by 2016 and a subsequent lens that will magnify neutron images by 10 times to achieve 1-µm resolution by 2018. If successful this will enable fuel cell researchers to measure water distributions with 1 µm resolution in 20 min as opposed to current 24 hours per image with the grating method.

Ensuring the accuracy of the data analysis techniques used to quantify the water content has been a continuing focus of the NIST fuel cell project. Previously the results of an extensive analysis of systematic effects present when measuring high resolution water distributions in fuel cell membranes identified multiple corrections that are required to do accurate measurements. One of the more significant contributions can be corrected in software using mathematical deconvolution of the data. This capability was added as a new feature in the data analysis software that is available to facility users. In addition an evaluation was made of the importance of this systematic correction to previous fuel cell data sets. It was determined that this would only amount to a 1% correction to the in-plane water distribution, which is a systematic error below the overall uncertainty in previous measurements.

CONCLUSIONS AND FUTURE DIRECTIONS

- NIST Neutron Imaging Facility continues to maintain a robust fuel cell user project with:
  - 11 publications and 8 presentations in 2013
  - Over 70 days of dedicated fuel cell beam time
- Fuel cell infrastructure now fully supports automotive-scale testing:
  - Developed in collaboration with GM
  - Test stand to control automotive-scale cells is available to users
  - NIST staff trained at GM to support calibration and use of the test stand
- Design of standard high resolution fuel cell is available to users:
  - Can use existing membranes from 50-cm^2 test sections
  - Seals well and maintains precise geometry for testing approaching 1-µm resolution
- With the goal to study catalysts, NIST continues to improve the image spatial resolution. New avenues toward resolving the MEA water content include:

  - Employing a grating method to achieve resolution approaching 1 μm with 12 hour acquisition time (end of 2014)
  - Developing a magnifying neutron lens to reach 1 μm with 20 min acquisition time (2018)
- Improve fuel cell high resolution image time:
  - Time resolution for through-plane water content measurements improved by a factor of 4 with 20 μm scintillator detector
  - Future neutron lens will increase time resolution by 50x to achieve image times of 10 s with 10 μm resolution
- Neutron image analysis and corrections:
  - Deblurring algorithms for images of the in-plane water content of fuel cells are demonstrated and published
- Future general improvements:
  - Second new cold neutron imaging facility will begin operation by 2015
  - Continue improvements to achieve 1-μm imaging:
    - Develop neutron lens
    - Improve grating method

FY 2014 PUBLICATIONS/PRESENTATIONS

1. O.F. Selamet, U. Pasaogullari, D. Spernjak, D.S. Hussey, D.L. Jacobson, and M.D. Mat, "Two-phase flow in a proton exchange membrane electrolyzer visualized *in situ* by simultaneous neutron radiography and optical imaging International", Journal of Hydrogen Energy **38** (14) 5823-5835 (2013).

2. J.D. Fairweather, D. Spernjak, A.Z. Weber, D. Harvey, S. Wessel, D.S. Hussey, D.L. Jacobson, K. Artyushkova, R. Mukundan, R.L. Borup, "Effects of Cathode Corrosion on Through-Plane Water Transport in Proton Exchange Membrane Fuel Cells", Journal of The Electrochemical Society **160** (9) F980-F993 (2013).

3. D. Liu, D. Hussey, M.V. Gubarev, B. D. Ramsey, D. Jacobson, M. Arif, D.E. Moncton, and B. Khaykovich, "Demonstration of achromatic cold-neutron microscope utilizing axisymmetric focusing mirrors", Applied Physics Letters **102** (18) 183508 (2013).

4. Hussey, D.S., E. Baltic, K.J. Coakley and D.L. Jacobson, "Improving quantitative neutron radiography through image restoration", NIMA **729** 316-321 (2013).

5. K.J. Coakley, D.F. Vecchia, D.S. Hussey, and D.L. Jacobson, "Neutron Tomography of a Fuel Cell: Statistical Learning Implementation of a Penalized Likelihood Method", IEEE Transactions On Nuclear Science, **60** (5) 3945-3954 (2013).

6. B.M. Wood, K. Ham, D.S. Hussey, D.L. Jacobson, A. Faridani, A. Kaestner, J.J. Vajo, P. Liu, T.A. Dobbins, L.G. Butler, "Real-time observation of hydrogen absorption by LaNi5 with quasi-dynamic neutron tomography", Nuclear Instruments and Methods in Physics Research Section B, 324 95-101 (2014).

7. Spernjak, D., G. Wu, J. Fairweather, D. Hussey, R. Mukundan, R. Borup & P. Zelenay, In situ measurement of flooding in thick Pt and PANI-derived catalyst layers in PEM fuel cells. Journal of the Electrochemical Society, In preparation (2014).

8. D.S. Hussey, D. Spernjak, G. Wu, D.L. Jacobson, D. Liu, B. Khaykovich, M.V. Gubarev, J.D. Fairweather, R. Mukundan, R. Lujan, R.L. Borup, "Neutron Imaging of Water Transport in Polymer-Electrolyte Membranes and Membrane-Electrode Assemblies", ECS Transactions **58** (1) 293-299 (2013).

9. Z. Lu, J. Waldecker, X. Xie, M.-C. Lai, D.S. Hussey, D.L. Jacobson, "Investigation of Water Transport in Perforated Gas Diffusion Layer By Neutron Radiography", ECS Transactions **58** (1) 315-324 (2013).

10. J.D. Fairweather, D. Spernjak, J. Spendelow, R. Mukundan, D.S. Hussey, D.L. Jacobson, R.L. Borup, "Evaluation of transient water content during PEMFC operational cycles by stroboscopic neutron imaging", ECS Transactions **58** (1) 301-307 (2013).

11. X. Liu, T.A. Trabold, J.J. Gagliardo, D.L. Jacobson, D.S. Hussey, "Neutron Imaging of Water Accumulation in the Active Area and Channel-to-Manifold Transitions of a PEMFC" ASME 2013 11th International Conference on Fuel Cell Science V001T01A010-V001T01A010 (2013).

12. Zijie Lu, James Waldecker, Xingbin Xie, Ming-Chia Lai, Daniel S Hussey, and David L Jacobson, "Investigation of Water Transport in Perforated Gas Diffusion Layer By Neutron Radiography", Abstract 1293, 224th ECS Meeting, San Francisco, CA, 2013.

13. Rangachary Mukundan, Dusan Spernjak, Roger Lujan, Joseph D. Fairweather, Daniel S Hussey, David L Jacobson, Andrew J. Steinbach, Adam Z. Weber, and Rod L Borup, "Neutron Imaging and Performance of PEM Fuel Cells With Nanostructured Thin Film Electrodes At Low Temperatures", Abstract 1292, 224th ECS Meeting, San Francisco, CA, 2013.

14. Joseph D. Fairweather, Dusan Spernjak, Jacob Spendelow, Rangachary Mukundan, Daniel S Hussey, David L Jacobson, and Rod L Borup, "Evaluation of Transient Water Content During PEMFC Operational Cycles By Stroboscopic Neutron Imaging", Abstract 1290, 224th ECS Meeting, San Francisco, CA, 2013.

15. Daniel S Hussey, David L Jacobson, Dazhi Liu, Boris Khaykovich, Mikhail V Gubarev, Dusan Spernjak, Gang Wu, Joseph D. Fairweather, Rangachary Mukundan, Roger Lujan, Piotr Zelenay, and Rod L Borup, "Neutron Imaging of Water Transport in Polymer-Electrolyte Membranes and Membrane-Electrode Assemblies", Abstract 1289, 224th ECS Meeting, San Francisco, CA, 2013.

16. Xinyu Huang, Hongying Zhao, and William A. Rigdon, "In Situ Observation of Membrane Degradation in PEM Fuel Cell Via Raman Spectroscopy", Abstract 1431, 224th ECS Meeting, San Francisco, CA, 2013.

17. Yasser Ashraf Gandomi and Matthew M. Mench, "Assessing the Limits of Water Management With Asymmetric Micro-Porous Layer Configurations", Abstract 1542, 224th ECS Meeting, San Francisco, CA, 2013.

18. Toshikazu Kotaka, Yuichiro Tabuchi, Ugur Pasaogullari, and Chao-Yang Wang, "The Influence of the Liquid Water Interaction Between Channel, GDL and CL On Cell Performance", Abstract 1456, 224th ECS Meeting, San Francisco, CA, 2013.

19. X. Liu, T.A. Trabold, J.J. Gagliardo, D.L. Jacobson, D.S. Hussey, "Neutron Imaging of Water Accumulation in the Active Area and Channel-to-Manifold Transitions of a PEMFC" ASME 2013 11th International Conference on Fuel Cell Science.

V.I.5 Enlarging the Potential Market for Stationary Fuel Cells through System Design Optimization

Genevieve Saur (Primary Contact),
Chris Ainscough, Jen Kurtz, Sam Sprik, Matt Post, Kristin Field, Eric Bonnema
National Renewable Energy Laboratory
15013 Denver West Parkway
Golden, CO 80401-3305
Phone: (303) 275-3783
Email: Genevieve.Saur@nrel.gov

DOE Manager
Jason Marcinkoski
Phone: (202) 586-7466
Email: Jason.Marcinkoski@ee.doe.gov

Subcontractor
Jack Brouwer, Dustin McLarty, Michael Ryan Sullivan, University of California, Irvine (UCI), Irvine, CA

Project Start Date: January 1, 2011
Project End Date: Project continuation and direction determined annually by DOE

Overall Objectives

Build an open-source tool (DG-BEAT[1]) that helps combined heat and power (CHP) fuel cell developers, end users, and other stakeholders to do the following for their systems, helping to drive economies of scale and cost reduction:

- Determine the appropriate sizing to reduce cost.
- Integrate to commercial building control and heating, ventilation and air conditioning systems to maximize durability.
- Compare performance relative to incumbent technologies.
- Determine optimum system configuration.
- Evaluate potential market penetration.

Fiscal Year (FY) 2014 Objectives

- Implement a control strategy which models fuel cell system response used for energy consumption calculations by accounting for system response lag.
- Implement a dispatch control for lowest greenhouse gas (GHG) emissions (CO_2) and criteria pollutants (ozone, SO_x, NO_x, PM10, CO), based on available regional electric grid emissions, and emissions profiles from stationary fuel cell systems.
- Identify and implement one additional set of commercial building energy usage profiles (16 types in 16 locations x 8,760 hours each, in 15-minute time steps).
- Deliver a compiled Windows executable of the model to the user's group, including 1,024 building energy load profiles.

Technical Barriers

This project addresses the following technical barriers from the Fuel Cells section of the Fuel Cell Technologies Office Multi-Year Research, Development, and Demonstration Plan:

(A) Durability

(B) Cost

(C) Performance

Technical Targets

This project is providing a tool to fuel cell manufacturers, end users, and other stakeholders to help them reduce the cost of fuel cell CHP installations by optimizing their sizing, combining them with hybridizing technologies such as thermal energy storage and batteries, dispatching them in cost-optimal ways, and investigating the fuel cell sizes and features to best address the national market. Relevant DOE targets (2020) are:

- Installed cost, natural gas: $1,500/kW
- Operating lifetime: 40,000-80,000 hours
- Electrical efficiency at rated power: >50%
- CHP energy efficiency: 90%

FY 2014 Accomplishments

- Implemented a non-predictive fuel cell load-following strategy that accounts for system lag. This will allow future improvements for optimization strategies.
- GHG and emissions reporting and minimization control strategies were implemented for CO_2, SO_2, and NO_x. The emissions reporting allows for a comparison of a stationary fuel cell integrated building system to a conventional building system. The GHG minimization control strategies sizes the fuel cell for emissions minimization of a specified pollutant.

[1] Distributed Generation Build-out Economic Assessment Tool

- New building profiles were implemented which cover 16 regions, 16 building types, and three vintages for 768 new profiles. These are added to a previous set of 512 building profiles for 1,280 total. The profiles include electricity, heating, and cooling demands in 15-minute time step intervals for a year, which allow for energy storage modeling with a fuel cell.
- Improvements were made to the fuel cell performance profiles, including additions of molten carbonate fuel cells and polymer electrolyte membrane fuel cells. The model can now simulate four separate fuel cell types.
- Implemented improvements to feedstock costs and time-of-use electricity pricing in 16 regions, as well as several net-metering methods for electricity sell-back to grid.

INTRODUCTION

This project aims to create an open-source software tool that allows fuel cell developers, their potential customers, and other stakeholders to evaluate the ability of fuel cell installations to save money relative to the grid/natural gas paradigm. The model includes 1,280 model building profiles covering the major American Society of Heating, Refrigerating and Air Conditioning Engineers climate zones in the United States.

The model can perform design optimizations on single fuel cells and building combinations or campuses of multiple buildings. In addition to fuel cells technologies that can be included in the buildings systems, the project scenario also includes chillers, energy storage technologies, and on-site renewables such as solar and wind.

APPROACH

The approach taken by the research team is to build a flexible, configurable model which allows users to create modules for the various components which make up a project scenario (fuel cells, energy storage, chillers, buildings and campuses). NREL has teamed with the University of California, Irvine, as a sub-contractor to leverage their extensive expertise in this area. Cost and sizing optimization can now be done for different control strategies utilizing the modules built. In addition, NREL is working cross-center within the lab, drawing extensively on the expertise of the commercial buildings research group within NREL to provide model building profiles.

RESULTS

The modeling effort this year focused on adding GHG emissions reporting and on refinements to other modules, which rounded out the features needed for future optimization, design, and analysis work.

The GHG emissions reporting covers CO_2, SO_2, and NO_x, and is based upon data from the Environmental Protection Agency Acid Rain Program and State Implementation Plans [1]. Hourly data allows the model to compare the fuel cell operation to the grid emissions. The hourly data compares well for most states to annual emissions factors from eGrid and is within 10% of the annual totals for 48 of the 50 states [2]. It is assumed that the fuel cell emissions can be compared to these grid factors when aggregated over a year. This hourly data is important due to differences in grid emissions by region and season (Figures 1 and 2). The emissions reporting has allowed modeling of GHG minimization control strategies whereby the fuel cell is dispatched based on day and night averages of grid emissions and is sized between the building peak and base load to minimize total annual emissions.

Several different functional methods for sizing and dispatching the fuel cell within the integrated building

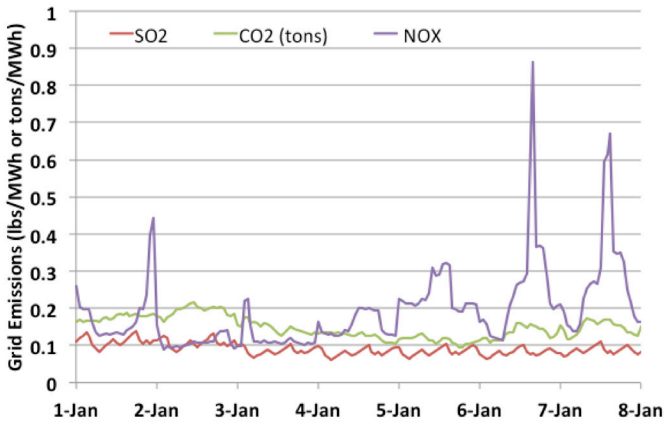

FIGURE 1. Example Grid Emissions Seasonal Variation, Winter

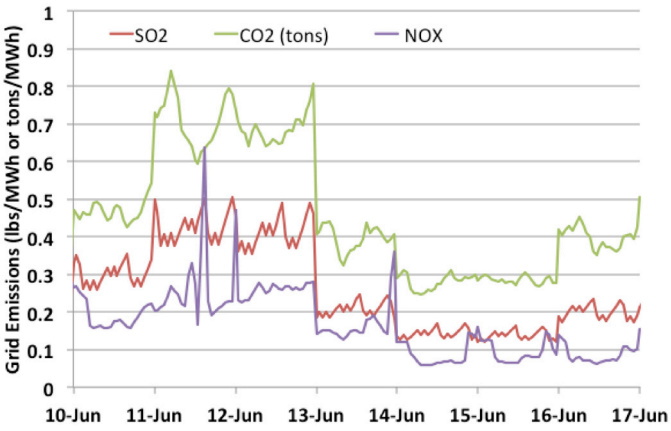

FIGURE 2. Example Grid Emissions Seasonal Variation, Summer

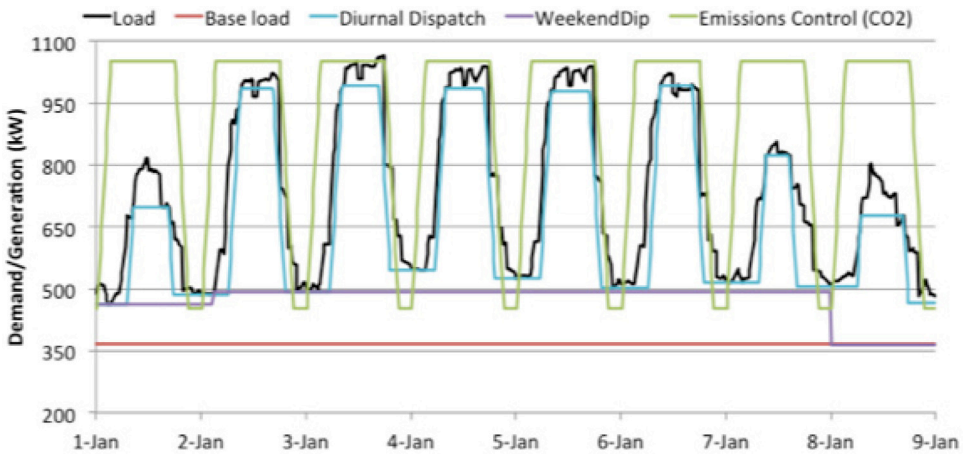

FIGURE 3. Example Fuel Cell Dispatch Strategies

system have been modeled. There are four sizing methods: fixed, 100% of summer peak demand, cost optimal, and emission minimizations. These are complemented by five fuel cell dispatch strategies that range from fixed usage (base load) to more structured usages (diurnal peak, weekend dip, emissions control) to full-load following (Figure 3).

The model can now do more detailed cost and emissions analyses (Figure 4) in which we can work towards a national survey of different types of building in the regions that span the United States.

CONCLUSIONS AND FUTURE DIRECTIONS

A strong model foundation is now in place for implementing component sizing optimization strategies and other future analysis. The model can now manage integration of fuel cells into building systems which can include chillers, energy storage technologies, and renewable energy systems. A number of sizing and control strategies are implemented. The new building profiles cover a significant percentage of the U.S. commercial building stock and will be invaluable for a national survey of fuel cell integration.

Future work for the remainder of FY 2014 and beyond could include:

- Assess requirements for an encompassing optimization strategy for sizing building components and implement dynamic control strategies.
- Implement a strategy for engaging the user's group in a more organized manner which includes regular beta software releases and collection of feedback for model development (both functionality and input data).
- Continue to refine and gather input data and develop a validation plan.

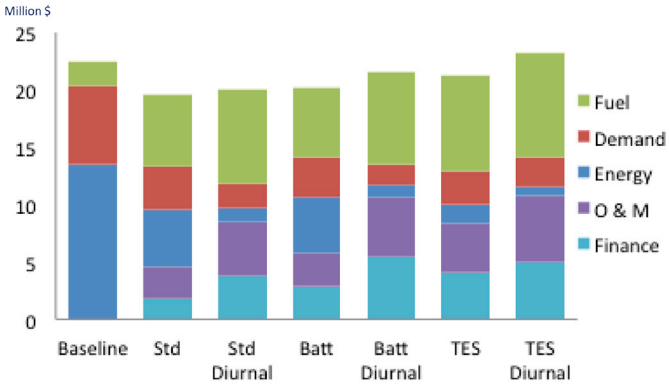

FIGURE 4. Example Cost Analysis Comparing Different Dispatch Strategies

- Investigate code requirements for including the OpenEI utility rate database.
- Work towards a national survey of buildings to help target where fuel cells may make the most sense and impact.

FY 2014 PUBLICATIONS/PRESENTATIONS

1. Wipke, K. "Modeling and Optimization of Commercial Buildings and Stationary Fuel Cell." Fuel Cell Seminar, published October 2013. (presentation)

REFERENCES

1. http://ampd.epa.gov/ampd

2. http://www.epa.gov/cleanenergy/energy-resources/egrid/index.html

V.I.6 Stationary and Emerging Market Fuel Cell System Cost Analysis – Material Handling Equipment

Vince Contini (Primary Contact), Fritz Eubanks, Mike Jansen, and Mike Heinrichs
Battelle
505 King Avenue
Columbus, OH 43201
Phone: (614) 424-7249
Email: continiv@battelle.org

DOE Managers
Donna Ho
Phone: (202) 586-8000
Email: Donna.Ho@ee.doe.gov
Reg Tyler
Phone: (720) 356-1805
Email: Reginald.Tyler@ee.doe.gov

Contract Number: DE-EE0005250/001

Project Start Date: September 30, 2011
Project End Date: September 30, 2016

Overall Objectives

The objective of this project is to assist the U.S. Department of Energy in developing fuel cell systems for stationary and emerging markets by developing independent cost models for manufacture and ownership.

- Identify the fundamental drivers of system cost and the sensitivity of the cost to system parameters.
- Help the DOE prioritize investments in research and development of components (e.g., metal bipolar plates versus composite graphite plates in polymer electrolyte membrane [PEM] fuel cells for low-volume markets) to reduce the costs of fuel cell systems while considering systems optimization.
- Identify manufacturing processes that must be developed to commercialize fuel cells.
- Provide insights into the optimization needed for use of off-the-shelf components in fuel cell systems.

Fiscal Year (FY) 2014 Objectives

- Finalize cost estimate of 1- and 5-kW solid oxide fuel cells (SOFC) for auxiliary power unit (APU) applications at annual production volumes of 100 units, 1,000 units, and 10,000 units.
- Finalize cost estimate of 1- and 5-kW PEM fuel cell for material handling equipment applications at annual production volumes of 100, 1,000, and 10,000 units.
- Initiate cost estimates of 1-, 5-, 10- and 25-kW PEM and SOFC fuel cell systems for primary power and combined heat and power (CHP) applications at annual production volumes of 100, 1,000, 10,000, and 50,000 units.

Technical Barriers

This project addresses the following technical barrier from the Fuel Cells section of the Fuel Cell Technologies Office Multi-Year Research, Development, and Demonstration Plan:

(B) Cost

Technical Targets

To widely deploy fuel cells, significant strides must be made in lowering the cost of components and systems without compromising reliability and durability. This cost analysis will

- Identify the fundamental drivers of component and system cost and the sensitivity of the cost to various component and system parameters
- Provide the DOE information on the impact of production volumes on lowering costs of fuel cells and the types of high-volume manufacturing processes that must be developed to enable widespread commercialization
- Provide insights into the optimization needed for use of off-the-shelf components in fuel cell systems to drive down system costs
- Analyze the lifecycle costs of owning and operating a fuel cell to estimate primary cost drivers to the end user in applicable markets.

FY 2014 Accomplishments

- Completed manufacturing cost analysis of 1-kW and 5-kW SOFC systems for APUs.
- Completed manufacturing cost analysis of 1-kW and 5-kW direct hydrogen PEM fuel cell systems for material handling applications.
- Detailed performance specifications and system requirements and completed preliminary system design of 1-, 5-, 10-, and 25-kW PEM and SOFC fuel cell systems for primary power and CHP applications.

Next Steps

In FY 2014/15, Battelle will:

- Complete full cost assessment of 1-, 5-, 10-, and 25-kW PEM and SOFC systems for primary power and CHP applications.

✧ ✧ ✧ ✧ ✧

APPROACH

Battelle will apply the established methodology used successfully on the previous fuel cell cost analysis study for the DOE (Battelle, 2011; Mahadevan, 2007; Stone, 2006). The technical approach consists of four steps—market assessment, system design, cost modeling, and sensitivity analysis (Figure 1). The first step characterizes the potential market and defines the requirements for system design. The second step involves developing a viable system design and associated manufacturing process vetted by industry. The third step involves building the cost models and gathering inputs to estimate manufacturing costs. Manufacturing costs will be derived using the Boothroyd-Dewhurst Design for Manufacture and Assembly software. Custom manufacturing process models will be defined where necessary and parametrically modeled based on knowledge of the machine, energy, and labor requirements for individual steps that comprise the custom process. The fourth step will evaluate the sensitivity of stack and system costs to various design parameters. In addition to the sensitivity analysis, we will conduct a lifecycle cost analysis to estimate total cost of ownership for the target application and markets.

RESULTS

Overall, the final cost was analyzed in four distinct categories: the capital cost of manufacturing equipment, the direct cost of material and assembly of the stack, the expense of balance-of-plant (BOP) hardware, and the final cost of complete system assembly and testing.

TABLE 1. 1-kW SOFC APU Fuel Cell System per Unit Cost Summary

Description	100 Units	1,000 Units	10,000 Units	50,000 Units
Total stack manufacturing cost, with scrap	$590	$511	$481	$473
Stack manufacturing capital cost	$4,757	$495	$69	$43
BOP	$9,597	$8,204	$7,383	$7,383
System assembly, test, and conditioning	$475	$451	$448	$448
Total system cost, pre-markup	$15,419	$9,661	$8,381	$8,347
System cost per net KW, pre-markup	$15,419	$9,661	$8,381	$8,347
Sales markup	50.00%	50.00%	50.00%	50.00%
Total system cost, with markup	$23,129	$14,491	$12,571	$12,520
System cost per net KW, with markup	$23,129	$14,491	$12,571	$12,520

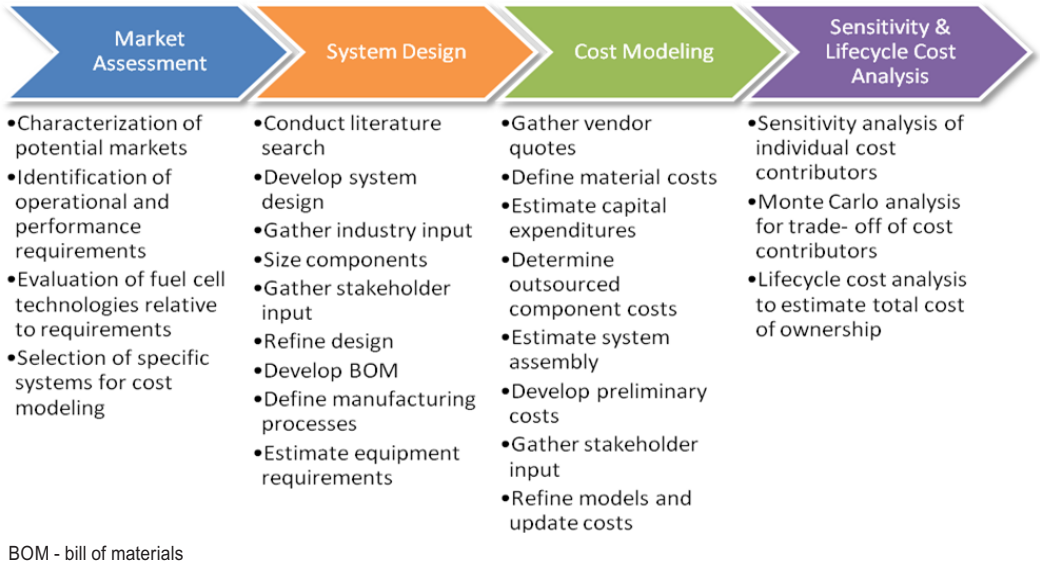

FIGURE 1. Battelle's Cost Analysis Methodology

TABLE 2. 5-kW SOFC APU Fuel Cell System per Unit Cost Summary

Description	100 Units	1,000 Units	10,000 Units	50,000 Units
Total stack manufacturing cost, with scrap	$1,476	$1,327	$1,267	$1,257
Stack manufacturing capital cost	$4,757	$495	$82	$73
BOP	$11,323	$9,802	$8,738	$8,738
System assembly, test, and conditioning	$481	$456	$454	$454
Total system cost, pre-markup	$18,037	$12,080	$10,541	$10,522
System cost per net KW, pre-markup	$3,608	$2,416	$2,108	$2,104
Sales markup	50.00%	50.00%	50.00%	50.00%
Total system cost, with markup	$27,056	$18,120	$15,812	$15,783
System cost per net KW, with markup	$5,411	$3,624	$3,162	$3,157

TABLE 3. 1-kW PEM MHE Fuel Cell System per Unit Cost Summary

Description	100 Units	1,000 Units	10,000 Units
Total stack manufacturing cost, with scrap	$985	$744	$628
Stack manufacturing capital cost	$4,337	$434	$62
BOP	$14,826	$11,859	$10,034
System assembly, test, and conditioning	$278	$255	$249
Total system cost, pre-markup	$20,426	$13,291	$10,973
System cost per net KW, pre-markup	$20,426	$13,291	$10,973
Sales markup	50.00%	50.00%	50.00%
Total system cost, with markup	$30,639	$19,937	$16,460
System cost per net KW, with markup	$30,639	$19,937	$16,460

A sales markup of 50% was integrated at the end and is called out separately in Tables 1-4. At high production volumes, the final ticket prices are estimated to be $12,520 and $3,157 per kW respectively for 1- and 5-kW SOFC APU systems and $16,460 and $4,401 per kW for the 1- and 5-kW PEM material handling equipment (MHE) systems. This work provides a detailed cost breakdown that helps identify key cost drivers and offers insight at various value propositions through the lifecycle cost analyses.

TABLE 4. 5-kW PEM MHE Fuel Cell System per Unit Cost Summary

Description	100 Units	1,000 Units	10,000 Units
Total stack manufacturing cost, with scrap	$2,219	$1,651	$1,337
Stack manufacturing capital cost	$4,337	$434	$96
BOP	$19,683	$15,594	$12,983
System assembly, test, and conditioning	$298	$264	$253
Total system cost, pre-markup	$26,537	$17,943	$14,669
System cost per gross KW, pre-markup	$5,307	$3,589	$2,934
Sales markup	50.00%	50.00%	50.00%
Total system cost, with markup	$39,806	$26,914	$22,004
System cost per gross KW, with markup	$7,961	$5,383	$4,401

CONCLUSIONS AND FUTURE DIRECTIONS

- The primary driver of overall system costs in both analyses is the BOP hardware, accounting for 62-91% of total system costs across the production volumes analyzed.
- For the SOFC APU, the complex nature of onboard fuel reforming and the high temperature requirements for SOFC operation keep the part count and material costs high. The SOFC stack cost is most sensitive to change in metal components, as the quantity of high-temperature steel makes up the bulk of the stack cost. BOP costs are most sensitive to heat transfer and power conversion equipment; specifically, the amount of heat transfer required to heat fuel feed streams, cool reformate for desulfurization, and reheat upstream of the stack is significant.
- The MHE BOP hardware is dominated by the battery, direct current (DC)/DC converter, hydrogen tank, and humidification system making up around 75% of the total BOP cost. The stack cost is most sensitive to change in current density and platinum loading.

FY 2014 PUBLICATIONS/PRESENTATIONS

1. F. Eubanks, V. Contini, G. Stout, M. Jansen, J. Smith. October 2013. Manufacturing Cost Analysis of SOFC Fuel Cells for APU Applications. Fuel Cell Seminar. Columbus, OH.

2. F. Eubanks, V. Contini, M. Jansen, G. Stout. June 2014. Stationary and Emerging Market Fuel Cell System Cost Analysis – Auxiliary Power Units. DOE Annual Peer Review. Washington, D.C.

V.I.7 A Total Cost of Ownership Model for PEM Fuel Cells in Combined Heat and Power and Backup Power Applications

Max Wei (Primary Contact), Hanna Breunig, Michael Stadler, Thomas McKone

Lawrence Berkeley National Laboratory (LBNL)
1 Cyclotron Road, MS 90R-4000
Berkeley, CA 94706
Phone: (510) 486-5220
Email: mwei@lbl.gov

DOE Managers

Donna Ho
Phone: (202) 586-8000
Email: Donna.Ho@ee.doe.gov

Reg Tyler
Phone: (720) 356-1805
Email: Reginald.Tyler@ee.doe.gov

Subcontractors

- University of California, Berkeley, CA
- Ballard Power Systems, Burnaby, British Columbia, Canada
- Strategic Analysis, Arlington, VA

Project Start Date: October 1, 2011
Project End Date: 2016

Overall Objectives

- Develop total-cost-of-ownership (TCO) modeling tool for design and manufacturing of fuel cell systems in emerging markets (e.g. co-generation and back-up power systems) for low-temperature proton exchange membrane (LT PEM), high-temperature (HT) PEM, and solid oxide fuel cell (SOFC) technologies
- Expand cost modeling framework to include life-cycle analysis and possible ancillary financial benefits, including carbon credits, health/environmental externalities, end-of-life recycling, and reduced costs for building operation
- Perform sensitivity analysis to key cost assumptions, externality valuation, and policy incentive structures

Fiscal Year (FY) 2014 Objectives

- Develop TCO modeling tool for HT PEM fuel cells in combined heat and power and stationary power applications
- Complete literature/patent summary and functional specifications SOFC systems in combined heat and power generation and stationary power

Technical Barriers

This project addresses the following technical barriers from the Fuel Cells section of the Fuel Cell Technologies Office Multi-Year Research, Development, and Demonstration Plan:

(B) Cost: Expansion of cost envelope to total cost of ownership including full life-cycle costs and externalities

Technical Targets

This project is conducting cost of ownership studies of LT PEM, HT PEM, and SOFC fuel cell systems in non-automotive applications. Insights gained from these studies can be applied toward the development of lower cost, higher volume manufacturing processes that can meet the following DOE combined heat and power system equipment cost targets listed in Table 1.

LT PEM: Although the 100-kW cost of $1,800/kW meets the 2015 target of $2,300/kW, the automated stack production processes and assumed high yields are more realistic in the 2020 timeframe. Compared to the 2020 targets, cost estimates for 10-kW and 100-kW exceed the target by 70% and 80%, respectively. (A 50% corporate markup is assumed for both system sizes.)

HT PEM: Although the 100-kW cost of $2,200/kW meets the 2015 target, the automated stack production processes and assumed high yields are more realistic in the 2020 timeframe. Compared to the 2020 targets, cost estimates for 10-kW and 100-kW exceed the target by 90% and 120%, respectively. (A 50% corporate markup is assumed for both system sizes.)

TABLE 1. Project Technical Targets

System	Units/yr	2015 Target	2020 Target	LT PEM direct cost	HT PEM direct cost	LT PEM cost with markup	HT PEM cost with markup
10-kW CHP System	50,000	$1,900/kW	$1,700/kW	$1,900	$2,100	$2,900	$3,200
100-kW CHP System	1,000	$2,300/kW	$1,000/kW	$1,200	$1,470	$1,800	$2,200

CHP – combined heat and power

FY 2014 Accomplishments

- Completed TCO model for LT PEM CHP and backup power applications
- Completed direct cost model for HT PEM CHP applications
- Completed literature/patent summary and functional specifications for SOFC systems in co-generation and stationary power

INTRODUCTION

The DOE has supported over the last decade several cost analysis studies for fuel cell systems for both automotive [1,2] and non-automotive systems [3,4]. These studies have primarily focused on the manufacturing costs associated with fuel cell system production. This project expands the scope and modeling capability from existing direct manufacturing cost modeling in order to quantify more fully the benefits of fuel cell systems by taking into account life-cycle assessment, air pollutant impacts and policy incentives. TCO modeling becomes important in a carbon constrained economy and in a context where health and environmental impacts are increasingly valued. TCO is also critical as an input to industry and governments decisions on funding research, development and deployment as well as an input to organizations and individuals who make long term investment decisions.

Three components of the TCO model are (1) direct manufacturing costs, (2) life-cycle or use- phase costs such as cost of operations and fuel, and (3) life-cycle impact assessment costs such as health and environmental impacts. FY 2014 has been focused on the development of a direct manufacturing cost model for HT PEM systems for application in CHP and work in SOFC CHP systems functional specifications and literature review of industry data and patent data.

APPROACH

Data for system designs and component costing is derived from (1) existing cost studies where applicable; (2) literature and patent sources; and (3) industry and national laboratory advisors. Vertically integrated manufacturing is assumed for stack components with high-speed roll-to-roll processes for gas diffusion layer/gas diffusion electrode/ catalyst-coated membrane components and largely purchased components for balance-of-plant components. Life-cycle or use-phase costing utilizes existing LBNL tools [5], a National Renewable Energy Laboratory database of commercial building electricity and heating demand profiles by building type and geographical region [6], and earlier CHP modeling work by one of the authors [7].

Life-cycle impact assessment is focused on use-phase impacts from energy use, carbon emissions and pollutant emissions [9]—specifically on particulate matter emissions since particulate matter is the dominant contributor to life-cycle impacts [10]. Health impact from particulate matter is disaggregated by geographical region using existing LBNL health impact models [11] and an estimation of the amount of displaced grid-based electricity and heating fuel for a fuel cell CHP system in that building type and geographical region.

RESULTS

A sampling of direct cost results is shown in Figures 1-3. Full details can be found in the publication Wei (2014). LT PEM 10-kW backup power system direct costs are found to be less than $1,000/kW above 1,000 units per year. A large declination in stack cost from 100 to 1,000 units per year is due to a sharp increase in tool utilization above 100 units per year. The catalyst-coated membrane is 43% of stack cost at 1,000 units per year increasing to 50% at 50,000 units per year. At the highest volume, stack cost is $240/kW. BOP is simplified relative to CHP systems with air cooling vs. liquid cooling for CHP systems.

Figures 2 and 3 show direct cost vs. annual manufacturing volume for 50-kW LT and HT PEM CHP systems, respectively. LT PEM system cost varies from $1,500 to $1,100/kW from 1,000 units per year to 50,000 units per year. The rate of cost reduction in the stack is about twice that of balance-of-plant components from 1,000 to 10,000 units per year (28% vs 14%), since stack components

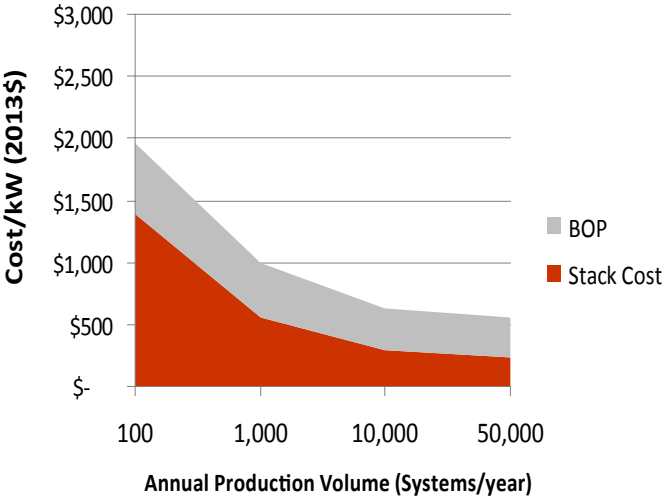

FIGURE 1. Direct Cost per kW for 10-kW LT PEM Backup Power System

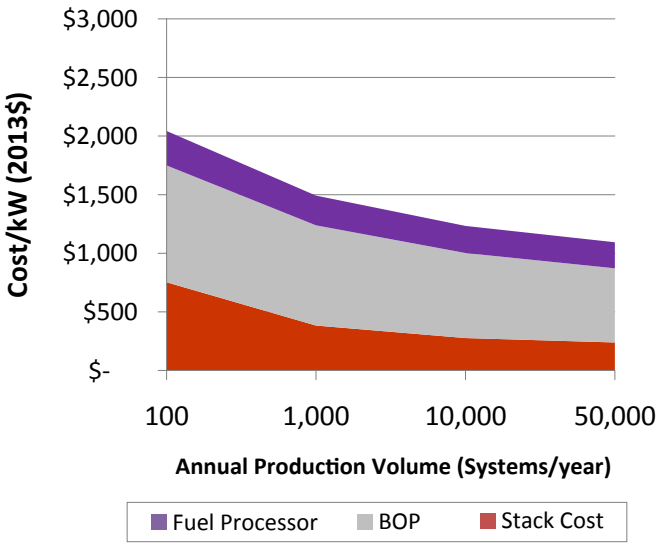

FIGURE 2. Direct Cost per kW for 50-kW LT PEM CHP System with Reformate Fuel

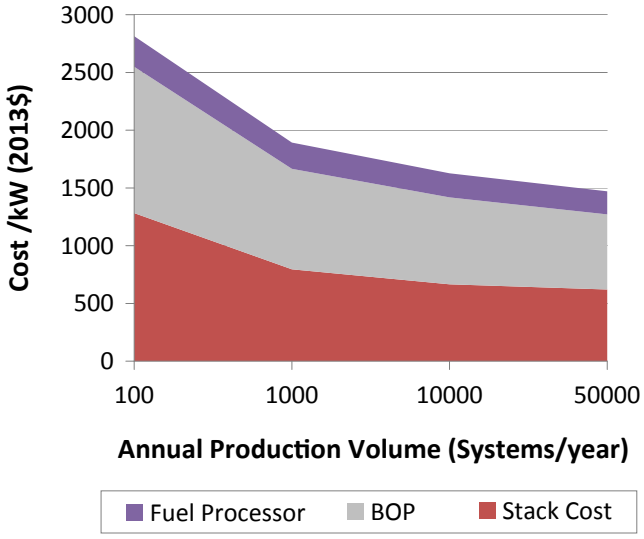

FIGURE 3. Direct Cost per kW for 50-kW HT PEM CHP System with Reformate Fuel

are assumed to achieve greater economies of scale e.g., higher tool utilization and increasing yield with higher volume, than purchased balance of plant components. Across the range of production volumes considered, the fuel cell stack cost constitutes 37% to 22% of total system cost.

At 50,000 systems per year, the 50-kW HT PEM system is projected to have 34% higher cost than the LT PEM CHP system despite slightly lower cost for the fuel processor and balance of plant. This is due to several factors: lower current density and higher cell area, higher platinum catalyst loading (0.7 vs. 0.5 mg/cm^2), more complex plate architecture, and slightly lower yield assumed due to less mature process technology. A compression-molded plate with a barrier layer to phosphoric acid is modeled for the HT PEM case for reliability and lifetime whereas injection molded plates are assumed for LT PEM CHP stacks. For HT PEM CHP across the range of production volumes considered, stack costs constitute 46% to 42% of overall system direct costs.

TCO cost of electricity for LT PEM is shown in Figure 4 for one building/geography pair (small hotel in Minneapolis). Other buildings and geographies were also modeling (hospitals, large and small office buildings) and several other cities across the U.S. (San Diego, Phoenix, Chicago, New York, and Miami). Figure 4 shows a waterfall chart of the cost of electricity starting from "levelized cost of electricity" (r=5%, 15-year system lifetime) and then successively including credits from offset heating fuel, carbon credits, and health and environmental externalities. Installed cost is taken to be $2,900/kW based on 100 MW of production per year, corporate markup of 50%, and an installation cost factor of 33%. In this particular case, heating fuel reduction contributes 5.5% savings, greenhouse gas (GHG), and health and environmental impacts contribute 23.4% savings, for an overall savings of 29% compared to the levelized cost of electricity. The TCO cost of electricity in this case is still slightly higher than the average commercial price of electricity in Minnesota ($0.092/kWh) but is much more competitive. Levelized cost of electricity is a strong function of fuel cost and capital cost, while TCO cost of electricity benefits from more fuel cell waste heat utilization, higher carbon price, and higher carbon intensity of displaced grid based electricity or conventional heating fuels.

CONCLUSIONS AND FUTURE DIRECTIONS

- Direct costs for LT PEM 10-kW backup power systems are found to be $1,959/kW at annual production volumes of 100 systems per year and $556/kW at 50,000 systems per year.
- For 100-kW CHP systems with reformate, the 2015 DOE cost target at 1,000 units year can be met with LT and HT PEM systems, but this volume of production is more realistic in the 2020 timeframe and the $1,000/kW cost target for 2020 is not met. For 10-kW CHP systems, 50,000 units per year, both PEM technologies exceed the cost target for both 2015 and 2020.
- Balance of plant is generally found to be the largest component of CHP system costs for LT and HT PEM systems. HT PEM CHP systems are projected to be higher cost than LT PEM systems due to lower power density, higher catalyst loading, more complex plate design, and lower process yield assumptions due to less overall technology maturity.

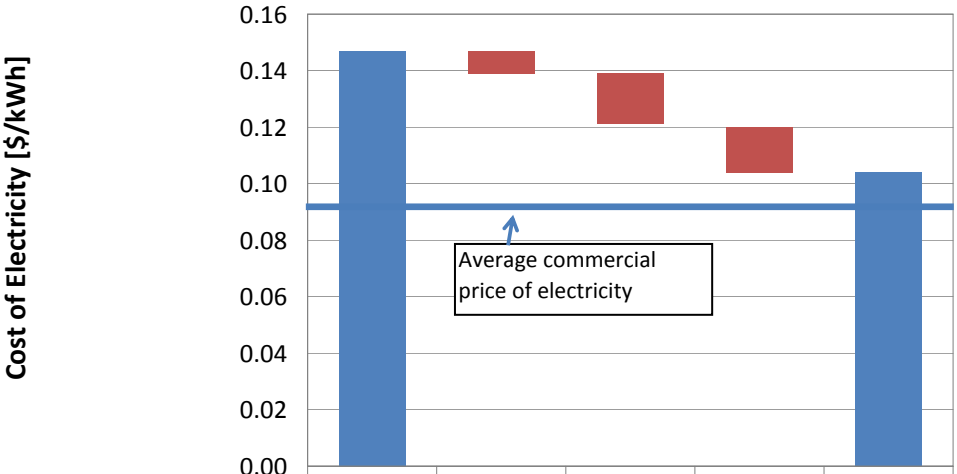

	Levelized Cost of Electricity	After Heating Savings per	After GHG Credit at $44/ton	After Environ-mental and	Cost of Electricity with TCO
Savings		$0.008	$0.018	$0.016	
O&M and Cap Replacement	$0.147	$0.139	$0.121	$0.104	$0.104

FIGURE 4. Total Cost Of Electricity Example for 50-kW LT PEM CHP System with Reformate Fuel in a Small Hotel in Minneapolis

- TCO including greenhouse gas and environmental and health externalities is very dependent on fuel costs, capital costs, waste heat utilization and the carbon intensity of displaced grid-based electricity and conventional heating fuels.
- The research team is refining the direct cost modeling and completing the TCO model for HT PEM CHP systems in the final quarter of FY 2014. SOFC direct cost modeling will be done in the fourth quarter of FY 2014 and the first quarter of FY 2015.
- The team is also completing an automated model for the LT and HT PEM TCO in the fourth quarter of FY 2014 which allows users to input cost assumptions and provides automated sensitivity analysis.

FY 2014 PUBLICATIONS/PRESENTATIONS

Publications

1. M. Wei 2014, Timothy Lipman, Ahmad Mayyas, Joshua Chien, Shuk Han Chan, David Gosselin, Hanna Breunig, Michael Stadler, Thomas McKone, Paul Beattie, Patricia Chong, Whitney G. olella, Brian D. James, "A Total Cost of Ownership Model for Low Temperature PEM Fuel Cells in Combined Heat and Power and Backup Power Applications," Lawrence Berkeley National Lab Report, July 2014.

Presentations

1. M. Wei, T. Lipman, A. Mayyas, S.H. Chan, D. Gosselin, H. Breunig, T. McKone, "A Total Cost of Ownership Model for Low Temperature PEM Fuel Cells in Combined Heat and Power and Backup power applications," Grove Fuel Cell Conference, Amsterdam, Netherlands, April 3-4, 2014.

2. D. Gosselin, M. Wei, "A Total Cost of Ownership Model for Low Temperature PEM Fuel Cells in Combined Heat and Power and Backup Power Applications," ASME 2014 12th Fuel Cell Science, Engineering and Technology Conference, Boston, MA, June 2014.

REFERENCES

1. James, Brian, Kalinoski, J., and K. Baum. Mass-Production Cost Estimation for Automotive Fuel Cell Systems. 2010 Annual Merit Review Proceedings, Department of Energy, Hydrogen and Fuel Cells Program. Washington, D.C. June 2010.

2. Sinha, Jayanti and Y. Yang. *Direct Hydrogen PEMFC Manufacturing Cost Estimation* for Automotive Applications. 2010 Annual Merit Review Proceedings, Department of Energy, Hydrogen and Fuel Cells Program. Washington, D.C. June 2010.

3. Mahadevan, Kathya , V. Contini, M. Goshe, J. Price, F. Eubanks, and F. Griesemer. Economic Analysis of Stationary PEM Fuel Cell Systems. 2010 Annual Merit Review Proceedings, Department of Energy, Hydrogen and Fuel Cells Program. Washington, D.C. June 2010.

4. James, B., Spisak, A., Colella, W. *Manufacturing Cost Analysis of Stationary Fuel Cell Systems*, Strategic Analysis Inc. Arlington VA, September 2012.

5. Stadler, Michael, Marnay, C., Gonçalo Cardoso, G. et. al. The Carbon Dioxide Abatement Potential of California's Mid-Sized Commercial Buildings. California Energy Commission, PIER Program. CEC-500-2010-050 (2011).

6. Deru, M., Field, K., Studer, D., Benne, K., Griffith, B., Torcellini, P., Liu, B., Halverson, M., Winiarski, D., Rosenberg, M., Yazdanian, M., Huang, J., Crawley, D. (2011). Reference Building Models of the National Building Stock. NREL Technical Report NREL/TP-5500-46861.

7. Lipman, Timothy E., Jennifer L. Edwards, and Daniel M. Kammen, "Fuel Cell System Economics: Comparing the Costs of Generating Power with Stationary and Motor Vehicle PEM Fuel Cell Systems," Energy Policy 32(1): 101-125 (2004)

8. ACI Technologies, Inc. Manufacturing Fuel Cell Manhattan Project, U.S. Government Contract No. N00014-08-D-0758, November 2011.

9. Van Rooijen, Jaap. A Life Cycle Assessment of the PureCell™ Stationary Fuel Cell System: Providing a Guide for Environmental Improvement, Center for Sustainable Systems, Report No. CSS06-09 University of Michigan, Ann Arbor, Michigan June 30, 2006.

10. National Research Council. Hidden Costs of Energy: Unpriced Consequences of Energy Production and Use. The National Academies Press: Washington, D.C., 2010.

11. Muller, N.Z., and R.O. Mendelsohn, The Air Pollution Emission and Policy Analysis Model (APEEP): Technical Appendix [online]. Yale University, New Haven, CT. December 2006. Available at: https://segueuserles.middlebury.edu/nmuller/APEEP_Tech_Appendix.pdf

V.J.1 Advanced Materials and Concepts for Portable Power Fuel Cells

P. Zelenay (Primary Contact), H. Chung, Y.S. Kim, J.H. Dumont, Y. Xu, U. Martinez, G. Wu

Materials Physics and Applications Division
Los Alamos National Laboratory
Los Alamos, NM 87545
Phone: (505) 667-0197
Email: zelenay@lanl.gov

DOE Manager

Nancy Garland
Phone: (202) 586-5673
Email: Nancy.Garland@ee.doe.gov

Subcontractors

- R.R. Adzic (PI), M. Li, M. Vukmirovic, K. Sasaki
  Brookhaven National Laboratory, Upton, NY
- Y. Yan (PI), J. Zheng
  University of Delaware, Newark, DE
- J.E. McGrath (PI), J. Rowlett, A. Shaver
  Virginia Polytechnic and State University, Blacksburg, VA
- A.M. Bonastre (PI), W. Hall, G. Hards, E. Price, J. Sharman, G. Spikes
  Johnson Matthey Fuel Cells (JMFC), Swindon, United Kingdom
- C. Böhm (PI)
  SFC Energy, Brunnthal, Germany
- K.L. More (PI), D. Cullen
  Oak Ridge National Laboratory, Oak Ridge, TN (no-cost partner)

Project Start Date: September 2010
Project End Date: August 2014

Overall Objective

Develop advanced materials (catalysts, membranes, electrode structures, membrane electrode assemblies [MEAs]) and fuel cell operating concepts capable of fulfilling cost, performance, and durability requirements established by DOE for portable power fuel cell systems; assure path to large-scale fabrication of successful materials.

Fiscal Year (FY) 2014 Objectives

- Optimize thrifted "advanced anode catalyst" (AAC) to achieve key direct methanol (MeOH) fuel cell (DMFC) performance goal of 150 mA cm^{-2} at 0.6 V with low Pt loadings (<1.0 mg cm^{-2} at anode).
- Scale up the synthesis of PtRu/CuNWs to a 10-mg batch and test in MEAs.
- Synthesize multi-block copolymers capable of delivering >200 mA cm^{-2} at 0.5 V in a single-cell DMFC test at 75°C.
- Develop alternative oxides and intermetallic Pt supports for ethanol (EtOH) oxidation.
- Improve mass activity of the ternary PtRuPd/C dimethyl ether (DME) oxidation catalyst from the FY 2013 performance of 37 A/g to 50 A/g at 0.5 V in a single-cell direct DME fuel cell test at 80°C.
- Complete DMFC testing of a short stack, utilizing components developed in the project.

Technical Barriers

This project addresses the following technical barriers in the Fuel Cells section of the Fuel Cell Technologies Office Multi-Year Research, Development, and Demonstration Plan [1]:

(A) Durability (catalysts, membranes, electrode layers)

(B) Cost (catalysts, MEAs)

(C) Performance (catalysts, membranes, electrodes, MEAs)

Technical Targets

Portable fuel cell research in this project focuses on the DOE technical targets specified in Tables 3.4.7a, 3.4.7b, and 3.4.7c in the Fuel Cells section 3.4.4 (Technical Challenges) of the Fuel Cell Technologies Office Multi-Year Research, Development, and Demonstration Plan [1]. Table 1 summarizes the latest DOE performance targets for portable power fuel cell systems in three power ranges.

Using DOE's Table 3.4.7 as a guide with relevance to portable power systems, the following specific project targets have been devised:

- System cost target: $5/W
- Performance target: Overall fuel conversion efficiency (η_Σ) of 2.0-2.5 kWh/L

In the specific case of a DMFC, the above assumption translates into a total fuel conversion efficiency (η_Σ) of 0.42-0.52, corresponding to a 1.6-2.0-fold improvement over state-of-the-art systems (ca. 1.250 kWh/L). Assuming fuel utilization (η_{fuel}) and balance-of-plant efficiency (η_{BOP}) of 0.96 and 0.90, respectively (efficiency numbers based on information obtained from DMFC systems developers), and using a theoretical voltage (V_{th}) of 1.21 V at 25°C, the cell voltage (V_{cell}) targeted in this project can be calculated as:

$$V_{cell} = V_{th}\,[\eta_\Sigma\,(\eta_{fuel}\,\eta_{BOP})^{-1}] = 0.6\text{-}0.7\ \text{V (depending on } \eta_\Sigma \text{ achieved)}$$

TABLE 1. Project Technical Targets

Technical Targets: Portable Power Fuel Cell Systems (< 2 W; 10-50 W; 100-250 W)				
Characteristics	**Units**	**2011 Status**	**2013 Targets**	**2015 Targets**
Specific power	**W/kg**	5; 15; 25	8; 30; 40	10; 45; 50
Power Density	**W/L**	7; 20; 30	10; 35; 50	13; 55; 70
Specific energy	**Wh/kg**	110; 150; 250	200; 430; 440	230; 650; 640
Energy density	**Wh/L**	150; 200; 300	250; 500; 550	300; 800; 900
Cost	**$/W**	150; 15; 15	130; 10; 10	70; 7; 5
Durability	**Hours**	1,500; 1,500; 2,000	3,000; 3,000; 3,000	5,000; 5,000; 5,000
Mean time between failures	**Hours**	500; 500; 500	1,500; 1,500; 1,500	5,000; 5,000; 5,000

Thus, the ultimate target of the material development efforts in the DMFC part of this project is to assure an operating single fuel cell voltage of ca. 0.60 V. Very similar voltage targets have been calculated for fuel cells operating on two other fuels, EtOH and DME.

FY 2014 Accomplishments

- Advanced anode catalysts that use much lower Pt loading compared to current state-of-the-art HiSPEC® 12100 PtRu/C catalyst (1.0 mg_{Pt} cm^{-2} *vs.* 2.7 mg_{Pt} cm^{-2}) were developed. Catalyst-coated membranes prepared by JMFC using the AAC were provided to SFC Energy for stack testing. In spite of much lower Pt loading, AAC exhibits better stability over 2,500 hours of stack operation than commercial catalyst without sacrificing performance.
- Tetramethyl bisphenol A (TM)-based multiblock copolymer systems with less than 30% water uptake and comparable proton conductivity to Nafion® were developed. MEAs using TM-based multiblock copolymers reached >200 mA/cm^2 at 0.5 V (75°C) with stable long-term performance without interfacial failure under DMFC accelerated stress test conditions.
- Direct DME fuel cell (DDMEFC) performance reached 0.220 A cm^{-2} at 0.5 V (an anode catalyst mass-specific activity of 55 A g^{-1}) thanks to the development of a new ternary $Pt_{55}Ru_{35}Pd_{10}$/C catalyst and optimization of DDMEFC operating conditions. This not only exceeds the FY 2014 performance target, but also is the first time that performance of the DDMEFC matches and outperforms that of state-of-the-art DMFCs.

INTRODUCTION

This multitask, multi-partner project targets advancements to portable fuel cell technology through the development and implementation of novel materials and concepts for enhancing performance, lowering cost, minimizing size and improving durability of fuel cell power systems for consumer electronics and other mobile and off-grid applications. The primary focus areas of the materials research in this project are: (i) electrocatalysts for the oxidation of MeOH, EtOH, and DME; (ii) innovative nanostructures for fuel cell electrodes; and (iii) hydrocarbon membranes for reduced MEA costs and enhanced fuel cell performance (fuel crossover, proton conductivity). In parallel with new materials, this project targets the development of various operational and materials-treatment concepts, concentrating among others on the improvements to the long-term performance of individual components and the complete MEA.

APPROACH

The two primary research goals of this project are: (i) development of binary and ternary catalysts for the oxidation of MeOH, EtOH, and DME, and (ii) synthesis of hydrocarbon polymers (multiblock copolymers, copolymers with cross-linkable functional groups) for lower cost and better fuel cell performance through reduced fuel crossover and increased protonic conductivity. Better understanding of the key factors impacting the performance of both catalysts and polymers is also pursued through characterization efforts including X-ray absorption spectroscopy, X-ray photoelectron spectroscopy, nuclear magnetic resonance and transmission electron microscopy.

Development of new catalysts and polymers is closely tied to electrode nanostructures tailored to minimize precious metal contents, maximize mass activity and enhance durability. The electrode-structure component of the efforts concentrates on two groups of materials: (i) solid-

metal nanostructures (e.g., nanowires and nanotubes) and (ii) carbon-based nanostructures acting as supports for metal catalysts.

In addition to the short-term testing and initial performance assessment, the catalysts, membranes, supports, electrode structures and MEAs developed in this project are subject to long-term performance (durability) testing. Performance-limiting factors and degradation mechanisms are being identified and, if possible, addressed. Fabrication and scale-up of viable catalysts, membranes, and supports are also being tackled through collaboration between partners in this project.

RESULTS

DMFC Catalysts—Further development of the AAC, thrifted binary PtRu/C catalyst first synthesized in FY 2012, continued in FY 2014 to meet the project milestone of 0.15 A cm^{-2} at 0.60 V through: (i) optimizing the Pt-to-Ru ratio to lower the onset potential of MeOH oxidation, (ii) using a lower carbon content to thin the electrode layer, and (iii) modifying the cell operation conditions (temperature, MeOH concentration). Among several Pt-to-Ru ratios, a 1:4 atomic ratio represented the optimum catalyst composition for fast dehydrogenation, efficient CO removal and low Ru crossover to the cathode. Additionally, increasing the Pt+Ru loading by 33% in AAC to thin the electrode had no effect on catalytic activity. When the cell temperature was increased to 88°C from 80°C, a gain of 20 mV at 150 mA cm^{-2} was obtained. With an increase in MeOH concentration from 0.5 M to 0.6 M, improvements in the current density at potentials lower than ca. 0.55 V were observed without any additional MeOH crossover loss. With these optimizations, a high performance of 0.56 V at 0.150 A cm^{-2} was achieved at 88°C, only 0.04 V away from the project target (Figure 1). Ten 50-cm^2 MEAs with optimized AAC were provided by JMFC to SFC Energy for stack testing. Noticeably, a decay rate of only 19 µV/h (per cell) was obtained, slightly lower than in commercial MEAs with much higher Pt loadings (Figure 2). This attests to AAC as a very promising catalyst with potential to enable DMFCs for higher power applications (such as kW-level power generators). A maximum stack voltage was reached after 70 hours of operation, and the

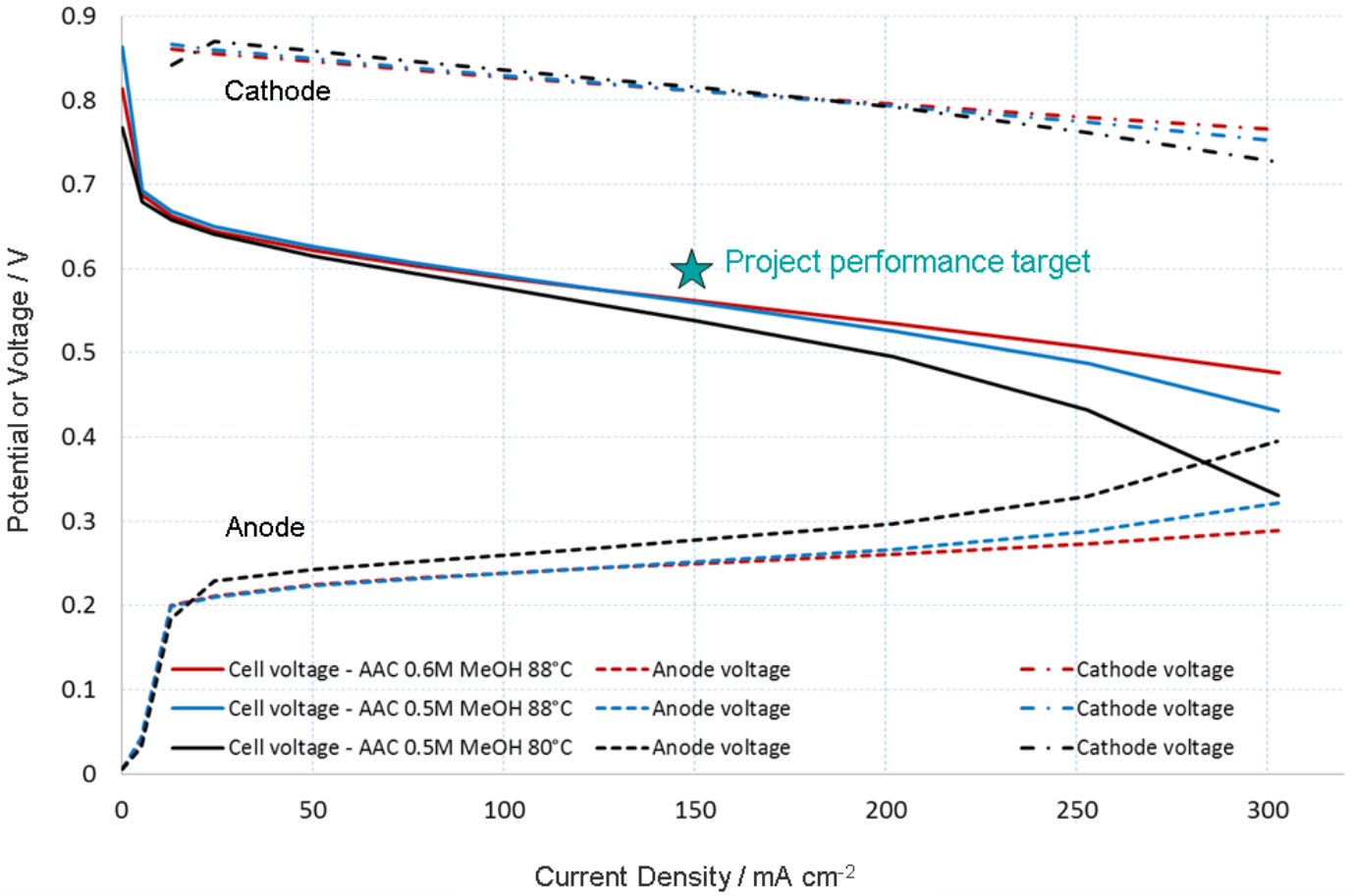

FIGURE 1. Polarization plots for AAC with catalyst loading 1.0 mg_{Pt} cm^{-2}, 0.5-0.6 M MeOH. Cathode - Pt/C catalyst loading 1.5 mg_{Pt} cm^{-2}, air (fuel cell), H_2 (anode polarization); Nafion® 115 membrane; cell temperature 80-88°C.

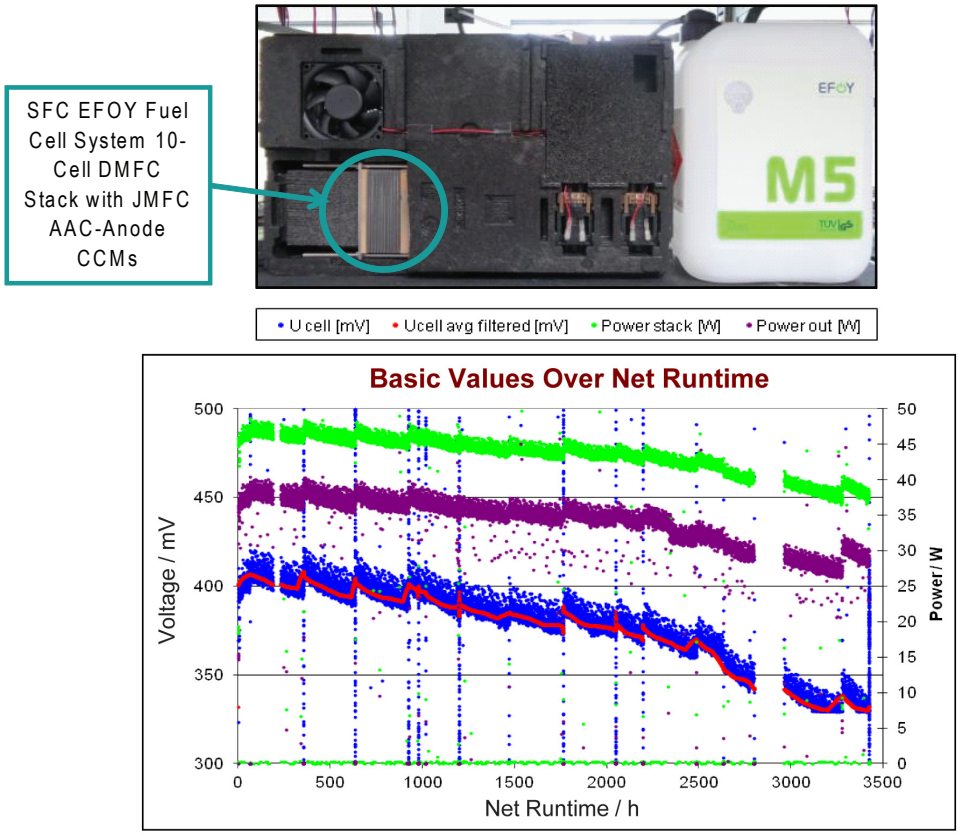

FIGURE 2. Durability Test of Ten-Cell DMFC Stack with JMFC AAC-Anode CCM

performance discontinuity observed around 2,800 hours of operation was due to pump failure.

Innovative Electrode Structures—In FY 2014, a successful scale up of PtRu/CuNWs from 5 mg to 19 mg per batch was achieved, accompanied by slightly higher MeOH oxidation activity. The cause of higher MeOH oxidation activity of PtRu/CuNWs compared to that of PtRu/C may be due to the facile removal of CO from the PtRu/CuNWs surface, as demonstrated by X-ray photoelectron spectroscopy Pt 4f and Ru 3p shifts.

Multiblock Copolymers for Better Interfacial Compatibility—We have focused this year on synthesizing multiblock copolymers with better interfacial compatibility with DMFC electrodes. It was achieved by reducing the membrane water uptake. Chemical modifications for this purpose included control of the fluorination level and of the bisphenol structure. We have successfully synthesized TM-based multiblock copolymers. This TM system had a water adsorption nearly half that of the dimethyl and bis A proton exchange membranes. MEAs using the highly hydrophobic TM system not only showed excellent DMFC performance, but met the FY 2014 performance milestone reaching >200 mA/cm^2 at 0.5 V (75°C). In addition, the TM-based multiblock copolymers showed good interfacial compatibility with Nafion®-bonded electrodes. Figure 3 shows the high-frequency resistance (HFR) of DMFC cells using three different membranes. The HFR of the cell using 6FPAEB-BPSH (water uptake = 57 vol%) constantly increases from 0.073 to 0.13 Ω cm^2 after 110 hours of the extended-term test. In contrast, the TM multi-block copolymer (water uptake = 23 vol%) shows stable HFR behavior during the entire 110 hour extended-term test. Nafion®, which has a water uptake of 39 vol%, also shows a stable HFR behavior, likely due to the synergistic effect of low water uptake and a highly fluorinated structure. These results confirm our hypothesis regarding interfacial delamination and TM-based multi-block copolymers, and have the potential to be applied in practical liquid-fueled fuel cell applications.

Ethanol Oxidation Catalysts—In FY 2014, combustion catalyst synthesis was developed as a way of forming multi-component catalysts in a single-step that were successfully deposited on gas diffusion layers. The ternary catalyst ($PtRhSnO_2$/C) synthesized by this method exhibited excellent activity and stability at 25°C and 60°C.

To solve the SnO_2 instability issues, which were recognized in FY 2013, several oxides and intermetallic compounds were studied as supports that can replace SnO_2. Among several oxides investigated (CeO_2, Ti_4O_7, ITO,

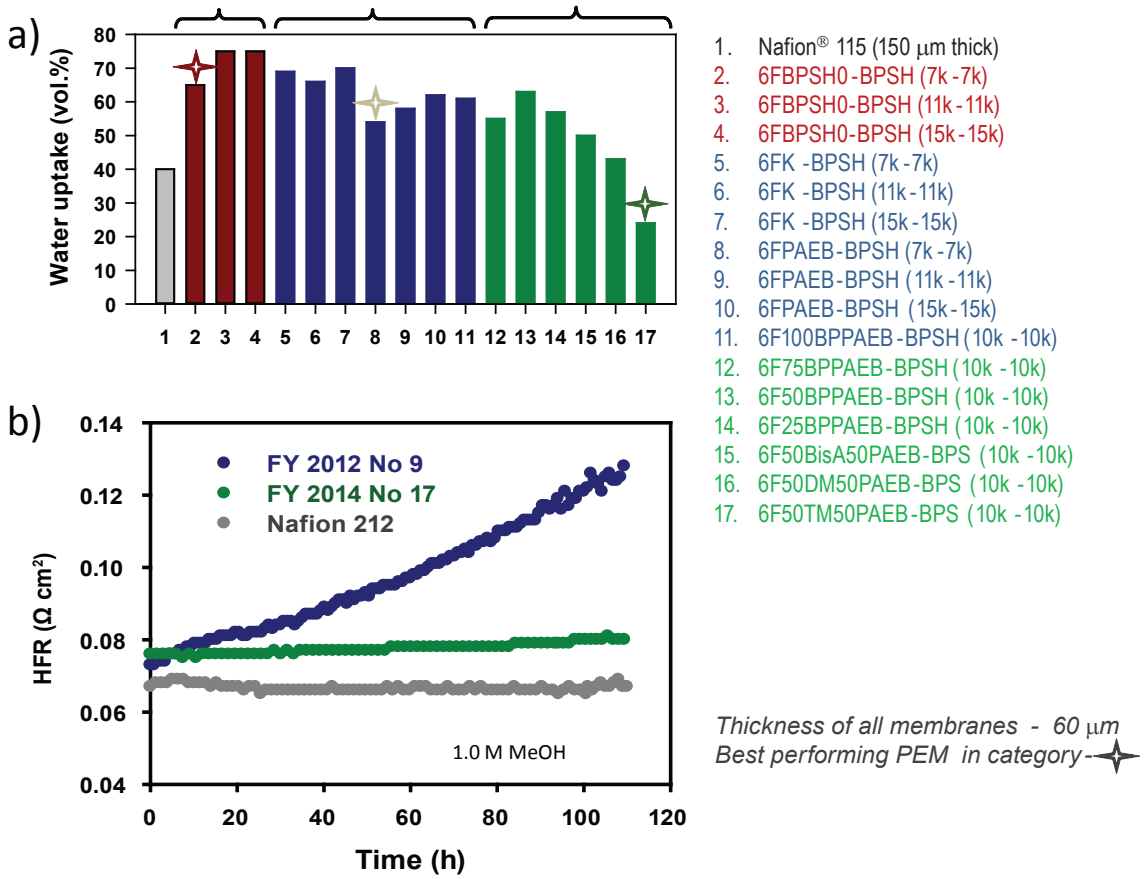

FIGURE 3. (a) Volumetric water uptake of mutiblock copolymers (best performing membranes for each year denoted as ✦), (b) its impact on DMFC durability. No. 9: FY 2012, membrane 6FPAEB-BPSH (11K-11K); No. 17: FY 2014 membrane 6F50TM50PAEB-BPS (10K-10k).

and IrO_x), IrO_x in particular was identified as a promising replacement for the SnO_2 in the ternary catalysts, and CeO_2 was also found to considerably enhance the activity of Pt_{ML}/Pd/C catalysts for EtOH oxidation. The intermetallic compound, PdAuCo, also exhibits better performance as a Pt_{ML} support than core-shell PdAuCo.

Dimethyl Ether Fuel Cell Research—Significant progress was made in MEA and fuel delivery system optimization. Thanks to these advancements, from FY 2013 to FY 2014, DDMEFC performance increased from 0.095 A cm^{-2} to 0.215 A cm^{-2} at 0.5 V, in spite of lowering the Pt-group metal anode loading by 25%. Based on density functional theory calculations, in FY 2013 we proposed the individual role of each metal in the ternary PtRuPd/C catalysts as follows: Pt—primary DME adsorption and dehydrogenation; Ru—source of oxidant for CO removal; Pd—C-O and C-H bond scission catalyst. In FY 2014, using two binary PtPd/C and PtRu/C catalysts, we experimentally demonstrated that Pd addition indeed results in higher current densities with the same onset potential observed with Pt, and Ru leads to a lower onset potential of DME oxidation. This finding allowed

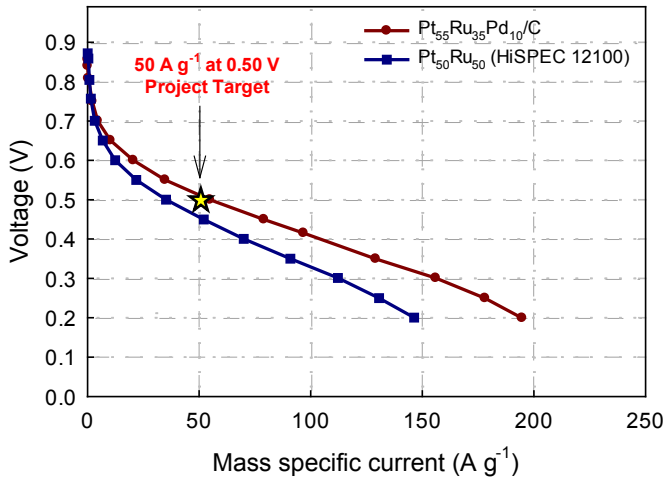

FIGURE 4. Polarization plots of DDMEFC. Anode: 4.0 mg_{PGM} cm^{-2} PtRuPd/C, HiSPEC® 12100, 40 sccm DME gas, 26 psig; cathode: 2.0 mg_{Pt} cm^{-2} Pt/C HiSPEC® 9100, 100 sccm air, 20 psig; Nafion® 212 membrane; cell temperature 80°C.

us to develop an advanced ternary $Pt_{55}Ru_{35}Pd_{10}$/C catalyst, more advanced than the $Pt_{45}Ru_{45}Pd_{10}$/C catalyst developed in FY 2013. DDMEFC performance measured with this catalyst reached a high current density of 0.220 A cm^{-2} (an anode catalyst mass-specific activity of 55 A g^{-1}) at 0.5 V, exceeding the FY 2014 performance target (Figure 4). Due to the new ternary $Pt_{55}Ru_{35}Pd_{10}$/C DME oxidation catalyst developments and optimization of the MEA and DDMEFC operation conditions over the project duration, DDMEFC performance has been improved by a factor of 2.5× in terms of current density at 0.5 V. This makes the performance of the latest-generation DDMEFC exceed that of the state-of-the-art DMFC (Figure 5).

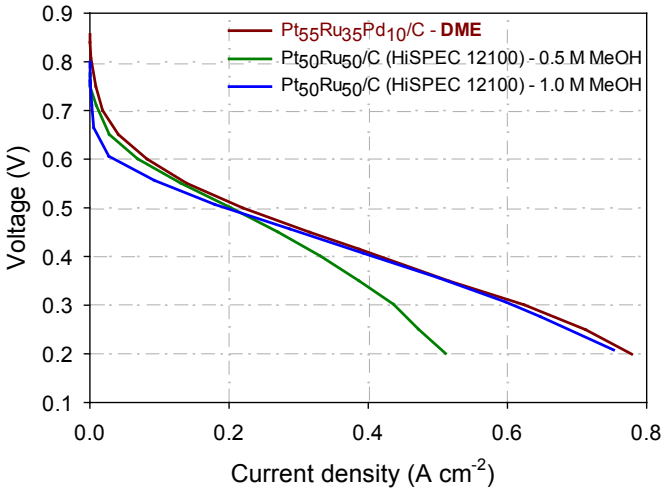

FIGURE 5. DDMEFC and DMFC performance comparison. Anode: 4.0 mg_{metal} cm^{-2} PtRuPd/C, HiSPEC® 12100, 40 sccm DME gas, 26 psig, 1.8 mL/min 0.5 M or 1.0 M MeOH, 0 psig; cathode: 2.0 mg_{Pt} cm^{-2} Pt/C HiSPEC® 9100, 100 sccm air, 20 psig; Nafion® 212 membrane (DME), Nafion® 115 membrane (MeOH); cell temperature 80°C.

CONCLUSIONS

- JMFC's AAC reached 0.150 A cm^{-2} at 0.56 V with low anode loading of 1.0 mg_{Pt} cm^{-2} (total 2.5 mg_{Pt} cm^{-2}).
- AAC-based catalyst-coated membranes prepared by JMFC were used for a 10-cell SFC Energy stack test. In spite of much lower Pt loading (1.0 mg_{Pt} cm^{-2} vs. 2.7 mg_{Pt} cm^{-2} of HiSPEC® 12100), AAC showed better stability over 2,500 hours of stack operation than commercial catalysts.
- Progress in MeOH catalyst development is viewed by SFC Energy as an enabling factor for higher power DMFC applications (i.e., power generators) that are currently not feasible due to the prohibitive catalyst cost.
- A high current density of 0.200 A cm^{-2} at 0.50 V (75°C) was achieved with TM-based multi-block copolymer. A 60-µm TM-based MEA showed lower resistance, MeOH crossover and water uptake than a Nafion® 115-based MEA—a DMFC industry standard.
- Significant progress in DME electrocatalysis with the development of ternary PtRuPd/C catalyst in conjunction with MEA and fuel delivery system optimization was demonstrated to result in a DDMEFC current density of 220 A cm^{-2} at 0.5 V (an anode catalyst mass-specific activity of 55 A g^{-1})—a 2.5-fold improvement in activity since project inception.
- The LANL DDMEFC was demonstrated to exceed state-of-the-art DMFCs across the entire range of current densities.
- Recent advancements in ethanol oxidation electrocatalysis at Brookhaven National Laboratory (Pt_{ML}/Au/C catalyst) led to a ca. 200 mV reduction in overpotential for EtOH oxidation relative to Pt/C.

FUTURE DIRECTIONS

- DMFCs: Complete current catalyst development efforts to meet the last remaining project milestone (0.15 A cm^{-2} at 0.60 V); develop MeOH oxidation catalysts free of intrinsically unstable components (possible formulations include two-dimensional platelets containing low-coordination atoms of precious metals and Au-core nanoparticles as supports); develop inks, gas diffusion layer treatments, optimize and assure manufacturability by a scalable production process for AAC targeting 50% Pt reduction in two years without performance/durability penalty (30% Pt reduction in FY 2015) and 500-W system.
- DDMEFCs: Complete development and optimization of the ternary PtRuPd catalyst for DME oxidation; implement multiblock copolymer membranes in DDMEFC-type MEAs; complete detailed study of DME crossover and its impact on DDMEFC performance.
- EtOH oxidation catalysis: Develop new-generation catalysts for EtOH oxidation, for example, catalysts on composites of stable oxides and lattice-expanded nanoparticles of precious metals; use in-fuel-cell stability and 12-electron selectivity as primary performance and selection criteria; perform assessment of direct EtOH fuel cell viability at the present state of ethanol oxidation catalysis.

SPECIAL RECOGNITIONS & AWARDS/ PATENTS ISSUED

1. Piotr Zelenay has been named a Fellow of The Electrochemical Society, 2014.

FY 2014 PUBLICATIONS

1. Yu Seung Kim, Kwan-Soo Lee, "Fuel Cell Membrane Characterizations", *Polym. Rev.*, in press.

2. Meng Li, Nebojsa S. Marinkovic, "In situ Infrared Spectroelectrochemistry: Principles and Applications", in *Infrared Spectroscopy: Theory, Developments and Applications*. Edited by Daniel Cozzolino. Nova Science Publishers, in press.

3. Qing Li, Gang Wu, Christina M. Johnston, Piotr Zelenay, "Direct Dimethyl Ether Fuel Cell with Much Improved Performance", *Electrocatalysis*, 2014, 10.1007/s12678-014-0196-z.

4. Jarret R. Rowlett, Yu Chen, Andrew T. Shaver, Gregory B. Fahs, Benjamin J. Sundell, Qing Li, Yu Seung Kim, Piotr Zelenay, Robert B. Moore, Sue Mecham, James E. McGrath, "Multiblock Copolymers Based Upon Increased Hydrophobicity Bisphenol A Moieties for Proton Exchange Membranes;" *J. Electrochem. Soc.* 161 (4) F535-F543 (2014).

5. Yijin Kang, Meng Li, Yun Cai, Matteo Cargnello, Rosa E. Diaz, Thomas R. Gordon, Noah L. Wieder, Radoslav R. Adzic, Raymond J. Gorte, Eric A. Stach, Christopher B. Murray, "Heterogeneous Catalysts Need Not Be so 'Heterogeneous': Monodisperse Pt Nanocrystals by Combining Shape-Controlled Synthesis and Purification by Colloidal Recrystallization", *J. Am. Chem. Soc.*, 135 (7), 2741-2747 (2013).

6. Qing Li, Yu Chen, Jarrett R. Rowlett, James E. McGrath, Nathan H. Mack, Yu Seung Kim, "Controlled Disulfonated Poly(Arylene Ether Sulfone) Multiblock Copolymers for Direct Methanol Fuel Cells", *ACS Appl. Mater. Interfaces*, 6, 5779-5788, 2014.

7. Meng Li, David A. Cullen, Kotaro Sasaki, Nebojsa S. Marinkovic, Karren L. More, Radoslav R. Adzic, "Ternary Electrocatalysts for Oxidizing Ethanol to Carbon Dioxide: Making Ir Capable of Splitting C-C bond", *J. Am. Chem. Soc.*, 135 (1), 132-141 (2013).

8. Hoon T. Chung, Joseph H. Dumont, Ulises Martinez, Piotr Zelenay, "Catalyst Development for Dimethyl Ether Electrooxidation", 225th Meeting of the Electrochemical Society, Orlando, Florida, May 11-16, 2014.

9. R.R. Adzic, "Platinum Monolayer Electrocatalysts: Tuning Their Properties by Core-shell Interactions", CEC 2014 Annual Workshop on Electrochemistry, University of Texas at Austin, Texas, February 8–9, 2014 (invited lecture).

10. R.R. Adzic, "Platinum Monolayer Electrocatalysts: Recent Improvements for the Oxygen Reduction Reaction and the Oxidation of Ethanol and Methanol", Electrochemical Conference on Energy and Environment, Shanghai, China, March 13–16, 2014 (invited keynote lecture).

11. Piotr Zelenay, "Development and Characterization of Catalysts for Fundamental Electrode Reactions in Polymer Electrolyte Fuel cells", Department of Chemistry, University of Warsaw, Warsaw, Poland, December 9, 2013 (invited lecture).

12. Jie Zheng, David Cullen, Yushan Yan, "PtRuCuNWs catalysts for methanol oxidation reaction in direct methanol fuel cells", 224th Meeting of the Electrochemical Society, San Francisco, California, October 27 – November 1, 2013.

13. Qing Li, Dusan Spernjak, Yu Seung Kim, Piotr Zelenay, Performance Stability of Carbon-Supported vs. Metal-Black DMFC Catalysts, 224th Meeting of the Electrochemical Society Meeting, San Francisco, California, October 27 – November 1, 2013.

14. Jie Zheng, Yushan Yan, "PtRu coated CuNWs as an efficient catalyst for methanol oxidation reaction", Center for Catalytic Science and Technology Annual Review, Newark, Delaware, October 10, 2013.

15. Jie Zheng, Yushan Yan, "PtRu coated CuNWs as an efficient catalyst for methanol oxidation reaction", SUNCAT Summer Institute 2013, Menlo Park, California, August 26, 2013 (poster).

REFERENCE

1. *Multi-Year Research, Development and Demonstration Plan: Section 3.4 Fuel Cells*, Fuel Cell Technologies Program, 2011. http://www1.eere.energy.gov/hydrogenandfuelcells/mypp/pdfs/fuel_cells.pdf

V.K.1 Power Generation from an Integrated Biomass Reformer and Solid Oxide Fuel Cell (SBIR Phase III)

Patricia Irving, Quentin Ming (Primary Contact)
InnovaTek, Inc.
3100 George Washington Way, Suite 108
Richland, WA 99354
Phone: (509) 375-1093
Email: ming@innovatek.com

DOE Manager
Donna Ho
Phone: (202) 586-8000
Email: Donna.Ho@ee.doe.gov

Contract Number: DE-EE0004535

Project Start Date: October 1, 2010
Project End Date: September 30, 2014

Overall Objectives

- Establish design to meet technical and operational needs for distributed energy production from renewable fuels
- Design, optimize, and integrate proprietary system components and balance of plant in a highly efficient system
- Demonstrate the technical and commercial potential of the technology for energy production, emissions reduction, and process economics

Fiscal Year 2014 Objectives

- Achieve 40% system operating efficiency with revised/optimized system design
- System performance proves superior energy efficiency and emissions reductions compared to conventional technology
- Analysis of process economics supports commercial feasibility

Technical Barriers

This project addresses the following technical barriers from the Fuel Cells section of the DOE Fuel Cell Technologies Office Multi-Year Research, Development, and Demonstration Plan:

(A) Durability

(B) Cost

(C) Performance

Technical Targets

InnovaTek's research plan addresses several DOE technical targets for stationary applications for 1-10 kW_e fuel cell power systems operating on natural gas [1]. Progress in meeting DOE's technical targets is provided in Table 1.

TABLE 1. Progress toward Meeting Technical Targets for Integrated Stationary 5-kW Fuel Cell Power Systems Operating on Reformate[a] from Bio-Derived Renewable Liquids

Characteristic	Units	2015 Target[c]	2020 Target	InnovaTek 2014 Status[d]
Electrical Energy Efficiency[b] @ rated power	%	42.5	>45%	42
Equipment Cost, 5-kW system	$/$kW_e$	1,700	1,500	1,722
Operating Lifetime	hr	40,000	60,000	1,000+
Start-up Time at 20°C ambient	min	30	20	10

[a] Includes fuel processor, stack, and all ancillaries.
[b] Regulated AC net/lower heating value of fuel
[c] For a fuel cell system using natural gas as fuel
[d] For a solid oxide fuel cell (SOFC) and fuel reformer system using bio-kerosene as fuel. InnovaTek lifetime test limited to 1,000 hours. Start-up time is for reformer only.

FY 2014 Accomplishments

- Completed design innovations to improve equipment lifetime, efficiency, and cost objectives.
- A heat exchanger was added to the distributed power generator as an option to increase efficiency and expand commercial applications.
- Manufactured a highly efficient 2.6-kW fuel processor for producing 22,776 kWh/yr of distributed power with a SOFC operating on natural gas or liquid biofuel.
- Manufactured critical parts using three-dimensional printing, an additive manufacturing approach that helps reduce equipment costs.
- Obtained 42% system efficiency.
- Completed analyses using the HOMER model and determined that cost of power using InnovaTek's technology operating on natural gas is competitive with current power prices.
- Completed initial system testing that confirms operational performance and began long-term performance evaluation.
- Supported two students and continued partnerships with Pacific Northwest National Laboratory, Washington

State University, Boeing, City of Richland, Impact Washington, Breakthrough Technologies Institute, and the Mid-Columbia Energy Initiative.

✧ ✧ ✧ ✧ ✧

INTRODUCTION

Alternative energy sources must be sought to meet energy demand for our growing economy and to improve energy security while reducing environmental impacts. In addition to facilitating the use of a renewable fuel source, cost and durability are among the most significant challenges to achieving clean, reliable, cost-effective fuel cell systems. Therefore, this project is focusing on lowering the cost and increasing the durability of a fuel cell distributed renewable energy system, while also assuring that its performance meets or exceeds that of competing technologies. Work was conducted to develop proprietary steam reforming technology that uses multiple fuel types, including renewable liquid bio-fuels, and to integrate the reformer with a SOFC. A highly efficient integrated system design with an SOFC was developed that reduces the loss of heat through effective thermal management. A third generation optimized system design was completed, components were fabricated, and a prototype 2.6-kW fuel processor was assembled and tested during this period to determine costs and performance.

APPROACH

The technological approach utilizes a steam reforming reactor to convert bio-fuel derived from lignocellulosic biomass to hydrogen rich reformate that fuels an integrated solid oxide fuel cell for power generation. The project has evolved through three developmental stages.

1. Optimization of SOFC and fuel processor integration – is completed using process simulation and analysis to optimize system design and produce a complete mass and energy balance for individual components of the system. Process flow and piping and instrumentation diagrams are prepared to analyze possible system configurations using MathCAD and FEMLAB models to simulate the process flow paths in the system.
2. Design for manufacturing and field operation – requires continued modeling and analysis such as failure modes and effects analysis and Design for Manufacturing and Assembly (DFMA®) and several iterations of component manufacturing and tests to compare design options. The dimensions, geometries and flow patterns defined from optimization modeling work completed in Stage 1 are translated into three-dimensional computer-aided design (CAD) images and drawings.
3. System demonstration and validation for commercial applications – is the current and final stage of the project. Two complete systems have been manufactured for demonstration to gain performance data necessary to validate the design, operation, and cost of the system.

RESULTS

System Design and Fabrication

The system design produced in 2013 was further optimized in 2014 using manufacturability and integrated product development concepts to achieve cost and performance targets for a pre-commercial fuel cell energy system. Various design concept alternatives were evaluated against DFMA® objectives to help reduce both capital equipment costs and maintenance cost while increasing lifetime and robustness. CAD and computational fluid dynamics modeling was used for cost effective development and analysis of design alternatives (Figure 1). All drawings, specifications, and price quotes were consolidated for subsystem components along with the specifications developed. This information formed the detailed design package for building a prototype system.

A bill of materials was prepared for all subsystems of the fuel cell power plant. This was used to obtain cost estimates for prototype fabrication and for volume production from potential vendors and fabricators. Suppliers were down-selected based on pricing and quality of products. A solid model of the integrated system was prepared (Figure 2) and used as a guide for system assembly. Compared to the 2012

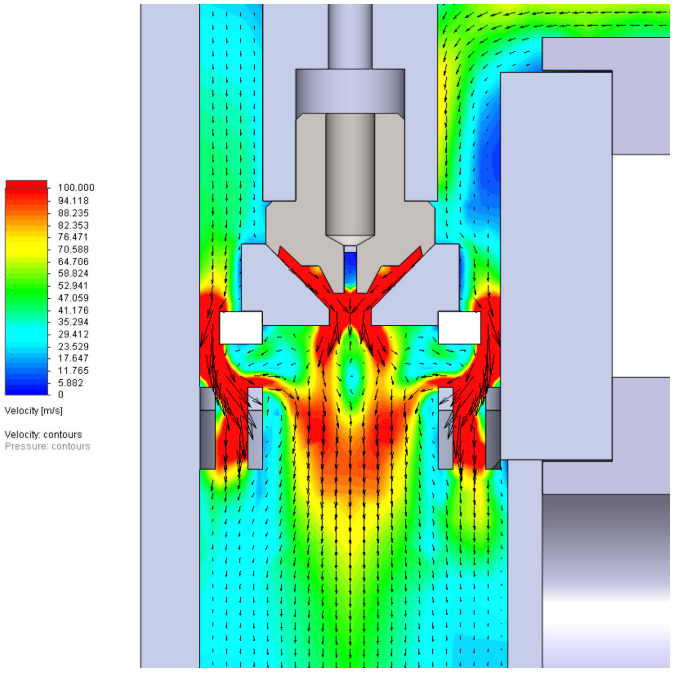

FIGURE 1. Computational fluid dynamics model results illustrating velocity and trajectory in InnovaTek's proprietary fuel injector/mixer.

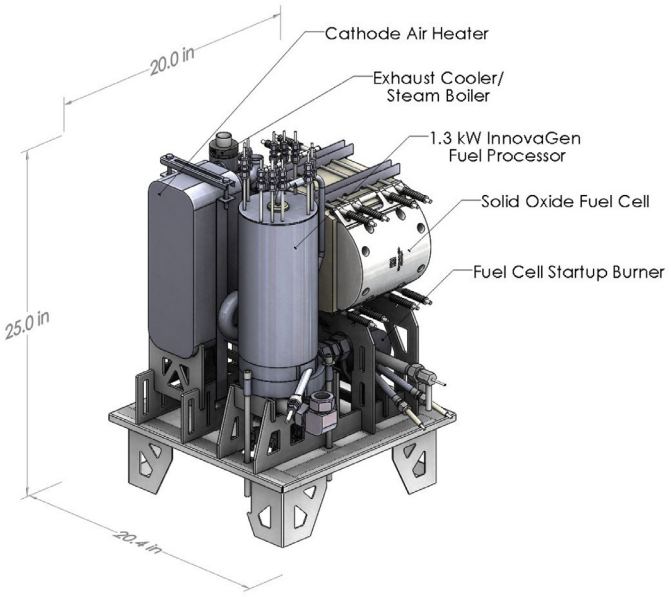

FIGURE 2. Solid model used for assembly of fuel cell power system components.

fuel processor prototype, part count was reduced by 63% and cost was reduced by 51% (Table 2).

Some of the critical parts for the system were manufactured using Direct Metal Laser Sintering and a three-dimensional printing process that fuses high-temperature metal powder. This process produces prototypes quickly and less expensively, thereby reducing non-recurring engineering costs. It also allows the creation of component geometries that cannot be prototyped by any other means.

TABLE 2. Fuel Processor Volume, Part and Cost Reduction

Prototype System	Number of Parts	Approx Volume (L)	Manufactured Cost[1] ($/kW)
2012	159	37.8	3,489
2013	66	11.3	2,388
2014	59	4.8	1,722

[1] Assumes production volume of 50,000 units/year

System efficiency, estimated at 42% (from 37.5% in 2012), was improved as a result of increased stack electrical efficiency, lower parasitic power due to lower stack pressure drop, less waste heat loss through improved thermal integration and heat transfer, and higher methane content in the reformate which reduced stack cooling needs.

Performance Testing

Initial performance of two manufactured prototype fuel processing systems was successful in producing hydrogen for 2.6-kW net power production in each system. In one of the prototypes an advanced catalyst structure was incorporated to improve heat and mass transfer. Performance test results indicate that the system with the structured catalyst starts up more rapidly, reforms efficiently at a significantly lower temperature, and produces more hydrogen per unit volume of fuel than the system with the pellet catalyst. These factors will improve system efficiency and lifetime. Several hundred hours of testing has been completed and longer term testing is continuing in order to determine durability and maintenance interval.

Cost Analysis

The HOMER model was used with data from our manufacturing cost analysis and system performance determinations to estimate cost of power using our technology. The results of these analyses indicate that the cost of power using InnovaTek 5-kW fuel cell generator operating on natural gas would be competitive at $0.096/kWh when volume production brings capital costs down.

CONCLUSIONS AND FUTURE DIRECTIONS

- On the basis of careful systems modeling and component integration using computer-aided design and thermal systems design an overall system electrical efficiency of about 42% is possible for InnovaTek's 5-kW distributed power system operating on natural gas or liquid biofuels.
- An optimized field-ready prototype system has been manufactured and is undergoing long-term durability and performance testing.
- Although an economic analysis indicates that cost of power from the 5-kW fuel cell distributed power system would be competitive, until there is a large scale market for small residential distributed energy, the technology is not economically viable.
- Therefore, early markets for auxiliary power units for trucks, marine systems, and military systems are being pursued.

FY 2014 PUBLICATIONS/PRESENTATIONS

1. Ming, Q., and Irving, P.M., The Role of the Fuel Cell System in Sustainable Power Generation, IEEE Conference on Technologies for Sustainability, Portland, OR, 1-2 August 2013.

2. Irving, P.M., Hybrid Power System for Sustainable Energy Production, oral presentation, DOE Clean Energy Technology Showcase, Stanford University, 15 April 2014.

REFERENCES

1. Fuel Cell Technologies Office Multi-Year Research, Development and Demonstration Plan, U.S. Department of Energy, Table 3.4.5. http://energy.gov/eere/fuelcells/downloads/fuel-cell-technologies-program-multi-year-research-development-and-10

V.L.1 Advanced Ionomers and MEAs for Alkaline Membrane Fuel Cells

Bryan Pivovar (Primary Contact), Dan Ruddy, Matt Sturgeon, Hai Long
National Renewable Energy Laboratory (NREL)
15013 Denver West Parkway
Golden, CO 80401
Phone: (303) 275-3809
Email: Bryan.Pivovar@nrel.gov

DOE Manager
David Peterson
Phone: (720) 356-1747
Email: David.Peterson@ee.doe.gov

Subcontractors
- Shimshon Gottesfeld, Dario Dekel: CellEra, Inc., Caesarea, Israel
- Krzysztof Lewinski, Mike Yandrasits, Steve Hamrock: 3M, St. Paul, MN
- Andy Herring, Mei-chen Kuo, Zachary Page-Belknap: Colorado School of Mines (CSM), Golden, CO

Project Start Date: April 22, 2013
Project End Date: April 22, 2015

Overall Objectives

- Synthesize novel perfluoro (PF) anion exchange membranes (AEMs) with high-temperature stability and high water permeability.
- Employ novel PF AEM materials in electrodes and as membranes in alkaline membrane fuel cells.
- Demonstrate high performance, durability, and tolerance to ambient carbon dioxide.

Fiscal Year (FY) 2014 Objectives

- Evaluate applicability of Grignard chemistry in linking hydroxide conducting head group (e.g. benzyltrimethylammonium, BTMA) to PF sulfonyl fluoride precursor polymer.
- Supply at least three novel PF AEMs to CellEra for fuel cell testing and characterization.
- Report alkaline membrane fuel cell (AMFC) performance of three novel membrane electrode assemblies (MEAs) using PF AEM materials.

Technical Barriers

This project addresses the following technical barriers from the Fuel Cells section (3.4.4) of the Fuel Cell Technologies Office Multi-Year Research, Development, and Demonstration Plan:

(A) Durability (of membranes and membrane electrode assemblies)

(B) Cost (of membranes and membrane electrode assemblies)

(C) Performance (of membranes and membrane electrode assemblies)

Technical Targets

This project will synthesize novel PF AEMs and ionomers and incorporate these MEAs for fuel cell testing. The project generally supports targets outlined in the Multi-Year Research, Development, and Demonstration Plan in application specific areas (portable, stationary, transportation). However, as AMFCs are at an earlier stage of development, specific target tables have not yet been developed. There are two tasks in the Technical Plan of the Multi-Year Research, Development, and Demonstration Plan for alkaline membranes, this project seeks to address both (Table 1).

TABLE 1. Alkaline Membrane Tasks

1.4	Demonstrate an anion-exchange membrane that retains 99% of original ion exchange capacity for 1,000 hours in hydroxide form at T >80°C. (2Q 2013)
3.8	Demonstrate anion-exchange membrane technologies in MEA/single cells with non-PGM catalysts that maintain performance higher than 350 mW/cm^2 for 2,000 hours at T >80°C. (4Q, 2016)

PGM – precious metal group

FY 2014 Accomplishments

- Demonstrated multiple PF AEM chemistries that have spacer groups separating cation from PF backbone.
- Synthesized significant quantities of polymers (>150 g).
- Delivered novel membranes for fuel cell testing.
- Developed and demonstrated novel Grignard chemistry to allow more facile functionalization.
- Polymers/membranes have been characterized using a variety of techniques including infrared (IR), nuclear magnetic resonance (NMR), thermogravimetric analysis (TGA), differential scanning calorimetry (DFT), conductivity, and water uptake.

INTRODUCTION

AMFCs are of interest primarily because they enable the use of non-Pt catalysts, the primary cost/supply limitation of proton exchange membrane fuel cells. AMFCs, therefore, offer the potential of greatly decreased polymer electrolyte fuel cell cost. Operating AMFCs under ambient carbon dioxide conditions remains a challenge due to carbonate formation. An approach that has shown promise for carbon dioxide tolerance is increased operating temperature. Unfortunately, the stability of cations and water management both become more difficult as temperature rises.

The use of perflourinated ionomers, similar to those used in proton exchange membrane systems, with tethered hydroxide conduction cation head groups should help improve water transport properties and offer exceptional chemical durability of the backbone. The significant advances demonstrated in AMFC systems have been accomplished primarily through improving water management and the bonding between membrane and electrode. Both issues can be tackled much more effectively when employing PF AEMs and ionomers. The project consists of three sub-tasks: synthesis of novel perfluorinated alkaline ionomers (NREL, CSM, 3M); developing membranes and dispersions (3M, NREL); and MEA fabrication and fuel cell testing (CellEra, 3M, NREL).

APPROACH

The team will focus on achieving higher-temperature, higher-power-density AMFC operation through implementation of novel alkaline PF membranes and ionomeric dispersions. The PF materials proposed are expected to enhance water transport capabilities and electrode performance/durability significantly, thereby enabling higher temperature and power density operation. The combination of high current density and operating temperature will improve the ability of these devices to tolerate ambient CO_2, potentially enabling complete tolerance to ambient CO_2. Starting with the sulfonyl fluoride form of current perfluoro ionomers we have identified and in several cases verified the ability to convert commercially available precursors into anion exchange polymers and membranes. The synthesized PF ionomers will be cast into membranes, made into polymeric dispersions, and characterized. The procedures will draw on existing membrane-making know-how and likely will be similar to that reported in the literature for Tosflex dispersion preparation. Most of the characterization performed on these materials is anticipated to be routine.

RESULTS

Due to the highly electron withdrawing polymer backbone, BTMA was chosen as a model cation as the benzyl group will act as a spacer unit, mitigating concerns regarding stability. Two linking strategies were explored in order to synthesize the PF AEMs, sulfonyl amide linkage and direct sulfonyl aryl linkage through a Grignard precursor (Figure 1). It was determined, through small molecule analogs (perfluoro-1-butanesulfonyl fluoride) and IR analysis of the resultant perfluoro polymer, that the proposed Grignard reaction (Figure 1) successfully links the desired head group (N,N-dimethylbenzylamine) with the PF sulfonyl fluoride precursor (PF-SFP) through a direct sulfonyl-aryl bond. Grignard chemistry was investigated due to its high degree of control and the ability to avoid sulfonamide linkages. However, DFT calculations (Figure 2) suggest enhanced stability of sulfonamide linkage (23.4 vs. 22.1 kcal/mol), and based on the ease of synthesis and membrane fabrication considerations; we have focused our efforts primarily on the aryl-amide linkage chemistry shown in both Figures 1 and 2.

Our initial attempts at membrane fabrication produced materials with less than optimum physical properties. Subsequent improvements in synthesis and casting have

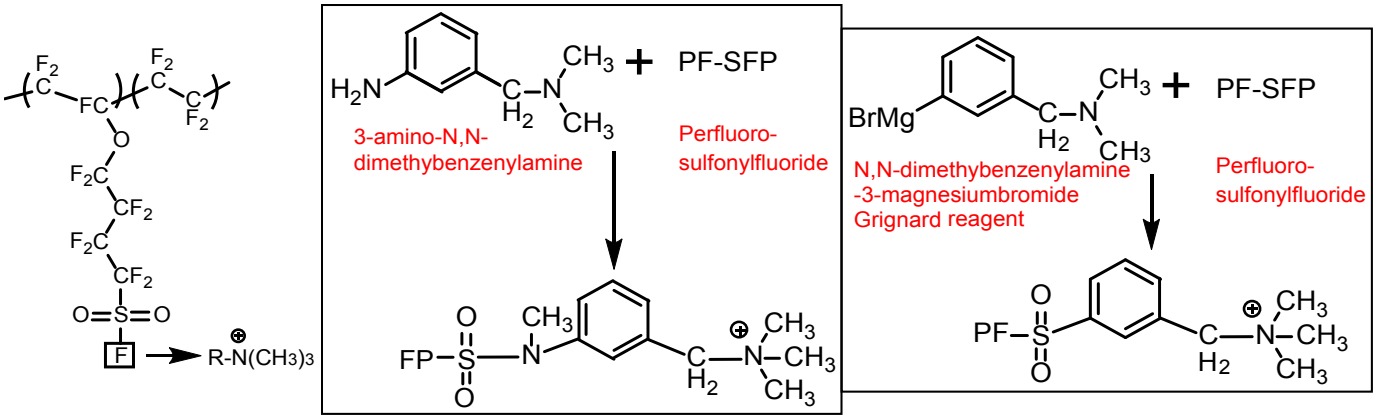

FIGURE 1. Strategies linking hydroxide conducting BTMA head group to PF-SFP (left) through amide (middle) and Grignard chemistries.

R	Linkage	DFT Hydroxide Stability (kcal/mol)		
		Benzyl CH_2	Ammonium CH_3	β elimination
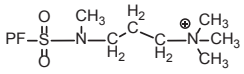	Amide	NA	24.7	19.7
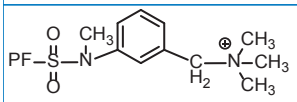	Amide	23.4	24.5	NA
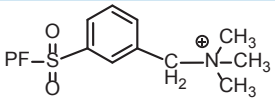	Aryl	22.1	24.1	NA

FIGURE 2. DFT studies of hydroxide stability of three initial target synthesis routes.

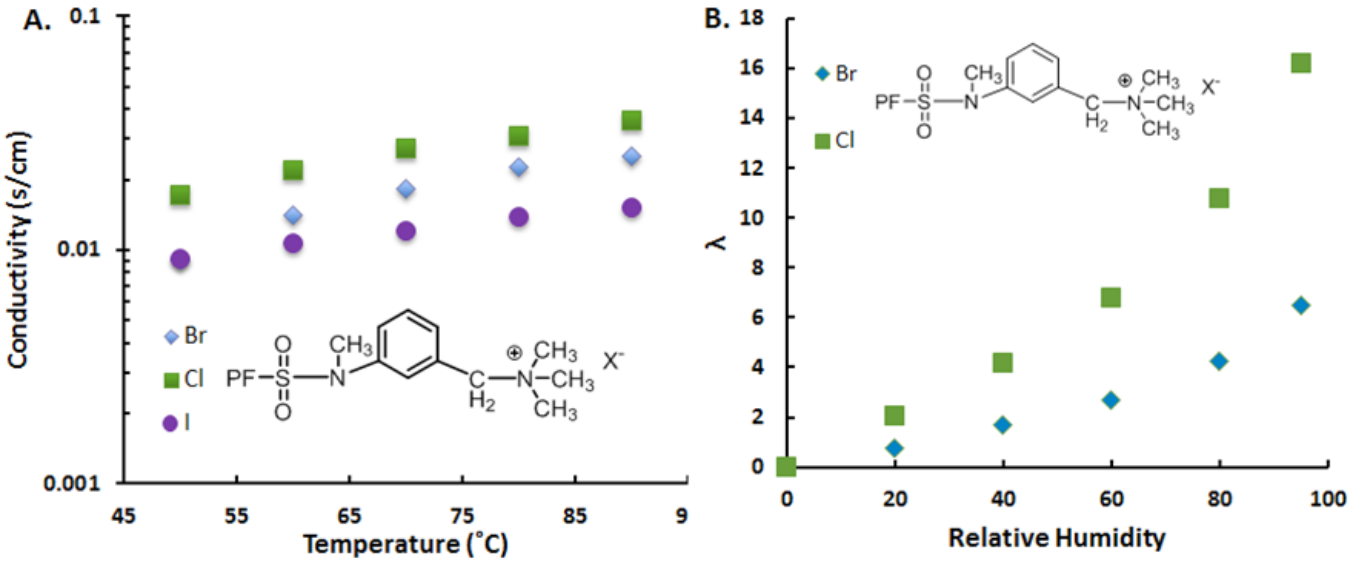

FIGURE 3. Conductivity (A) and water update data (B) of PF-AEM films consisting of a perfluoro sulfonyl polymer backbone and a BTMA cationic head group, X represents various counter-anions synthesized through anion exchange techniques.

more recently been achieved and we anticipate future work in this area to be accomplished with greatly improved materials properties. We have focused our efforts on scaled up synthesis (we have synthesized more than 150 g of polymer) and improved reactant purity. NREL has focused primarily on scale up and increased reactant purity. Colorado School of Mines has focused on scale up, membrane casting conditions, and characterization of membrane properties. 3M has focused on membrane casting and is targeting membranes 4 inches wide in sheets up to 2 m long for initial membrane fabrication. The availability of this material to the research community will allow the advancement of PF AEM technology to be greatly accelerated. CellEra has begun AMFC testing using materials from the project.

Figure 3 shows the conductivity and water uptake of three different films. It is expected that the hydroxide forms of the materials (avoided to date to minimize complications of carbonate formation and remove degradation concerns) will exhibit even greater conductivities. The materials properties for both conductivity and water uptake presented in Figure 3 and measured elsewhere in the project are reasonably consistent with expectation of a PF AEM. The amide-linked PF AEM was sent to CellEra for AMFC testing. Initial AMFC results showed poor performance when PF AEMs were employed as membranes, probably due to the relatively poor mechanical properties of the initial samples. When used as electrode ionomers, fuel cell performance was equivalent or slightly improved compared to state-of-the-art hydrocarbon ionomers. However, mass transport issues occurred within these initial tests, possibly due to unoptimized electrode structures.

CONCLUSIONS AND FUTURE DIRECTIONS

The project has demonstrated multiple PF AEM chemistries that have spacer groups separating cation

from PF backbone. We have synthesized significant quantities of polymers (>150 g). We have developed and demonstrated novel Grignard chemistry to allow more facile functionalization of the PF-SFP. Polymers/membranes have been characterized using a variety of techniques including IR, NMR, TGA, DSC, conductivity, and water uptake.

- Membrane Synthesis:
  - Scaling up of established chemistry, focus on aryl amide linkage.
- Characterization:
  - Expand membrane characterization to include OH^- form and more complete data set including titration to evaluate ion exchange capacity. Durability testing of membranes.
- Dispersion/Solution Preparation:
  - Ability to form or optimize solution/dispersions for electrodes and membrane fabrication. Higher temperature processing. Increase number of solvents investigated.
- Fuel Cell Testing

FY 2014 PUBLICATIONS/PRESENTATIONS

1. Pivovar, B. "Past, Current, and Future Research in Polymer Electrolyte Fuel Cells." Presented at Purdue University, West Lafayette, IN, April 3, 2014.

2. Pivovar, B. "Past, Current, and Future Research in Polymer Electrolyte Fuel Cells." Presented at Iowa State University, Department of Chemical and Biological Engineering, Ames, IA, September 19, 2013.

3. Pivovar, B. "Fuel Cell R&D at NREL." Presented at Los Alamos National Laboratory, August 16, 2013.

4. Pivovar, B. "Alkaline Membrane Fuel Cells, Current R&D and Future Potential." Presented at Transport Processes in Energy Systems, Cornell University, Ithaca, NY, August 7, 2013.

5. Pivovar, B. "Alkaline Membrane Work at NREL." Presented at University of Surrey, Guildford, England, May 16, 2013.

V.M.1 Best Practices and Benchmark Activities for ORR Measurements by the Rotating Disk Electrode Technique

Shyam S. Kocha[1] (Primary Contact), Jason W. Zack,[1] Kazuma Shinozaki,[1] Svetlana Pylypenko,[1] Vojislav Stamenkovic[2] (co-PI), Yijin Kang,[2] Dongguo Li,[2] Deborah Myers[3] (co-PI), Nancy Kariuki,[3] Tammi Nowicki[3]

National Renewable Energy Laboratory[1]
Fuel Cell Group
Phone: (303) 275-3284
Email: shyam.kocha@nrel.gov

Argonne National Laboratory (ANL)[2]
Energy Conversion and Storage Group

Argonne National Laboratory[3]
(Hydrogen and Fuel Cell Materials Group)

DOE Manager
David Peterson
Phone: (720) 356-1747
Email: David.Peterson@ee.doe.gov

Project Start Date: October 1, 2013
Project End Date: September 30, 2014

Overall Objectives

To aid DOE by establishing protocols and best practices for rotating disk electrode (RDE) measurements which would allow for more reliable oxygen reduction reaction (ORR) activity comparisons to be made in the area of electrocatalyst development.

Technical Barriers

This project addresses the following technical barriers from the Fuel Cells section of the Fuel Cell Technologies Office Multi-Year Research, Development, and Demonstration Plan:

(A) Durability and (C) Performance

- Best practices/protocol for electrocatalyst screening not standardized
- Benchmark activity for baseline Pt/C electrocatalysts for comparison to novel electrocatalysts not available
- Common/standard Pt/C catalysts not accessible
- Reproducibility of results

Fiscal Year (FY) 2014 Accomplishments

- Established a standard protocol and test methodology for measurement of electrochemical area (ECA), ORR activity, and durability.
- Evaluated three electrocatalysts using identical protocols and electrode preparation in three laboratories for ECA, ORR activity.
- Compared and verified ECA, ORR activity and durability for reproducibility between labs.

INTRODUCTION

The need for large amounts of materials and the complexity and cost of fabricating fuel cells have led to the widespread use of RDE measurements in aqueous acidic electrolyte to study the activity and stability of nano-materials used in proton exchange membrane fuel cell electrode catalysts. In addition to eliminating the need to fabricate membrane electrode assemblies (MEAs), as the first step in the catalyst evaluation process, RDE measurements also allow precise control over the potential of the fuel cell nano-catalysts and eliminate the influence of other cell components, such as the membrane, gas diffusion layer, and the opposing electrode on the initial performance and performance decay of the nano-catalyst of interest.

Several groups over the last few years have reported discrepancies in activity values reported between research groups and also improvements in technique that allowed for higher and more reproducible activity [1-3]. DOE worked with NREL and ANL to issue a Request for Information (RFI) on best practices for RDE measurements for ORR activity. The purpose of the RFI was to solicit feedback from catalyst developers, researchers, manufacturers, end users, and other stakeholders on use of RDE experiments for characterization/screening of the activity and durability of proton exchange membrane fuel cell electrocatalysts. DOE also organized a webinar on RDE to disseminate preliminary information and solicit input on RDE testing [5]. Lastly, the Catalysis Working Group (CWG) and Durability Working Group (DWG) joint meeting was held at NREL with one of the objectives being the discussion of responses to the RDE RFI [6]. The overarching goal is to develop best practices/protocols to enable consistency in procedures and minimize variability in results from different laboratories so that novel catalysts can be accurately benchmarked.

APPROACH

Our approach is to establish protocols and best practices for ink dispersion/film deposition/drying for RDE measurements to allow for more precise and reproducible data and reliable comparisons to be made by electrocatalyst development groups when evaluating novel synthesized catalysts in small quantities.

Briefly, the approach involves obtaining electrocatalytic activity measurements for:

- 2–3 commercially obtainable Pt/C electrocatalysts
- in which the activity is measured for a high degree of statistical reproducibility
- with the same protocol and ink formulation and having the catalysts tested in three laboratories

RESULTS

Protocols were established based on a large number of experiments conducted at NREL and based on discussions with the CWG and DWG and responses to the DOE RFI on RDE testing [6]. A number of sources for perchloric acid was also evaluated to determine the grades that had the least amount of impurities that contaminate platinum catalysts. The schematic and details of the conditioning, ECA and ORR activity protocols are detailed in Figure 1 a), b), and c). These protocols were used as a standard for all studies. The Pt/C catalyst specifications obtained from the three manufacturers is detailed in Figure 2.

Poly-Pt was used as a sensor of the cleanliness of the RDE electrochemical cell prior to conducting measurements on the three electrocatalysts from three catalyst suppliers (TKK, JM, Umicore) in three laboratories (NREL and two labs at ANL). The average ORR activity of poly-Pt at NREL was found to be 2.80 $mA/cm^2_{Pt} \pm 0.20$ and are comparable to some of the highest values reported in the literature. A specific activity of poly-Pt that was greater than ~2.0 mA/cm^2_{Pt} was found to be necessary in order to qualify the cell as having impurity levels below an acceptable limit in which the ORR activity of Pt-based catalysts could be measured with reasonable accuracy. Furthermore, the

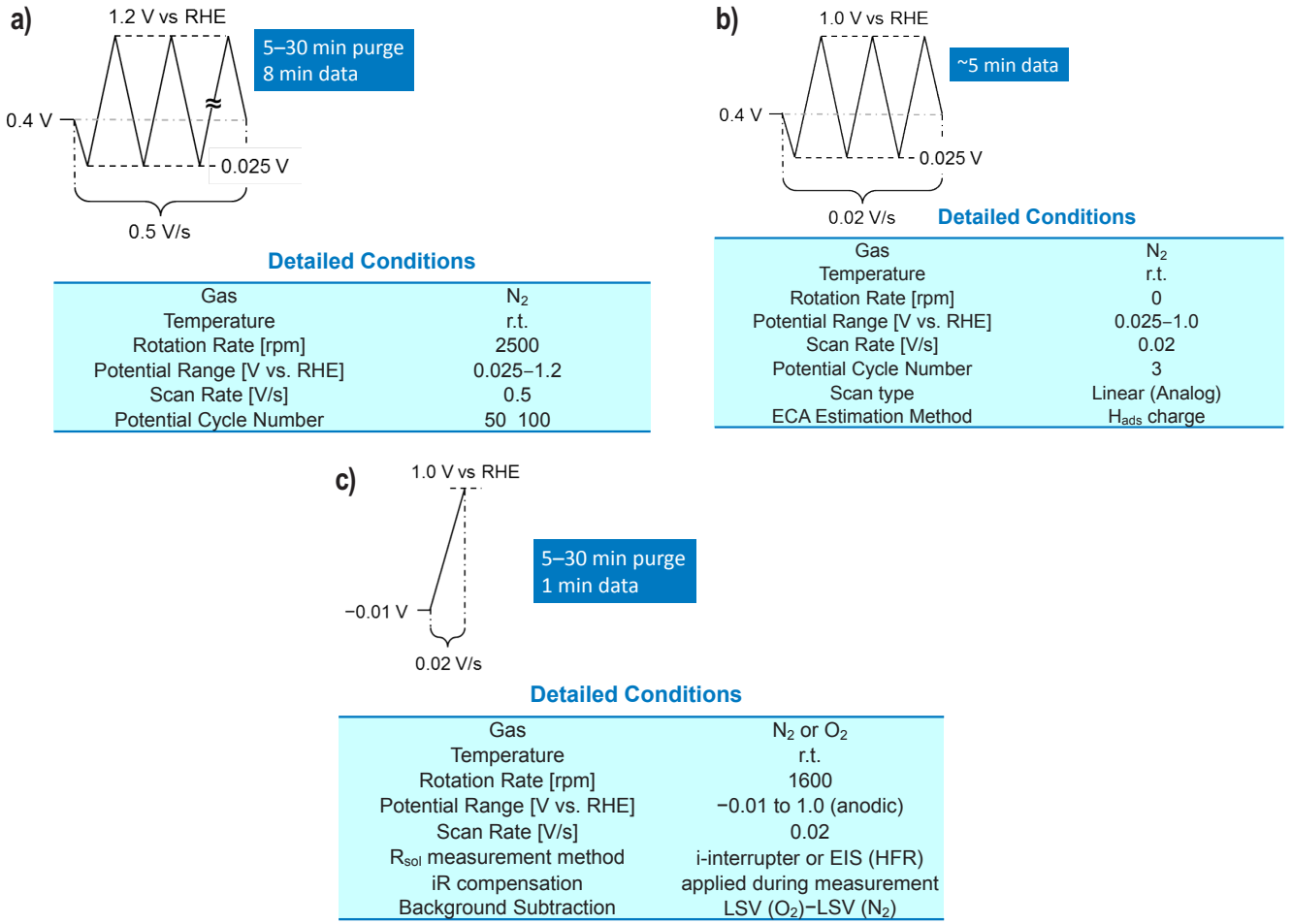

Detailed Conditions

Gas	N_2
Temperature	r.t.
Rotation Rate [rpm]	2500
Potential Range [V vs. RHE]	0.025–1.2
Scan Rate [V/s]	0.5
Potential Cycle Number	50 100

Detailed Conditions

Gas	N_2
Temperature	r.t.
Rotation Rate [rpm]	0
Potential Range [V vs. RHE]	0.025–1.0
Scan Rate [V/s]	0.02
Potential Cycle Number	3
Scan type	Linear (Analog)
ECA Estimation Method	H_{ads} charge

Detailed Conditions

Gas	N_2 or O_2
Temperature	r.t.
Rotation Rate [rpm]	1600
Potential Range [V vs. RHE]	−0.01 to 1.0 (anodic)
Scan Rate [V/s]	0.02
R_{sol} measurement method	i-interrupter or EIS (HFR)
iR compensation	applied during measurement
Background Subtraction	LSV (O_2)−LSV (N_2)

FIGURE 1. a) Schematic and details of conditioning protocol; b) Schematic and details of ECA protocol; c) Schematic and details of ORR activity protocol.

1. Pine Instruments

Poly-Pt disk
Dia 5 mm; 0.196 cm^2
Thickness: 4 mm
Roughness: ~1.1–1.3

2. Tanaka (TKK)

TEC10E50E; Pt wt%: 46.4
Support: Carbon Black
TEM average particle size: ~2.5 nm
(samples from 3 catalyst batches evaluated)

3. Johnson Matthey (JM)

Pt wt%: 37.6
Support Ketjen EC 300J
CO Chemisorption area: 81 m^2/g_{Pt}
XRD crystallite size: <2 nm

4.Umicore

Elyst Pt50 0550; Pt wt%: 47.2
Support: Carbon Black
XRD crystallite size: ~4.9 nm
BET-surface: 365 m^2/g_{Pt}

Manufacturer specifications for electrocatalysts under study.

FIGURE 2. Pt/C specifications from catalyst maufacturers.

activity of poly-Pt was found to be invariant for about an hour of repeated cycling (not shown). Figure 3 compares the ORR activity of poly-Pt measured in the three laboratories. Note that different electrochemical cells were employed at the three laboratories, but identical protocols and electrode surface preparations were employed.

Subsequently, using identical standardized protocols (Figure 1) and a standardized electrode preparation method of spin coating [2-3] two of the three electrocatalyst materials from TKK, JM, and Umicore were evaluated in the three laboratories. A comparison of the ORR mass activity between laboratories for the two catalysts indicates acceptable reproducibility as shown in Figure 4.

CONCLUSIONS AND FUTURE DIRECTIONS

- A standard RDE testing protocol and standard electrode preparation method were deveioped for making RDE measurements relevant for PEM fuel cell cathode electrocatalysis development. These techniques were verified and found to be reproducible across three laboratories.
- Finalize a strategy on the logistics of potentially distributing/shipping ~1 g of electrocatalyst material (no charge) to those groups that are awarded a new electrocatalyst related project in upcoming DOE Funding Opportunity Announcements over the next 5 years.
- Disseminate the results of the study (best practices for RDE and benchmark activity values) so that it is accessible to the scientific community and the general public.

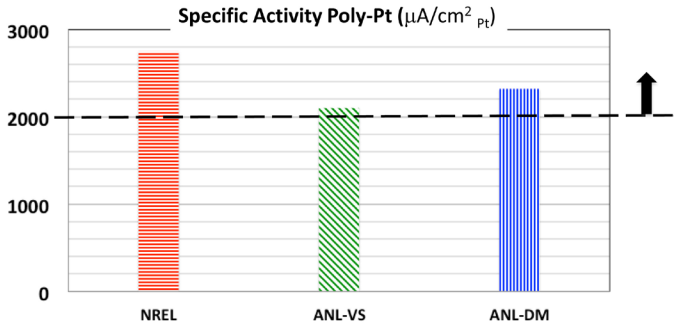

FIGURE 3. Comparison of specific activity between laboratories of poly-Pt in 0.1M $HClO_4$ at 25°C and 100 kPa conducted at 20 mV/s in the anodic sweep.

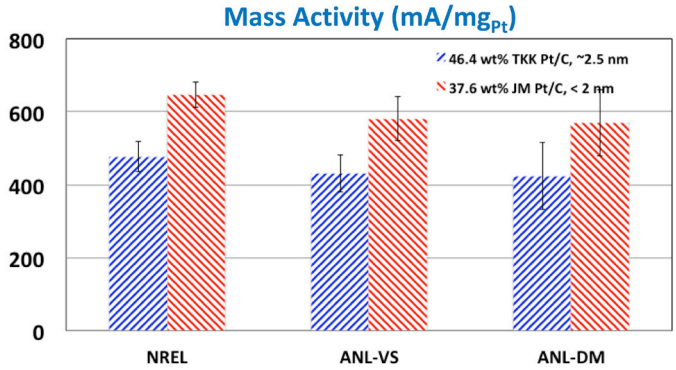

FIGURE 4. Comparison of mass activity between laboratories of 2 Pt/C electrocatalysts in 0.1M $HClO_4$ at 25°C and 100 kPa conducted at 20 mV/s in the anodic sweep.

FY 2014 PUBLICATIONS/PRESENTATIONS

1. Kocha, Shyam S., Jason W. Zack, Shaun M. Alia, K.C. Neyerlin, and Bryan S. Pivovar. "Influence of Ink Composition on the Electrochemical Properties of Pt/C Electrocatalysts." ECS Transactions 50, no. 2 (2013): 1475-1485.

2. Garsany, Yannick, Irwin L. Singer, and Karen E. Swider-Lyons. "Impact of film drying procedures on RDE characterization of Pt/VC electrocatalysts." Journal of Electroanalytical Chemistry 662, no. 2 (2011): 396-406.

3. Shinozaki, Kazuma, Bryan S. Pivovar, and Shyam S. Kocha. "Enhanced Oxygen Reduction Activity on Pt/C for Nafion-free, Thin, Uniform Films in Rotating Disk Electrode Studies." ECS Transactions 58, no. 1 (2013): 15-26.

4. Catalysis Working Group (CWG) and Durability Working Group (DWG) Meetings, Co-Chairs: Piotr Zelenay, Nancy Garland and Deborah Myers, Rod Borup, presented by Kocha, S.S. "Influence of Ink Composition on the Electrochemical Properties of Pt/C Electrocatalysts." Honolulu, Hawaii, 2012.

5. DOE Webinar: Shyam S. Kocha, Yannick Garsany, Deborah Myers, Chair: Dimitrios Papageorgopoulos, 'Testing Oxygen Reduction Reaction Activity with the Rotating Disc Electrode. Technique', http://www1.eere.energy.gov/hydrogenandfuelcells/pdfs/webinarslides_rde_technique_031213.pdf.

6. Catalysis Working Group (CWG) meeting and Durability Working Group (DWG) meeting at NREL/DOE Field Office, December 2013.

VI.0 MANUFACTURING R&D

VI.0 Manufacturing R&D Sub-Program Overview

INTRODUCTION

The Manufacturing Research and Development (R&D) sub-program supports activities needed to reduce the cost of manufacturing hydrogen and fuel cell systems and components. Manufacturing R&D will enable the mass production of components in parallel with technology development and will foster a strong domestic supplier base. The sub-program's R&D activities address the challenges of moving today's technologies from the laboratory to high-volume, pre-commercial manufacturing to drive down the cost of hydrogen and fuel cell systems. The sub-program focuses on the manufacturing of components and systems that will be needed in the early stages of commercialization. Research investments are focused on reducing the cost of components currently used or planned for use, as well as reducing overall processing times. Progress toward targets is measured in terms of reductions in the cost of producing fuel cells, increased manufacturing processing rates, and growth of manufacturing capacity.

In Fiscal Year (FY) 2014, manufacturing projects continued in the following areas:

- Reduction in the number of assembly steps for membrane electrode assemblies (MEAs)
- Use of component quality control to measure catalyst loading and detect defects in catalyst-coated membranes
- Fabrication technologies for high-pressure composite storage tanks

GOAL

The goal of the Manufacturing R&D sub-program is to develop innovative technologies and processes that reduce the cost of manufacturing fuel cells and systems for hydrogen production, delivery, and storage.

OBJECTIVES[1]

Key objectives for Manufacturing R&D include:

- Develop manufacturing techniques to reduce the cost of automotive fuel cell stacks at high volume (500,000 units/year) from the 2008 value of $38/kW to $20/kW by 2020.
- Develop fabrication and assembly processes to produce onboard vehicle hydrogen storage systems achieving: 1.8 kWh/kg (5.5 wt% H_2) and 1.3 kWh/L (40 g H_2/L) at a cost of $12/kWh ($400/kg H_2 stored) or less by 2017.
- Support efforts to reduce the cost of manufacturing components and systems to produce hydrogen at <$4/gasoline gallon equivalent (2007 dollars) (untaxed, delivered, and dispensed) by 2020.

FY 2014 TECHNOLOGY STATUS AND ACCOMPLISHMENTS

Presently, fuel cell systems are fabricated in small quantities. The cost of 10-kW, low-temperature polymer electrolyte membrane (PEM) fuel cell systems for backup power is projected to be ~$3,700/$kW_{net}$ at a volume of 100 systems per year.[2] For automotive applications using today's technology, the cost of an 80-kW PEM fuel cell system is projected to be $55/kW for high-volume manufacturing (500,000 systems/year).[3] Projected costs include labor, materials, and related expenditures, but do not account for manufacturing R&D investment.

FY 2014 saw a number of advancements in the manufacture of fuel cells and hydrogen storage systems, including:

Electrode Deposition

MEA materials were coated on a roll-to-roll process following minor equipment modifications to direct coat a membrane layer on top of a cathode layer using a modified backer over 100 meters of intermediate. Optimization of a direct-coated 3-layer MEA is in progress. Gore's state-of-the-art thin, durable reinforced membranes have been demonstrated in a roll-to-roll 3-layer process. (W. L. Gore & Associates, Inc.)

[1] Note: Targets and milestones were recently revised; therefore, individual project progress reports may reference prior targets.
[2] http://www.hydrogen.energy.gov/pdfs/review14/fc098_wei_2014_o.pdf
[3] http://hydrogen.energy.gov/pdfs/14014_fuel_cell_system_cost_2014.pdf

High-Pressure Storage

Composite weight was reduced by 5.7% from the previous design by reducing automated fiber placement (AFP) dome cap layers and optimizing filament winding layup. The Aft AFP dome cap design had a dip, potentially causing composite voids, and the burst pressure was 90% of the requirement, exceeding 157.5 MPa (2.25 x 70 MPa). Quantum filled the dip on the AFP dome cap of Vessel 15 with carbon fiber woven fabric rings, and the vessel achieved 103% of required burst pressure in mid cylinder. Quantum confirmed that the in-house software is sufficient for hybrid design. Vessel 16 achieved a target cycle test count of 15,000. (Quantum Fuel Systems Technologies Worldwide, Inc.)

Component and Stack Quality Control Measurement

Infrared/direct current equipment was assembled on an industrial electrode coating line at Ion Power. The National Renewable Energy Laboratory (NREL) collected data on three coating runs (defects created in wet coating, defects created in semi-dry coating, and simulated process defects) and it successfully detected defects at speed at the drying oven exit. The defects included die line, scratches (tens of μm wide x few mm long), added material (~1 mm droplet/lump), as well as start/stop operation. NREL demonstrated its new Infrared/Reactive Impinging Flow technique with a moving gas diffusion electrode sheet. (NREL)

Workshop

The Fuel Cell Technologies Office along with other Offices within Energy Efficiency and Renewable Energy, held a cross-cutting workshop on quality control/metrology to leverage diagnostic capabilities and identify synergies and opportunities across other technology offices.[4]

Funding Opportunity Announcement (FOA)

EERE/FCTO released a FOA focused on "*Clean Energy Supply Chain and Manufacturing Competitiveness Analysis for Hydrogen and Fuel Cell Technologies*" on May 20, 2014. DOE funding is up to $2M. The topics included outreach to develop strategies and new approaches to facilitate development and expansion of the domestic supply chain of hydrogen and fuel cell related components in the U.S. and global manufacturing competitive analysis for hydrogen and fuel cell-related technologies.

BUDGET

The FY 2015 budget request for the Fuel Cell Technologies Office includes $3 million for Manufacturing R&D. The FY 2014 appropriation for Manufacturing R&D was $3 million (see chart next page).

FY 2015 PLANS

In FY 2015, the Manufacturing R&D sub-program will:

- Initiate new projects on supply chain development and global manufacturing competitiveness analysis in collaboration with the DOE's Clean Energy Manufacturing Initiative
- Correlate size of defects generated during membrane and/or MEA fabrication to loss of fuel cell performance
- Build and test a fuel cell stack with a cell fabricated using a new 3-layer MEA manufacturing process
- Continue to use predictive modeling and single and segmented cell test methods to assist diagnostic development
- Develop novel defect detection and infrared detection of the thermal response of material
- Expand implementation of defect diagnostic techniques on industry production lines to original equipment manufacturers

The Fuel Cell Technology Office plans to release an FOA that includes topics on hydrogen and fuel cell R&D manufacturing in FY 2015, with awards subject to appropriation and announced later in the fiscal year. The sub-program will continue to coordinate with other agencies (including the National Institute of Standards and Technology and the U.S. Department of Defense) and with other technology offices within Energy Efficiency and Renewable Energy to identify synergies and leverage efforts.

[4] http://energy.gov/eere/fuelcells/eere-quality-control-workshop

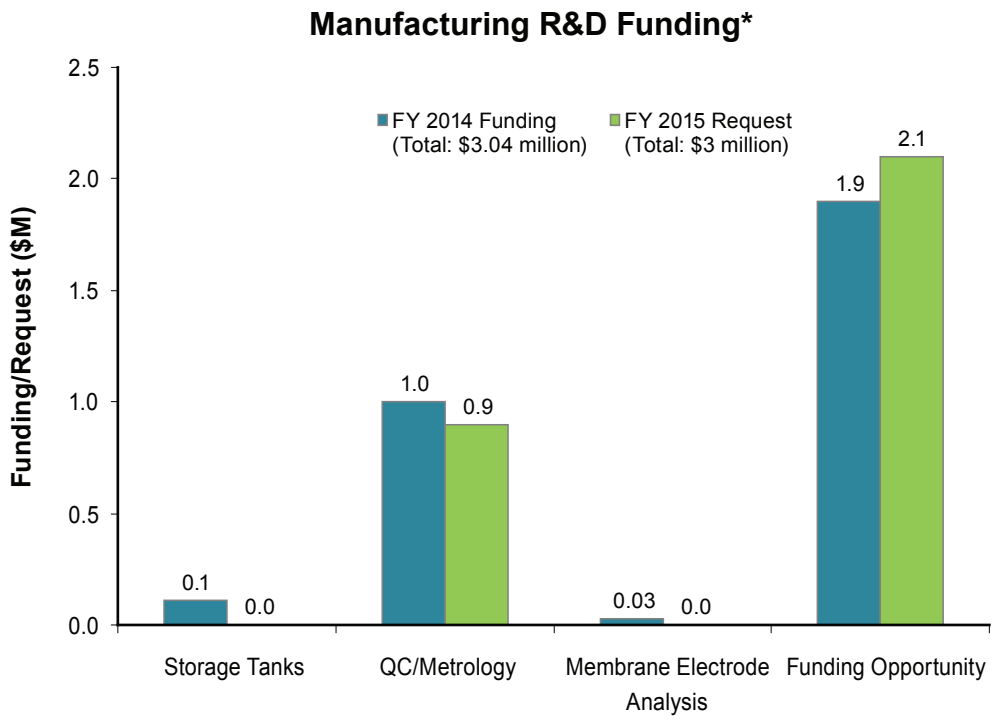

* Subject to appropriations, project go/no-go decisions, and competitive selections. Exact amounts will be determined based on research and development progress in each area and the relative merit and applicability of projects competitively selected through planned funding opportunity announcements.

Nancy Garland
Manufacturing R&D Project Manager
Fuel Cell Technologies Office
Office of Energy Efficiency and Renewable Energy
U.S. Department of Energy
1000 Independence Ave., SW
Washington, D.C. 20585-0121
Phone: (202) 586-5673
Email: Nancy.Garland@ee.doe.gov

VI.1 Fuel Cell Membrane Electrode Assembly Manufacturing R&D

Michael Ulsh (Primary Contact), Guido Bender
National Renewable Energy Laboratory (NREL)
15013 Denver West Parkway
Golden, CO 80401
Phone: (303) 275-3842
Email: michael.ulsh@nrel.gov

DOE Manager
Nancy Garland
Phone: (202) 586-5673
Email: Nancy.Garland@ee.doe.gov

Partners
- Lawrence Berkeley National Laboratory (LBNL), Berkeley, CA
- Colorado School of Mines, Golden, CO
- New Jersey Institute of Technology, Newark, NJ
- Automotive Fuel Cell Cooperation, Burnaby, BC
- General Motors, Pontiac, MI
- Ion Power, New Castle, DE
- W.L. Gore and Associates, Elkton, MD

Project Start Date: July 16, 2007
Project End Date: Project continuation and direction determined annually by DOE

Overall Objectives

- Evaluate and develop in-line diagnostics for cell and component quality control and validate diagnostics in-line
- Investigate the effects of membrane electrode assembly (MEA) component manufacturing defects on MEA performance and durability to understand the required performance of diagnostic systems and contribute to the basis of knowledge available to functionally determine manufacturing tolerances for these materials
- Use established models to predict the effects of local variations in MEA component properties, and integrate modeling of the operational and design characteristics of diagnostic techniques into the design and configuration of in-line measurement systems
- These objectives have strong support from the industry. Specifically, the outcomes of the 2011 NREL/DOE Hydrogen and Fuel Cell Manufacturing R&D Workshop and the Office of Naval Research-funded Manufacturing Fuel Cell Manhattan Project confirmed the importance of continued development of in-line quality control techniques for cell manufacturing. Our specific development activities have been and will continue to be fully informed by direct input from industry. As new technologies emerge and as the needs of the industry change, the directions of this project will be adjusted.

Fiscal Year 2014 Objectives

- Implement the infrared/direct-current (IR/DC) diagnostic on a production electrode coating line
- Make a Go/No-Go decision for further work to implement the capacitance technique for electrode ionomer-to-carbon ratio on moving sheet material
- Demonstrate the IR/reactive impinging flow (IR/RIF) technique on the research web-line

Technical Barriers

This project addresses the following technical barriers from the Manufacturing R&D section (3.5) of the Fuel Cell Technologies Office Multi-Year Research, Development, and Demonstration Plan:

(A) Lack of High-Volume Membrane Electrode Assembly Processes

(E) Lack of Improved Methods of Final Inspection of MEAs

(K) Low Levels of Quality Control.

Contribution to Achievement of DOE Manufacturing Milestones

This project contributes to the achievement of the following DOE milestone from the Manufacturing R&D section (3.5) of the Fuel Cell Technologies Office Multi-Year Research, Development, and Demonstration Plan:

- Milestone 6.4: Demonstrate methods to inspect full MEAs and cells prior to assembly into stacks (4Q, 2014).

FY 2014 Accomplishments

NREL accomplished the following in FY 2014:

- Implemented our IR/DC technique on industry partner Ion Power's production electrode coating line and demonstrated successful detection of intentionally created defects and process variability at their process conditions
- Used the coated sheets made during the Ion Power implementation on our research web-line to identify IR/DC excitation conditions for successful detection of electrode defects at speeds up to 60 foot per minute (fpm)
- Demonstrated the sensitivity of our IR/RIF technique to variations in electrode platinum loading and defects

- Performed modeling of the impinging flow dynamics of the IR/RIF technique to help understand the effects of the main process variables and process configuration
- Designed, fabricated, and installed new hardware to enable the demonstration of the IR/RIF technique on our research web-line with gas diffusion electrode (GDE) sheet material
- Demonstrated detection of a variety of membrane-electrode sub-assembly defects, including debris and scratches, using our optical reflectance technique
- Performed detailed studies of the capacitance technique and recommended a No-Go decision to move forward with testing using moving materials
- Continued collaboration with our industry partners, including the last of DOE's competitively awarded Manufacturing R&D projects, in accordance with our project charter
- Led the planning and organization of, and hosted a workshop on in-line quality control for two-dimensional engineered surfaces, which focused on identifying needs and synergies across DOE Office of Energy Efficiency and Renewable Energy technologies (e.g., solar, fuel cells, batteries, building materials, and window films)

INTRODUCTION

In FY 2005–2007, NREL provided technical support to DOE in developing a new key program activity: manufacturing R&D for hydrogen and fuel cell technologies. This work included a workshop on manufacturing R&D, which gathered inputs on technical challenges and barriers from the fuel cell industry, and subsequent development of a roadmap for manufacturing R&D. In late FY 2007, NREL initiated a project to assist the fuel cell industry in addressing these barriers, initially focusing on in-line quality control of MEA components.

Defects in MEA components differ in type and extent depending on the fabrication process used. The effects of these defects also differ, depending on size, location in the cell relative to the reactant flow-field, cell operating conditions, and which component contains the defect. Understanding the effects of these different kinds of defects is necessary in order to specify and/or develop diagnostic systems with the accuracy and data acquisition/processing rates required for the speed and size scales of high-volume continuous manufacturing methods. Furthermore, predictive capabilities for manufacturers are critical to assist in the development of tolerances and to enable assessment of the effects of material and process changes.

APPROACH

NREL and its partners are addressing the DOE manufacturing milestones listed above by evaluating, developing, and validating (in-line) diagnostics that will support the use of high-volume manufacturing processes for the production of MEAs and MEA component materials. Prioritization of this work is based on inputs from our industry partners on their critical manufacturing quality control needs. We are focusing on diagnostic capabilities not addressed by commercially available in-line systems; in particular we are evaluating methods to make areal rather than point measurements such that discrete defects can be identified. We are also developing test methodologies to study the effects of the size and/or extent of each important type of variability or defect. These results will assist our industry partners in validating manufacturing tolerances for these materials, ultimately reducing scrap rates and cost, and improving supply chain efficiency. Finally, predictive models are being used at LBNL to understand the operational and design characteristics of diagnostic techniques by simulating the behavior of MEA components in different excitation modes. These results are being fed back to our design effort in configuring the diagnostics for in-line implementation. MEA models are also being utilized to understand the in situ behavior of defected MEAs to guide and further elucidate experiments.

RESULTS

As noted in the approach section, our ultimate goal is to transfer in-line inspection techniques to industry. Taking another step in that direction, our major accomplishment over the past year was the implementation of our IR/DC technique on Ion Power's production electrode coating line. We set up our equipment directly on their line and operated it while they coated under standard production conditions. Figure 1 shows an example of the successful demonstration, in this case detection of a thin scratch in the electrode. While all of the defects were intentionally created or allowed to occur, many of the defects were fairly ubiquitous for the coating technique used, for example the "die line" in Figure 1. We then extended the value of this demonstration by taking the coated sheets back to NREL and running them on our research web-line to identify IR/DC excitation conditions (i.e. voltage set-points) for higher line speeds. All of the defects created in the electrode sheets were detected at speeds up to 60 fpm; an example of this is given in Figure 2, where the same defects are detected over a factor of six increase in speed.

Another important effort was advancing our reactive excitation technique for detection of GDE defects closer to a web-line demonstration. Formerly referred to as reactive flow-through, we renamed the technique to RIF (reactive impinging flow) to capture the open-environment conditions

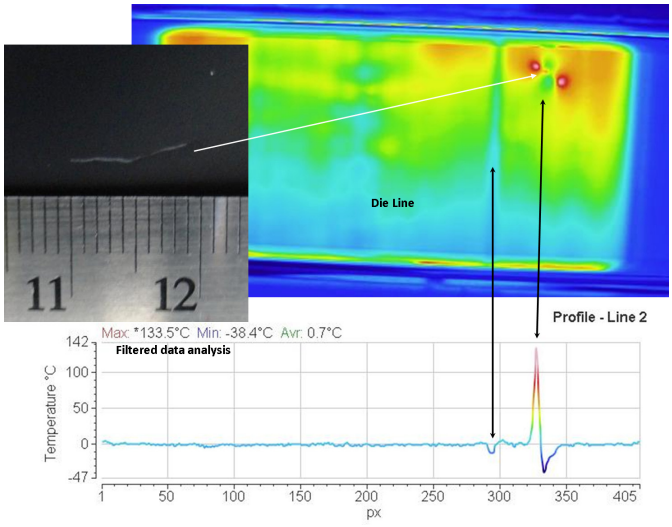

FIGURE 1. IR/DC data from demonstration on Ion Power coating line, showing detection of scratch in electrode surface and die line.

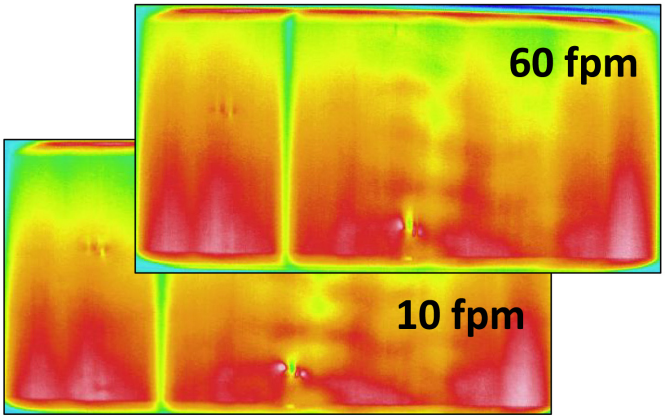

FIGURE 2. IR/DC data from Ion Power coated sheets run on NREL web-line, showing detection of defects over a range of speed.

under which it now operates. Using commercially available GDEs as well as materials fabricated in-house with our automated ultrasonic spraying system, we explored the sensitivity of the technique to platinum loading and different sizes and extents of defects. Figure 3 shows a sample with different sizes of electrode bare spots on the GDE, and the infrared thermographic line data indicating detection of those defects. These studies were performed at speeds up to 30 fpm. In support of these studies, our partners at LBNL developed new steady-state and transient models of the technique. These models are providing insights into the physics of the impinging flow that will help us optimize operating conditions and system configuration. Finally, new hardware was designed, fabricated, and installed in preparation for demonstration of the IR/RIF technique on our research web-line by the end of the fiscal year.

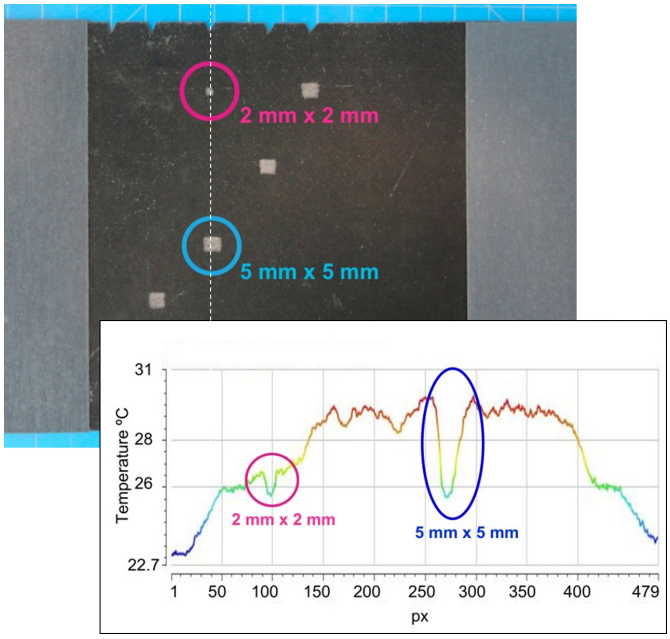

FIGURE 3. Commercial GDE sample with created defects of different size, and detection of those defects using IR/RIF at 30 fpm (2% H_2 and 1% O_2 in N_2, 1 mm knife-to-GDE gap, 20 slpm flow).

In other work, we performed detailed studies of an exploratory measurement using capacitance (via ex situ alternating current impedance) as an indicator of the electrode ionomer-to-carbon ratio. While some of the results were promising, we were not able to show sufficient sensitivity to small changes in ionomer-to-carbon ratio or acceptable repeatability of the data, which ultimately led to a No-Go decision for further work at this time. We also continued to apply our optical reflectance technique to different MEA and sub-assembly configurations of interest to our industry partners. As many of these partners scale up their manufacturing processes for commercialization (e.g., for automotive fuel cells), optimization of MEA components and configurations leads to new structures on which to validate these techniques. Known defects such as carbon powder debris on surfaces and inadvertent scratches on membranes during handling and assembly were detected.

FUTURE DIRECTIONS

- Apply our toolbox of techniques to industry-relevant MEA constructions and sub-assemblies, particularly focusing on near-term commercialization opportunities such as scale up of automotive fuel cells
- Use modeling and experimental studies to refine and improve the performance of the IR/RIF technique for GDE defect detection

- Continue to use predictive modeling and single and segmented cell test methods to study the effects of as-manufactured defects on MEA performance and lifetime using standard or accelerated stress tests
- Continue to work toward the implementation of more of our techniques on industry production lines

FY 2014 PUBLICATIONS AND PRESENTATIONS

1. Ulsh, M. "Fuel Cell MEA Manufacturing R&D." DOE Hydrogen Program Annual Merit Review, Washington, D.C., June 2014.

2. Das, P.K.; Weber, A.Z.; Bender, G.; Manak, A.; Bittinat, D.; Herring, A.M.; Ulsh, M. "Rapid detection of defects in fuel-cell electrodes using infrared reactive-flow-through technique." *Journal of Power Sources* (261), 2014; pp. 401-411.

3. Bender, G.; Felt, W.; Ulsh, M. "Detecting and localizing failure points in proton exchange membrane fuel cells using IR thermography." *Journal of Power Sources* (253), 2013; pp. 224-229.

4. Reshetenko, T.V.; St-Pierre, J.; Rocheleau, R. "Effects of local GDL gas permeability variations on spatial PEMFC performance." *Journal of Power Sources* (241), 2013; pp. 597-607.

5. Bittinat, D.C.; Bender, G.; Ulsh, M. "Defect detection in fuel cell gas diffusion electrodes using infrared thermography." ECS Fall Meeting, San Francisco, CA, October, 2013. *ECS Transactions* (58:1), 2013; pp. 495-503.

6. Reshetenko, T.V.; St-Pierre, J.; Artyushkova, K.; Rocheleau, R.; Atanassov, P.; Bender, G.; Ulsh, M. "Multi-analytical study of the PTFE content local variation of the PEMFC gas diffusion layer." *Journal of the Electrochemical Society* (160:11), 2013; pp. F1305-F1315.

VI.2 Manufacturing of Low-Cost, Durable Membrane Electrode Assemblies Engineered for Rapid Conditioning

F. Colin Busby
W.L. Gore & Associates, Inc (Gore)
Gore Electrochemical Technologies Team
201 Airport Road
Elkton, MD 21921
Phone: (410) 392-3200
Email: CBusby@WLGore.com

DOE Managers
Nancy Garland
Phone: (202) 586-5673
Email: Nancy.Garland@ee.doe.gov
Jesse Adams
Phone: (720) 356-1421
Email: Jesse.Adams@ee.doe.gov

Contract Number: DE-FC36-086018052

Subcontractors
- UTC Power, South Windsor, CT
- University of Delaware, Newark, DE
- University of Tennessee, Knoxville, TN

Project Start Date: October 1, 2008
Project End Date: December 30, 2014

Objectives

- The overall objective of this project is to develop a unique, high-volume manufacturing processes that will produce low-cost, durable, high-power density 5-layer (5-L) membrane electrode assemblies (MEAs) that minimize stack conditioning:
- Manufacturing process scalable to fuel cell industry MEA volumes of at least 500k systems/year.
- Manufacturing process consistent with achieving \$9/kW_e DOE 2017 transportation MEA cost target.
- The product made in the manufacturing process should be at least as durable as the MEA made in the current process for relevant automotive duty cycling test protocols.
- The product developed using the new process must demonstrate power density greater or equal to that of the MEA made by the current process for relevant automotive operating conditions.
- Product form is designed to be compatible with high-volume stack assembly processes: 3-layer (3-L) MEA roll-good (anode electrode + membrane + cathode electrode) with separate rolls of gas diffusion media.
- The stack break-in time should be reduced to 4 hours or less.

Phase 2 Objectives

- Low-cost MEA R&D
  - New 3-L MEA Process Exploration
    - Investigate equipment configuration for low-cost MEA production
    - Investigate raw material formulations
    - Map out process windows for each layer of the MEA
  - Mechanical Modeling of Reinforced 3-L MEA
    - Use model to optimize membrane reinforcement for 5,000+ hour durability and maximum performance
    - Develop a deeper understanding of MEA failure mechanisms
  - 5-L Heat and Water Management Modeling
    - Optimization of gas diffusion membrane thermal, thickness, and transport properties to enhance the performance of thin, reinforced membranes and unique properties of direct-coated electrodes using a validated model
  - MEA Conditioning
  - Evaluate potential for new process to achieve DOE cost targets prior to process scale up (Go/No-Go Decision)
- Scale Up
  - Equipment setup
  - Optimization
    - Execute designed experiments which fully utilize University of Delaware and University of Tennessee modeling results to improve the new MEA process and achieve the highest possible performance and durability
- Stack Validation

Technical Barriers

This project addresses the following technical barriers from the Manufacturing section of the Fuel Cell Technologies Office Multi-Year Research, Development, and Demonstration Plan:

(A) Lack of High-Volume Membrane Electrode Assembly Processes

Contribution to Achievement of DOE Manufacturing Milestones

This project will contribute to achievement of the following DOE milestones from the Fuel Cells section of the Fuel Cell Technologies Office Multi-Year Research, Development, and Demonstration Plan:

- RD&D Plan Section 3.4, Task 10.1: Test and evaluate fuel cell systems and components such as MEAs, short stacks, bipolar plates, catalysts, membranes, etc. and compare to targets. (3Q, 2011 thru 3Q, 2020)
- RD&D Plan Section 3.4, Task 10.2: Update fuel cell technology cost estimate for 80 kW transportation systems and compare it to targeted values. (3Q, 2011 thru 3Q, 2020)

FY 2014 Accomplishments

- Direct Coating Process Development
  - The primary path for the new 3-L MEA process has succeeded in incorporating the previously modeled process improvements which indicated potential for a 25% reduction in high-volume 3-L MEA cost.
  - Pilot-scale demonstration of the new 3-L MEA process is nearing completion:
    - Current density of un-optimized direct-coated electrodes is equivalent to or better than current commercial electrodes over a robust range of automotive operating conditions.
    - Gore has demonstrated mechanical durability of an 8-micron expanded polytetrafluoroethylene (ePTFE) reinforced membrane. In previous testing, GORE™ MEAs exceeded 2,000 hours of accelerated mechanical durability testing, which has been equated to achieving 9,000 hours of membrane durability in an 80°C automotive duty cycle. This exceeds the DOE 2015 membrane durability target of 5,000 hours. Gore's 8-micron ePTFE reinforced membrane technology has been successfully incorporated into the lab-scale new 3-L MEA process.
- Modeling tasks at the University of Delaware and University of Tennessee are complete.

✧ ✧ ✧ ✧ ✧

INTRODUCTION

Over the past 20 years, great technical progress has been made in the area of improving power density and durability of fuel cell stacks, so much so that most of the requisite technical targets are now within reach. Yet, three major technical challenges remain. First and foremost is meeting the cost targets. The second challenge is producing components that are amenable for use in a high-speed, automotive assembly line. One impediment to this latter goal is that stack components must currently go through a long and tedious conditioning procedure before they produce optimal power. This so-called "break-in" can take many hours, and can involve quite complex voltage, temperature and/or pressure steps. These break-in procedures must be simplified and the time required reduced, if fuel cells are to become a viable power source. The third challenge is to achieve the durability targets in real-world operation. This project addresses all three challenges: cost, break-in time, and durability for the key component of fuel cell stacks: MEAs.

APPROACH

The overall objective of this project is to develop unique, high-volume manufacturing processes for low-cost, durable, high-power density 3-L MEAs that require little or no stack conditioning. In order to reduce MEA and stack costs, a new process will be engineered to reduce the cost of intermediate backer materials, reduce the number and cost of coating passes, improve safety and reduce process cost by minimizing solvent use, and reduce required conditioning time and costs. MEA mechanical durability will be studied and optimized using a combination of ex situ mechanical property testing, non-linear mechanical model optimization, and in situ accelerated mechanical durability testing. Fuel cell heat and water management will be modeled to optimize electrode and gas diffusion membrane thermal, geometric, and transport properties and interactions. Unique enabling technologies that will be employed in new process development include:

- Direct coating which will be used to form at least one membrane–electrode interface.
- Gore's advanced ePTFE membrane reinforcement and advanced perfluorinated sulfonic acid ionomers which enable durable high-performance MEAs.
- Advanced fuel cell testing and diagnostics.

RESULTS

Low-Cost MEA Process Development

- Primary path (Figure 1)
  - Process step 1: Coat bottom electrode on low-cost, non-porous backer
  - Process step 2: Direct coat reinforced membrane on top of the bottom electrode

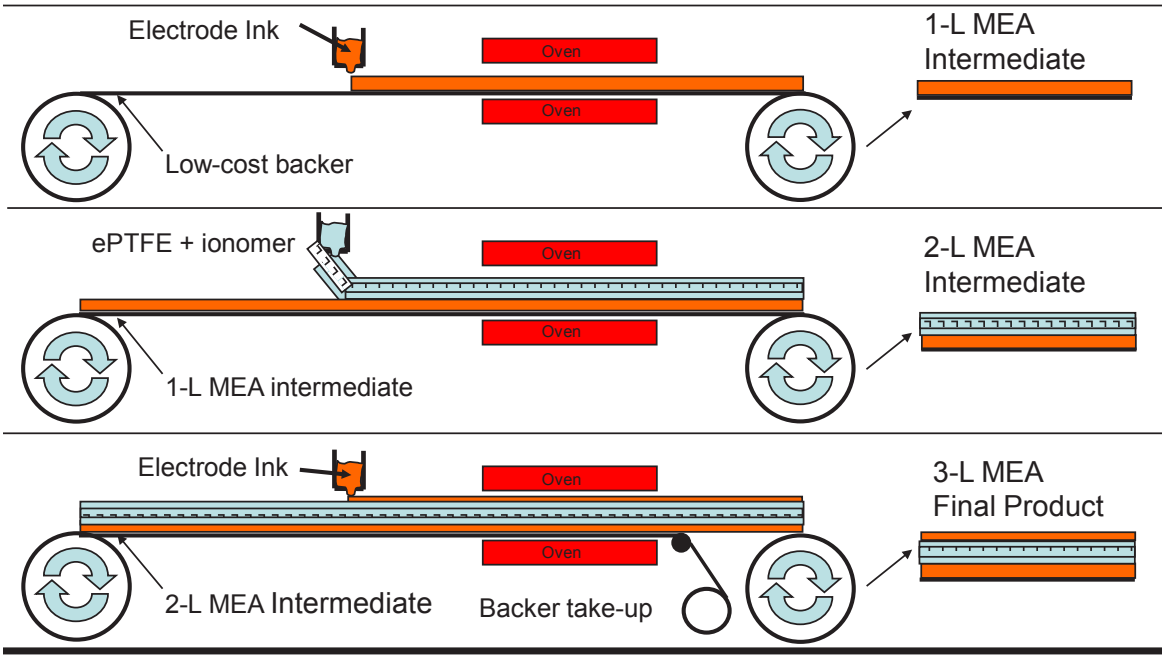

FIGURE 1. Low-Cost MEA Manufacturing Process

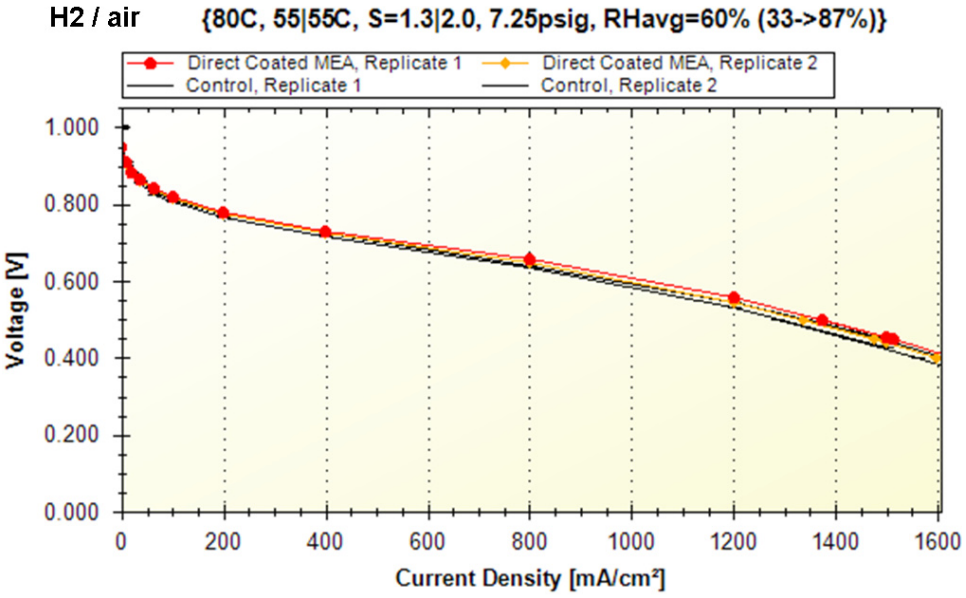

RH - relative humidity

FIGURE 2. Direct-Coated MEA Performance

  - Process step 3: Direct coat top-side electrode on top of the reinforced membrane
- Figure 2 indicates performance of a direct coated MEA compared with a control MEA made with the commercial process.
- Figure 3 demonstrates the advantage of thin Gore membranes in hot, dry operating conditions.

Mechanically Durable 8-µm Reinforced Membrane

Gore has successfully incorporated a mechanically durable 8-µm reinforced membrane into the current primary path process. The 8-µm membrane construction has demonstrated high performance due to reduced resistance and increased water back-diffusion (see Figure 3). In previous testing, GORE™ MEAs exceeded 2,000 hours of

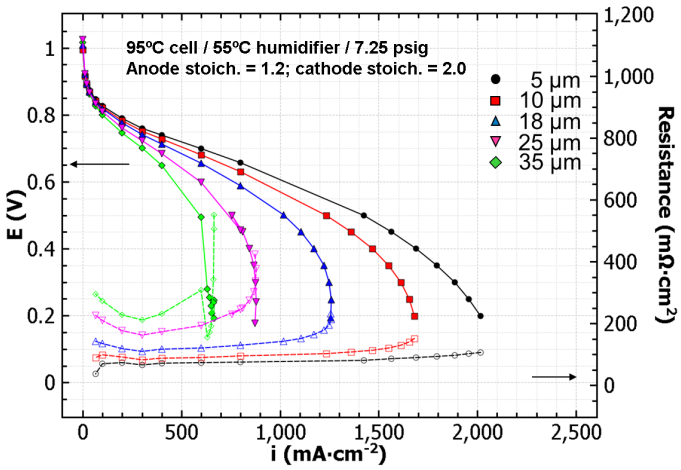

FIGURE 3. Performance Comparison of Thin, Mechanically Durable Reinforced Membranes

accelerated mechanical durability testing, which has been equated to achieving 9,000 hours of membrane durability in an 80°C automotive duty cycle. This exceeds the DOE 2015 membrane durability target of 5,000 hours. The accelerated mechanical durability testing protocol is summarized below:

Tcell (C)	Pressure (kPa)	Flow (Anode/Cathode, cc/min)
80	270	500 N_2/1,000 N_2

Cycle between dry feed gas and humidified feed gas (sparger bottle temp = 94˚C)
Dry feed gas hold time: 15 seconds
Humidified feed gas hold time: 5 seconds
For further protocol information, see: W. Liu, M. Crum, ECS Transactions **3**, 531-540 (2007)

CONCLUSIONS AND FUTURE DIRECTIONS

The combination of Gore's advanced materials, expertise in MEA manufacturing, and fuel cell testing with the mechanical modeling experience of University of Delaware and the heat and water management experience of University of Tennessee enables a robust approach to development of a new low-cost MEA manufacturing process.

Future work will focus on stack validation as well as accelerated stress testing to ensure that durability of the new, direct-coated MEAs is equivalent to or better than the current commercial control MEA.

GORE and designs are trademarks of W.L. Gore & Associates, Inc.

FY 2014 PUBLICATIONS/PRESENTATIONS

1. 2014 Hydrogen Program Annual Merit Review: mn004_ busby_2014_o.pdf.

2. "Time-Dependent Mechanical Behavior of Proton Exchange Membrane Fuel Cell Electrodes" Z. Lu, M.H. Santare, A.M. Karlsson, F.C. Busby, P. Walsh, *J. Power Sources*, 245, p. 543-552 (2014).

VI.3 Development of Advanced Manufacturing Technologies for Low-Cost Hydrogen Storage Vessels

Mark Leavitt
Quantum Fuel Systems Technologies Worldwide, Inc.
25242 Arctic Ocean Drive
Lake Forest, CA 92630
Phone: (949) 399-4584
Email: mleavitt@qtww.com

DOE Managers
Nancy Garland
Phone: (202) 586-5673
Email: Nancy.Garland@ee.doe.gov
Jesse Adams
Phone: (720) 356-1421
Email: Jesse.Adams@ee.doe.gov

Contract Number: DE-FG36-08GO18055

Subcontractors
- Boeing Research and Technology, Seattle, WA
- Pacific Northwest National Laboratory (PNNL), Richland, WA

Project Start Date: September 26, 2008
Project End Date: March 31, 2014

Overall Objectives

Develop new methods for manufacturing Type IV pressure vessels for hydrogen storage with the objective of lowering the overall product cost by:

- Optimizing composite usage through combining traditional filament winding (FW) and advanced fiber placement (AFP) techniques.
- Exploring the usage of lower-strength, higher-modulus fibers on the outer layers of FW.
- Building economic and analytical models capable of evaluating FW and AFP processes including manufacturing process variables and their impact on vessel mass savings, material cost savings, processing time, manufacturing energy consumption, labor and structural benefits.
- Studying polymer material degradation under high-pressure hydrogen environment to optimize storage volume.

Fiscal Year (FY) 2014 Objectives

- Design hybrid vessel with the latest version of mWind software.
- Pass all critical tests to the hybrid design per EC79/2009 standard.
- Improve manufacturing quality of AFP dome caps.
- Complete cost model for hybrid vessel manufacturing.
- Perform polymer liner material testing with in situ tensile rig and compare results.

Technical Barriers

The project addresses the following technical barriers from the Manufacturing R&D section (3.5) of the Fuel Cell Technologies Office Multi-Year Research, Development, and Demonstration Plan:

(M) Lack of Low-Cost Carbon Fiber

(N) Lack of Low-Cost Fabrication Techniques for Storage Tanks

Contribution to Achievement of DOE Manufacturing R&D Milestones

This project will contribute to achievement of the following DOE milestone from the Manufacturing R&D section of the Fuel Cell Technologies Office Multi-Year Research, Development, and Demonstration Plan:

- Milestone 7.2: Develop fabrication and assembly processes for high pressure hydrogen storage technologies that can achieve a reduction of 10% off the baseline cost of $18/kWh for Type IV, 700 bar tanks. (4Q, 2015)

FY 2014 Accomplishments

- Passed burst test with latest vessel design at 162.5 MPa, exceeding the minimum requirement by more than 3%.
- Passed ambient cycle, accelerated stress rupture and impact damage tests, which are critical to the hybrid design.
- Upgraded fiber creel system by Boeing to manufacture higher quality AFP dome caps.
- Saved 32% in mass and 27% in cost with latest design compared to baseline (all FW) vessel resulting in $20.7/kWh and 1.93 kWh/kg.
- Revealed high-density poly-ethylene (HDPE) ultimate tensile strength (UTS) decreases with increasing hydrogen pressure up to tested pressure of 5,000 psi.

INTRODUCTION

The goal of this project is to develop an innovative manufacturing process for Type IV high-pressure hydrogen storage vessels, with the intent to significantly lower manufacturing costs. The development is to integrate the features of high-precision AFP and commercial FW while satisfying design requirements.

APPROACH

Based on the latest in-house software developed for generating finite element analysis models of composite shells with option of using AFP methods, vessel design was completed for Boeing to build the AFP dome caps and Quantum to complete the vessel with FW. The design was tested in five different tests that are critical to the hybrid design. This project serves as a proof of concept that hybrid vessels can significantly reduce mass and save cost.

RESULTS

Vessel Build and Testing

Vessel 14: At the time of writing the 2013 annual report, Vessel 14 was being built with the latest design from the mWind software. During winding, a convex surface was observed between two layers of the AFP aft dome cap that would result in bridging of fiber. Chopped fiber with resin was used to fill in the gap. To ensure sufficient compaction to minimize the amount of voids, computed tomography (CT) scan on the vessel was planned before the burst test, but the equipment was not available. Nevertheless, a high-speed camera was utilized to help understand the burst mode for future design improvements if necessary.

The vessel achieved a burst pressure of 141.3 MPa (20,499 psi), short of the 157.5 MPa (22,844 psi) burst requirement. The rupture initiated from the aft dome area, which is consistent with the location that chopped fiber was applied. Although the dome cap was filled to avoid fiber bridging across the convex surface, the amount of void content in chopped fiber is unknown and may have contributed to lower translation efficiency at those locations.

Vessels 15 and 16: From observing the failure mode of Vessel 14, there was sufficient confidence that the vessel would have passed the test if there were no convex surface in the dome cap. Due to project timing, no extra time was available to redesign the aft dome cap to eliminate the convex surface. Carbon fiber woven rings of various sizes were used to fill in the convex surface for the next winds. Further, both Vessels 15 and 16 were wound on the winding machine at the same time because there was no need to develop new winding patterns.

Upon installing the woven rings, a very small amount of chopped fiber with resin was still necessary to eliminate all fiber bridging. A CT scanner was available this time. Figure 1 shows the CT scan result of Vessel 15, which indicates minimal voids at locations where woven rings and chopped fiber were used.

One of the two vessels was designated for burst test, and the other was for ambient cycle test. From previous experience in this project, a release film is necessary to be placed between the liner and composite, so they do not bond physically during composite cure.

A burst pressure of 162.5 MPa (23,572 psi), exceeding the minimum burst requirement of 157.5 MPa was achieved on Vessel 15. The composite mass was 51.5 kg, which translates to a 32% mass savings from the baseline vessel (composite mass of 76 kg). The failure mode was mid cylinder, as shown in Figure 2. Vessel 16 completed 15,000 cycles between 10% and 125% of service pressure without developing a leak or rupture.

Vessels 17 and 18: From the positive results on the previous two tests, two additional vessels were manufactured at the same time again using the same design. Vessel 17 was built for the accelerated stress rupture test, which evaluates the compatibility of the filament wound and advanced fiber placement resin systems (QT and Boeing) to transfer load between AFP and FW layers and determine if there

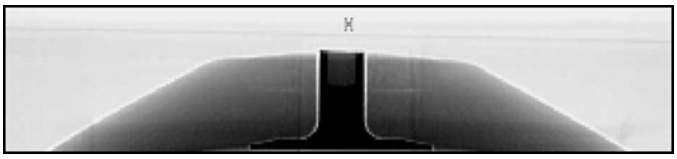

FIGURE 1. CT Scan of Vessel 15 Aft Dome

FIGURE 2. Vessel 15 Post Burst Test

is a resin creep issue with discontinuous winding. The test was performed at 125% of service pressure (87.5 MPa or 12,691 psi) at 85°C (185°F), which is the upper design limit temperature of the vessel, for 1,000 hours. The vessel was kept inside an environmental chamber, which was then placed inside a pit to protect personnel from injuries in case of rupture during test. Burst test was then performed after the 1,000-hour hold to evaluate the vessel's residual strength. The minimum requirement is 85% of the nominal working pressure times the burst pressure ratio (85% x 70 MPa x 2.25), which is equivalent to 133.9 MPa (19,421 psi).

After the 1,000-hr hold, the vessel successfully passed the test by rupturing at 153.0 MPa (22,191 psi), exceeding the minimum requirement. When compared with the virgin burst result (162.5 MPa or 23,572 psi) of Vessel 16, there is a 5.8% reduction in burst pressure.

The results showed that the vessel design was capable of resisting creep degradation at the test conditions even though

1) two different resin systems were used on the hybrid design and
2) the Boeing resin using in AFP was under-cured due to liner processing temperature limitation.

Vessel 18 was built for the impact damage test. The purpose of the test was to evaluate the vessel's resistance to impact damage even with a 32% reduction of composite in mass. The foam domes and foam rings designed for the baseline (all FW) vessel were used on this particular vessel to prepare for the test. Since the hybrid design reduced the vessel diameter significantly, the foam domes were modified to fit onto the vessel. Foam dome material was removed to fit them over the smaller composite domes, as shown in Figure 3. In addition, the inside curvatures of the two halves of the foam dome had to be forced to conform to the composite dome profile. However, a perfect conformance was not possible due to the stiffness of the foam domes. Some air gaps were present as a result. In addition to the less-than-ideal foam domes, the composite domes were much thinner as a result of the hybrid design. This further affected the outcome of the impact damage test.

FIGURE 3. Vessel 18 with Foam Domes Modified from Baseline Vessel

Upon impact, deformations and cracks were observed on the foam domes. They were most likely caused by air gap between the foam domes and composite. This was inevitable when complete conformance was not achievable. During post impact cycle testing, the vessel developed a leak after 11,658 cycles, exceeding the requirement of 3,000 cycles.

Vessel 19: The last vessel built was for extreme temperature pressure cycle testing, which evaluates the compatibility of two resin systems to transfer load between AFP and FW layers effectively.

After conditioning the vessel for 48 hours at 85°C, the vessel completed 3,679 fill cycles before rupturing on the aft end. The pre-mature rupture showed that the load transfer mechanism could have been compromised with higher operating temperature and pressure cycling. With only a few inches of AFP and FW overlapping on both ends of the vessel for load transfer, this location could have been weakened under cycling by the under-cured AFP resin. The cure temperature was limited due to the liner processing temperature restrictions. Because of the rupture, the low extreme temperature portion of the test could not be performed.

Upgrading Fiber Creel System

The final control logic was integrated into the upgraded creel system at Boeing. This controller allows the linear potentiometers that are associated with each individual dancer arm to send information back to the motor that it is affixed to, creating a more-refined tension control system. Each motor controls an individual tow; thus, each of the six tows is controlled independently of each other. Each motor will output the correct torque for its particular lane so that tension across all six tows is consistent, regardless of differences in drag from lane to lane.

The motors also allow the material to be wound back up or re-spooled when the head articulates in a manner which creates slack. Having this function keeps the material from coming into contact with any unwanted or foreign materials, while keeping consistent tension on the tows at all times.

Vessel Manufacturing Cost Modeling

The vessel manufacturing cost model was updated to evaluate the mass and cost savings of the Vessel 15 design. Cost comparison between the baseline vessel and the hybrid vessel designs 1, 7 and 15 was completed. Each of these vessel designs exceeded the burst pressure requirement during testing. The calculations assume a carbon fiber price at $13/lb. The improvement of Vessel 15's

design was significant—32% mass savings and 27% cost savings compared to the baseline filament wound vessel. In comparison, Vessel 7 only achieved 23% mass savings and 17% cost savings compared to the baseline vessel.

Hydrogen Testing of Polymer Liner Materials

After completion of the build and debugging the in situ tensile rig in 2013 by PNNL, the in situ frame was tested in air numerous times, and the stress/strain curves were cross-correlated with identical samples and strain rates in a standard tensile test frame equipped with a strain gauge. This allowed PNNL to obtain the "effective" gauge length of the polymer samples. Samples used were miniature tensile "dog-bone" geometry from ASTM International standards with the tabs reduced for the miniature grips. A procedure for reproducibly mounting the samples and setting the solenoid initial displacement was developed during this air testing to ensure high reproducibility. Even so, some tests showed either minor, or major jumps in the stress/strain curves at low strain within the elastic limit that are likely caused by "sticking" somewhere in the system and indicates some minor design modifications are needed. Due to limited funding, a larger number of samples was tested instead, and tests with major jumps in the stress/strain curve that indicated sticking were disregarded. After analysis, minor inflections in the stress strain curve in the elastic limit were considered acceptable for analysis of the UTS degradation in high-pressure hydrogen.

Testing occurred in a high-pressure hydrogen autoclave at pressures of 4,000 psi, 4,500 psi, and 5,000 psi. This represents the upper safe working limit of the autoclave. Multiple tests were carried out at each pressure. Tests exhibiting no inflections (signs of mechanical sticking) in the stress/strain curve are shown in Figure 4. From simple

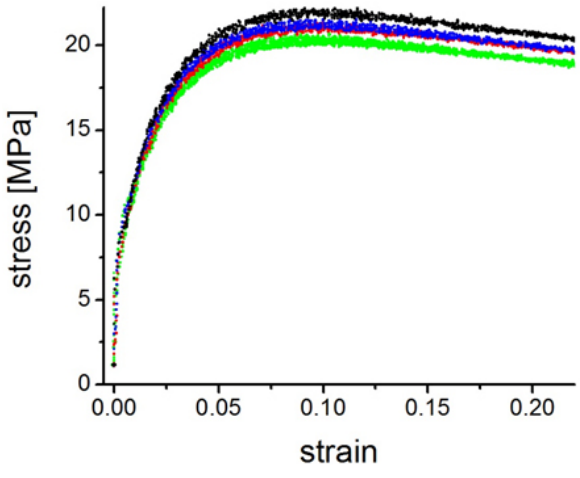

FIGURE 4. Stress/Strain Curves for HDPE Samples Tested in Air (black) and in High-Pressure Hydrogen at 4,000 psi (blue), 4,500 psi (red) and 5,000 psi (green)

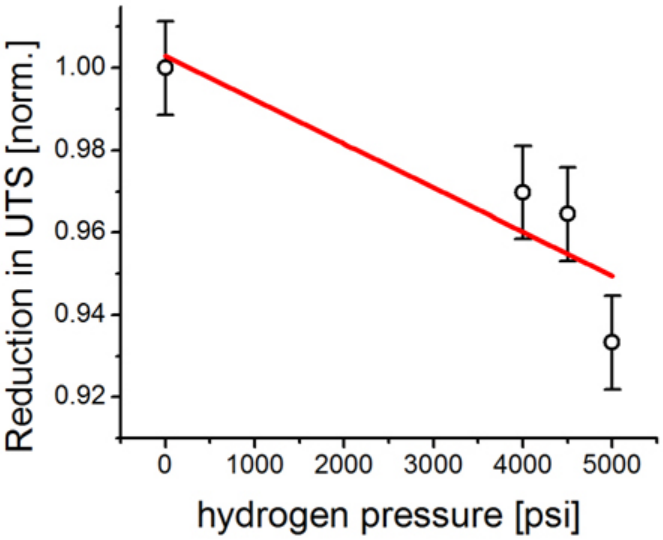

FIGURE 5. UTS Data Showing Marked Decrease with Increasing Hydrogen Pressure

examination of these curves, it appears that changes in the modulus are minimal, but there is a clear decrease in the UTS with increasing hydrogen pressure.

The data around the UTS demonstrating a clear decrease in the UTS of up to nearly 10% as compared to in air at 5,000 psi hydrogen. This marked decrease is similar to what was seen in ex situ measurements previously performed by PNNL. Again, these data are only those with no inflections in the elastic region. Figure 5 shows the average UTS as a function of hydrogen pressure. There appears to be a potentially non-linear behavior to the data with the UTS decreasing at more after 4,500 psi, but that cannot be confirmed without further testing at higher pressures not attainable with the current autoclave system.

CONCLUSIONS AND FUTURE DIRECTIONS

- Achieved significant mass (32%) and cost (27%) savings with hybrid design, comparing to all FW baseline vessel.
- The latest vessel design passed 80% of all tests that are critical to the hybrid design.
- Improved AFP dome caps achieved high consistency from part to part.
- mWind software is sufficiently accurate for hybrid vessel development based on test results.
- Modify AFP layup to avoid using woven fiber rings and chopped fiber as filler.
- Improve fit between AFP dome caps and boss/liner to improve fatigue performance.

- Extend the FW and AFP load transfer interface to improve cycle durability in the extreme temperature pressure cycle test.
- Investigate the potential non-linear UTS behavior of HDPE in hydrogen at pressures higher than 4,500 psi.

FY 2014 PUBLICATIONS/PRESENTATIONS

1. Development of Advanced Manufacturing Technologies for Low Cost Hydrogen Storage Vessels, Annual Merit Review and Peer Evaluation Meeting, Department of Energy, June 16–20, 2014, Washington, D.C.

VII. TECHNOLOGY VALIDATION

VII.0 Technology Validation Sub-Program Overview

INTRODUCTION

The Technology Validation sub-program demonstrates, tests, and validates hydrogen and fuel cell technologies and uses the results to provide feedback to the Fuel Cell Technologies Office's research and development (R&D) activities.

Continuing efforts include the real-world evaluation of fuel cell bus technologies at various transit authorities and monitoring performance of fuel cells in stationary power, backup power, and material handling equipment (MHE) applications. New data collection projects awarded include light-duty fuel cell electric vehicles (FCEVs), hydrogen stations, hybrid electric medium-duty trucks, rooftop backup power, and advanced hydrogen refueling components.

GOAL

The goal of the Technology Validation sub-program is to validate the state of the art of fuel cell systems in transportation and stationary applications as well as hydrogen production, delivery, and storage systems and assess technology status and progress to determine when technologies should be moved to the market transformation phase.

OBJECTIVES

The objectives of the Technology Validation sub-program are to:

- Validate hydrogen FCEVs with greater than 300-mile range and 5,000 hours fuel cell durability by 2019.
- Validate a hydrogen fueling station capable of producing and dispensing 200 kg H_2/day (at 5 kg/3 min; 700 bar) to cars and/or buses by 2019.
- Validate commercial stationary fuel cells against 2015 system targets (50,000 h, 45% electrical efficiency) by 2017.
- Validate durability of auxiliary power units against 2015 fuel cell system target (15,000 h, 35% electrical efficiency) by 2017.
- Validate large-scale systems for grid energy storage that integrate renewable hydrogen generation and storage with fuel cell power generation—operating for more than 10,000 hours, with a round-trip efficiency of 40% by 2020.

FISCAL YEAR (FY) 2014 TECHNOLOGY STATUS AND ACCOMPLISHMENTS

Fuel Cell Bus Evaluation

During FY 2014, data from four fuel cell electric bus (FCEB) demonstrations at three transit agencies were collected and analyzed; AC Transit (Oakland, California), SunLine (Thousand Palms, California), and BC Transit (Whistler, Canada). The objective of this effort is to determine the status of fuel cell systems for buses and to aid other fleets with the implementation of next generation FCEBs. Fuel cell buses continue to show improved fuel economy (ranging from 1.8 to 2.4 times higher) compared to baseline (diesel and compressed natural gas) buses in similar service. Fuel economy for the FCEBs ranged from 5.8 miles/diesel gallon equivalent (DGE), up to 7.3 miles/DGE (for an average of 6.8 miles/DGE), approaching the Federal Transit Administration's performance target for FCEB fuel economy of 8 miles/DGE. The top three fuel cell powerplants accumulated operating hours reported by the National Renewable Energy Laboratory (NREL) for these buses were 16,419, 11,908, and 9,903. A measure of reliability—the miles between road calls—was found to be 48% higher than first generation buses. FCEB availability demonstrated a 20% improvement, increasing from 57% to 69%. The highest percentage of road calls realized was not associated with the fuel cell system itself. The majority of the road calls were due to bus-related general maintenance, batteries, and hybrid propulsion systems, while fuel cell-related issues made up approximately 2% to 17% of the road calls. (NREL)

Hydrogen Component Validation

The main objectives of this project include the independent validation and systems integration of commercial and advanced prototype hydrogen production, compression, dispensing, and fuel cell technologies. In FY 2014, the project focused on performing highly accelerated life testing of diaphragm hydrogen compressors, which aims to

reproduce component failures and correlates these failures to real-world usage. The project team has partnered with compressor manufacturers to instrument, monitor, and analyze compressor performance in a relevant accelerated-testing environment. The team will also be identifying failure modes and working with manufacturers to improve reliability of future designs while collaborating with national laboratories to improve diaphragm compressor modeling. Compressor performance (power and pressure data) has been analyzed and mapped. (NREL and Pacific Northwest National Laboratory)

Hydrogen Station Analysis

The objective of this project is to collect data from state-of-the-art hydrogen fueling facilities, such as those operated by the California Air Resources Board, Proton OnSite, and the Gas Technology Institute, providing valuable feedback on data related to hydrogen infrastructure. (NREL)

- California Air Resources Board's Newport Beach, California station features onsite generation of 100 kg H_2/day through a small-scale natural gas steam methane reformer, demonstrating the footprint and equipment arrangement of such a retail facility. Evaluation results will be used to make recommendations on how to optimize discrete station components. The station is operational and additional data collection hardware is installed and calibrated. A full data set is expected by January 2015.
- Proton OnSite's fully containerized station deployments (SunHydro #1 located in Wallingford, Connecticut and SunHydro #2 located in Braintree, Massachusetts) demonstrate advanced technologies, including (1) higher-pressure (57 bar) hydrogen generation with electrochemical compression, (2) higher-efficiency generation with lower resistance electrolyte and advanced catalyst, (3) higher capacity composite storage, and (4) advanced packaging concepts for reduced footprint. This project goes beyond data collection; it aims to validate the first full-scale demonstration of a high-pressure water electrolyzer. The new high-pressure electrolyzer has been built and data monitoring is underway at the SunHydro #1 station. Design is complete and construction is underway at the SunHydro #2 station.
- Gas Technology Institute has partnered with Linde to demonstrate 100 kg H_2/day refueling stations in four Northern California locations (Foster City, Cupertino, Mountain View, West Sacramento) and a Southern California location (San Juan Capistrano), where new 900-bar ionic compression technology is utilized. The West Sacramento and San Juan Capistrano stations are expected to be installed and commissioned by the third and fourth quarters of 2014, respectively.
- California State University, Los Angeles is operating a 30-60 kg H_2/day, electrolyzer-based hydrogen station powered by renewable electricity on its campus to test, collect data on, and validate hydrogen refueling architecture and individual components in a real-world operating environment. The station was commissioned in May 2014. Performance evaluation data are being provided. The project also serves educational purposes, as it provides a "living lab" environment for engineering and technology students.

Stationary Fuel Cell Evaluation

This project informs the sub-program, the public, fuel cell manufacturers, and other stakeholders about the performance of stationary fuel cell systems operating under real-world conditions while reporting on the baseline, progress, and technical challenges. Operation, maintenance, and safety data are collected and analyzed quarterly for stationary fuel cell systems. In FY 2014, installation data from California's Self Generation Incentive Program were collected for 317 fuel cell-based units (totaling 131 MW, cumulative). Natural gas was seen as the most popular fuel choice, but there was a small resurgence of biomass projects in late 2013. The mean availability of the fuel cell systems was 93%, with about 35% of systems having availability over 95%. The mean electrical efficiency of the fuel cells was 27%, with less than 3% of the systems analyzed with over 35% electrical efficiency (based on higher heating value). Average installed cost was found to be $10,200/kW and $6,700/kW with incentives. (NREL)

Early Markets Analysis

Early market application of fuel cell technologies includes validating MHE and backup power fuel cell performance through analysis and reporting of real-world operation and value proposition metrics.

By the fourth quarter of 2013, 852 backup power units were operating as part of the Technology Validation sub-program. These units were found to be operating with average availability of about 99.5% in 23 states. Reasons for unsuccessful starts include an e-stop signal, no fuel, and other system failures. A backup power cost of ownership

analysis was also conducted. When the fuel cell backup power units were operated for 72 hours, the cost of ownership of the fuel cell system, without incentives, was found to be approximately 1.2 times higher than that of a diesel generator and more than five times lower than that of a battery system. In the same runtime scenario, but when incentives were considered, the cost of ownership of the fuel cell system was found to be approximately equal to that of the diesel generator and more than six times lower than that of a battery system.

By the fourth quarter of FY 2013, 490 MHE fuel cell units were operating as part of the Technology Validation sub-program, filling up on average in 2.3 minutes, and operating an average of 4.4 hours between fills. Among components related to the infrastructure, hydrogen compressors were consistently found to be a leading category for monthly maintenance hours. Control electronics is not as consistent but was also found to be a leading maintenance category. (NREL)

Hydrogen Fueling Infrastructure Research and Station Technology (H2FIRST)

This project is a new effort with a goal of ensuring FCEV customers have a positive fueling experience relative to conventional gasoline/diesel stations as vehicles are rolled out in the near term and transition to advanced fueling technology beyond 2017. The focus of this project is on station components and systems using core laboratory capabilities and leveraging resources to maximize impact. H2FIRST coordinates with industry, academic, and government partners, and also with H2USA. Five project teams have been organized: Station Performance Testing, Dispenser/Components, Reference Station Design, Hydrogen Contamination Detector, and Technical Assistance. A reference station matrix is also being developed for targets and metrics. This project is coordinated between the Technology Validation; Safety, Codes and Standards; and Hydrogen Delivery sub-programs. (NREL and Sandia National Laboratories, SNL)

Fuel Cell Electric Vehicle Analysis

Six major auto manufacturers (General Motors, Honda, Hyundai, Mercedes-Benz, Nissan, and Toyota) were awarded $5.5M to demonstrate advanced light-duty FCEVs, and data will be collected from up to 90 vehicles. The first composite data product will be published to NREL's website in December 2014.

Fuel Cell Hybrid Electric Medium-Duty Trucks

Two new projects were selected to demonstrate fuel cell hybrid electric medium-duty trucks.

FedEx Express partnered with Smith Electric Vehicles for the deployment and demonstration of an 80-kWh eTruck outfitted with a 10-kW fuel cell, extending the truck's range from 56 miles to 150 miles. The vehicles will be deployed at the FedEx Memphis, Tennessee headquarters and locations throughout the Los Angeles, California metro area. FedEx will make use of already existing hydrogen refueling infrastructure; a station currently installed at the Memphis site as well as several retail hydrogen refueling stations around the Los Angeles area. FedEx Express uses approximately 40,000 vehicles in its fleet, which could potentially be replaced with fuel cell hybrid vehicles. With fuel cells, the vehicles could save 196 million gallons diesel fuel and associated emissions per year. (FedEx Express and Smith Electric Vehicles)

The Center for Transportation and the Environment partnered with the University of Texas Center for Electromechanics, Electric Vehicles International, Hydrogenics USA, Valence Technology, and the United Parcel Service of America, Inc. (UPS) to develop, validate, and deploy 17 fuel cell hybrid battery electric walk-in delivery vans for parcel delivery service, which will be able to achieve an extended range of 150 miles. In the initial phase, one demonstration vehicle will be deployed for six months at a UPS facility in California for real-world validation. In the second phase, UPS will operate the additional 16 vehicles for over three years at two or more distribution centers throughout the state of California, making use of the already existing hydrogen fueling station infrastructure. Fuel cell hybrid vehicles could potentially take the place of ~46,000 diesel walk-in vans in UPS' fleet alone. With fuel cells the vehicles could save 120 million gallons of diesel fuel and associated emissions per year. (Center for Transportation and the Environment, University of Texas, Electric Vehicles International, Hydrogenics USA, Valence Technology, and UPS)

Cryogenic Pressurized Hydrogen Storage and Delivery

The use of a 100-kg H_2/hr, 875-bar high-pressure liquid hydrogen pump is being investigated and validated. Factors like fill density, electricity consumption, and refuel time will be evaluated during long-term testing. Liquid hydrogen pumps have the potential to increase hydrogen storage density (and vehicle driving range) by up to 30%,

while enabling five-minute refueling and minimizing delivery costs. The high-pressure pump is installed and operational, and validation testing is underway. (Lawrence Livermore National Laboratory)

High-Pressure Hydrogen Bulk Delivery

An advanced tube trailer based on high-pressure (8,500 psi or 590 bar) composite over-wrapped pressure vessel technology is being developed and tested to validate its performance under real-world conditions. Up to 920 kg of hydrogen can be stored in a single trailer, providing up to three times the capacity increase of conventional steel tank trailers. High-pressure composite hydrogen storage can lower existing hydrogen fueling costs by 30% to 60%, and can ultimately eliminate the need for some of the onsite compression. The new composite hydrogen trailer supply also provides the advantage of significantly lowering hydrogen fueling station site preparation costs, equipment costs, operating costs, and hydrogen product costs. (Air Products and Chemicals, Inc. and Structural Composite Industries)

BUDGET

The funding portfolio for Technology Validation enables the sub-program to continue to collect and analyze data from fuel cells operating in transportation and stationary applications, as well as hydrogen production and delivery technologies. In FY 2014, $6 million in funding was appropriated for the Technology Validation sub-program, and $6 million was requested for FY 2015 (subject to congressional appropriations).

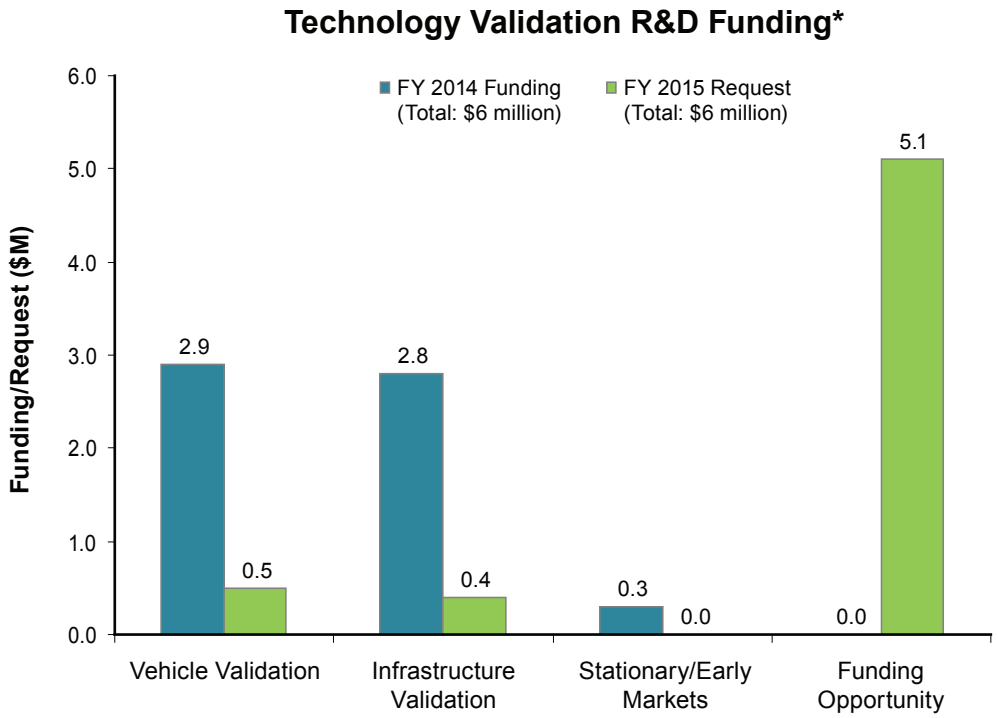

* Subject to appropriations, project go/no-go decisions and competitive selections. Exact amounts will be determined based on R&D progress in each area and the relative merit and applicability of projects competitively selected through planned funding opportunity announcements.

FY 2015 PLANS

In FY 2015, the Technology Validation sub-program will continue its detailed evaluations of fuel cell buses, FCEVs, hydrogen fueling stations, hybrid electric medium-duty trucks, rooftop back-up power, advanced hydrogen refueling components, stationary power deployments, and early market applications. Potential future funding opportunities (expected in the Fall of 2014) may emphasize hydrogen refueling station and components validation, and may also include validation of stationary and early market fuel cells, subject to appropriations.

In coordination with the Hydrogen Delivery and Safety, Codes and Standards sub-programs, a key focus in FY 2015 will be the H2FIRST project, a collaborative project between SNL and NREL coordinated with the H2USA Stations Working Group. H2FIRST includes research, development and validation tasks to support critical needs for hydrogen fueling stations, to help ensure a positive user experience relative to conventional vehicle fuels as commercialization of light-duty vehicles begins. H2FIRST project tasks include Reference Station Design, Hydrogen Contamination Detectors, and the Hydrogen Station Equipment Performance testing device development. The Hydrogen Station Equipment Performance device will be capable of testing hydrogen station fueling performance against the SAE International Standard SAE J2601 fueling protocol. Additionally, the Technology Validation sub-program will coordinate with the Office of Energy Efficiency and Renewable Energy's crosscutting grid integration activities to identify areas of synergy and potential applications for hydrogen and fuel cells.

Jason Marcinkoski
Technology Validation Project Manager
Fuel Cell Technologies Office
Office of Energy Efficiency and Renewable Energy
U.S. Department of Energy
1000 Independence Ave., SW
Washington, D.C. 20585-0121
Phone: (202) 586-7466
Email: Jason.Marcinkoski@ee.doe.gov

VII.1 Technology Validation: Fuel Cell Bus Evaluations

Leslie Eudy (Primary Contact), Matthew Post
National Renewable Energy Laboratory (NREL)
15013 Denver West Parkway
Golden, CO 80401
Phone: (303) 275-4412
Email: leslie.eudy@nrel.gov

DOE Manager
Jason Marcinkoski
Phone: (202) 586-7466
Email: Jason.Marcinkoski@ee.doe.gov

Project Start Date: 2003
Project End Date: Project continuation and direction determined annually by DOE

Overall Objectives

- Validate fuel cell electric bus (FCEB) performance and cost compared to DOE and U.S. Department of Transportation (DOT) targets and conventional technologies.
- Coordinate with the DOT's Federal Transit Administration (FTA) on the data collection for the National Fuel Cell Bus Program (NFCBP) and with international work groups to harmonize data-collection methods and enable the comparison of a wider set of vehicles.

Fiscal Year (FY) 2014 Objectives

- Document performance results from each current FCEB demonstration site.
- Complete an annual status report comparing results from the different demonstrations.

Technical Barriers

This project addresses the following technical barriers from the Technology Validation section of the Fuel Cell Technologies Office Multi-Year Research, Development, and Demonstration Plan:

(A) Lack of Fuel Cell Electric Vehicle and Fuel Cell Bus Performance and Durability Data

(D) Lack of Hydrogen Refueling Infrastructure Performance and Availability Data

Contribution to Achievement of DOE Technology Validation Milestones

This project has contributed to achievement of the following DOE milestone from the Technology Validation section of the Fuel Cell Technologies Office Multi-Year Research, Development, and Demonstration Plan:

- Milestone 2.3: Validate fuel cell electric vehicles achieving 5,000-hour durability (service life of vehicle) and a driving range of 300 miles between fuelings. (4Q, 2019)

  By the end of May 2014, NREL had documented 24 FCEB fuel cell systems with operation in excess of 8,000 hours. One of these systems has logged more than 16,800 hours in service, and a second system has surpassed 11,900 hours. Bus fuel economy is dependent on duty cycle. Based on in-service fuel economy values between 4 and 6.5 miles per kilogram, the hybrid FCEBs currently in service can achieve a range between 200 and 310 miles per fill.

FY 2014 Accomplishments

- Published reports on performance and operational data covering 24 full-size FCEBs in revenue service in the United States and Canada.
- Documented more than 16,800 hours on a single fuel cell power plant.

INTRODUCTION

Transit agencies continue to aid the FCEB industry in developing and optimizing advanced transportation technologies. These in-service demonstration programs are a vital part of the process to validate the performance of fuel cell systems in buses and to determine issues that require resolution. Using fuel cells in a transit application can help accelerate the learning curve for the technology because of the high mileage accumulated in short periods of time. During the last year, the project teams have made progress in improving fuel cell durability, availability, and reliability. More work is still needed to meet the performance needs of transit agencies, lower capital and operating costs, and transition the maintenance to transit staff.

APPROACH

NREL uses a standard evaluation protocol to provide:

- Comprehensive, unbiased evaluation results of advanced-technology vehicle development and operations

- Evaluations of hydrogen infrastructure development and operation
- Descriptions of facility modifications required for the safe operation of FCEBs
- Detailed FCEB performance and durability results to validate status against technical targets, educate key stakeholders, and further DOE goals.

The evaluation protocol includes collecting operation and maintenance data on the bus and infrastructure. The analysis, which consists of economic, technical, and safety factors, focuses on performance and use, including progress over time and experience with vehicle systems and supporting infrastructure. The data are compared to DOE/FTA technical targets and to conventional-technology baseline buses in similar service.

RESULTS

During FY 2014, NREL collected and analyzed data on the following four FCEB demonstrations at three transit agencies in the United States and Canada:

- Zero Emission Bay Area (ZEBA) Demonstration—five Bay Area transit agencies led by AC Transit (Oakland, California) are demonstrating twelve 40-foot Van Hool buses with US Hybrid[1] fuel cells in a Siemens hybrid system. The hybrid system was integrated by Van Hool and uses lithium ion batteries from EnerDel.
- Advanced Technology (AT) FCEB Project—SunLine (Coachella Valley area, California) is operating one New Flyer 40-foot bus with Blueways hybrid system, Ballard fuel cell, and lithium phosphate batteries from Valence. This bus was the pilot bus from the BC Transit demonstration.
- American Fuel Cell Bus (AFCB) Project—in December 2012 SunLine began operating an ElDorado 40-foot bus with a BAE Systems hybrid propulsion system using Ballard fuel cells and lithium ion batteries from A123. This project is part of FTA's NFCBP.
- British Columbia Transit (BC Transit) Fuel Cell Bus Demonstration—BC Transit conducted a 5-year demonstration of a fleet of FCEBs in Whistler, Canada. The fleet consisted of 20 New Flyer 40-foot buses with Bluways hybrid systems, Ballard fuel cells, and lithium phosphate batteries from Valence.

All of these buses are fuel-cell-dominant hybrid buses. The first two of these evaluations were funded by DOE, the third was covered by funding from FTA, and the BC Transit evaluation was funded by the California Air Resources Board. NREL published results from each of these demonstrations. A summary of selected results is included in this report.

[1] In 2013 US Hybrid acquired all the transit fuel cell assets originally owned by UTC Power.

NREL completed reports on operational and performance data from these FCEBs and from conventional baseline buses at each agency. The results are also compared to technical targets for FCEB performance established by DOE/FTA and published in a Fuel Cell Technologies Program Record in September 2012 [1]. Tables 1 through 3 provide a summary of the reported results from the operation at each agency, including data from the baseline buses.

TABLE 1. 2014 Summary Data Results for ZEBA FCEBs

Vehicle data	FCEB	Diesel
Number of buses	12	3
Data period (month, year)	Sep 11 – Dec 13	Sep 11 – Dec 13
Number of months	20	20
Total fleet miles	620,452	224,879
Average miles per month	2,095	4,249
Total fuel cell hours	69,407	–
Fuel economy (mi/kg)	6.46	–
Fuel economy (mi/diesel gal equivalent)	7.30	4.05
Average speed (mph)	8.9	–
Availability (%)	72	81

TABLE 2. 2014 Summary Data Results for BC Transit FCEBs

Vehicle data	FCEB	Diesel
Number of buses	20	–
Data period (month, year)	Apr 11 – Mar 14	–
Number of months	36	–
Total fleet miles	1,700,928	–
Average miles per month	2,612	–
Total fuel cell hours	150,556	–
Fuel economy (mi/kg)	3.97	–
Fuel economy (mi/diesel gal equivalent)	4.48	4.28
Average speed (mph)	14.2	–
Availability (%)	64	–

One key challenge for the fuel cell bus industry is increasing the durability and reliability of the fuel cell system to meet FTA life cycle requirements for a full-size bus—12 years or 500,000 miles. DOE and FTA have set an early fuel cell power plant (FCPP) performance target of 4–6 years (or 25,000 hours) durability for the fuel cell propulsion system, which would be approximately half the life of the bus. The FCPP would be rebuilt or replaced at that time—similar to what transit agencies typically do for diesel engines. Last year, NREL reported on FCPPs that had accumulated hours in excess of 13,000. These FCPPs have continued to accumulate hours in service. The addition of BC Transit to the analysis provides data on an additional 22 FCPPs (20 FCPPs plus

TABLE 3. 2014 Summary Data Results for SunLine FCEBs

Vehicle data	AFCB	AT FCEB	CNG
Number of buses	1	1	5
Data period (month, year)	Mar 11 – Dec 13	May 10 – Dec 13	May 10 – Dec 13
Number of months	22	44	44
Total fleet miles	58,366	58,101	962,247
Average miles per month	2,653	1,320	4,374
Total FC hours	3,779	4,939	–
Fuel economy (mi/kg)	6.50	5.52	–
Fuel economy (mi/diesel gal equivalent)	7.34	6.24	3.22
Average speed (mph)	15.4	11.7	15.7
Availability (%)	66	55	85

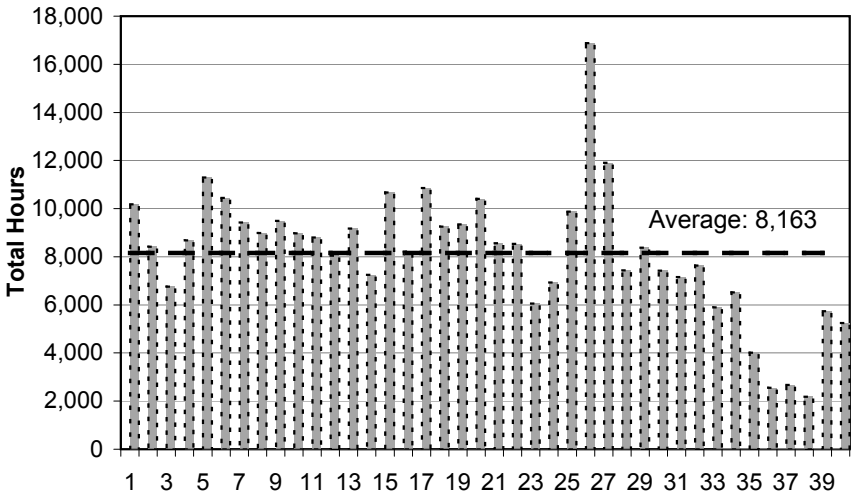

FIGURE 1. Total Fuel Cell Hours Accumulated on Each FCPP

2 spares). Figure 1 shows the total hours accumulated on individual FCPPs for the projects tracked by NREL since 2012. The average of 8,163 hours is shown on the graph as a dashed line. As of May 2014, the highest-hour FCPP had surpassed 16,800 hours. Of the 40 total FCPPs included in the graph, 60% (24) have surpassed 8,000 hours of operation. This shows significant improvement in durability toward meeting the 25,000-hour target.

One of the performance targets for FCEBs is to demonstrate fuel economy that is two times that of conventional bus technology. The FCEBs included in this report showed fuel economy improvements ranging from 5% to 128% compared to conventional buses, depending on duty cycle. Figure 2 shows the fuel economy of the buses at each of the three transit agencies in miles per diesel gallon equivalent. (Note that the baseline buses at SunLine are compressed natural gas [CNG] buses.) These data show that the FCEBs are demonstrating fuel economy values up to two times those of the baseline buses. The FCEBs at BC Transit demonstrated lower fuel economy than that typically shown at other locations. Several factors contribute to the lower numbers, including FCEB design strategy, an oversized heater, and a harsh duty cycle (extreme grades, seasonal crush loadings, cold temperatures, and wet conditions).

One measure of reliability for the transit industry is miles between roadcall (MBRC). Figure 3 provides a summary of MBRC for the four FCEB demonstrations and includes the MBRC for the bus as a whole, MBRC for the propulsion system, and MBRC for the fuel cell system. The targets for each category are included on the chart. For comparison, the MBRC results for two first-generation FCEB demonstrations are included on the graph.[2] Table 4 provides the average MBRC for the first- and second-

[2] 1st-gen 1: previous-generation Van Hool buses at AC Transit, SunLine, and Connecticut Transit; 1st-gen 2: non-hybrid Gillig/Ballard buses operated at Santa Clara Valley Transportation Authority in San Jose, California.

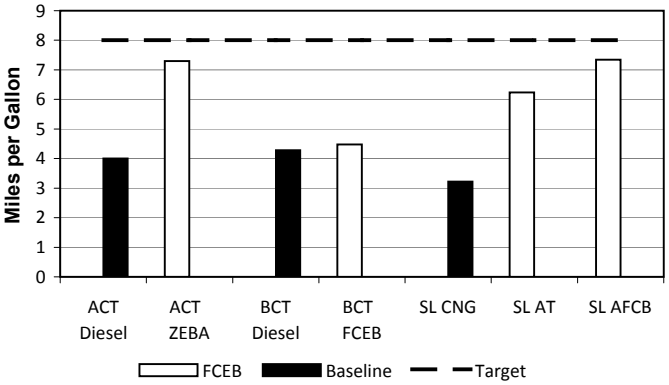

FIGURE 2. Fuel Economy Comparison by Fleet (Diesel Equivalent)

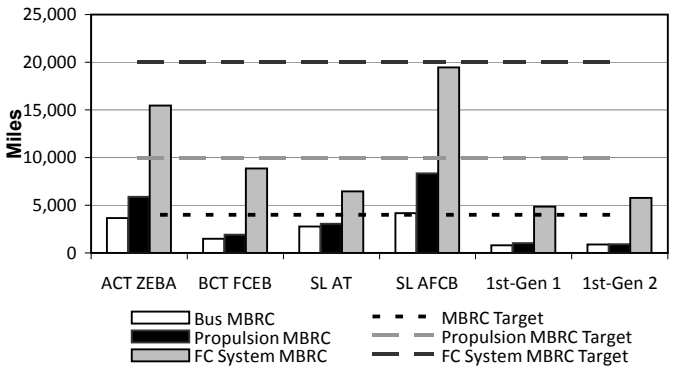

FIGURE 3. Miles Between Roadcall Comparisons by Fleet

generation FCEBs. Reliability has shown a marked increase over that of the earlier-generation buses; however, there are still improvements to be made to meet the targets. Roadcalls due to bus-related issues—such as problems with doors, air conditioning, and windshield wipers—made up 24% of the total failures. Fuel-cell-related issues made up approximately 17% of the roadcalls during the period.

TABLE 4. Comparison of Current MBRC to First-Generation FCEBs

	Total MBRC	Propulsion MBRC	FC System MBRC
1st-gen average	1,263	1,555	7,710
2nd-gen average	1,863	2,523	9,554
Percent improvement	48%	62%	24%

CONCLUSIONS AND FUTURE DIRECTION

Fuel cell propulsion systems in buses have continued to show progress in increasing the durability and reliability of FCEBs and the primary components. The current technology already meets fuel economy targets and is showing promise to exceed the fuel cell durability target. Table 5 summarizes the current status compared to the DOE/DOT performance targets. For fuel cell buses to match the current performance standard of diesel buses, the following needs to happen:

- Continuing operation to validate durability and reliability of the fuel cell systems and other components to match transit needs
- Optimizing the propulsion system to maximize operation and resolve integration issues
- Transferring all maintenance work to transit personnel
- Lowering the costs of purchasing, operating, and maintaining buses and infrastructure
- Integrating hydrogen fueling procedures into the existing fueling process
- Transferring the lead role for fuel cell system integration to transit bus builders.

TABLE 5. 2013 Summary of Progress Toward Meeting DOE/DOT Targets

	Units	2014 Status	2016 Target	Ultimate Target
Bus lifetime	Years/miles	5/100,000[a]	12/500,000	12/500,000
Power plant lifetime	Hours	1,000–16,500[a]	18,000	25,000
Bus availability	%	55–72	85	90
Roadcall frequency (Bus / fuel cell system)	Miles between road call	1,500–4,000 / 6,000–19,000	3,500/15,000	4,000/20,000
Operation time	Hours per day / days per week	19/7	20/7	20/7
Maintenance cost	$/mile	0.39–1.60	0.75	0.40
Fuel economy	Miles per diesel gallon equivalent	4.5–7.3	8	8
Range	Miles	220–310	300	300

[a] Accumulation of miles and hours to date—not end of life.

Future work by NREL includes:

- Continuing data collection, analysis, and reporting on performance data for FCEBs in service at the following sites:
  - ZEBA FCEB demonstration led by AC Transit
  - SunLine
  - Birmingham-Jefferson County Transit Authority in Birmingham, Alabama
  - Capital Metro, Austin, Texas
  - Additional sites as funding allows
- Investigating reliability, durability, and life cycle of FCEBs as a part of ongoing evaluations
- Coordinating with FTA to collect data on the demonstrations funded under the NFCBP
- Coordinating with national and international FCEB demonstration sites.

FY 2014 PUBLICATIONS/PRESENTATIONS

1. L. Eudy, *Technology Validation: Fuel Cell Bus Evaluations*, Presentation at the DOE Hydrogen and Fuel Cells Program Annual Merit Review, Washington, DC, June 2014.

2. L. Eudy, M. Post, *Zero Emission Bay Area (ZEBA) Fuel Cell Bus Demonstration: Third Results Report*, National Renewable Energy Laboratory, Golden, CO, NREL/TP-5400-60527, May 2014.

3. L. Eudy, M. Post, *BC Transit Fuel Cell Bus Project Evaluation Results: Second Report*, National Renewable Energy Laboratory, Golden, CO, NREL/TP-5400-62317, September 2014.

4. L. Eudy, C. Gikakis, *Fuel Cell Buses in U.S. Transit Fleets: Current Status 2013*, National Renewable Energy Laboratory, Golden, CO, NREL/TP-5400-60490, December 2013.

5. L. Eudy, K. Chandler, *American Fuel Cell Bus Project: First Analysis Report*, Federal Transit Administration, Washington, DC, FTA Report No. 0047, December 2013.

6. L. Eudy, *FCEB Validation: Overview and Status*, Presentation for the California Fuel Cell Partnership Bus Team meeting, December 2013.

7. L. Eudy, *Technology Validation of Zero-Emission Buses*, Presentation at the California Air Resources Board ZBus Workshop, September 2013.

REFERENCES

1. Fuel Cell Technologies Program Record #12012, September 2012, www.hydrogen.energy.gov/pdfs/12012_fuel_cell_bus_targets.pdf.

VII.2 Stationary Fuel Cell Evaluation

Genevieve Saur (Primary Contact), Jennifer Kurtz, Chris Ainscough, Mike Peters
National Renewable Energy Laboratory (NREL)
15013 Denver West Parkway
Golden, CO 80401-3305
Phone: (303) 275-3783
Email: Genevieve.Saur@nrel.gov

DOE Manager
Jason Marcinkoski
Phone: (202) 586-7466
Email: Jason.Marcinkoski@ee.doe.gov

Project Start Date: October 2011
Project End Date: Project continuation and direction determined annually by DOE

Overall Objectives

Independently assess, validate, and report operation targets and performance under stationary fuel cell system real operating conditions.

Fiscal Year (FY) 2014 Objectives

- Analysis of data quarterly as available.
- Publication of 28 technical stationary fuel cell composite data products (CDPs) biannually.
- Update of a public website for dissemination of CDPs.

Technical Barriers

This project addresses the following technical barriers from the Technology Validation section of the Fuel Cell Technologies Office Multi-Year Research, Development, and Demonstration Plan:

(B) Lack of Data on Stationary Fuel Cells in Real-World Operation - Address gaps in knowledge as stationary fuel cell installations have increased.

(E) Codes & Standards - Provide data and context to codes and standards activities.

Contribution to Achievement of DOE Technology Validation Milestones

This project will contribute to achievement of the following DOE milestones from the Technology Validation section of the Fuel Cell Technologies Office Multi-Year Research, Development, and Demonstration Plan:

- Milestone 1.1: Complete validation of residential fuel cell micro CHP (combined heat and power) systems that demonstrate 40% efficiency and 25,000 hour durability. (4Q, 2015)
- Milestone 1.2: Complete validation of commercial fuel cell CHP systems that demonstrate 45% efficiency and 50,000 hour durability. (4Q, 2017)

FY 2014 Accomplishments

- Individual CDPs were disseminated by a website (http://www.nrel.gov/hydrogen/proj_fc_systems_analysis.html) in September 2013 and April 2014.
- The project published an updated and expanded set of CDPs in November 2013 and May 2014, which included three new operational CDPs as well as expanded analysis of differentiated capacities and comparison to other incumbent technologies—28 CDPs in total.
- The project presented stationary CDP results at the Fuel Cell Seminar, October 2013.

INTRODUCTION

This project aims to provide status on stationary fuel cell systems to inform DOE, the public, fuel cell manufacturers, and other stakeholders. This is the only technology validation project working directly on technical barrier (B): Lack of Data on Stationary Fuel Cells in Real-World Operation.

APPROACH

The project's data collection plan builds on other technology validation activities. Data (operation, maintenance, and safety) are collected on site by the project partners for the fuel cell system(s) and infrastructure. NREL receives the data quarterly and stores, processes, and analyzes the data in NREL's National Fuel Cell Technology Evaluation Center (NFCTEC).

The NFCTEC is an off-network room with access for a small set of approved users. An internal analysis of all available data is completed quarterly, and a set of technical CDPs is published every six months. The CDPs present aggregated data across multiple systems, sites, and teams in order to protect proprietary data and summarize the performance of hundreds of fuel cell systems.

A review cycle is completed before the publication of CDPs. The review cycle includes providing detailed data products of individual system and site performance results

to the individual data provider. Detailed data products also identify the individual contribution to CDPs. The NREL Fleet Analysis Toolkit is an internally developed tool for data processing and analysis structured for flexibility, growth, and simple addition of new applications. Analyses are created for general performance studies as well as application- or technology-specific studies.

RESULTS

California's Self-Generation Incentive Program (SGIP) has helped deploy 317 fuel cell systems, for a total of 131 MW, since 2001. These fuel cell deployments have shown that fuel cells may be applied with a wide variety of fuels, including renewable biogas from landfill, biomass, and digester sources. Natural gas is the dominate fuel type, accounting for 74% of projects and 66% of the capacity. Since 2011, electric-only fuel cell projects have been increasing at a rate (number and capacity) greater than other competing technologies, which include gas turbines, internal combustion turbines, microturbines, and pressure reduction turbines (Figure 1). Deployment numbers have increased even in a climate of declining incentive. As such, 23 new fuel cell projects were accepted into the SGIP between the second quarter of 2013 and the fourth quarter of 2013 for a proposed capacity of 10 MW. To date, 75% of the fuel cell projects are completed and 11% of fuel cell projects have qualified for performance-based incentives, which were implemented in 2011.

The average unit costs in the SGIP are significantly higher than the DOE target of $1,500/kW. The overall average unit cost is $10,189/kW without incentives and $6,722/kW with incentives. The average range, when differentiating by capacities (0-50 kW, 51-200 kW, 201-400 kW, 401+ kW), is $9,524-$10,932/kW without incentives and $5,587-$8,299/kW with incentives. Generally, larger projects (those with larger capacities) have lower unit costs and also receive more incentives (Figure 2), but very few SGIP projects meet the DOE target costs.

This year the NFCTEC has also begun collecting operations data from several sites. Submission is voluntary and the data is limited. The mean availability of the systems analyzed was 93%, with almost 65% of systems showing more than 90% availability (Figure 3). This is less than the DOE target for commercial stationary power of 97%, but it is showing high availability of systems with the limited data. The systems had a mean electrical efficiency of 27% based on the higher heating value of hydrogen, with more than 65% having 25%-35% electrical efficiency based on the higher heating value of hydrogen (Figure 4). This converts to a mean of 32% based on lower heating value and about 65% of systems having 30%-41% lower heating value electrical efficiency. This is lower than the 2015 DOE target of 43% lower heating value for electrical efficiency for commercial systems. However, the data is limited and covers multiple fuel cell capacity ranges, across several stationary applications, and is not steady-state data. These factors contribute to the lower electrical efficiencies seen.

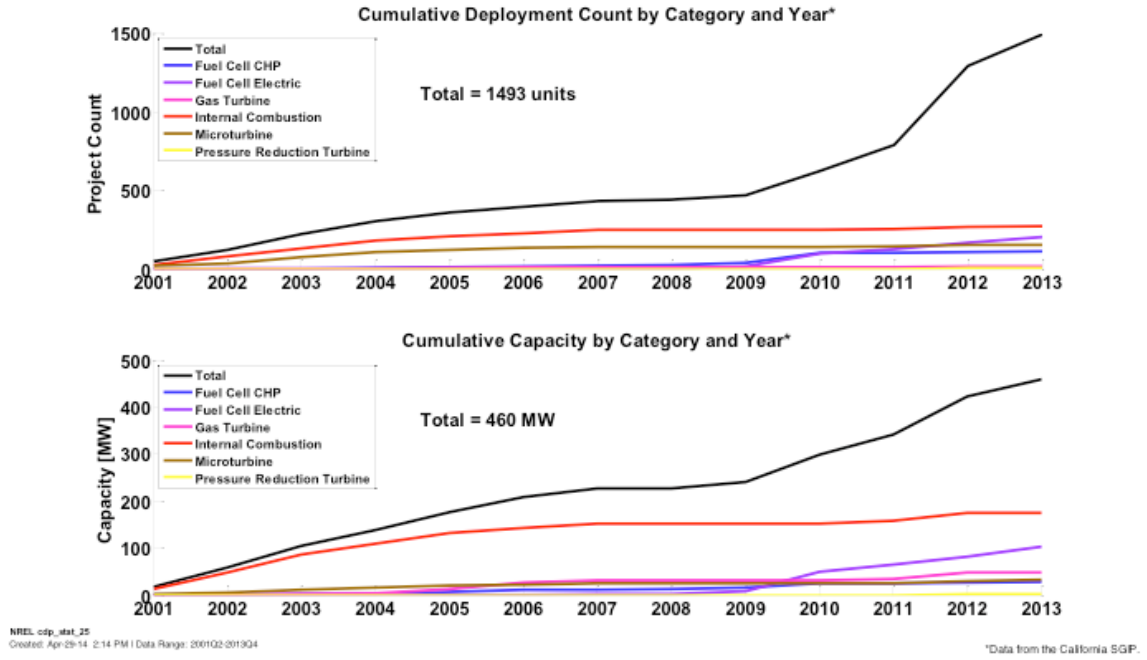

FIGURE 1. Cumulative Deployment of Fuel Cells Versus Competing Technologies

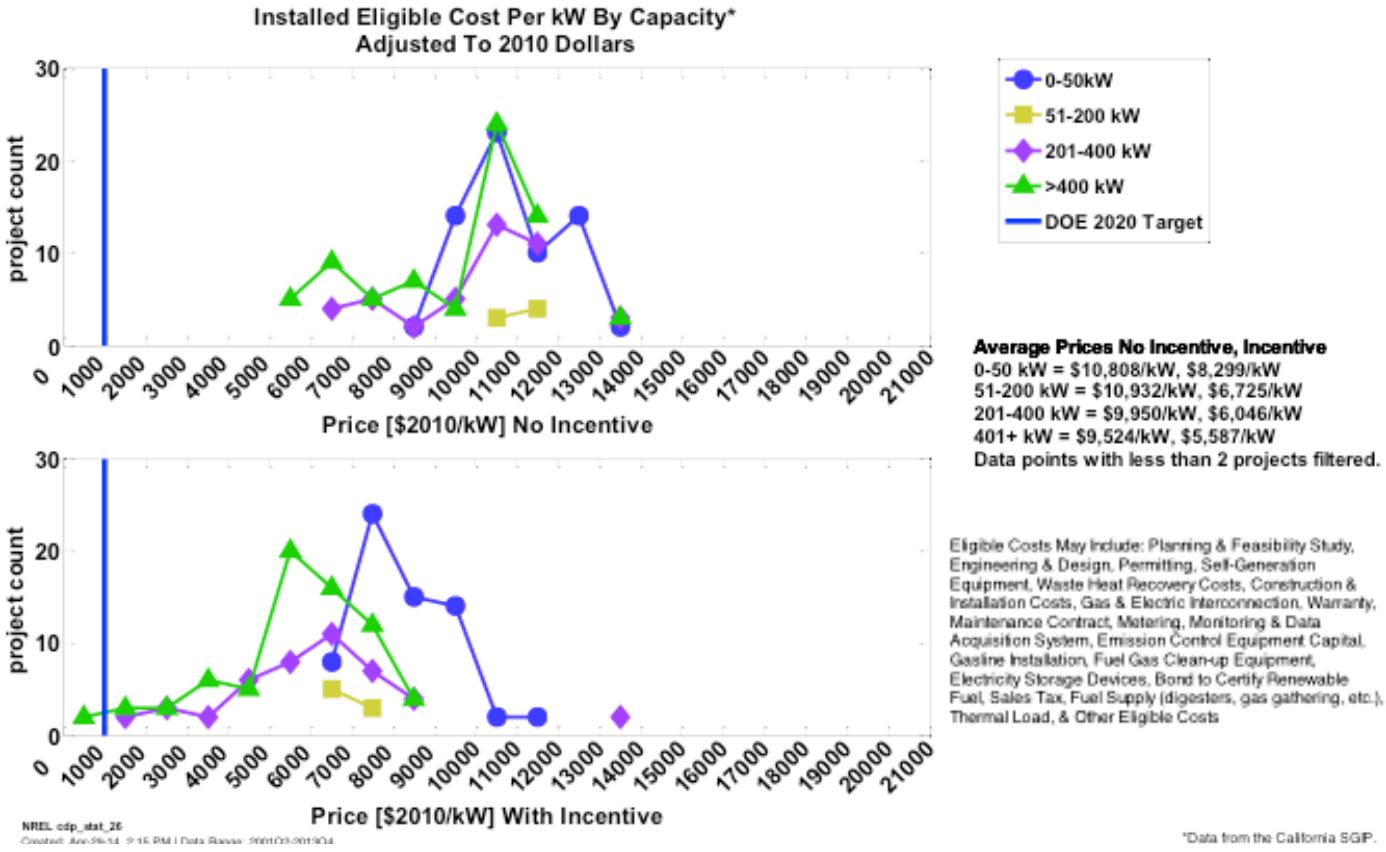

FIGURE 2. Eligible Installed Fuel Cell Unit Costs by Capacity

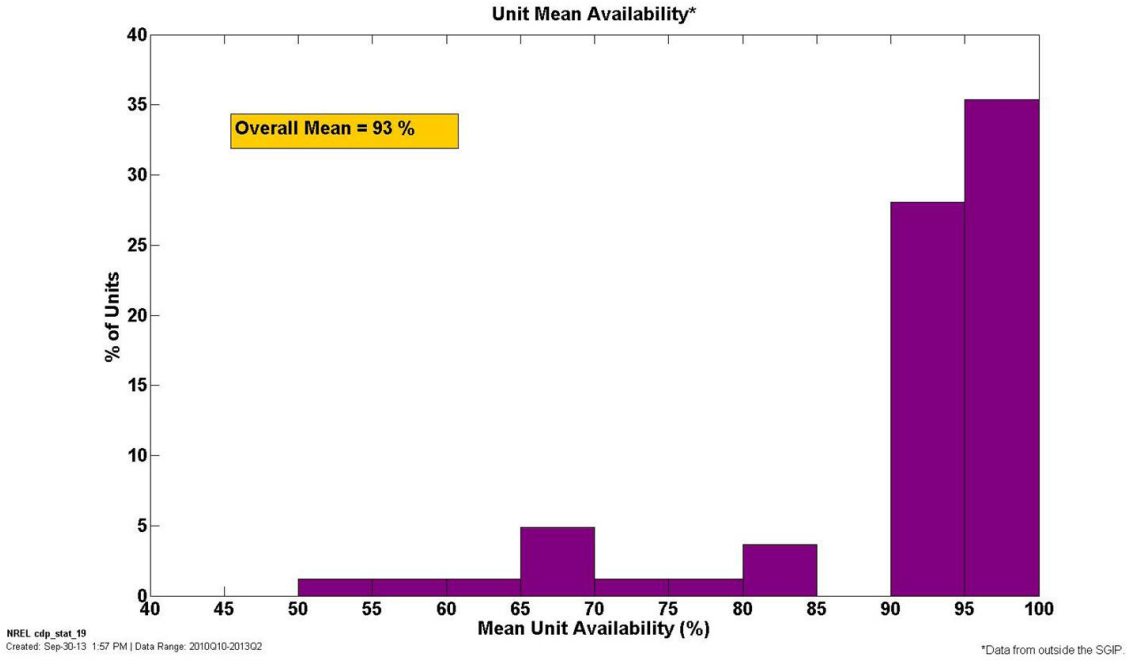

FIGURE 3. Stationary Fuel Cell Availability

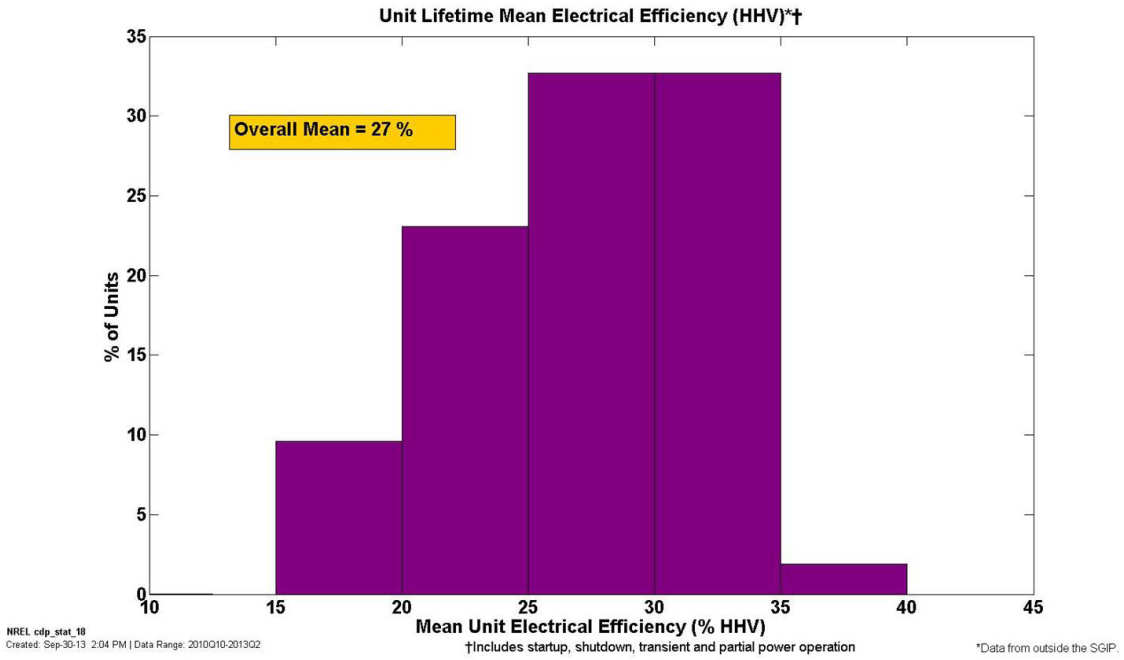

FIGURE 4. Stationary Fuel Cell Electrical Efficiency

Operations data continues to be collected for future iterations of the CDPs.

A total of 25 deployment CDPs have been published using California SGIP data as well as three new operations CDPs covering stoppages, availability, and electrical efficiency. All CDPs are available at http://www.nrel.gov/hydrogen/proj_fc_systems_analysis.html.

CONCLUSIONS AND FUTURE DIRECTIONS

The California SGIP has been very successful in installing fuel cell systems. In recent years, fuel cell projects have been installed in greater numbers than other competing technologies, despite generally higher installed costs and decreasing incentive spending. This early-market rollout is important for the stationary fuel cell industry in terms of real-world experience, especially as the SGIP program is slated to end January 1, 2016.

Operations data has been limited, but the NFCTEC is exploring more avenues to validate DOE performance targets.

Activities for the remainder of FY 2014 will include the following:

- FY 2014 Q4: Update all CDPs with current data from the SGIP and voluntary operations data submissions.
- Expand analysis to include new CDPs that address further segmentation of the data (CHP/non-CHP, competing technologies, fuel sources) and trends over time.
- Look into other data partners (state and federal programs, original equipment manufacturers) for additional data relevant to DOE targets.

FY 2014 PUBLICATIONS/PRESENTATIONS

1. Saur, G., Kurtz, J., Ainscough, C., Peters, M. "TV016: Stationary Fuel Cell Evaluation." Annual Merit Review meeting, Washington, DC, June 2014. (presentation)

2. Saur, G., Kurtz, J., Ainscough, C., Peters, M. "Stationary Fuel Cell System Composite Data Products: Data through Quarter 4 of 2013." Golden, CO: National Renewable Energy Laboratory, published May 2014. (report)

3. Ainscough, C., Saur, G. "VII.2 Stationary Fuel Cell Evaluation." DOE FY13 Annual Merit Review Proceedings, Washington, DC, published December 2013. (report)

4. Ainscough, C., Kurtz, J., Peters, M., Saur, G. "Stationary Fuel Cell System Composite Data Products: Data through Quarter 2 of 2013." Golden, CO: National Renewable Energy Laboratory, published November 2013. (report)

5. Wipke, K. "Evaluation of Stationary Fuel Cell Deployments, Costs, and Fuels." Fuel Cell Seminar, published October 2013. (presentation)

VII.3 Hydrogen Recycling System Evaluation and Data Collection

Rhonda Staudt
H2Pump LLC
11 Northway Lane North
Latham, NY 12110
Phone: (518) 783-2241
Email: Rhonda.staudt@h2pumpllc.com

DOE Managers
Jason Marcinkoski
Phone: (202) 586-7466
Email: Jason.Marcinkoski@ee.doe.gov
Jim Alkire
Phone: (720) 356-1426
Email: James.Alkire@ee.doe.gov

Contract Number: DE-EE0006091

Project Start Date: January 2013
Project End Date: December 2015

Overall Objectives

The objective of this project is to demonstrate the product readiness and to quantify the benefits and customer value proposition of H2Pump's Hydrogen Recycling System (HRS-100™) by installing and analyzing the operation of multiple prototype 100 kg per day systems in real world customer locations. The data gathered will be used to measure reliability and to demonstrate the value proposition to customers. H2Pump will install, track, and report multiple field demonstration systems in industrial heat treating and semi-conductor applications. The customer demonstrations will be used to develop case studies and showcase the benefits of the technology to drive market adoption. The objectives of the project are to:

- Validate commercial assumptions around the Hydrogen Recycling Agreement including customer assumptions and system performance.
- Build case studies of the HRS-100™ in customer operations that can be used as credible demonstrations quantifying the operating cost savings, emissions reduction and production efficiency improvement.
- Expand the Beta test fleet into additional customer environments to accelerate learning, problem identification, resolution and reduce the risk of product launch.
- Provide data to National Renewable Energy Laboratory (NREL) for in-depth analysis of system performance characteristics and identify areas for improved data gathering and perform causal analysis. All of the data acquired by the systems will be made available to the NREL. The minimum data includes stack voltage and current, system power, and hydrogen flow rate. Data frequency can be no less than a one minute interval. Maintenance and repair logs will also be provided to NREL, specifying time, maintenance item, or reason for repair. NREL will also be provided with gas analyses to help determine whether certain gases result in higher degradation.
- Prepare and test commercial infrastructure elements such as installation, commissioning, reporting, operation, and maintenance.

Fiscal Year (FY) 2014 Objectives

- Modified Statement of Project Objectives will include a new objective: H2Pump will perform extensive furnace exhaust gas stream analyses at each site and implement solutions to mitigate contaminates.
- Execute Go/No-Go review.
- Install and commission the remaining three systems in the fourth quarter of 2014 and provide data to NREL to perform degradation calculations.

Technical Barriers

This project addresses the following technical barriers from the Technology Validation section of the Fuel Cell Technologies Office Multi-Year Research, Development, and Demonstration Plan:

(D) Lack of Hydrogen Refueling Infrastructure Performance and Availability Data

(G) Hydrogen from Renewable Resources

FY 2014 Accomplishments

- Completed the development and deployment of a database tool to track system performance and store lifetime data.
- Identified furnace exhaust contaminates at Pall, Rome Strip Steel, and Ulbrich deployment sites through extensive gas sampling and analysis by an external lab.
- Implemented solutions at Pall and Rome Strip Steel for containment of sulfur compounds, CO, and other contaminates harmful to the pumping stack.
- Implemented automatic controls at Pall, increasing the daily recycle rate by three times.

- Provided data to NREL quarterly to assess system performance. Demonstrated less than 10 kWh/kg at most operating points.

INTRODUCTION

Hydrogen is used in numerous industrial applications including metallurgical and semiconductor processing. Hydrogen intensive metal heat treating applications include stainless steel annealing, brazing, and metal production from ore. Each industrial application uses hydrogen for different purposes; however, in general, hydrogen is used to create an oxygen-free reducing atmosphere and is not consumed by the industrial process. H2Pump has developed a unique hydrogen recycling solution capable of reclaiming nearly 100 kg per day from such industrial processes.

Figure 1 shows how the HRS integrates with a typical industrial furnace or semi-conductor manufacturing tool. The HRS receives the furnace or tool exhaust that is normally flared or exhausted to atmosphere. The HRS requires certain utilities including electricity, water, and nitrogen. The heart of the HRS system is the electrochemical pump stack. The electrochemical process involves the extraction of hydrogen from a gas stream containing hydrogen, followed by the formation of "new" hydrogen. This transformational approach is accomplished without mechanical compression. The new hydrogen is returned to the original process.

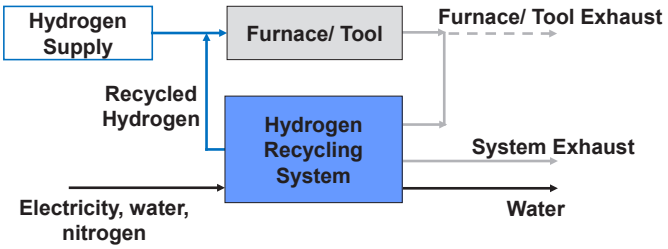

FIGURE 1. Integration of a Hydrogen Recycling System with an Industrial Process

The HRS-100™ system design is shown in Figure 2. The main subsystems and components include incoming gas clean-up, humidification, the pump stack, power supply, heat rejection and the dryer. Most heat treating processes require a very low dew point in the hydrogen supply. To ensure adequate quality of the recycled product, H2Pump measures the dew point of the product before returning the hydrogen to the customer's process.

APPROACH

H2Pump is fortunate to have the support of the New York State Energy Research and Development Authority as a cost sharing partner in this project. The New York State Energy Research and Development Authority award funds 50% of the system material cost, the installation cost, the ongoing operation, and maintenance costs of the demonstration. The DOE award shares the costs of the systems, the database development and the analysis performed by NREL.

A total of seven systems are planned to be installed and monitored during the project. The first step is establishing the site requirements and installation plan. Activities to uncover site specific issues, including potential gas contaminates are undertaken early in the planning process. Mitigation plans are put in place for known contaminates, and the systems are

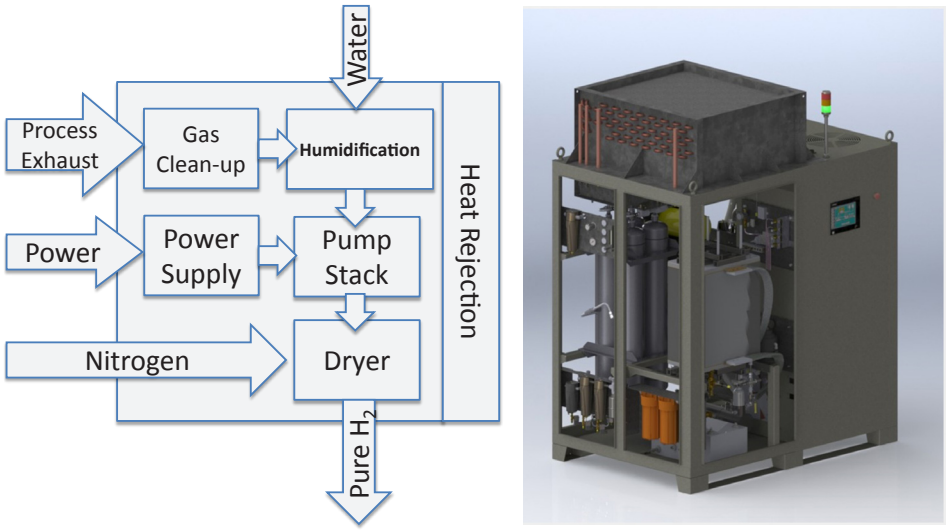

FIGURE 2. HRS-100™ Subsystems and Components

installed and commissioned. Following commissioning, the system will be monitored and the data logs will be given to NREL for analysis (Figure 3).

RESULTS

As of the writing of this report, H2Pump has completed exhaust gas sampling and analyses for the three sites shown in Figure 4 and implemented proprietary solutions for additional gas cleanup prior to the HRS-100™. The solutions include adsorbents for sulfur removal, catalytic CO reduction and oil clean-up. The implementation of control methods for auto-start and ramp-up has greatly increased the recycle rate. Under manual operation, the system at Pall Corporation only operated during daytime hours often missing a second or third shift since the system had to be remotely started and manually ramped up. With the implementation of exhaust sensing and controls, the daily recycle rate has increased 10 fold. The system output still depends on the customer's operating schedule but no longer requires remote intervention. Additionally, the gas sampling showed the presence of trace amounts of sulfur in the exhaust that may have been contaminating the stack. The stack in the Pall system has never been replaced indicating that the solution for sulfur removal was effective and did not permanently damage the stack.

H2Pump has implemented promising gas management solutions at Ulbrich and Rome Strip Steel and is awaiting verification of the efficacy of the solutions.

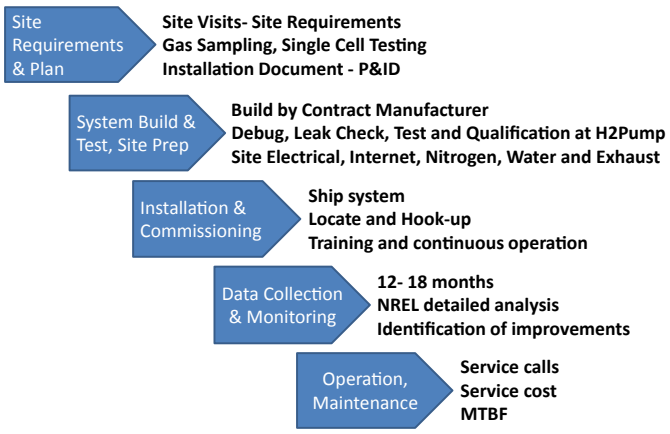

MTBF - mean time between failure

FIGURE 3. Site Installation and Monitoring Steps

CONCLUSIONS AND FUTURE DIRECTIONS

The site planning and commissioning steps are proving to be the most critical and time intensive part of the project. Revising the Statement of Project Objectives to include greater focus on identifying and mitigating the harmful or poisonous constituents in the furnace exhaust

FIGURE 4. Recycling Demonstration at Pall Corporation, Ulbrich Specialty Strip Mill, and Rome Strip Steel

gas has dramatically improved the system performance. For the remaining three installations in the second budget period of the program, greater emphasis will be placed on understanding the exhaust gas composition and implementing and refining solutions.

SPECIAL RECOGNITIONS & AWARDS/ PATENTS ISSUED

1. Granted US Patent 8,663,448 B2 on March 4, 2014, *Hydrogen Furnace System and Method*, Glenn Eisman.

2. Granted US Patent 8,734,632 B1 on May 27, 2014 *Hydrogen Furnace System and Method*, Glenn Eisman.

FY 2014 PUBLICATIONS/PRESENTATIONS

1. 2014 U.S. DOE Hydrogen and Fuel Cells Program and Vehicle Technologies Program Annual Merit Review and Peer Evaluation Meeting, June 16–20, 2014, Washington, D.C.

VII.4 Hydrogen Component Validation

Danny Terlip (Primary Contact), Kevin Harrison, Michael Peters, Misho Penev
National Renewable Energy Laboratory (NREL)
15013 Denver W Pkwy
Golden, CO 80401
Phone: (303) 827-9811
Email: danny.terlip@nrel.gov

DOE Manager
Jason Marcinkoski
Phone: (202) 586-7466
Email: Jason.Marcinkoski@ee.doe.gov

Subcontractors
Spectrum Automation Controls Inc., Arvada, CO

Project Start Date: April 1, 2013
Project End Date: Project continuation and direction determined annually by DOE

Overall Objectives

- Improve hydrogen compressor reliability
- Operate a compressor in a highly accelerated lifecycle testing environment to reproduce failures on a short time scale
- Correlate findings with real-world data
- Work with manufacturer to improve design and reduce downtime

Fiscal Year (FY) 2014 Objectives

- Integrate PDC 4-Series compressor into the existing Wind-to-Hydrogen system at the National Wind Technology Center
- Demonstrate unattended operation with appropriate safety systems and controls
- Operate system for 350 hours (assuming no major failures)

Technical Barriers

This project addresses the following technical barriers from the Technology Validation section of the Fuel Cell Technologies Office Multi-Year Research, Development, and Demonstration Plan:

(D) Lack of Hydrogen Refueling Infrastructure Performance and Availability Data

Contribution to Achievement of DOE Technology Validation Milestones

This project will contribute to achievement of the following DOE milestones from the Technology Validation section of the Fuel Cell Technologies Office Multi-Year Research, Development, and Demonstration Plan:

- Milestone 3.4: Validate station compression technology provided by delivery team. (4Q, 2018)

FY 2014 Accomplishments

- Integrated compressor system with the existing hydrogen, electrical, and cooling systems at the Wind-to-Hydrogen site at the National Wind Technology Center
- Commissioned system with manufacturer and conducted Readiness Verification with NREL staff
- Operated system with attendant for 80 hours (including one seal failure and replacement)
- Completed initial performance analysis of power versus pressure profile and study of hydraulic oil pressure for troubleshooting

INTRODUCTION

Data from the National Fuel Cell Technology Evaluation Center shows that hydrogen compressors are responsible for the most scheduled and unscheduled maintenance in both material handling and fuel cell electric vehicle infrastructure. With the expected increase in hydrogen demand from the 2015-2017 vehicle roll-out in California, increased reliability is critical to ensure the success of hydrogen refueling stations.

Based on real-world operation, it is understood that compressor reliability is an issue. However, there is a lack of detailed compressor reliability data and analysis available for root cause investigation and reliability improvements. This research aims to operate the compressor in an accelerated manner, though similar to what is experienced in the field to capture performance data, reproduce failures and investigate the causes.

APPROACH

Integration of the compressor with the Wind-to-Hydrogen system enables the accelerated reliability testing in a full system that includes hydrogen production to vehicle dispensing. A specific test plan was developed for the

compressor operation in a system configuration. This enables a detailed analysis on compressor reliability without ignoring potential influences that the overall system may also have on compressor reliability. This research will identify failure modes of a compressor in a shorter time frame than would be experienced in the field by operating at higher duty cycles. NREL is targeting 4,500 hours of system operation and 17,000 kg of compressed hydrogen over a 12 month period. Specifications for the PDC4-Series compressor are provided in Table 1.

TABLE 1. PDC4-Series Compressor Specifications

Parameter	Specification (Normal Operation)	Unit
Inlet Pressure	100	psig
Inlet Temperature	100	°F
Outlet Pressure	6000	psig
Capacity	20	SCFM
Stages	2	
Maximum Crankshaft Speed	425	rpm

psig – pounds per square inch gage; SCFM – standard cubic feet per minute; rpm – revolutions per minute

Two systems, a recirculation loop and remote control, were implemented to support the highly accelerated testing. The recirculation loop is pressure regulated piping that was installed between the compressor supply and discharge system. With this loop in place it is not necessary to continuously produce hydrogen when operating the compressor. The control system is capable of switching the compressor suction from the low-pressure storage tanks to the recirculation loop. The remote control system allows a user to start and stop the compressor from anywhere with internet access. This allows for operation cycles much longer than the standard work day.

A critical part of this research is the collaborative deep-dive analysis of failures with the compressor manufacturer. It will be performed as failures occur and the results will be communicated to the manufacturer in an effort to improve overall compressor reliability. The compressor has additional instrumentation to capture various operational parameters such as power consumption, pressure and temperature that will aid in the failure analysis, but also be used to characterize compressor performance and improve Pacific Northwest National Laboratory compressor modeling. Data collected will inform DOE on performance data of compressors.

RESULTS

Data collected on the compressor is listed in Table 2.

The flow rate versus discharge pressure is one example of the type of analysis on data collected. Station designers must consider the discharge rate of a compressor when sizing the various components at a station. Figure 1 shows data for discharge pressures from 3,600 psig to 6,000 psig, a typical operating range at hydrogen stations.

TABLE 2. Compressor Data Collection

Parameter	Frequency
Motor Current	1 Minute
Motor Voltage	1 Minute
Motor Apparent Power	1 Minute
1st Stage Inlet Pressure	10 seconds
1st Stage Outlet Pressure	10 seconds
1st Stage Inlet Temperature	10 seconds
1st Stage Outlet Temperature	10 seconds
2nd Stage Inlet Pressure	10 seconds
2nd Stage Outlet Pressure	10 seconds
2nd Stage Inlet Temperature	10 seconds
2nd Stage Outlet Temperature	10 seconds
Coolant Water Inlet Temperature	10 seconds
Coolant Water Outlet Temperature	10 seconds
Operational Hours	10 seconds
Ambient Temperature	10 seconds
Crankcase Oil Temperature	10 seconds
Crankcase Oil Injection Pump Pressure	10 seconds
Leak Detection Pressure	10 seconds
Process Filter Pressure	10 seconds
1st Stage Oil Pressure	0.00004 seconds
2nd Stage Oil Pressure	0.00004 seconds

Power consumption data is also collected when the compressor is operating. A power meter captures both voltage and current waveforms using transducers. The unit calculates real and reactive power, as well as the power factor. This data is captured simultaneously with pressure data to analyze the relationship between power consumption and discharge pressure.

When initially analyzed, the power data was extremely variable and thus unusable. Several diagnostic techniques were utilized to determine the cause of such a large variation. An example of this variation was captured with a high-speed oscilloscope and is shown in Figure 2. It was discovered that at a constant discharge pressure of 4,500 psig, the current draw fluctuated between 17 and 33 A_{max}, but the voltage was very stable. A periodic cycle of fluctuation was found every 150 ms. The frequency of compression cycles was obtained from the manufacturer and corresponded directly with current variations. Thus, it was reasoned that the variable motor current was a result of the motion of the

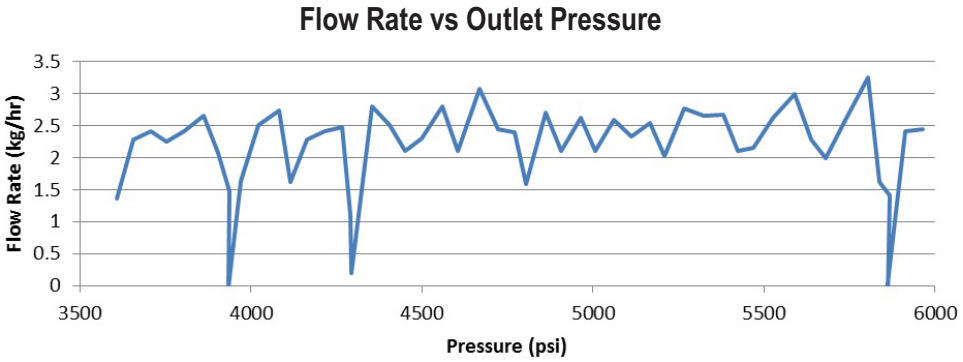

FIGURE 1. Flow rate in kg/hr is plotted against discharge pressure in psig. It can be seen that an average flow rate is experienced across various discharge pressures.

FIGURE 2. An oscilloscope was placed on the motor supply circuit to show voltage (cyan) to be uniform and current (yellow) to be variable over multiple periods.

piston driven by the motor. This was later confirmed with the manufacturer.

To make the power data usable, an averaging scheme was applied to the current and the resultant is now used to calculate power consumption. An example of the power versus pressure data is provided in Figure 3. The amount of power required by the compressor motor increased monotonically with the discharge pressure. A nearly 3.5 kVA range was recorded over the 3,000-6,000 psig range. The compressor motor is rated to 30 HP, or 26 kVA. In the upper range of discharge pressures, the compressor was observed to be consuming a maximum of 18.9 kVA which is 72% of rated power.

At the 60-hour operation mark, the compressor system experienced a failure. The second stage discharge check valve o-ring was partially destroyed and caused a hydrogen leak. The failure was discovered when a loud noise of gas escaping was heard with each compression cycle. The system had to be shut down manually while the problem

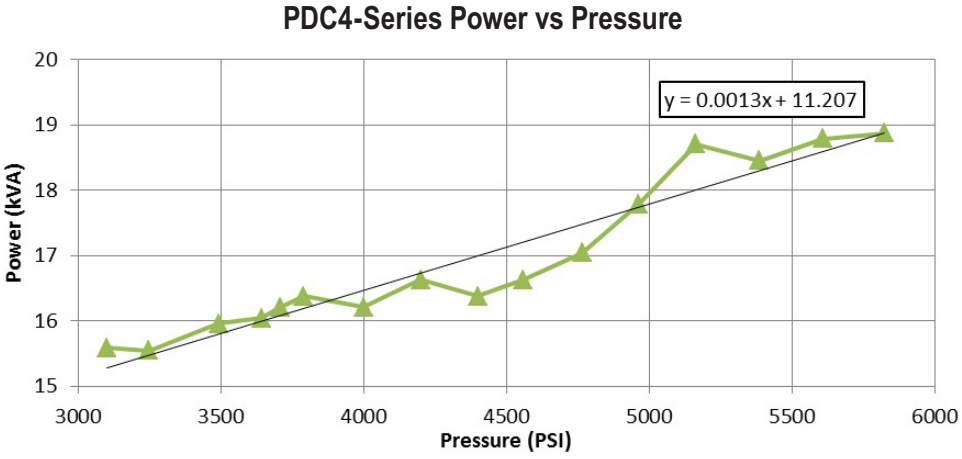

FIGURE 3. One critical piece of performance data is the power consumed by the compressor over a range of discharge pressures. This graph shows the average measured power for various discharge pressures with a line of best fit.

was diagnosed and repaired. The failed part was removed, documented and explained to the manufacturer. The other check valve o-rings were inspected and contained no damage. The compressor was then run to verify proper operation. The system is operational and at the time of this report, no other failures have occurred. Figure 4 shows the o-ring after it was removed from the compressor.

FIGURE 4. The seal on the second stage discharge check valve failed and required replacement at 60 hours.

The check valves are recessed about 8” into the head making access difficult. The repair procedure required very long skinny tools to reach the check valves. NREL has a set of dental tools that were used to grasp the valve and pull it out. Total downtime was one week, most of which elapsed while waiting for guidance and spare parts from the manufacturer. Actual repair time was about three hours.

The tedious nature of the procedure and difficulty for field operators was communicated to the manufacturer. A product of the conversations with the manufacturer was the acknowledgement that this is a common problem and typically observed with large ambient temperature cycling. The failure took place in April, during which Colorado experienced days with temperatures up to 70 degrees and days of snow. One lesson learned from this failure is the importance of having spare o-rings for all components on hand.

CONCLUSIONS AND FUTURE DIRECTIONS

- Significant knowledge and expertise of mechanical and electrical systems in classified environments is required to incorporate this component into a hydrogen system.
- Compressor performance study is valuable as multiple parties have contacted NREL team for data.
- Future research will focus on long duty cycle testing and failure analysis.
- A robust performance characterization will be formed as more data is collected.

FY 2014 PUBLICATIONS/PRESENTATIONS

1. “Hydrogen Component Validation,” Harrison, Kevin; Terlip, Danny; Peters, Michael; Penev Michael. 2014 DOE Annual Merit Review. 16 June 2014. Washington, D.C.

VII.5 Validation of an Advanced High-Pressure PEM Electrolyzer and Composite Hydrogen Storage, With Data Reporting, for SunHydro Stations

Larry Moulthrop (Primary Contact), Luke Dalton
Proton Energy Systems d/b/a Proton OnSite
10 Technology Drive
Wallingford, CT 06492
Phone: (203) 678-2188
Email: lmoulthrop@protononsite.com

DOE Managers
Jason Marcinkoski
Phone: (202) 586-7466
Email: Jason.Marcinkoski@ee.doe.gov
Jim Alkire
Phone: (720) 356-1426
Email: James.Alkire@ee.doe.gov

Contract Number: DE-EE0005887

Subcontractors
- SunHydro LLC, Wallingford, CT
- Air Products and Chemicals, Incorporated (APCI), Allentown, PA

Project Start Date: December 1, 2012
Project End Date: December 31, 2014 (Go/No-Go decision for next phase)

Overall Objectives

- Validate energy savings of up to 11 kWh/kg hydrogen through system and stack advancements
- Double usable hydrogen storage per unit volume by increasing pressure cycling range
- Provide advanced packaging design to reduce station footprint
- Collect and report station performance for up to 24 months

Fiscal Year (FY) 2014 Objectives

- Build full-scale advanced cell stack for stack portion of energy savings
- Install system upgrades for reduced dryer losses for system portion of energy savings
- Install and commission higher addressable capacity hydrogen storage tubes
- Complete analysis of codes and standards for advanced packaging arrangement
- Complete instrumentation of station and initiate reporting of station performance

Technical Barriers

This project addresses the following technical barriers from the Technology Validation section of the Fuel Cell Technologies Office Multi-Year Research, Development, and Demonstration Plan:

(C) Hydrogen Storage

(D) Lack of Hydrogen Refueling Infrastructure Performance and Availability Data

(E) Codes and Standards

Technical Targets

Advanced Electrolysis-Based Fueling Systems

There is not a specific target table in the Technology Validation section of the Multi-Year Research, Development, and Demonstration Plan specific to Hydrogen Refueling Infrastructure. This project is conducting technology validation of improved cell stack, system, and storage components for an electrolysis-based hydrogen refueling station. These improvements will support the following targets:

- Reduce station energy use by up to 11 kWh/kg
- Reduce the storage volume by 50% per kg of hydrogen dispensed
- Package a station based on proton exchange membrane (PEM) electrolysis within a 12-m International Organization for Standardization (ISO) container

FY 2014 Accomplishments

- Built and operated full-scale cell stack utilizing advanced manufacturing process
- Upgraded SunHydro#1 to 55-bar operation at generator and compressor
- Commissioned higher addressable capacity composite hydrogen storage tubes
- Acquired compression, storage and dispensing section of SunHydro#2
- Installed and utilized hydrogen station data acquisition system at SunHydro#1
- Reported hydrogen energy usage data to the Fuel Cell Electric Vehicle Infrastructure Composite Data Product database

INTRODUCTION

This project primarily leverages Proton's SunHydro#1 station in Wallingford, CT, with access to over 100 kg/day in generation capacity, and a new containerized SunHydro#2 station deploying to Braintree, MA, for technology validation of improved components for hydrogen fueling stations (Figure 1). Our compact, containerized SunHydro™ station design embodied by SunHydro#2 can address initial demand for small, manufactured hydrogen fueling infrastructure in a manner that affords rapid, scalable deployment. The SunHydro station product 'skid', integrating hydrogen generation, compression, storage, and dispensing in an intermodal transport ISO container, mitigates significant site permitting issues by virtue of its small 40' x 8' footprint and an innovative application of hydrogen code that drastically reduces required clearances.

Proton and SunHydro LLC are continuing down this pathway to demonstrate advanced generation/compression/storage component technologies, including: 1) higher pressure hydrogen generation with electrochemical compression, 2) higher efficiency generation with lower resistance electrolyte and advanced catalyst, 3) higher addressable capacity composite storage, and 4) advanced packaging concepts for reduced footprint.

APPROACH

These hydrogen fueling improvements will be accomplished based on the following approaches. For higher pressure/higher efficiency PEM cell stacks, Proton has recently qualified a 30% reduction in PEM membrane thickness for 15- and 30-bar hydrogen generator product lines. Furthermore, Proton has been developing advanced catalyst materials and processes that simultaneously reduce the cost of the product and improve the electrochemical performance. A 55-bar militarized cell stack design will be built using the thinner material and advanced catalyst deposition to show the performance improvement at full scale compared to previous technology stacks. We will upgrade a commercial 30-bar C series electrolyzer to operate at 55 bar by strengthening the gas drying components. An increase in hydrogen generation pressure from 30 bar to 55 bar can improve hydrogen fueling system efficiency in two areas—hydrogen gas drying and dried hydrogen compression into station storage. The dryer purge losses can be expected to decrease substantially since the water vapor concentration at 55 bar will be about 55% of the concentration at 30 bar. Higher dry hydrogen pressure into the station mechanical compressor will result in better combined compression energy and higher throughput capability.

FIGURE 1. SunHydro#1 and SunHydro#2 Stations

For higher addressable capacity storage and reduced station footprint, Proton will install and validate new compact Type II composite storage tubes and apply fresh interpretations of hydrogen safety code to design a complete fueling station within the compact footprint of an ISO container. Proton will apply these new rules to the design of SunHydro#2 station. The impact of all performance improvements will be reported through instrumentation of the station before and after the design changes. The impact of new compact station arrangements will be reported in site approval time and in station operability data.

RESULTS

Task 1.0 Validate Full-Scale 57-bar Higher Efficiency PEM Cell Stack

During the previous FY, work on the full-scale 57-bar higher efficiency PEM cell stack progressed from build planning to successful system level testing. Multiple iterations of platform specific tooling to interface with the electrode fabrication equipment to hone the process was procured. Separator plates with advanced coating for durability at high-pressure operation and the balance-of-stack embodiment hardware culminated in a completely assembled stack that passed acceptance test procedure midway through the FY. During green-run testing, cell voltage was higher than expected when compared to previous sub-scale testing. As this was the first manufacturing run at this scale with the advanced fabrication process, a review of manufacturing steps of both full- and sub-scale cells was initiated to discern any differences that may exist. It was determined that the desired catalyst loading point was not achieved during membrane electrode assembly fabrication. Efficiency gains from this first scale up fabrication run of the advanced cell stack manufacturing techniques were not yet realized on this full-scale sample. However, even with this reduced loading, cell stack performance to date has matched the existing production cell stack and efficiency gains may still be achieved in future iterations of the manufacturing scale up.

Task 2.0 Validate Full-Scale 57-bar, 65-kg/day Hydrogen Generator

The build of the Proton C Series hydrogen generator that is the test bed for the advanced cell stack was completed in late 2012 and supplies the hydrogen used by the SunHydro#1 station at Proton. The hydrogen gas management portion of Proton's commercial C series 30-bar pressure hydrogen generator is comprised primarily of proprietary design hydrogen/water phase separator and a pressure swing absorber (PSA). Proton engineering completed a mechanical design analysis of these components in FY 2013 to learn that only minor changes to valve seats, retaining bolts, orifices, and pressure sensors were needed to operate at 55 bar. These modifications were designed to easily revert back to 30-bar operation to assist with any factory testing as required. Upon a successful system acceptance test procedure, work culminated with tuning the PSA regeneration steps to maximize the efficiency gains allowed by higher operating pressures. Initial work cut the waste purge gas usage by 40%, however future tuning of the overall PSA cycle will be performed and validated during the next FY.

Task 3.0 Validate Higher Addressable Capacity Composite Hydrogen Storage Tubes

Within FY 2014, there were numerous delays on the delivery of the advanced storage tubes due to manufacturing difficulties and extended qualification processes. During this time, Proton engaged third party professional engineers to perform an assessment of the existing concrete pad in preparation for the addition of the new storage tubes. The assessment determined no modifications would be needed. A similar assessment of stability and seismic requirements found that both the site and tube stacking arrangement were adequate as well. Late in the FY, the storage tubes were delivered and promptly installed at the SunHydro#1 station. These tubes allow for deeper pressure cycling providing a higher addressable storage capacity. This capability was demonstrated during commissioning with the sequential filling of five vehicles, an increase over the previous capability of the SunHydro#1 station of only slightly more than two. Validation of the increase will be performed in the next FY.

Task 4.0 Validate Compressor Increased Throughput Capacity With 57-bar Input

During early work on this validation, Proton began drafting the techniques and computer models to calculate the anticipated increased throughput capacity of the compressor. With the successful completion of Task 2.0 and 3.0, validation of the anticipated increased throughput capacity of the compressor is anticipated to be completed early in the next FY.

Task 5.0 Hydrogen Station Safety Operation Procedure and EX Zone Review

Chapters 7 and 13 of the National Fire Protection Association (NFPA) 2 "Hydrogen Technologies Code" were used to determine hazardous equipment zones and methods to mitigate code-directed separation distances to develop the novel compact component layout and model in Task 6.0 with respect to classified and non-classified areas [1]. Following procedure and zone review, Proton's efforts shifted to actively working the site permitting for SunHydro#2 based on our compact arrangement and addressing several Massachusetts specific issues. A plan set is being generated to address these issues and a permit application for the 46 kilograms of hydrogen to be stored in the SunHydro#2 high-pressure

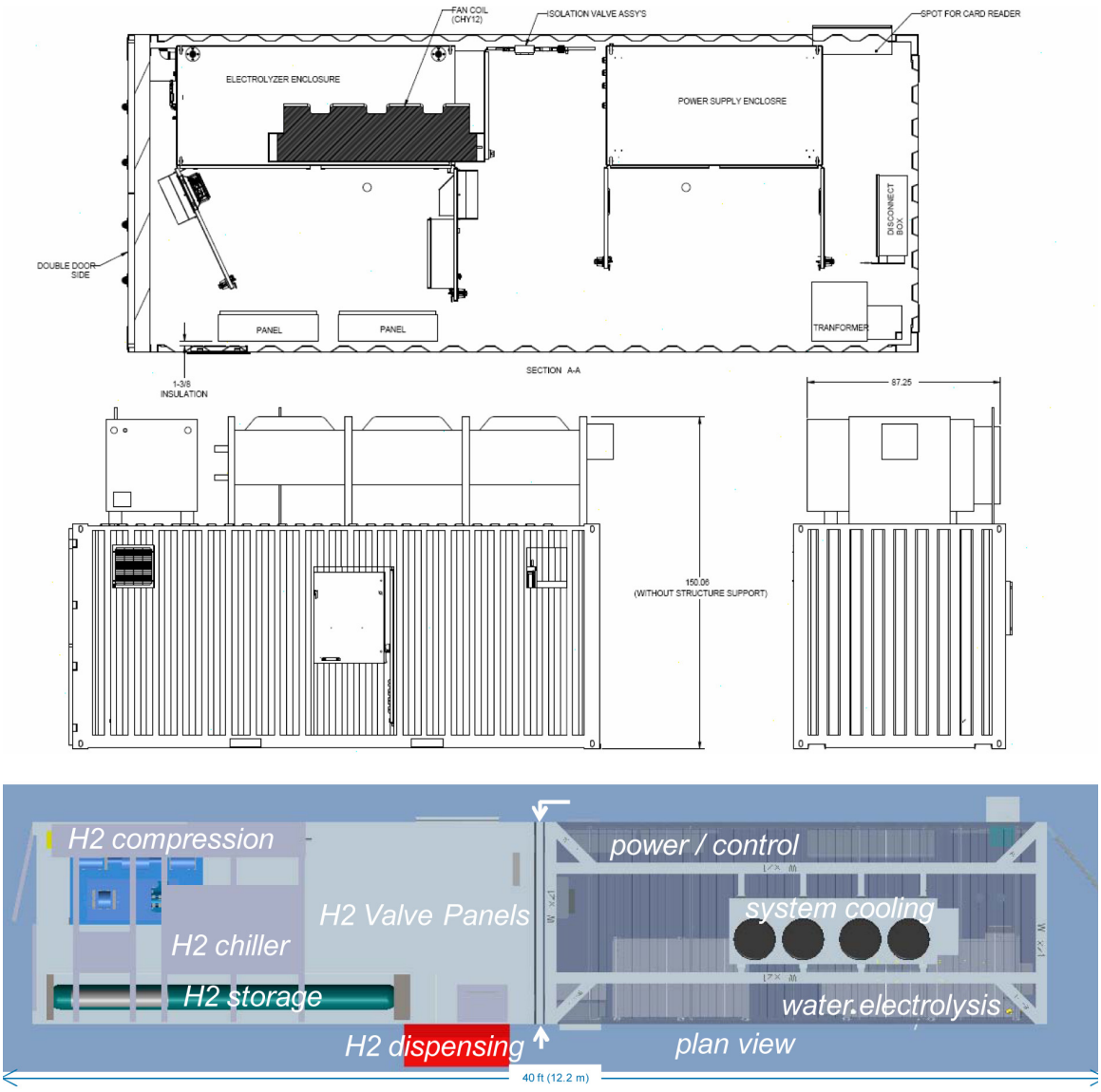

FIGURE 2. Arrangement, Hydrogen Generator Container Section and SunHydro Concept

composite storage tubes has been prepared for review by the appropriate authorities during the next FY.

Proton is an industry member of the NFPA 2 Hydrogen Technologies Code technical committee, and has a representative on the Hydrogen Safety Panel. The technical committee is preparing the 2016 edition of NFPA 2. The Hydrogen Safety Panel, with Proton support, has contributed to a draft public comment concerning hydrogen equipment in enclosures that was reviewed at the second draft meeting for the NFPA 2 committee. Creating specific code to address hydrogen processing equipment and storage in pre-fabricated intermodal enclosures will help code officials with permitting compact containerized hydrogen fueling stations.

Task 6.0 Validate Novel Compact and Non-EX Rated Component Arrangements

Work on a compact fueling station arrangement for the SunHydro#2 station progressed through all design phases during the previous FY (Figure 2). Procurement of a completely fabricated compression, storage, and dispensing container and all major components of the generation container then followed. Proton's analysis of compact hydrogen station component arrangements under this work shows an advantage to using the non-classified area immediately around our PEM hydrogen generator to house almost all electrical power and control equipment. Further, NFPA 2 hydrogen code permits reduction of separation distances to near zero when a 2-hour rated firewall

is interposed. Our arrangement shows significant space saving advantages in placing this firewall in between the non-classified electrolyzer generator container space and the classified container space that houses compression, storage, and a built-in dispenser. This approach will be validated to meet the 8' x 40' goal in the SunHydro#2 station when installed in the next FY.

Task 7.0 Hydrogen Station Data Acquisition System and Task 8.0 Quarterly Operation Data Reporting

Before reporting any data to the DOE for Task 8.0, a comprehensive data acquisition system needed to be specified and installed. This included the specification and selection of the power meter sensing equipment and associated signal conditioning equipment. Furthermore, detailed design effort was needed to define the component architecture to acquire, buffer, and transfer the power data to a file type accessible for data manipulation. The selected architecture utilizes a programmable logic controller to totalize the data from the power meters. These signals are also connected to the SunHydro programmable logic controller to provide a single collection point for energy usage and vehicle fill data. The SunHydro#1 data acquisition system generated data for two reports to the Fuel Cell Electric Vehicle Infrastructure Composite Data Product during the previous FY.

CONCLUSIONS AND FUTURE DIRECTIONS

Future Directions

- Show measurable reduction in dryer purge loss of SunHydro#1 with 57 bar hydrogen generation
- Validate SunHydro#1 dispensing capacity increase
- Validate compressor improvement or increased throughput capacity with 57-bar inlet pressure
- Install and validate novel compact and non-EX rated component arrangement of SunHydro#2
- Install data acquisition for SunHydro#2
- Continue reporting operational data to Fuel Cell Electric Vehicle Infrastructure Composite Data Product database

FY 2014 PUBLICATIONS/PRESENTATIONS

1. AMR 2014 Moulthrop TV-012

REFERENCES

1. NFPA 2 Hydrogen Technologies Code, NFPA, 1 Batterymarch, Quincy, MA.

VII.6 Forklift and Backup Power Data Collection and Analysis

Jennifer Kurtz (Primary Contact), Sam Sprik, Genevieve Saur, Matt Post, and Mike Peters
National Renewable Energy Laboratory (NREL)
15013 Denver West Parkway
Golden, CO 80401-3305
Phone: (303) 275-4061
Email: Jennifer.Kurtz@nrel.gov

DOE Manager
Jason Marcinkoski
Phone: (202) 586-7466
Email: Jason.Marcinkoski@ee.doe.gov

Project Start Date: October 2012
Project End Date: Project continuation and direction determined annually by DOE

Overall Objectives

- Study fuel cell systems operating in material handling equipment (MHE), backup power, portable power, and stationary power applications; the project includes approximately 1,000 deployed fuel cell systems
- Perform an independent assessment of technology in "real-world" operation conditions, focusing on fuel cell systems and hydrogen infrastructure
- Support market growth through reporting on technology status to key stakeholders and performing analyses relevant to the markets' value propositions

Fiscal Year (FY) 2014 Objectives

- Conduct quarterly analysis of operation and maintenance data for fuel cell systems and hydrogen infrastructure
- Prepare bi-annual technical composite data products (CDPs)
- Publish a project completion report of status and performance of fuel cell backup power systems
- Complete performance analyses on durability, reliability, and infrastructure utilization

Technical Barriers

This project addresses the following technical barriers from the Technology Validation section of the Fuel Cell Technologies Office Multi-Year Research, Development, and Demonstration Plan:

(D) Lack of Hydrogen Refueling Infrastructure Performance and Availability Data

(E) Codes and Standards

Contribution to Achievement of DOE Technology Validation Milestones

This project contributes to the achievement of the following DOE milestone from the Technology Validation section of the Fuel Cell Technologies Office Multi-Year Research, Development, and Demonstration Plan:

- Milestone 4.3 Report safety event data and information from ARRA (American Recovery and Reinvestment Act) projects. (3Q 2013)

FY 2014 Accomplishments

- Created or updated 32 backup power CDPs that were published every six months and included analysis results about deployment, fuel cell operation, fuel cell reliability, infrastructure operation, U.S. grid outage statistics, and cost of ownership.
- Summarized the backup power deployment of 1.99 MW of installed capacity and 852 systems operating in 23 states with an average of 4–6 kW capacity per site.
- Analyzed backup power operation (detailed data analysis of a subset) of 2,578 starts, 99.5% uninterrupted operation rate, 65 hours continuous demonstrated runtime, and 1,749 cumulative operation hours.
- Completed a backup power cost of ownership analysis that included cost estimates for capital, permitting and installation, maintenance, and fuel for multiple runtime scenarios for fuel cell, battery, and diesel systems. In the 72-hour runtime scenario, the cost of ownership of the fuel cell system, without incentives, is approximately 1.2 times higher than that of a diesel generator and more than 5 times lower than that of a battery system. In the same runtime scenario, the cost of ownership of the fuel cell system, with incentives, is approximately equal to that of the diesel generator and more than 6 times lower than that of a battery system.
- Analyzed mean time between interrupted operation (MTBIO) for the fuel cell backup power systems. The majority of systems (94%) did not experience any interrupted operation during the analysis period, and for the systems that experienced one or more of the 13 interrupted starts, the median MTBIO was 465 calendar days.

- Created or updated 75 MHE CDPs that were published every six months and included analysis results about deployment, fuel cell operation, fuel cell reliability, fuel cell safety, fuel cell durability, fuel cell maintenance, infrastructure operation, infrastructure safety, infrastructure maintenance, infrastructure reliability, and cost of ownership.
- Summarized the MHE operation and deployment of 490 units operating for more than 2 million hours and 329,834 hydrogen fills for 275,520 kilograms dispensed.
- Validated fill time to be less than 3 minutes, a key factor in the successful value proposition of fuel cell forklifts.
- Studied MHE durability against a long-term goal of 20,000 hours. Using an interim target of 10,000 hours, more than 50% of the fuel cell stacks have a projected voltage degradation time to 10% loss that is greater than 10,000 hours.
- Reported on the maximum operation hours, greater than 16,600, accumulated by one system.
- Studied MHE infrastructure utilization, which averages between 25% and 40% daily utilization, with maximum daily utilization demonstrated at more than 300 kg of hydrogen.
- Continued to evaluate data voluntarily supplied to the National Fuel Cell Technology Evaluation Center (NFCTEC), although MHE awards have all officially completed.

INTRODUCTION

The U.S. Department of Energy designated more than $40 million in ARRA funds for the deployment of up to 1,000 fuel cell systems. This investment is enabling fuel cell market transformation through development of fuel cell technology, manufacturing, and operation in strategic markets where fuel cells can compete with conventional technologies. The strategic markets include MHE, backup power, stationary power, and portable power, and the majority of the deployed systems are in the MHE and backup power markets. NREL is analyzing operational data from these key deployments to better understand and highlight the business case for fuel cell technologies and report on the technology status.

The project includes both end users and system developers: Air Products, FedEx, GENCO, Nuvera Fuel Cells,[1] Plug Power, ReliOn,[1,2] Sprint,[1] and Sysco Houston. The evaluation focused on fuel cell stack durability, reliability, refueling, safety, and value proposition. The deployment partners provided approximately $53 million in industry cost share [1]. In addition to the ARRA co-funded fuel cell backup power demonstrations, DOE supported additional demonstration projects with other federal agencies through Interagency Agreements. The Department of Defense and the Federal Aviation Administration are two agencies with fuel cell backup power demonstrations that also submitted operational and deployment data to NREL. All results covered in this report, unless specified as strictly ARRA, will include both ARRA and Interagency Agreement fuel cell backup power sites. Almost all sites (~98%) were co-funded through ARRA.

[1] Projects have completed, according to the award agreement.
[2] ReliOn was acquired by Plug Power as of April 2014, just before preparation of this report. The brand name is being retained by Plug Power.

APPROACH

The project's data collection plan builds on other technology validation activities. Operation, maintenance, and safety data for fuel cell system(s) and accompanying infrastructure are collected on site by project partners. NREL receives the data quarterly and stores, processes, and analyzes the data in NREL's NFCTEC. The NFCTEC is an off-network room with access provided to a small set of approved users. An internal analysis of all available data is completed quarterly, and a set of technical CDPs is published every six months. Publications are uploaded to NREL's technology validation website [2] and presented at industry-relevant conferences. The CDPs present aggregated data across multiple systems, sites, and teams in order to protect proprietary data and summarize the performance of hundreds of fuel cell systems and thousands of data records. A review cycle is completed before the CDPs are published. This review cycle includes providing detailed data products (DDPs) of individual system- and site-performance results to the specific data provider. DDPs also identify the individual contribution to the CDPs. The NREL Fleet Analysis Toolkit is an internally developed tool for data processing and analysis structured for flexibility, growth, and simple addition of new applications. Analyses are created for general performance studies as well as application- or technology-specific studies.

RESULTS

Over approximately a two-year period, 1,330 fuel cell units (Figure 1) were deployed in stationary power, MHE, auxiliary power, and backup power applications with ARRA co-funding awarded through DOE's Fuel Cell Technologies Office. This surpassed an ARRA objective of deploying up to 1,000 fuel cell units.

As of December 2013, 852 fuel cell units were deployed in backup power applications. The prime backup power ARRA awards were to Sprint-Nextel and ReliOn, with a small number of demonstrations to Plug Power. Other project partners included PG&E; AT&T; Robins Air Force Base; Fort

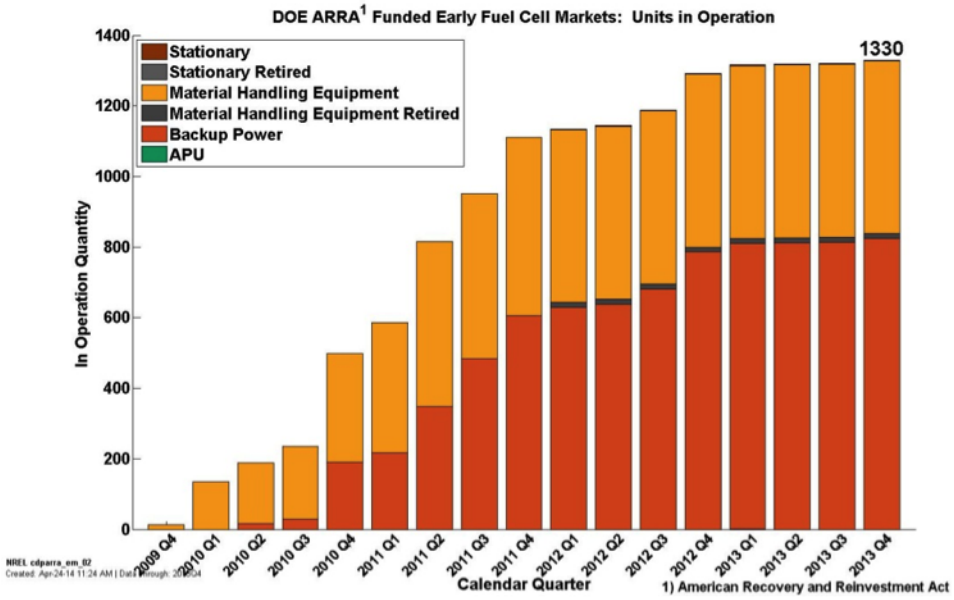

FIGURE 1. Early Market Fuel Cell Deployments Funded Through ARRA

Irwin; IdaTech (recently acquired by Ballard); Altergy; Air Products and Chemicals, Inc.; Champion Energy; Ericsson Services, Inc.; A&E Firms; Black & Veatch; and Burns & McDonnell.

Performance in backup power applications is related to the reliability and availability of the fuel cell backup system, the operating characteristics of the fuel cell, and the specific site. Degradation of the fuel cell performance is less of an issue due to the few hours that are accumulated in most backup power applications. These early market deployments did not provide monitoring of the voltage and current to estimate performance degradation; however, voltage degradation is being studied in other early market applications such as material handling and vehicles, and that analysis is expected to provide feedback for other fuel cell applications. The economics of backup power applications has three major factors: 1) the initial capital investment; 2) the opportunity costs of system downtime, which hinge on the reliability and availability of the backup system; and 3) the ongoing operating costs related to ongoing maintenance activities and fuel delivery cost. Other factors that can impact backup system selection are noise, emissions, and environmental issues, especially when considering urban versus rural installations.

The deployed fuel cell backup power units are being used in the field for backup of telecommunication towers, a vital service in emergencies. Detailed operation data are available for 136 of the units participating in the study from August 2009 through December 2013. During that time, the monitored units logged 1,764 hours of runtime. Much of that runtime was conditioning runs, which are used during regular system checks, especially after long periods of no operation, to maintain the health and reliability of the fuel cell. During the monitoring period, there were 2,583 uninterrupted operations and only 13 unsuccessful starts, resulting in a 99.5% availability value. For the purpose of this analysis, an operation is the system operating after a prompt to start. This prompt may either be for a routine system check or because of a grid outage. An interrupted operation is counted if the system did not start when requested or if the system did not complete the full operation period requested. We are not studying operation data on all of the DOE-sponsored deployments in order to keep the cost of data collection logistics to a minimum and the number of units deployed per the funding at a maximum.

An additional way to study the backup power system reliability is with MTBIO. The MTBIO averages all of the operation periods, in calendar days, based on interrupted operation events. As shown in Figure 2, the majority of systems (94%) did not experience an interrupted operation during this evaluation period. Of the 6% of systems that did experience an interrupted operation, the median MTBIO was 465 days. Each system had an MTBIO value, and there was not a weighting based on the total calendar period that the system was installed and operational. That is, a system recently installed may have a low MTBIO because of an early failure.

Backup power is a more intermittent service compared to other applications such as stationary power or vehicle power. The total operating times tend to be very low with long periods of inactivity. However, backup power for key infrastructure elements can aid emergency response during major storms or other devastating events and prevent loss of productivity, time, and money for other grid incidents.

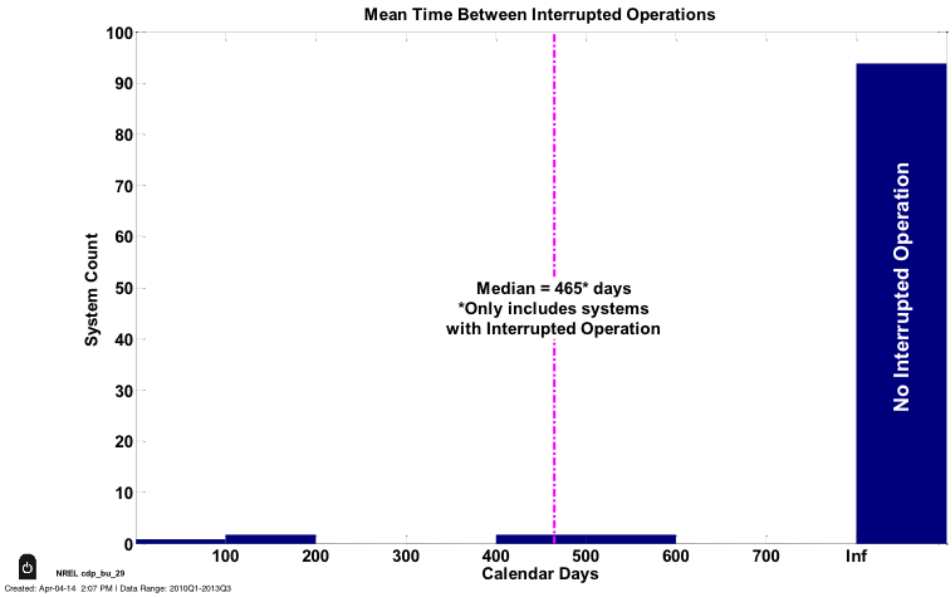

FIGURE 2. Mean Time Between Interrupted Operation for Backup Power Systems

The value is in the service backup power provides; however, understanding how the units are operated and needed will help in designing better systems that meet those requirements.

A benefit of fuel cell backup power is the ability for extended run times even if most outages are much shorter. The longest demonstrated continuous run time for a telecommunication tower fuel cell backup unit was 65 hours—close to 3 days; however, the average run time was only 42 minutes. During Hurricane Sandy (10/29/2012 through 11/12/2012), 122 ARRA-installed sites were located in the impact area from the Federal Emergency Management Agency Modeling Task Force analysis [3]. Not all of the systems were submitting detailed operation data to NFCTEC. Of the systems that were reporting data, five sites in New Jersey reported operation during Hurricane Sandy for a total of 112 hours of operation.

General performance metrics for backup power operators are reliability, cost, run time, and emissions. The cost of ownership data request included site description, system description, requirements, capital cost, operating and maintenance cost, and operating lifetime for fuel cells, batteries, and diesel systems. NREL completed a detailed cost of ownership analysis and published the results through CDPs and a report. Backup power operation can vary widely based on region, end user, and site-specific requirements, so a number of assumptions are made to compare three different backup power technologies (diesel, battery, and fuel cell) operating in similar circumstances in four run time scenarios (8, 52, 72, and 176 hours). Each run time scenario assumes the system operates for a specific amount of hours annually; for example. a system in the 72-hour scenario operates for 72 hours a year. The 72 hours could be accumulated through many shorter-run operations or through one continuous operation. It is important to note that the actual use of a telecommunication system is not as simple, nor as prescribed, as these run time scenarios.

Figure 3 displays the annualized cost estimates for each run time scenario and technology. The battery cost of ownership increases significantly with the higher run time scenarios, and this technology is unlikely to be a truly stand-alone solution for situations that require high run times. The fuel cell system with incentives[3] (denoted FC* in figures) is cost-competitive with the diesel generator, particularly in the 8-hour, 52-hour, and 72-hour run time scenarios. The fuel cell system has a higher efficiency and less frequent maintenance schedule than the diesel generator does, and the incentives offset the higher capital and installation costs.

As of December 2013, 490 fuel cell forklifts were in operation with one project (14 fuel cell forklifts) having completed the demonstration period. The prime forklift ARRA awards were to FedEx Freight East, GENCO, Nuvera Fuel Cells, and Sysco of Houston. The MHE fuel cell systems accumulated more than 2 million hours by the end of 2013. High operation hours on the 490 systems indicate these systems are successfully performing and making an impact at the high-productivity facilities. These end-user facilities have had experience with battery and propane lifts and expected the fuel cell systems to meet and exceed performance expectations in a few key areas for both the retrofit and

[3] "The credit is equal to 30% of expenditures, with no maximum credit. However, the credit for fuel cells is capped at $1,500 per 0.5 kilowatt (kW) of capacity. Eligible property includes fuel cells with a minimum capacity of 0.5 kW that have an electricity-only generation efficiency of 30% or higher" [4].

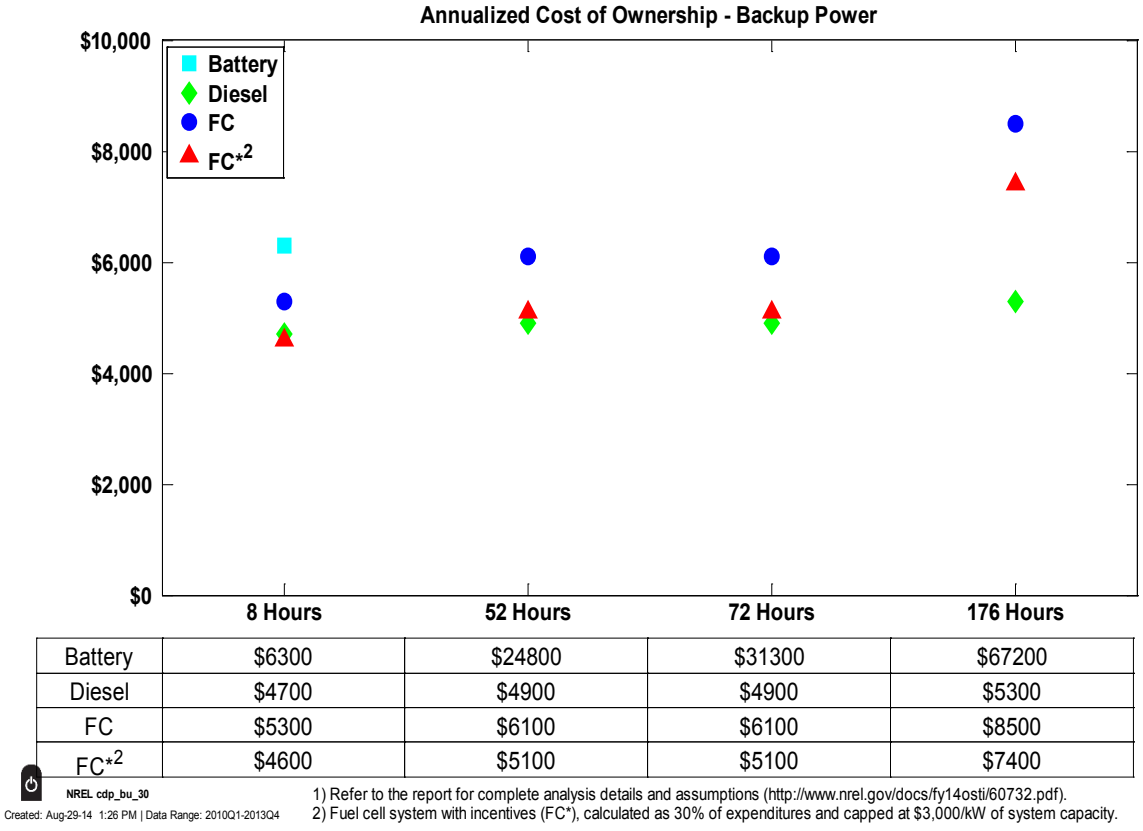

	8 Hours	52 Hours	72 Hours	176 Hours
Battery	$6300	$24800	$31300	$67200
Diesel	$4700	$4900	$4900	$5300
FC	$5300	$6100	$6100	$8500
FC*2	$4600	$5100	$5100	$7400

1) Refer to the report for complete analysis details and assumptions (http://www.nrel.gov/docs/fy14osti/60732.pdf).
2) Fuel cell system with incentives (FC*), calculated as 30% of expenditures and capped at $3,000/kW of system capacity.

FIGURE 3. Annualized Cost-of-Ownership Technology Comparison for Multiple Run Time Scenarios (battery cost is only plotted for the 8-hour scenario)

greenfield sites. These key performance areas include fill amount, operation per fill, operation per day (and year), mean time between failure, and voltage degradation (or fuel cell operation durability). These areas were studied in detail for each system, fleet, and lift classification.

The ultimate durability of fuel cell MHE is still being determined and will continue to be tracked by NREL. This is a key metric to the value proposition—if MHE are unable to meet the expectations of 2–3 times the life of a battery system (3,000–5,000 hours), the value proposition may be in jeopardy. The majority of systems are currently projected to experience 10% voltage decay past 10,000 hours of operation. It is important to note that the 10% level is a benchmark only and does not necessarily represent end-of-life for the fuel cell stack, and certainly not for the entire power plant, of which the stack is only one part.

Among components related to the infrastructure, hydrogen compressors contributed the highest number of maintenance events and maintenance labor hours, as well as the greatest number of hydrogen leaks. The next three categories that lead in unscheduled maintenance events are control electronics, dispenser, and air system. Figure 4 depicts the maintenance labor hours per month for these four categories. Over a three-year period, maintenance hours for compressors and dispensers are fairly consistent. Over this same period, the control electronics and air system maintenance hours are most sporadic. This analysis has helped set up the NFCTEC analysts for a future review that looks more closely at these maintenance trends, possible reasons for the trends, and identification of research and development gaps.

CONCLUSIONS AND FUTURE DIRECTIONS

- The ARRA co-funded deployment of early-market systems has enabled a significant amount of industry growth and lessons learned. The deployment of 1,330 fuel cell units, the majority in the backup power and forklift applications, exceeded the ARRA target of 1,000 fuel cell units. Additionally, the deployment vitalized the industry in several ways, including quantification and validation of fuel cell systems. The successful deployments show the technical viability of a cleaner, efficient, and effective alternative to the incumbent backup power technologies.
- A reduction in capital and installation costs will result in a stronger value proposition for fuel cell systems as backup power solutions. The cost and difficulty

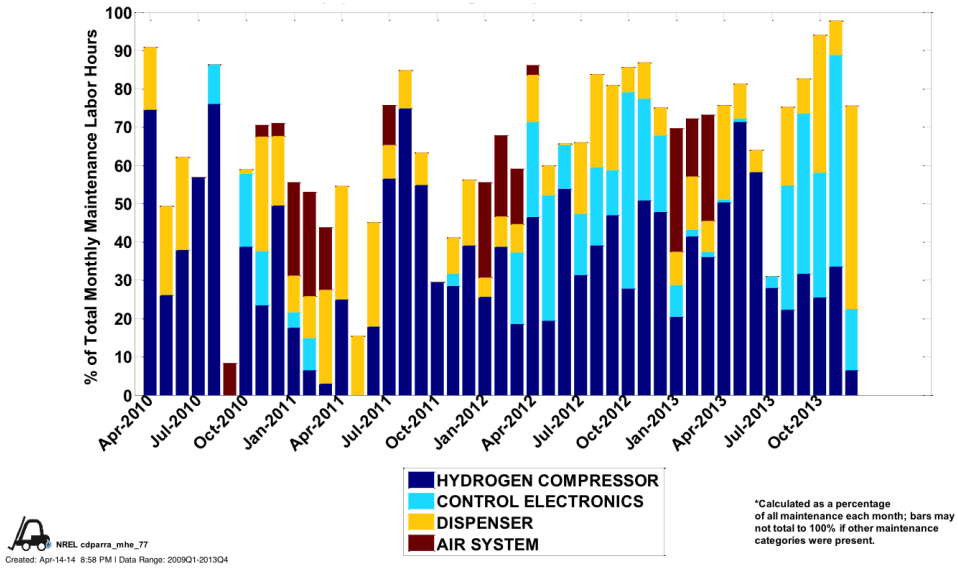

FIGURE 4. Maintenance Labor Hours per Month for Four Categories

associated with the permitting of hydrogen systems are other areas that require development for widespread deployment of fuel cell systems. These permitting challenges can vary greatly across the country and can be addressed by the consistent implementation of codes and standards.

FY 2014 PUBLICATIONS/PRESENTATIONS

1. Kurtz, J.; Sprik, S.; Ainscough, C.; Saur, G. "Backup Power Cost of Ownership Analysis and Incumbent Technology Comparison." Golden, CO: National Renewable Energy Laboratory, expected in August 2014. (report)

2. Kurtz, J.; Sprik, S.; Post, M., Peters, M. "Forklift and Backup Power Data Collection and Analysis." 2014 DOE Hydrogen and Fuel Cells Program and Vehicle Technologies Office Annual Merit Review and Peer Evaluation Meeting, June 2014. (poster presentation)

3. Kurtz, J.; Sprik, S.; Ainscough, C.; Saur, G.; Post, M.; Peters, M. "ARRA Material Handling Equipment Composite Data Products: Data Through Quarter 4 of 2013." Golden, CO: National Renewable Energy Laboratory, June 2014. (CDP report)

4. Kurtz, J.; Sprik, S.; Ainscough, C.; Saur, G.; Post, M.; Peters, M. "Spring 2014 Composite Data Products: Backup Power." Golden, CO: National Renewable Energy Laboratory, June 2014. (CDP report)

5. Kurtz, J.; Sprik, S. "National Fuel Cell Technology Evaluation Centers." DOE webinar, March 11, 2014. (presentation)

6. Kurtz, J.; Sprik, S.; Ainscough, C.; Saur, G.; Post, M.; Peters, M. "ARRA Material Handling Equipment Composite Data Products: Data Through Quarter 2 of 2013." Golden, CO: National Renewable Energy Laboratory, November 2013. (CDP report)

7. Kurtz, J.; Sprik, S.; Ainscough, C.; Saur, G.; Post, M.; Peters, M. "Fall 2013 Composite Data Products: Backup Power." Golden, CO: National Renewable Energy Laboratory, December 2013. (CDP report)

8. Kurtz, J.; Sprik, S.; Ainscough, C.; Saur, G.; Post, M.; Peters, M. "U.S. Department of Energy-Funded Performance Validation of Fuel Cell Material Handling Equipment." UK Hydrogen and Fuel Cell Association webinar, November 27, 2013. (presentation)

9. Kurtz, J.; Sprik, S.; Ainscough, C.; Saur, G.; Post, M.; Peters, M. "Hydrogen Fuel Cell Performance in Key Early Markets of MHE and Backup Power." 2013 Fuel Cell Seminar, October 23, 2013. (presentation)

10. Kurtz, J. "National Fuel Cell Technology Evaluation Center." Golden, CO: National Renewable Energy Laboratory, September 2013. (fact sheet)

REFERENCES

1. *Highlights from U.S. Department of Energy's Fuel Cell Recovery Act Projects*. Washington, DC: U.S. Department of Energy, February 2014. http://energy.gov/eere/fuelcells/downloads/highlights-us-department-energys-fuel-cell-recovery-act-projects.

2. "Fuel Cell and Hydrogen Technology Validation." Golden, CO: National Renewable Energy Laboratory. http://www.nrel.gov/hydrogen/proj_tech_validation.html.

3. "FEMA MOTF Hurricane Sandy Impact Analysis." FEMA Modeling Task Force Web Map, 2014. http://fema.maps.arcgis.com/home/webmap/viewer.html?webmap=307dd522499d4a44a33d7296a5da5ea0.

4. "Database of State Incentives for Renewables and Efficiency." U.S. Department of Energy, 2014. http://www.dsireusa.org/incentives/incentive.cfm?Incentive_Code=US02F&re=1&ee=1.

VII.7 Fuel Cell Electric Vehicle Evaluation

Jennifer Kurtz (Primary Contact), Sam Sprik, and Mike Peters
National Renewable Energy Laboratory (NREL)
15013 Denver West Parkway
Golden, CO 80401-3305
Phone: (303) 275-4061
Email: Jennifer.Kurtz@nrel.gov

DOE Manager
Jason Marcinkoski
Phone: (202) 586-7466
Email: Jason.Marcinkoski@ee.doe.gov

Project Start Date: October 2012
Project End Date: Project continuation and direction determined annually by DOE

Overall Objectives

- Validate hydrogen fuel cell electric vehicles (FCEVs) in a real-world setting
- Identify current status and evolution of the technology

Fiscal Year (FY) 2014 Objectives

- Complete the first round of processing and analyses of data from all six FCEV original equipment manufacturers (OEMs)
- Identify the first three composite data products (CDPs) for the first publication
- Submit the first CDP set for initial review by the OEM partners
- Conduct reviews of the individual data analyses with the OEMs

Technical Barriers

This project addresses the following technical barriers from the Technology Validation section of the Fuel Cell Technologies Office Multi-Year Research, Development, and Demonstration Plan:

(A) Lack of Fuel Cell Electric Vehicle and Fuel Cell Bus Performance and Durability Data

Contribution to Achievement of DOE Technology Validation Milestones

This project contributes to the achievement of the following DOE milestones from the Technology Validation section of the Fuel Cell Technologies Office Multi-Year Research, Development, and Demonstration Plan:

- Milestone 2.3: Validate fuel cell electric vehicles achieving 5,000-hour durability (service life of vehicle) and a driving range of 300 miles between fuelings (4Q, 2019)

FY 2014 Accomplishments

- Completed processing and analyses for data from five out of six OEM partners; the topics included fuel economy, range, voltage degradation, driving behavior, and fueling behavior.
- Analyzed more than 26,000 files in calendar year 2013.
- Rebranded the Hydrogen Secure Data Center to the National Fuel Cell Technology Evaluation Center (NFCTEC).
- Conducted site visits with all six OEM partners.
- Finalized data collection and analysis plans.

INTRODUCTION

Under FOA-625, the U.S. Department of Energy has funded projects for the collection and delivery of FCEV data to NREL for analysis, aggregation, and reporting. Multiple real-world sites and customers are included in this FCEV demonstration project. This activity addresses the lack of on-road FCEV data and seeks to validate improved performance and longer durability from comprehensive sets of early FCEVs, including first-production vehicles. NREL's objective in this project is to support DOE in the technical validation of hydrogen FCEVs under real-world conditions. This is accomplished through evaluating and analyzing data from the FCEVs to identify the current status of the technology, compare it to DOE program targets, and assist in evaluating progress between multiple generations of technology, some of which will include commercial FCEVs for the first time.

The project includes six OEMs: General Motors, Mercedes-Benz, Hyundai, Nissan, Toyota, and Honda. The latter three OEMs are part of one award managed by Electricore. Up to 90 vehicles are expected to supply data over potentially two phases, with particular attention on fuel cell stack durability and efficiency, vehicle range and fuel economy, driving behavior, maintenance, on-board storage, refueling, and safety.

APPROACH

The project's data collection plan builds on other technology validation activities. Operation, maintenance, and safety data for fuel cell system(s) and accompanying infrastructure are collected on site by project partners. NREL receives the data quarterly and stores, processes, and analyzes the data in NREL's NFCTEC. The NFCTEC is an off-network room with access provided to a small set of approved users. An internal analysis of all available data is completed quarterly and a set of technical CDPs is published every six months. Publications are uploaded to NREL's technology validation website [1] and presented at industry-relevant conferences. The CDPs present aggregated data across multiple systems, sites, and teams in order to protect proprietary data and summarize the performance of hundreds of fuel cell systems and thousands of data records. A review cycle is completed before the CDPs are published. This review cycle includes providing detailed data products (DDPs) of individual system- and site-performance results to the specific data provider. DDPs also identify the individual contribution to the CDPs. The NREL Fleet Analysis Toolkit (NRELFAT) is an internally developed tool for data processing and analysis structured for flexibility, growth, and simple addition of new applications. Analyses are created for general performance studies as well as application- or technology-specific studies.

RESULTS

The FY 2014 activities focused on integrating new OEM data into NRELFAT for processing and analyses. The analyses are built around the following topics: durability, deployment, operation, system specifications, range, fuel economy, efficiency, fill performance, reliability, drive and fill behaviors, power and energy management, transients, and benchmarking. Site visits were completed with all OEM partners and the frequency of data delivery has moved from start-up to regular.

In calendar year 2013 (Figure 1), more than 26,000 trip data files were analyzed. These data sets have been aggregated twice for internal NFCTEC review of the bulk performance data and in preparation of the first publication of CDPs in the fall of 2014. The cumulative data file size is nearly 5.5 GB. Because not all of the partners have supplied data and per NFCTEC process, the details of these analyses have not yet been published. Individual results have been reviewed at least once with the partners that have supplied data. In lieu of published results, Figure 2 is included as a snapshot of the processing user interface of NRELFAT for a fake partner called EcoCar. This interface includes the different processing options (right hand check boxes), archiving to store each data delivery and analysis cycle, and CDP setup and processing. Data from all six partners are expected to be integrated and working within NRELFAT by the end of FY 2014.

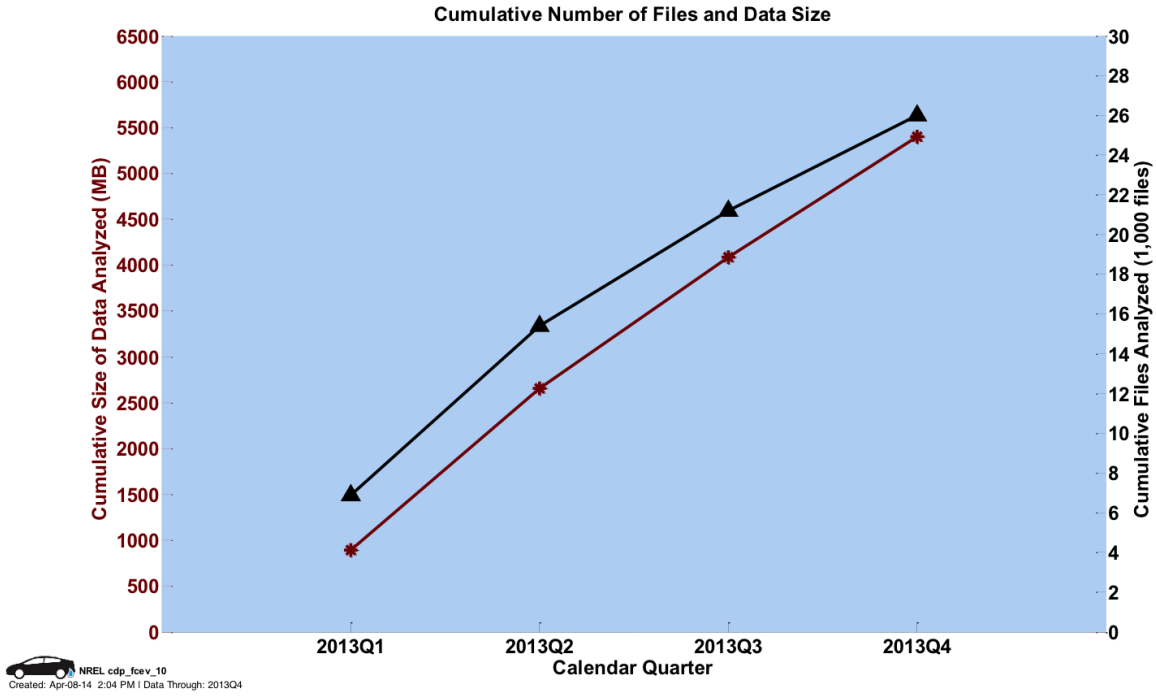

FIGURE 1. FCEV Data File Count and Size Analyzed in 2013 by NFCTEC

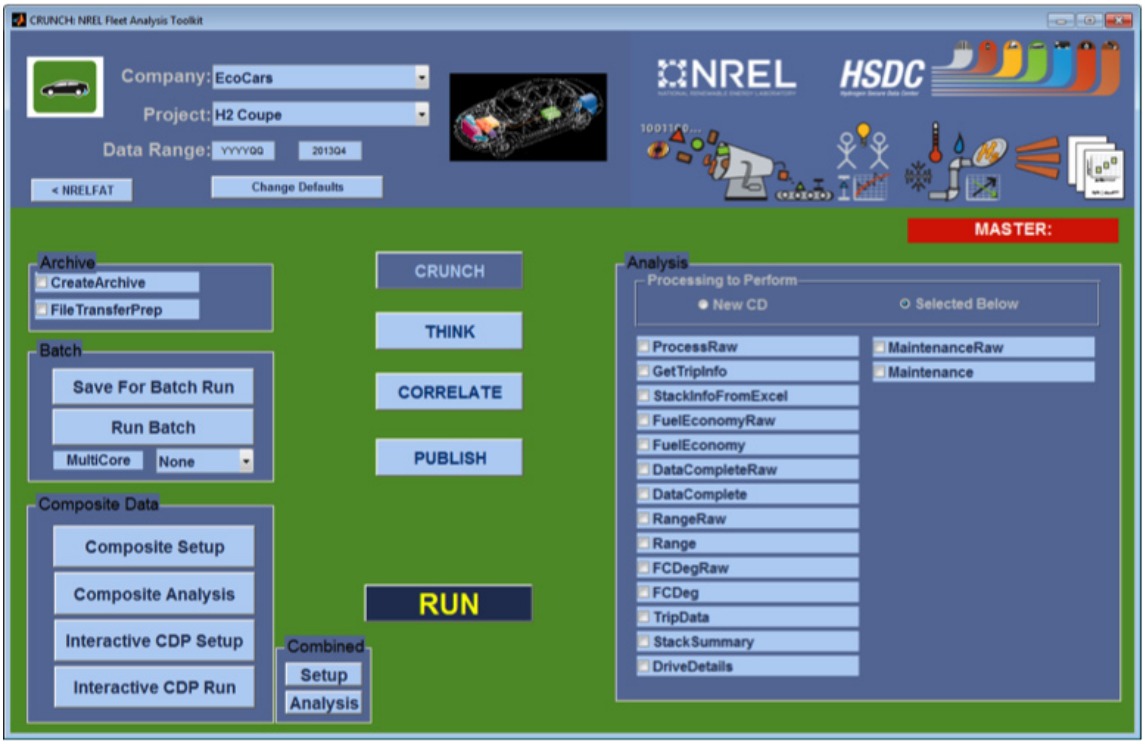

FIGURE 2. NRELFAT Crunch NFCTEC User Interface for Example of Data Processed

NREL supported project kick-off and one-on-one meetings to gain consensus on the methods for data transfer and the steps for building and maintaining trust, such as test data transfers and review process and schedule.

The architectures for fuel cell hours, vehicle miles, calendar time between fills, distance between fills, and fuel economy CDPs were created. CDPs were created with fake data for the purpose of discussion prior to publication (Figure 3).

CONCLUSIONS AND FUTURE DIRECTIONS

- NREL has received and processed initial data from five out of six OEMs. The remaining OEM is expected to deliver the first data by August.
- The regular CDP publication schedule is anticipated to begin in the fall of 2014.

FY 2014 PUBLICATIONS/PRESENTATIONS

1. Kurtz, J.; Sprik, S.; Peters, M. "Fuel Cell Electric Vehicle Evaluation." 2014 DOE Hydrogen and Fuel Cells Program and Vehicle Technologies Office Annual Merit Review and Peer Evaluation Meeting, June 2014. (poster presentation)

2. Kurtz, J., Sprik, S. "National Fuel Cell Technology Evaluation Center." DOE webinar, March 11, 2014. (presentation)

3. Kurtz, J.; Sprik, S.; Wipke, K.; Saur, G. "Technology Validation of Fuel Cell Vehicles and Their Hydrogen Infrastructure." 2013 Fuel Cell Seminar, October 2013. (presentation)

REFERENCES

1. "Fuel Cell and Hydrogen Technology Validation." Golden, CO: National Renewable Energy Laboratory. http://www.nrel.gov/hydrogen/proj_tech_validation.html.

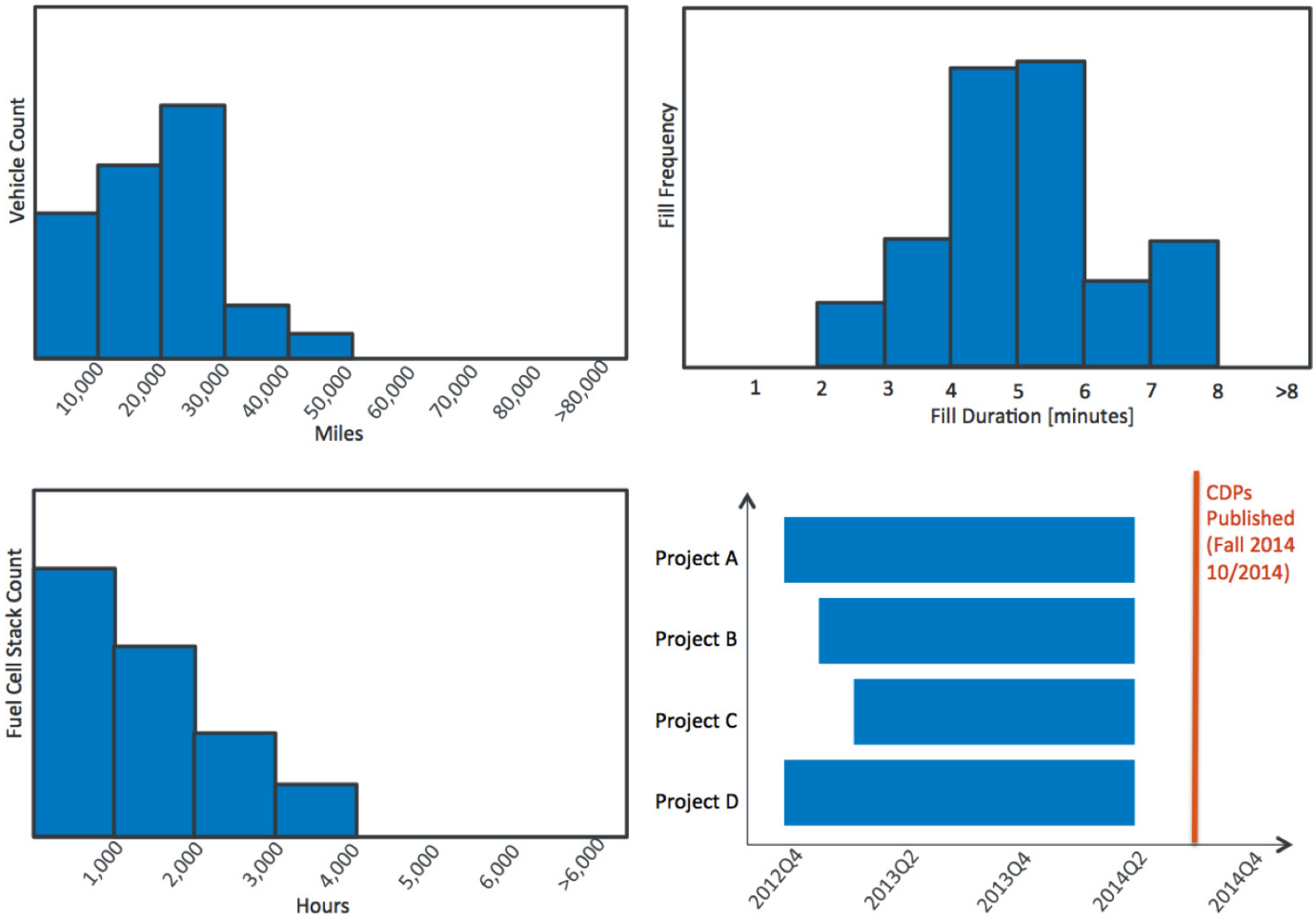

FIGURE 3. Fake CDP Examples for Metadata (e.g., start date), Fuel Cell Stack Hours, Vehicle Miles, and Calendar Days between Fills

VII.8 Next Generation Hydrogen Infrastructure Evaluation

Sam Sprik (Primary Contact), Jennifer Kurtz, Genevieve Saur, Matt Post, and Mike Peters
National Renewable Energy Laboratory (NREL)
15013 Denver West Parkway
Golden, CO 80401-3305
Phone: (303) 275-4431
Email: sam.sprik@nrel.gov

DOE Manager
Jason Marcinkoski
Phone: (202) 586-7466
Email: Jason.Marcinkoski@ee.doe.gov

Project Start Date: October 1, 2011
Project End Date: Project continuation and direction determined annually by DOE

Overall Objectives

- Study current, state-of-the-art hydrogen fueling stations. Analyze efficiency, performance, cost, and reliability of station components and systems from existing stations.
- Perform an independent assessment of technology in real-world operating conditions, focusing on hydrogen infrastructure for on-road vehicles.

Fiscal Year (FY) 2014 Objectives

- Collect data from state-of-the-art hydrogen fueling facilities funded by DOE Funding Opportunity Announcement (FOA) 626 and others, such as those funded by the State of California, to enrich the analyses and composite data products (CDPs) on hydrogen fueling originally established by the Learning Demonstration project.
- Work with codes and standards activities and fueling facility owners/operators to benchmark performance of the fueling events relative to current SAE International procedures.
- Perform analysis and provide feedback on sensitive data from hydrogen infrastructure for industry and DOE. Aggregate these results for publication.
- Participate in technical review meetings and site visits with industry partners to discuss results from NREL's analysis.
- Maintain an accurate database (location and status) of all online hydrogen stations in the United States, and provide periodic updates to other online resources, specifically NREL's Alternative Fuels Data Center (AFDC) station locator, the Fuel Cell and Hydrogen Energy Association, the California Fuel Cell Partnership, and FuelCells.org.

Technical Barriers

This project addresses the following technical barrier from the Technology Validation section of the Fuel Cell Technologies Office Multi-Year Research, Development, and Demonstration Plan:

(D) Lack of Hydrogen Refueling Infrastructure Performance and Availability Data

Contribution to Achievement of DOE Technology Validation Milestones

This project will contribute to achievement of the following DOE milestones from the Technology Validation section of the Fuel Cell Technologies Office Multi-Year Research, Development, and Demonstration Plan:

- Milestone 4.4: Complete evaluation of 700-bar fast fill fueling stations and compare to SAE J2601 specifications and DOE fueling targets. (3Q, 2016)

FY 2014 Accomplishments

- Internally processed and analyzed quarterly infrastructure data in the National Fuel Cell Technology Evaluation Center (NFCTEC) for inclusion in CDPs every six months.
- Created new fall 2013 and spring 2014 CDPs based on available data.
- Updated NREL's internal database of stations and their locations and submitted updates to the AFDC.
- Provided assistance in filling out and modifying templates for those providing infrastructure data.
- Gathered and provided updates on stations under the DOE FOA 626-funded projects.
- Updated NREL Fleet Analysis Toolkit code to accept data in multiple formats from stations outside the DOE FOA 626 stations.
- Analyzed data from station provider outside DOE FOA 626-funded projects.
- Participated in the California Fuel Cell Partnership working group meetings and H2USA hydrogen fueling station working group.
- Presented this project at Fuel Cell Seminar 2013 and at the 2014 Annual Merit Review.

INTRODUCTION

In the past decade, approximately 60 hydrogen fueling stations supported a few hundred fuel cell electric vehicles (FCEVs) in the United States. Of these stations, 25 supported the 183 DOE Learning Demonstration vehicles. As original equipment manufacturers are ramping up FCEV bus, forklift, and car production, there is an effort to build additional stations, increase individual station fueling output, and cluster stations to cover the area where vehicles are located.

California has been a leader in supporting hydrogen infrastructure with a goal of a 100-station network. There are now nine public stations in California with 17 more in near-term development. To further support the rollout of FCEVs coming in 2015-2017 and beyond, the California Energy Commission proposed awards for PON-13-607 in May of 2014. This would fund 28 new stations and a mobile refueler with more than $46 million of state money through the California Energy Commission's Alternative and Renewable Fuel and Vehicle Technology Program. These stations are expected to be included in subsequent evaluations and would bring the California public station count to 54.

Keys to success for improving hydrogen fueling availability are selecting the fueling location, ensuring public access, and providing adequate output to support the vehicles. Developing multi-use facilities that can serve cars, buses, and/or forklifts may help the economics and capacity utilization. Hydrogen output from existing and upcoming facilities varies from 12 to 140 kg/day, with most new fueling facilities being in the 100 kg/day range. There is an effort to focus on clusters of stations near population centers in the Los Angeles area. Using available biogas resources from landfills and wastewater treatment plants for hydrogen production is one way to make use of a renewable feedstock and to lower greenhouse gas emissions. As more vehicles come online, all fueling facilities will need to be accessible to anyone with a hydrogen vehicle. Long construction lead times need to be accounted for when planning for the upcoming stations. As these optimized fueling facilities are developed, there is a need to continue data collection and analysis to track the progress and determine future technology development needs.

APPROACH

The emphasis of this project is documenting the innovations in hydrogen fueling and how it will meet vehicle customer needs. This includes analysis that captures the technology capability (such as back-to-back filling capability, impact of pre-cooling temperature, and radio-frequency identification of vehicles to allow unique fueling profiles) as well as the customer perspective (such as fueling times and rates, safety, and availability). Individual components, such as compressors, will be evaluated with the available data to establish current status and research needs. Station locations will be evaluated within the context of both available vehicles and future vehicles and their fueling patterns. NREL will also use the analysis results to support DOE in identifying trends from the data that will help guide DOE's R&D activities.

Data analysis will be performed on sensitive industry hydrogen fueling data in NREL's National Fuel Cell Technology Evaluation Center and recommendations will be provided to DOE on opportunities to refocus or supplement R&D activities. Aggregation of the analyzed data allows for creation of composite results for public dissemination and presentation. Some existing CDPs from the previous learning demonstration will be updated with new data, as appropriate. All this involves working with industry partners to create and publish CDPs that show the current technology status without revealing proprietary data. Feedback to industry takes form in detailed data products (protected results) and provides direct benefit to them from the NREL analysis performed on their data. We will continue exercising the fueling analysis functionality of the NREL Fleet Analysis Toolkit to preserve and archive a snapshot of the analysis results from each quarter. This allows a deeper level of results to be stored in an easy-to-access form within the NFCTEC.

Using unique analysis capabilities and tools developed at NREL, researchers are providing valuable technical recommendations to DOE based on real-world experiences with the technology. NREL will continue to provide multiple outputs in the form of CDPs and presentations and papers at technical conferences.

RESULTS

The hydrogen station locations in the United States can be seen in Figure 1. As stations are built or retired, updates are made to the internal database and shared with others, including the AFDC. There are currently 52 stations in the United States and 12 are considered open to the public, with most of those in California. This year, enough stations started reporting data to NREL to make data aggregation possible in the form of CDPs, which were publicly available through presentations at Fuel Cell Seminar and the DOE Annual Merit Review. Results were also published on NREL's website.

Although the primary goal of the early stations is for coverage, we still want to show how the stations are being used in regards to capacity utilization and usage patterns. The capacity utilization CDPs have been presented and can be found on the NREL website. The amount of dispensed hydrogen per day of the week (Figure 2) shows more filling is happening Monday through Friday than on Saturday and Sunday. The highest station shows an average of 33 kg/day

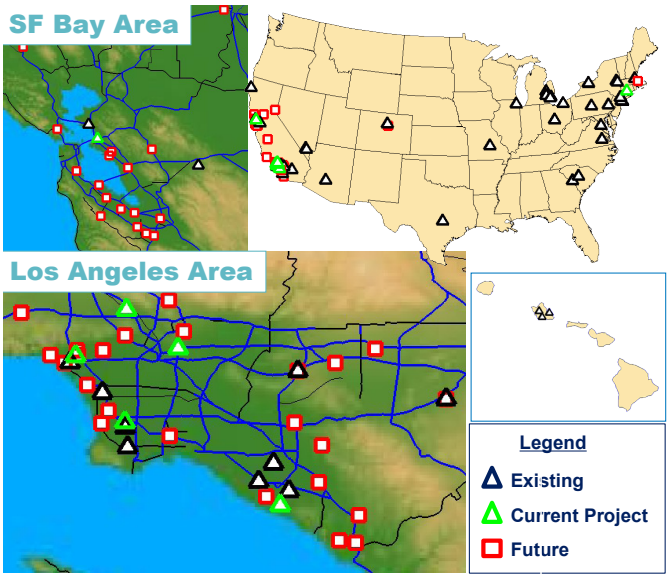

"Current Projects" are projects providing data as part of the DOE Technology Validation sub-program.

FIGURE 1. Hydrogen Station Locations

on Thursdays. The number of fills per day (Figure 3) at each station range from 3 to 11 on average with maximum daily fills at each station ranging from 7 to 30 fills per day. The amount of hydrogen dispensed per fill (Figure 4) is 2.46 kg on average ranging mostly between 1.5 and 3.5 kg. Some of the lower amounts in the histogram are due to incomplete fills where the station stops the fill for various reasons. A preliminary look at maintenance by equipment type (Figure 5) shows that hydrogen compressors are the primary items needing maintenance both in terms of number of events and hours. Dispenser maintenance, safety items (e.g., false alarms and sensors) and thermal management are the next highest items in terms of number of maintenance events. As more data comes in there will be more analysis focusing on usage, reliability, and performance of the stations.

CONCLUSIONS AND FUTURE DIRECTIONS

As new stations come online or are updated, their performance and availability will affect how successfully they support the current and upcoming fleet of fuel cell vehicles. Continual data collection, analysis, and feedback

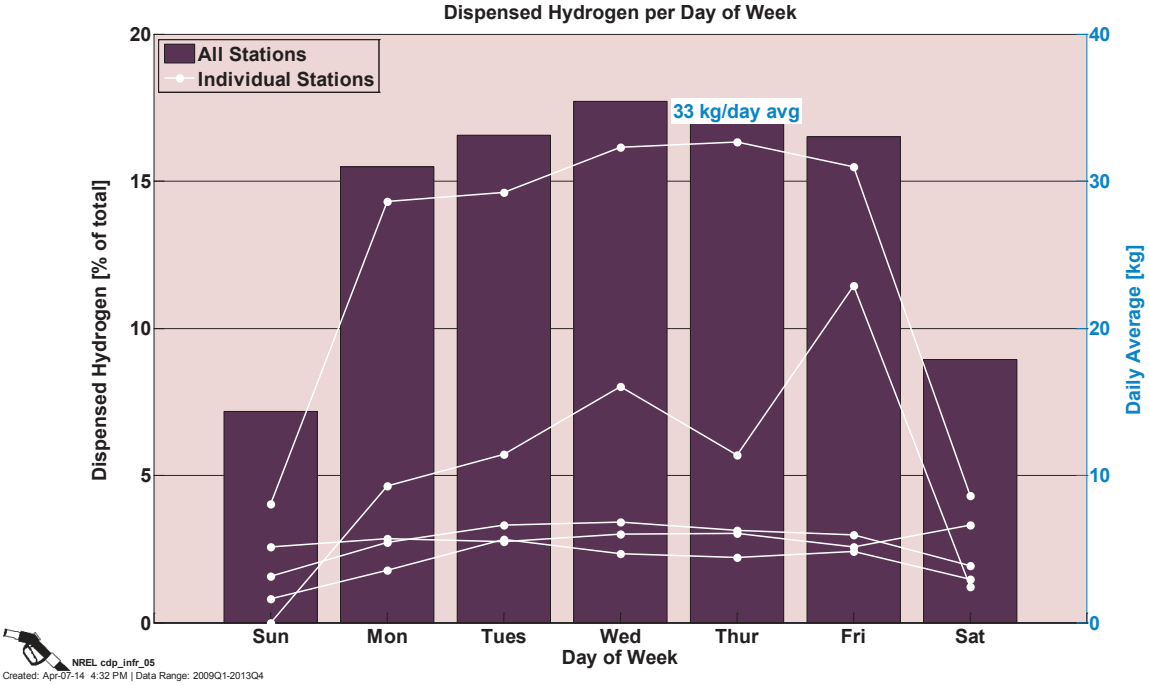

FIGURE 2. Dispensed Hydrogen per Day of Week

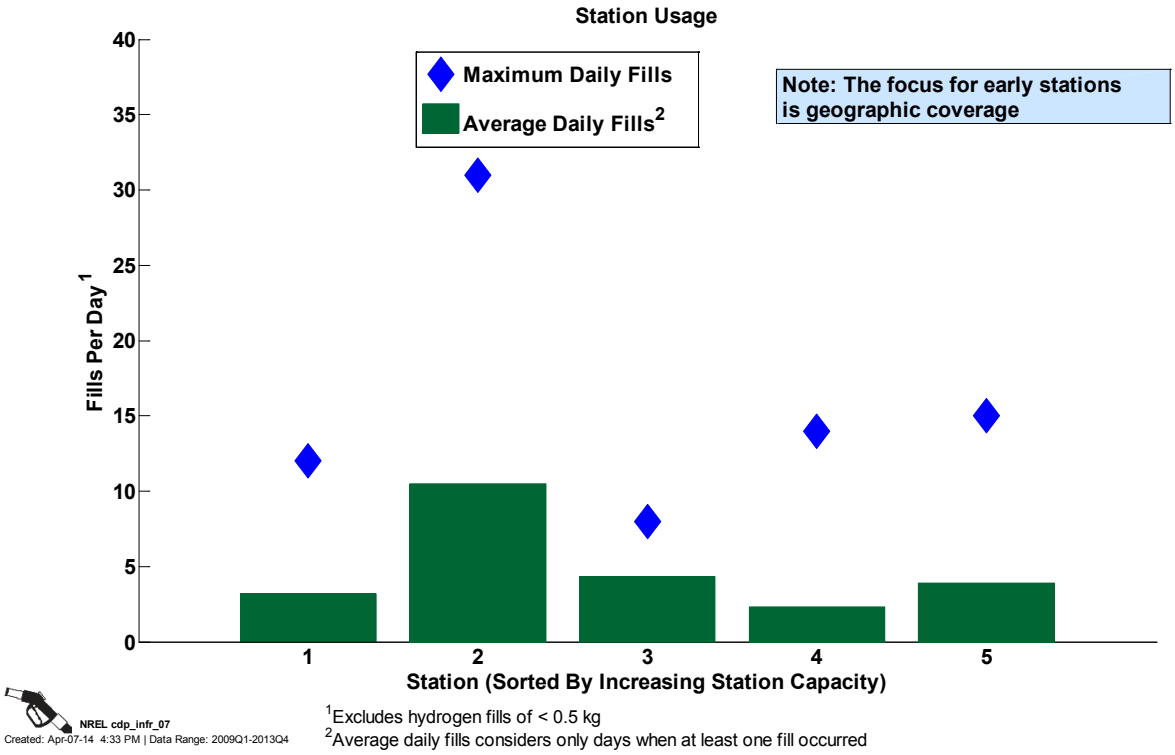

FIGURE 3. Station Usage – Number of Fills per Day

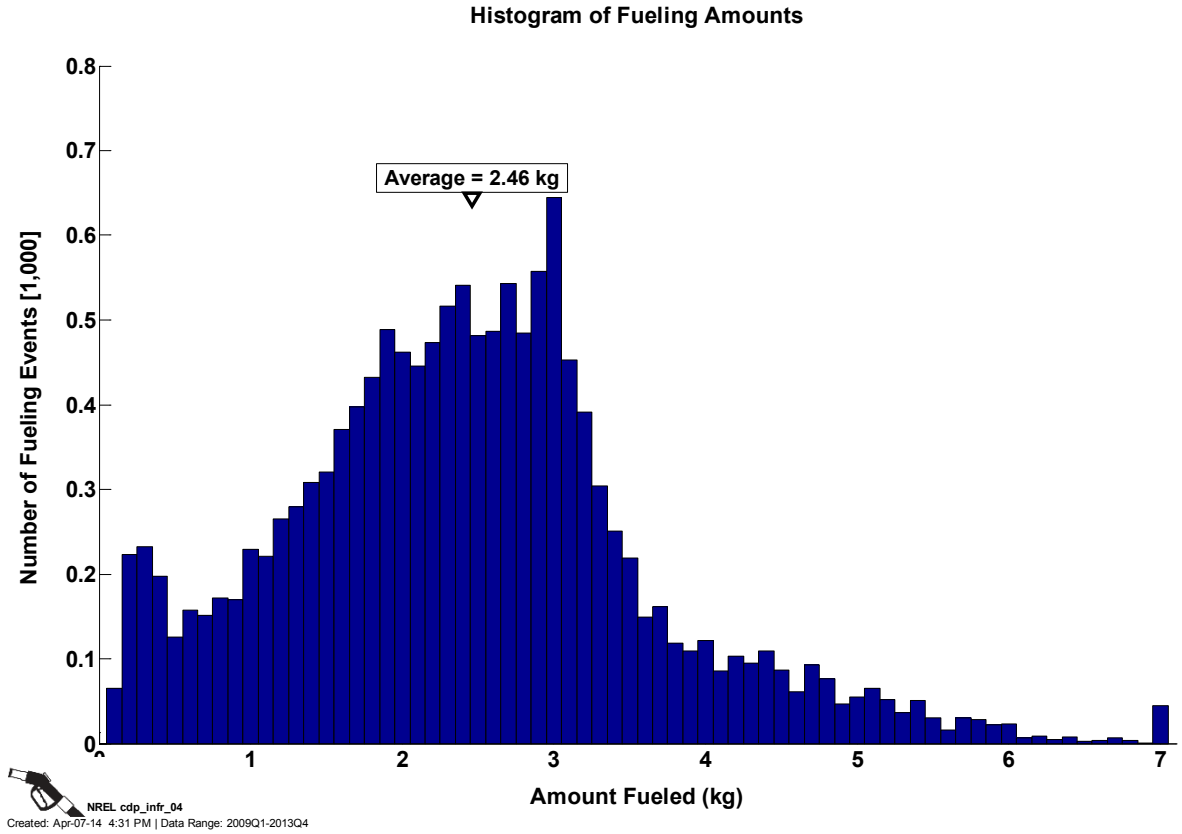

FIGURE 4. Histogram of Fueling Amounts

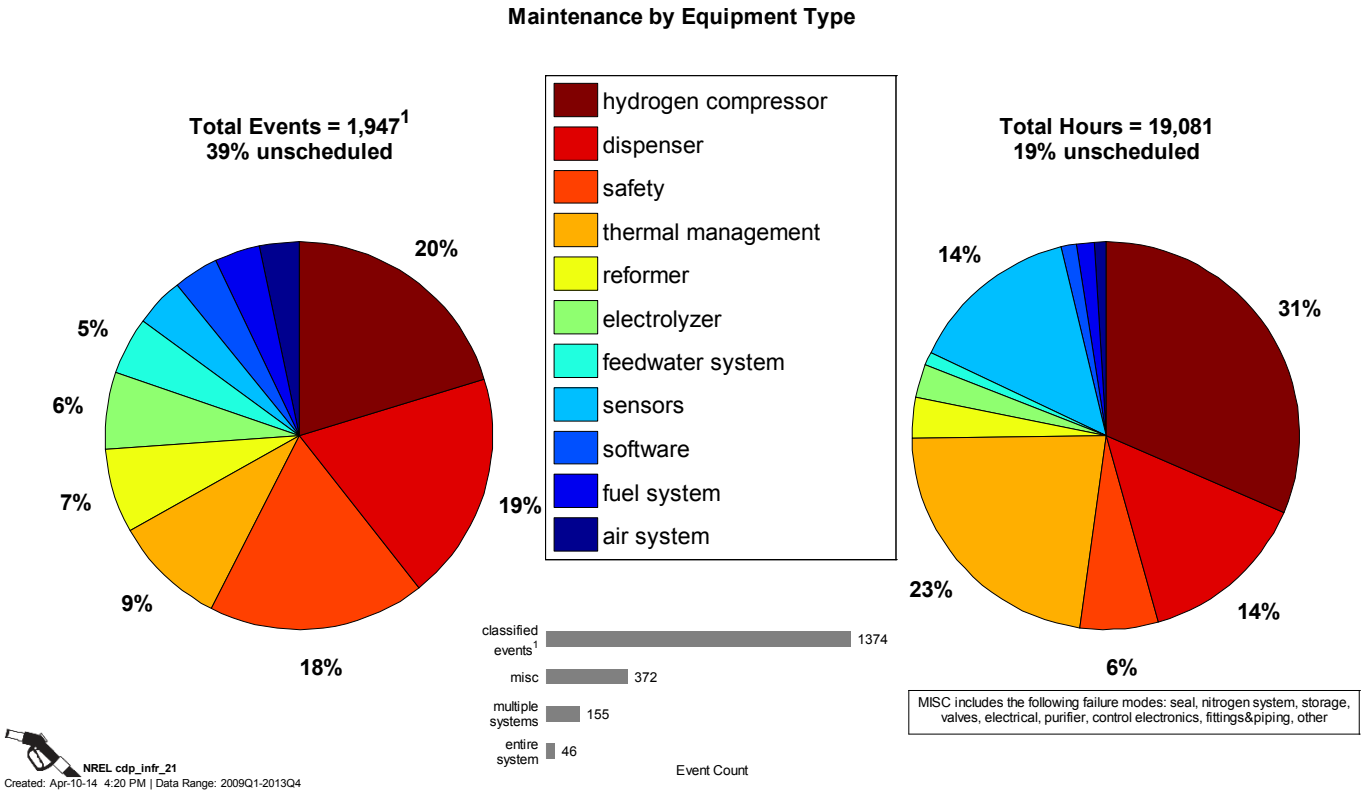

FIGURE 5. Maintenance by Equipment Type

will provide DOE and the hydrogen and fuel cell community with awareness of the technology readiness and identify research areas for improvement. Few stations had been providing data during this project startup but more of the stations have reported data in 2014, making it possible to start aggregating the data in CDPs without revealing individual station identity and to identify general trends in the industry. As more data become available from more stations and as more FCEVs enter the market, there will be an increase in data analysis possibilities to validate the technology for hydrogen infrastructure.

FY 2014 PUBLICATIONS/PRESENTATIONS

1. S. Sprik, J. Kurtz, M. Peters. "TV017: Hydrogen Station Data Collection and Analysis," 2014 DOE Annual Merit Review and Peer Evaluation Meeting, June 2014, Washington, D.C. (Poster Presentation)

2. S. Sprik, J. Kurtz, K. Wipke, G. Saur, C. Ainscough. "Technology Validation of Fuel Cell Vehicles and Their Hydrogen Infrastructure," 2013 Fuel Cell Seminar, October 2013, Columbus, OH. (Oral Presentation)

3. CDPs and past publications are available on the Hydrogen Infrastructure section of NREL's Technology Validation website: http://www.nrel.gov/hydrogen/proj_tech_validation.html.

VII.9 Data Collection and Validation of Newport Beach Hydrogen Station Performance

Michael J. Kashuba
California Air Resources Board
1001 I Street, P.O. Box 2815
Sacramento, CA 95812
Phone: (916) 323-5123
Email: mkashuba@arb.ca.gov

DOE Managers
Jason Marcinkoski
Phone: (202) 586-7466
Email: Jason.Marcinkoski@ee.doe.gov
Jim Alkire
Phone: (720) 356-1426
Email: James.Alkire@ee.doe.gov

Contract Number: DE-EE0005889

Subcontractor
Hydrogenics Corporation, Torrance, CA

Project Start Date: October 2012
Project End Date: March 2015

Overall Objective

- Specify and install correct instrumentation to increase the amount of data collected
- Validate new data and conduct initial analysis
- Increase overall station/equipment up time
- Reduce non-scheduled maintenance visits
- Make component optimization recommendations
- Check/validate station optimization

Fiscal Year (FY) 2014 Objectives

- Specify and install correct instrumentation to increase the amount of data collected
- Validate new data and conduct initial analysis

Technical Barriers

This project addresses the following technical barriers from the Technology Validation section of the Fuel Cell Technologies Office Multi-Year Research, Development, and Demonstration Plan:

(D) Lack of Hydrogen Refueling Infrastructure Performance and Availability Data

(F) Centralized Hydrogen Production from Fossil Resources

Contribution to Achievement of DOE Technology Validation Milestones

This project will contribute to achievement of the following DOE milestone from the Technology Validation section of the Fuel Cell Technologies Office Multi-Year Research, Development, and Demonstration Plan:

- Milestone 3.2: Validate novel hydrogen compression technologies or systems capable of >200 kg/day that could lead to more cost-effective and scalable (up to 500 kg/day fueling station solutions for motive applications. (4Q, 2014)

FY 2014 Accomplishments

- Specified 16 pieces of instrumentation to effectively increase data collection
- Researched and applied experience gained from installation of a similar suite of sensors at a nearby electrolyzer station to this station in order to plan a more streamline installation

INTRODUCTION

The hydrogen fueling station located at 1600 Jamboree Road in Newport Beach, CA was designed and built to refuel light-duty fuel cell electric vehicles (FCEVs). The station features the onsite generation of hydrogen through a small-scale natural gas steam methane reformer (SMR). All the hydrogen related equipment was added to an existing retail gasoline/diesel station. The station is an early demonstration of what the footprint and equipment arrangement of a retail onsite SMR facility might look like (Figure 1).

Only a few hundred FCEVs are on the road in California. As a result, hydrogen throughput is relatively low at the few early pre-commercial hydrogen stations that are currently open. As a result the stations are underutilized. This project aims to collect additional data to allow the operator to potentially adjust various station component and operational parameters in order to improve the overall efficiency of the station and lower operation and maintenance costs and to help improve air quality and reduce greenhouse gas emissions.

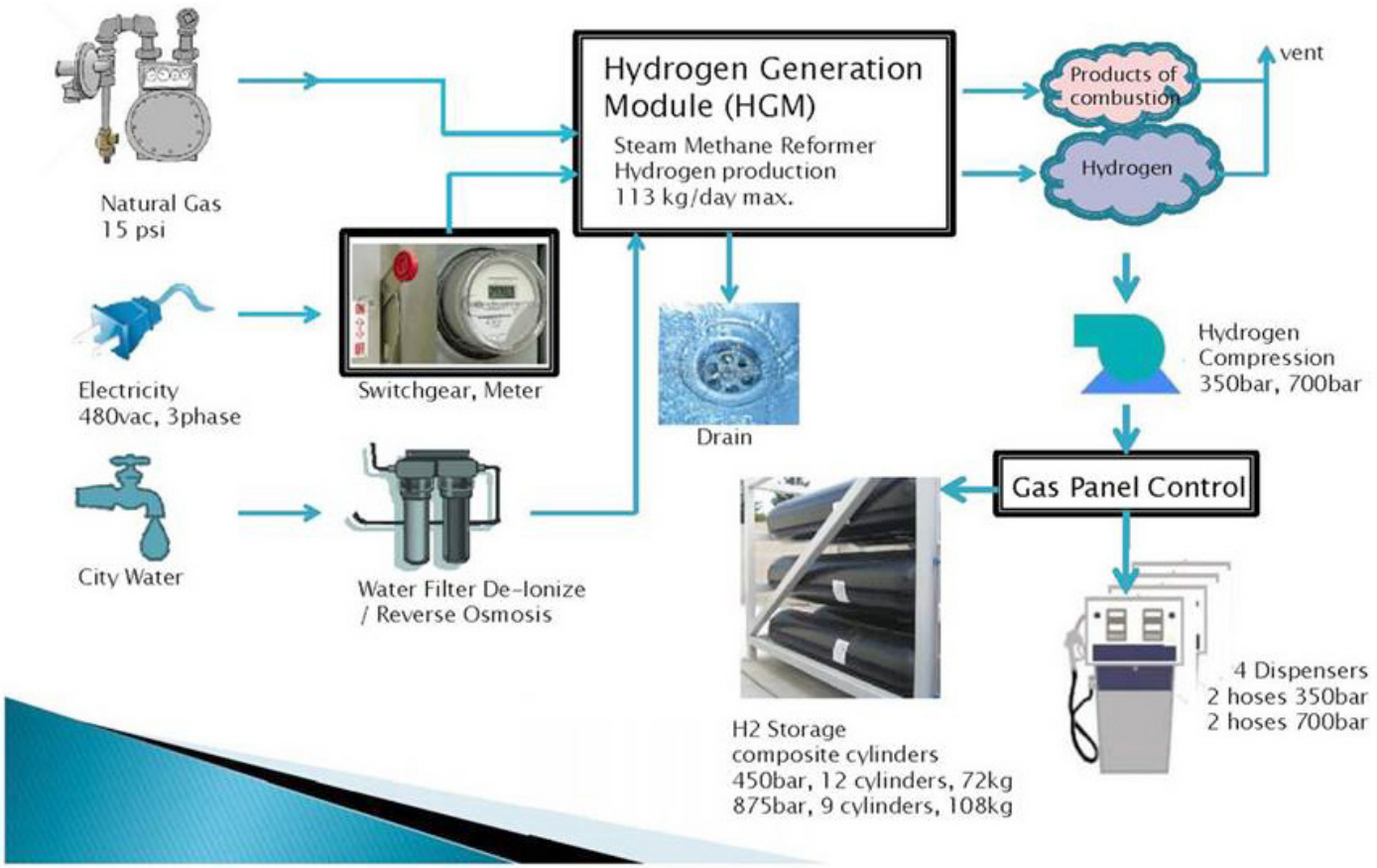

FIGURE 1. Newport Beach Hydrogen SMR Station Simplified Process Diagram

APPROACH

The first phase of the project involves specifying and installing the correct instrumentation to increase the amount of data collected. This involves installing three mass flow meters, two hour meters, nine power meters, and two water flow meters. The new data collected will be validated and the initial analysis will be conducted (Figures 2 and 3).

The second phase of the project aims to improve the efficiency of the station. The intent is to increase the overall station and equipment up time and reduce non-scheduled maintenance visits. The data collected will be used to make recommendations on how to optimize discrete station components. The recommendations will be acted upon, and continually monitored to validate the optimization of the station.

RESULTS

The results of this project have yet to be derived.

CONCLUSIONS AND FUTURE DIRECTIONS

Data collection will begin in the third quarter of 2014. Research is expected to continue as planned until 2015.

FY 2014 PUBLICATIONS/PRESENTATIONS

1. 2014 DOE Annual Merit Review "Newport Beach Hydrogen Station Key Performance Indicators, Project ID # TV023, Michael J. Kashuba, California Air Resources Board.

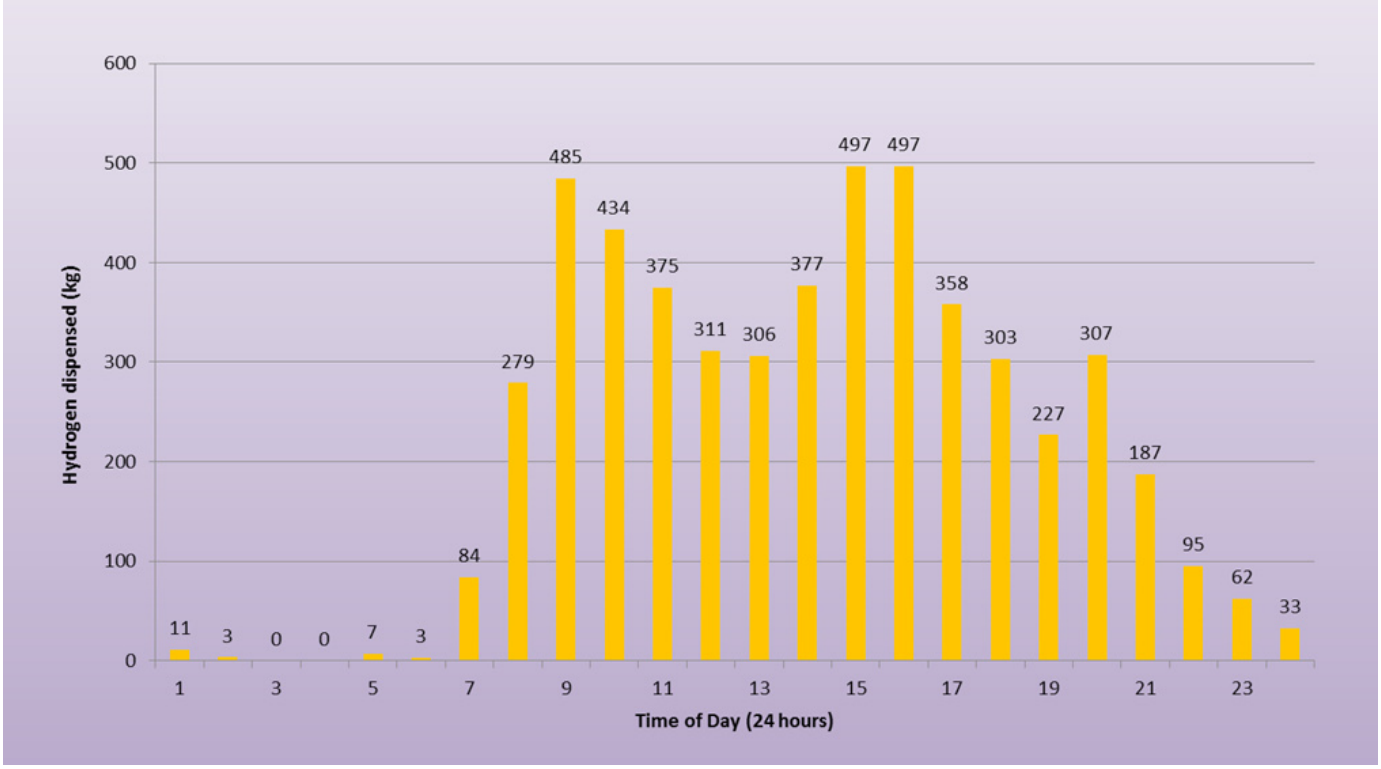

FIGURE 2. Data showing fueling patterns at the Newport Beach Hydrogen station show a similarity to the typical "double peak" that traditional fuel stations experience. Units are in cumulative kilograms dispensed per period over the history of the station. This information will be used to optimize the SMR, and compression operation.

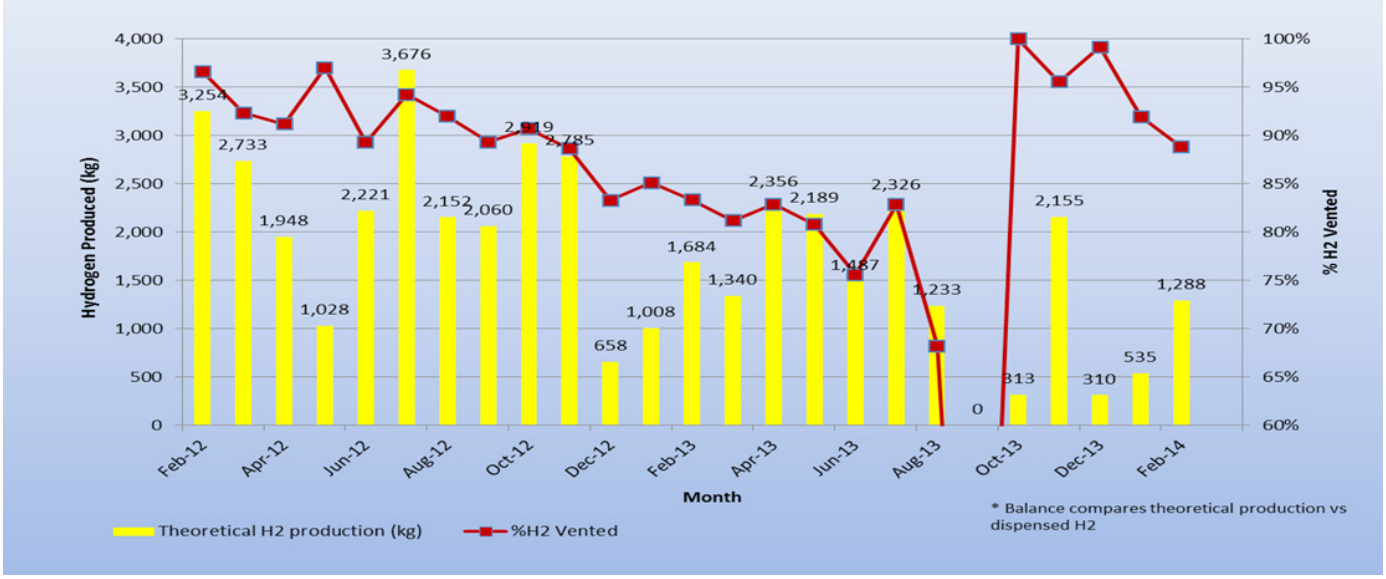

FIGURE 3. Mass balance comparing kilograms produced at the station plotted against percent vented due to a combination of relative lack of demand and overproduction.

VII.10 California State University, Los Angeles Hydrogen Refueling Facility Performance Evaluation and Optimization

David Blekhman
California State University, Los Angeles (CSULA)
Los Angeles, CA 90032
Phone: (323) 343-4569
Email: blekhman@calstatela.edu

DOE Managers
Jason Marcinkoski
Phone: (202) 586-7466
Email: Jason.Marcinkoski@ee.doe.gov
James Alkire
Phone: (720) 356-1426
Email: James.Alkire@ee.doe.gov

Contract Number: DE-EE0005890

Subcontractor
Hydrogenics Corporation, Mississauga, ON, Canada

Project Start Date: October 1, 2012
Project End Date: September 30, 2016

Overall Objectives

Technical Objectives

- Test, collect data, and validate hydrogen refueling architecture deployed at CSULA and its individual components in a real-world operating environment
- Provide the performance evaluations data to the National Fuel Cell Technology Evaluation Center (NFCTEC) at the National Renewable Energy Laboratory (NREL)
- Contribute to the development of new industry standards
- Develop and implement fueling station system performance optimization

Educational Objectives

- Conduct outreach and training activities promoting the project and hydrogen and fuel cell technologies
- Provide a living-lab environment for engineering and technology students pursuing interests in hydrogen and fuel cell technologies

Fiscal Year (FY) 2014 Objectives

- Complete design and install data collection system for the station and its major components
- Start regular collection of station performance data and submission of quarterly reports to NREL

Technical Barriers

This project addresses the following technical barriers from the Fuel Cell Technologies Office Multi-Year Research, Development, and Demonstration Plan:

Hydrogen Production

(L) Operations and Maintenance

(M) Control and Safety

Technology Validation

(D) Lack of Hydrogen Refueling Infrastructure Performance and Availability Data

Contribution to Achievement of DOE Hydrogen Production and Technology Validation Milestones

This project will contribute to achievement of the following DOE milestones from the Hydrogen Production and Technology Validation sections of the Fuel Cell Technologies Office Multi-Year Research, Development, and Demonstration Plan:

Hydrogen Production

- Milestone 2.6: Verify the total capital investment for a distributed electrolysis system against the 2015 targets using H2A. (Q2, 2016)
- Milestone 2.7: Verify 2015 distributed hydrogen production levelized cost target through pilot scale testing coupled with H2A analysis to project economies of scale cost reduction. (Q3, 2017)

Technology Validation

- Milestone 3.4: Validate station compression technology provided by delivery team. (4Q, 2018)

FY 2014 Accomplishments

This is the first year of the project with its accomplishments listed in the following:

- Completed installation and calibration of data acquisition equipment
- Developed automated data collection, storage and retrieval including NREL format reports
- Started regular reporting to NREL

- Upgraded station with a buffer volume to improve high-pressure end of fill
- Hosted grand-opening of the CSULA hydrogen research and fueling facility

INTRODUCTION

The CSULA hydrogen station deploys the latest technologies with the capacity to produce and dispense 60 kg/day, sufficient to fuel 15-20 vehicles. The station utilizes a Hydrogenics electrolyzer, first and second stage compressors enabling 350- and 700-bar fueling and 60 kg of hydrogen storage. The station is grid-tied and to be supplied by 100% renewable power.

In addition to collecting data per NREL specifications, the comprehensive data collection enhances research opportunities in evaluating and optimizing performance of the hydrogen fueling facility.

APPROACH

To enable effective data collection on the station performance, the team utilizes significant number of sensors and meters installed at the station. A software package has been developed to achieve maximum automation in data collection and reporting per NREL requirements.

As data is collected and analyzed for a period of time, the station performance will be evaluated for potential optimization and other technical enhancements. The goals would be to reduce maintenance cost, reduce hydrogen costs and improve user experience.

RESULTS

As part of the project, a large number of meters and sensors were installed throughout the station, see Figure 1. They were calibrated and wired into the programmable logic controller equipment. The data is stored into a Microsoft SQL database that can be quarried for reports per time periods and per meter of interest including populating the NREL quarterly reports and other research sub-projects, see Figure 2.

CONCLUSIONS AND FUTURE DIRECTIONS

The project has achieved the goals set for its first phase to complete data acquisition and enable report generation. In addition, most of the individual equipment is power metered allowing further research into performance efficiency not only of the entire facility but also its equipment.

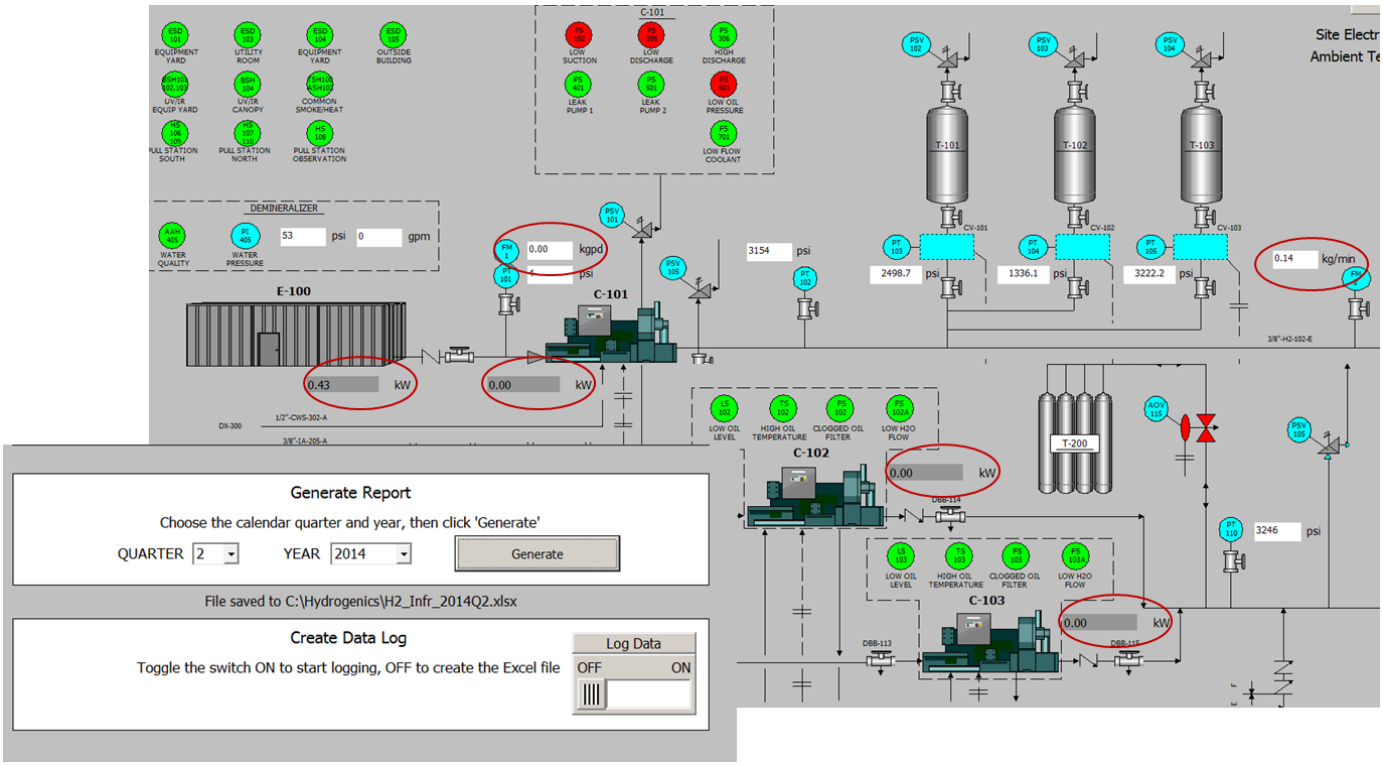

FIGURE 1. One of the Programmable Logic Controller Station Interfaces with New Meters (Circled Red) and the Screen with Report Generation Request

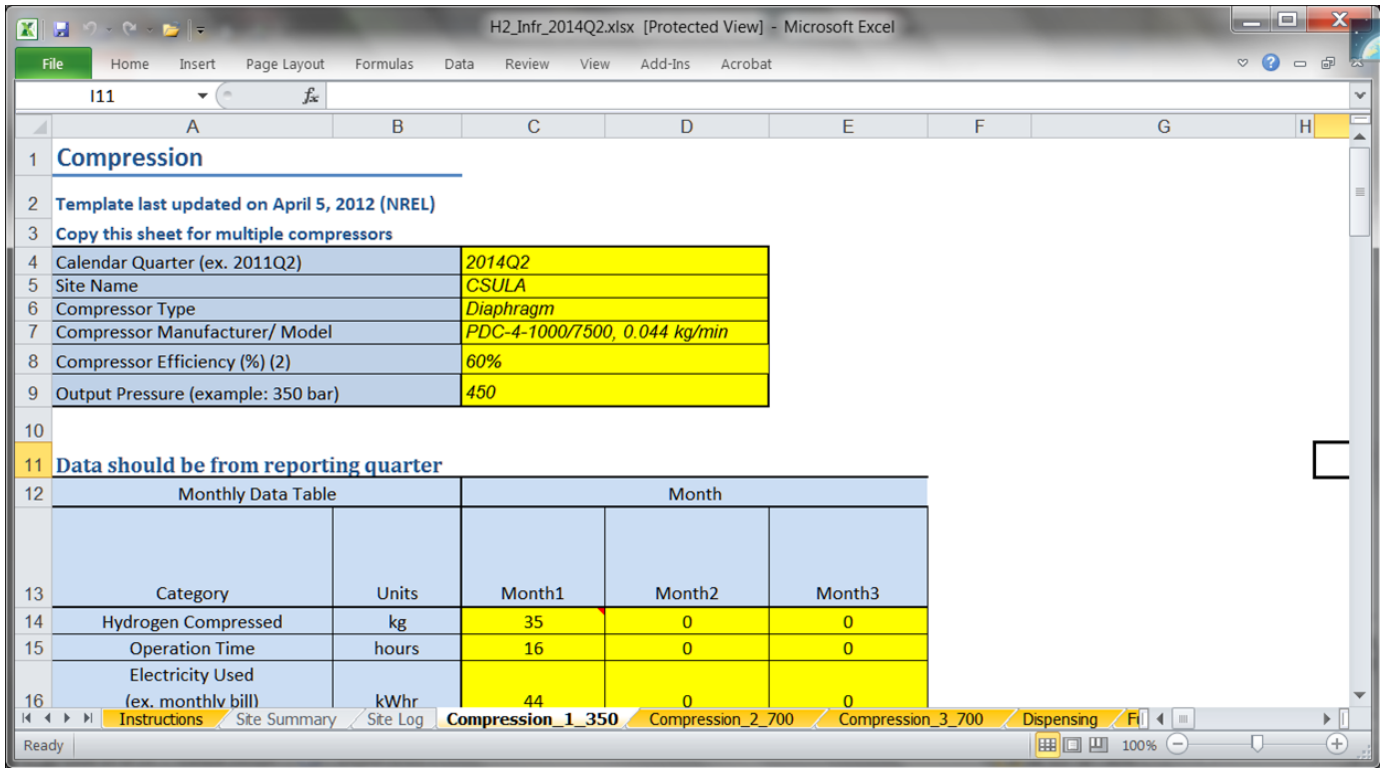

FIGURE 2. Example of an NREL Report with Multiple Tabs Populated Automatically

VII.11 Performance Evaluation of Delivered Hydrogen Fueling Stations

Mike Tieu
Gas Technology Institute (GTI)
1700 S Mt. Prospect Rd.
Des Plaines, IL 60018
Phone: (847) 768-0940
Email: michael.tieu@gastechnology.org

DOE Managers
Jason Marcinkoski
Phone: (202) 586-7466
Email: Jason.Marcinkoski@ee.doe.gov
Jim Alkire
Phone: (720) 356-1426
Email: James.Alkire@ee.doe.gov

Contract Number: DE-EE0005886

Subcontractor
Linde Gas LLC, Heyward, CA

Project Start Date: March 1, 2013
Project End Date: March 31, 2017

Overall Objectives

- Integrate non-intrusive data collection systems at five 100-kg/day delivered liquid hydrogen fueling stations located in California for 24-month performance period.
- Submit complete sets of the National Renewable Energy Laboratory (NREL) Hydrogen Station Data Templates to the National Fuel Cell Technology Evaluation Center (NFCTEC).
- Provide useful data to accurately benchmark and characterize station capacity, utilization, maintenance, and safety.

Fiscal Year (FY) 2014 Objectives

- Complete station assessments to confirm station sites and subsequent designs are adequate to ensure project deliverables are achievable.
- Complete engineering design review and data collection system design (mechanical, electrical, and software development) for first two station locations.
- Procure materials. Assemble and test system prior to deployment.
- Install and retrieve data of the first two project sites before the end of the year.

Technical Barriers

- Unforeseen construction permitting issues experienced by station developer.
- General construction delays experienced by the station developer.
- Efficient communications performance between GTI data collection equipment and functioning station equipment inherent to the stations' operations.

This project addresses the following technical barriers from the Technology Validation section of the Fuel Cell Technologies Office Multi-Year Research, Development, and Demonstration Plan:

(A) Lack of Fuel Cell Electric Vehicle and Fuel Cell Bus Performance and Durability Data

(D) Lack of Hydrogen Refueling Infrastructure Performance and Availability Data

This project will contribute to the achievement of the following milestones from the Technology Validation section of the Fuel Cell Technologies Program Multi-Year Research, Development, and Demonstration Plan:

- Milestone 3.2: Validate novel hydrogen compression technologies or systems capable of >200 kg/day that could lead to more cost-effective and scalable (up to 500 kg/day) fueling station solutions for motive applications (4Q, 2014). The stations currently being constructed will incorporate Linde's patented ionic fluid compressor. This technology utilizes a liquid piston to compress gas rather than a diaphragm or metal piston used in conventional compressor technologies. Linde is optimistic that this technology can be cost-effectively scaled to larger capacity stations in the future.
- Milestone 3.4: Validate station compression technology provided by the delivery team (4Q, 2018). (See Milestone 3.2)
- Milestone 3.8: Validate reduction of cost of transporting hydrogen from central production to refueling sites to <$0.90/gallon gasoline equivalent (4Q, 2019). This project will yield data directly aiding to develop baseline benchmarking and measure improved cost of delivery of liquid hydrogen to fueling stations in California.
- Milestone 4.4: Complete evaluation of 700-bar fast-fill fueling stations and compare to SAE International (SAE) J2601 specifications and DOE fueling targets (3Q, 2016). This project will supply data to the NFCTEC that aid the program in the characterization of the stations' storage and delivery capacities, compression performance, fueling transactional data, operational cost, maintenance,

and safety. Data supplied will provide points of direct comparison to SAE fueling standards and DOE fueling targets.

FY 2014 Accomplishments

- Initiated and completed a no-cost time extension in order to reflect delays in construction experienced by the California Energy Commission (CEC) project funding.
- Station assessments were completed for the first two fueling station locations. The assessments produced confirmation to the project team that a data collection plan with multiple options to achieve project objectives was feasible.
- Engineering design review and data collection system design (mechanical, electrical, and software development) was completed.
- Materials were procured. Data collection system assembly and system testing was completed prior to deployment.
- The additional three stations within project scope have been awarded to Linde by the CEC. Final approval of funding allocation is expected in the third quarter of 2014.

INTRODUCTION

The objective of this project is to collect, organize, and report on operational, transactional, safety, and reliability data for five hydrogen fueling stations located in California. Goals of the project are as follows. 1) The data collected will be statistically meaningful and the stations will have sufficient throughput and vehicle fueling frequency to minimize data aberrations. 2) The data collected will be accurate. 3) The data collected will be comprehensive and timely.

This project will directly assist the DOE in assessing the readiness level of current infrastructure and state-of-the-art technologies utilized to support planned fuel cell vehicle deployment within the next five years. The data and observations collected during the performance period of this project will provide NREL with information detailing the operational costs, efficiencies, and reliability of the delivered hydrogen fueling station design. Furthermore, the Linde design utilizes the patented IC90 ionic fluid compressor package; through this project GTI will provide the performance data which will enable the DOE and original equipment manufacturer to evaluate re-world efficiencies further gauging the technology's adequacy in this application. This system is a first of its kind utilized for hydrogen fueling applications in the United States.

APPROACH

Hydrogen station data will be submitted quarterly to the NFCTEC at NREL using the appropriate hydrogen station data templates. GTI's project partner, The Linde Group, is currently developing delivered hydrogen fueling stations under programs sponsored by the CEC. The sites will be accessible to the public for fueling consumer fuel cell vehicles, commercial vehicles, or government-owned vehicles. All five of the sites will be developed at existing or at new sites along with conventional gasoline stations operated by major, branded fuel providers. This provides the project with vehicle fueling data from a broad, cross-section of "real-world" vehicle applications. The station sites were selected to provide convenient, consumer-friendly vehicle fueling for drivers of fuel cell vehicles. Development of each of these stations has the support of vehicle original equipment manufacturers and each site has passed stringent location selection requirements of the CEC to ensure the stations will be utilized by a high volume of fuel cell vehicle operators.

The data collection system will utilize a variety of methods in order to provide the entire data requirements set forth by NREL. This system will utilize the existing control architecture of the compressor and dispenser equipment as well as monitor and record signals from a set of installed instrumentation that will supplement information required that is not already captured inherently by the stations' operating system. There are multiple descriptive (opposed to measured data) deliverables that will be taken "manually" and submitted to GTI for processing and formatting prior to delivery to NREL. Manually collected data templates include:

- NREL Site Log: recording safety drills, training, or public meetings
- Storage & Delivery: compiling liquid hydrogen supplies delivery quantities and cost
- Fuel Log: transferring transactional data from monthly reports emanating from fuel management system
- Maintenance: station maintenance and operations reporting
- Hydrogen Cost: Collection of utility bills
- Safety: station environmental, health, and safety reporting
- Hydrogen Quality: SAE quality analysis completed annually and submitted

GTI will collaborate with Linde and create a reporting/submittal process to collect this type of data required to populate the NREL templates.

RESULTS

The project team's efforts in 2014 yielded an encouraging path forward that will enable the team to make

meaningful contributions to program objectives. The group has reviewed and verified the feasibility of extracting all the data required to complete technology validation of delivered hydrogen stations. Table 1 shows the accumulation of data signals identified as a result of engineering drawing reviews and discussion with project partners.

TABLE 1. Electrical Signal Input List for Delivered Hydrogen Fueling Station

Instrument Tag	Location	Signal Type	Range	Channel	Triggering	Instrument Description	Installation
LT-85-1-B	Liquid Hydrogen Level	Analog	4-20 mA	ILIM-7_0A	10 min	Endress Hauser, PMD55, differential pressure transmitter, 0 - 40" water column range.	This is an existing piece of instrumentation, the signal can be shared by Linde and GTI through a signal isolation board.The isolation board would be installed inside the Tel-Tank Enclosure located in the communications panel on site.
FT-1	Flow Meter Located on Inlet Piping	Analog	4-20 mA	ILIM-7_0B	1 sec (During operation) else 5 min	Sierra Meters, Quadra Therm 780 i, inline thermal mass flow meter, max flow: 40 kg/hr.	Device to be installed at inlet, meter would be purchased by GTI and installed inside the IC90 compressor enclosure by located in DWG #: 12406-T-D-102-01 by GTI in the field.
FT-1	Flow Meter Located on Inlet Piping	Pulse	VDC	DI-A	1 sec (During operation) else 5 min	Sierra Meters, Quadra Therm 780 i, inline thermal mass flow meter, max flow: 40 kg/hr.	See above
FT-301	Flow Meter Located on 350 -700 Bar Dispenser Line	Quantum PLC	SCADA		1 sec (During fueling) else...	By Quantum	This is an existing piece of instrumentation, the signal can be shared by Linde through the web based SCADA system installed by the dispenser manufacturer.
CT-1	Current Transmitter-IC90 Compressor	Analog	4-20 mA	ILIM-7_0E	1 sec (During operation) else 5 min	Powertek, RCTrms, rogowski coil current transducer,0- 250 Amp range.	The current transducer would be purchased by GTI and installed by GTI on-site inside a pressurized enclosure. GTI has shown this transducer in the IC90 enclosure in DWG#: 12406-T-D-102-01.
CT-2	Current Transmitter-Dispenser	Analog	4-20 mA	ILIM-7_0F	1 sec (During oepration) else 5 min	CR Magnetics, Split Core current transducer, 0-20 Amp range.	The current transducer would be purchased by GTI and installed by GTI on-site into a pressurized enclosure. GTI has shown this transducer in the Dispenser enclosure in DWG#: 12406-T-D-104-01.
CT-3	Current Transmitter-Refrigeration Loop	Analog	4-20 mA	ILIM-7_0G	1 sec (During operation) else 5 min	Powertek, RCTrms, rogowski coil current transducer,0- 50 Amp range.	The current transducer would be purchased by GTI and installed by GTI on-site inside a pressuized enclosure. GTI has shown this transducer in the IC90 enclosure in DWG#: 12406-T-D-102-01.
CT-4	Current Transmitter-Refrigeration Loop	Analog	4-20 mA	ILIM-7_0H	1 sec (During operation) else 5 min	Powertek, RCTrms, rogowski coil current transducer,0- 10 Amp range.	The current transducer would be purchased by GTI and installed by GTI on-site inside a pressuized enclosure. GTI has shown this transducer in the IC90 enclosure in DWG#: 12406-T-D-102-01.
TE-1	Ambient Temperature	Thermocouple	Type T	AI-A	10 min	Smart Sensor, type T thermocouple, -328 to 662 deg F range.	The thermocouple would be purchased by GTI and installed by GTI in GTI panel. GTI has shown this temp element in the GTI enclosure in DWG#: 12406-T-D-104-01.
TS-302	Pre-Cool Hydrogen Temperature (HE0XX-Outlet)	Quantum PLC	SCADA		1 sec (During fueling) else...	By Linde	This is an existing piece of instrumentation, the signal can be shared through web based SCADA link.
TS-312	Pre-Cool Hydrogen Temperature (350 Bar-Outlet)	Quantum PLC	SCADA		1 sec (During fueling) else...	By Linde	This is an existing piece of instrumentation, the signal can be shared through web Ibased SCADA ink.
TT-3	Pre-Cool Hydrogen Temperature (HE092-Outlet)	Thermocouple	Type T	ILIM-7_0C	1 sec (During fueling) else 5 min	Honeywell, STT173, temperature transmittter, -328 to 662 deg F programmed range.	The thermocouple would be purchased by GTI and installed by GTI on-site. GTI request that Linde contractors provide taps to install instrumentation. GTI has shown this temp element in the field tubing in DWG#: 12406-T-D-104-01.
TT-4	Hydrogen Temperature (HE092-Inlet)	Analog	4-20mA	ILIM-7_0D	1 sec (during fueling) else 5 min	Honeywell, STT173, temperature transmittter, -328 to 662 deg F programmed range.	The thermocouple would be purchased by GTI and installed by GTI on-site. GTI request that Linde contractors provide taps to install instrumentation. GTI has shown this temp element in the IC90 Compressor Enclosure in DWG#: 12406-T-D-103-02. The first two units will be surface mounted and covered by pipe insulation/wrap.
PT-50A20PT026	Pressure Storage Vessel 1	Quantum PLC	SCADA		1 sec (During fueling) else...	By Linde	This is an existing piece of instrumentation, the signal can be shared by Linde through the web based SCADA system installed by the dispenser manufacturer.
PT-50B20PT026	Pressure Storage Vessel 2	Quantum PLC	SCADA		1 sec (During fueling) else...	By Linde	This is an existing piece of instrumentation, the signal can be shared by Linde through the web based SCADA system installed by the dispenser manufacturer.
PT-50C20PT026	Pressure Storage Vessel 3	Quantum PLC	SCADA		1 sec (During fueling) else...	By Linde	This is an existing piece of instrumentation, the signal can be shared by Linde through the web based SCADA system installed by the dispenser manufacturer.
PT-311	Pressure Transmitter-350 Bar Side	Quantum PLC	SCADA		1 sec (During fueling) else...	By Linde	This is an existing piece of instrumentation, the signal can be shared by Linde through the web based SCADA system installed by the dispenser manufacturer.
PT-302	Pressure Transmiter - 700 Bar Side	Quantum PLC	SCADA		1 sec (During fueling) else...	By Linde	This is an existing piece of instrumentation, the signal can be shared by Linde through the web based SCADA system installed by the dispenser manufacturer.

The data collection plan, system design, and software developed during FY 2014 will be used as a template for all subsequent station installations for the remainder of the project. The team's front-end development efforts will ensure a standardized system can be utilized through the duration of the project performance period. Figure 1 depicts the software programming that is utilized in order to program the data loggers to collect and automatically store data in remote servers for further analysis. Standardization of the design should decrease time and resources spent fabricating and deploying the systems while allowing the team to focus on the quality and completeness of data submitted to the NFCTEC. Figure 2 shows the standardization of project team design by making a side by side comparison of conceptual to actual data collection modules.

Furthermore, the project team has secured funding for the remaining sites listed in the project's scope of work. This ensures that the amount of data flowing into the data center is an adequate and appropriate representation of the delivered hydrogen station design methodology. Geographic diversity and multiple locations should provide an aggregate representation of the stations' performance and operational characteristics. The additional funding allocated to Budget Period 2 will enable the team to obtain and supply the database with accurate representation and characterization of the readiness of delivered hydrogen methodology as a vehicular fuel supply.

CONCLUSIONS AND FUTURE DIRECTIONS

- Installation and commissioning of the first station system will occur in the third quarter of 2014 at West Sacramento, CA site location.
- Installation and commissioning of the second system will occur in the fourth quarter of 2014 at San Juan Capistrano, CA site location.
- Produce the complete sets of data for the first two project sites at the end of each quarter after startup and commissioning is completed.
- Obtain approval to continue project efforts into Budget Period 2.

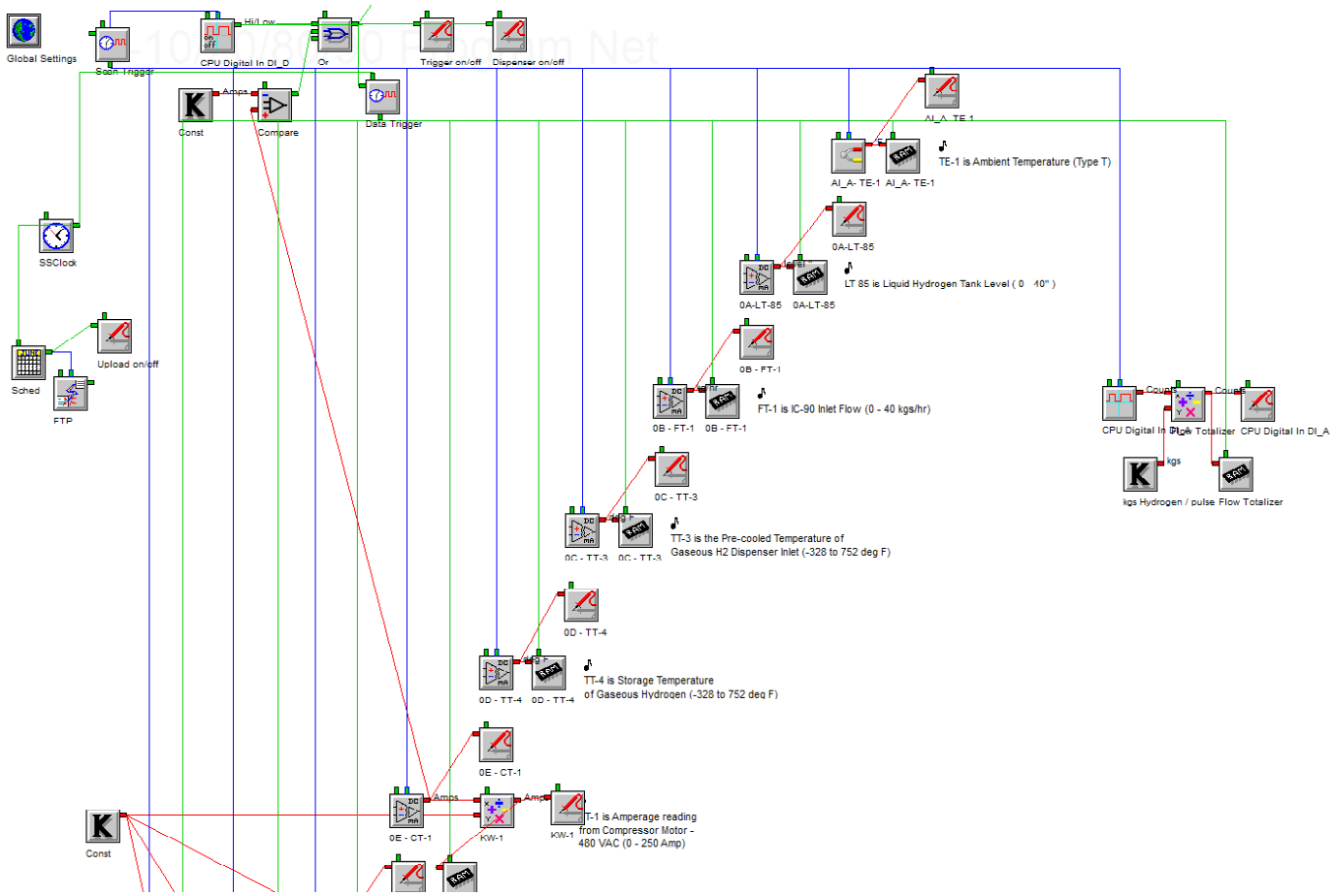

FIGURE 1. Logic Beach Hyperware Software Programming

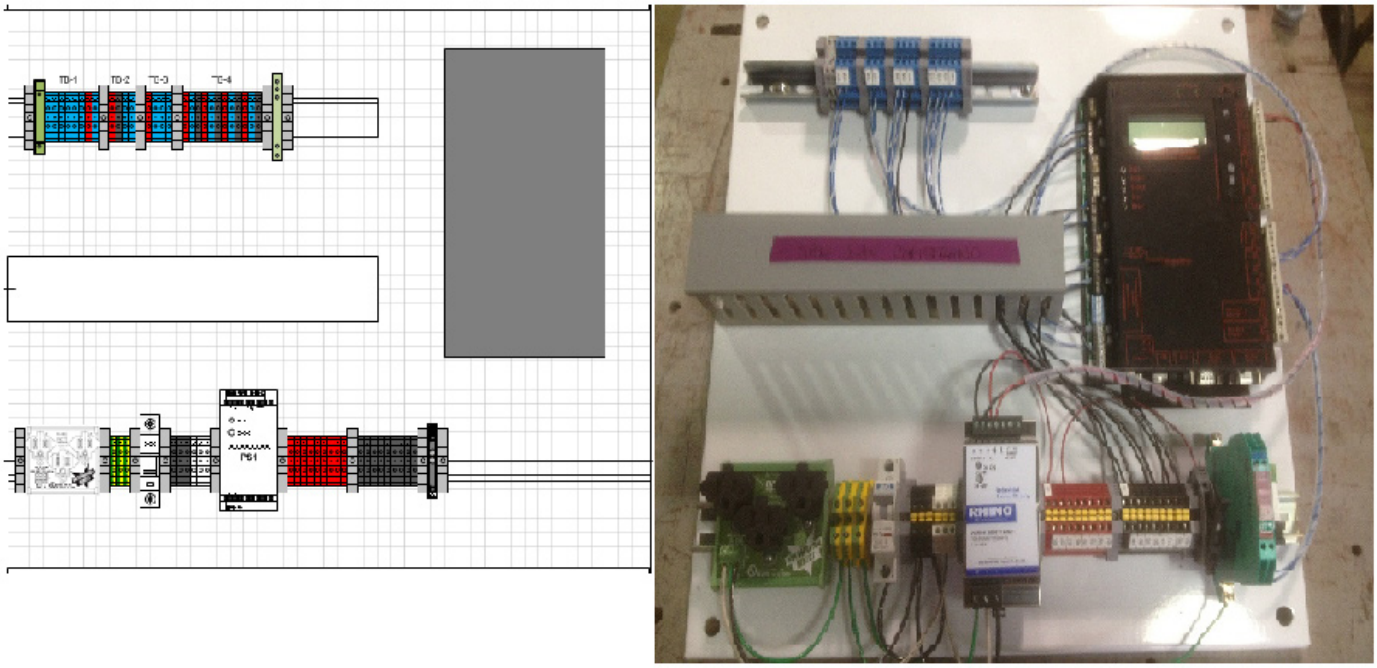

FIGURE 2. Conceptual (Left) and Actual (Right) Hardware

FY 2014 PUBLICATIONS/PRESENTATIONS

1. tv025_tieu_2014_o.pptx – Oral Presentation 2014 AMR.

VII.12 Hydrogen Fueling Infrastructure Research and Station Technology

Brian Somerday (Primary Contact), Jennifer Kurtz[1]
Sandia National Laboratories (SNL)
PO Box 969
Livermore, CA 94550
Phone: (925) 294-3141
Email: bpsomer@sandia.gov
[1]National Renewable Energy Laboratory (NREL)

DOE Manager
Jason Marcinkoski
Phone: (202) 586-7466
Email: Jason.Marcinkoski@ee.doe.gov

Project Start Date: March 2014
Project End Date: Project continuation and direction determined annually by DOE

Overall Objectives

- Reduce the installation cost of hydrogen fueling stations to be competitive with conventional liquid fuel stations
- Improve the availability, reliability, and cost while ensuring the safety of high-pressure components
- Focus a flexible and responsive set of technical experts and facilities to help solve today's urgent challenges and the unpredicted needs
- Enable distributed generation of renewable hydrogen in a broader energy ecosystem

Fiscal Year (FY) 2014 Objectives

- Establish relationship structure between Hydrogen Fueling Infrastructure Research and Station Technology (H2FIRST) and hydrogen fueling station technology stakeholders (e.g., industry, state agencies)
- Coordinate capabilities between NREL and SNL for effective application in R&D activities
- Commence work on reference station design activity to show trade-offs between component selection and design by identifying gaps and generating example designs through industry feedback and modeling
- In cooperation with technology stakeholders, form project teams focused on high-priority technical needs with aim of initiating R&D activities

Technical Barriers

This project addresses the following technical barriers from the Technology Validation section of the Fuel Cell Technologies Office Multi-Year Research, Development, and Demonstration Plan:

(C) Hydrogen Storage

(D) Lack of Hydrogen Refueling Infrastructure Performance and Availability Data

(E) Codes and Standards

This project addresses the following technical barriers from the Hydrogen Delivery section of the Fuel Cell Technologies Office Multi-Year Research, Development, and Demonstration Plan:

(B) Reliability and Costs of Gaseous Hydrogen Compression

(K) Safety, Codes, and Standards, Permitting

This project addresses the following technical barriers from the Hydrogen Safety, Codes, and Standards section of the Fuel Cell Technologies Office Multi-Year Research, Development, and Demonstration Plan:

(A) Safety Data and Information: Limited Access and Availability

(C) Safety is Not Always Treated as a Continuous Process

(G) Insufficient Technical Data to Revise Standards

Contribution to Achievement of DOE Delivery, Technology Validation, and Safety, Codes and Standards Milestones

This project will contribute to achievement of the following DOE milestones from the Technology Validation and Safety, Codes and Standards sections of the Fuel Cell Technologies Office Multi-Year Research, Development, and Demonstration Plan:

- Technology Validation Milestone 3.2: Validate novel hydrogen compression technologies or systems capable of >200 kg/day that could lead to more cost-effective and scalable (up to 500 kg/day) fueling station solutions for motive applications. (4Q, 2014)
- Technology Validation Milestone 3.4: Validate station compression technology provided by delivery team. (4Q, 2018)
- Technology Validation Milestone 4.4: Complete evaluation of 700-bar fast fill fueling stations and compare to SAE J2601 specifications and DOE fueling targets. (3Q, 2016)
- Safety, Codes and Standards Milestone 2.19: Validate inherently safe design for hydrogen fueling infrastructure. (4Q, 2019)

- Safety, Codes and Standards Milestone 3.3: Reduce the time required to qualify materials, components, and systems by 50%, relative to 2011) with optimized test method development. (1Q, 2017)
- Hydrogen Delivery Milestone 2.8: By 2015, reduce the cost of hydrogen delivery from the point of production to the point of use for emerging regional consumer and fleet vehicle markets to <$4/gge. (4Q, 2015)

FY 2014 Accomplishments

- Designed and released a request for quotation for the procurement of a hydrogen station equipment performance (HyStEP) testing device.
- Simulated over 100 station concepts through the H2A Refueling Station Analysis Model. The station parameters included design capacity, peak performance, number of hoses, fill configuration, and hydrogen delivery method. The simulation output includes fuel cost, capital cost, and return on investment and is used to support the future work of selecting and fully defining 3–5 reference stations.
- Gathered information to support draft requirements for an in-line hydrogen contaminant detector. Environmental requirements (e.g. temperature, pressure, and location) and contaminant requirements (e.g. likely contaminants from production techniques, process upsets, and maintenance activities) are considered.
- Established H2FIRST Coordination Panel, populated from the H2USA Hydrogen Fueling Station Working Group, to:
  - Provide industry perspective on R&D needs to support hydrogen infrastructure growth
  - Perform bi-yearly reviews of the H2FIRST project progress and impact
  - Identify potential project partners
  - Participate as project partners
  - Providing feedback to H2FIRST principal investigators on the impact of H2FIRST projects relative to H2FIRST goals and objectives
- Coordinated expertise and capabilities at the National Renewable Energy Laboratory and Sandia National Laboratories through a Memorandum of Understanding between the two institutions to address the technology challenges related to hydrogen refueling stations.
- Identified high-priority and near-term technical activities and formed project teams with industry and state agencies to support them. Formed five initial project activities and teams that included:
  - Station Acceptance: accelerate station acceptance by developing, validating, and implementing test methods and hardware for capacity and performance testing of commercial hydrogen stations
  - Research Dispenser: reduce cost and improve reliability through component and fueling technique enhancements
  - Reference Stations: improve station components and design by identifying gaps and generating example designs through industry feedback and modeling
  - Technical Assistance: provide a flexible, responsive set of technical experts and facilities to solve urgent/unexpected challenges for hydrogen stations
  - Hydrogen Contaminant Detector: develop a cost effective, deployable, inline fuel quality system that can be installed at stations to prevent damage to fuel cell vehicles

Future Directions

- In reference station task, establish peer reviewed designs for three to five station types
- Initiate at least one R&D task from each identified priority area Station Acceptance, Research Dispenser, and Hydrogen Contaminant Detector teams
- Foster active collaboration between H2FIRST and other DOE projects
- Convene H2FIRST Coordination Panel at Fuel Cell Seminar (November 2014) to review H2FIRST tasks, provide feedback, and identify additional high-priority technical needs
- Complete the final validation of the HyStEP device prior to pre-deployment testing at a commercial station

Special Recognitions & Awards/Patents Issued

1. Jennifer Kurtz, DOE Hydrogen and Fuel Cells Program Awards, Technology Validation, 2014.

2. Brian Somerday and Chris San Marchi, DOE Hydrogen and Fuel Cells Program Awards, Hydrogen Delivery and Safety, Codes and Standards, 2014.

VII.13 Demonstration of SOFC Generator Fueled by Propane to Provide Electrical Power to Real World Applications

Norman Bessette
Acumentrics Corporation
20 South West Park
Westwood, MA 02090
Phone: (781) 461-8251
Email: nbessette@acumentrics.com

DOE Manager
Ned Stetson
Phone: (202) 586-9995
Email: Ned.Stetson@ee.doe.gov

Contract Number: DE-EE0000479

Project Start Date: May 15, 2013
Project End Date: June 30, 2014

Objectives

- Develop a 1,000-W Cart-Based Portable Generator (fueled by propane) for powering multi-camera sites and in-field auxiliaries
- Develop a 250-W Man-Portable Generator (fueled by propane) for powering single camera sites
- Deliver two 1,000-W and two 250-W Generators
- Demonstrate the unit at several NASCAR races

Relevance to the American Recovery and Reinvestment Act (ARRA) of 2009 Goals:

- This project provided job growth as well as reinforce high-tech engineering and technician jobs by expanding the product line of remote power solid oxide fuel cell (SOFC) units.
- This project helps the DOE meet its goals of emission reduction and widespread adoption of fuel cells as a viable commercial remote power product.
- This project is funding development activities that will lead to near-term commercialization of fuel cell technology in multiple applications where internal combustion engine-based generators have significant drawbacks.

Technical Barriers

This project addresses the following technical barriers for SOFCs outlined by the DOE:

- Specific power and energy density
- Transportability
- Use of commercially available fuel
- Improved ruggedness and shock and vibration capabilities

Technical Targets and Milestones

The following were the technical targets for the project:

- Demonstrate propane consumption at or below 2 lbs/10 hr operational period.
- Allow powering of television cameras for entire 4-day race period.
- Demonstrate near 50% reduction in volume and weight of present SOFC remote power product.

Accomplishments

During this abbreviated project the following accomplishments were achieved:

- A remote power 250-W (RP250) unit was designed, built, and tested with nearly 50% reduction in weight and volume.
- Two RP1000 and RP250 units were delivered to NASCAR for powering of television cameras.
- Operation of over 4 days on a single 20-lb propane bottle was demonstrated.
- Powering of multiple broadcast cameras was demonstrated with no resulting delays or interference in broadcast.

INTRODUCTION

Small gasoline generators tend to be noisy and low in efficiency with excessive emissions. In addition, they tend to have a low reliability which limits their effectiveness in powering the latest generation of high-tech equipment. A perfect example of such is the powering of broadcast cameras for NASCAR events held throughout the year. Presently, NASCAR has 38 races in a season where each race can require 30 cameras for broadcast which are presently powered by Honda gasoline generators. These generators are very inefficient and require frequent refueling throughout a race event making them both an environmental and safety risk.

Acumentrics Corporation, after years of support from the DOE, has been fielding remote power generators that are highly efficient and provide high power quality to power just such equipment. The challenge for the Acumentrics product is it normally is a stationary product and operates its entire life in one location. Likewise, the unit is somewhat large and heavy for a continual redeployment type of operation. This project demonstrated the advancements to overcome these two barriers and allow this product to now be deployed for more mobile applications.

APPROACH

This project was focused on size reduction and ruggedization of the existing Acumentrics remote power products which have been substantially supported by DOE over the years. The remote RP250 unit was put through the most aggressive redesign with a goal of nearly 50% in volume and weight. All components from balance of plant, electronics, and enclosure to fuel cell stack had to be considered. The design also had to be accommodating for a remote propane tank to allow for fueling at any NASCAR site as well as provide multiple electrical output connections and configurations.

The RP1000 unit had to be modified for trailer mount capability as well as onboard fuel storage. The unit required electrical changes as well as integration of a rugged uninterruptable power source to assure power to critical camera equipment was never compromised. Ease of onboard fuel change and refueling was also needed to be considered in the design as well as ease of transportability from one NASCAR race to another.

RESULTS

To achieve the desired replacement of gasoline generators for sensitive camera equipment at NASCAR events, the Acumentrics RP family of units needed to be redesigned and modified for size, weight, and ruggedness. This objective was achieved in slightly less than 12 months time with high satisfaction from NASCAR personnel. Figure 1 shows the resulting size of the new RP250 unit next to the older RP250 unit as well as the RP1000 unit.

Table 1 shows the resulting size and weight of each of the resulting units. As one can see, the RP250 lite (RP250L) is now 47% reduced in volume than its predecessor as well as 58% lighter. This reduction from 300 lbs to 127 lbs now allows it to fall into the two-man portable range as opposed to requiring some form of material handling equipment.

What is also worth noting is the comparison of size and weight of the RP250L to the incumbent unit utilized at races, the Honda 3000. The Honda 3000 has a volume of 17.5” x 21.9” x 25.8” or 5.72 cubic feet while the RP250L comes in at 20” x 15.5” x 32” or 5.74 cubic feet and therefore taking up the same volume. The weight of the Honda is 134 lbs while the RP250L comes in at 127 lbs or 5% less.

FIGURE 1. Size Reduction of the RP250L

TABLE 1. Size and Weight of RP Units

Model	L (in)	W (in)	H (in)	Wt(lbs)
RP250L	32	20	15.5	127
RP250	39	22	22	300
RP1000	39	28	25	350

Upon completion of the design and internal testing, the unit next needed to be demonstrated at a NASCAR event and proven to adequately power broadcast cameras. This was first demonstrated at a NASCAR event in January called the Rolex24 which is a 24 hour non-stop race. Figure 2 shows the unit in operation with a standard propane tank found on similar propane appliances. This unit powered the broadcast camera as well as the articulating arm at the end of the boom crane as well as an LCD display for the video operator. All associated in-rush currents as well as other transients were handled with ease and the operator never knew there was a different power source. The NASCAR operators were also impressed that when the noise died down on the race track they could not hear the generator and only knew they still had power by looking at their monitor screen.

After successfully demonstrated the capabilities of the unit at this race, the units were returned to Acumentrics and some minor modifications were made for mobility and transportability based on NASCAR recommendations. The units were then redeployed for what NASCAR calls their “speed weeks” which culminated in the racing of the Daytona 500 in late February. Figures 3 and 4 show the units in operation powering a camera high above the race track on the infield. During this two-week period all units deployed ran flawlessly with no interruptions in broadcasts.

FIGURE 2. Powering a Broadcast Camera at the Rolex24

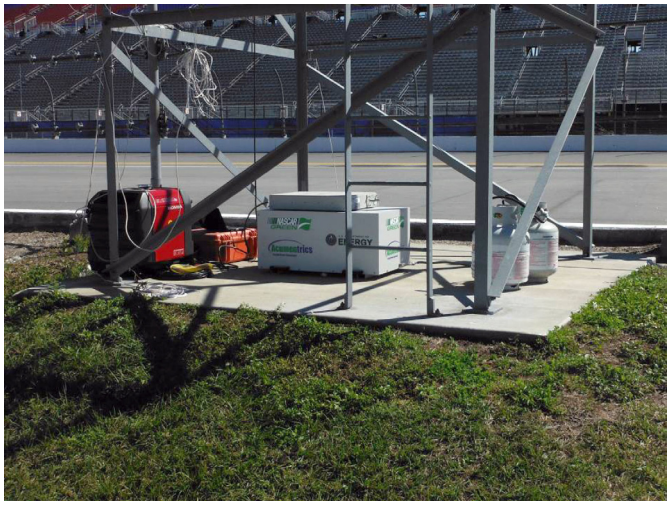

FIGURE 3. Daytona 500 Camera Power

Performance of these units was also exceptional and well above that achieved by the standard Honda 3000. During normal race events, staff are required to refuel each generator after every 4-5 hours during the day. Over a 4-day race period this can result in 8-10 total refuel calls on a fleet of up to 30 generators. These generators also consume over 20 gallons of gasoline each during that four day event. This results in a high price as well as safety concern considering the transport of gasoline in close proximity to spectators.

The RP250L gave NASCAR a huge increase in energy efficiency and emission reduction as well as reduced need for labor support. Each of these units demonstrated the capability to operate over 4-day race periods on a single 20-lb propane bottle normally seen on gas grills. This also allowed for fueling only at the start of the broadcast period and removal after the 4-day event. Considering just fuel costs, a fleet of

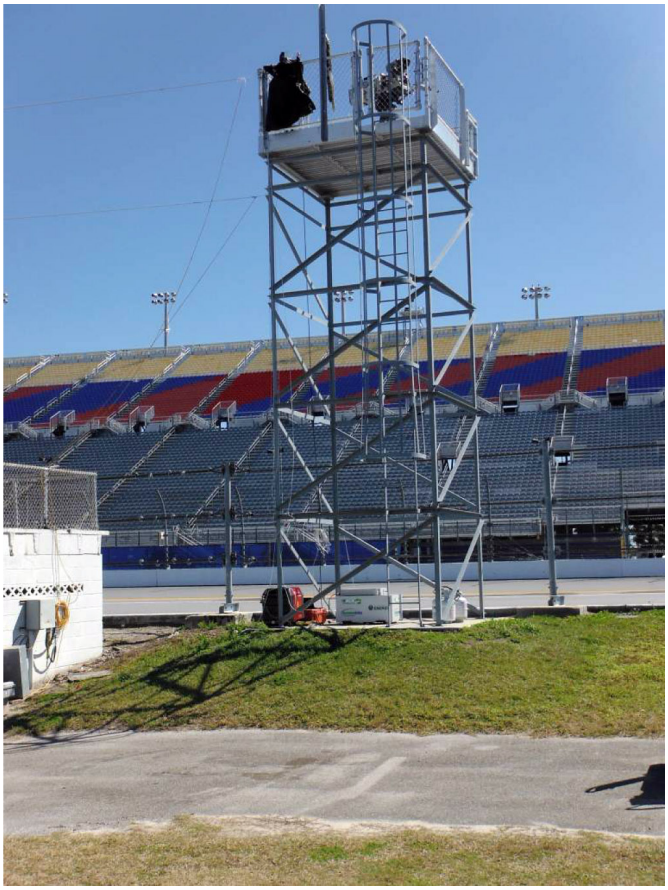

FIGURE 4. Daytona 500 Camera Power

30 units would consume close to $2,200 in gasoline for the Honda while only needing $150 of propane for the RP250L. This translates into close to $100,000 savings for a NASCAR Sprint series season.

This RP250L has now been added to the family of products offered by Acumentrics for remote power generation and is now being considered by those with mobile power needs as well as federal agencies involved in surveillance and monitoring.

CONCLUSIONS AND FUTURE DIRECTIONS

The newly re-designed Acumentrics remote power product has been successfully demonstrated to power sensitive broadcast equipment in real world conditions. Size and weight reductions have been realized as well as the specified fuel savings have been demonstrated. Future work would entail a more integrated fueling system as well as refinement of remote monitoring. Further data on market conditions and customer needs will drive refinement and sales in other remote power markets.

FY 2014 PUBLICATIONS/PRESENTATIONS

1. Demonstration of SOFC Generator Fueled by Propane to Provide Electrical Power to Real World Applications (AMR Presentation 6/19/2014).

VII.14 Accelerating Acceptance of Fuel Cell Backup Power Systems

Jim Petrecky
Plug Power
968 Albany-Shaker Road
Latham, NY 12110
Phone: (518) 817-9124
Email: James_Petrecky@plugpower.com

DOE Manager
Reg Tyler
Phone: (720) 356-1805
Email: Reginald.Tyler@ee.doe.gov

Subcontractor
IdaTech, Bend, OR

Project Start Date: June 2009
Project End Date: May 2014

Objectives

- Create new jobs as well as save existing ones; spur economic activity
- Accelerate the commercialization and deployment of fuel cells, fuel cell manufacturing, installation, maintenance, and support services
- Demonstrate market viability and increase market pull of fuel cell systems within our government customers/ partners

Relevance to the American Recovery and Reinvestment Act (ARRA) of 2009 Goals

- Jobs created at Plug Power including engineering, testing, sales, marketing, program management
- Commercialization and enablement of the fuel cell supply chain, including DANA, BASF, 3M, etc. as well as collaborations with other partners such as IdaTech and site installation support subcontractors
- Increased distributed power generation through the deployment of 20 GenSys systems
- Improved reliability and efficiency of mission critical backup power (>72 hours)
- Decrease fossil fuel dependencies for power generation

Technical Barriers

- Obtaining permitting from utility companies to operate fuel cells in a grid parallel (grid tied) configuration.

The following body of work was provided to the utility, however, the utility decided it was not sufficient.

  - Generating Facility Interconnection Application
  - Scope of Work for Fuel Cell Installation
  - Project Scope
  - Description of Work
  - Proposed Location and Build Layout
  - Concrete Pad Detail
  - Equipment Grounding Detail
  - Location of Fuel Cell Systems, Gas Piping, and Electrical Components
  - Site Electrical Wiring Diagram
  - Inverter Electrical Wiring Diagram
  - Equipment List and Specification
  - Contractor Requirements
  - Building Plans for Original Construction of Building (Host Site)
  - Map of Existing Renewable Energy Currently Installed at Host Base
  - Safety Plan and Emergency Procedure for GenSys Fuel Cell Fleet at Host Base

- The following was requested before permitting would be available:
  – Entire map of site host's interconnected generation–A complete and comprehensive single line diagram of the entire generating facility's electrical configuration will be required. This application requires substantially more detailed information to ensure compliance of all tariffs and standards.
  – Single Line Diagram—comprehensive diagram of the complete electrical configuration of the entire facility
  – Three Line Diagram—detailed protection study; phase and polarity identification
  – Elementary Diagram—comprehensive representation of the entire facility containing information of all components electrically connected
  – Plot Plan Drawing—needs update to include physical location and distances of all components
  – Relay Diagram—diagrams and written descriptions regarding protective relays that will be used to detect faults or abnormal operating conditions for distribution system

  - Proposed Relay Settings—demonstrate how the unscheduled and uncompensated export of real power from a generating facility for a duration exceeding two seconds but less than 60 seconds will be accomplished; for the proposed transfer switch, details to ensure that the automatic transfer switch and scheme comply with Rule 21 requirements
  - Relay test report will be required once the proposed relay settings have been reviewed and approved by protection engineering

Technical Targets and Milestones

- Install 20 fuel cells for backup power at two site hosts by September 2012
- Backup power >72 hours

Accomplishments

- Successful installation, commissioning, and decommissioning of the first fleet of 10 GenSys units at Site Host 1, resulting in the following metrics for backup power:
  - 13,506 operating hours
  - 39.07 MW-hr electricity produced
- A network outage simulation occurred at Site Host 1 on January 19, 2013. The fuel cells powered the lighting in the building without issue. The commercial utility power was turned off and within ~20 s, the relays transferred and lighting was restored by fuel cell system power. Network outage simulation was roughly 30 minutes.
- Successful installation, commissioning, and decommissioning of the first fleet of 10 GenSys units at Site Host 2, resulting in the following metrics for backup power:
  - 15,187 operating hours
  - 15.6 MWe-hr electricity produced
- A network outage simulation occurred at Site Host 2 on April 8. The fuel cells powered the lighting in the building without issue.

✧ ✧ ✧ ✧ ✧

INTRODUCTION

Extending the amount of backup power that is available to U.S. agencies provides flexibility to their emergency planning. If an outage occurs due to a natural disaster, for example, these agencies have more time to react to the issue at hand instead of applying resources to regaining power. The intent of this project is to demonstrate two fleets of backup power fuel cells as a validate solution for backup power requirements of greater than 72 hours.

APPROACH

The approach for extended backup is the merging of two Plug Power products—the GenCore and GenSys systems. By combining the field experience of the GenCore in backup applications with the long runtime of the GenSys system, extended backup is achieved, see Figure 1.

FIGURE 1. Approach

RESULTS

As outlined in the Accomplishment sections, the fleet of 10 GenSys units at Site Host 1 was successful in providing backup power and continuing to maintain power to the facilities through a network outage simulation.

A list of future work has been compiled based on the field experience in operating this micro fleet. This list includes the definition of failure modes, failure signatures/symptoms for future work to create early detection and recovery methods (Figure 2):

- Reactive Processing: Anode tailgas oxidizer timeout waiting for catalyst activation
- Controls and Electronics: Electronic board failures, some possible connection to software.
- Reactive Processing: Loss of fuel flow (related to flow meter/valve issues)
- Thermal Management: Coolant leak, loss of coolant
- Reactive Processing: Anode air pump failed to start, known issue
- Reactive Processing: Gas leak during commissioning

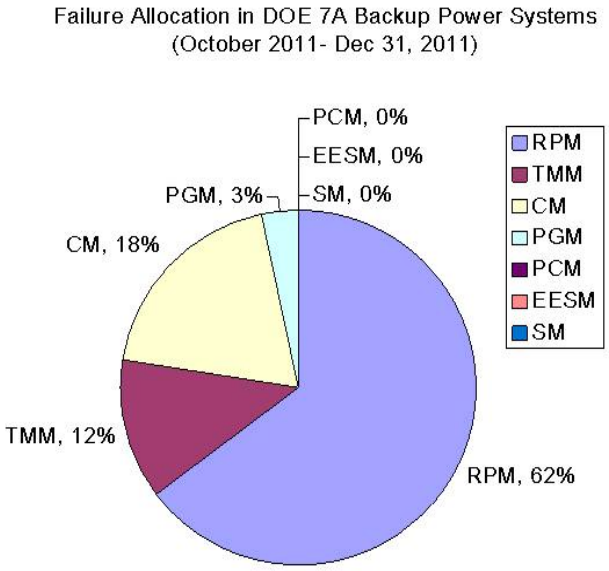

RPM - reactive processing; TMM - thermal management;
CM - controls & electronics; PGM - power generation; PCM - power controls;
EESM - electrical energy storage; SM - structure

FIGURE 2. Failure Allocation

- Controls and Electronics: Unknown, attributed to electronic boards
- Reactive Processing: Fuel flow issue with occasional dropout or flow spikes
- Power Generation Module: Max low cell trips, stack protection due to either CO or cell performance
- Reactive Processing: Desulfurization needed excessive time for conditioning/equilibration.
- Controls and Electronics: Firmware update and boot failure

CONCLUSIONS AND FUTURE DIRECTIONS

- Permitting is a case-by-case situation. Working with the utility for one site host was a straightforward process provided that the application requirements were met. Working with the utility for the second site host has been extremely problematic and has caused very significant delays. It is difficult to project the timing requirements for permitting, therefore future direction is to start the permitting process as soon as possible in any project.
- More charges may impact grid-parallel backup value propositions. Utilities are now charging a standby charge. The total line items of charges are as follows:
  - Customer Charge (flat)
  - Energy Charge—different rates for time of use (on peak, mid peak, off peak)
  - Demand Charge—related to the maximum amount of energy used
  - Standby Charge—"…represents the entire reserved capacity needed for SCE to serve the customer's load regularly served by the customer's generating facility when such facility experiences a partial or complete outage."
- This Standby Charge will likely affect the value propositions for backup, intermittent, or potentially other alternative power sources by adding another charge to what is expected to be removed from the grid.

FY 2014 PUBLICATIONS/PRESENTATIONS

1. H2RA007_PETRECKY_2014_o (Annual Merit Review).

VII.15 H2-FCEV Commercialization - Facilitating Collaboration, Obtaining Real World Expertise, and Developing New Analysis Tools

Bill Elrick (Primary Contact), Nico Bouwkamp
California Fuel Cell Partnership (CaFCP)
3300 Industrial Blvd., Suite 1000
West Sacramento, CA 95691
Phone: (916) 371-2870
Email: belrick@cafcp.org

DOE Manager
Jason Marcinkoski
Phone: (202) 586-7466
Email: Jason.Marcinkoski@ee.doe.gov

Project Start Date: January 1, 2012
Project End Date: December 31, 2016

Overall Objective

- Facilitate and support the early commercial market launch of fuel cell electric vehicles (FCEVs) in California (CA)
- Track, synthesize, analyze and report latest hydrogen infrastructure implementation progress and challenges
- Conduct regular stakeholder meetings to present and discuss challenges and progress in a collaborative manner
- Conduct education and outreach directly to conventional fuel providers via existing networks

Fiscal Year (FY) 2014 Objectives

- Increase participation in hydrogen-FCEV industry funding opportunities and activities
- Expand Station Operational System Status (SOSS) to a more capable platform to increase usability and early-customer confidence
- Include additional hydrogen stations in SOSS when these stations come online
- Complete a stakeholder-approved national emergency responder (ER) template to be used as guidance among U.S. Department of Energy and other ER activities
- Complete "train-the-trainer" outreach to successfully initiate the national ER template

Technical Barriers

This project addresses the following technical barriers from the Technology Validation, Education and Outreach, and Market Transformation sections of the Fuel Cell Technologies Office Multi-Year Research, Development, and Demonstration Plan:

Technology Validation

(D) Lack of Hydrogen Refueling Infrastructure Performance and Availability Data

(E) Codes and Standards

Education and Outreach

(A) Lack of Readily Available, Objective, and Technically Accurate Information

(C) Disconnect Between Hydrogen Information and Dissemination Networks

Market Transformation

(A) Inadequate standards and complex and expensive permitting procedures

(D) Market uncertainty around the need for hydrogen infrastructure versus timeframe and volume of commercial fuel cell application

FY 2014 Accomplishments

Collaboration and Communication

- Integrated Station Profiles, Station Report Cards and other reports into a new Hydrogen Station *Smartsheet*, used by California Governor's Office of Business and Economic Development (GO-Biz) Zero Emission Vehicle Infrastructure Project Manager to track progress of all state-funded hydrogen station development—which serves car manufacturers with coordinating the rollout of FCEVs, state agencies with assessing progress for future actions, and educating all stakeholders.
- Facilitated extensive discussions within CaFCP meetings and among industry stakeholders on CA funding programs, station development, implementation progress, challenges and needs, leading to improved request for proposal requirements that increasingly align with FCEV fueling performance requirements, future infrastructure needs and customer needs.

Conventional Fuel Provider Engagement

- Developed new "Stations" micro-site to meet (indicated) informational needs of fuel retailer/marketer community: http://cafcp.org/toolkits/stations
- Based on CaFCP input, the National Association of Convenience Stores (NACS)/Fuels Institute published an

article in NACS/FI Magazine titled "No Longer a Pipe Dream", August 2013 edition

- Exhibited at Western Petroleum Marketers Association Conference, February 2014
- Presented on CA FCEVs and hydrogen infrastructure progress, exhibited, and conducted FCEV ride-n-drive at Society of Independent Gasoline Marketers of America Spring Conference, April 2014
- Exhibited at Pacific Oil Conference, September 2013
- Presented on CA FCEVs and hydrogen infrastructure progress at Fuels Institute, April 2014.

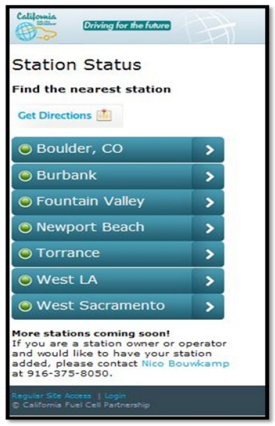

FIGURE 1. SOSS 2.0 Interface

- Conducted one-on-one hydrogen and FCEV educational meetings with ~25 regional fuel retailers and marketers
- Facilitated stakeholder response to CA hydrogen infrastructure funding through industry outreach and discussions; with 10 different companies submitting responses for 61 different station applications (versus four companies submitting nine station applications in previous solicitation)

Consumer Confidence and FCEV Usability

- Two new stations were added to SOSS—Emeryville and Richmond
- Secured strong automaker interest to accelerate and expand original SOSS statement of work and timeline

National Emergency Response Program

- Completed draft national ER training outline, including concept buy-in of major industry stakeholders
- New hydrogen-FCEV online training module added to National Fire Protection Association website, in collaboration with national outline project
- Developed new "Fire and Safety" micro-site for first responder community to meet informational needs: http://cafcp.org/toolkits/safety

INTRODUCTION

The CaFCP has worked since 1999 to bring together all stakeholders involved in the introduction of FCEVs in the market and facilitate collaboration between these. Through this collaboration, outreach communications have been be harmonized, interested conventional industry stakeholders became directly engaged, consumers were educated about FCEV and hydrogen technologies, and emergency responders became better informed in their efforts to provide emergency response services.

APPROACH

As a public/private stakeholder group, the CaFCP approach is to leverage active participation and commitment from all sectors to advance hydrogen-FCEV commercialization.

- Collaboration and Communication Tools
  - Support shortening the implementation timeline for hydrogen stations based on conclusions drawn from average station implementation progress reported in the CA station *Smartsheet*
- Directly Engage Conventional Fuel Providers
  - Conduct hydrogen-FCEV education and outreach
  - Increase conventional fuel provider participation in hydrogen-FCEV station development, solicitations, stakeholder discussions and industry activities
- Increase Consumer Confidence and FCEV Usability
  - Expand and upgrade SOSS to become more capable and user-friendly
  - Include new hydrogen stations when online, to increase customer satisfaction with FCEVs
- Establish a Harmonious National ER Program
  - Develop a stakeholder-based national ER outline and share this with national entities involved in recommendations for ER training programs' curriculum
  - Complete "train-the-trainer" outreach to initiate program

RESULTS

- Project reporting documents used by lead CA agency as basis for new station status and tracking *Smartsheet*
- Leveraged both CaFCP member and larger stakeholder meetings to facilitate collaborative discussion and progress leading to better aligned request for proposal station funding requirements for station infrastructure rollout

- Successfully reached conventional fuel retailers and marketers via four major industry conferences, with led to an interest in participating in the hydrogen FCEV industry
- 2014 California station funding solicitation saw 2.5x more respondents applying for over 6x more station projects compared to the 2013 solicitation
- Developed targeted micro-websites for fuel retailer/marketer and fire/safety market stakeholders
- Added two additional hydrogen stations to SOSS
- Completed initial draft of national emergency response outline with buy-in from the primary industry stakeholders

CONCLUSIONS AND FUTURE DIRECTIONS

Significant progress has been achieved through expanded collaboration and communication across market segments, resulting in announcements by multiple car manufacturers about availability of their FCEVs to consumers. Conventional fuel providers are becoming increasingly more involved and aware, and consumers starting to see the expansion of the number of hydrogen stations. At a national level, emergency response organizations recognized the need for a cohesive and comprehensive training guidance. To continue the progress made towards the full commercialization of FCEVs in the market, more work needs to be done, as summarized in the following list of activities.

- Continue updates and further refinement of industry and station reports, including new hydrogen station *Smartsheet* – to continue coordination of FCEV manufacturer rollout strategy and work towards shortening the implementation timeline of hydrogen stations. Expand usage and awareness of *Smartsheet* to enable broader stakeholder use and value.
- Continue direct outreach to fuel retailers and marketers
  - Support NACS/Fuels Institute concept proposal to develop hydrogen-FCEV industry review related to retail fuels market (Fall 2014)
  - Leverage Los Angeles location of Pacific Oil Conference for extensive hydrogen and FCEV sessions, ride-n-drive, etc (September 2014)
    - Present at future fuel provider industry events to inform conventional gasoline station operators about hydrogen as a fuel; NACS (October 2014), Western Petroleum Marketers Association (February 2015), Society of Independent Gasoline Marketers of America Spring conference (date to be determined)
- Add all recently funded CA hydrogen stations (seven in 2013, 28 in 2014) to SOSS when online
  - Work with stakeholders to upgrade SOSS platform from SOSS 2.0 (station-to-station set of assumptions/definitions) to SOSS 3.0 in which all station operators provide station information based on the same set of assumptions/definitions
- Work with ER stakeholders to complete the national emergency response outline
  - Present concept at National Fire Protection Association conference (June 2014), Continuing Challenge (September 2014), and Corona Auto-X (April 2015)
  - Conduct "train-the-trainer" sessions using the consensus national outline content
  - Conduct annual assessment and review of national program(s) to evaluate existence and consistency of content about hydrogen and FCEVs.
  - Support DOE efforts to expand use of the national emergency response outline as the source of authority on the subject, including annual reviews to expand value.

FY 2014 PUBLICATIONS/PRESENTATIONS

1. "Stations" micro-site for fuel retailer/marketer community http://cafcp.org/toolkits/stations.

2. "Fire and Safety" micro-site for first responder community http://cafcp.org/toolkits/safety.

3. Fuels Institute article "No Longer a Pipe Dream" in August 2013 NACS Magazine: http://www.nacsonline.com/magazine/PastIssues/2013/August2013/Pages/Feature10.aspx.

4. Station Profiles (September/ December 2013, March / May 2014) http://cafcp.org/sites/files/20140211_H2-Station-profiles.pdf.

5. "Input on the DRAFT Solicitation for Hydrogen Fuel Infrastructure - Comments of the California Fuel Cell Partnership" submitted to the California Energy Commission Docket 12-HYD-01 on 10/16/2013.

6. Presentation "H2 FCVs: Beginning the Commercial Launch" at SIGMA conference 4/9/2014.

7. Presentation "H2 FCVs: Beginning the Commercial Launch" at Fuels Institute Spring Meeting 4/15/2014.

VIII. SAFETY, CODES & STANDARDS

VIII.0 Safety, Codes & Standards Sub-Program Overview

INTRODUCTION

The Safety, Codes and Standards (SCS) sub-program identifies research and development (R&D) needs and performs high-priority R&D to provide an experimentally validated, fundamental understanding of the relevant physics, critical data, and safety information needed to define the requirements for technically sound and defensible codes and standards. This information is used to facilitate and enable the widespread deployment and commercialization of hydrogen and fuel cell technologies. In FY 2014, the sub-program continued to identify and evaluate safety and risk management measures that can be used to define the requirements and close the gaps in codes and standards in a timely manner.

The SCS sub-program promotes collaboration among government, industry, codes and standards development organizations, universities, and national laboratories in an effort to harmonize regulations, codes, and standards (RCS) both internationally and domestically. Communication and collaboration among codes and standards stakeholders, Federal government, industry, national labs, and trade associations is emphasized in order to maximize the impact of the sub-program's efforts and activities in international RCS development.

GOALS

The SCS sub-program's key goals are to provide the validated scientific and technical basis required for the development of codes and standards, to promulgate safety practices and procedures to allow for the safe deployment of hydrogen and fuel cell technologies, and to ensure that best safety practices are followed in Hydrogen and Fuel Cells Program activities.

OBJECTIVES

The sub-program's key objectives are to:

- Conduct materials R&D to provide the technical underpinning to enable fault tolerant system designs for use with hydrogen infrastructure rollout by 2015.
- Conduct a quantitative risk assessment study to address indoor refueling requirements to be adopted by code developing organizations (e.g., National Fire Protection Association [NFPA] and International Code Council [ICC]) by 2015.
- Support and facilitate development and promulgation of essential codes and standards by 2015 to enable widespread deployment and market entry of hydrogen and fuel cell technologies and completion of all essential domestic and international RCS by 2020.
- Ensure that best safety practices underlie research, technology development, and market deployment activities supported through DOE-funded projects.
- Develop and enable widespread sharing of safety-related information resources and lessons-learned with first responders, authorities having jurisdiction, and other key stakeholders.

FY 2014 TECHNOLOGY STATUS AND ACCOMPLISHMENTS

The SCS sub-program has made significant progress related to infrastructure codes such as supporting the integration of the NFPA 2: Hydrogen Technologies Code into the International Fire Code and the publication of several component standards related to hydrogen dispensers (i.e., CSA HGV 4.1, 4.2, 4.4, 4.5, and 4.6). In FY 2014, the CSA Compressed Hydrogen Materials Compatibility (CHMC1) standard for metals was also published, establishing a test method for evaluating material compatibility in compressed hydrogen applications. In addition, the international testing of Type IV tanks—conducted by the RCS Working Group of the International Partnership for Hydrogen and Fuel Cells in the Economy (IPHE) determined that temperature increases in tanks are system dependent and that temperature increases on a per cycle basis are independent of cycle rate. Lastly for codes and standards support, sub-program efforts supported the standardization and publication of two SAE International standards: J2799 Standard

for 70 MPa Compressed Hydrogen Surface Vehicle Fuelling Connection Device and Optional Vehicle to Station Communications and J2601 Standard Fueling Protocols for Light-Duty Gaseous Hydrogen Surface Vehicles.

The SCS sub-program continues to utilize the expertise of the Hydrogen Safety Panel to disseminate relevant information and implement safe practices pertaining to the operation, handling, and use of hydrogen and fuel cell technologies in sub-program-funded projects. The Safety Panel, with over 400 years of combined experience in the hydrogen industry, provides recommendations on the safe conduct of Federally-funded project work as well as lessons-learned and best practices that can be of broad benefit to the sub-program. The sub-program continues to share current safety information and knowledge with the community.

In addition, extensive external stakeholder input—from the fire-protection community, academia, automobile manufacturers, and energy, insurance, and aerospace sectors—is used to create and enhance safety knowledge tools for emergency responders and authorities having jurisdiction. The sub-program has renewed its emphasis on ensuring the continual availability of safety knowledge tools, distributed via an array of media outlets to reach the largest number of safety personnel possible. For FY 2014, the sub-program's training for code officials and first responders has reached more than 30,000 through our on-line and classroom training.

The sub-program continues to support R&D to provide the technical basis for codes and standards development, with projects in a wide range of areas including fuel specification, separation distances, materials and components compatibility, and hydrogen sensor technologies. Utilizing the results from these R&D activities, the sub-program continues to actively participate in discussions with standards development organizations such as the NFPA, ICC, SAE International, the CSA Group, and the International Organization for Standardization (ISO) to promote domestic and international collaboration and harmonization of RCS.

The following websites provide additional, up-to-date information relevant to the status of the sub-program's activities:

- Technical Reference for Hydrogen Compatibility of Materials (www.ca.sandia.gov/matlsTechRef/)
- Hydrogen Lessons Learned Database (www.h2tools.org/lessons, formerly www.h2incidents.org)
- Hydrogen Bibliographic Database (www.hydrogen.energy.gov/biblio_database.html)
- Hydrogen Safety Best Practices Manual (www.h2bestpractices.org/)
- Hydrogen Safety Training for Researchers (www-training.llnl.gov/ training/hc/HS5094DOEW/index.html#)
- Introduction to Hydrogen for Code Officials (www.hydrogen.energy.gov/training/code_official_training/)
- Hydrogen Safety for First Responders (www.hydrogen.energy.gov/firstresponders.html)
- H2 Tools (http://h2tools.org/)

The SCS sub-program continued to make progress in several key areas, including the following:

Hydrogen Behavior, Risk Assessment, and Materials Compatibility:

- Developed a metric to evaluate hydrogen codes and standards and benchmarked sub-program activity to show progress in enabling technology development. (Sandia National Laboratories, SNL)
- Completed an initial test matrix to measure for fatigue life of stainless steel 21Cr-6Ni-9Mn in 103 MPa hydrogen gas, satisfying the need to quantitatively evaluate methods published in the CSA CHMC1 standard and to generate qualification data for lower-cost stainless steels. (SNL)
- Finalized design requirements for the variable-temperature testing in a hydrogen gas system. (SNL)
- Organized and held a workshop on codes and standards quantitative risk assessment to build stakeholder awareness of risk and identify barriers limiting industry use of quantitative risk assessment approaches and tools. (SNL)

Hydrogen Quality:

- Improved sensitivity of analyzer using different electrode configurations, demonstrated a proof of concept for hydrogen sulfide (H_2S) analyzer using a platinum black electrode with an observed response to 10 ppb H_2S, and demonstrated clean-up techniques following H_2S exposure. (Los Alamos National Laboratory, LANL)

Coordination of Codes and Standards Development, Domestic and International:

- Developed new permitting and codes and standards training modules for hydrogen technologies deployment and presented in-person training sessions for deployment of hydrogen infrastructure in key jurisdictions including Huntington Beach, California and Culver City, California. (National Renewable Energy Laboratory, NREL)

Component Testing:

- Designed and built apparatus for high-pressure hydrogen component- and system-level testing to understand root cause failure modes and provide guidance for best practices. Test planning will take place in FY 2015. (NREL)
- Published peer review report "Pressure Relief Devices for High-Pressure Gaseous Storage Systems: Applicability to Hydrogen Technology" to provide information on best practices for hydrogen component design and selection. (NREL)

Hydrogen Safety Panel, Databases, Props, and First Responders:

- Released a first-of-its kind iPad/iPhone app to enhance utility and integration of the safety knowledge tools with other safety planning resources. Since May 2014, there have been more than 940 downloads of the app. (Pacific Northwest National Laboratory, PNNL)
- Developed training material for first responders and code officials, having educated over 30,000 first responders and code officials to-date (online and in-person). (PNNL)
- Participated in 13 project reviews (including safety plan and design review activities) for projects in fuel cell and hydrogen storage R&D. (PNNL)

Hydrogen Sensors:

- Completed an initial study in collaboration with the Joint Research Council quantifying the impact of potential chemical interferences, as identified in the ISO 26140 standard on hydrogen sensors, using major hydrogen sensor platform types. This included an impact assessment of selected sensor poisons on various platform types. (NREL)
- Researched and quantified the sensor requirements for preparing existing repair facilities to accommodate hydrogen vehicles. (NREL)
- Identified hydrogen refueling test sites for real-world sensor validation of solid-state electrochemical sensors to promote commercialization of the sensor. (LANL)

Hydrogen Fueling Infrastructure Research and Station Technology (H2FIRST):

- In coordination with the Technology Validation and Delivery sub-programs, the office established the H2FIRST project with significant input from the SCS sub-program. Current H2FIRST projects are focusing on station acceptance/qualification, reference station design, and fuel contamination detectors. (NREL and SNL)

Other Workshops and Reports:

- Convened industry experts for the Hydrogen Contamination Detector workshop at SAE International offices in Troy, Michigan. Participants such as fuel suppliers, component manufacturers, national labs, and automakers discussed near-term performance requirements, long-term R&D needs, and proposed solutions which will be detailed in a forthcoming workshop report.
- Published the report "Safety, Codes and Standards for Hydrogen Installations: Metrics Development and Benchmarking" to inform the siting and deployment of hydrogen refueling stations. This report describes the development and benchmarking of a metric specific to hydrogen codes relevant for hydrogen refueling stations: "number of fueling stations that can readily accept hydrogen." (SNL)
- Held the 2nd International Workshop on Hydrogen Infrastructure and Transportation at Toyota's headquarters in Torrance, California. Participants from the U.S., Europe, Germany, Scandinavia, and Japan gathered to communicate progress, share experiences and best practices, and identify solutions on key issues facing hydrogen refueling infrastructure which will be detailed in a forthcoming workshop report.

BUDGET

The SCS sub-program received an appropriation of $7.0 million in FY 2014. This allowed for sustained progress in key R&D and codes and standards development work. The FY 2015 budget request includes $7.0 million for Safety, Codes and Standards, which will ensure continuity in key R&D and focus areas as shown below.

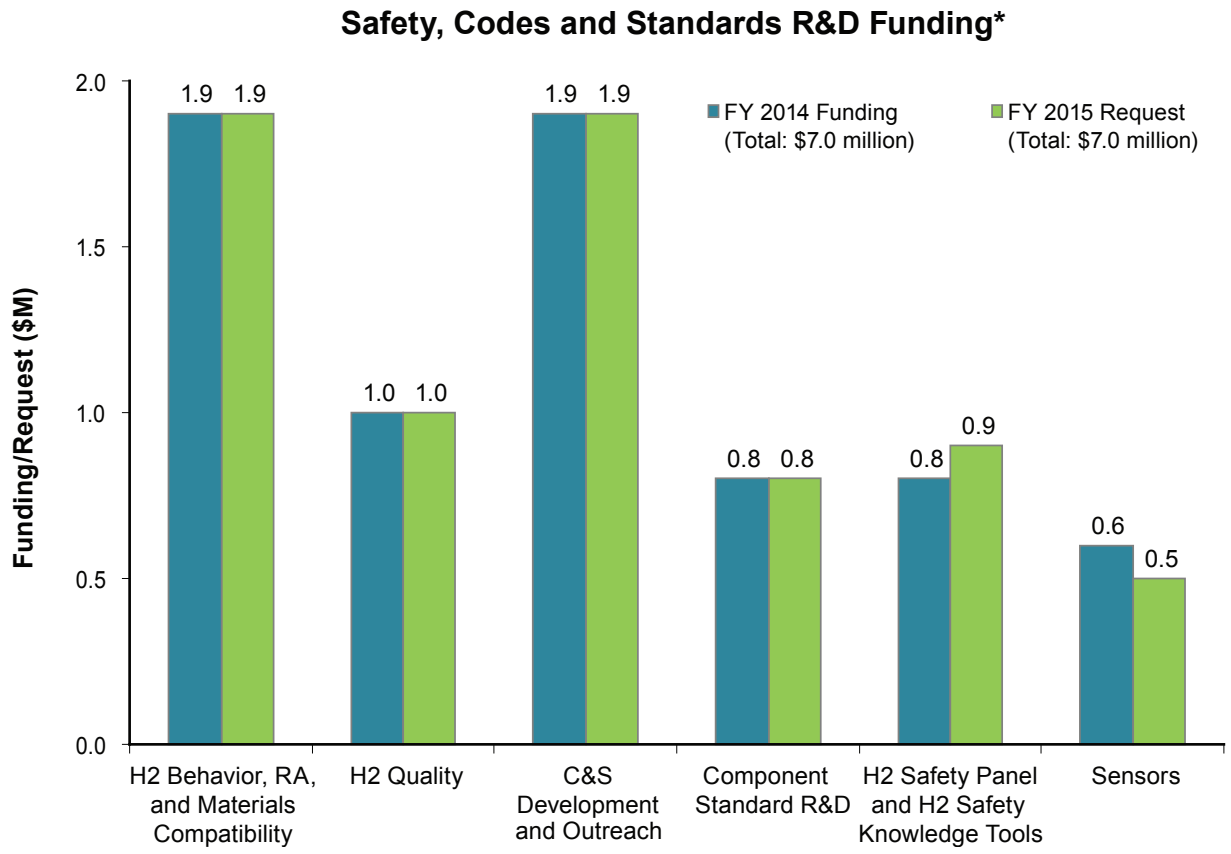

* Subject to appropriations, project go/no-go decisions, and competitive selections. Exact amounts will be determined based on research and development progress in each area.

FY 2015 PLANS

The SCS sub-program will continue to work with codes and standards development organizations to develop technical information and performance data to enhance hydrogen-specific codes and standards. To address these needs, the sub-program will continue to support a rigorous technical R&D program—including assessment of materials compatibility for component designs and high-pressure tank cycle testing—and continue to promote a performance-based quantitative risk assessment approach to assess risks and establish protocols to identify and mitigate risk. Future work will also focus on facilitating the permitting of hydrogen fueling stations and early market applications and testing, measurement, and verification of hydrogen fuel specifications.

The sub-program will also continue to promote the domestic and international harmonization of test protocols for qualification and certification as well as the harmonization of RCS for hydrogen fuel quality and other key international standards. This will be enabled by working with the appropriate domestic and international organizations such as the NFPA, ICC, SAE International, CSA Group, and ISO. The sub-program will also continue to participate in IPHE's RCS Working Group and the International Energy Agency's Hydrogen Implementing Agreement, both of which are engaged in hydrogen safety work.

Charles “Will” James
Safety, Codes & Standards Project Manager
Fuel Cell Technologies Office
Office of Energy Efficiency and Renewable Energy
U.S. Department of Energy
1000 Independence Ave., SW
Washington, D.C. 20585-0121
Phone: (202) 287-6223
Email: Charles.James@ee.doe.gov

VIII.1 Fuel Cell Technologies National Codes and Standards Development and Outreach

Carl Rivkin (Primary Contact), Robert Burgess, William Buttner
NREL
15301 Denver Parkway West
Golden, CO 80401
Phone: (303) 275-3839
Email: carl.rivkin@nrel.gov

DOE Manager
Will James
Phone: (202) 287-6223
Email: Charles.James@ee.doe.gov

Project Start Date: October 1, 2002
Project End Date: Project continuation and direction determined annually by DOE

Overall Objectives

- Support the deployment of hydrogen technologies for hydrogen fuel cell vehicles and stationary applications
- Make critical safety information readily available through webinars, training sessions, safety reports, and technical presentations
- Inform key stakeholders of the safety, codes and standards requirements for the safe use of hydrogen technologies
- Work with potential infrastructure developers to accelerate the deployment of hydrogen fueling stations and other key infrastructure
- Identify and resolve safety issues associated with hydrogen technologies infrastructure

Fiscal Year (FY) 2014 Objectives

- Publish a paper on progress and accomplishments in the development of codes and standards
- Support the development of the next edition of National Fire Protection Association (NFPA) 2 Hydrogen Technologies Code by leading the LH2 Task Group and acting as Principal Committee member
- Present webinars on Codes and Standards Progress and Hydrogen Components
- Publish updated National Permit Guide for hydrogen fueling stations
- Present Codes and Standards information at California hydrogen technologies deployments meetings and workshops
- Implement Continuous Codes and Standards Improvement Process by evaluating field data to determine codes and standards development priorities
- Provide in-person training to code officials and project developers in key jurisdictions in California and other locations where infrastructure projects are planned

Technical Barriers

This project addresses the following technical barriers from the Safety, Codes and Standards section of the Fuel Cell Technologies Office Multi-Year Research, Development, and Demonstration Plan:

(A) Safety Data and Information: Limited Access and Availability

(D) Lack of Hydrogen Knowledge by AHJs (authorities having jurisdiction)

(F) Enabling National and International Markets Requires Consistent RCS

(G) Insufficient Technical Data to Revise Standards

(H) Insufficient Synchronization of National Codes and Standards

(I) Lack of Consistency in Training of Officials

(K) No Consistent Codification Plan and Process for Synchronization of R&D and Code Development

(L) Usage and Access Restrictions

Contribution to Achievement of DOE Safety, Codes and Standards Milestones

This project will contribute to achievement of the following DOE milestones from the Safety, Codes and Standards section of the Fuel Cell Technologies Office Multi-Year Research, Development, and Demonstration Plan:

- Milestone 4.4: Complete National Codes and Standards Chronological Development Plan. (4Q, 2014)
- Milestone 4.5: Complete fueling station codes and template. (4Q, 2014)
- Milestone 4.6: Completion of standards for critical infrastructure components and systems. (4Q, 2014)
- Milestone 4.7: Complete risk mitigation analysis for advanced transportation infrastructure systems. (1Q, 2015)

- Milestone 4.8: Revision of NFPA 2 to incorporate advanced fueling and storage systems and specific requirements for infrastructure elements such as garages and vehicle maintenance facilities. (3Q, 2016)
- Milestone 4.9: Completion of GTR Phase 2. (1Q, 2017)

FY 2014 Accomplishments

- NREL provided broad coordination of codes and standards development by:
  - Supporting Codes and Standards Tech Team – develop and maintain the 2020 plan for defining and tracking codes and standards work required for deployment of hydrogen fuel cell vehicles and making presentations on sensors and codes and standards development activities
  - Acting as liaison between codes and standards development committees to assist in coordination between fire codes and standards development projects
  - Developed a plan for the NFPA Liquefied Hydrogen Task Group to evaluate the setback distances for and safety mitigation measures in NFPA 55 and NFPA 2
- NREL coauthored "Regulations, Codes and Standards for Hydrogen Technologies - A Historical Overview," a paper that will be drafted by the end of FY 2014
- Developed new Permitting and Codes and Standards training modules for hydrogen technologies deployment
- Presented in-person training sessions for Deployment of Hydrogen Infrastructure in key jurisdictions including Huntington Beach, CA and Culver City, CA

INTRODUCTION

The fundamental purpose of this work is to support the safe deployment of hydrogen technologies. To achieve this objective codes and standards must be in place to protect public safety and any significant safety issues must be resolved.

The work under this project has helped develop a national set of codes and standards to safely deploy hydrogen technologies. Additionally, key safety issues have been identified and are in the process of being resolved. Safety, codes and standards information has been distributed to interested parties using a variety of techniques including webinars, NREL technical reports, workshops, in-person presentations, and Web-based products.

APPROACH

The project approach has been to involve as many key stakeholders as possible in codes and standards development and coordination and outreach activities to achieve maximum effectiveness. These stakeholders include industry partners, standards development organizations, research organizations including other national laboratories, AHJs, local government in locations where projects will be deployed, and trade organizations involved in technology development and deployment.

RESULTS

Figure 1 illustrates the progress that has been made toward developing the key codes and standards required to deploy hydrogen technologies. The reference of NFPA 2 Hydrogen Technologies Code in the International Fire Code and the planned adoption by the State of California of NFPA 2 effectively creates a national hydrogen code. This

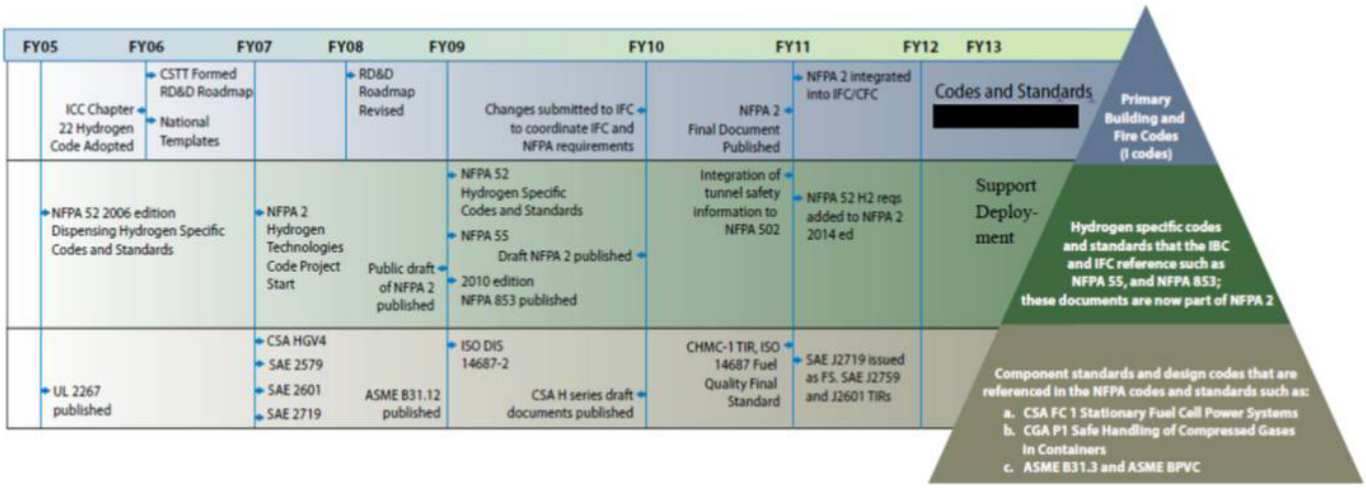

FIGURE 1. Progress in Codes and Standards Development

simplification and coordination of code requirements will make it easier to develop permit applications, review and approve applications, and ensure a high level of public safety. This accomplishment helps meet several DOE milestones including 4.4 and 4.8.

The next step in this codes and standards development process after the promulgation of the baseline set of codes and standards is monitoring the field performance of these documents, determining where modifications are required, and supporting the implementation of those modifications. This helps DOE meet milestone 4.5.

This modification process is illustrated in Figure 2. The process consists of evaluating field deployment of hydrogen technologies through use of NREL data and site visits, determining whether there are issues with codes and standards based on this information, and developing modified codes and standards requirements to resolve these issues. This process also integrates NREL laboratory research activities involving hydrogen technologies safety by using this research to address codes and standards issues.

NREL developed updated codes and standards training modules and provided in-person training for code officials and project developers in key jurisdictions. This work will be ongoing as deployment of infrastructure increases.

NREL supported the work of H2USA by participating as a member of the Market Acceleration Working Group. This participation included developing a generic slide presentation that will be used when introducing hydrogen technologies to organizations that may play a role in the support and development of hydrogen infrastructure.

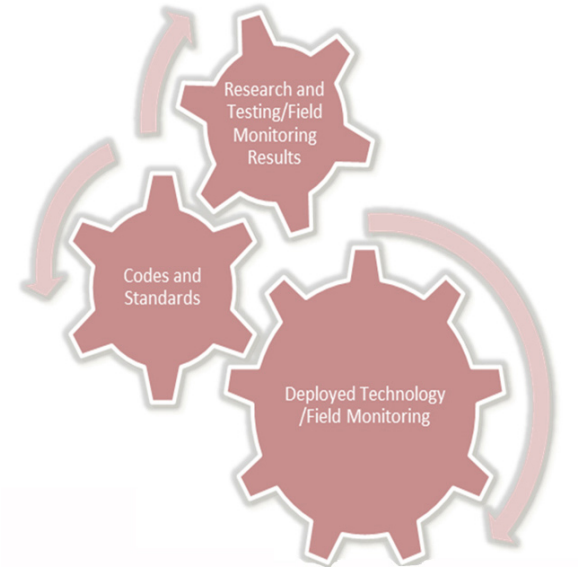

FIGURE 2. Continuous Codes and Standards Improvement

NREL will support testing required to develop Federal Motor Vehicle Safety Standards required to implement the Global Technical Regulation in the United States. This supports DOE milestone 4.9.

NREL has acted as Task Group Leader for a LH2 task group that will develop new requirements for bulk liquefied hydrogen and associated safety mitigation measures for the next edition of NFPA 55. The supports DOE Milestone 4.9.

CONCLUSIONS AND FUTURE DIRECTIONS

Conclusions

Codes and Standards

- Codes and standards development support will continue through direct support of standards development organizations by NREL staff participation on or operation of coordination committees
- Ongoing coordination of the fire and building codes and key hydrogen codes and standards is a priority
- Field deployment information will help set codes and standards development priorities

Outreach

- Deployment support will be focused on infrastructure at locations with project activity and concrete deployment plans, for example jurisdictions in California
- These goals can only be accomplished through collaborations with key stakeholders at all levels
- NREL will continue to support deployment of hydrogen and fuel cell technologies through technical reports, webinars, safety reviews, and the Web-based information compendium
- NREL will work with H2USA to support the efforts of key organizations involved in infrastructure deployment

Future Directions

Codes and Standards Coordination/Continuous Codes and Standards Improvement

Continue work to coordinate codes and standards on a smaller scale with special focus on taking information from deployment projects back to code development committees.

- Resolve infrastructure codes and standards issues such as hydrogen setback distances in NFPA codes
- Continue coordination between National Fire Codes and International Code Council codes
- Support efforts to adopt NFPA 2 Hydrogen Technologies Codes (and other key codes) such as the work done by

the California Fire Marshal's Office to adopt NFPA 2 earlier than adoption of the IFC would dictate

Outreach

- Continue to publish NREL technical reports, deliver webinars, and provide Web-based information on key safety issues required to support hydrogen technologies deployment
- Assist code officials, project developers, and other interested parties in use of new codes and standards and safety information through outreach activities, with special focus on key jurisdictions such as California
- Work with interested parties to provide information to assist in infrastructure deployment
- Provide in-person codes and standards training in key locations such as California and other zero-emission vehicle states
- Work with H2USA to support infrastructure development

FY 2014 PUBLICATIONS/PRESENTATIONS

1. Deployment of Hydrogen Infrastructure May 19,2014 Huntington Beach, CA

2. Deployment of Hydrogen Infrastructure May 27, 2014 Culver City, CA

3. Regulations, Codes and Standards (RCS) for Hydrogen Technologies- A Historical Overview projected September 2014.

VIII.2 Component Standard Research and Development

Robert Burgess (Primary Contact), Arlen Kostival, Jacquelyn Lewis, William Buttner, Carl Rivkin
National Renewable Energy Laboratory (NREL)
15013 Denver West Parkway
Golden, CO 80401
Phone: (303) 275-3823
Email: robert.burgess@nrel.gov

DOE Manager
Will James
Phone: (202) 287-6223
Email: Charles.James@ee.doe.gov

Project Start Date: October 1, 2012
Project End Date: Project continuation and direction determined annually by DOE.

Overall Objectives

- Accelerate development of codes and standards required for commercialization of hydrogen technologies.
- Codify standards language that is based on the latest scientific knowledge by providing analytical, technical and contractual support.
- Contribute directly to codes and standards committee efforts to identify technology gaps, then work to define research and development needs required to close those gaps.
- Build laboratory testing capability and conduct research and development aimed at providing the basis for improved code language.
- Collaborate with industry, university and government researchers to develop improved analytical and experimental capabilities.

Fiscal Year (FY) 2014 Objectives

- Coordinate infrastructure research and development support through interface with H2USA and H2FIRST organizations.
- Generate report on pressure relief valve technologies to provide industry with latest information on proper hydrogen design and system application.
- Conduct webinar on component testing activities and lessons learned, primary target audience is component designers and system suppliers.
- Build industry partnerships to conduct high pressure hydrogen component and system level testing designed to understand root cause failure modes and to provide guidance for engineering best practices.
- Work in partnership with National Institute of Standards and Technology Fluid Metrology Group and state agencies to advance knowledge of hydrogen metrology methods for hydrogen dispensing weights and measures.
- Facilitate utilization of the new DOE Energy Systems Integration Facility (ESIF) laboratory space by identifying best use of laboratory and testing capabilities and by supporting ESIF user facility designation through interface with DOE/NREL user facility personnel.

Technical Barriers

This project addresses the following technical barriers identified in the Safety Codes and Standards section of the Fuel Cell Technologies Office Multi-Year Research, Development, and Demonstration (MYRD&D) Plan:

(A) Safety Data and Information: Limited Access and Availability

(C) Safety is Not Always Treated as a Continuous Process

(F) Enabling National and International Markets Requires Consistent RCS

(G) Insufficient Technical Data to Revise Standards

(H) Insufficient Synchronization of National Codes and Standards

(J) Limited Participation of Business in the Code Development Process

(K) No Consistent Codification Plan and Process for Synchronization of R&D and Code Development

Contribution to Achievement of DOE Hydrogen Safety, Codes and Standards Milestones

This project contributes to achievement of the following DOE milestones from the Hydrogen Safety, Codes and Standards section of the Fuel Cell Technologies Office's MYRD&D Plan:

- Milestone 2.3: Publish protocols for identifying potential failure modes. (2Q, 2013)
- Milestone 2.11: Publish draft protocol for identifying potential failure modes and risk mitigation. (4Q, 2014)
- Milestone 2.15: Develop holistic design strategies. (4Q, 2017)
- Milestone 2.19: Validate inherently safe design for hydrogen fueling infrastructure. (4Q, 2019)

- Milestone 3.1: Develop, validate, and harmonize test measurement protocols. (4Q, 2014)
- Milestone 4.1: Complete determination of safe refueling protocols for high pressure systems. (1Q, 2012)
- Milestone 4.3: Identify and evaluate failure modes. (3Q, 2013)

FY 2014 Accomplishments

- Published NREL peer review report "Pressure Relief Devices for High-Pressure Gaseous Storage Systems: Applicability to Hydrogen Technology" to provide information on best practices for hydrogen component design and selection.
- Prepared presentation materials for hydrogen component webinar. Webinar plans are being finalized, dates in the fourth quarter of FY 2014 are being considered. The webinar addresses hydrogen component design, performance and operational topics.
- Represented DOE and NREL at interagency meetings with National Institute of Standards and Technology on the subject of hydrogen metrology with the purpose of supporting state weights and measures inspectors as they are preparing to issue use permits for the sale of hydrogen at public dispensers.
- Designed and built apparatus for high-pressure hydrogen component and system level testing designed to understand root cause failure modes and to provide guidance for best practices. Test planning for FY 2015.
- Hosted the National Fire Protection Association (NFPA) joint document review meetings for NFPA 2 Hydrogen Technologies Committee and NFPA 55 Industrial and Medical Gas Committee.
- Coordination of component activities with H2USA and H2FIRST, facilitating national laboratory support of hydrogen infrastructure projects.

INTRODUCTION

Hydrogen safety, codes and standards topics have been identified in the DOE MYRD&D Plan as a subject area where significant barriers need to be addressed. Developing robust codes and standards helps to ensure that hydrogen systems are safe and reliable, thereby enabling the acceptance and growth of hydrogen technologies. NREL is providing research and development support to these codes and standards through validation testing, analytical modeling, and product commercialization efforts. NREL has been tasked with these responsibilities as defined in the DOE MYRD&D Plan.

APPROACH

Hydrogen safety is being addressed by first identifying safety concerns, then developing appropriate test and analysis tasks that provide a technical basis for improved engineering best practices. Safety concerns are being compiled by direct discussion with key stakeholders, by leveraging existing data available through NREL's Technology Validation Program and by utilizing public outreach activities such as workshops and webinars. Identified safety concerns are prioritized, and then research and development tasks are aligned with the highest risk safety concerns. In general, the risk is defined by the combination of the severity and the likelihood of occurrence. Research and development (R&D) results are then published for general use by stakeholders. Information is further disseminated through NREL outreach activities. Published results are also being used as a basis for improved hydrogen codes and standards.

NREL is participating on relevant codes and standards committees to help identify gaps and define research and development needs to close those gaps. Working at the committee level allows us to quickly identify areas that need R&D support and to work directly with the technical experts in planning a path forward. This process is instrumental in avoiding delays and setbacks in the development of new codes and standards and in the revision of existing codes and standards. R&D support is being used to establish codes and standards language with solid technical basis.

RESULTS

NREL has been working toward identifying safety gaps and supporting R&D efforts for developing new and improved hydrogen codes and standards. Results reported here are for efforts specifically directed at component level standards and identified hydrogen safety concerns.

Codes and Standards Technical Committee Support – NREL provided development support for the SAE International (SAE) J2601 (Fueling Protocols for Light Duty Gaseous Hydrogen Surface Vehicles) fueling protocols by providing technical basis for several key sections of the document. This includes the hot soak conditions form NREL's Technology Validation data that was used as worst case assumptions for onboard system temperatures when formulating the non-communication fill tables. SAE J2601 has successfully passed balloting and is now available through SAE publications as of July 2014. NREL also supported NFPA 2 Hydrogen Technologies Code by hosting the joint meeting with NFPA 55 in July 2014. These two standards are on a synchronized revision schedule to simplify hydrogen content improvements.

NREL Hydrogen Component Webinar (Fourth Quarter FY 2014) – NREL has completed presentation materials for a component webinar. Presentation material

is currently being reviewed by DOE for a fourth quarter presentation date. The webinar provides valuable input for component suppliers and system developers.

Pressure Relief Valve Report (NREL report no. TP-5400-60175, November, 2013) – This NREL report, peer reviewed by industry, compiles information on the proper design, installation and operation of pressure safety devices in hydrogen service. Addressing safety concern by providing relevant best practices information will help to prevent future failures during field operation.

Pressure Relief Valve Failure Mode Demonstration – NREL is conducting a qualitative reliability test failure mode investigation by using the high-pressure testing capability at NREL. This test is designed to replicate a known field failure mode under laboratory controlled conditions and to provide insight into the necessary and sufficient conditions required to produce a component level failure. Testing hardware has been designed and assembled and is currently undergoing system check out testing with a planned test start date by the end of FY 2014 with continued testing into FY 2015.

Component Crosscutting Accomplishments – NREL is conducting DOE-funded component tasks under other subprograms including hose/dispenser and compressor testing. In FY 2014 NREL also completed a work for others task for the California Department of Food and Agriculture to construct a device for evaluating hydrogen metrology methods. These efforts have provided an opportunity to leverage safety codes and standards objectives through crosscutting activities. These activities include regulations, codes, and standards guidance for defining test protocols and design requirements. The safety codes and standards program is also benefiting from component test results that are the technical basis for improved code requirements.

Research and Development Outreach Activities – Numerous outreach activities were conducted in conjunction with the DOE/NREL safety, codes and standards activities. Outreach activities are used as a resource in soliciting industry feedback and identifying priorities for research and development tasks. Outreach tasks include contribution to key technical committees and working groups at H2USA, H2FIRST, California Fuel Cell Partnership and work with other key stakeholders.

CONCLUSIONS AND FUTURE DIRECTION

NREL has identified numerous opportunities to further improve the inherent safety of high-pressure hydrogen systems that are designed to serve fuel cell electric vehicle markets. These opportunities must be pursued through a variety of means, including failure mode testing investigations, root cause analysis and codes and standards development. Future direction will include R&D activities that utilize existing ESIF laboratory facilities for component and system level testing.

FY 2014 PUBLICATIONS/PRESENTATIONS

1. "Component Standard Research and Development", DOE Annual Merit Review, June 18th, 2014.

2. "Pressure Relief Devices for High-Pressure Gaseous Storage Systems: Applicability to Hydrogen Technology", NREL Technical Report TP-5400-60175, A. Kostival, C. Rivkin, W. Buttner, R. Burgess, Nov 2013.

VIII.3 Hydrogen Safety, Codes and Standards: Sensors

Eric L. Brosha[1] (Primary Contact), William Penrose[3], Leta Woo[2], Robert S. Glass[2] (Secondary Contact), Tommy Rockward[1], and Rangachary Mukundan[1]

[1]Los Alamos National Laboratory (LANL)
MS D429, P.O Box 1663
Los Alamos, NM 87545
Phone: (505) 665 4008
Email: brosha@lanl.gov

[2]Lawrence Livermore National Laboratory (LLNL)
L-103, P.O. Box 808, 7000 East Avenue
Livermore, CA 94550
Phone: (925) 423 7140
Email: glass3@llnl.gov

[3]Custom Sensor Solutions, Inc.
11786 N. Dragoon Springs Drive
Oro Valley, AZ 85737
Phone: (520) 544-7523
Email: wpenrose@customsensorsolutions.com

DOE Manager
Will James
Phone: (202) 287-6223
Email: Charles.James@ee.doe.gov

Project Start Date: October 1, 2008
Project End Date: Project continuation and direction determined annually by DOE

Overall Objectives

- Develop a low-cost, and low-power electrochemical hydrogen safety sensor for a wide range of infrastructure and vehicle applications with focus on high durability and reliability
- Continually advance test prototypes guided by materials selection, sensor design, electrochemical R&D investigation, fabrication, and rigorous life testing
- Disseminate packaged sensor prototypes and control systems to DOE laboratories and commercial parties interested in testing and fielding advanced prototypes for cross-validation
- Evaluate manufacturing approaches for commercialization
- Engage an industrial partner and execute technology transfer

Fiscal Year (FY) 2014 Objectives

- Identify operating H_2 refueling station partners in California for placement of first field trial unit(s)
- Compose field trials plan of action/indemnity agreement for commercial partners
- Design new integrated control/signal electronics and National Electrical Manufacturers Association (NEMA)-compliant packaging for field trials deployment
- Obtain commercial-off-the-shelf data wireless data system and pre-test field trials system in the laboratory for remote sensor interrogation
- Develop control software for sensor control, data logging, event logging
- Test first field trials unit and prepare for locating on site

This project addresses the following technical barriers from the Safety, Codes and Standards section of the Fuel Cell Technologies Office Multi-Year Research, Development, and Demonstration Plan:

(A) Safety Data and Information: Limited Access and Availability

(C) Safety is Not Always Treated as a Continuous Process

(K) No Consistent Codification Plan and Process for Synchronization of R&D and Code Development

(L) Usage and Access Restrictions

Technical Targets

Technical targets vary depending on the application [1,2], but in general include:

- Sensitivity: 1-4 vol% range in air
- Accuracy: ± 1% full scale in the range of 0.04-4 vol %
- Response Time: <1 min at 1% and <1 sec at 4%; recovery <1 min
- Temperature operating range: -40°C to 60°C
- Durability: Minimal calibration or no calibration required for over sensor lifetime (as defined by particular application)
- Cross-Sensitivity: minimal interference to humidity, H_2S, CH_4, CO, and volatile organic compounds

FY 2014 Accomplishments

- Demonstration hydrogen refueling sites in California were identified, and approved by station operators for test, and preparations to begin field trials development and testing commenced.
- Codes and standards guided planning for field trials work.
  - LLNL indemnity agreement written with Class 1/Div 2 standards used as guidance.

- LANL and Custom Sensor Solutions developed new electronics specifically for field trials units.
  - Packaged sensor mounts directly to impedance buffer circuit and heater control circuit simplified and optimized specifically to commercially prepared sensor substrate element (ESL ElectroScience, Inc.).
- Field trials unit designed to use commercial, off-the-shelf wireless transmitters/receivers to simplify deployment at testing site.
- A certified LabVIEW developer identified to provide data logging software (Agile Engineering/Zircoa Inc.)
  - Provisions to wirelessly log sensor output for up to three sensors simultaneously. User defined sampling rate, averaging, recording rate, and event threshold triggering.
- LANL conducted a site survey at Hydrogen Frontier LLC (Burbank) and identified desirable areas to locate field trial units. The best location was found to be inside the enclosure for the dispensing island. Known area of leaks and the housing is the location one of the filling station's commercial H_2 sensors.
- LLNL researchers surveyed AC Transit site and preparations for on-site testing were made. Testing at the AC Transit site did not go forward.
- NEMA-8 enclosures identified and internal layout fixed of field trials units.
- Five Custom Sensor Solutions sensor boards acquired in FY 2014 along with enough wireless units and NEMA-8 enclosures to assemble up to three test units by the end of FY 2014.

INTRODUCTION

Recent developments in the search for sustainable and renewable energy coupled with the advancements in fuel cell-powered vehicles have augmented the demand for hydrogen safety sensors initially to be placed at refueling sites and developed for incorporation onboard vehicles [2]. There are several sensor technologies that have been developed to detect hydrogen, including deployed systems to detect leaks in manned space systems and hydrogen safety sensors for laboratory and industrial usage. Among the several sensing methods commercially available or under development, electrochemical devices that utilize high-temperature-based ceramic electrolytes have been shown to be robust, potentially low cost, have high sensitivity and good selectivity, the latter exemplified by tolerance to changes in humidity, and are more resilient to electrode or electrolyte poisoning [3-9]. The desired sensing technique should meet a detection threshold of 1% (10,000 ppm) H_2 and response time of ≤1 min [10], which is a target for infrastructure and vehicular uses. Further, a review of electrochemical hydrogen sensors by Korotcenkov et. al [11] and the report by Glass et al. [10,12] suggest the need for inexpensive, low-power, and compact sensors with long-term stability, minimal cross-sensitivity, and fast response. This view has been largely validated and supported by the fuel cell and hydrogen infrastructure industries by the NREL/DOE Hydrogen Sensor Workshop held on June 8, 2011 [13]. Many of the issues preventing widespread adoption of best-available hydrogen sensing technologies available today outside of cost, derive from excessive false positives and false negatives arising from unstable sensor baseline; both of these problems necessitate the need for unacceptable frequent calibration [13].

As part of the Hydrogen Codes and Standards project, LANL and LLNL are working together to develop and test inexpensive, zirconia-based, electrochemical (mixed potential) sensors for hydrogen detection in air. Previous work conducted at LLNL showed [9] that indium tin oxide (ITO) electrodes produced a stable mixed potential response in the presence of up to 5% of H_2 in air with very low response to CO_2 and water vapor. The sensor also showed desirable characteristics with respect to response time and resistance to aging, and degradation due to thermal cycling.

In this investigation, the development and testing of an electrochemical hydrogen (H_2) sensor prototype based on ITO/yttria-stabilized zirconia (YSZ)/platinum (Pt) configuration is detailed. The device fabricated using commercial ceramic sensor manufacturing methods on an alumina substrate with an integrated Pt resistance heater to achieve precise control of operating temperature while minimizing heterogeneous catalysis and loss of hydrogen sensitivity. Targeting fuel cell vehicle infrastructure, the safety sensor was subjected to interference studies, temperature cycling, operating temperature variations, and long-term testing now exceeding over 6,000 hrs for some sensor configurations. In FY 2011, FY 2012, and FY 2013 the mixed potential electrochemical technology was independently validated at the hydrogen safety sensor-testing lab at the National Renewable Energy Laboratory (NREL) in three separate rounds of testing. In each round, two packaged pre-commercial prototypes were tested against a standard testing protocol including the effects changes in ambient temperature, pressure, humidity, and oxygen partial pressure and sensor resistance to cross-interferences such as CO, CO_2, CH_4, and NH_3. In general, NREL testing showed a fast response to H_2 with exceptional low-level sensitivity and high signal-to-noise, very little deviation in sensor response to changes in ambient conditions such as humidity and barometric pressure, and minimal response to some common interference gases. However, potential weaknesses were found in the first two rounds of testing such as changes in sensor calibration with ambient temperature changes and complete sensor failure under the most harsh operating environment tested (anaerobic conditions, which

would only happen under extremely unusual conditions) were identified. These last NREL-identified performance issues were ameliorated in FY 2013 and FY 2014. In FY 2013, a more chemically robust electrode was tested in a wide range of oxygen partial pressures (rich conditions to 100% O_2). The $La_{0.8}Sr_{0.2}CrO_3$ perovskite electrode will be incorporated into new ESL ElectroScience, Inc. devices and tested within work planned for FY 2015.

FY 2014 work focused primarily on the design, development, and testing of hardware required for field testing deployment at hydrogen refueling stations in California. In addition to technical work, pursuit of an indemnity agreement, commercial partner outreach, and planning for adherence to codes and standards in designing the prototype units were accomplished. In order to facilitate deployment at on site locations, a wireless means of transmitting sensor data was adopted. This extra step will represent a very small addition to package cost since low-cost commercial-off-the-shelf wireless systems are readily available. Of course, going wireless makes it unnecessary to run lengths of wiring through runs of explosion proof conduits, which is a very large cost increase for station operators. A new circuit board design was prepared by Custom Sensor Solutions, Inc. that combined the high impedance buffer circuit and sensor heater control board into one streamlined unit. The first of the new boards were delivered in May 2014 and testing and circuit revisions/optimization continued through June. At the end of June, all of the components were integrated into a commercially sourced, NEMA Class 8 enclosure and systems testing began in July in the laboratory (wireless portion excluded pending approval by DOE/National Nuclear Security Administration [NNSA]/LANL Security and Safeguards procedures).

A dedicated LabVIEW-based software program was developed by a certified LabVIEW developer (Agile Engineering with software/wireless communications testing performed by Zircoa Inc.). This executable code was designed to accommodate up to three independent, wireless hydrogen sensors at each deployment location. Given the exposure to outdoor environment at the primary California testing site, a ruggedized industrial computer with solid-state storage was selected and daily performance of the field trials unit will be carried out using remote access communication via the Internet.

The salient features of the hydrogen sensor prototype developed by LANL and LLNL are (a) low power consumption; (b) compactness to fit into critical areas for some applications; (c) simple operation; (d) fast response; (e) a direct voltage read-out circumventing the need for complicated signal processing; (f) a low-cost sensor platform; (g) excellent stability and reproducibility all of which are conducive to commercialization using common ceramic manufacturing methods; (h) low cost; and (i) technology readily lends itself to mass manufacturing protocols

RESULTS

(a) Layout and design, prototype testing of field trials electronics: In FY 2013, the principal goal for the third round of NREL testing was to test performance of the LANL/LLNL hydrogen safety sensor prototype with active temperature feedback and control. The variation in sensor output voltage with temperature is well known since the response of mixed potential sensors is governed by electrode kinetics and the electrochemical reactions are a strong function of temperature. The small changes in the sensor Pt heater resistance was used to provide feedback to a heater control circuit designed and constructed for this project by Custom Sensor Solutions (Tucson, AZ). Figure 1 shows an actual photograph of the electronic control for field trials operation. This new circuit board combines the constant resistance power supply with the high-impedance buffer that protects the sensor from stray currents from data acquisition boards and permits control of baseline offset and amplifier gain. This circuit uses a voltage output from a simple analog bridge to add/subtract to the heater voltage using the resistance from the sensor's Pt resistive heater as the control point. It is a very simple circuit and mode of operation that effectively maintained sensor temperature despite large changes in ambient temperature (over 90°C range tested in NREL test protocol during Round 3 testing FY 2013) or local changes in sensor element temperature due to heat generated by hydrogen combustion. This will be very important as will be discussed below: the location of the hydrogen refueling stations are in Southern California and the facility locations for sensor deployment are within enclosures exposed to direct

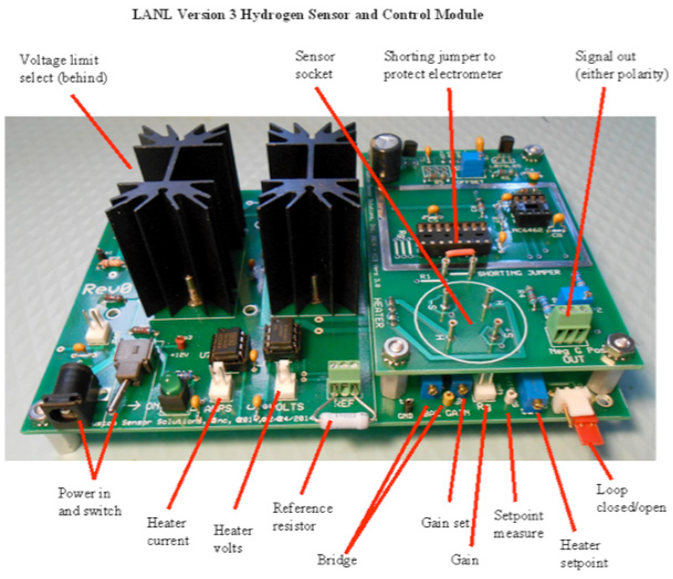

FIGURE 1. Field trials control electronics designed and constructed by Custom Sensor Solutions. This board simplifies the circuitry that maintains constant sensor temperature while adding the high impedance buffer and providing a direct-to-board mounting of the sensor package.

sunlight and internal temperatures can easily vary by 30°C throughout the course of a day in the summer.

(b) Identification of commercial California filling station partner and on-site inspection/evaluation for siting field trials units: In late FY 2013 several potential hydrogen-filling locations were identified in the State of California. LLNL took the lead in preparing a draft indemnity agreement that outlined purpose, explanation of technology, goals, and path forward for commencing with testing and collecting a database of field trials hydrogen sensor units. Contact was made with Dan Poppe of Hydrogen Frontier Inc. (Glendale, CA) and arrangements were made to visit the Burbank filling station facility in April 2014. A survey of the facility and identification of potential sites to locate field trials sensor units was accomplished. Figure 2 shows a collage of photographs and shows areas where there are known hydrogen leaks or potential for hydrogen accumulation. Other important observations were sources of power and location of existing commercial H_2 detectors (optical/thermal/chemical, etc.). FY 2015 will commence with operation of a LANL-built field trial unit inside the dispensing island (left, Figure 2).

(c) Ignition probability experiments (in mixtures up to 20% H_2 in air) performed at LANL using actual sensor and packaging: Concerns raised by reviewers during prior Annual Merit Review briefings and at Safety, Codes and Standards Tech Team presentations about the possibility of the LANL/LLNL mixed potential sensor acting as an ignition source were addressed this year and as part of the compilation of information for the indemnity agreement draft document. Because the sensor technology is a derivative of the automotive oxygen lambda sensor, the electrolyte is a stabilized zirconium oxide and as such, the temperature of the electrolyte must be raised to at least 400°C for normal operation. Although this temperature is below the autoignition temperature of hydrogen, the preferable temperature set point is 475–500°C and this approaching the autoignition temperature and if, in the event of a circuit failure, cross this threshold. (Protective voltage limits – user selectable – were built into the heater power circuit so this event can be mitigated by proper set-up of the field trials unit before deployment.) A flame arrestor was incorporated into the ceramic sensor package and an operating device was tested in H_2/air mixtures up to 20 vol% at LANL. Safety Standard for Hydrogen and Hydrogen Systems 1740.16 was consulted as guidance vis-à-vis specific information regarding flame arrestor specifications for hydrogen. Figure 3 illustrates the test apparatus that was built in an outdoor hydrogen facility at LANL. An existing Integrated Work Document was modified to permit working with flammable mixtures of hydrogen and air and these mixtures were introduced into a chamber with a packaged sensor (open-ended stainless steel tube). The power supply output voltage was monitored (tracking heat of combustion effects on sensor element during hydrogen exposure) as well as the temperature fore, aft, and at the mixing junction by three Type K thermocouples. The ignition of the flammable gas could be inferred by observing a spike

FIGURE 2. Photographs taken on site at the Burbank Hydrogen Frontier location. Although four suitable locations were identified, the location inside the hydrogen dispensing island enclosure (left and top/bottom center) was deemed the most desirable for single sensor unit deployment. Locations for test units to access 24-V direct current power were also identified (lower right).

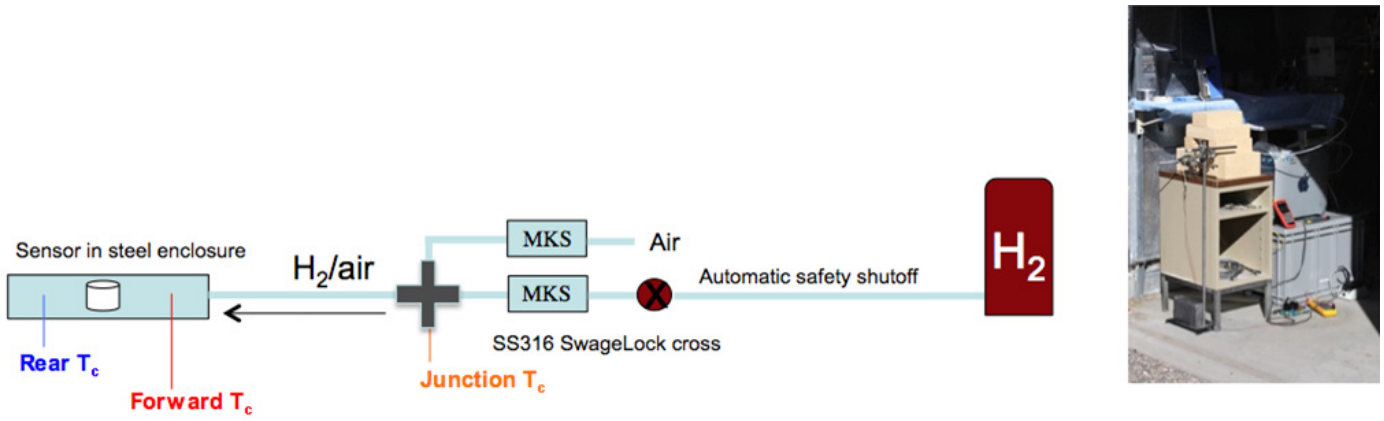

FIGURE 3. An open outdoor facility at LANL was used to test packaged, working LANL/LLNL H_2 sensors in flammable mixtures of hydrogen and air.

in temperature. The experiments were conducted with, and without the presence of the flame arrestor and while the sensor was being overdriven by the applied voltage (sensor glowing orange, well above operating temperature) and at no time was there a deviation in the temperature of the thermocouples signifying ignition of the flammable mixture. The apparatus was tested using a flame and ignition was observed, followed by flame propagation to the final thermocouple location and the automatic safety system terminated hydrogen flow to the experiment.

In the final experiment, the sensor was placed into a standard Plexiglas® test chamber and 10 vol% H_2/air was introduced for 15–20 minutes. The lid was not held in place as was normal procedure so rapid venting and pressure release would be permitted if ignition occurred. No ignition was observed as was expected given the results of the flow experiments conducted earlier. Figure 4 shows a photograph of the static test cell used in this final experiment.

(d) Design of NEMA-8 enclosures and component integration/testing: In the final work conducted in FY 2014, a prototype field trials sensor unit was constructed using commercially sourced NEMA-8 enclosures and hardware. The lack of free space in explosion proof electrical conduits at the Hydrogen Frontier facility in Burbank precluded running new cables to provide power the sensor and electronics, and providing a means to send the sensor signal back to the data acquisition computer. Therefore, an inexpensive commercial wireless system was adopted (Omega Engineering). The field trial unit was constructed that placed the sensor/heater control and the wireless transmitter into a single NEMA-8 enclosure. Provisions were made to power the unit either by 120-V AC or by 24-V DC (as will be the case at the Burbank facility). A schematic of a deployed three-sensor network is also shown in Figure 5. Testing of the field trial unit is underway at LANL the time this report was assembled.

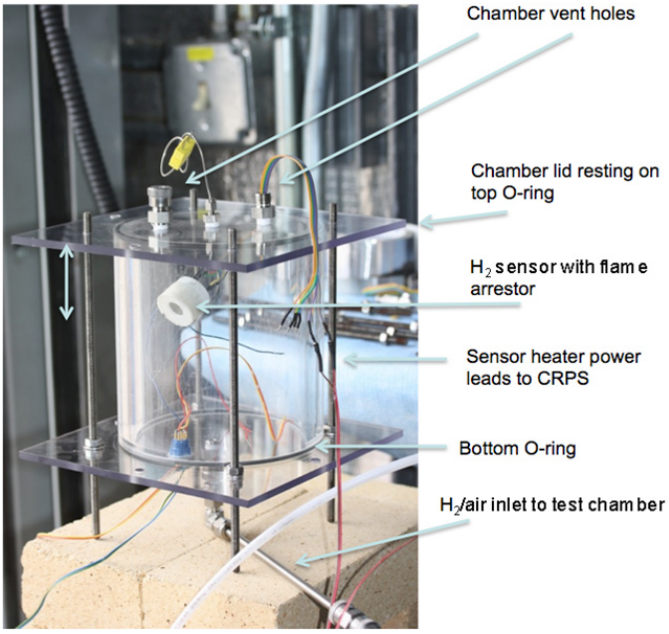

FIGURE 4. 10 vol% H_2 in air was introduced into a sensor test cell with sensor set at normal operating temperature inside the ceramic package that incorporates a flame arrestor. No ignition was observed during exposures up to 20 minutes. A Custom Sensor Solutions Constant Resistance Power Supply (CRPS) was used to maintain the sensor element at a normal operating temperature throughout the experiment.

The outdoor location and large temperature swings together with vibration, dust, and wildlife exposure, fires, etc. precluded the use of consumer computer equipment. An Advantech solid-state computer was selected and control software was custom designed by Agile Engineering and Zircoa Inc. Agile developed the software (executable LabVIEW program) and Zircoa tested the software and wireless systems. LANL is presently awaiting permission to test and use the wireless systems and is adhering to DOE/NNSA security requirements.

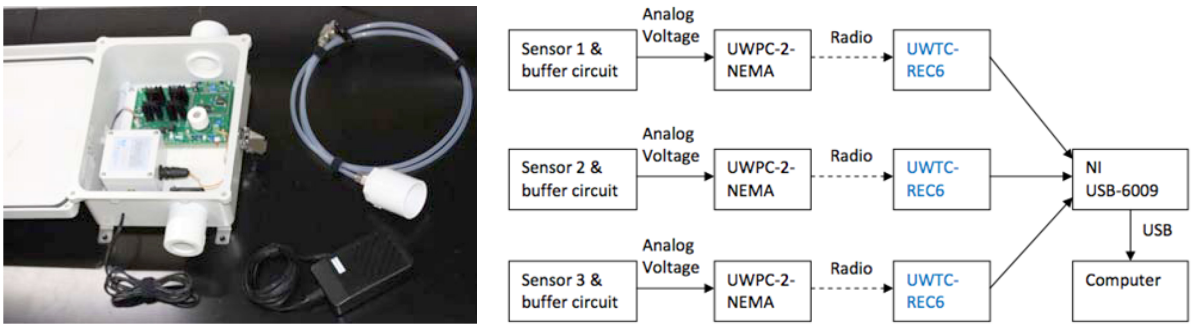

FIGURE 5. (left) Photograph of the first field trials LANL/LLNL hydrogen safety sensor unit and (right) a schematic of operation of a deployed, three-sensor system using a single industrial computer to log sensor voltage and calculated H_2 concentration.

(e) Establish design specifications for improved sensor platform and next generation electrode material from commercial partner ESL ElectroScience: All hydrogen sensors fabricated for use in this project over the past two years came from substrates prepared by ESL ca. 2011-2012. A new ceramic tape was used for the platform that may permit a very small amount of leakage current between heater circuit and sensor circuit. This leakage current prevents the LANL/LLNL H_2 sensor and impedance buffer circuits from operating at peak performance. A new batch of sensor platforms will be fabricated using higher performance tapes together with an insulating base coat. Moreover, an improved sensor design will be tested that utilizes the working electrode material reported last year the will easily entertain continued sensor operation in anaerobic conditions that NREL tested for in FY 2013. The use of a lanthanum chromite-based electrode will also permit the fabrication of the complete sensor in a single, two-step commercial firing approach that will significantly reduce fabrication costs and labor. Discussions with ESL began in the summer of FY 2014.

CONCLUSIONS

- The FY 2014 milestones were completed this year.
- A viable hydrogen safety sensor technology has been developed on an advanced sensor platform that continues to improve. An advanced hydrogen sensor prototype was fabricated on an alumina substrate with ITO and Pt electrodes and YSZ electrolyte with an integrated Pt heater to achieve precise operating temperature and minimize heterogeneous catalysis.
- New electronic control circuits were designed and fabricated that simplified the analog constant resistance power supply that maintains precise sensor Pt heater resistance (and therefore maintains precise temperature) and combines the high impedance buffer circuit that permits use of inexpensive National Instruments NI-6009 USB-DAQ unit to acquire sensor signal. Impedance buffer was designed to directly accept LANL sensor packaging to eliminate need for pigtail wires and to reduce noise and improve reliability.
- The prototype field trials system was situated inside a NEMA-8 enclosure guided by Class 1/Div. 2 standards along with wireless transmitter and supporting hardware. A means for one-time calibration was devised and tested.
- A model off-site field test plan for DOE federal laboratories developing project-funded technology, including insurance and indemnity that is required was drafted by LLNL. The experimental verification of intrinsic safety for the technology conducted at LANL was included as an appendix. In these experimental tests, ignition probability experiments in atmospheres up to 20 vol% H_2 in air were tested with naked sensors (no flame arrestor cap). At no time did a LANL/LLNL hydrogen sensor ignite flammable hydrogen mixtures with/without flame arrestor in place and at/well above normal sensor operating temperature in either dynamic static conditions.
- Several testing sites were identified in California. Discussions began in the end of FY 2013 with Dan Poppe at Hydrogen Frontier LLC. LANL research staff visited Hydrogen Frontier in April 2014 and three locations within the Burbank facility were identified as potential locations to site experimental field trials test units. As space within the explosion-proof wiring conduits was largely unavailable, a wireless system of operation was selected. Operational challenges identified include: high heat within cabinets (outdoor facility) and large temperature swings, vibration, insects, spiders, wind, water, potential for brush fires, flooding and nesting birds. Location ruled out the original plan to use a consumer laptop computer for data acquisition. A hardened, industrial computer was selected along with means to remotely interrogate sensor operation on a daily basis.
- In FY 2015, the California South Coast Air Quality Management District has tentatively agreed to co-fund the field test work (Board approval of proposal likely

in September) and two additional sites are the refueling stations at South Coast Headquarters in Diamond Bar and at the new station at California State University, Los Angeles.

- Systems integration and testing were started at LANL in June 2014 with target of August to complete initial testing of the first field trial unit.

FUTURE DIRECTIONS

- Build, test, and optimize design of field trial units (to extent permitted by resources).
- Site sensor unit(s) at Hydrogen Frontier in Burbank California South Coast Air Quality Management District, and potentially one additional location.
- Collate and analyze data from remote location.
- Set up mock field trials unit and experiments (NREL collaboration desired).
- Perform limited field testing.
- Seek out and engage potential partners for sensor testing and technology commercialization.
- Use data from deployed units to improve future field trial units.

COLLABORATION AND COORDINATION WITH COMMERCIAL PARTNERS AND OTHER INSTITUTIONS

- Los Alamos National Laboratory
- Lawrence Livermore National Laboratory
- Custom Sensor Solutions, Inc.
- Hydrogen Frontier, Inc.
- National Renewable Energy Laboratory
- ESL ElectroScience, Inc.
- Agile Engineering/Zircoa, Inc.

FY 2014 PUBLICATIONS AND PRESENTATION

1. P.K. Sekhar, Jie Zhou, Mathew B. Post, Leta Woo, William J. Buttner, William R. Penrose, Rangachargy Mukundan, Cortney R. Kreller, Robert S. Glass, Fernando H. Garzon, and Eric L. Brosha, "Independent Testing of Hydrogen Prototype Sensors," *Int. J. of Hydrogen Energy* **39** (2014) 4657-4663.

REFERENCES

1. W.J. Buttner, M.B. Post, R. Burgess, C. Rivkin, *Int. J. Hydrogen Energy*, **36**, 2462 (2011).

2. L. Boon-Brett, J. Bousek, G. Black, P. Moretto, P. Castello, T. Hübert, and U. Banach, Identifying performance gaps in hydrogen safety sensor technology for automotive and stationary applications, International Journal of Hydrogen Energy, 35 (2010), 373-384.

3. H.Iwahara, H.Uchida, K.Ogaki and H.Nagato, Nernstian Hydrogen Sensor Using $BaCeO_3$-Based, Proton-Conducting Ceramics Operative at 200-900^0 C, Journal of The Electrochemical Society, 138 (1991), 295-299.

4. Y. Tan and T.C. Tan, Characteristics and Modeling of a Solid State Hydrogen Sensor, The Journal of Electrochemical Society, 141 (1994), 461-466.

5. Z.Samec, F.Opekar, and G.J.E.F. Crijns, Solid-state Hydrogen Sensor Based on a Solid-Polymer Electrolyte, Electroanalysis, 7 (1995), 1054-1058.

6. Y-C.Liu, B-J. Hwang, and I.J.Tzeng, Solid-State Amperometric Hydrogen Sensor Using Pt/C/Nafion Composite Electrodes Prepared by a Hot-Pressed Method, Journal of The Electrochemical Society, 149 (2002), H173-H178.

7. L.B. Kriksunov, and D.D. Macdonald, Amperometric hydrogen sensor for high-temperature water, Sensors and Actuators B, 32 (1996), 57-60.

8. G.Lu, N.Miura, and N.Yamazoe, High-temperature hydrogen sensor based on stabilized zirconia and a metal oxide electrode, Sensors and Actuators B, 35-36 (1996), 130-135.

9. L.P. Martin and R.S. Glass, Hydrogen Sensor Based on Yttria-Stabilized Zirconia Electrolyte and Tin-Doped Indium Oxide Electrode, Journal of The Electrochemical Society, 152 (2005), H43-H47.

10. R.S. Glass, J. Milliken, K. Howden, R. Sullivan (Eds.), Sensor Needs and Requirements for Proton-Exchange Membrane Fuel Cell Systems and Direct-Injection Engines, 2000, pp. 7 – 15. DOE, UCRL-ID-137767.

11. G.Korotcenkov, S.D.Han and J.R.Stetter, Review of Electrochemical Hydrogen Sensors, Chemical Review, 109 (2009), 1402-1433.

12. L.P. Martin and R.S. Glass, Electrochemical Sensors for PEMFC Vehicles, presented at The 2004 DOE Hydrogen, Fuel Cells, and Infrastructure Technologies Program Review, Philadelphia, PA (May 27, 2004).

13. NREL/DOE Hydrogen Sensor Workshop, June 8, 2011, Chicago IL. http://www.hydrogen.energy.gov/pdfs/progress11/viii_3_burgess_2011.pdf

14. F.H.Garzon, R.Mukundan, and E.L.Brosha, Solid state mixed potential gas sensors: theory, experiments and challenges, Solid State Ionics, 136-137 (2000), 633-638.

15. P.K.Sekhar, E.L.Brosha, R.Mukundan, M.A.Nelson and F.H.Garzon, Application of Commercial Automotive Sensor Manufacturing Methods for NO_x/NH_3 Mixed Potential Sensors for Emission Control, ECS Transactions. 19 (2009), 45-49.

VIII.4 R&D for Safety, Codes and Standards: Materials and Components Compatibility

Chris San Marchi (Primary Contact),
Brian Somerday
Sandia National Laboratories (SNL)
P.O. Box 969
Livermore, CA 94551-0969
Phone: (925) 294-4530
Email: cwsanma@sandia.gov

DOE Manager
Will James
Phone: (202) 287-6223
Email: Charles.James@ee.doe.gov

Project Start Date: October 1, 2003
Project End Date: Project continuation and direction determined annually by DOE

Overall Objectives

- Optimize the reliability and efficiency of test methods for structural materials and components in hydrogen gas
- Generate critical hydrogen compatibility data for structural materials to enable technology deployment
- Create and maintain information resources such as the "Technical Reference for Hydrogen Compatibility of Materials"
- Demonstrate leadership in the international harmonization of standards for qualifying materials and components for high-pressure hydrogen service

Fiscal Year (FY) 2014 Objectives

- Demonstrate fatigue life measurements in gaseous hydrogen
- Determine boundary conditions for hosting "open-source" database of materials and materials properties in gaseous hydrogen
- Complete integration of automated gas-distribution manifold; establish cost estimates for variable-temperature testing hardware
- Foster growth of international collaboration and leadership on materials science of hydrogen embrittlement, in particular within the International Institute for Carbon-Neutral Energy Research (I2CNER)
- Leverage the partnership with the Japanese National Institute of Advanced Industrial Science and Technology (AIST) to supplement fracture testing database to influence materials testing standards; establish a roadmap for next phase collaboration with AIST (2015-2018)

Technical Barriers

This project addresses the following technical barriers from the Safety, Codes and Standards section (3.8) of the Fuel Cell Technologies Office Multi-Year Research, Development, and Demonstration Plan:

(A) Safety Data and Information: Limited Access and Availability

(F) Enabling national and international markets requires consistent RCS (regulations, codes and standards)

(G) Insufficient Technical Data to Revise Standards

Contribution to Achievement of DOE Safety, Codes and Standards Milestones

This project will contribute to achievement of the following DOE milestones from the Safety, Codes and Standards section of the Fuel Cell Technologies Office Multi-Year Research, Development, and Demonstration Plan:

- Milestone 2.9: Publish technical basis for optimized design methodologies of hydrogen containment vessels to account appropriately for hydrogen attack. (4Q, 2013)
- Milestone 2.16: Demonstrate the use of new high-performance materials for hydrogen applications that are cost-competitive with aluminum alloys. (4Q, 2017)
- Milestone 2.3: Implement validated mechanism-based models for hydrogen attack in materials. (4Q 2016)
- Milestone 3.3: Reduce the time required to qualify materials, components, and systems by 50% relative to 2011 with optimized test method development. (1Q 2017)
- Milestone 3.4: Develop hydrogen material qualification guidelines including composite materials. (Q4, 2017)
- Milestone 4.8: Completion of the GTR Phase 2. (1Q, 2017)
- Milestone 5.2: Update materials compatibility technical reference. (4Q, 2011-2020)
- Milestone 5.4 Develop and publish database for properties of structural materials in hydrogen gas. (2Q, 2013)

FY 2014 Accomplishments

- Completed the initial test matrix to measure fatigue life of the stainless steel 21Cr-6Ni-9Mn in 103 MPa hydrogen gas. This testing satisfies the need to quantitatively evaluate methods recently published in the the Compressed Hydrogen Material Compatibility standard (CHMC1) from the CSA Group and to generate qualification data for lower-cost stainless steels.
- Completed review and gap analysis of "Polymers for Hydrogen Infrastructure and Vehicle Fuel Systems" (report no. SAND2013-8904) in collaboration with the Hydrogen Delivery program element.
- Finalized design requirements and the procurement process for the variable-temperature testing in a hydrogen gas system.
- Devised a plan with international partner AIST to propose test methods to ASTM International for performing rising-displacement fracture threshold testing of structural metals in hydrogen gas.

INTRODUCTION

A principal challenge to the widespread adoption of hydrogen infrastructure is the lack of quantifiable data on its safety envelope and concerns about additional risk from hydrogen. To convince regulatory officials, local fire marshals, fuel suppliers, and the public at large that hydrogen refueling is safe for consumer use, the risk to personnel and bystanders must be quantified and minimized to an acceptable level. Such a task requires strong confidence in the safety performance of high-pressure hydrogen systems. Developing meaningful materials characterization and qualification methodologies in addition to enhancing understanding of performance of materials is critical to eliminating barriers to the development of safe, low-cost, high-performance high-pressure hydrogen systems for the consumer environment.

APPROACH

The Materials and Components Compatibility project leverages decades of experience in high-pressure hydrogen systems, well-developed industry partnerships, and a core capability in hydrogen-materials interactions anchored by the Hydrogen Effects on Materials Laboratory to focus on three critical activities: (1) optimize materials characterization methodologies, (2) generate critical hydrogen compatibility data for materials to enable technology deployment, and (3) provide international leadership by assembling and maintaining a technical reference that is populated with vetted data and includes a technical assessment of the data and its application.

RESULTS

Fatigue Life Measurements in Gaseous Hydrogen

Fatigue life assessment is a common design methodology that has only recently received attention in the context of qualifying materials for hydrogen service. In particular, the revised CHMC1 standard from CSA Group describes a materials qualification pathway that uses notched fatigue tests to qualify materials for hydrogen service.

Notched fatigue tests in high-pressure gaseous hydrogen were demonstrated at SNL for an austenitic stainless steel, 21Cr-6Ni-9Mn. Testing results (Figure 1) show a significant effect of high-pressure gaseous hydrogen (103 MPa) on the fatigue cycles to failure for nominally the same applied stress cycle. The results are also compared to previous testing in air with a more acute notch showing that the fatigue life in hydrogen is greater than for tests in air with a more acute notch. The significance of these results is not yet clear, as more data is necessary to clarify the trends. In general, the testing has shown that the testing configuration in gaseous hydrogen is feasible and provides basic trends that are

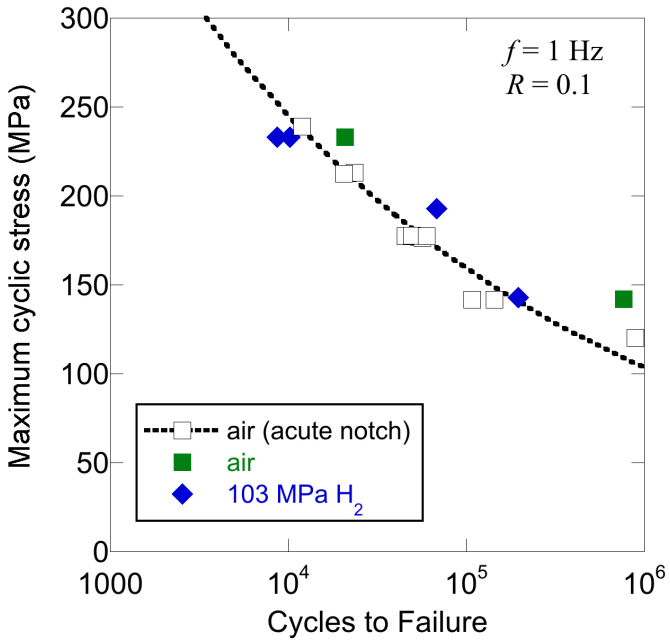

FIGURE 1. Stress amplitude cycles to failure plot for notched cylindrical fatigue tests, comparing tests in gaseous hydrogen with tests in air; open symbols represent tests in air with an acute notch, while closed symbols represent specimens with a notch as called out in CSA CHMC1.

consistent with expectations (e.g., power-law-like relationship between stress and cycles to failure).

Fatigue life assessment (e.g., using notched tensile fatigue tests) is anticipated to aid the qualification of lower cost materials for generic high-pressure hydrogen service; however, more work is necessary to demonstrate reproducibility and evaluate the effects of notch acuity in these tests. The effect of frequency must also be considered for fatigue testing, but has not been explored in this testing configuration.

"Open-Source" Database of Material Properties in Gaseous Hydrogen

Access to reliable and searchable materials properties measured in gaseous hydrogen is a significant limitation to selection of materials for hydrogen service. As part of the continued effort to provide access to materials selection information, Sandia teamed with Pacific Northwest National Laboratory to review the state of the art of polymeric materials in hydrogen systems, an effort jointly funded by the Hydrogen Delivery and the Safety, Codes and Standards programs. The resulting report included an extensive review of data and test methods for evaluating polymers in gaseous hydrogen and high pressure as well as an analysis of major gaps in knowledge and data related to selection of polymers for hydrogen service. Additionally, SNL is exploring methods to augment the Technical Reference for Hydrogen Compatibility of Materials (http://www.sandia.gov/matlsTechRef/) with a database of materials properties for both metals and polymers. As part of the Material Data Management Consortium (MDMC), an industry consortium organized by Granta Design, Sandia has engaged support for building the schema for incorporation of environmental variables in the Granta MI database structure with the aim of a comprehensive hydrogen effects in materials database. Discussions with Granta and individuals from MDMC suggest a precedent for data exchange using Web-based interface built on Granta database tools, such as Granta MI. Granta is the leader in materials information/database management solutions. Additional discussion is required to quantify the cost of maintaining an open platform for dissemination of materials properties measured in gaseous hydrogen.

System for Variable-Temperature Testing in Hydrogen Gas

Materials qualification for hydrogen fueling applications requires the measurement of materials properties, especially fatigue properties, in high-pressure gaseous hydrogen and low temperature. It is well known, for example, that certain materials such as austenitic stainless steels are most susceptible to hydrogen embrittlement at temperatures near 233 K (-50°C). Facilities for testing materials under the combined influence of variable temperature and high pressure do not exist nationally. Sandia maintains a core capability in hydrogen embrittlement of structural materials, in which the Hydrogen Effects on Materials Laboratory is the central asset. This laboratory features several specialized systems for measuring the mechanical properties of materials in high-pressure gaseous hydrogen; however, fatigue evaluation of materials is limited to testing at room temperature. Work is underway to add variable temperature testing to the fatigue testing capabilities in the Hydrogen Effects on Materials Laboratory.

The major components of the apparatus for variable-temperature testing in hydrogen has have been acquired. The final procurements are being made with investment from both Fuel Cell Technologies Office and the National Nuclear Security Administration. The Advancing Materials Testing in Hydrogen Gas workshop hosted by Sandia in March 2013 was instrumental in focusing attention on an internal cooling mechanism for the pressure vessel. A prototype cooling mechanism was designed and tested under ambient conditions. This mechanism is relatively simple in concept, consisting primarily of a copper-cooling block in contact with a stainless steel tube carrying cryogenic fluid (Figure 2a). This prototyping activity demonstrated that the target temperature of 223 K (-50^{o}C) could be attained at a cylindrical stainless steel test specimen surrounded by the copper-cooling block. In parallel with this successful prototyping, a student intern at Boise State simulated the temperature distribution in the concept pressure vessel with internal cooling mechanism. Example results from these SolidWorks simulations are displayed in Figure 2b.

Once operational, this system will provide system designers with data necessary to develop robust, cost-effective low-temperature hydrogen systems for storage and dispensing applications.

International Collaboration with I2CNER

Significant resources are being invested around the world in hydrogen material research. I2CNER is one of the premier organizations dedicated to the advancement of hydrogen materials science. Through coordination of hydrogen materials science research in the U.S. and Japan, hydrogen technology can be accelerated. Dr. Brian Somerday leads the Hydrogen Materials Compatibility division of I2CNER, providing a direct link between hydrogen embrittlement studies across the Pacific. Dr. Somerday co-organized several high-profile events for I2CNER in FY 2014:

- Coordination meeting for the Hydrogen Materials Compatibility division at Yufuin, Japan, to promote interaction within the division and refine the research roadmap of the division (December 2013)
- The Joint HYDROGENIUS and I2CNER International Workshop on Hydrogen-Materials Interactions at the International Hydrogen Energy Development Forum in Fukuoka, Japan (January 31, 2014)

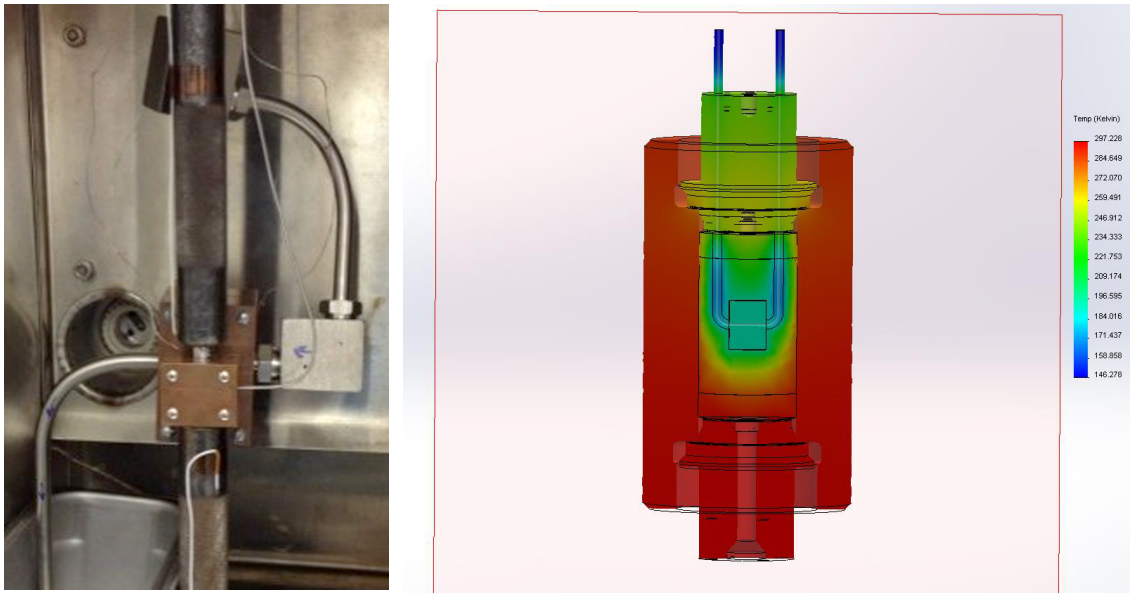

FIGURE 2. (a) Prototype cooling mechanism consisting of copper cooling block with stainless steel tubing carrying cryogenic fluid. (b) SolidWorks simulation of temperature distribution in pressure vessel with internal cooling mechanism.

Leveraging Partnership at AIST

International harmonization of methods for qualifying materials for hydrogen service is widely recognized as critical to the deployment of hydrogen technologies. Sandia interacts broadly with international partners to promote unified test methods, including research collaboration with staff from AIST (who visit Sandia regularly). The Sandia team hosted the SNL-AIST Workshop on High-Pressure Hydrogen Storage Systems in January 2014. The main outcomes of the workshop were (i) a plan for proposing revision of ASTM testing standards to include special requirements for testing gaseous hydrogen, (ii) identification of opportunities for risk analysis around materials and pressure vessels, and (iii) extension of materials testing activities in gaseous hydrogen. Future testing activities are contingent on budgets. Figure 3 shows the foundational data generated collectively by SNL and AIST; these data are anticipated to influence testing standards, such as those from ASTM International. Several papers were prepared jointly by SNL and AIST to be presented at the ASME 2014 Pressure Vessel and Piping Division Conference.

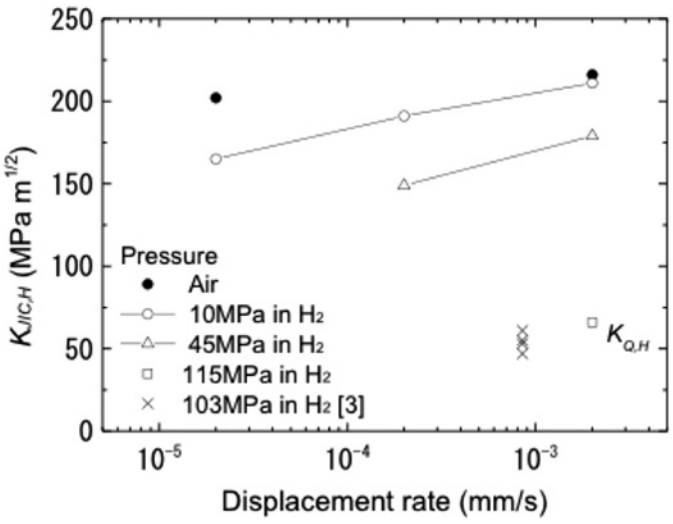

FIGURE 3. Rising-displacement fracture thresholds measured for SA372 Grade J pressure vessel steel in air and high-pressure hydrogen gas. Data points in plot represent measurements from both SNL (cross symbols) and AIST (other symbols).

CONCLUSIONS AND FUTURE DIRECTIONS

- Fatigue life testing on the stainless steel 21Cr-6Ni-9Mn in 103 MPa hydrogen gas has two potential impacts, quantitative evaluation of methods recently published in the CSA CHMC1 standard and qualification data for a lower-cost stainless steel.
- Progress in developing the variable-temperature testing system bolsters the core capability for materials characterization in high-pressure hydrogen and assures critical testing can be performed on technologically pivotal materials such as stainless steels.
- International partnerships with I2CNER and AIST provide access to basic science related to materials behavior in hydrogen and data that enable the development of international standards for materials testing and component qualification.

- (future) Formalize schema for material property database in Granta MI.
- (future) Commission variable-temperature testing in hydrogen gas system to integrate subsystems and demonstrate functionality.
- (future) Continue critical evaluation of test methods in CSA CHMC1, including rate effects (AIST collaboration) and "safety factor method" option.
- (future) Develop R&D project with industry partner(s) to evaluate and improve resistance of high-strength structural metals to hydrogen-assisted fracture.

SPECIAL RECOGNITIONS & AWARDS/ PATENTS ISSUED

1. Brian Somerday and Chris San Marchi, DOE Hydrogen and Fuel Cells Program Awards, Hydrogen Delivery and Safety, Codes and Standards, 2014.

FY 2014 PUBLICATIONS/PRESENTATIONS

1. C. San Marchi and B.P. Somerday, "Comparison of stainless steels for high-pressure hydrogen service" (PVP2014-2881), accepted for ASME 2014 Pressure Vessel and Piping Division Conference, Anaheim CA, 20–24 July 2014.

2. T. Iijima, B. An, C. San Marchi, B.P. Somerday, "Measurement of fracture properties for ferritic steel in high-pressure hydrogen gas" (PVP2014-28815), accepted for ASME 2014 Pressure Vessel and Piping Division Conference, Anaheim CA, 20–24 July 2014.

3. B. An, T. Iijima, C. San Marchi, B.P. Somerday, "Micromechanisms of hydrogen-assisted cracking in super duplex stainless steel investigated by scanning probe microscopy" (PVP2014-28181), accepted for ASME 2014 Pressure Vessel and Piping Division Conference, Anaheim CA, 20–24 July 2014.

4. (invited) J. Ronevich, B. Somerday, C. San Marchi, H. Jackson, and K. Nibur, "Fracture Resistance of Hydrogen Precharged Stainless Steel GTA Welds", SteelyHydrogen 2014: Second International Conference on Metals & Hydrogen, Ghent, Belgium, May 2014.

5. (invited) B. Somerday, "Technological and Industrial Progress in Hydrogen and Fuel Cells in the U.S.", International Hydrogen Energy Development Forum 2014, Fukuoka, Japan, Jan. 2014.

6. C. San Marchi and B.P. Somerday, "Design philosophies for high-pressure hydrogen storage systems". Presented at the AIST-SNL Workshop on High Pressure Hydrogen Storage Systems, Livermore CA, January 24, 2014 (SAND2014-0538P).

7. H.F. Jackson, C. San Marchi, D.K. Balch, B.P. Somerday, "Effect of low temperature on hydrogen-assisted crack propagation in 304L/308L austenitic stainless steel fusion welds". Corros Sci 77 (2013) 210-221.

8. C. San Marchi, B.P. Somerday, K.A. Nibur, "Development of methods for evaluating hydrogen compatibility and suitability", accepted to Intern J Hydrogen Energy.

9. L.A. Hughes, B.P. Somerday, D.K. Balch, C. San Marchi, "Hydrogen compatibility of austenitic stainless steel tubing and orbital tube welds", accepted to Intern J Hydrogen Energy.

10. R.R. Barth, K.L. Simmons, C. San Marchi, "Polymers for Hydrogen Infrastructure and Vehicle Fuel Systems: Applications, Properties and Gap Analysis" SAND2013-8904 (October 2013).

11. C. San Marchi, B.P. Somerday, K.A. Nibur, "Measuring fracture properties in gaseous hydrogen", presented at International Workshop on Hydrogen Embrittlement in Natural Gas Pipelines, Seoul, Korea, November 27, 2013 (SAND2013-10058P).

12. C. San Marchi, "Hydrogen transport in metals", invited presentation at Korean Research Institute of Standards and Science, Daejeon, Korea, November 2013 (SAND2013-10059P).

13. C. San Marchi, K.A. Nibur, "Materials qualification for hydrogen service using CSA CHMC1", presented at to Japanese stakeholders during informational meeting at SNL/CA, November 8, 2013 (SAND2013-9607P).

14. M. Dadfarnia, B.P. Somerday, P.E. Schembri, P. Sofronis, J.W. Foulk, III, K.A. Nibur, and D.K. Balch, "On Modeling Hydrogen Induced Crack Propagation Under Sustained Load", *JOM*, 2014, in press.

15. B.P. Somerday and M. Barney, "Measurement of Fatigue Crack Growth Relationships in Hydrogen Gas for Pressure Swing Adsorber Vessel Steels", *Journal of Pressure Vessel Technology*, 2014, accepted for publication.

Sandia National Laboratories is a multi-program laboratory managed and operated by Sandia Corporation, a wholly owned subsidiary of Lockheed Martin Corporation, for the U.S. Department of Energy's National Nuclear Security Administration under contract DE-AC04-94AL85000.

VIII.5 Hydrogen Fuel Quality

T. Rockward (Primary Contact), C. Quesada, F. Garzon, and R. Mukundan
P.O Box 1663
Los Alamos National Laboratory (LANL)
Los Alamos, NM 87545
Phone: (505) 667-9587
Email: trock@lanl.gov

DOE Manager
Will James
Phone: (202) 287-6223
Email: Charles.James@ee.doe.gov

Project Start Date: October 2006
Project End Date: Project continuation and direction determined annually by DOE

Overall Objectives

To support the Hydrogen Safety, Codes and Standards Program through:

- Participation in working group 12 providing leadership to hydrogen fuel quality efforts
- Performing the research and development needed to develop science-based codes and standards
- Develop tools that can remove safety and hydrogen fuel quality barriers to the commercialization of fuel cells

Fiscal Year (FY) 2014 Objectives

- To carry out the duties of ASTM International (ASTM) sub-committee chair for D03.14 gaseous hydrogen fuel efforts.
- To test an operating fuel cell using membrane electrode assemblies (MEAs) with ultra-low platinum loadings with impurity mixture at the levels indicated in the international standard for hydrogen fuel quality 14687-2 document (International Organization for Standardization [ISO] TC197 WG12) [1]/SAE International (SAE) J2719 [2].
- To demonstrate improved sensitivity of electrochemical analyzer to carbon monoxide.
  - Report results to the DOE
- ·To demonstrate proof-of-concept electrochemical analyzer capable of detecting low levels (few ppb) of H_2S in hydrogen fuel.
  - Report results to the DOE

Technical Barriers

This project addresses the following technical barriers from the Hydrogen Safety, Codes and Standards (section 3.7.5) of the Fuel Cell Technologies Office Multi-Year Research, Development, and Demonstration Plan:

(F) Enabling National and International Markets Requires Consistent RCS (regulations, codes and standards)

(G) Insufficient Technical Data to Revise Standards

(H) Insufficient Synchronization of National Codes and Standards

(K) No Consistent Codification Plan and Process for Synchronization of R&D and Code Development

FY 2014 Accomplishments

- Contributions to ASTM
  - Sub-committee Chair D03.14
  - Coordinated test labs for Inter-Laboratory Study (ILS) 775, ASTM D7649 - Test Method for Determination of Trace CO_2, Ar, N_2, O_2 and H_2O in Hydrogen Fuel by Jet Pulse Injection and GC/MS Analysis. Chaired an ASTM national meeting.
- In-line Fuel Quality Analyzer
  - Improved sensitivity of analyzer to CO using different electrode configuration
  - Proof of concept demonstrated for H_2S analyzer using a platinum black electrode:
  - Observed response to 10 ppb H_2S
  - Demonstrated clean-up techniques after H_2S exposure

  a). Impurity testing with ultra-low platinum MEAs
  - Completed testing with ISO mixture at various relative humidities (RHs)
  - Measured impedance spectra during exposure to ISO mixture
  - Tested MEAs for CO tolerance varying the concentrations (i.e. 0.2, 0.5, and 1.0 ppm CO); results showed a similar decay as our baseline. Experiments will be revisited.

  b). DOE/Japan Automobile Research Institute (JARI) and European Union (EU) Collaboration
  - Visited the JARI test facility
  - Conducted baseline measurements using LANL MEAs with 0.05 and 0.10 mg Pt/cm^2 at the anode and cathode, respectively

- Completed tests using JARI MEAs with two different Pt loadings (MEA #1: 0.05/0.1 mg Pt/cm^2 and MEA #2: 0.3/0.3 mg Pt/cm^2 for the anode and cathode, respectively)
- Initiated collaboration with VTT Technical Research Centre of Finland
- Began installing anode recirculation system for fuel quality testing
- Discussed international round-robin tests between JARI/EU/DOE

INTRODUCTION

The work performed in this project has been partitioned into four tasks: a) contributions to ASTM standards development, b) in-line fuel quality analyzer development, c) R&D for fuel quality standards development, and d) international collaborations.

The international team (ISO TC197 WG-12) for "development of a hydrogen fuel product specifications for use in proton exchange membrane fuel cell applications for road vehicles"; (ISO 14687-2:2012) [1] indicates acceptance levels of several contaminants. Although these contaminants are at sub-ppm levels, their effect on fuel cell performance is uncertain, especially since the total platinum content in the fuel cell MEA has been continuously lowered. Previously conducted fuel cell tests with the fuel specification indicated that ammonia, carbon monoxide and hydrogen sulfide were the critical constituents most harmful to proton exchange membrane fuel cell performance and/or its durability.

Science-based standards have been established; however, there is still a need to provide the tools necessary to implement this standard. LANL is helping this effort by providing leadership to ASTM in developing methods to determine the impurity content in the fuel. While steam reforming natural gas will make hydrogen affordable and available, it will produce trace amounts of CO and H_2S. The ISO has a maximum allowance of 0.2 ppm for CO and 4 ppb for H_2S [1]. Although the hydrogen grade should be certified, it would be invaluable to have in-line analyzers to protect expensive fuel cell systems and components from these contaminants. LANL demonstrated proof-of-concept for an in-line fuel quality analyzer using various concentrations of CO at or below the levels in the aforementioned standard. Our goal is to provide a quick and cheap method of detection at various points in the supply chain.

APPROACH

R&D for Fuel Quality Standards

Tests were conducted on 50-cm^2 MEAs using a total platinum loading of 0.15 mg/cm^2. The MEAs were supplied by Ion Power with an anode loading of 0.03 mg Pt/cm^2, and cathode loading of 0.12 mg Pt/cm^2, and a membrane thickness of 25 μm. The gas diffusion layers used were SIGRACET® 25BC manufactured by SGL.

In one set of experiments, the MEAs were subjected to approximately 200 hours of exposure to the ISO mixture (critical contaminants) at 100% and 50% RH in an operating fuel cell. In yet another set of experiments, we varied the CO concentration while keeping the dosage constant in order to quantify the MEA's CO tolerance level.

In-line Fuel Quality Analyzer

The interaction of either H_2S or carbon monoxide in a hydrogen stream over a platinum surface results in inhibition of hydrogen dissociation, and inherently lower current output that can be measured as increasing resistance of the system. The fuel quality analyzer is composed of a active area MEA ≤5 cm^2 with platinum-based electrodes. The electrodes were modified in order to improve the analyzer's sensitivity and selectivity to adsorbates. More specifically, we employed a low surface area platinum electrode sputtered on carbon cloth, Pt black (Alfa Aesar HiSPEC™ 1000 by Johnson Matthey), or PtRu (Pt: 30 wt%, Ru: 23.3 wt%, by TKK, Japan) loaded with 0.1 mg Pt/cm^2 as our working electrode in the experiments.

The counter electrode is either a PtRu electrode or a high surface area BASF Pt-Vulcan carbon with 0.2 mg Pt/cm^2. All MEAs were hot pressed on to Nafion® 117 membrane (thickness ≈180 μm), a much thicker membrane than the traditional fuel cell membranes (thickness <50 μm) for enhanced stability and sensitivity. The PtRu or the BASF high surface area electrode was positioned as the counter/reference electrode and exposed to ultra-high purity hydrogen only, while the adsorbates were introduced at the working electrode. Stripping voltammetry is used to verify the presence of either CO or H_2S, their amount, and to oxidize those species off the electrode's surface, which inherently doubles as a regenerating tool for subsequent measurements.

Here, we report the response of a modified platinum-type electrode to ppb levels of H_2S. This 5-cm^2 MEA had a working electrode prepared from a catalyst ink made of unsupported-catalyst powder (~6.3 nm particle size) and Nafion® solution (5%, 1,100 equivalent weight). The absence of a carbon support and the large initial Pt particle size are desirable for an electrode to be durable and have a low active surface area that is ultra sensitive to adsorbates.

RESULTS

Contributions to ASTM Standards Development

Sub-Committee Chair; Officer Duties: The sub-committee chair is responsible for preparing items for Sub- and Main-Committee ballots, resolving negative votes on the website, hosting meetings and recording minutes. Furthermore, the duties include registration of work items, organizing collaboration areas, submitting items for ballot, scheduling virtual meetings, handling negatives and comments, and organizing ILS.

On-Going Standards Development: The D03 Subcommittee D03.14 on Hydrogen and Fuel Cells is responsible for developing standards, specifications, practices, and guidelines relating to hydrogen used in energy generation or as feed gas to low-, medium- and high-temperature fuel cells. One current standard being developed under ASTM D03.14 is "Test Method for Determination of Trace CO_2, Ar, N_2, O_2 and H_2O in Hydrogen Fuel by Jet Pulse Injection and GC/MS Analysis."

ILS: The ultimate goal of ILS is to enhance the quality of ASTM standard test methods by assisting technical committees as they develop precision statements backed by high-quality laboratory data for their test method, so as to incorporate at least a repeatability statement.

In FY 2014, LANL scientists coordinated test labs for ILS 775 (ASTM D7649) through several conference calls. We also provided a data reporting format for compiling the ILS results.

In-Line Analyzer Development

As describe in FY 2013, the analyzer is designed to be operated as a hydrogen pump, with hydrogen flowing on both sides. A potentiostat is used to probe the electrode with a voltage and to measure the current response from hydrogen oxidizing on one side and protons reducing on the other. When plotted as current versus voltage, the inverse of the slope of the resulting line gives the resistance of the cell that is strongly affected by any poisoning of the Pt electrode. Hydrogen pump experiments were performed at 30°C and 100% RH using 100 sccm of hydrogen gas at each electrode without any applied backpressure to obtain a baseline. The working electrode was then exposed to either CO or H_2S, and the experimental details and results are listed in the sub-sections following.

a) Carbon Monoxide Exposure

We previously reported that the standard Pt electrode does get poisoned over time and decreasing the Pt loading and/or the Pt surface area can dramatically improve sensitivity to impurities. We studied various electrode conventions, and probed their responses to 200, 100, 50 and 25 ppb CO. We measured the analyzer response during the first 5 minutes of exposure using 1 minute increments and again at 1, 3, 5 and 7 hours. The shorter increments were chosen for employing the analyzer at a hydrogen filling station, while the longer periods could satisfy on-board fuel monitoring in the anode re-circulation loop.

Our experimental results from the three different working electrode configurations were successfully utilized in increasing the analyzer sensitivity. Each of the three electrodes was exposed to 200, 100, 50, and 25 ppb CO for 7 hours. The PtRu electrode did not respond to the sub-ppm levels of CO. However, the Pt black electrode did, and an observable increase in analyzer resistance occurred between 1 and 3 hours when exposed to 200 ppb CO, and less than 5 hours when exposed to 100 ppb of CO. This electrode did not respond (no change in resistance) when exposed to 50 ppb CO for up to 7 hours. Therefore the tolerance of this electrode lies in the region between 50 and 100 ppb CO. The sputtered electrode responded to each of the CO concentrations, and thus was the most sensitive of the three electrodes. For example, it responded to 100 ppb CO in less than an hour and to 25 ppb in less than 3 hours. The analyzer

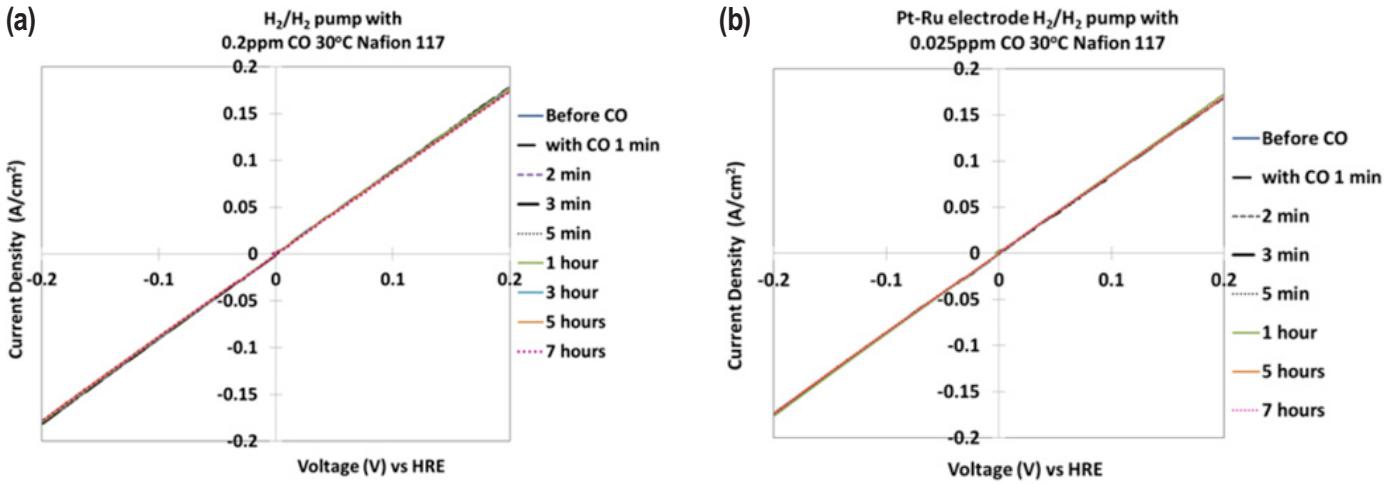

FIGURE 1. (a) and (b) show the impact of varying CO concentration on a Pt-Ru working electrode of the electrochemical analyzer.

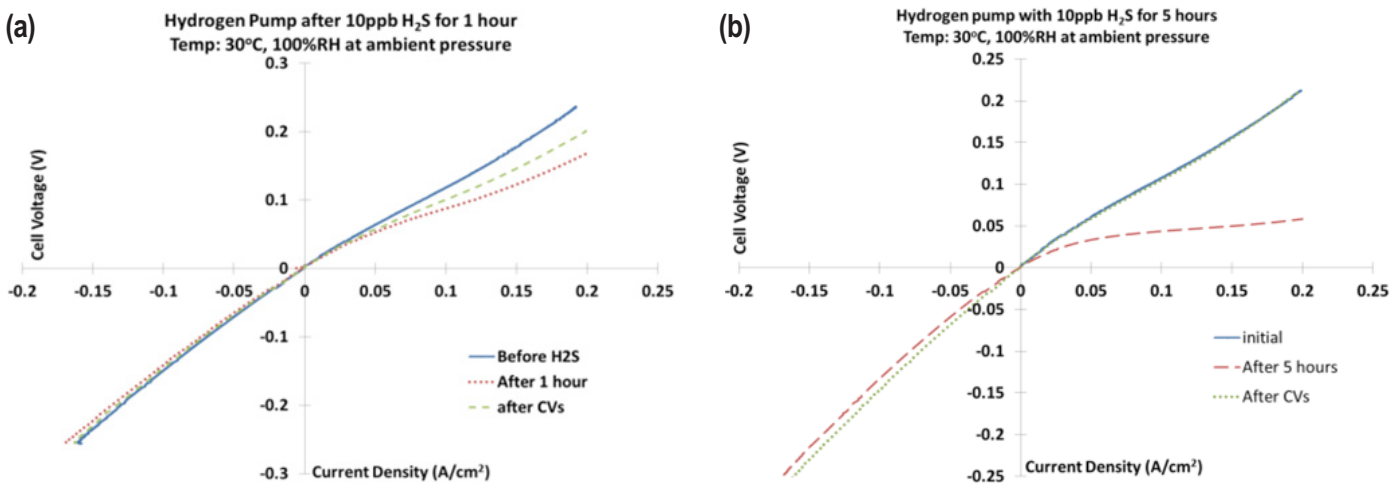

FIGURE 2. (a) and (b) demonstrate the impact of 10 ppb H_2S for 1-hr and 5-hr exposure times on a Pt black working electrode of the electrochemical analyzer.

sensitivity improved, as we hypothesized, with lower surface area electrodes. In fact, the sputtered electrode's response time was 5 times faster than the Pt black in the presence of 100 ppb CO. Figure 1 (a) and (b) show the family of current-voltage curves during exposure to 200 ppb and 25 ppb CO on the surface of a PtRu working electrode. The resistance of each remained constant throughout the duration of the experiments. This is typical for the PtRu, which can typically tolerate CO levels that exceeds the ISO concentration level for longer than 7 hours. These results indicate that by using a PtRu electrode as a psedo reference electrode and a sputtered Pt electrode as a working electrode we can design an analyzer that is sensitive to CO concentrations up to an order of magnitude lower than the current SAE CO standards (200 ppb)

b). Hydrogen Sulfide Exposure

We completed our FY 2014 milestone, which was to demonstrate the proof of concept of the analyzer to respond in the presence of 10 ppb H_2S. The current-voltage curves and cyclic voltammograms (CVs) before and after exposing the working electrode to H_2S were measured. Figure 2 shows an increase in the H_2 pumping resistance in the presence of H_2S. After four CV sweeps to 1.0 V, some of the H_2S was removed from the surface of the Pt and the H_2 pump resistance indicated a partial recovery. Figure 2 illustrates the effect of the 10 ppb H_2S over 5 hours and shows an increased degree of poisoning (larger increase in resistance) which can be completely recovered after 4 potential sweeps to 1.1 V followed by four more potential sweeps to 1.4 V. The observed resistance change is the direct result of H_2S adsorbing onto active platinum sites preventing hydrogen dissociation from occurring. Figure 2(a) and (b) demonstrate the impact of 10 ppb H_2S at 30°C, after 1 and 5 hour exposures. In Figure 2(a) the performance of the analyzer does not fully recover after CVs were run to 1.1 V, however after increasing our

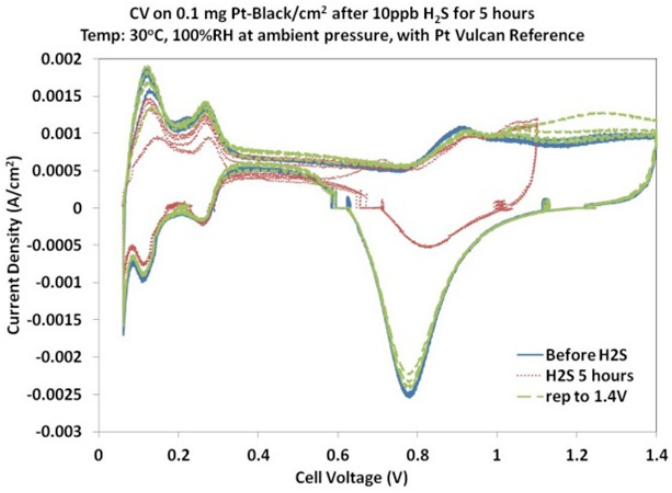

FIGURE 3. illustrates a CV of the working electrode after exposure to 10 ppb H_2S and cycled up to 1.1 V and subsequently to 1.4 V.

voltage to 1.4 V the performance returns to its original state (shown in Figure 2(b). Figure 3 illustrates the decrease in the hydrogen desorption from the Pt surface due to H_2S adsorption and its recovery after the H_2S is desorbed at the higher potentials. These results indicate that the high voltage (>1.4 V) cleaning can be utilized to reset the analyzer after prolonged H_2S exposures, while low voltage (0.6–1.0 V) can be utilized to impart selectivity to CO vs. H_2S.

R&D for Fuel Quality Standards

We completed 200 hours of tests with the ISO mixture in the hydrogen fuel stream. We used low-loaded anodes (0.03 mg-Pt/cm^2) to comply with existing DOE Pt loading targets. Fuel cells were run at 80°C, using two different RHs,

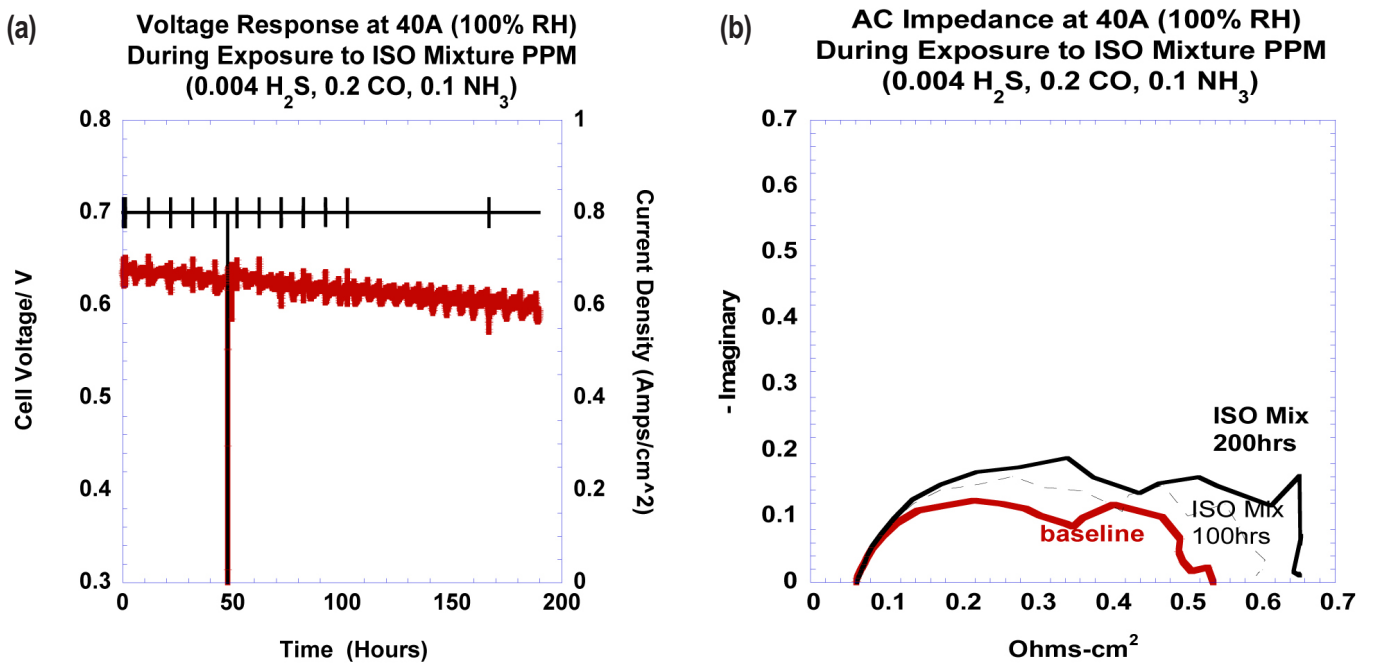

FIGURE 4. (a) shows the voltage response of an fuel cell operated at 1 A/cm^2 during exposure to 0.004 ppm H_2S, 0.2 ppm CO, and 0.1 ppm NH_3 and (b) captures its impedance spectra during the time of exposure using 0.05 and 0.1 mg Pt/cm^2 at the anode and cathode, repsectively.

with the current held at 0.8 A/cm^2. Total impedance spectra were also obtained throughout the experiments. Figures 4(a) and (b) highlight the voltage response over time of fuel cells operated at 100% RH and 30 psig back pressure and the impedance curves respectively. At 100% RH, we observed a voltage decay of 56 mV, while tests at 50% RH showed a 120 mV loss. Additional tests were conducted using MEAs with identical platinum loadings in the presence of low concentrations of CO with a focus on obtaining a tolerance level for CO. Tests were conducted using three different CO concentrations (0.2 ppm, 0.5 ppm, and 1.0 ppm). We observed a voltage decay rate similar to our baseline in each of these experiments. CVs were obtained to probe the platinum surface after each exposure. and indicated that CO was present at both electrodes, even though we intended to expose the anode only. We are currently examining this issue to determine other possible sources of CO contamination (humidifier bottles, etc..) before quantifying the CO tolerance of this low Pt-loaded MEA.

CONCLUSIONS AND FUTURE DIRECTIONS

In FY 2014, we improved the sensitivity of the analyzer to respond to 100 ppb CO in under an hour and less than 3 hours to 25 ppb CO. We also demonstrated the response of the analyzer to 10 ppb H_2S, which is 2.5 times the ISO level. However, we intend to reduce the platinum loading further to enhance both sensitivity and response time to both CO and H_2S.

In FY 2014 LANL continued to provide leadership to the ASTM Subcommittee D03.14 on Hydrogen and Fuel Cells. In FY 2014, LANL, JARI, and the EU established a working relationship. This collaboration will focus on fuel quality and durability. LANL will work on the following tasks in FY 2015.

- Continue providing leadership to ASTM efforts
- Improve response time and sensitivity of the electrochemical analyzer to CO and H_2S
- Develop a robust design for an analyzer to be utilized in a H_2 stream at a fueling station
- Perform tests with ultra-low platinum loading and state-of-the-art materials using the ISO concentration levels in DOE drive cycles using anode re-circulating systems
- Understand CO and H_2S recovery mechanisms in state-of-the-art MEAs
- Continue DOE/JARI/EU/LANL collaboration that incorporates durability and drive cycle tests in the presence of impurities

COLLABORATORS/PARTNERS

- Working Group-12 Members
- Japanese Automotive Research Institute
- European Union
- ASTM

- Air Liquide
- California Fuel Cell Partnership
- CONSCI

REFERENCES

1. Organization, I.S., *Hydrogen fuel — Product specification — Part 2: Proton exchange membrane (PEM) fuel cell applications for road vehicles*, in *ISO TC 197*2012, ISO copyright office: Case postale 56 • CH-1211 Geneva 20.

2. SAE J2719: Hydrogen Fuel Quality for Fuel Cell Vehicles, www.sae.org

VIII.6 R&D for Safety Codes and Standards: Hydrogen Release Behavior and Risk Assessment

Chris San Marchi (Primary Contact), Katrina Groth, Chris LaFleur, Ethan Hecht, Isaac Ekoto
Sandia National Laboratories
P.O. Box 969
Livermore, CA 94551-0969
Phone: (925) 294-4880
Email: cwsanma@sandia.gov

DOE Manager
Will James
Phone: (202) 287-6223
Email: Charles.James@ee.doe.gov

Project Start Date: October 1, 2003
Project End Date: Project continuation and direction determined annually by DOE

Overall Objectives

- Build tools to enable industry-led codes and standards (C&S) revision and safety analyses to be based on a strong science and engineering basis.
- Develop and validate hydrogen behavior physics models to address targeted gaps in knowledge.
- Develop hydrogen-specific quantitative risk assessment (QRA) tools and methods to support regulations, codes and standards decisions and to enable performance-based design (PBD) code-compliance option.
- Eliminate barriers to deployment of hydrogen fuel cell technologies through scientific leadership in codes and standards development efforts.

Fiscal Year (FY) 2014 Objectives

- Develop version 1 of an integrated hydrogen-specific risk assessment toolkit (HyRAM) to enable sustained use of QRA by a broad range of users.
- Initiate research activity with industrial partners to use QRA tool to implement and validate performance-based compliance approach of National Fire Protection Association (NFPA) 2 Chapter 5.
- Develop technical plan and partnerships for building experimental test platform for hydrogen release behavior at cryogenic temperatures.
- Conduct modeling and experimental activities to develop and validate reduced order modeling of jet flame behavior and deflagration overpressures.
- Provide expert perspective on QRA and behavior models to relevant codes and standards committees to promote the adoption of science-based methods.

Technical Barriers

This project addresses the following technical barriers from the Hydrogen Safety, Codes and Standards section of the Fuel Cell Technologies Office Multi-Year Research, Development, and Demonstration Plan:

(A) Safety Data and Information: Limited Access and Availability

(F) Enabling National and International Markets Requires Consistent Regulations, Codes and Standards

(G) Insufficient Technical Data to Revise Standards

(L) Usage and Access Restrictions (parking structures, tunnels and other usage areas)

Contribution to Achievement of DOE Safety, Codes and Standards Milestones

This project will contribute to achievement of the following DOE milestones from the Safety, Codes and Standards section of the Fuel Cell Technologies Office Multi-Year Research, Development, and Demonstration Plan:

- Milestone 2.8: Publish risk mitigation strategies. (2Q, 2014)
- Milestone 2.7: Provide critical understanding of hydrogen behavior relevant to unintended releases in enclosures. (4Q, 2013)
- Milestone 2.10: Understand flame acceleration leading to transition to detonation. (4Q, 2014)
- Milestone 2.11: Publish a draft protocol for identifying potential failure modes and risk mitigation. (4Q 2014)
- Milestone 2.13: Develop and validate simplified predictive engineering models of hydrogen dispersion and ignition. (4Q 2015)
- Milestone 2.19: Validate inherently safe design for hydrogen fueling infrastructure. (4Q, 2019)
- Milestone 4.7: Complete risk mitigation analysis for advanced transportation infrastructure systems. (1Q, 2015)
- Milestone 4.8: Revision of NFPA 2 to incorporate advanced fueling storage systems and specific requirements for infrastructure elements such as garages and vehicle maintenance facilities. (3Q, 2016)

FY 2014 Accomplishments

- Report: developed a metric to evaluate the development of hydrogen codes and standards and benchmarked program activity to show progress in enabling technology deployment
- Workshop: organized and led hydrogen C&S QRA user workshop to help build stakeholder awareness of risk and to identify barriers that limit industry use of QRA
- Developed an integrated reduced-order behavior model for predicting overpressures associated with transient hydrogen releases for use in risk-informed C&S development.
- Developed a detailed project plan to research and model the behavior of unintended releases of hydrogen at cold and cryogenic temperatures
- Updated existing reduced-order flame radiation models with large scale, downstream flame radiation behavior to improve prediction of downstream heat flux

INTRODUCTION

DOE has identified safety, codes, and standards as a critical barrier to the deployment of hydrogen, with key barriers related to the availability and implementation of technical information in the development of RCS. This project provides the technical basis for assessing the safety of hydrogen fuel cell systems and infrastructure using QRA and physics-based models of hydrogen behavior. The risk and behavior tools that are developed in this project are motivated by and shared directly with the committees revising relevant codes and standards, thus forming the scientific basis to ensure that code requirements are consistent, logical, and defensible.

APPROACH

This work leverages Sandia's unique experimental and modeling capabilities and combines these efforts with stakeholder engagement and international leadership. The behavior of hydrogen releases is examined using state-of-the-art diagnostics in the Turbulent Combustion Laboratory. Results of these experiments are used to develop and validate predictive engineering tools for flame initiation, flame sustainment, radiation patterns, and overpressures. The resulting behavior models provide the foundation for QRA modeling efforts, which include scenario analysis, consequence modeling, and quantification of risk. These integrated hydrogen behavior and QRA models are then applied to relevant technologies and systems to provide insight into the risk level and risk mitigation strategies with the aim of enabling the deployment of fuel cell technologies through revision of hydrogen safety, codes, and standards.

RESULTS

Develop Version 1 of HyRAM

Code committees and industry are both interested in using QRA to enable code development and code compliance for hydrogen systems. Gaps and limited availability of QRA tools for hydrogen form a barrier to this goal. This core research activity addresses the hydrogen QRA tool gap by integrating validated models and data into a Windows®-based engineering tool with a graphical user interface. This tool is called HyRAM, Hydrogen Risk Assessment Models.

Figure 1 is a flowchart that shows the various modules used within HyRAM. Initial elements of the flowchart were independently developed in Matlab®. The unified HyRAM tool replaces this array of independent modules to enable broader application of QRA by stakeholders. The modular architecture and open-source license set the stage for future development activities to occur collaboratively with other research organizations. HyRAM version 1 contains graphical user interfaces for "QRA mode," which enables end-to-end use of the HyRAM modules to calculate risk from jet flames for user-defined gaseous hydrogen systems. Toolkit priorities are based on published proceedings of the QRA user workshop held in June 2013. Version 1 of HyRAM, which is to be completed at the end of 2014, can be used to quantify the likelihood and thermal consequences associated with jet fires from gaseous releases from user-defined hydrogen installations. Future development activities include enabling stand-alone use of behavior models for consequence calculations and the addition of new consequence calculations (such as overpressure) to expand the type of infrastructure that can be modeled in HyRAM.

Cold and Cryogenic Hydrogen Behavior Research

Bulk liquid hydrogen storage has the benefit of a higher storage potential that enables greater station throughput over similarly sized gaseous systems. However, validated models of liquid hydrogen releases—critical information needed for risk-based strategies—do not exist, due to a lack of adequate data from science-based test platforms with full control over release boundary conditions. Sandia developed a detailed project plan to research and model the behavior of unintended releases of hydrogen at cold and cryogenic temperatures. Additionally, under a Cooperative Research and Development Agreement with industry, we have begun designing an experimental platform for generating the missing data. The preliminary design is shown in Figure 2. After installation and performance-testing of the cryogenic hydrogen release laboratory are complete (targeted for late 2015), the laboratory will be used to develop comprehensive data sets

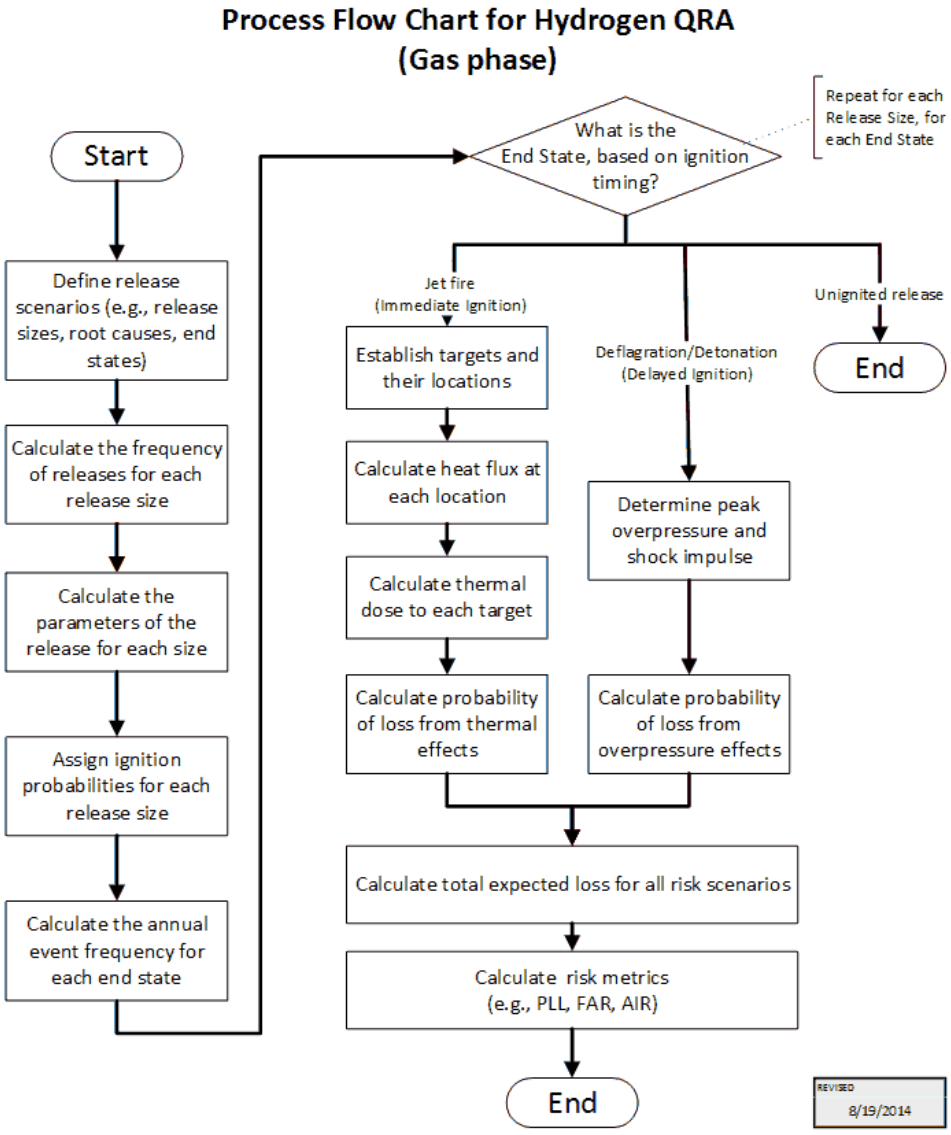

FIGURE 1. Flowchart of modules contained in the HyRAM toolkit. Modules can be used end-to-end, as illustrated in this figure, or in stand-alone calculations.

relevant to releases from liquid hydrogen storage systems similar to those located at commercial fueling stations. This will enable development and experimental validation of cold-plume release models that can be integrated into QRA and safety assessments to enable deployment of liquid hydrogen infrastructure.

Hydrogen Behavior Modeling and Experimental Validation

Ongoing research occurring over the past decade at Sandia has resulted in the development and validation of numerous scientific models of the behavior of gaseous hydrogen releases. During FY 2014, the jet flame model was updated to account for downstream buoyancy behavior that was observed during experimental validation activities. This and other physical models (products of several years of research in this program) are being consolidated, modularized, and documented for integration into the HyRAM toolkit. Gaseous hydrogen jet dispersion models and jet flame models (along with the required sub-models, e.g., notional nozzle models) were formalized and integrated into HyRAM during FY 2014. Ongoing activity includes a first-order overpressure model suitable for integrating into HyRAM in the FY 2015 timeframe. Several of these models and their sub-models require additional validation data and further refinement, including the overpressure model, the notional nozzle model, and models of liquid hydrogen behavior. Additionally, we are planning experiments to reduce the ambiguity in the notional nozzle (under-expanded jet) model in collaboration with a student from Tsinghua University.

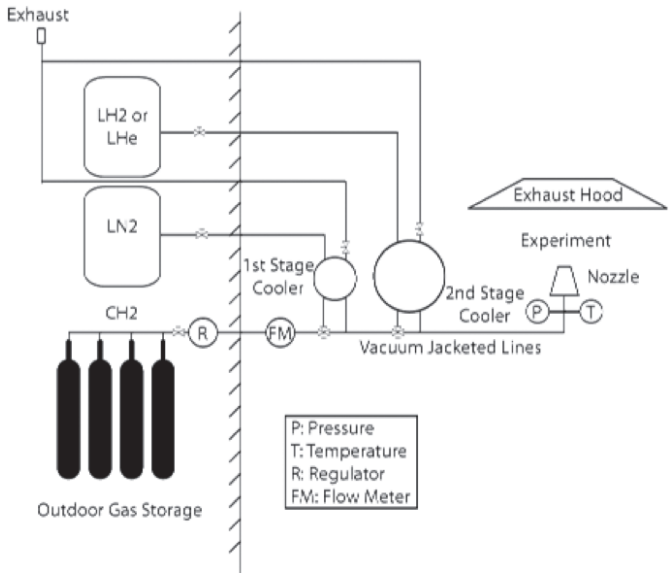

FIGURE 2. Cryogenic release laboratory design—gaseous hydrogen is cooled in two stages, by liquid nitrogen and then liquid hydrogen, before release.

Develop Design Brief to Enable Performance-Based Compliance Option

NFPA 2, Hydrogen Technologies Code, allows for the use of PBD for hydrogen facilities as a means of complying with the code without strict adherence to the prescriptive code requirements. While HyRAM can be used as a means of evaluating the risk of alternate designs, it can also be used to quantitatively evaluate risks associated PBD options. The establishment and demonstration of PBD option will directly increase the availability of locations for hydrogen fueling stations, reduce the effort required by industry to use the PBD approach and lay the groundwork for similar QRA-backed design processes for other alternative fuels. In order to initiate real-world application of science-based risk analysis, a Cooperative Research and Development Agreement was initiated with a major hydrogen fueling station provider.

Figure 3 depicts the approach of the application of QRA to the design of both a representative commercial hydrogen refueling station and a real-world station. The HyRAM software will be used to calculate the risk metrics for a station that is fully compliant with the prescriptive code requirements in order to establish a baseline for these metrics for a specific station configuration. In the next phase of work, a station design with key modifications to the prescriptive requirements will be evaluated with input from the industry partner. This mock PBD will then be vetted with in the fire protection and hydrogen industries with the aim of identifying best practices for implementing PBD methods. Following this, a real-world station with a key modification backed by a performance-based design will be processed through the permitting process for a hydrogen station in California.

Codes and Standards Participation

- CSA Group HGV 4.9 – Hydrogen fueling station guidelines have been edited and reorganized and are ready for industry review before they become a CSA Group standard.
- Hydrogen Safety Panel – Sandia participated in several hydrogen safety plan reviews for innovative industrial hydrogen implementations as well as participating in the revision of the hydrogen event data collection fields.
- NFPA 2 – Sandia participated in the second draft meeting of the 2016 version of NFPA 2 Hydrogen Technologies Code. Sandia also actively participated in the reactivation of the NFPA 2 liquid hydrogen separation distances task group, which began work on revision of the prescriptive requirements for the next revision cycle of the code.

CONCLUSIONS AND FUTURE DIRECTIONS

- Project impact is demonstrated by benchmarking metric: "Number of sites that can readily accept hydrogen"
  - (future) Re-evaluate benchmark to evaluate R&D investments at key project milestones and to ensure continued alignment with program goals.
- A template for implementing the performance-based approach in NFPA2 Chapter 5 is the next step for increasing the number of sites that can readily accept hydrogen.
  - (future) Demonstrate PBD option and work the PBD brief through a permitting process to demonstrate acceptance of a PBD approach by an authority having jurisdiction.
- HyRAM provides a standardized platform for developing and integrating hydrogen QRA and consequence models into codes and standards.
  - (future) Add reduced order overpressure model and features to enable PBD.
  - (future) Formalize rules for user-defined models and international harmonization of methodology.
- Improved physics-based models of hydrogen behaviors (e.g., jet flame model, multi-source radiation model) improves the fidelity of risk calculations.
  - (future) Improve the accuracy of the sub-models, particularly the notional nozzle model, through targeted experiments.

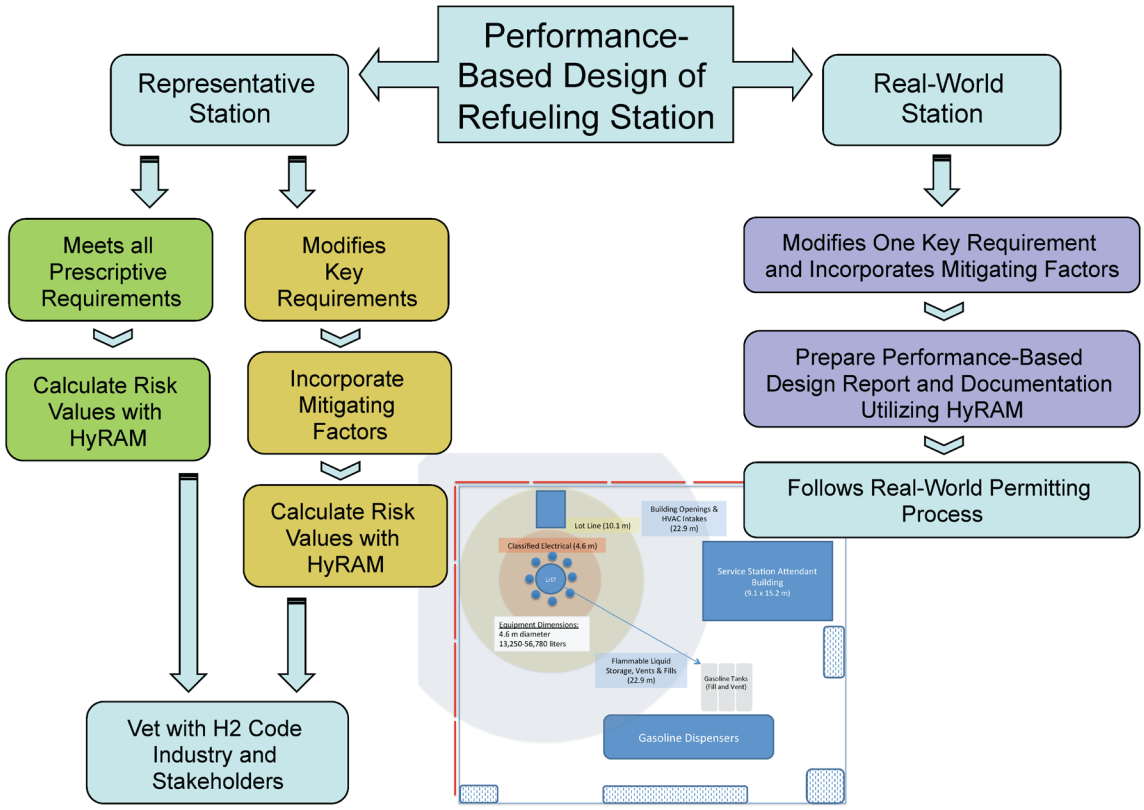

FIGURE 3. Overview of PBD Application of QRA

- An integrated, reduced-order overpressure model enables the calculation of overpressure in HyRAM and fills a key gap in modeling hydrogen deflagrations.
  - (future) Add overpressure model into HyRAM in the early FY 2015 timeframe.
  - (future) Validate model accuracy and make improvements as needed.
- The storage of liquefied hydrogen is limited by the existing code requirements and predictive behavior models for liquefied hydrogen releases.
  - (future) Construct experimental platform for characterizing the unintended release of liquid-vapor mixed-phase hydrogen releases (with support from industry).

Sandia National Laboratories is a multi-program laboratory managed and operated by Sandia Corporation, a wholly owned subsidiary of Lockheed Martin Corporation, for the U.S. Department of Energy's National Nuclear Security Administration under contract DE-AC04-94AL85000.

FY 2014 PUBLICATIONS/PRESENTATIONS

1. A.C. LaFleur, K. Groth, A.B. Muna. "Application of Quantitative Risk Assessment (QRA) to Hydrogen Fueling Infrastructure for FCEVs." Presentation at the 2014 ASME 12th Fuel Cell Science, Engineering and Technology Conference, Boston, MA, July 2014.

2. K. Groth "Hydrogen behavior and Quantitative Risk Assessment." Presentation at the 2014 DOE Hydrogen Fuel Cell Technologies Program Annual Merit Review, Washington, DC. June 2014.

3. K. Groth. "Hydrogen QRA & HyRAM Toolkit Introduction" Presentation at side-meeting on Hydrogen Risk Assessment at DOE Hydrogen Fuel Cell Technologies Program Annual Merit Review, Washington, DC. June 2014.

4. A.C. LaFleur, A.B. Muna, "Hydrogen Fueling Station Performance-Based Approach." Presented at 20th Hydrogen Safety Panel (HSP) meeting, Golden, CO, May 2014.

5. K.M. Groth. "Hydrogen QRA & HyRAM Toolkit Introduction" Presented at 20th Hydrogen Safety Panel (HSP) meeting, Golden, CO, May 2014.

6. A.V. Tchouvelev, K.M. Groth, P. Benard, T Jordan. "A Hazard Assessment Toolkit For Hydrogen Applications." *Proc World Hydrogen Energy Conference* (WHEC 2014), 2014.

7. K.M. Groth, A.V. Tchouvelev, "A toolkit for integrated deterministic and probabilistic risk assessment for hydrogen infrastructure*." Proc Int Conf Probabilistic Safety Assessment and Management (PSAM 12)*, June 2014.

8. I.W. Ekoto, A.J. Ruggles, L.W. Creitz, J.X. Li. "Updated Jet Flame Radiation Modeling with Corrections for Buoyancy". *Int. J. of Hydrogen Energy*, Accepted in 2014.

9. A.J. Ruggles, I.W. Ekoto. "Experimental investigation of nozzle aspect ratio effects on underexpanded hydrogen jet release characteristics*," International Journal of Hydrogen Energy*, Accepted March 2014.

10. K.M. Groth, J.L. LaChance, A.P. Harris. "Design-stage QRA for indoor vehicular hydrogen fueling systems". *Proc of the European Society for Reliability Annual Meeting (ESREL 2013).*

11. A.P. Harris, D.E. Dedrick, A.C. LaFleur and C. San Marchi, "Safety, Codes and Standards for Hydrogen Installations: Hydrogen Fueling System Footprint Metric Development." SAND2014-3416, Sandia National Laboratories, April 2014.

12. A.C. LaFleur, "Risk and Reliability Analysis" presented at AIST-SNL workshop on High Pressure Hydrogen Storage Systems, January 24, 2014.

13. K.M. Groth, "Sandia H2 Quantitative risk assessment (QRA) activities." Presented to DOE H2 CSTT, December 19, 2013.

14. A. Harris. "Survey of Materials Selection Information for Hydrogen Service" Presented to US DOE Hydrogen Safety Panel meeting, December 11, 2013.

15. A. Harris. "Leak Rate Standard Working document" Presented to US DOE Hydrogen Safety Panel meeting, December 11, 2013.

16. A. Harris. "Results from a case study of separation distances in support of program performance metric development for US DOE EERE FCTO" Presented to California Fuel Cell Partnership, December 4, 2013.

17. K.M. Groth, "SNL QRA toolkit and SNL-HySafe workshop." Presented to International Energy Agency Hydrogen Implementing Agreement Task 31 experts workshop (IEA HIA), October 15, 2013.

18. I.W. Ekoto, A.J. Ruggles, L.W. Creitz, J.X. L. "Updated Jet Flame Radiation Modeling with Corrections for Buoyancy." Proc Int Conf Hydrogen Safety, Brussels, Belgium, September 2013.

19. A.J. Ruggles, I.W. Ekoto. "Experimental investigation of nozzle aspect ratio effects on underexpanded hydrogen jet release characteristics." *Proc Int Conf Hydrogen Safety*, Brussels, Belgium, September 2013.

20. I.W. Ekoto. "Hydrogen release and deflagration experiments within a scaled, ventilated warehouse." Presented at HyIndoor Advanced Research Workshop, Brussels, Belgium, September 12, 2013.

21. I.W. Ekoto, "Simulation of hydrogen-air deflagrations within ventilated warehouse enclosures." Presented at HyIndoor Advanced Research Workshop, Brussels, Belgium, September 12, 2013.

22. K.M. Groth, "Design-stage QRA for indoor vehicular hydrogen fueling systems." Presented at the European Society for Reliability Annual Meeting (ESREL 2013), Amsterdam, 2013.

VIII.7 Hydrogen Emergency Response Training for First Responders

Nick Barilo
Pacific Northwest National Laboratory (PNNL)
P.O. Box 999
Richland, WA 99354
Phone: (509) 371-7894
Email: nick.barilo@pnnl.gov

DOE Manager
Will James
Phone: (202) 287-6223
Email: Charles.James@ee.doe.gov

Subcontractors
- Jennifer Hamilton, California Fuel Cell Partnership, West Sacramento, CA
- Volpentest HAMMER Federal Training Center, Richland, WA

Project Start Date: October 2004
Project End Date: Project continuation and direction determined annually by DOE

Overall Objectives

A properly trained first responder community is critical to the successful introduction of hydrogen fuel cell applications and their role in transforming how we use energy. This project supports the implementation of hydrogen and fuel cell technologies by providing technically accurate hydrogen safety and emergency response information to first responders.

Fiscal Year (FY) 2014 Objectives

Develop and conduct reviews of the National Emergency Response Education Program training template and slide package.

Technical Barriers

This project addresses the following technical barriers from the Safety, Codes and Standards (SCS) section 3.7.5 and Education (ED) section 3.8.5 of the Fuel Cell Technologies Office Multi-Year Research, Development, and Demonstration Plan:

(A) Safety Data and Information: Limited Access and Availability (SCS)

(D) Lack of Hydrogen Knowledge by AHJs (Authorities Having Jurisdiction) (SCS)

(E) Lack of Hydrogen Training Materials and Facilities for Emergency Responders (SCS)

(A) Lack of Readily Available, Objective and Technically Accurate Information (ED)

(D) Lack of Educated Trainers and Training Opportunities (ED)

Contribution to Achievement of DOE Safety, Codes and Standards and Education Milestones

This project will contribute to achievement of the following DOE milestones from the Safety, Codes and Standards section 3.7.7 and Education section 3.8.7 of the Fuel Cell Technologies Office Multi-Year Research, Development, and Demonstration Plan:

- 5.3 Enhance hydrogen safety training props and deliver classroom curriculum for emergency response training. (4Q, 2012) (SCS)
- 1.1 Update "Introduction to Hydrogen Safety for First Responders" course. (Biannually) (ED)

FY 2014 Accomplishments

- Several drafts of the slide package for the National Hydrogen Emergency Response Education Program have been prepared, reviewed and updated in anticipation of public release. A training template has been completed to guide program use and future enhancements.
- The PNNL project team interacted several times with the European Commission-funded HyResponse project to establish a collaborative effort on first responder training.
- The project team contributed to a PNNL-led planning session of diverse organizations and expertise to consider what electronic safety resource tools would benefit the next phase of hydrogen and fuel cell commercialization. The draft report identifies and recognizes the importance of new resource tools to meet the needs of a high priority user group—the first responder community [1].
- An educational session, "Hydrogen and Fuel Cell Vehicles: Educating Emergency Responders," was conducted at the 2014 NFPA Conference & Expo to expand outreach efforts and audiences as part of this project [2].

INTRODUCTION

Safety in all aspects of a future hydrogen infrastructure is a top priority, and safety concerns influence all DOE hydrogen and fuel cell projects. Despite the most concerted effort, however, no energy system can be made 100% risk-free. Therefore, for any fuel and energy system, a suitably trained emergency response force is essential to a viable infrastructure. The Fuel Cell Technologies Office has placed a high priority on training of emergency response personnel, not only because these personnel need to understand how to respond to a hydrogen incident, but also because firefighters and other emergency responders are influential in their communities and can be a positive force in the introduction of hydrogen and fuel cells into local markets.

This project employs the Occupational Safety and Health Administration and National Fire Protection Association frameworks for hazardous materials emergency response training to provide a tiered hydrogen safety education program for emergency responders. The effort started with development and distribution of the awareness-level online course in FY 2006–2007. An operations-level classroom curriculum was developed in FY 2008–2009, including the design, construction and operation of a fuel cell vehicle prop for hands-on training. In addition, PNNL has implemented outreach efforts to key stakeholder groups to not only facilitate delivery of training to a broad audience, but to consider new and relevant resources and approaches for meeting an important need.

APPROACH

PNNL works with subject matter experts in hydrogen safety and first responder training to develop, review, and revise all training materials as needed. The PNNL project team works with DOE to inform stakeholder groups of training opportunities and to provide "live" training when appropriate. The online awareness-level course is also available as a CD and provides the student with a basic understanding of hydrogen properties, uses, and appropriate emergency response actions. The operations-level classroom/hands-on prop-based course was initially presented at the Volpentest HAMMER Federal Training Center in Richland, WA. Subsequently, the operations-level course has been delivered at several offsite fire training centers in California and Hawaii to reach larger audiences in areas where hydrogen and fuel cell technologies are being deployed (see Table 1).

New approaches are needed to meet the specific needs of first responders and presentation styles of training organizations and to complement numerous existing training programs. The National Hydrogen and Fuel Cell Emergency Response Education Program will help ensure a consistent source of accurate information and current knowledge. As part of this program, a training template will be developed as a resource and guide for the delivery of a variety of training regimens to various audiences.

RESULTS

Drafts of the slide package for the National Hydrogen and Fuel Cell Emergency Response Education Program were completed and distributed to stakeholders and training organizations for review and feedback. In parallel, a training template was developed that will be integral to the first version of the program. Working meetings were held in Washington, D.C. in June 2014 during the DOE Hydrogen Program Annual Merit Review and Peer Evaluation Meeting for PNNL and California Fuel Cell Partnership staff to review all program draft materials, identify improvements, suggest edits and establish actions to complete the first version of slide package. An updated template/slide package was released to the full project team in mid-July for further review.

PNNL and DOE staff met with U.S. Fire Administration staff at the National Fire Academy, Emmitsburg, MD on November 15, 2013 to discuss our work on first responder

TABLE 1. Deployment of Operations-Level First Responder Training

Agency	Location	Date	Trained
HAMMER Federal Training Center	Richland, WA	2009-2010	66
Rio Hondo Community College	Santa Fe Springs, CA	August 2010	103
Orange County Fire Authority	Irvine, CA	August 2010	92
Sunnyvale Department of Public Safety	Sunnyvale, CA	September 2010	110
San Joaquin Defense Logistics Agency	Stockton, CA	June 2011	41
Los Angeles City Fire Department	Los Angeles, CA	January 2012	128
Los Angeles County Fire Department	San Dimas, CA	March 2012	170
Honolulu Fire and Federal Fire-HI	Honolulu, HI	February 2013	155
HI County Fire and Volcanoes National Park	Hilo, HI	February 2013	135
		Total	**1000**

training and identify potential areas of collaboration. The U.S. Fire Administration is a strong proponent of first responder training on hydrogen and fuel cells, and sees a definite need for these resources and wishes to assist with the program. Follow-up interactions are planned.

The need for first responder training resources has been well recognized internationally, and the value of collaboration in meeting those needs is also well understood. For example, to fill a need in the European-based hydrogen and fuel cell program, the HyResponse project was initiated in 2013 to develop a comprehensive, standardized hydrogen safety training program for emergency personnel. Discussion with HyResponse project staff was initiated at the 2013 International Conference on Hydrogen Safety and continued during a teleconference meeting on March 26, 2014 with HyResponse project leads [3,4].

PNNL hosted Lieutenant Colonel Bertrand Cassou, a division chief in the French Academy for Fire, Rescue and Civil Protection Officers, and Franck Verbecke, hydrogen reliability and safety product manager at AREVA, during the week of April 21, 2014. The visit provided an opportunity to discuss how PNNL's hydrogen first responder training program, which supports DOE's Hydrogen and Fuel Cells Program, and the HyResponse team can collaborate for mutual benefit. The possible exchange of videos and virtual reality training resources to enhance each program's content was discussed. During the visit, PNNL demonstrated the hands-on, live-fire vehicle prop that is used for its operations-level first responder training curriculum as well as other PNNL capabilities that could support such collaboration. PNNL also invited local fire department officers to witness the live prop demonstrations. Subsequent to that visit, DOE and PNNL accepted invitations to speak at the HyResponse project's International Workshop on Hydrogen Safety Training for First Responders, at the French Academy for Fire, Rescue and Civil Protection Officers, Aix-en-Provence, France, September 3-4, 2014 [5].

CONCLUSIONS AND FUTURE DIRECTIONS

It is critical that training materials for the awareness-level and operations-level courses be kept accurate and current. To remain vital and useful, such resources require concerted efforts beyond general maintenance. Relevance to the community being served and value to the individual user/attendee are key attributes for these resources.

The National Hydrogen and Fuel Cell Emergency Response Education Program is expected to become the focal point for delivering training resources under this project. In that spirit, it is vital that feedback from presenters and audiences to the developers and content stewards be collected, assessed and acted on to ensure that new and updated training content and techniques are incorporated into the program. Outreach and collaboration will be essential to future work.

FY 2014 PUBLICATIONS/PRESENTATIONS

1. Barilo, N.F., "Hydrogen Emergency Response Training for First Responders," DOE Hydrogen Program Annual Merit Review and Peer Evaluation Meeting, Washington, DC, June 18, 2014.

REFERENCES

1. Barilo, N.F., "Electronic Safety Resource Tools – Supporting Hydrogen and Fuel Cell Commercialization," Draft PNNL report, August 2014.

2. Elmore, M.R., "Hydrogen and Fuel Cell Vehicles: Educating Emergency Responders," NFPA Conference and Expo, Las Vegas, NV, June 9–12, 2014.

3. Hamilton, J.J., "Development of a Hydrogen and Fuel Cell Vehicle Emergency Response National Template," International Conference on Hydrogen Safety, Brussels, Belgium, September 10, 2013.

4. Verbecke, F., Vesy, B., Lopez, M., Molkov, V., Reijalt, M., Dey, R., Maranne, E. and Dang-Nhu, G., "European Hydrogen Safety Training Platform for First Responders: HyResponse Project," international Conference on Hydrogen Safety, Brussels, Belgium, September 9–11, 2013.

5. Weiner, S.C., "First Responder Training – Resources and Future Direction," PNNL-SA-104297, International Workshop on Hydrogen Safety Training for First Responders, ENSOSP, Aix-en-Provence, France, September 3–4, 2014.

VIII.8 Hydrogen Safety Panel and Hydrogen Safety Knowledge Tools

Nick Barilo
Pacific Northwest National Laboratory (PNNL)
P.O. Box 999
Richland, WA 99354
Phone: (509) 371-7894
Email: nick.barilo@pnnl.gov

DOE Manager
Will James
Phone: (202) 287-6223
Email: Charles.James@ee.doe.gov

Subcontractors
- Addison Bain, NASA (ret), Melbourne, FL (completed Panel service in December 2013)
- David J. Farese, Air Products and Chemicals, Inc., Allentown, PA
- William C. Fort, Shell Global Solutions (ret), Fairfax, VA
- Larry Fluer, Fluer, Inc., Paso Robles, CA
- Don Frikken, Becht Engineering, St. Louis, MO
- Aaron Harris, Air Liquide, Houston, TX
- Richard A. Kallman, City of Santa Fe Springs, CA
- Larry Moulthrop, Proton OnSite, Wallingford, CT
- Glenn W. Scheffler, GWS Solutions of Tolland, LLC, Tolland, CT
- Andrew J. Sherman, Powdermet Inc., Euclid, OH
- Ian Sutherland, General Motors, Warren, MI
- Robert G. Zalosh, Firexplo, Wellesley, MA

Project Start Date: 2004
Project End Date: Project continuation and direction determined annually by DOE

Overall Objectives

- Provide expertise and recommendations to DOE and help identify safety-related technical data gaps, best practices and lessons learned.
- Help DOE integrate safety planning into funded projects to ensure that all projects address and incorporate hydrogen and related safety practices.
- Collect information and share lessons learned from hydrogen incidents and near misses with a goal of preventing similar safety events from occurring in the future.
- Capture vast and growing knowledge base of hydrogen experience and make it publicly available to the "hydrogen community" and stakeholders.

Fiscal Year (FY) 2014 Objectives

- Conduct ongoing safety assessments of DOE projects through project reviews and site visits.
- Develop a Panel position on the safety of hydrogen systems installed in outdoor enclosures.
- Increase number of records in database by encouraging "incident owners" to share lessons learned with the hydrogen community.
- Enhance utility of the safety knowledge tools.

Technical Barriers

This project addresses the following technical barriers from the Hydrogen Safety, Codes and Standards section of the Fuel Cell Technologies Office Multi-Year Research, Development, and Demonstration Plan:

(A) Safety Data and Information: Limited Access and Availability

(C) Safety is Not Always Treated as a Continuous Process

(D) Lack of Hydrogen Knowledge by AHJs (Authorities Having Jurisdiction)

(G) Insufficient Technical Data to Revise Standards

Contribution to Achievement of DOE Safety, Codes and Standards Milestones

This project contributes to achievement of the following DOE tasks and milestones from the Hydrogen Safety, Codes and Standards section (3.7) of the Fuel Cell Technologies Office Multi-Year Research, Development, and Demonstration Plan:

- Task 1: Address Safety of DOE R&D (research and development) Projects (ongoing)
- Task 5: Dissemination of Data, Safety Knowledge and Information (ongoing)
- Milestone 5.1: Update safety bibliography and incidents databases. (4Q, 2011–2020)

FY 2014 Accomplishments

- Conducted the 19th Hydrogen Safety Panel (HSP) meeting in Washington, D.C., December 10–12, 2013, and the 20th meeting at the National Renewable Energy Laboratory in Golden, CO, May 13–15, 2014.
- Participated in 13 project reviews (including safety plan and design review activities) since July 1, 2013 for projects in fuel cell and hydrogen storage R&D.

- Completed an HSP white paper, "Safety of Hydrogen Systems Installed in Outdoor Enclosures" [1].
- Authored an *NFPA Journal* (National Fire Protection Association) article focusing on hydrogen safety, which highlighted the HSP and DOE's Hydrogen Emergency Response Training for First Responders.
- Presented an educational session at the 2014 NFPA Conference & Expo, Las Vegas, NV, on June 10, 2014.
- Led a planning session in April 2014 of 20 organizations/stakeholders to consider what electronic safety would benefit the next phase of hydrogen and fuel cell commercialization.
- Added four new safety event records to "H2Incidents.org" since the 2013 Annual Merit Review and Peer Evaluation Meeting, for a total of 214 records currently in the database.
- Released a first-of-its-kind iPad/iPhone app to enhance the utility and integration of the safety knowledge tools (h2incidents.org and h2bestpractices.org) with other safety planning resources.

INTRODUCTION

Safety is essential for realizing the "hydrogen economy"—safe operation in all of its aspects from hydrogen production through storage, distribution and use; from research, development and demonstration to deployment and commercialization. As such, safety is given paramount importance in all facets of the research, development, demonstration and deployment work of the DOE Fuel Cell Technologies (FCT) Office. This annual report summarizes activities associated with two projects, the Hydrogen Safety Panel and Hydrogen Safety Knowledge Tools.

Recognizing the nature of the DOE FCT program and the importance of safety planning, the HSP was formed in December 2003 to bring a broad cross-section of expertise from the industrial, government and academic sectors to help ensure the success of the program as a whole. The experience of the Panel resides in industrial hydrogen production and supply, hydrogen R&D and applications, process safety and engineering, materials technology, risk analysis, accident investigation and fire protection. The Panel provides expertise and recommendations on safety-related issues and technical data gaps, reviews individual DOE-supported projects and their safety plans and explores ways to bring best practices and lessons learned to broadly benefit the FCT program. The Panel is currently composed of 15 members having over 400 years of industry and related experience (see Table 1 for FY 2014 Panel membership).

TABLE 1. Hydrogen Safety Panel

Nick Barilo, Project Manager	PNNL
Bill Fort, Chair	Shell Global Solutions (ret)
David Farese	Air Products and Chemicals
Larry Fluer	Fluer, Inc.
Don Frikken	Becht Engineering
Aaron Harris	Sandia National Laboratories
Richard Kallman	City of Santa Fe Springs, CA
Chris LaFleur*	Sandia National Laboratories
Miguel Maes	NASA White Sands Test Facility
Larry Moulthrop*	Proton OnSite
Glenn Scheffler	GWS Solutions of Tolland, LLC
Andrew Sherman	Powdermet Inc.
Ian Sutherland	General Motors
Steven Weiner	PNNL
Robert Zalosh	Firexplo

* New Panel members

The widespread availability and communication of safety-related information are crucial to ensure the safe operation of future hydrogen and fuel cell technology systems. The entire hydrogen community benefits if hydrogen safety-related knowledge is openly and broadly shared. To that end, PNNL continues to improve the safety knowledge software tools and develop new techniques for disseminating this information. This report covers the Hydrogen Lessons Learned database (http://h2tools.org/lessons/), the Hydrogen Safety Best Practices online manual (http://h2bestpractices.org), the Hydrogen Tools iPad and iPhone apps as well as efforts to identify the need for new electronic resources. These resources are key to reaching, educating and informing stakeholders whose contributions will help enable the deployment of new hydrogen and fuel cell technologies.

APPROACH

The HSP strives to raise safety consciousness most directly at the project level through organizational policies and procedures, safety culture and priority. Project safety plans are reviewed to encourage thorough and continuous attention to safety aspects of the specific work being conducted. Panel-conducted safety reviews focus on engagement, learning, knowledge-sharing and active discussion of safety practices and lessons learned, rather than as audits or regulatory exercises. Through this approach, DOE and the HSP are trying to achieve safe operation, handling and use of hydrogen and hydrogen systems for all DOE projects.

The Hydrogen Lessons Learned database (h2tools.org/lessons/) facilitates open sharing of lessons learned from

hydrogen safety events to help prevent similar events in the future. DOE-funded project teams and others are encouraged to voluntarily submit records of incidents and near-misses, along with specific lessons learned. The addition of new records is also pursued by actively seeking news reports on hydrogen events, searching existing databases and encouraging self-submittals by "incident owners."

Hydrogen Safety Best Practices (H2bestpractices.org) is an easy-to-use, Web-based manual focusing on the safe use of hydrogen. It has been compiled from learnings and observations from HSP site visits, safety plan reviews, and other work, and available reference materials tailored specifically to working with hydrogen. Links are provided to other Web-based resources and supporting information to enhance the usefulness of this resource. Experts from the HSP, national laboratories, and other subject matter experts contribute and review new material added to the site. PNNL staff members, with assistance from the HSP, respond to user questions and comments.

RESULTS

The 19th and 20th meetings of the Hydrogen Safety Panel were held in Washington, D.C., December 10–12, 2013, and Golden, CO, May 13–15, respectively. The meetings provided opportunities to consider timely and relevant safety issues and provide direct input to the FCT Office. Details of the topics discussed and outcomes of the meetings can be found in the meeting minutes [2,3]. Two Panel task groups were formed at the 19th meeting to 1) perform a risk assessment of hydrogen equipment enclosures and 2) evaluate the current NREL Secure Data Center composite data products and templates to allow the Panel to better utilize the actual safety-related data and information reported by project teams in support of safety learnings. A Panel task group was formed during the 20th meeting to review the document, "Safety Planning Guidance for Hydrogen and Fuel Cell Projects," dated April 2010, and propose improvements based on the Panel's recent experiences with demonstration projects and early engagement activities.

A white paper report, "Safety of Hydrogen Systems Installed in Outdoor Enclosures," was issued in November 2013 [1]. The paper resulted from observations and considerations stemming from the Panel's work on early market applications. The paper focused on hydrogen system components that are installed in outdoor enclosures and proposed that a technical basis be developed to enable code bodies to write requirements for the range of enclosures from the smallest to the largest. A Panel task group was formed to follow up the white paper with a risk assessment on enclosures. Results from the task group's activities in April/May 2014 supported public comments submitted to the NFPA 2, "Hydrogen Technologies Code" technical committee in support of changes for the 2016 edition of the code.

During the past year the Panel has provided various safety review and support to projects as noted in Table 2. Since 2004, the Panel has participated in 399 project reviews (including safety plans, site visits reviewed, follow-up interviews and design review activities). Three of these projects utilized the early project involvement approach discussed in the FY 2013 annual progress report [4]. The results of those reviews were impactful by identifying significant project issues early enough to allow consideration by project teams.

Sharing and disseminating safety information and knowledge continues to be an important aspect of HSP work. For example, PNNL authored an *NFPA Journal* article focusing on hydrogen safety, which highlights the Panel and DOE's Hydrogen Emergency Response Training for First Responders [18]. The *NFPA Journal* is the official magazine of the National Fire Protection Association and reaches all

TABLE 2. HSP Project Safety Work since July 1, 2013

Work	Project Title	Contractor
Safety plan review [5]	Cryogenic Pressure Vessel Refueling	Lawrence Livermore National Laboratory (LLNL)
Safety plan reviews [6,7]	Fuel Cell Auxiliary Power Unit for Refrigerated Trucks	Nuvera
Project design review [8]	Energy Systems Integration Facility Fueling Station	National Renewable Energy Laboratory
Project design review [9]	Lawrence Livermore National Laboratory Cryogenic Refueling and Testing Facility	Lawrence Livermore National Laboratory
Safety plan reviews [10,11]	Demonstration of a Fuel Cell-powered Transport Refrigeration Unit	Plug Power
Safety plan reviews [12]	Fuel Cell Powered Airport Ground Support Equipment Deployment	Plug Power
Safety plan review [13]	Marine Corps Base Hawaii Hydrogen Fueling Station	Hawaii Natural Energy Institute
Safety plan reviews [14]	High Performance, Durable, Low Cost Membrane Electrode Assemblies for Transportation Applications	3M
Safety plan review [15]	New Fuel Cell Membranes with Improved Durability and Performance	3M
Project design review [16]	Maritime Fuel Cell Generator Project	Sandia National Laboratories
Safety plan review [17]	Fuel Cell Hybrid Electric Drayage Truck Demonstration Project	Vision Motor Corp

association members (70,000 individuals in 100 countries). PNNL also presented the educational session, "Design to Operation: Integrating Safety into Hydrogen and Fuel Cell Projects," at the 2014 NFPA Conference & Expo, Las Vegas, NV, on June 10, 2014 [19]. The session focused on activities for integrating safety into a hydrogen project and the resources available to designers, AHJs and first responders.

International collaboration is important to PNNL's hydrogen safety work. PNNL participated in a European/U.S. bilateral webinar, "What Can We Learn from Hydrogen Safety Event Databases?," held during the 5th International Conference on Hydrogen Safety in Brussels, Belgium on September 10, 2013 [20]. The webinar brought lessons learned and related knowledge to the forefront of the hydrogen community. PNNL also offered highlights of accomplishments of the HSP and other international collaborations through two presentations [21,22]:

- "Deploying Fuel Cell Systems: What Have We Learned?," which examines safety considerations in early market applications for hydrogen and fuel cell systems.
- "Advancing the Hydrogen Safety Knowledge Base," a white paper of the IEA Hydrogen Implementing Agreement Task 31 describing the value created and knowledge enhanced through member collaborations.

PNNL completed its work as leader for Task 31/Subtask D – Knowledge Analysis, Dissemination and Use and submitted the subtask final report [23].

During FY 2014 PNNL also focused on enhancing the HSP's role as a safety resource for enabling the widespread acceptance of hydrogen using branding (see Figure 1). Branding serves two primary functions:

- The consistent and appropriate use of branding will strengthen recognition of the Panel and its reputation as a safety resource
- Branding will validate that information is coming from a reliable and credible source

The branding is being implemented across the entire PNNL hydrogen safety project, including the HSP, Safety Knowledge Tools and First Responder Training.

The safety knowledge tools (Hydrogen Lessons Learned database and Hydrogen Safety Best Practices online manual) continue to see a steady number of users. To increase visibility and broaden the audience, the project has integrated information from the websites into a mobile application. The "Hydrogen Tools" app was released to the iPad and iPhone in September 2013 and adds value by combining information from the websites (h2tools.org/lessons/ and H2bestpractices.org) and other project resources (safety planning guidance and a safety checklist), calculators and related tools. The mobile app also allows users to search across the incidents and database resources and the best practices can be viewed offline.

FIGURE 1. Hydrogen Safety Panel Logo

During the development of the Hydrogen Tools app, the question was raised: "Do we have the right tools to support this next phase toward hydrogen and fuel cell commercialization?" PNNL conducted a planning session in Los Angeles, CA on April 1, 2014 to consider what electronic safety tools would benefit the next phase of hydrogen and fuel cell commercialization. A diverse, 20-person team led by an experienced facilitator considered the question as it applied to the eight most relevant user groups. The planning session revealed areas where users of safety information could benefit from a new approach to safety knowledge resources. Three example high-impact tools include:

- A hydrogen safety portal – a nexus for safety information and professional networking that integrates electronic safety resources into one location. A portal could integrate existing resources to facilitate accessibility (and display) from a single, *trustworthy* source, increasing their visibility and value.
- A codes and standards guide – a tool to guide the user through questions relating to application, topics and subtopics to help them identify the applicable requirements in a timely manner.
- Peer networking tools – tools to allow users to to discuss relevant hydrogen safety and code application topics with counterparts.

Implementing these tools will be a transformative step toward disseminating safety information and enabling fuel cell commercialization. A summary document will be made available near the end of FY 2014.

In June 2014, "H2incidents.org" was renamed "Hydrogen Lessons Learned (H2LL)," and relocated to a new Internet address, "h2tools.org/lessons/." These changes facilitate broader acceptance of the resource and make it part of the hydrogen safety portal.

CONCLUSIONS AND FUTURE DIRECTIONS

The HSP will continue to focus on how safety knowledge, best practices and lessons learned can be brought to bear on the safe conduct of project work and the deployment of hydrogen technologies and systems in applications of interest and priority in the DOE FCT Office.

The Panel can also be used more broadly as an asset for safe commercialization by reaching out to new stakeholders and users involved in early deployment activities.

The project will undertake a number of initiatives over the next year, including:

- Support project activities with the focus on early engagement, including kickoff meetings, safety plan reviews, site visits and other relevant interactions with project teams.
- Expand the Panel's visibility through a web page and integration into key social media tools.
- Work with DOE to strengthen contract language to support HSP early involvement in projects and a commitment to NFPA 2 implementation; and submit proposed changes to DOE project safety planning through an update to the document, "Safety Planning Guidance for Hydrogen and Fuel Cell Projects."
- Identify opportunities to support H2USA (H2USA is a public-private partnership to promote the commercial introduction and widespread adoption of fueled fuel cell electric vehicles across the United States with a mission to address hurdles to establishing hydrogen fueling infrastructure).
- Submit a draft hydrogen certification guide to DOE.
- Achieve an appropriate mix of safety expertise and perspective to perform safety reviews and address relevant issues. PNNL will continue to evaluate the Panel membership to maintain its leadership role in hydrogen safety.
- Seek opportunities to share safety knowledge with new audiences to facilitate the safe deployment of hydrogen and fuel cell technologies.

Hydrogen safety knowledge tools help remove barriers to the deployment and commercialization of hydrogen and fuel cell technologies. While feedback on the existing resources has been positive, a concerted effort beyond just general maintenance is necessary to remain relevant and impactful to the community being served. Working toward that goal, in FY 2014 the project will:

- Develop a "Hydrogen Tools" portal that combines existing hydrogen safety resources into one centralized and integrated website.
- Support the development of new tools identified during the April 2014 planning session.

FY 2014 PUBLICATIONS

1. Weiner, S.C., Fassbender, L.L., Blake, C., Aceves, S., Somerday, B.P. and Ruiz, A., "Web-Based Resources Enhance Hydrogen Safety Knowledge," PNNL-SA-82812, International Journal of Hydrogen Energy, Volume 38 (2013), pp 7583-7593.

2. Barilo, N., "The H Factor," *NFPA Journal*, May/June 2014, available online at http://www.nxtbook.com/nxtbooks/nfpa/journal_20140506/index.php#/80.

REFERENCES

1. Barilo, N.F., "Safety of Hydrogen Systems Installed in Outdoor Enclosures," PNNL-22960, November 2013.

2. Barilo, N.F. to C. James et al., "Minutes for the 19th Hydrogen Safety Panel Meeting," January 23, 2014.

3. Barilo, N.F. to C. James et al., "Minutes for the 20th Hydrogen Safety Panel Meeting," June 17, 2014.

4. 2013 Annual Progress Report, "VIII.9 Hydrogen Safety Panel and Hydrogen Safety Knowledge Tools," available online at http://www.hydrogen.energy.gov/pdfs/progress13/viii_9_barilo_2013.pdf.

5. Barilo, N.F. to Adams, J. and Stetson, N., "Safety Plan Review for the LLNL's Cryogenic Pressure Vessel Refueling Project," July 31, 2013.

6. Weiner, S.C. to Brooks, K.P., "'Demonstration of Fuel Cell-Based Auxiliary Power Unit for Refrigerated Trucks' - Safety Plan Review by the Hydrogen Safety Panel," October 12, 2013.

7. Barilo, N.F. to Brooks, K.P., "Hydrogen Safety Panel Review of the Nuvera APU Updated Safety Plan," March 24, 2014.

8. Fort, W.C. to Kurtz, J., "NREL ESIF Fueling Facility Review," March 10, 2014.

9. Barilo, N.F. to Adams, J. and Guillaume, P., "Hydrogen Safety Panel Review of LLNL Cryogenic Refueling and Testing Facility," March 12, 2014.

10. Barilo, N.F. to Brooks, K.P., "Hydrogen Safety Panel Comments of TRU GenDrive Preliminary Safety Plan," February 24, 2014.

11. Barilo, N.F. to Alkire, J.T., "Comments on Plug Power's Responses," June 23, 2014.

12. Barilo, N.F. to Alkire, J., "Re: Draft Safety Plan for Plug Power GSE Project," March 23, 2014.

13. Barilo, N.F. to Ewan, M., "Hydrogen Safety Panel Review of the HNEI Project Management Safety Plan (Marine Corps Base Hawaii Hydrogen Fueling Station)," April 7, 2014.

14. Barilo, N.F. to Kleen, G., "Hydrogen Safety Panel Review of the Safety Plan for High Performance, Durable, Low Cost Membrane Electrode Assemblies for Transportation Applications," March 25, 2014.

15. Barilo, N.F. to Peterson, D., "Hydrogen Safety Panel Review of the Safety Plan for the 3M Project 'New Fuel Cell Membranes with Improved Durability and Performance' (EE0006362)," May 8 2014.

16. Barilo, N.F. to Pratt, J., "Hydrogen Safety Panel Comments on the Maritime Fuel Cell Generator Project Preliminary Design," May 21, 2014.

17. Barilo, N.F. to Choe, B. "Hydrogen Safety Panel Review of the Fuel Cell Hybrid Electric Drayage Truck Safety Plan," June 23, 2014.

18. Barilo, N., "The H Factor," NFPA Journal®, May/June 2014, available online at http://www.nxtbook.com/nxtbooks/nfpa/journal_20140506/index.php#/80.

19. Barilo, N.F., "Design to Operations: Integrating Safety into Hydrogen and Fuel Cell Projects," 2014 NFPA Conference & Expo, Las Vegas, NV, June 10, 2014, available online at http://www.nfpa.org/~/media/2B0101A61A9346C595C7BB77A3A74A06.pdf.

20. Weiner, S.C., "What Can We Learn from Hydrogen Safety Event Databases? – H2Incidents.org," Webinar presented at the International Conference on Hydrogen Safety, Brussels, Belgium, September 10, 2013.

21. Barilo, N.F. and Weiner, S.C., "Deploying Fuel Cell Systems: What Have We Learned?" PNNL-SA-94975, International Conference on Hydrogen Safety, Brussels, Belgium, September 9–11, 2013.

22. Weiner, S.C., "Advancing the Hydrogen Safety Knowledge Base," PNNL-SA-91531, International Conference on Hydrogen Safety, Brussels, Belgium, September 9–11, 2013 (accepted for IJHE publication).

23. Weiner, S.C. to Hoagland, W. "Task 31 Final Report for Subtask D – Knowledge Analysis, Dissemination and Use," March 31, 2014.

VIII.9 NREL Hydrogen Sensor Testing Laboratory

William Buttner (Primary Contact), Ian Bloomfield, Kevin Hartmann, Robert Burgess, Carl Rivkin
National Renewable Energy Laboratory
15013 Denver West Parkway
Golden, CO 80401-3305
Phone: (303) 275-3903
Email: William.Buttner@nrel.gov

DOE Manager
Will James
Phone: (202) 287-6223
Email: Charles.James@ee.doe.gov

Subcontractor
Element One, Boulder Colorado

Project Start Date: October 1, 2013
Project End Date: Project continuation and direction determined annually by DOE

Overall Objectives

- Quantify performance of commercial hydrogen sensors relative to DOE metrics
- Support development and assess performance of advanced sensor technologies
- Support development and updating of hydrogen sensor codes and standards
- Support infrastructure deployment by providing expert guidance on the use of hydrogen sensors
- Educate the hydrogen community on the proper use of hydrogen sensors

Fiscal Year (FY) 2014 Objectives

- Support Department of Transportation/National Highway Safety Administration (DOT/NHTSA) on the development of the Federal Motor Vehicle Safety Standard (FMVSS) for hydrogen fuel cell vehicles, especially with regards to hydrogen detection requirements identified in the Global Technical Regulation (GTR) for hydrogen-powered vehicles.
- Quantify performance metrics of developmental sensor technologies supported by DOE, including technologies from private organizations and national laboratories.
- Support infrastructure deployment by providing sensor testing capability and guidance to stakeholders.
- Support of NREL component testing and facility upgrades with sensors for both safety and quantitation of hydrogen releases.
- Quantify hydrogen safety sensor requirements for repair facilities
- Coordinate domestic activities in a collaborative European Union (EU)—United States (U.S.) sensor research program, performed in Europe under the auspices of H2Sense [1], which is a European program funded through the Fuel Cell and Hydrogen Joint Undertaking. The EU partners include the Bundesanstalt für Materialforschung und -prüfung (Federal Institute for Materials Research and Testing; BAM, Berlin Germany), the Joint Research Centre (JRC) Institute for Energy and Transport (Petten, the Netherlands), and private companies.

Technical Barriers

This project addresses the following technical barriers identified in the Hydrogen Safety, Codes and Standards section of the Fuel Cell Technologies Office Multi-Year Research, Development, and Demonstration Plan:

(A) Safety Data and Information: Limited Access and Availability

(C) Safety is Not Always Treated as a Continuous Process

(F) Enabling National and International Markets Requires Consistent Regulations, Codes and Standards

(G) Insufficient Technical Data to Revise Standards

(H) Insufficient Synchronization of National Codes and Standards

(K) No Consistent Codification Plan and Process for Synchronization of R&D and Code Development

Contribution to Achievement of DOE Safety, Codes and Standards Milestones

This project will contribute to achievement of the following DOE milestones from the Hydrogen Safety, Codes and Standards section of the Fuel Cell Technologies Office Multi-Year Research, Development, and Demonstration Plan:

- Milestone 2.12: Develop leak detection devices for pipelines. (4Q, 2015)
- Milestone 2.15: Develop holistic design strategies. (4Q, 2017)
- Milestone 2.19: Validate inherently safe design for hydrogen fueling infrastructure. (4Q, 2019)

- Milestone 3.1: Develop, validate, and harmonize test measurement protocols. (4Q, 2014)
- Milestone 4.9: Completion of GTR Phase 2. (1Q, 2017)
- Milestone 5.1: Update safety bibliography and incidents databases. (4Q, 2011-2020)

FY 2014 Accomplishments

- Implemented five formal agreements with industrial partners. The majority of the agreements pertain to use of sensors to facilitate infrastructure deployment, with some support of new advanced sensor technology development.
- Quantified the sensor requirements for preparing existing repair facilities to accommodate hydrogen vehicles.
- Initiated collaboration with DOT/NHTSA to provide technical support pertaining to hydrogen detection requirements specified in the GTR. This activity supports the development of the FMVSS.
- Completed a study quantifying the limitations of using oxygen sensors to quantify hydrogen releases; the results were published in the International Journal of Hydrogen Energy.
- In collaboration with the JRC, completed an initial study quantifying the impact of potential chemical interferences, as identified in the ISO 26140 standard on hydrogen sensors [2], on the major hydrogen sensor platform types. The impact of selected sensor poisons on various platform types was also completed.
- Published the results of an assessment of the impact of miniaturization via micro-machining on hydrogen sensor performance in collaboration with the JRC and the University of Quebec.
- Working with an automotive original equipment manufacturer, initiated the development of an SAE hydrogen sensor evaluation protocol standard or annex for use on-board hydrogen vehicles.

INTRODUCTION

Safety is a major concern for the emerging hydrogen infrastructure. A reliable safety system is comprised of various elements that can include intrinsic design features (e.g., pressure control systems), engineering controls (e.g., sample size minimization), and the use of hydrogen sensors to monitor for releases. Both the International Fire Code (IFC) 2009 and National Fire Protection Association 2 require hydrogen sensors for numerous applications, and accordingly sensors will be mandatory in all jurisdictions that adopt either the IFC or National Fire Protection Association 2. To assure the availability of reliable safety sensors, NREL established the sensor testing laboratory. The NREL sensor test facility provides stakeholders (e.g., sensor developers and manufacturers, end users and code officials) a resource for an independent, unbiased evaluation of hydrogen sensor technologies. Test protocols are guided by the requirements in national and international sensor standards, as well as sensor performance targets established by DOE. In addition to laboratory assessment of sensor performance, a critical mission of the NREL sensor testing laboratory is to educate end users on the proper use of hydrogen sensors. This is achieved, in part, through topical studies designed to illustrate fundamental properties and limitations of various hydrogen sensor technologies, and through outreach activity such as participation on standards development organizations committees and workshops, conference and webinar presentations. The NREL sensor laboratory also facilitates deployment by partnering with end-users to assist in the design and deployment of their sensor system. Within the past year, the NREL sensor laboratory has formalized five agreements with industrial partners, with an emphasis evaluating sensors in support of deployment.

APPROACH

Evaluation of hydrogen safety sensors is an on-going activity at NREL and supports both sensor developers and end-users. The goal of the sensor laboratory is to assure that stakeholders in the hydrogen community have the sensor technology they need. The NREL sensor test apparatus was designed with advanced capabilities, including parallel testing of multiple hydrogen sensors, sub-ambient to elevated temperature, sub-ambient to elevated pressure, active humidity control and accurate control of gas parameters with multiple precision digital mass flow meters operating in parallel. Extended long-term stability testing of sensors is also available. The test apparatus is fully automated for control and monitoring of test parameters and for data acquisition with around-the-clock operation capability. Selected sensors are subjected to an array of tests to quantify the impact of variation of environmental parameters and chemical matrix on performance. Although standard test protocols have been developed [3], these can be adapted for specialized requirements. Results are reported back to the developer or manufacturer to support their future development work[1]. NREL sensor testing also supports end-users by qualifying sensor technology for their application and by educating the hydrogen community on the proper use of hydrogen sensors. The importance of hydrogen safety sensors has been internationally recognized, and the NREL sensor laboratory closely collaborates with international test

[1] It is the policy of the NREL sensor laboratory to treat test results as proprietary, and thus results pertaining to specific clients will not be disclosed without permission.

laboratories, sensor developers, and standards development organizations.

RESULTS

To support hydrogen deployment, the NREL Sensor Test Facility strives to assure the availability of hydrogen sensors to meet stakeholder needs. This is achieved in part by providing an unbiased assessment of performance to sensor developers and manufacturers as well as end users. NREL has also performed numerous topical studies aimed at educating the hydrogen community on the proper use of hydrogen sensors. Results reported here summarize major studies completed in FY 2014 on the characterization and use of hydrogen sensors.

Support of the FMVSS/GTR in collaboration with DOT/NHTSA: Recently the GTR defining safety requirements for hydrogen vehicles was formally implemented. To harmonize international regulations on the safety features of hydrogen vehicles, the GTR is to serve as the basis for the FMVSS in the U.S., which is currently being prepared by NHTSA; prior to formal implementation the draft FMVSS will be open to review and comment by stakeholders. The GTR has several requirements on allowable hydrogen levels external to the vehicle fuel system, including maximum hydrogen in vehicle compartments and allowable maximum hydrogen concentration in tail pipe emissions. Previously, the NREL sensor laboratory worked with DOT/NHTSA to develop a means to verify compliance to the GTR allowable hydrogen concentrations in vehicle compartments following crash tests [4]. The NREL sensor laboratory is expanding its partnership with NHTSA by providing expert advice on sensor technology and to develop analytical methods to verify compliance to the various GTR requirements (e.g., verification of compliance to the GTR tailpipe emission requirement). The NREL sensor laboratory also provides recommendation pertaining to modification of the GTR; for example NREL has recommended removing the GTR explicit endorsement of the use of oxygen sensors to measure hydrogen releases in vehicle compartments. During the Annual Merit Review, the NREL sensor laboratory organized an open meeting with NHTSA and stakeholders including representatives of original equipment manufacturers to review the GTR and the process for developing and implementing the FMVSS.

Hydrogen Safety Sensor Requirements for Vehicle Repair Facilities: The IFC 2009 edition has specific safety requirements pertaining to repair facilities for hydrogen vehicles, including the use of hydrogen detection systems. Thus, existing repair facilities will likely need modifications so as to accommodate hydrogen vehicles, and an integrated design for repair facilities is being explored for this purpose. One aspect of the upgrade will be the use of hydrogen sensors. The NREL sensor laboratory is working with KPA, LLC and Toyota Motor Sales USA on the deployment of a robust hydrogen sensor system as part of the integrated design. In this project, the sensor requirements for use in a repair facility were identified. Several commercial sensor models were identified as potential candidates and are currently being evaluated for long-term stability via an extended 6-month deployment in an actual vehicle repair facility. At the end of the 6-month deployment the overall performance of the candidate sensors will be assessed by the NREL sensor laboratory, and recommendations on the best sensor type for this application will be provided.

International Collaborations (topical studies): Over the past several years, the NREL sensor laboratory has formally collaborated with the sensor test facility at the JRC under the auspices of a Memorandum of Agreement. Under the Memorandum of Agreement, NREL and JRC initiated numerous topical studies aimed at educating the hydrogen community on the proper use of hydrogen sensors. In the past year, the results of several of these topical studies were presented at international conferences and published in the open literature. Included was the publication in the International Journal of Hydrogen Energy of the assessment of the use of oxygen sensors to monitor oxygen displacement as a means to quantify hydrogen releases. Also there is an on-going topical study on the impact of interferants (e.g., a chemical that produce a false positive or negative response on a sensor) and poisons (e.g., a chemical the permanently alters the behavior of a sensor). The results of the interferent testing were presented at the 2013 International Conference on Hydrogen Safety and published in the International Journal of Hydrogen Energy in 2014. Preliminary results on the impact poisons were presented at the 2014 World Hydrogen Energy Conference.

In FY 2014, sensor collaboration expanded to include BAM through an agreement between the Fuel Cell and Hydrogen Joint Undertaking and DOE, which represented the first U.S.-EU project with common objectives. The objectives included:

- To evaluate the capability of current sensors to detect hydrogen and to validate performance through independent laboratory tests.
- To ascertain the needs of facility designers, safety engineers, product designers, etc., with respect to their requirements on how hydrogen sensors should perform in different applications and under which conditions.
- To identify ways to facilitate hydrogen sensor innovation by removing barriers which currently hinder sensor use and commercialization.
- To facilitate the safe use and implementation of hydrogen as an alternative fuel by ensuring correct use of effective hydrogen detection devices.

NREL led the U.S. activity, while the JRC and BAM lead the program in the EU. The EU activity operated under the auspices of H2Sense [1], which was led by BAM and the JRC but included participation by numerous private sensor companies. NREL supported H2Sense as a keynote speaker at the H2Sense Sensor workshop, and through telecoms, program reviews, sensor evaluations, final report (pending), and future work plans.

Sensor Testing and Evaluation: Sensor testing and evaluation remains a core activity within the NREL sensor laboratory, and is performed for customers with both mature as well as developing sensor technology. DOE supported several sensor development programs with private industry and other national laboratories. The NREL sensor laboratory continues to provide the resources necessary to quantify sensor performance. Results of Los Alamos National Laboratory/Lawrence Livermore National Laboratory sensor evaluations were published in the International Journal of Hydrogen Energy. NREL also partnered with two private companies developing sensor technologies with DOE support.

NREL Hydrogen Component Testing Program: The NREL sensor laboratory is an integral element in the NREL component testing program [5,6]. Hydrogen detection is necessary for safety, an indicator for early detection of a pending component failure, and to quantify hydrogen releases. The NREL sensor laboratory has already provided sensors for the pressure relief device testing and performance assessment and calibration of the hydrogen sensors for the hose test [6].

CONCLUSIONS AND FUTURE DIRECTIONS

In the next year, the NREL sensor laboratory will build off its current accomplishment and capabilities via two main avenues—continued evaluation of commercial and developing sensor technologies and support of deployment by expanded collaborations with end users of sensors.

- End-User Support to Support Deployment
  - Guidance on the use of hydrogen sensors in infrastructure deployments, including repair facilities and fueling facilities
  - DOT/NHTSA on the Hydrogen Vehicle FMVSS and compliance to the GTR
  - Sensor performance testing protocol standards for vehicles
  - Barriers to sensor certification and the impact
- Manufacture/Developer Support
  - Commercial and developmental sensor technology performance validation
  - Assessment of wide area monitoring/distributed sensor technology (as a topical study with the JRC)
  - Sensors and analytical methods for the detection of contaminants in hydrogen fuel.

FY 2014 PUBLICATIONS/PRESENTATIONS

Journal Articles and Proceedings Papers

1. "An Assessment on the Quantification of Hydrogen Releases Through Oxygen Displacement Using Oxygen Sensors" W. Buttner, M. Post, R. Burgess, C. Rivkin, L. Boon-Brett, V. Palmisano; in press International Journal of Hydrogen Energy (2014).

2. "Evaluation of Selectivity and Resistance to Poisons of Commercial Hydrogen Sensors", V. Palmisano, L. Boon-Brett, W. Buttner, M. Post, R. Burgess, C. Rivkin, in press International Journal of Hydrogen Energy (2014).

3. "Assessment of Commercial Micro-machined Hydrogen sensors to guide the Next Generation" H. El Matbouly, F. Domingue, V. Palmisano, L. Boon-Brett, M.B. Post, C. Rivkin, R. Burgess, and W.J. Buttner; International Journal of Hydrogen Energy 39 (2014) 4664-4673.

4. "Independent Testing and Validation of Prototype Hydrogen Sensors" Sekhar, Praveen K.; Zhou, Jie; Post, Matthew B.; Woo, Leta**;** Buttner, William J.; Penrose, William R.; Mukundan, Rangachary; Kreller, Cortney R.; Glass, Robert S.; Garzon, Fernando H; Brosha, Eric; International Journal of Hydrogen Energy (2014), 39, 4657-4663.

5. "Selectivity and Resistance to Poisons of Commercial Hydrogen Sensors", E. Weidner, L. Boon-Brett, C. Bonato, F. Harskamp, P. Moretto, M. Post, R. Burgess, C. Rivkin, W.J. Buttner, published in the Proceedings of the World Hydrogen Energy Conference, Seoul, Korea (June 16–19,2014)

Reports

1. "U.S. Hydrogen Sensor Standards and their Impact on Infrastructure Implementation", Kathleen O'Malley, William J. Buttner, H. Lopez, Julie Cairns, Robert Burgess, Carl Rivkin, and Robert Wichert, to be published as an NREL Technical Report (2014).

Presentations

1. "NREL Hydrogen Sensor Testing Laboratory", William Buttner, Carl Rivkin, Robert Burgess, and Ian Bloomfield, DOE Annual Merit Review, June 18th, 2014

2. "NREL Webinar – Hydrogen Component Testing", Robert Burgess, William Buttner, Mike Peters, to be completed Q4 FY2014.

3. "Selectivity and Resistance to Poisons of Commercial Hydrogen Sensors", E. Weidner, L. Boon-Brett, C. Bonato, F. Harskamp, P. Moretto, M. Post, R. Burgess, C. Rivkin, W.J. Buttner, presented at the World Hydrogen Energy Conference, Seoul, Korea (June 16–19, 2014)

4. "An Assessment on the Quantification of Hydrogen Releases Through Oxygen Displacement Using Oxygen Sensors" W. Buttner, M. Post, R. Burgess, C. Rivkin, L. Boon-Brett, V. Palmisano; International Conference on Hydrogen Safety, Belgium (September 9–11, 2013) Belgium.

5. "Evaluation of Selectivity and Resistance to Poisons of Commercial Hydrogen Sensors", V. Palmisano, L. Boon-Brett, W. Buttner, M. Post, R. Burgess, C. Rivkin, International Conference on Hydrogen Safety, Belgium (September 9-11, 2013) Belgium.

6. "Very Low-Cost Visual and Wireless Sensors for Reliable Hydrogen Gas Leak Detection", W. Hoagland, D. Benson, R. Smith, W. Buttner, International Conference on Hydrogen Safety, Belgium (September 9-11, 2013) Belgium.

7. (Invited Talk) "Applications for H2 Sensors—US Practices and Perspective" W. Buttner, C. Rivkin, R. Burgess, I. Bloomfield, H2Sense Hydrogen Sensor Workshop (September 12, 2013) Belgium.

REFERENCES

1. H2Sense, see http://www.h2sense.bam.de/en/home/index.htm, accessed July 30, 2014.

2. "ISO 26142 Hydrogen Detector for Stationary Apparatus"

3. "Standard Hydrogen Test Protocols for the NREL Sensor Testing Laboratory" NREL Brochure (See http://www.nrel.gov/hydrogen/pdfs/53079.pdf, accessed July 30, 2014).

4. "Onboard Hydrogen/Helium Sensors in Support of the Global Technical Regulation: An Assessment of Performance in Fuel Cell Electric Vehicle Crash Tests" M.B Post, R. Burgess, C. Rivkin, W. Buttner, K. O'Malley, and A. Ruiz, NREL Technical Report NREL/TP 5600-56177 (2012) (See http://www.nrel.gov/docs/fy12osti/56177.pdf, assessed July 30, 2014).

5. "Component Standard Research and Development", R. Burgess, A. Kostival, W. Buttner, C. Rivkin, DOE Annual Merit Review (June 18th, 2014), Washington, D.C.

6. "700 Bar Hydrogen Dispenser Hose Reliability Improvement" K. Harrison, H. Dinh, M. Peters, DOE Annual Merit Review (June 17, 2014) Washington, D.C.

VIII.10 Hands-On Hydrogen Safety Training

Salvador M. Aceves (Primary Contact),
Gregg Holtmeier, Vernon Switzer
Lawrence Livermore National Laboratory (LLNL)
7000 East Avenue, L-792
Livermore, CA 94550
Phone: (925) 422 0864
Email: saceves@llnl.gov

DOE Manager
Will James
Phone: (202) 287-6223
Email: Charles.James@ee.doe.gov

Project Start Date: October 1, 2010
Project End Date: Project continuation and direction determined annually by DOE

Overall Objectives

- Maintain and update Web-based safety training materials for researchers running hydrogen laboratory experiments
- Teach hands-on safety training to personnel in charge of hydrogen systems

Fiscal Year (FY) 2014 Objectives

Prepare class materials for hands-on safety training

Technical Barriers

This project addresses the following technical barriers from the Hydrogen Safety, Codes and Standards section of the Fuel Cell Technologies Office Multi-Year Research, Development, and Demonstration Plan:

(D) Lack of Hydrogen Knowledge by AHJs (authorities having jurisdiction)

(E) Lack of Hydrogen Training Materials and Facilities for Emergency Responders

Contribution to Achievement of DOE Safety, Codes & Standards Milestones

This project will contribute to achievement of the following DOE milestone from the Hydrogen Safety, Codes and Standards section of the Fuel Cell Technologies Office Multi-Year Research, Development, and Demonstration Plan:

- Milestone 5.3: Enhance hydrogen safety training props and deliver classroom curriculum for emergency response training. (4Q, 2012)

FY 2014 Accomplishments

- Completed two modules of classroom training for hands-on hydrogen safety class
- Registered over 300 completions in Web-based hydrogen safety class (www.h2labsafety.org)

INTRODUCTION

LLNL has been conducting hydrogen research for more than 50 years, starting with national security applications and continuing with energy research. For many of these years, LLNL was designated as the pressure safety training facility for the whole DOE complex and other government institutions. Many technicians and researchers visited LLNL to receive training on many aspects of pressure safety, including hydrogen technology, cryogenics, leak detection, and vacuum technology.

This unique training expertise is still available and is now being applied for hydrogen energy research through the development of training materials that may contribute to safe operation within the many institutions working on hydrogen technology.

APPROACH

We are developing a two-pronged approach to hydrogen safety training:

- Researchers conducting laboratory experiments can benefit from basic training on hydrogen and pressure safety. This Web-based training can be completed in ~4 hours.
- Technical personnel in charge of setting up experimental equipment require comprehensive hands-on training on all aspects of hydrogen systems. This extensive training is planned for three full days.

RESULTS

Publicly released in 2010, the Web-based hydrogen safety class (www.h2labsafety.org) reached 300 total completions this year and it is standard training material in many universities, government institutions, and private companies. The class is, however, not well publicized, and targeted advertisement may contribute to more widespread utilization.

In addition to the Web-based fundamentals class, we are developing a hands-on hydrogen safety class for pressure

operators. This comprehensive training will be conducted during a three-day session at LLNL, or at remote institutions if appropriate facilities (classroom, compressed gas supply, and pressure testing laboratory) exist.

The hands-on training class starts with a full day of classroom instruction covering essential topics of pressure system assembly and operation (Table 1). Classroom instruction focuses on identifying hazards, safety precautions, personal protective equipment, and pressurized hydrogen system components and their function. This class greatly expands the descriptions from the online hydrogen safety class, going into detailed operational information about every component in pressure systems, describing their inner functionality, applicability, and recommended use.

Days two and three will be spent in the laboratory for practical application of the classroom information from day one. On day two, students will be handed a safety document and instructed to assemble the pressure system described therein. Students will have to select, inspect and install pressure components, bend tube, install pipe and compression fittings, and assemble the entire system.

On day three this system will be leak checked with a mass spectrometer helium leak detector with a leak rate of no more than 10^{-5} atm-cc/sec helium. The pressure system will then be connected to the data acquisition system and pressure tested remotely at 150% of the maximum allowable working pressure. The last leak test will be conducted using liquid leak detection fluid at the system's maximum operating pressure. Finally, the students will operate the system to reach a desired pressure.

The hands-on class is nearly complete. Two of the five modules for classroom instruction (Table 1) have been completed (Figures 1 and 2). Preliminary versions of the remaining three modules are being completed and reviewed.

TABLE 1. Hands-on safety class structure. Modules 3 and 5 are now complete and preliminary versions of the others are being completed and reviewed.

Modules	
Day 1	**Classroom Teaching**
	Concepts, Hazards Personal Protective Equipment Gas Cylinders CGA fittings supply manifolds flash arrestors Pressure Reducing Regulators Gauges/Pressure Transducers Relief Devices Valves Flash Arrestors Fittings (VCR, bite, NPT, VCO, DIN) Tubing and Piping Quiz
Day 2	**Pressure System Assembly**
	Given a system schematic and description, select components, inspect and install, cut and bend tube, apply various fittings, and assemble full system
Day 3	**System Leak Test and Operation**
	Leak test using a mass spectrometer leak detector; setup data acquisition; conduct remote pressure test; leak test at maximum operating pressure using leak detection fluid; operate system to reach a desired pressure.

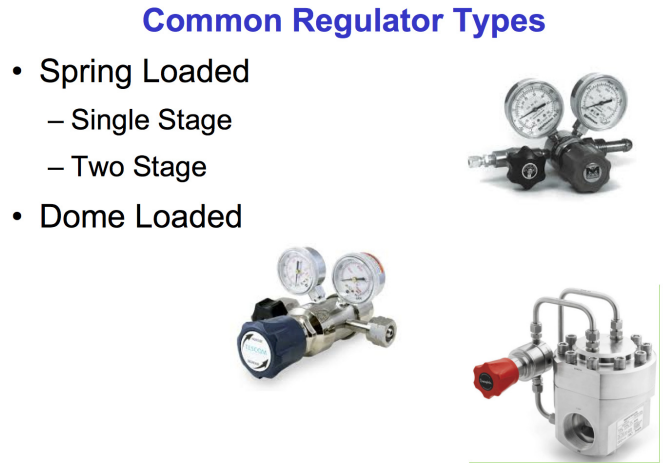

FIGURE 1. Example Page from the "Pressure Reducing Regulators" Module of the Classroom Training Section for the Hands-On Hydrogen Safety Class

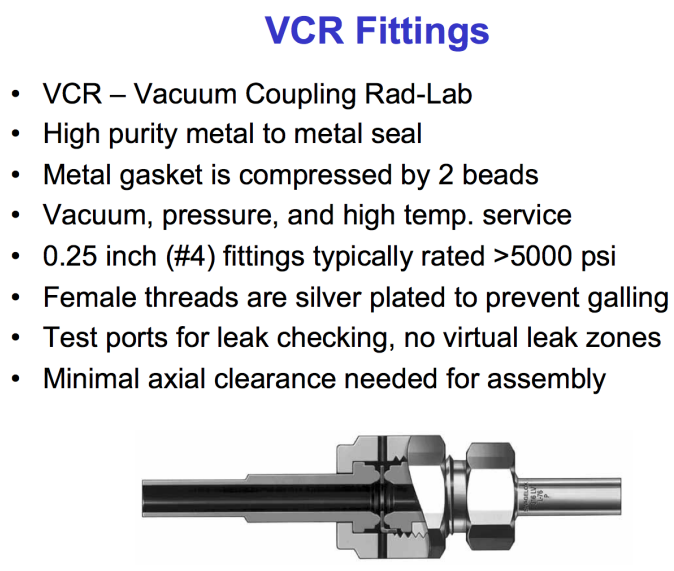

FIGURE 2. Example Page from the "Fittings, Tubing, and Piping" Module of the Classroom Training Section for the Hands-On Hydrogen Safety Class

CONCLUSIONS AND FUTURE DIRECTIONS

LLNL is contributing to safe hydrogen operations by developing instructional materials for researchers and technical operators:

- Laboratory researchers can obtain basic hydrogen safety information from a four-hour Web-based class (free online access at http://www.h2labsafety.org/) addressing hydrogen fundamentals: properties, pressure and cryogenic safety, emergency response, and codes and standards.
- Technical operators in charge of building and testing experimental hydrogen equipment require more in-depth information than provided by the Web-based class. We are therefore preparing a three-day hands-on safety class that presents detailed information for installation, testing, and operation of hydrogen pressurized systems. The hands-on class includes a full day of classroom instruction followed by two days of laboratory work where students assemble, test, and operate a pressure system based on a schematic and component description.

We anticipate completing the hands-on safety class and performing a peer review of the class before releasing it to the public.

FY 2014 PUBLICATIONS/PRESENTATIONS

1. Modeling of sudden hydrogen expansion from cryogenic pressure vessel failure, Petitpas, G. and Aceves, S.M., International Journal of Hydrogen Energy, Vol. 38, pp. 8190-8198, 2013.

2. Web-Based Resources Enhance Hydrogen Safety Knowledge, Weiner, S.C., Fassbender, L.L., Blake, C., Aceves, S.M., Somerday, B.P., and Ruiz, A., International Journal of Hydrogen Energy, Vol. 38, pp. 7583-7593, 2013.

3. Hydrogen Safety Training for Researchers And Technical Personnel, Aceves, S.M., Espinosa-Loza, F., Petitpas, G., Ross, T.O and Switzer, V.A., International Journal of Hydrogen Energy, Vol. 37, pp. 17497-17501, 2012.

IX. MARKET TRANSFORMATION

IX.0 Market Transformation Sub-Program Overview

INTRODUCTION

The purpose of the Market Transformation sub-program is to spur market growth for domestically produced hydrogen and fuel cell systems. The Market Transformation sub-program is conducting activities to help promote and implement commercial and pre-commercial hydrogen and fuel cell systems in real-world operating environments and to provide feedback to research programs, U.S. industry manufacturers, and potential technology users. By supporting increased technology use in key early markets, this sub-program helps to identify and overcome non-technical barriers to commercial deployment and to reduce the life-cycle costs of fuel cell power by helping to achieve economies of scale. These early market deployments will also address other market acceptance factors resulting in further expansion of market opportunities.

The Market Transformation sub-program aims to replicate past successes in material handling equipment (MHE) (e.g., lift trucks) and emergency backup power applications that were part of the American Reinvestment and Recovery Act. For example, Market Transformation has new projects in applications including fuel cell-powered airport ground support baggage tractors and fuel cell electric medium-duty hybrid trucks for parcel delivery applications. These projects are highly leveraged, with an average of more than half of the projects' funds being provided by DOE's industry partners. Partners providing resources to these projects have shown a high level of interest in exploring these applications and markets, and this level of industry interest is very promising for the potential growth of the domestic fuel cell industry. Market Transformation also partners with other federal agencies and stakeholders to deploy fuel cell systems in applications such as marine cargo transport operations. Affordable hydrogen fuel in accessible locations is another key goal; Market Transformation is supporting this by a landfill-gas-to-hydrogen project at a working manufacturing facility and using renewable power to electrolyze water on another project.

GOAL

Market Transformation activities provide financial and technical assistance for the use of hydrogen and fuel cell systems in early market applications, with the key goals of achieving sales volumes that will enable cost reductions through economies of scale, supporting the development of a domestic industry, and providing feedback to testing programs, manufacturers, and potential technology users.

OBJECTIVES

The objectives of the Market Transformation sub-program are to:

- Evaluate performance against target metrics for emergency backup power, MHE, and light commercial/residential power systems and provide feedback to component suppliers regarding cost reduction opportunities.
- Test emerging approaches to grid management using renewable hydrogen.
- Advance the knowledge and expertise of waste-to-energy fuel, shipboard and truck auxiliary power units, fuel cell electric truck parcel delivery, and aviation ground support applications through targeted testing and evaluation efforts in coordination with the Technology Validation sub-program, and in partnership with the U.S. Navy, the U.S. Marine Corps, and civilian agencies such as the U.S. Department of Transportation's Maritime and Federal Aviation Administrations.
- Identify lessons learned from commercial use performance and promote the development of the most effective and applicable practices for hydrogen and fuel cell technologies.
- Conduct market transformation deployment projects to enable total life-cycle cost and performance of fuel cell-powered lift trucks and emergency backup power systems to be on par with conventional technologies by 2020.

FISCAL YEAR (FY) 2014 TECHNOLOGY STATUS AND ACCOMPLISHMENTS

Fuel cells have been enjoying growing success in key early markets, particularly in MHE (e.g., lift trucks) and backup power applications. The sub-program's early market deployment efforts—including Market Transformation funding and Recovery Act funding—have successfully catalyzed a significant level of market activity in these areas, which has been accompanied by substantial reductions in the price of fuel cells. The sub-program is actively pursuing additional opportunities for effective stimulation of market activity. Ongoing activities and additional areas of interest include the following:

- **Micro-CHP (combined heat and power):** To evaluate the market viability of fuel cells for small facilities, the sub-program is working with fuel cell developers and system users to demonstrate micro-CHP systems at five commercial facilities with 10 fuel cells deployed. Performance data was collected and analyzed for an average of 3,000 hours per system. Fuel cell technology changes were made specifically using phosphoric acid in place of high temperature polymer electrolyte membrane fuel cells. Also, a business case analysis was completed and reported. (Pacific Northwest National Laboratory, PNNL)
- **Hydrogen Energy Storage:** This project is supporting the demonstration of a hydrogen energy storage system as a grid management tool. While hydrogen produced from the system could be used in a variety of value-added applications, the initial phase of the project will use the hydrogen in fuel cell buses operated by the County of Hawaii Mass Transportation Agency and the National Park Service. This year partnering arrangements were finalized in preparation for installing and operating the system. (Naval Research Laboratory and the State of Hawaii)
- **South Carolina Landfill Gas Purification:** The sub-program has completed the demonstration of the business case and technical viability of using landfill gas as a source of renewable hydrogen production, using BMW's assembly plant in South Carolina as the host site. This project represents a first-of-its-kind landfill gas-to-hydrogen production project in the nation and is expected to serve as a model for future adoption of renewable biogas as a feedstock for hydrogen production. (South Carolina Hydrogen and Fuel Cell Alliance)
- **Ground Support Vehicles Demonstration:** This project is demonstrating the value proposition of using fuel cell-powered tow tractors as a cost-competitive and more energy-efficient solution compared to incumbent internal combustion engine-powered ground support vehicles. This effort will address concerns regarding the weatherproofing of fuel cell-powered ground support vehilces and enable end users at an operator terminal to accomplish their daily tasks while reducing consumption of gasoline and diesel fuels. This project was kicked off in Latham, New York, in March of 2013 and has completed systems design developments and prototype testing in preparations for building 15 units, and installing refueling equipment, and operating ground support vehicles at the Federal Express site in Memphis, Tennessee. (Plug Power)
- **Refrigerated Truck Auxiliary Power Units:** This project is demonstrating the use of fuel cell-powered refrigeration onboard food delivery trucks to reduce petroleum use and greenhouse gas emissions. Design development has been accomplished and a prototype unit has been assembled and is being tested. (PNNL)
- **Fuel Cells in Hybrid Electric Trucks:** The sub-program modeled the cost-benefit tradeoffs of adding a fuel cell to double the range of in production battery electric vehicles. A solicitation resulted in two projects being selected for demonstration of the parcel delivery transportation service application. (FedEx Express and United Parcel Service)

BUDGET

FY 2014 appropriation for Market Transformation was $3 million, and $3 million was requested in FY 2015.

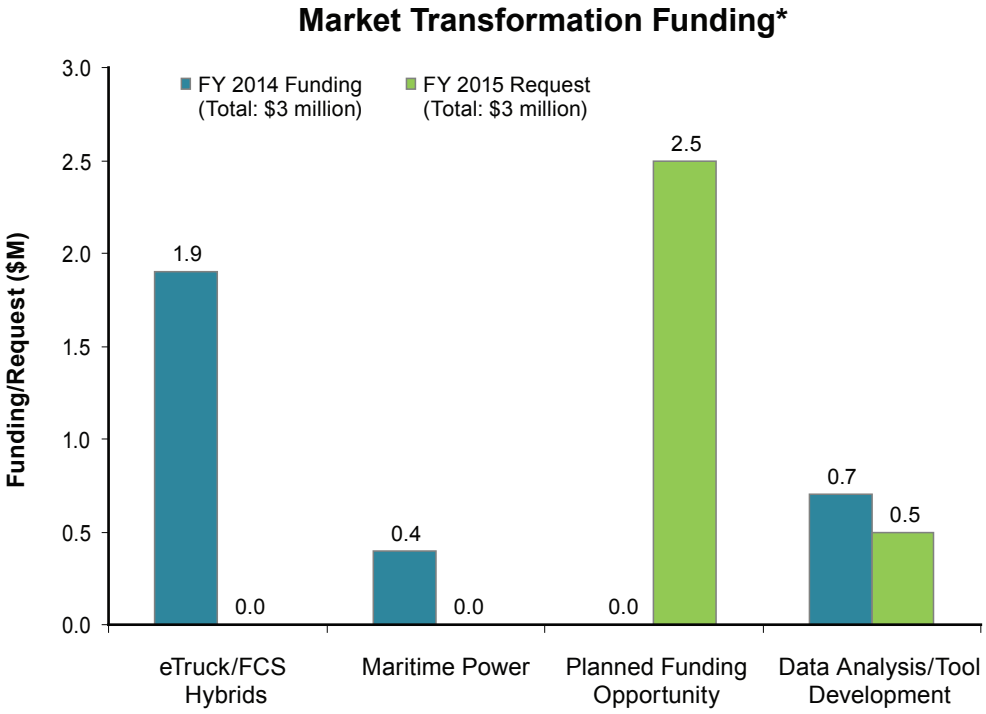

* Subject to appropriations, project go/no-go decisions, and competitive selections. Exact amounts will be determined based on progress in each area.

FY 2015 PLANS

In FY 2015, the sub-program will continue to document lessons learned associated with previously funded projects, including the strategies developed for market entry and for risk management with respect to safety, environmental, and siting requirements. Business analyses and case studies will be developed for new applications. Collection and evaluation of data from these projects will provide the basis for verifying the business cases for various early market fuel cell systems, as well as providing an assessment of the performance of these integrated systems. Data will be made publicly available so that more potential customers will become aware of the benefits of integrated hydrogen and fuel cell systems. In addition, a near-term priority will be to continue collaborating with other federal agencies—in accordance with existing interagency cooperative agreements such as the DOE-Department of Defense memorandum of understanding—to increase the use of fuel cells in market-ready applications and to increase awareness of the benefits of these deployments. A potential new activity that could be initiated subject to Congressional appropriations is the development and deployment of fuel cell and battery-powered hybrid light-duty vehicles for parcel delivery or passenger transportation applications.

Pete Devlin
Market Transformation Project Manager
Fuel Cell Technologies Office
Office of Energy Efficiency and Renewable Energy
U.S. Department of Energy
1000 Independence Ave., SW
Washington, D.C. 20585-0121
Phone: (202) 586-4905
Email: Peter.Devlin@ee.doe.gov

IX.1 Fuel Cell Combined Heat and Power Commercial Demonstration

Kriston P. Brooks (Primary Contact),
Atefe Makhmalbaf
Pacific Northwest National Laboratory
P.O. Box 999/K6-28
Richland, WA 99352
Phone: (509) 372-4343
Email: Kriston.brooks@pnnl.gov

DOE Manager
Peter Devlin
Phone: (202) 586-4905
Email: Peter.Devlin@ee.doe.gov

Subcontractor
ClearEdge Power, Hillsboro, OR

Project Start Date: August 2010
Project End Date: Project continuation and direction determined annually by DOE

Overall Objectives

- Deploy and monitor combined heat and power (CHP) fuel cell systems in the range of 5-50 kWe in commercial applications.
- Evaluate the engineering, economics, and environmental impact to provide end-users with an independent assessment of the technology.
- Monitor the long-term performance of the systems. As funding allows, we have a contract in place to monitor the systems for five years.
- Demonstrate the viability of the technology to potential customers by developing a business case.

Fiscal Year (FY) 2014 Objectives

- Monitor fuel cell performance with new M5 systems and compare their performance to the previous CE5 systems,
- Finalize business case for micro-CHP fuel cell systems (FCSs) and incorporate comments from an industrial review.

Technical Barriers

This project addresses the following technical barriers for Market Transformation from the Fuel Cell Technologies Office Multi-Year Research, Development, and Demonstration Plan:

(F) Inadequate user experience for many hydrogen and fuel cell applications

(H) Utility and other key industry stakeholders lack awareness of potential renewable hydrogen storage application

(I) Lack of cross cutting information on how to use hydrogen and fuel cell systems in combination with energy efficiency and renewable energy technologies with existing projects

Technical Targets

Applicable DOE 2015 Technical Targets for 1-10 kWe CHP fuel cell systems (FCSs) operating on natural gas:

- Electrical efficiency at rated power = 38.4% (higher heating value)
- System equipment cost, 5 kW = $1,700/kW
- Degradation with cycling = 0.5%/1,000 hrs
- Operating Lifetime = 40,000 hrs
- System Availability = 98%

FY 2014 Accomplishments

- Completed “Business Case for a Micro-Combined Heat and Power Fuel Cell System in Commercial Applications” (PNNL-22831).
- Completed evaluation of the performance of the 15 CE5 systems. These original polybenzimidazole (PBI)-based fuel cell systems have been shut down. Ten of these systems have been replaced with new phosphoric acid-based fuel cell M5 systems.
- Performed a comparison between the CE5 and M5 data. Results indicate an increase in electrical and heat output, availability and efficiency as a result of this upgrade.
- Determined heat utilization for systems with augmented instrumentation. As a result of this analysis, the augmented instrumentation on the systems at Roger’s Garden was moved to Oakland Hills Tennis Club where the heat was being better utilized.
- After operating for more than 14,600 hours each over the last two years, the 15 CE5 systems were shut down and replaced with new improved M5 systems.
- As of June 30, 2014, 10 M5 systems have been installed and operated for more than 3,100 hours each.

INTRODUCTION

PNNL provides support to the Market Transformation program with the objective to aid in the development of the fuel cell and associated hydrogen markets. The strategy is to identify near-term niche markets where fuel cells have potential, work with the DOE and stakeholders to develop activities in those areas, analyze the business case, and present the results to the community.

APPROACH

The objective of this project is to demonstrate micro-CHP FCSs and assess their performance to help determine and document market viability. In FY 2012, PNNL worked with a vendor to provide 5-kWe CHP systems, called CE5, at several small industrial buildings. The CE5 used high-temperature PEM fuel cells (PBI) as their basis. Data from these systems were collected for approximately two years. At the end of FY 2013 and early FY 2014, these CE5 systems were shut down and 10 of them were replaced with new M5 systems. The M5 provides similar power but the fuel cell is based on phosphoric acid technology. The gathered information from these new systems was compared to the original CE5s in terms of heat and power produced, system efficiency, and reliability.

This project also developed a business case that could be provided to industry to estimate the size of the market and its growth potential, identify possible niche markets, and compare the micro-CHP FCS with its alternatives in terms of economics, engineering and environmental impact. It has also utilized techno-economic-environmental optimization models to analyze the business case for micro-CHP FCSs. Model results elucidated competitive strengths of this technology by building type, load curve, and climate. Analyses under this effort incorporated market characteristics that will strengthen the business case such as electricity and gas prices and impacts of power outages.

RESULTS

Demonstration Evaluation

During the last year the original CE5 units installed in the demonstration sites were shut down and replaced with new M5 units as shown in Table 1. These M5 units operate based on phosphoric acid fuel cell technology originally developed by UTC power. In addition to the fuel cell upgrade, the M5 systems have front access to simplify repair and permit the systems to be located adjacent to each other. They are also grid independent, allowing them to load follow in the event of a power outage. As of June 30, 2014, averages of 3,100 hours of data were collected from each of these 10 new systems. While significantly less than the 14,700 hours of data collected with the CE5 systems, comparisons can be made between the two units.

TABLE 1. Micro-CHP Fuel Cell System Demonstration Site Information

Partner/Site	Location	Number of Systems	Data Collection Start Date	Days of Operation as of 3/1/14	Date of M5 Upgrade
College	Portland, OR	2	9/2011	771	2/2014
Nursery	Corona Del Mar, CA	3	11/2011	921, 731, 731	7/2013 2/2014
Recreation	Oakland, CA	5	12/2011	749, 742, 742, 732, 874	8/2013 1/2014
Grocery	San Francisco, CA	5	3/2012	487 (Not running)	Not Upgraded

A comparison of the average data analyzed for both the CE5 and M5 systems are shown in Table 2. The values provided are averages for all operating systems. These values can be compared to the manufacturer stated value for each parameter. The net electric power, heat recovery and heat recovery for the M5 system is very close to the manufacturer stated values. In contrast, the set point of the CE5 was reduced from 5 kWe and 4 kWe during the demonstration to provide better system stability. As a result, the manufacturer stated efficiency was not being met. The CE5 did provide a higher water temperature than the M5, although both are lower than the manufacturer stated value.

TABLE 2. Performance Comparison of New M5 System to Original CE5 System

Parameter	Unit	Manufacturer Stated Value	Average Value for CE5 Systems	Average Value for M5 Systems
Number of Operating Units	--	--	15	10
Average Net Electric Power Output	kWe	5.0	4.1	4.9
Average Net Heat Recovery	kWt	5.5	4.6	5.6
Temperature Heated Water to Site	°C	Up to 65	50.5	42.9
Average Net System Electric Efficiency	%	36	32	35
Average Net System Heat Recovery Efficiency	%	40	37	40
Overall Net System Efficiency	%	76	70	76
Availability	%	--	93	97

The most significant difference is a comparison of the efficiency with respect to time (see Figure 1). The

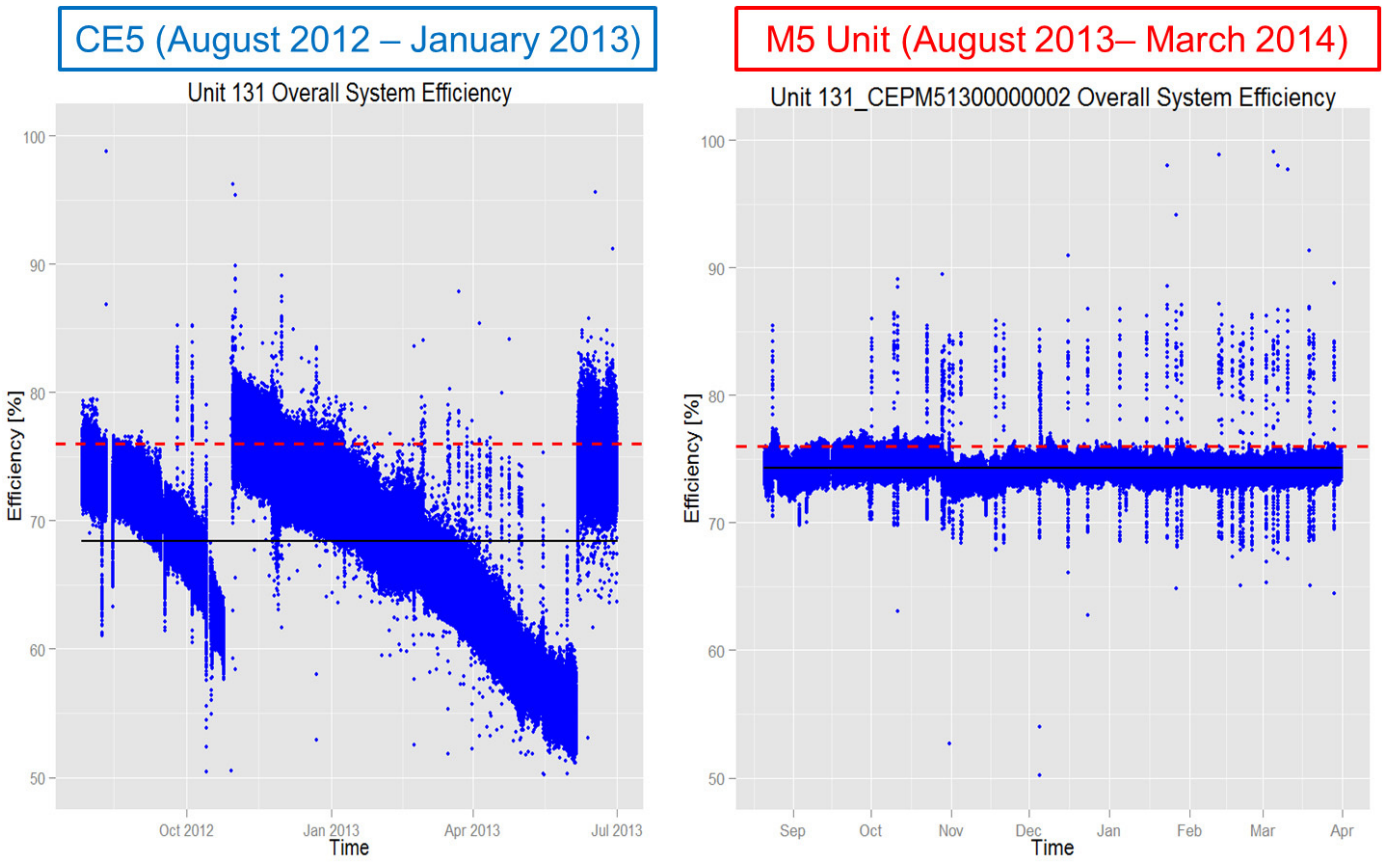

FIGURE 1. Comparison of Efficiencies between One CE5 System and its Replacement M5 System

efficiency of the Roger's Garden CE5 was compared to that of the M5 that replaced it. The efficiency of the CE5 continuously decreases over time while the M5 does not. The discontinuities represent system shut down and part replacement. During a similar period of time, the M5 shows no significant change in the efficiency. These results highlight the significant benefit of the M5 system and its phosphoric acid fuel cell relative to the PBI system.

Additional monitoring equipment was installed at two sites to gather data on the electricity and heat that was being utilized by the facility relative to the amount being produced. All of the electricity and nearly all of the heat (greater than 90%) produced by the CHP FCS was being used by the grocery store. Although all of the electricity was being used by the plant nursery, none of its heat was being utilized. As a result of this discovery, the additional monitoring equipment at the nursery was moved to the recreation facility where the heat would be used to warm the pools and saunas.

Business Case

A business case was developed for the 5-50 kWe CHP fuel cell system. In this business case the primary drivers were described in terms of system siting and market. Locations with high spark spread provide a good indication of areas where the economics for fuel cell systems can be promising. Spark spread indicates locations with high electricity prices and low natural gas prices. These locations provide a justification for the additional costs required to install and operate a distributed power source such as a micro-CHP FCS rather than use power from the grid. Figure 2 indicates that the cost of electricity relative to natural gas is generally high in the Northeast, Midwest, California, and the noncontiguous states of Alaska and Hawaii [1,2].

In addition to a high spark spread, there are economic drivers for high heat utilization. If both the electricity and heat generated by the micro-CHP FCS can be utilized, a better business case can be achieved. Using sample businesses in DOE's commercial reference building models and evaluating them with the Energy Plus Software over the course of the year, the highest utilization of heat was found to be 69% for a small hotel in Boston. Schools and small hospitals also have high utilization in Boston and Chicago as compared to relatively low heat utilization found at quick-service restaurants and office buildings in places like San Francisco.

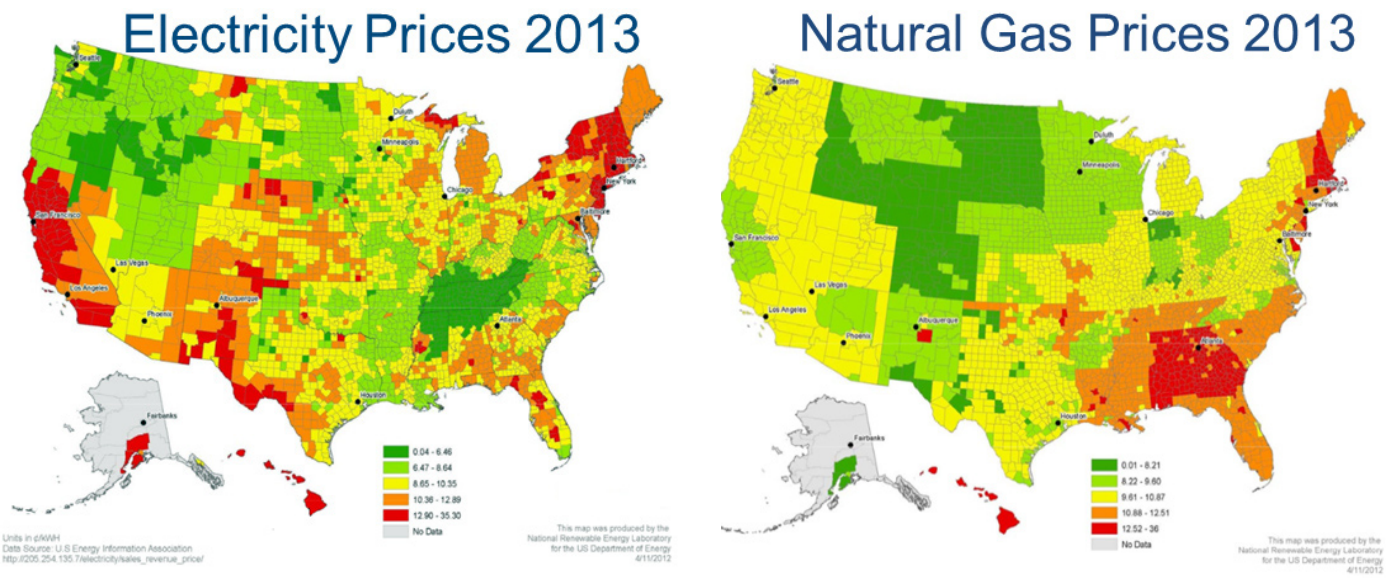

FIGURE 2. Electricity and Natural Gas Prices for 2013 based on EIA Data

The benefits of distributed power such as a micro-CHP FCS was also evaluated by estimating the yearly cost of grid interruptions for a small facility with modest outages. SAIC estimated that the commercial outage value of service would be $40-68/kWh [3]. For only three hours of total facility interruptions, an annual cost of the outages would be $12,000. Information technology intensive businesses could be much higher and have been documented as high as $100,000/hr for power interruptions [4].

By using available information on the expected growth of micro-CHP FCSs and estimating the decrease in system cost as a function of higher global capacity, the projected future cost of these systems can be estimated. Systems both with and without government incentives were considered at four different locations (see Figure 3). Results indicate that although the systems may not be cost competitive now, with continued increases in the electricity costs and reduced system cost associated with higher installed capacity, and benefits from continued research and development, the cost per unit of installed heat and power are expected to decrease by 40%. If this is the case and current government incentives continue, a fuel cell system may become economical in 2017.

CONCLUSIONS AND FUTURE DIRECTIONS

The conclusions of the fuel cell CHP work for FY 2014 are as follows:

- Performed a comparison between the M5 and CE5 in terms of initial power, efficiency and reliability. The

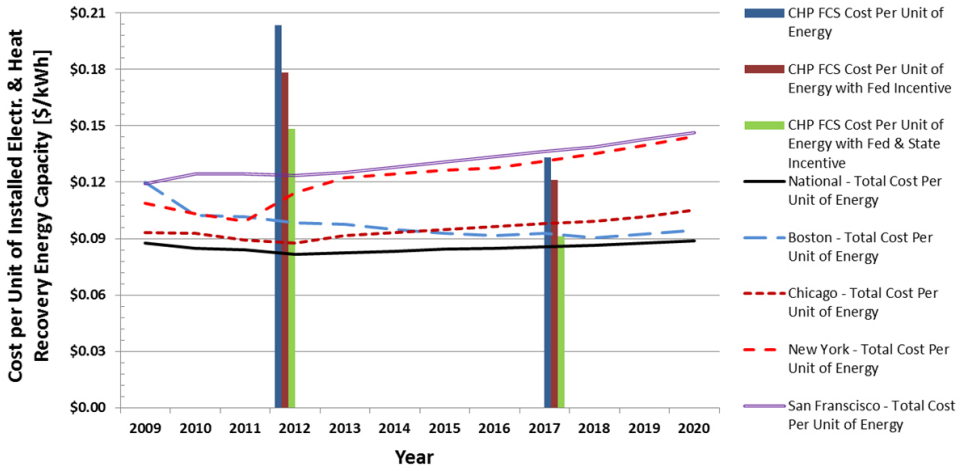

FIGURE 3. Current and Projected Future Costs of a Micro-CHP Fuel Cell

results indicate significant improvement in power and heat produced, efficiency and reliability.

- Additional monitoring equipment installed in Roger's Garden indicated that the heat being generated by the CHP was not being used.

The future work for the fuel cell CHP work in FY 2015 is as follows:

- Future work will continue to monitor the micro-CHP systems and analyze the long-term performance of the M5 systems.
- Future work will also assist ClearEdge in evaluating the trade-offs between higher water temperature and reduced efficiency.
- Business case will be updated to include the life-cycle costs for the new M5 systems and an evaluation of other possible markets.

SPECIAL RECOGNITIONS & AWARDS

1. Received Poster Award for 2013 at the Fuel Cell Seminar & Exposition, Columbus, OH, October 24, 2014.

FY 2014 PUBLICATIONS/PRESENTATIONS

Publications

1. Brooks KP, A Makhmalbaf, DM Anderson, SP Pilli, V Srivastava, and JF Upton. 2013. *Business Case for a Micro-Combined Heat and Power Fuel Cell System*, PNNL-22831, Pacific Northwest National Laboratory, Richland, WA.

2. Brooks KP, A Makhmalbaf, DM Anderson, SP Pilli, V Srivastava, and JF Upton, 2014, "Business Case for a Micro-Combined Heat and Power Fuel Cell System in Commercial Applications," Unpublished, Submitted to Journal of Fuel Cell Science & Technology, May 2014.

Presentations

1. Makhmalbaf, A.; Pilli, S.; Brooks, K, "Independent Analysis of Real-Time Performance Data from Co-Generative Fuel Cell Systems Installed in Commercial Buildings," Invited speaker to the Interagency Working Group, Washington, D.C., March 18 2014.

2. Brooks, K.P.; Pilli, S.; Anderson, D.; Srivastava, V.; Makhmalbaf, A.; "Economic and Engineering Assessment of Combined Heat and Power Fuel Cell Systems Installed in Commercial Buildings," 2013 AIChE Annual Meeting, San Francisco, CA, November 4, 2013.

3. Brooks, K.P.; Pilli, S.; Anderson, D.; Srivastava, V.; Makhmalbaf, A.; "Economic and Engineering Assessment of Combined Heat and Power Fuel Cell Systems Installed in Commercial Buildings," Fuel Cell Seminar & Energy Exposition, Columbus, OH, October 22, 2013.

4. Pilli, S.; Brooks, K.P.; Anderson, D.; Srivastava, V.; Makhmalbaf, A.; "Micro Fuel Cell Combined Heat And Power Commercial Demonstration," Fuel Cell Seminar & Exposition, Columbus, OH, October 24, 2013.

5. Makhmalbaf, A.; Brooks, K.P .; Pilli, S.; Srivastava, V.; Foster, N.; "Lesson Learned from Technical and Economic Performance Assessment and Benefit Evaluation of CHP-FCS," 2014 ACEEE Summer Study on Energy Efficiency in Buildings, to be presented Aug 2014.

REFERENCES

1. U.S. Energy Information Administration (EIA), 2012a, "Electricity, State Electricity Profiles." Available at: http://www.eia.gov/electricity/state/.

2. U.S. Energy Information Administration (EIA), May 2013, "U.S. Price of Natural Gas Sold to Commercial Consumers," Available at: http://www.eia.gov/dnav/ng/hist/n3020us3A.htm, Accessed Jun 12, 2013.

3. Centolella P, "Estimates of the Value of Uninterrupted Service for The Mid-West Independent System Operator." SAIC, Available at: http://www.hks.harvard.edu/hepg/Papers/2010/VOLL%20Final%20Report%20to%20MISO%20042806.pdf.

4. Vision Solutions (2008), "Assessing the Financial Impact of Downtime: Understand the factors that contribute to the cost of downtime and accurately calculate its total cost in your organization." visionsolutions.com, Available at: http://www.strategiccompanies.com/pdfs/Assessing%20the%20Financial%20Impact%20of%20Downtime.pdf.

IX.2 Landfill Gas-to-Hydrogen

Russ Keller
SCRA Applied R&D dba Advanced Technology International
5300 International Blvd.
Charleston, SC 29418
Phone: (843) 760-4358
Email: russ.keller@scra.org

DOE Managers
Pete Devlin
Phone: (202) 586-4905
Email: Peter.Devlin@ee.doe.gov
Greg Kleen (Project Phases 1 and 2)
Phone: (720) 356-1672
Email: Gregory.Kleen@ee.doe.gov

Contract Number: DE-FG36-08GO18113 (Project Phases 1 and 2)
Contract Number: 4F-31542 (Project Phase 3)

Subcontractors
- Gas Technology Institute (GTI), Des Plains, IL
- Ameresco, Inc., Framingham, MA

Project Start Date: March 1, 2011
Project End Date: September 30, 2014

Overall Objectives

- Validate that a financially viable business case exists for a full-scale deployment of commercially available equipment capable of converting landfill gas (LFG) to hydrogen under the specific BMW operating environment.
- Validate that commercially available clean-up and reformation equipment can convert BMW's LFG to hydrogen at purity levels consistent with fuel cell industry standards.
- Conduct an operational verification of fuel cell material handling equipment (MHE) performance and durability operating on LFG-supplied hydrogen.

Fiscal Year (FY) 2014 Objectives

- Complete troubleshooting gas clean-up system to achieve methane output purity consistent with steam methane reformer inlet requirements.
- Operate project equipment to achieve J2719 hydrogen purity standards for fuel cell operations, and demonstrate repeatability of achieving these results over time to check for potential impact of seasonal variations in LFG composition.
- Conduct operational trial where actual pieces of MHE are fueled with LFG-sourced hydrogen.

Technical Barriers

This project addresses the following technical barriers from the Technical Validation section of the Fuel Cell Technologies Office Multi-Year Research, Development, and Demonstration Plan:

(F) Centralized Hydrogen Production from Fossil Resources

(G) Hydrogen from Renewable Resources

Technical Targets

There are no specific technical targets associated with this particular project. Rather, the landfill gas-to-hydrogen project will focus on validating that integrated systems comprised of commercially available equipment can deliver cost-competitive hydrogen from an initial LFG source under real-world operating conditions.

FY 2014 Accomplishments

- Corrected gas clean-up system performance and produced hydrogen that satisfied all J2719 overall hydrogen purity and individual trace constituent standards.
- Demonstrated repeatability of the results over a three month period.
- Conducted operational trial using three pieces of in-service MHE at the BMW Manufacturing Company's X5 assembly hall (completed August 2014).

INTRODUCTION

BMW Manufacturing Company incorporated more than 100 pieces of fuel cell-powered MHE into a new assembly line that become operational 2010. While BMW currently is purchasing hydrogen services from an established industrial gas supplier, they strongly desire a future option where they could produce their own hydrogen, preferably from a renewable source—and ideally as a follow-on effort from their nationally acclaimed 2002 landfill methane project. BMW's original landfill gas project was implemented in December 2002, and the infrastructure currently allows for collecting and cleaning methane gas from the Palmetto

Landfill near Spartanburg, SC, transporting it through a 9.5-mile pipeline to the BMW plant, removing siloxane contaminants on-site, compressing and then using it as fuel for gas turbine electrical generators.

Assessments by BMW of the available quantity of LFG beyond that currently devoted to electrical power generation confirm that, should the LFG-to-hydrogen production initiative prove viable, there would be sufficient LFG available to fuel the entire BMW MHE fleet in both their existing and new facilities. Subsequent management decisions by BMW leadership after commencing this project have raised the on-site fuel cell MHE inventory to more than 300 units, representing a 100% site-wide conversion from battery power to fuel cell power.

APPROACH

The over-arching objective of this effort is to validate there is a viable business case for BMW to move forward with a full-scale LFG-to-hydrogen conversion operation should the proposed LFG-to-hydrogen conversion technology prove financially and technically viable. The project would execute in three distinct phases: (1) conduct a feasibility study to examine the potential cost-competitiveness of hydrogen generated from LFG through a capital investment in commercially available equipment compared with hydrogen delivered at current market prices; (2) deploy and test a pilot-scale system (LFG clean-up and hydrogen production) to demonstrate the technical feasibility of converting BMW's unique LFG composition to hydrogen at purity levels consistent with fuel cell industry standards; and (3) provide "real world" validation of this approach via an operational trial designed to demonstrate fuel cell-powered MHE performance and durability are consistent between LFG-sourced hydrogen and hydrogen supplied by an industrial gas provider.

Successfully meeting the project objectives will give BWM leadership the confidence to move forward with scale up should they so choose. Additionally, this effort will lay the groundwork for proving the business case for future adopters. As of this writing, two different private sector organizations have approached the project team, expressing interest in potentially adapting the project's results to LFG-to-hydrogen business opportunities in their respective locations.

RESULTS

The project commenced officially on June 17, 2011, with the first phase of an anticipated three phases. This initial phase was an economic feasibility study and business case analysis designed to assess whether a capital equipment investment in on-site LFG clean-up and methane conversion to hydrogen would enable production of hydrogen at or below the cost of having hydrogen delivered to the host site by an industrial gas company. This study completed on October 26, 2011, and was delivered to BMW management. BMW approved the study's conclusions on November 21, 2011, and authorized the project team to proceed to the second phase of the project. A copy of the feasibility study has been provided to DOE.

The "bottom line" conclusion from the feasibility study was that, at BMW's anticipated "full-scale" hydrogen production requirement, the existing LFG supply, front-end gas clean-up equipment at the BMW facility and on-site production of hydrogen using LFG as the hydrocarbon feedstock appears to be cost competitive, if not advantageous, vs. hydrogen sourced from vendors, produced offsite, and transported to the facility.

Implication for DOE Fuel Cell Technology Program: Although the analysis presented within the feasibility study is specific to the LFG equipment and constituents at the BMW facility, the basic principles of hydrocarbon feedstock clean-up and reformation to hydrogen should apply to other LFG sources, as well as to agricultural waste streams, wastewater systems, digester gases, and other process off-gases.

During FY 2014 the project team successfully overcame the technical challenges with the performance of the gas cleanup system that had stymied progress in FY 2013. Once sufficiently pure methane was recoverable, the subsequent performance of the steam methane reformation equipment produced hydrogen that met or exceeded every J2719 hydrogen purity standard for use in fuel cell equipment, as summarized in Table 1.

In 2013 the Environmental Protection Agency began a comprehensive review of its current incentive policies regarding "qualified" renewable transportation fuels. Initial decisions from these reviews have extended the existing renewable fuels incentives to transportation fuels derived from LFG. It now seems likely that hydrogen derived from these "renewable" transportation fuel feedstocks also should qualify for similar incentives. The economic advantages that flow from such a determination concerning cost competitiveness will become more pronounced at the higher daily production levels, and also might serve to lower the economic competitiveness threshold to smaller daily hydrogen production volumes.

CONCLUSIONS AND FUTURE DIRECTIONS

- A capital equipment investment in LFG cleanup and steam-methane reformation, amortized over a 10-year or greater period of time, is cost-competitive vs. delivered hydrogen for daily hydrogen demand signals of 500 kg or greater.
- The cost competitiveness of this solution will improve notably should final Environmental Protection Agency renewable transportation fuels definitions be expanded

TABLE 1. LFG-to-Hydrogen Project Results

Constituent	Specification	17 Oct 2013	14 Jan 2014
	(umol/mol)		
Total Hydrocarbons	2	1.4	1.2
Oxygen	5	<5	<5
Helium	300	<10	<10
Nitrogen	100	<5	<5
Argon	1	<1	<1
Carbon Dioxide	2	<0.4	<0.4
Carbon Monoxide	0.2	0.011	0.047
Total Sulfur	0.004	0.00072	0.0002
Hydrogen Fuel Index		99.99985%	99.99988%

to qualify transportation fuels derived from LFG (the methane itself and hydrogen derived from this methane).

- Fuel cell–quality hydrogen can be produced reliably from a LFG source with commercially available equipment.
- Future directions:
  - BMW makes business decision on whether to move forward with full-scale deployment of these technologies as the primary source of hydrogen for its MHE fleet.
  - Follow-on adopters conduct their own business case analyses, unique to their circumstances, and move forward consistent with those results.

FY 2014 PUBLICATIONS/PRESENTATIONS

1. EPA Landfill Methane Outreach Program Conference, 22 January 2014

2. DOE Annual Merit Review – 19 June 2014

IX.3 Hydrogen Energy Systems as a Grid Management Tool

Richard (Rick) E. Rocheleau (PI),
Mitch Ewan (Primary Contact)
Hawaii Natural Energy Institute (HNEI)
School of Ocean and Earth Science and Technology
University of Hawaii at Manoa
1680 East-West Road, POST 109
Honolulu, HI 96822
Phone: (808) 956-2337; (808) 956-8346
Email: ewan@hawaii.edu; rochelea@hawaii.edu

DOE Manager
Pete Devlin
Phone: (202) 586-4905
Email: Peter.Devlin@ee.doe.gov

Technical Advisor
Karen Swider-Lyons
Naval Research Laboratory
Phone: (202) 404-3314
Email: karen.lyons@nrl.navy.mil

Contract Number: DE-EE0002811

Project Start Date: September 30, 2010
Project End Date: September 29, 2015

Overall Objectives

- Demonstrate the use of electrolyzers to mitigate the impacts of intermittent renewable energy by regulating grid frequency
- Characterize performance/durability of commercially available electrolyzers under dynamic load conditions
- Supply hydrogen to fuel cell shuttle buses operated by County of Hawaii Mass Transit Agency, and Hawaii Volcanoes National Park
- Conduct performance/cost analysis to identify benefits of integrated system including grid ancillary services and off-grid revenue streams
- Evaluate effect on reducing overall hydrogen costs offset by value-added revenue streams

Fiscal Year (FY) 2014 Objectives

- Finalize Puna Geothermal Ventures (PGV) agreement.
- Develop a project hydrogen safety plan.
- Engage the DOE Hydrogen Safety Panel to support hydrogen safety including equipment installation, project hydrogen safety plans, outreach to the authorities having jurisdiction, and first responder training.
- Respond to questions posed by the public on the draft Environmental Assessment for the installation of a hydrogen system at the PGV power plant on the Island of Hawaii prepared in FY 2012 and complete the final draft of the Environmental Assessment.
- Install site improvements and utilities at the PGV geothermal plant to support the operation of the hydrogen system.
- Install, commission, and operate the hydrogen system at PGV.
- Purchase a F-450 diesel truck to tow the tube trailer.
- Install a 350-bar hydrogen fuel dispenser at the County of Hawaii Mass Transit Agency (MTA) base yard in Hilo.
- Supply hydrogen for a fuel cell electric vehicle (FCEV) shuttle bus for local community bus service operated by the County of Hawaii MTA.
- Characterize performance/durability of the Proton proton exchange membrane electrolyzer under dynamic load conditions.
- Conduct performance/cost analysis to identify benefits of integrated systems including grid services and off-grid revenue streams.

Technical Barriers

This project addresses non-technical issues that prevent full commercialization of fuel cells and hydrogen infrastructure as indicated in the following sections of the July 2013 amendments to the Fuel Cell Technologies Office Multi-Year Research, Development, and Demonstration Plan:

Section 3.1.5 - Hydrogen Production Technical Barriers

(H) Footprint

(J) Renewable Electricity Generation Integration (for central)

(M) Control & Safety

Section 3.2.5 - Hydrogen Delivery Technical Barriers

(A) Lack of Hydrogen Carrier and Infrastructure Options Analysis

(B) Reliability and Costs of Gaseous Hydrogen Compression

(E) Gaseous Hydrogen Storage and Tube Trailer Delivery Costs

(I) Other Fueling Sites/Terminal Operations

(K) Safety, Codes, and Standards, Permitting

Section 3.3.5 - Hydrogen Storage Technical Barriers

(B) System Costs

(C) Efficiency

(F) Codes and Standards

(H) Balance-of-Plant (BOP) Components

(I) Dispensing Technology

Section 3.7.4 - Hydrogen Safety, Codes, and Standards

(D) Lack of Hydrogen Knowledge by AHJs (authorities having jurisdiction)

Section 3.8.5 – Education and Outreach

(D) Lack of Educated Trainers & Training Opportunities

Section 3.9.5 – Market Transformation Barriers

(A) Inadequate Standards and Complex and Expensive Permitting Procedures

(B) High Hydrogen Fuel Infrastructure Capital Costs for Polymer Electrolyte Membrane (PEM) Fuel Cell Applications

(C) Inadequate Private Sector Resources Available for Infrastructure Development

(F) Inadequate User Experience for Many Hydrogen and Fuel Cell Applications

(G) Lack of Knowledge Regarding the Use of Hydrogen Inhibits Siting

(H) Utility and other Key Industry Stakeholders Lack Awareness of Potential Renewable Hydrogen Storage Application

(J) Insufficient Numbers of Trained and Experienced Servicing Personnel

(K) Inadequate Installation Expertise

(L) Lack of Qualified Technicians for Maintenance

(M) Lack of Certified Service Providing Organizations for Installation and Maintenance

Technical Targets

No specific technical targets have been set.

FY 2014 Accomplishments

- Procured two Powertech 450-bar tube trailers to transport hydrogen from PGV to the County of Hawaii MTA bus yard in the town of Hilo, and Hawaii Volcanoes National Park
- Contracted the Hawaii Center for Advanced Transportation Technologies to convert an ElDorado bus to an FCEV utilizing a Hydrogenics fuel cell power system
- Prepared draft responses to public comments
- Executed operations and maintenance contract to support daily operation of the hydrogen systems with Select Engineering Services
- Developed a draft Memorandum of Agreement with the County of Hawaii MTA
- Continued to work with PGV to progress Memorandum of Agreement; obtained PGV investor approval for the project

INTRODUCTION

While solar and wind resources offer a major opportunity for supplying energy for electrical grid electricity production and delivery systems, their variability and intermittency can raise challenges for the cost-effective and high-reliability integration of these renewable sources on electrical grids. In Hawaii, the curtailment and grid management-related challenges experienced by these renewable sources are a challenge at today's level of generation capacity, and these costs will hinder the substantive additional penetration of electricity generation supplied by these renewable resources. Hydrogen production through electrolysis may provide an opportunity to mitigate curtailment and grid management costs by serving as a controllable load allowing real-time control in response to changes in electricity production. The renewable hydrogen product can also create new and incremental revenue streams to the power producers through the sale of hydrogen products to customers outside of the electricity delivery system. Accordingly, hydrogen energy production at a utility scale offers the potential for increasing the levels of variable renewable energy that can be harnessed by the power producers or systems operators.

APPROACH

A four-step process is required to evolve island energy systems:

- Develop and validate rigorous analytic models for electricity and transportation
- Develop and model scenarios for the deployment of new energy systems including additional renewables
- Identify and analyze mitigating technologies (demand side management, storage, smart grid, advanced controls, forecasting, future gen) to address systems integration (grid stability) and institutional issues
- Conduct testing and evaluation to validate potential solutions to facilitate utility acceptance

Under separate and ongoing DOE and industry-funded efforts, HNEI has been conducting energy roadmapping and technology validation to identify economically viable technologies to transform island energy infrastructures. A full network model incorporating generator governors and automatic generator control was developed that provided the following capabilities:

- Transient stability simulation looks at challenging times with fluctuating renewables to check transient stabilities; and
- Long-term dynamic simulation.

Frequency variability due to wind fluctuation of the Big Island grid was used as the initial test of the models. The Big Island grid has the following characteristics:

- 100 to 200 MW with early evening peak
- 30 MW wind
- 38 MW regulated geothermal
- Significant and growing photovoltaics.

To explore the potential of the hydrogen production opportunity, this project will evaluate the value proposition of using utility-scale electrolyzers to both regulate the grid and use excess electricity from renewables to make hydrogen for various products. In this initial phase of the project, an electrolyzer will be installed at the PGV geothermal plant on the Big Island. In this first phase, it will not be connected to the grid. The electrolyzer will be operated in a dynamic mode designed to simulate future operation as a grid-connected variable load that can be quickly ramped up and down to provide frequency regulation. Data will be collected to analyze the ability of the electrolyzer to ramp up and down, and to determine its durability and performance under dynamic operating conditions (Figure 1). The hydrogen produced by the system will be used to fuel one hydrogen-fueled bus operated by the County of Hawaii MTA. A schematic of the project concept is shown in Figure 2.

RESULTS

- Completed the manufacture of three Powertech 450-bar tube trailers used to transport hydrogen from PGV to the County of Hawaii MTA bus yard in the town of Hilo, and Hawaii Volcanoes National Park (Figure 3).
- Contracted the Hawaii Center for Advanced Transportation Technologies to convert an ElDorado bus to a FCEV utilizing a Hydrogenics fuel cell power system (Figure 4).
- Prepared draft responses to Draft Environmental Assessment Finding of No Significant Impact comments submitted by the public.
- Executed operations and maintenance contract to support daily operation of the hydrogen systems with Select Engineering Services.

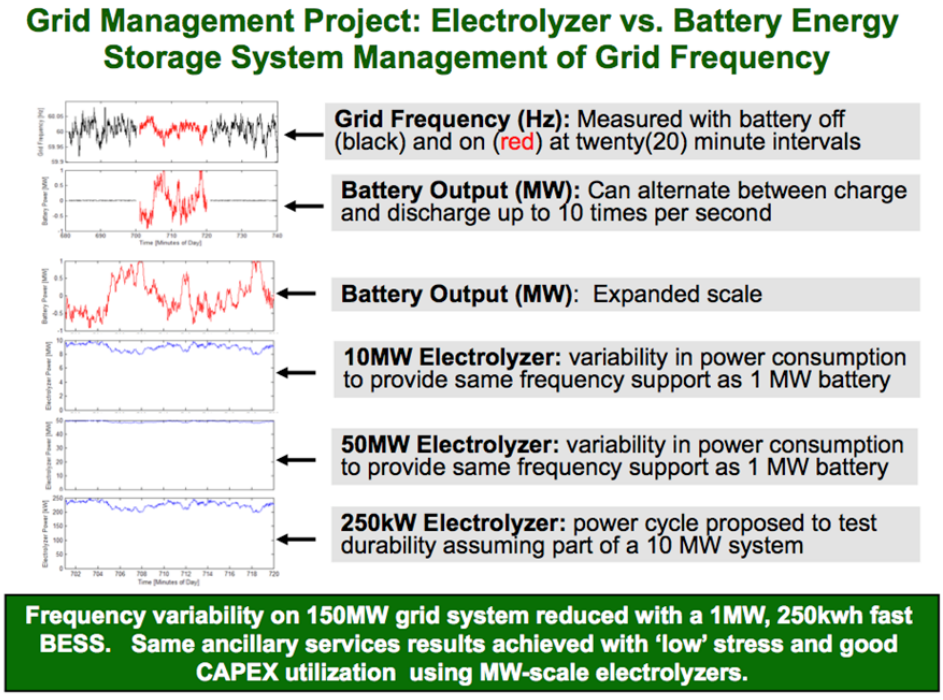

FIGURE 1. Comparison of a Battery Energy Storage System with a Dynamically Operated Electrolyzer Managing Grid Frequency

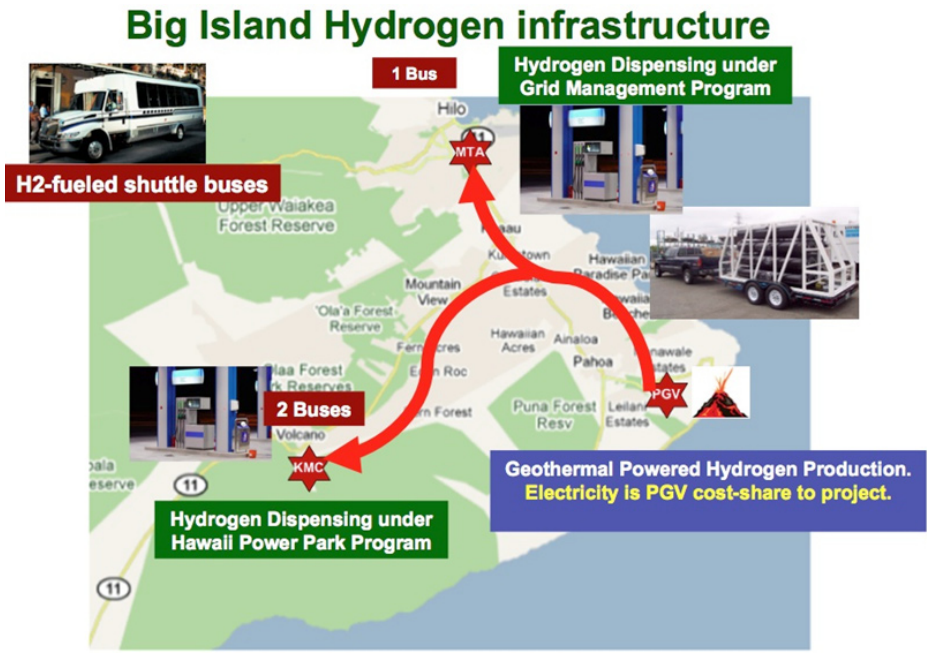

FIGURE 2. Hydrogen Production and Delivery System

FIGURE 3. Powertech Hydrogen Transport Trailers Ready for Delivery to Hawaii

FIGURE 4. First Hawaii Volcanoes National Park Bus Assembled in Honolulu by US Hybrid

- Developed a draft Memorandum of Agreement with the County of Hawaii MTA.
- Continued to work with PGV to progress Memorandum of Agreement; obtained PGV investor approval for the project.
- Completed design and fabrication of a fuel cell power system air filtration test stand (Figure 5). Used the test stand to quantify the adsorption capacity and breakthrough characteristics of commercial air filters that will be used in fuel cell electric buses at Hawaii Volcanoes National Park on the Island of Hawaii. This data will be used in collaboration with a "smart" onboard sensor system to prevent poisoning of the fuel cell power plant by the highly toxic environmental conditions. This test station has also been used over the past year to characterize and aid in the development of novel air purification materials, allowing HNEI to develop novel air filtration materials that are competitive with state of the art air filtration materials in both adsorption performance and cost.

CONCLUSIONS AND FUTURE DIRECTIONS

- Equipment and infrastructure need to be installed and operated before any results can be obtained and evaluated.
- Future work involves the procurement, installation, and operation of the following:

FIGURE 5. Fuel Cell Power System Air Filtration Test Station

- Installing hydrogen production systems and infrastructure at the PGV geothermal site
- Installing hydrogen dispensing systems and infrastructure at the County of Hawaii MTA bus depot site in Hilo
- Procuring and operating a 26-passenger fuel cell electric bus
- Operating the electrolyzer and hydrogen systems at the PGV and County of Hawaii MTA sites
- Transporting hydrogen in hydrogen transport trailers from the production site to dispensing sites at Hawaii Volcanoes National Park and County of Hawaii MTA
- Collecting and analyzing hydrogen system and FCEV bus performance data
- Preparing performance reports and sharing it with project sponsors and industry
- Conducting outreach activities with the public to inform them about hydrogen technologies.

A major project challenge to the timely deployment of hydrogen infrastructure and equipment necessary to conduct operations has been the amount of time required to develop legal agreements to address liability issues. This is approaching four years in this project. This in turn has required our requesting no-cost extensions to extend the project to meet operational test duration requirements. This represents a large investment in outreach and education of all parties concerned including the legal profession, risk managers, first responders, and authorities having jurisdiction.

FY 2014 PUBLICATIONS/PRESENTATIONS

1. Ewan M., Oral presentation to an NREL sponsored workshop "Electrolytic Hydrogen Production Workshop", Golden, CO, February 28, 2014.

2. Ewan M., Oral presentation to US DOE & Industry Canada sponsored workshop "Hydrogen Energy Storage for Grid and Transportation Services", Sacramento, CA, May 14–15, 2014.

3. Ewan M., Rocheleau, R., Oral presentation at US DOE Annual Merit Review, "Hydrogen Energy Systems as a Grid Management Tool", Washington, DC, June 19, 2014.

IX.4 Ground Support Equipment Demonstration

Jim Petrecky
Plug Power
968 Albany-Shaker Road
Latham, NY 12110
Phone: (518) 817-9124
Email: James_Petrecky@plugpower.com

DOE Managers
Pete Devlin
Phone: (202) 586-4905
Email: Peter.Devlin@ee.doe.gov
Jim Alkire
Phone: (720) 356-1426
Email: James.Alkire@ee.doe.gov

Contract Number: DE-EE0006093

Project Start Date: January 2013
Project End Date: December 2016

Overall Objectives

- To create a hydrogen fuel cell-based solution as a cost-competitive and more energy-efficient baggage tow tractors (airport vehicle) compared to the incumbent internal combustion engine-powered vehicles.
- To enable airport end users to accomplish their daily tasks with a hydrogen fuel cell solution while reducing consumption of gasoline and diesel fuels, reducing U.S. demand for petroleum.
- To demonstrate lower carbon emissions with fuel cells.
- To demonstrate a value proposition that shows decreased energy expenditures when compared to diesel-powered airport vehicles.

The project objectives are listed in Table 1.

Fiscal Year (FY) 2014 Objectives

- Plug Power develops the 80-V fuel cell product for baggage tow tractor
- Testing with Charlatte CT5E baggage tow tractor
- Factory acceptance test to demo equivalent operation as battery/internal combustion engine tow tractors
- Plug Power conducts site planning to install hydrogen at host site
- Start of the demonstration

Technical Barriers

- Upsizing GenDrive architecture from current 48-V product to 80-V
- Outdoor application – need for weatherproofing

Technical Targets

Technical targets for this project are listed in Table 2.

FY 2014 Accomplishments

- Fuel cell testing
- Alpha prototype demonstration
- Beta prototype demonstration in Charlatte CT5E tug
- Safety planning—fuel cell/hydrogen infrastructure
- Site planning/coordination with FedEx Express for hydrogen preperation/permits
- DOE event at Plug Power demonstrating the technology
- Site planning at Memphis

✧ ✧ ✧ ✧ ✧

TABLE 1. Specific Project Objectives and Expectations

DOE Project Objectives	Plug Power-FedEx Project Expectations
Reduce petroleum consumption	Each BTT uses ~2 gal/hr. Total BTT run time of 15 BTT's over 2 years will be upwards of **175,200 gallons of diesel fuel reduced.**
Reduce emissions at airports	AT 9.8 kg CO2 per gal of diesel, there will be upwards of **1717 metric tonnes of CO2 eliminated at airports.**
Operate 10 hrs/day & 5,000+ hours	BTT operation occurs during two shifts: day (10AM-2 PM) and night (10PM-2AM). The total clock day is 10AM-2PM (16 hours). **Actual BTT activity is 8 hours per day. Total run time of 15 BTT's over 2 years will be upwards of 87,600 fleet hours.**
Towing capability of 3,000 to 6,000 lbs.	The BTT will be able to tow 4 FedEx containers each weighing 40,000 lbs. The corresponding **drawbar capacity of the fuel cell-powered BTT is 5,000 lbs.**
Accelerated development of FC-powered GSE	**Fleet of 15 80V fuel cell systems in real world application in 2013 gaining significant field experience while allowing a premier BTT end user to evaluate for larger deployments.**

BTT - baggage tow tractor; FC - fuel cell; GSE - ground support equipment

TABLE 2. Project Technical Targets

Comparison of BTT Specifications (Fuel Cells vs. Diesel and Battery)					
Specifications	**Units**	**Current GenDrive (48V MHE)**	**Proposed GenDrive (80V BTT)**	**Diesel[1] (Tug MA Model)**	**Battery (80V)**
Startup Time[2]	min @ 0 °C	0	0	15	0
Maximum Output Power (kW)[3]	kW	10	~20	36.5 - 64[4]	10 @ 5 hrs
Minimum Output Power (kW)[5]	kW	0	0	3.6 - 6.4	
Energy Storage Capacity @ Rated Efficiency[6]	kW-hr	26.7	37.1	147.1	29
Run Time[7]	hrs	~ 8	8-10 (full shift)	7.75	~ 4-6
Operating Temperature Range[8]	deg C	-22°–104°F	-22°–140°F	See note 8.	-4°–140°F
Durability (power degradation with time)[9]	%	10%	10%	Minimal	80%
Fuel Cell Stack and Battery Voltage Degradation[10]	%	0%	0%	-	14%
Cycle Life	cycles	NA	NA	NA	1000 - 1200
Electrical Efficiency	%	45%	45%	20%	58% from grid
Refueling / Recharging Time	minutes	2	2	5	480
Availability	%	> 95% (~98.5%)	> 95% (~98.5%)	> 80%	> 95%
Scheduled Maintenance[11]	hrs	2,000	1,000	1000	200
Estimated Mean Time Between Failure (MTBF)[12]	hrs	425	250-500	250	1000
Emissions (CO) Level @ BTT	kg CO / unit	0	0	9.8 / gallon	0

[1] Diesel Tug MA model used a representative diesel BTT. This is a very popular model in used in the BTT market.
[2] Diesel generally need to be started for 15 to 20 minutes before usage at freezing or below. (Customer engagement interviews)
[3] Maximum output for batteries is rated at 5 hours. Battery capacity assumed to be 625 A-hr.
[4] Net brake hp at governed RPM. The range represents the different engines that can be selected.
[5] No minimum turndown for GenDrive or battery. Minimum turndown for diesel engines is typically 10% of rated power.
[6] Energy Storage * Efficiency = Storage Capacity. Diesel BTT holds 15.5 gallons. Diesel has 37.95 kW-hr per gallon. Hydrogen has 33 kW-hr per kg.
[7] Run time for diesel is calculated by dividing 15.5 gallon tank by 2 gallons per hour consumption. Significant energy is consumed by idlng.
[7] The batteries and fuel cell don't need as much energy onboard because energy is only consumed when needed (little idling) and due to regenerative braking.
[8] See note 2. Diesel engine needs to warm up before usage in freezing temps. Available energy run time drops by 40-60% in freezing conditions.
[8] At very cold temps, diesel engines use resistive heaters in the intake manifold to warm the inlet air for starting or until the engine is warm.
[8] Diesel fuel is also prone to waxing or gelling in cold weather. Number 2 diesel begins to cloud at 32 deg F due to the paraffin in the fuel solidifying.
[9] By definition, battery voltage (power) degrades to 20% of the state of charge at fully charged condition.
[10] Fuel cells are able to maintain output voltage throughout the shift. Batteries will drop 14% from 100% state of charge (SOC) to 20% SOC.
[11] Scheduled maintenance for fuel cells is air filter replacement. This will increase in frequency for BTT from MHE due to additional contaminants at airport.
[11] Diesel engine maintenance include oil changes, oil filters, and air filters. Battery maintenance include equalization charges once per month at a minimum.
[12] Demonstration-level fuel cells will have roughly 10 maintenance calls per year. This is expected to decrease to 5-6 with field experience

INTRODUCTION

This project will deploy 15 fuel cell-powered units for two years at FedEx Express's busiest airport. The project is planned for two phases. The first is a one-year development phase where Plug Power develops, builds and tests the 80-V (~20 kW) fuel cell system for the BTT application. The second is a two-year demonstration where a fleet of BTTs are integrated into Charlatte CT5E electric tow tractors and deployed at the FedEx locations under real world conditions. The fuel cell fleet will be fueled by a GenFuel hydrogen compression, storage, and dispensing solution.

APPROACH

Plug Power will design an 80-V fuel cell system as a drop in place replacement of an electric Charlatte tug (see Figure 1).

Hydrogen will be supplied to the tugs via GenFuel hydrogen infrastructure, which will provide onsite hydrogen at 350 bar to be dispensed directly to the fuel cell in the tug (see Figure 2).

- Definition of Requirements – complete
- Alpha Prototype – complete
- BTT Beta Builds – Q3 2014
- BTT Testing and Certification – Q3 2014
- Site Preparation – Q2, Q3 2014

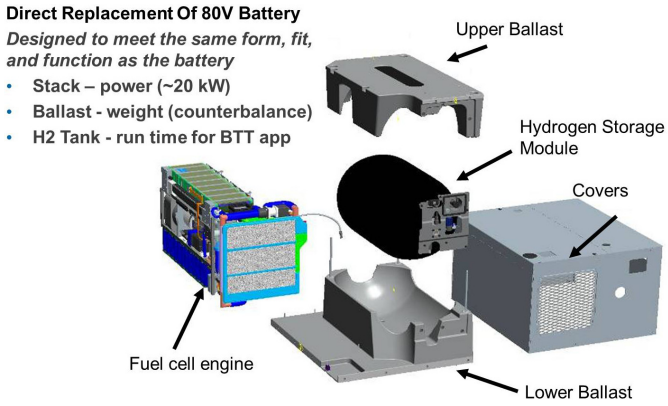

FIGURE 1. Direct Replacement of 80-V Battery

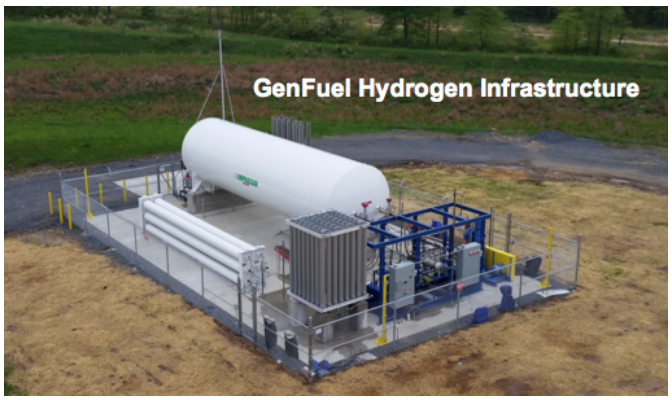

FIGURE 2. Hydrogen Solution

- Commissioning – Q4 2014
- Demonstration – Q4 2014 to Q4 2015
- Assessment after Year 1 – Q4 2015
- Demonstration – Q4 2015 to Q4 2016
- Assessment after Year 2 – Q4 2016

RESULTS

The kickoff of the project occurred on March 27, 2013. Results will be communicated in quarterly reports later this year.

CONCLUSIONS AND FUTURE DIRECTIONS

The demonstration of 15 BTT units at Memphis will begin in Q4 2014.

IX.5 Maritime Fuel Cell Generator Project

Joe Pratt
Sandia National Laboratories
PO Box 969, MS-9051
Livermore, CA 94551
Phone: (925) 294-2133
Email: jwpratt@sandia.gov

DOE Manager
Pete Devlin
Phone: (202) 586-4905
Email: Peter.Devlin@ee.doe.gov

Subcontractors
Hydrogenics, Mississauga, Ontario, Canada

Project Start Date: September 15, 2013
Project End Date: December 31, 2015

Overall Objectives

- Lower the technology risk of future port fuel cell deployments by providing performance data of hydrogen proton exchange membrane (PEM) fuel cell technology in this environment.
- Lower the investment risk by providing a validated business case assessment for this and future potential projects.
- Enable easier permitting and acceptance of hydrogen fuel cell technology in maritime applications by assisting U.S. Coast Guard (USCG) and the American Bureau of Shipping (ABS) develop hydrogen and fuel cell codes and standards.
- Act as a stepping stone for more widespread shipboard fuel cell auxiliary power unit (APU) deployments.
- Reduce port emissions with this and future deployments.

Fiscal Year (FY) 2014 Objectives

- Familiarize maritime code and safety offices with the project and concept of hydrogen fuel cells in maritime applications.
- Produce preliminary prototype design and review with ABS, USCG, and the Hydrogen Safety Panel.
- Produce data collection and analysis plan.
- Develop hydrogen supply plan in close coordination with existing resources

Technical Barriers

This project addresses the following technical barriers from the Market Transformation section of the Fuel Cell Technologies Office Multi-Year Research, Development, and Demonstration Plan:

(A) Inadequate standards and complex and expensive permitting procedures

(E) A lack of flexible, simple, and proven financing mechanisms

(F) Inadequate user experience for many hydrogen and fuel cell applications

Technical Targets

No specific technical targets have been set.

FY 2014 Accomplishments

- Established partnership team and held project kick-off
- Collaboratively determined prototype functional specifications
- Made progress towards hydrogen supply arrangements
- Engaged maritime code and safety authorities and defined requirements
- Engaged Hydrogen Safety Panel to ensure safety is integrated into the project
- Produced preliminary prototype design and received design basis approval from USCG

INTRODUCTION

Fuel costs and emissions in maritime ports are an opportunity for transportation energy efficiency and emissions reduction efforts. For example, a 2004 study showed the Port of Los Angeles had average daily emissions exceeding that of 500,000 vehicles [1]. Diesel fuel costs continue to rise as low-sulfur limits are imposed, making power generation more expensive for fleets. Hydrogen fuel cells have the potential meet the electrical demands of vessels in the port as well as supply power for other port uses such as yard trucks, forklifts and other material handling specialty equipment. Validation of the commercial value proposition of both the application and the hydrogen supply infrastructure is the next step towards widespread use of hydrogen fuel cells in the maritime environment, and is determined by meeting

necessary equipment and operating costs and customer expectations such as reliability, form, and function.

Sandia National Laboratories' recent report, "Vessel Cold-Ironing Using a Barge Mounted PEM Fuel Cell: Project Scoping and Feasibility," identified several opportunities for demonstrating technical and commercial viability of a fuel cell in the maritime environment [2]. One identified opportunity is in Honolulu Harbor at the Young Brothers Ltd. (YB) wharf. YB provides barge transport of goods between Oahu and the Hawaiian neighbor islands and is an ideal demonstration location because of their high fuel costs and corporate interest in low-emission, low-environmental impact solutions. YB uses refrigerated containers ("reefers") which are kept cold while on the dock and on the barge by using dedicated diesel generators mounted inside mobile 20-foot containers. Sandia's report concluded that it is technically feasible to build a containerized hydrogen fuel cell generator to replace the diesel generator in YB operations.

APPROACH

This project develops and demonstrates a nominally, 100-kW, integrated fuel cell prototype for marine applications. This project brings together industry partners in this prototype development as a first step towards eventual commercialization of the technology. To be successful, the project incorporates interested industry and regulatory stakeholders: an end user, technology supplier and product integrator, and land- and maritime-based safety and code authorities. Project costs will be shared by the primary stakeholders in the form of funds, in-kind contribution, and material/equipment either loaned or donated to the project. Funding provided by the Department of Transportation, Maritime Administration (MARAD) is used to provide assistance with the integrated system and packaging designs, data collection and assistance during the demonstration period, and technical assistance and project management throughout the project. In addition some MARAD funds will be used to purchase specialized equipment needed to construct the prototype. DOE funds will be used to provide overall project management, technical design assistance, and deployment facilitation, and used via subcontract to the prototype manufacturer for the design, build, and testing of the final product.

The project has four phases:

1. Establishment and specification (Sept. 2013-Dec. 2013)
2. Detailed design and engineering (Jan. 2014-June 2014)
3. Prototype fabrication/site construction (July 2014-March 2015)
4. Deployment (on-site demonstration) and analysis (April 2015-December 2015)

RESULTS

The Maritime Fuel Cell Project team consists of eleven partners, and their roles are shown in Table 1.

The functional specifications of the unit were decided upon by all partners, considering technical capabilities, and focused on operational requirements and end-user needs. These include:

TABLE 1. Project Partners and Roles

Partner		Project Roles
U.S. DEPARTMENT OF ENERGY	**DOE**	Sponsorship, steering, H_2 supply coordination
	DOT/MARAD	Sponsorship, steering, and facilitation of maritime relationships
YOUNG BROTHERS Your Neighbor Island Partner FOSS	**Young Bros. & Foss Maritime**	Site preparations, prototype operation and routine maintenance
HYDROGENICS SHIFT POWER | ENERGIZE YOUR WORLD	**Hydrogenics *(sub w/ cost share)***	Design, engineer, build, commission, and support prototype unit
HNEI Hawai'i Natural Energy Institute University of Hawai'i at Mānoa	**HNEI**	Hydrogen supply logistics facilitation
ABS	**ABS**	Prototype design to maritime product standards
SECTOR HONOLULU	**US Coast Guard**	Review and acceptance of prototype design and operation
Pacific Northwest NATIONAL LABORATORY	**PNNL H_2 Safety Program**	Prototype and project safety review by HSP; hydrogen emergency response training for first responders
Sandia National Laboratories	**Sandia**	Management and coordination, H_2 materials and systems expertise, tech/business data collection and analysis

- Performance
  - 240 volt alternating current, 3-phase power, at least 100 kW continuous at the plugs
  - Hybrid battery/ultracap for inrush current
  - 10-12 hrs/day on the dock and at least 28 hr on the barge
  - 60-90 kg of H_2 stored at 5,000 psi
- Size and Weight
  - 20-foot hi-cube shipping container; 81,000 lb max weight
- Environmental
  - Ambient temperature +2°C to +40°C
  - Tolerate rain, wave wash, salt water intrusion during operation
  - Tolerate side-to-side movement in 20-foot seas during operation
  - Handled as ordinary container (not operating when moved)

Hydrogen supply arrangements are being made. Current options include utilizing current hydrogen production and dispensing assets on Oahu that will need to be relocated, importing liquid or gaseous hydrogen from the mainland, or installation of new generation and dispensing equipment at or near the deployment site.

The USCG has reviewed the conceptual design of the prototype and will issue a design basis letter which notes that they agree with the concepts, codes, and standards proposed and allows the project team to proceed with detailed design. Because neither USCG nor ABS have existing codes, standards, or rules regarding the use of hydrogen onboard vessels, the project is assisting them with their development.

PNNL's Hydrogen Safety Program is participating in the project in two ways. First, the Hydrogen Safety Panel has reviewed the conceptual design twice and provided valuable feedback for the project team to consider during the design phase. Second, DOE is also working to provide hydrogen safety training to all Young Bros. operations personnel in Oahu, Molokai, and Lanai, the local Hawaii fire station in Oahu (where the unit will be operating on the dock and refueled), and first responders at sea.

CONCLUSIONS AND FUTURE DIRECTIONS

The Maritime Fuel Cell Project is a wholly collaborative effort with early and continuous stakeholders feedback that is breaking down non-technical barriers to hydrogen and fuel cell use. Future work includes:

- Finalize hydrogen supply arrangements
- Finalize data collection and analysis plan
- Begin prototype build
- Finish prototype build, factory test, on-site commissioning, and training
- Finish site preparations and conduct on-site hydrogen safety training
- Begin deployment testing and collect operational and cost data
- Continue to use the leverage for education and outreach both in Hawaii and in the worldwide maritime/port community

FY 2014 PUBLICATIONS/PRESENTATIONS

1. D. Dedrick, "Reducing Emissions at Ports and Advancing Hydrogen Fuel Infrastructure," presented at the California Fuel Cell Partnership Executive Board Meeting, April 15, 2014.

2. J. Pratt, "Fuel Cell Power for Refrigerated Containers: Towards Cleaner and Cheaper Maritime Power," presented at the Ship Operations Cooperative Program Spring Summit, Galveston, TX, May 13–14, 2014.

3. J. Pratt, "Applying Hydrogen and Fuel Cells to Maritime Ports," presented at the California Hydrogen Business Council Spring Summit, Long Beach, CA, May 5, 2014.

4. J. Pratt, "Maritime Fuel Cell Generator Project," presented at the DOE Annual Merit Review, Washington, DC, June 16–20, 2014.

REFERENCES

1. D. Bailey, T. Plenys, G.M. Solomon, T.R. Campbell, G.R. Feuer, J. Masters, and B. Tonkonogy, "Harboring Pollution - Strategies to Clean Up U.S. Ports," National Resources Defense Council, NY, August, 2004.

2. J.W. Pratt and A.P. Harris, "Vessel Cold Ironing Using a Barge Mounted PEM Fuel Cell: Project Scoping and Feasibility," Sandia National Laboratories, Report SAND2013-0501, available at http://energy.gov/eere/fuelcells/downloads/vessel-cold-ironing-using-barge-mounted-pem-fuel-cell-project-scoping-and.

IX.6 Fuel Cell-Based Auxiliary Power Unit for Refrigerated Trucks

Kriston P. Brooks
Pacific Northwest National Laboratory (PNNL)
P.O. Box 999/K6-28
Richland, WA 99352
Phone: (509) 372-4343
Email: Kriston.brooks@pnnl.gov

DOE Manager
Pete Devlin
Phone: (202) 586-4905
Email: Peter.Devlin@ee.doe.gov

Project Start Date: April 1, 2013
Project End Date: December 31, 2015

Overall Objectives

Demonstrate the viability of fuel cell-based transport refrigeration units (TRUs) for refrigerated Class 8 trucks by:

- Identify companies and partnerships to support multiple demonstrations.
- Develop system designs that meet or exceed the cooling capacity of the current diesel engine-based devices.
- Evaluate the value proposition for such systems by developing business cases for their use.
- Demonstrate the fuel cell-based TRUs with multiple 400-hour commercial demonstrations with food distribution companies making actual deliveries at a variety of locations and with varying routes.
- Analyze the data resulting from these demonstrations and provide an independent assessment of the technology.

Fiscal Year (FY) 2014 Objectives

- Compete and place subcontracts with two fuel cell vendors
- Develop business cases to analyze the system's market viability
- Size the systems to provide adequate power to meet the expected door openings and ambient temperatures
- Develop prototype systems and test over the expected range of conditions
- Address interfaces with trailer, refueling system, and TRU

Technical Barriers

This project addresses the following technical barriers for Market Transformation from the Fuel Cell Technologies Office Multi-Year Research, Development, and Demonstration Plan:

- (E) Inadequate private funds available for new projects
- (F) Inadequate user experience for fuel cell applications
- (H) Lack of awareness of applications

FY 2014 Accomplishments

- Set up subcontracts with Nuvera and Plug Power as the two system integrators. These subcontracts also include TRU manufacturers and demonstration partners.
- Both Nuvera and Plug Power teams have accomplished the following:
  - Developed business cases assessing the market, interviewing customers, and demonstrating the economics of the value proposition.
  - Defined the power requirements for the fuel cell-powered TRU system either with data collection at potential sites and modeling anticipated ambient temperatures and door openings.
  - Addressed the interface issues of refueling and electrical connections with the TRU.
  - Prepared safety plans including either a preliminary hazards analyses or a design failure modes and effects analysis.
  - Performed initial testing on a bench-top system.

INTRODUCTION

Fuel cells can provide clean, efficiency auxiliary power for vehicles that have significant power demands when the primary motive-power engines are not running. Currently, primary engines are often kept running solely to provide electrical power for those auxiliary loads, an inefficient practice that wastes fuel, increases emissions, and results in increased engine wear. Fuel cell-based auxiliary power units represent a possible solution to replace the need for operating a diesel engine. Heavy-duty refrigerated trucks are one such application that uses a diesel engine to power the TRU. By replacing the diesel engine in the TRU with a fuel cell, recent environmental mandates can be addressed, noise restrictions in urban areas, especially at night can be overcome, and the uncertainty of diesel prices can be resolved.

APPROACH

As part of DOE's Fuel Cell Technologies Office, Market Transformation seeks to increase the number of commercial products that use fuel cells, expand the fuel cell market, and promote early adoption of hydrogen and fuel cell technologies. One application that appears promising is the use of fuel cells to power the TRUs on refrigerated heavy-duty trucks. PNNL has been tasked to identify and subcontract with two fuel cell vendors and assist them in developing fuel cell-based auxiliary power unit prototypes that will power such TRUs. The demonstration systems will not be a final sellable product, but the project will demonstrate the feasibility of such systems by developing a business case and testing each demonstration system.

This project involves the major players in the TRU and food distribution arena, allowing them to become familiar with fuel cell technologies. The two major producers of TRUs in the U.S., Carrier Transicold and Thermo King, are partners with the subcontracts on this project. Significant players in food distribution, Sysco and HEB, are the demonstration partners. Four demonstrations are currently proposed in New York and Texas. These partners have been involved in the development of the business cases. They have assisted in sizing the system power to ensure that it provides similar levels as that produced by the diesel engine. This power data was developed by experimental measurements or modeling. Each team is required to address the issues with infrastructure, compliance with applicable regulations, and road worthiness. This aspect of the work is still ongoing.

At each stage of the system development, PNNL and DOE have Go/No-Go decisions to ensure the design is adequate. Once the systems have completed their acceptance testing and commissioning on the trailers, they will be evaluated in real-life delivery routes with the food distributors. Data on the fuel cell, TRU, route, and environmental conditions will be collected and analyzed by PNNL to provide an independent assessment of the systems' performance.

RESULTS

As part of the business case development of a "Voice of the Customer" was conducted. It involved interviews with six food service distribution and grocery companies, representing the functions of warehousing, fleet operations and maintenance, engineering, and senior management. These interviews provide indications of what is important to the customer and some of the important considerations in developing a fuel-cell based TRU. The results indicate that "return on investment is the biggest driver after safety"—the commercial product must be cost effective. Additionally, they found that "being a sustainability leader is critical to corporate image"—such reductions in fossil fuel use are expectations of the customers. The study also elucidated that "noise from diesel engines is unacceptable in an increasing number of settings where food is delivered, including densely residential areas, underground parking, hotels, hospitals and nursing homes." In addition, diesel price uncertainty is a major concern.

The business case also evaluated the economics of the system by comparing a current diesel-powered TRU with the fuel cell-powered version. The parameters of fuel cell incremental cost, diesel pricing and hydrogen pricing were evaluated assuming a 20-kW fuel cell with a 12-year trade cycle and 2,000 hours of operation. Federal investment tax credit for fuel cell systems is also included in Table 1. As can be seen in the results of the table, the price per unit of hydrogen is a major driver in making the system economical. This can be achieved as the overall consumption of hydrogen is increased, thus spreading the high cost of its infrastructure across a larger number of systems.

TABLE 1. Sample Value Proposition Analysis for the Fuel Cell TRU System

Hydrogen	TRU Incremental Cost	Diesel $4.00	Diesel $6.00	Diesel $8.00
Hydrogen $2.50	$21,000	$ 21,888	$ 57,399	$ 92,980
Hydrogen $4.00	$21,000	$ 9,297	$ 44,878	$ 80,459
Hydrogen $6.00	$21,000	$ (21,990)	$ 13,592	$ 49,173
Hydrogen $8.00	$21,000	$ (53,276)	$(17,695)	$ 17,887
Hydrogen $10.00	$21,000	$ (84,563)	$(48,981)	$(13,400)
Hydrogen $12.00	$21,000	$(115,849)	$(80,268)	$(44,686)

The maximum power requirements for the systems were estimated based on data logging of actual deliveries or based on modeling. Plug Power collected data at Sysco Long Island and Sysco Houston to during loading, driving and deliveries to determine the maximum power required for the systems. A sample data collection log for Sysco Long Island is shown in Figure 1. Nuvera in contrast developed a model with assistance from Thermo King to evaluate the maximum power requirements. The model was impacted by ambient temperature and includes loading, initial pull-down and then a series of door openings. In both cases, the output requirements for these systems were determined to be ~20 kWe.

Both the Carrier and Thermo King have selected systems that have an electric standby option that allows the compressor to be run either with a diesel engine or with external 480 VAC power. Power from the fuel cell would be fed to the TRU through this 480 VAC line. Both designs for the demonstrations will leave the diesel engine in place and install the fuel cell system underneath the belly of the trailer. By leaving the diesel engine in place, it can act as a backup in the event there is an issue with the fuel cell and prevent damage to the temperature-sensitive cargo being distributed during the demonstrations. With a commercial fuel cell

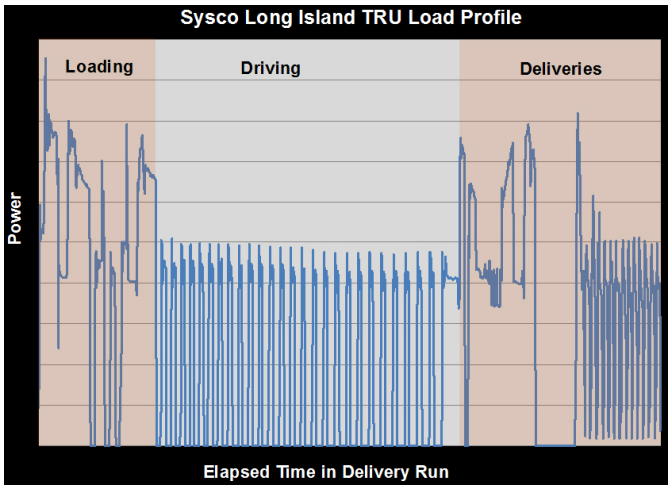

FIGURE 1. Sample TRU Load Profile developed by Sysco Long Island for Plug Power

product, the fuel cell and its ancillary equipment would replace the diesel engine. Early indications are that there is sufficient space for such an exchange.

Currently both subcontractors have developed their fuel cell systems and have tested them over the range of conditions expected for the TRU. These prototype systems are bench-top units as shown in Figure 2. They have not been packaged, but work is underway to develop these packages and prepare them for the vibration, impacts, and weather extremes expected during commercial operation.

CONCLUSIONS AND FUTURE DIRECTIONS

The conclusions of the fuel cell TRU development work for FY 2014 are as follows:

- Nuvera and Plug Power have developed business cases that indicate positive rates of return are possible with sufficient hydrogen usage volume.
- Nuvera and Plug Power have determined the power requirements for their systems at approximately 20 kWe. Based on available experimental and modeling data, these systems appear to be adequate to support TRU operation over a range of ambient conditions and anticipated door opening scenarios.

The future work for the fuel cell TRU development work in FY 2015 is as follows:

- Future work includes developing the packaged system and addressing on-road issues such as vibration, safety and weather extremes. The systems will then be demonstrated with commercial deliveries.

FY 2014 PUBLICATIONS

Media Interest Articles

1. Burke, Jack; "Future Cooling Trend?" Diesel Progress, October 2013.

2. Piellisch, Rich; "Hydrogen Fuel Cells for Reefer Trucks," Fleets & Fuels, August 2013.

3. Flatt, Courtney; "A Greener Way To Cool Your Foods On The Way To The Grocery Store," NPR, The Salt, September 2013, http://www.npr.org/blogs/thesalt/2013/09/03/218592685/a-greener-way-to-cool-your-foods-on-the-way-to-the-grocery-store.

4. Beaudry, David; "Cool that's Also Clean: Fuel Cells for Refrigerated Trucks," TruckingInfo.com, November 2013, http://www.truckinginfo.com/channel/products/article/story/2013/11/cool-that-s-also-clean-fuel-cells-for-refrigerated-trucks.aspx

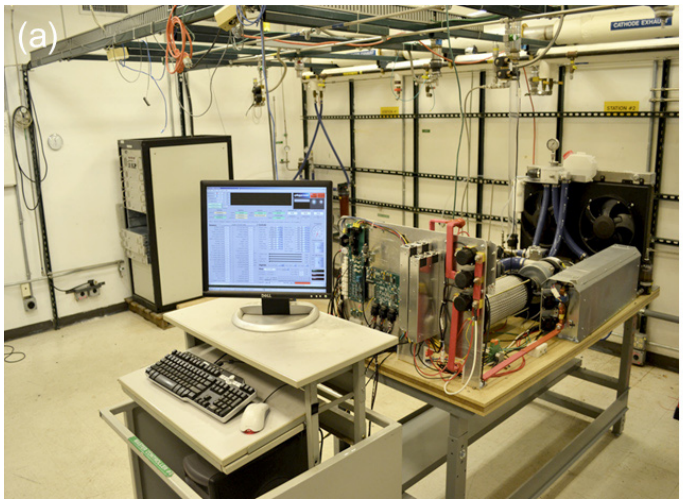

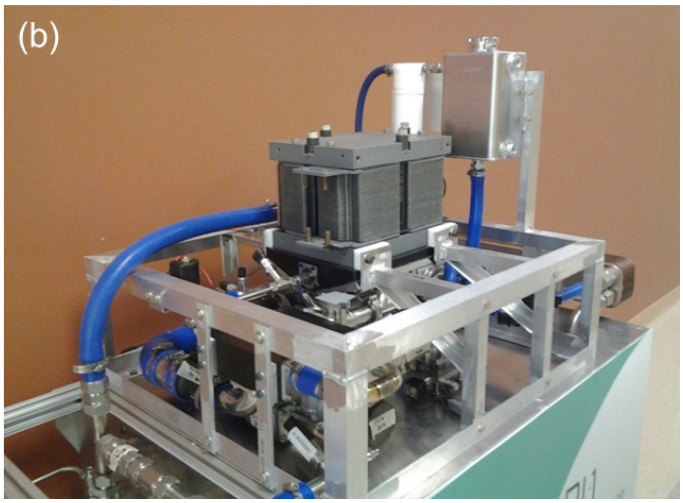

FIGURE 2. Prototype Testing Systems for (a) Plug Power and (b) Nuvera

5. Phys.org, "Refrigerated trucks to keep their cool thanks to fuel cell technology" (8/23/2013) http://phys.org/news/2013-08-refrigerated-trucks-cool-fuel-cell.html

6. EcoSeed, Hydrogen & Fuel Cells, "Fuel cell powered refrigeration trucks being developed and tested by P.N.N.L." (8/29/2013) http://www.ecoseed.org/renewables/hydrogen-fuel-cells/16961-fuel-cell-powered-refrigeration-trucks-being-developed-and-tested-by-p-n-n-l

7. Work Truck Magazine, "Fuel-Cell Technology Keeps Refrigerated Trucks from Losing Their Cool" (9/6/2013) http://www.worktruckonline.com/channel/green-fleet/news/story/2013/09/fuel-cell-technology-keeps-refrigerated-trucks-from-losing-their-cool.aspx?prestitial=1

X. SYSTEMS ANALYSIS

X.0 Systems Analysis Sub-Program Overview

INTRODUCTION

The Systems Analysis sub-program supports decision-making by providing a greater understanding of technology gaps, options and risks, and the contribution of individual technology components to the overall system. Examples include fuel production to utilization and the interaction of components and their effects on the system. Analysis is also conducted to assess cross-cutting issues, such as integration of hydrogen and fuel cells with the electrical sector for energy storage.

The Systems Analysis sub-program made several significant contributions to the Fuel Cell Technologies Office (FCTO) during Fiscal Year (FY) 2014. The cost reduction of hydrogen refueling infrastructure was examined, the impact of improving the fuel cell efficiency and the impact on fuel cell electric vehicle (FCEV) performance was studied, and opportunities to apply hydrogen for energy storage and electrical grid applications were evaluated. The JOBS and economic impacts of Fuel Cells (JOBS FC) model continues to be enhanced by Argonne National Laboratory (ANL) and RCF Economic and Financial Consulting (RCF), by adding the capability to assess employment impacts of infrastructure development for the early market penetration of FCEVs. Infrastructure analyses were conducted to better understand early market hurdles such as cash flow, station utilization, and low-volume cost-reduction strategies. The Greenhouse gases, Regulated Emissions and Energy use in Transportation model is being enhanced to evaluate greenhouse gas (GHG) emissions and petroleum use on a well-to-wheels life-cycle basis for hydrogen pathways, and to include water consumption analysis capability in the model to conduct life-cycle analysis of various hydrogen production pathways.

GOAL

The goal of the Systems Analysis sub-program is to provide system-level analysis to support hydrogen and fuel cell technology development and technology readiness by evaluating technologies and pathways, including resource and infrastructure issues, guiding the selection of research, development, and demonstration projects, and estimating the potential value of research, development, and demonstration efforts.

OBJECTIVES

- Complete analysis of milestones and technology targets, including risk analysis, independent reviews, financial evaluations, and environmental analysis to identify technology gaps and risk mitigation strategies by 2015.
- Complete analysis of FCTO performance, cost status, and potential for use of fuel cells in a portfolio of commercial applications by 2017.
- Complete analysis of the potential for hydrogen, stationary fuel cells, fuel cell vehicles, and other fuel cell applications such as material handling equipment to become cost competitive by 2019. The analysis will address necessary resources, hydrogen production, transportation infrastructure, performance of stationary fuel cells and vehicles, and the system effects resulting from the growth of fuel cell market shares in the various sectors of the economy.
- Provide milestone-based analysis, including risk analysis, independent reviews, financial evaluations, and environmental analysis to support FCTO's needs prior to technology readiness.
- Periodically update the life-cycle energy, petroleum use, GHG and criteria emissions analysis for technologies and pathways for FCTO to include technological advances or changes.

FY 2014 TECHNOLOGY STATUS AND ACCOMPLISHMENTS

The Systems Analysis sub-program focuses on examining the economics, benefits, opportunities, and impacts of fuel cells and renewable fuels with a consistent, comprehensive, analytical framework. Analysis conducted in FY 2014 included socio-economic impacts such as increased employment from early market infrastructure development, life-cycle analysis of various vehicle platforms including FCEVs with the Bio-Energy Technologies and Vehicle Technologies Offices, hydrogen use for energy storage, fuel cell system cost impact to improve fuel cell efficiency,

life cycle impacts of water use of hydrogen production pathways, identification of early markets for fuel cells and opportunities to reduce cost through various mechanisms, and options to reduce infrastructure cost through the application of tri-generation fuel cell systems.

Develop and Maintain Models and Systems Integration

ANL, with assistance from RCF, continues to estimate job creation as a result of DOE FCTO projects and created the JOBS H2 model to estimate employment and revenue impacts of infrastructure development to support the early market penetration of FCEVs. The JOBS H2 model uses the same model structure and input-output methodology as developed for the JOBS FC model to estimate changes in industry expenditures as a result of hydrogen fueling infrastructure deployment and calculates the effects of those changes throughout the economy. Version 1.0 of the model was released for public use in June 2014 and includes the economic impacts along the supply chain for infrastructure deployment and user-specified analyses at the state, regional, or national level and is available for download at http://jobsmodels.es.anl.gov. (ANL and RCF)

The model is being used to assess the employment impacts of infrastructure development for the early market introduction of FCEVs. Figure 1 illustrates that the infrastructure development of 25 hydrogen fueling stations for five years will create or retain approximately 2,400 jobs. Note that jobs will start to decline once the station construction is completed but operation-related jobs will be retained.

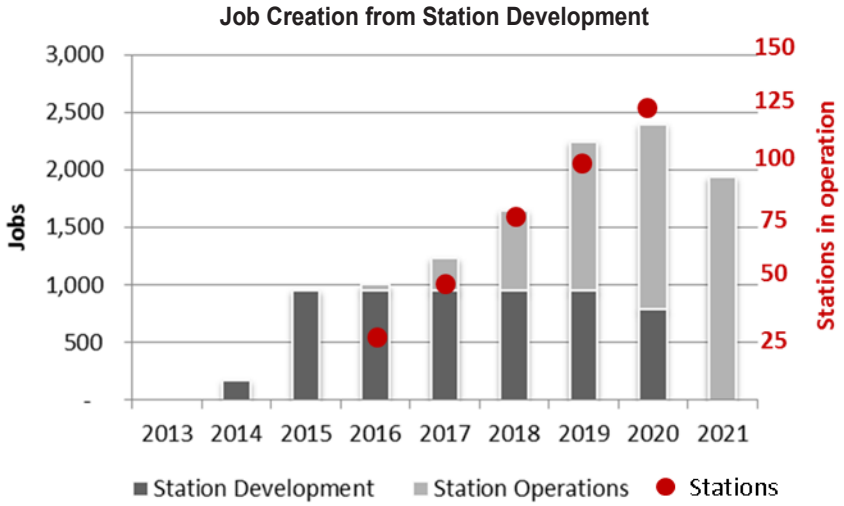

FIGURE 1. (Source: ANL)

Water Life-Cycle Analysis

Enhancements to the Greenhouse gases, Regulated Emissions and Energy use in Transportation Model's life-cycle analysis capabilities were continued in FY 2014 to examine water consumption for hydrogen production and delivery pathways from natural gas, water electrolysis, and other fuels such as gasoline and ethanol. The analysis includes the water use assessment of pathway components including feedstocks such as natural gas and crude oil, and energy use such as electricity. Also, the water use for growing biofeedstocks such as corn and cellulosic sources are included in the model. Converting these conventional and new feedstocks to fuels require additional water consumption. Similarly, water is needed for heat rejection in thermo-electric power generation cycles. Producing hydrogen from electricity (via electrolysis), natural gas (via steam methane reforming), or biomass (via gasification) requires additional use of water as a feed for the conversion process as well as for cooling. The results of the analysis shown in Figure 2 exhibit that water for irrigation, cooling water for electricity generation, and evaporation associated with hydropower generation has the greatest impact on life cycle water consumption of 85% ethanol/15% gasoline (E85) fuel, and hydrogen fuel cell and electric vehicles. (ANL)

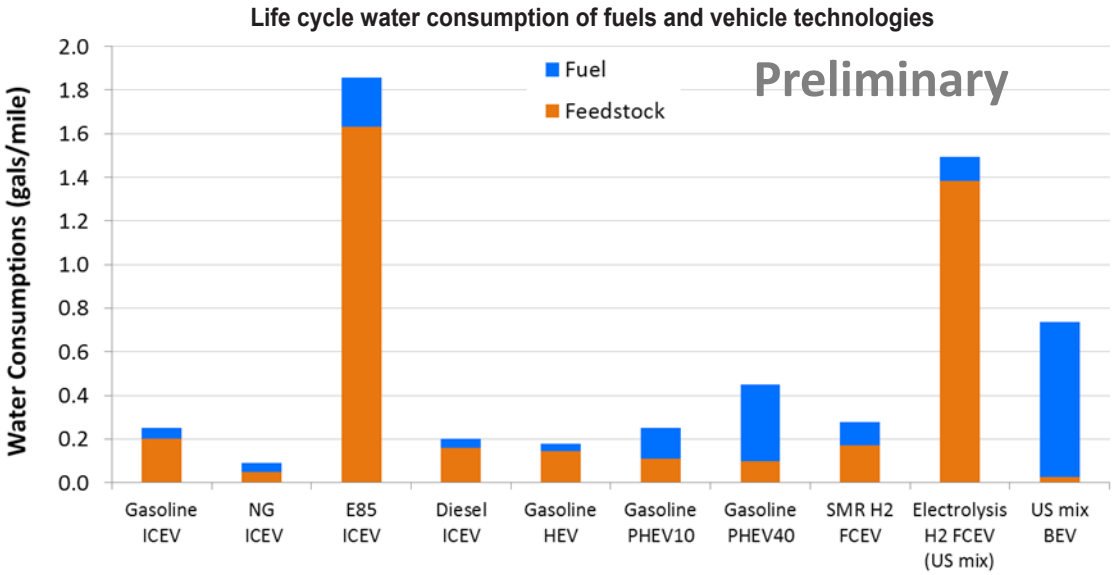

ICEV – internal combustion engine vehicle; NG – natural gas; HEV – hybrid electric vehicle; PHEV10 – plug-in hybrid electric vehicle with 10-mile all-electric range; PHEV40 – plug-in hybrid electric vehicle with 40-mile all-electric range; SMR – steam methane reformer; H2 – hydrogen; BEV – battery electric vehicle

FIGURE 2. (Source ANL)

Studies and Analysis

Global and domestic market analysis of the fuel cell markets for portable, stationary power, and transportation applications continue to be assessed. The analysis identified increased growth in the fuel cell market in the domestic and international markets. As exhibited in Figure 3, the fuel cell market remains strong with over 35,000 systems shipped in 2013, an increase of greater than 25% over 2012. (Navigant Research)

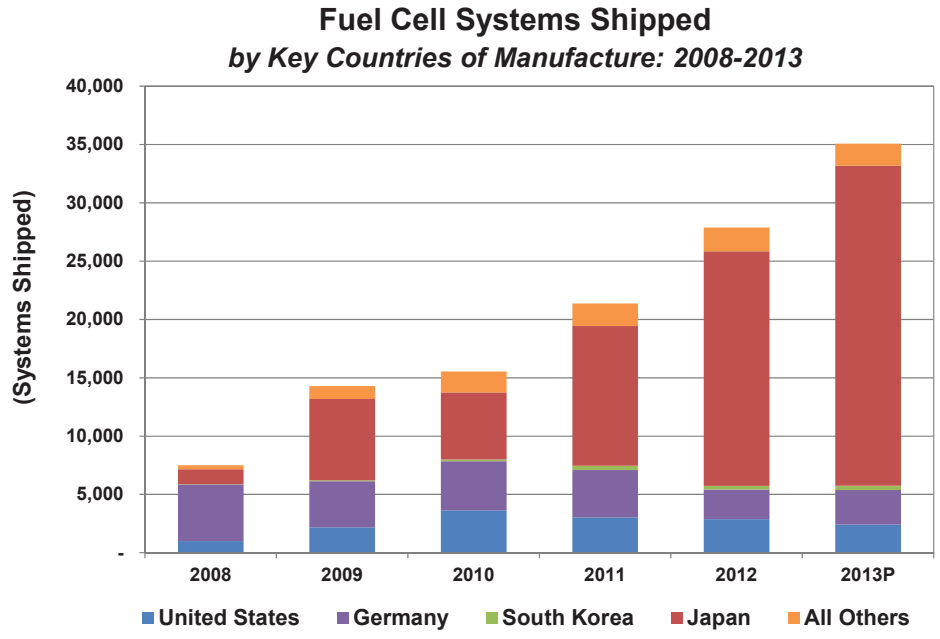

FIGURE 3. (Source Navigant Research)

Research also shows a continued growth in revenues from the fuel cells of greater than 44% from 2012 to 2013 to over $1.3 billion as exhibited in Figure 4.

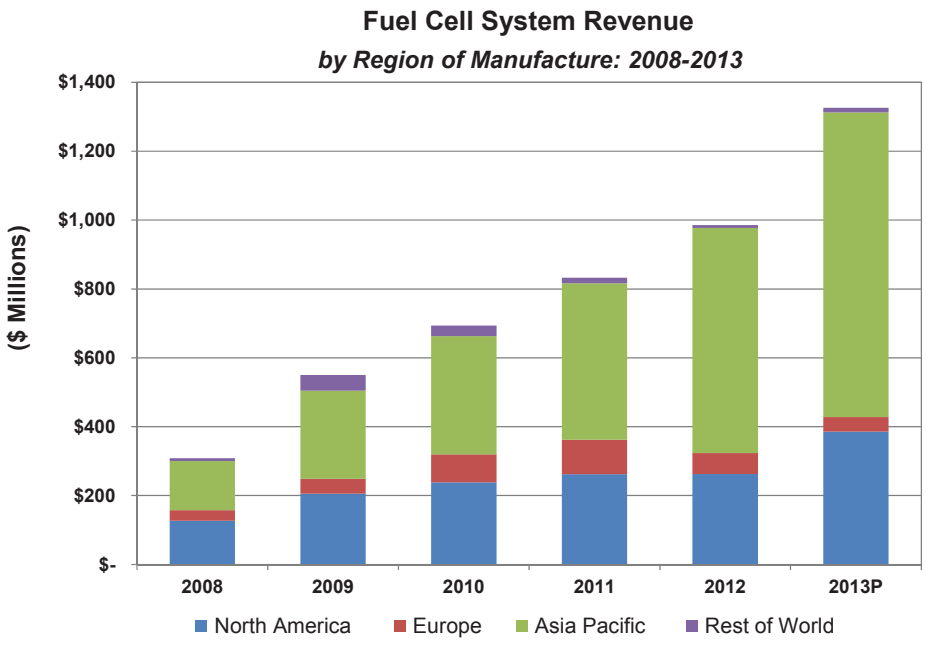

FIGURE 4. (Source Navigant Research)

Infrastructure Analysis

Fueling Pressure Analysis

Although the sub-program recognizes that market entry will focus on infrastructure to accommodate 700-bar hydrogen storage tanks, the impact of pressure on cost is valuable for assessing potential future scenarios. The dispensing options which would refuel a 700-bar-rated FCEV tank at various pressures (350, 500 and 700 bar) were examined, to evaluate the cost impact on the delivery system. The project assessed the performance of the refueling system and the impact of fueling pressure and pre-cooling requirements on the tank fill time and refueling cost. The refueling costs for station capacities of 200 kg/day, 400 kg/day and 750 kg/day are shown in Figure 5. The refueling cost savings with the lower fueling pressures is much greater for smaller station capacities compared to the larger stations. Greater cost savings would be realized in early FCEV markets where the deployed stations are of small capacities and the utilization of the station is expected to be low with a slow initial vehicle deployment rate. (ANL)

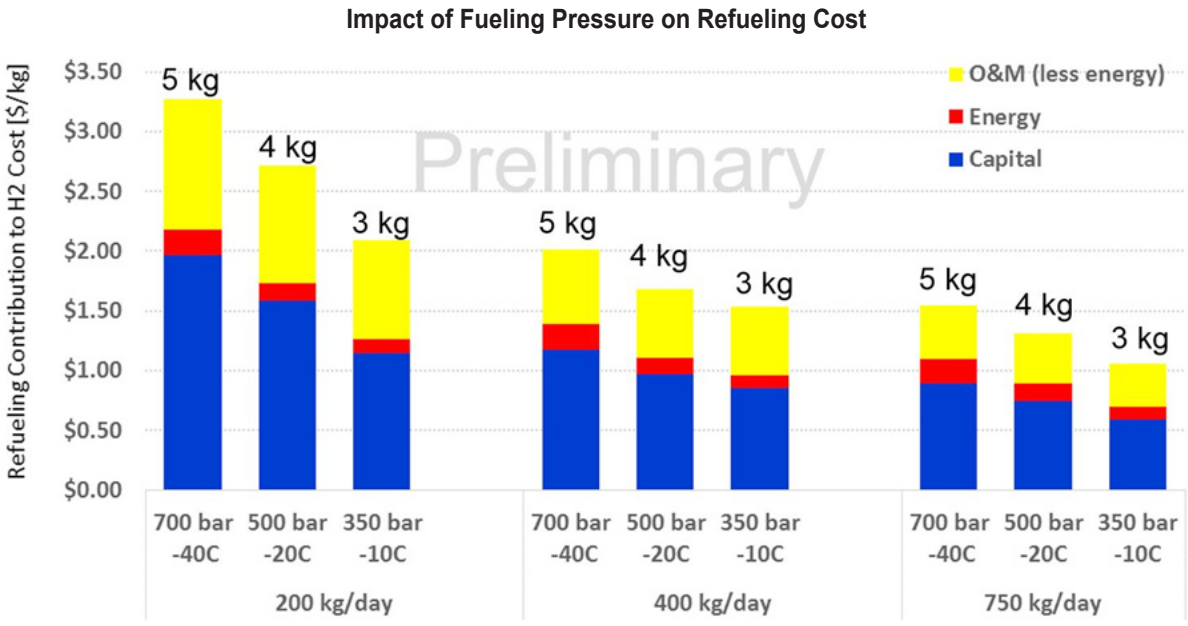

O&M – operations and maintenance

FIGURE 5. (Source ANL)

Environmental Analysis

Vehicle Portfolio Life Cycle Analysis

Analysis was conducted in collaboration with the Office of Energy Efficiency and Renewable Energy's (EERE) Bioenergy Technologies Office, Vehicles Technologies Office, national laboratories, and industry stakeholders to examine the life-cycle GHG emissions and energy use of multiple hypothetical low-carbon pathways for various fuels and vehicle configurations. Major inputs to the calculation of GHG emissions included the fuel economy of each vehicle and fuel production pathway efficiency. The data and major assumptions and results are documented in the following Hydrogen and Fuel Cells Program Record #14006: http://hydrogen.energy.gov/pdfs/14006_cradle_to_grave_analysis.pdf. The results of the analysis show that GHG emissions could be reduced by improving the efficiency of the vehicles but the major contribution of the GHG emissions will result from reducing the carbon content of the fuel. Also, a portfolio of fuels and advanced vehicle technologies will be needed to achieve significant GHG emission reductions from the transportation sector (Figure 6).

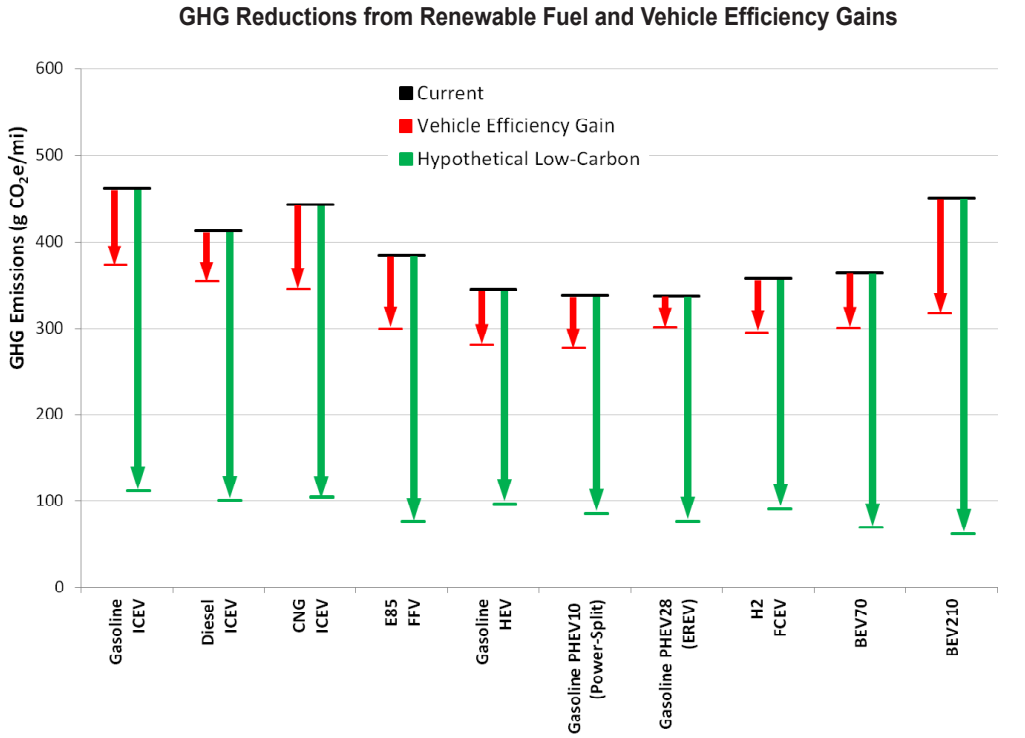

CNG – compressed natural gas; PHEV28 – plug-in hybrid electric vehicle with 28-mile all-electric range; EREV – extended-range electric vehicle; BEV70 – battery electric vehicle with 70-mile range; BEV120 – battery electric vehicle with 120-mile range

FIGURE 6. (Source FCTO)

Energy Storage Analysis

Hydrogen and Fuel Cell Application for Electrical Grid Energy Storage

The use of hydrogen generated from an electrolyzer via renewable energy, such as wind, for energy storage and dispatched to the electrical grid was examined. The analysis found that the operating flexibility of electrolyzers acting as demand response devices is fast enough (sub-second) and can be maintained long enough for them to participate in energy, capacity, and ancillary service electricity markets. Hydrogen and fuel cell technologies have the ability to generate fuel for FCEVs and supply electricity to the grid through arbitrage and ancillary services. The system economics showed the optimum regime occurs when hydrogen production equipment is designed to provide grid services and fuel for FCEVs. Also, the optimum hydrogen energy storage system was found to have a rated storage capacity for supplying ~3-16 hours of fuel and electricity for grid services; additional storage capacity is not more valuable in ancillary grid services markets (Figure 7). (National Renewable Energy Laboratory, NREL)

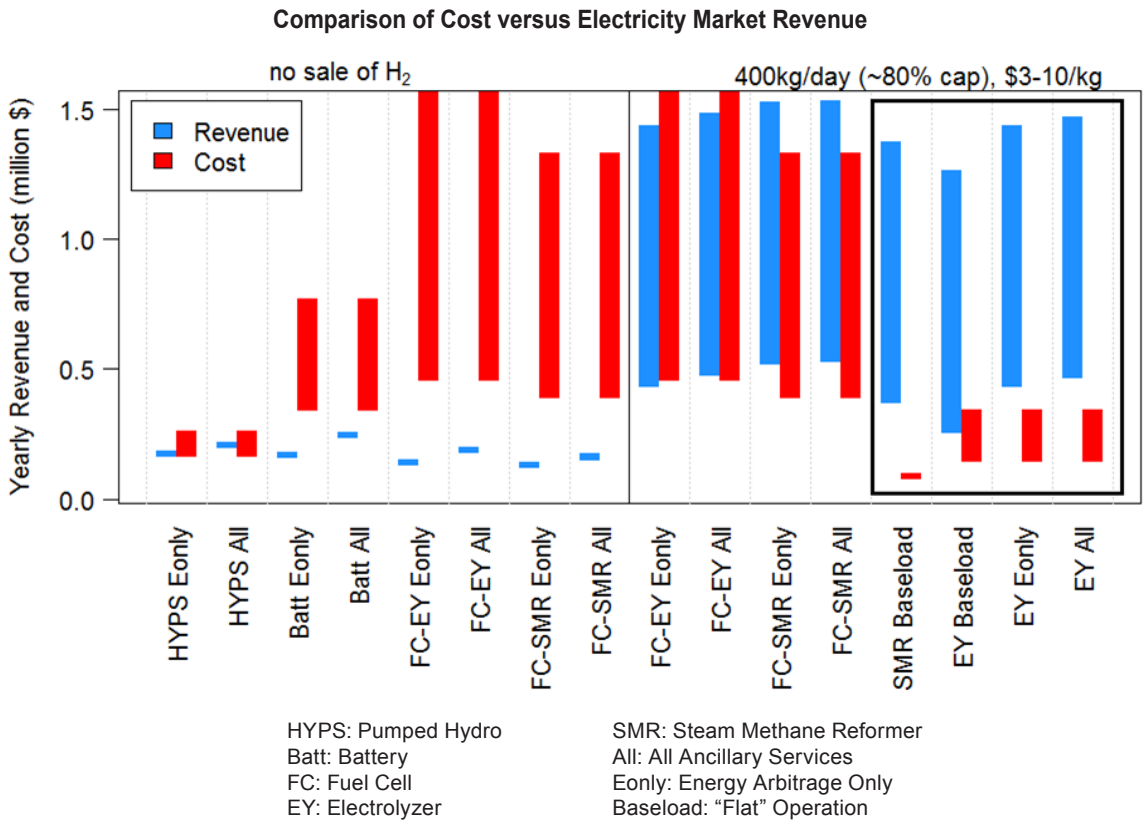

FIGURE 7. (Source NREL)

Impact of Fuel Cell System Peak Efficiency on Fuel Consumption and Cost

The impact of different fuel cell targets on the vehicle energy consumption and cost were studied using the Autonomie model and compared to conventional gasoline internal combustion powertrains. In addition, the impact of fuel cell system improvements on the potential onboard storage requirements and cost were analyzed. The findings of the study indicate the fuel economy of the FCEV could be improved by 10-14% by increasing the fuel cell peak efficiency from 60 to 68%. When the FCEV improvements are compared to a conventional vehicle, the FCEV fuel economy was found to be five times higher than the conventional vehicle in the 2030 timeframe (Figure 8). (ANL)

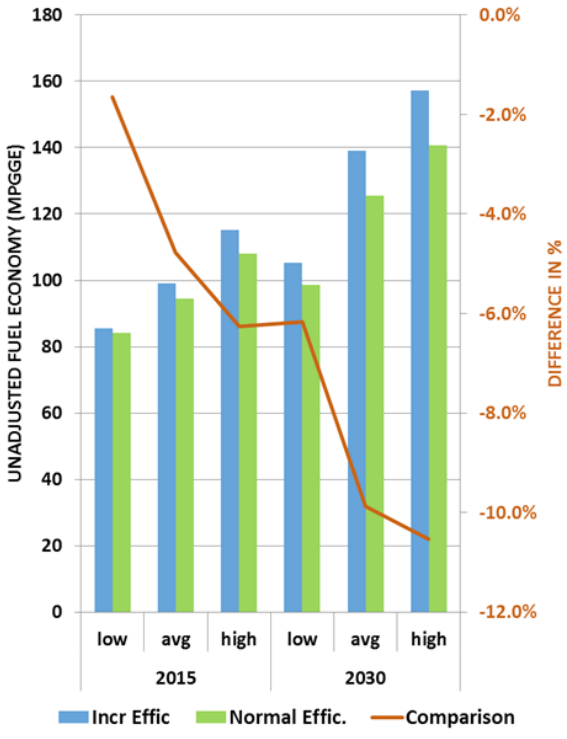

FIGURE 8. (Source ANL)

Analysis of the Levelized Costs of Electricity (LCOE) from Combined Heat & Power (CHP) and Solar Photovoltaic (PV) Technologies

The LCOE associated with for stationary fuel cells were compared to other conventional technologies in CHP applications, and renewable technologies such as solar PV technologies. In this analysis, the systems in CHP service had a capacity of 200-500 kW and the PV and micro fuel cells had a capacity of 7 kW. Fuel cells in the CHP service had a LCOE of $0.065-$0.085/kWh which is comparable to the LCOE of conventional technologies. In the case of the micro systems, the micro fuel cell had a LCOE range of $0.08-$0.13/kWh which is comparable to an average

solar PV LCOE of ~$0.105/kWh (Figure 9). The details of the analysis, which was peer reviewed by EERE's Solar Technologies Office and the NREL, are provided in the following Hydrogen and Fuel Cells Program Record #14003: http://hydrogen.energy.gov/pdfs/14003_lcoe_from_chp_and_pv.pdf

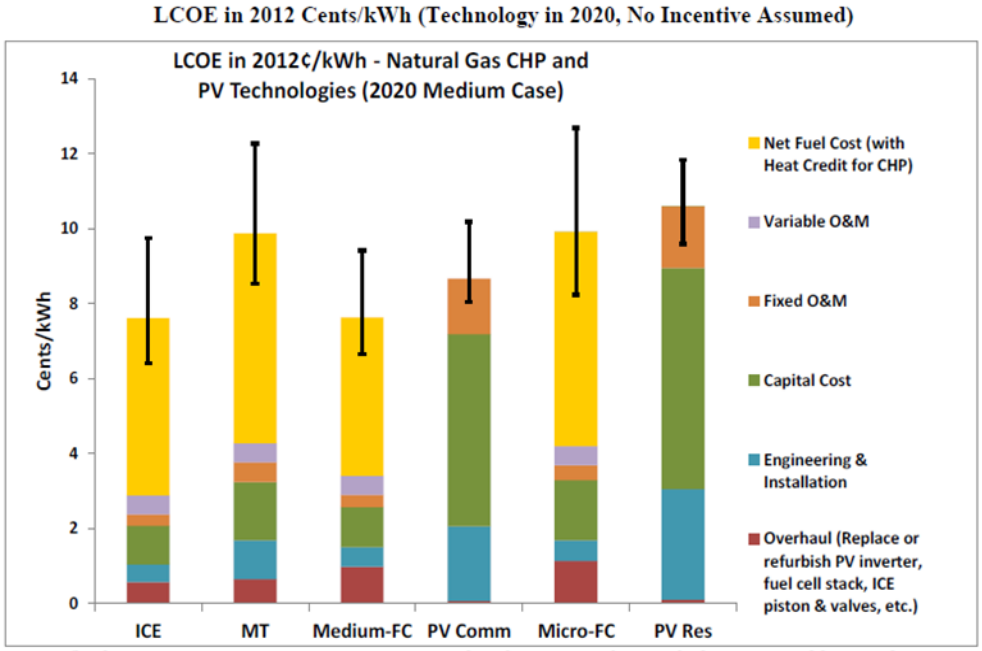

FIGURE 9. (Source FCTO)

Commercial Products and Patents Resulting from DOE Sponsored R&D

The commercial benefits of FCTO were analyzed by tracking the commercial products and technologies and patents developed from R&D funding. The benefits of DOE-funded projects continue to grow. Over 499 patents were awarded and 45 products were commercialized by 2014 as a result of research funded by FCTO in the areas of storage, production, delivery, and fuel cells which will be highlighted in the FY 2014 Pathways to Commercial Success Report. (Pacific Northwest National Laboratory, PNNL)

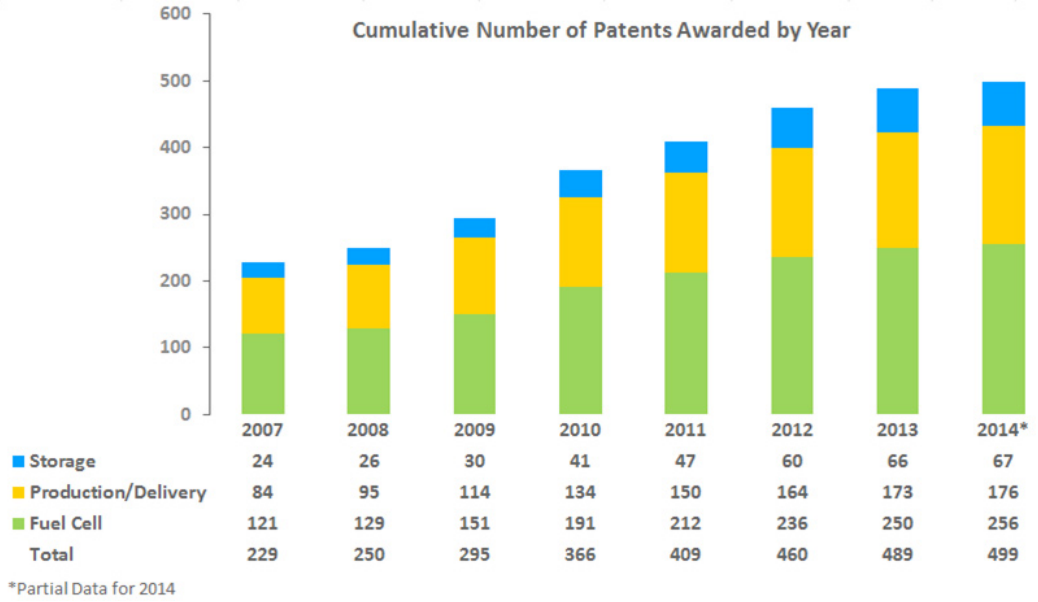

FIGURE 10. (Source PNNL)

BUDGET

The budget for the Systems Analysis sub-program is consistent with the goals and objectives of FCTO and is responsive to assessing hydrogen and fuel cell applications for light-duty transportation applications, as well as energy storage, stationary power generation, and specialty applications. The FY 2015 budget request includes funding for early fuel cell and hydrogen market and infrastructure analysis, as well as environmental life-cycle analysis, overall sub-program analysis of targets and technology gap assessment, market impact analysis, socio-economic analysis of fuel

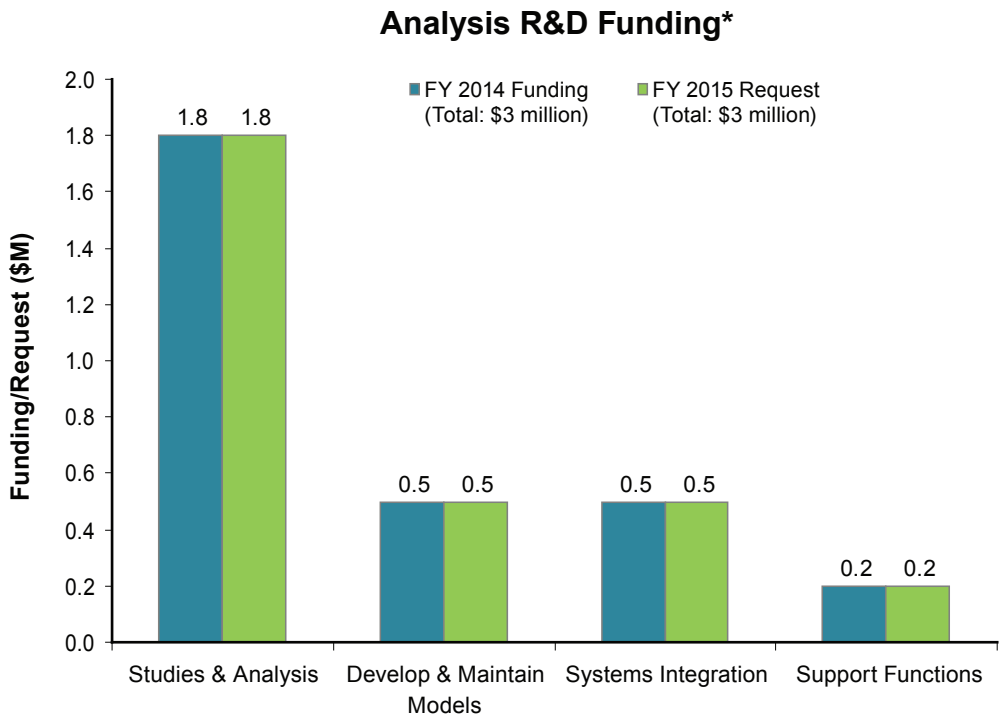

* Subject to appropriations, project go/no-go decisions, and competitive selections. Exact amounts will be determined based on research and development progress in each area.

cells and hydrogen infrastructure, market segmentation of fuel cell vehicles in the light-duty vehicle fleet, and business analysis of opportunities to reduce the cost of infrastructure for early market penetration of FCEVs. New opportunities for energy storage and integration with existing energy supply networks such as natural gas transmission will continue to be evaluated.

FY 2015 PLANS

The Systems Analysis activity for FY 2015 will focus on conducting analyses to determine technology gaps for fuel cell systems and infrastructure for fuel cell vehicles, benefits and opportunities for new onboard storage options and utilizing fuel cells for energy storage and transport. Analysis will be focused on business case studies of hydrogen supply infrastructure for the early market penetration of fuel cell vehicles, understanding the tradeoffs and regional impacts of fuel cells with other alternative fuels, light-duty vehicle life cycle costs for multiple platforms, socio-economic impacts of job creation based on hydrogen supply infrastructure development, and the market segmentation of light-duty fuel cell vehicles. The FY 2014 appropriation included $3 million for Systems Analysis; the FY 2015 request is $3 million. The budget request for FY 2015 reflects the focus on early market analysis, fuel cell technology evaluations, renewable fuel benefits, as well as water resource and infrastructure analysis.

Fred Joseck
Systems Analysis Project Manager
Fuel Cell Technologies Office
Office of Energy Efficiency and Renewable Energy
U.S. Department of Energy
1000 Independence Ave., SW
Washington, D.C. 20585-0121
Phone: (202) 586-7932
Email: Fred.Joseck@ee.doe.gov

X.1 Analysis of Optimal Onboard Storage Pressure for Hydrogen Fuel Cell Vehicles

Zhenhong Lin (Primary Contact), Changzheng Liu
Oak Ridge National Laboratory
2360 Cherahala Boulevard
Knoxville, TN 37932
Phone: (865) 946-1308
Email: linz@ornl.gov

DOE Manager
Fred Joseck
Phone: (202) 586-7932
Email: Fred.Joseck@ee.doe.gov

Project Start Date: October 1, 2012
Project End Date: Project continuation and direction determined annually by DOE

Overall Objectives

- Optimize delivered hydrogen pressure
- Analyze sensitivity of optimal pressure
- Compare different pressure options for California

Fiscal Year (FY) 2014 Objectives

- Include onboard storage cost in optimization
- Optimize with cluster infrastructure strategy
- Update station costs
- Represent refueling annoyance
- Capture early adopter preferences
- Conduct California case studies

Technical Barriers

This project addresses the following technical barriers from the Hydrogen Storage section of the Fuel Cell Technologies Office Multi-Year Research, Development, and Demonstration Plan:

(B) System Cost

(F) Codes and Standards

(K) System Life-Cycle Assessments

This project also addresses the following technical barrier from the Market Transformation section:

(B) High hydrogen fuel infrastructure capital costs for polymer electrolyte membrane fuel cell applications

Contribution to Achievement of DOE Milestones

This project will contribute to achievement of the following DOE milestones from the Hydrogen Storage and Market Transformation sections of the Fuel Cell Technologies Office Multi-Year Research, Development, and Demonstration Plan:

- Storage 3.3: Transportation: Complete economic evaluation of cold hydrogen storage against targets. (4Q, 2015)
- Storage 3.6: Update early market storage targets. (4Q, 2017)
- Storage 3.7: Transportation: Complete analysis of onboard storage options compared to ultimate targets. (4Q, 2020)
- Market Transformation 1.13: Deploy, test, and develop business cases for renewable hydrogen energy systems for power, building, and transportation sectors. (1Q, 2015)

FY 2014 Accomplishments

- Developed the hydrogen optimal pressure and its user interface as an Excel Visual Basic for Applications tool that solves for optimal pressure under a wide range of user-specified market and technological parameters.
- Expanded the optimization to reflect onboard storage capital cost, refueling annoyance, and cluster strategy. Analyzed optimality within the pressure span of 350-700 bar.
- Found lower pressure (350 or 500 bar) more desirable for certain cluster strategy scenarios and higher pressure (700 bar) generally more desirable for connector stations.
- Recommended 700 bar even with a cluster strategy for early adopters due to their possible higher time value.
- Recommended continued improvement of onboard storage technologies to facilitate deployment of higher pressure that enables longer driving range.
- Quantified tradeoffs between fuel availability and driving range, which have important implications for fuel cell vehicle design and hydrogen infrastructure deployment.
- Found most sensitive factors of optimal pressure: time value, driving intensity and city density (time to nearest station).

- Identified needs for further research that focuses on consumer segmentation and integration with consumer choice models.

INTRODUCTION

The pressure of hydrogen delivered to hydrogen vehicles can be an important parameter that has great impact on the delivered cost of hydrogen and the range limitation obstacle of hydrogen vehicles. On one hand, higher hydrogen pressure allows more hydrogen to be stored onboard, enabling a longer driving range between hydrogen refills, but the cost of hydrogen supply infrastructure, and therefore the delivered cost of hydrogen, will be higher. While lower hydrogen pressure shortens the driving range and results in higher refueling frequency, the delivered hydrogen cost can be lower. Also importantly, the lower capital cost of low-pressure stations will encourage investment activities in developing more stations, resulting in better refueling convenience for consumers.

The objectives of this project are:

- Develop an optimization model to identify the delivered pressure of hydrogen that reflects tradeoff among hydrogen cost, infrastructure capital cost requirement, driving range, refueling frequency and refueling convenience. The motivation of optimization is to maximize consumer acceptance of hydrogen vehicles.
- Analyze and recommend the delivered hydrogen pressure as a function of technology cost, regional geography, hydrogen demand and driving patterns.

APPROACH

The optimization method is formulated to reflect tradeoff between consumer refueling convenience, onboard storage cost and infrastructure costs. Higher pressure increases hydrogen storage and driving range between hydrogen refills, but increases the cost of delivery and storage infrastructure (therefore increase the cost of hydrogen) and the capital cost of the onboard storage system. Both region-wide optimal infrastructure roll-out strategies and cluster strategies are considered.

Specifically, the optimal pressure is solved for by equating the marginal value of increased range due to increased pressure to the sum of the marginal hydrogen delivered cost and the marginal onboard storage capital cost, also due to increased pressure. This is equivalent to minimization of combined costs of refueling inconvenience, onboard storage system and stations. The marginal value of increased range due to higher pressure is measured by reduction of net present value of total refueling time over five years. Refueling time includes access time to station (depends on availability), refueling time at station and annoyance amplification. The marginal cost of increased pressure includes the resulting increased cost of pumps, tanks, and energy use. Based on discussions with the Fuel Pathways Integration Technical Team of U.S.DRIVE and the published work by University of California, Davis, the DOE's H2A model and the National Household Travel Survey 2009, these parameter assumptions are assumed for the baseline: mid-size fuel cell vehicles (FCVs) with 60 miles per gasoline gallon equivalent (mpgge), a representative driver who drives 13,000 miles per year and values refueling travel time at $50/hour, a dispenser linger time at 2.4 minutes, hydrogen filling rate at 1.6 kg/min, $3.27/kg of delivered hydrogen cost at 700 bar at 200 kg/day and $2.21/kg at 350 bar at 200 kg/day, both with full utilization (based on H2A models), and Southern California as the regional context and the city of Santa Monica in California as the cluster strategy context.

RESULTS

The optimal pressure is found to be lower with the cluster strategy than with the region roll-out strategy. Cluster strategy allows a small number of stations to achieve a high level of refueling convenience and thus increases tolerance for a low-pressure-caused short driving range and avoids the situation of many underutilized or scale uneconomical stations. As shown in Figure 1, three stations and 1,000 FCVs, if spread out in a large metropolitan region, would demand 700 bar or higher. Three stations in a large region is too inconvenient and the value of longer range from higher pressure exceeds the incremental cost from 350 to 700 bar. The same three stations and 1,000 FCVs, if clustered in a small city, would lead to the optimal pressure around 350 bar. Three stations in a small city is convenient enough so that the additional cost of higher pressure fails to justify the additional convenience benefit of a longer range.

Improvement of onboard storage is needed for higher hydrogen pressure and longer driving range. High-pressure onboard storage is more expensive due to the higher per-kWh cost and a larger amount of hydrogen stored. Optimal pressure for one 150-kg/day station supporting 150 FCVs in Santa Monica is estimated to be 374 bar, or 540 bar if onboard storage cost is ignored (Figure 2). Reducing onboard storage cost (from R&D progress) can lead to higher optimal pressure (a, c unchanged, d curve shifting down and b curve up on Figure 2) and longer driving range.

Higher pressure may be more desirable for early adopters possibly with high time value. Higher pressure enables longer driving range, reduces refueling frequency, and thus saves annual refueling time. Refueling inconvenience cost is proportional to value of time, which may vary greatly among consumers. Assuming one 150 kg/day station supporting 150 FCVs driven in Santa Monica, optimal pressure changes

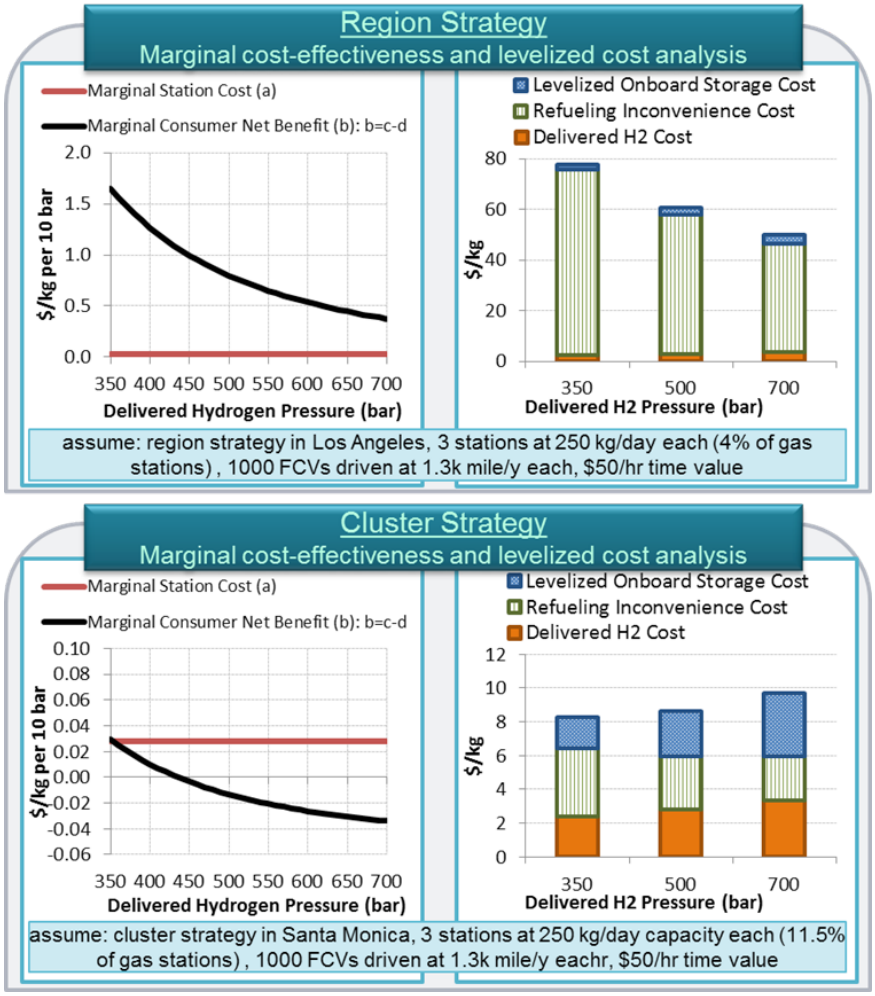

FIGURE 1. Optimize Pressure for Region and Cluster Strategies

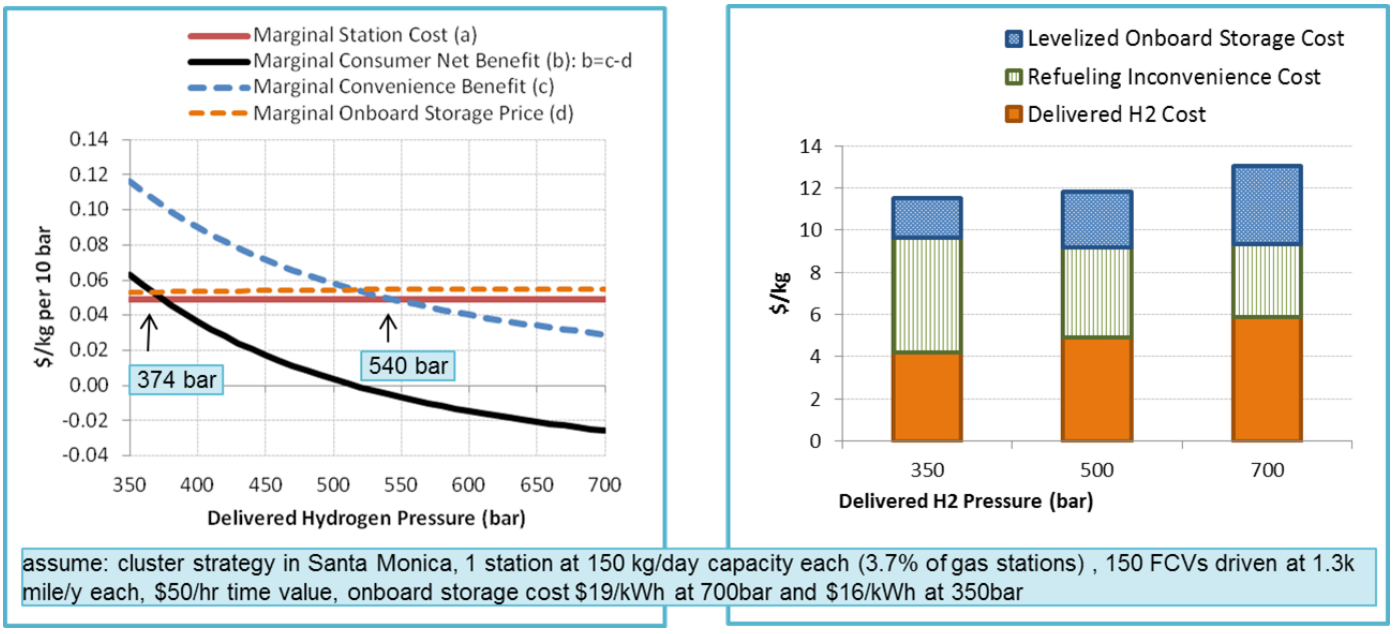

FIGURE 2. Effect of Onboard Storage Cost on Optimal Pressure

from 375 bar to over 700 bar when refueling travel time value increases from $50/hour to $200/hour (Figure 3). This illustrates the importance of segmenting early adopters by income and other demographic attributes that may affect time value.

Under scenarios constructed to reflect compliance with the zero-emission vehicle (ZEV) mandate in California, lower pressure is found to be desirable for the cluster strategy and higher pressure for the region strategy. For three 3-year periods, 636, 3,442 and 25,000 FCVs are assumed to be adopted, supported by 8, 12, and 48 stations at 100, 200, and 350 kg/day, respectively (Table 1). In the region strategy, these vehicles and stations are assumed to spread over the Southern California region. In the cluster strategy, they are assumed to concentrate in 4, 6, and 12 Santa Monica-like areas during the three periods, respectively. Even though the total numbers of vehicles and stations are the same, the refueling convenience differs between the two roll-out strategies, which leads to difference in optimal pressure. In Figure 4, cluster and region roll-out strategies are compared in terms of the optimal pressure, the best of three (350/500/700 bar) and the non-optimality regret of choosing one of the three, for the three ZEV mandate compliance periods. Optimal pressure under the region strategy is found to be well over 700 bar for all three periods. Under the cluster strategy, optimal pressure is estimated to be 412, 525 and 503 bar, respectively. If limited to the above three pressure levels, the best choice appears to be 350 bar during the 1st period and 500 bar during the 2nd and 3rd periods under the cluster strategy, and 700 bar during all three periods under the region strategy. The non-optimality regret is found between $0.1/kg and $1.7/kg hydrogen under the cluster strategy, depending on which non-optimal pressure is chosen, but is more significant with the region strategy, ranging from $2.6/kg to $41/kg hydrogen.

TABLE 1. ZEV Compliance Assumptions

	ZEV-Year1-3	ZEV-Year4-6	ZEV-Year7-9
FCVs on road	636	3,442	25,000
Average Station Size (kg/d)	100	200	350
Station Utilization	47%	85%	88%
Cluster Strategy			
Clusters	4	6	12
FCVs On Road/Cluster	159	574	2,083
Stations/Cluster	2	2	4
Percent of Gas Stations	7.7%	7.7%	15.4%
Region Strategy			
Stations in the region	8	12	48
Percent of Gas Stations	0.13%	0.20%	0.80%

Sensitivity analysis of optimal pressure is completed on seven parameters—time value, driving intensity, time to nearest station, onboard storage cost, station cost, pressure incremental station cost, and station scaling factor. Each parameter is varied by 20% at either direction from the reference case, for which assumptions include:

- Cluster strategy, 574 FCVs and two stations at 200 kg/day each
- Time value ($100/hour)
- Driving intensity (13,000 mile/yr)
- Time to nearest station (3.6 min)

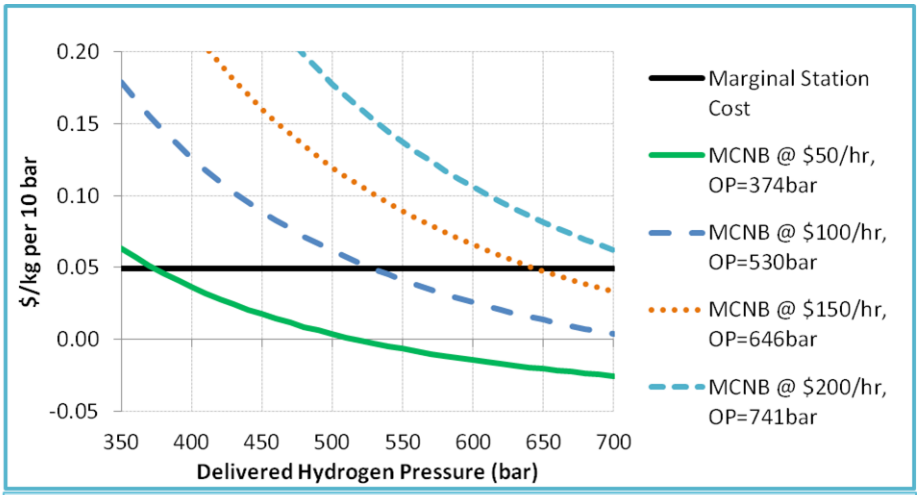

assume: cluster strategy in Santa Monica, 1 stations at 150 kg/day capacity each (3.7% of gas stations) , 150 FCVs driven at 1.3k mile/yr each, onboard storage cost $19/kWh at 700bar and $16/kWh at 350bar. Refueling travel time value varies from $50/hour to $200/hour, which is further multiplied by a refueling annoyance factor of 3.5.

FIGURE 3. Marginal Cost-Effectiveness by Travel Time Value

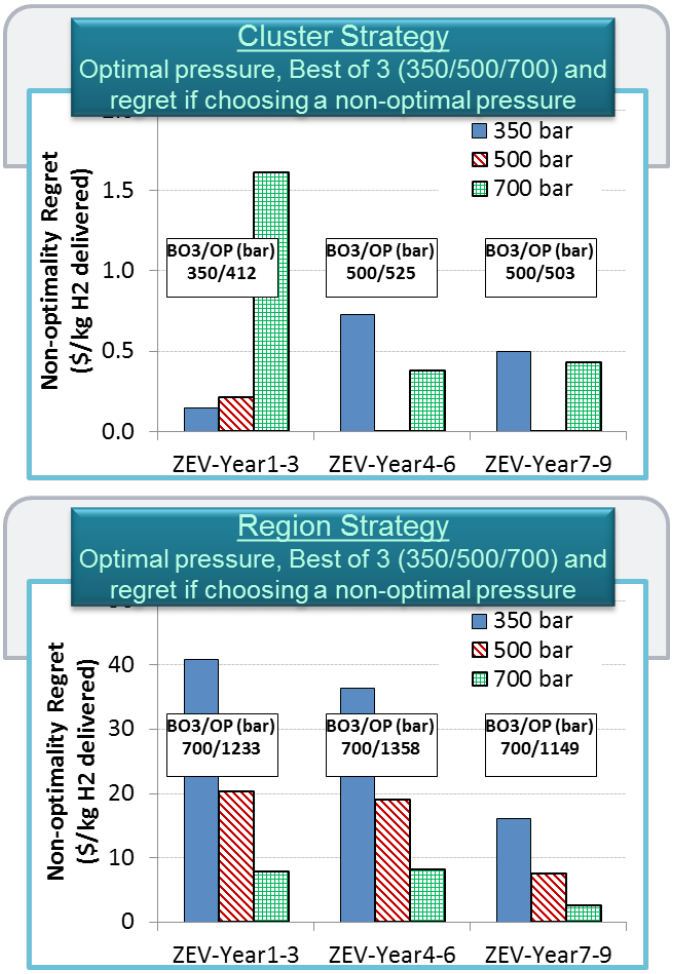

FIGURE 4. Optimal Pressure and Non-Optimality Regret under ZEV

- Onboard storage cost ($16/kg and $19/kg at 350/700 bar)
- Station cost ($3.27/kg at 83% utilization of 240 kg/d at 700 bar)
- Pressure incremental station cost (8.3%/100 bar)
- Station scaling factor (-0.608)

As shown in Figure 5, optimal pressure is most sensitive to time value, driving intensity and time to the nearest station, suggesting needs for consumer segmentation. It is also highly sensitive to onboard storage cost, implying that storage R&D can help adoption of high delivered pressure.

Clearly, there is a tradeoff between delivered pressure and fuel availability. More stations makes each refueling trip shorter and thus can reduce the need for a longer range that is enabled by higher pressure. The contour lines on Figure 6 visualize such tradeoffs between the optimal pressure and the hydrogen fuel availability, under the assumptions of the cluster strategy, 574 FCVs and two stations at 200 kg/day each. As shown, optimal pressure is 500 bar at 15% fuel availability and about 450 bar at 20% fuel availability, assuming $150/hour time value. The contour line shifts downward if lower time value is assumed, meaning lower optimal pressure for the same fuel availability or lower fuel availability for the same pressure.

CONCLUSIONS AND FUTURE DIRECTIONS

The FY 2014 work of this project has led to new understandings of the issue. The 700-bar pressure level was found by this project during FY 2013 to be more desirable in most scenarios including the California near-term plan. With inclusion of onboard storage cost, the cluster strategy and

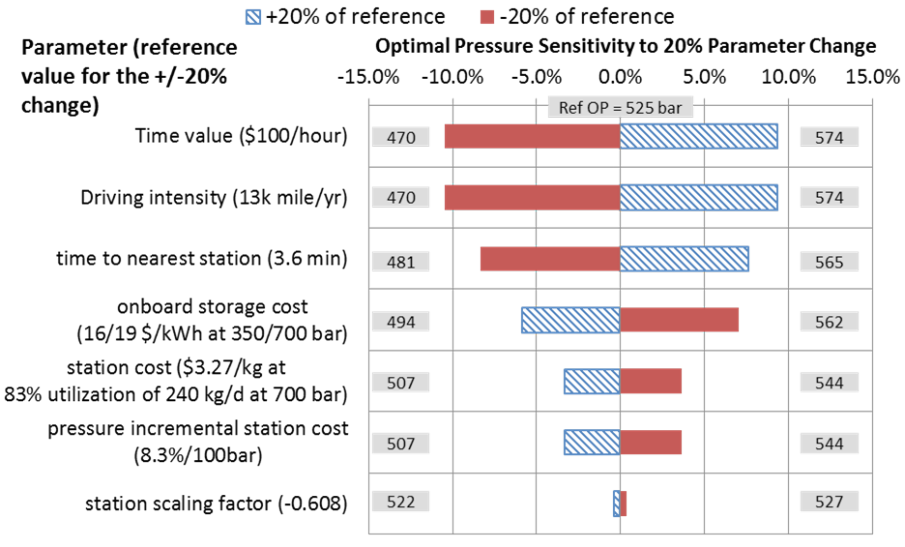

FIGURE 5. Sensitivity of the Optimal Pressure

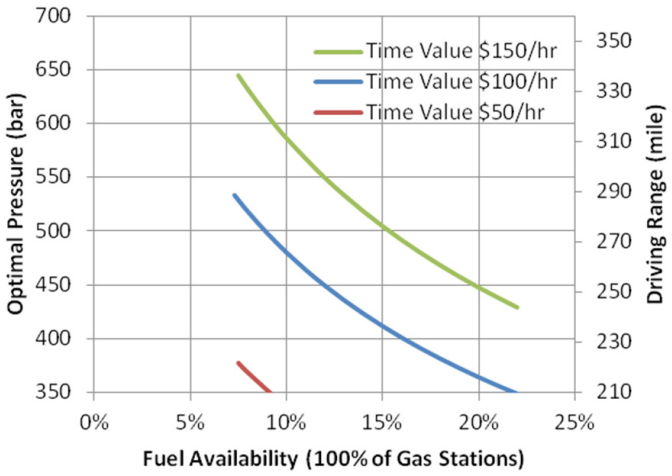

FIGURE 6. Pressure and Fuel Availability Tradeoff

refueling annoyance, the FY 2014 results suggest that 700 bar may not be the optimal, especially under cluster strategy and the current onboard storage cost. 350 bar and 500 bar appear superior in ZEV scenarios with the cluster strategy.

FY 2014 progress includes:

- Added storage cost to the objective function (only including station cost and inconvenience cost in FY 2013)
- Represented both cluster and region strategies
- Developed a friendly user-interface
- Analyzed optimal pressure under cases reflecting ZEV
- Conducted sensitivity analysis

In-depth optimal pressure analysis for early adopters and integration with consumer choice models is recommended. More research is needed on identifying the optimal pressure for early adopters, for maximizing FCV market acceptance and for standardization concerns. Uncertainty of key parameters also deserves more analysis.

FY 2014 PUBLICATIONS/PRESENTATIONS

1. Zhenhong Lin, Changzheng Liu, and David Greene. Analysis of Optimal On-Board Storage Pressure for Hydrogen Fuel Cell Vehicles. Presented at the 2014 DOE Annual Merit Review meeting.

X.2 Employment Impacts of Infrastructure Development for Hydrogen and Fuel Cell Technologies

Marianne Mintz
Argonne National Laboratory
9700 S. Cass Ave.
Argonne, IL 60439
Phone: (630) 252-5627
Email: mmintz@anl.gov

DOE Manager
Fred Joseck
Phone: (202) 586-7932
Email: Fred.Joseck@ee.doe.gov

Subcontractor
RCF Economic and Financial Consulting, Inc., Chicago, IL

Project Start Date: October 2012.
Project End Date: Project continuation and direction determined annually by DOE

Overall Objectives

- Facilitate early market deployment of fuel cells (FCs) by developing a downloadable, user-friendly tool to estimate economic impacts associated with the deployment of FCs and related infrastructure.
- Develop a consistent framework to identify opportunities to enhance the economic impact of FC production and deployment by better understanding where and how impacts occur and how infrastructure deployment produces economic benefits.
- Meet stakeholder needs for estimating impacts of FC and infrastructure deployment on state, regional and national employment, earnings, and economic output.

Fiscal Year (FY) 2014 Objectives

- Document the methodology and approach to estimating economic impacts of deploying hydrogen fueling infrastructure for early FC markets.
- Launch JOBS H2 (JOBS and economic impacts of Hydrogen) model.
- Examine sensitivity of job creation to modeling assumptions.

Challenges/Technical Barriers

This project addresses the following technical barriers from the Systems Analysis section of the Fuel Cell Technologies Office Multi-Year Research, Development, and Demonstration Plan:

(A) Future Market Behavior

(E) Unplanned Studies and Analysis

Contribution to Achievement of DOE Systems Analysis Milestones

This project contributes to achieving the following milestones for the Systems Analysis section of the Fuel Cell Technologies Office Multi-Year Research, Development, and Demonstration Plan:

- Milestones 2.2–2.6: Develop and maintain models and tools
- Milestones 1.7, 1.10 and 1.14: Perform studies and analyses of job impacts

FY 2014 Accomplishments

- Completed design and development of the JOBS H2 model. Launched JOBS H2 1.0 in a DOE-sponsored webinar on June 24, 2014.
- Continued close collaboration with stakeholders, hydrogen and fuel cell producers and other researchers via a series of teleconferences and webinars. Demonstrated beta version of the JOBS H2 (JOBS and economic impacts of Hydrogen) model to this group to (a) gain further insight into infrastructure development cost, deployment and other issues, (b) validate defaults, and (c) obtain feedback on desired functionality, granularity, and outputs.
- Developed a new website (http://jobsmodels.es.anl.gov) which contains documentation and publications related to both the hydrogen infrastructure model (JOBS H2) and the earlier JOBS FC (JOBS and economic impacts of Fuel Cells) model. Developed user resources for the site, including print documentation of JOBS FC, a set of video user guides to demonstrate the use of JOBS H2, and links to DOE-sponsored webinars.

✧ ✧ ✧ ✧ ✧

INTRODUCTION

The project is developing and applying a computer model to estimate economic impacts of deploying FCs and associated infrastructure in early markets. Insights from this work will assist Fuel Cell Technologies Office

and its stakeholders in estimating employment and other economic impacts from DOE technology development and in identifying FC markets and regions that are most likely to generate jobs and economic activity.

In earlier work, Argonne National Laboratory and RCF Economic & Financial Consulting designed and implemented a tool to calculate state, regional and national economic impacts of FC production, installation, and utilization in early markets. Known as JOBS FC (JOBS and economic impacts of Fuel Cells) that tool is a user-friendly, spreadsheet-based model. In FY 2013, work began on a companion tool, JOBS H2, using the same methodology. FY 2014 activities focused on beta testing, launching, and conducting sensitivity analyses of JOBS H2.

APPROACH

JOBS H2 is an Excel-based model that estimates economic impacts of activities associated with hydrogen station deployment based on user-specified scenarios. Activities include station design, engineering and permitting; site preparation; equipment production, shipping and installation; station operation and maintenance (O&M); and hydrogen production and delivery. The model calculates economic impacts along supply chains and from induced or ripple effects using input-output relationships from the U.S. Department of Commerce Bureau of Economic Analysis' Regional Input-output Modeling System. JOBS H2 can be run with default values (based on stakeholder input and engineering estimates from the published literature) or user inputs.

RESULTS

Model Development

JOBS H2 calculates the effect of hydrogen infrastructure deployment on any of 60 geographies—50 states, nine census regions, or the nation as a whole—by adjusting dollar flows among economic sectors within the relevant geography. As hydrogen infrastructure is deployed, those expenditures send dollars up the supply chain for station equipment (e.g., compressor packages, dispensers) and hydrogen fuel, as well as to the relevant supply chains for system integrators, installers, fuel suppliers and businesses providing O&M services. In the aggregate, the resulting web of transactions represents a nascent hydrogen retailing sector. Purchases include not only the hydrogen itself, but all transactions required to install, fuel and operate the station.

To demonstrate the model's capability, an illustrative scenario under which 25 stations are deployed for each of five years was postulated. As shown in Figure 1 under such a steady-state scenario, station development jobs rise quickly (to ~1,000 per year). As stations come online, jobs shift to new station development projects. However, if station development ceases, jobs associated those activities also cease. On the other hand, station operation jobs are not created until stations begin operation. These jobs rise steadily as more stations come online. Once all 125 stations in the illustrative scenario are online, station operation jobs level off at ~1,900/year.

Sensitivity Analysis

To examine the model's sensitivity a middle or base case was postulated along with upper and lower bounds for key parameters. These assumptions are shown in Table 1.

TABLE 1. Base Case Assumptions for Sensitivity Analyses

	Base Case Value		Lower Value	Upper Value
Station Size	200 kg/day		100 kg/day	400 kg/day
Station cost	$2.15 MM		$1.1 MM	$4.3 MM
Local shares	Installation & site prep	100%	0%	100%
	Equipment	50%	0%	100%
	Design & engineering	50%	0%	100%
	Station O&M	100%	0%	100%
	Hydrogen fuel	50%	0%	100%
Station utilization	50%		20%	80%

Employment impacts of expenditures associated with station development and operation are shown in Figures 2 and 3, respectively. Station development jobs are most sensitive to the proportion or share of expenditures that are spent in the region of interest, as well as to total expenditures. In the most extreme case shown, employment approximately triples. While station operation jobs are also sensitive to local shares, station throughput (a function of utilization and size) are also important. Note that station development jobs tend to be less numerous and of shorter duration than operational jobs which continue as long as the station remains in operation.

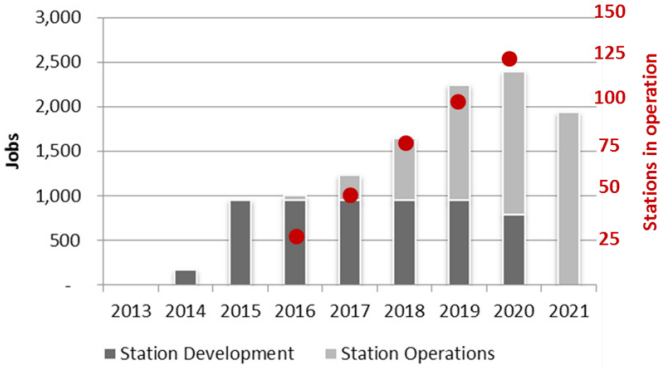

FIGURE 1. Station Development and Station Operation Jobs Associated with Deploying 25 Stations per Year for Six Years under an Illustrative Scenario

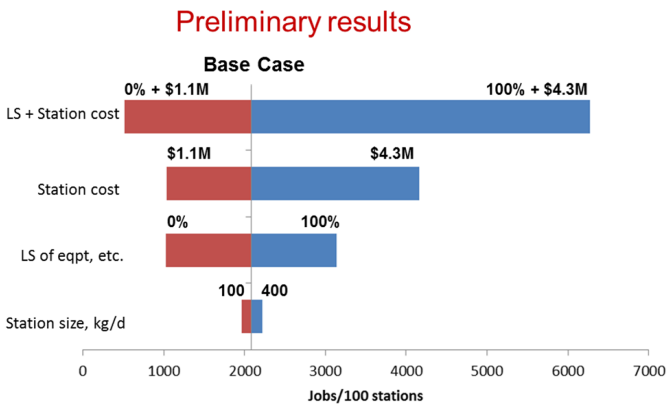

FIGURE 2. Station Development Jobs as a Function of Station Size, Cost and Local Share (LS) of Expenditures

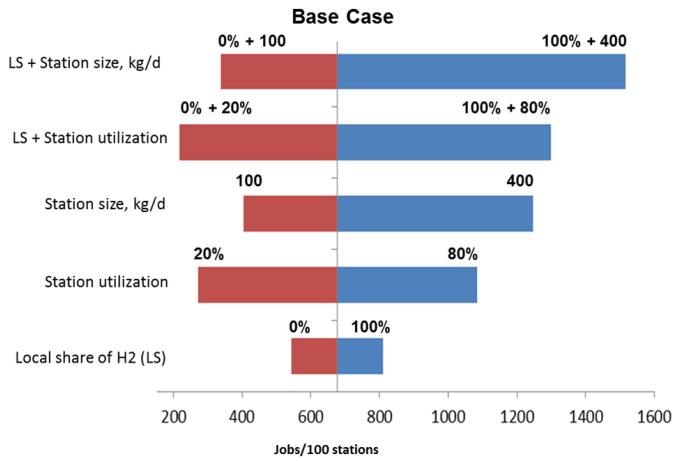

FIGURE 3. Station Operation Jobs as a Function of Station Size, Utilization and Local Share of Expenditures

User Resources

Stakeholders have been heavily involved in the development of JOBS H2. An advisory group consisting of representatives from the hydrogen and FC industry, station developers and state/local agencies assisted in data validation, requirements specification/review of the user interface, and beta testing of JOBS H2. Outreach included one-on-one conversations, webinars, and a website (http://jobsmodels.es.anl.gov). The latter features user access to a free downloadable copy of JOBS H2, along with video user guides, links to DOE-sponsored webinars, and copies of publications/presentations.

CONCLUSIONS AND FUTURE DIRECTIONS

FY 2014 work focused on development of the JOBS H2 model. Work included outreach to stakeholders to develop and validate input data and refine the user interface; model testing and quality assurance via a series of webinars, beta tests and sensitivity analyses; and model launch. FY 2015 work will build on these efforts, incorporating stakeholder recommendations for enhancements to the functionality and scope of the model, as well as developing estimates of employment impacts to support ongoing infrastructure deployment programs.

Potential future model enhancements include adding a capability to show uncertainty in results, expanding hydrogen delivery and dispensing options, and analyzing the impacts of alternative hydrogen station rollout scenarios.

FY 2014 PUBLICATIONS/PRESENTATIONS

1. Mintz, M., J. Gillette, C. Mertes and E. Stewart, *Employment Impacts of Hydrogen Infrastructure Deployment: Methodology and Initial Results,* Argonne National Laboratory, ANL/ESD-13/15, Sept. 2013.

2. Mintz, M., J. Gillette, C. Mertes and E. Stewart, *JOBS and Economic Impacts of Fuel Cells (JOBS FC) Model Documentation,* Argonne National Laboratory, ANL/ESD-13/14, Dec. 2013.

3. Mintz, M., *Employment Impacts of Hydrogen Fueling Infrastructure*, Alternative Clean Transportation (ACT) Expo, Long Beach, CA, May 8, 2014.

4. Mintz, M., C. Mertes and E. Stewart, *Employment and Economic Impacts of Hydrogen Station Deployment,* EERE webinar, June 24, 2014 (http://energy.gov/eere/fuelcells/2014-webinar-archives#date062414).

X.3 Pathway Analysis: Projected Cost, Life-Cycle Energy Use and Emissions of Future Hydrogen Technologies

Todd Ramsden (Primary Contact), Victor Diakov, Neil Popovich
National Renewable Energy Laboratory
15013 Denver West Pkwy.
Golden, CO 80401
Phone: (303) 275-3704
Email: todd.ramsden@nrel.gov

DOE Manager
Fred Joseck
Phone: (202) 586-7932
Email: Fred.Joseck@ee.doe.gov

Project Start Date: June 1, 2013
Project End Date: September 30, 2014

Overall Objectives

- Conduct cost and lifecycle energy and emissions analyses of full future-technology hydrogen pathways to evaluate hydrogen cost, energy requirements and greenhouse gas (GHG) emissions
- Provide detailed reporting of assumptions and data used to analyze hydrogen production, delivery, and dispensing technologies, enabling consistent and transparent understanding of results
- Report on upstream energy and feedstock usage and GHG emissions on a full lifecycle basis, including vehicle cycle and well-to-wheels fuel cycle
- Understand lifecycle costs, energy and emissions of hydrogen technologies to inform R&D decision-making process
- Evaluate potential of future hydrogen technologies to meet the hydrogen cost target of <$4/kg
- Validate the Fuel Cell Technologies Office's (FCTO's) Macro-System Model (MSM) and its underlying component models (in particular, the H2A Production model, the Hydrogen Delivery Scenario Analysis Model, and the Greenhouse gases, Regulated Emissions and Energy use in Transportation [GREET] model) through industry review

Fiscal Year (FY) 2014 Objectives

- Finalize an evaluation of nine complete hydrogen production, delivery, and dispensing pathways based on the cost and performance of future hydrogen technologies expected to be available in the 2020 to 2030 timeframe, assessing the impact technology improvements will have on lifecycle cost, energy use, and emissions
- Conduct detailed sensitivity analyses, including cost, energy use, and emissions analyses based on a fuel cell electric vehicle (FCEV) on-road fuel economy of 58 miles per gallon-equivalent (gge) and 68 miles/gge (mpgge)
- Complete technical report on the analysis, providing a detailed reporting of hydrogen cost and capital costs of the full hydrogen pathways to support FCEVs, upstream energy and feedstock usage and GHG emissions
- Initiate a companion pathway analysis to consider emerging renewable hydrogen production technologies

Technical Barriers

This project addresses the following technical barriers from the Systems Analysis section of the Fuel Cell Technologies Office Multi-Year Research, Development, and Demonstration Plan:

(B) Stove-Piped/Siloed Analytical Capability

(C) Inconsistent Data, Assumptions and Guidelines

(D) Insufficient Suite of Models and Tools

Contribution to Achievement of DOE Systems Analysis Milestones

This project will contribute to achievement of the following DOE milestones from the Systems Analysis section of the Fuel Cell Technologies Office Multi-Year Research, Development, and Demonstration Plan:

- Milestone 1.12: Complete an analysis of the hydrogen infrastructure and technical target progress for technology readiness. (4Q, 2015)
- Milestone 1.13: Complete environmental analysis of the technology environmental impacts for hydrogen and fuel cell scenarios and technology readiness. (4Q, 2015)
- Milestone 1.15: Complete analysis of program milestones and technology readiness goals - including risk analysis, independent reviews, financial evaluations, and environmental analysis - to identify technology and risk mitigation strategies. (4Q, 2015)
- Milestone 1.18: Complete life cycle analysis of vehicle costs for fuel cell electric vehicles compared to other vehicle platforms. (4Q, 2019)

- Milestone 2.2: Annual model update and validation. (4Q, 2011 through 4Q, 2020)
- Milestone 3.4: Review Hydrogen Threshold Cost status. (4Q, 2014; 4Q, 2017; 4Q, 2020)

FY 2014 Accomplishments

- Estimated the lifecycle costs, energy use, and emissions from nine future-technology hydrogen fuel pathways, including a total cost of fuel cell vehicle ownership that considers the cost of hydrogen fuel and FCEV purchase and operating costs. Distributed hydrogen production from natural gas reformation pathway resulted in lowest costs, with costs of $0.07 per mile driven for hydrogen fuel and total vehicle ownership and operational cost of $0.69 per mile (in a mature market).
- Nine future-technology hydrogen production, delivery and dispensing pathways analyzed, providing evaluations of well-to-wheels (WTW) costs, energy use and GHG emissions
  - Estimated the cost of hydrogen in a mature market, with costs ranging from $3.80/kg-$H_2$ for the distributed natural gas reformation pathway to almost $7.50/kg for the distributed ethanol reforming pathway.
  - Estimated the total fuel-cycle (WTW) and lifecycle GHG emissions of all pathways, including upstream fuel- and feedstock-related emissions and vehicle production-related emissions. The central wind electrolysis pathway had the lowest WTW emissions, with emissions of about 40 g CO_2-equivalent per mile. The lowest cost pathway – distributed natural gas reforming – yielded 250 g CO_2/mi at 68 mpgge fuel economy (300 g CO_2/mi at 58 mpgge).
- Extensive industry review of overall results, modeling results, and input parameters, providing external validation of the MSM and the related component models.
- Conducted an initial assessment of emerging-technology renewable hydrogen production pathways.

INTRODUCTION

DOE's FCTO had identified a need to understand the cost, energy use, and emissions tradeoffs of various hydrogen fuel infrastructure technologies under consideration for fuel cell vehicles. This study assesses nine complete hydrogen production, delivery, and dispensing scenarios based on the cost and performance of future hydrogen technologies expected to be available in the 2020 to 2030 timeframe, assessing the impact technology improvements will have on lifecycle cost, energy use, and emissions. The study considers the potential of future hydrogen technologies if they were brought to commercial scale in a mature fuel cell vehicle market; it is not an assessment of transition scenarios where equipment may not be fully utilized. The future-technology pathway analysis is a companion analysis of current-technology hydrogen pathways published in 2014 (publication 1).

This study will help FCTO evaluate the potential of future hydrogen technologies to meet the cost target of <$4/kg for dispensed hydrogen. By providing a common framework for modeling using consistent data and assumptions, this study provides a detailed and transparent understanding of hydrogen technologies and will assist FCTO with goal setting and R&D decisions. Finally, this analysis will aid in understanding and assessing technology needs and progress, potential environmental impacts, and the energy-related economic benefits of various hydrogen pathways.

APPROACH

This study evaluated nine hydrogen production, delivery, and dispensing pathways expected to be available in the 2020-2030 timeframe, assessing the impact technology improvements will have on hydrogen cost, energy requirements and GHG emissions (see Table 1). Considering plausible hydrogen production and delivery scenarios for mature hydrogen transportation-fuel markets combined with market penetration of hydrogen fuel cell vehicles, the study uses a common set of assumptions to provide a consistent assessment of all pathways. Major assumptions include:

- 2025 start-up year for hydrogen fuel infrastructure
- Future (2020-2030) hydrogen technologies, projected to a commercial scale
- Costs reported in 2007$
- 40-year analysis period for central production; 20-year analysis for distributed cases
- Feedstock and utility costs from the Annual Energy Outlook 2009, based on national averages
- On-road FCEV fuel economy of 58 mpgge (with sensitivity analyses at 68 mpgge)
- Urban demand area with a population of 1.25 million (nominally Indianapolis)
- 15% FCEV penetration
- Mid-sized FCEV, chassis comparable to conventional vehicle
- 15,000 miles/year vehicle miles traveled per FCEV
- Hydrogen dispensed for 700 bar, high-pressure storage (except cryo-compressed case)

TABLE 1. Future-Technology Hydrogen Pathways Evaluated

Path	Production Feedstock / Technology	Delivery Mode	Dispensing Mode
1	Natural Gas Reforming	Distributed Production	700 bar, gaseous
2	Ethanol Reforming	Distributed Production	700 bar, gaseous
3	Grid Electrolysis	Distributed Production	700 bar, gaseous
4	Natural Gas Reforming	Gaseous H_2 in Pipelines	700 bar, gaseous
5	Natural Gas Reforming	Gaseous H_2 Truck	700 bar, gaseous
6	Natural Gas Reforming	Liquid H_2 Truck	700 bar, gaseous
7	Natural Gas Reforming	Liquid H_2 Truck	Cryo-compressed
8	Natural Gas Reforming with CCS	Gaseous H_2 in Pipelines	700 bar, gaseous
9	Wind Electrolysis	Gaseous H_2 in Pipelines	700 bar, gaseous

CCS - carbon capture and storage

The analysis was conducted using the MSM, which acts as a central transfer station, linking together the H2A Production model, HDSAM, GREET, and the Cost-Per-Mile tool. Making use of the discounted cash flow, rate of return features of H2A Production and HDSAM, the MSM provides cost results in terms of a levelized cost of hydrogen (incorporating a 10% real rate of return on investments) in a $/kg basis. The MSM also outputs well-to-pump, pump-to-wheels, and well-to-wheels efficiencies, GHG emissions, and energy use for each pathway. Emissions and energy use results include upstream energy use required for feedstock production, processing, and delivery.

RESULTS

The MSM evaluation of the nine future-technology hydrogen pathways presents the cost of hydrogen and the performance of the pathways in terms of total energy use, fossil energy use, and GHG emissions. For all pathways evaluated, the key assumptions, modeling parameters, and analysis inputs were reviewed by industry partners through the U.S. DRIVE Fuel Pathway Integration Technical Team. Figure 1 shows the levelized cost of hydrogen from the nine different pathways. DOE's FCTO has set a hydrogen cost target of <$4/gge. $4.00 per gge (approximately equivalent to 1 kg of hydrogen), dispensed at the pump. The distributed natural gas reformation pathway is expected to meet this target, with a projected hydrogen cost of $3.80/kg. To achieve the $4/gge target, DOE has a hydrogen production target of $2/kg. The hydrogen pathways evaluation shows that central natural gas production will achieve this target (production cost of $1.95/kg) and distributed natural gas reformation will approach this target with a production cost of $2.20/kg. Hydrogen station compression, storage, and dispensing costs for 700-bar dispensing (not including delivery) range from under $1.00/kg to about $1.60/kg.

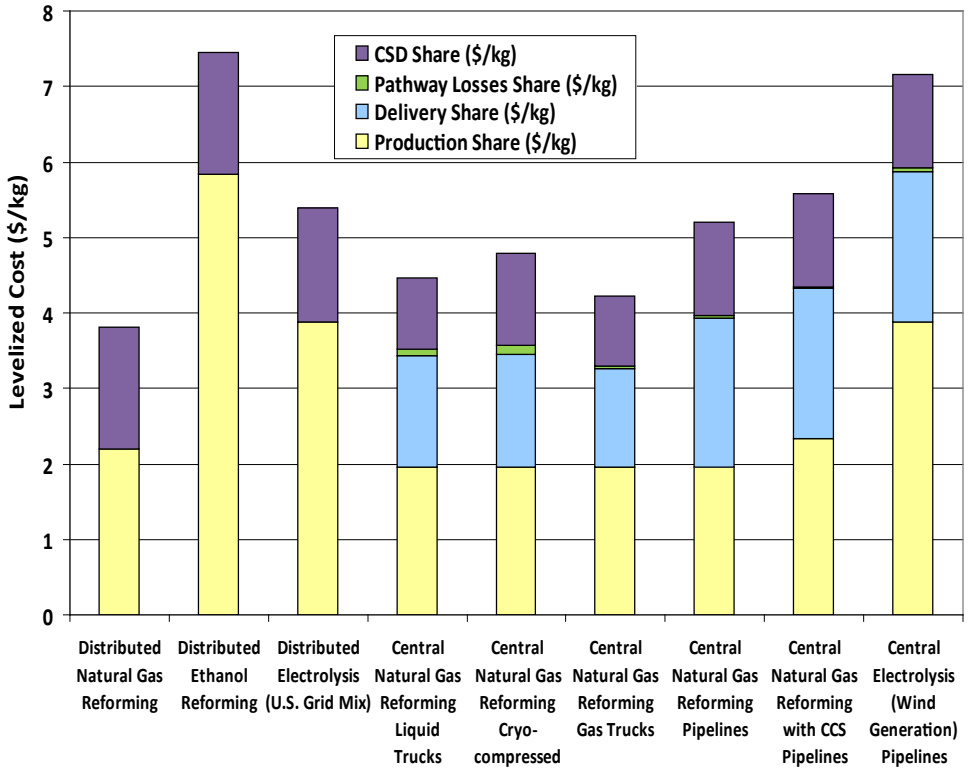

FIGURE 1. Cost of Dispensed Hydrogen from All Pathways

The study also evaluated the total cost of FCEV ownership including the costs of the hydrogen fuel and the costs of vehicle purchase and operation. The lowest cost of FCEV ownership resulted from hydrogen fuel produced and dispensed from the distributed natural gas reformation pathway. Assuming a 5-year ownership period and fuel economy of 58 mpgge, the distributed natural gas pathway resulted in total ownership costs of $0.69 per mile. With fuel costs of $0.066/mi, the cost of hydrogen fuel represents 10% of ownership costs. The purchase of the FCEV (represented as finance and depreciation costs) accounts for about 50% of ownership costs.

Figure 2 illustrates that for a 58 mpgge FCEV, all the pathways (except the distributed electrolysis pathway) result in GHG emissions (on a gram CO_2-equivalent per mile basis) lower than 300 g/mile, demonstrating a significant improvement over a conventional gasoline vehicle. Figure 2 also shows that when a higher fuel economy of 68 mpgge is considered, all of the pathways except distributed electrolysis result in GHG emissions lower than 250 g/mile and three pathways have GHG emissions lower than 100 g/mile. Distributed electrolysis has high GHG emissions when compared to the other hydrogen pathways because of the assumed electricity grid mix (the U.S. average grid mix is assumed). Hydrogen production from the central natural gas with carbon sequestration case has increased production costs over the other natural gas production pathways, but the additional costs for sequestration yield a significant reduction in WTW GHG emissions. Of the four options for delivering hydrogen from a centralized production plant, pipeline delivery has the lowest GHG emissions and lowest petroleum use. The two liquid truck delivery options have higher GHG emissions because of the high electricity consumption of the liquefaction process (the U.S. average grid mix is assumed).

CONCLUSIONS AND FUTURE DIRECTIONS

The lifecycle analysis shows that of the nine future-technology hydrogen production, delivery, and dispensing pathways investigated, only the distributed natural gas reformation pathway can achieve the $4/gge DOE target, although the central natural gas reformation with truck delivery cases approach the target. From an emissions perspective, almost all pathways demonstrate significant improvements in WTW GHG emissions compared to conventional gasoline vehicles.

In the latter part of FY 2014 and FY 2015, the hydrogen pathways analysis will be extended to consider emerging hydrogen production, delivery, and onboard vehicle storage technologies. This will include an assessment of high-

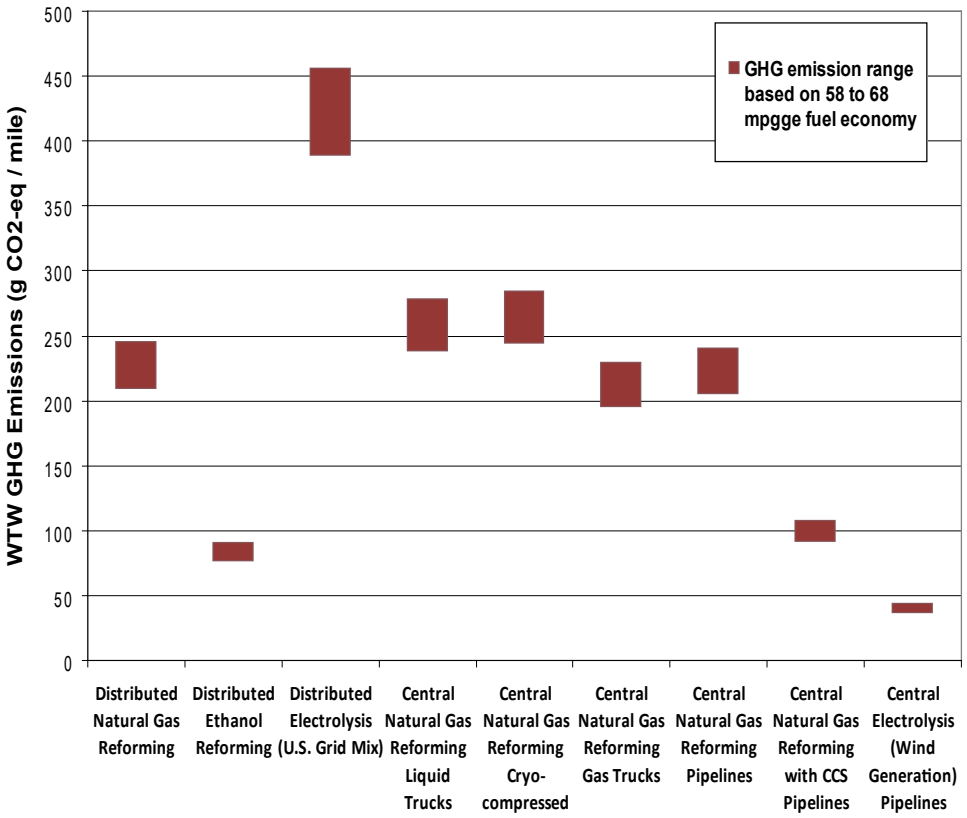

FIGURE 2. WTW Greenhouse Gas Emissions from All Pathways

pressure gaseous truck delivery and emerging renewable hydrogen production technologies such as photo-biological production, photo-electrochemical production, and solar thermo-chemical production. These evaluations of emerging hydrogen technologies will help to assess the potential of lowering hydrogen delivery costs and to evaluate the potential of a wider range of renewable hydrogen production pathways.

FY 2014 PUBLICATIONS/PRESENTATIONS

1. Ramsden, T., Ruth, M., Diakov, V., Laffen, M., and Timbario, T., 2013. *Hydrogen Pathways: Updated Cost, Well-to-Wheels Energy Use, and Emissions for the Current Technology Status of Ten Hydrogen Production, Delivery, and Distribution Scenarios*, National Renewable Energy Laboratory, Technical Report NREL/TP-6A10-60528 (March), Golden, CO.

2. Todd Ramsden, 2013 [presentation]. *Pathways Analysis: Future Technology Hydrogen Production, Delivery & Dispensing Pathways*. U.S. DRIVE Fuel Pathway Integration Technical Team Meeting, Chevron, San Ramon, CA (October).

3. Todd Ramsden, 2014 [presentation]. *Hydrogen Pathway Analysis Project: Future Technologies*. U.S. DRIVE Production, Delivery and Fuel Pathway Integration Joint Technical Team Meeting, Argonne National Laboratory, Lemont, IL (April).

4. Todd Ramsden, 2014 [presentation]. *Pathway Analysis: Projected Cost, Lifecycle Energy Use and Emissions of Future Hydrogen Technologies*. 2014 DOE Hydrogen and Fuel Cell Technologies Program Annual Merit Review, Washington, D.C.

X.4 Life-Cycle Analysis of Water Use for Hydrogen Production Pathways

Amgad Elgowainy (Primary Contact),
David Lampert, Hao Cai, May Wu, Jennifer Dunn,
Jeongwoo Han and Michael Wang
Argonne National Laboratory
9700 South Cass Avenue
Argonne, IL 60439
Phone: (630) 252-3074
Email: aelgowainy@anl.gov

DOE Manager
Fred Joseck
Phone: (202) 586-7932
Email: Fred.Joseck@ee.doe.gov

Project Start Date: April 2013
Project End Date: September 2015

Overall Objectives

Incorporate water consumption as a new sustainability metric for evaluating hydrogen as a transportation fuel for use in fuel cell electric vehicles (FCEVs) and other fuel/vehicle systems on a life-cycle basis.

Fiscal Year (FY) 2014 Objectives

- Provide a platform for evaluating and comparing hydrogen production pathways and other transportation fuels on a life-cycle basis.
- Develop water consumption factors for various processes along the fuel cycles of hydrogen, gasoline, natural gas, ethanol, and electricity production.
- Incorporate the water consumption factors into the Greenhouse gases and Regulated Emissions, and Energy use in Transportation (GREET) model to evaluate life-cycle water consumption for hydrogen production from steam methane reforming (SMR) and water electrolysis, and compare them to those for gasoline and other major transportation fuels.

Technical Barriers

This project directly addresses Technical Barriers C, D and E in the Systems Analysis section of the Fuel Cell Technologies Office Multi-Year Research, Development, and Demonstration Plan. These barriers are:

(C) Inconsistent Data, Assumptions and Guidelines

(D) Insufficient Suite of Models and Tools

(E) Unplanned Studies and Analysis

Technical Targets

This project expands the GREET model to include water consumption factors for the various life-cycle stages of hydrogen and other fuels, and to compare the life-cycle water consumption of the various fuel/vehicle systems on a consistent basis.

Contribution to Achievement of DOE System Analysis Milestones

This project contributes to achievement of the following DOE milestones from the Systems Analysis section of the Fuel Cell Technologies Office Multi-Year Research, Development, and Demonstration Plan:

- Milestone 1.13: Complete environmental analysis of the technology, environmental impacts for hydrogen and fuel cell scenarios and technology readiness. (4Q, 2015)
- Milestone 2.2: Annual model update and validation. (4Q, 2011 through 4Q, 2020)

FY 2014 Accomplishments

- Developed water consumption factors for hydrogen production processes via SMR and water electrolysis.
- Developed water consumption factors for petroleum fuels, natural gas, corn ethanol, and various electricity generation technologies.
- Incorporated water consumption as a new sustainability metric in the GREET model.
- Evaluated and compared the life-cycle water consumption for various fuel/vehicle systems, including hydrogen use in FCEVs.

✧ ✧ ✧ ✧ ✧

INTRODUCTION

One emerging sustainability metric of interest to the life-cycle analysis of alternative fuel/vehicle systems is water consumption. The production of most energy feedstocks and fuels require significant water use. Fossil feedstock sources such as natural gas, crude oil and oil sands require the use of water and steam for extraction, processing, refining and upgrading. Similarly, biofeedstocks such as corn, need water for growth. Converting these feedstocks to fuels requires additional water consumption. Producing electricity at thermal power plants requires a substantial amount of water to cool the equipment and complete the power cycle. A large amount of water evaporation is reported from water reservoirs used for hydropower generation.

Water withdrawal is the water uptake from a source by any given process, while water consumption is the withdrawal amount minus the amount returned to the same withdrawal source. Argonne developed water consumption factors for petroleum fuels (e.g., gasoline and diesel), conventional natural gas and shale gas, corn ethanol, hydrogen production via SMR and water electrolysis, and various electric power generation technologies. Water consumption factors for hydrogen production were developed from data provided by industrial sources. Water consumption factors for hydrogen production included water rejection during the preproduction treatment processes, steam use in the SMR process, water use as a feedstock for the electrolysis process, and water consumption with the various cooling technologies.

RESULTS

Table 1 shows the water consumption factors for hydrogen production via SMR and electrolysis in central production and distributed locations. The water rejection rate of reverse osmosis water treatment is assumed to be lower with production scale. The cooling technology is assumed to be cooling tower for large-scale central production and closed-loop dry cooling for small-scale distributed production. The cooling tower water circulation rate is approximately 0.1 gpm per each kg/h hydrogen production. We assumed that 3% of the circulating water is required as makeup water to compensate for blow down, evaporation, and drifting losses.

TABLE 1. Water Consumption Factors for Central and Distributed Hydrogen Production (gal/kg hydrogen)

Production Technology	SMR		Electrolysis	
Production Scale	**Central**	**Distributed**	**Central**	**Distributed**
Reverse Osmosis Treatment	1.3*	4**	1.3*	4**
Production Process	4 (3.9−4.2)	4 (3.9−4.2)	4 (3.6–5.4)	4 (3.6–5.4)
Cooling	0.2‡	0‡‡	0.2‡	0‡‡
Total	5.7	8	5.7	8

* 25% water rejection rate
** 50% water rejection rate
‡ Cooling tower with 3% of circulating water as makeup water and 0.1 gpm of circulating water per kg hydrogen/h production
‡‡ Closed-loop dry cooling

Table 2 shows the water consumption factors for various fuels and power generation technologies. It is noted that the water consumption factor for hydropower generation is large, mainly due to the evaporation from the large surface area of the water reservoir. The water consumption rate by the U.S. average generation mix is significantly impacted by the large water factor for hydropower even though the share of hydropower generation in the U.S. average generation mix is only 6.5%.

Table 3 shows the life-cycle water consumption per gallon of gasoline equivalent (gge) for petroleum gasoline, natural gas and corn ethanol. The table shows a wide range of water consumption for corn ethanol with the low end representing states that rely on rain fall (green water) for corn growth, while the high end represents states that depend on irrigation. The reported average water consumption in Tables 1–3 represents the production weighted average for each of the fuel production pathways.

TABLE 2. Water Consumption Factors for Electric Power Generation (gal/kWh)

	Water factor (range)
Natural gas	0.21 (0.2−0.7)
Coal	0.52 (0.1−1.1)
Biomass	0.40 (0.1−1.0)
Nuclear	0.58 (0.4−0.7)
Hydropower	18 (14−100)
U.S. Mix	1.6

TABLE 3. Life-Cycle Water Consumption of Petroleum, Natural Gas and Corn Ethanol (gal/gge)

Fuel	Water consumption (range)
Gasoline	5.4 (1.3−9)
Natural gas	0.7 (0.3–1.2)
Corn ethanol	55 (2.2−300)

Figure 1 shows the life-cycle water consumption for hydrogen production via SMR and water electrolysis. The impact of the electricity generation technology employed in the electrolysis pathway is obvious in Figure 1, with the U.S. average generation mix resulting in water consumption of 75 gallons per kg of hydrogen, while wind electrolysis consumes only 5 gallons per kg of hydrogen. With the interest in low-carbon hydrogen for powering future FCEVs, the latter is the likely pathway for hydrogen production via electrolysis. Figure 2 shows the life-cycle water consumption per mile for various fuel/vehicle systems for the midsize vehicle class. Figure 2 reflects 25 miles per gge (mpgge) fuel economy for gasoline, compressed natural gas (CNG) vehicles, and E85 (i.e., 85% ethanol blend with gasoline by

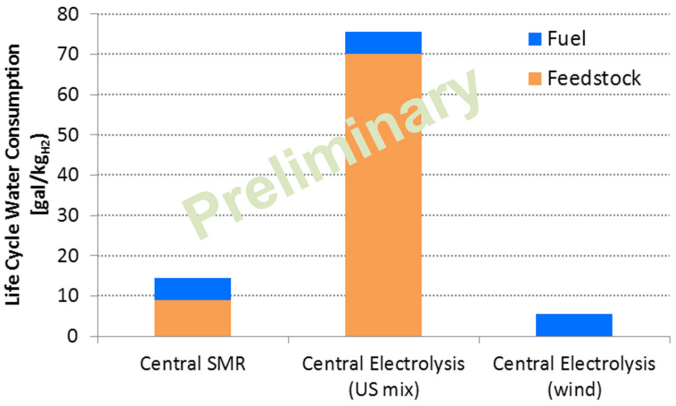

FIGURE 1. Life Cycle Water Consumption for Hydrogen Production via SMR and Electrolysis

volume), 29 mpgge for diesel vehicles, 35 mpg for gasoline hybrid electric vehicles (HEVs), 52 mpgge for hydrogen FCEVs, and 85 mpgge for battery electric vehicles (BEVs). Figure 2 shows the significant impact of the large water consumption factors of corn ethanol and U.S. electricity mix on the E85, hydrogen via electrolysis, and BEV pathways.

CONCLUSIONS AND FUTURE DIRECTIONS

Argonne expanded the GREET model to include water consumption factors for major transportation fuel pathways, including petroleum fuels, natural gas, electricity, corn ethanol and hydrogen, and completed the assessment of water consumption for hydrogen production from SMR and electrolysis. Irrigation water for farming, cooling water for electricity, and evaporation associated with hydropower generation have the greatest impact on life-cycle water consumption of E85 and electric vehicles. Water consumption factors are developed in GREET for the production of hydrogen, baseline petroleum fuels, and other fuels that are commonly used as feedstocks, blendstocks or process fuels (e.g., electricity, diesel, natural gas, corn ethanol, etc.) in the various pathways within the GREET model. The life-cycle water consumption analysis needs to be expanded to include additional hydrogen production pathways and alternative transportation fuel/vehicle systems.

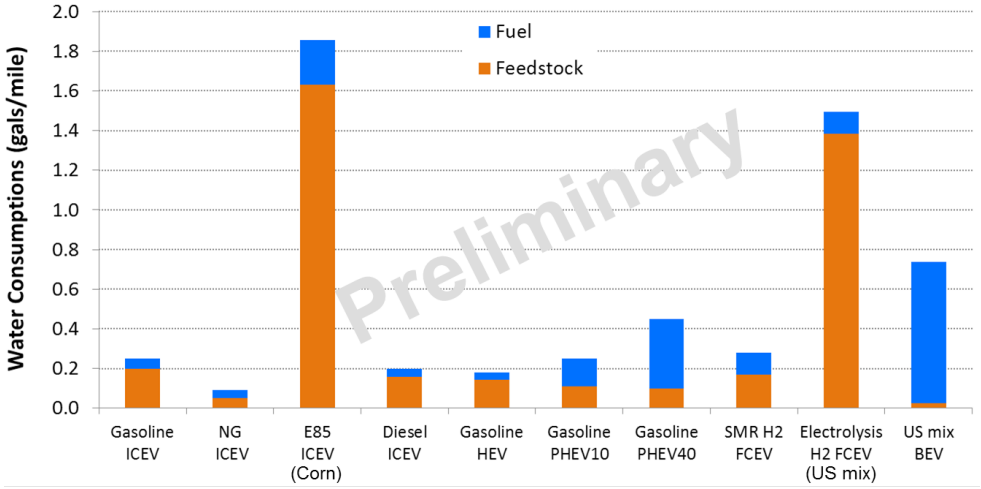

ICEV - internal combustion engine vehicle; PHEV10 - plug-in hybrid electric vehicle, 10-mile all-electric range; PHEV40 - plug-in hybrid electric vehicle, 40-mile all-electric range

FIGURE 2. Life Cycle Water Consumption for Alternative Fuel/Vehicle Systems

X.5 Impact of Fuel Cell System Peak Efficiency on Fuel Consumption and Cost

Ayman Moawad (Primary Contact),
Aymeric Rousseau
Argonne National Laboratory
9700 South Cass Avenue
Argonne, IL 60439-4815
Phone: (630) 252-2849
Email: amoawad@anl.gov

DOE Manager
Fred Joseck
Phone: (202) 586-7932
Email: Fred.Joseck@ee.doe.gov

Project Start Date: October 1, 2013
Project End Date: September 30, 2014

Overall Objectives

- Quantify the fuel displacement and cost of advanced fuel cell systems.
- Evaluate benefits of aggressive fuel cell system peak efficiency compared to the current target of 60% from an energy consumption and cost point of view.

Fiscal Year (FY) 2014 Objectives

- Study the impact of different fuel cell system targets on the vehicle energy consumption and cost using Autonomie.
- Develop specific fuel cell systems using high fidelity GCTool model for different mass activity to understand the impact of higher efficiency on component design and cost versus linear scaling approach.
- Build vehicle simulations using the individual component assumptions.
- Run the simulations and present detailed analysis related to energy consumption, cost, component sizing and vehicle weight, hydrogen tank effects, etc.
- Understand the impact of the fuel cell system and hydrogen storage performance and cost requirements compared to other powertrain technologies to ensure successful commercialization path.
- Provide guidance for long-term requirements for peak power and onboard hydrogen weight.

Technical Barriers

This project addresses the following technical barriers from the System Analysis section of the Fuel Cell Technologies Office Multi-Year Research, Development, and Demonstration Plan:

(A) Future Market Behavior

(C) Inconsistent Data, Assumptions and Guidelines

(D) Insufficient Suite of Models and Tools

(E) Unplanned Studies and Analysis

Contribution to Achievement of DOE Systems Analysis Milestones

This project will contribute to achievement of the following DOE milestones from the Fuel Cells section of the Fuel Cell Technologies Office Multi-Year Research, Development, and Demonstration Plan:

- Milestone 1.1: Complete an analysis of the hydrogen infrastructure and technical target progress for hydrogen fuel and vehicles. (2Q, 2011)
- Milestone 1.11: Complete analysis of the impact of hydrogen quality on the hydrogen production cost and the fuel cell performance for the long range technologies and technology readiness. (2Q, 2015)
- Milestone 1.12: Complete an analysis of the hydrogen infrastructure and technical target progress for technology readiness. (4Q, 2015)
- Milestone 1.16: Complete analysis of program performance, cost status, and potential use of fuel cells for a portfolio of commercial applications. (4Q, 2018)
- Milestone 1.17: Complete analysis of program technology performance and cost status, and potential to enable use of fuel cells for a portfolio of commercial applications. (4Q, 2018)
- Milestone 2.2: Annual model update and validation. (4Q, 2011 through 4Q, 2020)

FY 2014 Accomplishments

- Full vehicle simulations were performed to assess the vehicle energy consumption and cost of current and future fuel cell vehicles compared to conventional powertrains for different fuel cell systems.
- Aggressive fuel cell system peak efficiency targets could increase fuel economy from 10 to 14% while slightly decreasing cost.

- Compared to current conventional vehicles, fuel cell vehicles achieve similar weight and a fuel economy up to 5 times higher by 2030 or 1.5 times higher (if compared to same year conventional powertrains).
- Current DOE targets for both fuel cell peak power (80 kW) and onboard hydrogen weight (5.6 kg) will exceed the requirements for most vehicle classes by 2030.

INTRODUCTION

Autonomie has been used by the U.S Department of Energy to evaluate the vehicle energy consumption and benefits of a wide range or powertrain configurations, component technologies and control strategies. In this study, the objective is to quantify the vehicle energy consumption and cost of fuel cell hybrid vehicles compared to conventional powertrains using two target scenarios: current and aggressive. The current scenario is based on a 60% peak efficiency fuel cell system while the aggressive scenarios relies on higher fuel cell system efficiencies (up to 68%).

APPROACH

To evaluate the fuel efficiency benefits of advanced powertrains, each vehicle is designed on individual component assumptions to meet the same vehicle technical specifications (i.e. acceleration, gradeability…). The fuel efficiency is then simulated on the Urban Dynamometer Driving Schedule (UDDS) and Highway Fuel Economy Test (HWFET). The vehicle costs are calculated using the aggregated cost of each component.

To properly assess the benefits of future technologies, different vehicle classes were considered: compact car, midsize car, small sport utility vehicle (SUV), medium SUV, and pickup truck. Different timeframes representing different set of assumptions were simulated. We will show in this report 2013 and 2030 timeframes. Additionally, to address uncertainties, a triangular distribution approach (low, medium, and high) was employed. For each component, assumptions (e.g., regarding efficiency, power density) were made, and three separate values were defined to represent the (1) 90th percentile, (2) 50th percentile, and (3) 10th percentile. A 90% probability means that the technology has a 90% chance of being available at the time considered. For each vehicle considered, the cost assumptions also follow the triangular uncertainty. The current study includes micro hybrids as they are introduced to substitute conventional vehicles starting from 2030 (medium uncertainty case).

RESULTS

The assumptions described below have been defined on the basis of inputs from experts and the U.S. DRIVE targets. Table 1 shows the different fuel cell system assumptions evolution overtime used as inputs to the simulation model.

The fuel cell system costs are driven by the following equation:

$$(1246.5 \bullet x \bullet S^{0.2583} + P \bullet \mathbf{y}) \bullet FC_{pwr} \bullet (\frac{FC_{pwr}}{80})^{z}$$

Where *x, y* and *z* are coefficients and *P* is the platinum price, *S* is the stack unit per year and FC_{pwr} is the fuel cell power. The costs are assumed for high production volumes (500,000 per year).

Table 2 shows the different hydrogen storage assumptions.

Vehicle Weight

The simulation results show that fuel cell vehicles' weight will be close to conventional vehicles of the same year by 2030 (Figure 1). The comparison of both fuel cell system target scenarios show aggressive fuel cell system peak efficiency impacts total vehicle weight by less than 1% compared to the constant 60% peak efficiency target. Most of the light weighting comes from onboard hydrogen weight reduction.

All the vehicles' hydrogen storage systems have been sized to provide a range of 320 miles on the combined driving cycle (UDDS and HWFET). Figure 2 shows that aggressive fuel cell system peak efficiency leads to 13%

TABLE 1. Fuel Cell System Assumptions

Parameter	Units	2013			2030		
		Low	Med	High	Low	Med	High
Specific Power FC* system	W/kg	400	400	400	580	660	740
Power Density	W/L	410	410	410	600	730	980
Peak FC Efficiency at 25% Rated Power (Aggressive Projection)	%	60	60	61	65	67	68
Peak FC Efficiency at 25% Rated Power (Constant Efficiency)	%	60	60	60	60	60	60
Platinum Price	$/Troy Oz	1,800	1,800	1,800	1,800	1,400	1,100

*FC – Fuel Cell System

TABLE 2. Hydrogen Storage Assumptions

Parameter	Units	2013			2030		
		Low	Med	High	Low	Med	High
System Gravimetric Capacity	Useable kWh/kg	1.41	1.41	1.41	1.5	1.67	1.96
	Useable kg H_2/kg of Tank System	0.042	0.042	0.042	0.045	0.050	0.059
System Volumetric Capacity	Useable kWh/L	0.947	0.947	0.947	1.27	1.5	1.6
	Useable kg H_2/L	0.028	0.028	0.028	0.038	0.045	0.048
Cost	$/Useable kg H_2	769	769	769	418	334	267
Percentage H_2 used in Tank	%	95	95	95	97	97	97
Range on combined, adjusted miles/ gasoline gallon equivalent	miles	320	320	320	320	320	320

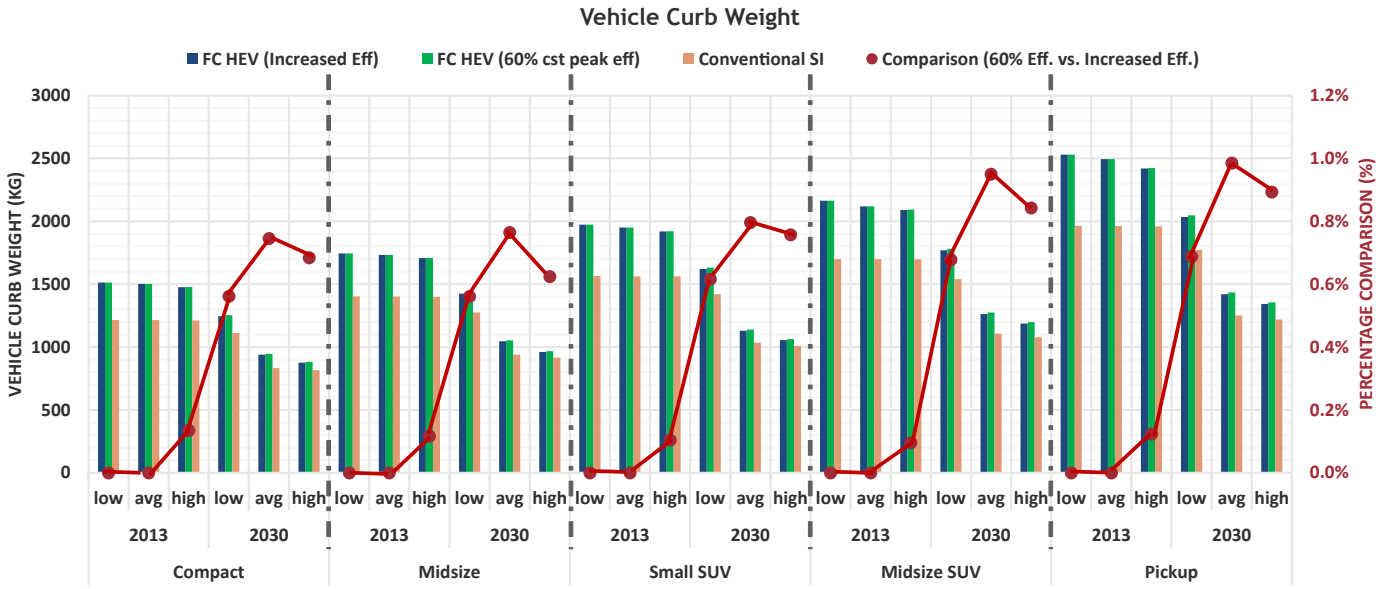

FIGURE 1. Vehicle Curb Weight (kg)

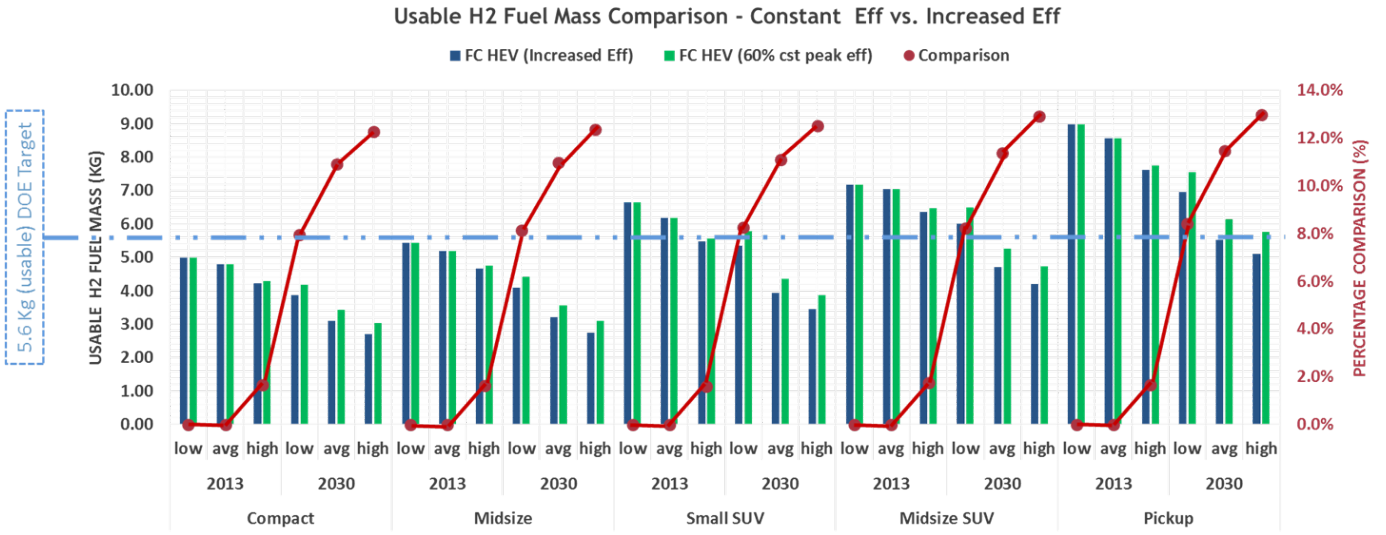

FIGURE 2. Hydrogen Usable Fuel Mass (Kg)

reduction in onboard hydrogen weight by 2030. One also notices that the shows that the current DOE target of 5.6 kg of usable hydrogen exceeds the range requirements for most vehicles by 2030.

Vehicle Energy Consumption

While aggressive fuel cell systems requirements have a small impact on vehicle weight, they do provide significant benefits on the vehicle energy consumption side. As shown in Figure 3, by 2030, advanced fuel cell systems will show about 12 to 13% of fuel economy benefit compared to the 60% peak efficiency case. When compared to the 2013 conventional reference vehicle, fuel cell hybrid electric vehicles (HEVs) could be up to 5 times more fuel efficient by 2030. Even with 60% fuel cell system peak efficiency targets, fuel cell HEVs still are up to 4 times more fuel efficient than today's conventional baseline.

As shown in Figure 4, when vehicle fuel cell HEV fuel economy gasoline equivalent ratios are compared to conventional of the same year, fuel cell HEVs fuel economy tend to get closer to the respective conventional gasoline vehicle of the same year (ratio closer to 1.5) versus a ratio of 2 in 2013. The fact that the ratios are decreasing with time points to the fact that advanced conventional vehicle energy

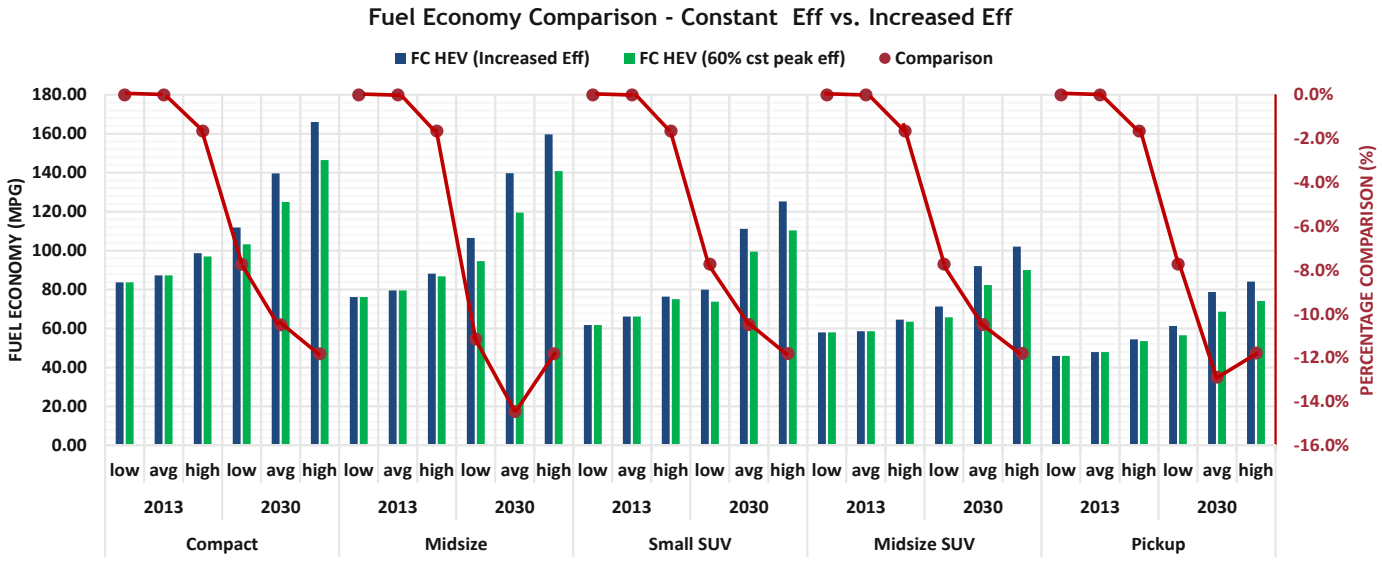

FIGURE 3. Vehicle Fuel Economy (MPGGE)

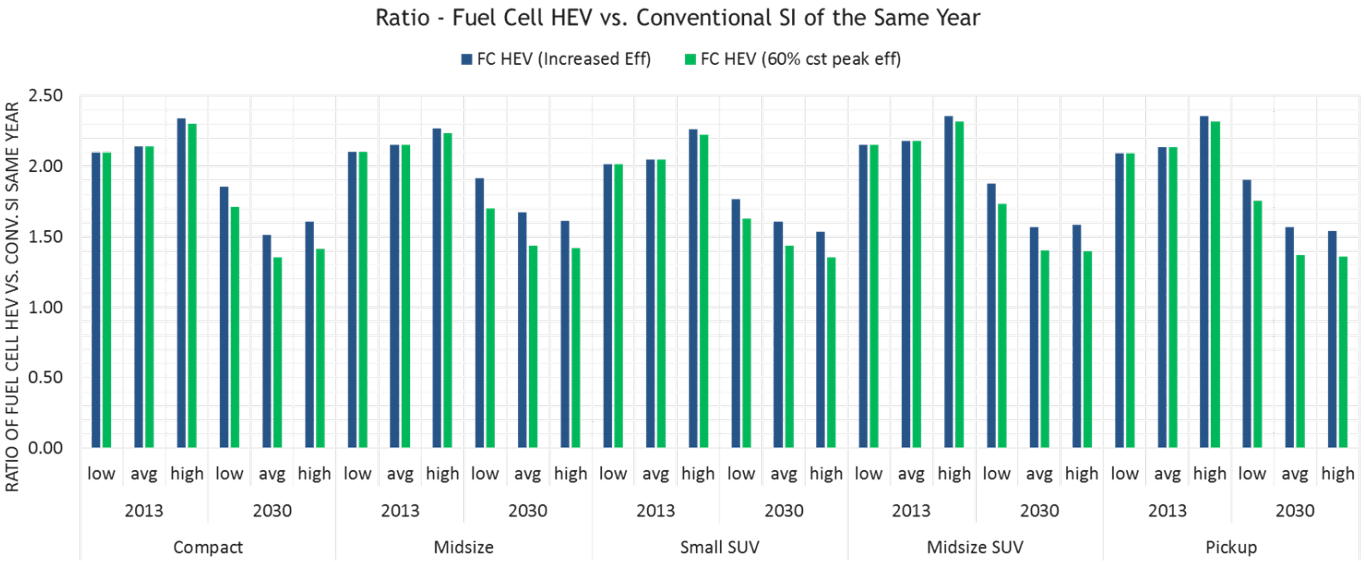

FIGURE 4. Ratio of Fuel Cell HEV vs. Conventional Gasoline of the Same Year

consumption is expected to improve faster than the one of fuel cell vehicles.

The previous trend can be explained by looking at individual system average efficiencies over the UDDS cycle. As shown in Figure 5, gasoline engines get more competitive as their average cycle efficiency significantly increases by 2030. Note that micro hybrids (start/stop systems) are introduced in 2030, which will also contribute to the reduction of the vehicle energy consumption ratio. The figure also shows that aggressive fuel cell peak efficiency targets (i.e. 68% vs. 60%) could provide up to 14% of fuel cell system average cycle efficiency increase on the UDDS cycle by 2030.

Figure 6 shows the fuel cell vehicle manufacturing cost of the different fuel cell systems considered. Manufacturer suggested retail price (MSRP) values have been computed, where the retail price equivalent value is set to 1.5 times the manufacturing cost. The results show that aggressive fuel cell

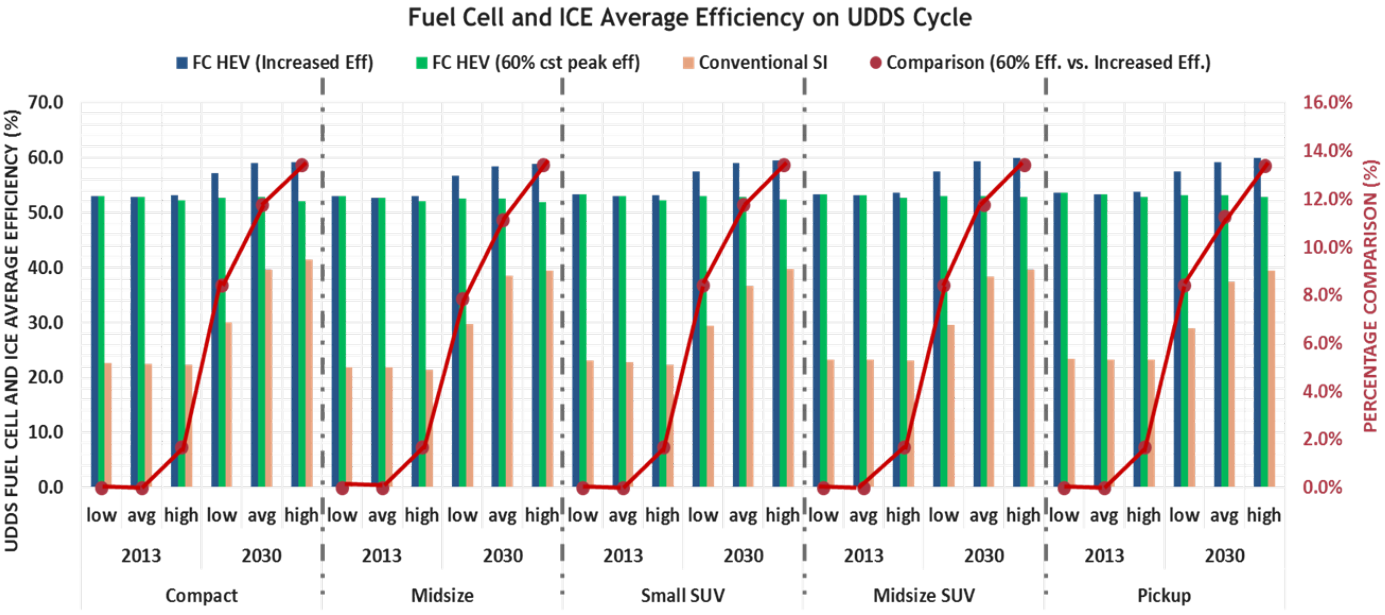

FIGURE 5. Fuel Cell and Engine Average Efficiency on the UDDS Cycle

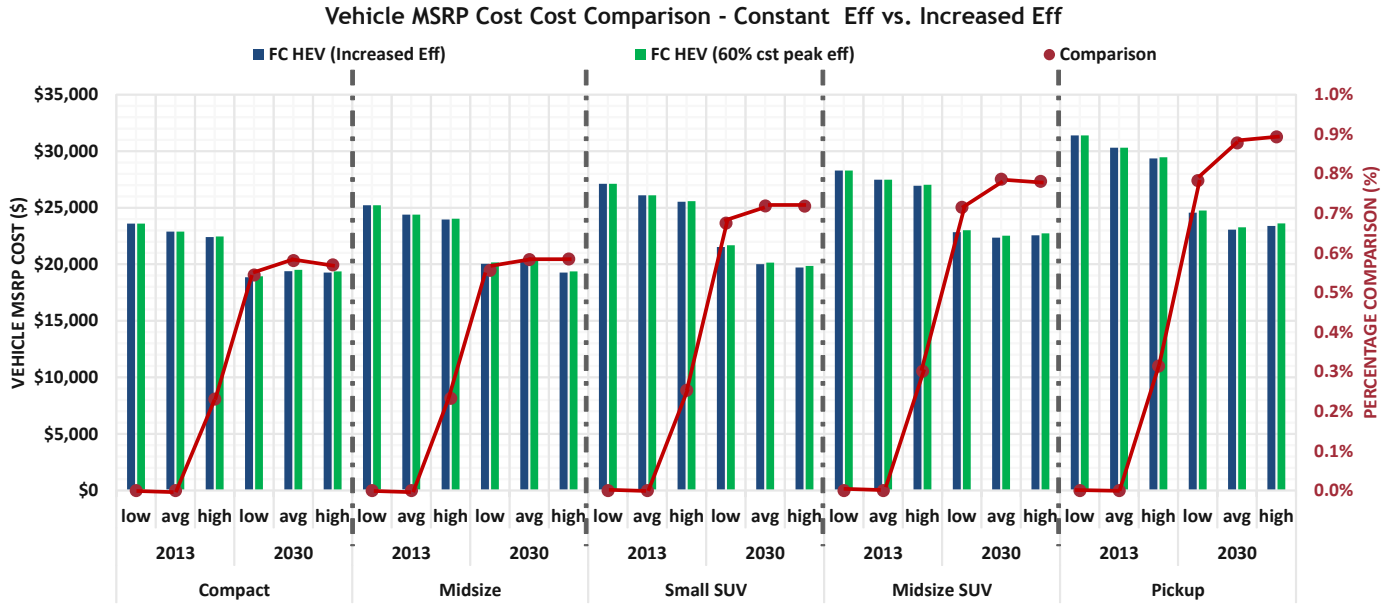

FIGURE 6. Fuel Cell Vehicle Cost

system peak efficiency could provide small cost benefit by 2030 (less than 1%).

CONCLUSIONS AND FUTURE DIRECTIONS

Full vehicle simulations were performed to assess the vehicle energy consumption and cost of fuel cell vehicles compared to conventional powertrains. Different timeframes (current and 2030) as well as fuel cell system peak efficiencies (constant 60% vs. aggressive cases up to 68%) were considered. The results showed that:

- Aggressive fuel cell system peak efficiency targets could increase fuel economy from 10 to 15% while slightly decreasing cost.
- The cost decrease is mostly due to the decrease of hydrogen tank cost (8 to 13%)
- Compared to conventional vehicles, fuel cell vehicles achieve similar weight and a fuel economy up to 4x higher by 2030.
- Current DOE targets for both fuel cell peak power (80 kW) and onboard hydrogen weight (5.6 kg) will exceed the requirements for most vehicle classes by 2030.

FY 2014 PUBLICATIONS/PRESENTATIONS

1. Aymeric Rousseau, "Impact of Fuel Cell System Efficiency on Vehicle Energy Consumption and Cost" Presentation at the Annual Merit Review.

X.6 Analysis of Incremental Fueling Pressure Cost

Amgad Elgowainy (Primary Contact) and Krishna Reddi
Argonne National Laboratory
9700 South Cass Avenue
Argonne, IL 60439
Phone: (630) 252-3074
Email: aelgowainy@anl.gov

DOE Manager
Fred Joseck
Phone: (202) 586-7932
Email: Fred.Joseck@ee.doe.gov

Project Start Date: October 2013
Project End Date: September 2014

Overall Objectives

Provide a platform for comparing impact of alternative refueling methods, fueling pressures, and pre-cooling temperatures on the refueling cost of hydrogen.

Fiscal Year (FY) 2014 Objectives

- Evaluate impact of fueling pressure on fill rate and refueling cost
- Incorporate implications of SAE International (SAE) J2601 refueling protocol in the modeling of hydrogen refueling stations (HRS)
- Identify cost drivers of various fueling technologies and configurations

Technical Barriers

This project directly addresses Technical Barriers A, D and E in the System Analysis section of the Fuel Cell Technologies Office Multi-Year Research, Development, and Demonstration Plan. These barriers are:

(A) Future Market Behavior

(D) Insufficient Suite of Models and Tools

(E) Unplanned Studies and Analysis

Technical Targets

The project employs the Hydrogen Station Cost Optimization and Performance Evaluation (H2SCOPE) simulation tool to simulate the performance of the refueling system and to investigate the impact of fueling pressure and pre-cooling requirement on the fill time and refueling cost. The project examines the tradeoff between the fueling pressure (fill amount) and refueling cost for a target fill time of three minutes.

Contribution to Achievement of DOE System Analysis Milestones

This project contributes to achievement of the following DOE milestone from the Systems Analysis section of the Fuel Cell Technologies Office Multi-Year Research, Development, and Demonstration Plan:

- Task 1.12: Complete an analysis of the hydrogen infrastructure and technical target progress for technology readiness. (4Q, 2015)
- Task 2.2: Annual model update and validation. (4Q, 2011 through 4Q, 2020)

FY 2014 Accomplishments

- A modeling framework (H2SCOPE) was developed to accurately evaluate various fueling pressures and pre-cooling temperatures.
- Evaluated the refueling times for various combinations of fueling pressures and pre-cooling temperatures.
- Evaluated the refueling costs for various combinations of fueling pressures, pre-cooling temperatures and station capacities.

INTRODUCTION

Previous studies have indicated that the compression, refrigeration and storage combined, accounts for more than 75% of the refueling equipment cost. Additionally, refrigeration and compression are the two major components with significant operation costs. While the refueling station compression and storage requirements depend on the fueling pressure, the cooling requirement depends on the pre-cooling temperature. The pre-cooling temperature largely decides the fill rate for a given fueling pressure and initial vehicle tank condition. In this project we studied the impact of the combinations of different fueling pressures and pre-cooling temperatures on the refueling cost of hydrogen.

The H2SCOPE simulation model was developed from first principles by solving the physical laws subject to a set of initial and boundary conditions. H2SCOPE tracks the temperature, pressure and mass at all the points from the hydrogen source to the vehicle's tank within a refueling station. The model provided the opportunity of examining the highest fill rate possible with any combination of fueling

pressure and pre-cooling temperature without exceeding the limits set by SAE J2601 protocol on pressure, temperature, and state of charge. The associated fueling costs were estimated for various combinations of fueling pressures and pre-cooling temperatures. The temperature rise inside the vehicle's tank is influenced by various parameters, including the tank's physical size and configuration, the tank thermal properties, and the initial conditions and boundary conditions of the tank system. The physical size, thermal properties, and initial conditions and boundary conditions of the fill process simulated by the H2SCOPE model are provided in Tables 1, 2 and 3, respectively.

TABLE 1. Vehicle Tank Characteristics

Tank Physical Properties	Fill Pressure (bar)		
	700	500	350
Capacity (kg)	5	4	3
Outer Diameter (inches)	19.5		
Thickness (inches)	1.83		
Tank Length (inches)	49.2		
Liner Thickness (inches)	0.2		
Volume (liters)	129		

TABLE 2. Vehicle Tank Thermal Properties

	Composite	Liner (Poly Ethylene)
Temperature Range (^{O}C)	-100 to 140	-100 to 140
Density (kg/m^3)	1,550	975
Specific Heat (J/kg-K)	500-1,500	1,000-3,000
Thermal Conductivity (W/m-K)	0.3-0.8	0.3-0.8
Thermal Diffusivity (cm^2/sec)	0.001-0.009	0.001-0.009

TABLE 3. Initial and Boundary Conditions of the Vehicle Tank System

Initial Pressure (bar)	20
Initial Temperature (Ambient, K)	298
Hot Soak Condition Temperature (K)	313
Maximum Pressure (bar)	875
Maximum Temperature (K)	358
Convective Heat Transfer Coefficient (W/m^{2}K)	325 (Inside), 5 (Outside)
Inlet (Dispensing) Temperature (K)	298, 273, 263, 253, 243, 233
Fill Strategy	Constant Pressure Ramp Rate

RESULTS

Figure 1 shows the minimum fill times possible for different fueling pressures at various pre-cooling temperatures while observing the limits specified by SAE J2601 fueling protocol. Figure 1 shows that for higher pre-cooling temperatures, the fueling pressures have greater impact on the fill duration. It also shows that the 700-bar refueling in Type IV tanks would require at least -30^{o}C pre-cooling to fill 5 kg within 3 minutes. Additionally, pre-cooling to -20^{o}C and -10^{o}C is required to fill the vehicle's tank within 3 minutes for fueling pressures of 500 bar and 350 bar, respectively. Figure 2 shows the estimated refueling costs for filling the vehicle's tank at different fueling pressures within 3 minutes for a 750 kg/day station. It can be seen from the figure that partial fill of a vehicle's tank (i.e., with lower fueling pressures), significantly reduces the refueling cost. These lower fueling costs are due to the reduced cooling, compression and storage costs at refueling stations with lower fueling pressures. Although more dispensers are required to satisfy the demand for the 350-bar refueling to maintain the same refueling position availability for customers, the increase in dispenser cost does not negate

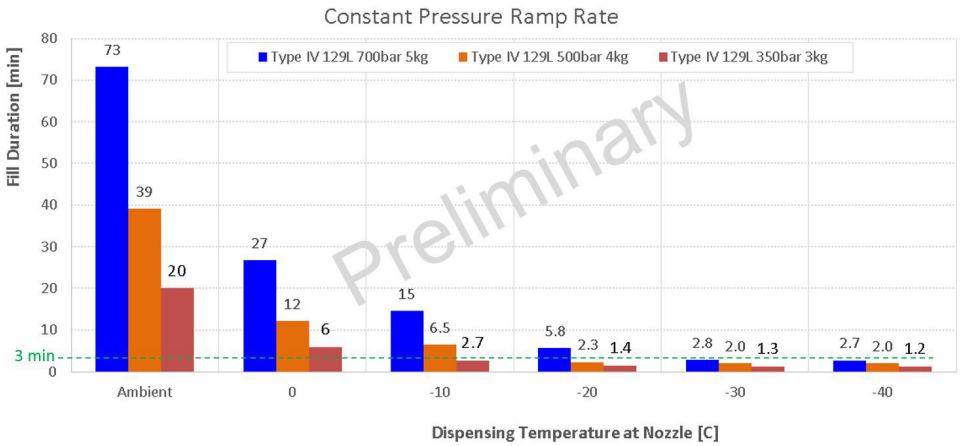

FIGURE 1. Estimated Fill Duration for Various Pre-Cooling Temperatures and Fueling Pressures

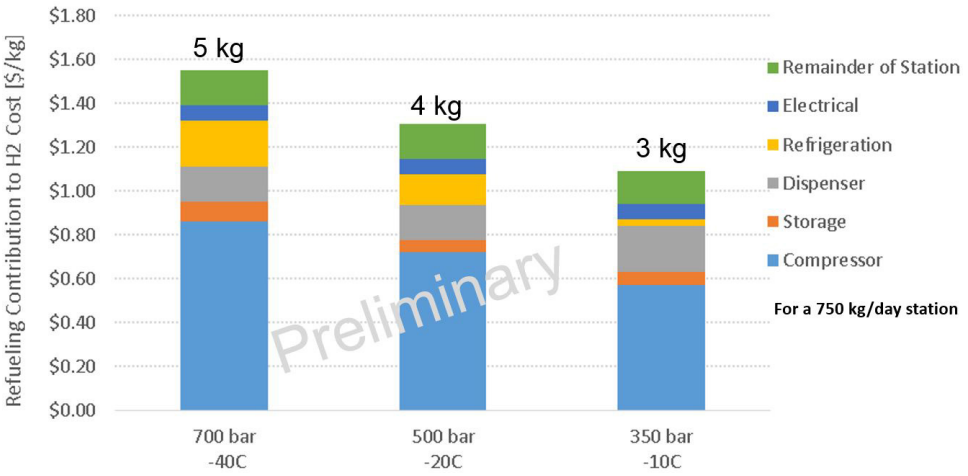

FIGURE 2. Estimated Refueling Cost by Component for Various Fueling Pressures at Same Fill Rate for a 750 kg/day Station

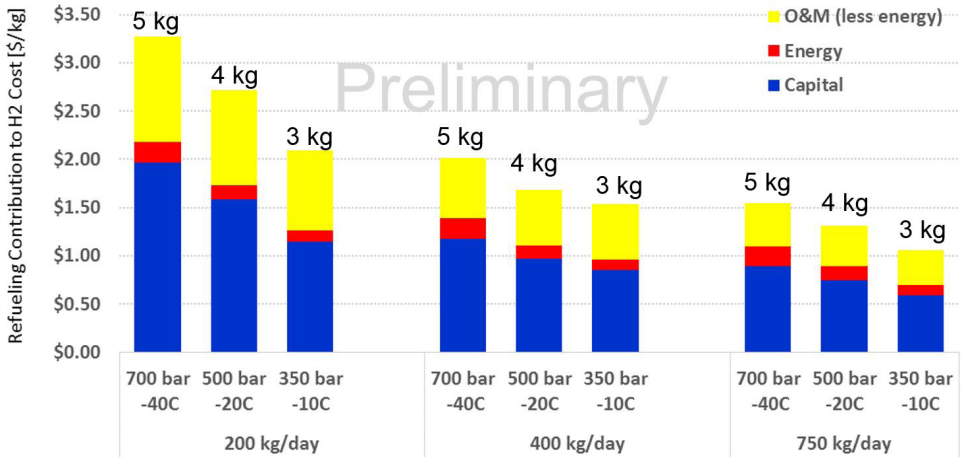

O&M - operations and maintenance

FIGURE 3. Estimated Refueling Cost for Various Fueling Pressures and Station Capacities for a Fill Time of Less Than 3 Minutes

the savings achieved from the reduction in the compression and storage and cooling costs. Figure 3 shows the refueling costs for station capacities of 200, 400 and 750 kg/day. The refueling cost savings with the lower fueling pressures is much greater for smaller station capacities compared to larger station. Greater cost savings would be realized in early fuel cell vehicle markets where the deployed stations are of small capacities and the utilization of such capacity is expected to be low with a slow initial vehicle deployment rate.

CONCLUSIONS AND FUTURE DIRECTIONS

The fueling pressure greatly impacts the fill duration, especially with higher pre-cooling temperatures. Filling the vehicle with lower pressures (partial fills) reduces the associated refueling costs. The reduction in refueling cost with lower fueling pressures is greater for lower station capacities and is primarily driven by the reduction is required compression, cooling and storage costs. In the future, the impact of station underutilization scenarios and the requirement of semi-continuous running of the pre-cooling equipment to satisfy the SAE J2601 time window need to be investigated to quantify the implication of various fueling pressures on refueling cost.

SPECIAL RECOGNITIONS & AWARDS/ PATENTS

Patent Application:

1. Elgowainy, A., Reddi, K., "ENHANCED METHODS FOR OPERATING REFUELING STATION TUBETRAILERS TO REDUCE REFUELING COST", Docket No.: ANL-IN-13-058,

submitted to United States Patent and Trademark Office on September 27th 2013.

FY 2014 PUBLICATIONS/PRESENTATIONS

1. Reddi, K., Mintz, M., Elgowainy, A., Sutherland, E., "Challenges and opportunities of hydrogen delivery via pipeline, tube-trailer, Liquid tanker and methanation-natural gas grid", Wiley (in press).

2. Reddi, K., Elgowainy, A., Sutherland, E., "Hydrogen Refueling Station Compression and Storage Optimization with Tube Trailer Deliveries" Accepted for publication at the International Journal of Hydrogen Energy.

3. Reddi, K., Elgowainy, A., Sutherland, E., Joseck, F., 2014, "Tube-Trailer Consolidation Strategy for Reducing Hydrogen Refueling Station Costs," submitted for publication at the International Journal of Hydrogen Energy.

X.7 Hydrogen Station Economics and Business (HySEB)—Preliminary Results

Zhenhong Lin (Primary Contact), Changzheng Liu
Oak Ridge National Laboratory
2360 Cherahala Boulevard
Knoxville, TN 37932
Phone: (865) 946-1308
Email: linz@ornl.gov

DOE Manager
Fred Joseck
Phone: (202) 586-7932
Email: Fred.Joseck@ee.doe.gov

Project Start Date: October 1, 2013
Project End Date: Project continuation and direction determined annually by DOE

Overall Objectives

- Develop a model that optimizes hydrogen station deployment for business success
- Analyze profitability, risk, and public-private partnership in hydrogen station deployment
- Develop more understanding of the hydrogen supply infrastructure and the interplay between infrastructure and fuel cell electric vehicle (FCEV) demand

Fiscal Year (FY) 2014 Objectives

- Develop a preliminary version of the Hydrogen Station Economics and Business (HySEB) model
- Analyze station network economics with the cluster strategy

Technical Barriers

This project addresses the following technical barriers from the Systems Analysis section of the Fuel Cell Technologies Office Multi-Year Research, Development, and Demonstration Plan:

(A) Future Market Behavior

(B) Stove-Piped/Siloed Analytical Capability

(D) Insufficient Suite of Models and Tools

Contribution to Achievement of DOE Systems Analysis Milestones

This project will contribute to achievement of the following DOE milestones from the Systems Analysis section of the Fuel Cell Technologies Office Multi-Year Research, Development, and Demonstration Plan:

- Milestone 1.12: Complete an analysis of the hydrogen infrastructure and technical target progress for technology readiness. (4Q, 2015)
- Milestone 1.15: Complete analysis of program milestones and technology readiness goals - including risk analysis, independent reviews, financial evaluations, and environmental analysis - to identify technology and risk mitigation strategies. (4Q, 2015)
- Milestone 1.16: Complete analysis of program performance, cost status, and potential use of fuel cells for a portfolio of commercial applications. (4Q, 2018)
- Milestone 1.19: Complete analysis of the potential for hydrogen, stationary fuel cells, fuel cell vehicles, and other fuel cell applications such as material handling equipment including resources, infrastructure and system effects resulting from the growth in hydrogen market shares in various economic sectors. (4Q, 2020)
- Milestone 2.2: Annual model update and validation. (4Q, 2011 through 4Q, 2020)

FY 2014 Accomplishments

- Developed a preliminary version of the HySEB model, which trades off infrastructure cost and fuel accessibility cost to find an optimal station deployment strategy that maximizes profitability for hydrogen station business.
- Completed the analysis of station network cash flow at the city level. Annual cash flow would be negative for about a decade. Building large stations first takes advantage of station economy of scale and delays the construction of additional stations for meeting fuel demand. Thus, compared with building small stations first, large-stations-first strategy has better cash flow and 8% lower system cost (the sum of infrastructure cost and fuel accessibility cost).
- Next-N-year net present value (NPV) is calculated to understand the risks perceived by investors and the relationship with investment planning horizon. It also builds a platform for analyzing public-private partnership in station economy.

INTRODUCTION

Deployment of the hydrogen supply infrastructure is one of most critical issues that must be addressed for a successful market transition to FCEVs. Not only must hydrogen refueling infrastructure be constructed, it must also be commercially viable and sell hydrogen to customers at retail prices that will encourage the continued expansion of the vehicle market. The objective of this project is to develop a station deployment optimization model and analyze station network economics, risk of investment, viable business strategies, public-private partnership, and the interaction with consumer demand for FCEVs. This project will help the Fuel Cell Technologies Office explore scenarios of station deployment and business models that enable commercially viable early hydrogen refueling infrastructure. Understanding how long, at what cost, and by what processes the U.S. can transition to a market-driven, self-sustaining hydrogen supply industry is highly relevant to industry confidence, investment risk management, government policy effectiveness, and R&D planning.

APPROACH

The HySEB model optimizes key deployment decisions to meet fuel demand by trading off infrastructure cost and fuel accessibility cost. Decision variables are when, where to build, and the size of stations. Fuel accessibility cost is relative to gasoline, measured by additional detour time in order to access hydrogen refueling stations. Apparently, early FCEV buyers would prefer high fuel availability (measured by the ratio of the number of hydrogen stations to the number of gasoline stations); however, to achieve high fuel availability in early commercialization implies deploying more small-sized stations and/or lower station utilization, which in turn leads to the loss of station scale economy and increased hydrogen cost. The model also considers driving pattern heterogeneity in order to more accurately estimate hydrogen fuel demand in the region of interest. Driving pattern data is obtained from the 2009 National Household Travel Survey. We classified California drivers into six groups: frequent driver and long commute (FLC), frequent driver and short commute, average driver and long commute, average driver and short commute, moderate driver and long commute, and moderate driver and short commute (MSC). For each driver group, fuel demand at location stations is calculated (assuming refueling at connector stations if daily driving distance is greater than a threshold value). A higher share of frequent drivers with long commute distance is expected to contribute more to local station business.

FCEV market penetration is assumed to be exogenous, constrained by the zero-emission-vehicle mandate. Station deployment scenarios are developed based on clustering strategy [1]. All station capital, operating and maintenance (O&M) costs, and efficiency data are consistent with Ref. [3] and the H2A model. Station network economics and investment risks at the city level are analyzed.

RESULTS

The project developed an Excel-based model, which takes input of FCEV attributes and penetration assumptions, driver characteristics including driving pattern, value of time, and discount rate, as well as infrastructure assumptions including station capital cost and O&M cost as a function of station size and type. The model outputs station deployment solutions (when and where to build and station size) and calculates cash flow and total system cost (infrastructure cost plus fuel accessibility cost). The model will be continuously expanded and improved with the goal to facilitate Fuel Cell Technologies Office discussions on economics and business models of early hydrogen refueling infrastructure.

Based on clustering strategy of station deployment [1], the case study focuses on station network in a cluster (a small city). The optimization algorithm is still under development. In FY 2014, the project is evaluating three station build-out scenarios which meet exogenous fuel demand: small station first (SSF), uniform-size station, and large station first (LSF). Total number of stations is a user input (it will be provided by the optimization model in the future work). The SSF scenario refers to deploying small-size stations first, then medium-size stations, and finally large stations. By contrast, the LSF scenario deploys larger stations first and smaller stations later. The scenarios are designed to examine the importance of station scale economy and timing of roll-out. Compared with small stations, large stations have better scale economy in terms of both capital cost and O&M cost but have lower utilization rate, particularly in the early market.

Cash flow analysis at the city level was conducted for all three scenarios (Figure 1 for the SSF scenario and Figure 2 for the LSF scenario). Positive cash flow includes hydrogen sales revenue and negative flow includes capital cost as a lump sum payment and annual O&M cost. Station owners endure net loss for about a decade before the break-even point. Figure 1 shows annual cash flow becomes positive around 2025 and cumulative flow is negative until 2029. Figure 2 for the LSF scenario shows slightly improved station economics—cumulative cash flow is already positive in 2027.

Next, we examined risks of investment and implications for public-private partnership (Figure 3). Since station cash flow is negative for at least a decade, investors' planning horizon is an important factor to determine how they perceive the risk of the investment. Figure 3 shows next-N-year NPV at each year, which is defined as NPV of the cash flows during the next N years. As expected, investment risk will be (perceived) smaller if the investors enter the market late or if they are more patient (indicated by a longer planning horizon). Comparing SSF and LSF scenarios, LSF

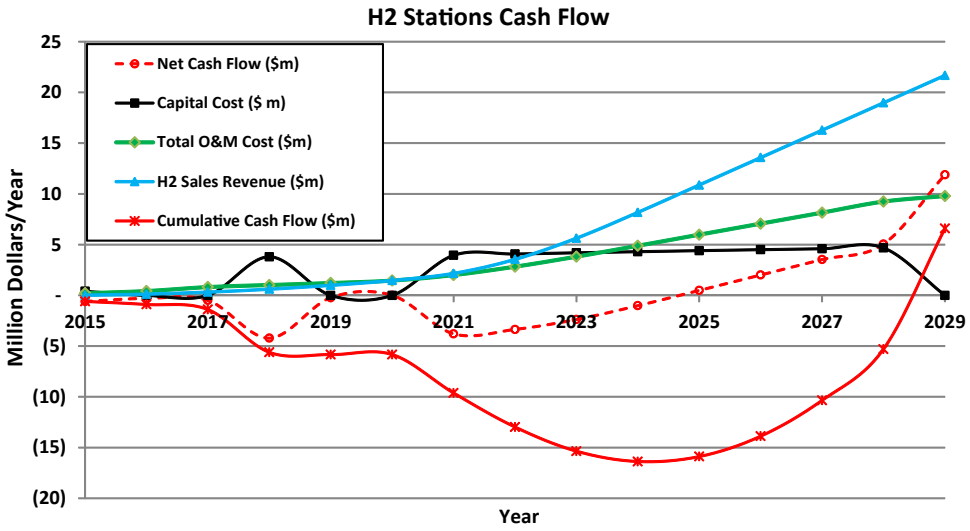

FIGURE 1. Hydrogen Stations Cash Flow for the SSF Strategy

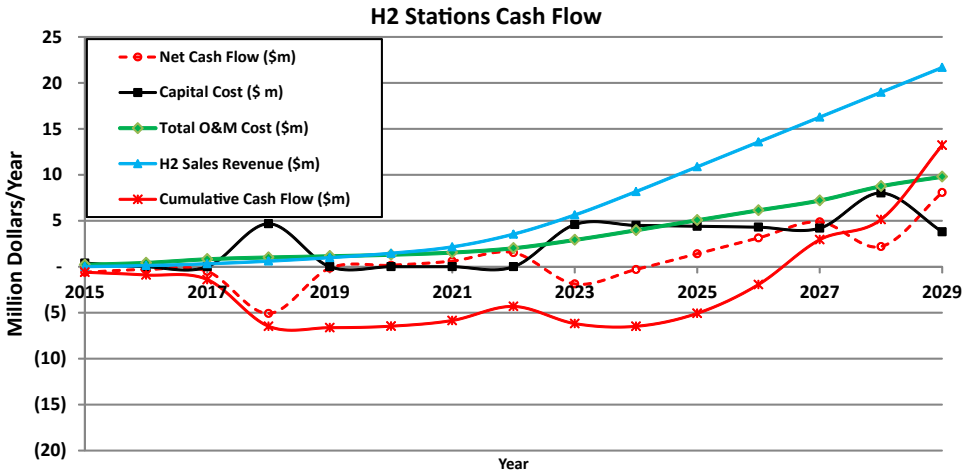

FIGURE 2. Hydrogen Stations Cash Flow for the LSF Strategy

has higher next-N-year NPV in the early period. LSF also has smaller government buy-down cost, which is defined as the cumulative sum of negative cash flows over the period. Namely, buy-down cost measures government subsidy cost if it wishes to pay for all losses before positive cash flows.

Table 1 shows total system cost (and infrastructure cost component in the parentheses) for the SSF and LSF scenarios under different assumptions of driving pattern. The reference driving pattern assumes drivers consists of 2% FLC, 2% frequent driver and short commute, 25% average driver and long commute, 25% average driver and short commute, 23% moderate driver and long commute, and 23% MSC. The percentage is calibrated to the 2009 National Household Travel Survey data. 100% FLC assumes early FCEV drivers are all frequent drivers with long commutes who have the highest fuel demand at local stations in the city, while 100% MSC assumes early FCEV drivers are all moderate drivers with short commutes who have the lowest fuel demand at local stations in the city. Table 1 shows the LSF scenario has lower system cost than the SSF scenario while the 100% FLC driving pattern leads to lower system cost than other mixes of driver groups.

TABLE 1. Total System Cost (and infrastructure cost component in the parentheses) for the SSF and LSF Scenarios

	Small Station First	Large Station First
Reference Driving Pattern	12.4 (9.2) $/kg	11.4 (7.8) $/kg
100% FLC	9.4 (5.9) $/kg	9.7 (6.4) $/kg
100% MSC	14.7 (11.7) $/kg	12.3 (8.5) $/kg

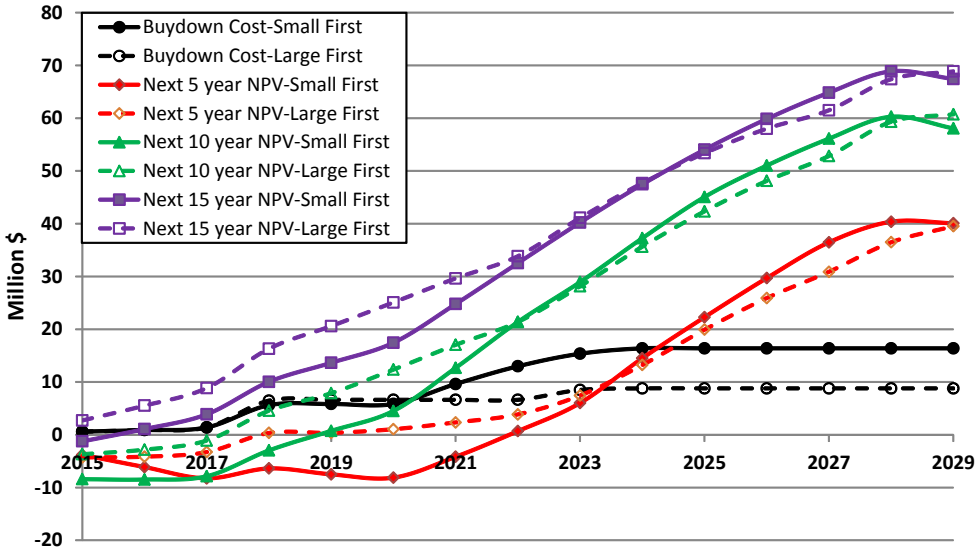

FIGURE 3. Buy-Down Cost and Next-N-Year NPV

CONCLUSIONS AND FUTURE DIRECTIONS

In summary, the project developed a preliminary version of the HySEB model that trades off infrastructure cost and fuel accessibility cost to find the optimal station deployment strategy. Cash flow analysis results suggest station networks at the city level may endure negative cash flows for about a decade. Station scale economy is important in planning station build-out, as illustrated by better cash flow and lower system cost of the LSF strategy. LSF delays the construction of additional stations for meeting early fuel demand. Investment risks perceived by investors would depend on their planning horizon, i.e., their investment patience. Limiting public subsidy would require more investor patience, and investors may be more patient if they perceive less technological and policy risk.

Future work will focus on model upgrade, uncertainty analysis, and public-private cost share mechanisms.

- Develop an optimization algorithm that identifies station placing and sizing strategy to minimize system cost
- Conduct uncertainty analysis, especially on fuel demand and station cost
- Integrate with consumer choice model and analyze the interplay between infrastructure and vehicle penetration by representing investor patience, risk, and hydrogen pricing
- Determine business viability for connector stations
- Conduct more analysis of public-private cost share mechanisms.

FY 2014 PUBLICATIONS/PRESENTATIONS

1. Zhenhong Lin, Changzheng Liu, and David Greene, Hydrogen Station Economics and Business (HySEB) -- Preliminary Results, 2014 DOE Fuel Cell Technologies Program Annual Merit Review June 17, 2014.

REFERENCES

1. Ogden, Joan M. and Michael A. Nicholas (2011) Analysis of a "Cluster" Strategy for Introducing Hydrogen Vehicles in Southern California. Energy Policy 39 (4), 1923–1938.

2. Joan Ogden, Design and Economics of an Early Hydrogen Refueling Network for California, 2013 DOE Fuel Cell Technologies Program Annual Merit Review, May 14, 2013.

X.8 Tri-Generation Fuel Cell Technologies for Location-Specific Applications

Kersey S. Manliclic, Brendan P. Shaffer (Primary Contact), Professor G. Scott Samuelsen
Advanced Power and Energy Program (APEP)
University of California, Irvine
Engineering Laboratory Facility, Bldg 323
Irvine, CA 92697-3550
Phone: (949) 824-7302 ext. 11127
Email: bps@apep.uci.edu

DOE Manager
Fred Joseck
Phone: (202) 586-7932
Email: Fred.Joseck@ee.doe.gov

Contract Number: XFC-4-23067-01

Project Start Date: January 1, 2014
Project End Date: January 1, 2015

Overall Objectives

Assess the potential number and location of tri-generation (Tri-Gen) fuel cell systems, producing electricity, high-quality waste heat, and hydrogen in an early fuel cell electric vehicle (FCEV) market scenario (circa 2015) in NY, NJ, CT, and MA:

- Consider use of natural gas and anaerobic digester gas as feedstock.
- Also consider the viability of the Tri-Gen units serving as a local hub for hydrogen production.

Fiscal Year (FY) 2014 Objectives

- Sensitivity studies:
  - Assess the effect that vehicle data sales selection/ market distribution has on the resulting necessary Tri-Gen and/or hydrogen refueling infrastructure.
- Complete the acquisition and cleanup of data regarding wastewater treatment plants (WWTP) and landfills.
- Complete the identification of Tri-Gen sites.
- Complete the identification of Tri-Gen central hubs.
- Estimate the hydrogen, electricity, and heat production from the aforementioned identified Tri-Gen sites.
- Conduct an economic analysis to compare cost of hydrogen across the different scenarios.

Technical Barriers

This project addresses the following technical barriers from the Systems Analysis section of the Fuel Cell Technologies Office Multi-Year Research, Development, and Demonstration Plan:

(A) Future Market Behavior

(B) Stove-piped/Siloed Analytical Capability

(E) Unplanned Studies and Analysis

This project will contribute to achievement of the following DOE milestones from the Systems Analysis section of the Fuel Cell Technologies Office Multi-Year Research, Development, and Demonstration Plan:

- Milestone 1.9: Complete analysis and studies of resource/feedstock, production/delivery, and existing infrastructure for technology readiness. (4Q, 2014)
- Milestone 1.12: Complete an analysis of the hydrogen infrastructure and technical target progress for technology readiness. (4Q, 2015)
- Milestone 1.13: Complete environmental analysis of the technology environmental impacts for hydrogen and fuel cell scenarios and technology readiness. (4Q, 2015)

FY 2014 Accomplishments

- Ascertained the locations of the WWTPs in NY, NJ, CT, and MA (~432 total).
- Ascertained the locations of the landfills in NY, NJ, CT, and MA (~96 total).
- Ascertained the locations of potential building heat and electrical loads in NY, NJ, CT, and MA via the U.S. Board on Geographic Names. These include schools, airports, hospitals, and so forth.
- Alternative vehicle sales data which serves as proxy for potential FCEV sales was combined with high resolution population data and used to determine an early FCEV market.
  - Subsequently, the number of hydrogen refueling stations to ensure 6-minute service coverage for that early FCEV market was determined.
- An initial analysis was completed which identifies favorable WWTPs and landfills to site a Tri-Gen system based on:
  - Covering the most alternative vehicle sales.
  - Serving as a central hub of hydrogen production and serving the most nearby hydrogen refueling stations as possible.

✧ ✧ ✧ ✧ ✧

FUTURE DIRECTIONS

- Refine the identification of WWTPs and landfills in the Northeast that would be favorable candidate sites for the deployment of Tri-Gen fuel cell systems operating on renewable biogas with an onsite hydrogen refueling station. Analysis will be repeated for the use of conventional natural gas.
- Refine the identification of WWTPs and landfills in the Northeast that could favorably serve as a central hub and provide hydrogen to nearby hydrogen refueling stations. The number of, and which specific hydrogen refueling stations that will be served by a given central hub site will be noted.
- Estimate the hydrogen, electricity, and heat production for the different Tri-Gen scenarios.
- An economic analysis will be done to compare the cost of hydrogen in the different scenarios considered (e.g., hub production versus onsite).

FY 2014 PUBLICATIONS/PRESENTATIONS

1. K.S. Manliclic, B.P. Shaffer (presenter), G.S. Samuelsen. Tri-Generation Fuel Cell Technologies for Location-Specific Applications. U.S. Department of Energy. 2014 Annual Merit Review. Washington D.C., June 8–12, 2014.

X.9 Electricity Market Valuation for Hydrogen Technologies

Josh Eichman (Primary Contact), Marc Melaina
National Renewable Energy Laboratory
15301 Denver West Parkway
Golden, CO 80401
Phone: (303) 275-3789; (303) 275-3836
Emails: Joshua.Eichman@NREL.gov; Marc.Melaina@nrel.gov

DOE Manager
Fred Joseck
Phone: (202) 586-7932
Email: Fred.Joseck@ee.doe.gov

Project Start Date: January 7, 2013
Project End Date: January 7, 2015

Overall Objectives

- Evaluate the ability of electrolyzers to bid into electricity markets
- Assess the value proposition for grid integration of hydrogen technologies
- Include hydrogen technologies into large-scale grid operation models

Fiscal Year (FY) 2014 Objectives

- Evaluate the ability of electrolyzers to bid into electricity markets
- Assess the value proposition for grid integration of hydrogen technologies
- Include hydrogen technologies into large-scale grid operation models

Technical Barriers

This project addresses the following technical barriers from the Systems Analysis section of the

Fuel Cell Technologies Office Multi-Year Research, Development, and Demonstration Plan:

(A) Future Market Behavior

(B) Stove-Piped/Siloed Analytical Capability

(D) Insufficient Suite of Models and Tools

Contribution to Achievement of DOE Systems Analysis Milestones

This project will contribute to achievement of the following DOE milestones from the System Analysis section of the Fuel Cell Technologies Office Multi-Year Research, Development, and Demonstration Plan:

- Milestone 1.5: Complete evaluation of hydrogen for energy storage and as an energy carrier to supplement energy and electrical infrastructure. (4Q, 2012)
- Milestone 1.9: Complete analysis and studies of resource/feedstock, production/delivery, and existing infrastructure for technology readiness. (4Q, 2014)

FY 2014 Accomplishments

- Determined, using operational data, that small (~40-kW) electrolyzers acting as demand response devices can respond sufficiently fast and for a long enough duration to participate in energy, capacity and ancillary service electricity markets.
- Created an optimization tool for analyzing the operation and economic competitiveness of hydrogen energy storage and demand response technologies.
- Performed an extensive review of methodology, inputs parameters and findings from industry and government stakeholders.
- Integrated the use of hydrogen storage and demand response technologies into a production cost model to determine grid system impacts.

INTRODUCTION

Hydrogen is a versatile element that can be used in a variety of applications including chemical and industrial processes, transportation and heating fuel as well as for electricity generation. Traditionally, hydrogen technologies focus on providing services to one sector; however, engaging multiple sectors has the potential to provide benefits to each sector and increase revenue potential. Additionally, electrolyzers are amenable to operation on renewable electricity so there is also the potential to reduce greenhouse gas and criteria pollutant emissions, while providing grid services.

Fuel cells and electrolyzers do not currently bid into the electricity market; however, dispatchable generation and loads are allowed to participate. There is potential to increase revenue by participating in electricity markets. The additional revenue received from dispatching the hydrogen technologies to support the grid can serve to increase the economic competitiveness of those technologies and accelerate the timetable for achieving the DOE hydrogen production cost targets.

APPROACH

This work involved three sequential activities: 1) Determine the requirements for participation in electricity markets and test electrolyzers to see if they are technically able to participate. Electrolyzers from the National Wind Technology Center were tested for response time, ramp-rate, turndown, startup time and shutdown time. 2) Develop an optimization tool capable of maximizing revenue from participation in electricity markets and the sale of hydrogen. This was done by modifying a price-taker model developed for analyzing energy storage to accommodate demand response devices and the sale of hydrogen. This tool was developed for the GAMS modeling environment and uses CPLEX as the solver. Historical prices from California in 2012 are used for energy, regulation, spinning and non-spinning reserve markets. With knowledge from the two previous steps for the most economic hydrogen system architectures, the final step is to 3) implement hydrogen technologies into a production cost model, PLEXOS. While the price-taker model presents the ideal operation to maximize profits the production cost model complements those results by calculating the optimal operation to support the larger grid system.

RESULTS

First, the operating flexibility of electrolyzers was tested using small (~40-kW) proton exchange membrane and alkaline electrolyzers. Electrolyzers acting as demand response devices can respond sufficiently fast and for long enough duration to participate in energy, capacity and ancillary service electricity markets. Furthermore, electrolyzers can be operated to support a variety of applications while also providing hydrogen for industrial processes, transportation fuel, or heating fuel. This opens new markets for electrolyzers and can aid in reaching the DOE hydrogen production cost targets by providing supplemental revenue streams. The results from the tests are summarized in the following and more details can be found in reference [1].

- Small electrolyzer systems begin changing their electricity demand within milliseconds of a set-point change
- The settling time after a set-point change is on the order of seconds
- Electrolyzers can reduce their electrical consumption for an unlimited amount of time
- Electrolyzers exhibit low part-load operation capabilities
- Electrolyzers can startup and shutdown in several minutes

Favorable operating properties and a variety of potential system architectures showcase the flexibility of hydrogen technologies. Figure 1 shows configurations for hydrogen equipment that we explore for economic competitiveness. Notice that multiple opportunities exist for each piece of

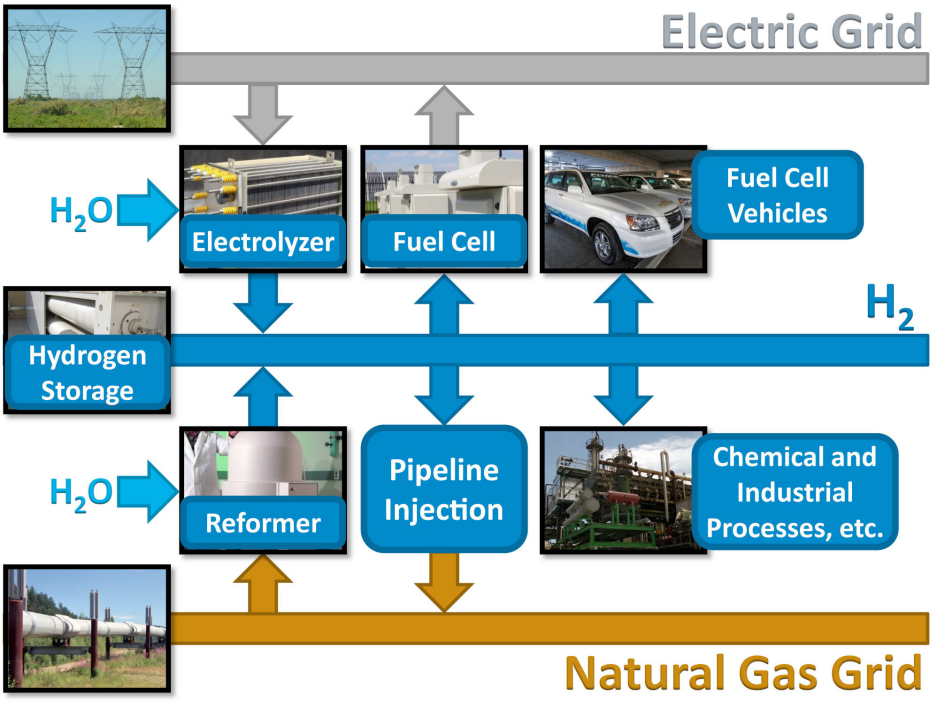

FIGURE 1. Hydrogen Technology Configurations[1]

[1] Picture sources (from top left by row), Path 26 Wikipedia GNU license; Matt Stiveson, NREL 12508; Keith Wipke, NREL 17319; Dennis Schroeder, NREL 22794; NextEnergy Center, NREL 16129; Warren Gretz, NREL 09830; David Parsons, NREL 05050; and Bruce Green, NREL 09408

equipment and depending on the configuration, multiple sectors become interconnected.

The maximum revenue achievable for each configuration was compared to the annualized cost to determine which systems are economically competitive (Figure 2). Hydrogen technologies (i.e., electrolyzer [EY], fuel cell [FC], and steam methane reformer [SMR]) are compared to conventional technologies (i.e., pumped hydro [HYPS] and lead acid batteries [batt]) and the competitiveness of not selling hydrogen (i.e., "no sale of H_2" means electricity-in, electricity-out devices) is compared to selling hydrogen at 80% capacity factor for the production equipment. List of assumptions can be found in Eichman, 2014 [Presentation 7]. Additionally, we compare different operation profiles including typical flat profile operation ("baseload"), providing only energy services ("Eonly") and providing both energy and ancillary services ("All")

It is clear that selling hydrogen can provide significantly more revenue than not selling hydrogen and strict electricity storage devices (e.g., electricity in, electricity out) using hydrogen are not competitive. In all cases, greater participation in electricity markets increased revenue. Devices providing both energy and ancillary services generate more revenue than devices only participating in energy markets. The demand response (i.e., last four on right) cases are particularly promising for hydrogen technologies. SMR is currently the widest used technology for hydrogen production and shows the greatest revenue margin but does not allow for integration with electricity markets. Electrolyzers are currently operated in baseload mode; however, there is significant value to capture from participating in electricity markets.

A sensitivity analysis is performed on the additional achievable value for increasing the energy capacity from 3 hours to 168 hours. Results for a fuel cell and electrolyzer storage device capable of providing both energy and ancillary services are presented in Figure 3. The revenue only slightly increases with additional capacity (i.e., 3.8% for $3/kg hydrogen and 1.2% for $10/kg hydrogen). This shows that more storage capacity is not necessarily more valuable in current energy and ancillary service markets. Aboveground steel tanks are used for storage so the cost increases linearly as the required storage capacity increases. Underground hydrogen storage could potentially reduce the cost for high volume storage; however, the revenue would not increase more on account of the storage technology used.

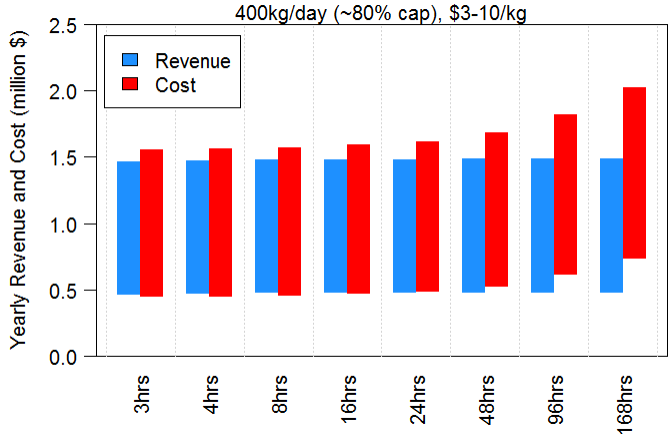

FIGURE 3. Storage Capacity Sensitivity Analysis

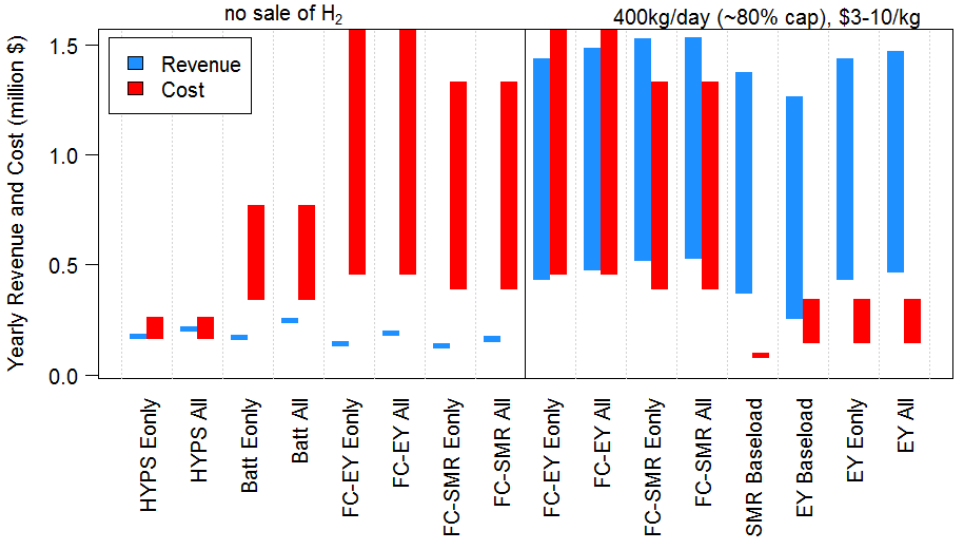

FIGURE 2. Comparison of Cost versus Electricity Market Revenue

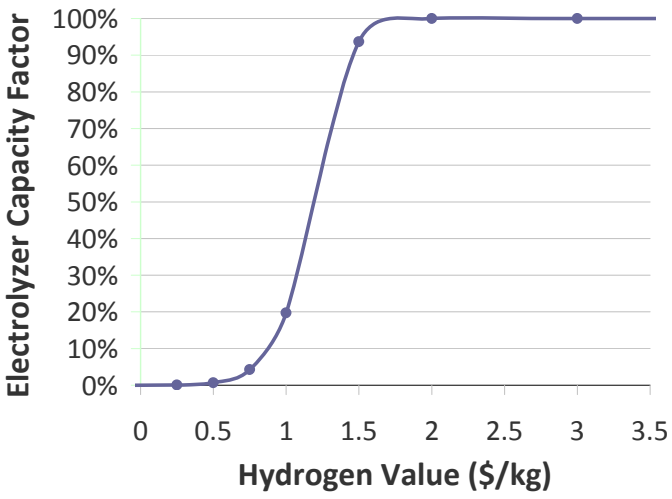

FIGURE 4. Electrolyzer Yearly Capacity Factor for Different Hydrogen Values from PLEXOS

We successfully integrated both hydrogen energy storage and demand response technologies into a production cost model. Figure 4 presents the electrolyzer yearly capacity factor with respect to hydrogen price. This shows how an electrolyzer operating as a demand response device changes operation with varying hydrogen sale price within California in 2022. With very low hydrogen prices, the grid receives the most value from participating in grid services but once the value of hydrogen is high enough, sale of hydrogen is more valuable than electricity (including arbitrage and ancillary services) and the capacity factor goes to 100%.

To the author's knowledge, this is the first time that hydrogen storage and demand response technologies have been integrated into a production cost model. The results offer great insight into the value of hydrogen from a utility or grid operator's point of view.

CONCLUSIONS AND FUTURE DIRECTIONS

This work bridges previously disconnected areas; that of hydrogen, and grid modeling and integration. From experimentally testing the operation parameters for electrolyzers it was found that they can respond sufficiently fast and for a long enough duration to participate in energy, capacity and ancillary service electricity markets. Knowing the flexibility of electrolyzers, we then explored the economic competitiveness of hydrogen technologies that participate in multiple sectors. We found 1) using hydrogen equipment to provide grid services has the potential to increase revenues beyond conventional operation, 2) the sale of hydrogen is important to achieve competitiveness; a strict electric storage device (electricity-in, electricity-out) is less competitive than technologies that sell hydrogen, and 3) additional energy storage capacity is not necessarily more competitive in current energy and ancillary service markets. Recognizing which configuration has the greatest potential can help to guide both industry and the DOE's decision making processes to maximize investments and to understand future market behavior.

One of the important factors that will impact the economics of having electrolyzers provide grid services is the impacts of variable operation on the operation and maintenance costs and lifetime of the equipment. This work did not consider the impacts of degradation on the stack or system; however, other NREL activities are exploring the impacts of variable electrolyzer operation on lifetime and stack performance. Economic comparisons were performed using California values for 2012, but looking at different years and different locations would improve the integrity of the results.

FY 2014 PUBLICATIONS/PRESENTATIONS

1. Eichman J., K. Harrison and M. Peters. (2014). "Novel Electrolyzer Applications: Providing more than just hydrogen," National Renewable Energy Laboratory. Golden, CO, NREL/TP-5400-61758 (In Review).

2. Eichman J., "Electricity Market Value for Fuel Cells and Electrolyzers," Presentation to FuelCell Energy on January 24, 2014.

3. Josh Eichman, "Electrolyzer Flexibility Study," Presentation to DOE FCTO on February 18, 2014.

4. Eichman J., "Electricity Market Value for Fuel Cells and Electrolyzers," Presentation to Xcel Energy on February 25, 2014.

5. Eichman J., "Electricity Market Valuation for Fuel Cells and Electrolyzers," Conference Presentation at ICEPAG in Irvine, California on April 2, 2014.

6. Eichman J., "H_2 Grid Integration: Tools and Analyses," Presentation at DOE/Industry Canada Hydrogen Energy Workshop in Sacramento, California on May 14, 2014.

7. Eichman J., "Electricity Market Valuation for Hydrogen Technologies," Presentation at the 2014 DOE Hydrogen and Fuel Cell Technologies Program Annual Merit Review on June 17, 2014.

REFERENCES

1. Eichman, J., K. Harrison and M. Peters. (2014). "Novel Electrolyzer Applications: Providing more than just hydrogen," National Renewable Energy Laboratory. Golden, CO, NREL/TP-5400-61758 (In Review).

XI. SMALL BUSINESS INNOVATION RESEARCH (SBIR) FUEL CELL TECHNOLOGIES OFFICE NEW PROJECTS AWARDED IN FY 2014

XI.0 Small Business Innovation Research (SBIR) Fuel Cell Technologies Office New Projects Awarded in FY 2014

The Small Business Innovation Research (SBIR) program provides small businesses with opportunities to participate in DOE research activities by exploring new and innovative approaches to achieve research and development (R&D) objectives. The funds set aside for SBIR projects are used to support an annual competition for Phase I awards of up to $225,000 each for about nine months to explore the feasibility of innovative concepts. Phase II R&D efforts further demonstrate the technologies to move them into the marketplace, and these awards are up to $1,500,000 over a two-year period. Small Business Technology Transfer (STTR) projects include substantial (at least 30%) cooperative research collaboration between the small business and a non-profit research institution.

Table 1 lists the SBIR Phase I and Table 2 lists the STTR Phase II projects awarded in FY 2014 related to the Hydrogen and Fuel Cells Program. Brief descriptions of each project follow.

TABLE1. FY 2014 SBIR Phase I Projects Related to the Hydrogen and Fuel Cells Program

	Title	Company	City, State
XI.1	Ionomer Dispersion Impact on Advanced Fuel Cell and Electrolyzer Performance and Durability	Giner, Inc.	Newton, MA
XI.2	Demonstration of a Prototype Fuel Cell-Battery Electric Hybrid Truck for Waste Transportation	US Hybrid	Torrance, CA
XI.3	Demonstration of a Prototype Fuel Cell Electric Truck for Waste Transportation	Vision Motor Corp.	Long Beach, CA
XI.4	Flexible Barrier Coatings for Harsh Environments	GVD Corporation	Cambridge, MA
XI.5	New Approaches to Improved PEM Electrolyzer Ion Exchange Membranes	Tetramer Technologies LLC	Pendleton, SC
XI.6	High-Performance Proton Exchange Membranes for Electrolysis Cells	Amsen Technologies LLC	Tucson, AZ
XI.7	High-Temperature High-Efficiency PEM Electrolysis	Giner, Inc.	Newton, MA

TABLE 2. FY 2014 SBIR Phase II Projects Related to the Hydrogen and Fuel Cells Program

	Title	Company	City, State
XI.8	Optimizing the Cost and Performance of Composite Cylinders for H2 Storage using a Graded Construction	Composite Technology Development, Inc.	Lafayette, CO
XI.9	Novel Structured Metal Bipolar Plates for Low-Cost Manufacturing	Treadstone Technologies, Inc.	Princeton, NJ
XI.10	Cryogenically Flexible, Low Permeability Thoraeus Rubber Hydrogen Dispenser Hose	NanoSonic, Inc	Pembroke, VA

PHASE I PROJECTS

XI.1 Ionomer Dispersion Impact on Advanced Fuel Cell and Electrolyzer Performance and Durability

Giner, Inc.
89 Rumford Avenue
Newton, MA 02466-1311

The project will develop advanced membrane and electrode components that may significantly enhance the durability and performance of proton exchange membrane fuel cells. Enhanced durability and performance will lead to more cost reduction and public acceptance of hydrogen vehicles. The widespread deployment of hydrogen vehicles will relieve the nation's heavy dependence on imported oil and reduce air pollutants.

XI.2 Demonstration of a Prototype Fuel Cell-Battery Electric Hybrid Truck for Waste Transportation

US Hybrid
445 Maple Avenue
Torrance, CA 90503-3807

The fuel cell refuse truck has no emissions, saves 17,000 barrels of imported oil with $4.2M fuel savings over its operational life and has less than three years return on investment. It is cleaner, quieter and friendlier to operate with a fuel cell power plant enabling mobility via renewable energy.

XI.3 Demonstration of a Prototype Fuel Cell Electric Truck for Waste Transportation

Vision Motor Corp.
2230 E. Artesia Blvd.
Long Beach, CA 90805

This project will prototype a Class 8 hydrogen fuel cell electric refuse truck that will be placed in demonstration service with the Santa Monica Publics Works Division in the City of Santa Monica, California. This project aims to measure and demonstrate operational cost effectiveness, emission reduction, and commercial viability of a heavy-duty fuel cell electric vehicle in the refuse service.

XI.4 Flexible Barrier Coatings for Harsh Environments

GVD Corporation
45 Spinelli Place
Cambridge, MA 02138

The project will develop a barrier coating for o-rings and other high-pressure hydrogen seals to prevent hydrogen from permeating the seal even at 200°C and 700 bar. They are partnered with Green Tweed and the Massachusetts Institute of Technology. The new barrier coating will reduce permeability of the seals by 10x compared to the uncoated seal baseline performance.

XI.5 New Approaches to Improved PEM Electrolyzer Ion Exchange Membranes

Tetramer Technologies LLC
657 S. Mechanic Street
Pendleton, SC 29670

Tetramer Technologies, LLC, has developed a new membrane molecular architecture, which has demonstrated equivalent or better performance to the current Nafion® materials under automotive fuel cell conditions at 50% lower cost. These attributes directly address the DOE high electrolyzer cost and performance issues. Key attributes of Tetramer's technology vs. the current Nafion® electrolyzer membranes are improved physical performance properties, 50% lower hydrogen permeability and equal or higher conductivity. This technology will provide thinner membranes which can lower costs and increase performance directly through decreased ionic resistance, and indirectly through the reduction of the overall cell potential. Tetramer's membranes can also provide 50% less hydrogen crossover loss, thus improving the electrolyzer yield and lowering costs.

XI.6 High-Performance Proton Exchange Membranes for Electrolysis Cells

Amsen Technologies LLC
1684 S. Research Loop, Suite 518
Tucson, AZ 85710

This project aims to develop high-performance ion-exchange membranes for proton exchange membrane electrolyzers based on a ternary material system. Such membranes shall have lower hydrogen permeability and higher proton conductivity than the state-of-the-art commercial membranes. Additionally, the new membrane shall have good water transfer capability, high tensile strength, and high stability under high-pressure electrolyzer operating conditions.

XI.7 High-Temperature High-Efficiency PEM Electrolysis

Giner, Inc.
89 Rumford Ave.
Newton, MA 02466

This project is a combined Phase I and Phase II award that will examine different membrane chemistries and additives in an effort to increase electrolyzer efficiency through a novel membrane electrode assembly (MEA). This MEA will be operated at higher than usual temperature and will withstand operation at high differential pressure through the use of this company's proprietary technology. Phase I will consist of fabricating membranes of various chemistries with the goal of increasing high-pressure efficiency. These membranes will be extensively characterized; with the top performers identified by the end of Phase I. Phase II will encompass short-term durability and performance testing of the membranes as electrolysis MEAs in moderate-pressure cells, with tasks for further membrane improvement from data gathered. Phase II ends with long-term durability testing of the top MEAs in multi-cell stack configurations and full (5,000 psi) pressure.

PHASE II PROJECTS

XI.8 Optimizing the Cost and Performance of Composite Cylinders for H2 Storage using a Graded Construction

Composite Technology Development, Inc.
2600 Campus Drive, Suite D
Lafayette, CO 80026-3359

Composite Technology Development will perform detailed design iterations using laminate analysis and finite element analysis to optimize the cost of a 700-bar hydrogen storage vessel using a graded construction (T700 on inside and textile polyacrylonitrile on outside). They will develop a model that incorporates accurate hoop strains with decreased radial/tangential ratios (increased wall thicknesses). They predict a cost savings of at least 25% over the current cost of Type IV 700-bar tanks. Composite Technology Development will also tailor fiber sizing and epoxy matrices that can harness the maximum achievable properties of the low-cost carbon fibers from Oak Ridge National Laboratory. Over the past 5–10 years, Oak Ridge National Laboratory has developed low-cost, textile-polyacrylonitrile funded by the DOE that has been qualified at intermediate strength which is what will be used in this project.

XI.9 Novel Structured Metal Bipolar Plates for Low-Cost Manufacturing

Treadstone Technologies, Inc.
201 Washington Road
Princeton, NJ 08540

The focus of this SBIR project is to develop a low-cost novel structured metal bipolar plate technology for low-temperature proton exchange membrane fuel cells for transportation applications. The innovative metal bipolar plate technique is aimed to meet industry revised performance and cost requirements for metal bipolar plates. This project goes beyond TreadStone's current low-cost metal plate technology that uses a very small amount of gold for low-temperature proton exchange membrane fuel cell applications. It will develop a gold-free metal plate coating technology that meets the revised requirements from industry, including: (i) gold-free coating; (ii) lower electrical contact resistance, and (iii) roll-to-roll coating on stainless steel foil strips, before stamping. In Phase II of the project, TreadStone plans to scale up this technology to roll-to-roll fabrication scale, and demonstrate the technology in a full-size, short stack in automobile fuel cells at Ford Motor. The proposed project is built on three pillars: (1) robust experimental evidence demonstrating the feasibility of our technology, (2) a team that consists of industrial leaders in fuel cell stack application, design, and manufactures; and (3) a low-risk, significant-milestone driven project that proves the feasibility of meeting project objectives. The implementation of this project will reduce the fuel cell stack metal bipolar separator plate cost which accounts 15-21% of the overall stack cost. The gold-free solution will reduce the cost risk associated with the rapid raising gold price of current metal plate technologies. The roll-to-roll processing capability will reduce the capital investment for the corrosion-resistant plate fabrication. In combination, all these improved plate attributes will help the market penetration of in current early stage of fuel cell commercialization.

XI.10 Cryogenically Flexible, Low Permeability Thoraeus Rubber Hydrogen Dispenser Hose

NanoSonic, Inc
158 Wheatland Drive
Pembroke, VA 24136

During Phase II, NanoSonic Inc. will work on developing a safe, reliable, and cost-effective hose for use at hydrogen refueling stations. The hose needs to perform in high pressure and cryogenic temperature environments while maintaining durability and low hydrogen permeability. The proposed technology utilizes NanoSonic's Thoraeus Rubber technology, that is comprised of multifunctional, low-glass-transition-temperature copolymer resins that are modified with alternating layers of nanoparticles with high and low atomic numbers for radiation resistance and electrostatic discharge protection for the hoses. These cost-effective, grounded hoses offer a unique business case in terms of cost savings through reduced replacement and maintenance compared to currently available hose materials. NanoSonic has six partners on the project including the National Renewable Energy Laboratory, Swagelok, and manufacturing partner, New England Wire Technology Inc.

XII. Acronyms, Abbreviations, and Definitions

~	Approximately
@	At
°C	Degrees Celsius
°F	Degrees Fahrenheit
Δ	Change, delta
ΔG	Gibbs free energy of reaction
ΔH	Enthalpy of reaction, Enthalpy of hydrogenation
ΔH°_{f}	Standard heat of formation
ΔK	Stress intensity factor
ΔP	Pressure drop, pressure change
≈	Equals approximately
>	Greater than
≥	Greater than or equal to
<	Less than
≤	Less than or equal to
µ	Micro (one-millionth; 0.000001)
µA	Microampere(s)
$\mu A/cm^2$	Microampere(s) per square centimeter
µc-Si	Microcrystalline silicon
µg	Microgram(s)
µCHP	Micro-combined heat and power
µCHX	Microscale combustor/heat exchanger
µm	Micrometer(s); micron(s)
µM	Micromolar
µmol	Micromole(s)
$\mu\Omega\text{-}cm^2$	Micro-ohm(s)-square centimeter
µV	Microvolt(s)
η	Viscosity
#	Number
Ω	Ohm(s)
Ω/cm^2	Ohm(s) per square centimeter
$\Omega\text{-}cm^2$	Ohm-square centimeter(s)
%	Percent
®	Registered trademark
$	United States dollars
^{11}B-NMR	Boron 11 nuclear magnetic resonance
1-D, 1D	One-dimensional
1Q	First quarter of the fiscal year
2-D, 2D	Two-dimensional
2Q	Second quarter of the fiscal year
3-D, 3D	Three-dimensional
3DSM	Dimensionally stable membrane with 3-dimensional porous support
3-L	Three-layer
3Q	Third quarter of the fiscal year
4Q	Fourth quarter of the fiscal year
5-L	Five-layer
6FBPS0	Hexafluoro biphenol sulfone
6FCN-x	Hexafluoro bisphenol A based disulfonated polybenzonitrile (H+ form) (x denotes degree of sulfonation)
6FK	Hexafluoro ketone; Partially fluorinated poly(arylene ether ketone)
6FPAEB	Hexafluoro bisphenol a benzonitrile
8YSZ	8 mol% yttria-stabilized zirconia
A	Ampere(s), amp(s)
Å	Angstrom(s)
AAC	Advanced anode catalyst
AB	Ammonia-borane, NH_3BH_3
ABH_2	Ammonium borohydride, NH_4BH_4
ABS	American Bureau of Shipping
AC	Alternating current; Activated carbon
A-CCC	Activated carbon composite catalyst
ACF	Activated carbon fibers
A/cm^2	Amps per square centimeter
ACN	Acetonitrile
ACNT	Aligned carbon nanotube
ADG	Anaerobic digester gas
AEM	Anion exchange membrane; Analytical electron microscopy
AEO	Annual Energy Outlook
AFDC	Alternative Fuels Data Center
AFM	Atomic force microscopy; Anti-ferromagnetic
AFP	Automated fiber placement
Ag	Silver
AGC	Activated graphitic carbon
AgCl	Silver chloride
A-h	Amp-hour(s)
AHJ	Authorities having jurisdiction
AISI	American Iron & Steel Institute
AIST	Japanese National Institute of Advanced Industrial Science and Technology
AK	Alkali
a.k.a.	Also known as

Al	Aluminum
Al_2O_3	Aluminum oxide
Al-AB	Aluminum-ammonia-borane
$AlCl_3$	Aluminum chloride
ALD	Atomic layer deposition
AlH_3	Aluminum hydride; Alane
ALS	Advanced Light Source at Lawrence Berkeley National Laboratory
ALT	Accelerated life test
AM	Air mass
AM 1.5	Air Mass 1.5 solar illumination
AM1.5G	Air Mass 1.5 Global (solar spectrum)
AMBH	Amine metal borohydride
AMC	Aminomethyl-cyclohexane
AMFC	Anion exchange membrane fuel cell; Alkaline membrane fuel cell
AMR	Annual Merit Review
AN	Acrylonitrile
ANL	Argonne National Laboratory
ANOVA	Analysis of variance
ANSI	American National Standards Institute
A_o	Arrhenius constant, ml/[cm^2-min-atm½]; Availability
APCI, APCi	Air Products and Chemicals, Inc.
APR	Aqueous-phase reforming
APU	Auxiliary power unit
AQMD	Air Quality Management District
Ar	Argon
AR	Areal resistance
ARPA-E	Advanced Research Projects Agency–Energy
ARRA	American Recovery and Reinvestment Act
As	Arsenic
ASAXS	Anomalous small-angle X-ray scattering
a-Si	Amorphous silicon
a-SiC	Amorphous silicon carbide
a-SiGe	Amorphous silicon germanium
a-SiN	Amorphous silicon nitride
ASME	American Society of Mechanical Engineers
ASPEN	Modeling software, computer code for process analysis
ASR	Area-specific resistance
AST	Accelerated stress test
ASTM	ASTM International, originally known as the American Society for Testing and Materials
AT	Ammonia triborane
at%	Atomic percent
atm	Atmosphere(s)
ATM-PP	Benzyl trimethyl ammonium functionalized poly(phenylene) anion exchange membrane
ATP	Adenosine triphosphate; Advanced Technology Program
ATPase	Adenosine triphosphatase
ATR	Autothermal reformer; Autothermal reforming; Attenuated total reflection
ATR-FTIR	Attenuated total reflectance Fourier transform infrared
a.u.	Arbitrary units
Au	Gold
AuS	Gold sulfide
$AuSnO_x$	Gold supported on hydrous tin oxide
$AuTiO_x$	Gold supported on titanium oxide
Autonomie	Plug-and-Play Powertrain and Vehicle Model Architecture and Development Environment software model by Argonne National Laboratory to support the rapid evaluation of new powertrain/propulsion technologies for improving fuel economy through virtual design and analysis in a math-based simulation environment
Avg	Average
AZO	Aluminum zinc oxide
^{11}B-NMR	Boron 11 nuclear magnetic resonance
B	Boron
B_2O_3	Boron oxide; Diboron trioxide
Ba	Barium
BAM	Bundesanstalt für Materialforschung und -prüfung (Federal Institute for Materials Research and Testing)
Bara	Bar absolute
barg	Bar gauge
BCC	Body-centered cubic
BCN	Boron carbon nitride
BDC	Benzenedicarboxylic acid
Be	Beryllium
BES	Basic Energy Sciences office within the DOE Office of Science
BESS	Battery energy storage system
BET	Brunauer-Emmett-Teller surface area analysis method
BEV	Battery electric vehicle
BFZ0	$BaFe_{0.975}Zr_{0.025}O_3$
BFZ1	$BaFe_{0.90}Zr_{0.10}O_3$
B-G	Boron doped graphitic material
BG-DW	65% bio-glycol-35% distilled water

B-H	Boron/hydrogen bond
B-H, BH, BH_4	Borohydride
BHP	Butyl perhydropyrolidine
Bi	Bismuth
BLASTP	Basic Local Alignment Search Tool – Protein
BM	Base metal
$bmimBF_4$	1-butyl-3-methyl-imidazolium tetrafluoroborate
bmimCl	1-butyl-3-methyl-imidazolium chloride
bmimOTf	1-butyl-3-methyl-imidazolium triflate
$bmimPF_6$	1-butyl-3-methyl-imidazolium hexafluorophosphate
BMPFFP	1-butyl-1-methyl-pyrrolidinium tris(pentafluoroethyl)trifluorophosphate
BN	Boron-nitrogen
BNH	Boron-nitrogen-hydrogen
BNHx	Dehydrogenated ammonia-borane
BNL	Brookhaven National Laboratory
BNNT	Boron nitride nanotubes
B-O	Any oxidized boron species, borate
Boc	Tert-butoxycarbonyl
BOC	Best of class
$B(OH)_3$	Boric acid
BOL	Beginning of life
BOP, BoP	Balance of plant
BOT	Beginning of test
BP	Bisphenol; Biphenyl
bpe	Bis(4-pyridyl)ethane
BPEE	1,2-bipyridylethene
BPDC	Biphenyl-4,4’-dicarboxylate
BPP	Bipolar plate
BPPPO	Biphenol-based phenyl phosphine oxide
BPPPO-35	Biphenol-based phenyl phosphine oxide copolymer, 35% molar fraction of disulfonic acid unit (35% level of sulfonation)
BPS	Ballard Power Systems
BPS	Bi Phenyl Sulfone
BPS100	Fully disulfonated poly(arylene ether sulfone)
BPSH	Block polysulfone ether polymer; Bi Phenyl Sulfone: H Form
BPSH-30	Biphenyl sulfone H form, 30% molar fraction of disulfonic acid unit (30% level of sulfonation)
BPSH-x	BiPhenyl based disulfonated polySulfone (H+ form) (x denotes degree of sulfonation)
BPVC	Boiler and Pressure Vessel Code
BPVE	Perfluorocyclobutane-biphenyl vinyl ether
BPVE-6F	Perfluorocyclobutane-biphenyl vinyl ether hexafluoroisopropylidene
BPy	2,2’-bipyridine
BPY	4,4’-bypyridine
bpydc	Bipyridine dicarboxylate
Br	Bromine
Br_2	Diatomic bromine
BTB	1,3,5-benzenetribenzoate
BTC	1,3,5-benzenetricarboxylate
BTE	4,4’,4’’-(benzene-1,3,5-triyltris(ethyne-2,1-diyl))tribenzoate
BTMA	Benzyltrimethylammonium
BTT	Benzene tris-tetrazole
BTTCD	Octa-carboxylate ligand
BTU, Btu	British thermal unit(s)
Bu_3SnCl	Tributyltin chloride
$Bu_3SnSnBu_3$	Hexabutyldistannane
BV	Benzyl viologen
BxHy	Polyhedral boranes
BZYC	$BaZr_{0.1}Ce_{0.7}Y_{0.1}Yb_{0.1}O_{3-\delta}$
C	Carbon; Couloumb
C_2H_4	Ethylene
C_2H_6	Ethane
C_3H_8	Propane
Ca	Calcium
CA	Carbon aerogel; Chronoamperometry
$CaBr_2$	Calcium bromide
$CaCO_3$	Calcium carbonate
CAD	Computer-aided design
CAE	Computer-assisted engineering
CAER	Center for Applied Energy Research
CaFCP	California Fuel Cell Partnership
CaI	*Clostridium acetobutylicum* hydrogenase
CaO	Calcium oxide
CARB	California Air Resources Board
CaS	Calcium sulfide
CaSFCC	California Stationary Fuel Cell Collaborative
CB	Conduction band; Carbon black
CBECS	Commercial Building Energy Consumption Survey
CbHS	Carbon-based hydrogen storage
CBM	Conduction band minimum
CBN	Carbon-boron-nitrogen
CBS	Casa Bonita strain; Complete basis set
cc	Cubic centimeter(s)

CCC	Carbon composite catalyst
CCD	Charge-coupled device; Catalyst coating on decal
CCDM	Catalyst coating on diffusion media
cc/g cat/hr	Cubic centimeter(s) per gram catalyst per hour
CcH2	Cryo-compressed hydrogen
CCHSS	Complex Compound Hydrogen Storage System
CCL	Cathode catalyst layer
CCM	Catalyst-coated membrane
cc/min, ccm	Cubic centimeters per minute
ccp	Cubic close-packing
CCS	Carbon capture and storage
CC&S	Carbon capture and sequestration
CCVJ	9-([E]-2-carboxy-2-cyanovinyl)julolidine
Cd	Cadmium
CD	Current density; Charge depleting; Cathode dewpoint
Cdl	Double layer capacitance
cDNA	Complementary DNA
CDO	Code development organization
CDP	Composite data product
CdS	Cadmium sulfide
C-DSM™	Chemically etched dimensionally stable membrane
Ce	Cerium
CEA	Commissariat à l'Energie Atomique
CEC	California Energy Commission
CEM	Compressor expander motor (module)
CeO_2	Ceric oxide
CF	Carbon fiber; Carbon foam
CFC	Chlorofluorocarbon
CFD	Computational fluid dynamics
CFF	Complex coolant fluid
cfm	Cubic feet per minute
CGA	Compressed Gas Association
CGH2	Compressed gaseous hydrogen
CGM	Charge-generating material
CGO	Cerium gadolinium oxide, Gd-doped CeO_2
CGS	Copper gallium diselenide, $CuGaSe_2$
$CGSe_2$	Copper gallium diselenide
CH	Chemical hydride; Chemical hydrogen
cH_2	Compressed hydrogen gas
CH_4	Methane
CHEX	Continuous catalytic heat exchanger
CHG	Compressed hydrogen gas
CHHP	Combined heat, hydrogen, and power
Chl	Chlorophyll
CHMC1	Test Method for Evaluating Material Compatibility for Compressed Hydrogen Applications–Phase I-Metals
CHP	Combined heat and power
CHPFC	Combined heat and power fuel cell
CHS	Chemical hydrogen storage
CHSCoE	Chemical Hydrogen Storage Center of Excellence
$CIGSe_2$	Copper indium gallium diselenide
CIGS	Copper indium gallium diselenide
Cl	Chlorine
CL	Catalyst layer; ε-caprolactone
C-L	Circumferential-longitudinal
cm	Centimeter
CM	Controls module
cm^2	Square centimeter
CMO	Conductive metal oxides
CMWNT	Carbon multi-walled nanotube
CN	Carbon-nitrogen
CNC	Carbon nanocage
CNF	Carbon nano-fiber
CNG	Compressed natural gas
CNT	Carbon nanotube
Co	Cobalt
CO	Carbon monoxide
CO_2	Carbon dioxide
CO_{2e}	Carbon dioxide equivalent
COD	Chemical oxygen demand
COE	Cost of electricity
COF	Covalent-organic framework
COF_2	Carbonyl fluoride
COGS	Cost of goods sold
COMSOL	Multiphysics modeling and engineering simulation software
COPV	Composite overwrapped pressure vessel
COS	Carbon oxysulfide; Carbonyl sulfide
COx	Oxides of carbon
c_p	Specific heat
cp	Commercial purity
cP	Centipoise
CpI	*Clostridium pasteurianum* [FeFe]- hydrogenase
CPMAS	Cross polarization magic angle spinning

CPO, CPOX	Catalytic partial oxidation
c.p.s.	Counts per second
CPU	Computer processing unit
CPV	Composite pressure vessel
Cr	Chromium
CRADA	Cooperative Research and Development Agreement
CRCC	Corrosion-resistant conducting catalytic
CRTP	Corrosion-resistant transparent protective
Cs	Cesium
C&S	Codes and standards
CSA	Canadian Standards Association; Cell stack assembly
CSMP	Cabot Superior MicroPowders
CSTT	Codes and Standards Tech Team
CSU	California State University
CSULA	California State University, Los Angeles
CT	Computed tomography; Compact tension
CTA	Charge transfer agent
CTAB	Cetyl trimethyl ammonium bromide
CTB	Cyclotriborazane
CTE	Coefficient of thermal expansion
CTS	Charge transfer salt
CTTRANSIT	Connecticut Transit
Cu	Copper
CU	University of Colorado
Cu_2O	Cuprous oxide
$CuBiW_2O_8$	Copper bismuth tungstate
CuBTC	Cu_3(1,3,5-benzenetricarboxylate [BTC])$_2(H_2O)_3$
cu in.	Cubic inch
$CuInGaS_2$	Copper indium gallium sulfide
CuNW	Copper nanowire
CuO	Cupric oxide; Copper(II) oxide
CuTDPAT	Cu_3(2,4,6-tris(3,5-dicarboxylphenylamino)-1,3,5-triazine)$(H_2O)_3$
$CuWO_4$	Copper tungstate
cu.yd.	Cubic yard(s)
CV	Cyclic voltammetry; Cyclic voltammogram
CVD	Chemical vapor deposition
CVS	Chemical vapor synthesis
CWG	Catalysis Working Group
CWRU	Case Western Reserve University
CY	Calendar year
CZO	Ceria-zirconia
d	Day(s)
D_2	Deuterium
D-A	Dubinin-Astakhov
DAC	Diamond anvil cell
DADB	Diammoniate of diborane, $[(NH_3)_2BH_2][BH_4]$
da/dN	Fatigue crack growth rate
DAKOTA	Design Analysis Kit for Optimization and Terascale Applications
DB	Diborane (B_2H_6)
dB(A)	Decibel(s) A scale
DBBPDSA	4, 4'-dibromobiphenyl 3, 3'-dislufonic acid, monomer
DBPDSA	1, 4-dibromo phenylene 2, 5-disulfonic acid
DC	Direct current
DCTDD	1,8-diazacyclotetradecane-2,7-dione
DDMEFC	Direct dimethyl ether fuel cell
DDP	Detailed Data Product
d_{DR}	Dubini-Radushkevich average micropore diameter
DDR	A zeolite structure code
DEF	Diethylformamide
Deg	Degree
DEGDBE	Diethylene glycol dibutyl ether
ΔB_a	The difference in magnetic induction at high and low applied magnetic fields
ΔG	Gibbs free energy of reaction
ΔH	Enthalpy of reaction; Enthalpy of hydrogenation
$\Delta H°_f$	Standard heat of formation
ΔK	Stress-intensity factor
ΔP	Pressure drop; Pressure change
ΔT	Temperature change
DEMS	Differential electrochemical mass spectroscopy
DFM	Design for manufacturing
DFMA®	Design for Manufacturing and Assembly
DFT	Density functional theory
DGDE	Di-ethylene glycol di-butyl ether
DHBC	2,5-dihydroxybenzene dicarboxylate
DI	Deionized; De-ionized water
DLC	Diamondlike carbon
dL/g	Deciliters per gram
DM	Diffusion media
DMA	Dimethylacetamide
DMAc	Dimethyl acetamide
DMC	Diffusion Monte Carlo; Direct manufactured cost

DMDF	2,5-dimethoxy 2,5-dihydrofuran
DMDS	Dimethyldisulfide
DME	Dimethyl ether; Dimethoxyethane
DMEA	Dimethlethylamine
DMEAA	Dimethlethylamine alane
DMF	n, n-di-methyl formamide
DMFC	Direct methanol fuel cell
$dmimMeSO_4$	1,3-dimethyl-imidazolium methylsulfate
dmpe	Dimethylphosphinoethane
DMPO	5,5-Dimethylpyrroline-N-oxide
DMSO	Dimethyl sulfoxide
DMT	Dimethyltrityl
DMTHF	Dimethyltetrahydrofuran
DNA	Deoxyribonucleic acid
DNG	Desulfurized natural gas
DNI	Direct normal insolation
dobdc	2,5-dioxido benzene-1,4-dicarboxylate
dobpdc	Dioxido-biphenyl-dicarboxylate
DOD	Depth of discharge; Department of Defense
DOE	Department of Energy
DOT	Department of Transportation
DP	Dew point
DRIFTs	Diffuse reflectance infrared Fourier transform spectroscopy
DSC	Differential scanning calorimetry; Dynamic scanning calorimetry
DSM™	Dimensionally stable membrane
DSM-MC	Distance scaling method Monte Carlo
DVBPC	Divinyl aryl ether monomer
DVD	Digital video disk
DVMT	Daily vehicle miles traveled
DWG	Durability Working Group
e^-	Electron
E	Activation energy, kJ/mol
E_0xE_1	Utilization efficiency of incident solar light energy
$E_{1/2}$	Half-wave potential
E85	85%-15% blend of ethanol with gasoline
Ea	Activation energy
EA	Environmental assessment
E_{ad}	Hydrogen adsorption heat
EAN	Ethylammonium nitrate
EASA	Electrochemically active surface area
E-BOP	Electrical balance of plant
EBSD	Electron backscatter diffraction
EC	European Commission; Electro-chemical; Evaporative-cooled; Efficiency of conversion; Electrochemical capacitance
ECA	Electrochemical area
ECB	Ethylcyclobutane
ECC	Electrochemical compressor; Engineered cementitious composite
ECE	Economic Commission for Europe
ECS	Equilibrium crystal shape
ECSA	Electrochemically active surface area; Electrochemical surface area; Effective catalyst surface area
ECV	Electrochemical capacitance voltage
ED	Ethylenediamine
EDA	Ethylene diamine; Energy decomposition analysis
EDAX	Manufacturer of energy dispersive X-ray hardware and software
EDBB	Ethylenediamine bisborane
EDC	Energy distribution curve
edmimCl	2-ethyl-1,3-dimethyl-imidazolium ethylsulfate
EDP	Electrophoretic deposition
EDS	Energy dispersive X-ray spectroscopy; Energy dispersive spectrum
EDTA	Ethylenediamine tetraacetic acid
EDX	Energy dispersive X-ray
EELS	Electron energy loss spectroscopy
EERE	U.S. DOE Office of Energy Efficiency and Renewable Energy
EFR-AHJ	Emergency first responder-authorities having jurisdiction
EFTE	Ethylene-tetrafluoroethylene
e.g.	*Exempli gratia*: for example
EGR	Exhaust gas recirculation
EHC	Electrochemical hydrogen compressor
EHS	Environmental Health and Safety
EIA	Energy Information Administration of the U.S. Department of Energy
EIGA IGC	European Industrial Gases Association/ Industrial Gases Council
EIHP	European Integrated Hydrogen Project
EIS	Electrochemical impedance spectroscopy
EISF	Elastic incoherent structure factor
ELAT®	Registered Trademark of De Nora North America, Inc., covers GDLs and GDEs
EMA	Effective medium approximation
EMF	Electromagnetic field

EMI	Electro magnetic interference
EMPA	Electron microprobe analysis
ENABLE	Energetic neutral atom beam lithography/ epitaxy
ENG	Expanded natural graphite
eNMR	Electrochemical nuclear magnetic resonance
EODC	Electro-osmotic drag coefficient
EOL	End of life
EOT	End of test
EPA	Environmental Protection Agency
EPD	Electrophoretic deposition
EPDM	Ethylene propylene diene monomer
EPHC	Ethylperhydrocarbazole
ePTFE	Expanded polytetrafluoroethylene
ER	Emergency responder
ERW	Electric resistance weld
ES	Energy storage
ESA	Electrochemical surface area
ESEM	Environmental scanning electron microscope
ESE(T)	Eccentrically loaded, single edge tension
ESIF	Energy Systems Integration Facility
et al.	*Et Alii:* and others
ETA	Event tree analysis
etc.	*Et cetera*: and so on
E-TEK	Division of De Nora North America, Inc.
ETFE	Ethylene-tetrafluoroethylene
ETFECS	Extended thin film electrocatalyst structures
EtOH	Ethanol
EU	European Union
eV	Electron volt
EVD	Extreme value distributions
EVOH	Ethylene vinyl alcohol
EVSE	Electric vehicle supply equipment
EW	Equivalent weight
EXAFS	Extended X-ray absorption fine structure analysis
EY	Electrolyzer
F	Fluorine
F	Faraday constant, the amount of electric charge in one mole of electrons (96,485.3383 coulomb/mole)
F^-	Fluorine ion
FA	Furfyl alcohol
FANS	Filter analyzer neutron spectroscopy
FAT	Fleet Analysis Toolkit; Factory acceptance test
FBMR	Fluidized bed membrane reactor
FC	Fuel cell
FCB	Fuel cell bus
FCC	Face-centered cubic; Fuel Cell Catalyst; Fluid catalytic cracking
FCEB	Fuel cell electric bus
FCEV	Fuel cell electric vehicle
FCI	Fixed capital investment
FC POWER	Fuel Cell Power Model
FCPP	Fuel cell power plant
FCS	Fuel cell system
FCSMR	Forecourt steam methane reformer (ing)
FCT	Fuel Cell Technologies
$FCTES^{QA}$	Fuel Cell Testing, Safety and Quality Assurance (an international effort to harmonize fuel cell testing procedures)
FCTO	Fuel Cell Technologies Office
FCTT	Fuel Cell Technical Team
FCV	Fuel cell vehicle
Fd	Ferredoxin
Fe	Iron
FE	U.S. DOE Office of Fossil Energy
Fe_2O_3	Ferric oxide
FEA	Finite element analysis
FEM	Finite element model
FEP	Fluorinated ethylene propylene; Teflon®
FESEM	Field emission scanning electron microscope
fg-ELAT	Fine gradient ELAT
FIB	Focused ion beam
FISIPE	Fibras Acrilicas Portugese
FLC	Frequent driver and long commute
FLiNaK	LiF-NaF-KF eutectic salt
FLP	Frustrated Lewis pair
Fluent	Computer code for computational fluid dynamics
FMEA	Failure modes and effects analysis
FMVSS	Federal Motor Vehicle Safety Standard
^{19}FNMR	^{19}Fluorine nuclear magnetic resonance
FNR	Ferredoxin NADP+ oxidoreductase
FOA	Funding Opportunity Announcement
FOM	Federated object model; Figure of merit
FPA	Fluoroalkyl phosphonic and phosphinic acids
fpi	Fins per inch
fpm	Feet per minute
FPS	Bis(4-fluorophenyl)sulfone; Fuel processing system

FRP	Fiber-reinforced composite piping; Fiber-reinforced polymer; Full rate production
FRR	Fluoride release rate
F-SPEEK	Fluorosulfonic acid of polyetheretherketone
FSW	Friction-stir welding
ft	Feet
FT	Fault tree
ft^2	Square feet
ft^3	Cubic feet
FTA	Federal Transit Administration
FT-IR, FTIR	Fourier transform infrared
FTIR-ATR	Fourier transform infrared attenuated total reflection
FTO	Fluorine-doped tin oxide
FTP, FTP-75	Federal Test Procedure
FWS	Fixed-window scan
FW	Formula weight; Filament winding
FWHM	Full width at half maximum
FY	Fiscal year
FZ	Fusion zone
g	Gram; acceleration of gravity
G	Graphite
Ga	Gallium
GaAs	Gallium arsenic
GADDS	General area diffraction system
gal	Gallon
GaP	Gallium phosphide
GB	Gigabyte
GC	Gas chromatograph; General computational
GC	Glassy, or vitreous carbon: a pure carbon that is amorphous (non-crystalline)
g/cc	Grams per cubic centimeter
GCLP	Grand-canonical linear programming
GCMC	Grand Canonical Monte Carlo
GCMS	Gas chromatograph-mass spectroscopy
GCNF	Graphitized carbon nano-fiber
GCNT	Graphitized carbon nanotubes
GCtool	Software package developed at ANL for analysis of fuel cells and other power systems
Gd	Gadolinium
GDC	Gadolinium-doped ceria
GDE	Gas diffusion electrode
GDL	Gas diffusion layer
GDM	Gas-diffusion media
GDS	Galvanodynamic scan
Ge	Germanium
GES	Giner Electrochemical Systems, LLC
GF	Glass fiber
GFC	Gas flow channel
GFP	Green fluorescent protein
GGA	Generalized gradient approximation
GGE, gge	Gasoline gallon equivalent
GH_2	Gaseous hydrogen
GHG	Greenhouse gas
GHSV	Gas hourly space velocity
GIS	Geographic information system
GJ	Gigajoule(s)
g/kW	Gram(s) per kilowatt
GLACD	Glancing angle co-deposition
GLAD	Glancing angle deposition
GLS	Gas-liquid separator
GLY	Glycerol
Glyme	Dimethoxyethane
gm	Gram(s)
GM	General Motors
gm/day	Gram(s) per day
g/min	Gram(s) per minute
GNF	Graphite nanofiber
GO	Graphene oxide
GODC	Graphene oxide derived carbon
GOF	Graphene-oxide framework
GPa	Gigapascal(s)
GPAT	Global Pathways Resource Analysis Tool
GPC	Gel permeation chromatography
GPS	Global positioning system
GPU	Gas permeation units
GRC	Glass-reinforced concrete
GREC	Graphite reinforced epoxy composite (IM6 continuously wound)
GREET	Greenhouse gases, Regulated Emissions and Energy use in Transportation model
GRPE	Working Party on Pollution and Energy
g/s	Grams per second
GS	Gas switching
GTI	Gas Technology Institute
GTR	Global Technical Regulations
GUI	Graphical user interface
GV	Gasoline vehicle
GVW	Gross vehicle weight
GW	An approximation permitting practical calculation of excitation energies in metals, semi-conductors and insulators

GWe, GW_e	Gigawatt(s) electric
h	Hour(s)
H	Hydrogen
H+	Proton
H^-	Hydride
H_2	Diatomic hydrogen
H2A	Hydrogen Analysis project sponsored by DOE
H_2BPyDC	2,2'-bipyridine-5,5'-dicarboxylic acid
H_2cat	Catechol, 1,2 dihydroxybenzene
H_2-FCS	Stationary fuel cell system designs that co-produce hydrogen
H2FIRST	Hydrogen Fueling Infrastructure Research and Station Technology
H_2(hfipbb)	4,4'-(hexafluoroisopropylidene)bis(benzoic acid)
H2I	Hawaii Hydrogen Initiative
H2-ICE, H_2 ICE	Hydrogen internal combustion engine
H_2Lib	Library of H_2 component models in Simulink®
H_2O	Water
H_2O_2	Hydrogen peroxide
H_2oba	4,4'-oxybis-benzoic acid
H2QWG	DOE Hydrogen Quality Working Group
H_2S	Hydrogen sulfide
H2SCOPE	Hydrogen Station Cost Optimization & Performance Evaluation
H_2SO_4	Sulfuric acid
H2V	Hydrogen vehicle
H_3BBC	1,3,5-tris(4'-carboxy[1,1'-biphenyl]-4-yl-) benzene
H_3BTB	4,4',4''-benzene-1,3,5-triyl-tribenzoic acid
H_3PO_4	Phosphoric acid
HAADF	High-angle annular dark-field
HAADF-STEM	High angle annular dark field scanning transmission electron microscopy
HAMMER	Hazardous Materials Management and Emergency Response
HATCI	Hyundai America Technical Center, Inc.
HAVO	Hawaii Volcanoes National Park
HAZ	Heat-affected zone
HAZID	Hazard Identification Analysis
HAZOP	Hazards and Operational Safety Analysis; Hazards and operability analysis
HB	Hydrazine borane
HBr	Hydrogen bromide
HBTU	o-Benzotriazol-1-yl-N,N,N',N'-tetramethyluronium hexafluorophosphate
HCC	Hybrid cathode catalyst
HCl, HCL	Hydrochloric acid; Hydrogen chloride
$HClO_4$	Perchloric acid
HCN	Hydrogen coordination number
HCNG	Hydrogen-compressed natural gas
HCO_3^-	Bicarbonate
hcp	Hexagonal close-packing
HC&S	Hawaiian Commercial and Sugar Company
HD	Deuterium hydride
HDF	Hydrogen dispensing facility
HDPE	High-density polyethylene
HDS	Hydrogen desulfurization
HDSAM	Hydrogen Delivery Scenario Analysis Model
He	Helium
HE	Hydrogen embrittlement
HEMA	2-hydroxylethyl methacrylate
HEN	Heat exchange network
HEPA	High efficiency particulate air filter
HER	Hydrogen evolution reaction
HES	Hydrogen energy station
HEV	Hybrid electric vehicle
HEX	Heat exchanger
HexCell	Hexagonal heat exchanger
Hf	Hafnium
HF	Hydrogen Fueler; Hydrofluorhydric acid; Hydrogen fluoride; Hartree-Fock
HFB	Hexafluorobenzene
HFC	Hydrogen fuel cell
HFCTF	Hawaii Fuel Cell Test Facility
HFCV	Hydrogen fuel cell vehicle
HFI	Hydrogen Fuel Initiative
HFP	Hexafluoropropylene
HFP	1,1,1,3,3,3 hexafluoro-2-propanol
HFR	High-frequency resistance
HFS	Hydrogen fueling station
HFSS	High-flux solar simulator
HFV	Hydrogen-fueled vehicle
HGEF	Hawaii Gateway Energy Center
HGM	Hydrogen Generation Module
HGMs	Hollow glass microspheres
HGV	Hydrogen gaseous vehicle
HHV	Higher heating value
HI	Hydrogen iodide, hydriodic acid

HIA	Hydrogen-induced amorphization; Hydrogen Implementing Agreement
HIAD	Hydrogen Incidents and Accidents Database
HIB	High-impedance buffer
HIC	Hydrogen-induced cracking
HICE	Hydrogen internal combustion engine
HiPCO, HiPCo	High-pressure carbon monoxide
HIPOC	Hydrogen Industry Panel on Codes
HIx	Blend of hydrogen iodide, iodine, and water
HIZ	Perhydro-indolizidine
HKUST	1 Cu_3(1,3,5-benzenetricarboxylate)$_2$
HLA	High level architecture
HMC	Hyundai Motor Company
HNEI	Hawaii Natural Energy Institute
HNO_3	Nitric acid
HOMO	Highest occupied molecular orbital
HOPG	Highly-ordered pyrolytic graphite
HOR	Hydrogen oxidation reaction
hp	Horsepower
HP	High pressure
HPA	Heteropoly acid
HPA-C	Heteropoly acid
HPC	Highly porous carbon
HPEP	Hydrogen Production Expert Panel
HPIT	Hydrogen-powered industrial truck
HPLC	High-performance liquid chromatography
HPPH	1,6-di(4-hydroxyl)phenylperfluorohexane
HPPS	*N,N*-diisopropylethylammonium 2,2-bis(*p*-hydroxyphenyl) pentafluoropropanesulfonate
HPRD	Hydrogen pressure relief device
HPTB	High Pressure Test Bay
HQS100	Hydroquinone sulfone
hr	Hour(s)
HRA	Home refueling appliance
HRS	Hydrogen refueling station
HR-STEM	High resolution scanning transmission electron microscopy
HRT	Hydraulic retention time
HRTEM	High-resolution transmission electron microscopy
HRXRT	High-resolution X-ray tomography
HS	Hydrogen sorption
HSAC	High surface area carbon
HSC	Database name derived from the letters for enthalpy, entropy, and heat capacity
HSCC	Hydrogen Station Cost Calculator
HSCoE	Hydrogen Sorption Center of Excellence
HSDC	Hydrogen Secure Data Center
HSE	High surface area electrode
HSECoE	Hydrogen Storage Engineering Center of Excellence
HSMCoE	Hydrogen Storage Material Center of Excellence
HSO_4	Bisulfate anion
HSP	Hydrogen safety plan
HSRP	Hydrogen Safety Review Panel
HSSIM	Hydrogen Storage SIMulator
HSU	Hydrogen separation unit
HT	High temperature
HTAC	Hydrogen and Fuel Cell Technical Advisory Committee
HTFC	High-temperature fuel cell
HTFSA	Trifluomethylsulfonic acid
HTGR	High-temperature gas-cooled reactor
HTHX	High-temperature heat exchanger
HTM	High-temperature membrane; Hydrogen transport membrane
HTMWG	High Temperature Membrane Working Group
H-T-NT	Hierarchical TiO_2 nanotubes
HTPEM	High-temperature polymer electrolyte membrane
HTWGS	High-temperature water-gas shift
HTXRD	High-temperature X-ray diffraction
HVAC	Heating, ventilation, and cooling
HWCVD	Hot-wire chemical vapor deposition
HWD	Hot wire deposition
HWFET	Highway Fuel Economy Test
HX	Heat exchanger
HyARC	Hydrogen Analysis Resource Center
HYDA	*Chlamydomonas reinhardtii* [FeFe] hydrogenase
HyDRA	Hydrogen Demand and Resource Analysis
Hydrofill™	GTI hydrogen dispenser filling control algorithm
HyPro, HYPRO	Analysis tool
HYPS	Pumped hydro
HyQRA	Hydrogen quantitative risk assessment
HyRAM	Hydrogen-specific risk assessment toolkit
HyS	Hybrid Sulfur
HySEB	Hydrogen Station Economics and Business
HYSYS®	Process simulation software by Aspentech, computer code for flowsheet analysis

HyTEx	Hydrogen Technical Experimental (database)
HyTRANS	DOE's market simulation model for the transition to hydrogen vehicles
Hz	Hertz
HZM	Hot zone module
i	Current density (mA/cm^2)
I	Current
I_2	Diatomic iodine
I2CNER	International Institute for Carbon-Neutral Energy Research
IBAD	Ion beam assisted deposition
IBS	Ion beam sputtering
I/C	Ionomer to catalyst; Ionomer to carbon
IC	Internal combustion
ICC	International Code Council
ICE	Internal combustion engine
ICEV	Internal combustion engine vehicle
ICMS	Integrated ceramic membrane system
ICP	Inductively coupled plasma
ICPAE	Inductively coupled plasma atomic emission
ICP-AES	Inductively coupled plasma atomic emission spectroscopy
ICP-MS	Inductively coupled plasma mass spectrometry
ICP-OES	Inductively coupled plasma optical emission spectroscopy
ICR	Interfacial contact resistance
ID	Inside diameter
i.e.	*id est*: that is
IE	Intelligent Energy
IEA	International Energy Agency
IEA-HIA	International Energy Agency Hydrogen Implementing Agreement
IEC	International Electrotechnical Commission; Ion exchange capacity, milliequivalents of acid groups per gram of material
IECV	Integrated end cap vessel
IEEE	Institute of Electrical and Electronics Engineers, Inc.
IET	Institute for Energy and Transport
IFC	International Fire Code
IGBT	Insolated-gate bipolar transistor
IGCC	Integrated gasification combined cycle
IGCC-CMR	Integrated gasification combined cycle-catalytic membrane reactor
IGCC-MR	Integrated gasification combined cycle-membrane reactor
IGCC-PBR	Integrated gasification combined cycle-paladium-based reactor
IGT	Institute of Gas Technology
IIC	Industrial, institutional, and commercial
IINS	Inelastic incoherent neutron scattering
IIT	Illinois Institute of Technology
IL	Ionic liquid
ILS	Inter-laboratory study(ies)
ILTA	Ionic liquids tethered to amineboranes
In	Indium
In., in	Inch
in^2	Square inch
INER	Institute of Nuclear Energy Research
INERI	International Nuclear Energy Research Initiative
InP	Indium phosphorus
INS	Inelastic neutron scattering
I-O	Input-output
IOS	Intelligent Optical Systems, Inc.
IP	Induction period; Intellectual property
IPA	Isopthalate; Isopropyl alcohol
IPCC	Intergovernmental Panel on Climate Change
IPCE	Incident photon conversion to electrons; Incident photon conversion efficiency
IPE	Integrated photovoltaic electrolysis
IPES	Inverse photoemission spectroscopy
IPHE	International Partnership for the Hydrogen Economy
IPNS	Intense Pulse Neutron Scattering Facility at Argonne National Laboratory
IQE	Internal quantum efficiency
IR	Infrared
iR	Internal resistance
Ir	Iridium
IRMOF	Isoreticular metal organic framework
IrO_x	Iridium oxide
IRR	Internal rate of return
IRRAS	Infrared reflection-absorption spectroscopy
ISIS	World's leading pulsed neutron and muon source located at the UK Rutherford Appleton Laboratory near Oxford
ISO	International Organization for Standardization
ISO TC197	International Standards Organization Technical Committee
ISS	Ion scattering spectroscopy
ITM	Ion transport membrane

ITO	Indium tin oxide
ITP	Indium tin phosphate
ITWS	Isothermal water splitting
IV	Current-voltage
J	Current; Joule(s)
JARI	Japan Automobile Research Institute
JHQTF	Joint Hydrogen Quality Task Force (U.S. Fuel Cell Council)
JM	Johnson Matthey
JMFC	Johnson-Matthey Fuel Cells, Inc.
JNAIST	Japanese National Institute of Advanced Industrial Science and Technology
JOBS FC	JOBS and economic impacts of Fuel Cells
JOBS H2	JOBS and economic impacts of Hydrogen
JPL	Jet Propulsion Laboratory
JRC	Joint Research Centre
J-V, JV	Current density-voltage
K	Sievert's constant, ml/[cm^2-min-atm½]; Kelvin, absolute temperature; Potassium
kÅ	1,000 angstroms
KAERI	Korea Atomic Energy Research Institute
KAIST	Korea Advanced Institute of Science and Technology
kA/m^2	Kilo-ampere(s) per square meter
kb	Kilo-base pair, a unit of measurement used in genetics equal to 1,000 nucleotides
KBr	Potassium bromide
kcal	Kilocalorie(s)
kcal/mol	Kilocalorie(s) per mole
KeV	Kilo electron volt(s)
kg	Kilogram(s)
kg/d	Kilogram(s) per day
kg/hr	Kilogram(s) per hour
kg/m^3	Kilogram(s) per cubic meter
KH	Potassium hydride
KHTC	Hydrotalcites; Potassium-promoted hydrotalcite
kHz	Kilohertz
K_{IH}	Fracture toughness measured in hydrogen gas
kJ	Kilojoule(s)
KJ	Ketjenblack
K_{JIC}	Fracture toughness
kJ/mol	Kilojoule(s) per mole
km	Kilometer(s)
KMC	Kinetic Monte Carlo
KOH	Potassium hydroxide
kPa	Kilopascal(s)
kph	Kilometer(s) per hour
ksi	1,000 pound-force per square inch
kT/y	Kiloton(s) per year
Kth, K_{th}	Fracture toughness threshold
K_{TH}	Hydrogen-assisted crack growth threshold
kVA	Kilovolt-amp(s) (units of apparent power)
kW	Kilowatt(s)
kWe, kW_e	Kilowatt(s) electric
kWh	Kilowatt-hour(s)
kWh/kg	Kilowatt-hour(s) per kilogram
kWh/L	Kilowatt-hour(s) per liter
kW/kg	Kilowatt(s) per kilogram
kWt	Kilowatt(s) thermal
L, l	Liter(s)
La	Lanthanum
LAGP	Lithium aluminum germanium phosphate
LAH	Lithium aluminum hydride ($LiAlH_4$)
λ	Lambda, hydration number
LAMH	Lithium amide and magnesium hydride
LAMOX	Lanthanum molybdenum oxide (*e.g.*, $La_2Mo_2O_9$)
LANL	Los Alamos National Laboratory
LAO	Lanthanum-modified alumina
LAPS	Large aperture projection scatterometer
LAS	Large aperture scatterometry
lb	Pound(s)
LBM	Lattice Boltzmann method
lbmol	Pound(s)-mole
LBNL	Lawrence Berkeley National Laboratory
LC	Liquid carrier; Low concentration
L-C	Longitudinal-circumferential
LCA	Life cycle assessment; Life-cycle analysis
LCC	Life cycle cost; $La_{0.7}Ca_{0.3}CrO_{3-\delta}$
LCH_2	Hydrogenated liquid carrier; Compressed hydrogen produced from liquid hydrogen
LCHPP	Low Cost Hydrogen Production Platform (DOE Program Title)
LCMS	Liquid chromatography-mass spectroscopy
LCOE	Levelized cost of electricity
L/D	Length to diameter ratio
LDV	Light-duty vehicle
LED	Light emitting diode
LEED	Low-energy electron diffraction
LEL	Lower explosion limit

LFG	Landfill gas
LFL	Lower flammability limit
L/h, l/h	Liter(s) per hour
LH2, LH_2	Liquid hydrogen
LHC	Light-harvesting chlorophyll
LHSV	Liquid hourly space velocity, h^{-1}
LHV	Lower heating value
Li	Lithium
LI	Leaching index
Li_3N	Lithium nitride
Li-AB	Lithium amidoborane, Li-NH_2-BH_3
$LiBH_4$	Lithium borohydride
LIBS	Laser-induced breakdown spectroscopy
LiH	Lithium hydride
LLC	Limited Liability Company; Lessons Learned Corner
LLNL	Lawrence Livermore National Laboratory
L/min, l/min	Liter(s) per minute
LMWO	Lanthanum molybdenum tungsten oxide (*e.g.*, $La_2Mo_{1.8}W_{0.2}O_{9-x}$)
LN_2	Liquid nitrogen
LNG	Liquefied natural gas
LOC	Liquid organic carrier
LOHC	Liquid organic hydrogen carrier
LP	Lattice parameter
LPG	Liquefied petroleum gas
LPM	Liter(s) per minute
LPR	Liquid-phase reforming
LQ*	Dehydrogenated liquid carrier
LQ*H2	Hydrogenated liquid carrier
L-R	Longitudinal-radial
LRIP	Low rate initial production
LRS	Laser raman spectroscopy
LS	Local share
LSAC	Low-surface-area carbon
LSC	Lanthanum strontium cobalt oxide, (La, Sr)CoO_3, strontium-doped lanthanum cobaltite, $La_{0.8}Sr_{0.2}CoO_{3+\delta}$
LSCF	Lanthanum strontium cobalt iron oxide, (La, Sr)(Co, Fe)O_3
LSCF7328	La-Sr-Cu-Fe-O
LSCM	Lanthanum strontium chromium manganese oxide, (La, Sr)(Cr, Mn)O_3
LSCr	Lanthanum strontium chromium oxide, (La, Sr)CrO_3
LSF	Large station first
LSM	Lanthanum strontium manganese
LSMO	Lanthanum strontium manganese oxide, (La, Sr)MnO_3, strontium-doped lanthanum manganite, $La_{0.8}Sr_{0.2}MnO_{3+\delta}$
LST	Lanthanum strontium titanium oxide, (La, Sr)TiO_3
LSV	Lanthanum strontium vanadate; Linear sweep voltammetry
LT	Low-temperature
LTDMS	Laser induced thermal desorption mass spectrometry
LUMO	Lowest unoccupied molecular orbital
m	Meter(s)
M	Mole, Molar; Million
m^2	Square meter(s)
m^2/g	Square meter(s) per gram
m^2/s	Square meter(s) per second
m^3	Cubic meter(s)
MA	Mass activity; methyl acrylate
MA3T	Market Acceptance of Advanced Automotive Technologies
μA	Microampere(s)
mA	Milliamp(s)
MA	Mass activity
M-AB	Metal ammonia-borane
MAB, M-AB	Metal amidoboranes
$\mu A/cm^2$	Microampere(s) per square centimeter
mA/cm^2	Milliamp(s) per square centimeter
MARAD	Maritime Administration
MARKAL	Market Allocation Model—A generic, multi-sector energy model developed by the Energy Technology Systems Analysis Program of the International Energy Agency
MAS	Magic angle spinning
MASC	Multi-acid side chain
MAS ^{11}B-NMR	Magic angle spinning boron-11 nuclear magnetic resonance spectroscopy
MAS-NMR	Magic angle spinning nuclear magnetic resonance
MATI	Modular Adsorption Tank Insert
MAWP	Maximum allowable working pressure
MB	Megabyte
MBE	Molecular beam epitaxy
MBMS	Molecular beam mass spectrometry
M-BOP	Mechanical balance of plant
MBRC	Miles between roadcall

MBWR	Modified Benedict Webb Rubin
MC	Monte Carlo; Methyl cellulose
mC^2	Multi-component composite (membrane)
MCB	Marine Corps Base
$mC\text{-}cm^{-2}$	Millicoulomb(s) per square centimeter
MCEL	Millenium Cell, Inc.
MCFC	Molten carbonate fuel cell
mCHP	Micro-combined heat and power
µCHP	Micro-combined heat and power
µCHX	Microscale combustor/heat exchanger
MCM	Mobile crystalline material
µc-Si	Microcrystalline silicon
MDC	Material-dependent components
MDES	Methyl-diethoxy silane
mdip	5,5′-methylene-di-isophthalate
MDMC	Material Data Management Consortium
m-dobdc	4,6-DiOxido Benzene 1,3-DiCarboxylate
MEA	Membrane electrode assembly
MeAB	Methylamine borane
MEAM	Modified embedded atom method
MEC	Microbial electrolysis cell; Minimum explosive concentration
MeCN	Acetonitrile
MEIC	Mixed electronic and ionic conducting (membranes)
MEMS	Micro-electro-mechanical systems
MeOH	Methanol
meq	Milliequivalents
meq/g	Milliequivalents/gram
MES	Microstructered electrode scaffold
MeV	Mega electron volt
mf	Mass fraction
Mg	Megagram(s)
µg	Microgram(s)
mg	Milligram(s)
$MgCl_2$	Magnesium chloride
mg/cm^2	Milligram(s) per square centimeter
MgH_2	Magnesium hydride
MgH_2@C	MgH_2 incorporated in carbon scaffold
MgO	Magnesium oxide
$Mg(OH)_2$	Magnesium hydroxide
$mgPt/cm^2$	Milligram(s) of platinum per square centimeter
MH, M-H	Metal hydride
MHC	Metal hydride-based compressor
MHCoE	Metal Hydride Center of Excellence
MHE	Material handling equipment
MHI	Methylperhydroindole
MHz	Megahertz
mi	Mile(s)
MIE	Minimum ignition energy
MIEC	Mixed ionic and electronic conduction
mi/kg	Mile(s) per kilogram
mil	Millimeter(s)
Mim	Methyl imidazole
min	Minute(s)
MIP	Mercury intrusion porosimetry
MIT	Massachusetts Institute of Technology
MiTi®	Mohawk Innovative Technologies Inc.
MJ	Megajoule(s)
mL, ml	Milliliter(s)
ML	Monolayer
µCHP	Micro-combined heat and power
µm	Micrometer(s); micron(s)
µM	Micromolar
mM	Millimolar
mm	Millimeter(s)
MMBtu	Million British thermal units
MM-FSW	Multi-pass, multi-layer friction stir welding
MMOF	Microporous metal-organic framework
mmol	Millimole(s)
µmol	Micromole(s)
MMSCFD	Million standard cubic feet/day
MMT	Million metric tonnes
Mn	Manganese
Mn_2O_3	Manganese oxide
M-N-H	Amide/imide
MnO	Manganese oxide
$\mu\Omega\text{-}cm^2$	Micro-ohm(s)-square centimeter
Mo	Molybdenum
MO	Molecular orbital; metal oxide
MOA	Memorandum of Agreement
MOF	Metal-organic framework
mol	Mole(s)
MOL	Middle of life
mol%	Mole percent
mol/min	Mole(s) per minute
mΩ	Milli-ohm(s)
MΩ	Mega-ohm(s)
$m\Omega/cm^2$	Milli-ohm(s) per square centimeter

MoPc	Molybdenum phthalocyanine
MOR	Methanol oxidation reaction
MPa	Megapascal(s)
MPG, mpg	Mile(s) per gallon
MPGGE	Miles per gasoline gallon equivalent
mph	Mile(s) per hour
MPHI	Methylperhydroindole
MPL	Micro-porous layer
MPMC	Massively Parallel Monte Carlo
mpy	Miles per year
MQMAS	Multiple quantum magic angle spinning
MR	Membrane reactor
MRCAT	Materials Research Collaborative Access Team
MREC	Microbial reverse-electrodialysis electrolysis cell
MRI	Magnetic resonance imaging
MRL	Manufacturing readiness level
ms	Millisecond(s)
MS	Mass spectroscopy; Mass spectrometry; More Stations
MSAC	Mid-range carbon support; Medium surface area carbon
MSC	Moderate driver and short commute
mS/cm	Milli-Siemen(s) per centimeter
MS-H_2	Hydrogen mass spectrometry
MSM	Macro-System Model
MSR	Membrane steam reformer
MSRI	Materials and Systems Research, Inc.
MSRP	Manufacturer suggested retail price
MSTF	Mesostructured thin films
MTA	Metric tonne per annum; Mass Transportation Agency
MTBIO	Mean time between interrupted operation
MTBF	Mean time between failure
MTBR	Mean time between repairs
M/TC	Metal-doped templated carbon
M-TCPP	M = Fe, Mn, Co, Ni, Cu, Zn, H2, tetrakis(4-carboxyphenyl)porphyrin
mtorr	Millitorr
μV	Microvolt(s)
mV	Millivolt(s)
MV	Methyl viologen
mW	Milliwatt(s)
MW	Megawatt(s); Molecular weight
mW/cm^2	Milliwatt(s) per square centimeter
MWCNT	Multiple-wall carbon nanotube
MWe	Megawatt(s) electric
MWh	Megawatt-hour(s)
MWNT	Multi-wall carbon nanotube
MWOE	Midwest Optoelectronics, LLC
MWth	Megawatt(s) thermal
MYPP	Multi-Year Program Plan (the Fuel Cell Technologies Office's Multi-Year Research, Development, and Demonstration Plan)
MYRDD, MYRD&DP	Multi-Year Research, Development and Demonstration Plan
N	Normal (e.g., 1N H_3PO_4 is 1 normal solution of phosphoric acid); Nitrogen atom; Newton (unit of force)
N112	Nafion® 1100 equivalent weight, 2 millimeter thick membrane
N_2	Diatomic nitrogen
N_2O	Nitrous oxide
Na	Sodium
NA	North American
Na_2S	Sodium sulfide
Na_3AlH_6	Trisodium hexahydroaluminate
$NaAlH_4$	Sodium aluminum hydride; Sodium tetrahydroaluminate; Sodium alanate
$NaBH_4$	Sodium borohydride
$NaBO_2$	Sodium metaborate
NACE	National Association of Corrosion Engineers
NaCl	Sodium chloride
NACS	North American Catalysis Society
NADH	(reduced) Nicotinamide adenine dinucleotide
NADP	Nicotinamide adenine dinucleotide phosphate
NADPH	Nicotinamide adeninine dinucleotide phosphate
Nafion®	Registered Trademark of E.I. DuPont de Nemours
NaH	Sodium hydride
NA NG	North American natural gas
NaOH	Sodium hydroxide
NAS	National Academy of Sciences
NASA	National Aeronautics and Space Administration
Nb	Niobium
Ncc	Normal cubic centimeters
N/cm^2	Newton(s) per square centimeter
NCNR	NIST Center for Neutron Research
ND	Not determined at this time

NDC	New delivery concept, Naphthalene-2,6-dicarboxylate
nDDB	N-dodecyl benzene
NDE	Non-destructive examination
NE	U.S. DOE Office of Nuclear Energy, Science, and Technology
NEB	Nudged elastic band
NEC	National Electrical Code
NEF	N-ethylformamide
NEMA	National Electrical Manufacturers Association
NEMS	National Energy Modeling System
NEPA	National Environmental Policy Act
NETL	National Energy Technology Laboratory
NEU	Northeastern University
NEXAFS	Near edge X-ray absorption fine structure
NFCBP	National Fuel Cell Bus Program
NFCRC	National Fuel Cell Research Center
NFCTEC	National Fuel Cell Technology Evaluation Center
NFM	Nanoporous framework material
Nfn-Pt/C	Nafion®-loaded Pt/C
NFPA	National Fire Protection Association
ng	Nanogram
NG	Natural gas; Next generation
NGCC	Natural gas combined cycle
NGNP	Next Generation Nuclear Plant
NGV	Natural gas vehicle
NH_3	Ammonia
NHA	National Hydrogen Association
NHE	Normal hydrogen electrode
NHFC4	National Hydrogen and Fuel Cells Codes and Standards Coordinating Committee
NHI	Nuclear Hydrogen Initiative
NHTSA	National Highway Traffic Safety Administration of the U.S. Department of Transportation
Ni	Nickel
NICC	Natural gas Infrastructure Component Cost model
NILS	Normal interstitial lattice sites
NiMH	Nickel metal hydride
NIR	Near infra-red
NIST	National Institute of Standards and Technology
NL	Normal liter(s)
NLDFT	Non-local density functional theory
nm	Nanometer(s)
NM	Noble metal
Nm^3	Normal cubic meter(s)
NMHC	Non-methane hydrocarbons
NMOC	Non-methane organic carbons
nmol	Nanomole(s)
NMP	N-methylpyrrolidone
NMR	Nuclear magnetic resonance
NMSU	New Mexico State University
NMT	New Mexico Tech
NNA	Non-North American
NNA NG	Non-North American natural gas
NNIF	NIST neutron imaging facility
NNSA	National Nuclear Security Administration
NO_2	Nitric oxide
NOA	Norland Optical Adhesive
nOB	N-octyl benzene
NOx, NO_x	Oxides of nitrogen
NP	Nanoparticle
NPB	Neopentyl benzene
NPC	Nanoporous carbon; Normalized photocurrent
NPD	Neutron powder diffraction
NPDF	Neutron powder diffraction
NPGM	Non-precious metal group
NPM	Nanostructured polymeric materials; Non-precious metal
NPMC	Non-precious metal catalyst
NPPD	n-phenyl-phenylenediamine
NPS	National Park Service
NPT	Normal pressure and temperature
NPV	Net present value
NR	Nanorod
NR_3	Tertiary amine
NRC	National Research Council
NREL	National Renewable Energy Laboratory
NRELFAT	NREL Fleet Analysis Toolkit
NRVS	Nuclear resonance vibrational spectroscopy
NSF	National Science Foundation
NSTF	Nano-structured thin-film
NSTFC	Nano-structured thin film catalyst
NT	Nanotube
NTCNA	Nissan Technical Center, North America
NTE	Negative thermal-expansion
N-T-NT	Nano-grass type titania nanotube
NV	Neutron vibrational

NVS	Neutron vibrational spectroscopy
NW	Nanowire
NWM	Natural Water Management, UTC Power's system and cell stack design which utilizes evaprotative cooling in the cell stack assembly
NYSERDA	New York State Energy Research and Development Authority
NZVI	Nano zerovalent iron
Ω	Ohm(s)
Ωcm^2	Ohm(s)-square centimeter
O	Oxygen
O_2	Diatomic oxygen
O/C	Oxygen-to-carbon ratio
OCP	Open circuit potential
OCSD	Orange County Sanitation District
OCV	Open-circuit voltage
o.d.,OD	Outer diameter
ODA	Oxygenated form of diamine
ODE	Ordinary differential equation
OEC	Oxygen evolving complex
OEM	Original equipment manufacturer
OER	Oxygen evolution reaction
OGMC	Ordered graphitic mesoporous carbon
OH^-	Hydroxyl radical
O&M	Operation and maintenance
OMC	Ordered mesoporous carbon
Ω	Ohm(s)
Ωcm^2	Ohm(s)-square centimeter
ONR	Office of Naval Research
ORF	Opening Reading Frame indicating the occurrence of a protein coding region in the DNA sequence
ORNL	Oak Ridge National Laboratory
ORNL-HTML	Oak Ridge National Laboratory High Temperature Materials Laboratory
ORR	Oxygen reduction reaction
OSC	Oxygen storage capability
OSHA	Occupational Safety and Health Administration
OSM	Optical scatterfield microscopy
o-SWNH	Oxidized single-walled nanohorn
OSU	Ohio State University; Oregon State University (Microproducts Breakthrough Institute)
OTM	Oxygen transport membrane
P	Phosphorus; Pressure
Pa	Pascal(s)
PA	Phosphoric acid, Phenylacetylene; Polyamide
PAA	Poly(acrylic acid); polyphthalamide
P&D	Pickup and delivery
PAD	Polymer-assisted deposition
PADD	Petroleum Administration for Defense District
PAES	Poly(arylene-ether-sulfone)
PAFC	Phosphoric acid fuel cell
P&ID	Piping and instrumentation diagram
PAN	Peroxyacetyl nitrate; Polyacrylonitrile
PANI	Polyaniline
PAN-MA	Polyacrylonitrile with methyl acrylate
PAN-VA	Polyacrylonitrile with vinyl acetate
PA/PBI	Phosphoric-acid-doped polybenzimidazole
PAR	Photosynthetically-active radiation
PAS	Photoactive semiconductor; Photo acoustic
Pb	Lead
PB	Polyborazylene; Pre-bridge
PBCTF	Pressurized Button Cell Test Facility
PBD	Performance-based design
PBI	Polybenzimidazole
PBPDSA	poly(biphenylene disulfonic acid)
P-C	Pressure-composition
PC	Polycarbonate
PCA	Pyrenecarboxylic acid; Principal component analysis
PCE	Perchloroethylene
PCF	Polycarbonate film
PCHD	Poly(cyclohexadiene)
PCI	Pressure-composition isotherm
PCL	Polycaprolactone
PCM	Power control module
PCN	Porous coordination network
P-C-P	Phosphorus-carbon-phosphorus
PCR	Polymerase chain reaction
PCS	Power conditioning system
PCT, P-C-T	Pressure-concentration-temperature
PCTFE	Polychlorotrifluoroethylene
Pd	Palladium
PDA	Phenyldiacetylene
PdAg	Palladium-silver alloy
Pd-ACF	Pd-modified activated carbon fibers
Pd-CR	Palladium-based chemical resistor

PdCu, Pd-Cu	Palladium-copper alloy
PdCuTM	Palladium copper transition metal
PDF	Probability density function; Pair distribution function
PdHg/CF	Carbon foam doped with palladium-mercury compound
PDI	Polydispersity index
Pd-MIS	Palladium-based metal-insulator-semiconductor
PDMS	Polydimethylsiloxane
PDS	Potentiodynamic scan
PDU	Process development unit
PE	Polyelectrolyte; Polyethylene
PEC	Photoelectrochemical; Photoelectrocatalyst; Photoelectrochemical cell
PECH	Polyepichlorohydrin
PECVD	Plasma-enhanced chemical vapor deposition
PED	Pulsed electrodeposition
PEDOT:ClO_4	Poly(3,4-ethylenedioxythiophene):perchlorate
PEEK	Polyether ether ether ketone
PEFC	Polymer electrolyte fuel cell; Proton exchange fuel cell
PEG	Polyethylene glycol
PEGMEMA	Monomethoxypoly(ethyleneglycol) methacrylate
PEGS	Prototype electrostatic ground state
PEI	Polyetherimide; Polyethylene imine
PEKK	Poly (ether ketone ketone)
PEM	Proton exchange membrane; Polymer electrolyte membrane
PEMFC	Polymer electrolyte membrane fuel cell; Proton exchange membrane fuel cell
PEN	Polyethylene naphthalate
PEO	Poly(ethylene oxide)
PES	Polyether sulfone; Proton Energy Systems, Inc.; Polyethersulfone
PET	Polyethylene teraphthalate
PetF1	*Synechocystis* host ferredoxin
PEV	Plug-in electric vehicle
PF	Perfluoro
PFA	Perfluoroalkoxy (a type of fluoropolymer; Polyfurfuryl alcohol
PFAC	PFA-derived carbon
PFAE	Perfluoroalkylether
PFC	Polymer electrolyte membrane fuel cell
PFCS	Poly-generative fuel cell systems
PFD	Process flow diagram
PFGB	Perfluorinated guanidine base
PFG-NMR	Pulse field gradient nuclear magnetic resonance
PFGSE	Pulse field gradient spin echo
PFGSE NMR	Pulsed field gradient spin echo nuclear magnetic resonance
PFIA	Perfluoroimide acid
PFPO	Perfluorinated propylene oxide
PFPO-PSS	Poly(perfluoropropylene oxide)-b-poly(styrene sulfonate)
PFSA	Perfluorinated sulfonic acid, perfluorosulfonic acid, poly(fluorosulfonic acid)
PF-SFP	PF sulfonyl fluoride precursor
PFSI	Perfluorosulfonate ionomer
PFSHQ	2-(5-fluorosulfonyl-3-oxaoctafluoropentyl)-1,4-dihydroxy-benzene
PG	Propylene glycol
PGAA	Prompt-gamma activation analysis
PGE	Platinum group element
PGM	Precious group metal; Platinum-group metal
PGSE	Pulsed-field gradient spin-echo
PGV	Puna Geothermal Ventures
pH	Power of the hydronium ion
p-H_2	Para-hydrogen
Ph_3SnCl	Triphenyltin chloride
$Ph_3SnSnPh_3$	Hexaphenyldistannane
PHA	Process hazard analysis; Preliminary hazard analysis
PHEC	Perhydro-ethylcarbazole
PHEV	Plug-in hybrid electric vehicle
PHI	Perhydro-indolizidine
PHIP	Para-hydrogen induced polarization
PHMI	Perhydro-methylindole
PhOH	Phenol
PI	Principal investigator
PI	Polyimide
P&ID	Piping and instrumentation diagram; Process and instrumentation diagram
PIL, pIL	Protic ionic liquid
PIM, pIM	Protic ionic membrane
pK_a	Acid dissociation constant
PLC	Programmable logic controller
PLLA	Poly-L-lactic acid
PLP	Prepared Lewis pair
PLRS	Planar laser Raleigh scatter
PLS	Polymer-layered silicate

PM	Precious metal such as platinum; Particulate matter
PMG	Glycidyl methacrylate-type copolymer
PMMA	Poly(methyl methacrylate)
PND	Polymerized nitrogen donor
PNNL	Pacific Northwest National Laboratory
pO_2	Oxygen partial pressure
POC	Proof of concept
POCOP	*P,P-bis*(1,1-dimethylethyl)-,3-[[*bis*(1,1-dimethylethyl)phosphino]oxy]phenyl ester
POF	Polymeric-organic framework; Porous organic framework
POM	Polyoxometallate
POP	Porous organic polymers
POSS	Polyhedral oligomeric silsesquioxane
POX	Partial oxidation
PP	Polyphosphazene; Polypropylene; Poly(phenylene)
PPA	Polyphosphoric acid; Polyphthalamide
ppb	Part(s) per billion
ppbv	Part(s) per billion by volume
PPDSA	Poly (p-phenylene disulfonic acid)
PPE	Porous polyethylene
PPI	Plug Power, Inc.; Pore(s) per inch
ppm, PPM	Part(s) per million
ppmv	Part(s) per million by volume
ppmw	Part(s) per million by weight
PPN	Porous polymer network
PPO	Phenyl phosphine oxide
PPOR	Metalloporphyrin porous organic polymer
P-POSS	Phosphonic acid polyhedral oligomeric silsesquioxane
PPS	Polyphenylene sulfide
PPSA	Poly (p-phenylene sulfonic acid)
PPSA	Partial pressure swing adsorption
PPSU	Polyphenylsulfone
PPy	Polypyrrole
Pr	Praseodymium
PR	Pressure ratio
PRA	Probabilistic risk assessment
PRD	Pressure relief device
PrOx	Preferential oxidation
PRSV	Peng-Robinson Stryjek-Vera
PS	Proton sponge (bis- (dimethyamino) naphthalene); Polysiloxane
PSA	Pressure swing adsorption, adsorber
PSAT	Powertrain Systems Analysis Toolkit, a vehicle simulation software package developed at Argonne National Laboratory
PSD	Particle size distribution, pore size distribution
PSEPVE	Perfluoro (4-methyl-3,6-dioxaoct-7-ene) sulfonyl fluoride
PSf	Poly(arylene ether sulfone)
psi, PSI	Pound(s) per square inch
PSI	Photosystem I
PSII	Photosystem II
psia	Pound(s) per square inch absolute
psid	Pound(s) per square inch differential
psig, PSIG	Pound(s) per square inch gauge
PSOFC	Planar solid oxide fuel cell
PSS	Porous stainless steel; Potentiostatic scan
PSU	Polysulfone
PSU	Pennsylvania State University
Pt	Platinum
PT	Phosphazene trimer
P-T	Pressure-temperature
Pt_3Co	Platinum-cobalt alloy
Pt_3Fe	Platinum-iron alloy
Pt_3Ni	Platinum-nickel alloy
PTA	Phosphotungstic acid
Pt/AC/BC/IRMOF-8	Isoreticular metal organic framework (MOF) doped with platinum supported on activated carbon, and further coupled to MOF with a bridging compound
Pt/AX-21	Pt-doped microporous carbon AX-21
Pt/C	Platinum/carbon
PTC	Production tax credit
PTFE	Teflon® – poly-tetrafluoroethylene
Pt-FePO	Platinum iron phosphate
PTM	Proton transport membrane
PtML	Platinum monolayer
Pt-MM	Platinum group mixed metal
Pt-NH	Platinum decorated carbon nano-horns
PtO	Platinum oxide
PtO_2	Platinum dioxide
PtRu	Platinum ruthenium
Pt-SWNH	Platinum decorated single-walled nanohorns
Pt-TaPO	Platinum tantalum phosphate
PTTPP	Poly-tetrakis(3,5-dithiophen-2-ylphenyl)-porphyrin
PTW	Pump to wheels

PV	Photovoltaic; Present value
PVA	Polyvinyl alcohol
PVC	Polyvinyl chloride
PVD	Physical vapor deposition
PVDC	Polyvinylidene chloride
PVDF	Polyvinylidene fluoride
PVP	Polyvinylpyrrolidone
PVPP	Polyvinyl pyridinium phosphate
PVT, P-V-T	Pressure-Volume-Temperature
PXRD	Powder X-ray diffraction
PyC	4-pyrazole carboxylate
PzDC	2,8-pyrazabole dicarboxylate
Q	Neutron momentum transfer
Q1, Q2, Q3, Q4	Quarters of the year
QC	Quality control
QCM	Quartz crystal microbalance
QE	Quantum efficiency
QENS	Quasielastic neutron scattering
QLRA	Qualitative risk analysis
QMC	Quantum Monte Carlo
QNS	Quasielastic neutron scattering
QRA	Quantitative risk assessment
qRT-PCR	Quantitative reverse transcriptase-polymerase chain reaction
*Q*st	Isosteric heat of adsorption
R	Universal or ideal gas constant, 8.314472 J · K^{-1} · mol^{-1}
RAMAN	A spectroscopic technique
RAS	Russian Academy of Sciences
RBS	Rutherford back scattering
RC	Resistance-capacitance; Research cluster
RCD	Rated current density
RCS	Regulations codes and standards
RCSWG	Regulations, Codes, and Standards Working Group
Rct	Charge transfer resistance
RCWA	Rigorous couples waveguide analysis
R&D	Research and development
RD&D, R,D&D	Research, development & demonstration
RDE	Rotating disk electrode
Re	Rhenium
ReaxFF	Reactive force field large-scale molecular dynamic calculations
REC	Renewable energy credit
RED	Reverse electrodialysis
REWP	Renewable Energy Working Party
Rf	Generic fluoroalkyl group
RF, rf	Radio frequency
RFC	Regenerative fuel cell
RFI	Request for Information
RFP	Request for proposals
RFT	Reactive flow-through
RGA	Residual gas analyzer (analysis)
Rh	Rhodium
RH	Relative humidity
RHE	Reference hydrogen electrode; Reversible hydrogen electrode
RHLC	Relative humidity/load cycle test
ρ_a	Apparent density of activated carbon
$\rho_{ad.H_2}$	Adsorbate hydrogen density in micropores
RIF	Reactive impinging flow
RIXS	Resonant inelastic X-ray scattering spectra
RMS	Root mean square
RNA	Ribo nucleic acid
RNG	Renewable natural gas
ROI	Return on investment
ROM	Rough order of magnitude
ROMP	Ring-opening metathesis polymerization
ROW	Right of way
RPC	Ruthenium-polypridyl complex
RPI	Rensselaer Polytechnic Institute
rpm	Revolution(s) per minute
RPN	Risk priority number
RPS	Renewable portfolio standard
RPSA	Rapic pressure swing adsorption
RR	Round robin
RRDE	Rotating ring disc electrode
RSOFC	Reversible solid oxide fuel cell
RT	Room temperature
RTD	Resistive temperature device
RTIL	Room temperature ionic liquid
RTO	Ruthenium-titanium oxide
Ru	Ruthenium
s	Second(s)
S	Siemen(s); Sulfur
-S	Sulfur-deprived
SA	Specific amperage; Surface area; Sulfur-ammonia thermochemical water-splitting cycle; System Architect

SAC	Super-activated carbon
SAE	SAE International, originally known as the Society of Automotive Engineers
SAFC	Solid acid fuel cell
SAH	Sodium aluminum hydride
SAM	Scanning Auger microscopy
SAMPE	Society for the Advancement of Material and Process Engineering
SANS	Small angle neutron scattering
SAS	Styrene-acrylonitrile-vinylsulfate
SASSP	Solvent assisted solid state processing
SAXS	Small angle X-ray scattering
SBAB	Sec-butylamineborane
S_{BET}	BET specific surface area
SBH	Sodium borohydride
SBIR	Small Business Innovation Research
Sc	Scandium
S/C	Steam to carbon ratio
SCC	Stress corrosion cracking
sccm, SCCM	Standard cubic centimeter(s) per minute
SCCV	Steel/concrete composite vessel
SCE	Saturated calomel electrode
SCF, scf	Standard cubic feet; Supercritical fluid
scfd	Standard cubic feet per day
SCFH, scfh	Standard cubic feet per hour
SCFM	Standard cubic feet per minute
S/cm	Siemen(s) per centimeter
SCOF	Single cell with open flowfield
SCR	Selective catalytic reduction; Semi-conductor rectifier
ScSZ	Scandia-stabilized zirconia
SD	Standard deviation; System dynamics
SDAPP	Sulfonated Diels-Alder polyphenylene
SDAPPe	Sulfonated Diels-Alder polyphenylene ether
SDC	Samarium-doped ceria
sDCDPS	3,3′-disulfonate-4,4′-dichlorodiphenylsulfone
SDE	SO_2-depolarized electrolyzer
SDO	Standards development organization
Se	Selenium
SE	Secondary electron; spectroscopic ellipsometry
sec	Second(s)
SECA	Solid State Energy Conversion Alliance
SECM	Scanning electrochemical microscope
SEM	Scanning electron microscopy; Scanning electron microscope
SEOS	Simple equation of state
SERA	Scenario Evaluation, Regionalization, and Analysis
SERC	Schatz Energy Research Center
SET	Surface energy treatment
SF	Safety factor; Polystyrene-b-PFPO
SF_6	Sulfur hexafluoride
SFA	Sulfonic acid
SFC2	$SrFeCo_{0.5}O_x$
SFM	$Sr_2Fe_{1.5}Mo_{0.5}O_{6-\delta}$
SFT	Sr-Fe-Ti oxide
SFTI	$Sr_{0.1}Fe_{0.9}Ti_{0.10}O_x$
SG	Shale gas
SGD	Spontaneous galvanic displacement; System gravimetric density
SGIP	Self-Generation Incentive Program
Sh	Sherwood
SHE	Standard hydrogen electrode
Si	Silicon
S-I	Sulfur-iodine
SI	Sulfur-iodine cycle; Spectrum image
Si^3N^4	Silicon nitride
SiC	Silicon carbide
SiCN	Silicon carbonitride
SIMS	Secondary ion emission spectroscopy
Si-NS	Silica nanosprings
SiO_2	Silicon dioxide
SIU	Southern Illinois University
sL	Standard liter (0°C, 1 atm)
SLAC	Stanford Linear Accelerator Center
SLMA	Sr- and Mn-doped $LaAlO_3$
SLMA2	$Sr_xLa_{1-x}Mn_yAl_{1-y}O_3$ perovskite compositions
SLPH	Standard liter(s) per hour
SLPM	Standars liter(s) per minute
slpm, slm, sL/min	Standard liter(s) per minute
SLT	Strontium-doped lanthanum titanate
SMART	Specific, measurable, attainable, relevant, timely
SMR	Steam methane reformer; Steam methane reforming
SMR-ECM	Steam methane reformer with electrochemical purifier
SMR-PSA	Steam methane reformer with pressure swing adsorption
SMT	Single-molecule trap

Sn	Tin
SNF	Silica nanofiber
SNG	Substitute natural gas
SNL	Sandia National Laboratories
SNLL	Sandia National Laboratory Livermore
SnO	Tin oxide
SnO_2	Tin dioxide
SNR	Signal-to-noise ratio
SNS	Spallation neutron source
SNTT	Spiral notch torsion test
SO_2	Sulfur dioxide
SO_3	Sulfur trioxide
SOC	State-of-charge
SOEC	Solid oxide electrolysis cell; Solid oxide electrolyzer cell
SOFC	Solid oxide fuel cell
SOFEC	Solid oxide fuel-assisted electrolysis cell
SOM	Solid-oxide oxygen-ion-conducting membrane
SORFC	Solid oxide regenerative fuel cell
SOTA	State of the art
SOW	Statement of work
SOx	Oxides of sulfur
sPAES	Sulfonated poly(arylene ether sulfone)
SPE	Solid phase epitaxial
SPEEK	Sulfonated poly(ether ether ketone)
SPEK	Sulfonated poly-etherketone-ketone
SPEKK	Sulfonated polyether(ether ketone ketone)
SPEX	Type of milling machine
SPM	Scanning probe microscope
sPOSS	Sulfonated octaphenyl polyhedral oligomeric silsesquioxanes
S-PPSU	Sulfonated polyphenylsulfone
SPS	Spark plasma sintering
sq. in.	Square inch(es)
Sr	Strontium
SR	Steam reformer; Steam reforming; Salinity ratio; Stoichometric ratio
SRNL	Savannah River National Laboratory
SrO	Strontium oxide
SRR	Solar receiver-reactor
$SrTiO_3$	Strontium titanate
SS	Stainless steel
SSA	Specific surface area
SSAWG	Storage System Analysis Working Group
SSC	Short side-chain; Structure, system, and component
SSF	Small station first
SSM	Sacrificial support method
SSNMR	Solid-state nuclear magnetic resonance
SSRL	Stanford Synchrotron Radiation Laboratory
SSWAG	Storage System Working Analysis Group
STCH	Solar thermochemical hydrogen
STEM	Scanning transmission electron microscopy
STH	Solar to hydrogen
STM	Scanning tunneling microscopy
STMBMS	Simultaneous thermogravimetric modulated beam mass spectrometer
STP	Standard temperature and pressure
STS	Scanning tunneling spectroscopy
STTP	Shared Technology Transfer Project
STTR	Small Business Technology Transfer
S_u	Ultimate tensile strength
SU/SD	Start-up/shut-down
SUNY-ESF	State University New York College of Environmental Science and Forestry
SV	Space velocity; surface validation
SVD	System volumetric density
SW	Square wave
SWCNH	Single-wall carbon nanohorn
SWCNT	Single-walled carbon nanotube
SWNH	Single-walled nanohorn
SWNT	Single-wall nanotube
SwRI®	Southwest Research Institute®
S_y	Yield strength
SUV	Sport utility vehicle
SYT	Yttrium-doped strontium titanate
T	Temperature
T, t	Ton, tonne
T	Tesla (unit of magnetic induction)
t	Time
T_{1bar}	Temperature at which equilibrium pressure of hydrogen is 1 bar for a hydrogen exchange reaction
Ta	Tantalum
TA	Terephthalic acid
TAG	Technical Advisory Group
TAMU	Texas A&M University
TaON	Tantalum oxynitride
TaPO	Tantalum phosphate
TBAB	Tetra-n-butylammonium bromide

$TBA_2B_{12}H_{12}$	Tetra-*n*-butylammonium dodecahydrododecaborate
TBABh	Tetra-n-butylammonium borohydride
TBA-PF_6	Tetra-*n*-butylammonium hexafluorophosphate
TBD	To be determined
TBMD	Tight-binding molecular dynamic
TC	Templated carbon; Thermocouple
TCCR	Transparent, conducting and corrosion resistant
TCD	Thermal conductivity detector
TCNE	Tetracyanoethylene
TCO	Transparent conductive oxide; Total cost of ownership
TDDFT	Time-dependent density functional theory
TDLAS	Tunable diode laser absorption spectroscopy
TDPAT	2,4,6-tris(3,5-dicarboxylphenylamino)-1,3,5-triazine
TDS	Transitional demand scenario
Te	Tellurium
te	Metric ton or tonne (1,000 kg)
TEA	Triethylamine
$TEA_2B_{12}H_{12}$	Triethylammonium dodecahydrododecaborate
TEAA	Triethylamine alane adduct
TEAB	Tetraethyl ammonium borohydride
TEAH	Tetraethylammonium hydroxide
TEAMS	tetraethylammonium methane sulfonic
TED	Triethylene-diamine
TEDA	Triethylenediamine
TEM	Transmission electron microscopy
TEOA	Triethanolamine
TEOM	Tapered element oscillating microbalance
TEOS	Tetra-ethoxy silane
tf	Thin film
Tf	Trifluormethane sufonate, or triflate anion (CF_3SO_3-)
TFA	Trifluoromethanesulfonic acid
TFAc	Trifluoroacetate
TFE	Tetrafluoroethylene
TFMPA	Trifluoromethylphosphonic acid
TFMSA	Trifluoromethane sulfonic acid
TF-RDE	Thin film rotating disk electrode
tf-Si	Thin-film silicon
TFSI	bis(Trifluoromethylsulfonyl)imide
TFVE	Trifluorovinyl ether
Tg, T_g	Glass transition temperature
TG	Thermogravimetric; Theory Group
TGA	Thermal gravimetric analysis; Thermogravimetric analysis; Thermogravimetric analyzer
TGA-DSC	Thermo-gravimetric analysis-differential scanning calorimetry
TGA-MS	Thermogravimetric analysis-mass spectrometer
TG-DTA	Thermo-gravimetric/differential thermal analyzer
THF	Tetrahydrofuran
Ti	Titanium
$TiCl_3$	Titanium trichloride
TiF_3	Titanium trifluoride
TiH_2	Titanium hydride
Ti-IRMOF-16	Titanium (Ti) intercalated IRMOF-16
TiO_2	Titanium dioxide (anatase)
Tip	2,4,6-triisopropylphenyl
TIVM	Toroidal intersecting vane machine
TKK	Tanaka Kikinzoku Kogyo K. K.
TLA, *Tla*	Truncated light-harvesting chlorophyll antenna
tla1	Mutant of the Tla1 gene (GenBank Assession No. AF534570)
tlaR	Mutant of unknown gene with a truncated light-harvesting chlorophyll antenna
tlaX	Mutant of unknown gene with a truncated light-harvesting chlorophyll antenna
TLCP	Thermotropic liquid crystal polymer
TM	Tetramethyl bisphenol A; Transition metal
TMA	Trimethylamine; Trimethylaluminum; Thermal mechanical analyzer
TMAA	Trimethylamine alane adduct
TMAB	Tetramethylammonium borohydride
TMAH	Tetramethylammonium hydroxide
TMB	Trimethylborate
TMEDA	Tetramethylethane-1,2-diamine; N^1,N^1,N^2,N^2-tetramethylethane-1,2-diamine
TMG	Tetramethyl guanidine
TM-N-C	Transition metal-doped nitrogen-carbon
TMOS	Tetramethoxy silane
TMPP	Tetramethoxyphenyl porphyrins
TMPS	Trimethoxyl phenyl silane
TMPyP	Tetramethylpyridylporphine
TNA	Titania nanotube array
TNT	Trinitrotoluene
TN-T	TiO_2 nanotubes
TOC	Total organic content

TOF	Turnover frequency
ToF-SIMS	Time-of-flight secondary ion spectroscopy
TPA	Tripropylamine; Temperature-programmed adsorption
TPAH	Tetra-n-propylammonium hydroxide
TPB	Triple phase boundary
TPD	Tonne(s) per day; tons/day
TPD	Thermally programmed desorption; Temperature-programmed desorption
TPDMS	Temperature-programmed desorption mass spectrometry
TPO	Temperature-programmed oxidation
TPP	Tetraphenyl porphyrin
TPPS	5,10,15,20-tetrakis(4-sulfonatophenyl) porphyrin
TPR	Temperature-programmed reduction
TPRD	Thermally-activated pressure relief device
TPS	3-(trihydroxysilyl)-1-propane-sulfonic acid
TPV	Through-plate voltage
TRA	Technology Readiness Assessment
TRAIN	TrainingFinder Realtime Affiliate Network
Tri-Gen	Tri-generation
TRL	Technology readiness level
TRO	RuO_2-TiO_2
Trityl	Chemical blocking group used to protect amines
tr. oz.	Troy ounce
TRU	Transport refrigeration units
TSWS	Temperature-swing water splitting
TVS	Twin Vortices Series
TW	Triangel wave
UC	University of California
UCB	University of California, Berkeley
UCF	University of Central Florida
UCI	University of California, Irvine
UCLA	University of California, Los Angeles
UCONN	University of Connecticut
UCSB	University of California, Santa Barbara
UDDS	Urban Dynamometer Driving Schedule
UEL	Upper explosive limit
UFL	Upper flammability limit
UGA	University of Georgia, Athens
UH	University of Hawaii
UHP	Ultra-high purity
UHV	Ultra-high vacuum
UIUC	University of Illinois, Urbana-Champaign
UL	Underwriters Laboratory
ULAM	Ultra-low-angle microtomy
ULSD	Ultra-low sulfur diesel
UM	University of Michigan
UMC	Unsaturated metal centers
UMC	Ultramicroporous carbon
UMCP	University of Maryland, College Park
UMSL	University of Missouri, St. Louis
UN	United Nations
UNB	University of New Brunswick
UNCC	University of North Carolina at Charlotte
UNECE	United Nations Economic Commission for Europe
UNLV	University of Nevada, Las Vegas
UNLVRF	UNLV Research Foundation
UNM	University of New Mexico
UNR	University of Nevada, Reno
UPD	Underpotential deposition
UP-DW	Ultra-pure distilled water
UPE	Ultra-high molecular weight polyethylene
UPL	Upper potential limit
UPS	Ultraviolet photoelectron spectroscopy
U.S.	United States
US06	Environmental Protection Agency vehicle driving cycle
USA	United States of America
USANS	Ultra-small angle neutron scattering
USAXS	Ultra-small angle X-ray scattering
USB	Universal serial bus
USC	University of South Carolina; University of Southern California
USCAR	United States Council for Automotive Research, U.S. Cooperative Automotive Research
USCG	United States Coast Guard
U.S. DRIVE	United States Driving Research and Innovation for Vehicle efficiency and Energy sustainability
USFCC	United States Fuel Cell Council
USM	University of Southern Mississippi
USTAG	U.S. Technical Advisory Group
UT	University of Toledo; University of Tennessee
UTC, UTC FC	United Technologies Corporation Fuel Cells
UTC	University of Tennessee, Chattanooga
UTCP	UTC Power
UTRC	United Technologies Research Center

UTS	Ultimate tensile strength
UV	Ultraviolet
UVL	Upper voltage limit
UV-vis	Ultraviolet-visual
UW	University of Washington
V	Vanadium; Volt
VA	Vinyl acetate
VAC	Volts alternating current
VACNTs	Vertically aligned carbon nanotubes
VANTA	Vertically aligned nanotube arrays
VASP	Vienna ab initio simulation package
VaTech	Virginia Polytechnic Institute and State University
VB	Valence band
VBM	Valence band minimum, Valence band maximum
VC	Vanadium carbide; Vulcan carbon; Volumetric capacity
VDC	Volts direct current
VDF	Vinylidene fluoride
VDOS	Vibrational density of states
vdW	van der Waals
vdW-DF	van der Waals density function
VFA	Volatile fatty acid
VFS	Vehicle fueling station
$V(H_2)$	Volumetric hydrogen adsorption capacity; Volumetric hydrogen storage capacity
VHSV	Volumetric hourly space velocity
VHTR	Very high temperature gas-cooled nuclear reactor
VHTS	Virtual high-throughput screening
VI	Venter Institute
V-I, V/I	Voltage–current
VIM/VAR	Vacuum induction melting/vacuum arc remelting
VIR	Voltage-current-resistance
VIS	Visible light at 400-700 nm
V_{mp}	Micropore volume
VMT	Vehicle miles traveled
VOC	Volatile organic compound, Voltage open circuit
Vol., vol.	Volume
vol%	Volume percent
V_{pore}	Total pore volume
VT	Virginia Tech
W	Tungsten; Watt(s)
WAXD	Wide-angle X-ray diffraction
WAXS	Wide angle X-ray scattering
WBS	Work breakdown schedule
WC	Tungsten carbon; Tungsten carbide
W/cm^2	Watt(s) per square centimeter
WDD	Water displacement desorption
We, W_e	Watt(s) electric
WG	Working group
WG-12	Working Group 12
WGS	Water-gas shift
WGSMR	Water-gas shift membrane reactor
WGSR	Water-gas shift reactor
Wh	Watt-hour(s)
$W(H_2)$	Gravimetric hydrogen storage capacity
W-h/kg	Watt-hour(s) per kilogram
W-h/L, Wh/liter, Wh/L	Watt-hour(s) per liter
WHSV	Weight hourly space velocity
Wind2H2	Wind to hydrogen demonstration project
W/kg	Watt(s) per kilogram
W/L, W/l	Watt(s) per liter
W/m-K, W/m.K, W/mK	Watt(s) per meter-Kelvin (unit of thermal conductivity)
WMO	World Meteorological Organization
WO_3	Tungsten trioxide
WO_x	Tungsten oxide
WP.29	Working Party 29 - World Forum for Harmonization of Vehicle Regulations
Wppm	Weight part(s) per million
WS	Water splitting
WSTF	White Sands Test Facility
wt	Weight
Wt	Watt(s) thermal
wt%, wt.%	Weight percent (percent by weight)
WT	Wild type
WTP	Well to pump; Water transport plate
WTPP	Well-to-power plant
WTT	Well-to-tank
WTW	Well-to-wheels
w/v	Weight by volume
WWTP	Waste water treatment plant
X-	an anionic ligand such as chloride
XAFS	X-ray absorption fine structure
XANES	X-ray absorption near-edge spectroscopy
XAS	X-ray absorption spectroscopy

XC72	High-surface-area carbon support made by Cabot
XES	X-ray emission spectroscopy
X_{O2}	Oxygen mole fraction
XPS	X-ray photoelectron spectroscopy, X-ray photon spectroscopy, X-ray photoemission spectroscopy, X-ray photoluminescence spectroscopy
XPS-UPS	X-ray photoelectron-ultraviolet photoelectron spectroscopy
XRD	X-ray diffraction
XRF	X-ray fluorescence
XRT	X-ray tomography
Y	Yttrium
YB	Young Brothers, Ltd.
yr, YR	Year
YSZ	Yttria-stablized zirconia
Z	Atomic number
ZEBA	Zero Emission Bay Area
ZEV	Zero emission vehicle
ZHS	Zinc hydroxystannate
ZIF	Zeolitic imidazolate framework
ZIO	Zirconium-doped indium oxide
ZMOF	Zeolite(-type) metal-organic framework
Zn	Zinc
ZnO	Zinc oxide
ZPE	Zero point energy
zpp	Zirconium phenyl phosphonate
Zr	Zirconium
ZrO_2	Zirconium dioxide
ZrSPP	Zirconium phosphate sulfophenylphosphonate
ZVI	Zerovalent iron

XIII. Primary Contacts Index

A

Aceves, Salvador. III-45, IV-136, VIII-54
Adams, Michael II-100
Adzic, Radoslav V-25
Ahluwalia, Rajesh. IV-11, V-167
Alptekin, Gokhan II-81
Anton, Don IV-22
Arif, Muhammad V-184
Armstrong, Neal II-85, II-123
Atanasoski, Radoslav V-9
Ayers, Katherine II-21, II-24

B

Baldwin, Don III-21
Barilo, Nick. VIII-40, VIII-43
Bessette, Norm VII-59
Blekhman, David VII-49
Borup, Rod V-105
Brooks, Kriston. IV-30, IX-7, IX-26
Brosha, Eric VIII-16
Burgess, Robert VIII-13
Busby, Colin VI-11
Buttner, William VIII-49

C

Cai, Mei. IV-52
Colon-Mercado, Hector II-45
Concepcion, Javier II-106
Contini, Vince. V-193

D

Deutsch, Todd II-48
Di Bella, Frank III-49
Dinh, Huyen V-128
Drost, Kevin IV-61

E

Eichman, Josh X-46
Elgowainy, Amgad III-11, X-27, X-36
Elrick, Bill. VII-66
Eudy, Leslie VII-9

F

Feng, Zhili. III-39

G

Garzon, Fernando V-30
Ghirardi, Maria. II-67
Goudy, Andrew. IV-95
Gregoire, John. II-119
Gu, Wenbin V-151

H

Harrison, Kevin II-17, III-58
Harvey, David V-122
Herring, Andrew. V-87
Heshmat, Hooshang III-16
Houle, Frances II-111

J

James, Brian II-11, IV-17, V-173
Jones, Anne. II-97, II-131

K

Kashuba, Michael VII-46
Keller, Russ. IX-12
Kim, Yu Seung V-91
King, Paul II-103, II-125
Kocha, Shyam. V-215
Kongkanand, Anusorn V-56
Kurtz, Jennifer V-118, VII-31, VII-37

L

Leavitt, Mark VI-15
Lin, Zhenhong X-13, X-40
Lipp, Ludwig. III-36
Liu, Shih-Yuan IV-105
Liu, Di-Jia V-74
Long, Jeffrey. IV-73
Lueking, Angela IV-79

M

Maness, Pin-Ching II-71, II-76
Markovic, Nenad V-19
McCrory, Charles II-134
McDaniel, Anthony II-39
McWhorter, Scott IV-140
Melis, Tasios II-63
Ming, Quentin. V-208

Mintz, Marianne X-19
Mittelsteadt, Cortney V-79, V-146
Moawad, Ayman X-30
More, Karren V-178
Moulthrop, Larry VII-26
Mukerjee, Sanjeev V-50
Mukundan, Rangachary V-111
Myers, Deborah V-100

N

Neale, Nathan II-92
Newhouse, Norman IV-65
Norris, Bob IV-118

O

Ogitsu, Tadashi II-58

P

Parilla, Phil IV-68
Petrecky, James VII-63, IX-20
Pfeifer, Peter IV-86
Pivovar, Bryan V-15, V-211
Polyansky, Dmitry II-108
Popov, Branko V-62
Pratt, Joe IX-23
Prezhdo, Oleg II-89
Prinz, Fritz II-128

R

Ramani, Vijay V-46
Ramsden, Todd X-22
Rawls, George III-24
Rivkin, Carl VIII-9
Rocheleau, Richard IX-15
Rockward, Tommy VIII-28
Rohatgi, Aashish III-54

S

San Marchi, Chris VIII-23, VIII-34
Saur, Genevieve V-190, VII-14
Semelsberger, Troy IV-43
Shaffer, Brendan X-44
Shaner, Matthew II-137
Sharp, Ian II-115
Simmons, Kevin IV-131
Somerday, Brian III-31, VII-57
Sprik, Sam VII-41
Staudt, Rhonda VII-18
Steinbach, Andrew V-95
St-Pierre, Jean V-133
Stretch, Dale V-162

T

Terlip, Danny VII-22
Thornton, Matthew IV-47
Tiede, David II-94
Tieu, Michael VII-52
Turner, John V-36

U

Udovic, Terry IV-100
Ulsh, Michael VI-7

V

van Hassel, Bart IV-36
Veenstra, Michael IV-56

W

Wagener, Earl V-158
Warren, Dave IV-124
Wasielewski, Michael II-141
Weber, Adam II-144, V-140
Wegrzyn, Jim IV-111
Wei, Max V-196
Weimer, Al II-33
Wolverton, Christopher IV-92

X

Xu, Hui II-28
Xu, Liwei II-53

Y

Yandrasits, Michael V-83

Z

Zelenay, Piotr V-69, V-201
Zidan, Ragaiy IV-114

XIV. Hydrogen and Fuel Cells Program Contacts

Sunita Satyapal
Director
Fuel Cell Technologies Office
Office of Energy Efficiency and Renewable Energy
U.S. Department of Energy
Phone: (202) 586-2336
Email: Sunita.Satyapal@ee.doe.gov

Rick Farmer
Operations Supervisor
Fuel Cell Technologies Office
Office of Energy Efficiency and Renewable Energy
U.S. Department of Energy
Phone: (202) 586-1623
Email: Richard.Farmer@ee.doe.gov

John Vetrano
Materials Sciences and Engineering Division
Basic Energy Sciences Program
Office of Science
U.S. Department of Energy
Phone: (301) 903-5976
Email: John.Vetrano@science.doe.gov

Guido B. DeHoratiis, Jr.
Division of Advanced Energy Systems
DOE Office of Fossil Energy
Phone: (202) 586-2795
Email: Guido.B.Dehoratiis@hq.doe.gov

Carl Sink
Office of Gas Cooled Reactor Technologies
DOE Office of Nuclear Energy
Phone: (301) 903-5131
Email: Carl.Sink@nuclear.energy.gov

HYDROGEN PRODUCTION AND DELIVERY

Sara Dillich
Hydrogen Production and Delivery Program Manager
Fuel Cell Technologies Office
Office of Energy Efficiency and Renewable Energy
U.S. Department of Energy
Phone: (202) 586-7925
Email: Sara.Dillich@ee.doe.gov

HYDROGEN STORAGE

Ned Stetson
Hydrogen Storage Program Manager
Fuel Cell Technologies Office
Office of Energy Efficiency and Renewable Energy
U.S. Department of Energy
Phone: (202) 586-9995
Email: Ned.Stetson@ee.doe.gov

FUEL CELLS

Dimitrios Papageorgopoulos
Fuel Cells Program Manager
Fuel Cell Technologies Office
Office of Energy Efficiency and Renewable Energy
U.S. Department of Energy
Phone: (202) 586-5463
Email: Dimitrios.Papageorgopoulos@ee.doe.gov

MANUFACTURING R&D

Nancy Garland
Manufacturing R&D Project Manager
Fuel Cell Technologies Office
Office of Energy Efficiency and Renewable Energy
U.S. Department of Energy
Phone: (202) 586-5673
Email: Nancy.Garland@ee.doe.gov

TECHNOLOGY VALIDATION

Jason Marcinkoski
Technology Validation Project Manager
Fuel Cell Technologies Office
Office of Energy Efficiency and Renewable Energy
U.S. Department of Energy
Phone: (202) 586-7466
Email: Jason.Marcinkoski@ee.doe.gov

SAFETY, CODES & STANDARDS

Charles James Jr.
(IPA) Safety, Codes & Standards Project Manager
Fuel Cell Technologies Office
Office of Energy Efficiency and Renewable Energy
U.S. Department of Energy
Phone: (202) 287-6223
Email: Charles.James@ee.doe.gov

EDUCATION

Gregory J. Kleen
Education Project Manager
Fuel Cell Technologies Office
Golden Field Office
U.S. Department of Energy
Phone: (720) 356-1672
Email: Gregory.Kleen@ee.doe.gov

MARKET TRANSFORMATION

Pete Devlin
Market Transformation Project Manager
Fuel Cell Technologies Office
Office of Energy Efficiency and Renewable Energy
U.S. Department of Energy
Phone: (202) 586-4905
Email: Peter.Devlin@ee.doe.gov

SYSTEMS ANALYSIS

Fred Joseck
Systems Analysis Project Manager
Fuel Cell Technologies Office
Office of Energy Efficiency and Renewable Energy
U.S. Department of Energy
Phone: (202) 586-7932
Email: Fred.Joseck@ee.doe.gov

AMERICAN RECOVERY AND REINVESTMENT ACT (ARRA) ACTIVITIES

Jim Alkire
Project Manager and Recovery Act Activities Lead
Fuel Cell Technologies Office
Office of Energy Efficiency and Renewable Energy
U.S. Department of Energy
Phone: (720) 356-1426
Email: James.Alkire@ee.doe.gov

XV. Project Listings by State

Alabama

IV.E.1 University of Alabama: Novel Carbon(C)-Boron(B)-Nitrogen(N)-Containing H2 Storage Materials IV-105

IV.F.3 Toray Composites America: Synergistically Enhanced Materials and Design Parameters for Reducing the Cost of Hydrogen Storage Tanks IV-131

Arizona

II.G.1 University of Arizona: Semiconductor Nanorod/Metal(Metal Oxide) Hybrid Materials: Characterization of Frontier Orbital Energies and Charge Injection Processes Using Unique Combinations of Photoemission Spectroscopies and Waveguide Spectroelectrochemistrie II-85

II.G.5 Arizona State: Electrochemical Characterization of the Oxygen-Tolerant Soluble Hydrogenase I from Pyrococcus furiosus II-97

II.G.13 University of Arizona: Center for Interface Science: Solar-Electric Materials (CISSEM) II-123

II.G.16 Arizona State: Artificial Hydrogenases: Utilization of Redox Non-Innocent Ligands in Iron Complexes for Hydrogen Production II-131

VIII.3 Custom Sensor Solutions: Hydrogen Safety, Codes and Standards: Sensors VIII-16

California

II.C.2 Sandia National Laboratories: Solar Hydrogen Production with a Metal Oxide-Based Thermochemical Cycle II-39

II.D.3 Lawrence Livermore National Laboratory: Characterization and Optimization of Photoelectrode Surfaces for Solar-to-Chemical Fuel Conversion II-58

II.E.1 University of California, Berkeley: Maximizing Light Utilization Efficiency and Hydrogen Production in Microalgal Cultures II-63

II.F.1 Sacramento Municipal Utility District : Bio-Fueled Solid Oxide Fuel Cells II-81

II.G.10 Lawrence Berkeley National Laboratory: Joint Center for Artificial Photosynthesis: An Overview II-111

II.G.11 Lawrence Berkeley National Laboratory: Joint Center for Artificial Photosynthesis: Corrosion Protection Schemes to Enable Durable Solar Water Splitting Devices. II-115

II.G.12 Caltech: Joint Center for Artificial Photosynthesis: High Throughput Experimentation for Electrocatalyst and Photoabsorber Discovery II-119

II.G.15 Stanford University: Center on Nanostructuring for Efficient Energy Conversion (CNEEC) II-128

II.G.17 Caltech: Joint Center for Artificial Photosynthesis: Benchmarking Electrocatalysts for the Oxygen Evolution Reaction II-134

II.G.18 Caltech: Joint Center for Artificial Photosynthesis: Si Microwire-Based Solar Water Splitting Devices II-137

II.G.20 Lawrence Berkeley National Laboratory: Joint Center for Artificial Photosynthesis: Modeling and Simulation Team II-144

III.5 Sandia National Laboratories: Hydrogen Embrittlement of Structural Steels III-31

III.7 Ben C. Gerwick Inc.: Vessel Design and Fabrication Technology for Stationary High-Pressure Hydrogen Storage. III-39

III.8 Lawrence Livermore National Laboratory: Preliminary Testing of LLNL/Linde 875-bar Liquid Hydrogen Pump III-45

III.8 Linde LLC: Preliminary Testing of LLNL/Linde 875-bar Liquid Hydrogen Pump III-45

III.9 HyGen Industries: Development of a Centrifugal Hydrogen Pipeline Gas Compressor III-49

IV.B.1 Jet Propulsion Laboratory: Hydrogen Storage Engineering Center of Excellence IV-22

IV.B.1 California Institute of Technology: Hydrogen Storage Engineering Center of Excellence IV-22

IV.C.1 H2 Technology Consulting LLC: Hydrogen Sorbent Measurement Qualification and Characterization IV-68

California (Continued)

IV.C.2 Lawrence Berkeley National Laboratory: Hydrogen Storage in Metal-Organic Frameworks IV-73

IV.D.1 University of California, Los Angeles: Design of Novel Multi-Component Metal Hydride-Based Mixtures for Hydrogen Storage IV-92

IV.F.4 Lawrence Livermore National Laboratory: Thermomechanical Cycling of Thin-Liner High-Fiber-Fraction Cryogenic Pressure Vessels Rapidly Refueled a by LH2 pump to 700 bar IV-136

IV.F.4 Linde LLC: Thermomechanical Cycling of Thin-Liner High-Fiber-Fraction Cryogenic Pressure Vessels Rapidly Refueled a by LH2 pump to 700 bar IV-136

IV.F.4 Spencer Composites Corporation: Thermomechanical Cycling of Thin-Liner High-Fiber-Fraction Cryogenic Pressure Vessels Rapidly Refueled a by LH2 pump to 700 bar. IV-136

V.D.1 Lawrence Berkeley National Laboratory: High-Performance, Durable, Low-Cost Membrane Electrode Assemblies for Transportation Applications V-95

V.E.1 Lawrence Berkeley National Laboratory: Durability Improvements through Degradation Mechanism Studies V-105

V.E.2 Lawrence Berkeley National Laboratory: Accelerated Testing Validation. V-111

V.G.1 Lawrence Berkeley National Laboratory: Fuel Cell Fundamentals at Low and Subzero Temperatures V-140

V.H.2 Electricore, Inc.: Roots Air Management System with Integrated Expander V-162

V.I.5 University of California, Irvine: Enlarging the Potential Market for Stationary Fuel Cells through System Design Optimization V-190

V.I.7 Lawrence Berkeley National Laboratory: A Total Cost of Ownership Model for PEM Fuel Cells in Combined Heat and Power and Backup Power Applications V-196

V.I.7 University of California, Berkeley: A Total Cost of Ownership Model for PEM Fuel Cells in Combined Heat and Power and Backup Power Applications V-196

VI.3 Quantum Fuel Systems Technologies Worldwide, Inc.: Development of Advanced Manufacturing Technologies for Low-Cost Hydrogen Storage Vessels. VI-15

VII.9 California Air Resources Board: Data Collection and Validation of Newport Beach Hydrogen Station Performance VII-46

VII.9 Hydrogenics Corporation: Data Collection and Validation of Newport Beach Hydrogen Station Performance VII-46

VII.10 California State University, Los Angeles: California State University Los Angeles Hydrogen Refueling Facility Performance Evaluation and Optimization VII-49

VII.11 Linde LLC: Performance Evaluation of Delivered Hydrogen Fueling Stations VII-52

VII.12 Sandia National Laboratories: Hydrogen Fueling Infrastructure Research and Station Technology. VII-57

VII.15 California Fuel Cell Partnership: H2-FCEV Commercialization - Facilitating Collaboration, Obtaining Real World Expertise, and Developing New Analysis Tools VII-66

VIII.3 Lawrence Livermore National Laboratory: Hydrogen Safety, Codes and Standards: Sensors VIII-16

VIII.4 Sandia National Laboratories: R&D for Safety, Codes and Standards: Materials and Components Compatibility VIII-23

VIII.6 Sandia National Laboratories: R&D for Safety Codes and Standards: Hydrogen Release Behavior and Risk Assessment VIII-34

VIII.7 California Fuel Cell Partnership: Hydrogen Emergency Response Training for First Responders VIII-40

VIII.8 Fluer, Inc.: Hydrogen Safety Panel and Hydrogen Safety Knowledge Tools VIII-43

VIII.8 City of Santa Fe Springs: Hydrogen Safety Panel and Hydrogen Safety Knowledge Tools. VIII-43

VIII.10 Lawrence Livermore National Laboratory: Hands-on Hydrogen Safety Training. VIII-54

IX.5 Sandia National Laboratories: Maritime Fuel Cell Generator Project IX-23

X.8 University of California, Irvine: Tri-Generation Fuel Cell Technologies for Location-Specific Applications X-44

Colorado

II.B.1 National Renewable Energy Laboratory: Renewable Electrolysis Integrated Systems Development and Testing . . . II-17

II.B.1 Spectrum Automation Controls: Renewable Electrolysis Integrated Systems Development and Testing . . . II-17

II.B.4 National Renewable Energy Laboratory: High-Performance, Long-Lifetime Catalysts for Proton Exchange Membrane Electrolysis . . . II-28

II.C.1 University of Colorado, Boulder: Solar-Thermal Redox-Based Water Splitting Cycles . . . II-33

II.C.2 University of Colorado, Boulder: Solar Hydrogen Production with a Metal Oxide-Based Thermochemical Cycle . . . II-39

II.C.2 Colorado School of Mines: Solar Hydrogen Production with a Metal Oxide-Based Thermochemical Cycle II-39

II.D.1 National Renewable Energy Laboratory: Semiconductor Materials for Photoelectrolysis . . . II-48

II.D.2 National Renewable Energy Laboratory: Critical Research for Cost-Effective Photoelectrochemical Production of Hydrogen . . . II-53

II.E.2 National Renewable Energy Laboratory: Biological Systems for Algal Hydrogen Photoproduction . . . II-67

II.E.3 National Renewable Energy Laboratory: Fermentation and Electrohydrogenic Approaches to Hydrogen Production . . . II-71

II.E.4 National Renewable Energy Laboratory: Probing O2-Tolerant CBS Hydrogenase for Hydrogen Production . . . II-76

II.F.1 TDA Research: Bio-Fueled Solid Oxide Fuel Cells . . . II-81

II.G.3 National Renewable Energy Laboratory: Oxidatively Stable Nanoporous Silicon Photocathodes for Photoelectrochemical Hydrogen Evolution . . . II-92

II.G.7 National Renewable Energy Laboratory: Photobiohybrid Solar Fuels . . . II-103

II.G.14 National Renewable Energy Laboratory: Photobiohybrid Solar Fuels Nanoparticle-Hydrogenase Complexes . . . II-125

III.11 National Renewable Energy Laboratory: 700-Bar Hydrogen Dispenser Hose Reliability Improvement . . . III-58

III.11 Spectrum Automation Controls: 700-Bar Hydrogen Dispenser Hose Reliability Improvement . . . III-58

IV.B.1 National Renewable Energy Laboratory: Hydrogen Storage Engineering Center of Excellence . . . IV-22

IV.B.5 National Renewable Energy Laboratory: System Design, Analysis, Modeling, and Media Engineering Properties for Hydrogen Energy Storage . . . IV-47

IV.C.1 National Renewable Energy Laboratory: Hydrogen Sorbent Measurement Qualification and Characterization . . . IV-68

V.A.2 National Renewable Energy Laboratory: Extended, Continuous Pt Nanostructures in Thick, Dispersed Electrodes . . . V-15

V.A.2 Colorado School of Mines: Extended, Continuous Pt Nanostructures in Thick, Dispersed Electrodes . . . V-15

V.A.6 National Renewable Energy Laboratory: Tungsten Oxide and Heteropoly Acid-Based System for Ultra-High Activity and Stability of Pt Catalysts in Proton Exchange Membrane Fuel Cell Cathodes . . . V-36

V.A.6 Colorado School of Mines: Tungsten Oxide and Heteropoly Acid-Based System for Ultra-High Activity and Stability of Pt Catalysts in Proton Exchange Membrane Fuel Cell Cathodes . . . V-36

V.A.6 University of Colorado, Boulder: Tungsten Oxide and Heteropoly Acid-Based System for Ultra-High Activity and Stability of Pt Catalysts in Proton Exchange Membrane Fuel Cell Cathodes . . . V-36

V.C.2 Colorado School of Mines: Advanced Hybrid Membranes for Next Generation PEMFC Automotive Applications . . . V-87

V.C.2 National Renewable Energy Laboratory: Advanced Hybrid Membranes for Next Generation PEMFC Automotive Applications . . . V-87

V.E.3 National Renewable Energy Laboratory: Fuel Cell Technology Status—Cost and Price Status . . . V-118

V.F.1 National Renewable Energy Laboratory: Effect of System Contaminants on PEMFC Performance and Durability . . . V-128

V.F.1 Colorado School of Mines: Effect of System Contaminants on PEMFC Performance and Durability . . . V-128

Colorado (Continued)

V.I.5 National Renewable Energy Laboratory: Enlarging the Potential Market for Stationary Fuel Cells through System Design Optimization . . . V-190

V.L.1 National Renewable Energy Laboratory: Advanced Ionomers and MEAs for Alkaline Membrane Fuel Cells . . . V-211

V.L.1 Colorado School of Mines: Advanced Ionomers and MEAs for Alkaline Membrane Fuel Cells . . . V-211

V.M.1 National Renewable Energy Laboratory: Best Practices and Benchmark Activities for ORR Measurements by the Rotating Disk Electrode Technique . . . V-215

VI.1 National Renewable Energy Laboratory: Fuel Cell Membrane Electrode Assembly Manufacturing R&D . . . VI-7

VII.1 National Renewable Energy Laboratory: Technology Validation: Fuel Cell Bus Evaluations . . . VII-9

VII.2 National Renewable Energy Laboratory: Stationary Fuel Cell Evaluation. . . . VII-14

VII.4 National Renewable Energy Laboratory: Hydrogen Component Validation . . . VII-22

VII.4 Spectrum Automation Controls: Hydrogen Component Validation . . . VII-22

VII.6 National Renewable Energy Laboratory: Forklift and Backup Power Data Collection and Analysis . . . VII-31

VII.7 National Renewable Energy Laboratory: Fuel Cell Electric Vehicle Evaluation . . . VII-37

VII.8 National Renewable Energy Laboratory: Next Generation Hydrogen Infrastructure Evaluation . . . VII-41

VIII.1 National Renewable Energy Laboratory: Fuel Cell Technologies National Codes and Standards Development and Outreach . . . VIII-9

VIII.2 National Renewable Energy Laboratory: Component Standard Research and Development . . . VIII-13

VIII.9 National Renewable Energy Laboratory: NREL Hydrogen Sensor Testing Laboratory . . . VIII-49

VIII.9 Element One: NREL Hydrogen Sensor Testing Laboratory . . . VIII-49

X.3 National Renewable Energy Laboratory: Pathway Analysis: Projected Cost, Life-Cycle Energy Use and Emissions of Future Hydrogen Technologies . . . X-22

X.9 National Renewable Energy Laboratory: Electricity Market Valuation for Hydrogen Technologies. . . . X-46

Connecticut

II.B.2 Proton OnSite: Economical Production of Hydrogen through Development of Novel, High-Efficiency Electrocatalysts for Alkaline Membrane Electrolysis . . . II-21

II.B.3 Proton OnSite: Low-Noble-Metal-Content Catalysts/Electrodes for Hydrogen Production by Water Electrolysis . . . II-24

II.F.1 FuelCell Energy, Inc.: Bio-Fueled Solid Oxide Fuel Cells . . . II-81

III.6 FuelCell Energy, Inc.: Electrochemical Hydrogen Compressor . . . III-36

III.6 Sustainable Innovations, LLC: Electrochemical Hydrogen Compressor . . . III-36

IV.B.1 United Technologies Research Center: Hydrogen Storage Engineering Center of Excellence . . . IV-22

IV.B.3 United Technologies Research Center: Advancement of Systems Designs and Key Engineering Technologies for Materials-Based Hydrogen Storage . . . IV-36

V.D.2 United Technologies Research Center: Rationally Designed Catalyst Layers for PEMFC Performance Optimization. . . . V-100

V.F.2 University of Connecticut: The Effect of Airborne Contaminants on Fuel Cell Performance and Durability . . . V-133

V.F.2 WPCSOL, LLC: The Effect of Airborne Contaminants on Fuel Cell Performance and Durability . . . V-133

V.G.1 United Technologies Research Center: Fuel Cell Fundamentals at Low and Subzero Temperatures . . . V-140

VI.2 UTC Power: Manufacturing of Low-Cost, Durable Membrane Electrode Assemblies Engineered for Rapid Conditioning . . . VI-11

VII.5 Proton OnSite: Validation of an Advanced High-Pressure PEM Electrolyzer and Composite Hydrogen Storage, with Data Reporting, for SunHydro Stations . . . VII-26

VII.5 SunHydro LLC: Validation of an Advanced High-Pressure PEM Electrolyzer and Composite Hydrogen Storage, with Data Reporting, for SunHydro Stations . . . VII-26

Connecticut (Continued)

VIII.8 Proton OnSite: Hydrogen Safety Panel and Hydrogen Safety Knowledge Tools VIII-43

VIII.8 GWS Solutions of Tolland, LLC: Hydrogen Safety Panel and Hydrogen Safety Knowledge Tools. VIII-43

Delaware

IV.D.2 Delaware State University: Hydrogen Storage Materials for Fuel Cell-Powered Vehicles. IV-95

IV.D.2 University of Delaware: Hydrogen Storage Materials for Fuel Cell-Powered Vehicles IV-95

V.A.2 University of Delaware: Extended, Continuous Pt Nanostructures in Thick, Dispersed Electrodes V-15

V.A.5 University of Delaware: The Science and Engineering of Durable Ultra-Low PGM Catalysts. V-30

V.E.1 Ion Power Inc.: Durability Improvements through Degradation Mechanism Studies V-105

V.E.2 Ion Power Inc.: Accelerated Testing Validation. V-111

V.J.1 University of Delaware: Advanced Materials and Concepts for Portable Power Fuel Cells V-201

VI.2 University of Delaware: Manufacturing of Low-Cost, Durable Membrane Electrode Assemblies Engineered for Rapid Conditioning. VI-11

Florida

VIII.8 Addison Bain: Hydrogen Safety Panel and Hydrogen Safety Knowledge Tools VIII-43

Georgia

II.G.6 University of Georgia: Hyperthermophilic Multiprotein Complexes and Pathways for Energy Conservation and Catalysis II-100

Hawaii

V.F.2 Hawaii Natural Energy Institute: The Effect of Airborne Contaminants on Fuel Cell Performance and Durability V-133

IX.3 Hawaii Natural Energy Institute: Hydrogen Energy Systems as a Grid Management Tool. IX-15

Illinois

II.B.2 Illinois Institute of Technology: Economical Production of Hydrogen through Development of Novel, High-Efficiency Electrocatalysts for Alkaline Membrane Electrolysis II-21

II.G.4 Argonne National Laboratory: Fundamental Design and Mechanisms for Solar Hydrogen Production in Natural and Artificial Photosynthetic Systems II-94

II.G.19 Northwestern University: Argonne-Northwestern Solar Energy Research (ANSER) Center II-141

III.1 Argonne National Laboratory: Hydrogen Delivery Infrastructure Analysis III-11

IV.A.1 Argonne National Laboratory: System Analysis of Physical and Materials-Based Hydrogen Storage Options IV-11

IV.D.1 Northwestern University: Design of Novel Multi-Component Metal Hydride-Based Mixtures for Hydrogen Storage. IV-92

V.A.1 Argonne National Laboratory: Durable Catalysts for Fuel Cell Protection during Transient Conditions V-9

V.A.3 Argonne National Laboratory: Nanosegregated Cathode Catalysts with Ultra-Low Platinum Loading. V-19

V.A.7 Illinois Institute of Technology: Synthesis and Characterization of Mixed-Conducting Corrosion-Resistant Oxide Supports V-46

V.A.12 Argonne National Laboratory: Non-PGM Cathode Catalysts using ZIF-Based Precursors with Nanonetwork Architecture. V-74

V.D.1 Argonne National Laboratory: High-Performance, Durable, Low-Cost Membrane Electrode Assemblies for Transportation Applications V-95

V.D.2 Argonne National Laboratory: Rationally Designed Catalyst Layers for PEMFC Performance Optimization. V-100

V.E.1 Argonne National Laboratory: Durability Improvements through Degradation Mechanism Studies. V-105

Illinois (Continued)

V.I.1 Argonne National Laboratory: Performance of Advanced Automotive Fuel Cell Systems with Heat Rejection Constraints . . . V-167

V.M.1 Argonne National Laboratory: Best Practices and Benchmark Activities for ORR Measurements by the Rotating Disk Electrode Technique . . . V-215

VII.11 Gas Technology Institute: Performance Evaluation of Delivered Hydrogen Fueling Stations . . . VII-52

IX.2 Gas Technology Institute: Landfill Gas-to-Hydrogen . . . IX-12

X.2 Argonne National Laboratory: Employment Impacts of Infrastructure Development for Hydrogen and Fuel Cell Technologies . . . X-19

X.2 RCF Economic and Financial Consulting, Inc.: Employment Impacts of Infrastructure Development for Hydrogen and Fuel Cell Technologies . . . X-19

X.4 Argonne National Laboratory: Life-Cycle Analysis of Water Use for Hydrogen Production Pathways . . . X-27

X.5 Argonne National Laboratory: Impact of Fuel Cell System Peak Efficiency on Fuel Consumption and Cost . . . X-30

X.6 Argonne National Laboratory: Analysis of Incremental Fueling Pressure Cost . . . X-36

Indiana

V.D.2 Indiana University Purdue University: Rationally Designed Catalyst Layers for PEMFC Performance Optimization . . . V-100

Maryland

IV.B.5 Mark Paster: System Design, Analysis, Modeling, and Media Engineering Properties for Hydrogen Energy Storage . . . IV-47

IV.C.2 National Institute of Standards and Technology: Hydrogen Storage in Metal-Organic Frameworks . . . IV-73

IV.D.3 National Institute of Standards and Technology: Neutron Characterization in Support of the DOE Hydrogen Storage Program . . . IV-100

V.D.1 Johns Hopkins University: High-Performance, Durable, Low-Cost Membrane Electrode Assemblies for Transportation Applications . . . V-95

V.I.4 National Institute of Standards and Technology: Neutron Imaging Study of the Water Transport in Operating Fuel Cells . . . V-184

VI.2 W. L. Gore & Associates, Inc.: Manufacturing of Low-Cost, Durable Membrane Electrode Assemblies Engineered for Rapid Conditioning . . . VI-11

Massachusetts

II.B.4 Giner, Inc.: High-Performance, Long-Lifetime Catalysts for Proton Exchange Membrane Electrolysis . . . II-28

III.9 Concepts NREC: Development of a Centrifugal Hydrogen Pipeline Gas Compressor . . . III-49

IV.E.1 Boston College: Novel Carbon(C)-Boron(B)-Nitrogen(N)-Containing H2 Storage Materials . . . IV-105

IV.E.1 Protonex Technology Corporation: Novel Carbon(C)-Boron(B)-Nitrogen(N)-Containing H2 Storage Materials . . . IV-105

V.A.8 Northeastern University: Development of Novel Non-PGM Electrocatalysts for Proton Exchange Membrane Fuel Cell Applications . . . V-50

V.A.9 Massachusetts Institute of Technology: High-Activity Dealloyed Catalysts . . . V-56

V.A.9 Northeastern University: High-Activity Dealloyed Catalysts . . . V-56

V.B.1 Giner, Inc.: Dimensionally Stable High Performance Membrane . . . V-79

V.G.2 Giner, Inc.: Transport in Proton Exchange Membrane Fuel Cells . . . V-146

V.G.2 Tech-Etch: Transport in Proton Exchange Membrane Fuel Cells . . . V-146

V.G.2 Ballard Material Products, Inc.: Transport in Proton Exchange Membrane Fuel Cells . . . V-146

VII.13 Acumentrics: Demonstration of SOFC Generator Fueled by Propane to Provide Electrical Power to Real World Applications . . . VII-59

Massachusetts (Continued)

VIII.8 Firexplo: Hydrogen Safety Panel and Hydrogen Safety Knowledge Tools VIII-43
IX.2 Ameresco, Inc.: Landfill Gas-to-Hydrogen IX-12

Michigan

IV.B.1 General Motors Company: Hydrogen Storage Engineering Center of Excellence IV-22
IV.B.1 Ford Motor Company: Hydrogen Storage Engineering Center of Excellence IV-22
IV.B.1 University of Michigan: Hydrogen Storage Engineering Center of Excellence IV-22
IV.B.6 General Motors Company: Thermal Management of Onboard Cryogenic Hydrogen Storage Systems IV-52
IV.B.7 Ford Motor Company: Ford/BASF-SE/UM Activities in Support of the Hydrogen Storage Engineering Center of Excellence. IV-56
IV.B.7 University of Michigan: Ford/BASF-SE/UM Activities in Support of the Hydrogen Storage Engineering Center of Excellence IV-56
IV.C.2 General Motors Company: Hydrogen Storage in Metal-Organic Frameworks IV-73
IV.D.1 Ford Motor Company: Design of Novel Multi-Component Metal Hydride-Based Mixtures for Hydrogen Storage IV-92
IV.F.3 Ford Motor Company: Synergistically Enhanced Materials and Design Parameters for Reducing the Cost of Hydrogen Storage Tanks IV-131
V.A.2 General Motors Company: Extended, Continuous Pt Nanostructures in Thick, Dispersed Electrodes V-15
V.A.7 Nissan Technical Center: Synthesis and Characterization of Mixed-Conducting Corrosion-Resistant Oxide Supports. V-46
V.A.8 Michigan State University: Development of Novel Non-PGM Electrocatalysts for Proton Exchange Membrane Fuel Cell Applications V-50
V.A.8 Nissan Technical Center: Development of Novel Non-PGM Electrocatalysts for Proton Exchange Membrane Fuel Cell Applications V-50
V.A.9 General Motors Company: High-Activity Dealloyed Catalysts V-56
V.C.1 General Motors Company: New Fuel Cell Membranes with Improved Durability and Performance V-83
V.C.2 Nissan Technical Center: Advanced Hybrid Membranes for Next Generation PEMFC Automotive Applications V-87
V.D.1 Michigan Technological University: High-Performance, Durable, Low-Cost Membrane Electrode Assemblies for Transportation Applications V-95
V.D.1 General Motors Company: High-Performance, Durable, Low-Cost Membrane Electrode Assemblies for Transportation Applications V-95
V.G.3 General Motors Company: Investigation of Micro- and Macro-Scale Transport Processes for Improved Fuel Cell Performance V-151
V.H.2 Kettering University: Roots Air Management System with Integrated Expander V-162
VIII.8 General Motors Company: Hydrogen Safety Panel and Hydrogen Safety Knowledge Tools VIII-43

Minnesota

II.B.4 3M Company: High-Performance, Long-Lifetime Catalysts for Proton Exchange Membrane Electrolysis II-28
V.A.1 3M Company: Durable Catalysts for Fuel Cell Protection during Transient Conditions V-9
V.A.3 3M Company: Nanosegregated Cathode Catalysts with Ultra-Low Platinum Loading. V-19
V.C.1 3M Company: New Fuel Cell Membranes with Improved Durability and Performance V-83
V.C.2 3M Company: Advanced Hybrid Membranes for Next Generation PEMFC Automotive Applications V-87
V.D.1 3M Company: High-Performance, Durable, Low-Cost Membrane Electrode Assemblies for Transportation Applications. V-95
V.G.1 3M Company: Fuel Cell Fundamentals at Low and Subzero Temperatures. V-140
V.L.1 3M Company: Advanced Ionomers and MEAs for Alkaline Membrane Fuel Cells V-211

Missouri

IV.C.4 University of Missouri: Multiply Surface-Functionalized Nanoporous Carbon for Vehicular Hydrogen Storage IV-86
VIII.8 Becht Engineering: Hydrogen Safety Panel and Hydrogen Safety Knowledge Tools VIII-43

Nebraska

III.3 Hexagon Lincoln: Development of High-Pressure Hydrogen Storage Tank for Storage and Gaseous Truck Delivery III-21
IV.B.1 Hexagon Lincoln: Hydrogen Storage Engineering Center of Excellence IV-22
IV.B.9 Hexagon Lincoln: Development of Improved Composite Pressure Vessels for Hydrogen Storage IV-65
IV.F.3 Hexagon Lincoln: Synergistically Enhanced Materials and Design Parameters for Reducing the Cost of Hydrogen Storage Tanks IV-131

Nevada

II.D.1 University of Nevada, Las Vegas: Semiconductor Materials for Photoelectrolysis II-48

New Jersey

IV.C.3 Rutgers University: Hydrogen Trapping through Designer Hydrogen Spillover Molecules with Reversible Temperature and Pressure-Induced Switching IV-79

New Mexico

IV.B.1 Los Alamos National Laboratory: Hydrogen Storage Engineering Center of Excellence IV-22
IV.B.4 Los Alamos National Laboratory: Chemical Hydride Rate Modeling, Validation, and System Demonstration IV-43
V.A.5 Los Alamos National Laboratory: The Science and Engineering of Durable Ultra-Low PGM Catalysts. V-30
V.A.5 University of New Mexico: The Science and Engineering of Durable Ultra-Low PGM Catalysts V-30
V.A.8 University of New Mexico: Development of Novel Non-PGM Electrocatalysts for Proton Exchange Membrane Fuel Cell Applications V-50
V.A.8 Pajarito Powder: Development of Novel Non-PGM Electrocatalysts for Proton Exchange Membrane Fuel Cell Applications V-50
V.A.8 Los Alamos National Laboratory: Development of Novel Non-PGM Electrocatalysts for Proton Exchange Membrane Fuel Cell Applications V-50
V.A.11 Los Alamos National Laboratory: Non-Precious Metal Fuel Cell Cathodes: Catalyst Development and Electrode Structure Design V-69
V.A.11 IRD Fuel Cells, LLC: Non-Precious Metal Fuel Cell Cathodes: Catalyst Development and Electrode Structure Design V-69
V.C.3 Los Alamos National Laboratory: Resonance-Stabilized Anion Exchange Polymer Electrolytes V-91
V.D.1 Los Alamos National Laboratory: High-Performance, Durable, Low-Cost Membrane Electrode Assemblies for Transportation Applications V-95
V.E.1 Los Alamos National Laboratory: Durability Improvements through Degradation Mechanism Studies V-105
V.E.2 Los Alamos National Laboratory: Accelerated Testing Validation. V-111
V.E.4 Los Alamos National Laboratory: Open-Source PEMFC-Performance and Durability Model Consideration of Membrane Properties on Cathode Degradation V-122
V.G.1 Los Alamos National Laboratory: Fuel Cell Fundamentals at Low and Subzero Temperatures V-140
V.J.1 Los Alamos National Laboratory: Advanced Materials and Concepts for Portable Power Fuel Cells V-201
VIII.3 Los Alamos National Laboratory: Hydrogen Safety, Codes and Standards: Sensors. VIII-16
VIII.5 Los Alamos National Laboratory: Hydrogen Fuel Quality VIII-28

New York

II.B.3 Brookhaven National Laboratory: Low-Noble-Metal-Content Catalysts/Electrodes for Hydrogen Production by Water Electrolysis . . . II-24

II.G.2 University of Rochester: Real-Time Atomistic Simulation of Light Harvesting and Charge Transport for Solar Hydrogen Production . . . II-89

II.G.8 Brookhaven National Laboratory: Heterogeneous Water Oxidation Catalysis With Molecular Catalysts . . . II-106

II.G.9 Brookhaven National Laboratory: Proton-Coupled Electron Transfer in Artificial Photosynthesis . . . II-108

III.2 Mohawk Innovative Technologies, Inc.: Oil-Free Centrifugal Hydrogen Compression Technology Demonstration . . . III-16

IV.E.2 Brookhaven National Laboratory: Aluminum Hydride: the Organo-Metallic Approach . . . IV-111

V.A.4 Brookhaven National Laboratory: Contiguous Platinum Monolayer Oxygen Reduction Electrocatalysts on High-Stability Low-Cost Supports . . . V-25

V.A.11 General Motors Company: Non-Precious Metal Fuel Cell Cathodes: Catalyst Development and Electrode Structure Design . . . V-69

V.A.11 University of Rochester: Non-Precious Metal Fuel Cell Cathodes: Catalyst Development and Electrode Structure Design . . . V-69

V.F.1 General Motors Company: Effect of System Contaminants on PEMFC Performance and Durability . . . V-128

V.G.3 Rochester Institute of Technology: Investigation of Micro- and Macro-Scale Transport Processes for Improved Fuel Cell Performance . . . V-151

V.G.3 University of Rochester: Investigation of Micro- and Macro-Scale Transport Processes for Improved Fuel Cell Performance . . . V-151

V.J.1 Brookhaven National Laboratory: Advanced Materials and Concepts for Portable Power Fuel Cells . . . V-201

VII.3 H2Pump LLC: Hydrogen Recycling System Evaluation and Data Collection . . . VII-18

VII.14 Plug Power Inc.: Accelerating Acceptance of Fuel Cell Backup Power Systems . . . VII-63

IX.4 Plug Power Inc.: Ground Support Equipment Demonstration . . . IX-20

Ohio

II.D.2 Midwest Optoelectronics, LLC: Critical Research for Cost-Effective Photoelectrochemical Production of Hydrogen . . . II-53

II.D.2 Xunlight Corporation: Critical Research for Cost-Effective Photoelectrochemical Production of Hydrogen . . . II-53

II.D.2 University of Toledo: Critical Research for Cost-Effective Photoelectrochemical Production of Hydrogen . . . II-53

V.I.6 Battelle: Stationary and Emerging Market Fuel Cell System Cost Analysis - Material Handling Equipment . . . V-193

VIII.8 Powdermet Inc.: Hydrogen Safety Panel and Hydrogen Safety Knowledge Tools . . . VIII-43

Oregon

IV.B.1 Oregon State University: Hydrogen Storage Engineering Center of Excellence . . . IV-22

IV.B.8 Oregon State University: Microscale Enhancement of Heat and Mass Transfer for Hydrogen Energy Storage . . . IV-61

VII.14 IdaTech, LLC: Accelerating Acceptance of Fuel Cell Backup Power Systems . . . VII-63

IX.1 ClearEdge Power: Fuel Cell Combined Heat and Power Commercial Demonstration . . . IX-7

Pennsylvania

II.C.2 Bucknell University: Solar Hydrogen Production with a Metal Oxide-Based Thermochemical Cycle . . . II-39

II.E.3 Pennsylvania State University: Fermentation and Electrohydrogenic Approaches to Hydrogen Production II-71

IV.C.3 Pennsylvania State University: Hydrogen Trapping through Designer Hydrogen Spillover Molecules with Reversible Temperature and Pressure-Induced Switching . . . IV-79

Pennsylvania (Continued)

V.A.3 University of Pittsburgh: Nanosegregated Cathode Catalysts with Ultra-Low Platinum Loading V-19
V.A.11 Carnegie Mellon University: Non-Precious Metal Fuel Cell Cathodes: Catalyst Development and Electrode Structure Design V-69
V.G.3 Pennsylvania State University: Investigation of Micro- and Macro-Scale Transport Processes for Improved Fuel Cell Performance V-151
VII.5 Air Products and Chemicals, Inc. : Validation of an Advanced High-Pressure PEM Electrolyzer and Composite Hydrogen Storage, with Data Reporting, for SunHydro Stations VII-26
VIII.8 Air Products and Chemicals, Inc.: Hydrogen Safety Panel and Hydrogen Safety Knowledge Tools VIII-43

Rhode Island

V.A.3 Brown University: Nanosegregated Cathode Catalysts with Ultra-Low Platinum Loading V-19

South Carolina

II.C.3 Savannah River National Laboratory: Electrolyzer Development for the HyS Thermochemical Cycle II-45
III.4 Savannah River National Laboratory: Fiber Reinforced Composite Pipeline III-24
IV.B.1 Savannah River National Laboratory: Hydrogen Storage Engineering Center of Excellence IV-22
IV.E.3 Savannah River National Laboratory: Electrochemical Reversible Formation of Alane IV-114
IV.F.5 Savannah River National Laboratory: Load-Sharing Polymeric Liner for Hydrogen Storage Composite Tanks IV-140
V.A.10 University of South Carolina: Development of Ultra-Low Platinum Alloy Cathode Catalysts for PEM Fuel Cells V-62
V.F.1 University of South Carolina: Effect of System Contaminants on PEMFC Performance and Durability V-128
V.G.2 University of South Carolina: Transport in Proton Exchange Membrane Fuel Cells V-146
V.H.1 Tetramer Technologies, LLC: New High-Performance Water Vapor Membranes To Improve Fuel Cell Balance-of-Plant Efficiency and Lower Costs (SBIR Phase II) V-158
IX.2 Advanced Technology International: Landfill Gas-to-Hydrogen IX-12

Tennessee

III.7 Oak Ridge National Laboratory: Vessel Design and Fabrication Technology for Stationary High-Pressure Hydrogen Storage III-39
IV.F.1 Oak Ridge National Laboratory: Melt Processable PAN Precursor for High-Strength, Low-Cost Carbon Fibers (Phase II) IV-118
IV.F.2 Oak Ridge National Laboratory: Development of Low-Cost, High-Strength Commercial Textile Precursor (PAN-MA) IV-124
IV.F.3 AOC, LLC: Synergistically Enhanced Materials and Design Parameters for Reducing the Cost of Hydrogen Storage Tanks IV-131
V.A.1 Oak Ridge National Laboratory: Durable Catalysts for Fuel Cell Protection during Transient Conditions V-9
V.A.2 Oak Ridge National Laboratory: Extended, Continuous Pt Nanostructures in Thick, Dispersed Electrodes V-15
V.A.3 Oak Ridge National Laboratory: Nanosegregated Cathode Catalysts with Ultra-Low Platinum Loading V-19
V.A.11 Oak Ridge National Laboratory: Non-Precious Metal Fuel Cell Cathodes: Catalyst Development and Electrode Structure Design V-69
V.C.1 Vanderbilt University: New Fuel Cell Membranes with Improved Durability and Performance V-83
V.E.1 Oak Ridge National Laboratory: Durability Improvements through Degradation Mechanism Studies V-105
V.E.2 Oak Ridge National Laboratory: Accelerated Testing Validation V-111
V.G.3 University of Tennessee: Investigation of Micro- and Macro-Scale Transport Processes for Improved Fuel Cell Performance V-151
V.I.3 Oak Ridge National Laboratory: Characterization of Fuel Cell Materials V-178

Tennessee (Continued)

VI.2 University of Tennessee: Manufacturing of Low-Cost, Durable Membrane Electrode Assemblies Engineered for Rapid Conditioning VI-11
X.1 Oak Ridge National Laboratory: Analysis of Optimal Onboard Storage Pressure for Hydrogen Fuel Cell Vehicles X-13
X.7 Oak Ridge National Laboratory: Hydrogen Station Economics and Business (HySEB)--Preliminary Results X-40

Texas

III.9 Texas A&M University: Development of a Centrifugal Hydrogen Pipeline Gas Compressor III-49
V.D.2 University of Texas at Austin: Rationally Designed Catalyst Layers for PEMFC Performance Optimization V-100
VIII.8 Air Liquide: Hydrogen Safety Panel and Hydrogen Safety Knowledge Tools VIII-43

Utah

III.7 MegaStir Technologies: Vessel Design and Fabrication Technology for Stationary High-Pressure Hydrogen Storage III-39

Virginia

II.A.1 Strategic Analysis, Inc.: Hydrogen Pathways Analysis for Polymer Electrolyte Membrane (PEM) Electrolysis II-11
IV.A.2 Strategic Analysis, Inc.: Hydrogen Storage Cost Analysis IV-17
IV.B.5 Strategic Analysis, Inc.: System Design, Analysis, Modeling, and Media Engineering Properties for Hydrogen Energy Storage IV-47
IV.F.1 Virginia Polytechnic Institute and State University: Melt Processable PAN Precursor for High-Strength, Low-Cost Carbon Fibers (Phase II) IV-118
IV.F.5 Virginia Polytechnic Institute and State University: Load-Sharing Polymeric Liner for Hydrogen Storage Composite Tanks IV-140
V.G.2 Virginia Polytechnic Institute and State University: Transport in Proton Exchange Membrane Fuel Cells V-146
V.I.2 Strategic Analysis, Inc.: Fuel Cell Transportation Cost Analysis V-173
V.I.7 Strategic Analysis, Inc.: A Total Cost of Ownership Model for PEM Fuel Cells in Combined Heat and Power and Backup Power Applications V-196
V.J.1 Virginia Polytechnic Institute and State University: Advanced Materials and Concepts for Portable Power Fuel Cells V-201
VIII.8 William C. Fort: Hydrogen Safety Panel and Hydrogen Safety Knowledge Tools VIII-43

Washington

III.7 Global Engineering and Technology: Vessel Design and Fabrication Technology for Stationary High-Pressure Hydrogen Storage III-39
III.10 Pacific Northwest National Laboratory: Investigation of H2 Diaphragm Compressors to Enable Low-Cost Long-Life Operation III-54
IV.B.1 Pacific Northwest National Laboratory: Hydrogen Storage Engineering Center of Excellence IV-22
IV.B.2 Pacific Northwest National Laboratory: Systems Engineering of Chemical Hydrogen Storage, Pressure Vessel, and Balance of Plant for Onboard Hydrogen Storage IV-30
IV.E.1 Pacific Northwest National Laboratory: Novel Carbon(C)-Boron(B)-Nitrogen(N)-Containing H2 Storage Materials IV-105
IV.F.3 Pacific Northwest National Laboratory: Synergistically Enhanced Materials and Design Parameters for Reducing the Cost of Hydrogen Storage Tanks IV-131

Washington (Continued)

V.K.1 InnovaTek, Inc.: Power Generation from an Integrated Biomass Reformer and Solid Oxide Fuel Cell (SBIR Phase III Xlerator Program) V-208
VI.3 Boeing Research and Technology: Development of Advanced Manufacturing Technologies for Low-Cost Hydrogen Storage Vessels VI-15
VI.3 Pacific Northwest National Laboratory: Development of Advanced Manufacturing Technologies for Low-Cost Hydrogen Storage Vessels VI-15
VIII.7 Pacific Northwest National Laboratory: Hydrogen Emergency Response Training for First Responders VIII-40
VIII.7 Hazardous Materials Management and Emergency Response Training and Eduction Center: Hydrogen Emergency Response Training for First Responders VIII-40
VIII.8 Pacific Northwest National Laboratory: Hydrogen Safety Panel and Hydrogen Safety Knowledge Tools VIII-43
IX.1 Pacific Northwest National Laboratory: Fuel Cell Combined Heat and Power Commercial Demonstration IX-7
IX.6 Pacific Northwest National Laboratory: Fuel Cell-Based Auxiliary Power Unit for Refrigerated Trucks IX-26

Washington, D.C.

V.A.9 George Washington University: High-Activity Dealloyed Catalysts V-56

Wisconsin

V.H.2 Eaton Corporation: Roots Air Management System with Integrated Expander V-162

Foreign Countries

Canada

IV.B.1 Université du Québec à Trois-Rivières: Hydrogen Storage Engineering Center of Excellence IV-22
V.A.1 Dalhousie University: Durable Catalysts for Fuel Cell Protection during Transient Conditions V-9
V.A.1 Automotive Fuel Cell Cooperation: Durable Catalysts for Fuel Cell Protection during Transient Conditions V-9
V.A.5 Ballard Fuel Cells: The Science and Engineering of Durable Ultra-Low PGM Catalysts V-30
V.A.11 University of Waterloo: Non-Precious Metal Fuel Cell Cathodes: Catalyst Development and Electrode Structure Design V-69
V.E.2 Ballard Power Systems: Accelerated Testing Validation V-111
V.E.4 Ballard Power Systems: Open-Source PEMFC-Performance and Durability Model Consideration of Membrane Properties on Cathode Degradation V-122
V.E.4 University of Calgary: Open-Source PEMFC-Performance and Durability Model Consideration of Membrane Properties on Cathode Degradation V-122
V.F.2 Ballard Power Systems: The Effect of Airborne Contaminants on Fuel Cell Performance and Durability V-133
V.G.1 McGill University: Fuel Cell Fundamentals at Low and Subzero Temperatures V-140
V.H.2 Ballard Power Systems: Roots Air Management System with Integrated Expander V-162
V.I.7 Ballard Power Systems: A Total Cost of Ownership Model for PEM Fuel Cells in Combined Heat and Power and Backup Power Applications V-196
VII.10 Hydrogenics Corporation: California State University Los Angeles Hydrogen Refueling Facility Performance Evaluation and Optimization VII-49
IX.5 Hydrogenics Corporation: Maritime Fuel Cell Generator Project IX-23

Germany

IV.B.7 BASF SE: Ford/BASF-SE/UM Activities in Support of the Hydrogen Storage Engineering Center of Excellence. . . . IV-56
IV.F.4 BMW: Thermomechanical Cycling of Thin-Liner High-Fiber-Fraction Cryogenic Pressure Vessels Rapidly Refueled a by LH2 pump to 700 bar IV-136
V.A.9 Technical University Berlin: High-Activity Dealloyed Catalysts V-56
V.J.1 SFC Energy: Advanced Materials and Concepts for Portable Power Fuel Cells V-201

Israel

V.L.1 CellEra, Inc.: Advanced Ionomers and MEAs for Alkaline Membrane Fuel Cells V-211

Japan

III.2 Mitsubishi Heavy Industries, Ltd: Oil-Free Centrifugal Hydrogen Compression Technology Demonstration III-16
III.7 Kobe Steel, LTD: Vessel Design and Fabrication Technology for Stationary High-Pressure Hydrogen Storage III-39

United Kingdom

V.A.9 Johnson Matthey Fuel Cells: High-Activity Dealloyed Catalysts V-56
V.D.2 Johnson Matthey Fuel Cells: Rationally Designed Catalyst Layers for PEMFC Performance Optimization. . . . V-100
V.J.1 Johnson Matthey Fuel Cells: Advanced Materials and Concepts for Portable Power Fuel Cells V-201

XVI. Project Listings by Organization

3M Company

II.B.4 High-Performance, Long-Lifetime Catalysts for Proton Exchange Membrane Electrolysis II-28
V.A.1 Durable Catalysts for Fuel Cell Protection during Transient Conditions V-9
V.A.3 Nanosegregated Cathode Catalysts with Ultra-Low Platinum Loading V-19
V.C.1 New Fuel Cell Membranes with Improved Durability and Performance V-83
V.C.2 Advanced Hybrid Membranes for Next Generation PEMFC Automotive Applications V-87
V.D.1 High-Performance, Durable, Low-Cost Membrane Electrode Assemblies for Transportation Applications V-95
V.G.1 Fuel Cell Fundamentals at Low and Subzero Temperatures V-140
V.L.1 Advanced Ionomers and MEAs for Alkaline Membrane Fuel Cells. V-211

Acumentrics

VII.13 Demonstration of SOFC Generator Fueled by Propane to Provide Electrical Power to Real World Applications VII-59

Addison Bain

VIII.8 Hydrogen Safety Panel and Hydrogen Safety Knowledge Tools. VIII-43

Advanced Technology International

IX.2 Landfill Gas-to-Hydrogen IX-12

Air Liquide

VIII.8 Hydrogen Safety Panel and Hydrogen Safety Knowledge Tools. VIII-43

Air Products and Chemicals, Inc.

VII.5 Validation of an Advanced High-Pressure PEM Electrolyzer and Composite Hydrogen Storage, with Data Reporting, for SunHydro Stations. VII-26
VIII.8 Hydrogen Safety Panel and Hydrogen Safety Knowledge Tools. VIII-43

Ameresco, Inc.

IX.2 Landfill Gas-to-Hydrogen IX-12

AOC, LLC

IV.F.3 Synergistically Enhanced Materials and Design Parameters for Reducing the Cost of Hydrogen Storage Tanks IV-131

Argonne National Laboratory

II.G.4 Fundamental Design and Mechanisms for Solar Hydrogen Production in Natural and Artificial Photosynthetic Systems II-94
III.1 Hydrogen Delivery Infrastructure Analysis III-11
IV.A.1 System Analysis of Physical and Materials-Based Hydrogen Storage Options IV-11
V.A.1 Durable Catalysts for Fuel Cell Protection during Transient Conditions V-9
V.A.3 Nanosegregated Cathode Catalysts with Ultra-Low Platinum Loading V-19
V.A.12 Non-PGM Cathode Catalysts using ZIF-Based Precursors with Nanonetwork Architecture V-74
V.D.1 High-Performance, Durable, Low-Cost Membrane Electrode Assemblies for Transportation Applications V-95

Argonne National Laboratory (Continued)

V.D.2 Rationally Designed Catalyst Layers for PEMFC Performance Optimization V-100
V.E.1 Durability Improvements through Degradation Mechanism Studies V-105
V.I.1 Performance of Advanced Automotive Fuel Cell Systems with Heat Rejection Constraints V-167
V.M.1 Best Practices and Benchmark Activities for ORR Measurements by the Rotating Disk Electrode Technique V-215
X.2 Employment Impacts of Infrastructure Development for Hydrogen and Fuel Cell Technologies X-19
X.4 Life-Cycle Analysis of Water Use for Hydrogen Production Pathways X-27
X.5 Impact of Fuel Cell System Peak Efficiency on Fuel Consumption and Cost X-30
X.6 Analysis of Incremental Fueling Pressure Cost X-36

Arizona State

II.G.5 Electrochemical Characterization of the Oxygen-Tolerant Soluble Hydrogenase I from Pyrococcus furiosus II-97
II.G.16 Artificial Hydrogenases: Utilization of Redox Non-Innocent Ligands in Iron Complexes for Hydrogen Production II-131

Automotive Fuel Cell Cooperation

V.A.1 Durable Catalysts for Fuel Cell Protection during Transient Conditions V-9

Ballard Fuel Cells

V.A.5 The Science and Engineering of Durable Ultra-Low PGM Catalysts V-30

Ballard Material Products, Inc.

V.G.2 Transport in Proton Exchange Membrane Fuel Cells V-146

Ballard Power Systems

V.E.2 Accelerated Testing Validation V-111
V.E.4 Open-Source PEMFC-Performance and Durability Model Consideration of Membrane Properties on Cathode Degradation V-122
V.F.2 The Effect of Airborne Contaminants on Fuel Cell Performance and Durability V-133
V.H.2 Roots Air Management System with Integrated Expander V-162
V.I.7 A Total Cost of Ownership Model for PEM Fuel Cells in Combined Heat and Power and Backup Power Applications V-196

BASF SE

IV.B.7 Ford/BASF-SE/UM Activities in Support of the Hydrogen Storage Engineering Center of Excellence IV-56

Battelle

V.I.6 Stationary and Emerging Market Fuel Cell System Cost Analysis - Material Handling Equipment V-193

Becht Engineering

VIII.8 Hydrogen Safety Panel and Hydrogen Safety Knowledge Tools VIII-43

Ben C. Gerwick Inc.

III.7 Vessel Design and Fabrication Technology for Stationary High-Pressure Hydrogen Storage III-39

BMW

IV.F.4 Thermomechanical Cycling of Thin-Liner High-Fiber-Fraction Cryogenic Pressure Vessels Rapidly Refueled a by LH2 pump to 700 bar IV-136

Boeing Research and Technology

VI.3 Development of Advanced Manufacturing Technologies for Low-Cost Hydrogen Storage Vessels VI-15

Boston College

IV.E.1 Novel Carbon(C)-Boron(B)-Nitrogen(N)-Containing H2 Storage Materials. IV-105

Brookhaven National Laboratory

II.B.3 Low-Noble-Metal-Content Catalysts/Electrodes for Hydrogen Production by Water Electrolysis II-24

II.G.8 Heterogeneous Water Oxidation Catalysis With Molecular Catalysts II-106

II.G.9 Proton-Coupled Electron Transfer in Artificial Photosynthesis II-108

IV.E.2 Aluminum Hydride: the Organo-Metallic Approach IV-111

V.A.4 Contiguous Platinum Monolayer Oxygen Reduction Electrocatalysts on High-Stability Low-Cost Supports V-25

V.J.1 Advanced Materials and Concepts for Portable Power Fuel Cells V-201

Brown University

V.A.3 Nanosegregated Cathode Catalysts with Ultra-Low Platinum Loading V-19

Bucknell University

II.C.2 Solar Hydrogen Production with a Metal Oxide-Based Thermochemical Cycle II-39

California Air Resources Board

VII.9 Data Collection and Validation of Newport Beach Hydrogen Station Performance VII-46

California Fuel Cell Partnership

VII.15 H2-FCEV Commercialization - Facilitating Collaboration, Obtaining Real World Expertise, and Developing New Analysis Tools VII-66

VIII.7 Hydrogen Emergency Response Training for First Responders VIII-40

California Institute of Technology

IV.B.1 Hydrogen Storage Engineering Center of Excellence IV-22

California State University, Los Angeles

VII.10 California State University Los Angeles Hydrogen Refueling Facility Performance Evaluation and Optimization. VII-49

Caltech

II.G.12 Joint Center for Artificial Photosynthesis: High Throughput Experimentation for Electrocatalyst and Photoabsorber Discovery II-119

II.G.17 Joint Center for Artificial Photosynthesis: Benchmarking Electrocatalysts for the Oxygen Evolution Reaction II-134

II.G.18 Joint Center for Artificial Photosynthesis: Si Microwire-Based Solar Water Splitting Devices II-137

Carnegie Mellon University

V.A.11 Non-Precious Metal Fuel Cell Cathodes: Catalyst Development and Electrode Structure Design V-69

CellEra, Inc.

V.L.1 Advanced Ionomers and MEAs for Alkaline Membrane Fuel Cells. V-211

City of Santa Fe Springs

VIII.8 Hydrogen Safety Panel and Hydrogen Safety Knowledge Tools. VIII-43

ClearEdge Power
IX.1 Fuel Cell Combined Heat and Power Commercial Demonstration IX-7

Colorado School of Mines
II.C.2 Solar Hydrogen Production with a Metal Oxide-Based Thermochemical Cycle II-39
V.A.2 Extended, Continuous Pt Nanostructures in Thick, Dispersed Electrodes. V-15
V.A.6 Tungsten Oxide and Heteropoly Acid-Based System for Ultra-High Activity and Stability of Pt Catalysts in Proton Exchange Membrane Fuel Cell Cathodes V-36
V.C.2 Advanced Hybrid Membranes for Next Generation PEMFC Automotive Applications V-87
V.F.1 Effect of System Contaminants on PEMFC Performance and Durability V-128
V.L.1 Advanced Ionomers and MEAs for Alkaline Membrane Fuel Cells. V-211

Concepts NREC
III.9 Development of a Centrifugal Hydrogen Pipeline Gas Compressor. III-49

Custom Sensor Solutions
VIII.3 Hydrogen Safety, Codes and Standards: Sensors VIII-16

Dalhousie University
V.A.1 Durable Catalysts for Fuel Cell Protection during Transient Conditions V-9

Delaware State University
IV.D.2 Hydrogen Storage Materials for Fuel Cell-Powered Vehicles IV-95

Eaton Corporation
V.H.2 Roots Air Management System with Integrated Expander. V-162

Electricore, Inc.
V.H.2 Roots Air Management System with Integrated Expander. V-162

Element One
VIII.9 NREL Hydrogen Sensor Testing Laboratory VIII-49

Firexplo
VIII.8 Hydrogen Safety Panel and Hydrogen Safety Knowledge Tools. VIII-43

Fluer, Inc.
VIII.8 Hydrogen Safety Panel and Hydrogen Safety Knowledge Tools. VIII-43

Ford Motor Company
IV.B.1 Hydrogen Storage Engineering Center of Excellence IV-22
IV.B.7 Ford/BASF-SE/UM Activities in Support of the Hydrogen Storage Engineering Center of Excellence. IV-56
IV.D.1 Design of Novel Multi-Component Metal Hydride-Based Mixtures for Hydrogen Storage IV-92
IV.F.3 Synergistically Enhanced Materials and Design Parameters for Reducing the Cost of Hydrogen Storage Tanks IV-131

FuelCell Energy, Inc.
II.F.1 Bio-Fueled Solid Oxide Fuel Cells. II-81
III.6 Electrochemical Hydrogen Compressor III-36

Gas Technology Institute
VII.11 Performance Evaluation of Delivered Hydrogen Fueling Stations VII-52
IX.2 Landfill Gas-to-Hydrogen IX-12

General Motors Company
IV.B.1 Hydrogen Storage Engineering Center of Excellence IV-22
IV.B.6 Thermal Management of Onboard Cryogenic Hydrogen Storage Systems IV-52
IV.C.2 Hydrogen Storage in Metal-Organic Frameworks. IV-73
V.A.2 Extended, Continuous Pt Nanostructures in Thick, Dispersed Electrodes. V-15
V.A.9 High-Activity Dealloyed Catalysts V-56
V.A.11 Non-Precious Metal Fuel Cell Cathodes: Catalyst Development and Electrode Structure Design V-69
V.C.1 New Fuel Cell Membranes with Improved Durability and Performance V-83
V.D.1 High-Performance, Durable, Low-Cost Membrane Electrode Assemblies for Transportation Applications V-95
V.F.1 Effect of System Contaminants on PEMFC Performance and Durability V-128
V.G.3 Investigation of Micro- and Macro-Scale Transport Processes for Improved Fuel Cell Performance. V-151
VIII.8 Hydrogen Safety Panel and Hydrogen Safety Knowledge Tools. VIII-43

George Washington University
V.A.9 High-Activity Dealloyed Catalysts V-56

Giner, Inc.
II.B.4 High-Performance, Long-Lifetime Catalysts for Proton Exchange Membrane Electrolysis II-28
V.B.1 Dimensionally Stable High Performance Membrane V-79
V.G.2 Transport in Proton Exchange Membrane Fuel Cells V-146

Global Engineering and Technology
III.7 Vessel Design and Fabrication Technology for Stationary High-Pressure Hydrogen Storage III-39

GWS Solutions of Tolland, LLC
VIII.8 Hydrogen Safety Panel and Hydrogen Safety Knowledge Tools. VIII-43

H2 Technology Consulting LLC
IV.C.1 Hydrogen Sorbent Measurement Qualification and Characterization IV-68

H2Pump LLC
VII.3 Hydrogen Recycling System Evaluation and Data Collection VII-18

Hawaii Natural Energy Institute
V.F.2 The Effect of Airborne Contaminants on Fuel Cell Performance and Durability V-133
IX.3 Hydrogen Energy Systems as a Grid Management Tool. IX-15

Hazardous Materials Management and Emergency Response Training and Eduction Center
VIII.7 Hydrogen Emergency Response Training for First Responders VIII-40

Hexagon Lincoln
III.3 Development of High-Pressure Hydrogen Storage Tank for Storage and Gaseous Truck Delivery III-21
IV.B.1 Hydrogen Storage Engineering Center of Excellence IV-22
IV.B.9 Development of Improved Composite Pressure Vessels for Hydrogen Storage IV-65

Hexagon Lincoln (Continued)

IV.F.3 Synergistically Enhanced Materials and Design Parameters for Reducing the Cost of Hydrogen Storage Tanks IV-131

Hydrogenics Corporation

VII.9 Data Collection and Validation of Newport Beach Hydrogen Station Performance VII-46

VII.10 California State University Los Angeles Hydrogen Refueling Facility Performance Evaluation and Optimization. VII-49

IX.5 Maritime Fuel Cell Generator Project IX-23

HyGen Industries

III.9 Development of a Centrifugal Hydrogen Pipeline Gas Compressor. III-49

IdaTech, LLC

VII.14 Accelerating Acceptance of Fuel Cell Backup Power Systems. VII-63

Illinois Institute of Technology

II.B.2 Economical Production of Hydrogen through Development of Novel, High-Efficiency Electrocatalysts for Alkaline Membrane Electrolysis II-21

V.A.7 Synthesis and Characterization of Mixed-Conducting Corrosion-Resistant Oxide Supports V-46

Indiana University Purdue University

V.D.2 Rationally Designed Catalyst Layers for PEMFC Performance Optimization. V-100

InnovaTek, Inc.

V.K.1 Power Generation from an Integrated Biomass Reformer and Solid Oxide Fuel Cell (SBIR Phase III Xlerator Program) V-208

Ion Power Inc.

V.E.1 Durability Improvements through Degradation Mechanism Studies V-105

V.E.2 Accelerated Testing Validation V-111

IRD Fuel Cells, LLC

V.A.11 Non-Precious Metal Fuel Cell Cathodes: Catalyst Development and Electrode Structure Design V-69

Jet Propulsion Laboratory

IV.B.1 Hydrogen Storage Engineering Center of Excellence IV-22

Johns Hopkins University

V.D.1 High-Performance, Durable, Low-Cost Membrane Electrode Assemblies for Transportation Applications V-95

Johnson Matthey Fuel Cells

V.A.9 High-Activity Dealloyed Catalysts V-56

V.D.2 Rationally Designed Catalyst Layers for PEMFC Performance Optimization. V-100

V.J.1 Advanced Materials and Concepts for Portable Power Fuel Cells V-201

Kettering University

V.H.2 Roots Air Management System with Integrated Expander. V-162

Kobe Steel, LTD

III.7 Vessel Design and Fabrication Technology for Stationary High-Pressure Hydrogen Storage III-39

Lawrence Berkeley National Laboratory

II.G.10 Joint Center for Artificial Photosynthesis: An Overview . . . II-111
II.G.11 Joint Center for Artificial Photosynthesis: Corrosion Protection Schemes to Enable Durable Solar Water Splitting Devices . . . II-115
II.G.20 Joint Center for Artificial Photosynthesis: Modeling and Simulation Team . . . II-144
IV.C.2 Hydrogen Storage in Metal-Organic Frameworks . . . IV-73
V.D.1 High-Performance, Durable, Low-Cost Membrane Electrode Assemblies for Transportation Applications . . . V-95
V.E.1 Durability Improvements through Degradation Mechanism Studies . . . V-105
V.E.2 Accelerated Testing Validation . . . V-111
V.G.1 Fuel Cell Fundamentals at Low and Subzero Temperatures . . . V-140
V.I.7 A Total Cost of Ownership Model for PEM Fuel Cells in Combined Heat and Power and Backup Power Applications . . . V-196

Lawrence Livermore National Laboratory

II.D.3 Characterization and Optimization of Photoelectrode Surfaces for Solar-to-Chemical Fuel Conversion . . . II-58
III.8 Preliminary Testing of LLNL/Linde 875-bar Liquid Hydrogen Pump . . . III-45
IV.F.4 Thermomechanical Cycling of Thin-Liner High-Fiber-Fraction Cryogenic Pressure Vessels Rapidly Refueled a by LH2 pump to 700 bar . . . IV-136
VIII.10 Hands-on Hydrogen Safety Training . . . VIII-54
VIII.3 Hydrogen Safety, Codes and Standards: Sensors . . . VIII-16

Linde LLC

III.8 Preliminary Testing of LLNL/Linde 875-bar Liquid Hydrogen Pump . . . III-45
IV.F.4 Thermomechanical Cycling of Thin-Liner High-Fiber-Fraction Cryogenic Pressure Vessels Rapidly Refueled a by LH2 pump to 700 bar . . . IV-136
VII.11 Performance Evaluation of Delivered Hydrogen Fueling Stations . . . VII-52

Los Alamos National Laboratory

IV.B.1 Hydrogen Storage Engineering Center of Excellence . . . IV-22
IV.B.4 Chemical Hydride Rate Modeling, Validation, and System Demonstration . . . IV-43
V.A.5 The Science and Engineering of Durable Ultra-Low PGM Catalysts . . . V-30
V.A.8 Development of Novel Non-PGM Electrocatalysts for Proton Exchange Membrane Fuel Cell Applications . . . V-50
V.A.11 Non-Precious Metal Fuel Cell Cathodes: Catalyst Development and Electrode Structure Design . . . V-69
V.C.3 Resonance-Stabilized Anion Exchange Polymer Electrolytes . . . V-91
V.D.1 High-Performance, Durable, Low-Cost Membrane Electrode Assemblies for Transportation Applications . . . V-95
V.E.1 Durability Improvements through Degradation Mechanism Studies . . . V-105
V.E.2 Accelerated Testing Validation . . . V-111
V.E.4 Open-Source PEMFC-Performance and Durability Model Consideration of Membrane Properties on Cathode Degradation . . . V-122
V.G.1 Fuel Cell Fundamentals at Low and Subzero Temperatures . . . V-140
V.J.1 Advanced Materials and Concepts for Portable Power Fuel Cells . . . V-201
VIII.3 Hydrogen Safety, Codes and Standards: Sensors . . . VIII-16
VIII.5 Hydrogen Fuel Quality . . . VIII-28

Mark Paster
IV.B.5 System Design, Analysis, Modeling, and Media Engineering Properties for Hydrogen Energy Storage IV-47

Massachusetts Institute of Technology
V.A.9 High-Activity Dealloyed Catalysts V-56

McGill University
V.G.1 Fuel Cell Fundamentals at Low and Subzero Temperatures V-140

MegaStir Technologies
III.7 Vessel Design and Fabrication Technology for Stationary High-Pressure Hydrogen Storage III-39

Michigan State University
V.A.8 Development of Novel Non-PGM Electrocatalysts for Proton Exchange Membrane Fuel Cell Applications V-50

Michigan Technological University
V.D.1 High-Performance, Durable, Low-Cost Membrane Electrode Assemblies for Transportation Applications V-95

Midwest Optoelectronics, LLC
II.D.2 Critical Research for Cost-Effective Photoelectrochemical Production of Hydrogen II-53

Mitsubishi Heavy Industries, Ltd
III.2 Oil-Free Centrifugal Hydrogen Compression Technology Demonstration. III-16

Mohawk Innovative Technologies, Inc.
III.2 Oil-Free Centrifugal Hydrogen Compression Technology Demonstration. III-16

National Institute of Standards and Technology
IV.C.2 Hydrogen Storage in Metal-Organic Frameworks. IV-73
IV.D.3 Neutron Characterization in Support of the DOE Hydrogen Storage Program IV-100
V.I.4 Neutron Imaging Study of the Water Transport in Operating Fuel Cells V-184

National Renewable Energy Laboratory
II.B.1 Renewable Electrolysis Integrated Systems Development and Testing II-17
II.B.4 High-Performance, Long-Lifetime Catalysts for Proton Exchange Membrane Electrolysis II-28
II.D.1 Semiconductor Materials for Photoelectrolysis II-48
II.D.2 Critical Research for Cost-Effective Photoelectrochemical Production of Hydrogen II-53
II.E.2 Biological Systems for Algal Hydrogen Photoproduction. II-67
II.E.3 Fermentation and Electrohydrogenic Approaches to Hydrogen Production. II-71
II.E.4 Probing O2-Tolerant CBS Hydrogenase for Hydrogen Production II-76
II.G.3 Oxidatively Stable Nanoporous Silicon Photocathodes for Photoelectrochemical Hydrogen Evolution II-92
II.G.7 Photobiohybrid Solar Fuels II-103
II.G.14 Photobiohybrid Solar Fuels – Nanoparticle-Hydrogenase Complexes II-125
III.11 700-Bar Hydrogen Dispenser Hose Reliability Improvement. III-58
IV.B.1 Hydrogen Storage Engineering Center of Excellence IV-22
IV.B.5 System Design, Analysis, Modeling, and Media Engineering Properties for Hydrogen Energy Storage IV-47
IV.C.1 Hydrogen Sorbent Measurement Qualification and Characterization IV-68

National Renewable Energy Laboratory (Continued)

V.A.2 Extended, Continuous Pt Nanostructures in Thick, Dispersed Electrodes . . . V-15
V.A.6 Tungsten Oxide and Heteropoly Acid-Based System for Ultra-High Activity and Stability of Pt Catalysts in Proton Exchange Membrane Fuel Cell Cathodes . . . V-36
V.C.2 Advanced Hybrid Membranes for Next Generation PEMFC Automotive Applications . . . V-87
V.E.3 Fuel Cell Technology Status—Cost and Price Status . . . V-118
V.F.1 Effect of System Contaminants on PEMFC Performance and Durability . . . V-128
V.I.5 Enlarging the Potential Market for Stationary Fuel Cells through System Design Optimization . . . V-190
V.L.1 Advanced Ionomers and MEAs for Alkaline Membrane Fuel Cells . . . V-211
V.M.1 Best Practices and Benchmark Activities for ORR Measurements by the Rotating Disk Electrode Technique . . . V-215
VI.1 Fuel Cell Membrane Electrode Assembly Manufacturing R&D . . . VI-7
VII.1 Technology Validation: Fuel Cell Bus Evaluations . . . VII-9
VII.2 Stationary Fuel Cell Evaluation . . . VII-14
VII.4 Hydrogen Component Validation . . . VII-22
VII.6 Forklift and Backup Power Data Collection and Analysis . . . VII-31
VII.7 Fuel Cell Electric Vehicle Evaluation . . . VII-37
VII.8 Next Generation Hydrogen Infrastructure Evaluation . . . VII-41
VIII.1 Fuel Cell Technologies National Codes and Standards Development and Outreach . . . VIII-9
VIII.2 Component Standard Research and Development . . . VIII-13
VIII.9 NREL Hydrogen Sensor Testing Laboratory . . . VIII-49
X.3 Pathway Analysis: Projected Cost, Life-Cycle Energy Use and Emissions of Future Hydrogen Technologies . . . X-22
X.9 Electricity Market Valuation for Hydrogen Technologies . . . X-46

Nissan Technical Center

V.A.7 Synthesis and Characterization of Mixed-Conducting Corrosion-Resistant Oxide Supports . . . V-46
V.A.8 Development of Novel Non-PGM Electrocatalysts for Proton Exchange Membrane Fuel Cell Applications . . . V-50
V.C.2 Advanced Hybrid Membranes for Next Generation PEMFC Automotive Applications . . . V-87

Northeastern University

V.A.8 Development of Novel Non-PGM Electrocatalysts for Proton Exchange Membrane Fuel Cell Applications . . . V-50
V.A.9 High-Activity Dealloyed Catalysts . . . V-56
II.G.19 Argonne-Northwestern Solar Energy Research (ANSER) Center . . . II-141
IV.D.1 Design of Novel Multi-Component Metal Hydride-Based Mixtures for Hydrogen Storage . . . IV-92

Oak Ridge National Laboratory

III.7 Vessel Design and Fabrication Technology for Stationary High-Pressure Hydrogen Storage . . . III-39
IV.F.1 Melt Processable PAN Precursor for High-Strength, Low-Cost Carbon Fibers (Phase II) . . . IV-118
IV.F.2 Development of Low-Cost, High-Strength Commercial Textile Precursor (PAN-MA) . . . IV-124
V.A.1 Durable Catalysts for Fuel Cell Protection during Transient Conditions . . . V-9
V.A.2 Extended, Continuous Pt Nanostructures in Thick, Dispersed Electrodes . . . V-15
V.A.3 Nanosegregated Cathode Catalysts with Ultra-Low Platinum Loading . . . V-19
V.A.11 Non-Precious Metal Fuel Cell Cathodes: Catalyst Development and Electrode Structure Design . . . V-69
V.E.1 Durability Improvements through Degradation Mechanism Studies . . . V-105

Oak Ridge National Laboratory (Continued)

V.E.2 Accelerated Testing Validation . . . V-111
V.I.3 Characterization of Fuel Cell Materials . . . V-178
X.1 Analysis of Optimal Onboard Storage Pressure for Hydrogen Fuel Cell Vehicles . . . X-13
X.7 Hydrogen Station Economics and Business (HySEB)--Preliminary Results . . . X-40

Oregon State University

IV.B.1 Hydrogen Storage Engineering Center of Excellence . . . IV-22
IV.B.8 Microscale Enhancement of Heat and Mass Transfer for Hydrogen Energy Storage . . . IV-61

Pacific Northwest National Laboratory

III.10 Investigation of H2 Diaphragm Compressors to Enable Low-Cost Long-Life Operation . . . III-54
IV.B.1 Hydrogen Storage Engineering Center of Excellence . . . IV-22
IV.B.2 Systems Engineering of Chemical Hydrogen Storage, Pressure Vessel, and Balance of Plant for Onboard Hydrogen Storage . . . IV-30
IV.E.1 Novel Carbon(C)-Boron(B)-Nitrogen(N)-Containing H2 Storage Materials . . . IV-105
IV.F.3 Synergistically Enhanced Materials and Design Parameters for Reducing the Cost of Hydrogen Storage Tanks . . . IV-131
VI.3 Development of Advanced Manufacturing Technologies for Low-Cost Hydrogen Storage Vessels . . . VI-15
VIII.7 Hydrogen Emergency Response Training for First Responders . . . VIII-40
VIII.8 Hydrogen Safety Panel and Hydrogen Safety Knowledge Tools . . . VIII-43
IX.1 Fuel Cell Combined Heat and Power Commercial Demonstration . . . IX-7
IX.6 Fuel Cell-Based Auxiliary Power Unit for Refrigerated Trucks . . . IX-26

Pajarito Powder

V.A.8 Development of Novel Non-PGM Electrocatalysts for Proton Exchange Membrane Fuel Cell Applications . . . V-50

Pennsylvania State University

II.E.3 Fermentation and Electrohydrogenic Approaches to Hydrogen Production . . . II-71
IV.C.3 Hydrogen Trapping through Designer Hydrogen Spillover Molecules with Reversible Temperature and Pressure-Induced Switching . . . IV-79
V.G.3 Investigation of Micro- and Macro-Scale Transport Processes for Improved Fuel Cell Performance . . . V-151

Plug Power Inc.

VII.14 Accelerating Acceptance of Fuel Cell Backup Power Systems . . . VII-63
IX.4 Ground Support Equipment Demonstration . . . IX-20

Powdermet Inc.

VIII.8 Hydrogen Safety Panel and Hydrogen Safety Knowledge Tools . . . VIII-43

Proton OnSite

II.B.2 Economical Production of Hydrogen through Development of Novel, High-Efficiency Electrocatalysts for Alkaline Membrane Electrolysis . . . II-21
II.B.3 Low-Noble-Metal-Content Catalysts/Electrodes for Hydrogen Production by Water Electrolysis . . . II-24
VII.5 Validation of an Advanced High-Pressure PEM Electrolyzer and Composite Hydrogen Storage, with Data Reporting, for SunHydro Stations . . . VII-26
VIII.8 Hydrogen Safety Panel and Hydrogen Safety Knowledge Tools . . . VIII-43

Protonex Technology Corporation

IV.E.1 Novel Carbon(C)-Boron(B)-Nitrogen(N)-Containing H2 Storage Materials IV-105

Quantum Fuel Systems Technologies Worldwide, Inc.

VI.3 Development of Advanced Manufacturing Technologies for Low-Cost Hydrogen Storage Vessels VI-15

RCF Economic and Financial Consulting, Inc.

X.2 Employment Impacts of Infrastructure Development for Hydrogen and Fuel Cell Technologies X-19

Rochester Institute of Technology

V.G.3 Investigation of Micro- and Macro-Scale Transport Processes for Improved Fuel Cell Performance V-151

Rutgers University

IV.C.3 Hydrogen Trapping through Designer Hydrogen Spillover Molecules with Reversible Temperature and Pressure-Induced Switching IV-79

Sacramento Municipal Utility District

II.F.1 Bio-Fueled Solid Oxide Fuel Cells II-81

Sandia National Laboratories

II.C.2 Solar Hydrogen Production with a Metal Oxide-Based Thermochemical Cycle II-39

III.5 Hydrogen Embrittlement of Structural Steels III-31

VII.12 Hydrogen Fueling Infrastructure Research and Station Technology VII-57

VIII.4 R&D for Safety, Codes and Standards: Materials and Components Compatibility VIII-23

VIII.6 R&D for Safety Codes and Standards: Hydrogen Release Behavior and Risk Assessment VIII-34

IX.5 Maritime Fuel Cell Generator Project IX-23

Savannah River National Laboratory

II.C.3 Electrolyzer Development for the HyS Thermochemical Cycle II-45

III.4 Fiber Reinforced Composite Pipeline III-24

IV.B.1 Hydrogen Storage Engineering Center of Excellence IV-22

IV.E.3 Electrochemical Reversible Formation of Alane IV-114

IV.F.5 Load-Sharing Polymeric Liner for Hydrogen Storage Composite Tanks IV-140

SFC Energy

V.J.1 Advanced Materials and Concepts for Portable Power Fuel Cells V-201

Spectrum Automation Controls

II.B.1 Renewable Electrolysis Integrated Systems Development and Testing II-17

III.11 700-Bar Hydrogen Dispenser Hose Reliability Improvement III-58

VII.4 Hydrogen Component Validation VII-22

Spencer Composites Corporation

IV.F.4 Thermomechanical Cycling of Thin-Liner High-Fiber-Fraction Cryogenic Pressure Vessels Rapidly Refueled a by LH2 pump to 700 bar IV-136

Stanford University

II.G.15 Center on Nanostructuring for Efficient Energy Conversion (CNEEC) II-128

Strategic Analysis, Inc.

II.A.1 Hydrogen Pathways Analysis for Polymer Electrolyte Membrane (PEM) Electrolysis II-11
IV.A.2 Hydrogen Storage Cost Analysis IV-17
IV.B.5 System Design, Analysis, Modeling, and Media Engineering Properties for Hydrogen Energy Storage IV-47
V.I.2 Fuel Cell Transportation Cost Analysis V-173
V.I.7 A Total Cost of Ownership Model for PEM Fuel Cells in Combined Heat and Power and Backup Power Applications V-196

SunHydro LLC

VII.5 Validation of an Advanced High-Pressure PEM Electrolyzer and Composite Hydrogen Storage, with Data Reporting, for SunHydro Stations VII-26

Sustainable Innovations, LLC

III.6 Electrochemical Hydrogen Compressor III-36

TDA Research

II.F.1 Bio-Fueled Solid Oxide Fuel Cells. II-81

Tech-Etch

V.G.2 Transport in Proton Exchange Membrane Fuel Cells V-146

Technical University Berlin

V.A.9 High-Activity Dealloyed Catalysts V-56

Tetramer Technologies, LLC

V.H.1 New High-Performance Water Vapor Membranes To Improve Fuel Cell Balance-of-Plant Efficiency and Lower Costs (SBIR Phase II). V-158

Texas A&M University

III.9 Development of a Centrifugal Hydrogen Pipeline Gas Compressor III-49

Toray Composites America

IV.F.3 Synergistically Enhanced Materials and Design Parameters for Reducing the Cost of Hydrogen Storage Tanks IV-131

United Technologies Research Center

IV.B.1 Hydrogen Storage Engineering Center of Excellence IV-22
IV.B.3 Advancement of Systems Designs and Key Engineering Technologies for Materials-Based Hydrogen Storage IV-36
V.D.2 Rationally Designed Catalyst Layers for PEMFC Performance Optimization. V-100
V.G.1 Fuel Cell Fundamentals at Low and Subzero Temperatures V-140

Université du Québec à Trois-Rivières

IV.B.1 Hydrogen Storage Engineering Center of Excellence IV-22

University of Alabama

IV.E.1 Novel Carbon(C)-Boron(B)-Nitrogen(N)-Containing H2 Storage Materials. IV-105

University of Arizona

II.G.1 Semiconductor Nanorod/Metal(Metal Oxide) Hybrid Materials: Characterization of Frontier Orbital Energies and Charge Injection Processes Using Unique Combinations of Photoemission Spectroscopies and Waveguide Spectroelectrochemistries II-85

II.G.13 Center for Interface Science: Solar-Electric Materials (CISSEM) II-123

University of Calgary

V.E.4 Open-Source PEMFC-Performance and Durability Model Consideration of Membrane Properties on Cathode Degradation V-122

University of California, Berkeley

II.E.1 Maximizing Light Utilization Efficiency and Hydrogen Production in Microalgal Cultures II-63

V.I.7 A Total Cost of Ownership Model for PEM Fuel Cells in Combined Heat and Power and Backup Power Applications V-196

University of California, Irvine

V.I.5 Enlarging the Potential Market for Stationary Fuel Cells through System Design Optimization V-190

X.8 Tri-Generation Fuel Cell Technologies for Location-Specific Applications X-44

University of California, Los Angeles

IV.D.1 Design of Novel Multi-Component Metal Hydride-Based Mixtures for Hydrogen Storage IV-92

University of Colorado, Boulder

II.C.1 Solar-Thermal Redox-Based Water Splitting Cycles II-33

II.C.2 Solar Hydrogen Production with a Metal Oxide-Based Thermochemical Cycle II-39

V.A.6 Tungsten Oxide and Heteropoly Acid-Based System for Ultra-High Activity and Stability of Pt Catalysts in Proton Exchange Membrane Fuel Cell Cathodes V-36

University of Connecticut

V.F.2 The Effect of Airborne Contaminants on Fuel Cell Performance and Durability V-133

University of Delaware

IV.D.2 Hydrogen Storage Materials for Fuel Cell-Powered Vehicles IV-95

V.A.2 Extended, Continuous Pt Nanostructures in Thick, Dispersed Electrodes V-15

V.A.5 The Science and Engineering of Durable Ultra-Low PGM Catalysts V-30

V.J.1 Advanced Materials and Concepts for Portable Power Fuel Cells V-201

VI.2 Manufacturing of Low-Cost, Durable Membrane Electrode Assemblies Engineered for Rapid Conditioning VI-11

University of Georgia

II.G.6 Hyperthermophilic Multiprotein Complexes and Pathways for Energy Conservation and Catalysis II-100

University of Michigan

IV.B.1 Hydrogen Storage Engineering Center of Excellence IV-22

IV.B.7 Ford/BASF-SE/UM Activities in Support of the Hydrogen Storage Engineering Center of Excellence IV-56

University of Missouri

IV.C.4 Multiply Surface-Functionalized Nanoporous Carbon for Vehicular Hydrogen Storage IV-86

University of Nevada, Las Vegas

II.D.1 Semiconductor Materials for Photoelectrolysis II-48

University of New Mexico

V.A.5 The Science and Engineering of Durable Ultra-Low PGM Catalysts. V-30

V.A.8 Development of Novel Non-PGM Electrocatalysts for Proton Exchange Membrane Fuel Cell Applications V-50

University of Pittsburgh

V.A.3 Nanosegregated Cathode Catalysts with Ultra-Low Platinum Loading V-19

University of Rochester

II.G.2 Real-Time Atomistic Simulation of Light Harvesting and Charge Transport for Solar Hydrogen Production II-89

V.A.11 Non-Precious Metal Fuel Cell Cathodes: Catalyst Development and Electrode Structure Design V-69

V.G.3 Investigation of Micro- and Macro-Scale Transport Processes for Improved Fuel Cell Performance. V-151

University of South Carolina

V.A.10 Development of Ultra-Low Platinum Alloy Cathode Catalysts for PEM Fuel Cells V-62

V.F.1 Effect of System Contaminants on PEMFC Performance and Durability V-128

V.G.2 Transport in Proton Exchange Membrane Fuel Cells V-146

University of Tennessee

V.G.3 Investigation of Micro- and Macro-Scale Transport Processes for Improved Fuel Cell Performance. V-151

VI.2 Manufacturing of Low-Cost, Durable Membrane Electrode Assemblies Engineered for Rapid Conditioning. VI-11

University of Texas at Austin

V.D.2 Rationally Designed Catalyst Layers for PEMFC Performance Optimization. V-100

University of Toledo

II.D.2 Critical Research for Cost-Effective Photoelectrochemical Production of Hydrogen II-53

University of Waterloo

V.A.11 Non-Precious Metal Fuel Cell Cathodes: Catalyst Development and Electrode Structure Design V-69

UTC Power

VI.2 Manufacturing of Low-Cost, Durable Membrane Electrode Assemblies Engineered for Rapid Conditioning VI-11

Vanderbilt University

V.C.1 New Fuel Cell Membranes with Improved Durability and Performance V-83

Virginia Polytechnic Institute and State University

IV.F.1 Melt Processable PAN Precursor for High-Strength, Low-Cost Carbon Fibers (Phase II) IV-118

IV.F.5 Load-Sharing Polymeric Liner for Hydrogen Storage Composite Tanks IV-140

V.G.2 Transport in Proton Exchange Membrane Fuel Cells V-146

V.J.1 Advanced Materials and Concepts for Portable Power Fuel Cells V-201

W. L. Gore & Associates, Inc.

VI.2 Manufacturing of Low-Cost, Durable Membrane Electrode Assemblies Engineered for Rapid Conditioning. VI-11

William C. Fort

VIII.8 Hydrogen Safety Panel and Hydrogen Safety Knowledge Tools. VIII-43

WPCSOL, LLC

V.F.2 The Effect of Airborne Contaminants on Fuel Cell Performance and Durability V-133

Xunlight Corporation

II.D.2 Critical Research for Cost-Effective Photoelectrochemical Production of Hydrogen II-53

U.S. DEPARTMENT OF
ENERGY

www.hydrogen.energy.gov